

# ORGANOMETALLICS

Volume 14, Number 8, August 1995

© Copyright 1995  
American Chemical Society

## Communications

### Synthesis, Structure, and Reactivity of the Iridium Hydrazido-Bridged Complex



Cesar H. Zambrano, Paul R. Sharp,\* and Charles L. Barnes

Department of Chemistry, University of Missouri—Columbia, Columbia, Missouri 65211

Received April 20, 1995<sup>®</sup>

**Summary:** The hydrazido-bridged iridium complex  $\text{Cp}^*\text{Ir}(\mu\text{-C}_6\text{H}_4\text{N-NC}_6\text{H}_4)\text{IrCp}^*$  (**1**;  $\text{Cp}^* = \text{C}_5\text{Me}_5$ ) reacts with  $\text{H}_2$  under pressure with oxidation of the N—N bond to give  $\text{Cp}^*\text{IrH}(\mu\text{-C}_6\text{H}_4\text{N=NC}_6\text{H}_4)\text{HrCp}^*$  (**3**) in its *cis* and *trans* forms. In the absence of hydrogen, **3** is converted back to **1** with reduction of the N=N bond. Complex **3** reacts with  $\text{CCl}_3\text{Br}$  to give only the *cis* isomer of  $\text{Cp}^*\text{IrBr}(\mu\text{-C}_6\text{H}_4\text{N=NC}_6\text{H}_4)\text{BrIrCp}^*$  (**4**). Complex **4** is also prepared by reaction of **1** with  $\text{HBr}$  or  $\text{Br}_2$ .

While there have been many reports involving the preparation and chemistry of early-transition-metal hydrazido complexes,<sup>1</sup> late-transition-metal derivatives (groups 9–11) are very scarce.<sup>2,3</sup> This paucity of late-metal hydrazido complexes, as well as the potentially rich chemistry that may be expected in these systems, prompted these investigations.<sup>3c</sup> Here, we report the

synthesis, structure, and reactivity of the hydrazido-bridged iridium complex  $\text{Cp}^*\text{Ir}(\mu\text{-C}_6\text{H}_4\text{N-NC}_6\text{H}_4)\text{IrCp}^*$  (**1**;  $\text{Cp}^* = \text{C}_5\text{Me}_5$ ) in which the hydrazido link contains two ortho-metallated phenyl rings.

Three different routes were found for the synthesis of **1** (Scheme 1). The reaction of the lithium salt  $\text{PhNHNLiPh}$  or  $\text{PhNLiNLiPh}$  with  $(\text{Cp}^*\text{IrCl}_2)_2$  gives low yields of **1**<sup>4</sup> along with a second product,  $\text{Cp}^*(\text{Cl})\text{Ir}(\eta^2\text{-C}_6\text{H}_4\text{N=NPh})$  (**2**).<sup>5</sup> Better yields are obtained when 1,2-diphenylhydrazine is reacted with iridium complexes bearing basic ligands. Whereas the reaction of  $\text{PhNHNHPh}$  with  $\text{Cp}^*\text{IrN}(t\text{-Bu})$ <sup>6</sup> gives **1** in moderate

(3) (a) Ramamoorthy, V.; Wu, Z.; Yang, Y.; Sharp, P. R. *J. Am. Chem. Soc.* **1992**, *114*, 1526. (b) Sharp, P. R.; Yang, Y.; Wu, Z.; Ramamoorthy, V. In *The Chemistry of the Copper and Zinc Triads*; Welch, A. J., Chapman, S. K., Eds.; The Royal Society of Chemistry: Cambridge, England, 1993; p 198. (c) Zambrano, C. H.; Barnes, C. L.; Sharp, P. R. Presented at the 205th National Meeting of the American Chemical Society, Denver, CO, April 1993, INOR 413, and 29th Midwest Regional Meeting of the American Chemical Society, Kansas City, KS, Nov 1994, INOR 130.

(4) Data for **1** are as follows. <sup>1</sup>H NMR ( $\text{C}_6\text{D}_6$ , 22 °C,  $\delta$  in ppm; aryl ring assignments were made with respect to the ipso C attached to N): 1.46 ( $\text{C}_5\text{Me}_5$ ), 8.47 (dd, 2 *m*-H, <sup>1</sup>J<sub>HH</sub> = 7.4 Hz, <sup>2</sup>J<sub>HH</sub> = 1.5 Hz), 8.16 (dd, 2 *o*-H, <sup>1</sup>J<sub>HH</sub> = 7.4 Hz, <sup>2</sup>J<sub>HH</sub> = 1.6 Hz), 7.17–7.28 (m, 4 *m*- and *p*-H). <sup>13</sup>C{<sup>1</sup>H} NMR ( $\text{C}_6\text{D}_6$ , 22 °C,  $\delta$  in ppm): 10.6 ( $\text{C}_5\text{Me}_5$ ), 88.3 ( $\text{C}_5\text{Me}_5$ ), 164.3, 158.8, 136.4, 124.4, 121.3, 120.2 (Ir— $\text{C}_6\text{H}_4\text{N}$ ). UV-vis (35 °C, toluene):  $\lambda(\text{max})$  600 nm ( $\epsilon = 1.17 \times 10^4 \text{ M}^{-1} \text{ cm}^{-1}$ ),  $\lambda$  672 nm ( $\epsilon = 1.10 \times 10^4 \text{ M}^{-1} \text{ cm}^{-1}$ ),  $\lambda$  432 nm ( $\epsilon = 9.34 \times 10^3 \text{ M}^{-1} \text{ cm}^{-1}$ ). Anal. Calcd for  $\text{Ir}_2\text{C}_{32}\text{H}_{38}\text{N}_2$ : C, 46.02; H, 4.59; N, 3.35. Found: C, 45.83; H, 4.64; N, 3.31.

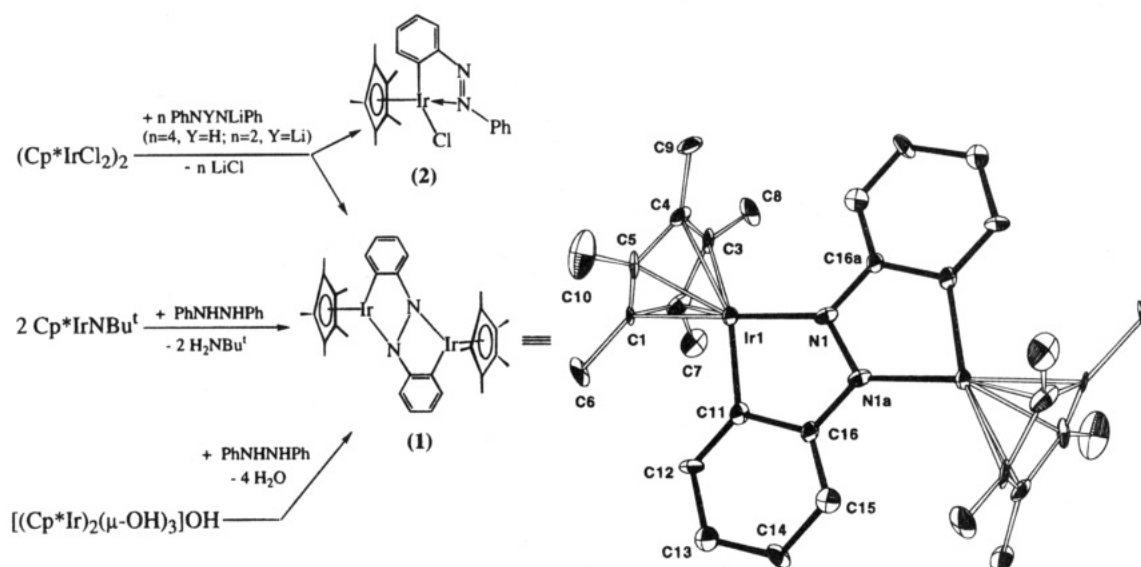
(5) See the supporting information.

<sup>®</sup> Abstract published in *Advance ACS Abstracts*, July 15, 1995.

(1) (a) Pelikan, P.; Boca, R. *Coord. Chem. Rev.* **1984**, *55*, 55. (b) Leigh, G. J. *Acc. Chem. Res.* **1992**, *25*, 177. (c) Dilworth, J. R.; Richards, R. L. In *Comprehensive Organometallic Chemistry*; Wilkinson, G., Stone, F. G. A., Abel, E. W., Eds.; Pergamon: Oxford, England, 1982; Chapter 60. (d) George, T. A.; Kaul, B. B.; Chen, Q.; Zubieta, J. *Inorg. Chem.* **1993**, *32*, 1706. (e) Vale, M. G.; Schrock, R. R. *Organometallics* **1993**, *12*, 1140 and references listed therein.

(2) (a) Ashley-Smith, J.; Green, M.; Mayne, N.; Stone, F. G. A. *J. Chem. Soc., Chem. Commun.* **1969**, 409. (b) Hussein, F. M.; Kasenally, A. S. *J. Chem. Soc., Chem. Commun.* **1972**, 3. (c) Ashley-Smith, J.; Green, M.; Stone, F. G. A. *J. Chem. Soc., Dalton Trans.* **1972**, 1805.

Scheme 1



yields, the reaction with  $[(\text{Cp}^*\text{Ir})_2(\mu\text{-OH})_3]\text{OH}^7$  produces **1** in yields greater than 90%.

Crystals of air-sensitive **1** were grown from hexane-layered THF solutions at  $-20^\circ\text{C}$ . An ORTEP view of **1** (hydrogen atoms omitted) is shown in Scheme 1.<sup>8</sup> The overall structure consists of two  $\text{Cp}^*\text{Ir}$  fragments bridged by a single 1,2-diphenylhydrazido ligand in which each aryl ring is ortho-metalated to each iridium atom. This binding mode of the hydrazido ligand results in the formation of one edge-shared (N–N) diaza metallacycle ring per metal atom. An important structural feature of this molecule is the N–N distance (1.419 Å, averaged), which falls well in the range observed for N–N single bonds.<sup>3a,9</sup> Also of importance are the bond angles around each of the nitrogen atoms, which add up to  $360^\circ$ . Since this structural feature invokes trigonal-planar nitrogen atoms, some degree of metal–ligand,  $d\pi\text{-}p\pi$  interaction can be conceived. Nevertheless, the iridium–nitrogen bond distances (1.96 Å, averaged) are not short compared with other Ir–N amido bonds.<sup>10</sup> The apparent lack of Ir–N ( $d\pi\text{-}p\pi$ ) interactions result in

16-electron, Ir(III) metal centers bound to nitrogen atoms which may show highly basic properties.<sup>11</sup> Because of the nucleophilic character of these atoms, an enhanced reactivity is expected. Unfortunately, reactions of **1** with electrophiles such as  $\text{CH}_3\text{I}$ ,  $\text{CH}_3\text{O}_3\text{SCF}_3$ , and  $\text{PhCH}_2\text{Cl}$  have only led to intractable products.

Compound **1** reacts with hydrogen under pressure (greater than 200 psi) to give a single product which is formulated as the iridium–hydride derivative  $\text{Cp}^*\text{IrH}(\mu\text{-C}_6\text{H}_4\text{N}=\text{NC}_6\text{H}_4)\text{HrCp}^*$  (**3**), present in two isomeric forms, *cis* and *trans* (Scheme 2).<sup>12</sup>  $^1\text{H}$  NMR ( $\text{C}_6\text{D}_6$ ) spectra show two sharp signals at  $-15.05$  and  $-15.92$  ppm, consistent with the presence of iridium hydrides. The integral ratio of these peaks is 0.6:1.0, suggesting that one conformational isomer is dominant. Two distinct  $\text{Cp}^*$  signals and two sets of aromatic peaks, one for each isomer, are also found in approximate ratios of 0.6:1.0. Assignment of a particular NMR resonance to either the *cis* or *trans* isomer was not possible, and spin saturation transfer as well as 2D-NOE experiments showed no appreciable isomeric exchange at 300 K.

(6) Gluek, D. S.; Wu, J.; Hollander, F. J.; Bergman, R. G. *J. Am. Chem. Soc.* **1991**, *113*, 2041.

(7) Bailey, P. M.; Maitlis, P. M. *J. Chem. Soc., Dalton Trans.* **1981**, 1997.

(8) Crystal data for **1**:  $\text{IrC}_{16}\text{H}_{19}\text{N}_4(\text{C}_{24}\text{H}_{24}\text{N}_4)$ , monoclinic, with  $a = 16.774(5)$  Å,  $b = 13.916(3)$  Å,  $c = 22.343(6)$  Å,  $\beta = 110.415(11)^\circ$ , and  $V = 4887.9(22)$  Å<sup>3</sup> for  $Z = 8$ , and  $M_r = 786.03$ ,  $d(\text{calcd}) = 1.630$  g/cm<sup>3</sup>. Data collection was done with an Enraf-Nonius CAD-4 diffractometer using Mo  $K\alpha$  radiation. Two independent molecules of **1**, located on inversion centers, were found in the unit cell. Additionally, two molecules of PhNHNHPh of crystallization were found per dimer. The space group was  $P2_1/c$ . Of 7066 measured reflections, 6797 were unique and 5706 had  $I > 2.0\sigma(I)$ . The structure was solved by direct methods. The last least-squares cycle gave  $R = 0.056$  and  $R_w = 0.094$  with  $(\Delta/\sigma)_{\text{max}} = 0.004$ . Selected bond distances (Å) and angles (deg) for **1** are as follows. Molecule 1 (ORTEP shown in Scheme 1): Ir(1)–C(3), 2.150(12); –C(4), 2.194(11); –C(5), 2.166(13); –C(11), 2.020(13); –N(1), 1.956(11); N(1)–N(1a), 1.402(19); N(1)–Ir(1)–C(11), 78.5(5); Ir(1)–N(1)–C(16a), 129.2(8); –N(1a), 121.5(8); C(16a)–N(1)–N(1a), 109.2(10). Molecule 2: Ir(2)–C(21), 2.189(14); –C(22), 2.189(12); –C(25), 2.142(12); –C(31), 2.037(12); –N(2), 1.961(11); N(2)–N(2b), 1.436(21); Ir(2)–N(2)–C(36b), 131.6(9); –N(2b), 120.5(9); C(36b)–N(2)–N(2b), 107.8(10) (a and b correspond to atoms across the inversion centers in molecule 1 and molecule 2, respectively).

(9) (a) Zambrano, C. H.; Fanwick, P. E.; Rothwell, I. P. *Organometallics* **1994**, *13*, 1174. (b) Schrock, R. R.; Glassman, T. E.; Vale, M. G.; Kol, M. *J. Am. Chem. Soc.* **1993**, *115*, 1760. (c) Matsumoto, K.; Hoshino, C.; Kawano, M. *Inorg. Chem.* **1992**, *31*, 5158.

(10) (a) Rahim, M.; White, C.; Rheingold, A. L.; Ahmed, K. J. *Organometallics* **1993**, *12*, 2401. (b) Dobbs, D. A.; Bergman, R. G. *J. Am. Chem. Soc.* **1993**, *115*, 3836. (c) Kolel-Veetil, M. K.; Rahim, M.; Edwards, A. J.; Rheingold, A. L.; Ahmed, K. J. *Inorg. Chem.* **1992**, *31*, 3877. (d) Finke, R. G.; Lyon, D. K.; Noyima, K.; Sur, S.; Mizuno, N. *Inorg. Chem.* **1990**, *29*, 1787. (e) Fryzuk, M. D.; Li, H.; McManus, N. T.; Paglia, P.; Rettig, S. J.; White, G. S. *Organometallics* **1992**, *11*, 2979. (f) Villanueva, L. A.; Abboud, K. A.; Boncella, J. A. *Organometallics* **1994**, *13*, 3921 and references cited therein.

(11) The trigonal-planar geometry of the nitrogens may be explained in terms of a delocalization of the lone pair over the ortho-metalated phenyl rings.<sup>10f</sup>

(12) Data for **3** are as follows.  $^1\text{H}$  NMR ( $\text{C}_6\text{D}_6$ ,  $27^\circ\text{C}$ ,  $\delta$  in ppm; aryl ring assignments were made with respect to the ipso C attached to N): most abundant isomer, 1.73 (s,  $\text{C}_5\text{Me}_5$ ),  $-15.92$  (s, IrH), 8.67 (m, 2 *m*-H), 8.25 (m, 2 *o*-H), 7.27 (m, 4 *m*- and *p*-H); less abundant isomer, 1.77 (s,  $\text{C}_5\text{Me}_5$ ),  $-15.05$  (s, IrH), 8.53 (m, 2 *m*-H), 8.20 (m, 2 *o*-H), 7.18 (m, 4 *m*- and *p*-H).  $^{13}\text{C}\{^1\text{H}\}$  NMR ( $\text{C}_6\text{D}_6$ ,  $27^\circ\text{C}$ ,  $\delta$  in ppm): most abundant isomer, 10.41 ( $\text{C}_5\text{Me}_5$ ), 93.1 ( $\text{C}_5\text{Me}_5$ ), 158.7, 162.9, 134.8, 129.2, 120.4 (Ir– $\text{C}_6\text{H}_4\text{N}$ ); less abundant isomer, 10.37 ( $\text{C}_5\text{Me}_5$ ), 92.3 ( $\text{C}_5\text{Me}_5$ ), 160.0, 162.3, 135.3, 129.3, 120.6 (Ir– $\text{C}_6\text{H}_4\text{N}$ ). IR (Nujol mull on NaCl plates):  $\nu(\text{Ir}–\text{H})$  2074 (m, br)  $\text{cm}^{-1}$ ; others, 1442 (s), 1305 (s), 1277 (s), 1230 (s), 1107 (s), 1024 (s), 750 (s)  $\text{cm}^{-1}$ . HRFAB-MS (*m/e*): for  $\text{C}_{32}\text{H}_{40}\text{N}_2^{191}\text{Ir}^{193}\text{Ir}$ ,  $[\text{M} + \text{H}]^+$  837.2521 (calcd 837.2508) for  $\text{C}_{32}\text{H}_{40}\text{N}_2^{193}\text{Ir}_2$ ,  $[\text{M} + \text{H}]^+$  839.2552 (calcd 839.2529). UV–vis ( $35^\circ\text{C}$ , toluene):  $\lambda(\text{max})$  590 nm ( $\epsilon = 1.03 \times 10^4$   $\text{M}^{-1}\text{cm}^{-1}$ ),  $\lambda$  362 nm ( $\epsilon = 7.33 \times 10^3$   $\text{M}^{-1}\text{cm}^{-1}$ ).





interesting structural features. Also under investigation is the mechanism involving the transformation of **3** into **1**.

**Acknowledgment.** We thank the Division of Chemical Sciences, Office of Basic Energy Sciences, Office of Energy Research, U.S. Department of Energy (Grant No. DE-FG02-88ER1388) for support of this work. We also thank Johnson-Matthey for a loan of  $\text{IrCl}_3 \cdot 3\text{H}_2\text{O}$ . The U.S. National Science Foundation provided a portion of the funds for the purchase of the X-ray (NSF Grant No. CHE-9011804) and NMR (Grant No. PCM-

9221835) instruments. We also thank Dr. W. Wycoff and Dr. H. Jimenez for their help in the spin saturation transfer and NOE NMR experiments.

**Supporting Information Available:** Text giving experimental details and spectroscopic data for **1–4**, text giving details of data collection and structure solution and tables of atomic coordinates, thermal parameters, and bond distances and angles for **1**, **2**, and **4**, and ORTEP drawings of **2** and **4** (30 pages). Ordering information is given on any current masthead page.

OM9502897

# Synthesis, Structure, and Reactivity of Electron-Deficient Complexes of Quinolines with Triosmium Clusters

Shariff E. Kabir,<sup>†</sup> Douglas S. Kolwaite,<sup>†</sup> Edward Rosenberg,<sup>\*,†</sup> Kenneth Hardcastle,<sup>‡</sup> Warren Cresswell,<sup>‡</sup> and John Grindstaff<sup>‡</sup>

Departments of Chemistry, The University of Montana, Missoula, Montana 59812, and California State University, Northridge, California 91330

Received November 21, 1994<sup>⊙</sup>

**Summary:** The reaction of  $Os_3(CO)_{10}(CH_3CN)_2$  with quinolines at 25 °C affords the series of complexes  $(\mu-H)(\mu-\eta^2-C_9H_4(R)R')Os_3(CO)_{10}$  ( $R = H, R' = H$  (**1a**);  $R = 4-CH_3, R' = H$  (**1b**);  $R = H, R' = 6-CH_3$  (**1c**)). These complexes are thermally decarbonylated to give the  $46e^-$  clusters  $(\mu-H)(\mu_3-\eta^2-C_9H_4(R)R')Os_3(CO)_9$  ( $R = H, R' = H$  (**2a**);  $R = 4-CH_3, R' = H$  (**2b**);  $R = H, R' = 6-CH_3$  (**2c**)). The reactivity of these novel electron-deficient clusters is reported.

The reactivity of aromatic nitrogen heterocycles toward transition-metal centers has been an active area of research due to the relevance of the complexes obtained in understanding catalytic hydrodenitrification.<sup>1–4</sup> The reactions of quinoline and tetrahydroquinoline with  $M_3(CO)_{12}$  ( $M = Ru, Os$ ) have been previously examined at elevated temperatures and gave complexes of the general type  $(\mu-H)(\mu-\eta^2-C_9H_5N)M_3(CO)_{10}$  ( $M = Ru, Os$ ) in which the C(2) carbon–hydrogen bond of the quinoline ring has oxidatively added to the cluster.<sup>1a,2a</sup> These compounds proved to be unreactive toward hydride donors and hydrogenation.<sup>1a,d,2b</sup> We have now reexamined the reaction of the quinolines  $C_9H_5(R)R'N$  with  $Os_3(CO)_{10}(CH_3CN)_2$  at ambient temperatures and find that the major product is the related compound  $(\mu-H)(\mu-\eta^2-C_9H_4(R)R')Os_3(CO)_{10}$  ( $R = H, R' = H$  (**1a**);  $R = 4-CH_3, R' = H$  (**1b**);  $R = H, R' = 6-CH_3$  (**1c**)), where the carbon–hydrogen bond at C(8) has oxidatively added to the cluster. Minor amounts of the previously reported isomeric compounds (**1a–c'**) are also formed (Scheme 1).<sup>5</sup> Complete assignment of the <sup>1</sup>H

NMR resonances for the new structural types reported herein was possible from established chemical shift patterns, peak multiplicities, and COSY data.<sup>6</sup> Compounds **1a–c** decarbonylate at elevated temperatures (100 °C) to give the deep green complexes  $(\mu-H)(\mu_3-\eta^2-C_9H_4(R)R')Os_3(CO)_9$  ( $R = H, R' = H$  (**2a**);  $R = 4-CH_3, R' = H$  (**2b**);  $R = H, R' = 6-CH_3$  (**2c**); see Scheme 1).<sup>7</sup> The solid-state structure of **2b** is shown in Figure 1; selected distances and bond angles are given in the figure caption.<sup>8</sup> The quinoline ring is bound to the cluster by coordination of the nitrogen lone pair and a three-center–two-electron bond with the C(8) carbon which bridges the same edge of the triangle as the  $\mu$ -hydride. It would appear from the structure of **2b** that both the hydride and C(8) have migrated to a different edge of the metal triangle. The aromatic nature of the rings remains relatively unperturbed, making **2b** a unique example of an electron-deficient trimetallic species containing a  $\mu_3$ -heterocyclic aromatic capping ligand. A related set of green electron-deficient clusters,  $(\mu-H)(\mu_3-\eta^2-Ph_2PCH_2(Ph)C_6H_4)Os_3(CO)_8$ , which also contains a bridging phenyl have been reported.<sup>9</sup> Like these clusters, **2a–c** react rapidly with carbon monoxide to give **1a–c** at 1 atm and ambient temperatures. Compounds **2a,b** also react rapidly with triphenylphosphine and triethyl phosphite, respectively. On the basis of their one- and two-dimensional <sup>1</sup>H and <sup>13</sup>C NMR, we can assign a structure where phosphine addition has occurred and is accompanied by a carbonyl migration to give  $(\mu-H)(\mu-\eta^2-C_9H_5RN)Os_3(CO)_9PR'_3$  ( $R = H, R' = Ph$  (**3a**);  $R = 4-CH_3, R' = OEt$  (**3b**)), in which the phosphine has substituted on the osmium atom bound to carbon, *cisoid* to the hydride, giving structures analogous to **1a,b**.<sup>11</sup>

(6) Bovey, F. A. *NMR Data Tables for Organic Compounds*; Wiley-Interscience: New York, 1967.

(7) <sup>1</sup>H NMR of **2a** at 400 MHz in CDCl<sub>3</sub>:  $\delta$  –12.06 (hydride), 9.28 (dd, H(2)), 7.13 (dd, H(3)), 8.05 (dd, H(4)), 8.45 (dd, H(5)), 7.21 (dd, H(6)), 8.60 (dd, H(7)). <sup>1</sup>H NMR of **2b** at 400 MHz in CDCl<sub>3</sub>:  $\delta$  –12.05 (hydride), 9.12 (d, H(2)), 6.95 (d, H(3)), 8.32 (dd, H(5)), 7.25 (dd, H(6)), 8.55 (dd, H(7)), 2.71 (s, CH<sub>3</sub>). <sup>1</sup>H NMR of **2c** at 400 MHz in CDCl<sub>3</sub>:  $\delta$  –12.15 (hydride), 9.17 (dd, H(2)), 7.07 (dd, H(3)), 7.95 (dd, H(4)), 7.98 (d, H(5)), 8.38 (d, H(7)), 2.60 (s, CH<sub>3</sub>). 100 MHz <sup>13</sup>C NMR for **2a** (carbonyl region in CDCl<sub>3</sub> at 0 °C):  $\delta$  191.32 (2C), 182.87 (1C), 180.64 ( $J_{C-H} = 2.1$  Hz, 2C), 178.51 ( $J_{C-H} = 3.8$  Hz, 2C), 175.09 ( $J_{C-H} = 9.8$  Hz, 2C).

(8) Crystal data and data collection and refinement details for **2b**:  $C_{19}H_9NO_9Os_3$ ,  $M_r = 965.87$ , monoclinic, Cc (No. 9),  $a = 16.034(3)$  Å,  $b = 10.556(2)$  Å,  $c = 14.000(3)$  Å,  $\beta = 114.86(3)^\circ$ ,  $V = 2150.0(7)$  Å<sup>3</sup>,  $Z = 4$ ,  $\lambda(Mo K\alpha) = 0.71073$  Å, Patterson method (SHELXS-86), 3420 independent absorption-corrected data,  $\theta$  range 2.38–30.98°,  $I_o \geq 2\sigma(I_o)$ , 288 (all non-H atoms anisotropic),  $R = 0.055$ ,  $R_w(F^2) = 0.118$ . The hydride position was calculated using the program HYDEX (Orpen, A. G. *J. Chem. Soc., Dalton Trans* 1980, 2509).

(9) Cartwright, S.; Lucas, J. A.; Dawson, R. H.; Foste, D. F.; Harding, M. M.; Smith, A. K. *J. Organomet. Chem.* 1986, 302, 403.

(10) Brown, M. P.; Dolby, P. A.; Harding, M. M.; Mathews, A. J.; Smith, A. K. *J. Chem. Soc., Dalton Trans.* 1993, 1671.

<sup>†</sup> The University of Montana.

<sup>‡</sup> California State University.

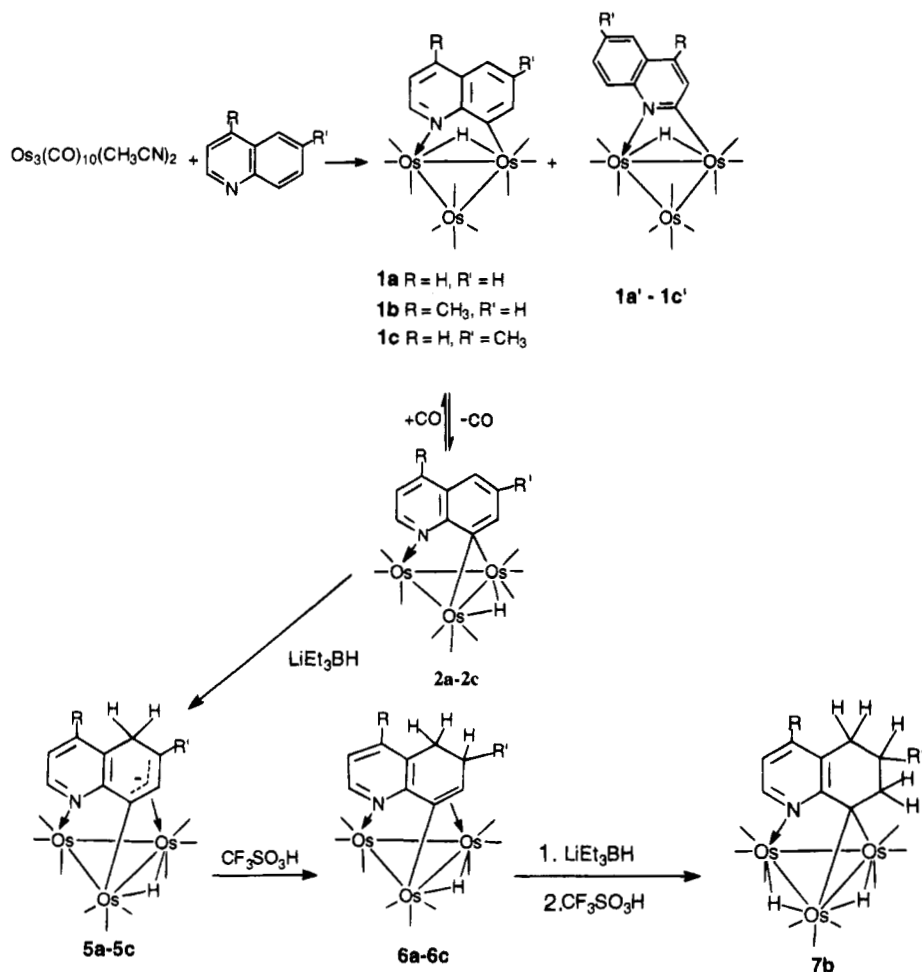
<sup>⊙</sup> Abstract published in *Advance ACS Abstracts*, July 1, 1995.

(1) (a) Fish, R. H.; Kim, J. J.; Steward, J. L.; Bushweller, J. H.; Rosen, R. K.; Dupon, J. W. *Organometallics* 1986, 5, 2193. (b) Fish, R. H.; Kim, H.; Fong, R. H. *Organometallics* 1991, 10, 770 and references therein. (c) Baralt, E.; Smith, S. J.; Hurwitz, J.; Horvath, I. T.; Fish, R. H. *J. Am. Chem. Soc.* 1992, 114, 5187. (d) Fish, R. H. In *Aspects of Homogeneous Catalysis*; Ugo, R., Ed.; Kluwer: Dordrecht, The Netherlands, 1990; pp 65–83.

(2) (a) Eisenstadt, A.; Giandomenico, C. M.; Frederick, M. F.; Laine, R. M. *Organometallics* 1985, 4, 2033. (b) Laine, R. M. *New J. Chem.* 1987, 11, 543.

(3) (a) Gray, S. D.; Smith, D. P.; Bruck, M. S.; Wigley, D. E. *J. Am. Chem. Soc.* 1992, 114, 5462. (b) Gray, S. D.; Fox, P. A.; Kingsborough, M. S.; Bruch, M. S.; Wigley, D. E. *Prepr.-Am. Chem. Soc. Div. Pet. Chem.*, 1993, 38, 706.

(4) Gates, B. C. *Catalytic Chemistry*; Wiley: New York, 1992; p 409.  
(5) <sup>1</sup>H NMR of **1a** at 400 MHz in CDCl<sub>3</sub>:  $\delta$  –12.56 (hydride), 9.42 (dd, H(2)), 7.16 (dd, H(3)), 8.15 (dd, H(4)), 7.25 (dd, H(5)), 7.37 (dd, H(6)), 8.51 (dd, H(7)). <sup>1</sup>H NMR of **1b** at 400 MHz in CDCl<sub>3</sub>:  $\delta$  –12.53 (hydride), 9.27 (d, H(2)), 7.01 (d, H(3)), 7.57 (dd, H(5)), 7.24 (dd, H(6)), 8.51 (dd, H(7)), 2.66 (s, CH<sub>3</sub>). <sup>1</sup>H NMR of **1c** at 400 MHz in CDCl<sub>3</sub>:  $\delta$  –12.71 (hydride), 9.30 (dd, H(2)), 7.10 (dd, H(3)), 8.03 (dd, H(4)), 7.15 (d, H(5)), 8.32 (d, H(7)), 2.66 (s, CH<sub>3</sub>). <sup>13</sup>C NMR of **1a** at 100 MHz (carbonyl region, CDCl<sub>3</sub>):  $\delta$  183.50 (1C), 182.69 (1C), 177.33 (1C), 177.16 ( $J_{C-H} < 1$  Hz, 1C), 177.08 ( $J_{C-H} = 3.8$  Hz, 1C), 176.74 ( $J_{C-H} = 4.6$  Hz, 1C), 176.35 ( $J_{C-H} = 12.1$  Hz, 1C), 175.64 (1C), 175.32 ( $J_{C-H} = 9.1$  Hz, 1C), 175.21 ( $J_{C-H} = 1.0$  Hz, 1C).

Scheme 1. Synthesis and Reactivity of  $4e^-$  Quinoline Complexes

Hydrogenation was of primary importance in our initial reactivity studies of **2a-c**, since there has been considerable attention given to the hydrogenation of quinolines and related aromatic nitrogen heterocycles.<sup>1-3</sup> Compound **2b** does react with  $H_2$  at 75 °C and 100 psi in hydrocarbon solvents to give good conversion (75%) to a mixture of isomeric trihydrides whose  $^1H$  NMR and  $^1H$  2D-COSY data are consistent with  $(\mu-H)_3(\mu-\eta^2-C_9H_5(4-Me)N)Os_3(CO)_9$  (**4b**) and  $H(\mu-H)_2(\mu-\eta^2-C_9H_5(4-Me)N)Os_3(CO)_9$  (**4b'** and **4b''**).<sup>12</sup> In sharp contrast to this observed reduction with  $H_2$  at the metal core, reaction of **2a-c** with 1 equiv of  $LiEt_3BH$  in  $CDCl_3$  or  $CD_2Cl_2$  results in regioselective nucleophilic attack at the C(5) of the quinoline ring to give the anionic complexes  $(\mu-H)(\mu-C_9H_5R(R')N)Os_3(CO)_9^-$  (**5a-c**; Scheme 1). Although we have not yet isolated these anions, their general structure is evident from the  $^1H$  NMR and the 2D-COSY data.<sup>13</sup> In compound **5a**, a broadened resonance of relative intensity 2 at 3.85 ppm is coupled to a

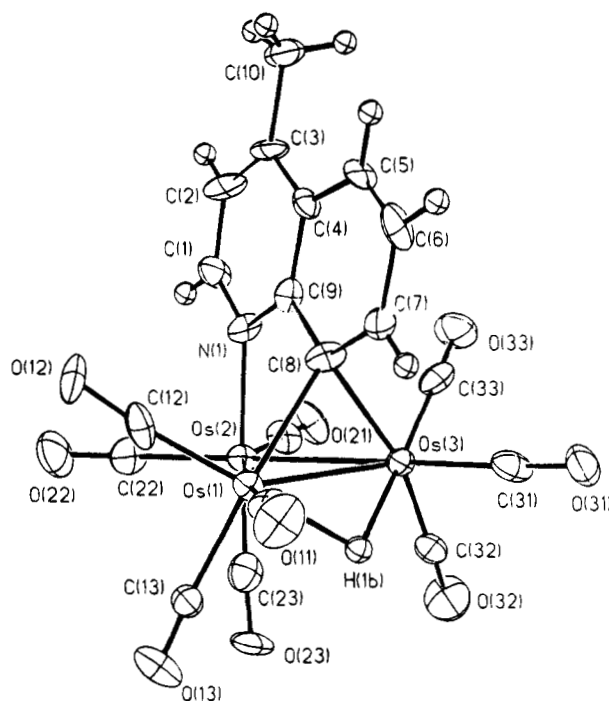


**Figure 1.** ORTEP drawing of **2b** showing the calculated position of the hydride. Selected bond distances (Å): Os(1)–Os(2), 2.764(1); Os(1)–Os(3), 2.770(1); Os(2)–Os(3), 2.781(1); Os(1)–C(8), 2.28(2); Os(3)–C(8), 2.32(2); Os(2)–Os(N), 2.13(2); C(8)–C(9), 1.42(3); C(7)–C(8), 1.40(3); C(6)–C(7), 1.40(4); C(9)–N(1), 1.37(2); C(1)–N(1), 1.32(3); C(1)–C(2), 1.36(3); C(2)–C(3), 1.43(4); C(4)–C(9), 1.42(3); C(3)–C(4), 1.37(3); C(4)–C(5), 1.45(2); C(5)–C(6), 1.29(3).

(11) (a)  $^1H$  NMR of **3a** at 400 MHz in  $CDCl_3$ :  $\delta$  -11.63 (d,  $J_{P-H}$  = 15.6 Hz, hydride), 9.44 (dd, H(2)), 7.11 (dd, H(3)), 8.10 (dd, H(4)), 7.16 (dd, H(5)), 6.76 (dd, H(6)), 7.90 (dd, H(7)).  $^1H$  NMR of **3b** at 400 MHz in  $CDCl_3$ :  $\delta$  -12.32 (d,  $J_{P-H}$  = 13.6 Hz, hydride), 9.29 (d, H(2)), 6.91 (d, H(3)), 7.37 (dd, H(5)), 7.13 (dd, H(6)), 8.45 (dd, H(7)), 2.60 (s,  $CH_3$ ). (b)  $^{13}C$  NMR of **3a** (in  $CDCl_3$ ):  $\delta$  (aromatic region) 160.57 (s, C(9)), 157.95 (s, CH), 152.00 (d, C(8),  $J_{P-C}$  = 9.9 Hz), 149.42 (d, C(7),  $J_{P-C}$  = 6 Hz), 140.47 (s, CH), 134.25 (d, C(1) of Ph,  $J_{P-C}$  = 49.3 Hz), 133.31 (d, CH of Ph,  $J_{P-C}$  = 10 Hz), 129.69 (d, CH(4) of Ph,  $J_{P-C}$  = 2 Hz), 127.89 (d, CH of Ph,  $J_{P-C}$  = 10 Hz), 127.68 (s, CH), 122.34 (s, CH), 119.71 (s, CH);  $\delta$  (carbonyl region) 185.73 (d,  $J_{P-C}$  = 6.1 Hz), 184.52 (s), 184.22 (s), 182.53 (dd,  $J_{P-C}$  = 4.5 Hz,  $J_{C-H}$  = 7.5 Hz), 177.95 (d,  $J_{C-H}$  = 13.7 Hz), 177.87 (s), 177.68 (d,  $J_{C-H}$  = 3.1 Hz), 176.54 (s). (c) Solid-state structural studies of **3a** and **3b** confirm the proposed structures for these compounds. Hardcastle, K. I.; Rosenberg, E.; Kolwaite, D. To be submitted for publication.

doublet of triplets at 4.19 ppm ( $J = 9.5$  and  $3.4$  Hz), which is in turn coupled to a doublet of triplets at 5.79 ppm ( $J = 9.5$  and  $<1.0$  Hz). An identical pattern is observed for **5b** but not for **5c**, where a broadened methylene resonance at 3.67 ppm, a methyl singlet at 1.40 ppm, and a slightly broadened singlet at 5.61 ppm are observed.<sup>13b</sup> That the methylene resonances in **5a–c** appear broadened could be due to a slow  $\sigma$ - $\pi$  interchange, perhaps via a  $\mu$ - $\eta^1$ -alkylidyne intermediate.<sup>13c</sup> Protonation of **5a–c** leads to quantitative conversion to the  $\sigma$ - $\pi$  vinyl structures ( $\mu$ -H)( $\mu$ - $\eta^2$ -C<sub>9</sub>H<sub>6</sub>R(R')Os<sub>3</sub>(CO)<sub>9</sub>) (**6a–c**), which have been isolated and characterized.<sup>14</sup> The structures of **6a–c** seem to rule out initial attack by H<sup>-</sup> at C(7) (Scheme 1), while the data for **5a–c** rule out initial attack at C(6). The regioselective nucleophilic attack by H<sup>-</sup> is unprecedented in complexes of aromatic nitrogen heterocycles which are not  $\pi$ -complexed to the metal center. A related regioselectivity has been observed in  $\pi$ -complexes of indole, ( $\eta^6$ -indole)ML (ML = RuCp<sup>+</sup>, Cr(CO)<sub>3</sub>).<sup>15</sup>

A second cycle of H<sup>-</sup>/H<sup>+</sup> leads to reduction of the 7,8-double bond in **6b** to yield the dihydride cluster ( $\mu$ -H)<sub>2</sub>( $\mu_3$ - $\eta^2$ -C<sub>9</sub>H<sub>7</sub>(4-CH<sub>3</sub>)N)Os<sub>3</sub>(CO)<sub>9</sub> (**7b**); Scheme 1).<sup>16</sup> In this second-stage reduction the sequence of attack of H<sup>-</sup>/H<sup>+</sup>

(i.e., on the metal core of the ring) is not clear and must await further mechanistic studies using labeled hydride and proton donors.

These results indicate that the site of nucleophilic attack by H<sup>-</sup> is at the 5-position of the quinoline ring regardless of the location or presence of a methyl substituent. Normally the site of electrophilic attack is the 5- and 8-positions, while nucleophilic attack is usually at the 2- and 4-positions in free quinolines. Nucleophilic attack and hydrogenation in previously reported mononuclear complexes of quinolines is also at the 2- and 4-positions.<sup>1d,3</sup> Thus, the electron-deficient bonding in **2a–c** has shifted reactivity toward nucleophilic reduction from the heterocyclic to the carbocyclic ring. In connection with this regioselective attack, it is interesting that the H(5) protons on **2a–c** all show a significant downfield shift (0.8–1.2 ppm) relative to **1a–c**. It should be mentioned that the treatment of **1a–c** with LiEt<sub>3</sub>BH showed no evidence of attack on the quinoline ring (by <sup>1</sup>H NMR), forming only a transient dihydride anion which liberated H<sub>2</sub> on protonation. Furthermore, the previously reported quinoline trisium and triruthenium complexes do not thermalize to give electron-deficient clusters such as **2a–c** and **1a–c** show no tendency to convert to **1a–1c'** at 100 °C under a CO atmosphere.<sup>17</sup> Given the very good yields of the transformations reported here, it should be possible to study the further reduction of complexes such as **4–6** and the mechanistic relationship between hydrogenation at the metal and reduction of the quinoline ring system. The general reactivity of **2a–c** and the anionic species **7** toward organic nucleophiles and electrophiles, respectively, should also be of interest as a means of selective functionalization of the quinoline ring system. These studies are currently commencing in our laboratories.

**Acknowledgment.** We gratefully acknowledge the National Science Foundation (Grant No. CHE9319062) and The University of Montana for research support and The National Science Foundation (Grant No. CHE9302468) for purchase of a 400 MHz NMR.

**Supporting Information Available:** Tables giving crystal data, atomic coordinates, anisotropic thermal parameters, and complete distances and angles for **2b** and text giving synthetic procedures, elemental analyses, and infrared spectra for **1a–c**, **2a–c**, **3a**, **3b**, **4b**, **6a–c** and **7b** (11 pages). Ordering information is given on any current masthead page.

OM9408831

(16) <sup>1</sup>H NMR of **7b** at 400 MHz in CDCl<sub>3</sub>:  $\delta$  -13.85 (d,  $J_{H-H} = 1.2$  Hz, hydride), -13.98 (d,  $J_{H-H} = 1.2$  Hz, hydride), 8.05 (d, H(2)), 6.28 (d, H(3)), 2.03 (s, CH<sub>3</sub>), 2.64 (m, CH<sub>2</sub>(5), CH<sub>2</sub>(7)), 1.68 (m, CH<sub>2</sub>(6)). <sup>13</sup>C NMR of **7b** at 100 MHz (in CDCl<sub>3</sub>): hydrocarbon regions  $\delta$  151.86 (CH), 145.20 (C), 134.819 (C), 132.50 (C), 129.03 (C), 120.43 (CH), 59.96 (CH<sub>2</sub>), 29.70 (CH<sub>2</sub>), 27.60 (CH<sub>2</sub>), 19.50 (CH<sub>3</sub>); carbonyl region  $\delta$  184.70, 180.20, 180.09, 175.82, 174.40, 172.25, 172.07, 170.93, 165.97.

(17) We subjected the 1,2- $\mu$ - $\eta^2$  quinoline complex first reported by Laine *et al.*<sup>2a</sup> to prolonged reflux in octane and detected no formation of **2a**. See ref 1a for the thermal behavior of the ruthenium analogs. We also refluxed **1a** in an atmosphere of CO for 4 h and noted no formation of **1a'**.

(12) <sup>1</sup>H NMR of **4b** (57% of mixture) at 400 MHz in CDCl<sub>3</sub>:  $\delta$  -13.40 (d,  $J_{H-H} = 3.6$  Hz, hydride), -13.62 (dd,  $J_{H-H} = 3.6$  Hz, 1, hydride), -13.86 (d,  $J_{H-H} = 1$  Hz, hydride), 8.80 (d, H(2)), 7.20 (d, H(3)), 7.72 (dd, H(5)), 6.97 (dd, H(6)), 8.00 (dd, H(7)), 2.66 (s, CH<sub>3</sub>). <sup>1</sup>H NMR of **4b'** (25%) at 400 MHz in CDCl<sub>3</sub>:  $\delta$  -9.04 (dd,  $J_{H-H} = 10$ , 3.2 Hz, hydride), -10.64 (d,  $J_{H-H} = 10$  Hz, hydride), -13.62 (d,  $J_{H-H} = 3.2$  Hz, hydride), 8.98 (d, H(2)), 7.08 (d, H(3)), 8.17 (dd, H(5)), 6.97 (dd, H(6)), 8.51 (dd, H(7)), 2.67 (s, CH<sub>3</sub>). <sup>1</sup>H NMR of **4b''** (18%) at 400 MHz in CDCl<sub>3</sub>:  $\delta$  -10.30 (s, hydride), -11.13 (d,  $J_{H-H} = 12.4$  Hz, hydride), -12.92 (d,  $J_{H-H} = 12.4$  Hz, hydride), 9.12 (d, H(2)), 7.15 (d, H(3)), 8.40 (dd, H(5)), 6.97 (dd, H(6)), 8.64 (dd, H(7)), 2.70 (s, CH<sub>3</sub>). The structures of **4b**, **4b'**, and **4b''** are also based, by analogy, on similar trihydride cluster structures obtained from the reaction of  $\mu_3$ -imidoyl trisium clusters with H<sub>2</sub>. See: Rosenberg, E.; Kabir, S. E.; Day, M.; Hardcastle, K. I.; Irving, M. *J. Cluster Sci.* **1994**, *5*, 481. Rosenberg, E.; Kabir, S. E.; Day, M.; Hardcastle, K. I. *Organometallics* **1994**, *12*, 4437.

(13) (a) To 20 mg (0.020 mmol) of **2a–c** in 0.6 mL of CD<sub>2</sub>Cl<sub>2</sub> in an NMR tube was added 20  $\mu$ L of a 1 M solution of LiBHET<sub>3</sub> in THF. <sup>1</sup>H NMR of the solution showed complete conversion to **5a–c**. In the case of **5a,b** the methylene resonance (CH<sub>2</sub>(5)) was obscured by the THF. The resonance was first detected by a COSY cross-peak with H(6) and then directly observed by evaporation of the solution under nitrogen and redissolution in CDCl<sub>3</sub>. (b) <sup>1</sup>H NMR of **5a** at 400 MHz in CDCl<sub>3</sub>:  $\delta$  -14.30 (s, hydride), 8.31 (dd, H(2)), 6.26 (dd, H(3)), 6.93 (dd, H(4)), 4.19 (dt, H(6)), 5.57 (dt, H(7)), 3.85 (br, CH<sub>2</sub>(5)). <sup>1</sup>H NMR of **5b** at 400 MHz in CDCl<sub>3</sub>:  $\delta$  -14.33 (s, hydride), 8.19 (d, H(2)), 6.12 (dd, H(3)), 4.21 (dt, H(6)), 5.79 (dt, H(7)), 1.78 (s, CH<sub>3</sub>), 3.74 (br, CH<sub>2</sub>(5)). <sup>1</sup>H NMR of **5c** at 400 MHz in CDCl<sub>3</sub>:  $\delta$  -14.22 (s, hydride), 8.27 (dd, H(2)), 6.18 (dd, H(3)), 6.88 (dd, H(4)), 5.61 (s, H(7)), 1.40 (s, CH<sub>3</sub>), 3.67 (s, CH<sub>2</sub>(5)). (c) The <sup>13</sup>C NMR in the carbonyl region of **5b** is consistent with a  $\sigma$ - $\pi$  vinyl interchange: <sup>13</sup>C of **5b** at 100 MHz  $\delta$  192.6 (2C), 187.9 (1C), 186.3 (2C, br), 183.5 (2C, br), 181.2 (2C, br).<sup>14</sup>

(14) (a) <sup>1</sup>H NMR of **6a** at 400 MHz in CDCl<sub>3</sub>:  $\delta$  -16.96 (s, hydride), 8.42 (dd, H(2)), 6.80 (dd, H(3)), 7.39 (dd, H(4)), 4.14 (t, H(7)), 2.55 (m, CH<sub>2</sub>(5)), 2.21 (m, CH<sub>2</sub>(6)). <sup>1</sup>H NMR of **6b** at 400 MHz in CDCl<sub>3</sub>:  $\delta$  -16.98 (s, hydride), 8.25 (d, H(2)), 6.63 (d, H(3)), 4.19 (t, H(7)), 2.08 (s, CH<sub>3</sub>), 2.57 (m, CH<sub>2</sub>(5)), 2.18 (m, CH<sub>2</sub>(6)). <sup>1</sup>H NMR of **6c** at 400 MHz in CDCl<sub>3</sub>:  $\delta$  -17.00 (s, hydride), 8.40 (dd, H(2)), 6.77 (dd, H(3)), 7.35 (dd, H(4)), 2.17 (m, H(6)), 3.71 (d, H(7)), 1.27 (d, CH<sub>3</sub>), 2.45 (m, CH<sub>2</sub>(5)). (b) <sup>13</sup>C NMR of **6a** at 100 MHz (in CDCl<sub>3</sub>): hydrocarbon region  $\delta$  171.05 (C), 153.02 (CH), 133.86 (CH), 132.67 (C), 122.98 (CH), 101.56 (C), 86.47 (C), 30.21 (CH<sub>2</sub>), 25.36 (CH<sub>2</sub>); carbonyl region  $\delta$  185.95 (2C), 181.91 (1C), 179.97 (2C), 178.81 (2C), 175.13 (2C). (c) The carbonyl region of **6a** indicates a symmetry plane for the cluster which is probably the result of a  $\sigma$ - $\pi$  interchange which is rapid on the NMR time scale at room temperature. See: Keister, J. F.; Shapley, J. R. *J. Organomet. Chem.* **1975**, *85*, C29.

(15) Gill, V. S.; Moriarty, R. M.; Ku, Y. Y.; Butler, J. R. *J. Organomet. Chem.* **1991**, *417*, 313.



# Addition of a Diphosphirenium Salt to Palladium(0) Complexes: The First Examples of Diphosphametallacyclobutenes

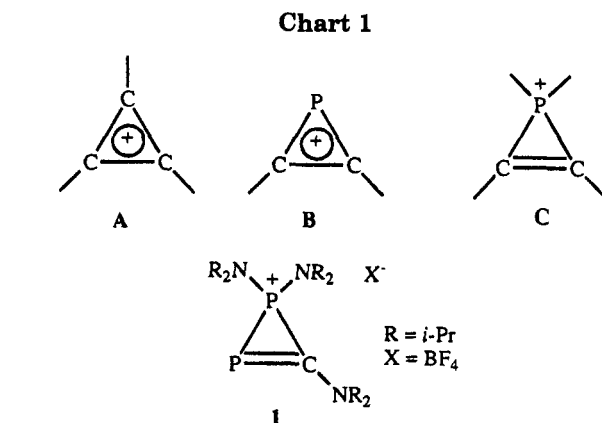
Yves Canac,<sup>†</sup> Michèle Soleilhavoup,<sup>†</sup> Louis Ricard,<sup>‡</sup> Antoine Baceiredo,<sup>†</sup> and Guy Bertrand<sup>\*†</sup>

Laboratoire de Chimie de Coordination du CNRS, 205 route de Narbonne, 31077 Toulouse Cédex, France, and Laboratoire de Chimie du Phosphore et des Métaux de Transition, DCPH, Ecole Polytechnique, 91128 Palaiseau Cédex, France

Received April 18, 1995<sup>®</sup>

**Summary:** *P*-Bis(diisopropylamino)-*C*-(diisopropylamino)diphosphirenium tetrafluoroborate (**1**) reacts with palladium tetrakis(triphenylphosphine), affording the tetrafluoroborate salt of 2,2-bis(triphenylphosphine)-1,3-diphospha-2-pallada(II)cyclobutene **2** in 70% yield. Exchange of the triphenylphosphine ligands occurs with diphenylmethylphosphine, dimethylphenylphosphine, trimethylphosphine, and 1,2-bis(diphenylphosphino)ethane, leading to the corresponding complexes **3–6** in good yields.

The interaction of transition-metal complexes with strained cyclopropenyl cations **A** has been widely studied.<sup>1–3</sup> Due to the aromatic and cationic character of **A**,<sup>4</sup> both the  $\eta^3$  and  $\eta^1$  ligations are to be expected,<sup>1,2</sup> but the  $\eta^2$  coordination mode with varying extents of intrusion of the metal into a C–C bond is the most fascinating.<sup>3</sup> The last kind of complexes represent points on the energy surface for the conversion of a metallatetrahedrane ( $\eta^3$ -cyclopropenyl) to a metallacyclobutadiene complex (complete insertion of the metal into the C–C bond),<sup>5</sup> a process which has been recognized to play an important role in alkyne metathesis.<sup>6</sup> In the phosphorus series, a stable nickel  $\eta^3$ -phosphirenium complex has recently been prepared by Nixon et al.;<sup>7</sup> this complexation mode has been explained by the aromatic character<sup>8</sup> of the three-membered phosphorus heterocycle **B**.<sup>9</sup> The ligation of the phosphirenium salts



**C**,<sup>10</sup> the related  $\sigma^4$ -phosphorus cation, has never been described, although it is quite likely that it would just behave as a simple olefin since the interaction between the cationic phosphorus center and the C=C double bond is weak.<sup>8a</sup> In contrast, several coordination modes are predictable for diphosphirenium salt **1**<sup>11</sup> (Chart 1), and here we report our preliminary results concerning the reactivity of this compound with palladium(0) complexes.

Treatment of a dichloromethane solution of diphosphirenium salt **1** with an equimolar amount of palladium tetrakis(triphenylphosphine), at  $-40$  °C, cleanly led to complex **2**, which was isolated as a yellow oil in 70% yield.<sup>12</sup> The low solubility in nonpolar solvents strongly argued for the ionic nature of **2**, which was confirmed by the presence of a sharp singlet at 0 ppm in the <sup>11</sup>B NMR spectrum due to BF<sub>4</sub><sup>-</sup>. The <sup>31</sup>P{<sup>1</sup>H} NMR spectrum revealed a multiplet at low field (+253 ppm) and a very complex signal at high field (+33.1 to +14.9 ppm) corresponding to one and three phosphorus nuclei, respectively. All attempts to solve the <sup>31</sup>P{<sup>1</sup>H} NMR spectrum or to obtain crystals suitable for an X-ray diffraction study failed. Therefore, we carried out

(8) (a) Mathey, F. *Chem. Rev.* **1990**, *90*, 997. (b) Maclagen, G. A. R. *Chem. Phys. Lett.* **1989**, *163*, 349.

(9) The first successful generation and characterization of a compound of type **B** has recently been reported: Laali, K. K.; Geissler, B.; Wagner, O.; Hoffmann, J.; Armbrust, R.; Einfeld, W.; Regitz, M. *J. Am. Chem. Soc.* **1994**, *116*, 9407.

(10) (a) Forgers, K. S.; Hogeveen, H.; Kingma, R. F. *Tetrahedron Lett.* **1983**, *24*, 643. (b) Breslow, R.; Doering, L. A. *Tetrahedron Lett.* **1984**, *25*, 1345. (c) Marinetti, A.; Mathey, F. *J. Am. Chem. Soc.* **1985**, *107*, 4700. (d) Vural, J. M.; Weissman, S. A.; Baxter, S. G.; Cowley, A. H.; Nunn, C. M. *J. Chem. Soc., Chem. Commun.* **1988**, 462.

(11) (a) Castan, F.; Baceiredo, A.; Fischer, J.; De Cian, A.; Comenges, G.; Bertrand, G. *J. Am. Chem. Soc.* **1991**, *113*, 8160. (b) Soleilhavoup, M.; Canac, Y.; Polozov, A. M.; Baceiredo, A.; Bertrand, G. *J. Am. Chem. Soc.* **1994**, *116*, 6149.

<sup>†</sup> Laboratoire de Chimie de Coordination du CNRS.

<sup>‡</sup> Ecole Polytechnique.

<sup>®</sup> Abstract published in *Advance ACS Abstracts*, July 1, 1995.

(1) See for examples: (a) Gowling, E. W.; Kettle, S. F. A. *Inorg. Chem.* **1964**, *3*, 604. (b) Shen, J.-K.; Tucker, D. S.; Basolo, F.; Hughes, R. P. *J. Am. Chem. Soc.* **1993**, *115*, 11312. (c) Lichtenberger, D. L.; Hoppe, L. M.; Subramanian, L.; Kober, E. M.; Hughes, R. P.; Hubbard, J. L.; Tucker, D. S. *Organometallics* **1993**, *12*, 2025. (d) Ditchfield, R.; Hughes, R. P.; Tucker, D. S.; Bierwagen, E. P.; Robbins, J.; Robinson, D. J.; Zakutansky, J. A. *Organometallics* **1993**, *12*, 2258. (e) Hughes, R. P.; Tucker, D. S.; Rheingold, A. L. *Organometallics* **1993**, *12*, 3069.

(2) (a) Gompper, R.; Bartmann, E.; Nöth, H. *Chem. Ber.* **1979**, *112*, 218. (b) DeSimone, D. M.; Desrosiers, P. J.; Hughes, R. P. *J. Am. Chem. Soc.* **1982**, *104*, 4842. (c) Gompper, R.; Bartmann, E. *Angew. Chem., Int. Ed. Engl.* **1985**, *24*, 209.

(3) (a) McClure, M. D.; Weaver, D. L. *J. Organomet. Chem.* **1973**, *54*, C59. (b) Tuggle, R. M.; Weaver, D. L. *Inorg. Chem.* **1972**, *11*, 2237. (c) Frisch, P. D.; Khare, G. P. *Inorg. Chem.* **1979**, *18*, 781. (d) Blunden, R. B.; Cloke, F. G. N.; Hitchcock, P. B.; Scott, P. *Organometallics* **1994**, *13*, 2917. (e) Hughes, R. P.; Tucker, D. S.; Rheingold, A. L. *Organometallics* **1994**, *13*, 4664.

(4) (a) Minkin, V. I.; Glukhovtsev, M. N.; Simkin, B. Ya. *Aromaticity and Antiaromaticity*; Wiley: New York, 1994. (b) Garratt, P. J. *Aromaticity*; Wiley: New York, 1986.

(5) (a) Jemmis, E. D.; Hoffmann, R. *J. Am. Chem. Soc.* **1980**, *102*, 2570. (b) Lin, Z.; Hall, M. B. *Organometallics* **1994**, *13*, 2878.

(6) Schrock, R. R. *Acc. Chem. Res.* **1986**, *19*, 342.

(7) Avent, A. G.; Cloke, F. G. N.; Flower, K. R.; Hitchcock, P. B.; Nixon, J. F.; Vickers, D. M. *Angew. Chem., Int. Ed. Engl.* **1994**, *33*, 2330.

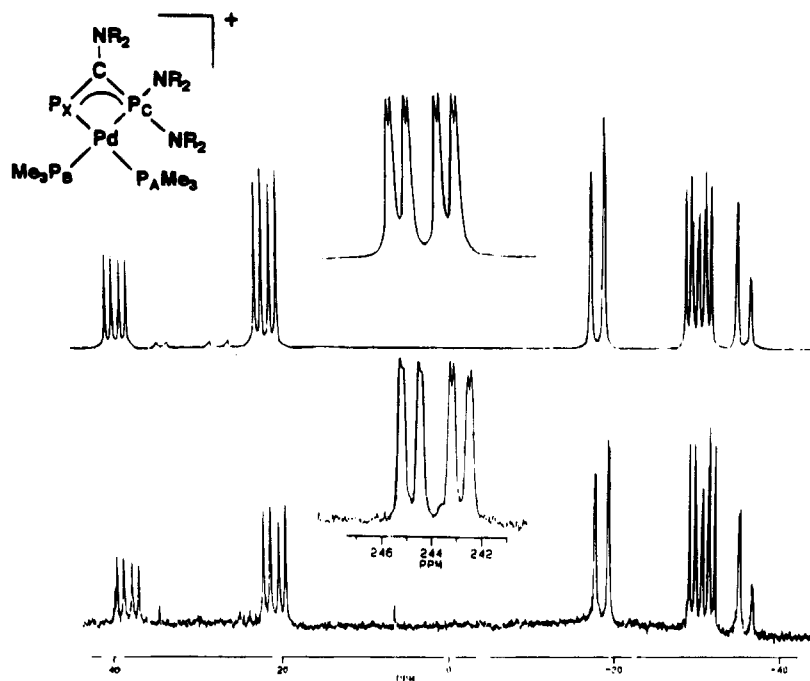


**Figure 1.** Experimental  $^{31}\text{P}\{^1\text{H}\}$  NMR spectrum (32.438 MHz) of **5** in  $\text{CDCl}_3$  at 298 K (bottom) and simulated spectrum (top) using  $\delta_A$  -30.8 ppm,  $\delta_B$  -26.1 ppm,  $\delta_C$  27.9 ppm,  $\delta_X$  244.6 ppm,  $J(\text{AB}) = 52$  Hz,  $J(\text{AC}) = 31$  Hz,  $J(\text{AX}) = 20$  Hz,  $J(\text{BC}) = 559$  Hz,  $J(\text{BX}) = 4$  Hz, and  $J(\text{CX}) = 57$  Hz.

exchange reactions of the triphenylphosphine ligands with a variety of other phosphines.

When diphenylmethylphosphine, dimethylphenylphosphine, or trimethylphosphine was added to complex **2**, clean reactions occurred leading to the corresponding complexes **3**, **4**, and **5**, which were isolated as yellow oils in near-quantitative yields.<sup>12</sup>

The  $^{31}\text{P}\{^1\text{H}\}$  NMR spectra of complexes **2–5** are similar and exhibit resonances of the type ABCX (Table 1). When the phosphine ligands are changed, the chemical shifts of the X (244–259 ppm) and C (25–32 ppm) parts change only slightly and therefore can be assigned to the phosphorus atoms arising from diphosphirenium salt **1**; moreover, the proton-coupled  $^{31}\text{P}$  NMR spectra demonstrate that  $\text{P}_C$  bears the amino groups. The simplest spectrum was obtained for complex **5** and is shown along with the simulated spectrum in Figure 1. The presence of an ABCX system excludes the  $\eta^1$  complex **D**, the two phosphines being magnetically equivalent. Since the value of the coupling constant between the phosphorus atom substituted by amino groups and one of the phosphine ligands is quite large ( $J_{\text{P}_B\text{P}_C} = 559$  Hz), the  $\eta^2$  complex of type **E** can also be excluded. Thus, the reasonable remaining possibility was a structure of type **F**, featuring a completely or partially opened diphosphirenium moiety

(12) Synthesis of complex **2**: To a dichloromethane solution (5 mL) of **1** (0.46 g, 1 mmol) at  $-40$  °C was added a stoichiometric amount of palladium tetrakis(triphenylphosphine) (1.10 g, 1 mmol). After the solution was warmed to room temperature, the solvent was removed in vacuo, and the residue was washed with toluene and ether, leading to complex **2** as a yellow oil (0.76 g, 70% yield). Synthesis of complexes **3–6**: To a dichloromethane solution (10 mL) of **2** (1.09 g, 1 mmol) at room temperature was added 2 equiv of phosphine (diphenylmethylphosphine (**3**), phenyldimethylphosphine (**4**), or trimethylphosphine (**5**)) or a stoichiometric amount of 1,2-bis(diphenylphosphino)ethane (**6**). After 30 min at room temperature, the solvent was removed in vacuo, and the residue was washed several times with toluene and ether to eliminate triphenylphosphine. Complexes **3** (0.82 g, 85% yield), **4** (0.69 g, 82% yield), and **5** (0.63 g, 88% yield) were obtained as yellow oils, and complex **6** (0.87 g, 90% yield) was obtained as orange crystals from a THF/ether solution.

**Table 1.**  $\delta(^{31}\text{P})$  Chemical Shifts (ppm) Obtained by Simulation of the Spectra of Complexes **2–6**

	$\delta_A$	$\delta_B$	$\delta_C$	$\delta_X$
<b>2</b>	+16	+19	+25	+253
<b>3</b>	-4.8	+4.2	+25.4	+259.0
<b>4</b>	-19.0	-14.5	+27.5	+250.0
<b>5</b>	-30.8	-26.1	+27.9	+244.6
<b>6<sup>a</sup></b>	+32	+32	+32	+249

<sup>a</sup> It has not been possible to solve the ABC part of the system observed for **6**; +32 is the center of the multiplet.

**Chart 2**

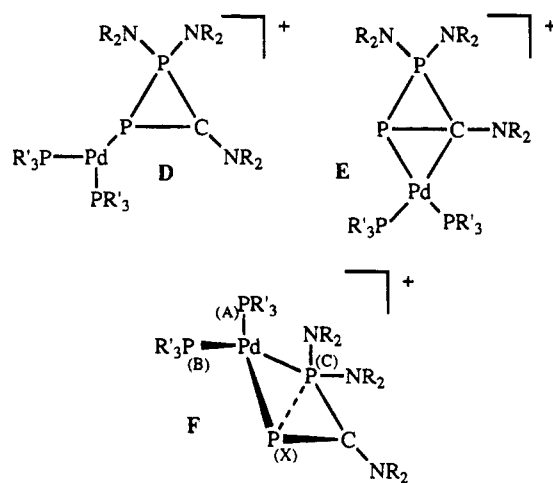
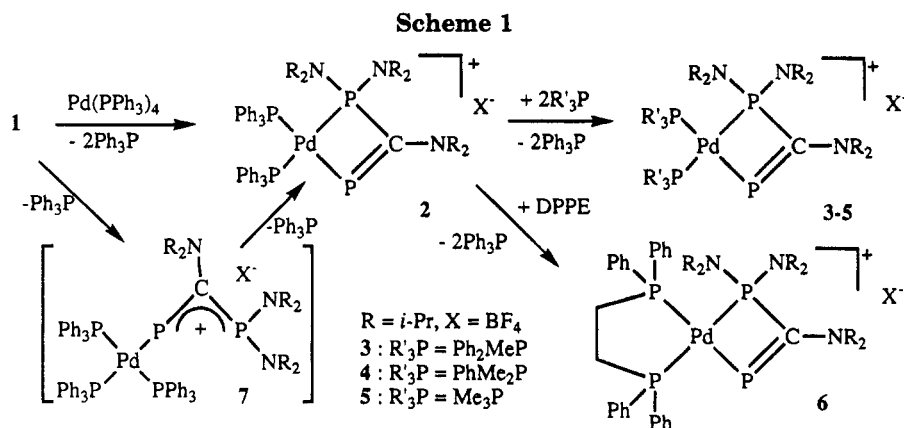


(Chart 2). Note that the value of the coupling constant between the two phosphorus atoms of the ring ( $J_{\text{P}_C\text{P}_X} = 57$  Hz) does not rule out a PP interaction, and the presence of only one large coupling constant ( $J_{\text{P}_B\text{P}_C} = 559$  Hz) is rather surprising, since two trans P–Pd–P arrangements are expected.

The exact structure of these complexes came from the reaction of **2** with 1,2-bis(diphenylphosphino)ethane,<sup>12</sup> since complex **6** was obtained in 90% yield as orange crystals (mp 169–171 °C) suitable for an X-ray analy-



sis.<sup>13</sup> The ORTEP view of the molecule is illustrated in Figure 2, along with the atom labeling and the pertinent metric parameters. No interaction between the cation and the anion ( $\text{BF}_4^-$ ) is observed. The P(1)–P(3) distance of 2.655(1) Å is longer than a normal P–P single bond, which is about 2.22 Å,<sup>14</sup> and is also longer than that observed in the related 1,3-diphospha-2,4-disilabicyclo[1.1.0]butane (2.34 Å).<sup>15</sup> Bond lengths do not always correlate with bond orders in a simple way; however, as the C(2) atom lies only 0.1899(34) Å out of the [P(1),Pd(1),P(3)] plane, we can rule out a bicyclic structure and therefore a P(1)–P(3) interaction. The palladium atom has a slightly distorted square-planar geometry (the value of the twist angle between the [P(1),Pd(1),P(3)] and [P(25),Pd(1),P(28)] planes is 16.44(7)°, probably due to the strain in the four-membered ring (P(1)–Pd–P(3), 70.27(3)°; P(1)–C(2)–P(3), 96.2(2)°), and can be considered as Pd(II). Since the P(1)–C(2) bond length (1.745(3) Å) falls in the range observed for C-amino-substituted phosphalkenes,<sup>16</sup> complex 6 and 2–5 have to be considered as the first examples of diphosphametallacyclobutene (Scheme 1).

It is quite likely that the mechanism leading to complexes 2–6 involves a nucleophilic attack of the

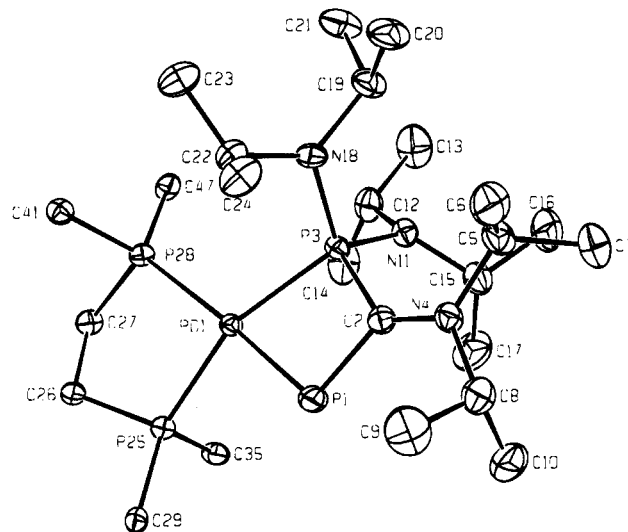


**Figure 2.** ORTEP view of complex 6. Selected bond lengths (Å) and bond angles (deg): Pd(1)–P(1), 2.317(1); Pd(1)–P(3), 2.2960(7); Pd(1)–P(25), 2.3228(7); Pd(1)–P(28), 2.382(1); P(1)–C(2), 1.745(3); P(3)–C(2), 1.821(4); C(2)–N(4), 1.349(5); P(3)–N(11), 1.686(3); P(3)–N(18), 1.691(3); P(1)–Pd(1)–P(3), 70.27(3); P(1)–Pd(1)–P(25), 95.78(3); P(1)–Pd(1)–P(28), 172.76(3); P(3)–Pd(1)–P(25), 160.45(4); P(3)–Pd(1)–P(28), 111.81(3); P(25)–Pd(1)–P(28), 83.78(3); Pd(1)–P(1)–C(2), 97.1(1); P(1)–C(2)–P(3), 96.2(2).

dicoordinated phosphorus atom of 1, as already observed with lithium salts,<sup>11b</sup> leading to  $\eta^1$ -coordinated 1,3-diphosphaallylic cations 7, which then undergo a ring closure (Scheme 1).<sup>17</sup>

**Acknowledgment.** Thanks are due to Prof. F. Mathey for providing us with X-ray facilities and to the CNRS for financial support of this work.

**Supporting Information Available:** Tables giving crystal and intensity collection data, positional and thermal parameters, interatomic distances and angles, and least-squares-plane equations (17 pages). Ordering information is given on any current masthead page.

OM950276T

(17) An alternative mechanism involving a direct insertion into the P–P bond of the  $(\text{R}_3\text{P})_2\text{Pd}$  fragment acting as a carbene<sup>15b</sup> has been suggested by a reviewer.

(13) Crystallographic data for 6 ( $\text{C}_{45}\text{H}_{66}\text{BF}_4\text{N}_3\text{P}_4\text{Pd}$ ) were collected at  $-150 \pm 0.5$  °C on an Enraf-Nonius CAD4 diffractometer using Mo K $\alpha$  radiation ( $\lambda = 0.71073$  Å) and a graphite monochromator. The crystal structure was solved and refined using the Enraf-Nonius MOLEN package. The compound crystallizes in space group  $P\bar{1}$  (No. 2), with  $a = 10.258(1)$  Å,  $b = 20.801$  Å,  $c = 24.435(2)$  Å,  $\alpha = 66.39(1)^\circ$ ,  $\beta = 88.14(1)^\circ$ ,  $\gamma = 88.38(1)^\circ$ ,  $V = 4773.90(91)$  Å<sup>3</sup>,  $Z = 4$ ,  $d_{\text{calc}} = 1.344$  g/cm<sup>3</sup>,  $\mu = 5.6$  cm<sup>-1</sup>, and  $F(000) = 2016$ . A total of 17 766 unique reflections were recorded in the range  $2^\circ \leq 2\theta \leq 50.0^\circ$ , of which 5289 were considered as unobserved ( $F^2 < 3.0\sigma(F^2)$ ), leaving 12 477 for solution and refinement. The structure was solved by Patterson methods, yielding a solution for the two palladium atoms. The two molecules contained in the asymmetric unit are identical. The hydrogen atoms were included as fixed contributions in the final stages of least-squares refinement while using anisotropic temperature factors for all other atoms. A non-Poisson weighting scheme was applied with a  $p$  factor equal to 0.08. The final agreement factors were  $R = 0.035$ ,  $R_w = 0.054$ , and  $\text{GOF} = 1.15$ .

(14) (a) Cowley, A. H. *Chem. Rev.* **1963**, *5*, 617. (b) Durig, J. R.; Carreira, L. A.; Odom, J. D. *J. Am. Chem. Soc.* **1974**, *96*, 2688.

(15) (a) Driess, M.; Fanta, A. D.; Powell, D. R.; West, R. *Angew. Chem., Int. Ed. Engl.* **1989**, *28*, 1038. (b) Fanta, A. D.; Driess, M.; Powell, D. R.; West, R. *J. Am. Chem. Soc.* **1991**, *113*, 7806.

(16) Markovski, L. N.; Romanenko, V. D.; Ruban, A. V. *The Chemistry of Acyclic Derivatives of Two-Coordinated Phosphorus*; Kirsanov, A. V., Ed.; Naukova Dumka: Kiev, Ukraine, 1988.

# Novel Alkylation–Annulation Reaction of Fischer Carbene Complexes<sup>†</sup>

Sk. Rasidul Amin,<sup>‡</sup> Sudhir S. Sawant,<sup>‡</sup> Vedavati G. Puranik,<sup>§</sup> and  
Amitabha Sarkar<sup>\*,‡</sup>

Divisions of Organic Chemistry (Synthesis) and Physical Chemistry,  
National Chemical Laboratory, Pune-411008, India

Received February 15, 1995<sup>®</sup>

**Summary:** Alkylation of aminocarbene complexes  $(CO)_5M=C(CH_3)(NHR)$  with dichloromethane or dibromomethane under PTC conditions triggers an annulation reaction leading to novel cyclic products. This is the first example of such reactivity of Fischer carbene complexes.

Fischer carbene complexes are often compared with esters or amides in terms of reactivity patterns,<sup>1</sup> viz. stabilization of  $\alpha$ -carbanion and consequent alkylation<sup>2</sup> or aldol reactions,<sup>3</sup> and participation of conjugated multiple bonds in Michael addition<sup>4</sup> or Diels–Alder reaction.<sup>5</sup> It has been recognized that the  $C=M(CO)_5$  fragment is far more electrophilic than a  $C=O$  function, and that is reflected in the  $pK_a$  of the  $\alpha$ -proton<sup>6</sup> as well as in the relative rate of Diels–Alder reactions.<sup>5</sup> Also, displacement of the alkoxy group of a Fischer carbene

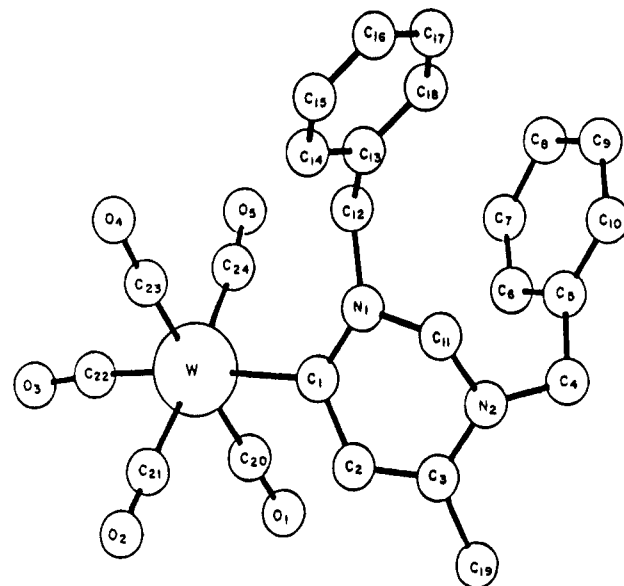


**Figure 1.** Crystal structure of **2a**. Important bond distances (Å) and angles (deg): W–C(1), 2.30(2); C(1)–C(2), 1.40(3); C(2)–C(3), 1.38(3); C(3)–N(2), 1.35; W–C(1)–N(1), 127.2(12); W–C(1)–C(2), 117.3(13); C(1)–N(1)–C(11), 114.3(14); C(1)–C(2)–C(3), 119.8(17); N(1)–C(11)–N(2), 110.2(14); C(2)–C(3)–N(2), 117.1(17); C(3)–N(2)–C(11), 111.2(16); N(1)–C(1)–C(2), 115.2(16).

complex by a different alcoholate or an amine,<sup>7</sup> which presumably proceeds *via* a tetrahedral intermediate, is reminiscent of ester exchange or ester aminolysis, respectively. Reaction of a carbon nucleophile at the carbene carbon leading to the displacement of the alkoxide group<sup>8</sup> parallels the synthesis of ketones from esters. In this report, we wish to describe the first example of an intramolecular aldol–dehydrometalation reaction involving the metal–carbene fragment of amino Fischer carbene complexes, in which the  $C=M$  bond behaves more like the  $C=O$  function of a ketone rather than that of an ester or an amide.

When a solution of the aminocarbene complex **1a** in dichloromethane was stirred with 50% aqueous NaOH and a catalytic amount of  $Bu_4NBr$  for 4 h at room temperature,<sup>2a,9</sup> a new product was formed, which was isolated by flash chromatography. Presence of a  $(CO)_5W=C$  fragment in this compound was confirmed

(7) (a) Casey, C. P.; Shusterman, A. *J. Organometallics* **1985**, *4*, 736. (b) Connor, J. A.; Fischer, E. O. *J. Chem. Soc. A* **1969**, 578.

(8) Casey, C. P.; Brukhardt, T. J.; Bunnell, C. A.; Calabrese, J. C. *J. Am. Chem. Soc.* **1977**, *99*, 2127.

(9) For the use of phase-transfer catalysis in Fischer carbene chemistry, see ref 2a and the following: (a) Veya, P.; Floriani, C.; Chiesi-Villa, A.; Rizzoli, C. *Organometallics* **1994**, *13*, 214. (b) Hoye, T. R.; Chen, K.; Vyvyan, J. R. *Organometallics* **1993**, *12*, 2806.

<sup>†</sup> NCL Communication No. 6227.

<sup>‡</sup> Division of Organic Chemistry (Synthesis).

<sup>§</sup> Division of Physical Chemistry.

<sup>®</sup> Abstract published in *Advance ACS Abstracts*, June 1, 1995.

(1) For reviews, see: (a) Wulff, W. D. In *Comprehensive Organic Synthesis*; Trost, B. M., Fleming, I., Eds.; Pergamon Press: Oxford, U. K.; 1991; Vol. 5. (b) Dötz, K. H. *Angew. Chem., Int. Ed. Engl.* **1984**, *23*, 587. (c) Dötz, K. H.; Fischer, H.; Hofmann, P.; Kreissel, F. R.; Schubert, U.; Weiss, K. *Transition Metal Carbene Complexes*; Verlag Chemie: Deerfield Beach, FL, 1984. (d) Wulff, W. D.; Tang, P. C.; Chan, K. S.; McCallum, J. S.; Yang, D. C.; Gilbertson, S. R. *Tetrahedron* **1985**, *41*, 5813. (e) Dötz, K. H. In *Organometallics in Organic Synthesis: Aspects of a Modern Interdisciplinary Field*; tom Dieck, H., de Meijere, A., Eds.; Springer-Verlag: Berlin, 1988. (f) Chan, K. S.; Peterson, G. A.; Brandvold, T. A.; Faron, K. L.; Challener, C. A.; Hyldahl, C.; Wulff, W. D. *J. Organomet. Chem.* **1987**, *334*, 9. (g) Wulff, W. D. In *Advances in Metal-Organic Chemistry*; Liebeskind, L. S., Ed.; JAI Press Inc.: Greenwich, CT, 1989; Vol. 1. (h) Brown, E. J. *Prog. Intermed. Chem.* **1980**, *27*, 1. (i) Semmelhack, M. F.; Bozell, J. J.; Keller, L.; Sato, T.; Spiess, E. J.; Wulff, W.; Zask, A. *Tetrahedron* **1985**, *41*, 5803. (j) Dötz, K. H. *Pure Appl. Chem.* **1983**, *55*, 1689. (k) Grotjahn, D. B.; Dötz, K. H. *Synlett* **1991**, 381. (l) Hegedus, L. S. *Pure Appl. Chem.* **1990**, *62*, 691.

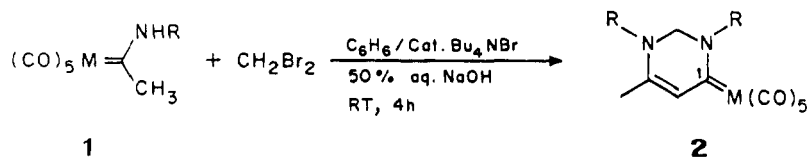
(2) (a) Amin, S. R.; Sarkar, A. *Organometallics* **1995**, *14*, 547. (b) Wulff, W. D.; Anderson, B. A.; Isaacs, L. D. *Tetrahedron Lett.* **1989**, *30*, 4061. (c) Xu, Y. C.; Wulff, W. D. *J. Org. Chem.* **1987**, *52*, 3263. (d) Alvarez, C.; Pacreau, A.; Parlier, A.; Rudler, H. *Organometallics* **1987**, *6*, 1057. (e) Casey, C. P.; Brunsvold, W. R. *J. Organomet. Chem.* **1976**, *118*, 309. (f) Casey, C. P.; Brunsvold, W. R. *J. Organomet. Chem.* **1975**, *102*, 175. (g) Casey, C. P.; Anderson, R. L. *J. Organomet. Chem.* **1974**, *73*, C28.

(3) (a) Wulff, W. D.; Anderson, B. A.; Toole, A. J. *J. Am. Chem. Soc.* **1989**, *111*, 5485. (b) Wulff, W. D.; Gilbertson, S. R. *J. Am. Chem. Soc.* **1985**, *107*, 503. (c) Casey, C. P. *CHEMTECH* **1979**, 378. (d) Casey, C. P.; Brunsvold, W. R. *J. Organomet. Chem.* **1974**, *77*, 345. (e) Casey, C. P.; Boggs, R. A.; Anderson, R. L. *J. Am. Chem. Soc.* **1972**, *94*, 8947.

(4) (a) Anderson, B. A.; Wulff, W. D.; Rahm, A. *J. Am. Chem. Soc.* **1993**, *115*, 4602. (b) Casey, C. P.; Brunsvold, W. R.; Scheck, D. M. *Inorg. Chem.* **1977**, *16*, 3059.

(5) (a) Bao, J.; Dragsich, V.; Wenglowksy, S.; Wulff, W. D. *J. Am. Chem. Soc.* **1991**, *113*, 9873. (b) Wang, S. L. B.; Wulff, W. D. *J. Am. Chem. Soc.* **1990**, *112*, 4550. (c) Wulff, W. D.; Bauta, W. E.; Kaesler, R. W.; Lankford, P. J.; Miller, R. A.; Murray, C. K.; Yang, D. C. *J. Am. Chem. Soc.* **1990**, *112*, 3642. (d) Wulff, W. D.; Yang, D. C. *J. Am. Chem. Soc.* **1984**, *106*, 7565.

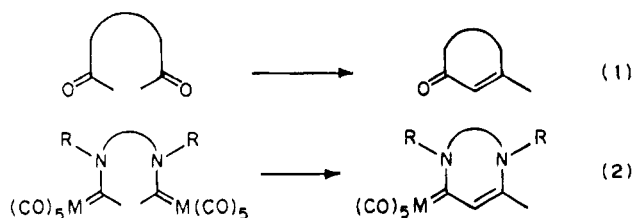
(6) (a) Gandler, J. R.; Bernasconi, C. F. *Organometallics* **1989**, *8*, 2282. (b) Casey, C. P.; Anderson, R. L. *J. Am. Chem. Soc.* **1974**, *96*, 1230.

Scheme 1<sup>a</sup>

M	R	M	R	Yield <sup>a</sup> (%)	<sup>13</sup> C (C-1) δ (PPM)
a : W	CH <sub>2</sub> Ph	a : W	CH <sub>2</sub> Ph	73	215.9
b : W	CH <sub>2</sub> CH=CH <sub>2</sub>	b : W	CH <sub>2</sub> CH=CH <sub>2</sub>	71	215.6
c : W	CH <sub>3</sub>	c : W	CH <sub>3</sub>	80	217.3
d : Cr	CH <sub>2</sub> Ph	d : Cr	CH <sub>2</sub> Ph	76	232.3
e : Cr	CH <sub>3</sub>	e : Cr	CH <sub>3</sub>	87	233.0

<sup>a</sup> Isolated yield based on recovered starting material (5–10%).

Scheme 2



by IR spectroscopy. The structure of this new complex was conclusively determined by X-ray crystallography (Figure 1).

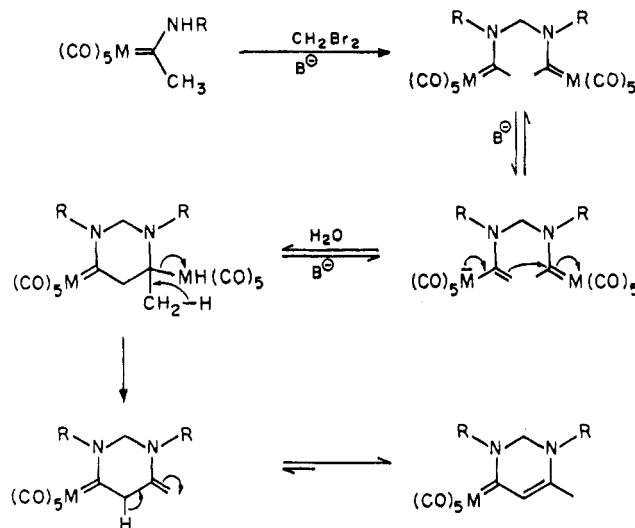
The complex **2a** was found to be a cyclic compound with an unusually electron-rich metal–carbene moiety. Clearly, this product resulted from the reaction of two molecules of the starting complex linked by a methylene group derived from dichloromethane. The <sup>1</sup>H NMR spectrum was readily interpreted on the basis of this structure. The singlet at 2.25 ppm was assigned to the vinylic methyl group. Of the two sets of benzylic methylene protons, one appeared together with the N–CH<sub>2</sub>–N protons as a singlet at 4.25 ppm and the other appeared as a singlet at 5.10 ppm. The olefinic proton appeared as a singlet at 6.60 ppm. The most deshielded <sup>13</sup>C NMR signal at 215.9 ppm was assigned to the carbene carbon, while the CO resonances appeared at 203.8 and 199.7 ppm. The carbene carbon is shielded by about 46 ppm compared to the amino carbene complex **1a**, the most shielded carbene carbon observed so far.<sup>10</sup>

A series of aminocarbene complexes **1b–e** undergoes a similar reaction with good to excellent yields (Scheme 1). It was found that replacement of dichloromethane (solvent) by an equivalent amount of dibromomethane in benzene significantly improved the yields.<sup>11</sup> Formation of the cyclic product **2e** from **1e** was also effected by the use of BuLi instead of NaOH at –78 °C.

(10) For a recent report on acyclic Fischer carbene complexes containing similar functional groups but prepared by an entirely different route, see: Stein, F.; Duetsch, M.; Pohl, E.; Herbst-Irmer, R.; de Meijere, A. *Organometallics* **1993**, *12*, 2556. The most shielded of the carbene carbons described therein appears at 258.75 ppm.

(11) Typical procedure: The carbene complex (*n* mmol) and tetrabutylammonium bromide (0.1*n* mmol) in benzene was treated with 50% aqueous NaOH and dibromomethane (*n* mmol). The mixture was stirred at room temperature under argon for 4 h. The reaction mixture was diluted with water, extracted with dichloromethane, dried, and concentrated under reduced pressure. The pure product was isolated by flash chromatography using dichloromethane (5–50%) in petroleum ether as the eluant.

Scheme 3



This novel annulation reaction has a close parallel in Robinson annulation<sup>12</sup> of carbocyclic systems, as represented in Scheme 2. In an annulation reaction (eq 1 of Scheme 2), a diketone can cyclize by an intramolecular aldol condensation followed by dehydration. In the present example, a possible intermediate bearing two (CO)<sub>5</sub>M=C(CH<sub>3</sub>)(NRR') functionalities undergoes a similar cyclization under mild conditions (eq 2). This is a unique reaction of Fischer carbene complexes. First, it implies facile formation of a carbanion adjacent to an aminocarbene function and its reaction with a C=M(CO)<sub>5</sub> group intramolecularly. Secondly, a dehydro-metalation is observed in preference to the expulsion of the amino group (as is common in acylation reactions). Such a reaction is characteristic of ketones or aldehydes in an aldol reaction and certainly not observed with esters or amides. Thus, the present reaction provides the first example of intramolecular *metalla-aldol*<sup>13</sup> reaction of Fischer carbene complexes.

A possible mechanism of this reaction is depicted in Scheme 3. Since (dialkylamino)carbene complexes did not undergo such a reaction, it is most probable that

(12) (a) Gawley, R. E. *Synthesis* **1976**, 777. (b) Jung, M. E. *Tetrahedron* **1976**, *32*, 3.

(13) We prefer the term "metalla-aldol", suggested by Prof. T. R. Hoye, to distinguish this reaction from closely related ones (see: Casey, C. P.; Brunsvold, W. R. *Inorg. Chem.* **1977**, *16*, 391). Here the C=M group not only acts as the electrophile for carbanion addition in an aldol fashion, it is also sacrificed in the subsequent dehydro-metalation step (akin to dehydration), which is a unique feature of this reaction.



N-alkylation by dihalomethane precedes cyclization. Thus, the first step is N-alkylation of the aminocarbene complex by dichloromethane to produce a bis-carbene complex. This was confirmed by the use of  $\text{CD}_2\text{Cl}_2$  as solvent, which resulted in the disappearance of the methylene singlet at 4.30 ppm in the  $^1\text{H}$  NMR spectrum of the product **2e** (Scheme 1). This complex can undergo an intramolecular aldol-type reaction in which a  $\text{C}=\text{M}$  bond is attacked by a proximate carbanion.  $\beta$ -Elimination followed by double-bond isomerization leads to the product.<sup>14</sup>

The feasibility of carbanion formation ( $\text{p}K_{\text{a}}$  of aminocarbene complexes is estimated<sup>4a</sup> to be about 20) under these conditions was substantiated by  $\text{D}_2\text{O}$  exchange ( $\text{CH}_2\text{Cl}_2/50\% \text{NaOD}$  in  $\text{D}_2\text{O}$  with catalytic amount of  $\text{Bu}_4\text{NBr}$ ) of methyl(benzylmethylamino)carbene tungsten complex. In 4.5 h, about 75% deuterium incorporation was observed.<sup>15</sup> Although C-alkylation of this complex could not be effected under similar conditions,

(14) Alternatively, one of the methylene protons might be lost in the dehydrometalation step, as suggested by one of the referees.

(15) There is also a noticeable change in the conformer ratio as observed in the  $^1\text{H}$  NMR spectrum, which is an indirect evidence for the deprotonation of the methyl group. An  $\alpha$ -carbanion competes with delocalization of the lone pair of nitrogen toward the  $\text{C}=\text{M}$  bond. This reduces the rotation barrier of  $\text{C}_{\text{carbene}}-\text{N}$  bond and facilitates conformational interchange.

intramolecular condensation reported herein probably occurs owing to favorable entropy.

Indeed, such a reaction is not common in amide chemistry, and this result shows that Fischer carbene complexes can display a wider range of reactivity than one anticipates merely in terms of analogy and precedents. The novel cyclization product has interesting structural features. In a way, the amino carbene complex **2** is also an enamine and thus constitutes an unusual push-pull system. The reactive sites of these complexes are located at the  $\text{C}=\text{M}$  bond as well as the enamine function. The chemistry of this new class of complexes as well as their heteroatom analogs is currently being explored.

**Acknowledgment.** We thank Prof. T. R. Hoye, University of Minnesota, U.S.A., and Dr. S. V. Pansare, NCL, for helpful comments. One of us (S.R.A.) thanks CSIR, New Delhi, for a Senior Research Fellowship.

**Supporting Information Available:** Spectral data ( $^1\text{H}$  and  $^{13}\text{C}$  NMR) of all compounds and tables giving details of X-ray analysis, atomic coordinates, thermal parameters, and bond lengths and bond angles of **2a** (20 pages). Ordering information is given on any current masthead page.

OM9501283

# Reaction of a Stannylyene with Carbon Disulfide: Formation of a Novel Tin-Containing 1,3-Dipole and Its Reactivity

Masaichi Saito, Norihiro Tokitoh, and Renji Okazaki\*

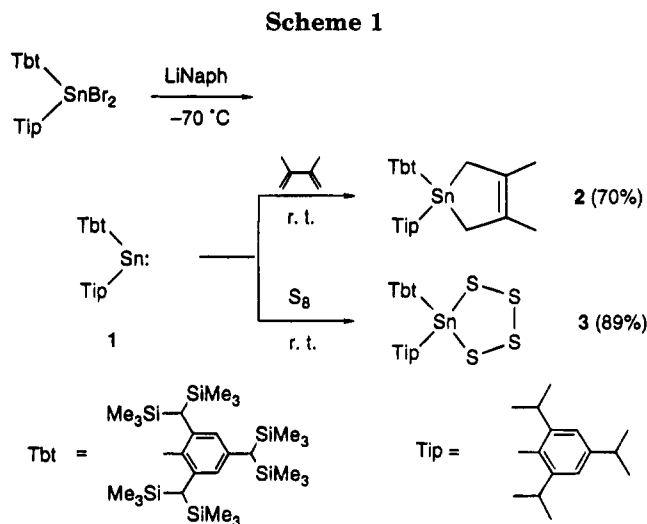
Department of Chemistry, Graduate School of Science, The University of Tokyo, 7-3-1 Hongo, Bunkyo-ku, Tokyo 113, Japan

Received April 26, 1995<sup>®</sup>

**Summary:** The reaction of the stannylyene  $Tbt(Tip)Sn:$  (**1**;  $Tbt = 2,4,6$ -tris[bis(trimethylsilyl)methyl]phenyl,  $Tip = 2,4,6$ -triisopropylphenyl), synthesized by reduction of  $Tbt(Tip)SnBr_2$  with lithium naphthalenide, with carbon disulfide in the presence of electron-deficient olefins, such as methyl acrylate, acrylonitrile, and methyl methacrylate, gave cycloadducts of the intermediary 1,3-dipole  $Tbt(Tip)Sn^-S-C^+=S$  (**4**). In the absence of the olefins, there was formed the unsymmetrical olefin  $Tbt(Tip)SnS_2C=CS_2C(=S)SSnTbt(Tip)$  (**8**), the structure for which was established by X-ray crystallography. Upon thermolysis, the olefin **8** underwent  $CS_2$  extrusion to afford the symmetrical olefin  $Tbt(Tip)SnS_2C=CS_2SnTbt(Tip)$  (**9**). The intermediary 1,3-dipole **4** showed  $\lambda_{max}$  at 608 nm and was stable up to ca.  $-30$  °C.

Recently, much attention has been focused on the low-coordinated compounds containing heavier group 14 elements (Si, Ge, Sn, and Pb), such as double-bond compounds and divalent species (higher homologues of a carbene). Although the divalent species containing silicon and germanium (silylene and germylene) have been well-investigated, the corresponding organotin compound (stannylyene) has been relatively less explored.<sup>1-4</sup>

It is well known that silylenes<sup>5</sup> and germylenes<sup>6</sup> form ylides in matrices with Lewis bases, such as ethers, sulfides, amines, alcohols, and carbonyl compounds. As for stannylenes, however, there have been only a few examples of ylides. For example, Ando et al. have proposed the formation of a stannylyene-thioketene ylide



by photolysis of an alkylidene-thiastannirane in a matrix at 77 K,<sup>7a</sup> while Veith et al. have reported the X-ray structural analysis of an ylide formed by the reaction of a stannylyene with *tert*-butylamine.<sup>7b</sup>

We have already reported the synthesis of the first stable stannanethione,  $Tbt(Tip)Sn=S$  ( $Tip = 2,4,6$ -triisopropylphenyl), via the kinetically stabilized diarylstannylyene  $Tbt(Tip)Sn:$  (**1**),<sup>3</sup> by taking advantage of an excellent steric protection group, 2,4,6-tris[bis(trimethylsilyl)methyl]phenyl (denoted as *Tbt*), developed by us.<sup>8</sup> In the course of our study on low-coordinated organotin compounds, we became interested in the reaction of a stannylyene with carbon disulfide which was expected to lead to the initial formation of a new type of ylide. In this paper, we present preliminary research on the formation and reactivity of a novel 1,3-dipole containing tin by the reaction of stannylyene **1**.

Although we previously reported the synthesis of the kinetically stabilized diarylstannylyene **1** by the reaction of stannous chloride with aryllithiums, the yield was not satisfactory.<sup>3</sup> We have now found that stannylyene

<sup>®</sup> Abstract published in *Advance ACS Abstracts*, July 15, 1995.

(1) For reviews, see: (a) Neumann, W. P. *Chem. Rev.* **1991**, *91*, 311. (b) Tsumuraya, T.; Batcheller, S. A.; Masamune, S. *Angew. Chem., Int. Ed. Engl.* **1991**, *30*, 902.

(2) For the first stable dialkylstannylyene, see: Kira, M.; Yauchibara, R.; Hirano, R.; Kabuto, C.; Sakurai, H. *J. Am. Chem. Soc.* **1991**, *113*, 7785.

(3) We have recently reported the first stable stannanethione in solution derived from a kinetically stabilized diarylstannylyene: Tokitoh, N.; Saito, M.; Okazaki, R. *J. Am. Chem. Soc.* **1993**, *115*, 2065.

(4) (a) For an X-ray structural analysis of bis[2,4,6-tris(trimethylsilyl)methyl]phenyl]stannylyene stabilized by the intramolecular coordination of fluorine atoms toward the tin atom, see: Grützmaier, H.; Pritzkow, H.; Edelmann, F. T. *Organometallics* **1991**, *10*, 23. (b) Very recently, the first X-ray structural analysis of bis(2,4,6-tri-*tert*-butylphenyl)stannylyene, a stable diarylstannylyene without any intramolecular coordination by heteroatoms, has been reported: Weidenbruch, M.; Schlaefke, J.; Schäfer, A.; Peters, K.; von Schnering, H. G.; Marsmann, H. *Angew. Chem., Int. Ed. Engl.* **1994**, *33*, 1846.

(5) (a) Gillette, G. R.; Noren, G. H.; West, R. *Organometallics* **1987**, *6*, 2617. (b) Ando, W.; Hagiwara, K.; Sekiguchi, A. *Organometallics* **1987**, *6*, 2270. (c) Ando, W.; Hagiwara, K.; Sekiguchi, A.; Sakakibara, A.; Yoshida, H. *Organometallics* **1988**, *7*, 558. (d) Gillette, G. R.; Noren, G. H.; West, R. *Organometallics* **1989**, *8*, 487.

(6) (a) Ando, W.; Itoh, H.; Tsumuraya, T.; Yoshida, H. *Organometallics* **1988**, *7*, 1880. (b) Ando, W.; Itoh, H.; Tsumuraya, T. *Organometallics* **1989**, *8*, 2759. (c) Ando, W.; Sato, S.; Tsumuraya, T. *Organometallics* **1989**, *8*, 161. (d) Ando, W.; Tsumuraya, T. *Organometallics* **1989**, *8*, 1467.

(7) (a) Ohtaki, T.; Kabe, Y.; Ando, W. *Organometallics* **1993**, *12*, 4. (b) Veith, M.; Schlemmer, G.; Sommer, M.-L. *Z. Anorg. Allg. Chem.* **1983**, *497*, 157.

(8) For the use of the *Tbt* group for kinetic stabilization of highly reactive species, see: (a) Okazaki, R.; Unno, M.; Inamoto, N. *Chem. Lett.* **1987**, 2293. (b) Okazaki, R.; Unno, M.; Inamoto, N.; Yamamoto, G. *Chem. Lett.* **1989**, 493. (c) Okazaki, R.; Unno, M.; Inamoto, N. *Chem. Lett.* **1989**, 791. For recent advances using the *Tbt* group, see: (d) Tokitoh, N.; Suzuki, H.; Okazaki, R.; Ogawa, K. *J. Am. Chem. Soc.* **1993**, *115*, 10428. (e) Tokitoh, N.; Suzuki, H.; Okazaki, R.; Ogawa, K. *J. Am. Chem. Soc.* **1994**, *116*, 11578. (f) Tokitoh, N.; Matsumoto, T.; Manmaru, K.; Okazaki, R. *J. Am. Chem. Soc.* **1993**, *115*, 8855. (g) Matsumoto, T.; Tokitoh, N.; Okazaki, R. *Angew. Chem., Int. Ed. Engl.* **1994**, *33*, 2316. (h) Matsuhashi, Y.; Tokitoh, N.; Okazaki, R.; Goto, M. *Organometallics* **1993**, *12*, 2573. (i) Tokitoh, N.; Matsuhashi, Y.; Shibata, K.; Matsumoto, T.; Suzuki, H.; Saito, M.; Manmaru, K.; Okazaki, R. *Main Group Met. Chem.* **1994**, *17*, 55.

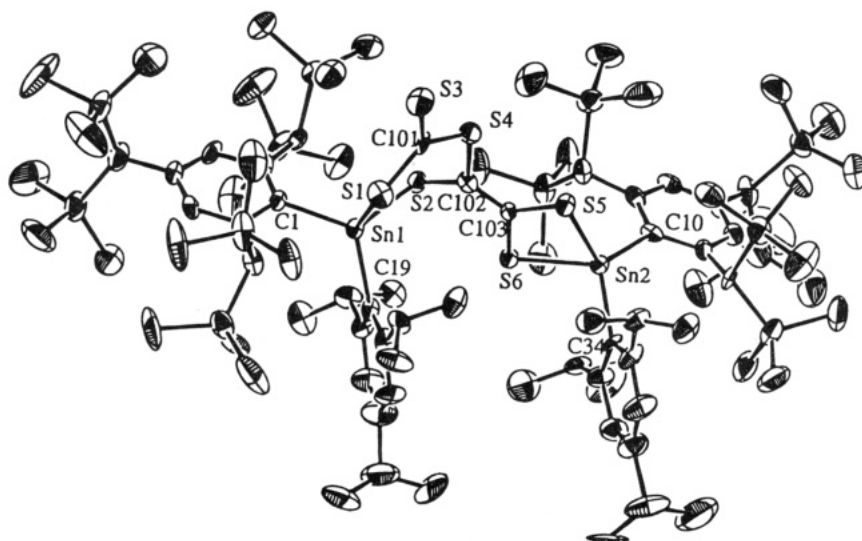
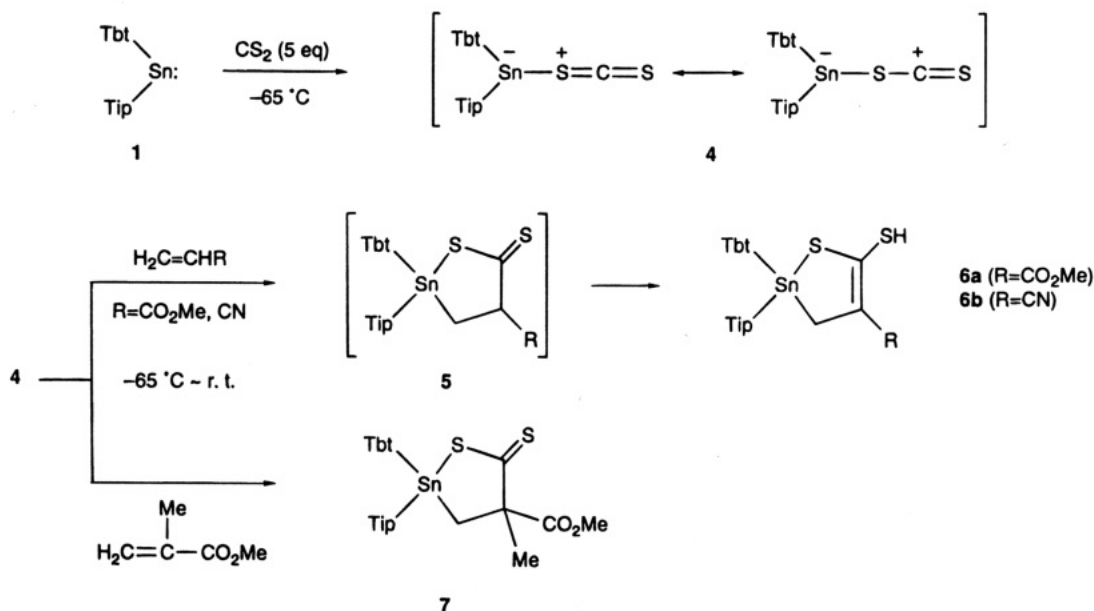


**Figure 1.** ORTEP drawing of  $\text{Tbt}(\text{Tip})\text{SnS}_2\text{C}=\text{CS}_2\text{C}(\text{=S})\text{SSn}(\text{Tip})\text{Tbt}$  (**8**) as a thermal ellipsoid plot (30% probability). Selected bond lengths (Å) and angles (deg):  $\text{Sn}(1)-\text{S}(1) = 2.484(6)$ ,  $\text{Sn}(1)-\text{S}(2) = 2.424(6)$ ,  $\text{Sn}(2)-\text{S}(5) = 2.460(5)$ ,  $\text{Sn}(2)-\text{S}(6) = 2.447(6)$ ,  $\text{C}(102)-\text{C}(103) = 1.35(2)$ ,  $\text{C}(101)-\text{S}(3) = 1.64(2)$ ;  $\text{S}(1)-\text{Sn}(1)-\text{S}(2) = 97.3(2)$ ,  $\text{S}(5)-\text{Sn}(2)-\text{S}(6) = 74.3(2)$ ,  $\text{S}(2)-\text{C}(102)-\text{S}(4) = 119(1)$ ,  $\text{S}(5)-\text{C}(103)-\text{S}(6) = 115(1)$ .

## Scheme 2



**1** can be easily and efficiently prepared by reaction of the corresponding dibromostannane with lithium naphthalenide in THF, as evidenced by the high-yield formation of trapping adducts with 2,3-dimethyl-1,3-butadiene and sulfur (Scheme 1).<sup>9</sup>

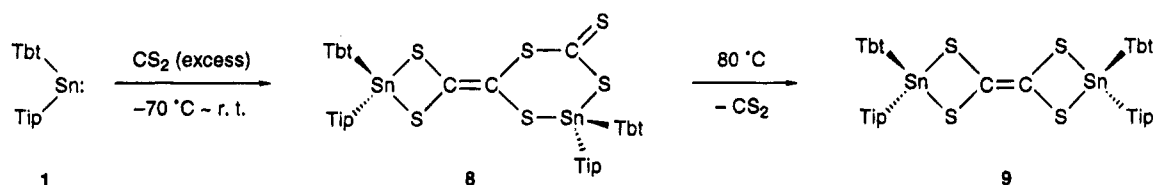
When carbon disulfide was added to a THF solution of stannylene **1** thus obtained, the solution turned deep blue-green. Monitoring of the reaction using UV-vis spectroscopy at  $-70^\circ\text{C}$  showed a new absorption at 608 nm assignable to the stannylene-carbon disulfide ylide **4**, which was substantially red-shifted from the absorption of stannylene **1** in hexane (561 nm).<sup>3</sup> This ylide

was quite stable at  $-70^\circ\text{C}$ , in contrast to the ylide of the stannylene with a thioketene which was observed in a 3-methylpentane matrix at 77 K.<sup>7a</sup>

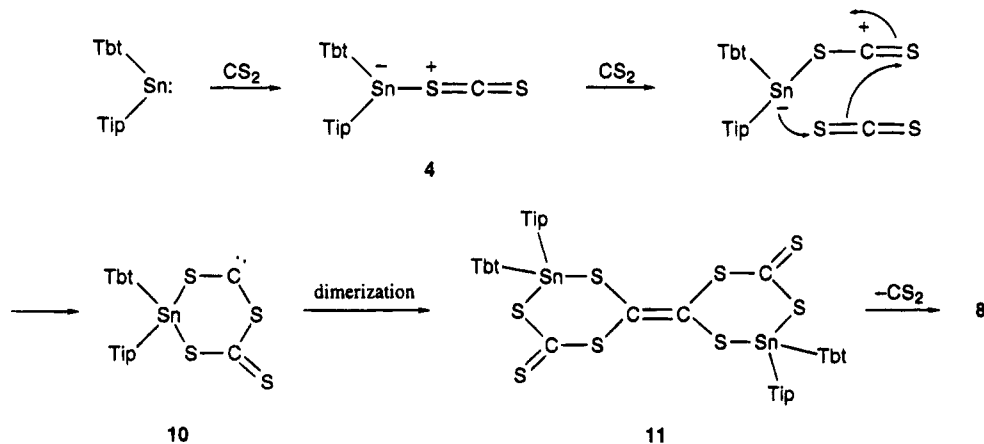
The stannylene-carbon disulfide ylide **4** was found to act as a novel 1,3-dipole by trapping experiments with some olefins. When carbon disulfide (5 equiv) was added to a THF solution of stannylene **1**, the solution turned blue-green, indicating the formation of **4**. Addition of an excess amount of methyl acrylate or acrylonitrile (*ca.* 10 equiv) to this solution at  $-65^\circ\text{C}$  resulted in the corresponding cyclic enethiol **6a** (40%) or **6b** (47%), respectively. These facts clearly show the initial formation of the stannylene-carbon disulfide ylide **4**, a novel 1,3-dipolar system, followed by trapping with the olefins to give the cycloadduct **5** and its enethiolization. The use of methyl methacrylate, having no proton for enethiol tautomerization, gave the corresponding 1,2-thiastannolane-5-thione **7** in 40% yield as a mixture of *cis* and *trans* isomers.<sup>10</sup> The formation of **6** and **7**

(9) General procedure for the preparation of diarylstannylene **1**: After addition of lithium naphthalenide (0.72 M in THF, 0.34 mL, 2.5 equiv), prepared from lithium (182 mg, 26.2 mmol) and naphthalene (2685 mg, 21.0 mmol) in THF (25 mL), to a THF solution (5 mL) of dibromostannane  $\text{Tbt}(\text{Tip})\text{SnBr}_2$  (102 mg, 0.098 mmol) at  $-70^\circ\text{C}$ , the reaction mixture was stirred for 30 min at this temperature. The mixture was gradually warmed to room temperature to give a THF solution of stannylene **1**.

## Scheme 3



## Scheme 4



represents the first unambiguous example of [2 + 3] cycloaddition reactions of a tin-containing 1,3-dipole with olefin.<sup>11</sup>

In the absence of trapping agents the reaction of stannylene **1** with an excess amount of carbon disulfide resulted in the formation of the chrome yellow unsymmetrical olefin **8** (77%), the structure of which was established by X-ray crystallographic analysis as shown in Figure 1.<sup>12</sup> The aryl substituents are found to be located in a *cis* fashion. Interestingly, thermolysis of **8** (80 °C) afforded the red, symmetrically substituted olefin **9**<sup>13</sup> in a quantitative yield via extrusion of carbon disulfide (Scheme 3). As mentioned above, the ylide **4** was quite stable at -70 °C. When methyl acrylate was added to a THF solution of **4** at -35 °C, **6a** was still obtained in 8% yield along with **8** (40%), suggesting that **4** was stable even at -35 °C in solution.

It is interesting that the mode of the present reaction of stannylene **1** with carbon disulfide is different from that of Jutzi's decamethylsilicocene, which reportedly affords a symmetrical cyclic thioester.<sup>14</sup> Although a detailed mechanism for the present reaction is not clear at present, we consider that it proceeds as shown in Scheme 4. The ylide **4** reacts with another carbon disulfide to give the dithiocarbene **10**, which then dimerizes, affording **11**. The dimer **11** is thermally unstable, probably due to steric repulsion between the very bulky aryl substituents as indicated by inspection of the molecular model, to decompose to **8** with loss of carbon disulfide as is observed in the thermolysis of **8**.

In conclusion, stannylene **1** reacted with carbon disulfide to give the novel 1,3-dipole **4** having its  $\lambda_{\max}$  at 608 nm. The 1,3-dipole **4** was trapped by electron-deficient olefins to give cycloadducts, whereas in the absence of the trapping agents, it underwent further reaction with carbon disulfide to give the olefin **8** with a new interesting structure.

(10) The two isomers (**7a** and **7b**) could be separated by TLC, although the assignment of stereochemistry was impossible (see the supporting information). In addition to **7**, there was also formed olefin **8** (10%) (for the structure of **8**, see Scheme 3).

(11) The formation of a 1:2 adduct of a stannylene with a thioketone was assumed to proceed via [3 + 2] cycloaddition of an intermediary ylide with a thioketone or insertion of a thioketone into the Sn-C bond of an intermediary thiastannirane.<sup>7a</sup>

(12) Crystal data for **8**: C<sub>94</sub>H<sub>172</sub>S<sub>6</sub>Si<sub>12</sub>Sn<sub>2</sub>,  $M_r = 2069.16$ , triclinic, space group  $P\bar{1}$ ,  $a = 18.220(7)$  Å,  $b = 22.989(6)$  Å,  $c = 17.485(5)$  Å,  $\alpha = 104.99(2)^\circ$ ,  $\beta = 115.31(2)^\circ$ ,  $\gamma = 73.92(3)^\circ$ ,  $V = 6277(4)$  Å<sup>3</sup>,  $Z = 2$ ,  $D_c = 1.095$  g cm<sup>-3</sup>,  $\mu = 6.47$  cm<sup>-1</sup>,  $R$  ( $R_w$ ) = 0.071 (0.087). The intensity data were collected on a Rigaku AFC5R diffractometer with graphite-monochromated Mo K $\alpha$  radiation ( $\lambda = 0.71069$  Å). The structure was solved by direct methods. The final cycle of full-matrix least-squares refinement was based on 6023 observed reflections ( $I > 3.00\sigma(I)$ ) and 976 variable parameters. Attempted structural refinement using space group  $P1$  (acentric) led to poorer results. Full details for the crystallographic analysis of **8** are described in the supporting information.

(13) We tentatively assign the *cis* configuration also to **9**.

(14) Jutzi, P.; Möhrke, A. *Angew. Chem., Int. Ed. Engl.* **1989**, *28*, 762. In the reaction of decamethylsilicocene with carbon disulfide, Jutzi has postulated the initial formation of a silathiiranethione. Although the involvement of a stannathiiranethione (either by itself or in equilibrium with ylide **4**) cannot be rigorously excluded also in the present reaction, we think that the reaction proceeds via **4** since the absorption at 608 nm is reasonably assignable to **4**.

**Acknowledgment.** This work was partially supported by a Grant-in-Aid for Scientific Research (No. 05236102) from the Ministry of Education, Science, and Culture of Japan. M.S. thanks Research Fellowships of the Japan Society for the Promotion of Science for Young Scientists. We are also grateful to Shin-etsu Chemical Co., Ltd., and Tosoh Akzo Co., Ltd., for generous gifts of chlorosilanes and alkyllithiums, respectively.

**Supporting Information Available:** Text giving the physical properties of **6**–**9** and crystallographic data with complete tables of bond lengths, bond angles, and thermal and positional parameters for **8** (54 pages). Ordering information is given on any current masthead page.

OM9503003





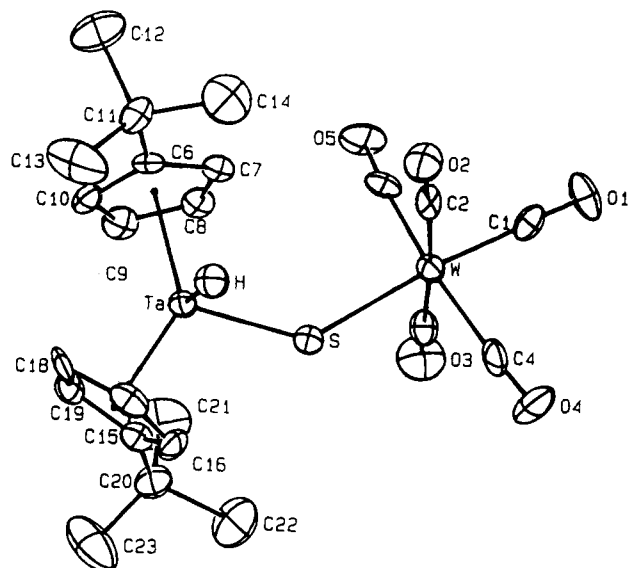


**Figure 1.** ORTEP drawing of  $(t\text{-BuC}_5\text{H}_4)_2\text{Ta}[\text{=S-W}(\text{CO})_5]\text{H}$  (**2c**). Selected distances (Å) and angles ( $^\circ$ ): Ta–S = 2.274(5), Ta–H = 1.74 (calcd), W–S = 2.554(4); W–S–Ta = 135.9(2), CP1–Ta–CP2 = 134.0.

resonance at  $\delta = 7.10$  is only shifted by about 0.4 ppm to higher field, whereas the corresponding resonance in  $[(\text{C}_5\text{H}_5)_2\text{Ta}(\text{CO})(\mu\text{-H})]\text{Cr}(\text{CO})_5$  is shifted by ca. 12 ppm to higher field.<sup>11</sup>

An X-ray diffraction analysis of  $\text{Cp}'_2\text{Ta}[\text{=S-W}(\text{CO})_5]\text{H}$  (**2c**)<sup>12</sup> confirms the bridging nature of sulfur (Figure 1). The Ta–S–W angle ( $135.9^\circ$ ) indicates an approximate  $sp^2$  hybridization of the sulfur atom. A relatively short Ta–S distance (2.274 Å) which is only slightly longer than those reported for  $\text{TaSCl}_3(\text{PhSCH}_2\text{-CH}_2\text{SPh})$  (2.204 Å) and  $\text{TaS}(\text{S}_2\text{CNEt}_2)_3$  (2.181 Å)<sup>13</sup> is consistent with a formal Ta=S double bond. The hydride ligand could not be found in the final difference Fourier map and has been placed in calculated position.<sup>14</sup>

(12) X-ray structure analysis of **2c**: A red crystal having the approximate dimensions  $0.2 \times 0.1 \times 0.1$  mm was used for unit cell measurements and intensity data collection, carried out at 296 K on an Enraf-Nonius CAD4 diffractometer with Mo K $\alpha$  radiation ( $\lambda = 0.71073$  Å). All calculations have been carried out by using the Enraf-Nonius Molen library. The structure was solved and refined by standard methods. **2c**: monoclinic, space group  $P2_1/n$  (No. 14),  $a = 12.238(2)$  Å,  $b = 18.258(3)$  Å,  $c = 12.831(2)$  Å,  $\beta = 116.23(1)^\circ$ ,  $V = 2572.0$  Å<sup>3</sup>,  $d_{\text{calc}} = 2.015$  g cm<sup>-3</sup>,  $Z = 4$ , and  $\mu = 88.75$  cm<sup>-1</sup>. An empirical absorption correction ( $\psi$  scan,  $\text{abs}_{\text{min}} = 77.9341$ ,  $\text{abs}_{\text{max}} = 99.7128$ ) was applied. All non-hydrogen atoms were refined with anisotropic temperature factors, and the hydrogen atoms were placed in calculated positions. These last atoms were ridden on the atoms bearing them and included in the final calculations with  $B_{\text{iso}}$  fixed at the values equal to  $1.3B_{\text{eq}}$  for the corresponding carbon atoms. Full-matrix least-squares refinement based on 1610 unique reflections with  $I > 1\sigma(I)$  converged at  $R = 0.030$ . Full details are given in the supporting information.

(13) Drew, M. G. B.; Rice, D. A.; Williams, D. M. *J. Chem. Soc., Dalton Trans.* **1984**, 845. Peterson, E. J.; von Dreele, R. B.; Brown, T. M. *Inorg. Chem.* **1978**, *17*, 1410. A discussion of short Ta–S bonds is given in: Tatsumi, K.; Inoue, Y.; Kawaguchi, H.; Kohsaka, M.; Nakamura, A.; Cramer, R. E.; VanDoorne, W.; Taogoshi, G. J.; Richmann, P. N. *Organometallics* **1993**, *12*, 352.

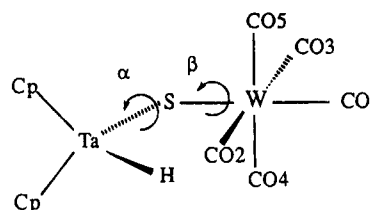
(14) The coordinates of the hydride ligand, needed for EHMO calculations, are proposed on the basis of typical geometries observed in bent tantalocenes  $\text{Cp}_2\text{TaX}_2$  by assuming the Ta–H bond length equal to 1.74 Å, the S–Ta–H angle of  $90^\circ$ , and the orthogonality of the  $\text{Cp}_1\text{-TaCp}_2$  and  $\text{STaH}$  planes.

(15) Hoffmann, R. *J. Chem. Phys.* **1963**, *39*, 1397. Mealli, C.; Proserpio, D. M. *J. Chem. Educ.* **1990**, *67*, 399.

(16) Lauher, J. W.; Hoffmann, R. *J. Am. Chem. Soc.* **1976**, *98*, 1729.

(17) The atomic parameters  $H_i$  used in this study were those contained in the DATA file of CACAO. Interatomic distances and bond angles were taken from the structure of **2c** reported here.

Scheme 1



EHMO calculations<sup>15</sup> on a model  $(\text{C}_5\text{H}_5)_2\text{Ta}[\text{=S-W}(\text{CO})_5]\text{H}$  show that the Ta=S  $\pi$  orbital is localized in the HTaS plane which corresponds to an usual donor interaction of the p atomic orbital of sulfur into the empty nonbonding orbital ( $1a_1$  in the Lauher–Hoffman model)<sup>16</sup> of Ta(V). For a  $sp^2$ -hybridized sulfur atom the ideal value of HTaS/TaSW dihedral angle should be equal to  $90^\circ$ . Such a value should lead to strong steric repulsions between one Cp' ligand and the  $\text{W}(\text{CO})_5$  fragment. Thus, the observed value is smaller ( $79.5^\circ$ ) and the largely opened TaSW angle ( $135.9^\circ$ ) confirms the presence of steric intramolecular repulsions. However, the molecular geometry of **2c** found in the solid state does not correspond to the structure expected on the basis of  $^1\text{H}$  NMR spectroscopy. The spectra recorded from room temperature to  $-75^\circ\text{C}$  (in acetone- $d_6$ ) exhibit one resonance for the t-Bu substituent and four signals for the  $\eta^5\text{-C}_5\text{H}_4$  protons. Such a pattern is consistent with a magnetic equivalence of both Cp' ligands and a symmetrical orientation of the  $\text{W}(\text{CO})_5$  fragment with respect to these ligands.

In order to clarify this apparent contradiction, additional EHMO calculations have been carried out<sup>17</sup> in a way that two dihedral angles  $\alpha$  (HTaS/TaSW) and  $\beta$  (TaSW/SWCO2) (Scheme 1) have been varied from  $0$  (endo) to  $180^\circ$  (exo geometry) and from  $0$  to  $90^\circ$ , respectively. The resulting minima of total energy are obtained for values of  $\alpha$  and  $\beta$  close to  $60$  and  $30^\circ$ , respectively. These results are in good agreement with the X-ray data:  $\alpha$  (HTaS/TaSW) =  $79.5^\circ$  and  $\beta$  (TaSW/SWCO2) =  $36.6^\circ$ .

Finally, it is important to note that the minimum of total energy for the conformation corresponding to the symmetrical structure suggested by  $^1\text{H}$  NMR ( $\alpha = 0^\circ$ ) is only 0.2 eV ( $\approx 19$  kJ/mol) higher than that for the stable conformation ( $\alpha = 60^\circ$ ). This means that the rotation of the  $\text{W}(\text{CO})_5$  fragment around the Ta=S bond may easily occur in solution.

In conclusion we have shown that the addition of  $\text{M}'(\text{CO})_5$  fragments to the Ta=S bond gives heterobimetallic compounds comprising an unsupported 4e sulfur bridge.  $^1\text{H}$  NMR investigations in solution and EHMO calculations are in agreement with a rotation around the Ta=S bond the energy barrier of which is relatively low.

**Supporting Information Available:** Plots of the total and minimal total energies of rotations around the Ta=S ( $\alpha$ ) and S–W ( $\beta$ ) bonds and tables of coordinates of non-hydrogen atoms, intramolecular distances and angles, hydrogen atom coordinates, isotropic and anisotropic temperature factors, and least-squares planes for **2c** (8 pages). Ordering information is given on any current masthead page.

OM9504680

# Synthesis and Reduction of the 9,10-Disilaanthracene Dimer

Wataru Ando,\* Ken Hatano, and Rie Urisaka

Department of Chemistry, University of Tsukuba, Tsukuba, Ibaraki 305, Japan

Received April 12, 1995<sup>⊗</sup>

**Summary:** 9,10-Dimethyl-9,10-disilaanthracene dimer (**2**) was prepared by treatment of 9,10-dihydro-9,10-disilaanthracene (**1a**) with 2 equiv of lithium. The reaction of **2** with excess lithium or potassium resulted in formation of 9,10-dilithio- or 9,10-dipotassio-9,10-dimethyl-9,10-disilaanthracene (**4a,b**), via the dianion **3**, in which one Si–Si bond has been cleaved. On treatment with  $\alpha,\omega$ -dichloropolysilanes, **4a** was converted into the corresponding cyclic compounds **6–9**, respectively.

The chemistry of 9,10-dihydroanthracenes with the silicon in position 9 and/or 10 has been considerably developed by Jutzi<sup>1</sup> and Bickelhaupt<sup>2</sup> and modified by Corey.<sup>3</sup> However, the anthracene dimer analogs with bridgehead silicon atoms have not been reported. We report herein the synthesis and reduction of the 9,10-dimethyl-9,10-disilaanthracene dimer, a silicon analog to the anthracene dimer.

Although the Wurtz coupling reaction of 9,10-dichloro-9,10-dimethyl-9,10-disilaanthracene (**1b**) with sodium in toluene at 110 °C formed bridged dimer **2** in only 7% yield, increased yields of **2** have been achieved by direct reaction of 9,10-dihydro-9,10-dimethyl-9,10-disilaanthracene (**1a**) with lithium.

Reaction of a cis/trans mixture (=45/55)<sup>4</sup> of **1a** (4.80 g, 20.0 mmol) with 2 equiv of lithium (0.28 g, 40.0 mmol) in THF (30 mL) containing 6 mL of TMEDA produces a yellow solution at room temperature over a reaction time of 48 h. After removal of unreacted lithium, the bridged dimer **2** was obtained in 61% yield (Scheme 1). The structure of dimer **2** has been confirmed by spectral data<sup>5</sup> and an X-ray analysis (Figure 1).<sup>6</sup> Although the

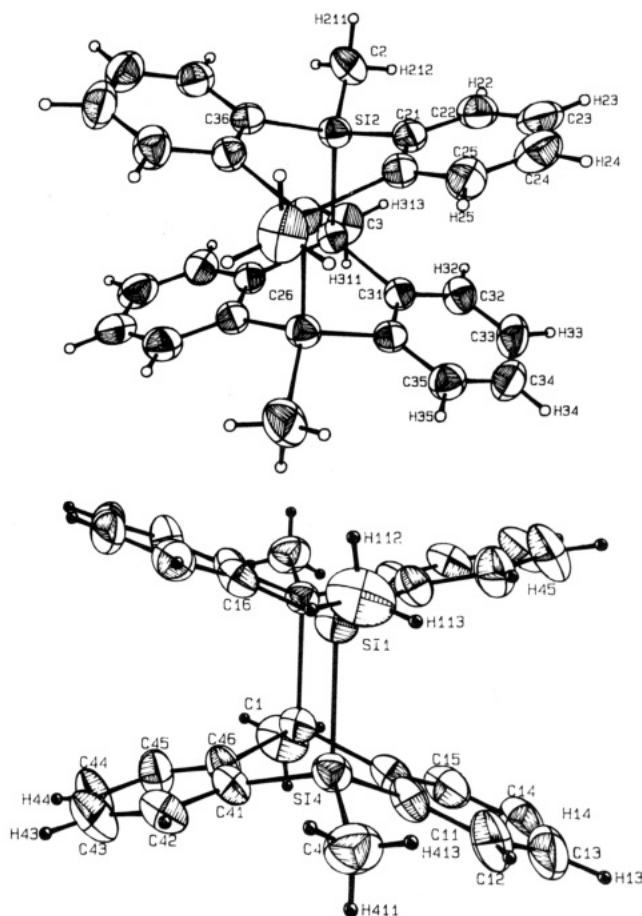


**Figure 1.** ORTEP drawings of 9,10-disilaanthracene dimer **2** showing the thermal ellipsoids at the 50% probability level. Important bond distances (Å) and angles (deg): Si(1)–Si(4) = 2.3710(9), Si(1)–C(1) = 1.867(3), Si(1)–C(16) = 1.884(2), Si(2)–Si(3) = 2.377(1), Si(2)–C(2) = 1.870(3), Si(2)–C(21) = 1.882(2); Si(4)–Si(1)–C(1) = 110.9(1), Si(4)–Si(1)–C(16) = 106.48(8), C(1)–Si(1)–C(16) = 111.8(1), C(16)–Si(1)–C(46) = 107.9(2), Si(3)–Si(2)–C(2) = 111.7(1), Si(3)–Si(2)–C(21) = 106.29, C(2)–Si(2)–C(21) = 111.7(1), C(21)–Si(2)–C(36) = 108.1(1).

exact nature of the intermediate produced from the dihydrosilanaanthracene remains uncertain, we tentatively suggest that is the silicon-centered 9,10-disilaanthracene biradical or its equivalent intermediate via electron transfer reactions.<sup>7</sup> Further studies concerning these question are in progress.

Stirring **2** (240 mg, 0.5 mmol) with an excess of lithium in THF at room temperature produced a green

(7) Spectroscopic studies of the yellow solution appearing at  $\lambda_{\max}$  349 nm did not support a clear assignment of the intermediate.

(8) The green compound probably is the 9,10-disilaanthracene anion radical. As a support for the existence of the anion radical, 9,10-dihydro-9,9,10-trimethyl-9,10-disilaanthracene was also obtained in 32% yield along with **1c**.

<sup>⊗</sup> Abstract published in *Advance ACS Abstracts*, July 15, 1995.

(1) (a) Jutzi, P. *Chem. Ber.* **1971**, *104*, 1455. (b) Jutzi, P. *Angew. Chem., Int. Ed. Engl.* **1975**, *14*, 232.

(2) (a) van den Winkel, Y.; van Baar, B. L. M.; Bickelhaupt, F.; Kulik, W.; Sierakowski, C.; Maier, G. *Chem. Ber.* **1991**, *124*, 185. (b) van den Winkel, Y.; van Baar, B. L. M.; Bastiaans, M. M.; Bickelhaupt, F. *Tetrahedron* **1990**, *46*, 1009. (c) Bickelhaupt, F.; van Mourik, G. L. *J. Organomet. Chem.* **1974**, *67*, 389.

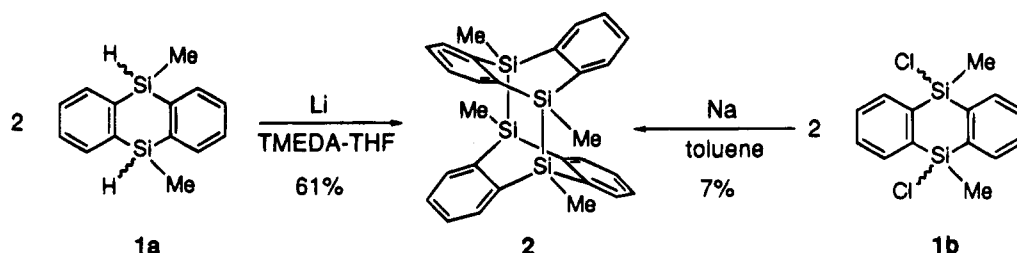
(3) (a) McCarthy, W. Z.; Corey, J. Y.; Corey, E. R. *Organometallics* **1984**, *3*, 255. (b) Corey, J. Y.; McCarthy, W. Z. *J. Organomet. Chem.* **1984**, *271*, 319.

(4) Welsh, K. M.; Corey, J. Y. *Organometallics* **1987**, *6*, 1393. This compound was prepared by Corey's procedure. The *cis/trans* ratio was determined by <sup>1</sup>H NMR spectroscopy.

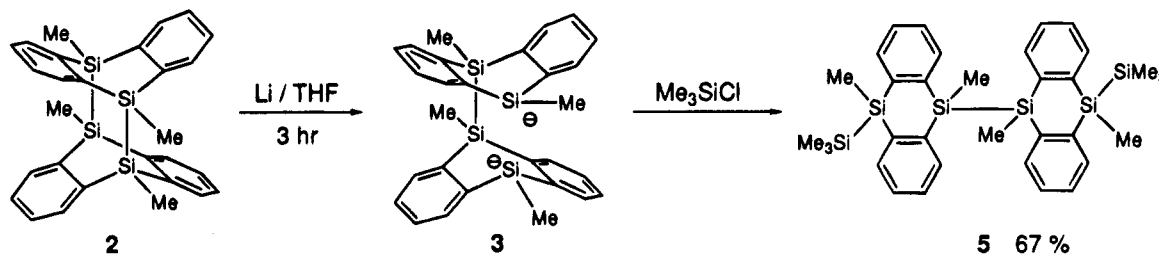
(5) **2**: colorless crystals; mp >300 °C; <sup>1</sup>H NMR (CDCl<sub>3</sub>, 300 MHz)  $\delta$  0.84 (s, 12H), 7.03 (dd,  $J = 5.1, 3.1$  Hz, 8H), 7.33 (dd,  $J = 5.1, 3.1$  Hz, 8H); <sup>13</sup>C NMR (CDCl<sub>3</sub>, 75 MHz)  $\delta$  -7.18, 127.08, 131.89, 143.47; <sup>29</sup>Si NMR (CDCl<sub>3</sub>, 60 MHz)  $\delta$  -27.91; mass *m/e* (%) 476 (100), 461 (56), 417 (67). Anal. Calcd for C<sub>28</sub>H<sub>28</sub>Si<sub>4</sub>: C, 70.52; H, 5.92. Found: C, 70.58; H, 5.88.

(6) Crystallographic data for **2**: fw 476.88, monoclinic,  $a = 14.157(1)$  Å,  $b = 10.765(1)$  Å,  $c = 18.469(2)$  Å,  $\beta = 110.25(1)^\circ$ ,  $V = 2640.6$  Å<sup>3</sup>, space group  $P2_1/a$ ,  $Z = 4$ ,  $\mu(\text{Mo K}\alpha) = 2.3$  cm<sup>-1</sup>,  $\rho(\text{calcd}) = 1.20$  g/cm<sup>3</sup>,  $R = 0.036$  ( $R_w = 0.036$ ). The 3954 independent reflections ( $2\theta \leq 52.6^\circ$ ;  $|F_o| \geq 3\sigma|F_o|$ ) were measured on an Enraf-Nonius CAD4 diffractometer using Mo K $\alpha$  irradiation and an  $\omega$ - $\theta$  scan. An empirical absorption correction based on a series of  $\psi$  scans was applied to the data (0.925/0.999). The structure was solved by direct methods, and hydrogen atoms were located and added to the structure factor calculations, but their positions were not refined.

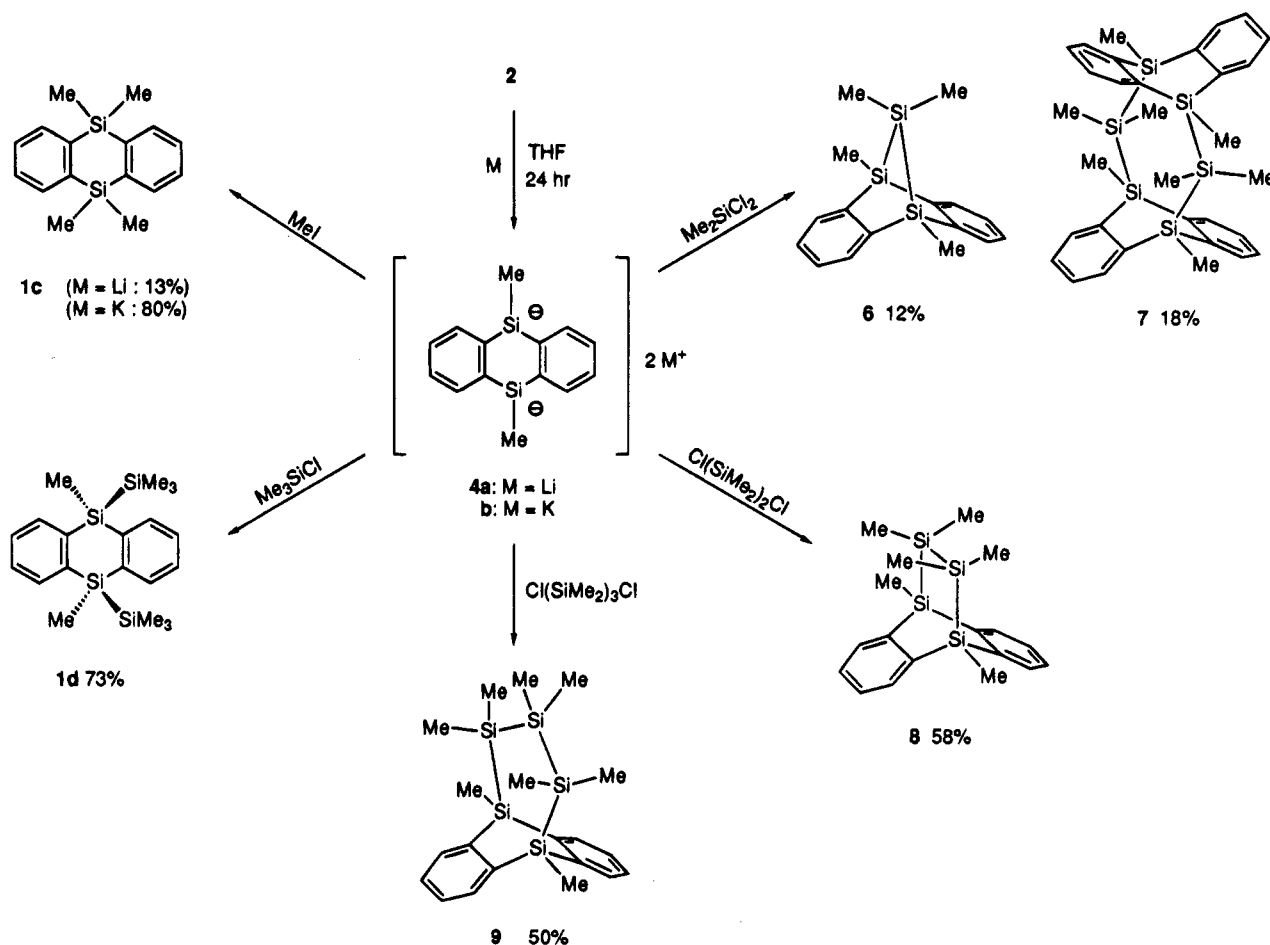
## Scheme 1. Preparations of 9,10-Disilaanthracene Dimer 2



## Scheme 2. Generation of Bis(9,10-dimethyl-9,10-disilaanthracen-9-yl) Dianion 3



## Scheme 3. Syntheses of 1c,d and 9,10-Bridged Polysila-9,10-disilaanthracenes 6–9



solution.<sup>8</sup> After removal of unreacted lithium and treatment with an excess of methyl iodide, 9,10-dihydro-9,9,10,10-tetramethyl-9,10-disilaanthracene (**1c**) was obtained in 13% yield. In a similar reaction, potassium was employed for the silicon-silicon bond cleavage of the dimer **2**. Treatment with methyl iodide followed; **1c** was produced in 80% yield (Scheme 3). It is noteworthy that the dimer **2** is easily reduced with potassium to afford dipotassium 9,10-disilaanthracenide (**4b**). <sup>29</sup>Si NMR chemical shifts for **4a,b** in THF-*d*<sub>8</sub> were

observed at -45.4 and at -42.8 ppm, respectively, a large upfield shift compared to other silyl anions (Ph<sub>3</sub>SiM, -9.0 (M = Li), -7.5 (M = K) ppm; Ph<sub>2</sub>MeSiM, -20.6 (M = Li), -18.5 (M = K) ppm).<sup>9</sup> The formation of these dianions **4** is strongly dependent upon the

(9) (a) Olah, G. A.; Hunadi, R. *J. Am. Chem. Soc.* **1980**, *102*, 6989. (b) Buncel, E.; Venkatachalam, T. K.; Eliasso, B.; Edlund, U. *J. Am. Chem. Soc.* **1985**, *107*, 303. (c) Edlund, U.; Buncel, E. In *Progress in Physical Organic Chemistry*; Taft, R. W., Ed.; Wiley: New York, 1993; Vol. 19, p 254.

solvent; it increased in THF and was suppressed in diethyl ether and dimethoxyethane (DME). In general, formation of silyl potassium reagents from disilanes has been accomplished by reaction with potassium alkoxide,<sup>10</sup> potassium hydride,<sup>11</sup> or Na–K alloy<sup>12</sup> and by treatment with potassium metal in liquid ammonia.<sup>13</sup> During the course of the reactions of **2** with an excess of lithium or potassium, the reaction mixture becomes a yellow suspension. Reaction of the yellow suspension with trimethylchlorosilane gave the bis(9,10-dimethyl-10-(trimethylsilyl)-9,10-disilaanthracen-9-yl) (**5**) in 67% yield (Scheme 2).<sup>14</sup> The molecular structure of the opened dimer **5** is shown in Figure 2.<sup>15</sup> Two methyl groups on the disilaanthracene unit of **5** are substituted in a *cis* configuration, respectively. Thus, the silicon–silicon bond cleavage of bridged dimer **2** with alkali metal proceeds with retention of configuration around the silicon atom. It is logical from these results that these dianions **4** are generated *via* one silicon–silicon bond-cleaved dianion (**3**).

The reactions of dipotassium disilaanthracenide (**4b**) with trimethylchlorosilane gave the expected adduct (**1d**) in 73% yield as one isomer.<sup>16</sup> The dipotassium (**4b**) also was treated with  $\alpha,\omega$ -dichloropolysilanes as shown in Scheme 3. The products were identified by means of <sup>1</sup>H, <sup>13</sup>C, and <sup>29</sup>Si NMR and mass spectra. The

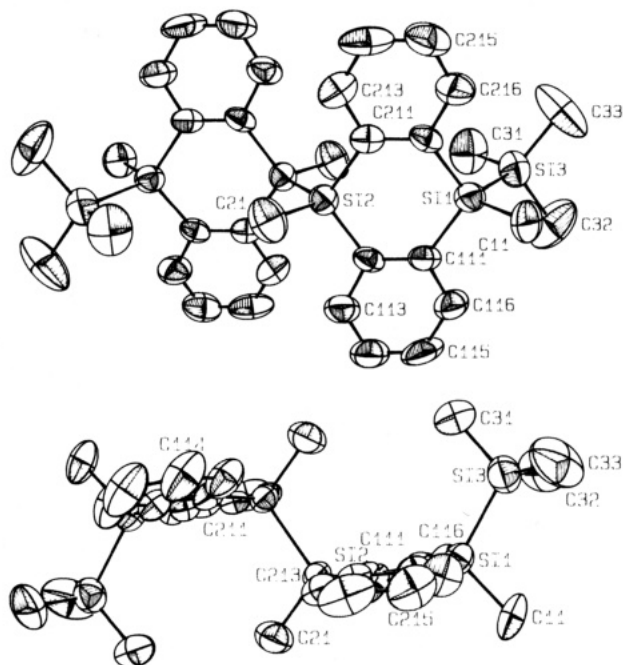


**Figure 2.** ORTEP drawings of opened dimer **5** showing the thermal ellipsoids at the 50% probability level. Important bond distances (Å) and angles (deg): Si(1)–Si(3) = 2.339(4), Si(1)–C(11) = 1.90(1), Si(1)–C(111) = 1.888(9), Si(2)–C(21) = 1.88(1), Si(2)–C(112) = 1.866(9), Si(3)–C(31) = 1.85(1); Si(3)–Si(1)–C(11) = 108.9(4), Si(3)–Si(1)–C(111) = 112.3(3), C(11)–Si(1)–C(111) = 106.9(4), C(111)–Si(1)–C(211) = 109.3(4), C(21)–Si(2)–C(112) = 109.6(5), C(112)–Si(2)–C(212) = 109.9(3).

reaction of **4b** with dimethyldichlorosilane gave the expected dimethylsilyl adduct **6** bonded to the 9- and 10-positions of the disilaanthracene and the dimeric compound **7** in 12% and 18% yields, respectively.<sup>17</sup> The corresponding 9- and 10-position adduct was obtained in good yield when the dipotassium species **4b** reacted with 1,2-dichlorotetramethyldisilane and 1,3-dichlorohexamethyltrisilane, respectively,<sup>18</sup> without formation of dimeric products. The formation of **6–9** clearly reveals that the generated dipotassium disilaanthracenide (**4b**) has a *cis* configuration.

It is clear that dipotassium 9,10-dimethyl-9,10-disilaanthracenide (**4b**), generated from the dimer **2** with potassium metal, can be a valuable intermediate for the synthesis of a great variety of *cis*-9,10-disilaanthracene derivatives.

**Acknowledgment.** This work was supported by a Grant-in-Aid for Scientific Research from the Ministry of Education, Science and Culture of Japan. We thank Prof. K. Okamoto for useful discussions and Shin-Etsu Chemical Co. Ltd. for a gift of organosilicon reagents.

**Supporting Information Available:** Text describing crystallographic procedures and tables of crystallographic data, atomic coordinates and thermal parameters, and bond lengths and angles for **2** and **5** (29 pages). Ordering information is given on any current masthead page.

OM9502650

(10) Sakurai, H.; Kira, M.; Umino, H. *Chem. Lett.* **1977**, 1265.

(11) Corriu, R. J. P.; Guerin, C. *J. Chem. Soc., Chem. Commun.* **1980**, 168.

(12) (a) Benkeser, R. A.; Landesman, H.; Foster, D. J. *J. Am. Chem. Soc.* **1951**, *74*, 648. (b) Gilman, H.; Wu, T. C. *J. Am. Chem. Soc.* **1951**, *73*, 4031.

(13) Wiberg, E.; Stecher, O.; Andrascheck, H. J.; Kreuzbichler, L.; Steude, E. *Angew. Chem., Int. Ed. Engl.* **1963**, *2*, 507.

(14) **5**: colorless crystals; <sup>1</sup>H NMR (300 MHz, CDCl<sub>3</sub>)  $\delta$  0.02 (s, 18H), 0.51 (s, 6H), 0.53 (s, 6H), 7.20–7.39 (m, 12H), 7.50 (d, *J* = 7.35 Hz, 4H); <sup>13</sup>C NMR (75 MHz, CDCl<sub>3</sub>)  $\delta$  -1.40, -0.71, -0.53, 127.55, 134.60, 135.17, 142.22, 143.54; <sup>29</sup>Si NMR (60 MHz, CDCl<sub>3</sub>)  $\delta$  -33.70, -33.55, -18.50; MS *m/z* (relative intensity) 622 (M<sup>+</sup>, 26), 550 (37). Anal. Calcd for C<sub>18</sub>H<sub>18</sub>Si<sub>4</sub>: C, 65.52; H, 7.44. Found: C, 65.49; H, 7.48.

(15) Crystallographic data for **5**: fw = 623.26, orthorhombic, *a* = 13.051(1) Å, *b* = 13.911(1) Å, *c* = 20.697(4) Å, *V* = 3757.4 Å<sup>3</sup>, space group *Pbca*, *Z* = 4,  $\mu$ (Mo K $\alpha$ ) = 2.4 cm<sup>-1</sup>,  $\rho$ (calcd) = 1.10 g/cm<sup>3</sup>, *R* = 0.065 (*R*<sub>w</sub> = 0.067). The 1287 independent reflections ( $2\theta \leq 21.7^\circ$ ;  $|F_o| \geq 3\sigma(F_o)$ ) were measured on an Enraf-Nonius CAD4 diffractometer using Mo K $\alpha$  irradiation and an  $\omega$ - $\theta$  scan. The structure was solved by direct methods, and hydrogen atoms were located and their positions and isotropic thermal parameters were refined.

(16) **1d**: <sup>1</sup>H NMR (300 MHz, CDCl<sub>3</sub>)  $\delta$  0.07 (s, 18H), 0.62 (s, 6H), 7.39 (dd, *J* = 3.3, 5.4 Hz, 4H), 7.56 (dd, *J* = 3.3, 5.4 Hz, 4H); <sup>13</sup>C NMR (75 MHz, CDCl<sub>3</sub>)  $\delta$  -1.60, -1.47, 127.61, 134.49, 143.17; <sup>29</sup>Si NMR (60 MHz, CDCl<sub>3</sub>)  $\delta$  -33.26, -18.31; MS *m/z* (relative intensity) 384 (M<sup>+</sup>, 94), 311 (M<sup>+</sup> - SiMe<sub>3</sub>, 82).

(17) **6**: <sup>1</sup>H NMR (300 MHz, C<sub>6</sub>D<sub>6</sub>)  $\delta$  0.04 (s, 6H), 0.79 (s, 6H), 7.17 (dd, *J* = 3.2, 5.3 Hz, 4H), 7.61 (dd, *J* = 3.2, 5.3 Hz, 4H); <sup>13</sup>C NMR (75 MHz, C<sub>6</sub>D<sub>6</sub>)  $\delta$  -11.80, -7.12, 127.17, 131.59, 147.90; <sup>29</sup>Si NMR (60 MHz, C<sub>6</sub>D<sub>6</sub>)  $\delta$  -25.65, -15.94; MS *m/z* (relative intensity) 296 (M<sup>+</sup>, 15). **7**: <sup>1</sup>H NMR (300 MHz, CDCl<sub>3</sub>)  $\delta$  0.44 (s, 12H), 0.53 (s, 12H), 7.00 (dd, *J* = 3.3, 5.5 Hz, 8H), 7.56 (dd, *J* = 3.3, 5.5 Hz, 8H); <sup>13</sup>C NMR (75 MHz, CDCl<sub>3</sub>)  $\delta$  -5.06, -1.72, 127.35, 134.20, 142.29; <sup>29</sup>Si NMR (60 MHz, CDCl<sub>3</sub>)  $\delta$  -50.04, -33.60; MS *m/z* (relative intensity) 592 (M<sup>+</sup>, 25), 519 (11).

(18) **8**: <sup>1</sup>H NMR (300 MHz, CDCl<sub>3</sub>)  $\delta$  0.56 (s, 12H), 0.80 (s, 6H), 7.28 (dd, *J* = 3.2, 5.4 Hz, 4H), 7.56 (dd, *J* = 3.2, 5.4 Hz, 4H); <sup>13</sup>C NMR (75 MHz, CDCl<sub>3</sub>)  $\delta$  -10.21, -7.33, 127.85, 132.33, 144.68; <sup>29</sup>Si NMR (60 MHz, CDCl<sub>3</sub>)  $\delta$  -58.33, -32.89; MS *m/z* (relative intensity) 354 (M<sup>+</sup>, 76), 339 (M<sup>+</sup> - Me, 43). Anal. Calcd for C<sub>18</sub>H<sub>18</sub>Si<sub>4</sub>: C, 62.36; H, 5.23. Found: C, 62.31; H, 5.28. **9**: <sup>1</sup>H NMR (300 MHz, CDCl<sub>3</sub>)  $\delta$  0.39 (s, 6H), 0.01 (s, 12H), 0.75 (s, 6H), 7.32 (dd, *J* = 3.3, 5.4 Hz, 4H), 7.57 (dd, *J* = 3.3, 5.4 Hz, 4H); <sup>13</sup>C NMR (75 MHz, CDCl<sub>3</sub>)  $\delta$  -7.21, -6.74, -6.58, 127.66, 133.03, 143.86; <sup>29</sup>Si NMR (60 MHz, CDCl<sub>3</sub>)  $\delta$  -46.39, -39.60, -30.98; MS *m/z* (relative intensity) 412 (M<sup>+</sup>, 47), 339 (61).

# Novel Synthesis of $\alpha$ -Stannyl Vinyl Ethers from Catalytic and Stoichiometric Fischer Carbene Anions

Frank E. McDonald,\*<sup>1</sup> Colleen C. Schultz, and Arnab K. Chatterjee

Department of Chemistry, Northwestern University, 2145 Sheridan Road, Evanston, Illinois 60208-3113

Received May 1, 1995<sup>§</sup>

**Summary:** Tributyltin triflate reacts with catalytic molybdenum carbene anion intermediates generated by alkynol cyclization, providing a novel and practical synthesis of  $\alpha$ -(tributylstannyl)dihydrofurans. Similar reactivity is observed with stoichiometric cyclic and acyclic chromium carbene anions.

$\alpha$ -Trialkylstannyl vinyl ethers have proven valuable in synthetic organic chemistry for a variety of carbon–carbon bond-forming reactions. For instance, they are commonly used as stable, storable precursors for the corresponding  $\alpha$ -lithio vinyl ether derivatives,<sup>2</sup> as well as the nucleophilic component for palladium-catalyzed couplings with unsaturated organic halides and sulfonates.<sup>3</sup> However, the usual preparation of  $\alpha$ -stannyl vinyl ethers requires highly reactive, pyrophoric bases for deprotonation of vinyl ether precursors.<sup>4</sup> In our studies of molybdenum pentacarbonyl catalyzed cyclizations of alkynols to dihydrofurans,<sup>5</sup> we have observed that a putative catalytic molybdenum carbene anion intermediate reacts with a variety of stoichiometric electrophiles, including trialkyltin electrophiles.

For instance, reaction of photogenerated molybdenum pentacarbonyl triethylamine (25 mol %) with alkynyl alcohol **1**<sup>6</sup> in the presence of 1 equiv of tributyltin chloride gives the 5-(tributylstannyl)-2,3-dihydrofuran **6** (45% yield), the unstannylated dihydrofuran (13%), and unreacted **1**; the preparative yield of **6** increases to 65% when the more highly electrophilic tributyltin triflate is employed (Table 1, entry 1).<sup>7</sup> The regiochemistry of this reaction contrasts with that observed with aldehyde electrophiles.<sup>5b</sup> This methodology is particularly valuable for preparation of substituted stannylated dihydrofurans **6** and **8** in a single step from alkynols **1** and **3**,<sup>8</sup> respectively.

Primary alkynol substrate **2** had previously appeared to be unreactive to molybdenum pentacarbonyl mediated cyclizations in the absence of tributyltin electrophiles, as the starting alkynol was largely recovered. We propose that electrophilic trapping apparently drives an unfavorable equilibrium between acyclic vinylidene carbene **11** and cyclic molybdenum carbene anion intermediates **12**; reaction of the anionic molybdenum atom with the stannyl electrophile forms the intermediate molybdenum stannyl species **13**, which reductively eliminates to the vinylstannanes **6–8** (Scheme 1).

As the corresponding reaction with stoichiometric Fischer-type carbenes had not been previously reported,<sup>9</sup> we then explored kinetic deprotonation of the chromium carbene **4**<sup>5a</sup> with *n*-butyllithium<sup>10</sup> followed by addition of tributyltin chloride, which also provided the  $\alpha$ -stannyl dihydrofuran **6** (Table 1, entry 4). The same product **6** is also obtained under mildly basic conditions (triethylamine, tributyltin triflate, ether, 20 °C; entry 5). This reaction is apparently general, as the acyclic

(7) Characterization data for **5**: IR (neat) 2961, 2081, 1915, 1454, 1258, 1032 cm<sup>-1</sup>; <sup>1</sup>H NMR (300 MHz, CDCl<sub>3</sub>)  $\delta$  4.76 (3H, s), 3.30 (2H, t, *J* = 7.5), 1.54–1.27 (4H, m), 0.90 (3H, t, *J* = 7.5); <sup>13</sup>C NMR (75 MHz, CDCl<sub>3</sub>)  $\delta$  362.7, 221.6, 215.4, 66.5, 61.7, 27.4, 21.4, 12.8; MS 292, 264, 236, 208, 180, 152, 107, 93, 80, 52; HRMS calcd for C<sub>11</sub>H<sub>12</sub>O<sub>6</sub>Cr 292.0039, found 292.0017. **6**: IR (neat) 3029, 2958, 2929, 2853, 1584, 1493, 1464, 1376, 1259, 1055, 937, 859, 697 cm<sup>-1</sup>; <sup>1</sup>H NMR (300 MHz, CDCl<sub>3</sub>)  $\delta$  7.37–7.18 (5H, m), 5.49 (1H, dd, *J* = 10.8, 8.0 Hz), 5.04 (1H, dd, *J* = 2.5, 2.0 Hz), 3.08 (1H, m), 2.57 (1H, ddd, *J* = 2.5, 8.0, 15.0), 1.71–0.88 (27H, m); <sup>13</sup>C NMR (75 MHz, CDCl<sub>3</sub>)  $\delta$  162.5, 144.4, 128.4, 127.3, 125.8, 110.7, 82.9, 39.2, 29.1, 27.3, 13.8, 9.7; MS *m/z* 436, 379, 351, 323, 275, 177, 145, 127, 117, 91, 45; HRMS calcd for C<sub>22</sub>H<sub>36</sub>O-<sup>120</sup>Sn 436.1788, found 436.1779. **7**: IR (thin film, CH<sub>2</sub>Cl<sub>2</sub>) 2953, 2655, 1561, 1464 cm<sup>-1</sup>; <sup>1</sup>H NMR (300 MHz, CDCl<sub>3</sub>)  $\delta$  5.06 (1H, t, *J* = 2.4 Hz), 4.22 (2H, t, *J* = 9.6 Hz), 2.56 (2H, dt, *J* = 2.4, 9.6 Hz), 1.58–0.82 (27H, m); <sup>13</sup>C NMR (75 MHz, CDCl<sub>3</sub>)  $\delta$  162.4, 111.5, 69.8, 29.9, 28.9, 27.2, 13.6, 9.5; MS *m/z* 303, 247, 191, 159, 121, 69, 41; HRMS calcd for C<sub>16</sub>H<sub>32</sub>O<sup>120</sup>Sn 360.1475, found 360.1467. **8**: IR (thin film, CH<sub>2</sub>Cl<sub>2</sub>) 2956, 2854, 1579, 1463 cm<sup>-1</sup>; <sup>1</sup>H NMR (300 MHz, CDCl<sub>3</sub>)  $\delta$  5.02 (1H, d, *J* = 2.4 Hz), 4.30 (1H, dd, *J* = 9.6, 9.0 Hz), 3.78 (1H, dd, *J* = 8.4, 7.6 Hz), 2.96 (1H, m), 1.61–0.87 (30H, m); <sup>13</sup>C NMR (75 MHz, C<sub>6</sub>D<sub>6</sub>)  $\delta$  162.4, 118.9, 77.4, 37.8, 29.5, 27.6, 21.1, 14.0, 10.0; MS *m/z* 372, 317, 261, 205, 173, 121, 83; HRMS calcd for C<sub>17</sub>H<sub>34</sub>O<sup>116</sup>Sn 370.1627, found 370.1602. **9**: IR (neat) 2697, 1616, 1463, 1366, 1210, 1146, 1101 cm<sup>-1</sup>; <sup>1</sup>H NMR (300 MHz, CDCl<sub>3</sub>)  $\delta$  5.23 (1H, t, *J* = 7.5), 3.45 (3H, s), 1.88 (2H, q, *J* = 7.5), 1.58–0.68 (32H, m); <sup>13</sup>C NMR (75 MHz, C<sub>6</sub>D<sub>6</sub>)  $\delta$  166.1, 111.4, 54.5, 32.3, 29.4, 27.6, 25.2, 13.8, 10.6; MS *m/z* 333, 301, 265, 235, 209, 177, 151, 121, 99, 57; HRMS calcd for C<sub>18</sub>H<sub>38</sub>O<sup>116</sup>Sn 386.1940, found 386.1951. The  $\alpha$ -stannyl vinyl ethers **6–9** are moderately sensitive to moisture and did not provide satisfactory combustion analyses.

(8) Gerard, F.; Miginiac, P. *Synth. Commun.* **1976**, *6*, 461.

(9) Addition of trialkylstannyl hydrides to group VIB Fischer carbenes gives  $\alpha$ -(alkoxyalkyl)stannanes. (a) Connor, J. A.; Rose, P. D.; Turner, R. M. *J. Organomet. Chem.* **1973**, *55*, 111. (b) Nakamura, E.; Tanaka, K.; Aoki, S. *J. Am. Chem. Soc.* **1992**, *114*, 9715. (c) Merlic, C. A.; Albanese, J. *Tetrahedron Lett.* **1995**, *36*, 1007, 1011. (d) From glycosylidiazirines: Uhlmann, P.; Nanz, D.; Bozo, E.; Vasella, A. *Helv. Chim. Acta* **1994**, *77*, 1430.

(10) Casey, C. P.; Brunsvold, W. R. *J. Organomet. Chem.* **1975**, *102*, 175.

\* Abstract published in *Advance ACS Abstracts*, August 1, 1995.

(1) Camille and Henry Dreyfus New Faculty Awardee, 1992–1997; Alfred P. Sloan Research Fellow, 1995–1997.

(2) (a) Soderquist, J. A.; Hsu, G. J.-H. *Organometallics* **1982**, *1*, 830. (b) Hanessian, S.; Martin, M.; Desai, R. C. *J. Chem. Soc., Chem. Commun.* **1986**, 926. (c) Lesimple, P.; Beau, J.-M.; Jaurand, G.; Sinay, P. *Tetrahedron Lett.* **1986**, *27*, 6201. (d) Behling, J. R.; Babiak, K. A.; Ng, J. S.; Campbell, A. L. *J. Am. Chem. Soc.* **1988**, *110*, 2641. (e) Paquette, L. A.; Oplinger, J. A. *Tetrahedron* **1989**, *45*, 107. (f) Kocienski, P.; Barber, C. *Pure Appl. Chem.* **1990**, *62*, 1933. (g) Boeckman, R. K.; Charette, A. B.; Asberom, T.; Johnston, B. H. *J. Am. Chem. Soc.* **1991**, *113*, 5337. (h) Bearder, J. R.; Dewis, M. L.; Whiting, D. A. *Synlett* **1993**, 805.

(3) (a) Stille, J. K. *Angew. Chem., Int. Ed. Engl.* **1986**, *25*, 508. (b) Schreiber, S. L.; Porco, J. A. *J. Org. Chem.* **1989**, *54*, 4721. (c) MacLeod, D.; Moorcroft, D.; Quayle, P.; Dorrity, M. R. J.; Malone, J. F.; Davies, G. M. *Tetrahedron Lett.* **1990**, *31*, 6077. (d) Zhang, H.-C.; Brakta, M.; Daves, G. D. *Tetrahedron Lett.* **1993**, *34*, 1571. (e) Friesen, R. W.; Loo, R. W.; Sturino, C. F. *Can. J. Chem.* **1994**, *72*, 1262.

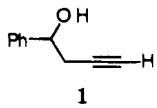
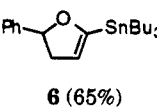
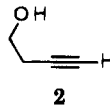
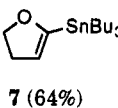
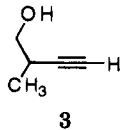
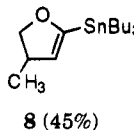
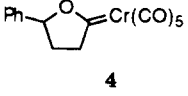
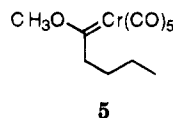
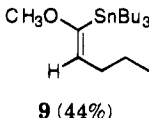
(4) For another alternative, see: Casson, S.; Kocienski, P. *Synthesis* **1993**, 1133.

(5) (a) McDonald, F. E.; Connolly, C. B.; Gleason, M. M.; Towne, T. B.; Treiber, K. D. *J. Org. Chem.* **1993**, *58*, 6952. (b) McDonald, F. E.; Schultz, C. C. *J. Am. Chem. Soc.* **1994**, *116*, 9363. (c) McDonald, F. E.; Gleason, M. M. *Angew. Chem., Int. Ed. Engl.* **1995**, *34*, 350.

(6) Brandsma, L. *Preparative Acetylenic Chemistry*, 2nd ed.; Elsevier: Amsterdam, 1988; p 67.

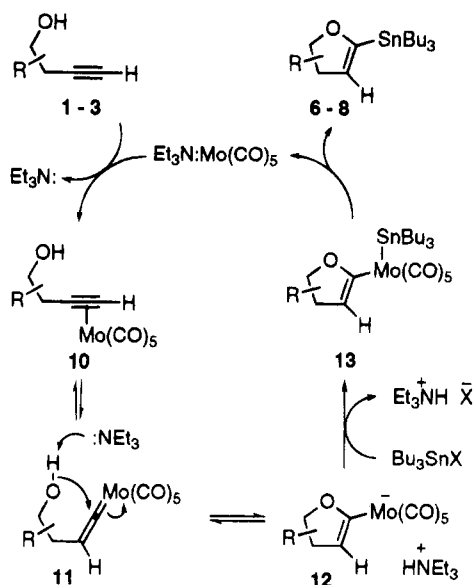


**Table 1. Reaction of Carbene Anions with Tributyltin Electrophiles<sup>a</sup>**

entry	substrate	conditions	product (purified yield)
1		A	 6 (65%)
2		A	 7 (64%)
3		A	 8 (45%)
4		B	6 (60%)
5	4	C	6 (58%)
6		C	 9 (44%)

<sup>a</sup> Procedure A: Mo(CO)<sub>6</sub> (0.25 mmol) was placed in a 18 × 150 mm borosilicate test tube; freshly distilled Et<sub>3</sub>N (3 mL) and Et<sub>2</sub>O (10 mL) were added and the contents dissolved by stirring. The reaction mixture was then photolyzed for 20 min under N<sub>2</sub>. The reaction vessel was removed from the light source, alkynyl alcohol 1–3 (1.0 mmol) was added, followed by *n*-Bu<sub>3</sub>SnOTf (1.0 mmol) in Et<sub>2</sub>O (2 mL), and the reaction mixture was stirred for 18 h. α-Stannyl dihydrofuran products 6–8 were isolated by evaporation of solvent followed by flash chromatography on silica gel (pentane/Et<sub>2</sub>O/1% Et<sub>2</sub>NH). Procedure B: Chromium carbene 4 was dissolved in THF and the solution was cooled to –78 °C. *n*-BuLi (1.0 equiv, 2.5 M in hexane) was added dropwise; after the mixture was stirred for 30 min *n*-Bu<sub>3</sub>SnCl was added and this reaction mixture was warmed to room temperature. α-Stannyl vinyl ether 6 was purified by evaporation of solvent followed by flash chromatography on silica gel (pentane/Et<sub>2</sub>O/1% Et<sub>2</sub>NH). Procedure C: Chromium carbenes 4 and 5 (0.5 mmol) were dissolved in freshly distilled Et<sub>3</sub>N (1 mL) and Et<sub>2</sub>O (5 mL), *n*-Bu<sub>3</sub>SnOTf (0.65 mmol) in Et<sub>2</sub>O (2 mL) was added, and the reaction mixture was stirred for 4 days. α-Stannyl vinyl ether products 6 and 9 were isolated by evaporation of solvent followed by flash chromatography on silica gel (pentane/Et<sub>2</sub>O/1% Et<sub>2</sub>NH).

chromium carbene 5 also gives the vinyl ether 9<sup>7</sup> as a single stereoisomer (entry 6).<sup>11</sup>

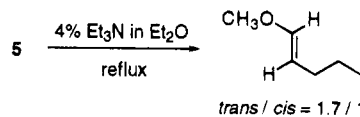
**Scheme 1**

In conclusion, these preparations of α-stannyl vinyl ethers represent a novel reaction pathway of Fischer carbene compounds. Further studies to extend the scope of these reactions and synthetic applications are in progress.

**Acknowledgment** is made to the donors of the Petroleum Research Fund, administered by the American Chemical Society, for partial support of this research. We also gratefully acknowledge financial support provided by Northwestern University and the Camille and Henry Dreyfus Foundation.

OM950316T

(11) (a) Stereochemistry for 9 is assigned as *Z* (tin *cis* to propyl), consistent with observed NOE enhancement of the vinylic hydrogen resonance ( $\delta$  5.23) upon irradiation of the methoxy protons ( $\delta$  3.45). The reaction of chromium carbene 5 with triethylamine in diethyl ether in the absence of tributyltin electrophile gives a mixture of vinyl ether isomers (*trans*,  $J_{H_1-H_2} = 13.0$  Hz; *cis*:  $J_{H_1-H_2} = 6.6$  Hz):



In contrast, Casey<sup>11b</sup> and Söderberg<sup>11c</sup> have observed predominant formation of *cis*-vinyl ethers and vinyl esters from chromium oxacarbene. (b) Casey, C. P.; Brunsvold, W. R. *Inorg. Chem.* **1977**, *16*, 391. (c) Söderberg, B. C.; Turbeville, M. J. *Organometallics* **1991**, *10*, 3951.

## Articles

## Group 4 Metal Mono-Dicarbollide Piano Stool Complexes. Synthesis, Structure, and Reactivity of $(\eta^5\text{-C}_2\text{B}_9\text{H}_{11})\text{M}(\text{NR}_2)_2(\text{NHR}_2)$ ( $\text{M} = \text{Zr}$ , $\text{R} = \text{Et}$ ; $\text{M} = \text{Ti}$ , $\text{R} = \text{Me}$ , $\text{Et}$ )

Daniel E. Bowen and Richard F. Jordan\*

Department of Chemistry, University of Iowa, Iowa City, Iowa 52242

Robin D. Rogers

Department of Chemistry, Northern Illinois University, DeKalb, Illinois 60115

Received March 13, 1995<sup>®</sup>

The amine elimination reaction of  $\text{C}_2\text{B}_9\text{H}_{13}$  and  $\text{Zr}(\text{NEt}_2)_4$  yields the mono-dicarbollide complex  $(\eta^5\text{-C}_2\text{B}_9\text{H}_{11})\text{Zr}(\text{NEt}_2)_2(\text{NHET}_2)$  (**1**), which has been shown to adopt a three-legged piano stool structure by X-ray crystallography. Crystal data for **1**: space group  $P2_1/c$ ,  $a = 10.704(4)$  Å,  $b = 11.066(3)$  Å,  $c = 20.382(8)$  Å,  $\beta = 99.20(3)^\circ$ ,  $V = 2383(1)$  Å<sup>3</sup>,  $Z = 4$ . Complex **1** undergoes facile ligand substitution by THF and 4-picoline, yielding  $(\eta^5\text{-C}_2\text{B}_9\text{H}_{11})\text{Zr}(\text{NEt}_2)_2(\text{THF})$  (**2**) and  $(\eta^5\text{-C}_2\text{B}_9\text{H}_{11})\text{Zr}(\text{NEt}_2)_2(4\text{-picoline})_2$  (**3**). Compound **3** exists as the four-coordinate species  $(\eta^5\text{-C}_2\text{B}_9\text{H}_{11})\text{Zr}(\text{NEt}_2)_2(4\text{-picoline})$  in  $\text{CH}_2\text{Cl}_2$  solution. Complex **1** reacts selectively with 2 equiv of  $[\text{NH}_2\text{Et}_2]\text{Cl}$ , yielding  $(\eta^5\text{-C}_2\text{B}_9\text{H}_{11})\text{ZrCl}_2(\text{NHET}_2)_2$  (**4**). Similarly, the reaction of  $\text{C}_2\text{B}_9\text{H}_{13}$  and  $\text{Ti}(\text{NR}_2)_4$  yields  $(\eta^5\text{-C}_2\text{B}_9\text{H}_{11})\text{Ti}(\text{NR}_2)_2(\text{NHR}_2)$  (**5**,  $\text{R} = \text{Me}$ ; **6**,  $\text{R} = \text{Et}$ ). Compounds **1–6** are potential precursors to group 4 metal  $(\eta^5\text{-C}_2\text{B}_9\text{H}_{11})\text{MR}_2\text{L}_n$  alkyl species.

## Introduction

Group 4 metal bent-metalocene  $\eta^5$ -dicarbollide species of general type  $(\eta^5\text{-C}_2\text{B}_9\text{H}_{11})(\text{C}_5\text{R}_5)\text{M}(\text{R})$  and  $(\eta^5\text{-C}_2\text{B}_9\text{H}_{11})(\text{C}_5\text{R}_5)\text{M}(\text{R})(\text{L})$  ( $\text{M} = \text{Ti}$ ,  $\text{Zr}$ ,  $\text{Hf}$ ;  $\text{L} = \text{labile ligand}$ ) undergo a variety of ligand exchange, insertion (alkenes, alkynes, etc.), and ligand C–H activation reactions characteristics of electrophilic metal alkyls.<sup>1,2</sup> The combination of an electron deficient, Lewis acidic metal center ( $d^0$ , 14-electron), a reactive M–R bond, and the presence of vacant coordination sites cis to the M–R bond promotes the coordination and activation of substrates by these complexes. These species are related to  $(\text{C}_5\text{R}_5)_2\text{M}(\text{R})^+$  ( $\text{M} = \text{group 4}$ , actinide)<sup>3</sup> and  $(\text{C}_5\text{R}_5)_2\text{M}(\text{R})$  ( $\text{M} = \text{group 3}$ , lanthanide)<sup>4</sup> complexes by formal replacement of a  $\text{Cp}^-$  ligand by the isolobal  $\text{C}_2\text{B}_9\text{H}_{11}^{2-}$  ligand, and to  $\text{Cp}_2\text{M}(\text{R})\text{X}$  species ( $\text{M} = \text{group 4}$ ) by replacement of a  $\text{Cp}^-$  and an  $\text{X}^-$  ligand by  $\text{C}_2\text{B}_9\text{H}_{11}^{2-}$ . A variety of other early transition metal bent-metal-

locene systems containing  $\eta^5$ -carboranyl ligands have been prepared.<sup>5,6</sup>

Group 4 metal mono-dicarbollide piano stool complexes of general type  $(\eta^5\text{-C}_2\text{B}_9\text{H}_{11})\text{MX}_2\text{L}_n$  ( $\text{L} = \text{labile ligand}$ ,  $n = 0–3$ ) are of interest because of the possibility of achieving higher levels of metal unsaturation and concomitant higher reactivity than in the bent-metalocene systems. For example, a  $d^0$   $(\eta^5\text{-C}_2\text{B}_9\text{H}_{11})\text{M}(\text{R})_2$  or  $(\eta^5\text{-C}_2\text{B}_9\text{H}_{11})\text{M}(\text{R})\text{X}$  complex is isolobal with group 4 metal  $(\text{C}_5\text{R}_5)\text{M}(\text{R})_2^+$  and  $(\text{C}_5\text{R}_4\text{SiR}_2\text{NR})\text{M}(\text{R})^+$  species,<sup>7,8</sup> which have been shown to coordinate arenes, undergo

(5) Group 3: (a) Bazan, G. C.; Schaefer, W. P.; Bercaw, J. E. *Organometallics* **1993**, *12*, 2126. (b) Marsh, R. E.; Schaefer, W. P.; Bazan, G. C.; Bercaw, J. E. *Acta Crystallogr.* **1992**, *C48*, 1416. (c) Oki, A. R.; Zhang, H.; Hosmane, N. S. *Organometallics* **1991**, *10*, 3964. Group 4: (d) Siriwardane, U.; Zhang, H.; Hosmane, N. S. *J. Am. Chem. Soc.* **1990**, *112*, 9637. (e) Hosmane, N. S.; Wang, Y.; Zhang, H.; Maguire, J. A.; Waldhoer, E.; Kaim, W.; Binder, H.; Kremer, R. K. *Organometallics* **1994**, *13*, 4156. (f) Jia, L.; Zhang, H.; Hosmane, N. S. *Acta Crystallogr.* **1993**, *C49*, 453. Group 5: (g) Uhrhammer, R.; Crowther, D. J.; Olson, J. D.; Swenson, D. C.; Jordan, R. F. *Organometallics* **1992**, *11*, 3098. (h) Uhrhammer, R.; Su, Y.; Swenson, D. C.; Jordan, R. F. *Inorg. Chem.* **1994**, *33*, 4398. (i) Houseknecht, K. L.; Stockman, K. E.; Sabat, M.; Finn, M. G.; Grimes, R. N. *J. Am. Chem. Soc.* **1995**, *117*, 1163. f-Element: (j) Fronczek, F. R.; Halstead, G. W.; Raymond, K. N. *J. Am. Chem. Soc.* **1977**, *99*, 1769. (k) Manning, M. J.; Knobler, C. B.; Khattar, R.; Hawthorne, M. F. *Inorg. Chem.* **1991**, *30*, 2009.

(6) For a recent review see: Saxena, A. K.; Hosmane, N. S. *Chem. Rev.* **1993**, *93*, 1081.

(7) (a) Pellecchia, C.; Immirzi, A.; Pappalardo, D.; Pelusa, A. *Organometallics* **1994**, *13*, 3773. (b) Pellecchia, C.; Immirzi, A.; Zambelli, A. *J. Organomet. Chem.* **1994**, *479*, C9. (c) Pellecchia, C.; Immirzi, A.; Grassi, A.; Zambelli, A. *Organometallics* **1993**, *12*, 4473. (d) Quyoum, R.; Wang, Q.; Tudoret, M.-J.; Baird, M. C.; Gillis, D. J. *J. Am. Chem. Soc.* **1994**, *116*, 6435. (e) Gillis, D. J.; Tudoret, M.-J.; Baird, M. C. *J. Am. Chem. Soc.* **1993**, *115*, 2543. (f) Crowther, D. J.; Jordan, R. F.; Baenziger, N. C. *Organometallics* **1990**, *9*, 2574.

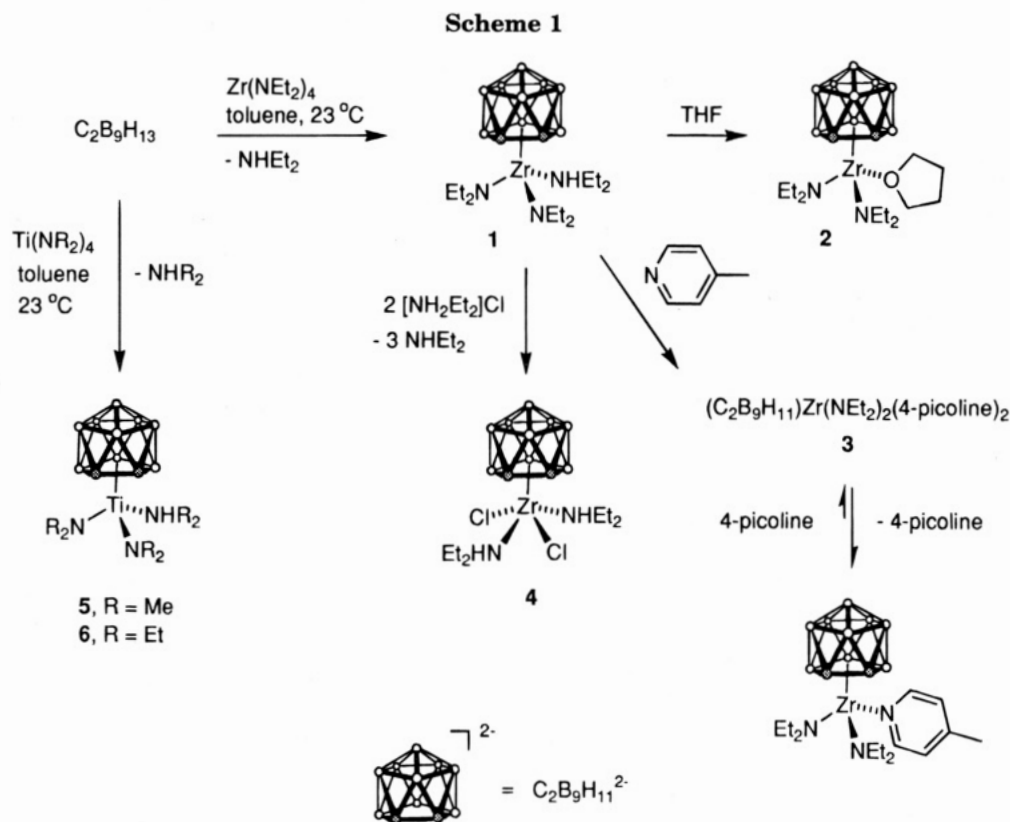
<sup>®</sup> Abstract published in *Advance ACS Abstracts*, June 15, 1995.

(1)  $\text{M} = \text{Zr}$ ,  $\text{Hf}$ : (a) Crowther, D. J.; Baenziger, N. C.; Jordan, R. F. *J. Am. Chem. Soc.* **1991**, *113*, 1455. (b) Jordan, R. F. *Makromol. Chem., Macromol. Symp.* **1993**, *66*, 121. (c) Jordan, R. F. *New Organometallic Models for Ziegler–Natta Catalysts*. In *Proceedings of the World Metalocene Conference*; Catalyst Consultants Inc.: 1993; pp 89–96.

(2)  $\text{M} = \text{Ti}$ : Kreuder, C.; Zhang, H.; Jordan, R. F. *Organometallics*, in press.

(3) Reviews: (a) Jordan, R. F. *Adv. Organomet. Chem.* **1991**, *32*, 325. (b) Marks, T. J. *Acc. Chem. Res.* **1992**, *25*, 57.

(4) Reviews and leading references (a) Watson, P. L.; Parshall, G. W. *Acc. Chem. Res.* **1985**, *18*, 51. (b) Thompson, M. E.; Bercaw, J. E. *Pure Appl. Chem.* **1984**, *56*, 1. (c) Schumann, H. *Angew. Chem., Int. Ed. Engl.* **1984**, *23*, 474. (d) Evans, W. J. *Adv. Organomet. Chem.* **1985**, *24*, 131. (e) Burger, B. J.; Thompson, M. E.; Cotter, D.; Bercaw, J. E. *J. Am. Chem. Soc.* **1990**, *112*, 1566. (f) Schaverien, C. J. *Adv. Organomet. Chem.* **1994**, *36*, 283.



clean olefin insertion reactions, and catalyze olefin polymerization, and with group 3 and lanthanide metal ( $\text{C}_5\text{R}_5\text{M}(\text{R})_2$  and  $\text{C}_5\text{R}_5\text{M}(\text{R})(\text{OR})$ ) species.<sup>9</sup> However, early metal piano stool complexes based on  $\eta^5$ -dicarbollide or related dianionic  $\eta^5$ -carboranyl ligands are rare, being restricted to several group 5 and lanthanide species, e.g.,  $(\eta^5\text{-C}_2\text{B}_9\text{H}_{11})\text{TaX}_3$  (X = Cl, Me),<sup>5g</sup>  $(\eta^5\text{-C}_2\text{B}_9\text{H}_{11})\text{M}(\text{THF})_4$  (M = Sm, Yb), and  $(\eta^5\text{-C}_2\text{B}_9\text{H}_{11})\text{Yb}(\text{DMF})_4$ .<sup>5k</sup> Here we report that amine elimination reactions provide a convenient entry to group 4 metal mono-dicarbollide complexes.

## Results and Discussion

**Synthesis of  $(\eta^5\text{-C}_2\text{B}_9\text{H}_{11})\text{Zr}(\text{NEt}_2)_2(\text{NHtEt}_2)$  (1).** The new chemistry we have developed is summarized in Scheme 1. The amine elimination reaction of  $\text{C}_2\text{B}_9\text{H}_{13}$  and  $\text{Zr}(\text{NEt}_2)_4$  proceeds readily in toluene at  $23^\circ\text{C}$ , yielding  $(\eta^5\text{-C}_2\text{B}_9\text{H}_{11})\text{Zr}(\text{NEt}_2)_2(\text{NHtEt}_2)$  (**1**) and 1 equiv of  $\text{NHtEt}_2$ . Compound **1** is soluble and reasonably stable in  $\text{CH}_2\text{Cl}_2$ ,<sup>10</sup> but is only sparingly soluble in toluene or hexane despite the presence of six ethyl groups. Accordingly, **1** is isolated as a yellow solid by recrystallization from  $\text{CH}_2\text{Cl}_2/\text{toluene}$ . The  $^{11}\text{B}$  NMR spectrum of

**1** contains five resonances in a 1/2/2/3/1 intensity ratio which are in the range observed for other early metal  $\eta^5$ -dicarbollide complexes and are shifted downfield from the resonances for  $\text{C}_2\text{B}_9\text{H}_{13}$  and  $\text{C}_2\text{B}_9\text{H}_{12}^-$  or  $\text{C}_2\text{B}_9\text{H}_{11}^{2-}$  salts.<sup>11</sup> The  $^1\text{H}$  NMR spectrum contains a singlet for the dicarbollide C–H hydrogens, which confirms the  $\text{C}_s$  symmetry implied by the  $^{11}\text{B}$  spectrum, and appropriate resonances for one  $\text{NHtEt}_2$  ligand (shifted from the free amine resonances) and two  $-\text{NEt}_2$  ligands. Two multiplets are observed for the  $\text{NH}(\text{CH}_2\text{CH}_3)_2$  methylene hydrogens, consistent with the expected diastereotopicity resulting from coordination of the amine to Zr. Collectively, these data are consistent with a three-legged piano stool structure for **1**. There is no evidence for exchange of the N–H proton between Zr– $\text{NEt}_2$  groups.

**Structure and Bonding in 1.** The molecular structure of **1** was determined by single-crystal X-ray diffraction (Figure 1, Tables 1–3). Compound **1** adopts a monomeric three-legged piano stool structure containing an  $\eta^5$ -dicarbollide ligand with amide and amine ligands in the basal positions. One amide group (N2) adopts a “perpendicular” orientation in which the C–N–C plane is roughly perpendicular to the dicarbollide bonding face and parallel to the N2–Zr–centroid plane (angle between C7–N2–C9 and N2–Zr–centroid planes,  $10.9^\circ$ ). The other amide (N3) lies in a “parallel” orientation such that the C–N–C plane is rotated ca.  $75^\circ$  from the perpendicular orientation (angle between C11–N3–C13 and N3–Zr–centroid planes,  $75.4^\circ$ ). The amine ligand adopts a rotational conformation which minimizes steric interactions with the remaining ligands. There is a

(8) Representative patent literature concerning use of  $(\text{C}_5\text{R}_4\text{SiR}_2\text{-NR})\text{M}(\text{R})^+$  species as olefin polymerization catalysts: (a) Canich, J. M. Eur. Pat. Appl. 420 436, 1991. (b) Canich, J. M.; Hlatky, G. G.; Turner, H. W. U.S. Patent 542 236, 1990. (c) Stevens, J. C.; Timmers, F. J.; Wilson, D. R.; Schmidt, G. F.; Nickias, P. N.; Rosen, R. K.; Knight, G. W.; Lai, S. Eur. Pat. 416 815, 1990. (d) Campbell, R. E. U.S. Patent 5 066 741, 1991. (e) LaPointe, R. E.; Rosen, R. K.; Nickias, P. N. Eur. Pat. 495 375, 1992.

(9) (a) van der Heijden, H.; Schaverien, C. J.; Orpen, A. G. *Organometallics* **1989**, *8*, 255. (b) van der Heijden, H.; Pasman, P.; de Boer, E. J. M.; Schaverien, C. J.; Orpen, A. G. *Organometallics* **1989**, *8*, 1459. (c) Schaverien, C. J. *J. Mol. Catal.* **1994**, *90*, 177. (d) Schaverien, C. J. *Organometallics* **1994**, *13*, 69.

(10) Complex **1** decomposes slowly (ca. 20% after 48 h at  $23^\circ\text{C}$ ) in  $\text{CH}_2\text{Cl}_2$  to a species tentatively identified as  $(\eta^5\text{-C}_2\text{B}_9\text{H}_{11})\text{Zr}(\text{Cl})(\text{NEt}_2)(\text{NHtEt}_2)$ .

(11) (a) Siedle, A. R.; Bodner, G. M.; Todd, L. J. *J. Organomet. Chem.* **1971**, *33*, 137. (b) Jutzi, P.; Galow, P.; Abu-Orabi, S.; Arif, A. M.; Cowley, A. H.; Norman, N. C. *Organometallics* **1987**, *6*, 1024. (c) Buchanan, J.; Hamilton, E. J. M.; Reed, D.; Welch, A. J. *J. Chem. Soc., Dalton Trans.* **1990**, 677.

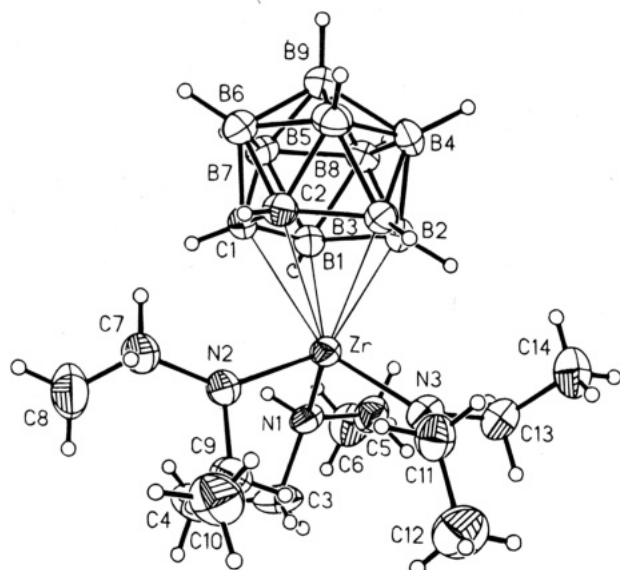


**Figure 1.** Molecular structure of  $(\eta^5\text{-C}_2\text{B}_9\text{H}_{11})\text{Zr}(\text{NEt}_2)_2\text{(NHEt}_2)$  (**1**).

**Table 1. Summary of Crystallographic Data for  $(\eta^5\text{-C}_2\text{B}_9\text{H}_{11})\text{Zr}(\text{NEt}_2)_2\text{(NHEt}_2)$  (**1**)**

compd	$(\eta^5\text{-C}_2\text{B}_9\text{H}_{11})\text{Zr}(\text{NEt}_2)_2\text{(NHEt}_2)$ ( <b>1</b> )
color/shape	colorless/fragment
empirical formula	$\text{C}_{14}\text{H}_{42}\text{B}_9\text{N}_3\text{Zr}$
fw	441.02
temp	291(2) K
cryst syst	monoclinic
space group	$P2_1/c$
unit cell dimens	$a = 10.704(4)$ Å, $b = 11.066(3)$ Å,
(25 reflns, $14^\circ < \theta < 25^\circ$ )	$c = 20.382(8)$ Å, $\alpha = 90^\circ$ ,
	$\beta = 99.20(3)^\circ$ , $\gamma = 90^\circ$
V	$2383.2(14)$ Å <sup>3</sup>
Z	4
density (calcd)	$1.229$ Mg m <sup>-3</sup>
abs coeff	$0.466$ mm <sup>-1</sup>
diffractometer/scan	Enraf-Nonius CAD-4/ $\omega$ -2 $\theta$
radiation/wavelength	Mo K $\alpha$ (graphite-monochromated)/ $0.710$ 73 Å
$F(000)$	928
cryst size	$0.40 \times 0.25 \times 0.20$ mm
$\theta$ range for data collection	$1.93^\circ$ – $24.99^\circ$
index ranges	$0 \leq h \leq 12$ , $0 \leq k \leq 13$ , $-24 \leq l \leq 23$
no. of standards/decay	3/2%
no. of reflns colld	4424
no. indep reflns	4195 ( $R_{\text{int}} = 0.0560$ )
refinement method	full-matrix least-squares on $F^2$
computing	SHELXS-85, SHELX-93
data/restraints/params	4176/0/244
goodness-of-fit on $F^2$	1.012
SHELX-93 wt params	0.0387, 0.3539
final R indices [ $I > 2\sigma(I)$ ]	$R_1 = 0.0386$ , $wR_2 = 0.0900$
R indices (all data)	$R_1 = 0.1088$ , $wR_2 = 0.1179$
largest diff peak and hole	$0.307$ and $-0.347$ e Å <sup>-3</sup>

slight asymmetry to the Zr–carborane bonding; i.e., the Zr–B2 and Zr–B3 bonds are slightly shorter than the remaining Zr–cage bonds. This may be ascribed to steric effects. The slight tipping of the cage (i.e., the lengthening of the Zr–C1, Zr–C2, and Zr–B1 bonds vs the Zr–B2 and Zr–B3 bonds) relieves steric interactions between the dicarbollide C–H units and the N2 amide group which lies directly beneath the C1–C2 bond, and between the B1–H unit and the amine ligand which lies directly beneath the B1–H bond. The steric interactions between the dicarbollide and N2 amide ligands are also manifested by the disparity in the angles at N2

**Table 2. Atomic Coordinates ( $\times 10^4$ ) and Equivalent Displacement Parameters ( $\text{\AA}^2 \times 10^3$ ) for **1****

atom	$x/a$	$y/b$	$z/c$	$U(\text{eq})^a$
Zr	2908(1)	2589(1)	670(1)	29(1)
N(1)	4915(3)	2557(3)	1345(2)	36(1)
N(2)	2043(4)	1255(3)	1130(2)	37(1)
N(3)	2283(3)	4218(3)	940(2)	38(1)
C(1)	3239(4)	897(4)	-187(2)	33(1)
C(2)	1878(4)	1453(4)	-375(2)	33(1)
C(3)	4925(5)	2410(5)	2080(2)	52(1)
C(4)	5146(7)	1144(5)	2301(3)	81(2)
C(5)	5769(4)	3561(4)	1206(2)	48(1)
C(6)	7154(5)	3288(5)	1413(3)	59(1)
C(7)	1623(5)	-7(4)	1005(2)	47(1)
C(8)	2302(6)	-935(5)	1473(3)	71(2)
C(9)	1765(4)	1679(4)	1777(2)	45(1)
C(10)	388(5)	1592(5)	1877(3)	66(2)
C(11)	973(4)	4353(4)	1052(2)	46(1)
C(12)	822(6)	4983(5)	1689(3)	73(2)
C(13)	2909(5)	5367(4)	860(2)	47(1)
C(14)	2239(5)	6186(4)	323(3)	57(1)
B(1)	4341(5)	1940(4)	-174(2)	31(1)
B(2)	3541(5)	3284(4)	-417(2)	34(1)
B(3)	1934(5)	2922(4)	-519(2)	34(1)
B(4)	2684(5)	3061(4)	-1230(3)	37(1)
B(5)	1571(5)	1888(5)	-1186(3)	40(1)
B(6)	2426(5)	549(5)	-957(2)	39(1)
B(7)	4036(5)	887(4)	-841(2)	36(1)
B(8)	4217(4)	2446(5)	-1013(2)	36(1)
B(9)	2994(5)	1577(5)	-1496(3)	40(1)

<sup>a</sup>  $U(\text{eq})$  is defined as one-third of the trace of the orthogonalized  $U_{ij}$  tensor.

**Table 3. Selected Bond Lengths (Å) and Angles (deg) for Compound **1****

Zr–Cent <sup>a</sup>	2.128(2)	Zr–N(3)	2.029(3)
Zr–N(2)	2.047(3)	Zr–N(1)	2.360(3)
Zr–B(3)	2.507(5)	Zr–B(2)	2.538(5)
Zr–C(2)	2.566(4)	Zr–B(1)	2.584(5)
Zr–C(1)	2.623(4)	C(1)–C(2)	1.571(6)
C–B <sup>b</sup>	1.69(3)	B–B <sup>b</sup>	1.77(1)
N(1)–Zr–Cent	112.6	N(2)–Zr–Cent	110.3
N(3)–Zr–Cent	123.5	N(3)–Zr–N(2)	108.9(2)
N(3)–Zr–N(1)	99.4(1)	N(2)–Zr–N(1)	99.1(1)
C(5)–N(1)–C(3)	111.3(3)	C(5)–N(1)–Zr	113.9(3)
C(3)–N(1)–Zr	116.3(3)	C(9)–N(2)–C(7)	110.8(3)
C(9)–N(2)–Zr	110.6(3)	C(7)–N(2)–Zr	138.7(3)
C(13)–N(3)–C(11)	113.4(4)	C(13)–N(3)–Zr	124.5(3)
C(11)–N(3)–Zr	119.9(3)		

<sup>a</sup> “Cent” denotes the centroid of the  $\eta^5$ -face of the dicarbollide ligand. <sup>b</sup> Average bond length.

(C7–N2–Zr,  $138.7(3)^\circ$ ; C9–N2–Zr,  $110.6(3)^\circ$ ) and by several close H–H contacts.<sup>12</sup> The Zr–centroid distance ( $2.128(2)$  Å) is ca.  $0.1$  Å longer than the corresponding distance in the bent-metallocene  $(\eta^5\text{-C}_2\text{B}_9\text{H}_{11})(\text{Cp}^*)\text{-ZrCMe=CMe}_2$  ( $2.04$  Å) but comparable to that in  $\{(\eta^5\text{-C}_2\text{B}_9\text{H}_{11})(\text{Cp}^*)\text{Zr}\}(\mu\text{-CH}_2)$  ( $2.09$  Å).<sup>1</sup>

The structural data clearly indicate that strong  $\text{N}_{\text{amide}}\text{-Zr}$   $\pi$ -donation is present in **1**. The amides are flat (sum of angles around N2 =  $360.1^\circ$ , N3 =  $357.8^\circ$ ), and the Zr– $\text{N}_{\text{amide}}$  distances ( $2.04$  Å, average) are at the short end of the range observed for other unsaturated Zr(IV) amide complexes in which N–Zr  $\pi$ -donation is present (ca.  $2.04$ – $2.17$  Å).<sup>13</sup> In particular, these Zr–N bond distances are comparable to those in the piano stool complexes  $\text{Cp}^*\text{Zr}(\text{N}^i\text{Pr}_2)\text{Cl}_2$  ( $2.00$  Å),<sup>14</sup> *meso*- $\{\mu$ -

(12) There are several close H–H contacts: H1A–H7A,  $2.17$  Å; H2A–H7A,  $2.20$  Å; H1–H1N1,  $2.28$  Å.

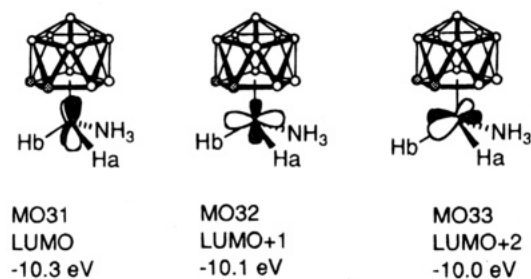


**Figure 2.** Key frontier orbitals of the model compound ( $\eta^5$ -C<sub>2</sub>B<sub>9</sub>H<sub>11</sub>)ZrH<sub>2</sub>(NH<sub>3</sub>) as determined by an extended Hückel molecular orbital analysis.

$\eta^5$ , $\eta^5$ -Me<sub>2</sub>Si(indenyl)<sub>2</sub>{Zr(NMe<sub>2</sub>)<sub>3</sub>}<sub>2</sub> (2.03–2.05 Å),<sup>15</sup> and, after correction for the difference in ionic radii of Ti(IV) vs Zr(IV),<sup>16</sup> Cp\*Ti(NMe<sub>2</sub>)<sub>3</sub> (1.92 Å).<sup>17</sup>

The orientations of the amide ligands are also consistent with the presence of strong N–Zr  $\pi$ -bonding. As noted above, the N2 amide group adopts a sterically unfavorable perpendicular orientation which directs one ethyl group directly toward the dicarbollide cage, while the N3 amide is rotated ca. 75° from this orientation. Qualitative inspection of space-filling models indicates that rotation of the perpendicular amide to relieve amide/dicarbollide steric interactions would not cause severe amide/amine or amide/amide steric interactions, and suggests that this orientational preference has an electronic origin. To identify the  $\pi$ -acceptor orbitals in ( $\eta^5$ -C<sub>2</sub>B<sub>9</sub>H<sub>11</sub>)ZrX<sub>2</sub>L piano stool species (X and L = anionic and neutral  $\sigma$ -donor ligands), we carried out an extended Hückel analysis of the model compound ( $\eta^5$ -C<sub>2</sub>B<sub>9</sub>H<sub>11</sub>)ZrH<sub>2</sub>(NH<sub>3</sub>).<sup>18</sup> As expected by analogy to Cp-ML<sub>3</sub> piano stool compounds,<sup>19</sup> this species has three low-lying empty Zr d orbitals (Figure 2). The LUMO (MO31, Figure 2) has  $\pi$ -symmetry with respect to the Ha site, with lobes suitable for overlap with the p orbital of an amide in the parallel orientation, and  $\delta$ -symmetry with respect to the Hb site. A second orbital (MO33, LUMO + 2) has  $\pi$ -symmetry with respect to both H sites, with lobes oriented for  $\pi$ -bonding with an amide in the

(13) Representative Zr(IV) amide complexes and average Zr–N distances. (a) Zr(NMe<sub>2</sub>)<sub>4</sub>, 2.07 Å (electron diffraction): Hagen, K.; Holwill, C. J.; Rice, D. A.; Runnacles, J. D. *Inorg. Chem.* **1988**, *27*, 2032. (b) (Me<sub>2</sub>N)<sub>3</sub>Zr( $\mu$ -NMe<sub>2</sub>)<sub>2</sub>Zr(NMe<sub>2</sub>)<sub>3</sub>, terminal Zr–N, 2.045(3)–2.108(3) Å: Chisholm, M. H.; Hammond, C. E.; Huffman, J. C. *Polyhedron* **1988**, *7*, 2515. (c) (Me<sub>2</sub>N)<sub>2</sub>Zr( $\mu$ -N<sup>t</sup>Bu)<sub>2</sub>Zr(NMe<sub>2</sub>)<sub>2</sub>, 2.06 Å: Nugent, W. A.; Harlow, R. L. *Inorg. Chem.* **1979**, *18*, 2030. (d) *rac*-Ethylenebis(indenyl)Zr(NMe<sub>2</sub>)<sub>2</sub>, 2.06 Å: Diamond, G. M.; Petersen, J. L.; Jordan, R. F. Unpublished results. (e) Cp<sub>2</sub>Zr(NC<sub>4</sub>H<sub>9</sub>)<sub>2</sub>, 2.17 Å: Bynum, R. V.; Hunter, W. E.; Rogers, R. D.; Atwood, J. L. *Inorg. Chem.* **1980**, *19*, 2368.

(14) Coalter, J. N.; Gunnoe, B.; Pupi, R. M.; Petersen, J. L. Unpublished results.

(15) Christopher, J. N.; Diamond, G. M.; Jordan, R. F.; Petersen, J. L. Manuscript in preparation.

(16) The ionic radius of Zr(IV) is ca. 0.1 Å larger than that of Ti(IV) in comparable coordination environments. Shannon, R. D. *Acta Crystallogr.* **1976**, *A32*, 751.

(17) Martin, A.; Mena, M.; Yelamos, C.; Serrano, R.; Raithby, P. R. *J. Organomet. Chem.* **1994**, *467*, 79.

(18) The model compound ( $\eta^5$ -C<sub>2</sub>B<sub>9</sub>H<sub>11</sub>)ZrH<sub>2</sub>(NH<sub>3</sub>) was constructed from **1** by replacement of the amide ligands by hydrides (Zr–H distance, 1.90 Å) and replacement of the amine ethyl groups by hydrogens (N–H distance, 0.90 Å). The bond angles and other atoms/distances are unchanged from **1**. Extended Hückel MO calculations were carried out on a CAChe system (CAChe Scientific Inc.), using the Alvarez parameter set. The HOMO of ( $\eta^5$ -C<sub>2</sub>B<sub>9</sub>H<sub>11</sub>)ZrH<sub>2</sub>(NH<sub>3</sub>) is a carborane-based orbital.

(19) (a) Albright, T. A.; Burdett, J. K.; Whangbo, M. H. *Orbital Interactions in Chemistry*; John Wiley and Sons: New York, NY, 1985; pp 384–387. (b) Bursten, B. E.; Clayton, R. H. *Organometallics* **1987**, *6*, 2004. (c) Legzdins, P.; Rettig, S. J.; Sanchez, L.; Bursten, B. E.; Gatter, M. G. *J. Am. Chem. Soc.* **1985**, *107*, 1411. (d) Lichtenberger, D. L.; Fenske, R. F. *J. Am. Chem. Soc.* **1976**, *98*, 50.

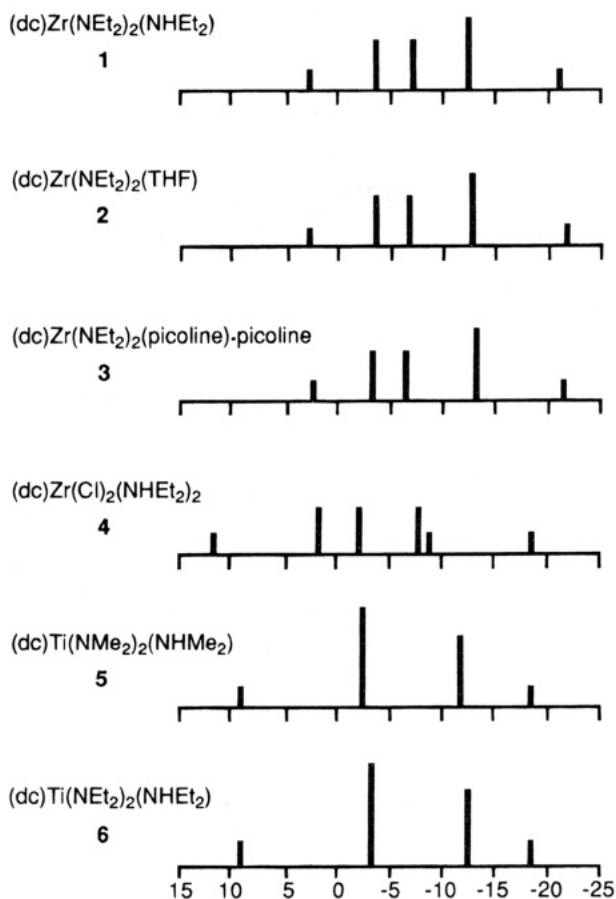


**Figure 3.** Schematic diagram of <sup>11</sup>B NMR spectra of **1**–**6**. The abbreviation “dc” indicates  $\eta^5$ -C<sub>2</sub>B<sub>9</sub>H<sub>11</sub>. The chemical shift scale is in ppm.

perpendicular orientation. The third frontier orbital, (MO32, LUMO + 1), has  $\pi$ -symmetry with respect to the Hb site, with lobes oriented for  $\pi$ -bonding with a parallel amide, but is expected to be less effective in  $\pi$ -bonding due to poorer overlap. This orbital has  $\delta$ -symmetry with respect to the Ha site. Thus, in an analogous ( $\eta^5$ -C<sub>2</sub>B<sub>9</sub>H<sub>11</sub>)Zr(NR<sub>2</sub>)<sub>2</sub>(NR<sub>3</sub>) species, one amide should adopt a parallel orientation in which  $\pi$ -donation to MO31 is maximized, while the other should adopt a near perpendicular orientation to allow  $\pi$ -donation to MO33 and to a lesser extent, MO32. This is what is observed in the solid state for **1**.

**Reactivity of 1.** Complex **1** may be converted to other mono-dicarbollide Zr(IV) complexes via ligand substitution and protonolysis reactions. Compound **1** reacts with neat THF to yield ( $\eta^5$ -C<sub>2</sub>B<sub>9</sub>H<sub>11</sub>)Zr(NEt<sub>2</sub>)<sub>2</sub>(THF) (**2**) and with excess 4-picoline to yield ( $\eta^5$ -C<sub>2</sub>B<sub>9</sub>H<sub>11</sub>)Zr(NEt<sub>2</sub>)<sub>2</sub>(4-picoline)<sub>2</sub> (**3**). The physical properties of **2** and **3** are similar to those of **1**, and both derivatives are isolated as yellow solids by recrystallization from CH<sub>2</sub>Cl<sub>2</sub>/toluene. The <sup>11</sup>B NMR spectrum of **2** is almost identical to that of **1** (Figure 3), consistent with a similar three-legged piano stool structure. The <sup>1</sup>H and <sup>13</sup>C NMR spectra of **2** contain THF resonances which are significantly shifted from those of free THF. The <sup>1</sup>H NMR and analytical data indicate that isolated **3** contains 2 equiv of 4-picoline per Zr. However, as illustrated in Figure 3, the <sup>11</sup>B NMR spectrum of **3** (CD<sub>2</sub>-Cl<sub>2</sub>) is almost identical to those of **1** and **2** and distinctly different from that of the five-coordinate complex ( $\eta^5$ -C<sub>2</sub>B<sub>9</sub>H<sub>11</sub>)ZrCl<sub>2</sub>(NHET<sub>2</sub>)<sub>2</sub> (**4**, *vide infra*). Additionally, the <sup>1</sup>H and <sup>13</sup>C chemical shifts for the dicarbollide C–H



units of **3** are very similar to those of **1** and **2** and quite different from those of **4**. The  $^1\text{H}$  NMR spectrum of **3** ( $\text{CD}_2\text{Cl}_2$ ) contains one set of 4-picoline resonances which are only slightly shifted from those of free 4-picoline and do not shift significantly or broaden when the temperature is lowered to 205 K.<sup>20</sup> Addition of 1 equiv of 4-picoline to this solution causes the 4-picoline resonances to shift back toward the free picoline values, but only a single set of 4-picoline resonances is observed down to 205 K. Collectively these observations establish that **3** undergoes nearly complete dissociation of one 4-picoline ligand in  $\text{CD}_2\text{Cl}_2$  solution and that exchange of free and coordinated 4-picoline is very rapid on the NMR time scale. Complex **1** reacts with excess  $\text{NHMe}_2$  to yield a mixture of unidentified products<sup>21</sup> but does not react with  $\text{Et}_2\text{O}$ .

The reaction of **1** with 2 equiv of  $[\text{NH}_2\text{Et}_2]\text{Cl}$  results in selective protonolysis of the Zr–amide bonds and formation of  $(\eta^5\text{-C}_2\text{B}_9\text{H}_{11})\text{ZrCl}_2(\text{NHEt}_2)_2$  (**4**), which is isolated as a yellow solid by recrystallization from  $\text{CH}_2\text{Cl}_2/\text{toluene}$ . The  $^{11}\text{B}$  NMR spectrum of **4** contains six resonances in a 1/2/2/1/1 intensity ratio which are shifted to somewhat lower field from the resonances of **1–3** and are consistent with an  $\eta^5$ -dicarbollide ligand in a  $C_s$ -symmetric structure. The  $^1\text{H}$  NMR spectrum of **4** contains two multiplets for the amine methylene hydrogens, and the  $^{13}\text{C}$  spectrum contains a single amine methylene carbon resonance. Collectively, these data are most consistent with a trans four-legged piano stool structure; in contrast, a cis structure would give rise to four  $^1\text{H}$  and two  $^{13}\text{C}$  ZrNH( $\text{CH}_2\text{CH}_3$ )<sub>2</sub> NMR resonances.<sup>22</sup> Complex **4** does not undergo ligand substitution by THF.

**Synthesis of  $(\eta^5\text{-C}_2\text{B}_9\text{H}_{11})\text{Ti}(\text{NR}_2)_2(\text{NHR}_2)$  Complexes.** The amine elimination approach also provides access to mono-dicarbollide Ti(IV) complexes. Thus the reaction of  $\text{C}_2\text{B}_9\text{H}_{13}$  with  $\text{Ti}(\text{NR}_2)_4$  in toluene at 23 °C yields  $(\eta^5\text{-C}_2\text{B}_9\text{H}_{11})\text{Ti}(\text{NR}_2)_2(\text{NHR}_2)$  (**5**, R = Me; **6**, R = Et). Compounds **5** and **6** are isolated as analytically pure red solids via simple removal of volatiles and hexane washing. The NMR properties of **5** and **6** are similar to those of **1** and are consistent with three-legged piano stool structures and the presence of a single amine ligand.

**Summary.** Amine elimination reactions of  $\text{C}_2\text{B}_9\text{H}_{13}$  and  $\text{M}(\text{NR}_2)_4$  compounds provide convenient access to  $(\eta^5\text{-C}_2\text{B}_9\text{H}_{11})\text{M}(\text{NR}_2)_2(\text{NHR}_2)$  complexes which adopt three-legged piano stool structures and can be converted to a variety of derivatives via ligand substitution or protonolysis reactions. We are currently attempting to exploit this chemistry in the synthesis of  $(\eta^5\text{-C}_2\text{B}_9\text{H}_{11})\text{M}(\text{R})_2\text{L}_n$  alkyl complexes.

(20)  $^1\text{H}$  NMR spectrum of free 4-picoline in  $\text{CD}_2\text{Cl}_2$ :  $\delta$  8.42 (d,  $J$  = 4 Hz, 2H), 7.09 (d,  $J$  = 4 Hz, 2H), 2.32 (s, 3H).

(21) The  $^{11}\text{B}$  NMR spectrum of this mixture contains high-field resonances characteristic of  $\text{C}_2\text{B}_9\text{H}_{12}^-$  species, suggesting that the amine elimination is reversible. Similarly, **1** undergoes hydrolysis, yielding  $\text{C}_2\text{B}_9\text{H}_{12}^-$  and other unidentified products.

(22) (a) These data are also accommodated by a cis structure which undergoes a dynamic process that collapses the expected four amine methylene resonances to two resonances, e.g., rapid interconversion with the trans isomer. This possibility is unlikely because the  $^1\text{H}$  NMR spectrum of **4** does not change significantly when the temperature is lowered to 205 K. Note that fast reversible amine dissociation would collapse the diastereotopic amine resonances of **4** to a single resonance; this is not observed at or below 295 K. (b) The spectrum of **4** containing free  $\text{NHEt}_2$  (2 equiv) exhibits resonances for free and coordinated  $\text{NHEt}_2$ .

## Experimental Section

**General Procedures.** All manipulations were performed on a high-vacuum line or in a Vacuum Atmospheres glovebox under a purified  $\text{N}_2$  atmosphere. Solvents were distilled from appropriate drying agents and stored under  $\text{N}_2$  or vacuum: hexane (Na/benzophenone), toluene (Na), THF (Na/benzophenone),  $\text{CH}_2\text{Cl}_2$  ( $\text{CaH}_2$ ),  $\text{CD}_2\text{Cl}_2$  ( $\text{CaH}_2$ ), 4-picoline (activated 3Å molecular sieves).  $\text{C}_2\text{B}_9\text{H}_{13}$  was prepared by the literature procedure,<sup>23</sup> and  $\text{Zr}(\text{NET}_2)_4$ ,  $\text{Ti}(\text{NMe}_2)_4$ , and  $\text{Ti}(\text{NET}_2)_4$  were prepared by a modification<sup>24</sup> of the literature procedures.<sup>13b,25</sup> NMR spectra were collected on a Bruker AMX-360 spectrometer in flame-sealed or Teflon-valved tubes.  $^1\text{H}$  and  $^{13}\text{C}$  chemical shifts are reported versus  $\text{Me}_4\text{Si}$  and were determined by reference to the residual solvent peaks. The  $^1\text{H}$  NMR spectra contain broad B–H resonances in the range  $\delta$  0–3 which are not listed.  $^{11}\text{B}\{^1\text{H}\}$  NMR spectra were referenced to external  $\text{BF}_3\cdot\text{Et}_2\text{O}$  ( $\delta$  0,  $\text{C}_6\text{D}_6$ ). Elemental analyses were performed by E + R Microanalytical Laboratory, Inc.

**$(\eta^5\text{-C}_2\text{B}_9\text{H}_{11})\text{Zr}(\text{NET}_2)_2(\text{NHEt}_2)$  (**1**).** A solution of  $\text{C}_2\text{B}_9\text{H}_{13}$  (1.78 g, 13.2 mmol) in toluene (25 mL) was added to a solution of  $\text{Zr}(\text{NET}_2)_4$  (5.01 g, 13.2 mmol) in toluene (40 mL), dropwise over a period of 10 min with vigorous stirring at 23 °C. The reaction mixture was stirred for 2 h, concentrated to ca. 20 mL under vacuum, and filtered, yielding a pale yellow solid and an orange filtrate. The solid was dried under vacuum overnight (4.06 g, 69.6%). Compound **1** was recrystallized from a concentrated  $\text{CH}_2\text{Cl}_2$  solution layered with toluene at –40 °C: mp 142–144 °C. Anal. Calcd for  $\text{C}_{14}\text{H}_{42}\text{B}_9\text{N}_3\text{Zr}$ : Z, 38.13; H, 9.60; N, 9.53. Found: C, 37.96; H, 9.42; N, 9.39.  $^1\text{H}$  NMR ( $\text{CD}_2\text{Cl}_2$ ):  $\delta$  3.59 (m, 8H,  $\text{NCH}_2$ ), 3.48 (br s, 1H, NH), 3.27 (dq,  $J$  = 14, 7, 3 Hz, 2H,  $\text{HNCH}_2$ ), 3.00 (dq,  $J$  = 14, 8, 7 Hz, 2H,  $\text{HNCH}_2$ ), 2.68 (br s, 2H, dicarbollide CH), 1.32 (t,  $J$  = 7 Hz, 6H,  $\text{HNCH}_2\text{CH}_3$ ), 1.09 (t,  $J$  = 7 Hz, 12H,  $\text{NCH}_2\text{CH}_3$ ).  $^{11}\text{B}\{^1\text{H}\}$  NMR ( $\text{CD}_2\text{Cl}_2$ ):  $\delta$  3.2 (1B), –4.1 (2B), –7.7 (2B), –12.9 (3B), –20.8 (1B).  $^{13}\text{C}\{^1\text{H}\}$  NMR ( $\text{CD}_2\text{Cl}_2$ ):  $\delta$  48.9 ( $\text{C}_2\text{B}_9\text{H}_{11}$ ), 44.1 ( $\text{HNCH}_2$ ), 42.5 ( $\text{NCH}_2$ ), 14.2 ( $\text{HNCH}_2\text{CH}_3$ ), 13.8 ( $\text{NCH}_2\text{CH}_3$ ).

**$(\eta^5\text{-C}_2\text{B}_9\text{H}_{11})\text{Zr}(\text{NET}_2)_2(\text{THF})$  (**2**).** A yellow solution of **1** (0.350 g, 0.790 mmol) in THF (15 mL) was stirred for 30 min at 23 °C. The volatiles were removed under vacuum, yielding a pale yellow solid which was left under vacuum for 1 h. The solid was dissolved in THF (15 mL), and the volatiles were immediately removed under vacuum. The pale yellow solid was dried under vacuum for 3.5 h (0.280 g, 80.2%). Compound **5** was recrystallized from a concentrated  $\text{CH}_2\text{Cl}_2$  solution layered with toluene at –40 °C: mp 150 °C. Anal. Calcd for  $\text{C}_{14}\text{H}_{39}\text{B}_9\text{N}_2\text{OZr}$ : C, 38.22; H, 8.94; N, 6.37. Found: C, 38.07; H, 8.97; N, 6.18.  $^1\text{H}$  NMR ( $\text{CD}_2\text{Cl}_2$ ):  $\delta$  4.31 (m, 4H, THF), 3.63 (q,  $J$  = 7 Hz, 8H,  $\text{NCH}_2$ ), 2.67 (br s, 2H, dicarbollide CH), 2.13 (m, 4H, THF), 1.09 (t,  $J$  = 7 Hz, 12H,  $\text{NCH}_2\text{CH}_3$ ).  $^{11}\text{B}\{^1\text{H}\}$  NMR ( $\text{CD}_2\text{Cl}_2$ ):  $\delta$  2.7 (1B), –4.0 (2B), –7.0 (2B), –12.9 (3B), –21.3 (1B).  $^{13}\text{C}$  NMR ( $\text{CD}_2\text{Cl}_2$ ):  $\delta$  76.1 (t,  $J$  = 151 Hz, THF), 49.1 (d,  $J$  = 159 Hz,  $\text{C}_2\text{B}_9\text{H}_{11}$ ), 42.7 (t,  $J$  = 131 Hz,  $\text{NCH}_2$ ), 26.0 (t,  $J$  = 134 Hz, THF), 14.5 (q,  $J$  = 124 Hz,  $\text{NCH}_2\text{CH}_3$ ).

**$(\eta^5\text{-C}_2\text{B}_9\text{H}_{11})\text{Zr}(\text{NET}_2)_2(4\text{-picoline})_2$  (**3**).** A 1:1 mixture of 4-picoline/ $\text{CH}_2\text{Cl}_2$  (8 mL total, ca. 40 mmol of 4-picoline) was added to a solution of **1** (0.500 g, 1.13 mmol) in  $\text{CH}_2\text{Cl}_2$  (10 mL) with vigorous stirring at 23 °C. The resulting yellow solution was stirred for 45 min. All volatiles were removed, and the resulting yellow solid was dried under vacuum for 1 h (0.585 g, 93.1%). Compound **6** was recrystallized from a concentrated  $\text{CH}_2\text{Cl}_2$  solution layered with toluene at –40 °C: mp 145 °C. Anal. Calcd for  $\text{C}_{22}\text{H}_{46}\text{B}_9\text{N}_4\text{Zr}$ : C, 47.68; H, 8.19; N, 10.11. Found: C, 47.54; H, 8.09; N, 9.94.  $^1\text{H}$  NMR ( $\text{CD}_2\text{Cl}_2$ ):  $\delta$  8.49 (d,  $J$  = 6 Hz, 4H, *o*-4-picoline), 7.27 (d,  $J$  = 6 Hz,

(23) See reference 5g and (a) Wiesboeck, R. A.; Hawthorne, M. F. *J. Am. Chem. Soc.* **1964**, *86*, 1642. (b) Plešek, J.; Hermanek, S.; Stibr, B. *Inorg. Synth.* **1963**, *22*, 231.

(24) Diamond, G. M.; Rodewald, S.; Jordan, R. F. *Organometallics* **1995**, *14*, 5.

(25) (a) Bradley, D. C.; Thomas, I. M. *J. Chem. Soc.* **1960**, 3857. (b) Bradley, D. C.; Thomas, I. M. *Proc. Chem. Soc. London* **1959**, 225.

4H, *m*-4-picoline), 3.66 (q,  $J = 7$  Hz, 8H,  $\text{NCH}_2$ ), 2.56 (br s, 2H, dicarbollide  $\text{CH}$ ), 2.42 (s, 6H, methyl, 4-picoline), 1.07 (t,  $J = 7$  Hz, 12H,  $\text{NCH}_2\text{CH}_3$ ).  $^{11}\text{B}\{^1\text{H}\}$  NMR ( $\text{CD}_2\text{Cl}_2$ ):  $\delta$  2.5 (1B), -4.0 (2B), -6.5 (2B), -13.0 (3B), -21.2 (1B).  $^{13}\text{C}\{^1\text{H}\}$  NMR ( $\text{CD}_2\text{Cl}_2$ ):  $\delta$  150.9 (*p*-C, 4-picoline), 149.8 (*o*-C, 4-picoline), 125.9 (*m*-C, 4-picoline), 49.4 ( $\text{C}_2\text{B}_9\text{H}_{11}$ ), 42.7 ( $\text{NCH}_2$ ), 21.4 (methyl, 4-picoline), 13.9 ( $\text{NCH}_2\text{CH}_3$ ).

( $^{17}\text{O}$ - $\text{C}_2\text{B}_9\text{H}_{11}$ ) $\text{ZrCl}_2(\text{NHEt}_2)_2$  (**4**). Solid [ $\text{H}_2\text{NEt}_2$ ] $\text{Cl}$  (1.00 g, 9.15 mmol) was added to a solution of **1** (2.03 g, 4.61 mmol) in  $\text{CH}_2\text{Cl}_2$  (25 mL) with vigorous stirring at 23 °C. The pale yellow solution was stirred for 2 h. The volatiles were removed under vacuum, and the resulting pale yellow solid was dried under vacuum for 1 h (2.02 g, 99.0%). Compound **4** was recrystallized from a concentrated  $\text{CH}_2\text{Cl}_2$  solution layered with toluene at -40 °C. Compound **4** is quite stable in air in  $\text{CH}_2\text{Cl}_2$  solution: mp 157–159 °C. Anal. Calcd for  $\text{C}_{10}\text{H}_{35}\text{B}_9\text{N}_2\text{Cl}_2\text{Zr}$ : C, 27.12; H, 7.97; N, 6.33. Found: C, 27.27; H, 7.84; N, 6.22.  $^1\text{H}$  NMR ( $\text{CD}_2\text{Cl}_2$ ):  $\delta$  3.40–3.45 (br m, 6H, dicarbollide  $\text{CH}$ ,  $\text{NCH}_2$ ), 3.04 (br s, 4H,  $\text{NCH}_2$ ), 2.86 (br s, 2H,  $\text{HN}$ ), 1.32 (t,  $J = 7$  Hz, 12H,  $\text{NCH}_2\text{CH}_3$ ),  $^{11}\text{B}\{^1\text{H}\}$  NMR ( $\text{CD}_2\text{Cl}_2$ ):  $\delta$  10.1 (1B), 1.8 (2B), -2.3 (2B), -7.8 (2B), -9.4 (1B), -14.7 (1B).  $^{13}\text{C}\{^1\text{H}\}$  NMR ( $\text{CD}_2\text{Cl}_2$ ):  $\delta$  59.0 (br s,  $\text{C}_2\text{B}_9\text{H}_{11}$ ), 48.0 (s,  $\text{NCH}_2$ ), 15.0 (s,  $\text{NCH}_2\text{CH}_3$ ).

( $^{17}\text{O}$ - $\text{C}_2\text{B}_9\text{H}_{11}$ ) $\text{Ti}(\text{NMe}_2)_2(\text{NHMe}_2)$  (**5**). A solution of  $\text{C}_2\text{B}_9\text{H}_{13}$  (1.20 g, 8.91 mmol) in toluene (25 mL) was added dropwise to a solution of  $\text{Ti}(\text{NMe}_2)_4$  (1.99 g, 8.90 mmol) in toluene (40 mL) over 30 min at 23 °C. The reaction mixture was stirred vigorously for 2.5 h, during which time a vacuum was periodically applied. The volatiles were moved under vacuum, and the maroon residue was triturated with hexane (50 mL). The hexane was removed under vacuum, and the resulting powder was heated under vacuum at 75 °C overnight, yielding a pale brick-red powder (2.72 g, 97.5%): mp 164–166 °C. Anal. Calcd for  $\text{C}_8\text{H}_{30}\text{B}_9\text{N}_3\text{Ti}$ : C, 30.64; H, 9.64; N, 13.40. Found: C, 30.48; H, 9.76; N, 13.20.  $^1\text{H}$  NMR ( $\text{CD}_2\text{Cl}_2$ ):  $\delta$  3.89 (br s, 1H,  $\text{HN}$ ), 3.43 (s, 12H,  $\text{NCH}_3$ ), 2.90 (br s, 2H, dicarbollide  $\text{CH}$ ), 2.68 (d,  $J = 6$  Hz, 6H,  $\text{HNCH}_3$ ).  $^{11}\text{B}\{^1\text{H}\}$  NMR ( $\text{CD}_2\text{Cl}_2$ ):  $\delta$  9.5 (1B), -3.1 (4B), -12.3 (3B), -17.9 (1B).  $^{13}\text{C}$  NMR ( $\text{CD}_2\text{Cl}_2$ ):  $\delta$  53.9 (d,  $J = 168$  Hz,  $\text{C}_2\text{B}_9\text{H}_{11}$ ), 49.3 (qq,  $J = 135$ , 6 Hz,  $\text{NCH}_3$ ), 41.8 (qp,  $J = 138$ , 5 Hz,  $\text{NHCH}_3$ ).

( $^{17}\text{O}$ - $\text{C}_2\text{B}_9\text{H}_{11}$ ) $\text{Ti}(\text{NEt}_2)_2(\text{NHEt}_2)$  (**6**). A solution of  $\text{C}_2\text{B}_9\text{H}_{13}$  (0.804 g, 5.98 mmol) in toluene (50 mL) was added to a solution of  $\text{Ti}(\text{NEt}_2)_4$  (2.01 g, 5.97 mmol) in toluene (30 mL), dropwise over 25 min at 23 °C with vigorous stirring. The deep maroon

reaction mixture was stirred overnight while a stream of  $\text{N}_2$  was bubbled through it. The volatiles were removed under vacuum, and the resulting pale brick red solid was triturated with hexane (50 mL) and dried under vacuum (1.96 g, 82.5%): mp 118–123 °C. Anal. Calcd for  $\text{C}_{14}\text{H}_{42}\text{B}_9\text{N}_3\text{Ti}$ : C, 42.28; H, 10.65; N, 10.57. Found: C, 42.05; H, 10.49; N, 10.36.  $^1\text{H}$  NMR ( $\text{CD}_2\text{Cl}_2$ ):  $\delta$  4.02 (m, 8H,  $\text{NCH}_2$ ), 3.37 (m, 2H,  $\text{NHCH}_2$ ), 3.17 (m, 1H,  $\text{HN}$ ), 2.90 (m, 2H,  $\text{HNCH}_2$ ), 2.87 (br s, 2H, dicarbollide  $\text{CH}$ ), 1.31 (t,  $J = 7$  Hz, 6H,  $\text{HNCH}_2\text{CH}_3$ ), 1.10 (t,  $J = 7$  Hz, 12H,  $\text{NCH}_2\text{CH}_3$ ).  $^{11}\text{B}\{^1\text{H}\}$  NMR ( $\text{CD}_2\text{Cl}_2$ ):  $\delta$  9.1 (1B), -3.3 (4B), -12.5 (3B), -17.9 (1B).  $^{13}\text{C}$  NMR ( $\text{CD}_2\text{Cl}_2$ ):  $\delta$  52.9 (d,  $J = 169$  Hz,  $\text{C}_2\text{B}_9\text{H}_{11}$ ), 47.9 (tq,  $J = 134$ , 4 Hz,  $\text{NCH}_2$ ), 47.5 (t,  $J = 138$  Hz,  $\text{HNCH}_2$ ), 15.9 (qq,  $J = 126$  Hz,  $J = 3$  Hz,  $\text{HNCH}_2\text{CH}_3$ ), 13.1 (qt,  $J = 126$ , 3 Hz,  $\text{NCH}_2\text{CH}_3$ ).

**X-ray Diffraction Study of 1.** Transparent colorless block-shaped crystals were obtained from a concentrated  $\text{CH}_2\text{Cl}_2$  solution of **1** layered with toluene at -40 °C. A single crystal was mounted in a thin-walled glass capillary under Ar and transferred to the goniometer. The space group was determined to be  $P2_1/c$  from the systematic absences. A summary of data collection and refinement parameters is given in Table 1. Least-squares refinement with isotropic thermal parameters led to  $R = 0.070$ . The geometrically constrained hydrogen atoms were placed in calculated positions ( $\text{C}-\text{H} = 0.95$  Å,  $\text{B}-\text{H} = 1.10$  Å,  $\text{N}-\text{H} = 0.90$  Å) and allowed to ride on the bonded atom with  $B = 1.2U_{\text{eq}}$ . The methyl hydrogen atoms were included as a rigid group with rotational freedom at the bonded carbon atom ( $\text{C}-\text{H} = 0.95$  Å,  $B = 1.2U_{\text{eq}}(\text{C})$ ). The C1, C2, and B1–B3 hydrogen atoms were located from a difference Fourier map and allowed to ride on the bonded atom with  $B = 1.2U_{\text{eq}}$ . Refinement of non-hydrogen atoms was carried out with anisotropic temperature factors. The final values of the positional parameters are given in Table 2.

**Acknowledgment.** This work was supported by the Department of Energy (DOE DE-GG02-88-ER13935).

**Supporting Information Available:** Tables of complete bond distances and angles, anisotropic displacement parameters, and hydrogen atom coordinates and an alternate view of **1** (7 pages). Ordering information is given on any current masthead page.

OM9501900



# Carbonyl Fluxionality in the *nido* Cluster $\text{Ru}_3(\text{CO})_9(\mu_3\text{-CO})(\mu_3\text{-NPh})$ . NMR Evidence and Mechanism for the Exchange of the Triply-Bridging CO with the Terminal CO Groups

D. Wang,<sup>1a,b</sup> H. Shen,<sup>1a,b,c</sup> M. G. Richmond,<sup>\*,1b,c</sup> and M. Schwartz<sup>\*,1b</sup>

Department of Chemistry and Center for Organometallic Research and Education, University of North Texas, Denton, Texas 76203-5068

Received March 6, 1995\*

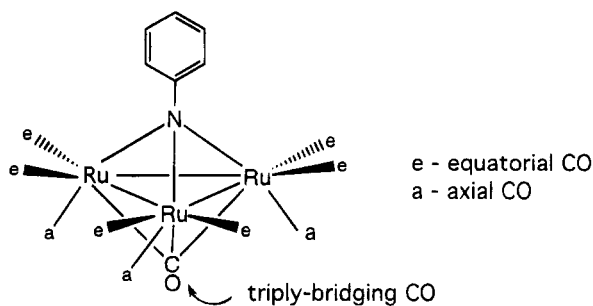
Variable-temperature  $^{13}\text{C}$  NMR studies on  $\text{Ru}_3(\text{CO})_9(\mu_3\text{-CO})(\mu_3\text{-NPh})$  reveal the presence of two distinct CO exchange processes that involve localized equatorial/axial carbonyl scrambling at each ruthenium vertex and exchange of the equatorial and triply-bridging CO groups. The kinetics and activation parameters for these exchange processes have been determined by both band shape analysis and 2D-EXSY experiments. The latter NMR method unequivocally rules out a sequence involving the direct exchange of the axial and triply-bridging CO groups. The somewhat faster of the two processes ( $\Delta G^\ddagger = 54.9$  (0.03) kJ/mol,  $\Delta H^\ddagger = 41.7$  (1.4) kJ/mol,  $\Delta S^\ddagger = -50$ (6) J/mol K) serves to equilibrate the equatorial/axial CO groups at each  $\text{Ru}(\text{CO})_3$  center, while the scrambling of the equatorial/triply-bridging CO groups displays comparable activation parameters ( $\Delta G^\ddagger = 58.1$ (0.14) kJ/mol,  $\Delta H^\ddagger = 45.4$  (3.4) kJ/mol,  $\Delta S^\ddagger = -49$ (14) J/mol K). Plausible mechanisms invoking a turnstile rotation and  $\mu_3\text{-CO} \rightarrow \mu_2\text{-CO}$  interconversions are presented and discussed relative to each CO exchange step.

## Introduction

The fluxional behavior of ancillary CO groups about polynuclear metal clusters has been extensively studied over the last two decades by variable-temperature  $^{13}\text{C}$  NMR spectroscopy.<sup>2</sup> Such studies have provided valuable insight into the relationship between the observed solid-state structure (X-ray) and the solution structure adopted by a given cluster. The observed ligand fluxionality has been proposed to function as a model for the movement of chemisorbed species on metallic surfaces.<sup>3</sup> The complete scrambling of terminal carbonyls about a cluster polyhedron generally proceeds via a series of terminal-to-bridge CO sequences, of which the one-for-one, two-center, and merry-go-round exchange processes represent the best known mechanisms.<sup>4</sup>

Our research groups have been interested in the NMR behavior of a wide variety of organometallic compounds, especially with regard to bonding considerations between a metal center(s) and different ancillary ligands,

as deduced by NMR spin-lattice ( $T_1$ ) measurements and quadrupole coupling constants (QCC's). For example, exploration of the dynamics of internal rotation of capping benzyldiene and phenylphosphinidene ligands in tri- and tetranuclear clusters has yielded useful information concerning the presence of  $\pi$  overlap between the phenyl groups of these ligands and the cluster framework.<sup>5</sup> Recently, we examined the rotation rates of the phenyl ligand in the imido-capped cluster  $\text{Ru}_3(\text{CO})_9(\mu_3\text{-CO})(\mu\text{-NPh})$  due to its isolobal relationship to the phenylphosphinidene fragment,<sup>6</sup> and we observed that all of the carbonyl groups undergo rapid exchange at most temperatures. Accordingly, we next conducted a more in-depth investigation into the exchange pathways operative for the carbonyl groups in  $\text{Ru}_3(\text{CO})_9(\mu_3\text{-CO})(\mu\text{-NPh})$ . The molecular structure of this cluster, with its three types of CO groups, is shown below.



\* Abstract published in *Advance ACS Abstracts*, June 15, 1995.

(1) (a) Robert A. Welch Predoctoral Fellow. (b) Department of Chemistry, University of North Texas. (c) Center for Organometallic Research and Education, University of North Texas.

(2) (a) Band, E.; Muetterties, E. L. *Chem. Rev.* **1978**, *78*, 639. (b) Evans, J. *Adv. Organomet. Chem.* **1977**, *16*, 319. (c) Aime, S.; Milone, L. *Prog. Nucl. Magn. Reson. Spectrosc.* **1977**, *11*, 183. (d) Cotton, F. A.; Hanson, B. E. In *Rearrangements in Ground and Excited States*; de Mayo, P., Ed.; Academic Press: New York, 1980; Vol. 2, Chapter 12.

(3) (a) Johnson, B. F. G.; Benfield, R. E. In *Transition Metal Clusters*; Johnson, B. F. G., Ed.; Wiley: New York, 1980; Chapter 7. (b) Johnson, B. F. G.; Rodgers, A. In *The Chemistry of Metal Cluster Complexes*; Shriver, D. F.; Kaesz, H. D.; Adams, R. D., Eds.; VCH Publishers: New York, 1990; Chapter 6.

(4) (a) Evans, J.; Johnson, B. F. G.; Lewis, J.; Matheson, T. W.; Norton, J. R. *J. Chem. Soc., Dalton Trans.* **1978**, 626. (b) Cotton, F. A.; Jamerson, J. D. *J. Am. Chem. Soc.* **1976**, *98*, 5396. (c) Stuntz, G. F.; Shapley, J. R. *J. Am. Chem. Soc.* **1977**, *99*, 607. (d) Washington, J.; Takats, J. *Organometallics* **1990**, *9*, 925. (e) Cotton, F. A.; Hanson, B. E.; Jamerson, J. D. *J. Am. Chem. Soc.* **1977**, *99*, 6588. (f) Adams, R. D.; Cotton, F. A. *J. Am. Chem. Soc.* **1973**, *95*, 6589.

(5) (a) Schwartz, M.; Richmond, M. G.; Chen, A. F. T.; Martin, G. E.; Kochi, J. K. *Inorg. Chem.* **1988**, *27*, 4698. (b) Wang, S. P.; Chen, A. F. T.; Richmond, M. G.; Schwartz, M. *J. Organomet. Chem.* **1989**, *371*, 81. (c) Yuan, P.; Richmond, M. G.; Schwartz, M. *Inorg. Chem.* **1991**, *30*, 588; 679. (d) Yuan, P.; Don, M.-J.; Richmond, M. G.; Schwartz, M. *Inorg. Chem.* **1991**, *30*, 3704.

(6) Wang, D.; Shen, H.; Richmond, M. G.; Schwartz, M. *Inorg. Chim. Acta* **1995**, in press.

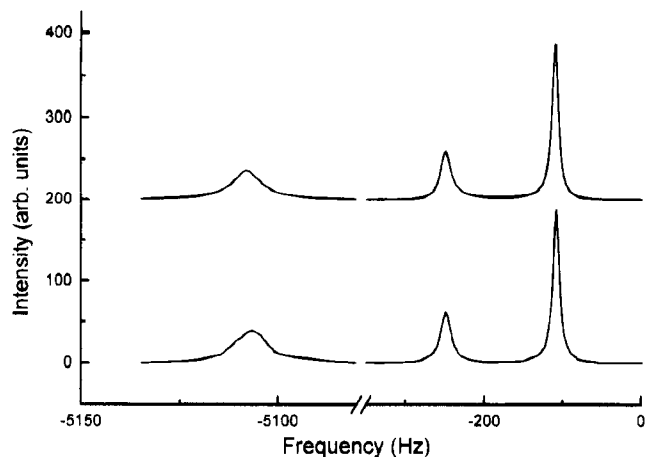


**Figure 1.** The experimental (lower) and calculated (upper)  $^{13}C$  NMR band shapes of  $Ru_3(CO)_9(\mu_3-CO)(\mu_3-NPh)$  in the carbonyl region at 250 K.

### Experimental Section

$Ru_3(CO)_{12}$  was synthesized from  $RuCl_3 \cdot nH_2O$  using the high-pressure carbonylation procedure of Bruce.<sup>7</sup> Nitrosobenzene and  $^{13}CO$  were purchased from Aldrich Chemical Co. and Isotec, respectively, and used as received. The imido cluster  $Ru_3(CO)_9(\mu_3-CO)(\mu_3-NPh)$  was prepared by using the thermolysis conditions reported by Gladfelter.<sup>8</sup>  $^{13}CO$ -enriched  $Ru_3(CO)_9(\mu_3-CO)(\mu_3-NPh)$  (ca. 15% enriched) was prepared from  $^{13}CO$ -enriched  $Ru_3(CO)_{12}$ .  $CD_2Cl_2$  and  $CDCl_3$  were bulb-to-bulb distilled from  $P_2O_5$  and then stored in Schlenk vessels equipped with Teflon stopcocks. All solvents and NMR tube preparations were carried out by using inert-atmosphere techniques.

All NMR spectra were obtained on a Varian VXR-300 FT-NMR spectrometer operating at 75.4 MHz. Temperature was regulated by cooled gas flow and measured from the control panel after calibration with a methanol NMR thermometer.<sup>9</sup>

Variable-temperature  $^{13}C$  NMR spectra in the carbonyl region were recorded on a natural abundance sample at various temperatures between 210 and 281 K. The spectra were digitized at intervals of 0.2 Hz, and the band shapes were fitted using the DNMR5 analysis program<sup>10</sup> adapted for use on a Solbourne 902/e computer with a Unix operating system.

$^{13}C$  2D-EXSY<sup>11</sup> spectra were obtained on  $^{13}C$ -enriched samples at 240 K using the standard pulse sequence  $[t_0 - \pi/2 - t_1 - \pi/2 - t_m - \pi/2 - t_2]_n$ . Spectra were acquired in both the absolute value and pure absorption modes.

Absolute value mode spectra were obtained at various mixing times,  $t_m$ , ranging from 0.01 to 0.6 s. The initial delay time,  $t_0$ , was 5 s. The spectral width in both the  $F_1$  and  $F_2$  dimensions was 6300 Hz.  $F_2$  contained 1024 words, and  $F_1$  had 64 words, zero-filled to 1024 points. The number of scans,  $n$ , per experiment ranged from 16 to 64; a four-term phase cycle was employed.<sup>11,12</sup>

Pure absorption mode spectra were obtained at mixing times of 0.05 and 0.10 s, with an initial delay of 8 s (approximately

**Table 1.** Temperature Dependence of Carbonyl Exchange Rates<sup>a,b</sup>

$T$	$k_{ea}$	$k_{eb}$	$k_{ab}$
281	224(3)		
270	140(2)	33(2)	0.012(3)
257	51(2)	9.2(0.7)	0.013(3)
250	23(3)	3.5(<0.1)	0(3)
236	8.3(<0.1)	1.6(4)	0.0083(5)
223	1.8(0.1)	0.3(0.01)	0.3(7)
$\Delta G^\ddagger$ (kJ/mol)	54.9(0.03)	58.1(0.14)	
$\Delta H^\ddagger$ (kJ/mol)	41.7(1.4)	45.4(3.4)	
$\Delta S^\ddagger$ (J/mol K)	-50(06)	-49(14)	

<sup>a</sup> Rate constants in units of  $s^{-1}$ . <sup>b</sup> Quantities in parentheses represent the standard deviations. <sup>c</sup> The activation free energy is calculated at the coalescence temperature (270 K).

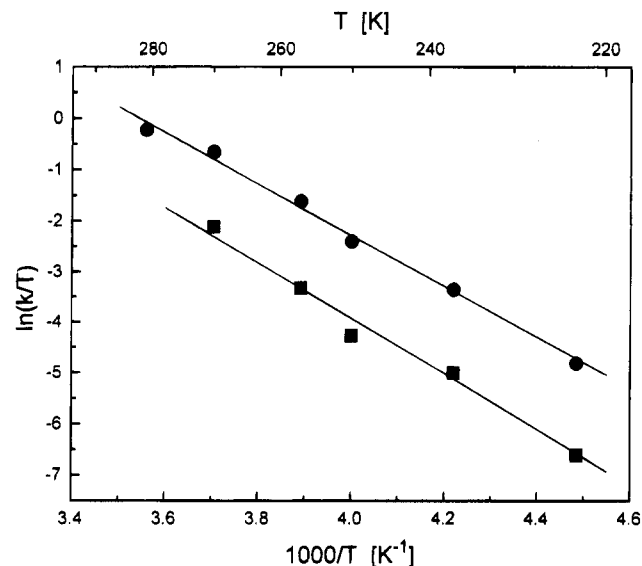


**Figure 2.** Dependence of the equatorial/axial,  $k_{ea}$  (●) and equatorial/bridging,  $k_{eb}$  (■) rate constants.

**Table 2.** Mixing Time Dependence of the Intensity Ratio,  $I_{ab}/I_{eb}$ , at 240 K

$t_m$ (s)	$I_{ab}/I_{eb}$	$t_m$ (s)	$I_{ab}/I_{eb}$
0.01	0.0	0.20	0.45
0.10	0.3	0.60	0.5

$4T_1$ ). The spectral width was 7663 Hz; the same number of words in each dimension were used as in the absolute intensity measurements. The number of scans per run ranged from 32 to 48, using a 16-term phase cycle.<sup>11,13</sup>

In both modes, the spectra were symmetrized prior to analysis. Spectral intensities were obtained using the "box integration" routine on the spectrometer, with several different box widths.

### Results

**Bandshape Analysis.** At low temperature (210 K), the carbonyl region of the  $^{13}C$  NMR spectrum of  $Ru_3(CO)_9(\mu_3-CO)(\mu_3-NPh)$  contains three peaks which appear (downfield from TMS) at 192.3 ppm (equatorial, e), 194.4 ppm (axial, a), and 260.0 ppm (triply-bridged, b) in the expected 6:3:1 intensity ratio. Upon increasing the temperature all three resonances broaden, and the equatorial-axial chemical shift difference diminishes

(13) States, D. J.; Haberkon, R. A.; Ruben, D. J. *J. Magn. Reson.* 1982, 48, 286.

(7) Bruce, M. I.; Jensen, C. M.; Jones, N. L. *Inorg. Synth.* 1989, 26, 259.

(8) Smieja, J. A.; Gladfelter, W. L. *Inorg. Chem.* 1986, 25, 2667.

(9) Duerst, R.; Merbach, A. *Rev. Sci. Instrum.* 1965, 36, 1896.

(10) Kleier, D. A.; Binsch, G. Program No. QCPE 365, Quantum Chemistry Program Exchange; Indiana University: Bloomington, IN 47405.

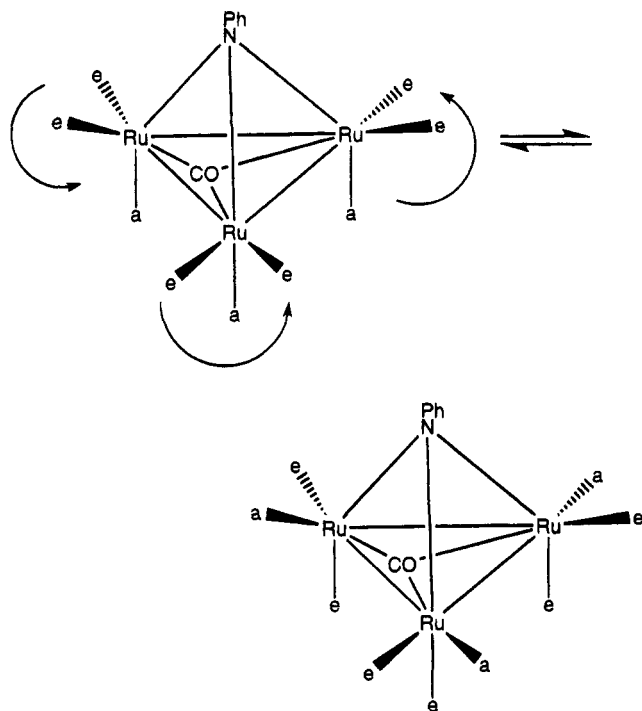
(11) (a) Jeener, J.; Meier, B. H.; Bachmann, P.; Ernst, R. R. *J. Chem. Phys.* 1979, 71, 4546. (b) Ernst, R. R.; Bodenhausen, G.; Wokaun, A., Eds. *Principles of Nuclear Magnetic Resonance in One and Two Dimensions*; Clarendon: Oxford, 1987; Chapter 9; (c) Willem, R. *Prog. Nucl. Magn. Reson. Spectrosc.* 1988, 20, 1. (d) Perrin, C. L.; Dwyer, T. *J. Chem. Rev.* 1990, 90, 935.

(12) Wider, G.; Macura, S.; Kumar, A.; Ernst, R. R.; Wüthrich, K. *J. J. Magn. Reson.* 1984, 56, 207.

Table 3. 2D-EXSY Intensities and Rate Constants at 240 K

intensity ( $I_{ij}$ )	$t_m = 0.05$ s			$t_m = 0.10$ s		
	e	j		e	j	
	e	a	b	e	a	b
	100.0	30.0	3.4	100.0	47.4	5.9
$i$	a	39.3	0.5	a	32.9	1.9
	b		21.1	b		17.9
$k_{ea}$ ( $s^{-1}$ )	7.4 $\pm$ 1.3			8.2 $\pm$ 2.1		
$k_{eb}$ ( $s^{-1}$ )	0.63 $\pm$ 0.09			0.60 $\pm$ 0.08		
$k_{ab}$ ( $s^{-1}$ )	-0.03 $\pm$ 0.1			0.05 $\pm$ 0.1		

Scheme 1



with peak coalescence at  $T = 270 \pm 2$  K. Above this temperature, the intensity of the bridging carbonyl peak is too low to be discerned from the level of the background. At the coalescence temperature, it is estimated that the equatorial/axial exchange rate constant is approximately  $k_{ea} = 136 \text{ s}^{-1}$ ,<sup>14,15</sup> in excellent agreement with the result obtained from complete band shape analysis (*vide infra*).

In a multisite-exchanging system, the absorption mode intensity,  $I(\nu)$ , is a function of a number of kinetic and NMR parameters,  $I(\nu) = f(\nu, C, \delta\nu_i, J_{ik}, T_{2i}, P_i, k_{ij})$ .<sup>16</sup> In this expression,  $C$  is a scaling constant,  $\delta\nu_i$  are the relative chemical shifts,  $J_{ik}$  are the scalar coupling constants,  $P_i$  represent the populations of each site,<sup>17</sup>  $T_{2i}$  are the spin-spin relaxation times, and  $k_{ij}$  are the exchange rate constants. One may neglect the scalar coupling constants in both the natural abundance and 15%-enriched  $^{13}\text{C}$  samples. The three rate constants required to characterize this system are  $k_{ea}$ ,  $k_{eb}$ , and  $k_{ab}$ ,

representing equatorial/axial, equatorial/bridging, and axial/bridging carbonyl exchange, respectively.

We have used the DNMR5 analysis program<sup>10</sup> to fit the carbonyl region band shapes as a function of temperature. The chemical shifts of the equatorial and axial peaks were constrained to values obtained by linear extrapolation from low temperatures at which there is no exchange; the chemical shift of bridging CO as well as the scaling constant, the relaxation times, and the three rate constants were varied to obtain the closest fit to experiment. A representative  $^{13}\text{C}$  NMR spectrum of  $\text{Ru}_3(\text{CO})_9(\mu_3\text{-CO})(\mu_3\text{-NPh})$  at 250 K is shown in Figure 1.

The resultant rate constants with their associated errors are presented in Table 1 and Figure 2. The two exchange rates involving the triply-bridging carbonyl were not obtained at the highest temperature, at which this resonance was too broad to be measurable. Activation free energies (at the coalescence temperature),  $\Delta G^\ddagger$ , enthalpies,  $\Delta H^\ddagger$ , and entropies,  $\Delta S^\ddagger$ , are given at the bottom of the table; the latter two quantities were obtained from a plot of  $\ln(k/T)$  vs  $1000/T$ .<sup>18</sup> As noted earlier, the equatorial/axial rate constant at the coalescence temperature (270 K) is quite close to the value obtained using the simple two-site exchange formula.<sup>9,10</sup>

One observes from Table 1 that  $k_{ea}$  is much greater than either  $k_{eb}$  or  $k_{ab}$ , indicating that the most efficient exchange pathway is that linking the equatorial and axial carbonyls. Most significantly, it was found that  $k_{ab}$  appears to be zero, to within experimental error, at all temperatures implying, somewhat surprisingly, that there is no direct exchange between the axial CO's and the triply-bridging CO, even though they are adjacent in the molecule.

**2D-EXSY Spectra. Axial/Bridging Exchange Rate Constant.** The above implication that there is no exchange pathway between the axial and bridging carbonyls is quite interesting, but may not be taken as definitive since both rate constants involving the latter CO are quite small. Hence, the result that  $k_{ab} \approx 0$  may represent an anomaly in the fitting process.

It has been shown in many systems<sup>11</sup> that 2D-EXSY spectra can be used to furnish unambiguous data on NMR rate constants. We have performed two series of experiments using this technique to investigate the carbonyl exchange pathways in  $\text{Ru}_3(\text{CO})_9(\mu_3\text{-CO})(\mu_3\text{-NPh})$ .

In the first series, we measured the relative intensities (in absolute value mode) of the axial/bridging to equatorial/bridging cross peaks. It may be shown<sup>11,19</sup>

(14) Sandström, J. *Dynamic NMR Spectroscopy*; Academic: New York, 1982.

(15) The rate constant at coalescence was estimated using eq 6.5 of ref 14, which assumes exchange between two unequally populated sites. The chemical shift difference between the equatorial and axial peaks at coalescence in the absence of exchange was obtained by extrapolation from low temperatures.

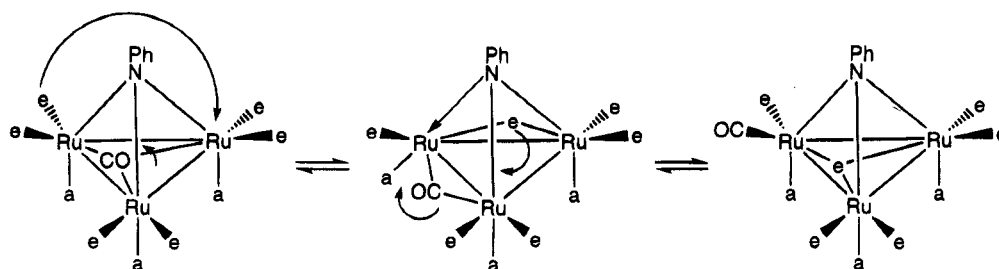
(16) Reference 14; Chapters 2 and 6.

(17)  $P_e = 0.6$ ;  $P_a = 0.3$ ;  $P_b = 0.1$ .

(18) Reference 14; Chapter 7.

(19) Kumar, A.; Wagner, G.; Ernst, R. R.; Wüthrich, K. *J. Am. Chem. Soc.* **1981**, *103*, 3654.

Scheme 2



that, in the limit of  $t_m \rightarrow 0$ ,  $I_{ij} \propto P_i k_{ij} t_m$ . Thus, one expects that at short  $t_m$  the ratio of the two cross peaks involving the bridging carbonyls will approach  $I_{ab}/I_{eb} = (p_a k_{ab})/(p_e k_{eb}) = 1/2 k_{ab}/k_{eb}$ . It may also be shown that the asymptotic long  $t_m$  limit of this ratio is independent of the relative rate constants and is given by  $I_{ab}/I_{eb} = p_a/p_e = 1/2$ .

The intensity ratio,  $I_{ab}/I_{eb}$ , as a function of  $t_m$  is displayed in Table 2. One observes that at long mixing times this ratio approaches the expected limiting value of 0.5 and that, most significantly, it diminishes to zero, to within experimental error, at the shortest value of  $t_m$ . Thus, one is led to conclude once again that  $k_{ab} \approx 0$ .

#### Quantitative Determination of Rate Constants.

Absolute value mode spectra cannot be used to obtain numerical values of the exchange rates since the equatorial/axial cross peak overlaps with the two diagonal peaks. We have repeated the EXSY experiments in the pure absorption mode for two values of the mixing time,  $t_m = 0.05$  and  $0.10$  s. These times were chosen to be long enough to observe all cross peaks but to be far from the asymptotic limit, in which the intensities are insensitive to the rate constants. The 2D-EXSY spectrum (not shown) at 240 K for  $t_m = 0.10$  s exhibits all cross peaks, including one between the axial and bridging carbonyls. However, it has been pointed out that the presence of a cross peak does *not* necessarily imply a direct exchange pathway between two sites but may be due, instead, to indirect exchange involving two or more paths involving the two sites.<sup>20,21</sup>

The matrix of 2D-EXSY intensities is given by  $\mathbf{I} = \mathbf{P} \exp(\mathbf{L}t_m)$ ,<sup>11</sup> in which  $\mathbf{P}$  is a vector containing the relative site populations<sup>22</sup> and  $\mathbf{L}$  is a matrix containing the exchange rate constants ( $k_{ij}$ ) and spin-lattice relaxation rates ( $R_{1i}$ ). For the three-site system studied here, this matrix is given by

$$\mathbf{L} = \begin{bmatrix} -R_{1e} - k_{ea} - & k_{ea} & k_{eb} \\ k_{eb} + \Delta & & \\ k_{ae} & -R_{1a} - k_{ae} - & k_{ab} \\ & k_{ab} + \Delta & \\ k_{be} & k_{ba} & -R_{1b} - k_{be} - \\ & & k_{ba} + \Delta \end{bmatrix} \quad (1)$$

The quantity  $\Delta$  in the diagonal terms of this equation represents an arbitrary additive constant dependent upon the scale factor used in the intensity array. One sees from eq 1 that the three independent rate con-

stants<sup>23</sup> in this system,  $k_{ea}$ ,  $k_{eb}$ , and  $k_{ab}$ , are equal to the off-diagonal elements in the  $\mathbf{L}$  matrix.

A method by which the expression relating the intensity to the exchange matrix can be inverted to furnish the  $\mathbf{L}$  directly has been detailed by several authors.<sup>20,24</sup> We have utilized this procedure using a matrix inversion program written in FORTRAN to obtain  $\mathbf{L}$  and, thus, the exchange rate constants at 240 K for both values of  $t_m$ . The intensities and resulting rate constants are presented in Table 3. Errors in the rate constant were estimated by estimating the error in each intensity, varying the intensities within the error limits, and then taking the rms sum of squared error in the rate constants.

It is satisfying to note that rate constants calculated at the two mixing times are in good agreement with each other as well as in reasonable qualitative agreement with values obtained using band shape analysis (at 237 K). As before,  $k_{ab} = 0$ , to within experimental error.

#### Discussion

The exchange of the axial/equatorial CO groups at each ruthenium  $Ru(CO)_3$  vertex is best considered to occur via a turnstile mechanism, as depicted in Scheme 1. In this exchange it is assumed that the localized scrambling at all three  $Ru(CO)_3$  moieties proceeds in a completely intranuclear fashion. This scheme is attractive due to the many examples of axial-equatorial CO exchange in a wide variety of polynuclear compounds.<sup>25</sup>

The more interesting CO exchange process that involves the net permutation of the triply-bridging and equatorial CO groups can be explained by the mechanism shown in Scheme 2. Here the concerted motion of the  $\mu_3$ -CO ligand to a  $\mu_2$ -CO ligand at a single Ru-Ru edge is accompanied by the conversion of one terminal CO group at a  $Ru(CO)_3$  center to a  $\mu_2$ -CO edge-bridging moiety. Related face-edge conversions involving CO ligands make this process attractive.<sup>26</sup> This intermediate may then collapse with reformation of the  $\mu_3$ -CO, which derives from the old equatorial CO (labeled e) group, and concomitant generation of the

(23) The six off-diagonal elements of this matrix are interrelated via the expressions  $p_i k_{ij} = p_j k_{ji}$  (eq 2.25 of ref 14).

(24) (a) Perrin, C. L.; Gipe, R. K. *J. Am. Chem. Soc.* **1984**, *106*, 4036. (b) Keepers, J. W.; James, T. L. *J. Magn. Reson.* **1984**, *57*, 404.

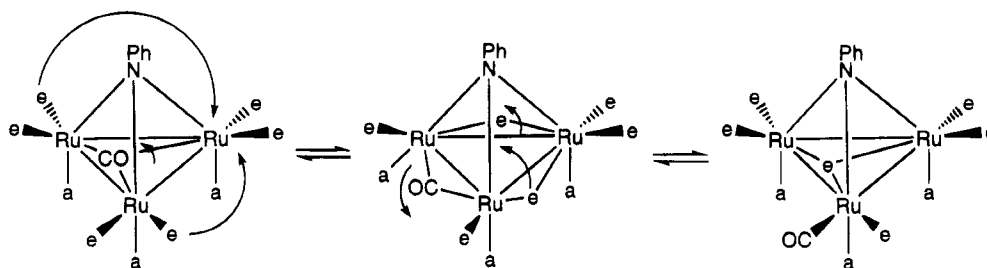
(25) (a) Milone, L.; Aime, S.; Randall, E. W.; Rosenberg, E. *J. Chem. Soc., Chem. Commun.* **1975**, 452. (b) Ewing, P.; Farrugia, L. J.; Rycroft, D. S. *Organometallics* **1988**, *7*, 859. (c) Cotton, F. A.; Hanson, B. E. *Inorg. Chem.* **1977**, *16*, 2820. (d) Alex, R. F.; Pomeroy, R. K. *J. Organomet. Chem.* **1985**, *284*, 379. (e) Deeming, A. J.; Donovan-Mtunzi, S.; Kabir, S. E. *J. Organomet. Chem.* **1985**, *281*, C43. (f) Cotton, F. A.; Hunter, D. L.; Lahuerta, P. *Inorg. Chem.* **1975**, *14*, 511. (g) Li, L.; D'Agostino, M. F.; Sayer, B. G.; McGlinchey, M. J. *Organometallics* **1992**, *11*, 477. (h) Aime, S.; Dastrú, W.; Gobetto, R.; Arce, A. *J. Organometallics* **1994**, *13*, 3737.

(20) Abel, E. W.; Coston, T. P. J.; Orrell, K. G.; Šik, V.; Stephenson, D. *J. Magn. Reson.* **1986**, *70*, 34.

(21) Farrugia, L. J.; Rae, S. E. *Organometallics* **1992**, *11*, 196.

(22)  $P_e = 0.6$ ;  $P_a = 0.3$ ;  $P_b = 0.1$ .

Scheme 3



required terminal CO group. The net result of these two transformations is the pairwise equilibration of an equatorial and triply-bridging CO group, which is mandated by the NMR data.

An alternative mechanism that leads to the exchange of the triply-bridging and equatorial CO groups through an intermediate involving three edge-bridging CO ligands is shown in Scheme 3.

Here migration of the  $\mu_3$ -CO to an edge-bridging position is accompanied by the concerted movement of a pair of equatorial CO groups to edge-bridging positions. The resulting intermediate, with its three  $\mu_2$ -CO ligands, is akin to the intermediate responsible for the in-plane "merry-go-round" process, a term originally coined by Muetterties.<sup>1a</sup> However, given the presence of the unique Ru(CO)<sub>3</sub> site in this intermediate, we do not favor the existence of an in-plane scrambling of the  $\mu_2$ -CO groups via a "merry-go-round" sequence.

Ru<sub>3</sub>(CO)<sub>9</sub>( $\mu_3$ -CO)( $\mu_3$ -NPh) represents a classical example of a cluster that cannot be adequately described by using an electron-precise formalism.<sup>27</sup> The presence of the  $\mu_3$ -CO ligand negates any possible two-center two-electron bonding argument in Ru<sub>3</sub>(CO)<sub>9</sub>( $\mu_3$ -CO)( $\mu_3$ -NPh). However, the bonding in this cluster is easily described by using the electron topology developed by Wade and Mingos.<sup>28</sup> Here Ru<sub>3</sub>(CO)<sub>9</sub>( $\mu_3$ -CO)( $\mu_3$ -NPh) may be regarded as a four-vertex *nido* cluster that possesses six

skeletal electron pairs (SEP). The proposed intermediates in Schemes 2 and 3 may also be regarded as *nido* clusters on the basis of their six SEP count. One major difference between these two schemes lies in an accurate electron-precise description of the intermediate edge-bridged cluster in Scheme 2, where the 2e donor bond from the capping amido group to the unique Ru(CO)<sub>2</sub> center is explicitly shown. Here each bond may be considered as electron precise, and for this reason we favor this scheme for the exchange of the  $\mu_3$ -CO and equatorial CO groups.

### Conclusions

It was found using (a) band shape analysis, (b) EXSY cross peak intensities as a function of  $t_m$ , and (c) complete EXSY rate constant determination, that the axial/bridging exchange rate constant,  $k_{ab}$ , vanishes, furnishing unambiguous evidence that there is no direct exchange pathway between these two sites. Either of two mechanisms, both involving the formation of edge-bridging  $\mu_2$ -CO moieties, can explain the observed exchange pathway.

**Acknowledgment.** The authors wish to thank the Robert A. Welch Foundation [Grants B-1039 (M.G.R.) and B-657 (M.S.)] and the University of North Texas Faculty Research Fund for financial support of this research.

OM950173A

(26) (a) Lawson, R. J.; Shapley, J. R. *Inorg. Chem.* **1978**, *17*, 772. (b) Roberts, D. A.; Harley, A. D.; Geoffroy, G. L. *Organometallics* **1982**, *1*, 1050. (c) Casey, C. P.; Widenhofer, R. A.; Hallenbeck, S. L.; Hayashi, R. K.; Gavney, J. A., Jr. *Organometallics* **1994**, *13*, 4720. (d) Robben, M. P.; Geiger, W. E.; Rheingold, A. L. *Inorg. Chem.* **1994**, *33*, 5615 and references therein.

(27) Mingos, D. M. P.; Wales, D. J. *Introduction to Cluster Chemistry*; Prentice Hall: Englewood Cliffs, NJ, 1990.

(28) (a) Wade, K. *Adv. Inorg. Chem. Radiochem.* **1976**, *18*, 1. (b) Mingos, D. M. P. *Acc. Chem. Res.* **1984**, *17*, 311.

# Oxygen Atom Transfer from Alkylperoxyl Radicals to Aromatic Tellurides

Lars Engman\*

*Institute of Chemistry, Department of Organic Chemistry, Uppsala University, Box 531, S-751 21 Uppsala, Sweden*

Joachim Persson

*Laboratory of Organic Chemistry, Department of Chemistry, Royal Institute of Technology, S-100 44 Stockholm, Sweden*

Gábor Merényi\* and Johan Lind\*

*Laboratory of Nuclear Chemistry, Department of Chemistry, Royal Institute of Technology, S-100 44 Stockholm, Sweden*

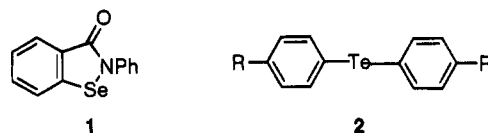
Received February 14, 1995<sup>®</sup>

The reactions of alkylperoxyl radicals with the diaryl tellurides bis(4-aminophenyl) telluride and bis(4-hydroxyphenyl) telluride were studied by pulse- and  $\gamma$ -radiolysis techniques in aqueous media. The diaryl tellurides served predominantly ( $\sim 70\%$ ) as one-electron reductants toward the  $\text{CCl}_3\text{OO}\cdot$  radical ( $k = 1.5 \times 10^9$  and  $2.5 \times 10^9 \text{ dm}^3 \text{ mol}^{-1} \text{ s}^{-1}$ , respectively), whereas they acted essentially ( $\geq 92\%$ ) as oxygen atom recipients in their reactions with the  $(\text{CH}_3)_2\text{C}(\text{OH})\text{CH}_2\text{OO}\cdot$  radical ( $k = 1.7 \times 10^8$  and  $3.7 \times 10^7 \text{ dm}^3 \text{ mol}^{-1} \text{ s}^{-1}$ , respectively), producing the corresponding diaryl telluroxides. The latter reaction mode was corroborated by the quantitative interception of a reducing  $\alpha$ -hydroxylalkyl radical, the product of  $\beta$ -scission of its precursor, the alkoxy radical  $(\text{CH}_3)_2\text{C}(\text{OH})\text{CH}_2\text{O}\cdot$ . On the basis of detailed energetic and mechanistic considerations the oxygen transfer is proposed to be a concerted one-step reaction without the intermediacy of an adduct.

## Introduction

Oxygen atom transfer from alkylperoxyl radicals has been observed to alkenes<sup>1</sup> and phosphines/phosphites.<sup>2,3</sup> In both of these cases the rate-determining steps appear to produce intermediate peroxyl radical adducts. With the phosphines/phosphites the rate constant of peroxyl radical addition has been found to be ca.  $10^4 \text{ dm}^3 \text{ mol}^{-1} \text{ s}^{-1}$  in isopentane solvent at room temperature.<sup>2</sup> Later, the  $\text{CCl}_3\text{OO}\cdot$  radical was shown to transfer an oxygen atom to indoles, again via the intermediacy of a peroxide adduct.<sup>4</sup> More recently, the  $\text{CCl}_3\text{OO}\cdot$  and  $\text{CHCl}_2\text{OO}\cdot$  radicals were shown<sup>5</sup> to participate simultaneously in a one-electron as well as a two-electron transfer process with  $(\text{CH}_3)_2\text{S}$  (DMS), where the latter reaction yielded  $(\text{CH}_3)_2\text{SO}$  (DMSO) directly. The reactivity of the pharmaceutically interesting organoselenium compound eb-selen (1) and structurally related analogues with halogenated alkylperoxyl radicals was also studied<sup>6</sup> recently. It was concluded that the organoselenium compounds served essentially as one-electron reductants in these systems. In a study<sup>7</sup> concerning the antioxidant activity in microsomal lipid peroxidation of 4,4'-substituted

diaryl tellurides 2, the most active compounds in the



series were shown to possess  $\text{IC}_{50}$  values as low as  $(3-6) \times 10^{-8} \text{ mol dm}^{-3}$ . This result prompted us to initiate a study of the reaction of alkylperoxyl radicals with aromatic tellurides. In the following we report on reactions of peroxyl radicals with diaryl tellurides involving oxygen atom transfer to tellurium.

## Experimental Section

Pulse radiolysis was performed at room temperature (22–23 °C) utilizing doses of 2–15 Gy/pulse corresponding to  $(1.2-9) \times 10^{-6} \text{ mol dm}^{-3}$  of radicals. The 7-MeV microtron accelerator<sup>8</sup> and the computerized optical detection system<sup>9</sup> have been described elsewhere. The cell used had an optical path length of 1 cm. Dosimetry was performed by means of an aerated  $10^{-2} \text{ mol dm}^{-3}$  KSCN solution taking<sup>10</sup>  $G_{\epsilon} = 2.23 \times 10^{-4} \text{ m}^2 \text{ J}^{-1}$  at 500 nm.  $\gamma$ -radiolysis was carried out in a

<sup>®</sup> Abstract published in *Advance ACS Abstracts*, June 15, 1995.  
 (1) Selby, K.; Waddington, D. J. *J. Chem. Soc. Perkin Trans. 2* **1980**, 65.  
 (2) Furimsky, C.; Howard, J. A. *J. Am. Chem. Soc.* **1973**, *96*, 369.  
 (3) Pomedimski, D. G.; Kirpichnikov, P. A. *J. Polym. Sci.* **1980**, *18*, 815.  
 (4) Shen, X.; Lind, J.; Eriksen, T. E.; Merényi, G. *J. Chem. Soc., Perkin Trans. 2* **1989**, 555.  
 (5) Schöneich, C.; Aced, A.; Asmus, K.-D. *J. Am. Chem. Soc.* **1991**, *113*, 375.  
 (6) Schöneich, C.; Narayanaswami, V.; Asmus, K.-D.; Sies, H. *Arch. Biochem. Biophys.* **1990**, *282*, 18.

(7) Andersson, C.-M.; Brattsand, R.; Hallberg, A.; Engman, L.; Persson, J.; Moldéus, P.; Cotgreave, I. A. *Free Radical Res.* **1994**, *20*, 401. See also: Cotgreave, I. A.; Moldéus, P.; Engman, L.; Hallberg, A. *Biochem. Pharmacol.* **1991**, *42*, 1481.  
 (8) Rosander, S. Thesis, The Royal Institute of Technology, Stockholm, Sweden, 1974; TRITAEPP-74-16, p 28.  
 (9) Eriksen, T. E.; Lind, J.; Reitberger, T. *Chem. Scr.* **1976**, *10*, 5.  
 (10) Fielden, E. M. In *The Study of Fast Processes and Transient Species by Electron Pulse Radiolysis*; Baxendale, J. H., Busi, F., Eds.; Reidel: Dordrecht, Holland, 1982; NATO Advanced Study Institutes Series pp 49–62.



$^{60}\text{Co}$   $\gamma$ -source at a dose rate of 0.27 Gy/s as determined by the Fricke dosimeter.<sup>10</sup> The solutions were made up in Millipore-deionized water.

Melting points (uncorrected) were determined by using a Büchi 510 melting point apparatus.  $^1\text{H}$  NMR spectra were obtained with a Bruker AC-F 250 instrument operating at 250 MHz and recorded for  $\text{CD}_3\text{OD}$  solutions containing tetramethylsilane as the internal standard. Elemental analyses were performed by Analytical Laboratories, Engelskirchen, Germany.

**Chemicals.** 2-Methyl-2-propanol (Merck, p.A.), 2-propanol (Aldrich, HPLC grade),  $\text{NaN}_3$  (Aldrich, 99%),  $\text{NaBr}$  (Aldrich, 99%),  $\text{HCO}_2\text{Na}$  (Aldrich, 99%+),  $\text{NaOH}$  (Aldrich, 99.99%),  $\text{H}_2\text{SO}_4$  (Merck, supra pure), and  $\text{NaB}_4\text{O}_7 \cdot 10\text{H}_2\text{O}$ ,  $\text{KH}_2\text{PO}_4$ , and  $\text{K}_2\text{HPO}_4$  (Merck, p.A.) were used as received.

Bis(4-aminophenyl) telluride and bis(4-hydroxyphenyl) telluride were prepared according to a literature procedure.<sup>11</sup>

**Bis(4-aminophenyl) Telluroxide.** To a solution of bis(4-aminophenyl) telluride (0.25 g, 0.80 mmol) in methanol (2 mL) at 0 °C was added *tert*-butyl hydroperoxide (110  $\mu\text{L}$ , 70%; 0.81 mmol). After 1 h the solvent was evaporated and the residue crystallized from  $\text{CH}_2\text{Cl}_2$ /hexane. The yield of bis(4-aminophenyl) telluroxide was 0.22 g (84%); mp 195–200 °C dec.  $^1\text{H}$  NMR:  $\delta$  6.78 (d, 2H), 7.51 (d, 2H). The analytical sample was obtained after heating at reduced pressure for 3 h (60 °C/ $10^{-2}$  mmHg). Anal. Calcd for  $\text{C}_{12}\text{H}_{12}\text{N}_2\text{TeO}$ : C, 43.96; H, 3.69. Found: C, 43.81; H, 3.81.

**Bis(4-hydroxyphenyl) Telluroxide.** To a boiling solution of bis(4-hydroxyphenyl) telluride (0.20 g, 0.64 mmol) in methanol (10 mL) was added *tert*-butyl hydroperoxide (90  $\mu\text{L}$ , 70%; 0.66 mmol). After 15 min hexane was added to cloudiness and the reaction mixture cooled to precipitate 0.12 g of bis(4-hydroxyphenyl) telluroxide. A second crop of the material (0.058 g) was obtained after further precipitation with hexane, corresponding to a total isolated yield of 85%.  $^1\text{H}$  NMR:  $\delta$  6.94 (d, 2H), 7.66 (d, 2H). The analytical sample (mp 197–200 °C dec) was obtained after heating at reduced pressure for 3 h (60 °C/ $10^{-2}$  mmHg). Anal. Calcd for  $\text{C}_{12}\text{H}_{10}\text{O}_3\text{Te}$ : C, 43.70; H, 3.06. Found: C, 43.78; H, 2.93. Bis(4-hydroxyphenyl) telluroxide has previously been reported twice in the literature: mp 93 °C<sup>12</sup> and mp 228 °C.<sup>13</sup> Both reports are probably in error.

## Results

**Preparation and Properties of Diaryl Tellurides and Diaryl Telluroxides.** Diaryl telluroxides are available by several methods, the most common ones involving oxidation (air, sodium periodate, *N*-haloimines, *m*-chloroperoxybenzoic acid, *tert*-butyl hypochlorite) of the corresponding diaryl telluride or hydrolysis of a suitable diaryltellurium(IV) derivative (dihalide, sulfonamide).<sup>14</sup> We found it convenient to prepare bis(4-aminophenyl) telluroxide (84%) and bis(4-hydroxyphenyl) telluroxide (85%) by oxidation of the respective diaryl tellurides with *tert*-butyl hydroperoxide in methanol. The required diaryl tellurides were previously prepared in our laboratories.<sup>11</sup> The study of organotellurium compounds by pulse radiolysis has received very little attention<sup>15</sup> to date. This is probably because organotellurium compounds have a reputation of being

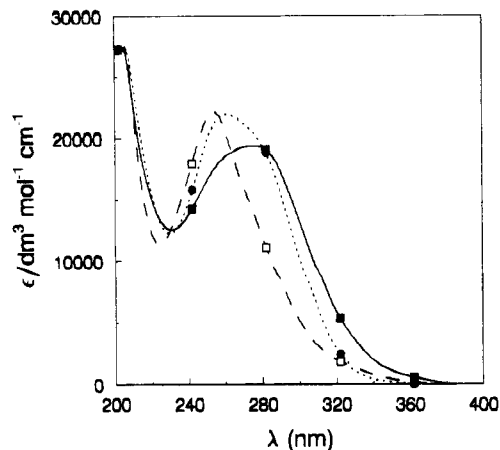
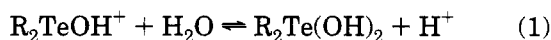


**Figure 1.** UV spectra of bis(4-aminophenyl) telluride(II) and telluroxide(IV) compounds in water: (●)  $(4\text{-NH}_2\text{C}_6\text{H}_4)_2\text{Te}$ , pH 7; (■)  $(4\text{-NH}_2\text{C}_6\text{H}_4)_2\text{TeOH}^+$ , pH 5; (□)  $(4\text{-NH}_2\text{C}_6\text{H}_4)_2\text{Te(OH)}_2$ , pH 8. The spectra were recorded with a wavelength step of 1 nm. The symbols are added for identification purposes only.

toxic and foul-smelling. In addition, most compounds are not sufficiently water soluble to be studied in aqueous solution, where the production of radical species in a pulse radiolysis experiment is fully controlled. The diaryl tellurides and diaryl telluroxides used in this study are all crystalline odorless materials with water solubilities in the range of  $10^{-4}$ – $10^{-3}$  mol  $\text{dm}^{-3}$ . Furthermore, the ultraviolet spectra of the diaryl tellurides are different from those of the corresponding diaryl telluroxides (see Figure 1). Thus, the solubility and UV properties of the selected organotellurium compounds make pulse radiolysis the method of choice for studying their interaction with peroxy radicals.

**Thermodynamic Properties of Aromatic Telluroxides.** When dissolved in water, diorganotellurium(IV) oxides ( $\text{R}_2\text{TeO}$ ) probably form the dihydroxides,<sup>16,17</sup> and their reported<sup>16,18</sup> basicity can be explained by equilibrium 1. The  $\text{p}K_1$  values of  $(4\text{-NH}_2\text{-C}_6\text{H}_4)_2\text{-}$



$\text{TeOH}^+$  and  $(4\text{-HO-C}_6\text{H}_4)_2\text{TeOH}^+$  are 5.85 and 5.75, respectively.<sup>19</sup> At pH values below 3.5 protonation occurs at the amino group of the  $(4\text{-NH}_2\text{-C}_6\text{H}_4)_2\text{TeOH}^+$  compound, but the exact value of this  $\text{p}K_a$  was not determined. Similarly,  $(4\text{-NH}_2\text{-C}_6\text{H}_4)_2\text{Te}$  is protonated below pH 4. To investigate the formation of the tellurium dihydroxide more quantitatively, dry  $\text{Ar}_2\text{TeO}$  was dissolved in water-free tetrahydrofuran (THF). The UV spectra of such solutions containing  $3 \times 10^{-5}$  mol  $\text{dm}^{-3}$   $(4\text{-NH}_2\text{-C}_6\text{H}_4)_2\text{TeO}$  or  $(4\text{-HO-C}_6\text{H}_4)_2\text{TeO}$  were found to change with the amount of added water, until they attained a final form above 0.1 mol  $\text{dm}^{-3}$  of  $\text{H}_2\text{O}$ . The final spectra were very similar to the corresponding aqueous spectra of  $\text{Ar}_2\text{Te(OH)}_2$ . The equilibrium con-

(11) Engman, L.; Persson, J.; Andersson, C. M.; Berglund, M. *J. Chem. Soc., Perkin Trans. 2* **1992**, 1309. See also: Engman, L.; Persson, J. *Organometallics* **1993**, *12*, 1068.

(12) Reichel, L.; Kirschbaum, E. *Justus Liebigs Ann. Chem.* **1936**, *523*, 211.

(13) Irgolic, K. J. In *Houben-Weyl, Methods of Organic Chemistry*; Klamann, D., Ed.; Georg Thieme Verlag: Stuttgart, Germany, 1990; Vol. E 12b, p 645.

(14) Reference 13, p 640.

(15) Bergman, J.; Eklund, N.; Eriksen, T. E.; Lind, J. *Acta Chem. Scand.* **1978**, *A32*, 455.

(16) Lederer, K. *Justus Liebigs Ann. Chem.* **1912**, *391*, 326.

(17) Compounds reported as diorganotelluroxides were sometimes formulated as hydrates,  $\text{R}_2\text{TeO} \cdot \text{H}_2\text{O}$ , and sometimes as diorganotellurium dihydroxides,  $\text{R}_2\text{Te(OH)}_2$ . Detty, M. R. *J. Org. Chem.* **1980**, *45*, 274. Uemura, S.; Fukuzawa, S. *J. Am. Chem. Soc.* **1983**, *105*, 2748.

(18) The basic character of diaryl telluroxides has recently found synthetic use in aldol condensations: Engman, L.; Cava, M. P. *Tetrahedron Lett.* **1981**, *22*, 5251. Akiba, M.; Lakshminantham, M. V.; Jen, K.-Y.; Cava, M. P. *J. Org. Chem.* **1984**, *49*, 4819.

(19) Engman, L.; Lind, J.; Merényi, G. *J. Phys. Chem.* **1994**, *98*, 3174.

Table 1. Rate Constants Determined in This Work

reacn	rate constant, dm <sup>3</sup> mol <sup>-1</sup> s <sup>-1</sup>
(CH <sub>3</sub> ) <sub>2</sub> (OH)CCH <sub>2</sub> OO• + (4-NH <sub>2</sub> -C <sub>6</sub> H <sub>4</sub> ) <sub>2</sub> Te → (4-NH <sub>2</sub> -C <sub>6</sub> H <sub>4</sub> ) <sub>2</sub> TeO + (CH <sub>3</sub> ) <sub>2</sub> (OH)CCH <sub>2</sub> O•	1.7 × 10 <sup>8</sup>
(CH <sub>3</sub> ) <sub>2</sub> (OH)CCH <sub>2</sub> OO• + (4-HO-C <sub>6</sub> H <sub>4</sub> ) <sub>2</sub> Te → (4-HO-C <sub>6</sub> H <sub>4</sub> ) <sub>2</sub> TeO + (CH <sub>3</sub> ) <sub>2</sub> (OH)CCH <sub>2</sub> O•	3.7 × 10 <sup>7</sup>
(CH <sub>3</sub> ) <sub>2</sub> (OH)COO• + (4-NH <sub>2</sub> -C <sub>6</sub> H <sub>4</sub> ) <sub>2</sub> Te → (4-NH <sub>2</sub> -C <sub>6</sub> H <sub>4</sub> ) <sub>2</sub> TeO + (CH <sub>3</sub> ) <sub>2</sub> (OH)CO•	1 × 10 <sup>7</sup>
CCl <sub>3</sub> OO• + (4-NH <sub>2</sub> -C <sub>6</sub> H <sub>4</sub> ) <sub>2</sub> Te → products	1.5 × 10 <sup>9</sup>
CCl <sub>3</sub> OO• + (4-HO-C <sub>6</sub> H <sub>4</sub> ) <sub>2</sub> Te → products	2.5 × 10 <sup>9</sup>
HOO• + (4-NH <sub>2</sub> -C <sub>6</sub> H <sub>4</sub> ) <sub>2</sub> Te → products	≤ 1.5 × 10 <sup>7</sup>
(4-NH <sub>2</sub> -C <sub>6</sub> H <sub>4</sub> ) <sub>2</sub> TeO + H <sub>2</sub> O → (4-NH <sub>2</sub> -C <sub>6</sub> H <sub>4</sub> ) <sub>2</sub> Te(OH) <sub>2</sub>	4 × 10 <sup>3</sup> (s <sup>-1</sup> )
(4-HO-C <sub>6</sub> H <sub>4</sub> ) <sub>2</sub> TeO + H <sub>2</sub> O → (4-HO-C <sub>6</sub> H <sub>4</sub> ) <sub>2</sub> Te(OH) <sub>2</sub>	4.5 × 10 <sup>3</sup> (s <sup>-1</sup> )
(4-NH <sub>2</sub> -C <sub>6</sub> H <sub>4</sub> ) <sub>2</sub> Te + H <sub>2</sub> O <sub>2</sub> → (4-NH <sub>2</sub> -C <sub>6</sub> H <sub>4</sub> ) <sub>2</sub> Te(OH) <sub>2</sub>	(1.3 ± 0.2) × 10 <sup>2</sup> (4.7 < pH < 9.2)

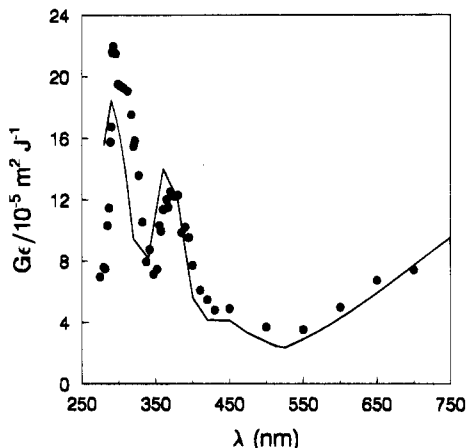
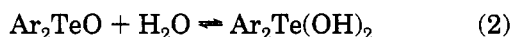


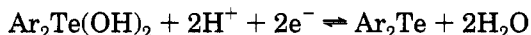
**Figure 2.** Transient spectra obtained by pulse radiolysis of bis(4-aminophenyl) telluride: (●) spectrum obtained in the reaction of CCl<sub>3</sub>OO• with (4-NH<sub>2</sub>-C<sub>6</sub>H<sub>4</sub>)<sub>2</sub>Te in an air-saturated 1/1 mixture (by volume) of 2-propanol and water containing 0.2 mol dm<sup>-3</sup> CCl<sub>4</sub>; (○) spectrum of the radical cation (4-NH<sub>2</sub>-C<sub>6</sub>H<sub>4</sub>)<sub>2</sub>Te<sup>•+</sup> produced by irradiation of a N<sub>2</sub>O-purged aqueous solution containing 2 × 10<sup>-4</sup> mol dm<sup>-3</sup> (4-NH<sub>2</sub>-C<sub>6</sub>H<sub>4</sub>)<sub>2</sub>Te and 10<sup>-2</sup> mol dm<sup>-3</sup> N<sub>3</sub><sup>-</sup>. This spectrum is scaled to G = 4.15 × 10<sup>-7</sup> mol J<sup>-1</sup> from G = 5.6 × 10<sup>-7</sup> mol J<sup>-1</sup>.

stants of hydrolysis, K<sub>2</sub>, in THF were found to be 20–30 dm<sup>3</sup> mol<sup>-1</sup> when Ar = 4-HO-C<sub>6</sub>H<sub>4</sub> and >100 dm<sup>3</sup> mol<sup>-1</sup> when Ar = 4-NH<sub>2</sub>-C<sub>6</sub>H<sub>4</sub>.



As will be argued further on, the K<sub>2</sub> values in water are probably similar for both Ar<sub>2</sub>TeO compounds and lie between 10 and 100 (where for H<sub>2</sub>O the mole fraction x = 1 is taken as the standard state).

The two-electron redox potential of the couple



has been determined<sup>19</sup> to be 0.65 ± 0.01 V vs NHE, irrespective of whether OH or NH<sub>2</sub> is the 4-substituent.

The invariance of <sup>2</sup>E<sup>0</sup> suggests similar Te=O bond strengths in Ar<sub>2</sub>TeO irrespective of the substituent on the phenyl ring.

**Reaction of Tellurides with the CCl<sub>3</sub>OO• Radical.** In a 1/1 (v/v) mixture of water and 2-propanol containing 0.2 mol dm<sup>-3</sup> CCl<sub>4</sub> and saturated with O<sub>2</sub> the CCl<sub>3</sub>OO• radical forms in quantitative yield upon pulse irradiation of the solution. Ar<sub>2</sub>Te reacts with CCl<sub>3</sub>OO• to form Ar<sub>2</sub>Te<sup>•+</sup> (rate constants in Table 1). The spectrum for Ar = 4-NH<sub>2</sub>-C<sub>6</sub>H<sub>4</sub> is shown in Figure 2. One-electron oxidation of (4-NH<sub>2</sub>-C<sub>6</sub>H<sub>4</sub>)<sub>2</sub>Te by N<sub>3</sub><sup>•</sup> in water yields the radical cation<sup>19</sup> (4-NH<sub>2</sub>-C<sub>6</sub>H<sub>4</sub>)<sub>2</sub>Te<sup>•+</sup>. Assuming similar extinction coefficients in water and the mixed solvent, the yield of the radical cation in the

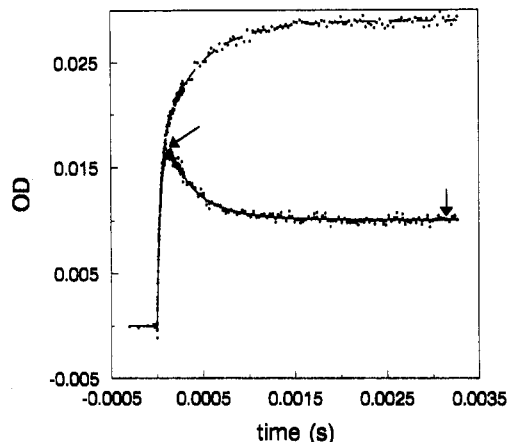
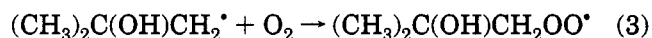
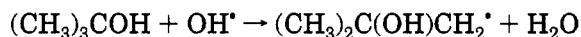
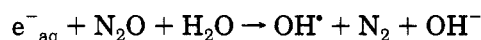
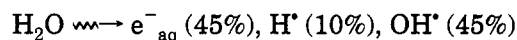


**Figure 3.** Observed optical time traces at 330 nm upon irradiation of aqueous solutions saturated with a 1/9 mixture (by volume) of O<sub>2</sub>/N<sub>2</sub>O containing 1 × 10<sup>-4</sup> mol dm<sup>-3</sup> (4-NH<sub>2</sub>-C<sub>6</sub>H<sub>4</sub>)<sub>2</sub>Te and 0.1 M 2-methyl-2-propanol: (upper) pH 5; (lower) pH 6.7. Initial concentration of radicals: 1.8 × 10<sup>-6</sup> mol dm<sup>-3</sup>. The points are experimental data, while the lines represent simulations (see text).

present case is calculated to be ca. 70% of the initial yield of CCl<sub>3</sub>OO•. The remaining 30% presumably undergoes an oxygen transfer reaction with (4-NH<sub>2</sub>-C<sub>6</sub>H<sub>4</sub>)<sub>2</sub>Te, to be discussed later.  $\gamma$ -radiolysis of such solutions showed Ar<sub>2</sub>TeO to be the only product (NMR, UV) almost up to complete conversion of Ar<sub>2</sub>Te. Extended irradiation caused changes in the aromatic groups.

**Reaction of Ar<sub>2</sub>Te with (CH<sub>3</sub>)<sub>2</sub>C(OH)CH<sub>2</sub>OO•.** When an aqueous solution containing 0.1 mol dm<sup>-3</sup> 2-methyl-2-propanol is purged with a gas mixture consisting of 80% N<sub>2</sub>O and 20% O<sub>2</sub> and is then e<sup>-</sup> beam irradiated, the following events take place:



With the rate constant k<sub>3</sub> ≈ 3 × 10<sup>9</sup> dm<sup>3</sup> mol<sup>-1</sup> s<sup>-1</sup> the peroxy radical forms within 4 μs with the yield G = 5.5 × 10<sup>-7</sup> mol J<sup>-1</sup> corresponding to ca. 90% of all radicals, the remaining 10%, deriving from the H<sup>•</sup> atoms, being HO<sub>2</sub><sup>•</sup>/O<sub>2</sub><sup>•-</sup>. When Ar<sub>2</sub>Te is added, transient absorptions are observed in the UV region. Typical transients are presented in Figure 3. The buildup rate of the transient is proportional to [Ar<sub>2</sub>Te], which shows it to be due to the initial attack of the peroxy radical on the telluride. By systematic variation of the

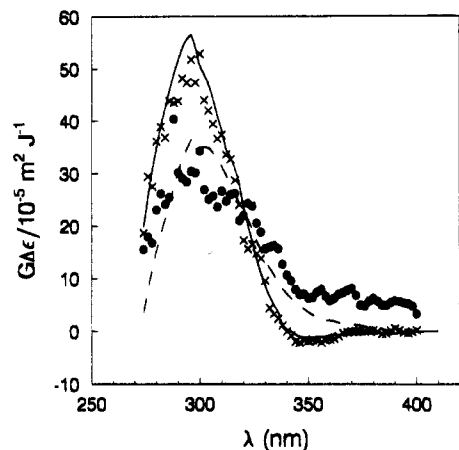
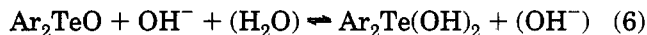
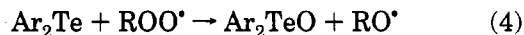


**Figure 4.** Transient spectra obtained by irradiating an aqueous solution at pH 6.7 saturated with a 1/9 mixture of O<sub>2</sub> and N<sub>2</sub>O, containing 2 × 10<sup>-4</sup> mol dm<sup>-3</sup> (4-NH<sub>2</sub>-C<sub>6</sub>H<sub>4</sub>)<sub>2</sub>Te and 0.1 mol dm<sup>-3</sup> 2-methyl-2-propanol with a dose of 13 Gy: (●) maximum signal (left arrow in Figure 3); (×) final absorbance (right arrow in Figure 3); (- - -) difference spectrum between (4-NH<sub>2</sub>-C<sub>6</sub>H<sub>4</sub>)<sub>2</sub>TeOH<sup>+</sup> and (4-NH<sub>2</sub>-C<sub>6</sub>H<sub>4</sub>)<sub>2</sub>Te multiplied by G = 4.15 × 10<sup>-7</sup> mol J<sup>-1</sup>; (-) difference spectrum between (4-NH<sub>2</sub>-C<sub>6</sub>H<sub>4</sub>)<sub>2</sub>Te(OH)<sub>2</sub> at pH 6.7 and (4-NH<sub>2</sub>-C<sub>6</sub>H<sub>4</sub>)<sub>2</sub>Te multiplied by G = 6.22 × 10<sup>-7</sup> mol J<sup>-1</sup>. The spectra are recorded at the time points marked by arrows in Figure 3.

concentrations of the tellurides at doses of 2 Gy, the rate constants presented in Table 1, were arrived at. Above pH ca. 6 a subsequent dose independent decay was observed, the rate of which was constant up to pH 7.5. Further increase of the pH accelerated this rate. Thus, at pH 9.22 only a small rapidly decaying signal remained. In Figure 4 are presented the spectra taken at times as marked by arrows in Figure 3. The full line corresponds to the difference spectrum between (4-NH<sub>2</sub>-C<sub>6</sub>H<sub>4</sub>)<sub>2</sub>Te(OH)<sub>2</sub> and (4-NH<sub>2</sub>-C<sub>6</sub>H<sub>4</sub>)<sub>2</sub>Te at pH 6.7 (from Figure 1) with allowance being made for equilibrium 1. The excellent spectral match shows (4-NH<sub>2</sub>-C<sub>6</sub>H<sub>4</sub>)<sub>2</sub>Te(OH)<sub>2</sub> to have formed within a few milliseconds. A similarly excellent match (not shown in Figure 4) was found at pH 5, where most of the telluroxide is in the (4-NH<sub>2</sub>-C<sub>6</sub>H<sub>4</sub>)<sub>2</sub>TeOH<sup>+</sup> form. On the basis of the pH dependence of the decay at pH > 6.3 and from the fact that the decay product is (4-NH<sub>2</sub>-C<sub>6</sub>H<sub>4</sub>)<sub>2</sub>Te(OH)<sub>2</sub>, we conclude that the process observed must be hydrolysis of the telluroxide (reaction 2 between pH 6 and 7.5). The spectrum at pH 6.7 in Figure 4, recorded at the time when the 330 nm absorbance has reached its maximum (see Figure 3), has a spectral shape that deviates from the difference spectrum between (4-NH<sub>2</sub>-C<sub>6</sub>H<sub>4</sub>)<sub>2</sub>TeOH<sup>+</sup> and (4-NH<sub>2</sub>-C<sub>6</sub>H<sub>4</sub>)<sub>2</sub>Te. Given that the absorbing species disappears through hydrolysis this spectrum should represent unhydrolyzed (4-NH<sub>2</sub>-C<sub>6</sub>H<sub>4</sub>)<sub>2</sub>TeO. In the 700 nm region, where both the radical cation (4-NH<sub>2</sub>-C<sub>6</sub>H<sub>4</sub>)<sub>2</sub>Te<sup>•+</sup> and the phenoxyl radical (4-O-C<sub>6</sub>H<sub>4</sub>)Te(C<sub>6</sub>H<sub>4</sub>-4-OH) absorb,<sup>19</sup> a slight absorbance is observed upon reaction of the parent tellurides with (CH<sub>3</sub>)<sub>2</sub>C(OH)CH<sub>2</sub>OO<sup>•</sup>. On the assumption that these absorbances belong to (4-NH<sub>2</sub>-C<sub>6</sub>H<sub>4</sub>)<sub>2</sub>Te<sup>•+</sup> or (4-O-C<sub>6</sub>H<sub>4</sub>)Te(C<sub>6</sub>H<sub>4</sub>-4-OH), it can be calculated that, at most, 8% of the peroxy radicals can bring about one-electron oxidation or hydrogen atom abstraction. The above observations can be explained by reaction 4 followed by reaction 2, 5, or 6.

In reaction 4 an alkoxy radical and unhydrolyzed



telluroxide Ar<sub>2</sub>TeO are formed. Ar<sub>2</sub>TeO is rapidly protonated below pH 6 or hydrolyzed by water or OH<sup>-</sup> above it to yield Ar<sub>2</sub>TeOH<sup>+</sup> or Ar<sub>2</sub>Te(OH)<sub>2</sub>. Apart from spectral evidence, the initial formation in reaction 4 of unhydrolyzed telluroxide, as opposed to Ar<sub>2</sub>TeOH<sup>+</sup> (which could be formed if H<sup>+</sup> or H<sub>2</sub>O were to participate in the elementary step), is supported by the lack of general acid catalysis on k<sub>4</sub>. Also, water is unlikely to act as a general acid,<sup>20</sup> it being a much weaker acid than Ar<sub>2</sub>TeOH<sup>+</sup>.

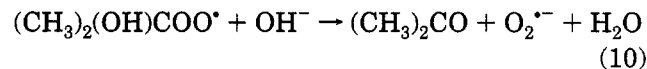
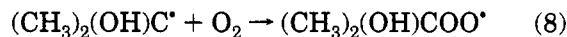
The relatively fast rate of the absorbance decay around pH 7 is consistent with reaction 2, given the strongly polar<sup>21</sup> (zwitterionic) character of the Te-O bond. This is to be contrasted with the hydration of carbonyl compounds, which occurs at rates several orders of magnitude slower. Note, however, that the acetyl (CH<sub>3</sub>C(O)) radical hydrates ca. 10<sup>6</sup> times more rapidly<sup>22</sup> than the parent acetaldehyde. Reaction 6 explains the acceleration of absorbance decay at higher pH. In order to find out whether protons could increase the yield of the radical cation, (4-HO-C<sub>6</sub>H<sub>4</sub>)<sub>2</sub>Te was reacted with (CH<sub>3</sub>)<sub>2</sub>C(OH)CH<sub>2</sub>OO<sup>•</sup> at pH 2. No radical cation formation could be discerned.

**Evidence for an Alkoxy Radical.** According to reaction 4, the telluroxide should form simultaneously with the alkoxy radical (CH<sub>3</sub>)<sub>2</sub>C(OH)CH<sub>2</sub>O<sup>•</sup>.

The latter species is expected to rapidly transform into a reductive radical either via a 1,2-hydrogen shift<sup>23,24</sup> or, more probably, through β-scission,<sup>25-28</sup> according to reaction 7.



The 1-hydroxy-1-methylethyl radical reacts rapidly with oxygen (reaction 8) to form a new peroxy radical, which expels O<sub>2</sub><sup>•-</sup> in reaction 9 or 10. k<sub>9</sub> and k<sub>10</sub> are 670



s<sup>-1</sup> and 5 × 10<sup>9</sup> dm<sup>3</sup> mol<sup>-1</sup> s<sup>-1</sup>,<sup>29</sup> respectively.

(20) Jencks, W. P. *J. Am. Chem. Soc.* **1972**, *94*, 4731.

(21) Jensen, K. A. *Z. Anorg. Allg. Chem.* **1943**, *250*, 268.

(22) Schuchmann, M. N.; von Sonntag, C. *J. Am. Chem. Soc.* **1988**, *110*, 5698.

(23) Berdnikov, V. M.; Bazhin, N. M.; Fedorov, V. K.; Polyakov, O. V. *Kinet. Katal.* **1972**, *13*, 1093.

(24) Gilbert, B. C.; Holmes, R. G. G.; Laue, H. A. H.; Norman, R. O. C. *J. Chem. Soc., Perkin Trans. 2* **1976**, 1047.

(25) Walling, C.; Wagner, P. J. K. *J. Am. Chem. Soc.* **1964**, *86*, 3368.

(26) Schuchmann, M. N.; von Sonntag, C. *J. Phys. Chem.* **1979**, *83*, 780.

(27) Mendenhall, G. D.; Stewart, R. C.; Scaiano, J. C. *J. Am. Chem. Soc.* **1982**, *104*, 5109.

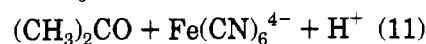
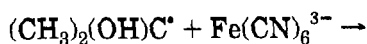
(28) Hiskey, M. A.; Brower, K. R.; Oxley, J. C. *J. Phys. Chem.* **1991**, *95*, 3955.

(29) Bothe, E.; Behrens, G.; Schulte-Frolinde, D. *Z. Naturforsch., B* **1977**, *32B*, 886.

Thus, at low pH the  $(\text{CH}_3)_2(\text{OH})\text{COO}^\bullet$  radical should be able to react with the telluride giving rise to more telluroxide. We produced specifically  $(\text{CH}_3)_2(\text{OH})\text{COO}^\bullet$  in the presence of  $(4\text{-NH}_2\text{-C}_6\text{H}_4)_2\text{Te}$ . While an accurate rate constant was difficult to obtain,  $(\text{CH}_3)_2(\text{OH})\text{COO}^\bullet$  appeared to react about 17 times more slowly than  $(\text{CH}_3)_2\text{C}(\text{OH})\text{CH}_2\text{OO}^\bullet$  with the telluride. The kinetics visualized in Figure 3 is consistent with a slow additional formation of telluroxide according to reaction 4 with  $(\text{CH}_3)_2(\text{OH})\text{COO}^\bullet$  as the peroxyl radical.

The size of the stable final absorbance at pH 5 did not vary linearly with the dose. At the lowest dose (2 Gy) one initial peroxyl radical gave rise to ca. two telluroxides, while at 13 Gy (Figure 3) this yield dropped to ca. one telluroxide per peroxyl radical. This is in keeping with competition between the two reaction modes of the peroxyl radicals, namely attack on  $\text{Ar}_2\text{Te}$  (i.e. reaction 4) and radical-radical combination. The lines drawn in Figure 3 are simulations utilizing the measured rate constants in Table 1 and the reaction sequence proposed in Scheme 1. From the literature the following rate constants of peroxyl radical combination were taken:  $2k((\text{CH}_3)_2\text{C}(\text{OH})\text{CH}_2\text{OO}^\bullet) = 8 \times 10^8 \text{ dm}^3 \text{ mol}^{-1} \text{ s}^{-1}$ ,<sup>29</sup>  $2k((\text{CH}_3)_2(\text{OH})\text{COO}^\bullet) = 1.1 \times 10^7 \text{ dm}^3 \text{ mol}^{-1} \text{ s}^{-1}$ ,<sup>30</sup> and  $k(\text{CH}_3\text{OO}^\bullet + \text{O}_2^{\bullet-}) = 2.5 \times 10^7 \text{ dm}^3 \text{ mol}^{-1} \text{ s}^{-1}$ .<sup>31</sup> The last rate constant was assumed for all  $\text{ROO}^\bullet + \text{O}_2^{\bullet-}$  reactions. For the remaining radical-radical reactions the rate constants were assumed to be  $10^9 \text{ dm}^3 \text{ mol}^{-1} \text{ s}^{-1}$ . The nice fit in Figure 3 lends credibility to the assumed reaction sequence.

During pulse radiolysis interception of the  $(\text{CH}_3)_2(\text{OH})\text{C}^\bullet$  radical or of  $\text{O}_2^{\bullet-}$  (at high pH) proved a difficult task. The standard reagent, tetranitromethane, reacted with the telluride upon mixing. The best alternative turned out to be  $\text{Fe}(\text{CN})_6^{3-}$ , which, however, has a rather poor molar absorbance. A  $4 \times 10^{-4} \text{ mol dm}^{-3}$  solution of  $\text{Fe}(\text{CN})_6^{3-}$  was added to a solution containing  $(4\text{-HO-C}_6\text{H}_4)_2\text{Te}$  ( $4 \times 10^{-4} \text{ mol dm}^{-3}$ ) at pH 4.6. A redox equilibrium, monitored at 420 nm, the absorbance maximum of  $\text{Fe}(\text{CN})_6^{3-}$ , was established within 1 min, resulting in an equilibrium mixture containing  $10^{-4} \text{ mol dm}^{-3} \text{ Fe}(\text{CN})_6^{3-}$ ,  $3 \times 10^{-4} \text{ mol dm}^{-3} \text{ Fe}(\text{CN})_6^{4-}$ ,  $2.5 \times 10^{-4} \text{ mol dm}^{-3}$  of  $(4\text{-HO-C}_6\text{H}_4)_2\text{Te}$ , and  $1.5 \times 10^{-4} \text{ mol dm}^{-3}$  of  $(4\text{-HO-C}_6\text{H}_4)_2\text{TeOH}^+$ . 2-Methyl-2-propanol ( $0.1 \text{ mol dm}^{-3}$ ) was added, and the solution was purged with a 9/1  $\text{N}_2\text{O}/\text{O}_2$  mixture. Upon pulse irradiation we observed a bleaching at 420 nm, the spectral maximum of  $\text{Fe}(\text{CN})_6^{3-}$ , corresponding to 38%  $\text{Fe}(\text{CN})_6^{4-}$  formed per initial radical. The rate of this bleaching was the same as the rate of telluroxide formation from  $(\text{CH}_3)_2\text{C}(\text{OH})\text{CH}_2\text{OO}^\bullet$  and telluride at the same concentration. The amount of the bleaching was halved upon doubling of the  $\text{O}_2$  concentration. This shows that in our oxidative system a reducing radical is formed. Assuming this radical to be  $(\text{CH}_3)_2(\text{OH})\text{C}^\bullet$  and taking into account the competition between reactions 8 and 11 ( $k_8 = 4.2 \times 10^9 \text{ dm}^3 \text{ mol}^{-1} \text{ s}^{-1}$ ),<sup>32</sup> we calculate that, following reaction 4, essentially all  $(\text{CH}_3)_2\text{C}(\text{OH})\text{CH}_2\text{OO}^\bullet$  radicals initially produced have been converted into  $(\text{CH}_3)_2(\text{OH})\text{C}^\bullet$ . These observations clearly support the initial formation of an alkoxyl radical in reaction 4.



$$k_{11} = 4.7 \times 10^9 \text{ dm}^3 \text{ mol}^{-1} \text{ s}^{-1} \quad (32)$$

In an alternative approach  $5 \times 10^{-4} \text{ mol dm}^{-3}$  each of  $(4\text{-HO-C}_6\text{H}_4)_2\text{Te}$  and  $(4\text{-HO-C}_6\text{H}_4)_2\text{TeOH}^+$  were pulse irradiated in the presence of  $0.1 \text{ mol dm}^{-3}$  2-methyl-2-propanol at pH 5 ( $\text{N}_2\text{O}/\text{O}_2 = 4/1$ ), the idea being that  $(\text{CH}_3)_2(\text{OH})\text{C}^\bullet$ , were it to form, would, in competition with reaction 8, reduce  $(4\text{-HO-C}_6\text{H}_4)_2\text{TeOH}^+$  to the Te(III) radical cation. The latter would then immediately deprotonate to form a phenoxyl radical. Indeed, we observed the buildup of the characteristic absorbance<sup>19</sup> of  $(4\text{-O}^\bullet\text{-C}_6\text{H}_4)\text{Te}(\text{C}_6\text{H}_4\text{-4-OH})$  at 700 and 370 nm. The competition between reaction 8 and the reduction of  $(4\text{-HO-C}_6\text{H}_4)_2\text{TeOH}^+$  by  $(\text{CH}_3)_2(\text{OH})\text{C}^\bullet$  was studied in a separate experiment where an  $\text{N}_2\text{O}/\text{O}_2$  (4/1) purged solution containing  $5 \times 10^{-4} \text{ mol dm}^{-3}$  telluroxide and  $0.1 \text{ mol dm}^{-3}$  2-propanol was pulse-irradiated at pH 5. The absorbances observed at the same wavelengths were almost identical with those seen in the previous experiment. We can thus infer the quantitative production of a reducing radical, as discussed above. To ascertain that the telluroxide did not react directly with peroxyl radicals, we have generated in separate experiments peroxyl radicals in the presence of millimolar concentrations of telluroxide. No reaction whatsoever could be discerned between the two species.

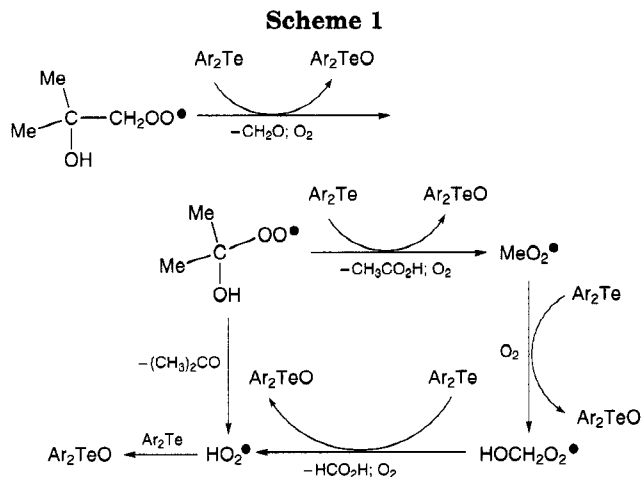
**$\gamma$ -Radiolysis of  $(4\text{-NH}_2\text{-C}_6\text{H}_4)_2\text{Te}$ .** Aqueous solutions  $10^{-4} \text{ mol dm}^{-3}$  in the telluride purged with 4/1  $\text{N}_2\text{O}/\text{O}_2$  and containing  $0.1 \text{ mol dm}^{-3}$  2-methyl-2-propanol at neutral pH were irradiated in a  $^{60}\text{Co}$   $\gamma$ -source. The sample was irradiated in consecutive time increments of 30 s, and after each increment the UV spectrum of the solution was recorded. By comparison with authentic spectra of telluroxide and telluride (see Figure 1) the quantitative conversion into telluroxide after sufficient irradiation could be confirmed. NMR measurements on spent solutions showed diaryl telluroxide as the sole tellurium product. Continued irradiation after 100% conversion did not destroy the  $\text{Ar}_2\text{TeO}$  formed. From the initial rate of conversion it follows that between 3.0 and 3.4 molecules of telluride are consumed for each  $(\text{CH}_3)_2\text{C}(\text{OH})\text{CH}_2\text{OO}^\bullet$  produced. Variation of the 2-methyl-2-propanol concentration did not affect this yield. Although we have not elaborated the details, the events can be accounted for by the sequence given in Scheme 1. Although not explicitly stated in scheme 1, the  $\text{CH}_3\text{O}^\bullet$  radical is expected to rapidly, i.e., with a rate exceeding  $10^5 \text{ s}^{-1}$ , convert into  $\text{CH}_2\text{OH}^\bullet$  by way of a 1,2-hydrogen shift, in analogy with findings in refs 23, 24, and 33. In a similar fashion, the alkoxy radical,  $\text{CH}_2\text{OH}(\text{O}^\bullet)$ , should rapidly transform into the reducing  $\text{CH}(\text{OH})_2$  radical. The ultimate peroxyl radical is superoxide. It was therefore important to assess its contribution to the formation of telluroxide. When oxygenated solutions containing  $0.1 \text{ mol dm}^{-3} \text{ HCO}_2^-$  (where all initial radicals are converted into  $\text{O}_2^{\bullet-}$ , the radiation chemical yield,  $G$ , of the latter being  $7.4 \times 10^{-7} \text{ mol J}^{-1}$ ) and  $10^{-4} \text{ mol dm}^{-3} \text{ Ar}_2\text{Te}$  at pH 6.7 were  $\gamma$ -irradiated, the  $G$  value of

(30) Ilan, Y.; Rabani, J.; Henglein, A. *J. Phys. Chem.* **1976**, *80*, 1558.

(31) von Sonntag, C.; Schuchmann, H.-P. *Angew. Chem., Int. Ed. Engl.* **1991**, *30*, 1229.

(32) Adams, G. E.; Willson, R. R. *Trans. Faraday Soc.* **1969**, *65*, 2981.

(33) Schuchmann, H.-P.; von Sonntag, C. *J. Photochem.* **1981**, *16*, 289.



produced telluroxide was found to be  $6.2 \times 10^{-7} \text{ mol J}^{-1}$ . Given that  $\text{H}_2\text{O}_2$  quantitatively oxidizes telluride to telluroxide (see below) and allowing for the molecular yield of  $\text{H}_2\text{O}_2$  ( $G(\text{H}_2\text{O}_2) = 7.3 \times 10^{-8} \text{ mol J}^{-1}$ ), the efficiency of telluroxide production by  $\text{O}_2^{\cdot-}$  is calculated to be  $0.74 \pm 0.04$ . In independent experiments  $\text{H}_2\text{O}_2$  was shown to rapidly oxidize  $(4\text{-NH}_2\text{-C}_6\text{H}_4)_2\text{Te}$  to its telluroxide. The rate constant, presented in Table 1, was unchanged between pH 4.5 and 9.2. Thus, in the  $\gamma$ -radiolysis experiments this reaction should have gone to completion by the time of analysis. Were  $\text{O}_2^{\cdot-}$  to be consumed exclusively through radical-radical combination, the yield of  $\text{H}_2\text{O}_2$  would amount to 0.5. Our measured yield of telluroxide being significantly higher than this figure, superoxide (presumably as  $\text{HO}_2^{\cdot}$ ) is implicated in a direct reaction with the telluride. In order to gain some more insight into this reaction,  $\text{HO}_2^{\cdot}$  was produced at pH 4.3 by pulse radiolysis of an  $\text{O}_2$ -saturated solution containing  $0.1 \text{ mol dm}^{-3} \text{ HCO}_2^-$  and  $10^{-4} \text{ mol dm}^{-3} (4\text{-NH}_2\text{-C}_6\text{H}_4)_2\text{Te}$ . A slow reaction between the telluride and  $\text{HO}_2^{\cdot}$  seemed to take place, judging by the changes in molar absorbancy around 320 nm. However, as we are in competition with radical-radical combination, the nature of the  $\text{HO}_2^{\cdot}$  reaction could not be unraveled beyond establishing an upper limit to its rate constant (see Table 1).

As can be seen in Scheme 1, the radiolytic degradation of 2-methyl-2-propanol in the presence of  $\text{O}_2$  and  $\text{Ar}_2\text{Te}$  is proposed to traverse five successive peroxy radical stages, including  $\text{HO}_2^{\cdot}/\text{O}_2^{\cdot-}$ . Were each of them to convert one telluride to telluroxide, the maximum yield of  $\text{Ar}_2\text{TeO}$  per initial radical would be 5. The experimental value of 3.0–3.4 is explained by  $(\text{CH}_3)_2(\text{OH})\text{COO}^{\cdot}$  participating in the competitive reactions 4 and 9, 10. Pulse radiolysis results suggest that at pH 6.7 in the presence of  $10^{-4} \text{ mol dm}^{-3} (4\text{-NH}_2\text{-C}_6\text{H}_4)_2\text{Te}$  reaction 4 is about as rapid as reactions 9, 10. Thus, the overall yield of  $(4\text{-NH}_2\text{-C}_6\text{H}_4)_2\text{TeO}$  during  $\gamma$ -irradiation should be  $1 + 0.74 + 3 \times 1/2 = 3.24$ , in fair agreement with experiment.

## Discussion

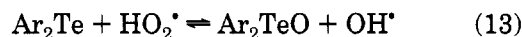
**Energetics of the Oxidation Reactions.** The rate of deprotonation of  $\text{Ar}_2\text{TeOH}^+$  by  $\text{OH}^-$  is surely diffusion-controlled<sup>34</sup> (ca.  $5 \times 10^9 \text{ dm}^3 \text{ mol}^{-1} \text{ s}^{-1}$ ). The microscopic reverse, i.e. the rate of protonation of  $\text{Ar}_2\text{-$

$\text{TeO}$  by  $\text{H}_2\text{O}$ , cannot be higher than the experimental rate of neutral hydrolysis of  $\text{Ar}_2\text{TeO}$  ( $\sim 4 \times 10^3 \text{ s}^{-1}$ ). It then follows that  $\text{p}K_{\text{a}}(12)$

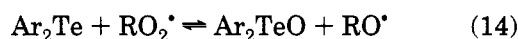


is 8 at most. In conjunction with the experimental  $K_1$  value, this yields  $K_2 \leq 10^2$ . The actual observation of the hydrolysis process according to eq 2 in pulse radiolysis sets 10 as the lower limit to  $K_2$ . Consequently,  $\Delta G^\circ_2 = -8 \pm 3 \text{ kJ mol}^{-1}$  and  ${}^2E^\circ(\text{Ar}_2\text{TeO}, 2\text{H}^+/\text{Ar}_2\text{Te}, \text{H}_2\text{O}) = 0.69 \pm 0.02 \text{ V}$  are obtained.

From this value,  $E^\circ((4\text{-NH}_2\text{-C}_6\text{H}_4)_2\text{Te}^{+}/(4\text{-NH}_2\text{-C}_6\text{H}_4)_2\text{-Te}) = 0.80 \text{ V}$ ,<sup>19</sup> and data in ref 35 the following free energies of oxidation reactions are calculated:



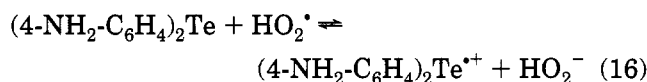
$$\Delta G^\circ_{13} = -84 \pm 6 \text{ kJ mol}^{-1}$$



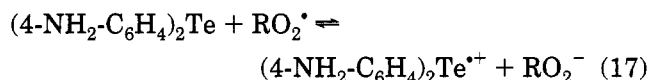
$$\Delta G^\circ_{14} = -125 \pm 17 \text{ kJ mol}^{-1}$$



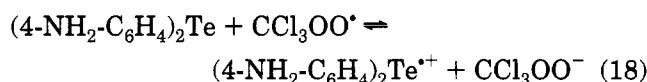
$$\Delta G^\circ_{15} = -125 \pm 34 \text{ kJ mol}^{-1}$$



$$\Delta G^\circ_{16} = 4.6 \pm 2.0 \text{ kJ mol}^{-1}$$



$$\Delta G^\circ_{17} = 3 \pm 5 \text{ kJ mol}^{-1}$$



$$\Delta G^\circ_{18} = -34 \pm 13 \text{ kJ mol}^{-1}$$

As  $E^\circ((4\text{-HO-C}_6\text{H}_4)_2\text{Te}^{+}/(4\text{-HO-C}_6\text{H}_4)_2\text{Te}) = 0.95 \text{ V}$ ,<sup>19</sup> the analogues of reactions 16–18 with  $(4\text{-HO-C}_6\text{H}_4)_2\text{Te}$  have  $\Delta G^\circ$  values that are more positive by  $15 \text{ kJ mol}^{-1}$ . However, given the facile deprotonation of the radical cation of the latter compound ( $\text{p}K_{\text{a}} = 2.5$ <sup>19</sup>), the one-electron-transfer reactions of  $(4\text{-HO-C}_6\text{H}_4)_2\text{Te}$  with the peroxy radicals, followed by proton transfer, amount to hydrogen atom transfer to yield neutral phenoxyl radical and hydroperoxide. Then we obtain the  $\Delta G^\circ$  values of  $-33$ ,  $-36$ , and  $-49 \text{ kJ mol}^{-1}$  for the hydrogen abstraction reactions of  $(4\text{-HO-C}_6\text{H}_4)_2\text{Te}$  with  $\text{HO}_2^{\cdot}$ ,  $\text{ROO}^{\cdot}$ , and  $\text{CCl}_3\text{OO}^{\cdot}$ , respectively. We recall that, despite the favorable energetics,  $\text{ROO}^{\cdot}$  essentially did not react via hydrogen abstraction with  $(4\text{-HO-C}_6\text{H}_4)_2\text{-Te}$ .

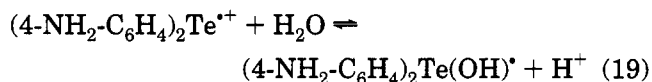
**Mechanism of the Reaction of Peroxy Radicals with Chalcogenides.** The present work testifies to the

(34) Eigen, M. *Angew. Chem., Int. Ed. Engl.* **1964**, *3*, 1.

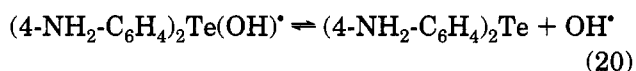
(35) Merényi, G.; Lind, J.; Engman, L. *J. Chem. Soc., Perkin Trans. 2* **1994**, 2551.

facile overall monooxygenation of diaryl tellurides by alkylperoxyl radicals. A mechanistically interesting question is whether oxygen transfer occurs by direct means or via a short-lived adduct. On the experimental side we note that not even in strongly acidic solutions (pH 2) did the  $(\text{CH}_3)_2\text{C}(\text{OH})\text{CH}_2\text{OO}^\bullet$  radical produce any noticeable amount of  $\text{Ar}_2\text{Te}^{+\bullet}$ . From known precedents<sup>4</sup> we reason that, had there been an  $\text{Ar}_2\text{Te}^\bullet\text{-OOR}$  adduct present, it would surely have undergone a proton-catalyzed decomposition into ROOH and  $\text{Ar}_2\text{Te}^{+\bullet}$  with a rate around  $10^9 \text{ dm}^3 \text{ mol}^{-1} \text{ s}^{-1}$ . In support of this we recall that the rate constant<sup>36</sup> of proton-catalyzed dehydration of  $(\text{CH}_3)_2\text{SOH}^\bullet$  is ca.  $10^{10} \text{ dm}^3 \text{ mol}^{-1} \text{ s}^{-1}$ , and such a rate is expected also for  $(\text{C}_6\text{H}_5)_2\text{TeOH}^\bullet$ , it having almost the same pseudobase<sup>19,37</sup>  $\text{p}K_a$  as  $(\text{CH}_3)_2\text{SOH}^\bullet$ . Clearly, the corresponding proton-catalyzed expulsion of ROOH from a  $(\text{C}_6\text{H}_5)_2\text{TeOOR}$  adduct should also proceed with a similar rate. We also note that the rate of  $\text{OH}^-$  expulsion from  $(\text{C}_6\text{H}_5)_2\text{TeOH}^\bullet$  is well above  $10^6 \text{ s}^{-1}$ . Given that the  $\text{p}K_a$  of ROOH is lower than that of  $\text{H}_2\text{O}$  by ca. 4 units, we expect the rate of  $\text{ROO}^\bullet$  expulsion from  $\text{TeOOR}$  to be at least  $10^7 \text{ s}^{-1}$ . These considerations set an upper limit of ca.  $10^{-7} \text{ s}$  to the lifetime of a presumptive  $\text{TeOOR}$  adduct. During such a short time no intermolecular events are likely to occur to an appreciable extent. In particular, nucleophilic attack on Te by a water molecule would seem to be all but precluded during this short time. Thus, even in the unlikely event (see further below) that an adduct existed on the pathway, its short lifetime would render its chemistry indistinguishable from that of a one-step oxygen atom transfer from  $\text{ROO}^\bullet$  to Te.

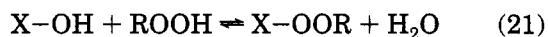
Equally important, however, are the following energetic considerations: in ref 19 the  $\text{p}K_a$  of pseudobase formation of  $(4\text{-H}_2\text{N-C}_6\text{H}_4)_2\text{Te}^{+\bullet}$  was measured to be 10.5:



From this value and  $E^\circ(4\text{-NH}_2\text{-C}_6\text{H}_4)_2\text{Te}^{+\bullet}/(4\text{-NH}_2\text{-C}_6\text{H}_4)_2\text{Te}$  the  $\Delta G^\circ_{20}$  value of the homolysis reaction below is calculated to be  $125 \text{ kJ mol}^{-1}$ .



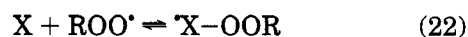
Now, judging by the Benson additivity rules,<sup>38</sup>  $\Delta G^\circ$  in water of the exchange reaction 21 should be  $0 \pm 13 \text{ kJ mol}^{-1}$ . This relation has good experimental support



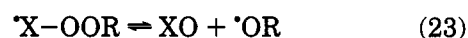
in cases where X is an alkyl<sup>39-42</sup> or acyl<sup>43</sup> group or even<sup>43-45</sup> a  $\text{SO}_3^-$  group. There is no reason why it

should not apply to cases where the X-OH and X-OOR species are radicals.<sup>46</sup> Qualitatively, the relation says that the difference in the bond strengths of HO-H and ROO-H,  $\sim 125 \text{ kJ mol}^{-1}$ , should be paralleled by a corresponding bond strength difference between HO-X and ROO-X. If we apply this relationship in combination with data in ref 35 to the presumptive chalcogenide-peroxyl radical adduct, where X =  $(4\text{-NH}_2\text{-C}_6\text{H}_4)_2\text{Te}$ , we obtain

$$\Delta G^\circ_{22} = \Delta G^\circ_{21} - \Delta G^\circ_{20} + 23.06\{E^\circ(\text{OH}^\bullet, \text{H}^+/\text{H}_2\text{O}) - E^\circ(\text{ROO}^\bullet, \text{H}^+/\text{ROOH})\} = -4 \pm 17 \text{ kJ mol}^{-1}$$



If we assume a  $T\Delta S^\circ_{22}$  value of ca.  $-33 \text{ kJ mol}^{-1}$ <sup>47</sup> and neglect  $\Delta S^\circ_{14}$  altogether, the enthalpy change



would turn out to be ca.  $-88 \text{ kJ mol}^{-1}$ , i.e., the strength of the O-O bond with respect to homolysis is *negative*. This is evidence against the presence of an adduct. Clearly, a local minimum cannot be excluded, but given that bond rupture hinges on a simple O-O vibration, it is hard to understand, how such an adduct could possess a finite lifetime.

Therefore, we believe the elementary step to be a one-step concerted oxygen atom transfer. Furthermore, from the variation of its rate constant with the substrate (cf. the rate of reaction of  $(\text{CH}_3)_2\text{C}(\text{OH})\text{CH}_2\text{OO}^\bullet$  with  $(4\text{-NH}_2\text{-C}_6\text{H}_4)_2\text{Te}$  and  $(4\text{-HO-C}_6\text{H}_4)_2\text{Te}$  in Table 1), we infer a polar transition state.

The rate of one-electron oxidation of  $(4\text{-NH}_2\text{-C}_6\text{H}_4)_2\text{Te}$  by  $(\text{CH}_3)_2\text{C}(\text{OH})\text{CH}_2\text{OO}^\bullet$  is rather slow (an upper limit of  $1.4 \times 10^7 \text{ dm}^3 \text{ mol}^{-1} \text{ s}^{-1}$  can be calculated from the maximum yield of the radical cation observed), in keeping with the essential thermoneutrality of reaction 17. In contrast,  $\text{CCl}_3\text{OO}^\bullet$  reacts predominantly by way of electron transfer with the diaryl tellurides, with close to diffusion-controlled rates. This is in keeping with the considerable exothermicity of reaction 18.

## Conclusions

In the present work the mechanism of reaction of peroxyl radicals with some diaryl tellurides was investigated. It was found that the organotellurium compounds served predominantly ( $\sim 70\%$ ) as one-electron reductants toward the  $\text{CCl}_3\text{OO}^\bullet$  radical, whereas they acted essentially ( $\geq 92\%$ ) as oxygen atom recipients in their reaction with the  $(\text{CH}_3)_2\text{C}(\text{OH})\text{CH}_2\text{OO}^\bullet$  radical. In the latter reaction the proposed oxygen transfer mechanism was corroborated by the favorable energetics calculated and the quantitative interception of a reducing  $\alpha$ -hydroxyl alkyl radical, the product of  $\beta$ -scission

(36) Schöneich, C.; Bobrowski, K. *J. Am. Chem. Soc.* **1993**, *115*, 6538.

(37) Manuscript in preparation.

(38) Benson, S. W. In *Thermochemical Kinetics, Methods for the Estimation of Thermochemical Data and Rate Parameters*, 2nd ed.; Wiley: New York, 1976.

(39) Sander, E. G.; Jencks, W. P. *J. Am. Chem. Soc.* **1968**, *90*, 6154.

(40) Dixon, J. E.; Bruce, T. C. *J. Am. Chem. Soc.* **1971**, *93*, 6592.

(41) Merényi, G.; Lind, J. *J. Am. Chem. Soc.* **1991**, *113*, 3146.

(42) Zhou, X.; Lee, Y.-N. *J. Phys. Chem.* **1992**, *96*, 265.

(43) Monger, J. N.; Redlich, O. *J. Phys. Chem.* **1956**, *60*, 797.

(44) Benson, S. W. *Chem. Rev.* **1978**, *78*, 23.

(45) Price, J. S.; Tasker, I. R.; Appelman, E. H.; O'Hare, P. A. G. *J. Chem. Thermodyn.* **1986**, *18*, 923.

(46) This can be seen, for instance, as follows: for  $\text{CH}_3\text{OH} + \text{H}_2\text{O}_2 \rightleftharpoons \text{CH}_3\text{OOH} + \text{H}_2\text{O}$ ,  $\Delta G^\circ \approx -13 \text{ kJ mol}^{-1}$  in water. Since the C-H bond strengths in  $\text{H-CH}_2\text{OH}$  and  $\text{H-CH}_2\text{OOH}$  should be similar (Nangia, P. S.; Benson, S. W. *J. Am. Chem. Soc.* **1980**, *102*, 3105), about the same  $\Delta G^\circ$  value is predicted for  $\text{CH}_2\text{OH} + \text{H}_2\text{O}_2 \rightleftharpoons \text{CH}_2\text{OOH} + \text{H}_2\text{O}$ .

(47) From compilations in ref 36  $\Delta S^\circ$  for a large number of gaseous association reactions similar to (22) is calculated to be close to  $-145 \text{ J mol}^{-1} \text{ K}^{-1}$ ; thus,  $T\Delta S^\circ \approx -42 \text{ kJ mol}^{-1}$  is obtained at room temperature in the gas phase. Upon transfer to water this value should, to a first approximation, increase by  $RT \ln(V_g/V_{aq})$ , where  $V_g$  and  $V_{aq}$  denote the molar volumes of a species in the gaseous ( $24.79 \text{ dm}^3 \text{ mol}^{-1}$ ) and aqueous ( $1 \text{ dm}^3 \text{ mol}^{-1}$ ) standard states, respectively.



of its precursor, the alkoxy radical. The rate constant of oxygen atom transfer from alkylperoxy radicals to diaryl tellurides was found to be on the order of  $10^7$ – $10^8$   $\text{dm}^3 \text{mol}^{-1} \text{s}^{-1}$ . These values exceed the corresponding rate constants between phosphites and peroxy radicals by ca. 4 orders of magnitude. This is a remarkable finding, considering that the latter reactions are more exothermic than the former by ca. 150  $\text{kJ mol}^{-1}$ . Kinetically, therefore, diaryl tellurides would

appear to be by far the most efficient two-electron reductants of peroxidic species known.

**Acknowledgment.** We are grateful to the Swedish Natural Science Research Council and the Swedish National Board for Technical Development for their financial support.

OM9501236

# Homoleptic Actinide Complexes with Chelating Diphosphinophosphido Ligands: New Mode of Reactivity with Carbon Monoxide and the X-ray Crystal Structure of $U\{P(CH_2CH_2PMe_2)_2\}_4$

Peter G. Edwards,\* Julian S. Parry, and Paul W. Read

Department of Chemistry, University of Wales Cardiff, P.O. Box 912, Cardiff, CF1 3TB, U.K.

Received September 14, 1994<sup>®</sup>

The tetrakis(dialkylphosphido) complexes  $M\{P(CH_2CH_2PMe_2)_2\}_4$  ( $M = Th, U$ ) are isolated in high yield from the reaction of  $MCl_4$  with 4 mol equiv of  $(Li^+ \text{ or } K^+)^-P(CH_2CH_2PMe_2)_2$  ( $(Li/K)PPP$ ). The uranium and thorium compounds are isostructural, although the thorium compound exhibits dimorphism. Detailed shape analysis indicates the structures of the three tetraphosphides conform to triangulated dodecahedra distorted toward bicapped trigonal prisms. The thorium compound is shown to be labile, exhibiting facile exchange of coordinated with uncoordinated tertiary phosphine functions, by  $^{31}P\{^1H\}$  NMR spectroscopy. The thorium compound reacts readily with CO to give a unique double-insertion product where CO is incorporated into a diphosphacarinol (diphospha secondary alcohol) derivative with two phosphido phosphorus atoms becoming bonded to the inserted carbon atom and the new  $P_2CO$  unit being  $\eta^3$ -bonded to thorium. Structural and spectroscopic data indicate a reduction in C–O bond order from 3 to 1 upon insertion. Hydrolysis liberates the free diphospha secondary alcohol, which is unstable with respect to P–C cleavage and aldehyde formation under mass-spectroscopic conditions. Alkenes with vinylic protons and phenols also react with the thorium tetraphosphide, which eliminates HPPP. The new compounds were characterized by analytical and spectroscopic techniques and by X-ray crystallography for the uranium complex.

## Introduction

There are very few authentic dialkylphosphido complexes of the actinides known. Prior to this study, the only other well-characterized examples of actinide dialkylphosphides reported were those of the type  $Cp_2Th(PR_2)_2$  ( $Cp = C_5H_5$ ;  $R = \text{alkyl}$ )<sup>1</sup> and  $Cp_2Th(PR_2)_2Ni(CO)_2$  ( $R = \text{alkyl}$ ).<sup>2</sup> The application of potentially multidentate amido and phosphido ligands containing ancillary neutral donors has been successful in stabilizing new classes of complexes with transition and lanthanide metals,<sup>3</sup> with one recent example for actinides.<sup>3b</sup> In this paper we discuss the synthesis, characterization, and structural analysis of the first homoleptic actinide phosphido complexes and report on their reactivities with carbon monoxide. We have recently reported preliminary results of the application of  $^-P(CH_2CH_2-$

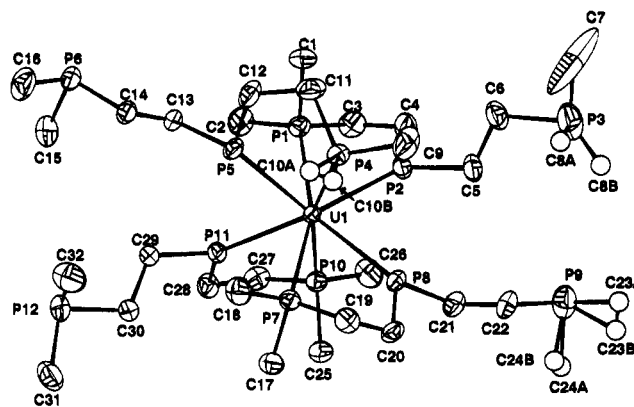


Figure 1. Molecular structure of  $U\{P(CH_2CH_2PMe_2)_2\}_4$  (1).

$PMe_2)_2$  (PPP) to the synthesis of thorium phosphides<sup>4</sup> and reactions with carbon monoxide.<sup>5</sup>

## Results and Discussion

The reactions discussed below and representations of the structures of the actinide compounds are collected in Scheme 1.

$U\{P(CH_2CH_2PMe_2)_2\}_4$  (1). The addition of 4 mol equiv of a standard solution of KPPP to  $UCl_4$  in PhMe/THF at  $-80^\circ C$  generates black solutions from which black crystals can be isolated in good yield from light petroleum ether. Interestingly, the interaction of 3 mol equiv of a standard solution of KPPP with  $UCl_3(THF)_x$

(5) Edwards, P. G.; Hursthouse, M. B.; Malik, K. M. A.; Parry, J. S. *J. Chem. Soc., Chem. Commun.* 1994, 1249.

\* To whom correspondence should be addressed.

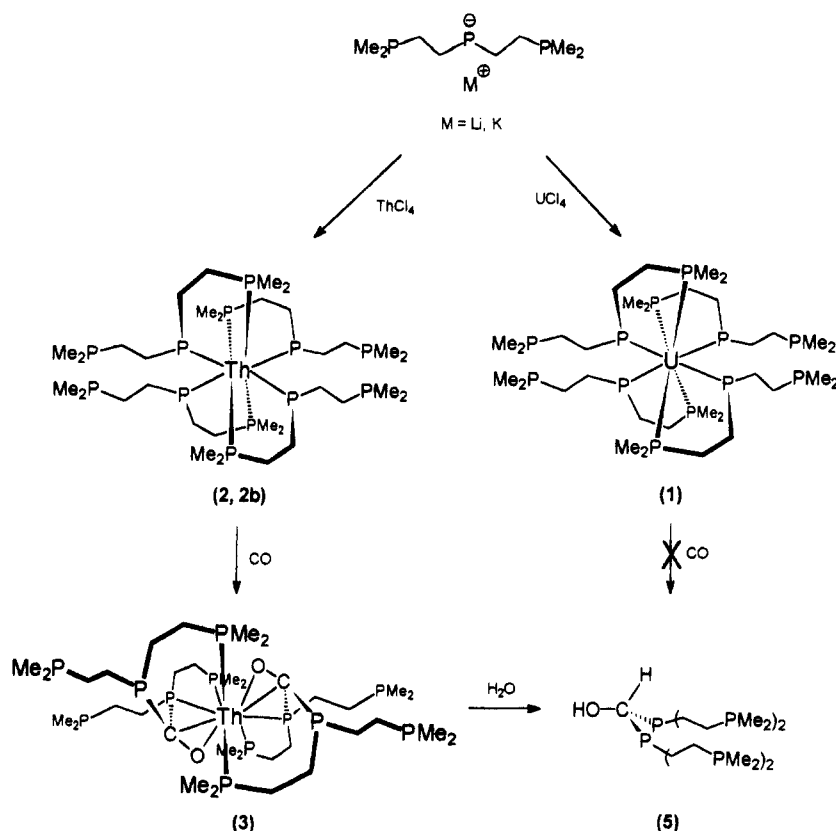
<sup>®</sup> Abstract published in *Advance ACS Abstracts*, June 15, 1995.

(1) Wroblewski, D. A.; Ryan, R. R.; Wasserman, H. J.; Salazar, K. V.; Paine, R. T.; Moody, D. C. *Organometallics* 1986, 5, 90.

(2) Ryan, R. R.; Paine, R. T.; Moody, D. C. *J. Am. Chem. Soc.* 1985, 107, 501.

(3) (a) Wills, A. R.; Edwards, P. G. *J. Chem. Soc., Dalton Trans.* 1989, 1253. Danopoulos, A. A.; Edwards, P. G. *Polyhedron* 1989, 8, 1339. Wills, A. R.; Edwards, P. G.; Harman, M.; Hursthouse, M. B. *Polyhedron* 1989, 1457. Al-Soudani, A.-R.; Batsanov, A.; Edwards, P. G.; Howard, J. A. K. *J. Chem. Soc., Dalton Trans.* 1994, 987. Fryzuk, M. D.; Haddad, T. S.; Berg, D. J. *Coord. Chem. Rev.* 1990, 99, 137. (b) Coles, S. J.; Edwards, P. G.; Hursthouse, M. B.; Read, P. W. *J. Chem. Soc., Chem. Commun.* 1994, 1967. (c) Edwards, P. G.; Howard, J. A. K.; Parry, J. S.; Al-Soudani, A.-R. *J. Chem. Soc., Chem. Commun.* 1991, 1385. (d) Danopoulos, A. A.; Edwards, P. G.; Harman, M.; Hursthouse, M. B.; Parry, J. S. *J. Chem. Soc., Dalton Trans.* 1994, 977. (e) Edwards, P. G.; Read, P. W.; Hursthouse, M. B.; Malik, K. M. A. *J. Chem. Soc., Dalton Trans.* 1994, 971.

(4) Edwards, P. G.; Harman, M.; Hursthouse, M. B.; Parry, J. S. *J. Chem. Soc., Chem. Commun.* 1992, 1469.

Scheme 1. Preparation and Reactions of Actinide Phosphides,  $M\{P(CH_2CH_2PMe_2)_2\}_4$  ( $M = Th, U$ )

affords an identical black crystalline material. The reaction of LiPPP with  $UCl_4$  and  $UCl_3(THF)_x$  gives the same compound in much lower yield; the lower solubility of potassium chloride vs that of lithium chloride in hydrocarbons and THF may help drive the reaction to a cleaner end point. Microanalysis confirms a tetrakis ligand formulation, and a negative chloride analysis is obtained with acidified silver nitrate. **1** represents the first structurally characterized uranium dialkylphosphide complex.

Uranium(IV) is paramagnetic ( $5f^2$ ), and  $^{31}P$  NMR signals have not been observed for any phosphorus atoms within the complex. Broad resonances are observed in the  $^1H$  NMR spectrum, from which detailed structural information cannot be inferred.

$Th\{P(CH_2CH_2PMe_2)_2\}_4$  (**2**). The reaction of 4 mol equiv of LiPPP or KPPP with  $ThCl_4$  in ethers or hydrocarbons affords red solutions from which red, petroleum ether soluble crystals of **2** may be isolated in good yield. Microanalysis confirms a tetrakis ligand formulation, and a negative chloride test is obtained with acidified silver nitrate. The room-temperature  $^{31}P\{^1H\}$  NMR spectrum of **2** contains two broad singlets at  $\delta$  83 ppm ( $\nu_{1/2} = ca. 100$  Hz) and  $\delta$  -34 ppm ( $\nu_{1/2} = ca. 400$  Hz) which are integrated in a ratio of 1:2, respectively. The former resonance is assigned to the phosphido phosphorus atoms and the latter to the tertiary phosphine atom, on the basis of chemical shift and signal intensity. The broadness of the resonances indicates that **2** is fluxional in solution. This is confirmed by variable-temperature  $^{31}P\{^1H\}$  NMR spectroscopy (Figure 2). Coalescence occurs at about 5 °C; below this temperature, new peaks appear in the regions expected for both coordinated and uncoordinated tertiary phosphine. At the low-temperature limit (-80 °C)

three resonances are observed of approximately equal signal intensity, which are assigned to coordinated phosphide ( $\delta$  71 ppm), coordinated tertiary phosphine ( $\delta$  -8 ppm), and uncoordinated tertiary phosphine ( $\delta$  -52 ppm). These resonances are still slightly broad ( $\nu_{1/2} = ca. 40$  Hz for all three peaks), and no P-P coupling is resolved. The spectra indicate that the fluxional nature of **2** is due to an exchange process involving the rapid exchange of coordinated with uncoordinated tertiary phosphines. The high-temperature (100 °C) spectrum shows a septet attributed to the phosphide ( $\delta$  89 ppm,  $\nu_{1/2} = ca. 45$  Hz) and a pentet for the tertiary phosphines ( $\delta$  -34 ppm,  $\nu_{1/2} = ca. 45$  Hz,  $J_{P-P} = 16$  Hz). As the sample is warmed through coalescence, the new peak due to the exchanging tertiary phosphines appears and sharpens at a position closer to the low-temperature position of uncoordinated than to that of coordinated tertiary phosphine. Indeed, the ratio of the distances at the high-temperature limit position to coordinated *versus* uncoordinated tertiary phosphine at the low-temperature limit is approximately 5:3, respectively. The spectra clearly show that this difference is not due to any linear chemical shift dependency on temperature (due to viscosity or other effects not associated with the fluxional behavior). The position of the tertiary phosphine resonance at the high-temperature limit implies that the tertiary phosphines have, on average, more uncoordinated than coordinated character, which may be attributed to an equilibrium between seven- and eight-coordinate species. Line shape analysis<sup>6</sup> allows estimation of  $\Delta G^\ddagger$  ( $49 \pm 3$  kJ mol<sup>-1</sup>). That the exchange process is intramolecular is confirmed by addition of the

(6) According to the method described by Crabtree in: Crabtree, R. H. *The Organometallic Chemistry of the Transition Metals*; Wiley: New York, 1988; pp 220-222.

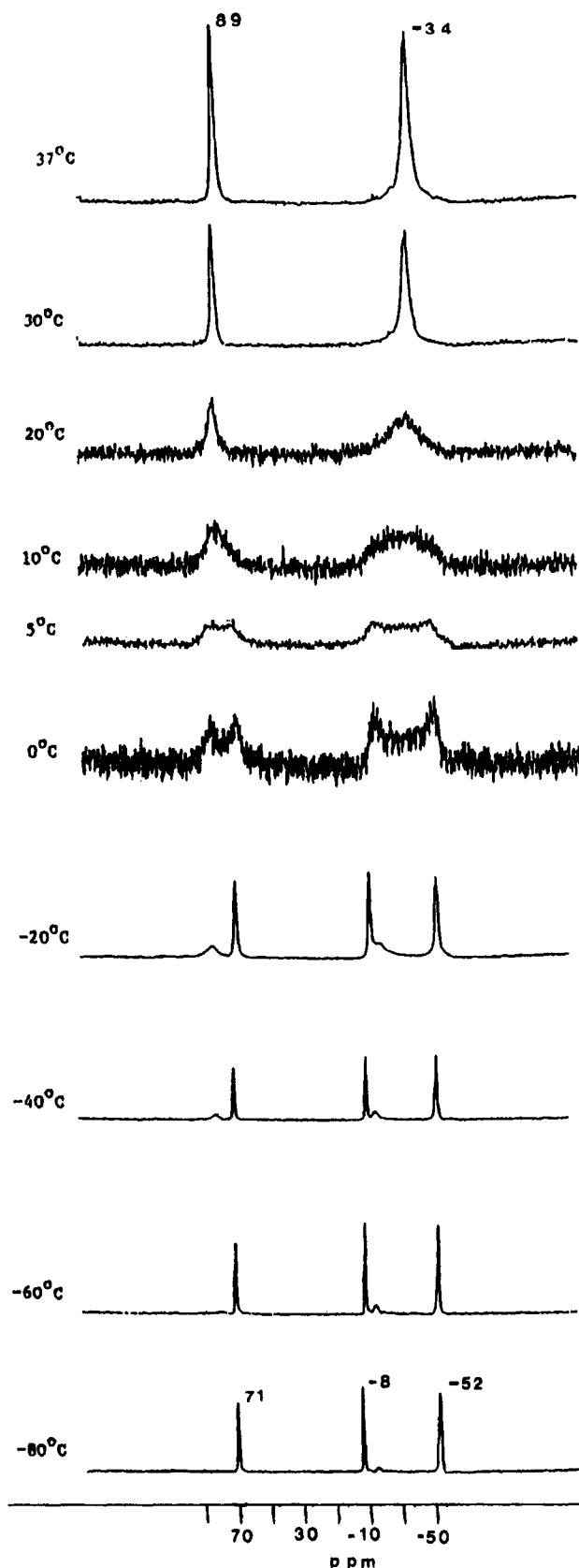


**Figure 2.** Variable-temperature  $^{31}\text{P}$  NMR spectra of  $\text{Th}\{\text{P}(\text{CH}_2\text{CH}_2\text{PMe}_2)_2\}_4$  (chemical shifts are in  $\delta$  (ppm)).

free secondary phosphine, HPPP, to the NMR sample.<sup>7</sup> Sharp resonances which are readily assigned to free HPPP<sup>3d</sup> ( $\delta_{\text{P tertiary}} -49.6$  ppm,  $\delta_{\text{P secondary}} -58.6$  ppm) are

(7) Variable-temperature  $^{13}\text{P}\{^1\text{H}\}$  NMR spectra for this experiment are presented in Figure 1 of the supporting information.

observed at all temperatures and are not involved in the fluxional process in **2**. At the low-temperature limit, the resonances assigned to pendant  $\text{PMe}_2$  functions in **2** are almost coincident with those of the tertiary phosphines in free HPPP, as would be expected.

In the hafnium dialkylphosphido  $\text{Cp}_2\text{Hf}\{\text{P}(\text{Cy})_2\}_2$ ,<sup>8</sup> two broad resonances at  $\delta$  270 and  $-15.3$  ppm, a difference of 285 ppm for two identical phosphido functions bonded to the same metal, were observed at the low-temperature limit ( $-126$  °C) in the  $^{31}\text{P}\{^1\text{H}\}$  NMR spectrum. These resonances were assigned to the planar and pyramidal phosphides, respectively, and the variable-temperature behavior was very reasonably interpreted as a rapid  $\sigma$  (pyramidal phosphorus)  $\leftrightarrow$   $\pi$  (planar phosphorus) interconversion at temperatures above  $-100$  °C, under which conditions a singlet is observed in an averaged position. In **2**, the position of the phosphido phosphorus signal is in a region similar to those observed for zirconium PPP complexes and the related hafnium complex above at ambient temperature; we have not observed coalescence of the phosphido resonance in **2** down to  $-80$  °C, where any planar  $\leftrightarrow$  pyramidal interchange would still be expected to be fast on the NMR time scale. However, this resonance shifts by some 18 ppm to lower field as the sample warms through coalescence, due to tertiary phosphine exchange, and is consistent with the phosphide becoming more  $\pi$  bonding in nature. This supposition is reasonable, since the loss of a  $\sigma$ -donating tertiary phosphine function from the coordination sphere of the thorium center results in the metal becoming more electron deficient and also allows more freedom for the phosphides to attain the planar geometry required in order to maximize  $\pi$  bonding.

The behavior of **2** is then consistent with a dissociative exchange of tertiary phosphines. This type of fluxionality, *i.e.* exchange of uncoordinated for coordinated tertiary phosphine, has not been observed in other transition-metal systems with this ligand,<sup>3c-e</sup> these other complexes are also relatively unreactive. The availability of an incipient coordination site within **2** is of particular interest and no doubt accounts for the unusual reactivity of the complex (*vide infra*).

**Structural Comparisons.** The X-ray single-crystal structure of **1** (Figure 1) shows that **1** and **2** are isostructural<sup>4</sup> with eight-coordinate uranium bonded to four tertiary phosphines and four phosphido phosphorus atoms. Bond lengths, angles, and atomic fractional coordinates are in Tables 1–3, respectively. There are several interesting features to note, since the complex allows a direct comparison of actinide–tertiary phosphine *vs* actinide–secondary dialkylphosphido bonding. The average  $\text{U}-\text{P}_{\text{phosphino}}$  bond length is considerably longer than the average  $\text{U}-\text{P}_{\text{phosphido}}$  bond length (averages 2.993(2) and 2.778(2) Å, respectively), as is to be expected.<sup>9</sup> In  $\text{Cp}_2\text{Hf}(\text{PEt}_2)_2$ , X-ray single-crystal diffraction studies showed that the two  $\text{M}-\text{P}$  bond lengths differ by 0.194(1) Å and that the phosphorus atom making the closer metal contact is planar.<sup>8</sup> These observations were interpreted as an increase in the degree of  $\pi$  bonding in one phosphido function relative to the other, and this behavior highlights the potential

(8) Baker, R. T.; Whitney, J. F.; Wreford, S. S. *Organometallics* **1983**, *2*, 1049.

(9) Domaille, P. J.; Foxman, B. M.; McNeese, T. J.; Wreford, S. S. *J. Am. Chem. Soc.* **1980**, *102*, 4114.

**Table 1. Selected Bond Lengths (Å) for  $U\{P(CH_2CH_2PMe_2)_2\}_4$** 

U(1)–P(2)	2.756(2)	P(5)–C(12)	1.854(7)
U(1)–P(11)	2.761(2)	P(6)–C(15)	1.797(9)
U(1)–P(5)	2.790(2)	P(6)–C(16)	1.837(9)
U(1)–P(8)	2.806(2)	P(6)–C(14)	1.843(6)
U(1)–P(7)	2.976(2)	P(7)–C(18)	1.818(7)
U(1)–P(10)	2.980(2)	P(7)–C(17)	1.820(7)
U(1)–P(1)	2.989(2)	P(7)–C(19)	1.841(7)
U(1)–P(4)	3.019(2)	P(8)–C(20)	1.838(7)
P(1)–C(1)	1.831(7)	P(8)–C(21)	1.859(6)
P(1)–C(2)	1.832(7)	P(9)–C(24B)	1.57(2)
P(1)–C(3)	1.834(7)	P(9)–C(24A)	1.81(2)
P(2)–C(4)	1.847(8)	P(9)–C(23B)	1.85(2)
P(2)–C(5)	1.850(7)	P(9)–C(22)	1.852(8)
P(3)–C(8B)	1.36(2)	P(9)–C(23A)	1.879(14)
P(3)–C(7)	1.61(2)	P(10)–C(25)	1.808(7)
P(3)–C(8A)	1.888(13)	P(10)–C(26)	1.825(8)
P(3)–C(6)	1.902(8)	P(10)–C(27)	1.830(7)
P(4)–C(9)	1.790(8)	P(11)–C(29)	1.858(6)
P(4)–C(11)	1.816(7)	P(11)–C(28)	1.867(7)
P(4)–C(10B)	1.84(2)	P(12)–C(32)	1.806(10)
P(4)–C(10A)	1.877(14)	P(12)–C(31)	1.817(9)
P(5)–C(13)	1.851(6)	P(12)–C(30)	1.842(6)

**Table 2. Selected Bond Angles (deg) for  $U\{P(CH_2CH_2PMe_2)_2\}_4$** 

P(2)–U(1)–P(11)	139.35(6)	C(9)–P(4)–C(11)	103.7(4)
P(2)–U(1)–P(5)	117.78(6)	C(9)–P(4)–C(10B)	86.3(9)
P(11)–U(1)–P(5)	73.08(5)	C(11)–P(4)–C(10B)	112.0(8)
P(2)–U(1)–P(8)	73.30(6)	C(9)–P(4)–C(10A)	102.7(6)
P(11)–U(1)–P(8)	122.75(6)	C(11)–P(4)–C(10A)	97.4(6)
P(5)–U(1)–P(8)	143.81(6)	C(9)–P(4)–U(1)	118.0(3)
P(2)–U(1)–P(7)	134.66(5)	C(11)–P(4)–U(1)	107.9(3)
P(11)–U(1)–P(7)	78.62(6)	C(10B)–P(4)–U(1)	125.8(7)
P(5)–U(1)–P(7)	93.07(6)	C(10A)–P(4)–U(1)	123.7(4)
P(8)–U(1)–P(7)	62.93(5)	C(13)–P(5)–C(12)	98.6(3)
P(2)–U(1)–P(10)	85.64(6)	C(13)–P(5)–U(1)	132.2(2)
P(11)–U(1)–P(10)	63.68(5)	C(12)–P(5)–U(1)	120.8(2)
P(5)–U(1)–P(10)	131.87(6)	C(15)–P(6)–C(16)	98.4(5)
P(8)–U(1)–P(10)	80.76(7)	C(15)–P(6)–C(14)	99.7(3)
P(7)–U(1)–P(10)	98.00(6)	C(16)–P(6)–C(14)	98.5(4)
P(2)–U(1)–P(1)	62.38(5)	C(18)–P(7)–C(17)	101.1(4)
P(11)–U(1)–P(1)	86.93(6)	C(18)–P(7)–C(19)	103.3(4)
P(5)–U(1)–P(1)	73.80(6)	C(17)–P(7)–C(19)	99.7(3)
P(8)–U(1)–P(1)	133.81(5)	C(18)–P(7)–U(1)	119.9(3)
P(7)–U(1)–P(1)	162.90(5)	C(17)–P(7)–U(1)	115.8(3)
P(10)–U(1)–P(1)	83.50(7)	C(19)–P(7)–U(1)	114.3(3)
P(2)–U(1)–P(4)	83.86(6)	C(20)–P(8)–C(21)	100.7(3)
P(11)–U(1)–P(4)	130.74(5)	C(20)–P(8)–U(1)	124.0(2)
P(5)–U(1)–P(4)	63.51(6)	C(21)–P(8)–U(1)	131.4(3)
P(8)–U(1)–P(4)	85.29(7)	C(24B)–P(9)–C(23B)	65.7(9)
P(7)–U(1)–P(4)	81.50(6)	C(24B)–P(9)–C(22)	70.4(6)
P(10)–U(1)–P(4)	164.48(4)	C(24A)–P(9)–C(22)	101.3(6)
P(1)–U(1)–P(4)	101.58(7)	C(23B)–P(9)–C(22)	99.8(6)
C(1)–P(1)–C(2)	100.5(4)	C(24A)–P(9)–C(23A)	109.6(7)
C(1)–P(1)–C(3)	99.9(4)	C(22)–P(9)–C(23A)	99.2(5)
C(2)–P(1)–C(3)	101.4(4)	C(25)–P(10)–C(26)	100.0(4)
C(1)–P(1)–U(1)	117.6(3)	C(25)–P(10)–C(27)	100.0(3)
C(2)–P(1)–U(1)	121.2(3)	C(26)–P(10)–C(27)	103.2(4)
C(3)–P(1)–U(1)	112.9(2)	C(25)–P(10)–U(1)	115.5(3)
C(4)–P(2)–C(5)	99.2(4)	C(26)–P(10)–U(1)	121.5(3)
C(4)–P(2)–U(1)	125.0(2)	C(27)–P(10)–U(1)	113.6(2)
C(5)–P(2)–U(1)	135.7(3)	C(29)–P(11)–C(28)	101.2(3)
C(8B)–P(3)–C(7)	134.9(11)	C(29)–P(11)–U(1)	134.5(2)
C(7)–P(3)–C(8A)	87.7(9)	C(28)–P(11)–U(1)	124.3(2)
C(8B)–P(3)–C(6)	130.2(10)	C(32)–P(12)–C(31)	98.6(5)
C(7)–P(3)–C(6)	91.4(6)	C(32)–P(12)–C(30)	100.0(4)
C(8A)–P(3)–C(6)	94.4(5)	C(31)–P(12)–C(30)	101.7(4)

electronic versatility of these ligands. Two of the phosphides in **1** are essentially planar, and two tend toward planarity.<sup>10</sup> By comparison with related transition-metal systems, it is reasonable to suggest that the planar phosphido phosphorus atoms are acting as  $\pi$

**Table 3. Atomic Coordinates and Equivalent Isotropic Displacement Parameters<sup>a</sup> ( $\text{Å}^2 \times 10^3$ ) for  $U\{P(CH_2CH_2PMe_2)_2\}_4$  (1)**

	x	y	z	U(eq)
U(1)	819(1)	1957(1)	2496(1)	34(1)
P(1)	2783(2)	2720(2)	3108(1)	48(1)
P(2)	586(2)	1807(2)	3595(1)	49(1)
P(3)	–2412(5)	2303(4)	4948(2)	137(2)
P(4)	–1783(2)	4503(2)	2461(1)	48(1)
P(5)	887(2)	4407(2)	1916(1)	52(1)
P(6)	3489(2)	6527(2)	983(1)	62(1)
P(7)	–713(2)	1469(2)	1611(1)	46(1)
P(8)	–891(2)	471(2)	2790(1)	47(1)
P(9)	–1766(3)	–1808(3)	4330(1)	90(1)
P(10)	2965(2)	–887(2)	2741(1)	44(1)
P(11)	2836(2)	1210(2)	1754(1)	43(1)
P(12)	3271(3)	2014(2)	–57(1)	69(1)
C(1)	2177(9)	4474(7)	3280(3)	70(2)
C(2)	4478(7)	2567(9)	2853(4)	75(2)
C(3)	3257(8)	1704(8)	3783(3)	65(2)
C(4)	1942(9)	1733(9)	4073(3)	72(2)
C(5)	–705(9)	1617(8)	4080(3)	70(2)
C(6)	–1164(9)	2675(10)	4446(4)	78(2)
C(7)	–2886(14)	3834(14)	5108(11)	313(17)
C(8A)	–3928(12)	3001(11)	4447(5)	60
C(8B)	–2968(24)	1310(23)	4989(10)	60
C(9)	–2966(9)	4533(9)	2987(5)	110(4)
C(10A)	–2957(15)	5323(14)	1846(6)	60
C(10B)	–3278(24)	5000(23)	1991(10)	60
C(11)	–1290(9)	5959(8)	2524(4)	80(3)
C(12)	–349(9)	6115(7)	2043(4)	85(3)
C(13)	2331(7)	4933(6)	1682(3)	48(2)
C(14)	2048(7)	5949(6)	1151(3)	53(2)
C(15)	4707(9)	4980(9)	777(4)	83(3)
C(16)	2843(11)	7515(10)	313(4)	94(3)
C(17)	138(8)	–147(7)	1348(3)	64(2)
C(18)	–1203(10)	2704(8)	992(3)	75(2)
C(19)	–2341(7)	1272(8)	1809(3)	61(2)
C(20)	–2041(7)	192(7)	2314(3)	55(2)
C(21)	–737(7)	–944(7)	3355(3)	58(2)
C(22)	–2091(8)	–840(8)	3637(3)	66(2)
C(23A)	–3598(15)	–1395(16)	4533(6)	60
C(24A)	–1033(17)	–3578(15)	4202(7)	60
C(23B)	–3417(20)	–2066(22)	4429(8)	60
C(24B)	–2051(16)	–2709(14)	3938(6)	60
C(25)	2631(8)	–2207(6)	2448(3)	59(2)
C(26)	3436(10)	–1768(8)	3432(3)	79(3)
C(27)	4629(7)	–1044(7)	2455(3)	58(2)
C(28)	4439(7)	–382(7)	1867(3)	56(2)
C(29)	3060(8)	1970(6)	1059(3)	53(2)
C(30)	2952(8)	1194(7)	606(3)	53(2)
C(31)	2873(11)	995(9)	–506(4)	91(3)
C(32)	1699(12)	3529(9)	–168(4)	109(4)

<sup>a</sup> U(eq) is defined as one-third of the trace of the orthogonalized  $U_{ij}$  tensor.

donors. This view is supported by comparisons with other systems in which planar *vs* pyramidal phosphorus atoms can be directly compared, as in the hafnium example above and in  $Zr_2Cl_3(PPP)_3$ ,<sup>3c</sup> where the terminal Zr–P<sub>phosphido</sub> bond is 0.237(3) Å shorter than the average Zr–P<sub>phosphino</sub> bond length. In the only example of a PPP complex where the phosphido phosphorus is pyramidal (*i.e.* Co(PPP)(PPP)<sub>2</sub>),<sup>3e</sup> PPP<sub>2</sub> = (Me<sub>2</sub>PCH<sub>2</sub>–CH<sub>2</sub>)<sub>2</sub>P–P(CH<sub>2</sub>CH<sub>2</sub>PMe<sub>2</sub>)<sub>2</sub>, where electronic saturation at Co precludes  $\pi$  donation from the phosphide to Co, the Co–P<sub>phosphido</sub> bond is longer than the (average) Co–P<sub>phosphino</sub> bond length (by approximately 0.14 Å). In the only other structurally characterized actinide phosphide (Cp<sub>2</sub>Th{P(Cy)<sub>2</sub>})<sub>2</sub><sup>1</sup> the phosphorus atoms are planar. In **1**, the degree of distortion from planarity is significant for P<sub>5</sub> and P<sub>8</sub> and may well be structurally imposed. In this case, dissociation of a tertiary phosphine would presumably help to alleviate this influence and allow the phosphido phosphorus atoms to attain a more

(10) Sums of angles (in degrees) around the phosphido phosphorus atoms: P(2), 359.9; P(5), 351.8; P(8), 356.1; P(11), 360.0.

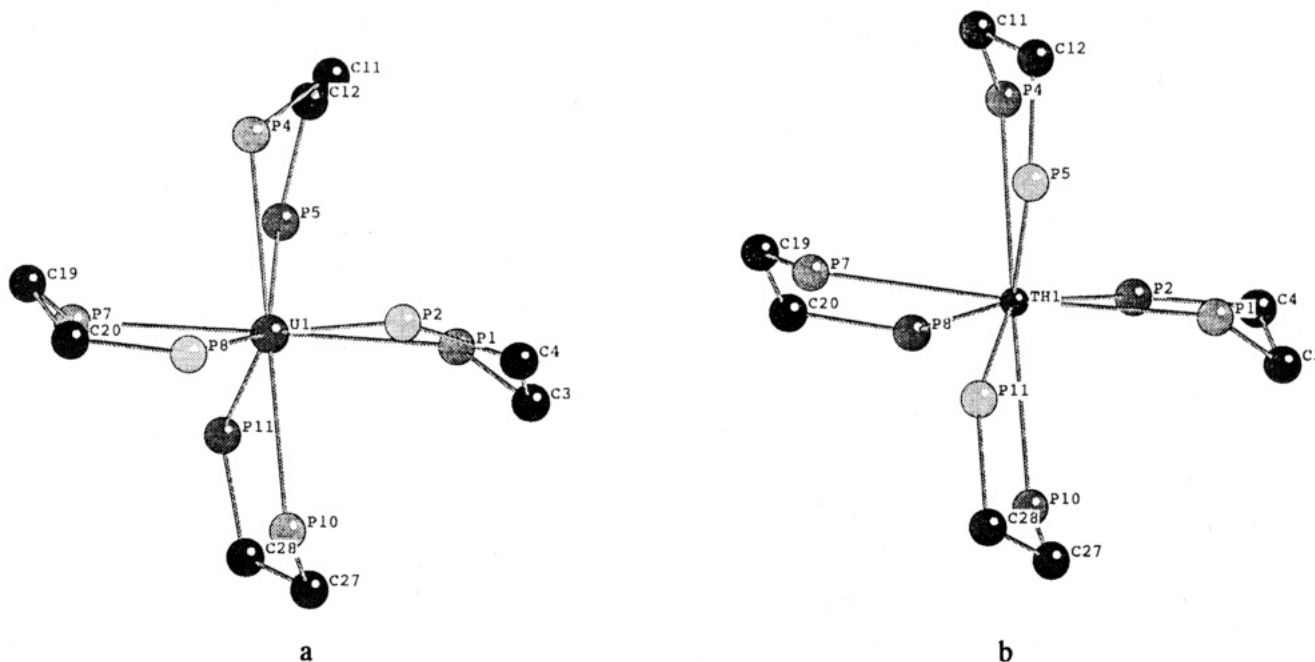


**Figure 3.** Inner coordination sphere and chelate conformations of  $M\{P(CH_2CH_2PMe_2)_2\}_4$  complexes (**1** and **2b**): (a) chelate conformation of **1** (the view is identical for the isostructural **2**); (b) chelate conformation for **2b**.

**Table 4.** Shape Parameters for  $M\{P(CH_2CH_2PMe_2)_2\}_4$  Complexes

polyhedron	$\delta'$ angle (deg)	$\phi$ angle (deg) <sup>a</sup>	structural data source (ref)
$D_{2d}$ dodecahedron	29.5, 29.5, 29.5, 29.5	0	14
$C_{2v}$ bicapped trigonal prism	0.0, 21.8, 48.2, 48.2	14.1	14
$D_{4d}$ antiprism	0.0, 0.0, 52.4, 52.4	24.5	14
U(PPP) <sub>4</sub> <sup>b</sup> ( <b>1</b> )	22.9, 24.8, 29.1, 43.2	11.5, 20.4	this work
Th(PPP) <sub>4</sub> , form a ( <b>2</b> )	23.8, 24.3, 29.1, 39.6	11.1, 28.7	4
Th(PPP) <sub>4</sub> , form b ( <b>2b</b> )	24.1, 27.9, 33.4, 38.4	15.3; 17.5	24

<sup>a</sup> Since triangulated dodecahedra have two interlocking trapezoidal planes whose corners are defined by pairs of A and B sites, the  $\phi$  angles for both these planes have been calculated. <sup>b</sup> PPP =  $^-P(CH_2CH_2PMe_2)_2$ .

rigorously planar geometry, as is implied by the NMR data. This feature may also indicate that the phosphido phosphorus atoms have the ability to achieve differing degrees of  $\pi$  bonding in these complexes.

The average uranium–phosphine bond length (2.993(2) Å) is significantly shorter than other reported uranium–phosphine bond lengths; e.g., the average U–P distance in  $U(OPh)_4(dmpe)_2$  is 3.104(6) Å<sup>11</sup> ( $dmpe = 1,2$ -bis(dimethylphosphino)ethane). It is not clear whether this difference is due to the relative bulk of the phenoxide functions preventing a closer approach of the  $dmpe$  ligand in the latter or the chelates containing the relatively short U–P<sub>phosphido</sub> bonds shortening the U–P<sub>phosphino</sub> bonds in the former. The chelate backbone from the phosphido phosphorus (P(5)) to the associated tertiary phosphine (P(4)) adopts a different conformation from the other three (Figure 3). P(5) is the phosphido that exhibits the greatest distortion from planarity, and the associated tertiary phosphine (P(4)) has a significantly longer metal–ligand interaction than the other three phosphines.

The thorium analogue can be crystallized from light petroleum ether as a mixture of two dimorphs (**2** and **2b**); both have been structurally characterized, and for the sake of the following comparisons, the numbering schemes of **1**, **2**, and **2b** are consistent. The coordination geometry of **2** is indistinguishable from that of **1** (Figure 1), as the two compounds are isostructural; a representation of the structures is shown in Scheme 1. Thus, all three compounds conform to  $MA_4B_4$  polyhedra, this

behavior having precedent in uranium and thorium complexes of the chelating ditertiary phosphine  $dmpe$ . The general structural features of **2** and **2b** are similar to those of **1** insofar as the Th–P<sub>phosphido</sub> bonds are consistently shorter than the Th–P<sub>phosphino</sub> bonds by approximately 0.2 Å (respective averages 2.895(5) and 3.075(5) Å for **2** and 2.883(2) and 3.095(2) Å for **2b**), and all phosphido phosphorus atoms tend toward planarity. In both thorium compounds, the average Th–P<sub>phosphido</sub> bond length is similar to that observed in  $Cp_2Th\{P(Cy)_2\}_2$  (2.87(2) Å)<sup>1</sup> and the average Th–P<sub>phosphino</sub> bond length (3.095(2) Å) is slightly shorter than that observed in  $(PhCH_2)_4Th(dmpe)$  (3.155(10) Å) (Ph =  $C_6H_5$ ).<sup>12</sup>

In the three tetraphosphides **1**, **2**, and **2b**, the coordination geometry around the metal atoms is difficult to identify by inspection of structural diagrams. A more accurate description of the  $MA_4B_4$  eight-coordinate structures may be obtained by analysis of the shape parameters  $\delta'$  and  $\phi$  defined by Porai-Koshits<sup>13</sup> and Muetterties<sup>14</sup> with the relatively longer bonds to the tertiary phosphines on the A sites and the phosphides in the B sites. These parameters for the three tetraphosphides are collected in Table 4. In all

(11) Edwards, P. G.; Andersen, R. A.; Zalkin, A. *J. Am. Chem. Soc.* **1981**, *103*, 7792.

(12) Edwards, P. G.; Andersen, R. A.; Zalkin, A. *Organometallics* **1984**, *3*, 293.

(13) Porai-Koshits, M. A.; Aslanov, L. A. *Zh. Strukt. Khim.* **1972**, *13*, 266.

(14) Muetterties, E. L.; Guggenberger, L. J. *J. Am. Chem. Soc.* **1974**, *96*, 1748.



**Table 5. Comparison of Metal–Ligand Bond Lengths (Å) in M{P(CH<sub>2</sub>CH<sub>2</sub>PMe<sub>2</sub>)<sub>2</sub>}<sub>4</sub> Complexes (1, 1b, and 2)**

	M = U (1)	M = Th, form a (1)	M = Th, form b (1b)
	Phosphides		
P(2)	2.756(2)	2.828(6)	2.886(1)
P(5)	2.790(2)	2.882(5)	2.901(2)
P(8)	2.806(2)	2.884(5)	2.883(2)
P(11)	2.761(2)	2.843(5)	2.862(1)
	Phosphines		
P(1)	2.989(2)	3.070(6)	3.097(2)
P(4)	3.019(2)	3.100(5)	3.085(1)
P(7)	2.976(2)	3.069(6)	3.105(2)
P(10)	2.989(2)	3.062(5)	3.094(2)

three compounds, the  $\delta'$  angles clearly indicate that the structures most closely conform to triangulated dodecahedra; the  $\phi$  angles, however, deviate considerably from the idealized value ( $0^\circ$ ) for a  $D_{2d}$  dodecahedron and indicate distortion from dodecahedral geometry toward either bicapped-trigonal-prismatic or square-antiprismatic geometry. Since two of the  $\delta'$  angles for an idealized square antiprism are zero, the structures are probably best described as distorted from dodecahedral toward bicapped trigonal prismatic, for which the smaller  $\phi$  angles for the actinide phosphides agree quite closely. By visual inspection, the inner coordination environments of the molecules appear to most readily fit a distorted trigonal prism capped by the phosphido atoms P(2) and P(5) with P(1), P(10), and P(11) forming one face and P(4), P(7), and P(8) forming the other of the two triangular faces of the prism. These planes are rotated with respect to each other away from idealized geometry and have a dihedral angle of  $8.5^\circ$ . The distortion is almost certainly caused by the constraints within the chelate rings preventing P(1) and P(4) from obtaining idealized positions. **2** and **2b** can be considered as conformational isomers, since in **2b** one of the chelate rings (the chelate from P(4) to P(5)) is puckered in an opposite direction from that in **2**. This is the major structural difference between the dimorphs and is more clearly shown in Figure 3a. In **1** and **2** the chelates described by P(10) to P(11) and P(4) to P(5) lie *syn* across the thorium atom, whereas in **2b** they lie *anti*.

The metal–ligand bond lengths (Table 5) are consistently shorter in the uranium compound than in the thorium compounds, indicating that the effective ionic radius of uranium is  $0.08 \text{ \AA}$  smaller than that of thorium in these complexes.<sup>15</sup>

**Th[CO{P(CH<sub>2</sub>CH<sub>2</sub>PMe<sub>2</sub>)<sub>2</sub>]<sub>2</sub>]<sub>2</sub> (3) and Th<sup>13</sup>CO{P(CH<sub>2</sub>CH<sub>2</sub>PMe<sub>2</sub>)<sub>2</sub>]<sub>2</sub> (4).** In the presence of CO<sub>2</sub>, NO<sub>2</sub>, CS<sub>2</sub>, H<sub>2</sub>, and CH<sub>3</sub>CN, **2** reacts to give intractable or otherwise unidentified products. However, the interaction of **2** with CO in hydrocarbons generates deep red solutions from which **3** can be isolated from light petroleum ether solutions in good yield. Microanalysis confirms the stoichiometry Th[CO{P(CH<sub>2</sub>CH<sub>2</sub>PMe<sub>2</sub>)<sub>2</sub>]<sub>2</sub>.

Upon reaction with CO, the resonances attributed to the phosphido phosphorus atoms in the <sup>31</sup>P{<sup>1</sup>H} NMR spectrum of **2** disappear. New resonances at higher field values accompany the formation of **3**, which only shows signals in regions commonly attributed to coordinated and uncoordinated tertiary phosphines (Figure

4a). The spectrum consists of a doublet of triplets ( $\delta$  2.9 ppm), an apparent quartet ( $\delta$  -16.4 ppm), a doublet ( $\delta$  -22.6 ppm), two poorly resolved doublets ( $\delta$  -23.3 and  $\delta$  -23.8 ppm), and two doublets at  $\delta$  -51 and -52.1 ppm. The resonances are integrated as 2:2:2:1:1:2:2, respectively, and therefore numerically account for all phosphorus atoms originally present in **2**. The last two resonances are readily assigned to uncoordinated tertiary phosphorus. Since the low-field signal is removed *ca.* 80 ppm upfield from the phosphido signals in **2**, it appears that CO insertion has occurred into all of the actinide–phosphide bonds, which would be expected to generate resonances in the region commonly assigned to tertiary phosphines. Two high-field resonances ( $\delta$  2.9 and -22.6 ppm) are assigned to the four new tertiary phosphines generated by the insertion of CO, with the former tentatively attributed to the two coordinated (CO) phosphines and the latter to the uncoordinated (CO) phosphines.

The <sup>31</sup>P{<sup>1</sup>H} NMR spectrum of the <sup>13</sup>C-enriched compound **4** (Figure 4b) enables assignment of the resonances. The resonance at  $\delta$  2.9 ppm becomes a complex symmetrical multiplet of at least 14 lines (separation of the outer lines 42 Hz), and the doublet at  $\delta$  -22.6 ppm becomes a doublet of doublets ( $J_{P-C} = 68 \text{ Hz}$ ). The spectrum of **4** clearly indicates that CO has inserted into two metal–phosphide bonds, since two different chemical shifts arise due to phosphorus atoms directly bonded to carbon (of CO). In order to account for the number of resonances, it also appears that the phosphorus atoms bonded to the inserted CO are at least pairwise equivalent; this in turn implies that two CO molecules have inserted. Since two PPP ligands appear to be bound (*via* the central phosphorus) to each carbon atom from CO, the difference in chemical shifts suggests that one phosphorus is coordinated to thorium and one is not, the latter being assigned to the higher field resonance ( $\delta$  -22.6 ppm) since it is in a region normally expected for similar higher alkyl tertiary phosphines (e.g. in HP(CH<sub>2</sub>CH<sub>2</sub>PEt<sub>2</sub>)<sub>2</sub>,  $\delta$ [P(tertiary)] -21.1 ppm).<sup>3d</sup> Unfortunately, there are no known similar compounds for comparison. The resonances at  $\delta$  -16.4, -23.3, and -23.8 ppm are assigned to the coordinated PMe<sub>2</sub> tertiary phosphines. The room-temperature spectrum also differs from that of **2** in that the resonances are sharp. When the temperature is lowered, the spectrum does not vary; however, at higher temperature a new broad signal appears at  $\delta$  -11 ppm, together with a universal loss of coupling information. This is attributed to coordinated tertiary phosphine and suggests that some exchange process(es) between coordinated and uncoordinated tertiary phosphines are occurring at elevated temperature.

The <sup>1</sup>H NMR spectrum of **3** consists of five doublets between  $\delta$  0.9 and 1.4 ppm with relative intensities 1:1:1:1:1. In addition there is a multiplet (of relative intensity 3) assigned to coincident methyl resonances centered at  $\delta$  0.98 ppm and broad multiplets attributed to methylene backbone protons. Since the <sup>31</sup>P{<sup>1</sup>H} NMR spectra indicate the tertiary PMe<sub>2</sub> functions are pairwise chemically equivalent between the two ligand systems, this must be true for the methyl protons. In view of this, the multiplicity of the methyl resonances in the proton NMR implies that they are diastereotopic, as is the case in the solid-state structure.

(15) The effective crystal radius of eight coordinate thorium is  $1.19 \text{ \AA}$ , compared with  $1.14 \text{ \AA}$  for uranium: Shannon, R. D. *Acta Crystallogr., Sect. A* **1976**, *32*, 751.

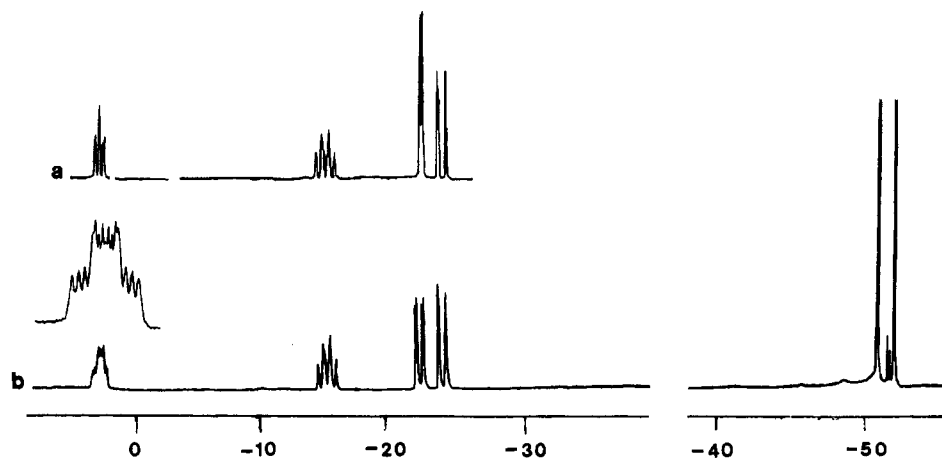


**Figure 4.**  $^{31}\text{P}$  NMR spectra of  $\text{Th}\{\text{CO}[\text{P}(\text{CH}_2\text{CH}_2\text{PMe}_2)_2]_2\}_2$  (**3**) (chemical shifts in  $\delta$  (ppm)): (a) natural-abundance  $^{13}\text{C}$ ; (b) isotopically enriched  $^{13}\text{C}$  with the low-field resonance expanded (inset). The resonances due to noncoordinated tertiary phosphine functions appear as in (a).

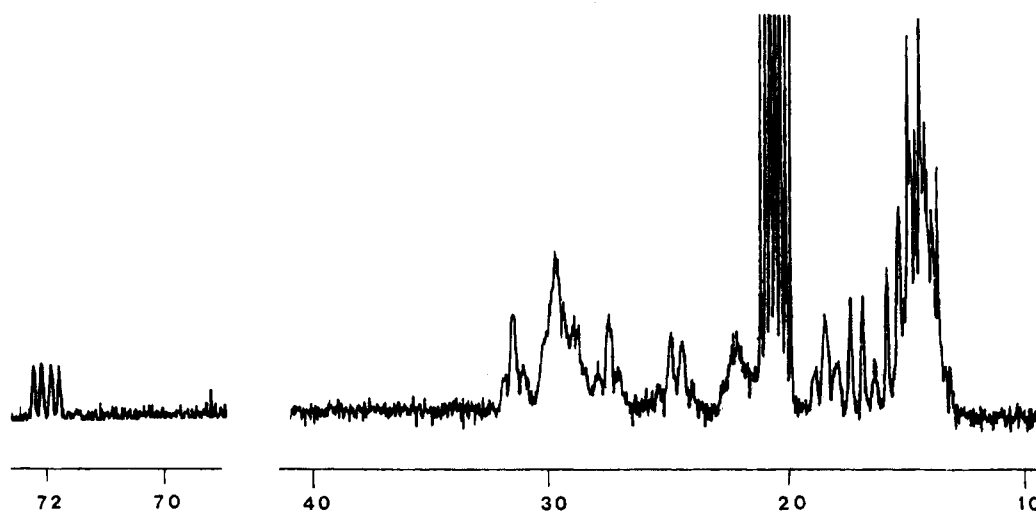


**Figure 5.**  $^{13}\text{C}$  NMR spectrum of  $\text{Th}\{\text{CO}[\text{P}(\text{CH}_2\text{CH}_2\text{PMe}_2)_2]_2\}_2$  (**3**) (chemical shifts in  $\delta$  (ppm)).

The  $^1\text{H}$  NMR spectrum of **4** is similar to that of **3** except that further coupling information ( $J_{\text{C-H}}$ ) is observed in the resonances due to the phosphine methyl protons.

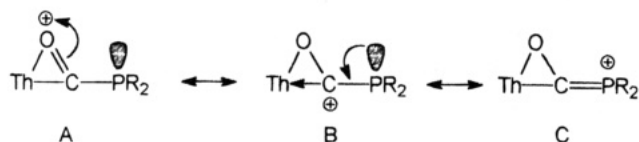
The  $^{13}\text{C}\{^1\text{H}\}$  NMR spectrum of **3** is complex in the aliphatic region, more so than for **2**. Resonances attributed to tertiary phosphine methyl carbons and to methylene backbone carbons are identified. A new resonance appears as a doublet of overlapping doublets at  $\delta$  72 ppm, where the separation of the outer lines is 110 Hz with each doublet having a different coupling constant ( $^1J_{\text{C-P}}$  is 68 and 42 Hz). It is only this resonance that is enhanced in the spectrum of the  $^{13}\text{C}$ -enriched analogue **4**, confirming its origin as the carbon from CO. The larger coupling constant is confirmed by and can be assigned to the noncoordinated phosphorus by comparison with the  $^{31}\text{P}\{^1\text{H}\}$  NMR spectrum, indicating that the C-P bond to the coordinated phosphorus is relatively weaker. This signal is in a position more commonly associated with secondary alcohol than carbonyl functions, *cf.*  $\delta$  3.3 ppm in the structurally characterized phosphidoacyl species  $(\eta^5\text{-Cp}^*)\text{HfCl}_2(\eta^2\text{-COP}^t\text{Bu}_2)$ .<sup>16</sup> The IR spectrum is consistent with a C-O

single bond ( $\nu_{\text{C-O}}$  1065  $\text{cm}^{-1}$ ). This assignment is confirmed by the expected isotopic shift in **4** ( $\nu_{^{13}\text{C-O}}$  1035  $\text{cm}^{-1}$ ).

The X-ray crystal structure of **3**<sup>5</sup> reveals that the solid-state and solution structures are consistent; this is represented in Scheme 1. The complex contains ten-coordinate thorium bonded to two dianionic (formally for Th(IV)) diphospha secondary alkoxy ligands generated as a result of CO insertion into M-PR<sub>2</sub> bonds. Only two CO molecules have inserted, each into two metal-phosphide bonds with reduction of the bond order in CO from 3 to 1. Each P<sub>2</sub>CO unit in the newly generated  $\{(\text{Me}_2\text{PCH}_2\text{CH}_2)_2\text{P}\}_2\text{CO}^{2-}$  ligand is  $\eta^3$ -bonded to the thorium atom (the hapticity assigned to the molecule refers to the linkages local to the inserted CO group) with one of the phosphorus atoms coordinated to thorium; for each phosphorus atom, one pendant dimethylphosphino donor remains coordinated to thorium and the other is uncoordinated. The bond lengths in each ThP<sub>2</sub>CO are consistent with Th-O, Th-C, and C-O single bonds. **3** represents only the second structurally characterized example of an insertion reaction into a M-P bond<sup>16,17</sup> (the first for an f-block metal), a new

(16) Roddick, D. M.; Santarsiero, B. D.; Bercaw, J. E. *J. Am. Chem. Soc.* **1985**, *107*, 4670.

(17) Smith, W. H.; Taylor, N. J.; Carty, A. J. *J. Chem. Soc., Chem. Commun.* **1976**, 896.

**Scheme 2. Possible Intermediates and Canonical Forms Involved in CO Insertion**


mode of insertion for CO, and the first instance of a  $\eta^3$  insertion product.

The reaction can be thought of as being driven by the coordination of oxygen to oxophilic thorium following dissociation of a tertiary phosphine, thereby generating an incipient coordination site in solution. The resultant polarizing of the C–O bond renders it susceptible to intramolecular nucleophilic attack by coordinated phosphine. Substantial contribution from the canonical form B is implicated (Scheme 2). It is noteworthy that the contribution from form C is not sufficient to prevent this process.

Surprisingly, **1** does not appear to react with CO even under more forcing conditions (70 °C, 7 atm). This relative lack of reactivity is under investigation.

**HC(OH){P(CH<sub>2</sub>CH<sub>2</sub>PMe<sub>2</sub>)<sub>2</sub>}<sub>2</sub> (**5**).** The addition of water to **3** generates a white precipitate (ThO<sub>2</sub>) and the grease **5**. In the <sup>31</sup>P{<sup>1</sup>H} NMR spectrum of **5**, a triplet of equally intense lines at  $\delta$  -50.7 ppm and a symmetrical five-line multiplet at  $\delta$  -17.1 ppm are observed in a ratio of 2:1, respectively. The former is assigned to the terminal tertiary phosphines on the basis of chemical shift and the latter to the internal phosphorus atoms. The spectrum can be explained in terms of an AA'BB'MM' spin system, indicating pairwise magnetically inequivalent dimethylphosphino groups A and B, where the only significant coupling constants are <sup>2</sup>J<sub>MM'</sub>, <sup>3</sup>J<sub>AM</sub>, <sup>3</sup>J<sub>BM</sub>, <sup>3</sup>J<sub>AM'</sub>, and <sup>3</sup>J<sub>BM'</sub>. The internal phosphorus atoms (MM') are then each coupled to one A and one B phosphorus atom and to each other, giving rise to a five-line pattern. The terminal phosphines are inequivalent, since rotation of the P–C bonds to the central prochiral carbon cannot generate equivalent positions for the tertiary phosphines on each side of the molecule. The spectrum can be satisfactorily simulated on this basis.<sup>18</sup> This suggests that the apparent quartet at  $\delta$  -16.4 ppm in the <sup>31</sup>P{<sup>1</sup>H} NMR spectrum of **4** may be assigned to the CO-bonded phosphorus atom that is not coordinated to thorium, the chemical shift difference being 0.7 ppm between coordinated and protonated ligand.

In the <sup>1</sup>H NMR spectrum the methyl protons are centered at  $\delta$  0.88 ppm as two doublets coupled to the pairwise inequivalent phosphorus atoms. The pattern is similar to that observed for the uncoordinated phosphorus methyl protons in **3**. The methylene backbone protons are located at  $\delta$  1.6 ppm as a broad multiplet. Doublets integrated as one proton appear at  $\delta$  4.28 and 2.16 ppm and are assigned to the unique carbon CH and OH protons, respectively. The latter resonance disappears after exchange with D<sub>2</sub>O, and the former collapses to a singlet (Figure 6).

In the <sup>13</sup>C{<sup>1</sup>H} NMR spectrum, the unique carbon is located at  $\delta$  72 ppm as a binomial triplet coupled to two equivalent phosphines (<sup>1</sup>J<sub>P–C</sub> = 29 Hz).

(18) NMR simulation using Bruker "PANIC" software generates the following parameters:  $\delta$ (A) -51.0 ppm,  $\delta$ (B) -50.9 ppm,  $\delta$ (M) -17.0 ppm, <sup>2</sup>J<sub>MM'</sub> = 5 Hz, <sup>3</sup>J<sub>AM</sub> = <sup>3</sup>J<sub>BM</sub> = <sup>3</sup>J<sub>AM'</sub> = <sup>3</sup>J<sub>BM'</sub> = 12 Hz, and all <sup>3</sup>J = 0.

The IR spectrum of **5** has a strong absorption assignable to  $\nu_{\text{O–H}}$  (3208 cm<sup>-1</sup>) and an absence of bands in the region associated with carbonyl  $\nu_{\text{C=O}}$  absorptions. The remainder of the spectrum is very similar to that of HPPP except for the absence of  $\nu_{\text{P–H}}$ . The mass spectrum of **5** (CI) does not show a molecular ion; the highest mass peak observed is at 238 amu, which is explained by the cleavage of HP(CH<sub>2</sub>CH<sub>2</sub>PMe<sub>2</sub>)<sub>2</sub> (mass 210 amu) from **5** (mass 448 amu), generating the aldehyde (Me<sub>2</sub>PCH<sub>2</sub>CH<sub>2</sub>)<sub>2</sub>PCHO of mass 238 amu.

**Reactions of Th{P(CH<sub>2</sub>CH<sub>2</sub>PMe<sub>2</sub>)<sub>2</sub>}<sub>4</sub> with Phenols and Alkenes.** The tetraphosphide **2** reacts with a number of reagents with acidic protons. From these reactions, no well-characterized materials were isolated pure in the solid state, although solution spectroscopy gives valuable insight into the reactivity of **2**.

The reaction with 2 mol equiv of phenol (per **2**) in hydrocarbons results in new resonances assigned to coordinated PPP in the <sup>31</sup>P{<sup>1</sup>H} NMR. The room-temperature <sup>31</sup>P{<sup>1</sup>H} NMR spectrum of the reaction product appears as a binomial five-line multiplet ( $\delta$  34.5 ppm) and a symmetrical triplet ( $\delta$  -10.96 ppm). This is consistent with an A<sub>4</sub>M<sub>2</sub> spin system, suggesting that the product is a monomeric bis(phenoxy) complex with two tridentate PPP ligands per thorium. The stoichiometry of the reaction was confirmed by titration of a solution of **2** with a solution of phenol. The elimination of HPPP continues until 2 mol equiv of phenol (per Th) is added. The further addition of phenol produces no more HPPP relative to the product (PhO)<sub>2</sub>Th(PPP)<sub>2</sub>.

Compound **2** also reacts with alkenes in hydrocarbons to generate colorless complexes that contain new resonances assigned to coordinated PPP in the <sup>31</sup>P{<sup>1</sup>H} NMR. The <sup>31</sup>P{<sup>1</sup>H} NMR spectrum of the product isolated from the reaction of ethene with **2** contains two broad resonances at  $\delta$  31 ppm ( $\nu_{1/2}$  = 274 Hz) and  $\delta$  4 ppm ( $\nu_{1/2}$  = 630 Hz) of equal intensity. Signals attributed to HPPP are also observed ( $\delta$  -52 and -60 ppm). Similar spectra are observed from the products of the reactions of **2** with propene or 2-methylbut-2-ene. No reaction occurs when 2,3-dimethylbut-2-ene is employed under similar conditions. This indicates that a vinylic proton  $\alpha$  to the carbon–carbon double bond is required for the reaction to proceed. Monitoring the reactions by <sup>31</sup>P{<sup>1</sup>H} NMR spectroscopy indicates that the reaction stoichiometry of alkene:**2** was 2:1, since the generation of HPPP, the other reaction product, was at a maximum when 2 mol equiv of alkene was added.

## Experimental Section

All manipulations were performed using a Vacuum Atmospheres HF-43-2 or Halco Engineering 140 FF glovebox, or using standard Schlenk techniques under purified nitrogen. Unless otherwise stated, all solvents were refluxed under nitrogen over sodium/benzophenone and were distilled immediately prior to use. Toluene was refluxed under nitrogen over sodium and was distilled immediately prior to use. Light petroleum ether had bp 40–60 °C. Perdeuterio solvents were refluxed over sodium (8 h) and distilled therefrom under nitrogen. ThCl<sub>4</sub> was dried by refluxing with thionyl chloride (5 d), washed repeatedly with dichloromethane (freshly distilled under nitrogen from CaH<sub>2</sub>) until the filtrate was colorless, and dried in vacuo (0.05 mmHg, 150 °C, 8 h). UCl<sub>4</sub> was prepared by following a modified literature route;<sup>19</sup> HPPP and LiPPP were prepared as previously described.<sup>3d</sup> KPPP was prepared by refluxing HPPP with excess K in light petroleum

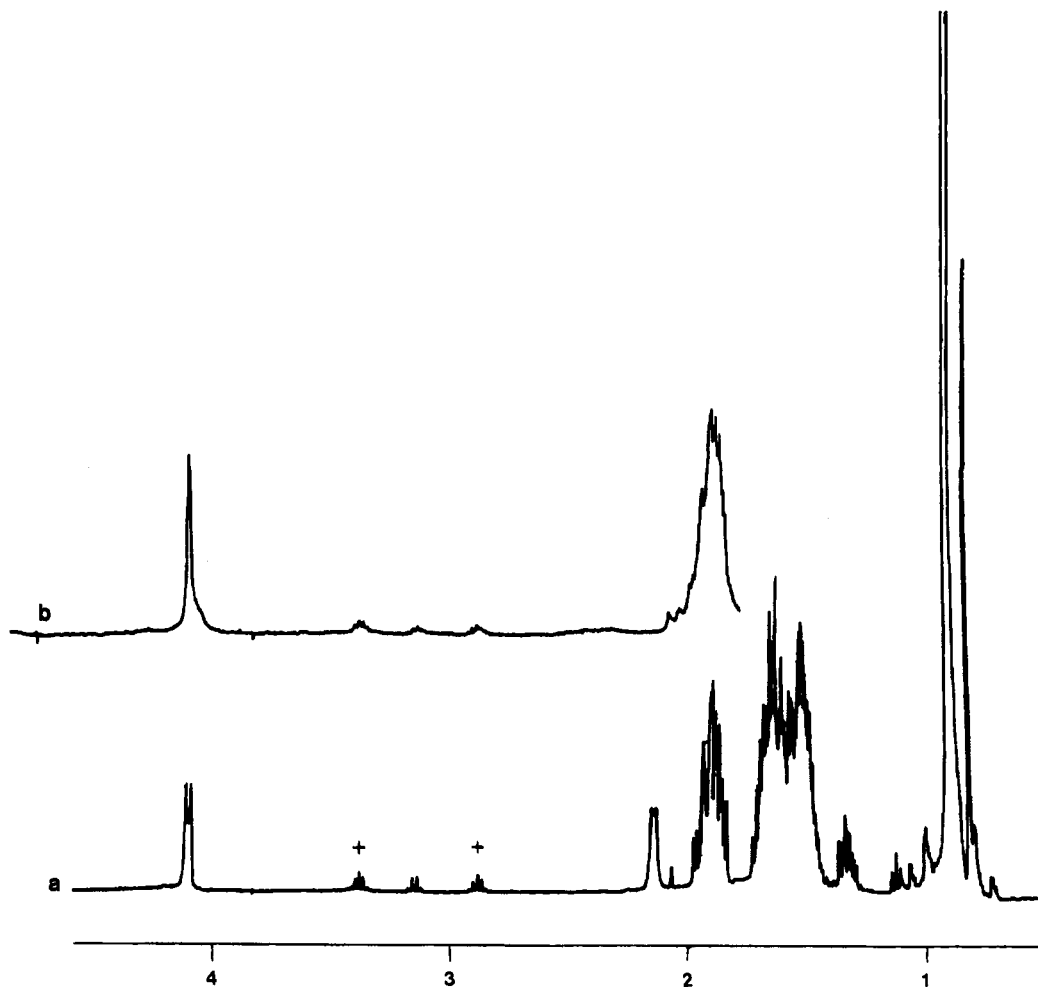


**Figure 6.**  $^1\text{H}$  NMR spectra of  $\text{HC(OH)(P(CH}_2\text{CH}_2\text{PMe}_2)_2)_2$  (**5**) (chemical shifts in  $\delta$  (ppm)): (a) before addition of  $\text{D}_2\text{O}$  (the peaks marked + are the P–H resonances of the HPPP impurity); (b) after addition of  $\text{D}_2\text{O}$ .

ether, followed by filtration, extraction into boiling toluene, and crystallization. Microanalyses were performed by CHN Analysis Ltd., Leicester, U.K. NMR data are quoted in ppm, and spectra were recorded on a JEOL FX90Q operating at 36.23 MHz (variable-temperature  $^{31}\text{P}$  and  $^1\text{H}$  in  $\text{C}_7\text{D}_8$ ,  $^{13}\text{C}\{^1\text{H}\}$  in  $\text{C}_6\text{D}_6$ ) or a Bruker WM360 operating at 145 MHz.  $^{31}\text{P}$  NMR spectra were referenced externally to 85%  $\text{H}_3\text{PO}_4$  ( $\delta$  0 ppm);  $^{13}\text{C}$  and  $^1\text{H}$  NMR spectra were referenced to solvent carbons ( $\text{C}_7\text{D}_8$ ,  $\delta$  137.5 ppm) or residual protons ( $\text{C}_7\text{D}_8$ ,  $\delta$  7.19 ppm). Melting points were recorded in sealed glass capillaries and are uncorrected.

**U{P(CH<sub>2</sub>CH<sub>2</sub>PMe<sub>2</sub>)<sub>2</sub>}<sub>4</sub> (1).** To a stirred solution of  $\text{UCl}_4$  in THF (0.14 M, 3  $\text{cm}^3$ ) at  $-80^\circ\text{C}$  was added KPPP in 4:1 toluene/THF (0.1687 M, 10  $\text{cm}^3$ ). The mixture was stirred for 8 h, during which time the color changed from green to black. The volatile materials were removed *in vacuo*. The resultant black solid was washed with cold ( $-80^\circ\text{C}$ ) light petroleum ether ( $2 \times 10 \text{ cm}^3$ ) and extracted with light petroleum ether ( $2 \times 50 \text{ cm}^3$ ). The black supernatant was evaporated to *ca.* 20  $\text{cm}^3$  and cooled ( $-20^\circ\text{C}$ ) for 4 h. **1** crystallizes as small black prisms in good yield (0.33 g, 72%). Mp:  $132\text{--}136^\circ\text{C}$ . Anal. Found: C, 34.7; H, 7.24. Calcd for  $\text{UP}_{12}\text{C}_{36}\text{H}_{80}$ : C, 35.8; H, 7.50. IR (Nujol,  $\text{cm}^{-1}$ ): 1305 (m), 1145 (s), 1121 (w), 1080 (m), 969 (m), 937 (w), 921 (m), 890 (w), 805 (m), 771 (m), 333 (w).  $^1\text{H}$  NMR ( $\delta_{\text{H}}$ , 89.5 MHz,  $\text{C}_7\text{D}_8$ ,  $20^\circ\text{C}$ ):  $-24.21$  (8H, s,  $\text{PCH}_2$ ),  $-25.87$  (8H, s,  $\text{PCH}_2$ ),  $-27.54$  (24H, br  $\nu_{1/2} = 45$  Hz,  $\text{PCH}_3$ ).

**Th{P(CH<sub>2</sub>CH<sub>2</sub>PMe<sub>2</sub>)<sub>2</sub>}<sub>4</sub> (2).**  $\text{ThCl}_4$  (0.54 g, 1.44 mmol) was suspended with stirring in diethyl ether (100  $\text{cm}^3$ ) and cooled

until frozen.  $\text{LiP(CH}_2\text{CH}_2\text{PMe}_2)_2$  (1.25 g, 5.78 mmol) in THF (10  $\text{cm}^3$ ) was then added. Initially a yellow color developed, which became red at  $-20^\circ\text{C}$ . The suspension was warmed to room temperature and then stirred (12 h). The solvents were removed *in vacuo*, and the red residue was washed with cold ( $-80^\circ\text{C}$ ) light petroleum ether ( $2 \times 10 \text{ cm}^3$ ). Extraction with light petroleum ether ( $3 \times 30 \text{ cm}^3$ ) and concentration of the filtrate to *ca.* 20  $\text{cm}^3$  followed by cooling ( $-20^\circ\text{C}$ , 1 h) afforded red crystals of **2** (0.66 g, 43%). Mp:  $132\text{--}136^\circ\text{C}$ . Anal. Found: C, 34.7; H, 7.90. Calcd for  $\text{ThP}_{12}\text{C}_{36}\text{H}_{80}$ : C, 35.9; H, 7.50. IR (Nujol,  $\text{cm}^{-1}$ ): 2023 (w), 1290 (m), 1145 (s), 1115 (w), 1075 (m), 960 (m), 930 (m), 910 (m), 885 (w), 805 (m), 765 (m), 330 (w).  $^{31}\text{P}\{^1\text{H}\}$  NMR ( $\delta_{\text{P}}$ , 36.23 MHz,  $\text{C}_7\text{D}_8$ ): 83 (br,  $\nu_{1/2} = 100$  Hz),  $-34$  (br,  $\nu_{1/2} = 400$  Hz).  $^1\text{H}$  NMR ( $\delta_{\text{H}}$ , 89.5 MHz,  $\text{C}_7\text{D}_8$ ): 2.6 (2H, br,  $\nu_{1/2} = 30$  Hz), 1.8 (2H, br,  $\nu_{1/2} = 30$  Hz), 1.3 (6H, s).

**Th[CO{P(CH<sub>2</sub>CH<sub>2</sub>PMe<sub>2</sub>)<sub>2</sub>]<sub>2</sub> (3).** A flask containing a solution of **2** (0.25 g, 0.23 mmol) in toluene (30  $\text{cm}^3$ ) was evacuated, filled with CO (to 5 psi above ambient pressure), and sealed. The solution was stirred at room temperature (8 h), during which time the color turned from red to purple. After removal of the volatile materials *in vacuo*, the residue was washed with cold ( $-80^\circ\text{C}$ ) light petroleum ether ( $2 \times 10 \text{ cm}^3$ ) and extracted with light petroleum ether ( $3 \times 30 \text{ cm}^3$ ). The purple supernatant was evaporated to *ca.* 15  $\text{cm}^3$  and cooled ( $-65^\circ\text{C}$ ) for 4 h. **3** crystallizes as red prisms in good yield (0.19 g, 73%). Mp:  $144\text{--}146^\circ\text{C}$ . Anal. Found: C, 35.9; H, 6.80. Calcd for  $\text{ThP}_{12}\text{C}_{38}\text{H}_{80}\text{O}_2$ : C, 36.3; H, 7.17. IR (Nujol,  $\text{cm}^{-1}$ ): 1305 (m), 1291 (w), 1280 (w), 1265 (m), 1210 (w), 1169 (m), 1155 (m), 1088 (s), 1063 (s), 969 (m), 937 (s), 921 (m), 890 (w), 844 (w), 805 (m), 771 (w), 670 (w), 523 (m).  $^{31}\text{P}\{^1\text{H}\}$  NMR

( $\delta_P$ , 145 MHz,  $C_6D_6$ ): 2.9 (2P, dt,  $J_{P-P} = 35$  and 14 Hz, respectively), -16.4 (2P, q,  $J_{P-P} = 35$  Hz), -22.6 (2P, d,  $J_{P-P} = 15$  Hz), -23.3 (1P, d,  $J_{P-P} = 6$  Hz), -23.8 (1P, d,  $J_{P-P} = 6$  Hz), -51.1 (2P, d,  $J_{P-P} = 15$  Hz), -52 (2P, d,  $J_{P-P} = 15$  Hz).  $^1H$  NMR ( $\delta_H$ , 360 MHz,  $C_6D_6$ ): 1.6 (16H, br m,  $\nu_{1/2} = 72$  Hz), 1.4 (3H, d,  $^2J_{P-H} = 3$  Hz), 1.13 (3H, d,  $^2J_{P-H} = 3$  Hz), 1.08 (3H, d,  $^2J_{P-H} = 3$  Hz), 1.03 (3H, d,  $^2J_{P-H} = 3$  Hz), 0.98 (3H, d,  $^2J_{P-H} = 3$  Hz), 0.94 (3H, d,  $^2J_{P-H} = 3$  Hz).

**Th**[ $^{13}CO\{P(CH_2CH_2PMe_2)_2\}_2$ ] (4). This procedure was identical with that for **3**, except for the use of enriched  $^{13}CO$  (in place of natural-abundance CO). For 0.35 g (0.33 mmol) of **2** in toluene (20 cm<sup>3</sup>), 30 cm<sup>3</sup> (1.3 mmol) of  $^{13}CO$  was used. **4** was crystallized as above. IR (Nujol, cm<sup>-1</sup>): 1305 (m, br), 1292 (m), 1278 (m), 1263 (m), 1209 (w), 1170 (m), 1155 (m), 1081 (s), 1035 (s), 967 (m), 937 (s), 921 (m), 892 (w), 846 (w), 807 (m), 771 (s), 669 (w), 523 (m).

**HC(OH)\{P(CH\_2CH\_2PMe\_2)\_2\}\_2** (**5**). Water (5 cm<sup>3</sup>) was added to a stirred solution of **3** (0.15 g, 0.14 mmol) in light petroleum ether (15 cm<sup>3</sup>), causing a pale yellow solution (organic phase) to develop. The organic phase was separated and dried (MgSO<sub>4</sub>, 2 h), following which the light petroleum ether was removed *in vacuo* to leave crude **5**. The deuterated analogue HC(OD)\{P(CH\_2CH\_2PMe\_2)\_2\}\_2 was prepared by H/D exchange by adding excess D<sub>2</sub>O to a sample of **5** in an NMR tube.

IR (liquid film, cm<sup>-1</sup>): 3208 (br), 2950 (s), 2920 (m), 2886 (s), 2801 (w), 1410 (s), 1280 (m), 1263 (m), 1248 (s), 1150 (s, br), 1081 (s, br), 1010 (s, br), 926 (s), 877 (w), 830 (w), 786 (s), 694 (s).  $^{31}P\{^1H\}$  NMR ( $\delta_P$ , 145 MHz,  $C_6D_6$ ): -17.1 (2P, m), -50.7 (4P, t).  $^1H$  NMR ( $\delta_H$ , 360 MHz,  $C_6D_6$ ): 4.28 (1H, d,  $J_{P-H} = 7$  Hz), 2.16 (1H, d,  $J_{P-H} = 7$  Hz), 1.60 (16H, br m,  $\nu_{1/2} = 94$  Hz), 0.88 (24H, dd,  $^2J_{P-H} = 2.4$  Hz).  $^{13}C\{^1H\}$  NMR ( $\delta_C$ , 90 MHz,  $C_6D_6$ ): 72 (1C, t,  $^1J_{P-C} = 29$  Hz). Other peaks are observed in the aliphatic region.

**Reactions of 2 with Phenols.** To a stirred solution of **2** (0.10 g, 0.09 mmol) in toluene (20 cm<sup>3</sup>) at -80 °C was added a solution of phenol in toluene (0.01 M, 18.7 cm<sup>3</sup>). The mixture was warmed to room temperature and stirred for 8 h. Removal of the volatile materials *in vacuo* and subsequent extraction of the residue with light petroleum ether (2 × 10 cm<sup>3</sup>) affords orange solutions from which orange crystals may be obtained. Reactions with substituted phenols were performed in a similar manner.  $^{31}P\{^1H\}$  NMR ( $\delta_P$ , 36.23 MHz,  $C_6D_6$ ): 34.5 (1P, m), -10.96 (2P, t).

**Reactions of 2 with Alkenes.** A flask containing a solution of **2** (0.10 g, 0.09 mmol) in toluene (20 cm<sup>3</sup>) was evacuated, filled with ethene (to 10 psi above ambient pressure), and sealed. The solution was stirred at room temperature for 8 h. After removal of the volatile materials *in vacuo*, the residue was extracted into light petroleum ether (2 × 15 cm<sup>3</sup>). Evaporation of the filtrate to ca. 5 cm<sup>3</sup> affords a purple material. Reactions with other alkenes were performed with the alkene being added as a 0.01 M solution to the reaction mixture *via* syringe.  $^{31}P\{^1H\}$  NMR ( $\delta_P$ , 36.23 MHz,  $C_6D_6$ ): 31 (br,  $\nu_{1/2} = 274$  Hz), 4 (br,  $\nu_{1/2} = 630$  Hz).

**X-ray Crystallography.** Crystals of **1** suitable for X-ray work were grown from petroleum ether and sealed under purified nitrogen in Lindemann capillaries.

**Crystal Data:** C<sub>32</sub>H<sub>80</sub>P<sub>12</sub>U,  $M_r = 1074.63$ , triclinic,  $a = 10.455(5)$  Å,  $b = 10.521(7)$  Å,  $c = 25.147(7)$  Å,  $\alpha = 81.43(3)^\circ$ ,  $\beta = 89.02(2)^\circ$ ,  $\gamma = 68.22(2)^\circ$ ,  $V = 2538(2)$  Å<sup>3</sup> (by least-squares refinement of diffractometer angles for 250 reflections within  $\theta = 2.22$ – $29.74^\circ$ ,  $\lambda = 0.71069$  Å), space group  $P\bar{1}$ ,  $Z = 2$ ,  $D_c =$

1.406 Mg m<sup>-3</sup>,  $F(000) = 1088$ ,  $\mu(Mo K\alpha) = 3.597$  mm<sup>-1</sup>, black air-sensitive prisms, crystal dimensions 0.20 × 0.15 × 0.08 mm<sup>3</sup>.

**Data Collection and Processing.**<sup>20</sup> Data collection was by a Delft Instruments FAST TV area detector diffractometer positioned at the window of a rotating anode generator using Mo K $\alpha$  radiation ( $\lambda = 0.71069$  Å). A total of 17 709 reflections were measured ( $2.22 \leq \theta \leq 29.74^\circ$ ; index ranges  $-14 \leq h \leq 14$ ;  $-11 \leq k \leq 13$ ;  $-33 \leq l \leq 25$ ), with two rejected for lying behind the backstop, giving rise to 11 664 unique reflections (merging  $R = 0.0378$ ).

**Structure Analysis and Refinement.** The structure was solved by direct methods (SHELX-S)<sup>21</sup> and refined by full-matrix least squares (SHELXL-93)<sup>22</sup> using all unique  $F_o^2$  data corrected for Lorentz and polarization factors. The non-hydrogen atoms were refined anisotropically. The hydrogen atoms were included in calculated positions with the  $U_{iso}$  values set at 1.2 times the  $U_{eq}$  values of the parent carbons. An empirical absorption correction was applied using DI-FABS<sup>23</sup> (minimum and maximum absorption correction factors were 0.869 and 1.284, respectively). The weighting scheme used was  $w = 1/\sigma^2(F_o)^2$ , which gave satisfactory agreement analyses. Final  $R1 = \Sigma(\Delta F)/\Sigma(F_o)$  and  $wR2 = \Sigma\{w(\Delta(F^2))^2\}/\Sigma\{w(F_o^2)^2\}^{1/2}$  values are 0.0563 and 0.1191, respectively, for 409 parameters and all 11 664 data ( $Q_{min}, Q_{max} = -0.99, 1.39$  e Å<sup>-3</sup>,  $(\Delta/\sigma)_{max} = -0.09$ ). The corresponding  $R$  indices for 6836 data with  $I > 2\sigma(I)$  are 0.0370 and 0.0930, respectively. Sources of scattering factors are given in ref 23. All calculations were performed on a 486DX2/66 personal computer. In the early difference maps and in subsequent refinement it became apparent that the terminal methyl groups (C(8), C(10), C(23), C(24)) exhibited positional disorder and could be satisfactorily modeled assuming two alternative atomic sites for these atoms with the following fractional occupancies: C(8A), 0.67; C(8B), 0.33; C(10A), 0.62; C(10B), 0.38; C(23A), 0.57; C(23B), 0.43; C(24A), 0.48; C(24B), 0.52.

**Acknowledgment.** We thank the SERC for studentships (J.S.P. and P.W.R.) and access to the mass spectrometry unit at University College Swansea. We are indebted to H. F. Lieberman and M. B. Hursthouse of this Department for help in the structural determination and S. J. Coles for help with calculating the shape parameters. We also thank A. Karaulov for MAP, an interactive molecular graphics program to aid in the crystal structure analysis of large molecules at atomic resolution (4000 atoms PC386-Pentium version 2.51, Jan 1994, Department of Chemistry, University of Wales, Cardiff CF1 3TB, U.K.).

**Supporting Information Available:** Tables giving anisotropic displacement parameters for the non-hydrogen atoms and hydrogen atom parameters for **1** and a figure giving variable-temperature  $^{31}P$  NMR spectra for **2** (4 pages). Ordering information is given on any current masthead page.

OM940719D

(21) Sheldrick, G. M. *Acta Crystallogr., Sect. A* **1990**, *46*, 467.

(22) Sheldrick, G. M. University of Gottingen, Gottingen, Germany, 1993.

(23) Walker, N. P. C.; Stuart, D. *Acta Crystallogr., Sect. A* **1983**, *39*, 158.

(24) Edwards, P. G.; et al. *Acta Crystallogr., Sect. C* **1995**, in press.

(20) Drake, S. R.; Hursthouse, M. B.; Malik, K. M. A.; Miller, S. A. *Inorg. Chem.* **1993**, *32*, 4653.

# Bifunctional Phosphines as Ligands and as Substrates: Synthesis of Iridium Hydrido, Carbonyl, Alkynyl, Vinyl, and Vinylidene Complexes from *i*-Pr<sub>2</sub>PCH<sub>2</sub>CH<sub>2</sub>X (X = OMe, NMe<sub>2</sub>), Including the X-ray Crystal Structure of an Unusual Cyclometalated Product<sup>†,1</sup>

Helmut Werner,\* Michael Schulz, and Bettina Windmüller

Institut für Anorganische Chemie der Universität Würzburg, Am Hubland,  
D-97074 Würzburg, Germany

Received February 9, 1995<sup>®</sup>

Treatment of [IrCl(C<sub>8</sub>H<sub>14</sub>)<sub>2</sub>]<sub>2</sub> (**5**) with *i*-Pr<sub>2</sub>PCH<sub>2</sub>CH<sub>2</sub>OMe (**6**) leads to the formation of the octahedral hydridoiridium(III) complex [IrHCl{κ<sup>2</sup>(C,P)-CH<sub>2</sub>OCH<sub>2</sub>CH<sub>2</sub>P*i*-Pr<sub>2</sub>{κ<sup>2</sup>(P,O)-*i*-Pr<sub>2</sub>PCH<sub>2</sub>CH<sub>2</sub>OMe}}] (**8**), which according to the X-ray structure analysis contains both a five- and a six-membered chelate ring. In contrast to **6**, the phosphinoamine *i*-Pr<sub>2</sub>PCH<sub>2</sub>CH<sub>2</sub>NMe<sub>2</sub> (**7**) reacts with **5** to give the expected square-planar iridium(I) compound *trans*-[IrCl{κ(P)-*i*-Pr<sub>2</sub>PCH<sub>2</sub>CH<sub>2</sub>NMe<sub>2</sub>}{κ<sup>2</sup>(P,N)-*i*-Pr<sub>2</sub>PCH<sub>2</sub>CH<sub>2</sub>NMe<sub>2</sub>}}] (**9**), which in solution at room temperature is nonfluxional on the NMR time scale. Reaction of **9** with CO yields four-coordinate *trans*-[IrCl(CO){κ(P)-*i*-Pr<sub>2</sub>PCH<sub>2</sub>CH<sub>2</sub>NMe<sub>2</sub>}<sub>2</sub>] (**10**), while on treatment of **9** with HCl in benzene the six-coordinate [IrHCl<sub>2</sub>{κ(P)-*i*-Pr<sub>2</sub>PCH<sub>2</sub>CH<sub>2</sub>NMe<sub>2</sub>}{κ<sup>2</sup>(P,N)-*i*-Pr<sub>2</sub>PCH<sub>2</sub>CH<sub>2</sub>NMe<sub>2</sub>}}] (**11**) is obtained. Compound **11** is also one of the products of the reaction of **9** with CH<sub>2</sub>Cl<sub>2</sub> which equally gives small quantities of the ionic bis(chelate) complex [IrCl<sub>2</sub>{κ<sup>2</sup>(C,P)-CH<sub>2</sub>NMe<sub>2</sub>CH<sub>2</sub>-CH<sub>2</sub>P*i*-Pr<sub>2</sub>}{κ<sup>2</sup>(P,N)-*i*-Pr<sub>2</sub>PCH<sub>2</sub>CH<sub>2</sub>NMe<sub>2</sub>}}]Cl (**12**). The chlorodihydrido and dichlorohydrido complexes [IrH(Cl)X{κ(P)-*i*-Pr<sub>2</sub>PCH<sub>2</sub>CH<sub>2</sub>OMe}{κ<sup>2</sup>(P,O)-*i*-Pr<sub>2</sub>PCH<sub>2</sub>CH<sub>2</sub>OMe}}] (**13**, X = H; **14**, X = Cl) are formed at room temperature almost instantaneously from **8** and H<sub>2</sub> or HCl, respectively. At 80 °C, the reaction of **8** (or **13**) with methyl acrylate and methyl vinyl ketone affords the hydrido(vinyl)iridium(III) derivatives [IrHCl{κ<sup>2</sup>(C,O)-CH=CHC(R)=O}{κ(P)-*i*-Pr<sub>2</sub>PCH<sub>2</sub>CH<sub>2</sub>OMe}}] (**15**, R = OMe; **16**, R = Me), whereas with HC≡CR the alkynyl(hydrido) compounds [IrH(C≡CR)Cl{κ(P)-*i*-Pr<sub>2</sub>PCH<sub>2</sub>CH<sub>2</sub>OMe}{κ<sup>2</sup>(P,O)-*i*-Pr<sub>2</sub>PCH<sub>2</sub>CH<sub>2</sub>OMe}}] (**17**, R = Ph; **18**, R = CO<sub>2</sub>Me) are obtained. Thermal or photochemical rearrangement of **17** and **18** leads to the formation of the isomeric vinylideneiridium(I) complexes *trans*-[IrCl(=C=CHR){κ(P)-*i*-Pr<sub>2</sub>PCH<sub>2</sub>CH<sub>2</sub>OMe}}] (**20**, **21**) in good yield. The octahedral alkynyl(vinyl) compound [IrCl(C≡CCO<sub>2</sub>Me)(CH=CHCO<sub>2</sub>Me){κ(P)-*i*-Pr<sub>2</sub>PCH<sub>2</sub>CH<sub>2</sub>OMe}{κ<sup>2</sup>(P,O)-*i*-Pr<sub>2</sub>PCH<sub>2</sub>CH<sub>2</sub>OMe}}] has been prepared from either **8** or **13** and excess HC≡CCO<sub>2</sub>Me. Chloride abstraction of **20** and **21** with AgSbF<sub>6</sub> affords the SbF<sub>6</sub> salts of the cationic complexes [Ir(=C=CHR){κ(P)-*i*-Pr<sub>2</sub>PCH<sub>2</sub>CH<sub>2</sub>OMe}{κ<sup>2</sup>(P,O)-*i*-Pr<sub>2</sub>PCH<sub>2</sub>CH<sub>2</sub>OMe}}]<sup>+</sup> (**22**, **23**), in which according to the X-ray structure analysis of **23** the vinylidene ligand and the methoxy unit are *trans* disposed.

## Introduction

We have recently shown that in contrast to P*i*-Pr<sub>3</sub> the related but potentially bidentate phosphine *i*-Pr<sub>2</sub>PCH<sub>2</sub>CH<sub>2</sub>OMe, which can form a strong and a weak bond to an electron-rich transition-metal center, behaves as a supporting ligand for the intramolecular conversion of a Ir(C<sub>2</sub>H<sub>4</sub>) to an isomeric IrH(CH=CH<sub>2</sub>) unit.<sup>2</sup> Whereas the equilibrium between the ethyleneiridium(I) complex **1** and the five-coordinate hydrido(vinyl)iridium(III) compound **2** lies mainly on the side of the olefin derivative, even in the presence of UV light, photolysis of the analogous starting material **3** in toluene proceeds rapidly and leads to the quantitative formation of the octahedral isomer **4** (Scheme 1).<sup>2</sup> The one-pot synthesis

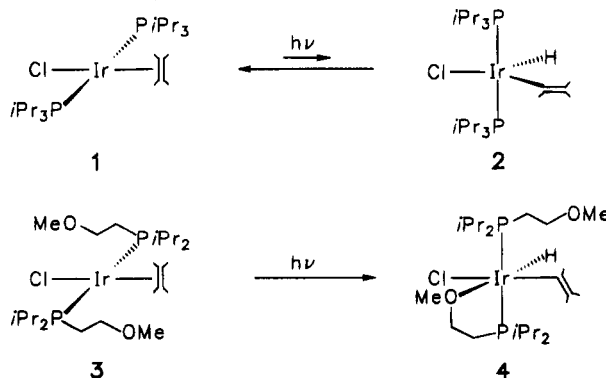
<sup>†</sup> Dedicated to Professor William C. Kaska on the occasion of his 60th birthday.

<sup>®</sup> Abstract published in *Advance ACS Abstracts*, July 1, 1995.

(1) (a) Studies on C–H Activation. 11. Part 10: Wecker, U.; Werner, H.; Peters, K.; von Schnering, H. G. *Chem. Ber.* **1994**, *127*, 1021–1029. (b) This work is part of the Ph.D. Thesis of M. Schulz, University of Würzburg, Würzburg, Germany, 1991.

(2) Schulz, M.; Werner, H. *Organometallics* **1992**, *11*, 2791–2795.

## Scheme 1

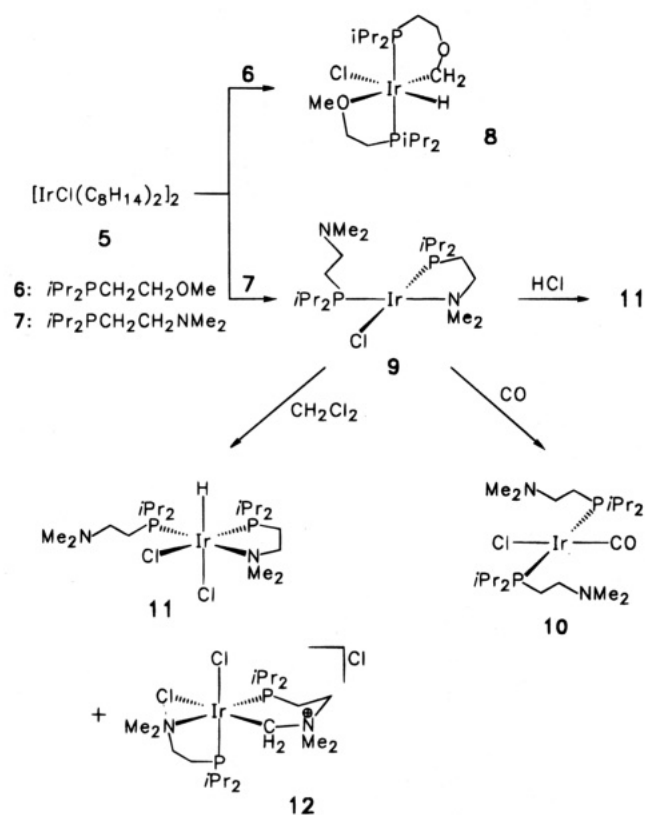


of **3** starts with the dimeric bis(cyclooctene)iridium compound [IrCl(C<sub>8</sub>H<sub>14</sub>)<sub>2</sub>]<sub>2</sub>, which reacts stepwise in an ether suspension at –50 °C with *i*-Pr<sub>2</sub>PCH<sub>2</sub>CH<sub>2</sub>OMe and C<sub>2</sub>H<sub>4</sub> to give the square-planar ethylene complex in excellent yield.

In this paper we report that, on treatment of [IrCl(C<sub>8</sub>H<sub>14</sub>)<sub>2</sub>]<sub>2</sub> with *i*-Pr<sub>2</sub>PCH<sub>2</sub>CH<sub>2</sub>OMe at room temperature



Scheme 2



in the absence of ethylene, a different reaction occurs, which leads via intramolecular C–H activation to a novel alkyl(hydrido)iridium(III) derivative. This compound reacts not only with  $\text{H}_2$  and HCl but also with terminal alkynes and activated olefins to yield a series of alkynyl(hydrido)-, alkynyl(vinyl)-, vinylidene-, and hydrido(vinyl)iridium complexes. Some preliminary results of this work have already been communicated.<sup>3</sup>

## Results and Discussion

**Reactions of  $[\text{IrCl}(\text{C}_8\text{H}_{14})_2]_2$  (5) with  $i\text{-Pr}_2\text{PCH}_2\text{CH}_2\text{OMe}$  (6) and  $i\text{-Pr}_2\text{PCH}_2\text{CH}_2\text{NMe}_2$  (7).** Treatment of a suspension of 5 in benzene with 4 equiv of the bifunctional phosphine 6 at room temperature results in a fairly rapid change of color from red-brown to yellow and, after chromatography on  $\text{Al}_2\text{O}_3$ , yields (88%) a pale yellow solid which is correctly analysed as  $[\text{IrCl}(\mathbf{6})_2]$ . However, in contrast to the corresponding rhodium complex  $[\text{RhCl}(\mathbf{6})_2]$ , which according to the X-ray structure analysis contains one *P*-monodentate and one chelating phosphine ligand,<sup>4</sup> the product from the reaction of 5 and 6 is not an analogous iridium(I) compound. This conclusion is supported not only by the significantly different properties (the rhodium complex  $[\text{RhCl}(\mathbf{6})_2]$  is thermally labile and highly air-sensitive, whereas compound 8 (see Scheme 2) can be handled for a short time in air) but more convincingly by the  $^1\text{H}$  NMR spectrum which displays a high-field signal at  $\delta$  –22.9 (doublet of doublets), typical for a metal-bonded

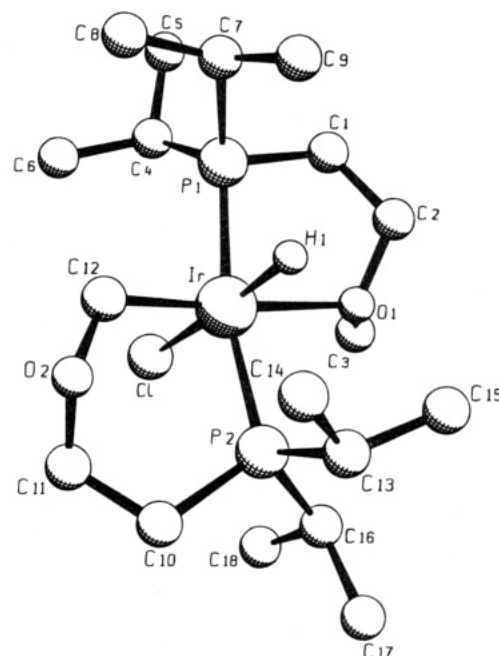


Figure 1. SCHAKAL drawing of complex 8.

Table 1. Selected Bond Distances and Angles with Esd's for Compound 8

Bond Distances (Å)			
Ir–P1	2.309(1)	Ir–H	1.77
Ir–P2	2.302(1)	O1–C2	1.444(6)
Ir–Cl	2.518(1)	O1–C3	1.430(7)
Ir–O1	2.339(4)	O2–C11	1.424(7)
Ir–C12	2.049(6)	O2–C12	1.425(7)
Bond Angles (deg)			
Cl–Ir–P1	92.07(2)	P2–Ir–O1	91.1(1)
Cl–Ir–P2	98.92(5)	P2–Ir–C12	91.5(2)
Cl–Ir–O1	90.6(1)	O1–Ir–C12	175.7(2)
Cl–Ir–C12	92.3(2)	Ir–O1–C2	106.9(3)
P1–Ir–P2	166.87(5)	Ir–O1–C3	121.5(3)
P1–Ir–O1	81.5(1)	Ir–C12–O2	120.2(4)
P1–Ir–C12	95.2(2)	C11–O2–C12	114.1(5)

hydrogen atom. Furthermore, all of the NMR spectra ( $^1\text{H}$ ,  $^{13}\text{C}$ ,  $^{31}\text{P}$ ) are not temperature-dependent, which would be expected if 8 were structurally related to  $[\text{RhCl}(\mathbf{6})_2]$ .

The straightforward assumption that compound 8 is an isomer of  $[\text{IrCl}(\mathbf{6})_2]$ , containing a hydride and a chelating  $i\text{-Pr}_2\text{PCH}_2\text{CH}_2\text{OCH}_2$  ligand instead of an intact  $i\text{-Pr}_2\text{PCH}_2\text{CH}_2\text{OMe}$  unit, has finally been confirmed by an X-ray structural investigation. As the SCHAKAL drawing (Figure 1) reveals, the iridium is coordinated in a somewhat distorted-octahedral fashion with the two phosphorus atoms in *trans* position. The bonding of the P–Ir–P axes (angle  $166.87(5)^\circ$ ) points to the direction of the smallest ligand (hydride) and probably originates from steric hindrance between the isopropyl units and the other groups in the basal plane as well as from the ring strain in the five- and six-membered chelate rings. The bond angles Cl–Ir–O1, Cl–Ir–C12, and Cl–Ir–P1 (see Table 1) are near to  $90^\circ$  and are thus in agreement with the octahedral geometry. The position of the metal-bonded hydride was taken from a difference-Fourier synthesis with all non-hydrogen atoms but could not be refined. The observed Ir–H bond length of 1.77 Å is similar to that found in other hydridoiridium(III) complexes.<sup>5</sup>

The distance between the metal and the carbon atom C12 (2.049(6) Å) is almost identical to that in the

(3) Schulz, M.; Werner, H. *Abstracts of Papers*, 29th International Conference in Inorganic Chemistry, University of Sussex, Brighton, U.K., 1991; P 74.

(4) Werner, H.; Hampp, A.; Peters, K.; Peters, E.-M.; Walz, L.; von Schnering, H.G. *Z. Naturforsch. B: Anorg. Chem., Org. Chem.* **1990**, *45*, 1548–1558.



vinyliridium compounds  $[\text{C}_5\text{Me}_5\text{IrH}(\text{CH}=\text{CH}_2)(\text{PMe}_3)]$  (2.054(4) Å)<sup>6</sup> and  $[\text{IrH}(\text{CH}=\text{CH}_2)\text{Cl}(\text{CO})(\text{Pi-Pr}_3)_2]$  (2.059(6) Å)<sup>2</sup> but somewhat longer than in the five-coordinate hydrido(phenyl) complex  $[\text{IrH}(\text{C}_6\text{H}_5)\text{Cl}(\text{Pi-Pr}_3)_2]$  (2.010(5) Å).<sup>7</sup> We note, however, that the bond length Ir–O1 (2.339(4) Å) is relatively long, which probably reflects the rather weak interaction between the CH<sub>3</sub>O oxygen and the metal center. The six-membered chelate ring containing the atoms C12 and O2 possesses a typical chair conformation with an Ir–P2 distance (2.302(1) Å) that is significantly shorter than in phosphine iridium complexes with *trans*-Ir(Pi-Pr<sub>3</sub>)<sub>2</sub> as a molecular unit.<sup>2,7,8</sup>

Regarding the structure of compound **8** in solution, we are convinced that the dominating species is the same as in the crystal. The supporting evidence for the proposed octahedral geometry (in benzene) includes the following: (1) the nonfluxionality of the molecule; (2) the nonequivalence of the two phosphorus atoms illustrated by the doublet-of-doublet splitting of the hydride signal in the <sup>1</sup>H and by the appearance of an AB pattern in the <sup>31</sup>P NMR; (3) the large P–P coupling between the two <sup>31</sup>P nuclei (349.5 Hz), which is most typical for *trans*-disposed phosphine ligands; and (4) the 2D-(H, C)-COSY spectrum of **8**, which allows correct assignment for the four <sup>13</sup>C NMR signals at δ 75.26, 67.66, 62.77, and 31.12 to the CH<sub>2</sub> and CH<sub>3</sub> carbon atoms of the ether-type units. The possibility that the metal center in **8** is five- and not six-coordinated (with the intact *i*-Pr<sub>2</sub>PCH<sub>2</sub>CH<sub>2</sub>OMe ligand being only *P*-bonded), as has been proposed by Dombek for the related cyclometalated species  $[\text{IrHCl}\{\kappa^2(\text{C},\text{P})\text{-CH}_2\text{-OCH}_2\text{PtBu}_2\}\{\kappa(\text{P})\text{-}t\text{Bu}_2\text{PCH}_2\text{OMe}\}]$ ,<sup>9</sup> can probably be excluded. In contrast to this complex, which is deep red, compound **8** is pale yellow like many other octahedral hydrido-iridium(III) derivatives.

The course of the reaction of **5** with the phosphino amine **7** is remarkably different to that of **5** with the phosphino ether **6**. From **5** and 4 equiv of **7** in benzene a yellow air-stable solid is obtained, which is correctly analysed as **9** (see Scheme 2). Since the <sup>31</sup>P NMR spectrum displays two well-separated doublets which show only a small P–P coupling of 17.6 Hz, we assume that **9** has a square-planar configuration with the two phosphorus atoms in *cis* position. However, in contrast to the analogous rhodium complex  $[\text{RhCl}(\text{6})_2]$  for which this geometry has been confirmed by X-ray analysis,<sup>4</sup> at room temperature compound **9** is nonfluxional on the NMR time scale. This is also substantiated by the appearance of two signals for the NCH<sub>3</sub> protons in the <sup>1</sup>H NMR spectrum, of which only one (at δ 2.62) shows P–H coupling.

While **9** is completely inert toward H<sub>2</sub> and ethylene, it reacts smoothly with CO in benzene at room temperature to give the square-planar monocarbonyl complex **10** in almost quantitative yield. According to the <sup>1</sup>H and <sup>31</sup>P NMR data, there is no doubt that the two

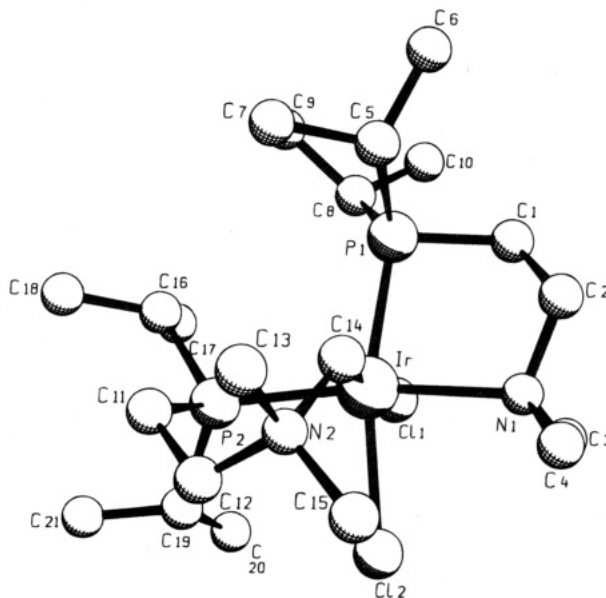


Figure 2. SCHAKAL drawing of complex **12**.

phosphinoamine ligands are equivalent and that the structure of compound **10** is very similar to that of *trans*- $[\text{IrCl}(\text{CO})(\text{Pi-Pr}_3)_2]$ .<sup>10</sup>

The reaction of **9** with HCl in benzene results in an oxidative addition and the formation of complex **11**. Like the starting material **9**, the dichloro(hydrido)iridium(III) derivative also possesses a rigid structure at room temperature with *cis*-disposed Pi-Pr<sub>2</sub> units. In agreement with this, the <sup>31</sup>P NMR spectrum displays two signals at δ 23.45 and –6.8 with a small P–P coupling (13.2 Hz) which, due to additional P–H coupling in off-resonance, appear as a doublet-of-doublets. The hydride signal in the <sup>1</sup>H NMR spectrum is equally a doublet-of-doublets, confirming the inequivalence of the phosphorus atoms.

Surprisingly, the octahedral dichloro(hydrido) complex **11** is also formed on treatment of **9** with dichloromethane. We made this serendipitous discovery in the course of our attempts to grow single crystals of **9** by diffusion of pentane into a saturated solution of the iridium(I) compound in CH<sub>2</sub>Cl<sub>2</sub>. With this procedure, a mixture of products is formed which contains **11** as the main component. When we stored the reaction mixture of **9** and CH<sub>2</sub>Cl<sub>2</sub>/pentane for a longer period of time, a small quantity of bright yellow crystals precipitated, which we investigated by X-ray crystallography. As Figure 2 reveals, the cationic complex **12** resembles compound **8** insofar as it also contains a five- and a six-membered chelate ring. In contrast to **8**, however, the two phosphorus atoms in **12** are *cis*-disposed, as are the two chloro ligands. The octahedral geometry around the metal center is considerably distorted, as is illustrated by the bond angles P1–Ir–Cl2 (165.34(6)°), P2–Ir–N1 (171.6(2)°), Cl1–Ir–Cl2 (173.8(2)°), and P1–Ir–P2 (103.26(7)°). The most remarkable feature, however, is the boat-type conformation of the Ir-containing six-membered ring, which could originate from the direction of the attack of the NMe<sub>2</sub> group of the nonchelated phosphinoamine ligand at the intermediately formed Ir–CH<sub>2</sub>Cl unit from the less hindered side of the molecule.

(5) (a) Bau, R.; Carroll, W. E.; Teller, R. G.; Koetzle, T. F. *J. Am. Chem. Soc.* **1977**, *99*, 3872–3874. (b) Garlaschelli, L.; Khan, S. I.; Bau, R.; Longoni, G.; Koetzle, T. F. *J. Am. Chem. Soc.* **1985**, *107*, 7212–7213.

(6) Stoutland, P. O.; Bergman, R. G. *J. Am. Chem. Soc.* **1988**, *110*, 5732–5744.

(7) Werner, H.; Höhn, A.; Dziallas, M. *Angew. Chem.* **1986**, *98*, 1112–1114; *Angew. Chem., Int. Ed. Engl.* **1986**, *25*, 1090–1092.

(8) Werner, H.; Dirnberger, T.; Schulz, M.; Ertel, T. S.; Hörner, W.; Bertagnolli, H. Submitted for publication.

(9) Dombek, B. D. *J. Organomet. Chem.* **1979**, *169*, 315–325.

(10) (a) Strohmeier, W.; Onada, T. Z. *Naturforsch. B: Anorg. Chem., Org. Chem.* **1968**, *23*, 1377–1379. (b) Werner, H.; Höhn, A. Z. *Naturforsch. B: Anorg. Chem., Org. Chem.* **1984**, *39*, 1505–1509.

**Table 2. Selected Bond Distances and Angles with Esd's for Compound 12**

Bond Distances (Å)			
Ir–Cl1	2.488(2)	Ir–C14	2.036(6)
Ir–Cl2	2.420(2)	N1–C2	1.504(9)
Ir–N1	2.264(6)	N2–C12	1.490(9)
Ir–P1	2.310(2)	N2–C14	1.527(9)
Ir–P2	2.305(2)		
Bond Angles (deg)			
Cl1–Ir–Cl2	88.63(6)	P1–Ir–P2	103.26(7)
Cl1–Ir–P1	82.23(6)	P1–Ir–N1	85.2(2)
Cl1–Ir–P2	92.67(6)	P1–Ir–C14	91.6(2)
Cl1–Ir–N1	88.6(2)	P2–Ir–N1	171.6(2)
Cl1–Ir–C14	173.8(2)	P2–Ir–C14	88.2(2)
Cl2–Ir–P1	165.34(6)	N1–Ir–C14	91.4(2)
Cl2–Ir–P2	88.53(6)	Ir–N1–C2	108.8(4)
Cl2–Ir–N1	88.6(2)	Ir–C14–N2	124.7(5)
Cl2–Ir–C14	97.5(2)	C12–N2–C14	113.3(5)

Despite the cationic nature of complex **12**, both the Ir–C and the Ir–P distances (Table 2) are nearly identical to those found in compound **8**. The bond length Ir–N1, however, is significantly shorter (2.264(6) Å) than the corresponding Ir–O1 distance in **8** (2.339(4) Å), which probably reflects the higher donor strength of the NMe<sub>2</sub> compared with the OCH<sub>3</sub> group.

With regard to the mechanism of formation of **11** and **12** from **8** and dichloromethane, we assume that initially oxidative addition of the substrate to the four-coordinate iridium(I) center takes place. There is ample evidence for this type of behavior in other square-planar d<sup>8</sup> systems as well as for the generation of [L<sub>n</sub>MH(Cl)] complexes from appropriate precursors [L<sub>n</sub>M] and CH<sub>2</sub>Cl<sub>2</sub>.<sup>11</sup> The formation of the six-membered chelate ring in compound **12** from the supposed intermediate containing a M–CH<sub>2</sub>Cl bond is also not without precedent since we have found that the half-sandwich type complex [C<sub>5</sub>H<sub>5</sub>RhCH<sub>2</sub>I{κ<sup>2</sup>(P,P)-Me<sub>2</sub>PCH<sub>2</sub>CH<sub>2</sub>PMe<sub>2</sub>}]<sup>+</sup>, prepared from [C<sub>5</sub>H<sub>5</sub>Rh(dmpc)] and CH<sub>2</sub>I<sub>2</sub>, isomerizes quantitatively in the presence of NEt<sub>3</sub> to give [C<sub>5</sub>H<sub>5</sub>RhI{κ<sup>2</sup>(C,P)-CH<sub>2</sub>PMe<sub>2</sub>CH<sub>2</sub>CH<sub>2</sub>PMe<sub>2</sub>}]<sup>+</sup>.<sup>12</sup>

**Reactions of the Cyclometalated Complex 8 with H<sub>2</sub> and HCl.** Although the spectroscopic data of compound **8** provide no hint that in solution it is in equilibrium with the square-planar isomer [IrCl(6)<sub>2</sub>], the octahedral iridium(III) complex nevertheless behaves as if it were a four-coordinate iridium(I) species. It reacts instantaneously with H<sub>2</sub> to yield the dihydrido derivative **13** (Scheme 3), which is obtained as a pale yellow, extremely air-sensitive oil. Since the IR spectrum of **13** shows two bands at 1112 and 1055 cm<sup>-1</sup> which are assigned to the asymmetric C–O–C stretching frequencies of a free and a coordinated ether functionality,<sup>13</sup> we assume that the iridium is six-coordinate with one monodentate and one bidentate *i*-Pr<sub>2</sub>PCH<sub>2</sub>CH<sub>2</sub>OMe ligand. The <sup>31</sup>P NMR spectrum, however, displays only one sharp singlet in C<sub>6</sub>D<sub>6</sub> (triplet in off-resonance due to P–H coupling), indicating that in solution at room temperature two isomers **A** and **C** exist, which interconvert rapidly (on the NMR time scale) via the five-coordinate species **B**. This proposal is also supported

by the <sup>1</sup>H NMR spectrum in which only one signal (δ –28.9, triplet with *J*(PH) = 15.4 Hz) appears at higher field. The Δ*G*<sup>‡</sup> value for the dynamic process shown in Scheme 3 is probably below 35 kJ/mol since only one very broad signal has been observed in the <sup>31</sup>P NMR spectrum (in toluene-*d*<sub>6</sub>) at –80 °C. For the analogous hydrido(vinyl)iridium(III) compound [IrH(CH=CH<sub>2</sub>)Cl(6)<sub>2</sub>], coalescence of the two <sup>31</sup>P NMR resonances occurs at –45 °C, which together with the difference in the chemical shift of the two signals results in a Δ*G*<sup>‡</sup> value of approximately 41 kJ/mol.<sup>2</sup>

Treatment of **8** with an equimolar amount of HCl in benzene equally leads to a rapid reaction in which the dichloro(hydrido)iridium(III) complex **14** is formed in excellent yield. Since the spectroscopic data of **13** and **14** resemble each other (IR, ν(CO)<sub>asym</sub> 1103 and 1045 cm<sup>-1</sup>; <sup>1</sup>H NMR at 25 °C, one high-field signal at δ –34.3 as a triplet with *J*(PH) = 13.2 Hz; <sup>31</sup>P NMR at 25 °C, one sharp singlet (doublet in off-resonance) at δ 17.5), we not only assume analogous structures but also similar fluxional behavior (see Scheme 3) of the two compounds in solution.

**Preparation of Hydrido(vinyl), Hydrido(alkynyl), and Alkynyl(vinyl) Complexes from 8.** In contrast to the formation of **13** and **14**, which is completed at 25 °C in a few minutes, the reactions of **8** with methyl acrylate and methyl vinyl ketone proceed much more slowly but finally yield the hydrido(vinyl)iridium complexes **15** and **16** almost quantitatively. Both compounds are pale yellow air-sensitive oily substances, the composition of which has been confirmed by elemental analysis. In contrast to **13** and **14**, the IR spectra of **15** and **16** display only one asymmetric C–O–C stretch at ca. 1120 cm<sup>-1</sup>, and thus there is no doubt that the phosphino ether ligands are not involved in chelate-type coordination. On the basis of the appearance of ν(C=O) bands at 1578 (for **15**) and 1539 cm<sup>-1</sup> (for **16**), which are significantly shifted to shorter wave numbers compared with free CH<sub>2</sub>=CHCO<sub>2</sub>Me and CH<sub>2</sub>=CHC(=O)CH<sub>3</sub>, respectively, we believe that the C=O group of the activated olefins is linked to the metal center and thus completes the octahedral coordination sphere. The structural proposal for **15** and **16** shown in Scheme 4 is fully consistent with the appearance of only one singlet resonance in the <sup>31</sup>P NMR spectra which in off-resonance is split into a doublet. It should be noted, however, that the <sup>1</sup>H NMR spectra of **15** and **16** (in contrast to those of **13** and **14**) display a broad multiplet for the PCHCH<sub>3</sub> protons of the *Pi*-Pr<sub>2</sub> units instead of two doublets-of-virtual-triplets. Due to the bonding of four different ligands in the equatorial plane, compounds **15** and **16** contain no mirror plane that passes through the two phosphorus atoms. The two molecules therefore possess four different prochiral centers, which makes all the phosphino CH<sub>3</sub> groups anisochronous and leads to an overlap of four virtually coupled signals.

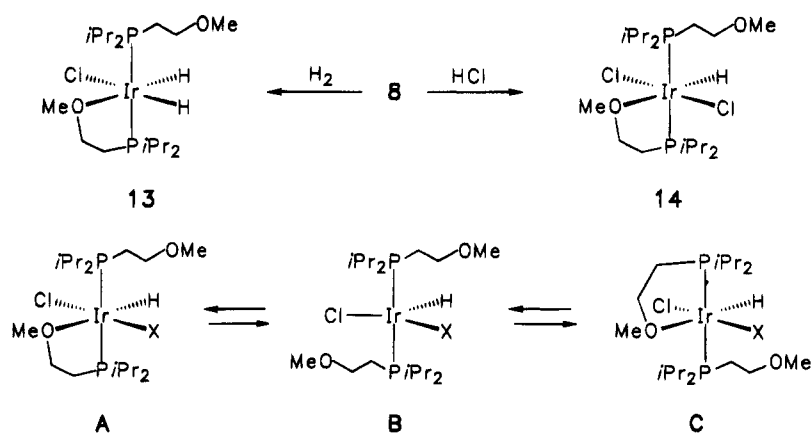
The octahedral hydrido(vinyl) complexes **15** and **16** are not only accessible from **8** but also on treatment of the dihydridoiridium(III) compound **13** with methyl acrylate or methyl vinyl ketone, respectively. In this case, the yield is 80%–85%. With regard to the mechanism of the reaction, we assume that displacement of the metal-bonded C=O unit by the substituted olefin occurs initially, which is followed by an insertion of the

(11) (a) Scherer, O. J.; Jungmann, H. J. *Organomet. Chem.* **1981**, *208*, 153–159. (b) Marder, T. B.; Fultz, W. C.; Calabrese, J. C.; Harlow, R. L.; Milstein, D. *J. Chem. Soc., Chem. Commun.* **1987**, 1543–1545.

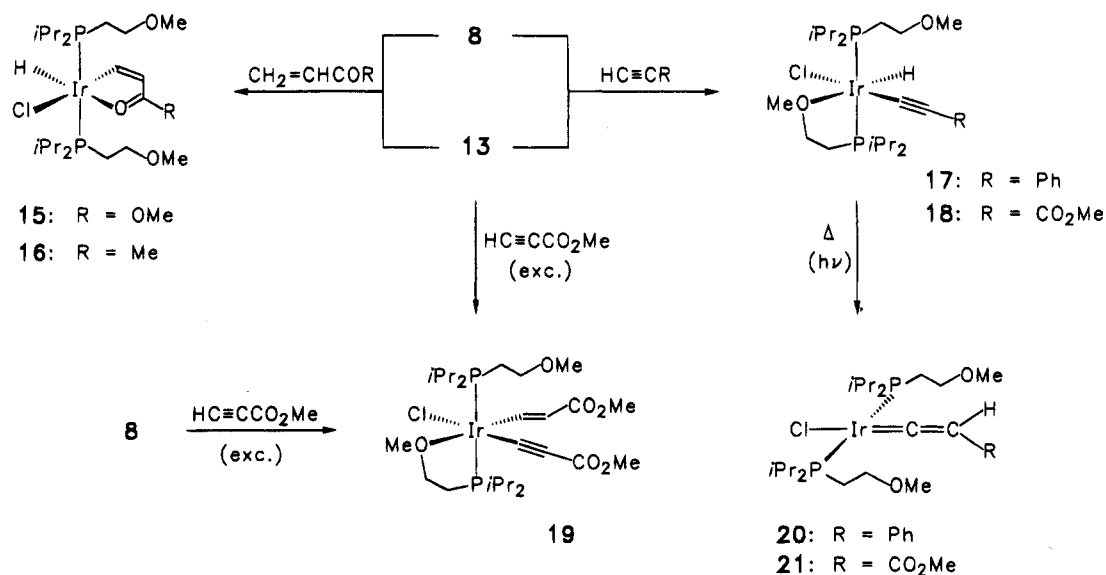
(12) Werner, H.; Hofmann, L.; Paul, W.; Schubert, U. *Organometallics* **1988**, *7*, 1106–1111.

(13) (a) Coutts, R. S. P.; Martin, R. L.; Wailes, P. C. *Aust. J. Chem.* **1971**, *24*, 2533–2540. (b) Lindner, E.; Mayer, H. A.; Wegener, P. *Chem. Ber.* **1986**, *119*, 2616–2630.

## Scheme 3



## Scheme 4



olefinic ligand into one of the Ir–H bonds. Reductive elimination of  $C_2H_5CO_2Me$  or  $C_2H_5C(=O)CH_3$  from the alkyl(hydrido)metal derivative would lead to the intermediate  $[IrCl(6)_2]$  which, after addition of a second molecule of  $CH_2=CHX$  ( $X = CO_2Me$ ,  $C(=O)Me$ ), gives the olefin complex *trans*- $[IrCl(CH_2=CHX)(6)_2]$ . Finally, this species intramolecularly rearranges via C–H activation to yield **15** and **16**, respectively. In this context, it should be mentioned that a similar reaction of bis-(phosphine)iridium(I) chlorides with  $CH_2=CHX$  to yield octahedral hydrido(vinyl)iridium(III) compounds has been established for  $L = Pi-Pr_3$ <sup>14</sup> and  $PPh_3$ <sup>14b,15</sup> and also for some related rhodium complexes.<sup>16</sup>

Terminal alkynes  $HC\equiv CR$  ( $R = Ph$ ,  $CO_2Me$ ) react rapidly with equimolar amounts of either **8** or **13** in benzene at room temperature to yield nearly quantitatively the alkynyl(hydrido)iridium(III) derivatives **17** and **18** (Scheme 4). At 25 °C, both compounds are fluxional in solution, which is illustrated by the appearance of one signal in the <sup>31</sup>P NMR and one sharp triplet resonance for the metal-bonded hydride ligand in the

<sup>1</sup>H NMR spectrum. That the two molecules, however, are not five-coordinate but contain one *P*-monodentate and one chelating phosphino ether unit is indicated by the IR spectra in which *two* asymmetric C–O–C stretching frequencies at 1105 and 1045  $cm^{-1}$  (for **17**) and at 1108 and 1038  $cm^{-1}$  (for **18**) have been observed. On the basis of the spectroscopic data, it cannot be decided whether the alkynyl or the hydride ligand is *trans* to Cl in **17** and **18**.

If compounds **8** and **13** are treated with an excess of methyl propiolate instead of 1 equiv, the alkynyl(vinyl)iridium(III) complex **19** is formed in about 60%–65% yield. Methyl acrylate has been detected as a byproduct in the reaction of **13** with  $HC\equiv CCO_2Me$ . In solution, compound **19** is less fluxional than the corresponding alkynyl(hydrido) derivative **18** and from the coalescence temperature (–3 °C in toluene-*d*<sub>8</sub>) and the difference in the chemical shift of the two signals in the low-temperature <sup>31</sup>P NMR spectrum, a  $\Delta G^\ddagger$  value of approximately 49 kJ/mol can be calculated. Compared with **13**, for which a  $\Delta G^\ddagger$  value of less than 35 kJ/mol has been estimated, the alkynyl(vinyl)iridium(III) complex is more rigid, which is probably due to a stronger Ir–OCH<sub>3</sub> bond than in the dihydridometal derivative. The *trans* configuration at the C=C double bond of the vinyl ligand in **19** is confirmed by the H–H coupling of

(14) (a) Werner, H.; Dirnberger, T.; Schulz, M. *Angew. Chem.* **1988**, *100*, 993–994; *Angew. Chem., Int. Ed. Engl.* **1988**, *27*, 948–950. (b) Dirnberger, T. Dissertation, University of Würzburg, Würzburg, Germany, 1990.

(15) Papenfuhs, B. Ph.D. Thesis, University of Würzburg, Würzburg, Germany, 1993.

(16) Dirnberger, T.; Werner, H. *Chem. Ber.* **1992**, *125*, 2007–2014.





is unusually short, which is probably the result of the *trans* arrangement of the strong  $\sigma$ -donating ether and the strong  $\pi$ -accepting vinylidene ligand. This bonding scheme also explains why the cationic compounds  $[\text{Ir}(\text{C}=\text{CHR})\{\kappa(P)\text{-}i\text{-Pr}_2\text{PCH}_2\text{CH}_2\text{OMe}\}\{\kappa^2(P,O)\text{-}i\text{-Pr}_2\text{PCH}_2\text{CH}_2\text{OMe}\}]^+$  are quite inert and do not react with  $\text{HC}\equiv\text{CPh}$  or  $\text{HC}\equiv\text{CCO}_2\text{Me}$  to give bis(vinylidene)iridium(I) species.

### Concluding Remarks

The work presented in this paper has confirmed that bifunctional ("hemilabile")<sup>21</sup> phosphines of the general composition  $\text{R}_2\text{PCH}_2\text{CH}_2\text{X}$  are not only useful ligands which temporarily are able to protect a free coordination site but can also behave as reacting substrates. Provided that X is  $\text{OCH}_3$  and the methoxy oxygen is coordinated to a transition metal that favors oxidative-addition reactions, metalation of the  $\text{OCH}_3$  group can occur to generate an alkyl(hydrido)metal derivative. Such an intramolecular C–H activation process involving a phosphino ether like  $i\text{-Pr}_2\text{PCH}_2\text{CH}_2\text{OMe}$  is certainly not limited to iridium since we have recently shown<sup>22</sup> that, in the coordination sphere of osmium, a  $\text{OCH}_3$  moiety can even be metalated *twice* to form a metal–carbene  $\text{M}=\text{CHO}$ – unit.

It is most interesting, however, that the substituents R at the phosphorus atom of the phosphino ethers seem to have a pronounced effect on the intramolecular metalation. While  $[\text{IrCl}(\text{C}_6\text{H}_{14})_2]_2$  (**5**) reacts with  $i\text{-Pr}_2\text{PCH}_2\text{CH}_2\text{OMe}$  (**6**) at room temperature to give the unexpected octahedral iridium(III) complex **8**, on treatment of  $[\text{IrCl}(\text{C}_8\text{H}_{12})_2]$  with  $\text{Cy}_2\text{PCH}_2\text{CH}_2\text{OMe}$  under nearly the same conditions the square-planar iridium(I) compound  $[\text{IrCl}\{\kappa(P)\text{-}\text{Cy}_2\text{PCH}_2\text{CH}_2\text{OMe}\}\{\kappa^2(P,O)\text{-}\text{Cy}_2\text{PCH}_2\text{CH}_2\text{OMe}\}]$  is formed.<sup>23</sup> There is also a difference in the case of C–H activation of  $\text{OCH}_3$  and  $\text{NCH}_3$  groups, because both **6** and **7** can be transformed with osmium as the metal center to  $\text{OCH}=\text{}$  and  $\text{NCH}=\text{}$  units,<sup>22</sup> whereas with iridium only a metalation of the phosphino ether takes place.

The final and really unusual facet of these studies is that the cyclometalated compound **8**, which is undoubtedly more thermodynamically stable both in the solid state and in solution than the hypothetical isomer  $[\text{IrCl}\{\kappa(P)\text{-}i\text{-Pr}_2\text{PCH}_2\text{CH}_2\text{OMe}\}\{\kappa^2(P,O)\text{-}i\text{-Pr}_2\text{PCH}_2\text{CH}_2\text{OMe}\}]$ , behaves like the isomeric four-coordinate species in the presence of substrates such as  $\text{H}_2$  and  $\text{HCl}$  (present work) and  $\text{CO}$  and  $\text{C}_2\text{H}_4$  (ref 2). These results (and also those obtained with activated olefins and terminal alkynes as substrates) indicate that the C–H activation process which leads to the formation of **8** is reversible, which is in complete analogy with the conversion of  $[\text{Ru}](\text{Pi-Pr}_3)$  to  $[\text{Ru}]\text{H}\{\kappa^2(C,P)\text{-}\text{CH}_2\text{CHMePi-Pr}_2\}$  ( $[\text{Ru}] = (\text{C}_6\text{H}_6)\text{Ru}$ )<sup>24</sup> but in contrast to the formation of  $[\text{Ir}]\text{H}(\text{CH}_3)$  from  $[\text{Ir}]$  and methane ( $[\text{Ir}] = (\text{C}_5\text{-}$

$\text{Me}_5)\text{Ir}(\text{CO})$ ,  $(\text{C}_5\text{Me}_5)\text{Ir}(\text{PMe}_3)$ ).<sup>25</sup> We are currently investigating whether a phosphino unit  $\text{PR}_2$  and/or a functional group X of a substituted phosphine  $\text{R}_2\text{P}(\text{CH}_2)_n\text{X}$  can also initiate or facilitate the C–H activation of the  $-(\text{CH}_2)_n-$  chain, and we will report on this work in due course.

### Experimental Section

All reactions were carried out under an atmosphere of argon by Schlenk tube techniques. The starting materials  $[\text{IrCl}(\text{C}_6\text{H}_{14})_2]_2$  (**5**),<sup>26</sup>  $i\text{-Pr}_2\text{PCH}_2\text{CH}_2\text{OMe}$  (**6**),<sup>4</sup> and  $i\text{-Pr}_2\text{PCH}_2\text{CH}_2\text{NMe}_2$  (**7**)<sup>4</sup> were prepared as described in the literature. The olefins  $\text{CH}_2=\text{CHC}(\text{O})\text{R}$  and alkynes  $\text{HC}\equiv\text{CR}$  were commercial products from Aldrich and Fluka. NMR spectra were recorded on Jeol FX 90 Q, Bruker AC 200, and Bruker AMX 400 instruments, and IR spectra were recorded on a Perkin-Elmer 1420 infrared spectrometer. Melting points were determined by DTA.

**Preparation of  $[\text{IrClH}\{\kappa^2(C,P)\text{-}\text{CH}_2\text{OCH}_2\text{CH}_2\text{Pi-Pr}_2\}\{\kappa^2(P,O)\text{-}i\text{-Pr}_2\text{PCH}_2\text{CH}_2\text{OMe}\}]$  (**8**).** A solution of **5** (108 mg, 0.12 mmol) in 10 mL of benzene was treated with **6** (90  $\mu\text{L}$ , 0.48 mmol) and stirred for 20 min at room temperature. The solvent was removed, the oily residue was dissolved in 3 mL of benzene, and the solution was chromatographed on  $\text{Al}_2\text{O}_3$  (neutral, activity grade V). With  $\text{C}_6\text{H}_6/\text{CH}_2\text{Cl}_2$  (2:3) a yellow fraction was eluted, from which a pale yellow, only moderately air-sensitive solid was isolated: yield 123 mg (88%); mp 70 °C decomp. Anal. Calcd for  $\text{C}_{18}\text{H}_{42}\text{ClIrO}_2\text{P}_2$ : C, 37.27; H, 7.30. Found: C, 36.98; H, 7.08. IR ( $\text{C}_6\text{H}_6$ ):  $\nu(\text{IrH})$  2167,  $\nu(\text{COC})_{\text{asym}}$  1050  $\text{cm}^{-1}$ .  $^1\text{H}$  NMR ( $\text{C}_6\text{D}_6$ , 200 MHz):  $\delta$  5.68 (dd,  $J(\text{PH}) = 10.1$  Hz,  $J(\text{HH}) = 5.8$  Hz, 1H of  $\text{IrCH}_2$ ), 5.42 (d, br,  $J(\text{HH}) = 5.8$  Hz, 1H of  $\text{IrCH}_2$ ), 3.77, 3.21 (both m,  $\text{PCH}_2\text{CH}_2$ ), 3.34 (s,  $\text{OCH}_3$ ), 2.78, 2.00 (both m,  $\text{PCHCH}_3$ ), 1.55, 1.41 (both m,  $\text{PCH}_2$ ), 1.49, 1.27, 1.12, 1.00 (all m,  $\text{PCHCH}_3$ ), –22.92 (dd,  $J(\text{PH}) = 17.2$  Hz,  $J(\text{P'H}) = 14.2$  Hz,  $\text{IrH}$ ).  $^{13}\text{C}$  NMR ( $\text{C}_6\text{D}_6$ , 50.2 MHz):  $\delta$  75.26 (s,  $\text{IrCH}_2\text{OCH}_2$ ), 67.66 (s,  $\text{PCH}_2\text{CH}_2\text{OCH}_3$ ), 62.77 (s,  $\text{OCH}_3$ ), 31.12 (s, br,  $\text{IrCH}_2$ ), 26.1–20.3 (m,  $\text{PCHCH}_3$  and  $\text{PCH}_2\text{CH}_2\text{OCH}_3$ ), 20.0–17.7 (m,  $\text{PCHCH}_3$ ).  $^{31}\text{P}$  NMR ( $\text{C}_6\text{D}_6$ , 36.2 MHz):  $\delta$  29.11, 6.72 (both d,  $J(\text{PP}) = 349.5$  Hz).

**Preparation of *cis*- $[\text{IrCl}\{\kappa^2(P,N)\text{-}i\text{-Pr}_2\text{PCH}_2\text{CH}_2\text{NMe}_2\}\{\kappa(P)\text{-}i\text{-Pr}_2\text{PCH}_2\text{CH}_2\text{NMe}_2\}]$  (**9**).** A solution of **5** (58 mg, 0.065 mmol) in 10 mL of benzene was treated with **7** (55  $\mu\text{L}$ , 0.26 mmol) and stirred for 10 min at room temperature. The solvent was removed, and the residue was recrystallized from pentane to give yellow, only moderately air-sensitive crystals: yield 57 mg (72%); mp 58 °C decomp. Anal. Calcd for  $\text{C}_{20}\text{H}_{48}\text{ClIrN}_2\text{P}_2$ : C, 39.62; H, 7.98; N, 4.62. Found: C, 40.43; H, 7.76; N, 4.33.  $^1\text{H}$  NMR ( $\text{C}_6\text{D}_6$ , 90 MHz):  $\delta$  2.7 (m,  $\text{PCH}_2\text{CH}_2$ ), 2.62 (d,  $J(\text{PH}) = 1.8$  Hz,  $\text{NCH}_3$ ), 2.11 (s,  $\text{NCH}_3$ ), 2.0–1.8 (m,  $\text{PCHCH}_3$  and  $\text{PCH}_2$ ), 1.5–0.9 (m,  $\text{PCHCH}_3$ ).  $^{31}\text{P}$  NMR ( $\text{C}_6\text{D}_6$ , 36.2 MHz):  $\delta$  41.24, 7.21 (both d,  $J(\text{PP}) = 17.6$  Hz).

**Preparation of *trans*- $[\text{IrCl}(\text{CO})\{\kappa(P)\text{-}i\text{-Pr}_2\text{PCH}_2\text{CH}_2\text{NMe}_2\}_2]$  (**10**).** A slow stream of CO was passed through a solution of **9** (43 mg, 0.07 mmol) in 5 mL of benzene at room temperature for 30 s. After the solution was stirred for 5 min, the solvent was removed, the oily residue was dissolved in 2 mL of benzene, and the solution was chromatographed on  $\text{Al}_2\text{O}_3$  (neutral, activity grade V). With benzene a yellow fraction was eluted, from which a yellow, almost air-stable solid was isolated: yield 41 mg (91%); mp 98 °C decomp. Anal. Calcd for  $\text{C}_{21}\text{H}_{48}\text{ClIrN}_2\text{OP}_2$ : C, 39.77; H, 7.63; N, 4.42. Found: C, 39.62; H, 7.80; N, 4.59. IR ( $\text{C}_6\text{H}_6$ ):  $\nu(\text{IrCO})$  1937  $\text{cm}^{-1}$ .  $^1\text{H}$  NMR ( $\text{C}_6\text{D}_6$ , 90 MHz):  $\delta$  2.85 (m,  $\text{PCH}_2\text{CH}_2$ ), 2.4–

(21) Jeffrey, J. C.; Rauchfuss, T. B. *Inorg. Chem.* **1979**, *18*, 2658–2666.

(22) Werner, H.; Weber, B.; Nürnberg, O.; Wolf, J. *Angew. Chem.* **1992**, *104*, 1079–1081; *Angew. Chem., Int. Ed. Engl.* **1992**, *31*, 1025–1027.

(23) (a) Lindner, E.; Meyer, S. *J. Organomet. Chem.* **1988**, *339*, 193–198. (b) Review: Bader, A.; Lindner, E. *Coord. Chem. Rev.* **1991**, *108*, 27–110.

(24) Werner, H.; Kletzin, H.; Roder, K. *J. Organomet. Chem.* **1988**, *355*, 401–417.

(25) (a) Hoyano, J. K.; McMaster, A. D.; Graham, W. A. G. *J. Am. Chem. Soc.* **1983**, *105*, 7190–7191. (b) Wax, M. J.; Stryker, J. M.; Buchanan, J. M.; Kovac, C. A.; Bergman, R. G. *J. Am. Chem. Soc.* **1984**, *106*, 1121–1122.

(26) van der Ent, A.; Onderdelinden, A. L. *Inorg. Synth.* **1973**, *14*, 92–95.

Table 4. Crystallographic Data for 8, 12, and 23

	C <sub>18</sub> H <sub>42</sub> ClIrO <sub>2</sub> P <sub>2</sub> (8)	C <sub>21</sub> H <sub>50</sub> Cl <sub>3</sub> IrN <sub>2</sub> P <sub>2</sub> (12)	C <sub>22</sub> H <sub>46</sub> F <sub>6</sub> IrO <sub>4</sub> P <sub>2</sub> Sb (23)
formula	C <sub>18</sub> H <sub>42</sub> ClIrO <sub>2</sub> P <sub>2</sub> (8)	C <sub>21</sub> H <sub>50</sub> Cl <sub>3</sub> IrN <sub>2</sub> P <sub>2</sub> (12)	C <sub>22</sub> H <sub>46</sub> F <sub>6</sub> IrO <sub>4</sub> P <sub>2</sub> Sb (23)
fw	580.15	691.17	864.52
cryst size, mm <sup>3</sup>	0.5 × 0.5 × 0.7	0.15 × 0.15 × 0.4	0.3 × 0.45 × 0.5
cryst syst	triclinic	orthorhombic	monoclinic
space group	P1 (No. 2)	Pna2 <sub>1</sub> (No. 33)	P2 <sub>1</sub> /n (No. 14)
cell dimens determn	24 reflns, 10° < θ < 15°	23 reflns, 10° < θ < 15°	25 reflns, 10° < θ < 16°
a, Å	7.852(1)	9.921(1)	13.167(2)
b, Å	9.529(2)	22.070(4)	16.956(2)
c, Å	15.747(3)	14.162(2)	14.534(2)
α, deg	78.67(2)		
β, deg	79.62(2)		99.32(1)
γ, deg	84.63(2)		
V, Å <sup>3</sup>	1134.2(4)	3100.8(7)	3201.9(8)
Z	2	4	4
d <sub>calcd</sub> , g cm <sup>-3</sup>	1.70	1.48	1.79
diffractometer		Enraf Nonius CAD4	
radiation (graphite monochromator)		Mo Kα (0.709 30 Å)	
temp, °C	-80 ± 1	-50 ± 1	20 ± 1
μ, cm <sup>-1</sup>	61.3	66.9	51.4
scan method	ω/θ	ω/θ	ω/θ
2θ(max), deg	44	50	44
tot no. of reflns scanned	3026	3107	4296
no. of unique reflns	2776	3107	3714
no. of obsd reflns	2638	2258	3088
no. of params refined	217	288	361
R	0.031	0.028	0.028
R <sub>w</sub>	0.039	0.031	0.030
refln:param ratio	12.16	7.84	8.55
resid electron density, e Å <sup>-3</sup>	1.00	1.30	1.14

2.1 (m, PCHCH<sub>3</sub> and PCH<sub>2</sub>), 2.27 (s, NCH<sub>3</sub>), 1.40, 1.23 (both dvt, N = 15.1 Hz, J(HH) = 6.8, PCHCH<sub>3</sub>). <sup>31</sup>P NMR (C<sub>6</sub>D<sub>6</sub>, 36.2 MHz): δ 32.68 (s).

**Preparation of [IrCl<sub>2</sub>H{κ<sup>2</sup>(P,N)-i-Pr<sub>2</sub>PCH<sub>2</sub>CH<sub>2</sub>NMe<sub>2</sub>}-κ(P)-i-Pr<sub>2</sub>PCH<sub>2</sub>CH<sub>2</sub>NMe<sub>2</sub>]} (11).** A solution of **9** (62 mg, 0.102 mmol) in 10 mL of benzene was treated with 0.32 mL of a 0.32 M solution of HCl in benzene (0.102 mmol) and stirred for 15 min at room temperature. The solvent was removed, and the pale yellow residue was washed repeatedly with pentane and dried in vacuo: yield 44 mg (67%); mp 82 °C decomp. Anal. Calcd for C<sub>20</sub>H<sub>49</sub>Cl<sub>2</sub>IrN<sub>2</sub>P<sub>2</sub>: C, 37.38; H, 7.69; N, 4.10. Found: C, 37.23; H, 7.86; N, 4.36. IR (C<sub>6</sub>H<sub>6</sub>): ν(IrH) 2232 cm<sup>-1</sup>. <sup>1</sup>H NMR (C<sub>6</sub>D<sub>6</sub>, 400 MHz): δ 3.75, 2.81 (both m, PCH<sub>2</sub>CH<sub>2</sub>), 2.58 (d, J(PH) = 2.0 Hz, NCH<sub>3</sub>), 2.4–2.1 (m, PCHCH<sub>3</sub>), 2.06 (s, NCH<sub>3</sub>), 1.93, 1.55 (both m, PCH<sub>2</sub>), 1.62 (dd, J(PH) = 16.0 Hz, J(HH) = 6.8, PCHCH<sub>3</sub>), 1.51 (dd, J(PH) = 15.4 Hz, J(HH) = 7.2, PCHCH<sub>3</sub>), 1.39 (dd, J(PH) = 15.2 Hz, J(HH) = 7.2, PCHCH<sub>3</sub>), 1.15 (dd, J(PH) = 14.0 Hz, J(HH) = 7.2, PCHCH<sub>3</sub>), 1.06 (dd, J(PH) = 11.2 Hz, J(HH) = 7.2, PCHCH<sub>3</sub>), 1.04 (dd, J(PH) = 12.4 Hz, J(HH) = 7.2, PCHCH<sub>3</sub>), 0.87 (dd, J(PH) = 16.0 Hz, J(HH) = 7.2, PCHCH<sub>3</sub>), 0.74 (dd, J(PH) = 12.0 Hz, J(HH) = 6.8, PCHCH<sub>3</sub>), -22.59 (dd, J(PH) = 19.8 Hz, J(PH) = 16.0 Hz, IrH). <sup>31</sup>P NMR (C<sub>6</sub>D<sub>6</sub>, 36.2 MHz): δ 23.45, -6.81 (both d, J(PP) = 13.2 Hz).

**Reaction of 5 with CH<sub>2</sub>Cl<sub>2</sub>.** Compound **9** (50 mg, 0.08 mmol) was dissolved in 1 mL of dichloromethane at room temperature, and the solution was layered with 1.5 mL of pentane. After it had been stored for 48 h, a small quantity of bright yellow crystals **12** precipitated, which were separated from the reaction mixture and dried in vacuo: yield ca. 10 mg.

**Preparation of [IrClH<sub>2</sub>{κ<sup>2</sup>(P,O)-i-Pr<sub>2</sub>PCH<sub>2</sub>CH<sub>2</sub>OMe}-κ(P)-i-Pr<sub>2</sub>PCH<sub>2</sub>CH<sub>2</sub>OMe]} (13).** A slow stream of H<sub>2</sub> was passed through a solution of **8** (95 mg, 0.164 mmol) in 10 mL of benzene at room temperature for 30 s. After the solution was stirred for 5 min, the solvent was removed, the oily residue was dissolved in 2 mL of benzene, and the solution was chromatographed on Al<sub>2</sub>O<sub>3</sub> (neutral, activity grade V). With C<sub>6</sub>H<sub>6</sub>/CH<sub>2</sub>Cl<sub>2</sub> (1:2) a yellow fraction was eluted, from which a pale yellow, very air-sensitive oil was isolated: yield 70 mg (73%). IR (C<sub>6</sub>H<sub>6</sub>): ν(IrH) 2260, ν(COC)<sub>asym</sub> 1112 and 1055 cm<sup>-1</sup>. <sup>1</sup>H NMR (C<sub>6</sub>D<sub>6</sub>, 90 MHz): δ 3.69 (m, PCH<sub>2</sub>CH<sub>2</sub>), 3.26 (s, OCH<sub>3</sub>), 2.20 (m, PCHCH<sub>3</sub>), 1.82 (m, PCH<sub>2</sub>), 1.16, 1.12 (both dvt, N = 14.3 Hz, J(HH) = 7.1, PCHCH<sub>3</sub>), -28.87 (t, J(PH) = 15.4 Hz,

IrH). <sup>31</sup>P NMR (C<sub>6</sub>D<sub>6</sub>, 36.2 MHz): δ 40.07 (s, t in off-resonance).

**Preparation of [IrCl<sub>2</sub>H{κ<sup>2</sup>(P,O)-i-Pr<sub>2</sub>PCH<sub>2</sub>CH<sub>2</sub>OMe}-κ(P)-i-Pr<sub>2</sub>PCH<sub>2</sub>CH<sub>2</sub>OMe]} (14).** A solution of **8** (47 mg, 0.08 mmol) in 5 mL of benzene was treated with 0.25 mL of a 0.32 M solution of HCl in benzene (0.08 mmol) and stirred for 5 min at room temperature. After the solvent was removed, the oily residue was dissolved in 2 mL of benzene, and the solution was chromatographed on Al<sub>2</sub>O<sub>3</sub> (neutral, activity grade V). With C<sub>6</sub>H<sub>6</sub>/CH<sub>2</sub>Cl<sub>2</sub> (2:1) a yellow fraction was eluted from which a pale yellow, moderately air-sensitive solid was isolated: yield 40 mg (80%); mp 96 °C decomp. Anal. Calcd for C<sub>18</sub>H<sub>43</sub>Cl<sub>2</sub>IrO<sub>2</sub>P<sub>2</sub>: C, 35.06; H, 7.03. Found: C, 35.49; H, 7.18. IR (C<sub>6</sub>H<sub>6</sub>): ν(IrH) 2275, ν(COC)<sub>asym</sub> 1103 and 1045 cm<sup>-1</sup>. <sup>1</sup>H NMR (C<sub>6</sub>D<sub>6</sub>, 90 MHz): δ 3.60 (m, PCH<sub>2</sub>CH<sub>2</sub>), 3.28 (s, OCH<sub>3</sub>), 2.75 (m, PCHCH<sub>3</sub>), 2.05 (m, PCH<sub>2</sub>), 1.30 (dvt, N = 14.2 Hz, J(HH) = 6.8, PCHCH<sub>3</sub>), 1.22 (dvt, N = 13.7 Hz, J(HH) = 6.8, PCHCH<sub>3</sub>), -34.31 (t, J(PH) = 13.2 Hz, IrH). <sup>31</sup>P NMR (C<sub>6</sub>D<sub>6</sub>, 36.2 MHz): δ 17.53 (s, d in off-resonance).

**Preparation of [IrClH{κ<sup>2</sup>(C,O)-CH=CHC(O)OMe}-κ(P)-i-Pr<sub>2</sub>PCH<sub>2</sub>CH<sub>2</sub>OMe]}<sub>2</sub> (15).** (a) A solution of **8** (43 mg, 0.074 mmol) in 5 mL of benzene was treated with methyl acrylate (0.1 mL) and stirred for 20 h at 80 °C. After the solution was cooled to room temperature, the solvent was removed, the oily residue was dissolved in 2 mL of benzene, and the resulting solution was chromatographed on Al<sub>2</sub>O<sub>3</sub> (neutral, activity grade V). With C<sub>6</sub>H<sub>6</sub>/CH<sub>2</sub>Cl<sub>2</sub> (1:2) a yellow fraction was eluted, from which a pale yellow, air-sensitive oil was isolated: yield 43 mg (88%). Anal. Calcd for C<sub>22</sub>H<sub>48</sub>ClIrO<sub>4</sub>P<sub>2</sub>: C, 39.66; H, 7.26. Found: C, 40.11; H, 7.49. IR (C<sub>6</sub>H<sub>6</sub>): ν(IrH) 2230, ν(C=O) 1578, ν(COC)<sub>asym</sub> 1110 cm<sup>-1</sup>. <sup>1</sup>H NMR (C<sub>6</sub>D<sub>6</sub>, 90 MHz): δ 10.55 (d, J(HH) = 7.8 Hz, IrCH=CH), 6.62 (d, J(HH) = 7.8 Hz, IrCH=CH), 3.85 (m, PCH<sub>2</sub>CH<sub>2</sub>), 3.69 (s, C(O)OCH<sub>3</sub>), 3.22 (s, OCH<sub>3</sub>), 2.38 (m, PCHCH<sub>3</sub>), 2.10 (m, PCH<sub>2</sub>), 1.30–0.95 (m, PCHCH<sub>3</sub>), -26.90 (t, J(PH) = 15.4 Hz, IrH). <sup>31</sup>P NMR (C<sub>6</sub>D<sub>6</sub>, 36.2 MHz): δ 11.95 (s, d in off-resonance). (b) The preparation of **15** from **13** (38 mg, 0.065 mmol) was performed analogously as described in (a): yield 36 mg (82%).

**Preparation of [IrClH{κ<sup>2</sup>(C,O)-CH=CHC(O)OMe}-κ(P)-i-Pr<sub>2</sub>PCH<sub>2</sub>CH<sub>2</sub>OMe]}<sub>2</sub> (16).** (a) A solution of **8** (47 mg, 0.081 mmol) in 5 mL of benzene was treated with methyl vinyl ketone (0.1 mL) and stirred for 20 h at 80 °C. After the solution was cooled to room temperature, the solvent was

removed, the oily residue was dissolved in 2 mL of benzene, and the resulting solution was chromatographed on  $\text{Al}_2\text{O}_3$  (neutral, activity grade V). With  $\text{C}_6\text{H}_6/\text{CH}_2\text{Cl}_2$  (1:2) a yellow fraction was eluted, from which a pale yellow, air-sensitive oil was isolated: yield 44 mg (83%). Anal. Calcd for  $\text{C}_{22}\text{H}_{48}\text{ClIrO}_3\text{P}_2$ : C, 40.64; H, 7.44. Found: C, 40.50; H, 7.76. IR ( $\text{C}_6\text{H}_6$ ):  $\nu(\text{IrH})$  2213,  $\nu(\text{C}=\text{O})$  1539,  $\nu(\text{COC})_{\text{asym}}$  1125  $\text{cm}^{-1}$ .  $^1\text{H}$  NMR ( $\text{C}_6\text{D}_6$ , 90 MHz):  $\delta$  11.00 (d,  $J(\text{HH}) = 7.1$  Hz,  $\text{IrCH}=\text{CH}$ ), 6.84 (d,  $J(\text{HH}) = 7.1$  Hz,  $\text{IrCH}=\text{CH}$ ), 3.80 (m,  $\text{PCH}_2\text{CH}_2$ ), 3.23 (s,  $\text{OCH}_3$ ), 2.40 (m,  $\text{PCHCH}_3$ ), 2.14 (s,  $\text{C}(\text{O})\text{CH}_3$ ), 1.93 (m,  $\text{PCH}_2$ ), 1.29–0.91 (m,  $\text{PCHCH}_3$ ), –23.80 (t,  $J(\text{PH}) = 15.9$  Hz,  $\text{IrH}$ ).  $^{31}\text{P}$  NMR ( $\text{C}_6\text{D}_6$ , 36.2 MHz):  $\delta$  12.36 (s, d in off-resonance). (b) The preparation of **16** from **13** (41 mg, 0.07 mmol) was performed analogously as described in (a): yield 39 mg (86%).

**Preparation of  $[\text{IrCl}(\text{C}=\text{CPh})\{\kappa^2(\text{P},\text{O})\text{-i-Pr}_2\text{PCH}_2\text{CH}_2\text{OMe}\}\{\kappa(\text{P})\text{-i-Pr}_2\text{PCH}_2\text{CH}_2\text{OMe}\}]$  (**17**).** (a) A solution of **8** (84 mg, 0.145 mmol) in 10 mL of benzene was treated with phenylacetylene (16  $\mu\text{L}$ , 0.145 mmol) and stirred for 5 min at room temperature. After the solvent was removed, the colorless solid was washed repeatedly with small amounts of pentane and dried in vacuo: yield 89 mg (90%); mp 108 °C decomp. Anal. Calcd for  $\text{C}_{26}\text{H}_{46}\text{ClIrO}_2\text{P}_2$ : C, 45.77; H, 7.09. Found: C, 46.10; H, 7.27. IR ( $\text{C}_6\text{H}_6$ ):  $\nu(\text{IrH})$  2280,  $\nu(\text{IrC}=\text{C})$  2096,  $\nu(\text{C}=\text{C})$  1595,  $\nu(\text{COC})_{\text{asym}}$  1105 and 1045  $\text{cm}^{-1}$ .  $^1\text{H}$  NMR ( $\text{C}_6\text{D}_6$ , 90 MHz):  $\delta$  7.27 (m,  $\text{C}_6\text{H}_5$ ), 3.64 (m,  $\text{PCH}_2\text{CH}_2$ ), 3.27 (s,  $\text{OCH}_3$ ), 2.78 (m,  $\text{PCHCH}_3$ ), 2.05 (m,  $\text{PCH}_2$ ), 1.43–1.08 (m,  $\text{PCHCH}_3$ ), –31.24 (t,  $J(\text{PH}) = 13.5$  Hz,  $\text{IrH}$ ).  $^{31}\text{P}$  NMR ( $\text{C}_6\text{D}_6$ , 36.2 MHz):  $\delta$  23.06 (s, d in off-resonance). (b) The preparation of **17** from **13** (61 mg, 0.105 mmol) was performed analogously as described in (a): yield 62 mg (87%).

**Preparation of  $[\text{IrCl}(\text{C}=\text{CO}_2\text{Me})\{\kappa^2(\text{P},\text{O})\text{-i-Pr}_2\text{PCH}_2\text{CH}_2\text{OMe}\}\{\kappa(\text{P})\text{-i-Pr}_2\text{PCH}_2\text{CH}_2\text{OMe}\}]$  (**18**).** (a) A solution of **8** (91 mg, 0.157 mmol) in 10 mL of benzene was treated with methyl propiolate (14  $\mu\text{L}$ , 0.157 mmol) and stirred for 5 min at room temperature. After the solvent was removed, the pale red residue was washed repeatedly with small amounts of pentane and dried in vacuo. According to the  $^{31}\text{P}$  NMR spectrum, the product contains small amounts of the corresponding vinylidene complex **23**: yield 93 mg (89%). IR ( $\text{C}_6\text{H}_6$ ):  $\nu(\text{IrH})$  2254,  $\nu(\text{IrC}=\text{C})$  2094,  $\nu(\text{COC})_{\text{asym}}$  1108 and 1038  $\text{cm}^{-1}$ .  $^1\text{H}$  NMR ( $\text{C}_6\text{D}_6$ , 90 MHz):  $\delta$  3.57 (m,  $\text{PCH}_2\text{CH}_2$ ), 3.42 (s,  $\text{C}(\text{O})\text{OCH}_3$ ), 3.23 (s,  $\text{OCH}_3$ ), 2.81 (m,  $\text{PCHCH}_3$ ), 1.96 (m,  $\text{PCH}_2$ ), 1.42–1.11 (m,  $\text{PCHCH}_3$ ), –30.50 (t,  $J(\text{PH}) = 15.8$  Hz,  $\text{IrH}$ ).  $^{31}\text{P}$  NMR ( $\text{C}_6\text{D}_6$ , 36.2 MHz):  $\delta$  11.95 (s, d in off-resonance). (b) The preparation of **18** from **13** (69 mg, 0.118 mmol) was performed analogously as described in (a): yield 71 mg (91%).

**Preparation of  $[\text{IrCl}(\text{CH}=\text{CHCO}_2\text{Me})(\text{C}=\text{CCO}_2\text{Me})\{\kappa^2(\text{P},\text{O})\text{-i-Pr}_2\text{PCH}_2\text{CH}_2\text{OMe}\}\{\kappa(\text{P})\text{-i-Pr}_2\text{PCH}_2\text{CH}_2\text{OMe}\}]$  (**19**).** (a) A solution of **8** (75 mg, 0.129 mmol) in 10 mL of benzene was treated with methyl propiolate (0.1 mL) and stirred for 15 min at room temperature. After the solvent was removed, the oily residue was dissolved in 2 mL of benzene, and the resulting solution was chromatographed on  $\text{Al}_2\text{O}_3$  (neutral, activity grade V). With  $\text{C}_6\text{H}_6/\text{CH}_2\text{Cl}_2$  (2:1) a yellow fraction was eluted, from which a pale yellow, air-sensitive oil was isolated: yield 59 mg (61%). Anal. Calcd for  $\text{C}_{26}\text{H}_{50}\text{ClIrO}_6\text{P}_2$ : C, 41.73; H, 6.74. Found: C, 42.18; H, 6.82. IR ( $\text{C}_6\text{H}_6$ ):  $\nu(\text{IrC}=\text{C})$  2094,  $\nu(\text{C}=\text{O})$  1675,  $\nu(\text{C}=\text{C})$  1612,  $\nu(\text{COC})_{\text{asym}}$  1115 and 1040  $\text{cm}^{-1}$ .  $^1\text{H}$  NMR ( $\text{C}_6\text{D}_6$ , 90 MHz):  $\delta$  10.21 (dt,  $J(\text{PH}) = 1.8$  Hz,  $J(\text{HH}) = 15.3$  Hz,  $\text{IrCH}=\text{CH}$ ), 6.86 (dt,  $J(\text{PH}) = 1.8$  Hz,  $J(\text{HH}) = 15.3$  Hz,  $\text{IrCH}=\text{CH}$ ), 3.54 (s,  $\text{CH}=\text{CHC}(\text{O})\text{OCH}_3$ ), 3.52 (m,  $\text{PCH}_2\text{CH}_2$ ), 3.47 (s,  $\text{C}=\text{CC}(\text{O})\text{OCH}_3$ ), 3.20 (s,  $\text{OCH}_3$ ), 2.87 (m,  $\text{PCHCH}_3$ ), 1.89 (m,  $\text{PCH}_2$ ), 1.40–1.02 (m,  $\text{PCHCH}_3$ ).  $^{31}\text{P}$  NMR ( $\text{C}_6\text{D}_6$ , 45 °C, 36.2 MHz):  $\delta$  3.37 (s). (b) The preparation of **19** from **13** (71 mg, 0.122 mmol) was performed analogously as described in (a): yield 58 mg (64%).

**Preparation of  $[\text{IrCl}(\text{C}=\text{CHPh})\{\kappa(\text{P})\text{-i-Pr}_2\text{PCH}_2\text{CH}_2\text{OMe}\}_2]$  (**20**).** (a) A solution of **17** (63 mg, 0.092 mmol) in 10 mL of benzene was stirred for 72 h at 80 °C. After the solution was cooled to room temperature, the solvent was

removed, the oily residue was dissolved in 2 mL of benzene, and the resulting solution was chromatographed on  $\text{Al}_2\text{O}_3$  (neutral, activity grade V). With  $\text{C}_6\text{H}_6$  a red fraction was eluted, from which a deep red air-sensitive oil was isolated: yield 34 mg (54%). Anal. Calcd for  $\text{C}_{26}\text{H}_{48}\text{ClIrO}_2\text{P}_2$ : C, 45.77; H, 7.09. Found: C, 45.35; H, 7.09. IR ( $\text{C}_6\text{H}_6$ ):  $\nu(\text{C}=\text{C})$  1630,  $\nu(\text{C}=\text{C}_{\text{Ph}})$  1592,  $\nu(\text{COC})_{\text{asym}}$  1108  $\text{cm}^{-1}$ .  $^1\text{H}$  NMR ( $\text{C}_6\text{D}_6$ , 90 MHz):  $\delta$  7.16 (m,  $\text{C}_6\text{H}_5$ ), 3.76 (m,  $\text{PCH}_2\text{CH}_2$ ), 3.06 (s,  $\text{OCH}_3$ ), 2.48 (m,  $\text{PCHCH}_3$ ), 2.46 (m,  $\text{PCH}_2$ ), 1.39 (dvt,  $N = 15.4$  Hz,  $J(\text{HH}) = 7.1$ ,  $\text{PCHCH}_3$ ), 1.09 (dvt,  $N = 14.1$  Hz,  $J(\text{HH}) = 7.0$ ,  $\text{PCHCH}_3$ ), –2.49 (t,  $J(\text{PH}) = 2.9$  Hz,  $\text{C}=\text{CH}$ ).  $^{13}\text{C}$  NMR ( $\text{C}_6\text{D}_6$ , 50.2 MHz):  $\delta$  263.10 (t,  $J(\text{PC}) = 13.1$  Hz,  $\text{Ir}=\text{C}=\text{C}$ ), 128.31, 128.17, 125.66, 124.84 (all s,  $\text{C}_6\text{H}_5$ ), 111.02 (s,  $\text{Ir}=\text{C}=\text{C}$ ), 69.45 (s,  $\text{PCH}_2\text{CH}_2\text{OCH}_3$ ), 57.96 (s,  $\text{OCH}_3$ ), 24.02 (vt,  $N = 28.7$  Hz,  $\text{PCHCH}_3$ ), 20.88 (vt,  $N = 26.4$  Hz,  $\text{PCH}_2\text{CH}_2\text{OCH}_3$ ), 19.94, 18.78 (both s,  $\text{PCHCH}_3$ ).  $^{31}\text{P}$  NMR ( $\text{C}_6\text{D}_6$ , 36.2 MHz):  $\delta$  23.02 (s). (b) A solution of **17** (66 mg, 0.097 mmol) in 13 mL of benzene was irradiated with a 125 W mercury vapor UV lamp (Phillips HPK) for 6 h at room temperature. After the solvent was removed, the solution was worked up as described in (a): yield 48 mg (72%).

**Preparation of  $[\text{IrCl}(\text{C}=\text{CHCO}_2\text{Me})\{\kappa(\text{P})\text{-i-Pr}_2\text{PCH}_2\text{CH}_2\text{OMe}\}_2]$  (**21**).** A solution of **13** (64 mg, 0.11 mmol) in 10 mL of benzene was treated with methyl propiolate (9.8  $\mu\text{L}$ , 0.11 mmol) and stirred for 5 h at 80 °C. After the solution was cooled to room temperature, the solvent was removed, the oily residue was dissolved in 2 mL of benzene, and the resulting solution was chromatographed on  $\text{Al}_2\text{O}_3$  (neutral, activity grade V). With  $\text{C}_6\text{H}_6$  a red fraction was eluted, which was brought to dryness in vacuo. A deep red air-sensitive solid was isolated, which was recrystallized from pentane at –78 °C: yield 59 mg (81%); mp 92 °C decomp. Anal. Calcd for  $\text{C}_{22}\text{H}_{46}\text{ClIrO}_4\text{P}_2$ : C, 39.78; H, 6.98. Found: C, 40.22; H, 7.14. IR ( $\text{C}_6\text{H}_6$ ):  $\nu(\text{C}=\text{O})$  1698,  $\nu(\text{C}=\text{C})$  1637,  $\nu(\text{COC})_{\text{asym}}$  1108  $\text{cm}^{-1}$ .  $^1\text{H}$  NMR ( $\text{C}_6\text{D}_6$ , 90 MHz):  $\delta$  3.76 (m,  $\text{PCH}_2\text{CH}_2$ ), 3.53 (s,  $\text{C}(\text{O})\text{OCH}_3$ ), 3.13 (s,  $\text{OCH}_3$ ), 2.49 (m,  $\text{PCH}_2$ ), 2.45 (m,  $\text{PCHCH}_3$ ), 1.27 (dvt,  $N = 15.6$  Hz,  $J(\text{HH}) = 7.3$ ,  $\text{PCHCH}_3$ ), 1.10 (dvt,  $N = 14.2$  Hz,  $J(\text{HH}) = 7.0$ ,  $\text{PCHCH}_3$ ), –2.09 (t,  $J(\text{PH}) = 2.5$  Hz,  $\text{C}=\text{CH}$ ).  $^{13}\text{C}$  NMR ( $\text{C}_6\text{D}_6$ , 50.2 MHz):  $\delta$  254.83 (t,  $J(\text{PC}) = 12.8$  Hz,  $\text{Ir}=\text{C}=\text{C}$ ), 151.69 (s,  $\text{C}(\text{O})\text{OCH}_3$ ), 103.12 (s,  $\text{Ir}=\text{C}=\text{C}$ ), 69.20 (s,  $\text{PCH}_2\text{CH}_2\text{OCH}_3$ ), 58.08 (s,  $\text{OCH}_3$ ), 50.29 (s,  $\text{C}(\text{O})\text{OCH}_3$ ), 24.04 (vt,  $N = 30.5$  Hz,  $\text{PCHCH}_3$ ), 20.40 (vt,  $N = 26.7$  Hz,  $\text{PCH}_2\text{CH}_2\text{OCH}_3$ ), 19.64, 18.43 (both s,  $\text{PCHCH}_3$ ).  $^{31}\text{P}$  NMR ( $\text{C}_6\text{D}_6$ , 36.2 MHz):  $\delta$  26.78 (s).

**Preparation of  $[\text{Ir}(\text{C}=\text{CHPh})\{\kappa^2(\text{P},\text{O})\text{-i-Pr}_2\text{PCH}_2\text{CH}_2\text{OMe}\}\{\kappa(\text{P})\text{-i-Pr}_2\text{PCH}_2\text{CH}_2\text{OMe}\}]\text{SbF}_6$  (**22**).** A solution of **20** (54 mg, 0.079 mmol) in 10 mL of dichloromethane was treated with a solution of  $\text{AgSbF}_6$  (27 mg, 0.079 mmol) in 3 mL of dichloromethane and stirred for 10 min at room temperature. The solution was filtered, and the solvent was removed from the filtrate. An oily residue was obtained, which was dissolved in 2 mL of dichloromethane, and 10 mL of ether was added slowly. A purple-red solid precipitated which was washed with ether and dried in vacuo: yield 61 mg (87%); mp 94 °C decomp. Anal. Calcd for  $\text{C}_{26}\text{H}_{48}\text{F}_6\text{IrO}_2\text{P}_2\text{Sb}$ : C, 35.38; H, 5.48. Found: C, 35.15; H, 5.68. IR ( $\text{CH}_2\text{Cl}_2$ ):  $\nu(\text{C}=\text{C})$  1667,  $\nu(\text{C}=\text{C}_{\text{Ph}})$  1592,  $\nu(\text{COC})_{\text{asym}}$  1104 and 1054  $\text{cm}^{-1}$ .  $^1\text{H}$  NMR ( $\text{CD}_2\text{Cl}_2$ , 90 MHz):  $\delta$  7.12 (m,  $\text{C}_6\text{H}_5$ ), 3.86 (m,  $\text{PCH}_2\text{CH}_2$ ), 3.48 (s,  $\text{OCH}_3$ ), 2.48 (m,  $\text{PCHCH}_3$ ), 2.25 (m,  $\text{PCH}_2$ ), 1.30, 1.28 (both dvt,  $N = 15.0$  Hz,  $J(\text{HH}) = 7.2$ ,  $\text{PCHCH}_3$ ), –1.62 (t,  $J(\text{PH}) = 2.6$  Hz,  $\text{C}=\text{CH}$ ).  $^{13}\text{C}$  NMR ( $\text{CD}_2\text{Cl}_2$ , 50.2 MHz):  $\delta$  275.88 (t,  $J(\text{PC}) = 13.1$  Hz,  $\text{Ir}=\text{C}=\text{C}$ ), 128.65, 126.44, 126.23 (all s,  $\text{C}_6\text{H}_5$ ), 111.50 (t,  $J(\text{PC}) = 4.4$  Hz,  $\text{Ir}=\text{C}=\text{C}$ ), 75.55 (s,  $\text{PCH}_2\text{CH}_2\text{OCH}_3$ ), 62.42 (s,  $\text{OCH}_3$ ), 25.78 (vt,  $N = 30.7$  Hz,  $\text{PCHCH}_3$ ), 20.40 (vt,  $N = 25.3$  Hz,  $\text{PCH}_2\text{CH}_2\text{OCH}_3$ ), 19.57, 18.63 (both s,  $\text{PCHCH}_3$ ).  $^{31}\text{P}$  NMR ( $\text{CD}_2\text{Cl}_2$ , 36.2 MHz):  $\delta$  39.96 (s).

**Preparation of  $[\text{Ir}(\text{C}=\text{CHCO}_2\text{Me})\{\kappa^2(\text{P},\text{O})\text{-i-Pr}_2\text{PCH}_2\text{CH}_2\text{OMe}\}\{\kappa(\text{P})\text{-i-Pr}_2\text{PCH}_2\text{CH}_2\text{OMe}\}]\text{SbF}_6$  (**23**).** This compound was prepared analogously as described for **22**, using **21** (58 mg, 0.087 mmol) and  $\text{AgSbF}_6$  (30 mg, 0.089 mmol) as starting materials: yield 65 mg (84%); mp 130 °C decomp. Anal. Calcd for  $\text{C}_{22}\text{H}_{46}\text{F}_6\text{IrO}_4\text{P}_2\text{Sb}$ : C, 30.57; H, 5.36. Found:



**Table 5. Positional Parameters and Their Esd's for 8**

atom	<i>x/a</i>	<i>y/b</i>	<i>z/c</i>	<i>B</i> <sub>eq</sub>
Ir	0.20688(4)	0.03441(4)	0.25186(2)	1.567(7)
Cl	-0.0782(3)	0.0333(2)	0.3551(2)	2.58(5)
P1	0.3280(3)	-0.1485(2)	0.3463(2)	1.76(5)
P2	0.1498(3)	0.2340(2)	0.1498(2)	1.88(5)
O1	0.3207(7)	0.1742(6)	0.3323(4)	2.0(1)
O2	0.0618(9)	-0.0394(7)	0.1015(4)	3.0(1)
C1	0.445(1)	-0.052(1)	0.4071(6)	2.5(2)
C2	0.479(1)	0.0997(9)	0.3553(6)	2.2(2)
C3	0.217(1)	0.226(1)	0.4053(6)	2.9(2)
C4	0.187(1)	-0.2571(9)	0.4378(6)	2.2(2)
C5	0.286(1)	-0.363(1)	0.5008(6)	3.2(2)
C6	0.048(1)	-0.329(1)	0.4074(7)	3.0(2)
C7	0.500(1)	-0.2773(9)	0.3057(6)	2.4(2)
C8	0.435(1)	-0.390(1)	0.2647(7)	3.5(2)
C9	0.645(1)	-0.198(1)	0.2410(7)	3.3(2)
C10	-0.014(1)	0.213(1)	0.0843(6)	2.8(2)
C11	-0.081(1)	0.064(1)	0.1104(7)	3.0(2)
C12	0.124(1)	-0.098(1)	0.1816(6)	2.6(2)
C13	0.339(1)	0.289(1)	0.0647(6)	2.5(2)
C14	0.409(1)	0.171(1)	0.0129(7)	3.7(3)
C15	0.482(1)	0.337(1)	0.1048(7)	3.6(3)
C16	0.077(1)	0.402(1)	0.1913(6)	2.6(2)
C17	0.077(1)	0.537(1)	0.1203(7)	3.5(2)
C18	-0.103(1)	0.390(1)	0.2490(7)	3.7(3)

**Table 6. Positional Parameters and Their Esd's for 12**

atom	<i>x/a</i>	<i>y/b</i>	<i>z/c</i>	<i>B</i> <sub>eq</sub>
Ir	0.03375(3)	0.07053(2)	0.000	1.654(5)
Cl1	0.0035(3)	0.0215(1)	-0.1568(2)	2.63(5)
Cl2	-0.1350(3)	0.1443(1)	-0.0447(2)	2.80(5)
Cl3	0.5201(4)	0.1586(2)	0.2289(2)	3.71(7)
Cl4	0.3189(6)	0.1650(2)	0.5237(6)	12.0(2)
Cl5	0.0259(5)	0.2463(2)	0.5001(7)	8.7(1)
P1	0.1529(3)	-0.0172(1)	0.0307(2)	1.82(5)
P2	0.1965(3)	0.1357(1)	-0.0564(2)	2.02(5)
N1	-0.1474(9)	0.0180(5)	0.0526(7)	2.6(2)
N2	0.0598(9)	0.1694(4)	0.1607(7)	2.3(2)
C1	0.012(1)	-0.0688(6)	0.0427(9)	2.9(2)
C2	-0.099(1)	-0.0387(5)	0.1005(9)	2.6(2)
C3	-0.241(1)	-0.0001(6)	-0.0240(9)	3.4(3)
C4	-0.232(1)	0.0505(6)	0.123(1)	3.7(3)
C5	0.238(1)	-0.0232(5)	0.1466(8)	2.4(2)
C6	0.270(1)	-0.0887(6)	0.1786(9)	3.6(3)
C7	0.365(1)	0.0173(6)	0.157(1)	3.4(3)
C8	0.259(1)	-0.0541(5)	-0.0608(9)	2.7(2)
C9	0.412(1)	-0.0539(6)	-0.046(1)	3.5(3)
C10	0.219(2)	-0.1192(7)	-0.083(1)	4.8(3)
C11	0.238(1)	0.1893(5)	0.0390(8)	2.4(2)
C12	0.113(1)	0.2122(5)	0.0883(8)	2.6(2)
C13	0.139(1)	0.1799(6)	0.2508(8)	3.4(3)
C14	0.072(1)	0.1030(5)	0.1319(7)	2.0(2)
C15	-0.083(1)	0.1872(6)	0.183(1)	3.1(3)
C16	0.362(1)	0.1039(6)	-0.0887(9)	2.8(2)
C17	0.360(1)	0.0777(6)	-0.1914(9)	3.3(3)
C18	0.486(1)	0.1434(7)	-0.073(1)	4.1(3)
C19	0.142(1)	0.1890(5)	-0.1494(8)	2.5(2)
C20	0.071(1)	0.1629(6)	-0.2346(9)	3.6(3)
C21	0.253(1)	0.2333(5)	-0.185(1)	3.4(3)

C, 30.76; H, 5.21. IR (CH<sub>2</sub>Cl<sub>2</sub>): ν(C=O) 1705, ν(C=C) 1638, ν(COC)<sub>asym</sub> 1106 and 1040 cm<sup>-1</sup>. <sup>1</sup>H NMR (CD<sub>2</sub>Cl<sub>2</sub>, 90 MHz): δ 3.85 (m, PCH<sub>2</sub>CH<sub>2</sub>), 3.63 (s, C(O)OCH<sub>3</sub>), 3.46 (s, OCH<sub>3</sub>), 2.58 (m, PCHCH<sub>3</sub>), 2.34 (m, PCH<sub>2</sub>), 1.32 (dvt, *N* = 15.6 Hz, *J*(HH) = 7.1, PCHCH<sub>3</sub>), -1.60 (t, *J*(PH) = 2.5 Hz, =C=CH). <sup>13</sup>C NMR (CD<sub>2</sub>Cl<sub>2</sub>, 50.2 MHz): δ 267.40 (t, *J*(PC) = 11.3 Hz, Ir=C=C), 211.26 (s, C(O)OCH<sub>3</sub>), 104.08 (s, Ir=C=C), 74.59 (s, PCH<sub>2</sub>CH<sub>2</sub>OCH<sub>3</sub>), 62.07 (s, OCH<sub>3</sub>), 51.47 (s, C(O)OCH<sub>3</sub>), 25.74 (vt, *N* = 31.4 Hz, PCHCH<sub>3</sub>), 20.35 (vt, *N* = 26.6 Hz, PCH<sub>2</sub>CH<sub>2</sub>OCH<sub>3</sub>), 19.41, 18.54 (both s, PCHCH<sub>3</sub>). <sup>31</sup>P NMR (CD<sub>2</sub>Cl<sub>2</sub>, 36.2 MHz): δ 35.59 (s).

**X-ray Structural Analyses of 8, 12, and 23.** Single crystals were grown from toluene/pentane (8), dichloromethane/pentane (12), and dichloromethane (29). Crystal data collec-

**Table 7. Positional Parameters and Their Esd's for 23**

atom	<i>x/a</i>	<i>y/b</i>	<i>z/c</i>	<i>B</i> <sub>eq</sub>
Ir	0.20897(2)	0.72791(2)	0.36084(2)	3.299(6)
Sb	0.26778(5)	0.52018(4)	0.84829(5)	5.65(2)
P1	0.0593(2)	0.7197(1)	0.4239(2)	4.33(5)
P2	0.3662(2)	0.7456(1)	0.3071(2)	3.95(5)
F1	0.2040(6)	0.4481(5)	0.9148(5)	11.0(2)
F2	0.3312(7)	0.5913(5)	0.7827(5)	12.3(2)
F3	0.325(1)	0.5588(9)	0.9588(8)	14.0(4)
F4	0.219(1)	0.480(1)	0.735(1)	14.3(5)
F5	0.156(1)	0.581(1)	0.843(2)	17.4(7)
F6	0.381(1)	0.462(1)	0.850(1)	19.8(7)
O1	0.3023(7)	0.4310(4)	0.4453(5)	8.0(2)
O2	0.3469(5)	0.5485(4)	0.5096(5)	6.3(2)
O3	0.1651(4)	0.8508(3)	0.3475(4)	5.2(1)
O4	0.3907(6)	0.2647(7)	0.9808(4)	7.0(2)
C1	0.2265(5)	0.6251(5)	0.3697(5)	3.6(2)
C2	0.2344(7)	0.5470(5)	0.3705(6)	4.6(2)
C3	0.2941(7)	0.5020(5)	0.4428(7)	5.4(2)
C4	0.407(1)	0.5108(7)	0.5884(8)	9.2(4)
C5	0.0207(7)	0.8234(5)	0.4300(7)	5.7(2)
C6	0.1110(8)	0.8766(5)	0.4221(7)	6.6(3)
C7	0.1257(8)	0.8830(6)	0.2583(8)	7.6(3)
C8	0.0676(8)	0.6842(6)	0.5442(7)	6.5(3)
C9	0.073(1)	0.5938(7)	0.5496(8)	10.0(4)
C10	0.1594(9)	0.7216(8)	0.6068(8)	9.2(4)
C11	-0.0491(7)	0.6706(6)	0.3517(7)	6.2(3)
C12	-0.0633(8)	0.7008(7)	0.2526(7)	7.3(3)
C13	-0.1505(7)	0.6769(8)	0.3922(9)	10.4(4)
C14	0.3992(7)	0.8482(5)	0.2834(6)	5.0(2)
C15	0.4088(7)	0.9059(5)	0.3639(7)	5.2(2)
C16	0.4165(9)	1.0428(6)	0.3859(8)	7.6(3)
C17	0.4736(6)	0.7058(5)	0.3909(7)	5.2(2)
C18	0.4714(8)	0.7332(6)	0.4895(7)	6.6(3)
C19	0.5792(7)	0.7164(7)	0.3624(9)	8.2(3)
C20	0.3746(7)	0.7012(5)	0.1936(7)	5.5(2)
C21	0.2840(8)	0.7268(6)	0.1205(7)	6.9(3)
C22	0.3828(8)	0.6105(6)	0.1948(7)	6.9(3)

tion parameters are summarized in Table 4. Intensity data were corrected for Lorentz and polarization effects. An empirical absorption correction was applied; the minimal transmissions were 77.2% (for 8), 95.3% (for 12), and 70.3% (for 23). The structures were solved by direct methods (SHELXS-86) for 8 and 23 and by the Patterson method (SHELXS-86, DIRDIF) for 12. In the case of 12, there is one molecule of CH<sub>2</sub>Cl<sub>2</sub> in the asymmetric unit. The SbF<sub>6</sub> anion of compound 23 reveals disorder in the octahedral plane with the disordered positions rotated by ca. 45° in the plane; a weighting factor of 0.4 was used for the refinement. The position of the metal-bonded hydrogen atom of 8 was taken from a difference-Fourier synthesis. The positions of all other hydrogen atoms were calculated according to ideal geometry (distance of C-H set at 0.95 Å) and were refined by the riding method. Atomic coordinates (see Tables 5-7) and anisotropic thermal parameters of the non-hydrogen atoms were refined by full-matrix least squares. For other details see Table 4.

**Acknowledgment.** We thank the Deutsche Forschungsgemeinschaft (SFB 347) and the Fonds der Chemischen Industrie for financial support, the Fonds in particular for a Doktorandenstipendium for M.S. We also gratefully acknowledge support by Mrs. A. Burger (experimental assistance), Dr. W. Buchner, Dr. M. Schäfer, and Mrs. M.-L. Schäfer (NMR spectra), Mrs. U. Neumann and Mr. C. P. Kneis (elemental analyses), and Degussa AG (chemicals).

**Supporting Information Available:** Drawings showing the atom-numbering schemes, and tables of crystal data, bond distances, bond angles, positional parameters, and general displacement parameter expressions of compounds 8, 12, and 23 (25 pages). Ordering information is given on any current masthead page.

OM950109T

# Formation and Structure of Coordinatively Unsaturated Cp\*Ir–Amino Acid Complexes. Kinetic and Thermodynamic Control in Highly Diastereoselective Complexation Reactions

D. B. Grotjahn\* and T. L. Groy†

Department of Chemistry and Biochemistry, Box 871604, Arizona State University, Tempe, Arizona 85287-1604

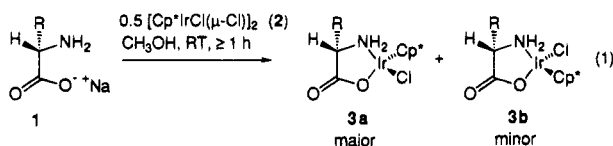
Received January 17, 1995\*

Amino acid derivatives bearing an electron-withdrawing group Z on N (Z = tosyl, CO<sub>2</sub>-CH<sub>2</sub>Ph, or acetyl) serve as (N,O)-chelating, dianionic ligands to the fragment Cp\*Ir. Six such complexes have been prepared, all of them coordinatively unsaturated yet air-stable. The structure of the *N*-tosylglycine derivative C<sub>19</sub>H<sub>24</sub>IrNO<sub>4</sub>S (**5a**) was analyzed at 20 °C. A planar chelate ring was revealed, and relatively short Ir–N and Ir–O bonds suggested stabilization of unsaturated Ir by  $\pi$ -donation. Crystals of the (*R*)-*N*-tosylphenylglycine complex C<sub>25</sub>H<sub>28</sub>IrNO<sub>4</sub>S (**5f**) were monoclinic. Some distortion of the chelate ring was seen, and both aryl rings were syn, the angle between their mean planes being 19°. Within seconds, red solutions of the unsaturated complexes **5** turn yellow on addition of ligands such as phosphines, CO, and primary aliphatic or heterocyclic amines. Ligands add to chiral complexes so as to place the amino acid side chain R and Cp\* cis to each other on the metallacycle, suggesting preferred approach of the ligand to **5** from the side opposite R. For one PMe<sub>3</sub> adduct this was shown to be the result of kinetic control ( $\geq 50:1$  selectivity at 25 °C) and thermodynamic control (40:1 selectivity after equilibration at 90 °C, half-life = 5 h). PPh<sub>3</sub> and amines exchange within minutes at 25 °C. The stereoselectivity of ligand addition was highest for smaller ligands. Comparing this result and previous work suggests that steric interactions between added ligand and the amino acid side chain R determine diastereoselectivity.

## Introduction

Amino acid–metal complexes have been the subject of innumerable studies,<sup>1</sup> prompted by the role of metals in biochemistry<sup>2</sup> and by the role of amino acids in producing chiral catalysts.<sup>3</sup> Transformation of amino acids into valuable enantiomerically pure organic compounds using organic reagents or main-group organometallics<sup>4</sup> are useful, but conversions using transition-metal catalysts or reagents appear to be unknown, motivating the following studies.

With very few exceptions,<sup>5</sup> amino acid–metal complexes<sup>1,6</sup> are coordinatively saturated. For example, interaction of *N*-unsubstituted amino acid salts **1** with [Cp\*IrCl( $\mu$ -Cl)]<sub>2</sub> (**2**) leads to 18-electron complexes **3** (eq 1), the stereogenic element of the amino acid producing



mixtures modestly enriched in diastereomer **3a** (from 50:50 up to 92:8).<sup>6a,b</sup> Here we report in full<sup>7</sup> that, under

\* X-ray crystal structures.

† Abstract published in *Advance ACS Abstracts*, June 1, 1995.

(1) (a) Laurie, S. H. *Amino Acids, Peptides and Proteins*. In *Comprehensive Coordination Chemistry*; Wilkinson, G., Ed.; Pergamon: Oxford, 1987, Vol. 2, pp 739–776. (b) Ioganson, A. A. *Russ. Chem. Rev.* **1985**, *54*, 277–292. (c) Sigel, H.; Martin, R. B. *Chem. Rev.* **1982**, *82*, 385–426.

(2) Metalloproteins: Structural Aspects. *Adv. Prot. Chem.* **1991**, *42*. Ibers, J. A.; Holm, R. H. *Science* **1980**, *209*, 223–235.

modified conditions, amino acid derivatives **4** (Scheme 1) bearing electron-withdrawing groups Z on N afford air-stable 16-electron species **5**, two members of which are characterized by X-ray diffraction. Furthermore, unlike ligand substitutions on **3** and related species, ligand addition reactions of chiral **5** proceed with high ( $\geq 25:1$ ) stereoselectivity. Additional experiments reported here define the range of ligands that bind to **5** and demonstrate the operation of kinetic and thermodynamic control in ligand binding, critical considerations in the design and use of asymmetric catalysts related to **4**.<sup>8</sup>

## Results

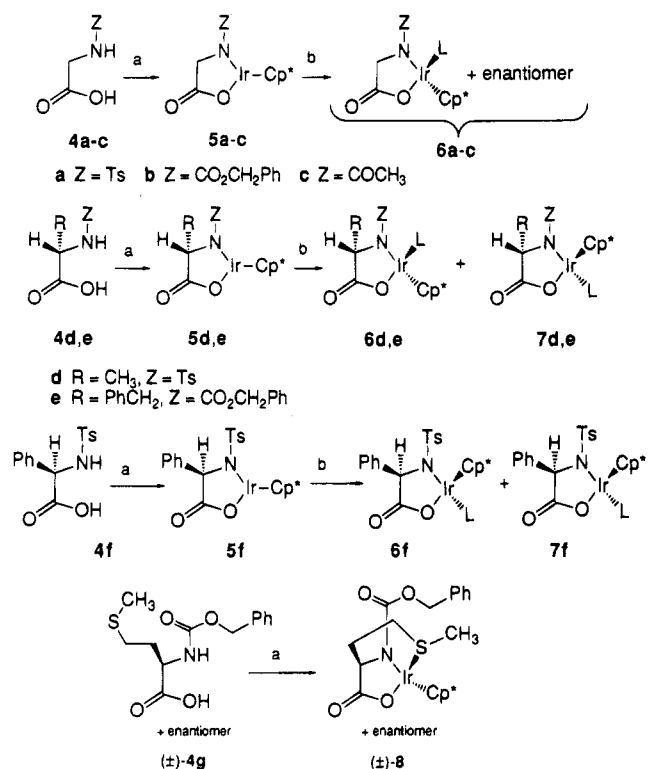
### Synthesis of **5a–f** and Crystallography of **5a** and **5f**. Our initial goal was to attach an amino acid to a

(3) (a) Brunner, H. *Top. Stereochem.* **1988**, *18*, 129–247. (b) *Chiral Catalysis: Asymmetric Synthesis*; Morrison, J., Ed.; Academic: Orlando, 1985; Vol. 5. (c) *Asymmetric Catalysis in Organic Synthesis*; Noyori, R., Ed.; Wiley: New York, 1994. (d) *Catalysis in Asymmetric Synthesis*; Ojima, I., Ed.; VCH: New York, 1993.

(4) (a) Reetz, M. T. *Angew. Chem., Int. Ed. Engl.* **1991**, *30*, 1531–1546. (b) Scott, J. W. Readily Available Chiral Carbon Fragments and Their Use in Synthesis. In *Asymmetric Synthesis*; Morrison, J. D., Scott, J. W., Eds.; Academic: Orlando, 1984; Vol. 4, pp 1–226.

(5) (a) To our knowledge, the only coordinatively unsaturated amino acid complexes reported are (CO)<sub>2</sub>Rh<sup>I</sup>(amino acidato) complexes, which undergo CO substitution by PR<sub>3</sub> and AsR<sub>3</sub>; Dowerah, D.; Singh, M. M. *J. Indian Chem. Soc.* **1980**, *57*, 368–371. Dowerah, D.; Singh, M. M. *J. Chem. Res., Synop.* **1979**, 38. Dowerah, D.; Singh, M. M. *Transition Met. Chem. (London)* **1976**, *1*, 294–295. (b) A dimeric Cp\*Rh–glycine amide complex (**16**) was recently suspected on the basis of <sup>1</sup>H NMR evidence of undergoing partial monomerization in solution to a species related to **5** (but formulated as rapidly epimerizing at Rh, **17a** + **17b**): Krämer, R.; Polborn, K.; Robl, C.; Beck, W. *Inorg. Chim. Acta* **1992**, *198–200*, 415–420.

Scheme 1



Legend: (a) K<sub>2</sub>CO<sub>3</sub>, [Cp\*IrCl(μ-Cl)]<sub>2</sub>, THF, or CH<sub>3</sub>CN, room temperature, 4–36 h; (b) ligand, CDCl<sub>3</sub> or C<sub>6</sub>D<sub>6</sub>, room temperature, ≤15 s.

metal as a chelating, dianionic ligand, which was anticipated to bind strongly to the metal center. Deprotonation at N was to be facilitated by N-substitution with an electron-withdrawing group Z,<sup>1</sup> as in sulfonamides, amides, and carbamates 4. Reported reactions of 2 and N-unsubstituted amino acid salts 1 were conducted in alcohol solvents.<sup>6a</sup> However, because amide and sulfonamide anions exhibit greater basicity in aprotic media,<sup>9</sup> and because hydrogen bonding attenuates nucleophilicity of anionic species,<sup>10</sup> we employed nonprotic media (THF or CH<sub>3</sub>CN) in reactions of 2 and amino acid derivatives 4<sup>11</sup> with the expectation that the coordination sphere of the metal in the product

(6 or 7, L = THF or CH<sub>3</sub>CN) would include a solvent molecule, which could be easily displaced as desired with other ligands. Thus, a nitrogen-saturated mixture of 4a, dimer 2,<sup>12</sup> and anhydrous K<sub>2</sub>CO<sub>3</sub> (molar ratio 1.00:0.50:2.0–3.0) in THF (initial orange color) was stirred for 24 h, during which time the color deepened to red. The residue remaining after rotary evaporation was diluted with CH<sub>2</sub>Cl<sub>2</sub> and filtered through Celite, and the filtrate was concentrated to afford a red foam in high yield. Similar results were obtained using CH<sub>3</sub>CN as solvent, although before turning red the mixture initially was yellow, presumably due to dissolution of 2 with formation of Cp\*Ir(Cl)<sub>2</sub>(CH<sub>3</sub>CN).<sup>13</sup>

Analytical data for the reaction product from 4a (Tables 1–3) pointed to chelation of the amino acid derivative: deprotonation at N was implicated by a <sup>1</sup>H NMR spectrum featuring a two-proton singlet, ascribable to the methylene protons, and deprotonation at both N and O was apparent from a lack of infrared absorption above 3100 cm<sup>-1</sup>. Furthermore, all analytical data, including elemental analysis, were consistent with the absence of coordination by reaction solvents THF or CH<sub>3</sub>CN, or even by N<sub>2</sub> in the product, suggesting structure 5a. However, the geometry at Ir remained unclear. Even at -90 °C, the <sup>1</sup>H NMR spectrum of 5a in CD<sub>2</sub>Cl<sub>2</sub> revealed a sharp two-proton singlet at δ 3.20 ppm for the methylene group, consistent with either an achiral structure or rapidly interconverting, enantiomeric, octahedral structures. Thus, the structural ambiguity surrounding 5a was settled by X-ray crystallographic analysis (Figure 1 and Tables 4, 10, and 11) on a crystal readily obtained by vapor diffusion of petroleum ether into a hot, undeoxygenated toluene solution of the compound. The planarity of the metallacycle is revealed by the position of the centroid of Cp\* only 0.022 Å away from the mean plane defined by the five atoms of the chelate ring. Furthermore, no atom of the chelate lies more than 0.029 Å away from the metallacycle mean plane. Compared with 18-electron 3,<sup>6a,b</sup> the Ir–N and Ir–O bonds are ca. 0.15 and 0.06 Å shorter, respectively, suggesting stabilization of the formally 16-electron metal by lone pairs on N and O, as proposed by Bergman and co-workers<sup>14</sup> in their structural analysis of 9. Additional evidence for π-do-

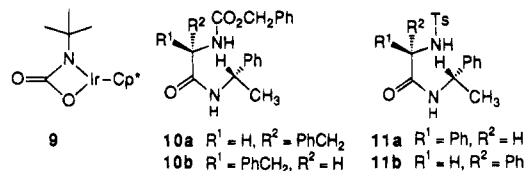
(6) (a) Krämer, R.; Polborn, K.; Wanjek, H.; Zahn, I.; Beck, W. *Chem. Ber.* **1990**, *123*, 767–778. (b) Carmona, D.; Mendoza, A.; Lahoz, F. J.; Oro, L. A.; Lamata, M. P.; San Jose, E. *J. Organomet. Chem.* **1990**, *396*, C17–C21. For amino acid chelate complexes to other organometallic fragments, see: (c) Dersnah, D. F.; Baird, M. C. *J. Organomet. Chem.* **1977**, *127*, C55–C58. (d) Sheldrick, W. S.; Heeb, S. *J. Organomet. Chem.* **1989**, *377*, 357–366. (e) Sheldrick, W. S.; Exner, R. *Inorg. Chim. Acta* **1990**, *175*, 261–268. (f) Werner, H.; Daniel, T.; Nürnberg, O.; Knaup, W.; Meyer, U. *J. Organomet. Chem.* **1993**, *445*, 229–235. (g) Sheldrick, W. S.; Gleichmann, A. *J. Organomet. Chem.* **1994**, *470*, 183–187. (h) Lippmann, E.; Krämer, R.; Beck, W. *J. Organomet. Chem.* **1994**, *466*, 167–174. (i) Bergs, R.; Sünkel, K.; Beck, W. *Chem. Ber.* **1993**, *126*, 2429–2432. (j) Shinoda, S.; Inoue, N.; Takita, K.; Saito, Y. *Inorg. Chim. Acta* **1982**, *65*, L21–L23. (k) Darenbourg, D. J.; Atnip, E. V.; Klausmeyer, K. K.; Reibenspies, J. H. *Inorg. Chem.* **1994**, *33*, 5230–5237. Cp<sub>2</sub>Ti(amino acid)<sub>2</sub> complexes: (l) Klapötke, T. M.; Köpf, H.; Tornieporth-Oetting, I. C.; White, P. S. *Angew. Chem., Int. Ed. Engl.* **1994**, *33*, 1518–1519. Klapötke, T. M.; Köpf, H.; Tornieporth-Oetting, I. C.; White, P. S. *Organometallics* **1994**, *13*, 3628–3633.

(7) Grotjahn, D. B.; Groy, T. L. *J. Am. Chem. Soc.* **1994**, *116*, 6969–6970.

(8) Deloux, L.; Srebnik, M. *Chem. Rev.* **1993**, *93*, 763–784 and references therein.

(9) Bordwell, F. G. *Acc. Chem. Res.* **1988**, *21*, 456–463. Dyumaev, K. M.; Korolev, B. A. *Russ. Chem. Rev.* **1980**, *49*, 1021–1032.

(10) March, J. *Advanced Organic Chemistry*, 4th ed.; Wiley: New York, 1992; p 349ff.



nation from N and O<sup>15,16</sup> in 5 will be discussed below. The other metrical parameters for 5a, in particular, the length of the carboxylato C–O double and single bonds,

(11) Compounds 4b, 4c, and 4e were purchased. N-Ts derivatives 4a and 4d (4f was made using a similar procedure): McChesney, F. W.; Swann, W. K. Jr. *J. Am. Chem. Soc.* **1937**, *59*, 1116–1118. (±)-4g: Dekker, C. A.; Fruton, J. S. *J. Biol. Chem.* **1948**, *173*, 471–477.

(12) White, C.; Yates, A.; Maitlis, P. M. *Inorg. Synth.* **1992**, *29*, 228.

(13) For CH<sub>3</sub>CN and [(COD)Ir(μ-Cl)]<sub>2</sub>, see: Day, V. W.; Klemperer, W. G.; Main, D. J. *Inorg. Chem.* **1990**, *29*, 2345–2355.

(14) Glueck, D. S.; Wu, J.; Hollander, F. J.; Bergman, R. G. *J. Am. Chem. Soc.* **1991**, *113*, 2041–2054.

(15) (a) Goldman, A. S.; Halpern, J. *J. Organomet. Chem.* **1990**, *382*, 237–253. (b) Lunder, D. M.; Lobkovsky, E. B.; Streib, W. E.; Caulton, K. G. *J. Am. Chem. Soc.* **1991**, *113*, 1837–1838.

Table 1. Yield, Color, Melting Points,<sup>a</sup> IR Data, and Elemental Analyses of Complexes Isolated

product	yield <sup>b</sup> (%)	appearance	IR $\nu_{C=O}$ (cm <sup>-1</sup> )	molecular formula (molecular wt)	anal. calcd, %			anal. found, %		
					C	H	N	C	H	N
<b>5a</b>	97	red foam	1684 (CH <sub>2</sub> Cl <sub>2</sub> , NaCl) 1684 (KBr)	C <sub>19</sub> H <sub>24</sub> IrNO <sub>4</sub> S (554.70)	41.14	4.36	2.53	41.95	4.47	2.38
<b>5b</b>	94	deep red solid <sup>c</sup>	1682, 1672 (KBr)	C <sub>20</sub> H <sub>24</sub> IrNO <sub>4</sub> (534.62)	44.93	4.52	2.62	44.40	4.44	2.61
<b>5c<sup>d</sup></b>	96	yellow solid	1653, 1570, 1553 (KBr) 1659, 1642 (CH <sub>2</sub> Cl <sub>2</sub> , NaCl)	(C <sub>14</sub> H <sub>20</sub> IrNO <sub>3</sub> ) <sub>n</sub> (n × 442.54)	38.00	4.52	3.17	38.17	4.83	2.64
<b>5d<sup>e</sup></b>	100	deep red powder	1678 (KBr)	C <sub>20</sub> H <sub>26</sub> IrNO <sub>4</sub> S (568.73)	42.24	4.61	2.46	42.46	4.79	2.25
<b>5e</b>	96	deep red solid <sup>f</sup>	1681, 1653 (KBr) 1668 (CH <sub>2</sub> Cl <sub>2</sub> , NaCl)	C <sub>27</sub> H <sub>30</sub> IrNO <sub>4</sub> (624.76)	51.91	4.84	2.24	52.38	4.98	2.20
<b>5f</b>	96	red foam <sup>g</sup>	1674 (KBr)	C <sub>25</sub> H <sub>28</sub> IrNO <sub>4</sub> S (630.79)	47.60	4.47	2.22	47.51	4.58	2.26
<b>6a-PMe<sub>3</sub></b>	89	yellow powder <sup>h</sup>	1650 (KBr)	C <sub>22</sub> H <sub>33</sub> IrNO <sub>4</sub> PS (630.77)	41.89	5.27	2.22	42.05	5.31	2.10
<b>6b-PMe<sub>3</sub><sup>i</sup></b> <b>6d-PMe<sub>3</sub></b>	95	pale yellow solid	1645 (CH <sub>2</sub> Cl <sub>2</sub> , NaCl) 1644 (KBr)	C <sub>23</sub> H <sub>35</sub> IrNO <sub>4</sub> PS (640.80)	42.84	5.47	2.17	42.58	5.48	1.97
<b>6e-PMe<sub>3</sub><sup>i</sup></b> <b>7e-PMe<sub>3</sub></b>	60	pale yellow crystals	1637 (CDCl <sub>3</sub> , NaCl) 1648 (KBr)	C <sub>30</sub> H <sub>39</sub> IrNO <sub>4</sub> P (700.84)	51.41	5.61	2.00	51.34	5.63	2.04
<b>6d-PMe<sub>2</sub>Ph</b>	100	pale yellow powder	1651 (KBr)	C <sub>28</sub> H <sub>37</sub> IrNO <sub>4</sub> PS (706.86)	47.58	5.27	1.98	46.67	5.32	1.94
<b>6d-PMePh<sub>2</sub></b>	92	yellow powder	1653 (KBr)	C <sub>33</sub> H <sub>39</sub> IrNO <sub>4</sub> PS (768.94)	51.55	5.11	1.82	51.64	5.19	1.83
<b>6a-PPh<sub>3</sub></b>	97	yellow powder	1661 (KBr)	C <sub>37</sub> H <sub>39</sub> IrNO <sub>4</sub> PS (816.99)	54.50	4.81	1.71	54.21	4.86	1.66
<b>6d-PPh<sub>3</sub><sup>j</sup></b>	88	yellow powder	1647 (KBr)	C <sub>38</sub> H <sub>41</sub> IrNO <sub>4</sub> PS (831.01)	54.92	4.97	1.69	53.87	4.97	1.90
<b>6a-CO</b> <b>6d-CO</b>	100 90	pale yellow powder pale yellow powder	2033, <sup>k</sup> 1671 (KBr) 2042, <sup>k</sup> 1669 (KBr)							
<b>(±)-6d-DMAP</b>	100	pale yellow solid	1643 (KBr)	C <sub>27</sub> H <sub>37</sub> IrN <sub>3</sub> O <sub>4</sub> S (691.90)	46.87	5.39	6.07	46.88	5.34	5.97
<b>6a-MeIm<sup>l,i</sup></b> <b>(±)-8</b>	98	yellow solid	1625 (CDCl <sub>3</sub> , NaCl) 1641 (br, KBr)	C <sub>23</sub> H <sub>32</sub> IrNO <sub>4</sub> S (610.81)	45.23	5.28	2.29	45.49	5.16	2.18

<sup>a</sup> In N<sub>2</sub>-filled, sealed capillaries. All compounds examined decomposed upon melting at temperatures dependent on how long sample was heated. Temperatures reported are for samples heated from 5–10 degrees below reported values. <sup>b</sup> Yields refer to material characterized by elemental analysis. <sup>c</sup> Mp 145–148 °C (decomp). <sup>d</sup> Structure in solution, see text. <sup>e</sup> Racemate obtained in 90% yield, exhibited identical spectral properties. <sup>f</sup> Mp 155–158 °C (decomp). <sup>g</sup> Mp 210 °C (decomp). <sup>h</sup> Mp 225 °C (decomp). <sup>i</sup> Not isolated. <sup>j</sup> Presumed to be admixed with **7d**-PPh<sub>3</sub>. <sup>k</sup>  $\nu_{C=O}$ . <sup>l</sup> MeIm = 1-methylimidazole.

are unexceptional. The nearest intermolecular contacts for the metal center are a carbonyl oxygen in a symmetry-related molecule at 5.47 Å, securing the assignment that in **5a** the metal center interacts only with the Cp\* and amino acid chelate ligands, both in solution and in the crystal.

Eventually, using similar synthetic procedures, other examples of complexes **5** were obtained as red solids or foams in ≥94% yield. Evidence presented below indicates that in these systems, red color is diagnostic for coordinative unsaturation. Products **5** are air-stable but solutions lose their red color when in contact with water, and chromatography of **5** over SiO<sub>2</sub> seems to destroy the complexes, presumably by hydrolysis. Occasionally in the synthesis of **5c** in THF the addition of Na<sub>2</sub>SO<sub>4</sub> was

required to achieve a red color, suggesting that water presumably produced in the neutralization of acid by carbonate ion interferes with the formation of **5c**. Alkoxide and amide ligands on late transition metals have been observed to act as hydrogen-bond acceptors,<sup>15,17</sup> and can exchange with the hydrogen bond donor.<sup>15,17</sup>

Base-catalyzed epimerization of amino acid derivatives can be a serious problem in peptide synthesis.<sup>18</sup> Therefore, evidence for the enantiomeric purity of chiral **5** was sought. The high susceptibility of phenylglycine derivatives to base-catalyzed racemization<sup>19</sup> suggested that the enantiomeric purity of **5f** would be an especially stringent test. Unfortunately, the application of chiral lanthanide shift reagents<sup>20</sup> led only to broadening of resonances in the <sup>1</sup>H NMR spectrum of chiral **5**. However, derivatization of the amino acid ligand in **5e**

(16) Reviews: (a) Bryndza, H. E.; Tam, W. *Chem. Rev.* **1988**, *88*, 1163–1188. (b) Fryzuk, M. D.; Montgomery, C. D. *Coord. Chem. Rev.* **1989**, *95*, 1–40. Alkoxide  $\pi$ -donation: (c) Hubbard, J. L.; McVicar, W. K. *Inorg. Chem.* **1992**, *31*, 910–913. (d) Poulton, J. T.; Sigalas, M. P.; Polting, K.; Streib, W. E.; Eisenstein, O.; Caulton, K. G. *Inorg. Chem.* **1994**, *33*, 1476–1485. (e) Bickford, C. C.; Johnson, T. J.; Davidson, E. R.; Caulton, K. G. *Inorg. Chem.* **1994**, *33*, 1080–1086. Amide complexes: (f) Villanueva, L. A.; Abboud, K. A.; Boncella, J. M. *Organometallics* **1994**, *13*, 3921–3931. (g) Rahim, M.; Ahmed, K. J. *Organometallics*, **1994**, *13*, 1751–1756. (h) Dewey, M. A.; Knight, D. A.; Arif, A.; Gladysz, J. A. *Chem. Ber.* **1992**, *125*, 815–824 and references therein. Amide complexes in which there appears to be no  $\pi$ -donation: (i) Joslin, F. L.; Johnson, M. P.; Mague, J. T.; Roundhill, D. M. *Organometallics* **1991**, *10*, 2781–2794.

(17) Simpson, R. D.; Bergman, R. G. *Organometallics* **1993**, *12*, 781–796.

(18) Kemp, D. S. In *The Peptides*; Gross, E., Meienhofer, J., Eds.; Academic: New York, 1979; Vol. 1, pp 315–383.

(19) Carpino, L. *J. Org. Chem.* **1988**, *53*, 875–878. Stroud, E. D.; Fife, D. J.; Smith, G. G. *J. Org. Chem.* **1983**, *48*, 5368–5369. Smith, G. G.; Sivakua, T. *J. Org. Chem.* **1983**, *48*, 627–634.

(20) Wenzel, T. J. *NMR Shift Reagents*; CRC Press: Boca Raton, Florida, 1987. *Nuclear Magnetic Resonance Shift Reagents*; Sievers, R. A., Ed.; Academic: New York, 1973. Hofer, O. *Top. Stereochem.* **1976**, *9*, 111–197.

**Table 2.**  $^1\text{H}$  NMR Data ( $\delta$ , ppm) for Coordinatively Unsaturated Complexes **5a**<sup>a</sup>

compd	solvent	$\text{C}_6(\text{CH}_3)_5$	CHR and R	Z
<b>5a</b>	$\text{CDCl}_3$	1.78 (s, 15H)	3.32 (s, 2H)	7.61 (~d, $J \approx 8$ , 2H) 7.23 (~d, $J \approx 8$ , 2H) 2.37 (s, 3H)
	$\text{CD}_2\text{Cl}_2^b$	1.81 (s, 15H)	3.25 (s, 2H)	7.65 (~d, $J \approx 8$ , 2H) 7.37 (~d, $J \approx 8$ , 2H) 2.41 (s, 3H)
	$\text{C}_6\text{D}_6$	1.25 (s, 15H)	3.78 (s, 2H)	7.73 (~d, $J \approx 8$ , 2H) 6.78 (~d, $J \approx 8$ , 2H) 1.91 (s, 3H)
<b>5b</b>	$\text{CDCl}_3$	1.70 (s, 15H)	3.63 (s, 2H)	7.24–7.38 (m, 5H) 5.16 (s, 2H)
<b>5c</b> <sup>c</sup>	$\text{CDCl}_3$	1.72 (s, 15H)	3.59 (s, 2H)	2.13 (s, 3H)
<b>5d</b>	$\text{CDCl}_3$	1.73 (s, 15H)	3.52 (q, $J = 7$ , 1H) 1.31 (d, $J = 7$ , 3H)	7.63 (d, $J = 8$ , 2H) 7.20 (d, $J = 8$ , 2H)
	$\text{C}_6\text{D}_6$	1.23 (s, 15H)	3.96 (s, 2H)	2.36 (s, 3H) 7.18–7.23 (m, 2H) 7.00–7.14 (m, 3H)
	$\text{CDCl}_3$	1.44 (s, 15H)	4.26 (dd, $J = 2.6, 6.0$ , 1H) 3.26 (dd, $J = 6.0, 13.3$ , 1H) 2.97 (dd, $J = 2.6, 13.3$ , 1H)	7.27–7.46 (m, 5H) <sup>d</sup> 7.08–7.16 (m, 3H) <sup>d</sup> 6.85–6.90 (m, 2H) <sup>d</sup>
<b>5e</b>	$\text{CDCl}_3$	1.84 (s, 15H)	4.60 (s, 1 H)	5.30 (d, $J = 12.3$ , 1H) 5.17 (d, $J = 12.3$ , 1H)
	$\text{CDCl}_3$	1.84 (s, 15H)	4.60 (s, 1 H) 6.98–7.08 (m, 5H)	7.39 (~d, $J \approx 8$ , 2 H) ~7.1 <sup>e</sup> 2.29 (s, 3H)

<sup>a</sup> Coupling constants in Hz, at 300 MHz at ambient probe temperature unless otherwise specified. Referenced to  $\text{CHCl}_3 = 7.24$  and  $\text{C}_6\text{HD}_5 = 7.15$  ppm, respectively. <sup>b</sup> 400 MHz,  $\text{CH}_2\text{Cl}_2 = 5.28$  ppm. <sup>c</sup> Red solution. <sup>d</sup> Resonances include those from Z and R groups. <sup>e</sup> Resonance obscured by signals for R = Ph.

or **5f** with (*S*)- $\alpha$ -methylbenzylamine gave mixtures of amides **10a/10b** and **11a/11b**,<sup>21</sup> respectively, in ratios of at least 20:1, signifying ee of at least 90%. An alternative, more sensitive method, based on coordination of an enantiomerically pure primary amine to Ir in **5**, indicated that **5f** and **5d** were obtained with ee of at least 96% and 99%, respectively.<sup>22</sup>

Evidence for intramolecular interaction of the (formally) unsaturated Ir center with an amino acid side chain was sought. On the basis of normal NMR chemical shifts for the phenyl protons and carbons of **5f**, the possibility of C–H agostic<sup>23</sup> or  $\eta^2$ -coordination<sup>24</sup> of the

phenyl substituent in **5f** seemed unlikely. Nevertheless, additional characterization of **5f**, which would also examine the general effect of a metallacycle substituent R on the geometry of the ring, was deemed desirable. The results of X-ray diffraction of a crystal of **5f**, obtained by vapor diffusion of petroleum ether into a xylenes solution, are presented in Figure 2 and Tables 5, 10 and 12. As in **5a**, the chelate ring is nearly planar (all five atoms are less than 0.018 Å from the mean chelate plane), although some distortion is suggested by the distances of the Cp\* centroid and S (0.083 and 0.362 Å, respectively) from that plane. The configuration of the stereogenic center established by derivatization to **11a/b** was verified by refinement of the Rogers  $\eta$  parameter to a value of 1.06(2).<sup>25</sup> The perpendicular distance of the Ir atom from the mean plane of the  $\text{C}_6\text{H}_5$  ring is only 0.22 Å, as required for agostic interaction, but the distance between Ir and H(9pa), the nearest hydrogen of the  $\text{C}_6\text{H}_5$  ring, is ca. 3.6 Å, which is further than the internuclear distance of metal and hydrogen in an unambiguous agostic interaction.<sup>23</sup> The orientation of the  $\text{C}_6\text{H}_5$  ring, though favorable for agostic interaction with Ir, may simply be a manifestation of  $\pi$ -stacking. Regardless, the syn arrangement of  $\text{C}_6\text{H}_5$  and  $\text{CH}_3\text{C}_6\text{H}_4$  substituents (angle between mean planes 19°) is an interesting contrast to the anti arrangement proposed for structurally uncharacterized boron-derived Lewis acids based on **4** and related species.<sup>8</sup>

**Coordination Chemistry of 5.** The deep red color of solutions of **5** fades to yellow within seconds after addition of a phosphine, unhindered amine, or CO. From all evidence gathered so far, the color change is diagnostic for coordinative saturation in these systems. The resulting glycine-derived complexes **6a–c** display  $^1\text{H}$  NMR signals (Tables 6 and 7) ascribable to two mutually coupled diastereotopic methylene protons, as expected for species containing a chiral center. Comparison of  $\nu_{\text{CO}} = 1684 \text{ cm}^{-1}$  for **5a** and  $\nu_{\text{CO}} = 1650 \text{ cm}^{-1}$  for the corresponding  $\text{PMe}_3$  adduct **6a–PMe}\_3** suggests reduced donation of electron density from O to Ir upon coordinative saturation. Further, whereas **5b** ( $\nu_{\text{CO}} = 1672 \text{ cm}^{-1}$ , br) shows a single set of resonances in its NMR spectrum at ambient temperatures, **6b–PMe}\_3** ( $\nu_{\text{CO}} = 1645 \text{ cm}^{-1}$ , br) shows two sets of absorptions, which coalesce at elevated temperatures (ca. 90 °C at 400 MHz). The ratio of the two species is solvent-dependent, changing from 1.6:1 in  $\text{CDCl}_3$  to 2.3:1 in  $d_8$ -toluene. These data point to the presence of rotameric forms of *N*-Cbz-substituted complex **6b–PMe}\_3** which interconvert slowly enough on the NMR time scale at ambient temperatures so as to show two sets of sharp resonances. Significantly, under similar conditions NMR spectra of **5b** exhibit only one set of sharp resonances, considered to be additional evidence for effective competition by the unsaturated Ir with the carbonyl group for electron density from N. Although activation parameters for rotation of the Cbz group were not determined in this study, the qualitative difference between the behavior of **6b–PMe}\_3** and **5b** resembles the difference between an acylated amine and an acylated pyrrole.<sup>26</sup>

(21) (a) Compounds **11a,b** are mentioned, but without detail: Clark, C. R.; Bouhadir, K.; Mayfield, C. A.; DeRuiter, J. *J. Chromatogr. Sci.* **1990**, *28*, 407–412. (b) Compound **10**: Herlinger, H.; Kleinmann, H.; Ugi, I. *Justus Liebig's Ann. Chem.* **1967**, *706*, 37–46.

(22) Grotjahn, D. B.; Joubran, C. *Tetrahedron: Asymmetry* **1995**, *6*, 745–752.

(23) Brookhart, M.; Green, M. L. H.; Wong, L.-L. *Prog. Inorg. Chem.* **1988**, *36*, 1–124. Crabtree, R. H.; Hamilton, D. G. *Adv. Organomet. Chem.* **1988**, *28*, 299–338.

(24) Li, C.-S.; Jou, D.-C.; Cheng, C.-H. *Organometallics* **1993**, *12*, 3945–3954 and references therein.

(25) Rogers, D. *Acta Crystallogr., Sect. A* **1981**, *A37*, 734–741.

(26) Stewart, W. E.; Siddall, T. H., III. *Chem. Rev.* **1970**, *70*, 517–551. Jackman, L. M. In *Dynamic Nuclear Magnetic Resonance Spectroscopy*; Jackman, L. M., Cotton, F. A., Eds.; Academic: New York, 1975; pp 203–252.

**Table 3.**  $^{13}\text{C}$  NMR Data ( $\delta$ , ppm) for Coordinatively Unsaturated Complexes **5**<sup>a</sup>

complex	C=O	C <sub>5</sub> (CH <sub>3</sub> ) <sub>5</sub>	C <sub>5</sub> (CH <sub>3</sub> ) <sub>5</sub>	CHR	R and Z <sup>b</sup>
<b>5a</b>	186.0	87.7	9.9	52.9	143.2 (C), 136.3 (C), 129.7 (CH), 127.4 (CH), 21.2 (CH <sub>3</sub> )
<b>5b</b>	187.3	87.3	9.7	53.7	161.0 (C), 137.0 (C), 128.6 (CH), 128.2 (CH), 128.2 (C), 22.0 (CH <sub>3</sub> )
<b>5c</b>	187.3	87.8	9.8	55.1	177.6 (C), 22.0 (CH <sub>3</sub> )
<b>5d</b>	189.2	87.7	9.8	59.8	142.8 (C), 139.0 (C), 129.5 (CH), 127.1 (CH), 23.0 (CH <sub>3</sub> ), 21.2 (CH <sub>3</sub> )
<b>5e</b>	188.6	86.8	9.4	64.6 <sup>c</sup>	160.4 (C), 137.5 (C), 137.1 (C), 130.7 (CH), 128.7 (CH), 128.3 (CH), 127.9 (CH), 126.1 (CH), 67.7, <sup>c</sup> 38.3
<b>5f</b>	186.2	88.0	9.9	68.0	142.4 (C), 138.5 (C), 138.1 (C), 129.0 (CH), 127.9 (CH), 127.4 (CH), 127.2 (CH), 126.8 (CH), 21.0 (CH <sub>3</sub> )

<sup>a</sup> In CDCl<sub>3</sub>, measured at ambient probe temperature at 75.5 MHz. Resonance for solvent = 77.00 ppm. <sup>b</sup> Assignments based on intensities and chemical shifts. <sup>c</sup> Assignments uncertain.

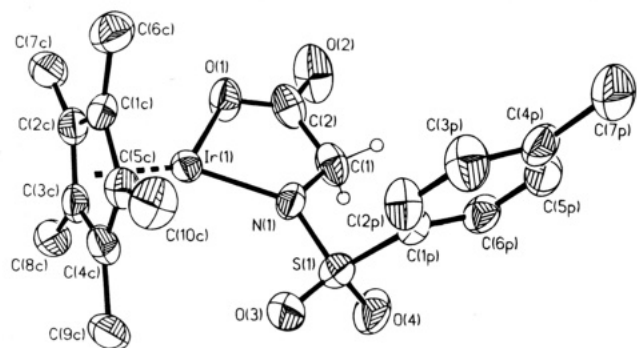


**Figure 1.** Molecular structure of **5a**, shown with 50% thermal ellipsoids. Hydrogen atoms other than those shown (assumed positions) are omitted for clarity.

**Table 4.** Bond Lengths (Å) and Selected Angles (deg) for **5a**

Ir(1)–N(1)	1.981(7)	Ir(1)–O(1)	2.030(6)
Ir(1)–C(1C)	2.136(8)	Ir(1)–C(2C)	2.162(8)
Ir(1)–C(3C)	2.138(7)	Ir(1)–C(4C)	2.177(8)
Ir(1)–C(5C)	2.145(8)	N(1)–C(1)	1.485(11)
N(1)–S(1)	1.629(7)	C(1)–C(2)	1.513(14)
C(2)–O(1)	1.281(11)	C(2)–O(2)	1.222(12)
C(1C)–C(2C)	1.425(12)	C(1C)–C(5C)	1.455(12)
C(1C)–C(6C)	1.489(13)	C(2C)–C(3C)	1.401(11)
C(2C)–C(7C)	1.508(12)	C(3C)–C(4C)	1.460(12)
C(3C)–C(8C)	1.504(13)	C(4C)–C(5C)	1.415(11)
C(4C)–C(9C)	1.500(12)	C(5C)–C(10C)	1.501(12)
S(1)–O(3)	1.429(7)	S(1)–O(4)	1.450(7)
S(1)–C(1P)	1.786(9)	C(1P)–C(2P)	1.360(13)
C(1P)–C(6P)	1.373(13)	C(2P)–C(3P)	1.363(14)
C(3P)–C(4P)	1.395(14)	C(4P)–C(5P)	1.383(13)
C(4P)–C(7P)	1.502(14)	C(5P)–C(6P)	1.380(14)
N(1)–Ir(1)–O(1)	80.3(3)	C(1)–C(2)–O(2)	119.5(9)
Ir(1)–O(1)–C(2)	118.5(6)	Ir(1)–N(1)–S(1)	131.3(4)
O(1)–C(2)–C(1)	115.8(8)	C(1)–N(1)–S(1)	113.2(5)
C(2)–C(1)–N(1)	109.8(7)	N(1)–S(1)–C(1P)	105.3(4)
C(1)–N(1)–Ir(1)	115.3(5)	O(3)–S(1)–O(4)	118.7(4)
O(1)–C(2)–O(2)	124.6(9)		

Racemic **4g** and **2** afford yellow ( $\pm$ )-**8** (98% yield) directly, showing the possibility of side chain coordination. Two sets of resonances are seen in the  $^1\text{H}$  NMR spectra of **8**. Because the ratio of the two species is 6:5 in CDCl<sub>3</sub> and 4:1 in C<sub>6</sub>D<sub>6</sub>, it is assumed that the difference between the two components is in the orientation of the Cbz group about the C–N bond and not in the undetermined configuration at S, which may in fact be changing rapidly on the NMR time scale at ambient probe temperature.<sup>27</sup>

Evaporation of a red solution of **5c** in CH<sub>2</sub>Cl<sub>2</sub> ( $\nu_{\text{CO}}$  = 1642, 1659 cm<sup>-1</sup>) leaves a yellow solid (in KBr  $\nu_{\text{CO}}$  =

**Table 5.** Bond Lengths (Å) and Selected Angles (deg) for **5f**

Ir(1)–N(1)	1.986(6)	Ir(1)–O(1)	2.022(9)
Ir(1)–C(1C)	2.135(15)	Ir(1)–C(2C)	2.168(8)
Ir(1)–C(3C)	2.125(9)	Ir(1)–C(4C)	2.149(8)
Ir(1)–C(5C)	2.154(9)	N(1)–C(1)	1.498(10)
N(1)–S(1)	1.634(6)	C(1)–C(2)	1.485(12)
C(1)–C(8P)	1.541(11)	C(2)–O(1)	1.280(12)
C(2)–O(2)	1.216(10)	C(1C)–C(2C)	1.395(17)
C(1C)–C(5C)	1.491(18)	C(1C)–C(6C)	1.506(18)
C(2C)–C(3C)	1.418(13)	C(2C)–C(7C)	1.528(14)
C(3C)–C(4C)	1.419(13)	C(3C)–C(8C)	1.486(16)
C(4C)–C(5C)	1.369(13)	C(4C)–C(9C)	1.485(14)
C(5C)–C(10C)	1.488(15)	S(1)–O(3)	1.449(10)
S(1)–O(4)	1.446(7)	S(1)–C(1P)	1.769(9)
C(1P)–C(2P)	1.383(14)	C(1P)–C(6P)	1.393(13)
C(2P)–C(3P)	1.420(15)	C(3P)–C(4P)	1.341(18)
C(4P)–C(5P)	1.371(18)	C(4P)–C(7P)	1.482(13)
C(5P)–C(6P)	1.427(14)	C(8P)–C(9P)	1.384(11)
C(8P)–C(13P)	1.380(12)	C(9P)–C(10P)	1.363(13)
C(10P)–C(11P)	1.315(18)	C(11P)–C(12P)	1.377(18)
C(12P)–C(13P)	1.429(16)		
N(1)–Ir(1)–O(1)	79.9(3)	C(1)–C(2)–O(2)	121.0(7)
Ir(1)–O(1)–C(2)	118.4(6)	Ir(1)–N(1)–S(1)	127.4(4)
O(1)–C(2)–C(1)	117.2(8)	C(1)–N(1)–S(1)	115.7(5)
C(2)–C(1)–N(1)	109.1(6)	N(1)–S(1)–C(1P)	108.3(4)
O(1)–N(1)–Ir(1)	115.4(4)	O(3)–S(1)–O(4)	117.5(4)
O(1)–C(2)–O(2)	121.8(8)		

1553, 1570, 1653 cm<sup>-1</sup>) which redissolves rapidly to give a red solution in noncoordinating solvents. These properties are consistent with interconversion of red **5c** in solution and a yellow dimer or oligomer in the solid, with the former possibility being favored on the basis of literature precedents.<sup>5b,28</sup> In addition, whereas dissolution of **5c** in CH<sub>2</sub>Cl<sub>2</sub> or THF affords a red solution, use of CH<sub>3</sub>CN yields a pale orange solution, presumably containing CH<sub>3</sub>CN complex **6c**–CH<sub>3</sub>CN.

**Diastereoselectivity of Ligand Additions.** It is anticipated that the stereochemical course of reactions at Ir in chiral **5** will depend on the diastereoselectivity of ligand additions to the metal. Addition of PMe<sub>3</sub> to a red solution of enantiomerically pure<sup>22</sup> (*S*)-alanine-derived complex **5d** within seconds gave a yellow solution, in which essentially a single set of sharp NMR resonances was seen. Integration established that the major product predominated over one or two minor components in a ratio of at least 25:1 (Table 8). NOE experiments indicated that, in the major product, the Cp\* and alanine side chain CH<sub>3</sub> group are syn, and the PMe<sub>3</sub> and methine H are syn, as in structure **6d**–PMe<sub>3</sub>. Similar color and spectral changes were observed when solutions of **5d**–**f** were treated with phosphines or CO. Moreover, NOE experiments on mixtures from **5d** + CO and **5f** + PMe<sub>3</sub> indicated a syn orientation of amino acid

(27) Reviews of the dynamics of coordinated thioethers: Jackson, W. G.; Sargeson, A. M. *Rearrange. Ground Excited States* **1980**, *2*, 273–378. Abel, E. W.; Bhargava, S. K.; Orrell, K. G. *Prog. Inorg. Chem.* **1984**, *32*, 1–118.

(28) Brown, L. D.; Itoh, K.; Suzuki, H.; Hirai, K.; Ibers, J. A. *J. Am. Chem. Soc.* **1978**, *100*, 8232–8238. Lindner, E.; Jansen, R.-M.; Mayer, H. A.; Hiller, W.; Fawzi, R. *Organometallics* **1989**, *8*, 2355–2360.



**Table 6.**  $^1\text{H}$  NMR Data ( $\delta$ , ppm) for  $\text{PMe}_3$  Adducts **6**– $\text{PMe}_3$  and **7**– $\text{PMe}_3$ <sup>a</sup>

compd	solvent	$\text{C}_5(\text{CH}_3)_5$	CHR and R	Z	L	
<b>6a</b> – $\text{PMe}_3$	$\text{CDCl}_3$	1.69 (d, $J = 2.1$ , 15H)	3.92 (d, $J = 16.5$ , 1H) 3.67 (d, $J = 16.5$ , 1H)	7.59 (~d, $J \approx 8$ , 2H) 7.17 (~d, $J \approx 8$ , 2H) 2.33 (s, 3H)	1.56 (d, $J = 11.0$ , 9H)	
<b>6b</b> – $\text{PMe}_3$	$\text{CDCl}_3$	major rotamer: <sup>b</sup>	4.51 (d, $J = 18.8$ , 1H) 1.53 (d, $J = 2.0$ , 15H)	7.18–7.36 (m, 5H) 5.13 and 4.86 (two d, $J = 11.5$ , each 1H)	1.26 (d, $J = 10.7$ , 9H)	
		minor rotamer: <sup>b</sup>	4.48 (d, $J = 18.5$ , 1H) 1.67 (d, $J = 2.1$ , 15H)	7.18–7.36 (m, 5H) 5.10 and 5.00 (two d, $J = 12.8$ , each 1H)	1.41 (d, $J = 10.9$ , 9H)	
	$d_8$ -toluene	major rotamer: <sup>c</sup>	4.75 (d, $J = 18.0$ , 1H) 1.34 (d, $J = 2.0$ , 15H)	4.06 (d, $J = 18.0$ , 1H)	6.98–7.5 <sup>d</sup> 5.23 and 5.20 (two d, $J = 12.7$ , each 1H)	1.05 (d, $J = 11.0$ , 9H)
		minor rotamer: <sup>c</sup>	4.96 (d, $J = 18.3$ , 1H) 1.18 (d, $J = 2.1$ , 15H)	3.08 (d, $J = 18.3$ , 1H)	6.98–7.5 <sup>d</sup> 5.26 and 4.84 (two d, $J = 11.5$ , each 1H)	0.87 (d, $J = 10.8$ , 9H)
<b>6c</b> – $\text{PMe}_3$	$\text{CDCl}_3$	1.67 (d, $J = 2.6$ , 15H)	4.25 (d, $J = 17.5$ , 1H) 3.94 (d, $J = 17.5$ , 1H)	2.04 (s, 3H)	1.45 (d, $J = 11.0$ , 9H)	
<b>6d</b> – $\text{PMe}_3$	$\text{CDCl}_3$	1.69 (d, $J = 2.1$ , 15H)	3.90 (q, $J = 7.0$ , 1H) 0.99 (d, $J = 7.0$ , 3H)	7.63 (~d, $J \approx 8$ , 2H) 7.17 (~d, $J \approx 8$ , 2H) 2.34 (s, 3H)	1.60 (d, $J = 11.1$ , 9H)	
<b>6e</b> – $\text{PMe}_3$	$\text{CDCl}_3$	major rotamer: <sup>e</sup>	4.45 (dd, $J = 3.9$ , 5.3, 1H) <sup>f</sup> 1.49 (d, $J = 2.2$ , 15H)	3.11 (dd, $J = 3.9$ , 13.0, 1H)	7.02–7.42 (m, 10H) <sup>f</sup> 5.17 and 4.89 (two d, $J = 11.6$ , each 1H)	1.21 (d, $J = 10.7$ , 9H)
		minor rotamer: <sup>e</sup>	4.46 (dd, $J = 5.5$ , 6.9, 1H) <sup>f</sup> 1.71 (d, $J = 2.2$ , 15H)	4.46 (dd, $J = 5.5$ , 6.9, 1H) <sup>f</sup>	7.02–7.42 (m, 10H) <sup>f</sup> 5.05 and 4.64 (two d, $J = 12.4$ , each 1H)	1.36 (d, $J = 10.9$ , 9H)
	$d_8$ -toluene	major rotamer: <sup>g</sup>	4.64 (dd, $J = 4.4$ , 7.5, 1H) <sup>f</sup> 1.39 (d, $J = 2.1$ , 15H)	3.24 (dd, $J = 7.5$ , 13.0, 1H) 3.13 (dd, $J = 4.4$ , 13.0, 1H)	7.58 (d, $J = 7.2$ , 2H) <sup>f</sup> 7.05–7.4 (m, 8H) <sup>f</sup> 5.21 and 4.94 (two d, $J = 12.2$ , each 1H)	0.98 (d, $J = 10.9$ , 9H)
		minor rotamer: <sup>g</sup>	4.77 (dd, $J = 3.4$ , 12.9, 1H) <sup>f</sup> 1.16 (d, $J = 2.0$ , 15H)	3.47 (dd, $J = 7.5$ , 13.0, 1H) 3.36 (dd, $J = 7.9$ , 12.9, 1H)	7.85 (d, $J = 7.2$ , 2H) <sup>f</sup> 7.05–7.4 (m, 8H) <sup>f</sup> 5.25 and 4.88 (two d, $J = 11.7$ , each 1H)	0.81 (d, $J = 10.7$ , 9H)
<b>7e</b> – $\text{PMe}_3$	$\text{CDCl}_3$	major rotamer: <sup>h</sup>	4.16 (dd, $J = 2.1$ , 6.1, 1H) <sup>f</sup> 1.55 (d, $J = 2.1$ , 15H)	3.94 (dd, $J = 6.1$ , 12.8, 1H)	7.25–7.4 (m, 5H) <sup>f</sup> 7.0–7.1 (m, 3H) 5.44 (d, $J = 11.8$ , 1H) 4.58 (d, $J = 11.8$ , 1H)	1.87 (d, $J = 11.0$ , 9H)
		minor rotamer: <sup>h,i</sup>	4.16 1.57 (d, $J = 2$ , 15H)	4.16	5.28 and 5.07 (two d, $J = 11.6$ , each 1H)	1.21 (d, $J = 11.0$ , 9H)
	$\text{C}_6\text{D}_6$	major rotamer: <sup>j</sup>	4.47 (dd, $J = 2.1$ , 6.2, 1H) <sup>f</sup> 1.15 (d, $J = 2.1$ , 15H)	4.63 (dd, $J = 6.2$ , 12.3, 1H) 3.91 (dd, $J = 2.1$ , 12.3, 1H)	7.95 (~d, $J = 7$ , 2H) <sup>f</sup> 7.36 (~d, $J = 7$ , 2H) 7.02–7.22 (m, 6H) 5.69 and 4.51 (two d, $J = 11.9$ , each 1H)	0.59 (d, $J = 10.9$ , 9H)
		minor rotamer: <sup>j</sup>	4.37 (dd, $J = 2$ , 5, 1H) <sup>f</sup> 1.24 (d, $J = 2$ , 15H)	~3.87 <sup>i</sup> 3.68 (dd, $J = 2$ , 12, 1H)	7.75 (~d, $J = 7$ , 2H) <sup>f</sup> 7.49 (~d, $J = 7$ , 2H) 7.02–7.22 (m, 6H) 5.51 and 5.21 (two d, $J = 12.2$ , each 1H)	0.92 (d, $J = 11.0$ , 9H)
<b>6f</b> – $\text{PMe}_3$	$\text{CDCl}_3$	1.70 (d, $J = 2.1$ , 15H)	4.97 (s, 1H) 6.9–7.02 (m, 5H)	7.14 (~d, $J \approx 8$ , 2H) 6.74 (~d, $J \approx 8$ , 2H) 2.16 (s, 3H)	1.76 (d, $J = 11.0$ , 9H)	
	$d_8$ -toluene	1.38 (d, $J = 2.1$ , 15H)	5.28 (s, 1H) 7.2–7.27 (m, 2H) 6.9–6.96 (m, 3H)	7.47 (~d, $J \approx 8$ , 2H) 6.57 (~d, $J \approx 8$ , 2H) 1.91 (s, 3H)	1.50 (d, $J = 11.0$ , 9H)	

<sup>a</sup> Coupling constants in Hz, at 300 MHz at ambient probe temperature unless otherwise specified. <sup>b</sup> Ratio of rotamers 1.6:1. <sup>c</sup> Ratio of rotamers 2.3:1. <sup>d</sup> Resonances overlapping with those of solvent. <sup>e</sup> Ratio of rotamers 1.2:1. <sup>f</sup> Resonances for R = PhCH<sub>2</sub> overlap with those for Z = PhCH<sub>2</sub>CO<sub>2</sub>. <sup>g</sup> Ratio of rotamers 1.7:1. <sup>h</sup> Ratio of rotamers 5:1. <sup>i</sup> Some resonances for minor rotamer not found or overlap with others. <sup>j</sup> Ratio of rotamers 3:1.

side chain R and Cp\* groups in the products, **6d**–CO and **6f**– $\text{PMe}_3$ , respectively. Eventually (vide infra), an authentic sample of a diastereomer in which R and Cp\* groups are trans to each other (**7e**– $\text{PMe}_3$ ) was synthesized independently, lending confidence to the assertion that **7e**– $\text{PMe}_3$  was not detectable (estimated 2% detection limit) in the addition of  $\text{PMe}_3$  to **5d**.

All available evidence indicates that ligand attack on **5** is preferred from the side of the metallacycle unhindered by R. Evidence presented below indicates that this preference is the result of both kinetic and thermodynamic control.

Initial attempts to synthesize an authentic sample of the minor (or undetectable) diastereomer from ligand addition reactions focused on preparation of **7d**– $\text{PMe}_3$ . Attempts to combine Cp\*IrCl<sub>2</sub>( $\text{PMe}_3$ )<sup>29</sup> (**12**) with **4d** using the conditions that worked in the synthesis of **5** (K<sub>2</sub>CO<sub>3</sub>, THF or MeCN) led to recovery of **12**, and use of Ag<sub>2</sub>CO<sub>3</sub> as base slowly led to a mixture in which **6d**– $\text{PMe}_3$  was the only species identifiable by  $^1\text{H}$  NMR as containing the Cp\*Ir( $\text{PMe}_3$ ) and TsNCHMe– units.



Table 7. <sup>1</sup>H NMR Data (δ, ppm) for Coordinatively Saturated Complexes **6** and **7**<sup>a</sup>

compd	solvent	C <sub>5</sub> (CH <sub>3</sub> ) <sub>5</sub>	CHR and R	Z	L
<b>6d</b> –PMe <sub>2</sub> Ph	CDCl <sub>3</sub>	1.45 (d, <i>J</i> = 2.2, 15H)	3.92 (q, <i>J</i> = 6.9, 1H) 1.00 (d, <i>J</i> = 6.9, 3H)	7.68 (~d, <i>J</i> ≈ 8, 2H) 7.19 (~d, <i>J</i> ≈ 8, 2H) 2.36 (s, 3H)	7.65–7.73 (m, 2H) 7.38–7.45 (m, 3H) 2.21 (d, <i>J</i> = 11.2, 3H) 1.56 (d, <i>J</i> = 11.1, 3H)
<b>6d</b> –PMePh <sub>2</sub> <sup>b</sup>	CDCl <sub>3</sub>	1.46 (d, <i>J</i> = 2.2, 15H)	3.75 (q, <i>J</i> = 7.0, 1H) 1.27 (d, <i>J</i> = 7.0, 3H)	7.13 (d, <i>J</i> = 8.2, 2H) 6.88 (d, <i>J</i> = 8.2, 2H) 2.23 (s, 3H)	7.90 (ddd, <i>J</i> = 11.6, 7.9, 2, 2H) 7.46–7.60 (m, 5H) 7.30–7.36 (m, 3H) 1.64 (d, <i>J</i> = 10.3, 3H)
<b>7d</b> –PMePh <sub>2</sub> <sup>b,c</sup>	CDCl <sub>3</sub>	1.49 (d, <i>J</i> = 2.4, 15H)	0.83 (d, <i>J</i> = 6.8, 3H) <sup>c</sup>	6.93 (d, <i>J</i> = 8.4, 2H) 6.77 (d, <i>J</i> = 8.4, 2H) 2.12 (s, 3H)	1.91 (d, <i>J</i> = 10.3, 3H) <sup>c</sup>
<b>6a</b> –PPh <sub>3</sub>	CDCl <sub>3</sub>	1.46 (d, <i>J</i> = 2.2, 15H)	3.82 (d, <i>J</i> = 16.5, 1H) 3.00 (d, <i>J</i> = 16.5, 1H)	7.01 (d, <i>J</i> = 8.2, 1H) 6.89 (d, <i>J</i> = 8.2, 1H) 2.26 (s, 3H)	6.9–7.8 (broad featureless resonances, 15H)
<b>6d</b> –PPh <sub>3</sub> <sup>d</sup>	CDCl <sub>3</sub>	1.50 (d, <i>J</i> = 2, 15H)	3.40 (q, <i>J</i> = 6.8, 1H) 1.46 (d, <i>J</i> = 6.8, 3H)	6.99 (d, <i>J</i> = 8, 2H) 6.88 (d, <i>J</i> = 8, 2H) 2.27 (s, 3H)	6.7–7.8 (broad)
<b>7d</b> –PPh <sub>3</sub> <sup>d</sup>	CDCl <sub>3</sub>	1.45 (d, <i>J</i> = 2, 15H)	4.05 (q, <i>J</i> = 7.0, 1H) 0.70 (d, <i>J</i> = 7.0, 3H)	6.84 (d, <i>J</i> = 8, 2H) 6.77 (d, <i>J</i> = 8, 2H) 2.24 (s, 3H)	6.7–7.8 (broad)
<b>6a</b> –CO	CDCl <sub>3</sub>	1.91 (s, 15H)	3.76 (d, <i>J</i> = 16.6, 1H) 3.51 (d, <i>J</i> = 16.6, 1H)	7.65 (d, <i>J</i> = 8.2, 2H) 7.22 (d, <i>J</i> = 8.2, 2H) 2.37 (s, 3H)	
<b>6d</b> –CO	CDCl <sub>3</sub>	1.89 (s, 15H)	4.04 (q, <i>J</i> = 7.0, 1H) 1.10 (d, <i>J</i> = 7.0, 3H)	7.67 (d, <i>J</i> = 8.2, 2H) 7.21 (d, <i>J</i> = 8.2, 2H) 2.36 (s, 3H)	
<b>6d</b> –PhCH <sub>2</sub> NH <sub>2</sub> <sup>e</sup>	CDCl <sub>3</sub>	1.69 (s, 15H)	3.95 (q, <i>J</i> = 7) 0.90 (d, <i>J</i> = 7)	7.63 (d, <i>J</i> = 8) 7.19 (d, <i>J</i> = 8) 2.37 (s, 3H)	3.8–4.6 (br) 7.25–7.38 (m, 5H) 3.98 (br s, 2H)
<b>6d</b> –PhCH <sub>2</sub> NH <sub>2</sub> <sup>f</sup>	CDCl <sub>3</sub>	1.61 (s, 15H)	3.94 (q, <i>J</i> = 7, 1H) 0.78 (d, <i>J</i> = 7, 3H)	7.63 (d, <i>J</i> = 8, 2H) 7.22 (d, <i>J</i> = 8, 2H) 2.38 (s, 3H)	7.25–7.38 (m, 5H) 4.52 (br s, 1H) 4.21 (br t, <i>J</i> ≈ 11, 1H) 4.08 (dt, <i>J</i> = 2, 12) ~3.94 (obscured by CHR)
<b>6f</b> –PhCH <sub>2</sub> NH <sub>2</sub>	CDCl <sub>3</sub>	1.60 (s, 15H)	5.0 (s) and see L	7.46 (d, <i>J</i> = 8, 2H) 6.94 (d, <i>J</i> = 8, 2H) 2.23 (s, 3H)	7.26–7.36 (m, 5H) 6.96–7.02 (m, 5H) 4.03 (sl br s, 2H)
(±)- <b>6d</b> –tBuNH <sub>2</sub> <sup>g</sup>	CDCl <sub>3</sub>	1.68 (s, 15H)	3.67 (q, <i>J</i> = 6.9, 1H) 1.15 (d, <i>J</i> = 6.9, 3H)	7.63 (d, <i>J</i> = 7.9, 2H) 7.21 (d, <i>J</i> = 7.9, 2H) 2.36 (s, 3H)	1.19 (s, 9H)
(±)- <b>6d</b> –tBuNH <sub>2</sub> <sup>g,h</sup>	CDCl <sub>3</sub>	1.64 (s, 15H)	3.64 (q, <i>J</i> = 7, 1H) 1.10 (d, <i>J</i> = 7, 3H)	7.60 (d, <i>J</i> = 7.5, 2H) 7.23 (d, <i>J</i> = 7.5, 2H) 2.36 (s, 3H)	4.33 (d, <i>J</i> = 12, 1H) ~3.6 1.20 (s, 9H)
(±)- <b>6d</b> –DMAP <sup>g,i,j</sup>	CDCl <sub>3</sub>	(s, 15H)			
(±)- <b>6d</b> –DMAP <sup>g,i,k</sup>	CDCl <sub>3</sub>	1.55 (s, 15H)	3.59 (q, <i>J</i> = 7, 1H) 1.28 (d, <i>J</i> = 7, 3H)	7.09 (d, <i>J</i> = 8, 2H) 6.90 (d, <i>J</i> = 8, 2H) 2.20 (s, 3H)	8.32 (d, <i>J</i> = 6, 2H) 6.32 (d, <i>J</i> = 6, 2H) 3.03 (s, 6H)
(±)- <b>7d</b> –DMAP <sup>g,i,k</sup>	CDCl <sub>3</sub>	1.33 (s, 15H)	4.02 (q, <i>J</i> = 7, 1H) 0.56 (d, <i>J</i> = 7, 3H)	7.56 (d, <i>J</i> = 8, 2H) 7.15 (d, <i>J</i> = 8, 2H) 2.33 (s, 3H)	8.17 (d, <i>J</i> = 6, 2H) 6.48 (d, <i>J</i> = 6, 2H) 3.09 (s, 3H)

<sup>a</sup> Coupling constants in Hz, at 300 MHz at ambient probe temperature unless otherwise specified. <sup>b</sup> Ratio of **6d**–PMePh<sub>2</sub> to **7d**–PMePh<sub>2</sub>, ca 20:1. <sup>c</sup> Some resonances for minor diastereomer not found or assumed to overlap with others. <sup>d</sup> Ratio of **6d**–PPh<sub>3</sub> to **7d**–PPh<sub>3</sub>, 6:1. Spectrum acquired at 63 °C at 500 MHz. At 25 °C, resonances for aryl protons of Ts in minor component were too broad to be discernible. <sup>e</sup> At 400 MHz. <sup>f</sup> At 400 MHz, –50 °C. <sup>g</sup> From racemic **5d**. <sup>h</sup> At 500 MHz, –50 °C. <sup>i</sup> Ratio of **6d**–DMAP to **7d**–DMAP, 6:1. <sup>j</sup> At 500 MHz. <sup>k</sup> At 500 MHz, –60 °C.

Alternatively, the dipotassium salt of **4d** was combined with Cp\*Ir(OTf)<sub>2</sub>(PMe<sub>3</sub>)<sup>30</sup> to give a mixture of products including **6d**–PMe<sub>3</sub> and several other Cp\*IrPMe<sub>3</sub>-containing species, as suggested by the appearance of doublets in the region δ 0.5–2 ppm. Neither crystallization nor chromatography allowed the isolation of significantly purified material from these experiments. Fortunately, the synthesis of **7e**–PMe<sub>3</sub> from **12** and **4e** under standard conditions (K<sub>2</sub>CO<sub>3</sub>, MeCN) proved straightforward, giving **6e**–PMe<sub>3</sub> and another compound in a ratio of 1:4 (total 98% yield). The success of this latter reaction may be attributed to greater basicity (and presumably nucleophilicity) of the deprotonated carbamate moiety compared with the sulfonamide analog. <sup>1</sup>H NMR spectral data for the major product suggested

that it had the same composition as **6e**–PMe<sub>3</sub>, and the yellow compound could be isolated in a pure form (60%–67% yield) by fractional crystallization. All analytical data point to structure **7e**–PMe<sub>3</sub> as a mixture of two rotamers. Significantly, the resonances observed for the new compound were not detectable (estimated lower limit of sensitivity, 2%) in the spectrum of the reaction of **5d** with PMe<sub>3</sub>.

The isolation of both diastereomers **6e**–PMe<sub>3</sub> and **7e**–PMe<sub>3</sub> allowed evaluation of thermodynamic and kinetic control of ligand binding. Heating a solution of **7e**–PMe<sub>3</sub> in C<sub>6</sub>D<sub>6</sub> at 80 °C led to a smooth conversion (half-life = ca. 14 h) to **6e**–PMe<sub>3</sub>, a process that was first-order in [**7e**–PMe<sub>3</sub>] over at least 3 half-lives. Similar behavior at 90 °C (half-life = 5 h) was seen, and the final ratio of **6e**–PMe<sub>3</sub> to **7e**–PMe<sub>3</sub> was found to be 40:1, corresponding to a free energy difference of 2.7 kcal

(30) Stang, P. J.; Huang, Y.-H.; Arif, A. M. *Organometallics* 1992, 11, 231–237.

**Table 8.**  $^{13}\text{C}$  NMR Data ( $\delta$ , ppm) for Coordinatively Saturated Complexes **6<sup>a</sup>**

complex	C=O	C <sub>5</sub> (CH <sub>3</sub> ) <sub>5</sub>	C <sub>5</sub> (CH <sub>3</sub> ) <sub>3</sub>	CHR	L	R and Z
<b>6a</b> -PMe <sub>3</sub>	185.1	91.3 (d, <i>J</i> = 2.3)	9.3	52.9	13.8 (d, <i>J</i> = 37.8)	141.4, 139.7, 129.2, 127.0, 21.1
<b>6b</b> -PMe <sub>3</sub> <sup>b</sup>	186.1 185.4	90.7 (d, <i>J</i> = 3.8, m) 90.5 (d, <i>J</i> = 3.4, M)	8.85 (m) 8.64 (M)	53.7 (M) 52.8 (m)	13.4 (d, <i>J</i> = 37, m) 12.6 (d, <i>J</i> = 37, M)	159.5 (C = O, M), 157.4 (C = O, m), 138.9, 138.1, 130.1, 128.6, 128.4, 128.3, 127.4, 67.0 (M), 66.2 (m)
<b>6c</b> -PMe <sub>3</sub>	185.3	90.5 (d, <i>J</i> = 3)	8.94	55.5	13.4 (d, <i>J</i> = 37)	172.3 (C = O), 22.3 (CH <sub>3</sub> )
<b>6d</b> -PMe <sub>3</sub>	188.4	91.3	9.3	57.8	14.2 (d, <i>J</i> = 37)	141.5, 140.4, 129.2, 127.4, 21.1, 20.3
<b>6e</b> -PMe <sub>3</sub> <sup>c</sup>	187.1 186.3	90.53 (d, <i>J</i> = 3) 90.45 (d, <i>J</i> = 3)	9.1, 8.7	65.2, <sup>d</sup> 64.3 <sup>d</sup>	13.2 (d, <i>J</i> = 36) 13.0 (d, <i>J</i> = 36)	140.1, 139.8, 138.6, 138.3, 130.4, 130.1, 129.9, 128.6, 128.3, 128.05, 128.01, 127.4, 125.93, 125.87, 66.8 <sup>d</sup> , 66.3 <sup>d</sup> , 42.9, 41.2
<b>6d</b> -PMe <sub>2</sub> Ph	188.6	91.5 (d, <i>J</i> = 3)	8.8	57.5	135.0 (d, <i>J</i> = 54, C) 130.9 (d, <i>J</i> = 10, CH) 130.7 (d, <i>J</i> = 3, CH) 128.5 (d, <i>J</i> = 10, CH) 14.4 (d, <i>J</i> = 36) 11.3 (d, <i>J</i> = 36)	141.7 (C), 139.9 (C), 129.3 (CH), 127.6 (CH), 21.2 (CH <sub>3</sub> ), 20.7 (CH <sub>3</sub> )
<b>6d</b> -PMePh <sub>2</sub>	188.4	92.3 (d, <i>J</i> = 3)	8.9	58.0	135.3 (d, <i>J</i> = 11.9), 132.1 (d, <i>J</i> = 9.2), 131.7 (d, <i>J</i> = 2), 130.4 (d, <i>J</i> = 2), 128.6 (d, <i>J</i> = 11.0), 128.3 (d, <i>J</i> = 11.1), 13.6 (d, <i>J</i> = 36)	140.9 (C), 139.3 (C), 128.8 (CH), 127.4 (CH), 21.3 (CH <sub>3</sub> ), 21.0 (CH <sub>3</sub> )
<b>6d</b> -PPh <sub>3</sub>	185.5	92.7 (d, <i>J</i> = 3)	9.1	52.18	134–136 (br), 130.6–132.4 (br), 128.2 (sl br d, <i>J</i> = 10)	140.5 (C), 138.6 (C), 127.1 (CH), 21.0 (CH <sub>3</sub> )
<b>6a</b> -CO	185.0	100.9	9.0	53.9	169.2	142.7 (C), 135.9 (C), 129.7 (CH), 128.1 (CH), 21.2 (CH <sub>3</sub> )
<b>6d</b> -CO	188.5	100.5	9.0	58.1	169.5	142.6 (C), 135.6 (C), 129.7 (CH), 128.0 (CH), 22.9, <sup>a</sup> 21.2 (CH <sub>3</sub> ) <sup>d</sup>
<b>6d</b> -PhCH <sub>2</sub> NH <sub>2</sub>	188.0	84.5	9.2	57.2	49.6 (br, NCH <sub>2</sub> )	<i>e</i> , <i>f</i>
<b>6d</b> -PhCH <sub>2</sub> NH <sub>2</sub> <sup>g</sup>	187.9	84.1	9.3	56.7	50.0 (NCH <sub>2</sub> )	<i>e</i> , <i>h</i>
<b>6f</b> -PhCH <sub>2</sub> NH <sub>2</sub>	185.6	84.6	9.0	64.3	49.4 <sup><i>e</i>,<i>i</i></sup> (br, NCH <sub>2</sub> )	21.1 <sup><i>e</i>,<i>i</i></sup>
(±)- <b>6d</b> - <i>t</i> BuNH <sub>2</sub> <sup>g</sup>	186.9	84.3	9.6	58.6	76.5 (NC), 31.0 (CH <sub>3</sub> )	142.0, 137.2, 129.3, 127.0, 21.5, 19.7
<b>6a</b> -MeIm	185.1	84.8	9.0	52.5	34.4 (NCH <sub>3</sub> ) <sup><i>e</i>,<i>j</i></sup>	21.1 <sup><i>e</i>,<i>j</i></sup>

<sup>a</sup> In CDCl<sub>3</sub>, measured at ambient probe temperature at 75.5 MHz. Referenced to  $^{13}\text{C}\text{DCl}_3 = 77.00$  ppm. Coupling constants in Hz.

<sup>b</sup> Where possible, peaks assigned to major (M) and minor (m) rotamer (ratio, 1.6:1) based on signal intensity. <sup>c</sup> Two rotamers, ratio 1.2:1.

<sup>d</sup> Assignment uncertain. <sup>e</sup> Other resonances could not be assigned to L, R, and Z with certainty. <sup>f</sup> 142.0, 139.6, 129.5, 129.3, 128.3 (br), 127.7, 21.2, 20.1. <sup>g</sup> At  $-50$  °C and 125.7 MHz. <sup>h</sup> 141.8, 138.7, 138.5, 129.2, 128.9, 128.5, 128.1, 127.3, 21.6, 20.0. <sup>i</sup> 141.7, 141.0, 139.2, 129.3, 129.0, 128.34, (br), 128.28 (br), 127.9, 127.54, 127.50, 126.5. <sup>j</sup> 141.0, 140.3, 138.8, 130.1, 129.1, 127.1, 121.1.

**Table 9.** Diastereoselectivity of Ligand Addition Reactions on **5**

reactants		ratio of <b>6:7</b>	ligand cone angle <sup>a</sup>
complex	ligand		
<b>5d</b>	PMe <sub>3</sub>	≥25:1	118
<b>5d</b>	PMe <sub>2</sub> Ph	≥25:11	122
<b>5d</b>	PMePh <sub>2</sub>	20:1	136
<b>5d</b>	PPh <sub>3</sub>	6:1	145
<b>5d</b>	CO	≥50:1	~95
<b>5e</b>	PMe <sub>3</sub>	≥50:1	118
<b>5f</b>	PMe <sub>3</sub>	≥50:1	118

<sup>a</sup> Reference 33a.

$\text{mol}^{-1}$  at 90 °C. At 80 °C, the observed rate constant,  $-0.044 \text{ h}^{-1}$ , was unaltered within experimental uncertainty in separate experiments conducted in the presence of added PMe<sub>3</sub> (1.0 equiv) or **5b** (0.54 equiv), but in the early stages of the latter experiment, as the amount of **7e**-PMe<sub>3</sub> decreased, **6b**-PMe<sub>3</sub> was formed at the expense of **6e**-PMe<sub>3</sub>. That isomerization involved inversion at Ir and not C was verified by the derivatization of the **6e**-PMe<sub>3</sub> produced in these experiments to amides **10a/b**, isolated in a ratio of at least 25:1. All results are consistent with isomerization of **7e**-PMe<sub>3</sub> via **5e** and free PMe<sub>3</sub>.

The addition of PPh<sub>3</sub> to **5a** produced a yellow solution

whose NMR spectrum exhibited sharp lines for all resonances except those attributable to the aryl protons of the PPh<sub>3</sub> ligand in **6a**-PPh<sub>3</sub>. NMR spectra of the yellow solution produced by adding PPh<sub>3</sub> to chiral **5d** showed two sets of resonances in a ratio of 6:1 at ambient temperature and at 63 °C. At the lower temperature, the resonances assigned to the PPh<sub>3</sub> ligand were very broad, but were sharpened somewhat at the higher temperature. The two apparent doublets for the AA'XX' spin system of the tosyl group of the minor component were only visible at 63 °C. Because of the smooth decrease in selectivity with increasing phosphine size in Table 9, it is assumed that the predominant isomer from reaction of **5d** and PPh<sub>3</sub> is **6d**-PPh<sub>3</sub>. In addition, rapid exchange of the bulky PPh<sub>3</sub> ligand was demonstrated by adding **5a** to a solution of **6d**-PPh<sub>3</sub> and **7d**-PPh<sub>3</sub> and observing within minutes the appearance of signals for **6a**-PPh<sub>3</sub> and **5d**.

Red solutions of **5** turn yellow on addition of a variety of primary aliphatic and heterocyclic amines, and decreased values for  $\nu_{\text{CO}}$  as well as changes in NMR spectra are consistent with amine complexation to Ir to produce single diastereomers. In most cases, broadened resonances, especially those ascribable to protons on the amine nitrogen and on the carbon adjacent to it,

**Table 10. Experimental Data for X-ray Diffraction Study of 5a and 5f**

compd	5a	5f
empirical formula	C <sub>19</sub> H <sub>24</sub> IrNO <sub>4</sub> S	C <sub>25</sub> H <sub>28</sub> IrNO <sub>4</sub> S
color and habit	ruby red needle	ruby red parallelepiped
cryst size (mm <sup>3</sup> )	0.10 × 0.15 × 0.45	0.15 × 0.25 × 0.30
cryst syst	monoclinic	monoclinic
space group	<i>P</i> 2 <sub>1</sub> / <i>n</i>	<i>P</i> 2 <sub>1</sub>
unit cell dimens	<i>a</i> = 7.2900(10) Å <i>b</i> = 12.137(2) Å <i>c</i> = 22.119(4) Å $\beta$ = 91.88(3)°	<i>a</i> = 8.221(3) Å <i>b</i> = 9.435(3) Å <i>c</i> = 15.896(5) Å $\beta$ = 91.03(3)°
volume	1955.9(10) Å <sup>3</sup>	1232.8(7) Å <sup>3</sup>
<i>Z</i>	4	2
fw	554.7	630.7
density (calcd)	1.884 Mg/m <sup>3</sup>	1.699 Mg/m <sup>3</sup>
abs coeff	6.956 mm <sup>-1</sup>	5.530 mm <sup>-1</sup>
<i>F</i> (000)	1080	620
radiation	Mo K $\alpha$ (graphite monochromated, $\lambda$ = 0.710 73 Å)	
temp (K)	298	298
2 $\theta$ range	3.5°–50.0°	3.5°–50.0°
scan type	$\omega$	$\omega$
scan speed	variable; 1.50°–14.65°/min in $\omega$	variable; 1.50°–14.65°/min in $\omega$
scan range ( $\omega$ )	1.60°	1.60°
std reflns	3 measd every 47 reflns	3 measd every 47 reflns
index ranges	–8 ≤ <i>h</i> ≤ 8, 0 ≤ <i>k</i> ≤ 14, 0 ≤ <i>l</i> ≤ 26	–9 ≤ <i>h</i> ≤ 9, –11 ≤ <i>k</i> ≤ 11, –18 ≤ <i>l</i> ≤ 18
reflns collected	3922	4810
indpdt reflns (%)	3467 ( <i>R</i> <sub>int</sub> = 1.90)	4810 ( <i>R</i> <sub>int</sub> = 6.65)
obsd reflns	2516 ( <i>F</i> > 4.0 $\sigma$ ( <i>F</i> ))	4252 ( <i>F</i> > 4.0 $\sigma$ ( <i>F</i> ))
absn corr	$\psi$ -scan of 6 reflns	$\psi$ -scan of 6 reflns
extincn corr	$\chi$ = –0.000 01(2), where <i>F</i> * = $F [1 + 0.002\chi F^2 / \sin(2\theta)]^{-1/4}$	0.000 00
hydrogen atoms	riding model, fixed isotropic <i>U</i>	riding model, fixed isotropic <i>U</i>
weighting scheme	$w^{-1} = \sigma^2(F) + 0.0004F^2$	$w^{-1} = \sigma^2(F) + 0.0010F^2$
no. of params refined	236	290
final <i>R</i> indices (obsd data, %)	<i>R</i> = 3.48, w <i>R</i> = 3.56	<i>R</i> = 2.99, w <i>R</i> = 3.77
<i>R</i> indices (all data)	<i>R</i> = 5.80, w <i>R</i> = 3.98	<i>R</i> = 3.65, w <i>R</i> = 3.99
goodness-of-fit	1.08	0.93
largest and mean $\Delta/\sigma$	0.359, 0.002 (only nonzero $\Delta/\sigma$ was for extinction corr)	0.004, 0.000
data-to-param ratio	10.7:1	14.7:1
largest difference peak	1.16 e Å <sup>-3</sup> (6 largest peaks <1.3 Å from Ir1)	1.89 e Å <sup>-3</sup> (3 largest peaks <1) Å from Ir1)
largest difference hole	–0.87 e Å <sup>-3</sup>	–0.92 e Å <sup>-3</sup>

suggested that rapid amine exchange is rapid even at ambient probe temperature. Chemical evidence to confirm this suspicion came from addition of a second unsaturated complex **5a** to a solution of **6f**–PhCH<sub>2</sub>NH<sub>2</sub>: within time of mixing, a new species, tentatively identified as **6a**–PhCH<sub>2</sub>NH<sub>2</sub>, was present. The acquisition of NMR spectra of amine adducts at temperatures well below ambient allowed the resolution of even the protons on nitrogen; see Figure 3 for these observations on **6d**–PhCH<sub>2</sub>NH<sub>2</sub>.

The clean isomerization of **7e**–PMe<sub>3</sub> to **6e**–PMe<sub>3</sub> over hours at 80 °C described above would suggest that amines, which apparently exchange within minutes at room temperature, should bind so as to produce a thermodynamically preferred syn orientation of R and Cp\* groups on the metallacycle. However, independent verification of this stereochemistry was sought through NOE experiments on amine adducts. The most successful of these attempts was performed at –60 °C on the mixture obtained from (±)-**5d** and DMAP (two isomers in a ratio of 6:1), giving results consistent with cis orientation of R = CH<sub>3</sub> and Cp\* in the major component, (±)-**6d**–DMAP. The importance of steric requirements in amine binding was shown by Me<sub>3</sub>N, which did not change the <sup>1</sup>H NMR spectrum or color of a solution of **5a** when added in equimolar amount, but when added in large excess (ca. 20 equiv) caused a color change to yellow and shifting of <sup>1</sup>H NMR signals.

**Table 11. Atomic Coordinates (×10<sup>4</sup>) and Equivalent Isotropic Displacement Coefficients (Å<sup>2</sup> × 10<sup>3</sup>) for 5a**

	<i>x</i>	<i>y</i>	<i>z</i>	<i>U</i> (eq) <sup>a</sup>
Ir(1)	1668(1)	780(1)	1607(1)	35(1)
N(1)	995(9)	2124(5)	1143(3)	41(2)
C(1)	–403(11)	2837(8)	1420(4)	51(3)
C(2)	–877(12)	2386(8)	2033(5)	55(3)
O(1)	–112(9)	1472(5)	2183(3)	56(2)
O(2)	–1989(9)	2874(6)	2337(4)	85(3)
C(1C)	3895(12)	–45(7)	2067(4)	41(3)
C(2C)	2277(11)	–687(7)	2131(3)	40(3)
C(3C)	1623(12)	–978(6)	1550(4)	41(3)
C(4C)	2876(11)	–561(7)	1102(4)	44(3)
C(5C)	4259(10)	33(7)	1425(4)	41(3)
C(6C)	5054(13)	465(8)	2558(4)	60(4)
C(7C)	1397(13)	–969(8)	2719(4)	53(3)
C(8C)	–61(13)	–1656(8)	1403(4)	57(3)
C(9C)	2729(14)	–787(8)	435(4)	60(3)
C(10C)	5921(12)	566(8)	1169(5)	61(4)
S(1)	1601(3)	2555(2)	481(1)	52(1)
O(3)	2810(10)	1749(5)	244(3)	64(3)
O(4)	–21(10)	2866(5)	124(3)	75(3)
C(1P)	2888(12)	3784(7)	625(4)	43(3)
C(2P)	4724(13)	3720(8)	749(4)	56(4)
C(3P)	5685(14)	4656(9)	885(5)	63(4)
C(4P)	4859(13)	5691(8)	912(4)	52(3)
C(5P)	3001(13)	5728(9)	766(4)	55(3)
C(6P)	2019(12)	4788(8)	619(4)	49(3)
C(7P)	5928(16)	6699(9)	1100(5)	77(5)

<sup>a</sup> Equivalent isotropic *U* defined as one-third of the trace of the orthogonalized *U*<sub>*ij*</sub> tensor.

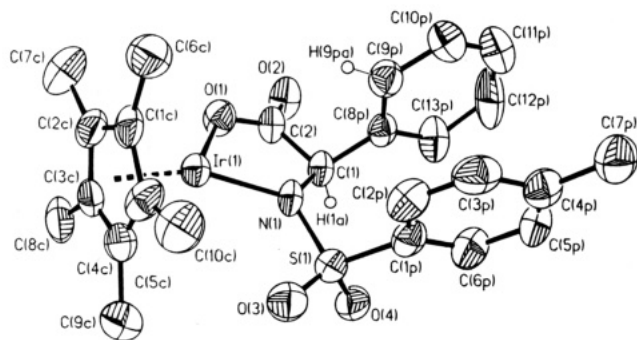


**Figure 2.** Molecular structure of **5f**, shown with 35% thermal ellipsoids. Hydrogen atoms other than those shown (assumed positions) are omitted for clarity.

**Table 12. Atomic Coordinates ( $\times 10^4$ ) and Equivalent Isotropic Displacement Coefficients ( $\text{\AA}^2 \times 10^3$ ) for **5f****

	x	y	z	$U(\text{eq})^a$
Ir(1)	2186(1)	5000	1474(1)	47(1)
N(1)	2887(7)	3916(7)	2489(4)	50(2)
C(1)	3414(9)	2422(9)	2330(5)	53(2)
C(2)	3213(10)	2104(8)	1419(5)	58(3)
O(1)	2734(11)	3118(9)	940(5)	62(3)
O(2)	3511(9)	933(6)	1143(4)	79(2)
C(1C)	2724(17)	6916(15)	821(10)	72(5)
C(2C)	1629(12)	6144(10)	322(5)	65(3)
C(3C)	204(10)	5925(10)	795(5)	65(3)
C(4C)	384(10)	6638(9)	1577(6)	65(3)
C(5C)	1890(12)	7254(9)	1622(6)	69(3)
C(6C)	4423(14)	7404(12)	631(9)	103(5)
C(7C)	1870(18)	5504(15)	-550(7)	121(6)
C(8C)	-1222(11)	5098(24)	483(7)	99(4)
C(9C)	-929(13)	6777(12)	2202(7)	90(4)
C(10C)	2476(17)	8206(12)	2310(8)	105(5)
S(1)	2576(3)	4326(3)	3471(1)	57(1)
O(3)	1773(10)	5693(10)	3482(5)	85(3)
O(4)	1761(7)	3153(8)	3870(3)	71(2)
C(1P)	4489(11)	4509(9)	3988(5)	60(3)
C(2P)	5528(13)	5612(12)	3801(6)	80(4)
C(3P)	7049(12)	5670(14)	4236(7)	94(4)
C(4P)	7543(12)	4703(17)	4804(5)	83(5)
C(5P)	6519(13)	3597(14)	4975(6)	84(4)
C(6P)	4962(13)	3478(12)	4570(5)	79(3)
C(7P)	9149(11)	4767(24)	5240(6)	109(6)
C(8P)	5180(9)	2112(8)	2614(5)	54(2)
C(9P)	6469(10)	2951(10)	2370(5)	65(3)
C(10P)	8041(12)	2633(13)	2582(7)	84(4)
C(11P)	8419(13)	1542(15)	3061(8)	95(5)
C(12P)	7195(15)	632(13)	3290(8)	114(5)
C(13P)	5526(12)	928(10)	3096(6)	77(3)

<sup>a</sup> Equivalent isotropic  $U$  defined as one-third of the trace of the orthogonalized  $U_{ij}$  tensor.

Although comparative NMR data for diastereomers **6** and **7** are rather limited due to the pronounced tendency to form **6**, several generalizations may be made. Particularly instructive is comparison of complexes derived from **5d**, because of lack of complications due to rotamerism or other conformational effects in the corresponding adducts. Looking at  $^1\text{H}$  NMR data for the pairs **6d**–/**7d**– $\text{PMePh}_2$ , **6d**–/**7d**–DMAP, and **6d**–/**7d**– $\text{PPh}_3$  (Table 7), one sees two trends: the doublet ascribable to the alanine methyl group appears at significantly higher field in the **7d** series, whereas the quartet for the amino acid methine is found at lower field in the **7d** series. Attempts to extend this generalization to the better-characterized **6e**–/**7e**– $\text{PMe}_3$  pair seem to fail, presumably because of unknown influence of the  $\text{CO}_2\text{CH}_2\text{Ph}$  and  $\text{CH}_2\text{Ph}$  groups in their (presumably) different conformations. Regardless, the consis-

tent trend seen for the **6d**–/**7d**–series lends confidence that the assigned stereochemistries are correct throughout.

## Discussion

Stabilization of coordinatively unsaturated metal centers by heteroatom lone pair donation is now a well-established phenomenon,<sup>15,16</sup> and serves to explain the stability and bonding in **5**. Metallacycles related to **5** include **9**,<sup>14</sup> **13** (Scheme 2),<sup>31a</sup> **14**,<sup>31b</sup> and others which also feature essentially planar metallacyclic rings. An apparent exception was presented by **15**, which was reported to be coordinatively unsaturated, yet bent;<sup>32a</sup> subsequently, however, it was shown that intermolecular Ru–C contact was responsible for the distortion.<sup>32b</sup>

Among amino acid-derived complexes, the structurally characterized dimeric  $\text{Cp}^*\text{Rh}$ –glycine amide complex **16** was suspected on the basis of  $^1\text{H}$  NMR evidence of undergoing partial monomerization in solution to **17**, a species related to **5**, but formulated as rapidly epimerizing at Rh (**17a** + **17b**).<sup>5b</sup> Given our results, we suggest that **16** actually dissociates to form achiral structure **18**, a behavior reminiscent of the interconversion of red **5c** in solution and a yellow dimer or oligomer in the solid.

As far as we are aware, the only isolated coordinatively unsaturated amino acid complexes other than **5** are represented by structure **19**.<sup>5a</sup> These Rh(I) species undergo ligand substitution and addition to give bisphosphine or bisarsine complexes in which the two new ligands are presumably trans to each other, thus precluding an evaluation of asymmetric induction of ligand addition. Recently, dramatic enhancement of CO substitution in **21a** and **21b** compared to **21c** was explained by N-deprotonation and resulting stabilization of an otherwise undetected five-coordinate intermediate.<sup>16k</sup>

One unique feature of chiral **5** is the high stereoselectivity of ligand addition. Results presented above demonstrate that, for the small phosphine  $\text{PMe}_3$ , the selectivity is a result of both kinetic and thermodynamic control. Increasing the number of phenyl groups on the phosphine erodes selectivity to the point that the large phosphine  $\text{PPh}_3$  adds with a selectivity of only 6:1. Moreover, the  $\text{PPh}_3$  ligand, unlike  $\text{PMe}_3$ , exchanges readily even at ambient temperature. The more limited data on additions of amines to **5** seems to show a similar trend based on amine size, and the behavior of chiral **5** towards phosphines and amines may be explained by the cone angles of the ligands.<sup>33</sup>

On the basis of the experience of organic chemistry of cyclic compounds,<sup>34</sup> the kinetic preference for ligand approach to Ir in **5** from the side opposite the amino acid side chain R is understandable. Less obvious is the thermodynamic preference for a cis orientation of the two larger groups ( $\text{Cp}^*$  and R) at the two stereogenic

(31) (a) Darensbourg, D. J.; Klausmeyer, K. K.; Mueller, B. L.; Reibenspies, J. H. *Angew. Chem., Int. Ed. Engl.* **1992**, *31*, 1503–1504. (b) Sellmann, D.; Wilke, M.; Knoch, F. *Inorg. Chem.* **1993**, *32*, 2534–2543. (c) Sellmann, D.; Ludwig, W.; Huttner, G.; Zsolnai, L. *J. Organomet. Chem.* **1985**, *294*, 199–207.

(32) (a) Kölle, U.; Kossakowski, J.; Raabe, G. *Angew. Chem., Int. Ed. Engl.* **1990**, *29*, 773–774. (b) Smith, M. E.; Hollander, F. E.; Andersen, R. A. *Angew. Chem., Int. Ed. Engl.* **1993**, *31*, 1294.

(33) (a) Tolman, C. A. *Chem. Rev.* **1977**, *77*, 313–348. (b) Seligson, A. L.; Troglor, W. C. *J. Am. Chem. Soc.* **1991**, *113*, 2520–2527.

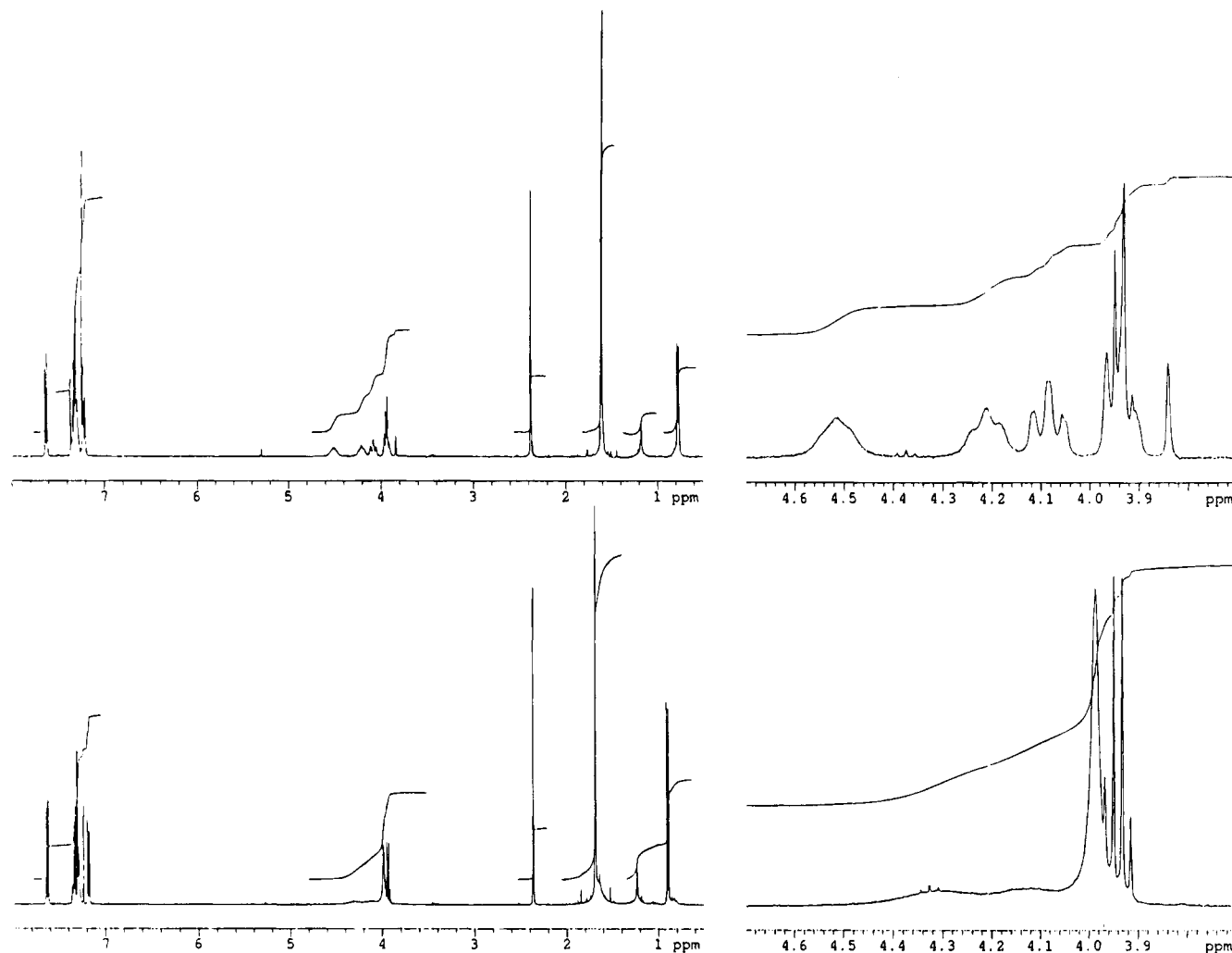


**Figure 3.**  $^1\text{H}$  NMR spectra of **6d**– $\text{PhCH}_2\text{NH}_2$  ( $\text{CDCl}_3$ , 400 MHz) at  $-50$  (upper) and  $25$  °C (lower).

centers. In this connection, we note that we have seen at least 50:1 thermodynamic preference for the *cis* isomer of **22** shown.<sup>35</sup> Presumably, the octahedral coordination environment about Ir in **6**, **7**, **22**, and related species makes the effective size of the metallocycle substituent L (in **6** or **7**) or chloride (in **22**) greater than that of Cp\*, which is tilted further away from the stereogenic carbon.

### Conclusions

Complexes **5** are unique coordinatively unsaturated derivatives of amino acids which enter into highly diastereoselective, rapid ligand addition reactions directed by steric interactions with nonpolar side chains, findings which we feel have relevance to design of both enantiomerically pure transition metal<sup>3</sup> and group 13<sup>8</sup> catalysts based on amino acids and related amides. Further applications of **5** and species related to it are under investigation.

### Experimental Section

**General.** Amino acids were from commercial sources. Amino acid derivatives **4a**, **4d**, **4f**, and racemic **4g**<sup>11</sup> and

iridium complexes **2**,<sup>12</sup> **12**,<sup>29</sup> and **14**<sup>30</sup> were synthesized according to published procedures. Amino acid derivatives **4b,c,e** were from commercial sources. Solvents  $\text{CH}_2\text{Cl}_2$ ,  $\text{CH}_3\text{CN}$ , toluene, and hexanes were reagent grade and used as received, whereas THF and diethyl ether were freshly distilled from blue Na–benzophenone mixtures. Phosphines were purchased, with the exception of  $\text{PMePh}_2$ , which was prepared.<sup>36</sup> Unless otherwise specified, all reactions were conducted under nitrogen atmosphere, using Schlenk line techniques or in an M. Braun inert atmosphere glovebox.

NMR solvents (Cambridge Isotope Labs)  $\text{C}_6\text{D}_6$ ,  $d_8$ -toluene, and  $\text{CD}_2\text{Cl}_2$  were used as received, but  $\text{CDCl}_3$  was passed through basic  $\text{Al}_2\text{O}_3$  before dissolving organometallic complexes. Solvents for NMR tube reactions were degassed by three freeze–pump–thaw cycles. Resealable NMR tubes featuring a Teflon threaded cap were manufactured by J. Young, Ltd.

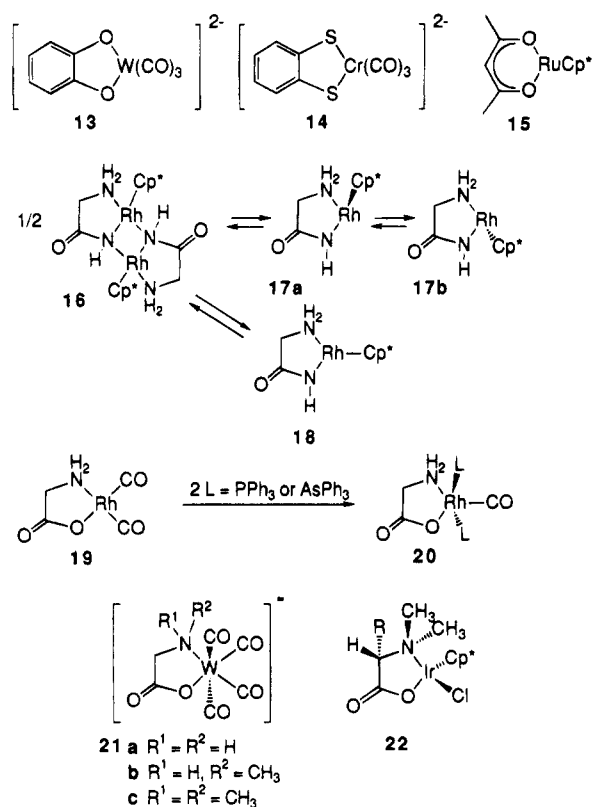
Infrared spectra were acquired on samples prepared in KBr pellets or as solutions held in NaCl cells. Either a Mattson Galaxy 2020 or a Nicolet 550 Magna FT-IR were used. NMR spectra were acquired at ambient probe temperatures of ca.  $25$  °C unless otherwise stated using a Varian Gemini 300, Unity Plus 400, Bruker 400, or Varian 500 MHz instrument.  $^1\text{H}$  NMR spectra are referenced to residual solvent peaks (ppm):  $\text{CHCl}_3$ , 7.24;  $\text{C}_6\text{HD}_5$ , 7.15;  $\text{CHD}_2\text{C}_6\text{D}_5$ , 2.09; and  $\text{CHDCl}_2$ , 5.28, respectively.  $^{13}\text{C}$  NMR spectra are referenced to  $\text{CDCl}_3$

(34) For example, the addition of nucleophiles to cyclic ketones: Huryn, D. M. In *Comprehensive Organic Synthesis*; Schreiber, S. L., Ed.; Pergamon: Oxford, 1991; Vol. 1, Chapter 1.2, pp 49–75, especially pp 67–68.

(35) Grotjahn, D. B. Unpublished results; *Abstracts of Papers*, 208th National Meeting of the American Chemical Society, Washington, DC, August 1994; American Chemical Society: Washington, DC, 1994; ORGN 325.

(36) Bianco, V. D.; Doronzo, S. *Inorg. Synth.* **1976**, *16*, 155–161.

Scheme 2



solvent resonance at  $\delta$  77.00 ppm. Elemental analyses were performed by Atlantic Microlabs, Norcross, GA.

**Synthesis of 5a (Representative Procedure).** Acetonitrile (10 mL) was added to  $[Cp^*IrCl(\mu-Cl)]_2$  (**2**) (99.0 mg, 0.124 mmol), *N-p*-toluenesulfonylglycine (**4a**) (57.4 mg, 0.250 mmol), and anhydrous  $K_2CO_3$  (72.8 mg, 0.527 mmol), and the resulting yellow mixture was deoxygenated by bubbling nitrogen through it for 10 min. After 5 h, the red mixture was concentrated by rotary evaporation. The residue was taken up in  $CH_2Cl_2$  (10 mL) and filtered through a pad of Celite on a glass frit. The filter cake was rinsed with additional  $CH_2Cl_2$  until filtrate was colorless. Combined filtrates were concentrated by rotary evaporation, and the red foamy residue was stored under high vacuum, leaving **5a** (133.8 mg, 97%).

The following compounds (**5b–f**) were isolated in a similar manner from the reactions indicated.

**5b:** From **2** (83.1 mg, 0.104 mmol), **4b** (43.9 mg, 0.210 mmol), and  $K_2CO_3$  (66.8 mg, 0.483 mmol) stirred in THF (15 mL) for 7 days was obtained **5b** (105.0 mg, 94%) as a deep red solid.

**5c** (structure in solution): From **2** (104.9 mg, 0.1317 mmol), **4c** (30.7 mg, 0.2621 mmol), and  $K_2CO_3$  (74.8 mg, 0.541 mmol) stirred in THF (10 mL) for 1.2 days was obtained a yellow solid (111.2 mg, 96%), identified as a dimer or oligomer of **5c**.

**5d:** From **2** (146.7 mg, 0.184 mmol), **4d** (89.8 mg, 0.369 mmol), and  $K_2CO_3$  (102.5 mg, 0.742 mmol) in THF (18 mL), deoxygenated for 10 min and stirred at room temperature for 1.8 days, was obtained **5d** as a deep red powder (207.5 mg, 99%).

**5e:** From **2** (45.0 mg, 0.0565 mmol), **4e** (33.9 mg, 0.113 mmol), and  $K_2CO_3$  (35.4 mg, 0.256 mmol) stirred in  $CH_3CN$  (3 mL) for 4 days was obtained **5e** (69.4 mg, 98%) as a deep red solid.

**5f:** From **2** (56.9 mg, 0.0714 mmol), **4f** (43.8 mg, 0.143 mmol), and  $K_2CO_3$  (43.0 mg, 0.311 mmol) in  $CH_3CN$  (7 mL) stirred at room temperature for 6 h was obtained **5f** (86.5 mg, 96%) as a red foam.

**Crystal Structures of 5a and 5f.** Crystallization occurred from hot toluene (**5a**) or xylenes (**5f**) by diffusion with

petroleum ether. Data were collected on a Siemens R3m/V autodiffractometer using graphite-monochromated Mo K $\alpha$  radiation, see Table 10. The structures were solved by Patterson synthesis using SHELXTL/PC, and the resulting structural parameters were refined by least-squares techniques. Anisotropic thermal parameters were refined for all non-hydrogen atoms, and fixed thermal parameters were used for the included hydrogens.

**Addition of  $PMe_3$  to 5a To Produce 6a- $PMe_3$ .** A J. Young resealable NMR tube was charged with **5a** (13.9 mg, 0.0251 mmol). In the glovebox, deoxygenated  $CDCl_3$  (1 mL) was filtered through basic  $Al_2O_3$  into the NMR tube, and  $PMe_3$  (2.8  $\mu$ L, 0.027 mmol) was added, causing the red color of the solution to turn to yellow upon mixing. After observation of NMR spectra, the solution was transferred to a flask and concentrated by rotary evaporation, and the yellow residue was triturated under a little  $Et_2O$  and pentane. Removal of the supernatant by pipet and storage of the residue under high vacuum left **6a- $PMe_3$**  (14.1 mg, 89%) as a yellow powder. nOe experiments on the product in  $CDCl_3$ : Irradiation of the signal at  $\delta$  2.33 (Ar- $CH_3$ ) resulted in a 21% enhancement of the d at 7.17. Irradiation of the d at 1.56 ppm ( $PMe_3$ ) produced enhancements in the d at 7.59 (3.6%), 3.92 (0.9%), and practically no change in the signal at 3.67 (0.05%). Irradiation of the d at 1.69 ppm ( $Cp^*-CH_3$ ) gave enhancements of the d at 7.59 (5.2%) and at 3.67 (1.8%) and led to a slight reduction of the d at 3.92 ppm (-0.3%), from which it was concluded that the methylene proton responsible for the d at 3.92 ppm is syn to  $PMe_3$ , whereas the proton resonating at 3.67 ppm is syn to  $Cp^*$ .

**6b- $PMe_3$ :** In the glovebox,  $PMe_3$  (2.4  $\mu$ L, 0.023 mmol) was added by syringe to a solution of **5b** (10.6 mg, 0.0198 mmol) in  $CDCl_3$  (0.7 mL) in a J. Young resealable NMR tube, whereupon the red color of the solution faded to yellow.  $^1H$  NMR showed two sets of signals, ascribed to a major and a minor rotamer in a ratio of 1.6:1.

**6c- $PMe_3$ :** As in the preparation of **6b- $PMe_3$** ,  $PMe_3$  (1.6  $\mu$ L, 0.015 mmol) was added by syringe to a solution of **5c** (6.6 mg, 0.015 mmol) in  $CDCl_3$  (1 mL).  $^{31}P\{^1H\}$  ( $CDCl_3$ , 202.3 MHz) -19.8 ppm.

**6d- $PMe_3$ :** In the glovebox,  $CDCl_3$  (1 mL) was filtered through basic  $Al_2O_3$  (4 cm in a pipet) into a J. Young resealable NMR tube containing **5d** (20.5 mg, 0.0360 mmol). Trimethylphosphine (4.0  $\mu$ L, 0.039 mmol) was added to the red solution, causing it to fade to yellow instantly.  $^1H$  and  $^{31}P\{^1H\}$  NMR spectra (the latter at 202.3 MHz, -17.0 ppm) indicated that a major compound was formed with a preponderance of at least 25:1 over minor, unidentified components as determined by integration of resonances in the range of  $\delta$  0.9–1.8 ppm. Concentration of the solution afforded **6d- $PMe_3$**  (22.0 mg, 95%) as a pale yellow solid.

**6e- $PMe_3$ :** Following the preparation of **6a- $PMe_3$** , a solution of **5e** (11.9 mg, 0.190 mmol) in  $CDCl_3$  (0.6 mL) was treated with  $PMe_3$  (2.2  $\mu$ L, 0.021 mmol), to give a solution of **6e- $PMe_3$**  as a mixture of two rotamers (1.2:1 in  $CDCl_3$ , 1.66:1 in *d*<sub>3</sub>-toluene) as evidenced by two sets of sharp signals.  $^{31}P\{^1H\}$  ( $C_6D_6$ , 161.9 MHz) -16.91 (major rotamer) and -17.37 (minor) ppm.

**Synthesis of 7e- $PMe_3$ .** Acetonitrile (3.5 mL) was added to **4e** (10.5 mg, 0.0351 mmol),  $Cp^*IrCl_2(PMe_3)$  (16.7 mg, 0.0352 mmol), and anhydrous  $K_2CO_3$  (11.1 mg, 0.080 mmol) and  $N_2$  was bubbled through the resulting yellow mixture for 5 min. After 1.8 days, the mixture was worked up as in the preparation of **5a**, leaving a pale yellow solid containing **7e- $PMe_3$**  and **6e- $PMe_3$**  (24.0 mg, 98%) in a ratio of 4:1 ( $^1H$  NMR). Recrystallization from THF-hexanes provided pure **7e- $PMe_3$**  (16.4 mg, 67%) as a pale yellow solid, existing as a mixture of rotamers in a ratio of 5:1 in  $CDCl_3$  and 3:1 in  $C_6D_6$ .  $^{31}P\{^1H\}$  ( $C_6D_6$ , 202.3 MHz) -23.33 (major rotamer) and -22.42 (minor) ppm.

**NOE characterization of 6f- $PMe_3$  in  $CDCl_3$ .** Irradiation of the multiplet at 6.9–7.02 ppm caused enhancement of



the resonances at 4.97 (13%) and 1.70 (1.0%) ppm. Irradiation of the singlet at 4.97 ppm led to enhancements of the signals at 7.14 (2.0%), 6.9–7.02 (2.6%), and 1.76 ppm (0.5%). Irradiation of the doublet at 1.76 ppm produced enhancement of the singlet at 4.97 ppm (12%), whereas irradiation of the doublet at 1.70 ppm led to insignificant enhancement of the singlet at 4.97 ppm (1.0%) and significant enhancement of the doublet at 7.14 (7.0%) and the multiplet at 6.9–7.02 ppm (4.6%). From these data it was concluded that the methine proton is syn to the  $\text{PMe}_3$  ligand, whereas the Ph substituent is syn to  $\text{Cp}^*$ .

**6d–PMe<sub>2</sub>Ph.** From addition of  $\text{PMe}_2\text{Ph}$  (2.7  $\mu\text{L}$ , 0.0190 mmol) to a solution of **5d** (10.5 mg, 0.0185 mmol) in  $\text{CDCl}_3$  (1 mL) in the glovebox was obtained **6d–PMe<sub>2</sub>Ph** (13.0 mg, quantitative) as a pale yellow powder.  $^{31}\text{P}\{^1\text{H}\}$  ( $\text{CDCl}_3$ , 202.3 MHz)  $-12.0$  ppm.

**6d–PMePh<sub>2</sub>.** After  $\text{PMePh}_2$  (6.1  $\mu\text{L}$ , 0.0328 mmol) was added by syringe to a solution of **5d** (18.4 mg, 0.0324 mmol) in  $\text{CDCl}_3$  (0.7 mL) in a J. Young NMR tube in the glovebox, the data reported in Tables 7 and 8 were obtained. The solution was poured through a plug of cotton in a pipet. The NMR tube and cotton were rinsed with  $\text{CH}_2\text{Cl}_2$  in small portions, and the residue left from concentration of the combined filtrates was triturated with  $\text{Et}_2\text{O}$ –pentane. The supernatant was removed by pipet, and the remaining yellow powder was dried in vacuo over  $\text{P}_2\text{O}_{10}$  to leave **6d–PMePh<sub>2</sub>** (22.9 mg, 92%).  $^{31}\text{P}\{^1\text{H}\}$  ( $\text{CDCl}_3$ , 202.3 MHz) 0.16 ppm. A small peak at  $-0.43$  ppm may be due to **7d–PMePh<sub>2</sub>**.

**6a–PPh<sub>3</sub>.** A solution of **5a** (22.0 mg, 0.0397 mmol) and  $\text{PPh}_3$  (10.8 mg, 0.0412 mmol) in an NMR tube in  $\text{CDCl}_3$  was worked up as in the preparation of **6d–PMePh<sub>2</sub>** above to give **6a–PPh<sub>3</sub>** (31.6 mg, 97%).  $^{31}\text{P}\{^1\text{H}\}$  ( $\text{CDCl}_3$ , 202.3 MHz) 12.97 ppm.

**6d–PPh<sub>3</sub>.** As in the preparation of **6a–PPh<sub>3</sub>**, **5d** (14.6 mg, 0.0257 mmol) and  $\text{PPh}_3$  (6.8 mg, 0.0259 mmol) gave a solution containing two species in a ratio of 6:1. On the basis of results with other phosphines and **5d**, the major and minor components are presumed to be **6d–PPh<sub>3</sub>** and **7d–PPh<sub>3</sub>**. Further workup left yellow powder (18.9 mg, 88%).  $^{31}\text{P}\{^1\text{H}\}$  ( $\text{CDCl}_3$ , 202.3 MHz) 12.50 (**6d–PPh<sub>3</sub>**) and 9.37 (**7d–PPh<sub>3</sub>**) ppm.

**6a–CO.**  $\text{CDCl}_3$  (1 mL) was filtered through basic  $\text{Al}_2\text{O}_3$  (2 cm in pipet) onto **5a** (8.5 mg, 0.0153 mmol) in a resealable J. Young NMR tube. CO was bubbled through the red solution through a syringe needle for 2 min; the red color faded to pale yellow within the first few seconds. Nitrogen was bubbled through the solution for 2 min.  $^1\text{H}$  and  $^{13}\text{C}$  NMR spectra showed the presence of a single compound. Concentration of the solution left **6a–CO** (8.9 mg, quantitative) as a slightly orangish powder.

**6d–CO.** As in the preparation of **6a–CO**, **6d** (9.8 mg, 0.0172 mmol) and CO in  $\text{CDCl}_3$  afforded a single compound, **6d–CO**, isolated as a pale orangish powder (9.2 mg, 90%).

( $\pm$ )-**6d–DMAP.** Racemic **5d** (11.7 mg, 0.0205 mmol) and DMAP (2.4 mg, 0.0196 mmol) were dissolved in  $\text{CDCl}_3$  (0.7 mL).  $^1\text{H}$  NMR spectra showed a mixture of two components in the yellow solution both at ambient temperature (some peaks broadened) and at  $-60$  °C. That DMAP exchange had been slowed sufficiently at  $-60$  °C was shown by enhancement (0.6%) of the downfield doublet for the DMAP protons upon irradiation of the  $\text{Cp}^*$  methyl resonance, and NOESY spectra showed a crosspeak between resonances ascribed to the  $\text{Cp}^*$  methyl protons and H-2 and H-6 of DMAP. NOE experiments showed weak (0.06%) enhancement of the  $\text{Cp}^*$  methyl protons on irradiation of the doublet ascribed to the alanine methyl group. Attempts at optimization of enhancements in this experiment and others on other amine adducts did not lead to more significant enhancements. Further workup as in preparation of **6d–PMe<sub>2</sub>Ph** left ( $\pm$ )-**6d–DMAP** (14.5 mg).

( $\pm$ )-**8.** A mixture of **2** (38.9 mg, 0.0488 mmol), ( $\pm$ )-**4g** (27.9 mg, 0.0984 mmol), and  $\text{K}_2\text{CO}_3$  (36 mg, 0.26 mmol) in THF (10 mL) was stirred at room temperature. After 1 day, the mixture displayed a yellow color which remained unchanged. After a total of 3.5 days, the mixture was worked up as in the

preparation of **5a** to afford ( $\pm$ )-**8** (58.3 mg, 98%) as a viscous yellow oil which slowly solidified.  $^1\text{H}$  NMR [major and minor isomers (M and m) in a ratio of 6:5 in  $\text{CDCl}_3$ ]  $\delta$  7.18–7.40 (m, 5 H for M + m), 5.28 (d,  $J = 12.0$  Hz, 1 H for m), 5.04 and 5.07 (two d,  $J = 13.0$  Hz, each 1 H for M), 4.86 (d,  $J = 12.0$  Hz, 1 H for m), 4.66–4.73 (m, 1 H for M + m), 2.31 (s, 3 H for M), 2.1–2.35 (m, 2 H for M + m), 2.12 (s, 3 H for m), 1.69 (s, 15 H for M), 1.50 ppm (s, 15H for m); partial  $^1\text{H}$  NMR [ $\text{C}_6\text{D}_6$ , major and minor rotamers (M and m) in a ratio of 4:1]  $\delta$  5.43 (d,  $J = 12.0$  Hz, 1 H for m), 5.39 (d,  $J = 12.5$  Hz, 1 H for M), 5.30–5.35 (m, 1 H for m), 5.21 (d,  $J = 12.5$  Hz, 1 H for M), 5.06–5.12 (m, 1 H for M), 4.99 (d,  $J = 12.0$  Hz, 1 H for m), 1.74 (s, 3 H for M), 1.55 (s, 3 H for m), 1.40 (s, 15 H for M), 1.12 ppm (s, 15 H for m); partial  $^{13}\text{C}$  NMR ( $\text{CDCl}_3$ , 300 MHz)  $\delta$  186.4 and 185.6 ( $\text{CCO}_2$ ), 159.7 and 157.6 ( $\text{NCO}_2$ ), 138.6 and 138.3, 88.7 and 88.3, 66.4 and 66.2, 61.4 and 60.1, 8.7 and 8.5 ppm.

**10b.** Dichloromethane (10 mL) was added to DCC (140.9 mg, 0.683 mmol) and the (*R*)-enantiomer of **4e** (195.1 mg, 0.652 mmol), and the resulting mixture was stirred for 10 min before (*S*)- $\alpha$ -methylbenzylamine (81.0 mg, 0.668 mmol) was added using  $\text{CH}_2\text{Cl}_2$  (2  $\times$  1 mL). After 80 min, the mixture was concentrated to dryness, the residue was taken up in  $\text{Et}_2\text{O}$ , and the resulting mixture was filtered. The white filter cake was washed with  $\text{Et}_2\text{O}$  (total 50 mL, in portions), and the combined filtrates were concentrated, leaving 261 mg of crude product. Purification by radial chromatography over a 2 mm  $\text{SiO}_2$  plate using  $\text{EtOAc}$ –petroleum ether (1:5 to 1:2) afforded **10b** (188.9 mg, 72%) as a white flaky solid. Mp 117.5–119.5 °C (lit. for enantiomer,<sup>21b</sup> 128–131 °C);  $^1\text{H}$  NMR ( $\text{CDCl}_3$ , 300 MHz)  $\delta$  7.05–7.35 (m, 15 H), 5.68 (sl br d,  $J = 7.3$  Hz, 1 H), 5.34 (br s, 1 H), 5.06 (s, 2 H), 4.95 (~quintet,  $J \approx 7$  Hz, 1 H), 4.32 (~q,  $J \approx 7$  Hz, 1 H), 3.15 (dd,  $J = 5.6, 13.5$  Hz, 1 H), 2.94 (dd,  $J = 8.2, 13.5$  Hz, 1 H), 1.225 ppm (d,  $J = 6.8$  Hz, 3 H). Anal. Calcd for  $\text{C}_{25}\text{H}_{26}\text{N}_2\text{O}_3$  (402.51): C, 74.60; H, 6.51; N, 6.96. Found: C, 74.73; H, 6.56; N, 6.95.

**10a.** By a procedure similar to that used for **10b**, **4e** (*S* configuration) (165.0 mg, 0.551 mmol), DCC (118.5 mg, 0.574 mmol), and (*S*)- $\alpha$ -methylbenzylamine (67.1 mg, 0.554 mmol) were reacted to produce **10a** (163.3 mg, 74%) as white solid. Significantly, **10a** exhibited the same  $R_f$  (0.6) as **10b** on  $\text{SiO}_2$  ( $\text{EtOAc}$ –petroleum ether, 1:2) and therefore would not be expected to be chromatographically separated under the conditions used to remove some impurities in derivatization reactions. Mp 177–180 °C (lit.,<sup>21b</sup> 187–188 °C); IR (KBr) 3295 (br, NH), 1692 and 1648  $\text{cm}^{-1}$  (C=O);  $^1\text{H}$  NMR ( $\text{CDCl}_3$ , 300 MHz)  $\delta$  7.00–7.35 (m, 15 H), 5.79 (sl br d,  $J = 8$  Hz, 1 H), 5.32 (br s, 1 H), 5.03 (d,  $J = 12.3$  Hz, 1 H), 5.08 (d,  $J = 12.3$  Hz, 1 H), 5.00 (quintet,  $J = 7.2$  Hz, 1 H), 4.31 (~q,  $J \approx 7$  Hz, 1 H), 3.07 (dd,  $J = 6.0, 13.6$  Hz, 1 H), 2.95 (dd,  $J = 8.0, 13.6$  Hz, 1 H), 1.35 ppm (d,  $J = 7.0$  Hz, 3 H). Anal. Calcd for  $\text{C}_{25}\text{H}_{26}\text{N}_2\text{O}_3$  (402.51): C, 74.60; H, 6.51; N, 6.96. Found: C, 74.02; H, 7.00; N, 7.33.

**11a.** Sulfonamide **4f** (280.0 mg, 0.917 mmol), HOBT (242.7 mg, 1.80 mmol), (*S*)- $\alpha$ -methylbenzylamine (115.3 mg, 0.951 mmol), and DCC (218.2 mg, 1.082 mmol) were allowed to react in THF. Chromatography and recrystallization afforded **11a** (351.2 mg, 94%) as a white solid. Mp 178–182 °C; IR (KBr) 3369, 3327, 3250 (N–H), 1656, 1644 (C=O)  $\text{cm}^{-1}$ ;  $^1\text{H}$  NMR ( $\text{CDCl}_3$ , 300 MHz)  $\delta$  7.56 (~d,  $J \approx 8$  Hz, 2 H), 7.08–7.38 (m, 7 H), 6.10 (sl br d,  $J \approx 8$  Hz, 1 H), 4.88 (d,  $J = 5.2$  Hz, 1 H), 4.95 (~quintet,  $J \approx 7$  Hz, 1 H), 4.75 (d,  $J = 5.2$  Hz, 1 H), 2.35 (s, 3 H), 1.29 ppm (d,  $J = 6.9$  Hz). Anal. Calcd for  $\text{C}_{23}\text{H}_{24}\text{N}_2\text{O}_2\text{S}$  (408.53): C, 67.62; H, 5.92; N, 6.86. Found: C, 67.34; H, 6.07; N, 7.05. A similar experiment starting with racemic **4f** afforded **11a** and **11b** in a ratio of 1:1 by  $^1\text{H}$  NMR. In the  $^1\text{H}$  NMR spectrum of the mixture, each of the four resonances in the region  $\delta$  4.7–6.1 and the doublet near 1.3 ppm appeared at different chemical shifts for **11a** and **11b**. The chemical shifts varied up to 0.1 ppm from sample to sample, but the chemical shift differences between resonances for **11a** and **11b**



did not change nearly as much, permitting determination of the ratio of the two diastereomers.

**Example of the Determination of the Enantiopurity of 5.** A solution of **5f** (27.6 mg, 0.0441 mmol) in CH<sub>2</sub>Cl<sub>2</sub> (2 mL) was treated successively with MeOH (36  $\mu$ L, 0.89 mmol) and Me<sub>3</sub>SiCl (22  $\mu$ L, 0.17 mmol), whereupon the solution turned orange. After 3 min, additional MeOH (2 mL) was added, followed by PPh<sub>3</sub> (11.9 mg, 0.0454 mmol; the presence of **2** seemed to interfere with subsequent reaction with (*S*)- $\alpha$ -methylbenzylamine, presumably by amine complexation). The mixture was concentrated, and the resulting residue (41 mg) was treated as in the preparation of **11a** with HOBT (12.6 mg, 0.0932 mmol), DCC (14.0 mg, 0.0679 mmol), and (*S*)- $\alpha$ -methylbenzylamine (5.8  $\mu$ L, 0.0450 mmol) in THF (5 mL). The crude product after workup (41 mg) contained **11a** and DCU (<sup>1</sup>H NMR), but peaks ascribable to **11b** could not be seen, indicating the presence of **11a** and **11b** in a ratio of at least 25:1.

**Acknowledgment.** We thank the Arizona State University Vice President for Research for partial support of this work, and Johnson Matthey Alfa/Aesar for a generous loan of iridium salts. Dr. Ron Nieman and Camil Joubran graciously performed NOE and VT NMR experiments, and the NSF (CHE-88-13109, CHE-92-14799, and BBS 88-04992) and Arizona State University provided funds for the requisite NMR instrumentation.

**Supporting Information Available:** Further details of the structure determinations of **5a** and **5f**, including a crystal-packing diagram for **5a** (64 pages). Ordering information is given on any current masthead page.

OM950028X

# Organotransition-Metal Metallacarboranes. 39. Arene-Capped Ruthenium–Carborane Tetradecker Sandwich Complexes<sup>1</sup>

Peter Greiwe,<sup>†</sup> Michal Sabat, and Russell N. Grimes\*

Department of Chemistry, University of Virginia, Charlottesville, Virginia 22901

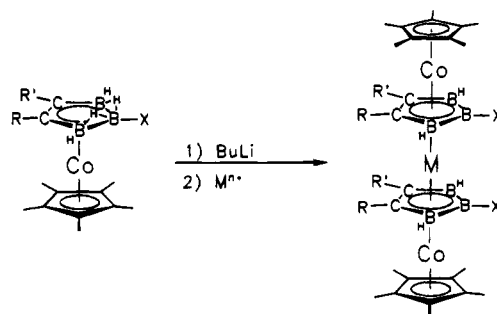
Received March 27, 1995<sup>®</sup>

A new family of C<sub>2</sub>B<sub>3</sub>-bridged tetradecker sandwich complexes, having cymene rather than cyclopentadienyl end rings, has been synthesized via reactions of metal ions with *nido*-(*p*-CHMe<sub>2</sub>C<sub>6</sub>H<sub>4</sub>Me)Ru(Et<sub>2</sub>C<sub>2</sub>B<sub>3</sub>H<sub>3</sub>-5-Y)<sup>-</sup> anions that are isoelectronic analogues of the *nido*-( $\eta^5$ -C<sub>5</sub>Me<sub>5</sub>)Co(Et<sub>2</sub>C<sub>2</sub>B<sub>3</sub>H<sub>3</sub>-5-Y)<sup>-</sup> synthons employed in earlier work. Bridge-deprotonation of CyRu(Et<sub>2</sub>C<sub>2</sub>B<sub>3</sub>H<sub>4</sub>-5-Y) (Cy = *p*-isopropyltoluene; **3**, Y = Me; **6**, Y = Cl), followed by treatment with CoCl<sub>2</sub> in THF and separation of the products on silica in air, afforded the tetradecker sandwiches [CyRu(2,3-Et<sub>2</sub>C<sub>2</sub>B<sub>3</sub>H<sub>2</sub>-5-Y)]<sub>2</sub>Co (**8a**, Y = Me; **8b**, Y = Cl) as the major products, isolated as air-stable paramagnetic green crystals in 40% and 55% yield, respectively. In addition, the minor products CyRu(Et<sub>2</sub>C<sub>2</sub>B<sub>3</sub>H<sub>2</sub>-5-Me)Co(Et<sub>2</sub>C<sub>2</sub>B<sub>3</sub>H<sub>2</sub>-5-Et)RuCy (**8c**) and CyRu(Et<sub>2</sub>C<sub>2</sub>B<sub>3</sub>H<sub>2</sub>-5-Cl)Co(Et<sub>2</sub>C<sub>2</sub>B<sub>3</sub>H<sub>3</sub>)RuCy (**8d**) were obtained. The formation of **8b** proceeds via a cobalt-protonated diamagnetic complex [CyRu(2,3-Et<sub>2</sub>C<sub>2</sub>B<sub>3</sub>H<sub>2</sub>-5-Cl)]<sub>2</sub>CoH (**7b**) which was isolated and characterized; **8a** is assumed to form via an analogous intermediate **7a** although this species was not isolated. A similar reaction of **3**<sup>-</sup> with NiCl<sub>2</sub> gave moderately air-stable, diamagnetic [CyRu(2,3-Et<sub>2</sub>C<sub>2</sub>B<sub>3</sub>H<sub>2</sub>-5-Me)]<sub>2</sub>Ni (**9**). Reactions of the anion of the B(4,5,6)-trimethyl complex CyRu(Et<sub>2</sub>C<sub>2</sub>B<sub>3</sub>Me<sub>3</sub>H<sub>2</sub>) with CoCl<sub>2</sub> and NiCl<sub>2</sub> generated the corresponding tetradecker products [CyRu(2,3-Et<sub>2</sub>C<sub>2</sub>B<sub>3</sub>Me<sub>3</sub>)]<sub>2</sub>Co (**10**) and [CyRu(2,3-Et<sub>2</sub>C<sub>2</sub>B<sub>3</sub>Me<sub>3</sub>)]<sub>2</sub>Ni (**11**) in low yields. The new compounds were characterized via <sup>1</sup>H and/or <sup>13</sup>C NMR, IR, UV–visible, and mass spectra, supported by X-ray crystal structure determinations on **8a**, **8c**, and **9**, which established the tetradecker sandwich geometry. The proton NMR spectrum of paramagnetic **8a** was completely assigned via the technique of correlated spectroscopy, involving generation of the diamagnetic anion **8a**<sup>-</sup> via stepwise reduction of the neutral compound. Crystal data for **8a**: Ru<sub>2</sub>CoClC<sub>34.5</sub>B<sub>6</sub>H<sub>59</sub>, space group *P* $\bar{1}$  (triclinic); *a* = 13.631(5) Å, *b* = 16.447(5) Å, *c* = 9.008(3) Å,  $\alpha$  = 100.07(3)°,  $\beta$  = 108.12(3)°,  $\gamma$  = 94.03(3)°; *Z* = 2; *R* = 0.038 for 5527 independent reflections. Crystal data for **8c**: Ru<sub>2</sub>Co<sub>2</sub>C<sub>35</sub>B<sub>6</sub>H<sub>60</sub>, space group *P*2<sub>1</sub>/*n* (monoclinic); *a* = 12.781(3) Å, *b* = 11.120(4) Å, *c* = 26.214(4) Å,  $\beta$  = 96.71°; *Z* = 4; *R* = 0.031 for 3052 observed reflections. Crystal data for **9**: Ru<sub>2</sub>NiC<sub>34</sub>B<sub>6</sub>H<sub>58</sub>, space group *P* $\bar{1}$  (triclinic); *a* = 12.577(7) Å, *b* = 14.330(6) Å, *c* = 11.671(7) Å,  $\alpha$  = 113.24(4)°,  $\beta$  = 111.71(4)°,  $\gamma$  = 83.24(4)°; *Z* = 2; *R* = 0.028 for 4073 independent reflections.

## Introduction

Transition metal sandwiches incorporating planar C<sub>2</sub>B<sub>3</sub> carborane rings form an extensive family of well-characterized organometallic complexes having 2–6 decks, many of which exhibit remarkable oxidative and thermal stability and are readily soluble in organic solvents.<sup>2,3</sup> Within this group, tetradecker sandwiches of the type [Cp\*Co(RR'C<sub>2</sub>B<sub>3</sub>H<sub>2</sub>X)]<sub>2</sub>M (Scheme 1; Cp\* =  $\eta^5$ -C<sub>5</sub>Me<sub>5</sub>) have been an object of detailed synthetic, structural, spectroscopic, and electrochemical investi-

## Scheme 1



M = Co, Ni, Ru

X = H, Cl, Br, I, Me, C(O)Me, CH<sub>2</sub>C≡CMe

R, R' = alkyl, H

<sup>†</sup> Visiting graduate student from the University of Bielefeld, Germany, 1993–1994. The assistance of Professor Peter Jutzi in arranging this visit is gratefully acknowledged.

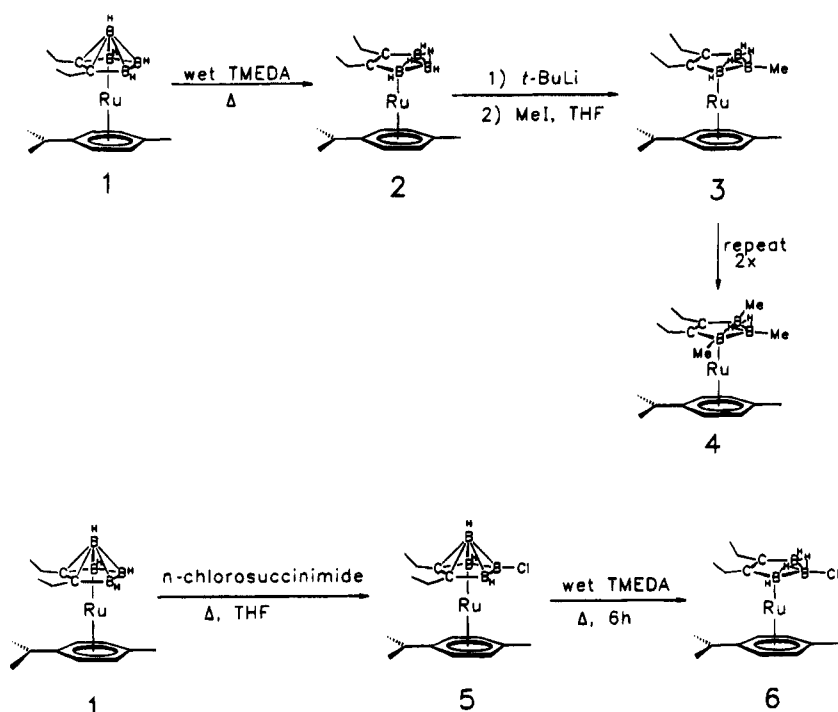
<sup>®</sup> Abstract published in *Advance ACS Abstracts*, July 1, 1995.

(1) (a) Part 38: Stockman, K. E.; Houseknecht, K. L.; Boring, E. A.; Sabat, M.; Finn, M. G.; Grimes, R. N. *Organometallics*, in press. (b) Part 37: Stephan, M.; Müller, P.; Zenneck, U.; Pritzkow, H.; Siebert, W.; Grimes, R. N. *Inorg. Chem.* **1995**, *34*, 2058. (c) Part 36: Houseknecht, K. L.; Stockman, K. E.; Sabat, M.; Finn, M. G.; Grimes, R. N. *J. Am. Chem. Soc.* **1995**, *117*, 1163. (d) Part 35: Stephan, M.; Hauss, J.; Zenneck, U.; Siebert, W.; Grimes, R. N. *Inorg. Chem.* **1994**, *33*, 4211.

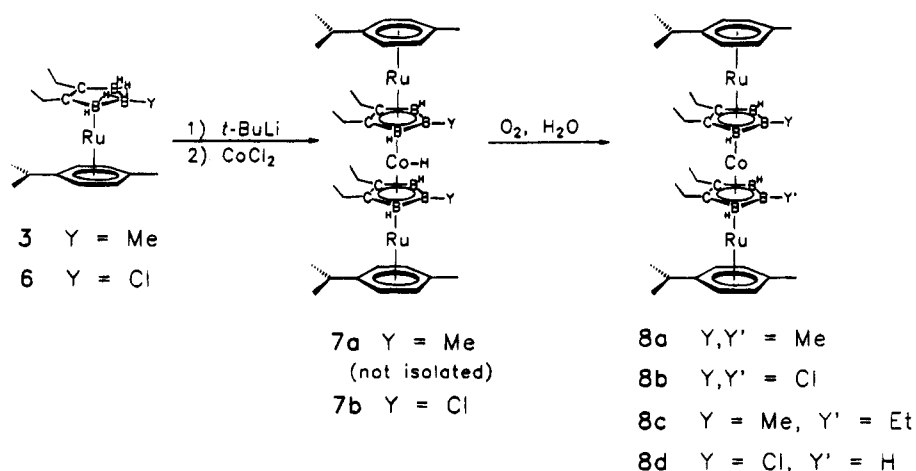
(2) Recent reviews: (a) Grimes, R. N. *Chem. Rev.* **1992**, *92*, 251. (b) Grimes, R. N. In *Current Topics in the Chemistry of Boron*; Kabalka, G. W., Ed.; Royal Society of Chemistry: Cambridge, 1994; 269.

gations.<sup>3a–d</sup> As shown in Scheme 1, these complexes are prepared via metal-stacking reactions involving *nido*-[Cp\*Co(RR'C<sub>2</sub>B<sub>3</sub>H<sub>2</sub>X)]<sup>-</sup> anions (generated by bridge-deprotonation of the neutral species) and transition metal cations at room temperature.<sup>3a</sup> This synthetic

Scheme 2



Scheme 3



route exploits the availability of the double-decker  $\text{Cp}^*\text{Co}(\text{RR}'\text{C}_2\text{B}_3\text{H}_4\text{X})$  starting materials,<sup>4</sup> which are routinely prepared in multigram quantity and are readily derivatized via substitution on the carborane ring.<sup>5</sup> Moreover, by employing bifunctional complexes that contain two  $\text{Co}(\text{RR}'\text{C}_2\text{B}_3\text{H}_4\text{X})$  units connected by multicyclic hydrocarbons such as  $(\text{C}_5\text{H}_4)_2$  (fulvalene) or  $(\text{C}_5\text{Me}_4)_2\text{C}_6\text{H}_4$ , this approach has been exploited in the synthesis of linked multisandwich oligomers.<sup>3b</sup>

It is apparent that other classes of stable carborane-

bridged tetradeckers should be accessible as well, and one would expect their electronic structures and properties to differ significantly from those of the well-established  $\text{Cp}^*\text{Co}$ -end-capped series. We were particularly interested in multideckers capped by arene ligands, which one would expect to be more reactive, hence more readily tailorable, than the relatively inert  $\text{Cp}^*$  groups. With this in mind, and also in order to explore possible alternative strategies for constructing multisandwich oligomers, we have developed a route to a new class of tetradeckers having  $\text{Ru}(\text{arene})$  end units that are isoelectronic and isolobal with  $\text{CoCp}^*$ . This paper describes the preparation and structural characterization of several such species.

## Results and Discussion

**Synthesis and Derivatization of Ruthenacarborane Double-Decker Complexes.** The starting point for this chemistry is the cymene-ruthenacarborane  $\text{CyRu}(\text{Et}_2\text{C}_2\text{B}_4\text{H}_4)$  ( $\text{Cy} = p\text{-isopropyltoluene}$ ) 1, a

(3) (a) Piepgrass, K. W.; Meng, X.; Hölscher, M.; Sabat, M.; Grimes, R. N. *Inorg. Chem.* **1992**, *31*, 5202. (b) Meng, X.; Sabat, M.; Grimes, R. N. *J. Am. Chem. Soc.* **1993**, *115*, 6143. (c) Pipal, J. R.; Grimes, R. N. *Organometallics* **1993**, *12*, 4452. (d) Pipal, J. R.; Grimes, R. N. *Organometallics* **1993**, *12*, 4459. (e) Wang, X.; Sabat, M.; Grimes, R. N. *J. Am. Chem. Soc.* **1994**, *116*, 2687.

(4) Davis, J. H., Jr.; Sinn, E.; Grimes, R. N. *J. Am. Chem. Soc.* **1989**, *111*, 4776.

(5) (a) Piepgrass, K. W.; Grimes, R. N. *Organometallics* **1992**, *11*, 2397. (b) Piepgrass, K. W.; Stockman, K. E.; Sabat, M.; Grimes, R. N. *Organometallics* **1992**, *11*, 2404. (c) Benvenuto, M. A.; Grimes, R. N. *Inorg. Chem.* **1992**, *31*, 3897. (d) Benvenuto, M. A.; Sabat, M.; Grimes, R. N. *Inorg. Chem.* **1992**, *31*, 3904.

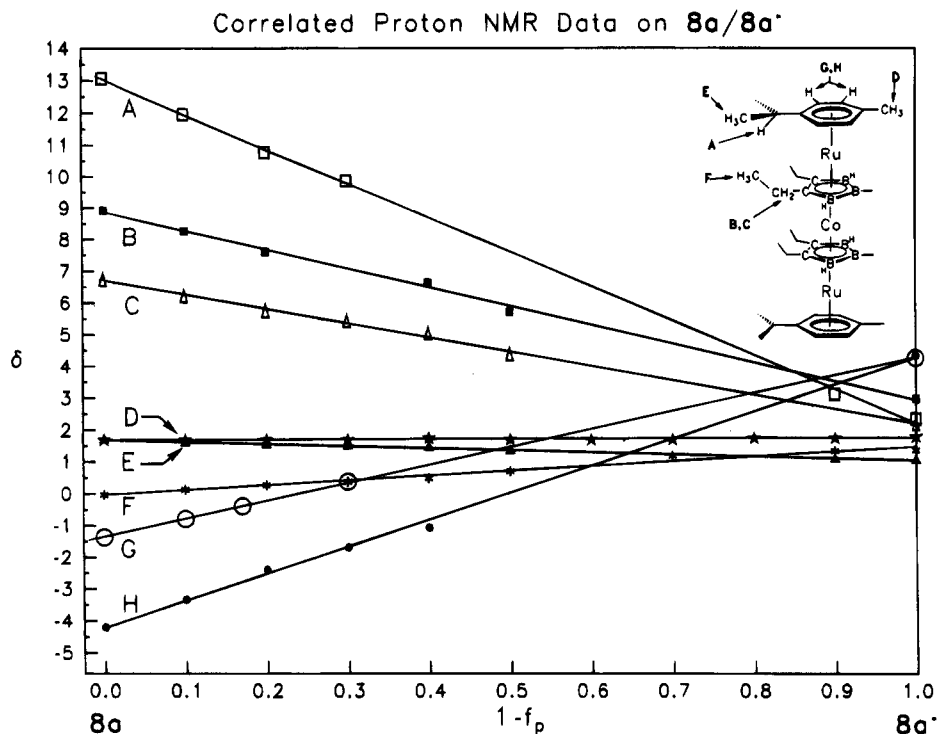


**Figure 1.** Correlation diagram for  $^1\text{H}$  NMR spectra of  $8\text{a}/8\text{a}^-$  in  $\text{CDCl}_3$ . Values of  $\delta$  (vertical axis) are plotted vs  $1 - f_p$  ( $f_p$  is the mole fraction of the paramagnetic component).

colorless, slightly air-sensitive oil first prepared by Davis et al.<sup>4</sup> (Scheme 2). Decapitation of this species with TMEDA affords *nido*- $\text{CyRu}(\text{Et}_2\text{C}_2\text{B}_3\text{H}_5)$  (**2**), an air-stable colorless complex that can be deprotonated and alkylated to yield mono- to tri-B-alkyl derivatives (e.g., **3** and **4**).<sup>6</sup> In the present work, the closo complex **1** was treated with *n*-chlorosuccinimide<sup>5b</sup> to generate regio-specifically (80% yield) the pale yellow *B*(5)-Cl complex **5**, which in turn was converted in refluxing TMEDA to the *nido* species *nido*- $\text{CyRu}(\text{Et}_2\text{C}_2\text{B}_3\text{H}_4\text{-5-Cl})$  (**6**), a colorless air-stable compound (Scheme 2). All of these double-decker ruthenacarborane sandwich species are oils at room temperature, readily separated via column chromatography on silica and characterized via multinuclear NMR and mass spectroscopy.

#### Synthesis of Tetradecker Sandwich Complexes.

As shown in Scheme 3, complexes **3** and **6** were bridge-deprotonated and reacted with 0.5 equiv of  $\text{CoCl}_2$ , producing in each case a dark orange-brown solution that turned green on exposure to air. Chromatographic separation of products on silica in air gave, respectively, the paramagnetic dimethyl and dichloro products  $[\text{CyRu}(\text{Et}_2\text{C}_2\text{B}_3\text{H}_2\text{-5-Y})_2\text{Co}]$  (**8a**,  $\text{Y} = \text{Me}$ ; **8b**,  $\text{Y} = \text{Cl}$ ). A minor side product of the synthesis of **8a**, having a mass 14 units higher than the latter complex, was identified by X-ray crystallography as a *B*(5)-methyl, *B*(5')-ethyl derivative (**8c**). The formation of this species implies the presence of small amounts of a *B*(5)-ethyl precursor complex, which may be generated from a  $[\text{Cp}^*\text{Co}(\text{Et}_2\text{C}_2\text{B}_3\text{H}_4\text{-5-CH}_2)]^-$  tautomer of the deprotonated **3**<sup>-</sup> anion and MeI during the synthesis of **3**.<sup>6</sup> Evidence of such tautomerism in an analogous system is seen in the preparation of  $\text{Cp}^*\text{Co}(\text{Et}_2\text{C}_2\text{B}_3\text{H}_4\text{-5-CH}_2\text{PPh}_2)$  via treatment of the  $[\text{Cp}^*\text{Co}(\text{Et}_2\text{C}_2\text{B}_3\text{H}_4\text{-5-Me})]^-$  anion with  $\text{PPh}_2\text{Cl}$ .<sup>7</sup>

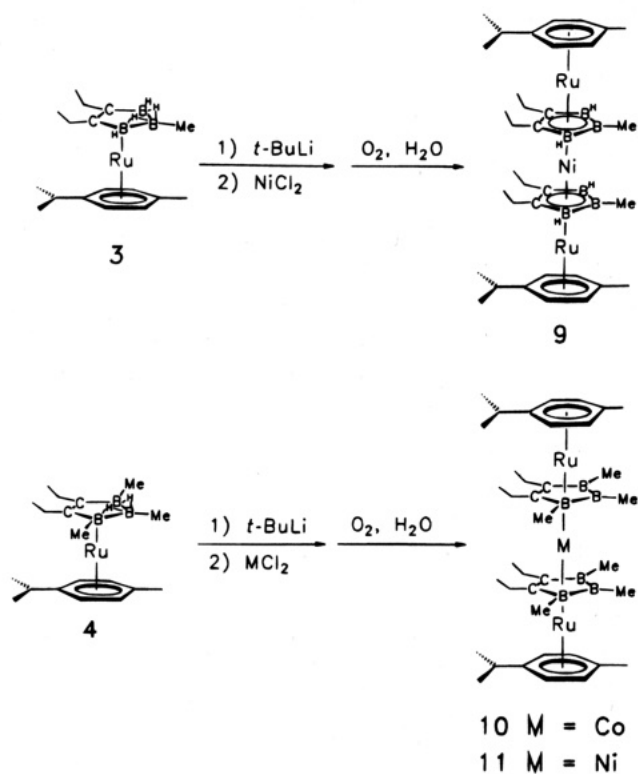
The synthesis of **8b** was accompanied by a paramagnetic monochloro product identified as  $\text{CyRu}(\text{Et}_2\text{C}_2\text{B}_3\text{H}_2\text{-5-Cl})\text{Co}(\text{Et}_2\text{C}_2\text{B}_3\text{H}_3)\text{RuCy}$  (**8d**). The proposed structures for these compounds are consistent with mass spectroscopic and UV-visible evidence, and X-ray diffraction studies of **8a** and **8c** (vide infra) confirmed the tetradecker sandwich geometry. The dichloro complex **8b** is generated via an isolable intermediate, **7b**, a dark brown diamagnetic 42-electron tetradecker complex containing a formal  $\text{Co(III)H}^{4+}$  unit that was characterized from NMR and mass spectra. The proton spectrum of this complex contains a high-field peak at  $\delta -6.66$  and a much smaller signal at  $-8.31$ , both of which are characteristic of metal-bound protons and can be assigned<sup>3b</sup> to  $\text{Co-H}$  and  $\text{Ru-H}$  hydrogens. This supports the likely possibility that isomers arising from protonation at two different metal sites are present in solution; indeed, the "extra" proton may in fact migrate between two or three metal centers, but the available data do not allow more definitive assignment. Conversion of **7b** to **8b** with loss of the metal-bound proton occurred quantitatively, with no decomposition, on exposure to silica in air. The synthesis of **8a** from **3** is assumed to follow a similar path via formation of a protonated intermediate **7a** as shown, but the latter compound was not isolated.

The  $^1\text{H}$  NMR spectra of **8a** and **8b** indicate that both species are paramagnetic, consistent with 41-valence-electron (ve) systems, and this was verified by the observation of ESR signals (X-band at  $-115$  K in frozen  $\text{CH}_2\text{Cl}_2$ ) indicating a single unpaired electron in each case. The presence of cobalt hyperfine structure in the spectra of both compounds establishes that the unpaired electron is at least partially associated with cobalt, corresponding to formal oxidation states of  $\text{Co(IV)}$  and  $\text{Ru(II)}$  in these species. This does not, however, preclude

(6) Davis, J. H., Jr.; Attwood, M. D.; Grimes, R. N. *Organometallics* 1990, 9, 1171.

(7) Wang, X. Ph.D. Thesis, University of Virginia, 1995.

Scheme 4



the possibility of some degree of electron-delocalization over the three metal centers, as has been seen in other multidecker systems. For example, the ESR spectrum of the closely related 29-electron cobalt–ruthenium triple-decker cation [CyRu(Et<sub>2</sub>C<sub>2</sub>B<sub>3</sub>H<sub>3</sub>)CoCp\*]<sup>+</sup>, a fully electron-delocalized species, exhibits cobalt hyperfine splitting,<sup>8</sup> yet, in the spectra of several 41-electron CoCoCo C<sub>2</sub>B<sub>3</sub>-bridged tetra-decker sandwiches that are also evidently electron-delocalized, on the basis of electrochemical data, no such feature is observed.<sup>3c</sup>

The proton NMR spectrum of **8a** was completely assigned via correlation with the spectrum of its 42-electron diamagnetic anion **8a**<sup>-</sup>, obtained by stepwise reduction of the neutral compound on repeated contact with a potassium mirror in the NMR tube as described in earlier publications.<sup>1b,d,9</sup> Least-squares plots of chemical shift vs 1 - *f*<sub>p</sub> (*f*<sub>p</sub> = mole fraction of the paramagnetic component) for the distinguishable proton signals in **8a** are shown in Figure 1. The chemical shifts of the paramagnetic neutral complex and the diamagnetic monoanion correspond to *f*<sub>p</sub> = 1 and 0, respectively. The *B*-methyl signal was not clearly observed in the paramagnetic spectra and is omitted from the diagram; this resonance was, however, identified in the spectrum of the monoanion as a singlet at δ 0.81. The trends evident in these plots can be compared with those found in earlier work on Cp\*Co-end-capped carborane-bridged multidecker sandwiches.<sup>1b,d,9a</sup> In the latter species, the protons closest to the paramagnetic metal center(s) tend to be most strongly affected by redox processes, exhibit-

(8) Merkert, J.; Davis, J. H., Jr.; Geiger, W.; Grimes, R. N. *J. Am. Chem. Soc.* **1992**, *114*, 9846.

(9) (a) Stephan, M.; Davis, J. H., Jr.; Meng, X.; Chase, K. P.; Hauss, J.; Zenneck, U.; Pritzkow, H.; Siebert, W.; Grimes, R. N. *J. Am. Chem. Soc.* **1992**, *114*, 5214. (b) Koehler, F. H.; Zenneck, U.; Edwin, J.; Siebert, W. *J. Organomet. Chem.* **1981**, *208*, 137. (c) Zwecker, J.; Kuhlmann, T.; Pritzkow, H.; Siebert, W.; Zenneck, U. *Organometallics* **1988**, *7*, 2316.

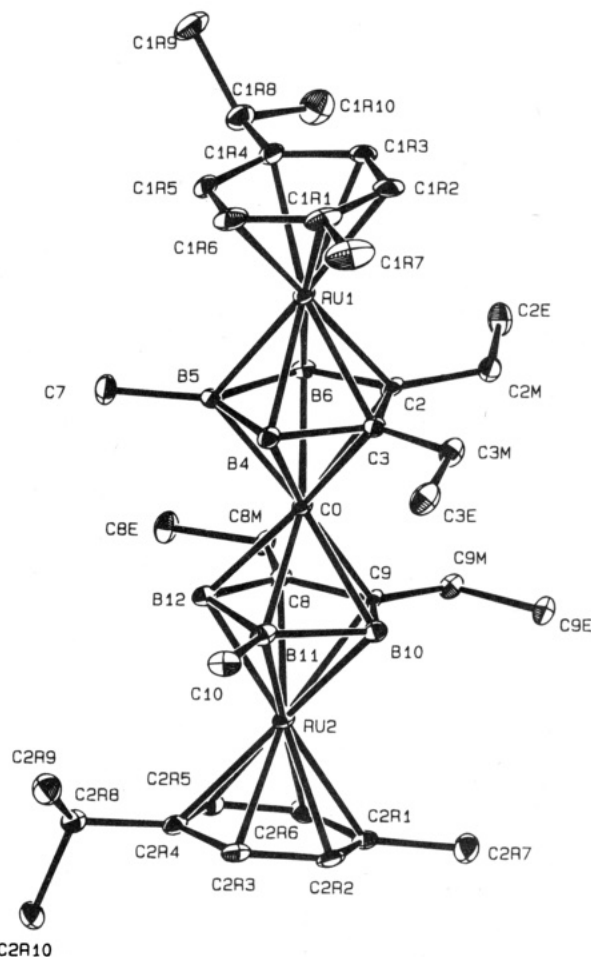
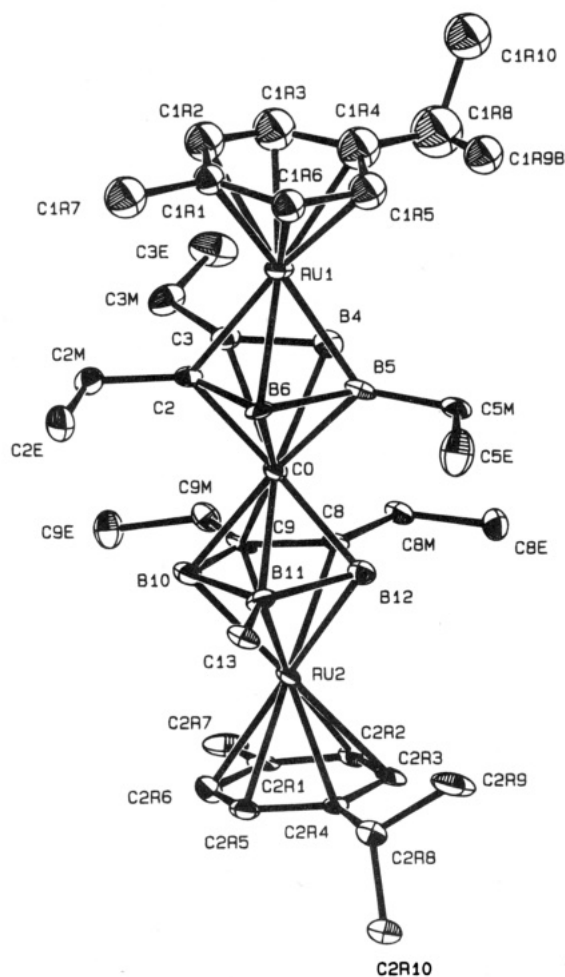


Figure 2. Molecular structure of [CyRu(Et<sub>2</sub>C<sub>2</sub>B<sub>3</sub>H<sub>2</sub>-5-Me)<sub>2</sub>Co] (**8a**).

ing the steepest slopes in the δ vs *f*<sub>p</sub> plots; conversely, the signals arising from the more remote protons generate nearly flat plots, showing little effect of the added electron. One finds similar correlations in the present case: the largest shifts observed on reduction occur in the isopropyl CH and ring proton resonances (plots A, G, and H), while the signals arising from the isopropyl CH<sub>3</sub> and ethyl CH<sub>3</sub> protons (E and F, respectively), which are more remote from the metals, are shifted only slightly. On the other hand, it is remarkable that the cymene tolyl (D) proton resonance is essentially unchanged in the paramagnetic vs diamagnetic species, in contrast to the isopropyl (A) signal, despite comparable Ru–H<sub>D</sub> and Ru–H<sub>A</sub> average distances. Conceivably, this effect can be accounted for by restricted rotation of the isopropyl group that holds hydrogen A in an orientation allowing significant interaction with the nearest metal (ruthenium), as shown; similar interactions of the individual D protons might be, in effect, averaged out by free rotation of the tolyl group and hence not observed.

Since the A protons are relatively far from cobalt, their sensitivity to the redox state of the complex suggests that some of the unpaired spin density is delocalized from the formal Co(IV) center onto the Ru atoms in **8a**, i.e., there is a partially occupied MO having both Co and Ru character. This would be consistent with the finding of cobalt hyperfine splitting in the ESR spectrum of **8a**, mentioned earlier, and also fits the pattern observed in the fully delocalized paramagnetic



**Figure 3.** Molecular structure of  $\text{CyRu}(\text{Et}_2\text{C}_2\text{B}_3\text{H}_2\text{-5-Me})\text{-Co}(\text{Et}_2\text{C}_2\text{B}_3\text{H}_2\text{-5-Et})\text{RuCy}$  (**8c**).

Co–Ru triple-decker cation referred to above. The nature and extent of electron-delocalization in these and other carborane-bridged multidecker sandwich systems are subjects of continuing investigations.

Treatment of the *B*(5)-methyl double-decker complex **3** with  $\text{NiCl}_2$  following deprotonation produced a dark greenish-brown solution which on workup via silica chromatography afforded the Ru–Ni–Ru tetradecker sandwich **9**, obtained in low yield as a dark green solid (Scheme 4). This compound is moderately air-stable, undergoing degradation on standing in air over several weeks. Characterization via  $^1\text{H}$  and  $^{13}\text{C}$  NMR, UV, IR, and mass spectra supported the proposed structure, and the tetradecker geometry was confirmed by a single-crystal X-ray diffraction study.

In order to probe steric inhibition of the tetradecker stacking reaction, we examined the reactivity of a peralkylated synthon, the *B*(4,5,6)-trimethyl complex **4**, toward metal reagents. Previous work involving formation of  $\text{C}_2\text{B}_3$ -bridged tetradeckers<sup>3a</sup> has not included substrates of this type in which all of the carborane ring atoms contain substituents, and it was of interest to see whether metal coordination is blocked in such cases. Accordingly, **4** was deprotonated with *n*-butyllithium and treated with  $\text{CoCl}_2$  or  $\text{NiCl}_2$ , which produced color changes similar to those obtained with the monosubstituted species as described above. Workup in air as before gave, in each case, a mixture of starting material

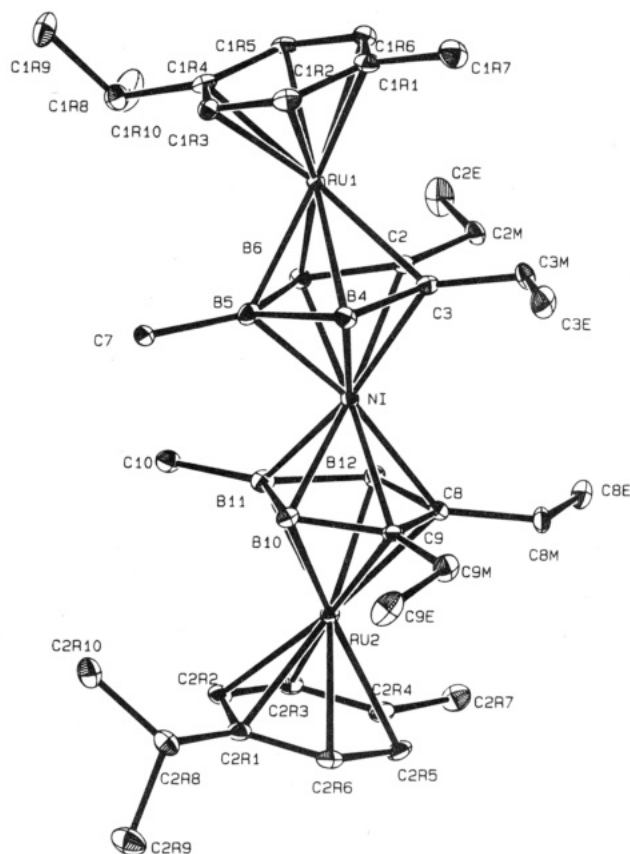


**Figure 4.** Molecular structure of  $[\text{CyRu}(2,3\text{-Et}_2\text{C}_2\text{B}_3\text{H}_2\text{-5-Me})_2\text{Ni}]$  (**9**).

(ca. 50% recovered) and one main product characterized as a hexamethyl derivative, **10** or **11**.

The slow formation and relatively low isolated yields of **10** and **11** (17% and 9%, respectively, based on **4** consumed) suggest that the alkyl groups do indeed sterically hinder the coordination of the carborane ring to metal ions. Electron donation from the alkyl substituents may also be an inhibiting factor, since previous studies have demonstrated that the construction of stable tetradecker sandwiches via metal stacking reactions of  $\text{Cp}^*\text{Co}(\text{Et}_2\text{C}_2\text{B}_3\text{H}_2\text{-5-X})^{2-}$  ions is facilitated by electron-withdrawing X groups.<sup>3a</sup> Nevertheless, the characterization data do support the proposed tetradecker structures for **10** and **11**, making these the first examples of fully substituted tetradecker sandwich metallocarboranes. Significantly, **10** and **11** are considerably less stable than the less substituted species **7–9**, rapidly decomposing on silica in air.

#### X-ray Crystallographic Studies of **8a,c** and **9**.

The molecular geometries of these complexes are depicted in Figures 2–4, data collection parameters and crystal data are presented in Table 1, bond distances and bond angles are listed in Tables 2–4, and tables of positional parameters as well as mean plane calculations are deposited as supporting information.

The molecular structural parameters of the three complexes **8a,c** and **9** can be compared with those obtained earlier on several  $\text{CoCp}^*$ -capped tetradeckers.<sup>3a</sup> As summarized in Table 5, the main features of these complexes display a basic similarity despite the variation in metals, substituent groups on boron, end ligands, and numbers of valence electrons. In all cases, the metals are essentially centered over the  $\text{C}_2\text{B}_3$  rings to



**Table 1. Experimental X-ray Diffraction Parameters and Crystal Data**

	<b>8a</b>	<b>8c</b>	<b>9</b>
empirical formula	Ru <sub>2</sub> CoClC <sub>34.5</sub> B <sub>6</sub> H <sub>59</sub>	Ru <sub>2</sub> Co <sub>2</sub> C <sub>35</sub> B <sub>6</sub> H <sub>60</sub>	Ru <sub>2</sub> NiC <sub>34</sub> B <sub>6</sub> H <sub>58</sub>
fw	835.2	806.8	792.53
cryst color, habit	black prism	black prism	dark green plate
cryst dimens (mm <sup>3</sup> )	0.46 × 0.32 × 0.28	0.46 × 0.36 × 0.32	0.48 × 0.28 × 0.18
space group	P $\bar{1}$	P2 <sub>1</sub> /n	P $\bar{1}$
a, Å	13.631(5)	12.781(3)	12.577(7)
b, Å	16.447(5)	11.120(4)	14.330(6)
c, Å	9.008(3)	26.214(4)	11.671(7)
α, deg	100.07(3)		113.24(4)
β, deg	108.12(3)	96.71	111.71(4)
γ, deg	94.03(3)		83.24(4)
V, Å <sup>3</sup>	1873	3700	1795
Z	2	4	2
μ, cm <sup>-1</sup> (Mo Kα)	13.13	12.56	13.60
transmissn factors	0.63–1.00	0.94–1.00	0.68–1.00
D <sub>calcd</sub> , g cm <sup>-3</sup>	1.481	1.448	1.466
2θ <sub>max</sub> , deg	50.0	46.0	46.0
reflins measd	6898	5470	4868
reflins obsd [I > 3σ(I)]	5527	3052	4073
R	0.038	0.031	0.028
R <sub>w</sub>	0.062	0.042	0.042
largest peak in final diff map, e Å <sup>-3</sup>	1.17	0.82	0.52

which they are coordinated, i.e., there are no cases of significant "ring slippage" in these systems. The intramolecular metal–metal distances (allowing for the larger covalent radius of Ru compared to Co and Ni), carborane C–C bond lengths, and metal–ring distances are closely similar in all of the structures.

Each stack is appreciably bent in the center, as measured by the deviation of the M–M'–M angle from linearity, but the degree of bending varies significantly, from 15° in the 40 ve Co–Ru–Co case<sup>3a</sup> and 14° in **9**, a 42 ve Ru–Ni–Ru system, to as little as 5–6° in the 41 ve Ru–Co–Ru species **8a** and **8c**. In all cases seen thus far, the bending is such as to increase the interligand distance between the Et–C–C–Et units on opposing carborane rings, although the steric interaction between these groups is also reduced in some instances by mutual rotation away from each other. This effect is also seen in the dihedral angles subtended by the four ring planes, which again exhibit their largest values in the Ru-centered sandwich. As discussed elsewhere, the nonparallel ring orientations in carborane-bridged multideckers can be ascribed to electronic causes related to the binding of the metal centers to the heterocyclic C<sub>2</sub>B<sub>3</sub> carborane rings. In the case of the 40-electron ruthenium-centered system, it is proposed that electron-deficiency at the formal Ru(IV) center produces closer Ru–boron contact and thus exacerbates the bending effect.<sup>3a</sup>

The wide variation in the rotational twist in these molecules defies simple rationalization, and may well be as much (or more) influenced by crystal-packing effects as by intramolecular steric or electronic factors. For example, in the Co–M'–Co series one sees a much smaller twist (27°) in the B,B'-diacetyl species than in the corresponding dichloro derivatives (75°), despite the considerably greater steric demands of acetyl vs chloro groups. In solution, relatively free rotation of the ring ligands on the intermetallic axes is assumed; NMR evidence, for example, is consistent in all cases with time-averaged C<sub>2v</sub> symmetry in which the four carborane C–ethyl groups are equivalent (except in the inherently asymmetric trichloro CoRuCo complex).

These findings do not reveal any particularly striking pattern of structural differences between the (arene)-

Ru-capped complexes reported in this paper and their Cp\*Co-capped analogues. Based on this very limited set of available structures, together with their close physical and chemical resemblance, one suspects that the stacked systems assembled from C<sub>2</sub>B<sub>3</sub> ring ligands and the formally isoelectronic (cymene)Ru and Cp\*Co units are not grossly dissimilar. It will be interesting to see if this impression is borne out as studies of tetradecker and other multidecker sandwich systems are extended to a broader range of compositions and molecular geometries.

## Experimental Section

**Instrumentation.** <sup>13</sup>C (75.5 MHz) and <sup>1</sup>H (300 MHz) NMR spectra were acquired on a GE QE300 spectrometer, and UV–vis spectra were recorded on a Hewlett-Packard 8452A diode array spectrophotometer with an HP Vectra computer interface. Infrared spectra were obtained on microcrystalline films on NaCl plates. Unit-resolution mass spectra of the bimetallic starting complexes **1a–f** and **2a–c** were obtained on a Finnegan MAT 4600 GC/MS spectrometer using perfluorotributylamine (FC43) as a calibration standard. In all cases, strong parent envelopes were observed, and the calculated and observed unit-resolution spectral patterns were in close agreement. Elemental analyses were obtained on a Perkin-Elmer 2400 CHN Analyzer using cyclohexanone-2,4-dinitrophenylhydrazone as a standard. In some cases, satisfactory microanalyses could not be obtained, but elemental composition and sample purity were established via combined multinuclear and mass spectra.

**Materials and Procedures.** Dichloromethane and *n*-hexane were anhydrous grade and were stored over 4A molecular sieves prior to use. THF was distilled from sodium–benzophenone immediately prior to use. Column chromatography was conducted on silica gel 60 (Merck), and thick-layer chromatography was carried out on precoated silica gel plates (Merck). Unless otherwise indicated, all syntheses were conducted under vacuum or an atmosphere of argon. Workup of products was conducted in air using benchtop procedures. The complex (CyRuCl<sub>2</sub>)<sub>2</sub> was prepared by the method of Bennett and Smith,<sup>10</sup> and the building-block compounds **1**, **2**, and **4** were obtained via literature routes.<sup>4,6</sup>

(10) Bennett, M. A.; Smith, A. K. *J. Chem. Soc., Dalton Trans.* **1974**, 233.

**Table 2. Bond Distances and Selected Bond Angles for [CyRu(Et<sub>2</sub>C<sub>2</sub>B<sub>3</sub>H<sub>2</sub>-5-Me)]<sub>2</sub>Co (8a)**

Bond Distances, Å			
Ru(1)-C(2)	2.193(4)	C(2)-B(6)	1.569(6)
Ru(1)-C(3)	2.205(4)	C(3M)-C(3)	1.513(6)
Ru(1)-C(1R1)	2.265(5)	C(3M)-C(3E)	1.510(7)
Ru(1)-C(1R2)	2.248(4)	C(3)-B(4)	1.596(6)
Ru(1)-C(1R3)	2.239(4)	C(7)-B(5)	1.587(6)
Ru(1)-C(1R4)	2.216(4)	C(8)-C(8M)	1.512(6)
Ru(1)-C(1R5)	2.180(4)	C(8)-C(9)	1.472(5)
Ru(1)-C(1R6)	2.202(5)	C(8)-B(12)	1.573(6)
Ru(1)-B(4)	2.207(5)	C(8M)-C(8E)	1.526(6)
Ru(1)-B(5)	2.234(5)	C(9M)-C(9)	1.502(6)
Ru(1)-B(6)	2.244(5)	C(9M)-C(9E)	1.534(6)
Ru(2)-C(8)	2.194(4)	C(9)-B(10)	1.551(7)
Ru(2)-C(9)	2.194(4)	C(10)-B(11)	1.577(7)
Ru(2)-C(2R1)	2.273(4)	C(1R1)-C(1R2)	1.409(8)
Ru(2)-C(2R2)	2.211(4)	C(1R1)-C(1R6)	1.420(7)
Ru(2)-C(2R3)	2.204(4)	C(1R1)-C(1R7)	1.502(7)
Ru(2)-C(2R4)	2.227(4)	C(1R2)-C(1R3)	1.421(7)
Ru(2)-C(2R5)	2.232(4)	C(1R3)-C(1R4)	1.409(6)
Ru(2)-C(2R6)	2.262(4)	C(1R4)-C(1R5)	1.426(7)
Ru(2)-B(10)	2.237(5)	C(1R4)-C(1R8)	1.520(7)
Ru(2)-B(11)	2.226(5)	C(1R5)-C(1R6)	1.412(7)
Ru(2)-B(12)	2.202(5)	C(1R8)-C(1R9)	1.536(6)
Co-C(2)	2.179(4)	C(1R8)-C(1R10)	1.519(7)
Co-C(3)	2.103(4)	C(2R1)-C(2R2)	1.414(7)
Co-C(8)	2.090(4)	C(2R1)-C(2R6)	1.412(7)
Co-C(9)	2.174(4)	C(2R1)-C(2R7)	1.531(6)
Co-B(4)	2.057(5)	C(2R2)-C(2R3)	1.430(7)
Co-B(5)	2.099(5)	C(2R3)-C(2R4)	1.433(6)
Co-B(6)	2.132(5)	C(2R4)-C(2R5)	1.410(7)
Co-B(10)	2.140(5)	C(2R4)-C(2R8)	1.513(6)
Co-B(11)	2.098(5)	C(2R5)-C(2R6)	1.420(6)
Co-B(12)	2.068(5)	C(2R8)-C(2R9)	1.505(7)
Cl(1)-C(1S)	1.85(2)	C(2R8)-C(2R10)	1.542(6)
Cl(2)-C(1S)	1.63(2)	B(4)-B(5)	1.783(7)
C(2M)-C(2)	1.515(6)	B(5)-B(6)	1.751(7)
C(2M)-C(2E)	1.502(7)	B(10)-B(11)	1.747(7)
C(2)-C(3)	1.464(6)	B(11)-B(12)	1.783(7)
Bond Angles, deg			
Ru(1)-C(2)-C(2M)	127.7(3)	C(8)-C(8M)-C(8E)	114.2(3)
Co-C(2)-C(2M)	133.4(3)	Ru(2)-C(9)-C(9M)	128.8(3)
C(2M)-C(2)-C(3)	119.3(4)	Co-C(9)-C(9M)	131.9(3)
C(2M)-C(2)-B(6)	127.3(4)	C(9)-C(9M)-C(9E)	114.6(4)
C(3)-C(2)-B(6)	113.4(4)	C(8)-C(9)-C(9M)	119.3(4)
C(2)-C(2M)-C(2E)	114.8(4)	C(8)-C(9)-B(10)	112.9(4)
Ru(1)-C(3)-C(3M)	129.1(3)	C(9M)-C(9)-B(10)	127.7(3)
Co-C(3)-C(3M)	130.2(3)	C(3)-B(4)-B(5)	105.6(4)
C(2)-C(3)-C(3M)	120.8(4)	C(7)-B(5)-B(4)	129.0(4)
C(2)-C(3)-B(4)	113.1(4)	C(7)-B(5)-B(6)	130.5(4)
C(3M)-C(3)-B(4)	126.1(4)	B(4)-B(5)-B(6)	100.4(3)
C(3)-C(3M)-C(3E)	115.9(4)	C(2)-B(6)-B(5)	107.3(4)
Co-C(8)-C(8M)	130.4(3)	Co-B(10)-B(11)	64.4(2)
Ru(2)-C(8)-C(8M)	128.0(3)	C(10)-B(11)-B(10)	130.3(4)
C(8M)-C(8)-C(9)	120.3(4)	C(10)-B(11)-B(12)	128.9(4)
C(8M)-C(8)-B(12)	125.6(3)	B(10)-B(11)-B(12)	100.8(4)
C(9)-C(8)-B(12)	114.1(4)	C(8)-B(12)-B(11)	104.8(3)

**Synthesis of CyRu(2,3-Et<sub>2</sub>C<sub>2</sub>B<sub>4</sub>H<sub>3</sub>-5-Cl) (5).** A 200-mg (0.55 mmol) sample of **1** was dissolved in ca. 60 mL of THF and placed in a 3-neck 100-mL flask which was fitted with a water-cooled condenser and a sidearm tip-tube charged with 150 mg (1.1 mmol) of *N*-chlorosuccinimide (NCS) and attached to an argon line and purged with argon. The NCS was tipped into the THF solution, and the mixture was refluxed for ca. 10 h under a flow of argon. The solution was stripped of solvent on a rotary evaporator, and the residue was taken up in 1:2 hexane/CH<sub>2</sub>Cl<sub>2</sub> and chromatographed on a silica column, affording one pale yellow major band, **5**, which was isolated in 80% yield (0.44 mmol) as a pale yellow oil. Minor bands were identified via mass spectroscopy as dichloro and trichloro derivatives of **1**. This reaction is very sensitive to temperature, concentration, and the NCS:1 ratio and requires continual monitoring by spot TLC analysis. MS: base peak at *m/z* 400, cutoff at *m/z* 405, corresponding to calcd spectrum for RuClC<sub>16</sub>B<sub>4</sub>H<sub>27</sub>. <sup>1</sup>H NMR (CDCl<sub>3</sub>, ppm relative to TMS): 5.335

**Table 3. Bond Distances and Selected Bond Angles for CyRu(Et<sub>2</sub>C<sub>2</sub>B<sub>3</sub>H<sub>2</sub>-5-Me)Co(Et<sub>2</sub>C<sub>2</sub>B<sub>3</sub>H<sub>2</sub>-5-Et)RuCy (8c)**

Bond Distances, Å			
Ru(1)-C(2)	2.194(5)	C(3)-B(4)	1.562(8)
Ru(1)-C(3)	2.191(5)	C(5M)-C(5E)	1.506(9)
Ru(1)-C(1R1)	2.277(6)	C(5M)-B(5)	1.584(8)
Ru(1)-C(1R2)	2.255(8)	C(8)-C(8M)	1.507(7)
Ru(1)-C(1R3)	2.177(8)	C(8)-C(9)	1.461(7)
Ru(1)-C(1R4)	2.199(9)	C(8)-B(12)	1.576(7)
Ru(1)-C(1R5)	2.182(7)	C(8M)-C(8E)	1.505(7)
Ru(1)-C(1R6)	2.229(6)	C(9)-C(9M)	1.507(7)
Ru(1)-B(4)	2.218(6)	C(9)-B(10)	1.559(8)
Ru(1)-B(5)	2.220(7)	C(9M)-C(9E)	1.506(7)
Ru(1)-B(6)	2.221(6)	C(1R1)-C(1R2)	1.36(1)
Ru(2)-C(8)	2.186(5)	C(1R1)-C(1R6)	1.378(8)
Ru(2)-C(9)	2.208(5)	C(1R1)-C(1R7)	1.54(1)
Ru(2)-C(2R1)	2.292(6)	C(1R3)-C(1R3)	1.31(1)
Ru(2)-C(2R2)	2.211(5)	C(13)-B(11)	1.569(7)
Ru(2)-C(2R3)	2.199(6)	C(1R3)-C(1R4)	1.37(1)
Ru(2)-C(2R4)	2.232(5)	C(1R4)-C(1R5)	1.51(1)
Ru(2)-C(2R5)	2.199(5)	C(1R4)-C(1R8)	1.57(1)
Ru(2)-C(2R6)	2.234(6)	C(1R5)-C(1R6)	1.432(8)
Ru(2)-B(10)	2.255(7)	C(1R8)-C(1R9A)	1.43(2)
Ru(2)-B(11)	2.237(7)	C(1R8)-C(1R9B)	1.15(2)
Ru(2)-B(12)	2.198(6)	C(1R8)-C(1R10A)	1.53(2)
Co-C(2)	2.110(5)	C(1R8)-C(1R10B)	1.86(2)
Co-C(3)	2.177(5)	C(2R1)-C(2R2)	1.410(8)
Co-C(8)	2.084(5)	C(2R1)-C(2R6)	1.428(8)
Co-C(9)	2.169(5)	C(2R1)-C(2R7)	1.476(9)
Co-B(4)	2.128(7)	C(2R2)-C(2R3)	1.425(8)
Co-B(5)	2.073(6)	C(2R3)-C(2R4)	1.417(7)
Co-B(6)	2.048(6)	C(2R4)-C(2R5)	1.417(7)
Co-B(10)	2.127(6)	C(2R4)-C(2R8)	1.499(7)
Co-B(11)	2.110(6)	C(2R5)-C(2R6)	1.405(8)
Co-B(12)	2.024(6)	C(2R8)-C(2R9)	1.518(8)
C(2)-C(2M)	1.522(7)	C(2R8)-C(2R10)	1.512(8)
C(2)-C(3)	1.493(7)	B(4)-B(5)	1.720(8)
C(2)-B(6)	1.559(8)	B(5)-B(6)	1.749(9)
C(2M)-C(2E)	1.499(8)	B(10)-B(11)	1.741(9)
C(3M)-C(3)	1.499(7)	B(11)-B(12)	1.783(8)
C(3M)-C(3E)	1.52(1)		
Bond Angles, deg			
Co-C(2)-C(2M)	129.2(4)	C(8)-C(8M)-C(8E)	114.9(4)
Ru(1)-C(2)-C(2M)	129.8(4)	Co-C(9)-C(9M)	132.9(4)
C(2M)-C(2)-C(3)	119.3(4)	Ru(2)-C(9)-C(9M)	128.4(4)
C(2M)-C(2)-B(6)	127.4(4)	C(8)-C(9)-C(9M)	120.1(4)
C(3)-C(2)-B(6)	113.3(4)	C(8)-C(9)-B(10)	112.5(4)
C(2)-C(2M)-C(2E)	113.8(4)	C(9M)-C(9)-B(10)	127.4(5)
Co-C(3)-C(3M)	134.1(4)	C(9)-C(9M)-C(9E)	114.5(4)
Ru(1)-C(3)-C(3M)	126.7(4)	C(3)-B(4)-B(5)	107.3(5)
C(2)-C(3)-C(3M)	120.4(5)	Co-B(5)-C(5M)	131.1(4)
C(2)-C(3)-B(4)	111.8(4)	B(4)-B(5)-B(6)	101.7(4)
C(3M)-C(3)-B(4)	127.8(5)	Ru(1)-B(5)-C(5M)	127.4(4)
C(3)-C(3M)-C(3E)	115.0(5)	C(2)-B(6)-B(5)	105.8(4)
C(5E)-C(5M)-B(5)	114.7(5)	C(9)-B(10)-B(11)	108.4(4)
Co-C(8)-C(8M)	130.5(3)	C(13)-B(11)-B(10)	130.1(5)
Ru(2)-C(8)-C(8M)	127.6(3)	C(13)-B(11)-B(12)	130.5(5)
C(8M)-C(8)-C(9)	120.9(4)	B(10)-B(11)-B(12)	99.4(4)
C(8M)-C(8)-B(12)	125.6(4)	C(8)-B(12)-B(11)	106.1(4)
C(9)-C(8)-B(12)	113.5(4)		

d (C<sub>6</sub>H<sub>4</sub>), 5.303 d (C<sub>6</sub>H<sub>4</sub>), 2.65 m (CHMe<sub>2</sub>), 2.30 m (ethyl CH<sub>2</sub>), 2.14 s (cymene tolyl CH<sub>3</sub>), 1.26 d (CH<sup>\*</sup>Me<sub>2</sub>), 1.18 m (ethyl CH<sub>3</sub>). <sup>13</sup>C NMR (CDCl<sub>3</sub>, ppm vs TMS): 107.9 (unsubstituted cymene ring carbons), 96.9 (unsubstituted cymene ring carbons), 84.2 (substituted cymene ring carbons), 81.7 (substituted cymene ring carbons), 31.9 (C<sup>\*</sup>HMe<sub>2</sub>), 24.3 (cymene tolyl CH<sub>3</sub>), 23.5 (ethyl CH<sub>2</sub>), 19.8 (isopropyl CH<sub>3</sub>), 15.9 (ethyl CH<sub>3</sub>).

**Synthesis of nido-CyRu(2,3-Et<sub>2</sub>C<sub>2</sub>B<sub>3</sub>H<sub>4</sub>-5-Cl) (6).** Complex **5** was decapitated in wet TMEDA (refluxing for 6 h) via the previously described procedure,<sup>5d</sup> affording **6** in 65%–70% yield as a pale yellow oil following chromatography on silica. MS: base peak at *m/z* 390, cutoff at *m/z* 395, corresponding to calcd spectrum for RuClC<sub>16</sub>B<sub>3</sub>H<sub>28</sub>. <sup>1</sup>H NMR (CDCl<sub>3</sub>, ppm relative to TMS): 5.32 m (C<sub>6</sub>H<sub>4</sub>), 2.71 m (CH<sup>\*</sup>Me<sub>2</sub>), 2.21 s (cymene tolyl CH<sub>3</sub>), 2.05 m (ethyl CH<sub>2</sub>), 1.90 m (ethyl CH<sub>2</sub>),

**Table 4. Bond Distances and Selected Bond Angles for [CyRu(2,3-Et<sub>2</sub>C<sub>2</sub>B<sub>3</sub>H<sub>2</sub>-5-Me)]<sub>2</sub>Ni (9)**

Bond Distances, Å			
Ru(1)-C(2)	2.225(4)	C(3M)-C(3)	1.518(5)
Ru(1)-C(3)	2.239(4)	C(3M)-C(3E)	1.525(5)
Ru(1)-C(1R1)	2.268(4)	C(3)-B(4)	1.553(6)
Ru(1)-C(1R2)	2.198(4)	C(7)-B(5)	1.593(6)
Ru(1)-C(1R3)	2.167(4)	C(8M)-C(8)	1.526(5)
Ru(1)-C(1R4)	2.209(4)	C(8M)-C(8E)	1.529(5)
Ru(1)-C(1R5)	2.238(4)	C(8)-C(9)	1.450(5)
Ru(1)-C(1R6)	2.252(4)	C(8)-B(12)	1.564(6)
Ru(1)-B(4)	2.236(4)	C(9M)-C(9)	1.521(5)
Ru(1)-B(5)	2.184(5)	C(9M)-C(9E)	1.515(6)
Ru(1)-B(6)	2.196(5)	C(9)-B(10)	1.558(6)
Ru(2)-C(8)	2.240(4)	C(10)-B(11)	1.587(6)
Ru(2)-C(9)	2.221(4)	C(1R1)-C(1R2)	1.411(6)
Ru(2)-C(2R1)	2.225(4)	C(1R1)-C(1R6)	1.418(5)
Ru(2)-C(2R2)	2.194(4)	C(1R1)-C(1R7)	1.509(6)
Ru(2)-C(2R3)	2.187(4)	C(1R2)-C(1R3)	1.388(6)
Ru(2)-C(2R4)	2.247(4)	C(1R3)-C(1R4)	1.434(5)
Ru(2)-C(2R5)	2.262(4)	C(1R4)-C(1R5)	1.421(5)
Ru(2)-C(2R6)	2.239(4)	C(1R4)-C(1R8)	1.509(6)
Ru(2)-B(10)	2.215(4)	C(1R5)-C(1R6)	1.415(6)
Ru(2)-B(11)	2.186(4)	C(1R8)-C(1R9)	1.524(6)
Ru(2)-B(12)	2.245(5)	C(1R8)-C(1R10)	1.510(6)
Ni-C(2)	2.173(4)	C(2R1)-C(2R2)	1.438(5)
Ni-C(3)	2.192(4)	C(2R1)-C(2R6)	1.418(5)
Ni-C(8)	2.187(4)	C(2R1)-C(2R8)	1.503(5)
Ni-C(9)	2.175(4)	C(2R2)-C(2R3)	1.421(5)
Ni-B(4)	2.117(4)	C(2R3)-C(2R4)	1.422(6)
Ni-B(5)	2.064(4)	C(2R4)-C(2R5)	1.408(5)
Ni-B(6)	2.062(4)	C(2R4)-C(2R7)	1.498(5)
Ni-B(10)	2.061(5)	C(2R5)-C(2R6)	1.420(5)
Ni-B(11)	2.077(5)	C(2R8)-C(2R9)	1.548(6)
Ni-B(12)	2.109(5)	C(2R8)-C(2R10)	1.528(6)
C(2M)-C(2)	1.502(5)	B(4)-B(5)	1.755(6)
C(2M)-C(2E)	1.506(5)	B(5)-B(6)	1.795(6)
C(2)-C(3)	1.465(5)	B(10)-B(11)	1.822(6)
C(2)-B(6)	1.559(6)	B(11)-B(12)	1.762(6)
Bond Angles, deg			
Ni-C(2)-C(2M)	132.7(3)	C(8)-C(8M)-C(8E)	114.3(3)
Ru(1)-C(2)-C(2M)	129.0(3)	Ni-C(9)-C(9M)	133.7(3)
C(2M)-C(2)-C(3)	120.6(3)	Ru(2)-C(9)-C(9M)	128.0(3)
C(2M)-C(2)-B(6)	126.4(3)	C(8)-C(9)-C(9M)	120.5(3)
C(3)-C(2)-B(6)	113.0(3)	C(8)-C(9)-B(10)	113.9(3)
C(2)-C(2M)-C(2E)	115.1(3)	C(9M)-C(9)-B(10)	125.6(3)
C(2)-C(3)-C(3M)	119.1(3)	C(9)-C(9M)-C(9E)	113.9(3)
C(2)-C(3)-B(4)	114.2(3)	C(3)-B(4)-B(5)	107.0(3)
C(3M)-C(3)-B(4)	126.7(3)	Ni-B(5)-C(7)	130.0(3)
Ni-C(3)-C(3M)	132.8(2)	Ru(1)-B(5)-C(7)	126.8(3)
Ru(1)-C(3)-C(3M)	129.9(3)	B(4)-B(5)-B(6)	99.5(3)
C(3)-C(3M)-C(3E)	115.1(3)	C(2)-B(6)-B(5)	106.3(3)
Ni-C(8)-C(8M)	133.0(3)	C(9)-B(10)-B(11)	105.7(3)
Ru(2)-C(8)-C(8M)	129.7(2)	Ni-B(11)-C(10)	131.7(3)
C(8M)-C(8)-C(9)	119.8(3)	Ru(2)-B(11)-C(10)	125.8(3)
C(8M)-C(8)-B(12)	125.8(3)	C(10)-B(11)-B(12)	130.7(3)
C(9)-C(8)-B(12)	114.4(3)	C(8)-B(12)-B(11)	106.8(3)

1.26 d (CHMe\*<sub>2</sub>), 1.07 m (CH<sub>2</sub>CH<sub>2</sub>). <sup>13</sup>C NMR (CDCl<sub>3</sub>, ppm vs TMS): 112.1 (unsubstituted cymene ring carbons), 101.3 (unsubstituted cymene ring carbons), 89.2 (substituted cymene ring carbons), 86.5 (substituted cymene ring carbons), 32.0 (C\*HMe<sub>2</sub>), 25.5 (cymene tolyl CH<sub>3</sub>), 23.7 (ethyl CH<sub>2</sub>), 20.0 (isopropyl CH<sub>3</sub>), 17.3 (ethyl CH<sub>3</sub>).

**Synthesis of [CyRu(2,3-Et<sub>2</sub>C<sub>2</sub>B<sub>3</sub>H<sub>2</sub>-5-Me)]<sub>2</sub>Co (8a) and CyRu(Et<sub>2</sub>C<sub>2</sub>B<sub>3</sub>H<sub>2</sub>-5-Me)Co(Et<sub>2</sub>C<sub>2</sub>B<sub>3</sub>H<sub>2</sub>-5-Et)RuCy (8c).** A 475-mg (1.22 mmol) sample of **3** was dissolved in ca. 75 mL of THF and placed in a 3-neck 100-mL flask containing a stir bar which was fitted with a septum and a sidearm tip-tube charged with 75 mg (0.58 mmol) of anhydrous CoCl<sub>2</sub> and attached to a vacuum line. Under argon, the mixture was cooled to -60 °C and 0.7 mL of 1.7 M (1.19 mmol) *tert*-butyllithium was added via syringe, producing an immediate color change from pale yellow to canary yellow. The solution was warmed to room temperature, stirred for 30 min, and cooled to 0 °C, and the cobalt salt was added via rotation of the sidearm. As it slowly dissolved, the color changed to dark

orange-brown. The mixture was warmed to room temperature and stirred overnight, after which it was opened to the air, causing a color change to dark green. The solution was stripped of solvent, and the residue was washed with CH<sub>2</sub>Cl<sub>2</sub> through a 2-cm silica column. The filtrate was evaporated to dryness and the residue was chromatographed in 2:1 hexane/CH<sub>2</sub>Cl<sub>2</sub>, giving a pale green band of unreacted **3** (190 mg, 40% recovery) and two dark green, nearly black bands. The first of these bands, which had a mass spectral parent ion (base peak) at *m/z* 808, was identified via X-ray crystallography as **8c**, 25 mg (0.031 mmol, 8.6% yield based on **3** consumed). The second band, having a parent ion at *m/z* 794, was **8a**, 108 mg (0.136 mmol, 37.8%). The proton NMR spectrum of paramagnetic **8a** was assigned via correlation with that of its diamagnetic anion **8a**<sup>-</sup> (vide supra and supporting information). <sup>1</sup>H NMR (CDCl<sub>3</sub>, ppm relative to TMS) for **8a**: 13.06 (CH\*Me<sub>2</sub>), 8.94 (ethyl CH<sub>2</sub>), 6.74 (ethyl CH<sub>2</sub>), 1.70 (CHMe\*<sub>2</sub>), -0.02 (ethyl CH<sub>3</sub>), -1.36 (C<sub>6</sub>H<sub>4</sub>), -4.19 (C<sub>6</sub>H<sub>4</sub>). For K<sup>+</sup>**8a**<sup>-</sup> in THF-*d*<sub>6</sub>: 4.34 m (C<sub>6</sub>H<sub>4</sub>), 4.26 m (C<sub>6</sub>H<sub>4</sub>), 2.98 m (ethyl CH<sub>2</sub>), 2.34 m (CH\*Me<sub>2</sub>), 2.19 m (ethyl CH<sub>2</sub>), 1.37 t (ethyl CH<sub>3</sub>), 1.06 d (CHMe\*<sub>2</sub>), 0.81 s (B-CH<sub>3</sub>). IR (cm<sup>-1</sup>) for **8a**: 2960 vs, 2925 vs, 2874 vs, 2495 vs, 1445 s, 1372 s, 1283 s, 1112 m, 1069 s, 1031 m, 874 m, 809 s; for **8c**, 2960 vs, 2926 vs, 2868 m, 2507 s, 2469 s, 2361 m, 2343 m, 1447 m, 1374 m, 1283 m, 1151 w, 1112 m, 1069 s, 1031 m, 940 w, 888 w, 856 w, 813 m. UV-visible absorptions (nm) for **8a**: 318 (100%), 594 (10%); for **8c**, 320 (100%), 594 (11%). Anal. Calcd for Ru<sub>2</sub>CoC<sub>34</sub>B<sub>6</sub>H<sub>58</sub> (**8a**): C, 51.51; H, 7.37. Found: C, 51.99; H, 7.19.

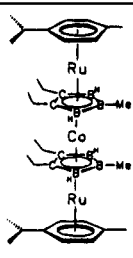
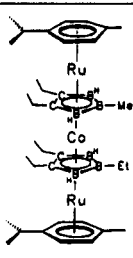
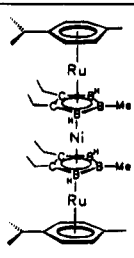
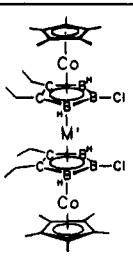
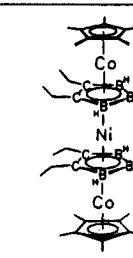
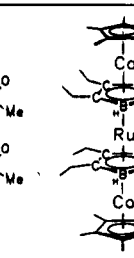
**Synthesis of [CyRu(2,3-Et<sub>2</sub>C<sub>2</sub>B<sub>3</sub>H<sub>2</sub>-5-Cl)]<sub>2</sub>CoH (7b), [CyRu(2,3-Et<sub>2</sub>C<sub>2</sub>B<sub>3</sub>H<sub>2</sub>-5-Cl)]<sub>2</sub>Co (8b), and CyRu(Et<sub>2</sub>C<sub>2</sub>B<sub>3</sub>H<sub>2</sub>-5-Cl)Co(Et<sub>2</sub>C<sub>2</sub>B<sub>3</sub>H<sub>3</sub>)RuCy (8d).** Following the same procedure as in the preceding synthesis, 225 mg (0.56 mmol) of **6** in 50 mL of THF was deprotonated with 1.06 mmol of *tert*-butyllithium and reacted with 40 mg (0.30 mmol) of CoCl<sub>2</sub> (added at -78 °C). After the solution had been stirred overnight at room temperature, the mixture was opened to the air and worked up as before. Chromatography on silica with 2:1 CH<sub>2</sub>Cl<sub>2</sub>/hexane gave three bands, the first of which was light brown unreacted **6** (70 mg, 0.18 mmol). The second band was dark brown diamagnetic **7b** (90 mg, 0.11 mmol, 55% based on **6** consumed). The last band eluted was red-orange paramagnetic **8d** (40 mg, 0.05 mmol, 25%), whose mass spectrum (parent base peak at *m/z* 801) indicated a monochlorinated tetraeder, i.e., with one less Cl atom than **8b**.

Exposure of **7b** in the same solvent mixture to air on a silica TLC plate for 36 h resulted in complete conversion of that compound to green paramagnetic **8b**, with no decomposition. MS for **7b**: base peak at *m/z* 835, cutoff at *m/z* 842 corresponding to calcd spectrum for Ru<sub>2</sub>CoCl<sub>2</sub>C<sub>32</sub>B<sub>6</sub>H<sub>53</sub>. <sup>1</sup>H NMR (CDCl<sub>3</sub>, ppm relative to TMS): 4.86 m (C<sub>6</sub>H<sub>4</sub>), 2.84 m (CH\*Me<sub>2</sub>), 2.16 m (ethyl CH<sub>2</sub>), 1.96 s (cymene tolyl CH<sub>3</sub>), 1.41 t (ethyl CH<sub>2</sub>), 1.16 d (CHMe\*<sub>2</sub>), -6.66 s (Co-H), -8.31 s (Ru-H?). <sup>13</sup>C NMR (CDCl<sub>3</sub>, ppm vs TMS): 106.8 (unsubstituted cymene ring carbons), 96.4 (unsubstituted cymene ring carbons), 83.8 (substituted cymene ring carbons), 81.1 (substituted cymene ring carbons), 31.7 (C\*HMe<sub>2</sub>), 27.2 (tolyl CH<sub>3</sub>), 23.4 (ethyl CH<sub>2</sub>), 19.4 (isopropyl CH<sub>3</sub>), 16.1 (ethyl CH<sub>3</sub>). IR (cm<sup>-1</sup>): 2961 vs, 2926 vs, 2870 vs, 2515 vs, 1476 m, 1447 s, 1377 s, 1319 w, 1279 w, 1055 w, 1032 w, 947 s, 847 m, 804 vs, 733 w. UV-visible absorptions (nm) for **8b**: 324 (100%), 590 (10%). Anal. Calcd for Ru<sub>2</sub>CoCl<sub>2</sub>C<sub>32</sub>B<sub>6</sub>H<sub>52</sub> (**8b**): C, 46.11; H, 6.29. Found: C, 45.93; H, 6.89.

MS for **8d**: base peak at *m/z* 801, cutoff at *m/z* 807 corresponding to calcd spectrum for Ru<sub>2</sub>CoClC<sub>32</sub>B<sub>6</sub>H<sub>53</sub>. UV-visible absorptions (nm): 316 (100%), 448 (10%), 738 (4%). IR (cm<sup>-1</sup>): 2961 vs, 2925 vs, 2868 s, 2515 vs, 2361 vs, 1458 m, 1375 s, 1319 w, 1262 w, 1055 w, 1032 w, 941 s, 889 m, 810 s, 669 m.

**Synthesis of [CyRu(2,3-Et<sub>2</sub>C<sub>2</sub>B<sub>3</sub>H<sub>2</sub>-5-Me)]<sub>2</sub>Ni (9).** Using an apparatus and procedure identical to that employed in the preparation of **8a**, a 390-mg (1.06 mmol) sample of **3** was dissolved in ca. 75 mL of THF and deprotonated with 1.14

Table 5. Comparison of Tetradecker Sandwich Structures

						
	8a	8c	9	M' = Co, Ni	M' = Co, Ni	M' = Co, Ni
ref						
no. of valence electrons	41	41	42	42 (Co-Ni-Co) <sup>c</sup> 41 (Co-Co-Co) <sup>c</sup>	42	40
M-M'-M angle (deg) <sup>d</sup>	175	174	166	172	171	165
dihedral angles (deg) <sup>e</sup>						
ring 1-ring 2	4.3	4.1	7.4	6.4	4.5	5.0
ring 2-ring 3	8.0	9.1	16.2	9.4	11.8	22.1
ring 3-ring 4	3.2	3.4	6.4	5.1	3.7	6.6
ring 1-ring 4	14.5	15.1	29.2	20.4	20.0	33.7
rotational twist (deg) <sup>f</sup>	95	98	48	75	27	89
M-M' distances (Å)	3.32, 3.32	3.31, 3.32	3.33, 3.33	3.19, 3.19	3.18, 3.19	3.30, 3.30
carborane C-C distances (Å)	1.46, 1.47	1.46, 1.49	1.47, 1.45	1.47, 1.48	1.44, 1.49	1.47, 1.46
M'-C <sub>2</sub> B <sub>3</sub> distances (Å) <sup>g</sup>	1.60, 1.59	1.58, 1.59	1.60, 1.60	1.61, 1.62	1.62, 1.62	1.76, 1.75
M-C <sub>2</sub> B <sub>3</sub> distances (Å) <sup>g</sup>	1.73, 1.72	1.73, 1.73	1.73, 1.73	1.58, 1.58	1.57, 1.58	1.56, 1.55
M-C <sub>n</sub> ring distances (Å) <sup>g</sup>	1.72, 1.73	1.72, 1.72	1.71, 1.71	1.67, 1.68	1.67, 1.68	1.69, 1.69

<sup>a</sup> This work. <sup>b</sup> Reference 3a. <sup>c</sup> Isomorphous structures. <sup>d</sup> M' = central metal, M = outer metals. <sup>e</sup> Top and bottom rings are 1 and 4, respectively, in each structure. <sup>f</sup> Dihedral angle between M'-B5-M and M'-B11-M planes. <sup>g</sup> Metal-ring perpendicular vectors.

mmol of *tert*-butyllithium at  $-60^{\circ}$ . After warming to  $0^{\circ}\text{C}$ , 75 mg (0.58 mmol) of  $\text{NiCl}_2$  was added from the sidearm and the reaction mixture turned green and finally dark greenish brown. After the mixture had been stirred overnight at room temperature, the solution was opened to the air and worked up as in the synthesis of **8a**. Chromatography on silica in 1:1 hexane/ $\text{CH}_2\text{Cl}_2$  gave a colorless band of unreacted **3** (175 mg, 45% recovery) and a major green band, as well as several smaller bands that were not collected. Further chromatography of the major band in 2.5:1 hexane/ $\text{CH}_2\text{Cl}_2$  afforded a major green fraction and three smaller bands, two green and one brown. The major band was dark green crystalline **9** (50 mg, 0.063 mmol, 22% yield based on **3** consumed), a moderately air-stable diamagnetic complex that decomposes in air over several weeks. MS: base peak at  $m/z$  793, cutoff at  $m/z$  800 corresponding to calcd spectrum for  $\text{Ru}_2\text{NiC}_{38}\text{B}_6\text{H}_{58}$ . Anal. Calcd for  $\text{Ru}_2\text{NiC}_{38}\text{B}_6\text{H}_{58}$ : C, 51.53; H, 7.38. Found: C, 51.97; H, 7.55.  $^1\text{H}$  NMR ( $\text{CDCl}_3$ , ppm relative to TMS): 4.77 m ( $\text{C}_6\text{H}_4$ ), 2.54 m ( $\text{CH}^*\text{Me}_2$ ), 2.29 m (ethyl  $\text{CH}_2$ ), 1.96 s (cymene tolyl  $\text{CH}_3$ ), 1.27 t (ethyl  $\text{CH}_3$ ), 1.21 s (B- $\text{CH}_3$ ), 1.16 d ( $\text{CHMe}^*_2$ ).  $^{13}\text{C}$  NMR ( $\text{CDCl}_3$ , ppm vs TMS): 106.8 (unsubstituted cymene ring carbons), 95.8 (unsubstituted cymene ring carbons), 82.8 (substituted cymene ring carbons), 80.1 (substituted cymene ring carbons), 32.2 ( $\text{C}^*\text{HMe}_2$ ), 23.7 (tolyl  $\text{CH}_3$ ), 23.4 (ethyl  $\text{CH}_2$ ), 19.5 (isopropyl  $\text{CH}_3$ ), 15.7 (ethyl  $\text{CH}_3$ ). IR ( $\text{cm}^{-1}$ ): 2961 vs, 2926 vs, 2870 vs, 2515 vs, 1476 m, 1447 s, 1377 s, 1319 w, 1279 w, 1055 w, 1032 w, 947 s, 847 m, 804 vs, 733 w. UV-visible absorptions (nm): 338 (100%), 386 (45%), 606 (5%), 656 (6%).

**Synthesis of [CyRu(2,3-Et<sub>2</sub>C<sub>2</sub>B<sub>3</sub>Me<sub>3</sub>)<sub>2</sub>Co] (10) and [CyRu(2,3-Et<sub>2</sub>C<sub>2</sub>B<sub>3</sub>Me<sub>3</sub>)<sub>2</sub>Ni] (11).** The above procedure was employed using 200 mg (0.50 mmol) of **4**, 0.50 mmol of *tert*-butyllithium, and 33 mg (0.25 mmol) of  $\text{CoCl}_2$  in ca. 50 mL of THF. Following deprotonation of the carborane complex,  $\text{CoCl}_2$  was added at  $-78^{\circ}\text{C}$  and the mixture was allowed to warm overnight, producing a color change to brownish-green. The solvent was stripped off, and the residue was dissolved in hexane and filtered through a standard medium-porosity frit under vacuum (the product decomposes on silica or alumina). A mass spectrum revealed the presence of the hexamethyl product **10** ( $m/z$  849) and an unidentified minor product ( $m/z$  656). Unreacted **4** (>50% recovery) and the lower

MW product were removed by sublimation in vacuo, leaving behind nonvolatile paramagnetic **10** as a dark green oil (18 mg, 0.02 mmol, ca. 17%). MS: base peak at  $m/z$  849, cutoff at  $m/z$  855 corresponding to calcd spectrum for  $\text{Ru}_2\text{CoC}_{38}\text{B}_6\text{H}_{66}$ . IR ( $\text{cm}^{-1}$ ): 2961 vs, 2926 vs, 2870 vs, 2486 m, 2361 vs, 1456 vs, 1375 s, 1292 vs, 1261 w, 1152 w, 1082 s, 1053 s, 1030 s, 966 w, 872 vs, 801 vs, 741 w, 667 m. UV-visible absorptions (nm): 334 (100%), 792 (7%).

The same method was followed using 600 mg (1.50 mmol) of **4**, 1.5 mmol of *tert*-butyllithium, and 98 mg (0.75 mmol) of  $\text{NiCl}_2$  in ca. 50 mL of THF. A similar workup procedure was employed except that the final filtration was done in  $\text{CH}_2\text{Cl}_2$  solution, giving **11** as a dark green oil (28 mg, 0.033 mmol, ca. 9%) with 50% recovery of starting complex **4**. MS: base peak at  $m/z$  849, cutoff at  $m/z$  855 corresponding to calcd spectrum for  $\text{Ru}_2\text{NiC}_{38}\text{B}_6\text{H}_{66}$ . IR ( $\text{cm}^{-1}$ ): 2959 vs, 2924 vs, 2868 vs, 1456 m, 1375 w, 1294 m, 1261 m, 1091 s, 1028 s, 864 m, 801 s. UV-visible absorptions (nm): 298 (35%), 360 (100%), 718 (5%).

**X-ray Structure Determinations.** Diffraction data were collected on a Rigaku AFC6S diffractometer at  $-100$ ,  $-120$ , and  $-110^{\circ}\text{C}$  for **8a**, **8c**, and **9**, respectively, using Mo  $K\alpha$  radiation ( $\lambda = 0.71069 \text{ \AA}$ ). Details of the data collections and structure determinations are listed in Table 1. For each crystal, the intensities of three standard reflections were monitored, showing no significant variation. Empirical absorption corrections were applied following  $\psi$  scanning of several reflections (transmission factors are reported in Table 1). All calculations were performed on a VAX station 3520 computer employing the TEXSAN 5.0 crystallographic software package.<sup>11</sup> The structures were solved by direct methods in SIR88.<sup>12</sup> Full-matrix least-squares refinement with anisotropic thermal displacement parameters was carried out for each structure, and the results are summarized in Table 1. The crystal lattice of **8a** contained two molecules of dichloromethane solvent per molecule of the complex, and high-temperature factors indicated that the molecular positions

(11) TEXSAN 5.0: Single Crystal Structure Analysis Software. Molecular Structure Corporation: The Woodlands, TX 77381; 1989.

(12) SIR88: Burla, M. C.; Camalli, M.; Cascarano, G.; Giacovazzo, C.; Polidori, G.; Spagna, R.; Viterbo, D. *J. Appl. Crystallogr.* **1989**, *22*, 389.

were only partially populated. In the final cycles, these atoms were refined using population parameters of 0.5 and isotropic thermal parameters.

In compound **8c** ring C(1R1)–C(1R10) was disordered; consequently, these carbon atoms were refined with isotropic thermal parameters. In addition, difference Fourier maps showed that the isopropyl group on this ring was disordered between two orientations. The carbon atoms belonging to these orientations were refined with occupancy factors of 0.6 and 0.4 for groups C(1R9A)–C(1R10A) and C(1R9B)–C(1R10B), respectively. The final difference Fourier maps for **8c** and **9** were essentially featureless. The map for **8a** showed a peak ca.  $1.1 \text{ e}/\text{\AA}^3$  high located in the vicinity of one of the disordered solvent molecules.

**Acknowledgment.** This work was supported by the National Science Foundation, Grant No. CHE 9322490, and the U.S. Army Research Office. We thank Dr. Yaning Wang for recording the ESR spectra and Dr. Eric Houser for the elemental analyses.

**Supporting Information Available:** Tables of atomic coordinates, isotropic and anisotropic displacement parameters, and calculated mean planes for **8a,c** and **9** (15 pages). Ordering information is given on any current masthead page.

OM9502244

**Solution Structures and Dynamics of  $\text{Ru}_4(\mu\text{-H})_4(\text{CO})_{12-x}\text{L}_x$   
( $x = 1-4$ ,  $\text{L} = \text{P}(\text{OEt})_3$ ,  $\text{PPh}_3$ ;  $x = 1, 2$ ,  $\text{L} = \text{AsPh}_3$ )  
Derivatives by VT Multinuclear NMR Spectroscopy.  
X-ray Structure Determination of  
 $\text{Ru}_4(\mu\text{-H})_4(\text{CO})_{10}(\text{P}(\text{OEt})_3)_2$**

Silvio Aime,<sup>\*,1a</sup> Mauro Botta,<sup>1a</sup> Roberto Gobetto,<sup>1a</sup> Luciano Milone,<sup>1a</sup>  
Domenico Osella,<sup>1a</sup> Robert Gellert,<sup>\*,1b</sup> and Edward Rosenberg<sup>\*,1c</sup>

*Dipartimento di Chimica Inorganica, Chimica Fisica e Chimica dei Materiali, Università di Torino, Via P. Giuria 7-9, 10125 Torino, Italy, Department of Chemistry, California State University, Northridge, California 91330, and Department of Chemistry, University of Montana, Missoula, Montana 59812*

Received March 23, 1995<sup>©</sup>

The addition of the catalyst  $(\text{FeCp}(\text{CO})_2)_2$  to the solution reactions of  $\text{Ru}_4(\mu\text{-H})_4(\text{CO})_{12}$  with  $\text{L}$  ( $\text{L} = \text{P}(\text{OEt})_3$ ,  $\text{PPh}_3$ ,  $\text{AsPh}_3$ ) affords the substitution derivatives  $\text{Ru}_4(\mu\text{-H})_4(\text{CO})_{12-x}\text{L}_x$  ( $x = 1-4$ ,  $\text{L} = \text{P}(\text{OEt})_3$ ,  $\text{PPh}_3$ ;  $x = 1, 2$ ,  $\text{L} = \text{AsPh}_3$ ) with good selectivity modulated by the carbonyl to ligand ratio and in satisfactory yield. Multinuclear variable temperature NMR studies at different temperatures show that the tri- and tetrasubstituted products are each obtained in only one isomeric form while for  $\text{L} = \text{P}(\text{OEt})_3$  the monosubstituted derivative exists as two isomers in solution. The disubstituted derivatives form only one isomer for  $\text{L} = \text{P}(\text{OEt})_3$ , whereas two isomers are observed for  $\text{L} = \text{PPh}_3$ ,  $\text{AsPh}_3$ . The stereochemical nonrigidity of the title compounds has been investigated, and correlations between solid-state and solution structures are discussed.

### Introduction

In the last two decades transition metal hydrido-carbonyl clusters have been the subject of several research efforts to elucidate their role in relevant catalytic processes.<sup>2</sup> In polymetallic systems the hydrido ligands exhibit different coordination modes, namely, terminal, edge- or face-bridging, and interstitial.<sup>3</sup> Usually a facile rearrangement takes place in solution, leading to rapid intramolecular exchange among the available coordination sites. There is an obvious interest in understanding the steric and electronic factors governing the preferential coordination sites of such hydrides and the factors affecting their mobility. The scrambling mechanisms involving hydrides are not as well defined as the corresponding processes related to carbonyl migrations. The experimental difficulties encountered in defining hydride fluxionality stem from the simplicity generally exhibited by the  $^1\text{H}$  NMR spectra of hydrido-carbonyl clusters; indirect information *via* the more complex  $^{13}\text{C}$  NMR spectra is usually sought. In particular, it is interesting to assess whether hydride motion is associated with that of other ancillary ligands. The  $\text{Ru}_4(\mu\text{-H})_4(\text{CO})_{12-x}\text{L}_x$

derivatives, archetypal electron precise (60e) tetrahedral clusters, represent suitable models for studying hydride dynamics and their relation to the dynamical properties of the ancillary ligands.

It is worthwhile to briefly summarize the solid-state structures determined for these derivatives: single-crystal X-ray diffraction studies have been carried out on  $\text{Ru}_4(\mu\text{-H})_4(\text{CO})_{12}$ ,  $\text{Ru}_4(\mu\text{-H})_4(\text{CO})_{11}(\text{P}(\text{OMe})_3)$ ,  $\text{Ru}_4(\mu\text{-H})_4(\text{CO})_{10}(\text{PPh}_3)_2$ , and  $\text{Ru}_4(\mu\text{-H})_4(\text{CO})_9(\text{PMe}_2\text{Ph})(\text{P}(\text{OC}_6\text{H}_4\text{-Me-}p)_3)(\text{P}(\text{OCH}_2)_3\text{CEt})$  clusters.<sup>4-6</sup> In these investigations the positions of the hydrides have not been located in the refined structures, but the usual assumption is that they bridge the four long Ru-Ru edges.<sup>7</sup> For all of these derivatives the unbridged (short) Ru-Ru bonds are opposite each other, forming a " $\text{Ru}_4\text{H}_4$ " core of  $D_{2d}$  symmetry. Furthermore, the P-donor ligands are always transoid to the same unbridged Ru-Ru edge. All of these features have been fully confirmed by combined X-ray and neutron diffraction analysis of  $\text{Ru}_4(\mu\text{-H})_4(\text{CO})_8(\text{P}(\text{OMe})_3)_4$ .<sup>8</sup> Incidentally, the  $\text{Ru}_4(\mu\text{-H})_4(\text{CO})_{10}(\text{Ph}_2\text{P}(\text{CH}_2)_n\text{PPh}_2)$  ( $n = 1-4$ ) geometries of both bridge- and chelate-isomers do not belong to this structural class, since three of the hydrides span the tetrahedral edges adjacent to a single Ru atom, forming a " $\text{Ru}_4\text{H}_4$ " core of  $C_s$  symmetry.<sup>9</sup>

<sup>©</sup> Abstract published in *Advance ACS Abstracts*, July 1, 1995.

(1) (a) Università di Torino. (b) California State University (Northridge). (c) University of Montana.

(2) (a) Kaesz, H. D.; Saillant, R. B. *Chem. Rev.* **1972**, *72*, 231. (b) Kaesz, H. D. *Chem. Br.* **1973**, *9*, 344. (c) Humphries, A. P.; Kaesz, H. D. *Prog. Inorg. Chem.* **1979**, *25*, 145. (d) Kaesz, H. D. *J. Organomet. Chem.* **1980**, *200*, 145. (e) Gladfelter, W. L.; Roesslet, K. J. In *The Chemistry of Metal Cluster Complexes*; Shriver, D. F., Kaesz, H. D., Adams, R. D., Eds.; VCH Publishers: New York, 1990; Chapter 7.

(3) (a) Bau, R.; Teller, R. G.; Kirtley, S. W.; Koetzle, T. F. *Acc. Chem. Res.* **1979**, *12*, 176. (b) Teller, R. G.; Bau, R. *Struct. Bonding (Berlin)* **1981**, *44*, 1.

(4) Wilson, R. D.; Mian Wu, S.; Love, R. A.; Bau, R. *Inorg. Chem.* **1978**, *17*, 1271.

(5) See footnote 24 in the following: Wilson, R. D.; Bau, R. *J. Am. Chem. Soc.* **1976**, *85*, 4687.

(6) Bruce, M. I.; Nicholson, B. K.; Patrick, J. M.; White, A. H. *J. Organomet. Chem.* **1983**, *254*, 361.

(7) (a) Orpen, A. G. *J. Organomet. Chem.* **1978**, *159*, C1. (b) Orpen, A. G. *J. Chem. Soc., Dalton Trans.* **1980**, 2509.

(8) Orpen, A. G.; Mc Mullen, R. K. *J. Chem. Soc., Dalton Trans.* **1983**, 463.



Interestingly, the  $\text{Ru}_4(\mu\text{-H})_4(\text{CO})_{12-x}(\text{P}(\text{OMe})_3)_x$  ( $x = 1-4$ ) series has already been investigated at the beginning of the application of the DNMR technique to the study of stereochemical nonrigidity in clusters.<sup>10</sup> From the  $^1\text{H}$  NMR data alone, a complete picture of the dynamics of these derivatives could not be extracted. Kaesz et al.<sup>10</sup> found that in each derivative the hydrides are equally coupled to all the phosphorous atoms at room temperature, and hence they are equivalent. This rapid scrambling implies that the coordination modes of such hydrides differ very little in energy. Corroboration of this hypothesis comes from the theoretical calculations on  $\text{Fe}_4(\mu\text{-H})_{4-x}(\text{CO})_{12-x}$  ( $x = 0-4$ ) model compounds<sup>11</sup> and from the isolation (by crystallization in slightly different conditions) of two structural isomers of the  $(\text{Ru}_4(\mu\text{-H})_3(\text{CO})_{12})^-$  anion.<sup>12</sup> Also we have recently shown that the hydrides are rapidly exchanging in  $\text{Ru}_4(\mu\text{-H})_4(\text{CO})_{12}$  even in the solid state.<sup>13</sup>

We have undertaken a multinuclear, variable temperature (VT) NMR study of the title compounds in order to examine how their solution structures compare to those reported in the solid state and whether isomerism can occur. We have also determined to some extent the processes that equilibrate the hydrides on the NMR time scale. In the course of our studies we uncovered that the single isomeric form observed for  $\text{Ru}_4(\mu\text{-H})_4(\text{CO})_{10}(\text{P}(\text{OEt})_3)_2$ , as well as the major isomers observed for  $\text{Ru}_4(\mu\text{-H})_4(\text{CO})_{10}(\text{PPh}_3)_2$  and  $\text{Ru}_4(\mu\text{-H})_4(\text{CO})_{10}(\text{AsPh}_3)_2$ , have a solution structure different from the solid-state structure reported for  $\text{Ru}_4(\mu\text{-H})_4(\text{CO})_{10}(\text{PPh}_3)_2$ .<sup>4</sup> This prompted us to carry out a single-crystal X-ray analysis of  $\text{Ru}_4(\mu\text{-H})_4(\text{CO})_{10}(\text{P}(\text{OEt})_3)_2$ .

## Results and Discussion

**Syntheses.** The thermal reaction of  $\text{Ru}_4(\mu\text{-H})_4(\text{CO})_{12}$  with Lewis bases (L) in the appropriate molecular ratios affords a mixture of the substitution products, namely,  $\text{Ru}_4(\mu\text{-H})_4(\text{CO})_{12-x}\text{L}_x$  ( $x = 1-4$ ). This requires chromatographic separation with consequent low yields. An improvement in the selectivity has been reported by Bruce et al.,<sup>14</sup> who employed sodium benzophenone ketyl (BPK) as a reaction promoter. We have obtained further increases in yield and selectivity by using  $(\text{FeCp}(\text{CO})_2)_2$  as a catalyst, as originally suggested by Coville et al. in substitution reactions of monometallic carbonyl complexes.<sup>15</sup> We have recently extended the use of such and other homologous bimetallic derivatives to substitution reactions of clusters in general.<sup>16</sup> We showed that

(9) (a) Shapley, G. R.; Richter, S. I.; Churchill, M. R.; Leshewycz, R. A. *J. Am. Chem. Soc.* **1977**, *99*, 7384. (b) Churchill, M. R.; Leshewycz, R. A. *Inorg. Chem.* **1978**, *17*, 1950. (c) Churchill, M. R.; Leshewycz, R. A.; Shapley, G. R.; Richter, S. I. *Inorg. Chem.* **1980**, *19*, 1277. (d) Puga, J.; Arce, A.; Braga, D.; Centritto, N.; Grepioni, F.; Castillo, R.; Ascanio, J. *Inorg. Chem.* **1987**, *26*, 867.

(10) Knox, S. A. R.; Kaesz, H. D. *J. Am. Chem. Soc.* **1971**, *93*, 4594. (11) Hoffmann, R.; Schilling, B. E. R.; Bau, R.; Kaesz, H. D.; Mingos, D. M. P. *J. Am. Chem. Soc.* **1978**, *100*, 6088.

(12) (a) Koeple, J. W.; Johnson, J. R.; Knox, S. A. R.; Kaesz, H. D. *J. Am. Chem. Soc.* **1975**, *97*, 3947. (b) Jackson, P. F.; Johnson, B. F. G.; Lewis, J.; Mc Partlin, M.; Nelson, W. J. *J. Chem. Soc., Dalton Trans.* **1986**, 1557.

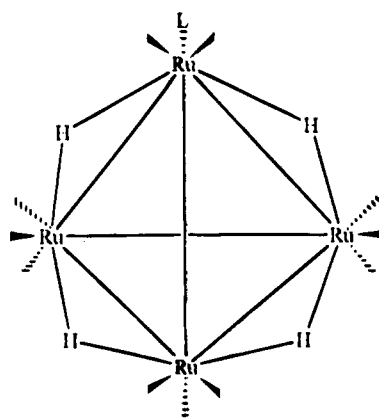
(13) Aime, S.; Gobetto, R.; Orlandi, A.; Groombridge, C. J.; Hawkes, G. E.; Mantle, M. D.; Sales, K. D. *Organometallics* **1994**, *13*, 2375.

(14) (a) Bruce, M. I.; Matison, J. G.; Nicholson, B. K.; Williams, M. L. *J. Organomet. Chem.* **1982**, *236*, C57. (b) Bruce, M. I.; Kehoe, D. C.; Matison, J. G.; Nicholson, B. K.; Rieger, P. H.; Williams, M. L. *J. Chem. Soc., Chem. Commun.* **1982**, 442.

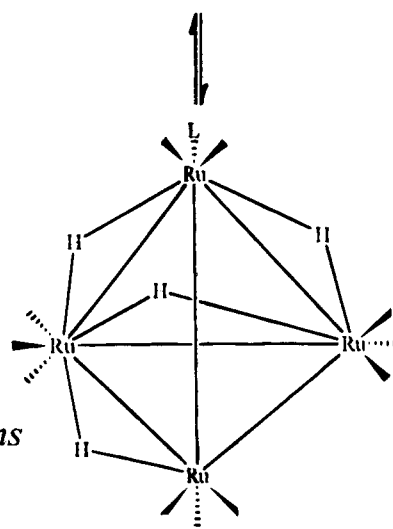
(15) Coville, N. J.; Albers, M. O.; Singleton, E. *J. Chem. Soc., Dalton Trans.* **1983**, 947.

Scheme 1

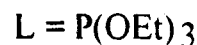
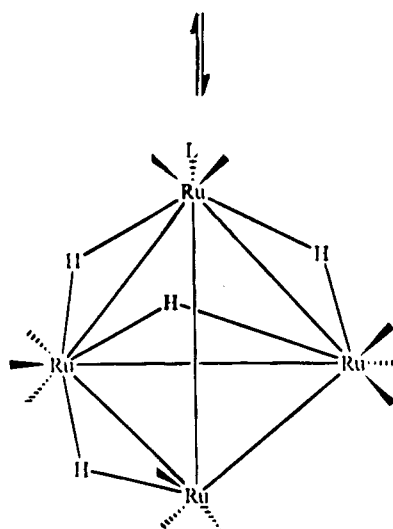
major  
(same as  
solid state)



minor  
(L and CO *trans*  
to same edge)



minor  
(2 CO *trans*  
to same edge)



these catalysts promote CO replacement through the formation, in solution, of labile metal-centered radicals. With this method satisfactory amounts of  $\text{Ru}_4(\mu\text{-H})_4(\text{CO})_{12-x}\text{L}_x$  ( $x = 1-4$ ,  $\text{L} = \text{P}(\text{OEt})_3$ ,  $\text{PPh}_3$ ;  $x = 1, 2$ ,  $\text{L} = \text{AsPh}_3$ ) derivatives are obtained, making feasible a multinuclear ( $^1\text{H}$ ,  $^{13}\text{C}$ ,  $^{31}\text{P}$ ) NMR study of these deriva-

(16) (a) Aime, S.; Botta, M.; Gobetto, R.; Osella, D. *Inorg. Chim. Acta* **1986**, *115*, 129. (b) Aime, S.; Botta, M.; Gobetto, R.; Osella, D. *Organometallics* **1985**, *4*, 1475.

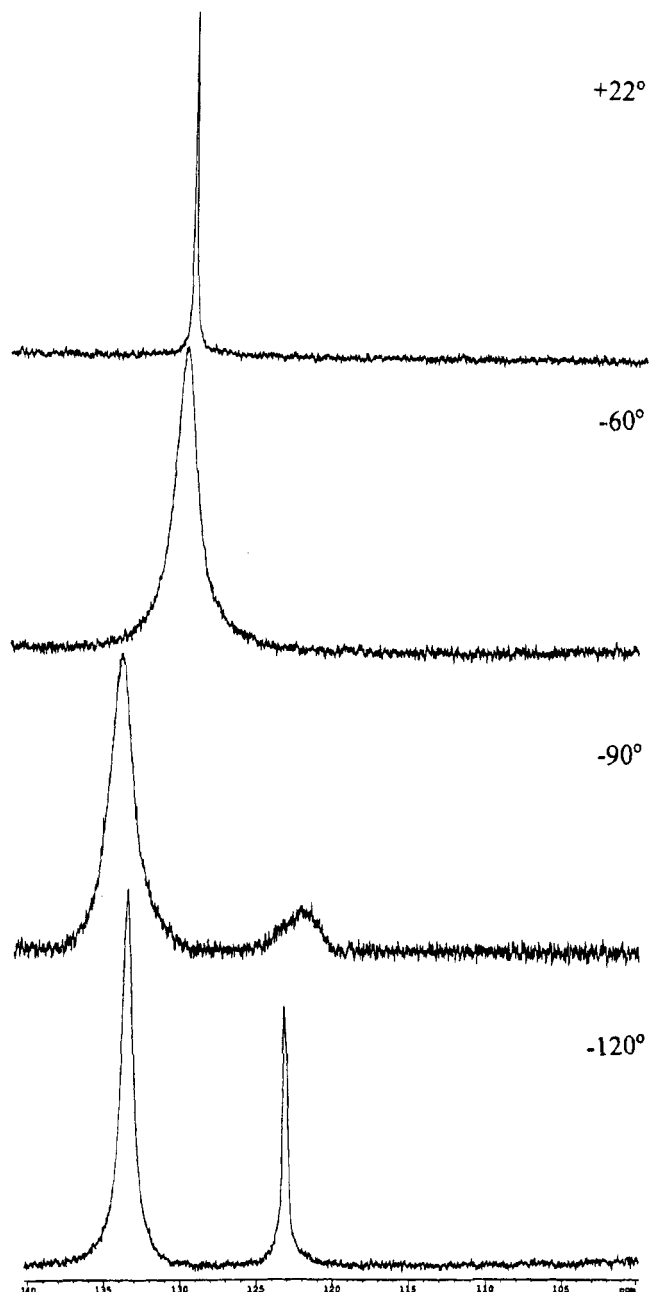


**Figure 1.** VT  $^{31}P$  NMR of **1a** ( $-120$  to  $22$  °C) in  $CD_2Cl_2$ /Freon-22 at 162 MHz.

tives. Only tri- and tetrasubstituted  $AsPh_3$  derivatives were not obtained in reasonable yields, probably because of the low basicity and/or the high steric bulk of such a ligand.

**Solution Structure and Dynamics of  $Ru_4(\mu-H)_4(CO)_{12-x}L_x$  Derivatives.**  $Ru_4(\mu-H)_4(CO)_{11}L$  ( $L = P(OEt)_3$ , **1a**;  $L = PPh_3$ , **1b**,  $L = AsPh_3$ , **1c**). The solid-state structure of  $H_4Ru_4(CO)_{11}P(OEt)_3$  (**1a**) has a plane of symmetry with the phosphine ligand transoid to an unbridged (short) metal–metal edge and the carbonyl groups staggered with respect to two of the three adjacent metal–metal edges (Scheme 1).<sup>4,5</sup> The VT  $^{31}P\{^1H\}$  NMR at 134 MHz reveals the presence of two isomers at 133.30 and 123.11 ppm at  $-120$  °C in a relative intensity of 3:1 which average to a single sharp resonance at 129.4 ppm at  $23$  °C (Figure 1). The VT  $^1H$  NMR of **1a** at  $-120$  °C shows two major resonances of equal intensity at  $-17.44$  and  $-18.32$  ppm and five minor resonances at  $-16.56$ ,  $-16.85$ ,  $-16.99$ ,  $-18.97$ ,

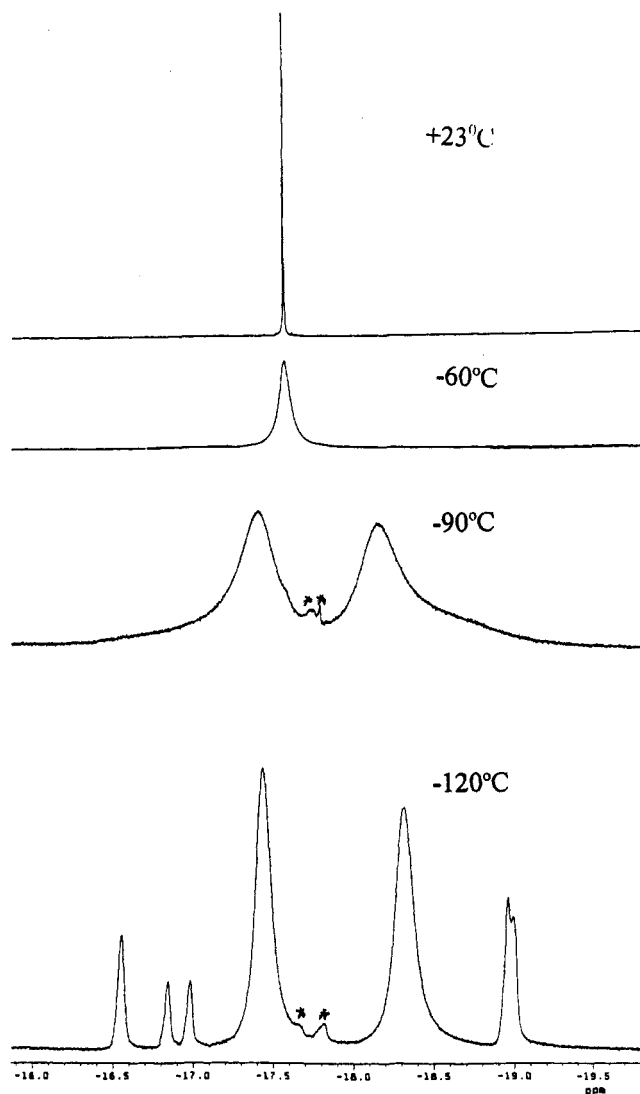


**Figure 2.** VT  $^1H$  NMR of **1a** ( $-120$  to  $22$  °C) in  $CD_2Cl_2$ /Freon-22 at 400 MHz (\* indicates impurity of **2a** and of  $H_4Ru_4(CO)_{12}$ ).

and  $-19.00$  ppm in a relative intensity of 1:0.5:0.5:1:1 (Figure 2). The combined relative intensity of these resonances compared with the major resonances is 1:3. From these data there appear to be a relatively symmetrical major isomer, which is probably the one found in the solid state, and a less symmetrical set of two minor isomers of equal population. These two minor isomers have the same phosphorous chemical shift and only one hydride with a resolvably different chemical shift. If one imposes the restriction that the phosphine ligand must be transoid to a nonbridged metal–metal edge<sup>4</sup> (*vide infra*), such a subset can be generated by edge migration of one hydride (Scheme 1). This less symmetrical isomer could exist in two very similar forms: one in which a carbonyl group is transoid to the same metal–metal bond as the phosphine ligand, and one in which it is transoid to the other nonbridged metal–metal bond (Scheme 1). These two isomers would be expected to have very similar phosphorous chemical shifts and similar proton chemical shifts for three of the four hydrides. Although we have no definitive proof for this explanation of the phosphorous and proton data, it does fit with the observed structural and dynamical behavior of the other complexes reported

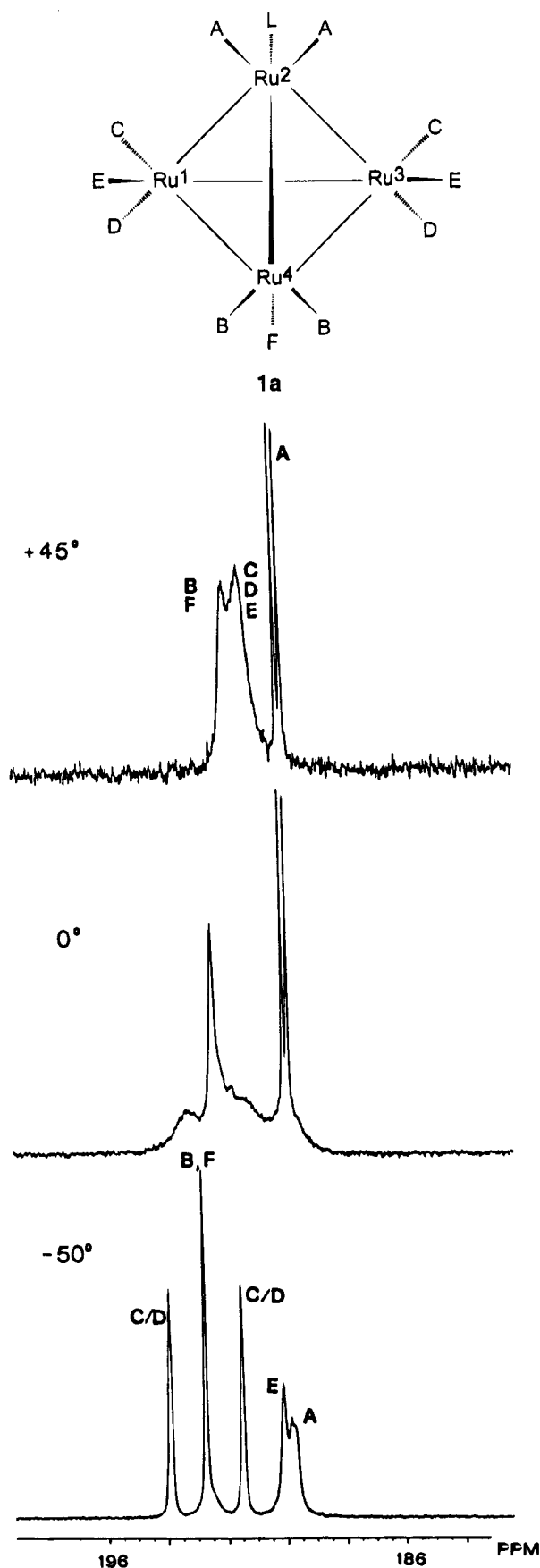


**Figure 3.** VT  $^{13}\text{C}\{^1\text{H}\}$  NMR spectra ( $-50$  to  $45^\circ\text{C}$ ) at 67.8 MHz of a  $\text{CDCl}_3$  solution of a  $^{13}\text{CO}$ -enriched (ca. 20%) sample of **1a** along with the proposed solution structure and labeling scheme of carbonyl ligands. The hydrides are omitted: they are in rapid exchange over the entire tetrahedron in this temperature range.

**Table 1.**  $^1\text{H}$  NMR Data for **1a–4b**

solvent (t, $^\circ\text{C}$ )		$\delta$ (ppm)
<b>1a</b>	$\text{CD}_2\text{Cl}_2/\text{fr-22}$ (25)	-17.5 (s, br)
<b>1b</b>	$\text{CDCl}_3$ (25)	-17.26 (d, $J_{\text{P-H}} = 4.4$ Hz)
<b>1c</b>	$\text{CDCl}_3$ (25)	-17.32 (s)
<b>2a</b>	$\text{CD}_2\text{Cl}_2$ ( $-75$ )	-17.6 (m, br, 1), -17.7 (m, br, 1), -17.8 (m, br, 2)
<b>2b</b>	acetone- $d_6$ ( $-40$ )	<b>2b'</b> -15.63 (t, 1, $J_{\text{P-H}} = 7.3$ Hz), -16.52 (d, 2, $J_{\text{P-H}} = 9.9$ Hz), -16.80 (s, 1)
<b>2c</b>	toluene- $d_8$ ( $-40$ )	<b>2b''</b> -16.31 (t, $J_{\text{P-H}} = 5.1$ Hz) <b>2c'</b> -15.47 (s, 1), -16.56 (s, 2), -17.0 (s, 1) <b>2c''</b> -16.34 (s)
<b>3a</b>	$\text{CDCl}_3$ ( $-50$ )	-17.0 (m, br, 2), -17.3 (m, br, 2)
<b>3b</b>	$\text{CDCl}_3$ (25)	-15.28 (m, 2), -16.16 (m, 2)
<b>4a</b>	$\text{CDCl}_3$ (25)	-17.52 (q, $J_{\text{C-P}} = 7.9$ Hz)
<b>4b</b>	$\text{CDCl}_3$ (25)	-15.50 (m, br)

**Table 2.**  $^{31}\text{P}$  NMR Data for **1a–4b**

solvent (t, $^\circ\text{C}$ )		$\delta$ (ppm)
<b>1a</b>	$\text{CDCl}_3$ (25)	124.8
<b>1b</b>	$\text{CDCl}_3$ (25)	43.8
<b>2a</b>	$\text{CDCl}_3$ (25)	134.7
<b>2b</b>	toluene- $d_8$ ( $-40$ )	<b>2b'</b> 42.3 <b>2b''</b> 42.7
<b>3a</b>	$\text{CDCl}_3$ (25)	142.5 (s, 2), 141.4 (s, 1)
<b>3b</b>	$\text{CDCl}_3$ ( $-20$ )	40.3 (s, 1), 39.8 (s, 2)
<b>4a</b>	$\text{CDCl}_3$ (25)	142.4
<b>4b</b>	$\text{CDCl}_3$ (25)	29.4

here. The VT  $^{13}\text{C}\{^1\text{H}\}$  NMR spectra of a  $^{13}\text{CO}$ -enriched sample of **1a** in the carbonyl region are reported in Figure 3 along with the solution structure and assignment. The pattern observed at  $45^\circ\text{C}$  consists of three resonances at 192.3 (s), 191.8 (s), and 190.5 (d,  $J_{\text{C-P}} = 11.0$  Hz) ppm in the integrated intensity ratio of 3:6:2. This pattern can be accounted for in terms of localized carbonyl exchange at Ru(1)–Ru(4). As the temperature is decreased, the peak of intensity 6 broadens, collapses into the base line, and finally ( $-50^\circ\text{C}$ ) emerges as three signals each of intensity 2 at 193.9, 191.5, and 190.1 ppm, respectively. The high-field signal partially overlaps with the doublet at 190.5 ppm. These features can be interpreted as a quenching of the localized exchange at the equivalent Ru(1) and Ru(3) moieties, which causes the differentiation within each pair of carbonyls C, D, and E. Importantly, during this temperature interval, the hydrides are rapidly scrambling over the entire tetrahedron. The  $^{13}\text{C}$  NMR of the carbonyl region of **1a** in  $\text{CD}_2\text{Cl}_2/\text{Freon-22}$  (1:1) measured at 100 MHz and  $-120^\circ\text{C}$  clearly shows that the hydride motion has been "frozen out" from the large number of partially overlapping resonances of different intensities observed. The spectrum is quite complex due to the population of the isomers discussed above, and no additional reasonable assignments can be made. The resonance of relative intensity 3 at 192.3 ppm (BFF, Figure 3) remains sharp down to  $-120^\circ\text{C}$ , at which point it partially resolves into several resonances. This is consistent with generation of the minor isomer set proposed above. These data clearly show that hydride motion over the cluster precedes localized carbonyl scrambling at Ru(1) and Ru(3) in **1a**. The homologous derivatives **1b** and **1c** exhibit in the  $45$  to  $-40^\circ\text{C}$  temperature range ( $\text{CDCl}_3$  solution) NMR features similar to those of **1a** (Tables 1–3). The hydrides are scrambling over the tetrahedron while all of the Ru(CO) $_3$  moieties are exhibiting a localized exchange. At low temperatures the scrambling processes at Ru(1) and

Table 3.  $^{13}C$  NMR data for 1a–4b

	solvent (t, °C)	$\delta$ , ppm
1a	$CDCl_3$ (-55)	193.8 (s, 2), 192.7 (s, 3), 191.5 (s, 2), 190.1 (s, 2), 189.7 (d, 2, $J_{P-H} = 7.7$ Hz)
1b	toluene- $d_8$ (-25)	195.1 (d, 2, $J_{P-H} = 7.7$ Hz), 193.3 (s, 2), 193.1 (s, 2), 192.1 (s, 2), 189.2 (s, 3)
1c	toluene- $d_8$ (-25)	195.4 (s, 2), 192.8 (s, 4), 192.0 (s, 2), 188.5 (s, 2), 197.4 (s, 1)
2a	$CDCl_3$ (-50)	195.1 (m, 4), 194.4 (s, 2), 194.0 (s, 2), 188.6 (d, 2, $J_{C-P} = 18.7$ Hz)
2b	toluene- $d_8$ (-47)	2b' 198.9 (d, 2, $J_{C-P} = 6.6$ Hz), 197.5 (d, 2, $J_{C-P} = 6.6$ Hz), 193.6 (s, 2), 193.0 (s, 2), 188.0 (d, 2, $J_{C-P} = 13.3$ Hz). 2b'' 198.4 (m, br, 4), 194.2 (s, 4), 189.0 (s, 2)
2c	toluene- $d_8$ (-47)	2c' 198.1 (s, 2), 196.7 (s, 2), 193.6 (s, 2), 192.8 (s, 2), 187.3 (s, 2) 2c'' 196.9 (s, 4), 193.2 (s, 4), 188.8 (s, 2)
3a	$CDCl_3$ (-50)	197.5 (m, 4), 195.9 (d, 2, $J_{C-P} = 8.8$ Hz), 195.0 (s, 2), 189.1 (d, 1, $J_{C-P} = 18.8$ Hz)
3b	$CDCl_3$ (-20)	199.9 (s, 2), 199.4 (d, 2, $J_{C-P} = 5.4$ Hz), 198.8 (s, 2), 194.7 (s, 2), 188.9 (d, 1, $J_{C-P} = 14.4$ Hz)
4a	$CDCl_3$ (25)	198.5
4b	$CDCl_3$ (25)	198.5

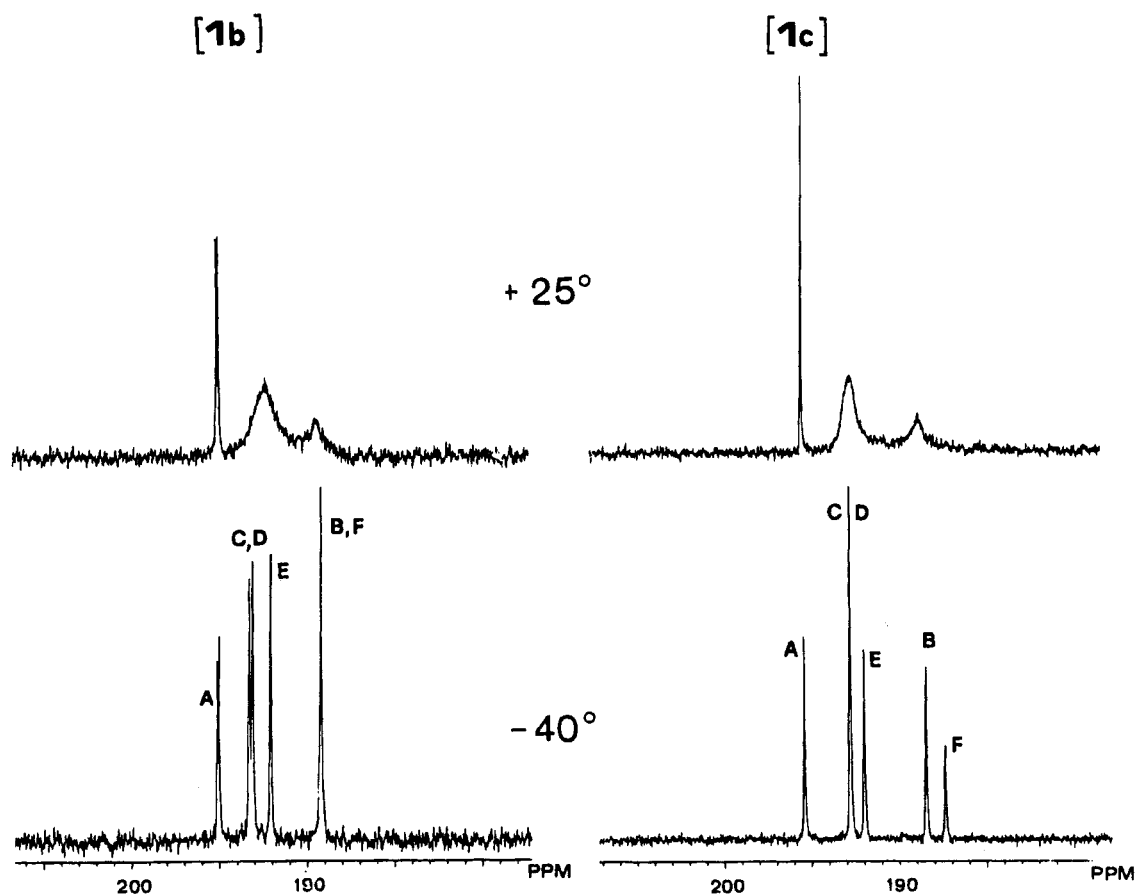
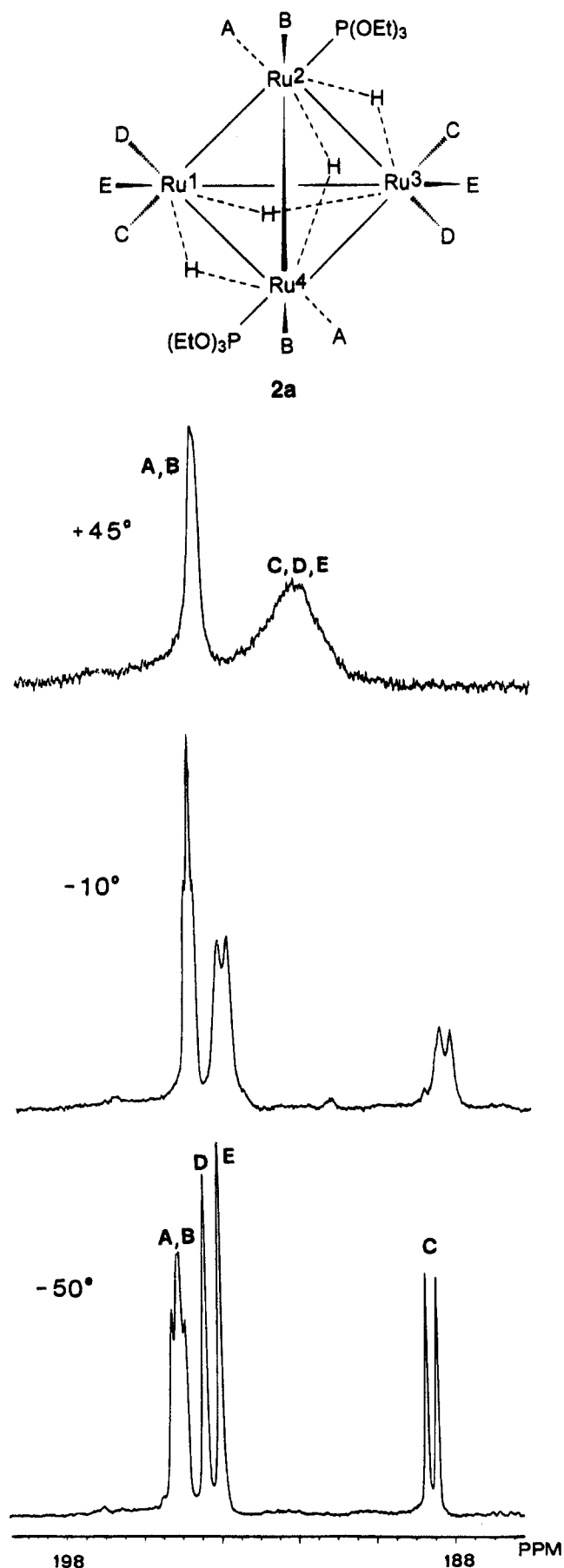


Figure 4. VT  $^{13}C\{^1H\}$  NMR spectra ( $-40$  to  $25$  °C) at 67.8 MHz of a toluene- $d_8$  solution of a  $^{13}CO$ -enriched (ca. 20%) sample of **1b** (left) and **1c** (right). The labeling scheme is identical to that of **1a** (Figure 1).

$Ru(3)$  units are frozen out, and this causes the differentiation of the C, D, and E carbonyls. In Figure 4 the VT  $^{13}C\{^1H\}$  NMR spectra in the carbonyl region of  $^{13}CO$ -enriched samples of **1b** and **1c** are reported along with the assignments. In **1c**, carbonyls BBF are rigid at  $-40$  °C, whereas they are rapidly exchanging in **1a** and **1b**. Further investigation at lower temperature was prevented by the low solubility of **1b** and **1c** in  $CD_2Cl_2$ /Freon-22.

$Ru_4(\mu-H)_4(CO)_{10}L_2$  ( $L = P(OEt)_3$ , **2a**;  $L = PPh_3$ , **2b**,  $L = AsPh_3$ , **2c**). The VT  $^{31}P\{^1H\}$  NMR spectra of **2a** show a singlet at 134.7 ppm throughout the temperature range 45 to  $-90$  °C. The VT  $^1H$  NMR spectra in the hydrido region exhibit a triplet at ambient temperature at  $-17.62$  ppm ( $J_{P-H} = 7.0$  Hz), which is split at  $-75$  °C into complex signals centered at ca.  $-17.6$  and  $-17.8$  ppm with an integrated intensity ratio of 1:3. The  $^{13}C\{^1H\}$  NMR spectrum in the carbonyl region at 45 °C shows a slightly broad resonance at 195.2 ppm and a

broad signal at ca. 193 ppm in an integrated intensity ratio of 4:6 (Figure 5). As the temperature is decreased, the broad resonance collapses into the base line and at  $-50$  °C is split into three peaks at 194.4 (s, 2), 194.1 (s, 2), and 188.6 (d, 2,  $J_{C-P} = 20.0$  Hz) ppm. Additionally, the downfield resonance is further resolved into two overlapping doublets. The high-field doublet is assigned to CO(C), and the overlapping doublets are assigned to CO(A) and CO(B). The NMR data suggest a solution structure different from the reported solid-state structure for  $Ru_4(\mu-H)_4(CO)_{10}(PPh_3)_2$ ; in particular, the phosphite ligands appear to be transoid to different unbridged Ru–Ru edges and not transoid to the same unbridged Ru–Ru edge, as found by Bau and co-workers. The proposed solution structure is supported by the results of the single-crystal X-ray structural determination of **2a** (*vide infra*). In the  $-50$  to 45 °C temperature interval, in which the hydrides are fluxional, primarily localized CO exchange occurs at each



**Figure 5.** VT  $^{13}\text{C}\{^1\text{H}\}$  NMR spectra ( $-50$  to  $45$   $^{\circ}\text{C}$ ) at 67.8 MHz of a  $\text{CDCl}_3$  solution of a  $^{13}\text{CO}$ -enriched (ca. 20%) sample of **2a** along with the proposed solution structure and labeling scheme for the carbonyl ligands.

Ru center. On the basis of the appearance of the  $45$   $^{\circ}\text{C}$  spectrum a higher energy delocalized exchange is also possible but cannot be proved due to the onset of decomposition at higher temperatures.

The IR spectrum of **2b** shows more  $\nu_{\text{CO}}$  bands than that of **2a** (Table 8), suggesting the presence of more than one isomer. The  $^{31}\text{P}\{^1\text{H}\}$  NMR spectrum at  $-40$   $^{\circ}\text{C}$  shows two broad singlets at 42.7 and 42.3 ppm in an integrated intensity ratio of 1:2. Furthermore, the  $^1\text{H}$  NMR spectrum at  $-40$   $^{\circ}\text{C}$  exhibits four resonances at  $-15.6$  (t,  $J_{\text{P-H}} = 7.3$  Hz),  $-16.3$  (t,  $J_{\text{P-H}} = 5.1$  Hz),  $-16.5$  (d,  $J_{\text{P-H}} = 9.9$  Hz), and  $-16.8$  (s) ppm, respectively (Figure 5). Three of these signals can be assigned to the hydrides H(A), H(B), and H(C) in the asymmetric isomer **2'b**. The triplet at  $-16.3$  ppm can be assigned to the hydrides of the isomer **2''b**, for which we propose a symmetric structure identical to that determined in the solid state, with the hydrides obviously involved in rapid scrambling. The ratio between the sum of the signals of **2'b** and those of **2''b** is 2:1, consistent with the  $^{31}\text{P}$  NMR results. Finally, the  $^{13}\text{C}\{^1\text{H}\}$  NMR low-temperature limiting spectrum ( $-30$   $^{\circ}\text{C}$ ) confirms the presence of **2b'** and **2b''** isomers (Figure 6). The pattern of the resonances of **2b'** is the same for **2a**, but with a larger separation between CO(A) and CO(B) doublets. The remaining peaks can be assigned within the symmetrical **2b''** structural scheme, with the hydrides exchanging over the entire tetrahedron. The integrated intensity ratio between the two sets of signals is again 2:1. Similar  $^1\text{H}$  and  $^{13}\text{C}$  NMR spectra are observed for **2c** (Tables 1 and 3), both in the number of signals and in the relative intensities.

**Discussion of the Structure of  $\text{Ru}_4(\mu\text{-H})_4(\text{CO})_{10}(\text{P}(\text{OEt})_3)_2$ , **2a**.** The geometry of **2a** is illustrated in Figure 7, including the location of all four bridging hydrides which were located but not included in the final least-squares refinement. Crystal data are given in Table 4, atomic coordinates in Table 5, and selected bond distances and angles in Table 6.  $\text{Ru}_4(\mu\text{-H})_4(\text{CO})_{10}(\text{P}(\text{OEt})_3)_2$  consists of a slightly distorted " $\text{H}_4\text{Ru}_4$ " core of  $D_{2d}$  symmetry. The ruthenium atoms Ru(2) and Ru(4) are each bound to a phosphito ligand and two terminal carbonyl groups, while the remaining ruthenium atoms Ru(1) and Ru(3) are each attached to three terminal carbonyl ligands. The " $\text{H}_4\text{Ru}_4\text{L}_2$ " core conforms to  $C_2$  symmetry with a noncrystallographic 2-fold axis passing through and bisecting the Ru(1)–Ru(3) and Ru(2)–Ru(4) vectors, respectively. The characteristic four "long" and two "short" Ru–Ru distances present in the molecule correspond to the  $\mu_2$ -H-bridged Ru–Ru bonds (Ru(2)–Ru(4) = 2.986(1) Å, Ru(1)–Ru(4) = 2.979(1) Å, Ru(2)–Ru(3) = 2.978(1) Å, Ru(1)–Ru(3) = 2.947(1) Å, averaging 2.973(1) Å), and to the unbridged Ru–Ru vectors with bond lengths of 2.798(1) Å for Ru(1)–Ru(2) and 2.786(1) Å for Ru(3)–Ru(4), averaging 2.792(1) Å. These observed distances are in good agreement with all previously reported phosphine and phosphite derivatives of  $\text{Ru}_4(\mu\text{-H})_4(\text{CO})_{12}$ .<sup>4-9</sup> The phosphito ligands adopt positions transoid to two different unbridged (short) Ru–Ru vectors with metal–phosphorus distances of 2.282(2) Å for Ru(2)–P(1) and 2.272(2) Å for Ru(4)–P(2) bond. The solid-state conformation of this molecule agrees with the solution structure assessed by multinuclear NMR methods. It is noteworthy to point out that the molecular geometry of this tetranuclear cluster

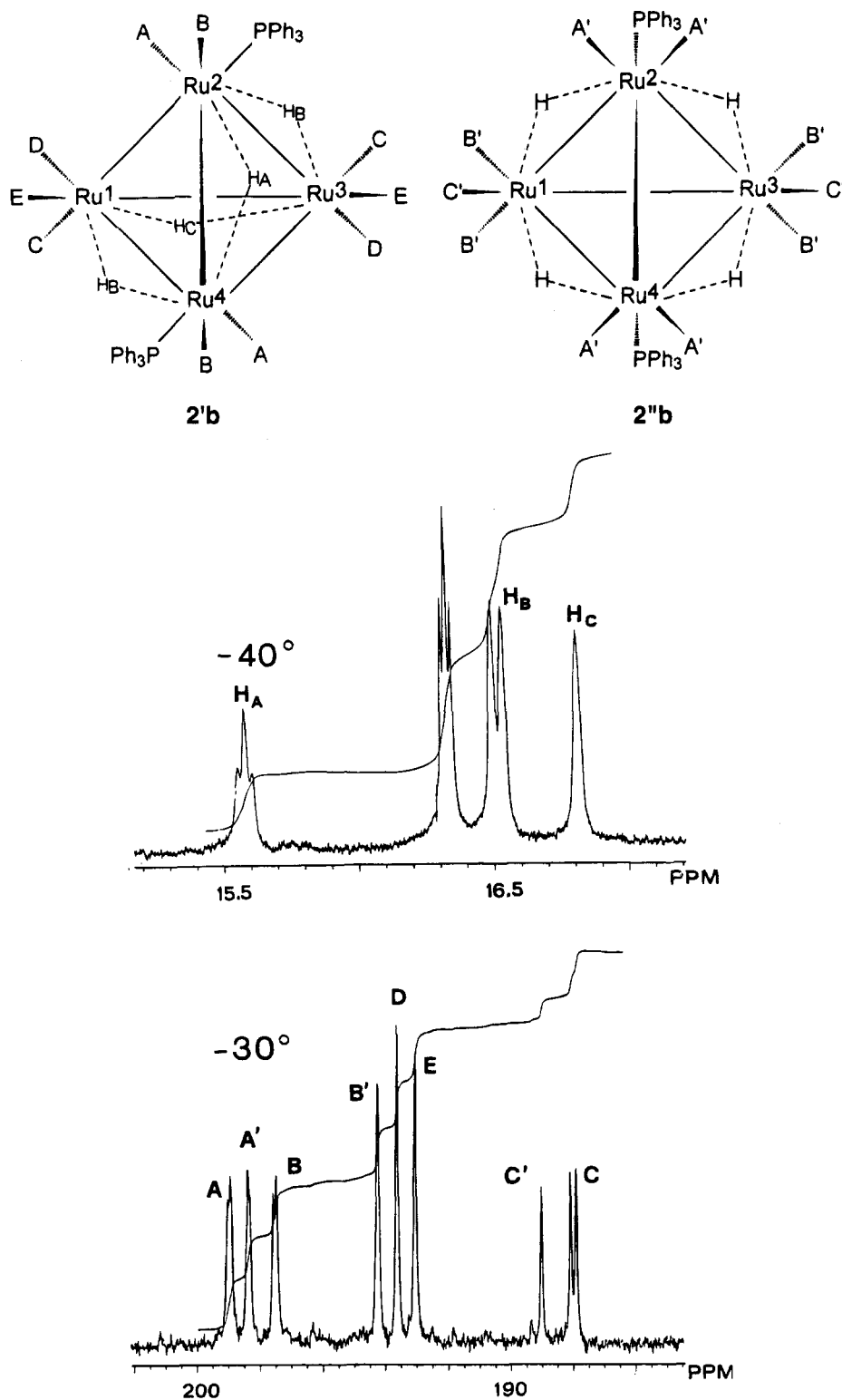


**Figure 6.**  $^1H$  NMR spectrum ( $-40\text{ }^\circ C$ ) at 270.0 MHz of an acetone- $d_6$  solution of **2b** (upper part) and  $^{13}C\{^1H\}$  NMR spectrum ( $-30\text{ }^\circ C$ ) at 67.8 MHz of toluene- $d_8$  solution of a  $^{13}C$ -enriched (ca. 20%) sample of **2b** (lower part) along with the proposed solution structure of the two isomers (**2'b** and **2''b**) and the labeling scheme for the carbonyl ligands.

is different than the solid-state structure of  $Ru_4(\mu-H)_4(CO)_{10}(PPh_3)_2$  in which the phosphine ligands are found transoid to the same short (unbridged) Ru–Ru bond. Additionally, the Ru–P bonds in the  $Ru_4(\mu-H)_4(CO)_{10}(PPh_3)_2$  structure are slightly longer, having an average value of 2.359(4) Å.<sup>4</sup> The 10 terminal carbonyl ligands are attached as  $Ru(CO)_3$  and  $Ru(CO)_2P$  moieties which are in a staggered conformation with respect to the metal–metal vectors (i.e., approximately bisecting the triangular  $Ru_3$  faces over which they protrude). The

Ru–C bonds along the unbridged edge of the cluster form angles that are closer to linear (averaging Ru–Ru–C = 171.6(2) $^\circ$ ) than those along  $\mu_2$ -H-bridged edges (averaging Ru–Ru–C = 151.1(3) $^\circ$ ). The carbonyl bond lengths range from 1.120(8) to 1.157(8) Å, averaging 1.139(8) Å, and their coordination is essentially linear (Ru–C–O = 176.8(6) $^\circ$ , average).

$Ru_4(\mu-H)_4(CO)_9L_3$  (L = P(OEt)<sub>3</sub>, **3a**; L = PPh<sub>3</sub>, **3b**). The  $^{31}P\{^1H\}$  NMR pattern of **3a**, consisting of two resonances at 142.5 and 141.5 ppm in a relative



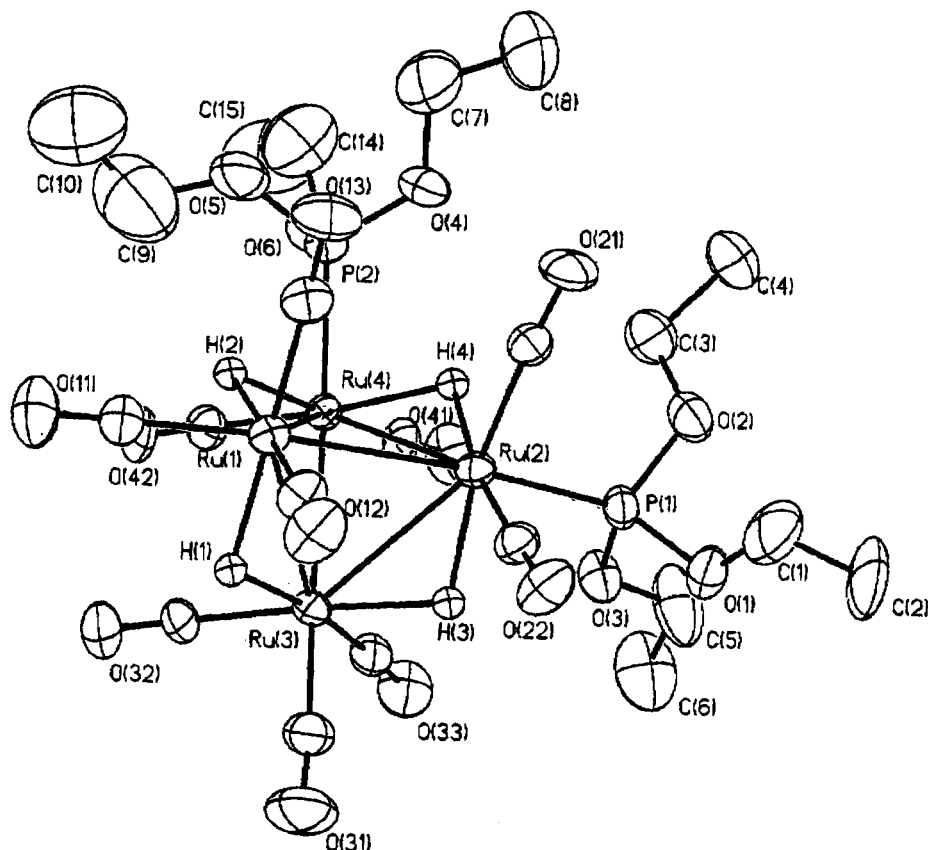


Figure 7. Molecular structure of **2a** along with the numbering scheme.

Table 4. Crystal Data: Collection and Refinement Parameters

formula	$(\mu\text{-H})_4\text{Ru}_4(\text{CO})_{10}[\text{P}(\text{OCH}_2\text{CH}_3)_3]_2$
$M_r$	1020.7
cryst syst, space group	triclinic, $P\bar{1}$ (No. 2)
$a$ , Å	11.253(3)
$b$ , Å	15.821(4)
$c$ , Å	11.048(4)
$\alpha$ , deg	100.33(3)
$\beta$ , deg	100.58(3)
$\gamma$ , deg	102.62(3)
$V$ , Å <sup>3</sup>	1837(1)
$Z$	2
$d_{\text{calcd}}$ , g/cm <sup>3</sup>	1.845
abs coeff, $\mu$ (cm <sup>-1</sup> )	17.28
data colln temp, °C	19.5(±1)
radiation ( $\lambda$ , Å)	Mo K $\alpha$ (0.71069)
monochromator	highly oriented graphite
scan mode	$\omega$ - $2\theta$ ("wandering $\omega$ ")
scan limits, deg	$2.5 < 2\theta \leq 50$
scan speed, deg/min	variable, 1.5–29.3
scan range, deg	1.0
bkgd, deg offset;	1.0/1.0
above K $\alpha_1$ /below K $\alpha_2$	
ratio bkgd/scan time	0.5
std reflns	(2, 8, 2); (0, 6, 0); (0, 7, 2)
no. of data colln	6731 ( $\pm h, \pm k, \pm l$ )
no. of indpt data	6614
no. of observns [ $F_o^2 > 3\sigma(F_o^2)$ ]	5682
no. of variables	397
$R^a$	0.033
$R_w^b$	0.050
GOF <sup>c</sup>	1.85
$(\Delta/\sigma)_{\text{max}}$	0.02

<sup>a</sup>  $R = \sum(|F_o| - |F_c|) / \sum|F_o|$ . <sup>b</sup>  $R_w = [\sum w(|F_o| - |F_c|)^2 / \sum w|F_o|^2]^{1/2}$ .  
<sup>c</sup>  $\text{GOF} = [\sum w(|F_o| - |F_c|)^2 / (N_{\text{observns}} - N_{\text{variables}})]^{1/2}$ .

intensity ratio of 2:1, remains unchanged from 45 to -90 °C. The <sup>1</sup>H NMR spectrum at room temperature in the hydride region exhibits a broad signal at -17.1 ppm, which at -35 °C splits into two unresolved multiplets

of equal intensity at -17.0 and -17.3 ppm (estimated  $\Delta G^\ddagger$  ca. 55 kJ mol<sup>-1</sup>).<sup>17</sup> At -40 °C the <sup>13</sup>C{<sup>1</sup>H} NMR spectrum in the carbonyl region exhibits four resonances at 197.5 (s, br, 4), 195.9 (d, 2,  $J_{\text{C-P}} = 8.8$  Hz), 195.0 (s, 2) and 189.1 (d, 1,  $J_{\text{C-P}} = 18.8$  Hz) ppm (Figure 8). The resonance at 197.5 ppm is due to the fortuitous overlap of two resonances, as is also seen in the <sup>13</sup>C NMR spectrum of **3b**. This overlap is resolved by changing solvents from CDCl<sub>3</sub> to toluene-*d*<sub>8</sub>. These NMR observations are consistent with a solution structure identical to the solid-state structure reported for Ru<sub>4</sub>( $\mu$ -H)<sub>4</sub>(CO)<sub>9</sub>(PMe<sub>2</sub>Ph)(P(OC<sub>6</sub>H<sub>4</sub>Me-*p*)<sub>3</sub>)(P(OCH<sub>2</sub>)<sub>3</sub>CET).<sup>6</sup> Increasing the temperature to 40 °C produces a broadening of the two upfield resonances CO(D) and CO(E) due to localized exchange at the unsubstituted Ru atom. Similar NMR features were observed for **3b** except that the resonances assigned to CO(A) and CO(B) are well separated, the hydrides are less fluxional than in **3a**, (i.e., two equal intensity hydride signals are observed in the room temperature spectrum), and CO(D) and CO(E) exchange at a higher temperature than in **3a**.

**Ru<sub>4</sub>( $\mu$ -H)<sub>4</sub>(CO)<sub>9</sub>L<sub>4</sub>** (L = P(OEt)<sub>3</sub>, **4a**; L = PPh<sub>3</sub>, **4b**). The derivative **4a** at room temperature exhibits a single resonance in both the <sup>31</sup>P{<sup>1</sup>H} NMR spectrum at 142.8 ppm and in the <sup>13</sup>C{<sup>1</sup>H} NMR spectrum (carbonyl region) at 198.5 ppm, respectively. These resonances remain unaltered down to -100 °C. This does not allow one to ascertain whether the carbonyls are rigid or are involved in fast localized exchange, owing to the high symmetry of the structure.<sup>8</sup> In the same temperature range the <sup>1</sup>H NMR spectra in the hydride region show

(17) Evaluated by using the approximate equation  $\Delta G^\ddagger = 4.57T_c(9.97 + \log T_c/\Delta\nu)$ . See: Kost, D.; Carlson, E. H.; Raban, M. J. *Chem. Soc., Chem. Commun.* **1971**, 656.

**Table 5. Atomic Coordinates for Ru<sub>4</sub>(μ-H)<sub>4</sub>(CO)<sub>10</sub>(P(OCH<sub>2</sub>CH<sub>3</sub>)<sub>3</sub>)<sub>2</sub>**

atom	x	y	z	B/B <sub>eq</sub>	atom	x	y	z	B/B <sub>eq</sub>
Ru(1)	0.44234(4)	0.35010(2)	0.14156(4)	3.61(1)	C(41)	0.5139(5)	0.0933(3)	0.2682(5)	4.44(15)
Ru(2)	0.37652(3)	0.28652(2)	0.34715(3)	3.21(1)	O(41)	0.5086(5)	0.0322(3)	0.3128(4)	6.68(15)
Ru(3)	0.27605(4)	0.16928(3)	0.08868(4)	3.49(1)	C(42)	0.5608(4)	0.1308(4)	0.0557(5)	4.90(17)
Ru(4)	0.52756(4)	0.19354(2)	0.20081(4)	3.32(1)	O(42)	0.5842(5)	0.0902(4)	-0.0293(4)	7.65(17)
P(1)	0.3271(1)	0.2022(1)	0.4871(1)	4.27(3)	O(1)	0.2148(4)	0.2171(3)	0.5513(4)	6.55(15)
P(2)	0.7350(1)	0.2502(1)	0.2917(1)	4.79(4)	O(2)	0.4288(4)	0.2130(3)	0.6127(4)	6.31(14)
C(11)	0.4833(6)	0.3789(4)	-0.0106(6)	5.00(17)	O(3)	0.2793(4)	0.0995(3)	0.4240(4)	5.54(12)
O(11)	0.5047(6)	0.4000(3)	-0.0975(5)	8.65(20)	C(1)	0.2241(11)	0.2906(7)	0.6473(11)	11.68(45)
C(12)	0.3285(6)	0.4221(4)	0.1544(6)	5.28(18)	C(2)	0.1478(12)	0.2762(9)	0.7294(10)	13.94(57)
O(12)	0.2592(5)	0.4654(4)	0.1557(6)	8.65(20)	C(3)	0.5522(7)	0.2028(6)	0.6099(7)	8.11(29)
C(13)	0.5755(6)	0.4390(4)	0.2544(6)	5.21(18)	C(4)	0.6272(9)	0.2302(8)	0.7444(8)	10.05(38)
O(13)	0.6581(5)	0.4937(3)	0.3200(5)	7.78(17)	C(5)	0.2471(11)	0.0327(6)	0.4970(8)	10.86(42)
C(21)	0.4943(5)	0.3766(4)	0.4741(5)	4.57(16)	C(6)	0.1977(12)	-0.0543(6)	0.4223(10)	11.52(44)
O(21)	0.5627(4)	0.4294(3)	0.5555(5)	6.65(15)	O(4)	0.7656(4)	0.3060(4)	0.4337(4)	8.76(20)
C(22)	0.2478(5)	0.3435(4)	0.3594(5)	4.58(16)	O(5)	0.8165(4)	0.3188(4)	0.2328(5)	7.41(17)
O(22)	0.1709(4)	0.3778(3)	0.3711(5)	7.52(17)	O(6)	0.8029(5)	0.1695(5)	0.2928(7)	10.73(27)
C(31)	0.1088(6)	0.1734(4)	0.0259(6)	5.64(19)	C(7)	0.8758(9)	0.3762(7)	0.4948(10)	10.73(39)
O(31)	0.0100(5)	0.1768(5)	-0.0182(6)	9.83(24)	C(8)	0.8882(9)	0.4025(7)	0.6236(10)	11.27(41)
C(32)	0.3071(6)	0.1235(4)	-0.0693(5)	5.15(17)	C(9)	0.8106(8)	0.3170(7)	0.1046(8)	9.38(34)
O(32)	0.3222(5)	0.0981(4)	-0.1653(4)	8.52(20)	C(10)	0.8891(22)	0.3912(9)	0.0827(12)	13.82(58)
C(33)	0.2426(5)	0.0556(4)	0.1229(5)	4.56(16)	C(14)	0.9250(10)	0.1694(10)	0.3092(13)	13.05(54)
O(33)	0.2152(5)	-0.0147(3)	0.1387(5)	7.13(16)	C(15)	0.9477(8)	0.0901(7)	0.2633(10)	9.50(35)

**Table 6. Selected Distances and Angles for Ru<sub>4</sub>(μ-H)<sub>4</sub>(CO)<sub>10</sub>(P(OCH<sub>2</sub>CH<sub>3</sub>)<sub>3</sub>)<sub>2</sub><sup>a</sup>**

Distances (Å)					
Ru(1)–Ru(2)	2.7984(6)	Ru(2)–P(1)	2.282(2)	Ru(4)–H(24)	1.82
Ru(1)–Ru(3)	2.9474(6)	Ru(2)–Ru(3)	2.9785(5)	Ru(4)–P(2)	2.272(2)
Ru(1)–Ru(4)	2.9788(6)	Ru(2)–Ru(4)	2.9859(5)	Ru–CO <sup>b</sup>	1.886(6)
Ru(1)–H(13)	1.73	Ru(3)–H(23)	1.74	C–O(CO) <sup>b</sup>	1.139(8)
Ru(1)–H(14)	1.76	Ru(3)–H(13)	1.74	P–O <sup>b</sup>	1.592(5)
Ru(2)–H(23)	1.78	Ru(3)–Ru(4)	2.7856(6)	O–C <sup>b</sup>	1.41(1)
Ru(2)–H(24)	1.78	Ru(4)–H(14)	1.81	C–C <sup>b</sup>	1.40(6)
Angles (deg)					
H(13)–Ru(1)–H(14)	95.3	H(13)–Ru(3)–Ru(1)	31.6		
H(13)–Ru(1)–Ru(2)	91.0	H(13)–Ru(3)–Ru(2)	84.9		
H(13)–Ru(1)–Ru(3)	31.9	Ru(4)–Ru(3)–Ru(1)	62.53(1)		
H(13)–Ru(1)–Ru(4)	80.6	Ru(4)–Ru(3)–Ru(2)	62.29(1)		
H(14)–Ru(1)–Ru(2)	92.2	Ru(1)–Ru(3)–Ru(2)	56.36(1)		
H(14)–Ru(1)–Ru(3)	82.7	H(14)–Ru(4)–H(24)	99.4		
H(14)–Ru(1)–Ru(4)	33.9	H(14)–Ru(4)–Ru(3)	86.8		
Ru(2)–Ru(1)–Ru(3)	62.38(1)	H(14)–Ru(4)–Ru(1)	33.0		
Ru(2)–Ru(1)–Ru(4)	62.15(1)	H(14)–Ru(4)–Ru(2)	85.4		
Ru(3)–Ru(1)–Ru(4)	56.07(1)	H(24)–Ru(4)–Ru(3)	93.2		
H(23)–Ru(2)–H(24)	108.4	H(24)–Ru(4)–Ru(1)	80.3		
H(23)–Ru(2)–Ru(1)	87.0	H(24)–Ru(4)–Ru(2)	33.5		
H(23)–Ru(2)–Ru(3)	31.6	P(2)–Ru(4)–Ru(3)	165.32(5)		
H(23)–Ru(2)–Ru(4)	82.8	P(2)–Ru(4)–Ru(1)	103.95(5)		
H(24)–Ru(2)–Ru(1)	86.3	P(2)–Ru(4)–Ru(2)	110.23(4)		
H(24)–Ru(2)–Ru(3)	87.7	Ru(3)–Ru(4)–Ru(1)	61.39(1)		
H(24)–Ru(2)–Ru(4)	34.3	Ru(3)–Ru(4)–Ru(2)	62.02(1)		
P(1)–Ru(2)–Ru(1)	165.77(4)	Ru(1)–Ru(4)–Ru(2)	55.96(1)		
P(1)–Ru(2)–Ru(3)	107.16(4)	Ru(1)–H(14)–Ru(4)	113.1		
P(1)–Ru(2)–Ru(4)	105.24(4)	Ru(1)–H(13)–Ru(3)	116.5		
Ru(1)–Ru(2)–Ru(3)	61.26(1)	Ru(2)–H(24)–Ru(4)	112.3		
Ru(1)–Ru(2)–Ru(4)	61.89(1)	Ru(3)–H(23)–Ru(2)	116.0		
Ru(3)–Ru(2)–Ru(4)	55.68(1)	O(3)–P(1)–O(2)	106.9(3)		
H(23)–Ru(3)–H(13)	104.0	Ru–C–O <sup>b</sup>	176.8(6)		
H(23)–Ru(3)–Ru(4)	89.8	O–P–O <sup>b</sup>	103.0(3)		
H(23)–Ru(3)–Ru(1)	83.1	Ru–Ru–C(CO, unbridged) <sup>b</sup>	171.6(2)		
H(23)–Ru(3)–Ru(2)	32.4	Ru–Ru–C(CO, H-bridged) <sup>b</sup>	151.1(3)		
H(13)–Ru(3)–Ru(4)	86.4				

<sup>a</sup> Numbers in parentheses are estimated standard deviations. <sup>b</sup> Average values.

an invariant quintet at -17.5 ppm ( $J_{H-P} = 8.0$  Hz), indicating that the hydrides are involved in a rapid scrambling that cannot be frozen out. Similar NMR features were observed for **4b**. The <sup>1</sup>H NMR spectra of **4a** and **4b** are similar to those reported for Ru<sub>4</sub>(μ-H)<sub>4</sub>(CO)<sub>8</sub>(P(OMe)<sub>3</sub>)<sub>4</sub>.<sup>10</sup>

### Conclusions

The motion of the hydride ligands in this class of compounds can be quenched only at very low temper-

atures, if at all, and the hydrides can adopt isomeric structures which differ by their relative disposition over the edges of the tetrahedron. The energy barrier for the hydride scrambling follows the order Ru<sub>4</sub>(μ-H)<sub>4</sub>(CO)<sub>12</sub> and Ru<sub>4</sub>(μ-H)<sub>4</sub>(CO)<sub>8</sub>(L)<sub>4</sub> << Ru<sub>4</sub>(μ-H)<sub>4</sub>(CO)<sub>12-x</sub>(L)<sub>x</sub> ( $x = 1-3$ ). This trend seems to indicate that charge imbalance causes stabilization of certain coordination modes of the hydrides, thus increasing the barrier for their intramolecular exchange. Localized exchange of the carbonyls takes place at approximately the same or



$Ru_4(\mu-H)_4(CO)_{12}$ , 6 mg (0.015 mmol) of  $(FeCp(CO)_2)_2$ , and 20 mL of cyclohexane under a nitrogen atmosphere. To the resulting suspension was added 0.025 mL (0.15 mmol) of  $P(OEt)_3$  by syringe. The mixture was heated to 45 °C for 2 h, at which time analytical TLC (silica gel, ether–hexane 1:4) showed complete consumption of the starting material. The deep orange solution was rotary evaporated, taken up in a minimum amount methylene chloride, and purified by preparative TLC (Kieselgel-60-PF254 or Merck commercial plates, 0.25 mm, ether–heptane 1:3). The major orange band, which moved slower than the starting material but faster than the catalyst, was isolated and recrystallized from chloroform–heptane at –20 °C to yield 65 mg (65%).

**Crystallographic Analysis of 2a.** Orange crystals of  $Ru_4(\mu-H)_4(CO)_{10}(P(OEt)_3)_2$ , **2a**, were obtained from a saturated *n*-heptane/ $CHCl_3$  (3:1 v/v) solution at 0 °C. The crystals were stable in air. A rectangularly shaped crystal (0.40 × 0.45 × 0.55 mm<sup>3</sup>) was used to obtain unit cell parameters and diffraction data. It was mounted along its greater dimension on the end of a thin glass fiber–brass pin assembly with epoxy and inserted into the head of a standard goniometer. All diffractions measurements were obtained on a P2<sub>1</sub> Siemens (Syntex) automated diffractometer, which was controlled by a Data General 1200 computer. The crystal was physically centered, and a rotation photograph was taken about the spindle ( $\varphi$ ) axis. Fifteen strong reflections well distributed in reciprocal space in the  $2\theta$  range 15–25° were selected and machine centered to obtain accurate cell parameters and an orientation matrix. Axial photographs taken along each unit cell dimension revealed no observable crystal defects and Laue symmetry consistent with a triclinic cell. Intensity data were collected by the  $\omega$ – $2\theta$  scan mode in 19 steps over a 1° scan range of  $\omega$ . The program was set such that three additional steps could be collected if the peak maximum was offset in either direction from the center of the scan range. Additional steps taken, if any, were retrieved from memory and used as the starting point for the following scan. The offset from the start of the scan was automatically reset to zero as new layers in *hkl* were encountered during data collection. Recentering of the crystal was found not to be necessary throughout data acquisition. The stability of the crystal and instrument was monitored by measuring the intensity of three standard reflections after every 100 intensity data. No significant (<4%) fluctuations were observed in their intensities over the period of data collection. The intensity of several strong reflections exceeded 50 000 counts s<sup>-1</sup> during the step scan, and for these no linear coincidence correction was possible.<sup>22</sup> The intensities of these reflections were recollected (along with multiple scans of the three standards) at the end of normal data acquisition at a lower power setting (40 kV/10 mA). The data were corrected for Lorentz and polarization effects, and an empirical absorption correction was applied using the  $\psi$ -scan technique.<sup>23</sup> The strong reflections were scaled to the main data set using a scale factor obtained from the intensity ratio of the standard

(22) Linear coincidence correction is made for reflections having intensities between 5 000 and 50 000 counts per second along any step of the scan using the approximation given by  $I = I_0 e^{-x}$ .

(23) Reflections close to  $\theta = 90^\circ$  or  $270^\circ$  are chosen, and the variations in their intensities are measured in increments of 10° of rotation about their diffraction vectors.

collected at the two different power settings. All data reduction was performed using the local program PROCESS. Additional details of data collection and refinement are listed in Table 4.

The structure was solved by standard heavy atom methods after direct methods (MULTAN-78)<sup>24</sup> failed to produce a reasonable starting model. The positions of the four Ru atoms were located from a three-dimensional Patterson map. Full-matrix least-squares refinement of their positional and isotropic thermal parameters along with a scale factor resulted in an  $R_F = 23.8\%$ . In subsequent structure factor difference Fourier cycles the two phosphorus atoms and the remaining 38 non-hydrogen atoms were successfully located. Refinement, with all non-hydrogen atom thermal parameters varied isotropically, converged to an  $R_F = 8.0\%$ . Further refinement, now treating the molecule as anisotropically vibrating atoms, resulted in an agreement factor  $R_F = 3.6\%$ ; a difference map calculated (using all observed data) at this stage yielded the positions of the four hydride ligands (peak heights varied from 0.75 to 0.54 e Å<sup>-3</sup>), and most of the hydrogen atom positions were calculated using idealized geometries<sup>25</sup> for the methylene and methyl groups (sp<sup>3</sup>). Final cycles of a full-matrix least-squares refinement included the hydrogen atoms, but their positions were not refined. The isotropic thermal parameters of the hydride ligands were set to  $B = 4.0 \text{ \AA}^2$ , while the hydrogen atoms of the phosphite ligand were fixed at a value 1.5 Å<sup>2</sup> larger than the isotropic temperature factor of the carbon atoms to which they are attached,  $B(H_i) = 1.5 + B(C_{i,iso})$ . The function minimized during least-squares refinement<sup>26</sup> was  $\sum_{hkl} w(|F_o| - |F_c|)^2$ , where  $w = 1/\sigma(F)^2$ ,  $\sigma(F) = \sigma(F_o^2)/2F_o$ , and  $\sigma(F_o^2) = [\sigma(I_{raw})^2 + (0.04F_o^2)^2]^{1/2}/Lp$ . Neutral atomic scattering factors and both real ( $\Delta f'$ ) and imaginary ( $\Delta f''$ ) components of anomalous dispersion for Ru atoms were calculated by standard procedures.<sup>27</sup> Final position parameters with esd values in parentheses are listed in Table 5.

**Acknowledgment.** We gratefully thank the NATO Science Program for a travel grant (L.M. and E.R.) and the NSF (E.R.) and the MURST (L.M.) for financial support. We also acknowledge Johnson-Matthey for a loan of  $RuCl_3$  and Mr. P. Loveday for high-pressure synthesis of  $Ru_3(CO)_{12}$ .

**Supporting Information Available:** Complete bond distances and angles and anisotropic thermal parameters (Tables 10 and 11) (6 pages). Ordering information is given on any current masthead page.

OM9502188

(24) Germain, G.; Main, P.; Woolfson, M. M. MULTAN: A system for computer programs for the automatic solution of crystal structures from X-ray diffraction data. *Acta Crystallogr., Sect. A* **1971**, *27*, 368.

(25) Churchill, M. R. *Inorg. Chem.* **1973**, *12*, 1213

(26) Major computations in this work were performed using the following computer programs: UCIGLS (least-squares refinement, a modified version of W. R. Busing and H. A. Levy's ORFLS), XXFT (fast Fourier transform of MULTAN), HPOSN (for calculated hydrogen positions), and ORTEP (modified thermal ellipsoid plotting program and calculations of all distances and angles with esd's). All calculations were performed on the CSUN data center Cyber 760/170 computer.

(27) Cromer, D. T.; Waber, J. T. *International Tables for X-ray Crystallography*; The Kynoch Press: Birmingham, England, 1974; Vol. IV, Tables 2.2B and 2.3.1.

# Coordination of Polythiaether Macrocycles to Metal Cluster Complexes. 3. Synthesis, Structure, and Dynamical Activity of the Cluster Complexes $\text{Ru}_3(\text{CO})_7(\mu\text{-CO})_2(1,1,1\text{-}\eta^3\text{-12S3})$ and $\text{Ru}_3(\text{CO})_7(\mu\text{-CO})_2(1,1,1\text{-}\eta^3\text{-9S3})$

Richard D. Adams\* and John H. Yamamoto

Department of Chemistry and Biochemistry, University of South Carolina,  
Columbia, South Carolina 29208

Received April 3, 1995\*

The compounds  $\text{Ru}_3(\text{CO})_7(\mu\text{-CO})_2(1,1,1\text{-}\eta^3\text{-12S3})$ , **1** (12S3 = 1,5,9-trithiacyclododecane), and  $\text{Ru}_3(\text{CO})_7(\mu\text{-CO})_2(1,1,1\text{-}\eta^3\text{-9S3})$ , **2** (9S3 = 1,4,7-trithiacyclononane), were obtained in 83% yields from the reactions of  $\text{Ru}_3(\text{CO})_{12}$  with 12S3 and 9S3, respectively. Both compounds were characterized crystallographically and were shown to possess  $\text{Fe}_3(\text{CO})_{12}$ -like structures having two bridging CO ligands across one of the Ru-Ru bonds and tridentate 12S3 and 9S3 ligands, respectively. Both compounds exhibit dynamical ligand activity on the NMR time scale at 25 °C. The dynamical activity of the CO ligands in **1** was characterized in detail by  $^{13}\text{C}$  NMR spectroscopy through a combination of variable temperature and EXSY magnetization transfer measurements. There is evidence for at least two mechanisms. The lowest temperature process can be explained by a series of bridge-terminal exchange processes involving the CO ligands. Compound **2** was transformed into the new compound  $\text{Ru}_2(\text{CO})_6(\mu\text{-}\eta^2\text{-SCH}_2\text{CH}_2\text{S})$ , **3** (16%), and the known compound  $\text{Ru}_3(\text{CO})_9(\mu\text{-}\eta^3\text{-SCH}_2\text{CH}_2\text{SCH}_2\text{-CH}_2\text{S})$ , **4** (32%), by degradation of the 9S3 ligand when solutions in THF solvent were heated to reflux. Crystal data for **1**: space group =  $P2_1/n$ ,  $a = 9.316(2)$  Å,  $b = 15.688(5)$  Å,  $c = 16.826(3)$  Å,  $\beta = 93.30(2)^\circ$ ,  $Z = 4$ , 2217 reflections,  $R = 0.032$ . For **2**: space group =  $P2_1/c$ ,  $a = 13.976(2)$  Å,  $b = 10.123(2)$  Å,  $c = 15.538(2)$  Å,  $\beta = 97.967(9)^\circ$ ,  $Z = 4$ , 1910 reflections,  $R = 0.025$ .

## Introduction

Polythiaether macrocycles have been shown to serve as effective ligands for the transition elements.<sup>1</sup> To date, however, there have been very few examples of metal carbonyl cluster complexes that contain polythia ether macrocycles as ligands.<sup>2-4</sup> We have recently described the reactions of the macrocycles 1,5,9-trithiacyclododecane (12S3), 1,5,9,13-tetrathiacyclohexadecane (16S4), and 1,4,7-trithiacyclononane (9S3) with  $\text{Ru}_6(\text{CO})_{17}(\mu_6\text{-C})^4$  and of 12S3 with  $\text{Ru}_5(\text{CO})_{15}(\mu_5\text{-C})$ .<sup>3</sup> When fully coordinated, these ligands exhibit a preference for the coordination of all three sulfur atoms to a single metal atom of the cluster.<sup>2-4</sup>

In previous studies the reaction of 12S3 with  $\text{Ru}_3(\text{CO})_{12}$  was found to yield higher nuclearity products formed by cluster fragmentation and reaggregation processes.<sup>2</sup> In contrast, the reaction of  $\text{Ru}_3(\text{CO})_{12}$  with

9S3 produced a degradation of the ligand.<sup>5</sup> We have found that both 12S3 and 9S3 react with  $\text{Ru}_3(\text{CO})_{12}$  under the conditions described herein to yield two analogous new compounds  $\text{Ru}_3(\text{CO})_7(\mu\text{-CO})_2(1,1,1\text{-}\eta^3\text{-12S3})$ , **1**, and  $\text{Ru}_3(\text{CO})_7(\mu\text{-CO})_2(1,1,1\text{-}\eta^3\text{-9S3})$ , **2**, in good yields that contain tridentate macrocyclic ligands. Compounds **1** and **2** were both characterized by X-ray crystallographic methods. Both compounds were also found to be dynamically active on the NMR time scale. Compound **1** was studied in detail by using a combination of variable temperature and EXSY  $^{13}\text{C}$  NMR spectroscopy. Pyrolysis of **2** was found to yield complexes via ligand degradation of the macrocyclic ligand with formation of the new compound  $\text{Ru}_2(\text{CO})_6(\mu_2\text{-}\eta^2\text{-SCH}_2\text{CH}_2\text{S})$ , **3**, and the known compound  $\text{Ru}_3(\text{CO})_9(\mu\text{-}\eta^3\text{-SCH}_2\text{CH}_2\text{SCH}_2\text{CH}_2\text{S})$ , **4**.<sup>5</sup>

## Experimental Section

**General Data.** Reagent grade solvents were dried with appropriate drying agents and stored over 4-Å molecular sieves. Macrocycle 9S3 was used as purchased from Aldrich.  $\text{Ru}_3(\text{CO})_{12}$  was used as purchased from Strem Chemicals, Inc.  $\text{Ru}_3(^{13}\text{C})_{12}$ <sup>6</sup> and 12S3<sup>7</sup> were prepared by the reported procedures. All reactions were performed under a nitrogen atmo-

(5) Rossi, S.; Kallinen, K.; Pursianinen, J.; Pakkanen, T. T.; Pakkanen, T. A. *J. Organomet. Chem.* **1992**, *440*, 367.

(6) James, B. R.; Rempel, G. L.; Teo, W. K. *Inorg. Synth.* **1976**, *14*, 45.

(7) Adams, R. D.; Falloon, S. B. *J. Am. Chem. Soc.* **1994**, *116*, 10540.

\* Abstract published in *Advance ACS Abstracts*, July 1, 1995.

(1) (a) Cooper, S. R., Ed. *Crown Compounds: Toward Future Applications*; VCH Publishers: New York, 1992. (b) Cooper, S. R.; Rawle, S. C. *Struct. Bonding (Berlin)* **1990**, *72*, 1. (c) Blake, A. J.; Schröder, M. *Adv. Inorg. Chem.* **1990**, *35*, 1. (d) Cooper, S. R. *Acc. Chem. Res.* **1988**, *21*, 141.

(2) Edwards, A. J.; Johnson, B. F. G.; Khan, F. K.; Lewis, J.; Raithby, P. R. *J. Organomet. Chem.* **1992**, *426*, C44.

(3) Adams, R. D.; Falloon, S. B.; McBride, K. T. *Organometallics* **1994**, *13*, 4870.

(4) Adams, R. D.; Falloon, S. B.; McBride, K. T.; Yamamoto, J. H. *Organometallics* **1995**, *14*, 1739.

sphere unless specified otherwise. Infrared spectra were recorded on a Nicolet 5DXB FTIR spectrophotometer. Chromatographic separations were performed in air on Analtech silica gel (0.25 mm) F<sub>254</sub> uniplates. Column separations were performed on silica gel (70–230 mesh, 60 Å) purchased from Aldrich. Elemental analyses were performed by Oneida Research Services, Whitesboro, NY.

**NMR Measurements.** One-dimensional <sup>1</sup>H and <sup>13</sup>C NMR spectra were obtained on a Bruker AM 500 spectrometer. The <sup>13</sup>C NMR spectra were recorded with the following parameters: spectrometer frequency, 125.759 MHz; sweep width, 38 461 Hz; data points, 128K; acquisition time, 1.7 s; delay, 500 ms; pulse width, 1.4 ms, where the 90° pulse width is 15.6 ms and 4096 scans. The temperatures of the variable temperature spectra were determined by MeOH calibration. The two-dimensional <sup>13</sup>C EXSY spectra were obtained on a Bruker AM 500 at –78 °C using the following parameters: spectrometer frequency, of 125.759 MHz; mixing time, 10.0 ms; sweep width, 100 00 Hz, with 2K data points in each dimension; acquisition time, 0.1025 s, with 8 scans per loop and 512 loops. Chemical shifts are reported in δ (ppm), and coupling constants *J* are reported in hertz. The one-dimensional exchange-broadened <sup>13</sup>C simulations were performed using the program EXCHANGE written by R. E. D. McClung of the Department of Chemistry at the University of Alberta on a 486 IBM compatible computer. Spin simulations were performed using the Bruker program Panic in the iteration mode on an Aspect 3000 computer.

**Synthesis of Ru<sub>3</sub>(CO)<sub>7</sub>(μ-CO)<sub>2</sub>(1,1,1-η<sup>3</sup>-12S3), 1.** In a typical experiment a 25.0-mg amount of Ru<sub>3</sub>(CO)<sub>12</sub> (0.039 mmol) and a 15.0-mg amount of 12S3 (0.063 mmol) were dissolved in 15 mL of hexane and then heated to reflux for 3.5 h. The solution was filtered hot, and a brown precipitate formed from the filtrate upon cooling. The precipitate was washed with two portions (1 mL each) of hexane and dried in vacuo to yield 25.5 mg of analytically pure Ru<sub>3</sub>(CO)<sub>7</sub>(μ-CO)<sub>2</sub>(1,1,1-η<sup>3</sup>-12S3), **1**, 83%. Unreacted Ru<sub>3</sub>(CO)<sub>12</sub> can be a minor contaminant without further purification by recrystallization. Analytical and spectral data for **1**: IR νCO (cm<sup>-1</sup>, in CH<sub>2</sub>Cl<sub>2</sub>, 2067 (s), 2022 (vs), 1993 (vs), 1971 (m), 1950 (m), 1719 (w); <sup>1</sup>H NMR (δ, in CD<sub>2</sub>Cl<sub>2</sub>), 3.03 (6H, ddd, <sup>2</sup>J<sub>H-H</sub> = 14.0, <sup>3</sup>J<sub>H-H</sub> = 8.5, <sup>3</sup>J<sub>H-H</sub> = 2.5), 2.30 (6H, ddd, <sup>2</sup>J<sub>H-H</sub> = 14.0, <sup>3</sup>J<sub>H-H</sub> = 8.0, <sup>3</sup>J<sub>H-H</sub> = 2.5), 2.72 (3H, dtt, <sup>2</sup>J<sub>H-H</sub> = 16.0, <sup>3</sup>J<sub>H-H</sub> = 8.5, <sup>3</sup>J<sub>H-H</sub> = 2.5), 2.46 (3H, dtt, <sup>2</sup>J<sub>H-H</sub> = 16.0, <sup>3</sup>J<sub>H-H</sub> = 8.0, <sup>3</sup>J<sub>H-H</sub> = 2.5). Anal. Calcd (found) for **1**: C, 27.80 (27.66); H, 2.32 (2.29).

**Synthesis of 1\*.** Ru<sub>3</sub>(<sup>13</sup>CO)<sub>9</sub>(1,1,1-η<sup>3</sup>-(SCH<sub>2</sub>CH<sub>2</sub>CH<sub>2</sub>)<sub>3</sub>), **1\***, was prepared by the procedure described above using Ru<sub>3</sub>(<sup>13</sup>CO)<sub>12</sub> with 99.99% <sup>13</sup>CO. Spectral data for **1\***: IR νCO (cm<sup>-1</sup>, in CH<sub>2</sub>Cl<sub>2</sub>), 2019 (m), 1974 (s), 1949 (vs), 1927 (sh), 1922 (sh), 1910 (w), 1680 (m); <sup>13</sup>C NMR of CO region (δ in ppm, in CD<sub>2</sub>Cl<sub>2</sub> solvent at –80 °C), 250.6 (2C), 206.7 (2C), 203.6 (2C), 200.2 (1C), 193.6 (1C), 190.4 (1C).

**Ru<sub>3</sub>(CO)<sub>7</sub>(μ-CO)<sub>2</sub>(1,1,1-η<sup>3</sup>-9S3), 2.** A 100.0-mg amount of Ru<sub>3</sub>(CO)<sub>12</sub> (0.156 mmol) and a 33.1-mg amount (0.184 mmol) of 9S3 were dissolved in 100 mL of hexane, and the solution was heated to reflux for 3 h. The solution was filtered hot, and a brown precipitate formed from the filtrate upon cooling. The precipitate was washed with two 1-mL portions of hexane to yield 95.1 mg of analytically pure Ru<sub>3</sub>(CO)<sub>7</sub>(μ-CO)<sub>2</sub>(1,1,1-η<sup>3</sup>-9S3), **2**, in 83% yield. Analytical and spectral data for **2**: IR νCO (cm<sup>-1</sup>, in CH<sub>2</sub>Cl<sub>2</sub>), 2068 (m), 2020 (s); 1988 (vs), 1951 (m), 1718 (w); <sup>1</sup>H NMR (δ, in CD<sub>2</sub>Cl<sub>2</sub> at 25 °C), 2.94 (6H, <sup>2</sup>J<sub>H-H</sub> = –14.02, <sup>3</sup>J<sub>H-H</sub> = 6.73, <sup>3</sup>J<sub>H-H</sub> = 6.91), 2.47 (6H, <sup>2</sup>J<sub>H-H</sub> = –14.02, <sup>3</sup>J<sub>H-H</sub> = 6.73, <sup>3</sup>J<sub>H-H</sub> = 6.91). Anal. Calcd (found) for **2**: C, 24.49 (24.45); H, 1.64 (1.73).

**Synthesis of 2\*.** Ru<sub>3</sub>(<sup>13</sup>CO)<sub>7</sub>(μ-CO)<sub>2</sub>(η<sup>3</sup>-9S3), **2\***, was prepared in 78% yield by the procedure described above by substituting Ru<sub>3</sub>(<sup>13</sup>CO)<sub>12</sub> for unlabeled Ru<sub>3</sub>(CO)<sub>12</sub>. Spectral data for **2\***: IR νCO (cm<sup>-1</sup>, in CH<sub>2</sub>Cl<sub>2</sub>), 2018 (m), 1972 (s), 1943 (vs), 1909 (m), 1685 (w); <sup>1</sup>H NMR (δ, in CD<sub>2</sub>Cl<sub>2</sub>), 2.94 (6H, <sup>2</sup>J<sub>H-H</sub> = –14.02, <sup>3</sup>J<sub>H-H</sub> = 6.73, <sup>3</sup>J<sub>H-H</sub> = 6.91), 2.47 (6H, <sup>2</sup>J<sub>H-H</sub> = –14.02, <sup>3</sup>J<sub>H-H</sub> = 6.73, <sup>3</sup>J<sub>H-H</sub> = 6.91); <sup>13</sup>C NMR (δ, in CD<sub>2</sub>Cl<sub>2</sub> at

**Table 1. Crystallographic Data for Compounds 1 and 2**

	1	2
empirical formula	Ru <sub>3</sub> S <sub>3</sub> O <sub>9</sub> C <sub>18</sub> H <sub>18</sub>	Ru <sub>3</sub> S <sub>3</sub> O <sub>9</sub> C <sub>15</sub> H <sub>12</sub>
fw	777.72	735.64
cryst syst	monoclinic	monoclinic
lattice param		
<i>a</i> (Å)	9.316(2)	13.976(2)
<i>b</i> (Å)	15.688(5)	10.123(2)
<i>c</i> (Å)	16.826(3)	15.538(2)
α (deg)	90.0	90.0
β (deg)	93.30(2)	97.967(9)
γ (deg)	90.0	90.0
<i>V</i> (Å <sup>3</sup> )	2455(1)	2177.1(4)
Space group	<i>P</i> 2 <sub>1</sub> / <i>n</i> (No. 14)	<i>P</i> 2 <sub>1</sub> / <i>c</i> (No. 14)
<i>Z</i> value	4	4
<i>D</i> <sub>calcd</sub> (g/cm <sup>3</sup> )	2.10	2.24
μ(Mo Kα), (cm <sup>-1</sup> )	20.72	23.87
temp (°C)	20	20
2θ <sub>max</sub> (deg)	45.0	43.0
no. of obsd ( <i>I</i> > 3σ( <i>I</i> ))	2217	1910
no. of variables	298	272
residuals: <i>R</i> , <i>R</i> <sub>w</sub> <sup>a</sup>	0.032; 0.031	0.025; 0.026
goodness of fit	1.32	1.21
indicator <sup>a</sup>		
max shift on final cycle	0.00	0.00
largest peak in final diff map (e/Å <sup>3</sup> )	0.59	0.49
abs cor; max/min	empirical; 1.0/0.84	empirical; 1.0/0.79

<sup>a</sup>  $R = \sum_{hkl} (|F_o| - |F_c|) / \sum_{hkl} |F_o|$ ;  $R_w = [\sum_{hkl} w(|F_o| - |F_c|)^2] / \sum_{hkl} w F_o^2$ ;  $w = 1/\sigma^2(F_{obs})$ ;  $GOF = [\sum_{hkl} (|F_o| - |F_c|/\sigma(F_{obs}))^2] / (n_{data} - n_{variables})$ .

–93 °C (CO)), 245.8 (2C), 208.1 (2C), 204.2 (2C), 199.5 (1C), 194.6 (1C), 190.5 (1C).

**Pyrolysis of 2.** A 100.0-mg amount of **2** (0.0136 mmol) was dissolved in dry THF and then heated to reflux for 16 h. The solvent was then removed in vacuo, and the residue was separated by TLC with a 1/1 CH<sub>2</sub>Cl<sub>2</sub>/hexane mixture. Two major bands were isolated in the following order: Ru<sub>2</sub>(CO)<sub>6</sub>(μ<sub>2</sub>-η<sup>2</sup>-SCH<sub>2</sub>CH<sub>2</sub>S), **3** (10.0 mg, 16%), and the known compound Ru<sub>3</sub>(CO)<sub>9</sub>(μ<sub>2</sub>-η<sup>2</sup>-SCH<sub>2</sub>CH<sub>2</sub>SCH<sub>2</sub>CH<sub>2</sub>S), **4** (31.1 mg, 32%).<sup>5</sup> Analytical and spectral data for **3**: IR νCO (cm<sup>-1</sup>, in hexane), 2087 (s), 2057 (vs), 2014 (vs), 2006 (vs), 1996 (s), 1965 (w); <sup>1</sup>H NMR (δ, in CDCl<sub>3</sub>): 2.37 (4H, s); MS, *m/e* 464–7(28); M<sup>+</sup>(for 2 <sup>102</sup>Ru) – (6 CO and 1 C<sub>2</sub>H<sub>4</sub>). The isotope distribution pattern for the parent ion indicates the presence of two ruthenium atoms.

**Crystallographic Analyses.** Crystals of **1** were grown by slow evaporation of solvent from a hexane/CH<sub>2</sub>Cl<sub>2</sub> solution at –14 °C. Crystals of **2** were grown by slow evaporation of solvent from acetone solutions at –14 °C. The crystals used for data collection were mounted in thin-walled glass capillaries. Diffraction measurements were made on a Rigaku AFC6S fully automated four-circle diffractometer using graphite-monochromated Mo Kα radiation. The unit cells were determined and refined from 15 randomly selected reflections obtained by using the AFC6 automatic search, center, index, and least-squares routines. Crystal data, data collection parameters, and results of the analyses are listed in Table 1. All data processing was performed on a Digital Equipment Corp. VAXstation 3520 computer by using the TEXSAN structure solving program library obtained from the Molecular Structure Corp., The Woodlands, TX. Neutral atom scattering factors were calculated by the standard procedures.<sup>8a</sup> Anomalous dispersion corrections were applied to all non-hydrogen atoms.<sup>8b</sup> Full matrix least-squares refinements minimized the function  $\sum_{hkl} w(F_o - F_c)^2$ , where  $w = 1/\sigma(F)^2$ ,  $\sigma(F) = \sigma(F_o^2)/2F_o$ , and  $\sigma(F_o^2) = [\sigma(I_{raw})^2 + (0.02I_{net}^2)^{1/2}]/Lp$ .

Compounds **1** and **2** both crystallized in the monoclinic crystal system. The space groups *P*2<sub>1</sub>/*n* and *P*2<sub>1</sub>/*c* for **1** and **2**,

(8) (a) *International Tables for X-ray Crystallography*; Kynoch Press: Birmingham, England, 1975; Vol. IV, Table 2.2B, pp 99–101; (b) Table 2.3.1, pp 149–150.



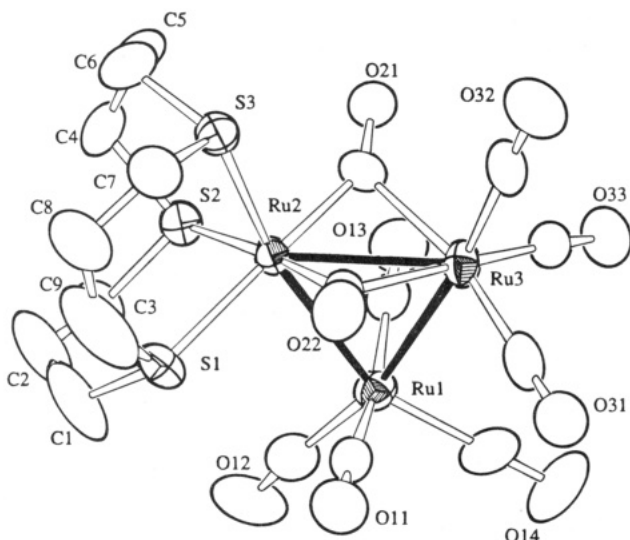


**Figure 1.** ORTEP diagram of  $\text{Ru}_3(\text{CO})_7(\mu\text{-CO})_2(1,1,1\text{-}\eta^3\text{-12S3})$ , **1**, showing 40% probability thermal ellipsoids.

respectively, were identified uniquely on the basis of systematic absences observed during the collection of data. Both structures were solved by a combination of direct methods (MITHRIL) and difference Fourier syntheses. All non-hydrogen atoms were satisfactorily refined with anisotropic thermal parameters. All hydrogen atom positions were calculated by assuming idealized geometries with C–H distances of 0.95 Å. The scattering contributions of the hydrogen atoms were added to the structure factor calculations, but their positions were not refined.

## Results and Discussion

The reaction of 12S3 with  $\text{Ru}_3(\text{CO})_{12}$  in refluxing hexane provided  $\text{Ru}_3(\text{CO})_7(\mu\text{-CO})_2(1,1,1\text{-}\eta^3\text{-12S3})$ , **1**, in 83% yield.<sup>5</sup> Compound **1** was characterized by single-crystal X-ray diffraction analysis, and an ORTEP drawing of its molecular structure is shown in Figure 1. Final atomic positional parameters are given in Table 2. Selected bond distances and angles are listed in Tables 3 and 4. The molecule consists of a triangular cluster of three ruthenium atoms with nine carbonyl ligands and one 12S3 ligand. All three sulfur atoms of the 12S3 ligand are coordinated to only one ruthenium, Ru(2). One sulfur atom, S(3), lies in the plane of the  $\text{Ru}_3$  triangle, and its ruthenium–sulfur distance,  $\text{Ru}(2)\text{--S}(3) = 2.381(2)$  Å, is significantly shorter than the other two,  $\text{Ru}(2)\text{--S}(1) = 2.448(2)$  Å and  $\text{Ru}(2)\text{--S}(2) = 2.440(2)$  Å. The structure of the 12S3 ligand is similar to that observed when it is complexed to metal ions<sup>9</sup> and to the metal atoms in cluster complexes.<sup>2–4</sup> Seven of the carbonyl ligands are of a linear terminal while two are strong semibridging ligands that bridge the  $\text{Ru}(2)\text{--Ru}(3)$  metal–metal bond. The arrangement of the bridging CO groups is thus similar to that found in the

**Table 2. Positional Parameters and  $B(\text{eq})$  for  $\text{Ru}_3(\text{CO})_9(1,1,1\text{-}\eta^3\text{-12S3})$ , **1****

atom	x	y	z	$B(\text{eq})$
Ru(1)	0.44339(7)	0.17226(5)	0.35598(4)	2.86(3)
Ru(2)	0.47810(7)	0.17014(4)	0.18657(4)	2.43(3)
Ru(3)	0.28850(7)	0.05935(4)	0.25289(4)	2.95(3)
S(1)	0.7409(2)	0.1664(1)	0.2022(1)	3.5(1)
S(2)	0.4705(2)	0.3256(1)	0.1834(1)	3.1(1)
S(3)	0.4669(2)	0.1493(1)	0.0462(1)	3.2(1)
O(11)	0.6920(7)	0.0443(4)	0.3600(4)	4.8(4)
O(12)	0.6234(8)	0.3133(5)	0.4358(5)	6.7(4)
O(13)	0.1920(7)	0.2971(4)	0.3204(4)	4.7(4)
O(14)	0.3208(9)	0.0912(5)	0.5018(4)	7.5(5)
O(21)	0.1669(6)	0.2135(4)	0.1514(4)	3.8(3)
O(22)	0.5624(7)	-0.0137(4)	0.1774(4)	4.6(3)
O(31)	0.3892(7)	-0.0910(4)	0.3589(5)	5.7(4)
O(32)	0.1156(7)	-0.0393(5)	0.1263(4)	5.8(4)
O(33)	0.0217(7)	0.1038(4)	0.3423(4)	5.1(4)
C(1)	0.823(1)	0.2649(7)	0.2285(9)	7.8(8)
C(2)	0.771(1)	0.3433(7)	0.2048(9)	7.5(7)
C(3)	0.629(1)	0.3776(6)	0.2257(6)	4.3(5)
C(4)	0.470(1)	0.3701(6)	0.0841(6)	4.4(5)
C(5)	0.385(1)	0.3191(6)	0.0215(5)	4.3(5)
C(6)	0.467(1)	0.2469(7)	-0.0121(5)	4.6(5)
C(7)	0.628(1)	0.0994(6)	0.0127(5)	4.6(5)
C(8)	0.771(1)	0.136(1)	0.0397(7)	7.9(8)
C(9)	0.822(1)	0.131(1)	0.117(1)	10(1)
C(11)	0.598(1)	0.0930(6)	0.3556(5)	3.5(4)
C(12)	0.559(1)	0.2622(7)	0.4031(6)	4.4(5)
C(13)	0.286(1)	0.2508(6)	0.3309(5)	3.4(4)
C(14)	0.367(1)	0.1229(7)	0.4485(6)	4.5(5)
C(21)	0.2661(9)	0.1765(5)	0.1786(5)	2.9(4)
C(22)	0.4958(9)	0.0449(6)	0.1952(5)	3.2(4)
C(31)	0.351(1)	-0.0346(6)	0.3190(6)	4.1(5)
C(32)	0.184(1)	-0.0035(6)	0.1732(6)	3.8(5)
C(33)	0.121(1)	0.0900(5)	0.3073(5)	3.6(5)

**Table 3. Intramolecular Distances for **1**<sup>a</sup>**

$\text{Ru}(1)\text{--Ru}(2)$	2.887(1)	$\text{S}(2)\text{--C}(3)$	1.796(9)
$\text{Ru}(1)\text{--Ru}(3)$	2.818(1)	$\text{S}(2)\text{--C}(4)$	1.811(9)
$\text{Ru}(2)\text{--Ru}(3)$	2.759(1)	$\text{S}(3)\text{--C}(6)$	1.82(1)
$\text{Ru}(2)\text{--S}(1)$	2.448(2)	$\text{S}(3)\text{--C}(7)$	1.81(1)
$\text{Ru}(2)\text{--S}(2)$	2.440(2)	$\text{O}(21)\text{--C}(21)$	1.163(9)
$\text{Ru}(2)\text{--S}(3)$	2.381(2)	$\text{O}(22)\text{--C}(22)$	1.16(1)
$\text{Ru}(2)\text{--C}(21)$	1.974(8)	$\text{O--C (av)}$	1.14(1)
$\text{Ru}(2)\text{--C}(22)$	1.976(9)	$\text{C}(1)\text{--C}(2)$	1.37(1)
$\text{Ru}(3)\text{--C}(21)$	2.226(9)	$\text{C}(2)\text{--C}(3)$	1.49(1)
$\text{Ru}(3)\text{--C}(22)$	2.222(9)	$\text{C}(4)\text{--C}(5)$	1.51(1)
$\text{Ru--C (av)}$	1.91(1)	$\text{C}(5)\text{--C}(6)$	1.50(1)
$\text{S}(1)\text{--C}(1)$	1.77(1)	$\text{C}(7)\text{--C}(8)$	1.50(1)
$\text{S}(1)\text{--C}(9)$	1.75(1)	$\text{C}(8)\text{--C}(9)$	1.36(2)

<sup>a</sup> Distances are in angstroms. Estimated standard deviations in the least significant figure are given in parentheses.

compound  $\text{Fe}_3(\text{CO})_{10}(\mu\text{-CO})_2$ , **5**,<sup>10</sup> but quite unlike that of  $\text{Ru}_3(\text{CO})_{12}$ , which has only terminal CO ligands.<sup>11</sup> The  $\text{Ru}(2)\text{--Ru}(3)$  bond is the shortest of the three metal–metal bonds, 2.759(1) Å versus 2.887(1) Å and 2.818(1) Å, which may be a result of the presence of the bridging carbonyl ligands. The transformation of two of the CO ligands to bridging positions in the conversion of  $\text{Ru}_3(\text{CO})_{12}$  to **1** is probably caused by the steric bulk of the 12S3 ligand. Previous studies have shown that increased steric interactions among the ligands in  $\text{M}_3$  clusters cause the CO groups to shift toward bridging positions.<sup>12</sup> There appears to be only one previous

(9) (a) Rawle, S. C.; Sewell, T. J.; Cooper, S. J. *Inorg. Chem.* **1987**, *26*, 3769. (b) Rawle, S. C.; Admans, G. A.; Cooper, S. R. *J. Chem. Soc., Dalton Trans.* **1988**, 93. (c) Cooper, S. R.; Rawle, S. C.; Hartman, J. R.; Hints, E. J.; Admans, G. A. *Inorg. Chem.* **1988**, *27*, 1209. (d) Dockal, E. R.; Jones, T. E.; Sokol, W. F.; Engerer, R. J.; Rorabacher, D. B.; Ochrymowycz, L. A. *J. Am. Chem. Soc.* **1976**, *98*, 4322. (e) Blower, P. J.; Clarkon, J.; Rawle, S. C.; Hartman, J. R.; Wolfe, R. E., Jr.; Yagbasan, R.; Bott, S. G.; Cooper, S. R. *Inorg. Chem.* **1989**, *28*, 4040. (f) Clarkon, J.; Yagbasan, R.; Blower, P. J.; Cooper, S. R. *J. Chem. Soc., Chem Commun.* **1989**, 1244.

(10) (a) Cotton, F. A.; Troup, J. M. *J. Am. Chem. Soc.* **1974**, *96*, 4155. (b) Braga, D.; Grepioni, F.; Farrugia, L. J.; Johnson, B. F. G. *J. Chem. Soc., Dalton Trans.* **1994**, 2911. (c) Wei, C. H.; Dahl, L. F. *J. Am. Chem. Soc.* **1969**, *91*, 1351.

(11) Churchill, M. R.; Hollander, F. J.; Hutchinson, J. P. *Inorg. Chem.* **1977**, *16*, 2655.

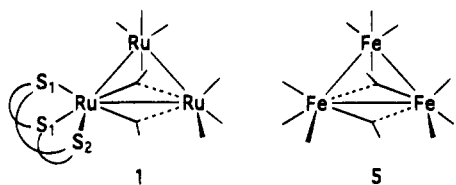
(12) Lauher, J. W. *J. Am. Chem. Soc.* **1986**, *108*, 1521.

**Table 4. Intramolecular Bond Angles for 1<sup>a</sup>**

Ru(2)–Ru(1)–Ru(3)	57.83(3)	Ru(2)–S(3)–C(6)	114.7(3)
Ru(1)–Ru(2)–Ru(3)	59.82(3)	Ru(2)–S(3)–C(7)	112.2(3)
Ru(1)–Ru(2)–S(1)	93.58(6)	C(6)–S(3)–C(7)	99.7(5)
Ru(1)–Ru(2)–S(2)	90.30(6)	S(1)–C(1)–C(2)	125(1)
Ru(1)–Ru(2)–S(3)	168.52(6)	C(1)–C(2)–C(3)	124(1)
Ru(3)–Ru(2)–S(1)	126.93(6)	S(2)–C(3)–C(2)	117.6(7)
Ru(3)–Ru(2)–S(2)	128.32(6)	S(2)–C(4)–C(5)	114.4(6)
Ru(3)–Ru(2)–S(3)	108.80(6)	C(4)–C(5)–C(6)	113.6(8)
S(1)–Ru(2)–S(2)	93.09(8)	S(3)–C(6)–C(5)	114.6(6)
S(1)–Ru(2)–S(3)	95.14(8)	S(3)–C(7)–C(8)	118.6(8)
S(2)–Ru(2)–S(3)	96.68(8)	C(7)–C(8)–C(9)	122(1)
C(21)–Ru(2)–C(22)	97.7(3)	S(1)–C(9)–C(8)	129(1)
Ru(1)–Ru(3)–Ru(2)	62.35(3)	Ru(2)–C(21)–Ru(3)	81.9(3)
C(21)–Ru(3)–C(22)	84.0(3)	Ru(2)–C(21)–O(21)	145.2(7)
Ru(2)–S(1)–C(1)	115.0(4)	Ru(3)–C(21)–O(21)	132.8(7)
Ru(2)–S(1)–C(9)	113.4(4)	Ru(2)–C(22)–Ru(3)	81.9(3)
C(1)–S(1)–C(9)	106.1(7)	Ru(2)–C(22)–O(22)	144.4(7)
Ru(2)–S(2)–C(3)	115.(3)	Ru(3)–C(22)–O(22)	133.3(7)
Ru(2)–S(2)–C(4)	113.8(3)	Ru–C–O (av)	176.0(9)
C(3)–S(2)–C(4)	98.6(4)		

<sup>a</sup> Angles are in degrees. Estimated standard deviations in the least significant figure are given in parentheses.

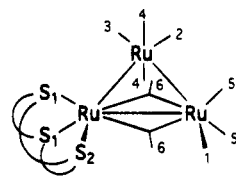
report of a triruthenium complex with the Fe<sub>3</sub>(CO)<sub>10</sub>(μ-CO)<sub>2</sub>-like structure, and that was for the tetraphosphite complex Ru<sub>3</sub>(CO)<sub>6</sub>[P(OMe)<sub>3</sub>]<sub>4</sub>(μ-CO)<sub>2</sub>.<sup>13</sup> However, close examination shows that the bridging ligands have an arrangement that is slightly different from that found in Fe<sub>3</sub>(CO)<sub>10</sub>(μ-CO)<sub>2</sub>. In particular, in Fe<sub>3</sub>(CO)<sub>10</sub>(μ-CO)<sub>2</sub> one bridging CO ligand is strongly bonded to each of the bridged iron atoms, **5**, while in **1** they are both strongly bonded to the ruthenium atom that contains the 12S3 ligand; see structural diagrams below, in which the dashed connections represent the longer M–C bonds.



The molecular symmetry in **1** is effectively C<sub>3</sub>. The <sup>1</sup>H NMR spectrum of **1** at 25 °C shows four resonances, δ (ppm) 3.03 (6H, ddd, J<sub>H–H</sub> = 14.0, J<sub>H–H</sub> = 8.5, J<sub>H–H</sub> = 2.5), 2.30 (6H, ddd, J<sub>H–H</sub> = 14.0, J<sub>H–H</sub> = 8.0, J<sub>H–H</sub> = 2.5), 2.72 (3H, dtt, J<sub>H–H</sub> = 16.0, J<sub>H–H</sub> = 8.5, J<sub>H–H</sub> = 2.5), and 2.46 (3H, dtt, J<sub>H–H</sub> = 16.0, J<sub>H–H</sub> = 8.0, J<sub>H–H</sub> = 2.5), which is consistent with a structure having three equivalent trimethylene groups between the three sulfur atoms. This is, however, inconsistent with the solid state structure and suggests that a dynamical averaging process might be occurring. This was confirmed by variable temperature measurements, which showed resonance broadenings at low temperatures, but since the resonances remain broad at the lowest recorded temperature, a mechanistic analysis of the dynamical process was not possible from the <sup>1</sup>H NMR data. However, a much more detailed analysis of the dynamical activity in **1** was obtained from a combination of variable temperature <sup>13</sup>C NMR spectra and 2-D EXSY experimental data performed at –78 °C. These measurements were made by using the 99.9% <sup>13</sup>CO-enriched compound **1**<sup>\*</sup>. A series of representative spectra taken

(13) Bruce, M. I.; Matison, J. G.; Patrick, J. M.; White, A. H.; Willis, A. C. *J. Chem. Soc. Dalton Trans.* **1985**, 1223.

at various temperatures is shown in Figure 2. At 25 °C only a broad singlet is observed at approximately +210 ppm, which is indicative of the presence of dynamical processes that lead to an averaging of all nine CO ligands. However, at –80 °C the rearrangements are slowed, and six slightly broadened singlets are observed at 250.6, 206.7, 203.6, 200.2, 193.6, and 190.4 ppm in the relative intensities 2:2:2:1:1:1. This spectrum is consistent with the solid state structure, and the following assignments have been made based, in part, upon known chemical shift patterns and the proposed mechanism of fluxionality which is described below. The resonance at 250.5 ppm (labeled 6) is assigned to the two equivalent bridging carbonyl ligands on the basis of its very low field shift. The two resonances of intensity 2 at 206.7 and 203.6 ppm are assigned to the equivalent pairs 4 and 5, respectively, see labeling scheme on the following figure.



The remaining resonances, 200.2, 193.6, and 190.4 ppm, are assigned to the CO ligands, 1, 2, and 3 in that order, although the assignments of 1 and 3 could be reversed.

A 2-D EXSY <sup>13</sup>C NMR spectrum (EXSY, exchange spectroscopy<sup>14</sup>) of **1** obtained at –78 °C using a 10-ms mixing time is shown in Figure 3. The advantage of the 10-ms mixing time is that it reveals important selectivities in the magnetization transfers. In particular, the cross peaks show that resonances 2, 4, 5, and 6 are exchanging among themselves, although a direct exchange between 2 and 6 was not observed. Resonances 1 and 3 are also exchanging, but they are not exchanging with the resonances 2, 4, 5, or 6. Interestingly, the cross peak between 5 and 6 is clearly smaller than the one between 4 and 6, and the cross peak between 2 and 4 is smaller than the one between 2 and 5. Although these cross peaks should not be quantitatively evaluated in terms of exchange rates, it is probably true that the smaller cross peaks do indicate qualitatively that exchange between those resonances is slower than that between those involving the larger cross peaks.<sup>15</sup> This is believed to be mechanistically significant as will be described below. At longer mixing times (e.g., 100 ms), exchange between all resonances was observed. This is consistent with the room temperature 1-D measurement which indicates that all CO resonances are averaged.

The data are consistent with the existence of at least two mechanisms for averaging of the CO ligands. The low-temperature mechanism was revealed by the 2-D EXSY measurement using the 10-ms mixing time. A mechanism that is consistent with this data is shown in Scheme 1. The proposed first step involves a pairwise shift, step a, of the bridging carbonyl ligands to terminal

(14) Sanders, J. K. M.; Hunter, B. K. *Modern NMR Spectroscopy*, 2nd ed.; Oxford University Press: New York, 1993; Chapter 7.

(15) (a) Farrugia, L. J. *Adv. Organomet. Chem.* **1990**, *31*, 301. (b) Farrugia, L. J.; Rae, S. E. *Organometallics* **1992**, *11*, 196. (c) Hawkes, G. E.; Lian, L. Y.; Randall, E. W.; Sales, K. D. *J. Magn. Reson.* **1985**, *65*, 173.

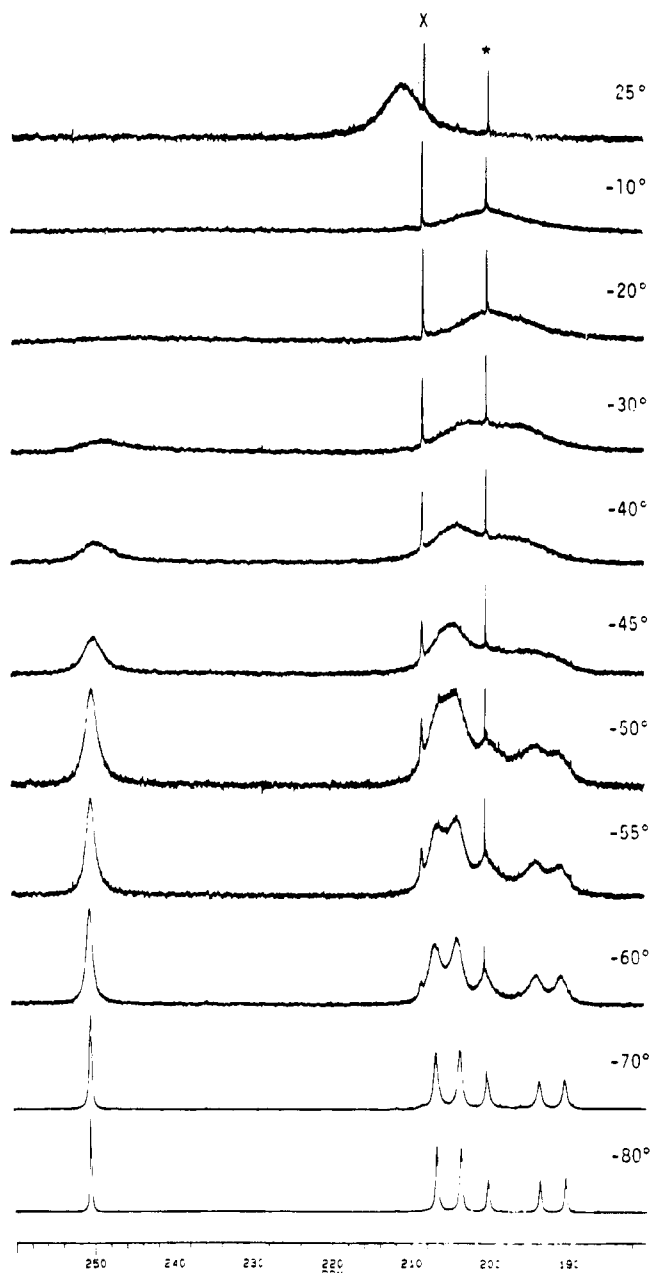


**Figure 2.**  $^{13}\text{C}$  NMR spectra for **1\*** recorded at several temperatures in  $\text{CD}_2\text{Cl}_2$ . The resonance marked with an X is a trace of unknown impurity. The resonance marked with an asterisk (\*) is a trace of  $\text{Ru}_3(\text{CO})_{12}$  impurity.

positions, one to each of the CO-bridged ruthenium atoms to yield the nonbridged tautomer **A**. The formation of a new double-CO-bridged structure **B** similar to **A** can occur by shifting the CO ligand 6 proximate to 12S3 ligand and the axial CO ligand 4 on the opposite side of the cluster into bridging positions across the other Ru–Ru bond to the 12S3-substituted ruthenium atom. In this one cycle of the rearrangement, one of the COs labeled 4 has moved into a 6 site, one of the COs labeled 6s remains a 6 while the other 6 has moved into a 4 site, the 2 and one of the 4s have assumed the two 5 sites and vice versa (note: all sites are referenced against the starting arrangement in **1** in Scheme 1), and 1 and 3 have been interchanged. These transformations are similar to the ones originally proposed by Cotton to explain the fluxionality in  $\text{Fe}_3(\text{CO})_{12}$ .<sup>10a</sup> A second pass, steps c and d, leads to the doubly bridged species **D** via

the nonbridged tautomer **C** in which one of the 5s has now assumed a bridging 6 site and a 4 has moved into the 2 site. A 5 and a 6 occupy the two 5 sites, 2 and 6 occupy the 4 sites, the bridging 4 is still in a bridging site, and 1 and 3 have been interchanged again. A third pass, steps e and f, leads to the doubly bridged species **F** via the nonbridged tautomer **E** in which the original CO labeled 2 has finally assumed a bridging site 6, a 4 and a 6 have assumed the two original 5 sites, a 4 and 5 occupy the two original 4 sites, 6 occupies the original 2 site, and 1 and 3 have been interchanged again. The pattern is established, and this can go on ad infinitum, but by this mechanism alone 1 and 3 will never exchange with 2, 4, 5, and 6 and vice versa. This is consistent with the 2-D EXSY result. It is worthwhile to trace the flow of the carbonyls 2, 4, and 5 through the bridging sites 6. The first new CO ligand to enter a bridging site is a 4. It is not until a second pass through the cycle that a 5 enters the 6 site, and it is not until the third pass that the CO originally labeled 2 enters a bridging site. This mechanism is also fully consistent with the 2-D EXSY results which indicate through the cross peaks that the carbonyls 4 are exchanging with 6 faster than the carbonyls 5, which in turn is faster than the carbonyl 2 for which no cross peak to 6 was observed at the 10-ms mixing time. The other cross peaks are similarly explained. This process also leads to interchange of the environments of the trimethylene groups on the 12S3 ligand.

Using this mechanism alone we have been able to obtain reasonable simulations of the exchange broadened spectra up to and including the spectrum recorded at  $-50^\circ\text{C}$ . An Eyring plot of those rates has yielded the activation parameters  $\Delta H^\ddagger = 7.8(5)$  kcal/mol,  $\Delta S^\ddagger = -9(1)$  eu, and  $\Delta G^\ddagger_{203} = 9.5$  kcal/mol. Above  $-50^\circ\text{C}$  the simulations became progressively poorer. We believe that this is due to the onset of one or more processes that leads to exchange of the CO ligands in the 1 and 3 sites with the others and vice versa. We have not been able to quantify the mechanisms of these high-temperature processes, and a variety of possibilities, ranging from localized tripod rotations at  $\text{Ru}(\text{CO})_3$  groups<sup>13</sup> to bimetallic pairwise bridge-terminal processes at the  $\text{Ru}_2(\text{CO})_8$  group in the nonbridged tautomers, could explain the observation that all CO ligands are finally averaged at the higher temperatures.

In summary, the dynamics of the lowest temperature ligand rearrangement of **1** can be explained by a series of pairwise opening and closing processes involving the bridging carbonyl ligands and the two Ru–Ru bonds adjacent to the 12S3-substituted ruthenium atom. This process is similar to those that have been proposed for  $\text{Fe}_3(\text{CO})_{10}(\mu\text{-CO})_2$ ,<sup>10a,16</sup> but is restricted to only two of the three metal–metal bonds as a result of the 12S3 ligand substitution.

The reaction of 9S3 with  $\text{Ru}_3(\text{CO})_{12}$  in refluxing hexane provided the new compound,  $\text{Ru}_3(\text{CO})_7(\mu\text{-CO})_2\text{-}(1,1,1\text{-}\eta^3\text{-9S3})$ , **2**, in 83% yield. Compound **2** was characterized by single-crystal X-ray diffraction analysis, and an ORTEP drawing of its molecular structure is shown in Figure 4. Final atomic positional parameters are given in Table 5. Selected bond distances and

(16) (a) Johnson, B. F. G.; Roberts, Y. V.; Parisini, E. *J. Chem. Soc., Dalton Trans.* **1992**, 2573 and references therein. (b) Johnson, B. F. G.; Bott, A. *J. Chem. Soc., Dalton Trans.* **1990**, 2437.

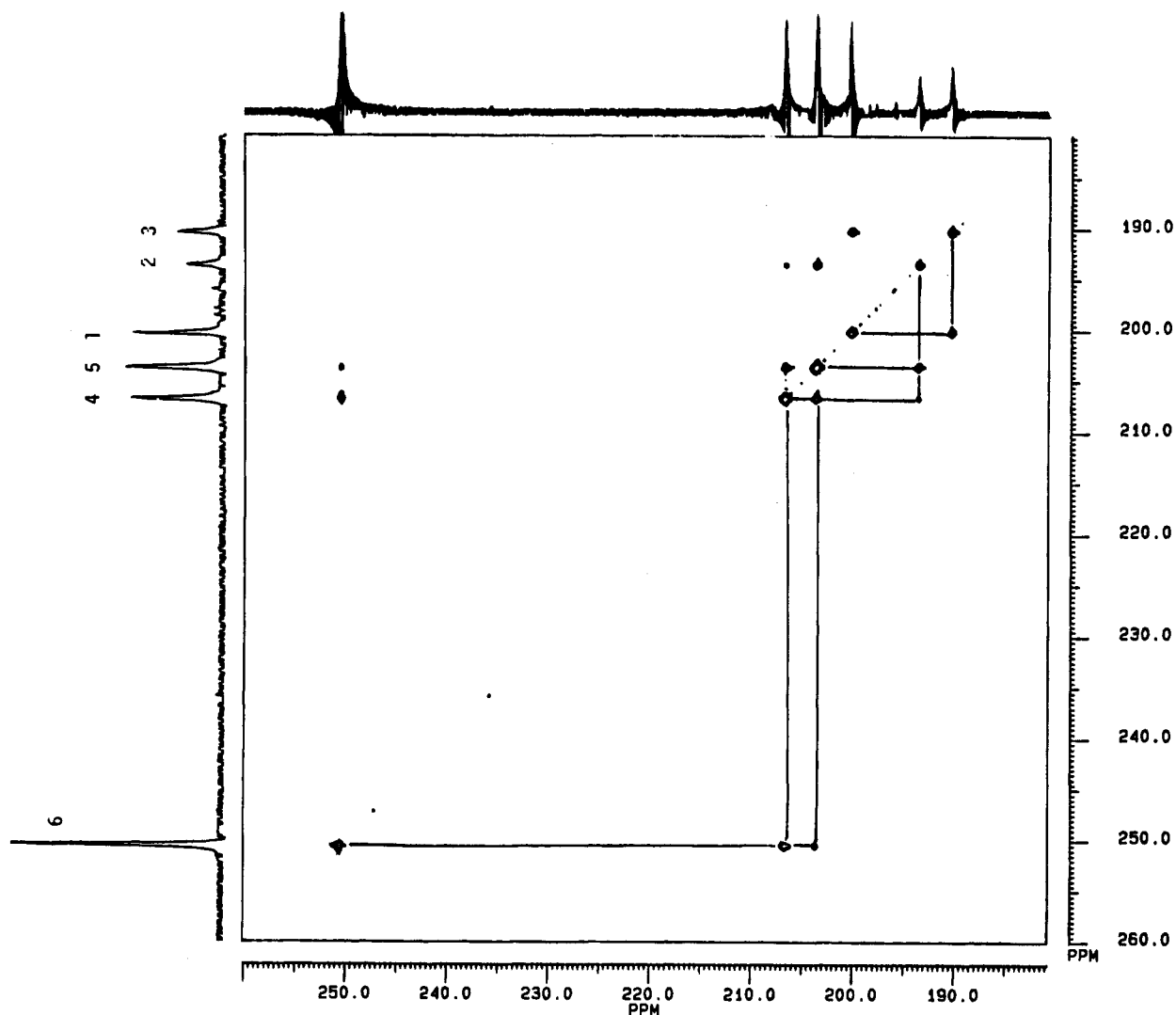
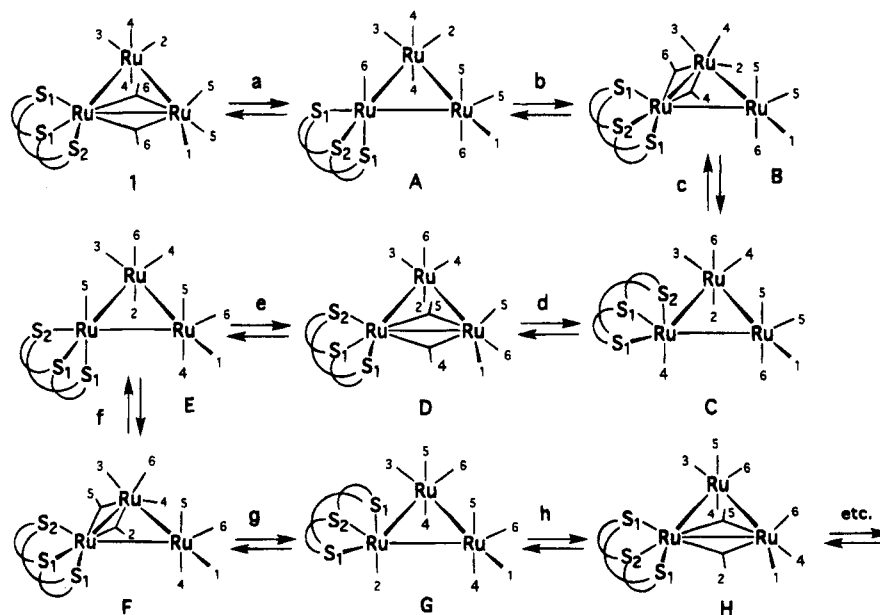


Figure 3. A 2-D  $^{13}\text{C}$  EXSY spectrum of  $1^*$  recorded at  $-78\text{ }^\circ\text{C}$  in the CO region using a 10-ms mixing time.

**Scheme 1. Lowest Temperature Mechanism for CO Ligand Exchange in 1**



angles are listed in Tables 6 and 7. The molecule is structurally similar to that of **1**. All three sulfur atoms of the 9S3 ligand are coordinated to only one ruthenium, Ru(2). The Ru–S distances in **2** are 0.03–0.05 Å shorter

than their counterparts in **1**, Ru(2)–S(3) = 2.352(2) Å, Ru(2)–S(1) = 2.393(2) Å, and Ru(2)–S(2) = 2.409(2) Å. The structure of the 9S3 ligand is similar to that found when it is complexed to metal ions<sup>1b,c</sup> and to the metal

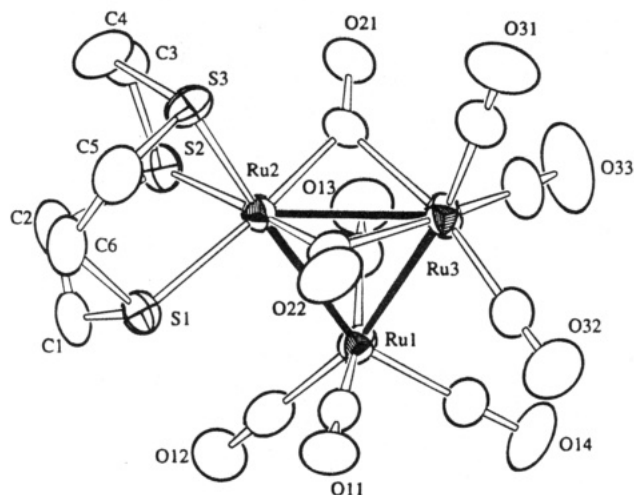


**Figure 4.** ORTEP diagram of  $\text{Ru}_3(\text{CO})_9(\mu\text{-CO})_2(1,1,1\text{-}\eta^3\text{-9S3})$ , **2**, showing 40% probability thermal ellipsoids.

**Table 5. Positional Parameters and  $B(\text{eq})$  for  $\text{Ru}_3(\text{CO})_9(1,1,1\text{-}\eta^3\text{-9S3})$ , **2****

atom	x	y	z	$B(\text{eq})$
Ru(1)	0.65281(4)	-0.16348(6)	0.76831(4)	2.58(3)
Ru(2)	0.77350(4)	0.05973(6)	0.81238(4)	2.29(3)
Ru(3)	0.80125(4)	-0.09146(6)	0.67156(4)	2.94(3)
S(1)	0.7840(1)	0.0248(2)	0.9657(1)	3.3(1)
S(2)	0.6470(1)	0.2139(2)	0.8320(1)	3.16(9)
S(3)	0.8833(1)	0.2349(2)	0.8438(1)	3.19(9)
O(11)	0.8092(4)	-0.3029(5)	0.8943(4)	4.8(3)
O(12)	0.5088(4)	-0.1740(6)	0.8990(4)	5.4(3)
O(13)	0.5214(4)	0.0267(6)	0.6527(4)	5.3(3)
O(14)	0.5911(4)	-0.4059(6)	0.6584(4)	6.1(3)
O(21)	0.7189(4)	0.1926(5)	0.6406(3)	4.4(3)
O(22)	0.9556(4)	-0.1015(5)	0.8406(4)	5.1(3)
O(31)	0.9694(5)	0.0254(7)	0.5924(4)	6.7(4)
O(32)	0.8709(5)	-0.3805(7)	0.6850(4)	6.7(4)
O(33)	0.6584(5)	-0.1051(9)	0.5036(4)	8.2(4)
C(1)	0.6704(6)	0.0876(9)	0.9916(5)	4.0(4)
C(2)	0.6383(5)	0.2184(9)	0.9492(5)	4.2(4)
C(3)	0.7079(6)	0.3678(8)	0.8217(5)	4.4(4)
C(4)	0.8111(6)	0.3794(7)	0.8650(6)	4.3(4)
C(5)	0.9373(5)	0.1949(8)	0.9546(5)	4.1(4)
C(6)	0.8663(5)	0.1549(8)	1.0140(5)	4.1(4)
C(11)	0.7533(6)	-0.2481(8)	0.8470(5)	3.3(4)
C(12)	0.5632(6)	-0.1690(8)	0.8516(5)	3.6(4)
C(13)	0.5730(6)	-0.0410(8)	0.6952(5)	3.5(4)
C(14)	0.6131(5)	-0.3153(8)	0.6997(5)	3.5(4)
C(21)	0.7465(5)	0.1056(8)	0.6881(5)	2.8(3)
C(22)	0.8828(6)	-0.0584(7)	0.8065(5)	3.0(4)
C(31)	0.9066(6)	-0.0191(8)	0.6221(5)	4.1(4)
C(32)	0.8459(6)	-0.2733(9)	0.6815(5)	3.7(4)
C(33)	0.7113(6)	-0.104(1)	0.5666(6)	4.6(5)

**Table 6. Intramolecular Distances for **2**<sup>a</sup>**

Ru(1)–Ru(2)	2.8460(8)	S(1)–C(6)	1.839(8)
Ru(1)–Ru(3)	2.8213(8)	S(2)–C(2)	1.842(8)
Ru(2)–Ru(3)	2.7416(8)	S(2)–C(3)	1.792(9)
Ru(2)–S(1)	2.393(2)	S(3)–C(4)	1.833(8)
Ru(2)–S(2)	2.409(2)	S(3)–C(5)	1.826(8)
Ru(2)–S(3)	2.352(2)	O(21)–C(21)	1.179(8)
Ru(2)–C(21)	1.971(7)	O(22)–C(22)	1.165(8)
Ru(2)–C(22)	1.952(8)	O–C (av)	1.140(8)
Ru(3)–C(21)	2.165(8)	C(1)–C(2)	1.52(1)
Ru(3)–C(22)	2.269(8)	C(3)–C(4)	1.51(1)
S(1)–C(1)	1.807(8)	C(5)–C(6)	1.50(1)

<sup>a</sup> Distances are in angstroms. Estimated standard deviations in the least significant figure are given in parentheses.

atoms in cluster complexes.<sup>4</sup> The two Ru–Ru bonds proximate to the ruthenium atom bearing the 9S3 ligand are shorter than those in **1**, Ru(2)–Ru(3) = 2.7416(8) Å and Ru(1)–Ru(2) = 2.8460(8) Å, but the

**Table 7. Intramolecular Bond Angles for **2**<sup>a</sup>**

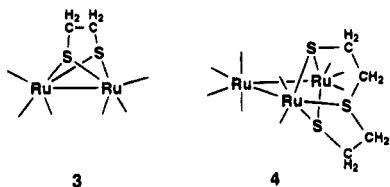
Ru(2)–Ru(1)–Ru(3)	57.86(2)	Ru(2)–S(2)–C(2)	106.9(3)
Ru(1)–Ru(2)–Ru(3)	60.62(2)	Ru(2)–S(2)–C(3)	100.7(3)
Ru(1)–Ru(2)–S(1)	94.27(5)	C(2)–S(2)–C(3)	99.4(4)
Ru(1)–Ru(2)–S(2)	97.13(5)	Ru(2)–S(3)–C(4)	106.2(3)
Ru(1)–Ru(2)–S(3)	175.26(6)	Ru(2)–S(3)–C(5)	101.6(3)
Ru(3)–Ru(2)–S(1)	135.74(5)	C(4)–S(3)–C(5)	100.0(4)
Ru(3)–Ru(2)–S(2)	130.55(5)	S(1)–C(1)–C(2)	115.2(5)
Ru(3)–Ru(2)–S(3)	115.23(6)	S(2)–C(2)–C(1)	110.6(5)
S(1)–Ru(2)–S(2)	85.10(7)	S(2)–C(3)–C(4)	117.6(6)
S(1)–Ru(2)–S(3)	87.52(7)	S(3)–C(4)–C(3)	112.0(6)
S(1)–Ru(2)–C(21)	170.8(2)	S(3)–C(5)–C(6)	114.7(5)
S(1)–Ru(2)–C(22)	90.9(2)	S(1)–C(6)–C(5)	111.8(5)
S(2)–Ru(2)–S(3)	87.38(7)	Ru(2)–C(21)–Ru(3)	82.9(3)
C(21)–Ru(2)–C(22)	98.3(3)	Ru(2)–C(21)–O(21)	142.2(6)
Ru(1)–Ru(3)–Ru(2)	61.52(2)	Ru(3)–C(21)–O(21)	134.8(6)
C(21)–Ru(3)–C(22)	84.0(3)	Ru(2)–C(22)–Ru(3)	80.6(3)
Ru(2)–S(1)–C(1)	103.6(3)	Ru(2)–C(22)–O(22)	148.0(6)
Ru(2)–S(1)–C(6)	104.4(3)	Ru(3)–C(22)–O(22)	131.3(6)
C(1)–S(1)–C(6)	100.2(3)	Ru–C–O (av)	177.0(9)

<sup>a</sup> Angles are in degrees. Estimated standard deviations in the least significant figure are given in parentheses.

third bond is slightly longer, Ru(1)–Ru(3) = 2.8213(8) Å. This can be explained by steric effects. The 9S3 ligand is slightly smaller than the 12S3 ligand, and therefore the proximate metal–metal bonds in **2** contract slightly. The bridging CO ligands in **2** exhibit an asymmetry pattern similar to that found in **1**. The <sup>1</sup>H NMR spectrum of **2** at room temperature shows two complex multiplets at  $\delta$  2.94 (6H, <sup>2</sup> $J_{\text{H-H}} = -14.02$ , <sup>3</sup> $J_{\text{H-H}} = 6.73$ , <sup>3</sup> $J_{\text{H-H}} = 6.91$ ), 2.47 (6H, <sup>2</sup> $J_{\text{H-H}} = -14.02$ , <sup>3</sup> $J_{\text{H-H}} = 6.73$ , <sup>3</sup> $J_{\text{H-H}} = 6.91$ ) ppm, indicating that all three ethylene groups are equivalent. The signs and magnitudes of the coupling constants were obtained by computer simulations. The existence of three equivalent ethylene groups is not consistent with the solid state structure but could be explained by a dynamical averaging process phenomenon similar to that observed in **1**. This was confirmed by low-temperature measurements in the <sup>1</sup>H NMR spectra of **2** and low-temperature <sup>13</sup>C NMR spectrum of **2**<sup>\*</sup> (99.9% enriched with <sup>13</sup>CO). The <sup>13</sup>C NMR spectrum of **2**<sup>\*</sup> in the CO region at –93 °C is similar to that of **1**<sup>\*</sup> and exhibits six resonances: 245.8 (2CO), 208.1 (2CO), 204.2 (2CO), 199.5 (1CO), 194.6 (1CO), and 190.5 (1CO) ppm. A series of resonance broadenings and averaging processes similar to those observed for **1**<sup>\*</sup> was also observed for **2**<sup>\*</sup>, but the broadenings occurred at slightly lower temperatures, which indicates slightly lower activation parameters. This is reflected in the slightly lower value of the free energy of activation,  $\Delta G^\ddagger_{203} = 9.2$  kcal/mol. From the Eyring plot,  $\Delta H^\ddagger = 8.6(5)$  kcal/mol and  $\Delta S^\ddagger = -3(1)$  eu. It is believed that the dynamical averaging processes in **2** are similar to those in **1**.

When heated to reflux in THF solvent for 16 h, compound **2** was transformed into two products: Ru<sub>2</sub>(CO)<sub>6</sub>(μ<sub>2</sub>-η<sup>2</sup>-SCH<sub>2</sub>CH<sub>2</sub>S), **3** (16% yield by degradation of the cluster) and the known compound Ru<sub>3</sub>(CO)<sub>9</sub>(μ<sub>2</sub>-η<sup>3</sup>-SCH<sub>2</sub>CH<sub>2</sub>SCH<sub>2</sub>CH<sub>2</sub>S), **4** (32% yield by degradation of the ligand). Compound **4** was obtained previously in a low yield (9%) from the reaction of Ru<sub>3</sub>(CO)<sub>12</sub> with 9S3 in refluxing THF solvent. Our studies suggest that **2** is probably an intermediate in the formation of **4**. The reaction involves a simple loss of ethylene. We have recently observed that the 9S3 ligand in the compound Ru<sub>6</sub>(CO)<sub>14</sub>(1,1,1-η<sup>3</sup>-9S3) also undergoes facile degradation by the elimination of ethylene to yield the complex Ru<sub>6</sub>(CO)<sub>14</sub>(μ<sub>3</sub>-η<sup>3</sup>-SCH<sub>2</sub>CH<sub>2</sub>SCH<sub>2</sub>CH<sub>2</sub>S)(μ<sub>5</sub>-C) that con-

tains a 3-thiapentanedithiolato ligand. The product **3** is believed to be analogous to the known compounds  $\text{Fe}_2(\text{CO})_6(\mu_2\text{-}\eta^2\text{-SCH}_2\text{CH}_2\text{S})^{17}$  and  $\text{Os}_2(\text{CO})_6(\mu_2\text{-}\eta^2\text{-SCH}_2\text{CH}_2\text{S})^{18}$  which have "sawhorse" structures.



**Acknowledgment.** This research was supported by the Office of Basic Energy Sciences of the U.S. Depart-

ment of Energy. We wish to thank Dr. A. R. Garber for assistance in obtaining the 2-D EXSY spectra.

**Supporting Information Available:** Tables of hydrogen atom positional parameters and anisotropic thermal parameters for the structural analyses (6 pages). Ordering information is given on any current masthead page.

OM950243D

(17) Shaver, A.; Fitzpatrick, P. J.; Steliou, K.; Butler, I. S. *J. Am. Chem. Soc.* **1979**, *101*, 1313.

(18) Adams, R. D.; Chen, L.; Yamamoto, J. H. *Inorg. Chim. Acta* **1995**, *229*, 47.



# Tetramethylammonium Pentacarbonyl[1-oxidoalkylidene]chromate(0) Salts as Acyl Anion Synthons in Michael Addition Reactions

Björn C. Söderberg,<sup>\*1</sup> Danny C. York, Elizabeth A. Harriston,  
H. John Caprara, and Ashley H. Flurry

Departments of Chemistry, West Virginia University, P.O. Box 6045,  
Morgantown, West Virginia 26506-6045, and University of South Alabama,  
Mobile, Alabama 36688

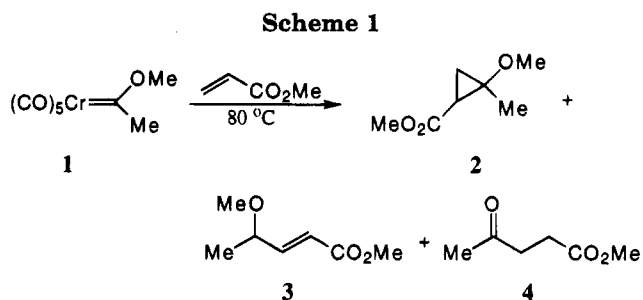
Received March 23, 1995<sup>⊗</sup>

Thermal and photolytic reactions of tetramethylammonium pentacarbonyl[1-oxidoalkylidene]chromate(0) salts with various electron-deficient alkenes have been investigated. Reaction of these electron-rich carbene complexes with 3-buten-2-one and methyl acrylate derivatives affords 1,4-dicarbonyl-substituted compounds, formal Michael addition products of an acyl anion and the alkene, in fair to good yield.

## Introduction

One of the very first synthetically useful reactions of alkoxy-substituted Fischer carbene complexes is the formal [2 + 1] cycloaddition reaction with electron-deficient alkenes providing functionalized donor-acceptor ("push-pull") substituted cyclopropanes as the major product.<sup>2,3</sup> Related cyclopropanation reactions have also been reported employing electron-rich alkenes such as enol ethers although under substantially different reaction conditions.<sup>4</sup> In addition to cycloaddition products, minor amounts of acyclic compounds derived from insertion into the  $\beta$ -CH bond of the alkene or by acid-catalyzed cleavage of the cyclopropane ring have been isolated in a few cases. For example, thermal reaction of pentacarbonyl[1-methoxyethylidene]chromium(0) (**1**) with methyl acrylate in 1,2-dichloroethane gave a 1:1:1 ratio of the cyclopropane **2**, the  $\beta$ -CH insertion product **3**, and methyl 4-oxopentanoate (**4**) in 72% yield (Scheme 1).<sup>2c</sup>

In contrast to the cyclopropanation reactions of "neutral" Fischer carbene complexes, we have recently observed that the electron-rich tetramethylammonium pentacarbonyl[1-oxidoethylidene]chromate(0) complex **5a** can be used as an acyl anion synthon. It was shown that formal Michael addition adducts are formed from reactions of **5a** with a number of  $\alpha,\beta$ -unsaturated ketones and esters.<sup>5,6</sup> For example, irradiation of a 0.1



M tetrahydrofuran solution of **5a** in the presence of methyl crotonate produced methyl 3-methyl-4-oxopentanoate (**6**) in 57% yield (Scheme 2). Although the yield of **6** was unchanged when the reaction was performed under a carbon monoxide atmosphere (6 atm), a significant amount of chromium hexacarbonyl can be isolated and recycled for the preparation of **5a**. Some amino-substituted chromium carbenes also afford formal Michael addition adducts upon reaction with electron deficient alkenes.<sup>2c</sup> For example, reaction of the dimethylamino-substituted complex **7** with methyl acrylate gave methyl 4-oxopentanoate (**4**) in excellent yield (Scheme 3).<sup>7</sup> A number of mechanistic formalisms can be entertained for the formation of **6**, and related 1,4-

(6) For reactions of other metal acylates with Michael acceptors forming 1,4-addition products, see the following. For nickel: (a) Corey, E. J.; Hegedus, L. S. *J. Am. Chem. Soc.* **1969**, *91*, 4926. (b) Semmelhack, M. F.; Keller, L.; Sato, T.; Spiess, E. *J. Org. Chem.* **1982**, *47*, 4382. (c) Hermanson, J. R.; Gunther, M. L.; Belletire, J. L.; Pinhas, A. R. *J. Org. Chem.* **1995**, *60*, 1900. For manganese: Hoye, T. R.; Rehberg, G. M. *Organometallics* **1990**, *9*, 3014. For cobalt: Hegedus, L. S.; Perry, R. J. *J. Org. Chem.* **1985**, *50*, 4955.

(7) Sierra, M. A.; Söderberg, B. C.; Lander, P. A.; Hegedus, L. S. *Organometallics* **1993**, *12*, 3769.

<sup>⊗</sup> Abstract published in *Advance ACS Abstracts*, July 1, 1995.

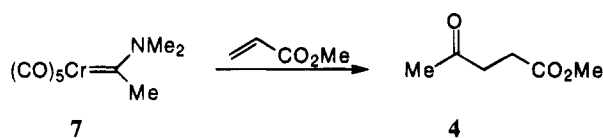
(1) Address all correspondence to West Virginia University.  
(2) For examples, see: (a) Wienand, A.; Reissig, H.-U. *Chem. Ber.* **1991**, *124*, 957. (b) Herndon, J. W.; Tumer, S. U. *J. Org. Chem.* **1991**, *56*, 286. (c) Wienand, A.; Reissig, H.-U. *Organometallics* **1990**, *9*, 3133. (d) Wienand, A.; Reissig, H.-U. *Tetrahedron Lett.* **1988**, *29*, 2315. (e) Buchert, M.; Reissig, H.-U. *Tetrahedron Lett.* **1988**, *29*, 2319. (f) Dorner, B.; Fischer, H.; Kalbfus, W. *J. Organomet. Chem.* **1974**, *81*, C 20. (g) Cooke, M. D.; Fischer, E. O. *J. Organomet. Chem.* **1973**, *56*, 279. (h) Dötz, K. H.; Fischer, E. O. *Chem. Ber.* **1972**, *105*, 1356. (i) Fischer, E. O.; Dötz, K. H. *Chem. Ber.* **1970**, *103*, 3966. (j) Fischer, E. O.; Dötz, K. H. *Chem. Ber.* **1970**, *103*, 1273.

(3) For a review on donor-acceptor-substituted cyclopropanes, see: Reissig, H.-U. *Top. Curr. Chem.* **1988**, *144*, 73.

(4) Dötz, K. H.; Fischer, E. O. *Chem. Ber.* **1972**, *105*, 3966. For a review on more recent work, see: Brookhart, M.; Studabaker, W. B. *Chem. Rev.* **1987**, *87*, 411.

(5) (a) Söderberg, B. C.; York, D. C.; Hoye, T. R.; Rehberg, G. M.; Suriano, J. A. *Organometallics* **1994**, *13*, 4501. (b) Presented in part by B.C.S. at the 205th ACS National Meeting, Denver, CO, 1993.

Scheme 3



dicarbonyl products discussed below, but at the present time these are only speculative.<sup>8</sup>

Several organic synthons are available for the introduction of acyl groups, but they all require an additional deprotection step.<sup>9</sup> It is conceivable that the easily prepared, highly crystalline tetramethylammonium pentacarbonyl[1-oxidoalkylidene]chromate(0) salts employing mild reaction conditions may offer some advantages over the presently available acyl synthons. Herein we report a more general study of the reaction of a number of alkyl- and aryl-substituted tetramethylammonium pentacarbonyl[1-oxidoalkylidene]chromate(0) salts with 3-buten-2-one and methyl acrylate derivatives.

### Results and Discussion

A selected number of isolated tetramethylammonium pentacarbonyl[1-oxidoalkylidene]chromate(0) complexes were reacted with 3-buten-2-one. Both alkyl- and aryl-substituted complexes, prepared by addition of the appropriate organolithium reagent to chromium hexacarbonyl followed by exchange of the counterion from lithium to tetramethylammonium, were examined. The reactions were performed in tetrahydrofuran under both photochemical conditions using a 450-W Conrad-Hanovia 7825 medium-pressure mercury lamp equipped with a Pyrex well as well as under thermal conditions at 75 °C (oil bath temperature). The results of these experiments are summarized in Table 1. A 1 to ~1.1 ratio of chromium complex to 3-buten-2-one was used for entries 1–3 and 5–15 (Table 1) producing in all instances only minute amounts (<5%) of oligomeric products as determined by GC-MS of the crude reaction mixtures. In most cases only one major product, together with chromium hexacarbonyl, was observed. The moderate yield isolated in several cases probably reflects the starting material's relatively low thermal stability. Decomposition of the chromium complexes at elevated temperatures is especially noticeable for the alkyl-substituted carbenes **5b–d**. These complexes show a visible decomposition, apparent by a slow color change from yellow-green to dark green after a few days, even when stored under a nitrogen atmosphere at –18 °C. As seen in Table 1, somewhat better yields are frequently obtained using photochemical conditions at ambient temperature compared to thermal conditions. This may also be a reflection of the thermal instability of the carbenes, at least for the alkyl-substituted complexes.  $\alpha$ -Substitution on the pendant alkyl chain appears to only moderately affect the isolated yield. The yield is reduced from 77% using **5a** having a methyl substituent to 56% using the bulky *tert*-butyl-substituted complex **5d** (entries 2 and 9).

In contrast to reactions employing near stoichiometric ratios of starting materials, a complex and hard to separate mixture of products was obtained by employing 5 equiv of 3-buten-2-one (entry 4). Again the only

**Table 1. Reaction of Tetramethylammonium Pentacarbonyl[1-oxidoalkylidene]chromate(0) Complexes with 3-Buten-2-one under Thermal and Photochemical Conditions**

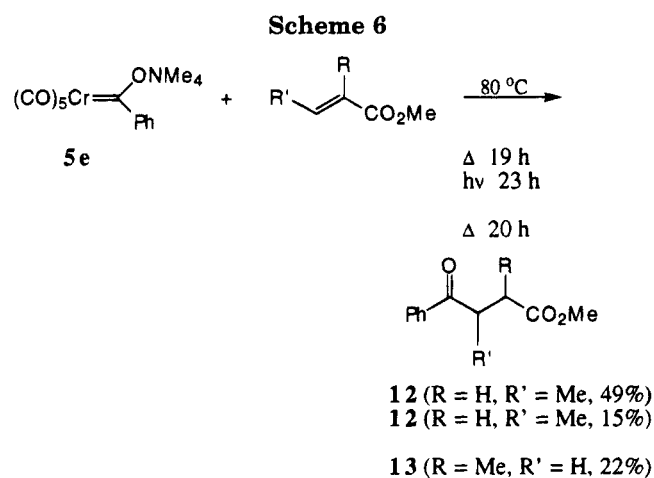
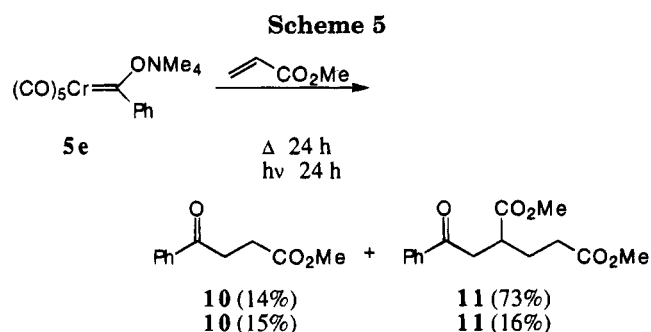
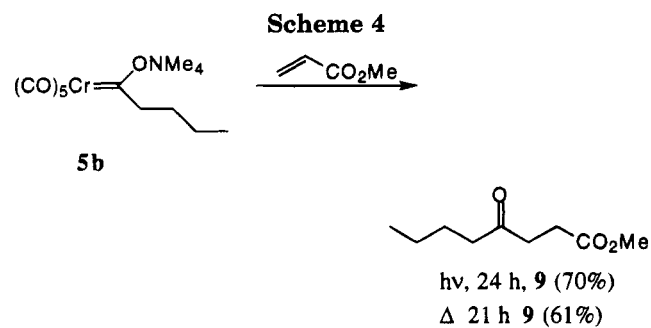
Entry	Carbene <sup>a</sup>	Conditions, time <sup>b</sup>	Diketone (yield) <sup>c</sup>
1	<b>5a</b>	h $\nu$ , 36 h	<b>8a</b> (75%) <sup>d</sup>
2	<b>5a</b>	$\Delta$ , 24 h	<b>8a</b> (77%) <sup>d</sup>
3	<b>5b</b>	h $\nu$ , 20 h	<b>8b</b> (59%)
4	<b>5b</b> <sup>e</sup>	h $\nu$ , 20 h	<b>8b</b> (47%)
5	<b>5b</b>	$\Delta$ , 22 h	<b>8b</b> (34%)
6	<b>5c</b>	h $\nu$ , 22 h	<b>8c</b> (73%)
7	<b>5c</b> <sup>e</sup>	$\Delta$ , 22 h	<b>8c</b> (59%)
8	<b>5d</b>	h $\nu$ , 23.5 h	<b>8d</b> (<44%) <sup>f</sup>
9	<b>5d</b>	$\Delta$ , 23.5 h	<b>8d</b> (<56%) <sup>f</sup>
10	<b>5e</b>	h $\nu$ , 24 h	<b>8e</b> (87%)
11	<b>5e</b>	$\Delta$ , 5.5 h	<b>8e</b> (57%)
12	<b>5f</b>	h $\nu$ , 24 h	<b>8f</b> (15%)
13	<b>5f</b>	$\Delta$ , 21 h	<b>8f</b> (47%)
14	<b>5g</b>	h $\nu$ , 24 h	<b>8g</b> (31%)
15	<b>5g</b>	$\Delta$ , 24 h	<b>8g</b> (20%)
16	<b>5h</b>	h $\nu$ , 24 h	<b>8h</b> (54%)
17	<b>5h</b>	$\Delta$ , 24 h	<b>8h</b> (53%)
18	<b>5h</b> <sup>g</sup>	$\Delta$ , 24 h	<b>8h</b> (86%)

<sup>a</sup> Isolated complexes, prepared by addition of the appropriate alkylolithium to a slurry of  $\text{Cr}(\text{CO})_6$  in diethyl ether followed by addition of  $\text{NMe}_4\text{Cl}$ , were used. <sup>b</sup> A 10% excess of 3-buten-2-one in THF was used unless otherwise stated. <sup>c</sup> Yield refers to pure isolated compounds. <sup>d</sup> Reference **5a**. <sup>e</sup> A 5-fold excess of 3-buten-2-one was used. <sup>f</sup> Contains minor amounts of unidentified byproducts. <sup>g</sup> A 10-fold excess of 3-buten-2-one was used. <sup>h</sup> EtOAc was used as solvent.

product isolated and characterized was the expected Michael adduct **8b**, albeit in a somewhat lower yield compared to standard conditions. Several other products were observed by <sup>1</sup>H NMR and GC-MS, none of

(8) For a mechanistic discussion, see ref 5a.

(9) Ager, D. J. In *Unpoled Synthons*; Hase, T. A., Ed.; Wiley Interscience: New York, 1987; p 19.



which could be purified or properly characterized. The less satisfying yield is probably caused by formation of oligomeric and/or polymeric material, evident from the substantial amount of insoluble material left in the reaction flask upon workup.

The reaction appears to be quite sensitive to electronic effects which was manifested in a substantial reduction in chemical yield for a series of aryl-substituted complexes (entries 10–15). In contrast to the parent phenyl-substituted complex **5e**, the more electron-rich 4-methylphenyl- and 4-methoxyphenyl-substituted complexes **5f** and **5g** gave a low yield of products. The reason for this reduction in yield is unclear.

Finally, somewhat in contradiction to the previously examined complexes, reaction of the cyclopropyl complex **5h** required a large excess of 3-buten-2-one (10 equiv) to give a satisfactory yield. Only very minute amounts of product were obtained using equimolar amounts of complex and alkene. For the reaction of **5h**, ethyl acetate was found to be a superior solvent compared to THF, and an 86% isolated yield of **8h** was obtained (entry 16). Although **8h** appeared to be spectroscopically pure, a satisfactory elemental analysis could not be obtained.

In addition to the reactions with 3-buten-2-one, treatment of a few selected chromium complexes with meth-

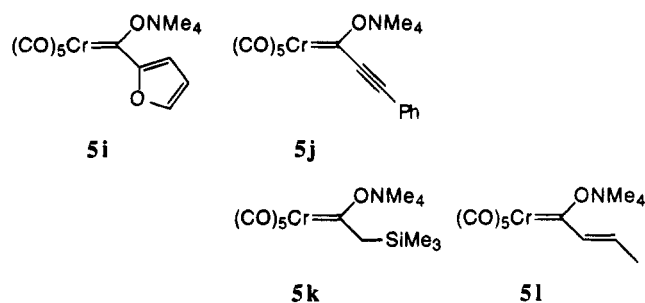


**Figure 1.**

yl, acrylate, methyl crotonate, and methyl methacrylate was briefly examined.<sup>10</sup> Thus, reaction of the *n*-butyl-substituted complex **5b** with methyl acrylate under both thermal and photochemical conditions gave the expected product **9** (Scheme 4).

A formal double Michael addition adduct **11** was isolated as the major product from either thermal or photochemical reaction of the phenyl-substituted complex **5e** with methyl acrylate (Scheme 5). In addition to **11**, a small amount of the 1:1 adduct **10** was isolated. Although commonly isolated as major products from reactions of the more reactive lithium pentacarbonyl[1-oxidoethylidene]chromate(0) salt with Michael acceptors, the formation of a 1:2 adduct has previously not been observed under photolytic reaction conditions using the corresponding tetramethylammonium salts. It should be noted that this formal double Michael addition has, to our knowledge, not been observed using "neutral" Fischer carbene complexes such as **1**. Reaction of the more sterically demanding Michael acceptors methyl crotonate and methyl methacrylate with **5e** again gave only 1:1 adducts in moderate yield (Scheme 6).

Some limitations to the reaction of these anionic Fischer carbene chromium complexes with Michael acceptors under the conditions described above have been identified. In contrast to the phenyl-substituted complexes **5e–g**, treatment of 3-buten-2-one with tetramethylammonium pentacarbonyl[2-(2-furyl)-1-oxido-methylidene]chromate(0) (**5i**) did not give any isolable products under either thermal or photochemical conditions. The starting material was completely consumed upon reaction of **5i** with 3-buten-2-one producing a complex mixture of unidentified products. Similar results were obtained from reaction of tetramethylammonium pentacarbonyl[3-phenyl-1-oxido-2-propynylidene]chromate(0) (**5j**) and tetramethylammonium pentacarbonyl[2-(trimethylsilyl)-1-oxidoethylidene]chromate(0) (**5k**) with 3-buten-2-one and tetramethylammonium pentacarbonyl[*trans*-1-oxido-2-butenylidene]chromate(0) (**5l**) with methyl crotonate (Figure 1).

In conclusion, transfer of an acyl group to electron-deficient alkenes is not restricted to the previously examined tetramethylammonium pentacarbonyl[1-oxidoethylidene]chromate(0) complex. Fair to good yields of 1,4-dicarbonyl compounds, formal Michael reaction adducts, can be isolated upon reaction of alkyl- and aryl-substituted tetramethylammonium pentacarbonyl[1-oxidoethylidene]chromate(0) with Michael acceptors under mild reaction conditions. For the synthesis of a given target molecule, the choice of reaction conditions (thermal or photochemical) is apparently not straight-

(10) For similar reactions of **5a** with methyl acrylate and methyl methacrylate, see ref 5a.

forward. Both conditions should probably be examined since the thermal stability of a given carbene, the electronics of the carbene, the rate of oligomerization/polymerization of the alkene, and further side reactions of the formed 1,4-diketone all affect the outcome of the reaction.

## Experimental Section

**General Procedures.** The tetramethylammonium pentacarbonyl[1-oxidoalkylidene]chromate(0) complexes were prepared according to literature procedures: tetramethylammonium pentacarbonyl[1-oxidoethylidene]chromate(0) (**5a**),<sup>11</sup> tetramethylammonium pentacarbonyl[1-oxidopentylidene]chromate(0) (**5b**),<sup>12</sup> tetramethylammonium pentacarbonyl[2-methyl-1-oxidobutylidene]chromate(0) (**5c**),<sup>13</sup> tetramethylammonium pentacarbonyl[2,2-dimethyl-1-oxidopropylidene]chromate(0) (**5d**),<sup>14</sup> tetramethylammonium pentacarbonyl[1-oxido-2-phenylmethylidene]chromate(0) (**5e**),<sup>11</sup> tetramethylammonium pentacarbonyl[1-oxido-1-(4-methoxyphenyl)methylidene]chromate(0) (**5f**),<sup>15</sup> tetramethylammonium pentacarbonyl[1-oxido-1-(4-methylphenyl)methylidene]chromate(0) (**5g**),<sup>16</sup> tetramethylammonium pentacarbonyl[1-cyclopropyl-1-oxido-methylidene]chromate(0) (**5h**),<sup>17</sup> tetramethylammonium pentacarbonyl[2-(2-furyl)methylidene]chromate(0) (**5i**),<sup>18</sup> tetramethylammonium pentacarbonyl[3-phenyl-1-oxido-2-propynylidene]chromate(0) (**5j**),<sup>19</sup> tetramethylammonium pentacarbonyl[1-oxido-2-(trimethylsilyl)ethylidene]chromate(0) (**5k**),<sup>16</sup> and tetramethylammonium pentacarbonyl[*trans*-1-oxido-2-butenylidene]chromate(0) (**5l**).<sup>20</sup>

Tetrahydrofuran (THF) was distilled from sodium benzophenone ketyl prior to use. All other chemicals used herein were obtained from commercial sources and used as received. All reactions were performed under a nitrogen atmosphere in oven-dried glassware.

NMR spectra were recorded in CDCl<sub>3</sub> at 90 MHz (<sup>1</sup>H) and 22.5 MHz (<sup>13</sup>C) using tetramethylsilane (<sup>1</sup>H, 0.00 ppm) or CDCl<sub>3</sub> (<sup>13</sup>C, 77.00 ppm) as internal standards. <sup>1</sup>H-<sup>1</sup>H coupling constants are reported as calculated from spectra; thus a slight difference between *J*<sub>a,b</sub> and *J*<sub>b,a</sub> is usually obtained. All melting points are uncorrected. Elemental analyses were performed by Atlantic Microlab Inc., Norcross, GA.

**Photolytic Conditions.** Nitrogen gas was bubbled through a solution of tetramethylammonium pentacarbonyl(1-oxidoalkylidene)chromate(0) salt in THF (0.10–0.20 M), in a threaded ACE pressure tube, for 5 min. The alkene was added via syringe; the reaction vessel was capped with a Teflon screw cap, and the mixture was irradiated (450-W Conrad-Hanovia 7825 medium-pressure mercury lamp, Pyrex well) for 20–36 h. The crude brown-green reaction mixture was filtered through a Celite pad (0.5 cm), and the pad was washed with THF. The solvent was removed on a rotary evaporator, and the solid residue was purified by short-path distillation or chromatography on silica gel. In some cases, the solid crude residue was dissolved in hexanes–EtOAc (1:1) and air oxidized

(sunlight) to remove any complex-bound chromium. The resulting clear solution containing a green-brown precipitate was filtered through a Celite pad (0.5 cm), and the pad was washed with hexanes–EtOAc (1:1). Solvent removal (rotary evaporator) and chromatography on silica gel afford the desired product.

**Thermal Conditions.** A solution of tetramethylammonium pentacarbonyl(1-oxidoalkylidene)chromate(0) salt in THF (0.033–0.15 M) in an airless flask equipped with a reflux condenser was flushed with N<sub>2</sub> for 5 min. The alkene was added via syringe, and the reaction mixture was heated at 75 °C (external bath temperature). The crude brown-green reaction slurry was filtered through a Celite pad (0.5 cm), and the pad was washed with THF. The solvent was removed on a rotary evaporator at water aspirator pressure, and the crude semisolid residue was purified by short-path distillation or chromatography on silica gel.

**2,5-Hexanedione (8a).** Irradiation of a solution of **5a** (618 mg, 2.00 mmol) and 3-buten-2-one (175 μL, 2.10 mmol) in 20 mL of THF for 36 h followed by air oxidation (sunlight, 45 min) gave, after filtration and solvent removal, **8a** (171 mg, 1.50 mmol, 75%) as a colorless oil. No further purification was necessary. Spectral data were in complete accordance with literature values.<sup>21</sup>

Thermolysis of a solution of **5a** (309 mg, 1.00 mmol) and 3-buten-2-one (92 μL, 1.10 mmol) in 10 mL of THF for 24 h followed by air oxidation (sunlight, 1 h) and chromatographical workup using hexanes–EtOAc (1:1) gave **8a** (88 mg, 0.77 mmol, 77%) as a colorless oil.

**2,5-Nonanedione (8a).** Irradiation of a solution of **5b** (702 mg, 2.00 mmol) and 3-buten-2-one (183 μL, 2.20 mmol) in 20 mL of THF for 20 h followed by filtration, solvent removal, and short-path distillation gave **8b** (184 mg, 1.18 mmol, 59%) as a colorless oil. Spectral data were in complete accordance with literature values.<sup>22</sup> Using a 5-fold excess of 3-buten-2-one under the same reaction conditions gave 47% of **8b** together with several unidentified products.

Thermolysis of a solution of **5b** (702 mg, 2.00 mmol) and 3-buten-2-one (183 μL, 2.20 mmol) in 20 mL of THF for 22 h followed by filtration, solvent removal, and short-path distillation gave **8b** (107 mg, 0.69 mmol, 34%) as a colorless oil.

**6-Methyl-2,4-octanedione (8c).** Irradiation of a solution of **5c** (355 mg, 1.01 mmol) and 3-buten-2-one (92 μL, 1.10 mmol) in 10 mL of THF for 24 h followed by filtration, solvent removal, and chromatography using hexanes–EtOAc (1:1) gave **8c** (115 mg, 0.74 mmol, 73%) as a colorless oil. Spectral data were in complete accordance with literature values.<sup>22</sup>

Thermolysis of a solution of **5c** (357 mg, 1.02 mmol) and 3-buten-2-one (92 μL, 1.10 mmol) in 10 mL of THF for 24 h followed by filtration, solvent removal, and chromatography using hexanes–EtOAc (1:1) gave **8c** (94 mg, 0.60 mmol, 59%) as a colorless oil.

**6,6-Dimethyl-2,5-heptanedione (8d).** Irradiation of a solution of **5d** (351 mg, 1.00 mmol) and 3-buten-2-one (92 μL, 1.10 mmol) in 10 mL of THF for 23 h followed by filtration, solvent removal, and short-path distillation gave **8d** (73 mg, 0.49 mmol, 49%) as a colorless oil. The product contains a small amount of impurity that could not be removed by distillation or chromatography. Spectral data of the major product were in complete accordance with literature values.<sup>6</sup>

Thermolysis of a solution of **5d** (351 mg, 1.00 mmol) and 3-buten-2-one (92 μL, 1.10 mmol) in 10 mL of THF for 23 h followed by filtration, solvent removal, and short-path distillation gave **8d** (88 mg, 0.56 mmol, 56%) as a colorless oil. The product contains a small amount of impurities that could not be removed.

**1-Phenyl-1,4-butanedione (8e).** Irradiation of a solution of **5e** (776 mg, 2.03 mmol) and 3-buten-2-one (186 μL, 2.20 mmol) in 10 mL of THF for 24 h followed by filtration, solvent removal, and air oxidation gave a yellow oil with a white

(11) Fischer, E. O.; Maasböl, A. *Chem. Ber.* **1967**, *100*, 2445.

(12) Thompson, D. K.; Suzuki, N.; Hegedus, L. D.; Satoh, Y. *J. Org. Chem.* **1992**, *57*, 1461.

(13) From chromium hexacarbonyl and *sec*-butyllithium followed by treatment of the intermediate lithium complex with tetramethylammonium chloride as described by Fischer and Maasböl in ref. 11.

(14) Murray, C. K.; Warner, B. P.; Dragisich, V.; Wulff, W. D. *Organometallics* **1990**, *9*, 3142.

(15) Vernier, J.-M.; Hegedus, L. S.; Miller, D. B. *J. Org. Chem.* **1992**, *57*, 6914.

(16) Fischer, E. O.; Selmayr, T.; Kreissl, F. R. *Chem. Ber.* **1977**, *110*, 2947.

(17) Connor, J. A.; Jones, E. M. *J. Organomet. Chem.* **1973**, *60*, 77.

(18) Connor, J. A.; Jones, E. M. *J. Chem. Soc.* **1971**, 1974.

(19) From chromium hexacarbonyl and lithium 2-phenylacetylde followed by treatment of the intermediate lithium complex with tetramethylammonium chloride as described by Fischer and Maasböl in ref. 11. See also: Duetsch, M.; Stein, F.; Lackmann, R.; Pohl, E.; Herbst-Irmer, R.; de Meijere, A. *Chem. Ber.* **1992**, *125*, 2051.

(20) Montgomery, J.; Wieber, G. M.; Hegedus, L. S. *J. Am. Chem. Soc.* **1990**, *112*, 6255.

(21) Monte, W. T.; Baizer, M. M.; Little, R. D. *J. Org. Chem.* **1983**, *48*, 803.

(22) Wijkens, P.; Vermeer, P. *J. Organomet. Chem.* **1986**, *301*, 247.

precipitate. The oil was purified by chromatography using hexanes–EtOAc (9:1) as eluent affording **8e** (311 mg, 1.77 mmol, 87%) as a colorless oil. Spectral data were in complete accordance with literature values.<sup>2c,23</sup>

Thermolysis of a solution of **5e** (1.855 g, 5.00 mmol) and 3-buten-2-one (625  $\mu$ L, 7.50 mmol) in 50 mL of THF for 5.5 h followed by filtration and solvent removal gave a green oil with a white precipitate. The oil was air oxidized (sunlight) for 1 h and refiltered followed by chromatographical workup using a sequence of hexanes–EtOAc mixtures (9:1; 8:2; 1:1) producing **8e** (498 mg, 2.83 mmol, 57%) as a colorless oil.

**1-(4-Methoxyphenyl)-1,4-butanedione (8f)**. Irradiation of a solution of **5f** (870 mg, 2.13 mmol) and 3-buten-2-one (183  $\mu$ L, 2.20 mmol) in 20 mL of THF for 24 h followed by filtration and solvent removal gave a green oil with a white precipitate. The oil was purified by chromatography using first hexanes–EtOAc (9:1) and then hexanes–EtOAc (8:2) affording **8f** (66 mg, 0.32 mmol, 15%) as colorless needles. Spectral data were in complete accordance with literature values.<sup>24</sup>

Thermolysis of a solution of **5f** (263 mg, 0.64 mmol) and 3-buten-2-one (64  $\mu$ L, 0.84 mmol) in 10 mL of THF for 16.5 h followed by filtration and solvent removal gave a green oil with a white precipitate. The oil was purified by chromatography using hexanes–EtOAc (8:2) giving **8f** (63 mg, 0.31 mmol, 47%) as colorless needles.

**1-(4-Methylphenyl)-1,4-butanedione (8g)**. Irradiation of a solution of **5g** (225 mg, 0.58 mmol) and 3-buten-2-one (55  $\mu$ L, 0.66 mmol) in 10 mL of THF for 24 h followed by filtration and solvent removal gave a green oil with a white precipitate. The oil was purified by chromatography using first hexanes–EtOAc (8:2) and then hexanes–EtOAc (8:2) affording **8g** (34 mg, 0.17 mmol, 31%) as a colorless oil. Spectral data were in complete accordance with literature values.<sup>25</sup>

Thermolysis of a solution of **5g** (213 mg, 0.55 mmol) and 3-buten-2-one (55  $\mu$ L, 0.66 mmol) in 10 mL of THF for 16.5 h followed by filtration and solvent removal gave a green oil with a white precipitate. The oil was purified by chromatography using hexanes–EtOAc (8:2) giving **8g** (21 mg, 0.11 mmol, 20%) as a colorless oil.

**5-Cyclopropyl-2,5-pentadione (8h)**. Irradiation of a solution of **5h** (340 mg, 1.01 mmol) and 3-buten-2-one (916  $\mu$ L, 11.0 mmol) in 10 mL of THF for 24 h followed by filtration and solvent removal gave a yellow oil with a white precipitate. The crude product was purified by chromatography using hexanes–EtOAc (1:1) as eluent affording **8h** (76 mg, 0.54 mmol, 54%) as a colorless oil.

Thermolysis of a solution of **5h** (336 mg, 1.00 mmol) and 3-buten-2-one (916  $\mu$ L, 11.0 mmol) in 10 mL of EtOAc for 24 h followed by filtration and solvent removal gave a green oil with a white precipitate. The oil was purified by chromatography using hexanes–EtOAc (8:2) as eluent producing **8h** (112 mg, 0.86 mmol, 86%) as a colorless oil. Similar thermolysis (70 °C) of a solution of **5h** (362 mg, 1.08 mmol) and 3-buten-2-one (916  $\mu$ L, 11.0 mmol) in 10 mL of THF for 24 h gave, after purification, **8h** (78 mg, 0.56 mmol, 52%) as a colorless oil: IR (film) 3000, 2920, 2860, 1685, 1380, 1100, 1080, 1020  $\text{cm}^{-1}$ ; <sup>1</sup>H NMR  $\delta$  2.9–2.6 (m, 4H), 2.19 (s, 3H, Me), 1.96 (m, 1H), 1.4–0.8 (m, 4H); <sup>13</sup>C NMR  $\delta$  209.1 (s), 207.2 (s), 36.8 (t), 36.6 (t), 29.9 (q), 20.5 (d), 10.7 (t, 2C); HRMS (CI, CH<sub>4</sub>) exact mass calcd for C<sub>8</sub>H<sub>13</sub>O<sub>2</sub> (M + 1) *m/z* 141.0916, obsd *m/z* 141.0919.

**4-Oxo-octanoic Acid Methyl Ester (9)**. Irradiation of a solution of **5b** (695 mg, 1.98 mmol) and methyl acrylate (198  $\mu$ L, 2.20 mmol) in 20 mL of THF for 24 h followed by filtration and solvent removal gave a green oil with a white precipitate. The oil was purified by chromatography using hexanes–EtOAc

(19:1) affording **9** (237 mg, 1.38 mmol, 70%) as a colorless oil. Spectral data were in complete accordance with literature values.<sup>26</sup>

Thermolysis of a solution of **5b** (698 mg, 1.98 mmol) and methyl acrylate (198  $\mu$ L, 2.20 mmol) in 20 mL of THF for 21 h followed by filtration and solvent removal gave a green oil with a white precipitate. The oil was purified by chromatography using hexanes–EtOAc (19:1) affording **9** (207 mg, 1.20 mmol, 61%) as a colorless oil.

**$\gamma$ -Oxobenzenebutanoic Acid Methyl Ester (10) and 2-(2-Phenyl-2-oxoethyl)pentanoic Acid Dimethyl Ester (11)**. Irradiation of a solution of **5e** (742 mg, 2.00 mmol) and methyl acrylate (360  $\mu$ L, 4.00 mmol) in 15 mL of THF for 24 h followed by filtration, solvent removal, and air oxidation gave a yellow oil with a white precipitate. The oil was purified by chromatography using hexanes–EtOAc (8:2) affording in order of elution **10** (59 mg, 0.31 mmol, 15%) and **11** (90 mg, 0.32 mmol, 16%) both as colorless oils.

Thermolysis of a solution of **5e** (742 mg, 2.00 mmol) and methyl acrylate (216  $\mu$ L, 2.40 mmol) in 15 mL of THF for 24 h followed by filtration, solvent removal, and air oxidation gave a yellow oil with a white precipitate. The oil was purified by chromatography using hexanes–EtOAc (8:2) affording in order of elution **10** (55 mg, 0.29 mmol, 14%) and **11** (243 mg, 0.87 mmol, 73%)<sup>27</sup> both as colorless oils. Spectral data were in complete accordance with literature values.<sup>28</sup> Spectral data for **11**: IR (film) 2940, 1715, 1665, 1430, 1175, 700  $\text{cm}^{-1}$ ; <sup>1</sup>H NMR  $\delta$  8.02 (dd, *J* = 7.5 and 2.1 Hz, 2H), 7.55 (m, 3H), 4.03 (m, 1H), 3.64 (s, 3H), 3.63 (s, 3H), 2.96 (dd, *J* = 16.8 and 8.7 Hz, 1H), 2.48 (dd, *J* = 16.9 and 5.4 Hz, 1H), 2.4–1.7 (m, 4H); <sup>13</sup>C NMR  $\delta$  202.0 (s), 173.0 (s), 172.4 (s), 136.3 (s), 133.3 (d), 128.7 (d, 2C), 128.4 (d, 2C), 51.8 (q), 51.6 (q), 40.5 (d), 35.4 (t), 31.0 (t), 27.1 (t). Anal. Calcd for C<sub>15</sub>H<sub>18</sub>O<sub>5</sub>: C, 64.73; H, 6.52. Found: C, 64.59; H, 6.58.

**$\gamma$ -Oxo- $\beta$ -methylbenzenebutanoic Acid Methyl Ester (12)**. Thermolysis of a solution of **5e** (1.13 g, 3.04 mmol) and methyl crotonate (636  $\mu$ L, 6.00 mmol) in 25 mL of THF for 19 h followed by filtration, solvent removal, and chromatography using hexanes–EtOAc (8:2) gave **12** (302 mg, 1.49 mmol, 49%) as a colorless oil. Spectral data were in complete accordance with literature values.<sup>29</sup>

Irradiation of a solution of **5e** (742 mg, 2.00 mmol) and methyl acrylate (360  $\mu$ L, 4.00 mmol) in 15 mL of THF for 23 h followed by filtration, solvent removal, and air oxidation gave a yellow oil with a white precipitate. The oil was purified by chromatography using hexanes–EtOAc (8:2), which gave **12** (59 mg, 0.31 mmol, 15%) as a colorless oil.

**$\gamma$ -Oxo- $\alpha$ -methylbenzenebutanoic Acid Methyl Ester (13)**. Thermolysis of a solution of **5e** (1.13 g, 3.04 mmol) and methyl methacrylate (641  $\mu$ L, 6.00 mmol) in 45 mL of THF for 20 h followed by filtration, solvent removal, and chromatography using hexanes–EtOAc (8:2) gave **13** (141 mg, 0.68 mmol, 22%) as a colorless oil. Spectral data were in complete accordance with literature values.<sup>30</sup>

**Acknowledgment.** Financial support for this research was obtained from the donors of the Petroleum Research Fund, administered by the American Chemical Society (PRF-ACS 24675-B1).

OM950216N

(26) Negishi, E.-I.; Chiu, K.-W.; Yoshida, T. *J. Org. Chem.* **1975**, *40*, 1676.

(27) The yield of **11** is based on methyl acrylate.

(28) Hegedus, L. S.; Darlington, W. H. *J. Am. Chem. Soc.* **1980**, *102*, 4980.

(29) Gajewski, J. J.; Conrad, N. D. *J. Am. Chem. Soc.* **1979**, *101*, 6693.

(30) Nakamura, E.; Aoki, S.; Sekeya, K.; Oshino, H.; Kuwajima, I. *J. Am. Chem. Soc.* **1987**, *109*, 8066.

(23) Stetter, H.; Schmitz, P. H.; Schreckenberger, M. *Chem. Ber.* **1977**, *110*, 1971.

(24) (a) Severin, T.; Kullmer, H. *Chem. Ber.* **1971**, *104*, 440. (b) Severin, T.; König, D. *Chem. Ber.* **1974**, *107*, 1449.

(25) Watanabe, S.; Fujita, T.; Suga, K.; Abe, H. *J. Appl. Chem. Biotechnol.* **1977**, *27*, 117.

# Mechanisms of Pyrolysis of Tricarbonylcyclopentadienylmanganese and Tricarbonyl(methylcyclopentadienyl)manganese

Douglas K. Russell,<sup>\*,†</sup> Iain M. T. Davidson, Andrew M. Ellis, Graham P. Mills, Mark Pennington,<sup>‡</sup> Ian M. Povey, J. Barrie Raynor, Sinan Saydam, and Andrew D. Workman

Department of Chemistry, University of Leicester, University Road, Leicester LE1 7RH, U.K.

Received December 15, 1994<sup>®</sup>

The mechanisms of the gas-phase pyrolysis of tricarbonylcyclopentadienylmanganese (**1**) and tricarbonyl(methylcyclopentadienyl)manganese (**2**) have been investigated using a combination of IR laser-powered homogeneous pyrolysis, stirred flow reactor kinetic measurements, and matrix isolation ESR spectroscopy. The observations are consistent with initial stepwise loss of CO, followed ultimately by release of  $\cdot\text{C}_5\text{H}_5$  (for **1**) or  $\cdot\text{C}_5\text{H}_4\text{CH}_3$  (for **2**); the hydrocarbon radicals then abstract hydrogen from unreacted starting material. For **1**, the resultant  $\cdot\text{C}_5\text{H}_4\text{Mn}$  unit undergoes intramolecular rearrangement, yielding ethyne and a second species tentatively identified as a manganese carbide. For **2**, the more rapid abstraction from the ring  $\text{CH}_3$  group results in formation of the fulvene  $\text{CH}_2\text{C}_5\text{H}_4$  followed by isomerization to benzene. These processes lead to heavy carbon contamination of deposited Mn films unless an alternative source of H atoms for abstraction by cyclopentadienyl radicals is present.

## Introduction

Tricarbonylcyclopentadienylmanganese (cymantrene,  $(\eta^5\text{-C}_5\text{H}_5)\text{Mn}(\text{CO})_3$ , **1**) and its methyl derivative (methylcymantrene,  $(\eta^5\text{-CH}_3\text{C}_5\text{H}_4)\text{Mn}(\text{CO})_3$ , **2**) serve as archetypal  $\eta^5$ -bonded compounds with **1** being among the earliest known and best characterized  $\eta$ -bonded systems.<sup>1</sup> They are both thermally stable, relatively volatile, low-melting solids or liquids. The physical properties and chemistry of **1** and its derivatives have been extensively investigated,<sup>2</sup> with major emphasis on the bonding and reactions of the cyclopentadienyl ring system. More recently, however, there has been some interest in the pyrolytic behavior of these compounds; **2** has found some application as an antiknock agent in gasoline,<sup>2,3</sup> and both **1** and **2** have been proposed as sources for magnetic dopants in processes such as metal organic chemical vapor deposition (MOCVD), metal organic vapor phase epitaxy (MOVPE), and molecular beam epitaxy (MBE).<sup>4</sup> Little is known about the mechanistic details of the pyrolysis of **1** and **2**. A recent quadrupole mass spectrometry study of the MOVPE of **2** has suggested that decomposition proceeds *via* successive loss of CO, followed by loss of  $\cdot\text{C}_5\text{H}_4\text{CH}_3$ , and an activation energy of 236 kJ mol<sup>-1</sup> for the process was

determined.<sup>5</sup> It is well-known from our own work on both main-group<sup>6</sup> and transition-metal complexes<sup>7</sup> that the investigation of the pyrolysis of organometallic compounds is fraught with difficulties, arising largely from the competition between homogeneous and surface reaction, and that observations must be interpreted with considerable caution. On the other hand, we have also shown that the judicious use of a range of techniques, particularly that of IR laser-powered homogeneous pyrolysis (IR LPHP), can disentangle these competing effects and provide reliable results.<sup>8</sup> In the present work, we report the application of these techniques to the pyrolysis of **1** and **2**, together with a mechanism consistent with the observations; a preliminary account of these investigations, together with those of related compounds, has appeared elsewhere.<sup>9</sup>

## Experimental Section

The experimental methods employed in the present study have been described in detail elsewhere, and hence only brief summaries of the more significant aspects are provided here. Except where noted below, analytical investigations (FTIR, NMR, GC-MS, and ESR) were conducted using commercial instrumentation in conjunction with comparison with authentic samples.

**Stirred Flow Reactor (SFR) Kinetic Measurements.** The SFR consists of a spherical quartz vessel of volume 10

<sup>\*</sup> Present address: Department of Chemistry, University of Auckland, Private Bag 92019, Auckland, New Zealand.

<sup>†</sup> Present address: School of Environmental Sciences, Nene College, Moulton Park, Northampton NN2 7AL, U.K.

<sup>®</sup> Abstract published in *Advance ACS Abstracts*, June 15, 1995.

(1) Piper, T. S.; Cotton, F. A.; Wilkinson, G. *J. Inorg. Nucl. Chem.* **1966**, *1*, 165.

(2) Treichel, P. M. In *Comprehensive Organometallic Chemistry*; Wilkinson, G., Stone, F. G. A., Abel, E. W., Eds.; Pergamon Press: Oxford, U.K., 1982; Chapter 29.

(3) *Dictionary of Organometallic Compounds*; Chapman and Hall: London, 1984; Volume 1.

(4) Pain, G. N.; Christiansz, G. I.; Dickson, R. S.; Deacon, G. B.; West, B. O.; McGregor, K.; Rowe, R. S. *Polyhedron* **1990**, *9*, 921.

(5) Sang, W.; Durose, K.; Brinkman, A. W.; Woods, J. *J. Cryst. Growth* **1991**, *113*, 1.

(6) Grady, A. S.; Mapplebeck, A. L.; Russell, D. K.; Taylorson, M. G. *J. Chem. Soc., Chem. Commun.* **1990**, 929. Grady, A. S.; Markwell, R. D.; Russell, D. K. *J. Chem. Soc., Chem. Commun.* **1991**, 14. Linney, R. E.; Russell, D. K. *J. Mater. Chem.* **1993**, *3*, 587.

(7) Davidson, I. M. T.; Pennington, M.; Russell, D. K.; Saydam, S. Unpublished work.

(8) Atiya, G. A.; Grady, A. S.; Jackson, S. A.; Parker, N.; Russell, D. K. *J. Organomet. Chem.* **1989**, *378*, 307.

(9) Davidson, I. M. T.; Ellis, A. M.; Mills, G. P.; Pennington, M.; Povey, I. M.; Raynor, J. B.; Russell, D. K.; Saydam, S.; Workman, A. D. *J. Mater. Chem.* **1994**, *4*, 13.



cm<sup>3</sup>, at the center of which is either a smaller perforated bulb or a simple jet inlet, which provides rapid mixing and thermal equilibration of the reactant. The reactor is housed in a conventional furnace capable of providing temperatures up to the softening temperature of the quartz. Rather than a continuous flow, reactant diluted in a carrier gas (N<sub>2</sub> or He) is admitted in a pulse or batch mode; this method confers both technical and economic advantages. Reaction in the vessel competes with the sweeping out of reagents and products, so that a controllable proportion of conversion may be achieved. Unreacted starting material and products may be analyzed directly *via* GC-MS or accumulated in cold traps for subsequent investigation. The output of the flame ionization or thermal conductivity detector of the GC may also be fed directly into a data-capture station for kinetic or other analysis. This kind of technique has been used with considerable success in the investigation of pyrolysis mechanisms of organosilicon compounds such as Me<sub>3</sub>SiSiMe<sub>3</sub>.<sup>10</sup>

**Infrared Laser-Powered Homogeneous Pyrolysis.** The majority of qualitative and analytical investigations were carried out using the method of IR LPHP. The experimental details and advantages of this technique have been described in an extensive review by Russell,<sup>11</sup> and its use in the investigation of a wide range of Al and Ga organometallic systems has been reported.<sup>12</sup> Briefly, static pyrolysis is conducted in a cylindrical Pyrex cell (length 10 cm, diameter 3.8 cm) fitted with ZnSe windows. The correct choice of window material is central to the success of the technique; in comparison with the cheaper alkali-metal halides, ZnSe has a higher optical transmission at the critical wavelength of 10 μm and greater mechanical strength. Most importantly, however, it is not hygroscopic, a point of crucial importance in the study of highly moisture sensitive materials. The cell is filled with up to 10 Torr of the vapor of the material under study, together with 10 Torr of SF<sub>6</sub>. For compounds of moderate volatility, such as **1** and **2**, liquid or solid can be condensed into the cell; this does not alter the basic features of the IR LPHP method but may introduce volatilization as a possible rate-limiting process. The contents of the cell are exposed to the output of a free-running continuous-wave CO<sub>2</sub> IR laser at power levels of a few watts. The laser radiation is strongly absorbed by the SF<sub>6</sub> and is rapidly converted into heat *via* very efficient inter- and intramolecular relaxation. The low thermal conductivity of the SF<sub>6</sub> ensures that this process results in a highly inhomogeneous temperature profile, in which the center of the cell may be heated up to 1500 K (above which the SF<sub>6</sub> itself decomposes), but where the cell walls remain at close to room temperature.

The technique has a number of advantages. The first is that pyrolysis is initiated unambiguously in the gas phase, eliminating entirely the complications frequently introduced by competing surface reaction. The second is that the primary products of pyrolysis are ejected into cool regions of the cell, where they are not subjected to further reaction. In favorable cases, these products may be collected as less volatile liquids (or even solids) and analyzed at leisure. On the other hand, the temperature of the pyrolysis is neither well-defined nor easy to measure, so that comparisons with conventional methods of pyrolysis must be made with care. Such indications as are available through studies of systems with well-known kinetic parameters (*e.g.* CH<sub>3</sub>CO<sub>2</sub>CH<sub>3</sub>) suggest that the overall cell reaction is dominated by that at the maximum temperature. In our laboratory, reaction is monitored in the first instance by *in situ* FTIR spectroscopy; further confirmation of the identity of products, and quantitative measurements of relative yields, can be accomplished by relative condensation into external vessels followed by NMR (usually

in toluene-*d*<sub>8</sub> as solvent), GC-MS, or elemental analysis, in conjunction with comparison with authentic samples.

**Matrix Isolation ESR Spectroscopy.** In order to identify free radicals produced in pyrolysis, reagents were pumped through a conventional resistively heated hot-wall quartz tube by means of mercury diffusion and rotary pumps at pressures much less than 1 Torr. Samples for study were contained in a vessel providing for variation of source temperature and flow rate or pressure (*via* a needle valve). Pyrolysis products were condensed onto a cold finger cooled to 77 K by liquid nitrogen; the whole cold finger assembly was removable for the examination of ESR or other spectra. ESR spectra were stored digitally on a computer for subsequent manipulation. Radicals could be trapped in a matrix of unreacted starting material or of a suitable inert host material such as adamantane; the latter usually provided more easily interpretable isotropic ESR spectra but did add another variable to the experimental conditions. Matrices sufficient to provide well-resolved ESR spectra could be condensed in 5–30 min, depending on the chemical system, flow rates, and pressures. Many of the ESR spectra observed arose from two or more species; these could be distinguished by judicious variation of the experimental conditions (temperature or pressure), followed by computer subtraction. The technique has been used successfully in the detection of many free radicals in organometallic pyrolyses, such as alkyl radicals from R<sub>3</sub>M (R = Me, Et, <sup>i</sup>Pr, <sup>t</sup>Bu, <sup>n</sup>Bu; M = Al, Ga, In).<sup>13</sup>

**Chemicals.** **1** was purchased from Aldrich Chemical Co. and **2** from Johnson Matthey. CD<sub>3</sub>Mn(CO)<sub>5</sub> was synthesized by modification of the literature method for CH<sub>3</sub>Mn(CO)<sub>5</sub>.<sup>14</sup> All compounds were purified by repeated trap-to-trap distillation before use and their purities checked by NMR or GC-MS.

## Results

**SFR Kinetic Measurements.** While **2** is a liquid at room temperature (boiling point 102 °C at 10 Torr), **1** is a moderately volatile solid.<sup>3</sup> For this reason, SFR studies (which require injection of a liquid sample) were carried out for **2** only at temperatures between 250 and 450 °C. Over this range, the pyrolysis produced free CO and 1- or 2-methylcyclopentadiene as the major gas-phase products detectable in the GC-MS system, with minor amounts of CH<sub>4</sub> and C<sub>5</sub>H<sub>6</sub> at higher temperatures. Measurable reaction rates were obtained between 284 and 361 °C. Formation of methylcyclopentadiene (measured by a flame ionization detector) and of CO (measured by a thermal conductivity meter) over this range followed first-order behavior (order 1.0 ± 0.1), as shown in Figure 1 for the formation of methylcyclopentadiene. In the lower part of the temperature range (284–342 °C), the overall Arrhenius parameters were log A = 16.1 ± 1.0 and E/kJ mol<sup>-1</sup> = 210 ± 11 for the formation of methylcyclopentadiene and log A = 15.4 ± 1.3 and E/kJ mol<sup>-1</sup> = 195 ± 14 for the formation of CO. The Arrhenius plots curved upward at higher temperature, indicating mechanistic complexity. The Arrhenius plot for the formation of methylcyclopentadiene at lower temperature is shown in Figure 2.

**IR LPHP Observations.** IR laser pyrolysis of **1** or **2** alone was carried out at laser powers ranging from 1.5 to 2.0 W. As described above, temperatures in the laser pyrolysis process are not well-defined; however, independent measurements of the rate of decomposition of CH<sub>3</sub>CO<sub>2</sub>CH<sub>3</sub> indicate that these powers generate

(10) Davidson, I. M. T.; Howard, A. V. *J. Chem. Soc., Faraday Trans. 1* **1975**, *71*, 69.

(11) Russell, D. K. *Chem. Soc. Rev.* **1990**, *19*, 407.

(12) Russell, D. K. *Coord. Chem. Rev.* **1992**, *112*, 131.

(13) Mills, G. P.; Raynor, J. B.; Russell, D. K.; Workman, A. D. Unpublished work.

(14) King, R. B. *Organomet. Chem. Synth.* **1965**, *1*, 147.

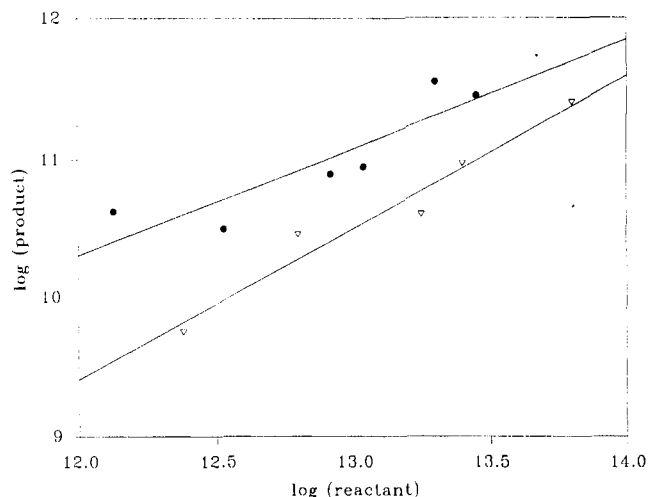


**Figure 1.** Order plot for the pyrolysis of  $\eta^5\text{-MeC}_5\text{H}_4\text{-Mn(CO)}_3$  (**2**) at 340 °C (●) and 290 °C (▽).

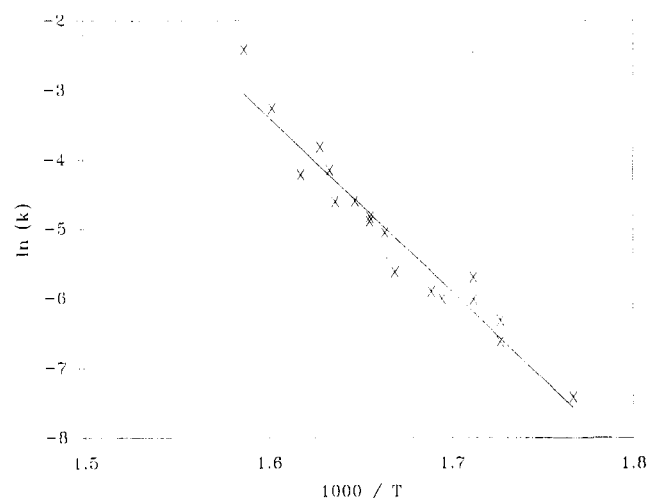


**Figure 2.** Arrhenius plot for the formation of  $\text{CH}_3\text{C}_5\text{H}_5$  from  $(\eta^5\text{-MeC}_5\text{H}_4)\text{Mn(CO)}_3$  (**2**).

maximum temperatures of between 250 and 350 °C.<sup>15</sup> For **1**, the postpyrolysis FTIR spectrum (see Figure 3) revealed substantial quantities of ethyne (sharp *Q*-branch at 729  $\text{cm}^{-1}$ ) in addition to the gas-phase products expected on the basis of the SFR results for **2**, *i.e.*, free CO (structured *P*- and *R*-branches near 2200  $\text{cm}^{-1}$ ) and cyclopentadiene (sharp *Q*-branches at 663 and 807  $\text{cm}^{-1}$ ). These identifications were confirmed by GC-MS and  $^1\text{H}$  NMR spectroscopy; the latter additionally yielded a molar ratio of close to 2:1 for  $\text{C}_2\text{H}_2$  and  $\text{C}_5\text{H}_6$ .

For **2**, the results were more complex. Although free CO and  $\text{C}_2\text{H}_2$  were again readily identified, assignment of other features in the FTIR spectrum proved less straightforward; in particular, there was little sign of the expected propyne. However, the  $^1\text{H}$  NMR spectrum clearly confirmed the production of both 1- and 2-methylcyclopentadiene (identified from the report of Mstislavsky *et al.*<sup>16</sup>) in equimolar amounts as well as much smaller amounts of  $\text{C}_2\text{H}_2$ , and also substantial quantities of benzene in the majority of experiments. Unfortunately, the resonances of both the methyl and alkynyl protons in  $\text{CH}_3\text{C}\equiv\text{CH}$  are coincidentally overlapped by

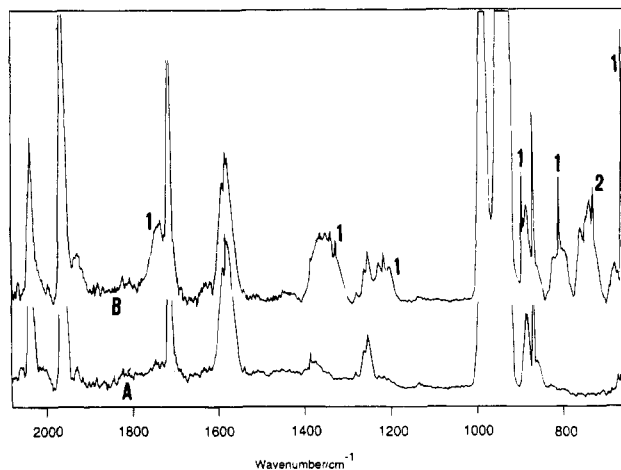


**Figure 3.** FTIR spectra of a mixture of 10 Torr of  $\text{SF}_6$  and the vapor pressure of  $\eta^5\text{-C}_5\text{H}_5\text{Mn(CO)}_3$  (**1**): (A) before pyrolysis; (B) after exposure to 1.5 W  $\text{CO}_2$  IR laser power for 5 min. Features identified arise (1) from  $\text{C}_5\text{H}_6$ , and (2) from  $\text{C}_2\text{H}_2$ ; unidentified features arise from starting material or  $\text{SF}_6$ .

those of  $\text{C}_2\text{H}_2$ , and  $^1\text{H}$  NMR cannot, therefore, be used to determine the proportion (if any) of propyne.

In order to provide further insight into the mechanism, **1** was copyrolyzed with perdeuterated pentacarbonylmethylmanganese ( $\text{CD}_3\text{Mn(CO)}_5$ , **3**). It is known from our previous work<sup>17</sup> that pyrolysis of **3** alone occurs at a temperature significantly lower (laser powers of 0.5 W) than that required for **1** or **2**, that the pyrolysis is initiated by homolysis of the  $\text{CD}_3\text{-Mn}$  bond, and that reaction proceeds *via* a free-radical process; the only significant hydrocarbon product is  $\text{CD}_4$ . Laser copyrolysis of a 1:1 mixture of **1** and **3** at a power of 0.6 W (*i.e.*, insufficient to initiate reaction of **1** alone) resulted in  $\text{CD}_3\text{H}$  (sharp *Q*-branches at 1036 and 2991  $\text{cm}^{-1}$ ) and  $\text{C}_2\text{H}_2$  as the only hydrocarbon products; significantly, neither the FTIR nor the  $^1\text{H}$  NMR spectra indicated the formation of  $\text{C}_5\text{H}_6$  or  $\text{CD}_4$ . At greater proportions of **3**, some  $\text{CD}_4$  was evident; at higher powers, variable quantities of  $\text{C}_5\text{H}_6$  could also be generated.

**Matrix Isolation ESR Results.** Matrix isolation ESR spectra were observed for pyrolysis temperatures between 250 and 400 °C. For both **1** and **2**, the appearance of the spectra depended on the precise conditions of pyrolysis temperature, flow rate, and pressure (*i.e.*, sample source temperature). Figure 4 illustrates spectra produced by pyrolysis of **1** at two different temperatures; Figure 5 illustrates spectra obtained by subtraction at different ratios of spectra similar to those of Figure 4 produced by pyrolysis of **2**.

It is very evident that the ESR spectra arising from pyrolysis of both **1** and **2** contain two major components, one isotropic and the other highly anisotropic. For **1**, the isotropic 1:5:10:10:5:1 sextet is readily identifiable as the  $\text{C}_5\text{H}_5$  radical;<sup>18</sup> for **2**, the isotropic component arises from more than one species and is discussed in detail below. The anisotropic component is very similar in the two spectra, the only discernible difference being that the low-field feature appears as a doublet in some spectra arising from **1** (as is evident in Figure 4).

(17) Davidson, I. M. T.; Mills, G. P.; Pennington, M.; Raynor, J. B.; Russell, D. K.; Saydam, S.; Workman, A. D. Unpublished work.

(18) Kira, M.; Watanabe, M.; Sakurai, H. *J. Am. Chem. Soc.* **1980**, *102*, 5202.

(15) Atiya, G. A. Ph.D. Thesis, University of Leicester, 1991.

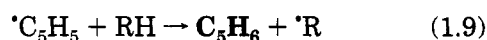
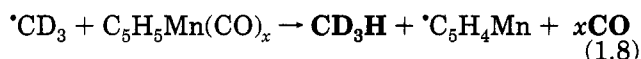
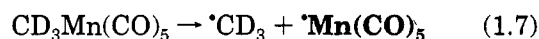
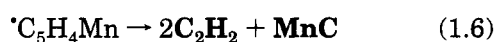
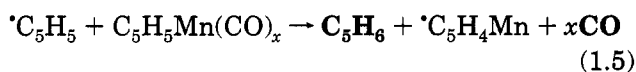
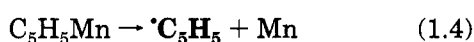
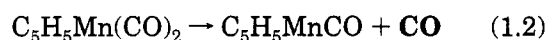
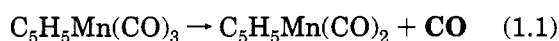
(16) Mstislavsky, V. I.; Korenevsky, V. A.; Sergeev, N. M.; Solkan, V. N. *Org. Magn. Reson.* **1976**, *8*, 368.

For comparison with the IR LPHP work, a copolyolysis of **1** and **3** was conducted at 220 °C, at which temperature pyrolysis of neither **1** nor **3** alone produced observable ESR spectra. This copolyolysis resulted in an ESR spectrum identical with the anisotropic component of Figure 4, with no trace of the isotropic contribution of the  $\cdot\text{C}_5\text{H}_5$  radical.

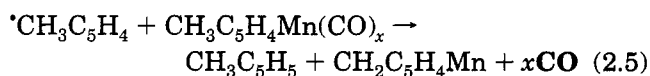
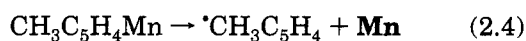
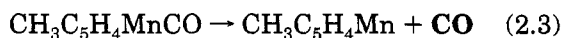
### Discussion and Conclusions

It is apparent that the overall mechanisms of pyrolysis of both **1** and **2** are complex; while the relatively high Arrhenius parameters for **2** indicate that the reactions are mainly homogeneous in the SFR system, there is little doubt that there will always be some contribution from surface reactions in pyrolyses of this type. However, all the observations for both **1** and **2** can be accommodated by the homogeneous reaction sequences shown in Schemes 1 and 2, where observed species are highlighted.

#### Scheme 1



#### Scheme 2



In contrast with the LPHP observations, in the SFR experiments on **2** no  $\text{C}_2\text{H}_2$  or  $\text{C}_6\text{H}_6$  is observed; this could

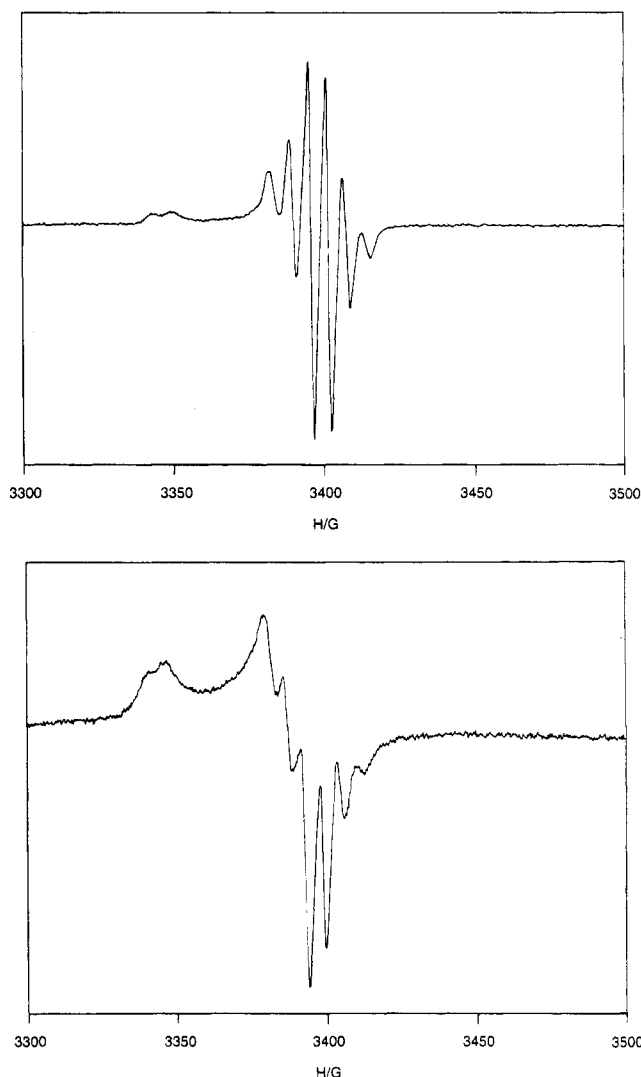


**Figure 4.** ESR spectra of the matrix-isolated products of pyrolysis of  $(\eta^5\text{-C}_5\text{H}_5)\text{Mn}(\text{CO})_3$  (**1**): (A, top) at 310 °C; (B, bottom) at 365 °C.

have been a result of a lower effective temperature in the SFR system, but it was more likely because the experiments were carried out at much lower pressures of **2**, thus reducing the competitiveness of the sequence (2.5) and (2.6) relative to (2.4). Furthermore, the extent of decomposition is sufficiently small in the SFR experiments that CO reassociation (the reverse of reactions 2.1–2.3) is likely to be insignificant. Consequently, the kinetic experiments for **2** could be described by a simplified mechanism consisting of (2.1)–(2.4), followed by any hydrogen abstraction process converting the  $\text{CH}_3\text{C}_5\text{H}_4$  radical to the observed  $\text{CH}_3\text{C}_5\text{H}_5$ .

This simplified scheme is broadly consistent with that proposed in the MOVPE study,<sup>5</sup> with initial loss of CO in reactions 2.1–2.3 being followed by slower dissociation of the Mn– $\text{C}_5\text{H}_4\text{CH}_3$  bond (reaction 2.4), but we can take the kinetic analysis further. In the work under MOVPE conditions, approximate kinetic measurements were made mass spectrometrically by following the decay of the  $(\text{MnC}_5\text{H}_4\text{CH}_3)^+$  ion. This measurement was complicated by fragmentation within the ionization chamber of the mass spectrometer, since it is well-known that the dominant species in the mass spectrum

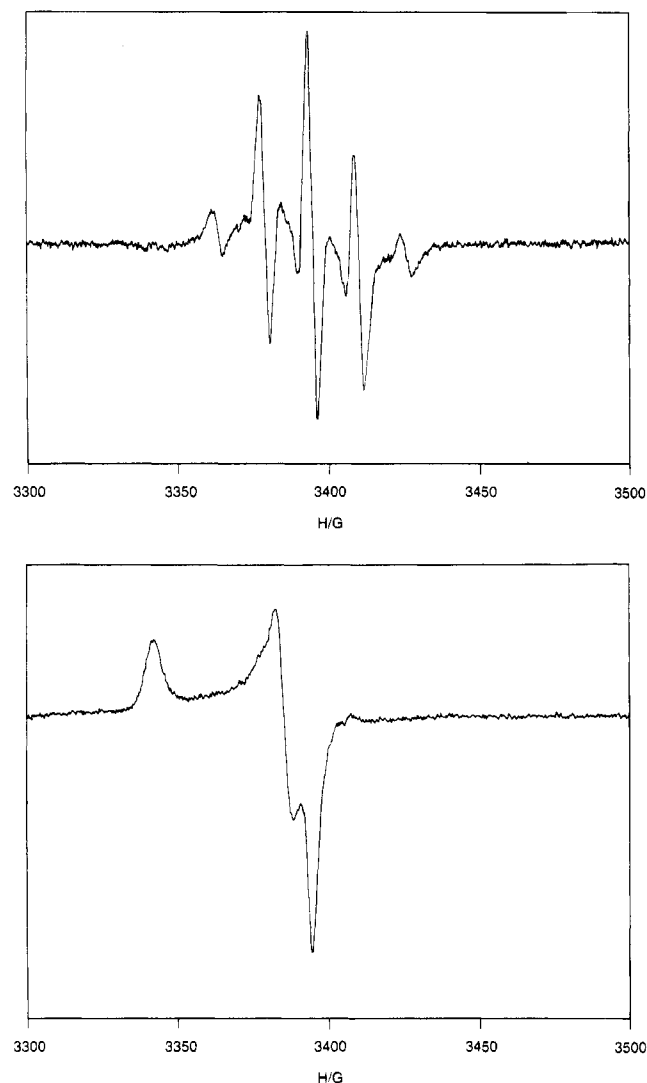


**Figure 5.** ESR spectra of the matrix-isolated products of pyrolysis of  $(\eta^5\text{-MeC}_5\text{H}_4)\text{Mn}(\text{CO})_3$  (**2**) at two different temperatures, computer subtracted to separate the isotropic (A, top) and anisotropic (B, bottom) contributions.

of the parent compound **1** is the  $(\text{MnC}_5\text{H}_5)^+$  ion.<sup>19</sup> In our system, this complication is avoided by the use of GC-MS, and we had the further advantage that the SFR technique allows separate measurement of the kinetics of formation of all stable products, CO and  $\text{CH}_3\text{C}_5\text{H}_5$  in this case.

The pyrolysis mechanism is complex, as indicated by the curvature of the Arrhenius plots observed in this work. It was undoubtedly even more complex in the MOVPE study,<sup>5</sup> especially as that pyrolysis was taken to much higher conversion than was our work, with rate constants as high as  $0.8 \text{ s}^{-1}$ . In these circumstances, with extensive secondary reactions, it is not appropriate to identify a single rate-determining step; the mechanism has to be considered as a whole. This we have done by analyzing the simplified scheme by numerical integration using the KINAL package.<sup>20</sup> This analysis requires Arrhenius parameters for the individual reactions; the estimation of A factors for reactions 2.1–2.4 is straightforward using published data,<sup>21</sup> but that of activation energies is much less so.

**Table 1.** Estimated Arrhenius Parameters for Scheme 2

reacn	log A <sup>a</sup>	E/kJ mol <sup>-1</sup>
2.1	15.5	205 <sup>b</sup>
2.2	15.5	150
2.3	15.5	150
2.4	14.5	150
2.5	8.0	40

<sup>a</sup> A factors in  $\text{s}^{-1}$  for first-order reactions and  $\text{dm}^3 \text{ mol}^{-1} \text{ s}^{-1}$  for second-order reactions. <sup>b</sup> Uncertainty in E is  $\pm 10 \text{ kJ mol}^{-1}$  for (2.1) and (2.4) and larger for (2.2) and (2.3) (these ranges reproduce observed rate constants to within a factor of 2).

Sang and co-workers<sup>5</sup> quote  $97.5$  and  $256.6 \text{ kJ mol}^{-1}$ , respectively, for the Mn–CO and Mn– $\text{C}_5\text{H}_4\text{CH}_3$  bond strengths; they associated the activation energy of  $236 \text{ kJ mol}^{-1}$  observed by them with reaction 2.4. However, we found that numerical integration with activation energies based on these bond strengths of  $97.5$  and  $256.6 \text{ kJ mol}^{-1}$  was completely inconsistent with the observed kinetic behavior for the formation of CO and  $\text{CH}_3\text{C}_5\text{H}_5$ . There is some confusion over the absolute values of bond dissociation energies in manganese carbonyls,<sup>21,22</sup> but there is good evidence for a much higher value for the first Mn–CO bond strength. For **1**, it has been measured<sup>23</sup> as  $195 \text{ kJ mol}^{-1}$  in solution, with a suggested gas-phase value of  $230 \text{ kJ mol}^{-1}$ ; the average Mn–CO bond energy has been estimated<sup>24</sup> at  $125 \text{ kJ mol}^{-1}$ .

Numerical integration with  $200 \text{ kJ mol}^{-1}$  for  $E_{2.1}$ ,  $150 \text{ kJ mol}^{-1}$  for  $E_{2.2}$  and  $E_{2.3}$ , and  $256 \text{ kJ mol}^{-1}$  for  $E_{2.4}$  gave excellent agreement with our observed Arrhenius parameters for the formation of CO, but those for the formation of  $\text{CH}_3\text{C}_5\text{H}_5$  were reproduced extremely poorly. We conclude that  $E_{2.4}$  is substantially lower than  $256 \text{ kJ mol}^{-1}$ , i.e., that the Mn– $\text{C}_5\text{H}_4\text{CH}_3$  dissociation energy is much lower in the Mn– $\text{C}_5\text{H}_4\text{CH}_3$  fragment than it is in the parent compound **2**. This reasonable conclusion is consistent with both our observation of the  $\text{C}_5\text{H}_5$  radical, and not the  $\text{MnC}_5\text{H}_5$  radical, in the pyrolysis of **1** and the observed significant difference between the first and second dissociation energies in sandwich compounds.<sup>25</sup> Accordingly, varying  $E_{2.4}$  by trial and error, we found that it had to be reduced to  $150 \text{ kJ mol}^{-1}$  in order to obtain good agreement with the experimental Arrhenius parameters for the formation of  $\text{C}_5\text{H}_5\text{CH}_3$ . The final Arrhenius parameters are given in Table 1. Thus, our kinetic study confirms that the first Mn–CO bond dissociation energy in **2** is at least  $200 \text{ kJ mol}^{-1}$  and provides an upper limit of  $150 \text{ kJ mol}^{-1}$  for the Mn– $\text{C}_5\text{H}_4\text{CH}_3$  dissociation energy in the Mn– $\text{C}_5\text{H}_4\text{CH}_3$  fragment.

The observation of free monomeric cyclopentadiene in the pyrolysis of **1** suggests that the major reaction pathway for loss of the  $\cdot\text{C}_5\text{H}_5$  radical is hydrogen abstraction, presumably from unreacted parent material (or perhaps some intermediate) as in (1.5), rather than dimerization. The fate of the resulting  $\cdot\text{C}_5\text{H}_4\text{Mn}$ -containing species cannot be determined with certainty,

(21) Smith, G. P. *Polyhedron* **1988**, *7*, 1605 and references therein.

(22) Connor, J. A.; Zafarani-Moattar, M. T.; Bickerton, J.; El Saied, N. I.; Suradi, S.; Carson, R.; Al Takhin, G.; Skinner, H. A. *Organometallics* **1982**, *1*, 1166.

(23) Klassen, J. K.; Selke, M.; Sorenson, A. A.; Yang, G. K. *J. Am. Chem. Soc.* **1990**, *112*, 1267.

(24) Chipperfield, J. R.; Sneyd, J. C. R.; Webster, D. E. *J. Organomet. Chem.* **1979**, *178*, 177.

(25) Robles, E. S.; Ellis, A. M.; Miller, T. A. *J. Phys. Chem.* **1992**, *96*, 8791.

(19) Winters, R. E.; Kiser, R. W. *J. Organomet. Chem.* **1965**, *4*, 190.

(20) Turanyi, T.; Berces, V. S.; Vadja, S. *Int. J. Chem. Kinet.* **1989**, *21*, 83. Turanyi, T. *J. Math. Chem.* **1990**, *5*, 203.

but it seems very likely that they are the source of the ethyne observed, as indicated in (1.6). The precise nature of the other product(s), designated "MnC" in (1.6), is not clear from our observations alone, but it is reasonable to assign the anisotropic ESR signal of Figure 4 to this species. In this context, it is of significance to note that MBE using **1** or **2** alone does result in the deposition of Mn very heavily contaminated with C<sup>26</sup> and that amorphous MnC is reported to exhibit magnetic behavior at or below room temperature.<sup>27</sup>

The results of the copyrolysis experiments are accounted for in reactions 1.7 and 1.8. <sup>13</sup>CD<sub>3</sub> radicals can be generated from **3** at temperatures much lower than those required for decomposition of **1** or **2**. These radicals are good hydrogen abstractors, as indicated by the generation of CD<sub>3</sub>H, and will therefore produce the <sup>55</sup>Mn species through a different route, as in reaction 1.8; this will then decompose as in (1.6). This is consistent with the production of C<sub>2</sub>H<sub>2</sub> in the absence of C<sub>5</sub>H<sub>6</sub> in the IR LPHP experiments and with the observation of the anisotropic ESR signal free of <sup>55</sup>Mn in the matrix isolation studies.

Finally, if the <sup>55</sup>Mn radicals are provided with an alternative and more available source of H atoms, they will preferentially abstract from the latter, as in (1.9), rather than parent material, as in (1.5). This will prevent formation of the <sup>55</sup>Mn system and in turn that of the MnC. This fact accounts for the greatly reduced C contamination observed in the MBE synthesis of MnAs from **2** and AsH<sub>3</sub>, since the H atoms in the latter are more readily abstracted than those in the former.<sup>26</sup>

The nature of the analogue of the abstraction reaction (2.5) in the pyrolysis of **2** is of considerable interest. The absence of 5-methylcyclopentadiene is not surprising, since equilibration of all three isomers *via* 1,5-H shifts is likely to be rapid at the temperature of the pyrolysis. Furthermore, by analogy with the fact that abstraction of H atoms from the CH<sub>3</sub> group of toluene is more facile than that of the ring protons, we expect to observe the products of the considerably more facile abstraction reaction from the CH<sub>3</sub> group, rather than the ring protons, of **2**. This results in a fulvene-type species, which will then rapidly rearrange to the observed benzene, as in (2.6).

The isotropic component of the ESR spectrum of the matrix-isolated products of pyrolysis of **2** consists of two components (Figure 5A). One is a well-resolved and strong 1:2:1 triplet with a hyperfine splitting of 16 G and a line width of 3.5 G; the second is a weaker and less well-resolved doublet of doublets with splittings of 40 and 25 G. The former we assign to a C-centered  $\pi$ -radical with the unpaired electron localized largely on the CH<sub>2</sub> group of a Me-deprotonated methylcyclopentadiene fragment. This assignment was confirmed by the results of Hückel molecular orbital calculations for the following radicals: **A**, the neutral five-electron radical <sup>55</sup>Mn-C<sub>5</sub>H<sub>4</sub>CH<sub>3</sub> (the monomethylated analogue of the <sup>55</sup>Mn radical); and **B**, the seven-electron radical anion <sup>55</sup>Mn-CH<sub>2</sub>C<sub>5</sub>H<sub>4</sub><sup>-</sup> (which serves as a prototype for radicals formed by H-abstraction from the methyl group); the results of these calculations are shown in Figure 6.

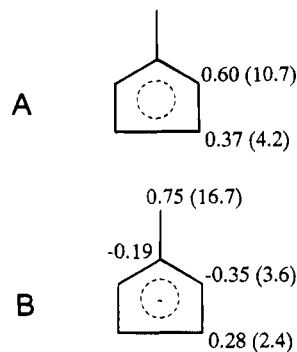


**Figure 6.** Hückel molecular orbital calculations for (A) <sup>55</sup>Mn-C<sub>5</sub>H<sub>4</sub>CH<sub>3</sub> and (B) <sup>55</sup>Mn-CH<sub>2</sub>C<sub>5</sub>H<sub>4</sub><sup>-</sup>. Numbers are Hückel coefficients and (in parentheses) predicted hyperfine splittings using a McConnell *Q*-factor of 29.9 G.

In Figure 6, the numbers in brackets are predicted hyperfine couplings for a McConnell *Q*-value of 29.9 G, the same as that for C<sub>5</sub>H<sub>5</sub>.<sup>28</sup> It is clear that radical **B** fits the experimental observations almost exactly. Coupling to the CH<sub>2</sub> protons matches the observed triplet splitting of 16 G very closely and is very similar to that found for the CH<sub>2</sub> protons in the benzyl radical.<sup>29</sup> The other predicted splittings are, not surprisingly, lost in the line width of 3.5 G. We cannot be certain whether this radical is bound to an Mn-containing unit, although the lack of anisotropy or Mn hyperfine splitting tends to suggest otherwise (the radical O<sub>2</sub>Mn(CO)<sub>5</sub>, with the unpaired electron located largely on O<sub>2</sub>, exhibits anisotropic Mn hyperfine structure of 8.3 and 6.4 G<sup>30</sup>). The observations are clearly inconsistent with both the calculations for the free <sup>55</sup>Mn-C<sub>5</sub>H<sub>4</sub>CH<sub>3</sub> radical (hyperfine splittings of 10.7 G for C2 and 4.2 G for C3) and previous observations of this species.<sup>18,31</sup> We conclude, therefore, the lower activation energy for the reaction (2.5) in the pyrolysis of **2** results in very rapid loss of the <sup>55</sup>Mn-C<sub>5</sub>H<sub>4</sub>CH<sub>3</sub> radical, with the result that only the abstraction product is observed in the ESR spectrum.

The fate of this abstraction product is clearly of interest. Since it is an isomer of benzene, it seems very likely that it is the origin of this product (which is never observed in the pyrolysis of **1**). The large hyperfine splittings of the secondary radical of Figure 5a suggest that it is a  $\sigma$ -radical, probably of the vinyl type <sup>55</sup>Mn-CH=CHR, arising from fragmentation of the <sup>55</sup>Mn-C<sub>5</sub>H<sub>4</sub>CH<sub>3</sub> rings. Hyperfine splittings from the  $\alpha$ - and  $\beta$ -protons in radicals of this type are very dependent on bond angles and *p*:*s* ratios in the orbital of the unpaired electron. Thus in the vinyl radical itself (R = H), couplings are 15.7 G ( $\alpha$ ), 68 G ( $\beta_1$ ), and 34 G ( $\beta_2$ ), whereas in the methylvinyl radical (R = Me), the couplings are 58 G ( $\beta_1$ ) and 38 G ( $\beta_2$ ).<sup>32,33</sup> It is unlikely that it is an allylic radical, since such species are  $\pi$ -radicals with a maximum hyperfine splitting of 15 G.<sup>31</sup>

The production of alkynes in the LPHP system, and their absence in SFR, merits additional comment. As

(28) Zandstra, P. J. *J. Chem. Phys.* **1964**, *40*, 612.

(29) Dixon, W. T.; Norman, R. O. C. *J. Chem. Soc.* **1964**, 4857.

(30) Mach, K.; Nováková, J.; Raynor, J. B. *J. Organomet. Chem.* **1992**, *439*, 341.

(31) Barker, P. J.; Davies, A. G.; Fisher, J. D. *J. Chem. Soc., Chem. Commun.* **1979**, 587.

(32) Fessenden, R. W.; Schuler, R. H. *J. Chem. Phys.* **1963**, *39*, 2147.

(33) Adrian, F. J.; Cochran, E. L.; Bowers, V. A. *Free Radicals in Organic Chemistry*; American Chemical Society: Washington, DC, 1962.

(26) Wright, P. J. Personal communication.

(27) Hauser, J. *J. Phys. Rev. B* **1980**, *22*, 2554.

described above, the very low reagent pressure in the SFR system is designed specifically to minimize surface reaction and also to result in low reactant conversion. Together, these will reduce alkyne production in comparison with the LPHP system, where longer residence times and higher pressures will increase the competitiveness of reactions 5. However, it is evident both from the nonlinear nature of Figure 2 and from other observations<sup>7,17</sup> that there may be a contribution from heterogeneous processes in the SFR system. It is likely that the stepwise CO loss of reactions 1–3 in Schemes 1 and 2 operates both in the gas phase and on the surface; what is likely to differ is the subsequent fate of abstraction products. That some closely related processes do occur on the surface is evident from the

heavy C contamination of Mn films<sup>26</sup> and the observation of the anisotropic ESR signals; however, it is very likely that any resultant alkyne undergoes further surface-catalyzed conversion, presumably into an involatile polymeric material.

**Acknowledgment.** We thank the SERC for their extensive support of this work, including equipment grants (to D.K.R., J.B.R., and I.M.T.D.), postdoctoral fellowships (to M.P., I.M.P., and A.D.W.), and a postgraduate studentship (to G.P.M.). We also gratefully acknowledge support from the Government of Turkey through a studentship to S.S.

OM9409579



# Isolation and Complete NMR and X-ray Crystallographic Characterization of an Unusual Pentadienyllutetium Complex,



Matthew B. Zielinski,<sup>\*,2a</sup> Donald K. Drummond,<sup>2b</sup> Pradeep S. Iyer,<sup>2a</sup>  
John T. Leman,<sup>2b</sup> and William J. Evans<sup>\*,2b</sup>

Unocal Corporation, P.O. Box 76, Brea, California 92621, and Department of Chemistry,  
University of California, Irvine, Irvine, California 92717

Received December 6, 1994<sup>®</sup>

From the metathesis reaction of (2,4-dimethylpentadienyl)potassium with lutetium trichloride (3:1 reaction stoichiometry) has been isolated a novel pentadienyllutetium complex,  $(\eta^5\text{-(CH}_3)_2\text{C}_5\text{H}_5)\text{Lu}(\eta^5\text{-}\eta^3\text{-(CH}_3)_2\text{C}_5\text{H}_5\text{CH}_2\text{CH}_2\text{CH(CH}_3)_3\text{C}_3\text{H}_3\text{(CH}_3))$  (**1**), which contains a dimeric chelate ligand derived from the end-to-end fusion of two 2,4-dimethylpentadienyl groups. The solid-state structure of **1** was established through single-crystal X-ray diffraction analysis. Resonances in the <sup>1</sup>H and <sup>13</sup>C NMR spectra were completely and unequivocally assigned by 2D NMR techniques and show the complex to be in an asymmetric conformation in solution.

## Introduction

Significant advances in the field of metal pentadienyl chemistry have been made within the past 10 years.<sup>3</sup> Much of this work has been stimulated by speculation that pentadienyl complexes may show unusual chemical reactivity by virtue of ready interconversion among any of three ligand–metal bonding modes, i.e.,  $\eta^1$ ,  $\eta^3$ , and  $\eta^5$ . Investigations have now led to the synthesis of a variety of transition-metal pentadienyl complexes which display the entire range of metal–ligand bonding interactions. In contrast, few pentadienyl–f-element complexes have been reported;<sup>4</sup> those which have been crystallographically characterized predominantly display  $\eta^5$ -pentadienyl–metal bonding.<sup>4a,b,f,g</sup> Our interest in the catalytic chemistry of organolanthanides with unusual hydrocarbyl ligation, as well as our desire to investigate the extent to which metal ion size will influence metal–pentadienyl bonding interactions, has led us to a further investigation of this area.

With the realization that coordination sphere oversaturation in trivalent organolanthanide chemistry can force complexes into higher reactivity manifolds,<sup>5</sup> our

immediate goal was to maximize steric crowding within a pentadienyllanthanide complex. Because of the considerable steric congestion already present within the only known homoleptic pentadienyllanthanide complex, tris( $\eta^5$ -2,4-dimethylpentadienyl)neodymium,<sup>4f</sup> we envisioned that substitution of a significantly smaller ionic radius lanthanide ion into a related synthetic sequence might effect pivotal changes in structure and/or reactivity. We chose to work with Lu<sup>3+</sup> because it is the smallest ionic radius lanthanide ion and because its diamagnetic character contributes to a simplification of NMR analysis. During the course of our study on the metathesis reaction of (2,4-dimethylpentadienyl)potassium with lutetium trichloride, an independent report on this system has appeared<sup>4g</sup> which describes the main product of this reaction,  $(\eta^5\text{-(CH}_3)_2\text{C}_5\text{H}_5)_2\text{Lu}(\eta^3\text{-(CH}_3)_2\text{C}_5\text{H}_5)$ . We report here the isolation of an unusual minor reaction product derived from the coupling of two pentadienyl ligands. Both X-ray crystallography and 2D NMR were used to characterize the complex. The power of the latter method for defining the organolanthanide structure in solution is clearly demonstrated.

## Experimental Section

The acute air and moisture sensitivity of each organometallic complex required that all synthetic procedures and subsequent manipulations be performed using vacuum line, Schlenk, or glovebox (Vacuum/Atmospheres HE-43 Dri-Lab with MO40 Dri-Train) techniques. Atmospheres of high-purity nitrogen or ultrahigh-purity argon were used in both Schlenk and glovebox operations.

**Materials.** Hexane and tetrahydrofuran (THF) were distilled from potassium benzophenone ketyl. Benzene-*d*<sub>6</sub> was vacuum-transferred from potassium benzophenone ketyl. Anhydrous lutetium trichloride (Cerac) was used as received. (2,4-Dimethylpentadienyl)potassium was prepared according to the literature<sup>6</sup> from dispersed potassium and 2,4-dimethyl-1,3-pentadiene (Aldrich).

<sup>®</sup> Abstract published in *Advance ACS Abstracts*, June 15, 1995.

(1) Reported in part at the California Catalysis Society Fall Meeting, Lake Arrowhead, CA, Oct 20–21, 1988.

(2) (a) Unocal Corporation. (b) University of California, Irvine.

(3) General reviews of this chemistry include: (a) Ernst, R. D. *Chem. Rev.* **1988**, *88*, 1255–1291. (b) Powell, P. In *Advances in Organometallic Chemistry*; West, R., Stone, F. G. A., Eds.; Academic Press: New York, 1986; Vol. 26, pp 125–164. (c) Ernst, R. D. *Acc. Chem. Res.* **1985**, *18*, 56–62. (d) Yasuda, H.; Nakamura, A. *J. Organomet. Chem.* **1985**, *285*, 15–29. (e) Ernst, R. D. *Struct. Bonding (Berlin)* **1984**, *57*, 1–53. Also see: (f) Bleeke, J. R.; Wittenbrink, R. J.; Clayton, T. W., Jr.; Chiang, M. Y. *J. Am. Chem. Soc.* **1990**, *112*, 6539–6545 and references cited therein.

(4) (a) Baudry, D.; Bulot, E.; Charpin, P.; Ephritikhine, M.; Lance, M.; Nierlich, M.; Vigner, J. *J. Organomet. Chem.* **1989**, *371*, 163–174. (b) Sieler, J.; Simon, A.; Peters, K.; Taube, R.; Geitner, M. *J. Organomet. Chem.* **1989**, *362*, 297–303. (c) Baudry, D.; Bulot, E.; Ephritikhine, M. *J. Chem. Soc., Chem. Commun.* **1989**, 1316–1317. (d) Baudry, D.; Bulot, E.; Ephritikhine, M. *J. Chem. Soc., Chem. Commun.* **1988**, 1369–1370. (e) Cymbaluk, T. H.; Liu, J.-Z.; Ernst, R. D. *J. Organomet. Chem.* **1983**, *255*, 311–315. (f) Ernst, R. D.; Cymbaluk, T. H. *Organometallics* **1982**, *1*, 708–713. (g) Schumann, H.; Dietrich, A. *J. Organomet. Chem.* **1991**, *401*, C33–C36.

(5) Evans, W. J. *Polyhedron* **1987**, *6*, 803–835.

(6) Yasuda, H.; Ohnuma, Y.; Yamauchi, M.; Tani, H.; Nakamura, A. *Bull. Chem. Soc. Jpn.* **1979**, *52*, 2036–2045.

**Physical Measurements.** Infrared spectra were recorded on a Perkin-Elmer Model 1430 spectrophotometer. Samples were prepared as Nujol mulls within the glovebox.  $^1\text{H}$  and  $^{13}\text{C}$  NMR spectra were obtained as described below. CH analyses were performed on a Carlo Erba EA 1108 elemental analyzer, and complexometric analysis for Lu was obtained as previously described.<sup>7</sup>

$(\eta^5\text{-(CH}_3)_2\text{C}_5\text{H}_5)\text{Lu}(\eta^5\text{-(CH}_3)_3\text{C}_5\text{H}_5\text{CH}_2\text{CH}_2\text{CH(CH}_3)_3\text{C}_3\text{H}_7\text{(CH}_3))$  (1). Into a 100-mL, three-necked, round-bottomed flask equipped with a spinbar, rubber septum, glass stopper, and gas inlet was placed 1.50 g (5.33 mmol) of anhydrous lutetium trichloride and 20 mL of THF. The assembly was attached to the Schlenk line, and the solution was stirred overnight to disperse the undissolved salt. A solution containing 2.15 g (16.0 mmol) of (2,4-dimethylpentadienyl)potassium in 30 mL of THF was slowly syringed into the rapidly stirred slurry of lutetium trichloride, previously cooled to  $-78^\circ\text{C}$ . Upon dropwise addition of the light amber potassium salt solution, a localized yellow color appeared momentarily and then dissipated. This occurred until approximately 1 mL of solution had been added. The yellow color then remained as the balance of the potassium salt was added. After complete addition, the solution was stirred for an additional 1.5 h. The cooling bath was then removed and the solution was warmed slowly to room temperature. During this period the solution gradually turned dark brown. After the mixture was stirred overnight, the solvent was vacuum-evaporated. The residue was extracted with hexane ( $4 \times 20$  mL), and the resulting extract was concentrated to a volume of ca. 30 mL. The solution was then cooled to  $-78^\circ\text{C}$  for 8 h, which resulted in the formation of olive-colored crystals. Using a double-ended filter, the crystals were separated from the mother liquor, which itself yielded a noncrystallizable, as yet uncharacterized, brown-black oil. The crystals were redissolved in a minimum amount of THF/hexane, and the solution was cooled to ca.  $-30^\circ\text{C}$  overnight. This resulted in the formation of pale orange-yellow crystals suitable for X-ray diffraction analysis; yield 0.13 g (5%). IR (Nujol mull): 3110 (vw), 3090 (w), 3080 (w), 3025 (w), 1525 (s, br), 1425 (sh), 1350 (w), 1340 (vw), 1320 (vw), 1290 (w), 1270 (w), 1250 (w-m), 1230 (w), 1210 (vw), 1180 (w), 1155 (vw), 1090 (w-m), 1060 (m), 1030 (m), 1015 (w), 990 (sh), 980 (w), 945 (w), 925 (w), 890 (w), 875 (w, br), 850 (w-m), 835 (w-m), 810 (s), 800 (w), 795 (w), 770 (s, br), 700 (sh), 690 (sh), 630 (m), 600 (w), and 565 (sh)  $\text{cm}^{-1}$ . Anal. Calcd for  $\text{LuC}_{21}\text{H}_{33}$ : C, 54.78; H, 7.22; Lu, 38.00. Found: C, 54.13; H, 7.28; Lu, 37.8.

**X-ray Crystallography of  $(\eta^5\text{-(CH}_3)_2\text{C}_5\text{H}_5)\text{Lu}(\eta^5\text{-(CH}_3)_3\text{C}_5\text{H}_5\text{CH}_2\text{CH}_2\text{CH(CH}_3)_3\text{C}_3\text{H}_7\text{(CH}_3))$  (1).** A single crystal of approximate dimensions  $0.20 \times 0.30 \times 0.40$  mm was sealed into a thin-walled glass capillary under an inert atmosphere ( $\text{N}_2$ ) and mounted on a Syntex P2<sub>1</sub> diffractometer. Subsequent setup operations (determination of accurate unit cell dimensions and orientation matrix) and collection of room temperature (296 K) intensity data were carried out using standard techniques similar to those of Churchill.<sup>8</sup> Details appear in Table 1.

All 4439 data were corrected for the effects of absorption and for Lorentz and polarization effects and placed on an approximately absolute scale by means of a Wilson plot. Any reflection with  $I(\text{net}) < 0$  was assigned the value  $|F_o| = 0$ . A careful examination of a preliminary data set revealed no systematic extinctions or any diffraction symmetry other than the Friedel condition. The centrosymmetric triclinic space group  $P\bar{1}$  ( $C_1^1$ ; No. 2) was chosen and later determined to be correct by successful solution of the structure.

All crystallographic calculations were carried out using either a modified version of the UCLA Crystallographic Computing Package<sup>9</sup> or the SHELXTL PLUS program set.<sup>10</sup>

**Table 1. Crystallographic Data for Complex 1**

formula: $\text{C}_{21}\text{H}_{33}\text{Lu}$
fw: 460.4
crystal syst: triclinic
space group: $P\bar{1}$
$a = 7.382(4) \text{ \AA}$
$b = 8.703(2) \text{ \AA}$
$c = 16.443(6) \text{ \AA}$
$\alpha = 78.54(2)^\circ$
$\beta = 84.74(4)^\circ$
$\gamma = 68.11(3)^\circ$
$V = 960.5(6) \text{ \AA}^3$
$Z = 2$
$D_{\text{calcd}} = 1.592 \text{ Mg/m}^3$
diffractometer: Syntex P2 <sub>1</sub>
radiation: Mo K $\alpha$ ( $\lambda = 0.710730 \text{ \AA}$ )
monochromator: highly oriented graphite
data collected: $+h, \pm k, \pm l$
scan type: $\theta-2\theta$
scan width: $1.2^\circ$
scan speed: $2.0^\circ \text{ min}^{-1}$ (in $\omega$ )
$2\theta_{\text{max}} = 55.0^\circ$
$\mu(\text{Mo K}\alpha) = 5.144 \text{ mm}^{-1}$
abs cor: semiempirical ( $\psi$ -scan method)
min/max transmissn: 0.4002/0.9352
no. of rflns collected: 4439
no. of rflns with $ F_o  > 0$ : 4380
no. of variables: 200
$R_F = 3.3\%$
$R_{wF} = 4.8\%$
goodness of fit: 1.23

The analytical scattering factors for neutral atoms were used throughout the analysis;<sup>11a</sup> both the real ( $\Delta f'$ ) and imaginary ( $i\Delta f''$ ) components of anomalous dispersion<sup>11b</sup> were included. The quantity minimized during least-squares analysis was  $\sum w(|F_o| - |F_c|)^2$ , where  $w^{-1} = \sigma^2(|F_o|) + 0.0007(|F_o|)^2$ .

The structure was solved by direct methods (MITHRIL)<sup>12</sup> and refined by full-matrix least-squares techniques (SHELXTL). Hydrogen atom contributions were included using a riding model with  $d(\text{C-H}) = 0.96 \text{ \AA}$  and  $U(\text{iso}) = 0.08 \text{ \AA}^2$ . Refinement of positional and anisotropic thermal parameters led to convergence with  $R_F = 3.3\%$ ,  $R_{wF} = 4.8\%$ , and  $\text{GOF} = 1.23$  for 200 variables refined against all 4380 unique data ( $R_F = 3.1\%$ ;  $R_{wF} = 4.6\%$  for those 4185 data with  $|F_o| > 6.0\sigma(|F_o|)$ ). A final difference-Fourier map was devoid of significant features;  $\rho(\text{max}) = 1.37 \text{ e \AA}^{-3}$ . Atomic coordinates and equivalent isotropic displacement coefficients are presented in Table 2.

**NMR Spectra of  $(\eta^5\text{-(CH}_3)_2\text{C}_5\text{H}_5)\text{Lu}(\eta^5\text{-(CH}_3)_3\text{C}_5\text{H}_5\text{CH}_2\text{CH}_2\text{CH(CH}_3)_3\text{C}_3\text{H}_7\text{(CH}_3))$  (1).**  $^1\text{H}$  and  $^{13}\text{C}$  NMR spectra were acquired at ambient temperature with an IBM AF-270 FT NMR narrow-bore spectrometer. All data processing was done on an Aspect-3000 computer using DISNMR standard software. A 5-mm dual-tuned probe was used to observe  $^1\text{H}$  and  $^{13}\text{C}$  nuclei at 270 and 68 MHz, respectively. The  $90^\circ$  pulse widths for  $^1\text{H}$  and  $^{13}\text{C}$  were 8.6 and 4.6  $\mu\text{s}$ , respectively, while the decoupler coil pulse length was measured to be 14.2  $\mu\text{s}$ . The lutetium complex was dissolved in benzene- $d_6$  solvent in a 5-mm Wilmad glass NMR tube, and the sample was sealed under vacuum. Chemical shifts are reported in ppm from TMS by setting the residual proton signal of the solvent at 7.15 ppm and the corresponding  $^{13}\text{C}$  solvent resonance at 128.0 ppm (Table 3).

Carbon signal multiplicities were determined using the  $J$ -modulated spin echo pulse sequence. A 2D  $^1\text{H}$  COSY spectrum was acquired using Jeener's two-pulse sequence,  $90^\circ\text{-t1-}45^\circ\text{-ACQ(t2)}$ , minimizing the diagonal peak intensi-

(9) UCLA Crystallographic Computing Package, University of California, Los Angeles, 1981. Strouse, C. Personal communication.

(10) Nicolet Instrument Corp., Madison, WI, 1988.

(11) (a) *International Tables for X-Ray Crystallography*; Kynoch Press: Birmingham, England, 1974; pp 99-101. (b) *Ibid.*, pp 149-150.

(12) Gilmore, C. J. *J. Appl. Crystallogr.* **1984**, *17*, 42-46.

(7) Evans, W. J.; Engerer, S. C.; Coleson, K. M. *J. Am. Chem. Soc.* **1981**, *103*, 6672-6677.

(8) Churchill, M. R.; Lashewycz, R. A.; Rotella, F. J. *Inorg. Chem.* **1977**, *16*, 265-271.

**Table 2. Atomic Coordinates ( $\times 10^4$ ) and Equivalent Isotropic Displacement Coefficients ( $\text{\AA}^2 \times 10^4$ ) for Complex 1<sup>a</sup>**

	x	y	z	U(eq)
Lu(1)	-2242.5(0.2)	347.4(0.2)	2205.9(0.1)	273.5(0.9)
C(1)	361(9)	-1464(7)	3336(3)	549(21)
C(2)	-164(7)	-2687(6)	3091(3)	469(17)
C(3)	-167(7)	-2961(6)	2291(3)	406(15)
C(4)	481(7)	-2203(6)	1517(3)	448(16)
C(5)	1181(8)	-921(8)	1419(4)	603(22)
C(6)	-974(10)	-3737(7)	3761(4)	741(24)
C(7)	256(10)	-2858(8)	771(4)	657(24)
C(8)	-1403(7)	2854(6)	1785(3)	454(17)
C(9)	-2849(7)	3468(5)	2387(3)	376(15)
C(10)	-2798(7)	2535(6)	3187(3)	434(17)
C(11)	-4231(10)	3020(8)	3887(3)	558(23)
C(12)	-5561(10)	1993(9)	4090(3)	607(25)
C(13)	-6885(8)	2158(8)	3381(3)	553(21)
C(14)	-5909(6)	1106(6)	2721(3)	402(16)
C(15)	-5981(6)	2044(5)	1896(3)	374(14)
C(16)	-5152(6)	1483(6)	1143(3)	385(15)
C(17)	-5375(9)	2847(7)	391(3)	557(21)
C(18)	-4531(9)	5100(6)	2112(3)	509(19)
C(19)	-3045(14)	2756(12)	4668(4)	951(47)
C(20)	-4972(7)	-585(6)	2951(3)	444(17)
C(21)	-4058(7)	-142(6)	1046(3)	450(17)

<sup>a</sup> Equivalent isotropic  $U$ , defined as one-third of the trace of the orthogonalized  $U_{ij}$  tensor.

**Table 3. 68 MHz  $^{13}\text{C}\{^1\text{H}\}$  and 270 MHz  $^1\text{H}$  NMR Data for Complex 1<sup>a</sup>**

no. <sup>c,d</sup>	carbon type <sup>e</sup>	chem shift ( $\delta$ , ppm) <sup>b</sup>	
		$^{13}\text{C}\{^1\text{H}\}$	$^1\text{H}^f$
1	CH <sub>2</sub>	81.1	3.68 (s, 1H), 2.68 (s, 1H)
2	C	147.3	
3	CH	90.0	4.73 (s, 1H)
4	C	145.2	
5	CH <sub>2</sub>	82.2	4.35 (s, 1H), 3.37 (s, 1H)
6	CH <sub>3</sub>	30.0	1.86 (s, 3H)
7	CH <sub>3</sub>	29.9	1.98 (s, 3H)
8	CH <sub>2</sub>	59.5	1.95 (m, 1H) 1.51 (d, 1H, $J = 4.6$ Hz)
9	C	151.3	
10	CH	80.9	3.58 (d, 1H, $J = 7.6$ Hz)
11	CH	33.8	2.46 (m, 1H)
12	CH <sub>2</sub>	44.3	1.75 (m, 1H), 1.25 (m, 1H)
13	CH <sub>2</sub>	41.5	2.73 (m, 1H), 1.93 (m, 1H)
14	C	155.0	
15	CH	98.0	4.63 (s, 1H)
16	C	149.0	
17	CH <sub>3</sub>	27.6	1.82 (s, 3H)
18	CH <sub>3</sub>	24.2	2.23 (s, 3H)
19	CH <sub>3</sub>	24.0	1.07 (d, 3H, $J = 6.6$ Hz)
20	CH <sub>2</sub>	73.0	3.12 (s, 1H), 3.01 (s, 1H)
21	CH <sub>2</sub>	76.0	2.95 (s, 1H), 2.61 (s, 1H)

<sup>a</sup> In benzene- $d_6$  solution under ambient conditions. <sup>b</sup> Chemical shifts ( $\delta$ ) are reported in ppm with respect to TMS. <sup>c</sup> Refer to carbon numbering scheme in Figure 1. <sup>d</sup> Signal assignments for atoms 1–7 were inferred from a combination of 2D NMR experiments and X-ray data. <sup>e</sup> Discerned from the  $J$ -modulated spin echo  $^{13}\text{C}$  experiment. <sup>f</sup> Multiplicities, integrations, and coupling constants are indicated in parentheses.

ties.<sup>13</sup> Thirty-two scans were collected over a spectral width of 2703 Hz for each of 256 time increments to give a matrix of  $1024 \times 1024$  data points. The recycle delay used was 2 s. The long-range COSY experiment used the pulse sequence of Bax and Freeman,<sup>14</sup>  $90^\circ-t_1-\Delta-45^\circ-\Delta-ACQ(t_2)$ , under the same conditions but with  $\Delta$  set to 80 ms to observe weak cross-peaks from long-range couplings. The free induction decays were multiplied by an unshifted sine squared bell function, and symmetrization was applied to the final spectrum.

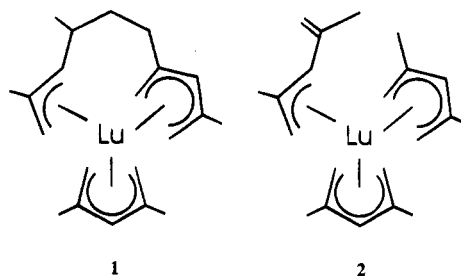
(13) Nagayama, K.; Kumar, A.; Wuthrich, K.; Ernst, R. R. *J. Magn. Reson.* **1980**, *40*, 321–334.

(14) Bax, A.; Freeman, R. *J. Magn. Reson.* **1981**, *44*, 542–561.

A 2D heteronuclear correlation spectrum (XHCORR)<sup>15</sup> was recorded using the pulse sequence  $90^\circ(\text{H})-1/2t_1-180^\circ(\text{C})-1/2t_1-D3-90^\circ(\text{C})90^\circ(\text{H})-d4-ACQ(t_2)$  (under proton decoupling). The acquisition involved 128 scans for each of 128  $t_1$  increments using a 3 s recycle delay. Delays D3 and D4 were optimized for  $J = 160$  Hz (i.e., set to 3.125 and 1.563 ms, respectively). The spectral widths used in the F1 and F2 domains were 2702 and 13 514 Hz, respectively. The  $t_2$  data were exponentially weighted using a line-broadening factor of 5 Hz and Fourier-transformed over 2048 data points. The  $t_1$  interferograms were modified with a shifted ( $\pi/4$ ) sine squared bell function before Fourier transformation over 256W data points as a magnitude spectrum. Finally, the pulse sequence that worked best for obtaining a long-range heteronuclear correlation spectrum of this complex was the modified version of XHCORR suggested by Krishnamurthy and Nunlist.<sup>16</sup> The sequence involves the elimination of the refocusing D4 delay and BB decoupling during acquisition. The D3 delay was optimized for long-range couplings of 8 Hz magnitude and set to be 62.5 ms. The number of scans was increased to 512 for each increment of  $t_1$ .

## Results and Discussion

A metathesis reaction involving the addition of 3 equivalents of (2,4-dimethylpentadienyl)potassium to a THF solution of lutetium trichloride at  $-78^\circ\text{C}$  led to a mixture of products. While removal of solvent from the reaction mixture and extraction with toluene has been reported<sup>4g</sup> to give ( $\eta^5$ -(CH<sub>3</sub>)<sub>2</sub>C<sub>5</sub>H<sub>5</sub>)<sub>2</sub>Lu( $\eta^3$ -(CH<sub>3</sub>)<sub>2</sub>C<sub>5</sub>H<sub>5</sub>) (2) in 46% yield, initial extraction with hexanes, a solvent in which 2 has limited solubility,<sup>4g</sup> affords a second product, ( $\eta^5$ -(CH<sub>3</sub>)<sub>2</sub>C<sub>5</sub>H<sub>5</sub>)Lu( $\eta^5$ : $\eta^3$ -(CH<sub>3</sub>)<sub>2</sub>C<sub>5</sub>H<sub>5</sub>CH<sub>2</sub>CH(CH<sub>3</sub>)C<sub>3</sub>H<sub>3</sub>(CH<sub>3</sub>)) (1). The solid-state structure of 1 was unequivocally determined through single-crystal X-ray diffraction analysis, which revealed the presence of a solitary 2,4-dimethylpentadienyl ligand and one chelate ligand resulting from the coupling of two 2,4-dimethylpentadienyl units. The complex displays one  $\eta^3$ -allyl and two  $\eta^5$ -pentadienyl bonding interactions, as are found in 2.<sup>4g</sup> The presence of preformed coupling product in the (2,4-dimethylpentadienyl)potassium starting material was ruled out through  $^1\text{H}$  NMR and IR analysis.



**Solid-State Structure of 1.** An ORTEP diagram of complex 1 is shown in Figure 1 with interatomic distances and angles presented in Table 4. Both the IR spectrum and X-ray crystallographic data are consistent with  $\eta^3$ -allyl and  $\eta^5$ -pentadienyl bonding modes. The strong IR absorption at  $1525\text{ cm}^{-1}$  clearly indicates delocalized C=C bond stretching within the unsaturated carbon frameworks of the complex. No localized C=C or C=C–C=C bond stretching absorptions are evident. Furthermore, least-squares analysis of the

(15) Bax, A.; Morris, G. A. *J. Magn. Reson.* **1981**, *42*, 501–505.

(16) Krishnamurthy, V. V.; Nunlist, R. *J. Magn. Reson.* **1988**, *80*, 280–295.

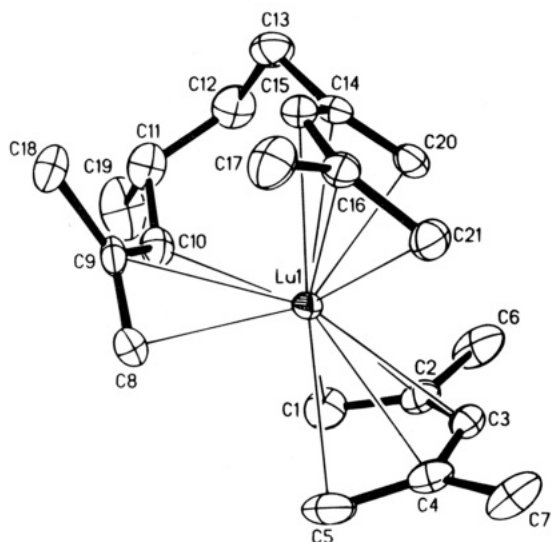


**Figure 1.** ORTEP diagram of complex **1**. Thermal ellipsoids are drawn at the 30% probability level.

**Table 4. Selected Interatomic Distances (Å) and Angles (deg) for Complex 1<sup>a</sup>**

Interatomic Distances			
Lu(1)–C(1)	2.620(6)	Lu(1)–C(2)	2.703(4)
Lu(1)–C(3)	2.693(4)	Lu(1)–C(4)	2.740(5)
Lu(1)–C(5)	2.677(6)	Lu(1)–C(8)	2.440(6)
Lu(1)–C(9)	2.656(5)	Lu(1)–C(10)	2.629(5)
Lu(1)–C(14)	2.636(5)	Lu(1)–C(15)	2.642(4)
Lu(1)–C(16)	2.658(5)	Lu(1)–C(20)	2.567(5)
Lu(1)–C(21)	2.614(6)	Lu(1)–Cent(1)	2.227
Lu(1)–Cent(2)	2.353	Lu(1)–Cent(3)	2.149
C(1)–C(2)	1.398(10)	C(2)–C(3)	1.383(8)
C(2)–C(6)	1.514(9)	C(3)–C(4)	1.439(7)
C(4)–C(5)	1.371(10)	C(4)–C(7)	1.497(9)
C(8)–C(9)	1.412(6)	C(9)–C(10)	1.398(6)
C(9)–C(18)	1.515(6)	C(10)–C(11)	1.504(7)
C(11)–C(12)	1.533(12)	C(11)–C(19)	1.551(11)
C(12)–C(13)	1.541(9)	C(13)–C(14)	1.515(8)
C(14)–C(15)	1.432(6)	C(14)–C(20)	1.362(7)
C(15)–C(16)	1.423(7)	C(16)–C(17)	1.508(7)
C(16)–C(21)	1.376(6)		
Interatomic Angles			
C(1)–C(2)–C(3)	127.1(5)	C(1)–C(2)–C(6)	116.7(5)
C(3)–C(2)–C(6)	116.0(6)	C(2)–C(3)–C(4)	130.8(5)
C(3)–C(4)–C(5)	125.4(5)	C(3)–C(4)–C(7)	115.0(6)
C(5)–C(4)–C(7)	119.6(5)	C(8)–C(9)–C(10)	120.9(4)
C(8)–C(9)–C(18)	117.5(4)	C(10)–C(9)–C(18)	121.5(4)
C(9)–C(10)–C(11)	126.8(4)	C(10)–C(11)–C(12)	113.8(6)
C(10)–C(11)–C(19)	107.6(6)	C(12)–C(11)–C(19)	108.8(5)
C(11)–C(12)–C(13)	115.2(5)	C(12)–C(13)–C(14)	115.5(4)
C(13)–C(14)–C(15)	114.8(4)	C(13)–C(14)–C(20)	119.2(5)
C(15)–C(14)–C(20)	125.8(5)	C(14)–C(15)–C(16)	129.8(4)
C(15)–C(16)–C(17)	115.7(4)	C(15)–C(16)–C(21)	126.9(4)
C(17)–C(16)–C(21)	117.3(4)		
Cent(1)–Lu(1)–Cent(2)	126.7	Cent(1)–Lu(1)–Cent(3)	128.9
Cent(2)–Lu(1)–Cent(3)	104.2		

<sup>a</sup> Cent(1) is the centroid of the unit defined by C(1)–C(2)–C(3)–C(4)–C(5), Cent(2) is the centroid of the unit defined by C(8)–C(9)–C(10), and Cent(3) is the centroid of the unit defined by C(20)–C(14)–C(15)–C(16)–C(21).

pentadienyl planes, defined by the five unsaturated carbon atoms of each pentadienyl array, indicates a high degree of planarity (maximum carbon atom deviation: 0.02 Å).

The pentadienyl units in complex **1** are oriented in a head-to-tail fashion,<sup>4f</sup> analogous to the arrangement of adjacent  $\eta^5$ -pentadienyl ligands in **2** and tris( $\eta^5$ -2,4-

dimethylpentadienyl)neodymium (**3**). The allyl group, however, with its syn alkyl bridge connection at C(10), is oriented head-to-head with respect to the chelate pentadienyl unit. This is in contrast to **2**, where a head-to-tail allyl-to-pentadienyl arrangement is found.<sup>4g</sup> Viewing complex **1** in perspective (Figure 1) shows this arrangement to minimize steric interaction among the C(17), C(18), and C(19) methyl groups and the alkyl bridge.

Complex **1** displays pseudotrigonal coordination as indicated by the incongruent (ligand centroid)–Lu–(ligand centroid) angles. Thus, the (allyl centroid)–Lu–(pentadienyl (chelate) centroid) angle (104.2°) is considerably narrower than either of the angles involving the centroid of the solitary pentadienyl ligand ((allyl centroid)–Lu–(pentadienyl centroid), 126.7°; (pentadienyl centroid)–Lu–(pentadienyl (chelate) centroid), 128.9°). The narrowness of the first angle clearly results from the restricted three-carbon bridge connecting the terminal  $\pi$  systems of the chelate ligand. The two remaining angles are necessarily much larger because of the placement of the solitary 2,4-dimethylpentadienyl ligand in a less congested area of the coordination sphere.

The solitary pentadienyl ligand of complex **1** displays the shortest metal–carbon bonds to the terminal carbon atoms C(1) (2.620(6) Å) and C(5) (2.677(6) Å). These distances are equivalent to the analogous bonds in **2** (2.63(1)–2.66(1) Å).<sup>4g</sup> The Lu–C(3) and Lu–C(2) bonds are intermediate in length (2.693(4) and 2.703(4) Å, respectively), while the Lu–C(4) bond is longest (2.740(5) Å). This trend is somewhat similar to that found in both the lutetium and neodymium complexes **2** and **3**, where the shortest bonds are to the anionic carbon atoms in the 1-, 3-, and 5-positions of each pentadienyl ligand. Carbons at these positions have formal electron charge densities derived from the three major resonance forms which describe the overall pentadienyl anion hybrid. Bond orders derived from these resonance contributors, however, would predict shorter external and longer internal carbon–carbon bond distances for the solitary pentadienyl ligand. Instead, the external C(1)–C(2) and C(4)–C(5) bonds (1.398(10) and 1.371(10) Å, respectively) as well as the internal C(2)–C(3) bond (1.383(8) Å) have similar lengths while the C(3)–C(4) bond (1.439(7) Å) is longer. These bond distances are, nevertheless, similar enough to confirm an  $\eta^5$  bonding mode. Failure to observe more systematic variations in metal–carbon and carbon–carbon bond distances, as found for the symmetrical complex **2**, is largely attributed to the unsymmetrical nature of **1**.

In the chelate pentadienyl ligand, metal–carbon bond lengths are again shortest for the terminal carbon atoms (Lu–C(20), 2.567(5) Å; Lu–C(21), 2.614(6) Å). The central Lu–C(15) bond (2.642(4) Å) is intermediate in length, as is the Lu–C(14) bond (2.636(5) Å). The Lu–C(14) bond is shorter than expected and may result from ligand distortion at C(14) brought about by attachment of the bridging unit; this presumably forces C(14) toward the metal as the allyl unit at the opposite end of the bridge is arranged for maximum coordination. Longest is the Lu–C(16) bond (2.658(5) Å). Carbon–carbon bond distances in this ligand clearly reflect bond orders derived from the major resonance forms contributing to the pentadienyl anion hybrid. Thus, the external

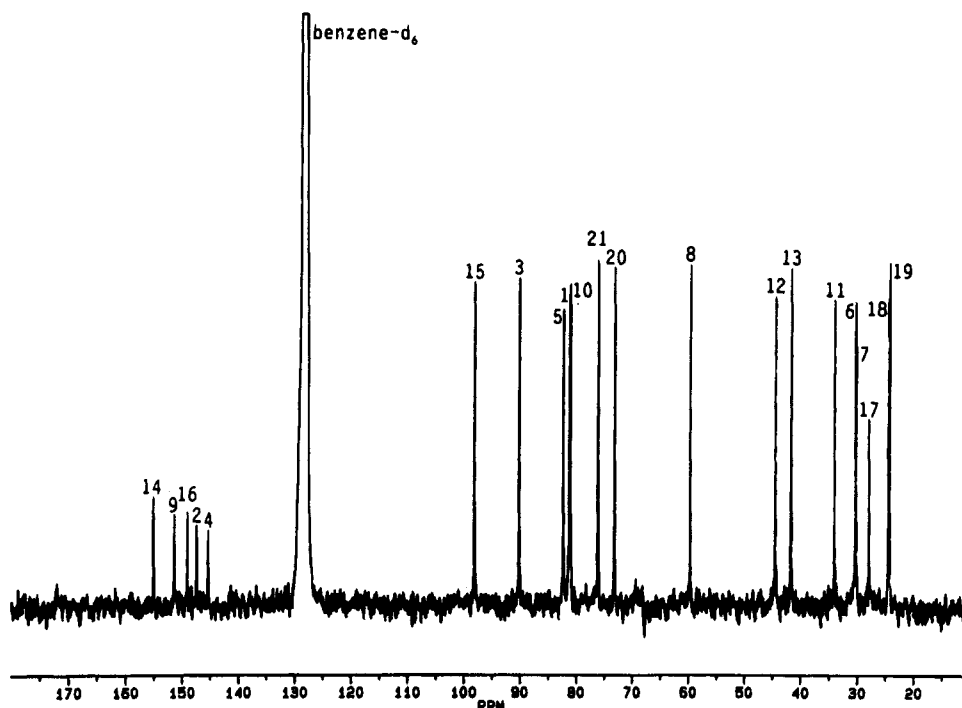


**Figure 2.** 68 MHz  $^{13}\text{C}\{^1\text{H}\}$  NMR spectrum of complex **1** in benzene- $d_6$  (ambient temperature). Refer to the numbering scheme in Figure 1.

pentadienyl carbon-carbon bonds (C(14)–C(20) and C(16)–C(21)) average 1.369(7) Å in length, which compares well with the 1.373(12) Å average length observed for the corresponding bonds in neodymium complex **2**. Similarly, the internal bonds C(14)–C(15) and C(15)–C(16) average 1.428(5) Å in length, compared with 1.421(12) Å for the internal bonds in **2**.

Within the allyl unit, carbon atom C(8) is bound more closely to lutetium (2.440(6) Å) than carbon atoms C(9) and C(10) (2.656(5) and 2.629(5) Å, respectively). In comparison, the average Lu-allyl distance in **2** is 2.59-(1) Å.<sup>4e</sup> The exceedingly short Lu–C(8) bond length is not the result of an  $\eta^1$  orientation of the allyl ligand, since the C(8)–C(9) and C(9)–C(10) bond distances (1.412(6) and 1.398(6) Å, respectively) are statistically equivalent. Rather, it is likely the result of steric constraints imposed by coordination of the chelating ligand. These results attest to an  $\eta^3$  bonding mode where greater formal charge density resides on the terminal allyl carbon atoms. The equivalent carbon-carbon bond distances further reflect the equivalence of the two major resonance structures describing the allyl anion hybrid. Related f-element allyl complexes **2**,  $(\text{C}_5\text{Me}_5)\text{U}(\eta^3\text{-2-methylallyl})_3$ ,<sup>17</sup> and  $(\text{C}_5\text{Me}_5)_2\text{Sm}(\eta^3\text{-allyl})$ <sup>18</sup> display similar trends.

The larger size of the pentadienyl ligand compared with the cyclopentadienyl ligand manifests itself in a longer average metal-carbon bond distance and shorter metal-(ligand centroid) distances. Thus, the average metal-carbon bond distance within the Lu-( $\eta^5$ -pentadienyl) framework of the solitary pentadienyl ligand in **1** is 2.69(4) Å compared with the mean Lu-( $\eta^5$ -cyclopentadienyl carbon) bond distance of 2.60 Å in the eight-

coordinate tris(cyclopentadienyl)lutetium system.<sup>19</sup> Metal-( $\eta^5$ -pentadienyl centroid) distances in **1** (pentadienyl (chelate) centroid, 2.149 Å; solitary pentadienyl centroid, 2.227 Å), on the other hand, are shorter than the corresponding metal-( $\eta^5$ -cyclopentadienyl centroid) distances (2.285 and 2.321 Å). Ligand size differences have effected similar results in the actinide complexes ( $\eta^5$ -2,4-dimethylpentadienyl) $\text{U}(\text{BH}_4)_3$  and ( $\eta^5$ -cyclopentadienyl) $\text{U}(\text{BH}_4)_3$ .<sup>4a</sup>

Interestingly, internal C–C–C bond angles within the pentadienyl units vary systematically. Those angles in which the central carbon atom bears an alkyl substituent are narrower than those angles which do not have a central carbon atom substituent. The same effect has been observed for **3**. The internal C–C–C bond angle of the methylallyl unit in **1** (120.9(4)°) is comparable to the average internal C–C–C bond angle for the methylallyl groups in  $(\text{C}_5\text{Me}_5)\text{U}(\eta^3\text{-2-methylallyl})_3$ <sup>17</sup> (120.3(7)°). This is in contrast to an internal angle of 125.6(20)° observed for the unsubstituted allyl unit in  $(\text{C}_5\text{Me}_5)_2\text{Sm}(\eta^3\text{-allyl})$ .<sup>18</sup>

**Solution Structure of 1.** It was of interest to determine if a complete NMR analysis of such a complicated ligand set could be accomplished with a lanthanide complex given the fluxionality and ligand redistribution equilibria common for these metals. The solution structure of **1** has been shown by NMR to correlate well with the solid-state structure. The proton-decoupled  $^{13}\text{C}$  and  $^1\text{H}$  NMR spectra of the complex, dissolved in benzene- $d_6$  solvent, are shown in Figures 2 and 3, respectively.

The  $^{13}\text{C}$  spectrum shows 21 resonances, consistent with the presence of 21 nonequivalent carbon nuclei making up the ligands about the lutetium metal center. Using the  $J$ -modulated spin echo  $^{13}\text{C}$  experiment, these

(17) Cymbaluk, T. H.; Ernst, R. D.; Day, V. W. *Organometallics* **1983**, *2*, 963–969.

(18) Evans, W. J.; Ulibarri, T. A.; Ziller, J. W. *J. Am. Chem. Soc.* **1990**, *112*, 2314–2324.

(19) Eggers, S. H.; Schultze, H.; Kopf, J.; Fischer, R. D. *Angew. Chem., Int. Ed. Engl.* **1986**, *25*, 656–657.

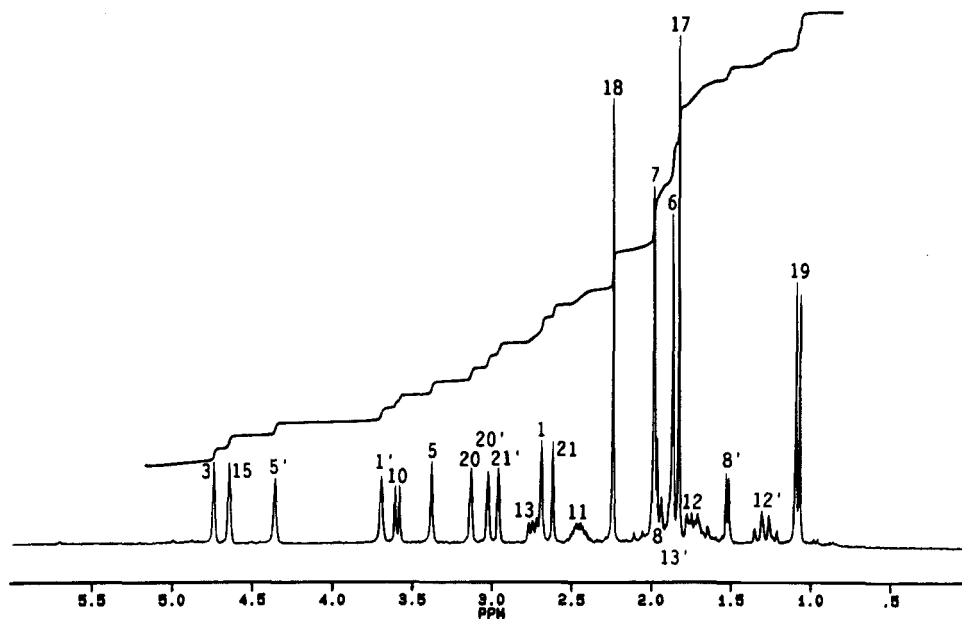


**Figure 3.** 270 MHz  $^1\text{H}$  NMR spectrum of complex **1** in benzene- $d_6$  (ambient temperature). Refer to the numbering scheme in Figure 1.

resonances were differentiated into sets of five methyl, seven methylene, four methine, and five quaternary carbon nuclei.

Evidence for the allyl/chelate-bridge substructure is readily apparent from the  $^1\text{H}$  NMR signal multiplicities observed for H(10) (doublet, 1H, 3.58 ppm), H(11) (multiplet, 1H, 2.46 ppm), and H(19) (doublet, 3H, 1.07 ppm) (Figure 3). These resonances provide the basis from which the remainder of the chelate ligand structure is established. Other proton resonances within the complex include four methyl group singlets (3H each) as well as ten other singlets which are integrated nominally as single protons. Six remaining single-proton resonances appear as multiplets which arise from methylenes H(8), H(12), and H(13).

Both  $^1\text{H}$  and  $^{13}\text{C}$  NMR spectra clearly reflect the asymmetric conformation of **1** in solution. No direct evidence for fluxional behavior involving the solitary pentadienyl ligand (e.g., 1,3- or 1,5-metal migrations) can be inferred under these conditions. This is in contrast to the room-temperature fluxional behavior noted for **2**.<sup>4g</sup> Nonfluxionality in **1** also is in contrast with the rapid room-temperature ligand oscillation reported for bis(2,4-dimethylpentadienyl) complexes of magnesium,<sup>20</sup> beryllium,<sup>21</sup> zinc,<sup>21</sup> nickel,<sup>22</sup> iron,<sup>3e</sup> and ruthenium<sup>3e</sup> but is more in line with the less fluxional behavior of bis(2,4-dimethylpentadienyl)titanium.<sup>3e</sup>

The complete assignment of all  $^1\text{H}$  and  $^{13}\text{C}$  resonances required further analyses by a combination of 2D NMR experiments. Using resonances H(10), H(11), and H(19) as unequivocal starting points, the proton coupling network was traced from the corresponding cross-peaks observed in COSY-45 and long-range COSY-45 spectra. The latter is shown in Figure 4. The long-range correlation proved particularly useful in assigning the four methyls, H(6), H(7), H(17), and H(18), that are

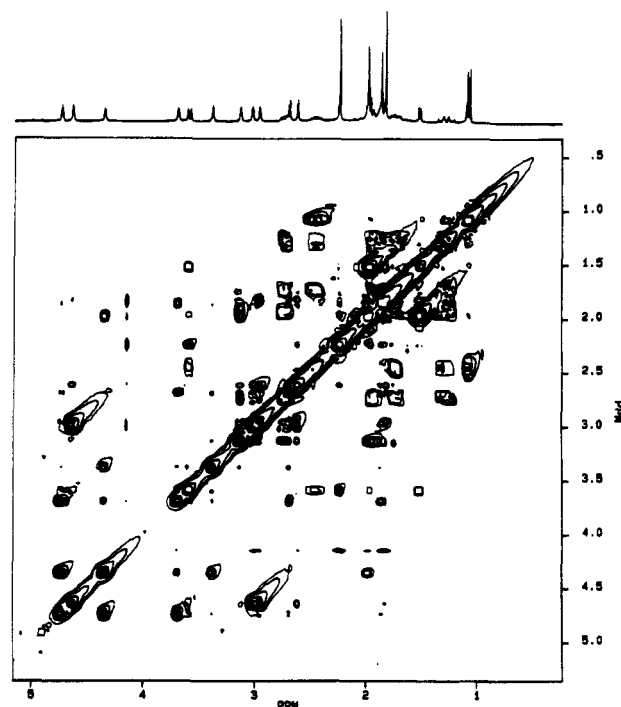


**Figure 4.** Long-range  $^1\text{H}$  COSY-45 spectrum of complex **1** in benzene- $d_6$ .

attached to quaternary carbons. The corresponding  $^{13}\text{C}$  resonances were assigned through a 2D heteronuclear correlation (XHCORR) study, shown in Figure 5. The spread of carbon frequencies in the f2 domain further helped corroborate and confirm the assignment of the nonequivalent methylene proton resonances, despite the fact that some were obscured by signal overlap in the  $^1\text{H}$  spectrum (e.g., H(8) and H(13)). Finally, the long-range analog of this experiment (not shown) helped in the assignment of the quaternary carbon signals and also provided further confirmation of all  $^1\text{H}$  and  $^{13}\text{C}$  signal assignments. The final outcome from these studies has been summarized in Table 3.

On the basis of the chemical shifts observed in both  $^{13}\text{C}$  and  $^1\text{H}$  NMR spectra, it is clear that the metal-

(20) Yasuda, H.; Yamauchi, M.; Nakamura, A.; Sei, T.; Kai, Y.; Yasuoka, N.; Kasai, N. *Bull. Chem. Soc. Jpn.* **1980**, *53*, 1089–1100.

(21) Yasuda, H.; Ohnuma, Y.; Nakamura, A.; Kai, Y.; Yasuoka, N.; Kasai, N. *Bull. Chem. Soc. Jpn.* **1980**, *53*, 1101–1111.

(22) Lehmkuhl, H.; Naydowski, C. *J. Organomet. Chem.* **1982**, *240*, C30–C32.



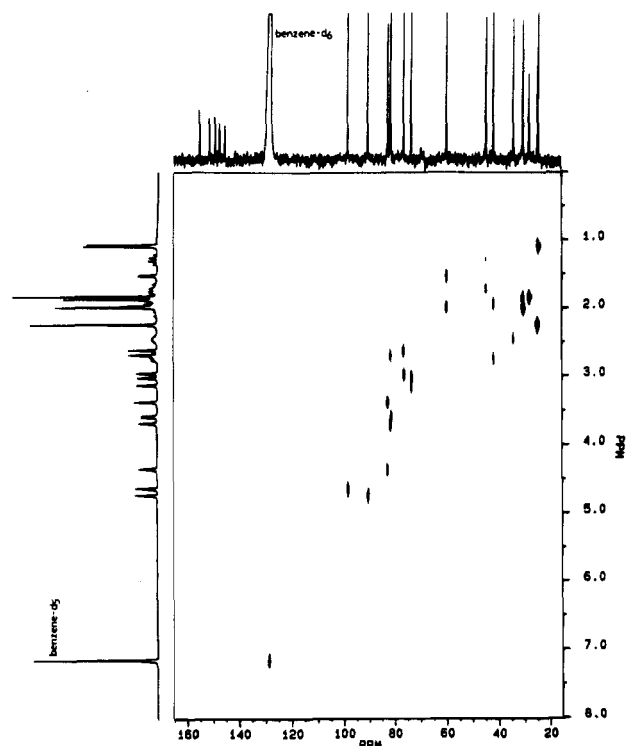


**Figure 5.** 2D  $^{13}\text{C}$ - $^1\text{H}$  heteronuclear correlation (XH-CORR) spectrum of complex **1** in benzene- $d_6$ .

carbon bonding hapticities observed in the solid state are also retained in the solution state. Establishing that the  $\eta^5$ -bound pentadienyl moieties are present in the "U" form, however, was less straightforward. The presence of alkyl substituents in the 2- and 4-positions precluded the observation of spin-spin coupling constants which have previously proven successful in establishing conformations of allyl and pentadienyl metal complexes in solution. Considering the large effective van der Waals radius of the methyl group (ca. 2.0 Å), it is nevertheless unlikely that the ligand would prefer either a "W" or "S" form in solution while adopting a "U" form in the solid state (vide supra).

Finally, the  $^{13}\text{C}$  chemical shifts of the anionic terminal methylene carbons show an interesting trend that can, at least in part, be related to their corresponding metal-carbon bond distances. For example, the C(1) and C(5) atoms of the solitary pentadienyl unit are 2.620(6) and 2.677(6) Å away from the lutetium metal center and show  $^{13}\text{C}$  resonances at 81.1 and 82.2 ppm, respectively. Carbons C(20) and C(21) are situated closer at 2.567(5) and 2.614(6) Å, respectively, and show corresponding  $^{13}\text{C}$  signals at 73.0 and 76.0 ppm that are relatively shielded. By far the shortest bond distance measured is that between lutetium and C(8) (2.440(6) Å), which also exhibits the most shielded resonance (59.5 ppm). Though bond distances measured in the solid state may be expected to change in solution, the observed trend is consistent with the expected relative charge densities at these carbon atoms. Similar effects arising on account of the relative importance of the resonance contributing structures are also evident when comparing the chemical shifts of the quaternary carbons (uncharged) with those of their neighbors which carry some negative charge.

These observations are especially interesting when comparing metal-carbon bond distances in transition-

metal pentadienyl complexes. Just as the shortest pentadienyl metal-carbon bonds in **1** and **2** are primarily to those carbons bearing formal electron charge density, the terminal pentadienyl metal-carbon bonds of the early-transition-metal complexes bis( $\eta^5$ -2,4-dimethylpentadienyl)vanadium<sup>23</sup> and bis( $\eta^5$ -2,4-dimethylpentadienyl)chromium<sup>24</sup> are also observed to be the shortest. Such bonding effects are attributable to the ionic character of these complexes. However, bis( $\eta^5$ -2,4-dimethylpentadienyl)iron<sup>25</sup> displays an opposite trend in which the shortest metal-carbon bonds are to the 2- and 4-carbon atoms. This behavior has been explained by the growing importance of back-bonding in later transition metal complexes.<sup>3a</sup> Back-bonding, as such, is inconsequential in f-block chemistry and does not play a role in describing the structures of **1** and **2**.

For transition-metal allyl complexes, it is more common that the central metal-carbon bond distance is shorter than the terminal allyl metal-carbon bond distances.<sup>26</sup> This is clearly opposite to that situation observed within the allyl framework of **1**, in which the shorter metal-carbon bonds are again to those carbons bearing formal electron charge density. These observations thus show that, steric constraints notwithstanding, charge plays a critical role in the architecture of lanthanide complex **1**.

**Factors Leading to the Formation of 1.** The dimeric chelate ligand in **1** clearly derives from the end-to-end fusion of two 2,4-dimethylpentadienyl groups. Although pentadienyl dimerizations have previously been observed in transition-metal chemistry,<sup>3a</sup> this is the first time that pentadienyl dimerization has been reported in the lanthanide series.

Dimerizations in transition-metal pentadienyl chemistry are believed to result from reorganizations involving unstable, non-18-electron intermediates. Since stabilities in organolanthanide chemistry are not formally governed by the inert-gas rule but, rather, are a function of electrostatic factors and coordination sphere saturation, it is likely that **1** originates, at least in part, from the steric overcrowding which results when three 2,4-dimethylpentadienyl ligands surround a lutetium center. This would appear reasonable, given that  $\text{Lu}^{3+}$  is significantly smaller in ionic radius compared with  $\text{Nd}^{3+}$ , whose coordination sphere is already fully saturated when  $\eta^5$ -complexed to three 2,4-dimethylpentadienyl ligands (vide supra). As reported earlier,<sup>4g</sup> one way to avoid the overcrowding of three  $\eta^5$ -pentadienyl ligands is to form the  $(\eta^5\text{-(CH}_3)_2\text{C}_5\text{H}_5)_2\text{Lu}(\eta^3\text{-(CH}_3)_2\text{C}_5\text{H}_5)$  complex, **2**. A parallel alternative route to a less

(23) Campana, C. F.; Ernst, R. D.; Wilson, D. R.; Liu, J.-Z. *Inorg. Chem.* **1984**, *23*, 2732-2734.

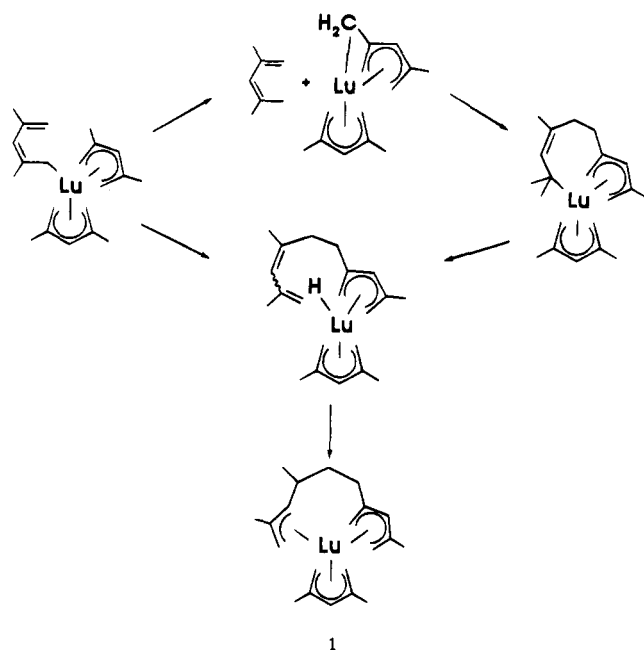
(24) Newbound, T. D.; Freeman, J. W.; Wilson, D. R.; Kralik, M. S.; Patton, A. T.; Campana, C. F.; Ernst, R. D. *Organometallics* **1987**, *6*, 2432-2437.

(25) Wilson, D. R.; Ernst, R. D.; Cymbaluk, T. H. *Organometallics* **1983**, *2*, 1220-1228.

(26) (a) Jolly, P. W. In *Comprehensive Organometallic Chemistry*; Wilkinson, G., Stone, F. G. A., Abel, E. W., Eds.; Pergamon Press: Oxford, England, 1982; Vol. 6, Chapter 37. (b) Maitlis, P. M.; Espinet, P.; Russell, M. J. H. In *Comprehensive Organometallic Chemistry*; Wilkinson, G., Stone, F. G. A., Abel, E. W., Eds.; Pergamon Press: Oxford, England, 1982; Vol. 6, Chapter 38. (c) Hartley, F. R. In *Comprehensive Organometallic Chemistry*; Wilkinson, G., Stone, F. G. A., Abel, E. W., Eds.; Pergamon Press: Oxford, England, 1982; Vol. 6, Chapter 39. (d) Putnik, C. F.; Welter, J. J.; Stucky, G. D.; D'Aniello, M. J., Jr.; Sosinsky, B. A.; Kirner, J. F.; Muetterties, E. L. *J. Am. Chem. Soc.* **1978**, *100*, 4107-4116. (e) Kaduk, J. A.; Poulos, A. T.; Ibers, J. A. *J. Organomet. Chem.* **1977**, *127*, 245-260. (f) Clarice, H. L. *J. Organomet. Chem.* **1974**, *80*, 155-173.



Scheme 1



crowded complex which is consistent with the propensity for  $\text{Lu}^{3+}$  to activate carbon-hydrogen bonds<sup>27</sup> involves a metal-assisted ligand reorganization leading to **1**.

Details of this process have not been investigated, but a route involving an  $\eta^1$ -complexed pentadienyl unit can be envisioned (see Scheme 1). Interligand proton abstraction by a terminally bound pentadienyl group could lead to a metallacyclic intermediate which upon diene reinsertion would generate a ligand-dimerized product.  $\beta$ -Hydrogen elimination followed by hydride addition

would then afford the final complex. Such transformations have precedent or have been proposed to occur in organolutetium chemistry: alkene insertion into Lu-C and Lu-H bonds,<sup>28</sup>  $\beta$ -hydrogen elimination,<sup>28</sup> and interligand proton abstraction.<sup>28e</sup>

### Conclusion

In contrast to the reaction of neodymium trichloride with the 2,4-dimethylpentadienyl anion which affords a simple tris( $\eta^5$ -2,4-dimethylpentadienyl) complex, the analogous reaction with lutetium trichloride leads to bis( $\eta^5$ -pentadienyl)  $\eta^3$ -allyl complexes. The predominant product of this reaction, ( $\eta^5$ -( $\text{CH}_3$ )<sub>2</sub> $\text{C}_5\text{H}_5$ )<sub>2</sub> $\text{Lu}(\eta^3$ -( $\text{CH}_3$ )<sub>2</sub>- $\text{C}_5\text{H}_5$ ),<sup>4g</sup> is accompanied by a complex resulting from coupling of 2,4-dimethylpentadienyl ligands to form a  $\text{C}_{14}$  unit. The solution and solid-state structures, as inferred from 2D NMR and X-ray analysis, have been shown to be in congruence.

**Acknowledgment.** We thank the Division of Chemical Sciences of the Office of Basic Energy Sciences of the Department of Energy for partial support of this work.

**Supporting Information Available:** Tables of anisotropic displacement coefficients, H-atom coordinates and isotropic displacement coefficients, complete interatomic distances and angles, and least-squares planes for **1** (8 pages). Ordering information is given on any current masthead page.

OM940926D

(28) (a) Jeske, G.; Lauke, H.; Mauermann, H.; Schumann, H.; Marks, T. J. *J. Am. Chem. Soc.* **1985**, *107*, 8111-8118. (b) Jeske, G.; Schock, L. E.; Swepston, P. N.; Schumann, H.; Marks, T. J. *J. Am. Chem. Soc.* **1985**, *107*, 8103-8110. (c) Jeske, G.; Lauke, H.; Mauermann, H.; Swepston, P. N.; Schumann, H.; Marks, T. J. *J. Am. Chem. Soc.* **1985**, *107*, 8091-8103. (d) Watson, P. L. *J. Am. Chem. Soc.* **1982**, *104*, 337-339. (e) Watson, P. L.; Roe, D. C. *J. Am. Chem. Soc.* **1982**, *104*, 6471-6473.

(27) Watson, P. L. *J. Am. Chem. Soc.* **1983**, *105*, 6491-6493.

# Synthesis of *ansa*-Titanocenes from 1,2-Bis(2-indenyl)ethane and Structural Comparisons in the Catalytic Epoxidation of Unfunctionalized Alkenes

Shawn R. Hitchcock, Janelle J. Situ, Jonathan A. Covell,  
Marilyn M. Olmstead, and Michael H. Nantz\*

Department of Chemistry, University of California, Davis, California 95616

Received March 30, 1995<sup>⊗</sup>

Novel *ansa*-titanocene dichlorides have been prepared from 1,2-bis(2-indenyl)ethane (**10**). Treatment of the dilithio salt of **10** with either methyl iodide or benzyl bromide gives the corresponding dialkylated bis(indene) in high yield. Titanium complexation of the dimethyl and dibenzyl bis(indene) derivatives affords [ethylenebis( $\eta^5$ -1-methyl-2-indenyl)]titanium dichloride (**14**) and [ethylenebis( $\eta^5$ -1-benzyl-2-indenyl)]titanium dichloride (**15**), respectively. In each case, the *ansa*-titanocene is obtained as a mixture of meso and racemic isomers. Treatment of the dilithio salt of **10** with trimethylsilyl chloride results in a mixture of bis(trimethylsilyl) derivatives. Attempted titanium complexation of the silylated bis(indene) mixture results in an intramolecular oxidative coupling of the C(3) and C(3') positions to yield a *trans*-6,7-dihydroindeno[2,1-*c*]fluorene derivative, **16**. [Ethylenebis( $\eta^5$ -2-indenyl)]titanium dichloride (**9**) is hydrogenated to yield [ethylenebis( $\eta^5$ -4,5,6,7-tetrahydro-2-indenyl)]titanium dichloride (**17**). The crystal structures of *rac*-**14** and **17** were determined by X-ray crystallography and are presented. Examination of ethylene-bridged bis(2-indenyl) *ansa*-titanocenes as catalysts for the epoxidation of unfunctionalized alkenes was conducted using the representative titanocenes **9**, **14**, **15**, and **17**. The catalytic ability of this new class of *ansa*-titanocenes in the epoxidation study was found in some cases to exceed the activity of existent titanocene complexes.

## Introduction

The development of chiral transition metal complexes as catalysts for stereoselective organic transformations is being widely pursued.<sup>1</sup> The successful application of chiral bridged-metallocenes of group IV transition metals in a wide variety of synthetic transformations including hydrogenation,<sup>2</sup> carbomagnesation,<sup>3</sup> olefin epoxidation,<sup>4</sup> olefin isomerization,<sup>5</sup> allylation of aldehydes,<sup>6</sup> ketone reduction,<sup>7</sup> and catalysis of Diels-Alder reactions<sup>8</sup> has further heightened the interest in this field. The most widely employed *ansa*-metallocene reagents thus far have been the [ethylenebis( $\eta^5$ -4,5,6,7-tetrahydro-1-indenyl)]titanium and -zirconium dichlorides (**1a,b**) first disclosed by Brintzinger.<sup>9</sup> The successful application of these C(1),C(1')

tethered bis(tetrahydroindenyl) complexes has resulted in the development of several new bis(indenyl)-derived ligands. Examples include the chiral complexes **2-6** (Chart 1).<sup>10-13</sup>

Recent attention has been drawn to the prospect of tethering indenyl rings through their respective C(2) positions (Chart 2). Halterman<sup>14</sup> and Bosnich<sup>14</sup> reported the first preparations of *ansa*-titanocene complexes containing tetrahydroindenyl ligands tethered via the C(2) positions. We have also focused our efforts in this area and have prepared the first ethylene-bridged example, [ethylenebis( $\eta^5$ -2-indenyl)]titanium dichloride (**9**).<sup>15</sup> We now describe the first synthesis of C(3)-alkylated, C(2)-tethered derivatives of 1,2-bis(2-indenyl)ethane and their use as ligands for *ansa*-titanocene formation. We also report the hydrogenation of complex **9** under ambient conditions to form the constitutional isomer of complex **1a**. The catalytic activity of these new *ansa*-titanocenes in the epoxidation of unfunctionalized alkenes has been examined, and the results of this study are presented herein.

<sup>⊗</sup> Abstract published in *Advance ACS Abstracts*, July 1, 1995.

(1) Halterman, R. L. *Chem. Rev.* **1992**, *92*, 965.

(2) (a) Willoughby, C. A.; Buchwald, S. L. *J. Am. Chem. Soc.* **1994**, *116*, 11703. (b) Broene, R. D.; Buchwald, S. L. *J. Am. Chem. Soc.* **1993**, *115*, 12569. (c) Willoughby, C. A.; Buchwald, S. L. *J. Am. Chem. Soc.* **1992**, *114*, 7562.

(3) (a) Morken, J. P.; Didiuk, M. T.; Hoveyda, A. H. *J. Am. Chem. Soc.* **1993**, *115*, 6997. (b) Hoveyda, A. H.; Morken, J. P. *J. Org. Chem.* **1993**, *58*, 4237.

(4) (a) Halterman, R. L.; Ramsey, T. L. *Organometallics* **1993**, *12*, 2879. (b) Colletti, S. L.; Halterman, R. L. *Tetrahedron Lett.* **1992**, *33*, 1005.

(5) Chen, Z.; Halterman, R. L. *J. Am. Chem. Soc.* **1992**, *114*, 2276. (6) (a) Collins, S.; Kuntz, B. A.; Hong, Y. *J. Org. Chem.* **1989**, *54*, 4154. (b) Sato, F.; Iijima, S.; Sato, M. *J. Chem. Soc., Chem. Commun.* **1981**, 180.

(7) (a) Carter, M. B.; Schiött, B.; Gutiérrez, A.; Buchwald, S. L. *J. Am. Chem. Soc.* **1994**, *116*, 11667. (b) Halterman, R. L.; Ramsey, T. M.; Chen, Z. *J. Org. Chem.* **1994**, *59*, 2642.

(8) (a) Jaquith, J. B.; Guan, J.; Wang, S.; Collins, S. *Organometallics* **1995**, *14*, 1079. (b) Hong, Y.; Kuntz, B. A.; Collins, S. *Organometallics* **1993**, *12*, 964.

(9) (a) Wild, F. R. W. P.; Zsolnai, L.; Huttner, G.; Brintzinger, H. H. *J. Organomet. Chem.* **1982**, *232*, 233. (b) Grossman, R. B.; Doyle, R. A.; Buchwald, S. L. *Organometallics* **1991**, *10*, 1501.

(10) Burk, M. J.; Colletti, S. L.; Halterman, R. L. *Organometallics* **1991**, *10*, 2998.

(11) Hollis, T. K.; Rheingold, A. L.; Robinson, N. P.; Whelan, J.; Bosnich, B. *Organometallics* **1992**, *11*, 2812.

(12) Bandy, J. A.; Green, M. L. H.; Gardiner, I. M.; Prout, K. J. *Chem. Soc., Dalton Trans.* **1991**, 2207.

(13) (a) Chen, Z.; Halterman, R. L. *J. Am. Chem. Soc.* **1992**, *114*, 2276. (b) Chen, Z.; Halterman, R. L. *Organometallics* **1994**, *13*, 3932.

(14) Ellis, W. W.; Hollis, T. K.; Odenkirk, W.; Whelan, J.; Ostrander, R.; Rheingold, A. L.; Bosnich, B. *Organometallics* **1993**, *12*, 4391.

(15) Nantz, M. H.; Hitchcock, S. R.; Sutton, S. C.; Smith, M. D. *Organometallics* **1993**, *12*, 5012.

Chart 1

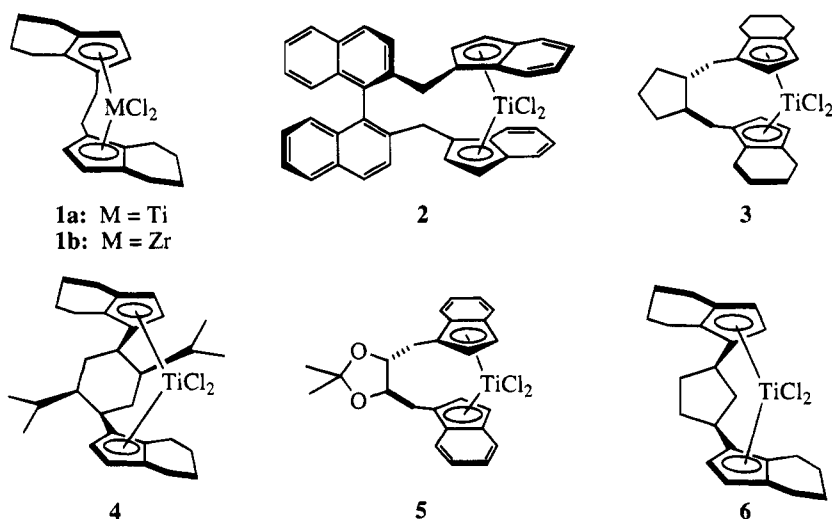
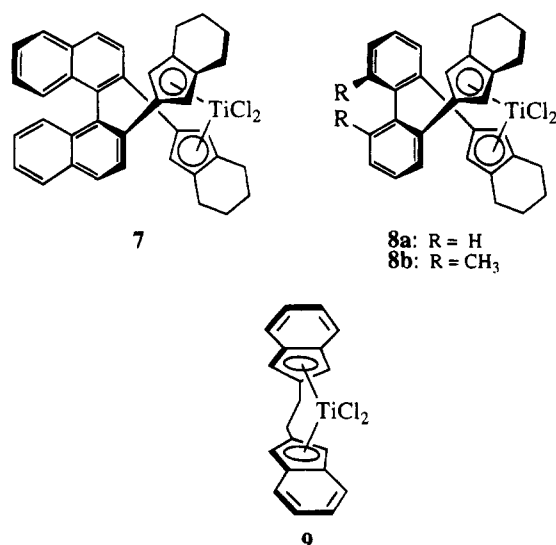


Chart 2



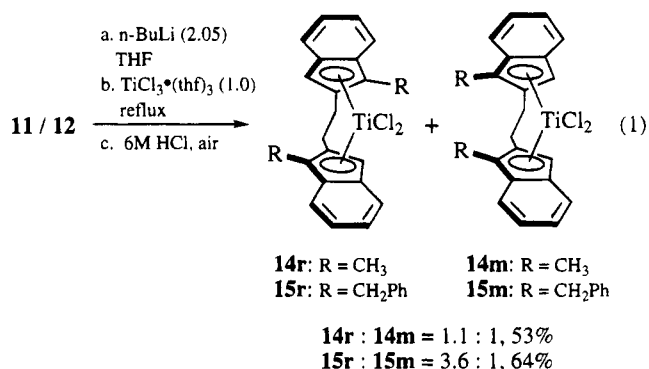
## Results and Discussion

Dialkylation of the bis(indenylide) dianion derived from 1,2-bis(2-indenyl)ethane (**10**)<sup>15</sup> would be anticipated to give rise to a prochiral ligand containing alkyl substituents proximal ( $\alpha$ ) to the ethylene bridge. Subsequent metal complexation of these dialkylated derivatives was expected to afford mixtures of racemic and meso *ansa*-metallocenes in varying ratios. Previous complexation studies on ethylene-bridged cyclopentadienyl ligands have shown that alkyl substituents in the positions alpha to the ethylene bridge slightly increase the racemic to meso diastereomeric ratio relative to ligands devoid of  $\alpha$ -substituents.<sup>16</sup> The dialkylation of **10** thus offers an opportunity to further examine the relationship between  $\alpha$ -substitution and the complexation diastereomeric ratio.

**Ligand Syntheses.** The dialkylation of **10** proved to be straightforward. The corresponding dilithio salt was formed by treatment of **10** with 2 equiv of *n*-BuLi in THF at low temperature. Subsequent addition of either methyl iodide or benzyl bromide afforded the dialkylated bisindenenes as diastereomeric mixtures con-

taining double-bond isomers. Treatment of the crude reaction mixtures according to the procedure of Friedrich and Taggart<sup>17</sup> (triethylamine at reflux) resulted in smooth equilibration of each mixture to give the C(3),C-(3') dimethyl and dibenzyl derivatives **11** and **12** in good yields (Scheme 1). Bis(silylation) of **10** was accomplished by reaction of the dilithio salt of **10** with trimethylsilyl chloride to give bis(indene) **13** as a 1:1 mixture of diastereomers. Treatment of **13** with triethylamine at reflux did not induce any appreciable isomerization of the allylic silane moiety to its bis(vinyl silane) isomer.

**Complexation.** The corresponding *ansa*-titanocenes were prepared using a similar technique employed for the preparation of the parent complex, **9**.<sup>15</sup> The dimethyl titanocene dichloride **14** was prepared by treatment of the dianion of **11** with  $\text{TiCl}_3 \cdot (\text{thf})_3$  followed by addition of 6 M HCl and subsequent aeration (eq 1). This

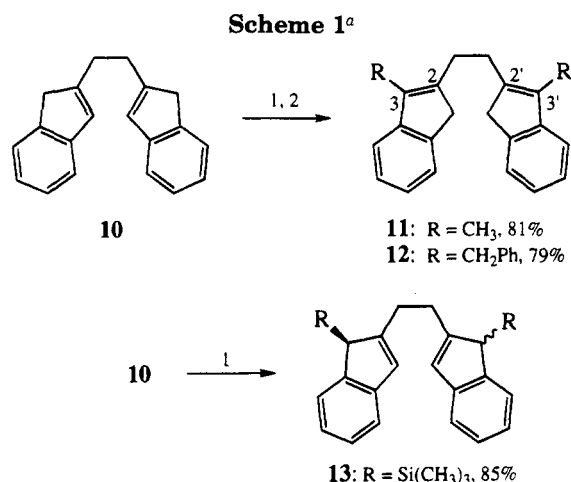


process yielded a mixture of the racemic and meso diastereomers, **14r** and **14m**, which were freed from polymeric byproducts via BioBead chromatography.<sup>18</sup> The racemic to meso diastereomeric ratio was 1.1:1.0. This ratio was readily determined from the <sup>1</sup>H NMR integral regions for the isolated and well-separated methyl singlets at  $\delta$  2.54 (racemic) and 2.40 (meso). The identities of the diastereomers were assigned by comparison of the <sup>1</sup>H NMR signals measured for the ethylene bridge hydrogens with analogous literature examples. Collins<sup>19</sup> has previously shown that the meso

(16) Collins, S. C.; Hong, Y.; Taylor, N. J. *Organometallics* **1990**, *9*, 2695.

(17) Friedrich, E. C.; Taggart, D. B. *J. Org. Chem.* **1975**, *40*, 720.

(18) BioBeads S-X1 were purchased from BioRad Laboratories.



<sup>a</sup> Legend: 1; (a) *n*-BuLi (2.05 equiv), THF, 0 °C, 1 h; (b) MeI (2.5 equiv) or BnBr (2.05 equiv) or (CH<sub>3</sub>)<sub>3</sub>SiCl (2.1 equiv). 2. Et<sub>3</sub>N, 80 °C, 3 h.

**Table 1. Chemical Shifts of the Ethylene Bridge Protons in Complexes 14 and 15**

titanocene	racemic diastereomer		meso diastereomer	
	$\delta$ (ppm) <sup>a</sup>	mult, integr	$\delta$ (ppm)	mult integr
<b>14r</b>	3.01–3.16	m, 2H		
	3.56–3.70	m, 2H		
<b>14m</b>			3.36	s, 4H
<b>15r</b>	3.03–3.07	m, 2H		
	3.63–3.67	m, 2H		
<b>15m</b>			3.32	s, 4H

<sup>a</sup> Spectra were recorded in CDCl<sub>3</sub> at 300 MHz.

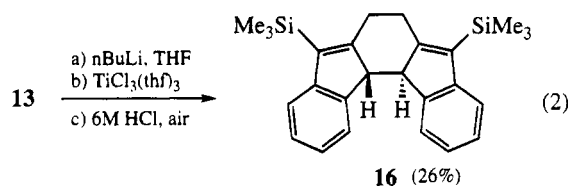
isomers of  $\alpha$ -substituted ethylene-bridged *ansa*-titanocenes exhibit a compact 4H multiplet corresponding to the ethylene bridge. The racemic isomers exhibit a distinctly separate pair of 2H multiplets for the ethylene bridge hydrogens. The chemical shift of the meso 4H signal typically is observed between the chemical shifts of the two racemic 2H multiplets. Table 1 summarizes the spectral data associated with the ethylene bridge in **14r** and **14m** to illustrate the relationship between multiplicity and stereochemistry, which was found to follow the literature trend.<sup>19</sup> The separation of titanocenes **14r** and **14m** could not be achieved by chromatography on silica gel as significant decomposition was observed. However, separation was effected by selective recrystallization from a dichloromethane–cyclohexane mixture. In this manner, pure **14r** was obtained, and the structural assignment was confirmed by X-ray crystallographic analysis. The low diastereoselectivity obtained in the complexation of **11**, the first example involving a C(2)-bridged C(1)-substituted indenylidene anion, is not unlike that observed in previous examples<sup>19,20</sup> of *ansa*-titanocene formation via complexation of bridged ligands possessing  $\alpha$ -substitution. The methyl substituents in **11** do not impart any significant thermodynamic bias to favor the transition toward racemic isomer formation, an observation that is consistent with the prevailing notion that the condensation of dianions with TiCl<sub>3</sub> proceeds along a kinetic path which likely will not reflect the relative stabilities of the eventual Ti(IV) metallocene dichlorides.<sup>19,21</sup>

(19) Collins, S.; Hong, Y.; Ramachandran, R.; Taylor, N. *J. Organometallics* **1991**, *10*, 2349.

(20) Burger, P.; Hortmann, K.; Diebold, J.; Brintzinger, H. H. *J. Organomet. Chem.* **1991**, *417*, 9.

Using the procedure outlined above, the dibenzyl ligand **12** was complexed to give titanocenes **15** in 64% yield. A diastereomeric ratio of 3.6:1.0 was determined from the <sup>1</sup>H NMR integral regions for the ethylene bridge resonances. The diastereomers were readily separated by selective recrystallization of **15r** from a toluene–cyclohexane mixture. The major diastereomer was assigned the racemic configuration on the basis of the <sup>1</sup>H NMR chemical shifts of the ethylene bridge (Table 1). The improvement in the racemic to meso diastereoselection on substitution of methyl with benzyl is the first indication that an increase in the size of the  $\alpha$ -substituent of ethylene-bridged enantiotopic ligands may be used to direct the diastereoselection of titanium complexation. This approach is complementary to previously reported methods devised to influence the complexation diastereoselectivity.<sup>14,22,23</sup>

Attempted complexation of the bis(trimethylsilyl) derivative **13**, an example in which the  $\alpha$ -substituent is larger<sup>24</sup> by comparison to **11** and **12**, led to a reaction mixture which included uncomplexed **13** and 5,8-bis-(trimethylsilyl)-6,7-dihydroindenof[2,1-c]fluorene, **16**.<sup>25</sup> Evidently, an intramolecular oxidative coupling of the



C(1) and C(1') positions occurs as a result of titanocene destabilization, presumably a consequence of steric repulsions involving the trimethylsilyl groups. Bosnich *et al.* have also observed this phenomenon during attempted complexation of a binaphthyl-strapped bis-(2-indenyl).<sup>14</sup> It was postulated that a C(1),C(1') bis(2-indenyl) diradical was formed from the corresponding dianion following Ti(IV) reduction. Subsequent intramolecular radical coupling led to the formation of a highly fused ring system. The *trans*-stereochemistry in **16** was assigned on the basis of X-ray crystallographic data obtained for this compound.<sup>26</sup>

**Hydrogenation of Titanocene 9.** The hydrogenation of strapped indenyl-based complexes is a well-documented method for obtaining the corresponding tetrahydroindenyl-based metallocenes.<sup>27</sup> Recently, Bosnich and co-workers reported the hydrogenation of 2-indenyl *ansa*-titanocene complexes under ambient pressure.<sup>28</sup> These conditions were applied to [ethylenebis( $\eta^5$ -2-indenyl)]titanium dichloride, the parent ti-

(21) Wiesenfeldt, H.; Reinmuth, A.; Barsties, E.; Evertz, K.; Brintzinger, H. H. *J. Organomet. Chem.* **1989**, *369*, 359.

(22) Sutton, S. C.; Nantz, M. H.; Parkin, S. R. *Organometallics* **1993**, *12*, 2248.

(23) For an excellent diastereoselective approach to the precursor of zirconocene **1b**, see: Diamond, G. M.; Rodewald, S.; Jordan, R. F. *Organometallics* **1995**, *14*, 5.

(24) For a comparison of the effective substituent radii of trimethylsilyl vs methyl, see: Bott, G.; Field, L. D.; Sternhell, S. *J. Am. Chem. Soc.* **1980**, *102*, 5618.

(25) The indenof[2,1-c]fluorene ring system has been previously reported, see: Straus, F.; Kühnel, R.; Haensel, R. *Ber.* **1933**, *66B*, 1847.

(26) Unpublished results; the X-ray crystallographic data for **16** will be presented elsewhere.

(27) Wild, F. R. W. P.; Wasiucionek, M.; Huttner, G.; Brintzinger, H. H. *J. Organomet. Chem.* **1985**, *288*, 63.

(28) Rheingold, A. L.; Robinson, N. P.; Whelan, J.; Bosnich, B. *Organometallics* **1992**, *11*, 1869.

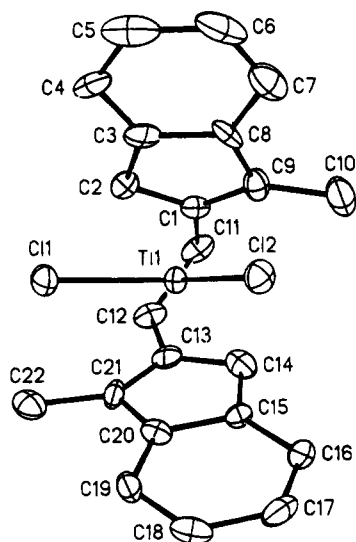
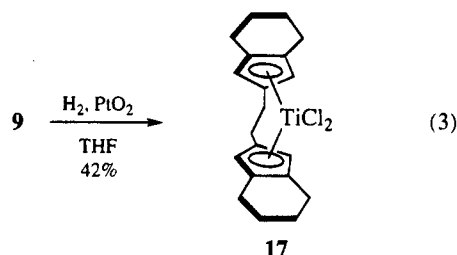


**Figure 1.** Molecular structure of compound **14r** with 50% probability ellipsoids depicted and H atoms removed for clarity.

titanocene of the ethylene bridged (2-indenyl) complexes (eq 3). The hydrogenation of **9** was conducted using



catalytic  $\text{PtO}_2$  in THF under ambient pressure to afford [ethylenebis( $\eta^5$ -4,5,6,7-tetrahydroindenyl)]titanium dichloride (**17**). Complex **17** was freed from  $\text{PtO}_2$  by filtration through a short BioBead column and purified by recrystallization from a mixture of  $\text{Et}_2\text{O}$  and  $\text{CH}_2\text{Cl}_2$ . The preparation of *ansa*-titanocene **17** represents the first synthesis of a constitutional isomer of Brintzinger's complex **1a**.

**Crystal Structures.** Titanocenes **14r** and **14m** were dissolved in the minimum amount of  $\text{CH}_2\text{Cl}_2$ , and cyclohexane was diffused slowly into the solution. After 16 h, this process led to growth of crystals that were enriched in one of the diastereomers. A second recrystallization gave crystals that were suitable for X-ray diffraction studies. The crystals were monoclinic and were assigned the space group  $P2_1/c$ . Two similar molecules were observed in the asymmetric unit of the structure, and both were determined to have the chiral, racemic configuration **14r**. The appearance of two very similar *ansa*-titanocenes in the unit cell has been observed previously by Collins *et al.*<sup>19</sup> Our discussion pertaining to **14r** will focus on only one of the molecules since the dimensions of the two are almost identical.<sup>29</sup> A thermal ellipsoid plot of **14r** is depicted in Figure 1, and the corresponding crystal data are listed in Table 2. The structural geometry about titanium is within expected values: the ( $\eta^5$ -centroid)-Ti-( $\eta^5$ -centroid) angle is determined as  $128.0^\circ$ , and the Cl-Ti-Cl bond angle

**Table 2.** Crystallographic Data for Titanocenes **14r** and **17**<sup>a</sup>

	<b>14r</b>	<b>17</b>
empirical formula	$\text{C}_{22}\text{H}_{20}\text{TiCl}_2$	$\text{C}_{20}\text{H}_{24}\text{TiCl}_2$
color; habit	dark block	red plates
cryst size ( $\text{mm}^3$ )	$0.16 \times 0.16 \times 0.18$	$0.06 \times 0.28 \times 0.36$
cryst syst	monoclinic	monoclinic
space group	$P2_1/c$	$P2_1/c$
unit cell dimens	$a = 27.676(8) \text{ \AA}$ $b = 11.347(3) \text{ \AA}$ $c = 11.660(4) \text{ \AA}$ $\beta = 101.27(2)^\circ$	$a = 19.029(7) \text{ \AA}$ $b = 7.045(2) \text{ \AA}$ $c = 13.167(4) \text{ \AA}$ $\beta = 101.27(3)^\circ$
volume	$3591(2) \text{ \AA}^3$	$1747.0(8) \text{ \AA}^3$
Z	8	4
fw	403.2	383.2
density (calcd)	$1.491 \text{ Mg/m}^3$	$1.457 \text{ Mg/m}^3$
abs coeff	$0.776 \text{ mm}^{-1}$	$0.792 \text{ mm}^{-1}$
$F(000)$	1664	800
$2\theta$ range	$0.0\text{--}45.0^\circ$	$0.0\text{--}50.0^\circ$
scan speed (constant)	$3.97 \text{ deg/min in } \omega$	$6.01 \text{ deg/min in } \omega$
scan range ( $\omega$ )	$0.80^\circ$	$0.80^\circ$
std refln	2 measd every 198 reflns	3 measd every 198 reflns
no. of reflns colld	4944	3405
no. of indep reflns	4688 ( $R_{\text{int}} = 2.87\%$ )	3059 ( $R_{\text{int}} = 6.09\%$ )
no. of obsd reflns	2890 ( $F > 4.0\sigma(F)$ )	2573 ( $F > 4.0\sigma(F)$ )
range of transmissn coeffs	$0.86\text{--}0.90$	$0.83\text{--}0.96$
soln	direct methods	direct methods
refinement method	full-matrix least-squares	full-matrix least-squares
weighting Scheme	$\sigma^2(F) + 0.0003F^2$	$\sigma^2(F) + 0.0007F^2$
factor minimized	$\sum w(F_o - F_c)^2$	$\sum w(F_o - F_c)^2$
no. of params refined	451	208
indices: $R_F, R_wF^f$	5.98%, 5.59%	3.72%, 4.18%
goodness of fit	1.36	1.21
largest diff peak	$0.96 \text{ e \AA}^{-3}$	$0.96 \text{ e \AA}^{-3}$
largest diff hole	$0.00 \text{ e \AA}^{-3}$	$-0.41 \text{ e \AA}^{-3}$

<sup>a</sup> Conditions: Siemens R3m/V diffractometer, Mo K $\alpha$  ( $\lambda = 0.71073 \text{ \AA}$ ), highly oriented graphite monochromator,  $T = 130 \text{ K}$ .  
<sup>b</sup> Siemens SHELXTL PLUS system: Sheldrick, G. M. SHELXTL, A Program For Crystal Structure Determination, Version 4.2; Siemens Analytical X-ray Instruments: Madison, WI, 1990. <sup>c</sup>  $R_F = \frac{\sum |F_o| - |F_c|}{\sum |F_o|}$ ;  $R_wF^f = \frac{\sum |F_o| - |F_c|w^{1/2}}{\sum |F_o|w^{1/2}}$ .

is  $96.2(1)^\circ$ . The indenyl rings bow out of planarity away from the  $\text{TiCl}_2$  moiety which is twisted  $14.5^\circ$  out of the cavity formed by the indenyl rings. The *ansa*-ligand is positioned around the plane containing  $\text{TiCl}_2$  in a  $\lambda$  conformation, and the angle between the normals to the cyclopentadienyl rings is  $63.2^\circ$ . These distortions cause the outer edges of the indenyl rings (C(5)-C(6) and C(17)-C(18)) to form a rectangular region directly in front of  $\text{TiCl}_2$  in which the two nonbonding distances are  $7.76 \text{ \AA}$  (C(5)-C(18)) and  $7.53 \text{ \AA}$  (C(6)-C(17)). This rectangular region is shifted to one side by  $0.22 \text{ \AA}$  (the second titanocene structure in the unit cell has the identical differential, but the size of the rectangular region is slightly larger). Atomic coordinates and selected bond lengths and angles for **14r** are listed in Tables 3-4.

Titanocene **17** was dissolved in the minimum amount of  $\text{CH}_2\text{Cl}_2$  to form a concentrated solution, and  $\text{Et}_2\text{O}$  was diffused slowly into the solution. This process led to the growth of very well defined crystals, and subsequent structural characterization was achieved by X-ray crystallography (Figure 2). The crystals were monoclinic and were assigned the space group  $P2_1/c$ . Selected data have been collected and are summarized in Tables 2, 5, and 6. The ( $\eta^5$ -centroid)-Ti-( $\eta^5$ -centroid) angle and the Cl-Ti-Cl angle were determined to be  $129.5$  and  $94.8(1)^\circ$ , respectively. Both of these measurements are well

(29) The supporting information for this article contains the X-ray data for both structures of **14r**.

**Table 3. Selected Bond Distances and Angles for Titanocene 14r<sup>a</sup>**

Bond Distances (Å)			
Ti(1)–Cl(1)	2.356(3)	Ti(1)–C(14)	2.297(9)
Ti(1)–Cl(2)	2.310(3)	Ti(1)–C(15)	2.512(8)
Ti(1)–C(1)	2.386(9)	Ti(1)–C(21)	2.475(9)
Ti(1)–C(2)	2.310(8)	C(20)–C(21)	1.441(12)
Ti(1)–C(3)	2.476(8)	C(5)–C(6)	1.404(17)
Ti(1)–C(9)	2.449(10)	C(6)–C(7)	1.348(15)
C(1)–C(2)	1.430(12)	C(5)–C(18)	7.76
C(2)–C(3)	1.439(13)	C(6)–C(17)	7.53
C(3)–C(4)	1.411(12)	Cent <sup>A</sup> –Ti	2.118
C(4)–C(5)	1.352(16)	Cent <sup>B</sup> –Ti	2.122

Bond Angles (deg)			
Cl(1)–Ti(1)–Cl(2)	96.2(1)	C(18)–C(19)–C(20)	117.6(8)
C(21)–C(13)–C(14)	108.4(7)	C(19)–C(20)–C(21)	130.9(8)
C(20)–C(21)–C(22)	125.1(8)	C(13)–C(21)–C(20)	108.1(7)
C(2)–C(1)–C(9)	108.8(8)	C(11)–C(12)–C(13)	108.4(7)
C(9)–C(10)–C(18)	124.4(8)	Cent <sup>A</sup> –Ti–Cent <sup>B</sup>	128.0

<sup>a</sup> Cent A and Cent B are the two centroids of the  $\eta^5$ -coordinated cyclopentadienyl rings.

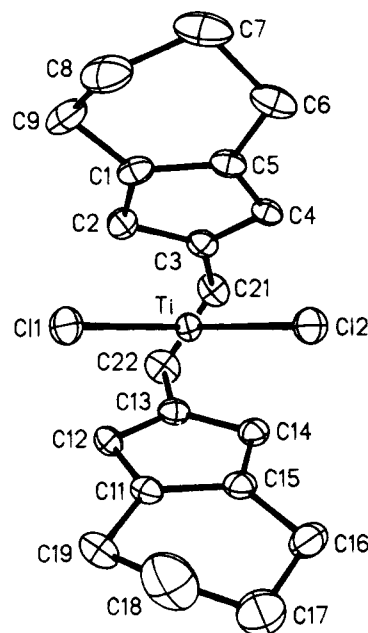
**Table 4. Atomic Coordinates ( $\times 10^4$ ) and Equivalent Isotropic Displacement Coefficients ( $\text{Å}^2 \times 10^3$ ) for Titanocene 14r**

atom	<i>x/a</i>	<i>y/b</i>	<i>z/c</i>	<i>U</i> (eq) <sup>a</sup>
Ti(1)	1175(1)	4726(1)	7261(1)	18(1)
Cl(1)	560(1)	6171(2)	6734(2)	28(1)
Cl(2)	1832(1)	6016(2)	7607(2)	26(1)
C(1)	1140(3)	2900(8)	6234(7)	22(3)
C(2)	789(3)	3715(8)	5615(7)	22(3)
C(3)	1061(3)	4586(8)	5106(7)	27(3)
C(4)	911(4)	5516(8)	4313(7)	30(4)
C(5)	1264(5)	6129(10)	3913(9)	50(5)
C(6)	1766(4)	5864(11)	4264(9)	46(5)
C(7)	1925(4)	5016(9)	5058(8)	37(4)
C(8)	1570(3)	4340(8)	5478(7)	25(3)
C(9)	1614(3)	3326(8)	6236(7)	26(3)
C(10)	2094(3)	2751(9)	6780(8)	43(4)
C(11)	997(3)	1816(8)	6812(7)	30(4)
C(12)	646(3)	2183(7)	7615(7)	25(3)
C(13)	863(3)	3219(8)	8318(7)	25(3)
C(14)	1378(3)	3392(8)	8759(7)	27(4)
C(15)	1438(3)	4451(8)	9431(7)	18(3)
C(16)	1850(3)	4988(8)	10174(7)	26(3)
C(17)	1780(4)	5981(9)	10725(7)	31(4)
C(18)	1313(3)	6546(8)	10578(7)	28(4)
C(19)	907(3)	6075(8)	9839(7)	26(3)
C(20)	969(3)	4990(7)	9285(7)	19(3)
C(21)	614(3)	4212(8)	8599(7)	24(3)
C(22)	64(3)	4385(8)	8367(7)	32(4)

<sup>a</sup> Equivalent isotropic *U* defined as one-third of the trace of the orthogonalized  $U_{ij}$  tensor.

within the range of values associated with ethylene-bridged *ansa*-titanocenes.<sup>30</sup> The overall structure of **17** is only slightly distorted from idealized  $C_2$  symmetry in that the  $\text{TiCl}_2$  moiety is twisted  $0.2^\circ$  out of the cavity formed by the tetrahydroindenyl ligands. The ethylene-bridged ligand adopts a  $\lambda$  configuration around the titanium center, and the edges (C(7)–C(8) and C(17)–C(18)) of the tetrahydroindenyl rings are oriented in a mesomeric fashion that is counterintuitive. The cavity dimensions, defined by the nonbonding nuclear distances between the carbons at the outer edges, are 7.037 Å (C(8) to C(18)) and 8.190 Å (C(7) to C(17)).

Studies by Brintzinger<sup>30</sup> seem to indicate that a purely  $C_2$  symmetric arrangement of an *ansa*-titanocene would cause synchronous steric interactions between the equatorial chloride ligands of the titanium and the  $\alpha$ -

**Figure 2.** Molecular structure of compound **17** with 50% probability ellipsoids depicted and H atoms removed for clarity.**Table 5. Selected Bond Distances and Angles for Titanocene 17<sup>a</sup>**

Bond Distances (Å)			
Ti–Cl(1)	2.340(1)	C(6)–C(7)	1.525(5)
Ti–Cl(2)	2.333(1)	C(7)–C(8)	1.511(6)
C(1)–C(2)	1.414(5)	C(11)–C(12)	1.421(4)
C(3)–C(4)	1.405(4)	C(12)–C(13)	1.402(4)
C(4)–C(5)	1.421(5)	C(13)–C(14)	1.420(4)
C(1)–C(9)	1.504(5)	Ti–Cent <sup>A</sup>	2.098
C(5)–C(6)	1.497(5)	Ti–Cent <sup>B</sup>	2.096

Bond Angles (deg)			
Cl(1)–Ti–Cl(2)	94.8(1)	C(13)–C(14)–C(15)	108.2(3)
C(2)–C(3)–C(4)	106.9(3)	C(15)–C(16)–C(17)	111.5(3)
C(1)–C(5)–C(6)	123.1(3)	C(16)–C(17)–C(18)	115.7(3)
C(6)–C(7)–C(8)	112.1(3)	C(17)–C(18)–C(19)	114.5(4)
C(12)–C(13)–C(14)	111.3(3)	C(19)–C(11)–C(15)	108.3(2)
C(12)–C(13)–C(14)	107.4(2)	Cent <sup>A</sup> –Ti–Cent <sup>B</sup>	129.5

<sup>a</sup> Cent A and Cent B are the two centroids of the  $\eta^5$ -coordinated cyclopentadienyl rings.

and  $\beta$ -substituents of the cyclopentadienyl rings. The distortion of *ansa*-titanocene complexes is usually manifested by ligand rotations about the  $\text{TiCl}_2$  moiety away from  $C_2$  symmetry in an effort to ameliorate these steric interactions. The structural distortions that are apparent in titanocenes **9**,<sup>31</sup> **14r**, and **17** follow this general behavior. Titanocenes **9** and **14r** have the  $\text{TiCl}_2$  moiety misaligned by consymmetric ligand rotations of  $19.2$  and  $14.5^\circ$ , respectively. In contrast, complex **17** exhibits only a slight consymmetric ligand rotation of  $0.2^\circ$ , which implies that dissymmetric ligand rotations prevail to alleviate the intramolecular steric interactions. These results suggest that the extent of the consymmetric misalignment is related to the inherent conformational flexibility of the ligand framework. The indenyl rings in complexes **9** and **14r** are structurally rigid, whereas complex **17** contains the more conformationally flexible tetrahydro-2-indenyl rings.

The dissymmetric structural distortions of the ethylene bridge in complexes **9**, **14r**, and **17** appear to be

(30) Burger, P.; Diebold, J.; Gutmann, S.; Hund, H.-U.; Brintzinger, H. H. *Organometallics* **1992**, *11*, 1319.

(31) Parkin, S.; Hitchcock, S. R.; Hope, H.; Nantz, M. H. *Acta Crystallogr.* **1994**, *C50*, 169.

**Table 6. Atomic Coordinates ( $\times 10^4$ ) and Equivalent Isotropic Displacement Coefficients ( $\text{\AA}^2 \times 10^3$ ) for Titanocene 17**

atom	<i>x/a</i>	<i>y/b</i>	<i>z/c</i>	<i>U(eq)</i> <sup>a</sup>
Ti	7477(1)	3784(1)	3992(1)	17(1)
Cl(1)	7511(1)	635(1)	4149(1)	28(1)
Cl(2)	7517(1)	4297(1)	5759(1)	26(1)
C(1)	6168(2)	2982(4)	2954(2)	24(1)
C(2)	6538(2)	3753(4)	2291(2)	24(1)
C(3)	6682(2)	5590(4)	2580(2)	22(1)
C(4)	6465(2)	5883(4)	3486(2)	21(1)
C(5)	6127(2)	4286(4)	3704(2)	23(1)
C(6)	5721(2)	3987(5)	4485(3)	33(1)
C(7)	5206(2)	2352(5)	4165(3)	44(1)
C(8)	5584(2)	756(5)	3852(3)	42(1)
C(9)	5793(2)	1171(5)	2853(3)	34(1)
C(11)	8825(2)	3205(4)	4316(2)	22(1)
C(12)	8422(2)	3429(4)	3199(2)	23(1)
C(13)	8166(2)	5216(4)	3024(2)	22(1)
C(14)	8351(2)	6062(4)	4049(2)	23(1)
C(15)	8790(2)	4832(4)	4844(2)	23(1)
C(16)	9220(2)	5155(5)	6011(3)	33(1)
C(17)	9747(2)	3608(6)	6495(3)	56(2)
C(18)	9479(3)	1819(6)	6085(3)	60(2)
C(19)	9279(2)	1613(5)	4882(3)	31(1)
C(21)	7040(2)	6926(4)	2033(2)	26(1)
C(22)	7747(2)	6069(4)	1959(3)	29(1)

<sup>a</sup> Equivalent isotropic *U* defined as one-third of trace of the orthogonalized  $U_{ij}$  tensor.

closely related to the degree of cyclopentadienyl substitution. X-ray diffraction studies<sup>31</sup> on complex **9** showed that the ethylene bridge exists in both the  $\delta$  and  $\lambda$  conformations, thus indicating a minimal barrier for interconversion of the two conformers. However, complexes **14r** and **17** exhibit a preference for the  $\lambda$  conformation while in the solid state. Evidently, the  $\alpha$ -substitution in complex **14r** diminishes the conformational equilibrium in the solid state and results in a preferential crystallization as a single conformer. Surprisingly, in the case of complex **17**, the addition of hydrogen to the indenyl ring diminishes the equilibrium between the two conformations in the solid state.

**Epoxidations.** Only a few investigations have examined the relationship between titanocene structure and reactivity,<sup>32</sup> and, to our knowledge, there have been no studies involving ethylene-bridged titanocenes as epoxidation catalysts.<sup>33</sup> The ability to obtain enantiomerically enriched *ansa*-titanocenes has thus stimulated interest in the use of these complexes as epoxidation catalysts. In this context, titanocenes **2** and **7** were recently employed by Halterman<sup>4</sup> in catalytic epoxidation experiments, and each was shown to be moderately effective.

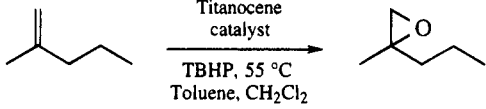
The successful preparation of the chiral titanocenes **14r** and **15r** prompted us to examine the catalytic reactivity of these complexes. We were initially concerned that the present ethylene-bridged 2-indenyl titanocenes might suffer immediate decomposition under the conditions required for olefin epoxidation.<sup>34</sup> Previous reports have noted an inherent instability of 2-indenyl titanocene dichlorides under protic condi-

(32) Colletti, S. L.; Halterman, R. L. *J. Organomet. Chem.* **1993**, *455*, 99 and references therein.

(33) The effect of binding titanocene dichlorides to a polymer support has been examined; see: (a) Lau, C. P.; Chang, B.-H.; Grubbs, R. H. Brubaker, C. H., Jr. *J. Organomet. Chem.* **1981**, *214*, 325. (b) Chang, B.-H.; Grubbs, R. H. Brubaker, C. H., Jr. *J. Organomet. Chem.* **1985**, *280*, 365.

(34) For a discussion pertaining to the stability of indenyl-based titanocenes, see: Samuel, E. *J. Organomet. Chem.* **1969**, *19*, 87.

**Table 7. Epoxidation of 2-Methyl-1-pentene<sup>a</sup>**

		
titanocene dichloride	no. of turnovers (alkene) <sup>b</sup>	no. of turnovers (epoxide) <sup>c</sup>
<b>1a</b>	19	15
<b>9</b>	23	20
<b>14r</b>	17	9
<b>15r</b>	12	9
<b>17</b>	18	10
<b>18</b>	14	13
<b>19</b>	18	16

<sup>a</sup> All reactions were conducted using 0.005 equiv of Ti catalyst and 1.10 equiv of TBHP; the reported turnover number was measured at 15 h. <sup>b</sup> In units of mmol of alkene consumed per mmol of Ti catalyst; calculated from a minimum of three experiments.

<sup>c</sup> In units of mmol of epoxide detected per mmol of Ti catalyst.

tions.<sup>4a,14</sup> The catalytic activities of the 2-indenyl *ansa*-titanocenes **9**, **14r**, and **15r** and the tetrahydro-2-indenyl *ansa*-titanocene **17** were examined in the epoxidation of 2-methyl-1-pentene using anhydrous *tert*-butylhydroperoxide according to previously described reaction conditions.<sup>4</sup> Additionally, to compare the effects of titanocene structure on catalytic reactivity, Brintzinger's complex (**1a**), bis(cyclopentadienyl)titanium dichloride (**18**), and [ethylenebis(cyclopentadienyl)titanium dichloride (**19**<sup>15,35</sup>)] were included in this study. Table 7 summarizes titanocene reactivity as a function of turnover number, which is calculated in relation to alkene consumption and in relation to epoxide formation.

We were gratified to find that the 2-indenyl titanocenes **9**, **14r**, and **15r** were as effective as existent *ansa*-titanocenes in the epoxidation of the representative alkene. The tetrahydro-2-indenyl complex **17** also exhibited similar reactivity in comparison to its isomer, titanocene **1a**. The differences between the turnover number based on alkene consumption and the turnover number based on epoxide formation presumably are due to epoxide consumption during the course of the reaction.<sup>36</sup> The modest turnover numbers found for titanocenes have been previously attributed to inactivation of the catalyst by formation of insoluble metal-oxygen-metal polymers<sup>33,37</sup> and ligand decomposition under the oxidative conditions.<sup>38</sup> The results in Table 7 seem to indicate that substitution of the cyclopenta-

(35) Brintzinger, H. H.; von Seyerl, J.; Huttner, G.; Smith, B. A. *J. Organomet. Chem.* **1979**, *173*, 175.

(36) In general, no volatile products other than the epoxide and *tert*-butyl alcohol were observed in >2% by GC analysis on the crude epoxidation mixture. For those entries where substantial differences were observed in the measured turnovers (alkene consumption *vs* epoxide formation), we speculate that titanocene-induced oligomerization of the epoxide may have occurred. The isolation and identification of postulated higher molecular weight side products remains to be investigated.

(37) Berry, M.; Davies, S. G.; Green, M. L. H. *J. Chem. Soc., Chem. Commun.* **1978**, 99.

(38) Sheldon, R. A. *J. Mol. Catal.* **1980**, *7*, 107.



dienyl rings and/or tethering the cyclopentadienyl rings do not have a large effect in circumventing the problems associated with catalyst inactivation. The use of more sterically encumbered ligands than those examined in the present study also has been shown to exhibit similar epoxidation turnovers.<sup>4</sup> In contrast, site isolation of the titanocene catalyst by attachment to a rigid polymer has been shown to increase the titanocene reactivity.<sup>33</sup>

The effect of varying alkene structure on 2-indenyl titanocene reactivity was examined using complex **9** (Table 8). The alkenes depicted in Table 8 were examined under reaction conditions identical to those in Table 7, and the catalyst reactivity was measured as a function of the turnover number based on alkene consumption. The results indicate that the representative 2-indenyl *ansa*-titanocene catalyzes the epoxidation of structurally different alkenes with approximately similar turnover capacity. The catalytic conversion of monosubstituted alkenes (entries a and b) was similar to the conversion observed for the *trans*-alkene substrate (entry e). Titanocene **9** exhibited the highest turnover rates with the *cis*-alkene substrates (entries c and d). The increase in *cis*-alkene consumption relative to the corresponding *trans*-alkene consumption (entry c vs entry e) may be explained in part by the absence of steric repulsions with at least one of the indenyl rings as the *cis*-alkene approaches the catalyst-oxidant species. In contrast, a *trans*-alkene, by virtue of the opposing substitution pattern of the  $\pi$  system, is expected to undergo steric interactions with both indenyl rings of the catalyst-oxidant species.<sup>39</sup>

### Conclusion

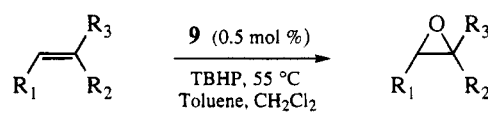
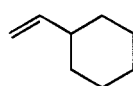
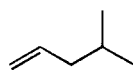
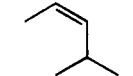
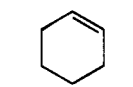
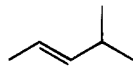
We have prepared the first examples of ethylene-bridged titanocenes in which the indenyl ligands are attached at the 2-position and have alkyl substituents in the 1-position. The assignment of stereochemistry in these complexes was related to the characteristic <sup>1</sup>H NMR chemical shifts which were found to be indicative of either a racemic or meso configuration. In contrast to the inherent instability previously associated with 2-indenyl *ansa*-titanocenes, the stability of the ethylene-bridged 2-indenyl *ansa*-titanocenes was sufficient for catalytic activity. The 2-indenyl *ansa*-titanocenes and a tetrahydro-2-indenyl derivative were shown to catalyze the epoxidation of structurally different unfunctionalized alkenes.

The chiral C<sub>2</sub> array formed on titanium complexation of  $\alpha$ -substituted ligands derived from 1,2-bis(2-indenyl)ethane potentially may be used in asymmetric synthesis. We anticipate the optical resolution of complexes **14r** and **15r** will provide catalysts for the asymmetric epoxidation of unfunctionalized alkenes.

### Experimental Section

All solvents and chemicals were reagent grade and were purified as required. THF and Et<sub>2</sub>O were distilled from sodium benzophenone ketyl immediately prior to use. CH<sub>2</sub>-Cl<sub>2</sub> was distilled from calcium hydride, and toluene was distilled from sodium. TiCl<sub>3</sub>(THF)<sub>3</sub> was prepared using the method of Manzer.<sup>40</sup> All reactions were conducted in either a

**Table 8. Epoxidation using Titanocene 9<sup>a,b</sup>**

		
entry	substrate	no. of turnovers
a		16
b		15
c		57
d		41
e		16

<sup>a</sup> The reported turnover number was measured at 15 h. <sup>b</sup> Turnover no. = mmol of alkene consumed per mmol of Ti catalyst, calculated from a minimum of three experiments using cyclohexane as the internal standard.

dry nitrogen or argon atmosphere using standard techniques. <sup>1</sup>H (300 MHz) and <sup>13</sup>C NMR (75 MHz) were recorded using a General Electric QE-300 spectrometer with residual undeuteriated solvent ( $\delta$  7.26 for CHCl<sub>3</sub>) or tetramethylsilane serving as the internal standard. Mass spectral analyses were conducted at the Facility for Advanced Instrumentation at the University of California, Davis. Elemental analyses were provided by Midwest Microlabs of Indianapolis, IN.

#### Preparation of 1,2-Bis(3-methylinden-2-yl)ethane (11).

To a solution of bisindene **10** (0.33 g, 1.3 mmol) in THF (5 mL) at 0 °C was added dropwise *n*-BuLi (1.1 mL of a 2.5 M solution in hexane, 2.8 mmol). After 30 min, the reaction was transferred via cannula into a solution of CH<sub>3</sub>I (0.18 mL, 2.9 mmol) in THF (2 mL) at 0 °C. The reaction was stirred for 15 h and was then quenched by the addition of saturated aqueous NaHCO<sub>3</sub> (10 mL). The reaction mixture was extracted with Et<sub>2</sub>O (2  $\times$  15 mL), and the combined organic extract was washed with brine (15 mL) and dried (MgSO<sub>4</sub>). The solvents were removed by rotary evaporation, and the residue was chromatographed (SiO<sub>2</sub>, cyclohexane, *R<sub>f</sub>* = 0.17) to yield 0.30 g (81%) of a mixture of double-bond isomers which included **11** (major isomer: <sup>1</sup>H NMR (CHCl<sub>3</sub>)  $\delta$  1.25 (d, *J* = 7.6 Hz, 6H), 2.65 (m, 4H), 3.26 (m, 2H), 6.43 (s, 2H), 7.15 (m, 8H)). A portion of this material was isomerized for complete characterization by heating a solution of the material (0.050 g, 1.3 mmol) in triethylamine (3 mL) at reflux for 2 h. The triethylamine was subsequently removed by rotary evaporation to give **11** in near-quantitative yield: mp 162–165 °C; <sup>1</sup>H NMR (CHCl<sub>3</sub>)  $\delta$  2.03 (s, 6H), 2.72 (s, 4 H), 3.34 (s, 4 H), 7.15 (t, *J* = 7.15 Hz, 2 H), 7.23–7.29 (m, 4 H), 7.40 (d, *J* = 7.3 Hz, 2 H); <sup>13</sup>C NMR (CHCl<sub>3</sub>)  $\delta$  10.1, 28.6, 40.2, 118.2, 123.1, 123.8, 126.1, 133.0, 141.8, 142.3, 147.2; IR (CHCl<sub>3</sub>) 3016, 1645, 1557, 1467, 1388, 1214, 758, 718 cm<sup>-1</sup>; EIMS *m/z* (relative intensity) 286 (M<sup>+</sup>, 6), 143 (M<sup>+</sup>/2, 100), 128 (M<sup>+</sup>/2 - CH<sub>3</sub>, 24). Anal. Calcd for C<sub>22</sub>H<sub>22</sub>: C, 92.26; H, 7.74. Found: C, 92.05; H, 7.52.

#### Preparation of 1,2-Bis(3-benzylinden-2-yl)ethane (12).

To a solution of bisindene **10** (0.336 g, 1.30 mmol) in THF (5 mL) at 0 °C was added dropwise *n*-BuLi (1.1 mL of a 2.5 M solution in hexane, 2.7 mmol). The reaction mixture was stirred 45 min, whereupon benzyl bromide (0.50 mL, 4.2 mmol)

(39) This rationale assumes that the epoxidation does not proceed via an edge-on approach of the alkene. For a mechanistic discussion of a titanium-catalyzed epoxidation, see: Carlier, P. R.; Sharpless, K. B. *J. Org. Chem.* **1989**, *54*, 4016 and reference 13 therein.

(40) Manzer, L. E. *Inorg. Synth.* **1982**, *21*, 135.

was added dropwise. The reaction mixture was then warmed to room temperature. After the mixture had been stirred 16 h, the reaction was quenched by addition of 10% HCl (10 mL). The reaction mixture was extracted with EtOAc (2 × 15 mL), and the combined organic extract was washed with brine (15 mL) and dried (MgSO<sub>4</sub>). The solvents were removed by rotary evaporation, and the residue was chromatographed (SiO<sub>2</sub>, cyclohexane, *R<sub>f</sub>* = 0.18) to yield 0.45 g (79%) of a mixture of double-bond isomers which included **12**. A portion of this material was isomerized for complete characterization by heating a solution of the material (0.084 g, 0.19 mmol) in triethylamine (3 mL) at reflux for 2 h. The triethylamine was subsequently removed by rotary evaporation to give **12** in near quantitative yield: mp 101–104 °C; <sup>1</sup>H NMR (CHCl<sub>3</sub>) δ 2.90 (s, 4H), 3.50 (s, 4H), 3.98 (s, 4H), 7.22–7.49 (m, 18H); <sup>13</sup>C NMR (CHCl<sub>3</sub>) δ 28.9, 31.2, 40.4, 119.2, 123.3, 123.9, 125.9, 126.0, 128.23, 128.3, 135.9, 142.4, 143.5, 146.2; IR (CHCl<sub>3</sub>) 3061, 3023, 2917, 1602, 1493, 771 cm<sup>-1</sup>; EIMS *m/z* (relative intensity) 438 (M<sup>+</sup>, 35), 347 (M<sup>+</sup> - C<sub>6</sub>H<sub>5</sub>CH<sub>2</sub>, 6), 219 (M<sup>+</sup>/2, 100); HRMS calcd for C<sub>34</sub>H<sub>30</sub>, 438.2347; found, 438.2319.

**Preparation of 1,2-Bis[1-(trimethylsilyl)inden-2-yl]ethane (13).** To a solution of bisindene **10** (0.18 g, 0.69 mmol) in THF (7 mL) at 0 °C was added dropwise *n*-BuLi (0.57 mL of a 2.5 M solution in hexanes, 1.5 mmol). After the solution had been stirred for 30 min, freshly distilled trimethylsilyl chloride (0.19 mL, 1.5 mmol) was added dropwise. The reaction was warmed to room temperature and stirred 12 h, whereupon the reaction was quenched by the addition of saturated aqueous NaHCO<sub>3</sub> (15 mL). The reaction mixture was extracted with EtOAc (2 × 25 mL), and the combined organic extract was washed with brine (15 mL) and dried (MgSO<sub>4</sub>). The solvents were removed by rotary evaporation. The residue was dissolved in toluene (1.5 mL) and chromatographed (SiO<sub>2</sub>, cyclohexane, *R<sub>f</sub>* = 0.27) to yield 0.24 g (85%) of **13** as a 1:1 mixture of diastereomers: <sup>1</sup>H NMR (CHCl<sub>3</sub>) δ -0.13 (s, 18H), 2.82–3.10 (m, 4H), 3.58 (s, 2H), 6.77 (s, 2H), 7.21 (apparent t, *J* = 7.4 Hz, 2H), 7.32 (apparent t, *J* = 7.4 Hz, 2H), 7.46–7.50 (m, 4H); <sup>13</sup>C NMR (CHCl<sub>3</sub>) δ -2.1, 31.3, 47.9, 120.0, 122.6, 122.9, 124.2, 124.8, 144.6, 144.8, 158.8; IR (CHCl<sub>3</sub>) 3059, 3041, 3018, 2952, 2922, 2898, 1606, 1462, 1249, 1011, 910, 841 cm<sup>-1</sup>; EIMS *m/z* (relative intensity) 402 (M<sup>+</sup>, 5), 201 (M<sup>+</sup>/2, 97), 73 (Si(CH<sub>3</sub>)<sub>3</sub>, 100); HRMS calcd for C<sub>26</sub>H<sub>34</sub>Si<sub>2</sub>, 402.2199; found, 402.2187.

**Preparation of *rac*- and *meso*-[Ethylenebis(1-methyl-η<sup>5</sup>-inden-2-yl)]titanium Dichlorides (14r and 14m).** To a degassed (N<sub>2</sub>) solution of bisindene **11** (0.335 g, 1.17 mmol) in THF (15 mL) at 0 °C was added dropwise *n*-BuLi (0.98 mL of a 2.5 M solution in hexane, 2.5 mmol). The reaction mixture was stirred for 45 min at 0 °C and then cooled to -25 °C, whereupon TiCl<sub>3</sub>(THF)<sub>3</sub> (0.45 g, 1.2 mmol) was added in one portion. After 5 min, the reaction mixture was gradually warmed to room temperature and was then heated at the reflux temperature for 4 h. The resultant dark brown reaction mixture was cooled to -78 °C, and 6.0 M HCl (1.7 mL) was added. The reaction was then gradually warmed to room temperature, whereupon dry air was bubbled vigorously into the reaction mixture to result in the partial precipitation of **14**. After 30 min of aeration, the solvents were removed by rotary evaporation and the residue was dissolved in CH<sub>2</sub>Cl<sub>2</sub> (30 mL). This solution was washed with H<sub>2</sub>O (3 mL) and dried (MgSO<sub>4</sub>). After filtration, the filtrate was concentrated by rotary evaporation to approximately one-half of the volume and passed through a short column of BioBeads SX-1. The collected solvent was removed *in vacuo* to yield 0.25 g (53%) of **14** as a 1.1:1.0 (*rac*:*meso*) mixture of diastereomers as determined by <sup>1</sup>H NMR integration on the mixture. Data for **14m**: <sup>1</sup>H NMR (CDCl<sub>3</sub>) δ 2.40 (s, 6H), 3.36 (s, 4H), 7.10 (s, 2H), 7.2 (m, 6H), 7.58 (d, *J* = 9 Hz, 2H). Data for **14r**: <sup>1</sup>H NMR (CDCl<sub>3</sub>) δ 2.54 (s, 6H), 3.01–3.16 (m, 2H), 3.56–3.70 (m, 2H), 6.20 (s, 2H), 7.20–7.28 (m, 4H), 7.34–7.38 (m, 2H), 7.51–7.58 (m, 2H). A portion of this material was dissolved in the minimum amount of CH<sub>2</sub>Cl<sub>2</sub>, and cyclohexane was added to

result in the selective crystallization of **14r** as determined by X-ray crystallographic analysis and corresponding spectral data: <sup>13</sup>C NMR (CDCl<sub>3</sub>) δ 12.8, 27.0, 105.5, 123.7, 124.1, 126.7, 126.9, 127.0, 132.4, 132.9, 137.2; IR (CHCl<sub>3</sub>) 2960, 1500, 1420, 1060 cm<sup>-1</sup>; EIMS *m/z* (relative intensity) 402 (M<sup>+</sup>, 15), 366 (M<sup>+</sup> - Cl, 28), 284 (M<sup>+</sup> - TiCl<sub>2</sub>, 81), 269 (M<sup>+</sup> - CH<sub>3</sub> - TiCl<sub>2</sub>, 32), 141 [(M<sup>+</sup> - CH<sub>3</sub> - TiCl<sub>2</sub>)/2, 100]; HRMS calcd for C<sub>22</sub>H<sub>20</sub>TiCl<sub>2</sub>, 402.0421; found, 402.0425.

**Preparation of *rac*- and *meso*-[Ethylenebis(1-benzyl-η<sup>5</sup>-inden-2-yl)]titanium Dichlorides (15r and 15m).** To a degassed (N<sub>2</sub>) solution of bisindene **12** (0.45 g, 1.0 mmol) in THF (12 mL) at 0 °C was added dropwise *n*-BuLi (0.88 mL of a 2.5 M solution in hexane, 2.2 mmol). The reaction mixture was stirred for 45 min at 0 °C and then cooled to -25 °C, whereupon TiCl<sub>3</sub>(THF)<sub>3</sub> (0.42 g, 1.13 mmol) was added in one portion. After 5 min, the reaction mixture was gradually warmed to room temperature and was then heated at the reflux temperature for 4 h. The resultant dark reaction mixture was cooled to -78 °C, and 6.0 M HCl (0.6 mL) was added. The reaction mixture was then gradually warmed to room temperature, whereupon dry air was bubbled vigorously into the reaction mixture to result in the formation of a brown-red precipitate. After 15 min, CH<sub>2</sub>Cl<sub>2</sub> (30 mL) was added to the reaction mixture to dissolve the precipitated material. The solution was washed with brine (5 mL) and dried (MgSO<sub>4</sub>). After filtration, the filtrate was concentrated by rotary evaporation to one-half of the volume and passed through a short column of BioBeads SX-1. The collected solvent was removed by rotary evaporation to yield 0.48 g of crude material. <sup>1</sup>H NMR examination of this material revealed a 3.6:1.0 (*rac*:*meso*) mixture of diastereomers contaminated with **12** (ca. 20%). Data for **15m**: <sup>1</sup>H NMR (CDCl<sub>3</sub>) δ 3.32 (s, 4H), 3.94 (1/2 ABq, *J* = 16 Hz, 2H), 4.59 (1/2 ABq, *J* = 16 Hz, 2H), 7.05–7.24 (m, 18H), 7.62 (d, *J* = 8.4 Hz, 2H). Data for **15r**: <sup>1</sup>H NMR (CDCl<sub>3</sub>) δ 3.03–3.07 (m, 2H), 3.63–3.67 (m, 2H), 4.17 (1/2 ABq, *J* = 16 Hz, 2H), 4.49 (1/2 ABq, *J* = 16 Hz, 2H), 6.36 (s, 2H, Cp), 7.24 (m, 14H), 7.39 (m, 2H), 7.56 (m, 2H). In practice, the precipitate that formed during the aeration step was collected and determined to be a 15:1 mixture of **15r**:**15m**. Recrystallization of this material from CH<sub>2</sub>Cl<sub>2</sub> and cyclohexane gave **15r** in essentially pure form: <sup>13</sup>C NMR (CDCl<sub>3</sub>) δ 27.6, 33.6, 105.0, 106.0, 124.22, 126.5, 126.6, 126.7, 127.3, 127.4, 128.0, 128.6, 128.7, 137.2, 140.0; IR (CHCl<sub>3</sub>) 3091, 3060, 3054, 1632, 1447, 730 cm<sup>-1</sup>; FAB-MS *m/z* (relative intensity) 555 (M + H, 13), 519 (M + H - Cl, 74), 483 (M + H - 2Cl, 48), 91 (tropyllium, 100); HRMS (FAB, M<sup>+</sup> - Cl) calcd for C<sub>34</sub>H<sub>28</sub>TiCl, 519.1359; found, 519.1353.

**Attempted Complexation of 13.** To a solution of **13** (0.19 g, 0.47 mmol) in THF (8 mL) at 0 °C was added dropwise *n*-BuLi (0.40 mL of a 2.5 M solution in hexanes, 1.0 mmol). The reaction mixture was cooled to -40 °C, and TiCl<sub>3</sub>(THF)<sub>3</sub> (0.18 g, 0.49 mmol) was added in one portion. After 5 min, the reaction mixture was warmed to room temperature, whereupon the reaction was heated to reflux for 4 h. The resultant dark reaction mixture was cooled to -78 °C, and 6.0 M HCl (0.25 mL) was added. The reaction was then gradually warmed to room temperature, whereupon dry air was bubbled vigorously into the reaction mixture. After 30 min, the solvents were removed by rotary evaporation. The residue was dissolved in CH<sub>2</sub>Cl<sub>2</sub> (10 mL) and filtered through a short pad of Celite. The filtrate was concentrated under vacuum to yield a residue that was recrystallized using a mixture of CH<sub>2</sub>Cl<sub>2</sub> and hexane. The needles which crystallized from this solvent mixture were collected (0.051 g) and were assigned the structure **16** on the basis of X-ray crystallographic analysis<sup>27</sup> and corresponding spectral data: <sup>1</sup>H NMR (CHCl<sub>3</sub>) δ 0.42 (s, 18H), 2.48 (m, 2H), 2.86 (s, 2H), 3.23 (s, 2H), 7.50 (m, 8H); EIMS *m/z* (relative intensity) 385 (M<sup>+</sup> - CH<sub>3</sub>, 35).

**[Ethylenebis(η<sup>5</sup>-4,5,6,7-tetrahydro-2-indenyl)]titanium Dichloride (17).** To a solution of complex **9** (0.75 g, 2.0 mmol) in THF (10 mL) at room temperature was added PtO<sub>2</sub> (0.048 g, 0.21 mmol). A hydrogen-containing balloon was

appended to the system through a septum adapter, and a hydrogen atmosphere was established via vacuum manifold manipulations. The reaction was stirred for 33 h before dilution with CH<sub>2</sub>Cl<sub>2</sub> (20 mL). The reaction mixture was loaded on a 35 mm × 40 mm column of BioBeads SX-1 and eluted with CH<sub>2</sub>Cl<sub>2</sub>. After 30 mL of solvent had eluted, the effluent was collected (ca. 70 mL) and the solvent was removed via rotary evaporation. The residue was recrystallized from CH<sub>2</sub>Cl<sub>2</sub> and Et<sub>2</sub>O to yield 325 mg (42%) of **17** as a red-gold solid: mp 327–331 °C; <sup>1</sup>H NMR (CDCl<sub>3</sub>) δ 1.60 (m, 4H), 1.85 (m, 4H), 2.51 (dt, *J* = 17.6, 5.2 Hz, 4H), 3.10 (m, 4H), 3.11 (s, 4H), 5.51 (s, 4H); <sup>13</sup>C NMR (CDCl<sub>3</sub>) δ 22.1, 25.2, 30.9, 112.4, 137.1, 137.6; IR (KBr) 3071, 2930, 2867, 2849, 1514, 1444 cm<sup>-1</sup>. Anal. Calcd for C<sub>20</sub>H<sub>24</sub>TiCl<sub>2</sub>: C, 62.69; H, 6.31. Found: C, 62.45; H, 6.28.

**Epoxidations.** All epoxidations were conducted as follows: A sealed tube fitted with a rubber septum was evacuated, flame-dried, and purged with argon. The tube was then charged with the alkene substrate (2.5 mmol) and cyclohexane (0.27 mL, 2.5 mmol). A small portion of the resultant solution (50 μL) was removed, diluted with toluene (4 mL), and analyzed by gas chromatography (Shimadzu GC-14A, J&W 30 m × 0.25 mm Durawax column) to record an internal standard chromatograph. To the reaction mixture was added *tert*-butylhydroperoxide (0.90 mL of a 2.8 M solution<sup>41</sup> in toluene, 2.5 mmol). The titanocene complex (0.012–0.014 mmol) was

subsequently added as a dilute (0.021–0.025 M) CH<sub>2</sub>Cl<sub>2</sub> solution. The rubber septum was replaced with a Teflon plug, and the reaction temperature was elevated to 55 °C. After 15 h, the reaction was stopped by cooling the mixture to room temperature. Analysis of the crude reaction mixture was performed using gas chromatography. No products other than the corresponding epoxide (determined by comparison to an authentic sample) were detected.

**Acknowledgment.** This work was supported by the University of California, Davis, Committee on Research. S.R.H. is the recipient of a NOBCCChE Procter & Gamble Graduate Fellowship, for which he is grateful. We thank Prof. Stephen L. Buchwald for a generous gift of *ansa*-titanocene **1a**. We also thank Ms. Ammie Kesse for technical assistance.

**Supporting Information Available:** Tables of X-ray crystallographic data for compounds **14r** and **17** (17 pages). Ordering information is given on any current masthead page.

OM950235X

(41) The *tert*-butylhydroperoxide concentration was determined according to the literature method, see: Hill, J. G.; Rossiter, B. E.; Sharpless, K. B. *J. Org. Chem.* **1983**, *48*, 3607.

# Synthesis and Nucleophilic Substitution of Highly Chlorinated Arene ( $\eta^5$ -Pentamethylcyclopentadienyl)ruthenium $\pi$ -Complexes

Alexa A. Dembek\* and Paul J. Fagan

DuPont Central Research and Development, Experimental Station,  
Wilmington, Delaware 19880-0328

Received March 15, 1995<sup>©</sup>

Facile synthesis of  $\text{Cp}^*\text{Ru}^+$  ( $\text{Cp}^*$  = pentamethylcyclopentadienyl)  $\pi$ -complexes of highly electron deficient aromatics, including 1,3,5-trichloro-, 1,2,4,5-tetrachloro-, pentachloro-, and hexachlorobenzene, is accomplished by the ligand exchange reaction with  $\text{Cp}^*\text{Ru}(\text{CH}_3\text{CN})_3^+\text{SO}_3\text{CF}_3^-$  in polar solvents under mild reaction conditions. The extraordinary activating ability of the  $\text{Cp}^*\text{Ru}^+$  moiety is demonstrated by rapid and quantitative nucleophilic substitution reactions of the 1,3,5-tri- and 1,2,4,5-tetrachlorobenzene  $\pi$ -complexes with potassium phenoxide, thiophenoxide, 4-aminophenoxide, 4-chlorophenoxide, and 4-fluorophenoxide. This methodology allows syntheses of highly substituted and functionalized aromatic compounds.

Nucleophilic displacement reactions on transition metal  $\pi$ -complexes of haloaromatics provides entry to novel functionalized arenes,<sup>1</sup> monomers that are inaccessible by traditional organic methodology<sup>2</sup> and metal-containing oligomers<sup>3</sup> and polymers.<sup>4</sup> Typically, the aromatic halide is a mono- or dichlorobenzene derivative, and the transition metal activating group is  $\text{Cr}(\text{CO})_3$ ,  $\text{CpFe}^+$  ( $\text{Cp}$  = cyclopentadienyl),  $\text{Mn}(\text{CO})_3^+$ ,  $\text{Cp-Ru}^+$ , or  $\text{Cp}^*\text{Ru}^+$  ( $\text{Cp}^*$  = pentamethylcyclopentadienyl).<sup>5</sup> However, facile solution routes to metallo  $\pi$ -complexes of more highly electron deficient arenes, such as aromatics with three or more halogen substituents, are largely unknown due to the decreased coordinating ability of the arene.

Considerable attention has recently been directed toward solution synthesis of perhalogenated  $\eta^5$ -cyclopentadienyl complexes due to their decreased susceptibility to oxidative decomposition.<sup>6</sup> In contrast, efforts to prepare perhalogenated  $\eta^6$ -arene complexes have

been limited primarily to metal atom synthesis.<sup>7</sup> One recent exception is a report on a solution lithiation/chlorination of  $(\eta^6\text{-C}_6\text{H}_5\text{Cl})\text{Cr}(\text{CO})_3$  to afford the homologs  $(\eta^6\text{-C}_6\text{H}_{6-n}\text{Cl}_n)\text{Cr}(\text{CO})_3$  ( $n = 1-6$ ), including  $(\eta^6\text{-C}_6\text{Cl}_6)\text{Cr}(\text{CO})_3$ .<sup>8</sup>

We now report the discovery that the cationic  $\text{Cp}^*\text{Ru}^+$  moiety overcomes the challenges of complexation to highly electron deficient aromatics and provides a versatile organometallic tool for construction of highly functionalized arene architectures.<sup>9</sup> We illustrate this methodology with the facile synthesis of  $\text{Cp}^*\text{Ru}^+$  complexes of highly electron deficient aromatics, including trichloro-, tetrachloro-, pentachloro-, and hexachlorobenzene. Remarkably, the trichloro- and tetrachlorobenzene  $\pi$ -complexes readily undergo rapid and quantitative nucleophilic substitution reactions which allow syntheses of highly substituted and functionalized aromatic compounds and offer opportunities for syntheses of novel organometallic dendrimer architectures.<sup>10</sup>

## Results and Discussion

**Synthesis and Characterization of  $\text{Cp}^*\text{Ru}^+$   $\pi$ -Complexes.** The outstanding  $\pi$ -complexing ability of the  $\text{Cp}^*\text{Ru}^+$  moiety<sup>11</sup> allows a surprisingly efficient and direct solution synthesis of highly electron deficient arene  $\pi$ -complexes based on tri-, tetra-, penta-, and hexachlorobenzene. These unique bonding features of

<sup>©</sup> Abstract published in *Advance ACS Abstracts*, June 15, 1995.

(1) (a) Pearson, A. J.; Park, J. G.; Yang, Y. S.; Chuang, Y. *J. Chem. Soc., Chem. Commun.* **1989**, 1363. (b) Pearson, A. J.; Park, J. G.; Zhu, P. Y. *J. Org. Chem.* **1992**, 57, 3583. (c) Pearson, A. J.; Zhu, P. Y.; Youngs, W. J.; Bradshaw, J. D.; McConville, D. B. *J. Am. Chem. Soc.* **1993**, 115, 10376.

(2) (a) Pearson, A. J.; Gelormini, A. M. *Macromolecules* **1994**, 27, 3675. (b) Pearson, A. J.; Gelormini, A. M. *J. Org. Chem.* **1994**, 59, 4561.

(3) (a) Abd-El-Aziz, A. S.; Schriemer, D. C.; de Denuis, C. R. *Organometallics* **1994**, 13, 374. (b) Abd-El-Aziz, A. S.; de Denuis, C. R. *J. Chem. Soc., Chem. Commun.* **1994**, 663.

(4) (a) Segal, J. A. *J. Chem. Soc., Chem. Commun.* **1985**, 1338. (b) Dembek, A. A.; Fagan, P. J.; Marsi, M. *Macromolecules* **1993**, 26, 2992. (c) Dembek, A. A.; Marsi, M. U.S. Patent 5350832, 1994. (d) Dembek, A. A.; Fagan, P. J.; Marsi, M. *Polym. Mater. Sci. Eng.* **1994**, 71, 158. (e) Percec, V.; Okita, S. *J. Polym. Sci., Part A* **1993**, 31, 923.

(5) For transition metal activated nucleophilic aromatic substitution, see: (a) Pearson, A. J. *Metallo-Organic Chemistry*; Wiley: New York, 1985; Chapter 9 and references therein. (b) Watts, W. E. *The Organic Chemistry of Metal-Coordinated Cyclopentadienyl and Arene Ligands Comprehensive Organometallic Chemistry*; Wilkinson, G., Stone, F. G. A., Abel, E., Eds.; Pergamon Press: Oxford, 1982; Vol. 8, Chapter 59 and references cited therein.

(6) (a) Curnow, O. J.; Hughes, R. P. *J. Am. Chem. Soc.* **1992**, 114, 5895. (b) Winter, C. H.; Han, Y. H.; Heeg, M. J. *Organometallics* **1992**, 11, 3169. (c) Winter, C. H.; Han, Y. H.; Ostrander, R. L. *Angew. Chem., Int. Ed. Engl.* **1993**, 32, 1161. (d) Han, Y. H.; Heeg, M. J.; Winter, C. H. *Organometallics* **1994**, 13, 3009.

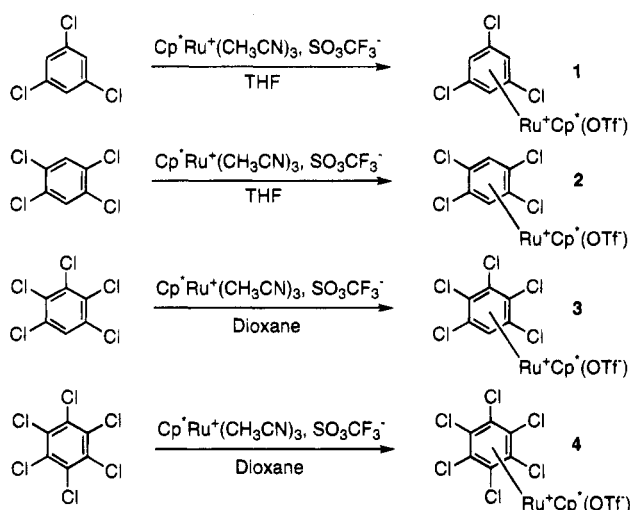
(7) (a) Trost, H. K. *Tailor-Made Metal-Organic Compounds: Technology and Chemistry of Metal Atom Synthesis*; VDI Verlag: Düsseldorf, Germany, 1992. (b) Blackborow, J. R. *Metal Vapour Synthesis in Organometallic Chemistry*; Springer-Verlag: New York, 1979. (c) McGlinchey, M. J. In *The Chemistry of the Metal-Carbon Bond*; Hartley, F. R., Patai, S., Eds.; Wiley: New York, 1982; p 539. (d) Marr, G.; Rockett, B. W. *Ibid.*, p 463. (e) Timms, P. L. *J. Chem. Educ.* **1972**, 49, 782.

(8) Gassman, P. G.; Deck, P. A. *Organometallics* **1994**, 13, 1934.

(9) Dembek, A. A. U.S. Patent 5,386,044, 1994.

(10) (a) Moulines, F.; Djakovitch, L.; Boese, R.; Gloaguen, B.; Thiel, W.; Fillaut, J. L.; Astruc, D. *Angew. Chem., Int. Ed. Engl.* **1993**, 32, 1075. (b) Liao, Y. H.; Moss, J. R. *J. Chem. Soc., Chem. Commun.* **1993**, 1774. (c) Alonso, B.; Cuadrado, I.; Morán, M.; Losada, J. *J. Chem. Soc., Chem. Commun.* **1994**, 2575.

Scheme 1



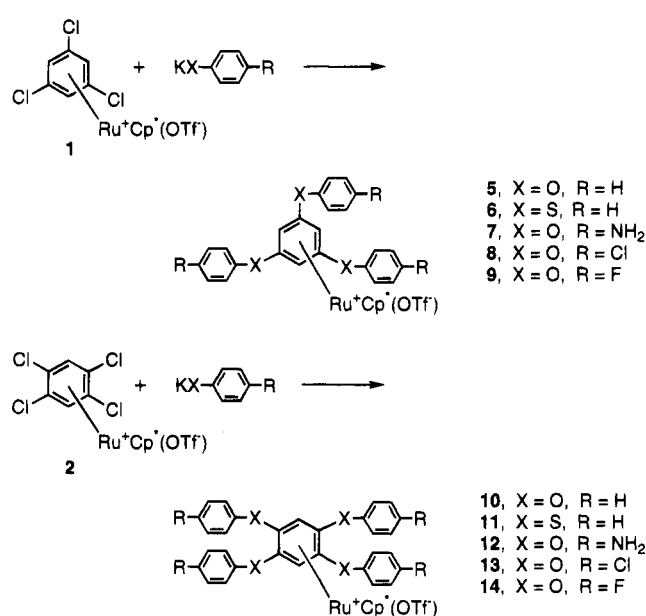
the Cp<sup>\*</sup>Ru<sup>+</sup> moiety are further accentuated considering that the corresponding Cr(CO)<sub>3</sub>, CpFe<sup>+</sup>, or Mn(CO)<sub>3</sub><sup>+</sup> π-complexes are inaccessible by direct solution reaction of the metal fragment precursor and the electron deficient aromatic.

Synthesis of Cp<sup>\*</sup>Ru<sup>+</sup> π-complexes 1–4 is accomplished simply by the ligand exchange reaction of [Cp<sup>\*</sup>Ru(CH<sub>3</sub>CN)<sub>3</sub>]<sup>+</sup>SO<sub>3</sub>CF<sub>3</sub><sup>−</sup> with an excess of the corresponding multichloroaromatic in polar solvents under mild reaction conditions (see Scheme 1). The tri- and tetrachlorobenzene Cp<sup>\*</sup>Ru<sup>+</sup> derivatives 1 and 2 are prepared in THF at 66 °C, while the more strongly electron deficient penta- and hexachlorobenzene Cp<sup>\*</sup>Ru<sup>+</sup> derivatives 3 and 4 are prepared in dioxane at 85 °C. Unoptimized reactions afford complexes 1–3 in good yield (62%–88%) and 4 in moderate yield (42%). The yields can be increased substantially if very large excesses (6–15 equiv) of the chloroaromatic are used.

<sup>1</sup>H and <sup>13</sup>C NMR spectra of compounds 1–4 confirm the Cp<sup>\*</sup>Ru<sup>+</sup> π-complexation. Specifically, <sup>1</sup>H NMR analysis shows a singlet resonance with characteristic upfield shifts for the coordinated arene in the range 7.21–7.81 ppm. Singlet resonances for the methyl group of the Cp<sup>\*</sup> ligand appear in the range 1.88–1.65 ppm. A progressive downfield shift in the complexed arene resonance and an upfield shift in the methyl group resonance of the Cp<sup>\*</sup> ligand are detected in both the <sup>1</sup>H and <sup>13</sup>C NMR spectra as the chloro substitution on the aromatic ring increases in the series 1–4. Positive-ion fast atom bombardment (FAB) mass spectral analyses and elemental microanalyses provide additional confirmation of the product structures.

Although the focus of this manuscript is on Cp<sup>\*</sup>Ru<sup>+</sup> π-complexation of chloroaromatic derivatives, we have also recently prepared the corresponding 1,3,5-tri-, 1,2,4,5-tetra-, and pentasubstituted fluorobenzene derivatives by ligand exchange with Cp<sup>\*</sup>Ru(CH<sub>3</sub>CN)<sub>3</sub><sup>+</sup>SO<sub>3</sub>CF<sub>3</sub><sup>−</sup>. The synthesis, characterization, and

Scheme 2



reactivity of these fluoroarene π-complexes will be presented separately.<sup>12</sup>

**Nucleophilic Substitution of Cp<sup>\*</sup>Ru<sup>+</sup> π-Complexes.** Investigation of nucleophilic displacement reactions of π-arenes 1–4 demonstrated the *extraordinary activating ability* of the Cp<sup>\*</sup>Ru<sup>+</sup> moiety. Surprisingly, tri- and tetrachlorobenzene π-complexes 1 and 2 undergo facile and *quantitative* nucleophilic displacement with preformed potassium salts of phenols or thiophenols in polar solvents under extremely mild reaction conditions. For example, reaction of [Cp<sup>\*</sup>Ru(η<sup>6</sup>-1,3,5-trichlorobenzene)]<sup>+</sup>SO<sub>3</sub>CF<sub>3</sub><sup>−</sup> (1) with potassium phenoxide or thiophenoxide (1.1 equiv/C–Cl bond) in THF, CH<sub>3</sub>CN, or DMSO solvent affords the trisphenoxy or tris thiophenoxy derivatives 5 and 6 (see Scheme 2). In a similar manner, reaction of [Cp<sup>\*</sup>Ru(η<sup>6</sup>-1,2,4,5-tetrachlorobenzene)]<sup>+</sup>SO<sub>3</sub>CF<sub>3</sub><sup>−</sup> (2) with potassium phenoxide or thiophenoxide affords the tetrakisphenoxy or tetrakis thiophenoxy derivatives 10 and 11. These reactions proceed rapidly to quantitative conversion at 25 °C as determined by <sup>1</sup>H NMR spectroscopy using THF-*d*<sub>8</sub>, CH<sub>3</sub>CN-*d*<sub>3</sub>, or DMSO-*d*<sub>6</sub> as the reaction solvent.

Reactions of penta- and hexachlorobenzene π-complexes 3 and 4 with potassium phenoxide or thiophenoxide afford a mixture of partially substituted products under mild reaction conditions. Note that the pentachlorobenzene π-complex 3 does undergo complete C–Cl substitution under forcing reaction conditions (CH<sub>3</sub>CN-*d*<sub>3</sub>, 75 °C, 16 h), as detected by <sup>1</sup>H NMR. Challenging C–Cl bond displacement on compounds 3 and 4 is likely due to a combination of factors, including (i) diminished ability of the Cp<sup>\*</sup>Ru<sup>+</sup> moiety to activate the remaining C–Cl bond(s) in the presence of multiple phenoxy or thiophenoxy groups on the aromatic ring and (ii) steric hinderance. Alkoxide or thioalkoxide nucleophiles may be more suitable candidates for displacement reactions on platforms 3 and 4.

Nucleophilic substitution of tri- and tetrachlorobenzene platforms 1 and 2 with potassium salts of *para*-substituted phenols offer new opportunities for synthesis of highly functionalized aromatic molecules. Scouting

(11) (a) Fagan, P. J.; Ward, M. D.; Caspar, J. V.; Calabrese, J. C.; Krusic, P. J. *J. Am. Chem. Soc.* **1988**, *110*, 2981. (b) Fagan, P. J.; Ward, M. D.; Calabrese, J. C. *J. Am. Chem. Soc.* **1989**, *111*, 1698. (c) Gill, T. P.; Mann, K. R. *Organometallics* **1982**, *1*, 485. (d) Glatzhofer, D. T.; Liang, Y.; Khan, M. A.; Fagan, P. J. *Organometallics* **1991**, *10*, 833. (e) Moriarty, R. M.; Gill, U. S.; Ku, Y. Y. *J. Organomet. Chem.* **1988**, *350*, 157. (f) Glatzhofer, D. T.; Liang, Y.; Funkhouser, G. P.; Khan, M. A. *Organometallics* **1994**, *13*, 315.

(12) Dembek, A. A.; Fagan, P. J. Manuscript in preparation.

reactions were initially carried out in deuteriated solvents (THF- $d_8$ , CH<sub>3</sub>CN- $d_3$ , and DMSO- $d_6$ ) to monitor the extent of reaction by <sup>1</sup>H NMR spectroscopy. As anticipated, the electronic characteristics of the *para* substituent correlate with the extent of reaction. Electron-donating substituents enhance the nucleophilic character of the phenoxide and therefore facilitate nucleophilic displacement while strong electron-withdrawing substituents retard reactivity. Similar reactivity trends are anticipated for the corresponding substituted potassium *thiophenoxides*.

Specifically, Cp\**Ru*<sup>+</sup>  $\pi$ -complexes **1** and **2** undergo complete C–Cl bond substitution with potassium 4-amino-, 4-chloro-, and 4-fluorophenoxide to afford fully derivatized products **7–9** and **12–14**, respectively (Scheme 2). The details of the syntheses are in the Experimental Section. In <sup>1</sup>H NMR scouting experiments, a variety of phenoxides with electron rich substituents in the *ortho*-, *meta*-, and *para*-positions afford complete nucleophilic substitution (additional examples include alkyl, aryl, alkoxy, and aryloxy substituents), illustrating the versatility of this methodology.

In contrast to the electron rich phenoxides, reactions of **1** and **2** with nucleophiles containing strong electron-withdrawing groups afford no chloro displacement using standard reaction conditions. Specific examples include potassium 4-cyano-, 4-(trifluoromethyl)-, 4-nitro-, 3-nitro-, and perfluorophenoxide, and the potassium salts of 2-hydroxy- and 4-hydroxypyridine. Under forcing conditions (long reaction time, high temperature, and large excess of potassium aryloxy), reactions with potassium 4-cyano- and 4-(trifluoromethyl)phenoxide nucleophiles are slow and incomplete, and mixtures of starting material and partially substituted products are detected by <sup>1</sup>H NMR.

Compounds **5–14** are isolated as air and moisture stable white solids in good yield (68%–96%). In all cases, the substitution reactions are quantitative by <sup>1</sup>H NMR, however, the isolated yields are always lower than 100% due to losses during product isolation and purification. Purification requires an aqueous extraction to remove the potassium chloride generated during reaction as well as excess potassium alkoxide or thioalkoxide. Since the cationic Cp\**Ru*<sup>+</sup> complexes are partially water soluble, product losses during purification are unavoidable. In general, the Cp\**Ru*<sup>+</sup> complexes are fully soluble in polar organic solvents.

<sup>1</sup>H and <sup>13</sup>C NMR spectra, positive-ion FAB mass spectral analyses and elemental microanalyses of Cp\**Ru*<sup>+</sup> products **5–14** confirm complete nucleophilic substitution (see Experimental Section). Compound **5** is representative of the series **5–14**. The <sup>1</sup>H NMR spectrum of **5** shows a singlet resonance for the Cp\**Ru*<sup>+</sup>  $\pi$ -complexed aromatic at 6.27 ppm, which is an upfield shift from the singlet resonance of the trichlorobenzene  $\pi$ -complex **1** at 7.21 ppm. The resonances of the phenoxy substituents are in the range 7.49–7.20 ppm and the methyl group of the Cp\* ligand is a singlet resonance at 1.98 ppm. The <sup>13</sup>C NMR spectrum shows two resonances for the central  $\pi$ -complexed aromatic at 126.5 and 73.0 ppm, four resonances for the phenoxy substituents at 155.2, 130.1, 124.9, and 118.4 ppm, and two resonances for the Cp\* ligand at 96.1 and 9.6 ppm. The positive-ion FAB mass spectrum of **5** shows the cation at  $m/z = 591$ .

It is interesting to note that no selectivity in C–Cl nucleophilic substitution is observed in reactions of [Cp\**Ru*( $\eta^6$ -1,3,5-trichlorobenzene)]<sup>+</sup>SO<sub>3</sub>CF<sub>3</sub><sup>–</sup> (**1**) with 1 equiv of potassium phenoxide or thiophenoxide in polar solvents at 25 °C. The <sup>1</sup>H NMR spectrum shows a series of resonances which correspond to an approximately statistical distribution of starting material (**1**), mono-, di-, and trisubstituted (**5**) Cp\**Ru*<sup>+</sup> species. This observation of equivalent C–Cl reactivity further supports the outstanding activating ability of the Cp\**Ru*<sup>+</sup> moiety. Similar behavior was observed previously using [Cp\**Ru*( $\eta^6$ -1,4-dichlorobenzene)]<sup>+</sup>SO<sub>3</sub>CF<sub>3</sub><sup>–</sup> as a monomer for nucleophilic substitution polymerizations.<sup>4b,c</sup> Reactions at low temperature to encourage selectivity were not studied.

At this time, the scope of nucleophiles (aliphatic amines, alkoxides, thioalkoxides, malonates, or cyanide) which can be used with these highly halogenated arene complexes has not been fully explored. However, nucleophiles that react cleanly with the corresponding mono- and dichloro Cp\**Ru*<sup>+</sup> arene complexes<sup>1,2,5</sup> will likely be successful with these tri- and tetrachloro analogs. Note that nucleophiles that do not react quantitatively may afford a complex mixture of products.

Decomplexation of the functionalized arene–Cp\**Ru*<sup>+</sup> complexes was explored by a variety of oxidative, ligand displacement, and photolytic methods and, in general, was challenging and highly inefficient. Specifically, the traditional arene displacement reactions (thermally in DMSO, 160 °C, 2 h, or photochemically in CH<sub>3</sub>CN, 450 W, 1 h) afford only partial decomplexation of complexes **5**, **6**, **8**, and **9** and no detectable decomplexation of complexes **7** and **10–14**. These results further accentuate the outstanding  $\pi$ -complexing ability of the Cp\**Ru*<sup>+</sup> moiety, especially to highly electron-rich aromatics such as the tri- and tetrafunctionalized products. Investigation of more rigorous decomplexation methods is planned.

**Opportunities for Highly Functionalized Aromatics.** Cp\**Ru*<sup>+</sup> activated nucleophilic substitution provides a unique route to highly functionalized aromatic small molecules and may offer opportunities for synthesis of soluble, metallomacromolecules with controlled architectures. The tris- and tetrakis-4-aminophenoxy-substituted derivatives **7** and **12** are particularly interesting compounds for branch points or cross-linking agents in polyamide and polyimide syntheses or cores for star polymers. Similarly, the 4-chloro- and 4-fluoro-substituted derivatives **8**, **9**, **13**, and **14** initiate the concept of a divergent approach to metallodendrimers.<sup>10</sup>

## Experimental Section

**General Procedures.** All procedures were carried out in a glovebox under a nitrogen atmosphere or in Schlenk-type glassware on a vacuum line. Tetrahydrofuran (THF) was dried and distilled from sodium metal under nitrogen before use. All other solvents, purchased as anhydrous grade from Aldrich, were stored over 3 Å molecular sieves under nitrogen before use. [Cp\**Ru*(CH<sub>3</sub>CN)<sub>3</sub>]<sup>+</sup>SO<sub>3</sub>CF<sub>3</sub><sup>–</sup> was prepared by using the procedures described previously.<sup>11b</sup> All potassium aryloxides or thioaryloxides were prepared by reaction of the corresponding phenol or thiophenol with potassium *tert*-butoxide (1.0 equiv) in THF at 66 °C for 6 h. The THF soluble salts were isolated by removal of the THF solvent in vacuo; the THF insoluble salts were collected by filtration under



nitrogen. All potassium salts were dried in vacuo at 60 °C for 16 h. All reagents (Aldrich) were used as received.  $^1\text{H}$  (300.0 MHz) and  $^{13}\text{C}$  (75 MHz) NMR spectra were recorded on a QE300 GE spectrometer using  $\text{DMSO-}d_6$  as solvent with tetramethylsilane as an external standard. Positive-ion atom fast atom bombardment (FAB) mass spectra were taken with a VG ZAB-E double-focusing instrument equipped with a Xe-gas ionization gun. Elemental analyses were performed by MicroAnalysis, Inc., Wilmington, DE.

**[Cp\*Ru( $\eta^6$ -1,3,5-trichlorobenzene)] $^+\text{SO}_3\text{CF}_3^-$  (1).** A 100 mL Schlenk flask was charged with 1,3,5-trichlorobenzene (1.64 g, 9.04 mmol, 1.15 equiv) and  $[\text{Cp}^*\text{Ru}(\text{CH}_3\text{CN})_3]^+\text{SO}_3\text{CF}_3^-$  (4.00 g, 7.87 mmol) in THF (70 mL). The reaction was stirred and heated at 66 °C for 16 h and cooled to room temperature. Diethyl ether (ca. 30 mL) was added to the solution to precipitate a white solid that was collected by filtration, washed twice with 10 mL portions of diethyl ether, and dried in vacuo. Yield: 72.5%.  $^1\text{H}$  NMR ( $\text{DMSO-}d_6$ ): 7.21 (s, 3 H, arene), 1.88 (s, 15 H,  $\text{CH}_3$ ) ppm.  $^{13}\text{C}$  NMR ( $\text{DMSO-}d_6$ ): 102.5, 98.7, 89.1, 8.5 ppm. MS (positive-ion FAB) cation,  $m/z$  calcd 416.95, found 417.07. Anal. Calcd for  $\text{C}_{17}\text{H}_{18}\text{Cl}_3\text{SO}_3\text{F}_3\text{Ru}$ : C, 36.02; H, 3.20. Found: C, 35.89; H, 3.12.

**[Cp\*Ru( $\eta^6$ -1,2,4,5-tetrachlorobenzene)] $^+\text{SO}_3\text{CF}_3^-$  (2).** Compound 2 was prepared by the same procedure described for 1 using 1.3 equiv of 1,2,4,5-tetrachlorobenzene. Yield: 78%.  $^1\text{H}$  NMR ( $\text{DMSO-}d_6$ ): 7.66 (s, 2 H, arene), 1.82 (s, 15 H,  $\text{CH}_3$ ) ppm.  $^{13}\text{C}$  NMR ( $\text{DMSO-}d_6$ ): 130.2, 99.3, 88.5, 8.0 ppm. MS (positive-ion FAB) cation,  $m/z$  calcd 450.9, found 450.9. Anal. Calcd for  $\text{C}_{17}\text{H}_{17}\text{Cl}_4\text{RuSO}_3\text{F}_3$ : C, 33.96; H, 2.85. Found: C, 33.83; H, 2.66.

**[Cp\*Ru( $\eta^6$ -pentachlorobenzene)] $^+\text{SO}_3\text{CF}_3^-$  (3).** A 50 mL Schlenk flask was charged with pentachlorobenzene (3.70 g, 14.80 mmol, 5 equiv) and  $[\text{Cp}^*\text{Ru}(\text{CH}_3\text{CN})_3]^+\text{SO}_3\text{CF}_3^-$  (1.50 g, 2.95 mmol) in dioxane (25 mL). The reaction was stirred and heated at 85 °C for 24 h. The solids that precipitated on cooling the reaction mixture to room temperature were collected by filtration and washed twice with 30 mL portions of toluene to remove unreacted pentachlorobenzene. The remaining solids were washed twice with 10 mL portions of diethyl ether and dried in vacuo. Yield: 73%.  $^1\text{H}$  NMR ( $\text{DMSO-}d_6$ ): 7.81 (s, 1 H, arene), 1.77 (s, 15 H,  $\text{CH}_3$ ) ppm.  $^{13}\text{C}$  NMR ( $\text{DMSO-}d_6$ ): 104.3, 103.9, 102.9, 100.1, 89.0, 7.8 ppm. MS (positive-ion FAB) cation,  $m/z$  calcd 484.87, found 484.87. Anal. Calcd for  $\text{C}_{17}\text{H}_{16}\text{Cl}_5\text{RuSO}_3\text{F}_3$ : C, 32.12; H, 2.54. Found: C, 31.85; H, 2.35.

**[Cp\*Ru( $\eta^6$ -hexachlorobenzene)] $^+\text{SO}_3\text{CF}_3^-$  (4).** Compound 4 was prepared by the same procedure described for 3 using hexachlorobenzene. Further purification was achieved by dissolving the solids in 15 mL of nitromethane and filtering the solution. Slow addition of ca. 5 mL of diethyl ether to the filtrate precipitated tan crystals that were collected by filtration, washed twice with 5 mL portions of diethyl ether, and dried in vacuo. Yield: 42%.  $^1\text{H}$  NMR ( $\text{DMSO-}d_6$ ): 1.65 (s,  $\text{CH}_3$ ).  $^{13}\text{C}$  NMR ( $\text{DMSO-}d_6$ ): 104.0, 100.8, 7.2 ppm. MS (positive-ion FAB) cation,  $m/z$  calcd 518.83, found 518.91. Anal. Calcd for  $\text{C}_{17}\text{H}_{15}\text{Cl}_6\text{RuSO}_3\text{F}_3$ : C, 30.47; H, 2.26. Found: C, 30.42; H, 2.14.

**[Cp\*Ru( $\eta^6$ -1,3,5-tris(phenoxy)benzene)] $^+\text{SO}_3\text{CF}_3^-$  (5).** A 50 mL Schlenk flask charged with 1 (0.30 g, 0.53 mmol) and potassium phenoxide (0.23 g, 1.75 mmol, 3.3 equiv) in  $\text{CH}_3\text{CN}$  (25 mL) was stirred at 25 °C for 1 h. To ensure complete substitution, the reaction was warmed at 60 °C for 1 h. The solvent was removed in vacuo, the residue was dissolved in methylene chloride (15 mL) and extracted with water ( $2 \times 20$  mL), and the organic layer was dried over magnesium sulfate. After filtration, the solvent was removed in vacuo and the residue was dissolved in acetonitrile (ca. 8 mL). Slow addition of diethyl ether (ca. 10 mL) precipitated a white solid that was collected by filtration and dried in vacuo. Yield: 86%.  $^1\text{H}$  NMR ( $\text{DMSO-}d_6$ ): 7.49–7.20 (m, 15 H, Ar H), 6.27 (s, 3 H, arene), 1.98 (s, 15 H,  $\text{CH}_3$ ) ppm.  $^{13}\text{C}$  NMR ( $\text{DMSO-}d_6$ ): 155.2, 130.1, 126.5, 124.9, 118.4, 96.1, 73.0, 9.6 ppm. MS (positive-

ion FAB) cation,  $m/z$  calcd 591.14, found 591.13. Anal. Calcd for  $\text{C}_{35}\text{H}_{33}\text{O}_6\text{SF}_3\text{Ru}$ : C, 56.83; H, 4.50. Found: C, 56.63; H, 4.50.

**[Cp\*Ru( $\eta^6$ -1,3,5-tris(thiophenoxy)benzene)] $^+\text{SO}_3\text{CF}_3^-$  (6).** Compound 6 was prepared by the same procedure described for compound 5 using potassium thiophenoxide as the nucleophile. Yield: 96%.  $^1\text{H}$  NMR ( $\text{DMSO-}d_6$ ): 7.44–7.42 (m, 15 H, Ar H), 5.88 (s, 3 H, arene), 1.86 (s, 15 H,  $\text{CH}_3$ ) ppm.  $^{13}\text{C}$  NMR ( $\text{DMSO-}d_6$ ): 133.2, 130.0, 129.6, 128.9, 103.9, 96.7, 85.5, 9.0 ppm. MS (positive-ion FAB) cation,  $m/z$  calcd 639.08, found 639.21. Anal. Calcd for  $\text{C}_{35}\text{H}_{33}\text{O}_3\text{S}_4\text{F}_3\text{Ru}$ : C, 53.35; H, 4.22. Found: C, 53.54; H, 4.27.

**[Cp\*Ru( $\eta^6$ -1,3,5-tris(4-aminophenoxy)benzene)] $^+\text{SO}_3\text{CF}_3^-$  (7).** A 50 mL Schlenk flask charged with 1 (0.30 g, 0.53 mmol) and potassium 4-aminophenoxide (0.31 g, 2.12 mmol, 4 equiv) in  $\text{CH}_3\text{CN}$  (25 mL) was stirred at 60 °C for 2 h. The excess potassium 4-aminophenoxide was filtered from the reaction mixture, and the solvent was removed in vacuo. The residue was dissolved in methylene chloride (25 mL) extracted with water ( $2 \times 25$  mL), and the organic layer was dried over magnesium sulfate. After filtration, the solvent was removed in vacuo and the residue was dissolved in THF (ca. 8 mL) with warming. Slow addition of diethyl ether (ca. 5 mL) precipitated a white solid that was collected by filtration and dried in vacuo at 80 °C for 4 h to remove coordinated  $\text{CH}_3\text{CN}$  solvent. Yield: 82%.  $^1\text{H}$  NMR ( $\text{DMSO-}d_6$ ): 6.86 (d,  $J = 8.9$  Hz, 6 H, Ar H), 6.56 (d,  $J = 8.9$  Hz, 6 H, Ar H), 5.79 (s, 3 H, arene), 1.92 (s, 15 H,  $\text{CH}_3$ ) ppm.  $^{13}\text{C}$  NMR ( $\text{DMSO-}d_6$ ): 146.6, 143.9, 129.0, 120.3, 114.7, 94.9, 68.8, 10.0 ppm. MS (positive-ion FAB) cation,  $m/z$  calcd 636.2, found 636.2. Anal. Calcd for  $\text{C}_{35}\text{H}_{36}\text{N}_3\text{O}_6\text{SF}_3\text{Ru}$ : C, 53.57; H, 4.62, N, 5.35. Found: C, 53.02; H, 4.41; N, 5.29.

**[Cp\*Ru( $\eta^6$ -1,3,5-tris(4-chlorophenoxy)benzene)] $^+\text{SO}_3\text{CF}_3^-$  (8).** Compound 8 was prepared by the same procedure described for compound 7 using potassium 4-chlorophenoxide as the nucleophile. A modification in the isolation and purification of 8 was that the mixed solvent system of methylene chloride/ethanol (80/20) was used for the extractions, since the product was not completely soluble in methylene chloride. Yield: 84%.  $^1\text{H}$  NMR ( $\text{DMSO-}d_6$ ): 7.53 (d,  $J = 9.1$  Hz, 6 H, Ar H), 7.30 (d,  $J = 9.1$  Hz, 6 H, Ar H), 6.49 (s, 3 H, arene), 1.96 (s, 15 H,  $\text{CH}_3$ ) ppm.  $^{13}\text{C}$  NMR ( $\text{DMSO-}d_6$ ): 154.4, 129.9, 128.6, 125.8, 119.9, 96.5, 73.9, 9.5 ppm. MS (positive-ion FAB) cation,  $m/z$  calcd 693.03, found 693.23. Anal. Calcd for  $\text{C}_{35}\text{H}_{30}\text{O}_6\text{SCl}_3\text{F}_3\text{Ru}$ : C, 49.86; H, 3.56. Found: C, 49.61; H, 3.27.

**[Cp\*Ru( $\eta^6$ -1,3,5-tris(4-fluorophenoxy)benzene)] $^+\text{SO}_3\text{CF}_3^-$  (9).** Compound 9 was prepared by the same procedure described for compound 7 using potassium 4-fluorophenoxide as the nucleophile. A modification in the isolation and purification of 9 was that the mixed solvent system of methylene chloride/ethanol (80/20) was used for the extractions, since the product was not completely soluble in methylene chloride. Yield: 81%.  $^1\text{H}$  NMR ( $\text{DMSO-}d_6$ ): 7.32–7.29 (m, 12 H, Ar H), 6.32 (s, 3 H, arene), 1.96 (s, 15 H,  $\text{CH}_3$ ) ppm.  $^{13}\text{C}$  NMR ( $\text{DMSO-}d_6$ ): 158.9 (d,  $^1J_{\text{CF}} = 341$  Hz), 151.6, 126.8, 120.3 (d,  $^3J_{\text{CF}} = 8.6$  Hz), 116.9 (d,  $^2J_{\text{CF}} = 23.7$  Hz), 96.3, 72.9, 9.7 ppm. MS (positive-ion FAB) cation,  $m/z$  calcd 645.12, found 645.44. Anal. Calcd for  $\text{C}_{35}\text{H}_{30}\text{O}_6\text{SF}_6\text{Ru}$ : C, 52.96; H, 3.81. Found: C, 52.95; H, 3.49.

**[Cp\*Ru( $\eta^6$ -1,2,4,5-tetrakis(phenoxy)benzene)] $^+\text{SO}_3\text{CF}_3^-$  (10).** A 50 mL Schlenk flask charged with 2 (0.25 g, 0.42 mmol) and potassium phenoxide (0.24 g, 1.83 mmol, 4.4 equiv) in  $\text{CH}_3\text{CN}$  (20 mL) was stirred at 25 °C for 3 h and at 60 °C for 1 h. The solvent was removed in vacuo, the residue was dissolved in methylene chloride (20 mL) and extracted with water ( $2 \times 25$  mL), and the organic layer was dried over magnesium sulfate. After filtration, the solvent was removed in vacuo and the residue was dissolved in THF (ca. 7 mL). Addition of diethyl ether (ca. 8 mL) precipitated a white solid that was collected by filtration and dried in vacuo at 60 °C for 2 h. Yield: 72%.  $^1\text{H}$  NMR ( $\text{DMSO-}d_6$ ): 7.40–7.09 (m, 20 H,



Ar H), 6.67 (s, 2 H, arene), 1.99 (s, 15 H, CH<sub>3</sub>) ppm. <sup>13</sup>C NMR (DMSO-*d*<sub>6</sub>): 156.0, 129.7, 124.2, 117.6, 117.0, 96.8, 76.2, 9.1 ppm. MS (positive-ion FAB) cation, *m/z* calcd 683.17, found 683.34. Anal. Calcd for C<sub>41</sub>H<sub>37</sub>RuSO<sub>7</sub>F<sub>3</sub>: C, 59.20; H, 4.48. Found: C, 59.35; H, 4.54.

**[Cp\**Ru*( $\eta^6$ -1,2,4,5-tetrakis(thiophenoxy)benzene)]<sup>+</sup>SO<sub>3</sub>CF<sub>3</sub><sup>-</sup> (11).** Compound 11 was prepared by a similar procedure described for compound 10 using potassium thiophenoxide. Yield: 83.1%. <sup>1</sup>H NMR (DMSO-*d*<sub>6</sub>): 7.44–7.38 (m, 20 H, Ar H), 5.60 (s, 2 H, arene), 1.83 (s, 15 H, CH<sub>3</sub>) ppm. <sup>13</sup>C NMR (DMSO-*d*<sub>6</sub>): 132.6, 130.1, 129.6, 128.9, 102.8, 96.8, 87.9, 8.8 ppm. MS (positive-ion FAB) cation, *m/z* calcd 747.08, found 747.06. Anal. Calcd for C<sub>41</sub>H<sub>37</sub>RuS<sub>5</sub>O<sub>3</sub>F<sub>3</sub>: C, 54.95; H, 4.16. Found: C, 54.91; H, 4.17.

**[Cp\**Ru*( $\eta^6$ -1,2,4,5-tetrakis(4-aminophenoxy)benzene)]<sup>+</sup>SO<sub>3</sub>CF<sub>3</sub><sup>-</sup> (12).** A 50 mL Schlenk flask charged with 2 (0.35 g, 0.58 mmol) and potassium 4-aminophenoxide (0.43 g, 2.91 mmol, 5 equiv) in CH<sub>3</sub>CN (15 mL) was stirred at 60 °C for 4 h. The excess potassium 4-aminophenoxide was filtered and washed with 5 mL of CH<sub>3</sub>CN and the CH<sub>3</sub>CN was removed in vacuo. The purple-colored residue was dissolved in methylene chloride (25 mL) and extracted with water (2 × 30 mL), and the organic layer was dried over magnesium sulfate. After filtration, the methylene chloride was removed in vacuo and the tan-colored residue was dissolved in THF (ca. 12 mL) with warming. Slow addition of diethyl ether (ca. 6 mL) precipitated a white solid that was collected by filtration and dried in vacuo at 90 °C for 4 h to remove coordinated CH<sub>3</sub>CN solvent. Yield: 68%. <sup>1</sup>H NMR (DMSO-*d*<sub>6</sub>): 6.88 (d, *J* = 8.9 Hz, 8 H, Ar H), 6.53 (d, *J* = 8.9 Hz, 8 H, Ar H), 5.94 (s, 2 H, arene), 1.91 (s, 15 H, CH<sub>3</sub>) ppm. <sup>13</sup>C NMR (DMSO-*d*<sub>6</sub>): 145.8, 145.7, 118.9, 118.0, 114.6, 95.4, 73.0, 9.5. MS (positive-ion FAB) cation, *m/z* calcd 743.22, found 743.41. Anal. Calcd for C<sub>41</sub>H<sub>41</sub>O<sub>7</sub>SN<sub>4</sub>F<sub>3</sub>Ru: C, 55.21; H, 4.63; N, 6.28. Found: C, 55.43; H, 4.78; N, 6.14 ppm.

**[Cp\**Ru*( $\eta^6$ -1,2,4,5-tetrakis(4-chlorophenoxy)benzene)]<sup>+</sup>SO<sub>3</sub>CF<sub>3</sub><sup>-</sup> (13).** Compound 13 was prepared by a

similar procedure described for compound 12 using potassium 4-chlorophenoxide. A modification in the isolation and purification of 13 was that the mixed solvent system of methylene chloride/ethanol (80/20) was used for the extractions, since the product was not completely soluble in methylene chloride. Isolation of 13 was achieved by addition of diethyl ether to a solution of the product in CH<sub>3</sub>CN/THF solvents to afford white solids. Yield: 71%. <sup>1</sup>H NMR (DMSO-*d*<sub>6</sub>): 7.44 (d, *J* = 9.1 Hz, 8 H, Ar H), 7.31 (d, *J* = 9.1 Hz, 8 H, Ar H), 7.00 (s, 2 H, arene), 1.97 (s, 15 H, CH<sub>3</sub>) ppm. <sup>13</sup>C NMR (DMSO-*d*<sub>6</sub>): 154.9, 129.6, 128.2, 118.7, 117.5, 97.3, 76.6, 9.1 ppm. MS (positive-ion FAB) cation, *m/z* calcd 819.02; found 819.22. Anal. Calcd for C<sub>41</sub>H<sub>33</sub>O<sub>7</sub>SCl<sub>4</sub>F<sub>3</sub>Ru: C, 50.79; H, 3.43. Found: C, 50.23; H, 3.36.

**[Cp\**Ru*( $\eta^6$ -1,2,4,5-tetrakis(4-fluorophenoxy)benzene)]<sup>+</sup>SO<sub>3</sub>CF<sub>3</sub><sup>-</sup> (14).** Compound 14 was prepared by a similar procedure described for compound 12 using potassium 4-fluorophenoxide. A modification in the isolation and purification of 14 was that the mixed solvent system of methylene chloride/ethanol (80/20) was used for the extractions, since the product was not completely soluble in methylene chloride. Isolation of 14 was achieved by addition of diethyl ether to a solution of the product in CH<sub>3</sub>CN/THF solvents to afford white solids. Yield: 79%. <sup>1</sup>H NMR (DMSO-*d*<sub>6</sub>): 7.32–7.19 (m, 16 H, Ar H), 6.79 (s, 2 H, arene), 1.98 (s, 15 H, CH<sub>3</sub>) ppm. <sup>13</sup>C NMR (DMSO-*d*<sub>6</sub>): 158.5 (d, <sup>1</sup>*J*<sub>CF</sub> = 240 Hz), 152.5, 118.6 (d, <sup>3</sup>*J*<sub>CF</sub> = 8.5 Hz), 117.9, 116.5 (d, <sup>2</sup>*J*<sub>CF</sub> = 23.6 Hz), 97.1, 76.3, 9.3 ppm. MS (positive-ion FAB) cation, *m/z* calcd 755.14, found 755.30. Anal. Calcd for C<sub>41</sub>H<sub>33</sub>O<sub>7</sub>SF<sub>7</sub>Ru: C, 54.49; H, 3.68. Found: C, 54.03; H, 3.60.

**Acknowledgment.** We thank Dr. J. Lazar for FAB mass spectral data, Dr. R. Burch and Dr. A. Feiring for insightful discussions, and J. M. Barker and R. Davis for technical assistance.

OM950198+

# Bimetallic Complexes with Chiral Molybdenum Centers and Bis( $\eta^5$ -cyclopentadienyl) Bridges: Interchange between Legs in Three-Legged Piano Stool Complexes

Mijail V. Galakhov, Alicia Gil, Ernesto de Jesús, and Pascual Royo\*

Departamento de Química Inorgánica, Universidad de Alcalá de Henares, Campus Universitario, 28871 Alcalá de Henares, Madrid, Spain

Received February 28, 1995<sup>®</sup>

Reactions of  $[\{\text{Mo}(\text{CO})_3\text{Cl}\}_2(\mu\text{-CpCp})]$  ( $\text{CpCp} = (\eta^5\text{-C}_5\text{H}_4)_2\text{SiMe}_2$  (**1a**) or  $(\eta^5\text{-C}_5\text{H}_3)_2(\text{SiMe}_2)_2$  (**1b**)) with  $\text{AgBF}_4$  and with 2-butyne in THF (THF = tetrahydrofuran) give  $[\{\text{Mo}(\text{CO})(\eta^2\text{-MeCCMe})_2\}_2(\mu\text{-CpCp})][\text{BF}_4]_2$  (**2a,b**). Addition of  $\text{PPh}_3$  or  $\text{PPh}_4\text{Cl}$  to **2a** or **2b** results in the substitution of one 2-butyne ligand at each Mo center by  $\text{PPh}_3$  or  $\text{Cl}^-$ , giving ionic  $[\{\text{Mo}(\text{CO})(\eta^2\text{-MeCCMe})(\text{PPh}_3)\}_2(\mu\text{-CpCp})][\text{BF}_4]_2$  (**3a,b**) or neutral  $[\{\text{Mo}(\text{CO})(\eta^2\text{-MeCCMe})\text{Cl}\}_2(\mu\text{-CpCp})]$  (**5**), respectively. Addition of dmpe (dmpe = dimethylphosphineethane) to **2a** gives the free carbonyl complex  $[\{\text{Mo}(\eta^2\text{-MeCCMe})(\text{dmpe})\}_2(\mu\text{-CpCp})][\text{BF}_4]_2$  (**4a**). Complexes **3** and **5** are obtained as a ca. 1:1 mixture of the *RS* isomer and the *RR,SS* racemate. The *RR,SS* racemate of **3a** can be obtained >90% pure by slow crystallization of the **3a** diastereomeric product mixture. In the absence of free ligands, conversion of *RR,SS-3a* into *RS-3a* is a first-order reaction with  $k = (8 \pm 1) \times 10^{-5} \text{ s}^{-1}$  and  $\Delta G^\ddagger = 94.6 \pm 0.2 \text{ kJ mol}^{-1}$  at 293 K, and the basic mechanism is likely to be intramolecular.

## Introduction

Recently, we have reported the use of bridged cyclopentadienyl ligands such as  $(\text{C}_5\text{H}_4)_2\text{SiMe}_2^1$  and  $(\text{C}_5\text{H}_3)_2(\text{SiMe}_2)_2^2$  as anchoring ligands for dinuclear molybdenum complexes. In the first part of this article we report the synthesis of the new complexes **2–5** which contain one or more 2-butyne ligands. In the second part we study by  $^1\text{H}$  NMR the kinetics of the ligand interchange in the three-legged piano stool complex **3a**. Observation by NMR of the interconversion between *cis* and *trans* isomers of the type  $\text{CpMX}_3\text{Y}$  or  $\text{CpMX}_2\text{Y}_2$  has formed an important part of their kinetic studies.<sup>3</sup> However, ligand interchange in mononuclear three-legged piano stool complexes of the type  $\text{CpMXYZ}$  interconverts *R* and *S* enantiomers, and cannot be monitored by NMR. In contrast, ligand interchange in dinuclear three-legged piano stool complexes such as **3a** interconverts diastereoisomers that give distinguishable NMR resonances.

## Results and Discussion

**Preparative Methods.** Complex **2a** is synthesized by reaction of **1a** with  $\text{AgBF}_4$ , in THF, and subsequent addition of excess 2-butyne (Scheme 1). Irradiation of the mixture with UV light increases the rate and yield of the reaction. Complex **2b** is synthesized by a similar method but is produced only in poor yields. Complexes **2a** and **2b** are obtained as yellow microcrystalline solids, stable for weeks in an inert atmosphere.

Addition of  $\text{PPh}_3$  to **2a** or **2b** results in the substitution of a single 2-butyne ligand at each molybdenum center, giving **3a** or **3b**. These are the only complexes obtained even when an excess of  $\text{PPh}_3$  is added. These results are similar to those reported for the mononuclear analogs,<sup>4</sup> for which steric effects have been invoked. In contrast, dmpe (dmpe = dimethylphosphineethane) replaces one 2-butyne and one carbonyl ligand at each molybdenum center in **2a**, giving **4a**, even when a deficiency of dmpe is used.

The neutral complex **5a** is obtained as a green solid by reaction of **2a** with  $\text{Ph}_4\text{PCl}$  in THF. The  $\text{BF}_4^-$  anion precipitates as  $[\text{Ph}_4\text{P}][\text{BF}_4]$ , and one 2-butyne ligand per molybdenum atom is replaced by a chloride ligand. Complexes **2–4** have molar conductivities between 160 and 200  $\text{ohm}^{-1} \text{ cm}^2 \text{ mol}^{-1}$ , consistent with the values expected for 1:2 electrolytes.<sup>5</sup>

**Structural Study.** Spectroscopic data for all complexes are given in the Experimental Section. The more valuable information is given by the cyclopentadienyl and the Me–Si resonances in the  $^1\text{H}$  NMR spectra, that appear in the range 4.23–7.98 and –0.91 to 0.67 ppm, respectively. In **2a** and **4a**, the Cp protons appear as an AA'BB' spin system and the Me resonances appear as a singlet. These data indicate the existence of two planes of symmetry (planes Me–Si–Me and cp–Si–cp; cp = centroid of the cyclopentadienyl ring) either in the structure of a rigid molecule or in the average structure of a fluxional molecule (Chart 1).<sup>1</sup> These planes of symmetry are also reflected in the  $^{13}\text{C}\{^1\text{H}\}$  NMR spectrum of **2a**, in which only three resonances are observed for the ring carbons, and in the  $^{31}\text{P}\{^1\text{H}\}$  NMR spectrum of **4a**, in which a single resonance is observed for the four phosphorus atoms of the two dmpe ligands in each molecule. An analogous situation is observed

<sup>®</sup> Abstract published in *Advance ACS Abstracts*, July 1, 1995.

(1) Gómez-Sal, P.; de Jesús, E.; Pérez, A. I.; Royo, P. *Organometallics* 1993, 12, 4633.

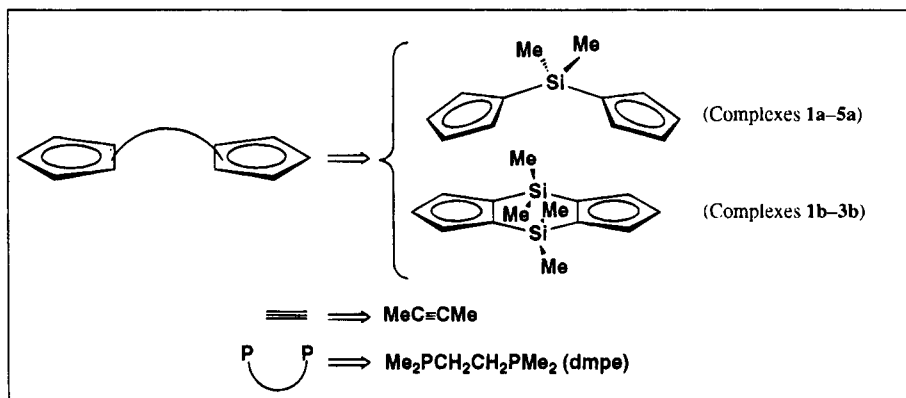
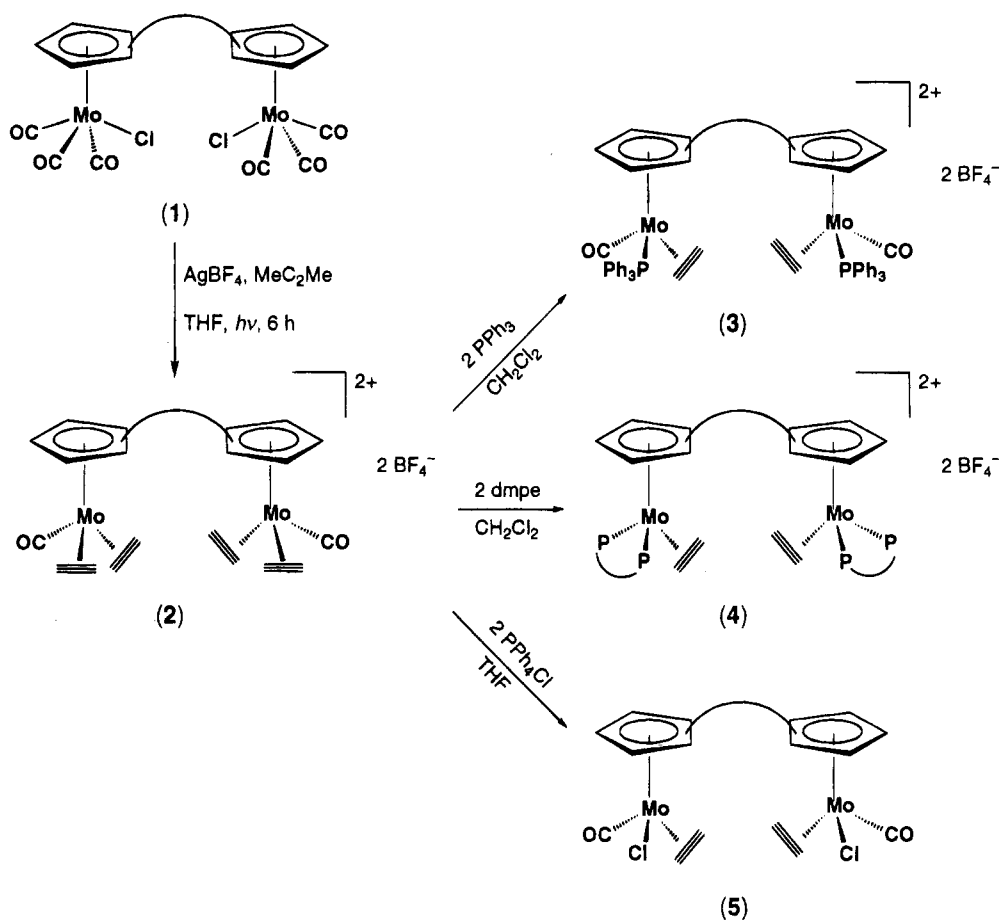
(2) Amor, F.; Gómez-Sal, P.; de Jesús, E.; Royo, P.; de Miguel, A. V. *Organometallics* 1994, 13, 4322.

(3) See for example: McLain, S. J.; Wood, C. D.; Schrock, R. R. *J. Am. Chem. Soc.* 1979, 101, 4558. Faller, J. W.; Anderson, A. S. *J. Am. Chem. Soc.* 1970, 92, 5852.

(4) Allen, S. R.; Baker, P. K.; Barnes, S. G.; Green, M.; Trollope, L.; Manojlovic-Muir, L.; Muir, K. W. *J. Chem. Soc., Dalton Trans.* 1981, 873.

(5) Geary, W. J. *Coord. Chem. Rev.* 1971, 7, 81.

Scheme 1



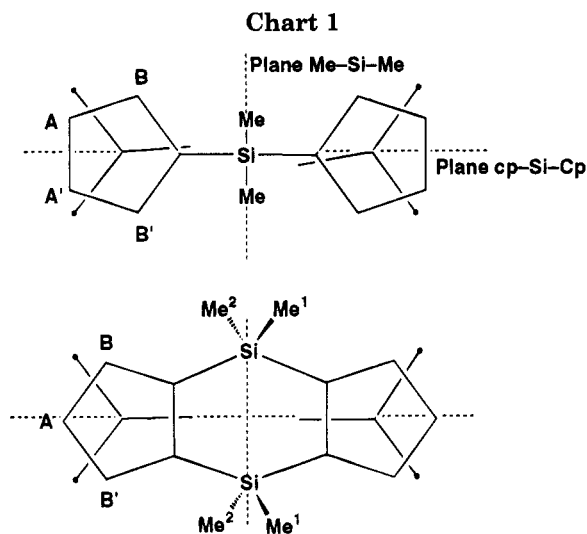
in **2b**, in which the cyclopentadienyl ring protons appear as an ABB' spin system and the Me-Si resonances appear as two singlets, one for the methyl groups above the ring plane and one for the methyl groups below the plane.

Molecules **3** and **5** each have two chiral molybdenum atoms and three stereoisomers: two are enantiomers to each other (*RR* and *SS*) and diastereoisomers with respect to the third (*RS*). *RS* and *SR* are the same isomer because the two Mo atoms are equivalent. The Me-Si groups of **3a** or **5a** appear in the  $^1\text{H}$  and  $^{13}\text{C}\{-^1\text{H}\}$  NMR spectra as two singlets assigned to the *RS* isomer which integrate as 1:1 and as an intense singlet assigned to the *RR,SS* racemate: the two Me-Si groups of the molecule are equivalent in the *RR* and *SS* isomers but not equivalent in the *RS* isomer (Chart 2). The Me-Si groups of **3b** appear in the  $^1\text{H}$  NMR spectrum as two resonances for the *RR,SS* racemate and

as four resonances for the *RS* isomer. In each case, the *RS* isomer and the *RR,SS* racemate are in a *ca.* 1:1 molar ratio.

At room temperature, **2a** and **2b** show separate resonances in the  $^1\text{H}$  NMR spectrum for the *endo* and *exo* methyl groups of the 2-butyne ligand, indicating that the ligand turns slowly through its bond to the metal. The 2-butyne of **3a** or **5a** appear as two resonances at low temperature which coalesce to a single resonance at 42 °C ( $\Delta G^\ddagger_{315\text{K}} = 57 \pm 5 \text{ kJ mol}^{-1}$ ) for **3a**, or 20 °C ( $\Delta G^\ddagger_{293\text{K}} = 56 \pm 5 \text{ kJ mol}^{-1}$ ) for **5a**. Analysis of the line shape for **3a** gives  $\Delta H^\ddagger = 73 \pm 5 \text{ kJ mol}^{-1}$  and  $\Delta S^\ddagger = 43 \pm 14 \text{ J K}^{-1} \text{ mol}^{-1}$ .

**Transformation of *RR,SS*-3a in *RS*-3a.** Isomer *RR,SS*-**3a** is isolated >90% pure ( $^1\text{H}$  NMR evidence) as prismatic purple crystals when **3a** is crystallized slowly in  $\text{CH}_2\text{Cl}_2$ /ether at -40 °C. *RR,SS*-**3a** transforms into *RS*-**3a** in a process that reaches equilibrium after



several hours in  $\text{CDCl}_3$ . The transformation was monitored by  $^1\text{H}$  NMR for  $10^{-3}$ – $10^{-2}$  M solutions of  $RR,SS$ -**3a** at  $20^\circ\text{C}$ .

In determination of the rate law (see Experimental Section for details), we assumed that the forward and reverse processes  $RR,SS\text{-}3a \rightleftharpoons RS\text{-}3a$  follow identical mechanisms and have the same rate constant  $k$ , in agreement with the measured equilibrium constant of *ca.* 1. The observed reaction rate corresponds to the contribution of both forward and reverse reactions, since the concentrations of  $RR,SS\text{-}3a$  and  $RS\text{-}3a$  during the measurements were close to the equilibrium concentrations. Under these conditions, the integrated rate law for a first order reaction is<sup>6</sup>  $[RR,SS] = \{(1 + e^{-2kt})/2\} [RR,SS]_0$  or  $\ln([RR,SS] - [RS]) = -2kt + \ln[RR,SS]_0$  in its logarithmic form. We have observed a linear dependence between  $\ln([RR,SS] - [RS])$  and time, and calculated a rate constant of  $(8 \pm 1) \times 10^{-5} \text{ s}^{-1}$  for the first order rate law ( $\Delta G^\ddagger_{293\text{K}} = 94.6 \pm 0.2 \text{ kJ mol}^{-1}$ ).

The process is accelerated by the addition of free  $\text{PPh}_3$  or CO but not by the addition of 2-butyne, equilibrium being reached in a matter of hours when no ligands are added, in minutes when CO is bubbled at 1 atm ( $k \approx 2 \times 10^{-3} \text{ s}^{-1}$ ), and in seconds when  $\text{PPh}_3$  ( $\approx 10^{-2} \text{ M}$ ) is added. The mechanism is likely to be associative in the presence of free  $\text{PPh}_3$  or CO (Scheme 2). In the absence of free  $\text{PPh}_3$  or CO an associative mechanism could be induced by traces of free ligand derived from impurities or decomposition. However, an associative mechanism and the observed first-order rate would only be compatible if we made the unlikely assumption that the trace concentration of free ligand was comparable in all the experiments regardless of changes in sample concentration or source. We therefore do not consider that this process makes a significant contribution to the overall rate. The observed first-order rate law is consistent with either an intramolecular or a dissociative mechanism. However, the addition of the efficient CO or  $\text{PPh}_3$  trap  $[\text{Pt}(\text{C}_2\text{H}_4)_2(\text{PPh}_3)]$  did not affect the reaction rate, making associative or dissociative pathways that require the presence of free ligands unlikely. The intramolecular route is therefore the more plausible mechanism for  $RR,SS$ - to  $RS\text{-}3a$  interconversion, although the dissociative or associative routes are not

excluded, at least in part, as the latter is the main mechanism when free ligands as CO or  $\text{PPh}_3$  are added.

## Experimental Section

**Reagents and General Techniques.** All reactions were carried out under an inert atmosphere (argon or nitrogen) using Schlenk and high-vacuum techniques. Solvents were dried and distilled under nitrogen: diethyl ether and tetrahydrofuran from sodium benzophenone ketyl; hexane from sodium;  $\text{CH}_2\text{Cl}_2$  over  $\text{P}_4\text{O}_{10}$ . Unless otherwise stated, reagents were obtained from commercial sources and used as received. IR spectra were recorded in Nujol mulls over the range  $4000$ – $200 \text{ cm}^{-1}$  on a Perkin-Elmer 583 spectrophotometer. IR data are given in  $\text{cm}^{-1}$ . The  $^1\text{H}$ ,  $^{31}\text{P}$ , and  $^{13}\text{C}$  NMR spectra were recorded at 299.95, 121.42, and 75.43 MHz, respectively, on a Varian Unity 300 spectrometer; chemical shifts, in ppm, are positive downfield relative to external  $\text{SiMe}_4$  for  $^1\text{H}$  and  $^{13}\text{C}$  and to external 85%  $\text{H}_3\text{PO}_4$  in  $\text{H}_2\text{O}$  for  $^{31}\text{P}$ . C, H, and N analyses were performed with a Perkin-Elmer 240-B instrument. Conductivity measurements were carried out in a WTW L42 instrument from acetone solutions *ca.*  $5 \times 10^{-4} \text{ M}$ .

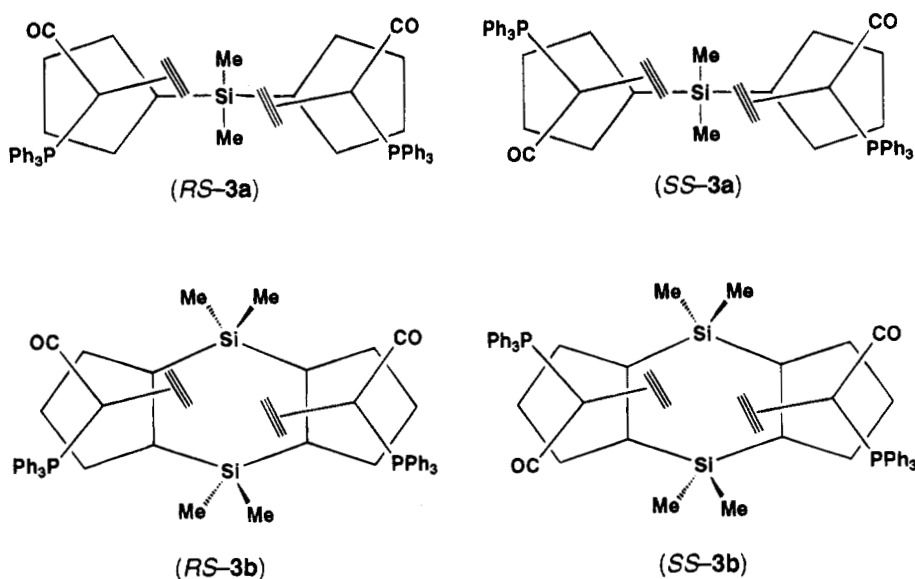
**Syntheses.** Complexes **1a**<sup>1</sup> and **1b**<sup>2</sup> were prepared according to reported methods.

**Preparation of  $[\{\text{Mo}(\text{CO})(\eta^2\text{-MeCCMe}_2)_2(\mu\text{-}(\eta^5\text{-C}_5\text{H}_4)_2\text{-SiMe}_2)][\text{BF}_4]_2$  (**2a**).**  $\text{AgBF}_4$  (0.29 g, 1.5 mmol) and a solution 1.42 M of 2-butyne in THF (4.0 mL, 5.7 mmol) were added at  $0^\circ\text{C}$  to a solution of **1a** (0.48 g, 0.77 mmol) in THF (50 mL). The mixture was irradiated with a UV lamp (Philips, HPK 125 W) over 6 h. The mixture was then filtered through Celite, and the solid extracted in a Soxhlet apparatus with  $\text{CH}_2\text{Cl}_2$  (100 mL) until colorless (*ca.* 8 h). The solution was concentrated *in vacuo* until a solid began to precipitate. Then diethyl ether (30 mL) was added, the mixture was filtered, and a yellow microcrystalline solid was obtained (0.35 g, 55%), which was washed with hexane ( $3 \times 30 \text{ mL}$ ). Anal. Calcd for  $\text{C}_{30}\text{H}_{38}\text{B}_2\text{O}_2\text{F}_8\text{Si}_2\text{Mo}_2$ : C, 43.7; H, 4.6. Found: C, 43.5; H, 4.6. Conductivity (acetone):  $\Lambda_M 225 \text{ ohm}^{-1} \text{ cm}^2 \text{ mol}^{-1}$ . IR (Nujol):  $\nu(\text{CO}) 2031$  vs.  $^1\text{H}$  NMR (acetone- $d_6$ ):  $\delta$  6.76, 6.28 (AA' and BB' parts of an AA'BB' spin system, 4 H,  $\text{C}_5\text{H}_4$ ), 3.11 (s, 6 H,  $\text{C}_2\text{Me}_2$ ), 2.81 (s, 6 H,  $\text{C}_2\text{Me}_2$ ), 0.28 (s, 4 H,  $\text{SiMe}_2$ ).  $^{13}\text{C}\{^1\text{H}\}$  NMR (acetone- $d_6$ ):  $\delta$  223.2 (s, CO), 164.7 (s,  $\text{C}_2\text{Me}_2$ ), 145.2 (s,  $\text{C}_2\text{Me}_2$ ), 111.4 (s,  $\text{C}_5\text{H}_4$ ), 108.1 (s,  $\text{C}_5\text{H}_4$ ), 98.1 (s,  $\text{C}_5\text{H}_4$ , C *ipso*), 20.0 (s,  $\text{C}_2\text{Me}_2$ ), 15.7 (s,  $\text{C}_2\text{Me}_2$ ), -2.1 (s,  $\text{SiMe}_2$ ).

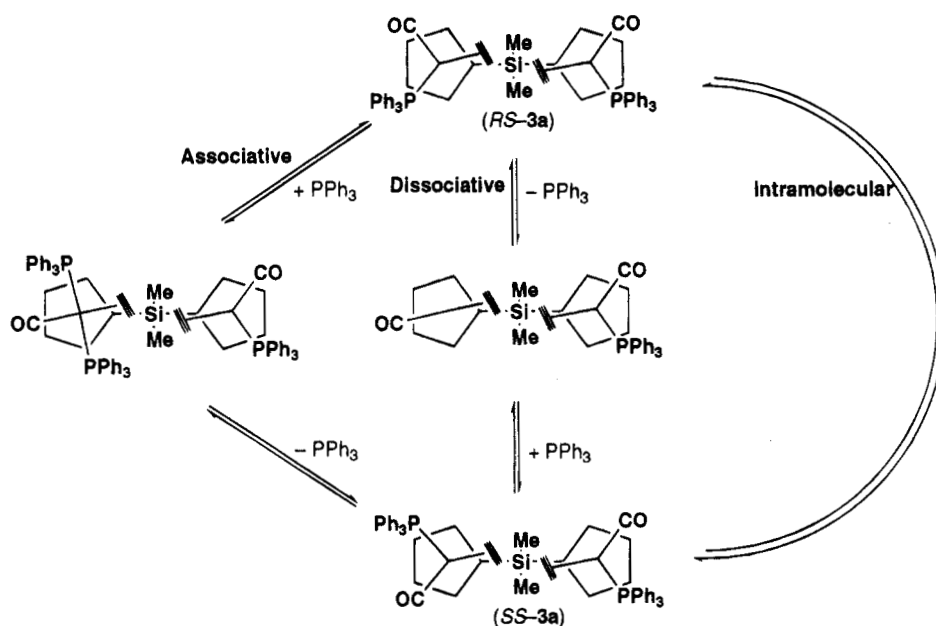
**Preparation of  $[\{\text{Mo}(\text{CO})(\eta^2\text{-MeCCMe}_2)_2(\mu\text{-}(\eta^5\text{-C}_5\text{H}_3)_2\text{-SiMe}_2)][\text{BF}_4]_2$  (**2b**).** This complex was prepared (0.25 g, 38%) by reaction of **1b** (0.50 g, 0.75 mmol),  $\text{AgBF}_4$  (0.29 g, 1.5 mmol) and a 1.42 M solution of 2-butyne in THF (4.0 mL, 5.7 mmol). Anal. Calcd for  $\text{C}_{32}\text{H}_{42}\text{B}_2\text{O}_2\text{F}_8\text{Si}_2\text{Mo}_2$ : C, 43.7; H, 4.8. Found: C, 43.9; H, 4.7. IR (Nujol):  $\nu(\text{CO}) 2028$  vs.  $^1\text{H}$  NMR (acetone- $d_6$ ):  $\delta$  7.98 (A part of an ABB' spin system, 1 H,  $\text{C}_5\text{H}_3$ ), 6.42 (BB' part of an ABB' spin system, 2 H,  $\text{C}_5\text{H}_3$ ), 3.18 (s, 6 H,  $\text{C}_2\text{Me}_2$ ), 2.90 (s, 6 H,  $\text{C}_2\text{Me}_2$ ), 0.52 (s, 3 H,  $\text{SiMe}_2$ ), 0.29 (s, 3 H,  $\text{SiMe}_2$ ).  $^{13}\text{C}\{^1\text{H}\}$  NMR (acetone- $d_6$ ):  $\delta$  225.3 (s, CO), 165.5 (s,  $\text{C}_2\text{Me}_2$ ), 143.8 (s,  $\text{C}_2\text{Me}_2$ ), 123.6 (s,  $\text{C}_5\text{H}_4$ ), 108.1 (s,  $\text{C}_5\text{H}_4$ ), 105.2 (s,  $\text{C}_5\text{H}_4$ , C *ipso*), 19.9 (s,  $\text{C}_2\text{Me}_2$ ), 15.4 (s,  $\text{C}_2\text{Me}_2$ ), 5.1 (s,  $\text{SiMe}_2$ ), -0.3 (s,  $\text{SiMe}_2$ ).

**Preparation of  $[\{\text{Mo}(\text{CO})(\eta^2\text{-MeCCMe}_2)(\text{PPh}_3)_2(\mu\text{-}(\eta^5\text{-C}_5\text{H}_4)_2\text{-SiMe}_2)][\text{BF}_4]_2$  (**3a**).**  $\text{PPh}_3$  (0.15 g, 0.56 mmol) was added to a suspension of **2a** (0.23 g, 0.28 mmol) in  $\text{CH}_2\text{Cl}_2$  (30 mL). The solution became progressively purple. Stirring was continued for 4 h followed by filtration. Solvent was removed *in vacuo* to yield a purple solid (0.27 g, 78%), which was washed with hexane ( $3 \times 30 \text{ mL}$ ) and dried *in vacuo*. Anal. Calcd for  $\text{C}_{58}\text{H}_{56}\text{B}_2\text{O}_2\text{F}_8\text{Si}_2\text{P}_2\text{Mo}_2$ : C, 56.1; H, 4.6. Found: C, 55.8; H, 4.5. Conductivity (acetone):  $\Lambda_M 200 \text{ ohm}^{-1} \text{ cm}^2 \text{ mol}^{-1}$ . IR (Nujol):  $\nu(\text{CO}) 1955$  s, br.  $^1\text{H}$  NMR ( $\text{CDCl}_3$ ) for  $RS\text{-}3a$ :  $\delta$  7.5–7.2 (30 H,  $\text{PPh}_3$ ), 6.23 (br, 2 H,  $\text{C}_5\text{H}_4$ ), 6.18 (br, 2 H,  $\text{C}_5\text{H}_4$ ), 6.02 (br, 2 H,  $\text{C}_5\text{H}_4$ ), 5.12 (br, 2 H,  $\text{C}_5\text{H}_4$ ), 3.15 (br, 6 H,  $\text{C}_2\text{Me}_2$ ), 2.60 (br, 6 H,  $\text{C}_2\text{Me}_2$ ), -0.61 (s, 3 H,  $\text{SiMe}_2$ ), 0.25 (s, 3 H,  $\text{SiMe}_2$ ); for  $RR,SS\text{-}3a$ :  $\delta$  7.49 (m, 18 H,  $\text{PPh}_3$ ), 7.26 (m, 12 H,  $\text{PPh}_3$ ), 6.27 (br, 2 H,  $\text{C}_5\text{H}_4$ ), 6.02 (br, 4 H,  $\text{C}_5\text{H}_4$ ), 5.12 (br, 2 H,  $\text{C}_5\text{H}_4$ ),

Chart 2



Scheme 2



3.15 (br, 6 H, C<sub>2</sub>Me<sub>2</sub>), 2.60 (br, 6 H, C<sub>2</sub>Me<sub>2</sub>), -0.11 (s, 6 H, SiMe<sub>2</sub>). <sup>13</sup>C{<sup>1</sup>H} NMR (CDCl<sub>3</sub>) for the 1:1 mixture of *RR,SS* and *RS* diastereoisomers: δ 230.8 (s, CO), 230.6 (s, CO), 128–135 (PPh<sub>3</sub> and C<sub>2</sub>Me<sub>2</sub>), 111.6 (s, C<sub>5</sub>H<sub>4</sub>), 111.4 (s, C<sub>5</sub>H<sub>4</sub>), 109.1 (s, C<sub>5</sub>H<sub>4</sub>), 108.8 (s, C<sub>5</sub>H<sub>4</sub>), 102.3 (s, C<sub>5</sub>H<sub>4</sub>), 102.2 (s, C<sub>5</sub>H<sub>4</sub>), 101.4 (s, C<sub>5</sub>H<sub>4</sub>), 95.5 (s, C<sub>5</sub>H<sub>4</sub>), 95.3 (s, C<sub>5</sub>H<sub>4</sub>), 23.5 (br, C<sub>2</sub>Me<sub>2</sub>), 20.1 (br, C<sub>2</sub>Me<sub>2</sub>), -0.8 (s, SiMe<sub>2</sub>, *RS* isomer), -2.4 (s, SiMe<sub>2</sub>, *RR,SS* isomer), -3.9 (s, SiMe<sub>2</sub>, *RS* isomer). <sup>31</sup>P{<sup>1</sup>H} NMR (CDCl<sub>3</sub>): δ 52.3 (s).

**Preparation of [(Mo(CO)(η<sup>2</sup>-MeCCMe)(PPh<sub>3</sub>)<sub>2</sub>]<sub>2</sub>(μ-(η<sup>5</sup>-C<sub>5</sub>H<sub>3</sub>)<sub>2</sub>(SiMe<sub>2</sub>)<sub>2</sub>)](BF<sub>4</sub>)<sub>2</sub> (3b).** This complex was prepared (0.14 g, 77%) by reaction of **2b** (0.12 g, 0.14 mmol) with PPh<sub>3</sub> (0.073 g, 0.28 mmol). Anal. Calcd for C<sub>60</sub>H<sub>60</sub>B<sub>2</sub>O<sub>2</sub>F<sub>8</sub>Si<sub>2</sub>P<sub>2</sub>Mo<sub>2</sub>: C, 55.6; H, 4.7. Found: C, 55.4; H, 4.7. IR (Nujol): ν(CO) 1951 s, br. <sup>1</sup>H NMR (CDCl<sub>3</sub>) for the 1:1 mixture of *RR,SS* and *RS* diastereoisomers: δ 7.5–7.2 (60 H, PPh<sub>3</sub>), 6.01 (A part of an ABB' spin system, 2 H, C<sub>5</sub>H<sub>3</sub>), 5.85 (BB' part of an ABB' spin system, 4 H, C<sub>5</sub>H<sub>3</sub>), 4.62 (BB' part of an ABB' spin system, 4 H, C<sub>5</sub>H<sub>3</sub>), 4.23 (A part of an ABB' spin system, 2 H, C<sub>5</sub>H<sub>3</sub>), 3.40 (br, 12 H, C<sub>2</sub>Me<sub>2</sub>), 2.57 (br, 12 H, C<sub>2</sub>Me<sub>2</sub>), 0.67 (s, 3 H, SiMe<sub>2</sub>, *RS* isomer), 0.62 (s, 3 H, SiMe<sub>2</sub>, *RS* isomer), 0.42 (s, 6 H, SiMe<sub>2</sub>, *RR,SS* isomer), 0.39 (s, 3 H, SiMe<sub>2</sub>, *RS* isomer), -0.02 (s, 6 H, SiMe<sub>2</sub>, *RR,SS* isomer), -0.91 (s, 3 H, SiMe<sub>2</sub>, *RS*

isomer). <sup>13</sup>C{<sup>1</sup>H} NMR (CDCl<sub>3</sub>) for the 1:1 mixture of *RR,SS* and *RS* diastereoisomers: δ 223.7 (s, CO), 223.6 (s, CO), 128–135 (PPh<sub>3</sub> and C<sub>2</sub>Me<sub>2</sub>), 117.9 (s, C<sub>5</sub>H<sub>3</sub>), 116.8 (s, C<sub>5</sub>H<sub>3</sub>), 111.1 (s, C<sub>5</sub>H<sub>3</sub>), 111.0 (s, C<sub>5</sub>H<sub>3</sub>), 110.5 (s, C<sub>5</sub>H<sub>3</sub>), 109.9 (s, C<sub>5</sub>H<sub>3</sub>), 108.4 (s, C<sub>5</sub>H<sub>3</sub>), 106.8 (s, C<sub>5</sub>H<sub>3</sub>), 106.5 (s, C<sub>5</sub>H<sub>3</sub>), 105.6 (s, C<sub>5</sub>H<sub>3</sub>), 25.6 (s, C<sub>2</sub>Me<sub>2</sub>), 20.2 (s, C<sub>2</sub>Me<sub>2</sub>), 4.4 (s, SiMe<sub>2</sub>, *RS* isomer), 2.9 (s, SiMe<sub>2</sub>, *RS* isomer), 2.3 (s, SiMe<sub>2</sub>, *RR,SS* isomer), 0.8 (s, SiMe<sub>2</sub>, *RR,SS* isomer), 0.4 (s, SiMe<sub>2</sub>, *RS* isomer), -1.4 (s, SiMe<sub>2</sub>, *RS* isomer). <sup>31</sup>P{<sup>1</sup>H} NMR (CDCl<sub>3</sub>): δ 52.3 (s).

**Preparation of [(Mo(η<sup>2</sup>-MeCCMe)(dmpe))<sub>2</sub>(μ-(η<sup>5</sup>-C<sub>5</sub>H<sub>4</sub>)<sub>2</sub>-SiMe<sub>2</sub>)](BF<sub>4</sub>)<sub>2</sub> (4a).** DMPE (0.26 mL, 0.56 mmol) was added to a suspension of **2a** (0.23 g, 0.28 mmol) in CH<sub>2</sub>Cl<sub>2</sub> (30 mL). The yellow solution became blue, and the solid dissolved. Stirring was continued for 1 h. Solvent was removed *in vacuo*, yielding a blue solid (0.20 g, 74%) which was washed with hexane (3 × 15 mL) and dried *in vacuo*. Anal. Calcd for C<sub>32</sub>H<sub>56</sub>B<sub>2</sub>F<sub>8</sub>Si<sub>2</sub>P<sub>4</sub>Mo<sub>2</sub>: C, 40.1; H, 6.1. Found: C, 40.5; H, 6.2. Conductivity (acetone): Λ<sub>M</sub> 209 ohm<sup>-1</sup> cm<sup>2</sup> mol<sup>-1</sup>. <sup>1</sup>H NMR (acetone-*d*<sub>6</sub>): δ 5.92, 5.42 (AA' and BB' parts of an AA'BB' spin system, 4 H, C<sub>5</sub>H<sub>4</sub>), 2.93 (s, 6 H, C<sub>2</sub>Me<sub>2</sub>), 2.05 (m, 4 H, PCH<sub>2</sub>), 1.48 (d, 6 H, PMe<sub>2</sub>, <sup>2</sup>J<sub>HP</sub> = 9.3), 1.45 (d, 6 H, PMe<sub>2</sub>, <sup>2</sup>J<sub>HP</sub> = 9.9), 0.21 (s, 3 H, SiMe<sub>2</sub>). <sup>31</sup>P{<sup>1</sup>H} NMR (acetone-*d*<sub>6</sub>): δ 51.7 (s).

**Preparation of [ $\{\text{Mo}(\text{CO})(\eta^2\text{-MeCCMe})\text{Cl}\}_2(\mu\text{-}(\eta^5\text{-C}_5\text{H}_5)_2\text{-SiMe}_2)_2$ ] (5a).**  $\text{PPh}_4\text{Cl}$  (0.18 g, 0.48 mmol) was added to a suspension of **2a** (0.20 g, 0.24 mmol) in THF (30 mL). The yellow solution became green. The solution was filtered, and the solvent was removed *in vacuo*. The green solid obtained (0.08 g, 54%) was washed with hexane ( $3 \times 10$  mL) and dried *in vacuo*. Anal. Calcd for  $\text{C}_{22}\text{H}_{26}\text{O}_2\text{Cl}_2\text{SiMo}_2$ : C, 43.1; H, 4.3. Found: C, 43.4; H, 4.2. IR (Nujol):  $\nu(\text{CO})$  1927 s, br.  $^1\text{H}$  NMR ( $\text{CDCl}_3$ ) for the 1:1 mixture of *RR,SS* and *RS* diastereoisomers:  $\delta$  6.14 (br, 4 H,  $\text{C}_5\text{H}_4$ ), 5.77 (br, 4 H,  $\text{C}_5\text{H}_4$ ), 5.70 (br, 4 H,  $\text{C}_5\text{H}_4$ ), 5.04 (br, 4 H,  $\text{C}_5\text{H}_4$ ), 3.19 (br, 24 H,  $\text{C}_2\text{Me}_2$ ), 0.35 (s, 3 H,  $\text{SiMe}_2$ , *RS* isomer), 0.10 (s, 6 H,  $\text{SiMe}_2$ , *RR,SS* isomer),  $-0.10$  (s, 3 H,  $\text{SiMe}_2$ , *RS* isomer).  $^{13}\text{C}\{^1\text{H}\}$  NMR ( $\text{CDCl}_3$ ) for the 1:1 mixture of *RR,SS* and *RS* diastereoisomers:  $\delta$  232.3 (s, CO), 200.9 (s,  $\text{C}_2\text{Me}_2$ ), 194.4 (s,  $\text{C}_2\text{Me}_2$ ), 114.7 (s,  $\text{C}_5\text{H}_4$ ), 114.2 (s,  $\text{C}_5\text{H}_4$ ), 109.0 (s,  $\text{C}_5\text{H}_4$ ), 108.3 (s,  $\text{C}_5\text{H}_4$ ), 101.6 (s,  $\text{C}_5\text{H}_4$ ), 101.4 (s,  $\text{C}_5\text{H}_4$ ), 99.3 (s,  $\text{C}_5\text{H}_4$ ), 22.3 (br,  $\text{C}_2\text{Me}_2$ ), 18.6 (br,  $\text{C}_2\text{Me}_2$ ),  $-1.0$  (s,  $\text{SiMe}_2$ , *RS* isomer),  $-1.2$  (s,  $\text{SiMe}_2$ , *RR,SS* isomer),  $-1.4$  (s,  $\text{SiMe}_2$ , *RS* isomer).

**Kinetic Study of the Transformation of *RR,SS-3a* in *RS-3a*.** All measurements were monitored at 20 °C in  $\text{CDCl}_3$  as a solvent. Five solutions were prepared at initial concen-

trations of *RS,SS-3a* in the range  $(2.53\text{--}8.43) \times 10^{-3}$  M. The relative concentration of *RS,SS-3a* and *RS-3a* was calculated by integration of the  $^1\text{H}$  NMR Me–Si resonances. For each sample, the concentrations were checked at least seven times in the 2–250 min interval, and  $\ln([\text{RR,SS}] - [\text{RS}])$  was plotted against time. In all the cases, fitting of data to a linear function by least-squares analysis gives  $R > 0.99$ . The rate constants  $k$  were obtained from the slopes of the lines, according to the first-order rate law  $\ln([\text{RR,SS}] - [\text{RS}]) = -2kt + \ln[\text{RR,SS}]_0$  (see Results and Discussion). The values obtained for  $k$  were in the range  $(7\text{--}10) \times 10^{-5} \text{ s}^{-1}$ , with  $8.4 \times 10^{-5} \text{ s}^{-1}$  as mean value and  $0.6 \times 10^{-5} \text{ s}^{-1}$  as standard error (five measurements). The free energy of activation ( $\Delta G^\ddagger = 94.6 \pm 0.2 \text{ kJ mol}^{-1}$ ) was estimated from the Eyring equation.<sup>7</sup>

**Acknowledgment.** We gratefully acknowledge financial support from the Comisión Asesora de Investigación Científica y Técnica (ref PB92/0178-C).

OM950162H

(7) Günther, H. *NMR Spectroscopy*, 1st ed.; John Wiley & Sons: Chichester, 1990; p 241.

# Subtle Balance between Various Phenanthroline Ligands and Anions in the Palladium-Catalyzed Reductive Carbonylation of Nitrobenzene

Petra Wehman, Vincent E. Kaasjager, Wim G. J. de Lange, Frantisek Hartl,  
Paul C. J. Kamer, and Piet W. N. M. van Leeuwen\*

*Van 't Hoff Research Institute, Department of Inorganic Chemistry, University of Amsterdam,  
Nieuwe Achtergracht 166, 1018 WV Amsterdam, The Netherlands*

Jan Fraanje and Kees Goubitz

*Laboratory of Crystallography, University of Amsterdam, Nieuwe Achtergracht 166,  
1018 WV Amsterdam, The Netherlands*

Received March 13, 1995<sup>®</sup>

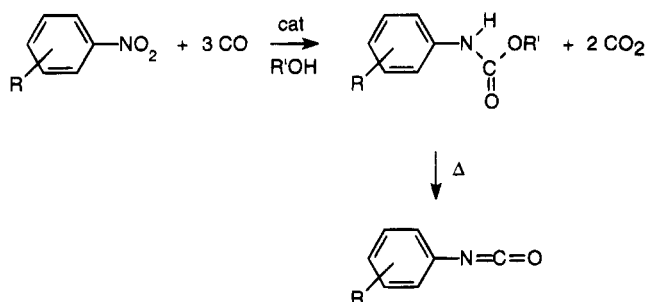
Palladium–phenanthroline catalyst systems for the reductive carbonylation of nitrobenzene in methanol yield methyl *N*-phenylcarbamate as the major product next to small amounts of *N,N'*-diphenylurea, aniline, and azoxybenzene. The influence of a series of 4,7-disubstituted 1,10-phenanthroline ligands (R = Cl, H, Me, MeO, and Me<sub>2</sub>N) in close correlation with two different noncoordinating anions (triflate or tetrafluoroborate) on the catalytic activity and selectivity was studied. Though all the rigid phenanthroline ligands afford stable catalyst precursors, no conversion into carbamate was obtained under the influence of the electron-withdrawing chloride substituents on the ligand. With the mildly electron-donating substituents H, Me, and MeO, high activities up to 311 mol/(mol/h) could be measured. A very subtle balance between the donating capacity of the ligand and the particular noncoordinating anion used was found. A cyclic voltammetric study established that the reduction of the originally Pd<sup>II</sup> species into a Pd<sup>0</sup> intermediate becomes more difficult with increasing donating capacity of the phenanthroline ligand. An X-ray structure was elucidated for Pd(phen)<sub>2</sub>(OTf)<sub>2</sub>. The Pd(phen)<sub>2</sub>(OTf)<sub>2</sub> crystals were triclinic, space group *P*1̄, *a* = 10.387(1) Å, *b* = 11.539(2) Å, *c* = 13.449(3) Å,  $\alpha$  = 70.53(1)°,  $\beta$  = 67.42(2)°,  $\gamma$  = 81.51(1)°, *Z* = 2, and final *R* = 0.045 for 6448 observed reflections.

## Introduction

Aromatic isocyanates and carbamates have become increasingly important ever since the work of O. Bayer in 1937 led to the formation of polyurethanes from diisocyanates and diols. Traditionally these isocyanates and carbamates are prepared via the phosgene route, in which a nitro compound is first catalytically hydrogenated to an amine. Subsequent reaction of the amine with phosgene yields the isocyanate, which can be converted into the carbamate by reaction with an alcohol. MDI, 1,1'-methylenebis(4-isocyanatobenzene), is the most widely applied diisocyanate nowadays, and it is produced by condensation of two molecules of aniline with formaldehyde prior to the reaction with phosgene.<sup>1–3</sup>

Because the reaction requires the use of the extremely toxic phosgene and because the reaction produces large quantities of HCl as a side product, two major disadvantages to the phosgene route, research is done on the reductive carbonylation of aromatic nitro compounds as an attractive alternative process for the production of isocyanates and carbamates. This way, an isocyanate is formed by direct reaction of the nitro function with

## Scheme 1. Reductive Carbonylation of Aromatic Nitro Compounds



CO, under the influence of a catalyst. If the reaction is performed in an alcohol a carbamate is formed as main product, which can be thermally degraded into the isocyanate (Scheme 1). The only waste product in this reaction is the relatively harmless CO<sub>2</sub>. This route can also be applied for the production of MDI by condensation of two of the carbamate molecules with formaldehyde, as was found by workers at the Atlantic Richfield Co. (Arco) and Asahi Chemical, independently, for ethyl *N*-phenylcarbamate.<sup>1,4</sup>

The catalyst system that is required for the reaction between the nitro function and CO can be based on group 8–10 metals. Ruthenium is a frequently applied

<sup>®</sup> Abstract published in *Advance ACS Abstracts*, July 1, 1995.

(1) Weissermel, K.; Arpe, H.-J. *Industrielle Organische Chemie*; VCH Verlagsgesellschaft mbH: Weinheim, Germany, 1988; 395.

(2) Braunstein, P. *Chem. Rev.* **1989**, *89*, 1927.

(3) Watanabe, Y.; Tsujii, Y.; Takeuchi, R.; Suzuki, N. *Bull. Chem. Soc. Jpn.* **1983**, *56*, 3343.

(4) Chono, M.; Fukuoka, S.; Kohno, M. *J. Cell. Plast.* **1983**, *385*.



metal, especially in mechanistic studies.<sup>5</sup> The most active and selective systems known use palladium as the active metal center, often applied as PdCl<sub>2</sub>. Although mechanistically less well clarified,<sup>6</sup> it is known that addition of a nitrogen-donor ligand to the palladium system is needed to obtain catalytic activity, and it was found that bidentate ligands are by far superior.<sup>7</sup> A catalyst system consisting of palladium and a bidentate nitrogen, phosphorus, arsenic, or antimony ligand for the reductive carbonylation of nitro compounds was patented in 1983, with the emphasis on the use of 1,10-phenanthroline and 1,3-bis(diphenylphosphino)propane (dppp).<sup>8</sup>

Mestroni et al. already reported the influence of the donating capacity of the bidentate ligand on the catalytic activity and selectivity. For [Pd(bidentate ligand)<sub>2</sub>]-[PF<sub>6</sub>]<sub>2</sub> the catalytic activity increases in the series 2,2'-bipyridine < 1,10-phenanthroline < 3,4,7,8-tetramethyl-1,10-phenanthroline.<sup>9</sup> The relatively high activity of the 1,10-phenanthroline ligands is probably caused by the rigidity of these ligands, in contrast to the more flexible 2,2'-bipyridine ligand in which free rotation around the linking bond is possible. This results in lower complexation constants for the bipyridine ligand.<sup>10</sup>

In a more detailed study on the influence of the donating capacity of the ligand on the catalytic activity and selectivity using 4,4'-disubstituted 2,2'-bipyridyl ligands, we found an absolute lack of conversion under the influence of electron-withdrawing substituents on the bipyridyl ligand. With the electron-donating substituents, on the other hand, only small differences were found.<sup>11</sup> A problem with these bipyridyl-palladium systems remained, however: the stability of the active species.

As part of our ongoing research, the effect of rigid 4,7-disubstituted 1,10-phenanthroline ligands (R = Cl, H, Me, MeO, and Me<sub>2</sub>N) on the palladium-catalyzed reductive carbonylation of aromatic nitro compounds was studied. With these ligands more stable catalyst systems could be obtained, compared to the bipyridine analogues. Higher catalytic activities were therefore expected, even under the influence of electron-withdrawing substituents on the phenanthroline ligand. The ligands were tested in combination with Pd(acetate)<sub>2</sub> and *p*-toluenesulfonic acid in the reductive carbonylation of nitrobenzene. Next to these *in situ* studies, Pd-phenanthroline complexes with noncoordinating anions have been prepared. Two different noncoordinating anions (OTf and BF<sub>4</sub>) have been used to study the exact influence of the anion on the catalytic activity and selectivity, in intimate interplay with the various ligands.

## Results and Discussion

**Synthesis of the Ligands.** Introduction of electron-withdrawing or electron-donating substituents at C(4)

(5) Skoog, S. J.; Campbell, J. P.; Gladfelter, W. L. *Organometallics* **1994**, *13*, 4137 and references cited therein.

(6) Leconte, P.; Metz, F.; Mortreux, A.; Osborn, J. A.; Paul, F.; Petit, F.; Pillot, A. *J. Chem. Soc., Chem. Commun.* **1990**, 1616 and references cited therein.

(7) Gupte, S.; Chaudhari, R. V. *J. Mol. Catal.* **1984**, *24*, 197.

(8) Drent, E.; van Leeuwen, P. W. N. M. Eur. Pat. EP 86281, 1983.

(9) Bontempi, A.; Alessio, E.; Chanos, G.; Mestroni, G. *J. Mol. Catal.* **1987**, *42*, 67.

(10) Sammes, P. G.; Yahioğlu, G. *Chem. Soc. Rev.* **1994**, 328.

(11) Wehman, P.; Dol, G. C.; Moorman, E. R.; Kamer, P. C. J.; Fraanje, J.; Goubitz, K.; van Leeuwen, P. W. N. M. *Organometallics* **1994**, *13*, 4856.

and C(7) (R = Cl, MeO, and Me<sub>2</sub>N) of 1,10-phenanthroline is not readily achieved because of the strong resistance of phenanthroline toward electrophilic reagents. This resistance cannot be easily overcome by oxidation at the nitrogen atom as in 2,2'-bipyridine.<sup>11</sup> Although 1,10-phenanthroline can be converted into 1,10-phenanthroline *N*-oxide under the influence of hydrogen peroxide in glacial acetic acid, it will not react to produce 1,10-phenanthroline *N,N'*-dioxide. This is probably caused by steric hindrance introduced by the first oxygen atom together with the relatively high stability of the conjugate acid of 1,10-phenanthroline *N*-oxide, which will be formed under the acidic conditions used in the oxidation. As a result only one of the heteroaromatic rings in this fused system will be activated toward substitution. Moreover, C(2) becomes the most activated position instead of the desired C(4), which is expressed in the relatively easy introduction of a cyano group at C(2) via this route by Corey et al.<sup>12</sup>

In contrast to other *N*-oxides like those of pyridine and 2,2'-bipyridine, the mono-oxidized 1,10-phenanthroline fails to undergo nitration. This rules out the possibility of a facile nucleophilic displacement of a thus introduced nitro group para to the *N*-oxide, a method we used with success for 2,2'-bipyridine 1,1'-dioxide. Nitration of plain 1,10-phenanthroline occurs in a high yield, but only at C(5).<sup>11-13</sup>

Activation of 1,10-phenanthroline by quaternization of the nitrogen atom by methyl iodide also results in substitution at C(2) only, as is shown by the synthesis of 2-chloro-1,10-phenanthroline by Halcrow et al.<sup>14</sup>

We therefore decided to use a Skraup-type synthesis of 1,10-phenanthroline with good leaving groups already present at the crucial carbon atoms in the starting materials, as is described by Snyder et al.<sup>15</sup> Starting from *o*-phenylenediamine and ethoxymethylenemalonate ester, 4,7-dihydroxy-1,10-phenanthroline can be prepared in four steps. The hydroxy groups that are initially positioned at the desired C(4) and C(7) atoms can be replaced by chloride substituents to afford 4,7-dichloro-1,10-phenanthroline (Cl<sub>2</sub>-phen, **1a**).<sup>15</sup> Cl<sub>2</sub>-phen (**1a**) is a convenient starting material for the preparation of other 4,7-disubstituted 1,10-phenanthroline ligands (R = MeO or Me<sub>2</sub>N; compounds **1d,e**, Scheme 2). Similar to the substitution of the nitro functions in 4,4'-dinitro-2,2'-bipyridine 1,1'-dioxide, the chloride substituents in Cl<sub>2</sub>-phen (**1a**) can be replaced by methoxy groups under the influence of sodium methoxide. Dimethylamino groups can be introduced by refluxing Cl<sub>2</sub>-phen (**1a**) in DMF, as has been previously described for halogenopyridines and -quinolines as well as for 4,4'-dichloro-2,2'-bipyridine 1,1'-dioxide.<sup>11,16</sup> A small percentage of 4-(dimethylamino)-7-chloro-1,10-phenanthroline remains present in the reaction mixture, which has to be removed by means of column chromatography. To separate the monosubstituted from the disubstituted product, careful elution in the absence of a base like triethylamine has to be used for the first half of the column. One side effect of this procedure, however, is

(12) Corey, E. J.; Borrer, A. L.; Foglia, T. *J. Org. Chem.* **1965**, *30*, 288.

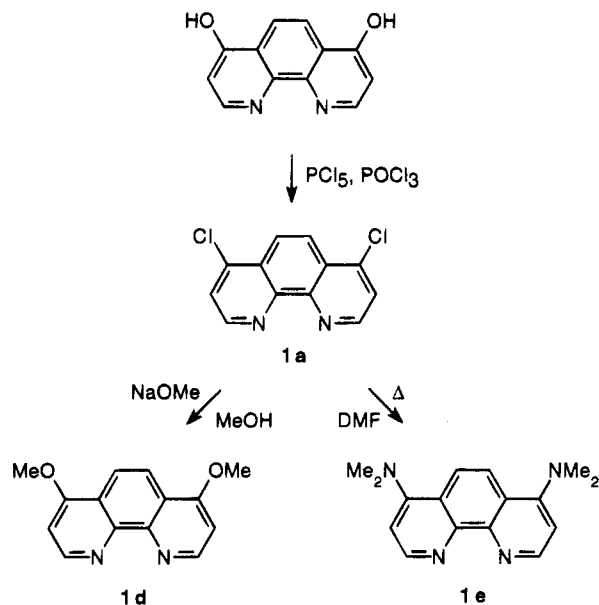
(13) Maerker, G. M.; Case, F. H. *J. Am. Chem. Soc.* **1958**, *80*, 2745.

(14) Halcrow, B. E.; Kermack, W. O. *J. Chem. Soc.* **1946**, 155.

(15) Snyder, H. R.; Freier, H. E. *J. Am. Chem. Soc.* **1946**, *68*, 1320.

(16) Heindel, N. D.; Kennewel, P. D. *J. Chem. Soc., Chem. Commun.* **1969**, 38.

**Scheme 2. Synthesis of the Substituted Phenanthroline Ligands with R = Cl, MeO, and Me<sub>2</sub>N**



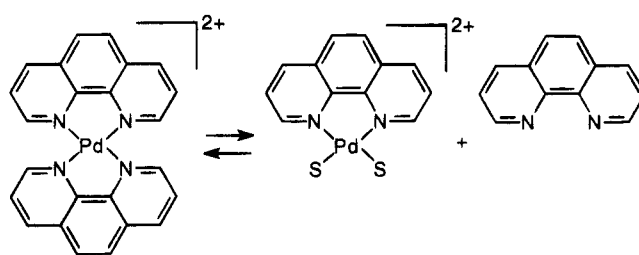
the partial protonation of the relatively alkaline (Me<sub>2</sub>N)<sub>2</sub>-phen compound (**1e**) by the slightly acidic silica gel. Therefore the product has to be dissolved in dichloromethane after purification by column chromatography and washed with a NaOH solution to obtain the fully deprotonated (Me<sub>2</sub>N)<sub>2</sub>-phen ligand (**1e**).

**Synthesis of the Complexes.** All phenanthroline complexes (**2a–c** and **3a–c**) had to be prepared from a tetrakis(acetonitrile) precursor Pd(CH<sub>3</sub>CN)<sub>4</sub>(Y)<sub>2</sub> (Y = OTf or BF<sub>4</sub>), as the Pd(phenanthroline ligand)Cl<sub>2</sub> complexes were essentially insoluble for all ligands other than unsubstituted phenanthroline (**1b**). For the substituted phenanthroline ligands this insolubility ruled out the convenient route in which the formed dichloride complex is subsequently reacted with silver triflate and 1 additional equiv of the ligand.

For the tetrafluoroborate anion the tetrakis(acetonitrile) precursor could be prepared from Pd metal and nitrosyl tetrafluoroborate in acetonitrile, according to the method of Hathaway and Underhill.<sup>17</sup> Though very moisture-sensitive, the resulting precursor complex is stable under inert atmosphere.

For the triflate anion, however, it was not possible to perform the same reaction because nitrosyl triflate is not available. We therefore tried a similar reaction to the one Hartley et al. performed with Pd(CH<sub>3</sub>CN)<sub>2</sub>Cl<sub>2</sub>, silver perchlorate, and dithioether ligands in acetonitrile.<sup>18</sup> The same procedure with Pd(benzonitrile)<sub>2</sub>Cl<sub>2</sub>, silver triflate, and phenanthroline ligands in benzonitrile failed to give the desired exchanges, while the same reaction in acetone resulted in the formation of Pd black. We were able though to prepare Pd(CH<sub>3</sub>CN)<sub>4</sub>(OTf)<sub>2</sub> through an exchange reaction between Pd(CH<sub>3</sub>CN)<sub>2</sub>Cl<sub>2</sub> and silver triflate in acetonitrile. The compound, however, remains sticky even after repeated azeotropic distillation with toluene. It is unstable as a semisolid compound under inert atmosphere. Probably partial

**Scheme 3. Equilibrium between a Bis(phenanthroline) and a Mono(phenanthroline) Complex**



dissociation of the acetonitrile occurs, resulting in the stickiness and eventually yielding Pd black. Only in an acetonitrile solution under inert atmosphere it is possible to store the compound at  $-20\text{ }^{\circ}\text{C}$  for several days, but best results are always obtained with a freshly prepared batch of Pd(CH<sub>3</sub>CN)<sub>4</sub>(OTf)<sub>2</sub>.

The exchange reactions between the various phenanthroline ligands and the tetrakis(acetonitrile) precursors Pd(CH<sub>3</sub>CN)<sub>4</sub>(Y)<sub>2</sub> (Y = OTf or BF<sub>4</sub>) proceed without difficulties. Only in the case of Pd(phen)<sub>2</sub>(OTf)<sub>2</sub> (**2b**) does a mixture of the bis(phenanthroline) complex **2b**, a mono(phenanthroline) complex, and free phenanthroline **1b** remain in solution next to the precipitation of the desired bis(phenanthroline) complex **2b**. This might suggest an equilibrium between the bis(phenanthroline) and the mono(phenanthroline) complexes, as is depicted in Scheme 3. The dissociation of one of the phenanthroline ligands (**1b**) is probably caused by the steric hindrance between the  $\alpha$ -hydrogens of the two ligands in the Pd(phen)<sub>2</sub>(OTf)<sub>2</sub> complex (**2b**), which will be discussed in more detail in the next section on the X-ray structural analysis of the complex. The resulting mono(phenanthroline) complex might be slightly stabilized by weak coordination of the triflate anions, as this behavior is not found for Pd(phen)<sub>2</sub>(BF<sub>4</sub>)<sub>2</sub> (**3b**). Due to their perfect symmetry, BF<sub>4</sub> anions are better noncoordinating anions than the triflate anions, which have a slight tendency to coordinate very weakly through the oxygen atoms of the SO<sub>3</sub> moiety.

If hexanes were added to the crude reaction mixture of Pd(phen)<sub>2</sub>(OTf)<sub>2</sub> (**2b**) as is done for all other complexes, the equilibrium of Scheme 3 is apparently disturbed due to the solubility of phenanthroline (**1b**) in hexanes. Various unknown complexes are formed, which results in broad signals in the <sup>1</sup>H-NMR spectrum, next to the known signals of the desired Pd(phen)<sub>2</sub>(OTf)<sub>2</sub> (**2b**).

Broadened NMR signals are also found for Pd(Cl<sub>2</sub>-phen)<sub>2</sub>(OTf)<sub>2</sub> (**2a**). Presumably, the same kind of equilibrium as drawn in Scheme 3 occurs for the relatively weakly coordinating Cl<sub>2</sub>-phen ligand (**1a**) in a coordinating solvent as DMSO-*d*<sub>6</sub>. Apparently coordination of the SO<sub>3</sub> moieties of the triflate anions is involved, as Pd-(Cl<sub>2</sub>-phen)<sub>2</sub>(BF<sub>4</sub>)<sub>2</sub> (**3a**) only shows sharp signals. The triflate complexes of the ligands with a higher donating capacity (**1c–e**) also give sharp signals, due to the better coordinating properties of these ligands.

**Molecular Structure of Pd(phen)<sub>2</sub>(OTf)<sub>2</sub> (**2b**).** The molecular structure of Pd(phen)<sub>2</sub>(OTf)<sub>2</sub> (**2b**) was determined to assure that it is possible for two phenanthroline ligands (**1b**) to coordinate to one Pd center, in spite of the easy dissociation of one of the ligands that is found by <sup>1</sup>H NMR (Scheme 3). We were also inter-

(17) Hathaway, B. J.; Underhill, A. E. *J. Chem. Soc.* **1962**, 2257, 2444.

(18) Hartley, F. R.; Murray, S. G.; Levason, W.; Souttler, H. E.; McAuliffe, C. A. *Inorg. Chim. Acta* **1979**, 35, 265.

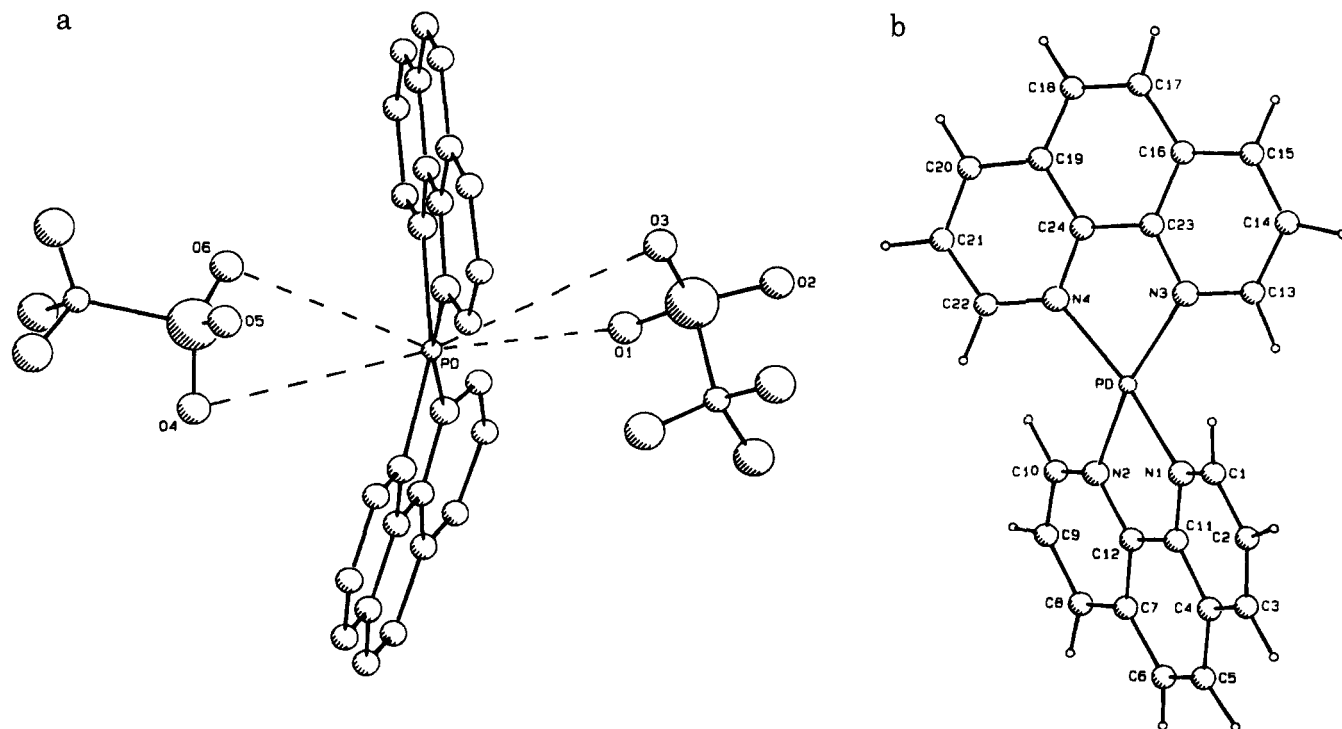


**Figure 1.** (a) ORTEP drawing of  $\text{Pd}(\text{phen})_2(\text{OTf})_2$  (**2b**), showing the relative orientation of the triflate anions with respect to the  $[\text{Pd}(\text{phen})_2]^{2+}$  cation. (b) ORTEP drawing of the  $\text{Pd}(\text{phen})_2$  moiety of  $\text{Pd}(\text{phen})_2(\text{OTf})_2$  (**2b**), depicting the applied numbering scheme.

**Table 1. Bond Distances (Å) of the Non-Hydrogen Atoms of  $\text{Pd}(\text{phen})_2(\text{OTf})_2$  (**2b**)<sup>a</sup>**

Pd–N(1)	2.044 (3)	C(11)–C(12)	1.421 (4)
Pd–N(2)	2.053 (3)	C(11)–N(1)	1.372 (4)
Pd–N(3)	2.058 (3)	C(12)–N(2)	1.367 (4)
Pd–N(4)	2.042 (3)	C(13)–C(14)	1.410 (7)
S(1)–C(25)	1.809 (7)	C(13)–N(3)	1.327 (5)
S(1)–O(1)	1.425 (5)	C(14)–C(15)	1.357 (7)
S(1)–O(2)	1.435 (4)	C(15)–C(16)	1.411 (8)
S(1)–O(3)	1.437 (4)	C(16)–C(17)	1.434 (8)
S(2)–C(26)	1.79 (1)	C(16)–C(23)	1.408 (6)
S(2)–O(4)	1.417 (6)	C(17)–C(18)	1.353 (9)
S(2)–O(5)	1.380 (6)	C(18)–C(19)	1.429 (7)
S(2)–O(6)	1.369 (6)	C(19)–C(20)	1.406 (7)
C(1)–C(2)	1.404 (5)	C(19)–C(24)	1.411 (6)
C(1)–N(1)	1.332 (4)	C(20)–C(21)	1.354 (8)
C(2)–C(3)	1.377 (6)	C(21)–C(22)	1.397 (7)
C(3)–C(4)	1.400 (5)	C(22)–N(4)	1.339 (5)
C(4)–C(5)	1.439 (6)	C(23)–C(24)	1.418 (6)
C(4)–C(11)	1.400 (5)	C(23)–N(3)	1.371 (5)
C(5)–C(6)	1.364 (5)	C(24)–N(4)	1.370 (5)
C(6)–C(7)	1.431 (5)	C(25)–F(1)	1.302 (9)
C(7)–C(8)	1.416 (5)	C(25)–F(2)	1.316 (8)
C(7)–C(12)	1.408 (5)	C(25)–F(3)	1.32 (1)
C(8)–C(9)	1.363 (6)	C(26)–F(4)	1.20 (1)
C(9)–C(10)	1.043 (6)	C(26)–F(5)	1.26 (1)
C(10)–N(2)	1.328 (4)	C(26)–F(6)	1.37 (2)

<sup>a</sup> Esd's in parentheses.

ested in the distances between the Pd center and the triflate anions, to see whether slight stabilization of the Pd cation by its anions would be plausible.

Two views of the molecular structure of  $\text{Pd}(\text{phen})_2(\text{OTf})_2$  (**2b**) are shown in Figure 1a,b. In Figure 1a the hydrogen atoms are omitted for the sake of clarity, but the relative orientation of the triflate anions is shown. In Figure 1b the numbering scheme of the  $\text{Pd}(\text{phen})_2$  moiety is depicted. The bond distances of the non-hydrogen atoms are listed in Table 1, whereas the bond angles of these atoms are given in Table 2.

Both phenanthroline units turned out to be similarly coordinated to the Pd center, with a mean Pd–N value

**Table 2. Bond Angles (deg) of the Non-Hydrogen Atoms of  $\text{Pd}(\text{phen})_2(\text{OTf})_2$  (**2b**)<sup>a</sup>**

N(1)–Pd–N(2)	80.7 (1)	C(15)–C(16)–C(17)	124.8 (4)
N(1)–Pd–N(3)	100.5 (1)	C(15)–C(16)–C(23)	117.0 (4)
N(1)–Pd–N(4)	168.7 (2)	C(17)–C(16)–C(23)	118.1 (5)
N(2)–Pd–N(3)	163.9 (2)	C(16)–C(17)–C(18)	121.4 (5)
N(2)–Pd–N(4)	101.1 (1)	C(17)–C(18)–C(19)	121.6 (5)
N(3)–Pd–N(4)	80.9 (1)	C(18)–C(19)–C(20)	124.6 (5)
C(25)–S(1)–O(1)	104.6 (3)	C(18)–C(19)–C(24)	117.8 (5)
C(25)–S(1)–O(2)	103.7 (3)	C(20)–C(19)–C(24)	117.5 (4)
C(25)–S(1)–O(3)	103.9 (3)	C(19)–C(20)–C(21)	119.5 (5)
O(1)–S(1)–O(2)	112.8 (2)	C(20)–C(21)–C(22)	120.3 (5)
O(1)–S(1)–O(3)	113.5 (3)	C(21)–C(22)–N(4)	122.2 (4)
O(2)–S(1)–O(3)	116.7 (3)	C(16)–C(23)–C(24)	120.3 (4)
C(26)–S(2)–O(4)	103.8 (5)	C(16)–C(23)–N(3)	122.8 (4)
C(26)–S(2)–O(5)	103.6 (5)	C(24)–C(23)–N(3)	117.0 (3)
C(26)–S(2)–O(6)	104.8 (5)	C(19)–C(24)–C(23)	120.7 (4)
O(4)–S(2)–O(5)	110.7 (4)	C(19)–C(24)–N(4)	122.3 (4)
O(4)–S(2)–O(6)	114.1 (4)	C(23)–C(24)–N(4)	117.0 (3)
O(5)–S(2)–O(6)	118.0 (5)	S(1)–C(25)–F(1)	112.3 (7)
C(2)–C(1)–N(1)	122.2 (3)	S(1)–C(25)–F(2)	111.8 (4)
C(1)–C(2)–C(3)	119.5 (3)	S(1)–C(25)–F(3)	110.9 (5)
C(2)–C(3)–C(4)	119.2 (3)	F(1)–C(25)–F(2)	107.7 (6)
C(3)–C(4)–C(5)	123.7 (3)	F(1)–C(25)–F(3)	107.5 (6)
C(3)–C(4)–C(11)	118.1 (3)	F(2)–C(25)–F(3)	106.4 (8)
C(5)–C(4)–C(11)	118.2 (3)	S(2)–C(26)–F(4)	119.3 (9)
C(4)–C(5)–C(6)	120.8 (4)	S(2)–C(26)–F(5)	114 (1)
C(5)–C(6)–C(7)	121.1 (4)	S(2)–C(26)–F(6)	107.3 (8)
C(6)–C(7)–C(8)	123.8 (3)	F(4)–C(26)–F(5)	116 (1)
C(6)–C(7)–C(12)	119.1 (3)	F(4)–C(26)–F(6)	96 (1)
C(8)–C(7)–C(12)	117.0 (3)	F(5)–C(26)–F(6)	99 (1)
C(7)–C(8)–C(9)	118.8 (4)	Pd–N(1)–C(11)	128.5 (3)
C(8)–C(9)–C(10)	120.7 (3)	Pd–N(1)–C(11)	113.0 (2)
C(9)–C(10)–N(2)	122.3 (4)	C(1)–N(1)–C(11)	118.3 (3)
C(4)–C(11)–C(12)	121.3 (3)	Pd–N(2)–C(10)	129.4 (3)
C(4)–C(11)–N(1)	122.3 (3)	Pd–N(2)–C(12)	112.3 (2)
C(12)–C(11)–N(1)	116.3 (3)	C(10)–N(2)–C(12)	117.6 (3)
C(7)–C(12)–C(11)	119.3 (3)	Pd–N(3)–C(13)	129.2 (3)
C(7)–C(12)–N(2)	123.5 (3)	Pd–N(3)–C(23)	112.2 (2)
C(11)–C(12)–N(2)	117.2 (3)	C(13)–N(3)–C(23)	118.2 (3)
C(14)–C(13)–N(3)	122.2 (4)	Pd–N(4)–C(22)	128.9 (3)
C(13)–C(14)–C(15)	119.9 (5)	Pd–N(4)–C(24)	112.8 (3)
C(14)–C(15)–C(16)	119.8 (4)	C(22)–N(4)–C(24)	117.9 (4)

<sup>a</sup> Esd's in parentheses.

of 2.049 Å. This value is in good agreement with the mean Pd–N distance in the Pd(phen)<sub>2</sub>(ClO<sub>4</sub>)<sub>2</sub> complex determined by Rund (2.051 Å)<sup>19</sup> and somewhat longer than the distance we found in the analogous Pd(bpy)<sub>2</sub>-(OTf)<sub>2</sub> complex (2.036 Å).<sup>11</sup> In contrast to these complexes, there appears to be a weak interaction between the Pd center and the anions in our Pd(phen)<sub>2</sub>(OTf)<sub>2</sub> complex (**2b**). Both triflate anions are oriented with their oxygen atoms toward the Pd center, and the shortest Pd–O distance is only 2.922 Å. Weak interactions between the Pd center and a nitrate anion in Pd-(bpy)<sub>2</sub>(NO<sub>3</sub>)<sub>2</sub>·2H<sub>2</sub>O were reported with a Pd–O distance of 3.089 Å.<sup>20</sup> Therefore we concluded that this is also the case in the Pd(phen)<sub>2</sub>(OTf)<sub>2</sub> complex (**2b**).

Mestroni et al. did not find any interaction between the highly symmetrical PF<sub>6</sub> anions and the Pd center in a Pd(phen)<sub>2</sub>(PF<sub>6</sub>)<sub>2</sub> complex.<sup>21</sup> This might suggest that the highly delocalized PF<sub>6</sub> and BF<sub>4</sub> anions are actually better noncoordinating anions than the triflate and nitrate anions, as was also implicated by our NMR studies. The Pd(phen)<sub>2</sub>(PF<sub>6</sub>)<sub>2</sub> complex by Mestroni also shows a different conformation of the Pd(phen)<sub>2</sub> cation itself. In this compound the steric repulsion between the α-hydrogen atoms (H<sub>2</sub> and H<sub>9</sub>) of the separate phenanthroline ligands is alleviated by a so-called "bow-step" conformation in which both ligands are slightly bowed, resulting in nonplanar structures of the ligands, while one of the ligands is lifted above the coordination plane and the other one is situated beneath this plane. The out of plane bending within one ligand is expressed in the angle that is found between the two equivalent parts of the ligand. In the Pd(phen)<sub>2</sub>(PF<sub>6</sub>)<sub>2</sub> complex a value of 13.4° is found for this angle,<sup>21</sup> which is much larger than the angles found in our Pd(phen)<sub>2</sub>-(OTf)<sub>2</sub> complex (**2b**) (5.3° and 3.7° for both phenanthroline ligands, respectively).

In the Pd(phen)<sub>2</sub>(OTf)<sub>2</sub> complex (**2b**), however, the steric crowding is relieved by a completely different, twist conformation. In this conformation a tetrahedral distortion of the square-planar PdN<sub>4</sub> skeleton occurs, resulting in one coordinating nitrogen atom above the coordination plane and one beneath it for each phenanthroline ligand (**1b**). This way a torsion angle between the two ligands is obtained, which amounts to 28.2° for Pd(phen)<sub>2</sub>(OTf)<sub>2</sub> (**2b**). The same conformation has already been found for Pd(phen)<sub>2</sub>(ClO<sub>4</sub>)<sub>2</sub>,<sup>19</sup> Pd(bpy)<sub>2</sub>-(OTf)<sub>2</sub>,<sup>11</sup> and Pd(bpy)<sub>2</sub>(NO<sub>3</sub>)<sub>2</sub>·2H<sub>2</sub>O<sup>20</sup> with torsion angles of 22.5, 24.3, and 33.2°, respectively.

The relatively large torsion angle in Pd(phen)<sub>2</sub>(OTf)<sub>2</sub> (**2b**) compared to the torsion angle in the closely related Pd(phen)<sub>2</sub>(ClO<sub>4</sub>)<sub>2</sub> system might be caused by the fact that the phenanthroline ligands are less bent in the triflate complex. Although the exact angles between the chemically equivalent parts of the phenanthroline ligands in the Pd(phen)<sub>2</sub>(ClO<sub>4</sub>)<sub>2</sub> complex are not given in ref 19, it can be deduced from the listed deviations of the ligand atoms from the plane through the cation that these angles in this complex are larger than the ones we have measured. As a result, less twisting of the ligands is needed to get to the same relief of steric hindrance.

From a comparison of the torsion angles and the Pd–N distances in Pd(phen)<sub>2</sub>(ClO<sub>4</sub>)<sub>2</sub> and Pd(bpy)<sub>2</sub>-

**Table 3. Reduction Potentials of Some Pd(bidentate ligand)<sub>2</sub>(Y)<sub>2</sub> Complexes and of the Corresponding Free Ligands<sup>a</sup>**

compd	E <sub>p,c</sub> (V) <sup>b</sup>
BIAN	-1.82
bpy	-2.60
phen	-2.55
Pd(BIAN) <sub>2</sub> (BF <sub>4</sub> ) <sub>2</sub>	-0.96
Pd(bpy) <sub>2</sub> (OTf) <sub>2</sub>	-1.31
Pd(Cl <sub>2</sub> -phen) <sub>2</sub> (OTf) <sub>2</sub> ( <b>2a</b> )	-1.17
Pd(phen) <sub>2</sub> (OTf) <sub>2</sub> ( <b>2b</b> )	-1.22
Pd(Me <sub>2</sub> -phen) <sub>2</sub> (OTf) <sub>2</sub> ( <b>2c</b> )	-1.27
Pd((MeO) <sub>2</sub> -phen) <sub>2</sub> (OTf) <sub>2</sub> ( <b>2d</b> )	-1.30
Pd(phen) <sub>2</sub> (BF <sub>4</sub> ) <sub>2</sub> ( <b>3b</b> )	-1.22
Pd(Me <sub>2</sub> -phen) <sub>2</sub> (BF <sub>4</sub> ) <sub>2</sub> ( <b>3c</b> )	-1.25

<sup>a</sup> See Cyclic voltammetry in the Experimental Section for the precise conditions. <sup>b</sup> E<sub>p,c</sub> (V) vs E<sub>1/2</sub> of Fc/Fc<sup>+</sup>.<sup>23</sup>

(NO<sub>3</sub>)<sub>2</sub>·2H<sub>2</sub>O, it was concluded that a larger torsion angle leads to a decrease of the Pd–N distance.<sup>19</sup> This view should be corrected, however, if the Pd(phen)<sub>2</sub>-(OTf)<sub>2</sub> complex (**2b**) is taken into account. Though this complex shows a larger torsion angle than the Pd(phen)<sub>2</sub>-(ClO<sub>4</sub>)<sub>2</sub> complex, there is no significant difference in Pd–N distances. This trend can also be found if Pd-(bpy)<sub>2</sub>(NO<sub>3</sub>)<sub>2</sub>·2H<sub>2</sub>O is compared with Pd(bpy)<sub>2</sub>(OTf)<sub>2</sub>.<sup>11,19</sup> Apparently, it is the difference in flexibility and donating capacity between the bipyridine and the phenanthroline ligands that causes the differences in Pd–N distances, instead of the different torsion angles.

Altogether, the molecular structure of Pd(phen)<sub>2</sub>(OTf)<sub>2</sub> (**2b**) has made it clear that there are actually two phenanthroline ligands (**1b**) coordinated to the Pd metal, but dissociation of one of these ligands is easily achieved due to the steric overcrowding in the complex. This property could be of importance for the catalytic activity of the complex, as it most probably has to lose one ligand before it can act as a catalyst.

**Cyclic Voltammetry.** Cyclic voltammograms of the Pd(R<sub>2</sub>-phen)(Y)<sub>2</sub> complexes (R = Cl, H, Me, or MeO and Y = OTf or BF<sub>4</sub>) were recorded in DMSO in order to study the influence of the 4,7-disubstituted 1,10-phenanthroline ligands on the Pd<sup>II</sup>/Pd<sup>0</sup> redox couple, which could play a crucial role in the catalytic reductive carbonylation of aromatic nitro compounds.

In addition, two other Pd(bidentate ligand)<sub>2</sub>(Y)<sub>2</sub> complexes were measured in the cyclic voltammetric study as reference compounds. In these reference complexes the bidentate ligands were either the α-diimine ligand bis(*p*-anisylimino)acenaphthene (BIAN)<sup>22</sup> or 2,2'-bipyridine. The electrode potentials, presented in Table 3, were measured against the standard Fc/Fc<sup>+</sup> couple.<sup>23</sup>

The reductions of all complexes under study were found at significantly more positive potentials with respect to those of the corresponding free ligands (Table 3). The difference between the reduction potentials of the free ligands was found to be much larger than the difference between the E<sub>p,c</sub> values of the complexes of the corresponding ligands. For all complexes the reduction was chemically totally irreversible, as was evidenced by complete absence of the anodic counterpeaks. At the same time no new anodic peaks, which might belong to reoxidation of some secondary reduction

(19) Rund, J. V.; Hazel, A. C. *Acta Crystallogr.* **1980**, B36, 3103.

(20) Chieh, P. C. *J. Chem. Soc., Dalton Trans.* **1972**, 1643.

(21) Geremia, S.; Randaccio, L.; Mestroni, G.; Milani, B. *J. Chem. Soc., Dalton Trans.* **1992**, 2117.

(22) van Asselt, R.; Elsevier, C. J.; Smeets, W. J. J.; Spek, A. L.; Benedix, R. *Recl. Trav. Chim. Pays-Bas* **1994**, 113, 88.

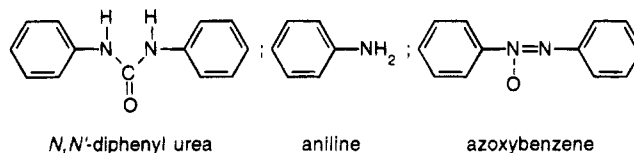
(23) Cagné, R. R.; Koval, C. A.; Lisensky, C. G. *Inorg. Chem.* **1980**, 19, 2854.

products, were observed on the reversed scans. If an excess of free ligand is added, resulting in the same ligand:Pd ratio as is used in the catalysis, the system becomes chemically slightly more reversible. This implies that the chemical irreversibility of the reduction is caused by dissociation of the phenanthroline ligands from the reduced Pd<sup>0</sup> species, which can be suppressed by the presence of an excess of ligand. All measurements on the complexes were strongly disturbed by sorption at the working electrode, which had to be polished with a 1 μm diamond paste before each repeated scan. This sorption might indicate the formation of Pd metal. The overall behavior of the Pd complexes resembles the reduction of some [Cu(bidentate ligand)<sub>2</sub>]<sup>+</sup> complexes (bidentate ligand = phen or bpy), which also occurred at relatively positive potentials and was only poorly reversible, ultimately leading to metallic copper.<sup>24</sup>

From the results it can be concluded that the irreversible reduction of the Pd(bidentate ligand)<sub>2</sub><sup>2+</sup> species is predominantly localized on the Pd<sup>II</sup> center rather than on the lowest π\* orbital of the bidentate ligands. In the case of a ligand-localized reduction the difference between the reduction potentials of Pd(BIAN)<sub>2</sub>(BF<sub>4</sub>)<sub>2</sub> and those of the phenanthroline complexes would have been expected to be roughly as large as for the free ligands, as was also observed for Re(CO)<sub>3</sub>Cl(bidentate ligand) and PtPh<sub>2</sub>(bidentate ligand) complexes containing 2,2'-bipyridine or 4,4'-bipyrimidine.<sup>25,26</sup>

Although the reduction is mainly localized on the metal center, an influence of the ligand is apparent, as can best be seen from the series of Pd(R<sub>2</sub>-phen)<sub>2</sub>(Y)<sub>2</sub> complexes. The results reveal that the reduction of the Pd(R<sub>2</sub>-phen)<sub>2</sub>(Y)<sub>2</sub> complexes becomes more negatively shifted in the order Cl<sub>2</sub>-phen < H<sub>2</sub>-phen < Me<sub>2</sub>-phen < (MeO)<sub>2</sub>-phen, i.e., with an increasing donating capacity of the R<sub>2</sub>-phen ligand. Cl<sub>2</sub>-phen (**1a**) is apparently the weakest σ-donor ligand in the series, and the Pd(Cl<sub>2</sub>-phen)<sub>2</sub><sup>2+</sup> species is consequently most easily reduced. For the catalysis this might imply that the conversion of nitrobenzene is readily initiated under the influence of a Cl<sub>2</sub>-phen ligand (**1a**). In contrast to the chemical irreversibility of the reduction observed in the cyclic voltammetric study, it is expected that, during the reductive carbonylation, the reduced Pd species are stabilized to some extent by the aromatic nitro substrate and CO, though this effect could not be found by cyclic voltammetric measurements on a CO-saturated solution and in the presence of a 5-fold excess of nitrobenzene. However, the high concentration of nitrobenzene and the high pressure of CO that are used in the catalysis cannot be mimicked in the cyclic voltammetric study. Under these more stabilizing conditions the reduced Pd<sup>0</sup>/Cl<sub>2</sub>-phen species is expected to be the relatively most stable species in the series of Pd(R<sub>2</sub>-phen)<sub>2</sub><sup>2+</sup> complexes, as Cl<sub>2</sub>-phen (**1a**) is apparently the weakest σ-donor ligand. This relatively high stability of the reduced Pd complex might well account for the low overall activity for the Cl<sub>2</sub>-phen systems, as was also found for the Cl<sub>2</sub>-

**Chart 1. Side Products in the Reductive Carbonylation of Nitrobenzene by a Pd/R<sub>2</sub>-phen Catalyst System**



bpy ligand.<sup>11</sup> Eventually, decomposition of the reduced Pd/Cl<sub>2</sub>-phen catalyst system into Pd black will occur.

**Catalysis.** With the 4,7-disubstituted 1,10-phenanthroline ligands (**1a–e**) two different types of catalytic systems have been used to study the influence of the ligand as well as the anions on the catalytic activity and selectivity in the reductive carbonylation of aromatic nitro compounds: (type 1) the catalyst is generated in situ from Pd(acetate)<sub>2</sub>, 6 equiv of one of the ligands, and 3 equiv of *p*-toluenesulfonic acid as cocatalyst; (type 2) a presynthesized complex Pd(ligand)<sub>2</sub>(Y)<sub>2</sub> (Y = OTf or BF<sub>4</sub>) is used in combination with 4 equiv of free ligand.

All reactions have been performed in methanol with nitrobenzene as a model substrate, resulting in methyl *N*-phenylcarbamate as the main product in all cases. The side products consisted mainly of *N,N'*-diphenylurea, next to some aniline and a small but significant amount of azoxybenzene (Chart 1). In comparable experiments with 4,4'-disubstituted 2,2'-bipyridyl ligands the urea derivative was mostly found to be the only important side product along with traces of aniline. No azoxybenzene was detected with these systems, and the selectivity could be very well expressed in the carbamate:urea ratio.<sup>11</sup> For the phenanthroline systems, however, the selectivity is given by a product distribution to show the amounts of urea derivative, aniline, and azoxybenzene relative to the amount of desired carbamate. Roughly speaking, we found that the selectivity toward the carbamate is reduced from 90%–95% with the bipyridyl systems<sup>11</sup> to 80%–85% under the influence of the phenanthroline ligands (**1a–e**).

Azoxybenzene has been reported before as an important product in the reductive carbonylation of nitrobenzene, especially with supported Pd on carbon or Al<sub>2</sub>O<sub>3</sub> systems in the presence of a phenanthroline ligand. Addition of 2,4,6-trimethylbenzoic acid has proven to reduce the amount of azoxybenzene in favor of the carbamate or isocyanate.<sup>27,28</sup> Bontempi et al. also found azoxybenzene as main product with their [Pd(3,4,7,8-tetramethyl-1,10-phenanthroline)<sub>2</sub>][BPh<sub>4</sub>]<sub>2</sub> catalyst complex. They claim a chelated Pd<sup>0</sup> carbonyl intermediate species to be responsible for the formation of azoxybenzene, as the same result could be obtained using a Pd<sup>0</sup> complex as catalyst precursor.<sup>9</sup>

In contrast to the bipyridine systems,<sup>11</sup> only the experiments with Cl<sub>2</sub>-phen (**1a**) yield a significant amount of Pd black at the end of the catalytic runs. Apparently the better coordinating properties of the phenanthroline ligands induce a higher degree of stabilization of catalytic intermediates, which is also expressed in a higher overall activity of the phenanthroline systems. If the phenanthroline ligands (**1a–e**) are applied under the same conditions as were used

(24) Federlin, P.; Kern, J. M.; Rastegar, A.; Dietrich-Buchecker, C.; Marnot, P. A.; Sauvage, J. P. *New J. Chem.* **1990**, *14*, 9.

(25) Kaim, W.; Kramer, H. E. A.; Vogler, C.; Rieker, J. *J. Organomet. Chem.* **1989**, *367*, 107.

(26) Vogler, C.; Schwederski, B.; Klein, A.; Kaim, W. *J. Organomet. Chem.* **1992**, *436*, 367.

(27) Alessio, E.; Mestroni, G. *J. Mol. Catal.* **1984**, *26*, 337.

(28) Cenini, S.; Ragaini, F.; Pizzotti, M.; Porta, F.; Mestroni, G.; Alessio, E. *J. Mol. Catal.* **1991**, *64*, 179.

**Table 4. Results of the Reductive Carbonylation of Nitrobenzene in Methanol with Pd(acetate)<sub>2</sub>/Ligand (1a-e)/*p*-tsa<sup>a</sup>**

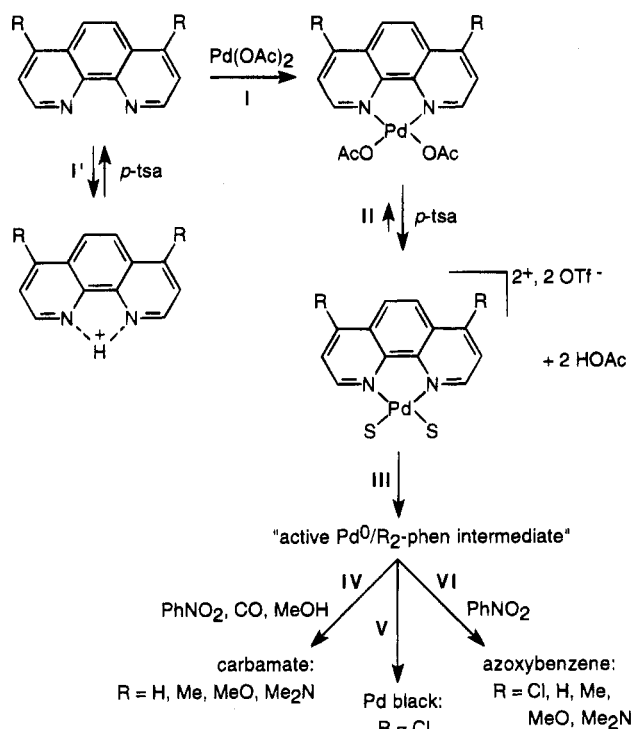
ligand	tof (mol/(mol/h))	product distribution (%) <sup>b</sup>			
		CA	UR	AN	AZOX
Cl <sub>2</sub> -phen ( <b>1a</b> )	26	0.0	0.0	85.7	14.3
H <sub>2</sub> -phen ( <b>1b</b> )	207	85.4	11.3	0.6	2.8
Me <sub>2</sub> -phen ( <b>1c</b> )	255	84.7	10.7	1.1	3.4
(MeO) <sub>2</sub> -phen ( <b>1d</b> )	249	82.6	10.8	0.0	6.3
(Me <sub>2</sub> N) <sub>2</sub> -phen ( <b>1e</b> )	105	80.2	5.9	0.0	13.9

<sup>a</sup> See Experimental Section for the precise conditions. <sup>b</sup> CA = methyl *N*-phenylcarbamate; UR = *N,N'*-diphenylurea; AN = aniline; AZOX = azoxybenzene.

for the bipyridine ligands, complete conversion of the substrate is reached within the 2 h of standard reaction time. To enable a comparison among the various phenanthroline ligands (**1a-e**) the concentration of Pd and the ligand: Pd ratio had to be reduced with respect to the bipyridine experiments.<sup>11</sup> Due to the higher stability of the phenanthroline catalyst systems, the reproducibility of the catalytic results was strongly improved, allowing us to confine to measurements in duplicate.

**Pd(acetate)<sub>2</sub>, a Phenanthroline Ligand, and *p*-Toluenesulfonic Acid.** In the catalytic runs of type I, with the in situ generated catalyst, the reaction conditions have deliberately been tuned to yield a conversion into carbamate of approximately 50% with H<sub>2</sub>-phen (**1b**) as the reference. As this required a ligand: Pd ratio of only 6 at a total Pd concentration of 0.002 M, the *p*-tsa: Pd ratio also had to be kept low (3) to maintain an excess of ligand with respect to the acid. The results of the in situ generated catalyst systems are listed in Table 4.

Even under the adjusted experimental conditions the phenanthroline systems are about twice as active as their corresponding bipyridine systems.<sup>11</sup> Throughout this work we use the average turnover frequencies (tof) to compare the activities of the catalysts. This is a reasonable method for these catalysts since the reactions are approximately 0 order in substrate concentration. The rate of conversion is constant unless the catalyst decomposes. The turnover frequencies obtained with H<sub>2</sub>-bpy and Me<sub>2</sub>-bpy (118 and 140 mol/(mol/h), respectively) are increased by a factor 1.8 if the ligands are replaced by their phenanthroline analogues H<sub>2</sub>-phen (**1b**) and Me<sub>2</sub>-phen (**1c**), while (MeO)<sub>2</sub>-phen (**1d**) is even 2.3 times as active as (MeO)<sub>2</sub>-bpy with a tof of 109 mol/(mol/h). This higher activity for the phenanthroline systems is most probably caused by the rigidity of these ligands. The differences between the phenanthroline and the bipyridine systems are less than the factor 5 observed by Mestroni et al. for the difference between Pd(1,10-phenanthroline)<sub>2</sub>(PF<sub>6</sub>)<sub>2</sub> and Pd(2,2'-bipyridine)<sub>2</sub>(PF<sub>6</sub>)<sub>2</sub>.<sup>9</sup> It should be pointed out, however, that Mestroni's experiments were carried out under completely different reaction conditions, resulting in far lower overall activities (tof = 90 and 18 mol/(mol/h), respectively). Furthermore, these experiments started with presynthesized catalyst complexes, thus omitting the acidic cocatalyst. As phenanthroline is a stronger base than bipyridine (pK<sub>b</sub> - values of 9.2<sup>12</sup> and 9.7,<sup>29</sup> respectively) the activity of the phenanthroline systems

**Scheme 4. Catalysis with the in Situ Generated Systems from Pd(acetate)<sub>2</sub>, R<sub>2</sub>-phen, and *p*-tsa**

is probably more influenced by the competition between Pd<sup>2+</sup> and H<sup>+</sup> for the ligand.

The variations among the R<sub>2</sub>-phen systems with R = H, Me, or MeO are smaller than in the case of the R<sub>2</sub>-bpy systems. The highest activity is found for Me<sub>2</sub>-phen (**1c**) (tof = 255 mol/(mol/h)), which might indicate that this ligand has the optimum donating capacity for the palladium-catalyzed reductive carbonylation of nitrobenzene. However, the influence of the amount of acid present in the reaction mixture in correlation with the basicity of the particular ligand has not been taken into account in this study. Yet this basicity will be decisive for the competition between reaction step I and the undesired side reaction step I' in Scheme 4. Previous results with the substituted bipyridine systems have shown that at least 2 equiv of *p*-tsa to Pd are required in order to replace the coordinating acetate anions with noncoordinating tosylate anions.<sup>11</sup> Because the phenanthroline ligands are applied in a 6-fold excess to palladium and an overall excess of ligand to acid is needed, only little variation of the amount of acid in the reaction mixture is possible. Still, the *p*-tsa: Pd ratio of 3 that is used could be most appropriate for Me<sub>2</sub>-phen (**1c**).

For (Me<sub>2</sub>N)<sub>2</sub>-phen (**1e**) a sharp decrease in the catalytic activity was observed. Though this could be caused by the high donating capacity of this ligand it is more likely to be a result of partial protonation of the amino function by the acidic cocatalyst. In view of the ready protonation of part of the ligand by slightly acidic silica gel, as was observed in the <sup>1</sup>H-NMR spectrum after column chromatography with the ligand, a strong acid as *p*-tsa should certainly be able to protonate the amino function. That way this highly electron-donating substituent is transformed into a strongly electron-withdrawing group.

From the results with Cl<sub>2</sub>-phen (**1a**) it is obvious that such electron-withdrawing substituents have a severe negative effect on the catalytic activity. Under the



**Table 5. Results of the Reductive Carbonylation of Nitrobenzene in Methanol with Pd(R<sub>2</sub>-phen)<sub>2</sub>(OTf)<sub>2</sub> (2a–e)/Ligand (1a–e)<sup>a</sup>**

ligand	tof (mol/(mol/h))	product distribution (%) <sup>b</sup>			
		CA	UR	AN	AZOX
Cl <sub>2</sub> -phen (1a)	11	0.0	0.0	100	0.0
H <sub>2</sub> -phen (1b)	234	83.5	7.2	2.5	6.9
Me <sub>2</sub> -phen (1c)	311	83.9	9.9	2.6	3.6
(MeO) <sub>2</sub> -phen (1d)	179	82.5	8.1	0.0	9.3
(Me <sub>2</sub> N) <sub>2</sub> -phen (1e)	95	67.8	5.7	8.0	18.3

<sup>a</sup> See Experimental Section for the precise conditions. <sup>b</sup> CA = methyl *N*-phenylcarbamate; UR = *N,N'*-diphenylurea; AN = aniline; AZOX = azoxybenzene.

influence of the chloride substituents only small amounts of aniline and azoxybenzene could be measured at the end of the catalytic runs. No conversion into carbamate at all was detected, but a large amount of Pd black was found. The overall turnover frequency therefore amounted to only 26 mol of nitrobenzene converted per mol of Pd catalyst per hour. As little aniline and azoxybenzene are formed it appears that a start has been made with the conversion of nitrobenzene, but the catalyst decomposes in some intermediate stage before the carbamate can be formed. In spite of the good coordinating properties of the rigid phenanthroline skeleton, the Cl<sub>2</sub>-phen ligand (1a) still seems not donating enough to fully stabilize the catalytic intermediates. An intermediate Pd<sup>0</sup>/Cl<sub>2</sub>-phen system, which is readily formed as is shown by the cyclic voltammetric study, might be able, however, to cause the formation of azoxybenzene as was described by Bontempi et al.<sup>9</sup> before it decomposes into Pd metal (reaction steps I–III, V, and VI in Scheme 4).

In contrast to Cl<sub>2</sub>-phen (1a), the (Me<sub>2</sub>N)<sub>2</sub>-phen (1e) system does not result in a large amount of Pd black at the end of the catalytic runs. Apparently, the equilibrium between the normal (Me<sub>2</sub>N)<sub>2</sub>-phen ligand (1e) and its protonated form is sufficient to prevent large-scale decomposition of the catalytic intermediates but does cause the decrease in catalytic activity.

The effect of the donating capacity of the active ligands on the selectivity of the catalyst toward carbamate turned out to be almost negligible. Only a very slight increase could be found in the sequence (Me<sub>2</sub>N)<sub>2</sub>-phen (1e) (selectivity toward carbamate, 80.2%) < (MeO)<sub>2</sub>-phen (1d) (82.9%) < Me<sub>2</sub>-phen (1c) (84.7%) < H<sub>2</sub>-phen (1b) (85.4%).

**Presynthesized Complexes Pd(ligand)<sub>2</sub>(Y)<sub>2</sub>, with Y = OTf or BF<sub>4</sub>.** Catalytic runs of type II with the presynthesized complexes have the advantage that no more *p*-tsa has to be added, as the complexes already contain noncoordinating anions. Results of the triflate complexes are collected in Table 5, while Table 6 gives the results obtained with the analogous tetrafluoroborate complexes.

Though the presynthesized complexes are generally more active than the corresponding in situ systems, the differences are smaller than those observed before for the bipyridine systems.<sup>11</sup> Therefore the experimental conditions need not be changed for the phenanthroline complexes with respect to the catalytic runs with the in situ systems, thus allowing a better comparison between the activities and selectivities of the two types of systems. The relatively small difference between the presynthesized complexes and the in situ systems for

**Table 6. Results of the Reductive Carbonylation of Nitrobenzene in Methanol with Pd(R<sub>2</sub>-phen)<sub>2</sub>(BF<sub>4</sub>)<sub>2</sub> (3a–e)/Ligand (1a–e)<sup>a</sup>**

ligand	tof (mol/(mol/h))	product distribution (%) <sup>b</sup>			
		CA	UR	AN	AZOX
Cl <sub>2</sub> -phen (1a)	37	0.0	0.0	91.1	8.8
H <sub>2</sub> -phen (1b)	247	86.7	8.3	1.2	3.8
Me <sub>2</sub> -phen (1c)	271	85.7	9.2	1.2	3.9
(MeO) <sub>2</sub> -phen (1d)	255	80.4	10.6	1.7	7.3
(Me <sub>2</sub> N) <sub>2</sub> -phen (1e)	207	79.1	8.3	0.0	12.5

<sup>a</sup> See Experimental Section for the precise conditions. <sup>b</sup> CA = methyl *N*-phenylcarbamate; UR = *N,N'*-diphenylurea; AN = aniline; AZOX = azoxybenzene.

the phenanthroline ligands compared to the bipyridine case is probably caused by the better coordinating properties of the phenanthroline ligands. This results in an easier formation of the active complex from Pd-(acetate)<sub>2</sub>, the ligand, and *p*-tsa (reaction steps I–III in Scheme 4).

Under the milder conditions the presynthesized phenanthroline complexes are still far more active than the bipyridine analogues. The smallest increase is found for the (Me<sub>2</sub>N)<sub>2</sub>-phen ligand (1e) which is only 1.5 times more active than its bipyridine analogue. However, with Me<sub>2</sub>-phen (1c) an increase by a factor of 4.6 is obtained, nearly resembling the enhancement found by Mestroni et al. for Pd(ligand)<sub>2</sub>(PF<sub>6</sub>)<sub>2</sub> (ligand = H<sub>2</sub>-phen and H<sub>2</sub>-bpy) under more favorable reaction conditions.<sup>9</sup>

From the turnover frequencies listed in the Tables 5 and 6 it becomes clear that the differences in activity between the various phenanthroline ligands are larger for the presynthesized complexes than for the in situ systems, which might be caused by the better defined starting systems. Within the triflate series the internal differences are even larger than within the series of BF<sub>4</sub> complexes. This might have to do with the very weak coordination of the triflate anions compared to the absolutely noncoordinating BF<sub>4</sub> anions. As one of the ligands presumably has to dissociate to create two vacant coordination sites for the catalysis, stabilization of the coordinatively unsaturated intermediate by a weak interaction with the triflate anions might have a positive effect in the case of the mildly donating phenanthroline ligands. For the ligands with a high donating capacity, on the other hand, vacant coordination sites are less readily available, and weak interaction with the anions would only reduce this availability even more (equilibrium of Scheme 3 in which S can be either an OTf anion or a solvent molecule in the case of the BF<sub>4</sub> complexes).

This complete picture of the donating capacity of the ligand and the degree of coordination of the anion results in the subtle balance that can be found between the ligand used and the particular noncoordinating anion that is needed to obtain the optimum activity. For instance, for Me<sub>2</sub>-phen (1c) best results are clearly obtained with the weakly coordinating triflate anions, while for (MeO)<sub>2</sub>-phen (1d) the tetrafluoroborate anions are the best choice.

For Cl<sub>2</sub>-phen (1a) again hardly any activity is observed, neither with the OTf anions nor with the BF<sub>4</sub> anions. No conversion into carbamate is found. Only traces of aniline and azoxybenzene can be detected, next to a large amount of Pd black. Although the Cl<sub>2</sub>-phen



ligand (**1a**) is coordinated to Pd at the beginning of the catalytic run, it is obviously not capable of stabilizing the intermediate Pd species, as was also found for the in situ generated systems.

All other phenanthroline ligands yield very stable catalyst systems, as was already observed with the in situ experiments of type I. For the presynthesized complexes the optimum activity is found at Me<sub>2</sub>-phen (**1c**) for both types of anion. As this was also the case with the in situ systems, it might suggest that Me<sub>2</sub>-phen actually has the optimum donating capacity for this process, independent of the anion or the presence of an acidic cocatalyst.

Of the active ligands (Me<sub>2</sub>N)<sub>2</sub>-phen (**1e**) always gives the lowest turnover frequency. As the acidic cocatalyst could be left out in the catalytic runs of type II, the amino function has to be present as a strongly electron-donating group in the presynthesized complexes. This means that under the influence of this substituent the electron density at the Pd center might be too high at some stage in the catalytic cycle. The inhibiting step, however, could also be the first dissociation of one of the ligands, which is hampered by the strong coordination of this (Me<sub>2</sub>N)<sub>2</sub>-phen ligand (**1e**).

The selectivity toward the carbamate appears to be rather unaffected by the system used. For the active ligands (**1b–e**) roughly the same selectivity is reached with the in situ generated systems and with both types of presynthesized complexes. For the Pd((Me<sub>2</sub>N)<sub>2</sub>-phen)<sub>2</sub>(Y)<sub>2</sub> complexes (**2e** and **3e**) a relatively low selectivity toward the carbamate is obtained, especially in the case of the triflate complex (**2e**). Because of the slow reactions with these catalysts a relatively high concentration of nitrene and nitroso intermediates might be present, resulting in an easy formation of azoxybenzene and reduction of the selectivity toward the carbamate.

## Conclusions

Phenanthroline ligands with moderately donating substituents (H, Me, or MeO) yield stable and active palladium catalyst systems for the reductive carbonylation of nitrobenzene. A subtle balance has been found between the ligand used and the particular noncoordinating anion for the optimum activity. The best catalyst among these systems consists of Pd(Me<sub>2</sub>-phen)<sub>2</sub>(OTf)<sub>2</sub> (**2c**).

Electron-withdrawing substituents like chloride on the phenanthroline ligand completely deactivate the catalyst, in spite of the good coordinating properties of the rigid phenanthroline skeleton.

## Experimental Section

**Materials and Analyses.** PdCl<sub>2</sub> and Pd(acetate)<sub>2</sub> were purchased from Degussa and used as received. All other chemicals were purchased from Aldrich or Janssen.

The solvents were purified prior to use. Acetone was distilled from anhydrous K<sub>2</sub>CO<sub>3</sub>; methanol, dichloromethane, DMF, DMSO, and acetonitrile from CaH<sub>2</sub> (5 g/L); chloroform from CaCl<sub>2</sub>; hexanes from sodium/benzoylbiphenyl; and toluene from sodium/benzophenone.

4,7-Dichloro-1,10-phenanthroline was synthesized as described in literature.<sup>15,30</sup> The 4,7-disubstituted 1,10-phenan-

throline ligands with R = methoxy and dimethylamino were prepared according to a modified literature procedure.<sup>11,16</sup>

Pd(acetonitrile)<sub>2</sub>Cl<sub>2</sub> was prepared analogously to Pd(benzonitrile)<sub>2</sub>Cl<sub>2</sub> in refluxing acetonitrile according to a literature procedure.<sup>31</sup> Pd(acetonitrile)<sub>4</sub>(BF<sub>4</sub>)<sub>2</sub> was prepared as described in literature.<sup>17</sup>

Column chromatography was performed using silica gel (Kieselgel 60, 70–230 mesh ASTM, purchased from Merck) as the stationary phase.

Infrared (IR) spectra were recorded on a Nicolet 510m FT-IR spectrophotometer. <sup>1</sup>H-NMR spectra were obtained on a Bruker AMX 300 instrument. Chemical shifts are given in ppm. TMS was used as reference with CDCl<sub>3</sub> as internal standard. Mass spectral data were recorded on a JEOL JMS SX/SX 102A four-sector mass spectrometer equipped with a JEOL MSMP7000 data system, using a nitrobenzyl alcohol matrix solution. Melting points were measured on a Gallenkamp melting point apparatus and are uncorrected. Elemental analyses were carried out by the Department of Micro Analysis, University of Groningen. Cyclic voltammetry measurements were performed with a PA4 (EKOM, Czech Republic) potentiostat in a vacuum-tight cyclic voltammetric cell, equipped with a Pt-disk electrode of 0.38 mm<sup>2</sup> apparent surface area, a Pt-gauze auxiliary electrode, and an Ag-wire as a pseudoreference electrode.

The reductive carbonylation of nitrobenzene was performed in a stainless steel (SS 316) 50 mL autoclave equipped with a glass liner, a gas inlet, a thermocouple, and a magnetic stirrer. CO 3.0 was purchased from Praxair and used as purchased. The results were analyzed by HPLC on a Gilson HPLC apparatus, using a Dynamax C18 column (eluent gradient: 45% water in methanol to 100% methanol in 20 minutes).

**Syntheses.** **4,7-Dimethoxy-1,10-phenanthroline ((MeO)<sub>2</sub>-phen) (1d).** To a freshly prepared solution of sodium methoxide (11 mmol) in 40 mL of methanol was added 250 mg of 4,7-dichloro-1,10-phenanthroline (Cl<sub>2</sub>-phen) (**1a**) (2.38 mmol). The reaction mixture was refluxed for 24 h, after which time it was concentrated under vacuum to approximately 15 mL. A 20 mL amount of ice water was added, resulting in the formation of a yellow precipitate. The suspension was stored overnight at +4 °C to assure complete precipitation of the product. The precipitate was filtered off, washed with 3 × 15 mL of water, and dried under vacuum. Yield: 502 mg of brown powder (2.09 mmol, 88%). IR (KBr): 1225 (s, C–O), 1028 (vs, C–O) cm<sup>-1</sup>. <sup>1</sup>H NMR (DMSO-*d*<sub>6</sub>): δ 8.89 (d, 2H, H<sub>2</sub> + H<sub>9</sub>), 8.16 (s, 2H, H<sub>5</sub> + H<sub>6</sub>), 7.25 (d, 2H, H<sub>3</sub> + H<sub>8</sub>), 4.12 (s, 6H, OCH<sub>3</sub>) ppm. Mp: 207–208 °C.

**4,7-Bis(dimethylamino)-1,10-phenanthroline (1e).** A suspension of 0.5 g of Cl<sub>2</sub>-phen (**1a**) (2.0 mmol) in 15 mL of DMF was refluxed under N<sub>2</sub> for 22 h. After the solvent was evaporated, the orange powder was treated with a mixture of 20 mL of 1 M NaOH and 25 mL of THF. The water layer was washed with 3 × 25 mL of THF. The combined THF fractions were dried over Na<sub>2</sub>SO<sub>4</sub>, and the solvent was evaporated. The crude product was purified by column chromatography, using 16% methanol in dichloromethane followed by 1% triethylamine and 16% methanol in dichloromethane as eluent. The product was dissolved in 16 mL of dichloromethane and washed with 2 × 10 mL of 1 M NaOH. The water layers were re-extracted with 2 × 15 mL of dichloromethane. The combined organic fractions were dried over Na<sub>2</sub>SO<sub>4</sub>, and the solvent was evaporated. Yield: 278 mg of beige powder (1.04 mmol, 52%). IR (KBr): 998 (m, C–N) cm<sup>-1</sup>. <sup>1</sup>H NMR (DMSO-*d*<sub>6</sub>): δ 8.88 (d, 2H, H<sub>2</sub> + H<sub>9</sub>), 7.95 (s, 2H, H<sub>5</sub> + H<sub>6</sub>), 6.98 (d, 2H, H<sub>3</sub> + H<sub>8</sub>), 3.05 (s, 12H, N(CH<sub>3</sub>)<sub>2</sub>) ppm. Mp: 143–145 °C.

**Pd(Cl<sub>2</sub>-phen)<sub>2</sub>(OTf)<sub>2</sub> (2a).** Pd(Cl<sub>2</sub>-phen)<sub>2</sub>(OTf)<sub>2</sub> (**2a**) was prepared from freshly synthesized Pd(CH<sub>3</sub>CN)<sub>4</sub>(OTf)<sub>2</sub>. A 98 mg amount of Pd(CH<sub>3</sub>CN)<sub>2</sub>Cl<sub>2</sub> (0.38 mmol) was dissolved under Ar in 15 mL of acetonitrile, and 194 mg of silver triflate (0.76

(31) Kharash, M. S.; Seyler, R. C.; Mayo, F. R. *J. Am. Chem. Soc.* **1938**, *60*, 882.

(30) Price, C. C.; Roberts, R. M. *J. Am. Chem. Soc.* **1946**, *68*, 1204.

mmol) was dissolved in 5 mL of acetonitrile under Ar in the dark. The silver triflate solution was added to the solution of  $\text{Pd}(\text{CH}_3\text{CN})_2\text{Cl}_2$ . The reaction mixture was stirred under Ar in the dark for 1 h. The yellow solution was decanted from the AgCl precipitate, and the solvent was evaporated. The resulting 216 mg of  $\text{Pd}(\text{CH}_3\text{CN})_4(\text{OTf})_2$  (0.38 mmol) was dissolved in acetone and used immediately in additional syntheses.

A solution of 91 mg of  $\text{Pd}(\text{CH}_3\text{CN})_4(\text{OTf})_2$  (0.16 mmol) in 5 mL of acetone was added dropwise to a solution of 80 mg of  $\text{Cl}_2$ -phen (**1a**) (0.32 mmol) in 15 mL of acetone and 10 mL of dichloromethane under Ar. The reaction mixture was stirred at room temperature for 16 h, after which time 20 mL of hexanes was added. The solvents were decanted, and the precipitate was washed with  $2 \times 5$  mL of toluene. The product was dried under vacuum. Yield: 99 mg of orange-yellow powder (0.11 mmol, 69%). IR (KBr): 1260 (vs,  $-\text{SO}_2\text{O}-$ ), 1028 (s, C-F)  $\text{cm}^{-1}$ .  $^1\text{H NMR}$  (MeOH- $d_4$ ):  $\delta$  9.28 (d, 2H,  $\text{H}_2 + \text{H}_9$ ), 8.75 (s, 2H,  $\text{H}_5 + \text{H}_6$ ), 8.47 (d, 2H,  $\text{H}_3 + \text{H}_8$ ) ppm. Anal. Calcd for  $\text{C}_{26}\text{H}_{12}\text{Cl}_4\text{F}_6\text{N}_4\text{O}_6\text{S}_2\text{Pd}$ : C, 34.59; H, 1.34. Found: C, 33.97; H, 1.49.

**$\text{Pd}(\text{phen})_2(\text{OTf})_2$  (2b).** To a freshly prepared solution of 183 mg of  $\text{Pd}(\text{CH}_3\text{CN})_4(\text{OTf})_2$  (0.32 mmol) in 10 mL of acetone under Ar was added dropwise a solution of 116 mg of phen (**1b**) (0.64 mmol) in 6 mL of acetone. The reaction mixture was stirred at room temperature for 1 h, after which time the supernatant was decanted from the precipitate. The precipitate was washed with  $2 \times 3$  mL of hexanes and dried under vacuum. To the supernatant was added 20 mL of hexanes, resulting in a new precipitate. The solvents were decanted, and the precipitate was washed with  $3 \times 2$  mL of toluene and dried under vacuum. Crystals were obtained from an unsaturated solution of the complex in 4 mL of methanol, to which 4 mL of hexanes was slowly added. After 3 days yellow crystals had grown in the solution. Overall yield: 168 mg of yellow powder (0.22 mmol, 69%). IR (KBr): 1260 (vs,  $-\text{SO}_2\text{O}-$ ), 1026 (s, C-F)  $\text{cm}^{-1}$ .  $^1\text{H NMR}$  (DMSO- $d_6$ ):  $\delta$  9.39 (d, 2H,  $\text{H}_2 + \text{H}_9$ ), 9.18 (d, 2H,  $\text{H}_4 + \text{H}_7$ ), 8.46 (s, 2H,  $\text{H}_5 + \text{H}_6$ ), 8.31 (dd, 2H,  $\text{H}_3 + \text{H}_8$ ) ppm. MS (FAB): 615 ( $\text{M}^+ - \text{OTf}$ ), 466 ( $\text{M}^+ - 2\text{OTf}$ ), 286 ( $\text{M}^+ - 2\text{OTf} - \text{phen}$ ). Anal. Calcd for  $\text{C}_{26}\text{H}_{16}\text{F}_6\text{N}_4\text{O}_6\text{S}_2\text{Pd}$ : C, 40.82; H, 2.11; N, 7.32. Found: C, 40.06; H, 2.21; N, 7.00.

**$\text{Pd}(\text{Me}_2\text{-phen})_2(\text{OTf})_2$  (2c).** The synthesis of  $\text{Pd}(\text{Me}_2\text{-phen})_2(\text{OTf})_2$  (**2c**) is analogous to the synthesis of  $\text{Pd}(\text{Cl}_2\text{-phen})_2(\text{OTf})_2$  (**2a**) with the following modifications. A freshly prepared solution of 34 mg of  $\text{Pd}(\text{CH}_3\text{CN})_4(\text{OTf})_2$  (0.06 mmol) in 2 mL of acetone was added dropwise to a solution of 25 mg of  $\text{Me}_2$ -phen (**1c**) (0.12 mmol) in 6 mL of acetone under Ar. No precipitate was formed until 20 mL of hexanes had been added. Yield: 34.5 mg of brown powder (0.04 mmol, 70%). IR (KBr): 1258 (vs,  $-\text{SO}_2\text{O}-$ ), 1028 (s, C-F)  $\text{cm}^{-1}$ .  $^1\text{H NMR}$  (DMSO- $d_6$ ):  $\delta$  9.15 (d, 2H,  $\text{H}_2 + \text{H}_9$ ), 8.46 (s, 2H,  $\text{H}_5 + \text{H}_6$ ), 8.02 (d, 2H,  $\text{H}_3 + \text{H}_8$ ), 3.05 (s, 6H,  $\text{CH}_3$ ) ppm. Anal. Calcd for  $\text{C}_{30}\text{H}_{24}\text{F}_6\text{N}_4\text{O}_6\text{S}_2\text{Pd}$ -toluene: C, 48.66; H, 3.53. Found: C, 48.24; H, 3.30.

**$\text{Pd}(\text{MeO})_2\text{-phen})_2(\text{OTf})_2$  (2d).**  $\text{Pd}(\text{MeO})_2\text{-phen})_2(\text{OTf})_2$  (**2d**) was prepared analogously to  $\text{Pd}(\text{Cl}_2\text{-phen})_2(\text{OTf})_2$  (**2a**). However, 96 mg of  $(\text{MeO})_2\text{-phen}$  (**1d**) (0.40 mmol) dissolved in 15 mL of acetone and 5 mL of dichloromethane was reacted with 114 mg of freshly prepared  $\text{Pd}(\text{CH}_3\text{CN})_4(\text{OTf})_2$  (0.20 mmol) in 8 mL of acetone under Ar. Yield: 97 mg of brown powder (0.11 mmol, 55%). IR (KBr): 1266 (vs,  $-\text{SO}_2\text{O}-$ ), 1221 (m, C-O-C), 1032 (s, C-F), 1028 (s, C-O-C)  $\text{cm}^{-1}$ .  $^1\text{H NMR}$  (DMSO- $d_6$ ):  $\delta$  9.07 (d, 2H,  $\text{H}_2 + \text{H}_9$ ), 8.31 (s, 2H,  $\text{H}_5 + \text{H}_6$ ), 7.65 (d, 2H,  $\text{H}_3 + \text{H}_8$ ), 4.35 (s, 6H,  $\text{OCH}_3$ ) ppm. Anal. Calcd for  $\text{C}_{30}\text{H}_{24}\text{F}_6\text{N}_4\text{O}_{10}\text{S}_2\text{Pd}$ : C, 40.71; H, 2.74. Found: C, 40.03; H, 2.72.

**$\text{Pd}(\text{Me}_2\text{N})_2\text{-phen})_2(\text{OTf})_2$  (2e).**  $\text{Pd}(\text{Me}_2\text{N})_2\text{-phen})_2(\text{OTf})_2$  (**2e**) was synthesized according to the synthesis of  $\text{Pd}(\text{Cl}_2\text{-phen})_2(\text{OTf})_2$  (**2a**), except that 85 mg of  $(\text{Me}_2\text{N})_2\text{-phen}$  (**1e**) (0.32 mmol) was used. The precipitate was washed with  $2 \times 5$  mL of chloroform as well as with  $2 \times 5$  mL of toluene. Yield: 94

mg of brown powder (0.10 mmol, 65 %). IR (KBr): 1266 (vs,  $-\text{SO}_2\text{O}-$ ), 1064 (w, C-N), 1026 (s, C-F)  $\text{cm}^{-1}$ .  $^1\text{H NMR}$  (DMSO- $d_6$ ):  $\delta$  8.40 (d, 2H,  $\text{H}_2 + \text{H}_9$ ), 8.04 (s, 2H,  $\text{H}_5 + \text{H}_6$ ), 7.04 (d, 2H,  $\text{H}_3 + \text{H}_8$ ), 3.45 (s, 12H,  $\text{N}(\text{CH}_3)_2$ ) ppm. Anal. Calcd for  $\text{C}_{34}\text{H}_{36}\text{F}_6\text{N}_8\text{O}_6\text{S}_2\text{Pd} \cdot 2\text{H}_2\text{O}$ : C, 42.75; H, 4.01; N, 11.73. Found: C, 42.85; H, 4.12; N, 11.51.

**$\text{Pd}(\text{Cl}_2\text{-phen})_2(\text{BF}_4)_2$  (3a).** A solution of 24.7 mg of  $\text{Cl}_2$ -phen (**1a**) (0.1 mmol) in 2 mL of acetone and 4 mL of dichloromethane under Ar was added dropwise to a solution of 22 mg of  $\text{Pd}(\text{CH}_3\text{CN})_4(\text{BF}_4)_2$  (0.05 mmol) in 2 mL of acetone under Ar. The reaction mixture was stirred at room temperature for 24 h, after which time 15 mL of hexanes was added. The solvents were decanted, and the precipitate was washed with  $3 \times 5$  mL of hexanes. The product was dried under vacuum. Yield: 28 mg of yellow powder (0.035 mmol, 70%). IR (KBr): 1061 (vs, br,  $\text{BF}_4$ )  $\text{cm}^{-1}$ .  $^1\text{H NMR}$  (DMSO- $d_6$ ):  $\delta$  9.30 (br, 2H,  $\text{H}_2 + \text{H}_9$ ), 8.67 (br, 2H,  $\text{H}_5 + \text{H}_6$ ), 8.55 (br, 2H,  $\text{H}_3 + \text{H}_8$ ) ppm. Anal. Calcd for  $\text{C}_{24}\text{H}_{12}\text{B}_2\text{Cl}_4\text{F}_8\text{N}_4\text{Pd} \cdot \text{H}_2\text{O}$ : C, 36.20; H, 1.77. Found: C, 36.52; H, 2.08.

**$\text{Pd}(\text{phen})_2(\text{BF}_4)_2$  (3b).**  $\text{Pd}(\text{phen})_2(\text{BF}_4)_2$  (**3b**) was synthesized analogously to  $\text{Pd}(\text{Cl}_2\text{-phen})_2(\text{BF}_4)_2$  (**3a**) with the following modifications: 144 mg of phen (**1b**) (0.8 mmol) in 10 mL of acetone was reacted with 178 mg of  $\text{Pd}(\text{CH}_3\text{CN})_2(\text{BF}_4)_2$  (0.4 mmol) in 15 mL of acetone under Ar. After the mixture had been stirred for 1 h, 30 mL of hexanes was added. The precipitate was washed with  $2 \times 5$  mL of toluene. Yield: 205 mg of yellow powder (0.32 mmol, 81%). IR (KBr): 1061 (vs, br,  $\text{BF}_4$ )  $\text{cm}^{-1}$ .  $^1\text{H NMR}$  (DMSO- $d_6$ ):  $\delta$  9.40 (d, 2H,  $\text{H}_2 + \text{H}_9$ ), 9.20 (d, 2H,  $\text{H}_4 + \text{H}_7$ ), 8.50 (s, 2H,  $\text{H}_5 + \text{H}_6$ ), 8.33 (dd, 2H,  $\text{H}_3 + \text{H}_8$ ) ppm. MS (FAB): 553 ( $\text{M}^+ - \text{BF}_4$ ), 466 ( $\text{M}^+ - 2\text{BF}_4$ ), 286 ( $\text{M}^+ - 2\text{BF}_4 - \text{phen}$ ). Anal. Calcd for  $\text{C}_{24}\text{H}_{16}\text{B}_2\text{F}_8\text{N}_4\text{Pd}$ : C, 45.01; H, 2.52; N, 8.75. Found: C, 44.24; H, 2.72; N, 8.63.

**$\text{Pd}(\text{Me}_2\text{-phen})_2(\text{BF}_4)_2$  (3c).**  $\text{Pd}(\text{Me}_2\text{-phen})_2(\text{BF}_4)_2$  (**3c**) was prepared as  $\text{Pd}(\text{Cl}_2\text{-phen})_2(\text{BF}_4)_2$  (**3a**), except that 20.8 mg of  $\text{Me}_2$ -phen (**1c**) (0.1 mmol) was dissolved in 3 mL of acetone and added to a solution of 22 mg of  $\text{Pd}(\text{CH}_3\text{CN})_4(\text{BF}_4)_2$  (0.05 mmol) in 2 mL of acetone under Ar. Yield: 34.5 mg of brown powder (0.04 mmol, 78%). IR (KBr): 1061 (vs, br,  $\text{BF}_4$ )  $\text{cm}^{-1}$ .  $^1\text{H NMR}$  (DMSO- $d_6$ ):  $\delta$  9.20 (d, 2H,  $\text{H}_2 + \text{H}_9$ ), 8.48 (s, 2H,  $\text{H}_5 + \text{H}_6$ ), 8.10 (d, 2H,  $\text{H}_3 + \text{H}_8$ ), 3.06 (s, 6H,  $\text{CH}_3$ ) ppm. Anal. Calcd for  $\text{C}_{28}\text{H}_{24}\text{B}_2\text{F}_8\text{N}_4\text{Pd} \cdot 2\text{H}_2\text{O}$ : C, 45.91; H, 3.86. Found: C, 45.29; H, 3.83.

**$\text{Pd}(\text{MeO})_2\text{-phen})_2(\text{BF}_4)_2$  (3d).**  $\text{Pd}(\text{MeO})_2\text{-phen})_2(\text{BF}_4)_2$  (**3d**) was prepared according to the synthesis of its triflate analogue **2d** with the following modifications: 66.6 mg of  $\text{Pd}(\text{CH}_3\text{CN})_4(\text{BF}_4)_2$  (0.15 mmol) in 5 mL of acetone under Ar was reacted with 72 mg of  $(\text{MeO})_2\text{-phen}$  (**1d**) (0.30 mmol) dissolved in 15 mL of acetone and 10 mL of dichloromethane. Yield: 84 mg of brown powder (0.11 mmol, 70%). IR (KBr): 1225 (m, C-O-C), 1081 (vs, br,  $\text{BF}_4$ )  $\text{cm}^{-1}$ .  $^1\text{H NMR}$  (DMSO- $d_6$ ):  $\delta$  9.08 (d, 2H,  $\text{H}_2 + \text{H}_9$ ), 8.35 (s, 2H,  $\text{H}_5 + \text{H}_6$ ), 7.66 (d, 2H,  $\text{H}_3 + \text{H}_8$ ), 4.38 (s, 6H,  $\text{OCH}_3$ ) ppm.

**$\text{Pd}(\text{Me}_2\text{N})_2\text{-phen})_2(\text{BF}_4)_2$  (3e).**  $\text{Pd}(\text{Me}_2\text{N})_2\text{-phen})_2(\text{BF}_4)_2$  (**3e**) was synthesized according to the synthesis of its triflate analogue **2e**. A solution of 133 mg of  $\text{Pd}(\text{CH}_3\text{CN})_4(\text{BF}_4)_2$  (0.30 mmol) in 7 mL of acetone was added dropwise to a solution of 160 mg of  $(\text{Me}_2\text{N})_2\text{-phen}$  (**1e**) (0.60 mmol) in 15 mL of acetone under Ar. Yield: 211 mg of brown powder (0.26 mmol, 85%). IR (KBr): 1061 (vs, br,  $\text{BF}_4$ )  $\text{cm}^{-1}$ .  $^1\text{H NMR}$  (DMSO- $d_6$ ):  $\delta$  8.43 (d, 2H,  $\text{H}_2 + \text{H}_9$ ), 8.08 (s, 2H,  $\text{H}_5 + \text{H}_6$ ), 7.08 (d, 2H,  $\text{H}_3 + \text{H}_8$ ), 3.45 (s, 12H,  $\text{N}(\text{CH}_3)_2$ ) ppm.

**X-ray Analysis. X-ray Structure Determination of  $\text{Pd}(\text{phen})_2(\text{OTf})_2$  (2b).** X-ray data for the pale yellow crystal were collected at room temperature on an Enraf-Nonius CAD-4 diffractometer with graphite-monochromated Mo  $\text{K}\alpha$  radiation. Crystallographic data are summarized in Table 7. Reflections were measured within the range  $-13 \leq h \leq 14$ ,  $-14 \leq k \leq 16$ , and  $0 \leq l \leq 18$ . The maximum value of  $(\sin \theta)/\lambda$  was 0.70  $\text{\AA}^{-1}$ . Two reference reflections (200 and 122) were measured every hour and showed no decrease during the 90 h of collection time. Unit cell parameters were refined with a least-squares fitting procedure, using 23 reflections with  $40 < 2\theta <$

**Table 7. Crystallographic Data for Pd(phen)<sub>2</sub>(OTf)<sub>2</sub> (2b)**

mol formula	C <sub>26</sub> H <sub>16</sub> F <sub>6</sub> N <sub>4</sub> O <sub>6</sub> S <sub>2</sub> Pd
mol wt	765.0
cryst syst	triclinic
space group	P1
temp	room temperature
radiation (λ, Å)	Mo Kα (0.710 69)
a, Å	10.387(1)
b, Å	11.539(2)
c, Å	13.449(3)
α, deg	70.53(1)
β, deg	67.42(2)
γ, deg	81.51(1)
V, Å <sup>3</sup>	2465.6(5)
Z	2
D <sub>calcd</sub> , g cm <sup>-3</sup>	1.56
F(000)	760
cryst dims, mm <sup>3</sup>	0.20 × 0.50 × 0.50
μ(Mo Kα), cm <sup>-1</sup>	8.81
no. of unique tot. data	8101
no. of unique obsd data	6448 ( <i>I</i> > 2.5σ( <i>I</i> ))
R	0.045
R <sub>w</sub>	0.064

41°. Corrections for Lorentz and polarization effects were applied. The Pd and S atoms were found by direct methods. The remainder of the non-hydrogen atoms was found in a subsequent  $\Delta F$  synthesis. The hydrogen atoms are calculated. Full-matrix least-squares refinement on *F*, anisotropic for the non-hydrogen atoms and isotropic for the hydrogen atoms, restraining the latter in such a way that the distance to their carrier remained constant at approximately 1.09 Å, converged to *R* = 0.045, *R*<sub>w</sub> = 0.064, and ( $\Delta/\sigma$ )<sub>max</sub> = 0.87. A weighting scheme  $w = (6.3 + F_{\text{obs}} + 0.0080F_{\text{obs}}^2)^{-1}$  was used. An empirical absorption correction (DIFABS)<sup>32</sup> was applied, with coefficients in the range 0.82–1.34. The secondary isotropic extinction coefficient<sup>33,34</sup> was refined to Ext = 0.02(2). A final difference Fourier map revealed a residual electron density between -0.7 and 1.1 e Å<sup>-3</sup>. Scattering factors were taken

(32) Walker, N.; Stuart, D. *Acta Crystallogr.* **1983**, A39, 158.

(33) Zachariasen, W. H. *Acta Crystallogr.* **1967**, A23, 558.

(34) Larson, A. C. The Inclusion of Secondary Extinction in Least-Squares Refinement of Crystal Structures. In *Crystallographic Computing*; Proceedings of an International Summer School organized by The Commission on Crystallographic Computing of the International Union of Crystallography, Ottawa, Canada, August 4–11, 1969; Ahmed, F. R., Hall, S. R., Huber, C. P., Eds.; Munksgaard: Copenhagen, 1970; p 291.

from refs 35 and 36. The anomalous scattering of Pd and S was taken into account. All calculations were performed with XTAL,<sup>37</sup> unless stated otherwise.

**Cyclic Voltammetry.** Cyclic voltammetry experiments were carried out in DMSO solutions at room temperature under N<sub>2</sub> with Bu<sub>4</sub>NPF<sub>6</sub> as supporting electrolyte. The solutions were all 10<sup>-3</sup> M in complex or free ligand and 10<sup>-1</sup> M in Bu<sub>4</sub>NPF<sub>6</sub>. The Fc/Fc<sup>+</sup> redox couple served as an internal standard for the determination of reduction potentials.<sup>23</sup> The cyclic voltammograms were recorded at a scan rate of 100 mV/s.

**Catalysis. Pd(acetate)<sub>2</sub>/Ligand/*p*-Toluenesulfonic Acid.** In a typical experiment using the in situ prepared catalyst system the autoclave was charged with 8 mL of methanol and 1.5 mL of nitrobenzene (14.6 mmol). A 4.5 mg amount of Pd(OAc)<sub>2</sub> (0.02 mmol) and 0.12 mmol of the ligand (6 equiv to Pd) were dissolved in this mixture. Subsequently, 2 mL of a 0.0295 M stock solution of *p*-tsa in methanol (0.06 mmol, 3 equiv to Pd) was added. The autoclave was pressurized with 60 bar of CO and heated to 135 °C within 35 min. The initial working pressure at 135 °C was approximately 80 bar. After 2 h, the autoclave was rapidly cooled down and the pressure was released.

**Pd(ligand)<sub>2</sub>(Y)<sub>2</sub>/Ligand (Y = OTf or BF<sub>4</sub>).** Experiments with the presynthesized complexes were carried out as described for the in situ combination in 10 mL of methanol, with 0.02 mmol of complex and 0.08 mmol of free ligand (resulting in an overall ligand:Pd ratio of 6). No *p*-tsa was added.

**Acknowledgment.** We thank the Innovation Oriented Research Programme (IOP-katalyse) for their financial support of this research.

**Supporting Information Available:** Listings of fractional atomic coordinates for the non-hydrogen and the hydrogen atoms and the anisotropic thermal parameters for Pd(phen)<sub>2</sub>(OTf)<sub>2</sub> (2b) (5 pages). Ordering information is given on any current masthead page.

OM950187G

(35) Cromer, D. T.; Mann, J. B. *Acta Crystallogr.* **1968**, A24, 321.

(36) *International Tables for X-ray Crystallography*; Kynoch Press: Birmingham, U.K., 1974; Vol. IV, p 55.

(37) Hall, S. R., Flack, H. D., Stewart, J. M., Eds. *XTAL3.2 Reference Manual*; Universities of Western Australia, Geneva, and Maryland: Perth, Australia, Geneva, Switzerland, and College Park, MD, 1992.

# Novel Ring Expansion Isomerism of a Fluorenylidene-phosphonium

Neil Burford,\* Jason A. C. Clyburne, Sergey V. Sereda, T. Stanley Cameron,\*  
James A. Pincock, and Michael Lumsden

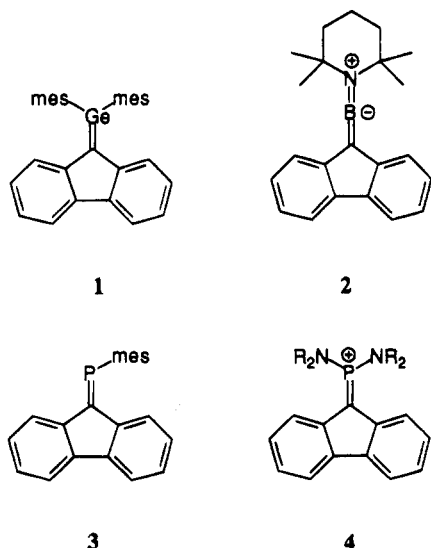
Department of Chemistry, Dalhousie University, Halifax, Nova Scotia B3H 4J3, Canada

Received February 13, 1995<sup>⊗</sup>

The synthesis and conclusive characterization of a series of fluorenyl- and fluorenylidene-tetraalkyldiaminophosphorus compounds (alkyl = ethyl and isopropyl) are described. The phosphines **6** are obtained by reaction of chlorodiaminophosphines with fluorenyllithium and are quantitatively oxidized to the phosphorane **7** by reaction with  $\text{CCl}_4$ . Crystal structures of the isopropyl derivatives are reported. (Crystal data for **6a**:  $\text{C}_{25}\text{H}_{37}\text{N}_2\text{P}$ ,  $M = 396.55$ ,  $P2_1/n$ ,  $a = 15.710(5) \text{ \AA}$ ,  $b = 9.66(1) \text{ \AA}$ ,  $c = 15.93(2) \text{ \AA}$ ,  $\beta = 91.48(6)^\circ$ ,  $V = 2417(7) \text{ \AA}^3$ ,  $Z = 4$ ,  $D_c = 1.089 \text{ Mg/m}^3$ ,  $R = 0.0538$ . For **7a**:  $\text{C}_{25}\text{H}_{36}\text{ClN}_2\text{P}$ ,  $M = 431.00$ ,  $P2_1/c$ ,  $a = 8.69(1) \text{ \AA}$ ,  $b = 16.24(1) \text{ \AA}$ ,  $c = 17.16(2) \text{ \AA}$ ,  $\beta = 96.0(1)^\circ$ ,  $V = 2409(8) \text{ \AA}^3$ ,  $Z = 4$ ,  $D_c = 1.188 \text{ Mg/m}^3$ ,  $R = 0.0481$ .) Contrary to previous reports (with  $\text{AlCl}_3$ ) reaction of the phosphoranes with  $\text{GaCl}_3$  gives the covalent complexes **7-GaCl<sub>3</sub>**. The ethyl derivative is stable, while the isopropyl derivative undergoes a quantitative isomerization to give 9-(diisopropylamino)-10-(diisopropyliminio)-9,10-dihydro-9-phosphaphenanthrene tetrachlorogallate **5** [ $\text{GaCl}_4$ ] via a novel ring expansion rearrangement. (Crystal data for **5** [ $\text{GaCl}_4$ ]:  $\text{C}_{25}\text{H}_{36}\text{Cl}_4\text{GaN}_2\text{P}$ ,  $M = 607.08$ ;  $P2_1/n$ ;  $a = 9.884(3) \text{ \AA}$ ;  $b = 21.189(4) \text{ \AA}$ ;  $c = 14.639(4) \text{ \AA}$ ;  $\beta = 95.12(2)^\circ$ ;  $V = 3054(2) \text{ \AA}^3$ ;  $Z = 4$ ;  $D_c = 1.320 \text{ Mg/m}^3$ ;  $R = 0.0393$ .)

## Introduction

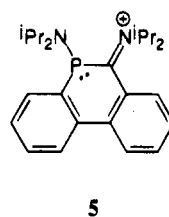
The fluorenylidene unit is an attractive substituent for the development of new bonding environments offering both steric and electronic stabilizing features. Consequently, it has been used for the isolation of the first stable methylenegermene **1**,<sup>1</sup> as well as compounds



containing low-coordinate environments for boron **2**<sup>2</sup> and phosphorus **3**.<sup>3</sup> The first alkenephosphonium cations **4** (fluorenylidene-phosphonium) were speculated as

the result of a halide ion abstraction from derivatives of fluorenylidene-phosphoranes on the basis of spectroscopic data.<sup>4</sup> These conclusions were refuted after comparison with the first structurally characterized example of an alkenephosphonium salt.<sup>5</sup>

We have re-examined two diamino-substituted phosphorus systems that have the potential to adopt structure **4** and report observations that are consistent with a covalent formulation. Moreover, promotion of an ionic structure in a polar solvent facilitates a novel quantitative isomerism to give the tricyclic iminiumphosphine salt **5** [ $\text{GaCl}_4$ ].



## Experimental Section

Fluorene and 1.6 M butyllithium in hexanes (Aldrich) were used as supplied.  $[\text{iPr}_2\text{N}]_2\text{PCL}$  and  $[\text{Et}_2\text{N}]_2\text{PCL}$  were prepared following literature procedures.<sup>6</sup>  $\text{GaCl}_3$  was sublimed under vacuum before use. Fluorenyllithium (0.25 M) was prepared *in situ* by adding BuLi in hexanes to a stirred solution (0 °C) of fluorene in ether.  $\text{CH}_2\text{Cl}_2$  and hexanes were dried over  $\text{CaH}_2$  and  $\text{P}_2\text{O}_5$  and stored in evacuated bulbs. Benzene was dried over sodium/benzophenone, and  $\text{CCl}_4$  was dried over  $\text{P}_2\text{O}_5$ . Solids were handled in a Vacuum Atmospheres nitrogen-filled

<sup>⊗</sup> Abstract published in *Advance ACS Abstracts*, July 1, 1995.

(1) Couret, C.; Escudié, J.; Satgé, J.; Lazraq, M. *J. Am. Chem. Soc.* **1987**, *109*, 4411–4412. Lazraq, M.; Escudié, J.; Couret, C.; Satgé, J.; Dräger, M.; Dammel, R. *Angew. Chem., Int. Ed. Engl.* **1988**, *27*, 828–829.

(2) Glaser, B.; Nöth, H. *Angew. Chem., Int. Ed. Engl.* **1985**, *24*, 416–417.

(3) van der Knaap, T.; Bickelhaupt, F. *Chem. Ber.* **1984**, *117*, 915–924.

(4) Appel, R.; Schmitz, R. *Chem. Ber.* **1983**, *116*, 3521–3523.

(5) Igau, A.; Baccaredo, A.; Grützmacher, H.; Pritzkow, H.; Bertrand, G. *J. Am. Chem. Soc.* **1989**, *111*, 6853–6854.

(6) King, R. B.; Sundaram, P. M. *J. Org. Chem.* **1984**, *49*, 1784–1789.

Table 1. Table of Crystallographic Data

compd	6a	7a	5[GaCl <sub>4</sub> ]
formula	C <sub>25</sub> H <sub>37</sub> N <sub>2</sub> P	C <sub>25</sub> H <sub>36</sub> ClN <sub>2</sub> P	C <sub>25</sub> H <sub>36</sub> Cl <sub>4</sub> GaN <sub>2</sub> P
<i>M</i>	396.55	431.00	607.08
cryst size/mm <sup>3</sup>	0.20 × 0.30 × 0.40	0.35 × 0.20 × 0.15	0.30 × 0.20 × 0.50
syst	monoclinic	monoclinic	monoclinic
space group	<i>P</i> 2 <sub>1</sub> / <i>n</i>	<i>P</i> 2 <sub>1</sub> / <i>c</i>	<i>P</i> 2 <sub>1</sub> / <i>n</i>
<i>a</i> /Å	15.710(5)	8.69(1)	9.884(3)
<i>b</i> /Å	9.66(1)	16.24(1)	21.189(4)
<i>c</i> /Å	15.93(2)	17.16(2)	14.639(4)
β/deg	91.48(6)	96.0(1)	95.12(2)
<i>V</i> /Å <sup>3</sup>	2417(7)	2409(8)	3054(2)
<i>Z</i>	4	4	4
<i>D</i> <sub>c</sub> /Mg m <sup>-3</sup>	1.089	1.188	1.320
<i>F</i> (000)	864	928	1256
μ/cm <sup>-1</sup>	1.210	2.351	13.18
no. of measd reflns	3768	3757	4677
no. of unique reflns	3619	3757	4388
no. of obsd reflns [ <i>I</i> > 3σ( <i>I</i> )]	1354	1437	1729
no. of params refined	262	263	299
100 <i>R</i>	5.38	4.81	3.93
100 <i>R</i> <sub>w</sub>	4.86	4.51	3.71
goodness of fit	2.47	2.04	1.73
max, min peak in difference map/e Å <sup>-3</sup>	0.32, -0.18	0.24, -0.22	0.46, -0.28

drybox. Reactions were performed in an evacuated (10<sup>-3</sup> Torr) reactor using established procedures.<sup>7</sup> Melting points were recorded on a Fisher-Johns apparatus and are uncorrected. Elemental analyses were performed by Beller Laboratories, Göttingen, Germany. Infrared spectra were recorded as Nujol mulls on CsI plates with a Nicolet 510P spectrometer. NMR spectra were recorded with a Bruker AC-250 spectrometer or a Nicolet AMX 400 spectrometer in 5 mm flame-sealed Pyrex tubes. All chemical shifts are reported in ppm relative to external standards, 85% H<sub>3</sub>PO<sub>4</sub> for <sup>31</sup>P, and TMS for <sup>1</sup>H and <sup>13</sup>C. Preparative procedures and characterization data for each compound are described below.

**[<sup>1</sup>Pr<sub>2</sub>N]<sub>2</sub>P-Fluorenyl 6a.** Fluorenyllithium was prepared *in situ* by slow addition of butyllithium in hexane (4.8 mL; 1.6 M) to fluorene (1.27 g, 7.64 mmol) in 30 mL of ether (0 °C). After it was stirred for 30 min, the bright yellow solution was added over ≈10 min to a stirred solution (0 °C) of [<sup>1</sup>Pr<sub>2</sub>N]<sub>2</sub>P-Cl in ≈30 mL of ether. Precipitation of LiCl occurred on warming to room temperature. Volatiles were removed *in vacuo*, the resulting solids were extracted with hexanes, and slow removal of the solvent gave pink crystals which were characterized as **6a**: yield 2.78 g, 7.02 mmol, 92%, mp 120–122 °C. Anal. Calcd: C, 75.72; H, 9.40; N, 7.06. Found: C, 75.80; H, 9.37; N, 6.89. IR (cm<sup>-1</sup>): 1343 m, 1297 s, 1192 m, 1175 s, 1155 m, 1117 m, 1092 m, 1018 m, 948 s, 865 m, 529 m, 520 s. NMR (CD<sub>2</sub>Cl<sub>2</sub>): <sup>31</sup>P{<sup>1</sup>H}, 71; <sup>1</sup>H, 7.86–7.27 (8 H, aromatic), 4.34 (s, 1H), 3.58–3.35 (multiplet, 4 H), 1.17 (d, <sup>3</sup>J<sub>HH</sub> = 7 Hz, 12 H), 0.77 (d, <sup>3</sup>J<sub>HH</sub> = 7 Hz, 12 H); <sup>13</sup>C{<sup>1</sup>H}, 126.7 (s), 126.5 (s), 126.3 (s), 119.7(s), 57.4 (d, <sup>1</sup>J<sub>PC</sub> = 35 Hz), 48.9 (d, <sup>2</sup>J<sub>PC</sub> = 13 Hz), 24.1 (d, <sup>3</sup>J<sub>PC</sub> = 7 Hz), 23.9 (d, <sup>3</sup>J<sub>PC</sub> = 7 Hz), quaternary carbons not observed. Reaction mixture: <sup>31</sup>P{<sup>1</sup>H}, 71 (quantitative).

**[Et<sub>2</sub>N]<sub>2</sub>P-Fluorenyl 6b.** Prepared in the same fashion as **6a**: yield, 1.27 g, 3.73 mmol, 50%, mp 121–123 °C. Elemental analysis not obtained, characterization made by comparison with **6a**. IR (cm<sup>-1</sup>): 1939 w, 1901 w, 1373 w, 1345 w, 1290 s, 1189 s, 1010 s, 904 s, 791 m, 776 m, 688 m, 661 m, 636 m, 504 m, 476 w, 427 w, 411 w. NMR (CD<sub>2</sub>Cl<sub>2</sub>): <sup>31</sup>P{<sup>1</sup>H}, 95; <sup>1</sup>H, 7.82–7.24 (8 H, aromatic), 4.75 (d, <sup>2</sup>J<sub>PH</sub> = 4 Hz, 1 H), 3.31–3.18 (multiplet, 8 H), 1.14 (t, <sup>3</sup>J<sub>HH</sub> = 7 Hz, 12 H); <sup>13</sup>C{<sup>1</sup>H}, 126.8, 126.6, 126.4, 119.7, 47.6 (d, <sup>1</sup>J<sub>PC</sub> = 21 Hz), 44.1 (d, <sup>2</sup>J<sub>PC</sub> = 17 Hz), 14.6 (d, <sup>3</sup>J<sub>PC</sub> = 4 Hz), quaternary carbons not observed.

**[<sup>1</sup>Pr<sub>2</sub>N]<sub>2</sub>P(Cl)=Fluorenylidene 7a.** CCl<sub>4</sub> (≈1 mL) was poured into a solution of **6a** (1.4 g, 3.6 mmol) in ≈20 mL of pentanes. The clear solution stood for 2 days at room tem-

perature, forming yellow block crystals. The supernatant was decanted from the crystalline material, and the crystals were washed with a small amount of pentanes and characterized as **7a** (0.47 g, 1.09 mmol, 30%); mp 207–209 °C (decomp). Anal. Calcd: C, 69.67; H, 8.42; N, 6.50. Found: C, 69.88; H, 8.38; N, 6.45. IR (cm<sup>-1</sup>): 1609 m, 1588 m, 1553 m, 1420 m, 1322 m, 1299 s, 1278 s, 1193 s, 1167 s, 1148 s, 1118 s, 1111 s, 889 m, 875 m, 855 m, 753 s, 694 s, 642 m, 599 m, 558 s, 542 s, 536 s, 525 m, 503 m, 469 s, 452 m, 425 m. NMR (CD<sub>2</sub>Cl<sub>2</sub>): <sup>31</sup>P{<sup>1</sup>H}, 53; <sup>1</sup>H (298 K), 8.33–7.31 (aromatic, 8 H), 3.84–3.60 (m, 4 H), 1.02 (d, <sup>3</sup>J<sub>HH</sub> = 7 Hz, 12 H), 0.98 (d, <sup>3</sup>J<sub>HH</sub> = 7 Hz, 12 H); <sup>13</sup>C{<sup>1</sup>H} (213 K), 140.7 (d, *J*<sub>PC</sub> = 21 Hz), 139.5 (d, *J*<sub>PC</sub> = 19 Hz), 130.7 (d, *J*<sub>PC</sub> = 18 Hz), 130.0 (d, *J*<sub>PC</sub> = 19 Hz), 122.8 (d, *J*<sub>PC</sub> = 29 Hz), 119.1 (d, *J*<sub>PC</sub> = 58 Hz), 118.2 (d, *J*<sub>PC</sub> = 68 Hz), 117.0 (d, *J*<sub>PC</sub> = 20 Hz), 66.3 (d, *J*<sub>PC</sub> = 201 Hz), aryl region is broad, at 293 K aryl region is broad, but alkyl region is sharp, 66.3 (d, *J*<sub>PC</sub> = 201 Hz), 50.0 (d, *J*<sub>PC</sub> = 4 Hz), 24.2 (d, *J*<sub>PC</sub> = 4 Hz), 23.4 (d, *J*<sub>PC</sub> = 4 Hz). Reaction mixture: <sup>31</sup>P{<sup>1</sup>H}, 53 (quantitative).

**[Et<sub>2</sub>N]<sub>2</sub>P(Cl)=Fluorenylidene 7b.** CCl<sub>4</sub> (≈1 mL) was added to a solution of **6b** (1.07 g, 3.14 mmol) in hexanes (25 mL), giving instantaneous precipitation. All volatiles were removed *in vacuo* and the yellow residue was recrystallized from benzene and characterized as **7b**, yield 1.10 g, 2.93 mmol, 90%, mp 103–104 °C. Elemental analyses were not obtained, and characterization was made by comparison with **7a**. IR (cm<sup>-1</sup>): 1610 m, 1588 m, 1557 w, 1421 s, 1356 s, 1326 s, 1289 s, 1234 m, 1203 s, 1153 s, 1115 m, 1095 m, 1061 s, 1035 s, 1022 s, 892 m, 788 s, 753 s, 704 s, 675 s, 597 w, 528 s, 504 m, 453 m, 422 m, 365 w, 332 w. NMR (CD<sub>2</sub>Cl<sub>2</sub>): <sup>31</sup>P{<sup>1</sup>H}, 58; <sup>1</sup>H, 8.09–7.09 (aromatic, 8 H), 3.52–3.20 (m, 8 H), 1.29 (t, *J*<sub>HH</sub> = 7 Hz, 12 H); <sup>13</sup>C{<sup>1</sup>H}, 124.4 (s), 118.7 (s), 117.8 (s), 64.5 (d, <sup>1</sup>J<sub>PC</sub> = 205 Hz), 40.8 (d, <sup>2</sup>J<sub>PC</sub> = 5 Hz), 13.5 (d, <sup>3</sup>J<sub>PC</sub> = 2 Hz), quaternary carbon nuclei were not observed.

**Reaction of [<sup>1</sup>Pr<sub>2</sub>N]<sub>2</sub>P(Cl)=Fluorenylidene 7a with GaCl<sub>3</sub>.** A solution of **7a** (0.21 g, 0.47 mmol) in benzene (≈20 mL) was added to a stirred solution of GaCl<sub>3</sub> (0.085 g, 0.47 mmol) in benzene (≈20 mL) in a 10 °C bath to give a white precipitate. After decantation of the solution, the solid was washed by back-distillation: mp 105 °C (decomp). IR (cm<sup>-1</sup>): 1305 m, 1195 m, 1165 m, 1149 m, 1140 m, 1110 m, 994 s, 972 s, 942 m, 799 m, 740 s, 681 m, 606 m, 558 m, 540 s, 366 s, 359 s, 345 s. NMR (CD<sub>2</sub>Cl<sub>2</sub>, -80 °C): <sup>31</sup>P{<sup>1</sup>H}, 71; <sup>13</sup>C and <sup>1</sup>H exhibit broad unresolved signals in the regions of those reported above. Solid state CP/MAS <sup>31</sup>P NMR 9.4 T: 72.2, 70.2, 68.7 (quadrupolar <sup>14</sup>N splitting). The white powder was (0.77 mmol) was dissolved in CH<sub>2</sub>Cl<sub>2</sub>/pentanes (75/25, ≈40 mL), and slow removal of solvent overnight yielded light pink crystals which were characterized as 9-(diisopropylamino)-10-

**Table 2. Positional Parameters and  $B(\text{eq})$  for 6a**

atom	<i>x</i>	<i>y</i>	<i>z</i>	$B(\text{eq})$
P(1)	0.4928(1)	0.1318(2)	0.6900(1)	3.5(1)
P(2)	0.5131(6)	0.147(1)	0.7807(5)	3.8(5)
N(1)	0.5172(3)	-0.0137(5)	0.7456(3)	3.9(3)
N(2)	0.5662(3)	0.2555(5)	0.7092(3)	3.8(3)
C(1)	0.3919(4)	0.1997(6)	0.7413(4)	4.1(3)
C(2)	0.3835(4)	0.2962(7)	0.8160(4)	4.1(4)
C(3)	0.4033(5)	0.2748(8)	0.9000(5)	6.0(5)
C(4)	0.3921(5)	0.382(1)	0.9566(4)	7.6(5)
C(5)	0.3589(6)	0.507(1)	0.9308(5)	7.5(5)
C(6)	0.3363(5)	0.5312(7)	0.8477(5)	5.7(4)
C(7)	0.3484(4)	0.4232(7)	0.7906(4)	4.1(4)
C(8)	0.3268(4)	0.4139(8)	0.7007(4)	4.2(4)
C(9)	0.2877(4)	0.5115(8)	0.6476(5)	5.6(4)
C(10)	0.2700(5)	0.474(1)	0.5656(6)	7.6(6)
C(11)	0.2913(5)	0.346(1)	0.5364(5)	7.2(6)
C(12)	0.3319(4)	0.2483(8)	0.5881(5)	5.6(4)
C(13)	0.3497(4)	0.2828(8)	0.6722(4)	4.0(4)
C(14)	0.5359(5)	-0.0323(9)	0.8350(5)	7.5(5)
C(15)	0.4670(5)	-0.1056(8)	0.8842(4)	7.0(5)
C(16)	0.6234(5)	-0.0938(8)	0.8550(5)	7.6(5)
C(17)	0.5035(5)	-0.1377(9)	0.6970(6)	8.3(6)
C(18)	0.5617(5)	-0.1617(8)	0.6268(5)	7.8(5)
C(19)	0.4131(6)	-0.1671(7)	0.6720(5)	7.8(5)
C(20)	0.6091(6)	0.2949(9)	0.6322(5)	7.6(5)
C(21)	0.5539(5)	0.3775(9)	0.5726(5)	8.9(5)
C(22)	0.6617(5)	0.189(1)	0.5923(5)	8.7(6)
C(23)	0.5962(6)	0.3277(8)	0.7836(5)	7.2(5)
C(24)	0.6838(5)	0.291(1)	0.8140(5)	9.1(6)
C(25)	0.5774(5)	0.4789(8)	0.7875(5)	8.6(6)

(diisopropylimino)-9,10-dihydro-9-phosphaphenanthrene tetrachlorogallate  $5[\text{GaCl}_4]$  (0.39 g, 0.64 mmol, 83%), mp 166–167 °C. Anal. Calcd: C, 49.46; H, 5.98; N, 4.61. Found: C, 49.23; H, 6.08; N, 4.54. IR ( $\text{cm}^{-1}$ ): 1582 s, 1195 s, 1167 s, 1138 s, 1113 s, 1017 s, 964 s, 874 m, 785 m, 758 s, 738 s, 687 m, 678 m, 517 m, 489 m, 456 m, 372 s. NMR ( $\text{CD}_2\text{Cl}_2$ , -80 °C):  $^{31}\text{P}\{^1\text{H}\}$ , 22;  $^1\text{H}$ , 8.03–7.17 (aromatic, 8 H), 4.79 (m, 1 H), 4.42 (m, 1 H), 3.22 (m, 1 H), 2.74 (m, 1 H), 2.01 (d,  $^3J_{\text{HH}} = 6.4$  Hz), 1.52 (d,  $^3J_{\text{HH}} = 6.1$  Hz), 1.44 (d,  $^3J_{\text{HH}} = 6.8$  Hz), 1.39 (d,  $^3J_{\text{HH}} = 6.0$  Hz), 1.07 (d,  $^3J_{\text{HH}} = 5.9$  Hz), 0.97 (d,  $^3J_{\text{HH}} = 5.9$  Hz), 0.48 (d,  $^3J_{\text{HH}} = 5.7$  Hz), -0.04 (d,  $^3J_{\text{HH}} = 6.0$  Hz) total integration 24 H;  $^{13}\text{C}\{^1\text{H}\}$ , 213.9 (d,  $^1J_{\text{PC}} = 89.2$  Hz, C=N), complex and unresolved. Reaction Mixtures:  $^{31}\text{P}\{^1\text{H}\}$ , 22 (quantitative).  $^{31}\text{P}\{^1\text{H}\}$  NMR studies of reactions between **7b** and  $\text{GaCl}_3$  in  $\text{CH}_2\text{Cl}_2$  reveal a single phosphorus-containing product (with a signal at  $\delta$  72) which remains unchanged for more than 1 month, but attempts at isolation produced oily materials. NMR studies of reactions between **7** and  $\text{HOSO}_2\text{CF}_3$  in  $\text{CD}_2\text{Cl}_2$  indicate quantitative formation of  $[(\text{Pr}_2\text{N})_2\text{P}(\text{Cl})\text{-fluorenyl}]\mathbf{8a}[\text{OSO}_2\text{CF}_3]$ ,  $^{31}\text{P}\{^1\text{H}\}$ , 71, and  $[(\text{Et}_2\text{N})_2\text{P}(\text{Cl})\text{-fluorenyl}]\mathbf{8b}[\text{OSO}_2\text{CF}_3]$ :  $^{31}\text{P}\{^1\text{H}\}$ , 72;  $^1\text{H}$ , 7.92–7.33 (8 H, aromatic), 5.74 (d,  $^2J_{\text{PH}} = 18$  Hz, 1 H), 3.17–2.93 (m, 8 H), 0.97 (t,  $J = 7$  Hz, 12 H);  $^{13}\text{C}\{^1\text{H}\}$ , 130.7 (d,  $J_{\text{PC}} = 3$  Hz), 128.7 (d,  $J_{\text{PC}} = 4$  Hz), 127.1 (d,  $J_{\text{PC}} = 4$  Hz), 121.6 (d,  $J_{\text{PC}} = 2$  Hz), 50.4 (d,  $^1J_{\text{PC}} = 89$  Hz), 42.1 (s), 12.5 (s), 12.4 (s). Multiplicity analysis (JMOD) confirms the assignment of the methine center.

### X-ray Crystallography

Crystals of  $5[\text{GaCl}_4]$ , **6a**, and **7a**, were obtained as described in the preparations of the compounds and were selected and mounted in Pyrex capillaries in the drybox. Unit cell parameters were obtained from the setting angles of a minimum of 16 carefully centered reflections having  $2\theta > 20^\circ$ ; the choice of space groups was based on systematically absent reflections and confirmed by the successful solution and refinement of the structures. All pertinent crystallographic data are summarized in Table 1.

Data were collected at room temperature ( $23 \pm 1$  °C) on a Rigaku AFC5R diffractometer using the  $\omega$ - $2\theta$  scan technique, and the stability of the crystals was monitored using three

**Table 3. Positional Parameters and  $B(\text{eq})$  for 7a**

atom	<i>x</i>	<i>y</i>	<i>z</i>	$B(\text{eq})$
Cl(1)	0.9978(2)	0.1301(1)	0.4849(1)	4.5(1)
P(1)	1.0162(2)	0.1962(1)	0.3821(1)	2.7(1)
N(1)	1.1880(6)	0.1710(3)	0.3596(3)	2.5(3)
N(2)	1.0098(6)	0.2946(3)	0.4094(3)	2.5(3)
C(1)	0.8624(8)	0.1699(4)	0.3177(4)	3.0(4)
C(2)	0.7895(9)	0.2204(5)	0.2562(4)	3.3(4)
C(3)	0.818(1)	0.3015(5)	0.2305(4)	4.9(4)
C(4)	0.728(1)	0.3328(5)	0.1663(5)	6.5(6)
C(5)	0.607(1)	0.2874(8)	0.1275(5)	7.5(7)
C(6)	0.578(1)	0.2087(7)	0.1515(6)	6.6(6)
C(7)	0.669(1)	0.1748(6)	0.2140(4)	4.2(5)
C(8)	0.787(1)	0.0890(5)	0.3105(4)	3.6(4)
C(9)	0.666(1)	0.0937(6)	0.2474(5)	4.4(5)
C(10)	0.570(1)	0.0246(7)	0.2272(6)	6.2(6)
C(11)	0.597(1)	-0.0464(7)	0.2689(7)	7.5(8)
C(12)	0.715(1)	-0.0526(6)	0.3287(6)	7.2(6)
C(13)	0.809(1)	0.0140(5)	0.3505(5)	5.3(5)
C(14)	0.872(1)	0.3156(4)	0.4513(4)	3.7(4)
C(15)	0.766(1)	0.3814(5)	0.4112(5)	6.0(5)
C(16)	0.909(1)	0.3355(5)	0.5366(5)	6.0(5)
C(17)	1.1459(9)	0.3494(4)	0.4102(4)	3.2(4)
C(18)	1.107(1)	0.4333(4)	0.3742(5)	5.7(5)
C(19)	1.243(1)	0.3600(5)	0.4886(4)	5.3(5)
C(20)	1.2213(9)	0.1495(4)	0.2787(4)	3.6(4)
C(21)	1.200(1)	0.2220(5)	0.2234(4)	5.3(5)
C(22)	1.137(1)	0.0743(5)	0.2430(5)	5.9(5)
C(23)	1.3229(9)	0.1599(4)	0.4209(4)	3.6(4)
C(24)	1.4648(9)	0.2088(5)	0.4029(4)	5.3(5)
C(25)	1.359(1)	0.0698(5)	0.4338(5)	6.4(5)

**Table 4. Positional Parameters and  $B(\text{eq})$  for  $5[\text{GaCl}_4]$** 

atom	<i>x</i>	<i>y</i>	<i>z</i>	$B(\text{eq})$
Ga(1)	0.2568(1)	-0.00658(5)	0.26644(7)	4.41(5)
Cl(1)	0.2365(3)	-0.0639(2)	0.3855(2)	9.9(2)
Cl(2)	0.2012(2)	0.0900(1)	0.2931(2)	8.2(2)
Cl(3)	0.4651(2)	-0.0077(1)	0.23112(2)	6.4(1)
Cl(4)	0.1238(3)	-0.0443(1)	0.1553(2)	7.9(2)
P(1)	0.8266(2)	-0.2057(1)	0.1404(1)	2.9(1)
N(1)	0.7488(6)	-0.3325(3)	0.1787(4)	3.0(3)
N(2)	0.7465(6)	0.1629(3)	0.0566(4)	3.2(3)
C(1)	0.7092(7)	-0.2749(4)	0.1591(5)	2.6(4)
C(2)	0.5627(7)	-0.2562(3)	0.1576(6)	2.6(4)
C(3)	0.4624(8)	-0.2810(4)	0.0950(6)	3.9(4)
C(4)	0.3305(9)	-0.2585(4)	0.0964(7)	4.9(5)
C(5)	0.2998(8)	-0.2130(5)	0.1561(7)	5.0(6)
C(6)	0.399(1)	-0.1877(4)	0.2167(6)	4.2(5)
C(7)	0.5350(8)	-0.2075(4)	0.2187(6)	3.1(4)
C(8)	0.6480(8)	-0.1763(3)	0.2777(5)	2.9(4)
C(9)	0.624(1)	-0.1500(4)	0.3617(7)	4.4(5)
C(10)	0.723(1)	-0.1170(4)	0.4147(6)	5.1(6)
C(11)	0.850(1)	-0.1109(4)	0.3832(6)	4.7(5)
C(12)	0.8773(8)	-0.1382(4)	0.3006(6)	3.5(5)
C(13)	0.7777(7)	-0.1706(4)	0.2462(5)	3.0(4)
C(14)	0.6540(8)	-0.1086(4)	0.0679(5)	3.6(4)
C(15)	0.5203(9)	-0.1140(4)	0.0073(6)	5.1(5)
C(16)	0.722(1)	-0.0459(4)	0.0533(6)	5.9(6)
C(17)	0.788(1)	-0.1726(4)	-0.0375(6)	4.7(5)
C(18)	0.739(1)	-0.2355(5)	-0.0751(6)	6.9(6)
C(19)	0.939(1)	-0.1648(6)	-0.0434(7)	8.4(8)
C(20)	0.8964(8)	-0.3527(4)	0.1835(6)	3.7(5)
C(21)	0.9539(8)	-0.3504(4)	0.0901(6)	4.6(5)
C(22)	0.9838(8)	-0.3184(4)	0.2578(6)	4.5(5)
C(23)	0.6530(8)	-0.3824(4)	0.2060(7)	4.2(5)
C(24)	0.649(1)	-0.4362(4)	0.1388(8)	7.3(6)
C(25)	0.692(1)	-0.4026(5)	0.3045(8)	7.4(7)

standard reflections; no significant decay was observed. Data were corrected for Lorentz and polarization effects; azimuthal scans of several reflections indicated no need for an absorption correction.

Structures were solved by direct methods<sup>8</sup> which revealed the positions of all non-hydrogen atoms. The non-hydrogen

(8) Busing, W. R., Martin, K. O.; Levy, H. A. ORFLS. A Fortran crystallographic least squares program. Report ORNL-TM-305; Oak Ridge National Laboratory: Oak Ridge, TN, 1962.

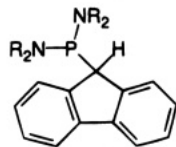


atoms were refined anisotropically. All of the hydrogen atoms were placed in geometrically calculated positions with a C–H distance of 0.95 Å. Their positions were not refined, and they were assigned fixed isotropic temperature factors with a value of  $1.2 \times B(\text{eq})$  of the atom to which it was bonded. The function minimized by full-matrix least squares was  $\sum w(\Delta|F|)^2$ ,  $w$  is the weight derived from counting statistics. Neutral atom scattering factors for non-hydrogen atoms were taken from Cromer and Waber,<sup>9</sup> and the scattering factors for hydrogen atoms were taken from Stewart, Davidson, and Simpson.<sup>10</sup> Anomalous dispersion effects were included in  $F_{\text{calc}}$ ;<sup>11</sup> the values for  $\Delta f'$  and  $\Delta f''$  were those of Cromer.<sup>12</sup> All calculations were performed using the TEXSAN<sup>13</sup> crystallographic software package of Molecular Structure Corporation.

In the structure of **6a** the phosphorus is pyramidal with interbond angles C(1)–P(1)–N(1), 103.8(3)°; C(1)–P(1)–N(2), 104.5(3)°, and N(1)–P(1)–N(2), 110.4(3)°. It is disordered with a second position P(2), roughly the mirror image of the pyramid, which gives the corresponding interbond angles to C(1), N(1), and N(2) of 100.0(5)°, 96.1(4)°, and 108.4(5)°, respectively. If the occupation of the two disordered sites P(1), P(2) is 80%:20%, then the thermal parameters of the two disordered phosphorus atoms are approximately equal ( $B(\text{eq}) = 3.5(1)$  and  $3.8(5)$ , respectively). The phosphorus atom can occupy these two disordered positions with minor adjustments of the position of C(1), N(1), and N(2) (P(1)–N(1)–C(14), etc.), there must be some significant adjustment in the position of at least one of the other substituents at these atoms. However, with disorder occupancies in the ratio of 4:1, these adjustments could not be reliably detected, and nonbonded contacts (particularly to C(14) and C(23)) to atom P(2) should be disregarded.

## Results and Discussion

**Fluorenylphosphine and Fluorenylidene-phosphorane Derivatives.** The fluorenylphosphorus linkage is readily obtained by the quantitative reaction of chlorodiaminophosphines with fluorenyllithium,<sup>3</sup> to give the fluorenyldiaminophosphines **6** as stable isolable



6

solids. Spectroscopic data are consistent with the observed crystal structure of **6a** illustrated in Figure 1, which shows a tetrahedral geometry for C(1) of the fluorenyl fragment. The average P–C bond length (1.99(7) Å) is comparable with those observed in pentamethylcyclopentadienylphosphorus compounds

(9) Cromer, D. T.; Waber, J. T. *International Tables for Crystallography*; The Kynoch Press: Birmingham, England, 1974; Vol. IV, Table 2.2A.

(10) Stewart, R. F.; Davidson, E. R.; Simpson, W. T. *J. Chem. Phys.* **1965**, *42*, 3175–3187.

(11) Ibers, J. A.; Hamilton, W. C. *Acta Crystallogr.* **1964**, *17*, 781–782.

(12) Cromer, D. T. *International Tables for X-ray Crystallography*; The Kynoch Press: Birmingham, England, 1974; Vol. IV, Table 2.3.1, pp 149–150 (Present distributor Kluwer Academic Publishers, Dordrecht).

(13) TEXSAN-TEXRAY Single-Crystal Structure Analysis Package, Version 5.0; Molecular Structure Corporation: The Woodlands, TX, 1989.

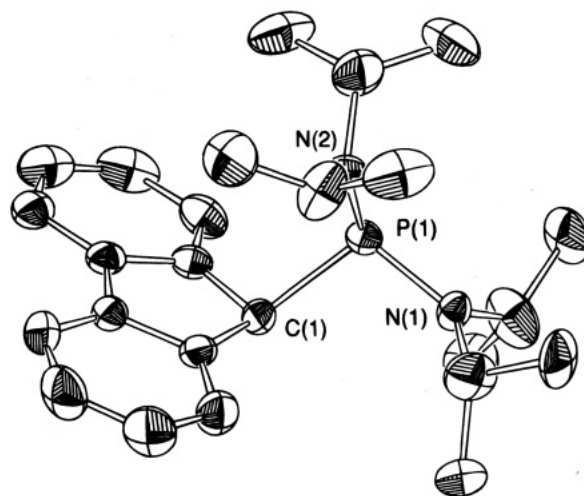


Figure 1. ORTEP view of  $[\text{Pr}_2\text{N}]_2\text{P}$ -fluorenyl **6a**.

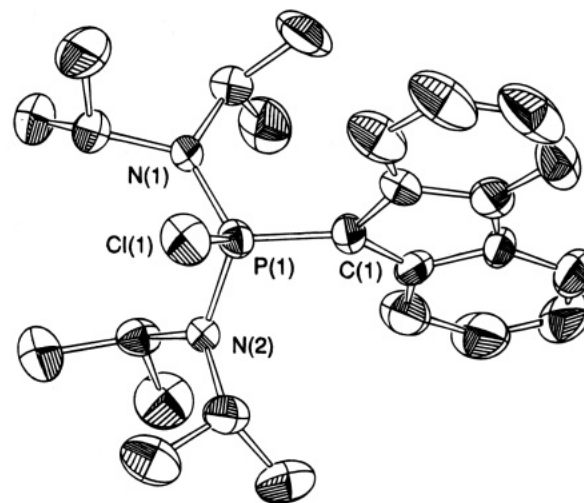


Figure 2. ORTEP view of  $[\text{Pr}_2\text{N}]_2\text{P}(\text{Cl})$ =fluorenylidene **7a**. Important bond lengths (Å) and angles (deg): P(1)–C(1), 1.698(7); P(1)–Cl(1), 2.085(3); P(1)–N(1), 1.634(6); P(1)–N(2), 1.668(5); Cl(1)–P(1)–N(1), 102.9(2); Cl(1)–P(1)–N(2), 104.4(2); Cl(1)–P(1)–C(1), 107.3(3); N(1)–P(1)–N(2), 111.4(3); N(1)–P(1)–C(1), 117.3(3); N(2)–P(1)–C(1), 112.1(3); P(1)–C(1)–(2), 126.4(6); P(1)–C(1)–C(8), 126.5(6); C(2)–C(1)–C(8), 106.9(6); Cl(1)–P(1)–C(1)–C(2) torsion angle, 151.5(6)°; Cl(1)–P(1)–C(1)–C(8) torsion angle, –33.7(7)°.

( $\text{Cp}^*\text{P}=\text{PCp}^*$ , 1.893(7) and 1.883(7) Å,<sup>14</sup> [ $\text{Cp}^*\text{P}=\text{P}(\text{N}(\text{H})-\text{Bu})[\text{AlCl}_4]$ , 1.990(2) Å<sup>15</sup>). Although each of these compounds exhibits ring whizzing by NMR spectroscopy in solution and in the solid state, the phosphorus atom is attached to a specific out-of-plane distorted carbon center of the  $\text{Cp}^*$  ring indicating a monohapto interaction. Recognizing fluorenyl as a derivative of cyclopentadienyl, **6a** may be considered an intimate ion-pair coordination complex involving the fluorenyl anion and the tetraisopropylidiaminophosphonium cation,  $[\text{Pr}_2\text{N}]_2\text{P}^+$ . However, the  $^{31}\text{P}$  NMR chemical shift for **6a** (71 ppm) is substantially upfield from that of the free cation ( $[(\text{Pr}_2\text{N})_2\text{P}][\text{GaCl}_4]^{31}\text{P}$ , 313 ppm)<sup>16</sup> but is comparable with the DBU complex ( $[(\text{Pr}_2\text{N})_2\text{PDBU}][\text{PF}_6]$ , 108 ppm).<sup>17</sup>

(14) Jutzi, P.; Meyer, U.; Krebs, B.; Dartmann, M. *Angew. Chem., Int. Ed. Engl.* **1986**, *25*, 919–921.

(15) Gudat, D.; Nieger, M.; Niecke, E. *J. Chem. Soc., Dalton Trans.* **1989**, 693–700.



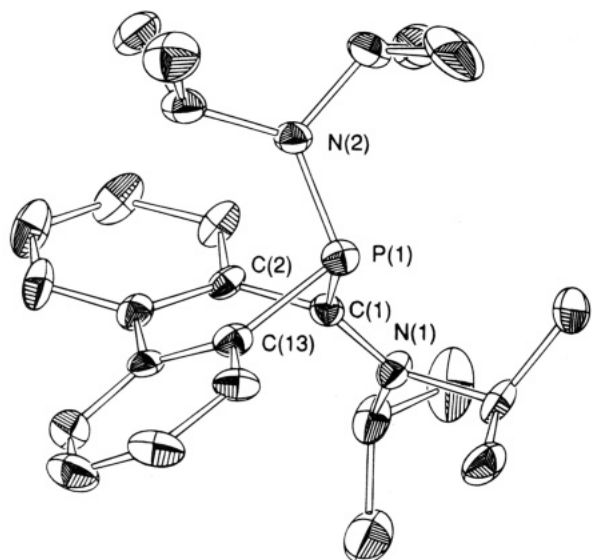
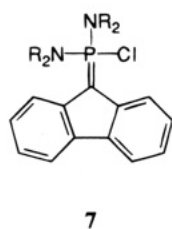


**Figure 3.** ORTEP view of cation **5**. Important bond lengths (Å) and angles (deg): P(1)–N(2), 1.667(6); P(1)–C(1), 1.905(8); P(1)–C(13), 1.822(8); N(1)–C(1), 1.305(9); N(2)–P(1)–C(1), 105.6(3); N(2)–P(1)–C(13), 105.0(3); C(1)–P(1)–C(13), 88.8(3);  $\Sigma$  angles at N(1), 359.9(6);  $\Sigma$  angles at N(2), 359.2(5);  $\Sigma$  angles at C(1), 359.8(6).

Both derivatives of **6** are quantitatively oxidized by  $\text{CCl}_4$ , as described by Appel,<sup>18</sup> to give the phosphoranes **7**.  $^1\text{H}$  and  $^{13}\text{C}$  NMR spectra show two types of isopropyl



groups for **7a**, implying restricted rotation about the N–P bond. At room temperature a single line is observed for the ethyl groups of **7b**, but this broadens on cooling implying a slowing down of a dynamic process, possibly a restriction of the N–P bond rotation. The X-ray crystal structure of **7a** (Figure 2) confirms the steric crowding and reveals a short P–C bond (1.698(7) Å), typical of methylenephosphoranes ( $^t\text{Bu}_2(\text{Cl})\text{P}=\text{CPh}_2$ ,<sup>19</sup> 1.673(5), 1.667(5), and 1.668(5) Å;  $\text{Ph}_3\text{P}=\text{C}(\text{cyclopropyl})$ ,<sup>20</sup> 1.696(6) Å;  $^i\text{Pr}_3\text{P}=\text{CMe}_2$ ,<sup>21</sup> 1.731(3) Å). The ylidic carbon center is planar (sum of the bond angles,  $360^\circ$ ), consistent with cyclopentadiene substituted phosphoranes.<sup>22</sup> Interestingly, the chlorine atom of **7a** is almost in the plane defined by the fluorenylidene substituent (Cl–P–C<sub>1</sub>–C<sub>2</sub> torsion,  $151.5(6)^\circ$ ; Cl–P–C<sub>1</sub>–C<sub>8</sub> torsion,  $-33.7(7)^\circ$ ). Such an

(16) Burford, N.; Losier, P.; Kyrimis, V.; Macdonald, C.; Bakshi, P. K.; Cameron, T. S. *Inorg. Chem.* **1994**, *33*, 1434–1439.

(17) Reed, R.; Reau, R.; Dahan, F.; Bertrand, G. *Angew. Chem., Int. Ed. Engl.* **1993**, *32*, 399–401.

(18) Appel, R.; Peters, J.; Schmitz, R. Z. *Anorg. Allg. Chem.* **1981**, *475*, 18–26.

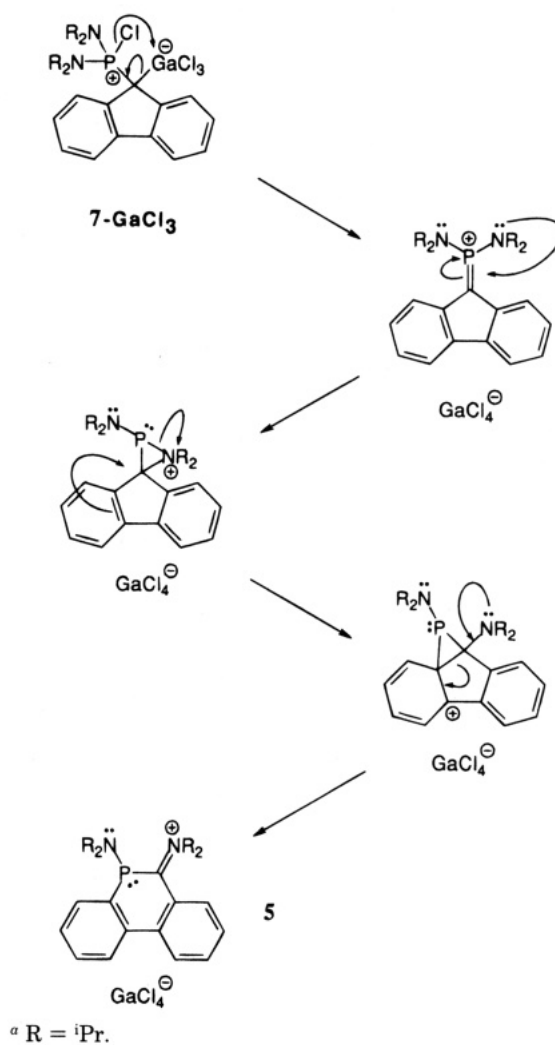
(19) Grützmacher, H.; Pritzkow, H. *Angew. Chem., Int. Ed. Engl.* **1992**, *31*, 99–101.

(20) Schmidbauer, H.; Schier, A.; Milewski-Mahrla, B.; Schubert, U. *Chem. Ber.* **1982**, *1155*, 722–730.

(21) Schmidbauer, H.; Schier, A.; Frazao, C.; Müller, G. *J. Am. Chem. Soc.* **1986**, *108*, 976–982.

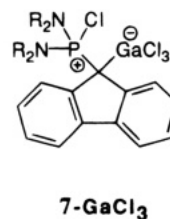
(22) Bacharach, S. M.; Nitsche, C. I. In *The Chemistry of Organophosphorus Compounds*; Hartley, F. R., Ed; Wiley & Sons: Toronto, 1994; Vol. 13, p 280.

## Scheme 1



arrangement precludes interaction between the  $\pi$ -network of the fluorenylidene and the  $\sigma^*$  orbital of the P–Cl bond (hyperconjugation), as speculated for other methylenephosphoranes  $^t\text{Bu}_2(\text{Cl})\text{P}=\text{CPh}_2$ , 2.195(2), 2.228(2), and 2.235(2) Å,<sup>19</sup> and is manifest in the short P–Cl bond of 2.085(3) Å.

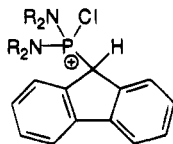
**Fluorenylphosphonium Derivatives.** Reactions of **7** with  $\text{GaCl}_3$  produce white solids, which are quantitatively precipitated from benzene and are soluble in polar solvents such as  $\text{CH}_2\text{Cl}_2$ . In contrast to previous observations for reactions of **7a** with  $\text{AlCl}_3$ ,<sup>4</sup> and the ionic structures observed for  $[\text{tBu}_2\text{P}=\text{C}(\text{SiMe}_3)_2][\text{AlCl}_4]$  from the reaction of  $^t\text{Bu}_2(\text{Cl})\text{P}=\text{C}(\text{SiMe}_3)_2$  with  $\text{AlCl}_3$ ,<sup>23</sup>  $^{31}\text{P}$  NMR chemical shifts in solution (**7a**– $\text{GaCl}_3$ , 71



ppm; **7b**– $\text{GaCl}_3$ , 72 ppm) and in the solid state (**7a**– $\text{GaCl}_3$ , 70 ppm) are comparable to the covalent pos-

(23) Grützmacher, H.; Pritzkow, H. *Angew. Chem., Int. Ed. Engl.* **1991**, *30*, 709–710.

phorane **7** precursor (53 ppm) and are substantially upfield from those of the established phosphonium cations (cf. [ ${}^i\text{Pr}_2\text{N}$ ] ${}_2\text{P}=\text{C}(\text{SiMe}_3)_2$ ] $^+$ , 130 ppm;<sup>5</sup> [ ${}^t\text{Bu}_2\text{P}=\text{CPh}_2$ ] $^+$ , 183 ppm<sup>19</sup>). Although it has not been possible to obtain informative  ${}^1\text{H}$  and  ${}^{13}\text{C}$  NMR data for **7a-GaCl<sub>3</sub>** or **7b-GaCl<sub>3</sub>** and recrystallization has been unsuccessful, we speculate the formation of coordination complexes involving a carbon-gallium coordinate bond, similar to those reported for other ylide/Lewis acid adducts.<sup>24</sup> Further convincing support for this phosphonium assignment is provided by the reactions of **7** with  $\text{HOSO}_2\text{CF}_3$  which give the corresponding phosphonium cations **8** exhibiting identical  ${}^{31}\text{P}$  NMR chemical shifts (**8a**, 71 ppm; **8b**, 72 ppm).



8

**Isomerism of a Fluorenylphosphonium.** Solutions of **7a-GaCl<sub>3</sub>** in  $\text{CH}_2\text{Cl}_2$  quickly become red, and a new  ${}^{31}\text{P}$  NMR signal appears at 21 ppm coincident with the loss of the signal at 71 ppm (reaction complete within 8 h). A red crystalline material isolated in high yield has been characterized as the tetrachlorogallate salt of the tricyclic iminumphosphine **5**. A crystallographic view of the cation is shown in Figure 3. The salt is isomeric with **7a-GaCl<sub>3</sub>** and is the result of heterolytic cleavage of the C-Ga and P-Cl bonds with subsequent formation of  $\text{GaCl}_4^-$ , a 1,3-shift of a tetra-

isopropylidamino substituent from phosphorus to the unique carbon of the fluorenyl substituent, and a reductive ring insertion of the phosphorus center into the C1-C2 bond of **7**. In Scheme 1, we provide a speculative mechanism with **4** undergoing a reductive cyclization through an ammonium center followed by a two-step insertion of the resulting phosphine center into the C1-C2 bond *via* an arenium intermediate. It should be noted that the oxime of fluorenone undergoes an analogous ring expansion in the Beckmann rearrangement.<sup>25</sup>

The isomerization of cation **4** is consistent with previous observations for tricoordinate phosphonium cations which undergo intramolecular electrocyclic ring closure,<sup>26</sup> adopt "covalent alternative" structures<sup>27</sup> or rearrange in other ways.<sup>19</sup> The quantitative rearrangement described here is unique in terms of the nature of the bonds broken and formed and is unprecedented in the chemistry of phosphorus ylides despite extensive studies.<sup>24</sup>

**Acknowledgment.** This work has been funded by the Natural Sciences and Engineering Research Council of Canada. We thank the Atlantic Region Magnetic Resonance Centre for the use of instrumentation.

**Supporting Information Available:** Tables of positional parameters, anisotropic thermal parameters, and intramolecular bond distances and angles for [ ${}^i\text{Pr}_2\text{N}$ ] ${}_2\text{P}$ -fluorenyl **6a**, [ ${}^i\text{Pr}_2\text{N}$ ] ${}_2\text{P}$ -fluorenylidene **7a**, and 9-(diisopropylamino)-10-(diisopropyliminio)-9,10-dihydro-9-phosphaphenanthrene tetrachlorogallate **5**[ $\text{GaCl}_4$ ] (34 pages). Ordering information is given on any current masthead page.

OM9501182

(25) Moore, F. J.; Huntress, E. H. *J. Am. Chem. Soc.* **1927**, *49*, 2618-2624.

(26) Heim, U.; Pritzkow, H.; Fleischer, U.; Grützmaier, H. *Angew. Chem., Int. Ed. Engl.* **1993**, *32*, 1359-1361.

(27) Burford, N.; Spence, R. E. v. H.; Richardson, J. F. *J. Chem. Soc., Dalton Trans.* **1991**, 1615-1619.

(24) *Ylides and Imines of Phosphorus*; Johnson, A. W., Ed.; Wiley: New York, 1993; p 153. Schmidbaur, H.; Fuller, H.-J.; Kohler, F. H. *J. Organomet. Chem.* **1975**, *99*, 353-357. Alcaraz, G.; Reed, R.; Baccaredo, A.; Bertrand, G. *J. Chem. Soc., Chem. Commun.* **1993**, 1354-1355.

# 47-Electron Organometallic Clusters. Synthesis, Characterization, and Reactivity toward Electrophiles/Oxidants of $\text{H}_2\text{Ru}_3(\text{RC}_2\text{R}')(\text{CO})_6(\text{PPh}_3)_3$ and Crystal Structures of $(\mu\text{-H})_2\text{Ru}_3(\mu_3\text{-}\eta^2\text{-EtCCEt})(\text{CO})_7(\text{PPh}_3)_2$ and $(\mu\text{-H})_2\text{Ru}_3(\mu_3\text{-}\eta^2\text{-EtCCEt})(\text{CO})_6(\text{PPh}_3)_3\cdot 3\text{CH}_2\text{Cl}_2$

Witold Paw, Charles H. Lake, Melvyn Rowen Churchill,\* and Jerome B. Keister\*

Department of Chemistry, University at Buffalo, State University of New York, Buffalo, New York 14260-3000

Received February 17, 1995\*

Electrochemical and chemical oxidations of 48-electron clusters  $(\mu\text{-H})_2\text{Ru}_3(\text{RCCR}')(\text{CO})_6(\text{PPh}_3)_3$  ( $\text{RCCR}' = \text{EtCCEt}, \text{HCCOEt}, \text{PhCCPh}$ ) give unstable radical cations. The radical cation derived from  $(\mu\text{-H})_2\text{Ru}_3(\text{EtCCEt})(\text{CO})_6(\text{PPh}_3)_3$  decomposes in the presence of halide sources primarily by disproportionation to  $[(\mu\text{-H})_2\text{Ru}_3(\mu\text{-X})(\text{EtCCEt})(\text{CO})_6(\text{PPh}_3)_3]^+$  ( $\text{X} = \text{F}, \text{Cl}$ ). Electrophilic additions using  $\text{Cl}_2$ ,  $\text{I}_2$ , and  $\text{CF}_3\text{CO}_2\text{H}$  give the analogous  $[(\mu\text{-H})_2\text{Ru}_3(\mu\text{-X})(\text{EtCCEt})(\text{CO})_6(\text{PPh}_3)_3]^+$  ( $\text{X} = \text{Cl}, \text{I}, \text{H}$ ). Although the 48/46-electron couple  $[\text{Fe}_3(\text{RCCR}')(\text{CO})_9]^{2-}/\text{Fe}_3(\text{RCCR}')(\text{CO})_9$  is well-documented, and the 46-electron cluster  $[\text{H}_2\text{Ru}_3(\text{HC}_2\text{CMe}_3)(\text{CO})_{9-n}(\text{PPh}_3)_n]^{2+}$  has been reported to be stable, there is no evidence for formation of 46-electron  $[\text{H}_2\text{Ru}_3(\text{RCCR}')(\text{CO})_6(\text{PPh}_3)_3]^{2+}$  by two-electron oxidation of  $(\mu\text{-H})_2\text{Ru}_3(\text{RCCR}')(\text{CO})_6(\text{PPh}_3)_3$ . Two crystal structures are reported. For the diphosphine derivative  $(\mu\text{-H})_2\text{Ru}_3(\text{EtCCEt})(\text{CO})_7(\text{PPh}_3)_2$ , the single Ru(1)–Ru(3) bond length is 2.757(2) Å while the hydrido-bridged distances are Ru(1)–Ru(2) = 2.889(2) Å and Ru(2)–Ru(3) = 2.993(2) Å. The EtCCEt ligand is  $\sigma$ -bonded to Ru(2) and Ru(3) (Ru(2)–C(2) = 2.118(8) Å and Ru(3)–C(1) = 2.123(8) Å) and  $\pi$ -bonded to Ru(1) (Ru(1)–C(1) = 2.338(7) Å and Ru(1)–C(2) = 2.295(9) Å). One  $\text{PPh}_3$  ligand occupies an equatorial site on Ru(1); the second occupies an axial site on Ru(2), trans to the Ru(2)–alkyne  $\sigma$ -bond. The single Ru(1)–Ru(3) bond length for  $(\mu\text{-H})_2\text{Ru}_3(\text{EtCCEt})(\text{CO})_6(\text{PPh}_3)_3\cdot 3\text{CH}_2\text{Cl}_2$  is 2.744(1) Å while the hydrido-bridged distances are Ru(1)–Ru(2) = 2.891(1) Å and Ru(2)–Ru(3) = 3.077(1) Å. The EtCCEt ligand is bonded in the same  $2\sigma, \pi$ -manner as for the previous structure. Two  $\text{PPh}_3$  ligands occupy those same two sites as in the diphosphine complex (equatorial on Ru(1), axial on Ru(2)), while the third occupies a close-to-equatorial site on Ru(3). Hydride ligands were located and refined in each structural study.

## Introduction

Electrochemical studies of organometallic clusters have received increasing attention because of the importance of odd-electron intermediates in many reaction mechanisms and also because of examples of structural changes of the metal cluster framework induced by electrochemical oxidations or reductions.<sup>1</sup> One couple for which structural rearrangement has been demonstrated is the  $\text{Fe}_3(\text{C}_2\text{R}_2)(\text{CO})_9/[\text{Fe}_3(\text{C}_2\text{R}_2)(\text{CO})_9]^{2-}$  system. The 46-electron cluster  $\text{Fe}_3(\text{C}_2\text{R}_2)(\text{CO})_9$  has a closo structure in which the C–C bond is perpendicular to one Fe–Fe bond, whereas the 48-electron cluster  $[\text{Fe}_3(\text{C}_2\text{R}_2)(\text{CO})_9]^{2-}$  has a nido structure with the C–C bond parallel to one Fe–Fe bond. Reduction of  $\text{Fe}_3(\text{C}_2\text{R}_2)(\text{CO})_9$  proceeds in two reversible 1-electron steps.<sup>2</sup> Very recently an example of a 46-electron triosmium alkyne cluster was reported, and the cyclic voltammogram of this compound displays a reversible two-electron reduction.<sup>3</sup> The reversible redox chemistry of the 46/48-electron clusters  $\text{M}_3(\text{C}_2\text{R}_2)(\text{CO})_9^{0/2-}$  suggested

that it might be possible to generate an analogous couple by oxidation of the 48-electron clusters  $\text{H}_2\text{Ru}_3(\text{C}_2\text{R}_2)(\text{CO})_9$  or substituted derivatives. In fact,  $[\text{H}_2\text{Ru}_3(\text{HC}_2\text{CMe}_3)(\text{CO})_{9-n}(\text{PR}_3)_n]^{2+}$  had been reported to be formed by protonation of  $\text{HRu}_3(\text{C}_2\text{CMe}_3)(\text{CO})_{9-n}(\text{PR}_3)_n$ .<sup>4</sup>

In this paper we report on the chemical and electrochemical oxidations of the 48-electron clusters  $\text{H}_2\text{Ru}_3(\text{RC}_2\text{R}')(\text{CO})_{9-n}(\text{PPh}_3)_n$ . The electronic properties of these clusters are expected to depend significantly upon the alkyne substituents R and R' and the degree of phosphine substitution. In earlier studies we showed that 1-electron oxidations of members of the series  $\text{H}_3\text{Ru}_3(\text{CX})(\text{CO})_{9-n}(\text{PPh}_3)_n$  ( $n = 0\text{--}3$ )<sup>5</sup> and  $\text{HRu}_3(\text{XCCR}')(\text{CO})_{9-n}(\text{PPh}_3)_n$  ( $n = 0\text{--}3$ )<sup>6</sup> produced moder-

(3) Osella, D.; Pospisil, L.; Fiedler, J. *Organometallics* 1993, 12, 3140.

(4) (a) Barner-Thorsen, C.; Rosenberg, E.; Saatjian, G.; Aime, S.; Milone, L.; Osella, D. *Inorg. Chem.* 1981, 20, 1592. (b) Rosenberg, E.; Anslin, E. V.; Barner-Thorsen, C.; Aime, S.; Osella, D.; Gobetto, R.; Milone, L. *Organometallics* 1984, 3, 1790.

(5) (a) Feighery, W. G. Ph.D. Thesis, State University of New York at Buffalo, 1990. (b) Feighery, W. G.; Allendoerfer, R. D.; Keister, J. B. *Organometallics* 1990, 9, 2424. (c) Churchill, M. R.; Lake, C. H.; Feighery, W. G.; Keister, J. B. *Organometallics* 1991, 10, 2384.

(6) (a) Yao, H. Ph.D. Thesis, State University of New York at Buffalo, 1994. (b) Yao, H.; McCargar, R. D.; Allendoerfer, R. D.; Keister, J. B. *Organometallics* 1993, 12, 4283.

\* Abstract published in *Advance ACS Abstracts*, July 1, 1995.

(1) (a) *Organometallic Radical Reactions*; Trogler, W. C., Ed.; Elsevier: Amsterdam, 1990. (b) Tyler, D. R. *Prog. Inorg. Chem.* 1988, 36, 125. (c) Geiger, W. E. *Prog. Inorg. Chem.* 1985, 33, 275.

(2) Osella, D.; Gobetto, R.; Montangero, P.; Zanello, P.; Cinquantini, A. *Organometallics* 1986, 5, 1247.

ately stable radical cations in which the stabilities of these radicals strongly depend upon the  $\pi$ -donor ability of the X group and the degree of phosphine substitution. Similar electronic stabilizations are expected for the alkyne clusters.

### Experimental Section

**Starting Materials.**  $\text{Ru}_3(\text{CO})_{12}$  was prepared as previously described.<sup>7</sup> Bis(triphenylphosphine)nitrogen(1+) chloride, [PPN]Cl, was purchased from Alfa Products. Tetrabutylammonium tetrafluoroborate, TBATFB, was prepared from tetrabutylammonium bromide and tetrafluoroboric acid, crystallized three times from ethyl acetate/pentane solution, and vacuum-dried. Tris(4-bromophenyl)ammonium hexachloroantimonate (TBPAHCA) was obtained from Aldrich. Tetrabutylammonium tetraphenylborate ( $\text{Bu}_4\text{NBPh}_4$ ) and tetrakis(3,5-bis(trifluoromethyl)phenyl)borate ( $\text{Bu}_4\text{NBAr}'_4$ , where  $\text{Ar}' = 3,5\text{-(CF}_3)_2\text{C}_6\text{H}_3$ ) were prepared from tetrabutylammonium bromide and sodium tetraphenylborate or sodium tetrakis(3,5-bis(trifluoromethyl)phenyl)borate, respectively.  $\text{NaBAR}'_4$  was prepared according to the literature procedure.<sup>29</sup>  $\text{FcPF}_6$  and  $\text{FcBAR}'_4$  ( $\text{Fc} = \text{ferrocenium}$ ) were obtained by oxidation of ferrocene with  $\text{H}_2\text{SO}_4$  and precipitation with  $\text{KPF}_6$  and with  $\text{NaBAR}'_4$ , respectively.

The clusters  $\text{H}_2\text{Ru}_3(\text{RCCR}')(\text{CO})_9$  ( $\text{R} = \text{R}' = \text{Et}$ ;  $\text{R} = \text{H}$ ,  $\text{R}' = \text{OEt}$ ) were prepared using the general halide-promoted synthesis reported by Lavigne et al.;<sup>8</sup> full details are included as supporting information.

**Solvents.** Tetrahydrofuran and dichloromethane were distilled from calcium hydride. Diethyl ether (Mallinckrodt) was taken from a freshly opened bottle. Acetonitrile (Baker), methanol (Baker), hexanes (Fisher), and cyclohexane (Fisher) were used without purification.

**General Considerations.** All reactions were carried out using standard Schlenk techniques. Products were isolated and purified by thin-layer chromatography (TLC) on silica gel with hexanes/dichloromethane mixtures as eluents and occasionally by recrystallization from methanol/dichloromethane solutions.

Elemental analyses were obtained from Galbraith Laboratories, Inc., or Oneida Research Services, Inc.

**Physical Methods of Characterization.** Infrared spectra in the carbonyl region were recorded with a Nicolet Magna 550 FTIR instrument with a Beckman 4250 spectrophotometer as cyclohexane solutions and were referenced with the  $2138.5\text{ cm}^{-1}$  absorption due to cyclohexane.  $^1\text{H}$  NMR spectra were obtained on Varian Gemini 300 or VXR-400s instruments (low temperature) in deuteriochloroform and with TMS as reference.  $^{31}\text{P}$  and  $^{19}\text{F}$  NMR spectra were obtained on a VXR-400s instrument in deuteriochloroform, and chemical shifts are referenced to ortho-phosphoric acid and  $\text{CFCl}_3$ , respectively. EPR spectra were recorded on an IBM/Bruker X-band ER200 SRC spectrometer with a microwave power of 20 mW in methylene chloride solution at 250 K. Mass spectra with field desorption (FD) or fast atom bombardment (FAB) were obtained on a VG 70-SE spectrometer.

**Electrochemistry.** All electrochemical experiments were performed on a BAS-100 electrochemical analyzer. Measurements were made in dichloromethane with a supporting electrolyte concentration of 0.1 M. The concentration of analyte was  $10^{-3}$  M. Electrodes used: working, 5 mm platinum disk; pseudo-reference, silver wire; auxiliary, platinum wire. For bulk electrolysis, a large Pt basket electrode was used. Compensation for  $iR$  drop was employed for all measurements. All potential values were referenced to the fer-

rocene/ferrocenium couple (0 V).<sup>9</sup> The potential reproducibility of the latter was checked before and after the actual measurement. Unless otherwise specified, the electrolyte is tetrabutylammonium tetrafluoroborate, TBATFB.

**Synthesis of  $\text{H}_2\text{Ru}_3(\text{EtC}_2\text{Et})(\text{CO})_7(\text{PPh}_3)_2$ .** A solution of 72 mg (0.11 mmol) of  $\text{H}_2\text{Ru}_3(\text{EtC}_2\text{Et})(\text{CO})_9$  in 15 mL of THF was added to a solution of 42 mg (0.38 mmol) of  $\text{Me}_3\text{NO}\cdot 2\text{H}_2\text{O}$  in 10 mL of acetonitrile. After 1 min  $\text{PPh}_3$  (90 mg, 0.34 mmol) was added. The solution was stirred under nitrogen for 2 h at room temperature, during which time the solution darkened (from yellow to orange). Then the solution was evaporated to dryness on a rotary evaporator and the products were separated by TLC. The reaction gave substantially one product, which tended to decompose on a plate. Because of this, a higher polarity eluent was used (50–100% dichloromethane/hexanes). The compound was crystallized from dichloromethane/methanol solution as orange crystals. Some were well-formed and suitable for X-ray analysis. Yield: 76 mg, 61%. Anal. Calcd for  $\text{C}_{49}\text{H}_{42}\text{O}_7\text{P}_2\text{Ru}_3$ : C, 53.12; H, 3.82. Found: C, 52.99; H, 3.83. IR ( $\text{C}_6\text{H}_{12}$ ): 2053 s, 2026 s, 1998 s, 1970 m, 1945  $\text{cm}^{-1}$ .  $^1\text{H}$  NMR ( $\text{CDCl}_3$ , 17 °C): 7.5–7.1 (m, 30H), 3.41 (s, br, 1H), 2.83 (s, br, 1H), 2.59 (s, br, 1H), 1.41 (t, 3H,  $J_{\text{HH}} = 7.2$  Hz), 1.30 (s, br, 1H), 1.03 (s, br, 3H), -14.7 (s, br, 1H), -19.8 (s, br, 1H) ppm.  $^1\text{H}$  NMR ( $\text{CDCl}_3$ , -20 °C): 7.5–7.0 (m, 30H), 3.40 (m, 1H), 2.85 (m, 1H), 2.54 (m, 1H), 1.38 (t, 3H,  $J_{\text{HH}} = 7.2$  Hz), 1.26 (m, 1H), 1.00 (t, 3H,  $J_{\text{HH}} = 7.2$  Hz), -14.80 (s, 1H), -19.95 (d, 1H,  $J_{\text{HP}} = 14.4$  Hz) ppm.  $^{31}\text{P}$  NMR ( $\text{CDCl}_3$ , 17 °C): 30.85 (s, 1P), 29.49 (s, 1P) ppm. MS (FAB):  $m/e$  1110 ( $^{102}\text{Ru}_3$ ). CV(100 mV/s): irreversible oxidation peak at  $E_{\text{p,a}} = +260$  mV.

**Synthesis of  $\text{H}_2\text{Ru}_3(\text{RC}_2\text{R}')(\text{CO})_6(\text{PR}_3)_3$ .** In a three-necked, round-bottomed flask equipped with an addition funnel and reflux condenser  $\text{H}_2\text{Ru}_3(\text{RC}_2\text{R}')(\text{CO})_9$  (e.g.,  $\text{R} = \text{R}' = \text{Et}$ ; 150 mg, 0.23 mmol) was dissolved in 50 mL of THF. The solution was heated to reflux, and then a degassed solution of 3 molar equiv (e.g., 86 mg, 0.77 mmol) of  $\text{Me}_3\text{NO}\cdot 2\text{H}_2\text{O}$  and >3 molar equiv (e.g. 0.94 mmol) of  $\text{PR}_3$  in THF was added dropwise over a 15 min period. The solution changed from yellow to orange-red. After 1 h the volume was decreased to ca. 3 mL by rotary evaporation. The solution was applied to a silica gel TLC plate, and the components were separated by TLC (dichloromethane/hexane 2:1).

**$\text{H}_2\text{Ru}_3(\text{EtC}_2\text{Et})(\text{CO})_6(\text{PPh}_3)_3$ .** Crystallization from dichloromethane/methanol gave red-orange crystals of the trisubstituted cluster in 80–90% yield. (Occasionally the formation of the disubstituted cluster in less than 10% yield was observed.) Some crystals were well-formed and suitable for X-ray analysis. After crystallization all samples contain a significant amount of dichloromethane (three molecules per cluster molecule in the crystal lattice). Drying under vacuum removes some of the solvent, but usually NMR spectra show the presence of residual dichloromethane. Anal. Calcd for  $\text{C}_{66}\text{H}_{57}\text{O}_6\text{P}_3\text{Ru}_3$ : C, 59.06; H, 4.28. Found (1): C, 57.06; H, 4.09. Found (2): C, 57.93; H, 4.28. Analyses are consistent with some content of dichloromethane: 0.7 equiv of dichloromethane for analysis 1 theoretical: C, 57.15; H, 4.20) and 0.4 equiv of dichloromethane for analysis 2 (theoretical: C, 57.94; H, 4.23). IR ( $\text{CH}_2\text{Cl}_2$ ): 2021 vw, 2005 s, 1965 w, 1957 w, 1943 m, 1918 vw  $\text{cm}^{-1}$ .  $^1\text{H}$  NMR ( $\text{CDCl}_3$ , 17 °C): 7.6–7.2 (m, 45H), 2.94 (m, 1H), 2.48 (m, 2H), 1.11 (t, 3H,  $J_{\text{HH}} = 6.9$  Hz), 0.86 (m, 1H), 0.57 (t, 3H,  $J_{\text{HH}} = 7.2$  Hz), -14.22 (s, 1H), -17.99 (t, 1H,  $J_{\text{HP}} = 11.2$  Hz) ppm.  $^1\text{H}$  NMR ( $\text{CDCl}_3$ , -50 °C): 7.6–7.0 (m, 45H), 2.88 (m, 1H), 2.36 (m, 2H), 1.06 (t, 3H,  $J_{\text{HH}} = 7.3$  Hz), 0.71 (m, 1H), 0.50 (t, 3H,  $J_{\text{HH}} = 6.8$  Hz), -14.26 (s, 1H), -18.02 (t, 1H,  $J_{\text{HP}} = 11.2$  Hz) ppm.  $^{31}\text{P}$  NMR ( $\text{CDCl}_3$ , 17 °C): 40.0 (d, 1P,  $J_{\text{PP}} = 28$  Hz), 29.0 (d, 1P,  $J_{\text{PP}} = 28$  Hz), 26.2 (s, 1P) ppm. MS (FAB):  $m/e$  1344 ( $^{102}\text{Ru}_3$ ). Intense ion signals at  $m/e$  1026 ( $^{102}\text{Ru}_3$ ) are assigned to  $\text{H}_2\text{Ru}_3(\text{EtC}_2\text{Et})(\text{CO})_4(\text{PPh}_3)_2^+$ . CV(100 mV/s): quasi-reversible couple, oxidation peak at  $E_{\text{p,a}} = 50$  mV.

(7) Dawes, J. L.; Holmes, J. D. *Inorg. Nucl. Chem. Lett.* **1971**, *7*, 847.

(8) Rivomanana, S.; Lavigne, G.; Lugan, N.; Bonnet, J. J.; Yanez, R.; Mathieu, R. *J. Am. Chem. Soc.* **1989**, *111*, 8959. (b) Rivomanana, S.; Lavigne, G.; Lugan, N.; Bonnet, J. *J. Organometallics* **1991**, *10*, 2285.

(9) Gagne, R. R.; Koval, C. A.; Lisensky, G. C. *Inorg. Chem.* **1980**, *19*, 2855.

**H<sub>2</sub>Ru<sub>3</sub>(EtC<sub>2</sub>Et)(CO)<sub>6</sub>(P(OCH<sub>3</sub>)<sub>3</sub>)<sub>3</sub>.** The yellow product was isolated in 90% yield after TLC. IR (C<sub>6</sub>H<sub>12</sub>): 2036 vw, 2019 vs, 1979 m, 1960 m cm<sup>-1</sup>. <sup>1</sup>H NMR (CDCl<sub>3</sub>, 17 °C): 3.60 (d, 27H, J<sub>HP</sub> = 12 Hz), 3.1 (s, br, 2H), 2.5 (s, br, 2H), 1.23 (t, 6H, J<sub>HH</sub> = 7.6 Hz), -16.0 (s, br, 1H), -20.5 (s, br, 1H) ppm. <sup>1</sup>H NMR (CDCl<sub>3</sub>, -40 °C): 3.61 (d, 18H, J<sub>HP</sub> = 12 Hz), 3.59 (d, 9H, J<sub>HP</sub> = 12 Hz), 3.22 (m, 1H), 3.08 (m, 1H), 2.49 (m, 1H), 2.29 (m, 1H), 1.22 (t, 6H, J<sub>HH</sub> = 7.2 Hz), -16.02 (t, br, 1H, J<sub>HP</sub> = 8 Hz), -20.56 (t, 1H, J<sub>HP</sub> = 13.6 Hz) ppm. <sup>31</sup>P NMR (CDCl<sub>3</sub>, -40 °C): -41.2 (br, 1P), -46.4 (s, br, 1P), -52.8 (br, 1P) ppm. CV (100 mV/s): irreversible oxidation, peak potential at E<sub>p,a</sub> = +10 mV.

**H<sub>2</sub>Ru<sub>3</sub>(EtOC<sub>2</sub>H)(CO)<sub>6</sub>(PPh<sub>3</sub>)<sub>3</sub>.** The product was isolated after TLC as an orange, oily, very difficult to crystallize product in 80% yield. IR (CH<sub>2</sub>Cl<sub>2</sub>): 2025 vw, 2005 s, 1965 m, 1939 m, 1913 vw cm<sup>-1</sup>. <sup>1</sup>H NMR (CDCl<sub>3</sub>, 17 °C): 7.6–7.1 (m, 45H), 5.48 (d, 1H, J<sub>HP</sub> = 9.3 Hz), 3.65 (m, 1H), 3.29 (m, 1H), 1.04 (t, 3H, J<sub>HH</sub> = 7 Hz), -14.31 (t, 1H, J<sub>HP</sub> = 7 Hz), -18.15 (t, 1H, J<sub>HP</sub> = 12 Hz) ppm. <sup>1</sup>H NMR (CDCl<sub>3</sub>, -50 °C): 7.6–7.1 (m, 45H), 5.49 (d, 1H, J<sub>HP</sub> = 9.3 Hz), 3.64 (m, 1H), 3.28 (m, 1H), 1.08 (t, 3H, J<sub>HH</sub> = 7.2 Hz), -14.30 (t, 1H, J<sub>HP</sub> = 7.6 Hz), -18.22 (tm, 1H, J<sub>HP</sub> = 12.6 Hz) ppm. <sup>31</sup>P NMR (CDCl<sub>3</sub>, 17 °C): 40.0 (d, 1P, J<sub>PP</sub> = 33 Hz), 32.6 (d, 1P, J<sub>PP</sub> = 33 Hz), 32.2 (s, 1P) ppm. MS (FAB): *m/e* (<sup>102</sup>Ru<sub>3</sub>). CV (100 mV/s): irreversible oxidation, peak potential at E<sub>p,a</sub> = 0 mV.

**H<sub>2</sub>Ru<sub>3</sub>(PhC<sub>2</sub>Ph)(CO)<sub>6</sub>(PPh<sub>3</sub>)<sub>3</sub>.** Yield: 20% (not optimized). IR (CH<sub>2</sub>Cl<sub>2</sub>): 2012 s, 1978 m, 1948 m, 1924 vw cm<sup>-1</sup>. <sup>1</sup>H NMR (CDCl<sub>3</sub>, 17 °C): 7.8–6.6 (m, 55H), -14.1 (s, br, 1H), -18.3 (s, br, 1H). <sup>31</sup>P NMR (CDCl<sub>3</sub>, 17 °C): 41.2 (br, 1P), 28.9 (s, 1P), 25.1 (br, 1P). FAB MS: *m/e* 1440 (<sup>102</sup>Ru<sub>3</sub>).

**Protonation of H<sub>2</sub>Ru<sub>3</sub>(EtC<sub>2</sub>Et)(CO)<sub>6</sub>(PPh<sub>3</sub>)<sub>2</sub>.** A sample of the cluster was placed in a NMR tube and a small excess of CF<sub>3</sub>COOH was added, causing a change of color from orange to yellow. <sup>1</sup>H NMR (CDCl<sub>3</sub>, 17 °C): 7.6–7.2 (m, 30H), 3.0 (s, br, 2H), 2.9 (s, br, 2H), 1.5 (s, br, 6H), -14.49 (br, 1H), -17.99 (s, br, 2H) ppm. <sup>1</sup>H NMR (CDCl<sub>3</sub>, -50 °C): 7.6–7.0 (m, 30H), methylene protons not seen, 1.54 (t, 3H, J<sub>HH</sub> = 7.0 Hz), 1.47 (t, 3H, J<sub>HH</sub> = 7.2 Hz), -14.48 (s, 1H), -15.7 (s, br, 1H), -20.4 (s, br, 1H) ppm. <sup>31</sup>P NMR (CDCl<sub>3</sub>, 25 °C): 28.0 (s, 2P) ppm. <sup>31</sup>P NMR (CDCl<sub>3</sub>, -50 °C): 31.6 (s, br, 1P), 24.8 (s, br, 1P) ppm. IR (CH<sub>2</sub>Cl<sub>2</sub>): 2113 m, 2072 vs, 2053 vs, 2021 m, br, 1998 w cm<sup>-1</sup>.

**Protonation of H<sub>2</sub>Ru<sub>3</sub>(EtC<sub>2</sub>Et)(CO)<sub>6</sub>(PPh<sub>3</sub>)<sub>3</sub>.** The addition of a small excess of trifluoroacetic acid to a solution of the cluster in CDCl<sub>3</sub> immediately caused a color change to dark brown, which slowly dissipated. However, the reaction was not complete (by NMR); therefore, another aliquot of acid was added. Again the same color changes were observed. The final solution was lighter than that of the starting solution. The <sup>1</sup>H NMR spectrum (hydride region) showed many signals, but only a few belonging to the main products. One set of signals, -14.49 (m, 1H) and -17.99 (s, br, 2H) ppm, was assigned to H<sub>3</sub>Ru<sub>3</sub>(EtC<sub>2</sub>Et)(CO)<sub>7</sub>(PPh<sub>3</sub>)<sub>2</sub><sup>+</sup>; a second of signals at -14.09 (m, 1H), -15.19 (dt, 1H, J<sub>HP</sub> = 28 Hz, J<sub>HP</sub> = 6 Hz), and -18.94 (t, 1H, J<sub>HP</sub> = 12.7 Hz) ppm was assigned to H<sub>3</sub>Ru<sub>3</sub>(EtC<sub>2</sub>Et)(CO)<sub>6</sub>(PPh<sub>3</sub>)<sub>3</sub><sup>+</sup>. The ratio of these products was estimated as 1:3.

**Reaction of H<sub>2</sub>Ru<sub>3</sub>(EtC<sub>2</sub>Et)(CO)<sub>6</sub>(PPh<sub>3</sub>)<sub>3</sub> with Cl<sub>2</sub>.** In a three-necked, round-bottomed flask equipped with gas inlet tubes 57 mg (0.042 mmol) of the cluster was dissolved in 100 mL of hexanes. The solution was cooled to 0 °C, and then chlorine was passed through it for 15 min. The color of the solution changed from orange-red to colorless, and a yellow solid deposited on the bottom. The solvent was withdrawn by pipet, and the solid was dried under vacuum. Yield: 55 mg (92%). IR and <sup>1</sup>H NMR spectra of the product are identical with those obtained for the product of the reaction with tris-(4-bromophenyl)ammoniumyl hexachloroantimonate (TBPAHCA) (vide infra). This suggests the formula H<sub>2</sub>Ru<sub>3</sub>(Cl)(EtC<sub>2</sub>Et)(CO)<sub>6</sub>(PPh<sub>3</sub>)<sub>3</sub><sup>+</sup>Cl<sup>-</sup>. We were unable to obtain a satisfactory elemental analysis.

**Oxidation of H<sub>2</sub>Ru<sub>3</sub>(EtC<sub>2</sub>Et)(CO)<sub>6</sub>(PPh<sub>3</sub>)<sub>3</sub> with Tris-(4-bromophenyl)ammoniumyl Hexachloroantimonate**

(TBPAHCA). To a solution of 84 mg (0.063 mmol) of the cluster in 40 mL of dichloromethane was added 56 mg (0.069 mmol) of TBPAHCA. The color changed rapidly to dark brown but after 15 min was light brown-yellow. The volume of the solution was decreased to 3 mL by vacuum evaporation, and it was then filtered into 50 mL of hexanes. A very light brown precipitate was collected by filtration, washed with hexanes, and dried in air. A second crystallization from dichloromethane/hexanes, followed by drying under vacuum for 2 days, afforded 80 mg of a very light brown solid, which is characterized as [H<sub>2</sub>Ru<sub>3</sub>(Cl)(EtC<sub>2</sub>Et)(CO)<sub>6</sub>(PPh<sub>3</sub>)<sub>3</sub>]<sup>+</sup>X<sup>-</sup>. The identity of the counteranion is unknown. IR (CH<sub>2</sub>Cl<sub>2</sub>): 2072 s, 2051 vs, 2020 m, 1982 m cm<sup>-1</sup>. <sup>1</sup>H NMR (CDCl<sub>3</sub>, 17 °C): 8.0–7.0 (m, 45H), 3.4 (s, br, 4H), 1.66 (t, 6H, J<sub>HH</sub> = 7.0 Hz), -12.22 (br d, 2H, J<sub>HP</sub> = 12.0 Hz) ppm. The spectra measured on 300 and 400 MHz instruments showed that the hydride signal is a doublet and not two singlets. <sup>1</sup>H NMR (CDCl<sub>3</sub>, -55 °C): 8.0–7.0 (m, 45H), 3.6 (m, 2H), 3.1 (m, 2H), 1.63 (t, 6H, J<sub>HH</sub> = 7.0 Hz), -12.22 (br d, 2H, J<sub>HP</sub> = 12.0 Hz) ppm. <sup>31</sup>P NMR (CDCl<sub>3</sub>, 17 °C): 29.7 (s, 1P), 17.5 (s, 2P) ppm. MS (FAB): the highest *m/e* envelope at 1379 (<sup>102</sup>Ru<sub>3</sub><sup>35</sup>Cl) corresponds to H<sub>2</sub>Ru<sub>3</sub>(Cl)(EtC<sub>2</sub>Et)(CO)<sub>6</sub>(PPh<sub>3</sub>)<sub>3</sub><sup>+</sup>, and an intense ion at *m/e* 1061 (<sup>102</sup>Ru<sub>3</sub><sup>35</sup>Cl) corresponds to H<sub>2</sub>Ru<sub>3</sub>(Cl)(EtC<sub>2</sub>Et)(CO)<sub>4</sub>(PPh<sub>3</sub>)<sub>2</sub><sup>+</sup>. The cluster decomposes slowly (appreciably within hours) in solution.

**Reaction of H<sub>2</sub>Ru<sub>3</sub>(EtC<sub>2</sub>Et)(CO)<sub>6</sub>(PPh<sub>3</sub>)<sub>3</sub> with I<sub>2</sub>: Synthesis of [H<sub>2</sub>Ru<sub>3</sub>(I)(EtC<sub>2</sub>Et)(CO)<sub>6</sub>(PPh<sub>3</sub>)<sub>3</sub>][BPh<sub>4</sub>].** H<sub>2</sub>Ru<sub>3</sub>(EtC<sub>2</sub>Et)(CO)<sub>6</sub>(PPh<sub>3</sub>)<sub>3</sub> (62 mg) was suspended in 50 mL of pentane. To that suspension was added 25 mg (2.1 equiv) of I<sub>2</sub> dissolved in 3 mL of dichloromethane. The mixture was stirred for 1 h. After this time the solution was almost clear with a slight pink tint and a brown precipitate was deposited on the walls. After the solution was decanted, the solid was dissolved in 3 mL of dichloromethane and then the solution was added dropwise to 50 mL of pentane. The resulting precipitate was collected by filtration, washed with pentane, and dried in air for 15 min. This afforded 65 mg of solid, most likely impure [H<sub>2</sub>Ru<sub>3</sub>(I)(EtC<sub>2</sub>Et)(CO)<sub>6</sub>(PPh<sub>3</sub>)<sub>3</sub>][I<sub>3</sub>]. The solid was dissolved in a minimum volume of methanol (ca. 5 mL), and then a solution of 30 mg of NaBPh<sub>4</sub> in 1.5 mL of methanol was added. Immediate precipitation occurred. The mixture was stored in the freezer overnight, and then the solid was filtered out, washed with 2 mL of cold methanol, and dried in air and then under vacuum. Final yield: 34 mg (41%). The same reaction can be performed in dichloromethane. Then, however, the product is less pure. Our purest (by <sup>1</sup>H NMR) sample failed to give a satisfactory elemental analysis. IR (CH<sub>2</sub>Cl<sub>2</sub>): 2069 s, 2044 vs, 2017 w, 1981 m cm<sup>-1</sup>. <sup>1</sup>H NMR (CDCl<sub>3</sub>, 17 °C): 7.8–6.8 (m, 65H), 3.39 (m, 4H), 1.60 (t, 6H, J = 7.2 Hz), -13.51 (dd, 2H, J<sub>HP</sub> = 11.2, 5.6 Hz) ppm. <sup>31</sup>P NMR (CDCl<sub>3</sub>, 17 °C): 25.4 (s, 1P), 16.3 (s, 2P) ppm. FAB MS: *m/e* 1471 (<sup>102</sup>Ru<sub>3</sub>).

**Reaction of H<sub>2</sub>Ru<sub>3</sub>(EtC<sub>2</sub>Et)(CO)<sub>6</sub>(PPh<sub>3</sub>)<sub>3</sub> with FcPF<sub>6</sub>: Synthesis of [H<sub>2</sub>Ru<sub>3</sub>(F)(EtC<sub>2</sub>Et)(CO)<sub>6</sub>(PPh<sub>3</sub>)<sub>3</sub>][PF<sub>6</sub>].** H<sub>2</sub>Ru<sub>3</sub>(EtC<sub>2</sub>Et)(CO)<sub>6</sub>(PPh<sub>3</sub>)<sub>3</sub> (72 mg) was dissolved in 40 mL of dichloromethane. Then 18 mg (1 equiv) of FcPF<sub>6</sub> was added as a solid. The solution rapidly turned dark brown but after 5 min became lighter and after 15 min returned to the original yellow-orange color. At this time the IR spectrum is quite clean. This solution was concentrated to 3 mL on a rotary evaporator and added dropwise into 50 mL of hexanes. The light brown solid was filtered out, washed with hexanes, and dried in air and then under vacuum. Yield: 58 mg (72%) (contains impurities). IR (CH<sub>2</sub>Cl<sub>2</sub>): 2072 s, 2056 m, 2050 m, 2020 m, 2007 w, 1977 m cm<sup>-1</sup>. <sup>1</sup>H NMR (CDCl<sub>3</sub>, 17 °C): 7.7–7.0 (m, 45H), 3.5 (s, br, 2H), 3.0 (s, br, 2H), 1.68 (t, 6H, J = 7.0 Hz), -11.25 (quasi-triplet, 2H) ppm. <sup>31</sup>P NMR (CDCl<sub>3</sub>, 17 °C): 146.0 (septet, 1P, J<sub>PF</sub> = 713 Hz), 29.3 (s, 1P), 13.7 (s, 2P) ppm. <sup>19</sup>F NMR (CDCl<sub>3</sub>, 17 °C): 75.1 (d, J<sub>PF</sub> = 713 Hz) ppm, no other resonance observed. FAB MS: *m/e* 1363 (<sup>102</sup>Ru<sub>3</sub>). Attempts to obtain an analytically pure sample failed.

**Synthesis of [H<sub>2</sub>Ru<sub>3</sub>(F)(EtC<sub>2</sub>Et)(CO)<sub>6</sub>(PPh<sub>3</sub>)<sub>3</sub>][BAR'<sub>4</sub>] Ar'** = 3,5-(CF<sub>3</sub>)<sub>2</sub>C<sub>6</sub>H<sub>3</sub>. H<sub>2</sub>Ru<sub>3</sub>(EtC<sub>2</sub>Et)(CO)<sub>6</sub>(PPh<sub>3</sub>)<sub>3</sub> (80 mg, 0.060

mmol) and 100 mg (0.30 mmol) of  $\text{Bu}_4\text{NBF}_4$  were dissolved in 20 mL of dichloromethane. The solution was cooled to 0 °C. Then 63 mg (0.060 mmol) of  $\text{FcBAR}'_4$  was added as a solid. The solution rapidly turned dark brown but after 15 min returned to the original yellow-orange color. At that time the IR spectrum still showed some starting material present; therefore, more oxidant was added. After 30 min the solution was evaporated to dryness, the residue was redissolved in ca. 4 mL of methanol, and the solution was combined with the solution of  $\text{NaBAR}'_4$  (2 equiv) in methanol. No precipitate was formed even after storing in the freezer overnight, but sonication resulted in a massive precipitation. The solid was separated out and dried under vacuum. Yield: 82 mg (62%). Spectroscopic data were identical with those of the  $\text{PF}_6$  salt. Crystals were grown by slow evaporation of a cooled (-20 °C) methanol solution. Anal. Calcd for  $\text{C}_{99}\text{H}_{69}\text{BF}_{24}\text{O}_6\text{P}_3\text{Ru}_3$ : C, 52.96; H, 3.13. Found: C, 53.16; H, 3.36.

**EPR Spectra of  $[\text{H}_2\text{Ru}_3(\text{RCCR})(\text{CO})_6(\text{PPh}_3)_3]^+$ .** To determine the EPR spectrum, the reaction of ferrocenium ion with  $\text{H}_2\text{Ru}_3(\text{RCCR})(\text{CO})_6(\text{PPh}_3)_3$  (R = Et, Ph) was performed at -20 °C. To a solution of 10 mg of the cluster in 5 mL of dichloromethane, maintained at -20 °C, was added 1 equiv of  $\text{FcPF}_6$ , and the cold solution was transferred to an EPR tube and was frozen in liquid nitrogen. The tube was deaerated by two freeze-pump-thaw cycles, sealed, and kept frozen until the EPR measurement. The EPR spectrum of the radical generated from  $\text{H}_2\text{Ru}_3(\text{EtCCEt})(\text{CO})_6(\text{PPh}_3)_3$  showed a single line with  $g = 2.105$ . Oxidation of  $\text{H}_2\text{Ru}_3(\text{PhC}_2\text{Ph})(\text{CO})_6(\text{PPh}_3)_3$  formed a radical with a slightly different  $g$  value, 2.097.

**Quantification of the Reaction of  $\text{H}_2\text{Ru}_3(\text{EtC}_2\text{Et})(\text{CO})_6(\text{PPh}_3)_3$  with  $\text{FcPF}_6$ .** The  $^1\text{H}$  NMR spectrum of a deuteriochloroform solution containing 20 mg of the cluster and 9 mg of  $\text{HRu}_3(\text{COCH}_3)(\text{CO})_{10}$  as an internal standard was recorded. Then the mixture was transferred to the Schlenk flask along with 20 mL of dichloromethane. To the solution was added 3.5 mg (ca. 0.7 equiv) of  $\text{FcPF}_6$ . After 30 min the solvent was evaporated and the  $^1\text{H}$  NMR spectrum was recorded. The alkyl and hydride signals of  $\text{H}_2\text{Ru}_3(\text{EtC}_2\text{Et})(\text{CO})_6(\text{PPh}_3)_3$  and the product were integrated separately against the standard. The integration showed the presence of 0.3 equiv of unreacted  $\text{H}_2\text{Ru}_3(\text{EtC}_2\text{Et})(\text{CO})_6(\text{PPh}_3)_3$ , 0.7 equiv of ferrocene, and 0.2 equiv of  $[\text{H}_2\text{Ru}_3(\text{F})(\text{EtC}_2\text{Et})(\text{CO})_6(\text{PPh}_3)_3]^+$ .

**Reaction of  $\text{H}_2\text{Ru}_3(\text{EtC}_2\text{Et})(\text{CO})_6(\text{PPh}_3)_3$  with  $\text{FcBAR}'_4$  ( $\text{Ar}' = 3,5\text{-}(\text{CF}_3)_2\text{C}_6\text{H}_3$ ).**  $\text{H}_2\text{Ru}_3(\text{EtC}_2\text{Et})(\text{CO})_6(\text{PPh}_3)_3$  (30 mg) was dissolved in 25 mL of dichloromethane. Then 23.5 mg (1 equiv) of  $\text{FcBAR}'_4$  was added as a solid. The solution turned brown immediately and remained dark for about 2 h. The reaction was monitored by IR spectroscopy. Initially a complete conversion of  $\text{H}_2\text{Ru}_3(\text{EtC}_2\text{Et})(\text{CO})_6(\text{PPh}_3)_3$  into a radical is observed (bands at 2079 vw, 2043 m, 2030 s, 2018 m, 1993 m, 1981 vw, 1968 vw, 1943 vw  $\text{cm}^{-1}$ ). After 1 h about 40% of the radical was still present. The final IR spectrum measured after 20 h did not show the presence of the initial product. The  $^1\text{H}$  NMR spectrum showed a mixture of many products.

**Reactions of the Radical Generated from  $\text{H}_2\text{Ru}_3(\text{EtC}_2\text{Et})(\text{CO})_6(\text{PPh}_3)_3$  with Nucleophiles, Including  $(\text{C}_2\text{H}_5\text{C})_2$ ,  $(\text{C}_2\text{H}_5\text{O}_2\text{CCH})_2$ ,  $\text{NH}(\text{CH}(\text{CH}_3)_2)_2$ ,  $\text{KOCMe}_3$ ,  $\text{PPh}_3$ ,  $\text{CH}_3\text{NC}$ ,  $\text{Bu}_4\text{NBF}_4$ , and  $[\text{PPN}]\text{Cl}$ .** In a typical experiment, 30 mg of  $\text{H}_2\text{Ru}_3(\text{EtC}_2\text{Et})(\text{CO})_6(\text{PPh}_3)_3$  was dissolved in 25 mL of dichloromethane. The radical was generated by the addition of 23.5 mg of  $\text{FcBAR}'_4$ . Then, within 5 min, 1 equiv (or a slight excess) of a nucleophile was added and the progress of the reaction was monitored by IR spectroscopy by comparison to the system without a nucleophile described above. In the case of  $\text{CH}_3\text{NC}$ ,  $\text{Bu}_4\text{NBF}_4$ , and  $[\text{PPN}]\text{Cl}$  a reaction was observed and additionally a different procedure for these reactions was used in which small aliquots of  $\text{FcBAR}'_4$  were added to solutions of  $\text{H}_2\text{Ru}_3(\text{EtC}_2\text{Et})(\text{CO})_6(\text{PPh}_3)_3$  with reagents. The addition of alkenes or alkynes to the solution of the radical did not change the decomposition pathway of the radical, and IR spectra of the solution containing alkene or alkyne resembled those collected in their absence. In the case of  $\text{PPh}_3$  initially the IR spectrum of  $\text{H}_2\text{Ru}_3(\text{EtC}_2\text{Et})(\text{CO})_6(\text{PPh}_3)_3$  appeared but then it

vanished and the final spectrum was the same as of the decomposition product. Reaction of the radical cation with diisopropylamine regenerated  $\text{H}_2\text{Ru}_3(\text{EtC}_2\text{Et})(\text{CO})_6(\text{PPh}_3)_3$  in 80% yield. The same product was formed with potassium *tert*-butoxide. For reactions with  $\text{MeNC}$ ,  $\text{Bu}_4\text{NBF}_4$  (electrolyte), or  $[\text{PPN}]\text{Cl}$  in each case  $\text{H}_2\text{Ru}_3(\text{EtC}_2\text{Et})(\text{CO})_6(\text{PPh}_3)_3$  was formed in ca. 50% yield, and for the last two reagents a second product was  $[\text{H}_2\text{Ru}_3(\text{EtC}_2\text{Et})(\text{X})(\text{CO})_6(\text{PPh}_3)_3]^+$ , where X = F, Cl, respectively. We were unable to characterize the product(s) of the reaction with  $\text{MeNC}$ .

**Quantification of the Reaction of  $\text{H}_2\text{Ru}_3(\text{EtC}_2\text{Et})(\text{CO})_6(\text{PPh}_3)_3$  with  $\text{FcBAR}'_4/[\text{PPN}]\text{Cl}$ .** In a Schlenk flask 20 mg of the cluster was dissolved in 1 mL of  $\text{CDCl}_3$  along with 26 mg of  $[\text{PPN}]\text{Cl}$  (3 equiv). Then, 10.5 mg (ca. 0.7 equiv) of  $\text{FcBAR}'_4$  was added as a solid. After 30 min the  $^1\text{H}$  NMR spectrum showed the formation of  $[\text{H}_2\text{Ru}_3(\text{Cl})(\text{EtC}_2\text{Et})(\text{CO})_6(\text{PPh}_3)_3]^+$  and ferrocene in the ratio 0.8:2. The amount of starting cluster remaining was 0.66 equiv. This reaction is very clean, and no side products were observed.

**Collection of X-ray Diffraction Data for  $(\mu\text{-H})_2\text{Ru}_3(\mu_3\text{-}\eta^2\text{-EtCCEt})(\text{CO})_7(\text{PPh}_3)_2$ .** An orange crystal with dimensions 0.65 mm  $\times$  0.20 mm  $\times$  0.17 mm was selected for the X-ray study. The crystal was sealed in a thin-walled capillary and was mounted and aligned on a Siemens R3m/V four-circle, single-crystal diffractometer as described previously.<sup>10</sup> Data were collected by the use of a coupled  $2\theta\text{-}\omega$  scan. Details of the data collection appear in Table 1. One form of data was collected (Mo K $\alpha$ ,  $\lambda = 0.71073$  Å,  $2\theta = 5.0\text{--}45.0^\circ$ ). A total of 6552 reflections were collected and were merged into a unique set of 6149 reflections ( $R_{\text{int}} = 1.56\%$ ). All data were corrected for Lorentz and polarization effects. An empirical absorption correction was applied to the data. The crystal belongs to the triclinic system. Intensity statistics and the far greater possibility of a synthetic crystal with  $Z = 2$  belonging to the centrosymmetric space group<sup>11</sup> each suggest that the space group will be  $P\bar{1}$  ( $C_i^1$ ; No. 2). This was confirmed by the successful solution of the structure in this centrosymmetric space group.

**Solution and Refinement of the Crystal Structure of  $(\mu\text{-H})_2\text{Ru}_3(\mu_3\text{-}\eta^2\text{-EtCCEt})(\text{CO})_7(\text{PPh}_3)_2$ .** All crystallographic calculations were carried out with the use of the Siemens SHELXTL<sup>12</sup> program package. The analytical scattering factors for neutral atoms were corrected for both the  $\Delta f'$  and  $i\Delta f''$  components of anomalous dispersion.<sup>13</sup> The structure was solved by the use of direct methods. Positional and anisotropic thermal parameters for all non-hydrogen atoms were refined. All organic hydrogen atoms were placed at calculated positions with  $d(\text{C-H}) = 0.96$  Å with the appropriate trigonal or staggered-tetrahedral geometry.<sup>14</sup> The isotropic thermal parameter of each organic hydrogen atom was set equal to the  $U_{\text{eq}}$  value for that carbon atom to which it was bound. The positional and isotropic thermal parameters of the hydridic hydrogen atoms were also refined.

Refinement of parameters was achieved through the minimization of the function  $\sum w(|F_o| - |F_c|)^2$ . The refinement of the model converged with  $R = 4.41\%$  and  $R_w = 4.78\%$  for 552 parameters refined against those 4306 reflections with  $|F_o| > 6\sigma$  and  $R = 6.95\%$  and  $R_w = 7.75\%$  for all data. The extreme features left on the difference-Fourier map were a peak of height 1.00  $e \text{ \AA}^{-3}$  and a negative feature of  $-0.90 e \text{ \AA}^{-3}$ . Atomic coordinates appear in Table 2.

**Collection of the X-ray Diffraction Data for  $(\mu\text{-H})_2\text{Ru}_3(\mu_3\text{-}\eta^2\text{-EtCCEt})(\text{CO})_6(\text{PPh}_3)_3 \cdot 3\text{CH}_2\text{Cl}_2$ .** A yellow crystal with dimensions 0.28 mm  $\times$  0.25 mm  $\times$  0.25 mm was selected for the X-ray study. The crystal was mounted, aligned, and

(10) Churchill, M. R.; Lashewycz, R. A.; Rotella, F. J. *Inorg. Chem.* **1977**, *16*, 265.

(11) Nowacki, W.; Matsumoto, T.; Edenharter, A. *Acta Crystallogr.* **1967**, *22*, 935.

(12) *Siemens SHELXTL PLUS Manual*, 2nd ed.; Siemens Analytical Instruments: Madison, WI, 1990.

(13) *International Tables for X-Ray Crystallography*; Kynoch Press: Birmingham, England, 1974; Vol. 4, pp 99-101, 149-150.

(14) Churchill, M. R. *Inorg. Chem.* **1973**, *12*, 1213.



**Table 1. Details on Data Collection for  $(\mu\text{-H})_2\text{Ru}_3(\mu_3\text{-}\eta^2\text{-EtCCet})(\text{CO})_7(\text{PPh}_3)_2$  and  $(\mu\text{-H})_2\text{Ru}_3(\mu_3\text{-}\eta^2\text{-EtCCet})(\text{CO})_6(\text{PPh}_3)_3\cdot 3\text{CH}_2\text{Cl}_2$** 

formula	$\text{H}_2\text{Ru}_3(\text{EtCCet})(\text{CO})_7(\text{PPh}_3)_2$	$\text{H}_2\text{Ru}_3(\text{EtCCet})(\text{CO})_6(\text{PPh}_3)_3\cdot 3\text{CH}_2\text{Cl}_2$
Crystal System	triclinic	triclinic
Space Group	$P\bar{1}$ (No. 2)	$P\bar{1}$ (No. 2)
unit cell dimens		
<i>a</i> (Å)	10.489(3)	14.032(2)
<i>b</i> (Å)	10.515(6)	15.512(2)
<i>c</i> (Å)	21.614(8)	16.644(2)
$\alpha$ (deg)	85.89(4)	77.506(11)
$\beta$ (deg)	89.09(3)	84.786(10)
$\gamma$ (deg)	79.16(4)	75.566(10)
vol (Å <sup>3</sup> )	2335(2)	3422.7(8)
<i>Z</i>	2	2
fw	1108.0	1597.0
density (calcd) (Mg/m <sup>3</sup> )	1.576	1.550
abs coeff (mm <sup>-1</sup> )	1.055	0.995
abs corr	semiempirical	semiempirical
min/max transmissn	0.5636/0.7892	0.7518/0.8389
2 $\theta$ range (deg)	5.0–45.0	5.0–45.0
index ranges	$-11 \leq h \leq 11, -11 \leq k \leq 0, -23 \leq l \leq 23$	$0 \leq h \leq 15, -16 \leq k \leq 16, -17 \leq l \leq 17$
no. of rflns collected	6552	9435
no. of obsd rflns ( $F > 0.3\sigma(F)$ )	6149 ( $R_{\text{int}} = 1.56\%$ )	8993 ( $R_{\text{int}} = 1.19\%$ )
no. of rflns ( $F > 6.0\sigma(F)$ )	4306	5555
no. of params refined	552	793
final <i>R</i> indices (obsd data) (%)	$R = 6.95, R_w = 7.75$	$R = 7.61, R_w = 6.71$
<i>R</i> indices (6 $\sigma$ data) (%)	$R = 4.41, R_w = 4.78$	$R = 4.00, R_w = 4.31$
goodness of fit	1.04	0.95
data to param ratio	11.1:1	11.3:1
largest diff peak (e/Å <sup>3</sup> )	1.00	1.14
largest diff hole (e/Å <sup>3</sup> )	-0.90	-1.05

treated similarly to that in the previous study. Details of the data collection appear in Table 1. One form of data (9435 reflections) was collected. These reflections were merged into a unique set containing 8993 reflections ( $R_{\text{int}} = 1.19\%$ ). This crystal also belongs to space group  $P\bar{1}$  in the triclinic system.

**Solution and Refinement of the Crystal Structure of  $(\mu\text{-H})_2\text{Ru}_3(\mu_3\text{-}\eta^2\text{-EtCCet})(\text{CO})_6(\text{PPh}_3)_3\cdot 3\text{CH}_2\text{Cl}_2$ .** Solution of the structure was carried out as described above. Refinement converged with  $R = 4.00\%$  and  $R_w = 4.31\%$  for those 5555 reflections with  $|F_o| > 6\sigma|F_o|$  and  $R = 7.61\%$  and  $R_w = 6.71\%$  for all 8993 independent reflections. A final difference-Fourier map showed features in the range of  $-1.05$  to  $1.14 \text{ e } \text{Å}^{-3}$ . The hydrogen atoms defining the hydride ligands were refined; all other hydrogen atoms were placed in idealized positions. Atomic coordinates appear in Table 3.

**Fenske–Hall Molecular Orbital Calculations.** Fenske–Hall calculations were performed using the program version 5.1.<sup>36</sup> Atomic positions for  $\text{H}_2\text{Ru}_3(\text{EtCCet})(\text{CO})_7(\text{PPh}_3)_2$  (this work;  $\text{PPh}_3$  ligands were replaced with CO ligands),  $\text{H}_2\text{Ru}_3(\text{MeOCCMe})(\text{CO})_9$ ,<sup>15b</sup> and  $\text{H}_2\text{Ru}_3(i\text{-Pr}_2\text{NCCH})(\text{CO})_9$ <sup>28</sup> (*i*-Pr was replaced with methyl) were taken from the crystal structures. Modifications of substituents ( $\text{PPh}_3$  to CO, *i*-Pr to Me) with the expected bond distances and angles were made for consistency. Atomic coordinates are available on request.

## Results

**Syntheses of Clusters of the Series  $\text{H}_2\text{Ru}_3(\text{RC}_2\text{R}')(\text{CO})_9$ .** The goal of this work was to examine the chemical and electrochemical oxidation of clusters  $\text{H}_2\text{Ru}_3(\mu_3\text{-}\eta^2\text{-XCCR})(\text{CO})_{9-n}\text{L}_n$ , in which X is a  $\pi$ -donor substituent such as alkoxy or amino. Although examples of the parent carbonyls had been prepared previously, the yields were poor, and di- and trisubstituted clusters had not been previously reported.

Lavigne and co-workers reported a halide-promoted synthesis for  $\text{H}_2\text{Ru}_3(\mu_3\text{-}\eta^2\text{-RCCR})(\text{CO})_9$  ( $R = \text{Et, Ph}$ ).<sup>8</sup> Using this method the yield of  $\text{H}_2\text{Ru}_3(\mu_3\text{-}\eta^2\text{-HCCOEt})$ -

$(\text{CO})_9$  was low, but still the procedure offers some advantages (time and ease) over methods of preparations of related clusters reported previously.<sup>15</sup> The procedure was ineffective for the electron-poor alkyne  $\text{C}_2(\text{CO}_2\text{Me})_2$  and also the electron-rich  $\text{Et}_2\text{NC}_2\text{Me}$ . Details are reported in the supporting information.

**Clusters of the Series  $\text{H}_2\text{Ru}_3(\text{RC}_2\text{R}')(\text{CO})_{9-n}(\text{PPh}_3)_n$  ( $n = 2, 3$ ).** Reactions of  $\text{H}_2\text{Ru}_3(\text{RCCR}')(\text{CO})_9$  ( $\text{RCCR}' = \text{EtCCet, PhCCPh, and HCCOEt}$ ) with  $\text{PPh}_3$  or  $\text{P(OMe)}_3$  ( $\text{EtCCet}$  only) in refluxing THF gave only the trisubstituted product. The use of  $\text{Me}_3\text{NO}$  to induce substitution with phosphines at room temperature gave a mixture of di- and trisubstituted clusters in various ratios. Products were characterized by <sup>1</sup>H and <sup>31</sup>P NMR, IR, and mass spectroscopy and in some cases elemental analysis. Crystal structures were obtained for  $\text{H}_2\text{Ru}_3(\text{EtCCet})(\text{CO})_7(\text{PPh}_3)_2$  and  $\text{H}_2\text{Ru}_3(\text{EtCCet})(\text{CO})_6(\text{PPh}_3)_3$ .

**Description of the Structure of  $(\mu\text{-H})_2\text{Ru}_3(\mu_3\text{-}\eta^2\text{-EtCCet})(\text{CO})_7(\text{PPh}_3)_2$ .** The unit cell consists of two molecules of  $(\mu\text{-H}_2)\text{Ru}_3(\text{EtCCet})(\text{CO})_7(\text{PPh}_3)_2$  which are separated by normal van der Waals distances. There are no anomalously short intermolecular contacts. Selected atomic distances are presented in Table 4. A diagram of the molecule, showing the atomic labeling scheme, is provided in Figure 1.

The core of the molecule is presented in Figure 2 and consists of three ruthenium atoms in a triangular arrangement. The two longer edges of the triangle ( $\text{Ru}(2)\text{-Ru}(3) = 2.993(2) \text{ Å}$  and  $\text{Ru}(1)\text{-Ru}(2) = 2.889(2) \text{ Å}$ ) are each bridged by hydride ligands. The third edge has a significantly shorter bond distance:  $\text{Ru}(1)\text{-Ru}(3) = 2.757(2) \text{ Å}$ . These distances are comparable to those in similar structures. In the structural study of  $(\mu\text{-H})\text{Ru}_3(\mu_3\text{-}\eta^3\text{-Me}_2\text{NCCHCMe})(\text{CO})_9$  the following  $\text{Ru-H-Ru}$  and  $\text{Ru-Ru}$  average bond distances were determined:  $2.968(1)$  and  $2.765(\pm 0.015) \text{ Å}$ , respectively.<sup>16</sup> The bond distances associated with  $(\mu\text{-H})\text{Ru}_3$

(15) (a) Jensen, C. M.; Kaesz, H. D. *J. Organomet. Chem.* **1987**, *330*, 133. (b) Churchill, M. R.; Fetinger, J. C.; Keister, J. B.; See, R. F.; Ziller, J. W. *Organometallics* **1985**, *4*, 2112.



**Table 2. Atomic Coordinates ( $\times 10^4$ ) and Equivalent Isotropic Displacement Coefficients ( $\text{\AA}^2 \times 10^3$ ) for  $(\mu\text{-H})_2\text{Ru}_3(\mu_3\text{-}\eta^2\text{-EtCCEt})(\text{CO})_7(\text{PPh}_3)_2$**

	<i>x</i>	<i>y</i>	<i>z</i>	<i>U</i> (eq) <sup>a</sup>
Ru(1)	2703(1)	1288(1)	2057(1)	31(1)
Ru(2)	3399(1)	3095(1)	2879(1)	31(1)
Ru(3)	4129(1)	205(1)	3088(1)	36(1)
H(12)	2549(95)	2346(88)	2492(44)	78(30)
H(23)	3597(66)	1598(62)	3373(32)	33(19)
P(4)	1626(2)	2561(2)	1196(1)	36(1)
P(5)	2020(2)	3777(2)	3755(1)	34(1)
O(11)	3384(6)	-1106(6)	1337(3)	69(3)
O(12)	259(6)	395(6)	2500(3)	66(3)
O(13)	2300(7)	-428(7)	4157(3)	77(3)
O(21)	5839(7)	3671(8)	3434(3)	81(3)
O(22)	3025(7)	5728(7)	2156(3)	68(3)
O(31)	4729(9)	-2594(7)	2738(4)	97(4)
O(32)	6526(7)	-136(8)	3894(4)	89(3)
C(1)	4927(7)	956(8)	2262(4)	39(3)
C(2)	4493(8)	2230(8)	2136(4)	41(3)
C(3)	5032(9)	3040(9)	1619(4)	50(3)
C(4)	6084(10)	3733(11)	1838(5)	74(4)
C(5)	5937(8)	89(9)	1884(4)	54(3)
C(6)	7280(9)	-39(13)	2157(5)	87(5)
C(11)	3137(8)	-184(9)	1604(4)	50(3)
C(12)	1185(8)	727(7)	2338(4)	38(3)
C(21)	4890(9)	3478(8)	3234(4)	47(3)
C(22)	3099(8)	4753(9)	2421(4)	45(3)
C(31)	4483(9)	-1526(10)	2857(4)	54(4)
C(32)	5637(9)	-7(9)	3582(5)	53(3)
C(33)	2919(9)	-187(9)	3746(5)	53(3)
C(411)	2476(8)	2581(8)	445(4)	40(3)
C(412)	3711(8)	1891(9)	387(4)	52(3)
C(413)	4355(9)	1887(10)	-194(4)	67(4)
C(414)	3783(10)	2600(10)	-684(5)	68(4)
C(415)	2534(9)	3271(10)	-639(4)	60(4)
C(416)	1880(8)	3268(9)	-86(4)	54(3)
C(421)	158(7)	2022(8)	948(4)	42(3)
C(422)	-977(8)	2900(10)	745(5)	61(4)
C(423)	-1999(8)	2420(13)	516(5)	72(5)
C(424)	-1934(10)	1117(13)	468(5)	74(5)
C(425)	-854(10)	255(12)	671(5)	73(4)
C(426)	163(8)	723(10)	904(4)	56(4)
C(431)	1043(8)	4268(8)	1321(4)	46(3)
C(432)	1437(10)	5313(9)	1000(4)	59(3)
C(433)	1020(11)	6576(10)	1141(6)	73(4)
C(434)	201(13)	6819(11)	1639(6)	91(5)
C(435)	-219(10)	5789(10)	1967(4)	59(3)
C(436)	188(9)	4577(9)	1835(4)	64(4)
C(511)	2908(7)	3859(8)	4461(4)	39(3)
C(512)	2614(8)	4882(9)	4846(4)	51(3)
C(513)	3284(10)	4905(11)	5377(4)	64(4)
C(514)	4255(10)	3891(12)	5553(4)	71(5)
C(515)	4577(10)	2827(11)	5188(5)	71(4)
C(516)	3903(9)	2842(9)	4647(4)	54(3)
C(521)	830(7)	2794(7)	4022(4)	39(3)
C(522)	25(8)	2440(8)	3583(4)	46(3)
C(523)	-962(8)	1788(9)	3776(5)	58(4)
C(524)	-1128(9)	1455(10)	4377(5)	63(4)
C(525)	-328(10)	1798(9)	4829(4)	61(4)
C(526)	626(8)	2479(8)	4647(4)	50(3)
C(531)	1021(7)	5409(7)	3652(4)	39(3)
C(532)	1627(9)	6420(8)	3438(4)	50(3)
C(533)	925(10)	7657(9)	3330(5)	61(4)
C(534)	-410(11)	7902(9)	3431(5)	66(4)
C(535)	-1000(10)	6924(9)	3652(5)	63(4)
C(536)	-307(9)	5663(9)	3753(4)	52(3)

<sup>a</sup> Equivalent isotropic *U*, defined as one-third of the trace of the orthogonalized *U<sub>i</sub>* tensor.

structures are significantly different from the metal-metal distances of  $\text{Ru}_3(\text{CO})_{12}$ , which average 2.854 Å.<sup>17</sup> The angles associated with the triruthenium core are

(16) Aime, S.; Osella, D.; Deeming, A. J.; Arce, A. J.; Hursthouse, M. B.; Dawes, H. M. *J. Chem. Soc., Dalton Trans.* **1986**, 1459.

(17) Churchill, M. R.; Hollander, F. J.; Hutchinson, J. P. *Inorg. Chem.* **1977**, *16*, 2655.

$\text{Ru}(2)\text{-Ru}(1)\text{-Ru}(3) = 64.0(1)^\circ$ ,  $\text{Ru}(1)\text{-Ru}(2)\text{-Ru}(3) = 55.9(1)^\circ$ , and  $\text{Ru}(1)\text{-Ru}(3)\text{-Ru}(2) = 60.2(1)^\circ$ .

The two hydride ligands are located bridging the  $\text{Ru}(1)\text{-Ru}(2)$  and  $\text{Ru}(2)\text{-Ru}(3)$  edges of the trimetallic core. The hydride ligand H(23) is associated with the longest Ru-Ru edge, occupies equatorial sites on Ru(2) and Ru(3), lies close to the triruthenium plane, and forms the angle  $\text{Ru}(2)\text{-H}(23)\text{-Ru}(3) = 121(4)^\circ$ . The other hydride ligand (H(12)) is situated on semiaxial sites of Ru(1) and Ru(2), with  $\text{Ru}(1)\text{-H}(12)\text{-Ru}(2) = 140(7)^\circ$ . As usual, those metal-metal bonds that are bridged by hydride ligands are substantially longer than nonbridged metal-metal distances.<sup>18-20</sup>

The EtCCEt ligand is coordinated to the triruthenium core in a  $\mu_3\text{-}\eta^2$  mode. This alkyne ligand is bonded through two Ru-C  $\sigma$ -bonds ( $\text{Ru}(2)\text{-C}(2) = 2.118(8)$  Å and  $\text{Ru}(3)\text{-C}(1) = 2.123(8)$  Å) and a delocalized Ru-ligand interaction ( $\text{Ru}(1)\text{-C}(1) = 2.338(7)$  Å and  $\text{Ru}(1)\text{-C}(2) = 2.295(9)$  Å).

Two  $\text{PPh}_3$  ligands are bonded to the triruthenium core. These ligands are associated with the following Ru-P distances:  $\text{Ru}(1)\text{-P}(4) = 2.380(2)$  Å and  $\text{Ru}(2)\text{-P}(5) = 2.430(2)$  Å. The  $\text{PPh}_3$  ligand based on P(4) occupies an equatorial site on Ru(1) and is located 0.156 Å from the plane formed by the three ruthenium atoms of the molecular core. The other  $\text{PPh}_3$  ligand occupies an axial site on ruthenium atom Ru(2) in a location trans to the capping alkyne ligand and has the slightly longer Ru-P distance.

Ru-CO bond lengths range from 1.871(10) Å to 1.965(10) Å. The shortest such distance ( $\text{Ru}(1)\text{-C}(11)$ ) is located trans to the  $\mu$ -hydride ligand H(13). The longest Ru-CO distance ( $\text{Ru}(3)\text{-C}(33) = 1.965(10)$  Å) is located trans to the alkyne  $\sigma$ -bound carbon atom C(1).

**Description of the Structure of  $(\mu\text{-H})_2\text{Ru}_3(\mu_3\text{-}\eta^2\text{-EtCCEt})(\text{CO})_6(\text{PPh}_3)_3\text{3CH}_2\text{Cl}_2$ .** The unit cell consists of two molecules of  $(\mu\text{-H})_2\text{Ru}_3(\mu_3\text{-}\eta^2\text{-EtCCEt})(\text{CO})_6(\text{PPh}_3)_3$  and six dichloromethane molecules of solvation, which are mutually separated by normal van der Waals distances. There are no anomalously short intermolecular contacts. Selected interatomic distances and angles are presented in Table 4. A diagram of the molecule, showing the atomic labeling scheme, is shown in Figure 3.

The triruthenium core of the cluster, shown in Figure 4, is similar to that of the related molecule  $(\mu\text{-H})_2\text{Ru}_3(\mu_3\text{-}\eta^2\text{-EtCCEt})(\text{CO})_7(\text{PPh}_3)_2$  and has the following Ru-Ru bond distances and Ru-Ru-Ru bond angles:  $\text{Ru}(2)\text{-Ru}(3) = 3.077(1)$  Å,  $\text{Ru}(1)\text{-Ru}(2) = 2.891(1)$  Å, and  $\text{Ru}(1)\text{-Ru}(3) = 2.744(1)$  Å;  $\text{Ru}(2)\text{-Ru}(1)\text{-Ru}(3) = 66.1(1)^\circ$ ,  $\text{Ru}(1)\text{-Ru}(2)\text{-Ru}(3) = 54.6(1)^\circ$ , and  $\text{Ru}(2)\text{-Ru}(3)\text{-Ru}(1) = 59.2(1)^\circ$ . This structure is related to the previous one by the substitution of a triphenylphosphine ligand for an equatorial carbonyl ligand on the third ruthenium atom, Ru(3). This substitution causes no major variations in the angles within the triruthenium core. These distortions from an equilateral triangle seem to be primarily influenced by the lengthening of

(18) Churchill, M. R.; DeBoer, B. G.; Rotella, F. J. *Inorg. Chem.* **1976**, *15*, 1843.

(19) Churchill, M. R. *Adv. Chem. Ser.* **1978**, *No. 167*, 36.

(20) Teller, R. G.; Bau, R. *Struct. Bonding (Berlin)* **1981**, *44*, 1.

(21) Churchill, M. R.; Buttrey, L. A.; Keister, J. B.; Ziller, J. W.; Janik, T. S.; Striejewske, W. S. *Organometallics* **1990**, *9*, 766.

(22) Deeming, A. J.; Arce, A. J.; Sanctis, A.; Day, M. W.; Hardcastle, K. I. *Organometallics* **1989**, *8*, 1408.

**Table 3. Atomic Coordinates ( $\times 10^4$ ) and Equivalent Isotropic Displacement Coefficients ( $\text{\AA}^2 \times 10^3$ ) for  $(\mu\text{-H})_2\text{Ru}_3(\mu_3\text{-}\eta^2\text{-EtCCet})(\text{CO})_6(\text{PPh}_3)_3\text{3CH}_2\text{Cl}_2$**

	<i>x</i>	<i>y</i>	<i>z</i>	<i>U</i> (eq) <sup>a</sup>		<i>x</i>	<i>y</i>	<i>z</i>	<i>U</i> (eq) <sup>a</sup>
Ru(1)	1035(1)	2112(1)	2618(1)	27(1)	C(512)	3797(6)	488(5)	3861(5)	47(3)
Ru(2)	2909(1)	2465(1)	1955(1)	29(1)	C(513)	3840(7)	-246(6)	4499(5)	58(4)
Ru(3)	1666(1)	3285(1)	3348(1)	29(1)	C(514)	4619(8)	-1017(6)	4537(6)	67(4)
H(12)	2339(54)	1668(48)	2664(43)	57(23)	C(515)	5324(7)	-1019(6)	3929(6)	62(4)
H(23)	2782(47)	3079(42)	2744(37)	37(19)	C(516)	5300(6)	-293(5)	3296(5)	48(3)
P(4)	723(1)	1055(1)	1882(1)	31(1)	C(521)	5278(5)	1158(5)	1619(5)	40(3)
P(5)	4478(1)	1527(1)	2475(1)	33(1)	C(522)	5900(6)	1688(6)	1197(5)	56(4)
P(6)	2004(1)	4655(1)	3502(1)	34(1)	C(523)	6465(7)	1455(7)	507(6)	69(4)
O(11)	1285(5)	869(4)	4296(4)	66(3)	C(524)	6412(7)	694(7)	253(6)	69(5)
O(12)	-1167(5)	2675(4)	2935(4)	69(3)	C(525)	5810(8)	175(7)	652(6)	70(4)
O(21)	4117(5)	3681(4)	876(4)	69(3)	C(526)	5233(6)	406(6)	1327(5)	49(3)
O(22)	3075(5)	1448(4)	569(4)	62(3)	C(531)	5253(5)	2083(5)	2935(5)	38(3)
O(31)	2607(6)	2104(4)	4927(4)	81(3)	C(532)	4944(6)	2973(5)	3022(5)	50(3)
O(32)	-238(5)	3389(4)	4355(4)	66(3)	C(533)	5565(7)	3362(7)	3350(7)	77(5)
C(1)	945(5)	3653(4)	2225(4)	30(3)	C(534)	6471(7)	2885(7)	3590(6)	66(4)
C(2)	1466(5)	3233(5)	1623(4)	31(3)	C(535)	6804(6)	1984(6)	3498(6)	58(4)
C(3)	1185(6)	3485(5)	722(5)	39(3)	C(536)	6183(6)	1596(6)	3180(5)	50(3)
C(4)	1716(7)	4156(7)	180(5)	66(4)	C(611)	2874(6)	5124(5)	2738(5)	42(3)
C(5)	-61(6)	4333(5)	2073(5)	43(3)	C(612)	3618(6)	5473(5)	2945(6)	52(4)
C(6)	13(6)	5305(5)	1693(5)	55(3)	C(613)	4192(7)	5872(6)	2314(7)	67(4)
C(11)	1188(6)	1323(5)	3657(5)	40(3)	C(614)	4005(8)	5952(6)	1504(7)	74(5)
C(12)	-336(6)	2463(5)	2801(5)	41(3)	C(615)	3285(8)	5602(6)	1299(6)	73(5)
C(21)	3622(6)	3264(5)	1298(5)	43(3)	C(616)	2717(7)	5191(5)	1914(5)	52(4)
C(22)	3006(5)	1829(5)	1092(5)	38(3)	C(621)	988(5)	5666(5)	3484(5)	36(3)
C(31)	2294(6)	2563(5)	4332(5)	45(3)	C(622)	75(6)	5586(6)	3839(6)	55(4)
C(32)	484(6)	3390(5)	3969(5)	40(3)	C(623)	-682(7)	6328(5)	3851(6)	63(4)
C(411)	-334(5)	559(5)	2326(5)	35(3)	C(624)	-592(7)	7183(6)	3499(6)	60(4)
C(412)	-1087(6)	499(6)	1866(5)	49(3)	C(625)	301(7)	7288(5)	3125(5)	57(4)
C(413)	-1786(6)	54(6)	2228(6)	59(4)	C(626)	1084(6)	6540(5)	3115(5)	42(3)
C(414)	-1785(6)	-335(5)	3057(6)	54(4)	C(631)	2570(6)	4598(5)	4471(4)	38(3)
C(415)	-1034(7)	-280(6)	3512(6)	57(4)	C(632)	2189(7)	5195(5)	4995(5)	49(3)
C(416)	-315(7)	154(6)	3157(5)	53(4)	C(633)	2637(8)	5130(7)	5710(6)	70(5)
C(421)	404(6)	1497(5)	796(4)	36(3)	C(634)	3485(9)	4484(8)	5925(7)	88(6)
C(422)	-416(6)	2231(6)	629(5)	55(4)	C(635)	3873(8)	3899(7)	5404(7)	83(5)
C(423)	-654(8)	2623(6)	-171(6)	67(4)	C(636)	3420(7)	3940(6)	4700(5)	59(4)
C(424)	-125(9)	2316(8)	-802(6)	78(5)	C(1S)	6368(11)	4414(12)	1206(12)	203(11)
C(425)	693(9)	1597(7)	-659(6)	71(5)	Cl(1A)	7078(3)	4965(3)	1964(3)	144(2)
C(426)	943(7)	1190(6)	150(5)	56(4)	Cl(1B)	7142(5)	3629(4)	1022(4)	205(4)
C(431)	1649(5)	-16(5)	1870(4)	36(3)	C(2S)	6923(12)	7553(13)	1422(10)	160(10)
C(432)	2545(6)	-180(5)	2229(5)	46(3)	Cl(2A)	5737(4)	7607(4)	1261(5)	258(5)
C(433)	3231(6)	-1005(6)	2274(6)	58(4)	Cl(2B)	7113(8)	7600(7)	2343(4)	316(7)
C(434)	3018(7)	-1678(6)	1949(6)	65(4)	C(3S)	2013(17)	8337(16)	4183(12)	221(16)
C(435)	2129(7)	-1529(6)	1596(6)	56(4)	Cl(3A)	2981(4)	7365(3)	4231(3)	156(3)
C(436)	1445(6)	-714(5)	1566(5)	48(3)	Cl(3B)	1252(4)	8496(4)	4899(3)	182(3)
C(511)	4531(5)	485(5)	3240(5)	37(3)					

<sup>a</sup> Equivalent isotropic *U* defined as one-third of the trace of the orthogonalized  $U_{ij}$  tensor.

the two Ru–(H)–Ru edges of the triruthenium core due to the hydride ligands' interaction.

Most of the structural features of this molecule are similar to those of  $(\mu\text{-H})_2\text{Ru}_3(\mu_3\text{-}\eta^2\text{-EtCCet})(\text{CO})_7(\text{PPh}_3)_2$ , which was described above, with the following exception. A total of three  $\text{PPh}_3$  ligands are associated with the triruthenium core. Those  $\text{PPh}_3$  ligands associated with phosphorus atoms P(4) and P(5) occupy sites similar to those of their counterparts in the structure of  $(\mu\text{-H})_2\text{Ru}_3(\mu_3\text{-}\eta^2\text{-EtCCet})(\text{CO})_7(\text{PPh}_3)_2$ . The  $\text{PPh}_3$  ligand associated with P(4) occupies an equatorial site on Ru(1), lying 0.052 Å from the  $\text{Ru}_3$  plane. The ligand containing the phosphorus atom P(5) occupies an axial site on Ru(2) trans to the  $\sigma$ -bond Ru(2)–C(2). The associated Ru–P bond distance Ru(2)–P(5) = 2.433(2) Å is the longest Ru–P distance in the molecule. The third  $\text{PPh}_3$  ligand occupies a close-to-equatorial site on ruthenium atom Ru(3). The phosphorus atom P(6) lies 0.845 Å from the plane formed by the three ruthenium atoms. The Ru(3)–P(6) bond distance is intermediate between

the other two ruthenium–phosphorus bonds in the molecule.

**IR and NMR Spectra.** The IR spectra of clusters  $\text{H}_2\text{Ru}_3(\text{EtCCet})(\text{CO})_6(\text{PPh}_3)_3$ ,  $\text{H}_2\text{Ru}_3(\text{EtOCCH})(\text{CO})_6(\text{PPh}_3)_3$ ,  $\text{H}_2\text{Ru}_3(\text{PhCCPh})(\text{CO})_6(\text{PPh}_3)_3$ , and  $\text{H}_2\text{Ru}_3(\text{EtCCet})(\text{CO})_6(\text{P(OMe)}_3)_3$  in the carbonyl region are very similar. The spectra of  $\text{H}_2\text{Ru}_3(\text{EtCCet})(\text{CO})_6(\text{PPh}_3)_3$  and  $\text{H}_2\text{Ru}_3(\text{EtOCCH})(\text{CO})_6(\text{PPh}_3)_3$  are essentially identical. This observation suggests that the complexes are isostructural.

A number of fluxional processes involving  $\text{H}_2\text{Ru}_3(\text{RC}_2\text{R}')(\text{CO})_9$  clusters have been identified.<sup>30</sup> Hydride migration between the three Ru–Ru edges is well-established. The alkyne ligand undergoes oscillation about the  $\text{Ru}_3$  face. The carbonyls undergo a 3-fold rotational process localized on each Ru atom. Because of the low symmetry of the  $\text{PPh}_3$ -substituted clusters fewer fluxional processes are observed.

The NMR spectra of the complexes in solution are consistent with the solid-state structures. For all

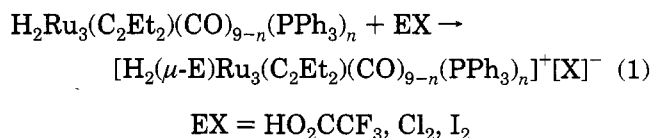
**Table 4. Selected Distances (Å) and Angles (deg) for  $(\mu\text{-H})_2\text{Ru}_3(\mu_3\text{-}\eta^2\text{-EtCCet})(\text{CO})_7(\text{PPh}_3)_2$  and  $(\mu\text{-H})_2\text{Ru}_3(\mu_3\text{-}\eta^2\text{-EtCCet})(\text{CO})_6(\text{PPh}_3)_3\cdot 3\text{CH}_2\text{Cl}_2$**

$\text{H}_2\text{Ru}_3(\mu_3\text{-}\eta^2\text{-EtCCet})(\text{CO})_7(\text{PPh}_3)_2$		$\text{H}_2\text{Ru}_3(\mu_3\text{-}\eta^2\text{-EtCCet})(\text{CO})_6(\text{PPh}_3)_3$	
(A) Ruthenium–Ruthenium Distances			
Ru(1)–Ru(2)	2.889(2)	Ru(1)–Ru(2)	2.891(1)
Ru(1)–Ru(3)	2.757(2)	Ru(1)–Ru(3)	2.744(1)
Ru(2)–Ru(3)	2.993(2)	Ru(2)–Ru(3)	3.077(1)
(B) Ruthenium–Hydride Distances			
Ru(1)–H(12)	1.49(9)	Ru(1)–H(12)	1.78(8)
Ru(2)–H(12)	1.58(10)	Ru(2)–H(12)	1.80(7)
Ru(2)–H(23)	1.82(6)	Ru(2)–H(23)	1.75(7)
Ru(3)–H(23)	1.63(6)	Ru(3)–H(23)	1.78(6)
(C) Ruthenium–Phosphorus Distances			
Ru(1)–P(4)	2.380(2)	Ru(1)–P(4)	2.388(2)
Ru(2)–P(5)	2.430(2)	Ru(2)–P(5)	2.433(2)
		Ru(3)–P(6)	2.360(2)
(D) Ruthenium–Alkyne Distances			
Ru(1)–C(1)	2.338(7)	Ru(1)–C(1)	2.313(7)
Ru(1)–C(2)	2.295(9)	Ru(1)–C(2)	2.287(7)
Ru(2)–C(2)	2.118(8)	Ru(2)–C(2)	2.131(6)
Ru(3)–C(1)	2.123(8)	Ru(3)–C(1)	2.106(7)
(E) Ruthenium–Carbonyl Distances			
Ru(1)–C(11)	1.871(10)	Ru(1)–C(11)	1.886(7)
Ru(1)–C(12)	1.878(8)	Ru(1)–C(12)	1.880(9)
Ru(2)–C(21)	1.875(9)	Ru(2)–C(21)	1.888(8)
Ru(2)–C(22)	1.917(9)	Ru(2)–C(22)	1.888(9)
Ru(3)–C(31)	1.890(10)	Ru(3)–C(31)	1.922(8)
Ru(3)–C(32)	1.891(10)	Ru(3)–C(32)	1.864(8)
Ru(3)–C(33)	1.965(10)		
(F) Carbon–Carbon in Alkyne Distances			
C(1)–C(2)	1.342(11)	C(1)–C(2)	1.368(10)
C(1)–C(5)	1.528(11)	C(1)–C(5)	1.541(9)
C(2)–C(3)	1.522(12)	C(2)–C(3)	1.528(10)
C(5)–C(6)	1.514(13)	C(5)–C(6)	1.529(11)
C(3)–C(4)	1.529(16)	C(3)–C(4)	1.521(13)
(G) Angles Associated with Molecular Triruthenium Core			
Ru(1)–Ru(2)–Ru(3)	55.9(1)	Ru(1)–Ru(2)–Ru(3)	54.6(1)
Ru(2)–Ru(3)–Ru(1)	60.2(1)	Ru(2)–Ru(3)–Ru(1)	59.2(1)
Ru(3)–Ru(1)–Ru(2)	64.0(1)	Ru(3)–Ru(1)–Ru(2)	66.1(1)
(H) Angles Associated with Hydride Ligands			
Ru(1)–H(12)–Ru(2)	140.2(65)	Ru(1)–H(12)–Ru(2)	107.2(32)
Ru(2)–H(23)–Ru(3)	120.6(43)	Ru(2)–H(23)–Ru(3)	121.1(42)

complexes separate  $^{31}\text{P}$  resonances are observed for each  $\text{PR}_3$  ligand at room temperature (albeit broad for some). For the trisubstituted complexes one large  $^{31}\text{P}$ – $^{31}\text{P}$  coupling of ca. 30 Hz is indicative of a *trans*- $\text{PRuRuP}$  arrangement as found in the crystal structure of  $\text{H}_2\text{Ru}_3(\text{EtCCet})(\text{CO})_6(\text{PPh}_3)_3$ . The hydride ligands are static on the NMR time scale at 17 °C. Signals for each of the nonequivalent methylene protons, typically between 4 and 2 ppm (in some compounds significant shielding due to ring currents of the  $\text{PPh}_3$  ligand causes substantial upfield shifts, e.g. to 0.71 ppm) are observed for  $\text{H}_2\text{Ru}_3(\text{EtCCet})(\text{CO})_6(\text{PPh}_3)_3$  and  $\text{H}_2\text{Ru}_3(\text{EtOCCH})(\text{CO})_6(\text{PPh}_3)_3$ , indicating static alkyne ligands; two broad resonances for two pairs of methylene protons and a single methyl resonance at 17 °C for  $\text{H}_2\text{Ru}_3(\text{EtCCet})(\text{CO})_6(\text{P(OMe)}_3)_3$  provide evidence for a fluxional process involving rotation of the  $\mu_3$ - $\text{EtCCet}$  ligand about the  $\text{Ru}_3$  face for this cluster, which averages the two methyl resonances and the resonances due to the two methylene groups.

**Electrophilic Additions: Characterizations of  $[\text{H}_2\text{Ru}_3(\mu\text{-X})(\text{EtCCet})(\text{CO})_{9-n}(\text{PR}_3)_n]^+$  ( $\text{X} = \text{H, I, Cl, F}$ ).** Electrophilic additions and oxidations are closely related. Electrophilic addition products are often intermediates or side products in oxidations. We therefore characterized the products of reactions of  $\text{H}_2\text{Ru}_3(\text{EtCCet})(\text{CO})_{9-n}(\text{PPh}_3)_n$ , ( $n = 2, 3$ ) with acids and of

$\text{H}_2\text{Ru}_3(\text{EtCCet})(\text{CO})_6(\text{PPh}_3)_3$  with halogens. In each case electrophilic addition products are formed (eq 1).



**Protonation Reactions.** Protonation of  $\text{H}_2\text{Os}_3(\mu_3\text{-}\eta^2\text{-HCCNEt}_2)(\text{CO})_9$ , which has a “basketlike” structure, was previously reported to form  $[\text{H}_3\text{Os}_3(\mu_3\text{-}\eta^2\text{-HCCNEt}_2)(\text{CO})_9]^+$ .<sup>23</sup> Protonation of  $\text{H}_2\text{Ru}_3(\text{EtC}_2\text{Et})(\text{CO})_7(\text{PPh}_3)_2$  with  $\text{CF}_3\text{COOH}$  is almost quantitative. The proposed structure is shown in Figure 5. The IR spectrum of the product solution shows a shift of the carbonyl stretches toward higher frequencies by ca. 50  $\text{cm}^{-1}$ , consistent with protonation of the metal framework. NMR spectroscopic characterization is also consistent with protonation at the Ru–Ru bond. At –50 °C two  $^{31}\text{P}$  resonances and three hydride resonances are observed. At room temperature the equivalence of two of the three hydrides, the equivalence of the two  $^{31}\text{P}$  nuclei, and the observation of broad methylene resonances and a single broad methyl resonance indicate that the two hydrides and  $\text{PPh}_3$  ligands are equilibrated via alkyne oscillation combined with 3-fold localized scrambling of CO and  $\text{PPh}_3$  ligands.

Protonation of  $\text{H}_2\text{Ru}_3(\text{EtC}_2\text{Et})(\text{CO})_6(\text{PPh}_3)_3$  forms  $[\text{H}_3\text{Ru}_3(\text{EtC}_2\text{Et})(\text{CO})_6(\text{PPh}_3)_3]^+$  but also a significant amount of  $[\text{H}_3\text{Ru}_3(\text{EtC}_2\text{Et})(\text{CO})_7(\text{PPh}_3)_2]^+$ . After NMR signals due to the latter ion are discounted, the remaining  $^1\text{H}$  and  $^{31}\text{P}$  resonances suggest a structure for the former shown in Figure 5. Proton addition to the Ru–Ru edge generates a cation having three inequivalent hydrides. There is no evidence for fluxionality in this case, and all hydride and  $^{31}\text{P}$  nuclei are inequivalent at room temperature. The  $^{31}\text{P}$ –hydride coupling constants are consistent with the proposed structure, with one large value (28 Hz) characteristic of a *trans* hydride–phosphine relationship and the remainder *cis*. The site of protonation is consistent with the expected character of the HOMO which is associated with the Ru–Ru bond of the neutral precursor.<sup>35</sup>

(23) (a) Adams, R. D.; Tanner, J. T. *Organometallics* **1988**, *7*, 2241. (b) Deeming, A. J.; Kabir, S. E.; Nuel, D.; Powell, N. I. *Organometallics* **1989**, *8*, 717.

(24) Nomikou, Z.; Halet, J.-F.; Hoffmann, R.; Tanner, J. T.; Adams, R. D. *Organometallics* **1990**, *9*, 588.

(25) Goudsmit, R. J.; Johnson, B. F. G.; Lewis, J.; Raithby, P. R.; Rosales, M. J. *J. Chem. Soc., Dalton Trans.* **1983**, 2257.

(26) Boyar, E.; Deeming, A. J.; Felix, M. S. B.; Kabir, S. E.; Adatia, T.; Bhusate, R.; McPartlin, M.; Powell, H. R. *J. Chem. Soc., Dalton Trans.* **1989**, 5.

(27) Adams, R. D.; Chen, G.; Tanner, J. T. *Organometallics* **1990**, *9*, 1530.

(28) Day, M.; Hajela, S.; Hardcastle, K. I.; McPhillips, T.; Rosenberg, E.; Botta, M.; Gobetto, R.; Milone, L.; Osella, D.; Gellert, R. W. *Organometallics* **1990**, *9*, 913.

(29) Brookhart, M.; Grant, B.; Volpe, A. F., Jr. *Organometallics* **1992**, *11*, 3920.

(30) Evans, J.; McNulty, G. S. *J. Chem. Soc., Dalton Trans.* **1981**, 2017.

(31) Sappa, E.; Tiripicchio, A.; Braunstein, P. *Chem. Rev.* **1983**, *83*, 203.

(32) (a) Schilling, B. E. R.; Hoffmann, R. *J. Am. Chem. Soc.* **1979**, *101*, 3456. (b) Halet, J. F.; Saillard, J. Y.; Lissilour, R.; McGlinchey, M. J.; Jaouen, G. *Inorg. Chem.* **1985**, *24*, 218.

(33) Song, L.; Troglor, W. C. *J. Am. Chem. Soc.* **1992**, *114*, 3355.

(34) Doherty, N. M.; Hoffman, N. W. *Chem. Rev.* **1991**, *91*, 553.

(35) Aime, S.; Bertocello, R.; Gobetto, R.; Granzozzi, G.; Osella, D. *Inorg. Chem.* **1986**, *25*, 4004.

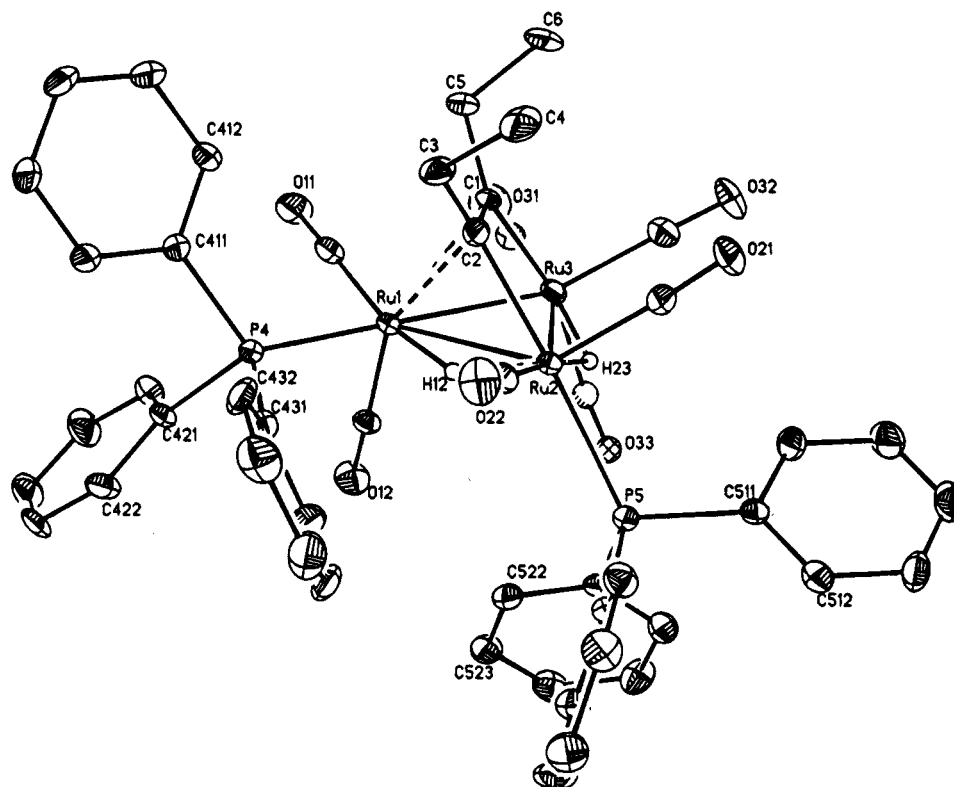


**Figure 1.** Labeling of atoms in the  $(\mu\text{-H})_2\text{Ru}_3(\mu_3\text{-}\eta\text{-EtCCEt})(\text{CO})_7(\text{PPh}_3)_2$  molecule (ORTEP2 diagram, organic H atoms omitted for clarity).

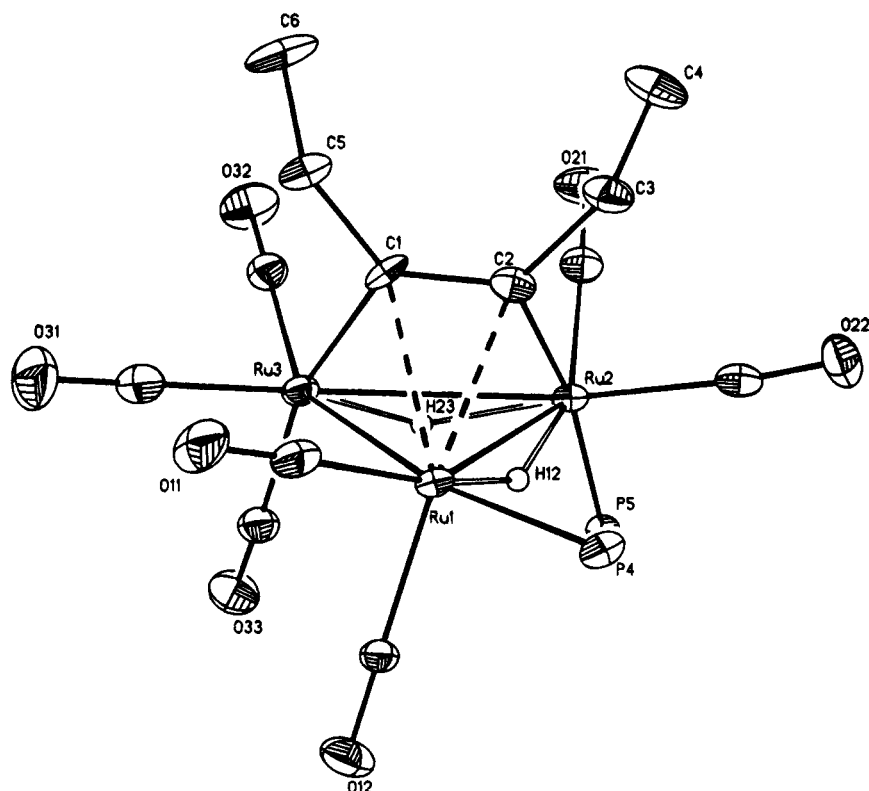


**Figure 2.** Core of the  $(\mu\text{-H})_2\text{Ru}_3(\mu_3\text{-}\eta\text{-EtCCEt})(\text{CO})_7(\text{PPh}_3)_2$  molecule.

**Halogen Additions.** The reaction of  $\text{H}_2\text{Ru}_3(\text{EtC}_2\text{Et})(\text{CO})_6(\text{PPh}_3)_3$  with  $\text{I}_2$  requires 2 equiv of iodine, most likely due to the formation of the  $\text{I}_3^-$  counterion; the product  $[\text{H}_2\text{Ru}_3(\text{I})(\text{EtC}_2\text{Et})(\text{CO})_6(\text{PPh}_3)_3][\text{BPh}_4]$  was isolated after ion exchange with  $\text{NaBPh}_4$ . Similarly, chlorine gas forms  $[\text{H}_2\text{Ru}_3(\text{Cl})(\text{EtC}_2\text{Et})(\text{CO})_6(\text{PPh}_3)_3]\text{Cl}$ . The cations  $[\text{H}_2\text{Ru}_3(\text{X})(\text{EtC}_2\text{Et})(\text{CO})_6(\text{PPh}_3)_3]^+$  (X =

Cl and F) were also formed by oxidations with tris-(4-bromophenyl)ammoniumyl hexachloroantimonate (TBAHCA) and  $\text{FcPF}_6$ , respectively (vide infra).

Although these cluster cations have not been previously reported, they are closely related to  $\text{PPN}[\text{Ru}_3(\mu\text{-Cl})(\mu_3\text{-}\eta^2\text{-PhCCPh})(\text{CO})_9]$  and  $\text{HRu}_3(\mu\text{-Cl})(\mu_3\text{-}\eta^2\text{-PhCCPh})(\text{CO})_9$ , which have been characterized by X-ray crys-



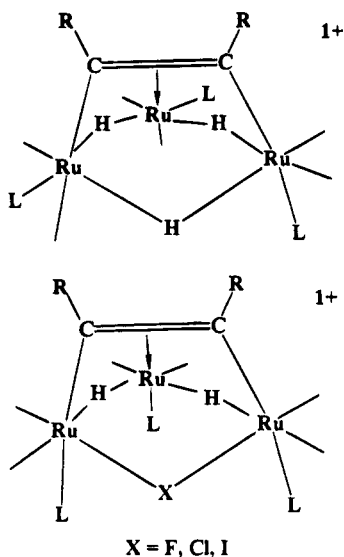


**Figure 5.** Proposed structures for  $[(\mu\text{-H})_2\text{Ru}_3(\mu\text{-X})(\text{EtCCEt})(\text{CO})_6(\text{PPh}_3)_3]^+$  (X = H, F, Cl, I).

appearance of the methylene resonance displays evidence for fluxionality involving the alkyne ligand. At room temperature the geminal methylene protons give two broad signals for  $[\text{H}_2\text{Ru}_3(\text{F})(\text{EtC}_2\text{Et})(\text{CO})_6(\text{PPh}_3)_3]^+$ , one broad signal for  $[\text{H}_2\text{Ru}_3(\text{Cl})(\text{EtC}_2\text{Et})(\text{CO})_6(\text{PPh}_3)_3]^+$ , which splits to two broad lines at  $-55^\circ\text{C}$ , and a quartet-like multiplet for  $[\text{H}_2\text{Ru}_3(\text{I})(\text{EtC}_2\text{Et})(\text{CO})_6(\text{PPh}_3)_3]^+$ . This implies that alkyne flipping is fastest for  $[\text{H}_2\text{Ru}_3(\text{I})(\text{EtC}_2\text{Et})(\text{CO})_6(\text{PPh}_3)_3]^+$  and slowest for  $[\text{H}_2\text{Ru}_3(\text{F})(\text{EtC}_2\text{Et})(\text{CO})_6(\text{PPh}_3)_3]^+$ .  $^{31}\text{P}$  NMR spectra each display two singlets in a 2:1 ratio.

The  $^{19}\text{F}$  NMR spectrum of  $[\text{H}_2\text{Ru}_3(\text{F})(\text{EtC}_2\text{Et})(\text{CO})_6(\text{PPh}_3)_3]\text{PF}_6$  displays the expected doublet due to the  $\text{PF}_6^-$  anion, but no other signal. The absence of fluoride ligand signals in the  $^{19}\text{F}$  NMR spectra of other metal fluoride complexes has been noted in other instances.<sup>34</sup>

Mass spectra display molecular ions for all three cluster cations.

**Electrochemistry of  $\text{H}_2\text{Ru}_3(\mu_3\text{-}\eta^2\text{-RCCR}')(\text{CO})_6(\text{PR}_3)_3$ .** In all cases cyclic voltammograms of  $\text{H}_2\text{Ru}_3(\text{RCCR}')(\text{CO})_6(\text{PR}_3)_3$  showed irreversible or almost irreversible oxidation processes. The oxidation potentials of  $\text{H}_2\text{Ru}_3(\text{HC}_2\text{OEt})(\text{CO})_6(\text{PPh}_3)_3$  ( $E_{p,a} = 0$  mV) and  $\text{H}_2\text{Ru}_3(\text{EtC}_2\text{Et})(\text{CO})_6(\text{PPh}_3)_3$  ( $E_{p,a} = 50$  mV) are nearly the same as that of ferrocene. The clusters of the closely related series  $\text{H}_3\text{Ru}_3(\text{CX})(\text{CO})_{9-n}(\text{PPh}_3)_n$  ( $n = 0\text{--}3$ )<sup>5</sup> and  $\text{HRu}_3(\text{XCRCR}')(\text{CO})_{9-n}(\text{PPh}_3)_n$  ( $n = 0\text{--}3$ )<sup>6</sup> display reversible CV waves (for the first oxidation process) and a significantly greater sensitivity of the oxidation potential to the  $\pi$ -donor ability of the hydrocarbyl substituents.<sup>5,6</sup> Because of its ready preparation only  $\text{H}_2\text{Ru}_3(\text{EtC}_2\text{Et})(\text{CO})_6(\text{PPh}_3)_3$  was examined in detail. Faster scan rates typically resulted in an increase in the  $i_p/c/i_{p,a}$  ratio for the couple (Figure 6). The Osteryoung square-wave voltammogram displayed quasi-reversible oxidation behavior, and the amplitude of the reduction current tended to increase with increasing frequency of pulses. This suggests that the irreversibility is due to follow-up chemical reactions of the radical cation.

Electrochemically generated odd-electron organometallic species are commonly unstable. Decomposition pathways include cluster fragmentation, atom abstraction, and disproportionation.<sup>1</sup> The isolation of  $\text{H}_2\text{-}$

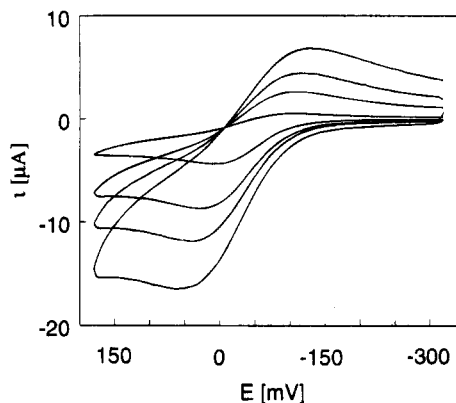


**Figure 6.** Cyclic voltammograms of  $\text{H}_2\text{Ru}_3(\text{EtCCEt})(\text{CO})_6(\text{PPh}_3)_3$  in 0.1 M TBATFB at scan rates of 100, 500, 1000, and 2000  $\text{mV s}^{-1}$ .

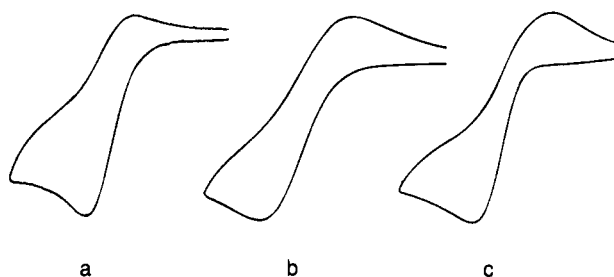


**Figure 7.** Cyclic voltammograms ( $100 \text{ mV s}^{-1}$ ) of  $\text{H}_2\text{Ru}_3(\text{EtCCEt})(\text{CO})_6(\text{PPh}_3)_3$  in 0.1 M  $[\text{NBu}_4][\text{BF}_4]$  (a),  $[\text{NBu}_4][\text{BPh}_4]$  (b), and  $[\text{NBu}_4][\text{BAR}'_4]$  (c) in dichloromethane.

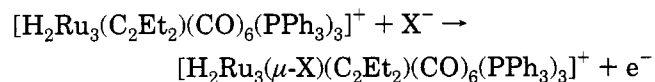
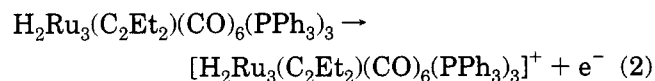
$\text{Ru}_3(\text{X})(\text{EtC}_2\text{Et})(\text{CO})_6(\text{PPh}_3)_3^+$ , where X = F and Cl, upon chemical oxidation of  $\text{H}_2\text{Ru}_3(\text{EtC}_2\text{Et})(\text{CO})_6(\text{PPh}_3)_3$  in the presence of a halide donor and especially the reaction with  $\text{FcPF}_6$ , which is discussed in the next section, led us to suspect that the electrochemical irreversibility might be due to a follow-up reaction of the oxidized species with the electrolyte. To test this hypothesis, we employed several electrolytes, including  $\text{Bu}_4\text{NBF}_4$ ,  $\text{Bu}_4\text{NPF}_6$ ,  $\text{Bu}_4\text{NSO}_3\text{CF}_3$ ,  $\text{Bu}_4\text{NBPh}_4$ , and  $\text{Bu}_4\text{NBAR}'_4$  ( $\text{Ar}' = 3,5\text{-(CF}_3)_2\text{C}_6\text{H}_3$ ). In the first three electrolytes, the cyclic voltammograms (Figure 7a) are virtually identical with very small  $i_p/c/i_{p,a}$  ratios. A cyclic voltammetry experiment using 0.1 M TBATFB at  $-20^\circ\text{C}$  gave the same result. With  $\text{Bu}_4\text{NBAR}'_4$  as electrolyte, a rather different cyclic voltammogram (Figure 7c) was obtained, having an  $i_p/c/i_{p,a}$  ratio of 0.81 but also a much greater  $\Delta E_p$  value, 320 mV. The most reversible voltammogram ( $\Delta E_p = 170$  mV) with comparable anodic and cathodic currents was obtained with  $\text{Bu}_4\text{NBPh}_4$  (Figure 7b), but in this case oxidation of the electrolyte began just ca. 100 mV beyond the cluster's oxidation and the voltammetric response was most likely slightly distorted. In conclusion, we were unable to see a reversible oxidation of  $\text{H}_2\text{Ru}_3(\text{EtC}_2\text{Et})(\text{CO})_6(\text{PPh}_3)_3$  but we clearly observed that the reversibility depended upon the electrolyte. It must be noted that the cyclic voltammogram of  $[\text{H}_2\text{Ru}_3(\text{F})(\text{EtC}_2\text{Et})(\text{CO})_6(\text{PPh}_3)_3]^+$  with  $\text{Bu}_4\text{NBF}_4$  as electrolyte displayed no redox processes under these experimental conditions.

The number of electrons,  $n$ , being transferred during the electrochemical oxidation of  $\text{H}_2\text{Ru}_3(\text{EtC}_2\text{Et})(\text{CO})_6(\text{PPh}_3)_3$  was a concern. Electrochemical oxidations of the 48-electron cluster series  $\text{H}_3\text{Ru}_3(\text{CX})(\text{CO})_6(\text{PPh}_3)_3$  and of  $\text{HRu}_3(\text{XCRCR})(\text{CO})_{9-n}(\text{PPh}_3)_n$  proceed via two 1-electron steps.<sup>5,6</sup> Electrochemical reduction of 46-

electron  $\text{Fe}_3(\text{Et}_2\text{C}_2)(\text{CO})_9$  also occurs through two 1-electron steps.<sup>2</sup> However, reduction of 46-electron  $\text{Os}_3(\text{Ph}_2\text{C}_2)(\text{CO})_7(\text{dppm})$  is a single 2-electron process.<sup>3</sup> Bulk electrolysis performed on  $\text{H}_2\text{Ru}_3(\text{EtC}_2\text{Et})(\text{CO})_6(\text{PPh}_3)_3$  failed to provide a definitive answer, as the current remained above 10% of the initial value even after charge corresponding to  $n = 3$  had been passed through the system; this is attributed to the formation of electroactive decomposition products. Normal pulse voltammetry was used to determine the value of  $nD^{1/2}$  from the limiting current,  $i_{\text{NP}} = (nFA D^{1/2} C) / (\pi^{1/2} t_p^{1/2})$ , where  $n$  is the number of electrons in the process,  $F$  is Faraday's constant,  $A$  is the electrode area,  $D$  is the diffusion coefficient of the cluster,  $C$  is the concentration of the cluster, and  $t_p$  is the pulse width. The value of the diffusion coefficient is estimated as  $5 \times 10^{-6} \text{ cm}^2 \text{ s}^{-1}$  on the basis of values for related clusters of similar size.<sup>5,6</sup> The slope of a plot of  $i$  vs  $t_p^{1/2}$  yielded the experimental value of  $nD^{1/2}$  as  $2.0 \times 10^{-3} \text{ cm s}^{-1/2}$ , consistent with  $n = 0.9$ . Qualitative comparison of anodic peak currents for  $\text{H}_2\text{Ru}_3(\text{HC}_2\text{OEt})(\text{CO})_6(\text{PPh}_3)_3$  and for  $\text{HRu}_3(\text{MeCCMeCOEt})(\text{CO})_6(\text{PPh}_3)_3$  (for which  $n$  was determined to be equal to 1)<sup>6</sup> also suggests that the electrochemical oxidation is a one-electron process.

The electrochemical irreversibility is partially due to the reactivity of the one-electron oxidation product toward species in solution, but other follow-up processes may also be involved. In the absence of electrolyte and with an unreactive counterion the radical has a significant lifetime (vide infra; minutes to hours). With our equipment we are unable to investigate the electrochemistry in the absence of a large excess of electrolyte.

**Characterization and Reactivity of the Radical Derived from  $\text{H}_2\text{Ru}_3(\text{EtC}_2\text{Et})(\text{CO})_6(\text{PPh}_3)_3$ .** Chemical oxidation is the best method for preparing significant quantities of radical cation clusters.  $\text{H}_2\text{Ru}_3(\text{EtC}_2\text{Et})(\text{CO})_6(\text{PPh}_3)_3$  is quite easily oxidized by a variety of one-electron oxidants, including  $\text{Ag}^+$ ,  $\text{NO}^+$ , and  $\text{Fe}(\text{o-phen})_3^{3+}$ , but most do not cleanly form the radical cation due to rapid follow-up reactions, presumably with the counteranion. Oxidation of  $\text{H}_2\text{Ru}_3(\text{EtC}_2\text{Et})(\text{CO})_6(\text{PPh}_3)_3$  with  $\text{FcPF}_6$  and with  $\text{TBPAC}$  produced the 50-electron clusters  $[\text{H}_2\text{Ru}_3(\mu\text{-X})(\text{EtC}_2\text{Et})(\text{CO})_6(\text{PPh}_3)_3]^+$  ( $\text{X} = \text{F}, \text{Cl}$ ), analogous to the products of electrophilic additions (eq 2).



In the absence of reactive anions, chemical oxidation of  $\text{H}_2\text{Ru}_3(\text{EtC}_2\text{Et})(\text{CO})_6(\text{PPh}_3)_3$  by common one-electron oxidants allowed the formation of the unstable radical cation. When  $\text{FcBAR}'_4$  ( $\text{BAR}'_4^-$  is less reactive than  $\text{PF}_6^-$ ) was used, the brown color due to the radical persisted in dichloromethane at 25 °C for about 2 h and after 1 h the IR bands of the radical still had significant intensities. The pattern of IR bands (Figure 8) is different than for  $\text{H}_2\text{Ru}_3(\text{EtC}_2\text{Et})(\text{CO})_6(\text{PPh}_3)_3$ , suggesting some structural changes upon oxidation. Structural differences between the radical cation and the 48-electron precursor could be due to a reorientation of the alkyne, but phosphine ligand reorientation is more

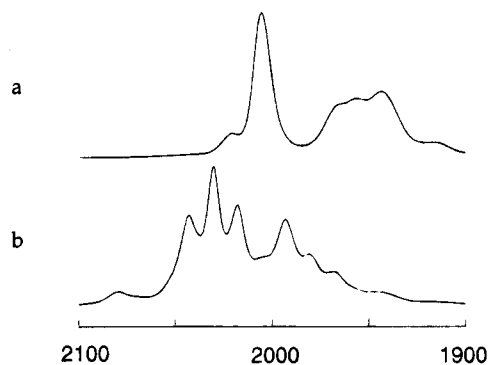


**Figure 8.** IR spectrum of the product (spectrum b) from  $\text{H}_2\text{Ru}_3(\text{EtCCEt})(\text{CO})_6(\text{PPh}_3)_3$  (spectrum a) and  $\text{Fc}[\text{BAR}'_4]$ .

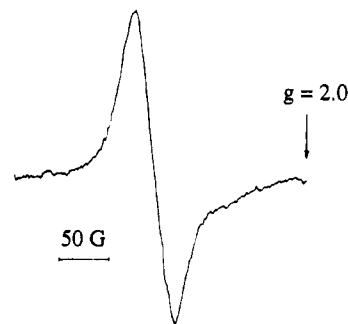


**Figure 9.** EPR signal of solution from  $\text{H}_2\text{Ru}_3(\text{EtCCEt})(\text{CO})_6(\text{PPh}_3)_3$  and  $\text{Fc}[\text{PF}_6]$ .

likely; such an isomerism upon oxidation was shown previously for  $\text{H}_3\text{Ru}_3(\text{CX})(\text{CO})_6(\text{PR}_3)_3$ ,<sup>5</sup> and it is notable that  $[\text{H}_2\text{Ru}_3(\mu\text{-X})(\text{EtC}_2\text{Et})(\text{CO})_6(\text{PPh}_3)_3]^+$  ( $\text{X} = \text{H}$  and  $\text{Cl}$ ) have different arrangements of phosphine ligands. The EPR spectrum (Figure 9) of the radical generated with  $\text{FcPF}_6$  showed a single line with  $g = 2.105$ , a result comparable to those obtained for  $\text{HRu}_3(\text{XCCRCR})(\text{CO})_{9-n}(\text{PPh}_3)_n$ .<sup>6</sup> Oxidation of  $\text{H}_2\text{Ru}_3(\text{PhC}_2\text{Ph})(\text{CO})_6(\text{PPh}_3)_3$  formed a radical with a slightly different  $g$  value, 2.097, indicating that the observed signal is due to an alkyne-containing species.

In the absence of halide sources the radical cation  $[\text{H}_2\text{Ru}_3(\text{EtC}_2\text{Et})(\text{CO})_6(\text{PPh}_3)_3]^+$  decomposes over a period of minutes to hours, yielding numerous, unidentified products. The IR spectrum of the solution following decomposition contains broad absorptions in the carbonyl region, and the NMR spectra contain many resonances of low intensities.

The improved stability of  $[\text{H}_2\text{Ru}_3(\text{EtC}_2\text{Et})(\text{CO})_6(\text{PPh}_3)_3]^-[\text{BAR}'_4]^+$  made it possible to probe its reactivity. The addition of alkenes or alkynes to the solution of the radical had no effect, and IR spectra of the solutions resembled that collected in absence of a nucleophile. In the case of  $\text{PPh}_3$ , initially the IR spectrum of  $\text{H}_2\text{Ru}_3(\text{EtC}_2\text{Et})(\text{CO})_6(\text{PPh}_3)_3$  appeared but the final spectrum was the same as that of the decomposition product. Reaction of the radical cation with diisopropylamine regenerated  $\text{H}_2\text{Ru}_3(\text{EtC}_2\text{Et})(\text{CO})_6(\text{PPh}_3)_3$  in 80% yield. The same product was formed with *tert*-butoxide. For reactions with  $\text{MeNC}$ ,  $\text{Bu}_4\text{NBF}_4$  (electrolyte), or  $[\text{PPN}]\text{Cl}$  in each case  $\text{H}_2\text{Ru}_3(\text{EtC}_2\text{Et})(\text{CO})_6(\text{PPh}_3)_3$  was formed in ca. 50% yield, and for the last two reagents a second product was  $[\text{H}_2\text{Ru}_3(\text{X})(\text{EtC}_2\text{Et})(\text{CO})_6(\text{PPh}_3)_3]^+$  ( $\text{X} = \text{F}, \text{Cl}$ ), respectively. We were unable to characterize the other product(s) of the reaction with  $\text{MeNC}$ .

The product of the oxidation of  $\text{H}_2\text{Ru}_3(\text{EtC}_2\text{Et})(\text{CO})_6(\text{PPh}_3)_3$  with tris(4-bromophenyl)ammonium hexachlo-



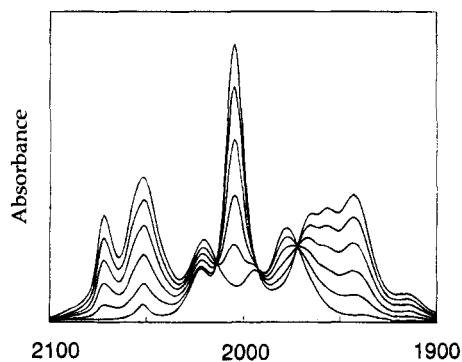


**Figure 10.** Infrared spectra taken during addition of aliquots of  $\text{FcBAR}'_4$  to  $\text{H}_2\text{Ru}_3(\text{EtC}_2\text{Et})(\text{CO})_6(\text{PPh}_3)_3$  in the presence of  $[\text{PPN}]\text{Cl}$ .

roantimonate (TBPAHCA) was  $[\text{H}_2\text{Ru}_3(\text{Cl})(\text{EtC}_2\text{Et})(\text{CO})_6(\text{PPh}_3)_3]^+[\text{X}]^-$ , verified by the FAB mass spectrum ( $m/e$  1379 ( $^{102}\text{Ru}_3^{35}\text{Cl}$ ), attributed to  $[\text{H}_2\text{Ru}_3(\text{Cl})(\text{EtC}_2\text{Et})(\text{CO})_6(\text{PPh}_3)_3]^+$ ) and comparison of the spectroscopic data with those of the product from the reaction with  $\text{Cl}_2$ . The identity of the counteranion is unknown, but it is believed to be  $\text{SbCl}_6^-$ . The cluster decomposes slowly in solution to give an unknown species, which on the basis of NMR spectra is probably the same as the decomposition product(s) from other reactions.  $\text{FcPF}_6$  and  $\text{H}_2\text{Ru}_3(\text{EtC}_2\text{Et})(\text{CO})_6(\text{PPh}_3)_3$  rapidly formed a brown solution, but after ca. 15 min a yellow solution containing  $[\text{H}_2\text{Ru}_3(\text{F})(\text{EtC}_2\text{Et})(\text{CO})_6(\text{PPh}_3)_3]^+$  was obtained (vide supra).

A different procedure for these reactions was used in which small aliquots of  $\text{FcBAR}'_4$  were added to the solutions of  $\text{H}_2\text{Ru}_3(\text{EtC}_2\text{Et})(\text{CO})_6(\text{PPh}_3)_3$  with the reagents. The IR spectra showed quite clean reactions with isosbestic points in the case of  $\text{Bu}_4\text{NBF}_4$  (Figure 10) and  $[\text{PPN}]\text{Cl}$ . The final IR spectra from these two reactions matched those of  $[\text{H}_2\text{Ru}_3(\text{F})(\text{EtC}_2\text{Et})(\text{CO})_6(\text{PPh}_3)_3]^+$  and  $[\text{H}_2\text{Ru}_3(\text{Cl})(\text{EtC}_2\text{Et})(\text{CO})_6(\text{PPh}_3)_3]^+$  (vide supra), and identities of fluoride and chloride clusters were confirmed by  $^1\text{H}$  NMR spectroscopy.

Halide-induced disproportionation of 17-electron mononuclear complexes is well-documented. The mechanism has been investigated.<sup>33</sup> We therefore expected that the stoichiometry of the oxidation in the presence of halide might conform to 2 equiv of oxidant/mol of cluster. However, both TBPAHCA and  $\text{FcPF}_6$  reacted with  $\text{H}_2\text{Ru}_3(\text{EtC}_2\text{Et})(\text{CO})_6(\text{PPh}_3)_3$  in 1:1 ratios, 1 equiv of the oxidant leading to the complete disappearance of  $\text{H}_2\text{Ru}_3(\text{EtC}_2\text{Et})(\text{CO})_6(\text{PPh}_3)_3$ . The addition of ca. 0.7 equiv of  $\text{FcPF}_6$  clearly left 0.3 equiv of unreacted  $\text{H}_2\text{Ru}_3(\text{EtC}_2\text{Et})(\text{CO})_6(\text{PPh}_3)_3$  and formed 0.7 equiv of ferrocene and 0.2 equiv of  $[\text{H}_2\text{Ru}_3(\text{F})(\text{EtC}_2\text{Et})(\text{CO})_6(\text{PPh}_3)_3]^+$ . Reactions of the radical cation with halides are proposed to occur by one-electron oxidation, followed by halide-induced disproportionation to form the 50-electron cationic halide cluster and 1 equiv of the starting material. This explanation is supported by a relatively low yield of  $[\text{H}_2\text{Ru}_3(\text{F})(\text{EtC}_2\text{Et})(\text{CO})_6(\text{PPh}_3)_3]^+$ , 0.2 equiv (theoretical amount 0.35 equiv if disproportionation and 0.7 equiv if a clean 1:1 reaction). In the absence of a halide donor, slower decomposition gives a mixture of uncharacterized products.

In the presence of chloride the disproportionation results in clean formation of  $[\text{H}_2\text{Ru}_3(\text{Cl})(\text{EtC}_2\text{Et})(\text{CO})_6(\text{PPh}_3)_3]^+$  and  $\text{H}_2\text{Ru}_3(\text{EtC}_2\text{Et})(\text{CO})_6(\text{PPh}_3)_3$ . The addition of 0.7 equiv of  $\text{FcBAR}'_4$  to the mixture of  $\text{H}_2\text{Ru}_3(\text{EtC}_2\text{Et})(\text{CO})_6(\text{PPh}_3)_3$

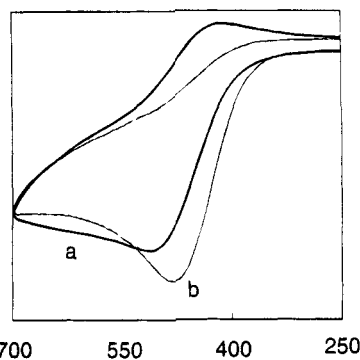


**Figure 11.** Cyclic voltammograms ( $100 \text{ mV s}^{-1}$ ) of  $\text{H}_2\text{Ru}_3(\text{EtC}_2\text{Et})(\text{CO})_6(\text{PPh}_3)_3$  (a) in 0.1 M TBATFB and (b) in 0.1 M TBATFB also containing 0.05 M  $[\text{PPN}]\text{Cl}$ .

$\text{Et}(\text{CO})_6(\text{PPh}_3)_3$  and excess  $[\text{PPN}]\text{Cl}$  resulted in the formation of  $[\text{H}_2\text{Ru}_3(\text{Cl})(\text{EtC}_2\text{Et})(\text{CO})_6(\text{PPh}_3)_3]^+$  and ferrocene in the ratio 0.8:2 (theoretical ratio 1:2 if disproportionation, 1:1 if only one-electron oxidation) and left 0.66 equiv of the starting cluster, matching very well the number predicted for disproportionation (0.30 equiv (unreacted) + 0.35 equiv (from disproportionation)). This reaction is very clean, and no side products were observed. The disproportionation seems to be evident also in cases where the addition of an excess of  $[\text{PPN}]\text{Cl}$  and  $\text{Bu}_4\text{NBF}_4$  to the solution of freshly generated radical causes the recovery of the starting cluster in ca. 50% yield as observed in IR spectra.

If electrolyte-induced disproportionation were occurring in the electrochemical experiments, then we would expect a two-electron oxidation. The effects of halide concentration upon the anodic current were investigated. Since  $\text{BF}_4^-$  and  $\text{PF}_6^-$  did not appear to be good halide donors (because the chemical synthesis with  $\text{FcPF}_6$  was relatively ineffective),  $[\text{PPN}]\text{Cl}$  was added to the solution. Cyclic voltammograms of  $\text{H}_2\text{Ru}_3(\text{EtC}_2\text{Et})(\text{CO})_6(\text{PPh}_3)_3$  at 100 and 200  $\text{mV s}^{-1}$  showed no difference in the anodic peak current when 0.05 M  $[\text{PPN}]\text{Cl}$  and 0.1 M  $\text{Bu}_4\text{NBF}_4$  was present compared to the current in 0.1 M  $\text{Bu}_4\text{NBF}_4$  alone, but the cathodic peak current was reduced to zero (Figure 11). The halide-assisted disproportionation is slow relative to the time scale of cyclic voltammetry.

**Fenske–Hall Molecular Orbital Calculations.** Previously reported calculations on  $\text{H}_2\text{M}_3(\text{RCCR})(\text{CO})_9$  show that the HOMO is associated with the unbridged metal–metal bond.<sup>35</sup> Fenske–Hall calculations were undertaken in order to estimate the effect of the alkyne substituents upon the oxidation potential. Crystallographic data were available for  $\text{H}_2\text{Ru}_3(\text{EtC}_2\text{Et})(\text{CO})_7(\text{PPh}_3)_2$  (this work; for consistency the  $\text{PPh}_3$  ligands were replaced with CO ligands),  $\text{H}_2\text{Ru}_3(\text{MeOCCMe})(\text{CO})_9$ ,<sup>15b</sup> and  $\text{H}_2\text{Ru}_3(i\text{-Pr}_2\text{NCCH})(\text{CO})_9$ <sup>28</sup> ( $i\text{-Pr}$  was replaced with methyl). Fenske–Hall calculations provided HOMO energies of  $-6.95$ ,  $-6.70$ , and  $-6.16$  eV, respectively. It was shown previously that  $\pi$  donation from hydrocarbyl substituents in  $\text{HRu}_3(\text{C}_3\text{R}_3)(\text{CO})_9$  significantly increases the energy of the HOMO:  $-7.04$  eV for  $\text{C}_3\text{Me}_3$ ,  $-6.90$  eV for  $\text{C}_3\text{Me}_2\text{OMe}$ , and  $-6.63$  eV for  $\text{C}_3(\text{H})\text{Me}(\text{NMe}_2)$ .<sup>6</sup> For both series there are good linear correlations of the HOMO energy with the substituent constant  $\sigma^+$  (Figure 12).<sup>37</sup> It was therefore expected that  $\pi$ -donor sub-

(36) Fenske–Hall program version 5.1, kindly provided by M. B. Hall, Department of Chemistry, University of Texas, Austin, TX.

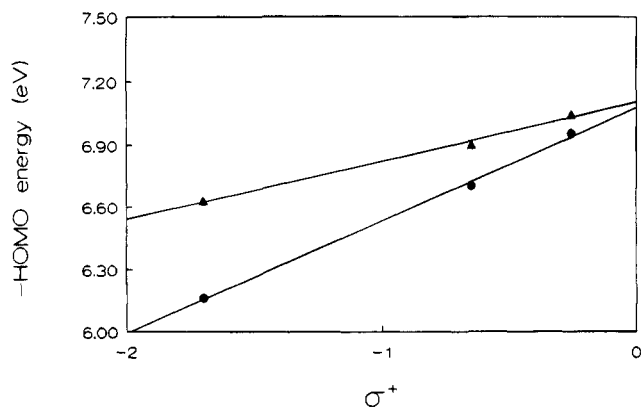


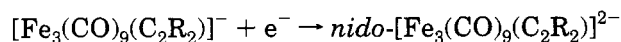
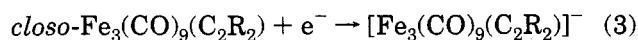
**Figure 12.** Plot of HOMO energy (calculated) for the series  $\text{HRu}_3(\text{XCCR}'\text{R}')(\text{CO})_9$  ( $(\text{X}, \text{R}, \text{R}') = (\text{NMe}_2, \text{H}, \text{Me}), (\text{Me}, \text{Me}, \text{Me}), (\text{MeO}, \text{Me}, \text{Me})$ ) and  $\text{H}_2\text{Ru}_3(\text{XCCR})(\text{CO})_9$  ( $(\text{X}, \text{R}) = (\text{NMe}_2, \text{H}), (\text{Me}, \text{Me}), (\text{MeO}, \text{Me})$ ) vs the  $\sigma^+$  substituent constant for X.

stituents would reduce the oxidation potentials of  $\text{H}_2\text{Ru}_3(\text{XCCR})(\text{CO})_{9-n}(\text{PPh}_3)_n$  in the same way that is found for  $\text{HRu}_3(\text{XCCR}'\text{R}')(\text{CO})_{9-n}(\text{PPh}_3)_n$ . However, no evidence for such a stabilization was found in the oxidation peak potentials (irreversible) for  $\text{H}_2\text{Ru}_3(\text{EtCCEt})(\text{CO})_6(\text{PPh}_3)_3$  and  $\text{H}_2\text{Ru}_3(\text{HCCOEt})(\text{CO})_6(\text{PPh}_3)_3$ .

### Discussion

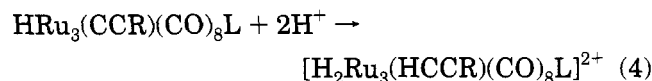
The structures and bonding of trimetallic alkyne clusters have been the subjects of many studies.<sup>23,24,32</sup> Two common coordination geometries of the  $\mu_3\text{-}\eta^2$ -alkyne are observed. For 48-electron clusters, such as  $[\mu_3\text{-}\eta^2\text{-Fe}_3(\text{RCCR})(\text{CO})_9]^{2-}$  and  $\text{H}_2\text{Ru}_3(\mu_3\text{-}\eta^2\text{-RCCR}')(\text{CO})_{9-n}(\text{PR}_3)_n$ , the alkyne is oriented parallel ( $\parallel$ ) to one metal-metal vector, creating a  $\text{M}_3\text{C}_2$  framework described as a square pyramid (or a nido structure based upon an octahedron). For 46-electron clusters, such as  $\text{Fe}_3(\mu_3\text{-}\eta^2\text{-RCCR})(\text{CO})_9$ , the alkyne is oriented perpendicular ( $\perp$ ) to a metal-metal bond so that the  $\text{M}_3\text{C}_2$  framework resembles a trigonal bipyramid (*closo*). In addition, 48-electron clusters in which the alkyne has a strong  $\pi$ -donor substituent exhibit distorted structures which have been described<sup>24</sup> as "basketlike", e.g.  $\text{H}_2\text{Os}_3(\mu_3\text{-}\eta^2\text{-HCCNR}_2)(\text{CO})_9$ ; an alternative description is that the structure is distorted from a nido structure based upon an octahedron toward an arachno structure by removing the  $\text{CNR}_2$  unit from the metal-carbon cluster framework. Fenske-Hall calculations show that the HOMO energies for these clusters should also increase linearly with the  $\pi$ -donor ability of the alkyne substituents.

Electrochemical reductions of 46-electron clusters with alkynes coordinated in  $\mu_3\text{-}\eta^2$  fashion can bring about rearrangement from the  $\mu_3\text{-}\eta^2(\parallel)$  mode to the  $\mu_3\text{-}\eta^2(\perp)$  mode and vice versa.<sup>2,3</sup> One couple for which structural rearrangement has been demonstrated is the  $\text{Fe}_3(\mu_3\text{-}\eta^2(\perp)\text{C}_2\text{R}_2)(\text{CO})_9/[\text{Fe}_3(\mu_3\text{-}\eta^2(\parallel)\text{C}_2\text{R}_2)(\text{CO})_9]^{2-}$  system. Reduction of  $\text{Fe}_3(\text{C}_2\text{R}_2)(\text{CO})_9$  proceeds in two reversible 1-electron steps (eq 3).<sup>2</sup> Very recently an



analogous 46-/48-electron couple,  $\text{Os}_3(\mu_3\text{-}\eta^2(\perp)\text{C}_2\text{R}_2)(\text{CO})_7(\text{Ph}_2\text{PCH}_2\text{PPh}_2)/[\text{Os}_3(\mu_3\text{-}\eta^2(\parallel)\text{C}_2\text{R}_2)(\text{CO})_7(\text{Ph}_2\text{PCH}_2\text{PPh}_2)]^{2-}$ , was reported.<sup>3</sup> The cyclic voltammogram of this couple displays a reversible two-electron process, and the 47-electron intermediate was proposed to contain a  $\mu_3\text{-}\eta^2(\parallel)$ -alkyne ligand.

Analogously, we thought that oxidation of the 48-electron clusters  $\text{H}_2\text{Ru}_3(\text{RCCR}')(\text{CO})_9$  and substituted derivatives might form the 46-electron clusters  $[\text{H}_2\text{Ru}_3(\text{RCCR}')(\text{CO})_9]^{2+}$ . On the basis of our previous studies of  $\text{H}_3\text{Ru}_3(\mu_3\text{-CX})(\text{CO})_{9-n}(\text{PR}_3)_n$  and  $\text{HRu}_3(\mu_3\text{-}\eta^3\text{-XCCR}'\text{R}')(\text{CO})_{9-n}(\text{PR}_3)_n$ , for which  $\pi$ -donor substituents stabilize radical cation oxidation products, we expected a similar stabilization for radical cations derived from oxidation of  $\text{H}_2\text{Ru}_3(\mu_3\text{-}\eta^2\text{-RCCR}')(\text{CO})_{9-n}(\text{PR}_3)_n$ . We hoped that it might be possible to electrochemically generate the 46-electron  $[\text{H}_2\text{Ru}_3(\mu_3\text{-}\eta^2\text{-RCCR}')(\text{CO})_{9-n}(\text{PR}_3)_n]^{2+}$ . Such a cluster,  $[\text{H}_2\text{Ru}_3(\text{HCCMe}_3)(\text{CO})_{9-n}(\text{PPh}_3)_n]^{2+}$ , had been generated by Rosenberg et al. by protonation of  $\text{HRu}_3(\text{CCMe}_3)(\text{CO})_{9-n}(\text{PPh}_3)_n$  ( $n = 0, 1$ ) in sulfuric acid (eq 4).



In fact, our results provide no evidence for the generation of  $[\text{H}_2\text{Ru}_3(\mu_3\text{-}\eta^2\text{-RCCR}')(\text{CO})_{9-n}(\text{PR}_3)_n]^{2+}$  by electrochemical or chemical oxidation, even though the 1-electron-oxidation potentials of the 48-electron clusters are relatively low. We attribute this to high reactivities of the 47-electron radical cations  $[\text{H}_2\text{Ru}_3(\mu_3\text{-}\eta^2\text{-RCCR}')(\text{CO})_{9-n}(\text{PR}_3)_n]^+$ , since the 46-electron clusters  $[\text{H}_2\text{Ru}_3(\text{HCCMe}_3)(\text{CO})_{9-n}(\text{PPh}_3)_n]^{2+}$  have been reported to be stable. Although this study has focused almost exclusively upon  $\text{H}_2\text{Ru}_3(\mu_3\text{-}\eta^2\text{-EtCCEt})(\text{CO})_6(\text{PPh}_3)_3$ , the electrochemical behavior of  $\text{H}_2\text{Ru}_3(\mu_3\text{-}\eta^2\text{-HCCOEt})(\text{CO})_6(\text{PPh}_3)_3$  suggests that there is no appreciable stabilization of the 47-electron cluster by  $\pi$ -donor substituents on the alkyne ligand.

One rationalization for the higher reactivity for the 47-electron clusters  $[\text{H}_2\text{Ru}_3(\mu_3\text{-}\eta^2\text{-RCCR}')(\text{CO})_{9-n}(\text{PR}_3)_n]^+$ , compared with  $[\text{H}_3\text{Ru}_3(\mu_3\text{-CX})(\text{CO})_{9-n}(\text{PR}_3)_n]^+$  and  $[\text{HRu}_3(\text{XCCR}'\text{R}')(\text{CO})_{9-n}(\text{PR}_3)_n]^+$ , is the different character of the SOMO. For  $\text{H}_3\text{Ru}_3(\text{CX})(\text{CO})_{9-n}(\text{PR}_3)_n$ , the HOMO has Ru-C bonding character, and for  $\text{HRu}_3(\text{XCCR}'\text{R}')(\text{CO})_{9-n}(\text{PR}_3)_n$  the HOMO is associated with metal-metal bonding but is delocalized over all three metal atoms. For  $\text{H}_2\text{Ru}_3(\text{XCCR})(\text{CO})_{9-n}(\text{PR}_3)_n$  the HOMO is associated with a single Ru-Ru bond and the greater positive charge density may make the Ru-Ru bond more susceptible to attack by nucleophiles.<sup>35</sup>

The chemistry of the oxidation of  $\text{H}_2\text{Ru}_3(\mu_3\text{-}\eta^2\text{-EtCCEt})(\text{CO})_6(\text{PPh}_3)_3$  is summarized in Figure 13. Chemical or electrochemical oxidation of  $\text{H}_2\text{Ru}_3(\mu_3\text{-}\eta^2\text{-EtCCEt})(\text{CO})_6(\text{PPh}_3)_3$  forms the 47-electron cation (most likely containing a  $\mu_3\text{-}\eta^2(\parallel)$ -alkyne), in which the unpaired electron occupies a Ru-Ru bonding orbital. The 47-electron cluster has a reasonable lifetime in the absence of reactive counterions (the electrolyte in the electrochemical experiments) but is not oxidizable to the stable 46-electron dication under our experimental conditions (perhaps because we have not used a powerful enough oxidant which does not also possess a reactive counterion). Loss of a metal-metal bonding electron destabilizes the 47-electron cluster both with respect to

(37) For  $\sigma^+$  values: Swain, C. G.; Lupton, E. C., Jr. *J. Am. Chem. Soc.* **1968**, *90*, 4328. Gordon, A. J.; Ford, R. A. *The Chemist's Companion*; Wiley: New York, 1972; p 152.

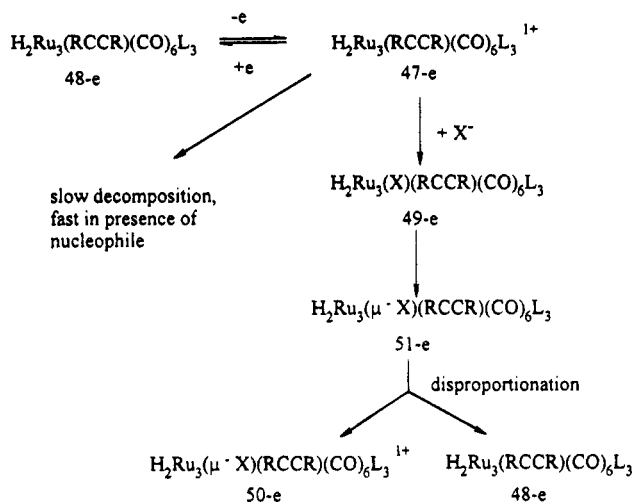


**Figure 13.** Reaction scheme for oxidation of  $\text{H}_2\text{Ru}_3(\text{EtCCEt})(\text{CO})_6(\text{PPh}_3)_3$ .

fragmentation and with respect to attack by halide; the positive charge will make halide attack much more favorable than is the case for anionic 47-electron analogs such as  $[\text{Fe}_3(\text{C}_2\text{R}_2)(\text{CO})_9]^-$ . Attack by halide may initially form the 49-electron neutral cluster containing a terminally coordinated halide ligand, but metal-metal bond cleavage can occur to form an unsaturated, neutral

cluster which is electrochemically inactive near the oxidation potential of  $\text{H}_2\text{Ru}_3(\text{EtCCEt})(\text{CO})_6(\text{PPh}_3)_3$ . Halide bridge formation, which would give the 51-electron product (1 electron more than necessary for a saturated cluster), may be then required before disproportionation can occur. Disproportionation is too slow on the electrochemical time scale to be observable but occurs efficiently in the preparative experiments in which  $[\text{H}_2\text{Ru}_3(\text{EtCCEt})(\text{CO})_6(\text{PPh}_3)_3]^+$  reacts with halide ions.

**Acknowledgment.** We wish to express our thanks to Dr. Robert Allendoerfer for his assistance with EPR spectra. This work was supported by Grant 92-13695 from the National Science Foundation (J.B.K.). Purchase of the Siemens R3m/V diffractometer was made possible by Grant 89-13733 from the Chemical Instrumentation Program of the National Science Foundation.

**Supporting Information Available:** Complete tables of bond lengths, bond angles, anisotropic displacement coefficients, and calculated H-atom coordinates for the two diffraction studies and text describing syntheses of  $\text{H}_2\text{Ru}_3(\text{RCCR})(\text{CO})_9$  (RCCR' = EtCCEt, HCCOEt) and attempted syntheses for RCCR' = HCCCMe<sub>3</sub>, C<sub>2</sub>(CO<sub>2</sub>Me)<sub>2</sub>, MeCCNEt<sub>2</sub> (15 pages). Ordering information is given on any current masthead page.

OM950131M

# Infrared Spectrum of Cyclopentadienyltrimethyltitanium(IV) and Investigation of the Methyl Group Geometry through Partial Deuteration Studies

G. Sean McGrady,\* Anthony J. Downs, and Janette M. Hamblin

*Inorganic Chemistry Laboratory, University of Oxford, South Parks Road,  
Oxford OX1 3QR, U.K.*

Donald C. McKean

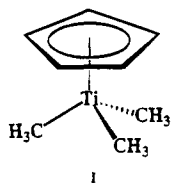
*Department of Chemistry, University of Edinburgh, West Mains Road,  
Edinburgh EH9 3JJ, U.K.*

Received March 1, 1995<sup>®</sup>

Infrared spectra have been recorded between 4000 and 200  $\text{cm}^{-1}$  for cyclopentadienyltrimethyltitanium(IV) in the forms  $\text{CpTi}(\text{CH}_3)_3$ ,  $\text{CpTi}(\text{CH}_2\text{D})_3$ ,  $\text{CpTi}(\text{CHD}_2)_3$ , and  $\text{CpTi}(\text{CD}_3)_3$  ( $\text{Cp} = \eta^5\text{-C}_5\text{H}_5$ ); measurements have been made (i) on the molecules isolated in solid  $\text{N}_2$  matrices at 14 K, (ii) on solutions of the compounds at room temperature, and (iii) on the annealed solid condensates at 77 K. Vibrational fundamentals of the  $\text{TiMe}_3$  fragment have been identified with particular reference to the  $\nu(\text{CH})$  and  $\nu(\text{CD})$  modes, which have been analyzed in terms of a harmonic local mode force field. The spectroscopic evidence is that the methyl groups, while unexceptional in their gross geometry, are asymmetric: with the molecule in the matrix-isolated or solution states, they feature one strong and two weak C-H bonds, but the pattern changes to one weak and two strong C-H bonds for the solid. The results offer a basis for comparison with the properties of other methyltitanium compounds, as well as a test of the utility of "isolated" C-H and C-D stretching frequencies. On the basis of the analysis, an  $\alpha$ -"agostic"  $\text{Ti} \cdots \text{H}-\text{C}$  interaction is proposed.

## Introduction

Cyclopentadienyltrimethyltitanium(IV),  $\text{CpTiMe}_3$ , where  $\text{Cp} = \eta^5\text{-C}_5\text{H}_5$ , **I**, has been known since 1960.<sup>1</sup>



The compound is not only extremely sensitive to attack by air and moisture but also thermally fragile, decomposing at temperatures above 0 °C. However, the appreciable volatility of the material, which sublimes *in vacuo* at ambient temperatures, affords a convenient means of transfer and purification.  $\text{CpTiMe}_3$  appears to have high catalytic activity, with reports of its involvement in Ziegler-Natta polymerization of propene,<sup>2</sup> cycloolefins,<sup>3</sup> and norbornene<sup>4</sup> and in the formation of highly syndiotactic polystyrene of controlled molecular weight.<sup>5</sup> Furthermore, species such as NO and  $\text{SO}_2$  are reported to insert into the  $\text{Ti}-\text{CH}_3$  bonds.<sup>6</sup> This reactivity of the molecule can be ascribed to steric

and electronic unsaturation at the titanium center (with a formal electron count of 12) and to the relatively high energy of the empty d orbitals on this center.

Rather surprisingly, in view of its catalytic behavior, there exists very little structural information about  $\text{CpTiMe}_3$ , although the related molecule  $\text{Cp}^*\text{TiMe}_3$  ( $\text{Cp}^* = \eta^5\text{-C}_5\text{Me}_5$ ) has been the subject of an electron-diffraction study.<sup>7</sup> The  $^1\text{H}$  NMR spectrum of a sample in toluene- $d_8$  solution shows two singlet resonances with relative intensities of 5:9 at temperatures as low as -60 °C. An early study included limited measurements of the vibrational properties in the low-frequency region, leading to the assignment of a few skeletal modes,<sup>8</sup> but as the measurements relate to a THF solution of the compound, there must be some doubts regarding the interpretation of the results, given the high Lewis acidity of the titanium center.

McKean *et al.* have shown that analysis of the vibrational frequencies associated with  $\text{CH}_3$ ,  $\text{CHD}_2$ , and  $\text{CD}_3$  derivatives can yield information about the geometry of the methyl group, including both C-H bond lengths and H-C-H angles.<sup>9</sup> Such results are derived from correlations between the "isolated" C-H stretching frequency,  $\nu^{\text{is}}(\text{CH})$ , displayed by  $\text{CHD}_2$  groups, with bond length or H-C-H angle, aided by harmonic local mode (energy-factored) force field calculations.<sup>10</sup> In addition,

<sup>®</sup> Abstract published in *Advance ACS Abstracts*, July 1, 1995.

(1) Giannini, U.; Cesca, S. *Tetrahedron Lett.* **1960**, *14*, 19.

(2) Chien, J. C. W.; Hsieh, J. T. T. *Coord. Polym.* **1975**, *305*.

(3) Okamoto, T.; Matsumoto, J.; Watanabe, M.; Maezawa, K. *PCT Int. Appl. WO 92 06,123*, 1992.

(4) Petasis, N. A.; Fu, D.-K. *J. Am. Chem. Soc.* **1993**, *115*, 7208.

(5) Takeuchi, T.; Tomotsu, N. *Jpn. Kokai Tokkyo Koho JP 05,271*, 337, 1993.

(6) Clark, R. J. H.; Stockwell, J. A.; Wilkins, J. D. *J. Chem. Soc., Dalton Trans.* **1976**, 120.

(7) Blom, R.; Rypdal, K.; Mena, M.; Royo, P.; Serrano, R. *J. Organomet. Chem.* **1990**, *391*, 47.

(8) Samuel, E.; Ferner, R.; Bigogno, M. *Inorg. Chem.* **1973**, *12*, 881.

(9) McKean, D. C. *Chem. Soc. Rev.* **1978**, *7*, 399; *Croat. Chem. Acta* **1988**, *61*, 447.

empirical correlations linking  $\nu^{is}(\text{CH})$  with the C–H bond dissociation energy,  $D^{\circ}_{\text{CH}}$ ,<sup>11</sup> and the mean M–C bond energy,  $D_{\text{MC}}$ ,<sup>12</sup> allow an assessment of the C–H and M–C bond strengths. A recent infrared study showed the value of this approach for defining the geometry of the methyl group in  $\text{MeTiCl}_3$ .<sup>13</sup>

Since part of the interest in these titanium compounds focuses on identifying different C–H bonds within the same methyl group, it is important to note that the time scale of the infrared experiment means that free rotation effects are not evident in the IR spectrum until the barrier to internal rotation is less than about 4 kJ mol<sup>-1</sup>. For barriers greater than this, the presence of two or three types of C–H bonds within the same methyl group is plain from the occurrence of two or three “isolated” C–H stretching bands in the spectrum of the  $\text{CHD}_2$  derivative.<sup>9</sup> The range of methyl compounds in which such nonequivalent C–H bonds may be identified is therefore greatly enlarged with respect to that accessible to NMR studies, and the IR method is well suited to systems such as  $\text{CpTiMe}_3$ , where the high catalytic activity suggests that C–H···M interactions, described as “agostic”,<sup>14</sup> may be important. In a recent NMR study of solutions containing  $\text{CpTi}(\text{CH}_2\text{D})_3$ , Green *et al.* measured the magnitude and sign of the coupling constant  $^2J(\text{H}–\text{D})$  and concluded that there was no NMR evidence of such an interaction.<sup>15</sup> The authors decided, however, that this technique is not well suited to the identification of agostic interactions in general.

Here we describe a detailed study of the IR spectra of the isotopomers  $\text{CpTi}(\text{CH}_3)_3$ ,  $\text{CpTi}(\text{CH}_2\text{D})_3$ ,  $\text{CpTi}(\text{CHD}_2)_3$ , and  $\text{CpTi}(\text{CD}_3)_3$  and draw on the results for the partially deuterated species to assess the geometry of the methyl groups. The availability of both  $\text{CHD}_2$ - and  $\text{CH}_2\text{D}$ -labeled species invites a subsidiary exploration to determine whether  $\nu^{is}(\text{CD})$  data from the latter constitute a reliable supplement to, or even a substitute for,  $\nu^{is}(\text{CH})$  data from the former.  $\nu^{is}(\text{CD})$  data have been used in earlier studies involving, for example, amines<sup>16</sup> and other species<sup>17</sup> but without any critical assessment of their quantitative significance. A parallel study of similarly substituted versions of  $\text{Me}_2\text{TiCl}_2$  will be reported elsewhere.<sup>18</sup>

## Experimental Section

**Preparation.**  $\text{CpTiMe}_3$  was prepared by the reaction of  $\text{CpTiCl}_3$  with methyl lithium in diethyl ether at  $-78$  to  $0$  °C.<sup>1</sup> On completion of the reaction, the ether was evaporated *in vacuo* at  $-45$  °C. The resulting yellow solid was purified by fractional sublimation *in vacuo*;  $\text{CpTiMe}_3$  was retained in a trap held at  $-45$  °C.

(10) McKean, D. C. *J. Mol. Struct.* **1984**, *113*, 251; **1976**, *34*, 181. McKean, D. C. *Spectrochim. Acta* **1973**, *29A*, 1559.

(11) McKean, D. C. *Int. J. Chem. Kinet.* **1989**, *21*, 445.

(12) McKean, D. C.; McQuillan, G. P.; Thompson, D. W. *Spectrochim. Acta* **1980**, *36A*, 1009.

(13) McKean, D. C.; McQuillan, G. P.; Torto, I.; Bednall, N. C.; Downs, A. J.; Dickinson, J. M. *J. Mol. Struct.* **1991**, *247*, 73.

(14) Brookhart, M.; Green, M. L. H. *J. Organomet. Chem.* **1983**, *250*, 395. Brookhart, M.; Green, M. L. H.; Wong, L. L. *Prog. Inorg. Chem.* **1988**, *36*, 1.

(15) Green, M. L. H.; Hughes, A. K.; Popham, N. A.; Stevens A. H. H.; Wong, L.-L. *J. Chem. Soc., Dalton Trans.* **1992**, 3077.

(16) Krueger, P. J.; Jan, J. *Can. J. Chem.* **1970**, *48*, 3229, 3236.

(17) Schultz, A. J.; Williams, J. M.; Schrock, R. R.; Rupprecht, G. A.; Fellmann, J. D. *J. Am. Chem. Soc.* **1979**, *101*, 1593.

(18) McGrady, G. S.; Downs, A. J.; McKean, D. C. To be published.

The partially deuterated species  $\text{CH}_2\text{DLi}$  and  $\text{CHD}_2\text{Li}$  were synthesized from the reaction of lithium metal with the corresponding methyl chloride, itself obtained from the reaction of  $\text{Bu}^n_3\text{SnD}$  with  $\text{CH}_2\text{BrCl}$  or  $\text{CHBr}_2\text{Cl}$ , respectively.<sup>15</sup>  $\text{CD}_3\text{Li}$  was prepared from  $\text{CD}_3\text{I}$ , which was derived from the reaction of  $\text{CD}_3\text{OD}$  with  $\text{PI}_3$ .<sup>19</sup> Use of the appropriate methyl lithium allowed the preparation of each of the isotopomers  $\text{CpTi}(\text{CH}_3)_3$ ,  $\text{CpTi}(\text{CH}_2\text{D})_3$ ,  $\text{CpTi}(\text{CHD}_2)_3$ , and  $\text{CpTi}(\text{CD}_3)_3$ . The purity of the product was checked by reference to the  $^1\text{H}$  NMR spectrum of a solution in toluene- $d_6$ .<sup>1</sup>

**Spectroscopic Measurements.** Infrared spectra were recorded in the region  $4000$ – $400$  cm<sup>-1</sup> for solid films of the compound formed by condensation of the vapor at  $77$  K and for solutions in  $\text{CCl}_4$  at ambient temperatures ( $0.5$  mm path length), using a Mattson “Galaxy” FT-IR spectrometer at a resolution of  $2$  and  $1$  cm<sup>-1</sup>, respectively. Solutions in  $\text{CCl}_4$  were opaque to IR radiation between  $700$  and  $820$  cm<sup>-1</sup>. The spectrum of a sample of each isotopomer isolated in an  $\text{N}_2$  matrix at  $14$  K was recorded over the range  $4000$ – $200$  cm<sup>-1</sup> using a Perkin-Elmer 580A dispersive spectrophotometer, at an optimum resolution of  $2.8$  cm<sup>-1</sup>. Because of the thermal frailty of the compound, freshly sublimed samples were used for each experiment. The difficulties apparent in handling such a reactive and thermally sensitive material for periods in excess of minutes at ambient temperatures meant that weak, extraneous absorptions probably arising from decomposition products could not be excluded from all of the spectra recorded for  $\text{CpTiMe}_3$ .

**Force Field Calculations.** Harmonic local-mode force field calculations were carried out on the internal vibrational modes of the methyl groups in  $\text{CpTiMe}_3$  using the program ASYM20.<sup>20</sup>

## Results

Infrared spectra were recorded for the following isotopomers of cyclopentadienyltrimethyltitanium(IV): (a)  $\text{CpTi}(\text{CH}_3)_3$ , (b)  $\text{CpTi}(\text{CH}_2\text{D})_3$ , (c)  $\text{CpTi}(\text{CHD}_2)_3$ , and (d)  $\text{CpTi}(\text{CD}_3)_3$ . In each case the spectrum of the isotopomer was measured (i) for the annealed solid condensate on a CsI window at  $77$  K, (ii) for a  $\text{CCl}_4$  solution at ca.  $298$  K, and (iii) for a solid  $\text{N}_2$  matrix at  $14$  K. Figure 1 shows the spectra of each of the matrix-isolated isotopomers in the region  $4000$ – $200$  cm<sup>-1</sup>, whereas Figure 2 shows the spectra of the isotopomers for each of the experimental conditions (i)–(iii) in the region  $3200$ – $2000$  cm<sup>-1</sup>.

Comparison of the spectra with one another and with those of related molecules, such as  $\text{Cp}_2\text{MMe}_2$  ( $\text{M} = \text{Ti}$ ,  $\text{Zr}$ , or  $\text{Hf}$ ),<sup>21</sup>  $\text{CpTiCl}_3$ , or  $\text{NaCp}$ , has allowed us to assign unambiguously the bands arising from the internal modes of the  $\eta^5$ -cyclopentadienyl ligand, and the relevant wavenumbers occurring above  $700$  cm<sup>-1</sup> are collected in Table 1. Table 2 then lists the modes associated with the  $\text{TiMe}_3$  moiety, also at wavenumbers exceeding  $700$  cm<sup>-1</sup>. Some weak absorptions in the spectra indicate the presence of impurities or decomposition products. In the case of the  $\text{CD}_3$  species, the band near  $2080$  cm<sup>-1</sup> observed in all three phases is close to a weak Cp combination frequency but is too intense to come from this source. The same is true of the band at  $1444$  cm<sup>-1</sup> displayed by the solid. Other likely impurity bands occur at  $2873$ ,  $2576$ ,  $2113$ ,  $1145$ ,  $1134$ ,  $1086$ , and  $914$  cm<sup>-1</sup> (the wavenumbers being those appropriate to the solid). Very weak bands at  $3010$  cm<sup>-1</sup>

(19) Douglass, I. B. *Int. J. Sulfur Chem.* **1973**, *8*, 441.

(20) Hedberg, L.; Mills, I. M. *J. Mol. Spectrosc.* **1993**, *160*, 117.

(21) McQuillan, G. P.; McKean, D. C.; Torto, I. *J. Organomet. Chem.* **1986**, *312*, 183.

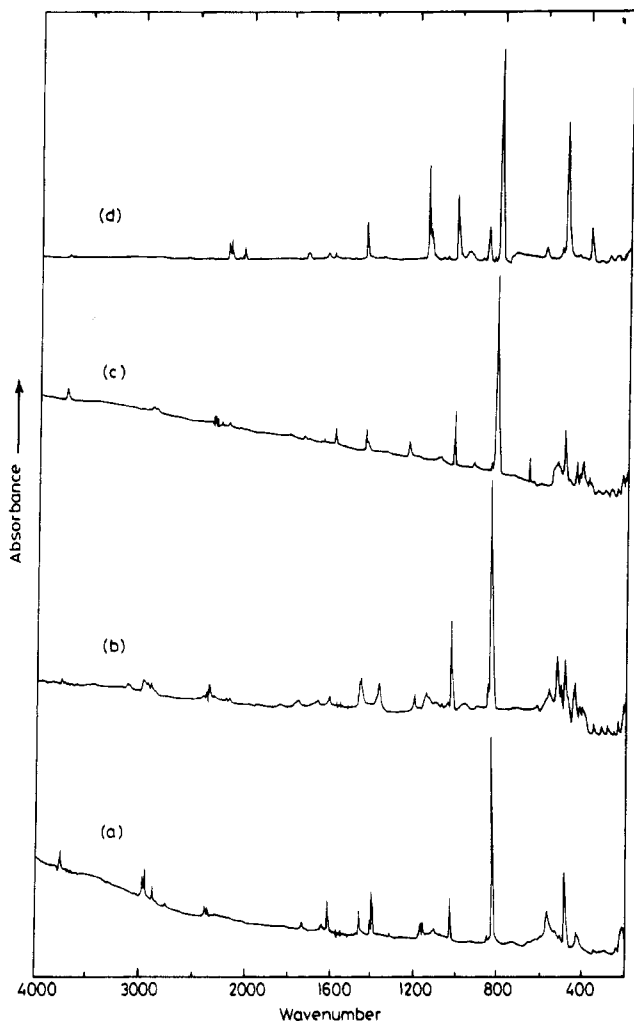


**Figure 1.** IR spectra (4000–200  $\text{cm}^{-1}$ ) of (a)  $\text{CpTi}(\text{CH}_3)_3$ , (b)  $\text{CpTi}(\text{CH}_2\text{D})_3$ , (c)  $\text{CpTi}(\text{CHD}_2)_3$ , and (d)  $\text{CpTi}(\text{CD}_3)_3$  isolated in an  $\text{N}_2$  matrix at 14 K.

( $\text{CH}_2\text{D}$ ) and 3015 and 2975  $\text{cm}^{-1}$  ( $\text{CHD}_2$ ) suggest traces of hydrocarbon impurity. The usual features due to atmospheric  $\text{H}_2\text{O}$  and  $\text{CO}_2$  are also present in the spectra of the solid condensates and carbon tetrachloride solutions; weak absorptions from these species are also evident in the matrix spectra.

**Analysis of the Spectra.** By reference to the results presented in Figures 1 and 2 and Table 2, the spectra of the molecules  $\text{CpTi}(\text{CH}_n\text{D}_{3-n})_3$  ( $n = 0-3$ ) lend themselves to the following analysis.

**Methyl Deformation and Other Bending Modes, Their Overtones and Combinations, and Lower Frequency Modes.** It is helpful to assign the methyl deformation and other bending modes before tackling the  $\nu(\text{CH})$  and  $\nu(\text{CD})$  regions of the spectrum. The  $\delta_{\text{as}}(\text{CH}_3)$  and  $\delta_{\text{s}}(\text{CH}_3)$  bands are readily located near 1390  $\text{cm}^{-1}$  and in the region 1130–1160  $\text{cm}^{-1}$ , respectively. As found previously for other methyltitanium compounds, these both occur at unusually low wavenumbers.<sup>13,21–23</sup> The mode  $\delta_{\text{as}}(\text{CD}_3)$  is expected to occur at ca. 1020  $\text{cm}^{-1}$ , but here it is obscured by strong absorption associated with the cyclopentadienyl group; the fundamental is visible only in the spectrum of an

$\text{N}_2$  matrix, appearing as a very weak band at ca. 1005  $\text{cm}^{-1}$ . Nevertheless, the overtone of this fundamental near 2000  $\text{cm}^{-1}$  is clearly in evidence in the spectra of all three phases. The  $\delta_{\text{s}}(\text{CD}_3)$  band appears at ca. 870  $\text{cm}^{-1}$ . We note a 13  $\text{cm}^{-1}$  splitting of the  $\delta_{\text{s}}(\text{CH}_3)$  band, attributed to  $A_1$  and  $E$  components and evident in the matrix and solution spectra; this is only slightly smaller than the 15  $\text{cm}^{-1}$  splitting found in  $\text{Me}_3\text{P}$ .<sup>24</sup> On the other hand, no similar splitting is displayed by the  $\delta_{\text{s}}(\text{CD}_3)$  band. For the  $\text{CH}_2\text{D}$  species, the mode  $\delta_{\text{s}}(\text{CH}_2)$  is identified with a band of medium intensity at ca. 1360  $\text{cm}^{-1}$ , the  $\text{CH}_2$  wagging mode with a band of similar intensity near 1200  $\text{cm}^{-1}$ , and the remaining deformation mode with a weak feature at ca. 975  $\text{cm}^{-1}$ . One of the deformation modes  $\delta(\text{CH})$  in the  $\text{CHD}_2$  isotopomer is located at ca. 1236  $\text{cm}^{-1}$  and the other at ca. 1089  $\text{cm}^{-1}$ , while the  $\delta_{\text{s}}(\text{CD}_2)$  mode appears at ca. 930  $\text{cm}^{-1}$ .

The overtone of  $\delta_{\text{as}}(\text{CH}_3)$  is found near 2740  $\text{cm}^{-1}$ , where an anharmonicity deficit  $2 \times \delta_{\text{as}}(\text{CH}_3) - 2\delta_{\text{as}}(\text{CH}_3)$  of 10–15  $\text{cm}^{-1}$  indicates a Fermi resonance shift of 26–21  $\text{cm}^{-1}$  due to interaction with  $\nu_{\text{s}}(\text{CH})$  at higher wavenumber. The intensity distribution between  $\nu_{\text{s}}(\text{CH}_3)$  and  $2\delta_{\text{as}}(\text{CH}_3)$ , particularly in the solution spectrum, is compatible with a shift of this magnitude. By contrast,  $\nu_{\text{s}}(\text{CD}_3)$  in the perdeuterated compound, which occurs near 2060  $\text{cm}^{-1}$ , appears to be much less affected by resonance with  $2\delta_{\text{as}}(\text{CD}_3)$  to lower wavenumber.

With regard to the spectrum of the  $\text{CH}_2\text{D}$  compound, assignment of the methyl bending modes near 970 and 1200  $\text{cm}^{-1}$  makes it likely that a combination will appear at ca. 2170  $\text{cm}^{-1}$ . Moreover, the overtone of the  $\text{CH}_2$  scissors mode near 1360  $\text{cm}^{-1}$ , though not observed, will also resonate with  $\text{CH}$  stretching fundamentals to higher wavenumber. For the  $\text{CHD}_2$  species, we must expect a combination  $1243 + 932 = 2175 \text{ cm}^{-1}$  and an overtone  $2 \times 1103 \text{ cm}^{-1}$ , both of which may interact with  $\nu(\text{CD})$  levels.

Assignment of vibrational features due to the  $\text{CH}_3$  moiety below 700  $\text{cm}^{-1}$  is rendered difficult by the complexity of the  $\text{CpTiMe}_3$  molecule and the presence in this region of numerous bands originating in the cyclopentadienyl ligand. The band associated with  $\rho(\text{CH}_3)$  is placed in the region of 480  $\text{cm}^{-1}$ , an energy lower than those of the corresponding features of  $\text{Cp}_2\text{TiMe}_2$ <sup>21</sup> and  $\text{CpTiMeCl}_2$ <sup>22</sup> but not as low as those found for  $\rho(\text{CH}_3)$  of  $\text{MeTiCl}_3$ <sup>13</sup> and  $\text{Me}_2\text{TiCl}_2$ .<sup>18</sup> As with  $\delta(\text{CH}_3)$ ,  $\rho(\text{CH}_3)$  modes occur at substantially lower energies in methyltitanium compounds than in most other methylmetal derivatives.<sup>23</sup> A band attributable to  $\rho(\text{CD}_3)$  is observed at 377  $\text{cm}^{-1}$  in the spectrum of the matrix-isolated  $\text{CD}_3$  derivative, whereas modes corresponding to  $\rho(\text{CH}_2\text{D})$  and  $\rho(\text{CHD}_2)$  are believed to occur near 470 and 430  $\text{cm}^{-1}$ , respectively.

The observation in the spectra of  $\text{CpTiMe}_3$  of two bands near 570 and 520  $\text{cm}^{-1}$  whose wavenumbers fall gradually with increasing deuteration of the methyl groups suggests that these arise from what are predominantly the skeletal fundamentals  $\nu_{\text{as}}(\text{TiC})$  and  $\nu_{\text{s}}(\text{TiC})$ , respectively. Assignment of the latter mode is in agreement with the conclusions drawn from an earlier Raman study, which placed this mode at 517  $\text{cm}^{-1}$ .<sup>8</sup> A fundamental approximating to the  $\text{Ti}-\text{Cp}$  stretching mode is expected to occur at ca. 350  $\text{cm}^{-1}$ ,

(22) Robertson, A. H. J. Ph.D. Thesis, University of Aberdeen, 1990.

(23) Williamson, R. L.; Hall, M. B. *J. Am. Chem. Soc.* **1988**, *110*, 4428.

(24) McKean, D. C.; McQuillan, G. P.; Murphy, W. F.; Zerbetto, F. *J. Phys. Chem.* **1990**, *94*, 4820.

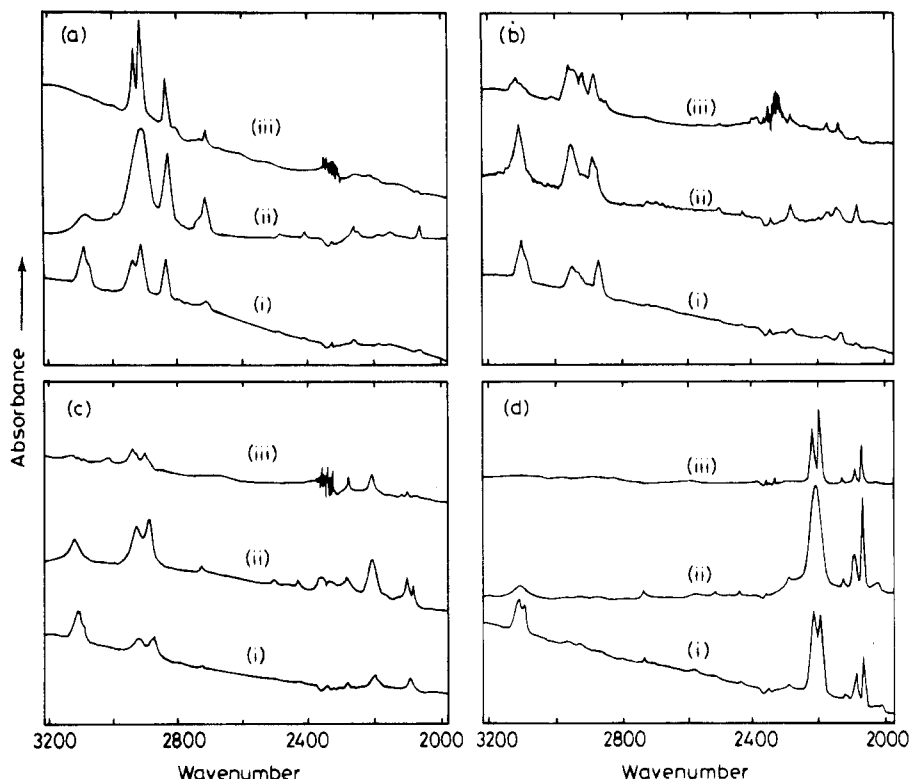


**Figure 2.** IR spectra (3200–2000  $\text{cm}^{-1}$ ) of (a)–(d) (see Figure 1): (i) solid condensate, 77 K; (ii)  $\text{CCl}_4$  solution, 298 K; (iii)  $\text{N}_2$  matrix, 14 K.

**Table 1. Wavenumbers (in  $\text{cm}^{-1}$ ) of the Absorptions in the Range 4000–700  $\text{cm}^{-1}$  Assigned to the Cyclopentadienyl Ligand in the  $\text{CpTiMe}_3$  Isotopomers<sup>a,b</sup>**

$\text{CpTi}(\text{CH}_3)_3$	$\text{CpTi}(\text{CH}_2\text{D})_3$	$\text{CpTi}(\text{CHD}_2)_3$	$\text{CpTi}(\text{CD}_3)_3$	assgnt <sup>c</sup>
3105 w	3105 w	3105 w	3104 w	
3092 w	3091 w	3097 w	3088 w	$\nu(\text{CH})$
2735 vw	2727 vw	2726 vw	2727 vw	$2 \times 1366$
n.o.	2504 vw	2505 vw	2508 vw	$1438 + 1067$
2430 vw	2432 vw	2429 vw	2432 vw	$1366 + 1067$
2284 vw	2284 vw	2282 vw	2282 vw	$1266 + 1019$
2208 vw	2209 vw	obs	obs	$1366 + 844$
2085 vw	2085 vw	2081 vw	2077 vw	$1067 + 1019$
1845 w, br	1845 w, br	1844 w, br	1824 vw	$1019 + 825$
1761 w, br	1759 w, br	1753 w, br	1735 vw, br	$904 + 825?$
1669 w, br	1666 w, br	1660 w, br	1643 w, br	$844 + 825$
1438 ms	1438 ms	1440 ms	1437 ms	$\nu(\text{CC}) (\text{E}_1)$
1366 w, br	1366 w	1366 w	1366 w	$\nu(\text{CC}) (\text{E}_2)$
1266 vw	1266 vw	1266 vw	1265 vw	$\delta_{\text{ip}}(\text{CH}) (\text{A}_2)$
1238 vw	1237 vw	obs	n.o.	?
1127 vw	1125 vw	1128 vw	1127 w, sh	$\nu(\text{CC}) (\text{A}_1)$
1067 vw	1066 vw	1067 vw	1066 vw	$\delta_{\text{op}}(\text{CH}) (\text{E}_2)$
1019 s	1019 s	1018 s	1018 s	$\delta_{\text{ip}}(\text{CH}) (\text{E}_1)$
973 w, br	973 w, br	973 w, br	n.o.	?
904 vw	903 vw	925 vw	914 vw	$\delta_{\text{ip}}(\text{CC}) (\text{E}_2)$
844 mw, sh	844 m, sh	845 mw, sh	846 mw	$\delta_{\text{op}}(\text{CH}) (\text{E}_1)$
825 vs	825 vs	822 vs	815 vs	$\delta_{\text{op}}(\text{CH}) (\text{A}_1)$

<sup>a</sup> Abbreviations: s, strong; m, medium; w, weak; v, very; sh, shoulder; br, broad; n.o., not observed; obs, obscured; ip, in-plane; op, out-of-plane. <sup>b</sup> Values quoted refer to the solid. <sup>c</sup> Based on an ( $\eta^5\text{-C}_5\text{H}_5$ )Ti moiety assumed to have local  $\text{C}_{5v}$  symmetry.

but it was not possible to fix this feature with any degree of certainty in any of the four isotopomers. The dearth of information available at wavenumbers lower than 400  $\text{cm}^{-1}$ , allied to the relative complexity of the  $\text{CpTiMe}_3$  molecule, militated against any attempt at a more detailed analysis of the low-energy regions of the spectra.

**C–H and C–D Stretching Regions.** The coupling between the C–H stretching modes of individual methyl

groups in  $\text{Me}_2\text{X}$  or  $\text{Me}_3\text{X}$  compounds has always proved to be negligible, as reflected, for example, by the observation that the spectra of  $\text{CH}_3(\text{CD}_3)_2\text{X}$  and  $(\text{CH}_3)_3\text{X}$  species are imperceptibly different in the C–H stretching region of the IR spectra.<sup>24</sup> There is no reason to suppose that the methyl groups in  $\text{CpTiMe}_3$  will behave differently. Additional complexity might arise, however, if the three groups were nonequivalent. Counteracting this would be a signal-averaging effect if the barrier to internal rotation about the Ti–CH<sub>3</sub> bonds were less, say, than 100  $\text{cm}^{-1}$ , but this seems unlikely if the C–Ti–C angle in  $\text{CpTiMe}_3$  is similar to that in  $\text{Cp}^*\text{TiMe}_3$ , namely 110.0°.<sup>7</sup>

With these considerations in mind, the identification and interpretation of the symmetric and antisymmetric  $\nu(\text{CH})$  and  $\nu(\text{CD})$  modes poses few problems, the assignments being set out in Table 2. Most noteworthy is the finding that the relevant bands form patterns which in all but two cases are in keeping with what would be expected of an asymmetric methyl group having just one plane of symmetry, i.e. belonging to the point group  $\text{C}_s$ , with two C–H bonds of one kind and one C–H bond of another kind. Thus, split  $\nu_{\text{as}}(\text{CH})$  and  $\nu_{\text{as}}(\text{CD})$  bands are seen in the solid and matrix spectra of the  $\text{CH}_3$  and  $\text{CD}_3$  versions of the compound, respectively, and the  $\text{CH}_2\text{D}$  and  $\text{CHD}_2$  versions each give rise to a pair of  $\nu_{\text{is}}$  bands. The two exceptions are the  $\nu_{\text{as}}(\text{CH})$  and  $\nu_{\text{as}}(\text{CD})$  bands in the solution spectra of the  $\text{CH}_3$  and  $\text{CD}_3$  compounds; both are single features, although broad enough to accommodate splittings of the magnitude observed in the other phases. Pending the further discussion of their contours (q.v.), we will assume that the breadth does indeed arise from such unresolved splitting.

**Analysis: Application of the Frequency Sum Rule.** The first stage in the analysis of the splittings displayed by the  $\nu(\text{CH})$  bands is to determine whether



**Table 2. Wavenumbers (in  $\text{cm}^{-1}$ ) of the IR Absorptions in the Range 4000–700  $\text{cm}^{-1}$  Assigned to the  $\text{TiMe}_3$  Moiety in the  $\text{CpTiMe}_3$  Isotopomers<sup>a</sup>**

molecule	mode <sup>b</sup>	solid film 77 K	$\text{CCl}_4$ soln 298 K	$\text{N}_2$ matrix 14 K	
$\text{CpTi}(\text{CH}_3)_3$	$\nu_{\text{as}}(\text{CH}_3)$	2959 m } 2934 m }	2935 br, mst	2952 mt } 2931 mst }	
	$\nu_{\text{s}}(\text{CH}_3)$	2859 mw	2856 m	2862 m	
	$2\delta_{\text{as}}(\text{CH}_3)$	2735 w	2738 w	2740 w	
	$\delta_{\text{as}}(\text{CH}_3)$	1385 mst	1387 mst	1398 m } 1389 mst }	
	$\delta_{\text{s}}(\text{CH}_3)$	1126 mw	1141 w ( $\text{A}_1$ ) } 1128 w ( $\text{E}$ ) }	1162 mw ( $\text{A}_1$ ) } 1149 mw ( $\text{E}$ ) }	
$\text{CpTi}(\text{CH}_2\text{D})_3$	$\nu_{\text{as}}(\text{CH}_2)$	2950 mw, br	2958 mw, br	2964 m } 2939 sh } (2926 mw?) }	
	$\nu_{\text{s}}(\text{CH}_2)$	2874 mw	2893 mw, br	2888 m } 2850 sh }	
	$\nu^{\text{is}}(\text{CD})$	2176 vw, br } 2136 mw }	2178 vw } 2150 vw }	2185 w } 2146 w }	
	$\delta_{\text{s}}(\text{CH}_2\text{D})$	1352 w, sh	1358 m	1358 m	
	$\text{CH}_2$ wag	1196 mw	1200 m	1199 m	
	$\delta(\text{CH}_2\text{D})$	973 w, br	969 vw	974 w, br	
	$\nu^{\text{is}}(\text{CH})$	2924 mw } 2873 mw }	2928 mw, br } 2891 mw, br }	2938 mw } 2900 w }	
$\text{CpTi}(\text{CHD}_2)_3$	$\nu_{\text{as}}(\text{CD}_2)$	2201 mw	2207 mw	2216 mw	
	$\nu_{\text{s}}(\text{CD}_2)$	2096 w	2105 w	2111 w	
	$\delta(\text{CH}) (\text{A}'')$	1232 mw	1236 mw	1243 m	
	$\delta(\text{CH}) (\text{A}')$	1095 mw, br	1086 w	1103 mw } 1089 mw }	
	$\delta_{\text{s}}(\text{CD}_2)$	923 w, br	934 mw	932 mw	
	$\text{CpTi}(\text{CD}_3)_3$	$\nu_{\text{as}}(\text{CD}_3)$	2206 m } 2186 m }	2201 mst	2211 mw } 2192 m }
		$\nu_{\text{s}}(\text{CD}_3)$	2055 w	2057 mst	2065 mw
$2\delta_{\text{as}}(\text{CD}_3)$		2005 w	2011 w	2010 vw	
$\delta_{\text{as}}(\text{CD}_3)$		obs	obs	1005 vw	
$\delta_{\text{s}}(\text{CD}_3)$		867 m	871 m	872 mst	

<sup>a</sup> Abbreviations: st, strong; m, medium; w, weak; v, very; sh, shoulder; br, broad; s, symmetric; as, antisymmetric; n.o., not observed; obs, obscured. <sup>b</sup> The split  $\nu_{\text{as}}$  bands are designated  $\nu_1$  and  $\nu_2$  in Table 4.  $\nu_{\text{s}}$  similarly becomes  $\nu_3$ .  $\nu_1$  and  $\nu_3$  are thus  $\text{A}'$  species;  $\nu_2$  is  $\text{A}''$ . A description of  $\nu_3$  as a *symmetric stretching* mode is therefore a slight misnomer.

**Table 3. Isolated CH and CD Stretching Frequencies ( $\text{cm}^{-1}$ ), Ratios, and Sum Rule Checks for  $\text{CpTiMe}_3$** 

param	$\text{N}_2$ matrix	$\Delta\nu$	$\text{CCl}_4$ soln	$\Delta\nu$	solid	$\Delta\nu$
$\nu^{\text{is}}(\text{CH})$ (1)	2938	}38	2928	}37	2924	}51
$\nu^{\text{is}}(\text{CH})$ (2)	2900		2891		2873	
$\sum \nu^{\text{is}}(\text{CH})$ ( $2 \times 1$ )	8771		8747		8721	
$\sum \nu^{\text{is}}(\text{CH})$ ( $2 \times 2$ )	8738		8710		8670	
$\sum \nu(\text{CH}_3)^{\text{c}}$	8720		8701		8726	
$\nu^{\text{is}}(\text{CD})$ (1)	2185	}39	2178	}28	2176	}40
$\nu^{\text{is}}(\text{CD})$ (2)	2146		2150		2136	
$\nu(\text{CH})/\nu(\text{CD})$ (1) <sup>b</sup>	1.3446		1.3444		1.3438	
$\nu(\text{CH})/\nu(\text{CD})$ (2) <sup>b</sup>	1.3514		1.3447		1.3450	
$\Delta\nu(\text{CH})/\Delta\nu(\text{CD})^{\text{b}}$		0.974		1.321		1.275

<sup>a</sup> After applying a Fermi resonance correction of  $25 \text{ cm}^{-1}$  to  $\nu_3(\text{CH}_3)$  (see Table 4). <sup>b</sup> Value expected from  $[g(\text{CH})/g(\text{CD})]^{1/2} = 1.347$  15, where  $g$  denotes the relevant  $G$  matrix element.

they arise from one strong bond and two weak bonds or *vice versa*. This is normally evident when the approximate sum rule for CH stretching frequencies (eq 1) is applied. Table 3 shows the results of the calcula-

$$\sum_3 \nu(\text{CH}_3) = \sum_3 \nu^{\text{is}}(\text{CH}) \quad (1)$$

tions. In summing the  $\text{CH}_3$  frequencies, we deduct  $25 \text{ cm}^{-1}$  from each  $\nu_{\text{s}}(\text{CH}_3)$  value to allow for the likely Fermi resonance with two  $\delta_{\text{as}}(\text{CH}_3)$  levels. The evidence from the matrix results indicates unequivocally the presence of one strong and two weak bonds. The same is true for the carbon tetrachloride solution results if we assume that the wavenumber of the  $\nu_{\text{as}}(\text{CH}_3)$  band ( $2935 \text{ cm}^{-1}$ ) is the mean of two values. According to the solid spectra, however, the reverse has to be the

case, with one weak and two strong bonds present. Although the bands here are broad, it is impossible to account for the  $44 \text{ cm}^{-1}$  discrepancy which results when one strong and two weak bonds are assumed.

In some circumstances, the relative intensities of the  $\nu^{\text{is}}$  bands can help to identify the numbers of strong and weak bonds (since the proportion of conformers with  $\text{H}_a$  present should be roughly twice that of the conformers with  $\text{H}_s$  present, where a and s indicate atoms out of or in the plane of symmetry, respectively). However, infrared intensities are notoriously variable, and the present results are in any case unsuitable for estimating their relative values.

Table 3 also illustrates a worrying feature of the  $\nu^{\text{is}}(\text{CH})$  and  $\nu^{\text{is}}(\text{CD})$  values and of the shifts which result. In the diatomic approximation, the ratio  $\nu^{\text{is}}(\text{CH})/\nu^{\text{is}}(\text{CD})$

should be given by the ratio of the square roots of the corresponding  $G$  elements,  $[g(\text{CH})/g(\text{CD})]^{1/2}$ , viz. 1.347 15. The effect of the small couplings involved in the  $\text{CH}_2\text{D}$  and  $\text{CHD}_2$  groups should be to make the observed ratios slightly larger than this figure. In the event, only one of the observed ratios—that for the lower frequency  $\nu^{\text{is}}(\text{CH})$  for the  $\text{N}_2$  matrix sample—fulfils this prediction. More disturbingly, the  $\Delta\nu^{\text{is}}$  splittings should also change in this way with the switch from C–H to C–D bonds, whereas the ratios shown in the table are all well below the expected values; this is particularly evident for the  $\text{N}_2$  matrix results ( $\Delta\nu^{\text{is}}(\text{CH}) = 38 \text{ cm}^{-1}$ ;  $\Delta\nu^{\text{is}}(\text{CD}) = 39 \text{ cm}^{-1}$ ). In part, the anomaly may derive from experimental error due to the widths of the bands involved, but the most likely source of the trouble is the intervention in the  $\nu(\text{CD})$  region of the  $\text{CH}_2\text{D}$  species by the combination  $1200 + 970 \text{ cm}^{-1}$ . This could both overlap with one of the  $\nu^{\text{is}}(\text{CD})$  bands and also be in resonance with either. The picture is further complicated by problems associated with the  $\nu(\text{CH})$  region of the  $\text{CHD}_2$  species. For we note that the lower energy band at  $2900 \text{ cm}^{-1}$  is accompanied by a shoulder at ca.  $2887 \text{ cm}^{-1}$  and the higher energy one at  $2938 \text{ cm}^{-1}$  is noticeably broad. The appearance of weak bands at  $3015$  and  $2975 \text{ cm}^{-1}$  suggests the presence of hydrocarbon impurity, and the latter may well be responsible for the above features associated with the  $\nu^{\text{is}}(\text{CH})$  bands.

**Harmonic Local Mode Force Fields.** The problems involved with assignment are further highlighted when we pass to the second stage of the analysis which involves a global treatment of all the C–H and C–D stretching fundamentals together, in isolation from all other vibrations in the molecule, and seeks refinement of a harmonic local mode force field. Such a treatment produces an “energy-factored” force field, more familiarly encountered in the analysis of carbonyl stretching vibrations in organometallic compounds.<sup>25</sup> The treatment has the advantage of yielding both diagonal and interaction stretch–stretch force constants and is particularly important when the methyl groups in question contain C–H bonds of differing strength. In the present case the local symmetry of the  $\text{CH}_3$  moieties is reduced from  $C_{3v}$  to  $C_s$ , resulting in two  $A'$  and one  $A''$  stretching vibrations instead of the  $\nu_{\text{as}}$  and  $\nu_s$  combinations. A diagnosis of the number of weak and strong bonds in the methyl group can then be made simply by identifying the symmetries of the split  $\nu_{\text{as}}(\text{CH}_3)$  modes.<sup>26</sup>

Table 4 shows the results of such calculations based on the results of the matrix and solution spectra. For the former spectra, nine frequencies appeared to be reasonably well defined and mutually compatible. These were assigned uncertainties in the range  $2\text{--}5 \text{ cm}^{-1}$ . The remaining ones were unweighted. The fit to  $\nu_1(\text{CH}_3\text{D}_2)$  is poor ( $\epsilon_\nu = 8.1 \text{ cm}^{-1}$ ), and that to  $\nu_3(\text{CH}_2\text{D}_a)$ , still worse ( $\epsilon_\nu = 17.3 \text{ cm}^{-1}$ ). While the former may reflect overlap with a weak impurity band, the latter is so wide of the mark as to cause one to query whether the band seen is due in fact not to  $\nu^{\text{is}}(\text{CH})$  but to the expected combination.

A further matter for concern is the failure to reproduce  $\nu_1$  in the  $\text{CH}_2\text{D}_a$  species, which is the more abundant of the two. By contrast, the value of  $\epsilon_\nu$  of 22.3

**Table 4. Harmonic Local Mode Refinements for the Methyl Groups in CpTiMe<sub>3</sub>**

group	mode	$\text{N}_2$ matrix, 14 K			$\text{CCl}_4$ soln, 298 K		
		$\nu_{\text{obs}}^a$	$\sigma_\nu^b$	$\epsilon_\nu^c$	$\nu_{\text{obs}}^a$	$\sigma_\nu^b$	$\epsilon_\nu^c$
$\text{CH}_3$	$\nu_1$	2952	2	0.3	2935		(2947.7)
	$\nu_2$	2931	2	2.4	2935		(2919.9)
	$\nu_3$	2837 <sup>d</sup>	5	0.6	2831 <sup>d</sup>	10	–0.5
$\text{CD}_3$	$\nu_1$	2211	2	–0.1	2201		(2211.2)
	$\nu_2$	2192	2	–2.3	2201		(2191.2)
	$\nu_3$	2060 <sup>d</sup>	3	–2.9	2052 <sup>d</sup>	5	0.2
$\text{CH}_2\text{D}_a^e$	$\nu_1$	2964		15.9	2958		14.1
	$\nu_2$	2888		10.7	2893		21.2
	$\nu_3$	2060 <sup>d</sup>	3	–2.9	2052 <sup>d</sup>	5	0.2
$\text{CH}_2\text{D}_s^e$	$\nu_1$	2926	2	–2.4	2958		38.1
	$\nu_2$	2888		22.4	2893		34.0
	$\nu_3$	2185		17.3	2178		12.2
$\text{CH}_a\text{D}_2^e$	$\nu_1$	2900	2	1.4	2891	2	0.0
	$\nu_2$	2216		8.3	2207		–0.2
	$\nu_3$	2111		2.1	2105		3.7
$\text{CH}_s\text{D}_2^e$	$\nu_1$	2938		8.1	2928	2	0.0
	$\nu_2$	2216		21.6	2207		15.8
	$\nu_3$	2111		12.0	2105		15.1
param		$\text{N}_2$ matrix		$\text{CCl}_4$ soln			
H–C–H ( $^\circ$ )		107		110			
$f_s$ (mdyn/Å)		4.6927(75)		4.6874(4)			
$f_a$ (mdyn/Å)		4.5924(36)		4.5689(4)			
$f'$ (mdyn/Å)		–0.0017(35)		0.0191(6)			

<sup>a</sup>  $\nu(\text{CD})$  data are divided by 1.011 before input, and output values multiplied by 1.011 for the  $\epsilon_\nu$  listing (see ref 21). <sup>b</sup> Uncertainty in  $\nu$ ; unweighted datum. <sup>c</sup>  $\epsilon_\nu = \nu_{\text{obs}} - \nu_{\text{calc}}$ . Values in parentheses are  $\nu_{\text{calc}}$ . <sup>d</sup> Fermi resonance corrections applied:  $-25 \text{ cm}^{-1}$  for  $\text{CH}_3$ ;  $-5 \text{ cm}^{-1}$  for  $\text{CD}_3$ . <sup>e</sup> The subscripts s and a denote C–H or C–D bonds lying respectively in or out of the plane of symmetry of the asymmetric methyl group.

$\text{cm}^{-1}$  for  $\nu_2$  for the less abundant  $\text{CH}_2\text{D}_s$  conformer probably indicates that the frequency listed, viz.  $2888 \text{ cm}^{-1}$ , applies only to the  $\text{CH}_2\text{D}_a$  conformer. With respect to  $\nu_1$ , the model cannot account for any  $\text{CH}_2\text{D}$  frequency which exceeds the highest  $\text{CH}_3$  one, so that the observed breach of this condition again suggests intervention from impurity.

In making each refinement, an H–C–H angle has to be assumed. Exploration of a range of likely angles showed only a slight sensitivity of the fit to the angle and the value finally selected,  $107^\circ$ , carries an uncertainty of  $2\text{--}3^\circ$ . If the wavenumber ratio of the anti-symmetric stretching modes of the  $\text{CH}_3$  and  $\text{CD}_3$  groups is used as an indicator of the angle (only  $\nu_2$  is appropriate for this purpose), the estimated H–C–H angle comes out to be  $103.4^\circ$ . However, the force field refinement gives a fit which is markedly worse with this value and, in addition, the value of the interaction force constant  $f'$  determined on this basis is anomalously negative ( $-0.027 \text{ mdyn/Å}$ ). Accordingly this source of information must be disregarded. That the value of  $f'$  for H–C–H =  $107^\circ$  is  $-0.002 \text{ mdyn/Å}$  suggests a greater likelihood of an angle which actually exceeds, rather than falls below,  $107^\circ$ .

In the attempt to fit the carbon tetrachloride solution results, only four band centers were sufficiently well defined to be utilized, and two of these,  $\nu_{\text{as}}(\text{CH}_3)$  and  $\nu_{\text{as}}(\text{CD}_3)$ , required Fermi resonance corrections of 25 and  $5 \text{ cm}^{-1}$ , respectively. With the assumption of one strong and two weak bond, the mean values of the two  $\nu_{\text{as}}(\text{CH}_3)$  and  $\nu_{\text{as}}(\text{CD}_3)$  frequencies predicted were very close to the centers of the broad bands seen in the spectra.

(25) See, for example: Nakamoto, K. *Infrared and Raman Spectra of Inorganic and Coordination Compounds*, 4th ed.; Wiley: New York, 1986.

(26) McKean, D. C.; Torto, I. J. *Mol. Struct.* **1982**, *81*, 51.

**Table 5. Comparison of  $\nu^{\text{is}}(\text{CH})$  and  $r_0(\text{CH})$  Values of CpTiMe<sub>3</sub> with Corresponding Parameters Reported for other Methyl–Metal Compounds**

molecule	$\nu^{\text{is}}(\text{CH})$ (cm <sup>-1</sup> )	$r_0(\text{CH})$ (Å) <sup>d</sup>	ref
CpTiMe <sub>3</sub> <sup>a</sup>	2943	1.098	this work
	2905 × 2	1.102	
CpTiMeCl <sub>2</sub> <sup>b</sup>	2958 × 2	1.096	22
	2918	1.100	
Cp <sub>2</sub> TiMe <sub>2</sub> <sup>b</sup>	2932 × 2	1.098	21
	2915	1.100	
MeTiCl <sub>3</sub> <sup>c</sup>	2952	1.096	13
Me <sub>2</sub> TiCl <sub>2</sub> <sup>c</sup>	2938	1.098	18
Cp <sub>2</sub> ZrMe <sub>2</sub> <sup>b</sup>	2904	1.101	21
Cp <sub>2</sub> HfMe <sub>2</sub> <sup>b</sup>	2900	1.102	21
MeMn(CO) <sub>5</sub> <sup>c</sup>	2955	1.096	40
MeRe(CO) <sub>5</sub> <sup>c</sup>	2935	1.098	40
Me <sub>2</sub> Zn <sup>c</sup>	2935	1.098	12
Me <sub>2</sub> Cd <sup>c</sup>	2948	1.097	12
Me <sub>2</sub> Hg <sup>c</sup>	2954	1.096	12
Me <sub>3</sub> Ga <sup>c</sup>	2940	1.097	41
Me <sub>3</sub> Tl <sup>c</sup>	2967	1.094	41
Me <sub>4</sub> Ge <sup>c</sup>	2954	1.096	42
Me <sub>4</sub> Sn <sup>c</sup>	2960	1.095	42
Me <sub>4</sub> Pb <sup>c</sup>	2978	1.093	42

<sup>a</sup> Values relate to an N<sub>2</sub> matrix containing the compound with the addition of 5 cm<sup>-1</sup> to give an empirical correlation with gas phase values. <sup>b</sup> Values relate to CCl<sub>4</sub> solution of the compound with the addition of 10 cm<sup>-1</sup> to give an empirical correlation with gas phase values. <sup>c</sup> Values relate to the gaseous molecule. <sup>d</sup> Calculated from eq 2.

However, the calculations gave a poor account of all the CH<sub>2</sub>D bands, including both the  $\nu^{\text{is}}(\text{CD})$  modes. The H–C–H angle chosen, viz. 110°, optimized the quality of the fit, but since this fit depended rather critically on the Fermi resonance shifts assumed, an uncertainty in the bond angle of ±3° is likely. No difference in the angle for the matrix-isolated and solution species can therefore be inferred. The marginally larger angle implied by the solution results does, however, illustrate the dependence on H–C–H of the interaction force constant  $f'$ .

We were unable to account for the spectra of the solid samples using a harmonic local mode analysis in any sensible manner. Whether this implies that the methyl groups are subject to significant additional interactions under these conditions must, however, remain a matter for speculation.

## Discussion

Despite difficulties in the detailed analysis outlined above, it is plain that we have in the molecule CpTiMe<sub>3</sub> a modest difference in C–H bond strength, in which a 40–50 cm<sup>-1</sup> change in  $\nu^{\text{is}}(\text{CH})$  may be translated *via* the correlation with  $r_0(\text{CH})$  (eq 2) into a 0.004–0.005 Å difference in bond length.<sup>9</sup>

$$r_0(\text{CH}) (\text{Å}) = 1.3982 - 0.0001023\nu^{\text{is}}(\text{CH}) (\text{cm}^{-1}) \quad (2)$$

Comparison of the results obtained from this study with the data obtained previously for the species CpTiMeCl<sub>2</sub><sup>22</sup> and Cp<sub>2</sub>TiMe<sub>2</sub>,<sup>21</sup> along with other methyl–metal derivatives (Table 5), is instructive for the light it sheds on the behavior of the CH<sub>3</sub> moiety when bonded to a metal center. The following points are evident.

1. All three of the cyclopentadienyltitanium derivatives CpTiMe<sub>3</sub>, CpTiMeCl<sub>2</sub>, and Cp<sub>2</sub>TiMe<sub>2</sub> exhibit asymmetric methyl groups. However, whereas the asymmetry for CpTiMeCl<sub>2</sub> and Cp<sub>2</sub>TiMe<sub>2</sub>, as well as other

methyl–metal compounds, involves one weak and two strong C–H bonds, CpTiMe<sub>3</sub> is unique among the compounds studied to date in displaying *one* strong and *two* weak C–H bonds. A second unusual feature is the apparent switch from *two* weak to *one* weak bond accompanying the move from the matrix or solution to the solid phase. Comparison of the values of  $\nu^{\text{is}}(\text{CH})$  associated with the CHD<sub>2</sub> versions of the cyclopentadienyl derivatives and of MeTiCl<sub>3</sub><sup>13</sup> and Me<sub>2</sub>TiCl<sub>2</sub><sup>18</sup> (each of which appears to be characterized by a single value of  $\nu^{\text{is}}(\text{CH})$ ) suggests that the stronger bonds comply with normal behavior, with  $\nu^{\text{is}}(\text{CH})$  and  $r_0(\text{CH})$  parameters generally in line with the values deduced from other methyl derivatives of titanium, the later transition metals, and the post-transition metals. Hence it is the *weaker* bonds that are anomalous. We have sought to correlate the source of the asymmetry with the groups lying  $\beta$  to the C–H bonds. In the methyltitanium compounds, these can be  $\eta^5\text{-C}_5\text{H}_5$ , other methyl groups, or chlorine. It is hard to see any regularities underlying the  $\beta$  effects, such as may be found, for example, in conventional organic compounds.<sup>9</sup> From the point of view of such organic compounds, it is curious that no distinction can be found between the C–H bonds in Me<sub>2</sub>TiCl<sub>2</sub>; slight asymmetries are certainly observed for Me<sub>2</sub>CH<sub>2</sub><sup>27</sup> and Me<sub>2</sub>SiH<sub>2</sub>.<sup>28</sup>

We considered two other explanations for the weakening of the C–H bonds in the methyl groups of the cyclopentadienyl derivatives. The first invokes steric crowding in the coordination sphere of the small titanium atom, while the second focuses on the electron deficiency of this center, leading to an agostic interaction with the electrons in the C–H bonds. In the series CpTiMe<sub>3</sub> (**1**), CpTiMeCl<sub>2</sub> (**2**), and Cp<sub>2</sub>TiMe<sub>2</sub> (**3**), steric crowding will decrease in the order **3** > **2** > **1**,<sup>29</sup> whereas electron deficiency might reasonably be expected to follow the order **1** > **2** > **3**. Table 6 details salient parameters for the species under consideration. There is no immediate correlation of the mean value,  $\nu^{\text{is}}(\text{CH}_{\text{av}})$ , or of  $\Delta\nu^{\text{is}}(\text{CH})$  (the difference between the two values) either with the degree of steric crowding about titanium or with the electron deficiency of the metal center. However, if we take into account the total weakening of C–H bonds in each molecule, a clearer picture emerges. Multiplying  $\Delta\nu^{\text{is}}(\text{CH})$  for each compound by the number of C–H bonds responsible for the lower value of  $\nu^{\text{is}}(\text{CH})$ ,  $\chi_{\text{CH}}$ , shows the effect to be much more marked in the 12-electron compound CpTiMe<sub>3</sub>, which has no ability to reduce its electron deficiency by classical  $\pi$ -donation from electron-rich substituents. Correlation of  $\nu^{\text{is}}(\text{CH})$  with the dissociation energy  $D^\circ_{\text{CH}}$ <sup>11</sup> implies a difference in strength between the stronger and weaker C–H bonds in CpTiMe<sub>3</sub> of about 14 kJ mol<sup>-1</sup>. Indeed, the spectroscopic properties bring the weaker bonds within, or close to, the regime of C–H bonds in organic molecules which are subject to significant weakening by electronic interactions, for example, with antiperiplanar lone pairs of electrons, as in Me<sub>2</sub>NH or Me<sub>2</sub>O.<sup>9</sup> It is not unreasonable therefore to suggest that an electronic interaction similar in magnitude occurs also in this cyclopentadienylmethyltitanium derivative, with removal of electron density from the C–H bonds into the empty d orbitals located mainly

(27) McKean, D. C. Unpublished results.

(28) Krömer, R.; Thiel, W. *Chem. Phys. Lett.* **1992**, *189*, 105.

(29) Tolman, C. A. *Chem. Rev.* **1977**, *77*, 313.

**Table 6. Comparison of  $\nu^{\text{is}}(\text{CH})$  and Related Parameters for Cyclopentadienyl Methyl Derivatives of Titanium(IV)<sup>a</sup>**

molecule	electron count on Ti	wavenumber (cm <sup>-1</sup> )			ref
		$\nu^{\text{is}}(\text{CH}_{\text{av}})$	$\Delta\nu^{\text{is}}(\text{CH})^b$	$\Delta\nu^{\text{is}}(\text{CH}) \times \chi_{\text{CH}}^c$	
CpTiMe <sub>3</sub> (1)	12	2918	38	228	this work
CpTiMeCl <sub>2</sub> (2)	12	2945	40	40	22
Cp <sub>2</sub> TiMe <sub>2</sub> (3)	16	2926	17	34	21

<sup>a</sup>  $\nu^{\text{is}}(\text{CH})$  values taken from Table 5. <sup>b</sup>  $\Delta\nu^{\text{is}}(\text{CH}) = \nu^{\text{is}}(\text{CH}_{\text{higher}}) - \nu^{\text{is}}(\text{CH}_{\text{lower}})$  for an asymmetric methyl group. <sup>c</sup>  $\chi_{\text{CH}}$  is the number of C-H bonds exhibiting  $\nu^{\text{is}}(\text{CH}_{\text{lower}})$ .

on the metal. The very existence of such an interaction in CpTiMe<sub>3</sub> may also give a clue to the absence of asymmetry in the methyl groups of Me<sub>2</sub>TiCl<sub>2</sub> (*vide supra*): extended Hückel MO calculations have indicated that such M··H-C agostic interactions are much more likely to occur in octahedrally, as opposed to tetrahedrally, ligated titanium systems.<sup>30</sup> The bonding in CpTiMe<sub>3</sub>, although formally involving a four-coordinate metal center, is much better described in terms of *pseudo*-octahedral coordination, with the 6-electron cyclopentadienide ligand straddling three vertices.<sup>31</sup>

2. The cyclopentadienyl methyl congeners of the heavier Group 4 metals, viz. Cp<sub>2</sub>ZrMe<sub>2</sub> and Cp<sub>2</sub>HfMe<sub>2</sub>,<sup>21</sup> each exhibit only one value of  $\nu^{\text{is}}(\text{CH})$ , yet this occurs at *lower* wavenumber than the  $\nu^{\text{is}}(\text{CH})$  values for the weaker C-H bonds in any of the titanium derivatives. This finding manifests the general tendency for C-H bonds in any family of methyl-transition metal compounds to become progressively weaker as the atomic number of the transition metal increases [cf. MeMn(CO)<sub>5</sub> and MeRe(CO)<sub>5</sub>, Table 5].

3. The correlation between  $\nu^{\text{is}}(\text{CH})$  and  $D^{\circ}_{\text{CH}}$  for methyl derivatives has been noted previously.<sup>11</sup> The difference between the highest and lowest reported  $\nu^{\text{is}}(\text{CH})$  values in Table 5 represents a difference of 6–7% in the C-H bond dissociation energy. This conclusion serves also to emphasize the comparative insensitivity of  $\nu^{\text{is}}(\text{CH})$  to variations in the strength and character of the C-H bond.

4. H-C-H angles in the range 107–110° are compatible with what is known about other organotitanium compounds, the best estimates coming from the NMR study<sup>15</sup> or from *ab initio* calculations.<sup>28,32</sup> The electron-diffraction study of Cp\*TiMe<sub>3</sub> yielded a Ti-C-H angle of 103.8°;<sup>7</sup> in terms of the model assumed (C<sub>3v</sub> local symmetry for the methyl group), this implies an H-C-H angle of 114.5°. We are confident that such an angle can be ruled out for CpTiMe<sub>3</sub> on the basis of our IR spectra, although these do not of course contain any direct information about the Ti-C-H angles.

5. The failure to resolve the  $\nu_{\text{as}}(\text{CH}_3)$  and  $\nu_{\text{as}}(\text{CD}_3)$  bands in the spectra of carbon tetrachloride solutions is puzzling. The appearance of these bands resembles that of the similar band displayed by MeMn(CO)<sub>5</sub> in solution.<sup>33</sup> For the manganese compound, however, the  $\nu^{\text{is}}(\text{CH})$  band of the CHD<sub>2</sub> version is also a singlet, although broad, behavior which contrasts with the splitting seen in the spectrum of the corresponding CpTiMe<sub>3</sub> derivative. Since the spectra of matrix-

isolated CHD<sub>2</sub>Mn(CO)<sub>5</sub> revealed only very small splittings of the  $\nu^{\text{is}}$  band, it may be concluded that the source of the broadening here is exclusively due to free internal rotation of the methyl group.<sup>33</sup> In molecules where there is both free internal rotation and also variation of  $\nu^{\text{is}}$  with torsional angle, two kinds of behavior are found. In toluene<sup>34,35</sup> and nitromethane<sup>35–38</sup> solutions,  $\nu_{\text{as}}(\text{CH}_3)$  splittings can be seen, but the spectrum of the gaseous molecule is dominated by a band whose frequency represents the *average* of a cyclical variation and whose intensity derives from the dipole moment change *parallel* to the top axis. This again cannot correspond to the CpTiMe<sub>3</sub> situation. Finally, we note that compounds of the type MeBX<sub>2</sub> show splitting in the  $\nu_{\text{as}}$  and also the  $\nu^{\text{is}}$  bands, the intensity of which appears to derive solely from a dipole change *perpendicular* to the top axis;<sup>39</sup> the last feature is reflected in the marked and unusual weakness of the  $\nu_{\text{s}}(\text{CH}_3)$  band. With CpTiMe<sub>3</sub>, however, the  $\nu_{\text{as}}/\nu_{\text{s}}$  intensity distribution is normal. All that can be said at the present time, therefore, is that the behavior of the IR bands due to CpTiMe<sub>3</sub> in carbon tetrachloride solution does not fall into any previously known category. Good quality *ab initio* calculations of the methyl torsional frequencies may yet help to throw light on the situation.

6. It will be evident from the difficulties experienced here in attempting simultaneously to fit  $\nu^{\text{is}}(\text{CH})$  and  $\nu^{\text{is}}(\text{CD})$  results that this investigation casts some doubt on the usefulness of  $\nu^{\text{is}}(\text{CD})$  results, at least for quantitative purposes. In extenuation, it may be said with some justification that the present molecule is not the most suitable one that could be chosen for this purpose and that comparative failure with CpTiMe<sub>3</sub> should not be taken to be symptomatic of the general inutility of  $\nu^{\text{is}}(\text{CD})$  studies. We are encouraged in this belief by the excellent consistency which has been found in our parallel study of another methyltitanium compound, Me<sub>2</sub>TiCl<sub>2</sub>;<sup>18</sup> such success may depend in part on the ability to study the spectra of the compound in the vapor phase.

**Acknowledgment.** We thank Jesus College, Oxford, U.K., for the award of a Junior Research Fellowship (to G.S.M.) and the SERC (now ESPRC) for funding which has enabled the purchase of equipment.

OM950165U

(34) Dempster, A. B.; Powell, D. B.; Sheppard, N. *Spectrochim. Acta* **1972**, *28A*, 373; **1975**, *31A*, 245.

(35) Cavagnat, D.; Lascombe, J. J. *Mol. Spectrosc.* **1982**, *92*, 141.

(36) Jones, W. J.; Sheppard, N. *Proc. R. Soc. London* **1968**, *A30*, 135.

(37) McKean, D. C.; Watt, R. A. *J. Mol. Spectrosc.* **1976**, *61*, 184.

(38) Cavagnat, D.; Brom, H.; Nugteren, P. R. *J. Chem. Phys.* **1987**, *87*, 801.

(39) McKean, D. C.; Becher, H. J.; Bramsiepe, F. *Spectrochim. Acta* **1977**, *33A*, 951.

(40) McKean, D. C.; McQuillan, G. P.; Thompson, D. W. *Spectrochim. Acta* **1980**, *36A*, 1009.

(41) McKean, D. C.; McQuillan, G. P.; Torto, I.; Morrison, A. R. *J. Mol. Struct.* **1986**, *141*, 457.

(42) Bürger, H.; Biedermann, S. *Spectrochim. Acta* **1972**, *28A*, 2283.

(30) Eisenstein, O.; Jean, Y. *J. Am. Chem. Soc.* **1985**, *107*, 1177.

(31) See, for example: Elschenbroich, Ch.; Salzer, A. *Organometallics: A Concise Introduction*, 2nd ed.; VCH: Weinheim, Germany, 1992.

(32) Jonas, V. Private communication.

(33) Firth, S.; Horton-Mastin, A.; Poliakov, M.; Turner, J. J.; McKean, D. C.; McQuillan, G. P.; Robertson, J. *Organometallics* **1989**, *8*, 2876.

# Solution Thermochemical Study of Ligand Steric Influences on Substitution Enthalpies in the $L_2Fe(CO)_3$ System

Chunbang Li, Edwin D. Stevens, and Steven P. Nolan\*

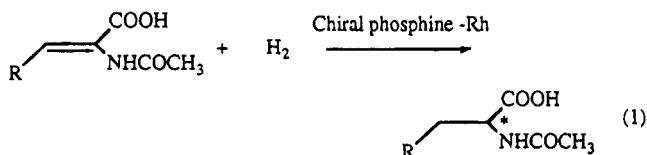
Department of Chemistry, University of New Orleans, New Orleans, Louisiana 70148

Received March 20, 1995\*

The enthalpies of reaction of  $(BDA)Fe(CO)_3$  ( $BDA = (C_6H_5)CH=CHO(CH_3)$ , benzylideneacetone) with a series of sterically demanding phosphine ligands, leading to the formation of  $(L)_2Fe(CO)_3$  complexes ( $L =$  phosphine) have been measured by solution calorimetry in THF at 50 °C. The range of reaction enthalpies spans some 7 kcal/mol. The overall relative order of stability established is as follows ( $PR_3$ ;  $-\Delta H$ , kcal/mol):  $PPh_3 < PCy_2Ph < PCyPh_2 < PCy_3 < P^iPr_3 < PPh_2Et < PBz_3$ . A quantitative analysis of ligand effect of the present and previously obtained data for  $L_2Fe(CO)_3$  complexes helps clarify the exact steric versus electronic ligand contributions to the enthalpy of reaction in this system. Results of a single-crystal diffraction study for the complex *diaxial*- $(PPh_2Cy)_2Fe(CO)_3$  (**2**) show the molecule to be monoclinic,  $P2_1/n$ , with  $a = 12.393(5)$  Å,  $b = 15.811(6)$  Å,  $c = 18.029(7)$  Å,  $\alpha = \gamma = 90^\circ$ ,  $\beta = 108.00(2)^\circ$ ,  $V = 43360(5)$  Å<sup>3</sup>,  $Z = 4$ ,  $d_{\text{calcd}} = 1.337$  g cm<sup>-3</sup>,  $n_{\text{obsd}} = 3130$ , and  $R = 0.052$ . Electronic effects are overwhelmingly important in this system, yet a steric threshold of 135° can be extracted from the QALE treatment which shows at which point steric factors begin to influence and contribute to the measured enthalpy of ligand substitution.

## Introduction

The importance of tertiary phosphine ligands in organometallic chemistry and catalysis is undeniable.<sup>1</sup> A large number of processes exhibit marked selectivity and reactivity differences according to the nature of the phosphine borne on the transition metal center.<sup>2</sup> A prototypical example of the importance of phosphine as an ancillary ligand is illustrated by the Noyori catalyst which mediates the asymmetric hydrogenation of olefins<sup>3</sup> (eq 1).



Kinetic, catalytic, and structural studies have been

\* Abstract published in *Advance ACS Abstracts*, July 15, 1995.

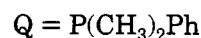
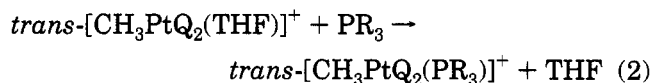
(1) Collman, J. P.; Hegedus, L. S.; Norton, J. R.; Finke, R. G. *Principles and Applications of Organotransition Metal Chemistry*, 2nd ed.; University Science: Mill Valley, CA, 1987.

(2) Pignolet, L. H., Ed. *Homogeneous Catalysis with Metal Phosphine Complexes*; Plenum: New York, 1983.

(3) Noyori, R. *Asymmetric Catalysis in Organic Synthesis*; Wiley and Sons, Inc.: New York, 1994, and references cited therein.

(4) For leading references in this area see: (a) Nolan, S. P. *Bonding Energetics of Organometallic Compounds*. In *Encyclopedia of Inorganic Chemistry*; J. Wiley and Sons: New York, 1994. (b) Hoff, C. D. *Prog. Inorg. Chem.* **1992**, *40*, 503-561. (c) Martinho Simões, J. A.; Beauchamp, J. L. *Chem. Rev.* **1990**, *90*, 629-688. (d) Marks, T. J., Ed. *Bonding Energetics in Organometallic Compounds*. *ACS Symp. Ser.* **1990**, No. 428. (e) Marks, T. J., Ed. *Metal-Ligand Bonding Energetics in Organotransition Metal Compounds*. *Polyhedron Symp.-in-Print*, **1988**, 7. (f) Skinner, H. A.; Connor, J. A. In *Molecular Structure and Energetics*; Liebman, J. F., Greenberg, A., Eds.; VCH: New York, 1987; Vol. 2, Chapter 6. (g) Skinner, H. A.; Connor, J. A. *Pure Appl. Chem.* **1985**, *57*, 79-88. (h) Pearson, R. G. *Chem. Rev.* **1985**, *85*, 41-59. (i) Mondal, J. U.; Blake, D. M. *Coord. Chem. Rev.* **1983**, *47*, 204-238. (j) Mansson, M. *Pure Appl. Chem.* **1983**, *55*, 417-426. (k) Pilcher, G.; Skinner, H. A. In *The Chemistry of the Metal-Carbon Bond*; Harley, F. R., Patai, S., Eds.; Wiley: New York, 1982; pp 43-90. (l) Connor, J. A. *Top. Curr. Chem.* **1977**, *71*, 71-110.

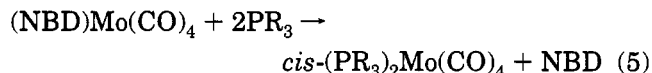
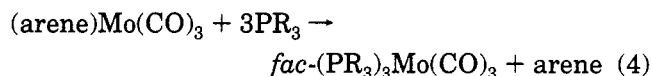
conducted on this and related catalytic systems.<sup>3</sup> In spite of the vast amount of information focusing on  $PR_3$ -transition metal complexes, few thermodynamic data regarding heats of binding of these ligands to metal centers exist.<sup>4,5</sup> Manzer and Tolman<sup>6</sup> have reported the solution calorimetry of square-planar platinum(II) complexes, shown in eq 2, for a series of phosphine ligands.



A similar series was then investigated for Ni(0) complexes<sup>7</sup> shown in eq 3. Detailed thermochemical inves-



tigations of two related Mo(0) systems have been reported by Hoff and co-workers<sup>8</sup> (eqs 4 and 5). At a



NBD = norbornadiene

more basic level of understanding lies the question of

(5) Nolan, S. P.; Lopez de la Vega, R.; Hoff, C. D. *Organometallics* **1986**, *5*, 2529-2537.

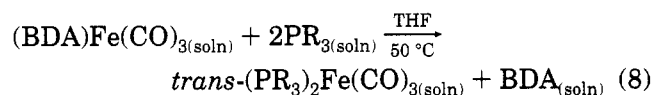
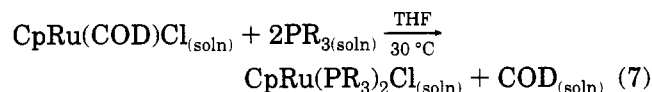
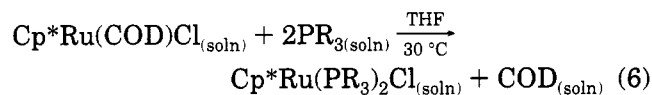
(6) Manzer, L. E.; Tolman, C. A. *J. Am. Chem. Soc.* **1975**, *97*, 1955-1986.

(7) Tolman, C. A.; Reutter, D. W.; Seidel, W. C. *J. Organomet. Chem.* **1976**, *117*, C30-C33.

(8) (a) Nolan, S. P.; Hoff, C. D. *J. Organomet. Chem.* **1985**, *290*, 365-373. (b) Mukerjee, S. L.; Nolan, S. P.; Hoff, C. D.; de la Vega, R. *Inorg. Chem.* **1988**, *27*, 81-85.

the relative importance of steric vs electronic ligand effects in organometallic systems bearing phosphine ligands.

We have addressed this question with the help of solution calorimetric techniques, having previously reported on the importance of enthalpy electronic and steric components for phosphine ligands binding to organogroup 8 systems:<sup>9,10</sup>



$\text{Cp} = \text{C}_5\text{H}_5$ ;  $\text{Cp}^* = \text{C}_5\text{Me}_5$ ;

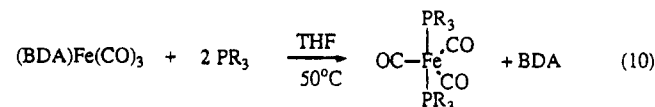
$\text{BDA} = \text{PhCH}=\text{CHCOMe}$ ;  $\text{PR}_3 = \text{tertiary phosphine}$

We recently extended this work to emphasize the importance of electronic factors in a series of para-substituted triphenylphosphine ligands within this (L)<sub>2</sub>-Fe(CO)<sub>3</sub> system<sup>10c</sup> (eq 9).



$\text{PR}_3 = \text{P}(\text{p-XC}_6\text{H}_4)_3$ ; X = H, Cl, F, Me, MeO, CF<sub>3</sub>

We now wish to complete the thermochemical investigation of this iron-based system by reporting on the thermochemical investigation of ligand substitution reactions of sterically demanding tertiary phosphine ligands (eq 10).



$\text{PR}_3 = \text{PCy}_2\text{Ph}$ ,  $\text{PCyPh}_2$ ,  $\text{PCy}_3$ ,  $\text{P}^i\text{Pr}_3$ ,  $\text{PPh}_2\text{Et}$ ,  $\text{PBz}_3$

## Experimental Section

**General Considerations.** All manipulations involving organoiron complexes were performed under inert atmospheres of argon or nitrogen using standard high-vacuum or Schlenk tube techniques or in a Vacuum/Atmospheres glovebox containing less than 1 ppm oxygen and water. Ligands were purchased from Strem Chemicals and used as received. Tetrahydrofuran was stored over sodium wire, distilled from sodium benzophenone ketyl, stored over Na/K alloy, and vacuum transferred into flame-dried glassware prior to use.

(9) For organoruthenium systems see: (a) Nolan, S. P.; Martin, K. L.; Stevens, E. D.; Fagan, P. J. *Organometallics* **1992**, *11*, 3947–3953. (b) Luo, L.; Fagan, P. J.; Nolan, S. P. *Organometallics* **1993**, *12*, 3405–3411. (c) Luo, L.; Zhu, N.; Zhu, N.-J.; Stevens, E. D.; Nolan, S. P.; Fagan, P. J. *Organometallics* **1994**, *13*, 669–675. (d) Li, C.; Cucullu, M. E.; McIntyre, R. A.; Stevens, E. D.; Nolan, S. P. *Organometallics* **1994**, *13*, 3621–3627. (e) Luo, L.; Li, C.; Cucullu, M. E.; Nolan, S. P. *Organometallics* **1995**, *14*, 1333–1338.

(10) For organoiron systems see: (a) Luo, L.; Nolan, S. P. *Organometallics* **1992**, *11*, 3483–3486. (b) Luo, L.; Nolan, S. P. *Inorg. Chem.* **1993**, *32*, 2410–2415. (c) Li, C.; Nolan, S. P. *Organometallics* **1995**, *14*, 1327–1332.

The organoiron complex (BDA)Fe(CO)<sub>3</sub> (**1**) was synthesized according to literature procedures.<sup>11</sup> Only materials of high purity as indicated by IR and NMR spectroscopies were used in the calorimetric experiments. Synthesis and characterization of iron tricarbonyl phosphine complexes have been previously reported.<sup>12,13</sup> Infrared spectra were recorded using a Perkin-Elmer FT Model 1760 spectrometer in 0.1 mm NaCl cells. NMR spectra were recorded using a Varian Gemini 300 MHz spectrometer. Calorimetric measurements were performed using a Calvet calorimeter (Setaram C-80) which was periodically calibrated using the TRIS reaction<sup>14</sup> or the enthalpy of solution of KCl in water.<sup>15</sup> The experimentally determined enthalpies for these two standard calibration reactions are the same within experimental error as literature values. This calorimeter has been previously described,<sup>16</sup> and typical procedures are described below. Experimental enthalpy data are reported with 95% confidence limits.

**<sup>1</sup>H NMR Titrations.** Prior to every set of calorimetric experiments involving a new ligand, an accurately weighed amount ( $\pm 0.1$  mg) of the organoiron complex was placed in a Wilmad screw-capped NMR tube fitted with a septum, and THF-*d*<sub>8</sub> was subsequently added. The solution was titrated with a solution of the ligand of interest by injecting the latter in aliquots through the septum with a microsyringe, followed by vigorous shaking. The reactions were monitored by <sup>1</sup>H NMR spectroscopy, and the reactions were found to be rapid, clean, and quantitative under experimental calorimetric conditions (50 °C). These conditions are necessary for accurate and meaningful calorimetric results and were satisfied for all organoiron reactions investigated. Only reactants and products were observed in the course of the NMR titration.

**Calorimetric Measurement for Reaction of (BDA)Fe(CO)<sub>3</sub> and Tricyclohexylphosphine.** The mixing vessels of the Setaram C-80 were cleaned, dried in an oven maintained at 120 °C, and then taken into the glovebox. A 20–30 mg sample of recrystallized (BDA)Fe(CO)<sub>3</sub> was accurately weighed into the lower vessel; it was closed and sealed with 1.5 mL of mercury. A 4 mL volume of a 25% stock solution of PCy<sub>3</sub> [1 g of PCy<sub>3</sub> in 25 mL of THF; >10:1 molar ratio of PCy<sub>3</sub>:BDAFe(CO)<sub>3</sub>] was then added, and the remainder of the cell was assembled, removed from the glovebox, and inserted into the calorimeter. The reference vessel was loaded in an identical fashion with the exception that no organoiron complex was added to the lower vessel. After the calorimeter had reached thermal equilibrium at 50.0 °C (about 2 h) the calorimeter was inverted thereby allowing the reactants to mix. After the reaction reached completion and the calorimeter had once again reached thermal equilibrium (ca. 2 h), the vessels were removed from the calorimeter, taken into the glovebox, and opened, and the infrared cell was filled under inert atmosphere. An infrared spectrum of each product was recorded using this IR cell filling procedure. Conversion to (PCy<sub>3</sub>)<sub>2</sub>Fe(CO)<sub>3</sub> was found to be quantitative under these reaction conditions. The enthalpy of reaction,  $-24.2 \pm 0.1$  kcal/mol, represents the average of five individual calorimetric determinations. The enthalpy of solution of (BDA)Fe(CO)<sub>3</sub><sup>10a</sup> ( $6.5 \pm 0.2$  kcal/mol) was then added to this value to obtain a value of  $-30.7 \pm 0.2$  kcal/mol for all species in solution.

**Synthesis.** (BDA)Fe(CO)<sub>3</sub> was synthesized according to the literature procedure.<sup>11</sup> The identities of all calorimetry prod-

(11) Howell, J. A. S.; Johnson, B. F. G.; Josty, P. L.; Lewis, J. J. *Organomet. Chem.* **1972**, *39*, 329–333.

(12) (a) Inoue, H.; Taki, T.; Heckmann, G.; Fluck, E. Z. *Naturforsch., B: Chem. Sci.* **1991**, *46*, 682–686. (b) Carroll, W. E.; Deeney, F. A.; Lalor, F. I. *J. Chem. Soc., Dalton Trans.* **1973**, 718–722.

(13) (a) Keiter, R. L.; Keiter, E. A.; Hecker, K. H.; Boecker, C. A. *Organometallics* **1988**, *7*, 2466–2469. (b) Darensbourg, D. J. *Inorg. Nucl. Chem Lett.* **1972**, *8*, 529–532.

(14) Ojelund, G.; Wadsö, I. *Acta Chem. Scand.* **1968**, *22*, 1691–1699.

(15) Kilday, M. V. *J. Res. Natl. Bur. Stand. (U.S.)* **1980**, *85*, 467–481.

(16) Nolan, S. P.; Hoff, C. D. *J. Organomet. Chem.* **1985**, *282*, 357–362.

**Table 1. Enthalpies of Substitution (kcal/mol) in the Reaction**

$$(BDA)Fe(CO)_3(soln) + 2L(soln) \xrightarrow[50^\circ C]{THF} (L)_2Fe(CO)_3(soln) + BDA(soln)$$

L	complex	$\nu_{CO}$ ( $cm^{-1}$ ) <sup>a</sup>	$-\Delta H_{rxn}$ <sup>b</sup>
AsPh <sub>3</sub>	(Ph <sub>3</sub> As) <sub>2</sub> Fe(CO) <sub>3</sub>	1886	10.2(0.2) <sup>c</sup>
P( <i>p</i> -CF <sub>3</sub> C <sub>6</sub> H <sub>4</sub> ) <sub>3</sub>	[( <i>p</i> -CF <sub>3</sub> C <sub>6</sub> H <sub>4</sub> ) <sub>3</sub> P] <sub>2</sub> Fe(CO) <sub>3</sub>	1899	22.4(0.3) <sup>d</sup>
AsEt <sub>3</sub>	(Et <sub>3</sub> As) <sub>2</sub> Fe(CO) <sub>3</sub>	1865	24.5(0.3) <sup>c</sup>
P( <i>p</i> -ClC <sub>6</sub> H <sub>4</sub> ) <sub>3</sub>	[( <i>p</i> -ClC <sub>6</sub> H <sub>4</sub> ) <sub>3</sub> P] <sub>2</sub> Fe(CO) <sub>3</sub>	1893	25.0(0.1) <sup>d</sup>
P( <i>p</i> -FC <sub>6</sub> H <sub>4</sub> ) <sub>3</sub>	[( <i>p</i> -FC <sub>6</sub> H <sub>4</sub> ) <sub>3</sub> P] <sub>2</sub> Fe(CO) <sub>3</sub>	1891	25.8(0.2) <sup>d</sup>
P(C <sub>6</sub> H <sub>5</sub> ) <sub>3</sub>	[(C <sub>6</sub> H <sub>5</sub> ) <sub>3</sub> P] <sub>2</sub> Fe(CO) <sub>3</sub>	1887	26.9(0.2) <sup>c</sup>
PCy <sub>2</sub> Ph	(PCy <sub>2</sub> Ph) <sub>2</sub> Fe(CO) <sub>3</sub>	1868	27.1(0.1) <sup>e</sup>
PCyPh <sub>2</sub>	(PCyPh <sub>2</sub> ) <sub>2</sub> Fe(CO) <sub>3</sub>	1879	27.5(0.1) <sup>e</sup>
P( <i>p</i> -CH <sub>3</sub> C <sub>6</sub> H <sub>4</sub> ) <sub>3</sub>	[( <i>p</i> -CH <sub>3</sub> C <sub>6</sub> H <sub>4</sub> ) <sub>3</sub> P] <sub>2</sub> Fe(CO) <sub>3</sub>	1884	28.2(0.3) <sup>d</sup>
P( <i>p</i> -CH <sub>3</sub> OC <sub>6</sub> H <sub>4</sub> ) <sub>3</sub>	[( <i>p</i> -CH <sub>3</sub> OC <sub>6</sub> H <sub>4</sub> ) <sub>3</sub> P] <sub>2</sub> Fe(CO) <sub>3</sub>	1882	30.1(0.2) <sup>d</sup>
PCy <sub>3</sub>	(PCy <sub>3</sub> ) <sub>2</sub> Fe(CO) <sub>3</sub>	1854	30.7(0.2) <sup>e</sup>
P <sup>i</sup> Pr <sub>3</sub>	(P <sup>i</sup> Pr) <sub>2</sub> Fe(CO) <sub>3</sub>	1860	31.6(0.1) <sup>e</sup>
PPh <sub>2</sub> Et	(PPh <sub>2</sub> Et) <sub>2</sub> Fe(CO) <sub>3</sub>	1881	32.7(0.1) <sup>e</sup>
PBz <sub>3</sub>	(PBz <sub>3</sub> ) <sub>2</sub> Fe(CO) <sub>3</sub>	1884	32.8(0.2) <sup>e</sup>
PPh <sub>2</sub> Me	(Ph <sub>2</sub> MeP) <sub>2</sub> Fe(CO) <sub>3</sub>	1878	34.1(0.3) <sup>c</sup>
PPhMe <sub>2</sub>	(PhMe <sub>2</sub> P) <sub>2</sub> Fe(CO) <sub>3</sub>	1875	37.3(0.3) <sup>c</sup>
PMe <sub>3</sub>	(Me <sub>3</sub> P) <sub>2</sub> Fe(CO) <sub>3</sub>	1871	38.9(0.2) <sup>c</sup>
P <sup>n</sup> Bu <sub>3</sub>	( <sup>n</sup> Bu <sub>3</sub> P) <sub>2</sub> Fe(CO) <sub>3</sub>	1865	41.7(0.3) <sup>c</sup>
PEt <sub>3</sub>	(Et <sub>3</sub> P) <sub>2</sub> Fe(CO) <sub>3</sub>	1867	42.4(0.2) <sup>c</sup>

<sup>a</sup> Infrared spectra were recorded in THF. <sup>b</sup> Enthalpy values are reported with 95% confidence limits. <sup>c</sup> Taken from ref 10a,b. <sup>d</sup> Taken from ref 10c. <sup>e</sup> This work.

ucts were determined by comparison with reported spectroscopic data<sup>12,13</sup> or with materials independently synthesized. A detailed synthetic procedure for new organoiron complexes is described below:

[(C<sub>6</sub>H<sub>11</sub>)<sub>2</sub>(C<sub>6</sub>H<sub>5</sub>)P]<sub>2</sub>Fe(CO)<sub>3</sub>. A 100 mL flask was charged with 105 mg (0.37 mmol) of (BDA)Fe(CO)<sub>3</sub> (BDA = benzylideneacetone), 204 mg (0.75 mmol) of PCy<sub>2</sub>Ph (dicyclohexylphosphine), and 20 mL of THF. This clear solution was stirred for 48 h at room temperature during which time the color of solution changed from red orange to orange. The solution was then evaporated to dryness in vacuum, the residue was taken up in a 5 mL of CH<sub>2</sub>Cl<sub>2</sub>/25 mL of pentane mixture, and crystals were grown from this solution by slow cooling. After filtration of the obtained yellow microcrystals and drying under vacuum, 140 mg (56%) of product was obtained. <sup>1</sup>H-NMR (THF-*d*<sub>6</sub>): 8.01 (m, 4H, -Ph), 7.43 (m, 6H, -Ph), 2.53 (m, 4H, -Cy), 2.16–2.13 (m, 4H, -Cy), 1.88–1.68 (m, 16H, -Cy), 1.55–1.20 (m, 20H, -Cy). <sup>1</sup>H-NMR (CDCl<sub>3</sub>): 7.91 (m, 4H, -Ph), 7.43 (m, 6H, -Ph), 2.41 (br, 4H, -Cy), 2.07 (m, 4H, -Cy), 1.89–1.68 (m, 16H, -Cy), 1.46–1.14 (m, 20H, -Cy). IR [ $\nu_{CO}$  (THF)]: 1867  $cm^{-1}$ . Anal. Calcd for C<sub>39</sub>H<sub>54</sub>FeO<sub>3</sub>P<sub>2</sub>: C, 67.99; H, 7.91. Found: C, 68.26; H, 7.83.

[(C<sub>6</sub>H<sub>5</sub>CH<sub>2</sub>)<sub>3</sub>P]<sub>2</sub>Fe(CO)<sub>3</sub>. A 100 mL flask was charged with 118 mg (0.41 mmol) of (BDA)Fe(CO)<sub>3</sub> (BDA = benzylideneacetone), 254 mg (0.836 mmol) of trisbenzylphosphine, and 25 mL of THF. Stirring the solution overnight at room temperature produces a color change of the solution from red orange to orange brown. After reduction the solution volume to 5 mL and addition of 25 mL pentane, the solution was left at room temperature where slow diffusion of pentane occurred through the THF layer. After filtration, this afforded 150 mg product (yield 57%) as greenish-yellow crystals. <sup>1</sup>H-NMR (THF-*d*<sub>6</sub>): 7.32–7.19 (m, 15H, -Ph); 3.27–3.25 (m, 6H, -CH<sub>2</sub>-). IR [ $\nu_{CO}$  (THF)]: 1884  $cm^{-1}$ . Anal. Calcd for C<sub>45</sub>H<sub>42</sub>FeO<sub>3</sub>P<sub>2</sub>: C, 72.17; H, 5.66. Found: C, 72.33; H, 5.56.

**Structure Determination of (PPh<sub>2</sub>Cy)<sub>2</sub>Fe(CO)<sub>3</sub> (2).** A rectangular light yellow crystal of **2**, grown by evaporation of a saturated CH<sub>2</sub>Cl<sub>2</sub>/pentane solution, having approximate dimensions 0.25 × 0.25 × 0.25 mm was selected and mounted on the end of a glass fiber using silicone high-vacuum grease, and cooled to 100(2) K in a stream of cold nitrogen gas on an Enraf-Nonius CAD 4 diffractometer. Cell dimensions were

**Table 2. Summary of Crystallographic Data for (PCyPh<sub>2</sub>)<sub>2</sub>Fe(CO)<sub>3</sub> (2)**

empirical formula	C <sub>39</sub> H <sub>42</sub> O <sub>3</sub> P <sub>2</sub> Fe
space group	<i>P</i> 2 <sub>1</sub> / <i>n</i>
unit cell dimensions	
<i>a</i> , Å	12.393(5)
<i>b</i> , Å	15.811(6)
<i>c</i> , Å	18.029(7)
$\alpha$ , deg	90
$\beta$ , deg	108.00(2)
$\gamma$ , deg	90
<i>V</i> , Å <sup>3</sup>	3360(5)
<i>Z</i> , molecule/cell	4
$d_{calcd}$ , g/cm <sup>3</sup>	1.337
$\mu$ (Mo), cm <sup>-1</sup>	5.766
monochromator	highly ordered graphite crystal
temp, K	100(2)
abs corr	empirical ( $\psi$ -scan method)
diffractometer	Enraf-Nonius CAD 4
scan type	$\theta$ - $2\theta$
data collcd	$-14 \leq h \leq 14, 0 \leq k \leq 18, 0 \leq l \leq 21$
$2\theta$ range, deg	4.0–50.0
no. of collcd reflns	5891
no. of indep reflns	5891
no. of obsd reflns ( $I > 3\sigma(I)$ )	3130
$R_F$ (obsd data), %	4.5
$R_{wF}$ , %	5.2
goodness of fit	1.6
no. of variables	561

**Table 3. Selected Bond Distances (Å) and Bond Angles (deg) for (PCyPh<sub>2</sub>)<sub>2</sub>Fe(CO)<sub>3</sub> (2)**

Bond Lengths <sup>a</sup>			
Fe–P(1)	2.218(1)	P(1)–C(4)	1.840(4)
Fe–P(2)	2.218(1)	P(1)–C(10)	1.850(4)
Fe–C(1)	1.780(5)	P(1)–C(16)	1.846(4)
Fe–C(2)	1.759(4)	P(2)–C(22)	1.831(5)
Fe–C(3)	1.773(5)	P(2)–C(28)	1.853(4)
C(1)–O(1)	1.141(5)	P(2)–C(34)	1.839(4)
C(2)–O(2)	1.174(5)	Cy C–C(ave)	1.502(8)
C(3)–O(3)	1.162(5)	Ph C–C(ave)	1.376(8)
Bond Angles <sup>a</sup>			
P(1)–Fe–P(2)	178.45(6)	C(4)–P(1)–C(10)	101.9(2)
P(1)–Fe–C(1)	89.5(1)	C(4)–P(1)–C(16)	102.5(2)
P(1)–Fe–C(2)	89.5(1)	C(10)–P(1)–C(16)	102.9(2)
P(1)–Fe–C(3)	88.8(1)	Fe–P(2)–C(22)	115.6(1)
P(2)–Fe–C(1)	89.1(1)	Fe–P(2)–C(28)	117.7(2)
P(2)–Fe–C(2)	88.6(1)	Fe–P(2)–C(34)	114.6(2)
P(2)–Fe–C(3)	92.5(1)	C(22)–P(2)–C(28)	102.6(2)
C(1)–Fe–C(2)	118.1(2)	C(22)–P(2)–C(34)	101.7(2)
C(1)–Fe–C(3)	120.0(2)	C(28)–P(2)–C(34)	102.4(2)
C(2)–Fe–C(3)	121.9(2)	Fe–C(1)–O(1)	178.5(4)
Fe–P(1)–C(4)	115.1(1)	Fe–C(2)–O(2)	177.8(4)
Fe–P(1)–C(10)	117.2(2)	Fe–C(3)–O(3)	176.8(4)
Fe–P(1)–C(16)	115.3(1)		

<sup>a</sup> Numbers in parentheses are the estimated standard deviations.

determined by least-squares refinement of the measured setting angles of 25 reflections with  $40^\circ < 2\theta < 50^\circ$  using Mo K $\alpha$  radiation. The structure was solved by direct methods (MULTAN80) and refined by full matrix least-squares techniques. Crystal data for **2** are summarized in Table 2 and selected bond distances and angles are listed in Table 3. Positional and equivalent isotropic thermal parameters are presented in Table 4. Figure 1 gives an ORTEP drawing of this molecule.

## Results

The (BDA)Fe(CO)<sub>3</sub> complex (BDA = PhCH=CHCOMe, benzylideneacetone) was selected as the entryway into the thermochemistry of the iron tricarbonyl system in view of the labile nature of the BDA ligand as illustrated

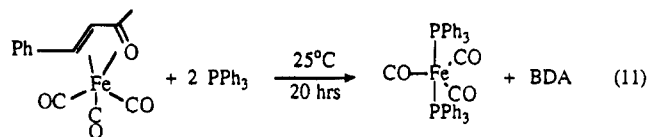


Table 4. Fractional Coordinates and Isotropic Thermal Parameters for (PCyPh<sub>2</sub>)<sub>2</sub>Fe(CO)<sub>3</sub> (2)<sup>a</sup>

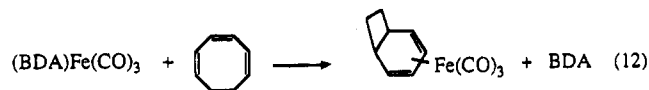
atom	x	y	z	B, Å <sup>2</sup>	atom	x	y	z	B, Å <sup>2</sup>
Fe	-0.02290(6)	0.21900(4)	0.22950(4)	1.76(1)	C(18)	-0.0364(6)	0.3606(4)	0.4730(3)	4.4(2)
P(1)	-0.1751(1)	0.27812(8)	0.24774(6)	1.79(2)	C(19)	-0.1097(5)	0.4193(4)	0.4833(3)	3.9(1)
P(2)	0.1281(1)	0.15667(8)	0.21263(7)	1.69(2)	C(20)	-0.2019(5)	0.4395(3)	0.4226(3)	3.6(1)
O(1)	-0.0217(3)	0.0934(3)	0.3486(2)	4.0(1)	C(21)	-0.2223(5)	0.3994(3)	0.3509(3)	2.9(1)
O(2)	-0.1492(3)	0.1751(2)	0.0680(2)	3.0(1)	C(22)	0.2410(4)	0.1289(3)	0.3020(3)	1.8(1)
O(3)	0.0931(3)	0.3815(2)	0.2744(2)	4.0(1)	C(23)	0.2681(4)	0.1839(3)	0.3654(3)	2.6(1)
C(1)	-0.0210(4)	0.1431(3)	0.3028(3)	2.5(1)	C(24)	0.3547(5)	0.1664(4)	0.4328(3)	3.0(1)
C(2)	-0.0983(4)	0.1943(3)	0.1322(3)	1.9(1)	C(25)	0.4140(5)	0.0912(4)	0.4296(3)	3.0(1)
C(3)	0.0496(4)	0.3164(3)	0.2558(3)	2.4(1)	C(26)	0.3867(5)	0.0358(3)	0.3786(3)	2.9(1)
C(4)	-0.2873(4)	0.2038(3)	0.2518(3)	1.9(1)	C(27)	0.3008(4)	0.0527(3)	0.3110(3)	2.4(1)
C(5)	-0.3140(4)	0.1356(4)	0.1983(3)	2.9(1)	C(28)	0.2062(4)	0.2144(3)	0.1558(3)	2.5(1)
C(6)	-0.4059(5)	0.0835(4)	0.1930(3)	3.1(1)	C(29)	0.1293(4)	0.2388(4)	0.0759(3)	2.9(1)
C(7)	-0.4733(5)	0.0986(4)	0.2379(3)	3.6(1)	C(30)	0.1960(5)	0.2727(5)	0.0252(3)	4.4(1)
C(8)	-0.4473(5)	0.1627(4)	0.2927(3)	3.8(1)	C(31)	0.2757(5)	0.3420(4)	0.0630(3)	4.2(1)
C(9)	-0.3574(4)	0.2170(4)	0.2970(3)	3.2(1)	C(32)	0.3487(5)	0.3204(5)	0.1442(3)	4.9(2)
C(10)	-0.2548(4)	0.3546(3)	0.1733(3)	2.2(1)	C(33)	0.2794(5)	0.2856(4)	0.1942(3)	4.4(1)
C(11)	-0.1803(5)	0.4159(4)	0.1492(3)	3.5(1)	C(34)	0.0993(4)	0.0541(3)	0.1622(3)	2.6(1)
C(12)	-0.24445(6)	0.4849(4)	0.0963(4)	4.3(2)	C(35)	0.0311(5)	-0.0020(4)	0.1822(4)	5.1(2)
C(13)	-0.3371(5)	0.4511(4)	0.0289(3)	3.7(1)	C(36)	0.0129(6)	-0.0822(5)	0.1483(5)	7.8(2)
C(14)	-0.4109(5)	0.3878(4)	0.0514(3)	3.6(1)	C(37)	0.0676(8)	-0.1082(4)	0.0997(4)	6.7(2)
C(15)	-0.3451(5)	0.3189(4)	0.1025(3)	3.7(1)	C(38)	0.1325(9)	-0.0532(5)	0.0780(4)	10.1(3)
C(16)	-0.1489(4)	0.3378(3)	0.3395(3)	2.3(1)	C(39)	0.1553(8)	0.0280(4)	0.1113(4)	7.6(2)
C(17)	-0.0552(5)	0.3193(4)	0.4031(3)	3.9(1)					

<sup>a</sup> Numbers in parentheses are the estimated standard deviations.

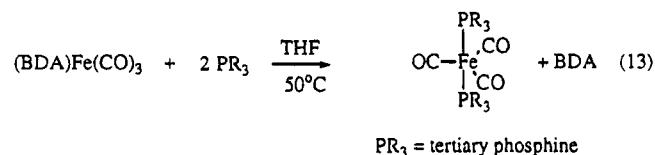
by Angelici and co-workers,<sup>17</sup> who have used this molecule in their synthetic efforts (eq 11). The labile



nature of the BDA complex has also previously been noted by Brookhart and co-workers in their use of this complex as a diene trapping agent<sup>18</sup> (eq 12).



We have recently reported the enthalpies of reaction of monodentate tertiary phosphines with the (BDA)Fe(CO)<sub>3</sub> complex<sup>10a-c</sup> as illustrated in eq 13.



We now extend this work to sterically demanding tertiary phosphine donors. All results involving monodentate phosphine ligands investigated for the present study, including those previously reported, are summarized in Table 1. A single-crystal structural study was carried out on one organoiron complex, **2**. Tables 2 and 4 give important bond distances and angles as well as positional parameters with an ORTEP drawing of the structure (Figure 4).

(17) Sowa, J. R.; Zanotti, V.; Facchin, G.; Angelici, R. J. *J. Am. Chem. Soc.* **1991**, *113*, 9185–92.

(18) (a) Graham, C. R.; Scholes, G.; Brookhart, M. *J. Am. Chem. Soc.* **1977**, *99*, 1180–1188. (b) Brookhart, M.; Nelson, G. O. *J. Organomet. Chem.* **1979**, *164*, 193–202.

## Discussion

With the exception of the few thermodynamic investigations reported by Muetterties<sup>19</sup> and Connor,<sup>20</sup> thermodynamic information focusing on organoiron systems remains scarce. Studies clearly separating steric from electronic contributions are also quite few in number.<sup>21,22</sup> In this section, thermochemical data for sterically demanding tertiary monodentate phosphine ligands are presented. These data enable a complete treatment of ligand effects within the L<sub>2</sub>Fe(CO)<sub>3</sub> system,<sup>23</sup> the nature of L ranging from sterically compact (PMe<sub>3</sub>) to spatially demanding (PCy<sub>3</sub>). A quantitative analysis of ligand effects (QALE) analysis is then described which shows the steric/electronic relationship existing in the present system.

**Sterically Demanding Monodentate Phosphines Ligands.** We have previously shown that the entryway into the thermochemistry of this system lies in the reaction of (BDA)Fe(CO)<sub>3</sub> with excess ligand as illustrated in reaction 14.<sup>10</sup> We now wish to show that this entryway can be extended to sterically demanding

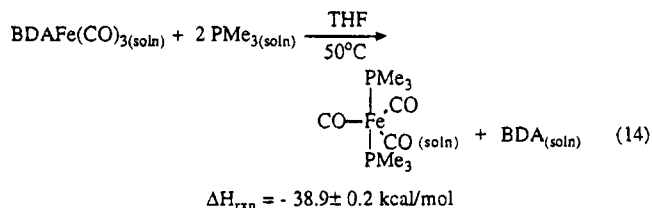
(19) Putnik, C. F.; Welter, J. J.; Stucky, G. D.; D'Aniello, M. J.; Sosinsky, B. A.; Kirner, J. F.; Muetterties, E. L. *J. Am. Chem. Soc.* **1978**, *100*, 4107–4109.

(20) (a) Brown, D. L. S.; Connor, J. A.; Leung, M. L.; Paz Andrade, M. I.; Skinner, H. A.; Zafarani-Moattar, M. T. *J. Organomet. Chem.* **1976**, *110*, 79–89. (b) Connor, J. A.; Demain, C. P.; Skinner, H. A.; Zafarani-Moattar, M. T. *J. Organomet. Chem.* **1979**, *170*, 117–130.

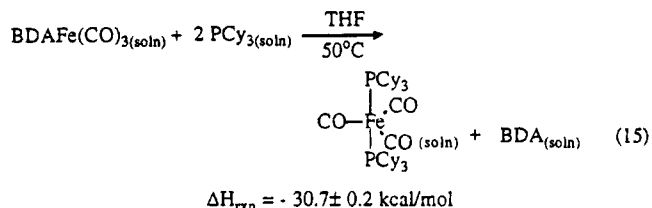
(21) (a) Rahman, M. M.; Liu, H.-Y.; Eriks, K.; Prock, A.; Giering, W. P. *Organometallics* **1989**, *8*, 1–7. (b) Liu, H.-Y.; Eriks, K.; Prock, A.; Giering, W. P. *Inorg. Chem.* **1989**, *28*, 1759–1763. (c) Poe, A. J. *Pure Appl. Chem.* **1988**, *60*, 1209–1216 and references cited. (d) Gao, Y.-C.; Shi, Q.-Z.; Kersher, D. L.; Basolo, F. *Inorg. Chem.* **1988**, *27*, 188–191. (e) Baker, R. T.; Calabrese, J. C.; Krusic, P. J.; Therien, M. J.; Troglor, W. C. *J. Am. Chem. Soc.* **1988**, *110*, 8392–8412. (f) Rahman, M. M.; Liu, H.-Y.; Prock, A.; Giering, W. P. *Organometallics* **1987**, *6*, 650–658.

(22) (a) Huynh, M. H. V.; Bessel, C. A.; Takeuchi, K. J. Presented at the 208th American Chemical Society Meeting; Abstract INOR 165. (b) Perez, W. J.; Bessel, C. A.; See, R. F.; Lake, C. H.; Churchill, M. R.; Takeuchi, K. J. Presented at the 208th American Chemical Society Meeting; Abstract INOR 166. (c) Ching, S.; Shriver, D. F. *J. Am. Chem. Soc.* **1989**, *111*, 3238–3243. (d) Lee, K.-W.; Brown, T. L. *Inorg. Chem.* **1987**, *26*, 1852–1856.

(23) The importance of organoiron complexes in stereochemical and chemical applications has been reviewed: Fatiadi, A. J. *J. Res. Natl. Stand. Technol.* **1991**, *96*, 1–113.



tertiary phosphine ligands (eq 15). A complete listing



of all thermochemical information thus far measured for monodentate ligands in this system is presented in Table 1. This rather extensive tabulation now allows for a detailed analysis of factors affecting the thermochemical stability of iron-phosphine bond enthalpy terms.

We have previously described the overwhelming importance of electronic effects in this system. The enthalpic trends in earlier contributions<sup>10a-c</sup> were described in terms of two-component relationships dealing exclusively with ligand substitution enthalpies and electronic terms quantifying the electronic donating ability of the phosphine ligand. Keeping in mind such considerations and enthalpy data listed in Table 1, it is surprising to find one of the most basic phosphines ( $PCy_3$ )<sup>24</sup> to have an unusually low enthalpy of ligand substitution. In the present data, involving sterically demanding phosphines, a simple linear relationship correlating the electronic factor associated with the phosphine ligand to the enthalpy of reaction cannot be obtained (Figure 1).

The poor correlation obtained (0.55) is taken to mean that the steric factor contributes in some amount to the magnitude of the ligand substitution reaction. It therefore appears that electronic arguments can explain the enthalpic trend to a point, beyond which both steric and electronic contributions must be considered. This argument has been presented qualitatively and semiquantitatively in a number of systems.<sup>21</sup>

#### Quantitative Analysis of Ligand Effects (QALE).

We now wish to consider the present data in quantitative terms with the help of a relationship and treatment proposed by Giering and Prock.<sup>25</sup> Giering and co-workers have partitioned relative importance of steric and electronic contributions using a variation of a treatment first proposed by Tolman.<sup>24</sup> These researchers have applied this treatment to a number of kinetic and thermodynamic data.<sup>21a,b,f,25</sup> If such a treatment is applied to the present data, the general eq 16 is obtained

$$-\Delta H_{rxn} = -(0.73 \pm 0.10)\chi - (0.46 \pm 0.03)(\theta - 135)\lambda - (1.69 \pm 0.38)E_{ar} + 46.28 \pm 0.78 \quad (16)$$

$$n = 16 \quad R^2 = 0.984$$

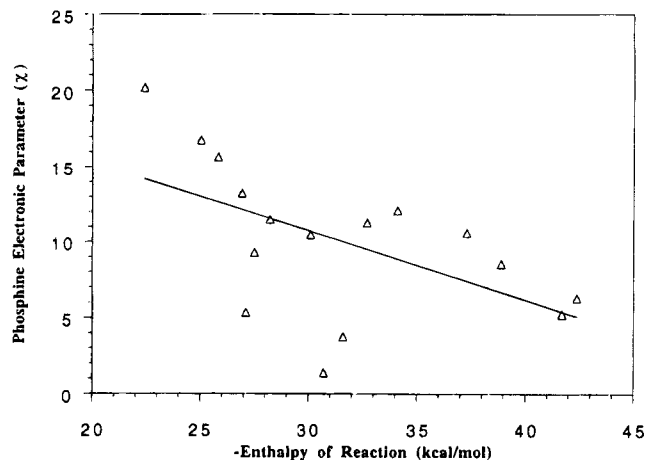


**Figure 1.** Enthalpy of reaction (kcal/mol) versus the phosphine electronic parameter ( $\chi$ ). Slope =  $-0.456$ ;  $R = 0.55$ .

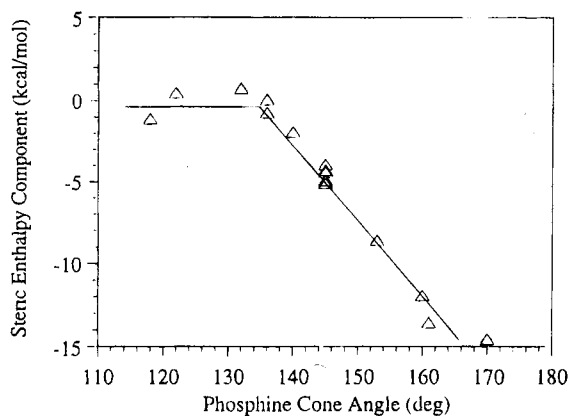


**Figure 2.** Steric enthalpy contribution (kcal/mol) versus phosphine cone angle (deg).

for 16 different phosphine reactions,<sup>26</sup> where  $\Delta H$  is the enthalpy of reaction (kcal/mol),  $\chi$  is the electronic parameter associated with a given phosphine ligand,  $\theta$  represents the phosphine steric factor,  $\lambda$  is a switching function that turns the steric effect when the size of the ligand exceeds the steric threshold (that is  $\lambda$  equals 0 when  $\theta$  is less than the steric threshold angle and  $\lambda$  equals 1 when  $\theta$  is greater than the threshold angle value), and  $E_{ar}$  is the phosphine aryl substituent contribution. All phosphine parameters values (with the exception of the enthalpy data) utilized in the treatment have previously been reported by Giering and Prock.<sup>25</sup> The correlation coefficient depicts the excellent fit of the data to this model. Once the general formula is derived, individual electronic and steric enthalpic contributions can be back-calculated. Doing this simple analysis affords the graphical representation of the enthalpic contribution associated with steric effects ( $\theta$ ) and is illustrated in Figure 2. Here, it can clearly be seen that a steric threshold of  $135^\circ$  is present in this system. This is taken to mean that phosphine ligands with cone angles greater than  $135^\circ$  will exhibit a steric contribution to the overall enthalpy of reaction. It should also be pointed out that since this is a thermodynamic study as opposed to a kinetic one, the analysis of the data

(25) (a) Fernandez, A. L.; Prock, A.; Giering, W. P. *Organometallics* **1994**, *13*, 2767-2772 and references cited. (b) Liu, H.-Y.; Eriks, K.; Prock, A.; Giering, W. P. *Organometallics* **1990**, *9*, 1758-1766.

(26)  $PBz_3$  has not been included in this analysis. Giering<sup>25</sup> has observed that this phosphine proves to be a problem in such analyses.

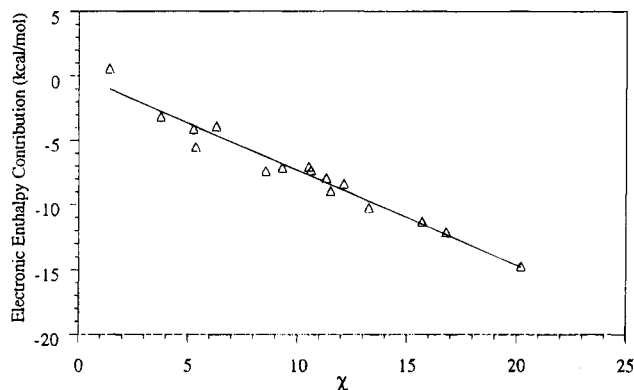


**Figure 3.** Electronic enthalpy contribution (kcal/mol) versus phosphine electronic parameter ( $\chi$ ). Slope =  $-0.733$ ;  $R = 0.98$ .

gives a view of  $L_2Fe(CO)_3$  that is independent of mechanism of formation. Thus, the steric threshold observed in the analysis must be attributed to nonlinear steric effects in  $L_2Fe(CO)_3$  and not to a change in mechanism or a change in the nature of the rate-determining step.

A simple electronic correlation (Figure 3) can also be established in a similar manner (by back-calculating the enthalpic electronic contribution) and shows a fairly good linear relationship denoting the principal electronic influences in this system. Observation of the steric threshold at  $135^\circ$  might be possible in different sets of data.<sup>27</sup> Accordingly, the infrared data reported in this contribution was examined for such a correlation using Giering's treatment. Regression analysis of the full set of data does not provide good results. It appears that a problem in this analysis is the loss of  $D_{3h}$  symmetry and the resulting distortion of the complex when  $PRR'_2$  ligands are used. The ORTEP of **2** nicely shows this distortion. In the  $D_{3h}$  symmetric systems  $(R_3P)_2Fe(CO)_3$ , the C–Fe–C bond angles are expected to be the same and the  $Fe(CO)_3$  group should be planar regardless of the ancillary ligand. The analysis of the IR data for these  $D_{3h}$  complexes<sup>28</sup> is excellent even in the absence of steric threshold limitation. This correlation is presented in eq 17. The best fit, however, the one with the

$$\nu(CO) = 1.688\chi - 0.0969\theta + 3.633E_{ar} + 68.04 \quad (17)$$

$$R^2 = 0.999$$

smallest standard deviation, is given by eq 18, where

$$\nu(CO) = 1.702\chi - 0.1266(\theta - 135)\lambda + 3.415E_{ar} + 56.35 \quad (18)$$

$$R^2 = 1.00$$

the steric threshold is identical to the one previously calculated for the enthalpy data. The reason behind the observed good fit of the data without the steric threshold constraint is the relatively small importance of steric effects in this system. The interpretation of the infrared data set analysis (an increase of the phosphine size past the steric threshold causes the carbonyl stretching frequency to shift to a lower wavenumber) might be

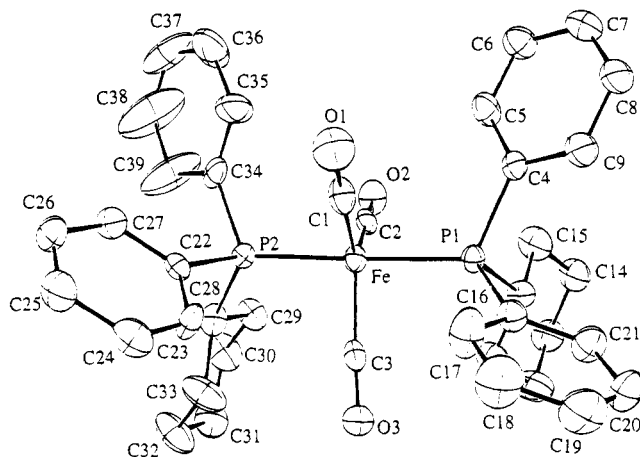


**Figure 4.** ORTEP drawing of  $(PCyPh_2)_2Fe(CO)_3$  with ellipsoids drawn at 50% probability.

explained in terms of diminished steric crowding of the first vibration state vs the ground state or, alternatively, as the phosphines are forced away from the iron center, there is an associated attenuation in the P–Fe  $\pi$  bonding, therefore resulting in an increase in electron density on the Fe available for back-donation with the carbonyl groups. This appears to be the first definitive evidence for phosphine–metal  $\pi$  bonding. More work aimed at elucidating the bonding factors present in this and related systems is currently underway.

#### Structural Features of $(PCyPh_2)_2Fe(CO)_3$ (**2**).

Figure 4 shows an ORTEP of  $(PCyPh_2)_2Fe(CO)_3$ ; the important bond lengths and angles are listed in Table 3. The iron complex is best considered a trigonal bipyramid with phosphine ligands occupying the apex in a mutually trans spatial arrangement (P–Fe–P bond angle of  $178.45(6)^\circ$ ) with a meridional arrangement of carbonyl groups (C–Fe–C average bond angle of  $120.0(2)^\circ$ ). In view of the steric demands associated with this ligand (cone angle  $153^\circ$ ) a slight distortion from pure  $D_{3h}$  might have been expected. In fact, it is slightly distorted from  $D_{3h}$  based on the Fe–C–O bond distances (see Table 3). The crystal structures of  $[(Me_2N)_3P]_2Fe(CO)_3$  (**3**)<sup>29</sup> and  $[P(OCH_2)_3]_2Fe(CO)_3$  (**4**)<sup>30</sup> indicate that  $(R_3P)_2Fe(CO)_3$  complexes of monodentate phosphines prefer to adopt trigonal-bipyramidal structures in which the phosphine ligands occupy trans axial positions. In these two complexes, the three Fe–CO bond lengths are 1.76 and 1.80 Å, respectively. This compares with Fe–C bond lengths of 1.780(5), 1.759(4), and 1.773(5) Å present in **2**, leading to a distortion from  $D_{3h}$  symmetry. The C–O bond lengths in **3** and **4** are 1.16 and 1.15 Å, respectively; whereas in **2**, C–O bond lengths of 1.141(5), 1.174(5), and 1.162(5) Å can be found. These important differences in individual bond lengths in **2** compared with the rather uniform bond length values found in the  $Fe(CO)_3$  moiety of **3** and **4** illustrate the deviation from ideal  $D_{3h}$  symmetry in **2**.<sup>31</sup>

(29) Cowley, A. H.; Davis, R. E.; Remadna, K. *Inorg. Chem.* **1981**, *20*, 2146–2152.

(30) Allison, D. A.; Clardy, J.; Verkade, J. G. *Inorg. Chem.* **1972**, *11*, 2804–2809.

(31) Casey and co-workers have observed structural distortion in a related  $Fe(CO)_3$  system involving chelating bidentate phosphine ligands: Casey, C. P.; Whiteker, G. T.; Campana, C. F.; Powell, D. R. *Inorg. Chem.* **1990**, *29*, 3376–3381.

(27) Giering, W. P. Private communication.

(28) All infrared data used for  $D_{3h}$  complexes can be found in Table 1. In addition a value for  $(P^tBu_3)_2Fe(CO)_3$  in THF of  $1852\text{ cm}^{-1}$  has been included in the treatment.

### Conclusion

The reported solution calorimetric investigation represents a detailed thermochemical study of organoiron complexes. Relative bond enthalpies are reported, and these help understand the donating ability of the ligands in the present system and the corresponding stabilizing effect on iron complexes. Moreover, a quantitative analysis of ligand effect analysis clearly shows the relative importance of steric and electronic factors in the present system at various phosphine steric requirements. This system to our knowledge is unique in that a complete ligand effect analysis can be performed on a large series of phosphine ligands therefore enabling a concise analysis of the relative importance of steric versus electronic effects. Studies focusing on enthalpic contributions associated with ligand substitution of

other ligands/ligand-types in this and related systems are presently underway.

**Acknowledgment.** The National Science Foundation (Grant CHE-9305492) and the Louisiana Board of Regents are gratefully acknowledged for support of this research. The Louisiana Board of Regents is also acknowledged for allocating funds allowing the purchase of FT-IR spectrometers. We are also indebted to Professor Warren Giering for helpful discussions.

**Supporting Information Available:** Tables of hydrogen coordinates and  $B$  values, selected distances and angles, anisotropic thermal parameters, and hydrogen bond distances for **2** (10 pages). Ordering information is given on any current masthead page.

OM950202H

# Molecular Dynamics of *dl*- and *meso*-Bis(indenyl)dimethylsilane: Reexamination of the Mechanism of Interconversion by Using Single Selective Inversion NMR

Suzie S. Rigby, Luc Girard, Alex D. Bain,\* and Michael J. McGlinchey\*

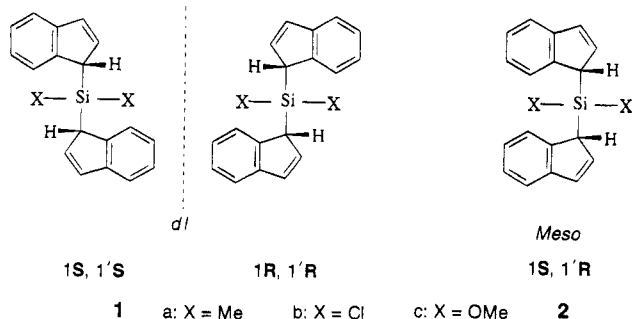
Department of Chemistry, McMaster University, Hamilton, Ontario L8S 4M1, Canada

Received March 8, 1995\*

In contrast to a previous report, it is found that the interconversion of *dl*-(indenyl)<sub>2</sub>SiMe<sub>2</sub>, **1a**, and its *meso* isomer, **2a**, proceeds through sequential [1,5]-suprafacial shifts and that there is only one mechanism operating at a detectable rate below ≈150 °C. Below 100 °C this process is too slow to be detected by NMR line-broadening methods, but it is readily followed by standard kinetic measurements. Above 100 °C, the rate of interconversion is conveniently measured by selective inversion NMR methods. The *iso*-indene intermediate, **3**, has been trapped as its double Diels–Alder adduct with TCNE showing that the rearrangement occurs relatively rapidly on the chemical time scale.

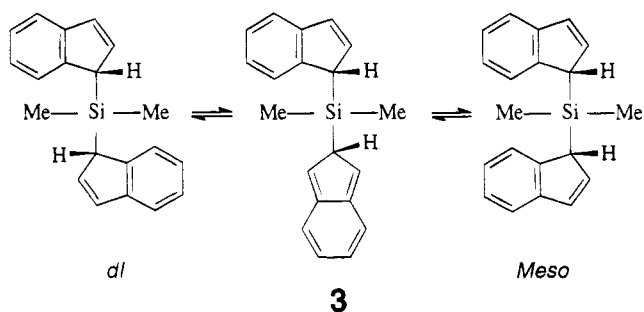
## Introduction

A recent report described the syntheses and molecular dynamics of a series of molecules of the type (indenyl)<sub>2</sub>SiX<sub>2</sub>, where X = Me, Cl, or MeO.<sup>1</sup> These molecules are important because of their relevance to stereospecific polymerizations of alkenes.<sup>2</sup> Moreover, (indenyl)<sub>2</sub>SiX<sub>2</sub> systems possess a particular stereochemical feature in that they can exist not only as the mixture of enantiomers, **1**, but also as the *meso* isomer **2**.



As noted previously, the *meso*-isomer, **2a**, has a single mirror plane (*C<sub>s</sub>* symmetry); the two methyl groups bonded to silicon are nonequivalent and yield a pair of singlets in either the <sup>1</sup>H or <sup>13</sup>C NMR regimes. In contrast, the *dl*-isomers, **1a**, have *C<sub>2</sub>* symmetry which renders these methyl groups chemical-shift equivalent, and a single CH<sub>3</sub> resonance is observed in either the <sup>1</sup>H or <sup>13</sup>C spectrum. The *dl*-compound, **1a**, is readily isolable by crystallization, and the rate of its conversion into **2a** is conveniently followed by monitoring the intensities of the <sup>1</sup>H NMR methyl resonances of **1a** and **2a**.

## Scheme 1. Interconversion of *dl*- and *meso*-Isomers **1a** and **2a** via *iso*-Indene **3**



One can readily envisage interconversion of the *dl*- and *meso*-isomers by successive [1,5]-suprafacial sigmatropic shifts of one (indenyl)SiMe<sub>2</sub> moiety over the surface of the five-membered ring of the other indenyl unit. As depicted in Scheme 1, the process would pass through the *iso*-indene intermediate **3**; indeed, such a [1,5]-shift mechanism has been the subject of detailed study by a number of groups,<sup>3–6</sup> and it has been firmly established that such migrations proceed with retention of configuration at the migrating silicon, germanium or tin center.<sup>7</sup> There is also the possibility of [1,5]-hydrogen shifts to give the 3-silyl isomer **4**, but this occurs only at elevated temperatures,<sup>1</sup> and isomer **4** can only be detected after prolonged heating at 200 °C (see Scheme 2).

The previous authors tried to evaluate the kinetic parameters for the *dl*-to-*meso* transformation by using conventional variable-temperature NMR measurements. At temperatures above 110 °C, the <sup>1</sup>H NMR methyl resonances in **1a** begin to broaden and, in principle, it

(3) (a) Rakita, P. E.; Davison, A. *Inorg. Chem.* **1969**, *5*, 1164. (b) Davison, A.; Rakita, P. E. *J. Organomet. Chem.* **1970**, *23*, 407.

(4) Larrabee, R. B.; Dowden, B. F. *Tetrahedron Lett.* **1970**, 915.

(5) Ashe, A. J., III. *Tetrahedron Lett.* **1970**, 2105.

(6) (a) Sergeev, N. M.; Grishin, Yu. K.; Lulikov, Yu. N.; Ustynyuk, Yu. A. *J. Organomet. Chem.* **1972**, *38*, C1. (b) Lulikov, Yu. N.; Sergeev, N. M.; Ustynyuk, Yu. A. *J. Organomet. Chem.* **1974**, *65*, 303.

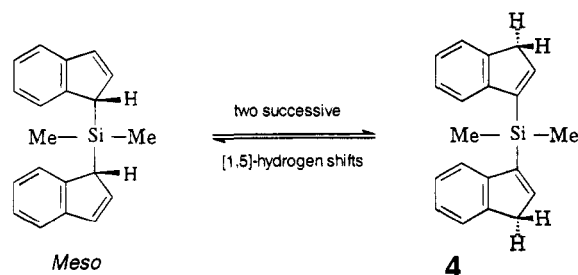
(7) (a) McMaster, A. D.; Stobart, S. R. *J. Am. Chem. Soc.* **1982**, *104*, 2109. (b) McMaster, A. D.; Stobart, S. R. *J. Chem. Soc., Dalton Trans.* **1982**, 2275. (c) Atwood, J. L.; McMaster, A. D.; Rogers, R. D.; Stobart, S. R. *Organometallics* **1984**, *3*, 1500.

\* Abstract published in *Advance ACS Abstracts*, June 15, 1995.

(1) Chen, Y.-X.; Rausch, M. D.; Chien, J. C. W. *Organometallics* **1993**, *12*, 4607.

(2) For reviews see: (a) Keii, T.; Soga, K., Eds. *Catalytic Olefin Polymerization*; Elsevier: New York, 1990. (b) Quirk, R. P., Ed. *Transition Metal Catalyzed Polymerizations: Ziegler–Natta and Metathesis Polymerizations*; Cambridge Press: New York, 1988. (c) Kaminsky, W.; Sinn, H. Eds. *Olefin Polymerization*; Springer-Verlag: Berlin, 1988.

**Scheme 2. Isomerization of 1a or 2a to 4 via [1,5]-Hydrogen Shifts**



may be possible to extract activation energies from these data. However, processes with such high activation energy barriers are at the upper limit of the line-broadening technique. Moreover, an attempt was made to follow the progress of the reaction below the temperature at which line-broadening became evident. A sample of the pure *dl*-compound, **1a**, was maintained at a given temperature, say 40 °C, for "about 15 min" and the measured intensity ratio of *dl*:*meso* methyl resonances was taken as the equilibrium constant at that particular temperature. The procedure was repeated at several temperatures, and these  $K_{eq}$  values were used to construct a  $\ln K_{eq}$  versus  $1/T$  plot.<sup>8</sup> The data obtained were interpreted in terms of the differing steric effects of the methyl, methoxy, and chloro substituents in **1a**, **1b**, and **1c**, respectively.<sup>1</sup> It was also claimed that since "the fluxional process" (presumably the [1,5]-silyl tropic shift) was only detectable by NMR line-broadening techniques at approximately 100 °C, then the interconversion of the *dl*- and *meso*-isomers, **1** and **2**, must occur via a different mechanism below this temperature.

The lack of kinetic data over a wide range of temperatures together with the proposal that **1** undergoes rearrangement by symmetry-forbidden [1,3]-silyl tropic shifts at relatively low temperatures prompted us to reinvestigate the molecular dynamics of this class of molecules.

## Results and Discussion

### The Interconversion of 1a and 2a below 100 °C.

In order to generate an Arrhenius (or Eyring) plot, one must have reliable rate data over a range of temperatures. This is readily accomplished by placing a pure sample of *dl*-(indenyl)<sub>2</sub>SiMe<sub>2</sub>, **1a**, dissolved in toluene-*d*<sub>6</sub>, in the probe of an NMR spectrometer at a constant temperature and regularly monitoring the intensities of the methyl peaks in **1a** and **2a**. By this means, one can obtain rate constants at a number of temperatures and evaluate the activation parameters. In this particular case, the barrier to interconversion of **1a** and **2a** is large, the rates are slow, and one does not reach equilibrium within 15 min, as assumed by the previous authors. Figure 1 illustrates the Eyring plot obtained by using our data; the  $\ln k/T$  values obtained at temperatures less than 100 °C are shown as open squares.

### The Interconversion of 1a and 2a above 100 °C.

As mentioned above, the use of peak coalescence methods to evaluate high activation energy barriers is not

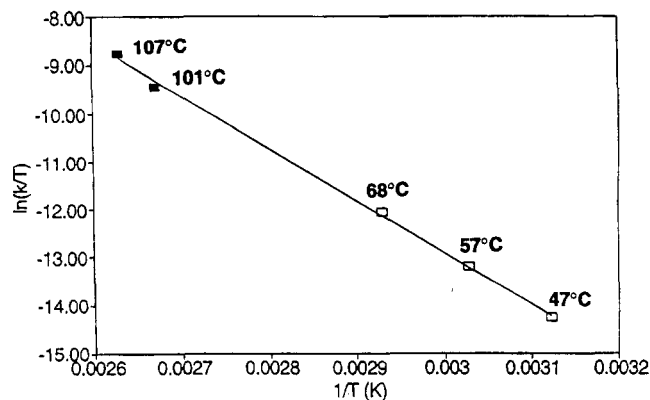


**Figure 1.** Eyring plot for the interconversion of *dl*- and *meso*-bis(indenyl)SiMe<sub>2</sub>, **1a** and **2a**, respectively.

the preferred option. Magnetization transfer techniques permit the measurement of exchange rates even when the processes are too slow to be monitored by conventional peak coalescence methods.<sup>9</sup> Thus exchange pathways can be elucidated by means of 2D NOESY spectra, and the rate constants are readily available from selective inversion recovery experiments.<sup>10</sup>

In the case at hand, a 2D NOESY experiment on a mixture of **1a** and **1b** at 100 °C reveals cross-peaks between the proton attached to the *sp*<sup>2</sup>-carbon at C(3) and the proton bonded to C(1), the *sp*<sup>3</sup>-carbon adjacent to silicon; it also shows cross-peaks between the *dl*-methyl resonance of **1a** and both methyl peaks of the *meso*-isomer, **1b**. Subsequently, the <sup>1</sup>H methyl signal attributable to *dl*-(indenyl)<sub>2</sub>SiMe<sub>2</sub>, **1a**, was selectively inverted and the return of that peak to equilibrium, and also those of the *meso*-methyl resonances, were monitored. The time dependence of the *z*-magnetization of each of these methyl peaks was fitted using a nonlinear least-squares program, and rate constants were extracted for several temperatures. The  $\ln k/T$  values for the temperature range above 100 °C are shown in Figure 1 as filled squares.

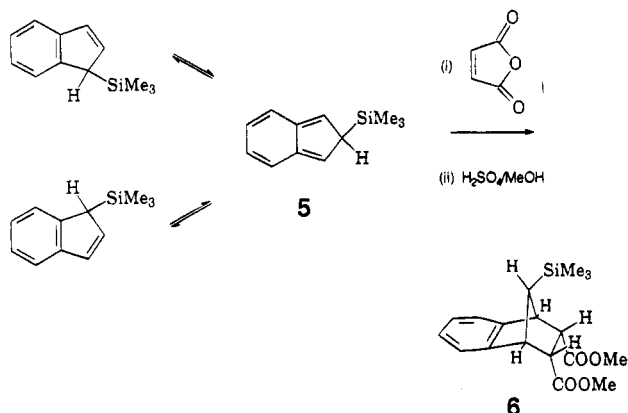
It is evident that the data over the entire temperature range studied (320–380 K) are fit by a single process with the following values:  $\Delta H^\ddagger = 21.9 \pm 0.5$  kcal mol<sup>-1</sup>,  $\Delta S^\ddagger = -7.2 \pm 1.4$  cal mol<sup>-1</sup> K<sup>-1</sup>, and  $\Delta G^\ddagger = 24.2 \pm 0.5$  kcal mol<sup>-1</sup> at 50 °C.<sup>11</sup> These results are consistent with the existence of a single migration mechanism, presumably the symmetry-allowed [1,5]-suprafacial sigmatropic shift of one (indenyl)SiMe<sub>2</sub> moiety relative to the other indenyl fragment. The earlier speculations<sup>1</sup> which invoked the symmetry-forbidden [1,3]-shift below 100 °C are thus unnecessary.<sup>12</sup> Moreover, as expected, molecular orbital calculations at the extended Hückel level show unequivocally that migration of a trimethylsilyl substituent over the five-membered ring of an indenyl group can proceed readily through an *iso*-indene intermediate. Indeed, placement of the Me<sub>3</sub>Si fragment over the center of the five-membered ring (as postulated by the authors of ref 1) is calculated to be strongly disfavored.

(9) (a) Forsén, S.; Hoffman, R. A. *J. Chem. Phys.* **1963**, *39*, 2982. (b) Forsén, S.; Hoffman, R. A. *J. Chem. Phys.* **1964**, *40*, 1189. (c) Hoffman, R. A.; Forsén, S. *J. Chem. Phys.* **1966**, *45*, 2049.

(10) Sanders, J. K. M.; Hunter, B. K. *Modern NMR Spectroscopy, A Guide for Chemists*; Oxford University Press: Oxford, 1987; pp 224–234.

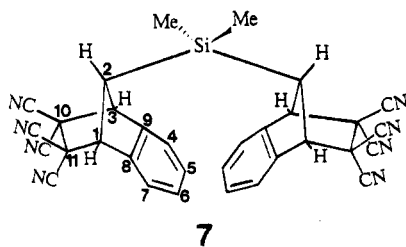
(11) This is in accord with earlier estimates of  $\approx 25$  kcal/mol for the migration barrier in R<sub>3</sub>Si-indene systems.<sup>3–6</sup>

(8) This was described as an Arrhenius plot; if done correctly, this would in fact have been a van't Hoff plot.

**Scheme 3. Diels–Alder Trapping of an *iso*-Indene Intermediate with Maleic Anhydride**


**Trapping of an *iso*-Indene Intermediate.** If the assumption of the intermediacy of an *iso*-indene structure, **3**, is correct, then one should be able to trap such a species as a Diels–Alder adduct. Some years ago, it was reported that 2-(trimethylsilyl)-*iso*-indene, **5**, could be intercepted by maleic anhydride, as depicted in Scheme 3; methanolysis of the resulting adduct afforded a diester, **6**, as characterized by its NMR spectrum.<sup>4</sup> Subsequently, it was reported that other Me<sub>3</sub>E-indenyl systems, where E = Ge or Sn, also underwent [1,5]-metallotropic shifts; moreover, in some cases, the *iso*-indene intermediates could be intercepted as their Diels–Alder adducts with tetracyanoethylene.<sup>6</sup>

When a mixture of **1a** and **2a** was stirred with an excess of tetracyanoethylene (TCNE) at room temperature for 72 h, the <sup>1</sup>H and <sup>13</sup>C NMR spectra indicated the disappearance of the starting materials and the formation of a molecule, **7**, with a remarkably symmetric structure. The aromatic rings exhibited only two CH environments, the bridgehead protons appeared as a doublet coupled to the methine triplet of the Me<sub>2</sub>Si–CH fragment, and the Me<sub>2</sub>Si moiety yielded a singlet. The mass spectrum of the isolated product indicated **7**



to be the adduct derived from the reaction of two TCNE's with one molecule of (indenyl)<sub>2</sub>SiMe<sub>2</sub>, and this assignment was confirmed by standard 1- and 2-D NMR techniques. The structure of the double Diels–Alder adduct **7** is shown with each TCNE positioned *anti* to the Me<sub>2</sub>Si substituent; this configuration has been found X-ray crystallographically for the mono Diels–Alder product derived from trimethylsilylindene and TCNE.<sup>13</sup>

In conclusion, we report that the isomerization of *dl*-(indenyl)<sub>2</sub>SiMe<sub>2</sub>, **1a**, to its *meso*-isomer, **2a**, proceeds through sequential [1,5]-suprafacial shifts. There is

only one mechanism operating at a detectable rate below ≈150 °C. At lower temperatures, this process is too slow to be detected by NMR line-broadening methods, but it is readily followed by standard kinetic measurements. Above 100 °C, the rate of interconversion is conveniently measured by selective excitation methods. The *iso*-indene intermediate, **3**, is easily trapped as its double Diels–Alder adduct showing that the rearrangement occurs relatively rapidly on the chemical time scale.

**Experimental Section**

All experiments were performed under an inert atmosphere of N<sub>2</sub> using standard Schlenk techniques. NMR spectra were recorded on a Bruker AC 300 spectrometer with a 7.65 T superconducting magnet, equipped with a Bruker B-VT 2000 temperature controller, and a 5 mm QNP probe. <sup>1</sup>H and <sup>13</sup>C data were obtained at 300.13 and 75.47 MHz, respectively. All spectra were recorded on spinning samples, locked to a solvent proton signal of the solvent, or to a <sup>13</sup>C solvent signal. Each temperature was measured by placing a copper–constantan thermocouple, contained in an NMR tube, into the probe. All FID's were transferred to an IBM PC using the program NMRLINK. Spectra were Fourier-transformed using the program NMR286.

**Bis(1-indenyl)dimethylsilane** was prepared by the method of Marechal.<sup>14</sup> The proton NMR chemical shifts correspond to those obtained by Chen and co-workers<sup>1</sup> both for the pure *dl* enantiomers and for the mixture of *meso* and *dl* diastereomers. The <sup>13</sup>C NMR spectra had not been fully assigned, and so these attributions were made by means of a <sup>1</sup>H–<sup>13</sup>C shift-correlated experiment. *dl* <sup>1</sup>H NMR (toluene-*d*<sub>8</sub>): δ 7.41 (d, <sup>3</sup>J = 7.6 Hz, 2H, H-4), 7.32 (d, <sup>3</sup>J = 7.5 Hz, 2H, H-7), 7.20 (d, <sup>3</sup>J = 7.6 Hz of d, <sup>3</sup>J = 7.5 Hz, 2H, H-5), 7.10 (d, <sup>3</sup>J = 7.5 Hz of d, <sup>3</sup>J = 7.6 Hz, 2H, H-6), 6.83 (d, <sup>3</sup>J = 5.3 Hz of d, <sup>3</sup>J = 1.0 Hz, 2H, H-3), 6.40 (d, <sup>3</sup>J = 1.9 Hz of d, <sup>3</sup>J = 5.3 Hz, 2H, H-2), 3.42 (s, 2H, H-1), –0.43 (s, 6H, CH<sub>3</sub>'s). *meso* <sup>1</sup>H NMR (toluene-*d*<sub>8</sub>): δ 7.39 (d, <sup>3</sup>J = 7.6 Hz, 2H, H-4), 7.32 (d, <sup>3</sup>J = 7.5 Hz, 2H, H-7), 7.20 (d, <sup>3</sup>J = 7.6 Hz of d, <sup>3</sup>J = 7.6 Hz, 2H, H-5), 7.10 (d, <sup>3</sup>J = 7.5 Hz of d, <sup>3</sup>J = 7.6 Hz, 2H, H-6), 6.79 (d, <sup>3</sup>J = 5.3 Hz of d, <sup>3</sup>J = 1.0 Hz, 2H, H-3), 6.26 (d, <sup>3</sup>J = 5.3 Hz of d, <sup>3</sup>J = 1.9 Hz, 2H, H-2), 3.42 (s, 2H, H-1), –0.21 (s, 3H, CH<sub>3</sub>), –0.59 (s, 3H, CH<sub>3</sub>).

*dl* <sup>13</sup>C NMR (toluene-*d*<sub>8</sub>): δ 145.2, 144.8 (C-8, C-9), 135.2 (C-2), 130.0 (C-3), 125.6 (C-5), 124.4 (C-6), 123.3 (C-7), 121.6 (C-4), 45.5 (C-1), –6.2 (CH<sub>3</sub>'s). *meso* <sup>13</sup>C NMR (toluene-*d*<sub>8</sub>): δ 145.2, 144.8 (C-8, C-9), 135.2 (C-2), 129.9 (C-3), 125.6 (C-5), 124.3 (C-6), 123.3 (C-7), 121.6 (C-4), 45.4 (C-1), –5.3, –7.1 (CH<sub>3</sub>'s). Mass spectrum: *m/z* 288 (10) ([M]<sup>+</sup>), 273 (5) ([M – CH<sub>3</sub>]<sup>+</sup>), 173 (100) ([M – C<sub>9</sub>H<sub>7</sub>]<sup>+</sup>), 145 (50) ([M – C<sub>9</sub>H<sub>7</sub>Si]<sup>+</sup>), 115 (15) ([C<sub>9</sub>H<sub>7</sub>]<sup>+</sup>).

**Trapping of *iso*-Indene **3** with Tetracyanoethylene.** A 100 mL two-necked round bottom flask was charged with ethyl acetate (50 mL), bis(1-indenyl)dimethylsilane (240 mg, 0.83 mmol), and tetracyanoethylene (380 mg, 2.97 mmol). The mixture was stirred under N<sub>2</sub> for 72 h. The Diels–Alder adduct was separated from excess TCNE by using flash chromatography on silica. Elution with CH<sub>2</sub>Cl<sub>2</sub> yielded the

(12) The fact that a kinetic process is too slow to be observed by using a particular spectroscopic technique does not mandate that it proceed by a different mechanism below the temperature at which becomes detectable.

(13) Stradiotto, M., Britten, J. F. Personal communication.

(14) Marechal, E.; Tortal, J. P. *C. R. Acad. Sci. Paris* **1968**, *267*, 467.



double Diels–Alder adduct, **7**, (200 mg, 0.37 mmol, 44%).  $^1\text{H}$  NMR (acetonitrile- $d_3$ ):  $\delta$  7.66–7.64 (m, 4H, H-7, H-4), 7.48–7.45 (m, 4H, H-5, H-6), 4.93 (d,  $^3J = 1.05$  Hz, 4H, H-1, H-3), 2.35 (t,  $^3J = 1.05$  Hz, 2H, H-2),  $-0.57$  (s, 6H,  $\text{CH}_3$ 's). The assignment of the proton signals was confirmed by NOE difference experiments.  $^{13}\text{C}$  chemical shifts were assigned on the basis of a  $^1\text{H}$ – $^{13}\text{C}$  shift-correlated experiment.  $^{13}\text{C}$  NMR (acetonitrile- $d_3$ ):  $\delta$  140.7 (C-8, C-9), 130.5 (C-5, C-6), 126.0 (C-7, C-4), 114.3, 112.5 (*exo* and *endo* nitriles), 60.5 (C-1, C-3), 51.3 (C-10, C-11), 49.4 (C-2),  $-3.8$  ( $\text{CH}_3$ 's). Mass spectrum:  $m/z$  544 (10) ( $[\text{M}]^+$ ), 416 (40) ( $[\text{M} - 4\text{CN}]^+$ ), 288 (45) ( $[\text{M} - 8\text{CN}]^+$ ).

**Selective Inversion Measurements.** The exchange rates in the slow exchange limit were measured by selective-inversion relaxation type experiments.<sup>15–17</sup> One part of the spectrum was perturbed using a 90–

$\tau$ –90 pulse sequence,<sup>18</sup> and then the return to equilibrium was monitored as in an inversion–recovery  $T_1$  experiment. In this case, selective inversion of a single line proved to be the best way of probing the relaxation, but this is by no means generally true.<sup>18</sup> A C programming language version of McClung's program SIFIT<sup>17</sup> was used to do a nonlinear least-squares fit to the experimental results, and to extract values for the rates. Typical errors in the rates are  $\pm 10\%$ .

**Acknowledgment.** We thank NSERC Canada for financial support.

**Supporting Information Available:** NOESY spectra and plots of experimental versus calculated data for  $^1\text{H}$  selective inversion recovery experiment for **1a,b** (2 pages). Ordering information is given on any current masthead page.

OM950183B

(15) Grassi, M.; Mann, B. E.; Pickup, B. T.; Spencer, C. M. *J. Magn. Reson.* **1986**, *69*, 92.

(16) Led, J. J.; Gesmar, H. *J. Magn. Reson.* **1982**, *49*, 444.

(17) Muhandiram, D. R.; McClung, R. E. D. *J. Magn. Reson.* **1987**, *71*, 187.

(18) Bain, A. D.; Cramer, J. A. *J. Magn. Reson.* **1993**, *A 103*, 217.

# Synthesis, X-ray Structure, and Dynamic NMR Investigation of Secondary Cymantrenyl- and Ferrocenylcarbenium Ions Stabilized by Heterobimetallic Cobalt–Molybdenum Clusters: $[(\text{MoCo}(\text{CO})_5\text{Cp})(\mu\text{-Mn}(\text{CO})_3\text{CpCHC}\equiv\text{CCH}_3)]^+\text{BF}_4^-$ and $[(\text{MoCo}(\text{CO})_5\text{Cp})(\mu\text{-FcCHC}\equiv\text{CCH}_3)]^+\text{BF}_4^-$

Mikhael A. Kondratenko,<sup>†,‡</sup> Marie-Noëlle Rager,<sup>†</sup> Jacqueline Vaissermann,<sup>§</sup> and Michel Gruselle<sup>\*,†</sup>

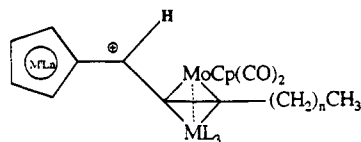
URA 403 CNRS, ENSCP, 11 rue P. et M. Curie, 75231 Paris Cédex 05, France, Laboratoire de chimie des métaux de transition, URA 419 CNRS, Université P. et M. Curie, 4 place Jussieu, 75252 Paris Cédex 05, France, and Laboratory for Organometallic Stereochemistry, INEOS, 28 Vavilov Street, 117813 Moscow, Russian Federation

Received February 10, 1995<sup>®</sup>

A solution-phase variable-temperature  $^1\text{H}$  NMR investigation was performed on  $[(\text{MoCo}(\text{CO})_5\text{Cp})(\mu\text{-Mn}(\text{CO})_3\text{CpCHC}\equiv\text{CCH}_3)]^+\text{BF}_4^-$  (**4**),  $[(\text{MoCo}(\text{CO})_5\text{Cp})(\mu\text{-FcCHC}\equiv\text{CCH}_3)]^+\text{BF}_4^-$  (**5b**), and  $[(\text{MoCo}(\text{CO})_5\text{Cp})(\mu\text{-FcCHC}\equiv\text{C}(\text{CH}_2)_4\text{CH}_3)]^+\text{BF}_4^-$  (**5c**). The NMR spectra were temperature dependent for **4** and for **5b,c**. The fluxional process could be ascribed to simple rotation around the  $\text{C}^+$ -cluster bond. In addition the X-ray structure of the complexes **4** and **5b** were determined. In all cases it appears that the molybdenum plays a major role in the stabilization of the positive charge.

## Introduction

We have previously described the synthesis<sup>1</sup> and structure<sup>2</sup> of the stabilized carbenium ion  $[(\text{Mo}_2\text{Cp}_2(\text{CO})_4)(\mu\text{-FcCHC}\equiv\text{C}(\text{CH}_2)_2\text{CH}_3)]^+\text{BF}_4^-$  (**5a**), where the



- (4)  $\text{ML}_3 = \text{Co}(\text{CO})_3$ ,  $n=0$ ,  $\text{M}'\text{Ln} = \text{Mn}(\text{CO})_3$   
 (5a)  $\text{ML}_3 = \text{MoCp}(\text{CO})_2$ ,  $n=2$ ,  $\text{M}'\text{Ln} = \text{FeCp}$   
 (5b)  $\text{ML}_3 = \text{Co}(\text{CO})_3$ ,  $n=0$ ,  $\text{M}'\text{Ln} = \text{FeCp}$   
 (5c)  $\text{ML}_3 = \text{Co}(\text{CO})_3$ ,  $n=4$ ,  $\text{M}'\text{Ln} = \text{FeCp}$

carbon atom bearing the positive charge is simultaneously adjacent to a ferrocenyl group and an acetylenic  $[\text{Mo}_2]$  cluster. Our NMR results, together with molecular structure data, have shown the competition between the ferrocenyl group and the dimolybdenum acetylenic cluster toward stabilization of the adjacent carbenium center. While the dimetallic cluster is the main contributor to the stabilization and is the center of the fluxional behavior of the molecules, the ferrocenyl group also seems to participate with its  $\pi$ -electronic system located on the substituted ring. In this case, we demonstrated that in acetone- $d_6$  solution, the cation **5a** is fluxional even at room temperature. Cooling the

solution to 248 K leads to the observation of two diastereomers equilibrating slowly on the NMR time scale. Two possible processes were invoked to explain these results as follows.

(1) A diastereomerization process of high activation energy was invoked, attributed to the following. (i) A suprafacial migration of the carbenium group occurs from one molybdenum to the other. In this mechanism the configuration of the carbenium ion is unchanged while the configuration of the cluster is inverted. (ii) A simple rotation occurs around the  $\text{C}^+$ -cluster bond. In this case the configuration of the cluster does not change but the carbenium center is inverted.

(2) An enantiomerization process was invoked (called antarafacial migration of the carbenium center) perhaps lower in activation energy than the diastereomerization processes, in which the configuration of the cluster and that of the carbenium center are simultaneously changed.

The stereochemical consequences of these mechanisms are shown in Figure 1.

In recent years, a number of tri- and dimetallic cluster cations have been synthesized and their variable-temperature NMR spectra have been investigated.<sup>3–5</sup> The mechanistic proposals described above are very useful for understanding the dynamic processes observed for these carbenium ions, but the mechanism which is actually operative has not been delineated. In one case,<sup>6</sup> simple rotation was demonstrated in the solid state for a tertiary homobinuclear  $[\text{Mo}_2]$  cation. The major difficulty in this differentiation is the local symmetry of the  $[\text{Mo}_2]$  acetylenic cluster.

\* To whom correspondence should be addressed.

<sup>†</sup> URA 403 CNRS.

<sup>‡</sup> INEOS.

<sup>§</sup> URA 419 CNRS.

<sup>®</sup> Abstract published in *Advance ACS Abstracts*, July 1, 1995.

(1) Troitskaya, L. L.; Sokolov, V. I.; Bakhmutov, V. I.; Reutov, O. A.; Gruselle, M.; Cordier, C.; Jaouen, G. *J. Organomet. Chem.* **1989**, *364*, 195.

(2) Cordier, C.; Gruselle, M.; Vaissermann, J.; Troitskaya, L. L.; Bakhmutov, V. I.; Sokolov, V. I.; Jaouen, G. *Organometallics* **1992**, *11*, 3826.

(3) Edidin, R. T.; Norton, J. R.; Mislow, K. *Organometallics* **1982**, *1*, 561.

(4) Padmanabhan, S.; Nicholas, K. M. *J. Organomet. Chem.* **1983**, *268*, C23.

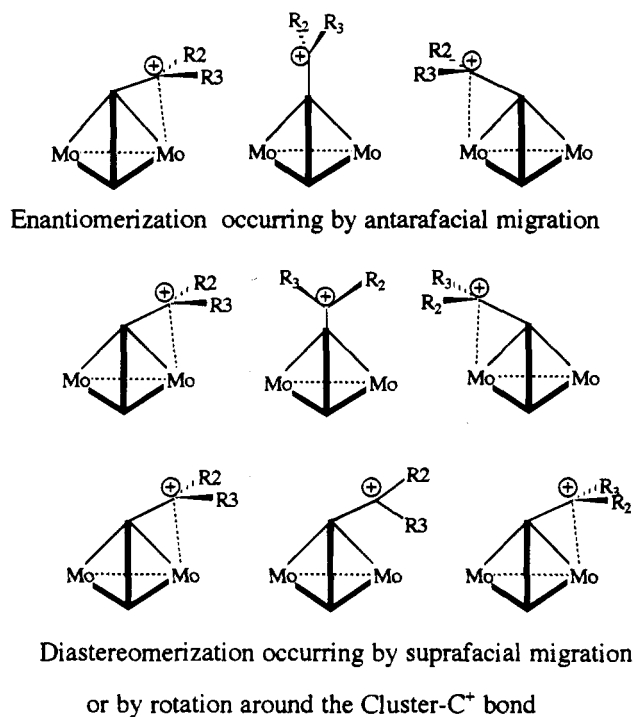


Figure 1.

Upon the building of a heterobinuclear complex by substitution of one of the ligands<sup>7</sup> or by substitution of one metallic vertex by another metal,<sup>8,9</sup> an intrinsically chiral cluster is obtained, as shown in Figure 2. In these cases it is not possible to observe an enantiomerization process, unless the cluster itself can isomerize. Nicholas<sup>10</sup> has reported an example of a carbenium ion stabilized by a chiral acetylenic cluster [Co<sub>2</sub>(CO)<sub>5</sub>PR<sub>3</sub>]; in this case it was demonstrated that the formation of the cation starting from diastereomeric alcohols is diastereoselective and controlled by kinetic factors. The ratio between *anti* and *syn* isomers depends on the nature of the substituents at the carbenium center and in the acetylenic position. The carbenium ion is preferentially stabilized by the phosphine-substituted cobalt vertex. For secondary cations, the initial [*anti*/*syn*] ratio is in favor of the *anti* isomer. For carbenium substituents such as methyl or phenyl, the cation initially

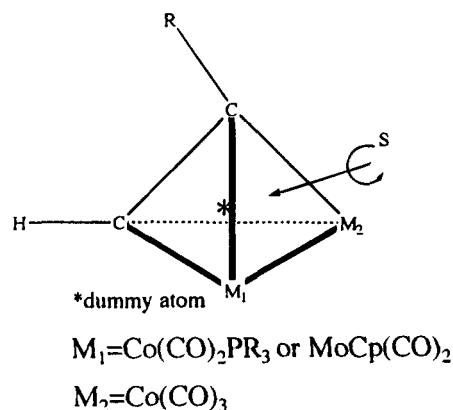


Figure 2. Determination of the configuration for a bimetallic acetylenic cluster.

formed isomerizes slowly to give a 1:1 [*anti*/*syn*] mixture. For larger substituents such as isopropyl or *tert*-butyl, the *anti* isomer is predominant and does not isomerize (Figure 3).

McGlinchey<sup>8b</sup> has established the diastereoselective formation of a binuclear [W-Co] stabilized secondary cation in solution, starting from diastereomerically pure secondary alcohol. No isomerization was observed from the mixture of initially formed cations, as shown in Scheme 1. For dicobalt hexacarbonyl propargylic secondary cations, Schreiber<sup>11</sup> has determined the *syn*/*anti* isomer ratios by integration of the corresponding resonances in the <sup>1</sup>H NMR spectra. Structural assignments were based on NOE experiments. The results show that the *syn* isomer is in all cases the major isomer. The ratio *syn*/*anti* depends on the bulkiness of the carbenium and alkynyl substituents (Figure 4).

The equilibration between *syn* and *anti* isomers occurs even at low temperature and is dependent on the R<sub>1</sub> and R<sub>2</sub> substituents for a secondary cation. These results are suggestive of thermodynamic control in the *syn*:*anti* ratio, while those obtained by Nicholas<sup>10</sup> result initially from kinetic control. In our own experiments<sup>9</sup> in the field of heterobimetallic [Mo-Co] clusters, we have prepared some stabilized cations and we have determined their structures. In all cases the carbenium center interacts with the molybdenum atom rather than cobalt as shown in Figure 5, and we do not observe isomerization of the cluster core. On the basis of these earlier results we report here on the fluxional processes observed for carbenium ions **4** and **5b,c**, which possess a chiral cluster in the α position.

## Results and Discussion

**Synthesis of 4 and 5b,c.** The carbenium ions **4** and **5b,c** were obtained as depicted in Scheme 2. Starting from either of the pure diastereomeric alcohols of [ $\eta^2, \eta^2$ -(1-cymantrenyl-2-butyn-1-ol)(CoMoCp(CO)<sub>5</sub>)] (**3a** or **3b**), we obtain at room temperature the same <sup>1</sup>H and <sup>13</sup>C NMR spectra in CH<sub>2</sub>Cl<sub>2</sub> solution attributed to [(MoCo(CO)<sub>5</sub>Cp)(μ-Mn(CO)<sub>3</sub>Cp)CHC≡CCH<sub>3</sub>]<sup>+</sup>BF<sub>4</sub><sup>-</sup> (**4**). The situation is the same for [(MoCo(CO)<sub>5</sub>Cp)(μ-Fc)CHC≡C(CH<sub>3</sub>)<sub>4</sub>]<sup>+</sup>BF<sub>4</sub><sup>-</sup> (**5b**) and [(MoCo(CO)<sub>5</sub>Cp)(μ-Fc)CHC≡C(CH<sub>2</sub>)<sub>4</sub>CH<sub>3</sub>]<sup>+</sup>BF<sub>4</sub><sup>-</sup> (**5c**). The cations **4** and **5b,c** were completely identified by spectroscopic techniques (NMR, IR) and by elemental analysis.

(11) Schreiber, S. L.; Klimas, M. T.; Sammakia, T. J. *J. Am. Chem. Soc.* **1987**, *109*, 5749.

(5) (a) Sokolov, V. I.; Barinov, V. I.; Reutov, O. A. *Izv. Akad. Nauk SSR Ser. Khim.* **1982**, 1992. (b) Meyer, A.; McCabe, D. J.; Curtis, D. *Organometallics* **1987**, *6*, 1491. (c) Barinov, V. I.; Reutov, O. A.; Polyanov, A. V.; Yanovsky, A. I.; Struchkov, Yu. T.; Sokolov, V. I. *J. Organomet. Chem.* **1991**, *418*, C24. (d) Cordier, C.; Gruselle, M.; Jaouen, G.; Bakhmutov, V. I.; Galakhov, M. V.; Troitskaya, L. L.; Sokolov *Organometallics* **1991**, *10*, 2303. (e) El Amouri, H.; Vaissermann, J.; Besace, Y.; Vollhardt, K. P. C.; Ball, G. E. *Organometallics* **1993**, *12*, 605. (f) El Amouri, H.; Besace, Y.; Vaissermann, J.; Jaouen, G.; McGlinchey, M. J. *Organometallics* **1994**, *13*, 4426. (g) El Hafa, H.; Cordier, C.; Gruselle, M.; Besace, Y.; McGlinchey, M. J.; Jaouen, G. *Organometallics* **1994**, *13*, 5149.

(6) Galakhov, M. V.; Bakhmutov, V. I.; Barinov, V. I. *Magn. Reson. Chem.* **1991**, *9*, 2972.

(7) (a) Bradley, D. H.; Khan, M. A.; Nicholas, K. M. *Organometallics* **1989**, *8*, 554. (b) D'Agostino, M. F.; Frampton, C. S.; McGlinchey, M. J. *Organometallics* **1990**, *9*, 2972. (c) Dunn, J. A.; Pauson, P. L. *J. Organomet. Chem.* **1991**, *419*, 383. (d) Verdaguer, X.; Moyano, A.; Pericás, M. A.; Riera, A.; Bernardes, V.; Greene, A. E.; Alvarez, A. A.; Piniella, J. F. *J. Am. Chem. Soc.* **1994**, *116*, 2153.

(8) (a) McGlinchey, M. J.; Mlekuz, M.; Bougeard, P.; Sayer, B. G.; Marinetti, A.; Saillard, J. Y.; Jaouen, G. *Can. J. Chem.* **1983**, *61*, 1319 and references cited. (b) D'Agostino, M. F.; Frampton, C. S.; McGlinchey, M. J. *J. Organomet. Chem.* **1990**, *394*, 145.

(9) Gruselle, M.; El Hafa, H.; Nikolski, M.; Jaouen, G.; Vaissermann, J.; Li, L.; McGlinchey, M. J. *Organometallics* **1993**, *12*, 4917.

(10) Bradley, D. H.; Khan, M. A.; Nicholas, K. M. *Organometallics* **1992**, *11*, 2598.

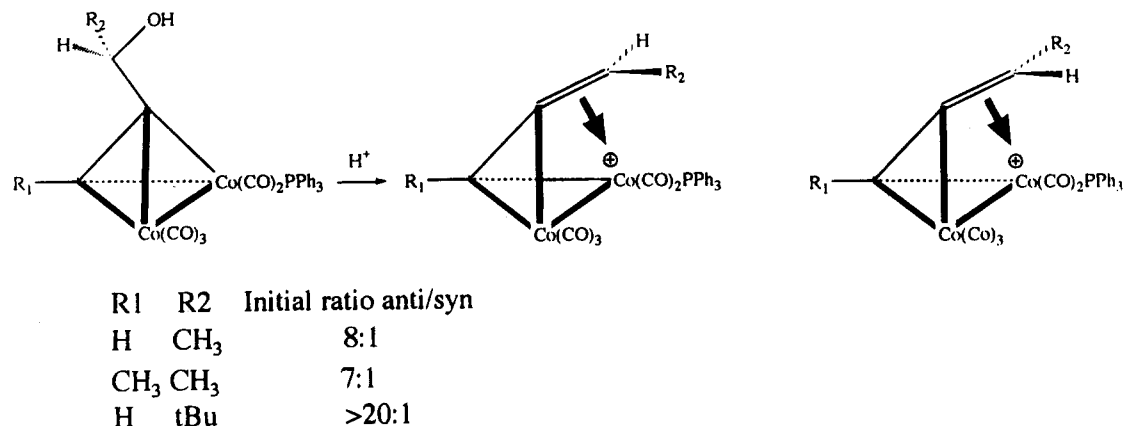


**Figure 3.** Diastereoselective formation of stabilized [Co–CoPPh<sub>3</sub>] carbenium ions from a pure diastereomeric alcohol.

### Scheme 1

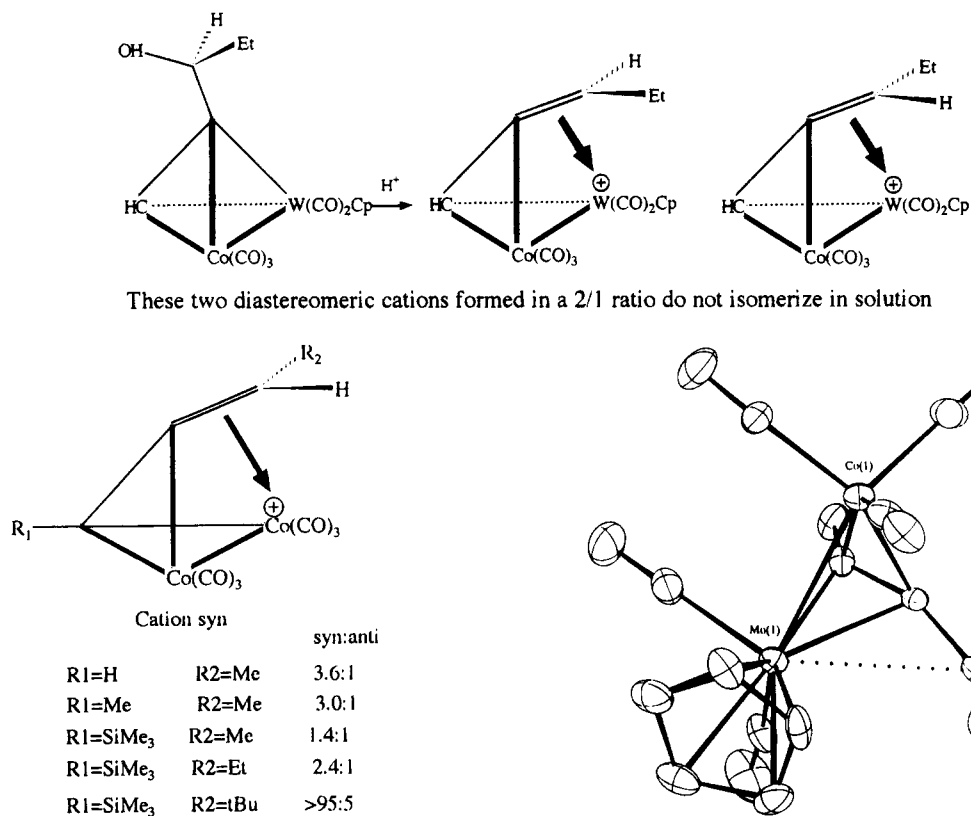


**Figure 4.** *Syn/anti* diastereoselective formation of [Co<sub>2</sub>] stabilized carbenium ions as a function of R1 and R2.

[ $\eta^2, \eta^3$ -(1-cymantrenyl-2-butyn-1-yl)ium](Co<sub>2</sub>(CO)<sub>6</sub>)]-BF<sub>4</sub> (**6**) was obtained from [Co<sub>2</sub>] complexed alcohol (**2**) in ether solution by the action of HBF<sub>4</sub>/Et<sub>2</sub>O. A green-brown solid precipitates. After being washed several times with ether, the powder was dissolved in CD<sub>2</sub>Cl<sub>2</sub> and its NMR spectrum was recorded. Surprisingly the product formed was identified as an ethoxy complex (**7**) resulting from an attack of the ether oxygen on the carbenium center (Scheme 3).

**Description of the Structures.** The X-ray crystal structures were performed using single crystals of **4** and **5b** obtained by the diffusion technique (Et<sub>2</sub>O–CH<sub>2</sub>Cl<sub>2</sub>). Crystal data, atomic coordinates, and selected interatomic distances are reported in Tables 1–3 and 4–6, respectively, for **4** and **5b**. CAMERON views are shown in Figure 6. The CAMERON views presented in Figure 6 reveal that the two structures are very similar. The relative configurations of the two chiral elements are

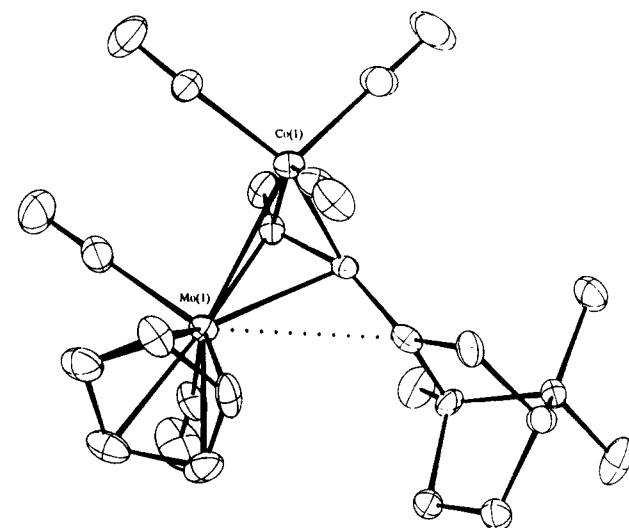
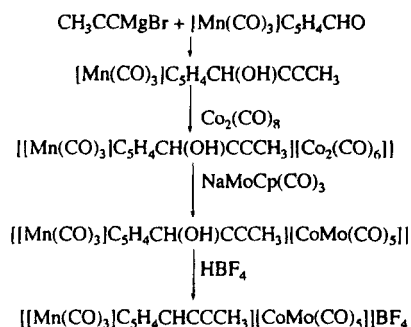


**Figure 5.** View of the [(2-propynylbornyl)Mo(CO)<sub>2</sub>CpCo(CO)<sub>3</sub>]<sup>+</sup> cation.

1*S*\*cluster*S*\*, which conforms with an *anti* configuration using the Nicholas's formalism. In each case the carbenium center leans toward the molybdenum vertex. The distances between C<sup>+</sup> and Mo are 2.66(1) and 2.726(4) Å for **4** and **5b**, respectively. For **4** the distance is similar compared to other secondary carbenium ions stabilized by homo-[Mo<sub>2</sub>] acetylenic clusters;<sup>12a</sup> for example the C<sup>+</sup>–Mo distance was 2.63 Å for **5a**.<sup>2</sup> For **5b** the result is close to those found for a tertiary cation.<sup>12b</sup> The molybdenum–cobalt, cobalt–carbon, and molybdenum–carbon distances within the tetrahedral cluster are 2.715, 1.95 (average), 2.15 (average) Å and

(12) (a) Gruselle, M.; Cordier, C.; Salmain, M.; El Amouri, H.; Guerin, C.; Vaissermann, J.; Jaouen, G. *Organometallics* **1990**, *9*, 2993. (b) Le Berre-Cosquer, N.; Kergoat, R.; L'haridon, P. *Organometallics* **1992**, *11*, 721.

### Scheme 2. Synthetic Pathway to the Carbenium Ions 4 and 5b,c



### Scheme 3. Reaction of the Carbenium Ion 6 with Diethyl Ether

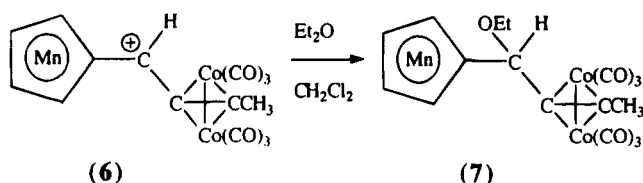


Table 1. Crystal Data for  $[\text{C}_{22}\text{H}_{13}\text{O}_8\text{MnCoMo}](\text{BF}_4)$  (4)

fw	701.95
<i>a</i> (Å)	8.998(4)
<i>b</i> (Å)	9.975(4)
<i>c</i> (Å)	14.916(5)
$\alpha$ (deg)	82.09(3)
$\beta$ (deg)	77.82(3)
$\gamma$ (deg)	78.139(3)
<i>V</i> (Å <sup>3</sup> )	1274(12)
<i>Z</i>	2
cryst system	triclinic
space group	$P\bar{1}$
linear abs coeff $\mu$ (cm <sup>-1</sup> )	16.49
density $\rho$ (g cm <sup>-3</sup> )	1.82
diffractometer	CAD4 Enraf-Nonius
radiation	Mo K $\alpha$ ( $\lambda = 0.71069$ Å)
scan type	$\omega/2\theta$
scan range (deg)	$0.8 + 0.345 \tan \theta$
$\theta$ limits (deg)	1–28
temp of measmnt	room temp
octants colld	–11, 11; –13, 13; 0, 19
no. of data colld	6369
no. of unique data colld	6138
no. of unique data used for refinement	3084, $(F_o)^2 > 3\sigma(F_o)^2$
<i>R</i> (int)	1.47
$R = \sum   F_o  -  F_c   / \sum  F_o $	0.0623
$R_w = \sum w( F_o  -  F_c )^2 / \sum wF_o^2$	0.0699, $w = 1.0$
abs corr	DIFABS (min = 0.578, max = 1.545)
extinction param ( $\times 10^{-6}$ )	no
goodness of fit <i>s</i>	3.29
no. of variables	343
$\Delta\rho_{\text{min}}$ (e/Å <sup>3</sup> )	–0.93
$\Delta\rho_{\text{max}}$ (e/Å <sup>3</sup> )	1.84

2.715, 1.94 (average), and 2.16 Å (average) for 4 and 5b, respectively. These values lie within the normal range for [Co–Mo] clusters<sup>13</sup> of this type. Finally we note that all the CO ligands are terminally bound.

**NMR Spectra.** The <sup>1</sup>H and <sup>13</sup>C NMR spectra of the starting complexed diastereomeric alcohols 3a and 3b are consistent with the presence of two chiral elements in the molecules. For the homobinuclear [Co<sub>2</sub>] complex 2, the spectra are consistent with the presence of one chiral element.

Table 2. Selected Interatomic Distances (Å) and Bond Angles (deg) for  $[\text{C}_{22}\text{H}_{13}\text{O}_8\text{MnCoMo}](\text{BF}_4)$

Mo(1)–Co(1)	2.715(2)	Mo(1)–C(2)	2.22(1)
Mo(1)–C(3)	2.11(1)	Mo(1)–C(11)	2.31(1)
Mo(1)–C(12)	2.28(1)	Mo(1)–C(13)	2.28(1)
Mo(1)–C(14)	2.34(1)	Mo(1)–C(15)	2.36(1)
Mo(1)–C(16)	2.03(1)	O(16)–C(16)	1.11(1)
Mo(1)–C(17)	2.01(1)	O(17)–C(17)	1.14(1)
Co(1)–C(2)	1.88(1)	Co(1)–C(3)	1.98(1)
Co(1)–C(18)	1.80(1)	O(18)–C(18)	1.14(2)
Co(1)–C(19)	1.75(2)	O(19)–C(19)	1.16(2)
Co(1)–C(20)	1.85(2)	O(20)–C(20)	1.10(2)
Mn(1)–C(21)	2.14(1)	Mn(1)–C(22)	2.12(1)
Mn(1)–C(23)	2.13(1)	Mn(1)–C(24)	2.14(1)
Mn(1)–C(25)	2.13(1)		
Mn(1)–C(26)	1.78(1)	O(26)–C(26)	1.15(2)
Mn(1)–C(27)	1.79(2)	O(27)–C(27)	1.15(2)
Mn(1)–C(28)	1.77(1)	O(28)–C(28)	1.14(1)
C(1)–C(2)	1.39(1)	C(2)–C(3)	1.36(1)
C(3)–C(4)	1.50(2)	C(1)–C(21)	1.45(1)
C(16)–Mo(1)–C(17)	82.3(5)	Mo(1)–C(16)–O(16)	177.1(12)
C(18)–Co(1)–C(19)	102.3(7)	Mo(1)–C(17)–O(17)	175.1(11)
C(18)–Co(1)–C(20)	103.3(7)	Co(1)–C(18)–O(18)	179.3(13)
C(19)–Co(1)–C(20)	98.1(7)	Co(1)–C(19)–O(19)	176.6(16)
C(26)–Mn(1)–C(27)	91.8(8)	Co(1)–C(20)–O(20)	175.9(17)
C(26)–Mn(1)–C(28)	91.6(7)	Mn(1)–C(26)–O(26)	178.3(17)
C(27)–Mn(1)–C(28)	90.9(6)	Mn(1)–C(27)–O(27)	179.8(16)
		Mn(1)–C(28)–O(28)	178.0(13)
C(2)–C(1)–C(21)	127.4(11)	C(1)–C(2)–C(3)	133.4(11)
C(2)–C(3)–C(4)	133.8(12)		

Table 3. Fractional Parameters for  $[\text{C}_{22}\text{H}_{13}\text{O}_8\text{MnCoMo}](\text{BF}_4)$

atom	<i>x/a</i>	<i>y/b</i>	<i>z/c</i>	<i>U</i> (eq) (Å <sup>2</sup> )
Mo(1)	0.1425(1)	0.19118(9)	0.15726(7)	0.0370
Co(1)	0.1834(2)	0.2728(2)	0.3153(1)	0.0512
Mn(1)	0.4889(2)	–0.2502(2)	0.3563(1)	0.0417
O(16)	–0.111(1)	0.030(1)	0.1372(8)	0.0803
O(17)	–0.144(1)	0.4327(9)	0.1646(7)	0.0739
O(18)	0.503(1)	0.316(1)	0.2509(8)	0.0876
O(19)	0.160(2)	0.218(2)	0.5142(9)	0.1175
O(20)	–0.007(2)	0.552(1)	0.311(1)	0.1016
O(26)	0.665(2)	–0.521(1)	0.4069(9)	0.1076
O(27)	0.195(2)	–0.349(2)	0.4160(9)	0.1086
O(28)	0.469(1)	–0.162(1)	0.5369(6)	0.0789
C(1)	0.249(1)	–0.031(1)	0.2617(7)	0.0448
C(2)	0.173(1)	0.092(1)	0.2965(7)	0.0449
C(3)	0.030(1)	0.169(1)	0.2959(8)	0.0458
C(4)	–0.128(2)	0.158(1)	0.3518(9)	0.0642
C(11)	0.396(1)	0.152(1)	0.0811(8)	0.0575
C(12)	0.308(2)	0.087(1)	0.039(1)	0.0601
C(13)	0.202(2)	0.181(2)	0.0017(9)	0.0627
C(14)	0.226(2)	0.310(1)	0.0149(9)	0.0629
C(15)	0.344(2)	0.293(1)	0.0642(9)	0.0554
C(16)	–0.020(2)	0.084(1)	0.1457(9)	0.0590
C(17)	–0.036(1)	0.349(1)	0.1595(8)	0.0499
C(18)	0.379(2)	0.300(1)	0.2753(9)	0.0605
C(19)	0.172(2)	0.243(2)	0.435(1)	0.0765
C(20)	0.068(2)	0.450(2)	0.311(1)	0.0741
C(21)	0.412(1)	–0.091(1)	0.2550(7)	0.0425
C(22)	0.484(2)	–0.215(1)	0.2132(8)	0.0543
C(23)	0.638(2)	–0.245(1)	0.2245(9)	0.0609
C(24)	0.665(1)	–0.146(1)	0.2745(9)	0.0597
C(25)	0.523(1)	–0.050(1)	0.2952(9)	0.0527
C(26)	0.596(2)	–0.414(2)	0.388(1)	0.0771
C(27)	0.310(2)	–0.310(2)	0.393(1)	0.0707
C(28)	0.474(2)	–0.196(1)	0.4663(8)	0.0547
B(1)	0.194(4)	0.686(2)	0.080(3)	0.0931
F(1)	0.099(1)	0.625(1)	0.058(1)	0.1183
F(2)	0.306(2)	0.606(1)	0.113(1)	0.1479
F(3)	0.135(3)	0.788(2)	0.123(2)	0.2023
F(4)	0.268(3)	0.742(4)	0.001(2)	0.3042

Protonation of 2 in CD<sub>2</sub>Cl<sub>2</sub> solution with HBF<sub>4</sub>/Et<sub>2</sub>O leads to the observation of a new <sup>1</sup>H NMR spectrum attributable to the carbenium ion 6 on the following

(13) Bailey, W. I., Jr.; Chisholm, M. H.; Cotton, F. A.; Rankin, L. A. *J. Am. Chem. Soc.* 1978, 100, 5764.

**Table 4. Crystal Data for [C<sub>24</sub>H<sub>18</sub>O<sub>5</sub>FeCoMo](BF<sub>4</sub>) (5b)**

fw	683.9
a (Å)	8.386(2)
b (Å)	10.272(3)
c (Å)	15.657(3)
α (deg)	94.35(2)
β (deg)	103.76(2)
γ (deg)	102.74(2)
V (Å <sup>3</sup> )	1266
Z	2
cryst system	triclinic
space group	P $\bar{1}$
linear abs coeff $\mu$ (cm <sup>-1</sup> )	17.5
density $\rho$ (g cm <sup>-3</sup> )	1.79
diffractometer	Philips PW 1100
radiation	Mo K $\alpha$ ( $\lambda$ = 0.710 69 Å)
scan type	$\omega/2\theta$
scan range (deg)	1.1 + 0.345 $\tan \theta$
$\theta$ limits (deg)	2–25
temp of measmnt	room temp
octants colld	–9, 9; –12, 12; 0, 18
no. of data colld	4620
no. of unique data colld	4416
no. of unique data used for refinement	3634, ( $F_o$ ) <sup>2</sup> > 3 $\sigma$ ( $F_o$ ) <sup>2</sup>
R(int)	1.42
$R = \sum   F_o  -  F_c   / \sum  F_o $	0.0306
$R_w = \sum w( F_o  -  F_c )^2 / \sum wF_o^2$	0.0322, $w = 1.0$
abs corr	DIFABS (min = 0.86, max = 1.15)
extinction param ( $\times 10^{-6}$ )	34
goodness of fit $s$	0.57
no. of variables	390
$\Delta\rho_{\min}$ (e/Å <sup>3</sup> )	–0.57
$\Delta\rho_{\max}$ (e/Å <sup>3</sup> )	1.00

**Table 5. Selected Interatomic Distances (Å) and Angles (deg) for [C<sub>24</sub>H<sub>18</sub>O<sub>5</sub>FeCoMo](BF<sub>4</sub>)**

Mo(1)–Co(1)	2.7150(7)	Mo(1)–C(2)	2.229(4)
Mo(1)–C(3)	2.125(4)	Mo(1)–C(11)	2.287(5)
Mo(1)–C(12)	2.315(5)	Mo(1)–C(13)	2.353(5)
Mo(1)–C(14)	2.363(5)	Mo(1)–C(15)	2.318(5)
Mo(1)–C(16)	2.020(5)	O(16)–C(16)	1.128(6)
Mo(1)–C(17)	2.021(5)	O(17)–C(17)	1.130(5)
Co(1)–C(2)	1.912(4)	Co(1)–C(3)	1.982(4)
Co(1)–C(18)	1.812(5)	O(18)–C(18)	1.133(6)
Co(1)–C(19)	1.832(5)	O(19)–C(19)	1.119(6)
Co(1)–C(20)	1.785(6)	O(20)–C(20)	1.125(6)
Fe(1)–C(21)	2.032(4)	Fe(1)–C(22)	2.033(5)
Fe(1)–C(23)	2.059(5)	Fe(1)–C(24)	2.056(5)
Fe(1)–C(25)	2.034(4)	Fe(1)–C(26)	2.040(7)
Fe(1)–C(27)	2.024(7)	Fe(1)–C(28)	2.022(6)
Fe(1)–C(29)	2.031(6)	Fe(1)–C(30)	2.027(6)
C(16)–Mo(1)–C(17)	84.3(2)	Mo(1)–C(16)–O(16)	177.6(4)
C(18)–Co(1)–C(19)	103.5(2)	Mo(1)–C(17)–O(17)	176.6(4)
C(18)–Co(1)–C(20)	101.9(3)	Co(1)–C(18)–O(18)	177.4(5)
C(19)–Co(1)–C(20)	100.6(2)	Co(1)–C(19)–O(19)	175.6(5)
C(2)–C(1)–C(21)	125.6(4)	Co(1)–C(20)–O(20)	175.8(5)
C(4)–C(3)–C(2)	134.3(4)	C(3)–C(2)–C(1)	140.2(4)

basis: disappearance of the hydroxyl proton, H<sub>1</sub> shifts from 5.49 to 7.50 ppm, H<sub>Cp</sub> shifts from respectively 5.00–4.76 and 4.74–4.71 ppm to 5.52 and 5.13 ppm, H<sub>3</sub> shifts from 2.64 to 3.03 ppm. These downfield shifts are suggestive of charge delocalization onto the [Co<sub>2</sub>] cluster and the cymentrene moieties.

For carbenium ions **4** and **5b,c**, all the <sup>1</sup>H NMR signals are shifted downfield compared to the starting alcohols. At room temperature, for example, the Cp–Mo signals are shifted from 5.46–5.45 to 5.67 ppm, 4.86–4.92 to 5.47 ppm, and 4.89–4.86 to 5.43 ppm, respectively, for **4** and **5b,c**.

At room temperature the <sup>1</sup>H NMR spectrum for **4**

**Table 6. Fractional Parameters for [C<sub>24</sub>H<sub>18</sub>O<sub>5</sub>FeCoMo](BF<sub>4</sub>)**

atom	x/a	y/b	z/c	U(eq) (Å <sup>2</sup> )
Mo(1)	0.10411(5)	0.75113(3)	0.84852(2)	0.0276
Co(1)	0.14402(8)	0.63024(6)	0.69733(4)	0.0342
Fe(1)	0.43883(8)	1.12168(6)	0.65976(4)	0.0356
O(16)	–0.1670(5)	0.9115(4)	0.8691(3)	0.0587
O(17)	–0.1967(5)	0.4998(3)	0.8377(3)	0.0534
O(18)	0.4995(5)	0.6289(5)	0.7754(3)	0.0659
O(19)	–0.0513(6)	0.3508(4)	0.6881(3)	0.0663
O(20)	0.1483(8)	0.6433(6)	0.5130(3)	0.0903
C(1)	0.2131(6)	0.9411(4)	0.7489(3)	0.0347
C(2)	0.1227(5)	0.8109(4)	0.7166(3)	0.0314
C(3)	–0.0310(5)	0.7253(4)	0.7127(3)	0.0331
C(4)	–0.2085(7)	0.7068(7)	0.6562(4)	0.0492
C(11)	0.2931(7)	0.9018(5)	0.9621(3)	0.0456
C(12)	0.1849(7)	0.8142(6)	1.007(3)	0.0479
C(13)	0.2099(7)	0.6842(5)	0.9869(3)	0.0458
C(14)	0.3362(6)	0.6907(5)	0.9405(3)	0.0436
C(15)	0.3875(6)	0.8251(5)	0.9252(3)	0.0440
C(16)	–0.0692(6)	0.8556(5)	0.8602(3)	0.0436
C(17)	–0.0854(6)	0.5881(4)	0.8433(3)	0.0370
C(18)	0.3621(7)	0.6295(5)	0.7473(3)	0.0459
C(19)	0.0282(6)	0.4555(5)	0.6935(3)	0.0439
C(20)	0.1420(8)	0.6339(6)	0.5833(4)	0.0573
C(21)	0.3875(6)	0.9969(4)	0.7497(3)	0.0349
C(22)	0.4874(7)	1.1279(5)	0.7937(3)	0.0437
C(23)	0.6414(7)	1.1536(5)	0.7698(3)	0.0485
C(24)	0.6410(6)	1.0427(5)	0.7106(3)	0.0433
C(25)	0.4856(6)	0.9457(5)	0.6976(3)	0.0382
C(26)	0.293(1)	1.0892(8)	0.5320(5)	0.0780
C(27)	0.448(1)	1.170(1)	0.5378(5)	0.0725
C(28)	0.473(1)	1.2839(8)	0.5946(7)	0.0721
C(29)	0.331(1)	1.2752(9)	0.6255(6)	0.0790
C(30)	0.2190(9)	1.153(1)	0.5871(6)	0.0720
B(1)	0.807(1)	0.7053(7)	0.0931(6)	0.0611
F(1)	0.745(1)	0.757(1)	0.0250(7)	0.1982
F(2)	0.8999(9)	0.8187(6)	0.1459(7)	0.1607
F(3)	0.6858(7)	0.6387(4)	0.1258(4)	0.1078
F(4)	0.9144(6)	0.6346(4)	0.0817(4)	0.0977

indicates a fluxional process in the intermediate exchange regime. All the signals are broadened. The situation is not as clear for **5b** and **5c** but in these cases the H<sub>1</sub> signal is slightly broadened. The spectra of the carbenium ions **4** and **5b,c** in CD<sub>2</sub>Cl<sub>2</sub> are temperature dependent, and this is best illustrated from the behavior of H<sub>1</sub> and H<sub>4</sub> (Figure 7). The evolution observed for the other protons is reported in Table 7.

It is clear that the evolution of the spectra, for these protons, from one signal to two signals, different in intensity, reveals the formation of two distinct diastereomers in the ratio 90/10 and 95/5, respectively, for **4** and **5b**. Protons H<sub>1</sub> in the less populated diastereomers of **4** and **5b** have resonances shown to be hardly shifted toward higher field that can be well compared in Table 8 with the data reported for the related [(Mo<sub>2</sub>Cp<sub>2</sub>(CO)<sub>4</sub>)-HCCCH(CH<sub>3</sub>)<sup>+</sup> secondary carbenium ion.<sup>14</sup> It seems to be obvious that the diastereomeric chemical shift differences in tables 7 and 8 observed for protons bound to the carbenium centers are caused by the different relative orientations of H<sub>1</sub> and the metal–metal bonds which have been correctly deduced for cation [(Mo<sub>2</sub>-Cp<sub>2</sub>(CO)<sub>4</sub>)-HCCCH(CH<sub>3</sub>)<sup>+</sup> from the solution and solid NMR data.<sup>14</sup> In addition it has been found that the less populated diastereomer of this cation exists only in solution whereas the structure of the more populated diastereomer corresponds to the solid state structure.<sup>14</sup> Thus these data allow us to propose that the more populated diastereomers of **4** and **5b** have the configurations found in the solid state.

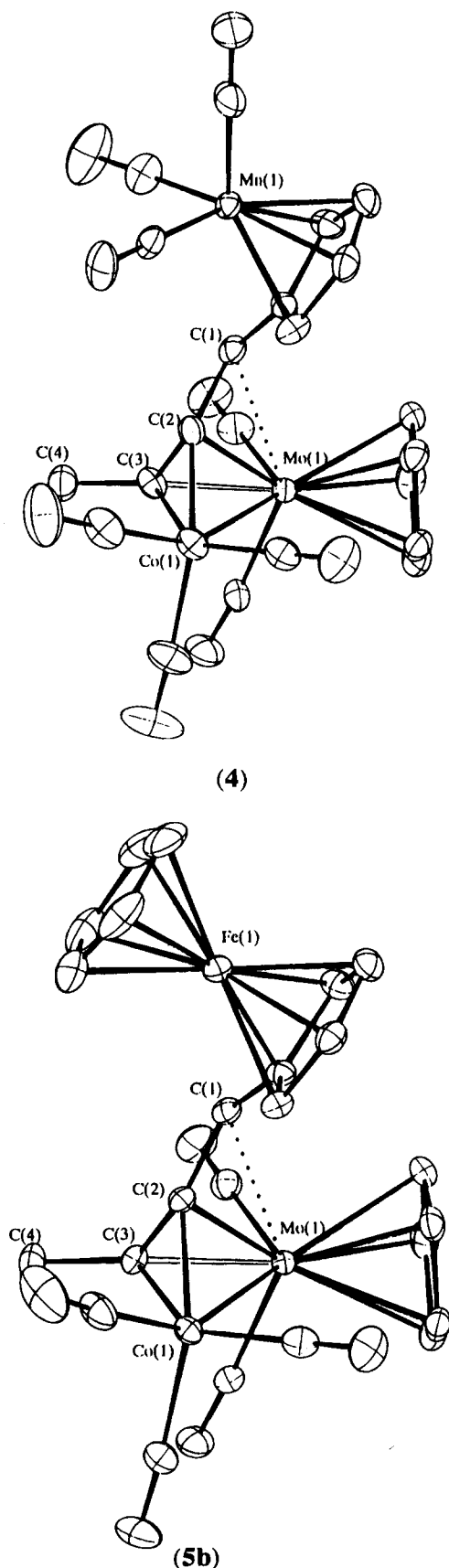


Figure 6. CAMERON view for **4** and **5b**.

In the case of the carbenium ions **4** and **5b**, the formation of two diastereomers equilibrating slowly on the NMR time scale is clearly a consequence of a slowing down of the rotational process around the C<sup>+</sup>-cluster bond. The energy associated with this process is calculated<sup>15</sup> as  $\Delta G^*_{283K} = 13.3 \pm 1 \text{ kcal}\cdot\text{mol}^{-1}$  and

$\Delta G^*_{253K} = 12.0 \pm 1 \text{ kcal}\cdot\text{mol}^{-1}$ , respectively, for **4** and **5b**. This result is close to that found for the diastereomerization process in the case of a secondary stabilized [Mo<sub>2</sub>] carbenium ion.<sup>2</sup>

These results show that the rotation around the C<sup>+</sup>-cluster bond is not as high in energy as postulated previously<sup>16</sup> and can explain the isomerization processes observed even at room temperature for secondary stabilized [M<sub>2</sub>] carbenium ions.

## Conclusion

Our NMR results and molecular structure data show the major role of the molybdenum atom in the stabilization of its adjacent carbenium center concurrently bonded to cobalt, iron, or manganese metallic atoms. In one case the fluxional process observed in the NMR spectra can be clearly attributed to a simple rotation around the C<sup>+</sup>-cluster bond. It seems that the isomerization of carbenium ions stabilized by homo- or heterobimetallic clusters is the consequence of two elementary processes which are (1) the rotation around the C<sup>+</sup>-cluster bond and (2) the antarafacial migration of the carbenium center from one metallic atom to the other and that the C<sup>+</sup>-cluster rotation can occur at lower energy.

## Experimental Section

All reactions were carried out under an inert atmosphere using standard Schlenk techniques. Solvents were distilled before use, Et<sub>2</sub>O and THF from Na-benzophenone and CH<sub>2</sub>Cl<sub>2</sub> from CaH<sub>2</sub>. The NMR spectra ( $\delta$ ) were recorded in solution on a Bruker AM250 and AC200 spectrometers, and IR on a Bomem IR-FT. Analyses were provided by "le service régional de microanalyse de l'Université Pierre et Marie Curie, Paris".

**X-ray Data for **4** and **5b**.** X-ray-quality crystals of the carbenium ion **4** and **5b** were obtained by the diffusion technique (Et<sub>2</sub>O-CH<sub>2</sub>Cl<sub>2</sub>). Intensity data were collected at room temperature on an Enraf-Nonius CAD4 diffractometer for compound **4** and on a Philips PW 1100 diffractometer for **5b** using Mo K $\alpha$  radiation. Accurate cell dimensions and orientation matrices were obtained from least-squares refinements of the setting angles of 25 well-defined reflections. No decay in the intensities of two standard reflections was observed during the course of data collection. The usual corrections for Lorentz and polarization effects were applied. Computations were performed by using the PC version of CRYSTALS.<sup>17</sup> Scattering factors and corrections for anomalous dispersion were taken from ref 18. The structures were resolved by direct methods SHELXS<sup>19</sup> and refined by least squares with anisotropic thermal parameters for all non-hydrogen atoms. For compound **4** hydrogen atoms were introduced as fixed contributors in theoretical positions and their coordinates were recalculated after each refinement. For compound **5b** hydrogen atoms were located on a Fourier

(15) Martin, M. L.; Martin, G. J.; Delpuech, J. J. *Practical NMR Spectroscopy (Dynamic NMR Experiments)*; Heyden and Son: London, 1981.

(16) (a) Schilling, B. E. R.; Hoffmann, R. *J. Am. Chem. Soc.* **1978**, *100*, 6274. (b) Schilling, B. E. R.; Hoffmann, R. *J. Am. Chem. Soc.* **1979**, *101*, 5764. (c) Girard, L.; Lock, P. E.; El Amouri, H.; McGlinchey, M. J. *J. Organomet. Chem.* **1994**, *478*, 189.

(17) Watkin, D. J.; Carruthers, J. R.; Betteridge, P. W. *Crystals User Guide*; Chemical Crystallography Laboratory; University of Oxford: Oxford, U.K., 1988.

(18) *International Tables for X-ray Crystallography*; Kynoch Press: Birmingham, U.K., 1974; Vol. IV.

(19) Sheldrick, G. M. SHELXS-86 Program for Crystal Structure Solution, University of Gottingen, 1986.



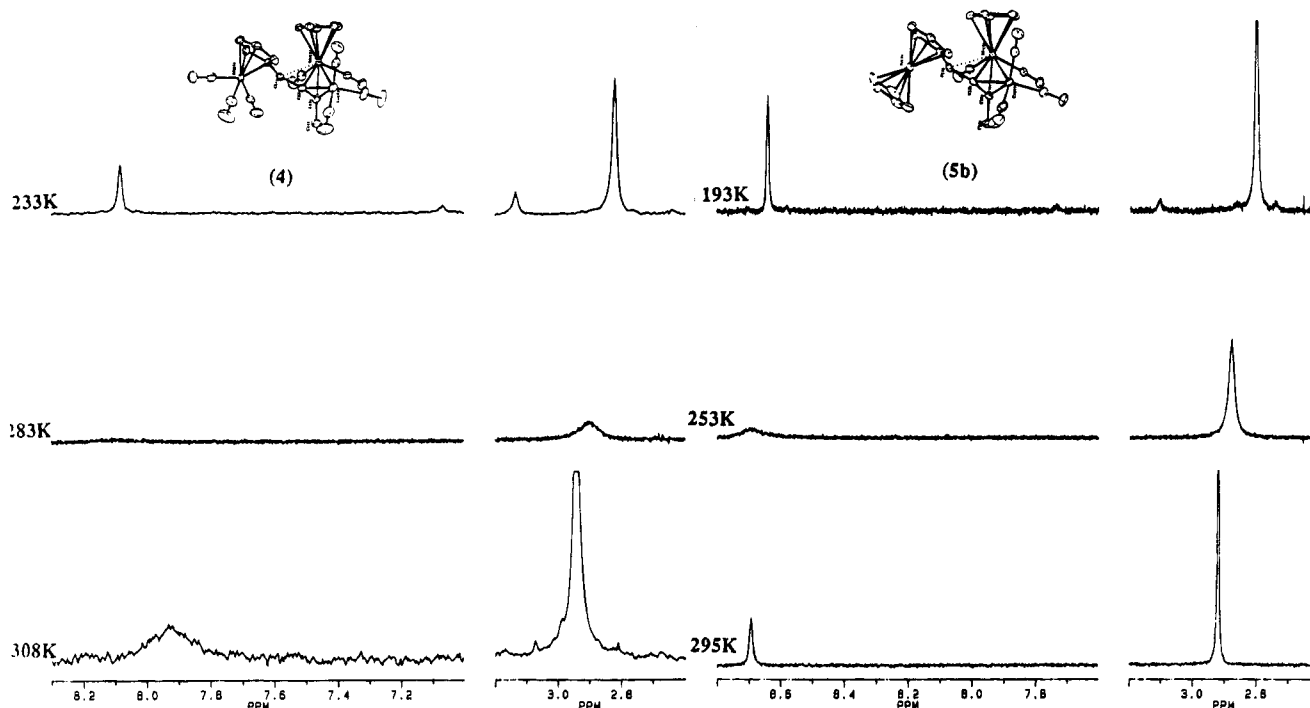


Figure 7. Sections of the variable-temperature 250 MHz  $^1\text{H}$  NMR spectra of **4** and **5b**, showing the peaks of H1 and H4.

Table 7. Comparative  $^1\text{H}$  NMR Chemical Shifts (ppm) for **4** and **5b** at Two Temperatures

	temp for <b>4</b>			temp for <b>5b</b>	
	293 K	233 K		295 K	193 K
H <sub>1</sub>	8.00	8.08 (s) major 7.08 (s) minor	H <sub>1</sub>	8.69 (s), 1H	8.64 (s), major 7.74 (s), minor
Mo(C <sub>5</sub> H <sub>5</sub> )	5.66	5.54 (s) major 5.87 (s) minor	Mo(C <sub>5</sub> H <sub>5</sub> )	5.47 (1), 5H	5.32 (s), major 5.71 (s), minor
Mn(C <sub>5</sub> H <sub>5</sub> )	5.95 5.04 4.97	5.92 (m) major 5.27 (m) major 5.07 (m) major 4.93 (m) major	Fe(C <sub>5</sub> H <sub>4</sub> -)	5.02 (t), 1H 4.99 (dd), 2H 4.86 (t), 1H	4.88 (t), major 4.91 (dd), major 4.73 (t), major
-CH <sub>3</sub>	2.92	2.92 (s) major 3.13 (s) minor	Fe(C <sub>5</sub> H <sub>5</sub> )	4.42 (s), 5H	4.33 (s), major
			-CH <sub>3</sub>	2.92 (s), 3H	2.80 (s), major 3.10 (s), minor

Table 8.  $^1\text{H}$  NMR Data for the Proton at C<sub>1</sub>

R1	R2	R3	M1	M2	$\delta$ , ppm	temp, K
CH <sub>3</sub>	CH <sub>3</sub>	H	Co	Mo	8.02	233 <sup>a</sup>
CH <sub>3</sub>	H	CH <sub>3</sub>	Co	Mo	7.08	233 <sup>a</sup>
CH <sub>3</sub>	CH <sub>3</sub>	H	Co	Mo	8.66	193 <sup>a</sup>
CH <sub>3</sub>	H	CH <sub>3</sub>	Co	Mo	7.75	193 <sup>a</sup>
H	CH <sub>3</sub>	H	Mo	Mo	6.36	187 <sup>b</sup>
H	H	CH <sub>3</sub>	Mo	Mo	5.80	187 <sup>b</sup>

<sup>a</sup> This work. <sup>b</sup> Reference 14.

difference map, and their coordinates were refined with an overall refinable isotropic thermal parameter.

**1-Cymantrenyl-2-butyn-1-ol (1).** The Grignard reagent was prepared from 1.45 g (13.25 mmol) of EtBr and 0.19 g (7.95 mmol) of Mg in 30 mL of Et<sub>2</sub>O. After the Grignard reagent was cooled to -40 °C, a solution of 1.24 g (5.3 mmol) of cymantrenyl aldehyde in 20 mL of ether was added dropwise, and the reaction was stirred for 2 h at this temperature. The solution was hydrolyzed at room temperature and the ethereal layer separated. After removal of the solvent in vacuum the residue was chromatographed on a silica gel column, using Et<sub>2</sub>O/pentane (1/1) as eluent. A 0.99 g amount of **2** was recovered in 68% yield.

$^1\text{H}$  NMR (CDCl<sub>3</sub>): 5.09 (1H, dd,  $J = 6-2$  Hz, H1); 5.01 (2H, dd,  $J = 14-2$  Hz, Cp); 4.63 (2H, m, Cp); 2.48 (1H, d,  $J = 6$  Hz, OH); 1.88 (3H, d,  $J = 2$  Hz, H4).  $^{13}\text{C}$  NMR (CDCl<sub>3</sub>): 224.5 (CO); 104.8 (C1'); 84.3-83.5-81.2-80.7 (C2', 3', 4', 5'); 82.7

(C2,3); 58.8 (C1); 3.3 (C4). IR (cm<sup>-1</sup>): 1935, 2022. Anal. Calcd for C<sub>12</sub>H<sub>9</sub>O<sub>4</sub>Mn: C, 52.94; H, 3.31. Found: C, 53.33; H, 3.42.

**[ $\eta^2, \eta^2$ -(1-cymantrenyl-2-butyn-1-ol)(Co<sub>2</sub>(CO)<sub>8</sub>)] (2).** To 0.33 g (1.21 mmol) of **1** in 10 mL of Et<sub>2</sub>O was added 0.41 g of Co<sub>2</sub>(CO)<sub>8</sub> (1.22 mmol). After the solvent was removed, the crude red oil was chromatographed on silica plates using pentane-Et<sub>2</sub>O (3/1) as eluent. A 0.47 g amount of **2** was recovered in 70% yield.

$^1\text{H}$  NMR (CDCl<sub>3</sub>): 5.49 (1H, d,  $J = 3$  Hz, H1); 5.00 (1H, dd,  $J = 2.6-1.0$  Hz, Cp); 4.76 (1H, dd,  $J = 2.6-1$  Hz, Cp); 4.74-4.71 (2H, t,  $J = 2.6$  Hz, Cp); 2.64 (3H, s, H4); 2.24 (1H, d,  $J = 3$  Hz, OH).  $^{13}\text{C}$  NMR (CDCl<sub>3</sub>): 224.2-199.2 (CO); 109.1 (C1'); 99.9-92.5 (C2,3); 80.2 (C2', 3', 4', 5'); 68.6 (C1); 20.8 (C4). IR (cm<sup>-1</sup>): 1934, 2022, 2053, 2093. Anal. Calcd for C<sub>15</sub>H<sub>9</sub>O<sub>9</sub>Co<sub>2</sub>Mn: C, 38.64; H, 1.79. Found: C, 39.48; H, 1.86.

**[ $\eta^2, \eta^2$ -(1-cymantrenyl-2-butyn-1-ol)(CoMoCp(CO)<sub>5</sub>)] (3a,b).** To a solution of 0.33 g (0.59 mmol) of **2** in 20 mL of THF was added a solution of NaMoCp(CO)<sub>3</sub> prepared as follows: 0.290 g of Mo<sub>2</sub>Cp<sub>2</sub>(CO)<sub>8</sub> (0.59 mmol) in 10 mL of THF was added to an amalgam (0.015 g of Na (1.15 mmol) with 2.3 g of Hg). The reaction is complete after 1 h at reflux. The solvent was removed, and the resulting red-brown oil was chromatographed on silica plates using Et<sub>2</sub>O-pentane (1/3) as eluent. Two products were separated, 0.18 g of the more polar (**3a**) and 0.20 g of the less polar compound (**3b**) in 95% yield.

$^1\text{H}$  NMR (CDCl<sub>3</sub>) (**3a**) 5.46 (5H, s, Cp-Mo); 5.20 (1H, d,  $J = 3$  Hz, H1); 4.91 (1H, m, Cp-Mn); 4.73 (1H, m, Cp-Mn), 4.68

(2H, m, Cp-Mn); 2.66 (3H, s, H4); 1.90 (1H, d,  $J = 3$  Hz, OH).  $^1\text{H}$  NMR ( $\text{CDCl}_3$ ) (**3b**): 5.45 (5H, s, Cp-Mo); 5.44 (1H, d,  $J = 3$  Hz, H1), 4.91 (1H, m, Cp-Mn), 4.68 (3H, m, Cp-Mn), 2.70 (3H, s, H4); 2.03 (1H, d,  $J = 3$  Hz, OH).  $^{13}\text{C}$  NMR ( $\text{CDCl}_3$ ) (**3a**): 225.9–224.7–223.4 (CO); 206.0 (CO broad); 110.6 (C1'); 97.9–91.4 (C2,3); 90.0 (Cp-Mo); 82.3–80.7–80.5 (Cp-Mn); 65.7 (C1); 20.3 (C4).  $^{13}\text{C}$  NMR ( $\text{CDCl}_3$ ) (**3b**): 226.0–224.2–221.2 (CO); 204.0 (CO broad); 109.3 (C1'); 98.5–91.6 (C2,3); 89.8 (Cp-Mo); 81.9–80.8–80.5–79.9 (Cp-Mn); 71.8 (C1); 25.5 (C4). IR  $\text{cm}^{-1}$  (**3a**): 1934, 1981, 1997, 2021, 2048. IR  $\text{cm}^{-1}$  (**3b**): 1935, 1980, 1998, 2020, 2048. Anal. Calcd for  $\text{C}_{17}\text{H}_{14}\text{O}_9\text{CoMoMn}$ : C, 41.77; H, 2.22. Found: C, 41.81; H, 2.22.

$[\eta^2, \eta^3\text{-}(1\text{-cymantrenyl-2-butyn-1-ylidium})(\text{CoMoCp}(\text{CO})_5)]\text{-BF}_4$  (**4**). To a solution of 0.09 g (0.142 mmol) of **3a** or **3b** in  $\text{Et}_2\text{O}$  was added 0.1 mL of  $\text{HBF}_4/\text{Et}_2\text{O}$  complex. The ochre precipitate formed was washed six times using  $\text{Et}_2\text{O}$  and dried under vacuum leading to 0.081 g (81% yield) of **4**.

$^1\text{H}$  NMR ( $\text{CD}_2\text{Cl}_2$ , 297 K) 8.00 (1H, broad, H1); 5.95 (2H, broad, MnCp); 5.67 (5H, broad, MoCp); 5.04 (1H, broad, MnCp); 4.97 (1H, sharp, MnCp); 2.92 (3H, broad, H4).  $^{13}\text{C}$  NMR (acetone- $d_6$ , 297 K): 224.6–220.6–218.8 (CO sharp); 200.0 (CO broad); 121.0–115.7 (broad); 96.0 (broad); 91.0–91.0 (sharp); 85.0 (broad); 23 (sharp). IR ( $\text{cm}^{-1}$ ): 1953, 2029, 2045, 2061, 2092. Anal. Calcd for  $\text{C}_{17}\text{H}_{13}\text{BF}_4\text{O}_8\text{CoMoMn}$ : C, 37.61; H, 1.85. Found: C, 37.92; H, 1.99.

$[\eta^2, \eta^3\text{-}(1\text{-ferrocenyl-2-butyn-1-ylidium})(\text{CoMoCp}(\text{CO})_5)]\text{-BF}_4$  (**5b**) and  $[\eta^2, \eta^3\text{-}(1\text{-ferrocenyl-2-octyn-1-ylidium})(\text{CoMoCp}(\text{CO})_5)]\text{-BF}_4$  (**5c**). The dicobalt-complexed alcohol precursors of **5b** and **5c** were prepared according to previous work.<sup>1</sup>

**5b,c**. The mixed [Co-Mo] alcohols were prepared starting from  $[\text{Co}_2]$  complexed alcohol; *vide supra*. The carbenium ion was obtained quantitatively as a violet powder by addition of  $\text{HBF}_4/\text{Et}_2\text{O}$  to an ethereal solution of the starting alcohol and crystallized in  $\text{Et}_2\text{O}/\text{CH}_2\text{Cl}_2$  mixture using the diffusion technique.

$^1\text{H}$  NMR ( $\text{CD}_2\text{Cl}_2$ ) (**5b**): 8.69 (1H, s); 5.47 (5H, s); 5.03 (1H, t,  $J = 3$  Hz); 5.01 (2H, m); 4.82 (1H, dd,  $J = 1\text{--}3$  Hz); 4.42 (5H, s); 2.92 (3H, s).  $^1\text{H}$  NMR ( $\text{CD}_2\text{Cl}_2$ ) (**5c**): 8.66 (1H, s); 5.43 (5H, s); 4.97 (3H, m); 4.92 (1H, m); 2.96 (2H, m); 1.72 (2H, m);

1.45 (4H, m); 0.96 (3H, t,  $J = 6.2$  Hz).  $^{13}\text{C}$  NMR ( $\text{CD}_2\text{Cl}_2$ ) (**5b**): 221.9; 214.2; 200.6; 139.6; 95.27; 77.6; 77.2; 73.5; 72.4; 23.5.  $^{13}\text{C}$  NMR (**5c**): 221.7; 215.2; 201.1; 135.3; 110.6; 108.7; 98.1; 78.3; 77.8; 76.5; 75.9; 71.9; 66.3; 37.2; 33.4; 31.9; 23.0; 14.5. IR ( $\text{cm}^{-1}$ ) (**5b**): 1931, 1989, 2045, 2055, 2083. IR ( $\text{cm}^{-1}$ ) (**5c**): 1931, 2044, 2055, 2082. Anal. Calcd for  $\text{C}_{24}\text{H}_{18}\text{BF}_4\text{O}_5\text{-CoMoFe}$  (**5b**): C, 42.00; H, 2.72. Found: C, 42.26; H, 2.63. Calcd for **5c**: C, 46.70; H, 3.62. Found: C, 45.63; H, 3.48.

$[\eta^2, \eta^3\text{-}(1\text{-cymantrenyl-2-butyn-1-ylidium})(\text{Co}_2(\text{CO})_6)]\text{-BF}_4$  (**6**). This compound was obtained *in situ* in the NMR probe using a solution of **2** in  $\text{CD}_2\text{Cl}_2$  with 2 drops of  $\text{HBF}_4/\text{Et}_2\text{O}$  complex.

$^1\text{H}$  NMR ( $\text{CD}_2\text{Cl}_2$ ): 7.50 (1H, s, H1); 5.52 (2H, m, Cp-Mn); 5.13 (2H, m, Cp-Mn); 3.03 (3H, s, H4).

$[\eta^2, \eta^2\text{-}(1\text{-cymantrenyl-2-butyn-1-ethoxy})(\text{Co}_2(\text{CO})_6)]$  (**7**).  $^1\text{H}$  NMR ( $\text{CDCl}_3$ ): 5.04 (1H, m); 4.99 (1H, s); 4.74 (1H, m), 4.72 (1H, m); 4.65 (1H, m); 3.82 (2H, dq,  $J = 7.2\text{--}1.2$  Hz); 1.29 (3H,  $J = 7.2$  Hz). IR ( $\text{cm}^{-1}$ ): 1933, 2021, 2051, 2090.

**NMR Experiments.** Variable-temperature NMR spectra were recorded on a Bruker AM250 spectrometer, using methylene chloride- $d_2$  as solvent. Chemical shifts are reported in ppm relative to TMS from the central peak of deuterio methylene chloride (5.3 ppm for  $^1\text{H}$  and 54 ppm for  $^{13}\text{C}$ ). Proton spectra were acquired at 250.133 MHz and carbon spectra at 62.896 MHz with a 5 mm dual frequency  $^1\text{H}/^{13}\text{C}$  probehead.  $^1\text{H}$  spectra were obtained in 32 scans in 32 K data points over a 3.5 kHz spectra width (4.7 s acquisition time). Temperatures quoted in Figure 7 are known with an accuracy of 2 K.

**Acknowledgment.** We thank the CNRS (France) for financial support and Dr. H. El Amouri for helpful discussion.

**Supporting Information Available:** Tables of bond distances and angles, hydrogen parameters, and anisotropic thermal parameters for **4** and **5b** (10 pages). Ordering information is given on any current masthead page.

OM950114X

# Palladium-Catalyzed Coupling Reactions in Superheated Water

Preshious Reardon, Sean Metts, Chad Crittendon, Pat Daugherty, and Edith J. Parsons\*

Department of Chemistry, Clemson University, Clemson, South Carolina 29634-1905

Received May 15, 1995<sup>⊗</sup>

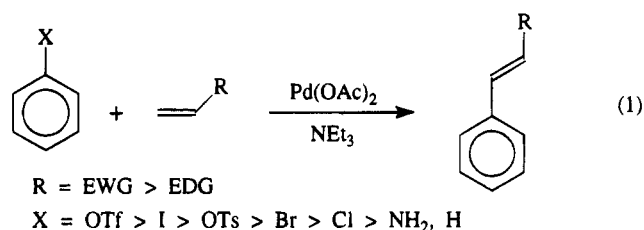
A series of Heck palladium-coupling reactions was carried out in superheated (260 °C) and supercritical (400 °C) water to determine their viability in these media. PdCl<sub>2</sub>, Pd(OAc)<sub>2</sub>, Pd(acac)<sub>2</sub>, Pd(dba)<sub>2</sub>, 30% Pd/C, (PPh<sub>3</sub>)<sub>2</sub>PdCl<sub>2</sub>, and (dppe)PdCl<sub>2</sub> performed indistinguishably as precatalysts for the coupling reaction of iodobenzene with styrene, therefore Pd(OAc)<sub>2</sub> was used for subsequent reactions. Removal of HX generated during the reaction was attempted with 10 bases: NEt<sub>3</sub>, (Pr<sup>i</sup>)<sub>2</sub>EtN, NaOAc, NaOH, NaHCO<sub>3</sub>, Na<sub>2</sub>CO<sub>3</sub>, NH<sub>4</sub>OAc, NH<sub>4</sub>OH, NH<sub>4</sub>HCO<sub>3</sub>, and (NH<sub>4</sub>)<sub>2</sub>CO<sub>3</sub>. Of these, the NH<sub>4</sub>HCO<sub>3</sub> was found to be the most effective. A series of aromatic compounds were examined in the superheated water system, using styrene as the alkene. The arenes C<sub>6</sub>H<sub>5</sub>I, C<sub>6</sub>H<sub>5</sub>Br, C<sub>6</sub>H<sub>5</sub>Cl, MesI, C<sub>6</sub>H<sub>5</sub>CHCHI, C<sub>6</sub>H<sub>5</sub>-CHCHBr, and C<sub>6</sub>H<sub>5</sub>OTf underwent coupling to styrene, while C<sub>6</sub>H<sub>5</sub>OTs, C<sub>6</sub>H<sub>6</sub>, p-CF<sub>3</sub>C<sub>6</sub>H<sub>4</sub>X (X = I, Br, Cl), and aniline derivatives did not. The alkenes C<sub>6</sub>H<sub>5</sub>CH=CH<sub>2</sub>, CH<sub>2</sub>=C(CH<sub>3</sub>)CO<sub>2</sub>-CH<sub>3</sub>, CH<sub>2</sub>=C(CH<sub>3</sub>)CO<sub>2</sub>H, CH<sub>2</sub>=CHCH<sub>2</sub>OH, CH<sub>2</sub>=CHCH<sub>2</sub>Br, and CH<sub>2</sub>=CHCH<sub>2</sub>Cl coupled to iodobenzene, while C<sub>4</sub>H<sub>9</sub>CH=CH<sub>2</sub>, C<sub>6</sub>H<sub>5</sub>C(CH<sub>3</sub>)=CH<sub>2</sub>, and C<sub>3</sub>H<sub>7</sub>CH(OH)CH=CH<sub>2</sub> did not. Styrene yielded predominantly stilbene, while the methacrylates yielded methylstyrene. The allyl substrates produced phenylpropanal, with small amounts of methylstyrene. The Heck couplings proceeded to approximately the same degree at 400 °C (supercritical) as at 260 °C. However, increased hydrogenation and hydrogenolysis side reactions and lower overall recoveries were observed at the higher temperature.

## Introduction

We have been developing superheated and supercritical water as a benign solvent system for carrying out organic syntheses.<sup>1,2</sup> In particular, we are exploring the applicability and scope of transition-metal-catalyzed transformations under these conditions. We previously demonstrated that cobalt-catalyzed alkyne cyclotrimerization reactions proceed readily in supercritical water, giving high yields of the desired benzene products.<sup>1a</sup> The facility with which the cyclization occurred suggested that other coupling reactions might also be amenable to supercritical water media. We therefore began exploring palladium-coupling reactions.

Palladium-coupling reactions in organic solvents are very versatile reactions which have found wide applicability in organic syntheses.<sup>3</sup> There is a breadth of reactions that fall under this heading, and new variations are continually being developed.<sup>4</sup> In our work, we opted to begin by studying palladium-catalyzed alkene-

arene coupling reactions which fall under the general heading of Heck arylation reactions (eq 1). These reac-



tions are relatively simple and proceed without transmetalation from main-group alkyl species, many of which are not expected to survive well in the superheated and supercritical water.

Water has a dielectric constant of 5 at its critical point, which means that it behaves similarly to diethyl ether ( $\epsilon = 4.3$  at room temperature).<sup>5</sup> One could therefore consider that the palladium-coupling reactions in nearcritical and supercritical water are simply being carried out in an ether-like solvent. However, supercritical conditions for water ( $T_c = 374$  °C,  $P_c = 218$  atm) are certainly not typical of traditional palladium-coupling reactions, which generally range from 25 to 100

\* Abstract published in *Advance ACS Abstracts*, July 1, 1995.

(1) (a) Jerome, K.; Parsons, E. J. *Organometallics* **1993**, *12*, 2991. (b) Myrick, M. L.; Kolis, J.; Parsons, E.; Chilke, K.; Lovelace, M.; Scrivens, W.; Holliday, R.; Williams, M. J. *Raman Spectrosc.* **1994**, *25*, 59. (c) Crittendon, R.; Parsons, E. J. *Organometallics* **1994**, *13*, 2587.

(2) Kuhlmann, B.; Arnett, E. M.; Siskin, M. J. *Org. Chem.* **1994**, *59*, 3098.

(3) (a) Heck, R. F. *Palladium Reagents in Organic Syntheses*; Academic Press: New York, 1985. (b) Colquhoun, H. M.; Holton, J.; Thompson, D. J.; Twigg, M. V. *New Pathways for Organic Synthesis*; Plenum Press: New York, 1984. (c) Davies, S. G. *Organotransition Metal Chemistry: Applications to Organic Synthesis*; Pergamon: New York, 1982. (d) Tsuji, J. *Organic Synthesis with Palladium Compounds*; Springer Verlag: New York, 1980. (e) Heck, R. F. *J. Am. Chem. Soc.* **1968**, *90*, 5526.

(4) For example, see: (a) Zhang, H.-C.; Daves, G. D. *Organometallics* **1993**, *12*, 1499. (b) Trost, B. M.; Shi, Y. *J. Am. Chem. Soc.* **1993**, *115*, 9421. (c) Oxawa, F.; Kubo, A.; Matsumoto, Y.; Hayashi, T.; Nishioka, E.; Yanagi, K.; Moriguchi, K. *Organometallics* **1993**, *12*, 4188. (d) Li, C.-S.; Jou, D.-C.; Cheng, C.-H. *Organometallics* **1993**, *12*, 3945.

(5) (a) Franck, E. U. *Pure Appl. Chem.* **1985**, *8*, 1065. (b) Frank, E. *Fluid Phase Equilib.* **1983**, *10*, 211. (c) *Supercritical Fluid Science and Technology*; Johnston, K. P., Penninger, J. M. L., Eds.; ACS Symposium Series 406; American Chemical Society: Washington, DC, 1989; Chapters 15-17. (d) Shaw, R. W.; Brill, T. B.; Clifford, A. A.; Eckert, C. A.; Franck, E. U. *Chem. Eng. News* **1991**, *69*(51), 26.

°C. Therefore, while many aspects of the Heck reaction proceed "identically" in superheated water and organic solvents, it is not surprising that differences in the reaction chemistry are also observed.

## Results

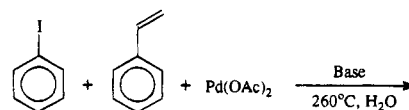
**Superheated Water Conditions.** A series of reactions were carried out in superheated water to determine the viability of, and optimum conditions for, the Heck palladium-coupling reaction in this medium. The reactions were carried out in stainless steel reactors at 260 °C for 20 min, including heat up time.

**Palladium Complexes and Bases.** PdCl<sub>2</sub>, Pd(OAc)<sub>2</sub>,<sup>6</sup> Pd(acac)<sub>2</sub>, Pd(dba)<sub>2</sub>, 30% Pd/C, (PPh<sub>3</sub>)<sub>2</sub>PdCl<sub>2</sub>, and (dppe)PdCl<sub>2</sub> were examined as precatalysts for the coupling reaction of iodobenzene with styrene. One-tenth of an equiv of palladium complex was added to each reaction, with the exception of the Pd/C. The expense and volume of this palladium metal catalyst required that it be used in much lower quantities (0.01 equiv of Pd). These palladium complexes did not significantly vary in their effectiveness at promoting the coupling. Less coupling was observed with the Pd/C; however, this may be due to the reduced amount of palladium present from this catalyst. Increasing the catalyst concentration (from 0.1 mmol up to 1.5 mmol) did slightly increase the yield of coupled products, although not proportionally. This may be due in part to mechanical difficulties such as clumping or clogging of the reactor at the higher amounts of palladium. An insoluble, black powder was obtained at the end of the PdCl<sub>2</sub> reactions and was analyzed by powder X-ray diffraction. Comparison with the JCPDS powder diffraction file showed palladium metal and Fe<sub>2</sub>O<sub>3</sub> (presumably from the 316 SS bomb)<sup>7</sup> (Figures S1 and S2).

Bases were added to the reaction mixture in an attempt to remove HX generated during the coupling reaction. Removal of this acid is necessary to halt palladium-catalyzed hydrogenation and hydrogenolysis of the starting materials and products. NEt<sub>3</sub>, (Pr<sup>i</sup>)<sub>2</sub>EtN, NaOAc, NaOH, NaHCO<sub>3</sub>, Na<sub>2</sub>CO<sub>3</sub>, NH<sub>4</sub>OAc, NH<sub>4</sub>OH, NH<sub>4</sub>HCO<sub>3</sub>, and (NH<sub>4</sub>)<sub>2</sub>CO<sub>3</sub> were examined. Of these, the NH<sub>4</sub>HCO<sub>3</sub> was found to be the most effective at halting these side reactions (Table 1). The amines NEt<sub>3</sub> and (Pr<sup>i</sup>)<sub>2</sub>EtN reacted inconsistently, occasionally resulting in a plethora of alkylated arene side products.

**Arene and Alkene Substrates.** A series of aromatic compounds was examined in the superheated water system, using styrene as the alkene. These arenes included haloarenes, phenyltriflate and tosylate, aniline derivatives, and benzene (Tables 2 and 3). The haloarenes underwent coupling, even when the halide was sterically protected by the methyl groups in mesityl iodide.  $\beta$ -Iodostyrene and  $\beta$ -bromostyrene, in which the halides are conjugated to the arene, also underwent coupling to styrene. The pseudohalide phenyltriflate underwent coupling, while the less active phenyltosylate and unactivated benzene did not. Attempts to further activate the iodo-, bromo-, and chlorobenzenes by adding an electron-withdrawing CF<sub>3</sub> group to the para position instead resulted in little reaction except loss of both

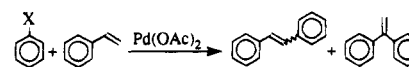
**Table 1. Effect of Various Bases on the Heck Coupling of Iodobenzene with Styrene in Superheated Water<sup>a</sup>**



Base				PhH	Ph-Ph
NEt <sub>3</sub>	28	0	42	0	19
(Pr <sup>i</sup> ) <sub>2</sub> EtN	30	3	33	0	13
NaOAc	12	2	75	0	2
NaOH	11	2	65	1	3
NaHCO <sub>3</sub>	18	2	56	2	2
Na <sub>2</sub> CO <sub>3</sub>	16	0	65	3	2
NH <sub>4</sub> OAc	16	2	72	1	2
NH <sub>4</sub> OH	15	0	76	0	2
NH <sub>4</sub> HCO <sub>3</sub>	25	0	58	0	0
(NH <sub>4</sub> ) <sub>2</sub> CO <sub>3</sub>	24	0	54	0	2

<sup>a</sup> Recoveries: 71%–108%. Internal standards: Ph<sub>2</sub>CH<sub>2</sub> or Ph<sub>3</sub>CH.

**Table 2. Ability of Arene Derivatives To Undergo Heck Coupling with Styrene<sup>a</sup>**



Coupled					Did Not Couple								

<sup>a</sup> All reactions included NH<sub>4</sub>HCO<sub>3</sub> in the reaction mixture except for the reactions involving aniline derivatives, which included HOAc instead.

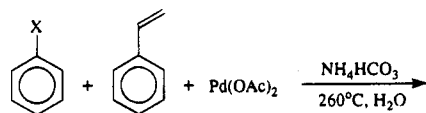
groups with formation of *p*-terphenyl (13%–17%). Acetic acid was added to the reactions involving aniline derivatives to assist in the C–N bond cleavage. However, none of the anilines underwent coupling whether or not excess acid was present, and only hydrogenation and hydrogenolysis side reactions were observed.

The activated alkenes styrene, methyl methacrylate, methacrylic acid, allyl alcohol, allyl bromide, and allyl chloride coupled to iodobenzene in the presence of Pd(OAc)<sub>2</sub> and NH<sub>4</sub>HCO<sub>3</sub> (Tables 4 and 5). Unactivated hexene did not undergo coupling, nor did the more sterically hindered  $\alpha$ -methylstyrene or 1-hexen-3-ol. Styrene yielded *cis*- and *trans*-stilbene and 1,1-diphenylethylene, of which *trans*-stilbene was the predominant olefinic product obtained. Methyl methacrylate and methacrylic acid each yielded  $\alpha$ - and  $\beta$ -methylstyrene, with *trans*- $\beta$ -methylstyrene predominating. Allyl alcohol, allyl bromide, and allyl chloride produced the aldehydes 3-phenylpropanal and 2-phenylpropanal, while the alcohol and bromide also produced small amounts of  $\alpha$ - and  $\beta$ -methylstyrene.

Side reactions observed with the alkenes included isomerization, oligomerization, and hydrogenation to the respective alkanes. Methyl methacrylate hydrolyzed to methacrylic acid in the presence of either acid or

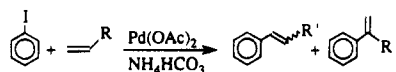
(6) Abbreviations: OAc, acetate; acac, acetylacetonate; dba, dibenzylidene acetone; dppe, 1,2-bis(diphenylphosphino)ethane.

(7) Powder diffraction file: Inorganic Phases; JCPDS, International Center for Diffraction Data, 1985.

**Table 3. Products from the Heck Coupling of Various Substituted Arenes with Styrene in Superheated Water<sup>a</sup>**

ArX				ArX		
PhI	21	0	3	28	15	0
PhBr	16	0	2	28	25	0
PhCl	16	1	1	32	26	0
PhOTf	5	0	0	24 <sup>b</sup>	35	0
MesI	10	0	0	24 <sup>c</sup>	12	0
PhCHCHI	14	0	0	15	25 <sup>d</sup>	16
PhCHCHBr	9	0	0	30	27	2

<sup>a</sup> Recoveries: 63–99%. Internal standards: Ph<sub>2</sub>CH<sub>2</sub> or Ph<sub>3</sub>CH.  
<sup>b</sup> PhOH, 5%. <sup>c</sup> MesH, 7%. <sup>d</sup> PhCH<sub>2</sub>CH<sub>3</sub>, 5%.

**Table 4. Ability of Alkenes To Undergo Heck Coupling with Iodobenzene**

Coupled	Did Not Couple

palladium. Double-bond migration was observed with 1-hexene, 1-hexene-3-ol, and allyl alcohol and resulted in the formation of 2- and 3-hexenes, 3-hexanone, and propanal, respectively. Allyl bromide and allyl chloride each produced a mixture of allyl alcohol and propanal. Oligomerization and polymerization of the alkene occurred to a small extent in many of the reactions.

**Supercritical Water Conditions.** The Heck reactions involving the various arenes and alkenes were also carried out in supercritical water at 400 °C (Tables 6–8). Little difference was observed in the amount of coupling obtained at 400 °C versus 260 °C. Hydrogenation and hydrogenolysis processes were favored by the supercritical conditions, however, leading to increased side products at this temperature. Overall recoveries were also lower at the higher temperature.

## Discussion

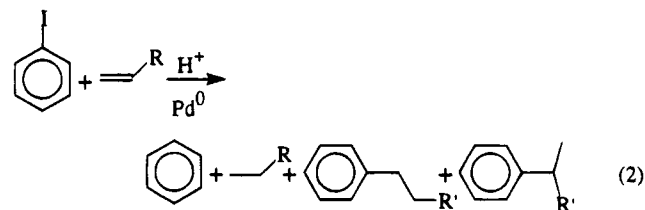
A generalized catalytic cycle for the palladium-coupling reactions in organic solvents is shown in Figure 1.

**Palladium Complexes.** The first step of the coupling reaction run under normal, organic conditions is reduction of the palladium precatalyst to palladium(0) with assistance from NEt<sub>3</sub>, PR<sub>3</sub>, or other reductants. In supercritical water, the palladium was readily reduced even in the absence of NEt<sub>3</sub> or PR<sub>3</sub>. The nature of the

reductant is uncertain at this time but may involve the walls of the reactor.

The coupling reaction did not appear to be sensitive to the nature of the palladium complex which was added. This may be the direct result of reduction of the palladium to palladium(0) or palladium metal, which then acted as a catalyst.<sup>8</sup> This possibility is supported both by the activity of the palladium-on-carbon catalyst and by the isolation of palladium metal at the end of the PdCl<sub>2</sub> reaction. The relatively low yields obtained from these reactions have been traced to deactivation of the catalyst, therefore efforts to construct or identify more stable palladium catalysts are continuing.

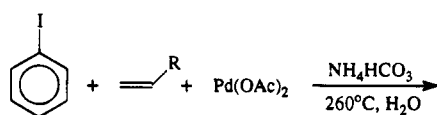
**Base.** The final step of the Heck coupling is a β-hydrogen elimination, which forms the alkylarene and also produces 1 equiv of acid (HI in the case of iodobenzene). In the organic systems a base is added to assist in the removal of the proton from the palladium and to neutralize this acid. The acid produced during the reaction had a much greater effect in the supercritical water system than is generally observed in organic solvents. The combination of acid and palladium catalyst resulted in facile hydrogenation of both the coupled products and the starting alkene, as well as hydrogenolysis of the arene substrate. The addition of HCl or HOAc to the system accentuated these hydrogenation processes (eq 2).



The addition of various bases to the reaction mixture did result in attenuation of the hydrogenation and hydrogenolysis activity, with NH<sub>4</sub>HCO<sub>3</sub> being the most efficient. The solubility of the ammonium salt in superheated and supercritical water may be a key to this base's activity, since the analogous NaHCO<sub>3</sub> was less effective. Although the solubilities of most salts are high in liquid water, their solubilities decrease dramatically as the critical point is approached<sup>9</sup> and the dielectric constant of the water decreases. Those salts which are soluble in weakly polar organic solvents are in turn more likely to be soluble in the superheated and supercritical water.

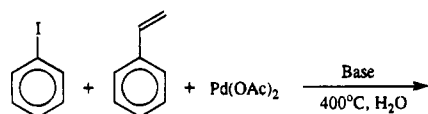
Trialkylamines were also examined as bases in the superheated water reactions and proved effective at promoting coupling of the alkene and arene. Solubility considerations may also account for these amines' effectiveness. However, the trialkylamines also consistently produced high yields of benzene from the iodobenzene and occasionally yielded significant amounts of other side products, as well. For example, in one NEt<sub>3</sub>

- (8) (a) Grushin, V. V.; Alper, H. *J. Am. Chem. Soc.* **1995**, *117*, 4305. (b) Stewart, S. K.; Whiting, A. *J. Organomet. Chem.* **1994**, *482*, 293. (c) Cho, C. S.; Uemura, S. *J. Organomet. Chem.* **1994**, *465*, 85. (d) Bumagin, N. A.; Sukhomlinova, L. I.; Tolstaya, T. P.; Beletskaya, I. P. *Dokl. Akad. Nauk* **1993**, *332*, 221. (e) Shieh, W.-C.; Carlson, J. A. *J. Org. Chem.* **1992**, *57*, 279. (f) Bumagin, N. A.; More, P. G.; Beletskaya, I. P. *J. Organomet. Chem.* **1989**, *371*, 397. (9) Gao, J. *J. Phys. Chem.* **1994**, *98*, 6049. (b) Armellini, F. J.; Tester, J. W. *Fluid Phase Equilib.* **1993**, *84*, 123. (c) Oelkers, E. H.; Helgeson, H. C. *Science* **1993**, *261*, 888. (d) Gloyna, E. F.; Li, L. *Waste Manage.* **1993**, *13*, 379.

Table 5. Products from the Heck Coupling of Various Alkenes with Iodobenzene in Superheated Water<sup>a</sup>

Alkene	Ph-CH2-CHO	Ph-CH(CH3)-CHO	Ph-CH=CH-R'	Ph-C(=O)-R'	PhI	CH2=CHR	PhH	Ph-CHO
	0	0	21 <sup>b</sup>	3 <sup>b</sup>	28	15 <sup>b</sup>	0	0
	0	0	16 <sup>c</sup>	12 <sup>c</sup>	25	16 <sup>d</sup>	0	0
	0	0	10 <sup>c</sup>	8 <sup>c</sup>	31	7 <sup>e</sup>	2	0
	12	3	1 <sup>c</sup>	2 <sup>c</sup>	18	7	2	3
	3	1	2 <sup>c</sup>	6 <sup>c</sup>	38	4 <sup>f</sup>	3	5
	3	0	0	0	47	5 <sup>f</sup>	5	2

<sup>a</sup> Recoveries: 65%–95%. Internal standards: Ph<sub>2</sub>CH<sub>2</sub> or Ph<sub>3</sub>CH. <sup>b</sup> R = R' = Ph. <sup>c</sup> R' = CH<sub>3</sub>. <sup>d</sup> CH<sub>2</sub>CHR = CH<sub>2</sub>C(CH<sub>3</sub>)CO<sub>2</sub>CH<sub>3</sub>. <sup>e</sup> CH<sub>2</sub>CHR = CH<sub>2</sub>C(CH<sub>3</sub>)CO<sub>2</sub>H. <sup>f</sup> R = CH<sub>2</sub>OH.

Table 6. Effect of Various Bases on the Heck Coupling of Iodobenzene with Styrene in Supercritical Water<sup>a</sup>

Base	Ph-CH=CH-Ph	Ph-CH2-CH2-Ph	Ph-CH=CH-Ph	Ph-CH2-CH2-Ph	PhH
NEt <sub>3</sub>	12	14	5	11	13
(Pr) <sub>2</sub> EtN	15	13	4	10	14
NaOAc	14	9	8	13	13
NaOH	11	6	8	9	10
NaHCO <sub>3</sub>	23	3	10	5	8
Na <sub>2</sub> CO <sub>3</sub>	17	3	12	4	14
NH <sub>4</sub> OAc	21	6	8	8	15
NH <sub>4</sub> OH	13	9	8	11	12
NH <sub>4</sub> HCO <sub>3</sub>	16	11	12	18	19
(NH <sub>4</sub> ) <sub>2</sub> CO <sub>3</sub>	19	7	5	4	13

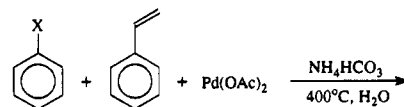
<sup>a</sup> Recoveries: 58%–103%. Internal standards: Ph<sub>2</sub>CH<sub>2</sub> or Ph<sub>3</sub>CH.

reaction, approximately 35% of the product mixture consisted of various alkyl benzene derivatives. This suggests that the amines may be susceptible to competing radical processes.<sup>10</sup>

**Arene Substrates.** The Heck reaction has been shown to occur under normal conditions with a variety of aromatic substrates.<sup>3,11</sup> Iodobenzene is the most reactive of the simple haloarenes, although electron-withdrawing substituents on the aromatic ring are known to increase the reactivity of the less active substrates.

(10) (a) Tsao, C. C.; Zhou, X. L.; Houser, T. J. *J. Supercrit. Fluids* **1992**, *5*, 107. (b) Houser, T. J.; Tsao, C.-C.; Dyla, J. E.; Van Atten, M. K.; McCarville, M. E. *Fuel* **1989**, *68*, 323.

(11) (a) Spencer, A. J. *Organomet. Chem.* **1984**, *270*, 115. (b) Spencer, A. J. *Organomet. Chem.* **1983**, *258*, 101.

Table 7. Products from the Heck Coupling of Various Substituted Arenes with Styrene in Supercritical Water<sup>a</sup>

ArX	Ar-CH=CH-Ph	Ar-CH2-CH2-Ph	Ar-CH=CH-Ph	ArX	Ph-CH=CH-Ph	ArH
PhI	15	2	1	3	9	15
PhBr	11	0	0	12	6	23
PhCl	9	1	1	26	14	17
PhOTf	3	0	0	5	8 <sup>b</sup>	0 <sup>c</sup>
MesI	7	0	0	4	2	17
PhCH2CHI	0	0	0	0	14	0
PhCH2CHBr	0	0	0	14	13	0

ArX	Ar-CH2-CH2-Ph	Ar-CH(Ph)-CH2-Ph	Ph-CH2-CH2-Ph	ArAr	Ph-C(=O)-CH2-Ph
PhI	8	4	18	4	4
PhBr	10	0	15	0	1
PhCl	1	0	8	0	2
PhOTf	0	3	3	0	2
MesI	1	0	6	0	6
PhCH2CHI	0	0	26	0	4
PhCH2CHBr	0	0	14	0	5

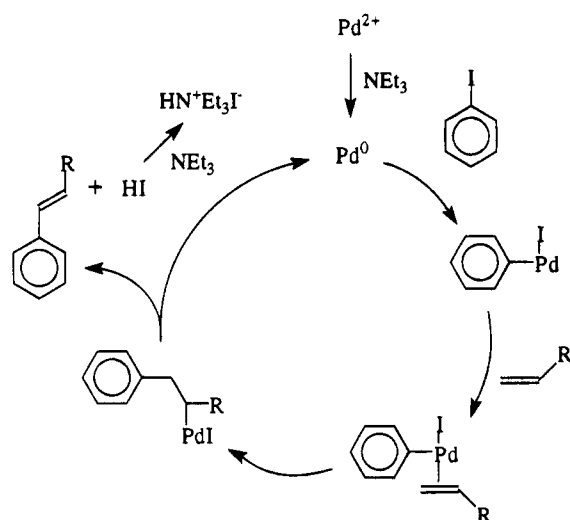
<sup>a</sup> Recoveries: 59%–83%. Internal standards: Ph<sub>2</sub>CH<sub>2</sub> or Ph<sub>3</sub>CH. <sup>b</sup> PhCH<sub>2</sub>CH<sub>2</sub>CF<sub>3</sub>, 9%. <sup>c</sup> PhOH, 32%.

In superheated water, little significant difference was observed in the degree to which the simple haloarenes coupled to styrene, although iodobenzene did give slightly higher yields of stilbene. The pseudohalides were less reactive than the halides, and phenyltosylate did not couple at all. This is not surprising, since the phenyltriflate and tosylate derivatives can undergo nonproductive hydrolysis reactions under the relatively harsh superheated water conditions. Benzene is not very active even under the best of organic conditions and did not couple at all in the superheated water. Attempts to activate the arene ring by placing an electron-withdrawing CF<sub>3</sub> group para to the halide were unsuccessful due to loss of both the CF<sub>3</sub> and the halide.

**Table 8. Products from the Heck Coupling of Various Alkenes with Iodobenzene in Supercritical Water<sup>a</sup>**

=CH-R	Ph-CH=CH-R'	Ph-CH=CH-R'	Ph-CH=CH-R'	Ph-CH=CH-R'	Ph-I	=CH-R	Ph-H	Ph-Ph	CH=O
	0	15 <sup>b,c</sup>	7 <sup>b</sup>	4 <sup>b</sup>	3	8 <sup>b,d</sup>	13	0	0 <sup>e</sup>
	0	5 <sup>f</sup>	1 <sup>f</sup>	0	1	99	22	3	0
	0	9 <sup>f</sup>	2 <sup>f</sup>	0	3	0	34	2	0
	4 <sup>h</sup>	0	2 <sup>f</sup>	0	0	0	28	0	8
	2 <sup>h</sup>	0	5 <sup>f</sup>	3 <sup>f</sup>	0	0	42	0	7
	2 <sup>h</sup>	0	3 <sup>f</sup>	1 <sup>f</sup>	4	2 <sup>i</sup>	23	1	3

<sup>a</sup> Recoveries: 48%–98%. Internal standards: Ph<sub>2</sub>CH<sub>2</sub> or Ph<sub>3</sub>CH. <sup>b</sup> R = R' = Ph. <sup>c</sup> Ph<sub>2</sub>CCH<sub>2</sub>, 1%. <sup>d</sup> PhCH<sub>2</sub>CH<sub>3</sub>, 16%. <sup>e</sup> PhCOCH<sub>3</sub>, 4%. <sup>f</sup> R' = CH<sub>3</sub>. <sup>g</sup> CH<sub>2</sub>CHR = CH<sub>2</sub>C(CH<sub>3</sub>)CO<sub>2</sub>CH<sub>3</sub>. <sup>h</sup> CH<sub>3</sub>CHPhCOH, 1%. <sup>i</sup> R = OH.

**Figure 1.** A Heck coupling reaction in organic media.

Haloarenes, in which the halide is conjugated to the aromatic ring via a styrene derivative, couple with appropriate alkenes in organic media.<sup>3c,12</sup> This coupling ability was also observed with  $\beta$ -iodostyrene and  $\beta$ -bromostyrene in superheated water.

The steric hindrance from the ortho methyl groups in mesityl iodide inhibited but did not halt its coupling with styrene. The coupled product, trimethylstilbene, was obtained, albeit in lower yield than the stilbene produced from unencumbered iodobenzene. In addition, significant amounts of mesitylene were obtained, which suggests that a small hydrogen can more easily access the protected carbon center than can a styryl group.

Aniline couples to styrene in low yields (19%–25%) under organic conditions and did not couple at all in the superheated water.<sup>3,13</sup> Attempts to change the electronic and steric profile of the amine as well as its leaving group ability were insufficient to activate these derivatives for the coupling reaction. The presence of acid, which is necessary to protonate the amine for activation as a leaving group, led to increased hydrogenation of the alkene provided in these reactions.

**Alkene Substrates.** Activated alkenes bearing electron-withdrawing groups couple the most readily to arenes in Heck reactions in organic solvents. However, coupling to unactivated alkenes has been observed under appropriate conditions. Sterically hindered alkenes do not coordinate well to the palladium center and therefore also do not readily couple.<sup>3</sup>

As was observed with the arene substrates, the reactions in superheated water were more sensitive to the nature of the alkene than were the corresponding reactions in organic solvents. Only activated alkenes underwent coupling, and unactivated hexene was not observed to couple to iodobenzene under any of the conditions examined. The reaction was also more sensitive to steric hindrance at the alkene than is generally observed in organic solvent systems, and no coupling was observed with the alkyl-substituted  $\alpha$ -methylstyrene or 1-hexen-3-ol.

**Nonhydrogenation Alkene Side Reactions.** Competing reactions involving the alkenes, in addition to the hydrogenations which were discussed above, were observed in several of the supercritical water reactions. In each case, these side reactions were minimized when the arene–alkene coupling was the most efficient. For example, oligomerization of the alkenes was observed, but occurred primarily in the reactions involving inactive arenes. Double-bond migration was also observed with the allylic alcohols 1-hexen-3-ol and allyl alcohol, and was followed by tautomerization to yield 3-hexanone and propanal, respectively. Furthermore, allyl bromide and allyl chloride underwent substitution to form allyl alcohol, which again produced propanal.

**Alkene Arylation.** Each of the active alkenes coupled with iodobenzene in the presence of Pd(OAc)<sub>2</sub> and NH<sub>4</sub>HCO<sub>3</sub> to give arylalkene products. The regio- and stereoselectivities of the styrene reactions generally mirrored those obtained under more traditional conditions.<sup>3,11</sup> However, secondary regioisomerization may occur during functional group loss, as discussed in the allyl alcohol section, below. The presence of NH<sub>4</sub>HCO<sub>3</sub> was necessary to prevent hydrogenation of the arylalkene products to their corresponding arylalkane derivatives. Although this hydrogenation could be maximized by adding additional acid, it was not synthetically

(12) Daves, G. D.; Hallberg, A. *Chem. Rev.* **1989**, *89*, 1433.(13) Akiyama, F.; Teranishi, S.; Fujiwara, Y.; Taniguchi, H. *J. Organomet. Chem.* **1977**, *140*, C7.



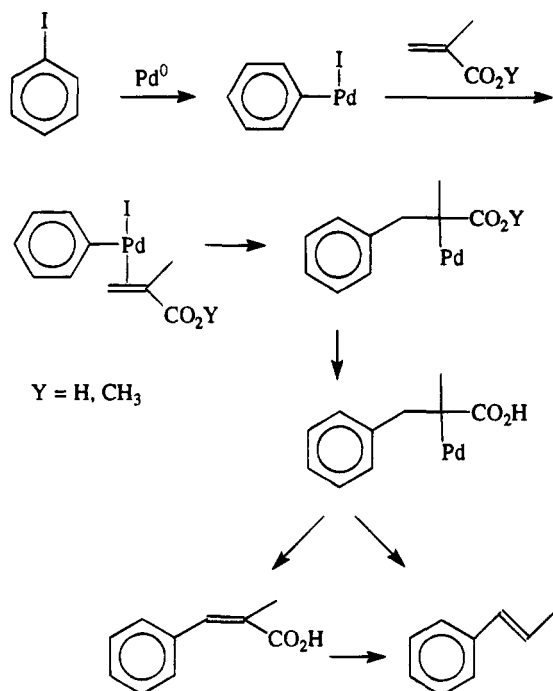


**Figure 2.** Possible decarboxylation sequence during the coupling of methyl methacrylate and iodobenzene.

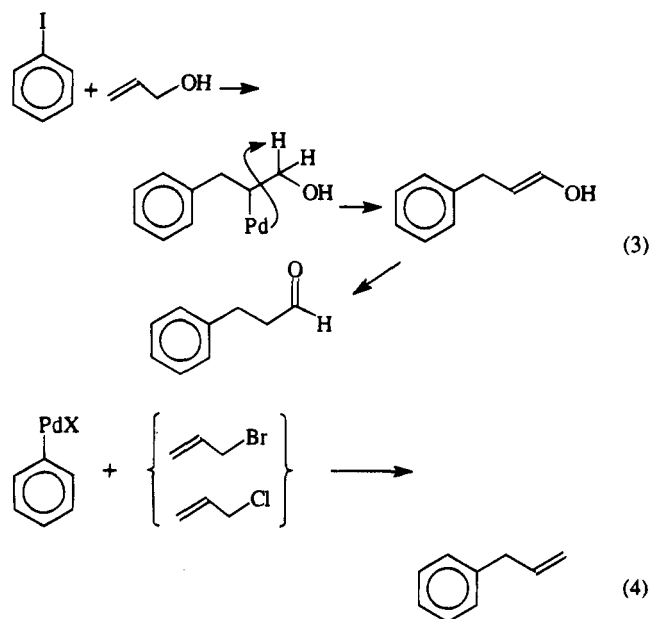
useful, since hydrogenation and hydrogenolysis of the starting substrates also competed.

**Methyl Methacrylate.** In organic solvents, methyl methacrylate couples to iodobenzene to give methyl  $\alpha$ -methylcinnamate, in which the ester functionality is preserved. In superheated water the ester is lost, giving  $\alpha$ - and  $\beta$ -methylstyrene. This outcome represents a route whereby superheated water permits coupling of an activated alkene with concomitant loss of its functionality to yield the product of a nonfunctionalized alkene (propene).

Decarboxylation most likely does not occur until after the migratory insertion step of the alkene-arene coupling, since unactivated alkenes are not observed to couple (Figure 2). The palladium may then remove the carboxylate either directly or in a separate step following release of the coupled product. *trans*-Cinnamic acid and methyl *trans*-cinnamate were reacted with Pd<sup>2+</sup> in water at 260 °C to see if the latter, two-step pathway could occur. These reactants each yielded ethylbenzene exclusively (no base was provided), indicating that independent removal of the carboxylate is possible in this system.<sup>14</sup> However, direct removal of the carboxylate can also be ruled out.

Hydrolysis of the ester may occur at any stage of the reaction. Methacrylic acid couples to form products that are essentially identical to those obtained from methyl methacrylate, indicating that hydrolysis prior to coupling would not alter the outcome of the observed reaction. The production of ethylbenzene from both *trans*-cinnamic acid and methyl *trans*-cinnamate, above, indicates that hydrolysis following coupling also would not alter the outcome of the reaction.

**Allyl Alcohol, Allyl Bromide, and Allyl Chloride.** Allyl alcohol couples with iodobenzene in organic solvents to yield an enol which tautomerizes to 3-phenylpropanal (eq 3). Allyl bromide and chloride, on the other hand, couple to phenylpalladium with loss of the halide to yield 3-phenylpropene (eq 4). In superheated water



these substrates produced 3-phenylpropanal accompanied by small amounts of 2-phenylpropanal. In addition, both the allyl alcohol and the allyl bromide yielded small amounts of  $\alpha$ - and  $\beta$ -methylstyrene. Thus, a common theme is observed in that the functional groups OH, Br, and CO<sub>2</sub>CH<sub>3</sub> can be lost to produce the unfunctionalized methylstyrene derivatives. In contrast, the more robust phenyl group of styrene is maintained in the product stilbenes.

The allyl halides both hydrolyze to allyl alcohol in superheated water, therefore, it is very likely that the small amounts of phenylpropanal produced under these conditions arise from this allyl alcohol, rather than from the allyl halides directly. The absence of any other coupling products from the allyl chloride may indicate that the chloride itself does not undergo Heck coupling in superheated water. However, the formation of methylstyrenes in the allyl bromide reaction suggests that direct coupling of the bromide may occur, analogous to its reaction in organic solvents. However, this is not definite, since the methylstyrene products are also produced in the allyl alcohol reaction.

One reasonable scenario for the formation of methylstyrene from the coupling of iodobenzene and allyl alcohol has cinnamyl alcohol formed from the coupling. This intermediate could then dehydroxylate to form methylstyrene or rearrange to the aldehyde. Cinnamyl alcohol was therefore placed under the reaction conditions.  $\beta$ -Methylstyrene was, in fact, obtained from the reaction, as was  $\alpha$ -methylstyrene. This represents both reduction of the cinnamyl alcohol and regioisomerization of the resulting alkene.

The observed regioisomerizations presumably involve a 1,2-phenyl shift. This type of isomerization has implications for each of the coupling reactions reported here; therefore, the other product alkenes, stilbene, and methylstyrene, were also reacted with palladium under

(14) (a) Tsao, C. C.; Zhou, Y.; Liu, X.; Houser, T. J. *J. Supercrit. Fluids* **1992**, *5*, 107. (b) Siskin, M.; Katritzky, A. R. *Science* **1991**, *11*, 231. (c) Siskin, M.; Brons, G.; Vaughn, S. N.; Katritzky, A. R.; Balasubramanian, M. *Energy Fuels* **1990**, *4*, 488. (d) Katritzky, A. R.; Luxem, F. J.; Siskin, M. *Energy Fuels* **1990**, *4*, 515. (e) Katritzky, A. R.; Luxem, F. J.; Siskin, M. *Energy Fuels* **1990**, *4*, 525.

typical reactions conditions. However, no regioisomerization of these alkenes was observed. This demonstrates that the isomerization requires an easily removable functional group on the coupled product. Regioisomerization probably accounts for the poor regioselectivities obtained from methyl methacrylate and methacrylic acid, as well as from the allyl alcohol.

**Supercritical Water.** The overall yields of coupled products did not significantly vary when the coupling reactions were run at 400 °C as opposed to 260 °C. The primary effect of the higher temperature was that the bases became ineffective at halting hydrogenation and hydrogenolysis processes. Overall recoveries were also slightly lower, suggesting that more of the substrates, particularly the alkenes, were either removed from the reaction mixture (through processes such as polymerization) or destroyed. The lack of increase in coupled products at the higher temperature provides additional evidence that the limitation in these reactions is deactivation of the coupling catalyst. However, the hydrogenation catalyst appears to continue functioning under these conditions.

### Summary

Palladium-catalyzed coupling of arenes with alkenes does occur in superheated and supercritical water. The reactions proceed similarly, but not identically, to their counterparts in traditional, organic solvents. The water-based couplings proceed relatively cleanly at 260 °C in the presence of  $\text{NH}_4\text{HCO}_3$ , although yields of the coupled products are limited by deactivation of the palladium catalyst. The reactions in SW are more sensitive to steric hindrance and electronic effects than are the analogous reactions in organic solvents. Also, SW promotes loss of the alkene's functionality to a much greater extent than do normal organic conditions. Bromide, chloride, carboxylate, and, to some extent, hydroxyl losses are all observed in superheated and supercritical water. Both the substrate and product alkenes in the SW are readily hydrogenated in the presence of acid. Hydrogenolysis and hydrogenation processes are halted at 260 °C by the addition of the

base  $\text{NH}_4\text{HCO}_3$ ; however, these side reactions are observed in all reactions at the higher temperature (400 °C).

### Experimental Section

Water was distilled from basic potassium permanganate. The reaction vessels consisted of coned and threaded 316 SS tubes, each fitted with an end cap, a valve, and a thermocouple. All parts were rated to 20 000 psi or greater and are commercially available from HiP.

Powder X-ray diffraction spectra were measured over the range 2–70° at a rate of 1°/min on a Scintag XDS/2000  $\theta$ – $\theta$  diffractometer using Cu K $\alpha$  radiation.

**Reactions.** Substrates (1.0 mmol each) and water (3.5 mL) were placed in the reactor along with the metal catalyst (0.1 mmol of  $\text{L}_2\text{PdX}_2$  [ $\text{L}_2\text{PdX}_2 = \text{PdCl}_2, \text{Pd}(\text{OAc})_2, \text{Pd}(\text{acac})_2, \text{Pd}(\text{dba})_2, (\text{PPh}_3)_2\text{PdCl}_2, (\text{dppf})\text{PdCl}_2$ ] or 0.01 equiv of Pd as 30% Pd/C) and acid (1.1 mmol of HOAc) or base (1.1 mmol of  $\text{NH}_4\text{HCO}_3$ ). The reactor was then sealed and placed in a tube furnace at a set temperature of 375 or 515 °C for 20 min. Monitoring the reaction with a thermocouple in the reactor showed final, actual temperatures of 260 (superheated) and 400 °C (supercritical). After the designated time period, the reactor was cooled under a stream of water and the contents were removed. The mixture was placed in a separatory funnel, and the organic layer was separated and dissolved in  $\text{CDCl}_3$ . The water layer was extracted with  $\text{CDCl}_3$ , and NMR spectra of both the water extract and the organic layer were obtained. Further analysis of these samples was obtained via GC/MS. Mass balances are listed as recoveries (see Tables 1–8). Occasional reactions were run in  $\text{D}_2\text{O}$ , and the water layer was analyzed directly.

**Acknowledgment.** P.R. wishes to acknowledge the National Science Foundation (CHE-9100387) for financial support. Support of this research by the EPA-EPSCoR program and by NSF (CHE-9403546) is also gratefully acknowledged. We would like to thank Prof. William T. Pennington for the powder X-ray diffraction spectra.

**Supporting Information Available:** Powder pattern and search match results for recovered palladium sample (2 pages). Ordering information is given on any current masthead page.

OM9503470

# Cyclopentadienylcobalt Coordination to Alkenylarenes: From 1,3-Diene Coordination to $\mu$ -Arene Cluster Complexes

Hubert Wadepohl,\* Till Borchert, Klaus Büchner, Michael Herrmann,  
Franz-Josef Paffen, and Hans Pritzkow

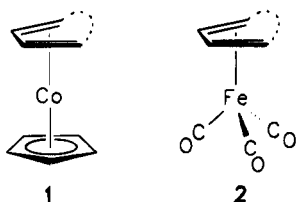
Anorganisch-Chemisches Institut der Ruprecht-Karls-Universität, Im Neuenheimer Feld 270,  
D-69120 Heidelberg, Germany

Received February 27, 1995<sup>®</sup>

Reaction of  $[\text{CpCo}(\text{C}_2\text{H}_4)_2]$ , **7**, with a number of alkenylnaphthalene derivatives  $\text{C}_{10}\text{H}_7\text{R}$  ( $\text{R} = 1\text{-CH=CH}_2$ ,  $2\text{-CH=CH}_2$ ,  $1\text{-CH=CHMe}$ , and  $1\text{-CH=CHPh}$ ) gave the mononuclear  $[\text{CpCo}\{\eta^4\text{-(alkenyl)naphthalene}\}]$  complexes **15a,b**, **16**, and **17**. In these complexes, two  $\pi$ -electrons each of the naphthalene nucleus and the olefinic side chain are involved in metal coordination. The crystal and molecular structure of the 1-vinyl derivative, **15a**, has been determined. Relevant crystal parameters are as follows: orthorhombic, space group  $Pcab$ ;  $Z = 8$ ;  $a = 8.206(1) \text{ \AA}$ ,  $b = 11.372(3) \text{ \AA}$ ,  $c = 28.067(7) \text{ \AA}$ ;  $wR2 = 0.131$  (based on 2308 unique reflections),  $R = 0.050$  (1374 reflections with  $I \geq 2\sigma(I)$ ). The distribution of carbon–carbon bond lengths indicates considerable electronic localization within the metal-coordinated part of the six-membered ring. Strong metal-to-ligand bonding is shown by equilibration of the carbon–carbon bonds within the 1,3-diene system. From *m*- and *p*-distyrylbenzene and **7** the dinuclear complexes  $[(\text{CpCo})_2(\eta^4\text{-}\eta^4\text{-distyrylbenzene})]$  **18a,b** were obtained. Here, coordination to each metal is in a 1,3-diene fashion via an olefinic double bond and a localized double bond of the central arene (phenylene) ring. In toluene, **18b** partially decomposed to form  $[(\text{CpCo})_3(\mu_3\text{-}\eta^2\text{:}\eta^2\text{:}\eta^2\text{-}p\text{-distyrylbenzene})]$ , **19**. Both **18b** and **19** were also formed from *p*-distyrylbenzene and  $[\text{CpCo}(\text{C}_6\text{Me}_6)]$ , **8**. Compound **19** is fluxional in solution; the barrier  $\Delta G^\ddagger$  for arene rotation was estimated to  $50 \text{ kJ mol}^{-1}$  at 250 K. From the reaction of  $\alpha$ -methylstyrene,  $\text{Cp}_2\text{Co}$ , and potassium, a minor amount of  $[\text{CpCo}\{1\text{-}3,8,9\text{-}\eta\text{-}(1\text{-Cp-}3\text{-Me-}1\text{-cobaltindenyl})\}]$  **20** was isolated. Compound **20** has been characterized by X-ray crystallography. Crystal data: tetragonal, space group  $I\bar{4}$ ;  $Z = 8$ ;  $a = 18.150(12) \text{ \AA}$ ,  $c = 9.307(5) \text{ \AA}$ ;  $wR2 = 0.100$  (based on 1878 unique reflections),  $R = 0.045$  (1373 reflections with  $I \geq 2\sigma(I)$ ).

## Introduction

The close similarity of the isoelectronic “conical” fragments  $(\text{CO})_3(\text{d}^n\text{-M})$  and  $\text{Cp}(\text{d}^{n+1}\text{-M})$  is well-known. On the basis of a simple frontier orbital treatment, the now very common term *isolobal* was coined to describe the relationship of such fragments and to understand its chemical consequences.<sup>1</sup> Particularly widespread are complexes **1** and **2** of the isolobal and isoelectronic fragments  $(\text{CO})_3\text{Fe}$  and  $\text{CpCo}$  with open-chain or cyclic conjugated dienes. Although in many cases **1** and **2** show quite similar structures and chemical reactivity, important differences do exist.



When styrene derivatives are treated with sources of  $(\text{CO})_3\text{Fe}$  (e.g.,  $[\text{Fe}(\text{CO})_5]$ ,<sup>2</sup>  $[(\text{CO})_3\text{Fe}(\text{cyclooctene})_2]^{3,4}$ ), the

iron becomes attached to the diene system formed by the vinyl group and one of the carbon–carbon bonds of the arene nucleus (Scheme 1). Structural<sup>4</sup> and spectroscopic<sup>2</sup> data as well as chemical reactivity<sup>2</sup> consistently indicate a loss of aromatic character of the coordinated arene in **4**. In many cases, **4** takes up a second  $(\text{CO})_3\text{Fe}$  fragment, and the *dinuclear* complex **5** is formed.<sup>2</sup> As shown by the crystal structure analysis of the *m*, $\alpha$ -dimethylstyrene derivative,<sup>5</sup> the two metals in **5** adopt the *anti* arrangement, one on each face of the styrene ligand. In marked contrast, *trinuclear* cluster complexes **6** with face-capping arene ligands are formed when ring or side-chain-substituted styrenes are treated with reactive sources of the  $\text{CpCo}$  moiety (e.g.,  $[\text{CpCo}(\text{C}_2\text{H}_4)_2]$ , **7**, and  $[\text{CpCo}(\text{C}_6\text{Me}_6)]$ , **8**).<sup>6</sup>

We have proposed a mechanism for this ligand assisted assemblage of the trinuclear metal cluster (Scheme 2).<sup>7</sup> As one of the first steps the formation of

(2) (a) Rae Victor; Ben-Shoshan, R.; Sarel, S. *Tetrahedron Lett.* **1970**, 49, 4253, 4257. (b) Rae Victor; Ben-Shoshan, R.; Sarel, S. *J. Chem. Soc., Chem. Commun.* **1970**, 1680. (c) Rae Victor; Ben-Shoshan, R.; Sarel, S. *J. Org. Chem.* **1972**, 37, 1930.

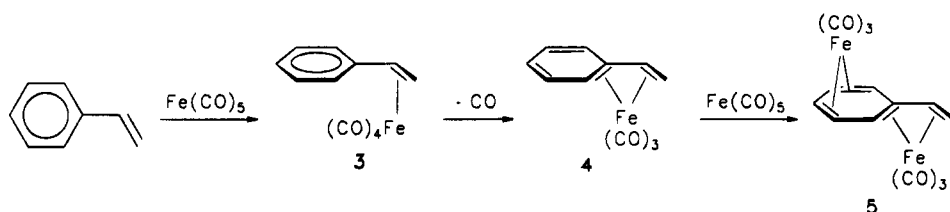
(3) Fleckner, H.; Grevels, F.-W.; Hess, D. *J. Am. Chem. Soc.* **1984**, 106, 2027.

(4) (a) Herrmann, W. A.; Weichmann, J.; Balbach, B.; Ziegler, M. L. *J. Organomet. Chem.* **1982**, 231, C69. (b) Adrianov, V. G.; Struchkov, Yu. T.; Babakhina, G. M.; Kritskaya, I. I.; Kravtsov, D. N. *Izv. Akad. Nauk SSSR, Ser. Khim.* **1985**, 590.

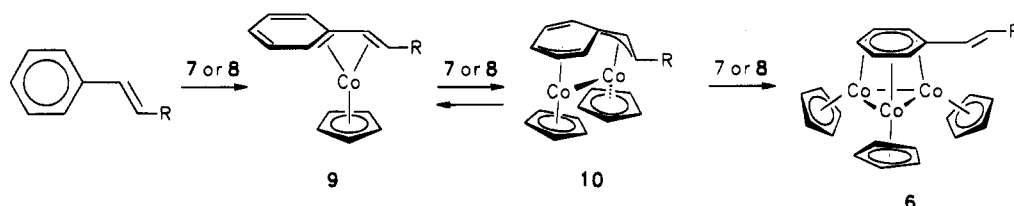
(5) Herbstein, F. H.; Reisner, M. G. *Acta Crystallogr.* **1977**, B33, 3304.

<sup>®</sup> Abstract published in *Advance ACS Abstracts*, July 1, 1995.  
(1) Elian, M.; Chen, M. M. L.; Mingos, D. M. P.; Hoffmann, R. *Inorg. Chem.* **1976**, 15, 1148.

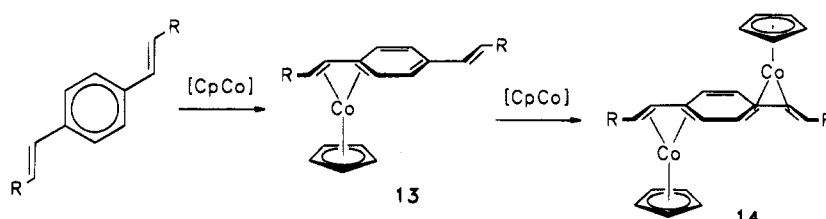
Scheme 1



Scheme 2



Scheme 3



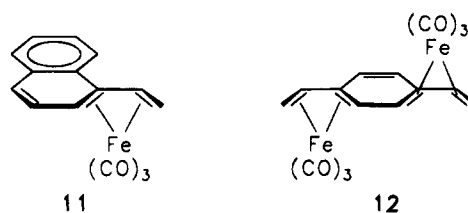
a mononuclear "diene" complex **9** with a  $\beta,\alpha,1,2-\eta^4$ -coordinated alkenylbenzene ligand was proposed. However, examples of such complexes with simple styrenes as ligands are conspicuously absent from the literature. We ourselves were unable to detect them during the one-pot syntheses of **6**. Likewise, in such cases where a  $\mu$ -arene cluster complex did not form with a particular substituted styrene ligand, neither **9** nor other mono- or dinuclear CpCo complexes were found.

From these results it seemed obvious that the mononuclear cobalt complexes **9** should be considerably less stable and more reactive than their iron analogs **4**. On the other hand, a few compounds have been reported with this type of coordination as a part of a more complicated oligonuclear structure, e.g.,  $[(\text{Cp}^*\text{Co})_3-(1,6,1',6'-\eta:2-5-\eta:2'-5'-\eta^4\text{-biphenyl})]^{18}$  and  $[(\text{CpCo})_2-(2,3,8,9-\eta:4-7-\eta-4,5,6,7-(\text{CF}_3)_4\text{-indene})]^{19}$ . Thus it did not seem impossible to stabilize more simple CpCo derivatives.

In this paper we present our studies of the ligand properties of alkenylnaphthalenes and distyrylbenzenes toward the CpCo moiety. These ligands were chosen because in each case a different kind of stabilization of the "diene" complex was anticipated:

(a) Compared to a monocyclic system, less resonance energy is lost when part of the extended  $\pi$ -system of a bicyclic arene coordinates to a metal. Furthermore, the more polyene-like nature of the condensed aromatic rings is expected to facilitate attack by a metal frag-

ment. This has been known to work in  $(\text{CO})_3\text{Fe}$  chemistry (complex **11**<sup>10</sup>). Some of our results have been mentioned in an earlier communication.<sup>7</sup>



(b) As an alternative, we hoped to trap **9** as a dinuclear complex, which, unlike the proposed intermediate **10**, would not easily proceed to the trinuclear **6**. Such a possibility exists with dialkenylbenzene ligands (Scheme 3). Addition of another CpCo fragment to the primary product **13** is expected to involve the free alkenyl group. Most of the resonance energy of the arene is lost in the first step, therefore formation of the dinuclear **14** from **13** should be more facile. In  $(\text{CO})_3\text{Fe}$  chemistry, introduction of a second vinyl group to styrene is already known to strongly enhance the tendency to form the bis( $\beta,\alpha,1,2-\eta^4$ ) complex **12**.<sup>11</sup> In addition, since the cobalt atoms are well separated from each other in **14**, this product was not expected to be on the reaction coordinate leading to a  $\mu_3$ -arene complex.

## Results

**Cyclopentadienylcobalt Complexes of Alkenyl-Substituted Naphthalenes. (a) Syntheses and Spectra.** When 1- or 2-vinylnaphthalene was gently heated with approximately equimolar amounts of  $[\text{CpCo}]$

(6) (a) Wadepohl, H.; Büchner, K.; Pritzkow, H. *Angew. Chem.* **1987**, *99*, 1294. (b) Wadepohl, H.; Büchner, K.; Herrmann, M.; Pritzkow, H. *Organometallics* **1991**, *10*, 861. (c) Wadepohl, H. *Angew. Chem.* **1992**, *104*, 253.

(7) Wadepohl, H.; Büchner, K.; Pritzkow, H. *Organometallics* **1989**, *8*, 2745.

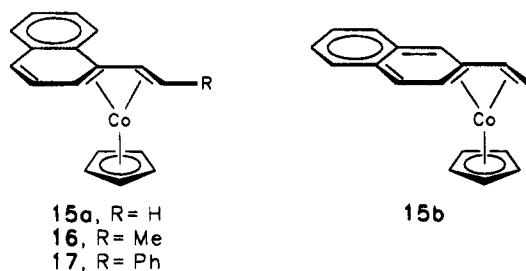
(8) Lehmkuhl, H.; Nehl, H.; Benn, R.; Mynott, R. *Angew. Chem.* **1986**, *98*, 628.

(9) Freeman, M. B.; Hall, L. W.; Sneddon, L. G. *Inorg. Chem.* **1980**, *19*, 1132.

(10) Manuel, T. A. *Inorg. Chem.* **1964**, *3*, 1794.

(11) (a) Manuel, T. A.; Stafford, S. L.; Stone, F. G. A. *J. Am. Chem. Soc.* **1961**, *83*, 3597. (b) Davis, R. E.; Pettit, R. *J. Am. Chem. Soc.* **1970**, *92*, 716.

(C<sub>2</sub>H<sub>4</sub>)<sub>2</sub>], **7**, greenish-brown solutions were obtained. The 1-vinylnaphthalene complex **15a** was obtained as dark



green crystals after cooling the reaction mixture. The 2-vinylnaphthalene complex **15b** crystallized much less readily and had to be separated from the by-products by column chromatography on deactivated alumina. [CpCo(1-propenylnaphthalene)] **16** was obtained in a similar manner. However, due to slow decomposition on the chromatography column, it proved to be impossible to completely separate **16** from traces of 1-(propen-1-yl)naphthalene.

In a mononuclear CpCo complex with 1-( $\beta$ -styryl)naphthalene as a ligand, the metal could be attached to the acyclic carbon-carbon double bond and part of either the naphthalenyl or the phenyl  $\pi$ -system. Only a single product, **17**, however, was formed from this ligand and **7**. Unfortunately, as in the case of **16**, slow decomposition during chromatography prevented the isolation of pure **17**, which was always contaminated with variable amounts of the free ligand.

The structures of the complexes **15**–**17** were established by NMR spectroscopic means and, in the case of **15a**, by single-crystal X-ray structure analysis. <sup>1</sup>H NMR spectroscopic data are given in Tables 1 and 2. The spectrum of **15a** was completely assigned by a series of <sup>1</sup>H–<sup>1</sup>H-decoupling experiments, those of **15b**–**17** by analogy. The metal coordination of the vinyl group reveals itself by a strong high-field shift of the two methylene proton resonances. These show a considerable chemical shift difference, H- $\beta_{endo}$  resonating at much higher field than H- $\beta_{exo}$ . The <sup>1</sup>H NMR spectra of **16** and **17** (Table 2) also present no difficulties. From the magnitude of the coupling constants <sup>3</sup>J(H- $\alpha$ –H- $\beta$ ) a *trans* configuration of the alkenyl double bonds can be assumed, as expected for steric reasons. In all cases, the proton on the metal coordinated carbon-carbon bond of the naphthalene ring (H-2 in **15a**, **16**, and **17**; H-1 in **15b**) resonates at high field. This is characteristic of an “outer” proton in a  $\eta^4$ -1,3-diene complex and indicates loss of aromatic character. The usual (high field) coordination shifts are also observed in the <sup>13</sup>C NMR spectra.

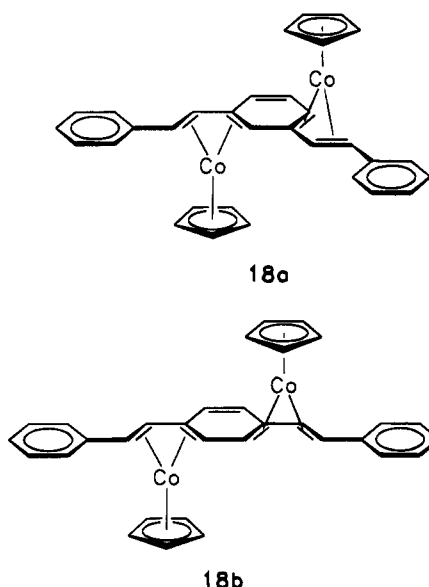
(b) **Crystal and Molecular Structure of [CpCo( $\beta,\alpha,1,2$ - $\eta$ -(1-vinylnaphthalene))], **15a**.** Single crystals of **15a** were obtained when the reaction mixture was slowly cooled to room temperature. Crystal details are given in the experimental section. The molecular structure of **15a** is shown in Figure 1. Positional and equivalent isotropic displacement parameters are given in Table 3; important bond lengths and angles are given in Table 4.

The crystal structure of **15a** consists of discrete molecules with no unusual intermolecular contacts. The vinyl group (C11, C12) and the carbon atoms C1 and C2 of the vinylnaphthalene ligand are bonded in a  $\eta^4$ -

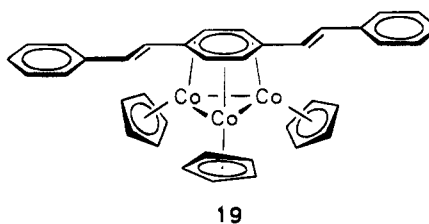
1,3-diene fashion to the cyclopentadienylcobalt fragment. Carbon-carbon bond lengths within the “diene” system are approximately equal. The substituents at the outer “diene” carbon atoms (C3, H2 and H12A, H12B) do not occupy positions in the plane defined by the “diene” system. The distortion is such that the *endo* substituents are moved away from and the *exo* substituents are moved toward the cobalt atom.

The cyclopentadienyl ring is approximately parallel to the “diene” plane, which is bent away from the naphthalene backbone (interplanar angle, 15.3(3)<sup>o</sup>). There is considerable bond localization in the metal-coordinated six-membered ring of the naphthalene bicycle as indicated by the short (double) bond C3–C4 (1.32(1) Å). The two fused six-membered rings of the vinylnaphthalene ligand are both essentially planar, with a dihedral angle of 4.2(3)<sup>o</sup> between the planes.

**Cyclopentadienylcobalt Complexes of *m*- and *p*-Distyrylbenzene.** Reaction of *m*-distyrylbenzene with excess (2–3 mol equiv) of **7** at 40 °C gave the red-brown dinuclear complex **18a** in about 65% yield. Complex **18a** is quite labile and decomposed on attempted chromatography.



The reaction of **7** with *p*-distyrylbenzene is much impeded by the very low solubility of this ligand in practically any solvent. When suspended in a solution of excess **7** in petroleum ether, the *p*-distyrylbenzene slowly dissolved and the color of the solution changed from orange to brown. From this mixture a 65% yield of the dinuclear **18b** was isolated by chromatography. During an attempt to recrystallize **18b** from toluene most of the complex decomposed predominantly to a new complex, **19**. The <sup>1</sup>H NMR spectrum of the mixture



indicated that **19** was a (CpCo)<sub>3</sub> cluster complex with a

**Table 1.**  $^1\text{H}$  NMR Spectral Data (200 MHz, in  $\text{C}_6\text{D}_6$ ) for the  $[\text{CpCo}(\eta^4\text{-Vinyl-naphthalene})]$  Complexes, **15a** and **15b**

	<b>15a</b>			<b>15b</b>		
	$\delta$	mult	$J(\text{HH})^a$ int	$\delta$	mult	$J(\text{HH})^a$ int
H-1				2.33	s	1
H- $\beta_{\text{endo}}$	-0.38	d	8.6	1	-0.41	dd 9.4/1.8
H-2	1.56	d	5.2	1		
H- $\beta_{\text{exo}}$	1.91	d	5.2	1	1.79	dd 6.6/1.8
Cp	4.16	s		5	4.12	s
H- $\alpha$	6.11	m		1	5.48	dd 9.2/6.7
H-3	6.78	m		1	6.92	d
H-4	6.93	m		1	7.42	d
arene-H	7.35-8.27	m		<i>b</i>	7.00-7.64	<i>m</i>

<sup>a</sup> In Hz. <sup>b</sup> Overlap with solvent signal.**Table 2.**  $^1\text{H}$  NMR Spectral Data (200 MHz, in  $\text{C}_6\text{D}_6$ ) for the  $[\text{CpCo}(\eta^4\text{-}(1\text{-CH=CHR})\text{naphthalene})]$  Complexes, **16** ( $\text{R} = \text{CH}_3$ ) and **17** ( $\text{R} = \text{Ph}$ )

	<b>16</b>			<b>17</b>		
	$\delta$	mult	$J(\text{HH})^a$ int	$\delta$	mult	$J(\text{HH})^a$ int
H- $\beta_{\text{endo}}$	0.3	m		1	1.09	d
H-2	1.47	"d"		1	1.85	d
Cp	4.10	s		5	3.93	s
H- $\alpha$	5.86	"d"		1	6.62	d
H-3	6.78	m		1	6.80	m
H-4	6.9	m		1	6.96	"d"
arene-H	7.1-8.3	m		<i>b</i>	7.14-7.20	<i>m</i>
					8.34	d
R	1.13	d	5.1	3	7.3-7.45	<i>m</i>

<sup>a</sup> In Hz. <sup>b</sup> Overlap with solvent signal.

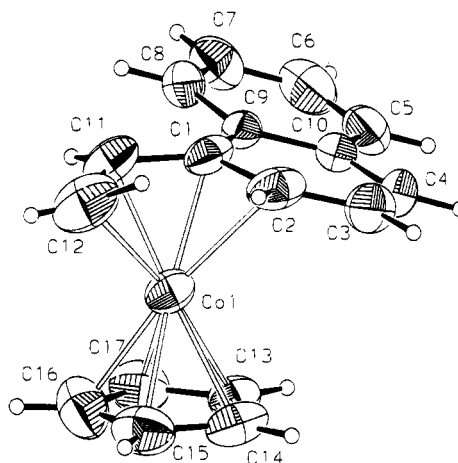
face-capping *p*-distyrylbenzene ligand. However, other decomposition products could not be completely removed from this sample.

The reaction was therefore repeated with  $[\text{CpCo}(\text{C}_6\text{-Me}_6)]$  **8** as a source of CpCo fragments. A mixture of **18b** and **19** was obtained, which could be separated by column chromatography into two fractions, consisting of pure **18b** (28% yield) and pure **19** (25% yield), respectively.

The structures **18a,b** are assigned to the dinuclear products on the basis of  $^1\text{H}$  (Table 5) and  $^{13}\text{C}$  NMR data. The coordination of two CpCo fragments to the ligand in each case is immediately evident from the integrals and, in the case of **18b**, from the high symmetry of the spectra. The spectra also show unambiguously that each CpCo group simultaneously bonds to an acyclic carbon-carbon double bond and to a part of the *central* arene ring of the ligands. As in **15-17**, the "outer" diene protons (H- $\beta,\beta'$  and H-2,4 in **18a**; H- $\beta,\beta'$  and H-2,3 in **18b**) are easily identified by their high field shifts (Table 5). The *trans* configuration of the C- $\alpha$ -C- $\beta$  bonds is revealed by the large coupling constants  $^3J(\text{H-}\alpha\text{-H-}\beta)$ . The  $^{13}\text{C}$  NMR resonances of the metal coordinated carbon atoms are also shifted to high field, again with  $\delta(\text{C}_{\text{outer}}) < \delta(\text{C}_{\text{inner}})$ .

The  $^1\text{H}$  NMR spectrum of **19** (Table 6) is typical of a  $(\text{CpCo})_3$  cluster bearing a face-capping arene ligand. Again, the symmetry of the spectra is only compatible with the cluster coordination of the central arene (phenylene) ring of the *p*-distyrylbenzene ligand. Chemical shifts ( $\delta(^1\text{H})$  and  $\delta(^{13}\text{C})$ , Table 7) and the coupling constant  $^3J(\text{H-}\alpha\text{-H-}\beta)$  exclude participation of the C- $\alpha$ -C- $\beta$  double bonds in the coordination to the metals. Once again, *trans* configuration of these bonds is implied by the magnitude of  $^3J(\text{H-}\alpha\text{-H-}\beta)$ .

When the solution is cooled, the Cp singlet resonance

**Figure 1.** Molecular structure of  $[\text{CpCo}(\beta,\alpha,1,2\text{-}(1\text{-vinyl})\text{naphthalene})]$ , **15a**, showing the crystallographic labeling scheme.**Table 3.** Atomic Coordinates ( $\text{\AA} \times 10^4$ ) and Equivalent Isotropic Displacement Parameters ( $\text{\AA}^2 \times 10^3$ ) for **15a**<sup>a</sup>

atom	x	y	z	$U_{\text{eq}}^a$
Co(1)	1928(1)	223(1)	786(1)	72(1)
C(1)	291(5)	1295(3)	1083(2)	71(1)
C(2)	-611(6)	388(4)	846(2)	91(2)
C(3)	-1457(7)	-445(5)	1135(3)	116(2)
C(4)	-1487(6)	-382(5)	1605(3)	118(2)
C(5)	-812(7)	680(6)	2356(3)	108(2)
C(6)	-135(7)	1616(7)	2586(2)	111(2)
C(7)	653(6)	2470(5)	2334(2)	97(2)
C(8)	795(5)	2383(4)	1848(2)	77(1)
C(9)	135(4)	1432(3)	1601(2)	65(1)
C(10)	-711(5)	563(4)	1859(2)	84(1)
C(11)	1449(7)	1916(4)	801(2)	90(2)
C(12)	1694(14)	1568(6)	319(2)	120(2)
C(13)	2597(5)	-1138(3)	1230(1)	84(1)
C(14)	2309(5)	-1546(3)	770(2)	98(2)
C(15)	3384(6)	-973(4)	464(1)	108(2)
C(16)	4336(5)	-212(4)	735(2)	111(2)
C(17)	3850(5)	-314(4)	1209(2)	99(2)

<sup>a</sup>  $U_{\text{eq}}$  is defined as one-third of the trace of the orthogonalized  $U_{ij}$  tensor.**Table 4.** Selected Bond Lengths ( $\text{\AA}$ ) and Angles (deg) for **15a** with Estimated Standard Deviations in Parentheses

Co(1)-C(1)	1.999(5)	Co(1)-C(2)	2.103(6)
Co(1)-C(11)	1.964(5)	Co(1)-C(12)	2.025(7)
Co(1)-C(13)··C(17)	2.025(4)··2.066(4)	C(1)-C(2)	1.436(6)
C(1)-C(9)	1.466(7)	C(1)-C(11)	1.426(7)
C(2)-C(3)	1.422(9)	C(3)-C(4)	1.324(10)
C(4)-C(10)	1.438(9)	C(5)-C(6)	1.361(9)
C(5)-C(10)	1.407(8)	C(6)-C(7)	1.363(8)
C(7)-C(8)	1.372(7)	C(8)-C(9)	1.395(6)
C(9)-C(10)	1.409(6)	C(11)-C(12)	1.427(9)
C(11)-C(1)-C(2)	116.3(5)	C(11)-C(1)-C(9)	123.8(4)
C(2)-C(1)-C(9)	119.4(5)	C(3)-C(2)-C(1)	117.7(5)
C(4)-C(3)-C(2)	122.8(6)	C(3)-C(4)-C(10)	121.7(6)
C(6)-C(5)-C(10)	121.5(6)	C(5)-C(6)-C(7)	120.2(6)
C(6)-C(7)-C(8)	120.3(6)	C(7)-C(8)-C(9)	121.2(5)
C(8)-C(9)-C(10)	118.7(5)	C(8)-C(9)-C(1)	122.8(4)
C(10)-C(9)-C(1)	118.5(4)	C(9)-C(10)-C(5)	118.1(5)
C(9)-C(10)-C(4)	119.3(6)	C(5)-C(10)-C(4)	122.6(6)
C(12)-C(11)-C(1)	119.2(7)		

in the  $^1\text{H}$  and  $^{13}\text{C}$  NMR spectra broadens and then splits into two components of unequal intensity (Figure 2). Likewise, two  $^{13}\text{C}$  resonances are observed at 210 K for the four CH carbons of the  $\mu_3$ -phenylene ring (Table 7). Unfortunately, the  $^1\text{H}$  NMR resonances of the  $\mu_3$ -

**Table 5.**  $^1\text{H}$  NMR Spectral Data (200 MHz, in  $\text{C}_6\text{D}_6$ ) for the  $[(\text{CpCo})_2(\eta^4\text{-distyrylbenzene})]$  Complexes, **18a** and **18b**.

18a				18b				
$\delta$	mult	$J(\text{HH})^a$	int	$\delta$	mult	$J(\text{HH})^a$	int	
H- $\alpha$	5.66	d	8.8	1	5.60	d	9.0	2
H- $\alpha'$	5.89	d	8.8	1				
H- $\beta$	1.01	d	8.8	1	0.95	d	8.8	2
H- $\beta'$	1.34	d	8.9	1				
H-2	2.58	s		1	1.92	s		<i>b</i>
H-3					1.92	s		<i>b</i>
H-4	1.38	d	5.4	1				
H-5	6.35	dd	9.0/5.4	1	6.86	s		<i>b</i>
H-6	6.89	d	9.2	1	6.86	s		<i>b</i>
Cp	4.16,	s		5	4.13	s		10
	4.22	s		5				
Ph	7.07–7.42	m		c	7.05–7.39	m		<i>c</i>

<sup>a</sup> In Hz. <sup>b</sup> Only one signal of intensity 2 for the two isochronous protons. <sup>c</sup> Overlap with solvent signal.

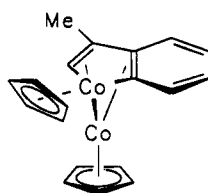
**Table 6.**  $^1\text{H}$  NMR Spectral Data (200 MHz, in  $\text{CD}_2\text{Cl}_2$ ) for the  $[(\text{CpCo})_3(\mu_3\text{-}\eta^2\text{-}\eta^2\text{-}p\text{-distyrylbenzene})]$  Complex, **19**

	293 K				230 K			
	$\delta$	mult	$J(\text{HH})^a$	int	$\delta$	mult	$J(\text{HH})^a$	int
$\mu$ -arene	4.87	s		4	4.79			<i>b</i>
Cp	4.92	s		15	4.79	"s"		<i>b</i>
					5.07	s		5
alkene	6.54	<i>c</i>	16.1	2	6.45	<i>c</i>	16.1	2
	6.72	<i>c</i>	16.1	2	6.70	<i>c</i>	16.1	2
Ph	7.28	m		10	7.26	m		10

<sup>a</sup> In Hz. <sup>b</sup> Overlapping peaks, total intensity 14. <sup>c</sup> AB system.

phenylene ring overlap with one of the two Cp resonances at low temperature. Other areas of the spectra are essentially independent of temperature.

**Reaction of  $\alpha$ -Methylstyrene with  $\text{Cp}_2\text{Co}/\text{Potassium}$ .** When an excess of  $\alpha$ -methylstyrene is treated with **7**, the cluster complex  $[(\text{CpCo})_3(\mu_3\text{-}\eta^2\text{-}\eta^2\text{-}\alpha\text{-methylstyrene})]$  is formed in good yield.<sup>7</sup> However, when CpCo fragments were generated *via* reductive degradation of cobaltocene with potassium<sup>12</sup> in the presence of  $\alpha$ -methylstyrene, mainly organic decomposition products were obtained. After careful chromatography of the reaction mixture, a minor organometallic product was isolated in very low yield. Structure **20** was assigned to this product on the basis of spectroscopic data and a single-crystal X-ray diffraction study (*vide infra*).

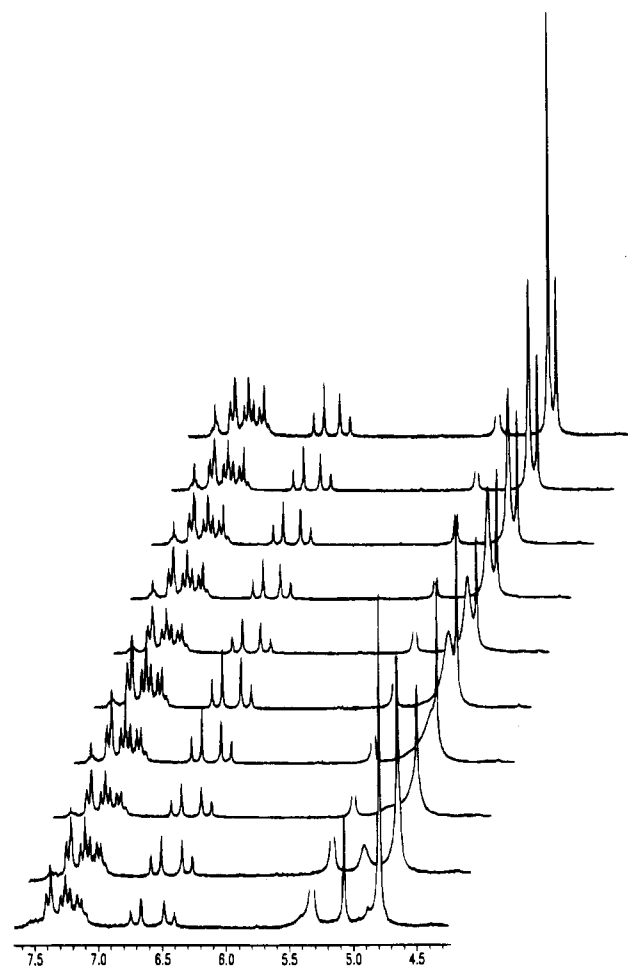
**20**

In the  $^1\text{H}$  and  $^{13}\text{C}$  NMR spectra there are two distinct resonances for the two chemically inequivalent CpCo groups. Unfortunately, not all of the resonances required for the benzocobaltole bicycle (five CH and three C) were detected in the carbon spectrum. This could be due to effects of the quadrupolar  $^{59}\text{Co}$  nucleus of the endocyclic CpCo group on the two carbon atoms (one C and one CH) which are  $\sigma$ -bonded to it. Similar observa-

**Table 7.**  $^{13}\text{C}\{^1\text{H}\}$  NMR Spectral Data (50.3 MHz, in  $\text{CD}_2\text{Cl}_2$ ) for the  $[(\text{CpCo})_3(\mu_3\text{-}\eta^2\text{-}\eta^2\text{-}p\text{-distyrylbenzene})]$  Complex, **19**.

	293 K		210 K	
	$\delta$	mult <sup>a</sup>	$\delta$	mult <sup>a</sup>
$\mu$ -arene	40.8	CH	40.8	CH
			44.0	CH
	56.1	C	58.5	C
Cp	83.5	CH	82.6	CH
			82.8	CH
C- $\beta$	121.0	CH	119.5	CH
Ph	125.7	CH	124.8	CH
	126.2	CH	125.9	CH
	129.1	CH	128.5	CH
	138.9	C	137.7	C
C- $\alpha$	138.9	CH	137.0	CH

<sup>a</sup> Determined by DEPT spectra.

**Figure 2.** Temperature dependent 200 MHz  $^1\text{H}$  NMR spectra of complex **19**. Temperatures are at (top to bottom) 297, 280, 275, 270, 265, 260, 255, 250, 240, and 220 K. The signal at  $\delta$  5.3 is due to solvent protons.

tions were made in complexes containing a cobaltapentalene bicyclic ring system.<sup>13</sup>

**Crystal and Molecular Structure of Cobalt Dimer **20**.** Deep green single crystals of **20** were obtained from *n*-hexane at  $-78$  °C. Crystal details are given in the Experimental Section. The molecular structure of **20** is shown in Figure 3. Positional and equivalent isotropic displacement parameters are given in Table 8;

(12) Jonas, K., Krüger, C. *Angew. Chem.* **1980**, *92*, 513.

(13) Wade, H.; Galm, W.; Pritzkow, H.; Wolf, A. *Angew. Chem.* **1992**, *104*, 1050.



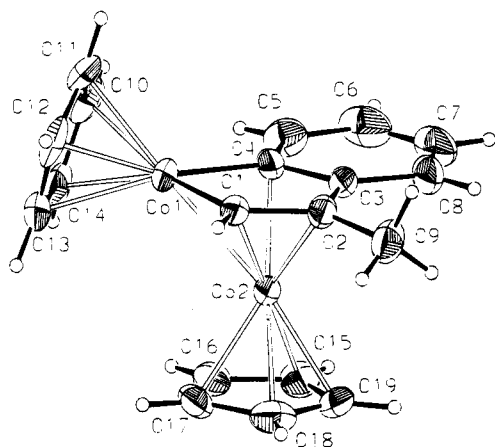


**Figure 3.** Molecular structure of [CpCo(1-3,8,9- $\eta$ -(1-Cp-3-Me-1-cobaltindenyl))], **20**, showing the crystallographic labeling scheme.

**Table 8. Atomic Coordinates ( $\text{\AA} \times 10^4$ ) and Equivalent Isotropic Displacement Parameters ( $\text{\AA}^2 \times 10^3$ ) for **20**<sup>a</sup>**

atom	x	y	z	$U_{\text{eq}}$
Co(1)	299(1)	2157(1)	7742(1)	45(1)
Co(2)	978(1)	2354(1)	9933(1)	41(1)
C(1)	292(5)	1520(5)	9329(9)	43(2)
C(2)	95(5)	1796(5)	10684(9)	47(2)
C(3)	-86(5)	2562(5)	10576(9)	50(2)
C(4)	20(5)	2861(5)	9165(9)	50(2)
C(5)	-118(5)	3629(5)	8980(13)	68(3)
C(6)	-369(6)	4048(6)	10084(19)	94(4)
C(7)	-456(6)	3742(8)	11471(16)	92(4)
C(8)	-315(5)	3022(6)	11766(12)	68(3)
C(9)	88(5)	1386(5)	12080(9)	70(3)
C(10)	-7(8)	2682(8)	5854(10)	81(3)
C(11)	-325(6)	1990(7)	5966(10)	76(3)
C(12)	240(8)	1456(6)	6008(9)	76(3)
C(13)	909(7)	1831(8)	5931(10)	81(3)
C(14)	765(7)	2572(8)	5847(10)	81(4)
C(15)	1723(5)	3131(6)	10600(12)	67(3)
C(16)	1923(5)	2848(6)	9252(11)	63(3)
C(17)	2030(5)	2088(6)	9393(11)	63(3)
C(18)	1908(5)	1892(7)	10833(13)	76(3)
C(19)	1712(5)	2548(6)	11555(11)	70(3)

<sup>a</sup>  $U_{\text{eq}}$  is defined as one-third of the trace of the orthogonalized  $U_{ij}$  tensor.

**Table 9. Selected Bond Lengths ( $\text{\AA}$ ) and Angles (deg) for **20a** with Estimated Standard Deviations in Parentheses**

Co(1)-C(1)	1.875(9)	Co(1)-C(4)	1.908(8)
Co(1)-C(10)···C(14)	2.027(9)···2.102(10)	Co(1)-Co(2)	2.410(2)
Co(2)-C(1)	2.040(9)	Co(2)-C(2)	2.020(8)
Co(2)-C(3)	2.056(8)	Co(2)-C(4)	2.094(9)
Co(2)-C(15)···C(19)	2.032(9)···2.062(10)	C(1)-C(2)	1.402(10)
C(2)-C(3)	1.432(12)	C(2)-C(9)	1.498(12)
C(3)-C(4)	1.433(12)	C(3)-C(8)	1.448(12)
C(4)-C(5)	1.427(12)	C(5)-C(6)	1.36(2)
C(6)-C(7)	1.41(2)	C(7)-C(8)	1.36(2)
C(1)-Co(1)-C(4)	82.2(4)	C(2)-C(1)-Co(1)	119.4(6)
C(1)-C(2)-C(3)	110.0(8)	C(1)-C(2)-C(9)	127.2(8)
C(3)-C(2)-C(9)	122.8(8)	C(2)-C(3)-C(4)	113.6(8)
C(2)-C(3)-C(8)	124.9(9)	C(4)-C(3)-C(8)	121.4(9)
C(5)-C(4)-C(3)	117.2(9)	C(5)-C(4)-Co(1)	128.1(8)
C(3)-C(4)-Co(1)	114.7(7)	C(6)-C(5)-C(4)	121.0(11)
C(5)-C(6)-C(7)	120.6(11)	C(8)-C(7)-C(6)	122.7(11)
C(7)-C(8)-C(3)	117.0(11)		

important bond lengths and angles are given in Table 9.

The crystal structure of **20** consists of discrete molecules with no unusual intermolecular contacts. Com-

plex **20** is best described as a cyclopentadienylcobalt complex of a  $\eta^5$ -benzocobaltole (or cobaltindenyl) ligand. The individual cobaltole and benzo rings are essentially planar (root mean square deviation from the best planes, 0.018 and 0.015  $\text{\AA}$ , respectively). The complete benzocobaltole is only slightly ( $1.9(3)^\circ$ ) folded along C3-C4. The noncoordinated part of the six-membered ring can be thought of as a diene unit (C5 to C8) with two short and one longer carbon-carbon bonds joined to the rest of the molecule by two longer (mean 1.44  $\text{\AA}$ ) such bonds. Within the cobaltole ring carbon-carbon bonds are of approximately equal length. The planes of the cobaltole and Cp rings are at angles of  $3.3(3)^\circ$  [Cp(Co2)] and  $77.1(3)^\circ$  [Cp(Co1)], respectively.

**Reaction of Alkenylnaphthalene Complexes **15a** and **17** with **7**.** The 1-vinyl- and 1-styrylnaphthalene complexes **15a** and **17** were treated with 1 additional equiv of **7** for several hours at room temperature.  $^1\text{H}$  NMR inspection of the mixtures indicated that no reaction had taken place. The mixtures were then heated to 45-60  $^\circ\text{C}$  for another 2-6 h. After workup, some of the starting **15a** and **17** was recovered, along with the ethylidyne hydrido cluster complex [H(CpCo)<sub>4</sub>(CMe)], the thermal decomposition product of **7**.<sup>14</sup>

## Discussion

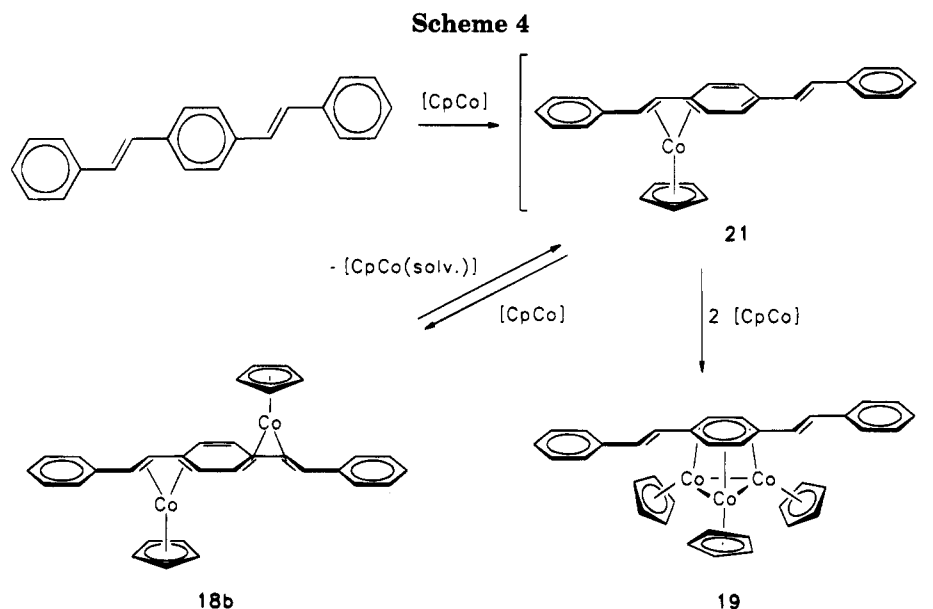
**CpCo( $\beta,\alpha,1,2-\eta$ -Alkenylnaphthalene) Complexes **15-17**.** The reactivity of CpCo with the alkenylnaphthalenes very nicely parallels that of the (CO)<sub>3</sub>Fe moiety. However, the CpCo complexes **15-17** appear to be less stable than their (CO)<sub>3</sub>Fe analogs. Unfortunately, no di- or trinuclear alkenylnaphthalene complexes could be prepared from the mononuclear products.

The molecular structure of [(CO)<sub>3</sub>Fe( $\beta,\alpha,1,2$ -(1-vinyl)naphthalene)] has been reported in the literature.<sup>11b</sup> In this complex, the carbon-carbon bond lengths within the vinylnaphthalene ligand are essentially identical to the corresponding distances in **15a**. Disruption of cyclic conjugation within the metal-coordinated six-membered ring is indicated by a pronounced alternation of carbon-carbon bond lengths. The distance C3-C4 (1.32(1)  $\text{\AA}$  in **15a**) is typical of a double bond. The other ring of the naphthalene, which is not directly coordinated to the metal, retains its aromaticity.

Extensive delocalization within the metal-coordinated diene substructure is indicated by the same length of the two "outer" and the one "inner" carbon-carbon bonds (C1-C2, C11-C12, and C1-C11 in **15a**). This is indicative of a bonding interaction with the metal of similar strength in both the iron and the cobalt complex. The range of cobalt-carbon distances (Table 4) indicates some asymmetry in the metal-to-diene bonding. A similar pattern was found in the (CO)<sub>3</sub>Fe complexes of  $\alpha$ -methylstyrene and 1,1-diphenylpropene.<sup>4</sup>

The substantial folding along C1-C2 of the vinylnaphthalene ligand is related to the out-of-plane distortion concerning the substituents at the outer diene carbon atoms. Such a distortion is commonly found in complexes of acyclic  $\eta^4$ -1,3-dienes. It was attributed to

(14) (a) Gambarotta, S.; Floriani, C.; Chiesi-Villa, A.; Guastini, C. *J. Organomet. Chem.* **1985**, 296, C6. (b) Wadepohl, H.; Pritzkow, H. *Polyhedron* **1989**, 8, 1939.



the steric interaction of the two *endo* substituents.<sup>15</sup> Naturally, these are not present in the cobaltindenyl ring system of **20**, and consequently the latter ligand is essentially flat.

During the reaction with  $\alpha$ -styrylnaphthalene, the CpCo fragment has a choice between getting attached to the acyclic double bond and part of the phenyl or naphthalenyl  $\pi$ -system. Only coordination of the condensed arene was found. This is in accord with our expectations, on the basis of the more localized  $\pi$ -system of the naphthalenyl residue.

**Dinuclear (18a,b) and Trinuclear (19) CpCo Complexes of *m*- and *p*-Distyrylbenzene.** The distyrylbenzenes were chosen as ligands because they offered a unique comparison of the reactivity of mono- and disubstituted benzene rings, which are both present in the molecule. Thus attack of CpCo could be envisaged involving either the terminal phenyl or the internal phenylene rings.

To some extent, the reactivity of the distyrylbenzenes with CpCo parallels that of divinylbenzene with  $(\text{CO})_3\text{Fe}$ .<sup>11</sup> In both cases dinuclear complexes are obtained. However, the observed formation of the  $\mu_3$ -arene cluster complex **19** is without precedence in iron carbonyl chemistry. It can be seen as a reflection of the better metal-metal-bonding capabilities<sup>1</sup> of the CpCo fragment.

Although, to our knowledge, mononuclear complexes of  $(\text{CO})_3\text{Fe}$  and CpCo with dialkenylbenzenes have not yet been isolated, such species are very likely formed initially. Addition of one metal fragment dramatically activates the ligand, and reaction with the second metal fragment is much faster. Therefore, the stationary concentration of a mononuclear intermediate like **21** is expected to be very low.

In the present case, dissimilar results are obtained with different sources of CpCo. When **7** is used in the reaction, **21** is trapped as the dinuclear complex **18**. With **8** and *p*-distyrylbenzene a mixture of **18a** and the  $\mu_3$ -arene cluster complex **19** is obtained. Without detailed knowledge of the mechanism of ligand exchange

reactions of **7** and **8**<sup>16</sup> we can only speculate about the different courses of reaction with *p*-distyrylbenzene (Scheme 4). A reasonable explanation of the experiments would be that the less reactive **7** picks coordination to the uncomplexed side chain in **21**, thereby selectively forming **18**. The more reactive **8** does not discriminate as well. Hence, along with **18a** the arene cluster complex **19** is formed, most probably *via* an intermediate analogous to **10**. It is interesting to note here that with stilbene (1,2-diphenylethene) as a ligand, only the cluster complex  $[(\text{CpCo})_3(\mu_3\text{-}\eta^2\text{:}\eta^2\text{:}\eta^2\text{-stilbene})]$  is formed in very good yield.<sup>6b</sup>

The formation of **19** when **18b** is allowed to stand in solution can be explained by dissociation of CpCo fragments from the latter. It has been suggested that these fragments are stabilized by binding to the arene ring of an aromatic solvent.<sup>17</sup> The very low solubility of the *p*-distyrylbenzene ligand, which precipitates out of the solution, could be the driving force for the stepwise dissociation of **18b**. Intermediate **21** will be reformed and can then be attacked by solvated CpCo fragments to eventually give the apparently more stable  $\mu_3$ -arene cluster complex **19**.

The dinuclear *m*-distyrylbenzene complex **18a** does not transform into a  $\mu_3$ -*m*-distyrylbenzene cluster complex on standing. This could be due to the much better solubility of the *m*-distyrylbenzene, and consequently the lesser tendency of **18a** to dissociate, in accord with the above arguments.

The complexes **18** have all the spectroscopic properties expected for  $\eta^4$ -1,3-diene complexes. In principle, **18a,b** could exist as two isomers, with the two CpCo groups in a *syn* or an *anti* arrangement with respect to the bridging phenylene ring. However, only one isomer was observed in both cases (**18a** and **18b**). For steric reasons we believe the CpCo groups to prefer the *anti* arrangement, in accord with the crystallographically established structure of  $[(\text{CO})_3\text{Fe}]_2(p\text{-divinylbenzene})$ .<sup>11b</sup>

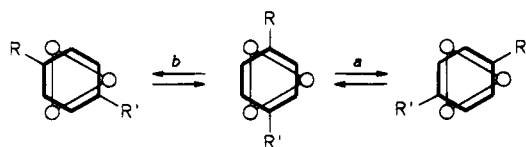
The temperature dependence of the NMR spectra of **19** can be explained by a hindered rotation of the  $\mu_3$ -

(15) Adams, C.; Cerioni, G.; Hafner, A.; Kalchauer, H.; v. Philipsborn, W.; Prew, R.; Schwenk, A. *Helv. Chim. Acta* **1988**, *71*, 1116.

(16) In both cases, dissociative and associative mechanisms are feasible.

(17) Barnes, C. E.; Orvis, J. A. *Organometallics* **1993**, *12*, 1016.

Scheme 5



arene ligand on top of the  $(\text{CpCo})_3$  cluster.<sup>18</sup> This dynamic process is typical for  $\mu_3$ -face-capping arene ligands.<sup>6,19</sup> At high temperature, rotation is fast on the NMR time scale, and hence an averaged resonance is observed in the  $^1\text{H}$  and  $^{13}\text{C}$  NMR spectra for the three CpCo groups. The four CH groups of the bridging phenylene ring are also averaged. When the temperature is lowered, a static  $\mu_3\text{-}\eta^2\text{:}\eta^2\text{:}\eta^2$  coordination of the ligand is attained. Disregarding rotations around single bonds and the rotational reorientation of the Cp rings around their binding axes (both of which should be very facile), the molecular symmetry corresponds to the (idealized) point group  $C_s$ . This is nicely reflected in the low-temperature spectra of **19** (Tables 6 and 7).

We have been able to prove that rotation of a  $\text{Co}_3$  face-capping monosubstituted arene proceeds in a series of  $60^\circ$  turns or 1,2-shifts of the metals around the  $\text{C}_6$  ring.<sup>6,19</sup> In the general case ( $R \neq R'$ , Scheme 5) the two possible  $60^\circ$  turns (clockwise, *a*, or counterclockwise, *b*) result in a complicated exchange pathway, e.g., for the Cp resonances. Because of the higher symmetry of **19** ( $R = R'$ ), *a* and *b* are degenerate, and we are, in effect dealing with a more simple two-site exchange process. The energy barrier can be estimated from the coalescence of the Cp resonances in the  $^1\text{H}$  NMR spectrum; with the formula valid for exchange of unequally populated singlets<sup>20</sup> and  $T_c = 250$  K, we obtain  $\Delta G^\ddagger(250 \text{ K}) = 50 \text{ kJ mol}^{-1}$ .

**$\pi$ -Complexation versus CH Activation of Alkenylbenzenes.** Under certain conditions, activation of CH bonds is a general reactivity pattern of the  $(\text{C}_5\text{R}_5)\text{Co}$  fragments.<sup>21,22</sup> For example, when treated with **7** or  $\text{Cp}_2\text{Co/K}$ , cycloolefins are dehydrogenated and incorporated as bridging cycloalkyne ligands into tri- and tetranuclear cluster complexes.<sup>23</sup> With vinylbenzenes, this kind of reactivity can be comparable to or even more facile than  $\pi$ -complexation of the arene and formation of a  $\mu$ -arene cluster complex.<sup>24</sup> In such cases, only the products of vicinal 1,2-dehydrogenation of the vinyl group, trinuclear  $\mu_3$ -alkyne cluster complexes, were found. The alternative geminal 1,1-dehydrogenation, possibly leading to a cluster bound vinylidene, has never yet been observed,<sup>22</sup> although in  $\text{Ru}_3$  and  $\text{Os}_3$  cluster chemistry such species are of comparable stability to the  $\mu$ -alkyne complexes.<sup>25</sup>

(18) Or vice versa, which amounts to the same.

(19) Wadepohl, H. In *The Synergy Between Dynamics and Reactivity at Clusters and Surfaces*; Farrugia, L. J., Ed.; NATO ASI Series, Kluwer: Dordrecht, The Netherlands, 1995; Vol. 465, pp 175–191.

(20) A  $60^\circ$  rotation (*a* or *b* in Scheme 5) does not suffice to equilibrate the Cp resonances. The rate constant  $k'$  calculated with the two-site exchange formula (Shanan-Atidi, H.; Bar-Eli, K. H. *J. Phys. Chem.* **1970**, *74*, 961) was therefore corrected to give the actual  $k$  for processes *a* and *b*. Because of the dependence of  $\Delta G^\ddagger$  on  $\ln(k)$  the influence on the former is small compared to the errors inherent in the coalescence method.

(21) Wadepohl, H. *Comments Inorg. Chem.* **1994**, *15*, 369.

(22) Wadepohl, H.; Gebert, S. *Coord. Chem. Rev.*, in press.

(23) Wadepohl, H.; Borchert, T.; Pritzkow, H. *J. Chem. Soc., Chem. Commun.*, in press.

(24) Wadepohl, H.; Borchert, T.; Büchner, K.; Pritzkow, H. *Chem. Ber.* **1993**, *126*, 1615.

$\alpha$ -Methylstyrene does not have vicinal olefinic hydrogens, therefore an alkyne complex cannot be formed. With **7** the only isolable product is the  $\mu_3$ -arene cluster complex  $[(\text{CpCo})_3(\mu_3\text{-}\eta^2\text{:}\eta^2\text{:}\eta^2\text{-}\alpha\text{-methylstyrene})]$ , which is formed in good yield.<sup>6</sup> This product is not obtained upon reaction of  $\alpha$ -methylstyrene with  $\text{Cp}_2\text{Co/K}$ , nor is a  $\mu$ -vinylidene cluster complex. Most of the ligand decomposes to intractable purely organic products. However, CH activation does take place to some extent, as shown by the formation of **20**. This time a vinylic CH bond and an aromatic CH bond are cleaved, and a benzocobaltole metallacycle is formed, which is further stabilized by the uptake of a second CpCo group, to give the final product **20**.

Complex **20** is similar to other systems with cobaltole ligands.<sup>26</sup> A  $\text{Cp}^*\text{Ir}$  complex of an iridiindenyl system was characterized by X-ray crystallography.<sup>27</sup> It shows a similar pattern of short and long carbon–carbon bonds in the metallacycle. The geometry of these complexes points to a considerable diminution of cyclic conjugation within the benzo rings.

## Conclusions

We have shown in the present work that the  $\eta^4$ -coordination mode of an alkenylarene to a CpCo fragment can indeed be stabilized. The coordination geometry of the “diene” unit in the  $\beta,\alpha,1,2\text{-}\eta\text{-}1$ -vinyl-naphthalene complexes of CpCo and  $(\text{CO})_3\text{Fe}$  is very similar. However, the mononuclear and dinuclear CpCo complexes are more labile than their  $(\text{CO})_3\text{Fe}$  analogs. Formation of trinuclear cluster complexes with the benzene nucleus of the alkenylarene in the  $\mu_3$ -face capping coordination mode is unique to CpCo; this is well accounted for by the electronic properties of the latter fragment.

## Experimental Section

**General Procedures.** All operations were carried out under an atmosphere of purified nitrogen or argon (BASF R3-11 catalyst) using Schlenk techniques. Solvents were dried by conventional methods. Petroleum ether refers to the fraction with bp.  $40\text{--}60^\circ\text{C}$ . The compounds  $[\text{CpCo}(\text{C}_2\text{H}_4)_2]$ , **7**,<sup>28</sup>  $[\text{CpCo}(\text{C}_6\text{Me}_6)]$ , **8**,<sup>28</sup> 1-vinylnaphthalene,<sup>29</sup> 1-propenylnaphthalene,<sup>30</sup> 1-styrylnaphthalene,<sup>31</sup> *m*-distyrylbenzene,<sup>32</sup> and *p*-distyrylbenzene<sup>33</sup> were prepared as described in the literature. Alumina used as a stationary phase for column chromatography was first heated for several days under vacuum and then treated with 5 mass % of water and stored under nitrogen. NMR spectra were obtained on Bruker AC 200 (200.1 MHz for  $^1\text{H}$ , 50.3 MHz for  $^{13}\text{C}$ ) and AC 300 (75.46 MHz for  $^{13}\text{C}$ ) instruments.  $^1\text{H}$  and  $^{13}\text{C}$  chemical shifts are reported vs  $\text{SiMe}_4$  and were determined by reference to internal  $\text{SiMe}_4$  or residual solvent peaks. The multiplicities of the  $^{13}\text{C}$  resonances were

(25) Lewis, J.; Johnson, B. F. G. *Pure Appl. Chem.* **1975**, *44*, 43. Deeming, A. J. *Adv. Organomet. Chem.* **1986**, *26*, 1.

(26) (a) Binger, P.; Martin, T. R.; Benn, R.; Rufinska, A.; Schroth, G. *Z. Naturforsch.* **1984**, *39b*, 993. (b) Sünkel, K. *J. Organomet. Chem.* **1990**, *391*, 247.

(27) McGhee, W. D.; Bergman, R. G. *J. Am. Chem. Soc.* **1988**, *110*, 4246.

(28) Jonas, K.; Deffense, E.; Habermann, D. *Angew. Chem.* **1983**, *95*, 729; *Angew. Chem. Suppl.* **1983**, 1005.

(29) Hashimoto, H.; Hida, M.; Miyano, S. *J. Organomet. Chem.* **1967**, *10*, 518.

(30) Kon, A. R.; Spickett, R. G. W. *J. Chem. Soc.* **1949**, 2725.

(31) Drefahl, G.; Lorenz, D.; Schnitt, G. *J. Prakt. Chem.* **1964**, *23*, 143.

(32) Blout, E. R.; Eager, V. W. *J. Am. Chem. Soc.* **1945**, *67*, 1315.

(33) Kauffmann, H. *Ber. Dtsch. Chem. Ges.* **1917**, *50*, 515.

determined using the DEPT or the *J*-modulated spin echo (JMOD) techniques; multiplicities determined by the latter method are indicated as odd (u) or even (g). Mass spectra were measured in the electron impact ionization mode (EI) at 70 eV or using chemical ionization (negative ions,  $\text{Cl}^-$ , or positive ions,  $\text{Cl}^+$ ) on Finnegan MAT 8230 and 4600 spectrometers. Elemental analyses were performed by Mikroanalytisches Labor Beller, Göttingen, Germany.

**Syntheses. [CpCo( $\beta,\alpha,1,2-\eta$ -(1-vinyl)naphthalene)], 15a.** A solution of 1.26 g (7.0 mmol) of **7** and 0.40 g (2.6 mmol) of 1-vinylnaphthalene in 60 mL of petroleum ether was stirred at room temperature. After 3 h, a dark grey precipitate was removed by filtration. Another 0.40 g sample of 1-vinylnaphthalene was added, and the mixture was refluxed for 5 h. When the reaction mixture was slowly cooled to  $-20^\circ\text{C}$ , dark green crystals precipitated, which were washed two times with cold petroleum ether to afford pure **15a** (0.45 g, 31%). The crystals became waxy within a few hours at room temperature.  $^{13}\text{C}\{^1\text{H}\}$  NMR (toluene- $d_6$ )  $\delta$  29.9 (C- $\beta$ ), 49.8 (C-2), 66.8 (C- $\alpha$ ), 80.6 (Cp), 90.7 (C-1), 122.5 (CH), 123.5 (CH), 126.4 (CH), 127.1 (CH), 127.6 (CH), 137.7 (CH); due to slow decomposition of the sample the signals due to some of the quaternary carbons were not observed. MS (EI) *m/e* (relative intensity) 278 ( $\text{M}^+$ , 100), 276 ( $[\text{M} - 2\text{H}]^+$ , 22), 211 (10), 189 ( $[\text{Cp}_2\text{Co}]^+$ , 10), 156 (6), 154 ( $\text{L}^+$ , 19), 153 ( $[\text{L} - \text{H}]^+$ , 30), 139 (6), 124 ( $[\text{CpCo}]^+$ , 65), 59 ( $\text{Co}^+$ , 13); L = vinylnaphthalene.

**[CpCo( $\beta,\alpha,2,1-\eta$ -(2-vinyl)naphthalene)], 15b.** A solution of 0.93 g (5.2 mmol) of **7** and 0.80 g (5.2 mmol) of 2-vinylnaphthalene in 60 mL of petroleum ether was stirred for 5 h at room temperature. The solution was then heated to gentle reflux for another 5 h. Removal of solvent under reduced pressure led to a brown oily residue, which was redissolved in a minimal amount of petroleum ether and chromatographed on alumina using the same solvent as a mobile phase. Solvent was removed under reduced pressure from the greenish-brown first fraction to give a brown solid. Recrystallization from petroleum ether afforded pure **15b** (0.55 g, 38%).  $^{13}\text{C}\{^1\text{H}\}$  NMR (JMOD,  $\text{C}_6\text{D}_6$ )  $\delta$  29.2 (u, C- $\beta$ ), 51.0 (g, C-1), 71.8 (g, C- $\alpha$ ), 80.8 (g, Cp), 91.8 (u, C-2), 114.0 (u, C), 123.4 (g, CH), 124.5 (g, CH), 126.1 (g, CH), 126.4 (g, CH), 127.6 (g, CH), 129.8 (g, CH), 144.4 (u, C). MS ( $\text{Cl}^-$ ) *m/e* (relative intensity) 278 ( $\text{M}^+$ , 100), 204 (9), 170 (9), 169 (57), 156 (16), 127 (31). Anal. Calcd (found): C, 73.39 (73.76); H, 5.43 (5.93).

**[CpCo( $\beta,\alpha,1,2-\eta$ -(1-propenyl)naphthalene)], 16.** A mixture of 0.93 g (5.17 mmol) of **7** and 0.84 g (5.17 mmol) of 1-(propen-1-yl)naphthalene in 50 mL of petroleum ether was stirred for 3 h at room temperature and then for 1 h at  $45^\circ\text{C}$ . The green-black solution was filtered, and the filtrate was chromatographed on alumina. With petroleum ether as a mobile phase a green fraction was obtained to give crude **16** after removal of solvent. Recrystallization from petroleum ether at  $-25^\circ\text{C}$  resulted in partial decomposition.

**[CpCo( $\beta,\alpha,1,2-\eta$ -(1-styryl)naphthalene)], 17.** A mixture of 0.88 g (4.89 mmol) of **7** and 1.04 g (4.52 mmol) of 1-( $\beta$ -styryl)naphthalene in 100 mL of petroleum ether was stirred for 15 h at room temperature and then for 3 h at  $45^\circ\text{C}$ . An intractable black solid was removed from the dark green solution by filtration. The filtrate was concentrated under reduced pressure. When the concentrate was cooled to  $6^\circ\text{C}$ , dark green crystals precipitated. The crude product was redissolved and chromatographed with petroleum ether/toluene (1:1, v:v) on alumina. A dark green fraction gave 1.02 g of **17**, which was still contaminated with styrylnaphthalene. Repeated recrystallization from petroleum ether at  $-25^\circ\text{C}$  gave a better product, but traces of styrylnaphthalene could not be completely removed.  $^{13}\text{C}\{^1\text{H}\}$  NMR ( $\text{C}_6\text{D}_6$ )  $\delta$  49.2 (C-2 or C- $\beta$ ), 49.8 (C- $\beta$  or C-2), 66.0 (C- $\alpha$ ), 82.0 (Cp), 88.6 (C-1), 122.9, 123.7, 124.8, 126.6, 127.3, 128.9, 134.4, 135.6, 137.6. MS (EI) *m/e* (relative intensity) 354 ( $\text{M}^+$ , 10), 289 ( $[\text{M} - \text{Cp}]^+$ ), 230 ( $\text{L}^+$ , 100), 215 (16), 202 (10), 189 ( $[\text{Cp}_2\text{Co}]^+$ , 5), 152 ( $[\text{L} - \text{C}_6\text{H}_5]^+$ , 17), 124 ( $[\text{CpCo}]^+$ , 3), 114 (18), 101 (10), 77 ( $[\text{C}_6\text{H}_5]^+$ ,

6), 66 (7); L = styrylnaphthalene. Anal. Calcd (found): C, 77.95 (75.71); H, 5.40 (5.37).

**[(CpCo) $_2$ ( $\beta,\alpha,1,2-\eta\beta',\alpha',3,4-\eta$ -(*m*-distyrylbenzene))], 18a.** A solution of 0.28 g (1.56 mmol) of **7** and 0.18 g (0.64 mmol) of *m*-distyrylbenzene in 60 mL of petroleum ether was heated for 7 h at  $40^\circ\text{C}$ . Complex **18a** (0.23 g, 67%) precipitated as a red-brown solid when the mixture was cooled to room temperature. Attempted chromatography of **18a** (alumina, toluene) or recrystallization from toluene resulted in decomposition. Distyrylbenzene was recovered nearly quantitatively.

**[(CpCo) $_2$ ( $\beta,\alpha,1,2-\eta\beta',\alpha',4,3-\eta$ -(*p*-distyrylbenzene))], 18b.** A 1.03 g (3.65 mmol) amount of *p*-distyrylbenzene was suspended in a solution of 1.79 g (9.94 mmol) of **7** in 120 mL of petroleum ether. After 2 h at room temperature the mixture was heated to  $35-45^\circ\text{C}$ . After about 6 h at this temperature the distyrylbenzene had completely dissolved, and the solution turned dark brown. After the solution cooled to room temperature a green intractable solid was removed by filtration, and the resulting solution was allowed to stand for 2 days. During that time a very small amount of brown crystals separated. Solvent was removed under reduced pressure from the mother liquor to give a dark solid residue and a small amount of red crystals (**7** by  $^1\text{H}$  NMR analysis). The solid was dissolved in a minimal amount of toluene and chromatographed on alumina. After removal of solvent from the first fraction, a pale green solid was obtained, which could not be redissolved in  $\text{C}_6\text{D}_6$  or THF. From the second brownish fraction **18b** (1.26 g, 65%) was obtained as a brownish-gray powder by crystallization at  $-20^\circ\text{C}$ . Mp, decomp above  $60^\circ\text{C}$ .  $^{13}\text{C}\{^1\text{H}\}$  NMR ( $\text{C}_6\text{D}_6$ )  $\delta$  48.4 (CH- $\beta,\beta'$  or CH-2,3), 56.7 (CH- $\beta,\beta'$  or CH-2,3), 72.8 (CH- $\alpha,\alpha'$ ), 82.5 (Cp), 85.9 (C-1,4), 124.6 (CH), 126.4 (CH), 126.9 (CH), 128.9 (CH), 146.3 (Ph- $\text{C}_{ipso}$ ). MS (EI) *m/e* (relative intensity) 282 ( $\text{L}^+$ , 100), 265 (10), 203 (17), 189 ( $[\text{Cp}_2\text{Co}]^+$ , 11), 178 (18), 141 (10). MS ( $\text{Cl}^+$ ) *m/e* (relative intensity) 283 ( $[\text{L} + \text{H}]^+$ , 100), 282 ( $\text{L}^+$ , 30), 269 (48), 193 (30), 189 ( $[\text{Cp}_2\text{Co}]^+$ , 36), 147 (18); L = distyrylbenzene.

**[(CpCo) $_3$ ( $\mu_3-1,2-\eta:3,4-\eta:5,6-\eta$ -(*p*-distyrylbenzene))], 19.** 0.21 g (0.75 mmol) of *p*-distyrylbenzene was added to a solution of 0.65 g (2.27 mmol) of **8** in 50 mL of THF. The mixture was stirred at room temperature for 4 h. After the solvent was removed under reduced pressure, a dark solid was obtained, which was redissolved in toluene, filtered, and chromatographed on alumina. Hexamethylbenzene was first eluted with petroleum ether. With toluene/petroleum ether (1:1, v:v) a brown fraction was obtained, which gave 110 mg (28%) of **18b** after removal of solvent. Another brown fraction was eluted with toluene/petroleum ether (2:1, v:v), from which 120 mg (25%) of **19** was obtained after removal of solvent and recrystallization. MS (EI) *m/e* (relative intensity) 282 ( $\text{L}^+$ , 100), 265 (10), 203 (12), 189 ( $[\text{Cp}_2\text{Co}]^+$ , 10), 178 (18), 141 (10); L = distyrylbenzene.

**[CpCo(1-3,8,9- $\eta$ -(1-Cp-3-Me-1-cobaltindenyl))], 20.** Note: Potassium powder is extremely pyrophoric; residues from filtration may ignite spontaneously in air. A 5.0 g (26.4 mmol) amount of cobaltocene was added to a suspension of 1.3 g (33.3 mmol) of potassium powder in 60 mL of diethyl ether at  $-50^\circ\text{C}$ . The slurry was slowly warmed to room temperature. A 20 mL aliquot of  $\alpha$ -methylstyrene was slowly (over approximately 0.5 h) added at around  $-10^\circ\text{C}$ . After 2 h at room temperature all volatiles were removed under reduced pressure. The residue was extracted with 100 mL of *n*-hexane and filtered. Most of the unreacted cobaltocene was removed from the filtrate by crystallization at  $-20^\circ\text{C}$ . The mother liquor was chromatographed on alumina. Residual cobaltocene was washed from the column with *n*-hexane. Complex **20** (40 mg, 1% after removal of solvent and recrystallization) was eluted with *n*-hexane/toluene (1:1, v:v) as the fourth, green fraction. The first two fractions (1.1 g of a red oil, 0.3 g of a light brown oil) did not show Cp peaks in the  $^1\text{H}$  NMR spectrum.  $^1\text{H}$  NMR ( $\text{C}_6\text{D}_6$ )  $\delta$  2.11 (s, 3H, Me), 4.23 (s, 5H, Cp), 4.83 (s, 5H, Cp), 6.76 ("t", 1H, H-5 or H-6), 6.89 ("t", 1H, H-6 or H-5), 7.21 (d, 1H, H-4 or H-7), 8.05 (s, 1H, H-2), 8.42 (d, 1H, H-7 or H-4).

**Table 10. Details of the Crystal Structure Determinations of [CpCo( $\beta,\alpha,1,2\text{-}\eta\text{-}(1\text{-Vinyl)naphthalene}$ )], **15a**, and [CpCo( $1\text{-}3,8,9\text{-}\eta\text{-}(1\text{-Cp-}3\text{-Me-}1\text{-cobaltindenyl})$ )] **20****

	<b>15a</b>	<b>20</b>
formula	C <sub>17</sub> H <sub>15</sub> Co	C <sub>19</sub> H <sub>18</sub> Co <sub>2</sub>
cryst habit, color	box, dark green	needle, dark green
cryst size [mm]	0.3 × 0.3 × 0.4	0.3 × 0.3 × 0.8
cryst system	orthorhombic	tetragonal
space group	<i>Pcab</i>	<i>I</i> $\bar{4}$
<i>a</i> (Å)	8.206(1)	18.150(12)
<i>b</i> (Å)	11.372(3)	
<i>c</i> (Å)	28.067(7)	9.307(5)
<i>V</i> (Å <sup>3</sup> )	2619(2)	3066(3)
<i>Z</i>	8	8
<i>M<sub>r</sub></i>	278.30	364.22
<i>d<sub>c</sub></i> (g cm <sup>-3</sup> )	1.411	1.574
<i>F</i> <sub>000</sub>	1152	1488
<i>μ</i> (Mo <i>Kα</i> ) (mm <sup>-1</sup> )	1.287	2.152
X-radiation, <i>λ</i> (Å)	Mo <i>Kα</i> , graphite monochromated, 0.710 69	
data collc temp	ambient	
2 $\theta$ range (deg)	3–50	3–55
<i>hkl</i> range	0–9, 0–13, 0–33	0–23, 0–23, 0–12
no. of reflns measd	2308	1878
unique	2308	1878
obsd ( <i>I</i> ≥ 2 $\sigma$ ( <i>I</i> ))	1374	1373
abs corr	empirical	
params refined/restraints	170/0	199/0
<i>G</i> <sub>oF</sub>	0.953	1.049
<i>R</i> values		
<i>R</i> (obsd reflns only)	0.050	0.046
<i>wR</i> <sub>2</sub> (all reflns)	0.131	0.100
( <i>w</i> = 1/[ $\sigma^2(F) + (AP)^2 + BP$ ])		
<i>A, B</i>	0.0735, 0	0.0393, 0.40
<i>P</i>		(max( <i>F</i> <sub>o</sub> <sup>2</sup> , 0) + 2 <i>F</i> <sub>c</sub> <sup>2</sup> )/3

<sup>13</sup>C{<sup>1</sup>H} NMR (C<sub>6</sub>D<sub>6</sub>)  $\delta$  19.1 (Me), 79.5 (Cp), 80.3 (Cp), 109.5 (C), 114.2 (C), 121.1 (CH), 127.9 (CH), 128.1 (CH), 153.0 (CH). MS (EI) *m/e* (relative intensity) 364 (M<sup>+</sup>, 100), 265 (7), 239 (28), 222 (12), 189 ([Cp<sub>2</sub>Co]<sup>+</sup>, 51), 124 ([CpCo]<sup>+</sup>, 22), 59 (Co<sup>+</sup>, 16). Anal. Calcd (found): C, 62.66 (62.61); H, 4.98 (5.13).

**Crystal Structure Determination of [CpCo( $\beta,\alpha,1,2\text{-}\eta\text{-}(1\text{-vinyl)naphthalene}$ )], **15a**, and [CpCo( $1\text{-}3,8,9\text{-}\eta\text{-}(1\text{-Cp-}3\text{-Me-}1\text{-cobaltindenyl})$ )] **20**.**

Single crystals were grown from petroleum ether (**15a**) or *n*-hexane (**20**) and mounted in Lindemann capillary tubes. Intensity data were collected on Syntex R3 (**15a**) or Siemens STOE (**20**) four circle diffractometers at ambient temperature and corrected for Lorentz, polarization, and absorption effects (Table 10). The structures were solved by the heavy atom method and refined by full-matrix least-squares based on *F*<sup>2</sup> using all measured unique reflections. All non-hydrogen atoms were given anisotropic displacement parameters.

Some of the hydrogen atoms (those on C2, C11, and C12 in **15a** and on C1 in **20**) were located from difference Fourier maps and refined with isotropic atomic displacement parameters. All other hydrogen atoms were input in calculated positions.

The cyclopentadienyl ring in **15a** was treated as a "variable metric" rigid regular pentagon. The carbon-carbon bond length within this group refined to 1.393(3) Å.

The calculations were performed using the programs SHELXS-86<sup>34</sup> and SHELXL-93.<sup>35</sup> Graphical representations were drawn with the ORTEP-II program.<sup>36</sup>

**Acknowledgment.** This work was supported by the Deutsche Forschungsgemeinschaft and the Fonds der Chemischen Industrie. H.W. gratefully acknowledges the award of a Heisenberg Fellowship. We thank Prof. R. N. Grimes (University of Virginia, U.S.A.) for some of the mass spectra.

**Supporting Information Available:** Tables listing anisotropic atomic displacement parameters, hydrogen atom coordinates, and complete bond distances and angles **15b** and **20** (18 pages). Ordering information is given on any current masthead page.

OM950161P

(34) Sheldrick, G. M. *Acta Crystallogr.* **1990**, *A46*, 467.

(35) Sheldrick, G. M. *SHELXL-93*; Universität Göttingen: Göttingen, Germany, 1993.

(36) Johnson, C. K. *ORTEP*, Report ORNL-5138; Oak Ridge National Laboratory: Oak Ridge, TN, 1965.

# Isomerization of Silyllallene

Hideaki Shimizu<sup>†</sup> and Mark S. Gordon\*

Department of Chemistry, Iowa State University, Ames, Iowa 50011

Received March 31, 1995<sup>®</sup>

The isomerization of silyllallene to seven of its isomers has been studied using *ab initio* molecular orbital theory. The energetics were obtained using quadratically convergent configuration interaction (QCISD(T)) with the 6-311G(d,p) basis set, at geometries optimized by second-order perturbation theory (MP2) with the 6-31G(d) basis set. Test calculations using multiconfiguration wave functions show that the configurational mixing is small; therefore, the single-configuration-based methods are reliable. In comparison to the isomerization of the parent allene, the silyl group was found to migrate more easily than the hydrogen. In particular, the 1,3-migration that converts silyllallene to silylpropyne has barriers of 55.8 and 52.9 kcal mol<sup>-1</sup> for the forward and backward reactions, respectively. These are roughly half of the 1,3-hydrogen migration barrier in allene.

## Introduction

Thermal isomerization of allene has been well studied experimentally<sup>1</sup> and understood thoroughly by a recent theoretical study<sup>2</sup> using multiconfigurational (MC) self-consistent field (SCF) and multireference configuration interaction (CI) calculations. The main path for the isomerization of allene to propyne is predicted to be allene (CH<sub>2</sub>=C=CH<sub>2</sub>) → vinylmethylene (CH<sub>2</sub>=CH-C(H):) → cyclopropene (c-CH=CH-CH<sub>2</sub>) → propylidene (CH<sub>3</sub>CH=C:) → propyne (CH<sub>3</sub>≡CH).

Silyllallenes have received much less attention than allene. Slutsky and Kwart carried out a kinetic study of (trimethylsilyl)allene isomerization<sup>3</sup> and investigated its mechanism. Recently there has been increasing interest in silyllallenes and in the synthetic use of silyllallene isomerization.<sup>4</sup> Also, silacycloallenes have been prepared and their thermal ring contractions and photochemistry have been studied.<sup>5,6</sup>

The purpose of this study is to compare the potential energy surfaces of allene and silyllallene using *ab initio* molecular orbital theory and to determine how the silyl group modifies the potential energy surface. In particular, how does silyl migration differ from hydrogen migration? One may follow the analog of the established allene isomerization mechanism as illustrated in Scheme 1. In this diagram, minima on the potential energy surface are indicated by a number (underlined

and in bold) beneath the structure. Transition states are indicated by a capital letter adjacent to the appropriate double arrow.

## Computational Methods

Since Scheme 1 includes some molecules for which a single-reference wave function may not be adequate, test calculations were performed using complete active space (CAS) MCSCF calculations (referred to as CASSCF),<sup>7</sup> in which we include all electronic configurations that arise from distributing 10 electrons among 10 orbitals (all electrons and orbitals excluding those in CH or SiH bonds). This amounts to correlating all CC and SiC bonds in the system. Geometry optimizations were carried out with second-order perturbation theory (MP2<sup>8</sup>) using the orbitals obtained from the Hartree-Fock (HF) wave function. The 6-31G(d) basis set<sup>9</sup> was used for both calculations.

In order to determine whether a stationary point is a minimum or a transition state, the matrix of energy second derivatives (Hessian) was calculated for each optimized geometry. Diagonalization of this matrix determines whether the structure is a minimum (no negative eigenvalues) or a transition state (one negative eigenvalue). The intrinsic reaction coordinates (IRC),<sup>10</sup> minimum energy paths connecting reactants and products through transition states, were followed to verify that each transition state does indeed connect the appropriate minima.

In order to obtain reliable energetics, higher level methods were employed for single-point energy calculations at the optimized geometries. Both full fourth-order perturbation theory (MP4SDTQ)<sup>11</sup> and quadratically convergent configuration interaction (QCISD(T))<sup>12</sup> calculations were performed at the MP2 geometries using the 6-311G(d,p) basis set.<sup>13</sup> The CASSCF calculations were done using GAMESS<sup>14</sup> and the MP2, MP4, and QCISD(T) calculations using Gaussian92.<sup>15</sup>

<sup>†</sup> Present address: Shin-Etsu Chemical Co., Ltd., 1-10, Hitomi, Matsuida, Gunma 379-02, Japan.

<sup>®</sup> Abstract published in *Advance ACS Abstracts*, July 15, 1995.

(1) (a) Sakakibara, Y. *Bull. Chem. Soc. Jpn.* **1964**, *37*, 1268. (b) Levush, S. S.; Abadzhiev, S. S.; Shevchuk, V. U. *Neftekhimiia* **1969**, *9*, 215. (c) York, E. J.; Dittmar, W.; Stevenson, J. R.; Bergman, R. G. *J. Am. Chem. Soc.* **1973**, *95*, 5680. (d) Bradley, J. N.; West, K. O. *J. Chem. Soc., Faraday Trans. 1* **1975**, *71*, 967. (e) Lifshitz, A.; Frenklach, M.; Burcat, A. *J. Phys. Chem.* **1975**, *79*, 1148. (f) Lifshitz, A.; Frenklach, M.; Burcat, A. *J. Phys. Chem.* **1976**, *80*, 2437. (g) Walsh, R. *J. Chem. Soc., Faraday Trans. 1* **1976**, *72*, 2137. (h) Bailey, I. M.; Walsh, R. *J. Chem. Soc., Faraday Trans. 1* **1978**, *74*, 1146. (i) Hopf, H.; Priebe, H.; Walsh, R. *J. Am. Chem. Soc.* **1980**, *102*, 1210.

(2) Yoshimine, M.; Pacansky, J.; Honjou, N. *J. Am. Chem. Soc.* **1989**, *111*, 4198-4209.

(3) Slutsky, J.; Kwart, H. *J. Am. Chem. Soc.* **1973**, *95*, 8678-8685.

(4) Robinson, L. R. Dissertation, DA8721925, 1987.

(5) Pang, Y.; Petrich, S. A.; Young, V. G., Jr.; Gordon, M. S.; Barton, T. J. *J. Am. Chem. Soc.* **1993**, *115*, 2534-2536.

(6) (a) Shimizu, T.; Hojo, F.; Ando, W. *J. Am. Chem. Soc.* **1993**, *115*, 3111. (b) Hojo, F.; Shimizu, T.; Ando, W. *Organometallics* **1994**, *13*, 3402.

(7) Møller, C.; Plesset, M. S. *Phys. Rev.* **1934**, *46*, 618.

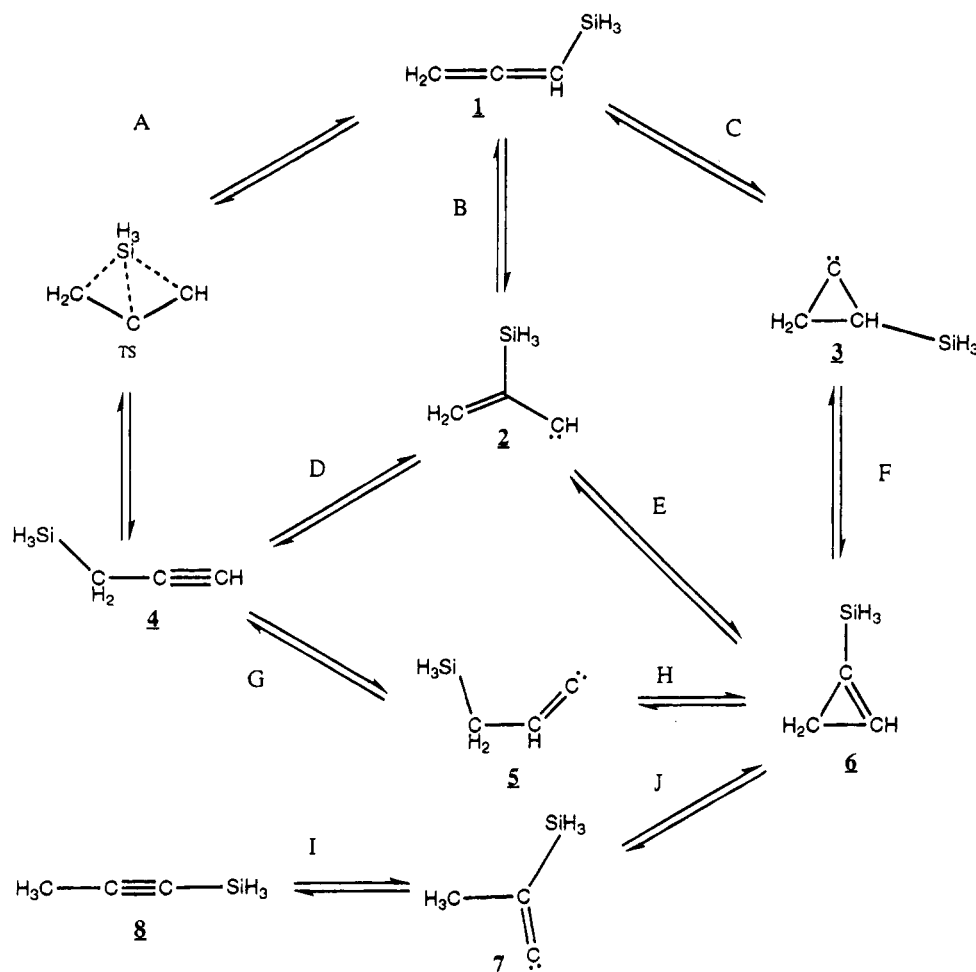
(8) (a) Ruedenberg, K.; Schmidt, M. W.; Gilbert, M. M.; Elbert, S. T. *Chem. Phys.* **1982**, *71*, 41, 51, 65. (b) Lam, B.; Schmidt, M. W.; Ruedenberg, K. *J. Phys. Chem.* **1985**, *89*, 2221.

(9) (a) H.; Ditchfield, R.; Hehre, W. J.; Pople, J. A. *J. Chem. Phys.* **1971**, *54*, 724-728. (b) C.; O.; Hehre, W. J.; Ditchfield, R.; Pople, J. A. *J. Chem. Phys.* **1972**, *56*, 2257-2261. (c) Si; Gordon, M. S. *Chem. Phys. Lett.* **1980**, *76*, 163-168. (d) Standard polarizations were used: H (*p* = 1.1), C (*d* = 0.8), O (*d* = 0.8), Si (*d* = 0.395).

(10) (a) Garrett, B. C.; Redmon, M. J.; Steckler, R.; Truhlar, D. G.; Baldrige, K. K.; Bartol, D.; Schmidt, M. W.; Gordon, M. S. *J. Phys. Chem.* **1988**, *92*, 1476-1488. (b) Gonzales, C.; Schlegel, H. B. *J. Phys. Chem.* **1990**, *94*, 5523-5527. (c) Gonzales, C.; Schlegel, H. B. *J. Chem. Phys.* **1991**, *95*, 5853-5860.

(11) Krishnan, R.; Frisch, M. J.; Pople, J. A. *J. Chem. Phys.* **1980**, *72*, 4244-4245.

Scheme 1. Silyllallene Isomerization Diagram

Table 1. Calculated Barriers for Allene and Silyllallene (kcal mol<sup>-1</sup>)<sup>a</sup>

path	direction	silyllallene QCISD(T) <sup>b</sup>	allene <sup>c</sup> MRCI <sup>d</sup>
A	1-TS	55.8	94.9 <sup>e</sup>
	4-TS	52.9	95.6 <sup>e</sup>
B	1-TS	64.8	65.8
	2-TS		12.1
E	2-TS		4.5
	6-TS	43.8	35.8
D	2-TS		18.9
	4-TS		72.9
C	1-TS	76.5	72.2
	3-TS	11.4	10.2
F	3-TS	4.2	14.9
	6-TS	49.1	54.5
G	4-TS	49.8	38.1
	5-TS		18.6
H	5-TS		-2.4
	6-TS	32.0	39.8
I	8-TS	66.5	38.1
	7-TS		18.6
J	7-TS		-2.4
	6-TS	37.5	39.8

<sup>a</sup> Labels and paths correspond to those in Scheme 1. <sup>b</sup> QCISD(T)/6-311G(d)//MP2/6-31G(d). <sup>c</sup> Reference 2. <sup>d</sup> MRCI/6-31G(d)/CASSCF(6,6)/6-31G(d). <sup>e</sup> All but path A for allene include ZPE correction.

## Results and Discussion

**Preliminary Considerations.** The geometries of the stationary points found on the silyllallene potential energy surface are shown in Figure 1. The relative

energies are summarized in Table 1, together with results for the allene isomerization for comparison. Note that several of the pathways (B-E, C-F, G-H, I-J) predicted in the earlier study<sup>2</sup> on the parent allene correspond to two-step processes. In the current work on silyllallene, only the G-H path is found to be a two-step process. All of the others merge into a single, concerted path.

One can assess the importance of performing a multiconfigurational (CASSCF) calculation by defining a simple index  $N_v$ , calculated as the sum of natural orbital occupation numbers in the restricted Hartree-Fock (RHF) virtual space. If the single-configuration RHF calculation is correct,  $N_v$  should be zero. Thus,  $N_v$  is an indicator of the importance of the additional configurations. The values calculated for  $N_v$ , using the CASSCF(10,10) wave function discussed in the previous section, on the MP2 potential energy surface are sum-

(12) Pople, J. A.; Head-Gordon, M.; Raghavachari, K. *J. Chem. Phys.* **1987**, *87*, 5968-5975.

(13) Krishnan, R.; Binkley, J. S.; Seeger, R.; Pople, J. A. *J. Chem. Phys.* **1980**, *72*, 650-654.

(14) GAMESS (General Atomic and Molecular Electronic Structure System): Schmidt, M. W.; Baldridge, K. K.; Boatz, J. A.; Elbert, S. T.; Gordon, M. S.; Jensen, J. H.; Koseki, S.; Matsunaga, N.; Nguyen, K. A.; Su, S.; Windus, T. L.; Dupuis, M.; Montgomery, J. A. *J. Comput. Chem.* **1993**, *14*, 1347-1363.

(15) Frisch, M. J.; Trucks, G. W.; Head-Gordon, M.; Gill, P. M. W.; Wong, M. W.; Foresman, J. B.; Johnson, B. G.; Schlegel, H. B.; Robb, M. A.; Replogle, E. S.; Gomperts, R.; Andres, J. L.; Raghavachari, K.; Binkley, J. S.; Gonzalez, C.; Martin, R. L.; Fox, D. J.; Defrees, D. J.; Baker, J.; Stewart, J. J. P.; Pople, J. A. Gaussian 92; Gaussian Inc., Pittsburgh, PA, 1992.



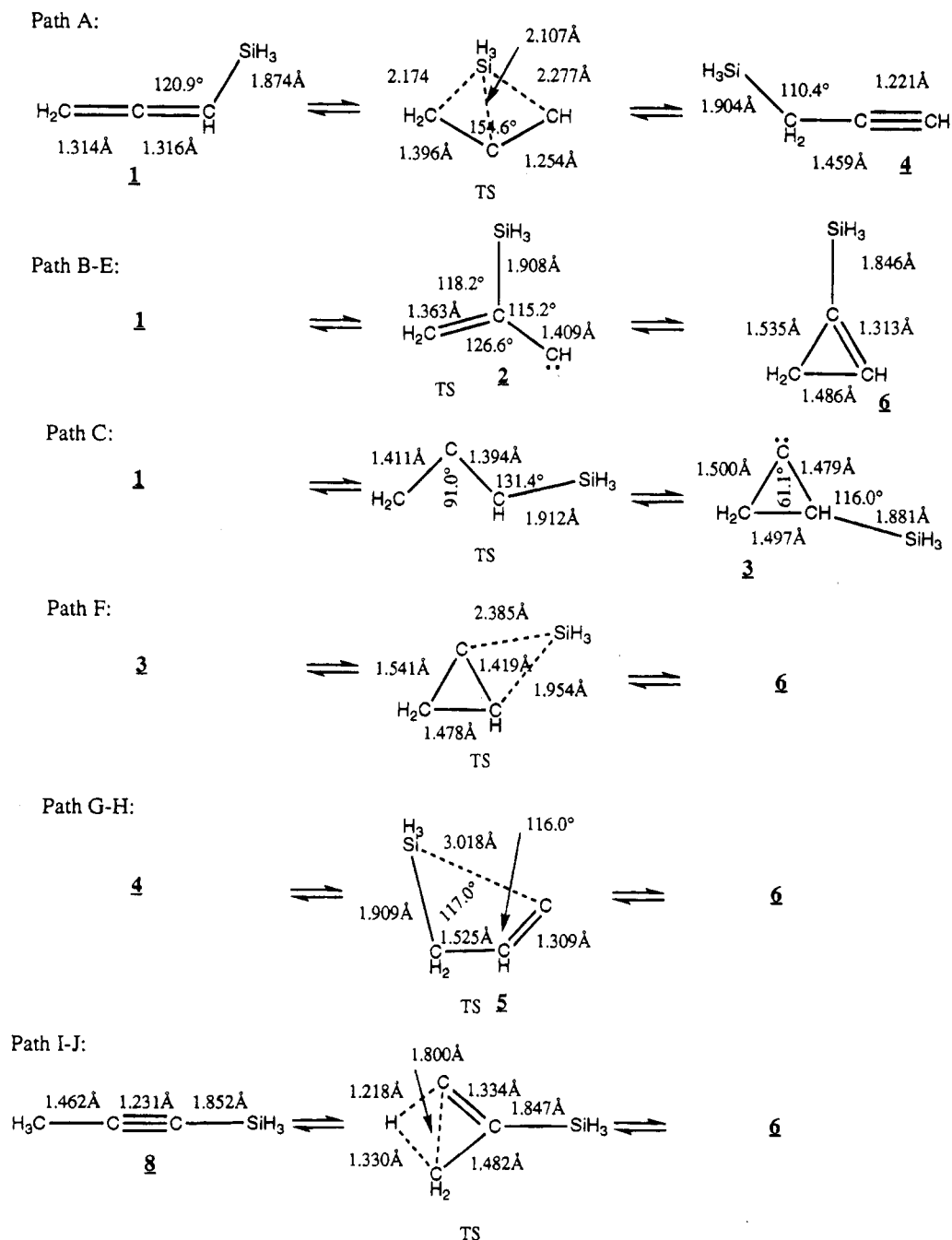


Figure 1. MP2/6-31G(d) geometries.

Table 2.  $N_v$  Values from CASSCF(10,10) for MP2-Optimized Geometries of Transition States

path	$N_v$	path	$N_v$
A	0.181	F	0.160
B-E	0.264	G-H	0.186
C	0.220	I-J	0.193

marized in Table 2. It is clear from the small values for  $N_v$ , that MP2-optimized geometries are likely to be reliable and that quantitative differences between the MP2 and CASSCF potential energy surfaces are likely to be due to the importance of dynamic correlation that is included to some extent in the MP2 energies, but not in the CASSCF results. Hence, the following discussion is based on QCISD(T) energies obtained at MP2-optimized geometries.

**Reaction Energetics.** Table 1 contains the reaction energetics calculated at the QCISD(T) level of theory,

using the MP2 geometries. A negative entry in this table means that although a transition state was identified at the level of theory used to determine stationary points, higher level single-point calculations reversed the relative energies of the minimum and apparent transition states. This may be taken as evidence that the transition state may disappear at the higher levels of theory.

Note that a transition state corresponding to process D on the allene reaction path was not found for silyllallene. This is not surprising, since structure 2 is itself predicted to be a transition state at the MP2 level of theory. Thus, it is likely that the competing lower energy 1,3-silyl shift (path A) is preferred.

The 1,3-silyl migration (path A) of silyllallene has a quite low (56 kcal mol<sup>-1</sup>) barrier (Table 1) compared to the 95 kcal mol<sup>-1</sup> barrier for hydrogen migration in the parent allene.<sup>2</sup> This activation energy of 56 kcal

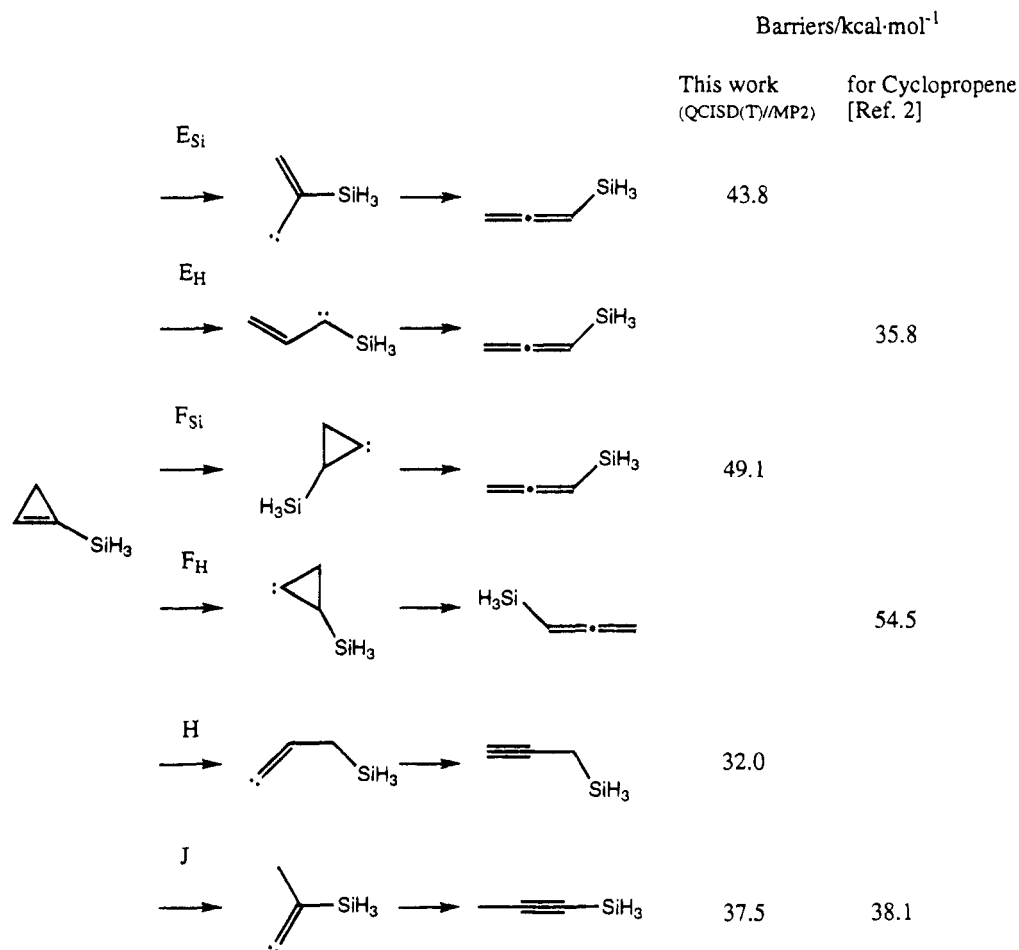


**Figure 2.** Possible reaction paths from silylcyclopropene and theoretical activation energies. The relevant path is indicated over the arrow.

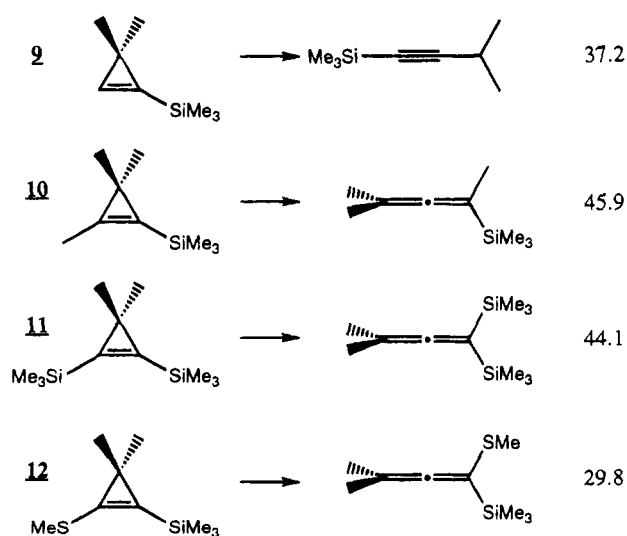


**Figure 3.** Experimental activation energies (kcal mol<sup>-1</sup>) of various silylcyclopropene derivatives.

mol<sup>-1</sup> is similar to the experimental value<sup>3</sup> of 49.9 kcal mol<sup>-1</sup> and is close to the 1,3-sigmatropic rearrangement activation energy of 50.2 kcal mol<sup>-1</sup> for allylsilane.<sup>16</sup>

Next, consider the pathways connecting **1** and **6** in Scheme 1. Paths B and E merge into a concerted reaction according to the MP2 calculations. The net QCISD(T) barrier height based on MP2 geometries (64.8 kcal mol<sup>-1</sup>) is very similar to that found for the parent

allene (65.8 kcal mol<sup>-1</sup>). The alternative pathway connecting **1** and **6**, via **3**, is predicted to have a net energy requirement of 76.5 kcal mol<sup>-1</sup>. This is slightly greater than the corresponding barrier (72.2 kcal mol<sup>-1</sup>) in allene.<sup>2</sup> Note that for the 1,2-migrations (paths F, B, and H), silyl migration tends to have a few kcal mol<sup>-1</sup> lower reaction barrier than that for hydrogen migration. This trend is consistent with the experimental evidence that silyl migrations are more facile than hydrogen migrations. This is reasonable, since C–Si bonds tend to be weaker (76 vs 100 kcal mol<sup>-1</sup>) and more polarizable than C–H bonds.

As noted earlier (see Table 1), MP2 predicts that structures **5** and **7** are transition states for concerted processes connecting **4** with **6** and **8** with **6**, respectively. The net energetic requirement for **4** → **6** is predicted to be somewhat higher (49.8 kcal mol<sup>-1</sup>) than that for the corresponding pathway in the parent allene (38.1 kcal mol<sup>-1</sup>). For the path (I–J) connecting **6** with **8**, the net barrier height is predicted to be 66.5 kcal mol<sup>-1</sup> at the QCISD(T)/MP2 level of theory. This is rather larger than the corresponding barrier in allene.<sup>2</sup>

Overall, the lowest energy path from silylallene (**1**) to 3-silylpropyne (**4**) occurs via a direct 1,3-silyl migration (A), with a barrier estimated to be about 56 kcal mol<sup>-1</sup>. The lowest energy path from silylallene to silylcyclopropene (**6**) occurs via transition state **2**, with an estimated barrier of about 65 kcal mol<sup>-1</sup>. To access

(16) Kwart, H.; Slutsky, J. *J. Am. Chem. Soc.* **1972**, *94*, 2515–2516.

silylacetylene (**8**) from silylcyclopropene requires 37.5 kcal mol<sup>-1</sup>.

**Comparison with Cyclopropene Isomerization Experiments.** There have been extensive studies of isomerizations of silylcyclopropenes.<sup>17</sup> This enables us to compare part of this study with experimental values for the reaction barriers of isomerization reactions. The various reactions starting from silylcyclopropene and the calculated barriers are shown in Figure 2, and the experimental activation energies for methylated analogs are shown in Figure 3. For **9**, the observed activation energy of 37.2 kcal mol<sup>-1</sup> is close to the calculated value for path J. Steric hindrance due to the methyl groups, as well as the intrinsic energy difference between Me<sub>3</sub>-SiCH<sub>2</sub>C≡CH and Me<sub>3</sub>SiC≡CCH<sub>3</sub>, may explain why path H, predicted to be the lowest energy path, is not found

experimentally. For compounds **10** and **11** path J is impossible, and the barrier for path H is again likely to be increased due to steric hindrance. Thus, the ring opening (path E) becomes the lowest energy path, and the observed activation energy (44.1 kcal mol<sup>-1</sup>) is again in good agreement with calculated value of 43.8 kcal mol<sup>-1</sup>. Although this reaction includes a 1,2-silyl migration in the latter stage, the transition state lies close to **2**, so that it is not affected by steric hindrance.

**Acknowledgment.** We thank Professors Thomas Barton and Robin Walsh for very helpful discussions about silylcyclopropenes. This work was supported by grants from the National Science Foundation (Grant No. CHE-9313717) and the Air Force Office of Scientific Research (Grant No. 93-0105). The calculations were performed on IBM RS 6000 computers generously provided by Iowa State University.

OM950238+

(17) (a) Walsh, R.; Untiedt, S.; Stohlmeier, M.; de Meijere, A. *Chem. Ber.* **1989**, *122*, 637-642. (b) Walsh, R.; Untiedt, S.; de Meijere, A. *Chem. Ber.* **1994**, *127*, 237-245.

# Mechanistic Aspects of a Highly Regioselective Catalytic Alkene Hydroformylation using a Rhodium Chelating Bis(phosphite) Complex

Bahram Moasser and Wayne L. Gladfelter\*

Department of Chemistry, University of Minnesota, Minneapolis, Minnesota 55455

D. Christopher Roe

Central Research and Development, E.I. du Pont de Nemours & Co., Inc., Experimental Station, P.O. Box 80328, Wilmington, Delaware 19880-0328

Received March 24, 1995\*

The rhodium-catalyzed hydroformylation of 1-octene using the bis(phosphite) ligand bbmb was studied using *in situ*, high-pressure  $^1\text{H}$  and  $^{31}\text{P}$  NMR and FT-IR spectroscopy. Four species,  $\text{Rh}(\text{bbmb})(\text{acac})$ ,  $\text{Rh}(\text{bbmb})(\text{CO})_2\text{H}$ , and two dimeric complexes, appeared sequentially during different stages of the catalysis when  $\text{Rh}(\text{acac})(\text{CO})_2$  was used as the catalyst precursor. These were independently synthesized and their reactivity studied. The major species present during catalysis was determined to be  $\text{Rh}(\text{bbmb})(\text{CO})_2\text{H}$  (**1**), which was fully characterized. This hydride complex was shown to be an effective alkene isomerization catalyst. Using magnetization transfer, the rate of exchange between **1** and the terminal and internal vinyl hydrogens of 3,3-dimethylbutene were 0.62 and 0.51  $\text{s}^{-1}$ , respectively. The rapid, reversible nature of the alkene insertion establishes that the regiochemistry of the final aldehyde is not determined at the alkene insertion step or any event prior to it. The dimeric species were shown to convert to **1** via reversible addition of dihydrogen.

## Introduction

Recently, the class of chelating bis(phosphite) ligands for organometallic complexes has received considerable attention. New reports involving the use of these ligands in regio-<sup>1,2</sup> and stereoselective<sup>3,4</sup> hydroformylation, as well as asymmetric hydrocyanation,<sup>5,6</sup> have appeared which demonstrate their potential utility. The closely related monosaccharide- and disaccharide-derived 1,2- and 1,3-diol phosphinites and phosphine phosphites have been utilized in asymmetric hydrocyanation<sup>7-10</sup> and asymmetric hydroformylation,<sup>11</sup> respectively, with success. With the perspective of catalysis in mind, a more careful study of this chemistry appeared warranted. There are numerous advantages of aryl bis(phosphite) modified catalysis over the currently employed phosphine methodology. These compounds show very good normal/iso (*n/i*) regioselectivity and they are fairly robust toward hydrolysis. Further-

more, they are readily available from the vast achiral/chiral diol synthetic methodology.

Here we report our study of the rhodium hydroformylation of 1-octene using the bis(phosphite) ligand bbmb (2,2'-bis[(1,1'-biphenyl-2,2'-diyl)phosphite]-3,3'-di-*tert*-butyl-5,5'-dimethoxy-1,1'-biphenyl), first developed by Billig, Abatjoglou and Bryant<sup>1</sup> (see figure 2). These workers observed very high regioselectivity in the bbmb-modified hydroformylation of propene with normal to iso ratios up to 50:1. Cuny and Buchwald extended the scope of the process, employing this critical bis(phosphite) ligand, to include the highly regioselective hydroformylation of a variety of functionalized terminal alkenes.<sup>12</sup> To probe the mechanism of this important reaction, we employed *in situ*, high-pressure spectroscopic studies to identify the critical species present under catalytic conditions. The hydroformylation of 1-octene was monitored by *in situ*, high-pressure  $^1\text{H}$  and  $^{31}\text{P}\{^1\text{H}\}$  NMR and FT-IR spectroscopy. The species that were observed in the catalysis were independently synthesized and characterized, and their stoichiometric and catalytic reactivity was studied.

## Results

**In Situ Spectroscopy.** Figure 1 shows the  $^1\text{H}$  and  $^{31}\text{P}\{^1\text{H}\}$  NMR spectra obtained during a typical catalysis in the high-pressure NMR tube.<sup>13</sup> Prior to the addition of  $\text{CO}/\text{H}_2$ , all rhodium was present as  $\text{Rh}(\text{bbmb})(\text{acac})$  (**2**). Upon addition of a 1:1 mixture of  $\text{CO}$  and  $\text{H}_2$  (20 atm, 2.1 mol % excess relative to alkene) **2** converted to  $\text{Rh}(\text{bbmb})(\text{CO})_2\text{H}$  (**1**) and alkene isomerization began.

\* Abstract published in *Advance ACS Abstracts*, July 1, 1995.  
 (1) Billig, E.; Abatjoglou, A. G.; Bryant, D. R. (Union Carbide) U.S. Patent 4,769,498, 1988.  
 (2) Kwok, T. J.; Wink, D. J. *Organometallics* **1993**, *12*, 1954.  
 (3) Sakai, N.; Nozaki, K.; Mashima, K.; Takaya, H. *Tetrahedron: Asymmetry* **1992**, *3*, 583.  
 (4) Buisman, G. J. H.; Kamer, P. C. J.; van Leeuwen, P. W. N. M. *Tetrahedron: Asymmetry* **1993**, *4*, 1625.  
 (5) Baker, M. J.; Pringle, P. G. *J. Chem. Soc., Chem. Commun.* **1991**, 1292.  
 (6) Baker, M. J.; Harrison, K. N.; Orpen, A. G.; Shaw, G.; Pringle, P. G. *J. Chem. Soc., Chem. Commun.* **1991**, 803.  
 (7) RajanBabu, T. V.; Casalnuovo, A. L. *J. Am. Chem. Soc.* **1992**, *114*, 6265.  
 (8) RajanBabu, T. V.; Casalnuovo, A. L. *Pure Appl. Chem.* **1994**, *66*, 1535.  
 (9) RajanBabu, T. V.; Ayers, T. A.; Casalnuovo, A. L. *J. Am. Chem. Soc.* **1994**, *116*, 4101.  
 (10) Casalnuovo, A. L.; RajanBabu, T. V.; Ayers, T. A.; Warren, T. H. *J. Am. Chem. Soc.* **1994**, *116*, 9869.  
 (11) Sakai, N.; Mano, S.; Nozaki, K.; Takaya, H. *J. Am. Chem. Soc.* **1993**, *115*, 7033.  
 (12) Cuny, G. D.; Buchwald, S. L. *J. Am. Chem. Soc.* **1992**, *115*, 2066.  
 (13) Roe, D. C. *J. Magn. Reson.* **1985**, *63*, 388.

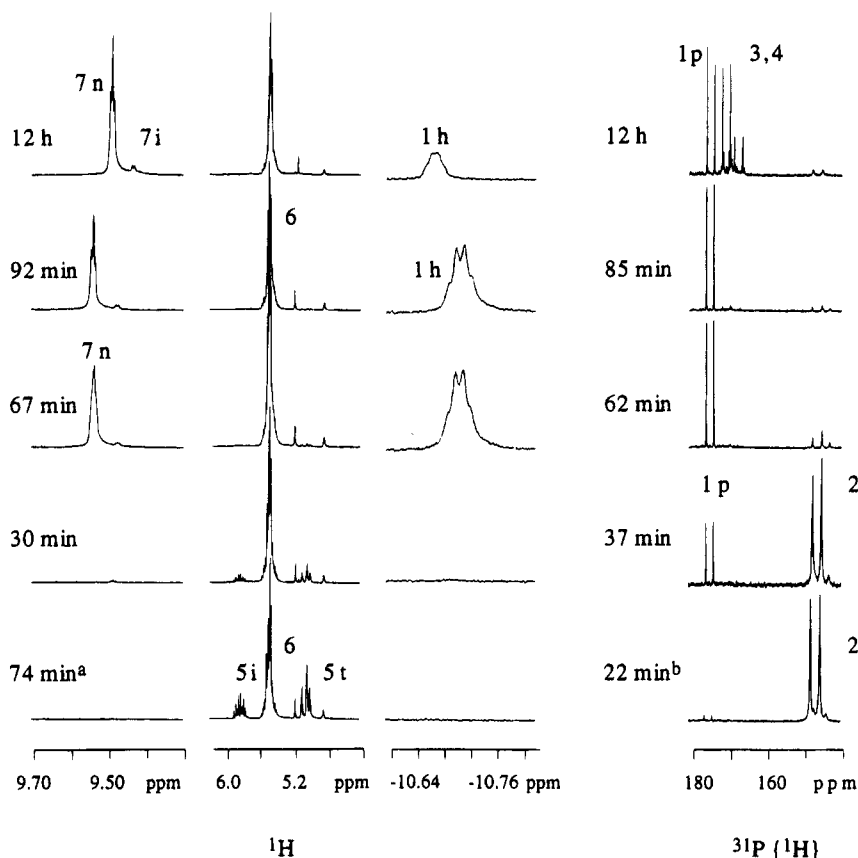


**Figure 1.** *In situ*  $^1\text{H}$  NMR (300 MHz) and  $^{31}\text{P}\{^1\text{H}\}$  NMR (121 MHz) spectra of the hydroformylation of 1-octene using  $\text{Rh}(\text{acac})(\text{CO})_2$  and  $\text{bbmb}$  in toluene- $d_8$ , initially under  $\text{N}_2$ , at 23 °C then under 300 psi of 1:1  $\text{CO}/\text{H}_2$ . Spectra were acquired at 60 °C unless otherwise stated. **1p** =  $\text{Rh}(\text{bbmb})(\text{CO})_2\text{H}$ ; **2** =  $\text{Rh}(\text{bbmb})(\text{acac})$ ; **3**, **4** =  $\text{Rh}_2(\text{bbmb})_2(\text{CO})_4$  + isomer. **5i** =  $\text{C}_6\text{H}_{13}\text{CHCH}_2$ ; **5t** =  $\text{C}_6\text{H}_{13}\text{CHCH}_2$ ; **6** = *cis*- $\text{C}_5\text{H}_{11}\text{CHCHCH}_3$ /*trans*- $\text{C}_5\text{H}_{11}\text{CHCHCH}_3$ ; **7n** = *n*- $\text{C}_8\text{H}_{17}\text{CHO}$ ; **7i** = *i*- $\text{C}_8\text{H}_{17}\text{CHO}$ ; **1h** =  $\text{Rh}(\text{bbmb})(\text{CO})_2\text{H}$ . Legend: (a) after 74 min, under  $\text{N}_2$ , at 23 °C. (b) Initially 40 °C.

Even in the presence of a very small amount of **1**, most of the 1-octene had isomerized to a mixture of internal alkenes. As more **1** was formed, isomerization continued and aldehyde formation began. Heating the tube to 60 °C quantitatively converted **2** to **1** after 95 min and raised the turnover rate. At the same time, the signal for the enolic proton of 2,4-pentanedione appeared at  $\delta$  15.91 (br s) in the  $^1\text{H}$  NMR spectrum. Only the vinyl signals of 2-octene were present as steady production of a 15:1 ratio of 1-nonanal/2-methyloctanal continued. The allylic methyl signals of *cis*- and *trans*-2-octene were integrated as a 1:1 ratio throughout the hydroformylation. As  $\text{H}_2$  was depleted at high conversions, two new species appeared in the  $^{31}\text{P}$  NMR spectrum, **3** and **4**, in a 4:1 ratio. We attribute these to two dimeric rhodium(0) species formed by the dinuclear reductive elimination of  $\text{H}_2$  from **1** (vide infra).

These observations were corroborated by the study of this reaction in a high-pressure IR autoclave. Initially, the  $\nu_{\text{CO}}$  region of the spectrum did not show any metal carbonyl or aldehyde absorptions. When the autoclave was charged with 1:1  $\text{CO}/\text{H}_2$  (40 atm, 60 °C), the signals due to **1** and aldehyde appeared with concomitant disappearance of the alkene  $\text{C}=\text{C}$  stretching signals. At longer times, signals from **3** and **4** appeared as the catalysis slowed down. Under these experimental conditions the turnover rate was 15 mol  $\text{L}^{-1} \text{h}^{-1}$ .

The conditions under which our *in situ* spectroscopic studies were performed differ from those described by Billig and co workers.<sup>1</sup> Under our experimental condi-

tions we do not observe any ligand degradation via hydrolysis or reaction with aldehyde, as determined by  $^{31}\text{P}$  NMR spectroscopy. Also, mass transfer of reactive gases from the head space of the NMR tube might not be efficient enough to replenish the solution, which is rapidly being depleted of  $\text{CO}$  and  $\text{H}_2$  by a highly active catalyst. Such mass transfer limited conditions would favor alkene isomerization. In the high pressure FT-IR experiments, in which there is efficient stirring (~1500 rpm) to overcome mass transfer limitations, however, it is difficult to quantify the degree of isomerization due to the overlap of multiple  $\text{C}=\text{C}$  stretching bands.

**Isolation and Characterization of  $\text{Rh}(\text{bbmb})(\text{CO})_2\text{H}$  and  $\text{Rh}_2(\text{bbmb})_2(\text{CO})_4$ .** The identification of the above species required their independent syntheses and characterization. Figure 2 shows the  $^1\text{H}$ ,  $^{31}\text{P}\{^1\text{H}\}$ , and  $^{13}\text{C}\{^1\text{H}\}$  NMR assignments of **1** that were obtained from the  $^{13}\text{C}$ -enriched compound. The IR spectrum in toluene of **1** exhibits two bands at 2074 and 2016  $\text{cm}^{-1}$  in the  $\nu_{\text{CO}}$  region and a hydride band at 1989  $\text{cm}^{-1}$ . These assignments were confirmed by preparation of  $\text{Rh}(\text{bbmb})(\text{CO})_2\text{D}$ , whose IR showed no absorption at 1989  $\text{cm}^{-1}$  and a slight shift to lower frequency in the other two bands. The decrease in the  $\nu_{\text{CO}}$  stretching frequencies upon deuteration corroborates the assignment of  $\nu_{\text{Rh}-\text{H}}$  as being lower in energy than  $\nu_{\text{Rh}-\text{CO}}$  and is consistent with previous observations.<sup>14</sup> Definitive assignment of  $\nu_{\text{Rh}-\text{D}}$ , however, was complicated by other

(14) Vaska, L. *J. Am. Chem. Soc.* **1966**, *88*, 4100.

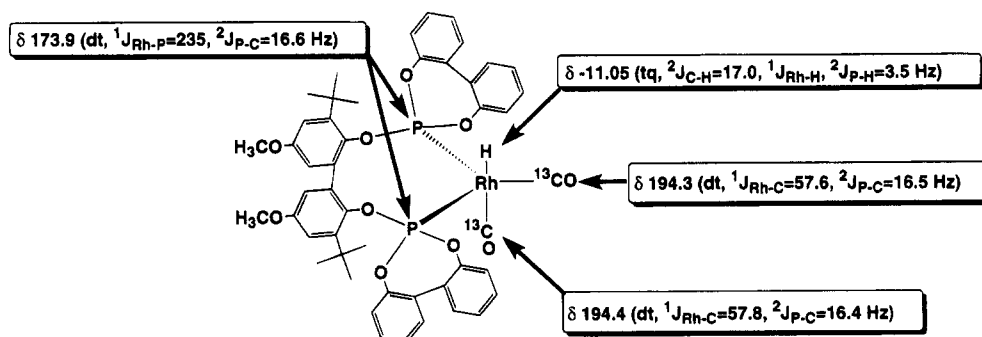
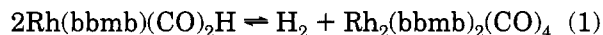


**Figure 2.**  $^{13}\text{C}\{^1\text{H}\}$  NMR (125 MHz),  $^{31}\text{P}\{^1\text{H}\}$  NMR (121 MHz), and  $^1\text{H}$  NMR (500 MHz) of  $\text{Rh}(\text{bbmb})(^{13}\text{CO})_2\text{H}$  in  $\text{CD}_2\text{Cl}_2$  at 23 °C.

features in the region of the spectrum anticipated from force constant calculations.

Heating a brown-red toluene solution of **1** under a purge of CO led to complete conversion to orange **3** and **4** in a constant 4:1 ratio. The  $^{31}\text{P}\{^1\text{H}\}$  NMR spectrum showed a pair of AA'A''A''XX' patterns similar to the patterns for A-frame dirhodium species,<sup>15–19</sup> and the  $^1\text{H}$  NMR spectrum did not contain any hydride signals. The IR spectrum indicated the presence of both terminal (2078 (m), 2052 (m), 2036 (msh), 2026 (ssh), 2011 (s), and 1968 (wsh)  $\text{cm}^{-1}$ ) and bridging (1865 (w), 1830 (w), 1802 (w), and 1734 (w)  $\text{cm}^{-1}$ ) carbonyls, and the FAB/MS was consistent with their formulation as two isomers of  $\text{Rh}_2(\text{bbmb})_2(\text{CO})_4$ . These data are insufficient to determine the structures of **3** or **4**, but the  $^{31}\text{P}$  NMR spectrum does favor structures that have the bis(phosphite) ligands bridging between the two rhodiums. A related chelating-to-bridging transformation was observed in the oxidative coupling of  $\text{Ru}(\text{bbmb})(\text{CO})_3$  to give  $[\text{Ru}_2(\text{bbmb})_2(\text{CO})_6]^{2+}$ ,<sup>20</sup> and the X-ray structural analysis of  $\text{Rh}_4(\text{bnpap})(\text{CO})_{10}$ <sup>21</sup> (bnpap = 2,2'-bis[(1,1'-biphenyl-2,2'-diyl)phosphite]-1,1'-binaphthyl) verifies the ability of bulky bis(phosphite) ligands to bridge between two metals. Reports of other dirhodium complexes that display AA'A''A''XX'  $^{31}\text{P}$  NMR patterns and that are structurally characterized have appeared in the case of  $[\text{Rh}(\text{dppe})\text{Cl}]_2(\mu\text{-Cl})_2(\mu\text{-CH}_2)$ <sup>22</sup> and  $[\text{Rh}(\text{dippe})]_2(\mu\text{-H})_2$ .<sup>23</sup> The  $^{31}\text{P}$  NMR data are not reported in sufficient detail to compare the important fine structural features of the spectra of these chelating rhodium diphosphine complexes to the ones in our study.

Solutions of a mixture of **3** and **4** react quantitatively with  $\text{H}_2$  or  $\text{H}_2/\text{CO}$  (20 atm) at 60 °C in 17 min to regenerate **1**. This facile reaction, represented in eq 1, is consistent with the chemistry of  $\text{Co}_2(\text{CO})_8$ <sup>24,25</sup> and  $\text{Rh}(\text{PPh}_3)_2(\text{CO})_2\text{H}$ .<sup>26</sup>



**Alkene Isomerization.** 1-Octene isomerization by **1** was rapid at 23 °C but short-lived in the absence of

CO and  $\text{H}_2$ . After 30 turnovers  $^{31}\text{P}$  NMR spectroscopy showed that **1** converted irreversibly (under these conditions) to an unidentified species. Addition of CO to the system slowed the rate of isomerization.

**Alkene Insertion into the Rh–H Bond.** To probe the intimate mechanistic process responsible for the regioselectivity of the overall reaction, we undertook a study of the rate of alkene insertion into the Rh–H bond. We chose 3,3-dimethylbutene as our representative alkene because (1) the possibility of isomerization did not exist, thus simplifying our analysis, and (2) the sterically disproportionate ends of the double bond provide a higher limit test of this effect. The exchange events shown in Scheme 1 were rapid enough at 23 °C, under vacuum, to measure using magnetization transfer experiments. Scheme 1 shows the exchange processes involving the four-spin system of the rhodium hydride and the internal, cis-terminal, and trans-terminal vinyl hydrogens of 3,3-dimethylbutene. The four sites involved in the exchange (shown in boxes) are the only observable species which are related by an underlying chemical mechanism (dashed lines), on the basis of well-established organometallic chemistry. The “outlined” H's represent the (spin) labeled hydrogens leading to the magnetization transfer.

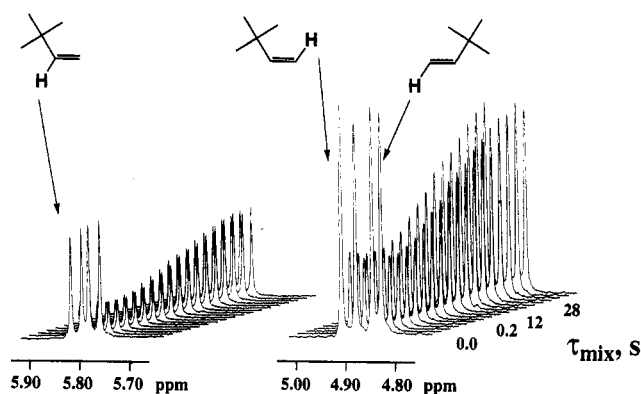
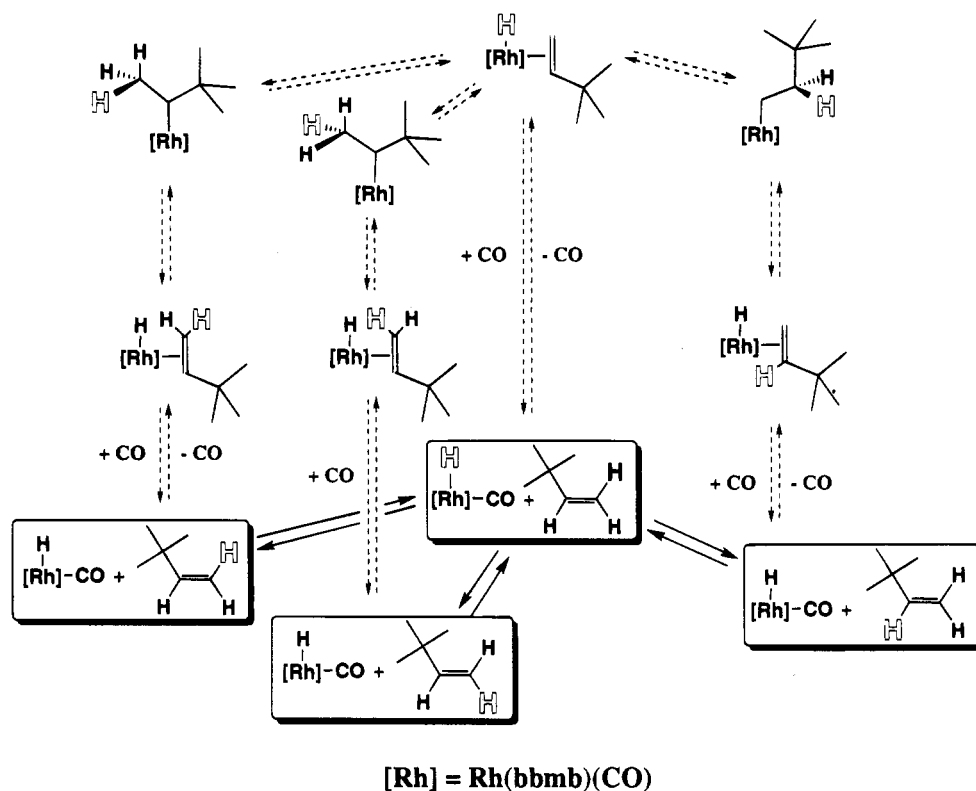
Consequently, exchange of Rh–H with the internal vinyl hydrogen of 3,3-dimethylbutene involves insertion of 3,3-dimethylbutene in a *terminal* manner, followed by  $\beta$ -hydride elimination of the geminal methylene hydrogen of the putative linear rhodium alkyl. Conversely, insertion of the alkene in an *internal* manner, leading to a branched rhodium alkyl, followed by scrambling of the terminal methyl hydrogens, brings about exchange of Rh–H with the terminal vinyl hydrogens of 3,3-dimethylbutene.

Figure 3 shows the vinylic region of the spectra during the experiment. The time-dependent  $z$ -magnetization of the four sites (three of which are shown here) shown in this figure were quantitatively expressed by a series of four coupled differential equations, derived from the Bloch equations modified for chemical exchange. Figure 4 shows plots of the areas of the internal and terminal vinyl hydrogens vs delay time after selective saturation of the rhodium hydrogen along with the best-fit solu-

- (15) Jenkins, J. A.; Cowie, M. *Organometallics* **1992**, *11*, 2767.  
 (16) Kramarz, K. W.; Eisenberg, R. *Organometallics* **1992**, *11*, 1997.  
 (17) Kubiak, C. P.; Woodcock, C.; Eisenberg, R. *Inorg. Chem.* **1982**, *21*, 2119.  
 (18) Mague, J. T.; Sanger, A. R. *Inorg. Chem.* **1979**, *18*, 2060.  
 (19) Shafiq, F.; Eisenberg, R. *Inorg. Chem.* **1993**, *32*, 3287.  
 (20) Moasser, B.; Gross, C.; Gladfelter, W. L. *J. Organomet. Chem.*, **1994**, *471*, 201.  
 (21) Moasser, B.; Gladfelter, W. L. Submitted for publication in *Inorg. Chim. Acta*.  
 (22) Ball, G. E.; Cullen, W. R.; Fryzuk, M. D.; James, B. R.; Rettig, S. J. *Organometallics* **1991**, *10*, 3767.  
 (23) Fryzuk, M. D.; Jones, T.; Einstein, F. W. B. *Organometallics* **1984**, *3*, 185.

- (24) Alemdaroglu, N. H.; Penninger, J. M. L.; Oltay, E. *Monatsh. Chem.* **1976**, *107*, 1043.  
 (25) Ungváry, F.; Markó, L. *J. Organomet. Chem.* **1980**, *193*, 383.  
 (26) Evans, D.; Yagupsky, G.; Wilkinson, G. *J. Chem. Soc. A* **1968**, 2660.

## Scheme 1. Spin Saturation Transfer Mechanism



**Figure 3.**  $^1\text{H}$  NMR (500 MHz) spectrum of the vinylic region showing magnetization transfer between  $\text{Rh}(\text{bbmb})(\text{CO})_2\text{H}$ , (1) and 3,3-dimethylbutene in  $\text{C}_6\text{D}_6$  at  $23^\circ\text{C}$ , using the selective saturation pulse sequence.

tions from the numerical integration. The  $k_{\text{exchange}}$ 's obtained from these calculations are shown in Figure 5.

Surprisingly, the rhodium hydride was found to exchange at nearly the same rate with the *cis*-terminal ( $0.62\text{ s}^{-1}$ ), *trans*-terminal ( $0.62\text{ s}^{-1}$ ), and the internal ( $0.51\text{ s}^{-1}$ ) vinyl hydrogens of 3,3-dimethylbutene even though the two sides of the double bond provide a sizeable steric contrast for the insertion step. In three separate experiments changing the concentration of alkene relative to rhodium from 1 to 5 to 10 equiv caused no change in rate of exchange. The rate independence of alkene concentration and the observation of 1 as the only rhodium species during the magnetization transfer experiment are supportive of dissociation of CO from 1 as the rate-determining step in the overall exchange mechanism (Scheme 1). Because initial binding of 3,3-dimethylbutene to rhodium is unlikely to predispose the reaction to any particular regioisomer

of the ultimate rhodium alkyl, it is the latter microscopic step (migratory insertion of alkene), among the complex series of events implied in Scheme 1, which is responsible for the small differences in the overall exchange rates. The stabilities of the intermediate rhodium alkyls are thus reflected in their transition states for insertion. In any event, it is the overall insertion of alkene whose rate is evaluated by this experiment and is relevant to the hydroformylation reaction.

## Discussion

The reaction between  $\text{Rh}(\text{acac})(\text{CO})_2$  and bbmb is rapid at room temperature giving  $\text{Rh}(\text{bbmb})(\text{acac})$ , (2), which subsequently converts smoothly to  $\text{Rh}(\text{bbmb})(\text{CO})_2\text{H}$ , (1) under catalytic conditions. It is clear from the *in situ*  $^1\text{H}$  NMR results that 1 is a very efficient alkene isomerization catalyst, effecting rapid isomerization even at very small concentrations. The isomerization of 1-octene, catalyzed by 1, was independently studied and shown to be first order in 1. The reaction proceeds to equilibrium at a fast rate, the equilibrium composition of the alkenes corresponding favorably with that predicted from calculations based on Benson's thermochemical data.<sup>27</sup> Under hydroformylation conditions, as observed by *in situ*  $^1\text{H}$  NMR spectra, most of the 1-octene was converted to *cis*- and *trans*-2-octene before hydroformylation began. These experiments, along with the saturation transfer results, demonstrate that the alkene insertion step is rapid, is reversible, and cannot be regioselective. Because mechanisms involving  $\pi$ -allyl type intermediates could not explain the exchange processes observed with 3,3-dimethylbutene,

(27) Benson, S. W.; Cruickshank, F. R.; Golden, D. M.; Haugen, G. R.; O'Neal, H. E.; Rodgers, A. S.; Shaw, R.; Walsh, R. *Chem. Rev.* **1969**, *69*, 279.



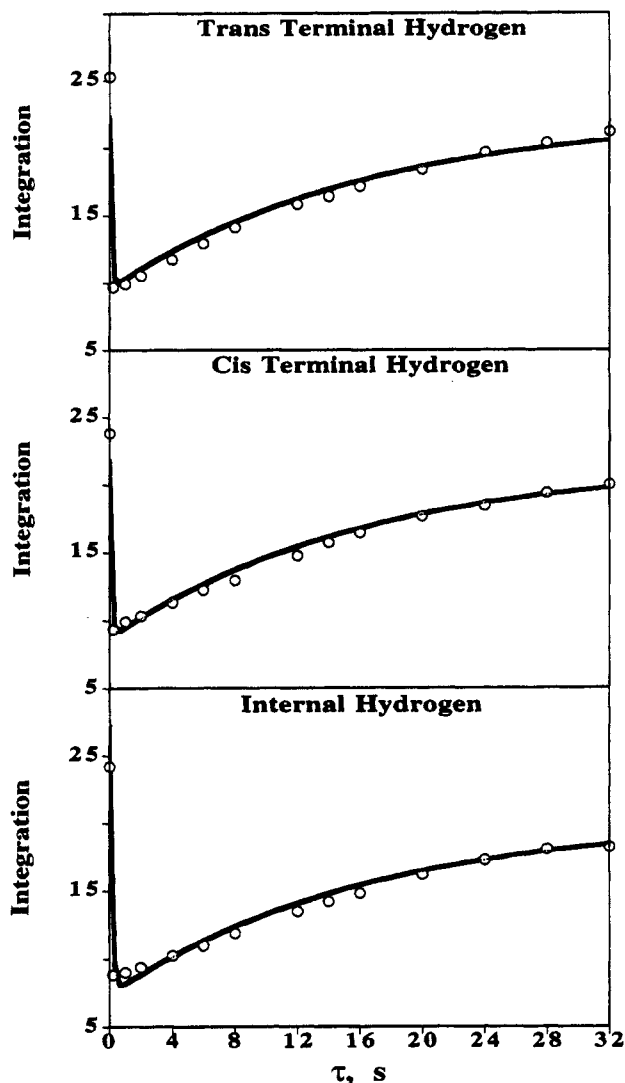


**Figure 4.** Integrated areas of the internal (bottom), trans-terminal (middle), and cis-terminal (top) hydrogens vs  $\tau_{\text{mix}}$ , the delay time after selective saturation of the hydride of  $\text{Rh}(\text{bbmb})(\text{CO})_2\text{H}$  (1).

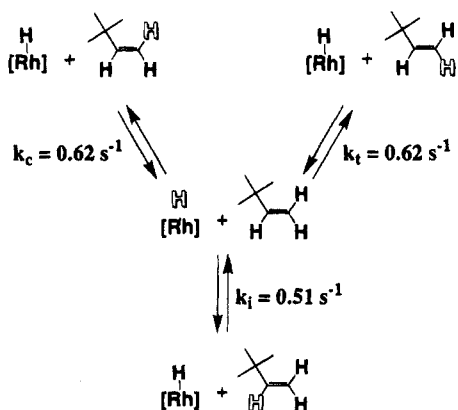
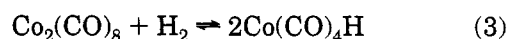
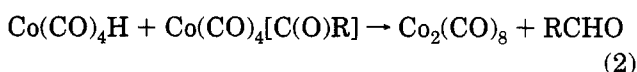


**Figure 5.**  $k_{\text{exchange}}$  for the internal ( $k_i$ ), trans-terminal ( $k_t$ ) and cis-terminal ( $k_c$ ) hydrogens of 3,3-dimethylbutene and  $\text{Rh}(\text{bbmb})(\text{CO})_2\text{H}$  (1).  $[\text{Rh}] = \text{Rh}(\text{bbmb})(\text{CO})_2$ .

we conclude that the hydride on  $\text{Rh}(\text{bbmb})(\text{CO})_2\text{H}$  is transferred to alkene via a migratory insertion/ $\beta$ -elimination mechanism. This contrasts with studies on cobalt systems in which isomerization has been shown to proceed without alkene elimination.<sup>28-31</sup>

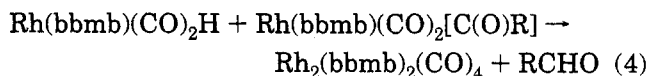
At this stage, we cannot predict which of the remaining steps in the catalytic cycle cause the high regioselectivity observed for bbmb-based catalysts. Considering that rhodium complexes containing bulky monodentate aryl phosphites do not exhibit comparably high regioselectivities,<sup>32,33</sup> the chelating nature of the ligand must be an important factor.

One of the difficulties in making such an assignment is the uncertainty in the mechanism itself. While there appears to be general agreement on the parts of the hydroformylation cycles, some important details remain controversial. Perhaps none has been more discussed than the nature of the aldehyde-forming step. Especially in cobalt-catalyzed reactions there is a substantial body of evidence supporting the binuclear reductive elimination reaction (eq 2) as playing at least a competing role in aldehyde formation.<sup>34-36</sup> One of the attractive aspects of this mechanism is that the activation of molecular hydrogen can be accomplished by the well-documented reaction shown in eq 3.<sup>24</sup>



Related reactions, involving rhodium complexed by several phosphine ligands, are not as likely to compete with effective mononuclear steps, and little evidence for the binuclear reductive elimination has been found. Only in situations especially designed to promote such steps is there a real suggestion that binuclear pathways might be competitive. These include coordinating two rhodiums in close proximity using a complex bridging phosphine ligand.<sup>37,38</sup> The possibility of binuclear reductive elimination in rhodium *mono*(phosphite) complexes has been considered.<sup>39</sup>

The equilibrium between  $\text{Rh}(\text{bbmb})(\text{CO})_2\text{H}$  and  $\text{Rh}_2(\text{bbmb})_2(\text{CO})_4$  (eq 1) occurs rapidly under mild conditions, and this similarity to the cobalt chemistry is striking. Both the small cone angle and the enhanced  $\pi$ -accepting ability of the phosphites (relative to phosphines) may enhance the rate of the binuclear reaction shown in eq 4. A catalytic cycle involving eq 1 as the



$\text{H}_2$  activation step and eq 4 as the aldehyde-producing step can avoid moving into the +3 oxidation state. The reduced basicity of phosphites vs phosphines could render the complex more disposed to proceed via such

(28) Piacenti, F.; Bianchi, M.; Frediani, P.; Matteoli, U.; Lomoro, A. *J. Chem. Soc., Chem. Commun.* **1976**, 789.

(29) Bianchi, M.; Piacenti, F.; Frediani, P.; Matteoli, U. *J. Organomet. Chem.* **1977**, 137, 361.

(30) Casey, C. P.; Cyr, C. R. *J. Am. Chem. Soc.* **1971**, 93, 1280.

(31) Casey, C. P.; Cyr, C. R. *J. Am. Chem. Soc.* **1973**, 95, 2248.

(32) Van Rooy, A.; Orij, E. N.; Kamer, P. C. J.; van Leeuwen, P. W. N. M. *Organometallics* **1995**, 14, 34.

(33) Trzeciak, A. M.; Ziólowski, J. J. *J. Mol. Catal.* **1988**, 48, 319.

(34) Kovács, I.; Ungváry, F.; Markó, L. *Organometallics* **1986**, 5, 209.

(35) Ungváry, F.; Markó, L. *Organometallics* **1983**, 2, 1608.

(36) Hoff, C. D.; Ungváry, F.; King, R. B.; Markó, L. *J. Am. Chem. Soc.* **1985**, 107, 666.

(37) Broussard, M. E.; Juma, B.; Train, S. G.; Peng, W.-J.; Laneman, S. A.; Stanley, G. G. *Science* **1993**, 260, 1784.

(38) Süß-Fink, G. *Angew. Chem., Int. Ed. Engl.* **1994**, 33, 67.

(39) Jongma, T.; Challa, G.; van Leeuwen, P. W. N. M. *J. Organomet. Chem.* **1991**, 421, 121.

a pathway. Further research is necessary first to determine whether such a reaction is possible and second whether it is fast enough to compete with mononuclear processes.

The normal to iso aldehyde regioselectivity for 1-octene hydroformylation, although high, is not as good as what was observed for propene by the Union Carbide group.<sup>1</sup> The choice of substrate and other differences in experimental conditions (e.g., catalyst concentration, ligand to metal ratios, batch vs continuous reactors, and mass transfer efficiencies) could easily account for such a discrepancy. The likelihood of bimetallic reaction pathways, for example, would be greater at higher rhodium concentrations and under mass transfer limited conditions.

### Conclusion

Rh(bbmb)(CO)<sub>2</sub>H, (**1**) was the predominant rhodium species present in the bbmb-modified hydroformylation of 1-octene starting with Rh(acac)(CO)<sub>2</sub>. Isomeric nonanals were formed in a constant n/i of 15:1 during this time. In the depleted H<sub>2</sub> regime of the catalysis, **1** was converted to a pair of closely related dimeric species, **3** and **4**. This equilibrium was independently studied, and it was shown that under CO or N<sub>2</sub> **1** was converted to a constant 4:1 ratio of **3** to **4**. This reaction was reversed by addition of H<sub>2</sub>. These observations raised the possibility of binuclear reductive elimination of aldehyde as the regiochemically significant element in the catalysis.

Isomerization of 1-octene to internal octenes was also rapid under hydroformylation conditions, even in the presence of small amounts of **1**. During the bulk of the catalysis, the substrate consisted entirely as a mixture of internal alkenes on the time scale of the NMR experiment. The 1-catalyzed isomerization of 1-octene was also rapid, although short-lived, under N<sub>2</sub>. The migratory insertion/deinsertion of 3,3-dimethylbutene into the Rh-H bond of **1** was studied using magnetization transfer experiments and found to be rapid and nonselective with regards to regiochemistry of the insertion step. The results require that aldehyde regioselectivity in the hydroformylation reaction be determined subsequent to the alkene insertion step.

### Experimental Section

**General Remarks.** The preparation and purification of materials were performed under prepurified nitrogen using standard Schlenk-type techniques. CP grade CO, <sup>13</sup>CO (99.2%), H<sub>2</sub>, and CO/H<sub>2</sub> (49.1% CO) were purchased from Matheson, Isotec, Genex, and Air Products, respectively. Rh(acac)(CO)<sub>2</sub>,<sup>40,41</sup> Rh<sub>2</sub>(CO)<sub>4</sub>(μ-Cl)<sub>2</sub>,<sup>42</sup> Rh<sub>2</sub>(C<sub>2</sub>H<sub>4</sub>)<sub>4</sub>(μ-Cl)<sub>2</sub>,<sup>43</sup> Rh(acac)(C<sub>2</sub>H<sub>4</sub>)<sub>2</sub>,<sup>44</sup> 2,4-pentanedione-d<sub>8</sub>,<sup>45</sup> and bbmb<sup>20</sup> were prepared according to reported procedures. 1-Nonyl aldehyde, 1-octene, and 3,3-dimethyl-1-butene were purchased from Aldrich and distilled prior to use. RhCl<sub>3</sub>·3H<sub>2</sub>O was obtained from Strem. Toluene, *o*-xylene, hexane, tetrahydrofuran, and Et<sub>2</sub>O were distilled from sodium benzophenone ketyl. *o*-Xylene used for IR studies was additionally distilled from sodium. Methylene

chloride was distilled from CaH<sub>2</sub>. Infrared spectra were recorded on a Mattson Polaris FTIR spectrometer equipped with an HgCdTe detector. <sup>1</sup>H, <sup>31</sup>P, and <sup>13</sup>C NMR were recorded at 300, 121, and 75 MHz, respectively, on a Varian VXR-300S spectrometer. Chemical shifts are reported in ppm and referenced to residual deuterated solvent signals for <sup>1</sup>H and <sup>13</sup>C NMR and external 85% H<sub>3</sub>PO<sub>4</sub> (δ 0.00 ppm) for <sup>31</sup>P NMR. Ultraviolet spectra were obtained on a HP 8452A diode array spectrometer at various dilutions and ε's were obtained from Beer's law plots. Low-resolution FAB mass spectra were obtained on a VG 7070E-HF instrument. Microanalyses were performed by M-W-H Laboratories. Melting points are uncorrected.

**Synthesis of Rh(bbmb)(acac).** Dissolution of Rh(acac)(CO)<sub>2</sub> and bbmb in toluene under N<sub>2</sub> led to effervescence and formation of yellow-green **2**. This was recrystallized from 5:1 PhCH<sub>3</sub>/hexane to yield a yellow-brown microcrystalline material in 85% yield. <sup>31</sup>P{<sup>1</sup>H} NMR (PhCH<sub>3</sub>, 121 MHz): δ 146.5 (d, 302 Hz). FAB/MS (*m/e*): [Rh(bbmb)(acac)]<sup>+</sup>, 988; [Rh(bbmb)]<sup>+</sup>, 889. Mp (sealed/N<sub>2</sub>): 110 °C dec.

**Synthesis of Rh(bbmb)(CO)<sub>2</sub>H.** Rh(bbmb)(acac) was generated in the manner described above. Exchanging the atmosphere with 1:1 CO/H<sub>2</sub> in the sealed flask for 45 min led to darkening of the solution to yellow, orange, red, and red-brown. Vacuum distillation of solvent gave a brown oil, which was recrystallized from 10:1 CH<sub>2</sub>Cl<sub>2</sub>/hexane. Methylene chloride was added, and the resulting solution was evaporated to dryness. A further three coevaporations with methylene chloride afforded tan-brown microcrystals of the monomeric rhodium(I) hydride Rh(bbmb)(CO)<sub>2</sub>H in 82% yield. <sup>1</sup>H NMR (C<sub>6</sub>D<sub>6</sub>, 300 MHz): δ 3.19 (s, Ar-OCH<sub>3</sub>), 1.60 (s, Ar-C(CH<sub>3</sub>)<sub>3</sub>), 6.8–7.4 (m, Ar-H<sub>n</sub>), -10.60 (dt, 3.5, 3.5 Hz, Rh-H). <sup>1</sup>H{<sup>31</sup>P} NMR (C<sub>6</sub>D<sub>6</sub>, 300 MHz): -10.60 (d, <sup>1</sup>J<sub>Rh-H</sub> = 3.5 Hz). <sup>31</sup>P{<sup>1</sup>H} NMR (C<sub>6</sub>D<sub>6</sub>, 121 MHz): δ 174.7 (d, 236 Hz). IR (PhCH<sub>3</sub>, cm<sup>-1</sup>): ν<sub>CO</sub>, 2074 (vs), 2016 (vs); ν<sub>Rh-H</sub>, 1989 (w). IR (KBr, cm<sup>-1</sup>): ν<sub>CO</sub>, 2090 (vs), 2016 (vs). Anal. Calcd for C<sub>48</sub>H<sub>45</sub>O<sub>10</sub>P<sub>2</sub>Rh: C, 60.89; H, 4.79; P, 6.54. Found: C, 61.03; H, 4.96; P, 6.33. FAB/MS (*m/e*): [Rh(bbmb)(CO)<sub>2</sub>]<sup>+</sup>, 945; [Rh(bbmb)(CO)]<sup>+</sup>, 917; [Rh(bbmb)H]<sup>+</sup>, 890; [Rh(bbmb)(CO)]<sup>-</sup>, 917; [Rh(bbmb)]<sup>-</sup>, 889. Mp (sealed/N<sub>2</sub>): 110 °C dec.

**Synthesis of Rh(bbmb)(CO)<sub>2</sub>D.** Rh(acac-*d*<sub>7</sub>)(CO)<sub>2</sub> was synthesized from 2,4-pentanedione-*d*<sub>8</sub> and Rh<sub>2</sub>(CO)<sub>4</sub>(μ-Cl)<sub>2</sub>.<sup>42</sup> Rh(bbmb)(CO)<sub>2</sub>D was synthesized in the same fashion as **1** using bbmb, Rh(acac-*d*<sub>7</sub>)(CO)<sub>2</sub> and 1:1 CO/D<sub>2</sub>, in C<sub>6</sub>D<sub>6</sub>. IR (CH<sub>2</sub>Cl<sub>2</sub>, cm<sup>-1</sup>): ν<sub>CO</sub>, 2056 (s), 2005 (s).

**Synthesis of Rh(bbmb)(<sup>13</sup>CO)<sub>2</sub>H.** Rh(bbmb)(<sup>13</sup>CO)<sub>2</sub>H was synthesized from Rh(acac)(<sup>13</sup>CO)<sub>2</sub> and bbmb, as described above, in 85% yield. IR (hexane, cm<sup>-1</sup>): ν<sup>13</sup>CO, 2035 (vs), ν<sup>12</sup>CO 2019 (vs). Rh(acac)(<sup>13</sup>CO)<sub>2</sub> was synthesized by condensing ~2 atm (1.6 mmol) of <sup>13</sup>CO onto an evacuated toluene solution of Rh(acac)(C<sub>2</sub>H<sub>4</sub>)<sub>2</sub> (120 mg, 0.46 mmol, 0.15 M) which had been subjected to three freeze-pump-thaw cycles. When the temperature was raised, the characteristic dichroism of the product appeared. Removal of solvent under vacuum and recrystallization from hexane gave 108 mg (0.42 mmol, 91%) of Rh(bbmb)(<sup>13</sup>CO)<sub>2</sub>. Rh(acac)(C<sub>2</sub>H<sub>4</sub>)<sub>2</sub><sup>44</sup> was obtained from Rh(C<sub>2</sub>H<sub>4</sub>)<sub>4</sub>(μ-Cl)<sub>2</sub> (71%), which was synthesized from RhCl<sub>3</sub>·3H<sub>2</sub>O, (39%).<sup>43</sup> Rh(bbmb)(<sup>13</sup>CO)<sub>2</sub>H was thus available from RhCl<sub>3</sub>·3H<sub>2</sub>O in a total 21% yield.

**Synthesis of Rh<sub>2</sub>(bbmb)<sub>2</sub>(CO)<sub>4</sub> and Isomer.** A red-brown toluene solution of **1** was stirred vigorously at 60 °C, under a purge of CO. <sup>31</sup>P{<sup>1</sup>H} NMR indicated complete conversion to orange **3** and **4** in a constant 4:1 ratio after 30 min. Recrystallization from 5:1 PhCH<sub>3</sub>/hexane afforded orange microcrystalline **3** and **4** in 93% yield. <sup>1</sup>H NMR (C<sub>6</sub>D<sub>6</sub>, 300 MHz): major isomer, δ 3.05 (s, Ar-OCH<sub>3</sub>), 1.45 (s, Ar-C(CH<sub>3</sub>)<sub>3</sub>), 6.6–7.7 (m, Ar-H<sub>n</sub>); minor isomer, δ 3.15 (s, Ar-OCH<sub>3</sub>), 1.46 (s, Ar-C(CH<sub>3</sub>)<sub>3</sub>), 6.6–7.7 (m, Ar-H<sub>n</sub>). <sup>31</sup>P{<sup>1</sup>H} NMR (C<sub>6</sub>D<sub>6</sub>, 121 MHz): major isomer, δ 170.4, <sup>1</sup>J<sub>Rh-P</sub> + <sup>2</sup>J<sub>Rh-P</sub> = 250.6 Hz; minor isomer, δ 167.2, <sup>1</sup>J<sub>Rh-P</sub> + <sup>2</sup>J<sub>Rh-P</sub> = 257.9 Hz. <sup>13</sup>C{<sup>1</sup>H} NMR (CD<sub>2</sub>Cl<sub>2</sub>, 75 MHz): major isomer (<sup>13</sup>CO enriched), 203.8, 187.1 (these are complex second-order multiplets similar to

(40) Varshavskii, Yu. S.; Cherkasova, T. G. *Russ. J. Inorg. Chem. (Engl. Transl.)* **1967**, *12*, 899.

(41) Bonati, F.; Wilkinson, G. *J. Chem. Soc.* **1964**, 3156.

(42) McCleverty, J. A.; Wilkinson, G. *Inorg. Synth.* **1991**, *28*, 84.

(43) Cramer, R. *Inorg. Synth.* **1990**, *28*, 26.

(44) Cramer, R. *Inorg. Synth.* **1974**, *15*, 14.

(45) Doyle, G.; Tobias, R. S. *Inorg. Chem.* **1968**, *7*, 2479.

those discussed in ref 18); minor isomer ( $^{13}\text{C}$ O enriched), 197 (br m), 182 (br m). IR ( $\text{PhCH}_3$ ,  $\text{cm}^{-1}$ ):  $\nu_{\text{CO}}$ , 2078 (m), 2052 (m), 2036 (msh), 2026 (ssh), 2011 (s), 1968 (wsh), 1865 (w), 1830 (w), 1802 (w), and 1734 (w). FAB/MS ( $m/e$ ):  $[\text{Rh}_2(\text{bbmb})_2(\text{CO})_4\text{K}]^+$ , 1929;  $[\text{Rh}(\text{bbmb})_2]^+$ , 1676;  $[\text{Rh}_2(\text{bbmb})(\text{CO})_4]^+$ , 1105;  $[\text{Rh}_2(\text{bbmb})]^+$ , 992; UV-vis ( $\text{CH}_2\text{CN}$ ;  $\lambda_{\text{max}}$ , nm ( $\epsilon$ ,  $\text{M}^{-1}\text{cm}^{-1}$ ): 326 (5890), 278 (13 434). Mp (sealed/ $\text{N}_2$ ): 125 °C dec.

**Reversible Interconversion of  $\text{Rh}_2(\text{bbmb})_2(\text{CO})_4$  and  $\text{Rh}(\text{bbmb})(\text{CO})_2\text{H}$ .** Stirring an orange toluene solution of  $\text{Rh}_2(\text{bbmb})_2(\text{CO})_4$ , under a purge of  $\text{H}_2$ , at 60 °C caused a color change to red-brown within 5 min.  $^{31}\text{P}\{^1\text{H}\}$  NMR shows complete conversion to  $\text{Rh}(\text{bbmb})(\text{CO})_2\text{H}$ , without decomposition. The same 4:1 mixture of dimers is re-formed as described above.

**Spin Saturation Transfer Experiment with  $\text{Rh}(\text{bbmb})(\text{CO})_2\text{H}$  and 3,3-Dimethyl-1-butene.** A rigorously anaerobic NMR sample was prepared in the following fashion. A 5 mm NMR tube was charged with 25 mg (0.026 mmol) of  $\text{Rh}(\text{bbmb})(\text{CO})_2\text{H}$  and evacuated. This was cooled to -78 °C, and approximately 3.5  $\mu\text{L}$  (2.3 mg, 1 equiv relative to Rh) of freshly distilled 3,3-dimethyl-1-butene and 0.45 mL of a  $\text{C}_6\text{D}_6$  (dried over  $\text{Na}^0/\text{Ph}_2\text{CO}$ ) were vacuum-distilled into the tube to form a final 58 mM solution. The NMR tube was flame-sealed under vacuum.

Spectra were acquired on a 500 MHz Varian Unity spectrometer over 2 h. A selective 90° saturating pulse was applied to the center of the Rh-H quartet, while the time dependencies of all the signals were monitored using a 90° nonselective pulse, applied at variable intervals ( $\tau_{\text{mix}}$ ) after application of the selective pulse. A delay of 10.0 s was used before application of each subsequent selective pulse to ensure thermal equilibration of all spin states. The nonselective observation pulse was 12.8  $\mu\text{s}$  long. The described pulse sequence ( $\text{RD}-\pi/2_{\text{sel}}-\tau_{\text{mix}}-\pi/2$ -acquisition) was used to acquire 18 spectra. A total of 16 scans were accumulated for each value of  $\tau_{\text{mix}}$ , from 0.00 to 32 s. The temperature was regulated at 23 °C, and spectra were acquired without sample spinning. The area under the internal and terminal alkene multiplets was determined in an absolute integration mode for each individual spectrum. Plots of these values vs  $\tau_{\text{mix}}$  provided the necessary data for determination of kinetic pseudo-first-order rates. Difference spectra from a "dummy" decoupling frequency showed no detectable effect on the intensity or integrals of the hydride or olefinic signals. Using longer preacquisition delays showed no change as well, ensuring complete relaxation of the nuclei within the given acquisition conditions. Higher selective pulse power levels also had no effect, guaranteeing complete saturation of the hydride signal. The extent of NOE contributions to the magnetizations of the vinylic hydrogens of 3,3-dimethyl-1-butene was evaluated using the method of Neuhaus.<sup>46</sup> Selective, prolonged, low-power saturation of individual lines of each multiplets was used to suppress selective population transfer and measure NOE exclusively. NOE effects measured using this highly sensitive method were found to be less than 2%.

The rate constants for the insertion of 3,3-dimethyl-1-butene into the rhodium-hydride bond of  $\text{Rh}(\text{bbmb})(\text{CO})_2\text{H}$  were determined by evaluating the set of coupled Bloch equations

modified for chemical exchange<sup>47</sup> describing the time dependence of the longitudinal magnetizations ( $\mathbf{M}(t)$ ) of a four-site system ( $\text{Rh}-\text{H}$ ,  $^i\text{BuCH}=\text{CH}_2$ ,  $\text{cis-}^i\text{BuCH}=\text{CHH}$ , and  $\text{trans-}^i\text{BuCH}=\text{CHH}$ ):

$$d\mathbf{M}(t)/dt = (\mathbf{K} + \mathbf{R})(\mathbf{M}(t) - \mathbf{M}^\circ)$$

Here,  $\mathbf{K}$  is the exchange matrix whose diagonal elements describe the rate of loss of magnetization ( $M_i$ ) from a given site and whose off-diagonal elements describe the rate of transfer of magnetization between different sites. Statistical effects were incorporated into  $\mathbf{K}$ , by means of a Kubo-Sack probability matrix.<sup>48</sup> The relaxation matrix,  $\mathbf{R}$ , contains the spin-lattice relaxation rates ( $1/T_1$ ) for the individual sites and  $\mathbf{M}^\circ$  contains the magnetizations of the exchanging species at thermal equilibrium. Individual  $T_1$ 's were measured under conditions of temperature, concentration, and medium identical with those in the spin saturation transfer experiment. A Runge-Kutta routine within *Mathematica*<sup>49</sup> was used to integrate the system of four differential equations. The parameters of initial intensities,  $\mathbf{M}(0)$ , equilibrium intensities,  $\mathbf{M}^\circ$ ,  $T_1$ 's and exchange rates were varied to provide a best fit to the experimental time-dependent magnetizations, which were plotted as absolute integrations of the  $^1\text{H}$  NMR signals.

**High-Pressure NMR and IR Experiments.** In a typical NMR experiment,  $\text{Rh}(\text{acac})(\text{CO})_2$  (17 mg, 0.066 mmol, 0.17 M, 18.7 ppt), bbmb (57 mg, 0.072 mmol, 0.18 M), and freshly distilled 1-octene (200  $\mu\text{L}$ , 143 mg, 1.27 mmol, 3.18 M) were dissolved in benzene- $d_6$ , in a  $\text{N}_2$ -filled glovebox, transferred to a high-pressure sapphire NMR tube, and sealed with a titanium alloy pressure valve.<sup>13</sup> The atmosphere in the tube was exchanged by several purge cycles from a 1:1  $\text{CO}/\text{H}_2$  tank and finally set to 20 atm. The tube was then placed in the probe of a 300 MHz Varian Unity spectrometer as expeditiously as possible. Spectra were acquired at various temperatures (see text) while the tube at was spun at  $\sim 26$  Hz.

Similarly, a cylindrical internal reflection cell<sup>50</sup> (a Parr autoclave embedded with a silicon crystal) was charged with  $\text{Rh}(\text{acac})(\text{CO})_2$  (139 mg, 0.54 mmol, 60 mM) and bbmb (425 mg, 0.54 mmol, 60 mM), to which a solution of 1-octene (4.2 mL, 3.0 g, 27 mmol, 3.0 M) in 4.8 mL of *o*-xylene was added under  $\text{N}_2$ , at ambient temperature. The autoclave was first purged with and finally set to 40 atm of 1:1  $\text{CO}/\text{H}_2$ . This corresponds to 28 mmol each of  $\text{CO}$  and  $\text{H}_2$  (based on head space calculations). The IR autoclave was placed in the external bench of a Mattson Polaris FTIR spectrometer, and the spectra were collected as the well-stirred solution ( $\sim 1500$  rpm) was heated at 60 °C. Background spectra at 60 °C and various  $\text{CO}$  pressures were recorded and used for spectral subtraction.

**Acknowledgment.** This work was supported by a grant from the National Science Foundation (Grant No. CHE-9223433).

OM9502190

(47) McConnell, H. M. *J. Chem. Phys.* **1958**, *28*, 430.

(48) Johnson, C. S., Jr.; Moreland, C. G. *J. Chem. Educ.* **1983**, *50*, 477.

(49) Wolfram Research, Inc., Champaign, IL.

(50) Moser, W. R.; Cnossen, J. E.; Wang, A. W.; Krouse, S. A. *J. Catal.* **1985**, *95*, 21.

(46) Neuhaus, D.; Sheppard, R. N.; Bick, I. R. *C. J. Am. Chem. Soc.* **1983**, *105*, 5996.

# Stabilization of 16-Electron Paramagnetic Organoiron Species versus Coordination of Dinitrogen. X-ray Crystal Structures of $[\text{Fe}(\eta^5\text{-C}_5\text{H}_5)(\text{N}_2)(\text{dippe})][\text{BPh}_4]$ , $[\text{Fe}(\eta^5\text{-C}_5\text{Me}_5)(\text{dippe})][\text{BPh}_4]$ , and $[\text{Fe}(\eta^5\text{-C}_5\text{H}_5)\text{Cl}(\text{dippe})][\text{BPh}_4]$ (dippe = 1,2-Bis(diisopropylphosphino)ethane)

Auxiliadora de la Jara Leal, Manuel Jiménez Tenorio, M. Carmen Puerta,\* and Pedro Valerga

Departamento de Ciencia de Materiales e Ingeniería Metalúrgica y Química Inorgánica, Facultad de Ciencias, Universidad de Cádiz, Apto. 40, 11510 Puerto Real, Cádiz, Spain

Received February 27, 1995<sup>⊗</sup>

The purple compound  $[\text{CpFeCl}(\text{dippe})]$  ( $\text{Cp} = \text{C}_5\text{H}_5$ ; dippe = 1,2-bis(diisopropylphosphino)ethane) reacts with dinitrogen and  $\text{Na}[\text{BPh}_4]$  in EtOH or MeOH, to furnish the novel half-sandwich end-on dinitrogen complex  $[\text{CpFe}(\text{N}_2)(\text{dippe})][\text{BPh}_4]$  (**1**). This compound is diamagnetic and dissociates dinitrogen reversibly in thf or acetone solution, to yield the paramagnetic complex  $[\text{CpFe}(\text{dippe})][\text{BPh}_4]$  (**2**). **1** and **2** are in equilibrium in acetone solution under dinitrogen. Thermodynamic parameters for such equilibrium have been estimated. The related complex  $[\text{Cp}^*\text{FeCl}(\text{dippe})]$  ( $\text{Cp}^* = \text{C}_5\text{Me}_5$ ) dissolves in MeOH or EtOH to yield only  $[\text{Cp}^*\text{Fe}(\text{dippe})]^+$ , and no dinitrogen uptake is observed. The X-ray crystal structure of  $[\text{Cp}^*\text{Fe}(\text{dippe})][\text{BPh}_4]$  (**3**) has been determined. The complexes **1–3** react with a variety of neutral donors L ( $\text{L} = \text{CNBu}^t$ , CO, MeCN) furnishing the corresponding adducts  $[\text{CpFe}(\text{L})(\text{dippe})][\text{BPh}_4]$  or  $[\text{Cp}^*\text{Fe}(\text{L})(\text{dippe})][\text{BPh}_4]$ , as expected. The insertion of  $\text{SnCl}_2$  into the Fe–Cl bond only occurs in  $[\text{FeCpCl}(\text{dippe})]$ , yielding  $[\text{CpFe}(\text{SnCl}_3)(\text{dippe})]$ . Both  $[\text{CpFeCl}(\text{dippe})]$  and  $[\text{Cp}^*\text{FeCl}(\text{dippe})]$  are readily oxidized by atmospheric oxygen in alcoholic solution to the corresponding  $\text{Fe}^{\text{III}}$  derivatives,  $[\text{CpFeCl}(\text{dippe})]^+$  and  $[\text{Cp}^*\text{FeCl}(\text{dippe})]^+$ , respectively. The X-ray crystal structure has been determined for  $[\text{CpFeCl}(\text{dippe})][\text{BPh}_4]$ .

## Introduction

It is well established that iron plays an important role in biological<sup>1</sup> as well as in nonbiological<sup>2</sup> nitrogen fixation. Its relevance has been enhanced recently, following an X-ray structural determination of the molybdenum-containing component of the enzyme nitrogenase<sup>3</sup> and the discovery of a nitrogenase that contains iron but no molybdenum or vanadium.<sup>1</sup> Despite these facts, relatively few dinitrogen complexes of iron are known. With very few exceptions, those reported contain tertiary phosphine as coligands. The methods for the preparation include abstraction of loosely bound ligands, displacement of dihydrogen in adducts of the type  $\text{Fe}(\eta^2\text{-H}_2)\text{L}_n$ , direct addition of dinitrogen to a coordinatively unsaturated metal complex, and reduction of a suitable precursor complex under dinitrogen. Thus, sodium tetraphenylborate abstracts chloride from both *trans*- $[\text{FeHCl}(\text{depe})_2]$  and *trans*- $[\text{FeCl}_2(\text{dmpe})_2]$  (*depe* = 1,2-bis(diethylphosphino)ethane; *dmpe* = 1,2-bis(dimethylphosphino)ethane) to yield the corresponding adducts *trans*- $[\text{FeH}(\text{N}_2)(\text{depe})_2][\text{BPh}_4]$ <sup>4</sup> and *trans*- $[\text{FeCl}(\text{N}_2)(\text{dmpe})_2][\text{BPh}_4]$ .<sup>5</sup> The labile dihydrogen ligand in the complexes  $[\text{FeH}_2(\text{H}_2)(\text{PETPh}_2)_3]$  and  $[\text{FeH}(\text{H}_2)(\text{dmpe})_2][\text{BPh}_4]$  is displaced by dinitrogen

furnishing  $[\text{FeH}_2(\text{N}_2)(\text{PETPh}_2)_3]^6$  and *trans*- $[\text{FeH}(\text{N}_2)(\text{dmpe})_2][\text{BPh}_4]$ ,<sup>7</sup> respectively. The five-coordinate, coordinatively unsaturated hydrides  $[\text{FeH}(\text{dppe})_2][\text{BPh}_4]$  and  $[\text{FeH}(\text{pp}_3)][\text{BPh}_4]$  ( $\text{pp}_3 = \text{P}(\text{CH}_2\text{CH}_2\text{PPh}_2)_3$ ) add dinitrogen yielding the hydrido dinitrogen complexes *trans*- $[\text{FeH}(\text{N}_2)(\text{dppe})_2][\text{BPh}_4]$ <sup>8</sup> and *cis*- $[\text{FeH}(\text{N}_2)(\text{pp}_3)][\text{BPh}_4]$ .<sup>9</sup> More recently, it has been reported that the reduction of  $[\text{FeCl}_2(\text{depe})_2]$  with sodium naphthalenide in tetrahydrofuran under dinitrogen affords the iron(0) dinitrogen complex  $[\text{Fe}(\text{N}_2)(\text{depe})_2]$ , which has been structurally characterized.<sup>10</sup> Besides these systems, there are some reports on the synthesis of half-sandwich bridging  $\text{N}_2$  complexes of the type  $[\{\text{CpFe}(\text{R}_2\text{PCH}_2\text{CH}_2\text{PR}_2)_2\}_2(\mu\text{-N}_2)]^{2+}$  ( $\text{Cp} = \text{C}_5\text{H}_5$ ;  $\text{R} = \text{Ph}, \text{Me}$ ).<sup>11,12</sup> These complexes are poorly characterized, and not much is known about their structure and properties. No half-

(4) Bancroft, G. M.; Mays, M. J.; Prater, B. E.; Stefanini, F. P. *J. Chem. Soc. A* **1970**, 2146. Bancroft, G. M.; Mays, M. J.; Prater, B. E. *J. Chem. Soc. A* **1970**, 956.

(5) Hughes, D. L.; Jiménez Tenorio, M.; Leigh, G. J.; Rowley, A. T. *J. Chem. Soc., Dalton Trans.* **1993**, 75.

(6) (a) Aresta, M.; Giannocaro, P.; Rossi, M.; Sacco, A. *Inorg. Chim. Acta* **1971**, 5, 115. (b) Kubas, G. J.; Caulton, K. G.; Van Der Sluys, L. D.; Eckert, J.; Eisenstein, O.; Hall, J. H.; Huffman, J. C.; Jackson, S. A.; Koetzle, T. F.; Vergamini, P. *J. Am. Chem. Soc.* **1990**, 112, 4831.

(7) Hills, A.; Hughes, D. L.; Jiménez Tenorio, M.; Leigh, G. J.; Rowley, A. T. *J. Chem. Soc., Dalton Trans.* **1993**, 3041.

(8) Giannocaro, P.; Rossi, M.; Sacco, A. *Coord. Chem. Rev.* **1972**, 8, 77. Giannocaro, P.; Sacco, A. *Inorg. Synth.* **1977**, 17, 69.

(9) Stoppioni, P.; Mani, F.; Sacconi, L. *Inorg. Chim. Acta* **1974**, 11, 227.

(10) Komiya, S.; Akita, M.; Yoza, A.; Kasuga, N.; Fukuoka, A.; Kai, Y. *J. Chem. Soc., Chem. Commun.* **1993**, 787.

(11) Sellmann, D.; Kleinschmidt, E. *Angew. Chem., Int. Ed. Engl.* **1975**, 14, 571.

<sup>⊗</sup> Abstract published in *Advance ACS Abstracts*, July 1, 1995.

(1) Joergen, R. D.; Bishop, P. E. *Microbiology* **1988**, 16, 1. Chisnell, J. R.; Premakumar, R.; Bishop, P. E. *J. Bacteriol.* **1988**, 170, 27.

(2) Leigh, G. J. *Acc. Chem. Res.* **1992**, 25, 177; Shilov, A. E. *New. J. Chem.* **1992**, 16, 213.

(3) Kim, J.; Rees, D. C. *Science* **1992**, 257, 1677.

sandwich complex of iron containing a terminal N<sub>2</sub> ligand is known. On the other hand, dinitrogen has shown in most cases to be unreactive toward direct protonation by acids, although there are some examples of dinitrogen reduction to ammonia and/or hydrazine mediated by dinitrogen complexes of iron.<sup>7,13–15</sup> Continuing our studies on the effects of bulky phosphine ligands on the binding and activation of small molecules, we have now shown that the complexes [CpFeCl(dippe)] and [Cp\*FeCl(dippe)]<sup>16</sup> have labile chloride ligands, which can be easily abstracted by Na[BPh<sub>4</sub>] in alcoholic solution to yield paramagnetic, coordinatively unsaturated species. In the case of the Cp derivative, this species reacts further with dinitrogen yielding the end-on dinitrogen complex [CpFe(N<sub>2</sub>)(dippe)][BPh<sub>4</sub>]. In this work we describe the synthesis, characterization, and reactivity of such compounds, including the structural aspects as well as the study of their behavior in solution.

### Experimental Section

All synthetic operations were performed under a dry dinitrogen atmosphere following conventional Schlenk or drybox techniques. Tetrahydrofuran, diethyl ether, and petroleum ether (boiling point range 40–60 °C) were distilled from the appropriate drying agents. All solvents were deoxygenated immediately before use. 1,2-Bis(diisopropylphosphino)ethane,<sup>17</sup> [Fe(C<sub>5</sub>H<sub>5</sub>)Cl(dippe)],<sup>16</sup> and [Fe(C<sub>5</sub>Me<sub>5</sub>)Cl(dippe)]<sup>16</sup> were prepared according to the literature. IR spectra were recorded in Nujol mulls on a Perkin-Elmer 881 spectrophotometer. NMR spectra were taken on Varian Unity 400 MHz or Varian Gemini 200 MHz equipment. Chemical shifts are given in ppm from SiMe<sub>4</sub> (<sup>1</sup>H and <sup>13</sup>C{<sup>1</sup>H}), 85% H<sub>3</sub>PO<sub>4</sub> (<sup>31</sup>P{<sup>1</sup>H}), or Sn<sup>n</sup>-Bu<sub>4</sub> (<sup>119</sup>Sn). Magnetic moments were measured in solution using the Evans method.<sup>18</sup> Microanalyses were by Dr. Manuel Arjonilla at the CSIC-Instituto de Ciencias Marinas de Andalucía or by Butterworth Laboratories, Middlessex, U.K.

**[Fe(C<sub>5</sub>H<sub>5</sub>)(N<sub>2</sub>)(dippe)][BPh<sub>4</sub>] (1).** To a solution of [FeCl(C<sub>5</sub>H<sub>5</sub>)(dippe)] (0.2 g, ca. 0.5 mmol) in MeOH (20 mL) under dinitrogen, an excess of Na[BPh<sub>4</sub>] (0.34 g, 1 mmol) dissolved in MeOH (10 mL) was added. The resulting mixture was stirred at room temperature for 1 h. During this time, a mustard-yellow precipitate is formed. It was filtered out, washed with ethanol and petroleum ether, and dried *in vacuo*. This product was recrystallized from THF/ethanol as amber-brown crystals suitable for X-ray diffraction. Yield: 0.21 g, 58%. Anal. Calcd for C<sub>43</sub>H<sub>57</sub>N<sub>2</sub>BF<sub>2</sub>FeP<sub>2</sub>: C, 70.06; H, 7.80; N, 3.83. Found: C, 70.1; H, 7.58; N, 3.4. IR: ν(N=N) 2112 cm<sup>-1</sup>. NMR: <sup>1</sup>H (acetone-*d*<sub>6</sub>), δ 5.061 (s, C<sub>5</sub>H<sub>5</sub>); <sup>31</sup>P{<sup>1</sup>H}, 98.37 (s). This compound coexists in acetone solution under dinitrogen with paramagnetic [Fe(C<sub>5</sub>H<sub>5</sub>)(dippe)<sub>2</sub>][BPh<sub>4</sub>] (2) as an equilibrium mixture.

**[Fe(C<sub>5</sub>H<sub>5</sub>)(dippe)][BPh<sub>4</sub>] (2).** This compound can be obtained by following a procedure analogous to that for 1, using an argon atmosphere instead of dinitrogen, although in rather

poor yield (25%). The following method has shown to be more efficient: [Fe(C<sub>5</sub>H<sub>5</sub>)(N<sub>2</sub>)(dippe)][BPh<sub>4</sub>] (1) (0.36 g, ca. 0.5 mmol) was dissolved in acetone (20 mL) under argon. An effervescence was observed, corresponding to the evolution of dinitrogen. Once the effervescence ceased, the mixture was stirred under argon at room temperature for 10 min. Then, the solution was concentrated to ca. 3–4 mL. Addition of petroleum ether afforded a brown precipitate, which was filtered out, washed with petroleum ether, and dried *in vacuo*. Yield: quantitative. Anal. Calcd for C<sub>43</sub>H<sub>57</sub>BF<sub>2</sub>FeP<sub>2</sub>: C, 73.5; H, 8.12. Found: C, 73.3; H, 8.26. μ<sub>eff</sub> 3.6 μ<sub>B</sub> (acetone-*d*<sub>6</sub>, 293 K). NMR (acetone-*d*<sub>6</sub>): <sup>1</sup>H, δ -37.2, -8.1, -0.8, 3.21, 17.3, 38.0 ppm.

**[Fe(C<sub>5</sub>Me<sub>5</sub>)(dippe)][BPh<sub>4</sub>] (3).** A solution of [FeCl(C<sub>5</sub>Me<sub>5</sub>)(dippe)] (0.49 g, 1 mmol) in deoxygenated MeOH (20 mL) under dinitrogen or argon was treated with an excess of Na[BPh<sub>4</sub>] (0.5 g) in MeOH (10 mL). A yellow-brown crystalline precipitate was immediately formed. The mixture was stirred for 15 min. Then, it was filtered out, washed with ethanol and petroleum ether, and dried *in vacuo*. It was recrystallized from hot acetone or an acetone/EtOH mixture. Yield: 0.46 g, 60%. Anal. Calcd for C<sub>48</sub>H<sub>67</sub>BF<sub>2</sub>FeP<sub>2</sub>: C, 72.7; H, 8.46. Found: C, 72.4; H, 8.31. μ<sub>eff</sub> 3.8 μ<sub>B</sub> (acetone-*d*<sub>6</sub>, 293 K). NMR (acetone-*d*<sub>6</sub>): <sup>1</sup>H, δ -42.60, -14.32, 3.80, 6.94, 7.47, 48.85.

**[Fe(C<sub>5</sub>H<sub>5</sub>)(CNBu<sup>t</sup>)(dippe)][BPh<sub>4</sub>] (4).** To a solution of [Fe(C<sub>5</sub>H<sub>5</sub>)Cl(dippe)] (0.2 g, ca. 0.5 mmol) in MeOH (20 mL) a slight excess of CNBu<sup>t</sup> (0.2 mL) was added. The purple solution changed immediately to yellow. It was stirred for 15 min at room temperature. Then Na[BPh<sub>4</sub>] (0.34 g) dissolved in ethanol (10 mL) was added. A yellow, crystalline precipitate was obtained. It was filtered out, washed with ethanol and petroleum ether, and dried *in vacuo*. The product was recrystallized from acetone/EtOH. Yield: 0.27 g 69%. This product can also be obtained by treatment of acetone solutions of 1 or 2 with CNBu<sup>t</sup>, followed by addition of EtOH, concentration, and cooling to -20 °C. Anal. Calcd for C<sub>48</sub>H<sub>66</sub>BF<sub>2</sub>FeNP<sub>2</sub>: C, 73.4; H, 8.41; N, 1.8. Found: C, 72.8; H, 8.75; N, 1.8. IR: ν(C≡N) 2084 cm<sup>-1</sup>. NMR (CDCl<sub>3</sub>): <sup>1</sup>H, δ 1.489 (s, CNC(CH<sub>3</sub>)<sub>3</sub>), 4.861 (t, *J*(H,P) = 1.2 Hz, C<sub>5</sub>H<sub>5</sub>); <sup>31</sup>P{<sup>1</sup>H}, 108.55 (s); <sup>13</sup>C{<sup>1</sup>H}, 19.168, 19.355, 19.440, 19.746 (s, P(CH(CH<sub>3</sub>)<sub>2</sub>)<sub>2</sub>), 23.554 (t, *J*(C,P) = 18.0 Hz, PCH<sub>2</sub>), 29.079 (t, *J*(C,P) = 12.8 Hz, P(CH(CH<sub>3</sub>)<sub>2</sub>)<sub>2</sub>), 29.674 (t, *J*(C,P) = 9.2 Hz, P(CH(CH<sub>3</sub>)<sub>2</sub>)<sub>2</sub>), 30.592 (s, C(CH<sub>3</sub>)<sub>3</sub>), 58.556 (s, C(CH<sub>3</sub>)<sub>3</sub>), 78.377 (s, C<sub>5</sub>H<sub>5</sub>), 164.853 (t, *J*(C,P) = 16.2 Hz, CNBu<sup>t</sup>).

**[Fe(C<sub>5</sub>Me<sub>5</sub>)(CNBu<sup>t</sup>)(dippe)][BPh<sub>4</sub>] (5).** This compound was obtained in a fashion analogous to that for 4, starting from either [Cp\*FeCl(dippe)] in MeOH or compound 3 in acetone. Yield: 74%. Anal. Calcd for C<sub>53</sub>H<sub>76</sub>BF<sub>2</sub>FeNP<sub>2</sub>: C, 74.4; H, 8.90; N, 1.6. Found: C, 75.4; H, 9.13; N, 1.42. IR: ν(C≡N) 2087 cm<sup>-1</sup>. NMR (CDCl<sub>3</sub>): <sup>1</sup>H, δ 1.537 (s, CNC(CH<sub>3</sub>)<sub>3</sub>), 2.052 (s, C<sub>5</sub>Me<sub>5</sub>); <sup>31</sup>P{<sup>1</sup>H}, 91.22 (s); <sup>13</sup>C{<sup>1</sup>H}, 10.652 (s, C<sub>5</sub>(CH<sub>3</sub>)<sub>5</sub>), 18.837, 18.845, 19.644, 20.766 (s, P(CH(CH<sub>3</sub>)<sub>2</sub>)<sub>2</sub>), 19.049 (t, *J*(C,P) = 19.9 Hz, PCH<sub>2</sub>), 24.506 (t, *J*(C,P) = 6.6 Hz, P(CH(CH<sub>3</sub>)<sub>2</sub>)<sub>2</sub>), 27.719 (t, *J*(C,P) = 12.7 Hz, P(CH(CH<sub>3</sub>)<sub>2</sub>)<sub>2</sub>), 30.049 (s, C(CH<sub>3</sub>)<sub>3</sub>), 57.57 (s, C(CH<sub>3</sub>)<sub>3</sub>), 89.77 (s, C<sub>5</sub>Me<sub>5</sub>), 170.23 (m, CNBu<sup>t</sup>).

**[Fe(C<sub>5</sub>H<sub>5</sub>)(CO)(dippe)][BPh<sub>4</sub>] (6).** CO was bubbled through a solution of [CpFeCl(dippe)] (0.2 g, ca. 0.5 mmol) in EtOH (20 mL). The solution changed its color from purple to yellow. An excess of Na[BPh<sub>4</sub>] (0.34 g) dissolved in EtOH (10 mL) was added, producing a yellow crystalline precipitate. It was filtered out, washed with EtOH and petroleum ether, and dried *in vacuo*. Yellow crystals were obtained upon recrystallization from acetone/EtOH. Yield: 0.28 g, 77%. Anal. Calcd for C<sub>44</sub>H<sub>57</sub>BF<sub>2</sub>FeOP<sub>2</sub>: C, 72.3; H, 7.81. Found: C, 72.6; H, 7.88. IR: ν(C=O) 1943 cm<sup>-1</sup>. NMR (CDCl<sub>3</sub>): <sup>1</sup>H, δ 5.29 (s, C<sub>5</sub>H<sub>5</sub>); <sup>31</sup>P{<sup>1</sup>H}, 106.5 (s); <sup>13</sup>C{<sup>1</sup>H}, 18.406, 18.500, 18.727, 19.176 (s, P(CH(CH<sub>3</sub>)<sub>2</sub>)<sub>2</sub>), 22.613 (t, *J*(C,P) = 18.4 Hz, PCH<sub>2</sub>), 28.151 (t, *J*(C,P) = 14.0 Hz, P(CH(CH<sub>3</sub>)<sub>2</sub>)<sub>2</sub>), 29.176 (t, *J*(C,P) = 9.0 Hz, P(CH(CH<sub>3</sub>)<sub>2</sub>)<sub>2</sub>), 83.118 (s, C<sub>5</sub>H<sub>5</sub>), 215.951 (t, *J*(C,P) = 25.4 Hz, CO).

**[Fe(C<sub>5</sub>Me<sub>5</sub>)(CO)(dippe)][BPh<sub>4</sub>] (7).** This compound was obtained in a fashion analogous to that for 6, starting from

(12) Silverthorn, W. E. *J. Chem. Soc., Chem. Commun.* **1971**, 1310. Green, M. L. H.; Silverthorn, W. E. *J. Chem. Soc., Dalton Trans.* **1973**, 301.

(13) Leigh, G. J.; Jiménez Tenorio, M. *J. Am. Chem. Soc.* **1991**, *113*, 5862.

(14) Bazhenova, T. A.; Kachapina, L. M.; Shilov, A. E.; Antipin, M. Yu.; Struchkov, Yu. T. *J. Organomet. Chem.* **1992**, *428*, 107.

(15) Bazhenova, T. A.; Shilova, A. K.; Deschamps, E.; Guiselle, M.; Levy, G.; Tchoubar, M. *J. Organomet. Chem.* **1981**, *222*, C1. Yamamoto, A.; Miura, Y.; Ito, T.; Chen, H.; Iri, K.; Ozawa, F.; Miki, K.; Sei, T.; Tanaka, N.; Kasai, N. *Organometallics* **1983**, *2*, 1429.

(16) Jiménez Tenorio, M.; Puerta, M. C.; Valerga, P. *Organometallics* **1994**, *13*, 3330.

(17) Fryzuk, M. D.; Jones, T.; Einstein, F. W. B. *Organometallics* **1984**, *3*, 185. Burt, T. A.; Chatt, J.; Hussain, W.; Leigh, G. J. *J. Organomet. Chem.* **1979**, *182*, 237.

(18) (a) Evans, D. F. *J. Chem. Soc.* **1959**, 2003. (b) Crawford, T. H.; Swanson, J. *J. Chem. Educ.* **1971**, *48*, 382.

either  $[\text{Cp}^*\text{FeCl}(\text{dippe})]$  in MeOH or compound **3** in acetone. Yield: 69%. Anal. Calcd for  $\text{C}_{49}\text{H}_{67}\text{BFeOP}_2$ : C, 73.0; H, 8.48. Found: C, 73.2; H, 8.60. IR:  $\nu(\text{C}=\text{O})$  1928  $\text{cm}^{-1}$ . NMR ( $\text{CDCl}_3$ ):  $^1\text{H}$ ,  $\delta$  2.040 (t,  $J = 2$  Hz,  $\text{C}_5\text{Me}_5$ );  $^{31}\text{P}\{^1\text{H}\}$ , 90.05 (s);  $^{13}\text{C}\{^1\text{H}\}$ , 18.306, 18.500, 18.657, 19.479 (s,  $\text{P}(\text{CH}(\text{CH}_3)_2)_2$ ), 21.764 (t,  $J(\text{C},\text{P}) = 16.6$  Hz,  $\text{PCH}_2$ ), 28.455 (t,  $J(\text{C},\text{P}) = 15.4$  Hz,  $\text{P}(\text{CH}(\text{CH}_3)_2)_2$ ), 29.176 (t,  $J(\text{C},\text{P}) = 8.5$  Hz,  $\text{P}(\text{CH}(\text{CH}_3)_2)_2$ ), 89.708 (s,  $\text{C}_5\text{H}_5$ ) (the signal corresponding to CO is not observed).

**$[\text{Fe}(\text{C}_5\text{H}_5)(\text{MeCN})(\text{dippe})][\text{BPh}_4]$  (8).** To a solution of  $[\text{CpFeCl}(\text{dippe})]$  (0.2 g, ca. 0.5 mmol) in 20 mL of methanol was added an excess of MeCN (2 mL). The color changed from purple to deep red. The solution was stirred for 15 min at room temperature. Then, the addition of an excess of Na- $[\text{BPh}_4]$  dissolved in 10 mL of MeOH produced a crystalline, red precipitate, which was filtered out, washed with ethanol and diethyl ether, and dried *in vacuo*. This compound was recrystallized from acetone/EtOH. Yield: 0.28 g, 76%. Anal. Calcd for  $\text{C}_{45}\text{H}_{60}\text{BFeNP}_2$ : C, 72.7; H, 8.08; N, 1.88. Found: C, 72.3; H, 8.20; N, 1.6. IR:  $\nu(\text{C}=\text{N})$  2256  $\text{cm}^{-1}$ . NMR ( $\text{CDCl}_3$ ):  $^1\text{H}$ ,  $\delta$  2.278 (s,  $\text{CH}_3\text{CN}$ ), 4.597 (t,  $\text{C}_5\text{H}_5$ ,  $J(\text{P},\text{H}) = 1.2$  Hz);  $^{31}\text{P}\{^1\text{H}\}$ , 101.3 (s);  $^{13}\text{C}\{^1\text{H}\}$ , 3.77 (s,  $\text{CH}_3\text{CN}$ ), 19.219, 19.508, 19.916 (s,  $\text{P}(\text{CH}(\text{CH}_3)_2)_2$ ), 22.823 (t,  $J(\text{C},\text{P}) = 17.3$  Hz,  $\text{PCH}_2$ ), 26.784 (t,  $J(\text{C},\text{P}) = 9.9$  Hz,  $\text{P}(\text{CH}(\text{CH}_3)_2)_2$ ), 28.722 (t,  $J(\text{C},\text{P}) = 9.9$  Hz,  $\text{P}(\text{CH}(\text{CH}_3)_2)_2$ ), 75.79 (s,  $\text{C}_5\text{H}_5$ ), 134.8 (s, MeCN).

**$[\text{Fe}(\text{C}_5\text{H}_5)(\text{MeCN})(\text{dippe})][\text{BPh}_4]$  (9).** To a solution of **3** (0.39 g, ca. 0.5 mmol) in 20 mL of acetone, MeCN (2 mL) was added, and the mixture was stirred for 15 min at room temperature. A red solution was obtained. EtOH (15 mL) was added. Concentration and cooling to  $-20$  °C afforded red crystals, which were filtered out, washed with petroleum ether, and dried *in vacuo*. Yield: 0.26 g, 65%. Anal. Calcd for  $\text{C}_{50}\text{H}_{70}\text{BFeNP}_2$ : C, 73.8; H, 8.61; N, 1.72. Found: C, 73.7; H, 8.63; N, 1.5. IR:  $\nu(\text{C}=\text{N})$  2238  $\text{cm}^{-1}$ . This product is paramagnetic.  $\mu_{\text{eff}} 4.0 \mu_{\text{B}}$ .

**$[\text{Fe}(\text{C}_5\text{H}_5)(\text{P}(\text{OPh})_3)(\text{dippe})][\text{BPh}_4]$  (10).** To a solution of  $[\text{CpFeCl}(\text{dippe})]$  (0.2 g, ca. 0.5 mmol) in 20 mL of MeOH an excess of  $\text{P}(\text{OPh})_3$  (3 mL) was added. A yellow-brown solution was obtained. The mixture was stirred for 15 min at room temperature. Then, an excess of Na- $[\text{BPh}_4]$  (0.34 g) in 10 mL of MeOH was added, and a yellow precipitate was obtained. The precipitate was filtered out, washed with EtOH and diethyl ether, and dried *in vacuo*. The product was recrystallized from acetone/EtOH. Yield: 0.37 g, 73%. Anal. Calcd for  $\text{C}_{61}\text{H}_{72}\text{BFeO}_3\text{P}_3$ : C, 72.3; H, 7.11. Found: C, 73.2; H, 7.46. NMR ( $\text{CDCl}_3$ ):  $^1\text{H}$ ,  $\delta$  4.838 (s,  $\text{C}_5\text{H}_5$ ), 7.025, 7.126, 7.232 (m,  $\text{P}(\text{OC}_6\text{H}_5)_3$ );  $^{31}\text{P}\{^1\text{H}\}$ , AX<sub>2</sub> spin system, 158.9 (t,  $\text{P}_A$ ), 103.9 (d,  $\text{P}_X$ ,  $J(\text{P}_A,\text{P}_X) = 81.8$  Hz);  $^{13}\text{C}\{^1\text{H}\}$ , 20.273, 20.426 (s br,  $\text{P}(\text{CH}(\text{CH}_3)_2)_2$ ), 21.803 (dt,  $J(\text{C},\text{P}_X) = 18.6$  Hz,  $J(\text{C},\text{P}_A) = 2.3$  Hz,  $\text{PCH}_2$ ), 32.513 (dt,  $J(\text{C},\text{P}_X) = 8.2$  Hz,  $J(\text{C},\text{P}_A) = 3.7$  Hz,  $\text{P}(\text{CH}(\text{CH}_3)_2)_2$ ), 34.111 (dt,  $J(\text{C},\text{P}_X) = 12.2$  Hz,  $J(\text{C},\text{P}_A) = 3.7$  Hz,  $\text{P}(\text{CH}(\text{CH}_3)_2)_2$ ), 76.58 (s,  $\text{C}_5\text{H}_5$ ), 121.076 (d,  $J(\text{C},\text{P}) = 3.6$  Hz,  $\text{P}(\text{OC}_6\text{H}_5)_3$ ), 130.123 (s,  $\text{P}(\text{OC}_6\text{H}_5)_3$ ), 151.87 (d,  $J(\text{C},\text{P}) = 17.1$  Hz,  $\text{P}(\text{OC}_6\text{H}_5)_3$ ).

**$[\text{Fe}(\text{C}_5\text{H}_5)(\text{SnCl}_3)(\text{dippe})]$  (11).** To a solution of  $[\text{CpFeCl}(\text{dippe})]$  (0.2 g, ca. 0.5 mmol) in 20 mL of dichloromethane, a slight excess of solid anhydrous  $\text{SnCl}_2$  (0.4 g) was added. The mixture was stirred overnight at room temperature. A magenta solution was obtained. The solution was filtered, in order to remove unreacted  $\text{SnCl}_2$ . The filtered solution was concentrated to a small volume (ca. 2 mL). Addition of petroleum ether (15 mL) produced a microcrystalline precipitate, which was filtered out, washed with petroleum ether, and dried *in vacuo*. Yield: 0.19 g, 64%. Anal. Calcd for  $\text{C}_{19}\text{H}_{37}\text{Cl}_3\text{FeP}_2\text{Sn}$ : C, 37.5; H, 6.08. Found: C, 37.7; H, 5.95. NMR ( $\text{CDCl}_3$ ):  $^1\text{H}$ ,  $\delta$  4.616 (t,  $J(\text{H},\text{P}) = 1.6$  Hz,  $\text{C}_5\text{H}_5$ );  $^{31}\text{P}\{^1\text{H}\}$ , 101.0 (s, with  $^{119}\text{Sn}/^{117}\text{Sn}$  satellites,  $J(\text{P},^{119}\text{Sn}) = 565$  Hz,  $J(\text{P},^{117}\text{Sn}) = 540$  Hz);  $^{13}\text{C}\{^1\text{H}\}$ , 19.540, 19.650, 19.727, 20.17 (s,  $\text{P}(\text{CH}(\text{CH}_3)_2)_2$ ), 23.130 (t,  $J(\text{C},\text{P}) = 19.4$  Hz,  $\text{PCH}_2$ ), 29.491 (t,  $J(\text{C},\text{P}) = 11.0$  Hz,  $\text{P}(\text{CH}(\text{CH}_3)_2)_2$ ), 32.106 (t,  $J(\text{C},\text{P}) = 15.0$  Hz,  $\text{P}(\text{CH}(\text{CH}_3)_2)_2$ ), 75.11 (s,  $\text{C}_5\text{H}_5$ );  $^{119}\text{Sn}$ , 48.7 (t,  $J(^{119}\text{Sn},\text{P}) = 565$  Hz, reference  $\text{Sn}^{\text{B}}\text{Bu}_4$ ).

**$[\text{FeCl}(\text{C}_5\text{H}_5)(\text{dippe})][\text{BPh}_4]$  (12).** A solution of  $[\text{CpFeCl}(\text{dippe})]$  (0.2 g, ca. 0.5 mmol) in 20 mL of MeOH was stirred in the air for 15 min at room temperature. The solution changed its color to dark red. Addition of an excess of Na- $[\text{BPh}_4]$  (0.34 g) in 10 mL of MeOH afforded a dark red, crystalline precipitate. It was filtered out, washed with EtOH and petroleum ether, and dried *in vacuo*. The product was recrystallized from a mixture dichloromethane/ethanol. Yield: 0.25 g, 67%. Anal. Calcd for  $\text{C}_{43}\text{H}_{57}\text{ClFeP}_2$ : C, 70.0; H, 7.73. Found: C, 70.2; H, 7.52.  $\mu_{\text{eff}} 2.4 \mu_{\text{B}}$ .

**$[\text{FeCl}(\text{C}_5\text{Me}_5)(\text{dippe})][\text{BPh}_4]$  (15).** This compound was obtained in the form of brown crystals, by following a procedure identical to that outlined above for compound **14**, starting from  $[\text{FeCp}^*\text{Cl}(\text{dippe})]$  in MeOH. Yield: 64%. Anal. Calcd for  $\text{C}_{48}\text{H}_{67}\text{ClFeP}_2$ : C, 71.3; H, 8.30. Found: C, 71.5; H, 8.47.  $\mu_{\text{eff}} 2.3 \mu_{\text{B}}$ .

**Experimental Determination of  $K_{\text{eq}}$  for the Equilibrium between  $[\text{CpFe}(\text{N}_2)(\text{dippe})]^+$  and  $[\text{CpFe}(\text{dippe})]^+$ , and of Its Dependence with Temperature.**  $K_{\text{eq}}$  was determined by following the procedure outlined in ref 18b, by measuring the effective magnetic moment  $\mu_{\text{eff}}$  for an acetone- $d_6$  solution of **1** of known concentration under dinitrogen. In such solution,  $\mu_{\text{eff}}$  range from zero (if only  $[\text{CpFe}(\text{N}_2)(\text{dippe})]^+$  is present) to  $3.6 \mu_{\text{B}}$  (if only  $[\text{CpFe}(\text{dippe})]^+$  is present). Intermediate values of the magnetic moment indicate a mixture of  $[\text{CpFe}(\text{N}_2)(\text{dippe})]^+$  and  $[\text{CpFe}(\text{dippe})]^+$ . The percentage of diamagnetic dinitrogen complex present can be calculated from the solution  $\mu_{\text{eff}}$  and the value of  $3.6 \mu_{\text{B}}$  for pure  $[\text{CpFe}(\text{dippe})]^+$ , according to the equation

$$\% \text{ diamagnetic species} = 100 \times [1 - (\mu_{\text{eff}}/3.6)^2]$$

The equilibrium constant for the process is

$$K_{\text{eq}} = \frac{\% \text{ paramagnetic}}{\% \text{ diamagnetic}}$$

The concentration of  $\text{N}_2$  in solution is assumed to be constant (equal to the solubility of  $\text{N}_2$  in acetone), since the experiment was conducted under a dinitrogen atmosphere in a  $\text{N}_2$ -saturated solvent. For this reason, it is included in the value of the calculated  $K_{\text{eq}}$ . By measurement of  $\mu_{\text{eff}}$  for the solution at different temperatures, the corresponding values of  $K_{\text{eq}}$  can be determined. A plot of  $\ln K_{\text{eq}}$  versus  $1/T$  allowed the calculation of  $\Delta H^\circ$  and  $\Delta S^\circ$  for the process.

**Experimental Data for the X-ray Crystal Structure Determinations.** A summary of crystallographic data for compounds **1**, **3**, and **12** is given in Table 1. X-ray measurements were made on crystals of the appropriate size, which were mounted onto a glass fiber and transferred to an AFC6S-Rigaku automatic diffractometer, using Mo  $K\alpha$  graphite-monochromated radiation. Cell parameters were determined from the settings of 25 high-angle reflections. Data were collected by the  $\omega$ -scan method. Lorentz, polarization, and absorption ( $\psi$ -scan method) corrections were applied. Decay was negligible during data collection for compound **3**, but deterioration corrections were applied in the case of compounds **1** (7.20%) and **12** (0.90%). Reflections having  $I > 3\sigma(I)$  were used for structure resolution. All calculations for data reduction, structure solution, and refinement were carried out on a VAX 3520 computer at the Servicio Central de Ciencia y Tecnología de la Universidad de Cádiz, using the TEXSAN<sup>19</sup> software system and ORTEP<sup>20</sup> for plotting. All the structures were solved by the Patterson method and anisotropically refined by full-matrix least-squares methods for all non-hydrogen atoms. Hydrogen atoms were included at idealized positions and not refined. Maximum and minimum peaks in the final difference Fourier maps were  $+0.87$  and  $-0.78 \text{ e } \text{Å}^{-3}$

(19) TEXSAN: Single-Crystal Structure Analysis Software, version 5.0; Molecular Structure Corp.: The Woodlands, TX, 1989.

(20) Johnson, C. K. ORTEP. A Thermal Ellipsoid Plotting Program; Oak Ridge National Laboratory: Oak Ridge, TN, 1965.







**Table 2. Positional Parameters and  $B(\text{eq})$  Values ( $\text{\AA}^2$ ) for  $[\text{Fe}(\text{N}_2)(\text{Cp})(\text{dippe})][\text{BPh}_4]$** 

atom	$x$	$y$	$z$	$B(\text{eq})$
Fe	0.3207(1)	0.1705(2)	0.16885(9)	3.3(1)
P(1)	0.2895(2)	0.3411(3)	0.1544(2)	3.5(2)
P(2)	0.1823(2)	0.1549(3)	0.2054(2)	4.1(2)
N(1)	0.3665(8)	0.194(1)	0.2472(6)	4.1(7)
N(2)	0.404(1)	0.206(1)	0.2953(7)	7(1)
C(1)	0.401(1)	0.155(1)	0.0867(8)	5(1)
C(2)	0.442(1)	0.107(1)	0.1399(8)	4.6(9)
C(3)	0.386(1)	0.024(1)	0.1595(8)	4.9(9)
C(4)	0.312(1)	0.028(1)	0.1207(8)	4.3(8)
C(5)	0.319(1)	0.111(2)	0.0753(7)	5(1)
C(10)	0.234(1)	0.380(1)	0.0765(7)	5.0(8)
C(11)	0.376(1)	0.443(1)	0.1694(8)	4.9(8)
C(12)	0.207(1)	0.369(1)	0.2144(7)	5.6(9)
C(20)	0.182(1)	0.118(1)	0.2933(7)	6(1)
C(21)	0.135(1)	0.286(1)	0.2082(8)	6(1)
C(22)	0.093(1)	0.084(1)	0.1631(8)	6(1)
C(101)	0.192(1)	0.487(1)	0.0809(8)	7(1)
C(102)	0.296(1)	0.381(1)	0.0183(7)	7(1)
C(111)	0.385(1)	0.478(1)	0.2400(9)	7(1)
C(112)	0.466(1)	0.407(1)	0.148(1)	8(1)
C(201)	0.233(1)	0.018(2)	0.3053(8)	8(1)
C(202)	0.088(1)	0.110(2)	0.3204(9)	10(1)
C(221)	0.087(1)	0.105(1)	0.091(1)	7(1)
C(222)	0.089(1)	-0.035(1)	0.1745(9)	8(1)
C(501)	0.6694(9)	0.216(1)	0.0401(6)	3.7(8)
C(502)	0.647(1)	0.326(1)	0.0395(8)	5(1)
C(503)	0.579(1)	0.359(1)	-0.003(1)	6(1)
C(504)	0.534(1)	0.296(2)	-0.0449(9)	6(1)
C(505)	0.554(1)	0.193(2)	-0.0470(8)	6(1)
C(506)	0.622(1)	0.158(1)	-0.0034(8)	4.9(8)
C(601)	0.745(1)	0.200(1)	0.1649(7)	3.6(7)
C(602)	0.668(1)	0.244(1)	0.1901(7)	4.7(8)
C(603)	0.662(1)	0.257(1)	0.2579(9)	5(1)
C(604)	0.731(2)	0.237(1)	0.2994(8)	6(1)
C(605)	0.809(1)	0.194(1)	0.2758(9)	6(1)
C(606)	0.814(1)	0.180(1)	0.2075(8)	4.9(8)
C(701)	0.766(1)	0.052(1)	0.0840(6)	3.8(7)
C(702)	0.843(1)	-0.000(1)	0.0723(8)	6(1)
C(703)	0.855(1)	-0.107(2)	0.0738(8)	7(1)
C(704)	0.786(2)	-0.171(1)	0.0871(7)	7(1)
C(705)	0.706(1)	-0.125(1)	0.0993(8)	6(1)
C(706)	0.698(1)	-0.018(1)	0.0988(6)	4.1(7)
C(801)	0.840(1)	0.238(1)	0.0572(6)	3.6(7)
C(802)	0.890(1)	0.313(1)	0.0892(7)	4.6(8)
C(803)	0.960(1)	0.367(1)	0.0611(8)	4.5(8)
C(804)	0.979(1)	0.343(2)	-0.0039(9)	6(1)
C(805)	0.930(1)	0.272(1)	-0.0367(7)	5(1)
C(806)	0.860(1)	0.218(1)	-0.0085(7)	4.9(8)
B	0.752(1)	0.179(1)	0.0854(7)	3.7(8)

**Table 3. Selected Bond Distances ( $\text{\AA}$ ) and Angles (deg) for Complex  $[\text{Fe}(\text{Cp})(\text{N}_2)(\text{dippe})][\text{BPh}_4]$** 

Bond Distances			
Fe-P(1)	2.251(4)	Fe-C(3)	2.13(1)
Fe-P(2)	2.269(4)	Fe-C(4)	2.07(1)
Fe-N(1)	1.76(1)	Fe-C(5)	2.07(1)
Fe-C(1)	2.13(1)	N(1)-N(2)	1.13(1)
Fe-C(2)	2.12(1)		
Angles			
P(1)-Fe-P(2)	86.3(1)	P(2)-Fe-C(3)	113.0(5)
P(1)-Fe-N(1)	91.5(4)	P(2)-Fe-C(4)	92.1(4)
P(1)-Fe-C(1)	96.4(5)	P(2)-Fe-C(5)	107.3(5)
P(1)-Fe-C(2)	121.0(5)	N(1)-Fe-C(1)	121.9(7)
P(1)-Fe-C(3)	159.6(4)	N(1)-Fe-C(2)	90.6(6)
P(1)-Fe-C(4)	141.1(6)	N(1)-Fe-C(3)	93.9(6)
P(1)-Fe-C(5)	103.9(5)	N(1)-Fe-C(4)	127.4(7)
P(2)-Fe-N(1)	92.8(4)	N(1)-Fe-C(5)	155.2(6)
P(2)-Fe-C(1)	145.1(6)	Fe-N(1)-N(2)	173(1)
P(2)-Fe-C(2)	152.3(5)		

is  $[\text{Fe}(\eta^5\text{-pentadienyl})(\text{PEt}_3)_2][\text{PF}_6]$ ,<sup>22</sup> which has been subjected to X-ray structure analysis. A magnetic moment of  $2.85 \mu_B$  for this compound indicates the presence of two unpaired electrons. It has been already mentioned that the dinitrogen adduct  $[\text{CpFe}(\text{N}_2)-$

(dippe)]<sup>+</sup> co-exists with the 16-electron complex  $[\text{CpFe}(\text{dippe})]^+$  as an equilibrium mixture in acetone or thf under dinitrogen. Thus, the <sup>1</sup>H NMR spectrum of **1** in acetone-*d*<sub>6</sub> under N<sub>2</sub> (Figure 2) displays signals corresponding to the diamagnetic cation  $[\text{CpFe}(\text{N}_2)(\text{dippe})]^+$  in the range 0–10 ppm. The C<sub>5</sub>H<sub>5</sub> resonance appears as one singlet at 5.06 ppm, whereas the phosphine protons appear as a series of overlapping multiplets. Besides these resonances, broad, paramagnetically shifted signals corresponding to the protons of the 16-electron cation  $[\text{CpFe}(\text{dippe})]^+$  are observed in the range -40 to +40 ppm. The <sup>31</sup>P{<sup>1</sup>H} NMR spectrum consists of one singlet at 98.4 ppm, due to the equivalent phosphorus atoms of the dinitrogen complex. No signal is observed for  $[\text{CpFe}(\text{dippe})]^+$ . Due to the occurrence of the equilibrium shown in eq 2 and to the presence of both diamagnetic and paramagnetic species, it was not possible to obtain the <sup>13</sup>C{<sup>1</sup>H} spectrum of compound **1**. The equilibrium constant  $K_{\text{eq}}$  for the process shown in eq 2 and its dependence with temperature have been determined by measuring the magnetic moment of acetone solutions of **1** under dinitrogen at different temperatures. This yielded a value of  $K_{\text{eq}} = 2.1$  at 20 °C. A van't Hoff plot (Figure 3) allowed the calculation of  $\Delta H^\circ$  and  $\Delta S^\circ$  for the process, the corresponding values being  $18.2 \pm 0.5 \text{ kJ mol}^{-1}$  and  $68 \pm 2 \text{ J mol}^{-1} \text{ K}^{-1}$ , respectively. These data suggest that the reaction in eq 2 is entropy driven and therefore that at high temperatures the equilibrium favors the formation of the paramagnetic 16-electron complex, whereas the addition of N<sub>2</sub> to **3** may be favored by lowering the temperature.

At variance with the behavior found for  $[\text{CpFeCl}(\text{dippe})]$ , which forms  $[\text{CpFe}(\text{N}_2)(\text{dippe})]^+$ , the related complex  $[\text{Cp}^*\text{FeCl}(\text{dippe})]$  ( $\text{Cp}^* = \text{C}_5\text{Me}_5$ )<sup>16</sup> dissolves in methanol or ethanol under dinitrogen yielding orange solutions from which only  $[\text{Cp}^*\text{Fe}(\text{dippe})][\text{BPh}_4]$  (**3**) can be isolated upon addition of Na[BPh<sub>4</sub>]. No dinitrogen uptake is observed. Compound **3** does not add N<sub>2</sub> at room temperature even under pressure (5 atm). It seems that the stronger donor properties of the C<sub>5</sub>Me<sub>5</sub> ligand, as well as its higher steric demands, preferentially stabilize the 16-electron complex to the detriment of the 18-electron dinitrogen adduct  $[\text{Cp}^*\text{Fe}(\text{N}_2)(\text{dippe})]^+$ , which does not seem to be a stable species. Compound **3** is paramagnetic and has an effective magnetic moment similar to that of **2** ( $3.8 \mu_B$ , Evans' method). The X-ray crystal structure of **3** has been determined and a view of the complex cation  $[\text{Cp}^*\text{Fe}(\text{dippe})]^+$  is shown in Figure 3. Final atomic coordinates are given in Table 4, and selected bond lengths and angles are in Table 5. The iron atom is in a formally five-coordinate environment. The Cp\* ring is pentahapto bonded, and the dippe ligand coordinates perpendicularly to the Cp\* plane (dihedral angle between the least-squares Cp\* plane and that defined by Fe-P(1)-P(2), 92.6°). The Fe-P separations found for this compound are longer than those in **1**, due possibly to the steric interactions of the phosphine isopropyl groups with the ring methyl substituents. These Fe-P bond lengths are also longer than in the Cp\* complex  $[\text{Cp}^*\text{FeH}_2(\text{dippe})][\text{BPh}_4]$ ,<sup>16</sup> although in this case iron is formally in the oxidation state +4, being smaller in size. The C<sub>5</sub> ring of the Cp\* ligand is planar, with the methyl substituents above this plane, displaced away from the iron atom. The X-ray

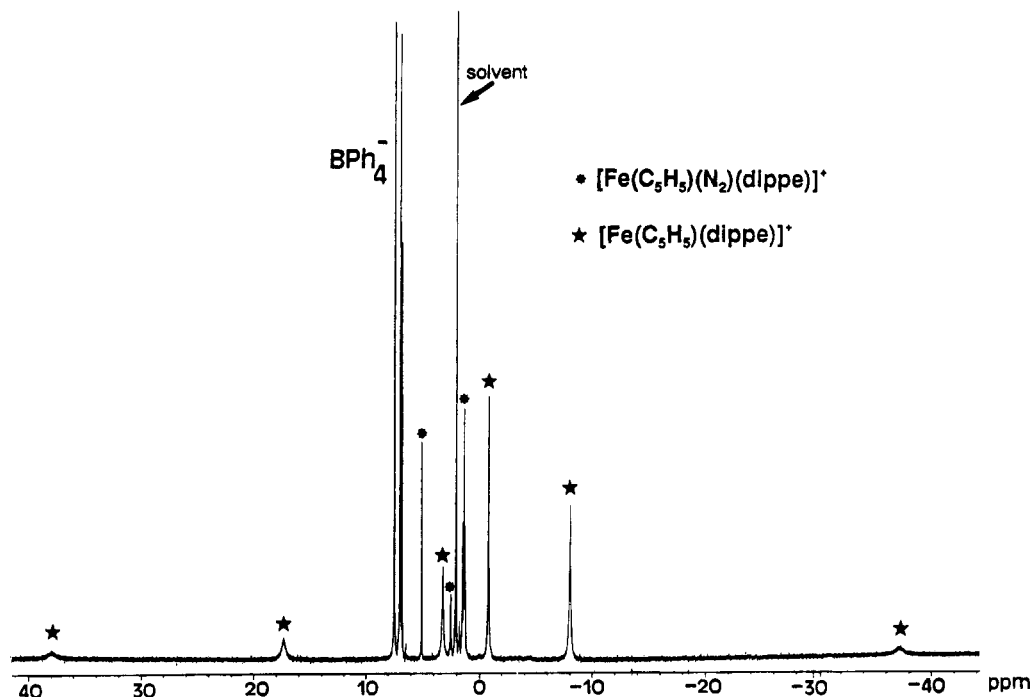


**Figure 2.**  $^1\text{H}$  NMR spectrum of **1** in acetone- $d_6$  under dinitrogen in the range  $-40$  to  $+40$  ppm, showing peaks corresponding to both  $[\text{CpFe}(\text{N}_2)(\text{dippe})]^+$  (\*) and  $[\text{CpFe}(\text{dippe})]^+$  (★).

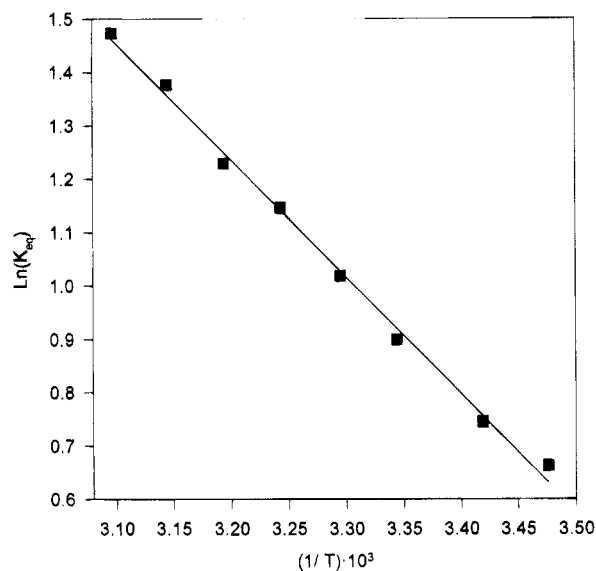


**Figure 3.** Plot of  $\ln K_{\text{eq}}$  versus  $1/T$  ( $\text{K}^{-1}$ ) for the equilibrium in acetone- $d_6$  solution between  $[\text{CpFe}(\text{N}_2)(\text{dippe})]^+$  and  $[\text{CpFe}(\text{dippe})]^+$  (eq 2) under dinitrogen.

crystal structure of **3** does not show any indications of stabilization by means of an intra- or intermolecular agostic interaction. This structure is closely related to that of the complex  $[\text{Fe}(\eta^5\text{-pentadienyl})(\text{PEt}_3)_2][\text{PF}_6]$ ,<sup>22</sup> which constitutes another example of a 16-electron paramagnetic organometallic compound of iron, in which there is no significant agostic interaction.

No ammonia or hydrazine was detected upon reaction of the dinitrogen adduct **1** with  $\text{HBF}_4$ . Furthermore, the complex decomposed, and the only species identified was the phosphonium salt  $[\text{Pr}_2\text{PCH}_2\text{CH}_2\text{P}^+\text{Pr}_2][\text{BF}_4^-]$ .

The complexes **1–3** react with a variety of neutral donors *L* furnishing the corresponding adducts  $[\text{CpFe}(\text{L})(\text{dippe})][\text{BPh}_4^-]$  or  $[\text{Cp}^*\text{Fe}(\text{L})(\text{dippe})][\text{BPh}_4^-]$  as expected. Thus, the reaction with  $\text{CNBu}^t$  afforded the complexes  $[\text{CpFe}(\text{CNBu}^t)(\text{dippe})][\text{BPh}_4^-]$  (**4**) and  $[\text{Cp}^*\text{Fe}$

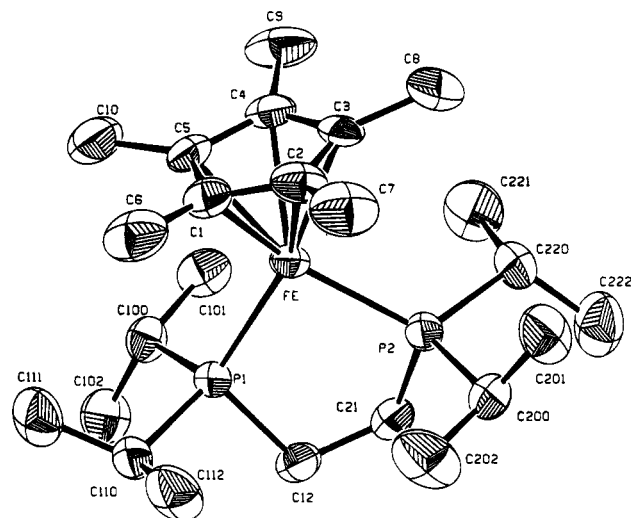


**Figure 4.** ORTEP drawing of the cation  $[\text{Cp}^*\text{Fe}(\text{dippe})]^+$ . Hydrogen atoms are omitted.

$(\text{CNBu}^t)(\text{dippe})][\text{BPh}_4^-]$  (**5**), respectively. In analogous fashion, the reaction with CO yielded  $[\text{CpFe}(\text{CO})(\text{dippe})][\text{BPh}_4^-]$  (**6**) and  $[\text{Cp}^*\text{Fe}(\text{CO})(\text{dippe})][\text{BPh}_4^-]$  (**7**). All these compounds can be also obtained directly from  $[\text{CpFeCl}(\text{dippe})]$  or  $[\text{Cp}^*\text{FeCl}(\text{dippe})]$  in MeOH, by addition of *L* and subsequent precipitation with  $\text{Na}[\text{BPh}_4^-]$ . Complexes **4–7** are crystalline, air-stable materials, which display one strong  $\nu(\text{C}\equiv\text{N})$  or  $\nu(\text{C}=\text{O})$  band in their respective IR spectra. The  $\nu(\text{C}\equiv\text{N})$  band appears at essentially the same wavenumber for both **4** and **5**, indicating that the isocyanide is acting mainly as a  $\sigma$ -donor. However, the  $\nu(\text{C}=\text{O})$  band in the  $\text{Cp}^*$  derivative **7** is at lower frequency than in the  $\text{Cp}$  complex **6**, as result of increased back-bonding, due possibly to the fact that the stronger donor properties of the  $\text{Cp}^*$  ligand provides a metal site which is more electron-rich. The  $^1\text{H}$ ,  $^{31}\text{P}\{^1\text{H}\}$ , and  $^{13}\text{C}\{^1\text{H}\}$  NMR spectra of these compounds are consistent with a "three-legged piano stool" structure, as has been found for **1** and for other half-

**Table 4. Positional Parameters and  $B(\text{eq})$  Values ( $\text{\AA}^2$ ) for  $[\text{Fe}(\text{Cp}^*)(\text{dippe})][\text{BPh}_4]$** 

atom	x	y	z	$B(\text{eq})$
Fe	0.31508(7)	0.05103(5)	0.25061(7)	2.51(4)
P(1)	0.4403(1)	0.0907(1)	0.1924(1)	2.59(8)
P(2)	0.3130(1)	0.1438(1)	0.3295(1)	2.73(9)
C(1)	0.3139(5)	-0.0487(4)	0.2457(6)	3.5(3)
C(2)	0.2665(6)	-0.0305(4)	0.3163(6)	4.0(4)
C(3)	0.1864(5)	0.0061(4)	0.2764(5)	3.5(4)
C(4)	0.1832(5)	0.0081(4)	0.1775(5)	3.5(4)
C(5)	0.2621(5)	-0.0245(3)	0.1576(5)	3.1(3)
C(6)	0.3927(6)	-0.0965(4)	0.2562(7)	5.7(5)
C(7)	0.2918(6)	-0.0517(5)	0.4174(6)	6.1(5)
C(8)	0.1098(6)	0.0279(4)	0.3249(7)	6.0(5)
C(9)	0.1027(6)	0.0349(4)	0.1056(7)	5.8(5)
C(10)	0.2804(6)	-0.0415(4)	0.0627(6)	5.7(5)
C(12)	0.4702(5)	0.1680(4)	0.2463(5)	3.7(4)
C(21)	0.3874(5)	0.1991(4)	0.2800(5)	3.5(4)
C(100)	0.4093(5)	0.1060(3)	0.0645(5)	3.1(3)
C(101)	0.3118(5)	0.1373(4)	0.0392(5)	4.1(4)
C(102)	0.4838(6)	0.1420(4)	0.0237(5)	4.7(4)
C(110)	0.5591(5)	0.0532(4)	0.2089(5)	3.6(4)
C(111)	0.5645(6)	-0.0003(4)	0.1425(6)	5.3(5)
C(112)	0.5936(6)	0.0328(5)	0.3113(6)	5.6(5)
C(200)	0.3650(5)	0.1416(4)	0.4570(5)	3.9(4)
C(201)	0.2985(6)	0.1133(5)	0.5145(5)	5.7(5)
C(202)	0.4602(6)	0.1080(5)	0.4750(6)	6.9(6)
C(220)	0.2022(5)	0.1886(4)	0.3252(5)	3.9(4)
C(221)	0.1522(6)	0.1978(5)	0.2235(7)	6.3(5)
C(222)	0.2146(6)	0.2506(4)	0.3799(6)	5.9(5)
C(601)	0.6161(5)	0.4288(3)	0.2114(5)	3.0(3)
C(602)	0.6073(5)	0.4627(3)	0.1278(5)	3.1(4)
C(603)	0.6247(5)	0.5265(4)	0.1237(6)	3.9(4)
C(604)	0.6525(6)	0.5593(4)	0.2057(7)	4.4(4)
C(605)	0.6635(6)	0.5282(4)	0.2900(6)	5.0(5)
C(606)	0.6462(5)	0.4643(4)	0.2925(5)	3.8(4)
C(701)	0.6944(5)	0.3140(4)	0.2085(5)	2.9(3)
C(702)	0.6954(5)	0.2542(4)	0.1695(6)	3.8(4)
C(703)	0.7771(7)	0.2207(4)	0.1676(6)	4.8(5)
C(704)	0.8630(6)	0.2461(5)	0.2052(6)	5.1(5)
C(705)	0.8869(5)	0.3042(5)	0.2453(6)	5.0(5)
C(706)	0.7849(5)	0.3378(4)	0.2479(5)	3.8(4)
C(801)	0.5636(5)	0.3358(3)	0.3141(5)	2.9(3)
C(802)	0.6051(5)	0.2882(3)	0.3752(5)	3.2(3)
C(803)	0.5754(6)	0.2743(4)	0.4580(5)	4.3(4)
C(804)	0.5026(7)	0.3072(5)	0.4852(6)	4.9(5)
C(805)	0.4595(6)	0.3538(4)	0.4261(7)	4.7(5)
C(806)	0.4902(6)	0.3679(4)	0.3451(6)	4.0(4)
C(901)	0.5123(5)	0.3333(3)	0.1227(5)	2.7(3)
C(902)	0.4167(5)	0.3254(3)	0.1290(5)	3.3(4)
C(903)	0.3489(5)	0.3105(4)	0.0479(7)	4.1(4)
C(904)	0.3730(6)	0.3041(4)	-0.0377(6)	4.3(4)
C(905)	0.4663(6)	0.3122(4)	-0.0465(5)	4.3(4)
C(906)	0.5330(5)	0.3261(4)	0.0331(5)	3.8(4)
B	0.5960(6)	0.3530(4)	0.2148(6)	2.8(4)

**Table 5. Selected Bond Distances ( $\text{\AA}$ ) and Angles (deg) for Complex  $[\text{Fe}(\text{Cp}^*)(\text{dippe})][\text{BPh}_4]$** 

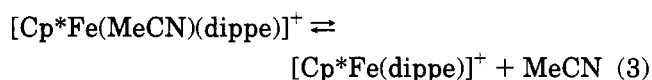
Bond Distances			
Fe-P(1)	2.290(2)	Fe-C(3)	2.178(7)
Fe-P(2)	2.292(2)	Fe-C(4)	2.192(7)
Fe-C(1)	2.133(8)	Fe-C(5)	2.149(7)
Fe-C(2)	2.162(8)		
Angles			
P(1)-Fe-P(2)	87.01(8)	P(2)-Fe-C(1)	151.7(2)
P(1)-Fe-C(1)	111.1(2)	P(2)-Fe-C(2)	116.2(2)
P(1)-Fe-C(2)	143.3(2)	P(2)-Fe-C(3)	101.8(2)
P(1)-Fe-C(3)	168.1(2)	P(2)-Fe-C(4)	120.8(2)
P(1)-Fe-C(4)	130.3(2)	P(2)-Fe-C(5)	157.9(2)
P(1)-Fe-C(5)	105.0(2)		

sandwich isocyanide and carbonyl derivatives of iron and ruthenium.<sup>23-25</sup> **1-3** also react with acetonitrile

(23) Rocco, A.; Paciello, R. A.; Manriquez, J. M.; Bercaw, J. E. *Organometallics* **1990**, *9*, 260.

(24) Morrow, J.; Catheline, D.; Desbois, M. H.; Manriquez, J. M.; Ruiz, J.; Astruc, D. *Organometallics* **1987**, *6*, 2605.

to yield the adducts  $[\text{CpFe}(\text{MeCN})(\text{dippe})][\text{BPh}_4]$  (**8**) and  $[\text{Cp}^*\text{Fe}(\text{MeCN})(\text{dippe})][\text{BPh}_4]$  (**9**), as deep red crystals. Both compounds exhibit one medium band near  $2250\text{ cm}^{-1}$  in their IR spectra, attributable to  $\nu(\text{C}\equiv\text{N})$  of the coordinated acetonitrile. The  $^1\text{H}$  NMR spectrum of **8** shows one singlet at 4.596 ppm, corresponding to the protons of the cyclopentadienyl ligand, and one singlet at 2.278 ppm, due to the acetonitrile protons. The  $^{31}\text{P}\{-^1\text{H}\}$  NMR spectrum consists of one singlet. These data, together with the  $^{13}\text{C}\{^1\text{H}\}$  NMR spectrum, support a "three-legged" piano-stool structure for this compound, as it has been suggested for the parent compounds  $[\text{CpFe}(\text{MeCN})(\text{dppe})][\text{BF}_4]$  and  $[\text{Cp}^*\text{Fe}(\text{MeCN})(\text{dppe})][\text{BF}_4]$ .<sup>27</sup> Whereas the NMR spectral properties of **8** are typical of a diamagnetic species, the  $\text{Cp}^*$  derivative **9** is paramagnetic in solution. It is well established that acetonitrile is a labile ligand, and sometimes their adducts exist in solution as equilibrium mixtures with free acetonitrile and the corresponding coordinatively unsaturated metal complex, as in the case of  $[\text{RuH}(\text{MeCN})(\text{dippe})_2][\text{BPh}_4]$ .<sup>26</sup> This might suggest that the paramagnetism of **9** arises from the existence of a dissociation process, similar to that found for the dinitrogen complex **1**, giving rise to the paramagnetic, 16-electron species  $[\text{Cp}^*\text{Fe}(\text{dippe})]^+$ , according to eq 3.



Two facts are against this: (1) The  $^1\text{H}$  NMR spectrum of **9** in acetone- $d_6$  consists of very broad features, different from the characteristic resonances of the cation  $[\text{Cp}^*\text{Fe}(\text{dippe})]^+$ , which are readily observable despite its paramagnetism. (2) The equilibrium shown in eq 3 would be shifted to the left in the presence of an excess of MeCN. However, the  $^1\text{H}$  NMR spectrum of **9** recorded in acetonitrile- $d_3$  indicates the presence of paramagnetic species. Furthermore, **9** in acetonitrile- $d_3$  solution has an effective magnetic moment of  $4.0\ \mu_{\text{B}}$ , and therefore this compound can be regarded as a paramagnetic, formally six-coordinate, 18-electron  $\text{Fe}^{\text{II}}$  organometallic complex. The effective magnetic moment of **9** is greater than the value of  $3.18\ \mu_{\text{B}}$  found for the unique paramagnetic, six-coordinate, 18-electron organometallic complex reported to date,  $[\text{Cp}^*\text{Fe}(\text{Me}_2\text{CO})(\text{dppe})][\text{CF}_3\text{SO}_3]$ .<sup>28</sup> This compound is assumed to have two unpaired electrons, corresponding to a spin-intermediate  $S = 1$  state, although the magnetic behavior could also result from the effective coexistence of  $S = 0$  and  $S = 2$  species. This may also happen in our case. It is interesting the fact that the Cp adduct **8** is diamagnetic whereas **9** is paramagnetic. This has also been observed in the dppe-acetone system, since  $[\text{CpFe}(\text{Me}_2\text{CO})(\text{dppe})][\text{PF}_6]$ <sup>11</sup> seems to be diamagnetic, at variance with  $[\text{Cp}^*\text{Fe}(\text{Me}_2\text{CO})(\text{dppe})][\text{CF}_3\text{SO}_3]$  which is paramagnetic, as it has been already mentioned. The complexes  $[\text{CpFe}(\text{MeCN})(\text{dppe})][\text{BF}_4]$  and  $[\text{Cp}^*\text{Fe}(\text{MeCN})(\text{dppe})][\text{BF}_4]$ <sup>27</sup> are also diamagnetic. The reasons for these differences in magnetic behavior remain unclear.

(25) Conroy-Lewis, F. M.; Simpson, S. J. *J. Organomet Chem.* **1987**, *322*, 221. Bruce, M. I.; Wallis, R. C. *Aust. J. Chem.* **1981**, *34*, 209.

(26) Jiménez Tenorio, M.; Puerta, M. C.; Valerga, P. *Inorg. Chem.* **1994**, *33*, 3515.

(27) Catheline, D.; Astruc, D. *Organometallics* **1984**, *3*, 1094.

(28) Hamon, P.; Toupet, L.; Hamon, J.-R.; Lapinte, C. *J. Chem. Soc., Chem. Commun.* **1994**, 931.

**Table 6. Positional Parameters and  $B(\text{eq})$  Values ( $\text{\AA}^2$ ) for  $[\text{Fe}(\text{Cp})(\text{Cl})(\text{dippe})][\text{BPh}_4]$** 

atom	$x$	$y$	$z$	$B(\text{eq})$
Fe(1)	0.3268(1)	0.1717(1)	0.17163(9)	2.87(9)
Cl	0.3920(3)	0.2122(3)	0.2699(2)	5.9(2)
P(1)	0.2922(3)	0.3423(3)	0.1555(2)	2.8(2)
P(2)	0.1876(2)	0.1575(3)	0.2086(2)	3.3(2)
C(1)	0.393(1)	0.028(1)	0.1613(7)	4.5(9)
C(2)	0.447(1)	0.106(1)	0.1410(7)	4.3(8)
C(3)	0.403(1)	0.155(1)	0.0872(7)	4.5(8)
C(4)	0.320(1)	0.106(1)	0.0785(7)	5(1)
C(5)	0.316(1)	0.025(1)	0.1251(8)	4.6(9)
C(12)	0.2132(9)	0.369(1)	0.2174(7)	3.9(7)
C(21)	0.141(1)	0.290(1)	0.2121(7)	4.7(8)
C(100)	0.235(1)	0.380(1)	0.0752(7)	4.2(8)
C(101)	0.189(1)	0.486(1)	0.0794(8)	6(1)
C(102)	0.294(1)	0.379(1)	0.0178(8)	6(1)
C(110)	0.3801(9)	0.442(1)	0.1669(6)	3.5(7)
C(111)	0.388(1)	0.487(1)	0.2370(7)	5.0(8)
C(112)	0.469(1)	0.405(1)	0.1462(8)	6(1)
C(200)	0.095(1)	0.085(1)	0.1655(7)	4.5(8)
C(201)	0.094(1)	-0.030(1)	0.1753(8)	7(1)
C(202)	0.087(1)	0.115(1)	0.0921(8)	7(1)
C(220)	0.191(1)	0.114(1)	0.2962(7)	4.5(8)
C(221)	0.244(1)	0.014(1)	0.3078(7)	6(1)
C(222)	0.102(1)	0.106(1)	0.3259(8)	7(1)
C(501)	0.768(1)	0.051(1)	0.0810(5)	2.7(6)
C(502)	0.846(1)	0.005(1)	0.0672(6)	3.6(8)
C(503)	0.859(1)	-0.104(1)	0.0705(7)	5(1)
C(504)	0.791(1)	-0.164(1)	0.0864(7)	5(1)
C(505)	0.710(1)	-0.125(1)	0.1007(7)	5(1)
C(506)	0.701(1)	-0.017(1)	0.0975(6)	4.2(8)
C(601)	0.6664(8)	0.215(1)	0.0357(6)	3.1(7)
C(602)	0.644(1)	0.321(1)	0.0315(7)	4.6(8)
C(603)	0.575(1)	0.359(1)	-0.0106(8)	5(1)
C(604)	0.530(1)	0.292(2)	-0.0514(7)	6(1)
C(605)	0.549(1)	0.187(1)	-0.0483(7)	6(1)
C(606)	0.617(1)	0.151(1)	-0.0063(7)	4.4(8)
C(701)	0.8377(9)	0.239(1)	0.0522(7)	3.3(7)
C(702)	0.8901(9)	0.314(1)	0.0867(6)	3.4(7)
C(703)	0.957(1)	0.366(1)	0.0599(7)	4.1(8)
C(704)	0.9798(8)	0.344(1)	-0.0031(7)	4.0(7)
C(705)	0.930(1)	0.273(1)	-0.0401(7)	4.0(8)
C(706)	0.862(1)	0.225(1)	-0.0127(6)	3.4(7)
C(801)	0.745(1)	0.204(1)	0.1621(7)	3.2(7)
C(802)	0.6685(9)	0.246(1)	0.1872(6)	3.2(7)
C(803)	0.661(1)	0.260(1)	0.2540(9)	5(1)
C(804)	0.729(1)	0.235(1)	0.2988(7)	5(1)
C(805)	0.804(1)	0.196(1)	0.2762(7)	5(1)
C(806)	0.8117(9)	0.179(1)	0.2096(7)	4.4(8)
B	0.754(1)	0.177(1)	0.0838(8)	3.4(8)

**Table 7. Selected Bond Distances ( $\text{\AA}$ ) and Angles (deg) for Complex  $[\text{Fe}(\text{Cp})\text{Cl}(\text{dippe})][\text{BPh}_4]$** 

Bond Distances			
Fe(1)–Cl	2.241(5)	Fe(1)–C(2)	2.13(1)
Fe(1)–P(1)	2.276(4)	Fe(1)–C(3)	2.13(1)
Fe(1)–P(2)	2.283(6)	Fe(1)–C(4)	2.07(1)
Fe(1)–C(1)	2.12(1)	Fe(1)–C(5)	2.11(1)
Angles			
Cl–Fe(1)–P(1)	89.5(2)	P(1)–Fe(1)–C(2)	122.3(5)
Cl–Fe(1)–P(2)	95.7(2)	P(1)–Fe(1)–C(3)	96.5(4)
Cl–Fe(1)–C(1)	95.8(5)	P(1)–Fe(1)–C(4)	105.3(5)
Cl–Fe(1)–C(2)	90.4(4)	P(1)–Fe(1)–C(5)	141.7(5)
Cl–Fe(1)–C(3)	120.4(5)	P(2)–Fe(1)–C(1)	114.3(5)
Cl–Fe(1)–C(4)	155.0(5)	P(2)–Fe(1)–C(2)	152.1(5)
Cl–Fe(1)–C(5)	128.8(5)	P(2)–Fe(1)–C(3)	143.8(5)
P(1)–Fe(1)–P(2)	85.1(2)	P(2)–Fe(1)–C(4)	105.3(5)
P(1)–Fe(1)–C(1)	159.1(5)	P(2)–Fe(1)–C(5)	91.3(4)

The reaction of complexes **1–3** with neutral donor molecules is controlled by the steric effects of the incoming ligand. Bulky molecules do not coordinate to the 16-electron complex **3**, which due to the presence of five methyl substituents at the cyclopentadienyl ring is more sterically demanding than compounds **1** and **2**. For instance,  $\text{P}(\text{OPh})_3$ , which has a large cone angle, does

not react at all with acetone or thf solutions of **3**, even under reflux. However, it reacts cleanly with **1**, **2**, or  $[\text{CpFeCl}(\text{dippe})]$  in MeOH yielding  $[\text{CpFe}(\text{P}(\text{OPh})_3)(\text{dippe})][\text{BPh}_4]$ , isolable as tetraphenylborate salt **10**. This is a yellow, crystalline, air-stable compound. Its  $^{31}\text{P}\{^1\text{H}\}$  NMR spectrum corresponds to an  $\text{AX}_2$  spin system and consists of one doublet at 103.9 ppm attributable to the two equivalent phosphorus atoms of the dippe ligand, coupled to one phosphorus atom of  $\text{P}(\text{OPh})_3$ , which appears as a triplet at 158.9 ppm,  $J(\text{P}_A, \text{P}_X) = 81.8$  Hz. The structure assumed for **10** is again the basic "three-legged piano stool", entirely unexceptional. Further differences between the reactivity of  $[\text{CpFeCl}(\text{dippe})]$  and  $[\text{Cp}^*\text{FeCl}(\text{dippe})]$  can be found in their reaction with  $\text{SnCl}_2$ . Both compounds react with anhydrous  $\text{SnCl}_2$  in  $\text{CH}_2\text{Cl}_2$ , but no characterizable product has been isolated in the case of the  $\text{Cp}^*$  derivative. However, the reaction of  $[\text{CpFeCl}(\text{dippe})]$  with  $\text{SnCl}_2$  yielded the magenta trichlorostannyl complex  $[\text{CpFe}(\text{SnCl}_3)(\text{dippe})]$  (**11**). This compound is formed by insertion of  $\text{SnCl}_2$  into the Fe–Cl bond, a process which is well-known and has been thoroughly studied,<sup>29,30</sup> due to the ability of the trichlorostannyl ligand to promote or modify the catalytic activity of transition metal complexes.<sup>31</sup> The  $^{31}\text{P}\{^1\text{H}\}$  NMR spectrum of **11** consists of one singlet, plus small satellites due to coupling of the phosphorus atoms to the NMR active  $^{117}\text{Sn}$  and  $^{119}\text{Sn}$  nuclei, with coupling constants  $J(\text{P}, ^{117}\text{Sn}) = 540$  Hz and  $J(\text{P}, ^{119}\text{Sn}) = 565$  Hz, respectively. Consistent with this, the  $^{119}\text{Sn}$  NMR spectrum of **11** displays one triplet due to coupling of the  $^{119}\text{Sn}$  nucleus with two equivalent phosphorus atoms of the phosphine ligand. Acetone or tetrahydrofuran solutions of **1–3** are very air-sensitive, turning dark brown when exposed to atmospheric oxygen. No product has been isolated from the reaction of any of these compounds with air. However, exposure to air of  $[\text{CpFeCl}(\text{dippe})]$  or  $[\text{Cp}^*\text{FeCl}(\text{dippe})]$  in methanol produced red-brown solutions, from which crystalline materials were isolated upon addition of  $\text{Na}[\text{BPh}_4]$ . These materials were identified as the  $\text{Fe}^{\text{III}}$ , 17-electron derivatives  $[\text{CpFeCl}(\text{dippe})][\text{BPh}_4]$  (**12**) and  $[\text{Cp}^*\text{FeCl}(\text{dippe})][\text{BPh}_4]$  (**13**). There is a growing interest in the chemistry of 17-electron organometallic complexes due to their relationship with the electron-transfer processes<sup>32</sup> and because their physical properties, such as conductivity, magnetism, and optical effects.<sup>33</sup> Half-sandwich  $\text{Fe}^{\text{III}}$  complexes have been prepared by oxidation of the corresponding  $\text{Fe}^{\text{II}}$  precursors, using different oxidizing agents, such as  $[\text{Cp}_2\text{Fe}][\text{PF}_6]$ ,<sup>16,21,34</sup>  $[\text{Ph}_3\text{C}][\text{PF}_6]$ ,<sup>35</sup> or atmospheric oxygen,<sup>21</sup> as it happens in our case. Dark

(29) Consiglio, G.; Morandini, F.; Ciani, G.; Sironi, A.; Kretschmer, M. *J. Am. Chem. Soc.* **1983**, *105*, 1391.

(30) Kaspar, J.; Sporgliarich, R.; Graziani, M. *J. Organomet. Chem.* **1982**, *231*, 71. Davies, J. A. *Organometallics* **1982**, *1*, 64.

(31) Davies, A. G.; Wilkinson, G.; Young, J. F. *J. Am. Chem. Soc.* **1963**, *85*, 1692. Cramer, R. D.; Jenner, E. L.; Lindsey, R. V.; Stolberg, V. G. *J. Am. Chem. Soc.* **1963**, *85*, 1961.

(32) Taube, H. *Angew. Chem., Int. Ed. Engl.* **1984**, *23*, 329. Astruc, D. *Angew. Chem., Int. Ed. Engl.* **1988**, *27*, 643.

(33) Parshall, G. V. *Organometallics* **1987**, *6*, 687. Green, M. L. H.; Qin, J.; O'Hare, D. *J. Organomet. Chem.* **1988**, *358*, 375. Miller, J. S.; Epstein, A. J.; Reiff, W. M. *Chem. Rev.* **1988**, *88*, 201.

(34) Hamon, P.; Toupet, L.; Hamon, J. R.; Lapinte, C. *Organometallics* **1992**, *11*, 1429. Connelly, N. G.; Gamasa, M. P.; Gimeno, J.; Lapinte, C.; Lastra, E.; Maher, J. P.; Le Narvor, N.; Rieger, P. H.; Rieger, A. L. *J. Chem. Soc., Dalton Trans.* **1993**, 2575.

(35) Guerschais, V.; Lapinte, C. *J. Chem. Soc., Chem. Commun.* **1986**, 663. Roger, C.; Toupet, L.; Lapinte, C. *J. Chem. Soc., Chem. Commun.* **1988**, 713.

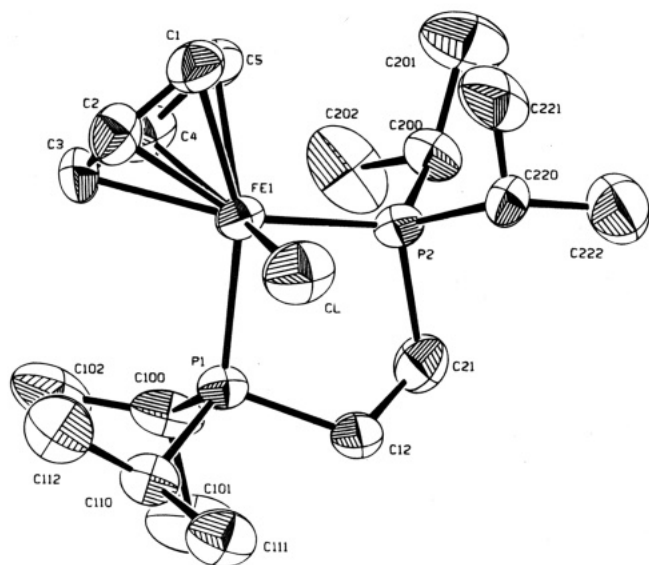


**Figure 5.** ORTEP drawing of the cation  $[\text{CpFeCl}(\text{dippe})]^+$ . Hydrogen atoms are omitted.

red **12** and brown **13** are both paramagnetic, as expected, having effective moment values of 2.40 and 2.30  $\mu_B$ , respectively, corresponding to one unpaired electron, and consistent with data reported in the literature for other half-sandwich  $\text{Fe}^{\text{III}}$  complexes, i.e.  $[\text{Cp}^*\text{Fe}(\text{CH}_3)(\text{dppe})][\text{PF}_6]$  (2.39  $\mu_B$ ),<sup>21</sup>  $[\text{Cp}^*\text{Fe}(\text{CH}_2\text{OCH}_3)(\text{dppe})][\text{PF}_6]$  (2.29  $\mu_B$ ),<sup>36</sup> or  $[\text{CpFeH}(\text{dippe})][\text{BPh}_4]$  (2.40  $\mu_B$ ).<sup>16</sup> The X-ray crystal structure of **12** was determined. Atomic coordinates and bond lengths and angles are listed in Tables 6 and 7. The molecular structure of the cation  $[\text{CpFeCl}(\text{dippe})]^+$  is shown in Figure 5. The structure consists of monomeric complex cations, with the expected "three-legged piano stool" arrangement, similar to that found for the related  $\text{Fe}^{\text{II}}$  complex  $[\text{Cp}^*\text{FeCl}(\text{dppe})]$ .<sup>21</sup>

(36) Morris, R. H. *Inorg. Chem.* **1992**, *31*, 1471. Jessop, P. G.; Morris, R. H. *Coord. Chem. Rev.* **1992**, *121*, 155.

The  $\text{Fe}-\text{Cl}$  distance of 2.241(5) Å is slightly shorter than the corresponding to the  $\text{Fe}^{\text{II}}$  derivative  $[\text{Cp}^*\text{FeCl}(\text{dppe})]$  (2.346(1) Å). This difference arises from the fact that  $\text{Fe}^{\text{III}}$  is smaller in size than the  $\text{Fe}^{\text{II}}$  cation rather than from the steric effects of the  $\text{Cp}^*$  ligand. The C5 ring of the cyclopentadienyl group is planar and is pentahapto bonded to the iron atom, with  $\text{Fe}-\text{C}$  separations in the range of those reported in the literature. All other bond lengths and angles, including the dippe ligand and the  $[\text{BPh}_4]^-$  anion, are also in the range expected, being unexceptional.

It is interesting to note that **1-3** react quantitatively with  $\text{H}_2$  to yield the hydrides  $[\text{CpFeH}_2(\text{dippe})][\text{BPh}_4]$  or  $[\text{Cp}^*\text{FeH}_2(\text{dippe})][\text{BPh}_4]$ . These compounds had been previously characterized as organoiron(IV) dihydrides, rather than iron(II) dihydrogen complexes, as inferred from NMR  $T_1$  measurements and the X-ray crystal structure of the  $\text{Cp}^*$  complex.<sup>16</sup> However, the value of 2112  $\text{cm}^{-1}$  found for  $\nu(\text{N}_2)$  in **1** suggests that, at least in this case, the dihydrogen adduct  $[\text{CpFe}(\text{H}_2)(\text{dippe})][\text{BPh}_4]$  should be stable, according to the criterion for the stability of the metal-dihydrogen bond proposed by Morris,<sup>36</sup> based upon the value of  $\nu(\text{N}_2)$  for the associated dinitrogen complex, and no homolytic splitting of dihydrogen should occur.

**Acknowledgment.** Suggestions from Prof. E. Carmona (Univ. de Sevilla) and Prof. G. J. Leigh (Univ. of Sussex), as well as financial support from the Ministerio de Educación y Ciencia of Spain (DGICYT, Project PB91-0741, Programa de Promoción General del Conocimiento), are gratefully acknowledged.

**Supporting Information Available:** Tables of X-ray crystallographic data, including atomic coordinates, isotropic thermal parameters, anisotropic thermal parameters, and interatomic distances and angles (39 pages). Ordering information is given on any current masthead page.

OM950151O

# Hypervalent Bond Formation in Halogeno(2-acylphenyl)bismuthanes

Toshihiro Murafuji,\* Takanori Mutoh, Kohichi Satoh, and Kazumi Tsunenari

Department of Chemistry, Faculty of Science, Yamaguchi University, Yoshida,  
Yamaguchi 753, Japan

Nagao Azuma

Department of Chemistry, Faculty of General Education, Ehime University,  
Matsuyama 790, Japan

Hitomi Suzuki\*

Department of Chemistry, Graduate School of Science, Kyoto University, Kyoto 606-01, Japan

Received March 28, 1995<sup>⊙</sup>

Hypervalent bond formation has been found to occur at bismuth as the hypervalent center. The transformation of (2-acetylphenyl)bis(4-methylphenyl)bismuthane (**2b**) to (2-acetylphenyl)bromo(4-methylphenyl)bismuthane (**3b**) brings about a noticeable change in the electronic nature of the carbonyl function in the 2-acetylphenyl group, which is sensitively reflected in the IR, <sup>1</sup>H, and <sup>13</sup>C NMR spectra of compound **3b**. These spectral changes may be rationalized in terms of the formation of a hypervalent O–Bi–Br bond through intramolecular coordination of the carbonyl oxygen atom to the bismuth center. X-ray crystallography of **3b** has confirmed this interpretation.

## Introduction

Hypervalent bond formation through intramolecular donor–acceptor interaction is a topic of growing interest in the chemistry of main group elements. Although many examples have hitherto been reported of the synthesis and characterization of such hypervalent compounds, most are concerned with those derived from

silicon,<sup>1</sup> tin,<sup>2</sup> sulfur,<sup>3</sup> phosphorus,<sup>4</sup> and tellurium.<sup>5,6</sup> Heavy members of the group 15 family have not yet received much attention.<sup>7</sup> Recently, we reported the synthesis of some chiral chlorobismuthanes stabilized by the intramolecular coordination of sulfonyl and dimethylamino groups and confirmed the occurrence of the hypervalent O–Bi–Cl and N–Bi–Cl bonds, respectively, in these compounds by X-ray crystallography.<sup>8–10</sup> In order to illustrate further the potential ability of heteroatom functions to form such a hypervalent bond, we have constructed a simple molecular model system bearing the bismuth atom as a hypervalent center. With this model system, one can readily visualize the formation of a hypervalent bond on the basis of infrared and <sup>1</sup>H and <sup>13</sup>C NMR spectra.

## Results and Discussion

When an organic functional group coordinates to a heteroatom center to form a hypervalent bond, there arises some electronic change within the group which should be sensitively reflected in its IR, <sup>1</sup>H, and <sup>13</sup>C

\* Abstract published in *Advance ACS Abstracts*, July 1, 1995.

(1) (a) Frolov, Yu. L.; Voronkov, M. G.; Gavrilova, G. A.; Chipanina, N. N.; Gubanova, L. I.; D'yakov, V. M. *J. Organomet. Chem.* **1983**, *244*, 107. (b) Kupce, E.; Liepins, E.; Lukevics, E. *J. Organomet. Chem.* **1983**, *248*, 131. (c) Corriu, R. J. P.; Kpoton, A.; Poirier, M.; Royo, G.; de Saxe, A.; Young, J. C. *J. Organomet. Chem.* **1990**, *395*, 1. (d) Corey, J. Y.; Rath, N. P.; John, C. S.; Corey, E. R. *J. Organomet. Chem.* **1990**, *399*, 221. (e) Gavrilova, G. A.; Chipanina, N. N.; Frolov, Yu. L.; Gubanova, L. I.; Voronkov, M. G. *J. Organomet. Chem.* **1991**, *418*, 291.

(2) (a) Kuivila, H. G.; Dixon, J. E.; Maxfield, P. L.; Scarpa, N. M.; Topka, T. M.; Tsai, K.-H.; Wursthorn, K. R. *J. Organomet. Chem.* **1975**, *86*, 89. (b) Weichmann, H.; Mugge, C.; Grand, A.; Robert, J. B. *J. Organomet. Chem.* **1982**, *238*, 343. (c) Jastrzebski, J. T. B. H.; Knaap, C. T.; van Koten, G. *J. Organomet. Chem.* **1983**, *255*, 287. (d) Jastrzebski, J. T. B. H.; Boersma, J.; van Koten, G. *J. Organomet. Chem.* **1991**, *413*, 43. (e) Swami, K.; Nebout, B.; Farah, D.; Krishnamurti, R.; Kuivila, H. G. *Organometallics* **1986**, *5*, 2370. (f) Ochiai, M.; Iwaki, S.; Takaoka, Y.; Nagao, Y. *Organometallics* **1989**, *8*, 1751. (g) van Koten, G.; Jastrzebski, J. T. B. H.; Noltes, J. G.; Pontenagel, W. M. G. F.; Spek, A. L. *J. Am. Chem. Soc.* **1978**, *100*, 5021. (h) Ochiai, M.; Iwaki, S.; Ukita, T.; Matsuura, Y.; Shiro, M.; Nagao, Y. *J. Am. Chem. Soc.* **1988**, *110*, 4606.

(3) (a) Akiba, K.-y.; Takee, K.; Ohkata, K. *J. Am. Chem. Soc.* **1983**, *105*, 6965. (b) Iwasaki, F.; Akiba, K.-y.; Ohkata, K. *J. Am. Chem. Soc.* **1983**, *105*, 445. (c) Akiba, K.-y.; Takee, K.; Shimizu, Y.; Ohkata, K. *J. Am. Chem. Soc.* **1986**, *108*, 6320. (d) Ohkata, K.; Ohnishi, M.; Yoshinaga, K.; Akiba, K.-y.; Rongione, J. C.; Martin, J. C. *J. Am. Chem. Soc.* **1991**, *113*, 9270.

(4) Verkade, J. G. *Acc. Chem. Res.* **1993**, *26*, 483 and references cited herein

(5) (a) Sadekov, I. D.; Maksimenko, A. A.; Minkin, V. I. *Khim. Geterotsikl. Soedin.* **1981**, *122*; *Chem. Abstr.* **1981**, *95*, 25027p. (b) Lohner, W.; Praefcke, K. *J. Organomet. Chem.* **1981**, *205*, 167. (c) Minkin, V. I.; Sadekov, I. D.; Maksimenko, A. A.; Kompan, O. E.; Struchkov, Yu. T. *J. Organomet. Chem.* **1991**, *402*, 331. (d) Abid, K. Y.; Al-Salim, N. I.; Greaves, M.; McWhinnie, W. R.; West, A. A.; Hamor, T. A. *J. Chem. Soc., Dalton Trans.* **1989**, 1697. (e) Maslakov, A. G.; McWhinnie, W. R.; Perry, M. C.; Shaikh, N.; McWhinnie, S. L. W.; Hamor, T. A. *J. Chem. Soc., Dalton Trans.* **1993**, 619.

(6) Piette, J. L.; Renson, M. *Bull. Soc. Chim. Belg.* **1970**, *79*, 367; *Chem. Abstr.* **1970**, *73*, 66200d.

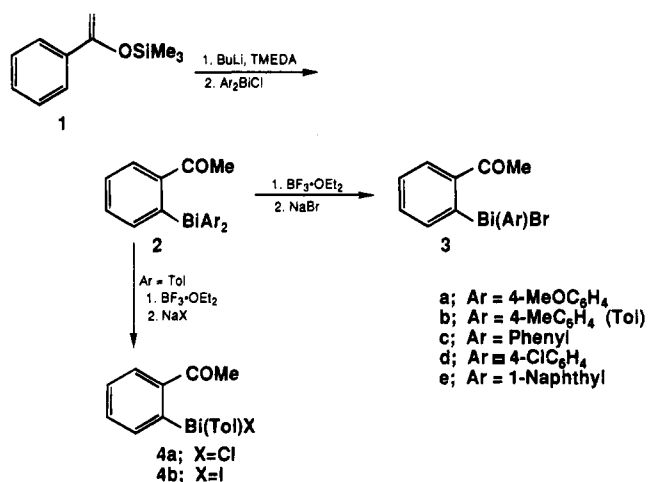
(7) (a) Dräger, M.; Schmidt, B. M. *J. Organomet. Chem.* **1985**, *290*, 133. (b) Ohkata, K.; Ohnishi, M.; Akiba, K.-y. *Tetrahedron Lett.* **1988**, *29*, 5401. (c) Ohkata, K.; Takemoto, S.; Ohnishi, M.; Akiba, K.-y. *Tetrahedron Lett.* **1989**, *30*, 4841. (d) Chen, X.; Yamamoto, Y.; Akiba, K.-y.; Yoshida, S.; Yasui, M.; Iwasaki, F. *Tetrahedron Lett.* **1992**, *33*, 6653. (e) Yamamoto, Y.; Chen, X.; Akiba, K.-y. *J. Am. Chem. Soc.* **1992**, *114*, 7906. (f) Yamamoto, Y.; Ohdoi, K.; Chen, X.; Kitano, M.; Akiba, K.-y. *Organometallics* **1993**, *12*, 3297. (g) Brau, E.; Falke, R.; Ellner, A.; Beuter, M.; Kolb, U.; Dräger, M. *Polyhedron* **1994**, *365*.

(8) Suzuki, H.; Murafuji, T.; Azuma, N. *J. Chem. Soc., Perkin Trans. 1* **1993**, 1169.

(9) Suzuki, H.; Murafuji, T.; Matano, Y.; Azuma, N. *J. Chem. Soc., Perkin Trans. 1* **1993**, 2969.

(10) Murafuji, T.; Suzuki, H.; Azuma, N. *Organometallics* **1995**, *14*, 1542.

Scheme 1



NMR spectra. On the basis of such an idea, we have designed a new type of triaryl bismuthane, compounds **2** and **5** with an acetyl or a formyl group *ortho* to the bismuth atom center. With these compounds, information about the carbonyl function obtained from IR,  $^1\text{H}$ , and  $^{13}\text{C}$  NMR spectra is expected to provide evidence for the formation of a hypervalent bond.<sup>11</sup>

**Synthesis.** The directed *ortho*-lithiation of benzaldehyde and acetophenone is an attractive synthetic route to compounds **2** and **5**. However, due to the reactive nature of the carbonyl function and the high acidity of  $\alpha$ -protons, both acetyl and formyl groups are not good directing substituents for *ortho*-lithiation. Piette and Renon reported the synthesis of butyl 2-formylphenyl telluride via the butyltellurenylation of 2-(diethoxymethyl)phenyllithium followed by deprotection.<sup>6</sup> However, this strategy is not applicable to the synthesis of compounds **2** and **5**, because the acid-catalyzed deprotection of acetal functionality after the introduction of bismuth atom leads to the concomitant cleavage of the bismuth-carbon bonds.

In order to overcome this difficulty, we chose the dilithiated compounds as starting materials (Schemes 1 and 2). They can be easily prepared from the reaction of trimethylsilyl enol ether of acetophenone and lithium  $\alpha$ -amino alkoxide of benzaldehyde, respectively, with butyllithium.<sup>12,13</sup> A variety of diarylchlorobismuthanes reacted smoothly with the dilithiated derivatives to afford the required products in acceptable yield. These results demonstrate that the dilithiation method is useful for the introduction of the 2-acylphenyl group to a metal center, particularly in the case where the metal-carbon bond is acid-sensitive. Compounds **2** and

Table 1.  $^{13}\text{C}$  NMR Spectra ( $\delta$ ) of Compounds **2b** and **3b**

carbon	<b>2b</b>	<b>3b</b>	$\delta_{3b} - \delta_{2b}$
C(1) <sup>a</sup>	159.8	175.8	16.0
C(2)	141.5	143.1	1.6
C(3)	132.2	135.1	2.9
C(4)	127.5	128.3	0.8
C(5)	135.0	138.5	3.5
C(6)	140.3	140.7	0.4
C(7)	201.1	208.7	7.6
C(8)	27.2	27.4	0.2
C(9) <sup>a</sup>	158.5	174.2	15.7
C(10)	137.7	137.1	-0.6
C(11)	131.2	132.5	1.3
C(12)	136.8	138.2	1.4
C(15)	21.5	21.5	0.0

<sup>a</sup> *Ipsso* carbon signals appear somewhat broadly.

**5** were converted to bromobismuthanes **3** and **6**, respectively, through fluoridearylation<sup>8</sup> with boron trifluoride-diethyl etherate and subsequent halogen exchange of the resulting fluorobismuthanes with sodium bromide. Chloro- and iodo-bismuthanes **4** and **7** were synthesized similarly via halogen exchange of the fluorobismuthanes with the respective alkali metal halides. In contrast to chlorobismuthane **4a**, chlorobismuthane **7a** was unstable and readily decomposed in solution to yield compound **8**.

**Spectral Characterization.** Spectral comparison of compound **2b** with **3b** clearly revealed an electronic change caused by the introduction of a bromine atom onto the bismuth atom. Compared with the parent bismuthane **2b** (1665  $\text{cm}^{-1}$ ), the IR spectrum of bromobismuthane **3b** showed a shift to lower frequency (40  $\text{cm}^{-1}$ ) of the carbonyl stretching vibration. The  $^{13}\text{C}$  NMR spectra of these compounds were also informative (Table 1). The carbonyl carbon signal of compound **3b** was observed at downfield region ( $\delta$  208.7). In addition, C(3) and C(5) atoms of compound **3b** suffered deshielding compared to the C(4) and C(6) atoms in the same ring, indicating the occurrence of a resonance interaction with the carbonyl function through the intramolecular Bi-O interaction. It is clear that the inductive effect of the bromine atom is transmitted to the carbonyl carbon atom mainly through the intramolecular Bi-O interaction rather than through the Bi-C(1) bond. This also is indicated by the downfield shift of the carbonyl carbon signal with increasing electronegativity of the halogen atom on bismuth (Table 2; **4a** versus **4b**). The chemical shift of the carbonyl carbon signal was not influenced by the nature of aryl group. All these observations are consistent with the formation of a hypervalent bond through the intramolecular coordination of the carbonyl group to bismuth-halogen. The

Scheme 2

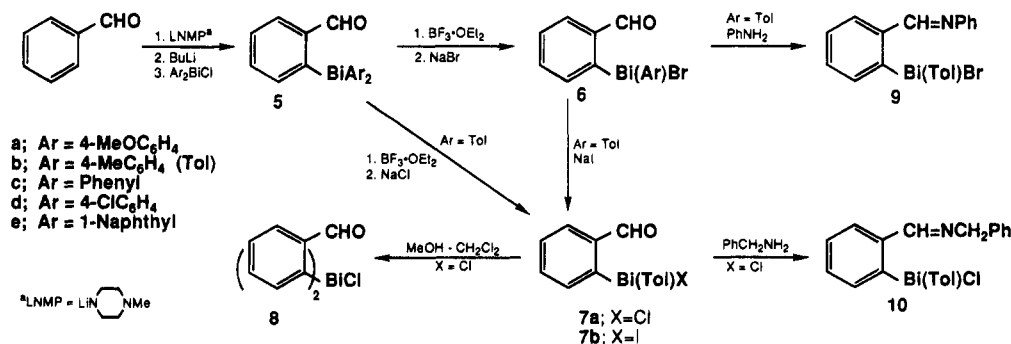




**Table 2. Influence of Halogen Atoms and Aryl Groups on the Chemical Shifts ( $\delta$ ) of the Carbonyl Carbon Atoms**

compound	chemical shift ( $\delta$ )	compound	chemical shift ( $\delta$ )
<b>2b</b>	201.1	<b>3a</b>	208.7
<b>3b</b>	208.7	<b>3c</b>	208.8
<b>4a</b>	209.2	<b>3d</b>	209.0
<b>4b</b>	207.5	<b>3e</b>	208.2

**Table 3. Chemical Shifts ( $\delta$ ) of the Ring Carbon Atoms Attached to the Bismuth**

compd	chemical shift ( $\delta$ )	
	phenylene ring	tolyl ring
<b>4a</b>	185.3	177.9
<b>3b</b>	175.8	174.2
<b>4b</b>	172.1	166.8
<b>2b</b>	159.8	158.5

signals of the *ipso* carbon atoms attached to the bismuth atom could be observed clearly in several cases (Table 3). Only recently has the chemical shift of the *ipso* carbon atom been assigned for triphenylbismuthane itself.<sup>14</sup>

The case with the 2-formylphenyl system was similar. The formyl proton signal of **6e** showed a downfield shift ( $\sim 0.4$  ppm) relative to that of **5e** due to enhanced polarization of the carbonyl group by the formation of the hypervalent bond. Despite the anticipated activation of the carbonyl carbon atom, the reaction of compound **6b** with aniline to form imine **9** proceeded quite slowly as compared with benzaldehyde (checked in a competitive experiment). This may be understood in terms of steric hindrance to the approach of the amine to the C=O group in **6b**.

Compounds **6** and **7a** are not so stable and slowly decompose on standing in air. Relative stability decreases in the order **6a,b** > **6c** > **6d,e** > **7a**. However, they can be stored without appreciable change under argon in a refrigerator. By treatment with benzylamine, compound **7a** could be isolated as a stable crystalline solid in the form of an imino-stabilized chlorobismuthane **10**. This may be taken as an example demonstrating the enhanced stability of the hypervalent N–Bi–Cl bond over the hypervalent O–Bi–Cl bond.

**Molecular Structures.** In order to confirm the formation of a hypervalent O–Bi–halogen bond, X-ray structure analysis was carried out for compound **3b** (Figure 1). As expected, the bismuth center was shown to have a distorted pseudotrigonal bipyramidal configuration similar to those of the sulfonyl- and dimethylamino-stabilized chlorobismuthanes,<sup>8–10</sup> where the carbon atoms C(1) and C(9) occupy the equatorial plane with a C(1)–Bi–C(9) angle of 95.1(4) $^\circ$  (Table 4). The apical positions of the pseudotrigonal bipyramid are occupied by the carbonyl oxygen and bromine atoms with an O–Bi–Br angle of 160.8(2) $^\circ$ . The lone pair of electrons is considered to occupy the remaining equatorial position. The intramolecular Bi–O distance (2.519(7) Å) is longer than the sum of the covalent radii (2.10

**Table 4. Selected Bond Lengths (Å) and Angles (deg) for Compound 3b with Estimated Standard Deviations in Parentheses**

bond lengths		bond angles	
Bi–C(1)	2.26(1)	O–Bi–Br	160.8(2)
Bi–C(9)	2.24(1)	C(1)–Bi–C(9)	95.1(4)
Bi–Br	2.746(1)	C(1)–Bi–Br	90.9(3)
Bi–O	2.519(7)	C(9)–Bi–Br	93.0(3)
O–C(7)	1.24(1)	C(1)–Bi–O	70.8(3)
		C(9)–Bi–O	83.0(3)
		C(7)–O–Bi	113.3(7)

Å) but is much shorter than that of the van der Waals radii (3.72 Å), in accord with the operation of a strong interaction between the bismuth and oxygen atoms. The Bi–Br bond length, 2.746(1) Å, is longer than the sum of the covalent radii (2.60 Å). All these observations support the formation of a hypervalent three-center four-electron bond over the oxygen, bismuth, and bromine atoms in compound **3b**.

## Experimental Section

**General Comments.** All reactions were carried out under nitrogen unless otherwise noted. Diethyl ether, hexane, and benzene were distilled from calcium hydride under nitrogen before use. Butyllithium was titrated against diphenylacetic acid. TLC was performed by using Merck precoated silica gel sheets 60F-254. Kieselgel 60 (Merck 9385) was used for column chromatography. Bismuth(III) chloride was purified by refluxing with thionyl chloride.  $^1\text{H}$  and  $^{13}\text{C}$  NMR spectra were recorded in  $\text{CDCl}_3$  on Hitachi R-250H (250 MHz) and Varian Gemini-200 (200 MHz) spectrometers with tetramethylsilane as an internal standard and are reported in  $\delta$ . Coupling constants  $J$  are given in Hz. IR spectra were obtained as KBr pellets on a Shimadzu FTIR-8100 spectrophotometer. Elemental analyses were performed at Microanalytical Laboratory, Institute for Chemical Research, Kyoto University, Japan.

**Preparation of (2-Acetylphenyl)diarylbi-muthanes 2.**  
**Typical Procedure 1.** Acetophenone trimethylsilyl enol ether **1** was prepared according to the reported procedure.<sup>15</sup> Chlorobis(4-methoxyphenyl)bismuthane (ca. 3 mmol) was generated by stirring tris(4-methoxyphenyl)bismuthane (1.06 g, 2 mmol) and bismuth(III) chloride (315 mg, 1 mmol) in diethyl ether (10 mL) for 1 h at room temperature. Lithiation of acetophenone trimethylsilyl enol ether was carried out by modifying the reported procedure.<sup>12</sup> To a stirred solution of TMEDA (1.36 mL, 9 mmol) in hexane (5 mL) was added dropwise at ice bath temperature butyllithium (9 mmol) followed by acetophenone trimethylsilyl enol ether **1** (576 mg, 3 mmol), and the mixture was stirred for 24 h at room temperature. To a suspension of the lithium compound thus obtained was added at room temperature an ethereal suspension of the above chlorobismuthane, and the resulting dark brown mixture was stirred for additional 15 min to complete the reaction. The mixture was quenched with brine (5 mL), benzene (10 mL) was added, and the insoluble polymeric substances were removed by filtration. The organic layer was separated and evaporated under reduced pressure to leave (2-acetylphenyl)bis(4-methoxyphenyl)bismuthane **2a** as a yellow oily residue. Attempted purification of this product by chromatography on silica gel using hexane–ethyl acetate (5:1) as the solvent led to extensive decomposition. Thus the oily residue was used without further purification for the synthesis of (2-acetylphenyl)bromo(4-methoxyphenyl)bismuthane, **3a**.

**Typical Procedure 2.** To a suspension of the lithium compound (ca. 3 mmol) derived from silyl enol ether **1** was added at room temperature a suspension of chlorobismuthane

(11) The intramolecular Bi–O interaction has previously been suggested for chlorobis[2-(isopropoxycarbonyl)ethyl]bismuthane: Nakamura, E.; Shimada, J.; Kuwajima, I. *Organometallics* **1985**, *4*, 641.

(12) Klein, J.; Medlik-Balan, A. *J. Org. Chem.* **1976**, *41*, 3307.

(13) (a) Comins, D. L.; Brown, J. D.; Mantlo, N. B. *Tetrahedron Lett.* **1982**, *23*, 3979. (b) Comins, D. L.; Brown, J. D. *Tetrahedron Lett.* **1983**, *24*, 5465. (c) Comins, D. L.; Brown, J. D. *J. Org. Chem.* **1984**, *49*, 1078.

(14) Ali, M.; McWhinnie, W. R.; West, A. A. *J. Chem. Soc., Dalton Trans.* **1990**, 899.

(15) House, H. O.; Czuba, L. J.; Gall, M.; Olmstead, H. D. *J. Org. Chem.* **1969**, *34*, 2324.

(ca. 3 mmol), prepared by stirring tris(4-methylphenyl)bismuthane (964 mg, 2 mmol) and bismuth(III) chloride (315 mg, 1 mmol) in diethyl ether (10 mL), and the resulting mixture was stirred for 15 min. Similar work up as described above gave (2-acetylphenyl)bis(4-methylphenyl)bismuthane, **2b**, as a yellow oil, which was purified by chromatography on silica gel using hexane-ethyl acetate (5:1) as the eluent and recrystallized from MeOH-CH<sub>2</sub>Cl<sub>2</sub> (5:1). Crystals: yield, 23%; mp 114–116 °C. <sup>1</sup>H NMR: 2.30 (6 H, s, Me), 2.61 (3 H, s, Me), 7.17 (4 H, d, *J*<sub>AB</sub> = 7.9, MeArH), 7.37–7.50 (2 H, m, MeCOArH), 7.57 (4 H, d, *J*<sub>AB</sub> = 7.9, MeArH), 7.94 (1 H, d, *J* = 7.3, MeCOArH), 8.13 (1 H, d, *J* = 7.3, MeCOArH). <sup>13</sup>C NMR: 21.5, 27.2, 127.5, 131.2, 132.2, 135.0, 136.8, 137.7, 140.3, 141.5, 158.5, 159.8, 201.1. IR: 1665, 1260, 790, 765, 600, 480 cm<sup>-1</sup>. Anal. Calcd for C<sub>22</sub>H<sub>21</sub>BiO: C, 51.8; H, 4.1. Found: C, 51.7; H, 4.0.

**(2-Acetylphenyl)diphenylbismuthane, 2c.** Crystals: yield, 23%; mp 96–98 °C (MeOH-CH<sub>2</sub>Cl<sub>2</sub> (5:1)). <sup>1</sup>H NMR: 2.63 (3 H, s, Me), 7.26–7.50 (8 H, m, ArH), 7.69 (4 H, d, *J* = 6.1, C<sub>6</sub>H<sub>5</sub>), 7.92 (1 H, d, *J* = 7.3, MeCOArH), 8.16 (1 H, d, *J* = 7.3, MeCOArH). <sup>13</sup>C NMR: 27.2, 127.3, 127.6, 130.3, 132.3, 135.2, 137.7, 140.4, 141.5, 201.2; *ipso* carbon signals were too weak to be assigned. IR: 1660, 1260, 760, 725, 700, 600 cm<sup>-1</sup>. Anal. Calcd for C<sub>20</sub>H<sub>17</sub>BiO: C, 49.8; H, 3.5. Found: C, 49.6; H, 3.5.

**(2-Acetylphenyl)bis(4-chlorophenyl)bismuthane, 2d.** Crystals: yield, 38%; mp 129–131 °C (MeOH-CH<sub>2</sub>Cl<sub>2</sub> (5:1)). <sup>1</sup>H NMR: 2.63 (3 H, s, Me), 7.30 (4 H, d, *J*<sub>AB</sub> = 7.9, ClArH), 7.40–7.60 (2 H, m, MeCOArH), 7.57 (4 H, d, *J*<sub>AB</sub> = 7.9, ClArH), 7.84 (1 H, d, *J* = 6.7, MeCOArH), 8.18 (1 H, d, *J* = 6.7, MeCOArH). <sup>13</sup>C NMR: 27.2, 128.0, 130.6, 132.6, 133.7, 135.5, 139.0, 140.2, 141.3, 201.4; *ipso* carbon signals were too weak to be assigned. IR: 1660, 1260, 1090, 1000, 800, 765, 710 cm<sup>-1</sup>. Anal. Calcd for C<sub>20</sub>H<sub>15</sub>BiCl<sub>2</sub>O: C, 43.6; H, 2.7. Found: C, 43.4; H, 2.7.

**Typical Procedure 3.** Chlorobis(1-naphthyl)bismuthane (ca. 3 mmol) was generated by stirring tris(1-naphthyl)bismuthane (1.18 g, 2 mmol) and bismuth(III) chloride (315 mg, 1 mmol) in CH<sub>2</sub>Cl<sub>2</sub> (10 mL) for 2 h at 45 °C and employed as an ethereal suspension after removal of CH<sub>2</sub>Cl<sub>2</sub> under reduced pressure. To a suspension of the lithium compound (ca. 3 mmol) derived from silyl enol ether **1** was added at room temperature a suspension of the above chlorobismuthane (ca. 3 mmol) in diethyl ether (10 mL), and the resulting mixture was stirred for 15 min. After the addition of brine (5 mL), the mixture was diluted with benzene (10 mL) and the insoluble substance was removed by filtration. The organic layer was separated and evaporated under reduced pressure to leave crude (2-acetylphenyl)bis(1-naphthyl)bismuthane, **2e**, as a yellow oil, which was purified by chromatography on silica gel followed by recrystallization from MeOH-CH<sub>2</sub>Cl<sub>2</sub> (5:1). Crystals: yield, 14%; mp 235–237 °C (decomp). <sup>1</sup>H NMR: 2.64 (3 H, s, Me), 7.23–7.32 (4 H, m, ArH), 7.43–7.50 (5 H, m, ArH), 7.78–7.93 (7 H, m, ArH), 8.12–8.21 (2 H, m, ArH). <sup>13</sup>C NMR: 27.1, 125.5, 125.8, 127.8, 127.9, 128.9, 129.0, 130.9, 132.4, 134.7, 135.3, 138.0, 139.1, 141.5, 157.7, 163.0, 200.9; one carbon peak could not be assigned due to weak signal response. IR: 1660, 1260, 785, 770 cm<sup>-1</sup>. Anal. Calcd for C<sub>28</sub>H<sub>21</sub>BiO: C, 57.7; H, 3.6. Found: C, 58.1; H, 3.6.

**Preparation of (2-Acetylphenyl)arylbromobismuthanes 3.** **Typical Procedure.** To a stirred mixture of crude compound **2a** (ca. 1 mmol) and benzene (3 mL) was added dropwise at ice bath temperature boron trifluoride-diethyl etherate (ca. 3 mmol), and after 5 min the reaction was quenched by the addition of saturated aqueous NaBr (3 mL). The organic layer was extracted with ethyl acetate (5 mL × 2), and the combined extracts were evaporated under reduced pressure to leave an oily residue, which was crystallized from MeOH-CH<sub>2</sub>Cl<sub>2</sub> (5:1) to afford (2-acetylphenyl)bromo(4-methoxyphenyl)bismuthane, **3a**, as crystals: yield, 12%; mp 153–155 °C. <sup>1</sup>H NMR: 2.69 (3 H, s, Me), 3.73 (3 H, s, OMe), 6.98 (2 H, d, *J*<sub>AB</sub> = 8.5, MeOArH), 7.66 (1 H, dt, *J* = 7.9 and 1.2,

MeCOArH), 7.97 (1 H, dt, *J* = 7.3 and 1.2, MeCOArH), 8.05 (2 H, d, *J*<sub>AB</sub> = 8.5, MeOArH), 8.25 (1 H, d, *J* = 7.9, MeCOArH), 9.21 (1 H, d, *J* = 7.3, MeCOArH). <sup>13</sup>C NMR: 27.4, 55.1, 117.5, 128.4, 135.1, 138.5, 138.7, 140.7, 143.1, 159.4, 169.0, 180.7, 208.7. IR: 1630, 1580, 1490, 1290, 1250, 1180, 810, 765 cm<sup>-1</sup>. Anal. Calcd for C<sub>15</sub>H<sub>14</sub>BiBrO<sub>2</sub>: C, 35.0; H, 2.7. Found: C, 34.7; H, 2.8.

**(2-Acetylphenyl)bromo(4-methylphenyl)bismuthane, 3b.** Crystals: yield, 83%; mp 174–176 °C (decomp) (MeOH-CH<sub>2</sub>Cl<sub>2</sub> (5:1)). <sup>1</sup>H NMR: 2.25 (3 H, s, Me), 2.69 (3 H, s, Me), 7.31 (2 H, d, *J*<sub>AB</sub> = 7.9, MeArH), 7.66 (1 H, t, *J* = 7.3, MeCOArH), 7.97 (1 H, t, *J* = 7.3, MeCOArH), 8.05 (2 H, d, *J*<sub>AB</sub> = 7.9, MeArH), 8.24 (1 H, d, *J* = 7.3, MeCOArH), 9.21 (1 H, d, *J* = 7.9, MeCOArH). <sup>13</sup>C NMR: 21.5, 27.4, 128.3, 132.5, 135.1, 137.1, 138.2, 138.5, 140.7, 143.1, 174.2, 175.8, 208.7. IR: 1625, 1550, 1300, 1280, 800, 765, 615, 480 cm<sup>-1</sup>. Anal. Calcd for C<sub>15</sub>H<sub>14</sub>BiBrO: C, 36.1; H, 2.8. Found: C, 36.2; H, 2.8.

**(2-Acetylphenyl)bromophenylbismuthane, 3c.** Crystals: yield, 87%; mp 146–148 °C (MeOH-CH<sub>2</sub>Cl<sub>2</sub> (5:1)). <sup>1</sup>H NMR: 2.69 (3 H, s, Me), 7.25 (1 H, t, *J* = 7.3, C<sub>6</sub>H<sub>5</sub>), 7.50 (2 H, t, *J* = 7.3, C<sub>6</sub>H<sub>5</sub>), 7.67 (1 H, t, *J* = 7.3, MeCOArH), 7.98 (1 H, t, *J* = 7.3, MeCOArH), 8.17 (2 H, d, *J* = 7.0, C<sub>6</sub>H<sub>5</sub>), 8.25 (1 H, d, *J* = 7.3, MeCOArH), 9.21 (1 H, d, *J* = 7.3, MeCOArH). <sup>13</sup>C NMR: 27.4, 128.2, 128.4, 131.7, 135.1, 137.1, 138.6, 140.7, 143.1, 177.3, 180.8, 208.8. IR: 1620, 1280, 770, 730 cm<sup>-1</sup>. Anal. Calcd for C<sub>14</sub>H<sub>12</sub>BiBrO: C, 34.7; H, 2.5. Found: C, 34.8; H, 2.4.

**(2-Acetylphenyl)bromo(4-chlorophenyl)bismuthane, 3d.** Crystals: yield, 86%; mp 157–159 °C (decomp) (MeOH-CH<sub>2</sub>Cl<sub>2</sub> (5:1)). <sup>1</sup>H NMR: 2.69 (3 H, s, Me), 7.40 (2 H, d, *J*<sub>AB</sub> = 7.9, ClArH), 7.68 (1 H, t, *J* = 7.3, MeCOArH), 7.99 (1 H, t, *J* = 7.3, MeCOArH), 8.09 (2 H, d, *J*<sub>AB</sub> = 7.9, ClArH), 8.25 (1 H, d, *J* = 7.9, MeCOArH), 9.19 (1 H, d, *J* = 7.9, MeCOArH). <sup>13</sup>C NMR: 27.4, 128.6, 131.7, 134.3, 135.2, 138.6, 138.7, 140.6, 143.1, 174.9, 180.4, 209.0. IR: 1630, 1280, 1085, 1005, 800, 765 cm<sup>-1</sup>. Anal. Calcd for C<sub>14</sub>H<sub>11</sub>BiBrClO: C, 32.4; H, 2.1. Found: C, 32.7; H, 2.1.

**(2-Acetylphenyl)bromo(1-naphthyl)bismuthane, 3e.** Crystals: yield, 82%; mp 225–227 °C (decomp) (MeOH-CH<sub>2</sub>Cl<sub>2</sub> (5:1)). <sup>1</sup>H NMR: 2.58 (3 H, s, Me), 7.43–7.53 (2 H, m, ArH), 7.61–7.75 (2 H, m, ArH), 7.85 (1 H, d, *J* = 8.6, ArH), 7.95 (1 H, d, *J* = 8.5, ArH), 8.05 (1 H, t, *J* = 7.9, ArH), 8.24 (1 H, d, *J* = 7.9, ArH), 8.48–8.55 (2 H, m, ArH), 9.26 (1 H, d, *J* = 7.3, MeCOArH). <sup>13</sup>C NMR: 27.2, 125.8, 126.2, 128.6, 128.7, 129.3, 129.7, 130.0, 135.1, 135.5, 138.4, 138.5, 141.0, 143.3, 179.1, 179.8, 208.2; one carbon signal was too weak to be assigned. IR: 1615, 1280, 790, 770 cm<sup>-1</sup>. Anal. Calcd for C<sub>18</sub>H<sub>14</sub>BiBrO: C, 40.4; H, 2.6. Found: C, 40.1; H, 2.7.

**(2-Acetylphenyl)chloro(4-methylphenyl)bismuthane, 4a.** To a stirred solution of compound **2b** (255 mg, 0.5 mmol) in benzene (3 mL) was added dropwise at ice bath temperature boron trifluoride-diethyl etherate (ca. 2 mmol). After 5 min, the mixture was quenched with brine (3 mL) and the organic layer was extracted with ethyl acetate (5 mL × 2). The combined extracts were evaporated under reduced pressure to leave an oily residue, which was crystallized from MeOH-CH<sub>2</sub>Cl<sub>2</sub> (5:1) to afford **4a** as crystals: yield 90%; mp 175–177 °C. <sup>1</sup>H NMR: 2.24 (3 H, s, Me), 2.68 (3 H, s, Me), 7.33 (2 H, d, *J*<sub>AB</sub> = 7.9, MeArH), 7.63 (1 H, t, *J* = 7.3, MeCOArH), 8.00 (1 H, t, *J* = 7.3, MeCOArH), 8.03 (2 H, d, *J*<sub>AB</sub> = 7.9, MeArH), 8.25 (1 H, d, *J* = 7.3, MeCOArH), 9.06 (1 H, d, *J* = 7.3, MeCOArH). <sup>13</sup>C NMR: 21.5, 27.4, 128.2, 132.4, 135.2, 136.4 (× 2), 138.1, 138.3, 143.1, 177.9, 185.3, 209.2. IR: 1625, 1550, 1280, 800, 765, 615, 480 cm<sup>-1</sup>. Anal. Calcd for C<sub>15</sub>H<sub>14</sub>BiClO: C, 39.6; H, 3.1. Found: C, 39.6; H, 3.1.

**(2-Acetylphenyl)iodo(4-methylphenyl)bismuthane, 4b.** To a stirred solution of compound **3b** (249 mg, 0.5 mmol) in benzene (3 mL) was added dropwise saturated aqueous NaI (3 mL). After 15 min, the organic layer was extracted with ethyl acetate (5 mL × 2). The combined extracts were evaporated under reduced pressure to leave an oily residue,

which was crystallized from MeOH-CH<sub>2</sub>Cl<sub>2</sub> (5:1) to afford **4b** as crystals: yield 89%; mp 148–150 °C. <sup>1</sup>H NMR: 2.25 (3 H, s, Me), 2.68 (3 H, s, Me), 7.25 (2 H, d, *J*<sub>AB</sub> = 7.9, MeArH), 7.70 (1 H, dt, *J* = 7.6 and 1.3, MeCOArH), 7.87 (1 H, dt, *J* = 7.4 and 1.3, MeCOArH), 8.07 (2 H, d, *J*<sub>AB</sub> = 7.9, MeArH), 8.23 (1 H, dd, *J* = 7.7 and 1.1, MeCOArH), 9.42 (1 H, dd, *J* = 7.7 and 1.1, MeCOArH). <sup>13</sup>C NMR: 21.6, 27.1, 128.5, 132.4, 134.5, 138.0, 138.2, 139.0, 143.1, 145.6, 166.7, 172.1, 207.5. IR: 1625, 1285, 800, 770, 480 cm<sup>-1</sup>. Anal. Calcd for C<sub>15</sub>H<sub>14</sub>BiO: C, 33.0; H, 2.6. Found: C, 33.0; H, 2.6.

**(2-Formylphenyl)bis(1-naphthyl)bismuthane, 5e.** *Ortho*-lithiated lithium α-amino alkoxide was generated according to the reported procedure<sup>13</sup> by adding lithium *N*-methylpiperazide (ca. 3 mmol) to benzaldehyde (3 mmol) in benzene (5 mL) and subsequently heating the solution with excess of butyllithium (9 mmol) at reflux for 12 h. To a suspension of the dilithiated compound (ca. 3 mmol) thus obtained in benzene (5 mL) was added dropwise at ice bath temperature a suspension of chlorobis(1-naphthyl)bismuthane (ca. 3 mmol) in diethyl ether (10 mL), and the resulting mixture was stirred for 15 min. This chlorobismuthane (ca. 3 mmol) was generated by stirring tris(1-naphthyl)bismuthane (1.18 g, 2 mmol) and bismuth(III) chloride (315 mg, 1 mmol) in CH<sub>2</sub>Cl<sub>2</sub> (10 mL) for 2 h at 45 °C and employed as an ethereal suspension after removal of CH<sub>2</sub>Cl<sub>2</sub> under reduced pressure. After the addition of brine (5 mL), the mixture was diluted with benzene (10 mL) and the insoluble polymeric substances were filtered off. The organic layer was separated and evaporated under reduced pressure to leave a yellow oil, which was purified by chromatography on silica gel using hexane-ethyl acetate (5:1) as the eluent to afford crude compound **5e**. Recrystallization from MeOH-CH<sub>2</sub>Cl<sub>2</sub> (5:1) gave pure product as crystals: yield, 17%; mp 170–172 °C. <sup>1</sup>H NMR: 7.24–8.15 (18 H, m, ArH), 10.18 (1 H, s, CHO). <sup>13</sup>C NMR: 125.6, 125.9, 128.1, 128.2, 128.9, 129.2, 130.7, 134.7, 136.3, 137.2, 138.1, 139.0, 141.1, 141.5, 156.7, 161.0, 195.0. IR: 1665, 1560, 1500, 1200, 790, 785, 770, 760 cm<sup>-1</sup>. Anal. Calcd for C<sub>27</sub>H<sub>19</sub>BiO: C, 57.0; H, 3.4. Found: C, 56.6; H, 3.3.

**Preparation of Arylbromo(2-formylphenyl)bismuthanes 6.** **Typical Procedure.** Chlorobis(4-methoxyphenyl)bismuthane (ca. 3 mmol) was generated by stirring tris(4-methoxyphenyl)bismuthane (1.06 g, 2 mmol) and bismuth(III) chloride (315 mg, 1 mmol) in diethyl ether (10 mL) for 1 h at room temperature. To a suspension of the *ortho*-lithiated lithium α-amino alkoxide (ca. 3 mmol) generated from benzaldehyde in benzene (5 mL) was added dropwise at ice bath temperature a suspension of the above chlorobismuthane (ca. 3 mmol), and the resulting mixture was stirred for 15 min. After the addition of brine (5 mL), the mixture was worked up in a manner as described in the preparation of **5e** to give a yellow oil containing compound **5a**, which was treated with boron trifluoride-diethyl etherate (ca. 3 mmol) in benzene (5 mL) at ice bath temperature. The reaction mixture was immediately quenched with saturated aqueous NaBr (3 mL). The organic layer was extracted with ethyl acetate (5 mL × 2), and the combined extracts were evaporated under reduced pressure to leave an oily residue, which was purified by chromatography on silica gel using hexane-ethyl acetate (5:1) as the eluent to afford crude bromo(2-formylphenyl)(4-methoxyphenyl)bismuthane **6a** as a yellow oil. Recrystallization from MeOH-CH<sub>2</sub>Cl<sub>2</sub> (5:1) gave pure product as crystals: yield, 16%; mp 125–127 °C. <sup>1</sup>H NMR: 3.73 (3 H, s, OMe), 6.99 (2 H, d, *J*<sub>AB</sub> = 8.6, MeOArH), 7.76 (1 H, t, *J* = 7.3, HCOArH), 7.96 (1 H, t, *J* = 7.3, HCOArH), 8.07 (2 H, d, *J*<sub>AB</sub> = 8.6, MeOArH), 8.22 (1 H, d, *J* = 7.3, HCOArH), 9.15 (1 H, d, *J* = 7.3, HCOArH), 10.67 (1 H, s, CHO). <sup>13</sup>C NMR: 55.1, 117.6, 128.7, 137.9, 138.9, 139.3, 141.1, 143.9, 159.6, 200.5; *ipso* carbon atoms were too weak to be observed. IR: 1640, 1575, 1490, 1285, 1245, 1210, 1180 cm<sup>-1</sup>. Anal. Calcd for C<sub>14</sub>H<sub>12</sub>BiBrO<sub>2</sub>: C, 33.5; H, 2.4. Found: C, 33.5; H, 2.4.

**Bromo(2-formylphenyl)(4-methylphenyl)bismuthane, 6b.** Crystals: yield, 24%; mp 139–141 °C (MeOH-CH<sub>2</sub>Cl<sub>2</sub> (5:1)). <sup>1</sup>H NMR: 2.25 (3 H, s, Me), 7.32 (2 H, d, *J*<sub>AB</sub> = 7.3, MeArH), 7.75 (1 H, t, *J* = 7.3, HCOArH), 7.95 (1 H, t, *J* = 7.3, HCOArH), 8.07 (2 H, d, *J*<sub>AB</sub> = 7.3, MeArH), 8.22 (1 H, d, *J* = 7.9, HCOArH), 9.15 (1 H, d, *J* = 7.3, HCOArH), 10.68 (1 H, s, CHO). <sup>13</sup>C NMR: 21.6, 128.7, 132.6, 137.3, 137.9, 138.4, 139.3, 141.1, 143.9, 174.3, 180.7, 200.6. IR: 1640, 1550, 1210, 800, 760, 475 cm<sup>-1</sup>. Anal. Calcd for C<sub>14</sub>H<sub>12</sub>BiBrO: C, 34.7; H, 2.5. Found: C, 34.8; H, 2.5.

**Bromo(2-formylphenyl)phenylbismuthane, 6c.** Crystals: <sup>16</sup> yield, 20%; mp 138–140 °C (MeOH-CH<sub>2</sub>Cl<sub>2</sub> (5:1)). <sup>1</sup>H NMR: 7.26–8.21 (8 H, m, ArH), 9.17 (1 H, d, *J* = 8.0, HCOArH), 10.69 (1 H, s, CHO). <sup>13</sup>C NMR: 128.3, 128.7, 131.8, 137.3, 137.9, 139.3, 141.0, 143.9, 177.1, 180.7, 200.6. IR: 1630, 1570, 1550, 1210, 850, 765, 735, 680, 665 cm<sup>-1</sup>.

**Bromo(4-chlorophenyl)(2-formylphenyl)bismuthane, 6d.** Crystals: <sup>16</sup> yield, 27%; mp 155–157 °C (MeOH-CH<sub>2</sub>Cl<sub>2</sub> (5:1)). <sup>1</sup>H NMR: 7.42 (2 H, d, *J*<sub>AB</sub> = 7.3, ClArH), 7.77 (1 H, t, *J* = 7.3, HCOArH), 7.98 (1 H, t, *J* = 7.3, HCOArH), 8.12 (2 H, d, *J*<sub>AB</sub> = 7.3, ClArH), 8.24 (1 H, d, *J* = 7.3, HCOArH), 9.14 (1 H, d, *J* = 7.3, HCOArH), 10.68 (1 H, s, CHO). <sup>13</sup>C NMR: 128.9, 131.8, 134.5, 138.0, 138.8, 139.5, 141.0, 143.8, 200.7; *ipso* carbon signals could not be assigned. IR: 1630, 1570, 1550, 1215, 1080, 1000, 855, 800, 760, 715, 665, 480 cm<sup>-1</sup>.

**Bromo(2-formylphenyl)(1-naphthyl)bismuthane, 6e.** Chlorobis(1-naphthyl)bismuthane (ca. 3 mmol) was generated by stirring tris(1-naphthyl)bismuthane (1.18 g, 2 mmol) and bismuth(III) chloride (315 mg, 1 mmol) in CH<sub>2</sub>Cl<sub>2</sub> (10 mL) for 2 h at 45 °C and was employed as an ethereal suspension after removal of CH<sub>2</sub>Cl<sub>2</sub> under reduced pressure. To a stirred suspension of the *ortho*-lithiated lithium α-amino alkoxide (ca. 3 mmol) generated from benzaldehyde in benzene (5 mL) was added dropwise at ice bath temperature a suspension of the above chlorobismuthane (ca. 3 mmol) in diethyl ether (10 mL), and the reaction mixture was stirred for additional 15 min. Similar work-up as described for **6a** afforded compound **6e**: crystals, <sup>16</sup> yield, 14%; mp 193–195 °C (decomp) (MeOH-CH<sub>2</sub>Cl<sub>2</sub> (5:1)). <sup>1</sup>H NMR: 7.44–7.53 (2 H, m, ArH), 7.66 (1 H, t, *J* = 6.7, ArH), 7.79 (1 H, t, *J* = 7.3 ArH), 7.86 (1 H, d, *J* = 7.9, ArH), 7.96 (1 H, d, *J* = 8.5, ArH), 8.03 (1 H, t, *J* = 7.9, ArH), 8.19 (1 H, d, *J* = 7.3, ArH), 8.49 (1 H, d, *J* = 8.5, ArH), 8.60 (1 H, d, *J* = 6.7, ArH), 9.21 (1 H, d, *J* = 7.3, HCOArH), 10.56 (1 H, s, CHO). Due to extensive decomposition of **6e** during the measurement of <sup>13</sup>C NMR, only one signal, at δ<sub>c</sub> 200.1, was assigned as the carbonyl carbon. IR: 1635, 1550, 1250, 1210, 845, 790, 770 cm<sup>-1</sup>.

**(2-Formylphenyl)iodo(4-methylphenyl)bismuthane, 7b.** To a solution of compound **6b** (242 mg, 0.5 mmol) in benzene (3 mL) was added saturated aqueous NaI (3 mL), and the resulting mixture was stirred for 15 min. The organic layer was extracted with ethyl acetate (5 mL × 2), and the combined extracts were evaporated under reduced pressure to leave an oily residue, which was crystallized from MeOH-CH<sub>2</sub>Cl<sub>2</sub> (5:1) to afford **7b** as crystals: yield, 88%; mp 141–143 °C. <sup>1</sup>H NMR: 2.25 (3 H, s, Me), 7.27 (2 H, d, *J*<sub>AB</sub> = 7.3, MeArH), 7.76–7.91 (2 H, m, HCOArH), 8.09 (2 H, d, *J*<sub>AB</sub> = 7.3, MeArH), 8.18 (1 H, *J* = 7.3, HCOArH), 9.36 (1 H, d, *J* = 7.7, HCOArH), 10.51 (1 H, s, CHO). <sup>13</sup>C NMR: 21.6, 128.7, 132.5, 137.6, 138.3, 138.5, 139.7, 143.7, 146.2, 199.5; *ipso* carbon signals were too weak to be assigned. IR: 1635, 1575, 1555, 1210, 950, 795, 750, 660, 480 cm<sup>-1</sup>. Anal. Calcd for C<sub>14</sub>H<sub>12</sub>BiIO: C, 31.6; H, 2.3. Found: C, 31.6; H, 2.3.

**Chlorobis(2-formylphenyl)bismuthane, 8.** To a suspension of the *ortho*-lithiated lithium α-amino alkoxide (ca. 3 mmol) derived from benzaldehyde in benzene (5 mL) was added dropwise at ice bath temperature a suspension of chlorobismuthane (ca. 3 mmol), generated from tris(4-methylphenyl)bismuthane (964 mg, 2 mmol) and bismuth(III) chloride (315 mg, 1 mmol) in diethyl ether (10 mL), and the

(16) This compound decomposed while waiting for elemental analysis.

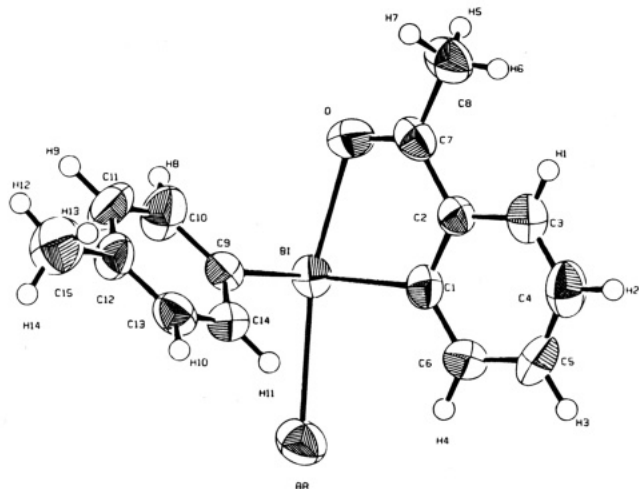


Figure 1.

Table 5. Positional Parameters and Isotropic Thermal Parameters ( $\text{\AA}^2$ ) for **3b**<sup>a</sup>

atom	x	y	z	$B(\text{eq})^b$
Bi	0.09598(5)	0.48044(3)	0.67273(3)	3.68(2)
Br	0.0101(1)	0.2652(1)	0.71497(8)	5.50(6)
O	0.2310(9)	0.6417(6)	0.6000(5)	4.7(4)
C(1)	0.190(1)	0.420(1)	0.5459(6)	3.8(5)
C(2)	0.264(1)	0.4995(8)	0.4958(6)	3.5(5)
C(3)	0.325(1)	0.467(1)	0.4159(7)	4.6(5)
C(4)	0.310(1)	0.316(1)	0.3861(7)	5.4(7)
C(5)	0.231(1)	0.281(1)	0.4329(8)	4.8(6)
C(6)	0.175(1)	0.310(1)	0.5138(7)	4.4(5)
C(7)	0.278(1)	0.617(1)	0.5275(7)	4.2(5)
C(8)	0.347(1)	0.707(1)	0.4749(7)	5.3(6)
C(9)	0.337(1)	0.4691(9)	0.7527(6)	3.5(4)
C(10)	0.391(2)	0.558(1)	0.8068(8)	6.4(7)
C(11)	0.536(2)	0.557(1)	0.8544(8)	6.4(7)
C(12)	0.647(1)	0.467(1)	0.8518(7)	4.5(5)
C(13)	0.593(1)	0.379(1)	0.7976(7)	4.5(6)
C(14)	0.446(1)	0.3788(9)	0.7493(7)	4.1(5)
C(15)	0.810(2)	0.469(1)	0.902(1)	7.4(8)
H(1)	0.3781	0.5215	0.3824	5.5
H(2)	0.3534	0.3401	0.3324	6.5
H(3)	0.2148	0.2072	0.4102	5.7
H(4)	0.1264	0.2542	0.5476	5.2
H(5)	0.2677	0.7643	0.4625	6.3
H(6)	0.3783	0.6770	0.4209	6.3
H(7)	0.4401	0.7387	0.5075	6.3
H(8)	0.3229	0.6219	0.8104	7.6
H(9)	0.5662	0.6194	0.8912	7.7
H(10)	0.6614	0.3153	0.7937	5.3
H(11)	0.4160	0.3162	0.7124	5.0
H(12)	0.8222	0.5369	0.9350	8.9
H(13)	0.8922	0.4649	0.8619	8.9
H(14)	0.8204	0.4066	0.9413	8.9

<sup>a</sup> Numerals in parentheses are estimated standard deviations.

<sup>b</sup>  $B(\text{eq}) = 1.33[a^2B_{11} + b^2B_{22} + c^2B_{33} + ab(\cos \gamma)B_{12} + ac(\cos \beta)B_{13} + bc(\cos \alpha)B_{23}]$ .

resulting mixture was stirred for 15 min. After the addition of brine (5 mL) and then benzene (10 mL), the insoluble polymeric substances were removed by filtration. The organic layer was separated and evaporated under reduced pressure to leave a yellow oily residue, which was purified by chromatography on silica gel using hexane–ethyl acetate (5:1) as the eluent to afford (2-formylphenyl)bis(4-methylphenyl)bismuthane, **5b**. A solution of **5b** in benzene (3 mL) was treated with boron trifluoride diethyl etherate (ca. 3 mmol) at ice bath temperature, and the resulting mixture was immediately quenched with brine (3 mL). The organic layer was separated and evaporated under reduced pressure to leave impure chloro-(2-formylphenyl)(4-methylphenyl)bismuthane **7a** as a yellow oily residue. Attempted recrystallization of this product from MeOH–CH<sub>2</sub>Cl<sub>2</sub> (5:1), however, resulted in the decomposition

to compound **8**: crystals, yield, 12%; mp 208–210 °C (decomp). <sup>1</sup>H NMR: 7.65 (2 H, t,  $J = 7.3$ , C<sub>6</sub>H<sub>4</sub>), 7.86 (2 H, t,  $J = 7.3$ , C<sub>6</sub>H<sub>4</sub>), 8.12 (2 H, d,  $J = 7.3$ , C<sub>6</sub>H<sub>4</sub>), 8.81 (2 H, d,  $J = 7.9$ , C<sub>6</sub>H<sub>4</sub>), 10.53 (2 H, s, CHO). IR: 1630, 1555, 1220, 1200, 855, 840, 755, 665 cm<sup>-1</sup>. Anal. Calcd for C<sub>14</sub>H<sub>10</sub>BiClO<sub>2</sub>: C, 37.0; H, 2.2. Found: C, 37.4; H, 2.4.

**Bromo(4-methylphenyl)[2-(N-phenylformimidoyl)phenyl]bismuthane, 9.** A stirred mixture of compound **6b** (484 mg, 1 mmol) and aniline (ca. 1.5 mmol) in benzene (3 mL) was heated at reflux for 4 h. The reaction mixture was evaporated to leave an oily residue, which was crystallized from MeOH to afford compound **9**: crystals, yield, 82%; mp 218–220 °C. <sup>1</sup>H NMR: 2.22 (3 H, s, Me), 7.13 (2 H, d,  $J = 6.7$ , C<sub>6</sub>H<sub>5</sub>), 7.22 (2 H, d,  $J_{AB} = 7.9$ , MeC<sub>6</sub>H<sub>4</sub>), 7.34–7.45 (3 H, m, C<sub>6</sub>H<sub>5</sub>), 7.70 (1 H, t,  $J = 7.3$ , C<sub>6</sub>H<sub>4</sub>CHN), 7.79 (1 H, t,  $J = 7.3$ , C<sub>6</sub>H<sub>4</sub>CHN), 8.00 (2 H, d,  $J_{AB} = 7.9$ , MeC<sub>6</sub>H<sub>4</sub>), 8.06 (1 H, d,  $J = 7.3$ , C<sub>6</sub>H<sub>4</sub>CHN), 9.22 (1 H, d,  $J = 7.3$ , C<sub>6</sub>H<sub>4</sub>CHN), 9.24 (1 H, s, CHN). IR: 1615, 1590, 1575, 1550, 1490, 1190, 920, 890, 795, 760, 710, 690, 545, 480, 425 cm<sup>-1</sup>. Anal. Calcd for C<sub>20</sub>H<sub>17</sub>BiBrN: C, 42.9; H, 3.1; N, 2.5. Found: C, 42.8; H, 3.0; N, 2.4.

**Chloro(4-methylphenyl)[2-(N-benzylformimidoyl)phenyl]bismuthane, 10.** Benzylamine (ca. 1.5 mmol) was added dropwise to a stirred mixture of crude chloro(2-formylphenyl)-(4-methylphenyl)bismuthane **7a** (ca. 1 mmol) and benzene (3 mL) at room temperature, and after 5 min the reaction was quenched by the addition of brine (1 mL). The organic layer was extracted with ethyl acetate (5 mL × 2), and the combined extracts were evaporated under reduced pressure to leave an oily residue, which was crystallized from MeOH–CH<sub>2</sub>Cl<sub>2</sub> (5:1) to afford compound **10**: crystals, yield, 69%; mp 210–212 °C. <sup>1</sup>H NMR: 2.25 (3 H, s, Me), 4.64 (1 H, d,  $J_{AB} = 14.0$ , CH<sub>2</sub>-Ph), 4.73 (1 H, d,  $J_{AB} = 14.0$ , CH<sub>2</sub>Ph), 7.14–7.41 (7 H, m, ArH), 7.62 (1 H, dt,  $J = 6.1$  and 1.2, C<sub>6</sub>H<sub>4</sub>CHN), 7.76 (1 H, dt,  $J = 6.0$  and 1.6, C<sub>6</sub>H<sub>4</sub>CHN), 7.85 (2 H, d,  $J_{AB} = 7.9$ , MeC<sub>6</sub>H<sub>4</sub>), 7.94 (1 H, dd,  $J = 6.1$  and 1.2, C<sub>6</sub>H<sub>4</sub>CHN), 8.99 (1 H, d,  $J = 7.3$ , C<sub>6</sub>H<sub>4</sub>CHN), 9.22 (1 H, s, CHN). IR: 1625, 1440, 1035, 800, 770, 755, 700, 480 cm<sup>-1</sup>. Anal. Calcd for C<sub>21</sub>H<sub>19</sub>BiClN: C, 47.6; H, 3.6. Found: C, 47.3; H, 3.6.

**X-ray Crystallography of Compound 3b.** A crystal of dimension 0.430 × 0.180 × 0.180 mm<sup>3</sup> grown from MeOH–CH<sub>2</sub>Cl<sub>2</sub> (5:1) at ambient temperature was used for X-ray crystallography.

**Crystal Data.** C<sub>15</sub>H<sub>14</sub>BiBrO:  $M = 499.16$ , monoclinic, space group  $P2_1/c$ ,  $a = 8.241(2)$  Å,  $b = 11.885(3)$  Å,  $c = 15.179(2)$  Å,  $\beta = 95.04(1)^\circ$ ,  $V = 1480.9(5)$  Å<sup>3</sup>,  $Z = 4$ ,  $D_{\text{calcd}} = 2.239$  g cm<sup>-3</sup>. Colorless prisms;  $\mu(\text{Mo K}\alpha)$ ,  $\lambda = 0.71069$  Å) = 145.29 cm<sup>-1</sup>. Intensity data were collected on a Rigaku AFC5R diffractometer with graphite–monochromated Mo K $\alpha$  radiation and a 12 KW rotating anode generator using the  $\omega$ – $2\theta$  scan technique to a maximum  $2\theta$ -value of 55.0°. Scans of  $(0.68 + 0.30 \tan \theta)^\circ$  were made at a speed of 16.0 deg min<sup>-1</sup> (in  $\omega$ ). Of the 3816 reflections that were collected, 3579 were unique ( $R_{\text{int}} = 0.082$ ). Data were corrected for Lorentz, polarization, and absorption effects. Empirical correction for the absorption was made based on azimuthal or  $\Psi$  scans<sup>17</sup> (transmission factors: 0.56–1.00). The correction for secondary extinction was applied (coefficient:  $4.997 \times 10^{-7}$ ). The structure was solved by the Patterson method.<sup>18</sup> The non-hydrogen atoms were refined anisotropically. The final cycle of full-matrix least-squares refinement was based on 1950 observed reflections ( $I > 3.00 \sigma(I)$ ) and 164 variable parameters and converged with unweighted and weighted agreement factors of  $R = 0.036$  and  $R_w = 0.034$ . The maximum and minimum peaks on the final difference Fourier map corresponded to 0.97

(17) North, A. C.; Phillips, D. C.; Mathews, F. S. *Acta Crystallogr., Sect. A*, **1968**, *24*, 351.

(18) Structure solution method: Calbrese, J. C. PHASE: Patterson Heavy Atom Solution Extractor. Ph.D. Thesis, University of Wisconsin–Madison, Madison, WI, 1972.

(19) Cromer, D. T.; Waber, J. T. *International Tables for X-ray Crystallography*; Kynoch Press: Birmingham, England, 1974; Vol IV. Table 2.2A.

(20) Ibers, J. A.; Hamilton, W. C. *Acta Crystallogr.* **1964**, *17*, 781.

and  $-1.00 \text{ e}/\text{\AA}^3$ , respectively. The weighting scheme,  $w = 1/\sigma^2(F_o)$ , was employed. Neutral atom scattering factors were taken from Cromer and Waber.<sup>19</sup> Anomalous dispersion effects were included in  $F_{\text{calcd}}$ ;<sup>20</sup> the values for  $\Delta f'$  and  $\Delta f''$  were those of Cromer.<sup>21</sup> All calculations were performed on a VAX station 3200 computer using the TEXSAN<sup>22</sup> crystallographic software package from the Molecular Structure Corporation. The ORTEP-II program<sup>23</sup> was used to obtain the drawing in Figure 1. Selected bond lengths, bond angles, and atomic coordinates are given in Tables 4 and 5.

**Acknowledgment.** The present work was supported by Grants-in-Aid for Scientific Research (Nos. 05236101 and 06740550) from the Ministry of Education, Science

---

(21) Cromer, D. T. *International Tables for X-ray Crystallography*; Kynoch Press; Birmingham, England, 1974; Vol. IV, Table 2.3.1.

and Culture of Japan. T.M. thanks Mr. T. Ikegami (Kyoto University) for the measurement of  $^{13}\text{C}$  NMR spectra.

**Supporting Information Available:** For **3b**, full details of crystal data, fractional atomic coordinates, bond lengths, bond angles, hydrogen coordinates, thermal parameters, and unit cell and PLUTO diagrams (19 pages). Ordering information is given on any current masthead page.

OM9502289

---

(22) TEXSAN-TEXRAY Structure Analysis Package, Molecular Structure Corp., The Woodlands, TX, 1985.

(23) Johnson, C. K.; ORTEP-II. Report ORNL-5138; National Technical Information Service, U.S. Department of Commerce: Springfield, VA, 1976.

# Synthesis, Characterization, and Reactivities of Diruthenium Complexes Containing a $\mu$ -Silane Ligand and Structural Studies of the $\mu$ -Silane Complex [Cp'Ru(CO)]<sub>2</sub>( $\mu$ - $\eta^2$ : $\eta^2$ -H<sub>2</sub>Si<sup>t</sup>Bu<sub>2</sub>)

Toshiro Takao, Shigeru Yoshida, and Hiroharu Suzuki\*

Department of Chemical Engineering, Faculty of Engineering, Tokyo Institute of Technology, O-okayama, Meguro-ku, Tokyo 152, Japan

Masako Tanaka

Research Laboratory of Resources Utilization, Tokyo Institute of Technology, 4259 Nagatsuta, Midori-Ku, Yokohama 226, Japan

Received November 14, 1994<sup>®</sup>

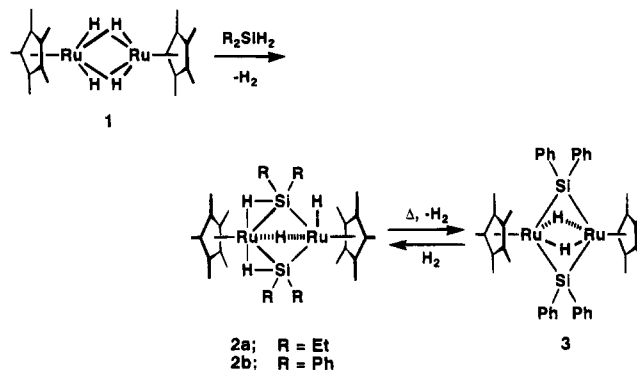
The diruthenium complex [Cp'Ru( $\mu$ -H)]<sub>2</sub>( $\mu$ - $\eta^2$ : $\eta^2$ -H<sub>2</sub>Si<sup>t</sup>Bu<sub>2</sub>) (**4**; Cp' =  $\eta^5$ -C<sub>5</sub>Me<sub>5</sub>), containing a  $\mu$ -silane ligand, was synthesized by the reaction of Cp'Ru( $\mu$ -H)<sub>4</sub>RuCp' (**1**) with <sup>t</sup>Bu<sub>2</sub>SiH<sub>2</sub>. The unusual coordination mode of di-*tert*-butylsilane was confirmed by means of <sup>1</sup>H, <sup>13</sup>C, and <sup>29</sup>Si NMR and IR spectroscopy. Treatment of **4** with 1 atm of CO affords a mixture of the  $\mu$ -silane complex [Cp'Ru(CO)]<sub>2</sub>( $\mu$ - $\eta^2$ : $\eta^2$ -H<sub>2</sub>Si<sup>t</sup>Bu<sub>2</sub>) (**5**) and the  $\mu$ -silyl complex [Cp'Ru(CO)]<sub>2</sub>( $\mu$ - $\eta^2$ -HSi<sup>t</sup>Bu<sub>2</sub>)(H) (**6**). The  $\mu$ -silane complex **5** is in equilibrium in solution with hydrido- $\mu$ -silyl species **6**. The equilibrium constant *K*, where *K* = [**6**]/[**5**], was determined to be 1.3 at 303 K in benzene-*d*<sub>6</sub>. Variable-temperature <sup>1</sup>H NMR measurements yielded thermodynamic parameters for conversion of **5** to **6**:  $\Delta H = 1.2 \pm 0.1$  kcal/mol and  $\Delta S = 4.5 \pm 0.1$  eu/mol. The reaction of **4** with 5 equiv of PhSiH<sub>3</sub> yields the mixed-bridge bis( $\mu$ -silyl) complex [Cp'Ru]<sub>2</sub>( $\mu$ - $\eta^2$ -HSi<sup>t</sup>Bu<sub>2</sub>)( $\mu$ - $\eta^2$ -HSiPhH)( $\mu$ -H)(H) (**7b**). When **4** is treated with 12 equiv of Et<sub>2</sub>SiH<sub>2</sub>, the mixed-bridge bis( $\mu$ -silyl) complex [Cp'Ru]<sub>2</sub>( $\mu$ - $\eta^2$ -HSi<sup>t</sup>Bu<sub>2</sub>)( $\mu$ - $\eta^2$ -HSiEtH)( $\mu$ -H)(H) (**7a**) is obtained via Si–C bond fission. The molecular structure of **5**, **7a**, and **7b** were determined by single-crystal X-ray diffraction studies.

## Introduction

In connection with hydrosilylation<sup>1</sup> or dehydrogenative coupling of primary or secondary silanes,<sup>2</sup> the reactions of silanes with transition-metal complexes have become of increased interest. In 1970, Graham and co-workers proposed a new coordination mode of hydrosilane, a two-electron–three-center (2e–3c) M–H–Si interaction, in CpMn(CO)<sub>2</sub>(H)SiPh<sub>3</sub> on the basis of X-ray diffraction studies.<sup>3</sup> Since this first example, a number of Si–H  $\sigma$ -complexes have been discovered and characterized by NMR<sup>4</sup> and photoelectron spectroscopy.<sup>5</sup> A Si–H  $\sigma$ -complex of manganese, MeCpMn(CO)<sub>2</sub>(H)-

SiPh<sub>2</sub>F, was structurally characterized by means of a neutron diffraction study by Schubert *et al.*<sup>4,6,7</sup>

In a previous communication, we reported the synthesis of the bis( $\mu$ -silyl) complexes [Cp'Ru( $\mu$ - $\eta^2$ -HSiR<sub>2</sub>)]<sub>2</sub>( $\mu$ -H)(H) (**2a**, R = Et; **2b**, R = Ph; Cp' =  $\eta^5$ -C<sub>5</sub>Me<sub>5</sub>), by the reaction of Cp'Ru( $\mu$ -H)<sub>4</sub>RuCp' (**1**) with R<sub>2</sub>SiH<sub>2</sub>.<sup>8</sup>



In this reaction, the ruthenium tetrahydride complex Cp'Ru( $\mu$ -H)<sub>4</sub>RuCp' (**1**), which readily generates unsatur-

(5) (a) Lichtenberger, D. L.; Rai-Chaudhuri, A. *J. Am. Chem. Soc.* **1989**, *111*, 3583. (b) Lichtenberger, D. L.; Rai-Chaudhuri, A. *Organometallics* **1990**, *9*, 1686. (c) Lichtenberger, D. L.; Rai-Chaudhuri, A. *Inorg. Chem.* **1990**, *29*, 975. (d) Lichtenberger, D. L.; Rai-Chaudhuri, A. *J. Am. Chem. Soc.* **1990**, *112*, 2492.

(6) Schubert, U.; Ackermann, K.; Wörle, B. *J. Am. Chem. Soc.* **1982**, *104*, 7378.

(7) Schubert, U. *Adv. Organomet. Chem.* **1990**, *30*, 151.

(8) Suzuki, H.; Takao, T.; Tanaka, M.; Moro-oka, Y. *J. Chem. Soc., Chem. Commun.* **1992**, 476.

<sup>®</sup> Abstract published in *Advance ACS Abstracts*, July 15, 1995.

(1) See, for example: (a) Ojima, I. In *The Chemistry of Organosilicon Compounds*; Patai, S., Rappoport, Z., Eds.; Wiley: New York, 1989; Chapter 25, p 1479. (b) Speir, J. L. *Adv. Organomet. Chem.* **1979**, *17*, 47.

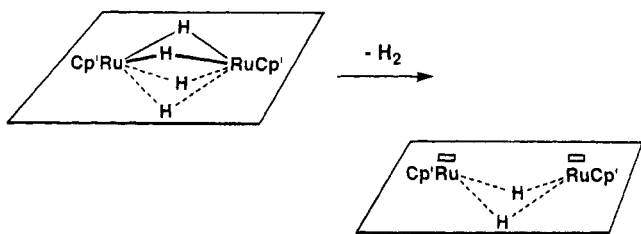
(2) (a) Aitken, C.; Harrod, J. F.; Samuel, E. *J. Organomet. Chem.* **1985**, *279*, C11. (b) Aitken, C.; Harrod, J. F.; Samuel, E. *J. Am. Chem. Soc.* **1986**, *108*, 4059. (c) Aitken, C.; Harrod, J. F.; Gill, U. S. *Can. J. Chem.* **1987**, *65*, 1804. (d) Aitken, C.; Barry, J.; Gauvin, F.; Harrod, J. F.; Malek, A.; Rousseau, D. *Organometallics* **1989**, *8*, 1732. (e) Harrod, J. F.; Ziegler, T.; Tschinke, V. *Organometallics* **1990**, *9*, 897. (f) Tilley, T. D. *Acc. Chem. Res.* **1993**, *26*, 22. (g) Woo, H.; Heyn, R. H.; Tilley, T. D. *J. Am. Chem. Soc.* **1992**, *114*, 5698. (h) Woo, H.; Walzer, J. F.; Tilley, T. D. *J. Am. Chem. Soc.* **1992**, *114*, 7047. (i) Woo, H.; Tilley, T. D. *J. Am. Chem. Soc.* **1989**, *111*, 3757. (j) Woo, H.; Tilley, T. D. *J. Am. Chem. Soc.* **1989**, *111*, 8043. (k) Forsyth, C. M.; Nolan, S. P.; Marks, T. J. *Organometallics* **1991**, *10*, 2543. (l) Corey, J. Y.; Chang, L. S.; Corey, E. R. *Organometallics* **1987**, *6*, 1595. (m) Yang, L. S.; Corey, J. Y. *Organometallics* **1989**, *8*, 1885. (n) Corey, J. Y.; Zhu, X.; Bedard, T. C.; Lange, L. D. *Organometallics* **1991**, *10*, 924.

(3) Graham, W. A. G. *J. Organomet. Chem.* **1986**, *300*, 81.

(4) (a) Schubert, U.; Müller, J.; Alt, H. G. *Organometallics* **1987**, *6*, 469. (b) Schubert, U.; Scholtz, G.; Müller, J.; Ackermann, K.; Wörle, B. *J. Organomet. Chem.* **1986**, *306*, 303.



ated sites on the same side of the molecular plane upon heating or treatment with a hydrogen acceptor, acts as a precursor of the active species for *bimetallic activation*.<sup>9</sup>

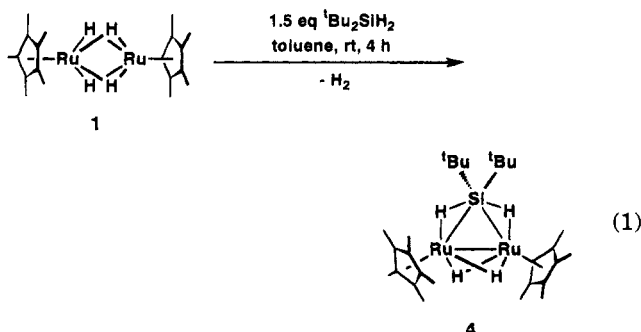


It is generally accepted that the  $(\eta^2\text{-X-Y})\text{-M}$  species are plausible intermediates in the oxidative addition of X-Y to the metal center. As far as silicon is concerned, there have been only a few examples of the oxidative addition of an Si-H bond via the well-characterized  $(\eta^2\text{-Si-H})\text{-metal}$  complex, while an equilibrium between  $(\eta^2\text{-H}_2)\text{M}$  and  $\text{M}(\text{H}_2)$  has been proved in the chemistry of  $\eta^2\text{-H}_2$  complexes on the basis of variable-temperature  $^1\text{H}$  NMR studies.<sup>10</sup>

We are interested in studying the interaction of silanes with dinuclear unsaturated species and transformation from  $(\eta^2\text{-Si-H})\text{-M}$  species into metal hydrido-silyl complex. In the reaction of  $\text{Cp}'\text{Ru}(\mu\text{-H})_4\text{RuCp}'$  (**1**) with  $^t\text{Bu}_2\text{SiH}_2$ , we have successfully isolated a dinuclear complex bridged by a  $\eta^2:\eta^2\text{-H}_2\text{Si}^t\text{-Bu}_2$  ligand. Here we describe in full detail its synthesis, characterization, and structure determination, as well as the oxidative addition of an agostic Si-H bond which forms a hydrido-silyl complex.

## Results and Discussion

When tetrahydride complex **1** was treated with  $^t\text{Bu}_2\text{SiH}_2$ , the mono( $\mu\text{-silane}$ ) complex  $[\text{Cp}'\text{Ru}(\mu\text{-H})]_2(\mu\text{-}\eta^2:\eta^2\text{-H}_2\text{Si}^t\text{Bu}_2)$  (**4**) was exclusively obtained, while a bis( $\mu\text{-silyl}$ ) complex was formed in the reaction of **1** with dihydrosilanes with less bulky substituents.<sup>8</sup> The reaction of complex **1** with 1.5 equiv of  $^t\text{Bu}_2\text{SiH}_2$  in toluene at room temperature for 4 h leads to the formation of mono( $\mu\text{-silane}$ ) complex **4**, which is isolated in 89% yield as a purple crystalline solid. Complex **4** is relatively stable to the air and moisture and is extremely soluble in nonpolar solvents, such as pentane or toluene. Complex **4** was fully characterized, and the  $\mu\text{-}\eta^2:\eta^2$  geometry of the  $^t\text{Bu}_2\text{SiH}_2$  ligand was confirmed on the basis of the  $^1\text{H}$ ,  $^{13}\text{C}$ , and  $^{29}\text{Si}$  NMR and IR spectral data.



In the  $^1\text{H}$  NMR spectrum of **4** measured at room temperature, three signals due to the Cp',  $^t\text{Bu}$ , and

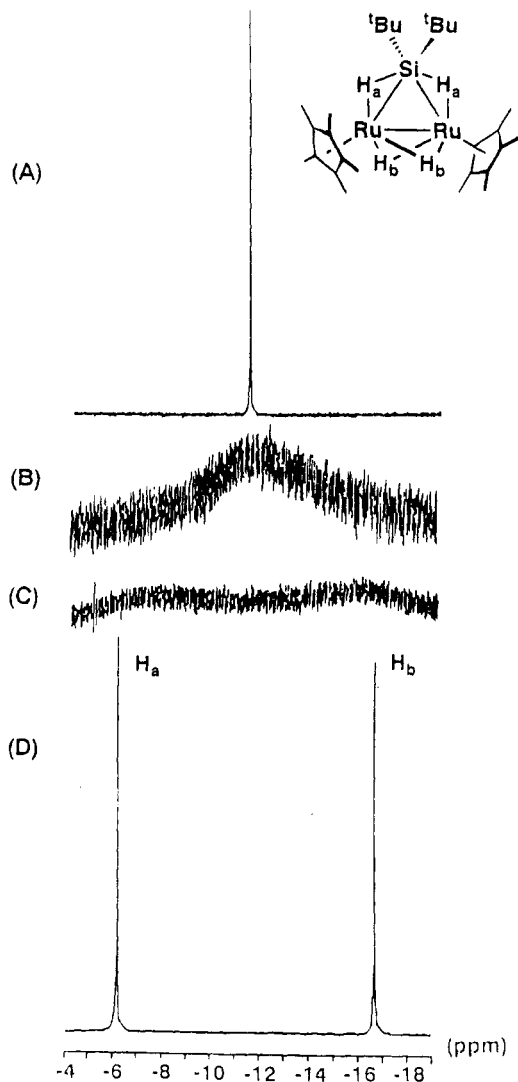


**Figure 1.** Variable-temperature  $^1\text{H}$  NMR spectra of  $[\text{Cp}'\text{Ru}(\mu\text{-H})]_2(\mu\text{-}\eta^2:\eta^2\text{-H}_2\text{Si}^t\text{Bu}_2)$  (**4**) showing hydride resonances: (A) 60 °C; (B) -50 °C; (C) -60 °C; (D) -120 °C.

hydride ligands are observed at  $\delta$  1.89, 1.11, and -11.12, respectively. Variable-temperature  $^1\text{H}$  NMR spectra shown in Figure 1 clearly establish the fluxionality of the hydride ligands in complex **4**. At ambient temperature, the four inequivalent hydrides are in time-averaged environments and a broad singlet resonance is observed at  $\delta$  -11.12. This resonance broadens and flattens at -60 °C. A sharp, low-temperature limiting spectrum is obtained at -120 °C. At this temperature, the resonance due to the hydride ligands is split into two singlet peaks at  $\delta$  -6.15 and -16.63. The signal at  $\delta$  -6.15 has satellite peaks due to a bonding interaction with silicon (Figure 2;  $^{29}\text{Si}$ , abundance 4.70%;  $J_{\text{Si-H}} = 75$  Hz). The coupling constant between  $^{29}\text{Si}$  and  $^1\text{H}$  often has been employed as a criterion for the magnitude of the Si-H bonding interaction, as has the Si-H distance as determined by neutron or X-ray diffraction studies (Table 1). The  $J_{\text{Si-H}}$  value for the  $\eta^2\text{-Si-H}$  ligand usually lies in the range of 20–140 Hz, intermediate between those of free silane ( $\sim 200$  Hz) and those characteristic of classical silyl hydrides ( $< 20$  Hz). Therefore, the signals at  $\delta$  -6.15 and -16.63 are assigned to the resonances due to hydride ligands with 2e-3c Ru-H-Si interactions ( $\text{H}_a$ ) and those bridging between two rutheniums ( $\text{H}_b$ ), respectively. We propose



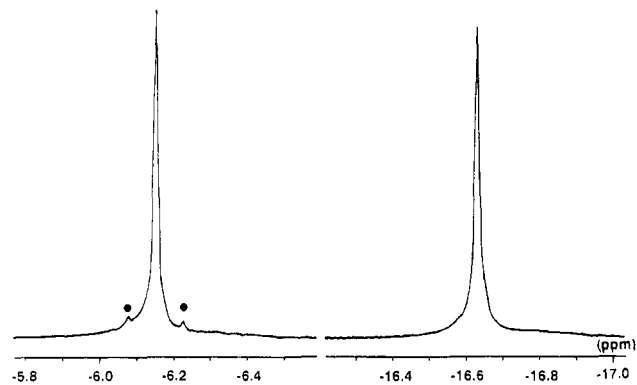


**Figure 2.**  $^1\text{H}$  NMR spectrum of  $[\text{Cp}'\text{Ru}(\mu\text{-H})]_2(\mu\text{-}\eta^2\text{:}\eta^2\text{-H}_2\text{-Si}^t\text{Bu}_2)$  (**4**) showing hydride resonances measured at  $-120^\circ\text{C}$ . The  $^{29}\text{Si}$  satellites are indicated (●).

an intramolecular site exchange of hydrides among two Ru–H–Si sites and two Ru–H–Ru sites to explain the VT-NMR data. From the line shape analysis of the variable-temperature  $^1\text{H}$  NMR data, the  $\Delta G^\ddagger$  value of this fluxional process was estimated at ca. 8.5 kcal/mol at the coalescence temperature (measured at 500 MHz), which is slightly smaller than those estimated for the bis( $\mu$ -silyl) complexes **2a** and **2b**.<sup>8</sup>

In the proton-coupled  $^{29}\text{Si}$  NMR spectrum of **4**, the  $J_{\text{Si-H}}$  coupling with the directly bound hydrogen atom apparently was not observed because it was not separable from the multiplet due to those with *tert*-butyl groups. When the butyl proton at  $\delta$  1.11 is irradiated, the  $^{29}\text{Si}$  signal appears at  $\delta$  75.5 as a quintet (Figure 3;  $J_{\text{Si-H}} = 34.2$  Hz). The coupling constant is about half of that of the satellite peaks observed in the  $^1\text{H}$  NMR spectrum measured at  $-120^\circ\text{C}$ . The above-mentioned site exchange of the hydride ligands is rapid compared to the NMR time scale at room temperature. The apparent coupling constant ( $J_{\text{Si-H}} = 34.2$  Hz) must, therefore, be an averaged value of those observed for each hydride site. The  $^{29}\text{Si}$  resonance of **4** ( $\delta$  75.5) shifts slightly upfield compared to those of the bis( $\mu$ -silyl) complexes **2a** and **2b** ( $\delta$  111.7 and 95.0, respectively).

The M–H–Si interaction is detectable by means of IR spectroscopy, as was found in the case of  $\eta^2\text{-H}_2$  complexes<sup>10</sup> or agostic C–H bonds.<sup>13</sup> Coordination of a Si–H  $\sigma$ -bond to a transition metal results in a weakening of the Si–H bond, and therefore, the stretching frequency of the Si–H bond decreases. Although there have been several reported examples of transition-metal complexes with M–H–Si 2e–3c interactions, most of them have carbonyl groups as supporting ligands. The M–H–Si stretching of them often is obscured by the

strong  $\nu(\text{CO})$  absorptions.<sup>7</sup> The  $\nu(\text{M-H-Si})$  values for the non-carbonyl complexes  $\text{Cp}_2\text{Zr}(\text{X})(\text{N}^t\text{BuSiMe}_2\text{H})$  (X = H, I, Br, Cl, F) have been reported recently by Berry and co-workers,<sup>14</sup> the zirconium complexes have Zr–H–Si stretching frequencies ranging from 1912 to 1998  $\text{cm}^{-1}$ , a red shift of ca. 100–200  $\text{cm}^{-1}$  compared with  $\nu(\text{Si-H})$  for uncoordinated  $\text{HN}^t\text{BuSiMe}_2\text{H}$  (2107  $\text{cm}^{-1}$ ). Stone *et al.* also reported the  $\nu(\text{Pt-H-Si})$  band for the dinuclear bis( $\mu$ -silyl)platinum complex  $[\text{Pt}(\text{PR}'_3)(\mu\text{-}\eta^2\text{-HSiR}_2)]_2$  (R = Ph, Me;  $\text{PR}'_3 = \text{PCy}_3, \text{PPh}_3, \text{PMe}^t\text{Bu}_2, \text{P}^i\text{-Pr}_2\text{Ph}$ ), to appear at ca. 1650  $\text{cm}^{-1}$ .<sup>15</sup>

In order to assign the Ru–H–Si stretching frequency, we synthesized an isotopomer of complex **4** by the reaction of  $\text{Cp}'\text{Ru}(\mu\text{-D})_4\text{RuCp}'$  (**1-d<sub>4</sub>**) with  $^t\text{Bu}_2\text{SiD}_2$ . The IR spectra of **4** and **4-d<sub>4</sub>** are shown in Figure 4. A broad absorption assignable to the stretching vibration of the agostic Ru–H–Si unit was observed at 1790  $\text{cm}^{-1}$  (spectrum A), which was confirmed by the fact that this broad absorption disappears in the spectrum of the deuterated complex **4-d<sub>4</sub>** and a new absorption of  $\nu(\text{Ru-D-Si})$  appears at 1290  $\text{cm}^{-1}$  (spectrum B). The differential spectrum (spectrum C) clearly shows the isotopic shift. This broad absorption was distinguished from that of a metal–hydride or a noncoordinated Si–H bond of a bridging silicon ligand. In the IR spectrum of  $[\text{Cp}'\text{Ru}]_2(\mu\text{-}\eta^2\text{-HSi}^t\text{Bu}_2)(\mu\text{-}\eta^2\text{-HSiPhH})(\mu\text{-H})(\text{H})$  (**7b**), obtained in the reaction of **4** with  $\text{PhSiH}_3$  (*vide infra*), the stretching vibration of the terminally bonded hydride  $\nu(\text{Ru-H})$  was observed at 2054  $\text{cm}^{-1}$  as a sharp absorption together with the broad absorptions of  $\nu(\text{Ru-H-Si})$  at 1813 and 1613  $\text{cm}^{-1}$ .  $\nu(\text{Si-H})$  values for the bridging silylene ligand (M–SiHR–M), however, have been observed in the range of 1955–2074  $\text{cm}^{-1}$ ,<sup>16,17</sup> and  $\nu(\text{Si-H})$  for **7b** is observed at 2036  $\text{cm}^{-1}$  as a relatively strong and sharp absorption. The significant low energy of  $\nu(\text{Ru-H-Si})$  of **4** (1790  $\text{cm}^{-1}$ ) compared with the  $\nu(\text{Si-H})$  value for  $^t\text{Bu}_2\text{SiH}_2$  (2116  $\text{cm}^{-1}$ )<sup>18</sup> indicates a distinct reduction in the Si–H bond order due to its coordination to the ruthenium centers.

An isotopic shift between  $\delta(\text{H-Si-H})$  and  $\delta(\text{D-Si-D})$  also was observed. The differential spectrum revealed that a relatively strong absorption of  $\delta(\text{H-Si-H})$  at 1050  $\text{cm}^{-1}$  was shifted to 760  $\text{cm}^{-1}$  by deuteration. The H–Si–H deformation mode showed a blue shift upon coordination; strong bands assignable to  $\delta(\text{H-Si-H})$  of the uncoordinated  $^t\text{Bu}_2\text{SiH}_2$  appeared at 928 and 851  $\text{cm}^{-1}$ ,<sup>18</sup> which were 100–200  $\text{cm}^{-1}$  lower than the  $\delta(\text{H-Si-H})$  value for **4**. The H–Si–H angle would be firmly fixed upon coordination to the ruthenium center

(9) (a) Suzuki, H.; Omori, H.; Lee, D. H.; Yoshida, Y.; Moro-oka, Y. *Organometallics* **1988**, *7*, 2243. (b) Suzuki, H.; Omori, H.; Moro-oka, Y. *Organometallics* **1988**, *7*, 279. (c) Suzuki, H.; Omori, H.; Lee, D. H.; Yoshida, Y.; Fukushima, M.; Tanaka, M.; Moro-oka, Y. *Organometallics* **1994**, *13*, 1129.

(10) See, for example: (a) Crabtree, R. H. *Angew. Chem., Int. Ed. Engl.* **1993**, *32*, 789. (b) Heinekey, D. M.; Oldham, W. J., Jr. *Chem. Rev.* **1993**, *93*, 913. (c) Jessop, P. G.; Morris, R. H. *Coord. Chem. Rev.* **1992**, *121*, 155. (d) Crabtree, R. H.; Luo, X.-L.; Michos, D. *Chemtracts: Inorg. Chem.* **1991**, *3*, 245. (e) Crabtree, R. H. *Acc. Chem. Res.* **1990**, *23*, 95. (f) Henderson, R. A. *Transition Met. Chem.* **1988**, *13*, 474. (g) Kubas, G. *Acc. Chem. Res.* **1988**, *21*, 120.

(11) (a) Takao, T.; Suzuki, H.; Tanaka, M. *Organometallics* **1994**, *13*, 2554. (b) Matthias, D.; Reigsys, M.; Pritzkow, H. *Angew. Chem., Int. Ed. Engl.* **1992**, *31*, 1510.

(12) (a) Jetz, W.; Graham, W. A. G. *Inorg. Chem.* **1971**, *10*, 1159. (b) Schubert, U. *Chem. Ber.* **1988**, *121*, 959.

(13) Brookhart, M.; Green, M. L. H. *J. Organomet. Chem.* **1983**, *250*, 395 and references cited therein.

(14) Procopio, L. J.; Carroll, P. J.; Berry, D. H. *J. Am. Chem. Soc.* **1994**, *116*, 177.

(15) Auburn, M.; Ciriano, M.; Howard, J. A. K.; Murray, M.; Pugh, N. J.; Spencer, J. L.; Stone, F. G. A.; Woodward, P. *J. Chem. Soc., Dalton Trans.* **1980**, 659.

(16) McDonald, R.; Cowie, M. *Organometallics* **1990**, *9*, 2468.

(17) (a) Tobita, H.; Kawano, Y.; Shimoi, M.; Ogino, H. *Chem. Lett.* **1987**, 2247. (b) Wang, W.; Hommeltoft, S. I.; Eisenberg, R. *Organometallics* **1988**, *7*, 2417. (c) Wang, W.; Eisenberg, R. *J. Am. Chem. Soc.* **1990**, *112*, 1833. (d) Herrmann, W. A.; Voss, E. *J. Organomet. Chem.* **1985**, *284*, 47. (e) Malisch, W.; Ries, W. *Angew. Chem., Int. Ed. Engl.* **1978**, *17*, 120. (f) Zarate, E. A.; Tessier-Youngs, C. A.; Youngs, W. J. *J. Am. Chem. Soc.* **1988**, *110*, 4968.

(18) IR spectra of the free silanes  $^t\text{Bu}_2\text{SiH}_2$  and  $^t\text{Bu}_2\text{SiD}_2$  were measured. A band for the stretching vibration of Si–H bonds appeared at 2116  $\text{cm}^{-1}$ , while that for Si–D was observed at 1533  $\text{cm}^{-1}$ . Absorptions assignable to  $\delta(\text{H-Si-H})$  appeared at 928 and 851  $\text{cm}^{-1}$ , which shifted to 677 and 569  $\text{cm}^{-1}$ , respectively, upon deuteration. Assignments of these absorption bands are corroborated by the literature: Kniseley, N.; Fassel, V. A.; Conrad, E. E. *Spectrochim. Acta* **1959**, 651.

Table 1.  $^{29}\text{Si}$  NMR Data of Hydridosilyl Complexes Having 2e–3c Interactions

entry no.	compd	$J_{\text{Si-M-H}}$ (Hz)	$^1J_{\text{Si-H}}$ (Hz)	ref
1	$[\text{Cp}_2\text{Ti}]_2(\mu\text{-H})(\mu\text{-}\eta^2\text{-HSiPhH})^a$	58	148	2b
2	$\text{Cp}_2\text{Zr}(\text{F})(\text{N}^t\text{BuSiMe}_2\text{H})$	135.4		14
3	$\text{Cp}_2\text{Zr}(\text{H})(\text{N}^t\text{BuSiMe}_2\text{H})$	113.2		14
4	$(\eta^5\text{-C}_6\text{Me}_6)\text{Cr}(\text{CO})_2(\eta^2\text{-HSiPh}_2\text{H})$	70.8	197	4a
5	$\text{Cr}(\text{CO})_3[\text{HSi}(\text{Mes})\text{P}(\text{Cy})_3]$	135.7		11b
6	$\text{MeCpMn}(\text{CO})(\text{PMe}_3)(\eta^2\text{-HSiNpPhH})^b$	69	208	4b
7	$\text{Cp}^*\text{Mn}(\text{CO})_2(\eta^2\text{-HSiPh}_2\text{H})^c$	65.4	200.3	4b
8	$\text{MeCpMn}(\text{CO})_2(\eta^2\text{-HSiPh}_2\text{H})$	63.5	205.2	4b
9	$\text{MeCpMn}(\text{CO})(\text{PMe}_3)(\eta^2\text{-HSiPh}_2\text{H})$	38	191	4b
10	$[\text{Cp}^*\text{Ru}(\mu\text{-H})]_2(\mu\text{-}\eta^2\text{-}\eta^2\text{-H}_2\text{Si}^t\text{Bu}_2)$	75		d
11	$[\text{Cp}^*\text{Ru}]_2(\mu\text{-}\eta^2\text{-HSiPh}_2)(\mu\text{-SiPh}_2\text{CH}=\text{CH}_2)(\mu\text{-H})(\text{H})$	53.6		11a
12	$[\text{Cp}^*\text{Ru}(\text{CO})]_2(\mu\text{-H})(\mu\text{-}\eta^2\text{-HSi}^t\text{Bu}_2)$	32.9		d
13	$[\text{Cp}^*\text{Ru}(\text{CO})]_2(\mu\text{-}\eta^2\text{-}\eta^2\text{-H}_2\text{Si}^t\text{Bu}_2)$	22.4		d
14 <sup>e</sup>	$\text{MeCpMn}(\text{CO})(\text{PMe}_3)(\text{H})(\text{SiCl}_3)$	20		12a
15 <sup>e</sup>	$\text{Cp}_2\text{W}(\text{H})\text{Si}(\text{SiMe}_3)_3$	3.5		12b

<sup>a</sup> Cp =  $\eta^5\text{-C}_5\text{H}_5$ . <sup>b</sup> MeCp =  $\eta^5\text{-CH}_3\text{C}_5\text{H}_4$ . <sup>c</sup> Cp' =  $\eta^5\text{-C}_5\text{Me}_5$ . <sup>d</sup> This work. <sup>e</sup> Compounds having no direct Si–H interaction.

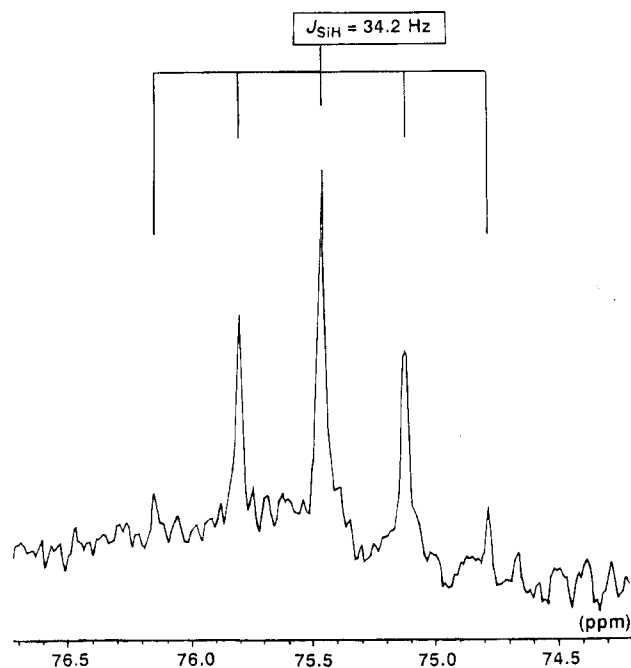


Figure 3.  $^{29}\text{Si}$  NMR spectrum of  $[\text{Cp}^*\text{Ru}(\mu\text{-H})]_2(\mu\text{-}\eta^2\text{-}\eta^2\text{-H}_2\text{Si}^t\text{Bu}_2)$  (**4**) measured at 20 °C upon irradiation at a resonance for the *tert*-butyl protons ( $\delta$  1.11).

in  $\mu\text{-}\eta^2\text{-}\eta^2$  geometry. The energy for the deformation vibration would, therefore, increase.

As far as the dinuclear  $\mu\text{-}\eta^2\text{-}\eta^2$ -silane complex is concerned, only two examples,  $[\text{Re}_2(\text{CO})_6(\mu\text{-}\eta^2\text{-}\eta^2\text{-H}_2\text{SiR}_2)]$  (R = Me, Ph)<sup>19a</sup> and  $[\text{Mn}_2(\text{CO})_6(\text{dppm})(\mu\text{-}\eta^2\text{-}\eta^2\text{-H}_2\text{SiPh}_2)]$ ,<sup>19b</sup> were reported prior to our work, while there have been several reported examples of a mononuclear silane complex. These complexes were characterized mainly on the basis of NMR studies. Although a single crystal of **4** suitable for the X-ray diffraction studies was not obtained,<sup>20</sup> all of the above data strongly indicate the coordination of  $^t\text{Bu}_2\text{SiH}_2$  in a  $\mu\text{-}\eta^2\text{-}\eta^2$  geometry. A structure determination of the  $\mu\text{-}\eta^2\text{-}\eta^2\text{-H}_2\text{Si}^t\text{Bu}_2$  ligand was performed by using a crystal of the analogous  $\mu$ -silane complex  $[\text{Cp}^*\text{Ru}(\text{CO})]_2(\mu\text{-}\eta^2\text{-}\eta^2\text{-H}_2\text{Si}^t\text{Bu}_2)$  (**5**) obtained by the reaction of **4** with CO. This is the first example of a structurally fully characterized dinuclear  $\mu\text{-}\eta^2\text{-}\eta^2$ -silane complex (*vide infra*).

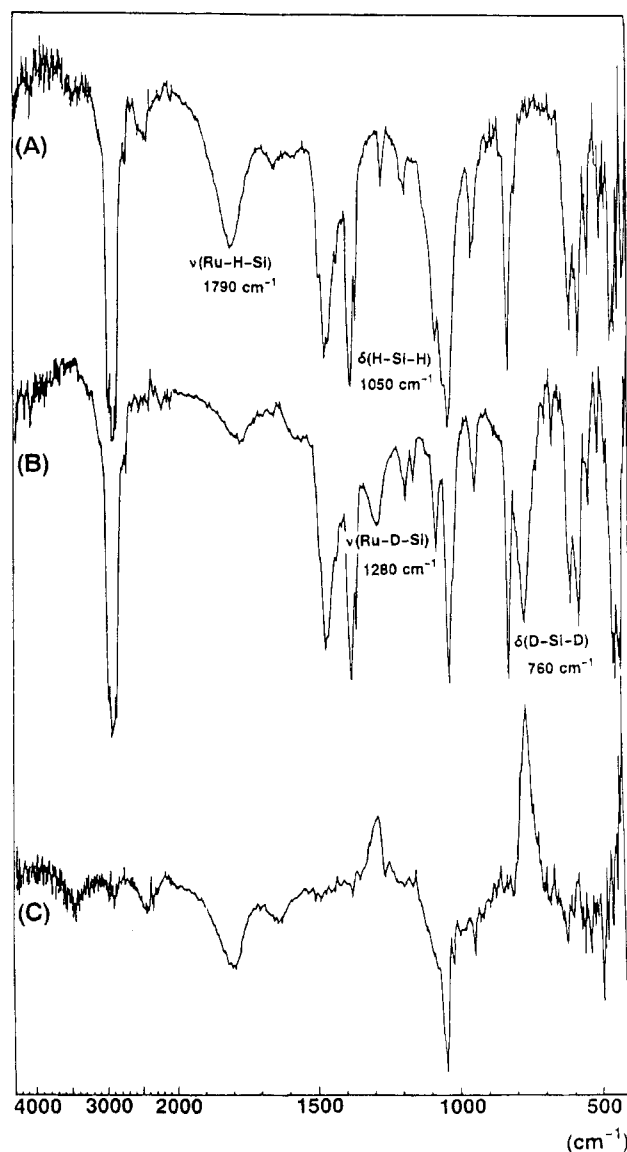
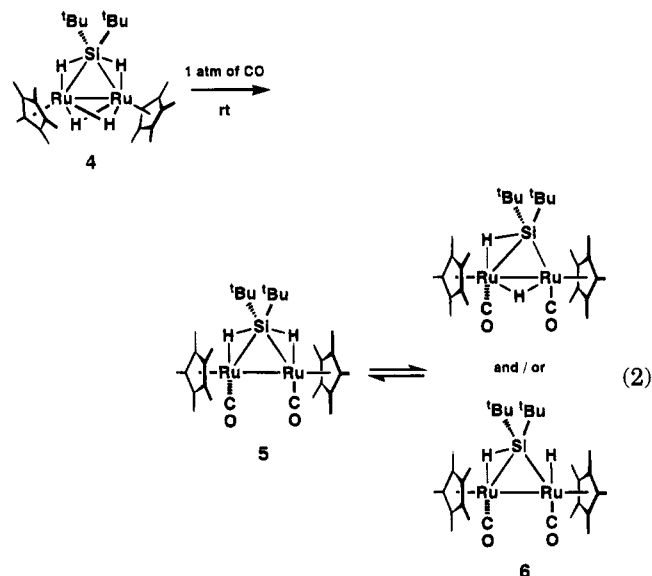


Figure 4. Infrared spectra of (A)  $[\text{Cp}^*\text{Ru}(\mu\text{-H})]_2(\mu\text{-}\eta^2\text{-}\eta^2\text{-H}_2\text{Si}^t\text{Bu}_2)$  (**4**) and (B)  $[\text{Cp}^*\text{Ru}(\mu\text{-D})]_2(\mu\text{-}\eta^2\text{-}\eta^2\text{-D}_2\text{Si}^t\text{Bu}_2)$  (**4-d<sub>4</sub>**) and (C) a differential spectrum of them.

**Reaction of the  $\mu$ -Silane Complex with CO.** Complex **4** reacts with 1 atm of CO at room temperature for 12 h to yield a mixture of the  $\mu$ -silane complex  $[\text{Cp}^*\text{Ru}(\text{CO})]_2(\mu\text{-}\eta^2\text{-}\eta^2\text{-H}_2\text{Si}^t\text{Bu}_2)$  (**5**; 43% yield based on  $^1\text{H}$  NMR) and the  $\mu$ -silyl complex  $[\text{Cp}^*\text{Ru}(\text{CO})]_2(\mu\text{-}\eta^2\text{-}$

(19) (a) Hoyano, J. K.; Elder, M.; Graham, W. A. G. *J. Am. Chem. Soc.* **1969**, *91*, 4568. (b) Elder, M. *Inorg. Chem.* **1970**, *9*, 762. (c) Carreño, R.; Ruiz, M. A.; Jeannin, Y.; Philoche-Levisalles, M. *J. Chem. Soc., Chem. Commun.* **1990**, 15.

HSi<sup>t</sup>Bu<sub>2</sub>(H) (**6**; 53%), together with a small amount of [Cp<sup>\*</sup>Ru(CO)<sub>2</sub>]<sub>2</sub> (4%) (eq 2).<sup>21</sup>



The structure of complex **5** was determined by X-ray crystallography using a single crystal obtained from pentane at  $-20\text{ }^{\circ}\text{C}$ . The structure of **5**, shown in Figure 5, clearly depicts the unique  $\mu\text{-}\eta^2\text{:}\eta^2$  geometry of the <sup>t</sup>Bu<sub>2</sub>SiH<sub>2</sub> ligand. The crystal data for **5** are given in the Experimental Section (Table 5), and selected bond lengths and bond angles are listed in Table 2.

Two terminal carbonyl groups are mutually *trans* with respect to the Ru(1)–Ru(2) vector. Two hydrogen atoms, H(1) and H(2), compose 2e–3c bonds between silicon and each ruthenium. The bridging silicon is separated from each ruthenium, Ru(1) and Ru(2), by 2.447(1) and 2.457(1) Å, respectively. These distances fall in the reported range for a Ru–Si single bond (2.288(11)–2.507(8) Å),<sup>11,22</sup> but they are comparatively long. Electron counting that keeps complex **5** diamagnetic requires a single bond between the two rutheniums, and the Ru(1)–Ru(2) distance of 2.9637(8) Å is comparable with that of Ru–Ru single bonds.<sup>22f,23</sup> The relatively acute Ru(1)–Si(1)–Ru(2) angle (74.38(4)<sup>o</sup>) also suggests a bonding interaction between the two rutheniums.<sup>24</sup>

The Si(1)–H(1) and Si(1)–H(2) distances, 1.77(3) and 1.75(3) Å, respectively, are reasonably longer than those reported for organosilicon compounds (1.48 Å).<sup>25</sup> This supports the decrease in the bonding interaction be-

(20) The  $\mu$ -silane complex **4** was crystallized from pentane at  $-20\text{ }^{\circ}\text{C}$  in the orthorhombic system, space group *Ama*2, with  $a = 17.832(5)$  Å,  $b = 19.780(7)$  Å,  $c = 8.674(3)$  Å, and  $Z = 4$ . Intensity data were collected at  $23\text{ }^{\circ}\text{C}$  on a Rigaku AFC-5R four-circle diffractometer with graphite-monochromated Mo K $\alpha$  radiation ( $\lambda = 0.710\text{ }69\text{ \AA}$ ) in the  $6.0^{\circ} < 2\theta < 50.0^{\circ}$  range. The intensity of the collected data were weak, and the quality of the data were not sufficiently good because the crystal gradually decomposed during data collection. The Ru atom positions were determined using Patterson methods. The remaining non-hydrogen atoms were located from successive difference Fourier map calculations and refined by using full-matrix least-squares techniques on  $F_o$ . The current  $R$  value is 0.067 for 2804 independent reflections with  $F_o > 5\sigma(F_o)$ . Although the refinement did not sufficiently converge, the X-ray data sufficiently elucidate the atom connectivity of the structure. The resulting structure of **4** is fully consistent with the data obtained from <sup>1</sup>H, <sup>13</sup>C, and <sup>29</sup>Si NMR spectroscopy. Bond lengths and angles of the Ru<sub>2</sub>Si core are as follows: Ru–Si = 2.51(1) Å, Ru–Ru = 2.755(5) Å; Ru–Si–Ru = 66.6(4)<sup>o</sup>, Ru–Ru–Si = 56.7(2)<sup>o</sup>.

(21) (a) Davison, A.; McCleverty, J. A.; Wilkinson, G. *J. Chem. Soc.* **1963**, 1133. (b) King, R. B.; Iqbal, M. Z.; King, A. D., Jr. *J. Organomet. Chem.* **1979**, 171, 53.

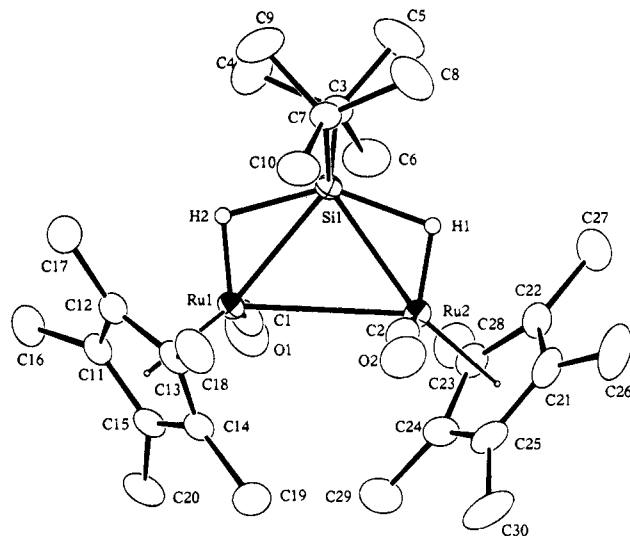


**Figure 5.** Molecular structure of [Cp<sup>\*</sup>Ru(CO)<sub>2</sub>]<sub>2</sub>( $\mu\text{-}\eta^2\text{:}\eta^2\text{-H}_2\text{-Si}^t\text{Bu}_2$ ) (**5**), with thermal ellipsoids at the 30% probability level.

**Table 2.** Selected Bond Lengths (Å) and Angles (deg) for **5**

Ru(1)–Ru(2)	2.9637(8)	Ru(2)–Si(1)	2.457(1)
Ru(1)–Si(1)	2.447(1)	Ru(2)–H(1)	1.44(4)
Ru(1)–H(2)	1.43(4)	Ru(2)–C(2)	1.829(4)
Ru(1)–C(1)	1.816(4)	Si(1)–H(1)	1.77(3)
Si(1)–H(2)	1.75(4)	Si(1)–C(7)	1.957(4)
Si(1)–C(3)	1.961(4)	C(2)–O(2)	1.153(5)
C(1)–O(1)	1.162(5)	Ru(2)–C(21)	2.201(4)
Ru(1)–C(11)	2.211(4)	Ru(2)–C(22)	2.276(4)
Ru(1)–C(12)	2.274(4)	Ru(2)–C(23)	2.345(4)
Ru(1)–C(13)	2.350(4)	Ru(2)–C(24)	2.309(4)
Ru(1)–C(14)	2.308(4)	Ru(2)–C(25)	2.254(4)
Ru(1)–C(15)	2.257(4)		
Ru(2)–Ru(1)–Si(1)	52.97(3)	Ru(1)–Ru(2)–Si(1)	52.66(3)
Ru(2)–Ru(1)–C(1)	83.6(1)	Ru(1)–Ru(2)–C(2)	84.8(1)
Ru(2)–Ru(1)–H(2)	97(1)	Ru(1)–Ru(2)–H(1)	97(1)
Si(1)–Ru(1)–C(1)	92.1(1)	Si(1)–Ru(2)–C(2)	93.6(1)
Si(1)–Ru(1)–H(2)	44(1)	Si(1)–Ru(2)–H(1)	45(1)
C(1)–Ru(1)–H(2)	95(1)	C(2)–Ru(2)–H(1)	92(1)
Ru(1)–Si(1)–Ru(2)	74.38(4)	C(3)–Si(1)–C(7)	107.1(2)
Ru(1)–C(1)–O(1)	170.7(4)	Ru(2)–C(2)–O(2)	168.5(4)

tween Si and H upon coordination to ruthenium. Although X-ray crystallography is not the best method to determine the location of the H atom attached to a heavy atom, the observed Si–H bond lengthening is consistent with the reduced  $J_{\text{Si-H}}$  coupling obtained by <sup>29</sup>Si NMR spectroscopy (*vide infra*).

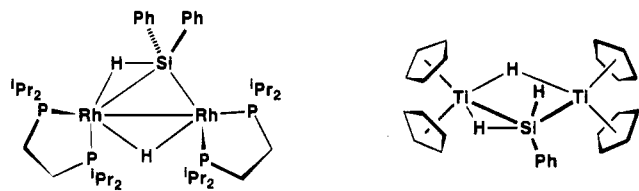
In the <sup>1</sup>H NMR spectrum of the mixture of **5** and **6**, three resonances arising from **5** appear at  $\delta$  1.89, 1.26,

(22) (a) Straus, D. A.; Tilley, T. D.; Rheingold, A. L.; Geib, S. J. *J. Am. Chem. Soc.* **1987**, 109, 5872. (b) Straus, D. A.; Zhang, C.; Quimbata, G. E.; Grumbine, S. D.; Heyn, R. H.; Tilley, T. D.; Rheingold, A. L.; Geib, S. J. *J. Am. Chem. Soc.* **1990**, 112, 2673. (c) Campion, B. K.; Heyn, R. H.; Tilley, T. D. *J. Chem. Soc., Chem. Commun.* **1992**, 1201. (d) Campion, B. K.; Heyn, R. H.; Tilley, T. D. *Organometallics* **1992**, 11, 3918. (e) Campion, B. K.; Heyn, R. H.; Tilley, T. D.; Rheingold, A. L. *J. Am. Chem. Soc.* **1993**, 115, 5527. (f) Crozat, M. M.; Watkins, S. F. *J. Chem. Soc., Dalton Trans.* **1972**, 2512. (g) Einstein, F. W. B.; Jones, T. *Inorg. Chem.* **1982**, 21, 987. (h) Klein, H.-P.; Thewalt, U.; Herrmann, G.; Süß-Fink, G.; Moinet, C. *J. Organomet. Chem.* **1985**, 286, 225. (i) Brookes, A.; Howard, J.; Knox, S. A. R.; Riera, V.; Stone, F. G. A.; Woodward, P. *J. Chem. Soc., Chem. Commun.* **1973**, 727. (j) Edwards, J. D.; Goddard, R.; Knox, S. A. R.; McKinney, R. J.; Stone, F. G. A.; Woodward, P. *J. Chem. Soc., Chem. Commun.* **1975**, 828. (k) Howard, J.; Woodward, P. *J. Chem. Soc., Dalton Trans.* **1975**, 59. (l) Harris, P. J.; Howard, J. A. K.; Knox, S. A. R.; McKinney, R. J.; Phillips, R. P.; Stone, F. G. A.; Woodward, P. *J. Chem. Soc., Dalton Trans.* **1978**, 403. (m) Djurovich, P. I.; Carroll, P. J.; Berry, D. H. *Organometallics* **1994**, 13, 2551.

and  $-13.60$ , which are assigned to the Cp',  $t$ Bu groups, and hydride ligands, respectively. Satellite peaks due to coupling with  $^{29}\text{Si}$  are observed besides the hydride signal. The  $^{29}\text{Si}$  NMR spectrum, measured with irradiation of  $t$ Bu protons, shows a triplet at  $\delta$  186.2 ( $J_{\text{Si-H}} = 22.4$  Hz). The  $J_{\text{Si-H}}$  coupling of 22.4 Hz is much smaller than that for **4** ( $J_{\text{Si-H}} = 75$  Hz), and this result also suggests the Si-H bond weakening, although a decrease in  $J_{\text{Si-H}}$  is not simply a reflection of the bond order.<sup>5a</sup> Coordination of CO instead of the hydride ligands would cause a reduction of the Si-H bond order and would result in a distinct weakening of the  $\eta^2$ -Si-H bond.

While the structure of **5** exhibits noncrystallographic  $C_2$  symmetry around the silicon atom, that of complex **6** does not. All of the  $^1\text{H}$  NMR signals for complex **6** are inequivalent as follows: Cp' ( $\delta$  1.98 and 1.73),  $t$ Bu ( $\delta$  1.42 and 1.41), and hydrides ( $\delta$   $-11.79$  and  $-14.40$ ). Moreover, satellite signals are observed only beside the hydride signal at  $\delta$   $-11.79$ . The  $^{29}\text{Si}$  resonance arising from **6** appears at  $\delta$  168.2 as a doublet of doublets ( $J_{\text{Si-H}} = 31.6$  and 7.9 Hz). It is noteworthy that the  $^{29}\text{Si}$  signal for **6** is observed as a doublet of doublets, while that for complex **5** is a triplet. The  $J_{\text{Si-H}}$  coupling of 31.6 Hz is common for the hydrides with  $2e-3c$  M-H-Si interactions, but that of 7.9 Hz is too small. Therefore, we can conclude that complex **6** adopts a mono( $\mu$ -silyl) form having a terminal (Ru-H) or bridging (Ru-H-Ru) hydride ligand.

Thus far, only two mono( $\mu$ -silyl) complexes have been characterized by means of X-ray diffraction studies. Fryzuk *et al.* have synthesized a dirhodium complex containing a  $\mu$ -diphenylsilyl ligand by the reaction of [(dippe)Rh( $\mu$ -H)]<sub>2</sub> (dippe = 1,2-bis(diisopropylphosphino)ethane) with 1 equiv of Ph<sub>2</sub>SiH<sub>2</sub>.<sup>26</sup> The dirhodium  $\mu$ -silyl complex [(dippe)Rh]<sub>2</sub>( $\mu$ - $\eta^2$ -HSiPh<sub>2</sub>)( $\mu$ -H) was shown to have a  $\mu$ -silyl ligand and a bridging hydride. Harrod *et al.* have determined the structure of [Cp<sub>2</sub>Ti]<sub>2</sub>( $\mu$ - $\eta^2$ -HSiPhH)( $\mu$ -H), which was obtained as an intermediate of the dehydrogenative coupling of phenylsilane using titanocene catalyst.<sup>2b</sup>

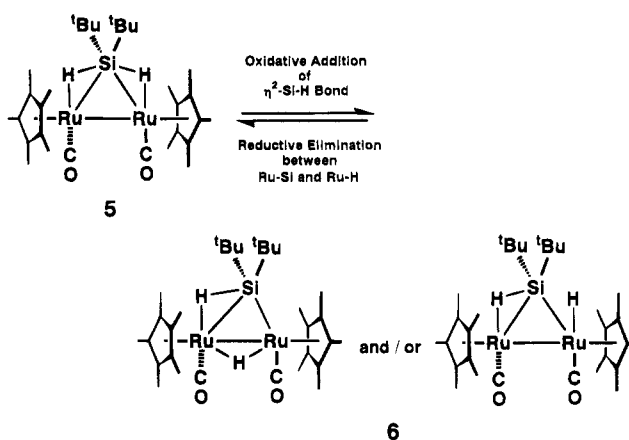


Remarkably, the  $\mu$ -silane complex **5** is in equilibrium in solution with the hydrido- $\mu$ -silyl complex **6** (Scheme 1). The solution of the isolated single crystal of **5** comes to an equilibrium with **6** in a few hours. Temperature-

(23) (a) Churchill, M. R.; Hollander, F. J.; Hutchinson, J. R. *Inorg. Chem.* **1977**, *16*, 2655. (b) Nucciarone, D.; Taylor, N. J.; Carty, A. J.; Tiripicchio, A.; Camellini, M. T.; Sappa, E. *Organometallics* **1988**, *7*, 118. (c) Parkins, A. W.; Fischer, E. O.; Huttner, G.; Regler, D. *Angew. Chem., Int. Ed. Engl.* **1970**, *9*, 633. (d) Bruce, M. I.; Cairns, M. A.; Cox, A.; Green, M.; Smith, M.; Woodward, P. *J. Chem. Soc. D* **1970**, 735. (e) Howard, J.; Knox, S. A. R.; Stone, F. G. A.; Woodward, P. *J. Chem. Soc. D* **1970**, 1477. (f) Howard, J.; Woodward, P. *J. Chem. Soc. A* **1971**, 3648.

(24) (a) Coleman, J. M.; Dahl, L. F. *J. Am. Chem. Soc.* **1967**, *89*, 542. (b) Stevenson, D. L.; Dahl, L. F. *J. Am. Chem. Soc.* **1967**, *89*, 3721. (c) Dahl, L. F.; deGil, E. R.; Feltham, R. D. *J. Am. Chem. Soc.* **1969**, *91*, 1653. (d) Connelly, N. G.; Dahl, L. F. *J. Am. Chem. Soc.* **1970**, *92*, 7470. (e) Connelly, N. G.; Dahl, L. F. *J. Am. Chem. Soc.* **1970**, *92*, 7472.

## Scheme 1



dependent behavior is observed for the two resonances (Figure 6), and the equilibrium constant  $K$ , where  $K = [\mathbf{6}]/[\mathbf{5}]$ , was determined on the basis of  $^1\text{H}$  NMR integration of the Cp' signals. The constant  $K$  is 1.3, 1.6, 1.8, and 2.0 at 30, 60, 90, and 110 °C, respectively. The constant  $K$  falls to 1.3 again on cooling down to 30 °C. These results yield the following thermodynamic parameters for the conversion of **5** to **6**:  $\Delta H = 1.2 \pm 0.1$  kcal/mol and  $\Delta S = 4.5 \pm 0.1$  eu/mol. While several examples of a tautomeric equilibrium between a nonclassical  $\eta^2$ -H<sub>2</sub> complex and a classical dihydride complex are known,<sup>10</sup> only one example has been reported for a Si-H bond, by Luo and Kubas.<sup>27</sup> They reported the first example of a tautomeric equilibrium between an  $\eta^2$ -SiH<sub>4</sub> complex and a hydrido-silyl species of molybdenum. As far as a dinuclear complex is concerned, the equilibrium between **5** and **6** is the first example of such tautomerism.

Reaction of the  $\mu$ -Silane Complex with PhSiH<sub>3</sub>.

As mentioned above, agostic Si-H bonds in the bis( $\mu$ -silyl) complex [Cp'Ru( $\mu$ - $\eta^2$ -HSiPh<sub>2</sub>)]<sub>2</sub>( $\mu$ -H)(H) (**2b**) oxidatively add to ruthenium to generate the bis( $\mu$ -silylene) complex [Cp'Ru( $\mu$ -SiPh<sub>2</sub>)( $\mu$ -H)]<sub>2</sub> (**3**) upon heating in solution.<sup>8</sup> This result strongly suggests that the reaction of Cp'Ru( $\mu$ -H)<sub>4</sub>RuCp' (**1**) with R<sub>2</sub>SiH<sub>2</sub>, which yields  $\mu$ - $\eta^2$ -silyl complexes **2**, proceeds by way of an agostic  $\mu$ - $\eta^2$ : $\eta^2$ -silane species.  $\mu$ -Silane complex **4** is, therefore, expected to react with a dihydrosilane to form the bis( $\mu$ -silyl) complex as a result of the oxidative addition of the  $\eta^2$ -Si-H bond. To test this possibility, we carried out the reaction of complex **4** with various hydrosilanes R<sub>n</sub>SiH<sub>4-n</sub>. The reaction of **4** with a less bulky silane such as PhSiH<sub>3</sub> or Et<sub>2</sub>SiH<sub>2</sub> proceeds to form the expected bis( $\mu$ -silyl) complex [Cp'Ru]<sub>2</sub>( $\mu$ - $\eta^2$ -HSi $t$ Bu<sub>2</sub>)( $\mu$ - $\eta^2$ -HSiPhH)( $\mu$ -H) or [Cp'Ru]<sub>2</sub>( $\mu$ - $\eta^2$ -HSi $t$ Bu<sub>2</sub>)( $\mu$ - $\eta^2$ -HSiEtH)( $\mu$ -H), respectively, while the reaction of **1** or **4** with an excess of  $t$ Bu<sub>2</sub>SiH<sub>2</sub> does not show any sign of the formation of the  $\mu$ -silyl complex.

$\mu$ -Silane complex **4** readily reacts with 5 equiv of phenylsilane at room temperature to yield the mixed-bridge bis( $\mu$ -silyl) complex [Cp'Ru]<sub>2</sub>( $\mu$ - $\eta^2$ -HSi $t$ Bu<sub>2</sub>)( $\mu$ - $\eta^2$ -HSiPhH)( $\mu$ -H)(H) (**7b**) (eq 3). This result demonstrates

(25) (a) Wells, A. F. In *Structural Inorganic Chemistry* 3rd ed.; Oxford University Press: London, England, 1962; p 696. (b) Baxter, S. G.; Mislou, K.; Blount, J. F. *Tetrahedron* **1980**, *36*, 605. (c) Allemand, J.; Gerdil, R. *Cryst. Struct. Commun.* **1979**, *8*, 927.

(26) Fryzuk, M. D.; Rosenberg, L.; Rettig, S. J. *Organometallics* **1991**, *10*, 2537.

(27) Luo, X.-L.; Kubas, G. J.; Burns, C. J.; Bryan, J. C.; Unkefer, C. J. *J. Am. Chem. Soc.* **1995**, *117*, 1159.

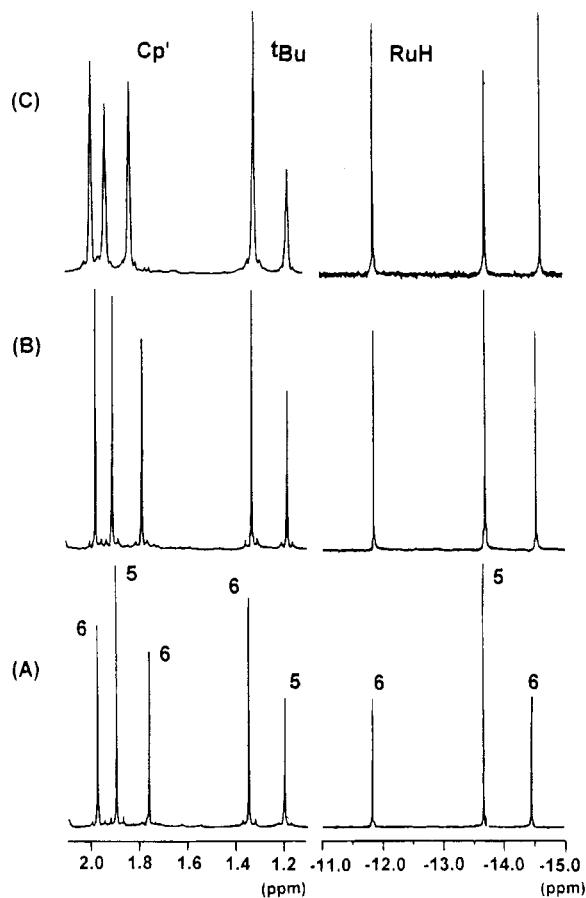
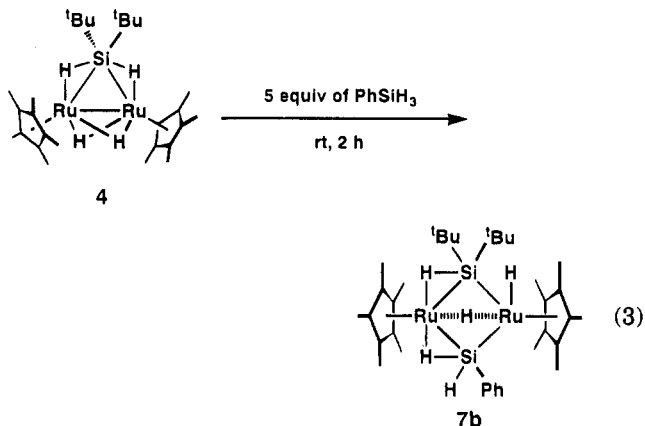


**Figure 6.**  $^1\text{H}$  NMR spectra of the mixture of  $[\text{Cp}'\text{Ru}(\text{CO})]_2(\mu\text{-}\eta^2\text{:}\eta^2\text{-H}_2\text{Si}^t\text{Bu}_2)$  (**5**) and  $[\text{Cp}'\text{Ru}(\text{CO})]_2(\mu\text{-}\eta^2\text{-HSi}^t\text{Bu}_2)(\text{H})$  (**6**): (A) 30 °C; (B) 60 °C; (C) 110 °C. Resonances for Cp' and *tert*-butyl groups are shown on the left side of the figure, and hydride resonances are displayed on the right side.



that bis( $\mu$ -silyl) complexes are formed by way of a  $\mu$ -silane intermediate in the reaction of **1** with secondary silanes. Complex **7b** can be isolated by crystallization from cold pentane and characterized by means of  $^1\text{H}$  and  $^{13}\text{C}$  NMR and IR spectroscopy and elemental analysis.

The  $^1\text{H}$  NMR measurement of **7b** at  $-90$  °C affords the low-temperature limiting spectrum. In the  $^1\text{H}$  NMR spectrum measured at  $-90$  °C, four resonances for hydride ligands are observed at  $\delta$   $-11.64$ ,  $-12.84$ ,  $-14.00$ , and  $-16.46$ . Among them, satellite peaks due to coupling with  $^{29}\text{Si}$  nuclei appear beside two signals at  $\delta$   $-11.64$  ( $J_{\text{Si-H}} = 26$  Hz) and  $\delta$   $-14.00$  ( $J_{\text{Si-H}} = 49$  Hz). They can, therefore, be attributed to the hydrides

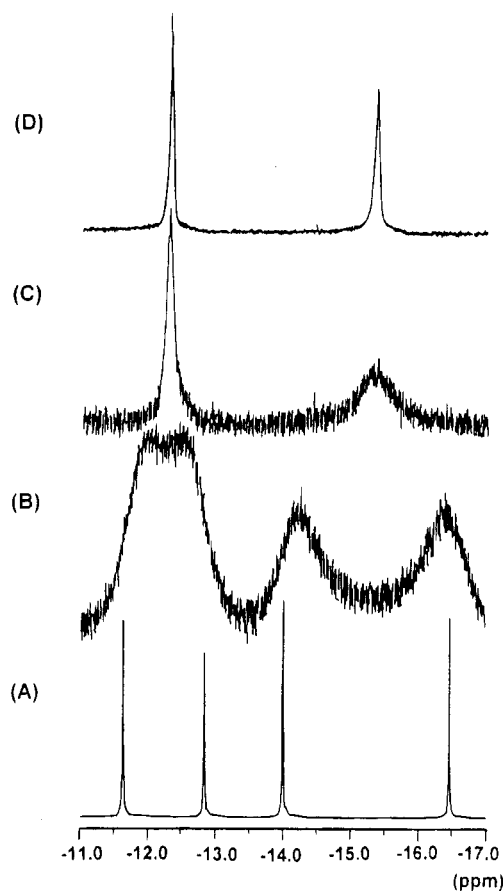


**Figure 7.** Variable-temperature  $^1\text{H}$  NMR spectra of  $[\text{Cp}'\text{Ru}]_2(\mu\text{-}\eta^2\text{-HSi}^t\text{Bu}_2)(\mu\text{-}\eta^2\text{-HSiPhH})(\mu\text{-H})(\text{H})$  (**7b**) showing the hydride resonances: (A)  $-90$  °C; (B)  $-9$  °C; (C) 20 °C; (D) 80 °C.

with Ru–H–Si 2e–3c interactions. The rest are assigned to terminal and bridging hydrides (Ru–H, and Ru–H–Ru). The  $^1\text{H}$  NMR spectra of the hydride region in Figure 7 demonstrate the fluxionality of **7b**. Two hydride signals at  $\delta$   $-11.64$  and  $-12.84$  coalesce into one signal ( $\delta$   $-12.30$ ) at  $-9$  °C, and the remaining two signals also coalesce ( $\delta$   $-15.45$ ) at  $0$  °C. Although the two newly appearing signals at  $\delta$   $-12.30$  (2H) and  $\delta$   $-15.45$  (2H) never coalesce in spite of further warming to 80 °C, the four hydride ligands exchange coordination sites, with one another. A  $^1\text{H}$  NMR spin saturation transfer experiment reveals a slow exchange of hydrides between the two sites: irradiation at  $\delta$   $-15.45$  resulted in a 50% decrease in the intensity of the proton signal at  $\delta$   $-12.30$  and *vice versa*.

The signals for the Cp' ligands are observed at  $\delta$  1.93 and 1.66 at  $-90$  °C. They broaden upon warming and coalesce at  $-28$  °C. The exact mechanism to account for this complicated temperature dependence of the spectra still has not been elucidated.

At room temperature, the resonance of the Si–H(terminal) group is observed at  $\delta$  6.30 as a sharp signal with satellite peaks ( $J_{\text{Si-H}} = 172$  Hz). The intensity of the Si–H resonance did not decrease upon irradiation at the hydride resonances. This result shows that the exchange process between Si–H(terminal) and Ru–H is negligible.

Two signals for *tert*-butyl groups on the bridging silicon are found at  $\delta$  1.24 and 1.05. This indicates complex **7b** has a butterfly structure, and the signals

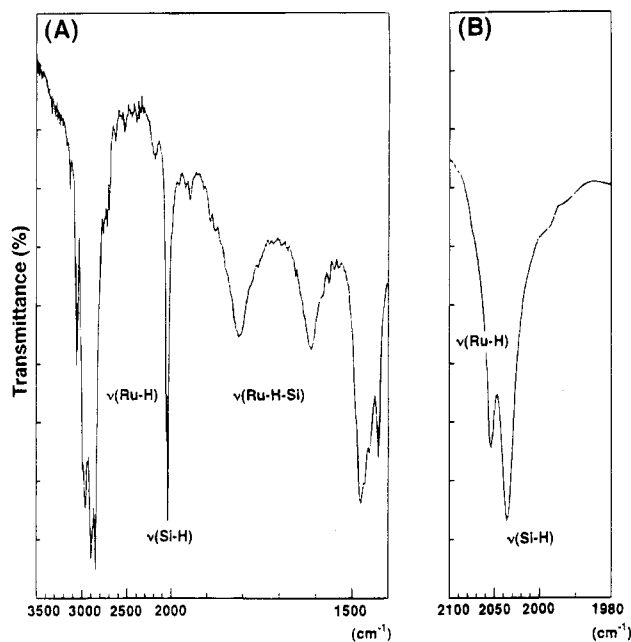


**Figure 8.** (A) Infrared spectrum of  $[\text{Cp}'\text{Ru}]_2(\mu\text{-}\eta^2\text{-HSi}^t\text{Bu}_2)(\mu\text{-}\eta^2\text{-HSiPhH})(\mu\text{-H})(\text{H})$  (**7b**). (B) Infrared region for the  $\nu(\text{Ru-H})$  and  $\nu(\text{Si-H})$  bands of **7b**.

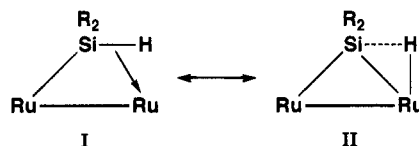
are assigned to the axial and equatorial  $t\text{Bu}$  groups of **7b**, respectively. We have observed that resonances for the substituents on the bridging silicon in the axial position appeared upfield from those for the equatorial position, seemingly because of the shielding effect of the  $\text{Cp}'$  ring.

In the IR spectrum of **7b**, two sharp bands were observed at 2054 and 2036  $\text{cm}^{-1}$  (Figure 8). A shoulder peak at 2054  $\text{cm}^{-1}$  is assigned to  $\nu[\text{Ru-H}(\text{terminal})]$ . For analogous  $\mu$ -silyl complexes **2a** and **2b**, the  $\nu[\text{Ru-H}(\text{terminal})]$  bands appear at 2066 and 2082  $\text{cm}^{-1}$ , respectively.<sup>8</sup> The other absorption at 2036  $\text{cm}^{-1}$  was relatively strong and was assignable to the stretching mode of the  $\text{Si-H}$  on bridging silicon, and this value falls in the reported range for the  $\nu(\text{Si-H})$  values of  $\text{M-SiHR-M}$  ligands (1955–2074  $\text{cm}^{-1}$ ).<sup>16,17</sup> In addition to these two sharp absorptions, two broad and characteristic absorptions of the  $\eta^2\text{-Si-H}$  bond were observed at 1813 and 1613  $\text{cm}^{-1}$ .<sup>28</sup>

The structure of the mixed-bridge bis( $\mu$ -silyl) complex **7b** determined by X-ray diffraction studies is displayed in Figure 9. Table 3 lists some of the relevant bond distances and angles.

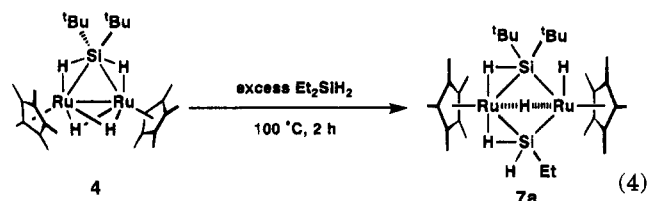
The  $\text{Ru}_2\text{Si}_2$  core forms a folded quadrilateral, as bis( $\mu$ -diethylsilyl) complex **2a** does.<sup>8</sup> Different  $\text{Ru-Si}$  bond lengths represent the existence of  $2e-3c$  interactions around  $\text{Ru}(2)$ ; the distance of the agostic bond  $\text{Ru}(2)-\text{Si}(1)$  (2.438(1) Å) is longer than that of  $\text{Ru}(1)-\text{Si}(1)$  (2.300(3) Å) by *ca.* 0.14 Å, and the distance of  $\text{Ru}(2)-\text{Si}(2)$  (2.675(1) Å) is *ca.* 0.30 Å longer than that of  $\text{Ru}(2)-\text{Si}(2)$  (2.375(1) Å). While the  $\text{Ru}(1)-\text{Si}(1)$  and  $\text{Ru}(1)-\text{Si}(2)$  distances lie in the reported range of  $\text{Ru-Si}$  single bonds (2.29–2.51 Å),<sup>22</sup> the  $\text{Ru}(2)-\text{Si}(2)$  distance of 2.675(1) Å is much longer. In contrast, the other agostic  $\text{Ru}(2)-\text{Si}(1)$  distance of 2.438(1) Å is shorter than that found in **2a** (average 2.56 Å).<sup>8</sup> This result is well consistent with the fact that two distinct  $\nu(\text{Ru-}$

$\text{Si})$  bands and two different  $J_{\text{Si-H}}$  values for the satellite peaks were observed in the IR spectrum and the low-temperature  $^1\text{H}$  NMR spectrum, respectively. The unusually long  $\text{Ru}(2)-\text{Si}(2)$  distance may be rationalized in terms of the great contribution of a  $\eta^2\text{-Si-H}$  complex such as resonance hybrid I.



The  $\text{Cp}'$  ligands of **7b** are bent away from  $\text{Si}(2)$  with respect to the  $\text{Ru}(1)-\text{Ru}(2)$  vector (Figure 10B). The phenyl group on  $\text{Si}(1)$  occupies the axial rather than the equatorial position (Figure 10A). This implies that the equatorial positions of bis( $\mu$ -silyl) complexes are sterically more congested by the two  $\text{Cp}'$  ligands than the axial positions.

**Reaction of the  $\mu$ -Silane Complex with  $\text{Et}_2\text{SiH}_2$ .** In the reaction of **4** with an excess of  $\text{Et}_2\text{SiH}_2$ , the mixed-bridge bis( $\mu$ -silyl) complex  $[\text{Cp}'\text{Ru}]_2(\mu\text{-}\eta^2\text{-HSi}^t\text{Bu}_2)(\mu\text{-}\eta^2\text{-HSiEtH})(\mu\text{-H})(\text{H})$  (**7a**) was unexpectedly obtained as a result of an unusual  $\text{Si-C}(\text{ethyl})$  bond fission (eq 4). The



reaction proceeds at 100 °C in a sealed tube to generate **7a** in 90% yield, together with a small amount (<5%) of bis( $\mu$ -diethylsilyl) complex **2a**. A notable feature of this reaction is the occurrence of  $\text{Si-C}(\text{alkyl})$  bond cleavage. While a number of examples of  $\text{Si-H}$  and  $\text{Si-C}(\text{aryl})$  bond cleavage by transition-metal complexes exist, successful examples of the  $\text{Si-C}(\text{alkyl})$  bond are scarce in the chemistry of mononuclear transition metal complexes.<sup>29,30</sup> Complex **7a** can be isolated from the reaction mixture by crystallization and characterized by means of  $^1\text{H}$  and  $^{13}\text{C}$  NMR and IR spectroscopy.

A single crystal of **7a** suitable for an X-ray diffraction study was obtained from pentane. Figure 11 displays the molecular structure of **7a**, and Table 4 lists the bond distances and angles. The structure shown in Figure 11 is fully consistent with the spectral data. The complex contains two  $\mu$ -silyl ligands. One of them is a  $\mu\text{-HSi}^t\text{Bu}_2$  and other is a  $\mu\text{-HSiH}^t\text{Et}$  ligand in which the bulky ethyl group occupies a less congested axial position.

Although the positions of the hydrogen atoms with agostic interactions among  $\text{Ru}$  and  $\text{Si}$  could not be determined by the difference Fourier synthesis, it can be concluded on the basis of the  $\text{Ru-Si}$  distances that two agostic hydrogens bridge  $\text{Ru}(1)$  and two silicon atoms. The  $\text{Ru}(1)-\text{Si}(1)$  and  $\text{Ru}(1)-\text{Si}(2)$  distances of 2.414(3) and 2.680(3) Å, respectively, are significantly longer than the values for  $\text{Ru}(2)-\text{Si}(1)$  (2.322(3) Å) and

(28) The  $\nu(\text{Ru-H-Si})$  bands of the bis( $\mu$ -silyl) complexes **2** were observed in the region of 1720–1790  $\text{cm}^{-1}$ : Takao, T.; Yoshida, S.; Suzuki, H.; Tanaka, M. Manuscript in preparation.

(29) Kakiuchi, F.; Furuta, K.; Murai, S.; Kawasaki, Y. *Organometallics* **1993**, *12*, 15.

(30) Hofmann, P.; Heiss, H.; Neiteler, P.; Müller, G.; Lachmann, J. *Angew. Chem., Int. Ed. Engl.* **1990**, *29*, 880.

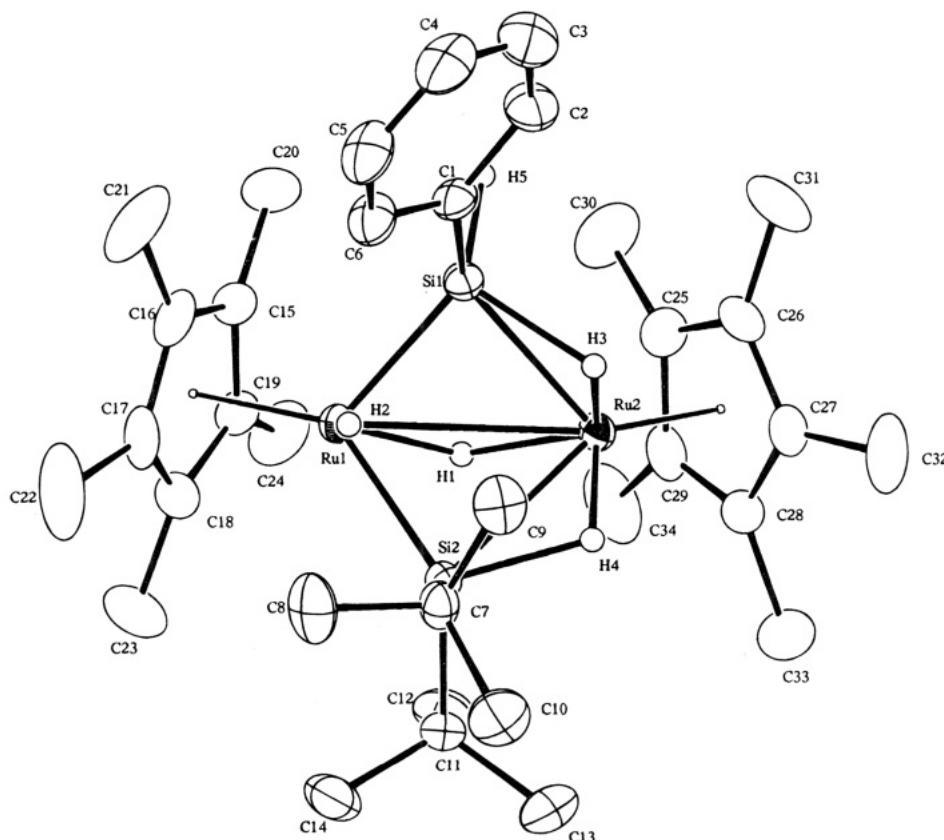


**Figure 9.** Molecular structure of  $[\text{CpRu}]_2(\mu\text{-}\eta^2\text{-HSi}^t\text{Bu}_2)(\mu\text{-}\eta^2\text{-HSiPhH})(\mu\text{-H})(\text{H})$  (**7b**), with thermal ellipsoids at the 30% probability level.

**Table 3. Selected Bond Lengths (Å) and Angles (deg) for 7b<sup>a</sup>**

Ru(1)–Ru(2)	2.9761(4)	Ru(2)–Si(1)	2.438(1)
Ru(1)–Si(1)	2.300(1)	Ru(2)–Si(2)	2.675(1)
Ru(1)–Si(2)	2.375(1)	Ru(2)–H(1)	1.76(3)
Ru(1)–H(1)	1.73(3)	Ru(2)–H(3)	1.64(3)
Ru(1)–H(2)	1.43(3)	Ru(2)–H(4)	1.64(3)
Si(1)–H(3)	1.89(3)	Si(2)–H(4)	1.77(3)
Si(1)–H(5)	1.50(3)	Si(2)–C(7)	1.951(4)
Si(1)–C(15)	1.902(4)	Si(2)–C(11)	1.944(4)
Ru(1)–C(15)	2.254(4)	Ru(2)–C(25)	2.216(4)
Ru(1)–C(16)	2.199(4)	Ru(2)–C(26)	2.178(4)
Ru(1)–C(17)	2.216(4)	Ru(2)–C(27)	2.182(4)
Ru(1)–C(18)	2.333(4)	Ru(2)–C(28)	2.256(4)
Ru(1)–C(19)	2.320(4)	Ru(2)–C(29)	2.280(4)
Cp(1)–Ru(1)–Ru(2)	146.9	Cp(2)–Ru(2)–Ru(1)	134.3
Si(1)–Ru(1)–Si(2)	94.80(4)	Si(1)–Ru(2)–Si(2)	84.50(3)
H(1)–Ru(1)–H(2)	116(1)	H(3)–Ru(2)–H(4)	75(1)
Si(1)–Ru(2)–H(3)	50.6(10)	Si(2)–Ru(2)–H(4)	39(1)
Ru(1)–Si(1)–Ru(2)	77.76(3)	Ru(1)–Si(2)–Ru(2)	71.94(3)
Ru(1)–Si(1)–H(5)	106(1)	Ru(1)–Si(2)–C(7)	120.0(1)
Ru(1)–Si(1)–C(1)	126.1(1)	Ru(1)–Si(2)–C(11)	118.9(3)
C(1)–Si(1)–H(5)	95(1)	C(7)–Si(2)–C(11)	109.7(2)
Ru(2)–H(3)–Si(1)	87(1)	Ru(2)–H(4)–Si(2)	103(2)

<sup>a</sup> CP(1) and CP(2) are the centroids of the C<sub>5</sub>Me<sub>5</sub> ligands.

Ru(2)–Si(2) (2.365(3) Å) and are consistent with a Ru–Si bond with a 2e–3c interaction.

Plausible reaction paths are shown in Scheme 2. These involve a direct Si–C(Et) activation by way of oxidative addition (path A) or an activation of the C–H bond at the  $\beta$ -position of the coordinated diethylsilane (path B). Coordination of diethylsilane and liberation of dihydrogen can be expected to yield the  $\eta^2$ : $\eta^2$ -silane species **A'** (path A) or **A''** (path B) by way of  $\eta^2$ -silane intermediate **A**. In the intermediate **A'**, diethylsilane is coordinated to both ruthenium centers through both

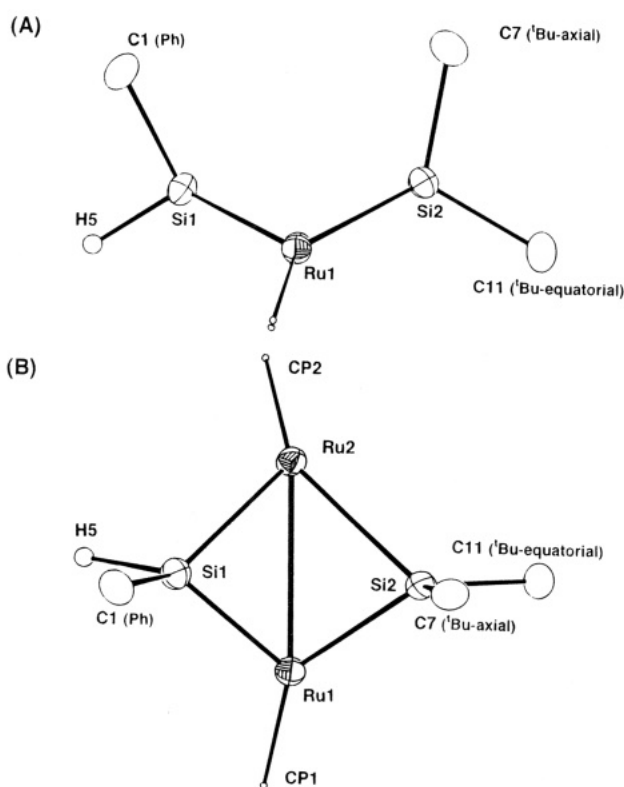


**Figure 10.** (A) View of the Ru<sub>2</sub>Si<sub>2</sub> core of **7b** along the Ru–Ru axis. (B) Another view of the Ru<sub>2</sub>Si<sub>2</sub> core, showing the bent form of the Cp' centroids.

Si–H and Si–C(ethyl)  $\sigma$  bonds while the silane is coordinated to the rutheniums through Si–H and C–H bonds in **A''**. Cleavage of the Si–C(ethyl) bond in **A'** as



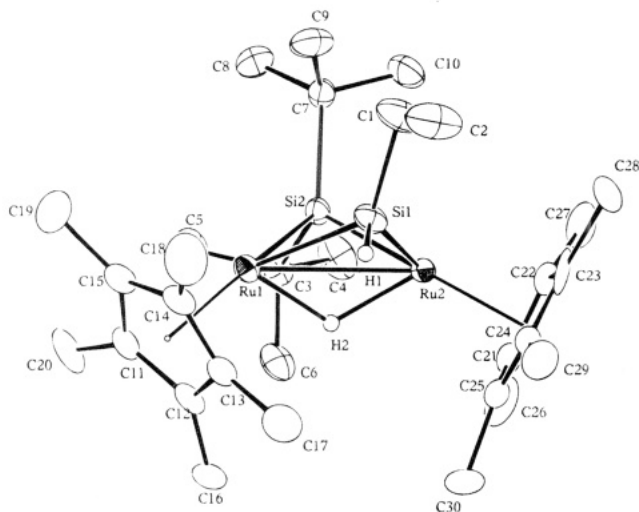


**Figure 11.** Molecular structure of  $[\text{CpRu}]_2(\mu\text{-}\eta^2\text{-HSiEtBu}_2)(\mu\text{-}\eta^2\text{-HSiEtH})(\mu\text{-H})(\text{H})$  (**7a**), with thermal ellipsoids at the 30% probability level.

a result of Si–C oxidative addition leads to the formation of **B**, which should undergo elimination of the ethyl group directly bound to ruthenium to generate **7a** together with ethylene. On the other hand, oxidative addition of a terminal C–H bond of the diethylsilane ligand in **A'** followed by the  $\beta$ -Si elimination and deinsertion of ethylene from the resulting ( $\beta$ -silylethyl)-ruthenium species **C** also can yield **7a**. Although formation of ethylene was expected in both reaction paths, we could not obtain definitive spectroscopic evidence for ethylene formation. However, the occurrence of important elementary steps, *i.e.* Si–C bond cleavage,<sup>29,30</sup> intramolecular  $\omega$ -C–H bond activation of the ligand,<sup>31</sup> and  $\beta$ -Si elimination,<sup>32</sup> are supported on the basis of previous results.

Although predominant cleavage of the Si–H bond over the Si–C(alkyl) bond by mononuclear late-transition metal complexes has been proved both experimentally<sup>29,30</sup> and theoretically,<sup>33</sup> Si–C(ethyl) bond cleavage exclusively takes place in the reaction of dinuclear complex **4** with diethylsilane. This result strongly suggests that one of the two ruthenium centers in **4** acts as a coordination site and that the second metal takes the role of an activation site. This is a typical example of the selective activation of an organic substrate in cooperation with two metal centers, *i.e.* bimetallic activation.

Another reaction path involves intramolecular ethyl migration from a silyl ligand to a terminal silylene ligand which is generated by way of oxidative addition of the second molecule of  $\text{Et}_2\text{SiH}_2$  and subsequent  $\alpha$ -H elimination (Scheme 3). Although 1,3-alkyl migration in the mononuclear silyl(silylene)–metal complexes has been established,<sup>34</sup> such a path including alkyl migration would be excluded in the reaction of **4** with  $\text{Et}_2\text{SiH}_2$ . The space between two rutheniums in the inter-

**Table 4.** Selected Bond Lengths (Å) and Angles (deg) for **7a**<sup>a</sup>

Ru(1)–Ru(2)	2.977(1)		
Ru(1)–Si(1)	2.414(4)	Ru(2)–Si(1)	2.322(3)
Ru(1)–Si(2)	2.680(3)	Ru(2)–Si(2)	2.365(3)
Ru(1)–H(2)	1.79	Ru(2)–H(2)	1.72
Si(1)–H(1)	1.47	Si(2)–C(3)	1.94(1)
Si(1)–C(1)	1.88(1)	Si(2)–C(7)	1.94(1)
Ru(1)–C(11)	2.28(1)	Ru(2)–C(21)	2.30(1)
Ru(1)–C(12)	2.28(1)	Ru(2)–C(22)	2.23(1)
Ru(1)–C(13)	2.22(1)	Ru(2)–C(23)	2.23(1)
Ru(1)–C(14)	2.15(1)	Ru(2)–C(24)	2.26(1)
Ru(1)–C(15)	2.18(1)	Ru(2)–C(25)	2.31(1)
CP(1)–Ru(1)–Ru(2)	140.5	CP(2)–Ru(2)–Ru(1)	149.8
Si(1)–Ru(1)–Si(2)	85.2(1)	Si(1)–Ru(2)–Si(2)	95.0(1)
Ru(1)–Si(1)–Ru(2)	77.9(1)	Ru(1)–Si(2)–Ru(2)	71.02(9)
Ru(1)–Si(1)–H(1)	104.6	Ru(1)–Si(2)–C(3)	111.7(4)
Ru(1)–Si(1)–C(1)	124.5(5)	Ru(1)–Si(2)–C(7)	120.4(4)
C(1)–Si(1)–H(1)	88.7	C(3)–Si(2)–C(7)	109.6(6)

<sup>a</sup> CP(1) and CP(2) are the centroids of the  $\text{C}_5\text{Me}_5$  ligands.

mediate **A** is occupied by two silicon ligands,  $\mu\text{-}\eta^2\text{-}\eta^2\text{-}^t\text{Bu}_2\text{SiH}_2$  and  $\eta^2\text{-Et}_2\text{SiH}_2$ , and is sterically very crowded. The steric congestion would therefore prevent access of the second molecule of  $\text{Et}_2\text{SiH}_2$  to one of the ruthenium centers. As mentioned above, an attempt to react  $\mu$ -silane complex **4** with  $^t\text{Bu}_2\text{SiH}_2$  resulted in complete recovery of **4**, whereas the reaction with the less bulky  $\text{Et}_2\text{SiH}_2$  proceeded on drastic heating. These results imply that there is not enough space between two ruthenium centers of **4** for two additional silane molecules to be accommodated.

**H/D Exchange Reaction.** While the  $\mu$ -silyl complex  $[\text{CpRu}(\mu\text{-}\eta^2\text{-HSiPh}_2)]_2(\mu\text{-H})(\text{H})$  (**2b**) undergoes oxidative addition of the agostic Si–H bonds to the ruthenium centers to yield the bis( $\mu$ -diphenylsilylene) complex  $[\text{CpRu}(\mu\text{-SiPh}_2)(\mu\text{-H})]_2$  (**3**) upon heating,<sup>8</sup> heating a solution of  $\mu$ -silane complex **4** does not result in formation of a dinuclear mono( $\mu$ -silyl) or mono( $\mu$ -silylene) complex via an oxidative addition of the agostic Si–H bonds.

When complex **4** was heated in  $\text{C}_6\text{D}_6$  at 80 °C, H/D exchange reaction between hydrides and  $\text{C}_6\text{D}_6$  proceeded slowly. After this heating was maintained for 2 weeks, four signals assignable to hydrides for complexes **4-d**<sub>0</sub>, **4-d**<sub>1</sub>, **4-d**<sub>2</sub>, and **4-d**<sub>3</sub> appeared at  $\delta$  –11.11, –11.38, –11.64, and –11.90, respectively (Figure 12). This result shows the occurrence of oxidative addition of the C–D bond of benzene-*d*<sub>6</sub>.

When the reaction of complex **1-d**<sub>4</sub> with  $^t\text{Bu}_2\text{SiH}_2$  was monitored by  $^1\text{H}$  NMR, a new hydride signal was initially found at  $\delta$  –11.64. Judging from the chemical shift, initial formation of **4-d**<sub>2</sub> was indicated. Prolonged reaction, however, resulted in a redistribution of deuterium. Namely, four signals of **4-d**<sub>0</sub>–**4-d**<sub>3</sub> also were observed as the H/D exchange reaction with

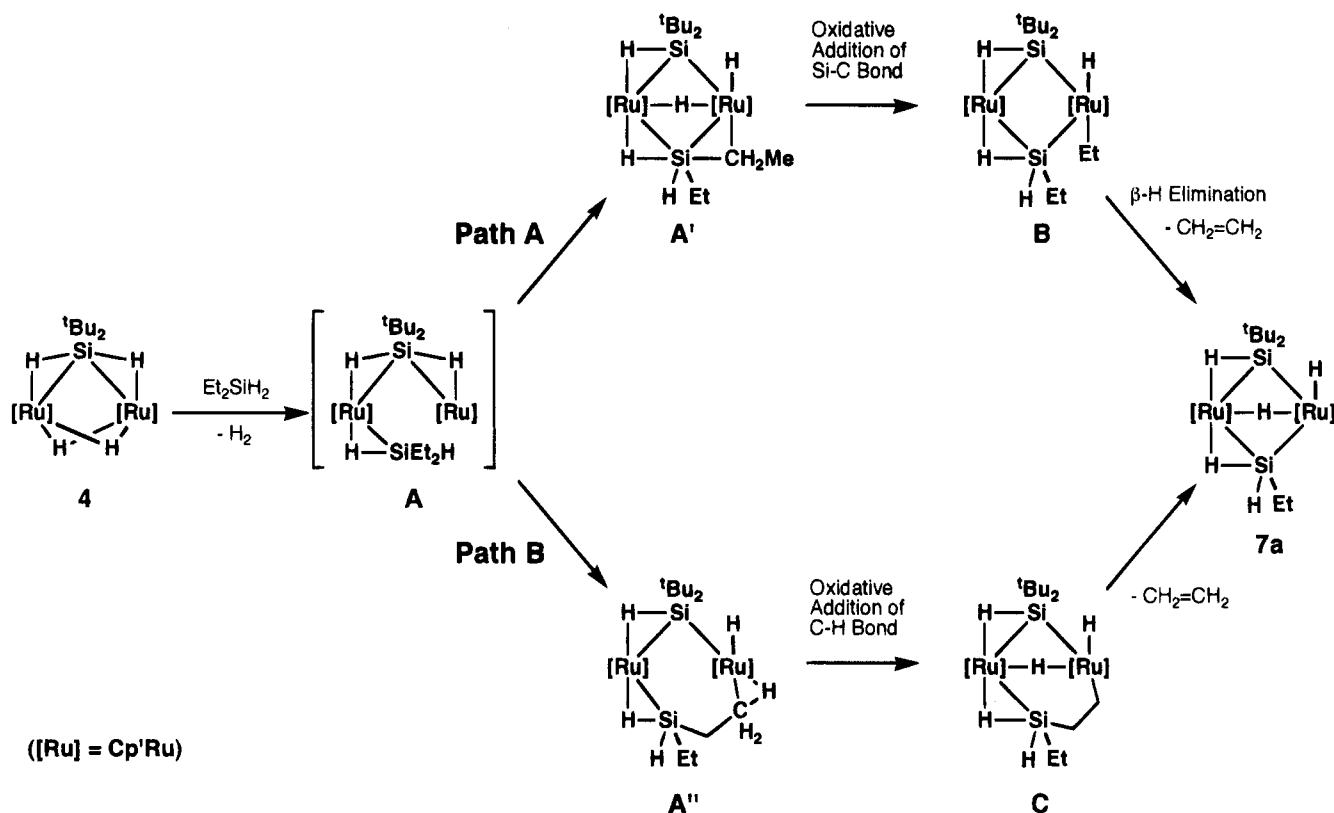
(31) See, for example: (a) Foley, P.; Whitesides, G. M. *J. Am. Chem. Soc.* **1979**, *101*, 2732. (b) Ibers, J. A.; DiCosimo, R.; Whitesides, G. M. *Organometallics* **1982**, *1*, 13. (c) Kletzin, H.; Werner, H. *Angew. Chem., Int. Ed. Engl.* **1983**, *22*, 873. (d) Bennett, M. A.; Huang, T.-A.; Latten, J. L. *J. Organomet. Chem.* **1984**, *272*, 189. (e) Bruno, J. W.; Marks, T. J. *J. Am. Chem. Soc.* **1982**, *104*, 7357. (f) Tulip, T. H.; Thorn, D. L. *J. Am. Chem. Soc.* **1981**, *103*, 2448.

(32) Wakatsuki, T.; Yamazaki, H.; Nakano, M.; Yamamoto, Y. *J. Chem. Soc., Chem. Commun.* **1991**, 703.

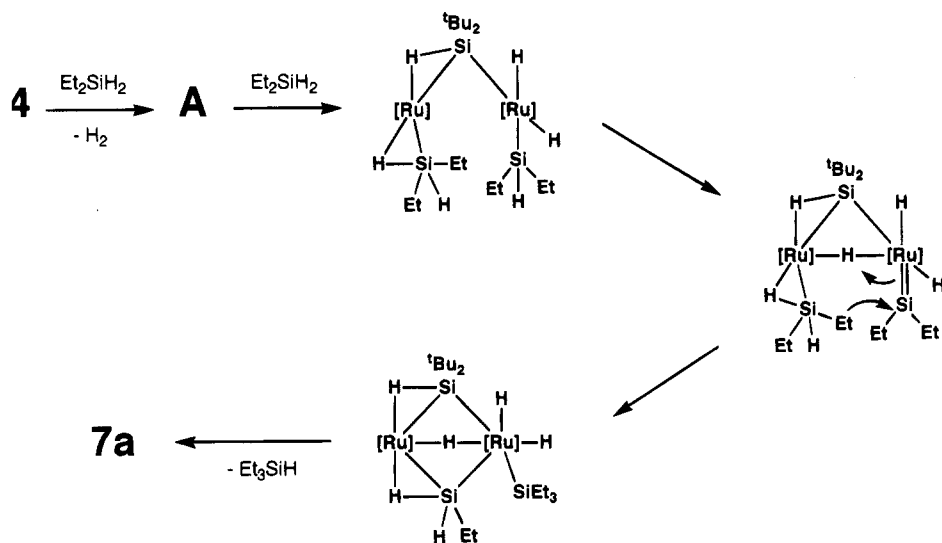
(33) Sakaki, S.; Ieki, M. *J. Am. Chem. Soc.* **1993**, *115*, 2373.

(34) (a) Pannell, K. H.; Cervantes, J.; Hernandez, C.; Cassias, J.; Vincenti, S. *Organometallics* **1986**, *5*, 1056. (b) Tobita, H.; Ueno, K.; Ogino, H. *Bull. Chem. Soc. Jpn.* **1988**, *61*, 2797. (c) Pannell, K. H.; Rozell, J. M., Jr.; Hernandez, C. *J. Am. Chem. Soc.* **1989**, *111*, 4482. (d) Pannell, K. H.; Wang, L.-J.; Rozell, J. M. *Organometallics* **1989**, *8*, 550. (e) Ueno, K.; Tobita, H.; Ogino, H. *Chem. Lett.* **1990**, 369. (f) Haynes, A.; George, M. M.; Haward, M. T.; Poliakov, M.; Turner, J. J.; Boag, N. M.; Green, M. *J. Am. Chem. Soc.* **1991**, *113*, 2011. (g) Jones, K. L.; Pannell, K. H. *J. Am. Chem. Soc.* **1993**, *115*, 11336. (h) Hernandez, C.; Sharma, H. K.; Pannell, K. H. *J. Organomet. Chem.* **1993**, *462*, 259. (i) Pannell, K. H.; Brun, M.-C.; Sharma, H.; Jones, K.; Sharma, S. *Organometallics* **1994**, *13*, 1075. (j) Grumbine, S. K.; Tilley, T. D. *J. Am. Chem. Soc.* **1994**, *116*, 6951. (k) Pestana, D. C.; Koloski, T. S.; Berry, D. H. *Organometallics* **1994**, *13*, 4173.

Scheme 2



Scheme 3



C<sub>6</sub>D<sub>6</sub> proceeded. H/D exchange between 4-*d*<sub>4</sub> and <sup>t</sup>Bu<sub>2</sub>SiH<sub>2</sub> was confirmed, and it was proved to proceed more rapidly than that of C<sub>6</sub>D<sub>6</sub> (75% conversion/80 °C/24 h).

### Conclusion

The  $\mu$ -silane complex [Cp'Ru( $\mu$ -H)]<sub>2</sub>( $\mu$ - $\eta^2$ : $\eta^2$ -H<sub>2</sub>Si<sup>t</sup>Bu<sub>2</sub>) (4) was obtained by the reaction of Cp'Ru( $\mu$ -H)<sub>4</sub>RuCp' (1) with di-*tert*-butylsilane. A unique  $\mu$ - $\eta^2$ : $\eta^2$  coordination of <sup>t</sup>Bu<sub>2</sub>SiH<sub>2</sub> was confirmed on the basis of <sup>1</sup>H, <sup>13</sup>C, and <sup>29</sup>Si NMR and IR spectra. Among these spectral data, relatively low coupling constants between Si and H observable at low temperature ( $J_{\text{Si-H}} = 75$  Hz) strongly indicated the existence of 2e-3c interactions.

Moreover, X-ray diffraction studies of [Cp'Ru(CO)]<sub>2</sub>( $\mu$ - $\eta^2$ : $\eta^2$ -H<sub>2</sub>Si<sup>t</sup>Bu<sub>2</sub>) (5) confirmed the  $\mu$ - $\eta^2$ : $\eta^2$  coordination of <sup>t</sup>Bu<sub>2</sub>SiH<sub>2</sub>.

Steric repulsion suppresses the coordination of the second molecule of <sup>t</sup>Bu<sub>2</sub>SiH<sub>2</sub>. This was confirmed by the reaction of 4 with less bulky silanes, such as PhSiH<sub>3</sub> or Et<sub>2</sub>SiH<sub>2</sub>, which yield mixed-bridge bis( $\mu$ -silyl) complexes 7b and 7a, respectively. These results demonstrate that  $\mu$ -silane complex 4 is best regarded as an intermediate in the formation of bis( $\mu$ -silyl) complexes.

Although the corresponding mono( $\mu$ -silylene) complex [Cp'Ru( $\mu$ -H)]<sub>2</sub>( $\mu$ -Si<sup>t</sup>Bu<sub>2</sub>) has never been obtained, an oxidative addition of one of the two  $\eta^2$ -Si-H bonds of 4 took place in the presence of PhSiH<sub>3</sub> and Et<sub>2</sub>SiH<sub>2</sub>. Also, the intra- and intermolecular H/D exchange reactions

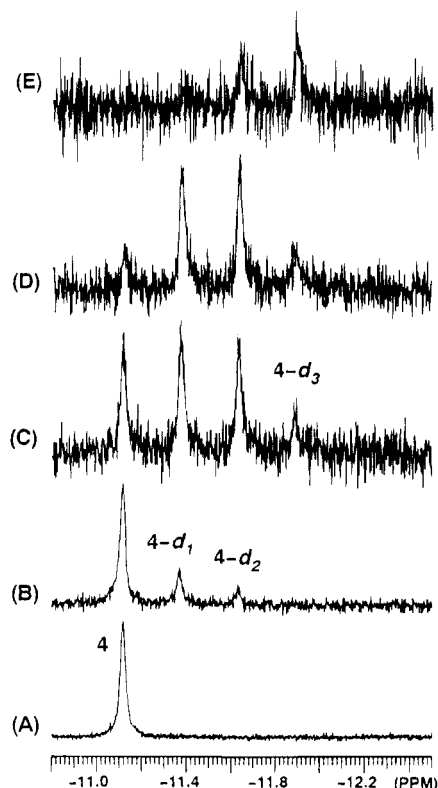


**Figure 12.**  $^1\text{H}$  NMR spectra of the hydride region in the H/D exchange reaction of **4** with benzene- $d_6$ : (A) 0 h; (B) 2 days; (C) 4 days; (D) 11 days; (E) 13 days.

of **4** distinctly indicate the occurrence of the oxidative addition of the  $\eta^2\text{-Si-H}$  bond of **4**.

### Experimental Section

**General Procedures.** All experiments were carried out under an argon atmosphere. All compounds were treated with Schlenk techniques. Reagent grade toluene was dried over sodium-benzophenone ketyl and stored under an argon atmosphere. Pentane was dried over phosphorus pentoxide and stored under an argon atmosphere. Benzene- $d_6$  and toluene- $d_8$  were used as received. Diethylsilane and phenylsilane were used as received, and di-*tert*-butylsilane and di-*tert*-butylsilane- $d_2$  were synthesized by the reduction of di-*tert*-butyldichlorosilane by  $\text{LiAlH}_4$  or  $\text{LiAlD}_4$  in diethyl ether, respectively. IR spectra were recorded on a JASCO FT/IR-5000 spectrophotometer.  $^1\text{H}$  and  $^{13}\text{C}$  NMR spectra were recorded on JEOL GX-500, JEOL EX-270, and Varian Gemini-3000 Fourier transform spectrometers with tetramethylsilane as an internal standard. Variable-temperature  $^1\text{H}$  NMR spectra were recorded on a JEOL GX-500.  $^{29}\text{Si}$  NMR spectra were recorded on a JEOL EX-270 with tetramethylsilane as an external standard under proton-decoupled conditions or were irradiated at a signal of *tert*-butyl groups under selective-decoupling conditions. Field-desorption mass spectra were recorded on a Hitachi GC-MS M80 high-resolution mass spectrometer. Elemental analyses were performed by the Analytical Facility at the Research Laboratory of Resources Utilization, Tokyo Institute of Technology. The dinuclear ruthenium tetrahydride complex  $[(\eta^5\text{-C}_5\text{Me}_5)\text{Ru}(\mu\text{-H})_4\text{Ru}(\eta^5\text{-C}_5\text{Me}_5)]$  (**1**) and  $[(\eta^5\text{-C}_5\text{Me}_5)\text{Ru}(\mu\text{-D})_4\text{Ru}(\eta^5\text{-C}_5\text{Me}_5)]$  (**1-d**) were prepared according to previously published methods.<sup>9</sup>

**X-ray Data Collection and Reduction.** X-ray-quality crystals of **5**, **7a**, and **7b** were obtained directly from the preparations described below and mounted on glass fibers. Diffraction experiments were performed on a Rigaku AFC-5R four-circle diffractometer with graphite-monochromated Mo K $\alpha$  radiation ( $\lambda = 0.71069 \text{ \AA}$ ) at  $23^\circ\text{C}$ . The lattice parameters

**Table 5.** Crystallographic Data for **5**, **7a**, and **7b**

	<b>5</b>	<b>7a</b>	<b>7b</b>
(a) Crystal Parameters			
formula	$\text{C}_{30}\text{H}_{50}\text{O}_2\text{Ru}_2\text{Si}$	$\text{C}_{30}\text{H}_{58}\text{Ru}_2\text{Si}_2$	$\text{C}_{34}\text{H}_{58}\text{Ru}_2\text{Si}_2$
cryst syst	triclinic	orthorhombic	monoclinic
space group	$P1$	$Pna2_1$	$P2_1/c$
$a, \text{ \AA}$	11.020(4)	17.064(4)	10.484(1)
$b, \text{ \AA}$	17.389(3)	11.396(3)	18.147(3)
$c, \text{ \AA}$	8.774(2)	16.782(3)	18.704(3)
$\alpha, \text{ deg}$	93.23(2)		
$\beta, \text{ deg}$	112.70(2)		97.68(1)
$\gamma, \text{ deg}$	87.47(3)		
$V, \text{ \AA}^3$	1548.1(8)	3263(2)	3526.6(8)
$Z$	2	4	4
$D_{\text{calcd}}, \text{ g cm}^{-3}$	1.444	1.378	1.366
temp, $^\circ\text{C}$	23.0	23.0	23.0
$\mu(\text{Mo K}\alpha), \text{ cm}^{-1}$	10.18	10.15	9.26
cryst dimens, mm	$0.4 \times 0.4 \times 0.1$	$0.4 \times 0.4 \times 0.2$	$0.3 \times 0.3 \times 0.2$
(b) Data Collection			
diffractometer	Rigaku AFC5R	Rigaku AFC5R	Rigaku AFC5R
radiation	Mo K $\alpha$ ( $\lambda = 0.71069 \text{ \AA}$ )	Mo K $\alpha$ ( $\lambda = 0.71069 \text{ \AA}$ )	Mo K $\alpha$ ( $\lambda = 0.71069 \text{ \AA}$ )
monochromator	graphite	graphite	graphite
scan type	$\omega/2\theta$	$\omega/2\theta$	$\omega/2\theta$
$2\theta_{\text{max}}, \text{ deg}$	50.0	50.0	55.0
scan speed, $\text{deg min}^{-1}$	16.0	16.0	16.0
reflins collected	5776	3259	8524
independent data	5465	3259	8098
independent data obsd	4741	2570	5649
(c) Refinement			
$R$	0.031	0.045	0.031
$R_w$	0.033	0.045	0.026
$p$ factor	0.03	0.01	0.01
variables	324	306	363
GOF	3.67	3.53	1.58

and orientation matrices were obtained and refined from 15 machine-centered reflections with  $24.4^\circ < 2\theta < 25.4^\circ$  for **5**, 19 machine-centered reflections with  $19.5^\circ < 2\theta < 20.5^\circ$  for **7a**, and 20 machine-centered reflections with  $19.4^\circ < 2\theta < 20.6^\circ$  for **7b**. Intensity data were collected using a  $\omega/2\theta$  scan technique; 3 standard reflections were recorded every 150 reflections. The data for **5**, **7a**, and **7b** were processed using the TEXSAN crystal solution package operating on a IRIS Indigo computer. Neutral atom scattering factors were obtained from the standard sources.<sup>35</sup> In the reduction of the data, Lorentz/polarization corrections and empirical absorption corrections based on azimuthal scans were applied to the data for each structure.

**Structure Solution and Refinement.** The Ru atom positions were determined using direct methods employing the MITHRIL direct-methods routines. In each case the remaining non-hydrogen atoms were located from successive difference Fourier map calculations. In all cases the non-hydrogen atoms were refined anisotropically by using full-matrix least-squares techniques on  $F$ . In the cases of **5** and **7b**, the positions of hydrogen atoms bonded to the Ru and silicon atoms were located by sequential difference Fourier synthesis and were refined isotropically. However, the positions of three of the four hydrogen atoms bound to the Ru atoms were not located from the difference Fourier map calculations in the case of **7a**. The positions of the one hydrogen atom bridging between two Ru atoms and of the hydrogen atom terminally bound to silicon were located but not refined. Crystal data and results of the analyses are listed in Table 5.

**Preparation of  $[(\eta^5\text{-C}_5\text{Me}_5)\text{Ru}(\mu\text{-H})_2(\mu\text{-}\eta^2\text{-}\eta^2\text{-H}_2\text{Si}^t\text{Bu}_2)]$  (**4**).** Toluene (20 mL) and  $\text{Cp}^*\text{Ru}(\mu\text{-H})_4\text{RuCp}^*$  (0.470 g, 0.986 mmol) were charged in a reaction flask. After 1.5 equiv of  $\text{H}_2$

(35) *International Tables for X-ray Crystallography*; Kynoch Press: Birmingham, U.K., 1975; Vol. 4.

Si<sup>t</sup>Bu<sub>2</sub> (0.29 mL, 1.61 mmol) was added, the solution was stirred for 4 h at 25 °C with vigorous stirring. The color of the solution changed from red to deep purple with slow generation of hydrogen. The solvent and remaining silanes were then evaporated under reduced pressure. The deep purple residual solid was dissolved in 7 mL of toluene, and the product was purified by the use of column chromatography on neutral alumina (Merck Art. No. 1097) with hexane/toluene. Removal of the solvent *in vacuo* afforded 0.546 g of purple solid (89% yield). <sup>1</sup>H NMR (300 MHz, 23 °C, C<sub>6</sub>D<sub>6</sub>):  $\delta$  1.89 (s, 30H, Cp'), 1.11 (s, 18H, <sup>t</sup>Bu), -11.12 (br, 4H, RuHRu and RuHSi). <sup>1</sup>H NMR (500 MHz, -120 °C, 1:5 toluene-*d*<sub>8</sub>/THF-*d*<sub>8</sub>):  $\delta$  1.90 (s, 30H, Cp'), 0.78 (s, 18H, <sup>t</sup>Bu), -6.15 (s, 2H, *J*<sub>Si-H</sub> = 75 Hz, RuHSi), -16.63 (s, 2H, RuHRu). <sup>13</sup>C NMR (75 MHz, 23 °C, C<sub>6</sub>D<sub>6</sub>):  $\delta$  85.7 (s, C<sub>5</sub>Me<sub>5</sub>), 32.3 (q, *J*<sub>C-H</sub> = 124.9 Hz, CMe<sub>3</sub>), 24.1 (s, CMe<sub>3</sub>), 12.8 (q, *J*<sub>C-H</sub> = 126.5 Hz, C<sub>5</sub>Me<sub>5</sub>). <sup>29</sup>Si NMR (99 MHz, 23 °C, toluene-*d*<sub>8</sub>):  $\delta$  75.5 (quintet, *J*<sub>Si-H</sub> = 34.2 Hz). IR (KBr, cm<sup>-1</sup>): 2974, 2952, 2884, 2854, 1790 br ( $\nu$ (Ru-H-Si)), 1468, 1377, 1050 ( $\delta$ (H-Si-H)), 1029, 816, 600. Anal. Calcd for C<sub>25</sub>H<sub>52</sub>Ru<sub>2</sub>Si: C, 54.36; H, 8.47. Found: C, 54.09; H, 8.57.

**Preparation of [( $\eta^5$ -C<sub>5</sub>Me<sub>5</sub>)Ru( $\mu$ -D)]<sub>2</sub>( $\mu$ - $\eta^2$ : $\eta^2$ -D<sub>2</sub>Si<sup>t</sup>Bu<sub>2</sub>)(**4-d**<sub>4</sub>).** Toluene (10 mL) and Cp'Ru( $\mu$ -D)<sub>4</sub>RuCp' (0.061 g, 0.13 mmol) were charged in a reaction flask. After 2.0 equiv of D<sub>2</sub>-Si<sup>t</sup>Bu<sub>2</sub> (0.05 mL, 0.25 mmol) was added, the solution was stirred for 4 h at 25 °C with vigorous stirring. The solvent and remaining silanes were then evaporated under reduced pressure. The deep purple residual solid was dissolved in 7 mL of hexane, and the product was purified by the use of column chromatography on neutral alumina (Merck Art. No. 1097) with hexane/toluene. Removal of the solvent *in vacuo* afforded 0.047 g of purple solid (60% yield). <sup>1</sup>H NMR (300 MHz, 23 °C, C<sub>6</sub>D<sub>6</sub>):  $\delta$  1.89 (s, 30H, Cp'), 1.11 (s, 18H, <sup>t</sup>Bu). IR (KBr, cm<sup>-1</sup>): 2960, 2920, 2854, 1468, 1375, 1280 br ( $\nu$ (Ru-D-Si)), 1029, 816, 760 ( $\delta$ (D-Si-D)), 601.

**Reaction of ( $\eta^5$ -C<sub>5</sub>Me<sub>5</sub>)Ru( $\mu$ -D)<sub>4</sub>Ru( $\eta^5$ -C<sub>5</sub>Me<sub>5</sub>)(**1-d**<sub>4</sub>) with Di-*tert*-butylsilane.** Benzene-*d*<sub>6</sub> (0.3 mL) and Cp'Ru( $\mu$ -D)<sub>4</sub>RuCp' (0.012 g, 0.025 mmol) were charged in an NMR tube. Four equivalents of <sup>t</sup>Bu<sub>2</sub>SiH<sub>2</sub> (0.019 mL, 0.097 mmol) was added; the reaction was then monitored by the use of <sup>1</sup>H NMR at room temperature. While the reaction rate was extremely slow when compared to the reaction carried in a Schlenk tube with vigorous stirring, all of **1-d**<sub>4</sub> was converted in 12 h. In the <sup>1</sup>H NMR measured after 15 min, a small hydride resonance was observed only at  $\delta$  -11.64 (conversion *ca.* 10%); four hydride signals assignable to **4**, **4-d**<sub>1</sub>, **4-d**<sub>2</sub>, and **4-d**<sub>3</sub> were observed after 12 h (conversion 100%). <sup>1</sup>H NMR (300 MHz, 23 °C, C<sub>6</sub>D<sub>6</sub>):  $\delta$  1.89 (s, 30H, Cp'), 1.11 (s, 18H, <sup>t</sup>Bu), -11.12 (br, **4**), -11.38 (br, **4-d**<sub>1</sub>), -11.64 (br, **4-d**<sub>2</sub>), -11.90 (br, **4-d**<sub>3</sub>). Intensity ratio of the hydride region to the Cp' signal is *ca.* 2.0H, and the ratio among **4**, **4-d**<sub>1</sub>, **4-d**<sub>2</sub>, **4-d**<sub>3</sub>, and **4-d**<sub>4</sub> was estimated at about 2:7:9:3:4. The reaction of **1** with <sup>t</sup>Bu<sub>2</sub>SiD<sub>2</sub> gave a similar result, though the ratio was slightly changed.

**Preparation of [( $\eta^5$ -C<sub>5</sub>Me<sub>5</sub>)Ru(CO)]<sub>2</sub>( $\mu$ - $\eta^2$ : $\eta^2$ -H<sub>2</sub>Si<sup>t</sup>Bu<sub>2</sub>)(**5**) and [( $\eta^5$ -C<sub>5</sub>Me<sub>5</sub>)Ru(CO)]<sub>2</sub>( $\mu$ - $\eta^2$ -HSi<sup>t</sup>Bu<sub>2</sub>)(**6**).** Toluene (10 mL) and [Cp'Ru( $\mu$ -H)]<sub>2</sub>( $\mu$ - $\eta^2$ : $\eta^2$ -H<sub>2</sub>Si<sup>t</sup>Bu<sub>2</sub>)(**4**; 0.081 g, 0.13 mmol) were charged in a reaction flask under 1 atm of carbon monoxide. After the solution was stirred for 12 h at 23 °C, the color changed from deep purple to light orange. Removal of the solvent under reduced pressure afforded a yellow solid mixture of **5** and **6** including 4% of [Cp'Ru(CO)( $\mu$ -CO)]<sub>2</sub> as a byproduct. Complexes **5** and **6** were extracted from the mixture by filtration with 5 mL of pentane three times. Removal of the solvent *in vacuo* afforded 0.066 g of the yellow solid mixture of **5** and **6** in the ratio of 1:1.2 (76% yield). Only **5** can be isolated from cold pentane as a yellow single crystal suitable for X-ray diffraction study, but it came to equilibrium within few hours when it was dissolved in benzene-*d*<sub>6</sub>. <sup>1</sup>H NMR (300 MHz, 23 °C, C<sub>6</sub>D<sub>6</sub>): **5**,  $\delta$  1.89 (s, 30H, Cp'), 1.26 (s, 18H, <sup>t</sup>Bu), -13.60 (s, 2H, *J*<sub>Si-H</sub> = 24 Hz, RuHSi); **6**,  $\delta$  1.98 (s, 15H, Cp'), 1.73 (s, 15H, Cp'), 1.42 (s, 9H, <sup>t</sup>Bu), 1.41 (s, 9H, <sup>t</sup>Bu), -11.79 (s, 1H, *J*<sub>Si-H</sub> = 36 Hz, RuHSi), -14.40 (s, 1H, RuHRu). <sup>13</sup>C{<sup>1</sup>H} NMR (69 MHz, 23 °C, C<sub>6</sub>D<sub>6</sub>): **5**,  $\delta$  211.1

(CO), 96.0 (C<sub>5</sub>Me<sub>5</sub>), 31.3 (CMe<sub>3</sub>), 28.1 (CMe<sub>3</sub>), 10.3 (C<sub>5</sub>Me<sub>5</sub>); **6**,  $\delta$  210.4 (CO), 205.7 (CO), 95.63 (C<sub>5</sub>Me<sub>5</sub>), 95.55 (C<sub>5</sub>Me<sub>5</sub>), 32.0 (CMe<sub>3</sub>), 31.7 (CMe<sub>3</sub>), 27.0 (CMe<sub>3</sub>), 26.8 (CMe<sub>3</sub>), 10.6 (C<sub>5</sub>Me<sub>5</sub>), 9.8 (C<sub>5</sub>Me<sub>5</sub>). <sup>29</sup>Si NMR (54 MHz, 23 °C, C<sub>6</sub>D<sub>6</sub>): **5**,  $\delta$  186.2 (t, *J*<sub>Si-H</sub> = 22.4 Hz); **6**,  $\delta$  168.7 (dd, *J*<sub>Si-H</sub> = 31.6, 7.9 Hz). IR (KBr, cm<sup>-1</sup>): **5** and **6**, 2976, 2894, 2854, 1928, 1905, 1869, 1479, 1379, 1027, 818. Anal. Calcd for C<sub>30</sub>H<sub>50</sub>O<sub>2</sub>Ru<sub>2</sub>Si: C, 53.55; H, 7.49. Found: C, 52.69; H, 7.45 (**5** and **6**).

**Preparation of [( $\eta^5$ -C<sub>5</sub>Me<sub>5</sub>)Ru]<sub>2</sub>( $\mu$ - $\eta^2$ -HSi<sup>t</sup>Bu<sub>2</sub>)( $\mu$ - $\eta^2$ -HSiEtH)( $\mu$ -H)(**7a**).** Benzene-*d*<sub>6</sub> and [Cp'Ru( $\mu$ -H)]<sub>2</sub>( $\mu$ - $\eta^2$ : $\eta^2$ -H<sub>2</sub>-Si<sup>t</sup>Bu<sub>2</sub>)(**4**; 0.031 g, 0.049 mmol) were charged in an NMR tube. After 20 equiv of diethylsilane (0.13 mL, 1.01 mmol) was added, the NMR tube was sealed. After the solution was heated in an oil bath at 100 °C for 2 h, the color changed from deep purple to red. The solvent and remaining silanes were then evaporated under reduced pressure in a flask. The orange residual oil was dissolved in 1 mL of pentane, and the product was purified by the use of column chromatography on neutral alumina (Merck Art. No. 1097) with hexane. Removal of the solvent *in vacuo* afforded 0.030 g of the orange solid of the mixture of **7a** together with [Cp'Ru( $\mu$ - $\eta^2$ -HSiEt)]<sub>2</sub>( $\mu$ -H)(**2a**) in the ratio of 10:1 (82% yield based on <sup>1</sup>H NMR). Complex **7a** can be isolated from cold pentane as a orange single crystal suitable for an X-ray diffraction study. A minor product was identified as **2a** by comparing the <sup>1</sup>H NMR chemical shift with that of an authentic sample alternatively synthesized. <sup>1</sup>H NMR (500 MHz, 60 °C, toluene-*d*<sub>8</sub>):  $\delta$  5.66 (br, 1H, *J*<sub>Si-H</sub> = 160 Hz, SiH), 1.87 (s, 30H, Cp'), 1.50 (m, 5H, Et), 1.28 (s, 9H, <sup>t</sup>Bu), 1.25 (s, 9H, <sup>t</sup>Bu), -12.83 (br, 2H, RuH), -15.50 (br, 2H, RuH). <sup>1</sup>H NMR (-90 °C):  $\delta$  5.64 (br, 1H, SiH), 1.94 (s, 15H, Cp'), 1.63 (s, 15H, Cp'), 1.6 -1.0 (m, 5H, Et), 1.6 -1.0 (m, 18H, <sup>t</sup>Bu), -12.32 (s, 1H, RuH), -13.26 (s, 1H, RuH), -14.29 (s, 1H, RuH), -16.67 (s, 1H, RuH). <sup>13</sup>C{<sup>1</sup>H} NMR (76 MHz, 23 °C, C<sub>6</sub>D<sub>6</sub>):  $\delta$  93.3 (C<sub>5</sub>Me<sub>5</sub>), 32.3 (CMe<sub>3</sub>), 32.4 (CMe<sub>3</sub>), 25.9 (CMe<sub>3</sub>), 24.9 (CMe<sub>3</sub>), 15.0 (-CH<sub>2</sub>CH<sub>3</sub>), 14.0 (-CH<sub>2</sub>CH<sub>3</sub>), 12.4 (C<sub>5</sub>Me<sub>5</sub>). IR (KBr, cm<sup>-1</sup>): 2964, 2906, 2850, 2062 m ( $\nu$ (Ru-H)), 2022 s ( $\nu$ (Si-H)), 1835 br ( $\nu$ (Ru-H-Si<sup>t</sup>Bu<sub>2</sub>)), 1659 br ( $\nu$ (Ru-H-SiEtH)), 1475, 1379, 1071, 1027, 812, 571. Anal. Calcd for C<sub>30</sub>H<sub>58</sub>Ru<sub>2</sub>Si<sub>2</sub>: C, 53.22; H, 8.63. Found: C, 53.02; H, 8.22. FD-MASS: *m/e* 678. The field desorption mass spectrum was measured, and the intensities of the obtained isotopic peaks for C<sub>30</sub>H<sub>58</sub>Ru<sub>2</sub>Si<sub>2</sub> agreed with the calculated values within experimental error.

**Preparation of [( $\eta^5$ -C<sub>5</sub>Me<sub>5</sub>)Ru]<sub>2</sub>( $\mu$ - $\eta^2$ -HSi<sup>t</sup>Bu<sub>2</sub>)( $\mu$ - $\eta^2$ -HSiPhH)( $\mu$ -H)(**7b**).** Toluene (10 mL) and [Cp'Ru( $\mu$ -H)]<sub>2</sub>( $\mu$ - $\eta^2$ : $\eta^2$ -H<sub>2</sub>Si<sup>t</sup>Bu<sub>2</sub>)(**4**; 0.074 g, 0.12 mmol) were charged in a reaction flask. After 5 equiv of phenylsilane (0.075 mL, 0.61 mmol) was added, the reaction solution was stirred for 2 h at room temperature. The color of the solution changed from deep purple to bright orange. The solvent and remaining silanes were then evaporated under reduced pressure. The orange residual oil was dissolved in 5 mL of pentane, and the product was purified by the use of column chromatography on neutral alumina (Merck Art. No. 1097) with hexane. Removal of the solvent *in vacuo* afforded 0.059 g of the orange solid of the mixture of **7b** (68% yield). <sup>1</sup>H NMR (500 MHz, 20 °C, toluene-*d*<sub>8</sub>):  $\delta$  8.2-7.1 (m, 5H, Ph), 6.29 (s, 1H, *J*<sub>Si-H</sub> = 172 Hz, SiH), 1.87 (s, 30H, Cp'), 1.24 (s, 9H, <sup>t</sup>Bu), 1.04 (s, 9H, <sup>t</sup>Bu), -12.31 (br, 2H, RuH), -15.35 (br, 2H, RuH). <sup>1</sup>H NMR (-90 °C):  $\delta$  8.2-7.1 (m, 5H, Ph), 6.37 (br, 1H, SiH), 1.93 (s, 15H, Cp'), 1.66 (s, 15H, Cp'), 1.5-1.0 (m, 18H, <sup>t</sup>Bu), -11.64 (s, 1H, *J*<sub>Si-H</sub> = 26 Hz, RuHSi), -12.84 (s, 1H, RuH or RuHRu), -14.00 (s, 1H, *J*<sub>Si-H</sub> = 49 Hz, RuHSi), -16.46 (s, 1H, RuH or RuHRu). <sup>13</sup>C{<sup>1</sup>H} NMR (76 MHz, 23 °C, C<sub>6</sub>D<sub>6</sub>):  $\delta$  144.6 (Ph ipso), 136.8 (Ph), 127.7 (Ph), 93.5 (C<sub>5</sub>Me<sub>5</sub>), 32.6 (CMe<sub>3</sub>), 32.1 (CMe<sub>3</sub>), 26.0 (CMe<sub>3</sub>), 25.0 (CMe<sub>3</sub>), 12.4 (C<sub>5</sub>Me<sub>5</sub>). IR (KBr, cm<sup>-1</sup>): 3062, 3048, 2958, 2900, 2850, 2054 ( $\nu$ (Ru-H)), 2036 ( $\nu$ (Si-H)), 1813 br ( $\nu$ (Ru-H-Si)), 1613 br ( $\nu$ (Ru-H-Si)), 1475, 1427, 1379, 1029, 880, 700. Anal. Calcd for C<sub>34</sub>H<sub>58</sub>Ru<sub>2</sub>Si<sub>2</sub>: C, 56.32; H, 8.06. Found: C, 56.04; H, 8.19.

**H/D Exchange Reaction of [Cp'Ru( $\mu$ -H)]<sub>2</sub>( $\mu$ - $\eta^2$ : $\eta^2$ -H<sub>2</sub>Si<sup>t</sup>Bu<sub>2</sub>)(**4**) with Benzene-*d*<sub>6</sub>.** Benzene-*d*<sub>6</sub> (0.3 mL) and [( $\eta^5$ -C<sub>5</sub>-

$\text{Me}_5\text{Ru}(\mu\text{-H})_2(\mu\text{-}\eta^2\text{-}\eta^2\text{-H}_2\text{Si}^t\text{Bu}_2)$  (**4**; 0.015 g, 0.024 mmol) were charged in an NMR tube; the tube was then sealed. When the mixture was heated in an oil bath at 80 °C for days, new peaks of hydride signals assignable to those for **4-d**<sub>1</sub>, **4-d**<sub>2</sub>, and **4-d**<sub>3</sub> appeared, each consecutively shifted 0.26 ppm upfield from that of **4**. Deuterium abstraction gradually proceeded, and those peaks finally disappeared after 2 weeks while the signal for Cp' groups did not show any observable changes during the reaction.

**H/D Exchange Reaction of 4-d<sub>4</sub> with Di-*tert*-butylsilane.** Di-*tert*-butylsilane (0.038 mL, 0.21 mmol) and  $[(\eta^5\text{-C}_5\text{Me}_5)\text{Ru}(\mu\text{-D})_2](\mu\text{-}\eta^2\text{-}\eta^2\text{-D}_2\text{Si}^t\text{Bu}_2)$  (**4-d**<sub>4</sub>; 0.013 g, 0.021 mmol) were dissolved in benzene-*d*<sub>6</sub> (0.3 mL). After the solution was charged in an NMR tube, the tube was sealed. Whereas the H/D exchange reaction did not proceed at room temperature, the signals for hydrides of **4**, **4-d**<sub>1</sub>, **4-d**<sub>2</sub>, and **4-d**<sub>3</sub> appeared upon heating in an oil bath at 80 °C for 24 h. The total intensity of those signals was *ca.* 3H to 30H of the Cp' signal at that time (conversion 75%), and a decrease in the intensity of the Si-H signal of  ${}^t\text{Bu}_2\text{SiH}_2$  was also observed. Prolonged heating resulted in a disappearance of both the Si-H signal

for  ${}^t\text{Bu}_2\text{SiH}_2$  and that for Ru-H. Deuterium distribution between C<sub>6</sub>D<sub>6</sub> occurred simultaneously.

**Acknowledgment.** This research was supported by fellowships of the Japan Society for the Promotion of Science for Japanese Junior Scientists and by a Grant-in-Aid for Scientific Research on Priority Area (Nos. 05225210 and 05236104) from the Ministry of Education, Science, and Culture. We thank Kanto Chemical Co., Inc., for generous gifts of pentamethylcyclopentadiene and several kinds of silanes.

**Supporting Information Available:** Text giving details of the data collection and reduction and the structure solution and refinement and tables of the crystal data and the data collection and refinement parameters, positional parameters, anisotropic thermal parameters, bond lengths and angles, and special contacts (45 pages). Ordering information is given on any current masthead page.

OM940859N

# Synthesis and Molecular Structures of the Mesitylindium Selenolates $[\text{Mes}_2\text{In}(\mu\text{-SeR})]_2$ ( $\text{R} = \text{Me}, \text{Ph}, \text{Mes}$ ) and $[\text{MeIn}(\mu\text{-SePh})(\text{SePh})]_\infty$ : Potential Precursors to Indium Chalcogenides

Hamid Rahbarnoohi, Rajesh Kumar, Mary Jane Heeg, and John P. Oliver\*

Department of Chemistry, Wayne State University, Detroit, Michigan 48202

Received March 13, 1995<sup>⊗</sup>

The reaction of trimesitylindium,  $\text{Mes}_3\text{In}$  ( $\text{Mes} = 2,4,6\text{-trimethylphenyl}$ ), with diselenides,  $\text{R}_2\text{Se}_2$  ( $\text{R} = \text{Me}, \text{Ph}$ ), at room temperature yields  $[\text{Mes}_2\text{In}(\mu\text{-SeR})]_2$  ( $\text{R} = \text{Me}$  (1),  $\text{Ph}$  (2)) and the corresponding selenoether,  $\text{MesSeR}$ . Under similar conditions, the reaction of  $\text{Me}_3\text{In}$  with  $\text{Ph}_2\text{Se}_2$  gives a rearranged product,  $[\text{MeIn}(\mu\text{-SePh})(\text{SePh})]_\infty$  (4).  $[\text{Mes}_2\text{In}(\mu\text{-SeMes})]_2$  (3) is obtained by the reaction of  $\text{Mes}_3\text{In}$  with elemental Se in refluxing toluene. The resulting derivatives have been characterized by  $^1\text{H}$ ,  $^{13}\text{C}$ , and  $^{77}\text{Se}$  NMR spectroscopy, and the structures of 2–4 have been determined by single-crystal X-ray diffraction techniques 2 and 3 form dimeric molecules with planar  $(\text{InSe})_2$  rings. 4 can be described as a spiral chain composed of alternate four-coordinate indium atoms and three-coordinate selenium atoms.

## Introduction

Our interest in the syntheses, structures, and dynamic properties of group 13–16 derivatives and their potential use as single-source precursors for group 13–16 materials has led us to prepare a number of new compounds and to characterize them by X-ray crystallography and NMR spectroscopy.<sup>1–8</sup> A number of other groups also have been investigating systems of this type. For example,  $[\text{Np}_2\text{In}(\mu\text{-SePh})]_2$ ,<sup>9</sup>  $\text{Np}_2\text{In}(\mu\text{-SePh})(\mu\text{-P-}t\text{-Bu}_2)\text{InNp}_2$ ,<sup>10</sup>  $[\text{Np}_2\text{Ga}(\mu\text{-TePh})]_2$ <sup>11</sup> ( $\text{Np} = \text{CH}_2\text{CMe}_3$ ) and  $[(t\text{-Bu})_2\text{Ga}(\mu\text{-SH})]_2$ <sup>12</sup> have been prepared, and Hoffman has reported the synthesis of several gallium and indium derivatives by reaction of  $\text{R}_2\text{E}_2$ ,  $\text{REH}$ , or  $(\text{R}_3\text{Si})_2\text{E}$  ( $\text{E} = \text{S}, \text{Se}$ ) with  $\text{X}_2\text{MR}$  ( $\text{X} = \text{Cl}, \text{Br}, \text{I}$ ) derivatives.<sup>13–16</sup> In a few cases, highly oriented thin films of  $\text{InS}$  and  $\text{GaS}$  have been prepared by MOCVD from organome-

tallic precursors of this type.<sup>17,18</sup> Similarly, it has been shown that the indium selenolates  $\text{R}_{3-n}\text{In}(\text{SeR}')_n$  can be used to produce  $\text{In}_x\text{Se}_y$  films.<sup>19</sup> We also have found that  $\text{In}(\text{ER})_3$  ( $\text{E} = \text{S}, \text{Se}$ ) complexes serve as precursors to previously unidentified phases of  $\text{In}_x\text{E}_y$  materials.<sup>20</sup> Much of the work on these organometallic precursors has appeared only recently and describes thiolate complexes of group 13 and, to a lesser extent, the selenolate and telluroate complexes.<sup>1,2,8–11,21–24</sup>

In this paper we report synthetic, solution, and X-ray studies on four new indium selenium derivatives,  $[\text{Mes}_2\text{In}(\mu\text{-SeMe})]_2$  (1),  $[\text{Mes}_2\text{In}(\mu\text{-SePh})]_2$  (2),  $[\text{Mes}_2\text{In}(\mu\text{-SeMes})]_2$  (3), and  $[\text{MeIn}(\mu\text{-SePh})(\text{SePh})]_\infty$  (4).

## Experimental Section

**General Experimental Procedures.** All solvents were purified and dried by standard techniques.<sup>25</sup> Argon gas was purified by passing it through a series of columns containing Deox catalyst (Alfa), phosphorus pentoxide, and sodium hydroxide. Elemental Se was purchased from Fairmount Chemicals.  $\text{Me}_2\text{Se}_2$  (Strem),  $\text{Ph}_2\text{Se}_2$  (Aldrich), and  $\text{Mes}_2\text{Se}_2$  (Alfa) were purchased and used as received. Trimesitylindium ( $\text{Mes}_3\text{In}$ )<sup>26</sup> and  $\text{Me}_3\text{In}$ <sup>27</sup> were prepared according to the published procedures. The compounds are both oxygen and water

(17) MacInnes, A. N.; Power, M. B.; Barron, A. R. *Chem. Mater.* **1992**, *4*, 11.

(18) MacInnes, A. N.; Cleaver, W. M.; Barron, A. R.; Power, M. B.; Hepp, A. F. *Adv. Mater. Opt. Electron.* **1992**, *1*, 229.

(19) Gysling, H. J.; Wernberg, A. A.; Blanton, T. N. *Chem. Mater.* **1992**, *4*, 900.

(20) Kampf, J.; Kumar, R.; Oliver, J. P.; Narula, C. K. To be submitted for publication.

(21) Cowley, A. H.; Jones, R. A.; Harris, P. R.; Atwood, D. A.; Contreras, L.; Burek, C. J. *Angew. Chem., Int. Ed. Engl.* **1991**, *30*, 1143.

(22) Power, M. B.; Ziller, J. W.; Barron, A. R. *Organometallics* **1992**, *11*, 2783.

(23) Power, M. B.; Ziller, J. W.; Tyler, A. N.; Barron, A. R. *Organometallics* **1992**, *11*, 1055.

(24) Uhl, W.; Schütz, U.; Hiller, W.; Heckel, M. *Organometallics* **1995**, *14*, 1073.

(25) Shriver, D. F.; Drezdson, M. A. *The Manipulation of Air-Sensitive Compounds*; Wiley: New York, 1986.

(26) Leman, J. T.; Barron, A. R. *Organometallics* **1989**, *8*, 2214.

(27) Foster, D. F.; Rushworth, S. A.; Cole-Hamilton, D. J.; Cafferty, R.; Harrison, J.; Parkes, P. J. *Chem. Soc., Dalton Trans.* **1988**, *7*.

<sup>⊗</sup> Abstract published in *Advance ACS Abstracts*, July 15, 1995.  
 (1) Oliver, J. P.; Kumar, R.; Taghiof, M. In *Coordination Chemistry of Aluminum*; Robinson, G. H., Ed.; VCH: New York, 1993; pp 167–195.  
 (2) Oliver, J. P.; Kumar, R. *Polyhedron* **1990**, *9*, 409.  
 (3) Ghazi, S. U.; Heeg, M. J.; Oliver, J. P. *Inorg. Chem.* **1994**, *33*, 4517.  
 (4) Rahbarnoohi, H.; Taghiof, M.; Heeg, M. J.; Dick, D. G.; Oliver, J. P. *Inorg. Chem.* **1994**, *33*, 6307.  
 (5) Keller, H.; Daran, J. C.; Lang, H. J. *Organomet. Chem.* **1994**, *482*, 63.  
 (6) Rahbarnoohi, H.; Kumar, R.; Heeg, M. J.; Oliver, J. P. *Organometallics* **1995**, *14*, 502.  
 (7) Taghiof, M.; Heeg, M. J.; Bailey, M.; Dick, D. G.; Kumar, R.; Hendershot, D. G.; Rahbarnoohi, H.; Oliver, J. P. *Organometallics* **1995**, *14*, 2903.  
 (8) Oliver, J. P. *J. Organomet. Chem.*, in press.  
 (9) Beachley, O. T., Jr.; Lee, J. C., Jr.; Gysling, H. J.; Chao, S.-H. L.; Churchill, M. R.; Lake, C. H. *Organometallics* **1992**, *11*, 3144.  
 (10) Beachley, O. T., Jr.; Chao, S.-H. L.; Churchill, M. R.; Lake, C. H. *Organometallics* **1993**, *12*, 5025.  
 (11) Banks, M. A.; Beachley, O. T., Jr.; Gysling, H. J.; Luss, H. R. *Organometallics* **1990**, *9*, 1979.  
 (12) Power, M. B.; Barron, A. R. *J. Chem. Soc., Chem. Commun.* **1991**, 1315.  
 (13) Hoffmann, G. G.; Faist, R. *J. Organomet. Chem.* **1990**, *391*, 1.  
 (14) Hoffmann, G. G. *Z. Naturforsch.* **1984**, *39B*, 352.  
 (15) Hoffmann, G. G.; Fischer, R. *Inorg. Chem.* **1989**, *28*, 4165.  
 (16) Hoffmann, G. G.; Fischer, R. *Phosphorus, Sulfur Silicon Relat. Elem.* **1989**, *41*, 97.

**Table 1. Selected Experimental Parameters for the X-ray Diffraction Study of the Compounds [Mes<sub>2</sub>In(μ-SePh)]<sub>2</sub> (2), [Mes<sub>2</sub>In(μ-SeMes)]<sub>2</sub> (3), and [MeIn(μ-SePh)(SePh)]<sub>∞</sub> (4)**

compd	[Mes <sub>2</sub> In(μ-SePh)] <sub>2</sub> (2)	[Mes <sub>2</sub> In(μ-SeMes)] <sub>2</sub> (3)	[MeIn(μ-SePh)(SePh)] <sub>∞</sub> (4)
formula	C <sub>48</sub> H <sub>54</sub> In <sub>2</sub> Se <sub>2</sub>	C <sub>54</sub> H <sub>66</sub> In <sub>2</sub> Se <sub>2</sub>	C <sub>13</sub> H <sub>13</sub> InSe <sub>2</sub>
mol wt	1018.47	1102.68	532.88
space group	<i>P</i> 2 <sub>1</sub> / <i>c</i> (No. 14)	<i>P</i> 1̄ (No. 2)	<i>P</i> 2 <sub>1</sub> / <i>n</i> (No. 14)
<i>a</i> (Å)	8.932(9)	12.702(5)	14.293(4)
<i>b</i> (Å)	22.732(10)	14.504(4)	10.671(1)
<i>c</i> (Å)	11.300(2)	16.381(5)	19.561(8)
α (deg)		93.48(2)	
β (deg)	103.750(10)	100.48(3)	93.02(3)
γ (deg)		99.01(3)	
<i>V</i> (Å <sup>3</sup> )	2228.6(11)	2919 (2)	2979.3(14)
<i>Z</i>	2 (dimers)	2 (dimers)	8
density (calcd) (g cm <sup>-3</sup> )	1.518	1.255	1.971
radiation type	Mo Kα (λ = 0.710 73 Å) graphite monochromator	Mo Kα (λ = 0.710 73 Å) graphite monochromator	Mo Kα (λ = 0.710 73 Å) graphite monochromator
temp (°C)	22	22	20
linear abs coeff (μ) (cm <sup>-1</sup> )	26.98	20.40	64.47
R <sup>a</sup>	3.27	8.1	12.21
R <sub>w</sub> <sup>b</sup>	6.95	9.0	7.01

$$^a R = \sum(|F_o| - |F_c|)/\sum|F_o|. \quad ^b R_w = [\sum w(|F_o| - |F_c|)^2/\sum w|F_o|^2]^{1/2}; \quad w^{-1} = s^2(F_o) + g(F_o)^2.$$

sensitive; therefore, standard Schlenk line and glovebox techniques were employed. All of the glassware used in the synthetic work was oven- and/or flame-dried. <sup>1</sup>H, <sup>13</sup>C, and <sup>77</sup>Se NMR spectra were recorded on either a QE-300 or a GN-300 NMR General Electric spectrometer. The <sup>1</sup>H and <sup>13</sup>C chemical shifts were referenced to benzene (δ 7.15 ppm for <sup>1</sup>H and δ 128.00 ppm for <sup>13</sup>C) while <sup>77</sup>Se (SF = 57.2208 MHz) was referenced to external Me<sub>2</sub>Se in CDCl<sub>3</sub>. Variable-temperature <sup>1</sup>H NMR spectra were recorded on a GN-300 NMR spectrometer in toluene-*d*<sub>8</sub> solutions and were referenced to the residual protic peak of toluene (<sup>1</sup>H, δ 2.09 ppm). Elemental analyses on selected compounds were performed by Galbraith Laboratories, Knoxville, TN. Melting points were recorded on a Haake-Buchler apparatus in sealed capillaries and are uncorrected. Mass spectra were run with a MS-80 AUTOCONSOLE (Kratos Analytical Instruments) mass spectrometer in the EI mode at 70 eV.

**Preparation of [Mes<sub>2</sub>In(μ-SeMe)]<sub>2</sub> (1).** Dimethyl diselenide (0.25 g, 1.33 mmol) was added dropwise from a syringe to 0.63 g (1.33 mmol) of Mes<sub>3</sub>In in 100 mL of hexane. The solution was stirred for 3 days at room temperature. The yellow precipitate resulting from the reaction was separated from the filtrate and recrystallized by redissolving it in approximately 20 mL of hot hexane/toluene (3/1, v/v) solvent, giving colorless crystals on cooling to room temperature: yield 75%; mp 281 °C. Anal. Calcd (found): C, 53.00 (52.88); H, 5.78 (5.67). <sup>1</sup>H NMR (C<sub>6</sub>D<sub>6</sub>; δ, ppm): 1.65 (s, 3H, Se-CH<sub>3</sub>), 2.14 (s, 6H, *p*-CH<sub>3</sub> of Mes), 2.59 (s, 12H, *o*-CH<sub>3</sub> of Mes), 6.77 (s, 4H, aryl of Mes); 2.10 (s, CH<sub>3</sub>), 6.98–7.14 (m, Ph) (toluene). <sup>13</sup>C{<sup>1</sup>H} NMR (C<sub>6</sub>D<sub>6</sub>; δ, ppm): 2.9 (Se-CH<sub>3</sub>), 21.1 (*p*-CH<sub>3</sub> of Mes), 26.5 (*o*-CH<sub>3</sub> of Mes), 127.8, 137.9, 144.7, 146.0 (aryl). <sup>77</sup>Se NMR (C<sub>6</sub>D<sub>6</sub>; δ, ppm): -123. Mass spectral data (EI mode): peaks at *m/e* 353, 119, 105, 92, 90 corresponding to fragments Mes<sub>2</sub>In<sup>+</sup>, Mes<sup>+</sup>, [MesH - Me]<sup>+</sup>, C<sub>7</sub>H<sub>8</sub><sup>+</sup>, [MesH - Me<sub>2</sub>]<sup>+</sup>.

**Preparation of [Mes<sub>2</sub>In(μ-SePh)]<sub>2</sub> (2).** Hexane (100 mL) was added to a mixture of Mes<sub>3</sub>In (0.75 g, 1.58 mmol) and Ph<sub>2</sub>Se<sub>2</sub> (0.50 g, 1.58 mmol). The solution was stirred for 3 days. The cream-colored precipitate resulting from the reaction was separated from the filtrate and recrystallized by dissolving it in approximately 20 mL of hot hexane/toluene (3/1) solvent, which gave colorless crystals on cooling: yield 80%; mp 245 °C. Anal. Calcd (found): C, 56.61 (56.35); H, 5.34 (5.23). <sup>1</sup>H NMR (C<sub>6</sub>D<sub>6</sub>; δ, ppm): 2.06 (s, 6H, *p*-CH<sub>3</sub> of Mes), 2.57 (s, 12H, *o*-CH<sub>3</sub> of Mes), 6.61 (s, 4H), 6.49 (m, 3H), 7.19 (m, 2H) (Ph+Mes); <sup>13</sup>C{<sup>1</sup>H} NMR (C<sub>6</sub>D<sub>6</sub>; δ, ppm): 21.1 (*p*-CH<sub>3</sub> of Mes), 26.6 (*o*-CH<sub>3</sub> of Mes), 126.5, 127.8, 128.2, 134.6, 137.8, 144.3, 147.8 (Ph + Mes). <sup>77</sup>Se NMR (C<sub>6</sub>D<sub>6</sub>; δ, ppm): -160. Mass spectral data (EI mode): peaks at *m/e* 624, 353, 246, 234, 157, 119, 105, 90 corresponding to fragments Mes<sub>2</sub>In<sub>2</sub>SePh<sup>+</sup>, Mes<sub>2</sub>

In<sup>+</sup>, Mes(Ph)Se<sup>+</sup>, Ph<sub>2</sub>Se<sup>+</sup>, PhSe<sup>+</sup>, Mes<sup>+</sup>, [MesH - Me]<sup>+</sup>, [MesH - Me<sub>2</sub>]<sup>+</sup>.

**Preparation of [Mes<sub>2</sub>In(μ-SeMes)]<sub>2</sub> (3).** A mixture of Mes<sub>3</sub>In (1.00 g, 2.12 mmol) and elemental Se (0.17 g, 2.12 mmol) was refluxed in 50 mL of toluene for 24 h, resulting in a yellow solution and the disappearance of the Se metal. The volume of the solution was reduced to approximately 20 mL. Colorless crystals were obtained after cooling the solution to 4 °C: yield 56%; mp 207–208 °C. <sup>1</sup>H NMR (C<sub>6</sub>D<sub>6</sub>; δ, ppm): 1.83 (s, 3H, *p*-CH<sub>3</sub> of SeMes), 2.04 (s, 6H, *p*-CH<sub>3</sub> of InMes), 2.47 (s, 6H, *p*-CH<sub>3</sub> of SeMes), 2.61 (s, 12H, *o*-CH<sub>3</sub> of InMes), 6.52 (s, 2H, SeMes), 6.65 (s, 4H, InMes); 2.10 (s, CH<sub>3</sub>), 6.98–7.14 (m, Ph) (toluene). <sup>13</sup>C{<sup>1</sup>H} NMR (C<sub>6</sub>D<sub>6</sub>; δ, ppm): 20.6 (*p*-CH<sub>3</sub> of SeMes), 21.0 (*p*-CH<sub>3</sub> of InMes), 25.9 (*o*-CH<sub>3</sub> of SeMes), 26.1 (*o*-CH<sub>3</sub> of InMes), 127.9, 129.0, 137.1, 137.7, 142.5, 144.0, 150.9 (SeMes + InMes). <sup>77</sup>Se NMR (C<sub>6</sub>D<sub>6</sub>; δ, ppm): -56. Mass spectral data (EI mode): peaks at *m/e* 433, 398, 353, 318, 234, 198, 120, 105, 92, 89 corresponding to fragments Mes<sub>2</sub>InSe<sup>+</sup>, Mes<sub>2</sub>Se<sub>2</sub><sup>+</sup>, Mes<sub>2</sub>In<sup>+</sup>, Mes<sub>2</sub>Se<sup>+</sup>, MesSe<sup>+</sup>, MesH<sup>+</sup>, [MesH - Me]<sup>+</sup>, C<sub>7</sub>H<sub>8</sub><sup>+</sup>, [MesH - Me<sub>2</sub>]<sup>+</sup>.

**Preparation of [MeIn(μ-SePh)(SePh)]<sub>∞</sub> (4).** A hexane solution (50 mL) of diphenyl diselenide (1.37 g, 4.38 mmol) was added to a solution (50 mL, hexane) of trimethylindium (0.70 g, 4.38 mmol) at 0 °C, and the mixture was stirred for 2 days. The light yellow precipitate which formed was separated by removal of the liquid with a cannula, and the solid was recrystallized from approximately 20 mL of a hexane/toluene (3/1) solvent mixture at room temperature: yield 45%; mp 127 °C. Anal. Calcd (found): C, 35.32 (35.18); H, 2.96 (3.08). In a subsequent reaction, Se<sub>2</sub>Ph<sub>2</sub> in hexane was added to a solution of Me<sub>3</sub>In in hexane (2/1) at -75 °C; the mixture was warmed to room temperature over 2 h and stirred for 2 days. The product was identical with that produced in the first reaction. It was isolated in near-quantitative yield and gave better quality crystals which were used for the X-ray diffraction study. The byproduct, MeSePh, was identified by GC/MS. <sup>1</sup>H NMR (C<sub>6</sub>D<sub>6</sub>; δ, ppm): 0.17 and 0.23 (s, 3H, CH<sub>3</sub>), 6.86 (m, 6H, Ph), 7.51 (m, 4H, Ph). <sup>13</sup>C{<sup>1</sup>H} NMR (C<sub>6</sub>D<sub>6</sub>; δ, ppm): -3.2 and -2.6 (s, CH<sub>3</sub>), 126.2, 127.1, 129.5, 135.9 (Ph). Mass spectral data (FAB mode): peaks at *m/e* 523, 287 corresponding to fragments MeIn(SePh)<sub>2</sub>Se<sup>+</sup>, MeInSePh<sup>+</sup>.

**X-ray Structure Determination of [Mes<sub>2</sub>In(μ-SeR)]<sub>2</sub> (R = Me (1), Ph (2), Mes (3)) and [MeIn(μ-SePh)(SePh)]<sub>∞</sub> (4).** X-ray-quality crystals of 2–4 were grown using the procedures described in the above. Suitable crystals were mounted in thin-walled capillary tubes in the drybox; the tubes were plugged with grease, removed from the drybox, flame-sealed, mounted on a goniometer head, and placed on a Nicolet P3/V diffractometer for data collection. 2 was monoclinic and assigned to the space group *P*2<sub>1</sub>/*c* (No. 14) on the basis of



**Table 2. Atomic Coordinates ( $\times 10^4$ ) and Isotropic Thermal Parameters ( $\times 10^3$ ) for the Non-Hydrogen Atoms of  $[\text{Mes}_2\text{In}(\mu\text{-SePh})_2]$  (**2**)**

atom	x	y	z	$U_{\text{eq}}^a$ ( $\text{\AA}^2$ )
In(1)	1437(1)	4742(1)	1464(1)	48(1)
Se(1)	1653(1)	5408(1)	-497(1)	50(1)
C(1)	2114(4)	5304(2)	3049(3)	49(1)
C(2)	3681(4)	5434(2)	3414(4)	56(1)
C(3)	4234(5)	5764(2)	4467(4)	67(1)
C(4)	3281(6)	5975(2)	5163(4)	69(1)
C(5)	1741(5)	5857(2)	4789(4)	68(1)
C(6)	1128(5)	5516(2)	3749(3)	56(1)
C(7)	4797(5)	5230(2)	2691(4)	75(1)
C(8)	3902(7)	6325(2)	6308(5)	108(2)
C(9)	-574(5)	5408(2)	3424(4)	78(1)
C(10)	2298(4)	3850(2)	1462(3)	52(1)
C(11)	3167(5)	3633(2)	685(4)	58(1)
C(12)	3629(6)	3050(2)	768(4)	72(1)
C(13)	3265(6)	2673(2)	1624(5)	79(1)
C(14)	2432(6)	2888(2)	2386(5)	76(1)
C(15)	1946(5)	3467(2)	2329(4)	61(1)
C(16)	3652(6)	4017(2)	-238(4)	82(2)
C(17)	3797(9)	2035(2)	1700(7)	131(3)
C(18)	1056(6)	3682(2)	3228(4)	80(2)
C(19)	1571(5)	6214(2)	30(4)	60(1)
C(20)	829(6)	6379(2)	889(5)	80(1)
C(21)	731(8)	6966(3)	1207(6)	116(2)
C(22)	1369(9)	7380(3)	572(10)	143(3)
C(23)	2116(9)	7224(3)	-279(8)	134(3)
C(24)	2253(6)	6627(2)	-557(6)	93(2)

$$^a U_{\text{eq}} = 1/3 \sum_i \sum_j U_{ij} a_i^* a_j^* \bar{a}_i \bar{a}_j.$$

systematic absences. **3** was triclinic and assigned to the space group  $P\bar{1}$  (No. 2) on the basis of successful refinement of the structure in this space group. **4** was solved in the monoclinic cell system space group  $P2_1/n$  (No. 14) on the basis of systematic absences. Lattice constants were verified by axial photographs. Data reduction was carried out with SHELXTL<sup>28</sup> or SHELXTL PC.<sup>29</sup> In each case, an empirical absorption correction, using psi-scans, was made. No correction for secondary extinction was made. Structure solution and refinement were performed using SHELXS-86,<sup>30</sup> SHELXL-93,<sup>31</sup> and SHELXTL PC.<sup>29</sup> Full-matrix least-squares refinement was carried out using SHELX-76<sup>32</sup> and SHELXTL PC.<sup>29</sup> Direct-methods routines produced acceptable solutions for the structures, yielding positions for most of the non-hydrogen atoms. The remaining atoms were located during subsequent refinement. The hydrogen atom positions in all compounds were calculated as riding on the carbon atoms to which they were bound. In **3**, the number of data were insufficient to refine the structure with all atoms anisotropic; therefore, only In and Se were refined anisotropically, and the phenyl rings were refined as rigid bodies. A region of solvent in the lattice of **3** remains unrefined due to the disorder of the solvent molecule, and some disorder of the carbon atoms of the mesityl rings necessitates an isotropic refinement of these atoms. Parameters from the crystal structure determinations are presented in Table 1. The atomic coordinates and isotropic thermal parameters for **2-4** are listed in Tables 2-4.

Efforts to obtain the structure of **1** were only partially successful. Repeated attempts were made to obtain suitable crystals, but no fully satisfactory crystals were obtained. A data set was collected and solved in space group  $P\bar{1}$ . The results are adequate to show that **1** consists of dimers in the solid state, but details of this structure must await a better data set.

(28) Sheldrick, G. M. *SHELXTL*; University of Göttingen: Göttingen, Federal Republic of Germany, 1978.

(29) *SHELXTL PC*; Siemens Analytical X-Ray Instruments, Inc.: Madison, WI, 1990.

(30) Sheldrick, G. M. *SHELX-86*; University of Göttingen: Göttingen, Federal Republic of Germany, 1986.

(31) Sheldrick, G. M. *SHELXL-93*; University of Göttingen: Göttingen, Federal Republic of Germany, 1993.

(32) Sheldrick, G. M. *SHELX-76*; University Chemical Laboratory: Cambridge, England, 1976.

**Table 3. Atomic Coordinates and Isotropic Thermal Parameters for the Non-Hydrogen Atoms of  $[\text{Mes}_2\text{In}(\mu\text{-SeMes})_2]$  (**3**)**

atom	x	y	z	$U_{\text{eq}}^a$ ( $\text{\AA}^2$ )
Molecule 1				
In(1)	0.0386(2)	0.0424(2)	0.8914(2)	0.069(1)
Se(1)	-0.0333(3)	-0.1192(2)	0.9535(2)	0.067(2)
C(1)	0.204(1)	0.062(2)	0.872(1)	0.07(1)
C(2)	0.266(1)	-0.008(2)	0.864(1)	0.09(1)
C(3)	0.368(1)	0.014(2)	0.844(1)	0.12(1)
C(4)	0.408(1)	0.106(2)	0.830(1)	0.17(2)
C(5)	0.346(1)	0.176(2)	0.838(1)	0.13(1)
C(6)	0.243(1)	0.154(2)	0.859(1)	0.09(1)
C(7)	0.224(3)	-0.102(3)	0.878(2)	0.11(1)
C(8)	0.515(5)	0.122(4)	0.795(4)	0.26(3)
C(9)	0.183(3)	0.228(3)	0.859(2)	0.12(1)
C(10)	-0.094(1)	0.068(2)	0.794(1)	0.07(1)
C(11)	-0.150(1)	0.143(2)	0.799(1)	0.07(1)
C(12)	-0.232(1)	0.154(2)	0.733(1)	0.09(1)
C(13)	-0.257(1)	0.090(2)	0.662(1)	0.08(1)
C(14)	-0.201(1)	0.016(2)	0.657(1)	0.07(1)
C(15)	-0.119(1)	0.005(2)	0.723(1)	0.06(1)
C(16)	-0.131(2)	0.210(2)	0.873(2)	0.08(1)
C(17)	-0.340(3)	0.103(3)	0.592(2)	0.13(1)
C(18)	-0.055(3)	-0.075(2)	0.715(2)	0.09(1)
C(19)	-0.168(2)	-0.178(2)	0.885(1)	0.07(1)
C(20)	-0.261(2)	-0.138(2)	0.869(1)	0.07(1)
C(21)	-0.352(2)	-0.184(2)	0.811(1)	0.10(1)
C(22)	-0.350(2)	-0.271(2)	0.771(1)	0.11(1)
C(23)	-0.257(2)	-0.311(2)	0.788(1)	0.11(1)
C(24)	-0.166(2)	-0.265(2)	0.845(1)	0.09(1)
C(25)	-0.269(3)	-0.048(2)	0.911(2)	0.09(1)
C(26)	-0.448(4)	-0.330(3)	0.715(3)	0.17(2)
C(27)	-0.071(3)	-0.311(3)	0.858(2)	0.13(1)
Molecule 2				
In(2)	0.1033(2)	0.6087(2)	0.4668(2)	0.079(1)
Se(2)	-0.1108(3)	0.5314(3)	0.4306(2)	0.087(2)
C(28)	0.124(2)	0.749(1)	0.530(2)	0.08(1)
C(29)	0.079(2)	0.815(1)	0.483(2)	0.08(1)
C(30)	0.102(2)	0.910(1)	0.513(2)	0.09(1)
C(31)	0.168(2)	0.938(1)	0.591(2)	0.11(1)
C(32)	0.213(2)	0.872(1)	0.638(2)	0.11(1)
C(33)	0.190(2)	0.777(1)	0.608(2)	0.08(1)
C(34)	0.018(3)	0.788(2)	0.391(2)	0.09(1)
C(35)	0.197(3)	1.042(3)	0.623(2)	0.12(1)
C(36)	0.231(3)	0.711(3)	0.661(2)	0.13(2)
C(37)	0.192(2)	0.588(1)	0.369(1)	0.07(1)
C(38)	0.304(2)	0.591(1)	0.393(1)	0.08(1)
C(39)	0.368(2)	0.586(1)	0.333(1)	0.09(1)
C(40)	0.321(2)	0.577(1)	0.248(1)	0.10(1)
C(41)	0.209(2)	0.574(1)	0.224(1)	0.08(1)
C(42)	0.145(2)	0.579(1)	0.284(1)	0.09(1)
C(43)	0.362(3)	0.598(2)	0.477(2)	0.09(1)
C(44)	0.388(3)	0.568(3)	0.185(2)	0.14(2)
C(45)	0.029(3)	0.576(2)	0.252(2)	0.11(1)
C(46)	-0.198(2)	0.620(1)	0.457(2)	0.07(1)
C(47)	-0.187(2)	0.662(1)	0.538(2)	0.08(1)
C(48)	-0.254(2)	0.726(1)	0.553(2)	0.12(1)
C(49)	-0.332(2)	0.747(1)	0.489(2)	0.11(1)
C(50)	-0.342(2)	0.705(1)	0.408(2)	0.10(1)
C(51)	-0.275(2)	0.641(1)	0.392(2)	0.10(1)
C(52)	-0.101(2)	0.649(2)	0.610(2)	0.08(1)
C(53)	-0.402(4)	0.814(3)	0.498(3)	0.20(2)
C(54)	-0.291(3)	0.594(3)	0.310(2)	0.13(2)

$$^a U_{\text{eq}} = 1/3 \sum_i \sum_j U_{ij} a_i^* a_j^* \bar{a}_i \bar{a}_j.$$

## Results and Discussion

**Syntheses.** The methane- and benzene selenolates of sterically hindered mesitylindium **1** and **2** can be prepared at room temperature by reduction of the Se-Se bond of the dichalcogenides  $\text{R}_2\text{Se}_2$  ( $\text{R} = \text{Me}, \text{Ph}$ ) with  $\text{Mes}_2\text{In}$  in hexane. The reaction likely proceeds through formation of a weakly associated addition complex similar to that proposed for the reaction of diselenides



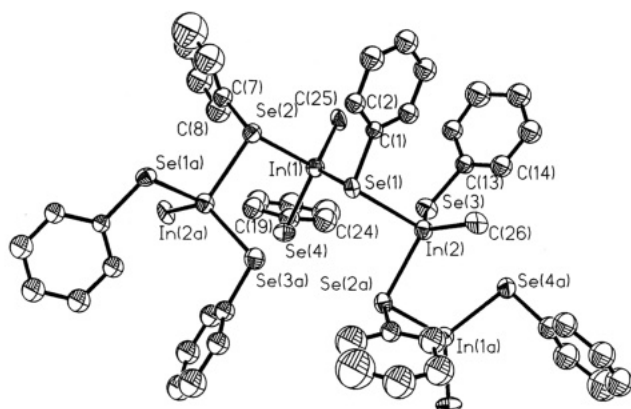


**Figure 3.** Diagram (30% thermal ellipsoids) of  $[\text{MesIn}(\text{SePh})(\mu\text{-SePh})]_{\infty}$  (**4**) showing the atom-labeling scheme. Hydrogen atoms have been omitted for clarity.

and bond angles are listed in Table 5. The gross features of the molecular structures of **2** and **3** are similar to those of related organoindium alkane- and arenethiolates and the tellurium derivatives. Efforts were also made to obtain the structure of **1**, but there were problems associated with crystal quality which could not be corrected. The data collected did indicate formation of a selenium-bridged dimer with a structure similar to those observed for **2** and **3**. The indium atoms are in a four-coordinate environment and are bonded to two mesityl groups and two bridging chalcogen atoms. The morphology of the crystals of the  $[\text{MeIn}(\text{SePh})_2]_n$  derivative initially obtained is a very thin sheet which suggests a two-dimensional layered structure. The idea of an extended array is supported by the FAB mass spectrum, which yielded fragments bound to three selenium moieties. When the compound was prepared under different conditions, the crystal morphology changed, yielding thicker, diamond-shaped crystals of **4**. These were used for the structural studies. The structure of **4** was solved in the monoclinic space group  $P2_1/n$  and has eight monomeric moieties per unit cell, arranged as a chain with alternating In and Se atoms along the screw axis. The indium is attached to one methyl unit and an uncoordinated SePh unit to complete its coordination. A packing diagram showing the arrangement of these chains in the lattice is shown in Figure 4. The spacing in these chains indicates no interaction between them. This result was unexpected because of the ease with which indium achieves higher coordination of 5 or 6 with sulfur or selenium ligands.

The In–C bond distances in the dimers range from 2.165 to 2.19 Å. In **4**, the In–C distance is slightly shorter at 2.141 Å. These distances are comparable to those found in related organoindium compounds.<sup>26,34</sup> The C–In–C angles in **2** and **3** fall into a very narrow range from 118.7 to 121.5°. The central core of the dimeric structures is composed of an  $(\text{InSe})_2$  four-membered ring which is strictly planar in **2** and **3**. A planar core is found in  $[\text{Mes}_2\text{In}(\mu\text{-Cl})_2]_2$ ,<sup>26</sup> but folded conformations are reported for  $[\text{Np}_2\text{In}(\mu\text{-SePh})_2]_2$ ,<sup>9</sup>  $\text{Np}_2\text{-In}(\mu\text{-SePh})(\mu\text{-P-}t\text{-Bu}_2)\text{InNp}_2$  (Np = neopentyl),<sup>10</sup> and  $[\text{Mes}_2\text{In}(\mu\text{-I})_2]_2$ .<sup>26</sup> The In–Se distances range from 2.705 to 2.737 Å in **2** and **3**. In **4**, three different In–Se bond distances are observed, two bridge bond distances of

2.633 and 2.726 Å and a distance of 2.541 Å for the terminal two-coordinate InSe bond. The bridge bond distances are similar to those reported for  $[\text{Np}_2\text{In}(\mu\text{-SePh})_2]_2$ <sup>9</sup> and  $\text{Np}_2\text{In}(\mu\text{-SePh})(\mu\text{-P-}t\text{-Bu}_2)\text{InNp}_2$  (Np = neopentyl)<sup>10</sup> but slightly longer than those for the bridging selenides observed in  $[\text{In}_4\text{Se}_{10}]^{8-}$  (average of 2.562 Å)<sup>35</sup> and  $[\text{In}_2\text{Se}_{21}]^{4-}$  (average of 2.67 Å) anions.<sup>36</sup> The terminal In–Se bond (2.541 Å) in **4** is shorter than the bridge bond distances but longer than the In–Se bond (2.396 Å) in  $\text{In}(\text{SeC}_6\text{H}_2\text{-}t\text{-Bu}_3\text{-}2,4,6)_3$ .<sup>37</sup> In related compounds with selenium bridging atoms, the In–Se bond distances have been reported as 2.584 Å for  $(\text{Ph}_3\text{P})_2\text{-CuIn}(\text{SeEt})_4$ ,<sup>38</sup> and 2.674 Å for  $[\{\text{Cp}(\text{CO})_2\text{Fe}\}_4\text{In}_4\text{Se}_4]$ .<sup>39</sup>

The view along the In–In axis shows that the two organic groups in **2** and **3** (Se–Se–R angles of 106 and 126.7°) are in the *anti* configuration. The bridging selenium atom has pyramidal geometry ( $\Sigma(\text{Se}) = 292.48^\circ$  (**2**), 323.7° (**3**, molecule 1), 323.1° (**3**, molecule 2)). The In–Se–In angles in **2** are substantially smaller than those found in the sterically hindered molecule **3** (96.9° (molecule 1, 98.3° molecule 2)), while the Se–In–Se angle of 90.24° in **2** is larger than the corresponding angles found in molecules 1 and 2 of **3**. In **4**, the bridging In–Se–In angles are all very similar and average 103.4°. The bridging Se atom is also in a more pyramidal configuration with the sum of the angles around it being 301.8°. The chain structure of this molecule is best seen in Figure 4, which shows the packing of the chains, and in Figure 5, which shows the core of the molecule.

**NMR Studies.** The <sup>1</sup>H and <sup>13</sup>C NMR spectral data for the complexes  $[\text{Mes}_2\text{In}(\mu\text{-SeR}')_n]$  (R = Me (**1**) Ph (**2**), Mes (**3**)) are presented in the Experimental Section. The <sup>1</sup>H resonances associated with the  $(\text{Mes})_2\text{In}$  moieties and with the SeR ligands are in appropriate integral ratios and are consistent with their formulation. Both the proton and the carbon chemical shifts of the mesityl ligands in all of the compounds are similar and are close to the values reported for related mesityl derivatives.

The presence of a planar conformation of the  $(\text{InSe})_2$  core with *anti* orientation of the bridging ligands in the structures of compounds **1–3** leads to the possibility that these derivatives may exhibit dissociation or conformation equilibria in solution. In solutions of **4**, the chain structure must be disrupted, giving rise to similar equilibria. In order to explore this possibility, we studied the effect of temperature and concentration on **3**. The resonances at 2.49 (*o*-CH<sub>3</sub>) and 2.34 (*p*-CH<sub>3</sub>) ppm are assigned to the  $(\text{Mes})_2\text{In}$  on the basis of a comparison of chemical shifts with those of a number of other mesitylindium derivatives<sup>4,6,34</sup> and with those of  $\text{Mes}_3\text{In}$ ,<sup>26</sup> in which the *para* methyl group chemical shift is in the range 2.02–2.17 ppm and the *ortho* methyl group is in the range of 2.34–2.73 ppm. The MesSe moiety has resonances at 1.98 (*o*-CH<sub>3</sub>) and 1.80 (*p*-CH<sub>3</sub>) ppm, assigned on the basis of their relative intensities. All of the resonances are reasonably sharp, indicating a single magnetic environment for each of the groups. The chemical shift of the *o*-methyl groups on

(35) Krebs, B.; Voelker, D.; Stiller, K.-O. *Inorg. Chim. Acta* **1982**, *65*, L101.

(36) Kanatzidis, M. G.; Dhingra, S. *Inorg. Chem.* **1989**, *28*, 2024.

(37) Ruhlandt-Senge, K.; Power, P. P. *Inorg. Chem.* **1993**, *32*, 3478.

(38) Hirpo, W.; Dhingra, S.; Sutorik, A. C.; Kanatzidis, M. G. *J. Am. Chem. Soc.* **1993**, *115*, 1597.

(39) Serzweiler, K.; Rudolph, F.; Brands, L. *Z. Naturforsch.* **1992**, *49B*, 470.

(34) Leman, J. T.; Ziller, J. W.; Barron, A. R. *Organometallics* **1991**, *10*, 1766.

**Table 5. Selected Bond Distances (Å) and Bond Angles (deg) for [Mes<sub>2</sub>In(μ-SePh)]<sub>2</sub> (2), [Mes<sub>2</sub>In(μ-SeMes)]<sub>2</sub> (3), and [MeIn(μ-SePh)(SePh)]<sub>∞</sub> (4)**

atoms	values for 2 and 3			values for 4	
	2	molecule 1	molecule 2	atoms	
Bond Distances					
In(1)··In(1)'	3.857(1)	4.067(3)	4.109(3)	2.640(3)	In(1)–Se(1) (b) <sup>a</sup>
In(1)–Se(1)	2.7272(7)	2.705(3)	2.717(4)	2.737(4)	In(1)–Se(2) (b)
In(1)–Se(1)'	2.7369(8)	2.728(3)	2.717(4)	2.541(4)	In(1)–Se(4) (t) <sup>a</sup>
				2.726(4)	In(2)–Se(1) (b)
				2.633(4)	In(2)–Se(2A) (b)
				2.542(3)	In(2)–Se(3) (t)
				2.141(26)	In(1)–C(25)
In(1)–C(1)	2.165(4)	2.16(2)	2.18(1)		
In(1)–C(10)	2.171(4)	2.19(2)	2.16(2)		
Bond Angles					
Se(1)–In(1)–Se(1)'	90.24(2)	83.1(1)	81.7(1)	83.7(1)	Se(1)–In(1)–Se(2) (b)
In(1)–Se(1)–In(1)'	89.75(2)	96.9(1)	98.3(1)	93.6(1)	Se(1)–In(2)–Se(2A) (b)
In(1)–Se(1)–C	97.64(12)	117.5(5)	114.1(8)	102.7(1)	In(1)–Se(1)–In(2) (b)
In(1)–Se(1)–C	105.09(14)	109.3(6)	110.7(6)	94.2(1)	In(1)–Se(2)–In(2A) (b)
				107.2(1)	Se(1)–In(1)–Se(4) (t)
				104.9(1)	Se(2)–In(1)–Se(4) (t)
				104.3(1)	Se(1)–In(2)–Se(3) (t)
				101.2(1)	Se(3)–In(2)–Se(2A) (t)
Cl–In1–C10	121.49(14)	120.7(6)	118.7(7)		
Σ of angles at Se	292.48	323.7	323.1	301.8	

<sup>a</sup> Legend: b = bridging selenium atom; t = terminal selenium atom.

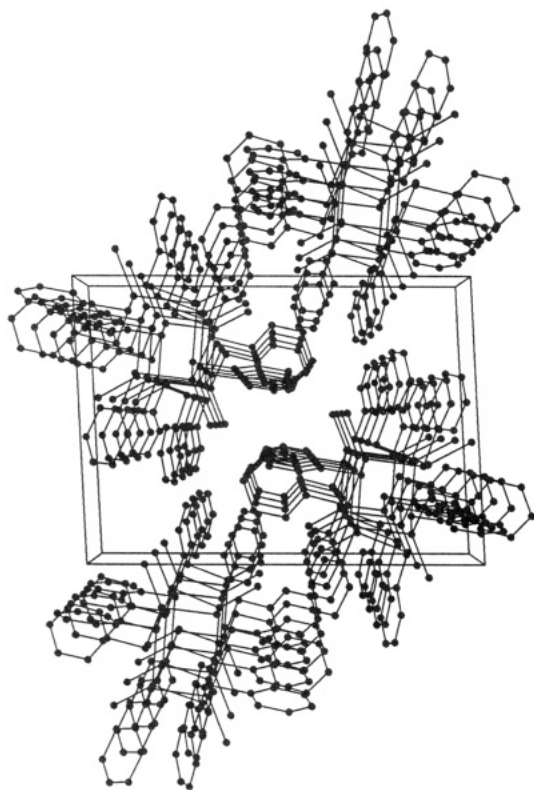


**Figure 4.** Packing diagram for 4 viewed along the z axis showing the arrangement of the chains in the lattice.

the Mes<sub>2</sub>In moiety was temperature dependent, shifting from 2.62 to 2.31 ppm over the range –85 to +105 °C. A small shift from 1.65 to 1.87 ppm also was observed for the *p*-methyl group on the SeMes moiety over this temperature range. The other chemical shifts remained invariant with temperature. It was observed that the *o*-methyl groups of mesityl moieties bound to indium and to selenium are broadened with increasing temperature. This was not explored further but is likely associated with rotational rates of the mesityl groups. We also studied the concentration dependence of the

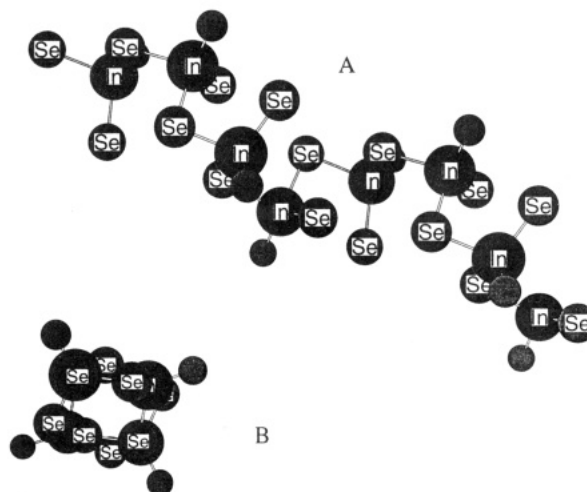


**Figure 5.** Diagrams of 4 showing the backbone of the chain: (A) view showing the chain perpendicular to the screw axis; (B) view of the chain down the screw axis. The phenyl groups have been omitted.

NMR spectra and found no effect over a 7-fold concentration range.

The <sup>77</sup>Se NMR spectra of the complexes show a single magnetic environment for the selenium atom in 1–3, but no <sup>77</sup>Se resonance was observed for 4. Failure to observe a <sup>77</sup>Se signal for 4 may be the result of exchange-broadened lines, but this was not established. The observed chemical shifts of –123 ppm for 1, –160 ppm for 2, and –56 ppm for 3 fall into the broad range observed for organometallic selenolates<sup>40</sup> and fall close to the values observed for the few group 13 selenolates reported. For example, in [(*t*-Bu)<sub>2</sub>Ga(μ-Se-*t*-Bu)]<sub>2</sub>, the δ value is 156 ppm,<sup>23</sup> in (*t*-BuGa-μ<sub>3</sub>Se)<sub>4</sub>, the values are δ –226.7 and –231.7 ppm,<sup>23</sup> and in a series of aluminum derivatives with SeR bridging groups, the range is from δ –247 to 372 ppm.<sup>33</sup>

(40) McFarlane, H. C. E.; McFarlane, W. In *NMR of Newly Accessible Nuclei*; Laszlo, P., Ed.; Academic Press: New York, 1983; Vol. 2, pp 275–99.

### Conclusion

The dimesitylindium selenolates have been prepared by the reaction of  $\text{Mes}_3\text{In}$  with dichalcogenides,  $\text{R}_2\text{Se}_2$ , under mild conditions. This synthetic route provides an alternative method to obtain these complexes, especially in those cases where the protic substrates,  $\text{RSeH}$ , are unstable. These derivatives are dimeric in the solid state. The pyramidalty decreases with increasing steric size of the ligand at the bridging selenium atom. This structural feature is in contrast to those of the oxygen-bridged structures, which generally adopt a planar configuration. The central ring is strictly planar with a *trans* orientation of the bridging ligands for **2** and **3**. With the structural data available, it is very difficult to make any prediction about the conformation of the core. It seems reasonable to state that the packing forces in the crystals may be partially responsible in determining the core geometry. Such homoleptic systems may serve as molecular precursors to  $\text{In}_x\text{Se}_y$  films by OMCVD.

The most surprising feature observed is in **4** where only one of the two selenium atoms is involved in bridge bond formation. It was anticipated that the second selenium group would coordinate to the indium atoms, forming a two- or three-dimensional lattice with five- or six-coordinate indium present. At this time we have no explanation for this unexpected behavior, but it seems unlikely that steric interactions play any significant role because of the small size of the methyl group.

**Acknowledgment** is made to the donors of the Petroleum Research Fund, administered by the American Chemical Society, for support of this research.

**Supporting Information Available:** Complete listings of experimental parameters for the X-ray study, bond distances and bond angles, anisotropic thermal parameters for the heavy atoms, and hydrogen atom positional parameters for **2-4** (16 pages). Ordering information is given on any current masthead page.

OM9501889



# Flow Reactors for Preparative Chemistry in Supercritical Fluid Solution: “Solvent-Free” Synthesis and Isolation of $\text{Cr}(\text{CO})_5(\text{C}_2\text{H}_4)$ and $(\eta^5\text{-C}_5\text{H}_5)\text{Mn}(\text{CO})_2(\eta^2\text{-H}_2)$

James A. Banister, Peter D. Lee, and Martyn Poliakoff\*

Department of Chemistry, University of Nottingham, Nottingham, England NG7 2RD

Received May 24, 1995<sup>®</sup>

We describe the use of supercritical flow reactors as a new but relatively straightforward approach to carrying out reaction chemistry in high-pressure fluids (<350 bar). Two photochemical flow reactors are described in detail, one reactor for the synthesis of  $\text{Cr}(\text{CO})_5(\text{C}_2\text{H}_4)$  from the reaction of  $\text{Cr}(\text{CO})_6$  with supercritical  $\text{C}_2\text{H}_4$  (sc $\text{C}_2\text{H}_4$ ), the other reactor for the generation of  $\text{CpMn}(\text{CO})_2(\eta^2\text{-H}_2)$  from  $\text{CpMn}(\text{CO})_3$  and  $\text{H}_2$  in supercritical  $\text{CO}_2$  (sc $\text{CO}_2$ ). Both compounds are isolated by rapid expansion of the supercritical solution. This is the first time that either compound has been isolated as a solid, and both are found to be not nearly as labile as had been anticipated. Indeed,  $\text{CpMn}(\text{CO})_2(\eta^2\text{-H}_2)$  is one of the simplest dihydrogen compounds so far to have been isolated, yet it is one of the more robust compounds, taking 2 h to react with moderately high pressures of  $\text{CO}$  or  $\text{C}_2\text{H}_4$ . Other reactions involving sc $\text{C}_2\text{H}_6$  as the fluid or  $\text{N}_2$  as the reactant (e.g., to form  $\text{CpMn}(\text{CO})_2\text{N}_2$ ) are described briefly. So far, the reactions have been carried out on a modest scale, ca. 20–40 mg per h, but this is more a limitation of the photochemistry rather than of the reactors themselves. All reactions are carried out without the use of any conventional organic solvents.

## Introduction

There has been an upsurge of interest in the use of supercritical fluids as media for reaction chemistry.<sup>1,2</sup> This interest has been stimulated in part by the possibility of using these fluids, particularly supercritical  $\text{CO}_2$  (sc $\text{CO}_2$ ), as environmentally acceptable substitutes for organic solvents. Equally important has been the promise of chemical results which would be difficult or even impossible to achieve by more conventional routes. Successful examples have included controlling the product distribution in the dimerization of isophorone,<sup>3</sup> the synthesis<sup>4</sup> of the tris(dinitrogen) complex,  $\text{CpRe}(\text{N}_2)_3$ , and the reaction<sup>5a</sup> of hex-3-yne with sc $\text{CO}_2$ . Nevertheless, whatever the attractions of supercritical fluids, the prospect of handling these high-pressure fluids has been quite discouraging for nonspecialist chemists. This paper describes how such reactions can be carried out relatively simply in miniature flow reactors.

Although synthetic chemists rarely use the term “batch processing,” most laboratory-scale synthetic chemistry involves batch reactions in flasks, Schlenk tubes, or similar containers. Given a suitable autoclave, a supercritical reaction can also be carried out as a batch process, but there are a number of problems not normally encountered in conventional solvents. For example, dissolving any solute in a fluid alters the critical temperature of that fluid, and, in general, each solute has a different effect.<sup>1</sup> The critical temperature is important because properties such as solvent power, dielectric constant, etc. are most easily tuned close to the critical point. Thus, in many experiments, it is crucial to maintain the reaction temperature close to critical. However, this can be difficult with a closed batch reactor because the critical temperature of the reaction mixture may change significantly as reactants are converted into products. More prosaic, but equally important, is the fact that small autoclaves can hold only small amounts of material, while large autoclaves filled with high-pressure fluids have considerable safety constraints associated with them.

Many of these difficulties are avoided by use of a flow reactor, in which the reaction is carried out as a continuous process and a significant throughput is achieved even though the total volume of the high-pressure system is small.<sup>6</sup> Scale-up of the reactor is less important than in a batch process because, within limits, a larger quantity of product can be obtained merely by running the flow reactor for a longer time. Furthermore, reaction conditions are much easier to control than in a batch reactor because the composition of the fluid at any particular point is constant as a

\* E-mail: Martyn.Poliakoff@Nottingham.ac.uk.

<sup>®</sup> Abstract published in *Advance ACS Abstracts*, July 1, 1995.

(1) For an excellent general introduction to supercritical fluids, see: McHugh, M. A.; Krukonis, V. J. *Supercritical Fluid Extraction: Principles and Practice*, 2nd ed.; Butterworth-Heinemann: Boston, 1994.

(2) For a recent review of reactions in supercritical fluids, see: Savage, P. E.; Gopalan, S.; Mizan, T. I.; Martino, C. J.; Brock, E. E. *Am. Inst. Chem. Eng. J.*, in press.

(3) Hrnjez, B. J.; Mehta, A. J.; Fox, M. A.; Johnston, K. P. *J. Am. Chem. Soc.* **1989**, *111*, 2662.

(4) (a) Howdle, S. M.; Grebenik, P.; Perutz, R. N.; Poliakoff, M. J. *Chem. Soc., Chem. Commun.* **1989**, 1517. (b) Howdle, S. M.; Healy, M. A.; Poliakoff, M. *J. Am. Chem. Soc.* **1990**, *112*, 4804.

(5) (a) Reetz, M. T.; Konen, W.; Strack, T. *Chimia* **1993**, *47*, 493.

(b) In a recent lecture, it was suggested that this reaction might have occurred as a multiphase reaction (i.e., between  $\text{CO}_2$  and catalyst, both dissolved in liquid hexyne) and not in sc $\text{CO}_2$ ; Dinjus, E. COST/Dechema Workshop, Lahnstein, Germany, April 1995.

(6) Tundo, P. *Continuous Flow Methods in Organic Synthesis*; Ellis Horwood: Chichester, U.K., 1991.

function of time. Most crucially, spectroscopic monitoring of the fluid can be used for optimization of the reaction conditions in *real time*.<sup>7</sup> In this paper, we give two examples of how such a reactor can be realized in practice. We describe the isolation of two organometallic compounds,  $\text{Cr}(\text{CO})_5(\text{C}_2\text{H}_4)$  and  $\text{CpMn}(\text{CO})_2(\eta^2\text{-H}_2)$ , both of which were previously believed to be too labile for isolation.

$\text{Cr}(\text{CO})_5(\text{C}_2\text{H}_4)$  is structurally the simplest  $d^6$  metal-alkene/carbonyl compound but has long been considered to be highly labile. Although  $\text{W}(\text{CO})_5(\text{C}_2\text{H}_4)$  has been known for many years,<sup>8</sup>  $\text{Cr}(\text{CO})_5(\text{C}_2\text{H}_4)$  was first identified (by IR spectroscopy) only quite recently, during the photolysis of  $\text{Cr}(\text{CO})_6$  in cryogenic liquid Xe solution.<sup>9</sup> Formation of *cis*-, and *trans*- $\text{Cr}(\text{CO})_4(\text{C}_2\text{H}_4)_2$  was also observed during this reaction, and shortly afterward Grevels and co-workers succeeded in isolating the *trans* isomer following the low-temperature photolysis of  $\text{Cr}(\text{CO})_6$  and  $\text{C}_2\text{H}_4$  in hydrocarbon solution.<sup>10</sup> Although Grevels et al. had also managed to isolate the closely related mono-olefin complex,  $\text{Cr}(\text{CO})_5(\text{cis-cyclohexene})$ ,<sup>11</sup>  $\text{Cr}(\text{CO})_5(\text{C}_2\text{H}_4)$  defied attempts to be isolated from alkane solution. Photochemical experiments in the gas phase confirmed that  $\text{Cr}(\text{CO})_5(\text{C}_2\text{H}_4)$  was also thermally labile under these conditions.<sup>12</sup> Indeed, Weitz and co-workers have exploited this lability<sup>13</sup> to obtain an estimate of the  $(\text{CO})_5\text{Cr}-(\text{C}_2\text{H}_4)$  bond dissociation energy,  $103 \pm 10 \text{ kJ mol}^{-1}$ . We recently published a preliminary report<sup>14</sup> of how  $\text{Cr}(\text{CO})_5(\text{C}_2\text{H}_4)$  can be isolated from supercritical  $\text{C}_2\text{H}_4$  ( $\text{scC}_2\text{H}_4$ ) at room temperature, and here we describe the procedure in full detail.

$\text{CpMn}(\text{CO})_2\text{H}_2$  was first detected by Leong and Cooper<sup>15</sup> at the end of a multistep route involving the dianion  $[\text{CpMn}(\text{CO})_2]^{2-}$ . However, like  $\text{Cr}(\text{CO})_5(\text{C}_2\text{H}_4)$ ,  $\text{CpMn}(\text{CO})_2\text{H}_2$  could not be isolated from the solvent (THF) in which it was prepared. Subsequently, the compound was generated in supercritical Xe ( $\text{scXe}$ ) solution<sup>4b,16</sup> by photolysis of  $\text{CpMn}(\text{CO})_3$  in the presence of  $\text{H}_2$ . The wavenumbers of its  $\nu(\text{C}-\text{O})$  bands and the ease with which the coordinated  $\text{H}_2$  was displaced by  $\text{N}_2$  led to the reformulation of the compound as the "non-classical" dihydrogen compound<sup>17</sup>  $\text{CpMn}(\text{CO})_2(\eta^2\text{-H}_2)$ . Isolation of pure  $\text{CpMn}(\text{CO})_2(\eta^2\text{-H}_2)$  is an important goal because structurally it is considerably simpler than most of the known dihydrogen compounds. Thus, both  $\text{Cr}(\text{CO})_5(\text{C}_2\text{H}_4)$  and  $\text{CpMn}(\text{CO})_2(\eta^2\text{-H}_2)$  are examples of a wider class of transition metal complexes with ligands

(i.e.,  $\text{C}_2\text{H}_4$  and  $\text{H}_2$ ) weakly bound to the metal. Such compounds are often quite simple to generate photochemically in solution, but they are extremely difficult to isolate as solids. The problems are both practical and psychological. Removal of the solvent usually leads to removal of the labile ligand as well, and the belief that such compounds are unstable often discourages further attempts at isolation.

In the following sections, we explain how these compounds can be generated in supercritical solution and how both of them can be isolated as solid compounds for the first time. First, we outline the general principles of our approach and describe the key components that are required. Then, we show how the method works in practice and describe very briefly some of the reactions, which can be obtained after  $\text{CpMn}(\text{CO})_2(\eta^2\text{-H}_2)$  has been isolated. Finally, the Experimental Section lists the precise experimental parameters, pressure, flow rates, etc., needed for the preparations. *It is important, even at this stage, to stress that the method is potentially far more general than the specific photochemical reactions described in this paper.* A broadly similar approach could be applied to a wide range of thermal and photochemical reactions in both inorganic and organic chemistry.

## Results

**Principles of the Flow Reactors.** Preliminary IR experiments in a miniature static cell with  $<1 \text{ mg}$  organometallic precursor have shown that both  $\text{Cr}(\text{CO})_5(\text{C}_2\text{H}_4)$  and  $\text{CpMn}(\text{CO})_2(\eta^2\text{-H}_2)$  can be generated in supercritical solution ( $\text{scC}_2\text{H}_4$ <sup>18</sup> and  $\text{scXe}$ ,<sup>16</sup> respectively), see eqs 1 and 2. Once formed, both compounds are stable in supercritical solution for several hours at room temperature. The problem is how to scale these reactions up and isolate the products.

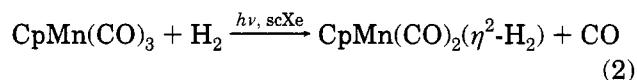
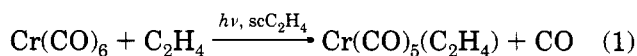


Figure 1 shows, very schematically, the flow reactors<sup>19</sup> used to prepare (a)  $\text{Cr}(\text{CO})_5(\text{C}_2\text{H}_4)$  and (b)  $\text{CpMn}(\text{CO})_2(\eta^2\text{-H}_2)$ . The two reactors are broadly similar; the principal difference is that  $\text{scC}_2\text{H}_4$  is both reactant and solvent for the synthesis of  $\text{Cr}(\text{CO})_5(\text{C}_2\text{H}_4)$  while the preparation of  $\text{CpMn}(\text{CO})_2(\eta^2\text{-H}_2)$  requires both a reactant,  $\text{H}_2$ , and a solvent,  $\text{scCO}_2$  (the original solvent<sup>16</sup>  $\text{scXe}$  is too expensive to be used in a flow reactor). In both cases, the organometallic reactant is a solid at room temperature and has to be dissolved into the flowing stream of supercritical fluid, although, as shown later, the methods of dissolving the two compounds differ in detail. The dissolved precursor then passes through a UV irradiation cell where the product,  $\text{Cr}(\text{CO})_5(\text{C}_2\text{H}_4)$  or  $\text{CpMn}(\text{CO})_2(\eta^2\text{-H}_2)$ , is generated. The high concentration of free  $\text{C}_2\text{H}_4$  or  $\text{H}_2$  in the solution minimizes any

(7) For reviews of vibrational spectroscopy in supercritical solution, see: (a) Buback, M. *Angew. Chem., Int. Ed. Engl.* **1991**, *30*, 641. (b) Poliakov, M.; Kazarian, S. G.; Howdle, S. M. *Angew. Chem., Int. Ed. Engl.*, in press.

(8) Stolz, I. W.; Dobson, G. R.; Sheline, R. K. *Inorg. Chem.* **1963**, *2*, 1264.

(9) Gregory, M. F.; Jackson, S. A.; Poliakov, M.; Turner, J. J., *J. Chem. Soc., Chem. Commun.* **1986**, 1175.

(10) Grevels, F.-W.; Jacke, J.; Özkar, S. *J. Am. Chem. Soc.* **1987**, *109*, 7536.

(11) Grevels, F.-W.; Skibbe, V. *J. Chem. Soc., Chem. Commun.* **1984**, 681.

(12) Weiller, B. H.; Grant, E. R. *J. Am. Chem. Soc.* **1987**, *109*, 1252.

(13) Wells, J. R.; House, P. G.; Weitz, E. *J. Phys. Chem.* **1994**, *98*, 8343.

(14) Banister, J. A.; Howdle, S. M.; Poliakov, M. *J. Chem. Soc., Chem. Commun.* **1993**, 1814.

(15) Leong, V. S.; Cooper, N. J. *Organometallics* **1988**, *7*, 2080.

(16) Howdle, S. M.; Poliakov, M. *J. Chem. Soc., Chem. Commun.* **1989**, 1099.

(17) For excellent reviews on dihydrogen complexes see: Jessop, P. G.; Morris, R. H. *Coord. Chem. Rev.* **1992**, *121*, 155. On hydrides: *Transition Metal Hydrides*; Ed. Dedieu, A., Ed.; VCH Publishers, Inc.: New York, 1992.

(18) Howdle, S. M.; Jobling, M.; Poliakov, M. *Supercritical Fluid Technology: Theoretical and Applied Approaches in Analytical Chemistry*; Bright, F. V., McNally, M. E., Eds.; ACS Symposium Series 488; American Chemical Society: Washington, DC, 1992; p 121.

(19) Preliminary reports of these reactors have been made in ref 14 and in the following: Poliakov, M.; Banister, J. A.; Lee, P. D.; Howdle, S. M. Proceedings of the 26th International Conference on Organometallic Chemistry, Brighton, U.K., July 1994; Abstract No. O14.



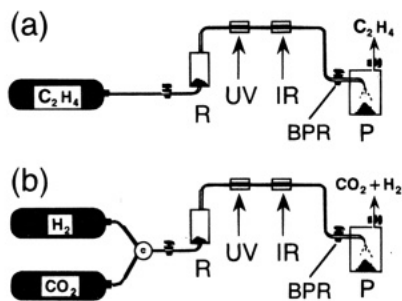


**Figure 1.** Schematic diagrams of flow reactors for the supercritical synthesis of (a)  $\text{Cr}(\text{CO})_5(\text{C}_2\text{H}_4)$  in  $\text{scC}_2\text{H}_4$  and (b)  $\text{CpMn}(\text{CO})_2(\eta^2\text{-H}_2)$  in an  $\text{scCO}_2/\text{H}_2$  mixture. The components of the two reactors are labeled as follows (from left to right): R, reservoir of solid reactant,  $\text{Cr}(\text{CO})_6$  or  $\text{CpMn}(\text{CO})_3$ ; UV, cell for photochemical reaction; IR, spectroscopic cell for monitoring the reaction; BPR, back-pressure regulator for reducing the pressure and precipitating the product; P, solid product,  $\text{Cr}(\text{CO})_5(\text{C}_2\text{H}_4)$  or  $\text{CpMn}(\text{CO})_2(\eta^2\text{-H}_2)$ . The full layouts of these reactors are shown in Figures 5 and 7, respectively.

decomposition of the product right up to the moment when the product reaches the back-pressure regulator (BPR in the figures), where it is isolated.

The key factor in the isolation of both compounds is the fact that solid materials can be precipitated extremely rapidly from supercritical fluid solution by a reduction in pressure. As the pressure is released, the fluid expands, solubility in the fluid decreases dramatically, and solutes are precipitated as finely divided powders, somewhat cooled below ambient temperature by the Joule–Thompson expansion of the gas. This so-called RESS process (rapid expansion of supercritical solution) has already been used as a route to finely divided materials,<sup>1</sup> but this is its first application to the isolation of labile compounds. RESS precipitation is not only more rapid than conventional methods of separating solute and solvent, e.g., rotary evaporation, but it also minimizes the chances of labile ligands being lost from the metal during precipitation.

Our aims, while developing these flow reactors, have been to keep the total volume to an absolute minimum on grounds of safety and to use commercially available equipment wherever possible, for simplicity. It can be seen from Figure 1 that there are three key components: (i) the UV photolysis cell, which must have high efficiency to minimize the amount of unaltered reactant passing through the system and contaminating the product; (ii) the IR cell for monitoring the reaction mixture and hence for optimizing the reaction conditions; and (iii) the back-pressure regulator, which not only maintains the pressure of the fluid but also controls the RESS precipitation of the product. In the next section, we discuss these three components further. Details of the other components of the reactors are given in the figure captions and in the Experimental Section at the end of the paper.

**Key Components. (a) Cells for IR Spectroscopy and for UV Photolysis.** We have previously described the miniature high-pressure spectroscopic cell, developed at Nottingham<sup>7b,20</sup> and illustrated in Figure 2a. This stainless steel cell has two  $\text{CaF}_2$  windows and two ports, and, although originally designed as a static cell, it can equally be used to monitor a flowing stream of fluid. Furthermore, the cell has a very low internal

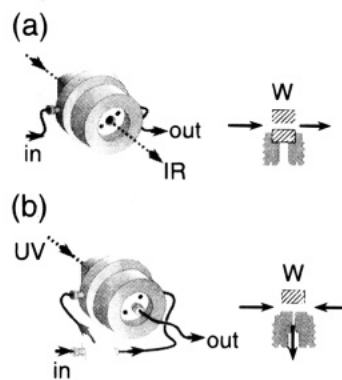


**Figure 2.** High-pressure flow cells for (a) IR spectroscopic monitoring of reaction mixture and for (b) UV irradiation to induce chemical reactions. For both cells, the smaller picture (on the right) shows more detail of the threaded inserts which carry (a) the second spectroscopic  $\text{CaF}_2$  window and (b) the outflow pipe for the reactant mixture. The figure is not drawn precisely to scale, nor are the general and detailed views on the same scale. The windows, W, are 15 mm in diameter, 10 mm thick, and have an unsupported diameter of 7 mm. The arrows indicate the direction of the fluid flow through the cell.

volume once it has been stripped of the valves, pressure gauge, etc. needed for stand-alone operation.

The same spectroscopic cell can also be used as a flow cell for UV irradiation, but it is rather inefficient because some of the fluid can flow through the cell without passing through the illuminated volume of the cell. A much more effective variant is shown in Figure 2b, where one of the windows has been replaced by a solid insert containing an extra port. With this third port fitted, all of the fluid necessarily flows through the illuminated zone in front of the remaining window, just before leaving the cell.<sup>21</sup> This ensures that photolysis is efficient but that the effects of secondary photolysis are minimized. Furthermore, by using all three ports, stagnation within the cell is minimized and the residence time is determined largely by the flow rate of the fluid.

**(b) Back-Pressure Regulation and Product Recovery.** Commercial back-pressure regulators (BPR) are generally of two types, electronically-controlled or mechanical. In a BPR, electronic control typically involves the use of a pressure transducer to control a solenoid or similar valve. In such a system, the pressure maintained in the system is more or less independent of the flow rate of the fluid through the system. By contrast, a mechanical BPR is fundamentally a sophisticated pressure relief valve, adjusted, for example, by altering the compression of a spring. Usually, the pressure maintained for a given setting of such a mechanical BPR depends at least partly on the flow rate; the greater the flow rate of the fluid, the higher

(20) (a) Poliakoff, M.; Howdle, S. M.; Healy, M. A.; Whalley, J. M. In *Proceedings of the International Symposium on Supercritical Fluids*, Nice, France, 1988; Perrut, M., Ed.; Societe Francaise de Chimie: Paris, 1988; p 967. (b) Howdle, S. M.; Poliakoff, M. In *Supercritical Fluids: Fundamentals for Applications*; Kiran, E., Levelt Sengers, J. M. H., Eds. NATO ASI Series E 273; Kluwer Academic Publications: Dordrecht, 1994; 527.

(21) A similar approach, replacing the window of a high-pressure cell with a port, has been used to modify a spectroscopic cell for use as a laser irradiation cell in a somewhat larger-scale high-pressure flow system for continuous free-radical polymerization. Brackermann, H.; Buback, M. *Makromol. Chem., Rapid Commun.* **1989**, *10*, 283.

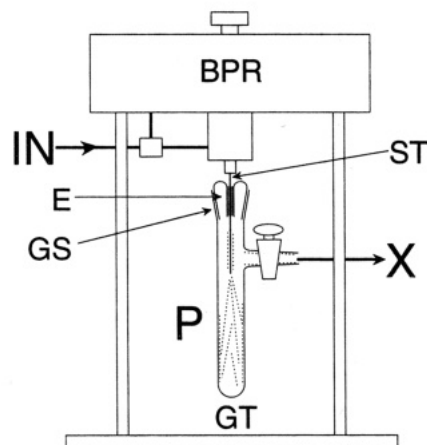


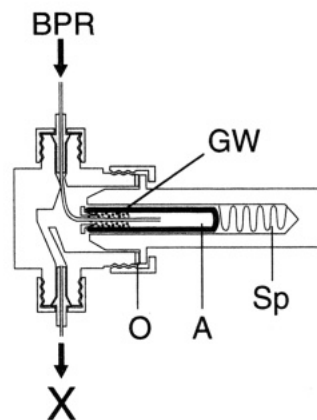
**Figure 3.** View of the back pressure regulator (Jasco Model 880-81) labeled BPR, as used in our flow reactors. In this figure, the BPR is fitted with a glass tube, GT, for collection of the solid product, P. The other parts are labeled as follows: IN, inlet pipe from the flow reactor; E, epoxy resin seal; ST, stainless steel tube; GS, ground glass stopper; X, exhaust for waste gases. Note that the operator is protected for accidental shattering of the glass by polycarbonate sheets (not illustrated) which form an enclosure around the sides of the frame, supporting the back-pressure regulator.

the pressure. We have chosen to use an electronic BPR (Jasco Model 880-81) in our flow reactors so that the pressure and the flow rate can be controlled independently. This is important because higher pressures increase solubility of the organometallics in the fluid while higher flow rates reduce the residence time in the photolysis cell.

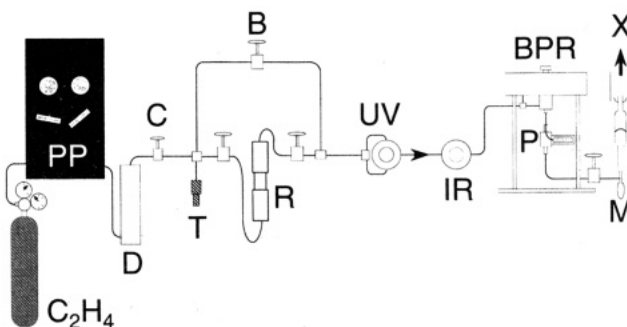
RESS precipitation generates extremely finely divided particles with relatively high velocities.<sup>1</sup> Compounds such as  $\text{Cr}(\text{CO})_5(\text{C}_2\text{H}_4)$  are quite toxic, and so care must be taken to collect the reaction product efficiently and more or less anaerobically. At the same time, the operator must be protected in the event of the collection vessel being inadvertently pressurized, for example, by a blockage in the downstream pipework. A simple recovery method is shown in Figure 3, in which the product is collected in a modified Schlenk tube and high-pressure protection is provided by polycarbonate (Lexan) sheets. This vessel, which was used in the isolation of  $\text{CpMn}(\text{CO})_2(\eta^2\text{-H}_2)$ , is easily adaptable to accommodate, for example, an NMR tube on the side of the tube.

Figure 4 shows a more sophisticated design, which was used in the isolation of  $\text{Cr}(\text{CO})_5(\text{C}_2\text{H}_4)$ . It comprises a glass collection ampule mounted inside a high-pressure holder which is constructed from the body of a surplus high-pressure valve. The efficiency of this design was tested in a simple experiment with  $\text{W}(\text{CO})_6$ ; it was found that 95% of the mass of  $\text{W}(\text{CO})_6$  placed in a high-pressure cell could be recovered by RESS using this collection vessel.<sup>22</sup>

**Isolation of  $\text{Cr}(\text{CO})_5(\text{C}_2\text{H}_4)$ .** Figure 1a gave a schematic outline of the flow reactor for generating and isolating  $\text{Cr}(\text{CO})_5(\text{C}_2\text{H}_4)$ , and the layout is shown in greater detail in Figure 5.  $\text{Cr}(\text{CO})_6$  is remarkably soluble<sup>18</sup> in  $\text{scC}_2\text{H}_4$ , and the principal problem is one of controlling the concentration of  $\text{Cr}(\text{CO})_6$  dissolved in the



**Figure 4.** View of a stainless steel vessel for attachment to the back-pressure regulator (BPR, see Figure 3) to collect solid product from the flow reactor. The parts are labeled as follows: A, glass ampule; GW, glass wool; O, PTFE O-ring; Sp, steel spring; X, exhaust for waste gases.



**Figure 5.** Layout of the flow reactor used for the photochemical generation and subsequent isolation of  $\text{Cr}(\text{CO})_5(\text{C}_2\text{H}_4)$  from  $\text{Cr}(\text{CO})_6$  in  $\text{scC}_2\text{H}_4$ . The components are labeled as follows (alphabetically): B, bypass valve; BPR, back-pressure regulator (Jasco Model 880-81); C, control valve;  $\text{C}_2\text{H}_4$ , ethene cylinder; D, 40 mL dead volume to dampen pressure fluctuations from the fluid pump; IR, infrared cell (see Figure 2a); M, soap-film flow meter; P, solid product,  $\text{Cr}(\text{CO})_5(\text{C}_2\text{H}_4)$  collected in the vessel shown in Figure 4; PP, pneumatic pump (NWA Model PM101); R, extraction vessel (Keystone 65503) containing the solid reactant,  $\text{Cr}(\text{CO})_6$ ; T, pressure transducer (RDP Electronics); UV, photolysis cell (see Figure 2b); X, exhaust vent. (Note that this figure is not drawn to scale.)

fluid. Control is necessary because too great a concentration of  $\text{Cr}(\text{CO})_6$  could result in inefficient photolysis. In this reactor, we have achieved the necessary control merely by adjusting the pressure and the flow rate of  $\text{scC}_2\text{H}_4$  through the extraction vessel containing  $\text{Cr}(\text{CO})_6$ . The concentration is monitored via IR at ca.  $4000\text{ cm}^{-1}$ , a region corresponding to the  $\nu(\text{C}-\text{O})$  combination bands of metal carbonyls, because absorptions of  $\text{scC}_2\text{H}_4$  almost completely mask the region (ca.  $2000\text{ cm}^{-1}$ ) in which the fundamental  $\nu(\text{C}-\text{O})$  absorptions occur.<sup>18</sup>

Although combination spectra are somewhat more complicated to interpret, use of the  $4000\text{ cm}^{-1}$  region has distinct advantages for this experiment because molar extinction coefficients are lower and, therefore,

(22) Buback and co-workers has exploited such differences in extinction coefficient to achieve extremely wide dynamic ranges for IR monitoring of reactions under high pressure.<sup>7a</sup> Monitoring the flow reactor in a spectroscopic region in which the fluid itself has little or no absorption has an additional benefit, namely, that the pressure of the fluid can be altered without significant changes in the "baseline" of the spectra.

(22) For additional details of this experiment and, more generally, of the development of these flow reactors, see: Banister, J. A. Ph.D. Thesis, University of Nottingham, Nottingham, U.K., 1994.

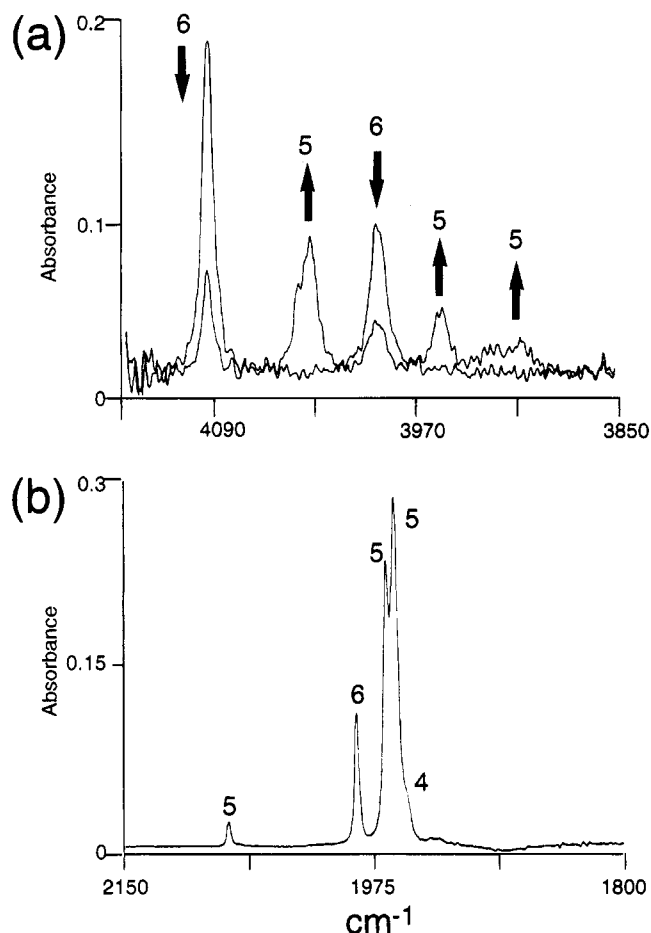


**Figure 6.** IR spectra illustrating the generation of  $\text{Cr}(\text{CO})_5(\text{C}_2\text{H}_4)$ : (a) two superimposed traces recorded in  $\text{scC}_2\text{H}_4$  prior to and during UV irradiation in the flow reactor (see Figure 5). Irradiation causes a decrease in the bands of  $\text{Cr}(\text{CO})_6$  labeled 6 and a corresponding growth in the bands labeled 5, assigned to  $\text{Cr}(\text{CO})_5(\text{C}_2\text{H}_4)$ , see Table 1. (b) IR spectrum of the solid product redissolved in  $n$ -heptane saturated with  $\text{C}_2\text{H}_4$  at room temperature. The bands are assigned to  $\text{Cr}(\text{CO})_6$ , 6,  $\text{Cr}(\text{CO})_5(\text{C}_2\text{H}_4)$ , 5, and  $\text{trans-Cr}(\text{CO})_4(\text{C}_2\text{H}_4)_2$ , 4. As explained previously,<sup>14</sup> the splitting of the strongest band labeled 5 indicates that  $\text{Cr}(\text{CO})_5(\text{C}_2\text{H}_4)$  has the  $\text{C}_2\text{H}_4$  group aligned parallel to one pair of CO groups as in structure 1,<sup>41</sup> in a way similar to that found crystallographically<sup>10</sup> for  $\text{trans-Cr}(\text{CO})_4(\text{C}_2\text{H}_4)_2$ , structure 2.

high concentrations of dissolved  $\text{Cr}(\text{CO})_6$  can be monitored with a cell of given optical pathlength.<sup>23</sup> Figure 6a illustrates spectra obtained in this region with our flow reactor. When the UV light is switched on, the two bands of  $\text{Cr}(\text{CO})_6$  drop substantially in intensity and at least three new bands are observed. Only a short time is required for a steady state to be established, and then the spectra remain almost unchanged as long as the UV irradiation is continued. During this time, a pale yellow and somewhat air-sensitive solid can be collected in the vessel attached to the back-pressure regulator. (Non-irradiated  $\text{Cr}(\text{CO})_6$  is snow white when collected under these conditions.) When this yellow solid is dissolved in  $n$ -heptane saturated with  $\text{C}_2\text{H}_4$ , the IR spectrum shows that the major component is  $\text{Cr}(\text{CO})_5(\text{C}_2\text{H}_4)$  with small amounts of  $\text{Cr}(\text{CO})_6$  and  $\text{trans-Cr}(\text{CO})_4(\text{C}_2\text{H}_4)_2$ , see Figure 6b and Table 1.

The spectrum of  $\text{Cr}(\text{CO})_5(\text{C}_2\text{H}_4)$  in solution is almost identical to that already assigned to the compound in

**Table 1.** Wavenumbers,<sup>a</sup>  $\text{cm}^{-1}$ , of  $\nu(\text{C}-\text{O})$  Fundamental and Combination Bands of  $\text{Cr}(\text{CO})_6$  and  $\text{Cr}(\text{CO})_5(\text{C}_2\text{H}_4)$  in  $\text{scC}_2\text{H}_4$  and in  $n$ -Heptane

species	$\text{scC}_2\text{H}_4^c$	$n$ -heptane	assignment
$\text{Cr}(\text{CO})_6$	2117.4 <sup>b</sup>	2115.5 <sup>b</sup>	$a_{1g}\nu(\text{C}-\text{O})$
	2023.6 <sup>b</sup>	2021.3 <sup>b</sup>	$e_g\nu(\text{C}-\text{O})$
		1986.4	$t_{1u}\nu(\text{C}-\text{O})$
	4099 (4104) <sup>d</sup>	(4101) <sup>e</sup>	$(a_{1g} + t_{1u})\nu(\text{C}-\text{O})$
	3994 (4010) <sup>d</sup>	(4007) <sup>e</sup>	$(e_g + t_{1u})\nu(\text{C}-\text{O})$
$\text{Cr}(\text{CO})_5(\text{C}_2\text{H}_4)$	2082.7 <sup>b</sup>	2077.6	$a_1\nu(\text{C}-\text{O})$
	2003.7 <sup>b</sup>	<sup>f</sup>	$a_2\nu(\text{C}-\text{O})$
		1966.1	$b_1\nu(\text{C}-\text{O})$
		1960.4	$(a_1/b_2)\nu(\text{C}-\text{O})$
	4035 (4047) <sup>g</sup>	(4034) <sup>e</sup>	$(a_1 + b_2)\nu(\text{C}-\text{O})$
	3955 (3964) <sup>g</sup>		$(a_2 + a_1/b_2)\nu(\text{C}-\text{O})$ <sup>e</sup>
	3905	(3926) <sup>e</sup>	$2b_1\nu(\text{C}-\text{O})$ <sup>e</sup>

<sup>a</sup> FTIR  $\pm 0.2 \text{ cm}^{-1}$ . <sup>b</sup> Data from FT-Raman spectrum.<sup>40</sup> <sup>c</sup> Band positions are modestly pressure dependent, i.e.,  $\pm 1 \text{ cm}^{-1}$ . <sup>d</sup> Wavenumbers calculated from the  $\text{scC}_2\text{H}_4$  FT-Raman and  $n$ -heptane IR data. <sup>e</sup> Wavenumbers calculated from the appropriate  $n$ -heptane data. <sup>f</sup> IR inactive. <sup>g</sup> Wavenumbers calculated from the  $\text{scC}_2\text{H}_4$  FT-Raman and  $n$ -heptane data for  $b_1$  and  $b_2$ .

previous studies.<sup>9,10</sup> The compound is quite air sensitive, but it is stable over relatively long periods in a sealed container at low temperatures (i.e.,  $-20^\circ\text{C}$ ). Once dissolved in  $n$ -heptane, it remains surprisingly stable, taking several hours to decompose. Thus,  $\text{Cr}(\text{CO})_5(\text{C}_2\text{H}_4)$  is not more reactive than the related  $\text{Cr}(\text{CO})_5(\text{cis-cyclooctene})$ , isolated previously by Skibbe and Grevels.<sup>11</sup>

The relative intensities of the  $\nu(\text{C}-\text{O})$  bands can be used to provide a semiquantitative measure of purity.<sup>14</sup> This analysis suggests that the solid product isolated in a number of different runs contained  $\text{Cr}(\text{CO})_5(\text{C}_2\text{H}_4)$  with purity between 80%–90%. The estimated purity was not particularly sensitive to the precise reaction conditions, and typical conditions are given in the Experimental Section.  $\text{Cr}(\text{CO})_5(\text{C}_2\text{H}_4)$  is considerably more soluble than  $\text{Cr}(\text{CO})_6$  in  $\text{scC}_2\text{H}_4$ . We attempted, therefore, to purify the crude product by extraction with  $\text{scC}_2\text{H}_4$  at relatively low pressure (e.g., 950 psi at  $25^\circ\text{C}$ ), conditions which should maximize the differences in solubility between  $\text{Cr}(\text{CO})_5(\text{C}_2\text{H}_4)$  and  $\text{Cr}(\text{CO})_6$ . Initially, the procedure appeared to be successful; when the spectrum of the flowing extract (not illustrated) was compared to that in the Figure 6a, the IR bands of  $\text{Cr}(\text{CO})_5(\text{C}_2\text{H}_4)$  were considerably more intense relative to those of  $\text{Cr}(\text{CO})_6$ . However, when the recovered solid was redissolved in  $n$ -heptane, there was disappointingly little difference from the spectrum of the raw product, Figure 6b. Thus, it is possible that limited decomposition occurs when the solid  $\text{Cr}(\text{CO})_5(\text{C}_2\text{H}_4)$  is dissolved in  $n$ -heptane and that the spectrum of the solution does not reflect the true composition of the original solid. Unfortunately, we could not confirm this because our attempts to record diffuse reflectance (DRIFTS) spectra of the solid material were defeated by the air-sensitivity of the compound.<sup>24</sup> Equally, FT-Raman spectroscopy, which can be used through the walls of a glass container without exposing the compound to air, was unsuccessful

(24) In theory, this air-sensitivity can be exploited to separate  $\text{trans-Cr}(\text{CO})_4(\text{C}_2\text{H}_4)_2$  from  $\text{Cr}(\text{CO})_5(\text{C}_2\text{H}_4)$  because exposure to air causes decomposition of  $\text{Cr}(\text{CO})_5(\text{C}_2\text{H}_4)$ , leaving  $\text{trans-Cr}(\text{CO})_4(\text{C}_2\text{H}_4)_2$  and residual  $\text{Cr}(\text{CO})_6$ . In practice, however, the overall yield of  $\text{trans-Cr}(\text{CO})_4(\text{C}_2\text{H}_4)_2$  is so low that the method has little practical value. By contrast solid  $\text{Cr}(\text{CO})_5(\text{C}_2\text{H}_4)$  appears to be relatively unreactive toward water. In one experiment, some of the solid product carried over into the soap solution in the bubble meter, M in Figure 5, and formed an emulsion, which remained pale yellow until exposed to air.

because the heating effect of the NIR laser led to blackening of the solid. We did, however, succeed in obtaining FT-Raman spectra of  $\text{Cr}(\text{CO})_5(\text{C}_2\text{H}_4)$  in  $\text{scC}_2\text{H}_4$  solution, but the spectra were weak and, sadly, only bands in the  $\nu(\text{C}-\text{O})$  region could be detected; nevertheless, we were able to locate the IR-inactive  $a_2$  mode, see Table 1.

Low-temperature photolysis has shown that photolysis of  $\text{Cr}(\text{CO})_5(\text{C}_2\text{H}_4)$ , **1**, leads to formation<sup>9</sup> of the relatively labile *cis*- $\text{Cr}(\text{CO})_4(\text{C}_2\text{H}_4)_2$ , **3**, before the more stable *trans*-isomer, **2**, is generated. It is possible that



a trace amount of this *cis*-isomer may be present in our crude product. Then, on dissolving the solid, decomposition of the *cis*-isomer might catalyze the partial decomposition of  $\text{Cr}(\text{CO})_5(\text{C}_2\text{H}_4)$ . Nevertheless, for whatever reason, decomposition in solution is more rapid than in the solid state. It is clear, therefore, that our synthetic route owes its success, at least in part, to the almost instantaneous precipitation of the solid product by the RESS procedure. We now describe how this flow reactor can be modified to generate  $\text{CpMn}(\text{CO})_2(\eta^2\text{-H}_2)$ .

**Isolation of  $\text{CpMn}(\text{CO})_2(\eta^2\text{-H}_2)$ .** The isolation of  $\text{CpMn}(\text{CO})_2(\eta^2\text{-H}_2)$  requires a reactor significantly more complicated than that used for  $\text{Cr}(\text{CO})_5(\text{C}_2\text{H}_4)$  because the synthesis involves *two* high-pressure gases,  $\text{H}_2$  and  $\text{CO}_2$ . Figure 7 shows the detailed layout of the reactor. Two related problems had to be overcome during the development of this reactor: (i) how to mix  $\text{H}_2$  efficiently on such small scale and (ii) how to avoid precipitation of  $\text{CpMn}(\text{CO})_3$  in the narrow pipework.<sup>25</sup>

The problem of mixing the gases was overcome by use of a commercially available dosage unit (see Experimental Section). The unit is plumbed in such a way that alternate pulses of  $\text{H}_2$  and  $\text{CO}_2$  pass into the flow system, and it is crucial to ensure that these pulses are properly mixed before the  $\text{CpMn}(\text{CO})_3$  is added to the fluid. Therefore, the gas mixture is passed through a mixing unit, the volume of which is significantly larger than the volume of the individual gas doses. Fortunately, the effectiveness of the mixing can be assessed by Raman spectroscopy because the  $S_1(1)$  rotational Raman band of  $\text{H}_2$  ( $586\text{ cm}^{-1}$ ) is significantly broader in  $\text{H}_2/\text{scCO}_2$  mixtures than in pure  $\text{H}_2$  gas at the same overall pressure.<sup>26</sup> The origin of the broadening has

(25) The viscosity of the fluid is so low that there is only a small pressure drop across the entire length of the reactor. However, with a saturated solution in a fluid close to its critical point, even a minor restriction in the pipework can quickly lead to total blockage, because solubility is related to fluid density. Close to the critical point, fluids are highly compressible and even a small reduction in pressure leads to a disproportionate drop in density. A minor restriction will lead to such a pressure drop. Material will precipitate, thereby restricting the pipework further and causing more precipitation until the tube is completely blocked.

(26) Howdle, S. M.; Bagratashvili, V. N. *Chem. Phys. Lett.* **1993**, *214*, 215. Howdle, S. M.; Stanley, K.; Popov, V. K.; Bagratashvili, V. N. *Appl. Spectrosc.* **1994**, *48*, 214.

(27) Separate accounts of the capillary spectroscopic cell<sup>7b</sup> and of these FT-Raman experiments have been published elsewhere: Bagratashvili, V. N.; Popov, V. K.; Robertson, D. G.; Howdle, S. M.; Poliakov, M.; George, M. W.; Walsh, E. Proceedings of the 3rd International Symposium on Supercritical Fluids, Strasbourg, France, 1994; Vol. 1 p 337.

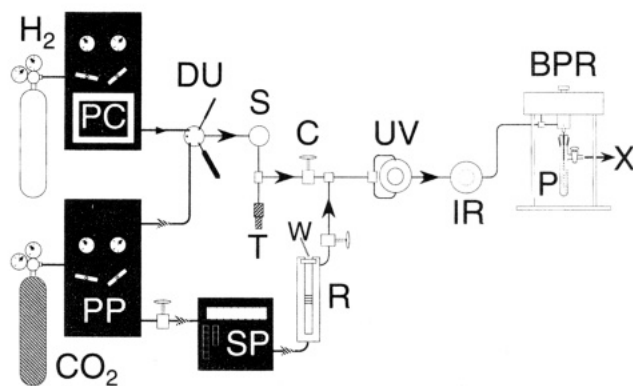


**Figure 7.** Layout of the reactor for the synthesis and isolation of  $\text{CpMn}(\text{CO})_2(\eta^2\text{-H}_2)$  from  $\text{CpMn}(\text{CO})_3$  and  $\text{H}_2$  in  $\text{scCO}_2$ . The photochemical section of the reactor is largely unaltered from that in Figure 5, but the gas-handling stage now includes two pumps and a mixing unit, and the method of adding  $\text{CpMn}(\text{CO})_3$  to the flowing fluid is different from that used for  $\text{Cr}(\text{CO})_6$ . The components are labeled as follows (alphabetically): BPR, back-pressure regulator (Jasco Model 880-81); C, control valve;  $\text{CO}_2$ , carbon dioxide cylinder (BOC SFC grade); DU, gas dosage unit (NWA);  $\text{H}_2$ , hydrogen cylinder; IR, infrared cell (see Figure 2a); P, solid product,  $\text{CpMn}(\text{CO})_2(\eta^2\text{-H}_2)$  collected in the vessel shown in Figure 3; PC, pneumatic compressor (NWA Model CU105); PP, pneumatic pump (NWA Model PM101); R, variable-volume cell<sup>28</sup> containing a solution of  $\text{CpMn}(\text{CO})_3$  in an  $\text{H}_2/\text{scCO}_2$  mixture; S, mixer with magnetic stirrer (Kontron M491); SP, syringe pump (Brownlee Lab Microgradient) containing  $\text{scCO}_2$  to drive the piston of the variable-volume cell; T, pressure transducer<sup>29</sup> (RDP Electronics); UV, photolysis cell (see Figure 2b); W, sapphire window of the variable-volume cell; X, exhaust vent. The arrows on the pipework are color-coded to make the gas flows clearer: cross-hatched arrows,  $\text{CO}_2$ ; small solid arrow,  $\text{H}_2$ ; large solid arrow,  $\text{CO}_2/\text{H}_2$  mixture. (Note that this figure is not drawn to scale.)

been discussed previously in the context of conventional Raman spectra.<sup>26</sup> In the present case, it was technically simpler to record FT-Raman spectra (Perkin-Elmer Model 2000) which confirmed that the gases were indeed mixed.<sup>27</sup> Once the efficiency of the mixing system had been established, FT-Raman monitoring was unnecessary for routine operation of the flow reactor, particularly because  $\text{H}_2$  can be detected indirectly by FTIR (see Figure 8). Thus, the FT-Raman cell is not included in the layout shown in Figure 7.

The addition of  $\text{H}_2$  to  $\text{scCO}_2$  reduces the solvent power of the mixture compared to that of  $\text{scCO}_2$  at the same overall pressure. Thus it is particularly important to control the concentration of  $\text{CpMn}(\text{CO})_3$  in the fluid because near-saturation can lead to precipitation and total blockage of the pipework.<sup>25</sup>  $\text{CpMn}(\text{CO})_3$  has a relatively high solubility in  $\text{scCO}_2$ , and the simple extraction vessel used with  $\text{Cr}(\text{CO})_6/\text{scC}_2\text{H}_4$  (see Figure 5) could not provide the delicate control which is needed. We decided, therefore, to make up a concentrated solution of  $\text{CpMn}(\text{CO})_3$  in a separate cell prior to the experiment and then to bleed this solution into the flow reactor. The rate of "bleed" could be controlled accurately by driving the solution with a syringe pump, with a programmable flow rate, see Experimental Section.

Once the  $\text{CpMn}(\text{CO})_3$  has been added to the flowing  $\text{scCO}_2/\text{H}_2$  stream, the remaining operations are similar to those of the  $\text{Cr}(\text{CO})_6/\text{scC}_2\text{H}_4$  reactor. Figure 8 gives



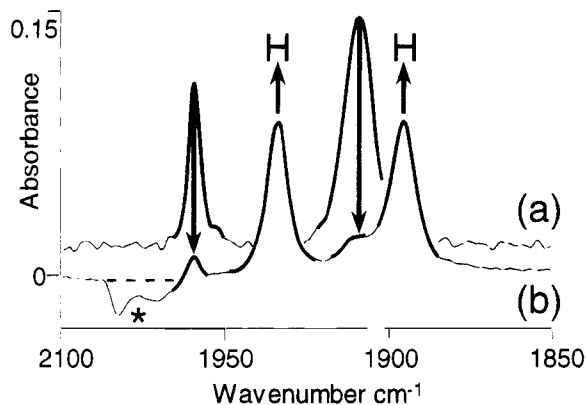


**Figure 8.** IR spectra illustrating the photochemical formation of  $\text{CpMn}(\text{CO})_2(\eta^2\text{-H}_2)$  in  $\text{scCO}_2/\text{H}_2$  solution. (a) Spectrum of  $\text{CpMn}(\text{CO})_3$  recorded in pure  $\text{scCO}_2$  without UV irradiation and (b) spectrum recorded during UV irradiation of  $\text{CpMn}(\text{CO})_3$  in flowing  $\text{scCO}_2/\text{H}_2$ . The bands are labeled as follows:  $\downarrow$ ,  $\text{CpMn}(\text{CO})_3$ ;  $\uparrow$ ,  $\text{CpMn}(\text{CO})_2(\eta^2\text{-H}_2)$ ; \*, absorption of  $\text{CO}_2$  itself which provides an indirect measure of the  $\text{H}_2$  concentration.<sup>30</sup> The absorbance scales of two spectra have been slightly offset for clarity. It is important to note that the conversion of  $\text{CpMn}(\text{CO})_3$  to  $\text{CpMn}(\text{CO})_2(\eta^2\text{-H}_2)$  is almost complete.

examples of IR spectra recorded with and without UV irradiation. These spectra show how almost all of the  $\text{CpMn}(\text{CO})_3$  can be destroyed by UV, leaving more or less pure  $\text{CpMn}(\text{CO})_2(\eta^2\text{-H}_2)$  to flow to the back-pressure regulator and the collection vessel. Even though crystalline  $\text{CpMn}(\text{CO})_3$  is pale yellow, powdered  $\text{CpMn}(\text{CO})_3$  deposited by RESS is almost white. By contrast, the reaction product is precipitated from the BPR as a yellow solid which melts to a dark, reddish-brown liquid close to room temperature.

Figure 9 shows the  $^1\text{H}$  NMR spectrum, obtained after dissolving this material in  $\text{C}_6\text{D}_6$ ; the resonances are similar to those reported earlier by Leong and Cooper<sup>15</sup> and confirm that the product is largely  $\text{CpMn}(\text{CO})_2(\eta^2\text{-H}_2)$  with a small amount of residual  $\text{CpMn}(\text{CO})_3$ . The resonance at  $-12.91$  ppm does not allow us to distinguish a dihydrogen complex rather than a dihydride, but the presence of dihydrogen has been confirmed by Waugh and Lawless<sup>31</sup> from  $\tau_1$  measurements and the spectrum of  $\text{CpMn}(\text{CO})_2(\eta^2\text{-HD})$  in  $\text{scXe}$ . Furthermore, the wavenumbers of the  $\nu(\text{C}-\text{O})$  bands are very close to those of  $\text{CpMn}(\text{CO})_2\text{N}_2$ , see Table 2, thus indicating

(28) Developed from an original design by McHugh. McHugh, M. A. Personal communication, 1994.

(29) As an additional safety measure, the electronic readout of the pressure transducer provides a signal which switches the dosage unit off should the pressure rise above a preset level.

(30) This absorption corresponds to a relatively weak combination band of  $\text{CO}_2$  itself. It appears to be "negative" in Figure 8b because the background spectrum for this experiment was deliberately recorded with pure  $\text{scCO}_2$  (i.e., without  $\text{H}_2$ ) while spectrum b was recorded in a  $\text{scCO}_2/\text{H}_2$  mixture at the same pressure. In these circumstances, there is an effective dilution of the  $\text{CO}_2$  by  $\text{H}_2$ , and the higher the concentration of  $\text{H}_2$ , the stronger is this negative band.

(31) These HD and  $\tau_1$  experiments were performed by generating  $\text{CpMn}(\text{CO})_3(\eta^2\text{-H}_2)$  in  $\text{scXe}/\text{H}_2$  *in situ* in the sapphire NMR tube: Cloke, F. G. N.; Lawless, G. A.; Waugh, M. P. Proceedings of the 26th International Conference on Organometallic Chemistry, Brighton, U.K., 1994; Abstract No. P363, to be published. We successfully transported a sample of  $\text{CpMn}(\text{CO})_3(\eta^2\text{-H}_2)$  prepared in our flow reactor to their laboratory in Brighton (ca. 200 miles away) to confirm that our sample was the same as theirs.

(32) George, M. W.; Haward, M. T.; Hamley, P. A.; Hughes, C.; Johnson, F. P. A.; Poliakov, M.; Popov, V. K. *J. Am. Chem. Soc.* **1993**, *115*, 2286.

(33) Kubas, G. J. *Acc. Chem. Res.* **1988**, *21*, 120.

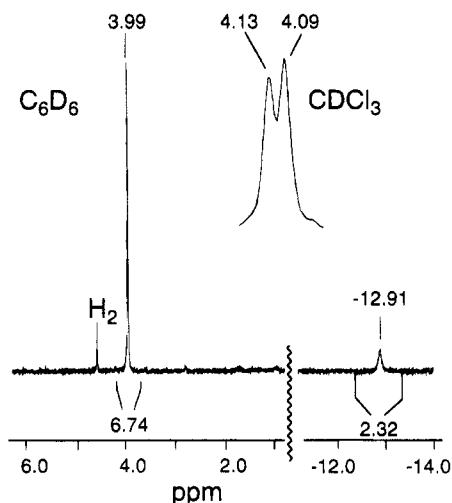


**Figure 9.**  $^1\text{H}$  NMR spectrum of crude  $\text{CpMn}(\text{CO})_2(\eta^2\text{-H}_2)$  dissolved in  $\text{C}_6\text{D}_6$  at room temperature. The spectrum was recorded with a relaxation delay time of 40 s. The resonance of residual  $\text{C}_6\text{D}_5\text{H}$  was used as a reference at 7.80 ppm. The spectrum is annotated with peak positions and integrated areas. In  $\text{C}_6\text{D}_6$ , there is an accidental coincidence of the chemical shifts of the Cp rings of  $\text{CpMn}(\text{CO})_3$  and  $\text{CpMn}(\text{CO})_2(\eta^2\text{-H}_2)$ . Thus, the presence of some  $\text{CpMn}(\text{CO})_3$  in the solution means that the areas of the resonances at 3.99 and  $-12.91$  ppm are in the ratio of 3:1 rather than the 2.5:1 expected for  $(\text{C}_5\text{H}_5)\text{Mn}(\text{CO})_2(\eta^2\text{-H}_2)$ . However, the inset peaks, obtained from a different sample of  $\text{CpMn}(\text{CO})_2(\eta^2\text{-H}_2)$ , show that  $^1\text{H}$  resonances of  $\text{CpMn}(\text{CO})_3$  and  $\text{CpMn}(\text{CO})_2(\eta^2\text{-H}_2)$  are easily resolved in  $\text{CDCl}_3$  solution.

**Table 2.** Wavenumbers,<sup>a</sup>  $\text{cm}^{-1}$ , of  $\text{CpMn}(\text{CO})_3$ ,  $\text{CpMn}(\text{CO})_2(\eta^2\text{-H}_2)$  and Related Compounds in  $\text{scCO}_2$  Solution

species	$\text{scCO}_2^b$	assignment
$\text{CpMn}(\text{CO})_3$	2030.7	$\text{a}_1\nu(\text{C}-\text{O})$
	1945.9	$\text{e}\nu(\text{C}-\text{O})$
$\text{CpMn}(\text{CO})_2(\eta^2\text{-H}_2)^c$	1986.1	$\text{a}'\nu(\text{C}-\text{O})$
	1922.8	$\text{a}''\nu(\text{C}-\text{O})$
	2173	$\text{a}'\nu(\text{N}-\text{N})$
$\text{CpMn}(\text{CO})_2(\text{C}_2\text{H}_4)^d$	1980.5	$\text{a}'\nu(\text{C}-\text{O})$
	1924.5	$\text{a}''\nu(\text{C}-\text{O})$
	1974.6	$\text{a}'\nu(\text{C}-\text{O})$
	1911.3	$\text{a}''\nu(\text{C}-\text{O})$

<sup>a</sup> FTIR  $\pm 0.2$   $\text{cm}^{-1}$ . <sup>b</sup> 500 psi of  $\text{N}_2 + \text{scCO}_2$  to a total pressure of 2200 psi. <sup>c</sup> No IR band assignable to the  $\nu(\text{H}-\text{H})$  vibration of the  $\eta^2\text{-H}_2$  group was detectable under these conditions. <sup>d</sup> 500 psi of  $\text{C}_2\text{H}_4 + \text{scCO}_2$  to a total pressure of 2200 psi.

that  $\text{CpMn}(\text{CO})_2(\eta^2\text{-H}_2)$  contains Mn(I) rather than Mn(III). Sadly, as with  $\text{Cr}(\text{CO})_5(\text{C}_2\text{H}_4)$ , our attempts to obtain FT-Raman spectra of  $\text{CpMn}(\text{CO})_2(\eta^2\text{-H}_2)$  were unsuccessful, partly because of the low melting point which caused the compound to flow away from the area of laser irradiation.

**Reactions of  $\text{CpMn}(\text{CO})_2(\eta^2\text{-H}_2)$ .** We have begun investigating some simple reactions of  $\text{CpMn}(\text{CO})_2(\eta^2\text{-H}_2)$  by precipitating the compound directly from the BPR into a high-pressure spectroscopic cell and then

(34) This slow rate of reaction was also observed in our original experiments<sup>16</sup> in  $\text{scXe}$ , but, at that time, the slowness was attributed to a residual pressure of  $\text{H}_2$  in the fluid. Now, it is clear that the rate is an inherent property of the compound. As yet, we have not pursued more quantitative kinetic measurements on these reactions because, although the spectroscopic monitoring is more than adequate for such measurement, the rather slow time scale of the reactions means that even trace amounts of impurity could have a profound effect on the measured rates.

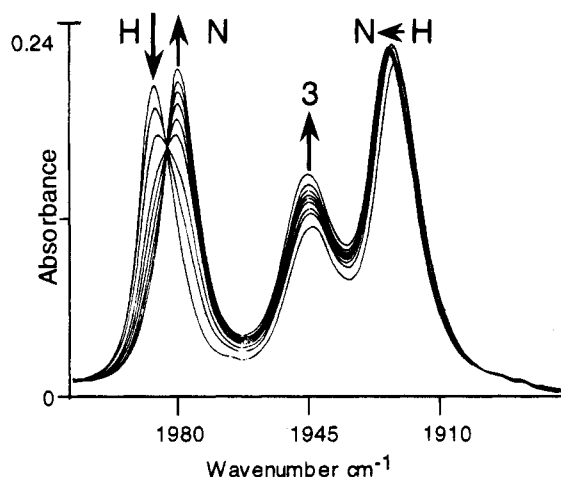


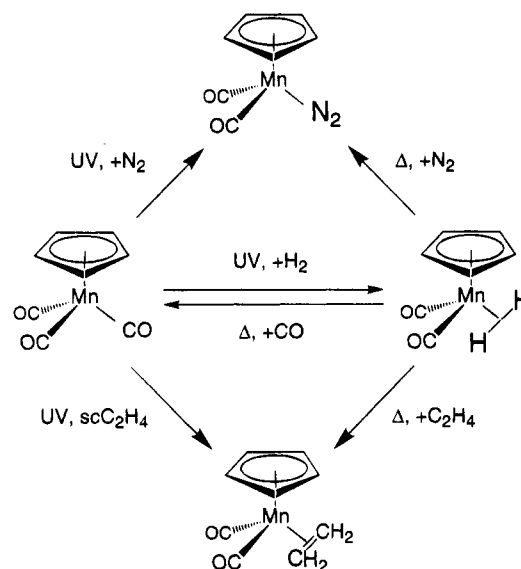
**Figure 10.** IR spectra in part of the  $\nu(\text{C}-\text{O})$  region, illustrating the *thermal* reaction of  $\text{CpMn}(\text{CO})_2(\eta^2\text{-H}_2)$  with  $\text{N}_2$  in  $\text{scCO}_2$  solution. The spectra were obtained by precipitating a sample of  $\text{CpMn}(\text{CO})_2(\eta^2\text{-H}_2)$  into a spectroscopic cell directly from the flow reactor. The cell was pressurized with  $\text{N}_2$  (500 psi) and  $\text{CO}_2$  was added to give a total pressure of 2200 psi. FTIR spectra were then recorded at 10 min intervals over a period of 90 min. The bands are labeled as follows: H,  $\text{CpMn}(\text{CO})_2(\eta^2\text{-H}_2)$ ; N,  $\text{CpMn}(\text{CO})_2\text{N}_2$ ; 3,  $\text{CpMn}(\text{CO})_3$ . Wavenumbers of the bands are listed in Table 2.

adding other reactants. The cell was pressurized with  $\text{scCO}_2$ , and the subsequent reactions were monitored by IR. Figure 10 shows a series of spectra recorded during the reaction with  $\text{N}_2$  and Scheme 1 summarizes the reactions studied so far. The most interesting feature of these reactions is that, qualitatively, they all occur at a similar rate, taking ca. 2 h to reach completion.<sup>34</sup> This suggests that the most probable rate-determining step is dissociation of the  $\text{Mn}-\text{H}_2$  bond.

Thus,  $\text{CpMn}(\text{CO})_2(\eta^2\text{-H}_2)$  appears to be one of the more stable dihydrogen complexes. By comparison,  $\text{CpV}(\text{CO})_3(\eta^2\text{-H}_2)$  has a half-life of only a few msec at room temperature<sup>32</sup> under 2 atm of pressure of  $\text{H}_2$  and even Kubas's prototypical compounds,<sup>33</sup>  $\text{M}(\text{CO})_3(\text{PCy}_3)_2(\eta^2\text{-H}_2)$ , have ca. 1 atm equilibrium vapor pressure of  $\text{H}_2$ . Furthermore,  $\text{CpMn}(\text{CO})_2(\eta^2\text{-H}_2)$  is one of the simplest dihydrogen complexes to be isolated so far. Above, we indicated that  $\text{Cr}(\text{CO})_5(\text{C}_2\text{H}_4)$  is stabilized, at least in part, by the solid state; in solution, it is much more reactive. By contrast, the stability of  $\text{CpMn}(\text{CO})_2(\eta^2\text{-H}_2)$  is not dependent on the solid state and melting the compound has little effect on its reactivity. Indeed, the closely related compound,  $(\text{C}_5\text{H}_4\text{Me})\text{Mn}(\text{CO})_2(\eta^2\text{-H}_2)$ , can be isolated from our flow reactor as liquid<sup>35</sup> and appears to be quite as robust as  $\text{CpMn}(\text{CO})_2(\eta^2\text{-H}_2)$ . Thus it is not obvious why  $\text{CpMn}(\text{CO})_2(\eta^2\text{-H}_2)$  should be so stable, and, in the absence of detailed structural parameters, one is left to argue by analogy.

The  $\text{CpMn}(\text{CO})_2$  fragment has good donor/acceptor orbitals and can form extremely strong bonds to 2-electron donors. Thus,  $\text{CpMn}(\text{CO})_3$  is one of the very few metal carbonyl compounds which does not undergo any thermal CO substitution reactions.  $\text{CpMn}(\text{CO})_2\text{N}_2$  was the first carbonyl dinitrogen complex to be isolated<sup>36</sup> and it remains one of the least reactive. The range of stable  $\text{CpMn}(\text{CO})_2(\eta^2\text{-H-SiR}_3)$  complexes constitute some the

### Scheme 1. Reactions in $\text{scCO}_2$



best examples of arrested oxidation of Si-H bonds.<sup>37</sup> Given such a context, it is perhaps not surprising that  $\text{CpMn}(\text{CO})_2$  should also form a very stable dihydrogen complex.

**Isolation of Other Compounds.** Both of the flow reactors, see Figures 5 and 7, can be used successfully for other photochemical reactions.  $\text{W}(\text{CO})_5(\text{C}_2\text{H}_4)$  and *trans*- $\text{W}(\text{CO})_4(\text{C}_2\text{H}_4)_2$  can be generated in the  $\text{scC}_2\text{H}_4$  reactor, and it has also been used to isolate  $\text{CpMn}(\text{CO})_2(\text{C}_2\text{H}_4)$ . We have not attempted to optimize the yields of these reactions, but even preliminary experiments gave encouraging yields. The  $\text{H}_2$  reactor works equally efficiently with  $\text{scC}_2\text{H}_6$  as the solvent but with the advantage that  $\text{C}_2\text{H}_6$  has a lower critical pressure than  $\text{CO}_2$  (4.88 vs 7.38 MPa). The reactor can therefore be used with a higher pressure of  $\text{H}_2$  without exceeding the total pressure rating of the apparatus. The same flow reactor can be used with  $\text{N}_2/\text{scCO}_2$  or  $\text{N}_2/\text{scC}_2\text{H}_6$  to isolate, for example,  $\text{CpMn}(\text{CO})_2\text{N}_2$ , more simply than by Sellmann's original route.<sup>36</sup>

We have previously shown that multiple substitution of CO by  $\text{N}_2$  is possible in supercritical solution,<sup>4</sup> e.g., in the formation of  $\text{CpRe}(\text{N}_2)_3$  from  $\text{CpRe}(\text{CO})_3$ . So far, we have not been able to scale such reactions up successfully in our flow reactor, presumably because the residence time in the photolysis cell is too short. We have also begun to explore the use of other metals. UV photolysis of  $(\text{C}_6\text{H}_5\text{Me})\text{Cr}(\text{CO})_3$  in  $\text{scCO}_2/\text{H}_2$  gives spectroscopic evidence for formation of  $(\text{C}_6\text{H}_5\text{Me})\text{Cr}(\text{CO})_2(\eta^2\text{-H}_2)$  in the flowing fluid,<sup>4b,38</sup> but, as yet, we have not succeeded in isolating the product. Unfortunately, this reaction has the added complication of  $\text{Cr}(\text{CO})_6$  appearing in significant quantities in the reactor.

### Experimental Section

**Safety Hazard!** *The experiments described in this paper involve the use of relatively high pressures and require equipment with the appropriate pressure rating. It is the responsibility of individual researchers to verify that their particular apparatus meets the necessary safety requirements. The indi-*

(35) Lee, P. D.; Seebald, S.; Poliakoff, M. To be published.

(36) Sellmann, D. *J. Angew. Chem., Int. Ed. Engl.* **1971**, *10*, 919.

(37) For a comprehensive review on silane complexes, see: Schubert, U. *Adv. Organomet. Chem.* **1990**, *30*, 151.

(38)  $(\text{C}_6\text{H}_5\text{Me})\text{Cr}(\text{CO})_2(\eta^2\text{-H}_2)$  has previously been detected in  $\text{scXe}$  solution in a static photolysis experiment.<sup>4b</sup>

vidual components, which we describe below, work well, but they are not necessarily the only equipment of this type available nor the most suitable for the purpose.

**Equipment (see also Main text). Fluid Pumps.**  $\text{scC}_2\text{H}_4$  and  $\text{H}_2$  are flammable, and so pneumatic operation is highly desirable for pumps and compressors. In the flow reactors, we have used a single-stage high compression ratio pump (Model PM101 from NWA GmbH, Lörrach, Germany) which incorporates a refrigeration unit to liquefy the  $\text{C}_2\text{H}_4$  or  $\text{CO}_2$  prior to pumping. Each time the pump refills, there is a momentary drop in the pressure of output. In the  $\text{scC}_2\text{H}_4$  reactor, the effects of these pulses were minimized by running the pump with a delivery pressure ca. 600 psi higher than needed for the experiment. The fluid was pumped into a 40 mL dead volume, D in Figure 5, with a high-pressure valve, C, to control the final output. This dead volume/control valve combination dampens out most of the pulsing. In the  $\text{CO}_2/\text{H}_2$  reactor, the flow of gas was necessarily pulsed because of the dosage unit (see below) with the result that pulsing of the pump was not important.  $\text{H}_2$  was compressed with a pneumatic double-stroke compressor (NWA Model CU105), which has an internal volume large compared to that of the flow reactor with the result that the supply of gas to the reactor was essentially continuous. The variable-volume cell was driven by a flow of pure  $\text{scCO}_2$ , pumped by a Brownlee Lab Microgradient syringe pump, which is electrically operated.

**Dosage Unit and Mixer.** This dosage unit, also supplied by NWA, consists of a pneumatically driven six-port valve (Rheodyne 7010) to which two short pieces of pipe are attached. These pieces are closed at one end and act as the dosage volumes for  $\text{H}_2$  and  $\text{CO}_2$  respectively. In operation, one volume is being filled with gas while the other is being vented to the line. As supplied, the unit has two dosage pipes of equal size. We have modified the unit so that the tube for  $\text{CO}_2$  has ca. 500 times the volume of the tube for  $\text{H}_2$ . The precise ratio of  $\text{H}_2:\text{CO}_2$  is then determined by the ratio of volumes and the supply pressures of the two gases. The gases are then passed through a magnetically stirred mixer (Kontron M491) to ensure thorough mixing of the gases. The mixer also acts as a relatively efficient pulse damper.

**Minor Components.** The variable-volume view cell used for the delivery of  $\text{CpMn}(\text{CO})_3$  is based on an original design by McHugh et al.<sup>28</sup> It consists of a 25 mL chamber with a piston driven by  $\text{scCO}_2$  and a sapphire window at one end for viewing the fluid inside. Our version is sealed with PTFE gaskets. The remaining components are largely based on those used for HPLC or capillary supercritical fluid chromatography. All pipework in the reactors is 1/16 in. o.d. stainless steel tubing and the valves are SSI 1/16th inch (Model LCT-43-90; a variety of similar valves are available from other manufacturers). Only the more important, valves are shown in Figures 5 and 7. Other components, such as the flow cells shown in figure 2, were machined to accept SSI fittings. Neither one of our flow reactors required heating; the critical temperature of  $\text{C}_2\text{H}_4$  is only 9 °C, and the mixtures of  $\text{H}_2/\text{scCO}_2$  used in these reactions also have critical temperatures below ambient.<sup>26</sup> The concentrations of dissolved organometallic were too low to affect the critical points of the fluids significantly.

**UV Photolysis Source.** A Cermax 300 W UV lamp was used with an OP2 cold mirror to remove visible and near-IR radiation. A crucial factor in the preparation of  $\text{CpMn}(\text{CO})_2(\eta^2\text{-H}_2)$ , was the use of a Pyrex glass filter,  $\lambda > 300$  nm, to remove the short-wavelength output of the lamp, which otherwise caused unacceptable decomposition of the product.

**IR Spectroscopy.** All IR spectra were recorded on a Nicolet Model 205 FTIR interferometer, which permits almost unlimited repetitive scanning. Spectra were obtained with 2 or 4  $\text{cm}^{-1}$  resolution. When needed, spectra were processed further on a Nicolet Model 620 Data Station.

**Materials.** All materials were used without further purification;  $\text{CpMn}(\text{CO})_3$  and  $\text{Cr}(\text{CO})_6$  (99%) from Aldrich;  $\text{CO}_2$

(SFC grade) from BOC;  $\text{H}_2$ ,  $\text{N}_2$ ,  $\text{C}_2\text{H}_4$  (99.8%), and  $\text{C}_2\text{H}_6$  (3.5 Grade) from Air Products.

**Preparation of  $\text{Cr}(\text{CO})_5(\text{C}_2\text{H}_4)$ .** The apparatus is set up as in Figure 5 but without the collection vessel between the back pressure regulator, BPR, and the bubble flow meter, M. The extraction vessel, R, is then filled with  $\text{Cr}(\text{CO})_6$  (>100 mg), and the valves on either side are closed.  $\text{C}_2\text{H}_4$  is flowed at low pressure (150 psi) through the bypass valve, B, to flush residual air from the system. The other valves are then opened so that the reservoir, R, is also flushed with  $\text{C}_2\text{H}_4$  (at these pressures  $\text{Cr}(\text{CO})_6$  is virtually insoluble in  $\text{C}_2\text{H}_4$ ). One valve is now closed and the BPR is set to an increased pressure, 1220 psi (i.e., supercritical). The control valve is adjusted to give a flow rate of ca. 200 mL of gas per min, measured at atmospheric pressure with the flow meter, M. For  $\text{C}_2\text{H}_4$ , this flow rate corresponds to a usage of ca. 0.5  $\text{mol h}^{-1}$  or 14  $\text{g h}^{-1}$ . A background FTIR spectrum is recorded (i.e.,  $\text{scC}_2\text{H}_4$  without  $\text{Cr}(\text{CO})_6$ ). B is closed, and the valves are opened so that  $\text{scC}_2\text{H}_4$  flows through R;  $\text{Cr}(\text{CO})_6$  now dissolves into the fluid. The concentration of  $\text{Cr}(\text{CO})_6$  is checked via FTIR, see Figure 6a, and the pressure is adjusted, if necessary, to obtain the required concentration of  $\text{Cr}(\text{CO})_6$ . The valves on R are closed, and B is reopened to flush  $\text{Cr}(\text{CO})_6$  out of the system. The gas flow is then stopped briefly, and the collection vessel (see Figure 4) is connected between the BPR and M. The gas flow is restarted, and any air is flushed from the collection vessel. B is closed, and the valves are opened so that  $\text{scC}_2\text{H}_4$  again flows through R. The UV lamp is then switched on, the extent of the UV photolysis is monitored via FTIR and, again, the conditions are adjusted if required to improve the overall conversion. Photolysis continues, and crude  $\text{Cr}(\text{CO})_5(\text{C}_2\text{H}_4)$  is collected, typically, at 40  $\text{mg h}^{-1}$ . The reactor is not truly continuous in operation because the stock of  $\text{Cr}(\text{CO})_6$  will eventually run out. The longest continuous operation has been ca. 2 h, but there is no reason why it should not be run longer because very little deposit builds up on the UV window. The collection vessel is then detached from the BPR, and product is removed in a glove box. (If  $\text{Cr}(\text{CO})_5(\text{C}_2\text{H}_4)$  is collected in the glass vessel, see Figure 3, the crude product can be worked up on a conventional Schlenk line.)

**Preparation of  $\text{CpMn}(\text{CO})_2(\eta^2\text{-H}_2)$ .** The reactor is set up as in Figure 7. The sapphire window, W, is removed from the variable volume cell, R, and ca. 130 mg of solid  $\text{CpMn}(\text{CO})_3$  is loaded into the cell which is then sealed (by replacing the window) and purged with  $\text{H}_2$ . With 200 psi of  $\text{H}_2$  still left in the cell, it was filled with  $\text{CO}_2$ , and the resulting solution of  $\text{CpMn}(\text{CO})_3$  in  $\text{H}_2/\text{CO}_2$  is stirred by using a magnet to agitate a magnetic flea inside the cell. The back-pressure regulator, BPR, is then set at 2500 psi, the  $\text{CO}_2$  pump, PP, at ca. 3050 psi, and the  $\text{H}_2$  compressor, PC, at ca. 2950 psi. The dosage unit, DU, is set to switch once every 0.70 s. The flow of fluid is then allowed to stabilize, and the BPR is adjusted to pulse regularly. A background IR spectrum is recorded, and the FTIR interferometer is started scanning repetitively (ca. 1 spectrum per min). The syringe pump, SP, is now used to pressurize the variable-volume cell behind the piston. The pressure output from the pump continues to rise until the forward pressure on the piston exceeds the friction from the O-rings, driving the piston forward and the solution of  $\text{CpMn}(\text{CO})_3$  into the flowing stream of  $\text{CO}_2/\text{H}_2$ . Once the pressure output from the Brownlee pump is stabilized, the flow rate is limited by the controlling software to a preset value (normally 100  $\mu\text{L min}^{-1}$ ). The UV lamp is turned on as soon as the  $\nu(\text{C}-\text{O})$  bands of  $\text{CpMn}(\text{CO})_3$  are detected in the FTIR spectrum. With care, the system can then be adjusted to give almost complete photolysis of  $\text{CpMn}(\text{CO})_3$  with  $\text{CpMn}(\text{CO})_2(\eta^2\text{-H}_2)$  as the sole product, detectable in by FTIR.  $\text{CpMn}(\text{CO})_2(\eta^2\text{-H}_2)$ , P, collects in the glass collection vessel attached to the BPR. The efficiency of collection is improved by cooling the vessel with ice. The reactor is then run until the photolysis is seen to be less efficient,<sup>39</sup> and the bands of unreacted  $\text{CpMn}$



(CO)<sub>3</sub> appear in the spectrum. Typically this occurs after 60–90 min. Yields of crude CpMn(CO)<sub>2</sub>(η<sup>2</sup>-H<sub>2</sub>) are 15–30 mg.

### Conclusions

In this paper, we have described two flow reactors that can be used to isolate new compounds. Both of the compounds, Cr(CO)<sub>5</sub>(C<sub>2</sub>H<sub>4</sub>) and CpMn(CO)<sub>2</sub>(η<sup>2</sup>-H<sub>2</sub>), were previously thought to be too labile for isolation as solids. Both have transpired to be surprisingly robust. Indeed, it is quite possible that non-supercritical routes will be found to these compounds, now that their stability is apparent. What these flow reactors do provide is quite a general approach to the synthesis of particular classes of compounds. Other C<sub>2</sub>H<sub>4</sub> compounds and other H<sub>2</sub> compounds should be accessible by similar procedures. Modifications of the reactor will lead to a whole range of new reactions.

Such modifications are straightforward because the design is inherently flexible. The reactors are built up of simple components, most of which are commercially available or easily machined. Other types of reactor can

(39) At the end of several runs, the cell was found to contain a pure white powder, sufficiently paramagnetic to be moved by a magnet. This powder was insoluble in organic solvents but soluble with effervescence in hydrochloric acid. It was amorphous by X-ray diffraction, decomposed to a brownish black solid on heating, and gave a DRIFTS spectrum consistent with [CO<sub>3</sub>]<sup>2-</sup>. This suggests that the solid was MnCO<sub>3</sub>. Precisely how this carbonate is formed is not known, but presumably it originates from traces of water present in the CO<sub>2</sub>, probably via transient formation of CpMn(CO)<sub>2</sub>(OH<sub>2</sub>). MnCO<sub>3</sub> was also formed during the reaction of CpMn(CO)<sub>3</sub> with N<sub>2</sub> in scCO<sub>2</sub> but not in the reaction of CpMn(CO)<sub>3</sub> and H<sub>2</sub> in scC<sub>2</sub>H<sub>6</sub>. Similarly, photolysis of (toluene)Cr(CO)<sub>3</sub> in H<sub>2</sub>/scCO<sub>2</sub> gave rise to a blue/green precipitate which decomposed at 258 °C (as measured by DSC), the same decomposition temperature as that of an authentic sample of Cr<sub>2</sub>(CO)<sub>3</sub>. For further discussion of the formation of carbonate complexes, see: Alvarez, R.; Carmona, E.; Galindo, A.; Gutiérrez, E.; Marin, J. M.; Monge, A.; Poveda, M. L.; Ruiz, C.; Savariault, J. M. *Organometallics* **1989**, *8*, 2430 and references therein.

(40) Robertson, D. G. Unpublished data, 1995.

(41) **Note Added in Proof.** For a very recent molecular modeling calculation on Cr(CO)<sub>5</sub>(C<sub>2</sub>H<sub>4</sub>) and related species, see: White, D. P.; Brown, T. L. *Inorg. Chem.* **1995**, *34*, 2718.

be developed merely by rearranging the basic components, much in the manner of a child's construction toy. Obvious extensions include the option of recycling the supercritical solvent or the replacement of the photochemical irradiation cell with a heated tube so that thermal reactions can be carried out.

Flow reactors have considerable advantages for safety, because the total volume under pressure is small and also because the fluid is free to expand thereby reducing the chances of an unanticipated build up of pressure. Of course, there are limitations to such a design. For example, in thermal reactions, the chemistry will take place under conditions of *constant pressure* rather than of *constant volume* which are found in a sealed autoclave. The precise consequences of this difference have yet to be explored. The scale of the reactions is still modest but the small size of the reactor combined with on-line spectroscopic monitoring means that even small quantities of compounds can be manipulated with a surprising degree of precision. Ultimately, the most appealing feature of the technique may be the possibility of carrying out synthetic chemistry in the total absence of conventional organic solvents.

**Acknowledgment.** We thank Mr. D. G. Robertson for obtaining the FT-Raman data on the Cr(CO)<sub>6</sub>/C<sub>2</sub>H<sub>4</sub> system. We are grateful to Dr. S. M. Howdle and Dr. P. Mountford for their help and guidance. We are pleased to acknowledge our fruitful collaboration with Dr. G. A. Lawless and Dr. M. P. Waugh via an EU COST program. We thank the EPSRC Clean Technology Unit for Grants No. GR/H95464 and No. GR/J95065 and for a Fellowship to M.P. We also thank the Royal Society, the Royal Academy of Engineering, BP Chemicals, and Zeneca Ltd. for support. We thank Dr. A. Banister, Dr. S. M. Critchley, Mr. J. G. Gamble, Dr. M. W. George, Mr. M. Guylar, Dr. M. Jobling, Mr. T. P. Lynch, Dr. K.-H. Pickel, Mr. K. Stanley, Professor J. J. Turner, and Dr. R. J. Watt for their help and advice.

OM9503813

# A Tetrachromium Complex from the Cage-Opening of $P_4S_3$ by Cyclopentadienylchromium Tricarbonyl. Synthesis, X-ray Crystal Structure, and Thermal Degradation of $Cp_4Cr_4(CO)_9(P_4S_3)$ . $CpCr(CO)_3H$ as a Byproduct<sup>†</sup>

Lai Yoong Goh,\* Wei Chen, and Richard C. S. Wong

Department of Chemistry, University of Malaya, 59100 Kuala Lumpur, Malaysia

K. Karaghiosoff

Institut für Anorganische Chemie, Universität München, Meiserstrasse 1, München D-80333, Germany

Received March 27, 1995<sup>®</sup>

The reaction of  $[CpCr(CO)_3]_2$  (**1**) with  $P_4S_3$  for 13 days at ambient temperature led to the isolation of  $Cp_4Cp_4(CO)_9(P_4S_3)$  (**2**, 66%),  $[CpCr(CO)_2]_2S$  (**3**, 13%),  $CpCr(CO)_2P_3$  (**4**, 2%), and  $CpCr(CO)_3H$  (**5**, 19%). In the presence of isoprene, **5** was not formed. Instead,  $[CpCr(CO)_2]_2$  (**8**, 4%) was obtained, alongside **2** (59%), **3** (5%), **4** (2%), and  $[CpCr(CO)_2]_2P_2$  (**6**, 3%). Under thermolytic conditions (60 °C for 3 h), the product composition changed to a mixture of **2** (30%), **3** (36%), **4** (0.4%), **5** (3%), **6** (1%), and  $Cp_4Cr_4S_4$  (**7**, 7%). The reaction of **8** with  $P_4S_3$  at 60 °C for 18 h yielded **3** (10%), **5** (34%), **6** (14%), and **7** (30%). The thermolysis of **2** at 80 °C for 3.5 h gave **3** (23%), **4** (10%), **6** (10%), and **7** (53%). The complexes were characterized spectroscopically and via thin layer chromatography versus authentic samples, where appropriate. The crystals of **2**, **4**, **5**, and recovered  $P_4S_3$  were also studied by X-ray diffraction analysis. Crystal data: **2** (dark brown crystals), space group triclinic  $P\bar{1}$ ,  $a = 12.074(1)$  Å,  $b = 12.880(3)$  Å,  $c = 14.451(5)$  Å,  $\alpha = 73.05(2)^\circ$ ,  $\beta = 73.21(1)^\circ$ ,  $\gamma = 78.67(1)^\circ$ ,  $Z = 2$ ,  $V = 2042.5(9)$  Å<sup>3</sup>; **5** (yellow polyhedron), space group monoclinic  $P2_1/n$ ,  $a = 10.982(2)$  Å,  $b = 7.284(1)$  Å,  $c = 11.844(2)$  Å,  $\alpha = 90.0^\circ$ ,  $\beta = 116.85(1)^\circ$ ,  $\gamma = 90^\circ$ ,  $Z = 4$ ,  $V = 845.3(2)$  Å<sup>3</sup>;  $P_4S_3$  (thick yellow needles), space group orthorhombic  $Pnma$ ,  $a = 10.596(2)$  Å,  $b = 9.6622(7)$  Å,  $c = 13.661(2)$  Å,  $Z = 8$ ,  $V = 1398.7(6)$  Å<sup>3</sup>.

## Introduction

For more than a decade, there has been sustained interest in the reactivity of main-group clusters toward transition metal fragments.<sup>1–4</sup> In particular, the cage molecules  $E_4X_3$  and  $E_4X_4$  from group 15 and 16 elements ( $E = P, As$ ;  $X = S, Se$ ) have featured prominently, on account of their diverse reaction pathways resulting in a rich structural variety of the resultant organometallic complexes. This area of work has been covered in a recent review by Di Vaira and Stoppioni.<sup>3</sup>

Having investigated the facile reactivity of the metal–metal-bonded complex  $[CpCr(CO)_3]_2$  toward  $X_8$  ( $X = S^5$  and  $Se^6$ ) and the  $E_4$  tetrahedra ( $E = P^{7,8}$  and  $As^9$ ), we

have extended the study to  $P_4S_3$ . Following a preliminary account,<sup>10</sup> we now describe the full details of our findings.

## Experimental Section

**General Procedures.** All reactions were carried out using conventional Schlenk techniques under an inert atmosphere of nitrogen or under argon in a Vacuum Atmospheres Dribox equipped with a Model HE 493 Dri-Train.

**Physical Measurements and Elemental Analysis.** <sup>1</sup>H and <sup>13</sup>C NMR spectra were measured on a JEOL FX100 (100 MHz) or JEOL JNM-GSX 270 (270 MHz) FT NMR spectrometer, with chemical shifts referenced to residual  $C_6H_6$  in benzene-*d*<sub>6</sub> or to  $(CH_3)_4Si$  in toluene-*d*<sub>8</sub>. <sup>31</sup>P NMR spectra were measured on a JEOL FX90Q FT (36.23 MHz) or JEOL JNM-GSX 270 (96.15 MHz) spectrometer and chemical shifts were referenced to external  $H_3PO_4$ . IR spectra in Nujol mulls or solution were measured in the range 4000–200  $cm^{-1}$  by means of a Perkin-Elmer 1600 FTIR instrument. Mass spectra were run on a VG ProSpec spectrometer. The VISIBLE spectrum of  $CrO_4^{2-}$  (for Cr analysis) was measured on a Beckmann DU-7 spectrometer.

Elemental S and P analyses were performed by the Analytical Unit of the Research School of Chemistry, Australian National University. C and H analyses were performed by the Industrial Research & Consultancy Unit of Universiti

<sup>†</sup> Presented in part at the Australian Symposium on Organometallic Chemistry, December 5–8, 1993, University of New England, Armidale, NSW, Australia, and at the 7th International Symposium on Inorganic Ring Systems, August 7–12, 1994, Banff, Canada.

<sup>®</sup> Abstract published in *Advance ACS Abstracts*, July 1, 1995.

(1) Scherer, O. *J. Angew. Chem., Int. Ed. Engl.* **1990**, *29*, 1104.

(2) Review: Dimaio, A.-J.; Rheinhold, A. L. *Chem. Rev.* **1990**, *90*, 169.

(3) Review: Di Vaira, M.; Stoppioni, P. *Coord. Chem. Rev.* **1992**, *120*, 259 and references cited therein.

(4) Brunner, H.; Nuber, B.; Poll, L.; Wachter, J. *Angew. Chem., Int. Ed. Engl.* **1993**, *32*, 1627.

(5) Goh, L. Y.; Hambley, T. W.; Robertson, G. B. *Organometallics* **1987**, *6*, 1051.

(6) Chen, W.; Goh, L. Y.; Sinn, E. *Organometallics* **1988**, *7*, 2020.

(7) Goh, L. Y.; Wong, R. C. S.; Chu, C. K.; Hambley, T. W. *J. Chem. Soc., Dalton Trans.* **1989**, 1951.

(8) Goh, L. Y.; Wong, R. C. S.; Sinn, E. *J. Chem. Soc., Chem. Commun.* **1990**, 1484; *Organometallics* **1993**, *12*, 888.

(9) Goh, L. Y.; Wong, R. C. S.; Mak, T. C. W. *Organometallics* **1991**, *10*, 875.

(10) Goh, L. Y.; Chen, W.; Wong, R. C. S. *Angew. Chem., Int. Ed. Engl.* **1993**, *32*, 1728.

Sains Malaysia. Chromium was analyzed as  $CrO_4^{2-}$  in an alkaline medium.<sup>11</sup>

**Solvents and Reagents.**  $[CpCr(CO)_3]_2$  (**1**) was synthesized as described by Manning<sup>12</sup> from chromium hexacarbonyl (99% purity from Aldrich Chemical Co.).  $CpCr(CO)_3H$  was prepared as reported by Baird.<sup>13</sup>  $P_4S_3$  purchased from Fluka was recrystallized from benzene before use. All solvents were dried over sodium/benzophenone and distilled before use. Celite (Fluka AG), silica gel (Merck Kieselgel 60, 35–70 and 230–400 mesh), and TLC plates (Merck Kieselgel  $^{60}F_{254}$ ) were dried at 150 °C overnight before chromatographic use.

**Reaction of  $[CpCr(CO)_3]_2$  with Tetraphosphorus Trisulfide,  $P_4S_3$ . (a) At Ambient Temperature.** A deep green suspension of **1** (100 mg, 0.25 mmol) and  $P_4S_3$  (55 mg, 0.25 mmol) in toluene (15 mL) was stirred at ambient temperature for 13 days. The resultant yellowish brown reaction mixture was filtered through Celite (1 cm  $\times$  1 cm disk, ca. 1 g), concentrated, absorbed onto silica gel (ca. 2 g), evacuated to dryness, and loaded onto a silica gel column (1.5 cm  $\times$  10 cm) prepared in *n*-hexane. Elution gave three fractions.

(i) Yellow eluate in *n*-hexane (50 mL): Concentration to ca. 2 mL and cooling at  $-28$  °C overnight yielded a fine pale yellow precipitate of unreacted  $P_4S_3$  (18 mg, 0.082 mmol, 32.7% recovery) and a mother liquor which required rechromatography as described below.

(ii) Dirty green eluate in *n*-hexane–toluene (2:1, 35 mL): Concentration to dryness yielded deep green crystalline solids of  $[CpCr(CO)_2]_2S$  (**3**) (12 mg, 0.032 mmol, 12.7% yield), identified by its  $^1H$  NMR ( $\delta(Cp)$  4.36 in benzene- $d_6$ )<sup>5,14</sup> and TLC against an authentic sample ( $R_f = 0.46$  with *n*-hexane–toluene (3:2) as eluent).

(iii) Reddish brown eluate in *n*-hexane–toluene (1:2, 45 mL): Concentration to dryness yielded dark brown crystalline solids of  $Cp_4Cr_4(CO)_9(P_4S_3)$  (**2**) (77 mg, 0.082 mmol, 66% yield).  $^1H$  NMR (benzene- $d_6$ ):  $\delta(Cp)$  4.58 (s), 4.61 (s), 4.76 (s), 4.77 (d,  $J = 1.5$  Hz) at 2–3 times the intensity at  $\delta(Cp)$  4.61 (s), 4.70 (s), 4.79 (d,  $J = 1.5$  Hz), and 4.86 (s).  $^{13}C$  NMR (benzene- $d_6$ ):  $\delta(Cp)$  91.71, 92.07, 92.72, 93.15. The  $^{31}P$  NMR spectrum in  $C_6D_6$  is shown in Figure 5a. IR:  $\nu(CO)$  2028 vs 1983 vs, 1969 vs, 1950 vs, 1942 vs, 1899 s, 1882 ssh, 1874 vs  $cm^{-1}$  (Nujol). Anal. Calcd for  $C_{28}H_{20}Cr_4O_9P_4S_3$ : C, 37.03; H, 2.14; Cr, 22.11; P, 13.17; S, 10.23%. Found: C, 36.03; H, 1.75; Cr, 22.40; P, 12.45; S, 10.20.

The mother liquor of fraction i above was rechromatographed on a silica gel column (1.5 cm  $\times$  5 cm). Elution with *n*-hexane (35 mL) gave a greenish yellow solution which, when concentrated to dryness, yielded fine yellow crystalline solids (30 mg), the  $^1H$  and  $^{31}P$  NMR spectra of which indicated a 3:1:8 molar mixture of  $P_4S_3$  (15% recovery),  $CpCr(CO)_2P_3$  (**4**) (2%), and  $CpCr(CO)_3H$  (**5**) (19%). This mixture was recrystallized from a small volume of THF–hexane for several days at  $-30$  °C to yield three types of crystals, distinguishable by their colors, viz. yellow  $P_4S_3$ , brownish-yellow **4**, and lemon yellow **5**. Selected crystals of these were subjected to X-ray diffraction analysis described below. These compounds were also identified by their spectral characteristics. Data for  $P_4S_3$  are as follows:  $^{31}P$  NMR (benzene- $d_6$ )  $\delta$  64.82 (q,  $J = 70$  Hz, 1 P, apical), 126.21 (d,  $J = 70$  Hz, 3 P, basal); MS  $m/z$  220 [ $P_4S_3$ ], 157 [ $P_3S_2$ ], 125 [ $P_3S$ ], 94 [ $P_2S$ ], 63 [PS]. For **4**:  $^1H$  NMR (benzene- $d_6$ )  $\delta(Cp)$  3.92;  $^{13}C$  NMR (benzene- $d_6$ )  $\delta(Cp)$  84.91;  $^{31}P$  NMR (benzene- $d_6$ )  $\delta$   $-285.6$ ; MS  $m/z$  266 [ $CpCr(CO)_2P_3$ ], 238 [ $CpCr(CO)P_3$ ], 210 [ $CpCrP_3$ ], 148 [ $CpCrP$ ], 145 [ $CrP_3$ ], 117 [ $CrP$ ].<sup>7</sup> For **5**:  $^1H$  NMR (benzene- $d_6$ )  $\delta(Cp)$  4.02,  $\delta(Cr-H)$   $-5.62$  (toluene- $d_8$ )  $\delta(Cp)$  4.09,  $\delta(Cr-H)$   $-5.63$ ;  $^{13}C$  NMR (benzene- $d_6$ )  $\delta(Cp)$  86.43; IR  $\nu(CO)$  2009 s and 1928 vs  $cm^{-1}$

(toluene), and 2018 s, 1946 s, and 1937 vs  $cm^{-1}$  (hexane);<sup>13</sup> MS  $m/z$  202 [ $CpCr(CO)_3H$ ], 174 [ $CpCr(CO)_2H$ ], 173 [ $CpCr(CO)_2$ ], 146 [ $CpCr(CO)H$ ], 145 [ $CpCr(CO)$ ], 118 [ $CpCrH$ ], 117 [ $CpCr$ ]. Additional elution with toluene (15 mL) gave a light brown solution which when dried yielded more yellow solids of  $P_4S_3$  (3 mg, 0.014 mmol, 5.5% recovery).

(b) At 60 °C. A deep green suspension of **1** (500 mg, 1.24 mmol) and  $P_4S_3$  (330 mg, 1.50 mmol) in toluene (30 mL) was stirred at 60 °C for 3 h. The resultant greenish brown mixture was filtered through a 2 cm  $\times$  1 cm disk of Celite. The concentrated filtrate absorbed onto silica gel (ca. 5 g) was evacuated to dryness and then loaded onto a silica gel column (1.5 cm  $\times$  15 cm) prepared in *n*-hexane. Five fractions were eluted.

(i) Yellow eluate in *n*-hexane (20 mL) followed by *n*-hexane–toluene (9:1, 25 mL): Cooling of the concentrated eluate (3 mL) at  $-28$  °C overnight yielded pale yellow needles of  $P_4S_3$  (45 mg, 0.20 mmol, 13.6% recovery). The mother liquor was rechromatographed on a silica gel column (1.5 cm  $\times$  8 cm). Elution with *n*-hexane–toluene (8:2, 50 mL) gave a yellow solution, the yellowish brown residue (60 mg) of which contained a 16:6:1 molar mixture of  $P_4S_3$ ,  $CpCr(CO)_3H$  (**5**), and  $CpCr(CO)_2P_3$  (**4**) with estimated yields of 13%, 3%, and 0.4%, respectively, based on its  $^{31}P$  and  $^1H$  NMR spectra.

(ii) Dirty green eluate in *n*-hexane–toluene (7:3, 40 mL) was eluted which when concentrated to dryness yielded deep green crystals of  $[CpCr(CO)_2]_2S$  (**3**) (170 mg, 0.45 mmol, 36.3% yield).

(iii) A magenta fraction in *n*-hexane–toluene (1:1, 30 mL) was eluted from which were obtained fine dark crystalline solids of  $[CpCr(CO)_2]_2P_2$  (**6**) (5 mg, 0.012 mmol, 1% yield), identified by its  $^1H$  NMR ( $\delta(Cp)$  4.15 in benzene- $d_6$ )<sup>7</sup> and TLC against an authentic sample ( $R_f = 0.41$  with *n*-hexane–toluene (3:2) as eluent).

(iv) A reddish brown fraction in toluene (40 mL) was eluted which yielded dark brown solids of  $Cp_4Cr_4(CO)_9(P_4S_3)$  (**2**) (130 mg, 0.14 mmol, 22.2% yield).

(v) A greenish brown fraction in ether (40 mL) was eluted which gave a brown residue (85 mg) consisting of **2** in admixture with  $Cp_4Cr_4S_4$  (**7**), identified by its  $^1H$  NMR ( $\delta(Cp)$  4.90 in benzene- $d_6$ )<sup>5,15</sup> and TLC against an authentic sample ( $R_f = 0.79$  with toluene–ether (3:2) as eluent) and an unidentified Cp-containing compound ( $\delta$  5.13). Rechromatography of this mixture on a silica gel column (1.5 cm  $\times$  10 cm) prepared in *n*-hexane–ether (1:1) gave a brown eluate in toluene (35 mL) which yielded brown residual solids of **2** (45 mg, 0.05 mmol, 8.1% yield), followed by a dirty green eluate in toluene–ether (9:1, 35 mL) which gave fine dark green solids of **7** (25 mg, 0.042 mmol, 6.8% yield).

(c) At Ambient Temperature in the Presence of Isoprene. A deep green mixture of **1** (80 mg, 0.20 mmol) and  $P_4S_3$  (44 mg, 0.20 mmol) in toluene (10 mL) containing ca. 10  $\mu$ L of isoprene was stirred at ambient temperature. After 9 days, the resultant dark brown product solution showed an approximately 40:5:1:2 molar mixture of **2**, **3**, **4**, and **6**, respectively, in its  $^1H$  NMR spectrum. Filtration on Celite removed a small amount of green insoluble solids. The ensuing chromatographic work up as in reaction a above, gave five fractions

(i) A pale yellow eluate in *n*-hexane (30 mL) which when concentrated to dryness yielded brownish yellow solids (16 mg). The solids were extracted with *n*-hexane (2  $\times$  5 mL), leaving behind unreacted  $P_4S_3$  (18 mg, 0.08 mmol, 41% recovery). Concentration of the extracts to dryness gave yellow flakes of **4** (ca. 2 mg, 0.007 mmol, 2% yield).

(ii) A dirty green eluate in *n*-hexane–toluene (4:1, 25 mL) which gave deep green crystalline solids of **3** (4 mg, 0.01 mmol, 5.3% yield).

(iii) A deep green eluate in *n*-hexane–toluene (3:1, 15 mL) which gave dark green solids of  $[CpCr(CO)_2]_2$  (**8**) (ca. 3 mg, 0.01 mmol, 4.4% yield).

(15) Chen, W.; Goh, L. Y.; Mak, T. C. W. *Organometallics* **1986**, *5*, 1977.

(11) Haupt, G. W. *J. Res. Nat. Bur. Stand.* **1952**, *48*, 414.  
 (12) Birdwhistle, R.; Hackett, P.; Manning, A. R. *J. Organomet. Chem.* **1978**, *157*, 239.  
 (13) Cooley, N. A.; MacConnachie, P. T. F.; Baird, M. C. *Polyhedron* **1988**, *7*, 1965.  
 (14) Greenhough, T. J.; Kolthammer, B. W. S.; Legzdins, P.; Trotter, J. *Inorg. Chem.* **1979**, *18*, 3543.

Table 1. Data Collection and Processing Parameters

molecular formula	Cp <sub>4</sub> Cr <sub>4</sub> (CO) <sub>9</sub> P <sub>4</sub> S <sub>3</sub> ·THF (2)	CpCr(CO) <sub>3</sub> H	P <sub>4</sub> S <sub>3</sub>
M <sub>r</sub>	1012.66	202.13	220.09
cryst color and habit	dark brown polyhedron	yellow polyhedron	thick yellow needles
cryst size (mm <sup>3</sup> )	0.1 × 0.15 × 0.2	0.46 × 0.43 × 0.2	0.3 × 0.3 × 0.21
unit cell parameters			
<i>a</i> (Å), α (deg)	12.074(1), 73.05(2)	10.982(2), 90.0	10.596(2)
<i>b</i> (Å), β (deg)	12.880(3), 73.21(1)	7.284(1), 116.85(1)	9.6622(7)
<i>c</i> (Å), γ (deg)	14.451(5), 78.67(1)	11.844(2), 90.0	13.661(2)
<i>V</i> (Å <sup>3</sup> ), <i>Z</i>	2042.5(9), 2	845.3(2), 4	1398.7(6), 8
<i>D<sub>x</sub></i> (Mg m <sup>-3</sup> )	1.646	1.588	2.090
cryst syst	triclinic	monoclinic	orthorhombic
space group	<i>P</i> 1̄	<i>P</i> 2 <sub>1</sub> / <i>n</i>	<i>Pnma</i>
radiation	Mo Kα	Mo Kα	Mo Kα
no. of reflns for lattice params	25	25	25
θ range for lattice params (deg)	12–15	15–16	14–16
abs coeff (mm <sup>-1</sup> )	1.365	1.312	1.806
temp (K)	300	300	300
diffractometer type	CAD4	CAD4	CAD4
collection method	<i>ω</i> -2θ	<i>ω</i> -2θ	<i>ω</i> -2θ
abs corr type	<i>ψ</i> -scan	<i>ψ</i> -scan	<i>ψ</i> -scan
abs corr ( <i>T</i> <sub>min</sub> , <i>T</i> <sub>max</sub> )	91.77, 99.76	89.40, 99.66	77.31, 98.45
no. of reflns measd	6208	1563	2478
no. of independent reflns	5788	1489	1302
θ <sub>max</sub> (deg)	25°	25°	25°
no. of obsd reflns	3221	1177	983
no. of std reflns (and interval)	3 (400)	3 (200)	3 (400)
criterion for obsd reflns	> 3σ( <i>I</i> )	> 3σ( <i>I</i> )	> 3σ( <i>I</i> )
variation of standards (% h <sup>-1</sup> )	-3.27 × 10 <sup>-1</sup>	-6.58 × 10 <sup>-1</sup>	-1.10 × 10 <sup>-1</sup>
<i>h</i>	0–12	-13 to 11	0–11
<i>k</i>	-15 to 15	0–8	0–12
<i>l</i>	-16 to 17	0–14	-8 to 0
<i>R</i>	0.048	0.052	0.044
<i>R<sub>w</sub></i>	0.057	0.126	0.052
no. of params refined	447	117	73
no. of reflns used in refinement	3221	1177	983
<i>S</i>	0.455	1.198	1.509
weighting scheme: <i>w</i> =	[σ( <i>F</i> ) <sup>2</sup> + 0.0004 <i>F</i> <sup>2</sup> + 1] <sup>-1</sup>	[σ <sup>2</sup> ( <i>F<sub>o</sub></i> ) <sup>2</sup> + (0.0600 <i>P</i> ) <sup>2</sup> + 0.4800 <i>P</i> ] <sup>-1</sup> <sup>a</sup>	[σ( <i>F</i> ) <sup>2</sup> ] <sup>-1</sup>
(Δσ) <sub>max</sub>	0	0.01	0.00
( <i>Q</i> ) <sub>max</sub> (e Å <sup>-3</sup> )	1.039	0.424	0.833

$$^a P = (F_o^2 + 2F_c^2)/3.$$

(iv) A light magenta eluate in *n*-hexane–toluene (2:1, 15 mL) which gave dark magenta solids of **6** (ca. 2 mg, 0.005 mmol, 2.5% yield).

(v) A reddish brown eluate in *n*-hexane–toluene (1:3, 40 mL) which gave fine dark brown crystalline solids of **2** (55 mg, 0.059 mmol, 58.9% yield). A greenish blue immovable band remained at the top of the column.

**Reaction of [CpCr(CO)<sub>2</sub>]<sub>2</sub> (8) with P<sub>4</sub>S<sub>3</sub>.** A deep green suspension of [CpCr(CO)<sub>2</sub>]<sub>2</sub> (50 mg, 0.145 mmol) and P<sub>4</sub>S<sub>3</sub> (32 mg, 0.145 mmol) in toluene (10 mL) was stirred at ambient temperature. No reaction was observed after 24 h. The reaction temperature was therefore raised to 60 °C, and the reaction proceeded to completion in ca. 18 h. The resultant dirty brown mixture was filtered through a 1.5 cm × 2 cm disk of Celite. The filtrate was concentrated, absorbed on silica gel (1.5 g), which was evacuated to remove solvent, and loaded onto a silica gel column (1.5 cm × 12 cm) prepared in *n*-hexane. Elution gave five fractions.

(i) A yellow eluate in *n*-hexane–toluene (4:1, 15 mL) which, when concentrated to dryness, yielded a brownish yellow residue (41 mg). Extraction with *n*-hexane (3 × 5 mL) left behind unreacted P<sub>4</sub>S<sub>3</sub> (13 mg, 0.06 mmol, 41% recovery). Concentration of the combined extracts to dryness yielded a brownish yellow solid (28 mg), the <sup>1</sup>H NMR spectrum of which showed a 2.7:1 molar mixture of CpCr(CO)<sub>3</sub>H (estimated 20 mg, 0.10 mmol, 34%) and CpCr(CO)<sub>2</sub>P<sub>3</sub> (estimated 8 mg, 0.03 mmol, 10%).

(ii) A green eluate in *n*-hexane–toluene (3:1, 20 mL) which gave dark green solids of [CpCr(CO)<sub>2</sub>]<sub>2</sub> (4 mg, 0.011 mmol, 8% recovery).

(iii) A magenta eluate in *n*-hexane–toluene (1:1, 25 mL) which gave dark magenta crystalline solids of [CpCr(CO)<sub>2</sub>]<sub>2</sub>P<sub>2</sub> (**6**) (8 mg, 0.02 mmol, 14% yield).

(iv) A dirty brownish green eluate in toluene–ether (1:1, 20 mL) which gave dark green solids of Cp<sub>4</sub>Cr<sub>4</sub>S<sub>4</sub> (13 mg, 22 mmol, 30% yield).

(v) A dark brown eluate in THF (20 mL) which gave an unidentified dark brown oily residue (9 mg).

**Thermolysis of Cp<sub>4</sub>Cr<sub>4</sub>(CO)<sub>9</sub>(P<sub>4</sub>S<sub>3</sub>) (2).** A stirred reddish brown solution of **2** (80 mg, 0.085 mmol) in toluene (15 mL) was maintained at 80 °C for 3.5 h. The resultant yellowish brown solution was concentrated to ca. 2 mL followed by addition of *n*-hexane (0.5 mL). Cooling at -28 °C overnight yielded fine dark green solids of Cp<sub>4</sub>Cr<sub>4</sub>S<sub>4</sub> (5 mg, 0.008 mmol, 9.4% yield) which was filtered. The mother liquor was concentrated to ca. 1 mL and loaded onto a silica gel column (1.5 cm × 17 cm) prepared in *n*-hexane. Four fractions were eluted.

(i) A yellow eluate in *n*-hexane–toluene (9:1, 35 mL) which when concentrated to dryness yielded brownish yellow crystals of CpCr(CO)<sub>2</sub>P<sub>3</sub> (**4**) (9 mg, 0.034 mmol, 10.0% yield), identified by its <sup>1</sup>H NMR (δ(Cp) 3.92 in benzene-*d*<sub>6</sub>)<sup>7</sup> and its TLC characteristics against an authentic sample (*R<sub>f</sub>* = 0.65 with *n*-hexane–toluene (3:2) as eluent).

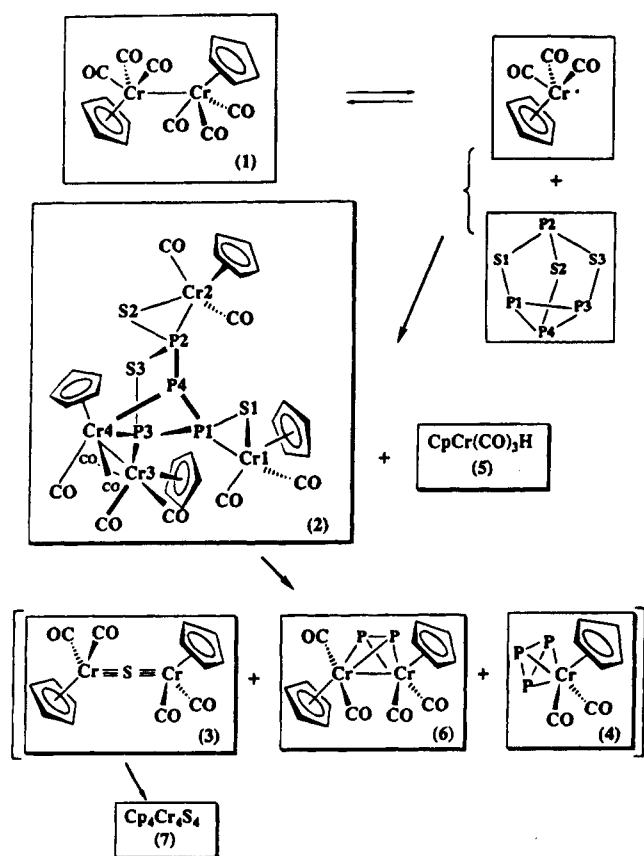
(ii) A dirty green eluate in *n*-hexane–toluene (3:1, 35 mL) which gave deep green crystals of [CpCr(CO)<sub>2</sub>]<sub>2</sub>S (**3**) (15 mg, 0.039 mmol, 23.3% yield).

(iii) A magenta eluate in *n*-hexane–toluene (1:3, 30 mL) which gave fine dark magenta solids of [CpCr(CO)<sub>2</sub>]<sub>2</sub>P<sub>2</sub> (**6**) (7 mg, 0.017 mmol, 10.1% yield).

(iv) A dirty brown eluate in ether (30 mL) which gave fine dark green solids of Cp<sub>4</sub>Cr<sub>4</sub>S<sub>4</sub> (**7**) (22 mg, 0.037 mmol, 43.5% yield).

**NMR Tube Experiments.** The following reactions were studied in C<sub>6</sub>D<sub>6</sub> in 5 mm NMR tubes via intermittent proton NMR spectral analysis: (a) reaction of a 2.4 mM solution of **1**

Scheme 1



with 0.5, 1, and 2 mol equiv, respectively, of  $P_4S_3$ , at 60 and 80 °C; (b) reaction of a 2.8 mM solution of  $[CpCr(CO)_2]_2$  with 0.5 and 1 mol equiv, respectively, of  $P_4S_3$  at 60 °C; (c) reaction of a 5 mM yellow solution of  $CpCr(CO)_3H$  with 1 mol equiv of  $P_4S_3$  for 18 h at 60 °C, and for 25 h at 80 °C, respectively; and (d) thermolysis of a 1 mM reddish brown solution  $Cp_4Cr_4(CO)_9(P_4S_3)$  (2) at 60 °C, both in the absence of  $P_4S_3$  and in the presence of 9 mol equiv of  $P_4S_3$ .

**Crystal Structure Analyses.** Single crystals of **2** were obtained as dark brown polyhedra from THF–ether after 3 weeks at –30 °C. Diffraction-quality single crystals of **5** (pale lemon yellow),  $P_4S_3$  (yellow), and **4** (brownish yellow) were selected from a mixture of crystals, obtained as described above, from a reaction at ambient temperature. Lemon yellow crystals of  $CpCr(CO)_3H$  were obtained from THF–hexane after a week at –30 °C. Details for the known structure of **4**<sup>7</sup> are not presented here, while those for the improved structure of  $P_4S_3$  molecule (previously determined four decades ago<sup>16</sup>) have been deposited as supporting information.

The crystals used for unit cell determination and data collection for **2** and  $P_4S_3$  were coated with epoxy glue while those of an authentic sample of  $CpCr(CO)_3H$  and the product **5** were sealed in glass capillaries to prevent decomposition in air. Details of the crystal parameters, data collection, and structure refinement are given in Table 1. Raw intensities were processed for Lorentz polarization effects and decay and corrected for absorption.<sup>17</sup> Structures of **2**, **5**, and  $P_4S_3$  were solved by the direct method MULTAN.<sup>18</sup> All non-hydrogen atoms were subjected to anisotropic refinement. Hydrogen atoms of the cyclopentadienyl rings were generated geo-

metrically each with a distance of 0.95 Å and was allowed to ride with  $B = 1.3$  times that of the parent atom. A disordered THF solvent molecule per molecule of **2** was found in the unit cell. The positional parameters for the five-membered ring were fixed while their displacement parameters were all refined as carbon atoms. Residual peaks in the final difference map account mainly for peaks around the THF molecules. The hydrogen atom in **5** cannot be located from the difference map. The crystal structure of  $CpCr(CO)_3H$  was solved by the heavy atom method from a Patterson synthesis, and all the remaining atoms were located from subsequent difference Fourier maps except for the hydrogen atoms on the Cp ring which were generated geometrically with riding mode on their respective parent C atoms. Two peaks were located near the Cr atoms at about 1.2 Å and were assigned as hydride and refined with occupancies of 0.5 each. The isotropic thermal parameters were reasonable and refinement concluded at  $R = 0.052$ . Computations for **2**, **5**, and  $P_4S_3$  were performed using the MolEN<sup>19</sup> package on a DEC MicroVax-II computer, while SHELXL93 programs were used for  $CpCr(CO)_3H$  on an IBM 486PC. Analytic expressions of atomic scattering factors were employed and anomalous dispersion corrections were incorporated.<sup>20</sup>

## Results and Discussion

**Reaction of  $[CpCr(CO)_3]_2$  (1) with  $P_4S_3$ .** The reaction of a suspension of yellow  $P_4S_3$  in a deep green toluene solution of 1 mol equiv of  $[CpCr(CO)_3]_2$  (1) for 13 days at ambient temperature, resulted in a yellowish brown mixture. Column chromatography of the product mixture on silica gel led to the isolation of unreacted  $P_4S_3$  (33%),  $Cp_4Cr_4(CO)_9(P_4S_3)$  (2) as dark brown crystals (66%),  $[CpCr(CO)_2]_2S$  (3) as deep green crystals (13%), and an inseparable mixture of  $CpCr(CO)_2(\eta^3-P_3)$  (4) as brownish yellow crystals (2%),  $CpCr(CO)_3H$  (5) as lemon yellow crystals (19%), and  $P_4S_3$  (15%) (yields of  $CpCr$  complexes are based on 1).

In the presence of isoprene, this reaction at ambient temperature for 9 days yielded **2** (59%), **3** (5.3%), **4** (2%), **6** (2.5%), and **8** (4.4%) with recovered  $P_4S_3$  (41%), but none of the hydride **5**.

A similar reaction at 60 °C for 3 h gave a substantially lower yield of **2** (30%) with increased yields of **3** (36%) and  $Cp_4Cr_4S_4$  (7) as dark green solids (6.8%), together with **4** (ca. 1%), **5** (3%),  $[CpCr(CO)_2]_2P_2$  (6) as magenta crystals (1%), and unreacted  $P_4S_3$  (13%). The apparent formation of **3**, **4**, **6**, and **7** at the expense of **2** is further demonstrated in a thermolysis study described below.

Although the elemental analysis of **5** is not attainable, its identity was unambiguously established via a crystal structure analysis, as well as a match of its spectral characteristics with those of a synthesized authentic sample as discussed below. In addition, thin-layer chromatography on Kieselgel  $^{60}F_{254}$  showed that compound **5** and the authentic  $CpCr(CO)_3H$  complex were identical species ( $R_f = 0.53$  with 3:2 *n*-hexane–toluene as eluent). The isolation of the hydride **5** is unexpected. It is significant that hydride formation was not observed in a reaction in the presence of isoprene, the reagent used for the synthesis of the dimer **1** from the hydride **5**.<sup>13</sup> One may envisage that its appreciable yield from the present reaction is a consequence of the cage effect of  $P_4S_3$  on the  $CpCr(CO)_3$  radical, rendering its reverse

(16) Leung, Y. C.; Waser, J.; Houten, S. Van; Vos, A.; Wiegers, G. A.; Wiebenga, E. H. *Acta Crystallogr.* **1957**, *10*, 574. Houten, S. Van; Vos, A.; Wiegers, G. A. *Recl. Trav. Chim. Pays-Bas* **1955**, *74*, 1167.

(17) North, A. C. T.; Philips, D. C.; Mathews, F. S. *Acta Crystallogr.* **1968**, *24A*, 351.

(18) MULTAN80. Main, P.; Fiske, S. J.; Hull, S. E.; Lessinger, L.; Germain, G.; DeClerq, J. P.; Woolfson, M. M. University of York: York, England, 1980.

(19) MolEn: An Interactive Structure Solution Procedure; Delft Instruments: Delft, The Netherlands, 1990.

(20) Cromer, D. T. *International Tables for X-ray Crystallography*; Kynoch Press: Birmingham, England, 1974; Vol. IV, Tables 2.2B and 2.3.1.

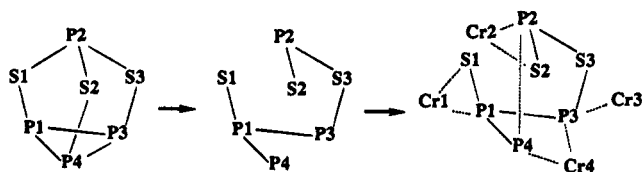


**Figure 1.** Bond cleavage and rearrangement of the  $P_4S_3$  cage.

dimerization unfavorable versus hydrogen atom abstraction from a hydrogen source. Slight formation of **1** with  $Ph_2S_2$ ,<sup>21</sup> though its identity was not recognized then, owing to the variability of the chemical shift of the Cp resonance.<sup>22c</sup> In this context, we note that atom transfer reactions constitute a common feature of transition metal-centered radicals.<sup>23</sup> Indeed, Baird has recently established the facile halogen atom abstraction from organic halides by  $CpCr(CO)_3$ .<sup>22</sup>

Consonant with the established facile thermal dissociation of the Cr–Cr bond in **1**<sup>24–29</sup> and the accumulating evidence suggesting that reactions of **1** generally proceed via its 17e monomeric derivative,<sup>13,24,25</sup> the role of  $CpCr(CO)_3$  is again implicated in this reaction (Scheme 1) as observed in our previous studies with group 15 and 16 nonmetals.<sup>5–9</sup> The radical cleavage of the P2–S1, P4–S2, and P3–P4 bonds of the  $P_4S_3$  cage, with subsequent cage rearrangement and concomitant coordination of  $CpCr(CO)_n$  ( $n = 2, 3$ ) fragments (Figure 1) will generate the molecular structure (Figure 2) described below.

**Reaction of  $[CpCr(CO)_2]_2$  (**8**) with  $P_4S_3$ .** No reaction was observed at ambient temperature. At 60 °C, the reaction with 1 mol equiv of  $P_4S_3$  almost reached completion (92%) in 18 h, giving  $CpCr(CO)_3H$  (**5**) in significant yield (34%), together with  $Cp_4Cr_4S_4$  (**7**) (30%) as the second major product. The formation of **5** in such a substantial yield does indeed constitute a novel feature of this reaction. Intramolecular carbonyl scrambling in  $[(CO)_2CpCr\equiv CrCp(CO)_2]$  must have occurred, either prior to or concurrent with  $M\equiv M$  bond dissociation to form  $CpCr(CO)_3$ . It seems that again the cage of the  $P_4S_3$  molecule plays a role in assisting the formation of the hydride, as suggested above.

There are two possible pathways to the ( $\eta^3$ - $P_3$ ) complex **4** (10%), the ( $u$ - $\eta^2$ - $P_2$ ) complex **6** (14%), and the sulfur cubane complex **7**. They may be formed directly from the fragmentation of the  $P_4S_3$  cage by the  $Cr\equiv Cr$  bonded complex **8** or they may be derived from the thermal degradation of a primary product such as  $Cp_4$ -

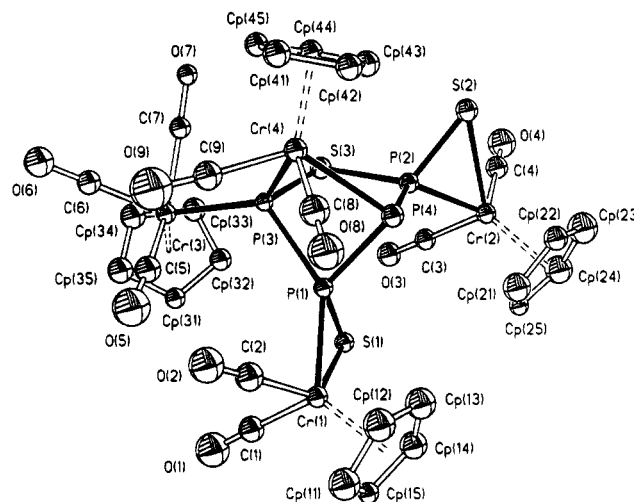


**Figure 2.** Molecular structure of **2**.

$Cr_4(CO)_9(P_4S_3)$  (**2**). The latter route would lead to the formation of  $[CpCr(CO)_2]_2S$  (**3**), as demonstrated in thermolytic studies described below. However, neither **2** nor **3** was observed despite careful monitoring in NMR tube experiments, suggesting that **2** is an unlikely primary product in the reaction. On a comparative note, it has been observed that the reaction of the  $Mo\equiv Mo$  complex  $[(C_5Me_5)Mo(CO)_2]_2$  with  $P_4S_3$  for 5 h in boiling toluene produced Mo complexes containing  $P_2S_3$  and  $P_4S$  ligands, in addition to the Mo analogues of **4** and **6**.<sup>30</sup>

**NMR Spectral Studies.** It was observed in NMR tube reactions of **1** with 0.5–2 mol equiv of  $P_4S_3$  at 60 °C for 3 h, that the yield (ca. 14%) of the hydride complex **5** was independent of the amount of  $P_4S_3$ . The reaction of **1** with 0.5 mol equiv of  $P_4S_3$  at 60 °C was complete within 4 h, giving as main products **2** (24%), **3** (14%), **5** (14%), and **7** (12%) with small amounts of **4** (6%) and **6** (7%) (cf. isolated yields of 30%, 36%, 3%, 7%, 0.4%, and 1%, respectively). Subsequently, **2** was observed to degrade to **3**, **4**, **6**, and predominantly **7**. The yield of **5** peaks at 3–4 h, ca. the time of completion of the reaction of **1**. The formation of  $CpCr(CO)_3H$  (**5**) from these reactions in  $C_6D_6$  seems to indicate that the hydridic H atom was derived from the Cp ligand, the only source of hydrogen atoms in the system. Investigations are currently under way to obtain definitive evidence for this suggestion.

At 80 °C, the reaction with one mol equiv of  $P_4S_3$  was complete within 1 h, yielding **2** (19%), **3** (21%), **4** (18%), **6** (16%), and **7** (18%). Within the next hour, all of **2** had degraded leading to slightly increased yields of **3** and **4** and a much higher yield of **7** (41%). At the end of 8 h, only **4** (23%) and **7** (68%) remained. As distinct from the reaction at 60 °C, there was no sign of the formation of the hydride **5** throughout the reaction. It may be envisaged that the enhanced rate of reaction of  $CpCr(CO)_3$  with  $P_4S_3$  is now competitive with that of its hydrogen atom abstraction, and the small amount of hydride that may be formed would react with  $P_4S_3$ . Indeed  $CpCr(CO)_3H$  was found to react with  $P_4S_3$  with a half-life of ca. 12 h at 60 °C (ca. 5 h at 80 °C) to give predominantly  $CpCr(CO)_2P_3$  (**4**) (ca. 3%) and  $Cp_4Cr_4S_4$  (**7**) (ca. 10%) with small amounts of  $[CpCr(CO)_2]_2$  and  $[CpCr(CO)_2]_2P_2$  as intermediate products.

(21) Goh, L. Y.; Tay, M. S. Unpublished observations.

(22) (a) Cooley, N. A.; Watson, K. A.; Fortier, S.; Baird, M. C. *Organometallics* **1986**, *5*, 2563. (b) Goulin, C. A.; Huber, T. A.; Nelson, J. M.; Macartney, D. H.; Baird, M. C. *J. Chem. Soc., Chem. Commun.* **1991**, 798. (c) MacConnachie, C. A.; Nelson, J. M.; Baird, M. C. *Organometallics* **1992**, *11*, 2521. (d) Huber, T. A.; Macartney, D. H.; Baird, M. C. *Organometallics* **1993**, *12*, 4715.

(23) Brown, T. L. Atom Transfer Reactions and Radical Chain Processes Involving Atom Transfer. In *Organometallic Radical Processes*; Trogler, W., Ed.; Elsevier: Lucerne, Switzerland, 1990.

(24) Goh, L. Y.; D'Aniello, M. J., Jr.; Slater, S.; Muettterties, E. L.; Tavanaiepour, I.; Chang, M. I.; Fredrich, M. F.; Day, V. W. *Inorg. Chem.* **1979**, *18*, 192.

(25) Baird, M. C. *Chem. Rev.* **1988**, *88*, 1217 and reference 40 therein.

(26) Adams, R. D.; Collins, D. E.; Cotton, F. A. *J. Am. Chem. Soc.* **1974**, *96*, 749.

(27) Madach, T.; Vahrenkamp, H. *Z. Naturforsch. B* **1978**, *33B*, 1301.

(28) McLain, S. J. *J. Am. Chem. Soc.* **1988**, *110*, 643.

(29) Goh, L. Y.; Lim, Y. Y. *J. Organomet. Chem.* **1991**, *402*, 209.

(30) Brunner, H.; Klement, U.; Meier, W.; Wachter, J.; Serhadle, O.; Ziegler, M. L. *J. Organomet. Chem.* **1987**, *335*, 339.

**Table 2. Atomic Coordinates and Their Equivalent Displacement Parameters for  $2^a$** 

atom	x	y	z	$B_{eq}$ (Å <sup>2</sup> )
Cr1	0.9669(1)	0.1427(1)	0.7459(1)	3.51(4)
Cr2	0.7739(1)	0.6350(1)	0.6664(1)	3.27(4)
Cr3	0.6101(1)	0.1827(1)	0.5715(1)	3.43(4)
Cr4	0.5347(1)	0.2363(1)	0.8763(1)	3.98(4)
S1	0.9265(2)	0.3135(2)	0.6192(2)	3.53(6)
S2	0.5665(2)	0.6216(2)	0.7671(2)	4.45(7)
S3	0.6059(2)	0.4341(2)	0.6271(2)	3.31(6)
P1	0.7961(2)	0.2554(2)	0.7332(2)	2.90(6)
P2	0.6668(2)	0.4930(2)	0.7225(2)	3.09(6)
P3	0.6257(2)	0.2624(2)	0.7025(2)	2.83(5)
P4	0.6938(2)	0.3469(2)	0.8428(2)	3.40(6)
O1	1.0422(8)	0.0423(7)	0.5732(6)	8.5(3)
O2	0.8308(7)	-0.0472(6)	0.8483(7)	7.6(3)
O3	0.8287(6)	0.5748(6)	0.4722(5)	5.2(2)
O4	0.6748(7)	0.8390(6)	0.5411(7)	7.5(3)
O5	0.7339(8)	-0.0154(6)	0.6870(6)	7.5(3)
O6	0.4526(6)	0.0115(6)	0.6186(6)	6.5(2)
O7	0.3714(6)	0.2997(7)	0.6402(6)	6.6(2)
O8	0.6860(7)	0.1018(8)	1.0123(6)	7.8(3)
O9	0.5310(9)	0.0148(6)	0.8545(7)	8.4(3)
C1	1.0117(9)	0.0817(9)	0.6401(8)	5.3(3)
C2	0.8822(9)	0.0273(8)	0.8052(8)	5.0(3)
C3	0.8080(8)	0.5971(8)	0.5480(7)	4.0(3)
C4	0.7099(9)	0.7619(8)	0.5913(8)	4.6(3)
C5	0.6861(9)	0.0614(7)	0.6489(8)	4.5(3)
C6	0.5134(9)	0.0775(8)	0.5995(8)	4.6(3)
C7	0.4624(8)	0.2558(8)	0.6157(8)	4.2(3)
C8	0.6282(9)	0.1560(9)	0.9581(8)	5.3(3)
C9	0.536(1)	0.1009(9)	0.8588(8)	5.1(3)
Cp11	1.0917(9)	0.056(1)	0.8322(9)	6.5(3)
Cp12	1.002(1)	0.116(1)	0.8914(8)	6.0(3)
Cp13	1.0071(9)	0.2235(9)	0.8457(8)	5.5(3)
Cp14	1.0964(9)	0.2345(9)	0.7609(8)	5.5(3)
Cp15	1.1485(9)	0.132(1)	0.7518(9)	6.6(4)
Cp21	0.9019(9)	0.5464(9)	0.7519(8)	5.7(3)
Cp22	0.8291(9)	0.615(1)	0.8029(8)	5.6(3)
Cp23	0.840(1)	0.7184(8)	0.7462(8)	6.1(3)
Cp24	0.9209(9)	0.713(1)	0.6554(9)	7.1(3)
Cp25	0.9581(9)	0.604(1)	0.6614(8)	6.3(3)
Cp31	0.7825(9)	0.1816(8)	0.4635(8)	4.8(3)
Cp32	0.7389(8)	0.2912(8)	0.4637(7)	4.3(3)
Cp33	0.6352(9)	0.3138(9)	0.4337(8)	5.2(3)
Cp34	0.6156(9)	0.2187(9)	0.4151(8)	5.5(3)
Cp35	0.7060(9)	0.1380(9)	0.4330(8)	5.3(3)
Cp41	0.368(1)	0.214(1)	0.9834(9)	6.6(4)
Cp42	0.419(1)	0.288(1)	1.0053(9)	7.4(4)
Cp43	0.426(1)	0.379(1)	0.925(1)	7.2(4)
Cp44	0.385(1)	0.360(1)	0.8532(9)	6.3(4)
Cp45	0.3466(9)	0.260(1)	0.890(1)	6.6(4)
C101*	0.123	0.777	0.887	19(1)
C102*	0.233	0.726	0.871	22(1)
C103*	0.038	0.703	0.907	21(1)
C104*	0.115	0.603	0.878	26(2)
C105*	0.219	0.629	0.862	26(2)

<sup>a</sup> Starred atoms were refined isotropically. Anisotropically refined atoms are given in the form of the isotropic equivalent displacement parameter, defined as follows:  $(4/3)[a^2B(1,1) + b^2B(2,2) + c^2B(3,3) + ab(\cos \gamma)B(1,2) + ac(\cos \beta)B(1,3) + bc(\cos \alpha)B(2,3)]$ .

The reaction of  $[CpCr(CO)_2]_2$  with  $P_4S_3$  is approximately doubled on increasing the amount of  $P_4S_3$  from 0.5–1.0 mol equiv ( $t_{1/2} \approx 1$  and 2 h, respectively, at 60 °C). After 18 h, the spectra showed 28 and 36% yields, respectively, of the hydride **5**, in close agreement with the isolated yields given earlier. The complexes **4**, **6**, and an unknown compound are formed in much lower yields, while **2** and **3** were not observed at all throughout the reaction.

The rate of thermal degradation of **2** is enhanced in the presence of excess  $P_4S_3$ ,  $t_{1/2}$  being approximately 1 h at 60 °C, compared to 3–4 h in the absence of  $P_4S_3$ . Primary products include **3**, **4**, and **6**, which at the end of 4 h reached ca. 10%, 7%, and 4%, respectively,

**Table 3. Bond Lengths (Å) and Bond Angles (deg) of  $2$** 

Bond Lengths			
Cr1–S1	2.486(3)	O8–C8	1.18(1)
Cr1–P1	2.298(3)	O9–C9	1.14(1)
Cr1–C1	1.82(1)	Cr3–Cp31	2.21(1)
Cr1–C2	1.83(1)	Cr3–Cp32	2.23(1)
Cr1–Cp11	2.17(1)	Cr3–Cp33	2.19(1)
Cr1–Cp12	2.18(1)	Cr3–Cp34	2.15(1)
Cr1–Cp13	2.21(1)	Cr3–Cp35	2.18(1)
Cr1–Cp14	2.23(1)	Cr4–P3	2.284(3)
Cr1–Cp15	2.20(1)	Cr4–P4	2.467(3)
Cr2–S2	2.517(3)	Cr4–C8	1.83(1)
Cr2–P2	2.266(3)	Cr4–C9	1.83(1)
Cr2–C3	1.83(1)	Cr4–Cp41	2.17(1)
Cr2–C4	1.84(1)	Cr4–Cp42	2.17(1)
Cr2–Cp21	2.19(1)	Cr4–Cp43	2.21(1)
Cr2–Cp22	2.19(1)	Cr4–Cp44	2.20(1)
Cr2–Cp23	2.17(1)	Cr4–Cp45	2.19(1)
Cr2–Cp24	2.15(1)	S1–P1	2.000(4)
Cr2–Cp25	2.16(1)	S2–P2	2.002(4)
Cr3–P3	2.468(3)	S3–P2	2.105(4)
Cr3–C5	1.88(1)	S3–P3	2.162(3)
Cr3–C6	1.84(1)	P1–P3	2.206(4)
Cr3–C7	1.87(1)	P1–P4	2.193(4)
O1–C1	1.16(1)	P2–P4	2.203(4)
O2–C2	1.16(1)	C101–C102	1.351
O3–C3	1.16(1)	C101–C103	1.444
O4–C4	1.13(1)	C102–C105	1.334
O5–C5	1.12(1)	C103–C104	1.522
O6–C6	1.15(1)	C104–C105	1.306
O7–C7	1.14(1)	$\langle C-C \rangle_{cp}$	1.38(2)
Bond Angles			
S1–Cr1–P1	49.24(9)	P3–Cr4–C8	114.3(4)
S1–Cr1–C1	83.8(4)	P3–Cr4–C9	78.8(4)
S1–Cr1–C2	129.3(4)	P4–Cr4–C8	74.8(4)
P1–Cr1–C1	107.1(4)	P4–Cr4–C9	131.6(4)
P1–Cr1–C2	88.8(4)	C8–Cr4–C9	81.0(6)
C1–Cr1–C2	83.9(6)	Cr1–S1–P1	60.5(1)
S2–Cr2–P2	49.14(9)	Cr2–S2–P2	58.9(1)
S2–Cr2–C3	114.7(3)	P2–S3–P3	97.6(1)
S2–Cr2–C4	83.8(4)	Cr1–P1–S1	70.3(1)
P2–Cr2–C3	83.3(3)	Cr1–P1–P3	142.3(1)
P2–Cr2–C4	115.8(4)	Cr1–P1–P4	124.6(1)
C3–Cr2–C4	80.8(5)	S1–P1–P3	118.1(2)
P3–Cr3–C5	79.4(3)	S1–P1–P4	123.2(2)
P3–Cr3–C6	121.5(4)	P3–P1–P4	83.4(1)
P3–Cr3–C7	73.8(3)	Cr2–P2–S2	72.0(1)
C5–Cr3–C6	78.1(5)	Cr2–P2–S3	122.7(1)
C5–Cr3–C7	125.9(5)	Cr2–P2–P4	124.8(2)
C6–Cr3–C7	77.3(5)	Cr4–P4–P2	107.2(1)
S2–P2–S3	114.9(2)	P1–P4–P2	90.9(1)
S2–P2–P4	115.5(2)	Cr1–C1–O1	179(1)
S3–P2–P4	103.9(1)	Cr1–C2–O2	176(1)
Cr3–P3–Cr4	133.8(1)	Cr2–C3–O3	179(1)
Cr3–P3–S3	99.7(1)	Cr2–C4–O4	177(1)
Cr3–P3–P1	120.7(1)	Cr3–C5–O5	173(1)
Cr4–P3–S3	110.2(1)	Cr3–C6–O6	179(1)
Cr4–P3–P1	89.9(1)	Cr3–C7–O7	178(1)
S3–P3–P1	97.7(1)	Cr4–C8–O8	178(1)
Cr4–P4–P1	88.1(1)	Cr4–C9–O9	175(1)
P3–Cr4–P4	74.2(1)	$\langle C-C \rangle_{cp}$	108(1)

together with a secondary product **7** (24%). In the presence of  $P_4S_3$ , the formation of the hydride **5** was observed, comprising 3%–4% of the total product composition throughout the reaction. This seems to support the above-mentioned hypothesis that the  $P_4S_3$  cage does play a role in the formation of the hydride from  $CpCr(CO)_3$  formed from homolysis of Cr–P and Cr–S bonds in **2**. After 18 h, the predominant product was **7** (ca. 60%), with minor amounts of **4** (4%) and **6** (2%) also being formed.

**Thermolysis of  $Cp_4Cr_4(CO)_9(P_4S_3)$  (**2**).** Thermolysis of a toluene solution of **2** for 3.5 h at 80 °C led to complete degradation to  $[CpCr(CO)_2]_2S$  (**3**),  $CpCr(CO)_2P_3$



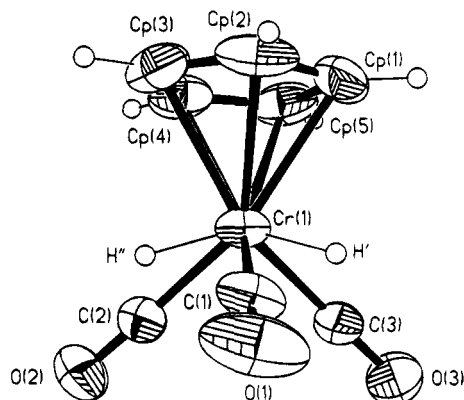


Figure 3. Molecular structure of  $\text{CpCr}(\text{CO})_3\text{H}$ .

Table 4. Atomic Coordinates ( $\times 10^4$ ) and Equivalent Isotropic Displacement Parameters ( $\text{\AA}^2 \times 10^3$ ) for  $\text{CpCr}(\text{CO})_3\text{H}^a$

atom	x	y	z	$U(\text{eq})$
Cr	4830(1)	-102(1)	2171(1)	63(1)
O1	7576(4)	317(6)	2339(7)	145(2)
O2	5534(4)	-3082(6)	4072(4)	114(1)
O3	4006(6)	-3179(5)	320(4)	138(2)
C1	6519(5)	148(6)	2265(6)	83(1)
C2	5266(5)	-1946(7)	3334(5)	74(1)
C3	4332(6)	-1998(6)	1032(5)	83(1)
Cp1	3431(7)	1963(9)	967(6)	104(2)
Cp2	4501(6)	2826(6)	2005(8)	101(2)
Cp3	4441(6)	2255(8)	3061(6)	100(2)
Cp4	3379(6)	1062(7)	2749(7)	94(2)
Cp5	2751(5)	872(7)	1479(7)	92(2)

<sup>a</sup>  $U(\text{eq})$  is defined as one-third of the trace of the orthogonalized  $U_{ij}$  tensor.

(4),  $[\text{CpCr}(\text{CO})_2]_2\text{P}_2$  (6), and  $\text{Cp}_4\text{Cr}_4\text{S}_4$  (7) in 23.3%, 9.9%, 10.1%, and 54.9% yields, respectively. This finding indicates that the reaction of 1 with  $\text{P}_4\text{S}_3$  produces primarily the complex 2, which degrades to the triply bonded  $\text{Cr}=\text{S}=\text{Cr}$  complex 3, and the ( $\mu$ - $\eta^2$ - $\text{P}_2$ ) complex 6 together with the cyclo- $\text{P}_3$  complex 4.<sup>7</sup> On the basis of our previous observations on the facile thermal transformation of 3 to the cubane complex 7 at room temperature<sup>5</sup> and 60 °C,<sup>15</sup> it is more likely that in this reaction 7 is derived from 3, rather than directly from 2. These reaction pathways are presented schematically in Scheme 1.

**Crystal Structures. Structure of 2.** The molecular structure is shown in Figure 2. Atomic coordinates and their equivalent isotropic displacement parameters are listed in Table 2. Selected bond lengths and bond angles are given in Table 3. It is apparent from a comparison of Figure 1 and the structure of 2 (Figure 2) that bond cleavages of the  $\text{P}_4\text{S}_3$  cage, as mentioned above, coupled with bond formation between P2 and P4 have led to the formation of a five-membered  $\text{P}_4\text{S}$  ring, namely  $\text{P3P1P4P2S3}$ , with two external S atoms as substituents at P1 and P2. Together with Cr4, this five-membered ring forms a bicyclo [2.1.1.] system, possessing common vertices at P3 and P4. In fact, the  $\text{P}_4\text{S}$  ring bridges four  $[\text{CpCr}(\text{CO})_n]$  ( $n = 2$  or 3) fragments via its four P atoms, its S atom not linked to any metal. Excepting Cr3, the other three Cr atoms are coordinated to two members of the  $\text{P}_4\text{S}_3$  system. It will be noted that P3 is the only P atom that links two Cr atoms, viz. Cr3 and Cr4, and is closer to the latter by 0.084 Å. Cr1 and Cr2 have similar ligand environments, both possessing a *pseudo*  $\eta^2$ -PS ligand. An earlier example of

Table 5. Bond Lengths (Å) and Angles (deg) for  $\text{CpCr}(\text{CO})_3\text{H}$

Bond Lengths			
Cr-C1	1.816(5)	O1-C1	1.131(6)
Cr-C2	1.826(5)	O2-C2	1.141(5)
Cr-C3	1.833(5)	O3-C3	1.143(6)
Cr-Cp3	2.156(5)	Cp1-Cp5	1.402(8)
Cr-Cp2	2.157(4)	Cp1-Cp2	1.408(8)
Cr-Cp1	2.163(5)	Cp2-Cp3	1.347(8)
Cr-Cp5	2.167(5)	Cp3-Cp4	1.365(8)
Cr-Cp4	2.171(4)	Cp4-Cp5	1.349(7)
Cr-H'	1.24(5)	Cr-Cp*	1.816(5)
Cr-H''	1.22(8)		
Bond Angles			
C1-Cr-C2	96.6(2)	O3-C3-Cr	179.2(6)
C1-Cr-C3	94.5(2)	Cp5-Cp1-Cp2	105.8(5)
C2-Cr-C3	83.7(2)	Cp3-Cp2-Cp1	107.5(5)
C1-Cr-H'	59(3)	Cp2-Cp3-Cp4	109.8(6)
C2-Cr-H'	128(2)	Cp5-Cp4-Cp3	108.1(5)
C3-Cr-H'	57(2)	Cp4-Cp5-Cp1	108.7(5)
C1-Cr-H''	82(4)	Cp <sup>a</sup> -Cr-C1	124.5(3)
C2-Cr-H''	37(4)	Cp <sup>a</sup> -Cr-C2	122.9(3)
C3-Cr-H''	119(4)	Cp <sup>a</sup> -Cr-C3	123.6(3)
H'-Cr-H''	138(5)	Cp <sup>a</sup> -Cr-H'	107(4)
O1-C1-Cr	179.1(6)	Cp-Cr-H''	107(4)
O2-C2-Cr	178.9(5)		

<sup>a</sup> Cp ring center.

$\eta^2$ -PS coordination has been established for the  $\text{Cr}(\text{CO})_5$  adduct of  $\text{Cp}^*_2\text{Mo}_2\text{P}_4\text{S}_3$ .<sup>30</sup> Each of the five-coordinate Cr atoms assumes a four-legged piano-stool geometry. The bonded P-P distances (average, 2.201 Å), significantly shorter than those in the  $\text{P}_4\text{S}_3$  cage (average, 2.232(2) Å), are very close to the single bond (2.21 Å) in  $\text{P}_4$  vapor.<sup>31</sup> The P-S distances (average, 2.067 Å) are also shorter than in the intact cage (average, 2.092(2) Å). The Cr-P distances (average, 2.282 Å) in the CrPS rings for Cr1 and Cr2 are significantly shorter than the other three Cr-P bonds (average, 2.440 Å), which fall within the range 2.341–2.494 Å observed for other CpCr-phosphorus complexes.<sup>7,8</sup> The Cr-S distances (2.486 and 2.517 Å) are longer than those observed in  $\text{Cr}(\mu$ - $\eta^2$ - $\text{S}_2$ ) and  $\text{Cr}(\mu$ - $\eta^1, \eta^2$ - $\text{S}_2$ ) complexes (range 2.348–2.466 Å).<sup>5</sup>

This is the first example of multiple bond-cleavage without fragmentation of the  $\text{P}_4\text{S}_3$  cage molecule by a transition metal complex. Previous examples of  $\text{P}_4\text{X}_3$  ( $\text{X} = \text{S}, \text{Se}$ ) as a ligand in transition metal complexes involve the coordination of the intact  $\text{P}_4\text{X}_3$  cages via its apical P atom [as represented by P2 in Figure 1], e.g., in *cis*-( $\text{P}_4\text{S}_3$ )<sub>2</sub> $\text{M}(\text{CO})_4$  ( $\text{M} = \text{Cr}, \text{Mo}, \text{W}$ ) and *cis*-( $\text{P}_4\text{S}_3$ )<sub>3</sub> $\text{M}'$ -( $\text{CO})_3$  ( $\text{M}' = \text{Cr}, \text{Mo}$ ),<sup>32</sup>  $\text{Mo}(\text{CO})_5(\text{P}_4\text{S}_3)$ <sup>33</sup> and  $(\text{np}_3)\text{Ni}(\text{P}_4\text{X}_3)$  ( $\text{X} = \text{S}, \text{Se}$ ;  $\text{np}_3 = [\text{N}(\text{CH}_2\text{CH}_2\text{PPh}_2)_3]$ ).<sup>34</sup> In the presence of the ligand triphos [1,1,1-tris(diphenylphosphino)methyl]ethane,  $\text{MeC}(\text{CH}_2\text{PPh}_2)_3$ , the reaction of  $\text{P}_4\text{X}_3$  ( $\text{X} = \text{S}, \text{Se}$ ) with  $\text{Co}(\text{BF}_4)_2 \cdot 6\text{H}_2\text{O}$ <sup>35,36</sup> and  $[\text{RhCl}(\text{COD})]_2$  (COD = cycloocta-1,5-diene)<sup>37</sup> had resulted in fragmentation of the  $\text{P}_4\text{X}_3$  cage, yielding the complexes [(triphos)- $\text{Co}(\text{P}_2\text{X})\text{BF}_4$ ] and [(triphos)Rh( $\text{P}_3\text{X}_3$ )], respectively. In its reaction with the  $\text{Mo}=\text{Mo}$  triply bonded complex  $[\text{Cp}^*\text{Mo}(\text{CO})_2]_2$  ( $\text{Cp}^* = \eta^5\text{-C}_5\text{Me}_5$ ), the  $\text{P}_4\text{S}_3$  cage like-

(31) Maxwell, L. R.; Hendricks, S. B.; Mosley, V. M. *J. Chem. Phys.* **1935**, *3*, 699.

(32) Jefferson, R.; Klein, H. F.; Nixon, J. F. *Chem. Commun.* **1969**, 536.

(33) Cordes, A. W.; Joyner, R. D.; Shores, R. D.; Dill, E. D. *Inorg. Chem.* **1974**, *13*, 132.

(34) Di Vaira, M.; Peruzzini, M.; Stoppioni, P. *Inorg. Chem.* **1983**, *22*, 2196; *J. Organomet. Chem.* **1983**, *258*, 373.

(35) Di Vaira, M.; Peruzzini, M.; Stoppioni, P. *J. Chem. Soc., Chem. Commun.* **1982**, 894; *J. Chem. Soc., Dalton Trans.* **1984**, 359.

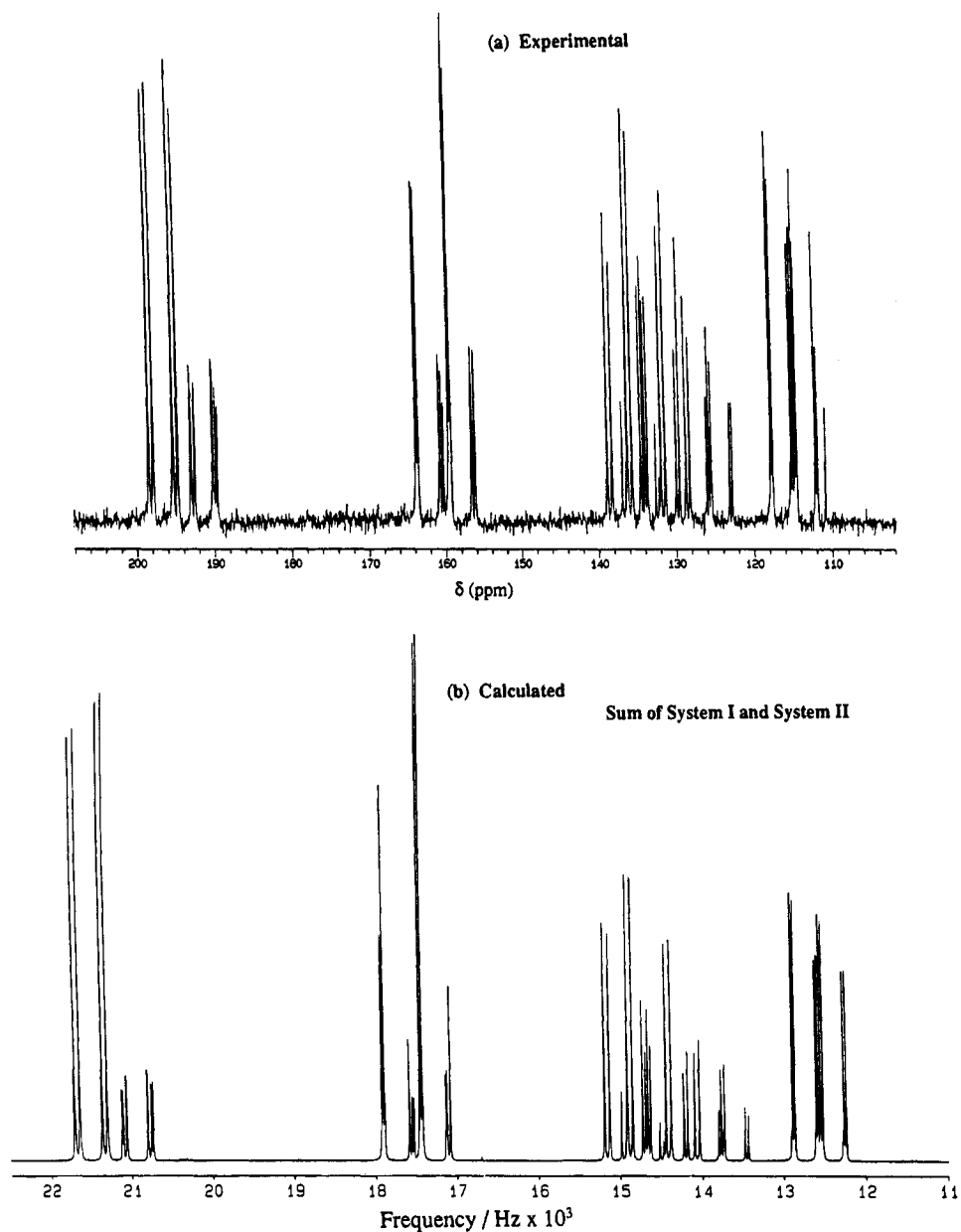


**Figure 4.** Experimental and calculated  $^{31}\text{P}$  NMR spectra of **2**.

wise underwent fragmentation, giving a mixture of  $\text{Cp}^*\text{Mo}(\text{CO})_2\text{P}_3$ ,  $\text{Cp}^*_2\text{Mo}_2(\text{CO})_4\text{P}_2$ ,  $\text{Cp}^*_2\text{Mo}_2\text{P}_2\text{S}_3$ , and  $\text{Cp}^*_2\text{Mo}_2\text{P}_4\text{S}_3$ .<sup>30</sup> In reactions with the  $d^8$  square-planar complexes  $\text{IrCl}(\text{CO})(\text{PPh}_3)_2$  (Vaska's complex) and  $\text{Pt}(\text{C}_2\text{H}_4)(\text{PPh}_3)_2$ , cleavage of a single P–P bond in the basal  $\text{P}_3$  triangle, led to the  $[\mu\text{-P}_4\text{S}_3]$ -bridged binuclear  $[\text{Ir}(\mu\text{-P}_4\text{S}_3)(\text{PPh}_3)\text{Cl}(\text{CO})]_2$ <sup>38</sup> and trinuclear  $[\text{Pt}(\mu\text{-P}_4\text{S}_3)(\text{PPh}_3)]_3$ <sup>39</sup> complexes, respectively. Slight cage rearrangement has been observed before in the insertion of a  $\text{Cr}(\text{CO})_5$  fragment into the isostructural nortricyclic homopolyatomic Zintl ion  $\text{As}_7^{3-}$ <sup>40</sup> and very recently of three  $\text{Ni}(\text{CO})$  fragments into  $\text{Sb}_7^{3-}$ <sup>41</sup> and a  $\text{Mo}(\text{CO})_3$  fragment into  $\text{Sb}_7^{2-}$ .<sup>42</sup> In this case, the extensive cage-

opening cum structural rearrangement of the neutral  $\text{P}_4\text{S}_3$  molecule is unprecedented and may be attributed to the unusual reactivity of the radical-like 17-electron  $\text{CpCr}(\text{CO})_3^*$  fragment, as was observed in the formation of the polycyclophosphidochromium cluster  $[\text{CpCr}(\text{CO})_2]_5\text{P}_{10}$  from elemental  $\text{P}_4$ .<sup>8</sup>

**Structure of  $\text{CpCr}(\text{CO})_3\text{H}$ .** Crystals of both the authentic sample of the hydride and the product **5** have been structurally determined, and the molecular structure is shown in Figure 3. Atomic coordinates and their equivalent isotropic displacement parameters are given in Table 4, and bonding parameters in Table 5. The CO ligands form the three legs of a piano stool configuration. Unlike the tungsten analogue,<sup>43</sup> in which there was a large OC–W–CO angle which can accommodate

(36) Di Vaira, M.; Mani, F.; Moneti, S.; Peruzzini, M.; Sacconi, L. *Inorg. Chem.* **1985**, *24*, 2230.

(37) Di Vaira, M.; Peruzzini, M.; Stoppioni, P. *J. Chem. Soc., Chem. Commun.* **1983**, 903.

(38) Ghilardi, C. A.; Midollini, S.; Orlandini, A. *Angew. Chem., Int. Ed. Engl.* **1983**, *22*, 790.

(39) Di Vaira, M.; Peruzzini, M.; Stoppioni, P. *J. Chem. Soc., Dalton Trans.* **1985**, 291.

(40) Eichhorn, B. W.; Haushalter, R. C.; Huffman, J. C. *Angew. Chem., Int. Ed. Engl.* **1989**, *28*, 1032.

(41) Charles, S.; Eichhorn, B. W.; Bott, S. G. *J. Am. Chem. Soc.* **1993**, *115*, 5837.

(42) Bolle, V.; Tremel, W. *J. Chem. Soc., Chem. Commun.* **1994**, 217.

(43) Johnson, P. L. *Diss. Abstr.* **1968**, *29*, B1626. Frenz, B. A.; Ibers, J. A. *Molecular Structures of Transition Metal Hydride Complexes*. In *Transition Metal Hydrides*; Muetterties, E. L., Ed.; Marcel Dekker, Inc.: New York, 1971.

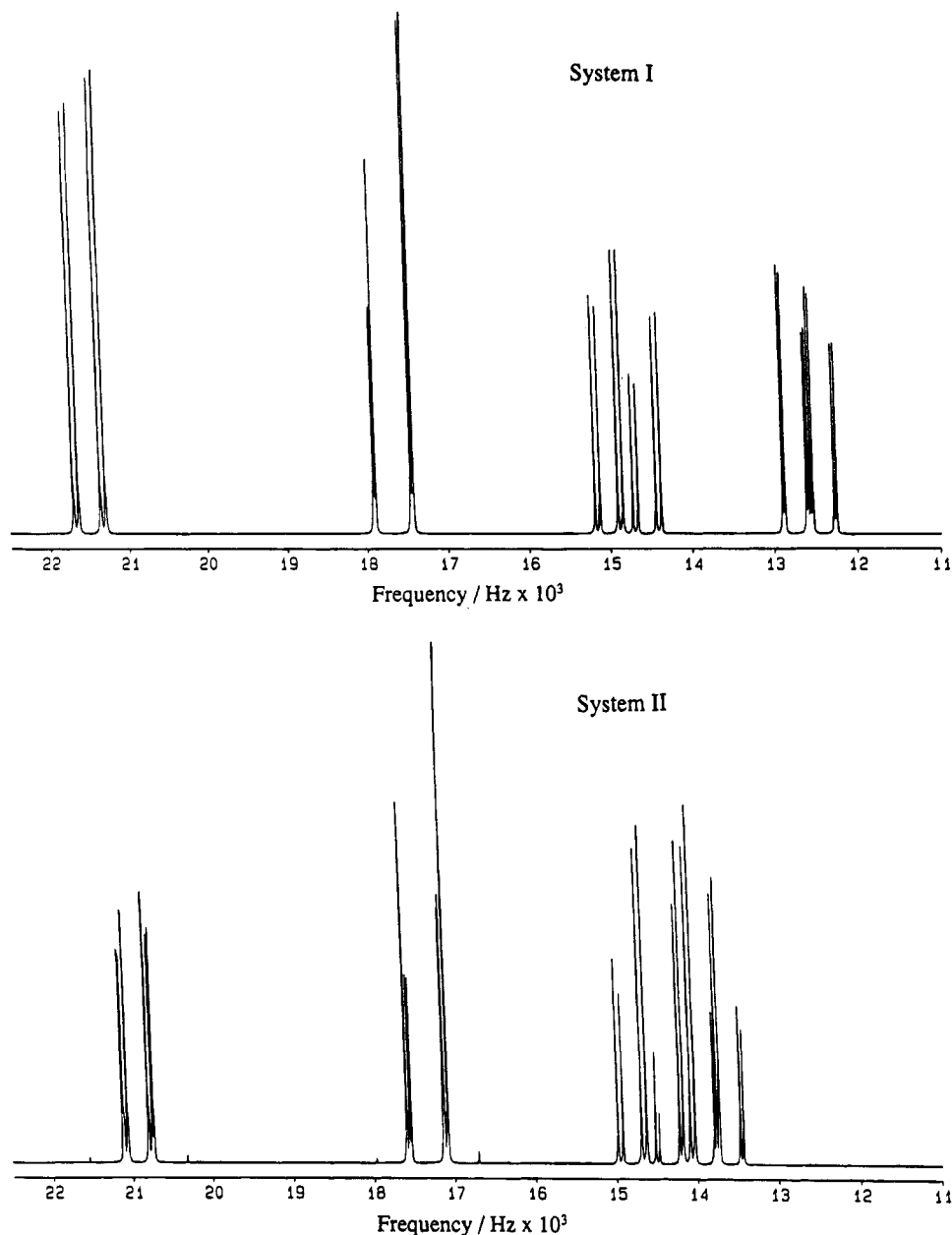


**Figure 5.** Calculated  $^{31}\text{P}$  NMR spectra for ABCD spin systems (I and II) for **2**.

a hydrogen atom, this hydride has two obtuse OC–Cr–CO angles and the one remaining acute angle. The hydrogen atoms are disordered at the two sites above the two obtuse angles, making H–Cr–Cp(center) angles of  $107(4)^\circ$ . The thermal parameters of all the atoms are quite high, consistent with the instability of the crystal. The Cr–H distances of 1.24(5) and 1.22(8) Å are within the sum of the covalent radii of Cr (1.18 Å) and hydrogen (0.2 Å).<sup>44</sup>

**Properties and Spectral Characteristics.** Complexes **3**, **4**, **6**, and **7** have been fully characterized from earlier work.<sup>5,7,14,15</sup> Dark brown crystals of **2** have been found to remain unchanged after several days in air. It is soluble in most organic solvents, except hexane, to give slightly air-sensitive reddish-brown solutions. In agreement with previous reports, the yellow hydride CpCr(CO)<sub>3</sub>H was found to be extremely air-sensitive in both the solid and solution state.

The proton NMR of **2** indicates an approximately 3:1 molar mixture of two isomers (isomer A,  $\delta(\text{Cp}) = 4.58(\text{s})$ , 4.61(s), 4.76(s), 4.77 (d,  $J = 1.5$  Hz); isomer B,  $\delta(\text{Cp})$  4.61 (s), 4.70 (s), 4.79 (d,  $J = 1.5$  Hz), and 4.86 (s)). A variable-temperature  $^1\text{H}$  NMR study in toluene-*d*<sub>8</sub> shows that isomer A is the predominant species below  $-30^\circ\text{C}$  ( $\delta(\text{Cp})$  4.39, 4.53, 4.63, and 4.71) and that rapid exchange of the four Cp rings at  $90^\circ\text{C}$  gives rise to a singlet at  $\delta$  4.77. The  $^{13}\text{C}$  NMR of the isomeric mixture shows Cp resonances at  $\delta$  90.39, 91.71 (the most intense peak, unresolved with  $\delta$  91.58 and 91.45), 92.07, 92.72, and 93.15.

The  $^{31}\text{P}$  NMR spectrum is complex and is illustrated in Figure 4a. Analysis shows that the signals belong to two ABCD spin systems (I and II) with an intensity ratio of approximately 3:1. Both spin systems have been successfully analysed using the LAOCN-5 computer program,<sup>45</sup> and their respective calculated spectra are

(44) Handy, L. B.; Treichel, P. M.; Dahl, L. F. *J. Am. Chem. Soc.* **1966**, *88*, 366.

(45) Cassidei, L.; Sciacovelli, O. QCPE Program No. 458. PC version: Tupper, K. J. Program QCMP049.

**Table 6.**  $^{31}\text{P}$  NMR Chemical Shifts<sup>a</sup> and Peak Frequencies of  $\text{Cp}_4\text{Cr}_4(\text{CO})_8(\text{P}_4\text{S}_3)$  (**2**)

obsd resonance peaks $\delta$ (PPM)	frequency (Hz)		assignment to ABCD spin system	obsd resonance peaks $\delta$ (PPM)	frequency (Hz)		assignment to ABCD spin system
	exptl	calcd			exptl	calcd	
198.34	21691.00	21693.98	I	136.95	14977.10	14976.76	II
	21691.00	21693.23			136.25	14900.80	14900.60
197.80	21632.30	21630.57		135.66	14836.20	14837.06	
	21632.30	21630.53			134.58	14718.90	14717.60
195.28	21356.40	21355.32		134.26	14683.70	14684.98	II
	21356.40	21355.28			133.99	14654.30	14654.95
194.69	21291.90	21292.53		133.67	14619.10	14621.72	II
	21291.90	21291.78			132.65	14507.60	14508.48
193.02	21109.90	21111.46	II	132.22	14460.60	14463.57	
192.92	21098.20	21097.51			132.01	14437.20	14435.10
192.49	21051.30	21052.60		131.42	14372.60	14372.35	
	21051.30	21048.31			130.02	14220.00	14216.70
190.13	20793.00	20793.63		129.59	14173.10	14171.68	
		20789.44			128.79	14085.00	14084.95
189.75	20752.00	20748.61		128.25	14026.30	14028.35	
189.48	20722.60	20726.18			126.11	13791.60	13793.07
163.78	17911.50	17912.87	I	125.84	13762.30	13762.82	
	17911.50	17912.13			125.62	13738.80	13736.47
163.56	17888.00	17885.52		125.52	13727.00	13724.37	
	17888.00	17885.48			123.15	13468.80	13471.05
160.77	17582.80	17584.36	II	122.83	13433.60	13432.59	
	17582.80	17580.06			117.84	12887.80	12886.74
160.45	17547.60	17545.90		117.57	12859.50	12860.09	
160.24	17524.10	17523.46			115.27	12606.10	12604.15
159.54	17447.80	17447.42	I	115.00	12576.80	12577.50	
	17447.80	17447.38			114.73	12547.40	12548.70
159.27	17418.50	17420.78		114.52	12523.90	12521.35	
	17418.50	17420.03			112.15	12265.70	12266.20
156.53	17119.20	17116.08	II	111.89	12236.40	12238.85	
156.10	17072.20	17077.62			110.87	12124.90 <sup>b</sup>	
	17072.20	17073.42					
138.82	15182.50	15183.10	I				
138.23	15117.90	15119.65					

<sup>a</sup> In  $\text{C}_6\text{D}_6$ , referenced to external 85%  $\text{H}_3\text{PO}_4$ . <sup>b</sup> Pertains to  $[\text{CpCr}(\text{CO})_2]_2\text{P}_2$  (**6**).

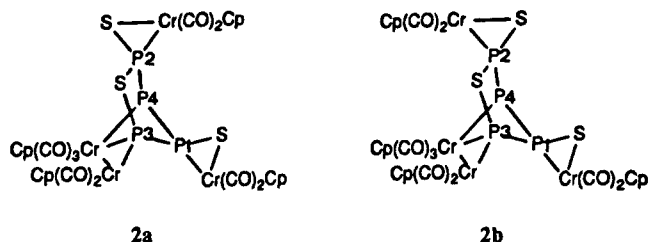
**Table 7.** Summary of NMR Parameters of Spin Systems I and II<sup>a</sup>

ABCD spin system I	ABCD spin system II
$\delta^{31}\text{P}$ : P <sub>3</sub> 196.5	$\delta^{31}\text{P}$ : P <sub>3</sub> 191.3
P <sub>2</sub> 161.5	P <sub>2</sub> 158.3
P <sub>4</sub> 135.2	P <sub>4</sub> 133.1
P <sub>1</sub> 115.0	P <sub>1</sub> 126.1
$^1J(\text{P}_3, \text{P}_1) = -339.9$	$^1J(\text{P}_3, \text{P}_1) = -330.5$
$^1J(\text{P}_4, \text{P}_1) = -284.9$	$^1J(\text{P}_4, \text{P}_1) = -293.9$
$^1J(\text{P}_2, \text{P}_4) = -467.4$	$^1J(\text{P}_2, \text{P}_4) = -478.3$
$^2J(\text{P}_3, \text{P}_2) < 1$	$^2J(\text{P}_3, \text{P}_2) = 3.8$
$^2J(\text{P}_3, \text{P}_4) = 65.3$	$^2J(\text{P}_3, \text{P}_4) = 72.3$
$^2J(\text{P}_2, \text{P}_1) = 31.6$	$^2J(\text{P}_2, \text{P}_1) = -26.6$

<sup>a</sup>  $J$  values given in hertz.

shown in Figure 5. The combined simulated spectrum for a 3:1 mixture, shown in Figure 4b, agrees remarkably well with the experimental spectrum (Figure 4a), with the exception of  $\delta$  110.87, which pertains to  $[\text{CpCr}(\text{CO})_2]_2\text{P}_2$  (**6**). The matching of experimental and calculated frequencies is given in Table 6. The spectrum of spin system I is nearly first order. In the case of spin system II, however, the signals of P<sub>1</sub> and P<sub>3</sub> get closer as compared to I, leading to a large value for  $J(\text{P}_1, \text{P}_3)/\nu_0\delta(\text{P}_1, \text{P}_3)$  and thus to a spectrum of high order. This affects also the signals of P<sub>2</sub> and P<sub>4</sub>, causing additional splittings.

The NMR parameters of I and II (Table 7) are quite similar. The large coupling constants indicate for both cases a P<sub>4</sub>-chain with the connectivity P<sub>3</sub>-P<sub>1</sub>-P<sub>4</sub>-P<sub>2</sub>

**Figure 6.** Proposed isomers corresponding to the two spin systems, I and II.

in agreement with the result of the X-ray structure determination of **2**. Thus most probably the two spin systems correspond to isomers having the same skeleton and differing only with respect to the configuration at P<sub>1</sub>, or more likely, at P<sub>2</sub> (e.g., **2a** and **2b** in Figure 6). The assignment of the  $^{31}\text{P}$ -NMR signals to the individual P atoms is based on the assumption that  $\delta^{31}\text{P}$  of the P atom with two Cr-neighbors appears at lower field than that of the P atom having one Cr- and one S-neighbor.

The EI and FAB mass spectra of **2** did not give any interpretable fragmentation pattern.

The spectral data of **5** were found to match closely those of a synthesized authentic sample of  $\text{CpCr}(\text{CO})_3\text{H}$ , viz.  $^1\text{H}$  NMR: (benzene- $d_6$ ),  $\delta(\text{Cp})$  4.06,  $\delta(\text{Cr}-\text{H})$  -5.62; (toluene- $d_8$ ),  $\delta(\text{Cp})$  4.10,  $\delta(\text{Cr}-\text{H})$  -5.63 (cf.  $\delta$  3.84 and -5.70, respectively).<sup>13</sup>  $^{13}\text{C}$  NMR: (benzene- $d_6$ ),  $\delta(\text{Cp})$  86.16; (toluene- $d_8$ ),  $\delta(\text{Cp})$  86.06. IR:  $\nu_{\text{CO}}$  2008 s, 1922 vs  $\text{cm}^{-1}$  (THF), and 2018 s, 1946 s, and 1937 vs  $\text{cm}^{-1}$

(*n*-hexanes) (cf.  $\nu_{\text{CO}}$  2010 s, 1922 vs br  $\text{cm}^{-1}$  (THF), and 2018 s, 1946 s, and 1936 vs  $\text{cm}^{-1}$  (hexanes)).<sup>13</sup> EI-MS:  $m/z$  202 [CpCr(CO)<sub>3</sub>H], 174 [CpCr(CO)<sub>2</sub>H], 173 [CpCr(CO)<sub>2</sub>], 146 [CpCr(CO)H], 145 [CpCr(CO)], 118 [CpCrH], and 117 [CpCr]. The apparent discrepancy in the  $\delta$ -(Cp) values is congruent with Baird's observation of a hydrogen atom exchange between the hydride and the CpCr(CO)<sub>3</sub>\* radical species, which results in coalescence of the Cp resonance of the dimer **1** with that of the hydride.<sup>22a,c</sup> In fact, we have observed that different samples of the product complex **5** possessed  $\delta$ (Cp) values in the range  $\delta$  4.02–4.26, with a corresponding increase in line width. This undoubtedly arose from some contamination with **1**, into which CpCr(CO)<sub>3</sub>H readily converts in the presence of trace amounts of air. It has been pointed out that the observed chemical shift and

line width of the coalesced resonance of **1** and its hydride is a weighted average of those of **1**, its monomer and hydride.<sup>22c</sup>

**Acknowledgment.** Support from the Malaysian IRPA R&D Grant No. 04-07-04-211 (L.Y.G.) and the University of Malaya, as well as from Universität München (K.K.), is gratefully acknowledged.

**Supporting Information Available:** Complete listings of anisotropic displacement parameters and bond lengths and angles for structures of **2**, CpCr(CO)<sub>3</sub>H, and P<sub>4</sub>S<sub>3</sub>, hydrogen coordinates and isotropic displacement parameters for CpCr(CO)<sub>3</sub>H, atomic coordinates of P<sub>4</sub>S<sub>3</sub>, details of NMR experiments, and a packing diagram of **2** (14 pages). Ordering information is given on any current masthead page.

OM950222J

# Intramolecular Transfer of CO from ( $\eta^6$ -arene)Cr(CO)<sub>3</sub> Complexes in Stille-Type Palladium-Catalyzed Cross-Coupling Reactions

Patrizia Caldirola, Ratan Chowdhury,<sup>†</sup> Anette M. Johansson,\* and Uli Hacksell

Organic Pharmaceutical Chemistry, Uppsala Biomedical Center, Uppsala University, Box 574, S-751 23 Uppsala, Sweden

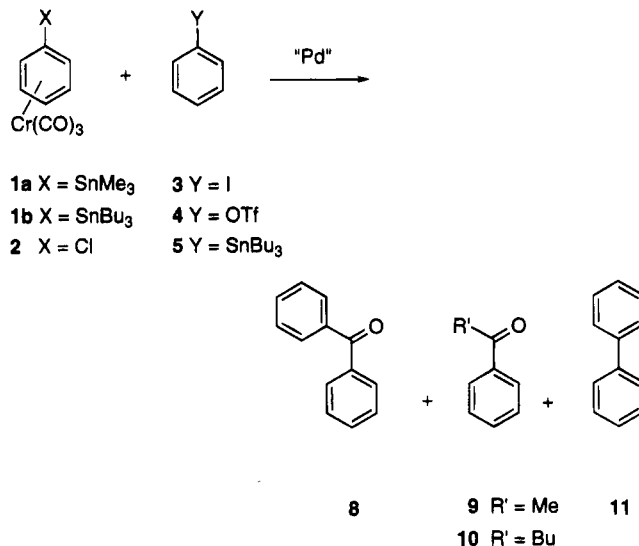
Received March 21, 1995<sup>©</sup>

Arylketones were formed from the Cr(CO)<sub>3</sub> complex of (trialkylstannyl)benzene or chlorobenzene by a palladium-catalyzed cross-coupling reaction in the absence of external CO. The Cr(CO)<sub>3</sub> moiety provides the required CO predominantly by an intramolecular mechanism. Products due to a direct coupling reaction were also observed. The influence of solvent, temperature, substrate, and catalyst on the relative amount of products due to both carbonylative coupling and direct coupling were studied.

## Introduction

We report that palladium(0)-catalyzed Stille<sup>1</sup> coupling reactions involving ( $\eta^6$ -arene)Cr(CO)<sub>3</sub> derivatives give carbonylated products in addition to cross-coupled products in the absence of an external source of CO. Pd-catalyzed studies on ( $\eta^6$ -arenes)Cr(CO)<sub>3</sub> have been previously reported to give carbonylated compounds only when CO was added as gas.<sup>2,3</sup> However, in the reactions of [ $\eta^6$ -(trimethylstannyl)benzene]Cr(CO)<sub>3</sub> (**1a**) or [ $\eta^6$ -(tributylstannyl)benzene]Cr(CO)<sub>3</sub> (**1b**) with iodobenzene (**3**) (Scheme 1) we observed products from two different types of reactions: (i) benzophenone (**8**) along with the alkyl aryl ketones acetophenone (**9**) or valerophenone (**10**),<sup>4</sup> resulting from carbonylative coupling, and (ii) biphenyl (**11**), arising from direct coupling. The observation of carbonylated products was not expected in the absence of external CO. In fact, neither an intermolecular nor an intramolecular version of such a reaction has been previously reported.<sup>5</sup> Therefore, we have studied this reaction in some detail using simple

## Scheme 1



reaction components and a variety of conditions (Scheme 1, Tables 1–6).

## Results and Discussion

Initially, the Stille-type palladium-catalyzed coupling reaction of iodobenzene (**3**) with Cr(CO)<sub>3</sub>-complexed organostannanes was explored. The organostannane–Cr(CO)<sub>3</sub> complex, **1a** or **1b**, was reacted with 1 or 2 equiv of **3** in the presence of a palladium catalyst in DMF at 100 °C (Scheme 1). After 24 h, the reactions were decomplexed by light (24 h), and the product distribution was determined by quantitative GC analysis. The amount of carbonylated product varied with the substrate, the catalyst, and the solvent (Table 1–2). In reactions using substrate **1a**, about equal amounts of the carbonylated **8** and **9** were formed; in addition, biphenyl (**11**) was formed, resulting in low ratios of **8**:**11**. Reactions performed under identical conditions with **1b** as substrate gave higher ratios of **8**:**11** and a low yield of **10** (Table 1). Slightly higher yields of **8** were obtained when 2 equiv of **3** was used.

The palladium-catalyzed reaction between **1b** and **3** was evaluated in several solvents (Table 2). The reac-

<sup>†</sup> Present address: Department of Chemical Engineering, Monash University, Clayton, Melbourne, Victoria 3168, Australia.

<sup>©</sup> Abstract published in *Advance ACS Abstracts*, July 15, 1995.

(1) Stille, J. K. *Angew. Chem., Int. Ed. Engl.* **1986**, *25*, 508–524.  
 (2) (a) Wright, M. E. *Organometallics* **1989**, *8*, 407–411. (b) Wright, M. E. *Macromolecules* **1989**, *22*, 3256–3259. (c) Uemura, M.; Nishimura, H.; Kamikawa, K.; Nakayama, K.; Hayashi, Y. *Tetrahedron Lett.* **1994**, *35*, 1909–1912.

(3) (a) Villemin, D.; Shigeo, E. *J. Organomet. Chem.* **1985**, *293*, C10–C12. (b) Scott, W. J. *J. Chem. Soc., Chem. Commun.* **1987**, 1755–1756. (c) Wright, M. E. *J. Organomet. Chem.* **1989**, *376*, 353–358. (d) Uemura, M.; Nishimura, H.; Hayashi, T. *J. Organomet. Chem.* **1994**, *473*, 129–137.

(4) (a) Milstein, D.; Stille, J. K. *J. Org. Chem.* **1979**, *44*, 1613–1618. (b) Labadie, J. W.; Stille, J. K. *J. Am. Chem. Soc.* **1983**, *105*, 6129–6137. (c) Gielen, M.; Nasielski, J. In *Organotin Compounds*; Sawyer, A. K., Ed; Dekker: New York, 1972; Vol. 3, pp 625–822.

(5) However, transition metal carbonyls [M(CO)<sub>n</sub>] have been used as carbonylating agents to prepare esters, amides, acids, or ketones from alkyl- and arylhalides in the presence or absence of carbon monoxide: (a) Thompson, D. J. In *Comprehensive Organic Synthesis*; Trost, B. M.; Fleming, I., Pattenden, G., Eds.; Pergamon Press: New York, 1991; Vol 3, pp 1015–1042. Co(CO)<sub>8</sub>; (b) Brunet, J.-J.; Sidot, C.; Caubere, P. *J. Org. Chem.* **1983**, *48*, 1166–1171. (c) Monflier, E.; Pellegrini, S.; Mortreux, A.; Petit, F. *Tetrahedron Lett.* **1991**, *32*, 4703–4704. Ni(CO)<sub>4</sub>; (d) Corey, E. J.; Hegedus, L. S. *J. Am. Chem. Soc.* **1969**, *91*, 1233–1234. (e) Tanaka, M. *Synthesis* **1981**, 47–48. Fe(CO)<sub>5</sub>; (f) Collman, J. P.; Winter, S. R.; Clark, D. R. *J. Am. Chem. Soc.* **1972**, *94*, 1788–1789. (g) Yamashita, M.; Mizushima, K.; Watanabe, Y.; Mitsudo, T.; Takegami, Y. *Chem. Lett.* **1977**, 1355–1358. (h) Reyne, F.; Brun, P.; Waegell, B. *Tetrahedron Lett.* **1990**, *31*, 4597–4600.

**Table 1. Palladium-Catalyzed Cross-Coupling Reaction Between [ $\eta^6$ -(Trialkylstannyl)benzene]Cr(CO)<sub>3</sub> (**1a,b**) and Iodobenzene (**3**) in DMF at 100 °C**

entry no.	$\eta^6$ -arene-Cr(CO) <sub>3</sub>	PhI (no. of equiv)	catalyst	products (yield %) <sup>a</sup>			
				<b>8</b>	<b>9</b>	<b>10</b>	<b>11</b>
1	<b>1a</b>	1	Pd(OAc) <sub>2</sub>	35	25		27
2	<b>1a</b>	2		31	25		30
3	<b>1b</b>	1		63		9	6
4	<b>1b</b>	2		83		18	12
5 <sup>b</sup>	<b>1b</b>	2		88		14	17
6	<b>1a</b>	1	(PPh <sub>3</sub> ) <sub>4</sub> Pd	44	24		13
7	<b>1a</b>	2		42	32		16
8	<b>1b</b>	1		72		7	5
9	<b>1b</b>	2		91		11	11
10 <sup>b</sup>	<b>1b</b>	2		81		7	10
11	<b>1a</b>	1	(PPh <sub>3</sub> ) <sub>2</sub> PdCl <sub>2</sub>	41	30		10
12	<b>1a</b>	2		49	20		14
13	<b>1b</b>	1		70		8	4
14	<b>1b</b>	2		81		11	4
15 <sup>b</sup>	<b>1b</b>	2		84		9	7
16	<b>1a</b>	1	(dba) <sub>3</sub> Pd <sub>2</sub> -(TFP) <sub>4</sub>	36	25		2
17	<b>1a</b>	2		42	23		3
18	<b>1b</b>	1		46		4	4
19	<b>1b</b>	2		63		5	4
20 <sup>b</sup>	<b>1b</b>	2		67		15	5

<sup>a</sup> Yield percentages were determined from quantitative GC analysis and were based on **1a** or **1b**. <sup>b</sup> The reactions were performed at 80 °C.

**Table 2. Effect of Different Solvents on the (PPh<sub>3</sub>)<sub>2</sub>PdCl<sub>2</sub>-catalyzed Reaction between [ $\eta^6$ -(Tributylstannyl)benzene]Cr(CO)<sub>3</sub> (**1b**) and Iodobenzene (**3**)<sup>a</sup>**

entry no.	solvent	temp (°C)	products (yield %) <sup>b</sup>		
			<b>8</b>	<b>10</b>	<b>11</b>
1	DMF	100	81	11	4
2	NMP <sup>c</sup>	100	73	12	1
3	THF	67	16	1	2
4	CH <sub>3</sub> CN	82	26	3	1

<sup>a</sup> The reactions were performed with 2 equiv of iodobenzene (**3**). <sup>b</sup> Yield percentages were determined by quantitative GC analysis and were based on **1b**. The results are the mean of two experiments. <sup>c</sup> NMP = *N*-methyl-2-pyrrolidinone.

tion was much more sluggish in THF and CH<sub>3</sub>CN as compared to DMF and NMP.<sup>6</sup> This effect may in part be related to the different boiling points of the solvents. However, also when reactions were performed at the same temperature (80–82 °C), the reaction in CH<sub>3</sub>CN was much less efficient than that in DMF (Tables 1–2). Since the carbonylated products **8** and **10** were also observed in solvents not containing a CO moiety (Table 2), we could reject the possibility that the CO in the carbonylated products would originate from the solvent. The sluggish reaction in CH<sub>3</sub>CN as compared to DMF or NMP may be related to a lower reaction rate because of increased stabilization of palladium complexes.<sup>7</sup>

The ability of different catalysts to catalyze the carbonylative coupling and the cross-coupling reactions of **1a** and **1b** with **3** was also studied (Table 1). The highest yield of **8** was obtained with (PPh<sub>3</sub>)<sub>2</sub>PdCl<sub>2</sub> and (PPh<sub>3</sub>)<sub>4</sub>Pd, whereas the use of tris(2-furyl)phosphine as ligand gave lower yields but increased the ratio of **8**:**11**. The presence of strongly stabilizing ligands does not

**Table 3. Cross-Coupling Reaction between [ $\eta^6$ -(Tributylstannyl)benzene]Cr(CO)<sub>3</sub> (**1b**) and Different Electrophiles with (PPh<sub>3</sub>)<sub>2</sub>PdCl<sub>2</sub> in DMF at 100 °C**

entry no.	compd	R	products (yield %) <sup>a</sup>		
			<b>A</b>	<b>B</b>	<b>C</b>
1	<b>3</b>	H	<b>8</b> 80 (81) <sup>b</sup>	<b>10</b> 6 (13) <sup>b</sup>	<b>11</b> N <sup>c</sup> (3) <sup>b</sup>
2	<b>6</b>	Me	<b>12</b> 80 (86) <sup>d</sup>	<b>13</b> 8 (10) <sup>d</sup>	<b>14</b> N (5) <sup>d</sup>
3	<b>7<sup>e</sup></b>	OMe	<b>15</b> 67	<b>16</b> 8	<b>17</b> N

<sup>a</sup> Yield percentages were based on isolated yields. <sup>b</sup> Yield percentages were determined by quantitative GC analysis. <sup>c</sup> N, not isolated. <sup>d</sup> Yield percentages were determined by <sup>1</sup>H NMR and were based on **1b**. <sup>e</sup> Benzophenone (**8**, 12%) was also formed.

seem to be crucial because carbonylated coupled products were also observed under "ligand-free" conditions using Pd(OAc)<sub>2</sub> as catalyst (Table 1, entries 1–5).

Both biphenyl and benzophenone might have been formed by (carbonylative) homocoupling reactions. Hence, in order to study the origin of the phenyl groups<sup>8</sup> in the products, we performed coupling reactions between **1b** and 4-iodotoluene (**6**, 2 equiv) and 4-iodoanisole (**7**, 2 equiv), respectively, in DMF using (PPh<sub>3</sub>)<sub>2</sub>PdCl<sub>2</sub> as catalyst (Table 3). The formation of 4-methylbenzophenone (**12**) and 4-methoxybenzophenone (**15**), respectively, as the main products established the carbonylative coupling as the predominant reaction pathway. 1-(4-Methylphenyl)- and 1-(4-methoxyphenyl)-1-pentanone (**13** and **16**) were also formed. The formation of biphenyl derivatives **14** and **17** confirmed that also homocoupling occurred.<sup>9</sup> Furthermore, **1b** may undergo a carbonylative homocoupling reaction because **8** (12%) was isolated from the reaction of **1b** with **7**.

The palladium-catalyzed carbonylation of **1b** was not restricted to the reaction with **3** but also worked well with phenyl triflate (**4**),<sup>10</sup> provided that LiCl (3 equiv) was added to the reaction mixture (Table 4).<sup>11</sup> The use of DMF or NMP as solvent in the (PPh<sub>3</sub>)<sub>2</sub>PdCl<sub>2</sub>-catalyzed reaction of **1b** and **4** (2 equiv) at 100 °C gave ketones **8** and **10** in highest yields. In addition, the cross-coupled **11** was obtained under these conditions.

(8) Migration of a phenyl group from the phosphine ligands to palladium is a phenomenon often observed in palladium-catalyzed cross-coupling reactions: (a) Fahey, D. R.; Mahan, J. E. *J. Am. Chem. Soc.* **1976**, *98*, 4499–4503. (b) Kong, K.-C.; Cheng, C.-H. *J. Am. Chem. Soc.* **1991**, *113*, 6313–6315. (c) O'Keefe, D. F.; Dannock, M. C.; Marcuccio, S. M. *Tetrahedron Lett.* **1992**, *33*, 6679–6688. (d) Segelstein, B. E.; Butler, T. W.; Chenard, B. L. *J. Org. Chem.* **1995**, *60*, 12–13.

(9) Clark, F. R. S.; Norman, R. O. C.; Thomas, C. B. *J. Chem. Soc., Perkin Trans. 1* **1975**, 121–125.

(10) Cr(CO)<sub>3</sub> complexes of aryl triflates have been used in palladium-catalyzed cross-coupling reactions with organostannanes or arylboranes, but only products from direct coupling have been reported: Gilbert, A. M.; Wulff, W. D. *J. Am. Chem. Soc.* **1994**, *116*, 7449–7450.

(11) (a) Ritter, K. *Synthesis* **1993**, 735–762. (b) Echavarren, A. M.; Stille, J. K. *J. Am. Chem. Soc.* **1988**, *110*, 1557–1565. (c) Saa', J. M.; Martorell, G.; Garcia-Raso, A. *J. Org. Chem.* **1992**, *57*, 678–685.

(6) Farina, V.; Krishnan, B.; Marshall, D. R.; Roth, P. G. *J. Org. Chem.* **1993**, *58*, 5434–5444.

(7) Davies, J. A.; Hartley, F. R. *Chem. Rev.* **1981**, 79–90.



**Table 4. Effect of Different Solvents on the (PPh<sub>3</sub>)<sub>2</sub>PdCl<sub>2</sub>-Catalyzed Reaction between (η<sup>6</sup>-(Tributylstannyl)benzene)Cr(CO)<sub>3</sub> (1b) and Phenyl Triflate (4)<sup>a</sup>**

entry no.	solvent	temp (°C)	products (yield %) <sup>b</sup>		
			8	10	11
1	DMF	100	59	34	21
2	NMP	100	53	38	13
3	THF	67	3	1	1
4	CH <sub>3</sub> CN	82	12	2	2

<sup>a</sup> The reactions were performed with 2 equiv of phenyl triflate (4). <sup>b</sup> Yield percentages were determined by quantitative GC analysis and were based on 1b.

**Table 5. Effect of Different Solvents and Temperatures on the (PPh<sub>3</sub>)<sub>2</sub>PdCl<sub>2</sub>-Catalyzed Reaction between (η<sup>6</sup>-Chlorobenzene)Cr(CO)<sub>3</sub> (2) and (Tributylstannyl)benzene (5)<sup>a</sup>**

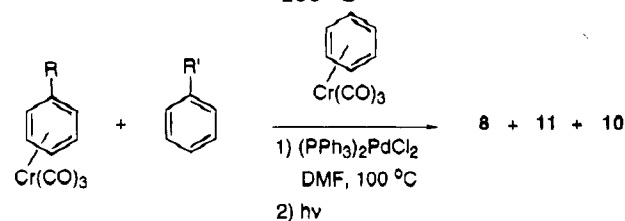
entry no.	solvent	temp (°C)	products (yield %) <sup>b</sup>	
			8	11
1 <sup>c</sup>	DMF	50	40	16
2	DMF	80	36	21
3	DMF	100	33	21
4	THF	67	30	43

<sup>a</sup> The reactions were performed with 2 equiv of (tributylstannyl)benzene (5). <sup>b</sup> Yield percentages were determined by quantitative GC analysis and were based on 2. The results are the mean of two experiments. <sup>c</sup> The reaction was stopped after 4 h.

In order to further explore the scope of the carbonylative coupling reaction, we studied the palladium-catalyzed coupling between (tributylstannyl)benzene (5) (2 equiv) and the Cr(CO)<sub>3</sub> complex of chlorobenzene (2) (Scheme 1). Complexation of chlorobenzene with the Cr(CO)<sub>3</sub> moiety increases its reactivity toward nucleophilic substitution and facilitates palladium-catalyzed cross-coupling reactions.<sup>12</sup> About equal amounts of 8 and 11 were formed (Table 5, entry 3). In comparison with the reaction between 1 and 3, the reaction between 2 and 5 seems to be more facile: experiments performed at 50 °C were complete in 4 h (Table 5, entry 1). The presence of stabilizing ligands was crucial for the formation of carbonylated compounds because very low yields were obtained under "ligand-free" conditions, *i.e.*, Pd(OAc)<sub>2</sub>.

The above results demonstrate that a CO moiety derived from (η<sup>6</sup>-arene)Cr(CO)<sub>3</sub> may be intra- or intermolecularly transferred to palladium in Stille-type couplings. To study this phenomenon further, we included an extra source of CO; the addition of 1 equiv of (η<sup>6</sup>-benzene)Cr(CO)<sub>3</sub> to a reaction mixture containing 1b and 3 (2 equiv) induced only a slight increase in the yield of benzophenone (Table 6). The palladium-catalyzed reaction of 2 with (tributylstannyl)benzene (5) (1 equiv) in the presence of (η<sup>6</sup>-benzene)Cr(CO)<sub>3</sub> (1 equiv) produced 8 (54%) and 11 (41%) in the same ratio as that obtained in the absence of (η<sup>6</sup>-benzene)Cr(CO)<sub>3</sub>.

We speculated that spontaneous decomposition of (η<sup>6</sup>-arene)Cr(CO)<sub>3</sub> might provide another source of CO. However, inspection of the <sup>1</sup>H NMR spectrum of a solution of 1b and (PPh<sub>3</sub>)<sub>2</sub>PdCl<sub>2</sub> (5 mol %) kept in DMF-d<sub>7</sub> at 100 °C for 4 h revealed no formation of decomposed products. In the presence of 3, however, 35% of 8 had formed after 4 h (GC). This indicates that the inserted CO does not emanate from spontaneously

**Table 6. Cross-Coupling Reaction between (η<sup>6</sup>-Arenes)Cr(CO)<sub>3</sub> (1b and 2) and Different Electrophiles (3 and 5) in the Presence of (η<sup>6</sup>-Benzene)Cr(CO)<sub>3</sub> with (PPh<sub>3</sub>)<sub>2</sub>PdCl<sub>2</sub> in DMF at 100 °C**

entry no.	R	R'	products (yield %) <sup>a</sup>		
			8	11	10
1	SnBu <sub>3</sub> (1b)	I (3)	91	20	11
2	Cl (2)	SnBu <sub>3</sub> (5)	54	41	nd <sup>b</sup>

<sup>a</sup> Yield percentages were determined by quantitative GC analysis and were based on 1b (entry 1) or 2 (entry 2). The results are the mean of three experiments. <sup>b</sup> Not detected.

**Table 7. Effect of Different Palladium Catalysts on the Reaction of (η<sup>6</sup>-Chlorobenzene)Cr(CO)<sub>3</sub> (2) with or without (Tributylstannyl)benzene (5)<sup>a</sup> in DMF at 100 °C**

entry no.	catalyst	5	products (yield %) <sup>b</sup>			
			8	11	<i>n</i>	
1	(PPh <sub>3</sub> ) <sub>4</sub> Pd	yes	24	24	2	
2		no	15	8	3	
3	(PPh <sub>3</sub> ) <sub>2</sub> PdCl <sub>2</sub>	yes	33	21	2	
4		no	17	8	3	
5	(dba) <sub>3</sub> Pd <sub>2</sub> -(TFP) <sub>4</sub>	yes	33	37	2	
6		no	14	3	3	

<sup>a</sup> The reactions were performed with 2 equiv of 5. <sup>b</sup> Yield percentages were determined by quantitative GC analysis and were based on 2. The results are the mean of *n* experiments.

decomplexed 1b but that it is transferred during the palladium-catalyzed reaction. The same results were obtained with substrate 2.

It is apparent that carbonylative homocoupling can occur because a substantial amount of 8 (14%–17%) was formed when the reactions were performed with substrate 2 in the absence of stannane (Table 7). Compound 8 was observed (TLC) before the photochemical decomposition. The formation of 8 in this reaction is difficult to rationalize since 8 is not a Stille coupling product. The reaction might have been promoted by the ability of CO and phosphine to reduce Pd.<sup>13,14</sup> In contrast, we could detect only minute amounts of 8 and 11 from homocoupling reactions of 3 and 1b, respectively.

Attempts to observe or isolate Cr(CO)<sub>3</sub>-complexed products from the reaction of 2 with 5 were unsuccessful. However, (η<sup>6</sup>-benzophenone)Cr(CO)<sub>3</sub><sup>15</sup> was isolated in <1% yield from the reaction of 1b with 3.<sup>16</sup>

In conclusion, we have found that (η<sup>6</sup>-arene)Cr(CO)<sub>3</sub> complexes undergo palladium-catalyzed carbonylative coupling reactions. These findings are in contrast to a number of investigations in which similar substrates<sup>2,3</sup>

(13) Schoenberg, A.; Bartoletti, I.; Heck, R. F. *J. Org. Chem.* **1974**, *39*, 3318–3326.

(14) Ozawa, F.; Kubo, A.; Hayashi, T. *Chem. Lett.* **1992**, 2177–2180.

(15) Holmes, J. D.; Jones, D. A. K.; Pettit, R. *J. Organomet. Chem.* **1965**, *4*, 324–331.

(16) (η<sup>6</sup>-Benzophenone)Cr(CO)<sub>3</sub>: <sup>1</sup>H NMR (270 MHz, CDCl<sub>3</sub>) δ 5.30 (app t, 2H), 5.60 (app t, 1H), 6.05 (dd, 2H), 7.48 (app t, 2H), 7.55 (app t, 1H), 7.78 (d, 2H).

(12) (a) Grushin, V. V.; Alper, H. *Chem. Rev.* **1994**, *94*, 1047–1062. (b) Fitton, F.; Rick, E. A. *J. Organomet. Chem.* **1971**, *281*, 187–191.

and, in one instance, similar reaction conditions<sup>2c</sup> were used, but in which no products resulting from a carbonylative coupling have been reported. Palladium-catalyzed cross-coupling reactions with **2** have been reported to give products from direct cross-coupling reactions and not from carbonylative couplings.<sup>3</sup> Palladium-catalyzed carbonylative couplings involving ( $\eta^6$ -arene)Cr(CO)<sub>3</sub> complexes have been reported in reactions in which a medium pressure of CO was applied.<sup>17</sup> However, our results are corroborated by a recent study by Uemura et al.<sup>18</sup> This group isolated a carbonylated product from a Suzuki cross-coupling reaction of a ( $\eta^6$ -arylhalide)Cr(CO)<sub>3</sub> complex.

The present results indicate a potential dual role of the Cr(CO)<sub>3</sub> moiety in palladium-catalyzed cross-coupling reactions; in addition to the established function in which the Cr(CO)<sub>3</sub> moiety modifies the reactivity of the arene and its substituents,<sup>19</sup> the Cr(CO)<sub>3</sub> moiety may also serve as a source of CO, leading to ketones. Ongoing studies focus on further establishing the scope and the limitations of this novel palladium-catalyzed carbonylative reaction.

### Experimental Section

**General Methods.** <sup>1</sup>H and <sup>13</sup>C NMR spectra were obtained on a JEOL JNM-EX 270 spectrometer with tetramethylsilane as internal standard. Infrared (IR) spectra were obtained on a Perkin-Elmer 1605 FT-IR spectrophotometer. Thin layer chromatography was performed on silica gel (Merck) mounted on aluminum cards with a fluorescent indicator (254 nm). Preparative chromatographic separations were achieved using silica gel (Merck) and various ratios of ether and light petroleum ether as eluent. The reaction mixtures were analyzed by capillary GC on a Carlo Erba 6000 instrument equipped with an SE 54 fused silica capillary column (25 m) and a Shimadzu 14-A instrument equipped with an NS-BDS capillary column (50 m). The elemental analyses (C, H, and N), which were performed by Analytische Laboratorien, Gummersbach, Germany, were within 0.4% of the theoretical values. Products were identified by comparison with authentic material. The estimations of the reaction yields were made by quantitative GC analysis using triglyme as internal standard (IS) and were based on peak-area measurements corrected with response factors of each component to be examined. All palladium-catalyzed coupling reactions were performed in sealed Micro Reaction Vessels under an atmosphere of nitrogen. All reactions involving ( $\eta^6$ -arene)Cr(CO)<sub>3</sub> complexes were performed in the dark. Decomplexation reactions were performed with a 300 W Osram bulb. Materials: Solvents and

arylhalides in the liquid state were dried, distilled,<sup>20</sup> and stored under a nitrogen atmosphere. ( $\eta^6$ -Chlorobenzene)Cr(CO)<sub>3</sub><sup>21</sup> (**2**) and phenyl triflate<sup>22</sup> (**4**) were prepared according to literature methods.

**Coupling Reactions:** All coupling reactions were performed in the same manner. Variations in stoichiometry, solvent, catalyst, temperature, and reaction time are specified in the tables. The following procedure is representative: [ $\eta^6$ -(tributylstannyl)benzene]Cr(CO)<sub>3</sub> (**1b**) (25 mg, 0.049 mmol), iodobenzene (**3**) (20 mg, 0.098 mmol), (PPh<sub>3</sub>)<sub>2</sub>PdCl<sub>2</sub> (1.72 mg, 0.0024 mmol, 5 mol %), triglyme (10 mg), and DMF (0.5 mL) were mixed in a 0.6 mL Micro Reaction Vessel under an atmosphere of nitrogen. The vessel was sealed, and the reaction mixture was stirred at 100 °C for 24 h. After filtration (Celite pad), the reaction mixture was decomplexed (24 h, light bulb, 300 W), filtered, and analyzed by quantitative GC analysis.

When the coupling reaction was performed with phenyl triflate (**4**), LiCl (3 equiv) was added to the reaction mixture.

The coupling reactions of 4-iodotoluene (**6**) and *p*-iodoanisole (**7**) with **1b** in a preparative scale (100 mg of **1b**) were performed as described above. The reaction products were isolated by flash column chromatography (SiO<sub>2</sub>; petroleum ether followed by petroleum ether-ether: **8** (6:1), **12** (6:1), and **15** (5:1)). The corresponding alkyl aryl ketones **10**, **13**, and **16** were also isolated, whereas the yields of biphenyls **11**, **14**, and **17** were determined by GC and <sup>1</sup>H NMR. The products were identified by comparison with authentic material.

[ $\eta^6$ -(Trimethylstannyl)benzene]Cr(CO)<sub>3</sub> (**1a**) and [ $\eta^6$ -(tributylstannyl)benzene]Cr(CO)<sub>3</sub> (**1b**) were prepared from (trimethylstannyl)benzene and (tributylstannyl)benzene, respectively, by refluxing in THF-Bu<sub>2</sub>O (1:9) in the presence of Cr(CO)<sub>6</sub>. Compound **1a** was isolated as a solid, mp 74–75 °C (lit.<sup>23</sup> 77–77.5 °C) whereas compound **1b** was isolated as an oil.<sup>24</sup>

**Stability Study of [ $\eta^6$ -(Tributylstannyl)benzene]Cr(CO)<sub>3</sub> (**1b**).** A mixture of complex **1b** (25 mg, 0.049 mmol) and (PPh<sub>3</sub>)<sub>2</sub>PdCl<sub>2</sub> (1.72 mg, 0.0024 mmol, 5 mol %) in DMF-*d*<sub>7</sub> (0.5 mL) was stirred at 100 °C for 4 h. The solution was cooled to room temperature and filtered (Celite pad) into an NMR tube. Analysis of the <sup>1</sup>H NMR spectrum showed no formation of (tributylstannyl)benzene.

The stability of  $\eta^6$ -(chlorobenzene)Cr(CO)<sub>3</sub> (**2**) was studied as described above for **1b**, with the exception that the reaction mixture was heated at 50 °C. The <sup>1</sup>H NMR spectrum showed no formation of chlorobenzene.

**Acknowledgment.** Financial support was obtained from the Swedish National Science Research Council.

**Supporting Information Available:** Tables giving additional results from experiments performed with substrates (a) **1b** and **3** or **4** and (b) **2** and **5**, using different solvents, catalysts, and temperature, and (c) homocoupling reactions of **1b** and of **3** with different catalysts (5 pages). Ordering information is given on any current masthead page.

OM950211Q

(20) *Purification of Laboratory Chemicals*; Parrin, D. D., Amarego, W. L. F., Eds.; Pergamon Press: New York, 1988.

(21) Mahaffy, C. A. L.; Pauson, P. L. *Inorg. Synth.* **1979**, *19*, 154–159.

(22) Stang, P. J.; Hanack, M.; Subramanian, R. F. *Synthesis* **1982**, 82–126.

(23) Seyferth, D.; Alleston, D. L. *Inorg. Chem.* **1963**, *2*, 417–418.

(24) Wright, M.; Lawson, L.; Baker, R. T.; Roe, C. *Polyhedron* **1992**, *11*, 323–329.

(17) (a) Mutin, R.; Lucas, C.; Thivolle-Cazat, J.; Dufaud, V.; Dany, F.; Basset, J.-M. *J. Chem. Soc., Chem. Commun.* **1988**, 896–898. (b) Dany, F.; Mutin, R.; Lucas, C.; Dufaud, V.; Thivolle-Cazat, J.; Basset, J.-M. *J. Mol. Catal.* **1989**, *51*, L15–L20. (c) Dufaud, V.; Thivolle-Cazat, J.; Basset, J.-M.; Mathieu, R.; Jaud, J.; Waissermann, J. *Organometallics* **1991**, *10*, 4005–4015. (d) Carpentier, J. F.; Petit, F.; Mortreux, A.; Dufaud, V.; Basset, J.-M.; Thivolle-Cazat, J. *J. Mol. Catal.* **1993**, *8*, 1–15.

(18) Uemura M.; Kamikawa, K. *J. Chem. Soc., Chem. Commun.* **1994**, 2697–2698.

(19) (a) Semmelhack, M. F.; Clark, G. R.; Garcia, J. L.; Harrison, J. J.; Thabtaranon, Y.; Wulff, W. D.; Yamashita, A. *Tetrahedron* **1981**, *37*, 3957. (b) Cavallo-Solladiè, A. *Polyhedron* **1985**, *4*, 901–927. (c) Jaouen, G. In *Transition Metal Organometallics*; Davies, S. G., Ed.; Academic Press: New York, 1978; Vol. 2, pp 65–120.

# Mixed-Ring and Indenyl Analogues of Molybdenocene and Tungstenocene: Preparation and Characterization

José R. Ascenso,<sup>†</sup> Cristina G. de Azevedo,<sup>†</sup> Isabel S. Gonçalves, Eberhardt Herdtweck,<sup>‡</sup> Domitília S. Moreno, Miguel Pessanha, and Carlos C. Romão\*

Instituto de Tecnologia Química e Biológica and Instituto Superior Técnico, R. da Quinta Grande 6, 2780 Oeiras, Portugal

Received February 13, 1995<sup>®</sup>

A stepwise route to derivatives of the molybdenocene, Cp<sub>2</sub>Mo, and analogue mixed-ring CpCp'Mo (Cp' = CpMe, Cp\*, Ind) fragments is described. Treatment of CpMo(η<sup>3</sup>-C<sub>5</sub>H<sub>5</sub>)(CO)<sub>2</sub> with HBF<sub>4</sub>·OEt<sub>2</sub> and C<sub>5</sub>H<sub>6</sub> forms [CpMo(η<sup>4</sup>-C<sub>5</sub>H<sub>6</sub>)(CO)<sub>2</sub>][BF<sub>4</sub>], which reacts with Ph<sub>3</sub>CBF<sub>4</sub> to give [Cp<sub>2</sub>Mo(CO)<sub>2</sub>][BF<sub>4</sub>]<sub>2</sub> and decarbonylates to [Cp<sub>2</sub>MoH(CO)][BF<sub>4</sub>]. These complexes are a convenient new entry into molybdenocene chemistry allowing ready access to other derivatives of the types [Cp<sub>2</sub>MoL<sub>2</sub>]<sup>2+</sup>, [Cp<sub>2</sub>MoXL]<sup>+</sup>, Cp<sub>2</sub>MoX<sub>2</sub>, and Cp<sub>2</sub>Mo(CO). Use of C<sub>5</sub>H<sub>5</sub>Me instead of cyclopentadiene allows the preparation of several mixed-ring, differentially substituted analogues of molybdenocene complexes, namely, [Cp(CpMe)MoCl(CO)][BF<sub>4</sub>], [Cp(CpMe)Mo(CO)<sub>2</sub>][BF<sub>4</sub>]<sub>2</sub>, [Cp(CpMe)Mo(NCMe)(CO)][BF<sub>4</sub>]<sub>2</sub>, and [Cp(CpMe)Mo(NCMe)<sub>2</sub>][BF<sub>4</sub>]<sub>2</sub>. Similar transformations of IndMo(η<sup>3</sup>-C<sub>3</sub>H<sub>5</sub>)(CO)<sub>2</sub>, through [IndMo(η<sup>4</sup>-C<sub>5</sub>H<sub>6</sub>)(CO)<sub>2</sub>][BF<sub>4</sub>], produce the indenyl substituted mixed-ring analogues of molybdenocene, [IndCpMo(CO)<sub>2</sub>][BF<sub>4</sub>]<sub>2</sub> and [IndCpMoH(CO)][BF<sub>4</sub>]. Substitution reactions of these complexes produce [IndCpMo(NCMe)(CO)][BF<sub>4</sub>]<sub>2</sub>, [IndCpMo(NCMe)<sub>2</sub>][BF<sub>4</sub>]<sub>2</sub>, [IndCpMoCl(CO)][BF<sub>4</sub>], [IndCpMoI(CO)][BF<sub>4</sub>], [IndCpMoCl(NCMe)][BF<sub>4</sub>], IndCpMoCl<sub>2</sub>, IndCpMoH<sub>2</sub>, and IndCpMo(SPh)<sub>2</sub>. The fluorenyl complex FluMo(η<sup>3</sup>-C<sub>3</sub>H<sub>5</sub>)(CO)<sub>2</sub> does not lead to a parallel chemistry. [Cp\*Mo(η<sup>4</sup>-C<sub>5</sub>H<sub>6</sub>)(CO)<sub>2</sub>][BF<sub>4</sub>] reacts with Ph<sub>3</sub>CBF<sub>4</sub> to give [Cp\*CpMo(CO)<sub>2</sub>][BF<sub>4</sub>]<sub>2</sub> and decarbonylates slowly to [Cp\*CpMoH(CO)][BF<sub>4</sub>], but [Cp\*Mo(η<sup>4</sup>-Cp\*H)(CO)<sub>2</sub>][BF<sub>4</sub>] is inert with respect to both reaction pathways. Prolonged photolysis of [Cp\*CpMo(CO)<sub>2</sub>][BF<sub>4</sub>]<sub>2</sub> gives [Cp\*CpMo(NCMe)(CO)][BF<sub>4</sub>]<sub>2</sub> and [Cp\*CpMo(NCMe)<sub>2</sub>][BF<sub>4</sub>]<sub>2</sub>. Deprotonation of [IndMo(η<sup>4</sup>-C<sub>5</sub>H<sub>6</sub>)(CO)<sub>2</sub>][BF<sub>4</sub>], [CpW(η<sup>4</sup>-C<sub>5</sub>H<sub>6</sub>)(CO)<sub>2</sub>][BF<sub>4</sub>], and [CpMo(η<sup>4</sup>-C<sub>5</sub>H<sub>6</sub>)(CO)<sub>2</sub>][BF<sub>4</sub>] with NEt<sub>3</sub> gives the ring-slipped complexes CpMo(η<sup>3</sup>-Ind)(CO)<sub>2</sub>, CpW(η<sup>3</sup>-Cp)(CO)<sub>2</sub>, and CpMo(η<sup>3</sup>-Cp)(CO)<sub>2</sub>, respectively. Oxidation of CpMo(η<sup>3</sup>-Ind)(CO)<sub>2</sub> gives the dication [IndCpMo(CO)<sub>2</sub>][BF<sub>4</sub>]<sub>2</sub>. Deprotonation of [CpM(η<sup>4</sup>-Cp\*H)(CO)<sub>2</sub>][BF<sub>4</sub>] occurs at one of the CH<sub>3</sub> substituents in a terminal position of the diene to give the allylic complexes [CpM{η<sup>3</sup>-C<sub>5</sub>(CH<sub>3</sub>)<sub>4</sub>H(CH<sub>2</sub>)}(CO)<sub>2</sub>] (M = Mo, W). The X-ray crystal structures of [IndCpMo(NCMe)(CO)][BF<sub>4</sub>]<sub>2</sub>, CpMo(η<sup>3</sup>-Ind)(CO)<sub>2</sub>, and [CpMo{η<sup>3</sup>-C<sub>5</sub>(CH<sub>3</sub>)<sub>4</sub>H(CH<sub>2</sub>)}(CO)<sub>2</sub>] are presented. The latter is present in an enantiomerically pure R form in the analyzed crystals.

## Introduction

Since the discovery of Cp<sub>2</sub>MH<sub>2</sub> (M = Mo, W), one of the earliest characterized transition metal hydrides,<sup>1</sup> the chemistry of molybdenocene and tungstenocene derivatives produced a number of examples of key complexes and reaction steps in organometallic chemistry. Among these reactions, acetylene insertion into the Mo–H bond,<sup>2</sup> α-hydride elimination,<sup>3</sup> and intermolecular C–H activation,<sup>4</sup> are the most important and pioneered their respective fields. The remarkable thermodynamic and kinetic stability of the Cp<sub>2</sub>M fragment

created the basis for reliable and extensive thermochemical studies on M–L bonds, including the important M–H and M–C bonds.<sup>5</sup>

Adding this stability to the fact that, with few exceptions, all the Cp<sub>2</sub>M derivatives are 18-electron complexes seems to explain the absence of catalytic insertion chemistry in these systems. In fact, compounds such as [Cp<sub>2</sub>MR(C<sub>2</sub>H<sub>4</sub>)]<sup>+</sup> (R = H, CH<sub>3</sub>) are typically quoted among the few stable *cis*-hydridoalkenes (or alkylalkenes) known.<sup>6</sup>

One way of changing this reactivity picture is by replacement of the Cp ligands by isoelectronic η<sup>5</sup>-dienyl congeners, heretofore referred to "Cp". In fact, the energy of the frontier orbitals will be changed and, in the case of η<sup>5</sup>-dienyl ligands prone to undergo ring-slippage to a η<sup>3</sup>-enyl coordination, new kinetically

\* Present address: Centro de Química Estrutural, Instituto Superior Técnico, 1096 Lisboa Codex, Portugal.

† Present address: Anorganisch-chemisches Institut, Technische Universität München, Lichtenbergstrasse 4, D-85747 Garching, Germany.

‡ Abstract published in *Advance ACS Abstracts*, July 15, 1995.

(1) Green, M. L. H.; McCleverty, J. A.; Pratt, L.; Wilkinson, G. J. *Chem. Soc.* **1961**, 4854.

(2) Nakamura, A.; Otsuka, S. *J. Molecular Catalysis* **1975**, *1*, 285 and references therein.

(3) (a) Cooper, N. J.; Green, M. L. H. *J. Chem. Soc., Dalton Trans.* **1979**, 1121. (b) Bullock, R. M.; Headford, C. E. L.; Kegley, S. E.; Norton, J. R. *J. Am. Chem. Soc.*, **1985**, *107*, 727.

(4) (a) Green, M. L. H.; Knowles, P. J. *J. Chem. Soc. A* **1971**, 1508. (b) Giannotti, C.; Green, M. L. H. *J. Chem. Soc., Chem Commun.* **1972**, 1114. (c) Cooper, N. J.; Green, M. L. H.; Mahtab, R. *J. Chem. Soc., Dalton Trans.* **1979**, 1557.

(5) Simões, J. A. M.; Dias, A. R. *Polyhedron* **1988**, *7*, 1531.

(6) Benfield, F. W. S.; Cooper, N. J.; Green, M. L. H. *J. Organomet. Chem.* **1974**, *76*, 49.

accessible pathways for substitution and other reactions may be opened. Indeed, the existence of such ring-slippage activation in photolyzed  $\text{Cp}_2\text{W}$  derivatives has been postulated by Green as a way of explaining some of the reactivity observed in the C–H activation reactions of tungstenocene.<sup>4</sup> The geometrical rearrangement of a bent to a parallel metallocene structure was proposed by Otsuka in order to account for the results of acetylene insertion reactions into  $\text{Cp}_2\text{MoH}_2$  bonds.<sup>2</sup> Of course, Cp replacement by Cp' might favor some of these transformations and help tune the reactivity of analogue  $\text{Cp}'_2\text{M}$  fragments.

In contrast to the case of group 4 metallocenes, in which the reactivity of the  $\text{MX}_4$  salts allows the simple introduction of Cp' substituents and even the easy preparation of a variety of symmetrical and unsymmetrical *ansa*-metallocenes from  $\text{LiCp}'$  reagents,<sup>7</sup> the situation is more complex in group 6 metallocenes. In fact, a similar preparation of  $\text{Cp}_2\text{WCl}_2$  from  $\text{WCl}_4(\text{DME})$  and  $\text{NaCp}$  was recently reported,<sup>8</sup> but it is doubtful that this method may be extended to the direct preparation of other  $\text{Cp}'_2\text{M}^{\text{IV}}\text{X}_2$  complexes, especially in the case of the more reducing Cp' anions. However, the presence of phosphine ligands capable of stabilizing lower oxidation states allowed the preparation of the molybdenocene analogue precursor  $(\eta^5\text{-Ind})(\eta^3\text{-Ind})\text{Mo}(\text{dppe})^9$  and the actual metallocene analogues  $(\eta^5\text{-2,4-Me}_2\text{C}_5\text{H}_5)_2\text{M}(\text{PR}_3)^{10}$  (M = Mo, W; R = Me, Et) from  $\text{MX}_n(\text{PR}_3)_m$  complexes and the diene anions.  $\text{Cp}^*\text{WCl}_2$  was obtained in 11% yield after a long and difficult sequence of steps,<sup>11</sup> and cocondensation of Mo vapor with  $\text{C}_5\text{Me}_6$  led to  $\text{Cp}^*\text{MoMe}_2$ .<sup>12</sup> A similar metal vapor synthesis starting with indene (IndH) gave a mixture of  $\text{Ind}_2\text{MoH}_2$ ,  $\text{IndMoH}(\eta^6\text{-IndH})$ , and  $\text{Mo}(\eta^6\text{-IndH})_2$  (Ind =  $\eta^5\text{-C}_9\text{H}_7$ ).<sup>13</sup>

A method of preparing differentially substituted tungstenocene complexes was elegantly developed by Cooper following earlier scattered reports on nucleophilic addition at the Cp rings of  $\text{Cp}_2\text{MX}_2$  complexes.<sup>14</sup> In spite of the interest of many of these species as chiral complexes, their reactivity remains essentially unchanged since only slight modifications of the electronic structure and energy of these  $\text{Cp}(\text{C}_5\text{H}_4\text{R})\text{WX}_2$  complexes are expected to occur relative to the parent  $\text{Cp}_2\text{WX}_2$ .

We have previously reported a stepwise preparation of molybdenocene<sup>15</sup> and tungstenocene<sup>16</sup> complexes which is easily extendable to mixed-ring analogues, e.g.,

(7) Llinas, G. H.; Day, R. O.; Rausch, M. D.; Chien, J. C. W. *Organometallics* **1993**, *12*, 1283 and references therein.

(8) Persson, C.; Andersson, C. *Organometallics* **1993**, *12*, 2370.

(9) Poli, R.; Mattamana, S. P.; Falvello, L. R. *Gazz. Chim. Ital.* **1992**, *122*, 315.

(10) (a) Stahl, L.; Hutchinson, J. P.; Wilson, D. R.; Ernst, R. D. *J. Am. Chem. Soc.* **1985**, *107*, 5016. (b) Ernst, R. D. *Chem. Rev.* **1988**, *88*, 1255.

(11) For the preparation of  $\text{Cp}^*\text{MX}_2$  (M = Mo, W) see: Cloke, F. G. N.; Day, J. P.; Green, J. C.; Morley, C. P.; Swain, A. C. *J. Chem. Soc. Dalton Trans.* **1991**, 789 and references therein.

(12) Green, J. C.; Green, M. L. H.; Morley, C. P. *J. Organomet. Chem.* **1982**, *233*, C4.

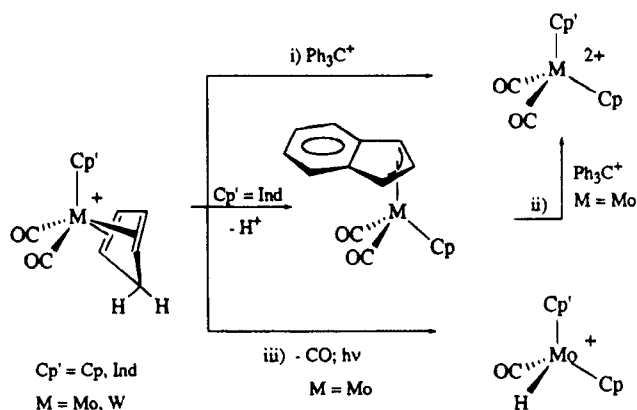
(13) VanDam, E. M.; Brent, W. N.; Silvon, M. P.; Skell, P. S. *J. Am. Chem. Soc.* **1975**, *97*, 465.

(14) (a) McNally, J. P.; Glueck, D. Cooper, N. J. *J. Am. Chem. Soc.* **1988**, *110*, 4838. (b) McNally, J. P.; Cooper, N. J. *J. Am. Chem. Soc.* **1989**, *111*, 4500. (c) Forschner, T. C.; Cooper, N. J. *J. Am. Chem. Soc.* **1989**, *111*, 7420.

(15) Ascenso, J. R.; de Azevedo, C. G.; Gonçalves, I. S.; Herdtweck, E.; Moreno, D. S.; Romão, C. C.; Zühlke, J. *Organometallics* **1994**, *13*, 429.

(16) Gonçalves, I. S.; Romão, C. C. *J. Organomet. Chem.* **1995**, *486*, 155.

Scheme 1



$[\text{CpIndM}(\text{CO})_2][\text{BF}_4]_2$  (M = Mo, W). This method is based on the transformations of the diene complexes  $[\text{Cp}'\text{M}(\eta^4\text{-diene})(\text{CO})_2]^+$  depicted in Scheme 1.

In this work we complete our previous report on the molybdenocene analogues  $[\text{CpIndMoL}_2]^{n+}$ <sup>15</sup> and present the extension of this route to the preparation of other mixed-ring formal analogues of molybdenocene and tungstenocene of general formula  $[\text{Cp}'\text{Cp}''\text{ML}_2]^{n+}$ .

## Results and Discussion

**1. Preparation of the  $[\text{Cp}'\text{Mo}(\eta^4\text{-diene})(\text{CO})_2]^+$  Complexes.** The family of the title complexes has played an important role in diene activation/function-alization and is well-known in the cases where  $\text{Cp}' = \text{Cp}$ , Ind, or  $\text{Cp}^*$ .<sup>17</sup> The general preparation involves NCMe displacement from  $[\text{Cp}'\text{Mo}(\text{CO})_2(\text{NCMe})_2]^+$ , which, in turn, is made from  $[\text{Cp}'\text{Mo}(\text{CO})_3]_2$  ( $\text{Cp}' = \text{Cp}$ , Ind)<sup>17a,b</sup> or  $\text{Cp}^*\text{Mo}(\text{CO})_3\text{Me}$ .<sup>17i</sup> In the case of the Cp and Ind derivatives, our approach uses the protonation of the allyl ligand in the  $\text{Cp}'\text{Mo}(\eta^3\text{-allyl})$  precursors, a rather general method for the opening of two adjacent coordination positions.<sup>18</sup> The method is particularly suitable for the  $[\text{Cp}'\text{Mo}(\text{CO})_2]^+$  derivatives since the corresponding allyl precursor,  $\text{Cp}'\text{Mo}(\eta^3\text{-C}_3\text{H}_5)(\text{CO})_2$  (**1**), is conveniently available from  $\text{Mo}(\eta^3\text{-C}_3\text{H}_5)\text{Cl}(\text{CO})_2(\text{NCMe})_2$ ,  $\text{C}_5\text{H}_6$ , and  $\text{NEt}_3$  in almost quantitative yield, as described for its W analogue.<sup>16</sup>

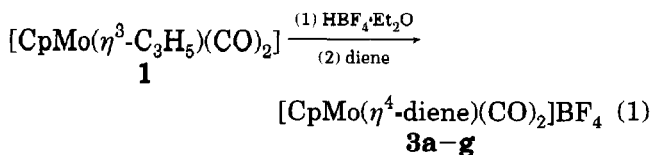
The protonation of  $\text{Cp}'\text{Mo}(\eta^3\text{-C}_3\text{H}_5)(\text{CO})_2$  with  $\text{HBF}_4 \cdot \text{Et}_2\text{O}$  in  $\text{CH}_2\text{Cl}_2$  to give a red solution of  $[\text{Cp}'\text{Mo}(\eta^2\text{-C}_3\text{H}_6)(\text{CO})_2(\text{FBF}_3)]$  (**2**) has been studied by Cutler and co-workers, who also showed that **2** reacts with several donors, L, to give  $[\text{Cp}'\text{Mo}(\text{CO})_2\text{L}_2][\text{BF}_4]$  (L =  $\text{PPh}_3$ , dppe).<sup>19</sup>

We found that, according to eq 1, addition of dienes to a solution of **2** leads to the rapid formation of the

(17) (a) Faller, J. W.; Murray, H. H.; White, D. L.; Chao, K. H. *Organometallics* **1983**, *2*, 400. (b) Pearson, A. J.; Khan, Md. N. I.; Clardy, J. C.; Cun-heng, H. *J. Am. Chem. Soc.* **1985**, *107*, 2748. (c) Green, M.; Greenfield, S.; Kersting, M. *J. Chem. Soc., Chem. Commun.* **1985**, 18. (d) Green, M.; Greenfield, S.; Kersting, M.; Orpen, A. G.; Rodrigues, R. A. *J. Chem. Soc., Chem. Commun.* **1987**, 97. (e) Baxter, J. S.; Green, M.; Lee, T. V. *J. Chem. Soc., Chem. Commun.* **1989**, 1595. (f) Pearson, A. J. *Adv. Met. Org. Chem.* **1989**, *1*, 1. (g) Pearson, A. J.; Mallik, S.; Mortezaei, R.; Perry, W. D.; Shively, R. J.; Youngs, W. J. *J. Am. Chem. Soc.* **1990**, *112*, 8034. (h) Norris, D. J.; Corrigan, J. F.; Sun, Y.; Taylor, N. J.; Collins, S. *Can. J. Chem.* **1993**, *71*, 1029. (i) Benyunes, S. A.; Binelli, A.; Green, M.; Grimshire, M. *J. Chem. Soc., Dalton Trans.* **1991**, 895. (j) King, R. B.; Bisnette, M. B. *Inorg. Chem.* **1965**, *4*, 475. (k) Bottrill, M.; Green, M. *J. Chem. Soc., Dalton Trans.* **1977**, 2365.

(18) Schrock, R. R.; Johnson, B. F. G.; Lewis, J. *J. Chem. Soc., Dalton Trans.* **1974**, 951.

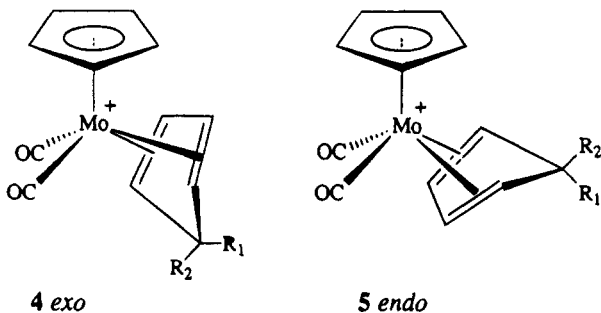
(19) Markham, J.; Menard, K.; Cutler, A. *Inorg. Chem.* **1985**, *24*, 1581.



[CpMo( $\eta^4$ -diene)(CO)<sub>2</sub>][BF<sub>4</sub>] cations **3a-g** presented in Chart 1. Of these, **3e**,<sup>17a</sup> **3f**,<sup>20</sup> and **3g**<sup>21</sup> have been reported in the literature.

Both conjugated and nonconjugated dienes coordinate readily to the [CpMo(CO)<sub>2</sub>]<sup>+</sup> fragment generated from **2**, and the product yields obtained largely exceed those reported for the similar reaction in diethyl ether for the cases of **3e** and **3g**. However, the reaction is not entirely general since C<sub>5</sub>Ph<sub>5</sub>H and pentaphenylcyclopentadienone (C<sub>5</sub>Ph<sub>4</sub>O) do not react with **2** whereas dimethylfulvene reacts sluggishly to give still unidentified products. Diene isomerization occurred in the formation of [CpMo( $\eta^4$ -CH<sub>2</sub>CHCHCHMe)(CO)<sub>2</sub>][BF<sub>4</sub>] (**3f**), which was prepared by treatment of **2** with the nonconjugated 1,4-pentadiene. A variable temperature <sup>1</sup>H NMR (VT <sup>1</sup>H NMR) study of **3f** showed it to be unambiguously identical to the piperylene complex described by Faller and Rosan.<sup>20</sup>

Variable temperature <sup>1</sup>H NMR shows that all complexes **3** are fluxional. The spectra obtained at room temperature are, in all cases, average spectra of the two conformers generated by the orientation of the coordinated diene relative to the Cp ring, as sketched in **4** (*exo* conformation) and **5** (*endo* conformation).



Detailed studies of this type of processes have been reported for similar complexes, like the butadiene derivatives [CpMo( $\eta^4$ -C<sub>4</sub>H<sub>4</sub>R<sub>2</sub>)(CO)<sub>2</sub>][BF<sub>4</sub>], that show that rotation around the Mo-diene axis is able to perform the observed interconversion of the conformers and that the *endo* conformation is thermodynamically preferred.<sup>20</sup> Lowering the temperature freezes this rotation, and the corresponding NMR spectra below ca. -50 °C show the presence of the two conformers in solutions of the new complexes **3a,c**. [CpMo( $\eta^4$ -C<sub>5</sub>Ph<sub>4</sub>H<sub>2</sub>)(CO)<sub>2</sub>][BF<sub>4</sub>] (**3d**) shows an average spectrum at room temperature, but no VT NMR studies were undertaken. At -80 °C one isomer of **3a** becomes slightly predominant, 52%, over the other, and, in agreement with the observations made for other [CpMo( $\eta^4$ -diene)(CO)<sub>2</sub>][BF<sub>4</sub>] complexes,<sup>20</sup> we assign the *endo* conformation to the former isomer. In the case of **3c** three conformers are observed. The two more abundant and interconvertible ones are assigned, on the basis of steric arguments, to the *exo* and *endo* conformers with the

**Chart 1. Diene Complexes of the Type [Cp'Mo( $\eta^4$ -diene)(CO)<sub>2</sub>][BF<sub>4</sub>]**

Cp'	Dienes						
	3a	3b	3c	3d	3e	3f	3g
	10a		10b				
	12		14				

bridgehead CH<sub>3</sub> group on the external face of the C<sub>5</sub>-Me<sub>5</sub>H ring as for **4** and **5**, R<sub>1</sub> = CH<sub>3</sub>, R<sub>2</sub> = H. They show the average bridgehead CH<sub>3</sub> doublet at  $\delta$  0.79 ppm. The third and minor isomer of **3c** (<5% by NMR integration at low temperature),  $\delta$  1.20 ppm for bridgehead CH<sub>3</sub> doublet, has a temperature independent spectrum between room temperature and -80 °C. We assign it to the *exo* conformer having the bridgehead CH<sub>3</sub> substituent facing the metal, as in **4**, R<sub>1</sub> = H, R<sub>2</sub> = CH<sub>3</sub>. In the case of **3b**, the NMR spectra are very complex due to the presence of coordinated isomers of the C<sub>5</sub>H<sub>5</sub>Me ligand, each one presenting two conformations, and were not thoroughly interpreted. The complexes **3a,b** are not very stable because they rearrange, upon CO loss, to molybdenocene-hydrido-carbonyl derivatives [Cp<sub>2</sub>MoH(CO)][BF<sub>4</sub>] as in path iii) of Scheme 1 (see below).

In a similar fashion, protonation of IndMo( $\eta^3$ -C<sub>3</sub>H<sub>5</sub>)(CO)<sub>2</sub> (**6**)<sup>22</sup> with HBF<sub>4</sub>·Et<sub>2</sub>O in CH<sub>2</sub>Cl<sub>2</sub>, at room temperature, gives a red solution which we assume to be due to the complex [IndMo( $\eta^2$ -C<sub>3</sub>H<sub>6</sub>)(CO)<sub>2</sub>(F<sup>-</sup>BF<sub>3</sub><sup>+</sup>)] (**7**) in keeping with the above mentioned formation of **2**. Accordingly, addition of Bu<sub>4</sub>NI or NCMe to **7** gives the known [IndMo(CO)<sub>2</sub>I]<sub>2</sub> (**8**)<sup>17j</sup> and [IndMo(CO)<sub>2</sub>(NCMe)<sub>2</sub>][BF<sub>4</sub>] (**9**),<sup>17c,h</sup> respectively, in very high yields. The latter complex is a very convenient starting material for the preparation of the diene derivatives [IndMo( $\eta^4$ -diene)(CO)<sub>2</sub>][BF<sub>4</sub>] (**10**), and in this way we prepared complexes **10a,b** (diene = C<sub>5</sub>H<sub>6</sub>, **10a**; C<sub>5</sub>Me<sub>5</sub>H, **10b**). As expected, **10a** has a fluxional structure due to rotation of the diene from the *endo* to the *exo* conformations. Only broadening of the AB spin system of the methylene protons of the C<sub>5</sub>H<sub>6</sub> ligand is observed at -70 °C. This contrasts with the behavior of the Cp congener **3c** in which the coalescence temperature is attained at -40 °C. It is a rather thermally and photochemically sensitive species with regard to CO loss and formation of [IndCpMoH(CO)][BF<sub>4</sub>] (see below). The fluxional behavior of **10b** is similar to that of **10a**, and at -70 °C only broadening of the bridgehead CHCH<sub>3</sub> protons is observed.

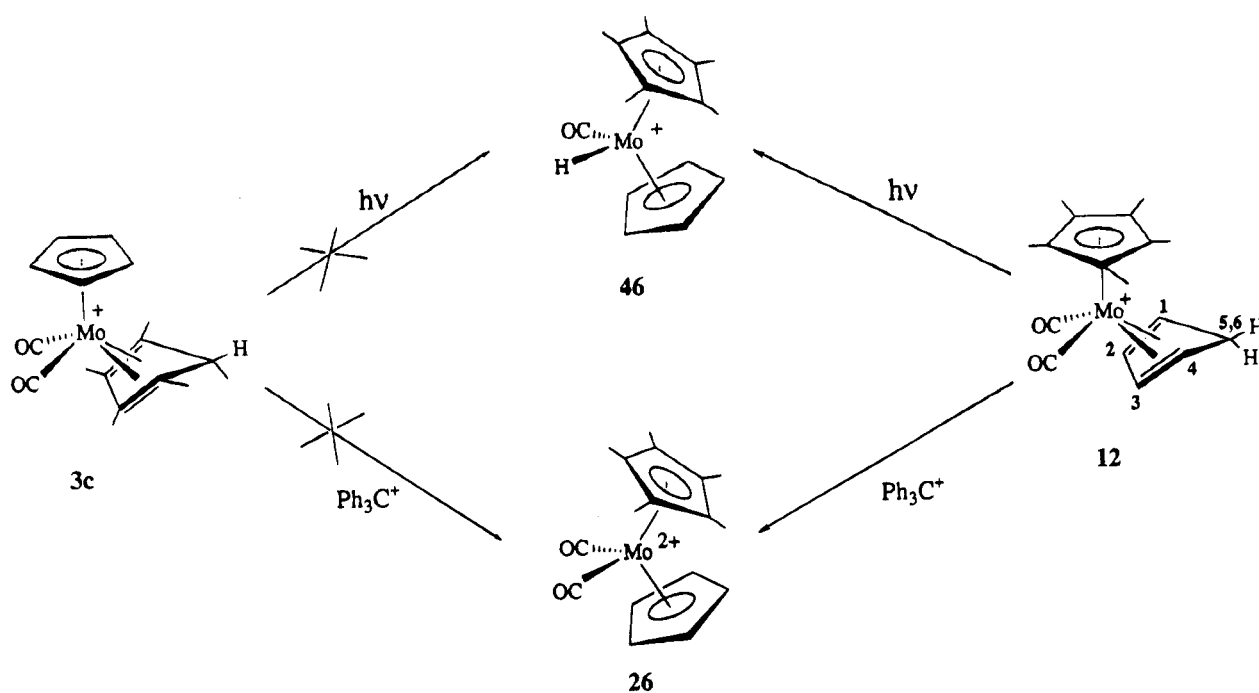
Reaction of fluorenyllithium with Mo( $\eta^3$ -C<sub>3</sub>H<sub>5</sub>)Cl(CO)<sub>2</sub>(NCMe)<sub>2</sub> gives the new FluMo( $\eta^3$ -C<sub>3</sub>H<sub>5</sub>)(CO)<sub>2</sub> (**11**) (Flu = fluorenyl,  $\eta^5$ -C<sub>9</sub>H<sub>13</sub>). From room temperature down to -70 °C only one set of signals is observed for

(20) Faller, J. W.; Rosan, A. M. *J. Am. Chem. Soc.* **1977**, *99*, 4858.

(21) Kryvikh, V. V.; Gusev, O. V.; Rybinskaya, M. I. *J. Organomet. Chem.* **1989**, *362*, 351.

(22) Faller, J. W.; Chen, C. C.; Mattina, M. J.; Jakubowski, A. J. *Organomet. Chem.*, **1973**, *52*, 361.

Scheme 2



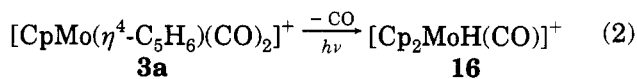
the allyl ligand. No further studies were made to ascertain whether this is due to the presence of only one isomer, presumably *endo*, or to very rapid fluxional averaging of the allylic protons. Unfortunately, the yield is rather low and the product very difficult to separate from unreacted fluorene. This fact has, so far, prevented the development of the chemistry of the  $[\text{FluMo}(\text{CO})_2]^+$  fragment and the preparation of mixed-ring derivatives, e.g.,  $[\text{FluCpMoL}_2]^{n+}$ . A similar situation occurred with the putative  $\text{Cp}^*\text{Mo}(\eta^3\text{-C}_3\text{H}_5)(\text{CO})_2$  ( $\text{Cp}^* = \text{C}_5\text{Ph}_4\text{H}$ ) and  $\text{Cp}^*\text{Mo}(\eta^3\text{-C}_3\text{H}_5)(\text{CO})_2$ , which could not be prepared from  $\text{Mo}(\eta^3\text{-C}_3\text{H}_5)\text{Cl}(\text{CO})_2(\text{NCMe})_2$  and  $\text{LiCp}^*$ ,  $\text{LiCp}^*$ ,  $\text{TiCp}^*$ , or  $\text{Cp}^*\text{SnBu}_3$ . Therefore, the complexes that are derived from the mixed-ring fragments  $\text{Cp}^*\text{CpMo}$  and  $\text{Cp}^*\text{CpMo}$  are only accessible from  $[\text{CpMo}(\eta^4\text{-C}_5\text{Ph}_4\text{H}_2)(\text{CO})_2][\text{BF}_4]$  (**3d**) and  $[\text{Cp}^*\text{Mo}(\eta^4\text{-C}_5\text{H}_6)(\text{CO})_2][\text{BF}_4]$  (**12**), the latter being readily available from  $[\text{Cp}^*\text{Mo}(\text{CO})_2(\text{NCMe})_2]^+$  (**13**) and  $\text{C}_5\text{H}_6$ , by a simple substitution reaction.<sup>17i</sup> For this purpose, an alternative high-yield (85%) preparation of **13** was developed. This takes advantage of the quantitative formation of  $\text{Cp}^*\text{MoH}(\text{CO})_3$  from  $\text{Mo}(\text{CO})_3(\text{NCMe})_3$  and  $\text{Cp}^*\text{H}$  in toluene, as described by Kubas.<sup>23</sup> The transformation of the hydride complex to  $\text{Cp}^*\text{MoI}(\text{CO})_3$  and further on to the desired **13** takes place in a series of steps in a convenient one-pot reaction, as described in the Experimental Section.

Reaction of **13** with  $\text{Cp}^*\text{H}$  gives  $[\text{Cp}^*\text{Mo}(\eta^4\text{-C}_5\text{Me}_5\text{H})(\text{CO})_2][\text{BF}_4]$  (**14**), a plausible precursor of the symmetric  $\text{Cp}^*_2\text{Mo}$  fragment (section 3, Scheme 2). Both complexes **12** and **14** have conformational flexibility of the same kind described for their cyclopentadienyl (**3a,c**) and indenyl (**10a,b**) analogues but with higher coalescence temperatures (ca.  $-10^\circ\text{C}$ ).

In a previous publication we showed that the chemistry described in Scheme 1 may be extended to the W analogues, starting from  $[\text{Cp}^*\text{W}(\eta^4\text{-C}_5\text{H}_6)(\text{CO})_2][\text{BF}_4]$  ( $\text{Cp}^*$

= Cp, Ind).<sup>16</sup> In order to extend this methodology to the preparation of the mixed-ring fragment  $\text{Cp}^*\text{CpW}$ ,  $[\text{Cp}^*\text{W}(\eta^4\text{-C}_5\text{Me}_5\text{H})(\text{CO})_2][\text{BF}_4]$  (**15**) was prepared by simply proceeding as in eq 1 but starting from  $\text{Cp}^*\text{W}(\eta^3\text{-C}_3\text{H}_5)(\text{CO})_2$  and adding  $\text{Cp}^*\text{H}$  as the diene. Fragment **15** also shows the same type of isomers as **3c**. At room temperature two bridgehead  $\text{CH}_3$  doublets are observed, the least abundant at  $\delta$  1.16 ppm and the more abundant at  $\delta$  0.75 ppm. The former is temperature invariant down to  $-40^\circ\text{C}$ , whereas the latter interconverts as shown by coalescence broadening at this temperature. The isomer assignment is similar to that described above for **3c**.

**2. Preparation of Molybdenocene Complexes  $[\text{Cp}_2\text{MoL}_2]^{n+}$  from  $[\text{CpMo}(\eta^4\text{-C}_5\text{H}_6)(\text{CO})_2][\text{BF}_4]$ .** As we have mentioned before, the preparation of the  $\text{Cp}_2\text{-Mo}$  fragment is possible by the appropriate transformations of the cyclopentadiene complex  $[\text{CpMo}(\eta^4\text{-C}_5\text{H}_6)(\text{CO})_2][\text{BF}_4]$  (**3a**) along paths i and iii of Scheme 1. Indeed, as already mentioned, **3a** easily decomposes in solution, under daylight, to give  $[\text{Cp}_2\text{MoH}(\text{CO})][\text{BF}_4]$  (**16**), eq 2.



Irradiation of a  $\text{CH}_2\text{Cl}_2$  solution of **3a** with a 60 W tungsten bulb accelerates the formation of **16**, and addition of  $\text{CHCl}_3$  to this mixture leads to formation of  $[\text{Cp}_2\text{MoCl}(\text{CO})][\text{BF}_4]$  (**17**) as a violet powder. Both complexes are known, and **16** has been previously prepared by protonation of the electron rich  $\text{Cp}_2\text{Mo}(\text{CO})$  (**18**), which is an important entry into molybdenocene chemistry.<sup>24,25</sup> It is worth noting that the corresponding

(24) Green, M. L. H.; MacKenzie, R. E.; Poland, J. S. *J. Chem. Soc., Dalton Trans.* **1976**, 1993.

(25) (a) Wong, K. L. T.; Thomas, J. L.; Brintzinger, H. H. *J. Am. Chem. Soc.* **1974**, *96*, 3694. (b) Geoffroy, G. L.; Bradley, M. G. *Inorg. Chem.* **1978**, *17*, 2410. (c) Jernakoff, P.; Cooper, N. J. *J. Am. Chem. Soc.* **1989**, *111*, 7424.

transformation of [CpW( $\eta^4$ -C<sub>5</sub>H<sub>6</sub>)(CO)<sub>2</sub>][BF<sub>4</sub>] into [Cp<sub>2</sub>-WH(CO)][BF<sub>4</sub>] is not feasible either under the same conditions or even under prolonged reflux (48 h) and visible irradiation in CH<sub>2</sub>Cl<sub>2</sub>/CHCl<sub>3</sub> mixtures. Again, stronger W–CO bonds may be held responsible for the blocking of this dissociatively induced reaction.

Additional irradiation of **17** in refluxing NCMe produces green [Cp<sub>2</sub>MoCl(NCMe)][BF<sub>4</sub>] (**19**),<sup>26</sup> which reacts with LiAlH<sub>4</sub> or NaBH<sub>4</sub> to give the dihydride Cp<sub>2</sub>MoH<sub>2</sub>, the parent compound for all the dihalides Cp<sub>2</sub>MoX<sub>2</sub>.<sup>27</sup>

Hydride abstraction from [CpMo( $\eta^4$ -C<sub>5</sub>H<sub>6</sub>)(CO)<sub>2</sub>][BF<sub>4</sub>] (**3a**) provides another possibility of generating the Cp<sub>2</sub>-Mo fragment (Scheme 1, path i). In fact, treatment of a solution of this complex, in CH<sub>2</sub>Cl<sub>2</sub>, with Ph<sub>3</sub>CBF<sub>4</sub> slowly yields a light yellow precipitate of the dication [Cp<sub>2</sub>Mo(CO)<sub>2</sub>][BF<sub>4</sub>]<sub>2</sub> (**20**). This complex shows the CO stretching vibrations at rather high wavenumbers (2139 and 2108 cm<sup>-1</sup>) and a remarkably deshielded Cp signal in the <sup>1</sup>H NMR ( $\delta$  6.69 ppm), as expected for a dicationic high oxidation state complex with weak back-bonding capabilities and as already ascertained in [Cp<sub>2</sub>Mo(CNMe)<sub>2</sub>]<sup>2+</sup> and [Cp<sub>2</sub>MoX(NCMe)]<sup>+</sup> complexes.<sup>28</sup> This activation of the coordinated CO in **20** explains its ready reaction with NaOH to give Cp<sub>2</sub>Mo(CO) in 82% yield, probably the most convenient and clean preparation of this compound to date. The lack of strong back-donation to coordinated CO in [Cp<sub>2</sub>Mo(CO)<sub>2</sub>][BF<sub>4</sub>]<sub>2</sub> (**20**) also explains its substitutional lability. Simple dissolution of **20** in NCMe forms [Cp<sub>2</sub>Mo(CO)(NCMe)][BF<sub>4</sub>]<sub>2</sub> (**21**) very rapidly. Under reflux and 60 W visible light irradiation in NCMe, total CO replacement is achieved and the known dication [Cp<sub>2</sub>Mo(NCMe)<sub>2</sub>][BF<sub>4</sub>]<sub>2</sub> is obtained in high yield.<sup>29</sup>

All of these transformations of [CpMo( $\eta^4$ -C<sub>5</sub>H<sub>6</sub>)(CO)<sub>2</sub>][BF<sub>4</sub>] provide convenient entries into the chemistry of molybdenocene, and, although it seems a complicated route for the preparation of these complexes, it must be noted that the transformations of CpMo( $\eta^3$ -C<sub>3</sub>H<sub>5</sub>)(CO)<sub>2</sub> (**1**) to [Cp<sub>2</sub>MoCl(NCMe)][BF<sub>4</sub>] (**19**) are easily performed in 80% overall yield, relative to **1**, with no other purification steps than filtrations or washings. In addition, this method may lead to different types of molybdenocene complexes like the electron rich d<sup>4</sup> Cp<sub>2</sub>-Mo(CO) or cationic d<sup>2</sup> derivatives, e.g., [Cp<sub>2</sub>Mo(CO)<sub>2</sub>][BF<sub>4</sub>]<sub>2</sub>, which are ideal precursors for a number of other products. So far, most of the molybdenocene chemistry has been derived from the dihalides Cp<sub>2</sub>MoX<sub>2</sub> by successive substitutions (leading to d<sup>2</sup> complexes) or reductions (leading to d<sup>4</sup> derivatives). Although advisable for large-scale preparations (ca. 25 g of product), the classical synthesis of the dihydride Cp<sub>2</sub>MoH<sub>2</sub> is a rather hard one.<sup>30</sup> On the other hand, the present method may be rapidly performed on a 1–2 g scale without any special equipment or skilled laboratory experience.

**3. Preparation of Mixed-Ring Molybdenocenes with One Alkyl-Substituted Cyclopentadienyl Ring, [CpCp'MoL<sub>2</sub>]<sup>n+</sup> (Cp' = MeCp, Cp\*).** In analogy with

the chemistry described in the previous section, solutions of the diene complex [CpMo( $\eta^4$ -C<sub>5</sub>H<sub>5</sub>Me)(CO)<sub>2</sub>][BF<sub>4</sub>] (**3b**) readily lose CO to give [Cp(CpMe)MoH(CO)][BF<sub>4</sub>] (hydride peak in NMR at  $\delta$  -8.09 ppm). This does not need to be isolated and may be more conveniently reacted *in situ* with Cl<sub>2</sub>(g) to give the corresponding chloride, [Cp(CpMe)MoCl(CO)][BF<sub>4</sub>] (**22**). Reaction of **3b** with Ph<sub>3</sub>CBF<sub>4</sub> (hydride abstraction) gives [Cp(CpMe)Mo(CO)<sub>2</sub>][BF<sub>4</sub>]<sub>2</sub> (**23**), which upon dissolution in NCMe forms [Cp(CpMe)Mo(NCMe)(CO)][BF<sub>4</sub>]<sub>2</sub> (**24**) and under further irradiation forms [Cp(CpMe)Mo(NCMe)<sub>2</sub>][BF<sub>4</sub>]<sub>2</sub> (**25**) in a reaction sequence similar to the one described for [CpMo( $\eta^4$ -C<sub>5</sub>H<sub>6</sub>)(CO)<sub>2</sub>][BF<sub>4</sub>] through to [Cp<sub>2</sub>Mo(CO)(NCMe)][BF<sub>4</sub>]<sub>2</sub> and [Cp<sub>2</sub>Mo(NCMe)<sub>2</sub>][BF<sub>4</sub>]<sub>2</sub>.

Given the simple preparation of monosubstituted cyclopentadienes C<sub>5</sub>H<sub>5</sub>R, this route seems to be a rapid way of building differentially substituted [Cp(C<sub>5</sub>H<sub>4</sub>R)-MoL<sub>2</sub>]<sup>n+</sup> complexes with a wide choice of R substituents. However, the changes in the properties of the cyclopentadiene upon increased substitution may lead to a different reactivity and eventually hinder the formation of CpCp'Mo fragments. This is best illustrated in the attempted preparation of the Cp\*CpMo fragment from [CpMo( $\eta^4$ -C<sub>5</sub>Me<sub>5</sub>H)(CO)<sub>2</sub>][BF<sub>4</sub>] (**3c**) summarized in Scheme 2.

Unlike **3a, b, c** is a very stable species in solution and does not evolve to the molybdenocene analogue complex, e.g., [Cp\*CpMoH(CO)]<sup>+</sup>, even under prolonged reflux (48 h) and visible light irradiation in CH<sub>2</sub>Cl<sub>2</sub>/CHCl<sub>3</sub> or NCMe/CCL<sub>4</sub> mixtures. Since it has been reported that oxidative additions of CpH and Cp\*H to M(CO)<sub>3</sub>(NCMe)<sub>3</sub> (M = Cr, Mo, W) have similar enthalpies, we assume that the higher stability of **3c** as compared to **3a** has a kinetic origin.<sup>23</sup> The increased Mo → CO back-donation expected on going from **3a** to **3c**, affecting the ease of CO dissociation, might decisively hamper the migration reaction.

An alternative method of generating the Cp\*CpMo fragment from [CpMo( $\eta^4$ -C<sub>5</sub>Me<sub>5</sub>H)(CO)<sub>2</sub>][BF<sub>4</sub>] (**3c**), would be H<sup>-</sup> abstraction with Ph<sub>3</sub>C<sup>+</sup>. This reaction, however, does not take place, probably due to the fact that the abstractable bridgehead H atom of C<sub>5</sub>Me<sub>5</sub>H faces the inner side of the molecule and is, therefore, inaccessible to the large, planar, trityl cation. In this situation, [Cp\*Mo(C<sub>5</sub>H<sub>6</sub>)(CO)<sub>2</sub>][BF<sub>4</sub>] (**12**) is left as the more obvious way of producing derivatives of the Cp\*CpMo fragment. In fact, although the photochemically activated migration pathway is found to be very slow for practical purposes, presumably due to difficult CO dissociation from **12**, H<sup>-</sup> abstraction with Ph<sub>3</sub>CBF<sub>4</sub> forms the off-white dication [Cp\*CpMo(CO)<sub>2</sub>][BF<sub>4</sub>]<sub>2</sub> (**26**) in quantitative yield. As expected, the  $\nu$ (CO) vibrations appear at lower wavelengths relative to [Cp<sub>2</sub>Mo(CO)<sub>2</sub>][BF<sub>4</sub>]<sub>2</sub> (**20**), indicating higher Mo → CO back-donation. This is also consistent with the slower rate of CO substitution, again when compared to **20**, to form [Cp\*CpMo(NCMe)(CO)][BF<sub>4</sub>]<sub>2</sub> (**27**) and [Cp\*CpMo(NCMe)<sub>2</sub>][BF<sub>4</sub>]<sub>2</sub> (**28**). While [Cp<sub>2</sub>Mo(NCMe)(CO)][BF<sub>4</sub>]<sub>2</sub> is formed upon dissolution of **20** in NCMe at room temperature, as indicated by NMR in d<sup>3</sup> NCMe, complete conversion of **26** to **27** in neat NCMe needs over 24 h at room temperature. Complexes like **26–28** certainly are adequate starting materials for the development of the chemistry of the Cp\*CpMo fragment, just

(26) Calhorda, M. J.; Carrondo, M. A. A. F. de C. T.; Dias, A. R.; Domingos, A. M. T.; Duarte, M. T. L. S.; Garcia, M. H.; Romão, C. C. *J. Organomet. Chem.* **1987**, *320*, 63.

(27) Cooper, R. L.; Green, M. L. H. *J. Chem. Soc. A* **1967**, 1155.

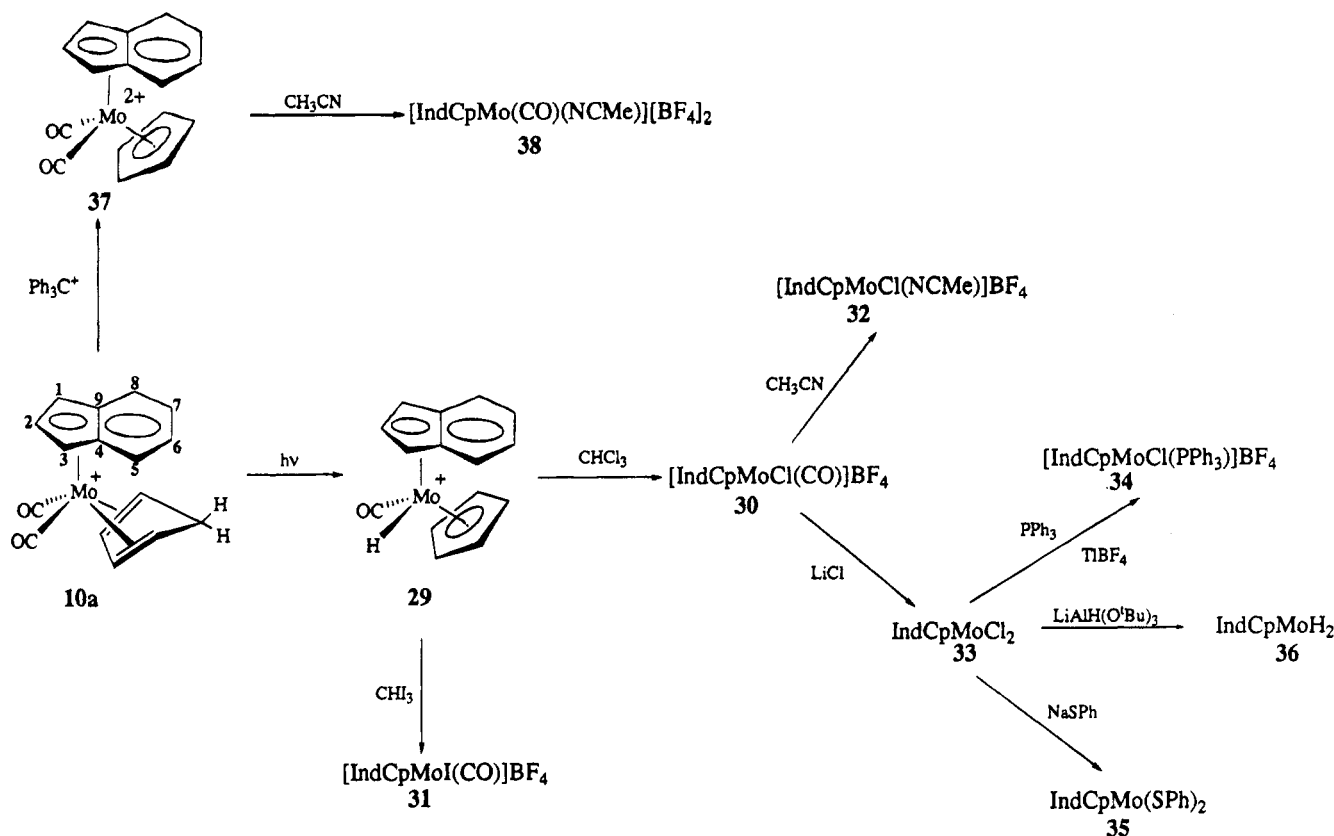
(28) Calhorda, M. J.; Dias, A. R.; Duarte, M. T.; Martins, A. M.; Matias, P. M.; Romão, C. C. *J. Organomet. Chem.* **1992**, *440*, 119.

(29) Aviles, T.; Green, M. L. H.; Dias, A. R.; Romão, C. C. *J. Chem. Soc., Dalton Trans.* **1979**, 1367.

(30) Green, M. L. H.; Knowles, P. J. *J. Chem. Soc., Perkin Trans. 1* **1973**, 989.



Scheme 3



as has been described above for  $[\text{Cp}_2\text{MoL}_2]^{n+}$  and below (section 4, Scheme 3) for the  $[\text{IndCpMoL}_2]^{n+}$  derivatives.

As might be expected from many of the preceding observations, the derivatives of the symmetrical fragment  $\text{Cp}^*\text{Mo}$  cannot be made from  $[\text{Cp}^*\text{Mo}(\eta^4\text{-C}_5\text{Me}_5\text{H})(\text{CO})_2][\text{BF}_4]$  (**14**) either by CO loss and H migration or  $\text{H}^-$  abstraction, and an alternative high-yield construction of this fragment remains to be found. The same applies to the fragment  $\text{Cp}^*\text{CpMo}$ , which could not be obtained from  $[\text{CpMo}(\eta^4\text{-C}_5\text{Ph}_4\text{H}_2)(\text{CO})_2][\text{BF}_4]$  using any of the reaction types presented in Scheme 1.

**4. Preparation of Mixed-Ring Molybdenocenes with One Indenyl Ring,  $[\text{IndCpMoL}_2]^{n+}$ .** The preparation of molybdenocenes and differentially alkyl-substituted molybdenocenes from **3a–d**, just described in sections 2 and 3, applies entirely to the preparation of mixed-ring, indenyl-substituted molybdenocenes. For this purpose, the starting material is  $[\text{IndMo}(\eta^4\text{-C}_5\text{H}_5)(\text{CO})_2][\text{BF}_4]$  (**10a**). It is rather thermally and photochemically sensitive toward CO loss and H migration, and, accordingly, it gives the corresponding carbonyl-hydride,  $[\text{IndCpMoH}(\text{CO})][\text{BF}_4]$  (**29**), in 92% isolated yield within 8 h of irradiation (60 W lamp) in  $\text{CH}_2\text{Cl}_2$ . This compound opens the way to a number of derivatives of the mixed-ring family  $[\text{IndCpMoL}_2]^{n+}$ , showing that its chemistry is largely parallel to the chemistry of the  $\text{Cp}_2\text{Mo}$  fragment itself. These simple, often practically quantitative transformations are summarized in Scheme 3 and result from straightforward substitution reactions.

The dichloride  $\text{IndCpMoCl}_2$  (**33**) is prepared from **30** by treatment with LiCl in acetone. Like  $\text{Cp}_2\text{MoCl}_2$ , **33** is practically insoluble, and we could not obtain any NMR spectrum. However, the IR spectra of both dichlorides are very similar. Treatment of **33** with

$\text{LiAlH}(\text{O}^i\text{Bu})_3$  in diethyl ether gives an orange solution from which the dihydride  $\text{IndCpMoH}_2$  (**36**) can be isolated in good yield. The complex is stable and sublimable under vacuum. The hydride signals appear at  $\delta -7.35$  ppm in the  $^1\text{H}$  NMR spectrum.

The preparation of both **33** and **36** is of central importance for the study of the chemistry of these mixed-ring analogues of molybdenocenes since these are the most important starting materials for the preparation of a series of derivatives, *e.g.*, alkyls, and for the test of catalytically important insertion reactions of the hydrides. These studies are in progress.

The  $^1\text{H}$  NMR spectra of the mixed-ring complexes in Scheme 3 is compatible with the  $\eta^5$ -coordination mode of the indenyl ligand. For the symmetrical  $\text{IndCpMo}(\text{SPh})_2$  (**35**) and  $\text{IndCpMoH}_2$  (**36**) the spectra present two resonances in the aromatic region at *ca.*  $\delta$  7.24 and 6.60 ppm ( $\text{H}_{5-8}$ ), a doublet between *ca.*  $\delta$  5.60 and 5.00 ppm ( $\text{H}_{1/3}$ ), and a triplet between *ca.*  $\delta$  5.30–4.90 ppm for  $\text{H}_2$ . This pattern is more complex in the cases of the asymmetric complexes  $[\text{IndCpMo}(\text{X})\text{L}]^+$  (**30–32** and **34**) as the resonances are doubled and occasionally superimposed, because the (normally equivalent) pairs of indenyl protons are now diastereotopic and, therefore, exhibit different chemical shifts.

Reaction of  $[\text{IndMo}(\eta^4\text{-C}_5\text{H}_5)(\text{CO})_2][\text{BF}_4]$  with  $\text{Ph}_3\text{CBF}_4$  gives the dication  $[\text{IndCpMo}(\text{CO})_2][\text{BF}_4]_2$  (**37**) characterized by  $\nu(\text{CO})$  stretching vibrations at 2129 and 2089  $\text{cm}^{-1}$ . The complex is rather insoluble in  $\text{CH}_2\text{Cl}_2$  and in acetone. Like in the related complexes  $[\text{Cp}_2\text{Mo}(\text{CO})_2][\text{BF}_4]_2$  and  $[\text{Cp}(\text{CpMe})\text{Mo}(\text{CO})_2][\text{BF}_4]_2$ , dissolution in acetonitrile leads to rapid substitution, forming  $[\text{IndCpMo}(\text{CO})(\text{NCMe})][\text{BF}_4]_2$  (**38**) and, more slowly, under visible light irradiation,  $[\text{IndCpMo}(\text{NCMe})_2][\text{BF}_4]_2$  (**39**). The molecular structure and atom-numbering

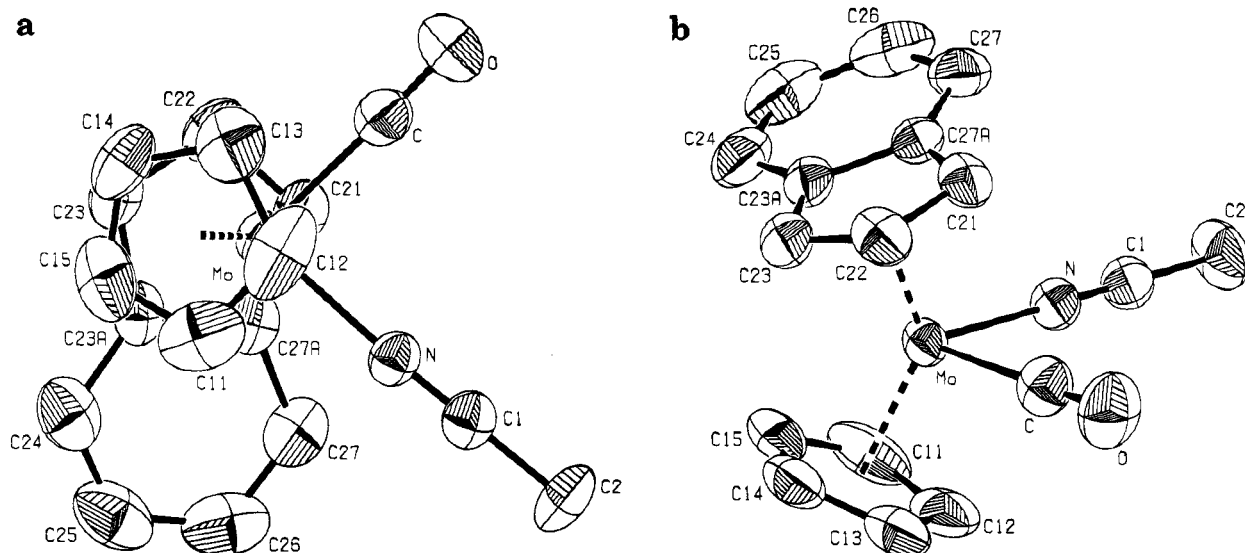


**Figure 1.** Molecular structure of the dication **38** showing 50% probability ellipsoids and the atom-labeling scheme: (a) top view; (b) side view. Hydrogen atoms are omitted for clarity.

**Table 1.** Selected Bond Distances (pm) and Angles (deg) for the Complexes **38**, **41**, and **47**

<b>38<sup>a</sup></b>		<b>41<sup>b</sup></b>		<b>47<sup>c</sup></b>	
M-C	202.5(3)	Mo-C	198.1(1)	Mo-C(1)	194.0(2)
Mo-N	211.9(2)	Mo-C(a)	198.1(1)	Mo-C(2)	194.1(2)
Mo-Cp	198	Mo-Cp	203	Mo-Cp	202
Mo-Cp*	199	Mo-All	211	Mo-All	208
O-C	111.9(3)	O-C	115.1(2)	O(1)-C(1)	115.8(3)
N-C(1)	112.9(3)	O(a)-C(a)	115.1(2)	O(2)-C(2)	116.0(2)
C(1)-C(2)	145.0(4)			C(23)-C(33)	133.8(3)
				C(23)-C(24)	152.2(2)
				C(24)-C(34)	153.8(3)
C-Mo-N	85.5(1)	C-Mo-C(a)	82.5(1)	C(1)-Mo-C(2)	82.8(1)
C-Mo-Cp	105.7	C-Mo-Cp	117.4	C(1)-Mo-Cp	117.9
C-Mo-Cp*	99.2	C-Mo-All	95.8	C(1)-Mo-All	91.7
N-Mo-Cp	106.0	C(a)-Mo-Cp	117.4	C(2)-Mo-Cp	119.1
N-Mo-Cp*	109.8	C(a)-Mo-All	95.8	C(2)-Mo-All	91.2
Cp-Mo-Cp*	137.6	All-Mo-Cp	134.5	All-Mo-Cp	138.5

<sup>a</sup> Cp denotes the centroid of C(11)–C(15). Cp\* denotes the centroid of C(21)–C(27)a, C(22), and C(25). <sup>b</sup> Cp denotes the centroid of C(11)–C(12)a. "All" denotes the centroid of C(21), C(22), and C(22)a. <sup>c</sup> Cp denotes the centroid of C(11)–C(15). "All" denotes the centroid of C(21).

scheme of **38** have been briefly communicated<sup>15</sup> but are presented here in Figure 1a (top view) and b (side view) for comparison purposes. Selected interatomic distances and angles are given in Table 1. To our knowledge, **38** is the first structurally characterized indenyl-substituted metallocene analogue of group 6 transition elements, the only other related examples being the ring-slipped metallocene precursors [Mo( $\eta^5$ -C<sub>9</sub>H<sub>7</sub>)( $\eta^3$ -C<sub>9</sub>H<sub>7</sub>)dppe]<sup>9</sup> and [Mo( $\eta^3$ -C<sub>9</sub>H<sub>7</sub>)( $\eta^5$ -C<sub>5</sub>H<sub>4</sub><sup>i</sup>Pr)(N<sup>t</sup>Bu)].<sup>31</sup> The crystal structure of **38** consists of discrete [IndCpMo(NCMe)(CO)]<sup>2+</sup> cations and two BF<sub>4</sub><sup>-</sup> anions at general positions in the unit cell. Both anions are disordered. The molybdenum atom is coordinated to two  $\eta^5$ -cyclopentadienyl rings, one of which is part of an indenyl system, to one carbonyl and to one acetonitrile ligand. The coordination geometry of the ring normals and the carbon and nitrogen atoms around the central metal atom is best described by a distorted tetrahedron. A projection onto the Mo, C and N plane (Figure 1a) shows that the Cp rings adopt an approximately eclipsed conformation. The metal atom lies 197.8 and 198.5 pm

from the best planes of the cyclopentadienyl rings, and no significant deviations from the generally observed metal to ligand bond distances and angles in other complexes of the type [CpCp'MoLL']<sup>2+</sup> are noteworthy.<sup>28,32,33</sup> For instance, the angle between the ring normals is 137.6° and compares with the analogous angles in the isoelectronic cations [Cp<sub>2</sub>Mo(THF)(CO)]<sup>2+</sup> (137.2(8)°),<sup>33</sup> [( $\eta^5$ -Ind)<sub>2</sub>V(CO)<sub>2</sub>]<sup>+</sup> (138.5(4)°), [Cp<sub>2</sub>V(CO)<sub>2</sub>]<sup>+</sup> (137.9(7)°), and [Cp<sub>2</sub>Ti(CO)<sub>2</sub>] (138.6(7)°).<sup>34</sup> The Mo–N and Mo–C distances are 211.9(2) and 202.5(3) pm, respectively, and the C–Mo–N bond angle is 85.5(1)°. The Cp part of the indenyl moiety tends to be a  $\eta^3 + \eta^2$  type ligand. Therefore, a small bending along the C21–C23 line with an angle of 5.1° is observed. C21 and C23 are not coplanar with the benzene ring and show 3 and 8 pm deviations from the best least-squares plane (2 pm maximum deviation in the benzene ring). A detailed

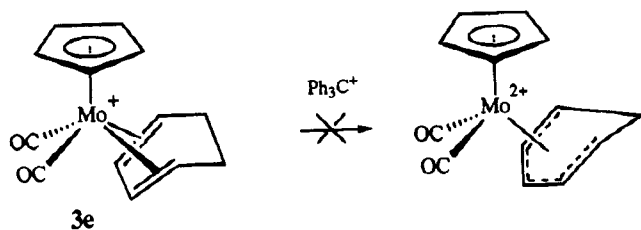
(31) (a) Green, J. C.; Green, M. L. H.; James, J. T.; Konidaris, P. C.; Maunder, G. H.; Mountford, P. *J. Chem. Soc. Chem. Commun.* **1992**, 1361. (b) Knox, R. J.; Prout, C. K. *Acta Crystallogr.* **1969**, B25, 2013.

(32) (a) Knox, R. J.; Prout, C. K. *Acta Crystallogr.* **1969**, B25, 2482. (b) McGilligan, B. S.; Wright, T. C.; Wilkinson, G.; Motevalli, M.; Hursthouse, M. B. *J. Chem. Soc., Dalton Trans.* **1988**, 1737. (c) Gowik, P.; Klapothke, T.; White, P. *Chem. Ber.* **1989**, 122, 1649. (d) Forder, R. A.; Gale, G. D.; Prout, K. *Acta Crystallogr.* **1975**, B31, 297.

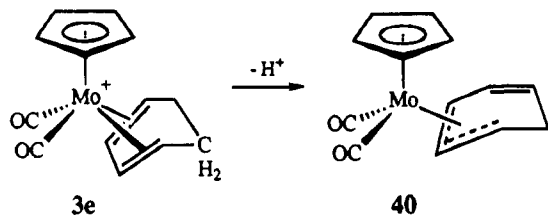
(33) Tsai, J.-C.; Khan, M.; Nicholas, K. M. *Organometallics* **1989**, 8, 2967.

(34) Bocarsly, J. R.; Floriani, C.; Chiesi-Villa, A.; Guastini, C. *Inorg. Chem.* **1987**, 26, 1871 and references cited therein.

Scheme 4



Scheme 5



discussion of the central coordination geometry of  $[\text{CpCp}'\text{MoLL}]^{n+}$  systems ( $n = 0, 1, 2$ ) will be given together with the discussion of compounds **41** and **47** in section 8.

**5. Attempted Preparations of "Open"  $[\text{Cp}(\eta^5\text{-dienyl})\text{MoL}_2]^{n+}$  Complexes.** In the previous sections we have shown that H migration or  $\text{H}^-$  abstraction from coordinated cyclopentadiene in  $[\text{Cp}'\text{Mo}(\eta^4\text{-C}_5\text{H}_6)(\text{CO})_2]^+$  complexes leads to a cyclopentadienyl ring in the mixed-ring  $[\text{Cp}'\text{Cp}'\text{MoH}(\text{CO})]^+$  and  $[\text{Cp}'\text{Cp}'\text{Mo}(\text{CO})_2]^+$  complexes, respectively. Application of this chemistry to other diene complexes might provide the opportunity of preparing "open" analogues of molybdocene. However, as exemplified in Scheme 4 for the cyclohexadiene derivative **3e** and as also tried for  $[\text{Cp}'\text{Mo}(\eta^4\text{-CH}_2\text{-CHCHCHMe})(\text{CO})_2][\text{BF}_4]$  (**3f**),  $\text{H}^-$  abstraction does not take place, and the starting materials are recovered after prolonged reaction times. H migration was also unsuccessful both on irradiation of **3e** and upon its decarbonylation with  $\text{Me}_3\text{NO}$ . Instead,  $[\text{Cp}'\text{Mo}(\eta^4\text{-C}_6\text{H}_8)(\text{NCMe})_2][\text{BF}_4]$  was formed.<sup>35</sup> Therefore, it seems reasonable to accept that  $\text{H}^-$  abstraction from a diene cation  $[\text{Cp}'\text{Mo}(\eta^4\text{-diene})(\text{CO})_2][\text{BF}_4]^+$  is the exception rather than the rule and that it is favored in the cyclopentadiene case by the resonance stabilization of the resulting  $\text{C}_5\text{H}_5$  ring.

**6. Preparation of Ring-Slipped Metallocene Congeners with  $\eta^3\text{-C}_5\text{H}_5$  and  $\eta^3\text{-C}_9\text{H}_7$  Ligands and Related Chemistry.** Deprotonation of the coordinated diene is a well-established reaction for all of these  $[\text{Cp}'\text{Mo}(\eta^4\text{-diene})(\text{CO})_2]^+$  complex cations, including the case of the butadiene derivative.<sup>17c</sup> Apart from the latter, this reaction leads to the formation of a pentadienyl ligand which, by force of the 18-electron rule, will only attain  $\eta^3$ -coordination to the  $\text{Cp}'\text{Mo}(\text{CO})_2$  fragment, forming  $[\text{Cp}'\text{Mo}(\eta^3\text{-pentadienyl})(\text{CO})_2]$  complexes. The typical example, in Scheme 5, is the efficient deprotonation of **3e** by  $\text{NEt}_3$ , forming  $\text{Cp}'\text{Mo}(\eta^3\text{-C}_6\text{H}_7)(\text{CO})_2$  (**40**).<sup>17g</sup> The  $\eta^5$ -indenyl analogue,  $\text{IndMo}(\eta^3\text{-C}_6\text{H}_7)(\text{CO})_2$ , has also been reported by Green.<sup>17c,h</sup>

Extension of this deprotonation reaction to cations containing the coordinated  $\eta^4\text{-C}_5\text{H}_6$  ring raises the possibility of producing complexes containing the rare

$\eta^3$ -cyclopentadienyl ring. In order to test this hypothesis, the deprotonation of  $[\text{IndMo}(\eta^4\text{-C}_5\text{H}_6)(\text{CO})_2][\text{BF}_4]$  was chosen as a simple and favorable example. Indeed, a simple situation is predictable in this case because the primary deprotonation product, namely,  $[\text{IndMo}(\eta^3\text{-C}_5\text{H}_5)(\text{CO})_2]$ , is expected to rearrange to the more stable ring-slipped isomer,  $[\text{Cp}'\text{Mo}(\eta^3\text{-C}_9\text{H}_7)(\text{CO})_2]$  (**41**).<sup>36a</sup> This is in fact the case, and **41** is prepared in high yield by  $\text{NEt}_3$  deprotonation of  $[\text{IndMo}(\eta^4\text{-C}_5\text{H}_6)(\text{CO})_2][\text{BF}_4]$ . Alternatively, **41** may also be prepared in very good yield from  $[\text{IndMo}(\text{CO})_2\text{I}]_2$  (**8**) and  $\text{TiCp}$ . It has the typical *cis*  $\nu(\text{CO})$  stretching vibrations at 1959 and 1888  $\text{cm}^{-1}$ , and the  $^1\text{H}$  NMR spectrum shows some temperature dependence with all expected signals appearing only at  $-65^\circ\text{C}$ . The indenyl signals at  $\delta$  6.75 (triplet;  $\text{H}_2$ ), 6.67–6.44 (multiplet;  $\text{H}_{5-8}$ ), and 5.20 ppm (doublet;  $\text{H}_{1/3}$ ) are consistent with a frozen, symmetrical structure. The complex is more flexible than its W analogue in which two conformers are observed at room temperature. The resonance of the  $\text{H}_2$  proton is unusually deshielded, like in the W analogue.<sup>16</sup> However, chemical shifts of ca.  $\delta$  7 ppm have been reported for this type of proton.<sup>36a</sup> The 18-electron rule prediction of a  $\eta^3$ -coordinated indenyl is also in agreement with the  $^{13}\text{C}$  NMR spectrum. In fact, the diagnostic resonance of the quaternary C4 and C9 carbons (C23 and C23a in Figure 2) appears at the remarkable downfield value of  $\delta$  151.10 ppm, in agreement with a highly slip-folded  $\eta^3$ -coordinated indenyl as actually observed in the X-ray crystal structure determination.<sup>16,36a,c</sup>

The molecular structure and atom numbering scheme of **41** are shown in Figure 2a (top view) and b (side view). Selected bond distances and angles are listed in Table 1. The crystal structure consists of discrete  $[(\eta^5\text{-Cp})(\eta^3\text{-Ind})\text{Mo}(\text{CO})_2]$  molecules in the unit cell. The molybdenum atom is linked with two carbonyl groups, one  $\eta^5$ -cyclopentadienyl ligand, and one  $\eta^3$ -indenyl ligand ( $\pi$ -allylic) which adopts an *endo* conformation with respect to the  $\text{Cp}'\text{Mo}(\text{CO})_2$  fragment. A mirror plane bisects the indenyl, the cyclopentadienyl, and the two carbonyl ligands (in Figure 2, numbers with "a" refer to the mirror-related atoms). The coordination geometry of the ring normals and the carbon atoms of the carbonyl groups around the central metal atom is best described by a distorted tetrahedron. A projection onto the  $\text{OC}-\text{Mo}-\text{CO}$  plane (Figure 2a) shows that the Cp rings adopt a strongly eclipsed conformation introduced by the mirror symmetry. Within the limits of error the  $\eta^5$ -Cp group is planar. The relevant metal-to-carbon distances range from 226.3(4) to 240.7(7) pm. The observed variation of the bond lengths is within the range typically found for metal-to-carbon distances in  $\eta^5$ -Cp complexes. The Cp part of the indenyl moiety acts as a  $\eta^3$ -( $\pi$ -allyl)ligand and is best regarded as being composed of an allylic (C21, C22, and C22a) fragment and a benzenoid (C23, C24, C25, C25a, C24a, and C23a) fragment. The planes defined by these two segments intersect with an angle of  $21.4^\circ$ . The metal-to-carbon bond distances range from  $\text{Mo}-\text{C21}$  (226.3(4) pm) to  $\text{Mo}-\text{C22}$  (238.1(2) pm), with the central carbon atom somewhat nearer to the metal than the terminal ones. Definitely outside the range generally accepted for

(35) Azevedo, C. G.; Galvão, A.; Romão, C. C. Unpublished results, 1995.

(36) (a) O'Connor, J.; Casey, C. P. *Chem. Rev.* **1987**, *87*, 307. (b) Marder, T. B.; Calabrese, J. C.; Roe, D. C.; Tulip, T. H. *Organometallics* **1987**, *6*, 2012. (c) Baker, R. T.; Tulip, T. H. *Organometallics* **1986**, *5*, 839.

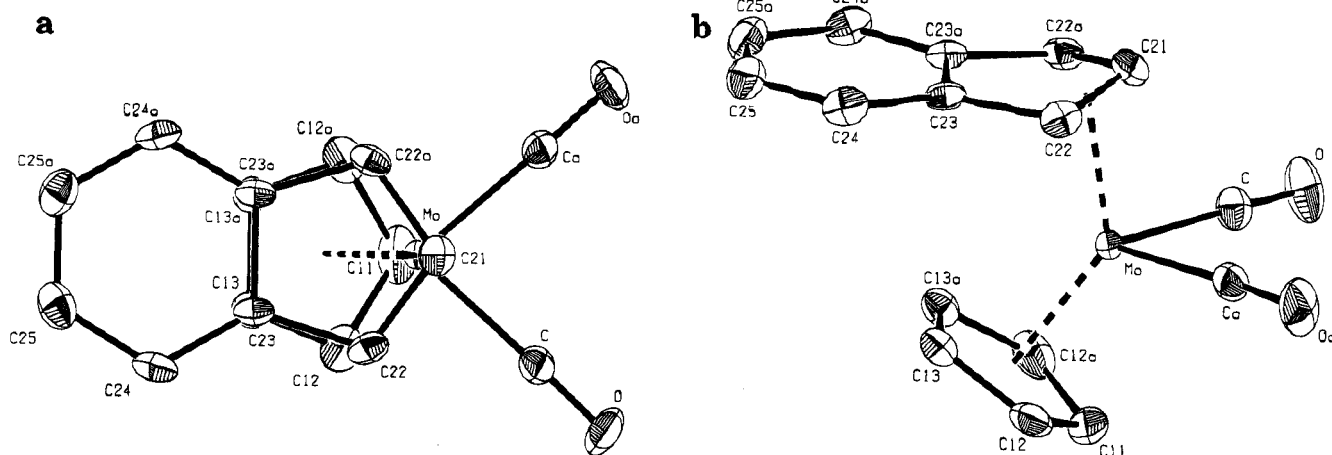


**Figure 2.** Molecular structure of **41** showing 50% probability ellipsoids and the atom-labeling scheme. (a) top view, (b) side view. Hydrogen atoms are omitted for clarity.

Mo–C bonds are the interatomic distances to the benzenoid atoms C23 and C23a within 299.6(4) pm. The metal atom lies 202.2 pm from the best planes through the cyclopentadienyl ring and 211.0 pm from C21, C22, and C22a. The angle between the normals is 137.9°. The Mo–C distance is 198.1(3) pm, and the C–Mo–C bond angle is 82.5(1)°. This overall geometry around the central metal atom is observed to be identical within small deviations in all other structurally characterized complexes of the  $[(\eta^5\text{-Cp})M(\eta^3\text{-}(\pi\text{-allyl})\text{Cp})(\text{CO})_2]$  type:  $[(\eta^5\text{-Ind})W(\eta^3\text{-Ind})(\text{CO})_2]$ ,<sup>37</sup>  $[(\eta^5\text{-Cp})W(\eta^3\text{-Cp})(\text{CO})_2]$ ,<sup>38</sup> and  $[(\eta^5\text{-Ind})V(\eta^3\text{-Ind})(\text{CO})_2]$ .<sup>39</sup>

In a formal sense,  $[(\eta^5\text{-Cp})(\eta^3\text{-Ind})\text{Mo}(\text{CO})_2]$  (**41**) is the 2-electron reduction product of  $[\text{IndCpMo}(\text{CO})_2][\text{BF}_4]_2$  (**37**), and conversely, oxidation of **41** should form **37**. Attempted reduction of **37** with Na/Hg as a suspension in THF was inconclusive. No reaction was observed, probably as the result of the insolubility of both reagents. However, oxidation of **41** with  $\text{Ph}_3\text{CBF}_4$ , in  $\text{CH}_2\text{Cl}_2$ , leads to quantitative formation of **37**. Therefore, the sequential deprotonation of  $[\text{IndMo}(\eta^4\text{-C}_5\text{H}_6)(\text{CO})_2][\text{BF}_4]$  (**10a**) followed by oxidation of **41** represents a third route for producing the mixed-ring fragment  $\text{IndCpMo}$ , i.e., the central reaction pathway of Scheme 1.

In view of this successful reaction we decided to reattempt the preparation of the well-characterized *trihaptocyclopentadienyl* complex  $[\text{CpW}(\eta^3\text{-C}_5\text{H}_5)(\text{CO})_2]$ <sup>38</sup> (**42**) by deprotonation of  $[\text{CpW}(\eta^4\text{-C}_5\text{H}_6)(\text{CO})_2][\text{BF}_4]$  (**43**), in spite of previously reported inconclusive results.<sup>16</sup> As a matter of fact, addition of excess  $\text{NEt}_3$  to a solution of **43**, in  $\text{CH}_2\text{Cl}_2$  at room temperature, gives a dark-blue solution. Treatment of the reaction mixture with toluene followed by concentration and filtration of the separated precipitate allows the isolation of the desired **42** in good yields, in the form of well-developed deep blue crystals as recrystallized from hexane/ether mixtures. The analytical, IR, and <sup>1</sup>H NMR data are in complete agreement with the data reported in the literature. The workup procedure must be performed as described in the Experimental Section otherwise

decomposition occurs to form  $[\text{Cp}_2\text{WH}(\text{CO})][\text{BF}_4]$  (**45**), as described below. It is, however, a rather simple procedure which allows the preparation of good quantities of this interesting molecule which has remained unstudied.

In the same vein, deprotonation of  $[\text{CpMo}(\eta^4\text{-C}_5\text{H}_6)(\text{CO})_2][\text{BF}_4]$  (**3a**) with  $\text{NEt}_3$ , in  $\text{CH}_2\text{Cl}_2$  solution at  $-70^\circ\text{C}$ , instantaneously produces a deep green solution. Workup of the reaction mixture at low temperature ( $-40^\circ\text{C}$ ) and with protection from light gives a bright green, hexane soluble product, **44**, which can be very easily crystallized from hexane/ether mixtures. This moderately temperature sensitive complex has two peaks in the CO stretching region of the IR spectrum, at 1950 and 1854  $\text{cm}^{-1}$ , typical of a *cis*  $\text{Mo}(\text{CO})_2$  geometry (KBr pellets and hexane solution). The disappearance of these peaks may be followed in hexane solution, at room temperature under laboratory light, and is concomitant with the appearance of a brown decomposition product and a peak at 1928  $\text{cm}^{-1}$  assigned to  $\text{Cp}_2\text{Mo}(\text{CO})$  (**18**). The <sup>1</sup>H NMR spectrum shows a singlet at  $\delta$  5.63 ppm that is distinctly different from the signal at  $\delta$  4.46 ppm reported for **18** but similar to the one observed for  $[\text{CpW}(\eta^3\text{-C}_5\text{H}_5)(\text{CO})_2]$  ( $\delta$  5.21 ppm). Therefore, both the IR and NMR data on **44** are very similar to the data reported for  $[\text{CpW}(\eta^3\text{-C}_5\text{H}_5)(\text{CO})_2]$ ,<sup>38</sup> and we assign it the formulation  $[\text{CpMo}(\eta^3\text{-C}_5\text{H}_5)(\text{CO})_2]$  (**44**). The singlet in the <sup>1</sup>H NMR spectrum shows the expected fluxional exchange between the two rings of different hapticity. Previous attempts to prepare this compound by several routes were unsuccessful, but, indeed, it is not much less stable than its W analogue.<sup>40</sup> Interestingly enough, reaction of  $[\text{CpMo}(\text{CO})_2]_2$  with  $\text{TiCp}$  gives **44** in reasonable yield. However, if deprotonation of  $[\text{CpMo}(\eta^4\text{-C}_5\text{H}_6)(\text{CO})_2][\text{BF}_4]$  is performed with NaH or  $\text{LiN}^i\text{Pr}_2$  in THF suspensions the initially deep blue-green solutions slowly turn brown. From the residue left after filtration and evaporation,  $\text{Cp}_2\text{Mo}(\text{CO})$  may be sublimed in low yield. Treatment of  $[\text{CpMo}(\eta^3\text{-C}_5\text{H}_5)(\text{CO})_2]$  with  $\text{HBF}_4\cdot\text{Et}_2\text{O}$  in  $\text{CH}_2\text{Cl}_2$  gives a yellow precipitate identified as  $[\text{CpMo}(\eta^4\text{-C}_5\text{H}_6)(\text{CO})_2][\text{BF}_4]$  by its IR spectrum.

We mentioned above that the deprotonation of  $[\text{CpW}(\eta^4\text{-C}_5\text{H}_6)(\text{CO})_2][\text{BF}_4]$  with  $\text{NEt}_3$  to give  $[\text{CpW}(\eta^3\text{-C}_5\text{H}_5)(\text{CO})_2]$  (**42**) is a rather simple procedure which allows the preparation of good quantities of this interesting molecule which has remained unstudied.

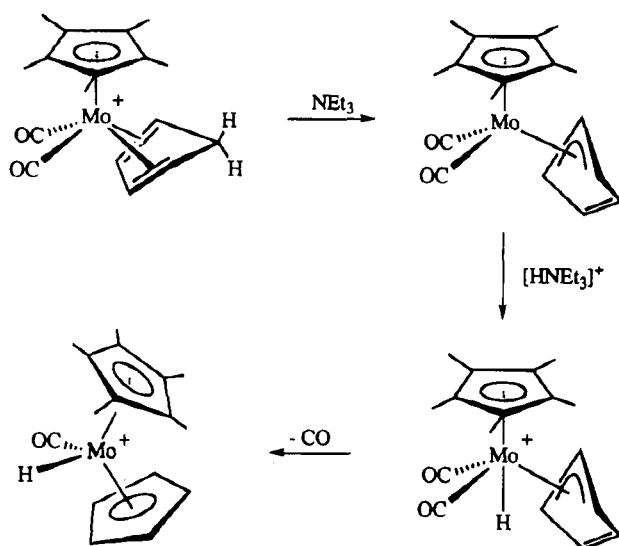
(37) Nesmeyanov, A. N.; Ustynyuk, N. A.; Makarova, L. G.; Andrianov, V. G.; Struchkov, Yu. T.; Andrae, S. *J. Organomet. Chem.* **1978**, *159*, 189.

(38) Huttner, G.; Brintzinger, H. H.; Bell, L. G.; Friedrich, P.; Bejenke V.; Neugebauer, D. *J. Organomet. Chem.* **1978**, *145*, 329.

(39) Kowaleski, R. M.; Rheingold, A. L.; Trogler, W. C.; Basolo, F. *J. Am. Chem. Soc.* **1986**, *108*, 2460.

(40) Bell, L. G.; Brintzinger, H. H. *J. Organomet. Chem.* **1977**, *135*, 173.

Scheme 6



(CO)<sub>2</sub>] has to be carried out carefully in order to avoid decomposition. Indeed, if the reaction mixture is taken to dryness without further treatment, the residue loses the blue color and becomes brown-orange. From this residue neither [CpW( $\eta^3$ -C<sub>5</sub>H<sub>5</sub>)(CO)<sub>2</sub>] nor Cp<sub>2</sub>W(CO) can be isolated. Instead, the known [Cp<sub>2</sub>WH(CO)][BF<sub>4</sub>] (**45**) is formed in high yield in an entirely reproducible manner. This was rather surprising considering the already noted unsuccessful transformation, [CpW( $\eta^4$ -C<sub>5</sub>H<sub>6</sub>)(CO)<sub>2</sub>][BF<sub>4</sub>] → [Cp<sub>2</sub>WH(CO)][BF<sub>4</sub>], induced by visible light irradiation and reflux,<sup>16</sup> and ruled out simple decomposition of the starting material, [CpW( $\eta^4$ -C<sub>5</sub>H<sub>6</sub>)(CO)<sub>2</sub>][BF<sub>4</sub>]. Furthermore, in an attempt to prepare [Cp\*Mo( $\eta^3$ -C<sub>5</sub>H<sub>5</sub>)(CO)<sub>2</sub>] by deprotonation of [Cp\*Mo( $\eta^4$ -C<sub>5</sub>H<sub>6</sub>)(CO)<sub>2</sub>][BF<sub>4</sub>] (**12**) with NEt<sub>3</sub>, a rather high yield of [Cp\*MoH(CO)][BF<sub>4</sub>] (**46**) was obtained. Again, as we noted above, the photochemical transformation of **12** in **46** is a slow, low-yield process. It then became evident that NEt<sub>3</sub> was somehow promoting this transformation. To confirm the genuine influence of NEt<sub>3</sub> on the reaction, 2 aliquots of a solution of **12** were prepared at room temperature under ordinary laboratory light. While one was left under these conditions, the other was immediately treated with NEt<sub>3</sub>. After 2 h, solution IR showed that most of the starting material was present unchanged in the untreated aliquot while virtually full conversion to **46** was achieved in the aliquot treated with NEt<sub>3</sub>. The results were confirmed by isolation and characterization of the complexes **12** and **46** from the untreated and treated aliquots, respectively. Careful comparison of the reaction conditions used for the preparation of [CpW( $\eta^3$ -C<sub>5</sub>H<sub>5</sub>)(CO)<sub>2</sub>] (**42**) with the conditions used for the preparation of both hydrido complexes **45** and **46** revealed that they were only formed when the reaction mixture is taken to dryness after treatment with NEt<sub>3</sub>. However, when the reaction mixture is taken to dryness only after addition of toluene and separation of the precipitated salts, **42** becomes the isolated product. On the basis of these observations, we propose that the [HNEt<sub>3</sub>]<sup>+</sup> is responsible for the transformation of the  $\eta^3$ -C<sub>5</sub>H<sub>5</sub> complexes into the hydrido-carbonyls as represented in Scheme 6.

The proposed initial step is deprotonation of the C<sub>5</sub>H<sub>6</sub> ring to form the  $\eta^3$ -C<sub>5</sub>H<sub>5</sub> ligand. This complex is then

protonated at the metal by the triethylammonium salt [HNEt<sub>3</sub>]<sup>+</sup> liberated in the first step. This protonation is a formal oxidation that will destabilize the M–CO bond, promoting CO dissociation. Return of  $\eta^3$ -C<sub>5</sub>H<sub>5</sub> to  $\eta^5$ -C<sub>5</sub>H<sub>5</sub> forms the final, stable, carbonyl–hydride 18-electron complexes **45** and **46**. The protonation at the metal is in obvious contradiction with the protonation of the  $\eta^3$ -C<sub>5</sub>H<sub>5</sub> ligand observed in the reaction of [CpMo( $\eta^3$ -C<sub>5</sub>H<sub>5</sub>)(CO)<sub>2</sub>] with HBF<sub>4</sub>·Et<sub>2</sub>O, which reforms the  $\eta^4$ -C<sub>5</sub>H<sub>6</sub> ligand. However, a competition between different protonation sites in the [CpM( $\eta^3$ -C<sub>5</sub>H<sub>5</sub>)(CO)<sub>2</sub>] (metal *vs* ligand; thermodynamic control *vs* kinetic control) complexes and/or divergent evolution pathways for the protonated species [CpM( $\eta^3$ -C<sub>5</sub>H<sub>5</sub>)H(CO)<sub>2</sub>]<sup>+</sup> is not difficult to anticipate and, depending on rather subtle differences, *e.g.*, Mo *vs* W and Cp\* *vs* Cp, leading to different observed final products. As mentioned above, the easy preparation of [CpW( $\eta^3$ -C<sub>5</sub>H<sub>5</sub>)(CO)<sub>2</sub>] and [CpMo( $\eta^3$ -C<sub>5</sub>H<sub>5</sub>)(CO)<sub>2</sub>] may allow a more detailed study of these and other similar reactions.

With these results in mind we decided to check whether the deprotonation of [CpMo( $\eta^4$ -C<sub>5</sub>Me<sub>5</sub>H)(CO)<sub>2</sub>][BF<sub>4</sub>] (**3c**) follows a similar route to give, presumably, Cp\*Mo( $\eta^3$ -C<sub>5</sub>H<sub>5</sub>)(CO)<sub>2</sub>. The reaction of **3c** with NEt<sub>3</sub> in CH<sub>2</sub>Cl<sub>2</sub> occurs readily to give the hexane soluble yellow complex **47**. The IR shows the presence of two *cis*-CO ligands, but the <sup>1</sup>H NMR spectrum is incompatible with Cp\*Mo( $\eta^3$ -C<sub>5</sub>H<sub>5</sub>)(CO)<sub>2</sub> since the bridgehead-substituted methylene group C(H)CH<sub>3</sub> was clearly present judging from the quartet ( $\delta$  2.45 ppm) and doublet ( $\delta$  0.93 ppm) assigned to H and CH<sub>3</sub>, respectively. Furthermore, three different CH<sub>3</sub> resonances were clearly observed. Crystal structure determination of **47** showed an unexpected result. The molecular structure, corresponding to the formula [CpMo{ $\eta^3$ -C<sub>5</sub>(CH<sub>3</sub>)<sub>4</sub>H(CH<sub>2</sub>)}(CO)<sub>2</sub>] (**47**), is represented in Figure 3a (top view) and b (side view). Selected bond angles and distances are given in Table 1.

The complex belongs to the general family of CpMo( $\eta^3$ -allyl)(CO)<sub>2</sub> complexes, of which there are many examples of structural determinations.<sup>41</sup> The geometry around the Mo atom is pseudotetrahedral with the two CO, the Cp, and the allylic ligands occupying the four formal coordination positions. The orientation of the allylic ligand with respect to the [MoCp(CO)<sub>2</sub>]<sup>+</sup> fragment is *exo*, and the bridgehead-substituted methylene at C24 has the proton facing the metal and the methyl (C34) facing the outside of the molecule. This fact certainly reflects the original coordination of Cp\*H which, for stereochemical reasons, occurs with the bridgehead H facing the metal (see **4** or **5**, R<sub>1</sub> = CH<sub>3</sub>, R<sub>2</sub> = H). The fully substituted allylic ligand is somewhat asymmetrically coordinated with the central carbon, C21, having the shorter distance to the Mo as seen in other Mo(II) allylic complexes.<sup>41</sup> Some degree of conjugation between the allyl and the exocyclic C–C double bond (C23–C33) is inferred from the C22–C23 bond length which is shorter than a typical C–C single bond (1.53(1) Å). Two other closely related examples of this type of ligand are described in the literature in the complexes **48**<sup>42a</sup> and **49**.<sup>42b</sup> In the case of **48**, however, the allylic ring presents an *endo* conformation relative to the [MoCp-

(41) (a) Faller, J. W.; Chodos, D. F.; Katahira, D. *J. Organomet. Chem.*, **1980**, *187*, 227. (b) Orpen, A. G.; Brammer, L.; Allen, F. H.; Kennard, O.; Watson, D. G.; Taylor, R. *J. Chem. Soc., Dalton Trans.* **1989**, S1.

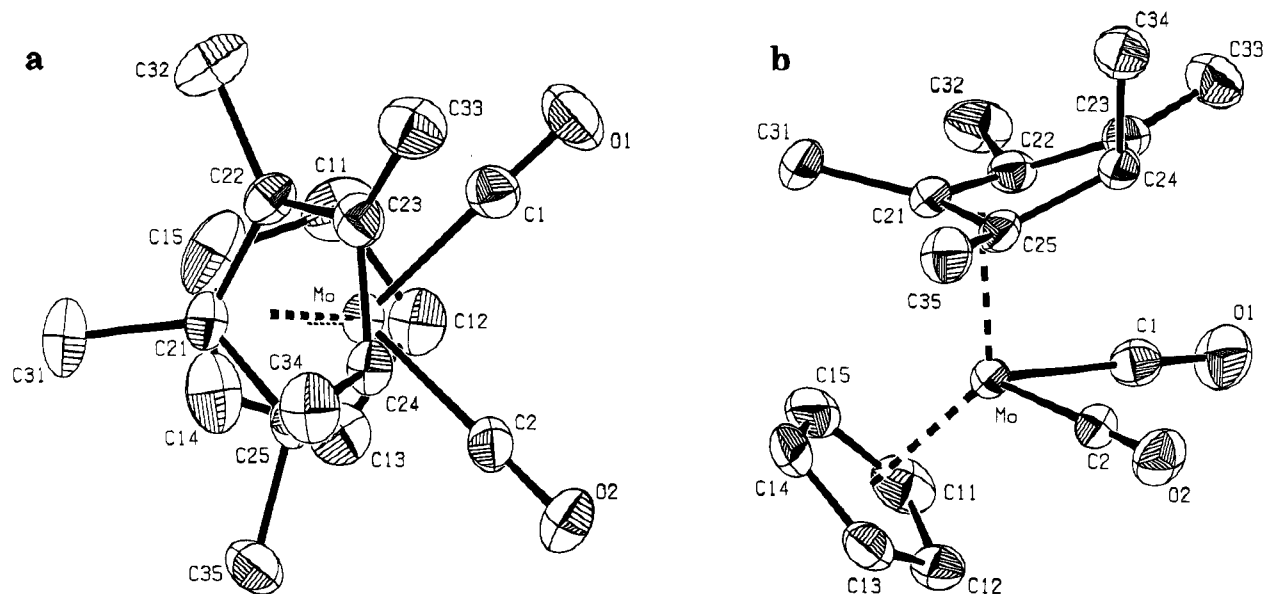
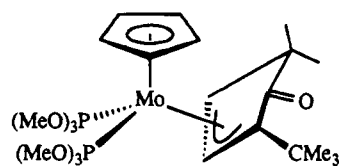


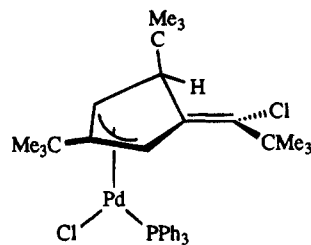
**Figure 3.** Molecular structure **47** showing 50% probability ellipsoids and the atom-labeling scheme: (a) top view, (b) side view. Hydrogen atoms are omitted for clarity.

(CO)<sub>2</sub>]<sup>+</sup> fragment but still keeps a shorter Mo–C distance for the central allylic carbon and also a short C–C bond between the allyl and the ketonic carbonyl group. This kind of conjugation has also been observed in the related CpRu(η<sup>3</sup>-CH<sub>2</sub>CHCHCHO)(CO) as pointed out in ref 17i. These effects are absent in the Pd complex **49**. The allylic ligand is chiral at C24. However, the <sup>1</sup>H NMR spectrum of a solution of the crystals of **47** shows the presence of only one isomer. Indeed, **47** crystallizes in the chiral space group *P*<sub>2</sub><sub>1</sub><sub>2</sub><sub>1</sub><sub>2</sub><sub>1</sub> with only one enantiomer in the unit cell. The chirality around atom C24 exhibits *R*-configuration.<sup>43,44</sup> From the chemical point of view there is no reason to produce only one enantiomer. Compounds **48** and **49** crystallize in the centrosymmetric space groups *P*<sub>2</sub><sub>1</sub>/*n* and *P*<sub>2</sub><sub>1</sub>/*c*, respectively, and have both enantiomers in the unit cell. Therefore, packing effects in the crystal may be responsible for the enantioselective crystallization. As a matter of fact, the <sup>1</sup>H NMR spectrum of a solution of **47**, obtained from the sticky residue resulting after hexane extraction of the reaction mixture, shows the presence of two isomers. Several recrystallizations are needed to obtain crystals of **47** as the ones used in the crystallographic experiments.

As expected, similar treatment of the tungsten analogue [CpW(η<sup>4</sup>-C<sub>5</sub>Me<sub>5</sub>H)(CO)<sub>2</sub>][BF<sub>4</sub>]<sup>-</sup> (**15**) with NEt<sub>3</sub> leads to the analogous [CpW{η<sup>3</sup>-C<sub>5</sub>(CH<sub>3</sub>)<sub>4</sub>H(CH<sub>2</sub>)}(CO)<sub>2</sub>] (**50**) in good yield. Again, only one isomer is present in the recrystallized solid, as evidenced by the <sup>1</sup>H NMR and IR spectra which are almost identical to the spectra of **47**. In both cases the allylic ligand was formed by deprotonation of one of the CH<sub>3</sub> groups substituting at



**48**



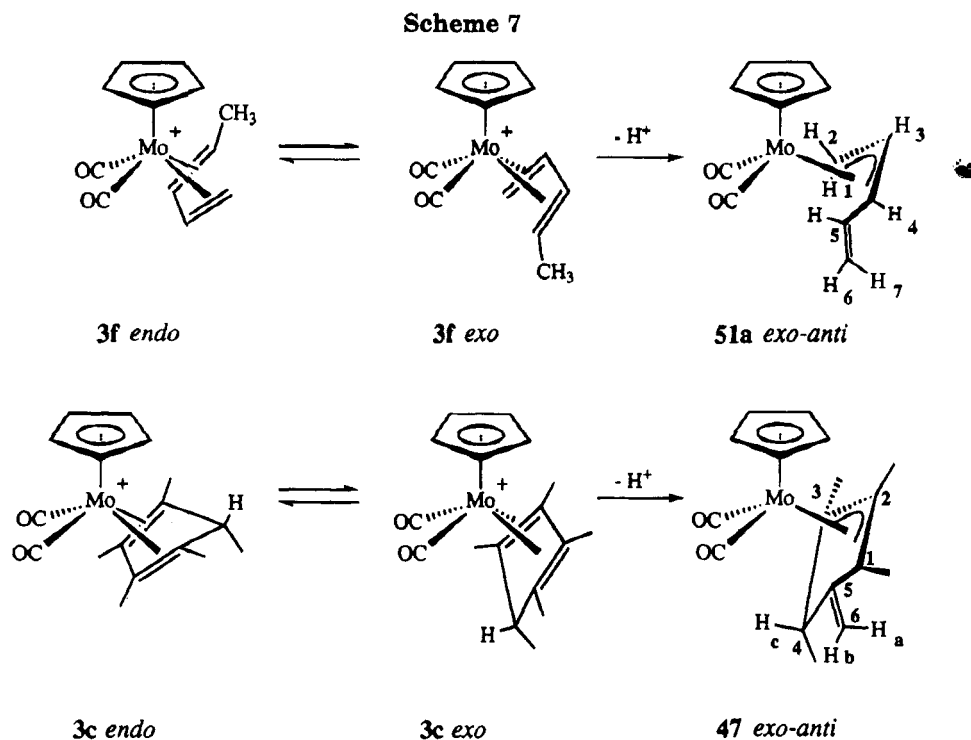
**49**

the diene skeleton of Cp\*H, leading to an *exocyclic* double bond, instead of taking place at the bridgehead C(H)CH<sub>3</sub> proton to form the aromatic C<sub>5</sub>Me<sub>5</sub><sup>-</sup> ring. Before attempting a discussion of this feature we will consider the result of the deprotonation of another complex containing a substituted diene, namely, the piperylene derivative **3f**. In this case, the hexane soluble yellow product has the expected formula CpMo-(η<sup>3</sup>-C<sub>5</sub>H<sub>7</sub>)(CO)<sub>2</sub> (**51a**). At -40 °C the <sup>1</sup>H NMR spectrum is sharp and reveals the presence of only one isomer since only one sharp Cp signal is observed. The signals of the pentadienyl ligand were assigned with the help of a COSY spectrum and selective peak irradiation. Both the values of the coupling constants, *J*<sub>34</sub> ≈ *J*<sub>23</sub> = 7.5 Hz and *J*<sub>13</sub> = 11.2 Hz, and the values of the chemical shifts of the vinyl group agree with the an *exo-anti*-η<sup>3</sup>-pentadienyl configuration, as they are clearly similar to the values reported for the analogues Cp\*Mo(*exo-anti*-η<sup>3</sup>-pentadienyl)(CO)<sub>2</sub><sup>17i</sup> and [MoBr(*exo-anti*-η<sup>3</sup>-penta-

(42) (a) Beevor, R. G.; Freeman, M. J.; Green, M.; Morton, C. E.; Orpen, A. G. *J. Chem. Soc., Dalton Trans.* **1991**, 3021. (b) Bailey, P. M.; Mann, B. E.; Segnitz, A.; Kaiser, K. L.; Maitlis, P. M. *J. Chem. Soc., Chem. Commun.* **1974**, 567.

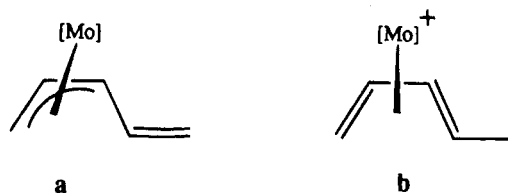
(43) IUPAC. *Nomenclature of Organic Chemistry, Sections A,B,C,D,E,F, and H, 1979 Edition*, Pergamon Press, Oxford, 1979; Section E: Stereochemistry.

(44) According to the Beilstein Institute in Frankfurt, Germany, **47** has the following systematic names: Beilstein system, dicarbonyl-(η<sup>5</sup>-cyclopentadienyl)-((4*R*)-*trans*-(1,2,3-η)-1,2,3,4-tetramethyl-5-methylene-cyclopent-1 → 3-enyl)molybdenum; Chemical Abstracts system, (4*R*)-*trans*-dicarbonyl(η<sup>5</sup>-2,4-cyclopentadien-1-yl)[(1,2,3-η)-1,2,3,4-tetramethyl-5-methylene-2-cyclopenten-1-yl]molybdenum.



dienyl)(CO)<sub>2</sub>(NCMe)<sub>2</sub>].<sup>45</sup> The broadening and loss of resolution observed in the <sup>1</sup>H NMR spectrum of **51a**, at room temperature, indicate the presence of some dynamic interconversion, most probably an *exo-anti* to *endo-anti* equilibrium which has been generally observed in CpMo(allyl)(CO)<sub>2</sub> complexes including CpMo(*syn*-η<sup>3</sup>-pentadienyl)(CO)<sub>2</sub>.<sup>46</sup> Accordingly, the IR spectrum (KBr pellet) has two pairs of peaks in the region of the CO stretching vibrations in agreement with the presence of two isomers both with a *cis*-Mo(CO)<sub>2</sub> arrangement. On the basis of steric arguments, the higher stability expected for the *exo-anti* isomer when compared to the *endo-anti* isomer may explain the presence of only the former already at -40 °C. Indeed, *anti* substitution strongly favors the *exo* conformers in CpMo(allyl)(CO)<sub>2</sub> complexes.<sup>20</sup> Alternative *anti-syn* isomerization seems less probable since the isomer exhibiting the *exo-syn* conformation, **51b**, has been prepared in different manners, has been fully characterized, and does not show this type of thermal isomerization at room temperature.<sup>45,46</sup>

If we now compare the deprotonations of **3c** and of **3f**, as shown in Scheme 7, it is obvious that they follow the same regiochemistry: in both cases the abstracted proton comes from the CH<sub>3</sub> substituent at the terminal position of the diene ligand. It has been pointed out by other authors that the bonds in acyclic pentadienyls coordinated to the [CpMo(CO)<sub>2</sub>]<sup>+</sup> fragment are best described in terms of the contribution of the two resonance hybrids **a** and **b**, and we have just mentioned some bond length evidence in **47** supporting this interpretation. Considering this resonance as a stabilization of the conjugate base of the diene complex [CpMo(η<sup>4</sup>-diene)(CO)<sub>2</sub>]<sup>+</sup> may explain the preferential deprotonation at the observed position.



Molecular orbital calculations designed to test these and other related aspects of conformational arrangements of allyl, diene, and pentadienyl ligands coordinated to the [CpMo(CO)<sub>2</sub>]<sup>+</sup> and related fragments are under way and will be published separately.

Experiments are under way to transform CpMo(η<sup>3</sup>-C<sub>5</sub>H<sub>7</sub>)(CO)<sub>2</sub> (**51a**) into the molybdenocene analogues bearing one "open" pentadienyl, e.g., photolysis to the known Cp(η<sup>5</sup>-pentadienyl)Mo(CO)<sub>2</sub><sup>46</sup> or oxidation to [Cp(η<sup>5</sup>-pentadienyl)Mo(CO)<sub>2</sub>]<sup>2+</sup>.

**7. Preparation of Ind<sub>2</sub>MoX<sub>2</sub> Derivatives.** As we have seen, the mixed-ring fragment IndCpMo is easily prepared from [IndMo(η<sup>4</sup>-C<sub>5</sub>H<sub>6</sub>)(CO)<sub>2</sub>][BF<sub>4</sub>] (**10a**) by any of the three routes shown in Scheme 1. In contrast with the W and V analogues [(η<sup>5</sup>-Ind)M(η<sup>3</sup>-Ind)(CO)<sub>2</sub>], which have been structurally characterized,<sup>37,39</sup> the preparation of derivatives of the symmetric Ind<sub>2</sub>Mo fragment remained unsuccessful for many an attempt. For example, reaction of [IndMo(CO)<sub>2</sub>I]<sub>2</sub> with LiInd or KInd does not produce the expected [(η<sup>5</sup>-Ind)Mo(η<sup>3</sup>-Ind)(CO)<sub>2</sub>] (**52**) in parallel with the preparation of [CpMo(η<sup>3</sup>-Ind)(CO)<sub>2</sub>]. However, the deprotonation approach works quite well giving the desired product. The reaction is performed by treatment of [IndMo(η<sup>2</sup>-C<sub>3</sub>H<sub>6</sub>)(CO)<sub>2</sub>(F<sub>3</sub>BF)] (**7**) with indene and NEt<sub>3</sub>. After extraction with hexane, **52** can be isolated in very good yield. The IR (two ν(CO) bands, 1929 and 1865 cm<sup>-1</sup>) and the <sup>1</sup>H NMR (three resonances with a 4:2:1 ratio) have the expected signals and are very similar to the spectra of [(η<sup>5</sup>-Ind)W(η<sup>3</sup>-Ind)(CO)<sub>2</sub>]. The reaction is remarkable insofar as the attempted isolation of any intermediate complex formed between **7** and indene failed to give any tractable

(45) Lee, G. H.; Peng, S. M.; Liu, F. C.; Mu, D.; Liu, R. S. *Organometallics* **1989**, *8*, 402.

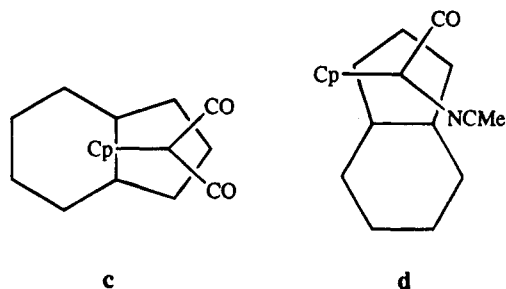
(46) Lee, G. H.; Peng, S. M.; Lee, T.-W.; Liu, R.-S. *Organometallics* **1986**, *5*, 2378. Lee, T.-W.; Liu, R.-S. *Organometallics* **1988**, *7*, 878.



or identifiable species. Therefore, we assume that deprotonation of any incipient species as [IndMo( $\eta^2$ -IndH)(CO)<sub>2</sub>]<sup>+</sup> occurs rather quickly and selectively to yield **52**.

**8. Further Considerations on the Basis of the Structures of Complexes 38, 41, and 47.** Table 1 summarizes the fundamental structural information concerning these three compounds, most of which has already been discussed in the appropriate sections above. However, a few points deserve a final comment.

In a general sense, both compounds [CpMo( $\eta^3$ -C<sub>9</sub>H<sub>7</sub>)(CO)<sub>2</sub>] (**41**) and [CpMo( $\eta^3$ -C<sub>5</sub>(CH<sub>3</sub>)<sub>4</sub>H(CH<sub>2</sub>))(CO)<sub>2</sub>] (**47**) may be considered as members of the large class of [CpMo( $\eta^3$ -allyl)(CO)<sub>2</sub>] complexes. From this point of view, their conformations, *endo*-**41** and *exo*-**47**, are somehow the "wrong" conformations. Indeed, a CSD search routine<sup>47</sup> with a CpMo(CO) fragment and a  $\eta^3$ -allyl ligand yields 38 hits (15 *endo*, 23 *exo*). From these data it is clear that the allyl ligands with substituents at the central carbon prefer the *endo* conformation. Therefore, **47** should be *endo* and not *exo* as observed. Conversely, the *exo* form is preferred when this central carbon atom remains unsubstituted.<sup>48</sup> This might erroneously predict an *exo* conformation for **41**. On the other hand, the observed structure of the latter can be correctly predicted by the "rule of thumb" introduced by Faller, Crabtree, and Habib.<sup>49</sup> This rule states that the preferred ring orientation of an indenyl ligand coordinated to a ML<sub>2</sub>L' fragment will place the six-membered ring *trans* to the ligands with higher *trans* influence. In the case of **41** the latter are the two CO's, resulting in the conformation shown schematically in **c**.



In [IndCpMo(CO)(NCMe)][BF<sub>4</sub>]<sub>2</sub> (**38**) the rule is more difficult to apply, but, as shown in **d**, the aromatic ring of the indenyl is still mainly oriented *trans* to the CO. In fact, **38** has a singular structural feature: the alignment of the indenyl ligand corresponds to that usually observed for group 4 transition metals.<sup>50</sup> [Ind<sub>2</sub>V(CO)<sub>2</sub>]<sup>+</sup>, which is isoelectronic with **38**, also shows the type of orientation depicted in **d**.<sup>34</sup> Compounds **41**, [Ind<sub>2</sub>W(CO)<sub>2</sub>]<sup>37</sup> and [Ind<sub>2</sub>V(CO)<sub>2</sub>],<sup>39</sup> on the contrary, show a vector bisecting both the indenyl group and the L-M-L angle. Crystal-packing forces, electronic effects in the  $\pi$ -electron system, or both factors may be responsible. Molecular orbital studies are under way.

(47) Allen, F. H.; Kennard, O.; Taylor, R. Systematic Analysis of Structural Data as a Research Technique in Organic Chemistry. *Acc. Chem. Res.* **1983**, *16*, 146.

(48) Only four exceptions were detected: *exo*, CSD-refcode, LANCAI; *endo*, CSD-refcodes, KIPWEL, VIBWOS, and VINLAF.

(49) Faller, J. W.; Crabtree, R. H.; Habib, A. *Organometallics* **1985**, *4*, 929.

(50) These statements are confirmed by a detailed CSD database search.

**Table 2. Slip Parameters<sup>a</sup> for [MoCp(Ind)(NCMe)(CO)][BF<sub>4</sub>]<sub>2</sub> (**38**), [Mo( $\eta^5$ -Cp)( $\eta^3$ -Ind)(CO)<sub>2</sub>] (**41**),**

**[CpMo( $\eta^3$ -C(Me)C(Me)C(Me)C(CH<sub>2</sub>)CH(Me))](CO)<sub>2</sub>] (**47**), and Related Compounds**

compd	$\Delta =  S $ , pm	$\sigma$ , deg	$\psi$ , deg	$\Delta(M-C)$ , pm	$\Omega$ , deg	ref
<b>38</b>						this work
$\eta^5$ -Cp	6.5	9.7	1.9	4	none	
$\eta^5$ -Ind	19.4	2.6	5.6	15	5.1	
<b>41</b>						this work
$\eta^5$ -Cp	12.0	0.6	3.4	9	2.1	
$\eta^3$ -ind	94.7	6.0	24.1	65	21.4	
<b>47</b>						this work
$\eta^5$ -Cp	7.0	8.8	2.0	4	0.5	
$\eta^3$ -ring	121.0	7.9	30.5	83	27.2	
(Ind) <sub>2</sub> V(I)						34
$\eta^5$ -ind 1	12.2	9.9	3.5	10	none	
$\eta^5$ -ind 2	7.9	5.0	2.3	7	none	
[(Ind) <sub>2</sub> V(CO) <sub>2</sub> ] <sup>+</sup>						34
$\eta^5$ -ind 1	19.2	27.9	5.6	13	none	
$\eta^5$ -ind 2	19.7	17.7	5.8	15	none	
(Ind) <sub>2</sub> V(CO) <sub>2</sub>						39
$\eta^5$ -ind	15.7	0.0	4.6	13	none	
$\eta^3$ -ind	79.8	1.5	20.9	56	12.0	
(Cp) <sub>2</sub> W(CO) <sub>2</sub>						38
$\eta^5$ -Cp	7.6	0	2.2	10	4.9 <sup>b</sup>	
$\eta^3$ -Cp	92.8	0	23.4	62	19.7	

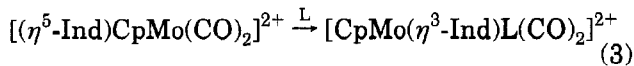
<sup>a</sup> Parameters are defined in refs 49 and 51. <sup>b</sup> Value may be incorrect.

At present we cannot offer a definitive explanation for the conformation presented in the crystal structure of **47**. Since the compound is structurally rigid, the conformation must originate during the proton abstraction step. The simple inspection of Scheme 7 does not reveal any particularly obvious stereochemical reason in favor of the H<sup>+</sup> abstraction from *exo*-**3c**, which, at room temperature, is simultaneously present in solution with *endo*-**3c**. We, therefore, believe that some subtle electronic effect is decisive for this regioselectivity, which, as shown in Scheme 7, is also present in the deprotonation of **3f**. However, since the thorough structural characterization of the other isomers of **47** formed in the reaction was not carried out, these suggestions must remain tentative.

A lot of experimental work showed that the reactivity toward substitution or elimination reactions of coordinatively saturated metal centers depends on the attached cyclopentadienyl or indenyl ligands. Both ligands are able to adapt their hapticity in response to the electronic pressure at the metal center. This tuning is best described in terms of ring-slippage parameters (Table 2), which are presented and compared with some values taken from the literature.<sup>49,51</sup> In general, the observed values for **38**, **41**, and **47** are consistent with those given in literature.<sup>49</sup> Detailed analyzes of the observed distortions are handicapped by the quality of the crystal data cited in literature. The slip-fold distortion of the indenyl ligand in **41** is rather large, as measured at  $\Omega = 21.4^\circ$ , but is smaller than the value of  $26^\circ$  reported for [IndW( $\eta^3$ -Ind)(CO)<sub>2</sub>].<sup>37</sup> Both are substantially smaller than the value of  $\Omega = 30.5^\circ$  observed for the typical allylic complex **47**.

(51) Honan, M. B.; Atwood, J. L.; Bernal, I.; Herrmann, W. A. *J. Organomet. Chem.* **1979**, *179*, 403.

The coordination of the indenyl ring in [IndCpMo(CO)(NCMe)][BF<sub>4</sub>]<sub>2</sub> (**38**) suggests an allyl-ene distortion due to the small but definite values of  $\Delta(M-C) = 15$  pm and  $\Omega = 5.1^\circ$ . Interestingly enough, the isoelectronic cation [Ind<sub>2</sub>V(CO)<sub>2</sub>]<sup>+</sup> presents similar values for  $\Delta(M-C)$  but does not show a slip-fold ( $\Omega = 0^\circ$ ). This apparent tendency for ring-slippage in **38** suggests that ligand association might be facile. Addition reactions to the dication **38**, of the type depicted in eq 3, are being



studied in order to test the validity of this hypothesis. After all, the possible catalytic implications of this addition reaction were the driving force for the preparation of indenyl analogues of molybdenocene and tungstenocene.

### Conclusions and Prospects

The stepwise preparation of molybdenocene and tungstenocene, and several of its analogues bearing *pentahaptocyclopentadienyl* ligands other than C<sub>5</sub>H<sub>5</sub>, is possible through simple transformations of the cations [Cp<sup>\*</sup>M(η<sup>4</sup>-C<sub>5</sub>H<sub>6</sub>)(CO)<sub>2</sub>][BF<sub>4</sub>]. Derivatives of the following fragments have been prepared in this way: Cp<sub>2</sub>M, Cp(CpMe)Mo, Cp<sup>\*</sup>CpM, IndCpM, and Ind<sub>2</sub>Mo (M = Mo, W). This family of compounds provides the chance to study the effects of fine modulation of the electronic and stereochemical properties of the metallocenes of Mo and W through cyclopentadienyl modification. So far, the simple substitution reactions performed on several of the reported complexes reveal a chemistry largely similar to the one of the unsubstituted, symmetric Cp<sub>2</sub>M metallocenes. However, rate enhancement of associatively activated insertions into IndCpM-H and IndCpM-C bonds is to be expected due to the "indenyl effect" and is now possible to study. Also interesting is the possibility of producing asymmetric, eventually stereogenic metal centers, e.g., CpCp<sup>\*</sup>MX<sub>2</sub>.

The deprotonation of [CpM(η<sup>4</sup>-C<sub>5</sub>H<sub>6</sub>)(CO)<sub>2</sub>][BF<sub>4</sub>] has provided an unexpectedly simple high-yield route into the preparation of ring-slipped species, including [CpM(η<sup>3</sup>-C<sub>5</sub>H<sub>5</sub>)(CO)<sub>2</sub>][BF<sub>4</sub>] (M = Mo, W), allowing the future study of the very rare η<sup>3</sup>-coordinated cyclopentadienyl ligand.

### Experimental Section

All preparations and manipulations were done with standard Schlenk techniques under an atmosphere of argon. Solvents were dried by standard procedures (THF and Et<sub>2</sub>O over Na/benzophenone ketyl; CH<sub>2</sub>Cl<sub>2</sub>, NCMe, and NCEt over CaH<sub>2</sub>), distilled under argon, and kept over 4Å molecular sieves (3Å for NCMe).

Microanalysis were performed by Mr. M. Barth of the Anorganisch-chemisches Institut of the Technical University of Munich, Germany, and at the ITQB. NMR spectra were measured on a Bruker CXP 300 spectrometer, and IR spectra were measured on a Unicam Mattson model 7000 FTIR spectrometer. Mo(CO)<sub>3</sub>(NCEt)<sub>3</sub>,<sup>52</sup> Ph<sub>3</sub>CBF<sub>4</sub>,<sup>53</sup> C<sub>5</sub>Ph<sub>4</sub>H<sub>2</sub>,<sup>54</sup> and LiC<sub>13</sub>H<sub>9</sub><sup>55</sup> were prepared as published.

**Preparation of CpMo(η<sup>3</sup>-C<sub>5</sub>H<sub>5</sub>)(CO)<sub>2</sub> (1).** Method a: Solid LiCp (0.50 g, 6.95 mmol) and [Mo(η<sup>3</sup>-C<sub>5</sub>H<sub>5</sub>)(CO)<sub>2</sub>(NCMe)<sub>2</sub>-Cl] (2.16 g, 6.95 mmol) were weighed in a Schlenk tube. The solid mixture was taken out of the glove box and cooled to -80 °C. Precooled THF (30 mL) was added and the temperature

was raised slowly to room temperature. Stirring was continued for 18 h, after which time the solution was taken to dryness. The residue was extracted with hexane at 40 °C for a few hours. The yellow extract solution obtained was concentrated, and a yellow powder was separated, which was recrystallized from hexane/Et<sub>2</sub>O at -30 °C. Yield 80%.

**Method b:** A solution of [Mo(η<sup>3</sup>-C<sub>5</sub>H<sub>5</sub>)(CO)<sub>2</sub>(NCMe)<sub>2</sub>Cl] (1.00 g; 3.22 mmol) in CH<sub>2</sub>Cl<sub>2</sub> (20 mL) was treated with excess C<sub>5</sub>H<sub>6</sub> (2 mL) and NEt<sub>3</sub> (1 mL). After 15 h at room temperature, the solution was taken to dryness and extracted with hexane. The extract was concentrated, and the yellow powder was precipitated in 82% yield.

Selected IR data (CH<sub>2</sub>Cl<sub>2</sub> solution, cm<sup>-1</sup>): 1946, 1859, vs, ν(CO). <sup>1</sup>H and <sup>13</sup>C NMR data are in agreement with ref 56.

**Preparation of [CpMo(η<sup>4</sup>-C<sub>5</sub>H<sub>6</sub>)(CO)<sub>2</sub>][BF<sub>4</sub>] (3a).** A solution of [CpMo(η<sup>3</sup>-C<sub>5</sub>H<sub>5</sub>)(CO)<sub>2</sub>] (0.50 g, 1.94 mmol) in CH<sub>2</sub>Cl<sub>2</sub> (20 mL) was treated with 1 equiv of HBF<sub>4</sub>·Et<sub>2</sub>O. After 10 min, excess C<sub>5</sub>H<sub>6</sub> (3 mL) was added to the purple red mixture and stirring continued for 2 h. The solution was concentrated to ca. 10 mL, and addition of Et<sub>2</sub>O precipitated a yellow complex, which was filtered and washed with Et<sub>2</sub>O. After recrystallization from CH<sub>2</sub>Cl<sub>2</sub>/Et<sub>2</sub>O, the product was isolated in 85% yield. Anal. Calcd for C<sub>12</sub>H<sub>11</sub>BF<sub>4</sub>O<sub>2</sub>Mo: C, 38.96; H, 3.00. Found: C, 38.82; H, 2.90. Selected IR (KBr, cm<sup>-1</sup>): 2810, m, ν(C-H<sub>exo</sub>); 2029, 1917, 1960, 1939, vs, ν(CO). <sup>1</sup>H NMR (Me<sub>2</sub>CO-d<sub>6</sub>, 300 MHz, room temperature, δ ppm): 6.56 (t, 2H, H<sub>2/3</sub>), 6.03 (s, 5H, Cp), 4.77 (m, 2H, H<sub>1/4</sub>), 3.87 (d, 1H, J(H<sup>5</sup>H<sup>6</sup>) = 14.58 Hz, H<sub>5</sub>), 3.53 (d, 1H, J(H<sup>6</sup>H<sup>5</sup>) = 14.58 Hz, H<sub>6</sub>) (see Scheme 2 for numbering).

**Preparation of [CpMo(η<sup>4</sup>-C<sub>5</sub>H<sub>5</sub>Me)(CO)<sub>2</sub>][BF<sub>4</sub>] (3b).** A solution of [CpMo(η<sup>3</sup>-C<sub>5</sub>H<sub>5</sub>)(CO)<sub>2</sub>] (0.50 g, 1.94 mmol) in CH<sub>2</sub>Cl<sub>2</sub> (20 mL) was treated with 1 equiv of HBF<sub>4</sub>·Et<sub>2</sub>O. After 10 min, excess C<sub>5</sub>H<sub>5</sub>Me (3 mL) was added and the reaction was left for an additional 2 h. After concentration to ca. 10 mL and addition of Et<sub>2</sub>O, the yellow complex separated. Additional recrystallization from CH<sub>2</sub>Cl<sub>2</sub>/Et<sub>2</sub>O gave the product in 87% yield. Anal. Calcd for C<sub>13</sub>H<sub>13</sub>BF<sub>4</sub>O<sub>2</sub>Mo: C, 40.66; H, 3.41. Found: C, 40.56; H, 3.40. Selected IR (KBr, cm<sup>-1</sup>) 2799, m, ν(C-H<sub>exo</sub>); 2043, 1987, vs, ν(CO).

**Preparation of [CpMo(η<sup>4</sup>-C<sub>5</sub>Me<sub>5</sub>H)(CO)<sub>2</sub>][BF<sub>4</sub>] (3c).** A solution of [CpMo(η<sup>3</sup>-C<sub>5</sub>H<sub>5</sub>)(CO)<sub>2</sub>] (0.50 g, 1.94 mmol) in CH<sub>2</sub>Cl<sub>2</sub> (20 mL) was treated with 1 equiv of HBF<sub>4</sub>·Et<sub>2</sub>O. A slight excess of C<sub>5</sub>Me<sub>5</sub>H was added after 10 min and after 2 more h, the solution was concentrated to ca. 5 mL. Addition of Et<sub>2</sub>O (20 mL) precipitated a microcrystalline yellow complex, which was filtered and washed with Et<sub>2</sub>O (2 × 10 mL) and further recrystallized from CH<sub>2</sub>Cl<sub>2</sub>/Et<sub>2</sub>O. Yield 90%. Anal. Calcd for C<sub>17</sub>H<sub>21</sub>BF<sub>4</sub>O<sub>2</sub>Mo: C, 46.39; H, 4.81. Found: C, 46.19; H, 4.80. Selected IR (KBr, cm<sup>-1</sup>): 2018, 1973, 1950, 1931, vs, ν(CO). <sup>1</sup>H NMR (Me<sub>2</sub>CO-d<sub>6</sub>, 300 MHz, room temperature, δ ppm): 5.87 (s, 5H, Cp), 3.44 (m, 1H, C<sub>5</sub>Me<sub>5</sub>H), 2.53 (s, 6H, C<sub>5</sub>Me<sub>5</sub>H), 1.97 (s, 6H, C<sub>5</sub>Me<sub>5</sub>H), 0.79 (d, 3H C<sub>5</sub>Me<sub>5</sub>H).

**Preparation of [CpMo(η<sup>4</sup>-C<sub>5</sub>Ph<sub>4</sub>H<sub>2</sub>)(CO)<sub>2</sub>][BF<sub>4</sub>] (3d).** A solution of [CpMo(η<sup>3</sup>-C<sub>5</sub>H<sub>5</sub>)(CO)<sub>2</sub>] (0.50 g, 1.94 mmol) in CH<sub>2</sub>Cl<sub>2</sub> (20 mL) was treated with 1 equiv of HBF<sub>4</sub>·Et<sub>2</sub>O. After 10 min, a slight excess of C<sub>5</sub>Ph<sub>4</sub>H<sub>2</sub> was added and the reaction was left for 6 h. After concentration to ca. 5 mL and addition of Et<sub>2</sub>O (15 mL), the yellow powder separated. This was filtered, washed with Et<sub>2</sub>O (2 × 10 mL), and recrystallized from CH<sub>2</sub>Cl<sub>2</sub>/Et<sub>2</sub>O. Yield 88%. Anal. Calcd for C<sub>36</sub>H<sub>27</sub>BF<sub>4</sub>O<sub>2</sub>Mo: C, 64.12; H, 4.04. Found: C, 64.00; H, 4.01. Selected IR (cm<sup>-1</sup>): in KBr, 2035, 1983, vs, ν(CO); in CH<sub>2</sub>Cl<sub>2</sub> solution, 2035, 1982. <sup>1</sup>H NMR (Me<sub>2</sub>CO-d<sub>6</sub>, 300 MHz, room temperature, δ ppm):

(52) Kubas, G. J. *Inorg. Synth.* **1991**, 27, 4.

(53) Olah, G. A.; Svoboda, J. J.; Olah, J. A. *Synthesis* **1972**, 544.

(54) Perevalova, E. G.; Grandberg, K. I.; Dyadchenko, V. P. and Baukova, T. V. *J. Organomet. Chem.* **1981**, 217, 403.

(55) Zeiger, R.; Rhine, W.; Stucky, G. D. *J. Am. Chem. Soc.* **1974**, 96, 5441.

(56) Luh, T.-Y. and Wong, C., S. *J. Organomet. Chem.*, **1985**, 287, 231.

(57) Benfield, F. W. S.; Green, M. L. H. *J. Chem. Soc., Dalton Trans.* **1974**, 1324.

7.7–6.99 (m, 20H, C<sub>5</sub>Ph<sub>4</sub>H<sub>2</sub>), 5.83 (d, 1H,  $J(\text{H}^{\text{H}}) = 13.59$  Hz, C<sub>5</sub>Ph<sub>4</sub>H<sub>2</sub>), 5.64 (s, 5H, Cp), 4.76 (d, 1H,  $J(\text{H}^{\text{H}}) = 13.59$  Hz, C<sub>5</sub>Ph<sub>4</sub>H<sub>2</sub>).

**Preparation of [CpMo( $\eta^4$ -C<sub>5</sub>H<sub>9</sub>)(CO)<sub>2</sub>][BF<sub>4</sub>] (3e).** A solution of [CpMo( $\eta^3$ -C<sub>3</sub>H<sub>5</sub>)(CO)<sub>2</sub>] (0.50 g, 1.94 mmol) in CH<sub>2</sub>Cl<sub>2</sub> (20 mL) was treated with 1 equiv of HBF<sub>4</sub>·Et<sub>2</sub>O. After 10 min, excess 1,3-cyclohexadiene (3 mL) was added, and the reaction was left for 2 h. After concentration to ca. 8 mL and addition of Et<sub>2</sub>O, the yellow product precipitated. After recrystallization from CH<sub>2</sub>Cl<sub>2</sub>/Et<sub>2</sub>O the yield was 90%. Selected IR data (CH<sub>2</sub>Cl<sub>2</sub> solution, cm<sup>-1</sup>): 2016, 1961, vs,  $\nu(\text{CO})$ . <sup>1</sup>H NMR data are in agreement with ref 17a.

**Preparation of [CpMo( $\eta^4$ -1,3-C<sub>5</sub>H<sub>9</sub>)(CO)<sub>2</sub>][BF<sub>4</sub>] (3f).** A solution of [CpMo( $\eta^3$ -C<sub>3</sub>H<sub>5</sub>)(CO)<sub>2</sub>] (0.50 g, 1.94 mmol) in CH<sub>2</sub>Cl<sub>2</sub> (20 mL) was treated with 1 equiv of HBF<sub>4</sub>·Et<sub>2</sub>O. Excess 1,4-pentadiene (2 mL) was added after 10 min, and the solution was left for 2 h. Upon concentration and addition of Et<sub>2</sub>O, the yellow complex is filtered, washed with Et<sub>2</sub>O, and recrystallized from CH<sub>2</sub>Cl<sub>2</sub>/Et<sub>2</sub>O. Yield 92%. Anal. Calcd for C<sub>12</sub>H<sub>13</sub>BF<sub>4</sub>O<sub>2</sub>Mo: C, 38.75; H, 3.52%. Found: C, 38.60; H, 3.46. Selected IR (KBr, cm<sup>-1</sup>) 2045, 1998, vs,  $\nu(\text{CO})$ . <sup>1</sup>H NMR data matched those published in ref 20.

**Preparation of [CpMo( $\eta^4$ -COD)(CO)<sub>2</sub>][BF<sub>4</sub>] (3g).** A solution of [CpMo( $\eta^3$ -C<sub>3</sub>H<sub>5</sub>)(CO)<sub>2</sub>] (0.50 g, 1.94 mmol) in CH<sub>2</sub>Cl<sub>2</sub> (20 mL) was treated with 1 equiv of HBF<sub>4</sub>·Et<sub>2</sub>O. After 10 min, excess cyclooctadiene (4 mL) was added and the reaction was left for 2 h. After concentration to ca. 10 mL and addition of Et<sub>2</sub>O (20 mL), the yellow crystalline product separated. After filtration and washing with Et<sub>2</sub>O, the product was recrystallized from CH<sub>2</sub>Cl<sub>2</sub>/Et<sub>2</sub>O. Yield 92%. Selected IR (KBr, cm<sup>-1</sup>): 2031, 1948, vs,  $\nu(\text{CO})$ . Anal. Calcd for C<sub>15</sub>H<sub>17</sub>O<sub>2</sub>MoBF<sub>4</sub>: C, 43.73; H, 4.16. Found: C, 43.56; H, 4.17. <sup>1</sup>H NMR (Me<sub>2</sub>CO-*d*<sub>6</sub>, 300 MHz, room temperature,  $\delta$  ppm): 6.06 (s, 5H, Cp), 5.89 (m (br), 4H, olefinic C<sub>8</sub>H<sub>12</sub>), 2.95–2.39 (m (br), 8H, aliphatic C<sub>8</sub>H<sub>12</sub>). The compound has been reported in ref 21 without detailed characterization.

**Preparation of [IndMo( $\eta^3$ -C<sub>3</sub>H<sub>5</sub>)(CO)<sub>2</sub>] (6).** A mixture of solid LiInd (0.60 g, 4.90 mmol) and [Mo( $\eta^3$ -C<sub>3</sub>H<sub>5</sub>)(CO)<sub>2</sub>(NCMe)<sub>2</sub>Cl] (1.52 g, 4.90 mmol) was weighed in the glovebox and later placed in a Schlenk tube in a cold bath at -80 °C. Precooled THF was slowly added, and the temperature was slowly raised to room temperature. After 18 h of total reaction time, the mixture was taken to dryness and the residue was extracted with warm hexane (40 °C) for a few hours. Concentration of the yellow solution gave a yellow powder, which could be further recrystallized from Et<sub>2</sub>O/hexane at -30 °C. Yield 85%. Similar results are obtained using KInd. Solution IR data (CH<sub>2</sub>Cl<sub>2</sub>, cm<sup>-1</sup>): 1946, 1861, vs,  $\nu(\text{CO})$ . <sup>1</sup>H NMR data are in agreement with the data described in ref 22.

**Preparation of [IndMo(CO)<sub>2</sub>]<sub>2</sub> (8).** A solution of [IndMo( $\eta^3$ -C<sub>3</sub>H<sub>5</sub>)(CO)<sub>2</sub>] (0.25 g, 0.81 mmol) in CH<sub>2</sub>Cl<sub>2</sub> (30 mL) was treated with 1 equiv of HBF<sub>4</sub>·Et<sub>2</sub>O. After 10 min, Bu<sub>4</sub>Ni (0.33 g, 0.90 mmol) was added and the reaction was left for 1 h. After concentration to ca. 5 mL and addition of ether, a ruby-red complex precipitated slowly. Yield 94%. <sup>1</sup>H NMR (Me<sub>2</sub>CO-*d*<sub>6</sub>, 300 MHz, room temperature,  $\delta$  ppm): 7.60 (m, 2H, H<sub>5-8</sub>), 7.30 (m, 2H, H<sub>5-8</sub>), 6.61 (d, 2H, H<sub>1/3</sub>), 5.80 (t, 1H, H<sub>2</sub>). IR and analytical data are in agreement with those reported in ref 17j).

**Preparation of [IndMo(NCMe)<sub>2</sub>(CO)<sub>2</sub>][BF<sub>4</sub>] (9).** A solution of [IndMo( $\eta^3$ -C<sub>3</sub>H<sub>5</sub>)(CO)<sub>2</sub>] (0.25 g, 0.81 mmol) in CH<sub>2</sub>Cl<sub>2</sub> (20 mL) was treated with 1 equiv of HBF<sub>4</sub>·Et<sub>2</sub>O. After 10 min, excess NCMe was added (5 mL) and the reaction was left for 1 h. The solvent was evaporated, and the residue was recrystallized from CH<sub>2</sub>Cl<sub>2</sub>/Et<sub>2</sub>O. Yield 96%. Analytical, IR, and <sup>1</sup>H NMR data (CH<sub>2</sub>Cl<sub>2</sub>-*d*<sub>2</sub>) are in agreement with those reported in ref 17k).

**Preparation of [IndMo( $\eta^4$ -C<sub>5</sub>H<sub>9</sub>)(CO)<sub>2</sub>][BF<sub>4</sub>] (10a).** A solution of [IndMo(NCMe)<sub>2</sub>(CO)<sub>2</sub>][BF<sub>4</sub>] (0.25 g, 0.57 mmol) in CH<sub>2</sub>Cl<sub>2</sub> (20 mL) was treated with an excess of C<sub>5</sub>H<sub>6</sub> (2 mL), and the reaction was stirred for 2 h. After concentration to

ca. 5 mL and addition of ether, a yellow complex precipitated slowly. Recrystallization from CH<sub>2</sub>Cl<sub>2</sub>/Et<sub>2</sub>O. Yield 86%. Anal. Calcd for C<sub>16</sub>H<sub>13</sub>BF<sub>4</sub>O<sub>2</sub>Mo: C, 45.75; H, 3.12. Found: C, 45.64; H, 3.08. Selected IR (Nujol, cm<sup>-1</sup>): 2050, 2018, 1973, vs,  $\nu(\text{CO})$ . <sup>1</sup>H NMR (CD<sub>2</sub>Cl<sub>2</sub>-*d*<sub>2</sub>, 300 MHz, room temperature,  $\delta$  ppm): 7.90–7.87 (m, 2H, H<sub>5-8</sub>), 7.46–7.44 (m, 2H, H<sub>5-8</sub>), 6.20 (d, 2H, H<sub>1/3</sub>), 5.61 (t, 1H, H<sub>2</sub>), 5.35 (s, 2H, H<sub>2/3</sub> of C<sub>5</sub>H<sub>6</sub>), 4.42 (s, 2H, H<sub>1/4</sub> of C<sub>5</sub>H<sub>6</sub>), 3.57 (d, 1H,  $J(\text{H}^{\text{H}}) = 14.53$  Hz, H<sub>5</sub> of C<sub>5</sub>H<sub>6</sub>), 3.05 (d, 1H,  $J(\text{H}^{\text{H}}) = 14.53$  Hz, H<sub>6</sub> of C<sub>5</sub>H<sub>6</sub>) (see Schemes 2 and 3 for numbering).

**Preparation of [IndMo( $\eta^4$ -C<sub>5</sub>Me<sub>5</sub>H)(CO)<sub>2</sub>][BF<sub>4</sub>] (10b).** A solution of [IndMo(NCMe)<sub>2</sub>(CO)<sub>2</sub>][BF<sub>4</sub>] (0.25 g, 0.57 mmol) in CH<sub>2</sub>Cl<sub>2</sub> (20 mL) was treated with an excess of C<sub>5</sub>Me<sub>5</sub>H (2 mL). After 4 h, the solution was evaporated to 5 mL and Et<sub>2</sub>O was added. The yellow product obtained was recrystallized from CH<sub>2</sub>Cl<sub>2</sub>/Et<sub>2</sub>O. Yield 86%. Anal. Calcd for C<sub>21</sub>H<sub>23</sub>BF<sub>4</sub>O<sub>2</sub>Mo: C, 51.46; H, 4.73. Found: C, 51.22; H, 4.58. Selected IR (KBr, cm<sup>-1</sup>): 2036, 2018, 1958, vs,  $\nu(\text{CO})$ . <sup>1</sup>H NMR (Me<sub>2</sub>CO-*d*<sub>6</sub>, 300 MHz, room temperature,  $\delta$  ppm): 7.82–7.80 (m, 2H, H<sub>5-8</sub>), 7.67–7.64 (m, 2H, H<sub>5-8</sub>), 6.24 (d, 2H, H<sub>1/3</sub>), 5.93 (t, 1H, H<sub>2</sub>), 3.35 (m, 1H, C<sub>5</sub>Me<sub>5</sub>H), 2.28 (s, 6H, C<sub>5</sub>Me<sub>5</sub>H), 1.70 (s, 6H, C<sub>5</sub>Me<sub>5</sub>H), 0.62 (d, 3H, C<sub>5</sub>Me<sub>5</sub>H).

**Preparation of [FluMo( $\eta^3$ -C<sub>3</sub>H<sub>5</sub>)(CO)<sub>2</sub>] (11).** A mixture of solid LiFlu (0.50 g, 2.90 mmol) and [Mo( $\eta^3$ -C<sub>3</sub>H<sub>5</sub>)(CO)<sub>2</sub>(NCMe)<sub>2</sub>Cl] (0.90 g, 2.9 mmol) was weighed in a Schlenk tube in the glovebox and later placed in a cold bath at -80 °C. Precooled THF was slowly added, and the temperature was slowly raised to room temperature. After 18 h, the mixture was taken to dryness and the residue was extracted with ether. The solution obtained was taken to dryness, and the residue was sublimed in order to eliminate the fluorene. The remaining residue was recrystallized from Et<sub>2</sub>O/pentane at -30 °C. Yield 21% (brownish yellow). Anal. Calcd for C<sub>16</sub>H<sub>14</sub>O<sub>2</sub>Mo: C, 60.35; H, 3.94. Found: C, 60.23; H, 4.08. Selected IR (KBr, cm<sup>-1</sup>): 1938, 1871, vs,  $\nu(\text{CO})$ ; in CH<sub>2</sub>Cl<sub>2</sub> solution, 1946, 1863, vs,  $\nu(\text{CO})$ . <sup>1</sup>H NMR (CDCl<sub>3</sub>-*d*<sub>1</sub>, 300 MHz, room temperature,  $\delta$  ppm): 7.73–7.67 (m, 4H, C<sub>13</sub>H<sub>9</sub>), 7.25–7.10 (m, 4H, C<sub>13</sub>H<sub>9</sub>), 6.40 (s, 1H, C<sub>13</sub>H<sub>9</sub>), 3.30 (m, 1H, *meso* of C<sub>3</sub>H<sub>5</sub>), 1.27 (d, 2H, *syn* of C<sub>3</sub>H<sub>5</sub>), 0.36 (d, 2H, *anti* of C<sub>3</sub>H<sub>5</sub>).

**Preparation of [Cp\*Mo( $\eta^4$ -C<sub>5</sub>H<sub>9</sub>)(CO)<sub>2</sub>][BF<sub>4</sub>] (12).** A solution of [Cp\*Mo(NCMe)<sub>2</sub>(CO)<sub>2</sub>][BF<sub>4</sub>] (0.50 g, 1.10 mmol) in CH<sub>2</sub>Cl<sub>2</sub> (30 mL) was reacted with an excess of C<sub>5</sub>H<sub>6</sub> (5 mL). After 15 h, the solution was concentrated and ether was added until precipitation of the yellow product occurred. The complex obtained was recrystallized from CH<sub>2</sub>Cl<sub>2</sub>/Et<sub>2</sub>O. Yield 88%. Anal. Calcd for C<sub>17</sub>H<sub>21</sub>BF<sub>4</sub>O<sub>2</sub>Mo: C, 46.36; H, 4.81. Found: C, 46.36; H, 4.80. Selected IR (KBr, cm<sup>-1</sup>): 2014, 1952, vs,  $\nu(\text{CO})$ ; in solution (CH<sub>2</sub>Cl<sub>2</sub>), 2037, 1985, vs,  $\nu(\text{CO})$ . <sup>1</sup>H NMR (Me<sub>2</sub>CO-*d*<sub>6</sub>, 300 MHz, room temperature,  $\delta$  ppm): 5.76 (s, 2H, H<sub>2/3</sub>), 4.53 (s, 2H, H<sub>1/4</sub>), 3.65 (d, 1H,  $J(\text{H}^{\text{H}}) = 12.3$  Hz, H<sub>5</sub>), 3.49 (d, 1H,  $J(\text{H}^{\text{H}}) = 12.3$  Hz, H<sub>6</sub>), 2.14 (s, 15H, Cp\*) (see Scheme 2 for numbering).

**Preparation of [Cp\*Mo(CO)<sub>2</sub>(NCMe)<sub>2</sub>][BF<sub>4</sub>] (13).** A suspension of Mo(CO)<sub>3</sub>(NCMe)<sub>3</sub> (3.80 g, 8.80 mmol) in toluene (80 mL) was treated with C<sub>5</sub>Me<sub>5</sub>H (1.22 g, 9.00 mmol) for 2 h at room temperature and then warmed to 60 °C until all of the starting material dissolved. The reaction mixture was then evaporated to dryness, and the residue was dissolved in CH<sub>2</sub>Cl<sub>2</sub>. This solution was then treated with CHI<sub>3</sub> (3.54 g, 9.00 mmol) and the mixture was taken to dryness after 1/2 h. The purple microcrystalline residue was washed with several small portions of Et<sub>2</sub>O, redissolved in NCMe (30 mL) and treated with TIBF<sub>4</sub> (1 equiv). After 15 h of reflux the dark red solution was separated from TII by filtration. The clear red solution was taken to dryness, and the residue was recrystallized from CH<sub>2</sub>Cl<sub>2</sub>/Et<sub>2</sub>O. Yield 85%. Spectroscopic and analytical data are in agreement with those reported in ref 17i).

**Preparation of [Cp\*Mo( $\eta^4$ -C<sub>5</sub>Me<sub>5</sub>H)(CO)<sub>2</sub>][BF<sub>4</sub>] (14).** A solution of [Cp\*Mo(NCMe)<sub>2</sub>(CO)<sub>2</sub>][BF<sub>4</sub>] (0.25 g, 0.55 mmol) in CH<sub>2</sub>Cl<sub>2</sub> (20 mL) was treated with excess of C<sub>5</sub>Me<sub>5</sub>H and concentrated to ca. 5 mL after 4 h. Addition of ether (15 mL) precipitated a microcrystalline yellow complex, which was

filtered, washed with ether (2 × 10 mL), and further recrystallized from CH<sub>2</sub>Cl<sub>2</sub>/Et<sub>2</sub>O. Yield 90%. Anal. Calcd for C<sub>22</sub>H<sub>31</sub>BF<sub>2</sub>O<sub>2</sub>Mo: C, 51.79; H, 6.12. Found: C, 51.60; H, 6.00. Selected IR (KBr, cm<sup>-1</sup>): 1994, 1969, 1933, 1906, vs, ν(CO). <sup>1</sup>H NMR (Me<sub>2</sub>CO-*d*<sub>6</sub>, 300 MHz, room temperature, δ ppm): 3.18 (m, 1H, C<sub>5</sub>Me<sub>5</sub>H), 2.47 (s, 6H, C<sub>5</sub>Me<sub>5</sub>H), 1.94 (s, 15H, Cp\*) 1.79 (m, 6H, C<sub>5</sub>Me<sub>5</sub>H), 0.79 (d, 3H C<sub>5</sub>Me<sub>5</sub>H).

**Preparation of [CpW(η<sup>3</sup>-C<sub>5</sub>H<sub>5</sub>)(CO)<sub>2</sub>][BF<sub>4</sub>] (15).** A solution of [CpW(η<sup>3</sup>-C<sub>5</sub>H<sub>5</sub>)(CO)<sub>2</sub>] (0.50 g, 1.44 mmol) in CH<sub>2</sub>-Cl<sub>2</sub> (20 mL) was treated with 85% HBF<sub>4</sub>·Et<sub>2</sub>O (1 equiv). After 10 min, an excess of C<sub>5</sub>Me<sub>5</sub>H was added and the mixture was left for 6 h. After concentration to ca. 5 mL and addition of Et<sub>2</sub>O (15 mL), the microcrystalline yellow precipitate was filtered, washed with Et<sub>2</sub>O (2 × 10 mL), and further recrystallized from CH<sub>2</sub>Cl<sub>2</sub>/Et<sub>2</sub>O. Yield 86%. Anal. Calcd for C<sub>17</sub>H<sub>21</sub>BF<sub>4</sub>O<sub>2</sub>W: C, 38.67; H, 4.00. Found: C, 38.42; H, 3.80. Selected IR (KBr, cm<sup>-1</sup>): 2012, 1956, 1940, 1921, vs, ν(CO). <sup>1</sup>H NMR (Me<sub>2</sub>CO-*d*<sub>6</sub>, 300 MHz, room temperature, δ ppm): 5.98 (s, 5H, Cp), 3.88 (m, 1H, C<sub>5</sub>Me<sub>5</sub>H), 2.75 (s, 6H, C<sub>5</sub>Me<sub>5</sub>H), 1.97 (s, 6H, C<sub>5</sub>Me<sub>5</sub>H), 0.75 (d, 3H C<sub>5</sub>Me<sub>5</sub>H).

**Preparation of [Cp<sub>2</sub>MoH(CO)][BF<sub>4</sub>] (16).** A solution of [CpMo(η<sup>4</sup>-C<sub>5</sub>H<sub>6</sub>)(CO)<sub>2</sub>][BF<sub>4</sub>] (0.20 g, 0.54 mmol) in CH<sub>2</sub>Cl<sub>2</sub> or acetone (20 mL) was stirred for ca. 8 h at room temperature. Concentration to ca. 10 mL and addition of ether produced a pale yellow powder, which was filtered, washed with ether (2 × 10 mL), and further recrystallized from CH<sub>2</sub>Cl<sub>2</sub>/Et<sub>2</sub>O. Yield 96%. Anal. Calcd for C<sub>11</sub>H<sub>11</sub>MoOBF<sub>4</sub>: C, 38.64; H, 3.24. Found: C, 38.52; H, 3.10. Selected IR (Nujol, cm<sup>-1</sup>): 2017, vs, ν(CO); 1849, m, ν(Mo-H). <sup>1</sup>H NMR (Me<sub>2</sub>CO-*d*<sub>6</sub>, 300 MHz, room temperature, δ ppm): 5.87 (s, 10H, Cp), -8.20 (s, 1H, Mo-H). Data for the PF<sub>6</sub><sup>-</sup> salt are reported in ref 57.

**Preparation of [Cp<sub>2</sub>MoCl(CO)][BF<sub>4</sub>] (17).** Method a: A solution of [Cp<sub>2</sub>MoH(CO)][BF<sub>4</sub>] (0.30 g, 0.88 mmol) in a mixture of CH<sub>2</sub>Cl<sub>2</sub>/CHCl<sub>3</sub> was irradiated with a 60 W tungsten bulb for ca. 8 h. The pink precipitate was filtered off and recrystallized from acetone/ether. Yield 96%.

Method b: Gaseous Cl<sub>2</sub> was bubbled through a solution of [Cp<sub>2</sub>MoH(CO)][BF<sub>4</sub>] (0.30 g, 0.88 mmol) in CH<sub>2</sub>Cl<sub>2</sub> for 1 min. The pink precipitate was filtered off and recrystallized from acetone/ether. Yield 98%. Selected IR (KBr, cm<sup>-1</sup>): 2045, vs, ν(CO). Anal. Calcd for C<sub>11</sub>H<sub>10</sub>MoOClBF<sub>4</sub>: C, 35.10; H, 2.68. Found: C, 35.10; H, 3.02. Data for the analogous [Cp<sub>2</sub>MoBr(CO)]PF<sub>6</sub> is given in ref 24.

**Preparation of [Cp<sub>2</sub>Mo(CO)] (18).** A solution of [Cp<sub>2</sub>Mo(CO)<sub>2</sub>][BF<sub>4</sub>]<sub>2</sub> (0.25 g, 0.55 mmol) in 20 mL of H<sub>2</sub>O was treated with a few drops of a saturated aqueous solution of NaOH. A green powder precipitated immediately and was recovered by filtration. It may be recrystallized from Et<sub>2</sub>O by slow evaporation. Yield 82%. Selected IR (hexane, cm<sup>-1</sup>): 1929, vs, ν(CO). <sup>1</sup>H NMR (C<sub>6</sub>H<sub>6</sub>-*d*<sub>6</sub>) 300 MHz, room temperature, δ ppm): 4.15 (s, Cp). These agree with the values reported in ref 25.

**Preparation of [Cp<sub>2</sub>Mo(NCMe)Cl][BF<sub>4</sub>] (19).** A solution of [Cp<sub>2</sub>MoCl(CO)][BF<sub>4</sub>] (0.25 g, 0.66 mmol) in NCMe (30 mL) was refluxed and irradiated with a 60 W tungsten lamp for 4 h. The final green solution was taken to dryness, and the residue was recrystallized from NCMe/Et<sub>2</sub>O at -30 °C. Yield 92%. Analytical and IR data agree with those reported in ref 26.

**Preparation of [Cp<sub>2</sub>Mo(CO)<sub>2</sub>][BF<sub>4</sub>]<sub>2</sub> (20).** A solution of [CpMo(η<sup>4</sup>-C<sub>5</sub>H<sub>6</sub>)(CO)<sub>2</sub>][BF<sub>4</sub>] (0.30 g, 0.81 mmol) in CH<sub>2</sub>Cl<sub>2</sub> was treated with a solution of Ph<sub>3</sub>CBF<sub>4</sub> (0.27 g, 0.81 mmol) in the same solvent. The reaction mixture became turbid, and after 4 h of stirring the off-white precipitate was filtered off and washed with CH<sub>2</sub>Cl<sub>2</sub> (10 mL) and Et<sub>2</sub>O (2 × 10 mL). Yield 80%. Anal. Calcd for C<sub>12</sub>H<sub>10</sub>B<sub>2</sub>F<sub>8</sub>O<sub>2</sub>Mo: C, 31.62; H, 2.21. Found: C, 31.50; H, 2.27. Selected IR (KBr, cm<sup>-1</sup>): 2139, 2108, vs, ν(CO). <sup>1</sup>H NMR (Me<sub>2</sub>CO-*d*<sub>6</sub>, 300 MHz, room temperature, δ ppm): 6.69 (s, 10H, Cp).

**Preparation of [Cp<sub>2</sub>Mo(CO)(NCMe)][BF<sub>4</sub>]<sub>2</sub> (21).** A solution of [Cp<sub>2</sub>Mo(CO)<sub>2</sub>][BF<sub>4</sub>]<sub>2</sub> (0.25 g, 0.55 mmol) in 20 mL of NCMe was stirred for 2 h at room temperature, in which time it became lemon yellow. After concentration to half the initial

volume and addition of ether, a crystalline precipitate separated, which was filtered off and washed with ether (2 × 10 mL). Yield 98%. Anal. Calcd for C<sub>13</sub>H<sub>13</sub>B<sub>2</sub>F<sub>8</sub>ONMo: C, 33.31; H, 2.80; N, 2.99. Found: C, 33.49; H, 2.93; N, 2.85. Selected IR (KBr, cm<sup>-1</sup>): 2075, vs, ν(CO); 2326, 2303, w, ν(N≡C). <sup>1</sup>H NMR (NCMe-*d*<sub>3</sub>, 300 MHz, room temperature, δ ppm): 6.32 (s, 10, Cp); 2.40 (s, 3H, NCMe).

**Preparation of [Cp<sub>2</sub>Mo(NCMe)<sub>2</sub>][BF<sub>4</sub>]<sub>2</sub> (21a).** A solution of [Cp<sub>2</sub>Mo(CO)(NCMe)][BF<sub>4</sub>]<sub>2</sub> (0.20 g, 0.43 mmol) in NCMe (20 mL) was refluxed and irradiated with a 60 W tungsten lamp for 6 h. After concentration to ca. 5 mL and addition of Et<sub>2</sub>O, a pink-red crystalline complex separated, which was filtered and washed with Et<sub>2</sub>O. Yield 96%. Selected IR (KBr, cm<sup>-1</sup>): 2291, 2314, m, ν(N≡C). Anal. Calcd for C<sub>14</sub>H<sub>16</sub>N<sub>2</sub>MoB<sub>2</sub>F<sub>8</sub>: C, 34.90; H, 3.35; N, 5.81. Found: C, 34.85; H, 3.21; N, 6.02. <sup>1</sup>H NMR (NCMe-*d*<sub>3</sub>, 300 MHz, δ ppm): 6.05 (s, 10H, Cp); 2.44 (s, 6H, NCMe). Similar data are reported in ref 29 for the analogous PF<sub>6</sub><sup>-</sup> salt.

**Preparation of [Cp(CpMe)MoCl(CO)][BF<sub>4</sub>] (22).** Gaseous Cl<sub>2</sub> was bubbled through a solution of [Cp(CpMe)MoH(CO)][BF<sub>4</sub>] (0.25 g, 0.70 mmol) in CH<sub>2</sub>Cl<sub>2</sub> for 1 min. The pink precipitate was filtered off and recrystallized from acetone/ether. Yield 90%. Anal. Calcd for C<sub>12</sub>H<sub>12</sub>BClF<sub>4</sub>OMo: C, 36.92; H, 3.10. Found: C, 36.81; H, 3.01. Selected IR (KBr, cm<sup>-1</sup>): 2042, vs, ν(CO). <sup>1</sup>H NMR (Me<sub>2</sub>CO-*d*<sub>6</sub>, 300 MHz, room temperature, δ ppm): 6.38 (s, 2H, C<sub>5</sub>H<sub>4</sub>Me), 6.14, 6.06 (m, 1H each, C<sub>5</sub>H<sub>4</sub>Me), 6.33 (s, 5H, Cp), 2.22 (s, 3H, C<sub>5</sub>H<sub>4</sub>Me).

**Preparation of [Cp(CpMe)Mo(CO)<sub>2</sub>][BF<sub>4</sub>]<sub>2</sub> (23).** A solution of [CpMo(η<sup>4</sup>-C<sub>5</sub>H<sub>5</sub>Me)(CO)<sub>2</sub>][BF<sub>4</sub>] (0.25 g, 0.65 mmol) in CH<sub>2</sub>Cl<sub>2</sub> was treated with a solution of Ph<sub>3</sub>CBF<sub>4</sub> (0.21 g, 0.65 mmol) in the same solvent. After 6 h of stirring, the off-white precipitate that formed was filtered off and washed with CH<sub>2</sub>-Cl<sub>2</sub> (10 mL) and Et<sub>2</sub>O (2 × 10 mL). Yield 90%. Anal. Calcd for C<sub>13</sub>H<sub>12</sub>B<sub>2</sub>F<sub>8</sub>O<sub>2</sub>Mo: C, 33.24; H, 2.57. Found: C, 33.08; H, 2.40. Selected IR (KBr, cm<sup>-1</sup>): 2135, 2106, vs, ν(CO). <sup>1</sup>H NMR (NCMe-*d*<sub>3</sub>, 300 MHz, room temperature, δ ppm): 6.49 (s, 2H, C<sub>5</sub>H<sub>4</sub>Me), 6.44 (s, 5H, Cp), 6.37 (s, 2H, C<sub>5</sub>H<sub>4</sub>Me), 2.40 (s, 3H, C<sub>5</sub>H<sub>4</sub>Me).

**Preparation of [Cp(CpMe)Mo(CO)(NCMe)][BF<sub>4</sub>]<sub>2</sub> (24).** A solution of [Cp(CpMe)Mo(CO)<sub>2</sub>][BF<sub>4</sub>]<sub>2</sub> (0.25 g) in 20 mL of NCMe was stirred for 15 h at room temperature, becoming lemon yellow. After concentration to half the initial volume and addition of ether, the crystalline precipitate that formed was filtered off and washed with ether (2 × 10 mL). Yield 90%. Anal. Calcd for C<sub>14</sub>H<sub>15</sub>B<sub>2</sub>F<sub>8</sub>NOMo: C, 34.83; H, 3.13; N, 2.90. Found: C, 34.53; H, 3.00; N, 2.61. Selected IR (KBr, cm<sup>-1</sup>): 2079, vs, ν(CO); 2330, 2303, w, ν(N≡C). <sup>1</sup>H NMR (NCMe-*d*<sub>3</sub>, 300 MHz, δ ppm): 6.27 (s, 5H, Cp), 6.32, 6.24, 6.19, 6.16 (s, 1H each, C<sub>5</sub>H<sub>4</sub>Me), 2.24 (s, 3H, C<sub>5</sub>H<sub>4</sub>Me), 2.20 (s, 3H, NCMe).

**Preparation of [Cp(CpMe)Mo(NCMe)<sub>2</sub>][BF<sub>4</sub>]<sub>2</sub> (25).** A solution of [Cp(CpMe)Mo(CO)(NCMe)][BF<sub>4</sub>]<sub>2</sub> (0.20 g) in NCMe (20 mL) was refluxed and irradiated with a 60 W tungsten lamp for 6 h. After concentration to ca. 5 mL and addition of Et<sub>2</sub>O, the pink-red crystalline complex that separated was filtered and washed with Et<sub>2</sub>O. Yield 96%. Anal. Calcd for C<sub>15</sub>H<sub>18</sub>B<sub>2</sub>F<sub>8</sub>N<sub>2</sub>Mo: C, 36.33; H, 3.66; N, 5.65. Found: C, 36.10; H, 3.50; N, 5.43. Selected IR (KBr, cm<sup>-1</sup>): 2322, 2293, w, ν(N≡C). <sup>1</sup>H NMR (NCMe-*d*<sub>3</sub>, 300 MHz, room temperature, δ ppm): 5.99 (s, 5H, Cp), 6.04, 5.79, 5.77, 5.76 (s, 1H each, C<sub>5</sub>H<sub>4</sub>-Me), 2.47 (s, 3H, C<sub>5</sub>H<sub>4</sub>Me), 2.44 (s, 6H, NCMe).

**Preparation of [Cp\*Mo(CO)<sub>2</sub>][BF<sub>4</sub>]<sub>2</sub> (26).** A solution of [Cp\*Mo(η<sup>4</sup>-C<sub>5</sub>H<sub>6</sub>)(CO)<sub>2</sub>][BF<sub>4</sub>] (0.20 g, 0.45 mmol) in CH<sub>2</sub>Cl<sub>2</sub> was treated with a solution of Ph<sub>3</sub>CBF<sub>4</sub> (0.15 g, 0.45 mmol) in the same solvent. After 4 h of stirring, an off-white precipitate was filtered off and washed with CH<sub>2</sub>Cl<sub>2</sub> (10 mL) and Et<sub>2</sub>O (2 × 10 mL). Yield 80%. Anal. Calcd for C<sub>17</sub>H<sub>20</sub>B<sub>2</sub>F<sub>8</sub>O<sub>2</sub>Mo: C, 38.83; H, 3.83. Found: C, 38.80; H, 3.80. Selected IR (KBr, cm<sup>-1</sup>): 2108, 2075, vs, ν(CO). <sup>1</sup>H NMR (Me<sub>2</sub>CO-*d*<sub>6</sub>, 300 MHz, room temperature, δ ppm): 6.17 (s, 5H, Cp), 2.30 (s, 15H, Cp\*).

**Preparation of [Cp\*Mo(CO)(NCMe)][BF<sub>4</sub>]<sub>2</sub> (27).** A solution of [Cp\*Mo(CO)<sub>2</sub>][BF<sub>4</sub>]<sub>2</sub> (0.10 g, 0.19 mmol) in 20 mL

of NCMe was stirred for 2 days at room temperature, becoming lemon yellow. After concentration to half the initial volume and addition of ether, the crystalline precipitate that was separated was filtered off and washed with ether (2 × 10 mL). Yield 81%. Anal. Calcd for C<sub>18</sub>H<sub>23</sub>B<sub>2</sub>F<sub>8</sub>NOMo: C, 40.12; H, 4.30; N, 2.60. Found: C, 40.32; H, 4.40; N, 2.75. Selected IR (KBr, cm<sup>-1</sup>): 2088, vs, ν(CO); 2332, 2288, w, ν(N≡C). <sup>1</sup>H NMR (NCMe-*d*<sub>3</sub>, 300 MHz, δ ppm): 5.34 (s, 5H, Cp), 2.34 (s, 3H, NCMe), 1.99 (s, 15H, Cp\*).

**Preparation of [Cp\*<sub>2</sub>CpMo(NCMe)<sub>2</sub>][BF<sub>4</sub>]<sub>2</sub> (28).** A solution of [Cp\*<sub>2</sub>CpMo(CO)(NCMe)][BF<sub>4</sub>]<sub>2</sub> (0.10 g, 0.19 mmol) in NCMe (15 mL) was refluxed and irradiated with a 60 W tungsten lamp for 25 h. After concentration to ca. 5 mL and addition of Et<sub>2</sub>O, the pink-red crystalline complex that was separated was filtered and washed with Et<sub>2</sub>O. Yield 94%. Anal. Calcd for C<sub>19</sub>H<sub>26</sub>B<sub>2</sub>F<sub>8</sub>N<sub>2</sub>Mo: C, 41.34; H, 4.75; N, 5.08. Found: C, 41.25; H, 4.86; N, 5.19. Selected IR (KBr, cm<sup>-1</sup>): 2318, 2297, 2289 w, ν(N≡C). <sup>1</sup>H NMR (NCMe-*d*<sub>3</sub>, 300 MHz, room temperature, δ ppm): 5.65 (s, 5H, Cp), 2.56 (s, 6H, NCMe), 1.90 (s, 15H, NCMe).

**Preparation of [IndCpMoH(CO)][BF<sub>4</sub>] (29).** A solution of [IndMo(η<sup>4</sup>-C<sub>5</sub>H<sub>6</sub>)(CO)<sub>2</sub>][BF<sub>4</sub>] (0.25 g, 0.64 mmol) in CH<sub>2</sub>Cl<sub>2</sub> (20 mL) was stirred for 8 h. The volume was halved, and ether was added to precipitate a yellow complex, which was filtered, washed with ether (2 × 10 mL), dried in vacuum, and recrystallized from CH<sub>2</sub>Cl<sub>2</sub>/Et<sub>2</sub>O. Yield 92%. Anal. Calcd for C<sub>15</sub>H<sub>13</sub>BF<sub>4</sub>OMo: C, 45.96; H, 3.34. Found: C, 45.81; H, 3.30. Selected IR (KBr, cm<sup>-1</sup>): 2019, vs, ν(CO); 1840, m, ν(hydride); in solution (CH<sub>2</sub>Cl<sub>2</sub>), 2023, vs, ν(CO). <sup>1</sup>H NMR (Me<sub>2</sub>CO-*d*<sub>6</sub>, 300 MHz, room temperature, δ ppm): 7.87–7.84 (m, 2H, H<sub>5-8</sub>), 7.53–7.50 (m, 2H, H<sub>5-8</sub>), 6.36 (s, 1H, H<sub>1/3</sub>), 6.32 (s, 1H, H<sub>1/3</sub>), 6.23 (t, 1H, H<sub>2</sub>), 5.56 (s, 5H, Cp), -7.16 (s, 1H, Mo–H).

**Preparation of [IndCpMoCl(CO)][BF<sub>4</sub>] (30).** A solution of [IndMo(η<sup>4</sup>-C<sub>5</sub>H<sub>6</sub>)(CO)<sub>2</sub>][BF<sub>4</sub>] (0.25 g, 0.60 mmol) in a mixture of CH<sub>2</sub>Cl<sub>2</sub>/CHCl<sub>3</sub> was irradiated for ca. 8 h with a 60 W tungsten bulb. The solution became violet, and a pink precipitate was separated, which was filtered, washed with ether, and recrystallized from acetone/ether. Yield 98%. Anal. Calcd for C<sub>15</sub>H<sub>12</sub>BF<sub>4</sub>OCIMo: C, 42.25; H, 2.83. Found: C, 42.26; H, 2.86. Selected IR (KBr, cm<sup>-1</sup>): 2044, vs, ν(CO); in solution (CH<sub>2</sub>Cl<sub>2</sub>), 2056, vs, ν(CO). <sup>1</sup>H NMR (Me<sub>2</sub>CO-*d*<sub>6</sub>, 300 MHz, room temperature, δ ppm): 8.18–8.15 (m, 1H, H<sub>5-8</sub>), 7.93–7.87 (m, 1H, H<sub>5-8</sub>), 7.81–7.75 (m, 1H, H<sub>5-8</sub>), 7.54–7.51 (m, 1H, H<sub>5-8</sub>), 6.84 (m, 1H, H<sub>1/3</sub>), 6.50 (t, 1H, H<sub>2</sub>), 6.43 (m, 1H, H<sub>1/3</sub>), 6.30 (s, 5H, Cp).

**Preparation of [IndCpMoI(CO)][BF<sub>4</sub>] (31).** A solution of [IndMo(η<sup>4</sup>-C<sub>5</sub>H<sub>6</sub>)(CO)<sub>2</sub>][BF<sub>4</sub>] (0.25 g, 0.60 mmol) in a mixture of CH<sub>2</sub>Cl<sub>2</sub>/CHCl<sub>3</sub> was irradiated for ca. 6 h with a 60 W tungsten bulb. The solution became dark red, and a violet precipitate was separated, which was filtered, washed with ether, and recrystallized from acetone/ether. Yield 96%. Anal. Calcd for C<sub>15</sub>H<sub>12</sub>BF<sub>4</sub>OIMo: C, 34.79; H, 2.34. Found: C, 34.74; H, 2.44. Selected IR (KBr, cm<sup>-1</sup>): 2048, vs, ν(CO). <sup>1</sup>H NMR (Me<sub>2</sub>CO-*d*<sub>6</sub>, 300 MHz, room temperature, δ ppm): 8.14–8.11 (m, 1H, H<sub>5-8</sub>), 7.82–7.72 (m, 2H, H<sub>5-8</sub>), 7.62–7.57 (m, 1H, H<sub>5-8</sub>), 7.03 (m, 1H, H<sub>1/3</sub>), 6.61 (m, 1H, H<sub>1/3</sub>), 6.43 (t, 1H, H<sub>2</sub>), 6.29 (s, 5H, Cp).

**Preparation of [IndCpMo(NCMe)Cl][BF<sub>4</sub>] (32).** A solution of [IndMoCp(CO)Cl][BF<sub>4</sub>] (0.50 g, 1.17 mmol) in NCMe (30 mL) was refluxed and irradiated with a 60 W tungsten lamp for 4 h. The resulting dark green solution was evaporated to dryness, and the solid residue was recrystallized from NCMe/Et<sub>2</sub>O at -30 °C. Yield 92%. Anal. Calcd for C<sub>16</sub>H<sub>15</sub>BF<sub>4</sub>CINMo: C, 43.73; H, 3.44; N, 3.19. Found: C, 43.83; H, 3.48; N, 3.28. Selected IR (KBr, cm<sup>-1</sup>): 2320, 2289, w, ν(N≡C). <sup>1</sup>H NMR (Me<sub>2</sub>CO-*d*<sub>6</sub>, 300 MHz, room temperature, δ ppm): 7.73–7.70 (m, 1H, H<sub>5-8</sub>), 7.59–7.55 (m, 3H, H<sub>5-8</sub>), 6.35 (d, 2H, H<sub>1/3</sub>), 6.08 (t, 1H, H<sub>2</sub>), 5.61 (s, 5H, Cp), 2.66 (s, 3H, NCMe).

**Preparation of [IndCpMoCl<sub>2</sub>] (33).** A solution of [IndCpMo(CO)Cl][BF<sub>4</sub>] (0.50 g, 1.17 mmol) in acetone (30 mL) was treated with excess LiCl, and the mixture was irradiated with

a 60 W tungsten lamp for 10 h. A purple precipitate formed slowly, and the solution became almost colorless. The precipitate was filtered, stirred with ethanol for 15 min, and washed again with Et<sub>2</sub>O (3 × 10 mL). Yield 92%. Anal. Calcd for C<sub>14</sub>H<sub>12</sub>Cl<sub>2</sub>Mo: C, 48.45; H, 3.48. Found: C, 48.16; H, 3.37.

**Preparation of [IndCpMoCl(PPh<sub>3</sub>)][BF<sub>4</sub>] (34).** A suspension of [IndCpMoCl<sub>2</sub>] (0.23 g, 0.66 mmol) in NCMe (20 mL) was treated with Ph<sub>3</sub>P (0.23 g, 0.66 mmol) and TIBF<sub>4</sub> (0.19 g, 0.66 mmol). The blue solution that formed was separated from TiCl<sub>4</sub> by filtration and evaporated to dryness. After being washed with Et<sub>2</sub>O, the residue was recrystallized from CH<sub>2</sub>Cl<sub>2</sub>/Et<sub>2</sub>O to give a blue microcrystalline complex. Yield 86%. Anal. Calcd for C<sub>32</sub>H<sub>27</sub>BClF<sub>4</sub>PMo: C, 58.17; H, 4.12. Found: C, 57.90; H, 4.12. <sup>1</sup>H NMR (Me<sub>2</sub>CO-*d*<sub>6</sub>, 300 MHz, room temperature, δ ppm): 7.64–7.49 (m, 19H, C<sub>6</sub>H<sub>5</sub> of Ph<sub>3</sub>P and H<sub>5-8</sub> of C<sub>9</sub>H<sub>7</sub>), 5.84 (m, 2H, H<sub>1/3</sub>), 5.71 (t, 1H, H<sub>2</sub>), 5.43 (s, 5H, Cp).

**Preparation of [IndCpMo(SC<sub>6</sub>H<sub>5</sub>)<sub>2</sub>] (35).** A solution of [IndCpMoCl<sub>2</sub>] (0.25 g, 0.72 mmol) in 20 mL of absolute EtOH was treated with C<sub>6</sub>H<sub>5</sub>SnA (0.19 g, 1.44 mmol). After 2 h, the solvent was evaporated in vacuo and the brown precipitate was extracted with CH<sub>2</sub>Cl<sub>2</sub>. After being concentrated and cooled a brown microcrystalline complex was isolated by filtration and dried under vacuum. Yield 85%. Anal. Calcd for C<sub>16</sub>H<sub>12</sub>O<sub>2</sub>Mo: C, 57.85; H, 3.64. Found: C, 57.88; H, 3.72. <sup>1</sup>H NMR (NCMe-*d*<sub>3</sub>, 300 MHz, room temperature, δ ppm): 7.22–6.89 (m, 14H, H<sub>5-8</sub> of C<sub>9</sub>H<sub>7</sub> and C<sub>6</sub>H<sub>5</sub>), 5.55 (d, 2H, H<sub>1/3</sub>), 5.26 (t, 1H, H<sub>2</sub>), 5.13 (s, 5H, Cp).

**Preparation of [IndCpMoH<sub>2</sub>] (36).** A suspension of IndCpMoCl<sub>2</sub> (0.50 g, 1.44 mmol) in THF (20 mL) was treated with 2 equiv of LiAlH(O<sup>t</sup>Bu)<sub>3</sub> at -10 °C for 2 h. The orange solution was filtered and taken to dryness. The residue was extracted with Et<sub>2</sub>O and recrystallized from hexane/Et<sub>2</sub>O (-30 °C). Yield 75%. Anal. Calcd for C<sub>14</sub>H<sub>14</sub>Mo: C, 60.44; H, 5.07. Found: C, 60.06; H, 4.91. Selected IR (KBr, cm<sup>-1</sup>): 1840, m, ν(Mo–H). <sup>1</sup>H NMR (Me<sub>2</sub>CO-*d*<sub>6</sub>, 300 MHz, room temperature, δ ppm): 7.25–7.20 (m, 2H, H<sub>5-8</sub>), 6.68–6.63 (m, 2H, H<sub>5-8</sub>), 4.93 (d, 2H, H<sub>1/3</sub>), 4.86 (t, 1H, H<sub>2</sub>), 4.30 (s, 5H, Cp), -7.35 (s, 2H, Mo–H).

**Preparation of [IndCpMo(CO)<sub>2</sub>][BF<sub>4</sub>]<sub>2</sub> (37).** Method a: A solution of [IndMo(η<sup>4</sup>-C<sub>5</sub>H<sub>6</sub>)(CO)<sub>2</sub>][BF<sub>4</sub>] (0.30 g, 0.71 mmol) in CH<sub>2</sub>Cl<sub>2</sub> was treated with a solution of Ph<sub>3</sub>CBF<sub>4</sub> (0.23 g, 0.71 mmol) in the same solvent. After 8 h of stirring, an off-white precipitate was filtered and washed with CH<sub>2</sub>Cl<sub>2</sub> (10 mL) and Et<sub>2</sub>O (2 × 10 mL). Yield 88%. Anal. Calcd for C<sub>16</sub>H<sub>12</sub>B<sub>2</sub>F<sub>8</sub>O<sub>2</sub>Mo: C, 37.99; H, 2.39. Found: C, 37.86; H, 2.36. Selected IR (cm<sup>-1</sup>): in KBr, 2129, 2089, vs, ν(CO); in Nujol, 2133, 2093. <sup>1</sup>H NMR (Me<sub>2</sub>CO-*d*<sub>6</sub>, 300 MHz, δ ppm): 8.28–8.25 (m, 2H, H<sub>5-8</sub>), 8.12–8.08 (m, 2H, H<sub>5-8</sub>), 7.55 (d, 2H, H<sub>1/3</sub>), 6.98 (t, 1H, H<sub>2</sub>), 6.79 (s, 5H, Cp).

Method b: A solution of [CpMo(η<sup>3</sup>-Ind)(CO)<sub>2</sub>] (0.20 g, 0.60 mmol) in CH<sub>2</sub>Cl<sub>2</sub> was treated with a solution of Ph<sub>3</sub>CBF<sub>4</sub> (0.40 g, 1.2 mmol) in the same solvent. The turbid reaction mixture was left stirring for 1 h, and the precipitate was recovered and washed as above. Yield 90%.

**Preparation of [IndCpMo(CO)(NCMe)][BF<sub>4</sub>]<sub>2</sub> (38).** [IndCpMo(CO)<sub>2</sub>][BF<sub>4</sub>]<sub>2</sub> (0.25 g, 0.49 mmol) was dissolved in NCMe (20 mL). After 2 h the solution was concentrated to 6 mL, and addition of Et<sub>2</sub>O precipitated the product. Further recrystallization from NCMe/Et<sub>2</sub>O gave the compound in 98% yield. Anal. Calcd for C<sub>17</sub>H<sub>15</sub>B<sub>2</sub>F<sub>8</sub>ONMo: C, 39.35; H, 2.91; N, 2.70. Found: C, 39.52; H, 2.73; N, 2.76. Selected IR (KBr, cm<sup>-1</sup>): 2323, 2303, w, ν(N≡C); 2050, vs, ν(CO). <sup>1</sup>H NMR (NCMe-*d*<sub>3</sub>, 300 MHz, room temperature, δ ppm): 7.97–7.92 (m, 2H, H<sub>5-8</sub>), 7.82–7.74 (m, 2H, H<sub>5-8</sub>), 6.93 (m, 1H, H<sub>1/3</sub>), 6.40 (t, 1H, H<sub>2</sub>), 6.22 (m, 1H, H<sub>1/3</sub>), 6.15 (s, 5H, Cp); 2.38 (s, 3H, NCMe).

**Preparation of [IndCpMo(NCMe)<sub>2</sub>][BF<sub>4</sub>]<sub>2</sub> (39).** A solution of [IndCpMo(CO)(NCMe)][BF<sub>4</sub>]<sub>2</sub> (0.25 g, 0.48 mmol) in NCMe (20 mL) was refluxed and irradiated with a 60 W tungsten bulb for 8 h. After concentration to 5 mL and addition of ether, the pink-red microcrystalline precipitate was



filtered off, washed with Et<sub>2</sub>O, and dried under vacuum. Yield 96%. Anal. Calcd for C<sub>18</sub>H<sub>18</sub>B<sub>2</sub>F<sub>8</sub>N<sub>2</sub>Mo: C, 40.65; H, 3.41; N, 5.27. Found: C, 40.69; H, 3.58; N, 5.20. Selected IR (KBr, cm<sup>-1</sup>): 2292, 2324, w, ν(N≡C). <sup>1</sup>H NMR (NCMe-d<sub>3</sub>, 300 MHz, δ ppm): 7.63 (s, 4H, H<sub>5-8</sub>); 6.34 (s, 3H, H<sub>1/3</sub> + H<sub>2</sub>); 5.85 (s, 5H, Cp); 2.47 (s, 6H, NCMc).

**Preparation of [CpMo(η<sup>3</sup>-C<sub>6</sub>H<sub>7</sub>)(CO)<sub>2</sub>] (40).** A solution of [CpMo(η<sup>4</sup>-C<sub>6</sub>H<sub>8</sub>)(CO)<sub>2</sub>][BF<sub>4</sub>] (0.25 g, 0.65 mmol) in CH<sub>2</sub>Cl<sub>2</sub> (20 mL) was treated with excess NEt<sub>3</sub> for 1 h. The resulting reaction mixture was then evaporated to dryness, and the residue was extracted with hexane. After being concentrated and cooled the yellow crystalline complex was isolated in 94% yield. A similar yield was obtained using NaH and THF instead of NEt<sub>3</sub> and CH<sub>2</sub>Cl<sub>2</sub>, respectively. The analytical, IR, and <sup>1</sup>H NMR data agree with those published in ref 17f).

**Preparation of [CpMo(η<sup>3</sup>-Ind)(CO)<sub>2</sub>] (41).** Method a: A solution of [IndMo(η<sup>3</sup>-C<sub>3</sub>H<sub>5</sub>)(CO)<sub>2</sub>] (1.20 g, 3.80 mmol) in CH<sub>2</sub>Cl<sub>2</sub> (30 mL) was treated with 85% HBF<sub>4</sub>·Et<sub>2</sub>O (1 equiv), and after 15 min Bu<sub>4</sub>NI (1.40 g, 3.80 mmol) was added to the red solution. After 2 h the reaction mixture was evaporated and redissolved in THF. TICp (1.20 g, 4.45 mmol) was added, and the reaction mixture was stirred for another 3 h and evaporated to dryness. Extraction of the residue with ether gave a ruby-red solution, which gave the crystalline product after concentration and prolonged cooling at -30 °C. Yield 81%. Anal. Calcd for C<sub>16</sub>H<sub>12</sub>O<sub>2</sub>Mo: C, 57.85; H, 3.64. Found: C, 57.88; H, 3.72. Selected IR (CH<sub>2</sub>Cl<sub>2</sub> solution, cm<sup>-1</sup>): 1965, 1886, vs, ν(CO). <sup>1</sup>H NMR (CDCl<sub>3</sub>-d<sub>1</sub>, 300 MHz, room temperature, δ ppm): 6.75 (t, 1H, H<sub>2</sub>), 6.68–6.66 (m, 2H, H<sub>5-8</sub>), 6.46–6.39 (m, 2H, H<sub>5-8</sub>), 5.20 (d, 2H, H<sub>1/3</sub>), 4.99 (s, 5H, Cp). <sup>13</sup>C (CDCl<sub>3</sub>-d<sub>1</sub>, 75 MHz, room temperature, δ ppm): 228.76, CO; 151.10, (C<sub>4/9</sub>); 122.55, (C<sub>5/8</sub>); 115.88, (C<sub>6/7</sub>); 105.58, (C<sub>2</sub>); 97.64, (Cp); 60.57, (C<sub>1/3</sub>).

Method b: A suspension of [IndMo(η<sup>4</sup>-C<sub>5</sub>H<sub>6</sub>)(CO)<sub>2</sub>][BF<sub>4</sub>] (0.50 g, 1.20 mmol) in THF (20 mL) was treated with excess NaH for 2 h. After filtration and evaporation to dryness, the complex was extracted into hexane and recrystallized by concentration and cooling. Yield 82%.

Method c: A solution of [IndMo(η<sup>4</sup>-C<sub>5</sub>H<sub>6</sub>)(CO)<sub>2</sub>][BF<sub>4</sub>] (0.50 g, 1.20 mmol) in CH<sub>2</sub>Cl<sub>2</sub> (20 mL) was treated with excess NEt<sub>3</sub> for 1 h. The red solution was evaporated to dryness, and the residue was extracted with ether to give the dark-red product in 88% yield.

**Preparation of [CpW(η<sup>3</sup>-C<sub>5</sub>H<sub>5</sub>)(CO)<sub>2</sub>] (42).** Treatment of a solution of [CpW(η<sup>4</sup>-C<sub>5</sub>H<sub>6</sub>)(CO)<sub>2</sub>][BF<sub>4</sub>] (0.50 g, 1.09 mmol) in CH<sub>2</sub>Cl<sub>2</sub> (20 mL) with NEt<sub>3</sub> gave an immediate color change to blue. Toluene (10 mL) was then added, and the mixture was evaporated until the compound was only dissolved in toluene. This solution was filtered and taken to dryness. Extraction of the residue with hexane gave a blue solution, which was concentrated and cooled to give the blue crystalline product. Yield 85%. Anal. Calcd for C<sub>12</sub>H<sub>10</sub>O<sub>2</sub>W: C, 38.95; H, 2.72. Found: C, 38.80; H, 2.69. Selected IR (cm<sup>-1</sup>): in KBr, 1942, 1923, 1853, 1830, vs, ν(CO); in CH<sub>2</sub>Cl<sub>2</sub> solution, 1946, 1850. <sup>1</sup>H NMR (CDCl<sub>3</sub>-d<sub>1</sub>, 300 MHz, room temperature, δ ppm): 5.21 (s, 10H, Cp).

**Preparation of [CpMo(η<sup>3</sup>-C<sub>5</sub>H<sub>5</sub>)(CO)<sub>2</sub>] (44).** A solution of [CpMo(η<sup>4</sup>-C<sub>5</sub>H<sub>6</sub>)(CO)<sub>2</sub>][BF<sub>4</sub>] (0.50 g, 1.20 mmol) in CH<sub>2</sub>Cl<sub>2</sub> (20 mL) was treated with excess NEt<sub>3</sub> at -30 °C. After 1/2 h the green solution was taken to dryness, and the residue was extracted with hexane. The green solution was then concentrated and cooled to give the green crystalline product. Yield 85%. Anal. Calcd for C<sub>12</sub>H<sub>10</sub>O<sub>2</sub>Mo: C, 51.08; H, 3.57. Found: C, 51.12; H, 3.70. Selected IR (cm<sup>-1</sup>): in KBr, 1952, 1933, 1851, 1838, vs, ν(CO); in Nujol, 1954, 1929, 1863, 1838. <sup>1</sup>H NMR (CDCl<sub>3</sub>-d<sub>1</sub>, 300 MHz, δ ppm): 5.63 (s, 10H, Cp).

**Preparation of [Cp\*Mo(η<sup>4</sup>-C<sub>5</sub>H<sub>6</sub>)(CO)<sub>2</sub>][BF<sub>4</sub>] (46).** A solution of [Cp\*Mo(η<sup>4</sup>-C<sub>5</sub>H<sub>6</sub>)(CO)<sub>2</sub>][BF<sub>4</sub>] (0.20 g, 0.45 mmol) in CH<sub>2</sub>Cl<sub>2</sub> (20 mL) was treated with excess NEt<sub>3</sub> (1 mL) at room temperature for 2 h. The resulting reaction mixture was then evaporated to dryness and the residue was washed with hexane. Yield 88%. Anal. Calcd for C<sub>16</sub>H<sub>21</sub>BF<sub>4</sub>O<sub>2</sub>Mo: C,

46.64; H, 5.14. Found: C, 46.72; H, 5.01. Selected IR (KBr, cm<sup>-1</sup>): 2008, vs, ν(CO); 1842, m, ν(Mo–H). <sup>1</sup>H NMR (Me<sub>2</sub>CO-d<sub>6</sub>, 300 MHz, room temperature, δ ppm): 5.55 (s, 5H, Cp), 2.21 (s, 15H, Cp\*), -7.87 (s, 1H, Mo–H).

**Preparation of [CpMo(η<sup>3</sup>-C<sub>5</sub>(CH<sub>3</sub>)<sub>4</sub>H(CH<sub>2</sub>)}(CO)<sub>2</sub>] (47).** Method a: A suspension of [CpMo(η<sup>4</sup>-C<sub>5</sub>Me<sub>5</sub>H)(CO)<sub>2</sub>][BF<sub>4</sub>] (0.50 g, 1.1 mmol) in THF (20 mL) was treated for 2 h with excess NaH. After filtration, the resulting yellow solution was taken to dryness, and the residue was extracted into hexane and taken to dryness to give a powder in 86% crude yield. The product may be recrystallized from hexane/Et<sub>2</sub>O mixtures by concentration and cooling to -30 °C. Crystals suitable for X-ray analysis and NMR spectra can be grown very slowly from MeOH/hexane mixtures. Anal. Calcd for C<sub>17</sub>H<sub>20</sub>O<sub>2</sub>Mo: C, 57.96; H, 5.72. Found: C, 57.98; H, 5.82. Selected IR (KBr, cm<sup>-1</sup>): 1921, 1847, vs, ν(CO). <sup>1</sup>H NMR (CDCl<sub>3</sub>-d<sub>1</sub>, 300 MHz, -40 °C, δ ppm): 5.26 (s, 5H, Cp), 4.42 (d, 1H, H<sub>a</sub>), 4.28 (d, 1H, H<sub>b</sub>), 2.45 (q, 1H, H<sub>c</sub>), 2.19 (s, 3H, <sup>2</sup>CH<sub>3</sub>), 1.74 (s, 6H, <sup>3</sup>CH<sub>3</sub> + <sup>1</sup>CH<sub>3</sub>), 0.93 (d, 3H, <sup>4</sup>CH<sub>3</sub>). <sup>13</sup>C (CDCl<sub>3</sub>-d<sub>1</sub>, 75 MHz, -40 °C): 237.11, 235.86 (CO); 161.07 (C<sub>5</sub>); 93.67 (Cp); 93.38 (C<sub>6</sub>); 82.91, 77.02, 74.27 (C<sub>1,2,3</sub>); 49.01 (C<sub>4</sub>); 23.15 (C<sub>4</sub>); 17.80, 17.27, 16.07 (C<sub>1,2,3</sub>) (see Scheme 7 for numbering).

Method b: A solution of [CpMo(η<sup>4</sup>-C<sub>5</sub>Me<sub>5</sub>H)(CO)<sub>2</sub>][BF<sub>4</sub>] (0.50 g, 1.1 mmol) in CH<sub>2</sub>Cl<sub>2</sub> (20 mL) was treated with excess NEt<sub>3</sub> for 1 h. The solution was evaporated to dryness, and the residue was extracted with ether to give the yellow product in 90% yield (crude mixture of isomers).

**Preparation of [CpW(η<sup>3</sup>-C<sub>5</sub>(CH<sub>3</sub>)<sub>4</sub>H(CH<sub>2</sub>)}(CO)<sub>2</sub>] (50).** A solution of [CpW(η<sup>4</sup>-C<sub>5</sub>Me<sub>5</sub>H)(CO)<sub>2</sub>][BF<sub>4</sub>] (0.25 g, 0.47 mmol) in CH<sub>2</sub>Cl<sub>2</sub> (20 mL) was treated with excess NEt<sub>3</sub> for 1 h. The solution was evaporated to dryness, and the residue was extracted with ether to give the yellow crude product in 90% yield. Larger crystals were obtained from MeOH/hexane. Anal. Calcd for C<sub>17</sub>H<sub>20</sub>O<sub>2</sub>W: C, 46.39; H, 4.58. Found: C, 46.50; H, 4.70. Selected IR (KBr, cm<sup>-1</sup>): 1915, 1840, vs, ν(CO). <sup>1</sup>H NMR (CDCl<sub>3</sub>-d<sub>1</sub>, 300 MHz, -40 °C, δ ppm): 5.24 (s, 5H, Cp), 4.33 (d, 1H, H<sub>a</sub>), 4.23 (d, 1H, H<sub>b</sub>), 2.69 (q, 1H, H<sub>c</sub>), 2.34 (s, 3H, <sup>2</sup>CH<sub>3</sub>), 1.73 (s, 6H, <sup>3</sup>CH<sub>3</sub> + <sup>1</sup>CH<sub>3</sub>), 0.96 (d, 3H, <sup>4</sup>CH<sub>3</sub>) (see Scheme 7 for numbering).

**Preparation of [CpMo(η<sup>3</sup>-C<sub>5</sub>H<sub>7</sub>)(CO)<sub>2</sub>] (51a).** A solution of [CpMo(η<sup>4</sup>-1,3-C<sub>5</sub>H<sub>8</sub>)(CO)<sub>2</sub>][BF<sub>4</sub>] (0.25 g, 0.67 mmol) in CH<sub>2</sub>Cl<sub>2</sub> (20 mL) was treated with excess NEt<sub>3</sub> for 1 h, and the resulting reaction mixture was evaporated to dryness. The residue was extracted with hexane, concentrated, and cooled to give the yellow crystalline complex in 85% yield. A similar yield was obtained using NaH and THF instead of NEt<sub>3</sub> and CH<sub>2</sub>Cl<sub>2</sub>, respectively. Anal. Calcd for C<sub>12</sub>H<sub>12</sub>O<sub>2</sub>Mo: C, 50.72; H, 4.26. Found: C, 50.73; H, 4.18. Selected IR (KBr, cm<sup>-1</sup>): 1937, 1859, vs, ν(CO). <sup>1</sup>H NMR (CDCl<sub>3</sub>-d<sub>1</sub>, 300 MHz, -40 °C, δ ppm): 5.33 (s, 5H, Cp), 5.06 (dd, 1H, H<sub>6</sub>), 4.78 (dd, 1H, H<sub>7</sub>), 4.49 (dd, 1H, H<sub>3</sub>), 4.30 (dt, 1H, H<sub>5</sub>), 4.21 (dt, 1H, H<sub>4</sub>), 2.84 (ddd, 1H, H<sub>2</sub>), 1.47 (dd, 1H, H<sub>1</sub>); J<sub>76</sub> = 1.7, J<sub>75</sub> = 9.9, J<sub>65</sub> = 16.5, J<sub>54</sub> = 10.5, J<sub>43</sub> = 7.5, J<sub>32</sub> = 7.5, J<sub>13</sub> = 11.2, J<sub>12</sub> = 2.7 Hz (see Scheme 7 for numbering).

**Preparation of [IndMo(η<sup>3</sup>-Ind)(CO)<sub>2</sub>] (52).** A solution of [IndMo(η<sup>3</sup>-C<sub>3</sub>H<sub>5</sub>)(CO)<sub>2</sub>] (1.20 g, 3.80 mmol) in CH<sub>2</sub>Cl<sub>2</sub> (30 mL) was treated with 1 equiv of HBF<sub>4</sub>·Et<sub>2</sub>O. After 10 min, C<sub>9</sub>H<sub>8</sub> was added (5 mL), and the solution was left for 8 h at room temperature and then treated with excess NEt<sub>3</sub> for 1 h. The resulting solution is taken to dryness and the residue was extracted with hexane to give an orange solution. Crystallization ensued after concentration and prolonged cooling at -30 °C. Yield 73%. Anal. Calcd for C<sub>20</sub>H<sub>14</sub>O<sub>2</sub>Mo: C, 62.31; H, 3.50. Found: C, 62.50; H, 3.67. Selected IR (Nujol, cm<sup>-1</sup>): 1967, 1878, vs, ν(CO). <sup>1</sup>H NMR (C<sub>6</sub>H<sub>5</sub>Me-d<sub>8</sub>, 300 MHz, room temperature, δ ppm): 6.69–6.66 (m, 8H, H<sub>5-8</sub>), 5.11 (d, 4H, H<sub>1/3</sub>), 4.80 (t, 2H, H<sub>2</sub>).

**X-ray Crystal Structure Analysis of 41 and 47.** Complex 41. Crystallographic data and a summary of data collection and refinement parameters are presented in Table 3. Unit cell parameters were determined by a least-squares fit of 20 reflections in the range 39.8–54.6° in 2θ. Intensity

**Table 3. Summary of Crystal Data and Details of Intensity Collection for [CpMo( $\eta^3$ -C<sub>9</sub>H<sub>7</sub>)(CO)<sub>2</sub>] (41) and**

	41	47
formula	C <sub>16</sub> H <sub>12</sub> MoO <sub>2</sub>	C <sub>17</sub> H <sub>20</sub> MoO <sub>2</sub>
fw	332.2	352.3
cryst syst	orthorhombic	orthorhombic
space group	<i>Pnma</i> (No. 62)	<i>P2<sub>1</sub>2<sub>1</sub>2<sub>1</sub></i> (No. 19)
cryst dimens, mm <sup>3</sup>	0.40 × 0.45 × 0.50	0.77 × 0.38 × 0.46
cryst color, habit	orange block	yellow prism
temp, K	208	193
<i>a</i> , pm	986.5(1)	743.2(1)
<i>b</i> , pm	1136.1(1)	1295.4(1)
<i>c</i> , pm	1150.5(4)	1602.8(2)
<i>V</i> , pm <sup>3</sup> × 10 <sup>6</sup>	1289.4	1543.1
<i>Z</i>	4	4
<i>d</i> <sub>calcd</sub> , g cm <sup>-3</sup>	1.711	1.516
radiation ( $\lambda$ , pm)	Cu K $\alpha$ (154.184)	Mo K $\alpha$ (71.073)
$\mu$ , cm <sup>-1</sup>	84.2	8.3
abs cor	Difabs	none
transm, min/max	0.823/1.354	
scan type	$\theta/2\theta$ scan	$\theta/2\theta$ scan
scan time, s	max 90	max 90
scan width, deg	(1.00 + 0.25 tan $\theta$ )	(1.13 + 0.20 tan $\theta$ )
$\theta$ <sub>max</sub> , deg	65	30
bkgd measurement	25% additional at each end of scan	
no. of rflns colld	1277 (+ <i>h</i> , + <i>k</i> , - <i>l</i> )	7591 (+ <i>h</i> , ± <i>k</i> , ± <i>l</i> )
<i>R</i> <sub>merge</sub> (on <i>I</i> )	no	0.020
no. of indpt reflns	1122	4485
no. of obsd rflns (NV)	1122, <i>I</i> > 0	4485, <i>I</i> > 0
no. of variables (NO)	115	261
data:variable ratio	9.8	17.2
<i>R</i> , <i>R</i> <sub>w</sub> <sup>a</sup>	0.021, 0.024	
<i>R</i> <sub>1</sub> , <i>wR</i> <sub>2</sub> <sup>b</sup>		0.021, 0.045
GOF	4.055	2.211
Flack param		-0.01(3)
weighting scheme	$w^{-1} = \sigma^2(F_o)$	$w^{-1} = \sigma^2(F_o^2)$
largest shift/err	< 0.001	< 0.001
max/min, e <sub>s</sub> Å <sup>-3</sup>	+0.38/-0.47	+0.40/-0.81

<sup>a</sup>  $R = \sum(|F_o| - |F_c|)/\sum|F_o|$ ,  $R_w = [\sum w(|F_o| - |F_c|)^2/\sum w|F_o|^2]^{1/2}$  and  $GOF = [\sum w(|F_o| - |F_c|)^2/(\text{NO} - \text{NV})]^{1/2}$ . <sup>b</sup>  $R_1 = \sum(|F_o| - |F_c|)/\sum|F_o|$ ,  $wR_2 = [\sum w(F_o^2 - F_c^2)^2/\sum w(F_o^2)^2]^{1/2}$  and  $GOF = [\sum w(F_o^2 - F_c^2)^2/(\text{NO} - \text{NV})]^{1/2}$ .

data were corrected for usual Lorentz and polarization effects; absorption correction was also applied. The structure was solved by the direct-method approach. Full-matrix least-squares refinement minimizing  $\sum w(|F_o| - |F_c|)^2$  was carried out with anisotropic thermal parameters for all non-hydrogen atoms. Hydrogen atoms were found in the difference Fourier map calculated from the model containing all non-hydrogen atoms and was refined freely with isotropic thermal parameters. All software and the sources of the scattering factors are contained in the STRUX-V system including the programs MULTAN 11/82, ORTEP II, PLATON-92'', PLUTON-92'', SCHAKAL, and SDP on a Micro-Vax 3100 computer. Coordinates and relevant structural parameters are given in Tables 4 and 1, respectively.

**Complex 45.** Crystallographic data and a summary of data collection and refinement parameters are presented in Table 3. Unit cell parameters were determined by a least-squares fit of 25 reflections in the range 39.7–49.8° in  $2\theta$ . Intensity data were corrected for usual Lorentz and polarization effects; a small decay was also corrected (161.3 h exposing time; 4.5% loss of intensity). The structure was solved by the direct-method approach. Full-matrix least-squares refinement minimizing  $\sum w(F_o^2 - F_c^2)^2$  was carried out with anisotropic thermal parameters for all non-hydrogen atoms. Hydrogen atoms were

**Table 4. Final Coordinates and Equivalent Isotropic Thermal Parameters of the Non-Hydrogen Atoms for 41**

atom	<i>x</i>	<i>y</i>	<i>z</i>	<i>U</i> <sub>eq</sub> (Å <sup>2</sup> ) <sup>a</sup>
Mo	0.23455(2)	1/4	0.47942(2)	0.0126(1)
O	0.0359(2)	0.4343(2)	0.3701(2)	0.0403(6)
C	0.1088(3)	0.3650(2)	0.4078(2)	0.0228(7)
C(11)	0.1281(4)	1/4	0.6575(3)	0.0319(11)
C(12)	0.2117(3)	0.1490(3)	0.6546(2)	0.0292(8)
C(13)	0.3481(2)	0.1880(2)	0.6541(2)	0.0209(7)
C(21)	0.3382(4)	1/4	0.3039(3)	0.0213(10)
C(22)	0.3947(2)	0.1495(2)	0.3606(2)	0.0201(7)
C(23)	0.5207(2)	0.1869(2)	0.4184(2)	0.0167(6)
C(24)	0.6271(3)	0.1259(2)	0.4679(2)	0.0235(7)
C(25)	0.7347(2)	0.1895(3)	0.5187(2)	0.0285(8)

<sup>a</sup>  $U_{eq}$  is defined as one-third of the trace of the orthogonalized  $U_{ij}$  tensor.

**Table 5. Final Coordinates and Equivalent Isotropic Thermal Parameters of the Non-Hydrogen Atoms for 47**

atom	<i>x</i>	<i>y</i>	<i>z</i>	<i>U</i> <sub>eq</sub> (Å <sup>2</sup> ) <sup>a</sup>
Mo	0.21086(2)	0.10205(1)	0.15827(1)	0.0227(1)
O(1)	-0.1026(3)	0.1810(1)	0.0480(1)	0.0495(5)
O(2)	-0.1016(2)	0.0191(1)	0.2676(1)	0.0411(4)
C(1)	0.0151(3)	0.1501(1)	0.0883(1)	0.0315(4)
C(2)	0.0151(2)	0.0493(1)	0.2262(1)	0.0281(4)
C(11)	0.3499(3)	0.2647(1)	0.1510(1)	0.0446(6)
C(12)	0.2604(3)	0.2561(1)	0.2286(1)	0.0364(5)
C(13)	0.3471(3)	0.1782(1)	0.2760(1)	0.0369(5)
C(14)	0.4887(3)	0.1381(2)	0.2277(2)	0.0433(6)
C(15)	0.4905(3)	0.1914(2)	0.1505(1)	0.0489(6)
C(21)	0.3298(2)	-0.0372(1)	0.0987(1)	0.0271(4)
C(22)	0.2333(2)	0.0084(1)	0.0305(1)	0.0287(4)
C(23)	0.0600(2)	-0.0462(1)	0.0220(1)	0.0288(4)
C(24)	0.0352(2)	-0.1122(1)	0.0998(1)	0.0257(4)
C(25)	0.1976(2)	-0.0808(1)	0.1530(1)	0.0249(3)
C(31)	0.5289(3)	-0.0574(2)	0.1021(2)	0.0410(6)
C(32)	0.3207(4)	0.0586(2)	-0.0434(1)	0.0446(6)
C(33)	-0.0497(3)	-0.0435(2)	-0.0441(1)	0.0419(6)
C(34)	0.0403(3)	-0.2278(1)	0.0778(1)	0.0391(5)
C(35)	0.2458(3)	-0.1435(1)	0.2289(1)	0.0370(5)

<sup>a</sup>  $U_{eq}$  is defined as one-third of the trace of the orthogonalized  $U_{ij}$  tensor.

found in the difference Fourier map calculated from the model containing all non-hydrogen atoms and were refined freely with isotropic thermal parameters. All software and the sources of the scattering factors are contained in the STRUX-V system including the programs MULTAN 11/82, ORTEP II, PLATON-92'', PLUTON-92'', SCHAKAL, SDP, and SHELXL-93 on a Micro-Vax 3100 computer. Coordinates and relevant structural parameters are given in Tables 5 and 1, respectively.

**Acknowledgment.** This work was financially supported by the Junta Nacional de Investigação Científica e Tecnológica (JNICT) under project PMCT/C/CEN/659/90. I.S.G. and D.S.M. thank JNICT for grants. We thank Prof. W. A. Herrmann, Technical University of Munich, for providing analytical facilities and mass spectra.

**Supporting Information Available:** Tables giving a structural report of X-ray data collection and refinement, atomic coordinates, thermal parameters, bond lengths, and bond angles, and a stereo cell plot (13 pages). Ordering information is given on any current masthead page.

OM950122D



# Thallium-Stabilized Silsesquioxides: Versatile Reagents for the Synthesis of Metallasilsesquioxanes, Including High-Valent Molybdenum-Containing Silsesquioxanes

Frank J. Feher,\* Kamyar Rahimian, Theodore A. Budzichowski, and Joseph W. Ziller

Department of Chemistry, University of California, Irvine, California 92717

Received June 8, 1995\*

The reactions of the incompletely-condensed silsesquioxanes ( $c\text{-C}_6\text{H}_{11}$ )<sub>7</sub>Si<sub>7</sub>O<sub>9</sub>(OH)<sub>3</sub> (**1a**), ( $c\text{-C}_6\text{H}_{11}$ )<sub>7</sub>Si<sub>7</sub>O<sub>9</sub>(OTMS)(OH)<sub>2</sub> (**2a**), ( $c\text{-C}_6\text{H}_9$ )<sub>7</sub>Si<sub>7</sub>O<sub>9</sub>(OTMS)(OH)<sub>2</sub> (**2b**), and ( $c\text{-C}_6\text{H}_{11}$ )<sub>7</sub>Si<sub>7</sub>O<sub>9</sub>(OTMS)<sub>2</sub>(OH) (**3a**) with thallium(I) ethoxide (1/1 Tl/OH) result in the formation of the corresponding Tl-substituted silsesquioxanes [( $c\text{-C}_6\text{H}_{11}$ )<sub>7</sub>Si<sub>7</sub>O<sub>9</sub>(OTl)<sub>3</sub>]<sub>n</sub> (**7a**), [( $c\text{-C}_6\text{H}_{11}$ )<sub>7</sub>Si<sub>7</sub>O<sub>9</sub>(OTMS)(OTl)<sub>2</sub>]<sub>n</sub> (**8a**), [( $c\text{-C}_6\text{H}_9$ )<sub>7</sub>Si<sub>7</sub>O<sub>9</sub>(OTMS)(OTl)<sub>2</sub>]<sub>n</sub> (**8b**), and [( $c\text{-C}_6\text{H}_{11}$ )<sub>7</sub>Si<sub>7</sub>O<sub>9</sub>(OTMS)<sub>2</sub>(OTl)]<sub>n</sub> (**9a**). These thallium-stabilized silsesquioxides are not prone to cycloelimination reactions or the formation of "ate" complexes. They are versatile anionic equivalents of incompletely-condensed silsesquioxanes which react with a variety of halide complexes, including POCl<sub>3</sub> and MoO<sub>2</sub>Cl<sub>2</sub>, to afford high yields of metallasilsesquioxanes.

Over the past several years incompletely-condensed silsesquioxanes<sup>1</sup> have attracted interest as models for silica,<sup>2,3a</sup> as ligands for main-group<sup>4</sup> and transition-metal elements,<sup>3b,5-7</sup> and as comonomers for silsesquioxane-siloxane polymers.<sup>8,9</sup> The key to success in all of these areas has been the development of a highly

efficient methodology for constructing and modifying structurally well-defined Si/O frameworks.

The recent discovery that Me<sub>4</sub>Sb-stabilized silsesquioxides (e.g., **4-6**) can be used as anionic equivalents of incompletely-condensed silsesquioxanes (e.g., **1a-3a**) provided an important tool for preparing metal-containing Si/O frameworks.<sup>2d,4b,c,d</sup> Unfortunately, the utility of these latent anions is somewhat limited because of their tendency to cycloeliminate and/or form anionic "ate" complexes when reacted with high-valent, electrophilic metal halide complexes (e.g., TiX<sub>4</sub>, MoO<sub>2</sub>Cl<sub>2</sub>, POCl<sub>3</sub>)<sup>2d</sup> (Chart 1).

In this paper we report the synthesis, characterization, and reactivity of thallium-stabilized silsesquioxides, which can be easily obtained from the reactions of incompletely-condensed silsesquioxanes (e.g., **1-3**) with thallium ethoxide (TlOEt). These thallium-stabilized silsesquioxides are versatile anionic equivalents of incompletely-condensed silsesquioxanes. They react with a variety of halide complexes to afford high yields of metallasilsesquioxanes, and they are not as prone as Me<sub>4</sub>Sb-stabilized silsesquioxides to cycloeliminate or form "ate" complexes.<sup>6</sup>

## Results and Discussion

**Synthesis and Characterization of Thallium-Stabilized Silsesquioxides.** The reactions of **1-3** with stoichiometric amounts of TlOEt (Tl/SiOH = 1:1, 25 °C, C<sub>6</sub>H<sub>6</sub>) afford excellent yields of thallium-containing silsesquioxanes. In each case, spectroscopic and analytical data indicate that all protons available from siloxy groups are completely replaced by thallium (Scheme 1).

(9) (a) Lichtenhan, J. D. *Comments Inorg. Chem.* **1995**, *17*, 115-30. (b) Lichtenhan, J. D.; Mantz, R. A.; Jones, P. F.; Carr, M. J. *Polym. Prepr.* **1994**, *35*, 523-4. (c) Haddad, T. S.; Lichtenhan, J. D. *Polym. Prepr.* **1994**, *35*, 708-9. (d) Lichtenhan, J. D.; Otonari, Y. A.; Carr, M. J. *Macromolecules*, submitted for publication. (e) Lichtenhan, J. D. *Silsesquioxane-Based Polymers*. In *The Polymeric Materials Encyclopedia: Synthesis, Properties and Applications*; CRC Press, Inc.: Boca Raton, FL, in press. (f) Haddad, T. S.; Lichtenhan, J. D. *J. Inorg. Organomet. Polym.*, in press.

\* Abstract published in *Advance ACS Abstracts*, July 15, 1995.

(1) For reviews concerning incompletely-condensed silsesquioxanes: (a) Voronkov, M. G.; Lavrent'yev, V. I. *Top. Curr. Chem.* **1982**, *102*, 199-236. (b) Burgy, H.; Calzaferri, G.; Herren, D.; Zhdanov, A. *Chimia* **1991**, *45*, 3-8. (c) Edelmann, F. T. *Angew. Chem., Int. Ed. Engl.* **1992**, *32*, 586.

(2) (a) Feher, F. J.; Newman, D. A.; Walzer, J. F. *J. Am. Chem. Soc.* **1989**, *111*, 1741-8. (b) Feher, F. J.; Newman, D. A. *J. Am. Chem. Soc.* **1990**, *112*, 1931-6. (c) Feher, F. J.; Budzichowski, T. A.; Blanski, R. L.; Weller, K. J.; Ziller, J. W. *Organometallics* **1991**, *10*, 2526-8. (d) Feher, F. J.; Budzichowski, T. A.; Rahimian, K.; Ziller, J. W. *J. Am. Chem. Soc.* **1992**, *114*, 3859-66.

(3) (a) Hambley, T. W.; Maschmeyer, T.; Masters, A. F. *Appl. Organomet. Chem.* **1992**, *6*, 253-60. (b) Field, L. D.; Lindall, C. M.; Maschmeyer, T.; Masters, A. F. *Aust. J. Chem.* **1994**, *47*, 1127-32.

(4) (a) Feher, F. J.; Budzichowski, T. A.; Weller, K. J. *J. Am. Chem. Soc.* **1989**, *111*, 7288-9. (b) Feher, F. J.; Weller, K. J. *Organometallics* **1990**, *9*, 2638-40. (c) Feher, F. J.; Weller, K. J. *Inorg. Chem.* **1991**, *30*, 880-2. (d) Feher, F. J.; Weller, K. J.; Ziller, J. W. *J. Am. Chem. Soc.* **1992**, *114*, 9686-8. (e) Feher, F. J.; Budzichowski, T. A.; Ziller, J. W. *Inorg. Chem.* **1992**, *31*, 5100-5.

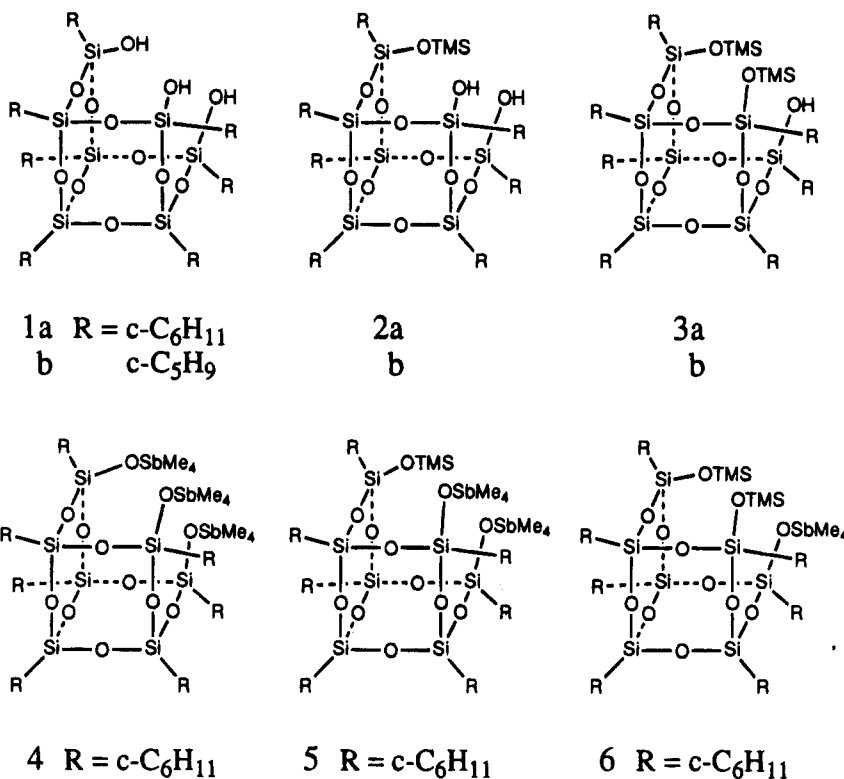
(5) (a) Feher, F. J.; Blanski, R. L. *J. Am. Chem. Soc.* **1992**, *114*, 5886-7. (b) Feher, F. J.; Blanski, R. L. *J. Chem. Soc., Chem. Commun.* **1990**, 1614-6. (c) Feher, F. J.; Walzer, J. F.; Blanski, R. L. *J. Am. Chem. Soc.* **1991**, *113*, 3618-9. (d) Liu, J.-C.; Wilson, S. R.; Shapley, J. R.; Feher, F. J. *Inorg. Chem.* **1990**, *29*, 5138-9. (e) Feher, F. J.; Walzer, J. F. *Inorg. Chem.* **1991**, *30*, 1689-94. (f) Feher, F. J. *J. Am. Chem. Soc.* **1986**, *108*, 3850-2. (g) Budzichowski, T. A.; Chacon, S. T.; Chisholm, M. H.; Feher, F. J.; Streib, W. *J. Am. Chem. Soc.* **1991**, *113*, 689-91. (h) Feher, F. J.; Walzer, J. F. *Inorg. Chem.* **1990**, *29*, 1604-11. (i) Feher, F. J.; Gonzales, S. L.; Ziller, J. W. *Inorg. Chem.* **1988**, *27*, 3440-2.

(6) A preliminary report of the synthesis and use of a thallium-containing silsesquioxane derived from **2b** has been recently reported: Feher, F. J.; Tajima, T. L. *J. Am. Chem. Soc.* **1994**, *116*, 2145-6.

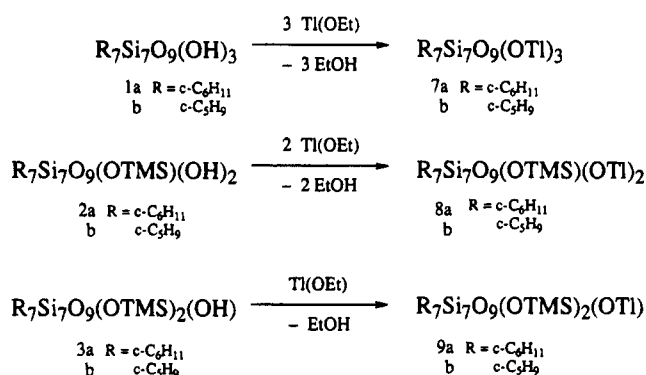
(7) (a) Winkhofer, N.; Roesky, H. W.; Noltmeyer, M.; Robinson, W. T. *Angew. Chem., Int. Ed. Engl.* **1992**, *31*, 599-601. (b) Herrmann, W. A.; Anwander, R.; Dufaud, V.; Schere, W. *Angew. Chem., Int. Ed. Engl.* **1994**, *33*, 1285-6. (c) Winkhofer, N.; Voigt, A.; Dorn, H.; Roesky, H. W.; Steiner, A.; Stalke, D.; Reller, A. *Angew. Chem., Int. Ed. Engl.* **1994**, *33*, 1352-3. (d) Gosink, H.-J.; Roesky, H. W.; Schmidt, H.-G.; Noltmeyer, M.; Irmer, E.; Herbst-Irmer, R. *Organometallics* **1994**, *13*, 3420-6.

(8) Lichtenhan, J. D.; Vu, N. Q.; Carter, J. A.; Gilman, J. W.; Feher, F. J. *Macromolecules* **1993**, *26*, 2141.

Chart 1

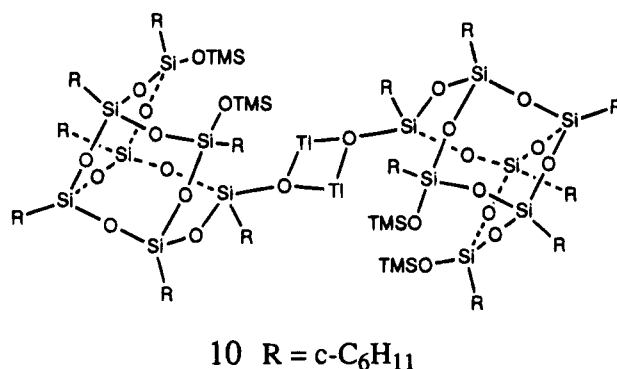


Scheme 1



Considering that Tl(I) has been observed to support coordination numbers ranging from 2 to 12,<sup>10,11</sup> the NMR spectra (25 °C, C<sub>6</sub>D<sub>6</sub>) for 7–9 are surprisingly simple. In each case, the spectra of the thallium-substituted product and the parent silsesquioxane exhibit the same multiplicity of <sup>29</sup>Si and methine (SiCH) <sup>13</sup>C resonances. For 7a, for example, both the <sup>29</sup>Si NMR spectrum and the (SiCH) region of the <sup>13</sup>C NMR spectrum exhibit three resonances with relative integrated intensities of 3:3:1. These results are consistent with structures analogous to 4–6, and it is convenient to view 7–9 as Tl-substituted derivatives of 1–3, but the structure of each molecule is undoubtedly more complex. In the case of 9a, a preliminary X-ray crystal structure<sup>12</sup> indicates that the molecule adopts a dimeric

structure with Tl in a relatively rare, two-coordinate, siloxy-bridged structure (i.e., 10). A dimeric structure



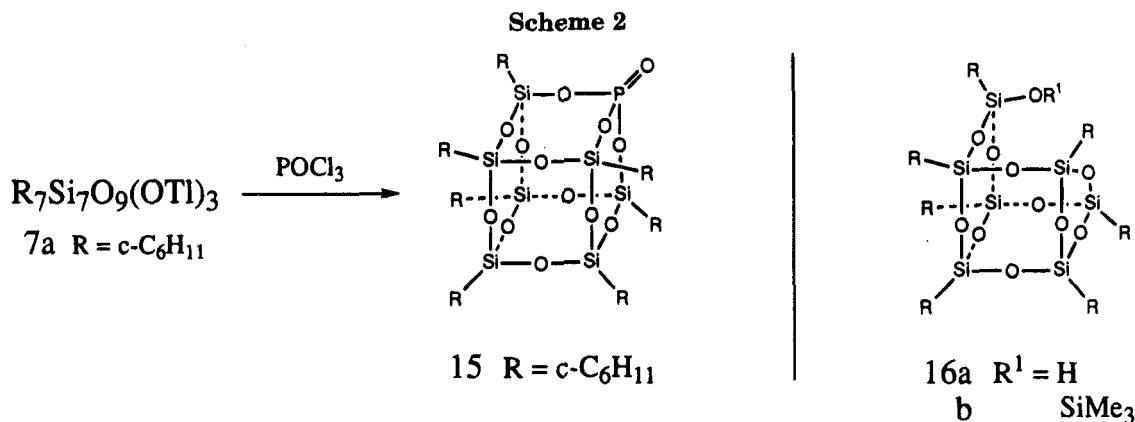
is also formed by 8b, but a preliminary X-ray structure<sup>13</sup> reveals a more complex siloxy-bridged structure with two- and three-coordinate Tl(I) ions. Unfortunately, it has not been possible to collect enough high-quality data

(12) (a) Complex 10 crystallizes from toluene/hexanes (–34 °C) as poorly diffracting, colorless plates in the monoclinic space group C2/c with  $a = 41.487(8)$  Å,  $b = 14.613(3)$  Å,  $c = 24.541(5)$  Å, and  $\beta = 109.79(3)^\circ$ . The asymmetric unit consists of one-half of the dimer shown, which is related to the other half by a 2-fold axis of rotation defined by the Tl–Tl vector. The structure was solved by direct methods (SHELXTL PLUS), and all non-hydrogen atoms were located by a series of difference-Fourier syntheses. The trimethylsilyl groups appear to be disordered. The current  $R_F$  is 9.5% (anisotropic parameters for Si, O, Tl; isotropic parameters for C). (b) Budzichowski, T. A., Ph.D. Thesis, University of California, Irvine, CA 1991.

(13) Complex 8b crystallizes from benzene/acetonitrile as very poorly diffracting crystals in the monoclinic space group P2<sub>1</sub>/n with  $a = 17.982(4)$  Å,  $b = 16.338(3)$  Å,  $c = 19.387(4)$  Å, and  $\beta = 113.80(3)^\circ$ . The solid-state structure, which contains two silsesquioxane fragments bridged by four Tl atoms, is very complex. The Si/O/Tl framework could be clearly identified, but severe X-ray damage to the crystal, disorder problems with cyclopentyl groups, and failures of the low-temperature unit prevented the collection of enough high-quality data to complete the structure: Feher, F. J.; Rahimian, K.; Ziller, J. W. Unpublished results.

(10) Lee, A. G. *Chemistry of Thallium*; Elsevier: Amsterdam, 1971, and references cited therein.

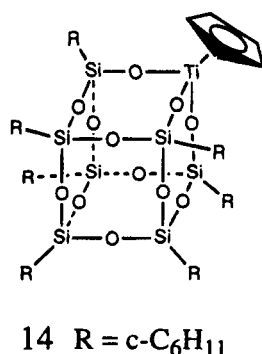
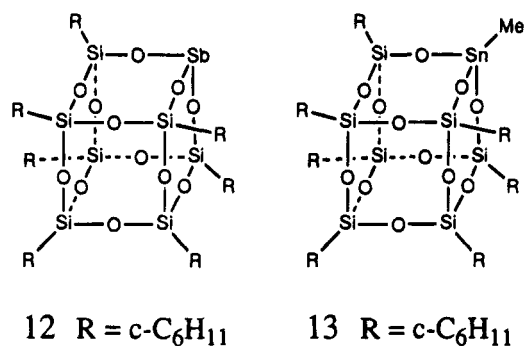
(11) Examples of coordination environments in Tl(I) alkoxides or siloxides: (a) Roesky, H. W.; Scholz, M.; Noltemeyer, M.; Edelmann, F. T. *Inorg. Chem.* **1989**, *28*, 3829–30. (b) Harvey, S.; Lappert, M. F.; Raston, C. L.; Skelton, B. W.; Srivastava, G.; White, A. H. *J. Chem. Soc., Chem. Commun.* **1988**, 1216–7. (c) Brown, I. D.; Faggianai, R. *Acta Crystallogr.* **1980**, *B36*, 1802–6 and references cited therein.



for satisfactory structural solutions. For reasons that are not yet apparent, these Tl-substituted silsesquioxanes produce either very poorly diffracting crystals (even at  $-100^\circ\text{C}$ ) or no crystals at all.<sup>14</sup>

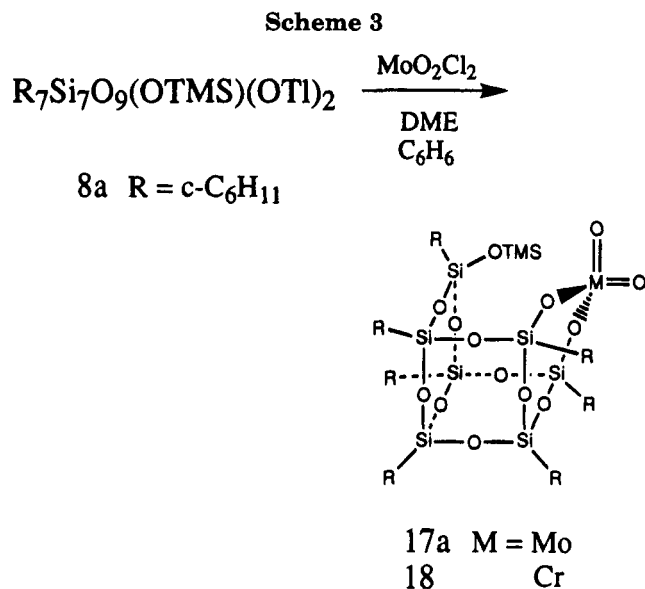
**Thallium-Stabilized Silsesquioxides as Anionic Equivalents of Incompletely-Condensed Silsesquioxanes.** Metathetical reactions between thallium-stabilized silsesquioxides and halide-containing reagents are very attractive because thallium halides have high lattice energies and are insoluble in almost all common laboratory solvents.<sup>15</sup> This minimizes any tendency for "ate" complex formation with Lewis acidic metal halides and allows TLX coproducts to be easily separated.

Thallium complex **7a** reacts quickly with a variety of halide-containing reagents (e.g., CpTiCl<sub>3</sub>, MeSnCl<sub>3</sub>, SbCl<sub>3</sub>) to afford high yields of metallasilsesquioxanes (i.e., **12**–**14**). In each case, the yield is quantitative by



(14) Tl-containing silsesquioxanes precipitate from many solvents as amorphous white powders. In those instances where well-formed crystals were obtained, diffraction intensities were very poor (even at  $-110^\circ\text{C}$ ) and X-ray damage to the crystals was severe.

(15) Wade, K.; Banister, A. J. In *Comprehensive Inorganic Chemistry*; Bailar, J. C., Emelus, H. J., Nyholm, R., Trotman-Dickenson, A. F., Eds.; Pergamon: Oxford, 1973; Vol. 1, pp 1127–37.



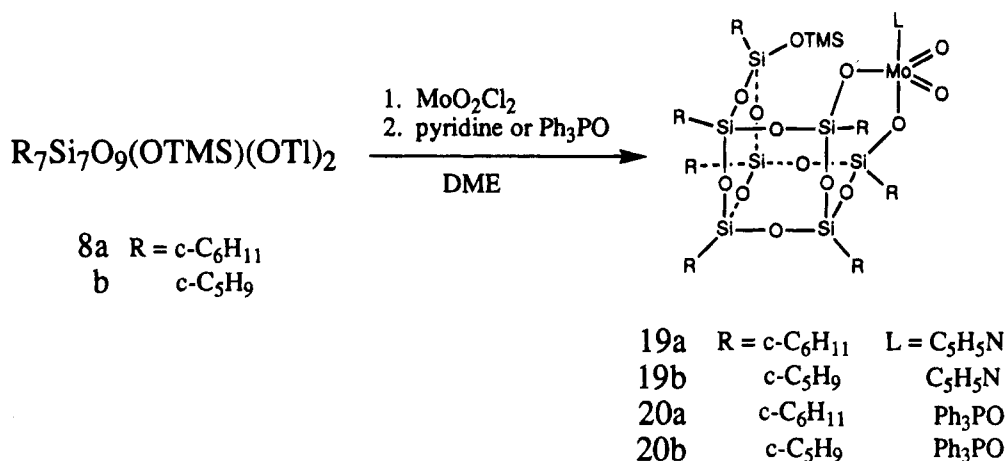
NMR spectroscopy and a crude product of very high purity can be obtained simply by removing the volatiles in vacuo, extracting the residue with benzene or hexane, and evaporating the solvent.

In contrast to Me<sub>4</sub>Sb-stabilized silsesquioxides **4** and **5**, which are prone to intramolecular condensation to **16** when reacted with reagents capable of producing good leaving groups on silicon,<sup>2d</sup> Tl-stabilized silsesquioxides react cleanly to afford high yields of metallasilsesquioxanes. For example, **7a** reacts with POCl<sub>3</sub> to afford a quantitative NMR yield of **15** (Scheme 2), while **4** produces a complex mixture of cyclocondensation products containing trivial amounts of **15**. Evidently, intramolecular attack at silicon is not very favorable for Tl-stabilized silsesquioxides.

**Synthesis and Characterization of Molybdenum-Containing Silsesquioxides.** The observation that **7a** reacts cleanly with POCl<sub>3</sub> to afford **15** prompted us to investigate the reaction of **8a** with MoO<sub>2</sub>Cl<sub>2</sub>, a reagent known to affect the cyclocondensation of **2a** and **5**.<sup>2d</sup> The reaction MoO<sub>2</sub>Cl<sub>2</sub> with **8a** in the presence of DME occurs rapidly upon mixing to precipitate TlCl and affords a quantitative NMR yield of a new Mo-containing silsesquioxane, which was assigned as **17a** on the basis of its <sup>95</sup>Mo NMR spectrum ( $\delta -70.6$ ,  $w_{1/2} = 220$  Hz) and the similarity between its <sup>13</sup>C NMR spectrum and the spectrum observed for **18** (Scheme 3).

Molybdate **17a** is extremely soluble in most organic solvents with which it does not react, and it is very sensitive to traces of water, which appear to catalyze

## Scheme 4



its cyclocondensation to the much less soluble **16b**. It can be obtained as a spectroscopically (<sup>1</sup>H and <sup>13</sup>C NMR) and analytically pure, amorphous white powder by extracting the crude reaction mixture with DME and evaporating the volatiles or by allowing DME to diffuse slowly into a pentane solution of **17a** at -35 °C.

The analogous reaction of **8b** with MoO<sub>2</sub>Cl<sub>2</sub> appears to follow a different course, and the <sup>13</sup>C NMR spectrum of the crude product is very complex. It is somewhat surprising that such a minor structural change could have such a dramatic effect, but similar results are occasionally observed when **1b** is substituted for **1a**.<sup>16</sup> In most instances, any apparent reactivity difference between cyclohexyl- and cyclopentyl-substituted silsesquioxanes can be traced to a large difference in product solubility, particularly if one derivative is so poorly soluble that its precipitation is the driving force for the reaction.<sup>15a</sup> However, the fact that no metallasilsesquioxanes precipitate from reactions of MoO<sub>2</sub>Cl<sub>2</sub> with **8a** and **8b** rules out this explanation and suggests that some other yet-to-be-determined factor is responsible for this difference in reactivity.

Molybdate **17a** reacts with strong Lewis bases to afford stable five-coordinate adducts. For example, the reactions of **17a** with pyridine and Ph<sub>3</sub>PO occur immediately upon mixing to afford quantitative NMR yields of **19a** and **20a**, respectively. Lewis adducts **19a** and **20a**, as well as stoichiometrically similar adducts which are formally derived from **17b**, can be prepared in "one pot" by reacting **8a** and **8b** with MoO<sub>2</sub>Cl<sub>2</sub> in the presence of pyridine or Ph<sub>3</sub>PO (Scheme 4). In all cases, the Lewis adducts adopt distorted trigonal bipyramidal structures with both oxo ligands located in the equatorial plane.

The pentane solvate of **19b** crystallizes as well-formed colorless crystals in the space group *P*( $\bar{1}$ ) with two molecules of **19b** and one molecule of pentane in the asymmetric unit. There are subtle structural differences due to differing cyclopentyl group conformations, but metrical data for both molecules are quite similar,

(16) A good example is the reaction of R<sub>7</sub>Si<sub>7</sub>O<sub>9</sub>(OH)<sub>3</sub> with Me<sub>3</sub>Al, (i-PrO)<sub>3</sub>Al or AlCl<sub>3</sub>/Et<sub>3</sub>N (see ref 4a). In the case of **1a**, these reactions provide virtually quantitative yields of [(*c*-C<sub>6</sub>H<sub>11</sub>)<sub>7</sub>Si<sub>7</sub>O<sub>12</sub>Al]<sub>2</sub>, which is poorly soluble and precipitates from the reaction mixture. No metallasilsesquioxanes precipitate from analogous reactions of **1b**, and all attempts to prepare [(*c*-C<sub>5</sub>H<sub>9</sub>)<sub>7</sub>Si<sub>7</sub>O<sub>12</sub>Al]<sub>2</sub> have been unsuccessful: Feher, F. J.; Budzichowski, T. A.; Weller, K. J.; Rahimian, K. Unpublished work.

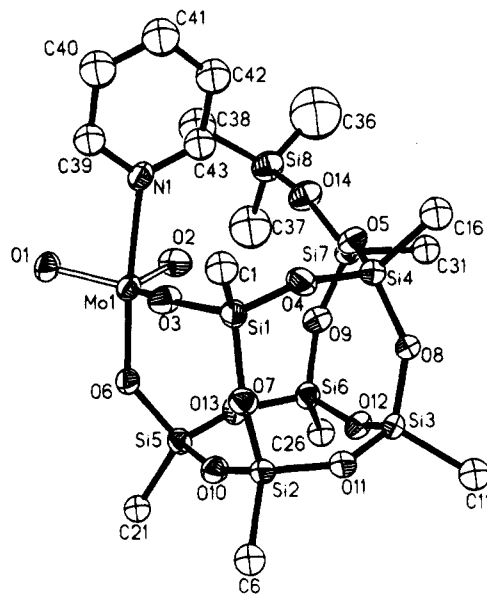


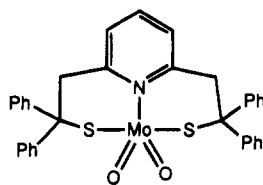
**Figure 1.** ORTEP drawing of **19b** with thermal ellipsoids plotted at the 50% probability level. For clarity, only one of the crystallographically independent molecules is shown, only the ipso carbon atoms (SiCH) of the cyclopentyl groups are shown, and the pentane of solvation is omitted. Selected interatomic distances (Å) and interbond angles (deg) are as follows: Mo1-N1, 2.283(9); Mo1-O1, 1.694(7); Mo1-O2, 1.694(5); Mo1-O3, 1.905(6); Mo1-O6, 1.903(7); Si1-O3, 1.621(7); Si5-O6, 1.627(7); other Si-O, 1.602-1.630; N1-Mo1-O1, 85.0(3); N1-Mo1-O2, 83.6(3); N1-Mo1-O3, 78.4(3); N1-Mo1-O6, 171.1(3); O1-Mo1-O2, 111.2(3); O1-Mo1-O3, 120.2(3); O1-Mo1-O6, 101.5(3); O2-Mo1-O3, 123.1(3); O2-Mo1-O6, 99.4(3); O3-Mo1-O6, 93.0(3); Mo1-O3-Si1, 150.2(4); Mo1-O6-Si5, 139.2(4); Si-O-Si, 141.3-159.1.

especially within the coordination sphere of Mo. The structure of **19b** is illustrated in Figure 1.

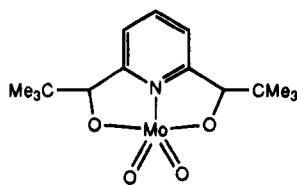
Dioxomolybdenum(VI) complexes generally adopt six-coordinate structures with mutually cis oxo ligands.<sup>17</sup> The first crystallographically characterized example of a five-coordinate dioxomolybdenum(VI) complex (**21**) was reported in 1984,<sup>18</sup> and the first five-coordinate dioxomolybdenum(VI) bis(alkoxide) (**22**) appeared shortly afterward.<sup>19</sup> The only other structurally characterized,

(17) Nugent, W. A.; Mayer, J. M. *Metal-Ligand Multiple Bonds*; Wiley-Interscience: New York, 1988, and references cited therein.

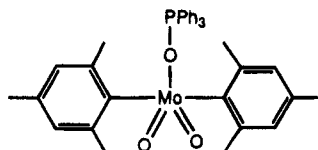
(18) Berg, J. M.; Holm, R. H. *J. Am. Chem. Soc.* **1984**, *106*, 3035-6.



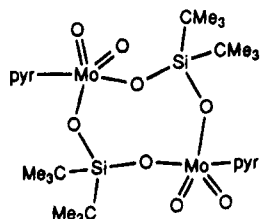
21



22



23



24

monomeric, five-coordinate dioxomolybdenum(VI) complex appears to be  $(2,4,6\text{-Me}_3\text{C}_6\text{H}_2)_2\text{MoO}_2(\text{CH}_2\text{PPh}_3)$  (**23**),<sup>20</sup> although an interesting bimetallic cluster with two five-coordinate dioxomolybdenum(VI) centers (i.e., **24**) is also known.<sup>21</sup>

In each of these cases the molecule adopts a distorted trigonal bipyramidal structure with oxo ligands situated in the equatorial plane. For **21** and **22**, coordination of a tridentate ligand forces the N-donor ligand to occupy a site within the equatorial plane; but in the case of **19b**, the pyridine ligand must occupy an axial site because chelation of the silsesquioxane framework requires mutually cis coordination sites. Axial coordination of pyridine is also observed in **24**.

At low temperature ( $\text{C}_7\text{D}_8$ ,  $-60\text{ }^\circ\text{C}$ ), the  $^{13}\text{C}$  NMR spectra of **19** and **20** are consistent with  $C_1$ -symmetric structures. In the case of **19b**, for example, there are seven methine (SiCH) resonances with equal intensity ( $\delta$  24.55, 23.50, 23.36, 23.09, 22.94, 22.67, 22.34). When the solution is warmed to  $25\text{ }^\circ\text{C}$ , two pairs of methine resonances coalesce to produce a pattern of five resonances with relative integrated intensities of 1:2:2:1:1 ( $\delta$  24.95, 23.85, 23.68, 23.00, 22.85). Any rapid process capable of transiently generating a  $C_s$ -symmetric silsesquioxane framework can produce the observed coalescence phenomena. Pseudorotation and reversible dissociation of pyridine are particularly attractive mechanisms because they quickly produce  $C_s$ -symmetric intermediates. However, small amounts of added pyridine or  $\text{Ph}_3\text{PO}$  (or any other Lewis base) greatly accelerate the dynamic process, and only one time-averaged set of resonances is observed for both the free and coordinated ligands. These observations strongly implicate the availability of an associative mechanism with six-coordinate, bis-ligand adducts.

### Conclusion

The reactions of incompletely-condensed silsesquioxanes with thallium(I) ethoxide afford high yields of the

corresponding Tl-substituted silsesquioxanes. These stable, hydrocarbon soluble compounds react with a variety of transition-metal and main-group halide complexes to afford high yields of metallasilsesquioxanes. Unlike  $\text{Me}_4\text{Sb}$ -substituted silsesquioxanes, which are prone to cycloelimination and/or the formation of anionic "ate" complexes when reacted with highly electrophilic metal halides,<sup>2d</sup> Tl-substituted silsesquioxanes appear to be generally useful for the synthesis of metallasilsesquioxanes. Tl-substituted silsesquioxanes are versatile anionic equivalents of incompletely-condensed silsesquioxanes.

### Experimental Section

**DANGER:** *Thallium-containing compounds are poisonous. The authors strongly recommend that any work with thallium-containing compounds be performed only by experienced technicians educated in the use, disposal, and hazards of thallium-containing compounds.*

General experimental procedures for the synthesis of **1–3**, as well as general protocol for the synthesis and characterization of silsesquioxanes and metallasilsesquioxanes, are described in refs 2a–d.  $\text{CDCl}_3$ , pyridine, and triethylamine were vacuum distilled ( $25\text{ }^\circ\text{C}$ , 0.1 Torr) from  $\text{CaH}_2$ .  $\text{C}_6\text{D}_6$ , toluene- $d_8$ , THF- $d_8$  and dimethoxyethane (DME) were vacuum distilled ( $25\text{ }^\circ\text{C}$ , 0.1 Torr) from sodium benzophenone ketyl. TIOEt (Aldrich) and  $\text{MoO}_2\text{Cl}_2$  (Alpha/Johnson-Matthey) were used without further purification.

**Synthesis of [(c-C<sub>6</sub>H<sub>11</sub>)<sub>7</sub>(Si<sub>2</sub>O<sub>12</sub>)Tl<sub>3</sub>] (**7a**):** Tl(OEt) (771 mg, 3.09 mmol) was added to a suspension of **1a** (1.00 g, 1.03 mmol) in toluene ( $\sim 25\text{ mL}$ ). All solids dissolved within 20 min. After the mixture had been stirred for 12 h, the solvent was removed in vacuo ( $25\text{--}45\text{ }^\circ\text{C}$ , 0.1 Torr) to afford a white microcrystalline solid, which was washed with hexanes ( $3 \times 15\text{ mL}$ ) and dried in vacuo ( $45\text{ }^\circ\text{C}$ , 0.1 Torr, 1 h) to afford 1.35 g (83%) of spectroscopically pure ( $^1\text{H}$ ,  $^{13}\text{C}$ ,  $^{29}\text{Si}$ ) **7a**. Analytically pure material can be obtained by recrystallization from toluene/hexanes ( $25$  to  $-34\text{ }^\circ\text{C}$ ) or by allowing acetonitrile to diffuse into a benzene solution of **7a**. Data for **7a**:  $^1\text{H}$  NMR (500.1 MHz,  $\text{C}_6\text{H}_6$ ,  $25\text{ }^\circ\text{C}$ ):  $\delta$  2.3–1.15 (br m's, 70H), 1.08 (m, 4H), 0.96 (m, 3H).  $^{13}\text{C}\{^1\text{H}\}$  NMR (125.03 MHz,  $\text{C}_6\text{H}_6$ ,  $25\text{ }^\circ\text{C}$ ):  $\delta$  28.66, 28.47, 28.17, 27.85, 27.71, 27.45, 27.42, 27.27 ( $\text{CH}_2$ );  $\delta$  27.03, 25.25, 23.90 (3:3:1 for CH).  $^{29}\text{Si}\{^1\text{H}\}$  NMR (99.35 MHz,  $\text{C}_6\text{H}_6$ ,  $25\text{ }^\circ\text{C}$ ):  $\delta$  -60.49, -66.31, -69.18 (3:1:3). MS (70 eV,  $200\text{ }^\circ\text{C}$ ; relative intensity):  $m/e$  1500 ( $\text{M}^+ - \text{C}_6\text{H}_{11}$ ; 40), 872 ( $\text{M}^+ - 3\text{TL} - \text{O} - \text{C}_6\text{H}_{11}$ ; 100). Anal. Calcd for  $\text{C}_{42}\text{H}_{77}\text{O}_{12}\text{Si}_7\text{Tl}_3$  (found): C, 31.85 (32.04); H, 4.90 (4.73). Mp:  $325\text{--}30\text{ }^\circ\text{C}$  (decomp).

**Synthesis of [(c-C<sub>6</sub>H<sub>11</sub>)<sub>7</sub>(Si<sub>2</sub>O<sub>11</sub>)(OTMS)Tl<sub>2</sub>] (**8a**):** Tl(OEt) (460 mg, 1.84 mmol) was added to a solution of **2a** (965 mg, 0.923 mmol) in toluene ( $\sim 25\text{ mL}$ ). After the mixture had been stirred for 3.5 h, the volatiles were evaporated in vacuo ( $25\text{ }^\circ\text{C}$ , 0.1 Torr, 3 h) to afford a white solid, which was washed with hexanes ( $3 \times 8\text{ mL}$ ) and dried ( $25\text{ }^\circ\text{C}$ , 0.1 Torr, 3 h) to afford 300 mg of **8a** as a white microcrystalline solid; a second crop (880 mg) was obtained by cooling the filtrate to  $-34\text{ }^\circ\text{C}$  for 2 days. The total yield of analytically pure material was 1.18 g (88%). Well-formed crystals may be obtained by recrystallization from toluene/hexanes ( $25$  to  $-34\text{ }^\circ\text{C}$ ). Data for **8a**:  $^1\text{H}$  NMR (500.1 MHz,  $\text{C}_6\text{H}_6$ ,  $25\text{ }^\circ\text{C}$ ):  $\delta$  2.3–0.8 (br m's, 77H), 0.358 (s,  $-\text{Si}(\text{CH}_3)_3$ , 9H).  $^{13}\text{C}\{^1\text{H}\}$  NMR (125.03 MHz,  $\text{C}_6\text{H}_6$ ,  $25\text{ }^\circ\text{C}$ ):  $\delta$  28.91, 28.77, 28.70, 28.51, 28.45, 28.26, 28.20, 28.12, 28.06, 27.94, 27.84, 27.80, 27.70, 27.65, 27.56, 27.48, 27.36 ( $\text{CH}_2$ );  $\delta$  27.26, 26.09, 25.46, 24.61, 23.94 (2:1:2:1:1 for CH);  $\delta$  2.74 ( $-\text{Si}(\text{CH}_3)_3$ ).  $^{29}\text{Si}\{^1\text{H}\}$  NMR (99.35 MHz,  $\text{C}_6\text{H}_6$ ,  $25\text{ }^\circ\text{C}$ ):  $\delta$  -60.70, -66.62, -66.69, -68.13, -68.90 (2:1:1:1:2 for  $\text{RSiO}_{3/2}$ );  $\delta$  8.53 ( $-\text{Si}(\text{CH}_3)_3$ ). MS (70 eV,  $200\text{ }^\circ\text{C}$ ; relative intensity):  $m/e$  943 ( $\text{M}^+ - \text{Tl}_2\text{O} - \text{C}_6\text{H}_{11}$ ; 100). Anal. Calcd for  $\text{C}_{45}\text{H}_{86}\text{O}_{12}\text{Si}_8\text{Tl}_2$  (found): C, 37.21 (37.65); H, 5.97 (5.98). Mp:  $125\text{--}130\text{ }^\circ\text{C}$  (decomp).

(19) Hawkins, J. M.; Dewan, J. C.; Sharpless, K. B. *Inorg. Chem.* **1986**, *25*, 1501–3.

(20) Lai, R.; Le Bot, S.; Baldy, A.; Pierrot, M.; Arzoumanian, H. J. *Chem. Soc., Chem. Commun.* **1986**, 1208.

(21) Gosink, H.-J.; Roesky, H. W.; Noltemeyer, M.; Schmidt, H.-G.; Freire-Erdbrugger, C.; Sheldrick, G. M. *Chem. Ber.* **1993**, *126*, 279–83.

**Synthesis of [(*c*-C<sub>5</sub>H<sub>5</sub>)<sub>7</sub>(Si<sub>7</sub>O<sub>11</sub>)(OTMS)Ti<sub>2</sub>] (8b):** Ti(OEt)<sub>2</sub> (2.26 g, 9.06 mmol) was added to a solution of **2b** (4.00 g, 4.22 mmol) in benzene (~125 mL). After the mixture had been stirred for 12 h, the volatiles were removed in vacuo (25 °C, 0.1 Torr, 3 h) to afford **8b** as a white solid. Well-formed crystals can be obtained by allowing CH<sub>3</sub>CN to diffuse into a benzene solution of **8b**. Yield: 4.00 g (70%). Data for **8b**: <sup>1</sup>H NMR (500.1 MHz, C<sub>6</sub>H<sub>6</sub>, 25 °C): δ 2.1–1.1 (br m's, 63H), 0.282 (s, 9H). <sup>13</sup>C{<sup>1</sup>H} NMR (125.03 MHz, C<sub>6</sub>H<sub>6</sub>, 25 °C): δ 29.23, 28.97, 28.46, 28.40, 28.31, 28.02, 27.88, 27.80, 27.54, 27.51, 27.37 (CH<sub>2</sub>); δ 26.20, 25.35, 24.23, 23.83, 23.21 (2:1:2:1:1 for CH); δ 2.62 (–Si(CH<sub>3</sub>)<sub>3</sub>). <sup>29</sup>Si{<sup>1</sup>H} NMR (99.35 MHz, C<sub>6</sub>H<sub>6</sub>, 25 °C): δ –59.06, –64.48, –64.99, –65.82, –66.52 (2:1:1:1:2 for RSiO<sub>3/2</sub>); δ 8.55 (–Si(CH<sub>3</sub>)<sub>3</sub>). Anal. Calcd for C<sub>38</sub>H<sub>72</sub>O<sub>12</sub>Si<sub>8</sub>Ti<sub>2</sub> (found): C, 33.70 (33.46); H, 5.36 (5.32). Mp: 197–203 °C (decomp).

**Synthesis of [(*c*-C<sub>6</sub>H<sub>11</sub>)<sub>7</sub>(Si<sub>7</sub>O<sub>10</sub>)(OTMS)<sub>2</sub>Ti] (9a):** Ti(OEt)<sub>2</sub> (33.5 mg, 0.134 mmol) was added to a solution of **3a** (150 mg, 0.134 mmol) in toluene/hexanes (1:1, ~4 mL) and cooled to –34 °C for 2 days. The crystalline solid which formed was collected by vacuum filtration, washed with hexanes (~2 mL), and dried in vacuo (45 °C, 0.01 Torr) overnight. Yield: 155 mg, 85%. Data for **9a**: <sup>1</sup>H NMR (500.1 MHz, C<sub>6</sub>H<sub>6</sub>, 65 °C): δ 2.2–0.8 (br m's, 77H), 0.455 (s, –Si(CH<sub>3</sub>)<sub>3</sub>, 18H). <sup>13</sup>C{<sup>1</sup>H} NMR (125.03 MHz, C<sub>6</sub>H<sub>6</sub>, 65 °C): δ 28.83, 28.68, 28.39, 28.31, 28.19, 28.13, 27.89, 27.80, 27.77, 27.73, 27.68, 27.43, 27.40, 27.36, 27.28 (CH<sub>2</sub>); δ 26.08, 25.88, 25.72, 23.95 (2:2:1:1 for CH); δ 3.02 (–Si(CH<sub>3</sub>)<sub>3</sub>). MS (70 eV, 200 °C; relative intensity): *m/e* 944 (M<sup>+</sup> –TiOTMS, –C<sub>6</sub>H<sub>11</sub>; 80), 466, and 451 (Ti decomposition fragments, 100%). Anal. Calcd for C<sub>48</sub>H<sub>95</sub>O<sub>12</sub>Si<sub>8</sub>Ti (found): C, 43.62 (43.79); H, 7.25 (7.11). Mp: 175–80 °C (decomp).

**Reactions of 7a with SbCl<sub>3</sub>, MeSnCl<sub>3</sub>, and (C<sub>5</sub>H<sub>5</sub>)TiCl<sub>3</sub>.**  
**Syntheses of 12–14:** The reactions of **7a** with SbCl<sub>3</sub>, MeSnCl<sub>3</sub>, and (C<sub>5</sub>H<sub>5</sub>)TiCl<sub>3</sub> were performed by adding the trichloride (1 equiv) to a solution of **7a** (~65 mg) in benzene (0.40 mL) in an NMR tube and stirring on a Vortex mixer for 1 h at 25 °C. Precipitation of TiCl<sub>4</sub> was noted immediately upon mixing. After the samples were centrifuged to settle TiCl<sub>4</sub> formed in the reaction, <sup>1</sup>H and <sup>13</sup>C{<sup>1</sup>H} NMR spectra of the reaction mixtures were identical in all respects to samples of **12–14** prepared by the Et<sub>3</sub>N-catalyzed reactions of **1a** with SbCl<sub>3</sub>, MeSnCl<sub>3</sub>, and (C<sub>5</sub>H<sub>5</sub>)TiCl<sub>3</sub>, respectively.<sup>2d</sup>

**[(*c*-C<sub>6</sub>H<sub>11</sub>)<sub>7</sub>(Si<sub>7</sub>O<sub>11</sub>)(OTMS)]Mo(=O)<sub>2</sub> (17a):** MoO<sub>2</sub>Cl<sub>2</sub> (213 mg, 1.033 mmol) was added to a solution of **8a** (1.500 g, 1.033 mmol) and 1,2-dimethoxyethane (~1 mL) in benzene (~50 mL). The solution was stirred for 1.5 h, filtered through Celite to remove TiCl<sub>4</sub>, and evaporated (25 °C, 0.1 Torr) to afford a white solid. Analytically pure material can be obtained by washing the crude product with DME and drying in vacuo (25 °C, 0.1 Torr) or by allowing DME to diffuse into a pentane solution of **17a** at –35 °C. Yield: 968 mg (80%). Analytically pure powder can also be obtained by allowing DME to diffuse into a pentane solution of **17a** at –35 °C. Data for **17a**: <sup>1</sup>H NMR (500.1 MHz, C<sub>6</sub>H<sub>6</sub>, 25 °C): δ 2.15–0.90 (br m's, 77H); 0.415 (s, –Si(CH<sub>3</sub>)<sub>3</sub>, 9H). <sup>13</sup>C{<sup>1</sup>H} NMR (125.03 MHz, C<sub>6</sub>H<sub>6</sub>, 25 °C): δ 27.99, 27.86, 27.83, 27.63, 27.59, 27.48, 27.45, 27.34, 27.17, 27.06, 26.92, 26.79 (CH<sub>2</sub>); 25.37, 24.66, 24.13, 23.55 (1:2:2:2 for CH); δ 2.01 (–Si(CH<sub>3</sub>)<sub>3</sub>). <sup>95</sup>Mo NMR (32.58 MHz, C<sub>6</sub>H<sub>6</sub>, 25 °C): δ –70.64 (w<sub>1/2</sub> = 220 Hz). Anal. Calcd for C<sub>45</sub>H<sub>86</sub>MoO<sub>14</sub>Si<sub>8</sub> (found): C, 46.13 (46.22); H, 7.40 (7.51). Mp: 90 °C (decomp).

**[(*c*-C<sub>6</sub>H<sub>11</sub>)<sub>7</sub>(Si<sub>7</sub>O<sub>11</sub>)(OTMS)]Mo(=O)<sub>2</sub>(C<sub>5</sub>H<sub>5</sub>N) (19a):** MoO<sub>2</sub>Cl<sub>2</sub> (75 mg, 0.377 mmol) was added to a solution of **8a** (548 mg, 0.377 mmol) and pyridine (0.031 mL, 0.377 mmol) in benzene (~25 mL). The solution was stirred for 1.5 h and filtered through Celite to remove TiCl<sub>4</sub>, and then the volatiles were removed in vacuo (25 °C, 0.1 Torr) to afford **19a** as an amorphous white solid. All attempts to effect recrystallization were unsuccessful because **19a** is extremely soluble in common organic solvents, but the product obtained in this fashion is pure by <sup>1</sup>H and <sup>13</sup>C NMR spectroscopy. Data for **19a**: <sup>1</sup>H NMR

(500.1 MHz, C<sub>6</sub>H<sub>6</sub>, 25 °C): δ 8.428 (d, J<sub>H–H</sub> = 5.1 Hz, *o*-C<sub>5</sub>H<sub>5</sub>N), 6.697 (t, J<sub>H–H</sub> = 6.2 Hz, *p*-C<sub>5</sub>H<sub>5</sub>N), 6.390 (t, J<sub>H–H</sub> = 6.5 Hz, *m*-C<sub>5</sub>H<sub>5</sub>N); 2.20–1.00 (br m's, 77H); 0.509 (s, –Si(CH<sub>3</sub>)<sub>3</sub>, 9H). <sup>13</sup>C{<sup>1</sup>H} NMR (125.03 MHz, C<sub>6</sub>H<sub>6</sub>, 25 °C): δ 149.08 (*o*-C<sub>5</sub>H<sub>5</sub>N), 138.54 (*m*-C<sub>5</sub>H<sub>5</sub>N), 124.73 (*p*-C<sub>5</sub>H<sub>5</sub>N); 28.09, 28.05, 28.00, 27.91, 27.79, 27.63, 27.45, 27.40, 27.36, 27.29, 27.25, 27.19 (CH<sub>2</sub>); 25.58, 25.03, 24.87, 23.86, 23.83 (1:2:2:1:1, CH); 2.10 (–Si(CH<sub>3</sub>)<sub>3</sub>). <sup>95</sup>Mo NMR (32.58 MHz, C<sub>6</sub>H<sub>6</sub>, 25 °C): δ –4.03 (w<sub>1/2</sub> = 790 Hz).

**[(*c*-C<sub>5</sub>H<sub>5</sub>)<sub>7</sub>(Si<sub>7</sub>O<sub>11</sub>)(OTMS)]Mo(=O)<sub>2</sub>(C<sub>5</sub>H<sub>5</sub>N) (19b):** MoO<sub>2</sub>Cl<sub>2</sub> (100 mg, 0.502 mmol) was added to a solution of **8b** (680 mg, 0.502 mmol) and pyridine (0.041 mL, 0.502 mmol) in benzene (~25 mL). The solution was stirred for 1.5 h, filtered through Celite to remove TiCl<sub>4</sub>, and evaporated to dryness (25 °C, 0.1 Torr) to afford **19b** as an amorphous white solid. Analytically pure product (434 mg, 75%) was obtained by cooling a pentane solution of **19b** to –35 °C. Data for **19b**: <sup>1</sup>H NMR (500.1 MHz, C<sub>6</sub>H<sub>6</sub>, 25 °C): δ 8.455 (d, J<sub>H–H</sub> = 4.4 Hz, *o*-C<sub>5</sub>H<sub>5</sub>N); 6.762 (t, J<sub>H–H</sub> = 7.3 Hz, *p*-C<sub>5</sub>H<sub>5</sub>N); 6.467 (t, J<sub>H–H</sub> = 6.6 Hz, *m*-C<sub>5</sub>H<sub>5</sub>N); 2.05–1.15 (br m's, C<sub>5</sub>H<sub>5</sub>, 63H); 0.470 (s, Si(CH<sub>3</sub>)<sub>3</sub>, 9H). <sup>13</sup>C{<sup>1</sup>H} NMR (125.03 MHz, C<sub>6</sub>H<sub>6</sub>, 25 °C): δ 149.10 (*o*-C<sub>5</sub>H<sub>5</sub>N), 138.40 (*m*-C<sub>5</sub>H<sub>5</sub>N), 124.59 (*p*-C<sub>5</sub>H<sub>5</sub>N); 28.30, 28.17, 28.13, 28.08, 27.94, 27.54, 27.51, 27.45, 27.39 (CH<sub>2</sub>); 24.94, 23.81, 23.64, 22.98, 22.82 (1:2:2:1:1, CH); 2.097 (–Si(CH<sub>3</sub>)<sub>3</sub>). <sup>95</sup>Mo NMR (32.58 MHz, C<sub>6</sub>H<sub>6</sub>, 25 °C): δ –3.48 (w<sub>1/2</sub> = 1500 Hz). Anal. Calcd for C<sub>49</sub>H<sub>77</sub>MoNO<sub>14</sub>Si<sub>8</sub>·0.5 pentane (found): C, 45.97 (45.30); H, 7.04 (6.83). Mp: 180 °C (decomp).

**[(*c*-C<sub>6</sub>H<sub>11</sub>)<sub>7</sub>(Si<sub>7</sub>O<sub>11</sub>)(OTMS)]Mo(=O)<sub>2</sub>(OPPh<sub>3</sub>) (20a):** MoO<sub>2</sub>Cl<sub>2</sub> (86 mg, 0.432 mmol) was added to a solution of **8a** (627 mg, 0.432 mmol) and (C<sub>6</sub>H<sub>5</sub>)<sub>3</sub>PO (120 mg, 0.432 mmol) in benzene (~25 mL). The solution was stirred for 1.5 h, filtered through Celite to remove TiCl<sub>4</sub>, and evaporated (25 °C, 0.1 Torr) to afford **20a** as an amorphous white solid. Analytically pure product (439 mg, 70%) was obtained by cooling a pentane solution of **20a** to –35 °C. Data for **20a**: <sup>1</sup>H NMR (500.1 MHz, C<sub>6</sub>H<sub>6</sub>, 25 °C): δ 7.698 (ddm, J<sub>H–P</sub> = 12 Hz, J<sub>H<sub>o</sub>–H<sub>m</sub></sub> = 8.5 Hz, *o*-C<sub>6</sub>H<sub>5</sub>, 6H), 7.040 (m, *m*- and *p*-C<sub>6</sub>H<sub>5</sub>, 9H), 2.20–1.00 (br m's, C<sub>6</sub>H<sub>11</sub>, 77H), 0.432 (s, –Si(CH<sub>3</sub>)<sub>3</sub>, 9H). <sup>13</sup>C{<sup>1</sup>H} NMR (125.03 MHz, C<sub>6</sub>H<sub>6</sub>, 25 °C): δ 132.61 (s, *p*-C<sub>6</sub>H<sub>5</sub>), 132.39 (d, J<sub>C–P</sub> = 9.7 Hz, *o*-C<sub>6</sub>H<sub>5</sub>), 130.07 (J<sub>C–P</sub> = 106.6 Hz, *ipso*-C<sub>6</sub>H<sub>5</sub>), 128.79 (d, J<sub>C–P</sub> = 13.6 Hz, *m*-C<sub>6</sub>H<sub>5</sub>); 28.13, 28.09, 28.06, 28.03, 28.00, 27.88, 27.83, 27.71, 27.65, 27.51, 27.48, 27.42, 27.37, 27.34, 27.25, 27.22 (CH<sub>2</sub>); 25.55, 25.11, 24.75, 23.92, 23.89 (1:2:2:1:1, CH); 2.11 (–Si(CH<sub>3</sub>)<sub>3</sub>). <sup>31</sup>P{<sup>1</sup>H} NMR (202.2 MHz, C<sub>6</sub>H<sub>6</sub>): δ 38.11. Anal. Calcd for C<sub>63</sub>H<sub>101</sub>MoO<sub>15</sub>PSi<sub>8</sub> (found): C, 52.18 (52.03); H, 7.02 (7.45). Mp: 152 °C (decomp).

**[(*c*-C<sub>5</sub>H<sub>5</sub>)<sub>7</sub>(Si<sub>7</sub>O<sub>11</sub>)(OTMS)]Mo(=O)<sub>2</sub>(OPPh<sub>3</sub>) (20b):** MoO<sub>2</sub>Cl<sub>2</sub> (100 mg, 0.502 mmol) was added to a solution of **8a** (680 mg, 0.502 mmol) and (C<sub>6</sub>H<sub>5</sub>)<sub>3</sub>PO (140 mg, 0.502 mmol) in benzene (~25 mL). The solution was stirred for 1.5 h, filtered through Celite to remove TiCl<sub>4</sub>, and evaporated (25 °C, 0.1 Torr) to afford **20b** as an amorphous white solid. Analytically pure product (508 mg, 75%) was obtained by cooling a pentane solution of **20b** to –35 °C. Data for **20b**: <sup>1</sup>H NMR (500.1 MHz, C<sub>6</sub>H<sub>6</sub>, 25 °C): δ 7.695 (ddm, J<sub>H–P</sub> = 12 Hz, J<sub>H<sub>o</sub>–H<sub>m</sub></sub> = 8.5 Hz, *o*-C<sub>6</sub>H<sub>5</sub>, 6H), 7.033 (m, 9H, *m*- and *p*-C<sub>6</sub>H<sub>5</sub>), 2.10–1.15 (br m's, C<sub>5</sub>H<sub>5</sub>, 63H), 0.410 (s, –Si(CH<sub>3</sub>)<sub>3</sub>, 9H). <sup>13</sup>C{<sup>1</sup>H} NMR (125.03 MHz, C<sub>6</sub>H<sub>6</sub>, 25 °C): δ 132.89 (d, J<sub>C–P</sub> = 9.6 Hz, *o*-C<sub>6</sub>H<sub>5</sub>), 132.59 (s, *p*-C<sub>6</sub>H<sub>5</sub>), 130.26 (d, J<sub>C–P</sub> = 106.6 Hz, *ipso*-C<sub>6</sub>H<sub>5</sub>), 128.76 (d, J<sub>C–P</sub> = 13.6 Hz, *m*-C<sub>6</sub>H<sub>5</sub>); 28.30, 28.22, 28.14, 28.00, 27.96, 27.54, 27.51, 27.40, 27.37, 27.32 (CH<sub>2</sub>), 24.89, 23.87, 23.04, 22.93 (1:4:1:1 for CH), 2.13 (–Si(CH<sub>3</sub>)<sub>3</sub>). <sup>31</sup>P{<sup>1</sup>H} NMR (202.2 MHz, C<sub>6</sub>H<sub>6</sub>): δ 33.36. Anal. Calcd for C<sub>56</sub>H<sub>87</sub>MoO<sub>15</sub>PSi<sub>8</sub> (found): C, 49.75 (49.75); H, 6.49 (6.48). Mp: 178 °C (decomp).

**Variable Temperature Study of 19a,b:** At low temperature (C<sub>7</sub>D<sub>8</sub>, –60 °C), the <sup>13</sup>C NMR spectra of **19a** and **19b** are consistent with C<sub>1</sub>-symmetric structures. At room temperature, the spectra are consistent with time-averaged C<sub>s</sub>-symmetric structures. In the case of **19b** there are seven methine (SiCH) resonances with equal intensity (δ 24.55, 23.50, 23.36, 23.09, 22.94, 22.67, 22.34). When the solution is warmed to 25 °C, two pairs of methine resonances coalesce

to produce a pattern of five resonances with relative integrated intensities of 1:2:2:1:1 ( $\delta$  24.95, 23.85, 23.68, 23.00, 22.85). The same time-averaged spectra can be obtained by adding pyridine (1 equiv) at low temperature.

**Variable Temperature Study of 20a,b:** At low temperature ( $C_7D_8$ ,  $-60$  °C), the  $^{13}C$  NMR spectra of **20a** and **20b** are consistent with  $C_1$ -symmetric structures. At room temperature, the spectra are consistent with time-averaged  $C_s$ -symmetric structures. In the case of **20b** there are seven methine (SiCH) resonances with equal intensity ( $\delta$  24.47, 24.44, 23.62, 23.17, 22.74, 22.65, 22.51). When the solution is warmed to 25 °C, two pairs of methine resonances coalesce to produce a pattern of four resonances with relative integrated intensities of 1:4:1:1 ( $\delta$  24.90, 23.91, 23.07, 22.96).

**X-ray Diffraction Study of 19b.** Crystals suitable for an X-ray diffraction study were obtained by crystallization from pentane. Crystal data for **19b** ( $C_{43}H_{77}NO_{14}Si_8Mo \cdot 0.5(C_5H_{12})$ , fw = 1188.8) are as follows: triclinic  $P\bar{1}$ ,  $a = 14.599(2)$  Å,  $b = 19.875(2)$  Å,  $c = 21.826(3)$  Å;  $\alpha = 96.752(10)^\circ$ ,  $\beta = 97.452(12)^\circ$ ,  $\gamma = 107.282(10)^\circ$ ,  $V = 5914.2(14)$  Å<sup>3</sup>;  $D_{\text{calcd}} = 1.335$  g/cm<sup>3</sup> ( $Z = 4$ ). A total of 16 311 unique reflections with  $4.0^\circ \leq 2\theta \leq 45.0^\circ$  were collected on a Nicolet R3m/V diffractometer at  $-110$  °C with use of graphite-monochromated Mo K $\alpha$  radiation. The

structure was solved by direct methods (SHELXTL PLUS). Full-matrix least-squares refinement of positional and thermal parameters (anisotropic for Si, O, C, Mo, N) led to convergence with a final R factor of 7.7 % for 777 variables refined against 10 895 data with  $|F_o| > 4.0\sigma(|F_o|)$ . All other details regarding the crystal structure are reported in the supporting information.

**Acknowledgment.** These studies were supported by the National Science Foundation (CHE-9011593 and CHE-9307750) and an NSF Presidential Young Investigator Award (CHE-8657262). Acknowledgment is also made to the donors of the Petroleum Research Fund, administered by the American Chemical Society, for partial support of this research.

**Supporting Information Available:** X-ray crystal data for **19b**, including experimental procedures, tables of crystal data, atomic coordinates, thermal parameters, bond lengths, and bond angles, and ORTEP figures (28 pages). Ordering information is given on any current masthead page.

OM950438L



# A Simple and Convenient Preparation of $[(\text{Ph}_3\text{P})_4\text{Rh}_2(\mu\text{-OH})_2]$ and Its Reactions with C–H, O–H, and M–H Acids

Vladimir V. Grushin, Vladimir F. Kuznetsov, Corinne Bensimon, and Howard Alper\*

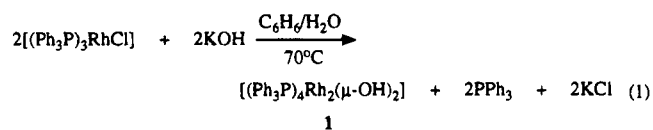
Department of Chemistry, University of Ottawa, 10 Marie Curie, Ottawa, Ontario, Canada K1N 6N5

Received March 21, 1995<sup>⊙</sup>

A simple and efficient procedure was developed for the preparation of  $[(\text{Ph}_3\text{P})_4\text{Rh}_2(\mu\text{-OH})_2]$ , **1**, from Wilkinson's catalyst and aqueous KOH under biphasic conditions (75–85% yield). Complex **1** reacted with cyclopentadiene, methyl malonate, and benzoic acid to give  $[\text{CpRh}(\text{PPh}_3)_2]$ ,  $[(\text{Ph}_3\text{P})_2\text{Rh}(\text{CH}(\text{COOMe})_2)]$ , and  $[(\text{Ph}_3\text{P})_2\text{Rh}(\mu\text{-PhCOO})]$ , respectively. Depending on the amount of formic acid, the reaction between **1** and HCOOH resulted in either decarboxylation and formation of  $[(\text{Ph}_3\text{P})_2\text{Rh}(\text{H})_2(\text{HCOO})]$  or dehydration affording *trans*- $[(\text{Ph}_3\text{P})_2\text{Rh}(\text{CO})(\text{HCOO})]$ , **6** both transformations being chemospecific. Treatment of **1** with  $[\text{CpM}(\text{CO})_3\text{H}]$  (M = Cr, Mo, W) gave heterobinuclear complexes,  $[(\text{Ph}_3\text{P})_2\text{Rh}(\mu\text{-CO})_2\text{M}(\text{CO})\text{Cp}]$ , in excellent yield. The structure of **6** was confirmed by X-ray analysis.

In 1988, Brune and co-workers<sup>1,2</sup> reported the isolation of a binuclear rhodium complex with two bridging hydroxo ligands,  $[(\text{Ph}_3\text{P})_4\text{Rh}_2(\mu\text{-OH})_2]$ , **1**. The complex was isolated in 26% yield from the reaction between  $[(\text{Ph}_3\text{P})_3\text{RhH}]$  and an aromatic imine in aqueous dioxane and characterized by elemental analysis, IR spectroscopy, and an X-ray diffraction of its benzene solvate,  $1 \cdot 2\text{C}_6\text{H}_6$ .<sup>2</sup> In the present paper we describe a simple and efficient preparation of **1** from Wilkinson's catalyst and alkali, its solution NMR characterization, and some applications for inorganic and organometallic synthesis. Interestingly, since the discovery of chlorotris(triphenylphosphine)rhodium in 1966,<sup>3</sup> there have been no reports on the reaction of the complex with alkali leading to **1**, although the reactivity of Wilkinson's catalyst toward various compounds has been studied quite extensively.<sup>4</sup>

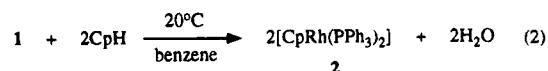
**Preparation of 1.** Treatment of Wilkinson's catalyst in benzene with 40% aqueous KOH results in clean formation of **1**, with 2 equiv of  $\text{PPh}_3$  per **1** being released in the process (eq 1). Reaction 1 is somewhat similar to



the synthesis of  $[(1,5\text{-COD})_2\text{Rh}_2(\mu\text{-OH})_2]$  from  $[(1,5\text{-COD})_2\text{Rh}_2(\mu\text{-Cl})_2]$  and KOH.<sup>5</sup> The alkaline hydrolysis of  $[(\text{Ph}_3\text{P})_3\text{RhCl}]$  and isolation of **1** should be conducted in an oxygen-free atmosphere, as **1** is quite air-sensitive in solution. Although **1** is more stable in the solid state (can be exposed to air for a few minutes without any

significant decomposition), the complex should be stored under nitrogen or argon. To reach completion, reaction 1 requires a few hours at 70 °C; it is convenient to follow the reaction progress by <sup>31</sup>P NMR of the organic phase. At early stages, the <sup>31</sup>P NMR spectra of the benzene layer exhibit a doublet at 57.3 ppm ( $J_{\text{P-Rh}} = 188$  Hz), due to **1**, and an ABX-type pattern of two doublets of doublets at 56.4 ppm ( $J_{\text{Rh-P}} = 175$  Hz;  $J_{\text{P-P}} = 51$  Hz) and 52.6 ppm ( $J_{\text{Rh-P}} = 214$  Hz;  $J_{\text{P-P}} = 51$  Hz), indicative of the intermediate formation of  $[(\text{Ph}_3\text{P})_4\text{Rh}_2(\mu\text{-OH})(\mu\text{-Cl})]$ . Therefore, reaction 1 involves stepwise substitution of chloro ligands for OH. Isolation of  $1 \cdot 2\text{C}_6\text{H}_6$  in 75–85% yield is achieved by concentration of the benzene layer, followed by addition of methanol. The <sup>1</sup>H NMR spectrum of **1** in benzene-*d*<sub>6</sub> consists of aromatic multiplets and a singlet at –2.2 ppm due to the hydroxo ligand. It is conceivable that the compound formulated as  $[(\text{Ph}_3\text{P})_3\text{Rh}(\text{OH})]_2$  was in fact the hydroxo dimer **1**. Even if  $[(\text{Ph}_3\text{P})_3\text{Rh}(\text{OH})]$  exists in the solid state, it should readily lose one phosphine ligand upon dissolution, resulting in the formation of **1**. In fact, <sup>31</sup>P NMR spectra of the benzene layer (reaction 1) containing **1** and  $\text{PPh}_3$  exhibited slightly broadened signals of both **1** (57.3 ppm) and the free ligand (–5 ppm), pointing to exchange processes. The latter likely involves mononuclear  $[(\text{Ph}_3\text{P})_3\text{Rh}(\text{OH})]$ .

**Reactions of 1 with C–H and O–H Acids.** Complex **1** readily reacts with cyclopentadiene in benzene, to give  $[\text{CpRh}(\text{PPh}_3)_2]$  in quantitative yield (eq 2).



Reaction 2 is similar to the recently developed preparation of relevant complexes,  $[\text{CpM}(\text{Ph})(\text{PR}_3)]$  (M = Pd, Pt), from the corresponding hydroxo dimers.<sup>7</sup> Clearly,

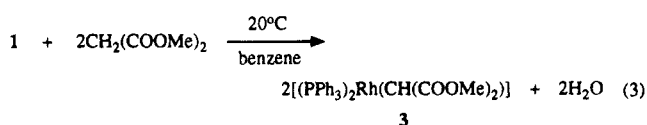
<sup>⊙</sup> Abstract published in *Advance ACS Abstracts*, July 1, 1995.  
 (1) Brune, H.-A.; Unsin, J.; Hemmer, R.; Reichhardt, M. *J. Organomet. Chem.* **1989**, *369*, 335.  
 (2) Brune, H.-A.; Hemmer, R.; Unsin, J.; Holl, K.; Thewalt, U. *Z. Naturforsch., B* **1988**, *43*, 487.  
 (3) Osborn, J. A.; Jardine, F. H.; Young, F. H.; Wilkinson, G. *J. Chem. Soc. A* **1966**, 171.  
 (4) Jardine, F. H. *Prog. Inorg. Chem.* **1981**, *28*, 63.  
 (5) Uson, R.; Oro, L. A.; Cabeza, J. A. *Inorg. Synth.* **1985**, *23*, 126.

(6) Gregorio, G.; Pregaglia, G.; Ugo, R. *Inorg. Chim. Acta* **1969**, *3*, 89.

(7) Grushin, V. V.; Bensimon, C.; Alper, H. *Organometallics* **1993**, *12*, 2737.

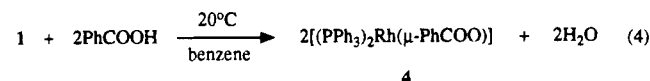
the synthesis of **2** from **1** and CpH possesses a number of obvious advantages over the known methods employing  $[\text{CpRh}(\text{PPh}_3)_2]_2$ <sup>8</sup> or  $[(\text{Ph}_3\text{P})_3\text{RhCl}]_2$ <sup>9</sup> and highly reactive organomagnesium and organosodium compounds. First, reaction 2 does not require dry, prepurified solvents. Bubbling  $\text{N}_2$  through commercially available solvent-grade samples of benzene for 10–15 min makes them sufficiently  $\text{O}_2$ -free for use in reaction 2. Second, the synthesis of **2** from Wilkinson's catalyst via **1** employs no organometallics whatsoever. Finally, isolation of **2** is exceedingly simple and efficient, affording the spectroscopically ( $^1\text{H}$  and  $^{31}\text{P}$  NMR)<sup>8,10</sup> pure **2** in over 90% yield. It is noteworthy that the number of reports on complex **2** are rather limited, despite its synthetic potential<sup>8,11</sup> and particularly interesting red-ox properties.<sup>12</sup>

Condensation of **1** with dimethyl malonate in benzene results in the quantitative formation of a new complex,  $[(\text{Ph}_3\text{P})_2\text{Rh}(\text{CH}(\text{COOMe})_2)]$ , **3** (eq 3), which was isolated



in 70% yield and characterized by elemental analysis and  $^1\text{H}$  and  $^{31}\text{P}$  NMR spectra. Unambiguous structural characterization of **3** failed, because all our attempts to obtain suitable for X-ray analysis crystals of the complex were unsuccessful. The  $^1\text{H}$ ,  $^{13}\text{C}$ , and  $^{31}\text{P}$  NMR spectra of **3** in benzene- $d_6$  (see Experimental Section) reveal pairwise equivalence of the two methyl groups, two carbonyl groups, and two phosphine ligands in **3**. Although three of the four different aromatic carbons in **3** appear as virtual triplets in the  $^{13}\text{C}$  NMR spectrum, this cannot be regarded as firm evidence for a trans-arrangement of the  $\text{PPh}_3$  ligands; in fact, similar patterns were observed in the  $^{13}\text{C}$  NMR spectra of **1** and **2** which, by definition, cannot have trans-phosphines. A *singlet* resonance from the CH carbon (66.9 ppm) indicates that there is no Rh–C bond in the molecule. Therefore, complex **3** likely has a chelating structure similar to that of (acetylacetonato)bis(triphenylphosphine)rhodium,  $[(\text{Ph}_3\text{P})_2\text{Rh}(\text{acac})]$ .<sup>13</sup>

Treatment of **1** with benzoic acid affords  $[(\text{Ph}_3\text{P})_2\text{Rh}(\mu\text{-PhCOO})]$ , **4**, which was quantitatively isolated as an air-sensitive red microcrystalline solid (eq 4). The  $\eta^2$ -



nature of the benzoato ligand in **4** follows from its IR spectra (see Experimental Section). In addition to IR data, the new complex **4** was characterized by elemental

analysis and  $^1\text{H}$  and  $^{31}\text{P}$  NMR spectra. It is known that Rh(I) carboxylates,  $[\text{L}_2\text{Rh}(\mu\text{-RCOO})]_n$ , are monomeric ( $n = 1$ ) when L = tertiary phosphine<sup>14</sup> but dimeric ( $n = 2$ ) if L = CO,  $\text{C}_2\text{H}_4$  or  $\text{L}_2 = \text{diene}$ .<sup>15</sup> The structure of  $[(i\text{-Pr}_3\text{P})_2\text{Rh}(\mu\text{-CH}_3\text{COO})]$  was established by X-ray analysis.<sup>14</sup>

**Transformations of 1 in the Presence of Formic Acid.** The reaction of **1** with benzoic acid, described above, is similar to those of  $[\text{L}_2\text{Pd}_2(\text{R})_2(\mu\text{-OH})_2]$ , where L = tertiary phosphine and R = alkyl or aryl, which give the corresponding organopalladium carboxylates.<sup>16–18</sup> Likewise, treatment of  $[(\text{Ph}_3\text{P})_2\text{Pd}_2(\text{R})_2(\mu\text{-OH})_2]$ , where R = Ph or Me, with formic acid gives rise to the (formato)palladium complexes which have been isolated and fully characterized.<sup>18</sup> Unexpectedly, the addition of HCOOH to **1** did not result in an isolable formato analogue of **4**,  $[(\text{Ph}_3\text{P})_2\text{Rh}(\mu\text{-HCOO})]$ .<sup>19</sup> In fact, the red color that is characteristic of the rhodium benzoate **4** did appear upon treatment of **1** with HCOOH in benzene but instantly vanished (in less than 1 s). Surprisingly, the reaction was very sensitive to the ratio of HCOOH to **1**.

When **1**, in benzene- $d_6$ , was treated with 4 molar equiv of HCOOH (2 mol of formic acid/1 mol of Rh), one major rhodium product (complex **5**) formed instantaneously in greater than 90% selectivity. Monitoring this reaction by  $^{13}\text{C}$  NMR ( $\text{H}^{13}\text{COOH}$  was used) revealed evolution of  $\text{CO}_2$  ( $\delta = 125.3$  ppm)<sup>21</sup> and no formation of CO. Although **5** was not isolated in pure form, it was reliably characterized in solution and formulated as  $[(\text{Ph}_3\text{P})_2\text{Rh}(\text{H})_2(\text{HCOO})]$ , on the basis of the following spectral data. A doublet of triplets at  $-21.0$  ppm ( $J_{\text{Rh-H}} = 23$  Hz;  $J_{\text{P-H}} = 17$  Hz) was observed in the  $^1\text{H}$  NMR spectrum of the reaction mixture, indicating the presence of hydrido ligand(s) and two equivalent phosphines in **5**. The doublet ( $\delta = 41.0$  ppm;  $J_{\text{Rh-P}} = 120$  Hz) observed in the  $^{31}\text{P}\{^1\text{H}\}$  spectrum became a doublet of triplets ( $J_{\text{Rh-P}} = 120$  Hz;  $J_{\text{H-P}} = 17$  Hz) with the same chemical shift, when the spectrum was measured with selective proton decoupling (*o*- $\text{C}_6\text{H}_5$ ). This experiment revealed the presence of two equivalent hydrido ligands in the coordination sphere of **5**. Finally, a singlet at 173 ppm in the  $^{13}\text{C}$  NMR spectrum that was obtained with a sample of **5** prepared from **1** and  $\text{H}^{13}\text{COOH}$  confirmed the presence of a formato ligand at the rhodium center. Thus, the reaction between **1** and 4 equiv of HCOOH proceeds in accordance with eq 5.

(14) Werner, H.; Schäfer, M.; Nürnberg, O.; Wolf, J. *Chem. Ber.* **1994**, *127*, 27.

(15) (a) Lawson, D. N.; Wilkinson, G. *J. Chem. Soc.* **1965**, 1900. (b) Reis, A. H., Jr.; Willi, C.; Siegel, S.; Tani, B. *Inorg. Chem.* **1979**, *18*, 1859. (c) Bianchi, F.; Gallazzi, M. C.; Porri, L.; Diversi, P. *J. Organomet. Chem.* **1980**, *202*, 99. (d) Arthurs, M. A.; Nelson, S. M. *J. Coord. Chem.* **1983**, *13*, 29. (e) Lahoz, F. J.; Martin, A.; Esteruelas, M. A.; Sola, E.; Serrano, J. L.; Oro, L. A. *Organometallics* **1991**, *10*, 1794.

(16) Ruiz, J.; Vicente, C.; Martí, J. M.; Cutillas, N.; García, G.; López, G. *J. Organomet. Chem.* **1993**, *460*, 241. See also: Ruiz, J.; Cutillas, N.; Torregrosa, J.; García, G.; López, G.; Chaloner, P. A.; Hitchcock, P. B.; Harrison, R. M. *J. Chem. Soc., Dalton Trans.* **1994**, 2353, and references cited therein.

(17) Grushin, V. V.; Alper, H. *J. Am. Chem. Soc.* **1995**, *117*, 4305.

(18) Grushin, V. V.; Bensimon, C.; Alper, H. *Organometallics*, in press.

(19) An octadiene complex with bridging formato ligands,  $[(1,5\text{-COD})_2\text{Rh}_2(\mu\text{-HCOO})_2]$ , has been isolated and reliably characterized.<sup>20</sup>

(20) Keim, W.; Becker, J.; Trzeciak, A. *J. Organomet. Chem.* **1989**, *372*, 447.

(21) Günther, H. *NMR Spectroscopy. An Introduction*; John Wiley and Sons: New York, 1980; p 398.

(8) Yamazaki, H.; Hagihara, N. *Bull. Chem. Soc. Jpn.* **1971**, *44*, 2260.

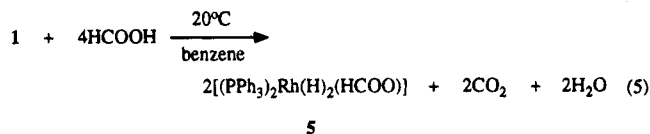
(9) Wakatsuki, Y. Japan Kokai 74 100,065, 1974; *Chem. Abstr.* **1975**, *82*, P 73183g.

(10) Haddleton, D. M.; Perutz, R. N. *J. Chem. Soc., Chem. Commun.* **1985**, 1372.

(11) Wakatsuki, Y.; Yamazaki, H.; Cheng, C. *J. Organomet. Chem.* **1989**, *372*, 437. Tewari, S. K.; Pandey, K. K. *Synth. React. Inorg. Met.-Org. Chem.* **1989**, *19*, 545. Wakatsuki, Y.; Yamazaki, H. *J. Organomet. Chem.* **1974**, *64*, 393.

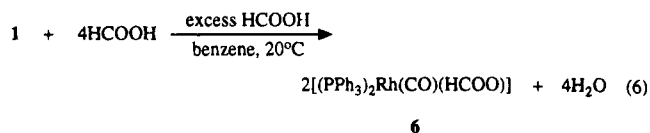
(12) McKinney, R. J. *J. Chem. Soc., Chem. Commun.* **1980**, 603.

(13) Barlex, D. M.; Hacker, M. J.; Kemmitt, R. D. W. *J. Organomet. Chem.* **1972**, *43*, 425. Mukhedkar, A. J.; Mukhedkar, V. A.; Green, M.; Stone, F. G. A. *J. Chem. Soc. A* **1970**, 3166.



When a 10-fold excess of HCOOH was added to a vigorously stirred benzene solution of **1** under the same conditions, no evolution of CO<sub>2</sub> or CO (<sup>13</sup>C-labeled HCOOH) took place. Instead of **5**, another complex, [(Ph<sub>3</sub>P)<sub>2</sub>Rh(CO)(HCOO)], **6**, was formed selectively and isolated in high yield. Complex **6** was previously described by Keim, Becker, and Trzeciak<sup>20</sup> and characterized by <sup>1</sup>H NMR and IR spectra. Here we report <sup>1</sup>H, <sup>13</sup>C, and <sup>31</sup>P NMR data for **6** (see Experimental Section) and its X-ray crystal structure (Figure 1). The structural parameters of **6** (Table 1) are very similar to those of the closely related bicarbonato complex, [(Ph<sub>3</sub>P)<sub>2</sub>Rh(CO)(OCO<sub>2</sub>H)].<sup>22</sup> In the solid state, **6** exhibits a square-planar arrangement of one carbonyl, one η<sup>1</sup>-formato, and two trans-triphenylphosphine ligands about the rhodium atom. Similar principal bond distances and angles were found for **6** and in its bicarbonato analogue. A negligible difference in the Rh–CO bond lengths (1.807(4) and 1.798(4) Å, respectively) indicates that formato and bicarbonato ligands possess similar trans-influences.

Equation 6 describes the reaction between **1** and excess HCOOH, resulting in **6**. Remarkably, while



reactions 5 and 6 selectively lead to totally different products, both equations display the *same* stoichiometry for the ratio of **1** to HCOOH. It seemed conceivable, therefore, that such a dramatic difference was due to the presence of extra H<sup>+</sup> which is somehow responsible for directing the reaction toward the formation of **6**. Indeed, treatment of **1** with a 10-fold excess of *acetic acid*, followed by addition of 4 equiv of HCOOH, gave rise to **6** without evolution of CO<sub>2</sub>.<sup>23</sup>

Both reactions 5 and 6 are quite facile, resulting in quantitative conversion of **1** within seconds. If an excess of formic acid is added to a solution of **5** obtained from **1** and 4 equiv of HCOOH, a sluggish reaction occurs leading to **6** in 15–20 h. Hydrogen is presumably a byproduct of the reaction between **5** and HCOOH.<sup>24</sup> Clearly, **5** cannot mediate the formation of **6** from **1** and excess formic acid as reaction 5 takes seconds, whereas the formation of **6** from the once formed **5** and HCOOH takes hours. Scheme 1 accounts for the observations

(22) Hossain, S. F.; Nicholas, K. M.; Teas, C. L.; Davis, R. E. *J. Chem. Soc., Chem. Commun.* **1981**, 268.

(23) The orange solution of **1** in benzene turned red immediately upon addition of AcOH, the resulting Rh complex being similar to **4** in both the color and <sup>31</sup>P NMR parameters (δ = 57.1 ppm; J<sub>Rh–P</sub> = 201 Hz). Treatment of the thus generated red Rh(I) acetate with HCOOH resulted in fast decoloration and formation of a new complex, whose <sup>31</sup>P NMR characteristics (δ = 32.3 ppm; J<sub>Rh–P</sub> = 132 Hz) were exactly as those observed for **6**. It is possible that the product was [(Ph<sub>3</sub>P)<sub>2</sub>Rh(CO)(AcO)] or its mixture with **6**. The acetate and formate complexes in the presence of AcOH could be undergoing fast (on the NMR time scale) exchange.

(24) Yoshida et al.<sup>25</sup> proposed that complexes [L<sub>2</sub>Rh(H)<sub>2</sub>(HCOO)] (L = *i*-Pr<sub>3</sub>P, Cy<sub>3</sub>P) mediated the formation of [L<sub>2</sub>Rh(CO)(HCOO)] from formic acid and [L<sub>3</sub>RhH] or [L<sub>4</sub>Rh<sub>2</sub>(H)<sub>2</sub>(μ-N<sub>2</sub>)].

(25) Yoshida, T.; Thorn, D. L.; Okano, T.; Ibers, J. A.; Otsuka, S. *J. Am. Chem. Soc.* **1979**, *101*, 4212.

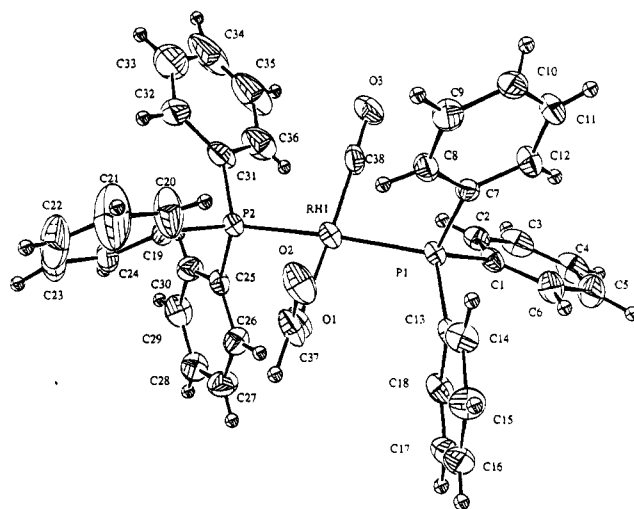


**Figure 1.** Structure of [(Ph<sub>3</sub>P)<sub>2</sub>Rh(CO)(HCOO)], **6**, showing the atom-labeling scheme. Selected bond distances, Å: Rh–P1, 2.3349(12); Rh–P2, 2.3207(12); Rh–O1, 2.082(3); Rh–C38, 1.807(4); O3–C38, 1.150(5). Selected bond angles, deg: P1–Rh–P2, 174.19(19); P1–Rh–O1, 91.27(8); P1–Rh–C38, 89.82(13); P2–Rh–O1, 87.34(8); P2–Rh–C38, 91.98(13); O1–Rh–C38, 175.62(16); Rh–C38–O3, 177.0(4); Rh–O1–C37, 115.8(3); O1–C37–O2, 127.0(4).

**Table 1. Crystallographic Data for [(Ph<sub>3</sub>P)<sub>2</sub>Rh(CO)(HCOO)] (6)**

formula	C <sub>38</sub> H <sub>31</sub> O <sub>3</sub> P <sub>2</sub> Rh
fw	696.40
cryst shape	cube
cryst dimens, mm	0.2 × 0.2 × 0.2
cryst system	monoclinic
lattice params	a = 16.870(6) Å b = 9.826(4) Å c = 20.265(5) Å β = 102.423(20)°
space group	P2 <sub>1</sub> /c
Z	4
V, Å <sup>3</sup>	3260.2(20)
d <sub>calc</sub> , g/cm <sup>3</sup>	1.419
T, K	163
radiation (λ, Å)	Mo Kα (0.709 30)
μ, mm <sup>-1</sup>	0.65
R (R <sub>w</sub> ), %	3.9 (4.8)

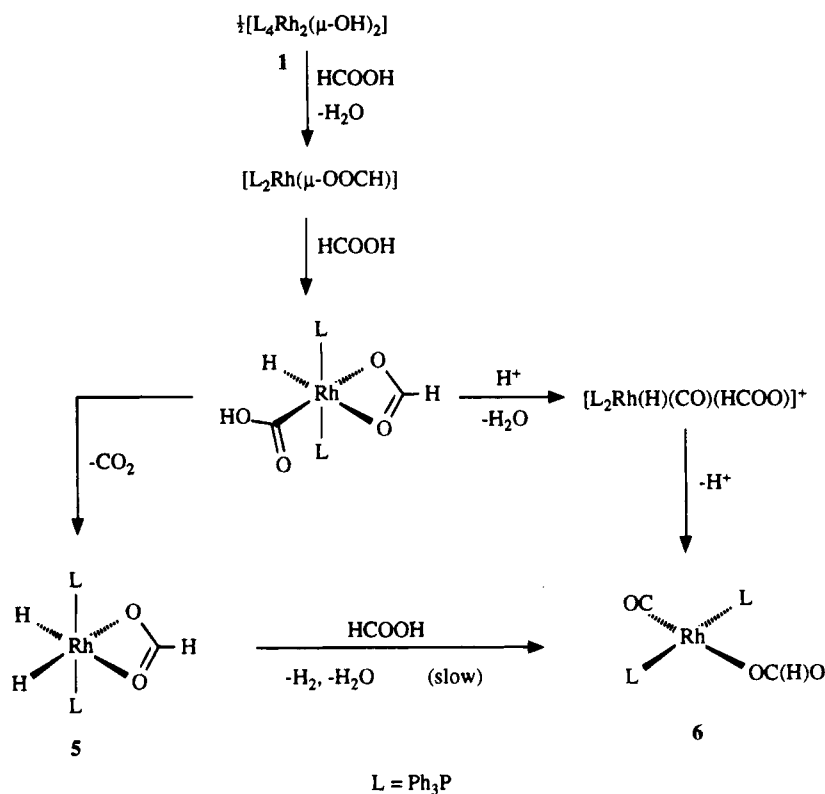
described in this section. The C–H bond of HCOOH oxidatively adds to the originally formed red Rh(I) formate, to give the rhodacarboxylic acid. The latter either loses a molecule of CO<sub>2</sub> giving rise to **5** or, in the presence of H<sup>+</sup>, undergoes dehydration and subsequent deprotonation affording **6**. Both decarboxylation and acid-promoted dehydroxylation reactions of metalla-carboxylic acids are well-documented processes.<sup>26</sup> It is noteworthy that some basic [L<sub>n</sub>MCOOH] compounds can be dehydroxylated even with weak acids, like AcOH.<sup>27</sup> Very complicated patterns were observed in the <sup>31</sup>P NMR spectra of samples obtained with **1** and less than 4 equiv of HCOOH. Molecules of the originally formed red Rh(I) formate may react with each other by oxidatively adding the coordinated formate ligand C–H bonds to the Rh centers.

**Reactions of **1** with M–H Acids.** The acidity of some transition metal hydrides has been reliably established and well-documented in a number of recent

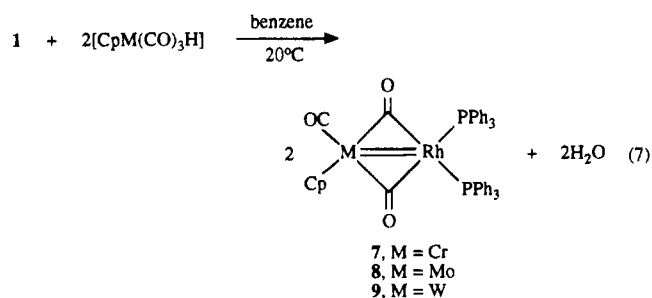
(26) Bennett, M. A. *J. Mol. Catal.* **1987**, *41*, 1.

(27) Deeming, A. J.; Proud, G. P. *J. Organomet. Chem.* **1986**, *301*, 385.

Scheme 1



reviews.<sup>28-31</sup> It was interesting to determine whether the hydroxo complex **1** can be "neutralized" with an M-H acid. To our knowledge, reactions between an L<sub>n</sub>MH and L'<sub>m</sub>M'OH have not been used for M-M' bond formation. Addition of acidic hydrides, [CpM(CO)<sub>3</sub>H], where M = Cr, Mo, and W (pK<sub>a</sub>(MeCN, 25 °C) = 13.3(1), 13.9(1), and 16.1(1), respectively),<sup>32</sup> to a benzene solution of **1** resulted in a facile reaction quantitatively leading to heterobinuclear complexes [(Ph<sub>3</sub>P)<sub>2</sub>Rh(μ-CO)<sub>2</sub>M(CO)Cp] (M = Cr (**7**), Mo (**8**), W (**9**)) containing a rhodium-metal double bond (eq 7). Complexes **7-9**



were isolated in good to excellent yield as analytically and spectroscopically pure compounds. The dark cherry-red chromium-rhodium complex **7** is new, whereas the Mo and W analogues **8** and **9** have been prepared and structurally characterized before.<sup>33,34</sup> With respect to

simplicity and efficiency, this method for the synthesis of **8** and **9** is far superior to one of the literature methods<sup>34</sup> and certainly comparable with the other.<sup>33</sup> In addition, workup of the reaction mixtures is exceptionally simple affording complexes **7-9** in analytically pure form without recrystallization. Comparison of the IR and <sup>1</sup>H and <sup>31</sup>P NMR spectra of **7** with those reported in the literature,<sup>33-35</sup> and obtained by us for **8** and **9**, suggests that **7** should be structurally similar to the Rh-Mo and Rh-W complexes. Like complex **9**,<sup>35</sup> **7** and **8** exhibit dynamic behavior in solution, with the barriers to the pseudorotation being even lower than that determined for the Rh-W compound (ΔG<sup>‡</sup> = 27.9 ± 0.8 kJ/mol at -108 ± 8 °C).<sup>35,36</sup>

We have also found that, like **9**,<sup>37</sup> complexes **7** and **8** reversibly absorb CO. The reactions are accompanied by an efficient and fast exchange between CO gas and all the three carbonyl ligands of the heterobinuclear complexes. Stirring dark-brown **9** in toluene under <sup>13</sup>CO for a few minutes, followed by bubbling N<sub>2</sub> through the resulting orange solution, gave [(Ph<sub>3</sub>P)<sub>2</sub>Rh(μ-<sup>13</sup>CO)<sub>2</sub>W-(<sup>13</sup>CO)Cp], in quantitative yield.<sup>38</sup> A very broad signal at ca. 20 ppm was observed in the 293 K <sup>31</sup>P NMR spectrum of the <sup>13</sup>CO-saturated solution of **9** in toluene-*d*<sub>6</sub>; the <sup>13</sup>C NMR pattern in the carbonyl region consisted of one broad resonance at 205.5 ppm. Cooling the sample to 193 K resulted in freezing the exchange

(28) Pearson, R. G. *Chem. Rev.* **1985**, *85*, 41.

(29) Kristjánssdóttir, S. S.; Norton, J. R. Acidity of Hydrido Transition Metal Complexes in Solution. In *Transition Metal Hydrides*; Dedieu, A., Ed.; VCH Pub.: New York, 1991; p 309.

(30) Jessop, P. G.; Morris, R. H. *Coord. Chem. Rev.* **1992**, *121*, 155.

(31) Grushin, V. V. *Acc. Chem. Res.* **1993**, *26*, 279.

(32) Moore, E. J.; Sullivan, J. M.; Norton, J. R. *J. Am. Chem. Soc.* **1986**, *108*, 2257.

(33) Carlton, L.; Lindsell, W. E.; McCullough, K. J.; Preston, P. N. *J. Chem. Soc., Dalton Trans.* **1984**, 1693.

(34) Hoskins, S. V.; James, A. P.; Jeffery, J. C.; Stone, F. G. A. *J. Chem. Soc., Dalton Trans.* **1986**, 1709.

(35) Lindsell, W. E.; Tomb, P. J. *J. Organomet. Chem.* **1989**, *378*, 245.

(36) No signal coalescence was observed in 160 K <sup>31</sup>P NMR spectra of **7** and **8** in 1:1 toluene-dichloromethane solutions.

(37) Carlton, L.; Lindsell, W. E.; McCullough, K. J.; Preston, P. N. *J. Chem. Soc., Dalton Trans.* **1987**, 2741.

(38) IR of the labeled Rh-W complex (KBr): 1826, 1726, 1699 cm<sup>-1</sup>. All three carbonyl stretches are 41-43 cm<sup>-1</sup> lower than those in nonlabeled **9**. <sup>13</sup>C NMR of the <sup>13</sup>CO-labeled **9** (toluene-*d*<sub>6</sub>, 20 °C), δ: 238.5 (J<sub>Rh-C</sub> = 16.7 Hz; J<sub>W-C</sub> = 185.5 Hz).

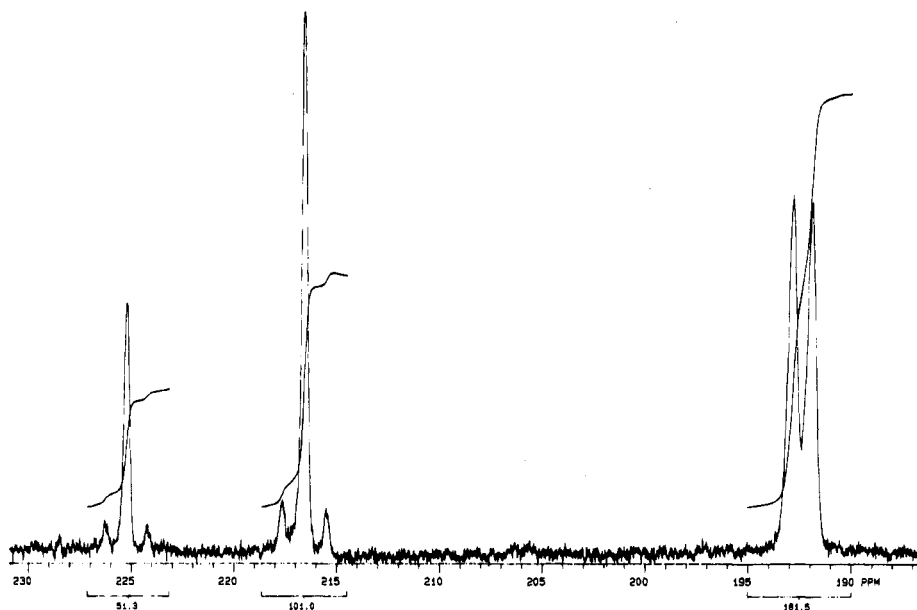
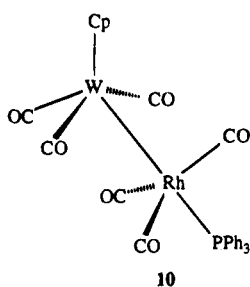


**Figure 2.** 193 K <sup>13</sup>C spectrum (carbonyl region) of the sample obtained by saturation with <sup>13</sup>CO a solution of **9** in toluene-*d*<sub>8</sub>, measured with *D*<sub>1</sub> = 30 s (see ref 39).

processes, and two 1:1 resonances were observed in the <sup>31</sup>P NMR spectrum. One of them, a sharp singlet at -7 ppm, was due to free PPh<sub>3</sub>; the other signal was a slightly broadened ( $\Delta_{1/2}$  = 35 Hz) doublet at 37.0 ppm with *J*<sub>Rh-P</sub> = 105 Hz. Hence, the reaction between **9** and CO led to elimination of one of the two phosphine ligands from the rhodium atom. The 193 K <sup>13</sup>C NMR spectrum of the same sample (Figure 2) exhibited three 1:2:3<sup>39</sup> carbonyl resonances at 225.2 (s, *J*<sub>W-C</sub> = 153.4 Hz), 216.6 (s, *J*<sub>W-C</sub> = 164.7 Hz), and 192.4 ppm (*J*<sub>Rh-C</sub> = 69.8 Hz). No tungsten satellites were observed for the upfield carbonyl signal which appeared at that temperature as a slightly distorted and broadened ( $\Delta_{1/2}$  = 36 Hz) doublet. Our NMR data suggest that the product of the reaction between **9** and CO should be formulated not as [Cp(CO)<sub>3</sub>WRh(CO)(PPh<sub>3</sub>)<sub>2</sub>]<sup>37</sup> but rather [Cp(CO)<sub>3</sub>WRh(CO)<sub>3</sub>(PPh<sub>3</sub>)], **10**, assuming the rotation around the W-Rh bond is unhindered.



In conclusion, an exceptionally simple and convenient method has been developed for the synthesis of [(Ph<sub>3</sub>P)<sub>4</sub>Rh<sub>2</sub>(μ-OH)<sub>2</sub>] from Wilkinson's catalyst and aqueous alkali under biphasic conditions. This binuclear hydroxo rhodium complex readily and cleanly reacts with various C-H, O-H, and M-H acids to give the corresponding compounds with the Rh-C, Rh-O, and Rh-M bonds.

### Experimental Section

Spectral measurements were carried using the following equipment: Varian Gemini-200 (<sup>1</sup>H NMR), Varian XL 300 (<sup>13</sup>C

and <sup>31</sup>P NMR), and Bomem MB-100 (FT-IR). A Rigaku AFC6S diffractometer was used for the single-crystal X-ray diffraction study. All chemicals including [CpM(CO)<sub>3</sub>]<sub>2</sub> (M = Mo, W) were purchased from Aldrich, Strem, Organometallics, and MSD Isotopes chemical companies. Wilkinson's catalyst, [(Ph<sub>3</sub>P)<sub>3</sub>RhCl],<sup>3,40</sup> [CpM(CO)<sub>3</sub>H] (M = Mo, W),<sup>41</sup> and Hg[CpCr(CO)<sub>3</sub>]<sub>2</sub><sup>42</sup> were prepared as described in the literature.

**Synthesis of [(Ph<sub>3</sub>P)<sub>4</sub>Rh<sub>2</sub>(μ-OH)<sub>2</sub>], **1**.** Wilkinson's catalyst (0.30 g; 0.32 mmol) was added to an oxygen-free mixture of KOH (2 g), water (3 mL), and benzene (12 mL), and the mixture was stirred under N<sub>2</sub> at 75 °C (oil bath) for 3 h. The orange, slightly opaque organic layer was filtered hot through cotton, the aqueous phase was washed with O<sub>2</sub>-free benzene (3 × 2 mL) and filtered, and the combined organic solutions were reduced in volume to ca. 2 mL. The remaining viscous dark-orange solution was treated with oxygen-free MeOH (2 mL), and the mixture was left for ca. 30 min until a considerable amount of 1·2C<sub>6</sub>H<sub>6</sub> precipitated as nice orange crystals. More MeOH (4 mL) was added, and the mixture was kept in an ice bath for 1 h. The crystals were separated, washed with MeOH (4 × 3 mL), and dried under vacuum. The yield of 1·2C<sub>6</sub>H<sub>6</sub> was 0.198 g (85%). <sup>1</sup>H NMR (benzene-*d*<sub>6</sub>),  $\delta$ : -2.2 (s, 2H, OH); 7.0 (m, 36H, 3,4,5-C<sub>6</sub>H<sub>5</sub>); 7.9 (m, 24H, 2,6-C<sub>6</sub>H<sub>5</sub>). <sup>13</sup>C NMR (benzene-*d*<sub>6</sub>),  $\delta$ : 127.7 (virtual t, *J* = 10.8 Hz); 129.0 (s); 135.5 (virtual t, *J* = 12.4 Hz); 137.5 (virtual t, *J* = 40.3 Hz). <sup>31</sup>P NMR (benzene-*d*<sub>6</sub>),  $\delta$ : 57.3 (d, *J*<sub>Rh-P</sub> = 188 Hz).

**Reaction of **1** with Cyclopentadiene.** A mixture of 1·2C<sub>6</sub>H<sub>6</sub> (0.123 g; 0.085 mmol), benzene (6 mL), and freshly cracked cyclopentadiene (0.4 mL) was stirred under N<sub>2</sub> for 24 h. All volatiles were removed under vacuum, and MeOH (5 mL) was added to the residual dark-brown oil, causing fast crystallization. After the mixture was kept in an ice bath for 1 h the well-shaped brown crystals were separated, washed with MeOH (3 × 2 mL), and dried under vacuum. The yield of **2** (1:1 benzene solvate)<sup>8</sup> was 0.124 g (95%). <sup>1</sup>H NMR (benzene-*d*<sub>6</sub>),  $\delta$ : 5.0 (s, 5H, C<sub>5</sub>H<sub>5</sub>); 6.9 (m, 18H, 3,4,5-C<sub>6</sub>H<sub>5</sub>); 7.7 (m, 12H, 2,6-C<sub>6</sub>H<sub>5</sub>).<sup>8</sup> <sup>13</sup>C NMR (benzene-*d*<sub>6</sub>),  $\delta$ : 88.5 (s); 127.5 (virtual t, *J* = 7.6 Hz); 131.0 (s); 135.3 (virtual t, *J* = 12.2 Hz); 140.7 (virtual t, *J* = 39.0 Hz). <sup>31</sup>P NMR (benzene-*d*<sub>6</sub>),  $\delta$ : 57.3 (d, *J*<sub>Rh-P</sub> = 222.5 Hz).<sup>10</sup>

**Reaction of **1** with Dimethyl Malonate.** A mixture of 1·2C<sub>6</sub>H<sub>6</sub> (0.10 g; 0.07 mmol), benzene (4 mL), and dimethyl malonate (0.12 g) was stirred under nitrogen until all the solid

(39) The same integration ratio was obtained when the <sup>13</sup>C NMR spectra were measured with *D*<sub>1</sub> = 10, 30, and 50 s.

(40) Osborn, J. A.; Wilkinson, G. *Inorg. Synth.* **1990**, *28*, 77.

(41) Fischer, E. O. *Inorg. Synth.* **1963**, *7*, 136.

(42) Burtlitch, J. M.; Ferrari, A. *Inorg. Chem.* **1970**, *9*, 563.

dissolved and then for an extra 1 h. The solution was reduced in volume to ca. 2 mL, and hexane ( $4 \times 1$  mL) was added portionwise to the residual solution. The orange crystals were separated, washed with hexane ( $3 \times 2$  mL), and dried under vacuum. The yield of **3** was 0.080 g (76%). Anal. Calcd for  $C_{41}H_{37}O_4P_2Rh$ : C, 64.9; H, 4.9. Found: C, 64.7; H, 4.8.  $^1H$  NMR (benzene- $d_6$ ),  $\delta$ : 2.7 (s, 6H,  $CH_3$ ); 5.1 (s, 1H, CH); 6.8 (m, 18H, 3,4,5- $C_6H_5$ ); 7.8 (m, 12H, 2,6- $C_6H_5$ ).  $^{13}C$  NMR (benzene- $d_6$ ),  $\delta$ : 50.6 (s); 66.9 (s); 127.9 (virtual t,  $J = 9.5$  Hz); 129.4 (s); 135.6 (virtual t,  $J = 11.4$  Hz); 136.7 (virtual t,  $J = 44.8$  Hz); 175.1 (s).  $^{31}P$  NMR (benzene- $d_6$ ),  $\delta$ : 58.4 (d,  $J_{Rh-P} = 200.5$  Hz). IR (KBr),  $cm^{-1}$ : 1618 (CO).

**Reaction of 1 with Benzoic Acid.** Benzoic acid (0.030 g; 0.25 mmol) was added to a stirring suspension of **1** (0.10 g; 0.08 mmol) in benzene (4 mL), and the mixture was stirred for a few minutes until all the solid dissolved and a clear, dark-red solution formed. The solution was reduced in volume to ca. 1 mL, treated with hexane (5 mL), and stirred until precipitation of a dark-red microcrystalline solid, which was washed with hexane and dried under vacuum. The yield of **4** was 0.107 g (92%). Anal. Calcd for  $C_{43}H_{35}O_2P_2Rh$ : C, 69.0; H, 4.7. Found: C, 68.6; H, 4.7.  $^1H$  NMR (benzene- $d_6$ ),  $\delta$ : 7.0 (m, 42H, 3,4,5- $C_6H_5$ ); 7.8 (m, 24H, 2,6- $C_6H_5$ ); 8.2 (m, 4H, 2,6- $C_6H_5COO$ ).  $^{31}P$  NMR (benzene- $d_6$ ),  $\delta$ : 57.1 (d,  $J_{Rh-P} = 201$  Hz). IR (KBr),  $cm^{-1}$ : 1602, 1378.

**Reactions of 1 with Formic Acid. Method a.** In a typical run, formic acid (1.8  $\mu$ L, 0.04 mmol or 4.5  $\mu$ L, 0.1 mmol) was introduced via a microsyringe needle into a standard 5-mm NMR tube charged with  $1\cdot 2C_6H_6$  (15 mg; 0.01 mmol) and  $O_2$ -free benzene- $d_6$  under  $N_2$  and equipped with a septum stopper. The mixture was intensively shaken for 10–15 s immediately after the formic acid was added, and NMR studies were subsequently run (see above).

**Method b.** Formic acid (0.16 g; 3.48 mmol) was added at once, and with vigorous stirring, to a mixture of  $1\cdot 2C_6H_6$  (0.115 g; 0.08 mmol) and benzene (5 mL). After the red color appeared and faded within 1 s and all solids dissolved, the yellow mixture was filtered through cotton, reduced in volume to ca. 1 mL, and left overnight. The precipitated crystals of **6** were separated, washed with benzene ( $2 \times 0.5$  mL), and dried under vacuum (yield 0.091 g). More **6** (0.010 g) was obtained by evaporation of the combined mother liquor and benzene washings and treatment with ether (3 mL). The overall yield of **6** was 0.101 g (91%).  $^{31}P$  NMR (benzene),  $\delta$ : 31.9 (d,  $J_{Rh-P} = 132$  Hz).  $^{13}C$  NMR (benzene- $d_6$ ),  $\delta$ : 129.0 (virtual t,  $J = 10.8$  Hz); 132.4 (s); 133.8 (virtual t,  $J = 44.0$  Hz); 135.6 (virtual t,  $J = 14.0$  Hz); 166.9 (s); 191.6 (dt,  $J_{Rh-C} = 68.7$  Hz,  $J_{P-C} = 17.0$  Hz). IR (KBr),  $cm^{-1}$ : 1969 (CO), 1611 (unsymmetric HCOO), 1291 (symmetric HCOO).

**Reaction of 1 with  $[CpCr(CO)_3H]$ .** A mixture of  $Hg\cdot [CpCr(CO)_3]_2$  (0.243 g; 0.40 mmol), THF (5 mL), and Na/K alloy (ca. 0.5 mL) was stirred for 1 h and filtered. The filtrate was reduced in volume to ca. 3 mL, treated with acetic acid (0.2 mL), stirred for 10 min, and taken to dryness under vacuum. Yellow-orange crystals of  $[CpCr(CO)_3H]$  were isolated from the residue by sublimation under vacuum and added to a mixture of **1** (0.051 g; 0.035 mmol) and benzene (3 mL). After the mixture was stirred for 5–10 min, the clear dark-cherry solution was reduced in volume to ca. 1 mL, diluted with MeOH (5 mL), and left for 40 min. The dark-purple crystals were separated and thoroughly washed with MeOH. The yield of **7** was (0.045 g (77%). The compound was found to be analytically and spectroscopically pure without recrystallization. Anal. Calcd for  $C_{44}H_{35}CrO_3P_2Rh$ : C, 63.8; H, 4.3. Found: C, 64.0; H, 4.3.  $^1H$  NMR (benzene- $d_6$ ),  $\delta$ : 4.5 (s, 5H,  $C_5H_5$ ); 6.9 (m, 18H, 3,4,5- $C_6H_5$ ); 7.6 (m, 12H, 2,6- $C_6H_5$ ).  $^{31}P$  NMR (benzene- $d_6$ ),  $\delta$ : 39.4 (d,  $J_{Rh-P} = 177$  Hz). IR (KBr),  $cm^{-1}$ : 1876, 1780, 1749.

**Reaction of 1 with  $[CpMo(CO)_3H]$ .** Solid  $[CpMo(CO)_3H]$  (0.035 g; 0.14 mmol) was added to a mixture of  $1\cdot 2C_6H_6$  (0.092 g; 0.06 mmol) and benzene (3 mL), and the mixture was stirred for 15–20 min until all solids dissolved. The solution was

reduced in volume to ca. 1 mL, diluted with MeOH (3 mL), and placed in an ice bath for 1 h. The precipitated **8** was separated, washed with MeOH ( $3 \times 4$  mL) and pentane ( $2 \times 3$  mL), and dried under vacuum. The yield of **8** was 0.070 g (73%). The compound was found to be analytically and spectroscopically pure without recrystallization. Anal. Calcd for  $C_{44}H_{35}MoO_3P_2Rh$ : C, 60.6; H, 4.0. Found: C, 60.9; H, 4.0.  $^1H$  NMR (benzene- $d_6$ ),  $\delta$ : 5.0 (s, 5H,  $C_5H_5$ ); 6.9 (m, 18H, 3,4,5- $C_6H_5$ ); 7.7 (m, 12H, 2,6- $C_6H_5$ ).  $^{31}P$  NMR (benzene- $d_6$ ),  $\delta$ : 38.1 (d,  $J_{Rh-P} = 175$  Hz). IR (KBr),  $cm^{-1}$ : 1873, 1776, 1748.

**Reaction of 1 with  $[CpW(CO)_3H]$ .** Solid  $[CpW(CO)_3H]$  (0.070 g; 0.21 mmol) was added to a mixture of  $1\cdot 2C_6H_6$  (0.130 g; 0.09 mmol) and benzene (5 mL), and the mixture was stirred for 15–20 min until all solids dissolved. Methanol (10 mL) was added to the resulting clear, dark-brown solution, and the mixture was kept in an ice bath for 1.5 h. Crystals of **9** were separated, washed with MeOH ( $4 \times 2$  mL) and pentane ( $3 \times 4$  mL), and dried under vacuum. The yield of **9** was 0.167 g (97%). The compound was found to be analytically and spectroscopically pure without recrystallization. Anal. Calcd for  $C_{44}H_{35}O_3P_2RhW$ : C, 55.0; H, 3.7. Found: C, 55.0; H, 3.6.  $^1H$  NMR (benzene- $d_6$ ),  $\delta$ : 4.9 (s, 5H,  $C_5H_5$ ); 6.9 (m, 18H, 3,4,5- $C_6H_5$ ); 7.7 (m, 12H, 2,6- $C_6H_5$ ).  $^{31}P$  NMR (benzene- $d_6$ ),  $\delta$ : 31.8 (d,  $J_{Rh-P} = 173$  Hz). IR (KBr),  $cm^{-1}$ : 1869, 1767, 1738.

**Single-Crystal Diffraction Study of 6.** Well-shaped, transparent, yellow crystals of **6** were obtained by layering a concentrated solution of **6** in chloroform with hexane. One of the crystals having approximate dimensions of  $0.2 \times 0.2 \times 0.2$  mm was mounted on a glass capillary. The measurements were made at  $-110$  °C with Mo K $\alpha$  radiation and a graphite monochromator. During the data collection, standard reflections were measured after every 150 reflections to check the stability of the crystal. No crystal decay was noticed. A total of 5577 reflections were measured. The unique set contained 5366 reflections. Using the criteria  $I > 2.5 \sigma(I)$ , where  $\sigma(I)$  is the estimated standard deviation derived from the counting statistics, 4060 out of 5366 reflections were used. The data were corrected for Lorentz and polarization effects.<sup>43</sup> No absorption correction was made.

The structure was solved by direct methods. All the atoms were refined anisotropically except the hydrogens. The hydrogen atoms were found by difference Fourier map. The final cycle of full-matrix least-squares refinement was based on 4060 observed reflections and 518 variable parameters. Weights based on counting statistics were used. The maximum and minimum peaks on the final Fourier map corresponded to 0.580 and  $-1.020$  e/Å<sup>3</sup>, respectively. All the calculations were performed using the NRCVAX crystallographic software package.<sup>44</sup>

**Acknowledgment.** We thank the Natural Sciences and Engineering Research Council of Canada (NSERC) for support for this research.

**Supporting Information Available:** X-ray crystallographic data for **6**, including text describing the experimental procedure, tables of crystal parameters, atomic coordinates, and thermal parameters, and ORTEP diagrams (13 pages). This material is contained in many libraries on microfiche, immediately follows this article in the microfilm version of the journal, and can be ordered from the ACS; see any current masthead page for ordering information.

OM950209Z

(43) Grant, D. F.; Gabe, E. J. *J. Appl. Crystallogr.* **1978**, *11*, 114.

(44) Gabe, E. J.; Lee, F. L.; Lepage, Y. *J. Appl. Crystallogr.* **1989**, *22*, 384.

# The Silylium Ion ( $R_3Si^+$ ) Problem: Effect of Alkyl Substituents R

Zuowei Xie,<sup>†</sup> Robert Bau,<sup>†</sup> Alan Benesi,<sup>‡</sup> and Christopher A. Reed<sup>\*,†</sup>

Departments of Chemistry, University of Southern California,  
Los Angeles, California 90089-0744, and Pennsylvania State University,  
State College, Pennsylvania 18602

Received June 12, 1995<sup>®</sup>

The X-ray structures of four  $R_3Si(Br_6-CB_{11}H_6)$  species have been determined ( $R_3 = Et_3$ ,  $i-Pr_3$ ,  $t-Bu_3$ , and  $t-Bu_2Me$ ).  $Br_6-CB_{11}H_6^-$  is a particularly weakly coordinating anion and leads to long Si–Br bond distances (ca. 2.43–2.48 Å). The developing silylium ion character in these species is reflected in the approach of the  $R_3Si^{\delta+}$  moiety toward planarity. The sum of the C–Si–C angles for each of the four derivatives lies in the range ca. 345–351°. The closest approach to 360° is found in the triisopropyl derivative, not the tri-*tert*-butyl derivative as might be anticipated from steric considerations. One of the isopropyl groups in the  $i-Pr_3$  derivative has its carbon atoms very nearly planar with the silicon atom. This is indicative of C–H bond hyperconjugative stabilization of the developing positive charge on silicon. An “inorganic” description would be in terms of an  $\alpha$ -agostic C–H interaction with the electron-deficient  $3p_z$  orbital on silicon. The results suggest that hyperconjugative stabilization of cationic character, although relatively unimportant compared to that for carbon in carbenium ions, is nevertheless not negligible for silicon. Solid state CPMAS  $^{29}Si$  NMR data are also reported. The chemical shifts lie in the 105–115 ppm downfield region as expected for silylium ion-like character in these  $R_3Si^{\delta+}(Br_6-CB_{11}H_6)^{\delta-}$  species.

## Introduction

The long-sought silylium ion,  $R_3Si^+$ , analogous to well-known carbenium ions<sup>1</sup> ( $R_3C^+$ ) has yet to be definitively characterized in condensed media.<sup>2–12</sup> The essential problem is one of excluding nucleophiles (solvent or anion) from bonding to silicon. An additional consideration is the choice of the substituent R in order to maximize the stability of  $R_3Si^+$ . In this paper we explore the effect of increasingly branched-chain aliphatic substituents on the degree of silylium ion character in trialkylsilyl compounds of the type  $R_3Si^{\delta+}-Y^{\delta-}$ , where Y is the carborane anion  $Br_6-CB_{11}H_6^-$ , currently perhaps the least nucleophilic anion known for silicon.<sup>2</sup> By emphasizing solid state data, particularly from X-ray crystallography, uncertainties about the role of solvent are removed. Ethers,<sup>13</sup> nitriles,<sup>14–16</sup> and, most recently

and interestingly, toluene<sup>3</sup> have been shown to be sufficiently nucleophilic that discrete and characterizable four-coordinate species of the type  $[R_3Si(solvent)]^+$  are formed, analogous to cations proposed earlier with a variety of nucleophiles<sup>17</sup> and characterized by X-ray structure in the case of pyridine.<sup>18</sup>

Part of the impetus behind the search for the elusive  $R_3Si^+$  ion is the desire to find silicon analogues of familiar electron-deficient and low-coordinate structures of carbon chemistry. The crystal structures of a number of carbocations are now known, although the first simple trialkylcarbenium ion,  $R_3C^+$ , was characterized only very recently ( $R = Me$ ).<sup>19</sup> It was stabilized by using somewhat lowered temperatures ( $<-20$  °C) and by using  $Sb_2F_{11}^-$  as a noncoordinating anion. Similar reaction conditions fail to produce free  $R_3Si^+$  ions because of silicon–fluorine bond formation.<sup>4</sup> This highlights one of the most important differences between carbon and silicon, namely, the greater ease with which silicon can increase its coordination number by binding hard nucleophiles, particularly fluoro and oxy anions. This is fundamentally related to the more electropositive nature of silicon, its more metal-like behavior, and its participation in more polar bonding.<sup>20</sup> The greater size of silicon relative to carbon (ca. 15%–50% longer bonds

<sup>†</sup> University of Southern California.

<sup>‡</sup> Pennsylvania State University.

<sup>®</sup> Abstract published in *Advance ACS Abstracts*, August 1, 1995.

(1) Olah, G. A. Nobel Lecture. *Angew. Chem., Int. Ed. Engl.* **1995**, in press.

(2) Reed, C. A.; Xie, Z.; Bau, R.; Benesi, A. *Science* **1993**, *262*, 402–404.

(3) Lambert, J. B.; Zhang, S.; Stern, C. L.; Huffman, J. C. *Science* **1993**, *260*, 1917–1919. Lambert, J. B.; Zhang, S.; Ciro, S. M. *Organometallics* **1994**, *13*, 2430–2443.

(4) Olah, G. A.; Heiliger, L.; Li, X.-Y.; Prakash, G. K. S. *J. Am. Chem. Soc.* **1990**, *112*, 5991–5995.

(5) Eaborn, C. *J. Organomet. Chem.* **1991**, *405*, 173–177.

(6) Lickiss, P. D. *J. Chem. Soc., Dalton Trans.* **1992**, 1333–1338.

(7) Schleyer, P. v. R.; Buzek, P.; Müller, T.; Apeloig, Y.; Siehl, H. U. *Angew. Chem., Int. Ed. Engl.* **1993**, *32*, 1471–1473.

(8) Crestoni, M. E.; Fornarini, S. *Angew. Chem., Int. Ed. Engl.* **1994**, *33*, 1094–1096.

(9) Olsson, L.; Cremer, D. *Chem. Phys. Lett.* **1993**, *215*, 433–443.

(10) Pauling, L. *Science* **1994**, *263*, 983.

(11) Strauss, S. H. *Chemtracts: Inorg. Chem.* **1993**, *5*, 119–124.

(12) Houk, K. N. *Chemtracts: Org. Chem.* **1993**, *6*, 360–363.

(13) Kira, M.; Hino, T.; Sakurai, H. *J. Am. Chem. Soc.* **1992**, *114*, 6697–6700.

(14) Xie, Z.; Liston, D. J.; Jelinek, T.; Mitro, V.; Bau, R.; Reed, C. A. *J. Chem. Soc., Chem. Commun.* **1993**, 384–386.

(15) Kira, M.; Hino, T.; Sakurai, H. *Chem. Lett.* **1993**, 153–156.

(16) Bahr, S. R.; Boudjouk, P. *J. Am. Chem. Soc.* **1993**, *115*, 4514–4519.

(17) Bassindale, A. R.; Stout, T. *Tetrahedron Lett.* **1985**, *26*, 3403–3406.

(18) Hensen, K.; Zengerly, T.; Pickel, P.; Klebe, G. *Angew. Chem., Int. Ed. Engl.* **1993**, *22*, 725–726.

(19) Hollenstein, S.; Laube, T. *J. Am. Chem. Soc.* **1993**, *115*, 7240–7245.

(20) Corey, J. Y. In *The Chemistry of Organic Silicon Compounds*; Patai, S.; Rappoport, Z., Eds.; Wiley-Interscience: New York, 1989; Vol. 1, pp 1–56.



in compounds)<sup>20</sup> must also be a factor. These comparisons suggest that attempts to attain charge separation of  $R_3Si-Y$  into a free silylium ion should stress anions  $Y^-$  that are large and soft rather than small and hard.

There has been considerable progress in the last decade in the development of new large and weakly coordinating anions.<sup>21,22</sup> For silicon, the most useful to date have proved to be perfluorotetraphenylborate ( $F_{20}-BPh_4^-$ )<sup>3,14,23</sup> and two brominated *closo*-carboranes, the 10-vertex pentabromo  $Br_5-CB_9H_5^-$  and the 12-vertex hexabromo  $Br_6-CB_{11}H_6^-$ .<sup>2,14</sup> The success of  $F_{20}-BPh_4^-$  can be ascribed to very strong  $sp^2 C-F$  covalent bonding and the consequent low nucleophilicity of the fluorine atoms. In addition, size, overall inertness, and good solubility characteristics are important. In situations where its coordination to metal centers has been established by X-ray crystallography,<sup>24</sup> bidentate coordination via fluorine atoms is observed. The success of bromocarboranes as weakly coordinating anions derives from the remarkable stability of *closo* (i.e., closed-shell)-carborane polyhedra and the increased inertness given to them by partial bromination.<sup>25</sup> In addition, the negative charge is delocalized over the entire polyhedron, albeit concentrated antipodal to the carbon, i.e., in the brominated region of the boron framework. With respect to stabilizing positive charge on silicon, a center which has been classified as hard,<sup>26</sup> the soft and polarizable bromine substituents may contribute a useful degree of soft/hard incompatibility. Although  $F_{20}-BPh_4^-$  and  $Br_6-CB_{11}H_6^-$  show roughly comparable nucleophilicity toward silicon,<sup>2</sup> the bromocarboranes have proven to be much superior in growing crystals for X-ray crystallography. Indeed, the structure of a solvent-free  $R_3Si(F_{20}-BPh_4)$  derivative has yet to be determined; concentrated solutions show a marked tendency to form oils. For this reason, our studies have mostly employed the brominated carboranes, chiefly  $Br_6-CB_{11}H_6^-$ .

Systematic studies on the relative stabilities of silylium ions have necessarily been restricted to gas phase experiments<sup>26</sup> and to theory.<sup>27</sup> There has been an emphasis on small silyl moieties, presumably because of volatility considerations in MS and ICR studies and computational feasibility in theoretical studies. The effect of heteroatom stabilization (O, N, etc.) has received considerable study but, when applied to silylium ion synthesis in the condensed phase, has usually led to reaction chemistry which thwarts the isolation of three-coordinate silicon.<sup>28-30</sup> In addition, conjugating substituents are generally found to be much less effective

in stabilizing charge at silicon relative to carbon because of longer bonds and diminished  $\pi$ -bonding. Thus, aryl substituents are not as effective in stabilizing silylium ions as they are in carbenium ions (e.g., trityl ion).<sup>32</sup> Nevertheless, gas phase electron-impact fragmentation studies on para-substituted aryl silanes show pronounced effects of electron-donating para substituents on the abundance of silylium ions,<sup>33</sup> and recent theory finds a 15 kcal mol<sup>-1</sup>  $\pi$ -stabilization effect of a phenyl group when coplanar rather than perpendicular to  $SiH_2^+$ .<sup>34</sup> Other studies leading to potentially stabilizing substituent effects have involved a silacyclopropenium ion approach,<sup>35</sup> tris(trimethylsilyl)methyl as a substituent,<sup>5</sup> attempts to exploit aromatization,<sup>36</sup> and an  $\alpha$ -halogen effect.<sup>36</sup> An additional observation regarding stabilizing effects in silylium ions is that hyperconjugation is much less effective for silicon than carbon.<sup>27,37</sup> Nevertheless, the present work provides experimental evidence that hyperconjugative stabilization is not negligible. A point of consideration when attempting to use gas phase data or theory as a guide to synthesis in the solution phase is the role of solvation. This is particularly true for ions because, in the gas phase, large size and polarizability are important for delocalizing the effect of a charge. On the other hand, in the solution phase, the close approach of solvent molecules to charge is important in controlling ionization phenomena and can sometimes lead to seemingly paradoxical results. For example, although  $F_{20}-BPh_4^-$  is slightly more nucleophilic than  $Br_6-CB_{11}H_6^-$  by the criterion of <sup>29</sup>Si downfield shift, in toluene solution the  $F_{20}-BPh_4^-$  compound ionizes more easily to  $[i-Pr_3Si(toluene)]^+$ .<sup>2</sup> This presumably arises from superior toluene solvation of free  $F_{20}-BPh_4^-$  relative to  $Br_6-CB_{11}H_6^-$ .

Another potential source of information about substituent stabilization in  $R_3Si^+$  is in the relative rates of solution reactions that are believed to proceed via silylium ions as intermediates.<sup>38</sup> Deductions from such data are valid only if the transition state has a high degree of silylium ion character. Bulky substituents can slow reactions by introducing reactant-like character into the transition state and this can mask their ability to stabilize developing charge. The trade-off between inductive effects and steric effects leads to relative rates of hydride abstraction from  $R_3SiH$  that are not particularly sensitive to the *n*-alkyl substituent.<sup>30</sup> The effect of para substituents in analogous reactions of arylsilanes are not as marked in solution studies<sup>30</sup> as might be expected from gas phase data.<sup>33</sup> Various Hammett and Taft relationships can be obtained from these types of studies, but the effects are not dramatic, and, as

(21) Strauss, S. H. *Chem. Rev.* **1993**, *93*, 927-942.

(22) Seppelt, K. *Angew. Chem., Int. Ed. Engl.* **1993**, *32*, 1025-1027.

(23) Lambert, J. B.; Zhang, S. *J. Chem. Soc., Chem. Commun.* **1993**, 383-384.

(24) Yang, X.; Stern, C. L.; Marks, T. J. *Organometallics* **1991**, *10*, 840-842.

(25) Xie, Z.; Jelinek, T.; Bau, R.; Reed, C. A. *J. Am. Chem. Soc.* **1994**, *116*, 1907-1913.

(26) Schwarz, H. In *The Chemistry of Organic Silicon Compounds*; Patai, S., Rappoport, Z., Eds.; Wiley-Interscience: New York, 1989; Vol. 1, pp 445-510.

(27) Apeloig, Y. In *The Chemistry of Organic Silicon Compounds*; Patai, S., Rappoport, Z., Eds.; Wiley-Interscience: New York, 1989; Vol. 1, pp 57-225.

(28) Corriu, R. J. P.; Henner, M. *J. Organomet. Chem.* **1974**, *74*, 1-28.

(29) Cowley, A. H.; Cushner, M. C.; Riley, P. E. *J. Am. Chem. Soc.* **1980**, *102*, 624-628.

(30) Mayr, H.; Basso, N.; Hagen, G. *J. Am. Chem. Soc.* **1992**, *114*, 3060-3066.

(31) Tokitoh, N.; Imakubo, T.; Okazaki, R. *Tetrahedron Lett.* **1992**, *33*, 5819-5822.

(32) Lambert, J. B.; Schulz, W. J., Jr. In *The Chemistry of Organic Silicon Compounds*; Patai, S., Rappoport, Z., Eds.; Wiley-Interscience: New York, 1989; Vol. 1, pp 1007-1014.

(33) Dube, G.; Chvalovsky, V. *Coll. Czech. Chem. Commun.* **1974**, *39*, 2621-2629; 2641-2650.

(34) Cremer, D.; Olsson, L.; Ottosson, H. *J. Mol. Struct. (THEOCHEM)* **1994**, *313*, 91-109.

(35) Robinson, L. R.; Burns, G. T.; Barton, T. J. *J. Am. Chem. Soc.* **1985**, *107*, 3935-3941.

(36) Olah, G. A.; Rasul, E.; Heiliger, L.; Bausch, J.; Prakash, G. K. S. *J. Am. Chem. Soc.* **1992**, *114*, 7737-7742.

(37) Basso, N.; Gors, S.; Popowski, E.; Mayr, H. *J. Am. Chem. Soc.* **1983**, *115*, 6025-6028.

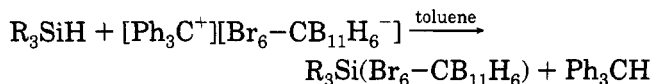
(38) For a review see: Chojnowski, J.; Stanczyk, W. *Adv. Organomet. Chem.* **1990**, *30*, 243-307.

pointed out by Mayr *et al.*,<sup>30</sup> caution is necessary in deriving thermodynamic properties from kinetic data.

Given the paucity of condensed phase structural data and the need to experimentally assess the relative merits of inductive,  $\pi$ -conjugative, hyperconjugative, polarization, steric, and solvation effects in stabilizing  $R_3Si^+$ , we have embarked on a systematic study of alkyl substituents using C–Si–C angles and <sup>29</sup>Si NMR downfield shifts as our criteria for relative silylium ion character. Along the series R = Et, *i*-Pr, *t*-Bu there is a confident expectation of increasingly favorable inductive, polarization, and steric effects.  $\pi$ -Conjugative effects are formally absent, and solvation effects are replaced by crystal-packing considerations in a solid state investigation. The unanticipated results concern the subtlety of hyperconjugative effects and the ineffectiveness of alkyl steric effects.

## Results and Discussion

**Synthesis.** The desired trialkylsilyl derivatives were prepared from the corresponding trialkylsilanes by formal hydride abstraction with the trityl salt of  $Br_6-CB_{11}H_6^-$ . Carefully dried toluene was used as solvent.



These conversions are essentially quantitative as judged by NMR scale experiments which showed triphenylmethane (<sup>1</sup>H,  $\delta$  5.6) as the only byproduct. Traces of minor amounts (<10%) of the corresponding silanols,  $R_3SiOH$ , could sometimes be detected by <sup>1</sup>H NMR and are ascribed to hydrolysis of the product by traces of water in the solvents and on the glassware surface. The alkyl groups used in this study included methyl, ethyl, isopropyl, and *tert*-butyl in various combinations. Reaction times appear to be correlated with the cumulative steric bulk of the silane, the *tri-tert*-butyl reaction requiring weeks to proceed to completion at room temperature. The reactions all gave pale yellow solutions from which nearly colorless crystals could be isolated in good yield by vapor diffusion with *n*-hexane. Slow diffusions typically gave single crystals suitable for X-ray diffraction at the first attempt.

**X-ray Structures.** Four trialkylsilyl derivatives of  $Br_6-CB_{11}H_6^-$  have now been characterized by X-ray crystallography: the *i*-Pr<sub>3</sub>Si derivative communicated earlier,<sup>2</sup> the corresponding *tri-tert*-butyl and triethyl homologues, and the mixed *t*-Bu<sub>2</sub>MeSi derivative. The triethyl derivative crystallizes with two independent molecules in the unit cell, designated triethyl and triethyl' for the purposes of this discussion, giving a total of five structures to compare. These are displayed in Figure 1. Key bond lengths and angles are given in Tables 1 and 2. Complete listings of metrical data are provided in the supporting information.

All structures show the same general features. They are unsolvated and ordered. The anion is bound to silicon via one bromine atom from the pentagonal belt of the carborane anion. There is no evidence of bidentate dibromo coordination as observed in related silver salts;<sup>25</sup> the next closest approach of a bromine atom to silicon is 4.92 Å to Br(8) in the triethyl' structure. The coordination of the carborane anion via a bromine atom

is not unexpected; they have formal lone pairs and are located toward the negative end of this dipolar anion. However, the symmetry-unique bromine atom located antipodal to carbon (i.e., in the 12-position) is expected to be more electron rich than those in the pentagonal belt (positions 7–11).<sup>25</sup> For example, the 12-position is the site of initial electrophilic attack in substitution reactions of the parent carborane  $CB_{11}H_{12}^-$ .<sup>39,40</sup> Also, in the tridentate coordination of  $Br_5-CB_9H_5^-$  to  $Ag^+$  in an iridium adduct<sup>25</sup> it is the bromine atom antipodal to carbon that has the shortest Ag–Br bond length. We believe that the pentagonal belt of bromine atoms in  $Br_6-CB_{11}H_6^-$  screens the lone pairs on the symmetry-unique bromine atom such that large Lewis acids like  $R_3Si^+$  cannot closely approach the 12-position. Coordination is thus preferentially directed to the 7–11 positions. This appears to be an important factor in explaining why  $Br_6-CB_{11}H_6^-$  is such a weakly coordinating anion.

**Bond Lengths.** The Si–Br bond lengths lie in the relatively narrow range 2.430(6)–2.479(9) Å (see Table 1). This suggests that, to a first approximation, the  $R_3Si$ –anion interaction is primarily determined by the coordinating ability of the anion and is relatively insensitive to the substituents on silicon. The triisopropyl derivative has the longest Si–Br distance. There is a correlation of Si–Br–B angle with the bulk of the substituents on silicon. The smallest is found in the triethyl derivative at 109.1(6)°, a value consistent with a possible prediction for  $sp^3$  orientation of the bromine lone pairs. The values increase from triethyl < triethyl' < triisopropyl < *di-tert*-butylmethyl up to the *tri-tert*-butyl derivative at 125.0(5)°, making the range quite large (16°). The largest Si–Br–B angle does not, however, correlate with the longest Si–Br bond. This suggests that electrostatic effects rather than covalency dominate the Si–Br interaction. The Si–Br–B angle is very "soft", and it is apparent that the anion can readily accommodate the differing steric and charge compensation requirements of the formal  $R_3Si^+$  cation.

The Si–Br bonds are long. They exceed that of  $Me_3SiBr^{41}$  by >0.23 Å. This reflects the low coordinating nucleophilicity of the carborane anion and the developing separation of charge,  $R_3Si^{\delta+}(Br_6-CB_{11}H_6)^{\delta-}$ . The Si–Br bonds are short compared to our expectation value for complete charge separation (ca. 3.5 Å), emphasizing that only partial silylium ion character has been achieved.

Another guide to the strength or weakness of the interaction of the anion with silicon is the distortion of the anion upon coordination. This can be probed by comparing the Br–B bond length of the coordinated bromine atom to those of equivalent, uncoordinated bromine atoms. In all cases, the coordinated B–Br bonds [1.99(2)–2.05(2) Å] are longer than the average of the uncoordinated bonds in the pentagonal belt [1.95(2) Å], but their extension outside of the range of uncoordinated bonds [1.92(2)–2.02(3) Å] is barely of statistical significance. Overall, the anion shows only a very small structural response to coordination. This

(39) Jelínek, T.; Plešek, J.; Mareš, F.; Heřmánek, S.; Stíbr, B. *Polyhedron* **1987**, 1981–1986.

(40) Jelínek, T.; Baldwin, P.; Scheidt, W. R.; Reed, C. A. *Inorg. Chem.* **1993**, 32, 1982–1990.

(41) Harmony, M. D.; Strand, M. R. *J. Mol. Spectrosc.* **1980**, 81, 308–315.

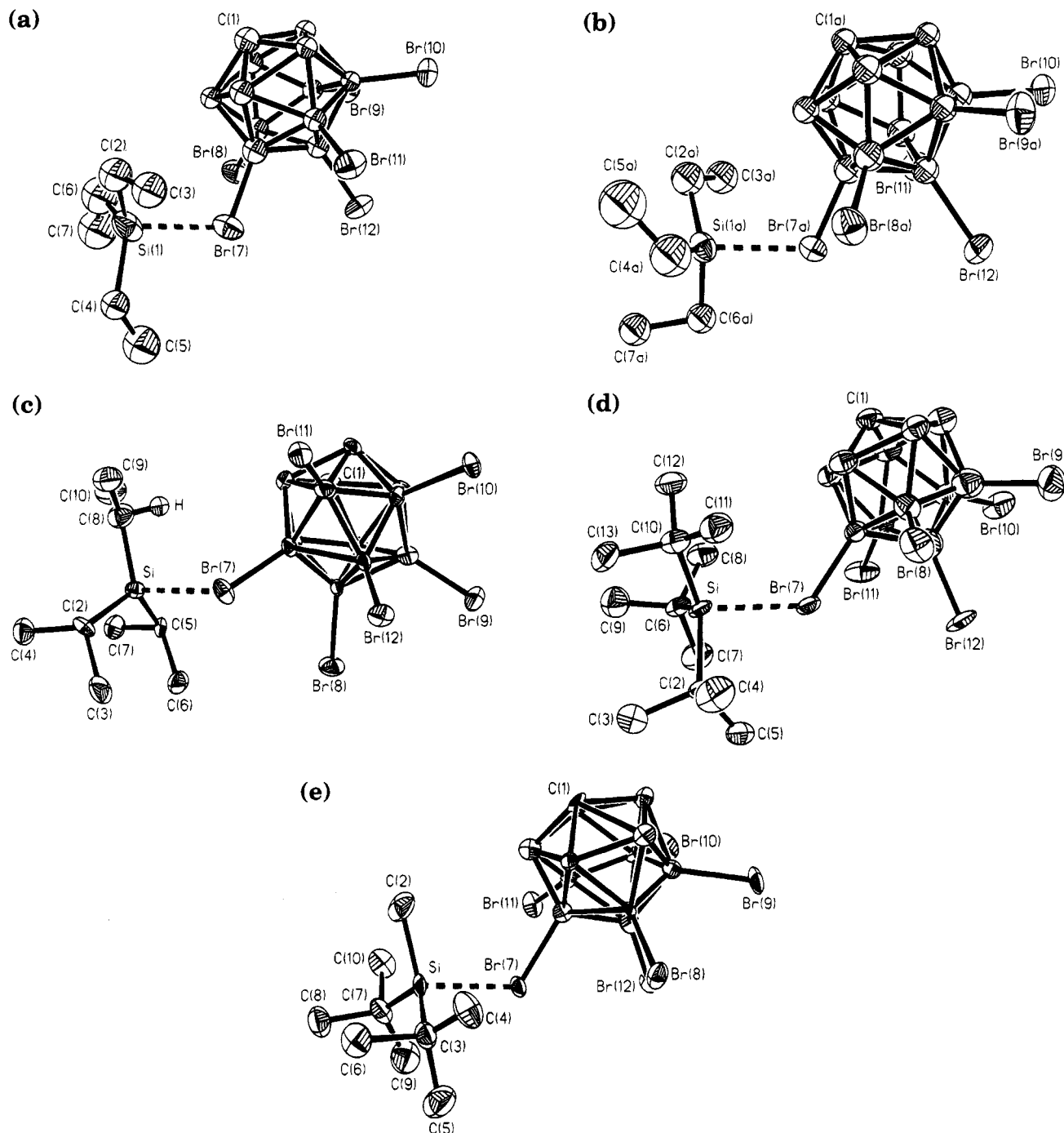


**Figure 1.** Perspective drawings of the five distinct molecules of  $R_3Si(Br_6-CB_{11}H_6)$  from the four X-ray crystal structures: (a) triethyl, (b) triethyl', (c) triisopropyl (d) tri-*tert*-butyl, and (e) di-*tert*-butylmethyl. The hydrogen atom in c is a calculated position.

reflects a relatively weak interaction with silicon and is consistent with a dominance of electrostatic rather than covalent character in the silicon-anion bonding.

**Bond Angles.** The developing silylium ion character in  $R_3Si(Br_6-CB_{11}H_6)$  is also reflected in the bond angles around silicon. Increasing C-Si-C angles to the substituents reflect the apparently gradual transition from the  $sp^3$  ideal of  $109.5^\circ$  for tetrahedral covalent silicon to the  $sp^2$  ideal of  $120^\circ$  expected for planar  $R_3Si^+$ . For this reason, it is useful to measure decreasing pyramidalicity in the  $R_3Si^{\delta+}$  moieties by following the approach of the average C-Si-C angle toward  $120^\circ$ . However, there is frequently quite a range in the three individual C-Si-C angles, with one of them sometimes  $>120^\circ$  (see Table 1). This suggests that the sum of the three

angles, rather than the average, is a somewhat preferable measure of approach to planarity ( $360^\circ$ ). In a perfect tetrahedron this sum is  $328.5^\circ$ . In  $Me_3SiBr$ ,<sup>41</sup> it is  $333.9^\circ$ . The out-of-plane distance of the silicon atom from the three bonded carbon atoms is another measure of approach of planarity. In  $Me_4Si$  this displacement is  $0.62 \text{ \AA}$ . In  $Me_3SiBr$ , it is  $0.56 \text{ \AA}$ . These displacements are also listed in Table 1 for the five structures.

Values for the mean and the sum of the C-Si-C angles range from  $115.0(10)$  to  $117.0(13)^\circ$  and from  $345.0(10)$  to  $351.0(13)^\circ$  respectively (see Table 1). The relatively narrow range suggests that, to a first approximation, these parameters are not particularly sensitive to the nature of the substituent. Rather, the strength of the cation-anion electrostatic interaction

Table 1. Summary of Key Geometrical Parameters for  $R_3Si(Br_6-CB_{11}H_6)$ 

param	triethyl	triethyl'	triisopropyl	tri- <i>tert</i> -butyl	di- <i>tert</i> -butylmethyl
Si-Br (Å)	2.444(7)	2.430(6)	2.479(9)	2.465(5)	2.466(12)
Si-Br-B (deg)	109.1(6)	111.3(5)	114.7(7)	125.0(5)	116.2(10)
B-Br <sub>coord</sub> (Å)	1.99(2)	2.01(2)	2.05(3)	2.04(2)	2.05(3)
B-Br <sub>uncoord</sub> (Å) <sup>a</sup>	1.92-1.98(2)	1.92-1.98(2)	1.93-2.02(3)	1.92-1.93(2)	1.94-2.00(4)
C-Si-C (deg) <sup>b</sup>	111.2(10) [2, 6]	113.4(10) [4a, 6a]	111.2(14) [2, 8]	115.1(7) [2, 10]	110.7(21) [2, 7]
	114.6(9) [2, 4]	117.4(8) [2a, 6a]	119.6(13) [5, 8]	115.9(6) [2, 6]	114.1(21) [2, 3]
	119.2(10) [4, 6]	118.2(9) [2a, 4a]	120.2(12) [2, 5]	117.7(7) [6, 10]	121.0(19) [3, 7]
ΣC-Si-C (deg)	345.0(10)	349.0(9)	351.0(13)	348.7(7)	345.8(21)
mean C-Si-C (deg)	115.0(10)	116.3(9)	117.0(13)	116.2(7)	115.3(21)
Si out of C <sub>3</sub> plane	0.419	0.348	0.300	0.371	0.408

<sup>a</sup> From pentagonal belt only (i.e., excludes 12-position). <sup>b</sup> Numbers in brackets identify the carbon atoms (see Figure 1).

Table 2. Table of Key Substituent Bond Distances and Angles in  $R_3Si(Br_6-CB_{11}H_6)$ 

Angles (deg)		Distances (Å)	
Triethyl			
Si-C(2)-C(3)	114.5(14)	Si-C(2)	1.85(3)
Si-C(4)-C(5)	116.6(13)	Si-C(4)	1.84(2)
Si-C(6)-C(7)	122.6(14)	Si-C(6)	1.80(2)
Triethyl'			
Si-C(2a)-C(3a)	114.6(13)	Si-C(2a)	1.82(2)
Si-C(4a)-C(5a)	120.7(20)	Si-C(4a)	1.85(2)
Si-C(6a)-C(7a)	109.2(11)	Si-C(6a)	1.86(2)
Triisopropyl			
Si-C(2)-C(3)	118.8(22)	Si-C(2)	1.86(3)
Si-C(2)-C(4)	110.0(17)		
C(3)-C(2)-C(4)	107.5(21)		
Si-C(5)-C(6)	113.9(19)	Si-C(5)	1.91(3)
Si-C(5)-C(7)	107.5(18)		
C(6)-C(5)-C(7)	108.8(23)		
Si-C(8)-C(9)	119.0(22)	Si-C(8)	1.80(3)
Si-C(8)-C(10)	128.2(28)		
C(9)-C(8)-C(10)	112.3(32)		
Tri- <i>tert</i> -butyl			
Si-C(2)-C(4)	114.9(10)	Si-C(2)	1.91(2)
Si-C(2)-C(5)	113.3(11)		
Si-C(2)-C(3)	108.3(9)		
Si-C(6)-C(7)	114.2(10)	Si-C(6)	1.87(2)
Si-C(6)-C(8)	113.9(9)		
Si-C(6)-C(9)	109.9(12)		
Si-C(10)-C(11)	114.6(10)	Si-C(10)	1.89(2)
Si-C(10)-C(12)	112.3(11)		
Si-C(10)-C(13)	106.5(10)		
Di- <i>tert</i> -butylmethyl			
		Si-C(2)	1.85(4)
Si-C(3)-C(4)	112.2(33)	Si-C(3)	1.85(4)
Si-C(3)-C(5)	113.2(34)		
Si-C(3)-C(6)	106.7(29)		
Si-C(7)-C(8)	108.9(33)	Si-C(7)	1.88(4)
Si-C(7)-C(9)	115.1(37)		
Si-C(7)-C(10)	108.6(30)		

may be the dominant factor in determining the geometry around silicon. The differences between the ethyl and the ethyl' structures can be taken as some measure of crystal-packing forces on the conformations of the substituents. Differences are small but can be as much as 0.02 Å in a particular bond length and ca. 2° in a particular bond angle.

The ranking of substituents in order of increasing mean or sum of C-Si-C angles or decreasing Si out-of-plane distance (Table 1) is triethyl ≤ di-*tert*-butylmethyl < tri-*tert*-butyl ≤ triethyl' < triisopropyl. The unexpected result is that the tri-*tert*-butyl derivative is not the highest ranking. One might have expected its slightly superior electron-releasing inductive effect to best stabilize the developing positive charge on silicon

and its superior steric bulk to push the carborane anion more distant. However, as discussed above, the Si-Br-B angle simply opens up to 125° to accommodate the bulky *tert*-butyl substituents.

**Bromonium versus Silylium Ion Character.** It has been suggested that these  $R_3Si(Br_6-CB_{11}H_6)$  species are bromonium ions.<sup>42</sup> The structural data do not, however, support this view. The formal representation of a bromonium ion is given as structure I in Figure 2. The C-Si-C angles reflect tetrahedrality at silicon (109°), and the bond angle at bromine is 109° (by VSEPR theory and X-ray structure).<sup>43</sup> The formal representation of a silylium ion is given as structure III in Figure 2. The C-Si-C angles reflect trigonal planarity (120°), and there is no Si-Br bond. The present  $R_3Si$ -(carborane) species are represented by structure II in Figure 2. The C-Si-C angles at averages of 115-117° are ca. 55%-70% along the trajectory from 109° in I to 120° in III, representing ca. 55%-70% development of silylium ion character. In addition, the wide range of Si-Br-B angles (109-125°), the long Si-Br bonds, and the minimal perturbation of the coordinated Br-B bond all reflect electrostatic bonding in a silylium ion rather than bromonium ion sense, i.e.,  $R_3Si^{\delta+}(Br_6-CB_{11}H_6)^{\delta-}$ . Thus, while bromonium ion character must be present to some extent, we conclude that it is minor compared to silylium ion character. Compounds should be named after their predominant structural and electronic form, and we suggest silylium "ion-like" as the most appropriate description. The silylium ion character of the present species is reflected in their reaction chemistry. They react with nucleophiles such as organic halides to form  $R_3SiX$  (X = halide) or water to give  $R_3Si(OH_2)^+$ .<sup>44</sup> We have yet to observe any property that might indicate predominant bromonium ion character, and in no circumstance have we observed B-Br bond cleavage. Rather, the bromocarborane moiety retains its weakly nucleophilic anionic character in all chemistry explored to date.

The above observations have led us to propose that there is a continuum of cation-anion interactions between partially covalent species of the type  $R_3SiY$  and the fully ionic silylium ion,  $R_3Si^+Y^-$ .<sup>2,45</sup> This principle has been adopted in recent theoretical papers<sup>34,46</sup> and is in marked contrast to carbocation chemistry where

(42) Olah, G. A.; Rasul, G.; Li, X.-Y.; Buchholz, H. A.; Sanford, G.; Prakash, G. K. S. *Science* **1994**, *263*, 983-984.

(43) Yanovskii, A. I.; Struchkov, Yu. T.; Grushin, V. V.; Tolstaya, T. P.; Demkina, I. I. *Zh. Strukt. Khim.* **1988**, *29*, 89-94.

(44) Xie, Z.; Bau, R.; Reed, C. A. *J. Chem. Soc., Chem. Commun.* **1994**, 2519-2520.

(45) Reed, C. A.; Xie, Z. *Science* **1994**, *263*, 985-986.

(46) Schleyer, P. v. R. Personal communication, 1994. Maerker, C.; Kapp, J.; Schleyer, P. v. R. Submitted for publication.

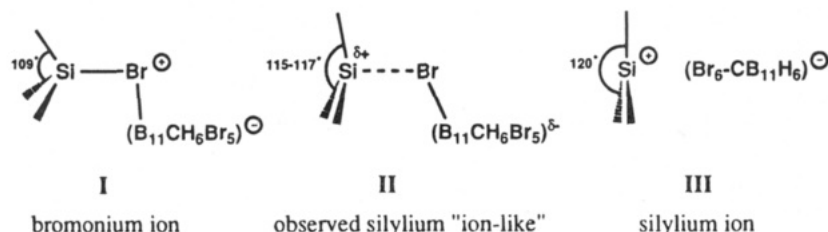


**Figure 2.** Structural representations of a bromonium ion (I), the present compounds (II) having a majority of silylium ion-like character, and a silylium ion (III).

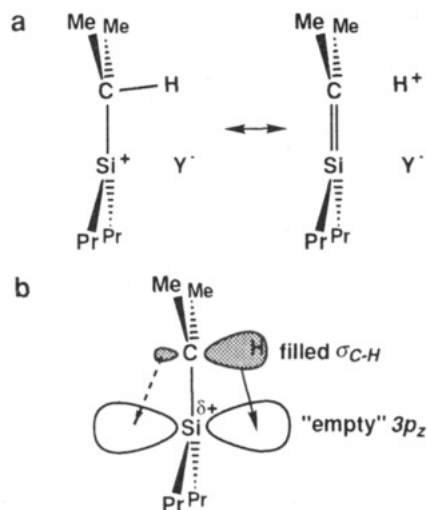


**Figure 3.** (a) Classical resonance representation of C-H bond hyperconjugative stabilization of cationic silicon. (b) Equivalent molecular orbital description. Shading is used to represent the filled orbital (not the sign of the wave function).

the distinction between covalent tetrahedral carbon and ionic trigonal carbenium ions is more "black and white".

**Hyperconjugation.** There are notable differences in the three isopropyl groups of *i*-Pr<sub>3</sub>Si(Br<sub>6</sub>-CB<sub>11</sub>H<sub>6</sub>) with respect to Si-C bond length and with respect to bond angles around their central carbon atoms. In particular, the shortest Si-C bond is to C(8), and this isopropyl carbon atom has the largest Si-C-C angles [119.0(22) and 128.2(28)°]. They far exceed the sp<sup>3</sup> ideal, and indeed, the C(8) isopropyl carbon atom is nearly planar. The sum of the angles around C(8) is 359.5 (3)° (see Table 2). This can be seen in the uppermost isopropyl group of Figure 1c. It is strongly suggestive of C-H bond hyperconjugation, giving double-bond character to the Si-C(8) bond and sp<sup>2</sup> character to the isopropyl carbon. The localized valence-bond representation is given in Figure 3a. The equivalent molecular orbital representation is given in Figure 3b. The filled  $\sigma_{C-H}^b$  orbital donates electron density into the developing empty 3p<sub>z</sub>-like orbital along the Si-Br direction. The pyramidalization at silicon means that this orbital will also have silicon 3s character. It is electron deficient because of the weak silicon-bromine bond. A more "inorganic" description would use the same molecular orbital representation of Figure 3b but would call it an  $\alpha$ -agostic C-H interaction.<sup>47</sup> Either way, a donor orbital and an acceptor orbital are identified, and the short Si-C bond and near-planarity of the isopropyl carbon atom substituents are rationalized. The calcu-

lated position of the isopropyl H atom (assuming trigonal pyramidal) does not place it in the same plane as the C(8)-Si-Br atoms, as might be expected for optimal  $\sigma_{C-H}^b/3p_z$  overlap. Rather, there is a torsional angle of 36° between the H-C and Si-Br vectors. This probably reflects a compromise engendered by the steric effect of the bromine atom. Its size prevents an ideal alignment of the C-H bond with the Si-Br bond. We have considered the possibility of an attractive interaction of the C<sup>δ-</sup>-H<sup>δ+</sup> dipole to the electron-rich bromine atom. Indeed, this is an expected consequence of hyperconjugation. There is no simple way to separate these two effects, although the lack of coplanarity of the C-H and Si-Br bonds suggests that the extended overlap of orbitals is more important than the attraction of localized partial charges at the atomic positions.

The steric effect of the bromine atom offers a possible explanation for why *tert*-butyl substituents show less structural manifestation of hyperconjugation than this particular isopropyl group. Hyperconjugative C-C bond approach to the Si-Br bond will be hindered by the bulk of the methyl group in a *tert*-butyl substituent relative to the H atom of an isopropyl substituent. Inspection of bond angles around silicon and the  $\alpha$ -carbon atoms in the di-*tert*-butylmethyl derivative, which has the opportunity for both C-C and C-H bond hyperconjugation, is less demonstrative of it. The three Si-C bonds are the same within experimental error and do not show the large range seen in the triisopropyl derivative. Similarly, the spread of Br-Si-C angles is only ~6° [101.1(15)-106.6(17)°]. It is not possible to determine the positions of the methyl group H atoms either from a X-ray data or by inference as was done for the isopropyl group. The spread of Si-C-C angles in the two *tert*-butyl groups is only ~8°, and no particular angle is far removed from sp<sup>3</sup> ideality (see Table 2). The lower angles might be interpreted as indicating C-C bond hyperconjugation, perhaps into the back lobe of the developing empty 3p<sub>z</sub> orbital on silicon, but overall, the dimensions of this compound suggest that hyperconjugative stabilization is distributed over a number of weak interactions among the three substituents rather than concentrated in one particular substituent as in the isopropyl case.

The two triethyl structures are somewhat more illustrative of hyperconjugation since there is a somewhat greater spread in the Si-C distances [1.80(2)-1.86(2) Å] and a larger range of Si-C-C angles [109.2(11)-122.6(14)°]. Like the isopropyl derivative, the shortest Si-C distance (to C(6) in the triethyl molecule) has the largest Si-C-C angle. This again suggests C-H hyperconjugation into the developing empty 3p<sub>z</sub> orbital on silicon but this time into the back lobe, *trans* to the Si-Br bond. The Br-Si-C(6) bond is 107.7 (8)°.

(47) Brookhart, M.; Green, M. L. H.; Wong, L.-L. *Prog. Inorg. Chem.* **1988**, *36*, 1-124.

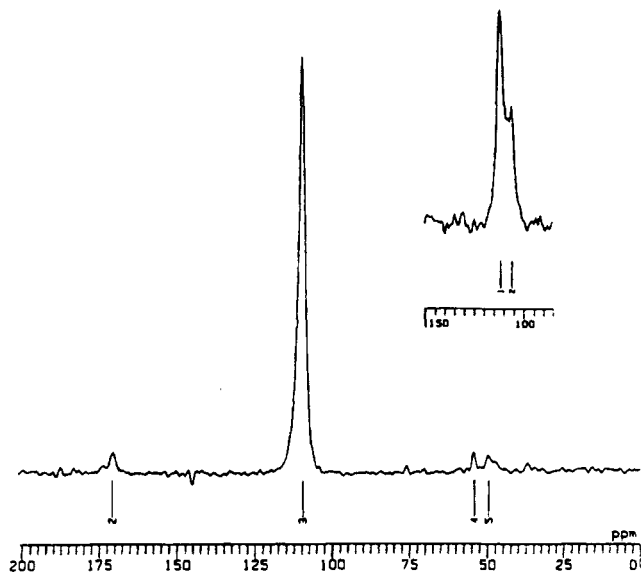


**Figure 4.** Solid state  $^{29}\text{Si}$  NMR spectrum of  $i\text{-Pr}_3\text{Si}(\text{Br}_6\text{-CB}_{11}\text{H}_6)$  and insert of the downfield portion for  $\text{Et}_3\text{Si}(\text{Br}_6\text{-CB}_{11}\text{H}_6)$ . Conditions: 110 mg sample, cross-polarization via spin lock with bilevel decoupling, pulse width  $5.35 \mu\text{s}$ , contact time 2.0 ms, pulse delay 2 s.

An ethyl substituent is quite unhindered as indicated by the variety of orientations of the ethyl groups in Figure 1a,b. Thus, they have the opportunity to engage in both C–H and C–C bond hyperconjugation. Evidence for C–C bond hyperconjugation would be a correlation of short Si–C bonds with *small* Si–C–C angles. This is not observed in any significant way (see Table 2). On the other hand, the correlation of the shortest Si–C bond with the *largest* Si–C–C angles (at least in the triethyl and triisopropyl structures) suggests that C–H hyperconjugation may be slightly more effective than C–C hyperconjugation in stabilizing the partial positive charge on silicon. This may reflect a closer energy match of the more polar C–H bond with the partially empty  $3p_z$  orbital on silicon.

**$^{29}\text{Si}$  NMR.** Downfield  $^{29}\text{Si}$  chemical shifts are the expected signature of developing silylium ion character in  $R_3\text{Si}^{\delta+}(\text{Br}_6\text{-CB}_{11}\text{H}_6^{\delta-})$  derivatives. We have determined these in the solid state by cross-polarization magic angle spinning techniques (CPMAS) for several reasons. Firstly, there is a practical reason. These derivatives are not very soluble in the only suitable solvent, benzene. Secondly, the possible coordination of solvent to form  $[\text{R}_3\text{Si}(\text{solvent})]^+$ , even if only to a small degree, complicates the interpretation of comparative data. Thirdly, we wanted to see if there is a correlation of downfield  $^{29}\text{Si}$  shift with X-ray measures of developing silylium ion character, particularly the mean C–Si–C angle.

A typical solid state  $^{29}\text{Si}$  spectrum is shown in Figure 4, and this one for the triisopropyl derivative. The only significant resonance occurs at 109.6 ppm downfield of tetramethylsilane. In a duplicate experiment from a different preparation we obtained an essentially identical sharp resonance at 110.0 ppm, indicating that the error in our quoted values is ca. 0.5 ppm. The  $t\text{-Bu}_2\text{Me}$  derivative gives a similar resonance at a chemical shift of 112.8 ppm. As expected from the two independent triethyl molecules seen in the X-ray structure, two  $^{29}\text{Si}$  resonances are seen in an  $\text{Et}_3$  sample, at 111.8 and 106.2 ppm. This is illustrated in the insert of Figure 4. To

date, we have been unable to obtain a comparable resonance for the tri-*tert*-butyl derivative perhaps due to the lack of hydrogen nuclei on  $\alpha$ -carbon atoms which may impractically change the time dependence of the cross-polarization compared to methyl, ethyl, or isopropyl substituents.

The small range of  $^{29}\text{Si}$  shifts in these  $R_3\text{Si}(\text{Br}_6\text{-CB}_{11}\text{H}_6)$  derivatives (106–113 ppm) is notable as is the lack of any discernable correlation with any particular X-ray structural parameter. The combined effects of three alkyl substituents on silicon, whether methyl, ethyl, isopropyl or *tert*-butyl, are apparently quite similar from an NMR chemical shift point of view. This supports the view developed earlier from our discussion of the silicon-bromine bonding that electrostatic considerations are the most important part of the trialkyl-silicon to carborane bonding. To a first approximation, the carborane anion dictates the degree of silylium ion character developed in the  $R_3\text{Si}^{\delta+}$  moiety and the R groups compensate accordingly. There is a possible parallel with carbocations where the  $^{13}\text{C}$  chemical shift for classical carbenium centers is rather insensitive to substituent. For example,  $\delta(^{13}\text{C})$  is essentially identical in  $\text{Me}_3\text{C}^+$  and  $\text{Et}_3\text{C}^+$  (335.2 and 336.8 ppm, respectively).<sup>48</sup> In the present trialkyl silicon derivatives the geometrical differences are apparently too small to produce a trend in  $\delta(^{29}\text{Si})$  and are matched by compensating electronic factors.

The downfield  $^{29}\text{Si}$  shifts (106–113 ppm) are the largest observed to date in a trialkylsilyl compound. The only comparable species is  $i\text{-Pr}_3\text{Si}(\text{F}_{20}\text{-BPh}_4)$ , whose solid state resonance is reported at 107.6 ppm.<sup>23</sup> For reference,  $[i\text{-Pr}_3\text{Si}(\text{toluene})]^+$  is ca. 94 ppm, and most other anions  $\text{Y}^-$  in comparable  $R_3\text{SiY}$  derivatives have  $^{29}\text{Si}$  chemical shifts in the range 30–55 ppm.<sup>4,14</sup> The silanes,  $R_3\text{SiH}$ , fall in the range 0–12 ppm for R = an alkyl group. Fully ionic planar  $R_3\text{Si}^+$  ions are expected to show  $\sim 300$  ppm downfield shifts.<sup>7,34,36,49,50</sup> Thus, the ca. 100 ppm downfield shifts of the  $R_3\text{Si}(\text{Br}_6\text{-CB}_{11}\text{H}_6)$  derivatives, relative to their silanes, are a clear indication of developing silylium ion character. Since there is no reason to expect  $^{29}\text{Si}$  shifts to scale linearly with any particular geometric parameter in  $R_3\text{Si}^{\delta+}\text{Y}^{\delta-}$  species, it is not presently possible to estimate "how much" silylium ion character the  $\sim 100$  ppm downfield shift represents. Interestingly, Schleyer<sup>46</sup> has shown by IGLO methods that the  $\sim 300$  ppm shift of  $R_3\text{Si}^+$  rapidly diminishes upon approach of weak nucleophiles. For example, when MeBr approaches  $\text{Me}_3\text{Si}^+$  to a Si $\cdots$ Br distance 2.46 Å (the same as that in the present bromocarborane species), the shift is calculated to be only 102 ppm. Thus, despite the fact that the downfield shifts of the present compounds fall well short of the predicted free silylium value, they may indicate a very high degree of silylium ion character.

## Conclusions

The very weak coordinating ability, the extreme chemical inertness, and the excellent crystallizing char-

(48) Olah, G. A.; Donovan, D. J. *J. Am. Chem. Soc.* **1976**, *99*, 5026–5039.

(49) Kutzelnigg, W.; Feischer, U.; Schindler, M. In *NMR; Basic Principles and Progress*; Diehl, P., Fluck, E., Gunther, H., Kosfeld, R., Selling, J., Eds.; Springer-Verlag: New York, 1991; Vol. 23, pp 228–231.

(50) Olah, G. A.; Field, L. *Organometallics* **1982**, *1*, 1485–1487.



**Table 3. Summary of Data and Intensity Collection Parameters for R<sub>3</sub>Si(Br<sub>6</sub>-CB<sub>11</sub>H<sub>6</sub>)**

R <sub>3</sub>	Et <sub>3</sub>	<i>i</i> -Pr <sub>3</sub>	<i>t</i> -Bu <sub>2</sub> Me	<i>t</i> -Bu <sub>3</sub>
formula	C <sub>7</sub> H <sub>21</sub> B <sub>11</sub> Br <sub>6</sub> Si	C <sub>10</sub> H <sub>27</sub> B <sub>11</sub> Br <sub>6</sub> Si	C <sub>10</sub> H <sub>27</sub> B <sub>11</sub> Br <sub>6</sub> Si	C <sub>13</sub> H <sub>33</sub> B <sub>11</sub> Br <sub>6</sub> Si
molecular wt (mol)	731.7	773.8	773.8	815.8
cryst syst	triclinic	triclinic	monoclinic	monoclinic
space group	<i>P</i> $\bar{1}$	<i>P</i> $\bar{1}$	<i>P</i> 2 <sub>1</sub> / <i>c</i>	<i>P</i> 2 <sub>1</sub>
<i>a</i> , Å	7.786(2)	11.124(8)	8.121(5)	8.208(2)
<i>b</i> , Å	16.212(3)	15.628(15)	23.351(23)	20.409(2)
<i>c</i> , Å	19.660(4)	8.000(9)	14.214(18)	8.648(2)
$\alpha$ , deg	110.70(3)	94.96(8)	90	90
$\beta$ , deg	97.62(3)	98.85(8)	96.18(8)	97.22(2)
$\gamma$ , deg	92.05(3)	76.30(7)	90	90
<i>V</i> , Å <sup>3</sup>	2291.8(9)	1333(2)	2680(5)	1437.2(5)
<i>Z</i>	4	2	4	2
calcd density (g cm <sup>-3</sup> )	2.12	1.93	1.93	1.89
radiation ( $\lambda$ , Å)	Cu K $\alpha$ (1.541 78)	Mo K $\alpha$ (0.710 69)	Mo K $\alpha$ (0.710 69)	Cu K $\alpha$ (1.541 78)
abs coeff	13.07	8.99	8.95	10.49
temp (K)	123	298	298	123
scan type	$\theta$ -2 $\theta$	$\omega$	$\omega$	$\omega$
index ranges	<i>h</i> , $\pm k$ , $\pm l$	<i>h</i> , $\pm k$ , $\pm l$	<i>h</i> , <i>k</i> , $\pm l$	<i>h</i> , $\pm k$ , $\pm l$
no. of independent reflns	4749	2993	2805	2873
no. of obsd reflns ( <i>F</i> > 3.0 $\sigma$ ( <i>F</i> ))	3194	1296	1072	2789 ( <i>F</i> > 4.0 $\sigma$ ( <i>F</i> ))
no. of params refined	271	255	255	279
final R indices	6.71	6.37	6.93	6.28

acteristics of the brominated carborane Br<sub>6</sub>-CB<sub>11</sub>H<sub>6</sub><sup>-</sup> make it the anion of choice at this time for approaching the long-sought silylium ion, R<sub>3</sub>Si<sup>+</sup>, in the solid state. By the criteria of angular approach to planarity and <sup>29</sup>Si downfield shifts, the present compounds are the closest approach to date. To a first approximation, the nature of R is less important than the low coordinative nucleophilicity of the anion. The degree of pyramidalization at silicon and the chemical shifts span only a small range of R = Me, Et, *i*-Pr, and *t*-Bu. A close examination of substituent geometries in five different R<sub>3</sub>Si(Br<sub>6</sub>-CB<sub>11</sub>H<sub>6</sub>) molecules suggests that hyperconjugative stabilization of the positive charge at silicon, while not dramatic, is nevertheless present. Moreover, C-H bond hyperconjugation seems to be slightly favored over C-C bond hyperconjugation. This suggests that an isopropyl substituent may be the alkyl group of choice in attempts to isolate fully ionic R<sub>3</sub>Si<sup>+</sup>. Steric bulk can obviously be a factor in helping separate the cation and anion, but the *tert*-butyl group is surprisingly ineffective.

Silicon is an important bridging element between organic and inorganic chemistry. To our knowledge, no one has previously pointed out that the C-H bond hyperconjugation concept of organic chemistry is the same as the  $\alpha$ -agostic C-H interaction concept of transition metal chemistry, when viewed in donor-acceptor molecular orbital terms. Both, of course, are manifestations of the modern chemical reality that we live in the age of weak interactions, and all bonds are significantly more delocalized than suggested by writing familiar valence bond structures. Mulliken defined hyperconjugation in 1939 as "conjugation over and above that usually recognized".<sup>51</sup> In 1983, Brookhart and Green defined agostic interactions specifically with regard to entropically-promoted interactions of C-H bonds with transition metals.<sup>47</sup> Both definitions were very important in attracting attention to phenomena that tended to be overlooked at the times they were introduced. The passage of time, however, diminishes the need for such exclusive or specific definitions. Having said this, it is important to add that the  $\beta$ -agostic effect (as opposed to the  $\alpha$ ) is a remote C-H bond donation which remains usefully distinguished

from the through-bond hyperconjugative effect. It remains to be seen whether a  $\beta$ -agostic effect will be found in silicon cations.

### Experimental Section

Solution NMR spectra were recorded on a Bruker WP-270 or Bruker AM-360 spectrometer using BF<sub>3</sub>·OEt<sub>2</sub> or Me<sub>4</sub>Si as external standard for <sup>11</sup>B or <sup>29</sup>Si, respectively, and are reported in ppm. Infrared spectra were recorded on an IBM IR/30S FT instrument. Elemental analyses were performed by Oneida Research Services, NY, or by Microanalytical Lab, Department of Chemistry, University of California, Berkeley. (*t*-C<sub>4</sub>H<sub>9</sub>)<sub>3</sub>-SiH,<sup>52</sup> (*t*-C<sub>4</sub>H<sub>9</sub>)<sub>2</sub>(CH<sub>3</sub>)SiH,<sup>52</sup> and [(C<sub>6</sub>H<sub>5</sub>)<sub>3</sub>C<sup>+</sup>][Br<sub>6</sub>-CB<sub>11</sub>H<sub>6</sub><sup>-</sup>]<sup>25</sup> were prepared by literature methods. All solvents were distilled from Na/benzophenone inside the glovebox. Other reagents were purchased from Aldrich and used as supplied. All experiments were performed with flame-dried glassware in a He atmosphere glovebox (O<sub>2</sub>, H<sub>2</sub>O < 0.5 ppm).

Solid state <sup>29</sup>Si NMR spectra were obtained at 294 K on a Chemagnetics CMX-300 spectrometer operating in the quadrature mode at 59.08 MHz. Cross-polarization with magic angle spinning (CPMAS) was used with a contact time of 2.0 ms to enhance the signal and shorten the relaxation time between successive transients. Typically, 5000-15 000 transients were acquired for each sample. Samples were sealed in glass rotor inserts designed by Wilmad Glass Co. to fit the zirconia Chemagnetics rotors. Tetrakis(trimethylsilyl)silane was used as an external reference.

(C<sub>2</sub>H<sub>5</sub>)<sub>3</sub>Si(Br<sub>6</sub>-CB<sub>11</sub>H<sub>6</sub>): (C<sub>2</sub>H<sub>5</sub>)<sub>3</sub>SiH (30.5 mg, 0.262 mmol) was added to a suspension of [Ph<sub>3</sub>C<sup>+</sup>][Br<sub>6</sub>-CB<sub>11</sub>H<sub>6</sub><sup>-</sup>] (124.7 mg, 0.145 mmol) in dry toluene (50 mL). The mixture was stirred at room temperature for 7 h to give a clear pale yellow solution. Concentration of the solution and *n*-hexane vapor diffusion resulted in colorless crystals (80.2 mg, 76%). <sup>11</sup>B NMR (C<sub>6</sub>D<sub>6</sub>): -1.40 (s, 1B), -9.65 (s, 5B), -20.03 (d, 5B). IR (KBr): 3057 w, 2960-2858 s, 2610 s, 1475 m, 1005 s, 860 s cm<sup>-1</sup>. Anal. Calcd for C<sub>7</sub>H<sub>21</sub>B<sub>11</sub>Br<sub>6</sub>Si: C, 11.49; H, 2.89. Found: C, 11.40; H, 3.00.

(*i*-C<sub>3</sub>H<sub>7</sub>)<sub>3</sub>Si(Br<sub>6</sub>-CB<sub>11</sub>H<sub>6</sub>): Under preparative conditions similar to above, a mixture of *i*-Pr<sub>3</sub>SiH (20.1 mg, 0.127 mmol) and [Ph<sub>3</sub>C<sup>+</sup>][Br<sub>6</sub>-CB<sub>11</sub>H<sub>6</sub><sup>-</sup>] (60.0 mg, 0.070 mmol) in dry toluene (25 mL) was stirred at room temperature overnight. Very pale yellow crystals (35.5 mg, 66%) were isolated by *n*-hexane diffusion. <sup>11</sup>B NMR (C<sub>6</sub>D<sub>6</sub>): -1.43 (s, 1B), -9.69 (s, 5B), -20.06 (d, 5B). IR (KBr): 3065 w, 2964-2865 s, 2612 s,

(51) Mulliken, R. S. *J. Chem. Phys.* **1939**, *7*, 339-352.(52) Doyle, M. P.; West, C. T. *J. Am. Chem. Soc.* **1975**, *97*, 3777-3782.



1480 m, 1010 s, 950 s, 860 vs, 830 m  $cm^{-1}$ . Anal. Calcd for  $C_{10}H_{27}B_{11}Br_6Si$ : C, 15.52; H, 3.52. Found: C, 15.59; H, 3.57.

**(*t*-C<sub>4</sub>H<sub>9</sub>)<sub>2</sub>(CH<sub>3</sub>)Si(Br<sub>6</sub>-CB<sub>11</sub>H<sub>6</sub>):** This was prepared in a similar manner to (*i*-C<sub>3</sub>H<sub>7</sub>)<sub>3</sub>Si(Br<sub>6</sub>-CB<sub>11</sub>H<sub>6</sub>), and pale yellow crystals were isolated in 71% yield. <sup>11</sup>B NMR (C<sub>6</sub>D<sub>6</sub>): -1.40 (s, 1B), -9.60 (s, 5B), -20.01 (d, 5B). IR (KBr): 3058 s, 2964-2861 s, 2610 s, 1470 m, 1003 s, 992 s, 933 m, 860 vs, 825 s  $cm^{-1}$ . Anal. Calcd for  $C_{10}H_{27}B_{11}Br_6Si$ : C, 15.52; H, 3.52. Found: C, 15.48; H, 3.50.

**(*t*-C<sub>4</sub>H<sub>9</sub>)<sub>3</sub>Si(Br<sub>6</sub>-CB<sub>11</sub>H<sub>6</sub>):** To a suspension of [Ph<sub>3</sub>C<sup>+</sup>][Br<sub>6</sub>-CB<sub>11</sub>H<sub>6</sub><sup>-</sup>] (150.0 mg, 0.175 mmol) in dry toluene (80 ml) was added (*t*-C<sub>4</sub>H<sub>9</sub>)<sub>3</sub>SiH (80.0 mg, 0.399 mmol). The mixture was stirred at room temperature for 2 weeks to give a colorless clear solution. Concentration of the solution and *n*-hexane vapor diffusion gave pale-yellow crystals (118 mg, 83%). <sup>11</sup>B NMR (C<sub>6</sub>D<sub>6</sub>): -1.42 (s, 1B), -9.63 (s, 5B), -20.00 (d, 5B). IR (KBr): 3057 w, 2960-2866 s, 2611 s, 1469 s, 1002 s, 953 s, 860 s, 816 m  $cm^{-1}$ . Anal. Calcd for  $C_{13}H_{33}B_{11}Br_6Si$ : C, 19.14; H, 4.08. Found: C, 19.10; H, 4.12.

**X-ray Structure Determinations.** All crystals were mounted in thin-walled glass capillaries using Paratone-N oil. Diffraction data were collected on a Siemens P4/RA or a Syntex P2<sub>1</sub> diffractometer under the conditions indicated in Table 3. Crystallographic examinations led to the cell constants and

space groups. Absorption correction procedures were applied to the intensity data. Structures were solved by direct methods using Siemens SHELXTL PC software or SHELX86.<sup>53</sup> In the final model, hydrogen atoms of the alkyl substituents were placed in idealized positions and most of non-hydrogen atoms were refined anisotropically. Data collection and refinement parameters are given in Table 3.

**Acknowledgment.** We thank the National Science Foundation (CHE 9407284 to C.A.R.) and the Research Corporation (R-171 to R.B.) for support.

**Supporting Information Available:** Further details of the X-ray crystal structure determinations, tables of bond lengths, bond angles, anisotropic thermal parameters, calculated hydrogen atomic coordinates, final atomic coordinates, and atom-numbering schemes for the four structures (44 pages). Ordering information is given on any current mast-head page.

OM9504462

(53) *Shelxtl PC*; Siemens Analytical X-ray Instruments, Inc.: Madison, WI, May 1990.

# Reactions of a Uranium(IV) Tertiary Alkyl Bond: Facile Ligand-Assisted Reduction and Insertion of Ethylene and Carbon Monoxide

Marc Weydert, John G. Brennan, Richard A. Andersen,\* and Robert G. Bergman\*

Department of Chemistry, University of California, and Chemical Sciences Division, Lawrence Berkeley Laboratory, Berkeley, California 94720

Received March 8, 1995<sup>®</sup>

Reaction of  $(\text{MeC}_5\text{H}_4)_3\text{UX}$  ( $\text{X} = \text{Cl}, \text{MeC}_5\text{H}_4$ ) with  $t\text{-BuLi}$  affords the tertiary alkyl complex  $(\text{MeC}_5\text{H}_4)_3\text{U}(t\text{-Bu})$ . Despite uranium(IV) generally being the preferred oxidation state in organometallic systems,  $(\text{MeC}_5\text{H}_4)_3\text{U}(t\text{-Bu})$  reacts with Lewis bases ( $\text{L} = \text{PMe}_3, \text{THF}, \text{RCN}, \text{RNC}$ ) to yield the reduced uranium(III) base adducts  $(\text{MeC}_5\text{H}_4)_3\text{U}(\text{L})$ . Carbon monoxide undergoes migratory insertion into the metal tertiary alkyl bond. The resulting acyl derivative decomposes at  $90^\circ\text{C}$  to yield insoluble uranium-containing products and a mixture of *tert*-butyltoluenes by ring expansion of a methylcyclopentadienyl ligand. Ethylene also undergoes migratory insertion into the metal tertiary alkyl bond. No subsequent insertion of ethylene into the metal carbon bond takes place after the first equivalent has inserted. In marked contrast, reaction of various  $(\text{MeC}_5\text{H}_4)_3\text{ThX}$  ( $\text{X} = \text{Cl}, \text{I}, \text{MeC}_5\text{H}_4, \text{O}-2,6\text{-Me}_2\text{C}_6\text{H}_3, \text{OTs}$ ) compounds with  $t\text{-BuLi}$  gave intractable materials. However, reaction of the cationic species  $[(\text{RC}_5\text{H}_4)_3\text{Th}](\text{BPh}_4)$  ( $\text{R} = \text{Me}_3\text{Si}, t\text{-Bu}$ ) with  $t\text{-BuLi}$  yields the new thorium hydrides  $(\text{RC}_5\text{H}_4)_3\text{ThH}$ .

## Introduction

Isolable metal tertiary alkyl compounds,  $\text{L}_n\text{M}-t\text{-Bu}$ , are quite scarce. In d-block organometallic chemistry, only a few compounds are known due to the ease of  $\beta$ -hydrogen elimination.<sup>1</sup> This fact is in contrast to that which is found in the main group and f-block metals. In the main group metal series, compounds such as  $\text{Li}-t\text{-Bu}$ ,  $\text{Be}(t\text{-Bu})_2$ , and  $\text{B}(t\text{-Bu})_3$  are thermally stable to temperatures in excess of  $100^\circ\text{C}$ .<sup>2</sup> Several cyclopentadienyl and anionic lanthanide derivatives of the type  $\text{Cp}_2\text{M}(t\text{-Bu})(\text{L})$  and  $[\text{Li}(\text{L})_x][\text{M}(t\text{-Bu})_4]$  are stable enough to be isolated and characterized at room temperature.<sup>3</sup>

This paper reports a study of the reactions of the isolable uranium tertiary alkyl compound  $(\text{MeC}_5\text{H}_4)_3\text{U}(t\text{-Bu})$ . The unsubstituted uranium complex,  $\text{Cp}_3\text{U}(t\text{-Bu})$ , was included among the tris(cyclopentadienyl) alkyl compounds,  $\text{Cp}_3\text{UR}$ , prepared by Marks.<sup>4</sup> The decomposition of this compound in toluene solution was reported to yield 97% isobutane and insoluble uranium-

containing products. This isolable compound appeared to be an attractive starting material because of the relatively large body of known chemistry of tris(cyclopentadienyl)uranium complexes, allowing a straightforward comparison of the behavior of a tertiary alkyl derivative to that of the primary and secondary alkyl derivatives. Our interest in preparing an isolable uranium tertiary alkyl derivative is derived from earlier studies in which we<sup>5</sup> and others<sup>6</sup> have used *tert*-butyllithium as a reducing agent for synthesis of some U(III) metallocenes from U(IV) halide precursors. In our experience, this is the most useful synthetic method for preparation of base-free  $(\text{RC}_5\text{H}_4)_3\text{U}$ , in which R is  $\text{Me}_3\text{Si}^{5a}$  or  $t\text{-Bu}$ .<sup>5b</sup> In these cases the *tert*-butyl compound,  $(\text{RC}_5\text{H}_4)_3\text{U}(t\text{-Bu})$ , presumably is formed but it decomposes to the trivalent metallocene. In contrast, U(IV) metallocenes with sterically small substituents on the cyclopentadienyl ring yield isolable *tert*-butyl derivatives,  $(\text{RC}_5\text{H}_4)_3\text{U}(t\text{-Bu})$ ,  $\text{R} = \text{H},^4 \text{Me}, \text{Et}$ . We chose to study the methylcyclopentadienyl compound rather than the unsubstituted or ethyl derivatives because of its higher solubility in hydrocarbon solvents and since the methylcyclopentadienyl ligand yields three sets of resonances in the  $^1\text{H-NMR}$  spectrum, an advantage in these paramagnetic systems. We also describe our attempts to prepare the analogous thorium *tert*-butyl compound since this alkyl has not been mentioned in the literature.<sup>7</sup>

<sup>®</sup> Abstract published in *Advance ACS Abstracts*, July 15, 1995.

(1) (a) Giering, W. P.; Rosenblum, M. *J. Organomet. Chem.* **1970**, *25*, C71-C73. (b) Kruse, W. *J. Organomet. Chem.* **1972**, *42*, C39-C42. (c) Bower, B. K.; Tennent, H. G. *J. Am. Chem. Soc.* **1972**, *94*, 2512-2514. (d) Bougeard, P.; McCullough, J. J.; Sayer, B. G.; McGlinchey, M. J. *Inorg. Chim. Acta* **1984**, *89*, 133-138. (e) Buchwald, S. L.; Kreutzer, K. A.; Fisher, R. A. *J. Am. Chem. Soc.* **1990**, *112*, 4600-4601.

(2) (a) Coates, G. E.; Wade, K. *Organometallic Compounds. The Main Group Elements*, 3rd ed.; Methuen: London, 1967; Vol. 2. (b) Nöth, H.; Taeger, T. *J. Organomet. Chem.* **1977**, *142*, 281-288.

(3) (a) Wayda, A. L.; Evans, W. J. *J. Am. Chem. Soc.* **1978**, *100*, 7119-7121. (b) Schumann, H.; Genthe, W.; Brucks, N. *Angew. Chem., Int. Ed. Engl.* **1981**, *20*, 119-120. (c) Evans, W. J.; Wayda, A. L.; Hunter, W. E.; Atwood, J. L. *J. Chem. Soc., Chem. Commun.* **1981**, 292-293. (d) Schumann, H.; Genthe, W.; Brucks, N.; Pickhardt, J. *Organometallics* **1982**, *1*, 1194-1200. (e) Schumann, H.; Reiser, F. W.; Dentlaff, M. *J. Organomet. Chem.* **1983**, *255*, 305-310. (f) Ye, C.; Qian, C.; Yang, X. *J. Organomet. Chem.* **1991**, *407*, 329-335.

(4) Marks, T. J.; Seyam, A. M.; Kolb, J. R. *J. Am. Chem. Soc.* **1973**, *95*, 5529-5539.

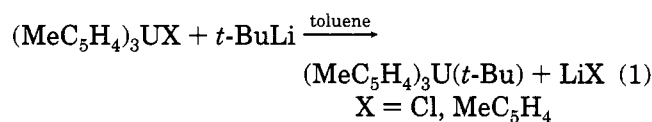
(5) (a) Brennan, J. G.; Andersen, R. A.; Zalkin, A. *Inorg. Chem.* **1986**, *25*, 1756-1760. (b) Stults, S. D.; Andersen, R. A.; Zalkin, A. *Organometallics* **1990**, *9*, 1623-1629.

(6) (a) Manriquez, J. M.; Fagan, P. J.; Marks, T. J.; Vollmer, S. H.; Day, C. S.; Day, V. W. *J. Am. Chem. Soc.* **1979**, *101*, 5075-5078. (b) Blake, P. C.; Lappert, M. F.; Taylor, R. G.; Atwood, J. L.; Hunter, W. E.; Zhang, H. *J. Chem. Soc., Chem. Commun.* **1986**, 1394-1395.

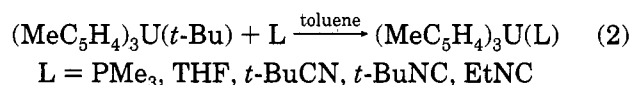
(7) Marks, T. J.; Wachter, W. A. *J. Am. Chem. Soc.* **1976**, *98*, 703-710.

## Results

As reported by Marks for the analogous cyclopentadienyl system,<sup>4</sup> addition of 1 equiv of *tert*-butyllithium to a toluene solution of  $(\text{MeC}_5\text{H}_4)_3\text{UCl}$  led to formation of  $(\text{MeC}_5\text{H}_4)_3\text{U}(t\text{-Bu})$ , which was isolated as dark green needles by crystallization from diethyl ether (eq 1).

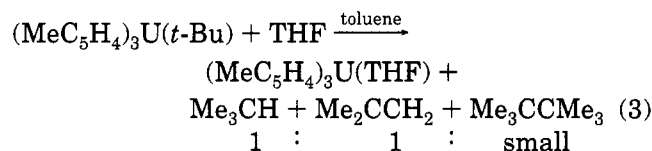


Alternatively,  $(\text{MeC}_5\text{H}_4)_3\text{U}(t\text{-Bu})$  was prepared with equal convenience starting from  $(\text{MeC}_5\text{H}_4)_4\text{U}$ . The tertiary alkyl compound was treated with a variety of Lewis bases to yield the reduced uranium(III) base adducts (eq 2). With the exception of THF, these reac-



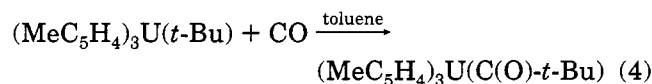
tions were fast at room temperature in toluene solution. At  $-80^\circ\text{C}$ , the reactions proceeded to completion within several hours to days. Qualitatively, the rate of reaction is correlated with the ability of the Lewis base to coordinate to the tris(methylcyclopentadienyl)uranium fragment; the better the base, in a thermodynamic sense,<sup>8</sup> the faster the rate of reaction. Furthermore, the rate of reaction increased with increasing concentration of a given Lewis base.

In the case of L = THF, the organic products of the reaction carried out in toluene were identified as isobutane and isobutene in approximately a 1:1 ratio; a small amount of hexamethylethane was also formed (eq 3).



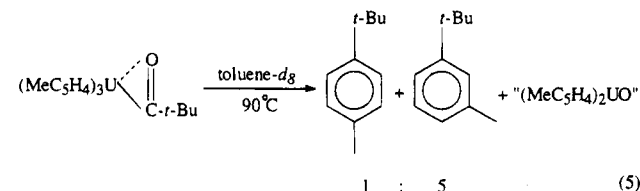
The identities of these compounds were confirmed by  $^1\text{H-NMR}$  spectroscopy and comparison to known standards by gas chromatography. Monitoring the reaction by  $^1\text{H-NMR}$  spectroscopy in the presence of an internal standard (cyclohexane) demonstrated that the conversion to  $(\text{MeC}_5\text{H}_4)_3\text{U}(\text{THF})$ , isobutane, and isobutene is essentially quantitative based on  $(\text{MeC}_5\text{H}_4)_3\text{U}(t\text{-Bu})$ . The unsubstituted and the ethyl derivative,  $(\text{RC}_5\text{H}_4)_3\text{U}(t\text{-Bu})$ , R = H, Et, showed qualitatively similar behavior toward THF.

Under 1 atm of carbon monoxide,  $(\text{MeC}_5\text{H}_4)_3\text{U}(t\text{-Bu})$  underwent migratory insertion of 1 equiv of CO to yield a tris(methylcyclopentadienyl)uranium(IV) acyl compound exhibiting a CO infrared stretching frequency at  $1490\text{ cm}^{-1}$  (eq 4). While investigating the variable



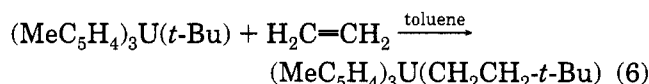
temperature  $^1\text{H-NMR}$  spectrum of the acyl derivative (Figure 1) in hopes of detecting a  $\eta^1-\eta^2$  equilibrium, we noticed that a decomposition reaction took place. In-

deed, when heated to  $90^\circ\text{C}$  in toluene- $d_8$  or methylcyclohexane- $d_{14}$  solution, the acyl derivative decomposed to yield *m*- and *p-tert*-butyltoluene in essentially quantitative yield and an insoluble organometallic residue, written as a metallocene oxo uranium compound although we have no evidence for its identity (eq 5). The



identity of the organic products was established by comparison to known commercial samples using GC and  $^1\text{H}$ - and  $^{13}\text{C}$ -NMR spectroscopy. No evidence of deuterium incorporation was detected in the resulting *m*- and *p-tert*-butyltoluene by GC-MS and NMR spectroscopy.

Under ethylene (210 psi), a toluene solution of  $(\text{MeC}_5\text{H}_4)_3\text{U}(t\text{-Bu})$  slowly reacted over a period of ca. 5 h to yield the ethylene monoinsertion product (eq 6).



This compound, tris(methylcyclopentadienyl)neohexyluranium, could be isolated as deep red-brown crystals from hexane. When a toluene solution of the neohexyl derivative was exposed to 220 psi of ethylene for 1 week, no evidence of additional insertion of ethylene into the metal-carbon bond could be detected. On the basis of  $^1\text{H-NMR}$  evidence, propylene also appears to insert into the uranium tertiary alkyl bond, although we have not been able to isolate the resulting oil as a pure substance.

A number of thorium compounds,  $(\text{MeC}_5\text{H}_4)_3\text{ThX}$  (X = Cl, I,  $\text{MeC}_5\text{H}_4$ , O-2,6- $\text{Me}_2\text{C}_6\text{H}_3$ ) were treated with *t*-BuLi in toluene solution. In each case, no immediate reaction could be observed. After longer reaction times (24–48 h), only a reduced yield of starting material was recovered from the reaction mixtures, while all the *t*-BuLi had been consumed and insoluble materials had formed. All the above mentioned compounds reacted cleanly with MeLi to form  $(\text{MeC}_5\text{H}_4)_3\text{ThMe}$  in good yield. In order to develop thorium compounds with better leaving groups, the iodide derivative was prepared by reaction of  $(\text{MeC}_5\text{H}_4)_3\text{ThCl}$  with (trimethylsilyl)iodide, and the 2,6-dimethylphenoxide derivative was prepared by treatment of  $(\text{MeC}_5\text{H}_4)_4\text{Th}$  with the phenol. The *p*-toluenesulfonate derivative,  $(\text{MeC}_5\text{H}_4)_3\text{Th}(\text{OTs})$ , was prepared by a similar protonation reaction from  $(\text{MeC}_5\text{H}_4)_4\text{Th}$  and *p*-toluenesulfonic acid. The tosylate reacted instantaneously with *t*-BuLi in toluene solution. The isolated reaction product, however, could not be unambiguously characterized due to its low solubility. The cationic complex  $[(\text{MeC}_5\text{H}_4)_3\text{Th}(\text{NMe}_3)](\text{BPh}_4)$  was prepared from  $(\text{MeC}_5\text{H}_4)_3\text{ThMe}$  and  $(\text{Me}_3\text{NH})(\text{BPh}_4)$ , as previously reported.<sup>9</sup> A suspension of this complex was treated with *t*-BuLi in hexane for 18 h. The only product that could be isolated from the reaction mixture was  $(\text{MeC}_5\text{H}_4)_4\text{Th}$  in low yield (25%). However, the bulkier base-free and hydrocarbon-soluble cations  $[(\text{RC}_5\text{H}_4)_3\text{Th}](\text{BPh}_4)$  (R =  $\text{Me}_3\text{Si}$ , *t*-Bu) gave clean reactions with *t*-BuLi at room temperature to yield the new

(8) (a) Brennan, J. G.; Stults, S. D.; Andersen, R. A.; Zalkin, A. *Inorg. Chim. Acta* **1987**, *139*, 201–202. (b) Brennan, J. G. Ph.D. Thesis, University of California, Berkeley, CA, 1985.

(9) Lin, Z.; Le Maréchal, J. F.; Sabat, M.; Marks, T. J. *J. Am. Chem. Soc.* **1987**, *109*, 4127–4129.

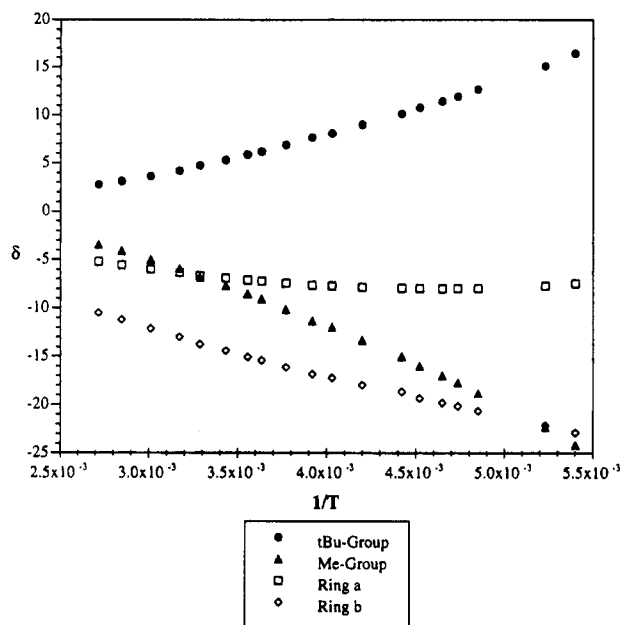
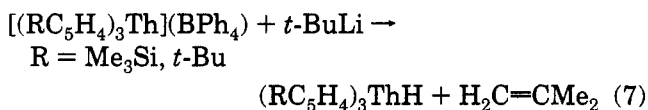


**Figure 1.** Plot of the  $^1\text{H}$  NMR chemical shifts of  $(\text{MeC}_5\text{H}_4)_3\text{U}(\text{C}(\text{O})-t\text{-Bu})$  in toluene- $d_8$  solution from +95 to  $-88^\circ\text{C}$ .

thorium hydride species  $(\text{RC}_5\text{H}_4)_3\text{ThH}$  (eq 7). When



these reactions were followed by  $^1\text{H}$ -NMR spectroscopy in benzene- $d_6$  solution, the formation of  $(\text{RC}_5\text{H}_4)_3\text{ThH}$  and isobutene in a 1:1 ratio could be observed, and impurities accounted for less than 5% of the consumed starting material.  $(\text{Me}_3\text{SiC}_5\text{H}_4)_3\text{ThH}$  could also be prepared from  $(\text{Me}_3\text{SiC}_5\text{H}_4)_3\text{ThCl}$  with 1 equiv of lithium triethylborohydride. However, the attempted hydrogenolysis of  $(t\text{-BuC}_5\text{H}_4)_3\text{ThMe}$  gave no reaction over *ca.* 8 h in toluene solution at 220 psi of hydrogen.

## Discussion

The tertiary alkyluranium complex  $(\text{MeC}_5\text{H}_4)_3\text{U}(t\text{-Bu})$  was prepared by addition of 1 equiv of *tert*-butyllithium to a toluene solution of the corresponding chloride  $(\text{MeC}_5\text{H}_4)_3\text{UCl}$  or alternatively to a toluene solution of  $(\text{MeC}_5\text{H}_4)_4\text{U}$ . The methylcyclopentadienyl derivative rather than the cyclopentadienyl analogue was chosen because it exhibits more convenient solubility properties. The methylcyclopentadienyl ligand also provides three  $^1\text{H}$ -NMR resonances rather than the single peak of the cyclopentadienyl ligand, thus facilitating the identification of paramagnetic uranium compounds by  $^1\text{H}$ -NMR spectroscopy. We have previously reported on the reactions of  $(\text{MeC}_5\text{H}_4)_3\text{U}(t\text{-Bu})$  with fluorocarbons.<sup>10</sup>

**Reactions with  $\sigma$ -Donor Ligands.** Thermolysis of  $(\text{MeC}_5\text{H}_4)_3\text{U}(t\text{-Bu})$  in the presence of dative ligands results in the cleavage of the tertiary metal-carbon bond. The nature of the dative ligand has a strong effect on the rate of this reaction. At room temperature  $(\text{MeC}_5\text{H}_4)_3\text{U}(t\text{-Bu})$  reacts instantaneously with  $\text{PMe}_3$  to give the reduced uranium(III) phosphine complex

$(\text{MeC}_5\text{H}_4)_3\text{U}(\text{PMe}_3)$ <sup>11</sup> in high yield. As has been established earlier, trimethylphosphine is a good  $\sigma$ -donor ligand toward the  $(\text{MeC}_5\text{H}_4)_3\text{U}$ -fragment.<sup>8</sup> However, the ease with which this reaction takes place is surprising, given that the uranium(IV)/uranium(III) reduction potential in these types of organometallic compounds is on the order of  $-1.5\text{ V}$ .<sup>12</sup> It should be noted that thermal decomposition of  $(\text{MeC}_5\text{H}_4)_3\text{U}(t\text{-Bu})$  in toluene solution in the absence of  $\text{PMe}_3$  requires higher temperatures and leads to an insoluble organometallic product. Treatment of this insoluble material with  $\text{PMe}_3$  in toluene solution does not result in formation of  $(\text{MeC}_5\text{H}_4)_3\text{U}(\text{PMe}_3)$ . Hence, the reaction of  $(\text{MeC}_5\text{H}_4)_3\text{U}(t\text{-Bu})$  with trimethylphosphine in toluene solution seems to involve direct interaction between the two reactants.

The weakest  $\sigma$ -donor ligand known to yield an isolable  $(\text{MeC}_5\text{H}_4)_3\text{U}(\text{L})$  complex is THF.<sup>8</sup> Thus,  $(\text{MeC}_5\text{H}_4)_3\text{U}(t\text{-Bu})$  was treated with 1 equiv of THF in toluene solution, and again formation of the reduced base adduct  $(\text{MeC}_5\text{H}_4)_3\text{U}(\text{THF})$  was observed. This behavior contrasts markedly with that of the analogous primary alkyl compounds, *e.g.*,  $\text{Cp}_3\text{UME}$  or  $\text{Cp}_3\text{U}(n\text{-Bu})$ , which dissolve in neat THF without appreciable reaction at room temperature. Even upon photolysis, formation of  $\text{Cp}_3\text{U}(\text{THF})$  is slow.<sup>13</sup> The reaction between  $(\text{MeC}_5\text{H}_4)_3\text{U}(t\text{-Bu})$  and THF is slower than its reaction with trimethylphosphine. With 1 equiv of THF in toluene solution at room temperature, the reaction is no longer instantaneous but goes to completion in *ca.* 1 day. This establishes that the rate of reaction depends on the  $\sigma$ -donor ability of the entering ligand L. Upon attempted dissolution of  $(\text{MeC}_5\text{H}_4)_3\text{U}(t\text{-Bu})$  in neat THF the donor complex  $(\text{MeC}_5\text{H}_4)_3\text{U}(\text{THF})$  is formed within minutes, although organometallic side products are formed as well. If several equivalents of THF are used in toluene or benzene solution, the rate of reaction increases with increasing concentration of THF. Thus the rate of reaction depends on the concentration of the entering  $\sigma$ -donor ligand. The organic reaction products isobutane, isobutene, and hexamethylethane are consistent with the displacement of a *tert*-butyl radical from the uranium metal center by the entering  $\sigma$ -donor ligand. We also prepared the analogous compounds  $\text{Cp}_3\text{U}(t\text{-Bu})$  and  $(\text{EtC}_5\text{H}_4)_3\text{U}(t\text{-Bu})$ . They both exhibit similar behavior toward THF. A detailed mechanistic study of this ligand-assisted metal-carbon bond homolysis will be reported elsewhere.<sup>14</sup>

**Reactions with Nitriles and Isocyanides.** In order to gain some insight into the preferred oxidation state in this system, the reaction of  $(\text{MeC}_5\text{H}_4)_3\text{U}(t\text{-Bu})$  was investigated with ligands known to form isolable  $(\text{MeC}_5\text{H}_4)_3\text{U}(\text{L})$  complexes<sup>8</sup> but which would also be capable of inserting into the metal-carbon bond and thus maintaining the tetravalent oxidation state of uranium. The reaction between  $(\text{MeC}_5\text{H}_4)_3\text{U}(t\text{-Bu})$  and *tert*-butylnitrile in toluene solution again resulted in formation of the uranium(III) complex  $(\text{MeC}_5\text{H}_4)_3\text{U}(\text{NC}-t\text{-Bu})$ . This may seem not too surprising as insertions

(11) Brennan, J. G.; Zalkin, A. *Acta Crystallogr., Sect. C: Cryst. Struct. Commun.* **1985**, *41C*, 1038-1040.

(12) Sonnenberger, D. C.; Gaudiello, J. G. *Inorg. Chem.* **1988**, *27*, 2747-2748.

(13) Klähne, E.; Gianotti, C.; Marquet-Ellis, H.; Folcher, G.; Fischer, R. D. *J. Organomet. Chem.* **1980**, *201*, 399-410.

(14) The details of this reaction are very complex and a detailed mechanism paper will be submitted shortly: Weydert, M.; Andersen, R. A.; Bergman, R. G. Manuscript in preparation.

(10) Weydert, M.; Andersen, R. A.; Bergman, R. G. *J. Am. Chem. Soc.* **1993**, *111*, 8837-8838.

of nitriles into metal-carbon bonds are relatively rare.<sup>15</sup> Though isocyanides readily insert into metal-carbon bonds,<sup>16</sup> *tert*-butyl isocyanide again reacted with  $(\text{MeC}_5\text{H}_4)_3\text{U}(t\text{-Bu})$  to form the uranium(III) base adduct. In contrast, *tert*-butylisocyanide will undergo migratory insertion into the metal-carbon  $\sigma$ -bond of  $\text{Cp}_3\text{UMe}$  and  $\text{Cp}_3\text{U}(n\text{-Bu})$ , yielding  $\eta^2$ -bound iminoacyl uranium(IV) compounds.<sup>17</sup> This difference highlights the unique reactivity of the tertiary alkyl compound.

In order to determine whether the increased steric bulk of the tertiary *vs* primary alkyl substituent affects the outcome of the reaction,  $(\text{MeC}_5\text{H}_4)_3\text{U}(t\text{-Bu})$  was reacted with a sterically small isocyanide. However, ethyl isocyanide also reacted with  $(\text{MeC}_5\text{H}_4)_3\text{U}(t\text{-Bu})$ , even at low temperature, to yield the uranium(III) base adduct  $(\text{MeC}_5\text{H}_4)_3\text{U}(\text{CNET})$ . These combined results suggest that the intrinsically preferred product for the reaction of  $(\text{MeC}_5\text{H}_4)_3\text{U}(t\text{-Bu})$  with isocyanides is the reduced base adduct and that steric factors play a minor role in determining the outcome of the reaction.

**Reaction with Carbon Monoxide.** Insertion of some small molecules into the uranium tertiary alkyl bond of  $(\text{MeC}_5\text{H}_4)_3\text{U}(t\text{-Bu})$  is nevertheless possible. Under 1 atm of carbon monoxide  $(\text{MeC}_5\text{H}_4)_3\text{U}(t\text{-Bu})$  is converted into the corresponding acyl compound. Its low IR stretching frequency of  $1490\text{ cm}^{-1}$  is consistent with the presence of an  $\eta^2$ -bonded acyl group. It should be noted that solution IR and solid state X-ray crystallographic data have been obtained for  $(\text{RC}_5\text{H}_4)_3\text{U}(\text{CO})$ <sup>18a</sup> and  $(\text{Me}_4\text{C}_5\text{H}_1)_3\text{U}(\text{CO})$ ,<sup>18b</sup> respectively. The insertion of carbon monoxide into the uranium-carbon bond has precedent in the  $\text{Cp}_3\text{UR}$  series, for which similar reactions have been reported for primary, secondary, and tertiary alkyl substituents.<sup>19</sup> The migratory insertion of carbon monoxide was reported to be reversible in the  $\text{Cp}_3\text{UR}$  series ( $\text{R} = \text{Me}, \text{Et}, i\text{-Pr}, n\text{-Bu}, t\text{-Bu}$ ) at temperatures above  $60^\circ\text{C}$ , as judged by the reported  $^1\text{H-NMR}$  spectra. In the present case, however, we see no evidence of reversibility for the carbon monoxide insertion into the metal-carbon  $\sigma$ -bond of  $(\text{MeC}_5\text{H}_4)_3\text{U}(t\text{-Bu})$ . We can offer no explanation of this apparent difference between the  $\text{Cp}_3\text{UR}$  and  $(\text{MeC}_5\text{H}_4)_3\text{UR}$  series.

In order to probe for a temperature-dependent  $\eta^1$ - $\eta^2$ -equilibrium for the acyl group, we investigated the variable temperature  $^1\text{H-NMR}$  spectrum of  $(\text{MeC}_5\text{H}_4)_3\text{U}(\text{C}(\text{O})-t\text{-Bu})$ , since a plot of  $\delta\text{ vs }1/T$  should follow Curie-Weiss behavior in the absence of temperature-dependent equilibria in solution.<sup>20</sup> A plot of the variable temperature  $^1\text{H-NMR}$  spectrum of  $(\text{MeC}_5\text{H}_4)_3\text{U}(\text{C}(\text{O})-t\text{-Bu})$  in toluene- $d_8$  solution is shown in Figure 1. A slight

deviation from linearity is apparent, and Curie-Weiss behavior is thus not strictly followed. The effect is most pronounced for the resonance that shows the smallest temperature dependence, ring resonance a. It is tempting to ascribe this behavior to the presence of a temperature-dependent  $\eta^1$ - $\eta^2$  equilibrium for the acyl group. However, a similar slight perturbation has been observed for a number of unrelated tris(cyclopentadienyl)uranium compounds, which we ascribe to the presence of temperature-dependent conformational equilibrium.<sup>21</sup> Figure 2 shows a superposition of the variable temperature  $^1\text{H-NMR}$  spectra of  $(\text{MeC}_5\text{H}_4)_3\text{U}(\text{C}(\text{O})-t\text{-Bu})$  in toluene- $d_8$  and in methylcyclohexane- $d_{14}$ . The curves follow the same qualitative behavior in both solvents, although a solvent effect on the chemical shift is apparent. Inspection of the ring resonance a, lower left graph of Figure 2c, shows that the temperature at which the curve reaches a minimum is lower in methylcyclohexane relative to toluene. This may be due to the greater viscosity of toluene relative to methylcyclohexane at low temperatures. Higher viscosity will result in higher internal pressure, which could change the conformational preferences of the molecule. These effects are small, but they are reproducible, so we think they reflect the energetic preference of one  $\text{MeC}_5\text{H}_4$ -ring conformation relative to the others. It is not possible to be more precise on the basis of the available data.

During these variable temperature  $^1\text{H-NMR}$  studies we discovered that, when samples of  $(\text{MeC}_5\text{H}_4)_3\text{U}(\text{C}(\text{O})-t\text{-Bu})$  in toluene- $d_8$  or methylcyclohexane- $d_{14}$  solution were heated to  $90^\circ\text{C}$  for 1 h, complete decomposition of the organometallic acyl compound occurred. No intermediate could be detected by  $^1\text{H-NMR}$  spectroscopy, and the only soluble products of these decomposition reactions were *tert*-butyltoluenes (eq 5), even in the saturated hydrocarbon solvent. A similar reaction has recently been reported by Ephritikhine and co-workers for the analogous  $\text{Cp}_3\text{U}(\text{C}(\text{O})\text{R})$  compounds.<sup>22</sup> These authors report that the reaction is promoted by the presence of a  $\sigma$ -donor ligand. They also established that the aromatic group originates from the cyclopentadienyl ring by incorporation of the acyl carbon into the six-membered ring. They attribute this peculiar reactivity to the oxycarbenoid character of the  $\text{Cp}_3\text{U}(\text{C}(\text{O})\text{R})$  complexes.

The present results indicate that, although this reaction may be accelerated by  $\sigma$ -donor ligands, their presence is not required for the reaction to proceed. The use of methylcyclopentadienyl ligands on uranium rather than cyclopentadienyl ligands leads to formation of alkyltoluenes rather than alkylbenzenes, and the regiochemistry of this reaction can be addressed. The decomposition of  $(\text{MeC}_5\text{H}_4)_3\text{U}(\text{C}(\text{O})-t\text{-Bu})$  in toluene- $d_8$  or in methylcyclohexane- $d_{14}$  at  $90^\circ\text{C}$  yields a mixture of *tert*-butyltoluenes. By GC and  $^1\text{H-NMR}$  spectroscopy, *m*-*tert*-butyltoluene and *p*-*tert*-butyltoluene were found in a 5:1 ratio, and no *o*-isomer was detected. This ratio differs from the reported thermodynamic equilibrium mixture of *tert*-butyltoluenes,<sup>23</sup> indicating some kinetic regioselectivity for the oxycarbene insertion into the methylcyclopentadienyl ring.

(21) Weydert, M. Ph.D. Thesis, University of California, Berkeley, CA, 1993.

(22) Villiers, C.; Adam, R.; Ephritikhine, M. *J. Chem. Soc., Chem. Commun.* **1992**, 1555-1556.

(23) Olah, G. A.; Meyer, M. W.; Overchuk, N. A. *J. Org. Chem.* **1964**, 29, 2310-2312.

(15) (a) Buchwald, S. L.; Watson, B. T.; Huffmann, J. C. *J. Am. Chem. Soc.* **1986**, 108, 7411-7413. (b) Buchwald, S. L.; Lum, R. T.; Dewan, J. C. *J. Am. Chem. Soc.* **1986**, 108, 7441-7442.

(16) Collman, J. P.; Hegedus, L. S.; Norton, J. R.; Finke, R. G. *Principles and Applications of Organotransition Metal Chemistry*; University Science Books: Mill Valley, CA, 1987; pp 377-378.

(17) (a) Dormond, A.; Elbouadili, A. A.; M6ise, C. *J. Chem. Soc., Chem. Commun.* **1984**, 749-751. (b) Zanella, P.; Paolucci, G.; Rosseto, F.; Benetello, F.; Polo, A.; Fischer, R. D.; Bombieri, G. *J. Chem. Soc., Chem. Commun.* **1985**, 96-98.

(18) (a) Brennan, J. G.; Andersen, R. A.; Robbins, J. L. *J. Am. Chem. Soc.* **1985**, 108, 335-336. (b) Parry, J.; Carmona, E.; Coles, S.; Hursthouse, M. *J. Am. Chem. Soc.* **1995**, 117, 2649-2650.

(19) Paolucci, G.; Rosseto, G.; Zanella, P.; Y6nli, K.; Fischer, R. D. *J. Organomet. Chem.* **1984**, 272, 363-383.

(20) (a) *NMR of Paramagnetic Molecules*; La Mar, G. N., Horrocks, W. de W., Holm, R. H., Eds.; Academic Press: New York, 1973. (b) Jahn, W.; Y6nli, K.; Oroschin, W.; Amberger, H.-D.; Fischer, R. D. *Inorg. Chim. Acta* **1984**, 95, 85-104. (c) Fischer, R. D. In *Fundamental and Technological Aspects of Organo-f-Element Chemistry*; Marks, T. J., Fraga, I. L., Eds.; Reidel Publishing Company: Dordrecht, 1985; pp 277-326.

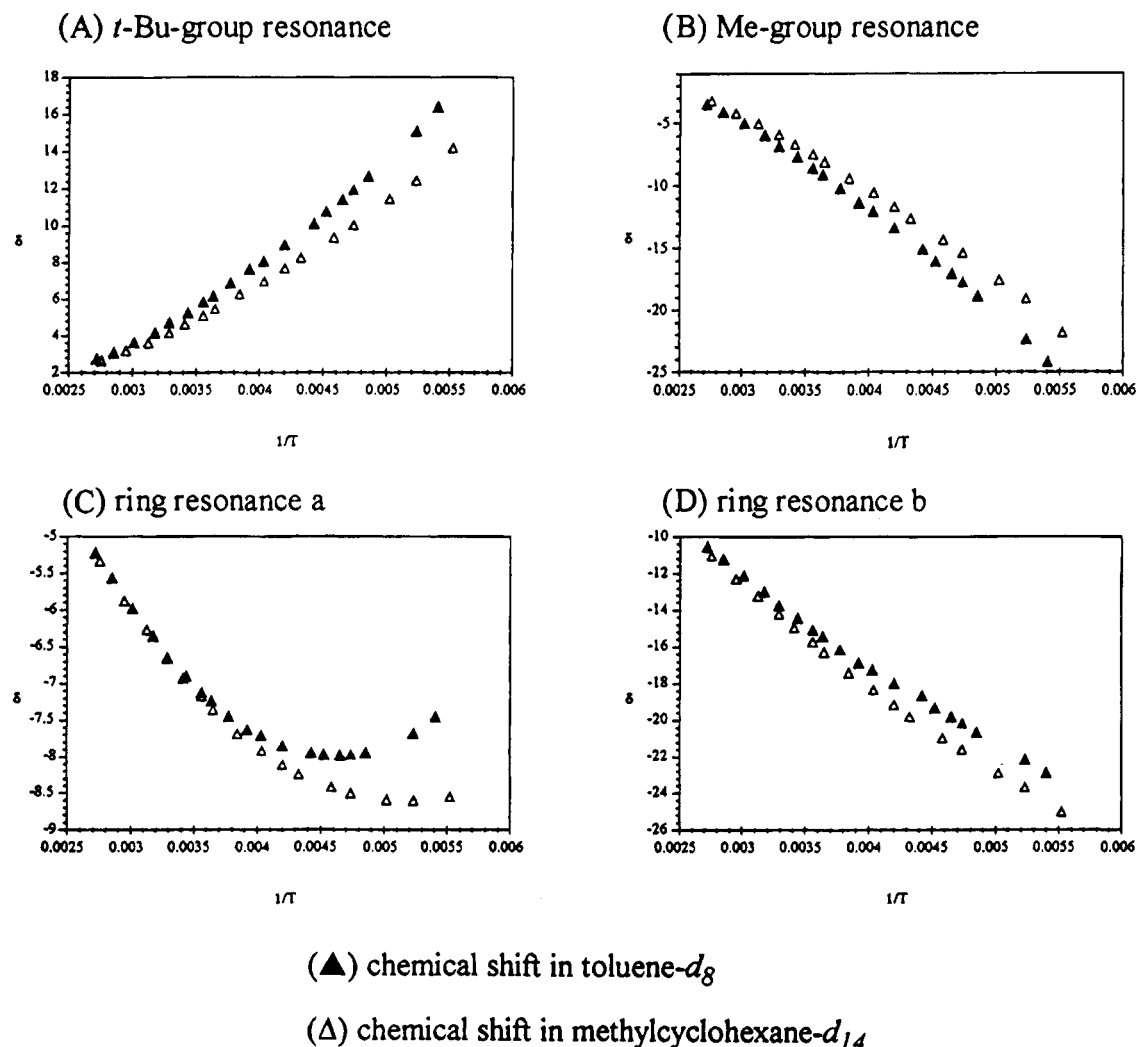


**Figure 2.** Plot of  $^1\text{H}$  NMR chemical shifts of  $(\text{MeC}_5\text{H}_4)_3\text{U}(\text{C}(\text{O})-t\text{-Bu})$  in toluene- $d_8$  solution from  $+95$  to  $-88$   $^\circ\text{C}$  and in methylcyclohexane solution from  $+90$  to  $-92$   $^\circ\text{C}$ .

**Reaction with Ethylene.** Under ethylene pressure,  $(\text{MeC}_5\text{H}_4)_3\text{U}(t\text{-Bu})$  in toluene solution yields the monoinsertion product,  $(\text{MeC}_5\text{H}_4)_3\text{U}(\text{CH}_2\text{CH}_2-t\text{-Bu})$ . The isolated monoinsertion product of ethylene is stable under 210 psi of ethylene for 1 week. No evidence for additional insertion into the primary metal-carbon bond of  $(\text{MeC}_5\text{H}_4)_3\text{U}(\text{CH}_2\text{CH}_2-t\text{-Bu})$  could be detected. This behavior is quite unusual for early transition metal alkyls since they normally either polymerize ethylene or do not react at all.<sup>24</sup> A few examples have been reported in which a single insertion of ethylene into a metal-carbon bond can be observed spectroscopically.<sup>25</sup> Recently, isolation of single-insertion products of  $\alpha$ -olefins into a zirconium-benzyl bond has been reported.<sup>26</sup> In the latter case, the ethylene insertion product could not be isolated and was only observed spectroscopically. In marked contrast,  $\text{Zn}(t\text{-Bu})_2$  cleanly inserts 2 equiv of ethylene, and the resulting  $\text{Zn}(\text{CH}_2\text{CH}_2-t\text{-Bu})_2$  can be isolated.<sup>27</sup> In the uranium *tert*-butyl compound, it is reasonable to postulate that the driving force for inser-

tion of ethylene is the relief of steric congestion around the uranium center in going from a tertiary to a primary alkyl group, which also results in the formation of a somewhat stronger primary *vs* tertiary alkyl uranium bond. For subsequent insertions, these driving forces are essentially lost, leading to a large difference between the rate of the first insertion step and the rate of chain growth therefrom.

The mechanism of the uranium reaction may not be that of normal migratory insertion. In keeping with the reactions of  $(\text{MeC}_5\text{H}_4)_3\text{U}(t\text{-Bu})$  with  $\sigma$ -donor ligands, initial attack of ethylene on the tertiary alkyl complex might lead to uranium-carbon bond homolysis and formation of a uranium(III) ethylene complex and a *tert*-butyl radical. Subsequent attack of the *tert*-butyl radical on the coordinated olefin would lead to the observed insertion product. This mechanism would also explain why no additional insertion of ethylene is observed, since ethylene can be viewed as trapping a radical pair, and for subsequent insertions, the primary alkyl radical is energetically much less accessible than the tertiary radical.

**Related Thorium Systems.** The results obtained with  $(\text{MeC}_5\text{H}_4)_3\text{U}(t\text{-Bu})$  encouraged us to attempt the preparation of the analogous thorium compound,  $(\text{MeC}_5\text{H}_4)_3\text{Th}(t\text{-Bu})$ . Since tetravalent thorium is much more difficult to reduce to trivalent thorium than is uranium, major differences in the reactivity between

(24) Cotton, F. A.; Wilkinson, G. *Advanced Inorganic Chemistry*, 5th ed.; Wiley-Interscience: New York, 1988; pp 1213-1216.

(25) (a) Watson, P. L. *J. Am. Chem. Soc.* **1982**, *104*, 337-339. (b) Burger, B. J.; Thompson, M. E.; Cotter, W. D.; Bercaw, J. E. *J. Am. Chem. Soc.* **1990**, *112*, 1566-1577.

(26) (a) Pellicchia, C.; Grassi, A.; Zambelli, A. *J. Chem. Soc., Chem. Commun.* **1993**, 947-949. (b) Pellicchia, C.; Grassi, A.; Zambelli, A. *Organometallics* **1994**, *13*, 298-302.

(27) Lehmkuhl, H.; Olbrysch, O. *Liebigs Ann. Chem.* **1975**, 1162-1175.

these two compounds are expected.<sup>28</sup> Ligand-assisted thorium-carbon bond homolysis should be much less favorable, and it is likely that insertions of unsaturated substrates into the thorium tertiary alkyl bond would be observed rather than reduction. The thorium-tertiary alkyl bond is likely to be somewhat more stable than the uranium analogue, as thorium-carbon bond strengths are generally *ca.* 5 kcal/mol higher than the analogous uranium-carbon bond strengths,<sup>29</sup> and tetravalent thorium is somewhat bigger than tetravalent uranium,<sup>30</sup> reducing steric congestion around the metal center. In sum, it is reasonable to expect that tris(cyclopentadienyl)thorium tertiary alkyl compounds will be more stable than the analogous uranium compounds. However, we have not been able to prepare the thorium analogue despite many attempts. Our initial strategy for synthesizing  $(\text{MeC}_5\text{H}_4)_3\text{Th}(t\text{-Bu})$  was to follow a procedure analogous to those that were successful for uranium. Surprisingly, no reaction was observed upon addition of 1 equiv of *t*-BuLi to a toluene solution of  $(\text{MeC}_5\text{H}_4)_3\text{ThCl}$ . Over short periods of time (*ca.* 1 h), only unreacted starting material was recovered. When the reaction mixture was stirred at room temperature for *ca.* 24 h, slow formation of a white precipitate was observed. However, upon workup, only starting material was recovered in *ca.* 35% yield. Presumably, the white precipitate observed is due to reaction of *t*-BuLi with toluene and/or the cyclopentadienyl ligands, resulting in an insoluble precipitate. In contrast, treatment of  $(\text{MeC}_5\text{H}_4)_3\text{ThCl}$  with 1 equiv of MeLi resulted in an immediate reaction to give  $(\text{MeC}_5\text{H}_4)_3\text{ThMe}$  in good yield. We reasoned that a leaving group better than chloride was needed on the tris(methylcyclopentadienyl)thorium fragment. Therefore,  $(\text{MeC}_5\text{H}_4)_3\text{ThI}$  was prepared, but again reaction of  $(\text{MeC}_5\text{H}_4)_3\text{ThI}$  with *t*-BuLi did not lead to the desired product, and  $(\text{MeC}_5\text{H}_4)_3\text{ThI}$  behaved similarly to  $(\text{MeC}_5\text{H}_4)_3\text{ThCl}$  upon reaction with *t*-BuLi and MeLi.

In order to eliminate at least the possibility that *t*-BuLi reacts with the aromatic solvent, toluene, we sought hexane-soluble starting materials. Like its uranium analogue,  $(\text{MeC}_5\text{H}_4)_4\text{Th}$  is moderately soluble in hexane. However, when a hexane or benzene solution of  $(\text{MeC}_5\text{H}_4)_4\text{Th}$  was treated with *t*-BuLi, no reaction was observed over several hours. Some precipitate formed over a longer reaction time, presumably by reaction of *t*-BuLi with the methylcyclopentadienyl rings, but only  $(\text{MeC}_5\text{H}_4)_4\text{Th}$  was recovered from the reaction mixture in lower yield. Again,  $(\text{MeC}_5\text{H}_4)_4\text{Th}$  reacted instantaneously with MeLi to give  $(\text{MeC}_5\text{H}_4)_3\text{ThMe}$  in good yield. The insolubility of lithium aryloxides in saturated hydrocarbons should provide a driving force for the reaction of  $(\text{MeC}_5\text{H}_4)_3\text{Th}(\text{OAr})$  with *t*-BuLi in hexane. We therefore prepared  $(\text{MeC}_5\text{H}_4)_3\text{Th}(\text{O}-2,6\text{-Me}_2\text{C}_6\text{H}_3)$ , but again when *t*-BuLi was added to a hexane solution of  $(\text{MeC}_5\text{H}_4)_3\text{Th}(\text{O}-2,6\text{-Me}_2\text{C}_6\text{H}_3)$ , no immediate reaction was observed. After the solution had been stirred at room temperature for 24 h, the only organometallic product recovered from the reaction mixture was  $(\text{MeC}_5\text{H}_4)_3\text{Th}(\text{O}-2,6\text{-Me}_2\text{C}_6\text{H}_3)$  in 53% yield.

Since sulfonates are good leaving groups, we prepared the *p*-toluenesulfonate derivative,  $(\text{MeC}_5\text{H}_4)_3\text{Th}(\text{OTs})$ . When *t*-BuLi was added to a toluene solution of  $(\text{MeC}_5\text{H}_4)_3\text{Th}(\text{OTs})$ , an immediate reaction occurred, and a small amount of white powder was isolated from this reaction. The material is only sparingly soluble in aromatic hydrocarbons, and thus only a marginal <sup>1</sup>H-NMR spectrum for this diamagnetic material could be obtained. The spectrum displayed only one set of resonances corresponding to a methylcyclopentadienyl ligand (5.94, AA'BB', 2H; 5.80, AA'BB', 2H; and 2.26 s, 3H), but no resonance attributable to a *tert*-butyl group was observed. Furthermore, when the solid material was exposed to ambient light for a prolonged period of time, it slowly turned dark-green. No such change took place when the material was protected from light. The solubility behavior and the <sup>1</sup>H-NMR spectrum are inconsistent with the formulation of a  $(\text{MeC}_5\text{H}_4)_3\text{Th}(t\text{-Bu})$  compound. Rather, the behavior is reminiscent of green  $\text{Cp}_3\text{Th}$ , reported by Marks as the product of the photodecomposition of  $\text{Cp}_3\text{ThR}$  compounds.<sup>31</sup> While the trivalent thorium compound was incompletely characterized largely due to its relative insolubility, it was reported to react with hydrogen to yield  $\text{Cp}_3\text{ThH}$ . This uncharacterized hydride was also reported to be poorly soluble and to revert back to green  $\text{Cp}_3\text{Th}$  upon photolysis or prolonged exposure to room light. The low solubility of the diamagnetic reaction product of  $(\text{MeC}_5\text{H}_4)_3\text{Th}(\text{OTs})$  with *t*-BuLi precludes finding the missing hydride resonance in the <sup>1</sup>H-NMR spectrum. Since actinide-hydride infrared stretching frequencies do not fall in a characteristic region, characterization of the white material by IR spectroscopy is ambiguous. The green material obtained after prolonged exposure of the white material to light did not give an EPR-signal, as a powder sample at 4 K. In light of these difficulties and the low yield, the subject was not pursued further. Finally, it should be noted that the white, isolated, and well-characterized thorium hydride  $[(\text{Me}_3\text{Si})_2\text{N}]_3\text{ThH}$  does not display any marked photosensitivity.<sup>32</sup> The dimeric compound  $(\text{Cp}^*_2\text{ThH}_2)_2$  also does not seem to be photochemically labile.<sup>33</sup>

We also prepared the cationic species,  $[(\text{MeC}_5\text{H}_4)_3\text{Th}(\text{NMe}_3)](\text{BPh}_4)$ , and investigated its reaction with *t*-BuLi. Unfortunately, this cation is insoluble in hydrocarbon solvents. We therefore treated  $[(\text{MeC}_5\text{H}_4)_3\text{Th}(\text{NMe}_3)](\text{BPh}_4)$  as a suspension in hexane with 1 equiv of *t*-BuLi. The only product that we could isolate from the reaction mixture was  $(\text{MeC}_5\text{H}_4)_4\text{Th}$  in low yield. Evidently, *t*-BuLi assisted cyclopentadienyl ligand redistribution. Since the cationic starting complex is insoluble, it and its reaction products are exposed to an excess of *t*-BuLi in solution. Hence a soluble cationic species might give rise to a cleaner reaction. The base-free cation,  $[(\text{Me}_3\text{SiC}_5\text{H}_4)_3\text{Th}](\text{BPh}_4)$ , was reported to be soluble in aromatic hydrocarbons.<sup>9</sup> Thus it would be an ideal substrate for investigation of its reaction with *t*-BuLi. Even though the bulkier substituents on the cyclopentadienyl ligands would destabilize a hypotheti-

(28) Morss, L. R. In *The Chemistry of the Actinide Elements*; Katz, J. J., Seaborg, G. T., Morss, L. R., Eds.; Chapman & Hall: London, 1986; Vol. 2, Chapter 17, pp 1278-1360.

(29) Bruno, J. W.; Stecher, H. A.; Morss, L. R.; Sonnenberger, D. C.; Marks, T. J. *J. Am. Chem. Soc.* **1986**, *108*, 7275-7280.

(30) (a) Shannon, R. D. *Acta Crystallogr., Sect. A* **1976**, *32B*, 751-767. (b) Shannon, R. D.; Prewitt, C. T. *Acta Crystallogr., Sect. B* **1969**, *25*, 925-946.

(31) (a) Kalina, D. G.; Marks, T. J.; Wachter, W. A. *J. Am. Chem. Soc.* **1977**, *99*, 3877-3879. (b) Bruno, J. W.; Kalina, D. G.; Mintz, E. A.; Marks, T. J. *J. Am. Chem. Soc.* **1982**, *104*, 1860-1869.

(32) (a) Turner, H. W.; Simpson, S. J.; Andersen, R. A. *J. Am. Chem. Soc.* **1979**, *101*, 2782-2782. (b) Simpson, S. J.; Turner, H. W.; Andersen, R. A. *J. Am. Chem. Soc.* **1979**, *101*, 7728-7729. (c) Simpson, S. J.; Turner, H. W.; Andersen, R. A. *Inorg. Chem.* **1981**, *20*, 2991-2995.

(33) Fagan, P. J.; Manriquez, J. M.; Maatta, E. A.; Seyam, A. M.; Marks, T. J. *J. Am. Chem. Soc.* **1981**, *103*, 6650-6667.



cal  $(RC_5H_4)_3Th(t-Bu)$  compound, only a weak interaction between the  $(RC_5H_4)_3Th$  moiety and the tetraphenylborate anion would have to be broken. The related base-free cation  $[(t-Bu)C_5H_4)_3Th](BPh_4)$  was prepared according to the methodology developed by Marks for the  $Me_3Si$  derivative. Reaction of the cation,  $[(RC_5H_4)_3Th](BPh_4)$ , with  $t-BuLi$  in toluene or hexane solution resulted in clean formation of  $(RC_5H_4)_3ThH$  in good yield. The observed  $^1H$ -NMR resonances ( $\delta$  12.81 and 13.98 for  $R = Me_3Si$  and  $t-Bu$ ) for the thorium-bound hydrides are quite characteristic for hydrides bound to elements in the left-hand side of the periodic table. The infrared spectra of the resulting  $(RC_5H_4)_3ThH$  species did not allow unambiguous assignment of the metal-hydride stretching frequencies, but the infrared stretching frequencies of the analogous uranium compounds, prepared by Ephritikhine, have been assigned by preparation of the corresponding deuterides  $(RC_5H_4)_3UD$ . The reported values for  $\nu(U-H)$  are 1395 and 1410  $cm^{-1}$  for  $(Me_3SiC_5H_4)_3UH$  and  $(t-BuC_5H_4)_3UH$ , respectively,<sup>34</sup> and the thorium hydrides show absorptions in this region, although we have not confirmed the assignments by labeling. When the reaction between  $[(RC_5H_4)_3Th](BPh_4)$  and  $t-BuLi$  was carried out in an NMR tube in benzene- $d_6$  and followed by  $^1H$ -NMR spectroscopy, the reaction was essentially quantitative. Furthermore, the only significant organic reaction product was isobutene, present in a 1:1 ratio with  $(RC_5H_4)_3ThH$ . No evidence of deuterium incorporation from solvent into the thorium-bound hydride or the isobutene could be detected. These observations strongly suggest that after initial formation of the long sought thorium tertiary butyl, a  $\beta$ -hydrogen elimination leads to formation of the stable, isolable thorium hydride.

Since for  $R = SiMe_3$  and  $t-Bu$  both  $(RC_5H_4)_3ThCl$  species are quite soluble in hexane, their reaction with  $t-BuLi$  in hexane solution was investigated to see if the cation was essential. No immediate reaction was observed when one equivalent of  $t-BuLi$  was added to hexane solutions of  $(RC_5H_4)_3ThCl$ . After *ca.* 1 h the formation of a precipitate was observed; after *ca.* 30 h, the mixture was evaporated to dryness and the residue was investigated by  $^1H$ -NMR spectroscopy. In both cases two compounds were present,  $(RC_5H_4)_3ThCl$  and  $(RC_5H_4)_3ThH$ . For the (trimethylsilyl)cyclopentadienyl system, the ratio of  $(RC_5H_4)_3ThCl$  to  $(RC_5H_4)_3ThH$  obtained was about 1:1, and in the *tert*-butylcyclopentadienyl system, the ratio was about 2:1. When these reactions were carried out in an NMR-tube in benzene- $d_6$  solution and monitored by  $^1H$ -NMR spectroscopy, integration relative to the solvent resonance showed that all the thorium-containing material was not conserved. Approximately 30–40% of the starting material was lost as insoluble precipitate. Within the accuracy of the integration, no deuterium incorporation into the thorium-bound hydride position was detected, and the organic products of the reactions were isobutene and isobutane. Furthermore, no substantial deuterium incorporation into the isobutane was detected. Hence, we conclude that the isobutane is formed by deprotonation of the cyclopentadienyl ligand by *tert*-butyllithium. Such a metalated cyclopentadienyl species would be expected to be fairly reactive and lead to subsequent reactions with the starting  $(RC_5H_4)_3ThCl$

compounds. This explains the loss of thorium-containing material observed during the reactions. The amount of isobutene is equivalent to the amount of  $(RC_5H_4)_3ThH$  formed. It is therefore tempting to assign the formation of  $(RC_5H_4)_3ThH$  to rapid  $\beta$ -hydrogen elimination from an intermediate  $(RC_5H_4)_3Th(t-Bu)$  species, also in this system. The analogous uranium chlorides show a markedly different behavior toward  $t-BuLi$ , since here reduction to trivalent uranium takes place, presumably by metal-carbon bond homolysis from an intermediate uranium tertiary alkyl.<sup>5</sup> The difference is consistent with the stability of uranium(III) relative to thorium(III).

## Conclusion

The results obtained show that in the absence of  $\beta$ -hydrogen elimination, the remarkable propensity of uranium tertiary alkyl compounds to reduce the metal to the next lower oxidation state by easily accessible metal-carbon bond homolysis can be exploited for the synthesis of reduced base adducts. This represents a marked contrast to the reactivity of the analogous primary alkyl compounds  $Cp_3UR$ . Nevertheless, a ligand  $L$  is required to assist metal-carbon bond homolysis and to stabilize the  $(MeC_5H_4)_3U$  fragment. For weak ligands (CO, ethylene) toward  $(MeC_5H_4)_3U$ , insufficient stabilization of the metal fragment is provided and insertion of the ligand into the metal-carbon bond becomes the preferred reaction pathway. This limits the synthetic usefulness of the ligand-assisted metal-carbon bond homolysis for the synthesis of reduced uranium(III) base adducts to ligands providing sufficient stabilization of the  $(MeC_5H_4)_3U$ -fragment. In contrast to the uranium systems, in which the chemistry is dominated by metal-carbon bond homolysis, reactions of analogous thorium compounds with  $t-BuLi$  are more complicated. The alkyllithium reagent can deprotonate the supporting ligands or act as an alkylating agent. Depending on the available leaving groups and the ancillary ligands, a subtle balance between those reactivity patterns takes place. When formed, a thorium tertiary alkyl complex seems to easily decompose by  $\beta$ -hydrogen elimination, leading to thorium hydrides, and this is a useful synthetic reaction.

## Experimental Section

**General Procedures.** Unless otherwise noted, materials were obtained from commercial suppliers and used without further purification. Toluene, tetrahydrofuran, diethyl ether, and hexane were distilled under nitrogen from potassium, sodium, or sodium/benzophenone immediately prior to use. Methylcyclohexane- $d_{14}$  and deuteriated aromatic solvents were heated at reflux over sodium and subsequently distilled from sodium under nitrogen. Uranium tetrachloride was treated with thionyl chloride at reflux for *ca.* 7 days, followed by washing the finely ground solid with methylene chloride until the extract was colorless and heating the powder under reduced pressure (1 mTorr) at *ca.* 150 °C for 24 h. Methylcyclopentadienyl sodium,<sup>35</sup> *tert*-butyl- and ethylisocyanide,<sup>36</sup>  $(MeC_5H_4)_3UCl$ ,<sup>37</sup>  $(MeC_5H_4)_3ThCl$ ,<sup>38</sup>  $(MeC_5H_4)_4Th$ ,<sup>38</sup>  $[(MeC_5H_4)_3-$

(35) Reynolds, L. T.; Wilkinson, G. J. *Inorg. Nucl. Chem.* **1959**, *9*, 86–92.

(36) Weber, W. P.; Gokel, G. W.; Ugi, I. K. *Angew. Chem., Int. Ed. English* **1972**, *11*, 530–531.

(37) (a) Fischer, R. D.; v. Ammon, R.; Kanellakopoulos, B. *J. Organomet. Chem.* **1970**, *25*, 123–137. (b) Fischer, R. D.; Siel, G. R. *Z. Anorg. Allg. Chem.* **1976**, *419*, 126–138.

(34) Berthet, J.-C.; Le Maréchal, J.-F.; Lance, M.; Nierlich, M.; Vigner, J.; Ephritikhine, M. *J. Chem. Soc., Dalton Trans.* **1992**, 1573–1577.

$\text{Th}(\text{NMe}_3)_3(\text{BPh}_4)_9$ ,  $[(\text{Me}_3\text{SiC}_5\text{H}_4)_3\text{Th}](\text{BPh}_4)_9$  and trialkylammonium tetraphenylborate salts were prepared as described previously.<sup>39</sup> *tert*-Butylcyclopentadiene was prepared according to literature procedure and used as the sodium salt in THF.<sup>40</sup> All compounds were handled using standard Schlenk techniques under a nitrogen or argon atmosphere or in an inert atmosphere dry box under argon.

Melting points were determined in sealed capillaries under argon using a Buchi melting point apparatus and are uncorrected. Infrared spectra were recorded as Nujol mulls between CsI or KBr plates on a Perkin-Elmer 580 or Mattson Sirius 100 instrument. <sup>1</sup>H-NMR spectra were measured at 89.56 MHz on a JEOL-FX90Q instrument equipped with Tecmag Libra software and are reported in  $\delta$  values relative to tetramethylsilane with positive values to high frequency. Samples for routine NMR spectroscopy were prepared in septum-capped NMR tubes in the drybox. Samples for quantitative NMR experiments were prepared in NMR tubes equipped with a J. Young Teflon valve in the drybox. Electron impact mass spectra were obtained with an Atlas MS-12 spectrometer operated by the Mass Spectrometry Laboratory operated by the College of Chemistry, University of California, Berkeley, CA. Elemental analyses were performed by the Microanalytical Laboratory operated by the College of Chemistry, University of California, Berkeley, CA. Analytical gas chromatography traces were obtained on a Hewlett-Packard HP-5790 instrument equipped with an HP-3390A integrator and an HP-19091B Option 112 ultrahigh-performance capillary column (cross-linked 5% phenylmethylsilicone: length, 25 m; i.d., 0.31 mm). GC-MS was performed with a Hewlett-Packard 5890 GC equipped with an HP 5970 series mass selective detector (70 eV) and JNW-Scientific column as above.

**(MeC<sub>5</sub>H<sub>4</sub>)<sub>3</sub>U(*t*-Bu):** (a) A solution of  $(\text{MeC}_5\text{H}_4)_3\text{UCl}$  (1.60 g, 3.13 mmol) was prepared in 60 mL of toluene. Upon addition of *t*-BuLi (3.14 mmol, 1.65 mL of a 1.90 M solution in hexane) the dark red-brown solution turned dark green within 1 min. After the reaction mixture had been stirred for 30 min the solvent was removed under reduced pressure. Proceeding under exclusion of light, the resulting solid was extracted with 65 mL of diethyl ether for 1 h. The diethyl ether solution was filtered, and the volume of the filtrate was reduced to ca. 20 mL. Cooling to  $-80^\circ\text{C}$  yielded dark green needles of  $(\text{MeC}_5\text{H}_4)_3\text{U}(\textit{t}\text{-Bu})$  (0.92 g, 58%), mp 224–228 °C (decomp). <sup>1</sup>H-NMR ( $\text{C}_6\text{D}_6$ ;  $30^\circ\text{C}$ ):  $\delta$  9.96 (s, 6H);  $-6.25$  (s, 6H);  $-8.98$  (s, 9H);  $-18.96$  (s, 9H) ppm. IR (CsI): 1260 (w), 1086 (w), 1040 (m), 845 (m), 814 (m), 773 (s), 720 (m), 400 (w), 330 (w)  $\text{cm}^{-1}$ . Anal. Calcd for  $\text{C}_{22}\text{H}_{30}\text{U}$ : C, 49.6; H, 5.68. Found: C, 49.9; H, 5.29.

(b) To a solution of  $(\text{MeC}_5\text{H}_4)_4\text{U}$  (2.00 g, 3.61 mmol) in 50 mL of toluene was added by syringe *t*-BuLi (3.70 mmol, 1.65 mL of a 2.24 M solution in hexane). The red brown solution rapidly turned dark green. The mixture was stirred for 45 min, and then the solvent was removed under reduced pressure. Proceeding under exclusion of light, the resulting solid was extracted with 100 mL of diethyl ether for 1 h. The diethyl ether solution was filtered, and the volume of the filtrate was reduced to ca. 40 mL. Cooling to  $-80^\circ\text{C}$  yielded dark green needles of  $(\text{MeC}_5\text{H}_4)_3\text{U}(\textit{t}\text{-Bu})$  (1.01 g, 52.6%). The materials obtained using methods a and b exhibited identical physical and spectroscopic properties.

**(MeC<sub>5</sub>H<sub>4</sub>)<sub>4</sub>U:** To a solution of  $\text{UCl}_4$  (1.89 g, 4.98 mmol) in 60 mL of tetrahydrofuran was added by cannula a solution of  $\text{Na}(\text{MeC}_5\text{H}_4)$  (2.05 g, 20.1 mmol) in 60 mL of tetrahydrofuran. Upon addition, the green uranium solution turned deep red. After the solution had been stirred for 24 h, the solvent was removed under reduced pressure. The resulting solid was extracted with 100 mL of toluene at  $65^\circ\text{C}$ . After filtration of the toluene extract at  $65^\circ\text{C}$ , the toluene was removed under

reduced pressure, yielding a deep red powder of  $(\text{MeC}_5\text{H}_4)_4\text{U}$  (2.08 g, 75.3%), mp 248–252 °C. <sup>1</sup>H NMR ( $\text{C}_6\text{D}_6$ ;  $30^\circ\text{C}$ ):  $\delta$  0.94 (s, 3H);  $-13.44$  (s, 2H);  $-14.84$  (s, 2H) ppm. IR (KBr): 1496 (w), 1255 (m), 1075 (w), 1042 (s), 914 (s), 874 (s), 850 (s), 799 (s), 774 (s), 612 (m), 598 (m)  $\text{cm}^{-1}$ . Anal. Calcd for  $\text{C}_{24}\text{H}_{28}\text{U}$ : C, 52.0; H, 5.10. Found: C, 51.8; H, 5.03. EIMS:  $\text{M}^+$ , 554 amu.

**(MeC<sub>5</sub>H<sub>4</sub>)<sub>3</sub>U(PMe<sub>3</sub>):** To a deep-green solution of  $(\text{MeC}_5\text{H}_4)_3\text{U}(\textit{t}\text{-Bu})$  (0.73 g, 1.4 mmol) in 50 mL of toluene was added 0.12 mL (1.5 mmol) of  $\text{PMe}_3$ . The reaction mixture instantly turned red. After the reaction mixture had been stirred for 24 h the solvent was removed under reduced pressure. The remaining solid was extracted with 50 mL of hexane. The hexane solution was filtered, and the volume of the filtrate was reduced to ca. 30 mL. Cooling to  $-80^\circ\text{C}$  yielded 0.29 g (39%) of  $(\text{MeC}_5\text{H}_4)_3\text{U}(\text{PMe}_3)$ , mp 228–232 °C (decomp). <sup>1</sup>H-NMR ( $\text{C}_6\text{D}_6$ ;  $31^\circ\text{C}$ ):  $\delta$   $-21.68$  (s, 9H);  $-21.18$  (s, 9H);  $-13.55$  (s, 6H);  $-12.68$  (s, 6H) ppm. The second resonance exchanges with added phosphine. IR (CsI): 1670 (w), 1650 (w), 1420 (s), 1303 (m), 1284 (s), 1260 (w), 1235 (m), 1033 (s), 945 (s), 865 (w), 816 (s), 767 (s), 740 (s), 719 (s), 660 (w), 635 (w), 605 (m), 330 (s), 210 (s)  $\text{cm}^{-1}$ . Anal. Calcd for  $\text{C}_{21}\text{H}_{30}\text{PU}$ : C, 45.7; H, 5.48. Found: C, 45.5; H, 5.52.

**(MeC<sub>5</sub>H<sub>4</sub>)<sub>3</sub>U(THF):** To a solution of  $(\text{MeC}_5\text{H}_4)_3\text{U}(\textit{t}\text{-Bu})$  (0.31 g, 0.58 mmol) in 25 mL of toluene was added 47  $\mu\text{L}$  (0.58 mmol) of THF. After the reaction mixture had been stirred for 28 h the solvent was removed under reduced pressure. The remaining solid was extracted with 50 mL of diethyl ether. The ether solution was filtered, and the volume of the filtrate was reduced to ca. 10 mL. Cooling to  $-80^\circ\text{C}$  yielded 0.12 g (36%) of  $(\text{MeC}_5\text{H}_4)_3\text{U}(\text{THF})$ . Characterization data have been reported previously.<sup>5a</sup>

**(MeC<sub>5</sub>H<sub>4</sub>)<sub>3</sub>U(NC-*t*-Bu):** To a solution of  $(\text{MeC}_5\text{H}_4)_3\text{U}(\textit{t}\text{-Bu})$  (0.83 g, 1.6 mmol) in 20 mL of toluene was added 180  $\mu\text{L}$  (1.64 mmol) of *t*-BuCN. The dark green solution turned red-brown over ca. 2 min, and a precipitate formed. The reaction mixture was stirred for 1 h, and then the solvent was removed under reduced pressure. The residual solid was extracted with 25 mL of diethyl ether. After filtration the volume of the ether extract was reduced in vacuo to ca. 10 mL. Cooling to  $-80^\circ\text{C}$  yielded dark brown crystals of  $(\text{MeC}_5\text{H}_4)_3\text{U}(\text{NC-}\textit{t}\text{-Bu})$  (0.25 g, 29%), mp 129–132 °C (decomp). <sup>1</sup>H-NMR ( $\text{C}_6\text{D}_6$ ;  $30^\circ\text{C}$ ):  $\delta$   $-5.49$  (s, 6H);  $-11.03$  (s, 9H);  $-12.28$  (s, 9H);  $-21.80$  (s, 6H) ppm. IR (CsI): 2220 (w), 1235 (m), 1205 (w), 1155 (w), 1055 (w), 1040 (w), 1025 (m), 925 (w), 865 (w), 845 (w), 810 (m), 760 (s), 740 (s), 610 (m), 325 (m)  $\text{cm}^{-1}$ . Anal. Calcd for  $\text{C}_{23}\text{H}_{30}\text{NU}$ : C, 49.5; H, 5.42; N, 2.51. Found: C, 49.2; H, 5.47; N, 2.64.

**(MeC<sub>5</sub>H<sub>4</sub>)<sub>3</sub>U(CN-*t*-Bu):** A solution of  $(\text{MeC}_5\text{H}_4)_3\text{U}(\textit{t}\text{-Bu})$  (0.96 g, 1.8 mmol) was prepared in 40 mL of toluene. Upon addition of *t*-BuNC (0.20 mL, 1.8 mmol) the dark green solution instantly turned dark purple. The reaction mixture was stirred for 40 min, and then the solvent was removed under reduced pressure. The residual solid was extracted with 30 mL of hexane. After filtration the volume of the hexane extract was reduced in vacuo to ca. 20 mL. Cooling to  $-20^\circ\text{C}$  yielded dark red needles of  $(\text{MeC}_5\text{H}_4)_3\text{U}(\text{CN-}\textit{t}\text{-Bu})$  (0.33 g, 33%), mp 100–102 °C (decomp). <sup>1</sup>H-NMR ( $\text{C}_6\text{D}_6$ ;  $30^\circ\text{C}$ ):  $\delta$   $-8.22$  (s, 6H);  $-10.20$  (s, 9H);  $-15.56$  (s, 9H);  $-19.20$  (s, 6H) ppm. IR (CsI): 3080 (w), 2720 (w), 2280 (w), 2140 (s), 1235 (m), 1195 (s), 1060 (w), 1040 (s), 1025 (s), 970 (w), 925 (s), 845 (w), 820 (s), 755 (s), 700 (w), 610 (m), 520 (m), 325 (s), 220 (m)  $\text{cm}^{-1}$ . Anal. Calcd for  $\text{C}_{23}\text{H}_{30}\text{NU}$ : C, 49.5; H, 5.42; N, 2.51. Found: C, 49.7; H, 5.49; N, 2.50.

**(MeC<sub>5</sub>H<sub>4</sub>)<sub>3</sub>U(CNEt):** (a) A solution of  $(\text{MeC}_5\text{H}_4)_3\text{U}(\textit{t}\text{-Bu})$  (0.44 g, 0.83 mmol) in 50 mL of toluene was cooled to  $-78^\circ\text{C}$ , and EtNC (0.06 mL, 0.82 mmol) was added. The mixture was stirred for 5 h at  $-78^\circ\text{C}$ , during which time the dark green solution gradually turned red. The solution was allowed to warm to room temperature while simultaneously removing the solvent under reduced pressure. The resulting solid was extracted with 25 mL of hexane. After filtration the volume of the hexane extract was reduced in vacuo to ca. 20 mL.

(38) Edwards, P. G.; Weydert, M.; Petrie, M. A.; Andersen, R. A. *J. Organomet. Chem.* **1994**, *213/214*, 11–14.

(39) Barker, B. J.; Sears, P. G. *J. Chem. Phys.* **1974**, *78*, 2687–2688.

(40) Leigh, T. *J. Chem. Soc.* **1964**, 3294–3302.

Cooling to  $-20\text{ }^{\circ}\text{C}$  yielded dark red needles of  $(\text{MeC}_5\text{H}_4)_3\text{U}(\text{CNEt})$  (0.14 g, 31%), mp  $59\text{--}60\text{ }^{\circ}\text{C}$ .  $^1\text{H-NMR}$  ( $\text{C}_6\text{D}_6$ ;  $30\text{ }^{\circ}\text{C}$ ):  $\delta$   $-8.46$  (s, 6H);  $-8.94$  (s, 3H);  $-16.04$  (s, 9H);  $-18.96$  (s, 6H);  $-60.51$  (s, 2H) ppm. IR (CsI):  $2155$  (s),  $1338$  (m),  $1090$  (w),  $1028$  (m),  $925$  (w),  $847$  (w),  $823$  (m),  $765$  (s),  $610$  (w),  $328$  (m),  $215$  (w)  $\text{cm}^{-1}$ . Anal. Calcd for  $\text{C}_{21}\text{H}_{26}\text{NU}$ : C, 47.6; H, 4.94; N, 2.64. Found: C, 47.3; H, 4.90; N, 2.16.

(b) To a solution of  $(\text{MeC}_5\text{H}_4)_3\text{U}(\text{THF})$  (0.69 g, 1.2 mmol) dissolved in diethyl ether (20 mL) was added by syringe EtNC (0.17 mL, 2.3 mmol). The diethyl ether was removed under reduced pressure after 5 min, leaving a red solid. Hexane was added, and the red solution was filtered and cooled to  $-20\text{ }^{\circ}\text{C}$ , yielding red needles (0.18 g, 28%). The materials obtained under methods a and b had identical physical and spectroscopic properties.

**$(\text{MeC}_5\text{H}_4)_3\text{U}(\text{C}(\text{O})\text{-}t\text{-Bu})$ :** A solution of  $(\text{MeC}_5\text{H}_4)_3\text{U}(t\text{-Bu})$  (0.89 g, 1.7 mmol) in 30 mL of toluene was transferred by cannula into a pressure bottle under 1 atm of nitrogen. Carbon monoxide (20 psi) was introduced into the pressure bottle. The deep-green solution was stirred for 4 h, during which time it gradually turned red. Then the pressure was released, and the solution was transferred by cannula to a Schlenk tube. The solvent was removed under reduced pressure, and the resulting solid was extracted with 35 mL of hexane. After filtration, the volume of the hexane extract was reduced in vacuo to ca. 25 mL. Cooling to  $-80\text{ }^{\circ}\text{C}$  yielded red needles of  $(\text{MeC}_5\text{H}_4)_3\text{U}(\text{C}(\text{O})\text{-}t\text{-Bu})$  (0.33 g). The volume of the mother liquor was reduced to ca. 5 mL, and cooling to  $-80\text{ }^{\circ}\text{C}$  yielded a second crop of  $(\text{MeC}_5\text{H}_4)_3\text{U}(\text{C}(\text{O})\text{-}t\text{-Bu})$  (0.11 g) (combined yield: 47%, mp  $72\text{--}76\text{ }^{\circ}\text{C}$ ).  $^1\text{H-NMR}$  ( $\text{C}_7\text{D}_8$ ;  $31\text{ }^{\circ}\text{C}$ ):  $\delta$   $4.74$  (s, 9H);  $-6.65$  (s, 6H);  $-6.83$  (s, 9H);  $-13.75$  (s, 6H) ppm. IR (CsI):  $1490$  (m),  $1305$  (w),  $1258$  (w),  $1237$  (w),  $1222$  (w),  $1068$  (w),  $1045$  (m),  $1030$  (m),  $970$  (w),  $927$  (m),  $885$  (w),  $843$  (w),  $762$  (s),  $718$  (m),  $600$  (m),  $389$  (m),  $330$  (m),  $229$  (m)  $\text{cm}^{-1}$ . Anal. Calcd for  $\text{C}_{23}\text{H}_{30}\text{OU}$ : C, 49.3; H, 5.39. Found: C, 49.2; H, 5.39.

**tert-Butyltoluenes:** GC ( $30\text{ }^{\circ}\text{C}$  for 2 min, then  $10\text{ }^{\circ}\text{C}/\text{min}$ ): *m*-(*t*-Bu) $\text{MeC}_6\text{H}_4$ , 12.63 min; *p*-(*t*-Bu) $\text{MeC}_6\text{H}_4$ , 12.72 min.  $^{13}\text{C}$ - $\{^1\text{H}\}$ -NMR (THF-*d*<sub>6</sub>; room temperature): *m*-(*t*-Bu) $\text{MeC}_6\text{H}_4$ , 151.1, 137.8, 128.8, 127.0, 126.7, 123.1, 35.1, 32.1, 22.1 ppm; *p*-(*t*-Bu) $\text{MeC}_6\text{H}_4$ , 148.2, 134.7, 128.8, 125.1, 34.3, 31.5, 20.8 ppm.  $^1\text{H-NMR}$  (THF-*d*<sub>6</sub>; room temperature): *m*-(*t*-Bu) $\text{MeC}_6\text{H}_4$ , 7.3–7.0 (m, 4H), 2.30 (s, 3H), 1.30 (s, 9H) ppm; *p*-(*t*-Bu) $\text{MeC}_6\text{H}_4$ , 7.14 (AA'BB', 4H), 2.25 (s, 3H), 1.30 (s, 9H) ppm.

**$(\text{MeC}_5\text{H}_4)_3\text{U}(\text{CH}_2\text{CH}_2\text{-}t\text{-Bu})$ :** In a pressure bottle a solution of  $(\text{MeC}_5\text{H}_4)_3\text{U}(t\text{-Bu})$  (0.76 g, 1.4 mmol) in 25 mL of toluene was stirred under an atmosphere of ethylene at 210 psi. The dark green solution gradually turned red. After 5 h the pressure was released, and the solution was transferred by cannula to a Schlenk flask. The solvent was removed under reduced pressure. The resulting solid was extracted with 50 mL of hexane. After filtration the volume of the hexane extract was reduced in vacuo to ca. 20 mL. Cooling to  $-80\text{ }^{\circ}\text{C}$  yielded red blocks of  $(\text{MeC}_5\text{H}_4)_3\text{U}(\text{CH}_2\text{CH}_2\text{-}t\text{-Bu})$  (0.19 g, 24%), mp  $78\text{--}81\text{ }^{\circ}\text{C}$ .  $^1\text{H-NMR}$  ( $\text{C}_6\text{D}_6$ ;  $30\text{ }^{\circ}\text{C}$ ):  $\delta$   $1.00$  (s, 6H);  $-2.35$  (s, 6H);  $-7.19$  (s, 9H);  $-13.27$  (s, 9H);  $-27.66$  (m br, 2H);  $-190.45$  (s br, 2H) ppm. IR (CsI):  $1360$  (w),  $1260$  (m),  $1080$  (m),  $1030$  (s),  $905$  (m),  $845$  (m),  $790$  (m),  $770$  (s),  $720$  (w),  $670$  (w),  $610$  (w),  $395$  (w),  $325$  (w),  $235$  (w)  $\text{cm}^{-1}$ . Anal. Calcd for  $\text{C}_{24}\text{H}_{34}\text{U}$ : C, 51.4; H, 6.11. Found: C, 51.1; H, 6.05.

**$(\text{MeC}_5\text{H}_4)_3\text{ThI}$ :** To a solution of  $(\text{MeC}_5\text{H}_4)_3\text{ThCl}$  (1.20 g, 2.38 mmol) in 140 mL of toluene was added by syringe (trimethylsilyl)iodide (0.80 mL, 5.6 mmol) freshly vacuum-transferred from copper. The reaction mixture was kept in the dark and heated to  $100\text{ }^{\circ}\text{C}$  under a slow stream of dinitrogen for 41 h. After the mixture had been cooled to room temperature, the solvent was removed under reduced pressure. The resulting solid was extracted with 50 mL of toluene at  $100\text{ }^{\circ}\text{C}$ . Following filtration, cooling of the toluene extract to  $-80\text{ }^{\circ}\text{C}$  yielded a white powder of  $(\text{MeC}_5\text{H}_4)_3\text{ThI}$  (0.33 g, 23%). The compound does not appear to melt up to  $260\text{ }^{\circ}\text{C}$ .  $^1\text{H-NMR}$  ( $\text{C}_6\text{D}_6$ ;  $30\text{ }^{\circ}\text{C}$ ):  $\delta$   $5.96$  (s, 4H);  $2.21$  (s, 3H) ppm. EIMS:  $\text{M}^+$ , 596 amu.

**$(\text{MeC}_5\text{H}_4)_3\text{ThMe}$ :** (a) To a suspension of  $(\text{MeC}_5\text{H}_4)_3\text{ThCl}$  (0.64 g, 1.3 mmol) in 100 mL of toluene was added by syringe

1.3 mL of MeLi (1.0 M solution in diethyl ether, 1.3 mmol). The resulting mixture was stirred at room temperature for 5 h, and then the solvent was removed under reduced pressure. The remaining solid was extracted with 90 mL of diethyl ether. After filtration the volume of the ether extract was reduced in vacuo to ca. 50 mL. Cooling to  $-80\text{ }^{\circ}\text{C}$  yielded white shiny plates of  $(\text{MeC}_5\text{H}_4)_3\text{ThMe}$  (0.32 g, 52%), mp  $225\text{--}230\text{ }^{\circ}\text{C}$  (decomp).  $^1\text{H-NMR}$  ( $\text{C}_6\text{D}_6$ ;  $30\text{ }^{\circ}\text{C}$ ):  $\delta$   $5.86$  (AA'BB', 6H);  $5.65$  (AA'BB', 6H);  $2.08$  (s, 9H);  $0.57$  (s, 3H) ppm.  $^{13}\text{C-NMR}$  ( $\text{C}_6\text{D}_6$ ;  $30\text{ }^{\circ}\text{C}$ ):  $\delta$   $116.99$  (d of m,  $^1J_{\text{C-H}} = 174\text{ Hz}$ );  $115.00$  (d of m,  $^1J_{\text{C-H}} = 162\text{ Hz}$ );  $42.54$  (q,  $^1J_{\text{C-H}} = 114\text{ Hz}$ );  $15.06$  (q,  $^1J_{\text{C-H}} = 127\text{ Hz}$ ) ppm. IR (KBr):  $1491$  (w),  $1400$  (w),  $1350$  (w),  $1242$  (w),  $1091$  (w),  $1064$  (w),  $1048$  (w),  $1031$  (m),  $864$  (m),  $846$  (s),  $834$  (s),  $797$  (s),  $774$  (s),  $617$  (w)  $\text{cm}^{-1}$ . Anal. Calcd for  $\text{C}_{19}\text{H}_{24}\text{Th}$ : C, 47.1; H, 5.00. Found: C, 47.1; H, 5.18. EIMS:  $\text{M} - \text{H}^+$ , 483 amu.

(b) To a solution of  $(\text{MeC}_5\text{H}_4)_3\text{Th}$  (0.13 g, 0.24 mmol) in 30 mL of diethyl ether was added by syringe 0.46 mL of MeLi (0.24 mmol, 0.52 M solution in diethyl ether). The reaction mixture was stirred for 5 h at room temperature. The solution was filtered, and the volume of the filtrate was reduced *in vacuo* to ca. 10 mL. Cooling to  $-80\text{ }^{\circ}\text{C}$  yielded white shiny plates of  $(\text{MeC}_5\text{H}_4)_3\text{ThMe}$  (50 mg, 43%). The materials obtained under methods a and b exhibited identical physical and spectroscopic properties.

**$(\text{MeC}_5\text{H}_4)_3\text{Th}(\text{O-}2,6\text{-Me}_2\text{C}_6\text{H}_3)$ :** A solution of  $(\text{MeC}_5\text{H}_4)_3\text{Th}$  (0.81 g, 1.5 mmol) in 35 mL of toluene was prepared. A solution of 2,6-dimethylphenol (0.18 g, 1.5 mmol) in 20 mL of toluene was added. The mixture was heated to  $70\text{ }^{\circ}\text{C}$  for 48 h. After the mixture was cooled to room temperature, the solvent was removed under reduced pressure. The resulting solid was extracted with 100 mL of hexane at  $55\text{ }^{\circ}\text{C}$ . After filtration the volume of the hexane extract was reduced *in vacuo* to ca. 80 mL. Cooling first to  $-20$  and then to  $-80\text{ }^{\circ}\text{C}$  yielded thin white needles of  $(\text{MeC}_5\text{H}_4)_3\text{Th}(\text{O-}2,6\text{-Me}_2\text{C}_6\text{H}_3)$  (0.61 g, 70%), mp  $150\text{--}152\text{ }^{\circ}\text{C}$ .  $^1\text{H-NMR}$  ( $\text{C}_6\text{D}_6$ ;  $30\text{ }^{\circ}\text{C}$ ):  $\delta$   $7.06$  (m, 2H);  $6.79$  (m, 1H);  $6.10$  (s, 12H);  $2.45$  (s, 6H);  $2.06$  (s, 9H) ppm. IR (KBr):  $1592$  (w),  $1493$  (w),  $1424$  (w),  $1413$  (w),  $1295$  (w),  $1271$  (s),  $1243$  (w),  $1227$  (s),  $1094$  (m),  $1070$  (w),  $1048$  (w),  $1032$  (w),  $931$  (w),  $860$  (m),  $833$  (w),  $798$  (w),  $795$  (w),  $781$  (w),  $767$  (s),  $741$  (w),  $710$  (m),  $614$  (w),  $539$  (m)  $\text{cm}^{-1}$ . Anal. Calcd for  $\text{C}_{25}\text{H}_{30}\text{OTh}$ : C, 52.9; H, 5.12. Found: C, 53.2; H, 5.07. EIMS:  $\text{M}^+$ , 590 amu.

**$(\text{MeC}_5\text{H}_4)_3\text{Th}(\text{O}_3\text{SC}_6\text{H}_4\text{Me})$ :** A solution of  $(\text{MeC}_5\text{H}_4)_3\text{Th}$  (1.36 g, 2.48 mmol) in 65 mL of toluene was prepared. A solution of *p*-toluenesulfonic acid (0.43 g, 2.5 mmol) in 20 mL of toluene was added by cannula. Upon addition the colorless thorium solution turned bright yellow. The bright yellow color then gradually receded over ca. 20 min, and the mixture was stirred at room temperature for an additional 20 h. The solution was filtered, and the volume of the filtrate was reduced in vacuo to ca. 20 mL. Cooling to  $-80\text{ }^{\circ}\text{C}$  yielded a white powder of  $(\text{MeC}_5\text{H}_4)_3\text{Th}(\text{O}_3\text{SC}_6\text{H}_4\text{Me})$  (0.87 g, 55%), mp  $124\text{--}129\text{ }^{\circ}\text{C}$  (decomp).  $^1\text{H-NMR}$  ( $\text{C}_6\text{D}_6$ ;  $30\text{ }^{\circ}\text{C}$ ):  $\delta$   $8.13$  (AA'BB', 2H);  $6.91$  (AA'BB', 2H);  $6.05$  (s, 12H);  $2.13$  (s, 9H);  $1.94$  (s, 3H) ppm. IR (KBr):  $1599$  (m),  $1495$  (m),  $1396$  (w),  $1259$  (s),  $1215$  (m),  $1162$  (s),  $1107$  (s, br),  $1035$  (s),  $1009$  (s),  $979$  (w),  $936$  (w),  $890$  (w),  $850$  (s),  $817$  (s),  $777$  (s),  $731$  (m),  $710$  (w),  $695$  (w),  $680$  (s),  $636$  (w),  $611$  (w),  $598$  (w),  $565$  (s),  $551$  (s)  $\text{cm}^{-1}$ . Anal. Calcd for  $\text{C}_{25}\text{H}_{28}\text{O}_3\text{STh}$ : C, 46.9; H, 4.41. Found: C, 47.0; H, 4.40. EIMS:  $\text{M} - \text{H}^+$ , 639 amu.

**$(\text{Me}_3\text{SiC}_5\text{H}_4)_3\text{ThH}$ :** (a) To a solution of  $[(\text{Me}_3\text{SiC}_5\text{H}_4)_3\text{Th}]\text{-[BPh}_4]$  (0.36 g, 0.37 mmol) in 80 mL of toluene was added by syringe *t*-BuLi (0.17 mL of a 2.24 M solution in hexane, 0.38 mmol). Within 1 min, the solution became cloudy. The reaction mixture was stirred at room temperature for 11 h, and then the solvent was removed under reduced pressure. The resulting solid was extracted with 30 mL of hexane. After filtration, the volume of the hexane extract was reduced in vacuo to ca. 5 mL. Cooling to  $-80\text{ }^{\circ}\text{C}$  yielded white crystals of  $(\text{Me}_3\text{SiC}_5\text{H}_4)_3\text{ThH}$  (0.15 g, 62%), mp  $87\text{--}89\text{ }^{\circ}\text{C}$ .  $^1\text{H-NMR}$  ( $\text{C}_6\text{D}_6$ ;  $30\text{ }^{\circ}\text{C}$ ):  $\delta$   $12.81$  (s, 1H);  $6.31$  (AA'BB', 6H);  $5.68$  (AA'BB', 6H);  $0.41$  (s, 27H) ppm. IR (KBr):  $1444$  (s),  $1415$  (m),  $1403$

(m), 1366 (m), 1311 (w), 1249 (s), 1191 (w), 1176 (s), 1093 (m), 1062 (m), 1041 (s), 902 (s), 885 (m), 860 (s), 834 (s), 810 (s), 796 (s), 783 (s), 774 (s), 756 (s), 688 (m), 635 (s), 629 (s), 596 (m), 523 (m)  $\text{cm}^{-1}$ . Anal. Calcd for  $\text{C}_{24}\text{H}_{40}\text{Th}$ : C, 44.7; H, 6.26. Found: C, 43.2; H, 6.37. EIMS:  $\text{M} - \text{H}^+$ , 643 amu.

(b) To a solution of  $(\text{Me}_3\text{SiC}_5\text{H}_4)_3\text{ThCl}$  (1.28 g, 1.88 mmol) in 40 mL of THF was added by syringe  $\text{Li}(\text{BHEt}_3)$  (2.0 mL of a 1.0 M solution in THF, 2.0 mmol). The reaction mixture was stirred at room temperature for 3 h. Then the solvent was removed under reduced pressure. The resulting oily solid was extracted with 50 mL of hexane. After filtration, the volume of the hexane extract was reduced to ca. 10 mL. Cooling to  $-80^\circ\text{C}$  yielded white crystals of  $(\text{Me}_3\text{SiC}_5\text{H}_4)_3\text{ThH}$  (0.32 g, 26%). The materials obtained using methods a and b exhibited identical physical and spectroscopic properties.

**$(t\text{-BuC}_5\text{H}_4)_3\text{ThCl}$ :** To a suspension of  $\text{ThCl}_4$  (2.76 g, 7.38 mmol) in 30 mL of THF was added by syringe  $\text{Na}(t\text{-BuC}_5\text{H}_4)$  (105 mL of a 0.22 M solution in THF, 23.1 mmol). The reaction mixture was stirred at room temperature for 48 h, the solvent was then removed under reduced pressure, and the resulting solid was extracted with 150 mL of hexane. After filtration, the saturated hexane extract was cooled to  $-20^\circ\text{C}$  and after 3 h to  $-80^\circ\text{C}$ , yielding colorless crystals of  $(t\text{-BuC}_5\text{H}_4)_3\text{ThCl}$  (1.56 g). The crystals were isolated by filtration and dried under reduced pressure. The reaction mixture residue was extracted with an additional 100 mL of hexane. After filtration, the second hexane extract was combined with the mother liquor from the first extraction, and the volume of the combined extracts was reduced to ca. 100 mL. Cooling to  $-80^\circ\text{C}$  yielded an additional 0.80 g of  $(t\text{-BuC}_5\text{H}_4)_3\text{ThCl}$ . Combined yield: 2.36 g (50.7%), mp  $160\text{--}163^\circ\text{C}$ .  $^1\text{H-NMR}$  ( $\text{C}_6\text{D}_6$ ;  $30^\circ\text{C}$ ):  $\delta$  6.21 (AA'BB', 2H); 5.98 (AA'BB', 2H); 1.37 (s, 9H) ppm. IR (KBr): 1482 (m), 1436 (w), 1397 (m), 1384 (m), 1365 (s), 1361 (s), 1356 (s), 1274 (s), 1199 (m), 1190 (m), 1154 (s), 1047 (m), 1037 (m), 1027 (m), 924 (m), 913 (m), 857 (m), 849 (m), 834 (s), 834 (s), 826 (m), 816 (m), 798 (s), 786 (s), 780 (s), 767 (s), 679 (m), 667 (m)  $\text{cm}^{-1}$ . Anal. Calcd for  $\text{C}_{27}\text{H}_{39}\text{ClTh}$ : C, 51.4; H, 6.24. Found: C, 51.3; H, 6.15. EIMS:  $\text{M}^+$ , 630 amu.

**$(t\text{-BuC}_5\text{H}_4)_3\text{ThMe}$ :** To a solution of  $(t\text{-BuC}_5\text{H}_4)_3\text{ThCl}$  (1.41 g, 2.23 mmol) in 50 mL of diethyl ether was added by syringe methyllithium (5.8 mL of a 0.40 M solution in diethyl ether, 2.3 mmol). The reaction mixture was stirred at room temperature for 4 h. The solvent was removed under reduced pressure. The resulting solid was extracted with 50 mL of hexane. After filtration, the volume of the hexane extract was reduced in vacuo to ca. 35 mL. Cooling to  $-80^\circ\text{C}$  yielded colorless blocks of  $(t\text{-BuC}_5\text{H}_4)_3\text{ThMe}$  (0.90 g, 66%), mp  $108\text{--}110^\circ\text{C}$ .  $^1\text{H-NMR}$  ( $\text{C}_6\text{D}_6$ ;  $30^\circ\text{C}$ ):  $\delta$  6.03 (AA'BB', 6H); 5.91 (AA'BB', 6H); 1.31 (s, 27H), 0.85 (s, 3H) ppm.  $^{13}\text{C-NMR}$  ( $\text{C}_6\text{D}_6$ ;  $30^\circ\text{C}$ ):  $\delta$  143.3 (m); 115.0 (d of m,  $^1J_{\text{C-H}} = 167\text{ Hz}$ ); 114.0 (d

of m,  $^1J_{\text{C-H}} = 165\text{ Hz}$ ); 42.2 (q,  $^1J_{\text{C-H}} = 114\text{ Hz}$ ); 33.1 (m); 32.3 (q of m,  $^1J_{\text{C-H}} = 125\text{ Hz}$ ) ppm. IR (KBr): 1480 (m), 1410 (w), 1395 (m), 1365 (s), 1355 (s), 1275 (s), 1195 (w), 1190 (w), 1155 (s), 1095 (m), 1050 (m), 1035 (m), 1020 (w), 925 (w), 910 (w), 845 (m), 825 (s), 820 (s), 815 (m), 790 (s), 780 (s), 770 (s), 760 (s), 675 (m), 670 (m)  $\text{cm}^{-1}$ . Anal. Calcd for  $\text{C}_{28}\text{H}_{42}\text{Th}$ : C, 55.1; H, 6.95. Found: C, 55.2; H, 6.97. EIMS:  $\text{M} - \text{Me}^+$ , 595 amu.

**$[(t\text{-BuC}_5\text{H}_4)_3\text{Th}][\text{BPh}_4]$ :** A solution of  $(t\text{-BuC}_5\text{H}_4)_3\text{ThMe}$  (0.47 g, 0.77 mmol) in 20 mL of THF was cooled to  $-60^\circ\text{C}$  and then added by cannula to a solution of  $(\text{Et}_3\text{NH})(\text{BPh}_4)$  (0.32 g, 0.76 mmol) in 10 mL of THF, also cooled to  $-60^\circ\text{C}$ . The reaction mixture warmed to room temperature and was then stirred at room temperature for 3 h. The solvent was removed under reduced pressure. The resulting solid was washed with 30 mL of hexane and dried under reduced pressure, yielding 0.64 g (92%) of  $[(t\text{-BuC}_5\text{H}_4)_3\text{Th}][\text{BPh}_4]$ , mp  $149\text{--}155^\circ\text{C}$ .  $^1\text{H-NMR}$  (THF- $d_6$ ;  $30^\circ\text{C}$ ):  $\delta$  7.31 (m, 8H); 6.85 (m, 12 H); 6.69 (AA'BB', 6H); 6.41 (AA'BB', 6H), 1.39 (s, 27H) ppm. IR (KBr): 1591 (w), 1580 (w), 1478 (s), 1430 (m), 1363 (s), 1342 (w), 1277 (m), 1240 (m), 1155 (m), 1066 (w), 1042 (m), 1033 (m), 1022 (w), 915 (w), 844 (m), 822 (m), 815 (m), 779 (s, br), 759 (m), 744 (m), 735 (s), 705 (s), 667 (w), 612 (m)  $\text{cm}^{-1}$ . Anal. Calcd for  $\text{C}_{51}\text{H}_{59}\text{BTh}$ : C, 66.9; H, 6.51. Found: C, 67.3; H, 6.71.

**$(t\text{-BuC}_5\text{H}_4)_3\text{ThH}$ :** A suspension of  $[(t\text{-BuC}_5\text{H}_4)_3\text{Th}][\text{BPh}_4]$  (0.50 g, 0.55 mmol) in 20 mL of hexane was cooled to  $-78^\circ\text{C}$ , and then  $t\text{-BuLi}$  (0.25 mL of a 2.24 M solution in hexane, 0.56 mmol) was added by syringe. The reaction mixture was warmed to room temperature, and the mixture was stirred at room temperature for 24 h. The solid was allowed to settle, and the solution was filtered. The volume of the filtrate was reduced in vacuo to ca. 10 mL. Cooling to  $-20^\circ\text{C}$  caused colorless crystals of  $(t\text{-BuC}_5\text{H}_4)_3\text{ThH}$  to appear (0.20 g, 61%), mp  $143\text{--}148^\circ\text{C}$ .  $^1\text{H-NMR}$  ( $\text{C}_6\text{D}_6$ ;  $30^\circ\text{C}$ ):  $\delta$  13.98 (s, 1H); 6.06 (AA'BB', 6H); 5.47 (AA'BB', 6H); 1.43 (s, 27H) ppm. IR (KBr): 1485 (s), 1437 (s), 1420 (s), 1393 (s), 1383 (s), 1363 (s), 1359 (s), 1278 (s), 1202 (m), 1190 (m), 1155 (s), 1049 (s), 1043 (s), 1023 (s), 915 (s), 842 (s), 825 (s), 818 (s), 784 (s), 773 (s), 762 (s), 676 (s), 613 (w), 578 (m), 571 (m)  $\text{cm}^{-1}$ . Anal. Calcd for  $\text{C}_{27}\text{H}_{40}\text{Th}$ : C, 54.3; H, 6.77. Found: C, 54.5; H, 6.94. EIMS:  $\text{M}^+$ , 596 amu.

**Acknowledgment.** This work was supported by the Director, Office of Energy Research, Office of Basic Energy Sciences, Chemical Sciences Division of the U.S. Department of Energy under Contract No. DE-AC03-76SF00098. We thank D. J. Schwartz for assistance with the NMR experiments.

OM9501790

## Agostic B-H→Ru Bonds in *exo*-Monophosphino-7,8-dicarba-*nido*-undecaborate Derivatives

Clara Viñas,<sup>†</sup> Rosario Nuñez,<sup>†</sup> Miquel A. Flores,<sup>†</sup> Francesc Teixidor,<sup>\*,†</sup>  
Raikko Kivekäs,<sup>‡</sup> and Reijo Sillanpää<sup>§</sup>

*Institut de Ciència de Materials de Barcelona, Campus de Bellaterra, Cerdanyola,  
08193 Barcelona, Spain, Inorganic Chemistry Laboratory, Box 6, University of Helsinki,  
FIN-00014 Helsinki, Finland, and Chemistry Department, University of Turku,  
FIN-20500 Turku, Finland*

Received January 3, 1995<sup>®</sup>

The reaction of [NMe<sub>4</sub>][7-PPh<sub>2</sub>-8-Me-7,8-C<sub>2</sub>B<sub>9</sub>H<sub>10</sub>] with RuCl<sub>3</sub>·H<sub>2</sub>O or RuCl<sub>2</sub>(DMSO)<sub>4</sub> leads to the formation of [Ru(7-PPh<sub>2</sub>-8-Me-7,8-C<sub>2</sub>B<sub>9</sub>H<sub>10</sub>)<sub>2</sub>]. Each carborane ligand is tridentate, forming one P-Ru bond and two B-H→Ru agostic bonds. The number of isomers obtained depends on the initial ruthenium form, giving one isomer (**1**) when RuCl<sub>3</sub>·H<sub>2</sub>O is used and two isomers (**1** and **2**) in the case of the DMSO derivative. No reaction is found with similar thiocarborane ligands [NMe<sub>4</sub>][7-SR-8-Me-7,8-C<sub>2</sub>B<sub>9</sub>H<sub>10</sub>] (R = Ph, Me), suggesting that the surrounding P<sub>2</sub>(BH)<sub>4</sub> is a better stabilizing system. The complexes have been characterized by an X-ray diffraction study.

### Introduction

The chemistry of ruthenium and its complexes plays an important role in fields such as catalysis<sup>1</sup> of organic reactions or, more recently, in the search for organic conductors<sup>2</sup> to be used as elements in electronic circuits. In such applications, stable, long-lasting molecules are demanded along with the desired specific properties. Phosphorus-, nitrogen-, or sulfur-containing ligands are usually involved in those complexes in order to fulfill these requirements. Since the discovery of carboranes, boron chemistry has provided new, versatile clusters which can bind transition metals, giving stable complexes that are of interest in the aforementioned applications.

Our research has been dealing with the chemistry of platinum-group metal complexes of 11 vertex *exo*-thiocarborane and *exo*-phosphinocarborane derivatives.<sup>3</sup> Besides the sulfur-metal and phosphorus-metal interaction, agostic B-H→M bonds have been found. In order to further explore the coordinating properties of

those B-H groups and study their dependence on the electron-rich element attached to the carborane cage, new metal complexes have been synthesized. In this paper we report the synthesis and structural characterization of two isomers of the first ruthenium carborane complex incorporating four B-H→Ru agostic bonds, which are provided by two *nido*-monophosphinocarborane anionic ligands.

### Results and Discussion

Monothioethers of the type indicated in Figure 1A have been proven to be tridentate<sup>4</sup> when they are bonded to Ru(II), which is a transition-metal ion that demands an octahedral geometry. The coordination takes place by means of the thioether group and boron atoms B(2) and B(11) through B-H→Ru agostic bonds. The 3-fold denticity of these compounds parallels that of dithioether species of a similar type indicated in Figure 1B. In that case coordination takes place via the two sulfur atoms and the B(3)-H→Ru agostic bond. Consequently the existence of one or two sulfur elements in the molecule does not modify the binding capacity of these *exo*-thioether 7,8-dicarba-*nido*-undecaborate derivatives, but it does modify the nature and number of the participating B-H groups. A further difference between mono- and dithioethers has been found upon their coordination to the moiety [Ru<sup>II</sup>Cl(PPh<sub>3</sub>)<sub>2</sub>]<sup>+</sup>. The monothioether alters the cage by removal of B(5), while the dithioethers leave the cage unaltered.<sup>5</sup>

The monothioether species offer the possibility of being separated into enantiomers and consequently being used as tricoordinating<sup>4</sup> (S, BH(2), BH(11)), or dicoordinating<sup>6</sup> (S, BH(11)) anionic chiral ligands in

(4) Teixidor, F.; Viñas, C.; Casabó, J.; Romerosa, A. M.; Rius, J.; Miravittles, C. *Organometallics* 1994, 13, 914.

(5) Teixidor, F.; Ayllón, J. A.; Viñas, C.; Kivekäs, R.; Sillanpää, R.; Casabó, J. *Organometallics* 1994, 12, 2751.

(6) Teixidor, F.; Viñas, C.; Flores, M. A. To be submitted for publication.

<sup>†</sup> Institut de Ciència de Materials de Barcelona, CSIC.

<sup>‡</sup> University of Helsinki.

<sup>§</sup> University of Turku.

<sup>®</sup> Abstract published in *Advance ACS Abstracts*, July 1, 1995.

(1) For recent applications see: (a) Darensbourg, D. J.; Joó, M.; Kannisto, M.; Kathó, A.; Reibenspies, J. H.; Daigle, J. *Inorg. Chem.* 1994, 33, 200 and references therein. (b) Gargulak, J. D.; Gladfelter, W. L. *Inorg. Chem.* 1994, 33, 253.

(2) (a) Sano, M.; Taube, H. *Inorg. Chem.* 1994, 33, 103 and references therein. (b) Sun, Y.; DeArmond, K. *Inorg. Chem.* 1994, 33, 2004. (c) Meyer, T. J.; Meyer, G. J.; Pfennig, B. W.; Schoonover, J. R.; Timpson, C. J.; Wall, J. F.; Kobusch, C.; Chen, X.; Peek, B. M.; Wall, C. G.; Ou, W.; Erickson, B. W.; Bignozzi, C. A. *Inorg. Chem.* 1994, 33, 3952.

(3) (a) Teixidor, F.; Rudolph, R. W. *J. Organomet. Chem.* 1983, 241, 301. (b) Viñas, C.; Butler, W. M.; Teixidor, F.; Rudolph, R. W. *Organometallics* 1984, 3, 503. (c) Viñas, C.; Butler, W. M.; Teixidor, F.; Rudolph, R. W. *Inorg. Chem.* 1986, 25, 4369. (d) Teixidor, F.; Rius, J.; Romerosa, A. M.; Miravittles, C.; Escriche, Ll.; Sanchez, E.; Viñas, C.; Casabó, J. *Inorg. Chim. Acta* 1990, 176, 287. (e) Teixidor, F.; Romerosa, A. M.; Rius, J.; Miravittles, C.; Casabó, J.; Viñas, C.; Sanchez, E. *J. Chem. Soc., Dalton Trans.* 1990, 525. (f) Teixidor, F.; Viñas, C.; Rius, J.; Miravittles, C.; Casabó, J. *Inorg. Chem.* 1990, 29, 149. (g) Teixidor, F.; Casabó, J.; Romerosa, A. M.; Viñas, C.; Rius, J.; Miravittles, C. *J. Am. Chem. Soc.* 1991, 113, 9895.

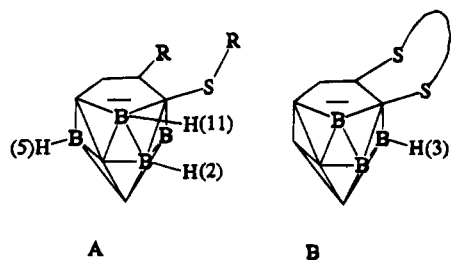


**Figure 1.** Schematic drawings of mono- and dithioether derivatives of 7,8-dicarba-*nido*-undecaborate.

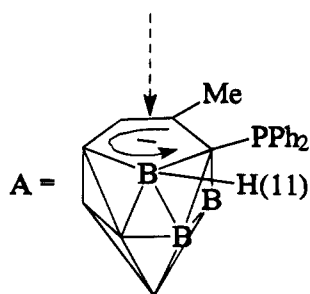


**Figure 2.** Schematic drawing of the 7-(diphenylphosphino)-8-methyl-7,8-dicarba-*nido*-undecaborate anion showing the A motif.

asymmetric catalysis. Due to the role phosphines play in catalysis, the arylphosphine equivalent to Figure 1A was synthesized (Figure 2). This would lead to a comparison of the coordinating capacity of the monothioethers versus monophosphine derivatives. The C-P bond in *exo*-phosphino-1,2-dicarba-*closo*-dodecaborane derivatives easily breaks in the partial degradation process; however, a procedure has been found which enables the synthesis of the ligands in the free state.<sup>7</sup>

The reaction of [7-PPh<sub>2</sub>-8-Me-7,8-C<sub>2</sub>B<sub>9</sub>H<sub>10</sub>]<sup>-</sup>, abbreviated as L<sub>Pn</sub><sup>-</sup>, with RuCl<sub>3</sub>·xH<sub>2</sub>O in a 2:1 ratio in ethanol produced a very low yield of yellow crystals with the stoichiometry Ru(L<sub>Pn</sub>)<sub>2</sub> (1). The low yield was attributed to the partial consumption of the phosphine ligand to produce the Ru(III) → Ru(II) conversion. The <sup>1</sup>H NMR spectra displays broad signals at -11.20 and -10.32 ppm, which are assigned to two sorts of B-H-Ru agostic bonds. Furthermore, the existence of a unique CH<sub>3</sub> peak at 1.51 ppm indicated that the two cages were symmetry-related. No other -CH<sub>3</sub> peaks were observed, which proved the isomeric purity of the crystalline material. The <sup>31</sup>P NMR also displayed only one signal at 22.93 ppm, in agreement with the sample's isomeric purity.

The 2:1, L<sub>Pn</sub><sup>-</sup>:Ru(II), stoichiometry and the hexacoordinating predisposition of Ru(II) presumes that each L<sub>Pn</sub><sup>-</sup> ligand has to be tricoordinating. This was expected in the event L<sub>Pn</sub><sup>-</sup> had a coordinating behavior comparable to that of [7-SR-8-Me-7,8-C<sub>2</sub>B<sub>9</sub>H<sub>10</sub>]<sup>-</sup>. The three coordinating sites could be provided by the -PPh<sub>2</sub> moiety and BH(11) and BH(2) fragments. Thus, as with the monothioether, the activation of two BH units had been made possible in this monophosphinocarborane derivative.

Earlier we did report<sup>4</sup> that the reaction of [7-SR-8-Me-7,8-C<sub>2</sub>B<sub>9</sub>H<sub>10</sub>]<sup>-</sup> with [RuCl<sub>2</sub>(PPh<sub>3</sub>)<sub>3</sub>] yielded the compound [RuCl{7-SR-8-Me-(5)-7,8-C<sub>2</sub>B<sub>8</sub>H<sub>10</sub>}(PPh<sub>3</sub>)<sub>2</sub>], where

(7) Teixidor, F.; Viñas, C.; Abad, M. M.; Nuñez, R.; Kivekäs, R.; Sillanpää, R. *J. Organomet. Chem.*, submitted for publication.

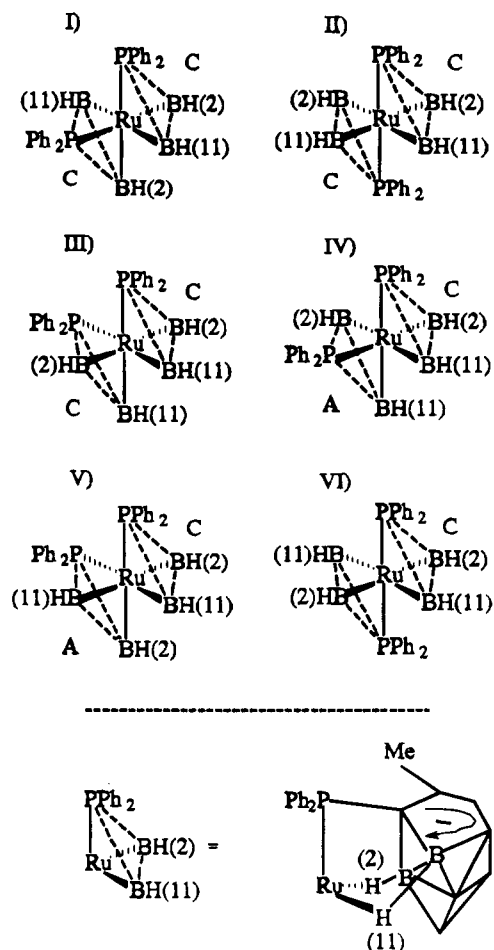
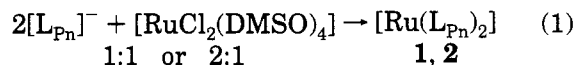


**Figure 3.** Isomers compatible with the formulation [Ru-(7-PPh<sub>2</sub>-8-Me-7,8-C<sub>2</sub>B<sub>9</sub>H<sub>10</sub>)<sub>2</sub>]. The bonding scheme shown at the bottom has been used. A stands for an anticlockwise and C for a clockwise motif following Figure 2.

the starting *nido*-carborane had been converted upon Ru complexation into an arachno species by the removal of B(5). This *nido* to *arachno* conversion could have taken place with the monophosphines as well; however, the <sup>11</sup>B NMR indicates the 11-vertex cage retention. Even more conclusive than the <sup>11</sup>B NMR spectrum is the lack of a quartet of doublets at ~-2.40 ppm, which we have found indicative of two B-H-B hydrogen bridges in the open face defined by five boron atoms in (5)-C<sub>2</sub>B<sub>8</sub> cages.

The low yield obtained in the former synthesis of (1) using RuCl<sub>3</sub>·xH<sub>2</sub>O was partially overcome by using [RuCl<sub>2</sub>(DMSO)<sub>4</sub>] as a source of Ru(II). The reaction is indicated in eq 1.



The product of this reaction and that formerly obtained with RuCl<sub>3</sub>·xH<sub>2</sub>O show a common [Ru(L<sub>Pn</sub>)<sub>2</sub>] stoichiometry, but the <sup>1</sup>H NMR of the [RuCl<sub>2</sub>(DMSO)<sub>4</sub>] reaction mixture displayed two peaks of unequal intensity in the -CH<sub>3</sub> region at 1.51 and 1.23 ppm. The first peak corresponded to the signal found in 1 following the RuCl<sub>3</sub> procedure, but the peak at 1.23 ppm should correspond to a new isomer. Consequently, the [RuCl<sub>2</sub>(DMSO)<sub>4</sub>] method has produced two isomers, which are 1 and 2. The <sup>31</sup>P NMR also shows two resonances at 22.93 and 36.53 ppm, the first corresponding to 1. The



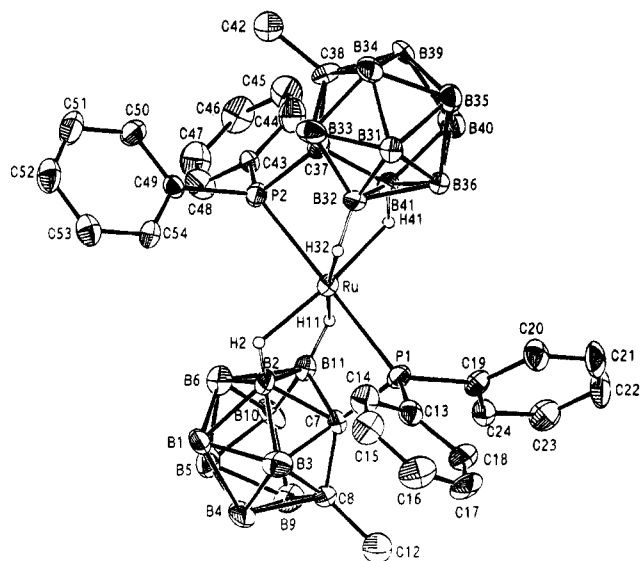


**Figure 4.** Simplified ORTEP view of  $[\text{Ru}(7\text{-PPh}_2\text{-8-Me-7,8-C}_2\text{B}_9\text{H}_{10})_2]\cdot 2(\text{Me})_2\text{CO}$  (**1**) showing 30% thermal ellipsoids.

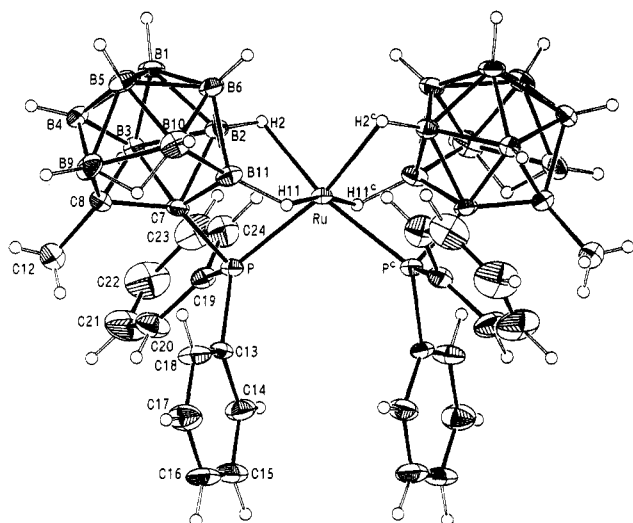


**Figure 5.** Simplified ORTEP view of  $[\text{Ru}(7\text{-PPh}_2\text{-8-Me-7,8-C}_2\text{B}_9\text{H}_{10})_2]\cdot 1.486\text{CHCl}_3$  (**2**) showing 30% thermal ellipsoids.

$^1\text{H}$  NMR in the negative area shows, in addition to the resonances assigned to **1**, two B–H–Ru signals at  $-5.55$  and  $-10.70$  ppm, which are attributed to the **2** isomer.

There are several isomers compatible with this stoichiometry, which are the result of the  $\text{PPh}_2$ ,  $\text{BH}(2)$ , and  $\text{BH}(11)$  disposition of one cluster when the second one is kept immobile around the Ru(II). In Figure 3 the possible isomers are represented. To make the representation clearer, only the intervening atoms are depicted. The structure of the ligating section is shown at the bottom of Figure 3. In the event the isomer is optically active, only one of the enantiomers is represented. This is the general situation, since optical isomers should be expected for I–V but not for VI in Figure 3. The capital letters C and A in the drawing stand for clockwise and anticlockwise motifs. To distinguish these, the CIP protocol has been used, in a view of the cluster through an axis moving down to the unique vertex as shown in Figure 2.

**Table 1.** Final Positional Parameters and Isotropic Thermal Parameters ( $\text{\AA}^2$ ) with Esd's in Parentheses for  $[\text{Ru}(7\text{-PPh}_2\text{-8-Me-7,8-C}_2\text{B}_9\text{H}_{10})_2]\cdot 2(\text{Me})_2\text{CO}$  (**1**)

	$x/a$	$y/b$	$z/c$	$U_{\text{eq}}^a$
Ru	0.96172(9)	0.3078(1)	0.63494(2)	0.0376(3)
P(1)	1.0811(3)	0.2092(4)	0.59588(7)	0.042(1)
B(1)	0.734(1)	0.241(1)	0.5600(3)	0.049(6)
B(2)	0.848(1)	0.259(1)	0.5890(3)	0.047(6)
B(3)	0.867(1)	0.151(2)	0.5559(3)	0.057(7)
B(4)	0.802(1)	0.237(2)	0.5229(3)	0.064(7)
B(5)	0.746(1)	0.394(2)	0.5361(3)	0.061(7)
B(6)	0.770(1)	0.402(2)	0.5778(3)	0.053(6)
C(7)	0.9709(9)	0.271(1)	0.5675(2)	0.040(5)
C(8)	0.9459(9)	0.254(1)	0.5306(2)	0.048(5)
B(9)	0.882(1)	0.394(2)	0.5176(3)	0.056(6)
B(10)	0.856(1)	0.504(2)	0.5519(3)	0.058(6)
B(11)	0.917(1)	0.406(1)	0.5836(3)	0.036(5)
C(12)	1.034(3)	0.180(3)	0.5103(7)	0.065(4)
C(13)	1.1011(9)	0.028(1)	0.5928(2)	0.045(5)
C(14)	1.023(1)	-0.060(1)	0.6072(3)	0.057(5)
C(15)	1.028(1)	-0.200(1)	0.6045(3)	0.069(6)
C(16)	1.112(1)	-0.256(1)	0.5864(3)	0.076(6)
C(17)	1.194(1)	-0.177(1)	0.5725(3)	0.067(5)
C(18)	1.190(1)	-0.032(1)	0.5751(3)	0.062(6)
C(19)	1.2152(9)	0.287(1)	0.5860(2)	0.041(4)
C(20)	1.318(1)	0.254(1)	0.6031(3)	0.061(6)
C(21)	1.418(1)	0.315(2)	0.5956(3)	0.081(6)
C(22)	1.425(1)	0.415(1)	0.5720(3)	0.074(6)
C(23)	1.328(1)	0.450(1)	0.5554(3)	0.066(6)
C(24)	1.2240(9)	0.387(1)	0.5623(3)	0.051(5)
P(2)	0.8438(3)	0.4146(3)	0.67264(7)	0.040(1)
B(31)	1.082(1)	0.136(1)	0.7195(3)	0.038(5)
B(32)	1.014(1)	0.218(2)	0.6863(3)	0.042(6)
B(33)	0.944(1)	0.211(2)	0.7225(3)	0.056(6)
B(34)	1.048(1)	0.235(2)	0.7528(3)	0.052(6)
B(35)	1.185(1)	0.262(1)	0.7354(3)	0.053(6)
B(36)	1.162(1)	0.243(2)	0.6931(3)	0.049(6)
C(37)	0.9540(9)	0.366(1)	0.7017(2)	0.037(4)
C(38)	0.971(1)	0.375(1)	0.7386(2)	0.047(5)
B(39)	1.107(1)	0.409(2)	0.7472(3)	0.057(7)
B(40)	1.185(1)	0.411(2)	0.7099(3)	0.057(6)
B(41)	1.072(1)	0.376(1)	0.6813(3)	0.035(5)
C(42)	0.873(2)	0.431(4)	0.7588(8)	0.063(4)
C(43)	0.8317(9)	0.601(1)	0.6739(2)	0.038(5)
C(44)	0.908(1)	0.678(1)	0.6912(3)	0.065(5)
C(45)	0.898(1)	0.821(1)	0.6907(3)	0.072(6)
C(46)	0.812(1)	0.884(1)	0.6738(3)	0.066(6)
C(47)	0.738(1)	0.806(1)	0.6571(3)	0.073(6)
C(48)	0.746(1)	0.665(1)	0.6568(3)	0.062(5)
C(49)	0.7027(9)	0.353(1)	0.6822(2)	0.037(4)
C(50)	0.636(1)	0.418(1)	0.7046(3)	0.059(5)
C(51)	0.529(1)	0.363(1)	0.7120(3)	0.069(6)
C(52)	0.489(1)	0.244(1)	0.6973(3)	0.065(6)
C(53)	0.555(1)	0.179(1)	0.6746(3)	0.060(5)
C(54)	0.6597(9)	0.236(1)	0.6676(3)	0.049(5)
O(55)	1.426(1)	0.873(1)	0.6467(3)	0.193(6)
C(56)	1.354(1)	0.797(2)	0.6531(4)	0.132(6)
C(57)	1.248(1)	0.823(2)	0.6692(4)	0.119(6)
C(58)	1.391(1)	0.647(2)	0.6425(3)	0.111(6)
O(59)	0.602(2)	-0.178(2)	0.5638(4)	0.340(8)
C(60)	0.548(2)	-0.173(3)	0.5371(4)	0.340(8)
C(61)	0.613(3)	-0.178(5)	0.5064(4)	0.340(8)
C(62)	0.420(2)	-0.160(5)	0.5360(7)	0.340(8)

$$^a U_{\text{eq}} = \frac{1}{3} \sum_i \sum_j U_{ij} a_i^* a_j^* \mathbf{a}_i \cdot \mathbf{a}_j$$

To unambiguously know the nature of compounds **1** and **2**, their X-ray analysis was necessary. Crystals suitable for X-ray analysis were obtained from recrystallization. The isomer II in Figure 3 was obtained pure in the  $\text{RuCl}_3$  reaction, while a mixture of isomers I and II was obtained by using  $[\text{RuCl}_2(\text{DMSO})_4]$ . In the second case, care was taken to examine a crystal not having the cell parameters of the former.

Figure 4 shows the molecular structure of compound **1**. Table 1 lists positional parameters, and Table 2 lists selected interatomic distances and angles. The Ru(II)



**Table 2. Selected Interatomic Distances (Å) and Angles (deg) with Esd's in Parentheses for [Ru(7-PPh<sub>2</sub>-8-Me-7,8-C<sub>2</sub>B<sub>9</sub>H<sub>10</sub>)<sub>2</sub>]<sub>2</sub>(Me)<sub>2</sub>CO (1)**

Ru–P(1)	2.373(3)	Ru–P(2)	2.358(3)
Ru–B(2)	2.34(1)	Ru–B(11)	2.39(1)
Ru–B(32)	2.38(1)	Ru–B(41)	2.38(1)
Ru–H(2)	1.88	Ru–H(11)	1.95
Ru–H(32)	1.94	Ru–H(41)	1.93
P(1)–C(7)	1.82(1)	P(1)–C(13)	1.79(1)
P(1)–C(19)	1.80(1)	P(2)–C(37)	1.80(1)
P(2)–C(43)	1.82(1)	P(2)–C(49)	1.81(1)
B(3)–C(7)	1.74(2)	B(3)–C(8)	1.74(2)
C(7)–C(8)	1.56(1)	C(7)–B(11)	1.62(2)
C(8)–B(9)	1.64(2)	C(8)–C(12)	1.53(3)
B(9)–B(10)	1.81(2)	B(10)–B(11)	1.76(2)
B(33)–C(37)	1.75(2)	B(33)–C(38)	1.76(2)
C(37)–C(38)	1.55(1)	C(37)–B(41)	1.64(2)
C(38)–B(39)	1.65(2)	C(38)–C(42)	1.53(3)
B(39)–B(40)	1.82(2)	B(40)–B(41)	1.79(2)
P(1)–Ru–P(2)	177.6(1)	C(8)–C(7)–B(11)	115.1(9)
H(2)–Ru–H(41)	172	C(7)–C(8)–B(9)	108.0(9)
H(11)–Ru–H(32)	173	C(7)–C(8)–C(12)	119(1)
Ru–P(1)–C(7)	83.8(4)	B(9)–C(8)–C(12)	121(1)
Ru–P(1)–C(13)	122.0(4)	C(8)–B(9)–B(10)	108.4(9)
Ru–P(1)–C(19)	121.0(4)	B(9)–B(10)–B(11)	102(1)
C(7)–P(1)–C(13)	111.7(5)	C(7)–B(11)–B(10)	106.5(9)
C(7)–P(1)–C(19)	108.4(5)	C(37)–B(33)–C(38)	52.2(7)
C(13)–P(1)–C(19)	106.7(5)	P(2)–C(37)–B(33)	105.2(7)
Ru–P(2)–C(37)	84.9(4)	P(2)–C(37)–C(38)	120.3(7)
Ru–P(2)–C(43)	120.5(4)	P(2)–C(37)–C(38)	135.9(8)
Ru–P(2)–C(49)	123.3(4)	P(2)–C(37)–B(41)	103.1(7)
C(37)–P(2)–C(43)	107.3(5)	C(38)–C(37)–B(41)	115.3(9)
C(37)–P(2)–C(49)	113.6(5)	C(37)–C(38)–B(39)	108.6(9)
C(43)–P(2)–C(49)	104.8(5)	C(38)–B(39)–B(40)	108.9(9)
C(7)–B(3)–C(8)	53.3(6)	C(37)–C(38)–C(42)	119(1)
P(1)–C(7)–B(2)	103.0(7)	B(39)–C(38)–C(42)	122(1)
P(1)–C(7)–B(3)	115.6(8)	B(39)–B(40)–B(41)	100.6(9)
P(1)–C(7)–C(8)	135.4(8)	C(37)–B(41)–B(40)	106.3(9)
P(1)–C(7)–B(11)	106.1(7)		

cation is coordinated octahedrally to two tridentate carborane cages, and two acetone molecules from recrystallization occupy empty places in the lattice. The phosphorus atoms are in trans positions, and BH(2)'s and BH(11)'s are in cis positions with the molecular symmetry C<sub>1</sub>. In the complex both clusters have the A configuration. The structure is the enantiomer to that of isomer II in Figure 3. However, as **1** crystallizes in a centrosymmetric space group, the crystal contains an equal amount of isomer II and its enantiomer with ligand configuration C.

Figure 5 shows the complex unit of compound **2**. Table 3 lists positional parameters, and Table 4 lists selected interatomic distances and angles. The molecular structure is essentially the same as for compound **1**. The Ru(II) cation is coordinated octahedrally to two tridentate carborane cages, and chloroform molecules occupy empty places in the lattice. The phosphorus atoms are in positions cis to each other, the BH(2)'s are trans to phosphorus atoms, and the BH(11)'s are trans to each other. The molecular symmetry is C<sub>2</sub> with Ru on the 2-fold axis. In the complex both ligands have the C configuration and the structure is equivalent to that of isomer I in Figure 3. However, as **2** crystallizes in a centrosymmetric space group, the crystal contains an equal amount of isomer I and its enantiomer with ligand configuration A.

A comparison of distances and angles of the two isomeric complex units reveals some significant differences. In **1** the Ru–P distances (2.373(3) and 2.358(3) Å) are clearly longer than in **2** (2.298(2) Å). The Ru–B(2) distance in **2** (2.436(8) Å) is slightly longer than

**Table 3. Final Positional Parameters and Isotropic Thermal Parameters (Å) with Esd's in Parentheses for [Ru(7-PPh<sub>2</sub>-8-Me-7,8-C<sub>2</sub>B<sub>9</sub>H<sub>10</sub>)<sub>2</sub>]<sub>2</sub>·1.486CHCl<sub>3</sub> (2)**

	<i>x/a</i>	<i>y/b</i>	<i>z/c</i>	<i>U</i> <sub>eq</sub> <sup>a</sup>
Ru	1/2	0.83192(7)	1/4	0.0258(3)
P	0.5072(1)	0.7112(2)	0.3394(1)	0.0298(7)
B(1)	0.5756(5)	1.0473(7)	0.4201(5)	0.042(4)
B(2)	0.5399(4)	0.9449(7)	0.3550(4)	0.032(3)
B(3)	0.5397(4)	0.9152(7)	0.4372(4)	0.034(3)
B(4)	0.6185(5)	0.9670(8)	0.4936(5)	0.041(4)
B(5)	0.6686(5)	1.0260(8)	0.4488(5)	0.045(4)
B(6)	0.6162(5)	1.0166(7)	0.3597(5)	0.037(4)
C(7)	0.5693(3)	0.8126(6)	0.3933(3)	0.031(3)
C(8)	0.6099(4)	0.8237(6)	0.4704(3)	0.039(3)
B(9)	0.6862(5)	0.8813(8)	0.4817(5)	0.047(4)
B(10)	0.6882(5)	0.9192(9)	0.3954(5)	0.049(4)
B(11)	0.6043(4)	0.8653(7)	0.3427(5)	0.036(4)
C(12)	0.6026(5)	0.7304(8)	0.5180(4)	0.066(4)
C(13)	0.5495(4)	0.5707(6)	0.3498(4)	0.035(3)
C(14)	0.5110(4)	0.4700(7)	0.3307(4)	0.053(4)
C(15)	0.5445(5)	0.3634(7)	0.3395(5)	0.065(4)
C(16)	0.6148(5)	0.3572(6)	0.3676(5)	0.067(5)
C(17)	0.6536(4)	0.4572(7)	0.3858(5)	0.062(4)
C(18)	0.6207(4)	0.5630(6)	0.3766(5)	0.052(4)
C(19)	0.4348(4)	0.6941(6)	0.3675(4)	0.039(3)
C(20)	0.4358(5)	0.6135(8)	0.4183(5)	0.064(4)
C(21)	0.3847(6)	0.6127(9)	0.4447(6)	0.095(7)
C(22)	0.3324(6)	0.690(1)	0.4240(6)	0.097(6)
C(23)	0.3304(5)	0.7713(9)	0.3766(6)	0.077(5)
C(24)	0.3820(4)	0.7723(8)	0.3481(5)	0.060(4)
Cl(1) <sup>b</sup>	0.6874(3)	0.6691(5)	0.7171(3)	0.153(3)
Cl(2) <sup>b</sup>	0.6125(3)	0.8793(5)	0.6808(2)	0.144(3)
Cl(3) <sup>b</sup>	0.7553(3)	0.8674(6)	0.7012(3)	0.172(4)
C(25) <sup>b</sup>	0.6931(8)	0.827(2)	0.7287(7)	0.118(9)

<sup>a</sup>  $U_{eq} = 1/3 \sum_i \sum_j U_{ij} a_i^* a_j^* a_i a_j$ . <sup>b</sup> Site occupation parameter 0.743(4).

**Table 4. Selected Interatomic Distances (Å) and Angles (deg) with Esd's in Parentheses for [Ru(7-PPh<sub>2</sub>-8-Me-7,8-C<sub>2</sub>B<sub>9</sub>H<sub>10</sub>)<sub>2</sub>]<sub>2</sub>·1.486CHCl<sub>3</sub> (2)**

Ru–P	2.298(2)	Ru–B(2)	2.436(8)
Ru–B(11)	2.363(8)	Ru–H(2)	2.01(7)
Ru–H(11)	1.69(4)	P–C(7)	1.806(6)
P–C(13)	1.818(7)	P–C(19)	1.805(9)
B(2)–H(2)	1.23(6)	B(3)–C(7)	1.74(1)
B(3)–C(8)	1.73(1)	C(7)–C(8)	1.538(9)
C(7)–B(11)	1.60(1)	C(8)–B(9)	1.65(1)
C(8)–C(12)	1.51(1)	B(9)–B(10)	1.88(2)
B(10)–B(11)	1.80(1)	B(11)–H(11)	1.27(4)
P–Ru–H(2)	84(2)	C(13)–P–C(19)	106.5(4)
P–Ru–H(11)	81(2)	C(7)–B(3)–C(8)	52.6(4)
P–Ru–P <sup>a</sup>	105.33(8)	P–C(7)–B(2)	103.1(4)
P–Ru–H(2) <sup>a</sup>	165(2)	P–C(7)–B(3)	117.8(5)
P–Ru–H(11) <sup>a</sup>	92(2)	P–C(7)–C(8)	135.4(6)
H(2)–Ru–H(11)	102(2)	P–C(7)–B(11)	102.6(5)
H(2)–Ru–H(2) <sup>a</sup>	89(3)	C(8)–C(7)–B(11)	117.3(6)
H(2)–Ru–H(11) <sup>a</sup>	87(2)	C(7)–C(8)–B(9)	108.7(7)
H(11)–Ru–H(11) <sup>a</sup>	169(2)	C(7)–C(8)–C(12)	119.3(6)
Ru–P–C(7)	86.7(2)	B(9)–C(8)–C(12)	120.6(6)
Ru–P–C(13)	121.8(3)	C(8)–B(9)–B(10)	107.7(6)
Ru–P–C(19)	120.9(2)	B(9)–B(10)–B(11)	99.4(7)
C(7)–P–C(13)	107.4(3)	C(7)–B(11)–B(10)	106.7(6)
C(7)–P–C(19)	110.7(4)		

<sup>a</sup> Symmetry code: 1 – *x*, *y*, 1/2 – *z*.

the Ru–B(2) distance in **1** and Ru–B(11) distances in **1** and **2**. In **1** the P–Ru–P angle value does not deviate much from linearity (177.6(1)°). In **2**, in which the phosphorus atoms are in a cis disposition, the P–Ru–P angle (105.33(8)°) is considerably opened compared to the ideal angle (90°) of an octahedral coordination sphere. The opening is not unexpected, taking into account the great differences in the Ru–H and Ru–P bond lengths. The angles around the phosphorus atoms

vary from 83.8(4) to 123.3(4)° for **1**, and from 86.7(2) to 121.8(3)° for **2**. In both structures the smallest values are for Ru–P–C(7) angles (83.8(3) and 84.9(4)° for **1** and 86.7(2)° for **2**), and the values are much smaller than the others, indicating angle strain at the phosphorus atoms caused by tridentate coordination of the carborane cages.

By using monophosphinocarboranes as the unique source of Ru(II) ligands, it has been possible to get the RuP<sub>2</sub>(BH)<sub>4</sub> motifs. To our knowledge, these molecules contain the largest number of BH units in the vicinity of a metal. Examples of molecules with a large number of BH units in the metal neighborhood are (OC)<sub>3</sub>Mn–B<sub>8</sub>H<sub>13</sub>,<sup>8</sup> (OC)<sub>3</sub>MnB<sub>3</sub>H<sub>8</sub>,<sup>9</sup> (PPh<sub>3</sub>)<sub>2</sub>ClRu(C<sub>2</sub>B<sub>9</sub>H<sub>10</sub>R<sub>2</sub>),<sup>10</sup> and CpZr(CH<sub>3</sub>)<sub>2</sub>(CB<sub>11</sub>H<sub>12</sub>),<sup>11</sup> all containing three BH units attached to the metal. The low bonding capacity of the BH groups is proved by the instability of some of those compounds. In contrast, **1** and **2** are fairly stable in the solid state as well as in solution. To have a comparison with the equivalent monothioethers, reactions similar to those described above leading to **1** and **2** have been conducted. In contrast, the reactions of [(7-SPh-8-Me-7,8-C<sub>2</sub>B<sub>9</sub>H<sub>10</sub>)]<sup>-</sup> (L<sub>SPh</sub><sup>-</sup>)<sup>12</sup> and [(7-SMe-8-Me-7,8-C<sub>2</sub>B<sub>9</sub>H<sub>10</sub>)]<sup>-</sup> (L<sub>SMe</sub><sup>-</sup>) with [RuCl<sub>2</sub>(DMSO)<sub>4</sub>] in different solvents (ethanol, THF, dimethoxyethane, toluene), at different stoichiometries (2:1, 1:1), and at different temperatures have yielded free ligand in every case. The lack of reaction was, initially, attributed to the difficulty of these anionic monothioethers in displacing chloride completely from transition-metal complexes. To overcome this difficulty, the ligands L<sub>SMe</sub><sup>-</sup> and L<sub>SPh</sub><sup>-</sup> were treated with [Ru(DMSO)<sub>6</sub>][ClO<sub>4</sub>]<sub>2</sub> or [Ru(DMSO)<sub>6</sub>][CF<sub>3</sub>SO<sub>3</sub>]<sub>2</sub>, two Ru(II) complexes with weak coordinating ligands in the form of perchlorate or trifluoromethanesulfonate salts. As before, only free ligand was found.

In summary, it can be concluded that metal coordination surroundings with four BH units have been found as RuP<sub>2</sub>(BH)<sub>4</sub> moieties. Furthermore, the binding capacity of *exo*-monothiocarborane derivatives L<sub>SMe</sub><sup>-</sup> and L<sub>SPh</sub><sup>-</sup> does not fully parallel that of the analogous *exo*-monophosphine L<sub>Pn</sub><sup>-</sup>. Therefore, the P<sub>2</sub>(BH)<sub>4</sub> surrounding is a better stabilizing system than S<sub>2</sub>(BH)<sub>4</sub>. On the other hand, the coordinating capability of the S(BH)<sub>2</sub> moiety is increased when two triphenylphosphine ligands and a chloride fulfill the Ru(II) octahedral environment.

## Experimental Section

Before use, methyl-*o*-carborane (Dexsil Chemical Corp.) was sublimed under high vacuum; [NMe<sub>4</sub>][7-PPh<sub>2</sub>-8-Me-7,8-C<sub>2</sub>B<sub>9</sub>H<sub>10</sub>] was prepared from 1-(diphenylphosphino)-2-methyl-1,2-dicarba-*closo*-dodecaborane according to the literature.<sup>7</sup> [RuCl<sub>2</sub>(DMSO)<sub>4</sub>], [Ru(DMSO)<sub>6</sub>][ClO<sub>4</sub>]<sub>2</sub>, and [Ru(DMSO)<sub>6</sub>][CF<sub>3</sub>SO<sub>3</sub>]<sub>2</sub> were synthesized according to the literature,<sup>13</sup> and RuCl<sub>3</sub>·xH<sub>2</sub>O was utilized as purchased. Ethanol was reagent grade.

(8) Calabrese, J. C.; Fischer, M. B.; Gaines, D. F.; Lott, J. W. *J. Am. Chem. Soc.* **1974**, *96*, 63186.

(9) Hildebrandt, S. J.; Gaines, D. F.; Calabrese, J. C. *Inorg. Chem.* **1978**, *17*, 790.

(10) Chizhevsky, I. T.; Lobanova, I. A.; Bregadze, V. I.; Petrovskii, P. V.; Antonovich, V. A.; Polyakov, A. V.; Yanovskii, A. I.; Struchkov, Y. T. *J. Chem. Soc., Mendeleev Commun.* **1991**, 47.

(11) Crowther, D. J.; Borkowsky, S. L.; Swenson, D.; Meyer, T. Y.; Jordan, R. F. *Organometallics* **1993**, *12*, 2897.

(12) Teixidor, F.; Viñas, C.; Flores, M. A. To be submitted for publication.

(13) Evans, P.; Spencer, A.; Wilkinson, G. *J. Chem. Soc., Dalton Trans.* **1973**, 204–209.

**Synthesis of [Ru(7-PPh<sub>2</sub>-8-Me-7,8-C<sub>2</sub>B<sub>9</sub>H<sub>10</sub>)<sub>2</sub>].** (a) To 25 cm<sup>3</sup> of deoxygenated methanol containing 428 mg (1.06 mmol) of [NMe<sub>4</sub>][7-PPh<sub>2</sub>-8-Me-7,8-C<sub>2</sub>B<sub>9</sub>H<sub>10</sub>] was added RuCl<sub>3</sub>·xH<sub>2</sub>O (48 mg, 0.197 mmol), and the mixture was refluxed for 6 h. A red solid precipitated in the warm mixture. The solution was concentrated to one-third of the initial volume. The red solid was separated by filtering under nitrogen, and then it was washed with deoxygenated methanol (10 cm<sup>3</sup>) and ethyl ether. Practically all the red solid dissolved in ethyl ether, forming a red solution. The solvent was eliminated to yield an orange-red solid, yield 15 mg (3%). FTIR (KBr): ν (cm<sup>-1</sup>) 2551, 2530 (B–H). <sup>1</sup>H FT NMR (250 MHz, CDCl<sub>3</sub>, 25 °C, TMS): δ -11.20 (br, 1, BHRu), -10.32 (q, 1, BHRu), -2.73 (br, 1, B–H–B), 1.51 (s, 3, CH<sub>3</sub>), 7.20–7.60 (m, 10, C<sub>aryl</sub>–H). <sup>11</sup>B FT NMR (128 MHz, CO(CD<sub>3</sub>)<sub>2</sub>, 25 °C, BF<sub>3</sub>·Et<sub>2</sub>O): δ 6.01 (d, <sup>1</sup>J(B,H) = 142 Hz, 1B), -10.33 (1B), -15.37 (1B), -17.05 (d, <sup>1</sup>J(B,H) = 141 Hz, 1B), -22.93 (d, <sup>1</sup>J(B,H) = 91 Hz, 1B), -23.49 (d, <sup>1</sup>J(B,H) = 122 Hz, 1B), -28.59 (2B), -38.76 (d, <sup>1</sup>J(B,H) = 141 Hz, 1B). <sup>31</sup>P{<sup>1</sup>H} FT NMR (101 MHz, CDCl<sub>3</sub>, 25 °C, H<sub>3</sub>PO<sub>4</sub>, 85%): δ 22.93 (s). Anal. Calcd for C<sub>30</sub>H<sub>46</sub>B<sub>18</sub>P<sub>2</sub>Ru: C, 47.00; H, 6.07. Found: C, 46.95; H, 6.03. From slow evaporation of an ethyl ether:acetone (5:1) solution of the solid, red microcrystals were obtained.

(b) To 20 cm<sup>3</sup> of deoxygenated ethanol containing 100 mg (0.25 mmol) of [NMe<sub>4</sub>][7-PPh<sub>2</sub>-8-Me-7,8-C<sub>2</sub>B<sub>9</sub>H<sub>10</sub>] was added [RuCl<sub>2</sub>(DMSO)<sub>4</sub>] (120 mg, 0.25 mmol), and the mixture was refluxed for 3 h. An orange solid precipitated in the warm mixture. The solution was cooled to -10 °C and the solid was separated by filtering, and then it was washed with deoxygenated ethanol (20 cm<sup>3</sup>); yield 20 mg (11%). FTIR (KBr): ν (cm<sup>-1</sup>) 2564, 2551, 2544 (B–H). <sup>1</sup>H FT NMR (250 MHz, CDCl<sub>3</sub>, 25 °C, TMS): δ -10.70 (br, 3, BHRu), -5.55 (br, 1, BHRu), -2.87 (br, 2, B–H–B), 1.23 (s, 3, CH<sub>3</sub>), 1.51 (s, 3, CH<sub>3</sub>), 7.11–7.60 (m, 20, C<sub>aryl</sub>–H). <sup>11</sup>B FT NMR (128 MHz, CDCl<sub>3</sub>, 25 °C, BF<sub>3</sub>·Et<sub>2</sub>O): δ 4.65 (2B), -10.31 (2B), -14.70 (2B), -17.51 (3B), -20.26 (2B), -23.84 (d, <sup>1</sup>J(B,H) = 122 Hz, 1B), -28.20 (2B), -30.47 (2B), -37.27 (1B), -38.25 (1B). <sup>31</sup>P{<sup>1</sup>H} FT NMR (101 MHz, CDCl<sub>3</sub>, 25 °C, H<sub>3</sub>PO<sub>4</sub>, 85%): δ 22.93 (s), 36.53 (s). Anal. Calcd for C<sub>30</sub>H<sub>46</sub>B<sub>18</sub>P<sub>2</sub>Ru: C, 47.00; H, 6.07. Found: C, 47.10; H, 6.12. Red and orange microcrystals were obtained from ethyl ether/chloroform (1:1).

**X-ray Data Collection for [Ru(7-PPh<sub>2</sub>-8-Me-7,8-C<sub>2</sub>B<sub>9</sub>H<sub>10</sub>)<sub>2</sub>·2(Me)<sub>2</sub>CO (1).** Single-crystal data collection was performed at ambient temperature on a Nicolet P3F diffractometer using graphite-monochromatized Mo Kα radiation. The unit cell parameters were determined by least-squares refinement of 18 carefully centered reflections. Owing to the width of the reflections and very long *c* axis, the individual reflections at high reflection angles could not be distinguished and numerous background imbalances were observed. Therefore, the data collection was terminated after collecting 8259 reflections. The data were then limited, and only reflections with 2θ<sub>max</sub> = 42° were included in the calculations. The data were corrected for decay (10%) and for absorption (*ψ* scan). Numerous attempts to prepare crystals of better quality failed. Crystallographic data are presented in Table 5.

**Structure Determination and Refinement of [Ru(7-PPh<sub>2</sub>-8-Me-7,8-C<sub>2</sub>B<sub>9</sub>H<sub>10</sub>)<sub>2</sub>·2(Me)<sub>2</sub>CO.** The structure was solved by direct methods by using the SHELXS86 program.<sup>14</sup> Least-squares refinements and all subsequent calculations were performed using the XTAL3.2 program system,<sup>15</sup> which minimized the function Σw(ΔF)<sup>2</sup> (1/w = σ<sup>2</sup>(F<sub>o</sub>)). One of the acetone molecules and all of the methyl groups were refined as rigid groups. The non-hydrogen atoms of the other acetone molecule were refined isotropically as individual atoms. The rest of the non-hydrogen atoms were refined with anisotropic temperature factors. The hydrogen atoms of the carborane

(14) Sheldrick, G. M. SHELXS86, Program for Crystal Structure Solution; University of Göttingen, Göttingen, Federal Republic of Germany, 1986.

(15) Hall, S. R.; Flack, H. D.; Stewart, J. M., Eds. *Xtal3.2 User's Guide*; Universities of Western Australia and Maryland, 1992.

**Table 5. Crystallographic Data for [Ru(7-PPh<sub>2</sub>-8-Me-7,8-C<sub>2</sub>B<sub>9</sub>H<sub>10</sub>)<sub>2</sub>] $\cdot$ 2(Me)<sub>2</sub>CO (1) and [Ru(7-PPh<sub>2</sub>-8-Me-7,8-C<sub>2</sub>B<sub>9</sub>H<sub>10</sub>)<sub>2</sub>] $\cdot$ 1.486CHCl<sub>3</sub> (2)**

	[Ru(L <sub>Ph</sub> ) <sub>2</sub> ] (1)	[Ru(L <sub>Ph</sub> ) <sub>2</sub> ] (2)
chem formula	C <sub>30</sub> H <sub>46</sub> B <sub>18</sub> P <sub>2</sub> Ru 2(CH <sub>3</sub> ) <sub>2</sub> CO	C <sub>30</sub> H <sub>46</sub> B <sub>18</sub> P <sub>2</sub> Ru 1.486CHCl <sub>3</sub>
fw	880.45	941.4
a (Å)	11.664(9)	20.674(3)
b (Å)	9.773(7)	11.539(2)
c (Å)	41.59(3)	20.976(3)
β (deg)	91.61(6)	110.92(1)
V (Å <sup>3</sup> )	4739(6)	4674(2)
Z	4	4
space group	monoclinic, P2 <sub>1</sub> /n (No. 14)	monoclinic, C2/c
T °C	23 °C	23
λ (Å)	0.710 69	0.710 69
ρ (g cm <sup>-3</sup> )	1.234	1.338
μ (cm <sup>-1</sup> )	4.2	6.8
transmissn coeff	0.903–1.000	0.91–1.000
R(F <sub>o</sub> )	0.067	0.066
R <sub>w</sub> (F <sub>o</sub> )	0.060	0.068

moieties (except H(10B) and H(40B)) and the phenyl hydrogen atoms were included in the calculations in fixed positions (B–H = 1.10 Å and C–H = 0.95 Å). The final *R* value was 0.067 (*R*<sub>w</sub> = 0.060). Neutral atomic scattering factors were those included in the programs.

**X-ray Data Collection for [Ru(7-PPh<sub>2</sub>-8-Me-7,8-C<sub>2</sub>B<sub>9</sub>H<sub>10</sub>)<sub>2</sub>] $\cdot$ 1.486CHCl<sub>3</sub> (2).** Single-crystal data collection was performed at ambient temperature on a Rigaku AFC5S diffractometer using graphite-monochromatized Mo Kα radiation. The unit cell parameters were determined by least-squares refinement of 25 carefully centered reflections. Crystallographic data are presented in Table 5.

**Structure Determination and Refinement of [Ru(7-PPh<sub>2</sub>-8-Me-7,8-C<sub>2</sub>B<sub>9</sub>H<sub>10</sub>)<sub>2</sub>] $\cdot$ 1.486CHCl<sub>3</sub>.** The structure was solved by direct methods<sup>16</sup> and successive Fourier map calculations. Refinements of the non-hydrogen atoms anisotropically resulted in abnormal thermal parameters and residual electron densities for the CHCl<sub>3</sub> solvent molecule, indicating that the solvent molecule is not fully occupied. Refinements yielded the value 0.743(4) for the population parameter of the solvent molecule. In the final refinements the non-hydrogen atoms were refined anisotropically and the hydrogen atoms bonded to the carborane moiety were refined isotropically. The phenyl hydrogen atoms and the hydrogen atom of the solvent molecule were included in the calculations in fixed positions with C–H = 0.95 Å. The final *R* value was 0.066 (*R*<sub>w</sub> = 0.068). Refinements were performed using the XTAL3.2 program system,<sup>15</sup> which minimized the function  $\sum w(|F_o| - |F_c|)^2$ , where  $w = 1/\sigma_F^2$ .

**Acknowledgment.** We are grateful to the Spanish agencies CICYT and CIRIT (QF92-4313) for financial support and to Suomen Kulttuurirahasto for a grant.

**Supporting Information Available:** Tables giving experimental details of the X-ray crystallographic analysis, positional and thermal parameters for hydrogen atoms, anisotropic thermal parameters, and interatomic distances and angles for [Ru(L<sub>Ph</sub>)<sub>2</sub>] (1) and [Ru(L<sub>Ph</sub>)<sub>2</sub>] (2) (29 pages). Ordering information is given on any current masthead page.

OM950003Y

(16) TEXSAN-TEXRAY: Single Crystal Structure Analysis Package, Version 5.0; Molecular Structure Corp., The Woodlands, TX, 1989.

# Synthesis of Half-Sandwich Iron Carboxyalkyls and Iron (Thiocarboxy)alkyls: Reaction of Cyclopentadienyldicarbonyliron with O- and S-Based Nucleophiles in the Presence of Triphenylphosphine

Ling-Kang Liu,<sup>\*,†,‡</sup> Uche B. Eke,<sup>†,§</sup> and M. Adediran Mesubi<sup>§</sup>

*Institute of Chemistry, Academia Sinica, Taipei, Taiwan 11529, ROC,  
Department of Chemistry, National Taiwan University, Taipei, Taiwan 10767, ROC, and  
Department of Chemistry, University of Ilorin, Ilorin, Nigeria*

Received April 18, 1995<sup>⊗</sup>

One equivalent of NaOMe is added to an equimolar mixture of  $(\eta^5\text{-C}_5\text{H}_5)\text{Fe}(\text{CO})_2\text{I}$  (**1**) and  $\text{PPh}_3$  after the addition of a few drops of *n*-BuLi, to take advantage of the catalytic formation of  $[(\eta^5\text{-C}_5\text{H}_5)\text{Fe}(\text{CO})_2(\text{PPh}_3)]^+\text{I}^-$  (**3**), which, upon formation, becomes the virtual reactant with  $\text{OMe}^-$ . The  $\text{OMe}^-$  reaction yields the methyl carboxylate  $(\eta^5\text{-C}_5\text{H}_5)\text{Fe}(\text{CO})(\text{PPh}_3)\text{C}(\text{O})\text{OMe}$  (**8Me**). A similar pattern is observed in the  $\text{OPh}^-$ ,  $\text{SMe}^-$ , and  $\text{SPh}^-$  reactions, resulting in the derivatives  $(\eta^5\text{-C}_5\text{H}_5)\text{Fe}(\text{CO})(\text{PPh}_3)\text{C}(\text{O})\text{OPh}$  (**8Ph**),  $(\eta^5\text{-C}_5\text{H}_5)\text{Fe}(\text{CO})(\text{PPh}_3)\text{C}(\text{O})\text{SMe}$  (**9Me**), and  $(\eta^5\text{-C}_5\text{H}_5)\text{Fe}(\text{CO})(\text{PPh}_3)\text{C}(\text{O})\text{SPh}$  (**9Ph**), respectively. The metalloesters exist simultaneously in the molecular form (**8R**) and the ionic form  $[(\eta^5\text{-C}_5\text{H}_5)\text{Fe}(\text{CO})_2(\text{PPh}_3)]^+\text{OR}^-$  (**10R**; R = Me, Ph) in solutions of medium polarity ( $\text{CHCl}_3$ ,  $\text{CH}_2\text{Cl}_2$ , and MeCN), whereas the S analogs exist only in the ionic form. In  $\text{CHCl}_3$ ,  $\text{CH}_2\text{Cl}_2$ , and MeCN solutions, the ratio of neutral **8Me** to ionic **10Me** is *ca.* (6.0–8.4):1, as judged from the NMR measurements. Nonetheless, the ratio of neutral **8Ph** to ionic **10Ph** is *ca.* (0.17–0.25):1.

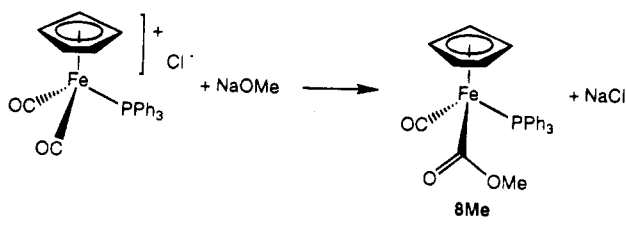
## Introduction

Transition-metal carboxylates and related derivatives are of great interest because they represent a series of proposed intermediates in metal carbonyl catalyzed water-gas shift reactions.<sup>1</sup> A number of years ago, Pettit *et al.* reported, among other derivatives, the preparation of  $(\eta^5\text{-C}_5\text{H}_5)\text{Fe}(\text{CO})(\text{PPh}_3)\text{C}(\text{O})\text{OMe}$  by treating the chloride salt of the cation  $(\eta^5\text{-C}_5\text{H}_5)\text{Fe}(\text{CO})_2(\text{PPh}_3)^+$  with equimolar amounts of the base NaOMe (Scheme 1).<sup>2</sup> Recently, Gibson *et al.* prepared the same compound by reacting the alkali-metal salts of  $(\eta^5\text{-C}_5\text{H}_5)\text{Fe}(\text{CO})(\text{PPh}_3)\text{CO}_2^-$  with electrophilic methylating agents, e.g., MeI and  $\text{Me}_3\text{OBF}_4$  (Scheme 2).<sup>3</sup> We report in this note the synthesis of the similar species  $(\eta^5\text{-C}_5\text{H}_5)\text{Fe}(\text{CO})(\text{PPh}_3)\text{C}(\text{O})\text{Nu}$  ( $\text{Nu}^- = \text{OMe}^-$ ,  $\text{OPh}^-$ ,  $\text{SMe}^-$ ,  $\text{SPh}^-$ ) by reacting the neutral  $(\eta^5\text{-C}_5\text{H}_5)\text{Fe}(\text{CO})_2\text{I}$  with  $\text{Nu}^-$  in the presence of  $\text{PPh}_3$ , albeit initiated with a small amount of *n*-BuLi.

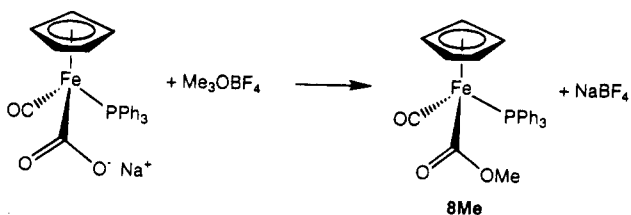
## Results and Discussion

The 1:1 mixture of  $(\eta^5\text{-C}_5\text{H}_5)\text{Fe}(\text{CO})_2\text{I}$  (**1**) and  $\text{PPh}_3$ , when stirred in THF at  $-78^\circ\text{C}$ , gives only  $(\eta^5\text{-C}_5\text{H}_5)\text{Fe}(\text{CO})(\text{PPh}_3)\text{I}$  (**2**) after several days, although in the literature it gives both **2** and  $[(\eta^5\text{-C}_5\text{H}_5)\text{Fe}(\text{CO})_2(\text{PPh}_3)]^+$

Scheme 1



Scheme 2



$\text{I}^-$  (**3**) under refluxing conditions.<sup>4</sup> In our earlier studies, the reactions of  $(\eta^5\text{-C}_5\text{H}_5)\text{Fe}(\text{CO})_2\text{X}$  (**4X**; X = Cl, Br, I) and  $\text{RLi}$  (R = *n*-Bu, Me, *i*-Bu, Ph) in the presence of  $\text{PPh}_3$  at  $-78^\circ\text{C}$  effectively change the bonding mode of the ring from  $\eta^5\text{-C}_5\text{H}_5$  to  $\eta^4\text{-RC}_5\text{H}_5$ .<sup>5</sup> It is noted that, shortly after *n*-BuLi (1–2 drops) is introduced into a 1:1 mixture of **1** and  $\text{PPh}_3$  in THF at  $-78^\circ\text{C}$ , the presence of a small amount of the cationic iron complex **3** and the dimer  $[(\eta^5\text{-C}_5\text{H}_5)\text{Fe}(\text{CO})_2]_2$  (**5**) is evident in the IR spectrum.<sup>5b</sup> Stirring of this mixture for 2 h without

(4) (a) Pandey, V. N. *Inorg. Chim. Acta* **1977**, *22*, L39 and references therein. (b) Alway, D. G.; Barnett, K. W. In *Inorganic and Organometallic Photochemistry*; Adv. Chem. Ser. 168; Wrighton, M. S., Ed.; American Chemical Society: Washington, DC, 1978; pp 115–131. (c) Zakrezevski, J. J. *Organomet. Chem.* **1991**, *412*, C23.

(5) (a) Luh, L.-S.; Liu, L.-K. *Bull. Inst. Chem., Acad. Sin.* **1994**, *41*, 39. (b) Liu, L.-K.; Luh, L.-S. *Organometallics* **1994**, *13*, 2816. (c) Liu, L.-K.; Luh, L.-S.; Eke, U. B. *Organometallics* **1995**, *14*, 440.

\* Academia Sinica.

† National Taiwan University.

‡ University of Ilorin.

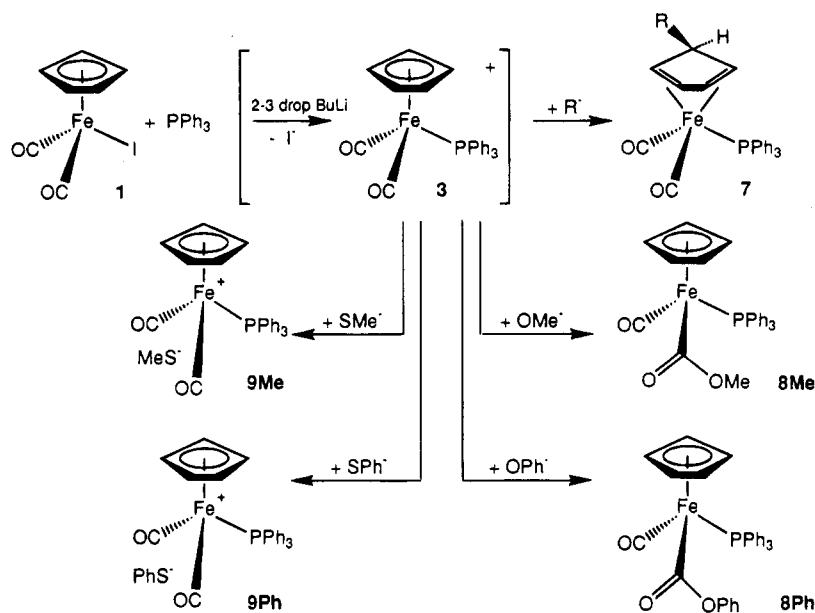
§ Abstract published in *Advance ACS Abstracts*, July 15, 1995.

(1) (a) Ford, P. C. *Acc. Chem. Res.* **1981**, *14*, 31. (b) Darensbourg, D. J.; Kudarowski, R. A. *Adv. Organomet. Chem.* **1983**, *22*, 129. (c) Ford, P. C.; Rokicki, A. *Adv. Organomet. Chem.* **1987**, *28*, 139.

(2) Grice, N.; Kao, S. S.; Pettit, R. *J. Am. Chem. Soc.* **1979**, *101*, 1627.

(3) (a) Gibson, D.; Ong, T.-S. *J. Am. Chem. Soc.* **1987**, *109*, 7191. (b) Gibson, D.; Ong, T.-S.; Ye, M. *Organometallics* **1991**, *10*, 1811. (c) Gibson, D.; Franco, J. D.; Harris, M. T.; Ong, T.-S. *Organometallics* **1992**, *11*, 1993.

Scheme 3



further addition of  $n\text{-BuLi}$  results in yellow precipitates of **3** (Scheme 3). The rationale here is that  $n\text{-BuLi}$  reduces **1** to the dimer **5** or to the radical  $(\eta^5\text{-C}_5\text{H}_5)\text{Fe}(\text{CO})_2^\bullet$  to act as a catalyst assisting the conversion of **1** and  $\text{PPh}_3$  to **3**. The iron-centered radicals are exceedingly reactive species, dimerizing at near-diffusion-controlled rates.<sup>6</sup> The catalytic ability of dimer **5** has been demonstrated in the replacement reaction of CO or  $\text{I}^-$  of **1** with ligands such as  $\text{PPh}_3$  and  $t\text{-BuNC}$ .<sup>7</sup>

Stirring an equimolar mixture of **1**,  $\text{PPh}_3$ , and  $\text{NaOMe}$  in THF overnight has been found to result in the recovery of starting materials. Yet, under the experimental conditions employed in this note, the addition of  $\text{NaOMe}$  to a 1:1 mixture of **1** and  $\text{PPh}_3$  follows the initiation by a few drops of  $n\text{-BuLi}$ , to take advantage of the catalytic formation of **3** that, upon formation, becomes the intermediate to react with  $\text{OMe}^-$ . The nucleophile  $\text{OMe}^-$  does not produce any detectable amounts of  $\eta^4$  species, different from the reaction (Scheme 3) of the lithiated C-based nucleophile  $\text{R}^-$  with **1** in the presence of  $\text{PPh}_3$ , which gives mainly  $(\eta^4\text{-exo-RC}_5\text{H}_5)\text{Fe}(\text{CO})_2\text{PPh}_3$  (**7**).<sup>5b</sup> Scheme 3 also shows the  $\text{OMe}^-$  reaction in which the isolated product (80.3–91.7%), slowly decomposing in solution, is found to be the methyl carboxylate  $(\eta^5\text{-C}_5\text{H}_5)\text{Fe}(\text{CO})(\text{PPh}_3)\text{C}(\text{O})\text{OMe}$  (**8Me**) on the basis of spectroscopic data. In the literature, **8Me** has been reported by Pettit *et al.* to be prepared from the reaction of the chloride salt of the cation  $[(\eta^5\text{-C}_5\text{H}_5)\text{Fe}(\text{CO})_2\text{PPh}_3]^+$  with equimolar  $\text{NaOMe}$  and by Gibson *et al.* to be prepared from the alkali-metal salts of  $(\eta^5\text{-C}_5\text{H}_5)\text{Fe}(\text{CO})\text{PPh}_3(\text{CO})_2^-$  with  $\text{Me}_3\text{OBf}_4$  or  $\text{MeI}$ . The preparation here involves the Pettit polarity in a modified way. With an initiation by a very small amount of  $n\text{-BuLi}$ , the neutral  $(\eta^5\text{-C}_5\text{H}_5)\text{Fe}(\text{CO})_2\text{I}$  reacts with  $\text{NaOMe}$  in the presence of  $\text{PPh}_3$  to give an excellent yield of **8Me**. The advantage here is that there is no

need to isolate the iodide salt  $[(\eta^5\text{-C}_5\text{H}_5)\text{Fe}(\text{CO})_2\text{PPh}_3]^+\text{I}^-$ , effectively making the preparation a one-flask procedure. A very similar pattern is observed in the  $\text{OPh}^-$ ,  $\text{SMe}^-$ , and  $\text{SPh}^-$  reactions, resulting in the derivatives  $(\eta^5\text{-C}_5\text{H}_5)\text{Fe}(\text{CO})(\text{PPh}_3)\text{C}(\text{O})\text{OPh}$  (**8Ph**),  $(\eta^5\text{-C}_5\text{H}_5)\text{Fe}(\text{CO})(\text{PPh}_3)\text{C}(\text{O})\text{SMe}$  (**9Me**), and  $(\eta^5\text{-C}_5\text{H}_5)\text{Fe}(\text{CO})(\text{PPh}_3)\text{C}(\text{O})\text{SPh}$  (**9Ph**), respectively. The sequence of adding the small amount of  $n\text{-BuLi}$  is important, however. An attempt to mix 1:1:1 **1**,  $\text{NaOMe}$ , and  $\text{PPh}_3$  and then introduce 2–3 drops of  $n\text{-BuLi}$  into the mixture failed to produce **8Me**.<sup>8</sup>

Table 1 lists the recorded IR  $\nu_{\text{CO}}$  stretching bands and NMR chemical shifts of **8R** ( $\text{R} = \text{Me}, \text{Ph}$ ) in  $\text{CHCl}_3$ ,  $\text{CH}_2\text{Cl}_2$ ,  $\text{MeCN}$ , and  $\text{C}_6\text{H}_6$  and of **9R** in  $\text{CHCl}_3$ . A relevant IR spectrum of **8Me** in  $\text{CH}_2\text{Cl}_2$  is presented in Figure 1. The existence of two forms in  $\text{CH}_2\text{Cl}_2$  solution is clear, the same features being also found in  $\text{CHCl}_3$  and  $\text{MeCN}$  solutions. The molecular metalloester  $(\eta^5\text{-C}_5\text{H}_5)\text{Fe}(\text{CO})(\text{PPh}_3)\text{C}(\text{O})\text{OMe}$  (**8Me**) has corresponding IR  $\nu_{\text{CO}}$  bands at 1940 (vs) and 1603 (s)  $\text{cm}^{-1}$  and the ionic form  $[(\eta^5\text{-C}_5\text{H}_5)\text{Fe}(\text{CO})_2\text{PPh}_3]^+\text{OMe}^-$  (**10Me**) has IR  $\nu_{\text{CO}}$  bands at 2058 (m) and 2014 (m)  $\text{cm}^{-1}$ . The complex **8Me** in  $\text{C}_6\text{H}_6$  exhibits in the IR spectrum  $\nu_{\text{CO}}$  bands at 1939 (s) and 1600 (s)  $\text{cm}^{-1}$ , corresponding to the ester form only. No evidence of the ionic form **10Me** could be found in the IR spectrum using  $\text{C}_6\text{H}_6$  as solvent. Gibson *et al.* has reported the solid DRIFTS IR spectra of **8Me** with  $\nu_{\text{CO}}$  bands at 1937 and 1594  $\text{cm}^{-1}$ .<sup>3b</sup> Pettit *et al.* has reported for **8Me** the existence of an ester in  $\text{C}_6\text{H}_6$ ,  $\text{CS}_2$ , and  $\text{CHCl}_3$  ( $\nu_{\text{CO}}$  bands at 1935 and 1605  $\text{cm}^{-1}$ ) and the existence of an ionic form in formamide ( $\nu_{\text{CO}}$  bands at 2080 and 2030  $\text{cm}^{-1}$ ).<sup>2</sup> The cation  $[(\eta^5\text{-C}_5\text{H}_5)\text{Fe}(\text{CO})_2(\text{PPh}_3)]^+$  with various counteranions shows characteristic  $\nu_{\text{CO}}$  bands at 2055 and 2010  $\text{cm}^{-1}$  ( $\text{I}^-$ , KBr disk),<sup>4a</sup> 2058 and 2013  $\text{cm}^{-1}$  ( $\text{I}^-$ , in  $\text{CH}_2\text{Cl}_2$ ),<sup>5b</sup> 2055 and 2010  $\text{cm}^{-1}$  ( $\text{PF}_6^-$ , in  $\text{CHCl}_3$ ),<sup>9</sup> and 2066–2070 and 2030–2033  $\text{cm}^{-1}$  ( $\text{Cl}^-$ ,  $\text{BF}_4^-$ ,  $0.5\text{PtCl}_6^{2-}$ , Nujol mulls).<sup>10</sup>

(6) (a) Caspar, J. V.; Meyer, T. J. *J. Am. Chem. Soc.* **1980**, *102*, 7794. (b) Moore, B. D.; Poliakov, M.; Turner, J. J. *J. Am. Chem. Soc.* **1986**, *108*, 1819. (c) Dixon, A. J.; George, M. W.; Hughes, C.; Poliakov, M.; Turner, J. J. *J. Am. Chem. Soc.* **1992**, *114*, 1719. (d) Kuskis, T.; Baird, M. C. *Organometallics* **1994**, *13*, 1551.

(7) (a) Coville, N. J.; Albers, M. O.; Ashworth, T. V.; Singleton, E. *J. Chem. Soc., Chem. Commun.* **1981**, 408. (b) Coville, N. J.; Darling, E. A.; Hearn, A. W.; Johnston, P. *J. Organomet. Chem.* **1987**, *328*, 375.

(8) In principle, the 1:1:1 mixture of **1**,  $\text{PPh}_3$ , and  $\text{NaOMe}$  in THF should produce **8Me** after addition of a small amount of  $n\text{-BuLi}$ . Due to the unavoidable presence of free  $\text{MeOH}$ , usually from the preparation of  $\text{NaOMe}$ , the third component ( $\text{NaOMe}$ ) should be introduced after the  $n\text{-BuLi}$  initiation. Otherwise, the residual  $\text{MeOH}$  would likely block out the intended reaction.

**Table 1. Recorded IR  $\nu_{\text{CO}}$  Bands,  $^1\text{H}$  NMR  $\delta$  Values, and  $^{31}\text{P}$  NMR  $\delta$  Values for  $(\eta^5\text{-C}_5\text{H}_5)\text{Fe}(\text{CO})(\text{PPh}_3)\text{C}(\text{O})\text{Nu}^a$** 

compd	solvent <sup>b</sup>	IR $\nu_{\text{CO}}$ , $\text{cm}^{-1}$	$^1\text{H}$ , $\delta$	$^{31}\text{P}$ , $\delta$	ratio <sup>c</sup>
<b>8Me</b>	$\text{CH}_2\text{Cl}_2$	2058 w, 2014 w <sup>d</sup>	7.40–7.62, 5.37, 3.43 <sup>d</sup>	63.34 <sup>d</sup>	1 <sup>d</sup>
		1940 vs, 1603 s	7.40–7.62, 4.49, 3.02	79.58	6.5
	$\text{CHCl}_3$	2053 m, 2013 m	7.35–7.58, 5.46, 3.46	61.78	1
		1941 vs, 1592 s	7.35–7.58, 4.47, 3.01	77.29	8.4
	MeCN	2058 w, 2015 w	7.50–7.65, 5.29, 3.28	67.14	1
$\text{C}_6\text{H}_6$	1937 w, 1617 vs	7.38–7.46, 4.49, 2.98	82.88	6.0	
	1939 vs, 1600 vs	7.1–7.7, 4.34, 3.31	78.51		
<b>8Ph</b>	$\text{CH}_2\text{Cl}_2$	2057 vs, 2014 vs	7.32–7.52, 5.31	63.42	1
		1952 m, 1602 w	7.32–7.52, 4.40	69.57	0.25
	$\text{CHCl}_3$	2055 s, 2014 s	7.24–7.44, 5.35	61.7	1
		1955 w, 1605 w	7.24–7.44, 4.31	67.8	0.17
	MeCN	2055 vs, 2013 vs	7.40–7.57, 5.29	67.10	1
$\text{C}_6\text{H}_6$	1952 m, 1626 w, br	7.40–7.57, 4.51	72.6	0.21	
	1944 m, 1554 w, br	7.40–7.93, 4.38	68.91		
<b>9Me</b>	$\text{CHCl}_3$	2056 vs, 2014 vs	7.4–7.6, 5.47, 1.66	61.7	
<b>9Ph</b>	$\text{CHCl}_3$	2057 vs, 2013 vs	7.33–7.56, 5.47	61.78	

<sup>a</sup> Conditions: [**8Me**] and [**8Ph**] = ca.  $10^{-4}$  M; [**9Me**] and [**9Ph**] = ca.  $10^{-5}$  M. Varying degrees of decomposition were observed in most of the solvents. <sup>b</sup> For  $^1\text{H}$  and  $^{31}\text{P}$  NMR measurements, the corresponding D solvents were employed. <sup>c</sup> Approximated by peak integration ratio in  $^1\text{H}$  NMR and peak height ratio in  $^{31}\text{P}$  NMR; estimated error 20%. <sup>d</sup> Data in italics correspond to the ionic forms.

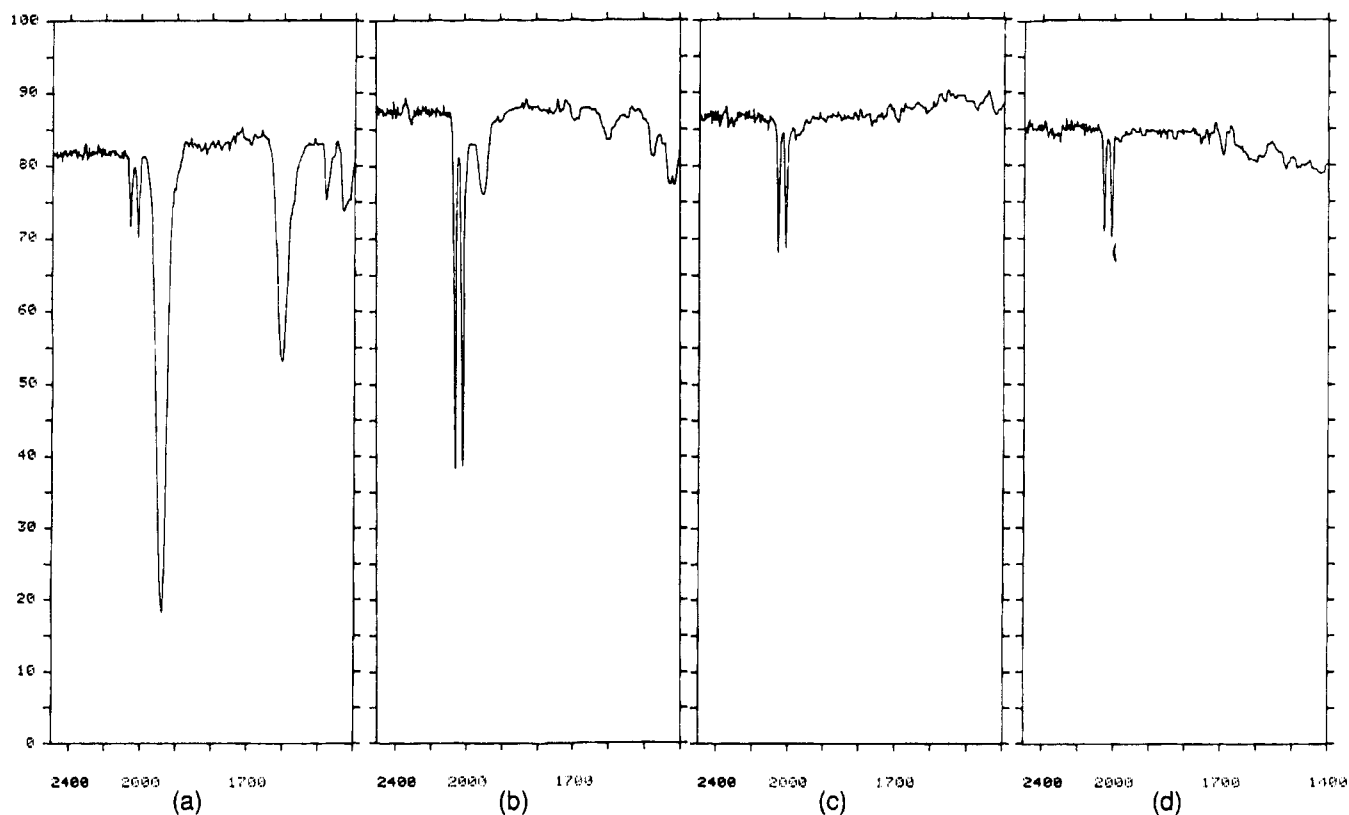


**Figure 1.** IR spectra ( $\nu_{\text{CO}}$  region, 2400–1400  $\text{cm}^{-1}$ ) in  $\text{CH}_2\text{Cl}_2$  for (a)  $(\eta^5\text{-C}_5\text{H}_5)\text{Fe}(\text{CO})(\text{PPh}_3)\text{C}(\text{O})\text{OMe}$  (**8Me**), (b)  $(\eta^5\text{-C}_5\text{H}_5)\text{Fe}(\text{CO})(\text{PPh}_3)\text{C}(\text{O})\text{OPh}$  (**8Ph**), (c)  $(\eta^5\text{-C}_5\text{H}_5)\text{Fe}(\text{CO})(\text{PPh}_3)\text{C}(\text{O})\text{SMe}$  (**9Me**), and (d)  $(\eta^5\text{-C}_5\text{H}_5)\text{Fe}(\text{CO})(\text{PPh}_3)\text{C}(\text{O})\text{SPh}$  (**9Ph**).

The IR data suggest that **8Me** in solution is in equilibrium (or in degradation). The interconversion between **8Me** and **10Me** in  $\text{CH}_2\text{Cl}_2$  must be slower than  $10^{-11}$  s, the IR time scale.<sup>11</sup> As the  $^1\text{H}$  NMR data of **8Me** in  $\text{CDCl}_3$ ,  $\text{CD}_2\text{Cl}_2$ , or  $\text{CD}_3\text{CN}$  clearly reveal a ratio for **8Me** to **10Me** of ca. (6.0–8.4):1, the exchange rate must be even slower than  $10^{-1}$  s, the slow limit with

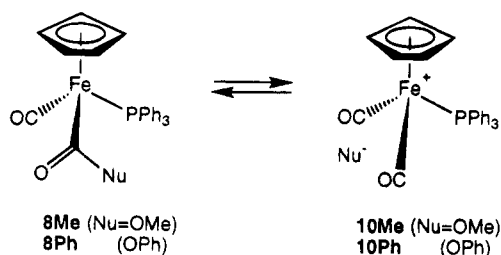
NMR kinetic techniques.<sup>11</sup> The  $^1\text{H}$  NMR data of **8Me** in  $\text{C}_6\text{D}_6$  reveal no resonances assignable to the ionic form, very reasonable if one takes into consideration of  $\text{C}_6\text{H}_6$  a medium of low polarity that keeps the cation and anion from single iron carboxylate, if any, a close pair. Davies *et al.* reported that the base-promoted migration of carboxyalkyl ligands of  $(\eta^5\text{-C}_5\text{H}_5)\text{Fe}(\text{CO})(\text{PPh}_3)\text{C}(\text{O})\text{OR}$  (**8R**; R = Me, *i*-Pr, *t*-Bu, 1-menthyl) from the Fe atom to the Cp ring is not stereospecific, the stereochemistry at Fe being scrambled.<sup>12</sup> The racemization of the Fe center may be partially affected by the equilibrium between the achiral form, ionic **10R**, and the chiral form, neutral **8R** (Scheme 4).

(9) Treichel, P. M.; Shubkin, R. L.; Barnett, K. W.; Reichard, D. *Inorg. Chem.* **1966**, *5*, 1177.

(10) Davison, A.; Green, M. L. H.; Wilkinson, G. *J. Chem. Soc.* **1961**, 3172.

(11) Drago, R. S. *Physical Methods in Chemistry*; Saunders: Philadelphia, PA, 1977.

Scheme 4



The OPh<sup>-</sup> reaction results in a slowly decomposing **8Ph** (45%), which has not been investigated previously in the literature. **8Ph** exhibits in its IR spectra  $\nu_{\text{CO}}$  bands attributed less to the molecular metalloester **8Ph** (1952–1955 (m-w), 1602–1626 (w) cm<sup>-1</sup>) and more to the cation **10Ph** (2055–2057 (vs-s), 2013–2014 (vs-s) cm<sup>-1</sup>) with CHCl<sub>3</sub>, CH<sub>2</sub>Cl<sub>2</sub>, and MeCN as solvents (Table 1). An IR spectrum ( $\nu_{\text{CO}}$  region) in CH<sub>2</sub>Cl<sub>2</sub> is also presented in Figure 1. The solubility of **8Ph** in C<sub>6</sub>H<sub>6</sub> is only sparse, and hence, the data from IR measurements are less reliable. Despite the solubility problem, the IR results suggest that only a very dilute concentration of molecular metalloester **8Ph** is present in C<sub>6</sub>H<sub>6</sub>. The NMR data also indicate that there is a much smaller population of neutral **8Ph** than that of ionic **10Ph**, the ratio being (0.17–0.25):1, which is the complete reverse of the NMR results for **8Me**. Apparently, the anion OPh<sup>-</sup> is relatively much more stable than the anion OMe<sup>-</sup> because of a built-in aromatic system which effectively delocalizes the negative charge. It is not unreasonable that **8Ph** in solution prefers an ionic form and **8Me** a neutral form.

The S analogs ( $\eta^5\text{-C}_5\text{H}_5\text{Fe}(\text{CO})(\text{PPh}_3)\text{C}(\text{O})\text{SR}$  (**9R**; R = Me, Ph) are obtained similarly by dropwise addition of the nucleophile SMe<sup>-</sup> or SPh<sup>-</sup> to the 1:1 mixture of **1** and PPh<sub>3</sub>, shortly after the mixture has been treated with 1–2 drops of *n*-BuLi. The yields are 82.7% for **9Me** and 45.0% for **9Ph**, both exhibiting decomposition in solution. The solubility of the S analogs is much worse than that of the O analogs. **9Me** and **9Ph** are virtually insoluble in C<sub>6</sub>H<sub>6</sub>. As indicated from the IR measurements shown in Table 1, **9Me** and **9Ph** in solution show IR  $\nu_{\text{CO}}$  bands mostly of the ionic form (see Figure 1). With CDCl<sub>3</sub> as solvent, **9Me** exhibits in <sup>1</sup>H NMR only resonances assignable to Ph, Cp, and Me protons and in <sup>31</sup>P NMR a single peak due to a cationic species; **9Ph** gives in <sup>1</sup>H NMR peaks for Ph and Cp and in <sup>31</sup>P NMR one peak, also cationic in nature.

In CHCl<sub>3</sub>, CH<sub>2</sub>Cl<sub>2</sub>, or MeCN, the equilibrium between metalloester and oxide salt is such that for the methyl ester the majority is the metalloester **8Me**, with a (6.0–8.4):1 ester to salt ratio and for the phenyl ester the majority is the oxide salt **10Ph** with a (0.17–0.25):1 ester to salt ratio. On the other hand, the equilibria for the S analogs **9R** favor only the thiolate salt, as judged from the spectroscopic evidence.

PhOH is a stronger acid than MeOH, and thiols are even stronger acids than alcohols. The pK<sub>a</sub> values of the conjugated acids<sup>13</sup> increase in the following order: PhSH < MeSH < PhOH < MeOH. The cation [ $\eta^5\text{-C}_5\text{H}_5\text{Fe}(\text{CO})_2\text{PPh}_3$ ]<sup>+</sup>, if considered as a Lewis acid,

would behave like a proton in the reaction with the conjugated bases. Therefore, **8Me** is more in the metalloester form than **8Ph**, as evidenced in the IR and NMR studies. That is, weak bases favor the ionic form and strong bases favor the ester. SMe<sup>-</sup> and SPh<sup>-</sup> are weaker bases than either OMe<sup>-</sup> or OPh<sup>-</sup>. Hence, it is not too surprising to see only ionic **9R** forms (R = Me, Ph) are present in solution for the S analogs. Furthermore, considering a C–O bond energy of 86 kcal/mol and a C–S bond energy of ca. 70 kcal/mol,<sup>14</sup> the ionization process for **8R** (Scheme 4, a C–O bond cleavage) is also kinetically more difficult.

## Experimental Section

**General Considerations.** All manipulations were performed under an atmosphere of prepurified nitrogen with standard Schlenk techniques. All solvents were distilled from an appropriate drying agent.<sup>15</sup> Infrared spectra were recorded in CH<sub>2</sub>Cl<sub>2</sub> using CaF<sub>2</sub> optics on a Perkin-Elmer 882 spectrophotometer. The <sup>1</sup>H NMR and <sup>13</sup>C NMR spectra were obtained on Bruker AC200/AC300 spectrometers, with chemical shifts reported in  $\delta$  values relative to the residual solvent resonance of CDCl<sub>3</sub> (<sup>1</sup>H, 7.24 ppm; <sup>13</sup>C, 77.0 ppm). The <sup>31</sup>P{<sup>1</sup>H} NMR spectra were obtained on Bruker AC200/AC300 spectrometers using 85% H<sub>3</sub>PO<sub>4</sub> as an external standard (0.00 ppm). The melting points (uncorrected) were determined on a Yanaco MPL melting-point apparatus. Compound **1** was prepared according to the literature procedure.<sup>16</sup> Other reagents were obtained from commercial sources (e.g. Aldrich, Merck) and used without further purification.

**Reaction of **1** and NaOMe in the Presence of PPh<sub>3</sub>.** Compound **1** (1.216 g, 4 mmol) and PPh<sub>3</sub> (1.049 g, 4 mmol) were dissolved in dry THF (100 mL) and cooled to –78 °C. On addition of 2–3 drops of *n*-BuLi, a yellow colloid was immediately observed. NaOMe (0.238 g, 4.4 mmol) in dry MeOH (5 mL) kept at –78 °C was added dropwise to the mixture from a pressure-equalizing dropping funnel. The mixture was stirred for 1 h at –78 °C before being warmed with continued stirring for a further 2 h. The resultant clear yellow-light brown solution was reduced to a small volume on a rotary evaporator. MeOH (10 mL) was added to the solution to precipitate golden yellow solids that were collected, washed with a small amount of cold water (5–10 mL), and repeatedly washed with diethyl ether (10 mL  $\times$  3). Yield of **8Me**: 1.51 g (80.3%). Alternatively in diethyl ether, the product could also be obtained by stirring the reactants as above. The product precipitated after 2–3 h and was collected and washed as described above. Yield: 1.70 g (91.7%). Mp: 112–114 °C. IR (CH<sub>2</sub>Cl<sub>2</sub>):  $\nu_{\text{CO}}$  2058 s, 2014 s, 1940 vs, 1604 s cm<sup>-1</sup>. <sup>31</sup>P NMR (CDCl<sub>3</sub>):  $\delta$  77.3 major, 61.8 minor (s, respectively). <sup>1</sup>H NMR (CDCl<sub>3</sub>):  $\delta$  7.35–7.58 (m, 15 h, Ph), 5.47 minor, 4.47 major (b, respectively, 5H, Cp), 3.46 minor, 3.01 major (s, respectively, 3H, Me, the  $\delta$  3.46 peak with 0.5–0.6 MeOH in excess by integration). MS (FAB): *m/z* 439 (M<sup>+</sup> – OMe). Anal. Calcd for C<sub>26</sub>H<sub>23</sub>FeO<sub>3</sub>P·0.5MeOH: C, 65.44; H, 5.19. Found: C, 65.41; H, 5.11.

**Reaction of **1** and NaOPh in the Presence of PPh<sub>3</sub>.** Compound **1** (0.608 g, 2 mmol) and PPh<sub>3</sub> (0.525 g, 2 mmol) were dissolved in dry THF (60.0 mL) and cooled to –78 °C.

(13) (a) March, J. *Advanced Organic Chemistry: Reactions, Mechanisms, and Structures*; McGraw-Hill: New York, 1968; pp 219–221. (b) *Organicum: Practical Handbook of Organic Chemistry*; Pergamon: Oxford, U.K., 1973; p 467. (c) Vollhardt, K. P. C. *Organic Chemistry*; Freeman: New York, 1987; p 339.

(14) Purcell, K. F.; Kotz, J. C. *Inorganic Chemistry*; Saunders: Philadelphia, PA, 1977; Chapter 6.

(15) Perrin, D. D.; Armarego, W. L. F.; Perrin, D. R. *Purification of Laboratory Chemicals*; Pergamon: Oxford, U.K., 1981.

(16) (a) Dombek, B. D.; Angelici, R. J. *Inorg. Chim. Acta* **1973**, *7*, 345. (b) Meyer, T. J.; Johnson, E. C.; Winterton, N. *Inorg. Chem.* **1971**, *10*, 1673. (c) *Inorg. Synth.* **1971**, *12*, 36. (d) *Inorg. Synth.* **1963**, *7*, 110.

(12) Abbot, S.; Baird, G. J.; Davies, S. G.; Dordor-Hedgecock, I. M.; Maberly, T. R.; Walker, J. C.; Warner, P. J. *Organomet. Chem.* **1985**, *289*, C13.



On addition of a few drops (2–3) of *n*-BuLi, an immediate cloudiness due to the yellow cationic  $[(\eta^5\text{-C}_5\text{H}_5)\text{Fe}(\text{CO})_2\text{PPh}_3]^+$  species was observed. NaOPh (0.232 g, 2 mmol), freshly prepared from methanolic solutions of phenol and sodium hydroxide according to the method of Kornblum and Lurie,<sup>17</sup> was taken up in dry MeOH (5.0 mL). After it was cooled to  $-78^\circ\text{C}$ , the solution was added dropwise to the stirred mixture of  $(\eta^5\text{-C}_5\text{H}_5)\text{Fe}(\text{CO})_2\text{I}$  and  $\text{PPh}_3$  over a period of 10 min. The mixture was then stirred for 1 h at  $-78^\circ\text{C}$  before being warmed to room temperature and stirred for a further 2 h. After filtration on a bed of Celite, the resultant brown filtrate was reduced to a small volume on a rotary evaporator.  $\text{Et}_2\text{O}$  (10.0 mL) was added to the solution to precipitate a brown solid material that was collected, washed with a small amount of cold water (5.0 mL), and repeatedly washed with  $\text{Et}_2\text{O}$  (10.0 mL  $\times$  3). Yield of **8Ph**: 0.48 g (45.0%). Mp:  $150^\circ\text{C}$  dec. IR ( $\text{CH}_2\text{Cl}_2$ ):  $\nu_{\text{CO}}$  2057 vs, 2014 vs, 1952 m, 1602 w  $\text{cm}^{-1}$ .  $^{31}\text{P}$  NMR ( $\text{CDCl}_3$ ):  $\delta$  67.8 minor, 61.8 major.  $^1\text{H}$  NMR ( $\text{CDCl}_3$ ):  $\delta$  7.24–7.44 (m, 20H, Ph), 5.35 major, 4.31 minor (s, respectively, 5H, Cp). MS (FAB):  $m/z$  439 ( $\text{M}^+ - \text{OPh}$ ).

#### Reaction of 1 and NaSMe in the Presence of $\text{PPh}_3$ .

Compound 1 (1.216 g, 4 mmol) and  $\text{PPh}_3$  (1.049 g, 4 mmol) were dissolved in dry THF (100 mL) and cooled to  $-78^\circ\text{C}$ . The addition of a few drops of *n*-BuLi gave yellow colloids instantly in the stirred mixture when NaSMe (0.280 g, 4.4 mmol; freshly generated by refluxing equivalent amounts of Na and MeSSMe<sup>18</sup> in THF for 1 h), dissolved in THF (25 mL) and cooled to  $-78^\circ\text{C}$ , was added dropwise over a 15 min

period. Stirred at  $-78^\circ\text{C}$  for 1 h, the reaction mixture was then continuously stirred overnight at room temperature under a stream of nitrogen. After the precipitate was filtered through a bed of Celite, the solvent was removed by rotary evaporation to obtain a dark paste that was shaken up in cold water (200 mL). The water layer was discarded. Diethyl ether (50 mL) was added to the semiliquid residue to precipitate slightly yellow solids which were filtered and washed with further amounts of ether. Yield of **9Me**: 1.61 g (82.7%). Mp:  $234^\circ\text{C}$  dec. IR ( $\text{CH}_2\text{Cl}_2$ ):  $\nu_{\text{CO}}$  2057 vs, 2015 vs, 1598 vs  $\text{cm}^{-1}$ .  $^{31}\text{P}$  NMR ( $\text{CDCl}_3$ ):  $\delta$  61.7.  $^1\text{H}$  NMR ( $\text{CDCl}_3$ ):  $\delta$  7.36–7.57 (m, 15H, Ph), 5.47 (s, 5H, Cp), 1.66 (s, 3H, Me). MS (FAB):  $m/z$  439 ( $\text{M}^+ - \text{SMe}$ ).

#### Reaction of 1 and NaSPh in the Presence of $\text{PPh}_3$ .

This procedure was carried out in a manner similar to that for the NaSMe analog. Yield of **9Ph**: 0.99 g, (45.0%). Mp:  $>200^\circ\text{C}$  dec. IR ( $\text{CH}_2\text{Cl}_2$ ):  $\nu_{\text{CO}}$  2057 vs, 2015 vs, 1735 m, 1585 vs  $\text{cm}^{-1}$ .  $^{31}\text{P}$  NMR ( $\text{CDCl}_3$ ):  $\delta$  61.8.  $^1\text{H}$  NMR ( $\text{CDCl}_3$ ):  $\delta$  7.37–7.57 (m, 20H, Ph), 5.47 (s, 5H, Cp). MS (FAB):  $m/z$  439 ( $\text{M}^+ - \text{SPh}$ ).

**Acknowledgment.** We are obliged to Academia Sinica and the National Science Council of the ROC for financial support.

OM9502805

(18) (a) *Organicum: Practical Handbook of Organic Chemistry*; Pergamon: Oxford, U.K., 1973; p 578. (b) Greene, T. W.; Wunts, P. G. P. *Protective Groups in Organic Synthesis*, 2nd ed.; Wiley: New York, 1991; p 302. (c) Lecher, H. *Chem. Ber.* **1915**, *48*, 254.

(17) Kornblum, N.; Lurie, A. P. *J. Am. Chem. Soc.* **1959**, *81*, 2705.

**Novel Reactions of the Rhenium Carbyne Complex  
 $[(\eta\text{-C}_5\text{H}_5)(\text{CO})(\text{COC}_2\text{HB}_{10}\text{H}_{10})\text{ReCC}_6\text{H}_5]$  with Metal  
 Carbonyl Compounds. Crystal Structures of  
 $[\text{ReFe}(\mu\text{-CC}_6\text{H}_5)(\mu\text{-CO})(\text{CO})_3(\eta\text{-C}_5\text{H}_5)(\text{COC}_2\text{HB}_{10}\text{H}_{10})]$  and  
 $[\text{ReCo}_2(\mu_3\text{-CC}_6\text{H}_5)(\mu\text{-CO})_2(\text{CO})_5(\eta\text{-C}_5\text{H}_5)(\text{C}_2\text{HB}_{10}\text{H}_{10})]$**

Bin Zhu,<sup>1a</sup> Yong Yu,<sup>1a</sup> Jiabi Chen,<sup>\*,1a</sup> Qiangjin Wu,<sup>1b</sup> and Qiutian Liu<sup>1b</sup>

*Laboratory of Organometallics Chemistry, Shanghai Institute of Organic Chemistry, Chinese Academy of Sciences, 345 Lingling Lu, Shanghai 200032, China, and Fujian Institute of Research on the Structure of Matter, Chinese Academy of Sciences, Fuzhou, Fujian 350002, China*

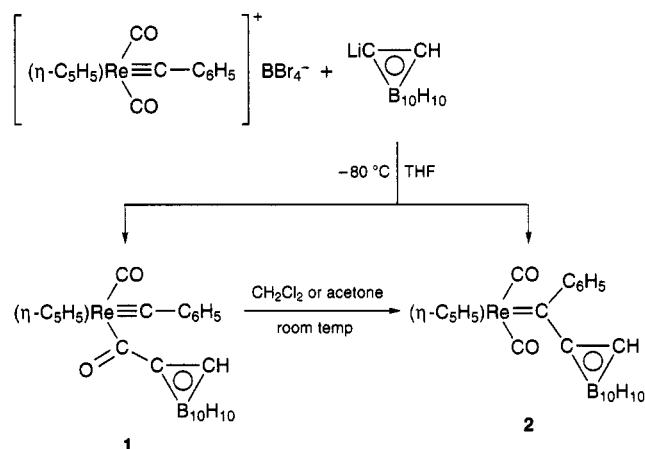
Received April 11, 1995<sup>®</sup>

The reactions of  $[(\eta\text{-C}_5\text{H}_5)(\text{CO})(\text{COC}_2\text{HB}_{10}\text{H}_{10})\text{Re}\equiv\text{CC}_6\text{H}_5]$  (**1**) with  $\text{Fe}_2(\text{CO})_9$  and  $\text{Co}_2(\text{CO})_8$  in THF at  $-5$  to  $+10$  °C gave the novel heteronuclear dimetal bridging carbyne complex  $[\text{ReFe}(\mu\text{-CC}_6\text{H}_5)(\mu\text{-CO})(\text{CO})_3(\eta\text{-C}_5\text{H}_5)(\text{COC}_2\text{HB}_{10}\text{H}_{10})]$  (**3**) and the heteronuclear trimetal bridging carbyne complex  $[\text{ReCo}_2(\mu_3\text{-CC}_6\text{H}_5)(\mu\text{-CO})_2(\text{CO})_5(\eta\text{-C}_5\text{H}_5)(\text{C}_2\text{HB}_{10}\text{H}_{10})]$  (**4**), respectively. The structures of **3** and **4** were established by X-ray crystallographic studies. The carboranyl group remained bonded to the Re atom via the formacyl group in **3** but was transferred from the formacyl group to the Co atom in **4**.

### Introduction

The current interest in the synthesis, structure, and chemistry of di- and trimetal bridging carbene or carbyne complexes stems from the possible involvement of these species in some reactions catalyzed by organometallic compounds.<sup>2,3</sup> Recently, we have reported the reaction between a cationic carbyne complex of rhenium,  $[(\eta\text{-C}_5\text{H}_5)(\text{CO})_2\text{Re}\equiv\text{CC}_6\text{H}_5]\text{BBr}_4$ , and nucleophiles containing a carbonyliron dianion which gives a dimetal bridging carbene complex.<sup>4</sup> We have also reported several novel olefin-coordinated dimetal bridging carbene or carbyne complexes by the reactions of olefin-ligated dimetal carbonyl compounds with aryllithium reagents followed by alkylation with  $\text{Et}_3\text{OBF}_4$ , a most direct, simple, and convenient method for the synthesis of dimetal bridging carbene or carbyne complexes.<sup>5–7</sup> A number of di- and trimetal bridging carbyne complexes have been synthesized by Stone et al. by reactions of alkylidyne complexes with low-valent metal species.<sup>8</sup> Stone et al. have reported the reaction of the monometal carbyne complex  $[(\eta\text{-C}_5\text{H}_5)(\text{CO})_2\text{W}\equiv\text{CC}_6\text{H}_4\text{CH}_3\text{-}p]$  with

### Scheme 1



$\text{Fe}_2(\text{CO})_9$ <sup>9</sup> and  $\text{Co}_2(\text{CO})_8$ <sup>10</sup> to give a heteronuclear dimetal bridging carbyne complex and a trimetal bridging carbyne complex, respectively.

Several years ago, we reported the reaction of a cationic carbyne complex of rhenium,  $[(\eta\text{-C}_5\text{H}_5)(\text{CO})_2\text{Re}\equiv\text{CC}_6\text{H}_5]\text{BBr}_4$ , with 1-lithio-*o*-carborane to afford the unexpected carbyne complex  $[(\eta\text{-C}_5\text{H}_5)(\text{CO})(\text{COC}_2\text{HB}_{10}\text{H}_{10})\text{Re}\equiv\text{CC}_6\text{H}_5]$  (**1**), in which a bulky icosahedral *o*-carboranyl moiety is bound to a CO to form a carboranylcarbonyl group, in addition to the expected carbene complex  $[(\eta\text{-C}_5\text{H}_5)(\text{CO})_2\text{Re}=\text{C}(\text{C}_2\text{HB}_{10}\text{H}_{10})(\text{C}_6\text{H}_5)]$  (**2**)<sup>11</sup> (Scheme 1). We are now interested in examining the reactivities of this novel carbyne complex **1** and investigating the effect of the bulky icosahedral carboranyl group on the reactions it undergoes. Thus, we have

<sup>®</sup> Abstract published in *Advance ACS Abstracts*, July 1, 1995.

(1) (a) Shanghai Institute of Organic Chemistry. (b) Fujian Institute of Research on the Structure of Matter (X-ray structure analysis).

(2) Rofer Depoeter, C. K. *Chem. Rev.* **1981**, *81*, 447.

(3) Wilkinson, S. G.; Stone, F. G. A.; Abel, E. W. *Comprehensive Organometallic Chemistry*; Pergamon Press: Oxford, U.K., 1982; Vol. 8, p 40.

(4) Chen, J.-B.; Yu, Y.; Liu, K.; Wu, G.; Zheng, P.-J. *Organometallics* **1993**, *12*, 1213.

(5) Chen, J.-B.; Li, D.-S.; Yu, Y.; Jin, Z.-S.; Wei, G.-C. *Organometallics* **1993**, *12*, 3885.

(6) Chen, J.-B.; Li, D.-S.; Yu, Y.; Chen, C.-G. *Organometallics* **1994**, *13*, 3581.

(7) Yu, Y.; Chen, J.-B.; Chen, J.; Zheng, P.-J. *Organometallics* **1993**, *12*, 4731.

(8) (a) Garcia, M. E.; Jeffery, J. C.; Sherwood, P.; Stone, F. G. A. *J. Chem. Soc., Dalton Trans.* **1987**, 1209. (b) Evans, D. G.; Howard, J. A. K.; Jeffery, J. C.; Lewis, D. B.; Lewis, G. E.; Grosse-Ophoff, M. J.; Parrott, M. J.; Stone, F. G. A. *J. Chem. Soc., Dalton Trans.* **1986**, 1723. (c) Ashworth, T. V.; Howard, J. A. K.; Stone, F. G. A. *J. Chem. Soc., Dalton Trans.* **1980**, 1609. (d) Abad, J. A.; Delgado, E.; Garcia, M. E.; Grosse-Ophoff, M. J.; Hart, I. J.; Jeffery, J. C.; Simmons, M. S.; Stone, F. G. A. *J. Chem. Soc., Dalton Trans.* **1987**, 41.

(9) Busetto, L.; Jeffery, J. C.; Mills, R. M.; Stone, F. G. A.; Went, M. J.; Woodward, P. *J. Chem. Soc., Dalton Trans.* **1984**, 101.

(10) Chetcuti, M. J.; Chetcuti, P. A. M.; Jeffery, J. C.; Mills, R. M.; Mittrachachon, P.; Pickering, S. J.; Stone, F. G. A.; Woodward, P. *J. Chem. Soc., Dalton Trans.* **1982**, 699.

(11) Chen, J.-B.; Lei, G.-X.; Xu, W.-H.; Zhang, Z.-Y.; Xu, X.-J.; Tang, Y.-Q.; *Sci. Sin., Ser. B* **1987**, *30*(1), 24.

Table 1. Crystal Data and Experimental Details for Complexes 3 and 4

	3	4
formula	C <sub>19</sub> H <sub>21</sub> O <sub>5</sub> B <sub>10</sub> ReFe	C <sub>21</sub> H <sub>21</sub> O <sub>7</sub> B <sub>10</sub> ReCo <sub>2</sub>
fw	679.53	797.57
space group	<i>Pbca</i> (No. 61)	<i>P</i> $\bar{1}$ (No. 2)
<i>a</i> (Å)	11.944(8)	9.850(7)
<i>b</i> (Å)	13.194(4)	11.733(6)
<i>c</i> (Å)	32.06(1)	13.639(9)
$\alpha$ (deg)	90	86.32(5)
$\beta$ (deg)	90	83.19(6)
$\gamma$ (deg)	90	66.76(7)
<i>V</i> (Å <sup>3</sup> )	5053(7)	1438(4)
<i>Z</i>	8	2
<i>d</i> <sub>calc</sub> (g/cm <sup>3</sup> )	1.79	1.84
cryst size (mm)	0.45 × 0.25 × 0.20	0.52 × 0.26 × 0.30
$\mu$ (Mo K $\alpha$ ) (cm <sup>-1</sup> )	54.56	54.34
radiation (monochromated in incident beam)	Mo K $\alpha$ ( $\lambda$ = 0.710 69 Å)	Mo K $\alpha$ ( $\lambda$ = 0.710 69 Å)
diffractometer	Enraf-Nonius CAD4	Enraf-Nonius CAD4
temperature (°C)	23	23
orientation rflns: no.; range (2 $\theta$ ), deg	25: 20.20–25.30	25; 13.93–15.30
scan method	2 $\theta$ - $\omega$	2 $\theta$ - $\omega$
data collec range, 2 $\theta$ (deg)	2–50	2–52
no. of unique data, total with <i>I</i> > 3 $\sigma$ ( <i>I</i> )	4984, 1218	5642, 4284
no. of params refined	155	370
correction factors: max, min (DIFABS)	1.433, 0.700	1.3182, 0.7667
<i>R</i> <sup>a</sup>	0.062	0.051
<i>R</i> <sub>w</sub> <sup>b</sup>	0.068	0.059
quality-of-fit indicator <sup>c</sup>	1.28	1.47
largest shift/esd, final cycle	0.14	0.01
largest peak, e/Å <sup>3</sup>	1.63	2.25

<sup>a</sup>  $R = \sum ||F_o| - |F_c|| / \sum |F_o|$ . <sup>b</sup>  $R_w = [\sum w(|F_o| - |F_c|)^2 / \sum w|F_o|^2]^{1/2}$ ;  $w = 1/\sigma^2(|F_o|)$ . <sup>c</sup> Quality of fit =  $[\sum w(|F_o| - |F_c|)^2 / (N_{\text{observns}} - N_{\text{Params}})]^{1/2}$ .

studied the reactions of complex **1** with Fe<sub>2</sub>(CO)<sub>9</sub> and Co<sub>2</sub>(CO)<sub>8</sub>. These gave the novel heteronuclear dimetal bridging carbyne complex and the heteronuclear trimetal bridging carbyne complex, respectively. This paper describes a detailed study of these reactions and the structural characterization of the products formed.

## Experimental Section

All manipulations were carried out under a prepurified N<sub>2</sub> atmosphere using standard Schlenk techniques. All solvents employed were dried by refluxing over appropriate drying agents and stored over 4 Å molecular sieves under an N<sub>2</sub> atmosphere. Tetrahydrofuran (THF) and diethyl ether (Et<sub>2</sub>O) were distilled from sodium benzophenone ketyl, petroleum ether (30–60 °C) from CaH<sub>2</sub>, and CH<sub>2</sub>Cl<sub>2</sub> from P<sub>2</sub>O<sub>5</sub>, while toluene was distilled from sodium. The neutral alumina (Al<sub>2</sub>O<sub>3</sub>; 100–200 mesh) used for chromatography was deoxygenated at room temperature under high vacuum for 16 h, deactivated with 5% w/w N<sub>2</sub>-saturated water, and stored under N<sub>2</sub>. [( $\eta$ -C<sub>5</sub>H<sub>5</sub>)(CO)(COC<sub>2</sub>HB<sub>10</sub>H<sub>10</sub>)Re≡CC<sub>6</sub>H<sub>5</sub>] (**1**) was prepared as previously described.<sup>11</sup> Fe<sub>2</sub>(CO)<sub>9</sub> and Co<sub>2</sub>(CO)<sub>8</sub> were purchased from Strem Chemicals, Inc.

The IR spectra were measured on a Zeiss Specord-75 and a Shimadzu IR-440 spectrophotometer. <sup>1</sup>H NMR spectra were recorded at ambient temperature in acetone-*d*<sub>6</sub> solution with TMS as the internal reference using a Varian-200 spectrometer. Electron ionization mass spectra (EIMS) were run on a Hewlett-Packard 5989A spectrometer. The melting points were determined in sealed, nitrogen-filled capillaries and are not corrected.

**Reaction of [( $\eta$ -C<sub>5</sub>H<sub>5</sub>)(CO)(COC<sub>2</sub>HB<sub>10</sub>H<sub>10</sub>)Re≡CC<sub>6</sub>H<sub>5</sub>] (**1**) with Fe<sub>2</sub>(CO)<sub>9</sub> To Give [ReFe( $\mu$ -CC<sub>6</sub>H<sub>5</sub>)( $\mu$ -CO)(CO)<sub>3</sub>( $\eta$ -C<sub>5</sub>H<sub>5</sub>)(COC<sub>2</sub>HB<sub>10</sub>H<sub>10</sub>)] (**3**).** To 42 mg (0.078 mmol) of **1** dissolved in 30 mL of THF at –10 °C was added 57 mg (0.156 mmol) of Fe<sub>2</sub>(CO)<sub>9</sub>. The mixture was stirred at –5 to 0 °C for 20 h, during which time the bright yellow solution gradually turned brown-red. After the solution was evaporated at 0 °C under vacuum to dryness, the residue was chromatographed on an alumina (neutral) column (1.6 × 10 cm) at –15 to –10

°C with petroleum ether/CH<sub>2</sub>Cl<sub>2</sub> (5:1) as the eluant. The brown-red band was eluted and collected. The solvent was removed from the brown-red eluate in vacuo, and the crude product was recrystallized from petroleum ether/CH<sub>2</sub>Cl<sub>2</sub> at –80 °C to give 40 mg (76%, based on **1**) of brown-red crystals of **3** (mp 100–102 °C dec). IR ( $\nu_{\text{CO}}$ ): in hexane, 2000 vs, 1990 vs, 1980 s, 1855 m cm<sup>-1</sup>; in KBr, 2020 vs, 1990 vs, 1975 s, 1855 m, 1575 cm<sup>-1</sup>. <sup>1</sup>H NMR (CD<sub>3</sub>COCD<sub>3</sub>):  $\delta$  7.50–7.00 (m, 5H, C<sub>6</sub>H<sub>5</sub>), 5.95 (s, 5H, C<sub>5</sub>H<sub>5</sub>), 4.55 (m, 1H, C<sub>2</sub>HB<sub>10</sub>H<sub>10</sub>), 3.20 (m, 10H, C<sub>2</sub>HB<sub>10</sub>H<sub>10</sub>). MS: *m/e* 483 [M<sup>+</sup> – H – 2CO – Fe(CO)<sub>3</sub>], 336 [C<sub>5</sub>H<sub>5</sub>ReFe(CO)]<sup>+</sup>, 308 [C<sub>5</sub>H<sub>5</sub>ReFe]<sup>+</sup>, 252 [C<sub>5</sub>H<sub>5</sub>Re]<sup>+</sup>, 143 [C<sub>2</sub>HB<sub>10</sub>H<sub>10</sub>]<sup>+</sup>. Anal. Calcd for C<sub>19</sub>H<sub>21</sub>O<sub>5</sub>B<sub>10</sub>ReFe: C, 33.58; H, 3.12. Found: C, 33.73; H, 3.05.

**Reaction of **1** with Co<sub>2</sub>(CO)<sub>8</sub> To Give [ReCo<sub>2</sub>( $\mu$ -CC<sub>6</sub>H<sub>5</sub>)( $\mu$ -CO)<sub>2</sub>(CO)<sub>5</sub>( $\eta$ -C<sub>5</sub>H<sub>5</sub>)(C<sub>2</sub>HB<sub>10</sub>H<sub>10</sub>)] (**4**).** To a stirred solution of **1** (50 mg, 0.093 mmol) in 30 mL of THF at –10 °C was added 175 mg (0.512 mmol) of Co<sub>2</sub>(CO)<sub>8</sub>. The mixture was warmed to 0 °C and stirred at 0–10 °C for 15 h, during which time the orange-red solution gradually turned dark red to dark brown. After vacuum removal of the solvents, the dark purple residue was chromatographed on Al<sub>2</sub>O<sub>3</sub> (neutral) at –15 to –10 °C with petroleum ether as the eluant. After elution of the unreacted Co<sub>2</sub>(CO)<sub>8</sub> from the column, a green-yellow band was eluted with petroleum ether/CH<sub>2</sub>Cl<sub>2</sub>/Et<sub>2</sub>O (10:1:1). The solvent was removed under vacuum, and the crude product was recrystallized from petroleum ether/CH<sub>2</sub>Cl<sub>2</sub> at –80 °C to yield 54 mg (73%, based on **1**) of blackish green crystals of **4** (mp 132 °C dec). IR ( $\nu_{\text{CO}}$ ): in hexane, 2050 vs, br, 1870 s cm<sup>-1</sup>; in KBr, 2080 vs, 2020 vs, 1918 s, 1870 s cm<sup>-1</sup>. <sup>1</sup>H NMR (CD<sub>3</sub>COCD<sub>3</sub>):  $\delta$  7.94 (m, 3H, C<sub>6</sub>H<sub>5</sub>), 7.55 (m, 2H, C<sub>6</sub>H<sub>5</sub>), 5.87 (s, 5H, C<sub>5</sub>H<sub>5</sub>), 3.99 (m, 1H, C<sub>2</sub>HB<sub>10</sub>H<sub>10</sub>), 3.39 (m, 10H, C<sub>2</sub>HB<sub>10</sub>H<sub>10</sub>). MS: *m/e* (based on <sup>187</sup>Re) 588 [M – C<sub>5</sub>H<sub>5</sub> – CC<sub>6</sub>H<sub>5</sub> – 2CO]<sup>+</sup>, 560 [M – C<sub>5</sub>H<sub>5</sub> – CC<sub>6</sub>H<sub>5</sub> – 3CO]<sup>+</sup>, 532 [M – C<sub>5</sub>H<sub>5</sub> – CC<sub>6</sub>H<sub>5</sub> – 4CO]<sup>+</sup>, 504 [M – C<sub>5</sub>H<sub>5</sub> – CC<sub>6</sub>H<sub>5</sub> – 5CO]<sup>+</sup>, 476 [M – C<sub>5</sub>H<sub>5</sub>CC<sub>6</sub>H<sub>5</sub> – 6CO]<sup>+</sup>, 423 [C<sub>5</sub>H<sub>5</sub>ReCo(CO)<sub>4</sub>]<sup>+</sup>, 395 [C<sub>5</sub>H<sub>5</sub>ReCo(CO)<sub>3</sub>]<sup>+</sup>, 308 [C<sub>5</sub>H<sub>5</sub>Re(CO)<sub>2</sub>]<sup>+</sup>, 280 [C<sub>5</sub>H<sub>5</sub>Re(CO)]<sup>+</sup>, 252 [C<sub>5</sub>H<sub>5</sub>Re]<sup>+</sup>, 143 [C<sub>2</sub>HB<sub>10</sub>H<sub>10</sub>]<sup>+</sup>. Anal. Calcd for C<sub>21</sub>H<sub>21</sub>O<sub>7</sub>B<sub>10</sub>ReCo<sub>2</sub>: C, 31.63; H, 2.65. Found: C, 31.47; H, 2.60.

**X-ray Crystal Structure Determinations of Complexes 3 and 4.** The single crystals of **3** and **4** suitable for an X-ray diffraction study were obtained by recrystallization from

Table 2. Positional Parameters and Their Estimated Standard Deviations<sup>a</sup> for **3** and **4**

atom	<b>3</b>				<b>4</b>			
	<i>x</i>	<i>y</i>	<i>z</i>	<i>B</i> (eq), Å <sup>2</sup>	<i>x</i>	<i>y</i>	<i>z</i>	<i>B</i> (eq), Å <sup>2</sup>
Re	-0.0935(1)	0.0552(1)	0.14402(1)	2.05(7)	0.45724(5)	0.14576(4)	0.22174(3)	2.47(2)
Fe	0.0878(6)	0.0488(6)	0.1933(2)	2.2(3)				
Co(1)					0.7448(1)	0.0113(1)	0.1723(1)	2.41(8)
Co(2)					0.6450(2)	0.2395(1)	0.1246(1)	3.2(1)
O(1)	-0.111(3)	0.211(2)	0.213(1)	5.1(9)	1.030(1)	0.0071(8)	0.2072(8)	5.5(7)
O(2)	0.157(3)	0.232(2)	0.242(1)	3.6(7)	0.824(1)	-0.087(1)	-0.0306(7)	6.6(8)
O(3)	0.288(3)	-0.077(3)	0.189(1)	5.0(9)	0.510(1)	-0.0694(7)	0.0906(6)	4.1(6)
O(4)	0.006(3)	-0.054(4)	0.268(1)	8(1)	0.324(1)	0.3028(7)	0.0438(6)	4.8(6)
O(5)	0.131(2)	0.123(2)	0.142(1)	2.3(6)	0.909(1)	0.2874(9)	0.147(1)	6.7(9)
O(6)					0.451(1)	0.5051(8)	0.138(1)	7.3(9)
O(7)					0.683(1)	0.2137(9)	-0.0925(7)	6.3(8)
C					0.647(1)	0.155(1)	0.2525(8)	2.9(6)
C(1)	-0.079(4)	0.149(3)	0.188(1)	3(1)	0.919(1)	0.009(1)	0.195(1)	3.6(8)
C(2)	0.135(3)	0.160(3)	0.224(1)	3(1)	0.791(1)	-0.0-47(1)	0.047(1)	4.0(8)
C(3)	0.216(4)	-0.021(3)	0.197(2)	3(1)	0.514(1)	0.008(1)	0.1379(8)	3.0(7)
C(4)	0.041(4)	-0.009(4)	0.238(2)	4(1)	0.389(1)	0.240(1)	0.1051(8)	3.3(7)
C(5)	0.038(4)	0.136(4)	0.121(2)	3(1)	0.808(2)	0.264(1)	0.136(1)	4(1)
C(6)	0.052(3)	0.216(3)	0.086(1)	1.8(9)	0.527(2)	0.405(1)	0.134(1)	5(1)
C(7)	-0.052(4)	0.286(4)	0.072(2)	4(1)	0.666(1)	0.222(1)	-0.010(10)	4.1(9)
C(10)	0.008(3)	-0.045(4)	0.159(1)	1.9(8)				
C(11)	0.025(2)	-0.157(3)	0.153(1)	0.4(7)	0.220(2)	0.230(3)	0.282(2)	11(2)
C(12)	0.021(3)	-0.198(3)	0.113(1)	0.4(8)	0.263(3)	0.110(3)	0.290(2)	10(3)
C(13)	0.049(3)	-0.302(4)	0.107(2)	2(1)	0.366(2)	0.065(1)	0.357(1)	7(1)
C(14)	0.064(3)	-0.0364(3)	0.140(2)	3(1)	0.387(1)	0.170(2)	0.386(1)	5(1)
C(15)	0.075(4)	-0.326(4)	0.181(2)	4(1)	0.292(3)	0.271(1)	0.340(2)	9(2)
C(16)	0.056(3)	-0.229(3)	0.185(1)	2(1)				
C(21)	-0.194(4)	-0.035(5)	0.095(2)	5(1)	0.687(1)	0.193(1)	0.3429(8)	3.0(7)
C(22)	-0.244(4)	-0.060(5)	0.139(2)	5(1)	0.637(1)	0.318(1)	0.368(1)	4.0(8)
C(23)	-0.285(3)	0.035(4)	0.151(2)	4(1)	0.671(1)	0.356(1)	0.450(1)	5(1)
C(24)	-0.265(4)	0.109(4)	0.119(2)	4(1)	0.753(2)	0.269(1)	0.516(1)	6(1)
C(25)	-0.219(4)	0.056(6)	0.087(2)	6(1)	0.803(2)	0.144(1)	0.497(1)	5(1)
C(26)					0.772(1)	0.107(1)	0.411(1)	4.0(8)
C(O1)					0.795(1)	-0.1646(8)	0.2396(7)	2.5(6)
C(O2)					0.792(1)	-0.280(1)	0.1785(8)	3.1(7)
B(1)	0.053(3)	0.337(4)	0.107(2)	1(1)	0.959(1)	-0.276(1)	0.192(1)	3.7(9)
B(2)	0.180(3)	0.271(3)	0.090(2)	1(1)	0.940(1)	-0.224(1)	0.313(1)	3.6(9)
B(3)	0.153(5)	0.184(6)	0.048(2)	5(2)	0.757(2)	-0.194(1)	0.362(1)	3.5(8)
B(4)	0.008(4)	0.194(4)	0.036(2)	2(1)	0.666(1)	-0.226(1)	0.273(1)	3.0(8)
B(5)	0.018(3)	0.412(3)	0.063(2)	1(1)	0.933(2)	-0.418(1)	0.199(1)	4(1)
B(6)	0.162(4)	0.394(4)	0.079(2)	2(1)	1.026(2)	-0.385(1)	0.290(1)	4(1)
B(7)	0.204(4)	0.308(5)	0.042(2)	4(1)	0.901(2)	-0.337(1)	0.394(1)	4(1)
B(8)	0.110(5)	0.258(5)	0.003(2)	4(1)	0.730(2)	-0.336(1)	0.370(1)	4(1)
B(9)	-0.026(5)	0.322(5)	0.022(2)	5(2)	0.750(2)	-0.388(1)	0.249(1)	4(1)
B(10)	0.114(4)	0.391(3)	0.017(2)	2(1)	0.896(2)	-0.455(1)	0.323(1)	4(1)

<sup>a</sup> Anisotropically refined atoms are given in the form of the isotropic equivalent parameter defined as  $4/3[a^2B(1,1) + b^2B(2,2) + c^2B(3,3) + ab(\cos \gamma)B(1,2) + ac(\cos \beta)B(1,3) + bc(\cos \alpha)B(2,3)]$ .

petroleum ether/toluene and petroleum ether/CH<sub>2</sub>Cl<sub>2</sub> solutions at -80 °C, respectively. The single crystals of approximate dimensions 0.45 × 0.25 × 0.20 mm for **3** and 0.52 × 0.26 × 0.30 mm for **4** were sealed in capillaries under an N<sub>2</sub> atmosphere. The X-ray diffraction intensity data for 4984 and 5642 independent reflections, of which 1218 and 4284 with  $I > 3\sigma(I)$  were observable, were collected with an Enraf-Nonius CAD4 diffractometer at 23 °C using Mo K $\alpha$  radiation within the ranges  $2^\circ \leq 2\theta \leq 50^\circ$  and  $2^\circ \leq 2\theta \leq 52^\circ$  for **3** and **4**, respectively. The intensity data were corrected for Lorentz and polarization factors. An empirical absorption correction was applied to the data for **3** and **4**.

The crystal structures of **3** and **4** were solved by direct methods to locate the metal atoms and then by difference Fourier maps to successively locate all the non-hydrogen atoms. The structure was refined with isotropic and anisotropic thermal parameters using the unique reflections with  $I > 3\sigma(I)$ . Final refinement converged to  $R = 0.062$  and  $R_w = 0.068$  for **3** and  $R = 0.051$  and  $R_w = 0.059$  for **4**. All the calculations were performed on a Micro-VAX 3100 computer using TEXSAN.

The details of the crystallographic data and the procedure used for data collection and reduction information for **3** and **4** are given in Table 1. The positional parameters and temperature factors for non-hydrogen atoms for **3** and **4** are presented

in Table 2. The selected bond lengths and selected bond angles for **3** and **4** are listed in Tables 3 and 4, respectively.

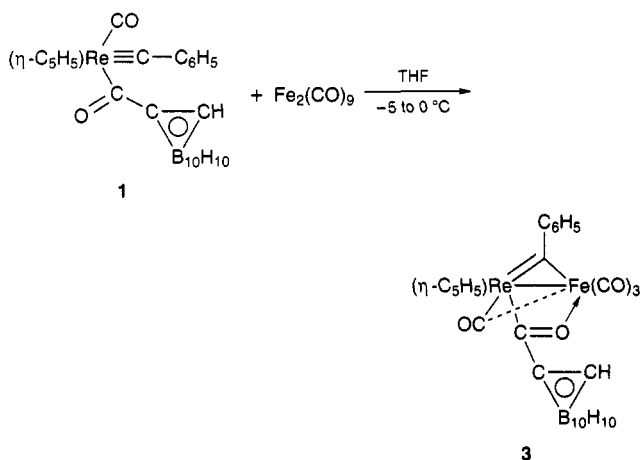
## Results and Discussion

**Reaction of  $[(\eta\text{-C}_5\text{H}_5)(\text{CO})(\text{COC}_2\text{HB}_{10}\text{H}_{10})\text{Re}\equiv\text{C-C}_6\text{H}_5]$  (**1**) with  $\text{Fe}_2(\text{CO})_9$  To Form  $[\text{ReFe}(\mu\text{-CC}_6\text{H}_5)(\mu\text{-CO})(\text{CO})_3(\eta\text{-C}_5\text{H}_5)(\text{COC}_2\text{HB}_{10}\text{H}_{10})]$  (**3**).** ( $\eta$ -Cyclopentadienyl)carbonyl(1-carboranylcarbonyl)(phenylcarbyne)-rhenium,  $[(\eta\text{-C}_5\text{H}_5)(\text{CO})(\text{COC}_2\text{HB}_{10}\text{H}_{10})\text{Re}\equiv\text{CC}_6\text{H}_5]$  (**1**), was treated with an excess of  $\text{Fe}_2(\text{CO})_9$  in THF at -5 to 0 °C for 20 h. After workup as described in the Experimental Section, the brown-red complex **3**,  $[\text{ReFe}(\mu\text{-CC}_6\text{H}_5)(\mu\text{-CO})(\text{CO})_3(\eta\text{-C}_5\text{H}_5)(\text{COC}_2\text{HB}_{10}\text{H}_{10})]$ , was isolated in 76% yield (Scheme 2). Complex **3** is readily soluble in polar organic solvents such as THF and CH<sub>2</sub>-Cl<sub>2</sub> but is only slightly soluble in nonpolar organic solvents such as petroleum ether. It is very sensitive to air and temperature in solution but stable for a short period on exposure as the solid to air at room temperature. Compound **3** is formulated as a heteronuclear dimetal bridging carbyne on the basis of its elemental analysis and IR, <sup>1</sup>H NMR, and mass spectra, as well as

**Table 3. Selected Bond Distances (Å)<sup>a</sup> for Complexes 3 and 4**

Complex 3					
Re-Fe	2.682(6)	Fe-C(2)	1.86(5)	C(12)-C(13)	1.42(5)
Re-C(10)	1.86(4)	Fe-C(10)	1.91(4)	C(13)-C(14)	1.35(6)
Re-C(1)	1.88(5)	Fe-O(5)	1.98(3)	C(14)-C(15)	1.42(6)
Re-C(5)	2.04(5)	O(1)-C(1)	1.22(5)	C(15)-C(16)	1.30(6)
Re-C(21)	2.31(5)	O(2)-C(2)	1.14(5)	C(21)-C(25)	1.37(8)
Re-C(24)	2.31(5)	O(3)-C(3)	1.16(5)	C(21)-C(22)	1.46(7)
Re-C(23)	2.31(4)	O(4)-C(4)	1.20(6)	C(22)-C(23)	1.40(6)
Re-C(22)	2.36(5)	O(5)-C(5)	1.31(5)	C(23)-C(24)	1.45(6)
Re-C(25)	2.37(5)	C(10)-C(11)	1.50(6)	Re-Cp(cen) <sup>b</sup>	2.00
Fe-C(1)	2.39(6)	C(11)-C(12)	1.39(5)	C(24)-C(25)	1.35(6)
Fe-C(4)	1.73(6)	C(11)-C(16)	1.45(5)	C(5)-C(6)	1.54(6)
Fe-C(3)	1.79(5)			C(6)-C(7)	1.62(5)
Complex 4					
Re-Co(1)	2.669(3)	Co(1)-C(2)	1.82(1)	C(11)-C(12)	1.30(4)
Re-Co(2)	2.688(2)	Co(1)-C(3)	2.39(1)	C(11)-C(15)	1.35(3)
Co(1)-Co(2)	2.531(3)	Co(1)-C(O1)	2.10(1)	C(12)-C(13)	1.37(3)
Re-C	2.01(1)	Co(2)-C(4)	2.57(1)	C(13)-C(14)	1.41(2)
Co(1)-C	1.92(1)	Co(2)-C(5)	1.76(1)	C(14)-C(15)	1.36(2)
Co(2)-C	1.95(1)	Co(2)-C(6)	1.83(1)	C-C(21)	1.48(1)
Re-C(3)	1.89(1)	Co(2)-C(7)	1.84(1)	C(21)-C(22)	1.40(1)
Re-C(4)	1.91(1)	O(1)-C(1)	1.11(1)	C(21)-C(26)	1.41(1)
Re-C(12)	2.21(2)	O(2)-C(2)	1.14(1)	C(22)-C(23)	1.35(2)
Re-C(11)	2.22(2)	O(3)-C(3)	1.17(1)	C(23)-C(24)	1.39(2)
Re-C(14)	2.27(1)	O(4)-C(4)	1.15(1)	C(24)-C(25)	1.38(2)
Re-C(13)	2.27(1)	O(5)-C(5)	1.16(1)	C(25)-C(26)	1.38(2)
Re-C(15)	2.28(2)	O(6)-C(6)	1.12(1)	C(O1)-C(O2)	1.64(1)
Co(1)-C(1)	1.77(1)	O(7)-C(7)	1.12(1)		

<sup>a</sup> Estimated standard deviations in the least significant figure are given in parentheses. <sup>b</sup> Cp(cen) denotes the centroid of the cyclopentadienyl group.

**Scheme 2**

the single-crystal X-ray diffraction study. In complex **3**, the carboranylcarbonyl ligand is bonded to the Re atom via a formacyl group. The oxygen atom of the acyl is coordinated to the Fe atom to satisfy an 18-electron configuration.

The IR spectrum and solution <sup>1</sup>H NMR spectrum of **3** are consistent with the structure in Scheme 2. The IR spectrum (KBr) in the  $\nu_{\text{CO}}$  region (Experimental Section) of **3** showed an absorption band at 1855  $\text{cm}^{-1}$  attributed to a bridging or semibridging carbonyl ligand, in addition to three strong terminal CO absorption bands at 2020, 1990, and 1975  $\text{cm}^{-1}$ , which is indicative of a  $(\text{CO})_3\text{FeRe}(\mu\text{-CO})$  moiety in **3**. The weak absorption band at 1575  $\text{cm}^{-1}$  which is characteristic of the carboranylcarbonyl ligand in **1** demonstrated that the acyl ligand has not been destroyed or converted in the reaction. As compared with starting material **1**, the intensity of the acyl absorption band in **3** is weakened, arising from the coordination of the oxygen atom of the formacyl ligand with the Fe atom. The <sup>1</sup>H NMR

spectrum of **3** showed the expected proton signals attributed to phenyl, cyclopentadienyl, and carboranyl groups.

An X-ray diffraction study was carried out in order to establish firmly the structure of **3**. As shown in Figure 1, **3** is a heteronuclear dimetal complex with a bridging carbyne ligand. The Re-Fe bond is bridged by the  $\text{CC}_6\text{H}_5$  group, giving a dimetallacyclopropene ring. The Re-Fe distance of 2.682(2) Å in **3** is slightly shorter than that found (2.7581(8) Å) in the dimetal bridging carbene complex  $[\text{ReFe}(\mu\text{-CHC}_6\text{H}_5)(\eta\text{-C}_5\text{H}_5)(\text{CO})_6]$ .<sup>4</sup> The alkylidene carbon asymmetrically bridges the Re-Fe bond ( $\text{Re-C}(10) = 1.86(4)$  Å,  $\text{Fe-C}(10) = 1.91(4)$  Å). The Re-C distance (1.86(4) Å) is significantly longer than the  $\text{Re}=\text{C}_{\text{carbyne}}$  bond in **1** (1.76(3) Å) and is close to the sum of covalent double-bond radii of Re and C (1.91 Å),<sup>12</sup> which indicates that Re is double-bonded to the carbyne carbon C(10). The Fe-C(10) distance (1.91(4) Å) not only is shorter than the Fe-C<sub>carbyne</sub> bond in the analogous carbyne complex  $[\text{FeMo}(\mu\text{-CC}_6\text{H}_4\text{CH}_3\text{-}p)(\text{CO})_6(\eta\text{-C}_5\text{H}_5)]$  (2.008 Å)<sup>8a</sup> but also is shorter than the average distance of the  $\mu\text{-C-Fe}$  bonds in diiron bridging carbene complexes  $[(\text{C}_8\text{H}_8)(\text{CO})_4\text{Fe}_2\{\mu\text{-C}(\text{OC}_2\text{H}_5)(\text{C}_6\text{H}_4\text{CF}_3\text{-}p)\}]$  (2.037 Å),<sup>5</sup>  $[\text{Fe}_2(\eta\text{-C}_5\text{H}_5)_2(\text{CO})_2(\mu\text{-CO})\{\mu\text{-C}(\text{OC}_2\text{H}_5)\text{C}_6\text{H}_5\}]$  (2.026 Å),<sup>6</sup> and  $[\text{Fe}_2(\eta\text{-C}_5\text{H}_5)_2(\text{CO})_2(\mu\text{-CO})\{\mu\text{-C}(\text{OC}_2\text{H}_5)\text{C}_6\text{H}_4\text{CF}_3\text{-}p\}]$  (2.004 Å).<sup>6</sup> It is close to the Fe-C<sub>carbene</sub> bond length in monoiron carbene complexes  $[(\text{CO})_4\text{Fe}=\text{C}(\text{OC}_2\text{H}_5)\text{C}_6\text{Cl}_5]$  (1.887(4) Å)<sup>13</sup> and  $[(\eta^4\text{-C}_{10}\text{H}_{16})(\text{CO})_2\text{Fe}=\text{C}(\text{OC}_2\text{H}_5)\text{C}_6\text{H}_4\text{CH}_3\text{-}o]$  (1.915(15) Å).<sup>14</sup> Therefore, we consider that there also exists partial double-bond character in the Fe-C(10) bond.

The distance between the carbyne carbon C(10) and phenyl group (C(10)-C(11) 1.50(6) Å) in **3** is longer than that found (1.43(4) Å) in **1**, which shows that the conjugation of the benzene ring with the carbyne bond in **3** is weakened. This is consistent with the fact that the proton signals of the phenyl group moved upfield in the <sup>1</sup>H NMR spectrum of **3** and the dihedral angle between the benzene ring plane and  $\text{ReFeC}(10)$  plane of 134.87°.

As anticipated from the IR spectrum, of five CO groups, three terminal CO's are attached to the Fe atom and the other two to the Re atom. Among the two CO groups bonded to the Re atom, one is a formacyl bonded to the carboranyl group with an Re-C(5) bond length of 2.04(5) Å. The bond angle of Re-C(5)-C(6) is 134°, greatly deviating from 120°, probably due to the steric bulk of the carboranyl group. The oxygen atom of the acyl is coordinated to the Fe atom, thus giving the Fe atom an 18-electron configuration. As a result, the bond length of C(5)-O(5) (1.31(5) Å) is much longer than that found (1.13(4) Å) in **1**. The other CO bonded to the Re atom is a semibridging carbonyl to the Fe atom ( $\text{Re-C}(1) = 1.88(5)$  Å,  $\text{Fe-C}(1) = 2.39(6)$  Å). In complex **3**, the carboranyl group is retained in the reaction, as can be visualized in the ORTEP diagram of **3** represented in Figure 1.

The mechanism for the formation of complex **3** (Scheme 2) is not yet clear. When  $\text{Fe}(\text{CO})_5$  was used instead of  $\text{Fe}_2(\text{CO})_9$  for the reaction under the same

(12) Tilzpatrick, P. J.; Page, Y. L.; Butler, I. S. *Acta Crystallogr.* **1987**, *B37*, 1052.

(13) Wang, T.-L.; Chen, J.-B.; Xu, W.-H.; Zhang, S.-W.; Pan, Z.-H.; Tang, Y.-Q. *Acta Chim. Sin.* **1987**, *1*, 85.

(14) Chen, J.-B.; Lei, G.-X.; Jin, Z.-S.; Hu, L.-H.; Wei, G.-C. *Organometallics* **1988**, *7*, 1652.

Table 4. Selected Bond Angles (deg)<sup>a</sup> for Complexes 3 and 4

Complex 3					
C(1)–Re–Fe	60(1)	C(1)–Re–C(21)	154(2)	C(5)–Re–C(21)	115(2)
C(5)–Re–Fe	67(1)	C(1)–Re–C(22)	123(2)	C(5)–Re–C(22)	154(2)
C(10)–Re–Fe	45(1)	C(1)–Re–C(23)	95(2)	C(5)–Re–C(23)	149(2)
C(21)–Re–Fe	144(1)	C(1)–Re–C(24)	98(2)	C(5)–Re–C(24)	113(2)
C(24)–Re–Fe	159(1)	C(1)–Re–C(25)	129(2)	C(5)–Re–C(25)	102(2)
C(23)–Re–Fe	137(1)	C(3)–Fe–C(10)	97(2)	C(1)–Fe–O(5)	83(2)
C(22)–Re–Fe	129(1)	C(3)–Fe–O(5)	95(2)	C(1)–Fe–C(2)	82(2)
C(25)–Re–Fe	165(1)	C(2)–Fe–C(10)	166(2)	C(1)–Fe–C(3)	178(2)
C(1)–Fe–Re	43(1)	C(2)–Fe–O(5)	88(2)	C(1)–Fe–C(4)	92(2)
C(4)–Fe–Re	104(2)	C(10)–Fe–O(5)	89(2)	C(1)–Fe–C(10)	84(2)
C(3)–Fe–Re	138(2)	C(5)–O(5)–Fe	106(3)	C(4)–Fe–C(3)	90(2)
C(2)–Fe–Re	122(1)	Re–C(1)–Fe	77(2)	C(4)–Fe–C(2)	90(2)
O(5)–Fe–Re	73.0(8)	O(1)–C(1)–Fe	126(2)	C(4)–Fe–C(10)	92(2)
C(10)–Fe–Re	44(1)	O(1)–C(1)–Re	156(4)	C(4)–Fe–O(5)	175(2)
C(10)–Re–C(1)	102(2)	O(2)–C(2)–Fe	175(4)	C(3)–Fe–C(2)	97(2)
C(10)–Re–C(5)	88(2)	O(3)–C(3)–Fe	161(5)	O(5)–C(5)–C(6)	112(4)
C(10)–Re–C(21)	99(2)	O(4)–C(4)–Fe	175(5)	O(5)–C(5)–Re	113(3)
C(10)–Re–C(24)	152(2)	C(11)–C(10)–Re	139(3)	C(6)–C(5)–Re	134(3)
C(10)–Re–C(23)	122(2)	C(11)–C(10)–Fe	131(3)	Cp(cen) <sup>b</sup> –Re–C(1)	123
C(10)–Re–C(22)	93(2)	Re–C(10)–Fe	91(2)	Cp(cen)–Re–Fe	162
C(10)–Re–C(25)	128(2)	C(12)–C(11)–C(10)	120(3)	Cp(cen)–Re–C(10)	122
C(1)–Re–C(5)	82(2)	C(16)–C(11)–C(10)	125(4)	Cp(cen)–Re–C(5)	130
Complex 4					
Co(1)–Re–Co(2)	56.40(7)	C–Re–C(11)	136(1)	C(5)–Co(2)–Co(1)	97.0(4)
Co(2)–Co(1)–Re	62.17(8)	C–Re–C(12)	142.6(8)	C(5)–Co(2)–Re	142.3(4)
Co(1)–Co(2)–Re	61.43(8)	C–Re–C(13)	107.8(7)	C(6)–Co(2)–Co(1)	157.8(5)
C–Re–Co(1)	45.8(3)	C–Re–C(14)	85.7(4)	C(6)–Co(2)–Re	99.1(5)
C–Re–Co(2)	46.3(3)	C–Re–C(15)	100.8(9)	C(7)–Co(2)–Co(1)	97.9(4)
C–Co(1)–Co(2)	49.6(3)	C(3)–Re–C(4)	83.6(4)	C(7)–Co(2)–Re	113.6(4)
C–Co(1)–Re	48.6(3)	C(3)–Re–C(12)	91.0(7)	C–Co(2)–C(5)	94.2(5)
C–Co(2)–Co(1)	48.6(3)	C(3)–Re–C(11)	117(1)	C–Co(2)–C(6)	111.0(6)
C–Co(2)–Re	48.1(3)	C(3)–Re–C(14)	132.6(6)	C–Co(2)–C(7)	145.4(5)
Co(1)–C–Co(2)	81.8(4)	C(3)–Re–C(13)	98.0(5)	C(5)–Co(2)–C(6)	92.9(6)
Co(1)–C–Re	85.6(4)	C(3)–Re–C(15)	149.1(7)	C(5)–Co(2)–C(7)	99.0(6)
Co(2)–C–Re	85.6(4)	C(4)–Re–C(12)	104(1)	C(6)–Co(2)–C(7)	100.1(6)
C(3)–Re–Co(1)	60.4(3)	C(4)–Re–C(11)	84.5(7)	C(21)–C–Co(1)	131.7(7)
C(3)–Re–Co(2)	95.0(3)	C(4)–Re–C(14)	135.4(6)	C(21)–C–Co(2)	124.1(7)
C(4)–Re–Co(1)	104.7(4)	C(4)–Re–C(13)	138.9(7)	C(21)–C–Re	131.2(8)
C(4)–Re–Co(2)	65.3(3)	C(4)–Re–C(15)	100.6(7)	O(1)–C(1)–Co(1)	178(1)
C(11)–Re–Co(1)	169.6(8)	C–Co(1)–C(1)	89.8(5)	O(2)–C(2)–Co(1)	178(1)
C(11)–Re–Co(2)	133(1)	C–Co(1)–C(2)	145.7(5)	O(3)–C(3)–Re	162(1)
C(12)–Re–Co(1)	137(1)	C–Co(1)–C(O1)	118.6(4)	O(3)–C(3)–Co(1)	121.1(8)
C(12)–Re–Co(2)	167(1)	C(1)–Co(1)–Fe	138.4(4)	Re–C(3)–Co(1)	76.0(4)
C(13)–Re–Co(1)	111.8(4)	C(1)–Co(1)–Co(2)	93.3(3)	O(4)–C(4)–Re	168(1)
C(13)–Re–Co(2)	153.7(6)	C(2)–Co(1)–Co(2)	96.6(3)	O(4)–C(4)–Co(2)	117.4(9)
C(14)–Re–Co(1)	115.4(4)	C(2)–Co(1)–Re	115.3(4)	Re–C(4)–Co(2)	72.1(3)
C(14)–Re–Co(2)	122.8(4)	C(O1)–Co(1)–Co(2)	167.5(3)	O(5)–C(5)–Co(2)	176(1)
C(15)–Re–Co(1)	143.8(8)	C(O1)–Co(1)–Re	107.6(3)	O(6)–C(6)–Co(2)	177(1)
C(15)–Re–Co(2)	114.7(5)	C(1)–Co(1)–C(2)	99.6(6)	O(7)–C(7)–Co(2)	177(1)
C–Re–C(3)	106.2(4)	C(1)–Co(1)–C(O1)	90.7(4)	C(22)–C(21)–C	122(1)
C–Re–C(4)	111.2(4)	C(2)–Co(1)–C(O1)	94.4(4)	C(26)–C(21)–C	123(1)

<sup>a</sup> Estimated standard deviations in the least significant figure are given in parentheses. <sup>b</sup> Cp(cen) denotes the centroid of the cyclopentadienyl group.

conditions, no product **3** was obtained and only starting materials were received. Interestingly, Stone et al. reported that the heteronuclear dimetal bridging carbyne complex  $[(\eta\text{-C}_5\text{H}_5)(\text{CO})_6\text{MFe}(\mu\text{-CC}_6\text{H}_4\text{CH}_3\text{-p})]$  (M = Mo, W) formed by the reaction of the carbyne complex  $[(\eta\text{-C}_5\text{H}_5)(\text{CO})_2\text{M}\equiv\text{CC}_6\text{H}_4\text{CH}_3\text{-p}]$  (M = Mo, W) with 1 equiv of  $\text{Fe}_2(\text{CO})_9$  can react further with an excess of  $\text{Fe}_2(\text{CO})_9$  to afford a heteronuclear trimetal bridging carbyne complex,  $[(\eta\text{-C}_5\text{H}_5)(\text{CO})_9\text{MFe}_2(\mu_3\text{-CC}_6\text{H}_4\text{CH}_3\text{-p})]$ .<sup>9</sup> However, in contrast with  $[(\eta\text{-C}_5\text{H}_5)(\text{CO})_6\text{MFe}(\mu\text{-CC}_6\text{H}_4\text{CH}_3\text{-p})]$ , complex **3** did not react with an excess of  $\text{Fe}_2(\text{CO})_9$  to give a heteronuclear trimetal bridging carbyne complex. This may be caused by the steric hindrance of the bulky carboranyl group, which serves to prevent further reaction of **3** with  $\text{Fe}_2(\text{CO})_9$ .

**Reaction of 1 with  $\text{Co}_2(\text{CO})_8$  To Form  $[\text{ReCo}_2(\mu_3\text{-CC}_6\text{H}_5)(\mu\text{-CO})_2(\text{CO})_5(\eta\text{-C}_5\text{H}_5)(\text{C}_2\text{HB}_{10}\text{H}_{10})]$  (**4**).** Similar to the reaction of **1** with  $\text{Fe}_2(\text{CO})_9$ , compound **1** was treated with an excess of  $\text{Co}_2(\text{CO})_8$  in THF at 0–10 °C

for 15 h. After removal of the solvent under vacuum, the residue was chromatographed on  $\text{Al}_2\text{O}_3$ , and the crude product was recrystallized from petroleum ether/ $\text{CH}_2\text{Cl}_2$  at –80 °C to give (Scheme 3) a 73% yield of the blackish green complex  $[\text{ReCo}_2(\mu_3\text{-CC}_6\text{H}_5)(\mu\text{-CO})_2(\text{CO})_5(\eta\text{-C}_5\text{H}_5)(\text{C}_2\text{HB}_{10}\text{H}_{10})]$  (**4**), which is sensitive to air and temperature in solution but is air-stable as the solid. On the basis of its elemental analysis, IR, <sup>1</sup>H NMR, and mass spectra, as well as single-crystal X-ray structure determination, it is corroborated that compound **4** is a novel heteronuclear trimetal bridging carbyne complex. Surprisingly, the carboranyl group has been transferred from the formacyl to a Co atom during the reaction.

The results of the structure analysis (Figure 2) confirmed that complex **4** is a heteronuclear trimetal bridging carbyne complex. However, the carboranyl group is directly bonded to the Co(1) atom, caused by migration of the carboranyl group from the formacyl to

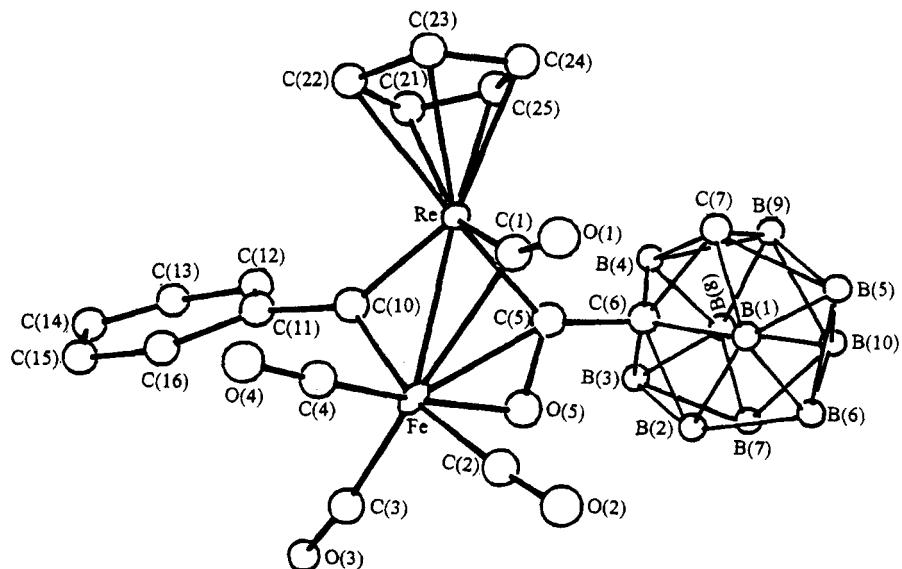


Figure 1. Molecular structure of **3** showing the atom-labeling scheme.

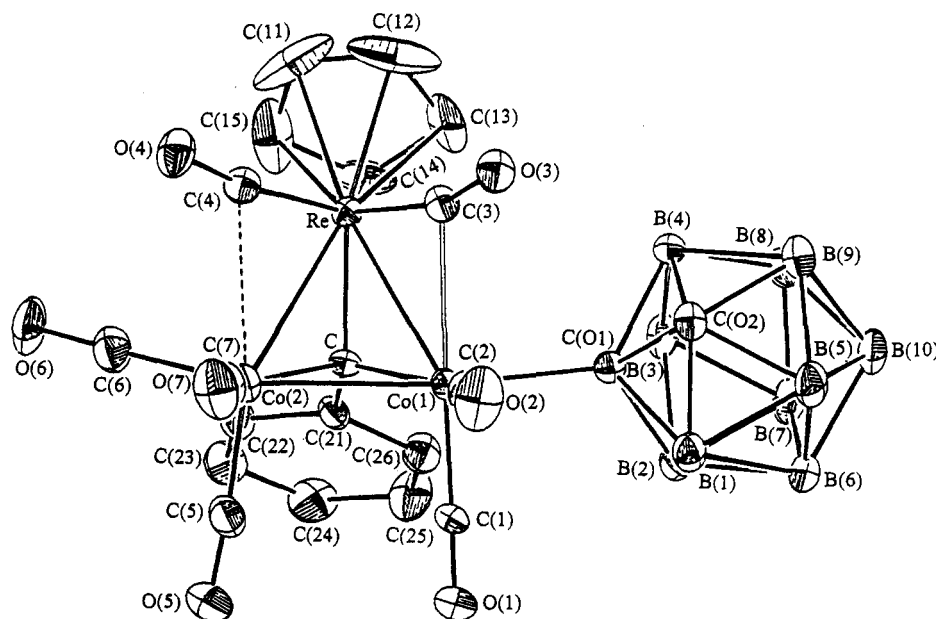
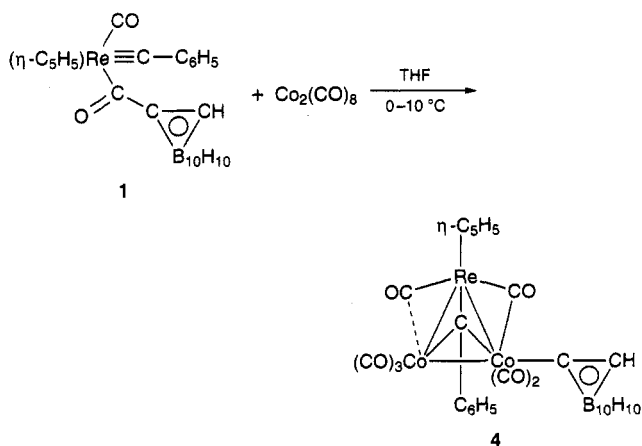


Figure 2. Molecular structure of **4** showing the atom-labeling scheme.

### Scheme 3



(2) construct an approximate isosceles triangle (Co(1)–Co(2) = 2.531(3) Å, Re–Co(1) = 2.669(3) Å, Re–Co(2) = 2.688(2) Å). The metal–metal bond lengths are closely related to that of the known complex [Co<sub>2</sub>Re(μ<sub>3</sub>-CC<sub>6</sub>H<sub>4</sub>Me-4)(CO)<sub>10</sub>] (Co–Co = 2.535(1) Å, average Re–Co = 2.70 Å).<sup>15</sup> The μ-C–Co and μ-C–Re distances are C–Co(1) = 1.92(1) Å, C–Co(2) = 1.95(1) Å, and C–Re = 2.01(1) Å, respectively, of which the C–Co bond lengths are comparable to that found (average C–Co = 1.89 Å) in [Co<sub>2</sub>Re(μ<sub>3</sub>-CC<sub>6</sub>H<sub>4</sub>Me-4)(CO)<sub>10</sub>],<sup>15</sup> while the C–Re bond length is significantly shorter than that in [Co<sub>2</sub>Re(μ<sub>3</sub>-CC<sub>6</sub>H<sub>4</sub>Me-4)(CO)<sub>10</sub>] (2.189(6) Å)<sup>15</sup> and is closer to the sum of covalent double-bond radii of Re and C (1.91 Å).<sup>12</sup>

The five carbonyl groups are terminally bound to both Co atoms, two to Co(1) and three to Co(2), and the two carbonyl groups bridge or semibridge the Re–Co bonds. Among two carbonyl groups bonded to the Re atom, one (C(3)O(3)) is a bridging carbonyl ligand with the Co(1)

the Co atom; the original formacyl is converted into a bridging CO or semibridging CO ligand.

The molecule of **4** possesses a trimetallatetrahedrane CC<sub>2</sub>Re core. The three metal atoms Re, Co(1), and Co-

(15) Jeffery, J. C.; Lewis, D. B.; Lewis, G. E.; Stone, F. G. A. *J. Chem. Soc., Dalton Trans.* **1985**, 2001.



atom, thus giving the Re and Co(1) atoms an 18-electron configuration. The C(3)O(3) ligand is asymmetrically bonded to the Re and Co(1) atoms (Re–C(3) = 1.89(1) Å, Co(1)–C(3) = 2.39(1) Å). The Re–C(3) distance (1.89(1) Å) is close to that of the Re–C(terminal CO) bond (1.90 Å) in **1**<sup>11</sup> and the Re–C(terminal CO) bond (average 1.97 Å) in [Co<sub>2</sub>Re(μ<sub>3</sub>-CC<sub>6</sub>H<sub>4</sub>Me-4)(CO)<sub>10</sub>]<sub>15</sub> while the Co(1)–C(3) bond length of 2.39(1) Å is much longer than the Co–C(terminal CO) bond lengths (average 1.80 Å) in **4**. The asymmetrical bridging carbonyl groups were also found in some di- and trimetal carbonyl compounds such as Fe<sub>2</sub>(CO)<sub>7</sub>dipy,<sup>16</sup> Fe<sub>3</sub>(CO)<sub>12</sub>,<sup>17</sup> and Fe<sub>3</sub>(CO)<sub>8</sub>(C<sub>4</sub>H<sub>8</sub>S)<sub>2</sub>.<sup>18</sup> Cotton et al. considered that this asymmetrical bridge linkage of the carbonyl group equilibrates electric charge on the two neighboring metal atoms.<sup>16</sup> In **4**, since the back-donation of d electrons from the Co(1) atom to the π\* back-bonding orbital of the bridging carbonyl group (C(3)O(3)) is weaker than that from the Re atom, the electric charge on the Re atom decreased and on the Co(1) atom increased relatively, thus giving the Re and Co(1) atoms in an electric charge equilibrium. Another carbonyl group bonded to the Re atom (C(4)O(4)) is a semibridging carbonyl group with the Co(2) atom (Re–C(4) = 1.91(1) Å, Co(2)–C(4) = 2.57(1) Å, which led the Re–C(4)–O(4) bond angle to be 168°, greatly deviating from 180° and closer to the bond angle of Re–C(3)–O(3) (162°). In [Co<sub>2</sub>Re(μ<sub>3</sub>-CC<sub>6</sub>H<sub>4</sub>Me-4)(CO)<sub>10</sub>] the average Re–C–O bond angle is 176°.<sup>15</sup>

Although the carboranyl group migrated, transferring from formacyl to the Co(1) atom, during the reaction, the structure of the carboranyl group in **4** is unchanged. The icosahedral carboranyl group has an average bond

angle of 60°, C(O1)–C(O2) = 1.64(1) Å, an average B–C distance of 1.70 Å, and an average B–B distance of 1.77 Å, which are close to those found in **1**<sup>11</sup> and **3**.

The spectroscopic data showed significant structural information for **4**, shown in Scheme 3. The IR spectrum (KBr) of **4** showed a semibridging CO absorption band at 1918 cm<sup>-1</sup> and a bridging CO absorption band at 1870 cm<sup>-1</sup>, in addition to terminal CO absorption bands at 2080 and 2020 cm<sup>-1</sup>. No absorption attributable to the acyl function was observed. These are consistent with the results of the X-ray diffraction determination of **4** (Figure 2). The <sup>1</sup>H NMR spectrum of **4** showed the expected proton signals of phenyl, cyclopentadienyl, and carboranyl groups. However, the chemical shift of the carboranyl protons is greatly different from those in **1** (δ<sub>CH</sub> 4.58 ppm, δ<sub>B<sub>10</sub>H<sub>10</sub></sub> 2.88 ppm). The C–H signal moved upfield (δ 3.99 ppm), and the B–H resonances moved downfield (δ 3.39 ppm), which suggested that the chemical environment of the carboranyl group in **4** is different from that in **1**. In **1** the carboranyl group is attached to the electron-poor acyl, but in **4** the carboranyl group is bonded to the electron-rich Co metal atom as shown in Figure 2, thus leading δ<sub>CH</sub> to move upfield and δ<sub>B<sub>10</sub>H<sub>10</sub></sub> to move downfield.

**Acknowledgment.** We thank the National Natural Science Foundation of China and the Science Foundation of the Chinese Academy of Sciences for support of this research.

**Supporting Information Available:** Tables of additional bond lengths and angles and least-squares planes for **3** and **4** (9 pages). Ordering information is given on any current masthead page.

OM9502594

(16) Cotton, F. A.; Troup, J. M. *J. Am. Chem. Soc.* **1974**, *96*, 1233.

(17) Cotton, F. A.; Troup, J. M. *J. Am. Chem. Soc.* **1974**, *96*, 4155.

(18) Cotton, F. A.; Troup, J. M. *J. Am. Chem. Soc.* **1974**, *96*, 5071.

**Organometallic Complexes for Nonlinear Optics. 2.<sup>1</sup>  
Syntheses, Electrochemical Studies, Structural  
Characterization, and Computationally-Derived  
Molecular Quadratic Hyperpolarizabilities of Ruthenium  
 $\sigma$ -Arylacetylides: X-ray Crystal Structures of  
 $\text{Ru}(\text{C}\equiv\text{CPh})(\text{PMe}_3)_2(\eta\text{-C}_5\text{H}_5)$  and  
 $\text{Ru}(\text{C}\equiv\text{CC}_6\text{H}_4\text{NO}_2\text{-4})(\text{L})_2(\eta\text{-C}_5\text{H}_5)$  ( $\text{L} = \text{PPh}_3, \text{PMe}_3$ )**

Ian R. Whittall and Mark G. Humphrey\*

*Department of Chemistry, Australian National University, Canberra, ACT 0200, Australia*

David C. R. Hockless

*Research School of Chemistry, Australian National University, Canberra, ACT 0200, Australia*

Brian W. Skelton and Allan H. White

*Department of Chemistry, University of Western Australia, Nedlands, WA 6907, Australia*

Received January 23, 1995<sup>©</sup>

A series of complexes  $\text{Ru}(\text{C}\equiv\text{CC}_6\text{H}_4\text{R-4})(\text{PR}'_3)_2(\eta^5\text{-C}_5\text{H}_5)$  ( $\text{R} = \text{H}$ ,  $\text{R}' = \text{Ph}$ , **1a**;  $\text{R} = \text{H}$ ,  $\text{R}' = \text{Me}$ , **1b**;  $\text{R} = \text{NO}_2$ ,  $\text{R}' = \text{Ph}$ , **2a**;  $\text{R} = \text{NO}_2$ ,  $\text{R}' = \text{Me}$ , **2b**) has been synthesized by reaction of  $\text{RuCl}(\text{PR}'_3)_2(\eta^5\text{-C}_5\text{H}_5)$  with 4- $\text{HC}\equiv\text{CC}_6\text{H}_4\text{R}$  and deprotonation of the intermediate metal vinylidene complex. The complexes are of the donor–acceptor type, giving enhanced second-order nonlinear optical responses. Correlations of spectroscopic data are consistent with increased electron density at the metal upon increasing the donor strength of the phosphine and with decreased electron density at the metal upon increasing the acceptor strength of the acetylide ligand. Electrochemical data are consistent with an  $\text{Ru}^{\text{II/III}}$  couple for **1a,b**, and **2a,b** whose oxidation potentials vary strongly with the donor and acceptor strengths of ligands, and a  $\text{NO}_2$ -centered LUMO for **2a,b**. Enhanced solvatochromic responses are observed on replacement of 4-H by 4- $\text{NO}_2$  on the acetylide ligand. Complexes **1b** and **2a,b** have been crystallographically characterized.  $\text{Ru}-\text{C}(1)$  distances for these complexes are among the shortest for ruthenium  $\sigma$ -acetylide complexes. Semiempirical calculations employing ZINDO were performed; the results are consistent with increased molecular quadratic hyperpolarizabilities for (i) increasing electron density at the metal center (replacing  $\text{PPh}_3$  by  $\text{PMe}_3$ ), (ii) increasing acceptor strength of the arylacetylide (replacing 4-H by 4- $\text{NO}_2$ ), (iii) decreasing  $\text{M}-\text{C}(\text{acetylide})$  bond length, and (iv) optimum orientation of the acetylide aryl group. Thus, the  $\text{RuL}_2(\eta^5\text{-C}_5\text{H}_5)$  behaves as an efficient *tunable* donor group.

### Introduction

New materials exhibiting large nonlinear optical responses are required for applications in photonics,<sup>2</sup> and with this in mind, a wide range of possible materials have been investigated.<sup>3</sup> A great deal of work has been carried out on inorganic crystals and, more recently, on organic molecules. For the latter in particular, investigations in the last few years have correlated hyperpolarizabilities with various molecular parameters including *inter alia* bond length alternation between adjacent carbon–carbon double and single bonds in a polyene chain,<sup>3n</sup> reduced aromaticity using heterocycles

or combining aromatic and quinonoidal rings,<sup>3n</sup> and progression from dipolar to octapolar systems.<sup>3n,o</sup>

Despite the significant advances in our understanding of organic materials, organometallic compounds are comparatively little explored, and little understood, and systematic structure–property investigations are lacking.<sup>1,4</sup> The most extensively studied system is that of ferrocenyl derivatives;<sup>4b–p</sup> however, the donor–acceptor interaction for these substituted ferrocenes is orthogonal to the MLCT axis, an unfavorable alignment. Recent work has suggested that the metal should be incorporated in the same plane as the  $\pi$ -system and that some metal–carbon multiple-bond character should be introduced to maximize second-order nonlinear optical response.<sup>4b</sup> Attention has turned to  $\sigma$ -acetylide complexes, which certainly satisfy the first design criterion, although the existence of  $\text{M}-\text{C}$  multiple bonding is problematic. In this regard, little work has been carried out on  $\sigma$ -acetylides bearing strong donor and/or acceptor

\* To whom correspondence should be addressed. Tel.: +61 6 249 2927. FAX: +61 6 249 0760. E-mail: Mark.Humphrey@anu.edu.au.

<sup>©</sup> Abstract published in *Advance ACS Abstracts*, July 1, 1995.  
(1) Part 1: Whittall, I. R.; Cifuentes, M. P.; Costigan, M. J.; Humphrey, M. G.; Goh, S. C.; Skelton, B. W.; White, A. H. *J. Organomet. Chem.* **1994**, *471*, 193.

(2) Eaton, D. F. *Science* **1991**, *253*, 281.

substituents to maximize second-order response. As part of a program directed at evaluating the second-order nonlinear optical responses of metal  $\sigma$ -acetylides, we have synthesized a systematically varied series of ruthenium  $\sigma$ -arylacetylides  $\text{Ru}(\text{C}\equiv\text{CC}_6\text{H}_4\text{R}-4)(\text{PR}'_3)_2(\eta^5\text{-C}_5\text{H}_5)$  involving phosphine ligand replacement and varying the nature of the  $\sigma$ -acetylide ligand ( $\text{R}' = \text{Ph}$ ,  $\text{R} = \text{H}$ , **1a**;  $\text{R}' = \text{Me}$ ,  $\text{R} = \text{H}$ , **1b**;  $\text{R}' = \text{Ph}$ ,  $\text{R} = \text{NO}_2$ , **2a**;  $\text{R}' = \text{Me}$ ,  $\text{R} = \text{NO}_2$ , **2b**). We report herein syntheses of the (nitrophenyl)acetylide complexes **2a,b**, electrochemical

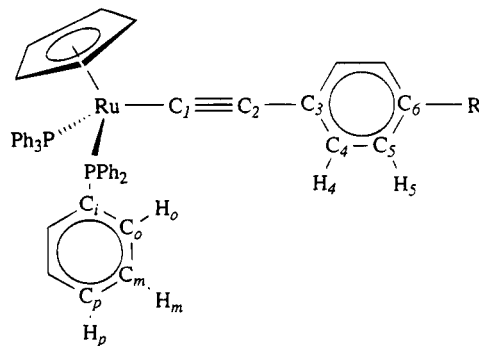


**Figure 1.** Numbering scheme for NMR spectral assignments;  $\text{R} = \text{H}_6$  or  $\text{NO}_2$ . Analogous scheme for trimethylphosphine complexes.

(3) See for example: (a) *Materials for Nonlinear Optics, Chemical Perspectives*; Marder, S. R., Sohn, J. E., Stucky, G. D., Eds.; American Chemical Society: Washington DC, 1991. (b) *Organic Materials for Non-linear Optics*; Hann, R. A., Bloor, D., Eds.; The Royal Society of Chemistry: London, 1989. (c) *Organic Materials for Non-linear Optics II*; Hann, R. A., Bloor, D., Eds.; The Royal Society of Chemistry: London, 1991. (d) *Organic Materials for Non-linear Optics III*; Ashwell, G. J., Bloor, D., Eds.; The Royal Society of Chemistry: Cambridge, 1993. (e) *Organic Molecules for Nonlinear Optics and Photonics*; Messier, J., Kajzar, F., Prasad, P. N., Eds.; Kluwer Academic Publishers: Dordrecht, 1991; Vol. 194, Series E. (f) *Nonlinear Optics of Organics and Semiconductors*; Kobayashi, T., Ed.; Springer-Verlag: Berlin, 1989. (g) *Nonlinear Optical Effects in Organic Polymers*; Messier, J., Kajzar, F., Prasad, P. N., Ulrich, D. R., Eds.; Kluwer Academic Publishers: Dordrecht, 1989; Vol. 162, Series E. (h) *Materials for Non-linear and Electro-optics 1989*; Lyons, M. H., Ed.; Institute of Physics: Bristol, U.K. 1989. (i) *Nonlinear Optical Properties of Organic and Polymeric Materials*; Williams, D. J., Ed.; American Chemical Society: Washington, DC, 1983; Vol. 233. (j) *Nonlinear Optical Properties of Organic Molecules and Crystals*; Chemla, D. S., Zyss, J., Eds.; Academic Press, Inc.: Orlando, FL, 1987; Vol. 1. (k) *Nonlinear Optical Properties of Organic Molecules and Crystals*; Chemla, D. S., Zyss, J., Eds.; Academic Press, Inc.: Orlando, FL, 1987; Vol. 2. (l) *Nonlinear Optical Properties of Polymers*; Heeger, A. J., Orenstein, J., Ulrich, D. R., Eds.; Materials Research Society: Pittsburgh, PA, 1988. (m) Williams, D. J. *Angew. Chem., Int. Ed. Engl.* **1984**, *23*, 690. (n) Marder, S. R.; Perry, J. W. *Adv. Mater.* **1993**, *5*, 804. (o) Zyss, J.; Ledoux, I. *Chem. Rev.* **1994**, *4*, 77.

(4) See: (a) Nalwa, H. S. *Appl. Organomet. Chem.* **1991**, *5*, 349. (b) Calabrese, J. C.; Cheng, L.-T.; Green, J. C.; Marder, S. R.; Tam, W. J. *Am. Chem. Soc.* **1991**, *113*, 7227. (c) Coe, B. J.; Jones, C. J.; McCleverty, J. A.; Bloor, D.; Cross, G. J. *Organomet. Chem.* **1994**, *464*, 225. (d) Yuan, Z.; Taylor, N. J.; Sun, Y.; Marder, T. B. *J. Organomet. Chem.* **1993**, *449*, 27. (e) Bandy, J. A.; Bunting, H. E.; Garcia, M. H.; Green, M. L. H.; Marder, S. R.; Thompson, M. E.; Bloor, D.; Kolinsky, P. V.; Jones, R. J. In *Organic Materials for Non-linear Optics*; Hann, R. A., Bloor, D., Eds.; Royal Society of Chemistry: London, 1989; pp 225–231. (f) Kanis, D. R.; Ratner, M. A.; Marks, T. J. *J. Am. Chem. Soc.* **1992**, *114*, 10338. (g) Winter, C. S.; Oliver, S. N.; Rush, J. D. *Optics Commun.* **1988**, *69*, 45. (h) Bunting, H. E.; Green, M. L. H.; Marder, S. R.; Thompson, M. E.; Bloor, D.; Kolinsky, P. V.; Jones, R. J. *Polyhedron* **1992**, *11*, 1489. (i) Coe, B. J.; Jones, C. J.; McCleverty, J. A.; Bloor, D.; Kolinsky, P. V.; Jones, R. J. *J. Chem. Soc., Chem. Commun.* **1989**, 1485. (j) Doisneau, G.; Balavoine, G.; Fillebeen-Khan, T.; Clinet, J.; Delaire, J.; Ledoux, I.; Loucif, R.; Puccetti, G. *J. Organomet. Chem.* **1991**, *421*, 299. (k) Ghosal, S.; Samoc, M.; Prasad, P. N.; Tufariello, J. T. *J. Phys. Chem.* **1990**, *94*, 2847. (l) Green, M. L. H.; Marder, S. R.; Thompson, M. E.; Bandy, J. A.; Bloor, D.; Kolinsky, P. V.; Jones, R. J. *Nature* **1987**, *330*, 360. (m) Houlton, A.; Jasim, N.; Roberts, R. M. G.; Silver, J.; Cunningham, D.; McArdle, P.; Higgins, T. *J. Chem. Soc., Dalton Trans.* **1992**, 2235. (n) Winter, C. S.; Oliver, S. N.; Rush, J. D. In *Organic Materials for Non-linear Optics*; Hann, R. A., Bloor, D., Eds.; Royal Society of Chemistry: London, 1989; pp 232–237. (o) Houlton, A.; Miller, J. R.; Silver, J.; Jassim, N.; Ahmet, M. J.; Axon, T. L.; Bloor, D.; Cross, G. H. *Inorg. Chim. Acta* **1993**, *205*, 67. (p) Marder, S. R.; Perry, J. W.; Tiemann, B. G.; Schaefer, W. P. *Organometallics* **1991**, *10*, 1896. (q) Marder, T. B.; Lasley, G.; Yuan, Z.; Fyfe, H. B.; Chow, P.; Stringer, G.; Jobe, I. R.; Taylor, N. J.; Williams, I. D.; Kurtz, S. K. In *Materials for Nonlinear Optics, Chemical Perspectives*; Marder, S. R., Sohn, J. E., Stucky, G. D., Eds.; American Chemical Society: Washington, DC, 1991; pp 605–615. (r) Kimura, M.; Abdel-Halim, H.; Robinson, D. W.; Cowan, D. O. *J. Organomet. Chem.* **1991**, *403*, 365. (s) Loucif-Sabi, R.; Delair, J. A.; Bonazzola, L.; Doisneau, G.; Balavoine, G.; Fillebeen-Khan, T.; Ledoux, I. *Mol. Eng.* **1992**, *2*, 221. (t) Dias, A. R.; Garcia, M. H.; Robalo, M. P.; Green, M. L. H.; Lai, K. K.; Pulham, A. J.; Klueber, S. M.; Balavoine, G. *J. Organomet. Chem.* **1993**, *453*, 241. (u) Myers, L. K.; Langhoff, C.; Thompson, M. E. *J. Am. Chem. Soc.* **1992**, *114*, 7560. (v) Laidlaw W. M.; Denning, R. G.; Verbiest, T.; Chaudard, E.; Persoons, A. *Nature* **1993**, *363*, 58. (w) Anderson, A. G.; Calabrese, J. C.; Tam, W.; Williams, I. D. *Chem. Phys. Lett.* **1987**, *134*, 392. (x) Mignani, G.; Krämer, A.; Puccetti, G.; Ledoux, I.; Soula, G.; Zyss, J.; Meyrueix, R. *Organometallics* **1990**, *9*, 2640. (y) Kanis, D. R.; Ratner, M. A.; Marks, T. J. *J. Am. Chem. Soc.* **1990**, *112*, 8203. (z) Kanis, D. R.; Ratner, M. A.; Marks, T. J.; Zerner, M. C. *Chem. Mater.* **1991**, *3*, 19.

studies on all four complexes together with correlations of their spectroscopic responses and solvatochromic behavior, X-ray structural studies on **1b** and **2a,b**, and semiempirical calculations of the molecular quadratic hyperpolarizabilities of **1a,b** and **2a,b**. To the best of our knowledge, these are the first structural studies on acetylide complexes bearing the prototypical organic acceptor group  $4\text{-C}_6\text{H}_4\text{NO}_2$  and the first report of computationally-obtained nonlinearities for metal  $\sigma$ -acetylides.

## Experimental Section

All reactions were carried out under an atmosphere of nitrogen with the use of standard Schlenk techniques, although no attempt was made to exclude air during workup of products. "Petrol" refers to a fraction of petroleum ether of boiling point range 60–80 °C. 4-Ethynylnitrobenzene was prepared from commercial 4-iodonitrobenzene (Aldrich) following the literature method.<sup>5</sup>  $\text{RuCl}(\text{L})_2(\eta^5\text{-C}_5\text{H}_5)$  and  $\text{Ru}(\text{C}\equiv\text{CPh})(\text{L})_2(\eta^5\text{-C}_5\text{H}_5)$  ( $\text{L} = \text{PPh}_3, \text{PMe}_3$ ) were prepared following literature methods.<sup>6</sup> Thin layer chromatography was carried out using 7749 Kieselgel 60 PF<sub>254</sub> (Merck) silica. Microanalyses were carried out at the Research School of Chemistry, Australian National University. Infrared spectra were recorded using a Perkin-Elmer 1725x FT-IR spectrometer. <sup>1</sup>H, <sup>13</sup>C, and <sup>31</sup>P NMR spectra were recorded using a Bruker AC 300 or a Varian Gemini-300 FT NMR spectrometer and are referenced to residual  $\text{CHCl}_3$  (7.24 ppm),  $\text{CDCl}_3$  (77.0 ppm), and external 85%  $\text{H}_3\text{PO}_4$  (0.0 ppm), respectively. NMR spectral assignments follow the numbering scheme shown in Figure 1.

UV–Visible spectra were recorded using a Hitachi U-3200 spectrophotometer. Electrochemical measurements were carried out using a Princeton Applied Research model 170 potentiostat. The supporting electrolyte was 0.7 M [<sup>n</sup>Bu<sub>4</sub>N][PF<sub>6</sub>] in distilled degassed  $\text{CH}_2\text{Cl}_2$ . Solutions ( $1 \times 10^{-3}$  M) were made under a purge of nitrogen and measured versus an Ag/AgCl reference electrode at –60 °C, such that the ferrocene/ferrocenium redox couple was located at 0.55 V.

**Spectroscopic Data for  $\text{Ru}(\text{C}\equiv\text{CPh})(\text{PPh}_3)_2(\eta^5\text{-C}_5\text{H}_5)$  (**1a**).** UV–Vis:  $\lambda_{\text{max}}$  (cyclohexane) 306,  $\epsilon$  40 000  $\text{M}^{-1} \text{cm}^{-1}$ ; (dimethylformamide) 313 nm. <sup>1</sup>H NMR: ( $\delta$ , 300 MHz,  $\text{CDCl}_3$ ) 4.29 (s, 5H,  $\text{C}_5\text{H}_5$ ), 7.07 (t,  $\text{H}_m$ ,  $J_{\text{HH}} = 7$  Hz), 7.18 (t,  $\text{H}_p$ ,  $J_{\text{HH}} = 7$  Hz), 7.47 (m, 12H,  $\text{H}_o$ ). Resonances for  $\text{H}_4$ ,  $\text{H}_5$ , and  $\text{H}_6$  are obscured by those of  $\text{H}_m$  and  $\text{H}_p$ . <sup>13</sup>C NMR: ( $\delta$ , 75 MHz,  $\text{CDCl}_3$ ) 85.1 (s,  $\text{C}_5\text{H}_5$ ), 114.4 (s,  $\text{C}_2$ ), 116.2 (t,  $\text{C}_1$ ,  $J_{\text{CP}} = 25$  Hz), 122.9 (s,  $\text{C}_6$ ), 127.2 (t,  $\text{C}_m$ ,  $J_{\text{CP}} = 5$  Hz), 127.6 (s,  $\text{C}_5$ ), 128.3 (s,

(5) Takahashi, S.; Kuroyama, Y.; Sonogashira, K.; Hagihara, N. *Synthesis* **1980**, 627.

(6) (a) Bruce, M. I.; Wallis, R. C. *Aust. J. Chem.* **1979**, *32*, 1471. (b) Bruce, M. I.; Hameister, C.; Swincer, A. G.; Wallis, R. C. *Inorg. Synth.* **1982**, *21*, 78.

$C_p$ ), 130.3 (s,  $C_3$ ), 130.5 (s,  $C_4$ ), 133.8 (t,  $C_6$ ,  $J_{CP} = 5$  Hz), 138.8 (m,  $C_1$ ).  $^{31}P$  NMR: ( $\delta$ , 121 MHz,  $CDCl_3$ ); 51.2.

**Spectroscopic Data for  $Ru(C\equiv CPh)(PMe_3)_2(\eta^5-C_5H_5)$  (**1b**).** UV-Vis:  $\lambda_{max}$  (cyclohexane) 307,  $\epsilon$  50 000  $M^{-1} cm^{-1}$ ; (dimethylformamide) 324 nm.  $^1H$  NMR: ( $\delta$ , 300 MHz,  $CDCl_3$ ); 1.48 (m, 18H,  $CH_3$ ), 4.69 (s, 5H,  $C_5H_5$ ), 6.92 (t, 1H,  $H_6$ ,  $J_{HH} = 7$  Hz), 7.09 (t, 2H,  $H_5$ ,  $J_{HH} = 7$  Hz), 7.19 (d, 2H,  $H_4$ ,  $J_{HH} = 7$  Hz).  $^{13}C$  NMR: ( $\delta$ , 75 MHz,  $CDCl_3$ ); 23.2 (m,  $CH_3$ ), 80.8 (s,  $C_5H_5$ ), 107.8 (s,  $C_2$ ), 121.4 (t,  $C_1$ ,  $J_{CP} = 25$  Hz), 122.8 (s,  $C_6$ ), 127.6 (s,  $C_5$ ), 130.3 (s,  $C_3$ ), 130.7 (s,  $C_4$ ).  $^{31}P$  NMR: ( $\delta$ , 121 MHz,  $CDCl_3$ ); 13.7. Crystals of **1b** suitable for diffraction analysis were grown by slow diffusion of hexane into a dichloromethane solution at  $-10$  °C.

**Synthesis of  $Ru(C\equiv CC_6H_4NO_2-4)(PPh_3)_2(\eta^5-C_5H_5)$  (**2a**).**  $RuCl(PPh_3)_2(\eta^5-C_5H_5)$  (160 mg, 0.22 mmol) and 4-ethynynitrobenzene (50 mg, 0.34 mmol) were refluxed in MeOH (15 mL) for 1 h and were then cooled. A solution of NaOMe in MeOH (5 mL, 0.102 M) was added, the mixture was stirred, and then the solvent was removed under reduced pressure. The product was isolated by thin layer chromatography (25% acetone:75% petrol eluant), affording a red powder (136 mg, 74%), mp 214 °C. Anal. Calcd for  $C_{49}H_{39}NO_2P_2Ru$ : C, 70.33; H, 4.70; N, 1.61. Found: C, 69.99; H, 4.92; N, 1.63. IR: (cyclohexane)  $\nu(C\equiv C)$  2063  $cm^{-1}$ . UV-Vis:  $\lambda_{max}$  (cyclohexane) 437,  $\epsilon$  85 000  $M^{-1} cm^{-1}$ ; (dimethylformamide) 476 nm.  $^1H$  NMR: ( $\delta$ , 300 MHz,  $CDCl_3$ ); 4.35 (s, 5H,  $C_5H_5$ ), 7.02 (d, 2H,  $H_4$ ,  $J_{HH} = 9$  Hz), 7.08 (t, 12H,  $H_m$ ,  $J_{HH} = 7$  Hz), 7.21 (t, 6H,  $H_p$ ,  $J_{HH} = 7$  Hz), 7.39 (m, 12H,  $H_o$ ), 8.00 (d, 2H,  $H_5$ ,  $J_{HH} = 9$  Hz).  $^{13}C$  NMR: ( $\delta$ , 75 MHz,  $CDCl_3$ ); 85.6 (s,  $C_5H_5$ ), 117.5 (s,  $C_2$ ), 123.6 (s,  $C_5$ ), 127.3 (t,  $C_m$ ,  $J_{CP} = 5$  Hz), 128.7 (s,  $C_p$ ), 130.4 (s,  $C_4$ ), 133.7 (t,  $C_o$ ,  $J_{CP} = 5$  Hz), 137.5 (s,  $C_3$ ), 138.4 (m,  $C_1$ ), 139.1 (t,  $C_l$ ,  $J_{CP} = 25$  Hz), 142.6 (s,  $C_6$ ).  $^{31}P$  NMR: ( $\delta$ , 121 MHz,  $CDCl_3$ ); 51.0. Crystals of **2a** suitable for diffraction analysis were grown by slow diffusion of methanol into dichloromethane solutions at 5 °C.

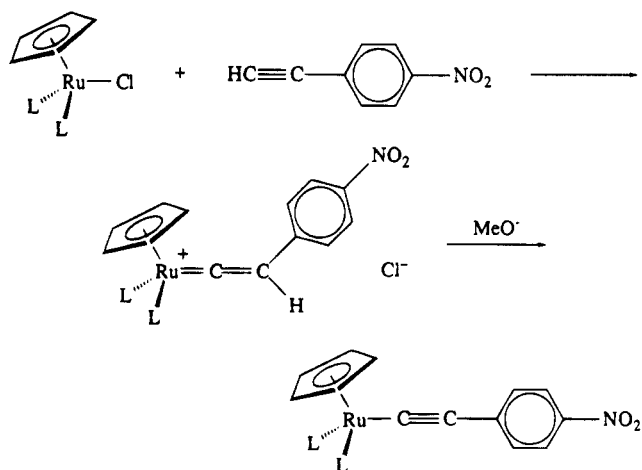
**Synthesis of  $Ru(C\equiv CC_6H_4NO_2-4)(PMe_3)_2(\eta^5-C_5H_5)$  (**2b**).**  $RuCl(PMe_3)_2(\eta^5-C_5H_5)$  (45 mg, 0.13 mmol) and 4-ethynynitrobenzene (28 mg, 0.19 mmol) were dissolved in MeOH (15 mL). The solution was refluxed for 30 min and was then cooled. A solution of NaOMe in MeOH (3 mL, 0.109 M) was added, the mixture was stirred, and then the solvent was removed under reduced pressure. The crude product was isolated by thin layer chromatography (25% acetone:75% petrol eluant) and then crystallized from hot hexane, affording purple crystals (31 mg, 53%), mp 150 °C. Anal. Calcd for  $C_{19}H_{27}NO_2P_2Ru$ : C, 49.14; H, 5.86; N, 3.02. Found: C, 49.07; H, 5.94; N, 2.87. IR: (cyclohexane)  $\nu(C\equiv C)$  2060  $cm^{-1}$ . UV-Vis:  $\lambda_{max}$  (cyclohexane) 440,  $\epsilon$  40 000  $M^{-1} cm^{-1}$ ; (dimethylformamide) 505 nm.  $^1H$  NMR: ( $\delta$ , 300 MHz,  $CDCl_3$ ); 1.48 (m, 18H,  $CH_3$ ), 4.73 (s, 5H,  $C_5H_5$ ), 7.14 (d, 2H,  $H_4$ ,  $J_{HH} = 9$  Hz), 7.97 (d, 2H,  $H_5$ ,  $J_{HH} = 9$  Hz).  $^{13}C$  NMR: ( $\delta$ , 75 MHz,  $CDCl_3$ ); 23.1 (m,  $CH_3$ ), 81.6 (t,  $C_5H_5$ ,  $J_{CP} = 2$  Hz), 111.5 (s,  $C_2$ ), 123.7 (s,  $C_3$ ), 130.5 (s,  $C_4$ ), 137.6 (s,  $C_3$ ), 142.3 (s,  $C_6$ ), 143.8 (t,  $C_1$ ,  $J_{CP} = 25$  Hz).  $^{31}P$  NMR: ( $\delta$ , 121 MHz,  $CDCl_3$ ); 13.5. Crystals of **2b** suitable for diffraction analysis were grown by slow cooling of a hot saturated solution in hexane.

**X-ray Crystallography.** Unique diffractometer data sets were measured within the specified  $2\theta_{max}$  limit (monochromatic radiation;  $\omega-2\theta$  scan mode) yielding  $N$  independent reflections.  $N_o$  of these with  $I > 3\sigma(I)$  were considered "observed" and were used in the full matrix least-squares refinements after absorption correction. Anisotropic thermal parameters were refined for the non-hydrogen atoms; ( $x$ ,  $y$ ,  $z$ , and  $U_{iso}$ )<sub>H</sub> were included, constrained at estimated values. Conventional residuals  $R$ ,  $R_w$  on  $|F|$  at convergence are given. Neutral atom complex scattering factors were used, computation with the teXsan<sup>7</sup> (**1b**) and XTAL 3.2<sup>8</sup> (**2a,b**) program systems. Pertinent results

(7) teXsan; Single Crystal Structure Analysis Software, Version 1.6c; Molecular Structure Corporation: The Woodlands, TX, 1993.

(8) Hall, S. R.; Flack, H. D.; Stewart, J. M. *The XTAL 3.2 Reference Manual*; Universities of Western Australia, Geneva, and Maryland: Nedlands, Australia, Geneva, Switzerland, and Baltimore, MD, 1992.

## Scheme 1



are given in the figures and tables; supporting information deposited comprises hydrogen and thermal parameters, and full non-hydrogen geometries. Individual variants are noted in Table 3.

**Computational Details.** Results were obtained using ZINDO<sup>9</sup> (June 1994 version) from Biosym Technologies, San Diego, CA, implemented on a Silicon Graphics INDY workstation without parameter manipulation or basis function alteration. Calculations used crystallographically-derived atomic coordinates<sup>10</sup> as input data. CI calculations included single excitations; basis set sizes were increased progressively for all calculations until convergence ( $\pm 2 \times 10^{-30}$   $cm^5 esu^{-1}$ ) in the computed  $\beta_{vec}$  value was reached (150–250 excited configurations).

## Results and Discussion

The new  $\sigma$ -(nitrophenyl)acetylide complexes were prepared following the same procedure as their previously reported phenylacetylide analogues.<sup>6a</sup> Thus, reaction of  $RuCl(L)_2(\eta^5-C_5H_5)$  ( $L = PPh_3, PMe_3$ ) with 4-ethynynitrobenzene in refluxing methanol afforded ruthenium vinylidene complexes which were not isolated but, instead, deprotonated *in situ* using methoxide solution to afford the  $\sigma$ -acetylide products,  $Ru(C\equiv CC_6H_4NO_2-4)(L)_2(\eta^5-C_5H_5)$  ( $L = PPh_3$ , **2a**;  $L = PMe_3$ , **2b**) (Scheme 1).

Complexes **2a,b** were characterized by IR,  $^1H$ ,  $^{13}C$ , and  $^{31}P$  NMR spectroscopies and satisfactory microanalyses. Characteristic  $\nu(C\equiv C)$  at 2063 (**2a**) and 2060 (**2b**)  $cm^{-1}$  in the solution IR spectra (cyclohexane solvent),  $\eta^5-C_5H_5$  resonances in the  $^1H$  ( $\delta$  4.35 (**2a**) and 4.73 (**2b**)) and  $^{13}C$  ( $\delta$  85.6 (**2a**) and 81.6 (**2b**)) NMR spectra,  $Ru-C$  in the  $^{13}C$  NMR spectra ( $\delta$  139.1 (**2a**) and 143.8 (**2b**)),  $Ru-C\equiv C$  in the  $^{13}C$  NMR spectra ( $\delta$  117.5 (**2a**) and 111.5 (**2b**)), and equivalent phosphine P in the  $^{31}P$  NMR spectra ( $\delta$  51.0 (**2a**) and 13.5 (**2b**)) were observed. It was of interest to ascertain the effect of ligand variance on the spectroscopic data; important resonances for **2a,b** together with those of **1a,b**, which were determined for comparative purposes, are collected in Table 1.

As can be seen, the cyclopentadienyl and phosphorus resonances are relatively insensitive to the nature of the  $\sigma$ -arylacetylide; replacement of H by  $NO_2$  at the 4-position of the aryl ring has little effect on the chemical shift. In contrast, the chemical shifts of the C(1) and, to a

(9) ZINDO User Guide; Biosym Technologies; San Diego, CA, 1994.

(10) For **1a**, see ref 13a; for **1b** and **2a,b**, see this work.

Table 1. NMR Data for 1a,b and 2a,b

	<sup>1</sup> H		<sup>13</sup> C		<sup>31</sup> P
	C <sub>5</sub> H <sub>5</sub>	C <sub>5</sub> H <sub>5</sub>	C(1)	C(2)	
Ru(C≡CPh)(PPh <sub>3</sub> ) <sub>2</sub> (η <sup>5</sup> -C <sub>5</sub> H <sub>5</sub> ) ( <b>1a</b> )	4.29	85.1	116.2	114.4	51.2
Ru(C≡CPh)(PMe <sub>3</sub> ) <sub>2</sub> (η <sup>5</sup> -C <sub>5</sub> H <sub>5</sub> ) ( <b>1b</b> )	4.69	80.8	121.4	107.8	13.7
Ru(C≡CC <sub>6</sub> H <sub>4</sub> NO <sub>2</sub> -4)(PPh <sub>3</sub> ) <sub>2</sub> (η <sup>5</sup> -C <sub>5</sub> H <sub>5</sub> ) ( <b>2a</b> )	4.35	85.6	139.1	117.5	51.0
Ru(C≡CC <sub>6</sub> H <sub>4</sub> NO <sub>2</sub> -4)(PMe <sub>3</sub> ) <sub>2</sub> (η <sup>5</sup> -C <sub>5</sub> H <sub>5</sub> ) ( <b>2b</b> )	4.73	81.6	143.8	111.5	13.5

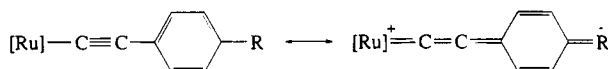


Figure 2.

lesser extent, the C(2) resonances are a function of aryl substituent; C(1) moves 22–23 ppm downfield and C(2) shifts 3–4 ppm downfield on replacement of H by NO<sub>2</sub>. Phosphine substitution of PPh<sub>3</sub> by the more electron-donating PMe<sub>3</sub> has the expected effect on cyclopentadienyl resonances (0.4 ppm downfield shift in the <sup>1</sup>H NMR, 4 ppm upfield shift in the <sup>13</sup>C NMR), consistent with increased cyclopentadienyl ring currents on increased electron density at the metal. Replacement of PPh<sub>3</sub> by PMe<sub>3</sub> shifts C(1) downfield by 5 ppm and C(2) upfield by 6 ppm, consistent with increased charge transfer from Ru to C(2) and the aryl ring; the shifts in the resonances are consistent with the possibility of some contribution of a vinylidene form (Figure 2).

The UV–visible spectra of complexes **1a,b** and **2a,b** are characterized by intense ( $\epsilon = 40\,000\text{--}85\,000\text{ M}^{-1}\text{ cm}^{-1}$ ) MLCT bands at lowest frequency. Replacement of the aryl 4-H by 4-NO<sub>2</sub> gives rise to a bathochromic shift, as expected, of 130 nm. The nitro-substituted complexes **2a,b** have much larger solvatochromic shifts (39 and 65 nm, respectively, proceeding from cyclohexane to dimethylformamide solvent) than their protio-analogues **1a,b** (7 and 17 nm, respectively), consistent with increased stabilization of the charge-separated form for the complexes bearing the strong acceptor functionality. Solvatochromism has been used to obtain quantitative second-order nonlinear optical responses using a two-state model.<sup>11</sup> While such an approach is not justified here, qualitative interpretations are possible, particularly as a systematically varied series of compounds exists. Replacing H by NO<sub>2</sub> and PPh<sub>3</sub> by PMe<sub>3</sub> (i.e., increasing the acceptor and donor strengths) is reflected in an increased solvatochromic shift and should result in an increased second-order nonlinear optical response. The absolute values of solvatochromic shift are large compared to those of other recently reported organometallic complexes (see, for example, ref 4m).

The electrochemical results obtained for complexes **1a,b**, and **2a,b** are gathered in Table 2. Correlations that may be drawn from this data are that (i) ruthenium is oxidized at potentials approximately 0.2 V lower upon replacement of PPh<sub>3</sub> by PMe<sub>3</sub>, i.e., upon increasing the donor strength of the phosphine; (ii) ruthenium is oxidized at potentials 0.2 V higher upon replacement of C≡CPh by C≡CC<sub>6</sub>H<sub>4</sub>NO<sub>2</sub>-4, i.e., upon increasing the acceptor strength of the acetylide; and (iii) the reversibility of the oxidation waves are greater for the complexes bearing PPh<sub>3</sub> rather than PMe<sub>3</sub> ligands. The data are consistent with an Ru<sup>II/III</sup> couple susceptible

Table 2. Cyclic Voltammetric Data for 1a,b and 2a,b

	$E^\circ$ (V) <sup>a</sup>	$i_{pc}/i_{pa}$
Ru(C≡CPh)(PPh <sub>3</sub> ) <sub>2</sub> (η <sup>5</sup> -C <sub>5</sub> H <sub>5</sub> ) ( <b>1a</b> )	0.55	0.7
Ru(C≡CPh)(PMe <sub>3</sub> ) <sub>2</sub> (η <sup>5</sup> -C <sub>5</sub> H <sub>5</sub> ) ( <b>1b</b> )	0.37	0.2
Ru(C≡CC <sub>6</sub> H <sub>4</sub> NO <sub>2</sub> -4)(PPh <sub>3</sub> ) <sub>2</sub> (η <sup>5</sup> -C <sub>5</sub> H <sub>5</sub> ) ( <b>2a</b> ) <sup>b</sup>	0.73	1.0
Ru(C≡CC <sub>6</sub> H <sub>4</sub> NO <sub>2</sub> -4)(PMe <sub>3</sub> ) <sub>2</sub> (η <sup>5</sup> -C <sub>5</sub> H <sub>5</sub> ) ( <b>2b</b> ) <sup>c</sup>	0.52	0.3

<sup>a</sup> At -60 °C vs Ag/AgCl in CH<sub>2</sub>Cl<sub>2</sub> with a rate of 100 mV s<sup>-1</sup> and a switching potential of 1.0 V. <sup>b</sup> Reduction wave at -1.08 V,  $i_{pc}/i_{pa} = 1.0$ . <sup>c</sup> Reduction wave at -1.10 V,  $i_{pc}/i_{pa} = 1.0$ .

to variation in the electron-donating properties of the ligands. Both complexes **2a,b** have fully reversible reduction waves at -1.08 and -1.10 V, respectively, which are assigned to reduction of the nitro substituent and which indicate that the LUMO for **2a,b** is localized at this substituent; theoretical studies by Kostic and Fenske<sup>12</sup> on Fe(C≡CH)(PH<sub>3</sub>)<sub>2</sub>(η<sup>5</sup>-C<sub>5</sub>H<sub>5</sub>) suggested that the LUMO is metal centered for  $\sigma$ -acetylide complexes of that type.

We have reported the structural characterization of **1a** in an earlier paper,<sup>13a</sup> and have completed X-ray diffraction studies on **1b** and **2a,b** to generate a set of structural data for complexes with systematic variation of substituents. Crystallographic data are collected in Table 3, atomic coordinates are collected in Tables 4 (**1b**), 5 (**2a**), and 6 (**2b**), bond lengths are in Table 7, and bond angles in Table 8. ORTEP plots are displayed in Figures 3 (**1b**), 4 (**2a**), and 5 (**2b**).

The structural data in Tables 7 and 8 permit comparisons, although the relative imprecision of the crystallographic determination of **2b** necessitates caution in interpreting its data. Ru–P distances elongate significantly on replacing C≡CPh by C≡CC<sub>6</sub>H<sub>4</sub>NO<sub>2</sub>-4 for the PPh<sub>3</sub> complexes but are suggestive of a contraction (if anything) for the analogous PMe<sub>3</sub> complexes. Not surprisingly, angles P(1)–Ru–P(2) are smaller for complexes **1b** and **2b** bearing the smaller phosphine.

(12) Kostic, N. M.; Fenske, R. F. *Organometallics* **1982**, *1*, 974.

(13) (a) Bruce, M. I.; Humphrey, M. G.; Snow, M. R.; Tiekink, E. R. T. *J. Organomet. Chem.* **1986**, *314*, 213. (b) Sato, M.; Shintate, H.; Kawata, Y.; Sekino, M. *Organometallics* **1994**, *13*, 1956. (c) Haquette, P.; Pirio, N.; Touchard, D.; Toupet, L.; Dixneuf, P. H. *J. Chem. Soc., Chem. Commun.* **1993**, 163. (d) Touchard, D.; Haquette, P.; Pirio, N.; Toupet, L.; Dixneuf, P. H. *Organometallics* **1993**, *12*, 3132. (e) Romero, A.; Peron, D.; Dixneuf, P. H. *J. Chem. Soc., Chem. Commun.* **1990**, 1410. (f) Echavarren, A. M.; López, J.; Santos, A.; Romero, A.; Hemoso, J. A.; Vegas, A. *Organometallics* **1991**, *10*, 2371. (g) Wisner, J. M.; Bartczak, T. J.; Ibers, J. A. *Inorg. Chim. Acta* **1985**, *100*, 115. (h) Montoya, J.; Santos, A.; López, J.; Echavarren, A. M.; Ros, J.; Romero, A. *J. Organomet. Chem.* **1992**, *426*, 383. (i) Jia, G.; Rheingold, A. L.; Meek, D. W. *Organometallics* **1989**, *8*, 1378. (j) Jia, G.; Gallucci, J. C.; Rheingold, A. L.; Haggerty, B. S.; Meek, D. W. *Organometallics* **1991**, *10*, 3459. (k) Consiglio, G.; Morandini, F.; Sironi, A. *J. Organomet. Chem.* **1986**, *306*, C45. (l) Kruger, G. J.; Ashworth, T. V.; Singleton, E. *Acta Crystallogr. A* **1981**, *37*, C220. (m) Sun, Y.; Taylor, N. J.; Carty, A. *J. Organometallics* **1992**, *11*, 4293. (n) Atherton, Z.; Faulkner, C. W.; Ingham, S. L.; Kakkar, A. K.; Khan, M. S.; Lewis, J.; Long, N. J.; Raithby, P. R. *J. Organomet. Chem.* **1993**, *462*, 265. (o) Torres, M. R.; Santos, A.; Ros, J.; Solans, X. *Organometallics* **1987**, *6*, 1091. (p) Sun, Y.; Taylor, N. J.; Carty, A. *J. Organomet. Chem.* **1992**, *423*, C43. (q) Helliwell, M.; Stell, K. M.; Mawby, R. J. *J. Organomet. Chem.* **1988**, *356*, C32. (r) Wakatsuki, Y.; Satoh, M.; Yamazaki, H. *Chem. Lett.* **1989**, 1585.

(11) Prasad, P. N.; Williams, D. J. *Introduction to Nonlinear Optical Effects in Molecules and Polymers*; John Wiley & Sons, Inc.: New York, 1991.

Table 3. Crystallographic Data for 1b and 2a,2b

	1b <sup>a,b</sup>	2a <sup>c</sup>	2b <sup>b,d</sup>
chemical formula	C <sub>19</sub> H <sub>23</sub> P <sub>2</sub> Ru	C <sub>49</sub> H <sub>39</sub> NO <sub>2</sub> P <sub>2</sub> Ru·0.36CH <sub>2</sub> Cl <sub>2</sub>	C <sub>19</sub> H <sub>27</sub> NO <sub>2</sub> P <sub>2</sub> Ru
fw	419.45	867.5	464.5
space group	Cc (No. 9)	C2/c (No. 15)	Pca2 <sub>1</sub> (No. 29)
a, Å	10.732(2)	28.00(2)	26.52(3)
b, Å	22.493(3)	20.555(4)	8.623(8)
c, Å	8.436(2)	18.349(5)	9.416(1)
α, deg	90	90	90
β, deg	101.38(2)	130.00(4)	90
γ, deg	90	90	90
V, Å <sup>3</sup>	1996.4(7)	8091(7)	2153(3)
ρ calcd, g cm <sup>-3</sup>	1.40	1.42	1.43
Z	4	8	4
radiation/λ, Å	Cu Kα/1.54178	Mo Kα/0.71073	Mo Kα/0.71073
T, K	213	295	295
μ, cm <sup>-1</sup>	78.20	5.6	8.9
size, mm <sup>3</sup>	0.12 × 0.28 × 0.12	0.58 × 0.20 × 0.20	0.03 × 0.09 × 0.58
A* (min, max)	1.00, 1.41	1.10, 1.20	1.03, 1.13
2θ <sub>max</sub> , deg	120.2	60	60
N	1540	11 786	3305
N <sub>o</sub>	1486	7233	1176
R <sup>e</sup>	0.031	0.060	0.062
R <sub>w</sub> <sup>f</sup>	0.039 <sup>g</sup>	0.063 <sup>h</sup>	0.058 <sup>h</sup>

<sup>a</sup> A linear correction factor was applied to the data to compensate for a uniform decrease of 5% in standard intensities over the course of data collection. <sup>b</sup> Residuals are quoted for the preferred chirality. <sup>c</sup> The material available was twinned, and the data set used was deconvoluted for such a specimen; a subset of the data was refined with an independent scale factor. Difference map artifacts were modelled in terms of a partly occupied CH<sub>2</sub>Cl<sub>2</sub> solvent located about a crystallographic 2-fold axis. The carbon was refined with an isotropic thermal parameter form, and the site occupancy for the molecule was refined to 0.36(1). <sup>d</sup> Limited data from a very small specimen would not support meaningful/stable refinement of anisotropic thermal parameter forms throughout in the context of a noncentrosymmetric space group, and C(1) was refined isotropically ( $n_v = 220$ ). Cyclopentadienyl thermal motion was very high. <sup>e</sup>  $R(F_o) = \sum(|F_o| - |F_c|)/\sum|F_o|$ . <sup>f</sup>  $R_w(F_o) = (\sum w(|F_o| - |F_c|)^2/\sum w F_o^2)^{1/2}$ . <sup>g</sup>  $w = 4F_o^2/\sigma^2(F_o^2)$ , where  $\sigma^2(F_o^2) = [\sigma^2(C + 4B) + (pF_o^2)^2/Lp^2]$  ( $\sigma$  = scan rate,  $C$  = peak count,  $B$  = background count,  $p = 0.027$  determined experimentally from standard reflections). <sup>h</sup> Statistical weights are derivative of  $\sigma^2(I) = \sigma^2(I_{diff}) + 0.0004\sigma^4(I_{diff})$ .

Table 4. Non-Hydrogen Atomic Coordinates and Equivalent Isotropic Displacement Parameters for Complex 1b

atom	x	y	z	B <sub>eq</sub> , Å <sup>2</sup>
Ru(1) <sup>a</sup>	0.9972	0.84238(2)	0.5003	1.97(1)
P(1)	0.8250(2)	0.85173(8)	0.2977(2)	2.26(4)
P(2)	1.1404(2)	0.85185(8)	0.3368(3)	2.45(4)
C(01)	1.0948(9)	0.9075(4)	0.685(1)	4.7(2)
C(02)	1.120(1)	0.8488(4)	0.751(1)	3.9(2)
C(03)	1.0048(9)	0.8243(4)	0.7626(9)	3.9(2)
C(04)	0.9056(9)	0.8651(5)	0.709(1)	4.1(2)
C(05)	0.961(1)	0.9171(4)	0.659(1)	5.0(2)
C(1)	0.9833(6)	0.7561(3)	0.4477(7)	2.2(1)
C(2)	0.9764(7)	0.7026(3)	0.4211(8)	2.3(1)
C(201)	0.9813(6)	0.6401(3)	0.3913(8)	2.1(1)
C(202)	0.9147(6)	0.5991(3)	0.4671(9)	2.8(2)
C(203)	0.9221(8)	0.5387(3)	0.4374(9)	3.4(2)
C(204)	0.9944(9)	0.5181(3)	0.334(1)	4.1(2)
C(205)	1.0623(8)	0.5576(4)	0.257(1)	3.8(2)
C(206)	1.0551(6)	0.6180(3)	0.2855(9)	2.8(2)
C(11)	0.8193(8)	0.8110(4)	0.1111(9)	3.5(2)
C(12)	0.6777(8)	0.8251(5)	0.354(1)	4.0(2)
C(13)	0.7787(8)	0.9261(4)	0.225(1)	4.5(2)
C(21)	1.1662(8)	0.7908(4)	0.2048(10)	3.4(2)
C(22)	1.3030(8)	0.8631(4)	0.446(1)	4.1(2)
C(23)	1.1231(9)	0.9160(4)	0.199(1)	4.4(2)

<sup>a</sup> Defines origin.

Distances and angles within the arylacetylide groups are not unusual (in particular, there is no obvious bond length alternation which would be expected for appreciable quinonoidal contribution), and distances and angles associated with the nitro substituents are also unexceptional. Our primary interest in these structural determinations is in variations in the Ru–C(1)–C(2)–C(201) bond length and angle data. For the PPh<sub>3</sub> complexes, replacement of aryl 4-H by aryl 4-NO<sub>2</sub> results in a possible slight decrease in Ru–C(1), C(1)–C(2), and C(2)–C(201). Marginal variations within the angles of the essentially linear Ru–C(1)–C(2)–C(201)

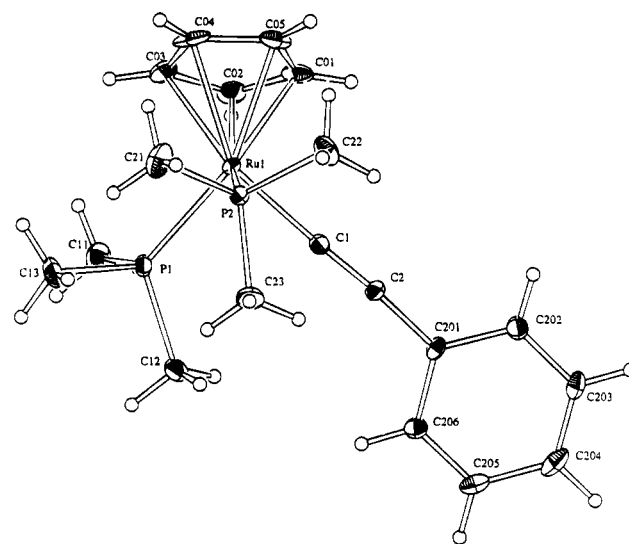
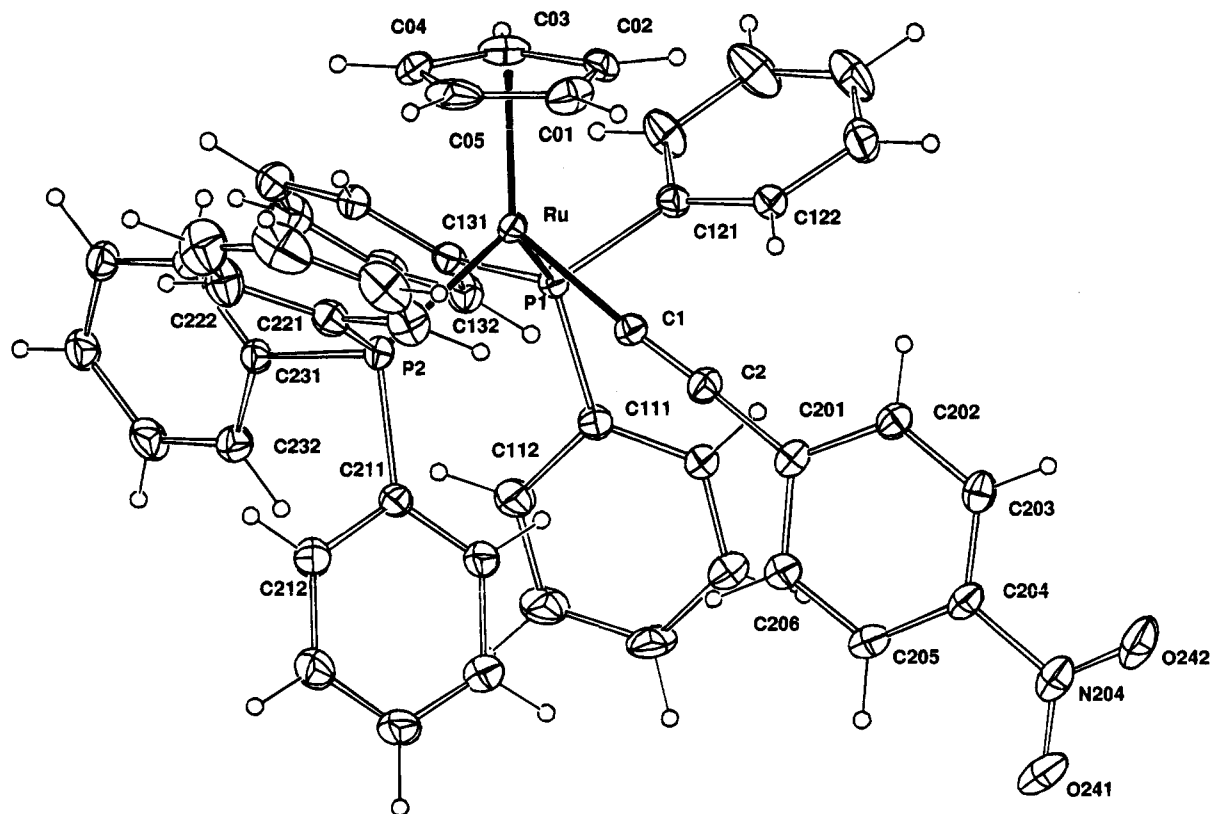


Figure 3. Molecular structure and atomic labeling scheme for 1b. The 20% thermal ellipsoids are shown for the non-hydrogen atoms; hydrogen atoms have arbitrary radii of 0.1 Å.

framework are also evident. Differences and trends, such as they are, are within crystallographic errors. Clearly, replacement of 4-H by the strong acceptor 4-NO<sub>2</sub> has made little if any difference to the ground state structure at Ru–C(1)–C(2)–C(201), and more data is required before further comment can be made.

A large number of mononuclear ruthenium  $\sigma$ -acetylide complexes have been characterized crystallographically, and important bond length and angle data are collected in Table 9, ordered by Ru–C(1) distance. The four complexes reported herein have some of the shortest Ru–C(1) interactions, the only substantively shorter being those of the imprecisely determined butadienyl



**Figure 4.** Molecular structure and atomic labeling scheme for **2a**. The 20% thermal ellipsoids are shown for the non-hydrogen atoms; hydrogen atoms have arbitrary radii of 0.1 Å.

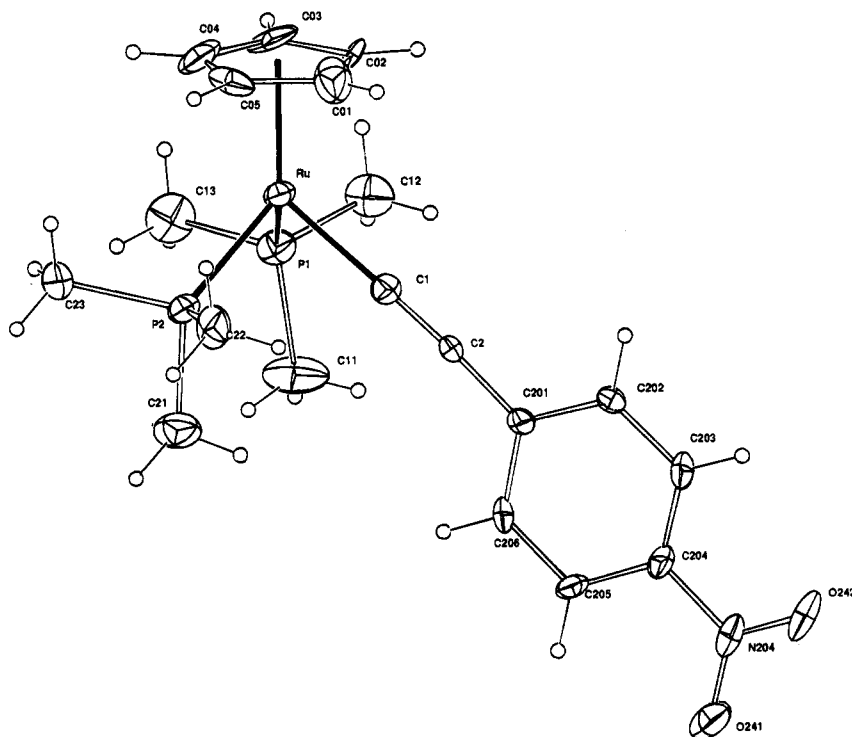


**Figure 5.** Molecular structure and atomic labeling scheme for **2b**. The 20% thermal ellipsoids are shown for the non-hydrogen atoms; hydrogen atoms have arbitrary radii of 0.1 Å.

$\text{Ru}(\text{C}\equiv\text{C}\equiv\text{C}(\text{OSiMe}_3)\text{Ph}_2)(\text{Cl})(\text{PMe}_3)(\text{C}_6\text{Me}_6)^{13\text{e}}$  and the parent acetylide  $\text{Ru}(\text{C}\equiv\text{CH})(\text{Cl})(\text{dppm})_2^{13\text{c,d}}$  average  $\text{Ru}-\text{C}(1)$  for complexes other than **1a,b** and **2a,b** is 2.04 Å. The  $\text{C}(1)-\text{C}(2)$  distances do not vary significantly across the series, with an average  $\text{C}(1)-\text{C}(2)$  distance for all other complexes of 1.20 Å. Significantly fewer  $\text{C}(2)-\text{C}(201)$  data have been reported, with an average

bond distance of 1.43 Å for previously reported complexes. Associated angles do not deviate from linearity for any of the complexes surveyed. Across the series, the new complexes reported herein have shorter  $\text{Ru}-\text{C}(1)$  and marginally longer  $\text{C}(1)-\text{C}(2)$ , consistent with the strong electron-donating ruthenium for **1a,b** and **2a,b**. Recent photoelectron spectroscopy measurements



**Table 5. Non-Hydrogen Atomic Coordinates and Equivalent Isotropic Displacement Parameters for Complex 2a**

atom	x	y	z	$U_{eq}, \text{\AA}^2$
Ru	0.24701(2)	0.82859(2)	0.16182(3)	0.0346(2)
P(1)	0.20547(6)	0.76351(6)	0.21049(9)	0.0368(8)
C(111)	0.2550(2)	0.7187(2)	0.3229(3)	0.043(3)
C(112)	0.2676(3)	0.7447(3)	0.4044(4)	0.060(4)
C(113)	0.3068(3)	0.7128(3)	0.4901(4)	0.075(5)
C(114)	0.3356(3)	0.6553(3)	0.4986(4)	0.076(5)
C(115)	0.3257(3)	0.6301(3)	0.4207(4)	0.069(5)
C(116)	0.2852(3)	0.6606(2)	0.3336(4)	0.052(4)
C(121)	0.1597(2)	0.6978(2)	0.1224(3)	0.042(3)
C(122)	0.1879(3)	0.6569(2)	0.1001(4)	0.049(3)
C(123)	0.1545(3)	0.6073(3)	0.0336(4)	0.062(5)
C(124)	0.0934(3)	0.6008(3)	-0.0119(5)	0.078(5)
C(125)	0.0630(3)	0.6414(4)	0.0065(5)	0.088(6)
C(126)	0.0964(3)	0.6903(3)	0.0741(4)	0.063(4)
C(131)	0.1491(2)	0.7993(2)	0.2182(3)	0.041(3)
C(132)	0.1232(3)	0.7643(3)	0.2506(4)	0.053(4)
C(133)	0.0788(3)	0.7927(3)	0.2528(4)	0.062(4)
C(134)	0.0599(3)	0.8564(3)	0.2225(4)	0.065(4)
C(135)	0.0855(3)	0.8909(3)	0.1918(4)	0.056(4)
C(136)	0.1290(2)	0.8628(2)	0.1885(3)	0.045(3)
P(2)	0.30947(6)	0.89660(6)	0.29085(9)	0.0404(8)
C(211)	0.3797(2)	0.8745(3)	0.4105(3)	0.047(3)
C(212)	0.4190(3)	0.9247(3)	0.4714(4)	0.063(4)
C(213)	0.4691(3)	0.9122(3)	0.5646(4)	0.077(4)
C(214)	0.4810(3)	0.8496(3)	0.6004(4)	0.074(4)
C(215)	0.4434(3)	0.7989(3)	0.5412(4)	0.070(4)
C(216)	0.3924(3)	0.8117(3)	0.4456(4)	0.052(3)
C(221)	0.3448(2)	0.9566(3)	0.2622(4)	0.049(3)
C(222)	0.3332(3)	1.0230(3)	0.2511(5)	0.065(5)
C(223)	0.3578(4)	1.0608(3)	0.2192(6)	0.088(6)
C(224)	0.3927(4)	1.0350(4)	0.1994(5)	0.093(6)
C(225)	0.4061(3)	0.9698(4)	0.2141(5)	0.084(5)
C(226)	0.3825(3)	0.9305(3)	0.2454(5)	0.067(4)
C(231)	0.2700(2)	0.9437(2)	0.3234(3)	0.040(3)
C(232)	0.2791(3)	0.9306(3)	0.4056(4)	0.052(4)
C(233)	0.2437(3)	0.9614(3)	0.4237(4)	0.062(4)
C(234)	0.2000(3)	1.0064(3)	0.3618(4)	0.060(4)
C(235)	0.1897(2)	1.0202(2)	0.2787(4)	0.052(4)
C(236)	0.2230(2)	0.9886(2)	0.2590(3)	0.046(3)
C(1)	0.3171(2)	0.7654(2)	0.2211(3)	0.041(3)
C(2)	0.3569(2)	0.7250(2)	0.2517(4)	0.047(3)
C(201)	0.4037(2)	0.6754(2)	0.2939(4)	0.047(3)
C(202)	0.4104(2)	0.6341(2)	0.2400(4)	0.046(3)
C(203)	0.4529(2)	0.5844(2)	0.2814(4)	0.048(4)
C(204)	0.4892(2)	0.5748(2)	0.3770(4)	0.046(3)
N(204)	0.5348(2)	0.5215(2)	0.4236(4)	0.062(3)
O(241)	0.5638(2)	0.5118(2)	0.5076(3)	0.083(3)
O(242)	0.5414(2)	0.4896(2)	0.3738(4)	0.087(4)
C(205)	0.4846(3)	0.6134(3)	0.4329(4)	0.063(4)
C(206)	0.4422(3)	0.6633(3)	0.3919(4)	0.063(4)
C(01)	0.2403(3)	0.8377(3)	0.0343(4)	0.060(4)
C(02)	0.1893(3)	0.8016(3)	0.0094(4)	0.068(4)
C(03)	0.1528(3)	0.8414(3)	0.0199(4)	0.063(4)
C(04)	0.1803(3)	0.9021(3)	0.0482(4)	0.066(4)
C(05)	0.2332(3)	0.8994(3)	0.0558(4)	0.080(4)
C1 <sup>a</sup>	0.5569(4)	0.7950(4)	0.3168(5)	0.328(9)
C(0) <sup>a,b</sup>	1/2	0.765(1)	1/4	0.22(1)

<sup>a</sup> Site occupancy factor = 0.714(8). <sup>b</sup> Isotropic thermal parameter.

on  $\text{Fe}(\text{C}\equiv\text{CR})(\text{CO})_2(\eta\text{-C}_5\text{H}_5)$  ( $\text{R} = \text{H}, \text{tBu}, \text{Ph}$ ) with a comparatively electron poor metal center have shown little evidence for metal-to-acetylide  $\pi^*$  back-bonding; it was suggested that compounds of the type  $\text{Ru}(\text{C}\equiv\text{CR})\text{-}(\text{PMe}_3)_2(\eta\text{-C}_5\text{H}_5)$  with a more electron rich metal should facilitate this interaction.<sup>14</sup> The trend across the tabulated structures is for a decrease in Ru-C(1) upon replacement of CO by electron-donating ligands. Lewis and co-workers have also recently noted a decrease in electron charge transfer to acetylide ligands upon

**Table 6. Non-Hydrogen Atomic Coordinates and Equivalent Isotropic Displacement Parameters for Complex 2b**

atom	x	y	z	$U_{eq}, \text{\AA}^2$
Ru <sup>a</sup>	0.59906(5)	0.7714(2)	0.5(-)	0.0446(4)
P(1)	0.6488(2)	0.5602(6)	0.492(1)	0.062(2)
C(11)	0.7076(9)	0.549(4)	0.596(4)	0.12(1)
C(12)	0.674(1)	0.527(3)	0.321(3)	0.09(1)
C(13)	0.6190(9)	0.376(2)	0.532(5)	0.10(2)
P(2)	0.5964(2)	0.8024(8)	0.7378(7)	0.051(2)
C(21)	0.6476(9)	0.755(4)	0.855(3)	0.09(1)
C(22)	0.5871(9)	1.002(3)	0.782(2)	0.08(1)
C(23)	0.5451(9)	0.711(4)	0.829(3)	0.09(1)
C(1) <sup>b</sup>	0.6628(6)	0.892(2)	0.508(4)	0.044(5)
C(2)	0.7027(7)	0.964(2)	0.515(3)	0.050(8)
C(201)	0.7496(7)	1.043(2)	0.531(2)	0.037(7)
C(202)	0.7620(7)	1.165(2)	0.440(2)	0.047(8)
C(203)	0.8076(8)	1.247(3)	0.454(2)	0.059(9)
C(204)	0.8400(7)	1.201(3)	0.559(2)	0.053(8)
N(204)	0.8862(6)	1.285(3)	0.578(2)	0.067(8)
O(241)	0.9158(5)	1.245(2)	0.675(2)	0.092(8)
O(242)	0.8946(5)	1.393(2)	0.503(4)	0.093(7)
C(205)	0.8288(7)	1.084(3)	0.652(2)	0.051(8)
C(206)	0.7833(8)	1.005(2)	0.635(3)	0.052(8)
C(01)	0.553(1)	0.950(4)	0.376(4)	0.09(1)
C(02)	0.5704(8)	0.821(5)	0.287(3)	0.10(2)
C(03)	0.5500(9)	0.682(4)	0.324(3)	0.11(2)
C(04)	0.5204(9)	0.714(4)	0.439(3)	0.08(1)
C(05)	0.5214(9)	0.868(4)	0.472(3)	0.08(1)

<sup>a</sup> Defines origin. <sup>b</sup> Isotropic thermal parameter.

**Table 7. Important Bond Lengths ( $\text{\AA}$ ) for Complexes 1a,b and 2a,b**

	1a <sup>a</sup>	1b	2a	2b
Ru-P(1)	2.229(3)	2.266(2)	2.297(2)	2.250(6)
Ru-P(2)	2.228(3)	2.269(2)	2.301(2)	2.256(6)
Ru-Cp	2.229(3)	2.242(7)	2.233(8)	2.29(3)
	2.228(3)	2.264(9)	2.221(6)	2.19(3)
	2.242(4)	2.235(8)	2.231(5)	2.24(3)
	2.251(4)	2.236(8)	2.261(5)	2.22(2)
	2.243(4)	2.231(7)	2.255(8)	2.24(3)
Ru-C(1)	2.017(5)	1.989(7)	1.994(5)	1.99(2)
C(1)-C(2)	1.214(7)	1.224(10)	1.202(8)	1.23(2)
C(2)-C(201)	1.462(8)	1.430(9)	1.432(7)	1.43(3)
C(201)-C(202)	<i>b</i>	1.40(1)	1.41(1)	1.39(3)
C(202)-C(203)	<i>b</i>	1.39(1)	1.370(7)	1.40(3)
C(203)-C(204)	<i>b</i>	1.36(1)	1.363(8)	1.36(3)
C(204)-C(205)	<i>b</i>	1.39(1)	1.37(1)	1.36(3)
C(205)-C(206)	<i>b</i>	1.38(1)	1.373(8)	1.40(3)
C(206)-C(201)	<i>b</i>	1.40(1)	1.400(8)	1.37(3)
C(204)-N(204)			1.468(6)	1.43(3)
N(204)-O(241)			1.211(8)	1.26(3)
N(204)-O(242)			1.23(1)	1.19(3)

<sup>a</sup> Reference 13a; atom labeling as per 1b and 2a,b in this work. <sup>b</sup> Constrained as a rigid group, C-C = 1.395  $\text{\AA}$ .

**Table 8. Important Bond Angles (deg) for Complexes 1a,b and 2a,b**

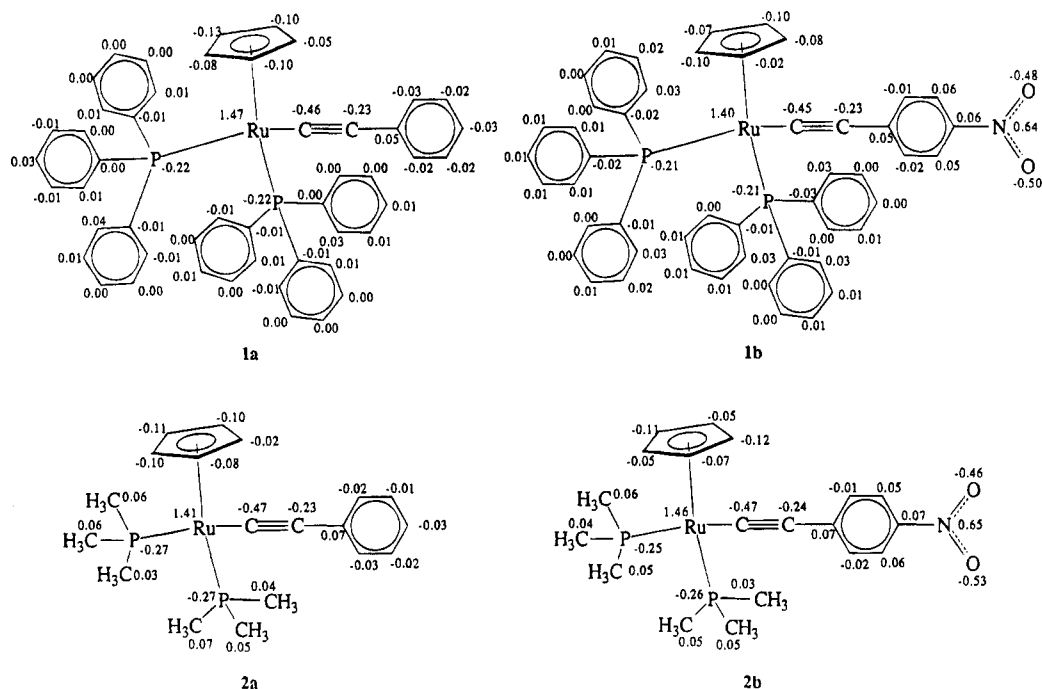
	1a <sup>a</sup>	1b	2a	2b
P(1)-Ru-P(2)	100.9(1)	94.70(8)	101.17(7)	98.4(4)
P(1)-Ru-C(1)	89.2(1)	84.7(2)	88.6(2)	85.8(5)
P(2)-Ru-C(1)	88.6(1)	89.2(2)	90.2(1)	86(1)
Ru-C(1)-C(2)	177.7(4)	177.7(6)	175.9(4)	178(2)
C(1)-C(2)-C(201)	170.6(5)	174.5(7)	175.0(9)	177(3)
C(203)-C(204)-N(204)			120.5(6)	119(2)
C(205)-C(204)-N(204)			117.5(5)	118(2)
C(204)-N(204)-O(241)			119.0(6)	119(2)
C(204)-N(204)-O(242)			117.0(5)	119(2)
O(241)-N(204)-O(242)			124.0(5)	122(2)

<sup>a</sup> Reference 13a, atom labeling as per 1b and 2a,b in this work.

replacement of phosphine by carbonyl by examining  $\nu(\text{C}\equiv\text{C})$  for a series of metal  $\sigma$ -acetylides.<sup>15</sup>

Crystallographically-obtained atomic coordinates for

(14) Lichtenberger, D. L.; Renshaw, S. K.; Bullock, R. M. *J. Am. Chem. Soc.* **1993**, *115*, 3276.

Figure 6. Mulliken population analyses of **1a,b** and **2a,b**.Table 9. Selected Bond Distances and Angles for Mononuclear Ruthenium  $\sigma$ -Acetylide Complexes

complex	Ru-C(1)	C(1)-C(2)	C(2)-C(201)	Ru-C(1)-C(2)	C(1)-C(2)-C(201)
Ru(C≡CH)(Cl)(dppe) <sub>2</sub> <sup>a,b</sup>	1.906(9)	1.162(9)		177.0(6)	
Ru(C≡CC≡CC(OSiMe <sub>3</sub> )Ph <sub>2</sub> (Cl)(PMe <sub>3</sub> )(C <sub>6</sub> Me <sub>6</sub> ) <sup>c</sup>	1.93(3)	1.26(4)	1.40(5)	174(3)	175(4)
<b>1b</b> <sup>d</sup>	1.989(7)	1.224(10)	1.430(9)	177.7(6)	174.5(7)
<b>2b</b> <sup>d</sup>	1.99(2)	1.23(2)	1.43(3)	178(2)	177(3)
[Ru(C≡CFc)(PPh <sub>3</sub> ) <sub>2</sub> ( $\eta$ -C <sub>5</sub> H <sub>5</sub> )] [PF <sub>6</sub> ] <sup>e</sup>	1.99(2)	1.19(3)	1.38(3)	173(2)	178(3)
<b>2a</b> <sup>d</sup>	1.994(5)	1.202(8)	1.432(7)	175.9(4)	175.0(9)
Ru(C≡CPh)(dppe)( $\eta$ -C <sub>5</sub> H <sub>5</sub> ) <sup>f</sup>	2.009(3)	1.204(5)	1.444(5)	178.1(3)	176.3(4)
[Ru(C≡CC <sub>6</sub> H <sub>13</sub> )(CO)(NC <sub>5</sub> H <sub>3</sub> ) <sub>2</sub> (PPh <sub>3</sub> ) <sub>2</sub> ][ClO <sub>4</sub> ] <sup>g</sup>	2.01(3)	1.13(5)	1.54(5)	175(3)	171(5)
<b>1a</b> <sup>h</sup>	2.016(3)	1.215(4)	1.456(4)	178.0(2)	171.9(3)
<b>1a</b> <sup>i</sup>	2.017(5)	1.214(7)	1.462(8)	177.7(4)	170.6(5)
[Ru(C≡CPh)(CNBu <sup>t</sup> ) <sub>3</sub> (PPh <sub>3</sub> ) <sub>2</sub> ][PF <sub>6</sub> ] <sup>j</sup>	2.03(3)	1.17(4)	1.46(4)	175(3)	178(4)
Ru(C≡CPh)( $\eta$ <sup>3</sup> -Ph <sub>3</sub> CHPh)(PhP(CH <sub>2</sub> CH <sub>2</sub> CH <sub>2</sub> PCy <sub>2</sub> ) <sub>2</sub> ) <sup>k</sup>	2.037(3)	1.205(5)	<i>t</i>	178.1(3)	<i>t</i>
Ru(C≡CPh)(Ph <sub>2</sub> PCHMeCHMePPh <sub>2</sub> )( $\eta$ -C <sub>5</sub> H <sub>5</sub> ) <sup>l</sup>	2.038(7)	1.172(9)	<i>t</i>	<i>t</i>	<i>t</i>
[Ru(C≡CPh)(PMe <sub>2</sub> Ph) <sub>4</sub> ][PF <sub>6</sub> ] <sup>m</sup>	2.051	1.203	<i>t</i>	<i>t</i>	<i>t</i>
Ru(C≡CC≡CSiMe <sub>3</sub> ) <sub>2</sub> (CO) <sub>2</sub> (PEt <sub>3</sub> ) <sub>2</sub> <sup>n</sup>	2.057(2)	1.226(2)	1.370(2)	176.5(2)	178.9(2)
Ru(C≡CPh) <sub>2</sub> (dppe) <sub>2</sub> <sup>o</sup>	2.061(5)	1.207(7)	1.434(7)	178.1(5)	174.4(6)
	2.064(5)	1.194(7)	1.449(8)	174.3(5)	168.3(6)
Ru(C≡CSiMe <sub>3</sub> ) <sub>2</sub> (CO) <sub>2</sub> (PEt <sub>3</sub> ) <sub>2</sub> <sup>n</sup>	2.062(2)	1.221(2)		178.1(1)	
Ru(C≡CCO <sub>2</sub> Me)(CO)(PPh <sub>3</sub> ) <sub>2</sub> (MeO <sub>2</sub> CC=CHCH=CHCO <sub>2</sub> Me) <sup>p</sup>	2.064(4)	1.203(5)	1.444(6)	179.6(3)	168.2(5)
Ru(C≡CPh)(CO) <sub>2</sub> (PEt <sub>3</sub> ) <sub>2</sub> <sup>q</sup>	2.074(3)	1.200(4)	1.438(4)	177.1(3)	<i>t</i>
Ru(C≡CH) <sub>2</sub> (CO) <sub>2</sub> (PEt <sub>3</sub> ) <sub>2</sub> <sup>q</sup>	2.078(1)	1.199(2)		179.8(1)	
Ru(C≡CC≡CH) <sub>2</sub> (CO) <sub>2</sub> (PEt <sub>3</sub> ) <sub>2</sub> <sup>q</sup>	2.078(2)	1.194(2)	1.386(3)	177.9(1)	176.9(2)
Ru(C≡CPh)(CO) <sub>2</sub> (PMe <sub>2</sub> Ph) <sub>2</sub> (C <sub>6</sub> H <sub>3</sub> MeC(O)C <sub>6</sub> H <sub>4</sub> Me) <sup>r</sup>	2.120(5)	1.192(7)	1.432(7)	176.2(5)	178.9(6)
Ru(C≡CBu <sup>t</sup> ) <sub>2</sub> (CO)(PPh <sub>3</sub> ) <sub>3</sub> <sup>r</sup>	<i>t</i>	<i>t</i>	<i>t</i>	<i>t</i>	<i>t</i>
Ru(C≡CBu <sup>t</sup> ) <sub>2</sub> (CO)(PPh <sub>3</sub> ) <sub>2</sub> (MeOH) <sup>s</sup>	<i>t</i>	<i>t</i>	<i>t</i>	<i>t</i>	<i>t</i>

<sup>a</sup> Reference 13c. <sup>b</sup> Reference 13d. <sup>c</sup> Reference 13e. <sup>d</sup> This work. <sup>e</sup> Reference 13b. <sup>f</sup> Reference 13a. <sup>g</sup> Reference 13f. <sup>h</sup> Reference 13g. <sup>i</sup> Reference 13h. <sup>j</sup> Reference 13i. <sup>k</sup> Reference 13j. <sup>l</sup> Reference 13k. <sup>m</sup> Reference 13l. <sup>n</sup> Reference 13m. <sup>o</sup> Reference 13n. <sup>p</sup> Reference 13o. <sup>q</sup> Reference 13p. <sup>r</sup> Reference 13q. <sup>s</sup> Reference 13r. <sup>t</sup> Not reported.

**1a,b** and **2a,b** have been used as input data for Mulliken population analyses using ZINDO; the results are displayed pictorially in Figure 6 and can be compared to the chemically intuitive charge density comparisons employed in spectral interpretation. Thus, for the series of complexes, a charge prediction at Ru of **2a** < **1a** < **2b** < **1b** is consistent with a phosphine donor strength PMe<sub>3</sub> > PPh<sub>3</sub> and an acetylide acceptor strength

(15) Khan, M. S.; Kakkar, A. K.; Ingham, S. L.; Raithby, P. R.; Lewis, J.; Spencer, B.; Whittmann, F.; Friend, R. H. *J. Organomet. Chem.* **1994**, *472*, 247.

(16) Suzuki, H. *Electronic Absorption Spectra and Geometry of Organic Molecules*; Academic Press: New York, 1967; p 9.

Table 10. Calculated  $\beta_{\text{vec}}$  ( $10^{-30}$  cm<sup>5</sup> esu<sup>-1</sup>,  $\hbar\omega = 0.65$  eV)

	$\beta_{\text{vec}}$
Ru(C≡CPh)(PPh <sub>3</sub> ) <sub>2</sub> ( $\eta$ <sup>5</sup> -C <sub>5</sub> H <sub>5</sub> ) ( <b>1a</b> )	2
Ru(C≡CPh)(PMe <sub>3</sub> ) <sub>2</sub> ( $\eta$ <sup>5</sup> -C <sub>5</sub> H <sub>5</sub> ) ( <b>1b</b> )	5
Ru(C≡CC <sub>6</sub> H <sub>4</sub> NO <sub>2</sub> -4)(PPh <sub>3</sub> ) <sub>2</sub> ( $\eta$ <sup>5</sup> -C <sub>5</sub> H <sub>5</sub> ) ( <b>2a</b> )	29
Ru(C≡CC <sub>6</sub> H <sub>4</sub> NO <sub>2</sub> -4)(PMe <sub>3</sub> ) <sub>2</sub> ( $\eta$ <sup>5</sup> -C <sub>5</sub> H <sub>5</sub> ) ( <b>2b</b> )	31

4-C≡CC<sub>6</sub>H<sub>4</sub>NO<sub>2</sub> >> C≡CPh, and with spectral data above. The Ru in **1b** bears an anomalously low +1.40 charge (expected about +1.52 from the trend in values), and its cyclopentadienyl group has a low -0.37 charge (expected -0.45), implying unusually large (for this system) Cp → M charge donation in **1b** to satisfy the

Table 11. Optical Spectral Data for 1a,b and 2a,b

	$\lambda_{\text{exp}}$ (nm)	$\epsilon$ ( $\text{M}^{-1} \text{cm}^{-1}$ )	$f_{\text{exp}}^a$	$\lambda_{\text{calcd}}$ (nm)	$f_{\text{calcd}}$
$\text{Ru}(\text{C}\equiv\text{CPh})(\text{PPh}_3)_2(\eta^5\text{-C}_5\text{H}_5)$ ( <b>1a</b> )	306	40 000	0.7	(315) 339	(0.06) 0.08
$\text{Ru}(\text{C}\equiv\text{CPh})(\text{PMe}_3)_2(\eta^5\text{-C}_5\text{H}_5)$ ( <b>1b</b> )	307	50 000	1.1	312	0.33
$\text{Ru}(\text{C}\equiv\text{CC}_6\text{H}_4\text{NO}_2\text{-4})(\text{PPh}_3)_2(\eta^5\text{-C}_5\text{H}_5)$ ( <b>2a</b> ) <sup>b</sup>	437	85 000	1.2	351	0.58
$\text{Ru}(\text{C}\equiv\text{CC}_6\text{H}_4\text{NO}_2\text{-4})(\text{PMe}_3)_2(\eta^5\text{-C}_5\text{H}_5)$ ( <b>2b</b> ) <sup>c</sup>	440	40 000	0.7	372	0.40

<sup>a</sup> Estimated as in ref 16.

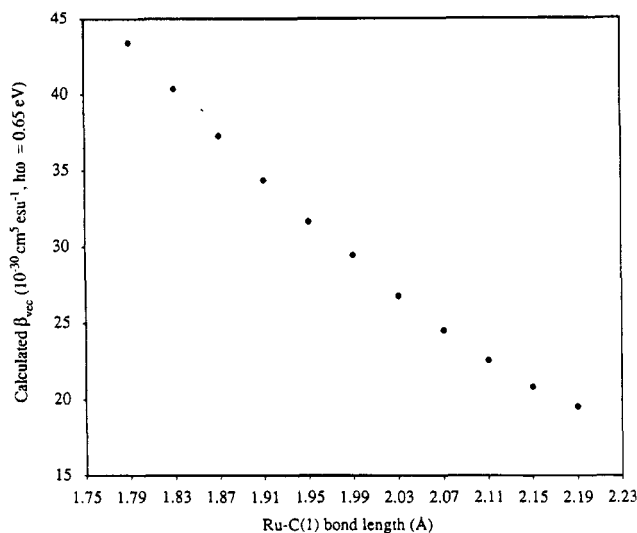


**Figure 7.** Effect of varying the Ru-C(1) bond length from the crystallographically-determined bond length of 1.99 Å on the calculated hyperpolarizability for  $\text{Ru}(\text{C}\equiv\text{CC}_6\text{H}_4\text{NO}_2\text{-4})(\text{PMe}_3)_2(\eta^5\text{-C}_5\text{H}_5)$  (**2b**).

electronic requirements. These results should be treated cautiously, there being no confirmatory evidence from spectral data. As well as the foregoing, no appreciable difference in ground state electron density at C(1) and C(2) is apparent across the series of complexes, from the Mulliken analysis.

Kanis *et al.* have reported molecular quadratic hyperpolarizabilities calculated using ZINDO for ferrocenyl, (arene)chromium tricarbonyl,<sup>4f,y</sup> and (pyridine)-tungsten pentacarbonyl<sup>4y</sup> as well as main group organometallic derivatives,<sup>4z</sup> and found that the ZINDO-derived second-order nonlinear optical responses were in excellent agreement with experiment. We have utilized our crystallographically-derived atomic coordinates to obtain  $\beta_{\text{vec}}$  for **1a,b** and **2a,b** using ZINDO; results are presented in Table 10. Whether such computationally-derived results accurately predict absolute responses for the ruthenium  $\sigma$ -acetylide chromophores is unknown; while we believe the *relative* NLO responses tabulated in Table 10 are realistic, the lack of accuracy in the simulation of the linear optical spectra (Table 11; although relative  $\lambda_{\text{max}}$  are reproduced, absolute values are incorrect) suggests that (i) comparison with ZINDO-derived organic NLO responses or (ii) treating these ZINDO results as having *absolute* rather than *relative* significance is not justified. A comparison of relative responses within the systematically varied organometallic chromophores as presented here does seem valid, however.

One attraction of organometallic chromophores as nonlinear optical materials is the opportunity to fine-tune the response by varying the coordination sphere of the metal; replacement of  $\text{PPh}_3$  by the stronger electron donor  $\text{PMe}_3$  ligands results in a small increase ( $(2\text{--}3) \times 10^{-30} \text{cm}^5 \text{esu}^{-1}$ ) in calculated quadratic

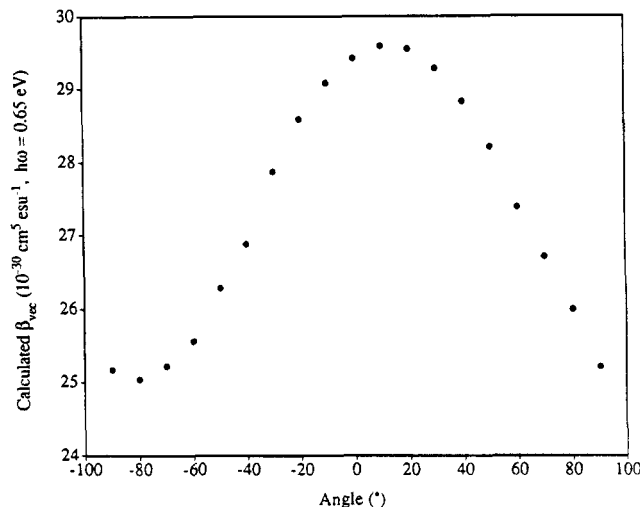


**Figure 8.** Effect of varying the acetylide ring angle from the crystallographically-determined position on the calculated hyperpolarizability for  $\text{Ru}(\text{C}\equiv\text{CC}_6\text{H}_4\text{NO}_2\text{-4})(\text{PMe}_3)_2(\eta^5\text{-C}_5\text{H}_5)$  (**2b**).

hyperpolarizability. Similarly, replacing  $\text{C}\equiv\text{CPh}$  by the strong acceptor  $\text{C}\equiv\text{CC}_6\text{H}_4\text{NO}_2\text{-4}$  increases  $\beta_{\text{vec}}$  by  $(26\text{--}27) \times 10^{-30} \text{cm}^5 \text{esu}^{-1}$ . Reported Ru-C(1) bond lengths for  $\sigma$ -bound ligands are in the range 1.8–2.2 Å. Varying Ru-C(1) for **2b** (Figure 7) results in a substantial increase in  $\beta_{\text{vec}}$  on decreasing Ru-C(1). As was mentioned above, complexes **1a,b** and **2a,b** have some of the shortest Ru-C(1) distances for ruthenium  $\sigma$ -acetylides. In the absence of any competing steric interactions, decreased Ru-C(1) distance and improved nonlinearity would be expected on replacing, for example, the cyclopentadienyl group by a pentamethylcyclopentadienyl group; a similar substitution with metallocenes resulted in an experimentally-determined increase in second-order nonlinearity.<sup>4b</sup> Extending this prescription,  $\sigma$ -ligands with formal multiple-bond character and decreased M-C bond length, such as vinylidene, carbene or carbyne, should afford complexes with enhanced nonlinearity. Effective coupling of the metal to the arylacetylide should be important in nonlinear optical response. We have probed this by rotating the aryl acetylide ligand in **2b** (Figure 8), in which a variation of less than 20% of computed response was found. This suggests that this aspect of the solid state packing of metal  $\sigma$ -acetylide materials should not critically influence their bulk susceptibilities; other factors (e.g., the proclivity of molecular dipoles to oppose) are more important.

## Conclusion

Metal  $\sigma$ -acetylide complexes are attracting increasing attention as potential nonlinear optical materials. A series of ruthenium  $\sigma$ -acetylide complexes, involving systematic variation in acetylide and coligands, has been synthesized as a model donor-acceptor system to

probe effects of structural variation on nonlinear optical merit. Trends in spectroscopic, structural, and electrochemical data and molecular quadratic hyperpolarizabilities have been examined; spectroscopic and electrochemical data are consistent with donor and acceptor strengths varying in a rational fashion, although structural data are unclear. Computationally-derived molecular quadratic hyperpolarizabilities increase on increasing the donor strength of the coligand, increasing the acceptor strength of the aryl substituent, and decreasing the M–C(acetylide) bond length; little dependence on orientation of the acetylide aryl group was found. Finally, the strong dependence of  $\beta_{\text{vec}}$  on the Ru–C(acetylide) bond length suggests that systems incorporating M–C multiple bonding (e.g., vinylidene, carbene, or carbyne) are worthy of investigation. Such complexes, together with  $\sigma$ -vinyl compounds and extended chain  $\sigma$ -acetylides, will be the subject of future reports.

**Acknowledgment.** We thank the Australian Research Council for support of this work and Johnson-Matthey Technology Centre for the loan of ruthenium salts. Dr. G. A. Heath and Mr. I. Kováček are thanked for help with electrochemical measurements. Dr. D. Ollis is thanked for access to an INDY workstation. I.R.W. is the recipient of an Australian Postgraduate Research Award (Industry), and M.G.H. holds an ARC Australian Research Fellowship.

**Supporting Information Available:** Final values of all refined atomic coordinates, all calculated atomic coordinates, all anisotropic and isotropic thermal parameters, all bond lengths and angles, and plots of ZINDO-derived  $\beta_{\text{vec}}$  as a function of the number of state basis functions (26 pages). Ordering information is given on any current masthead page.

OM9500477

# Hydride Complexes of Ruthenium and Related Metals: Preparation and Structures of $\text{Cp}(\text{PMe}_3)_2\text{RuH}$ and $[\text{Cp}(\text{PMe}_3)_2\text{RuH}_2]\text{BF}_4$

Frederick R. Lemke\*

*Department of Chemistry, Ohio University, Athens, Ohio 45701-2979*

Lee Brammer\*

*Department of Chemistry, University of Missouri—St. Louis, 8001 Natural Bridge Road,  
St. Louis, Missouri 63121-4499*

Received February 23, 1995\*

The reaction of  $\text{Cp}(\text{PMe}_3)_2\text{RuCl}$  with either KOMe in MeOH or  $\text{LiAlH}_4$  in  $\text{Et}_2\text{O}$  produces the hydride  $\text{Cp}(\text{PMe}_3)_2\text{RuH}$  (**1**) in high yield. Protonation of **1** with HX quantitatively generates the dihydrides  $[\text{Cp}(\text{PMe}_3)_2\text{RuH}_2]\text{X}$  ( $\text{X} = \text{Cl}$  (**2**),  $\text{BF}_4$  (**3**),  $\text{B}[3,5-(\text{CF}_3)_2\text{C}_6\text{H}_3]_4$  (**4**)). The spectroscopic data on **3** indicate a classical dihydride configuration with no evidence for a dihydrogen tautomer. The  $\text{p}K_a$  of **3** in  $\text{CH}_2\text{Cl}_2$  is 13.9, and the contribution of the ancillary ligands to the  $\text{p}K_a$  value is discussed. X-ray crystal structures of hydride **1** and dihydride **3** have been determined. Hydride **1** exhibits a “three-legged piano stool” geometry, while the cation of **3** exhibits a “four-legged piano stool” geometry, consistent with the classical dihydride configuration. A comparison of the structures of **1** and **3** with related  $\text{d}^6$   $\text{Cp}'\text{L}_2\text{MH}$ ,  $\text{d}^4$   $\text{Cp}'\text{L}_2\text{MH}_2$ , and  $\text{d}^6$   $\text{Cp}'\text{L}_2\text{M}(\eta^2\text{-H}_2)$  complexes ( $\text{Cp}' = \eta^5\text{-C}_5\text{H}_5$ ,  $\eta^5\text{-C}_5\text{Me}_5$ ,  $\eta^5\text{-C}_5\text{H}_5\text{Me}$ ) reveals several general structural trends. First, the angle between the  $\text{Cp}'$  plane and the  $\text{ML}_2$  plane lies in the range  $59\text{--}79^\circ$  (mean  $67.6(13)^\circ$ ) for  $\text{d}^6$   $\text{Cp}'\text{L}_2\text{MH}$  complexes but is in the range  $86\text{--}90^\circ$  (mean  $87.6(4)^\circ$ ) for  $\text{d}^4$   $\text{Cp}'\text{L}_2\text{MH}_2$  complexes and has a mean value of  $56.1(8)^\circ$  for known  $\text{d}^6$   $\text{Cp}'\text{L}_2\text{M}(\eta^2\text{-H}_2)$  complexes. Second, the angle between the M–H vector and the normal to the  $\text{ML}_2$  plane is generally less than  $10^\circ$  (mean  $7.9(12)^\circ$ ) for the  $\text{d}^6$   $\text{Cp}'\text{L}_2\text{MH}$  complexes, while in  $\text{d}^4$   $\text{Cp}'\text{L}_2\text{MH}_2$  complexes the M–H vector is shifted toward the  $\text{ML}_2$  plane, increasing this angle by ca.  $20^\circ$  (mean  $30.0(20)^\circ$ ). The corresponding angle in  $\text{d}^6$   $\text{Cp}'\text{L}_2\text{M}(\eta^2\text{-H}_2)$  complexes has a mean value of  $15.5(18)^\circ$ . Third, the L–M–L' angles in  $\text{d}^6$   $\text{Cp}'\text{L}_2\text{MH}$  complexes (range  $84\text{--}101^\circ$ , mean  $93.0(19)^\circ$ ) are typically smaller than the corresponding angles in  $\text{d}^4$   $\text{Cp}'\text{L}_2\text{MH}_2$  complexes (range  $101\text{--}111^\circ$ , mean  $107.2(10)^\circ$ ).

## Introduction

For many years there has been great interest in transition metal hydrides because of their unusual reactivity and their involvement in many stoichiometric and catalytic processes.<sup>1–6</sup> Recently, ruthenium(II) hydrides of the type  $\text{Cp}'\text{L}_2\text{RuH}$  ( $\text{Cp}' = \text{C}_5\text{H}_5$  (Cp),  $\text{C}_5\text{Me}_5$  (Cp\*);  $\text{L} = \text{CO}$ ,  $\text{PR}_3$ ,  $\text{PAR}_3$ ;  $\text{L}_2 =$  diphosphines) have been the focus of considerable interest. The reactivity of  $\text{Cp}'\text{L}_2\text{RuH}$  is largely dependent on the ancillary ligands.  $\text{Cp}(\text{PMe}_3)_2\text{RuH}$  reacts with electron-deficient chlorosilanes  $\text{R}_3\text{SiCl}$  ( $\text{SiR}_3 = \text{SiCl}_3$ ,  $\text{SiHCl}_2$ ,  $\text{SiMeCl}_2$ ,  $\text{SiMeHCl}$ , and  $\text{SiMe}_2\text{Cl}$ ) to form the ruthenium silyl complexes  $\text{Cp}(\text{PMe}_3)_2\text{RuSiR}_3$  and the ruthenium dihydride  $[\text{Cp}(\text{PMe}_3)_2\text{RuH}_2]\text{Cl}$ , while  $\text{Cp}(\text{PPh}_3)_2\text{RuH}$ , under similar conditions, shows no reactivity with chlorosilanes.<sup>7</sup> This difference in reactivity was attributed to

the enhanced electron donor ability of  $\text{PMe}_3$  compared to  $\text{PPh}_3$ . Protonation of  $\text{Cp}'\text{L}_2\text{RuH}$  has proven to be a useful route to cationic ruthenium(II) dihydrogen complexes  $[\text{Cp}'\text{L}_2\text{Ru}(\eta^2\text{-H}_2)]^+$  and/or cationic ruthenium(IV) dihydride complexes  $[\text{Cp}'\text{L}_2\text{RuH}_2]^+$ .<sup>8–16</sup> The nature of the ancillary ligands dictates the protonation product. Electron-withdrawing ligands, like CO, favor dihydrogen formation while electron-donating ligands, like  $\text{C}_5\text{Me}_5$  and  $\text{PMe}_3$ , favor dihydride formation; many protonation reactions lead to equilibrium mixtures of the two tautomers.

In contrast to this great interest in the hydrides of ruthenium, very few have been the subject of a crystallographic investigation. In this paper, we report the synthesis and  $^1\text{H}$  NMR spectra of the electron-rich

(8) Conroy-Lewis, F. M.; Simpson, S. J. *J. Chem. Soc., Chem. Commun.* **1986**, 506–507.

(9) Conroy-Lewis, F. M.; Simpson, S. J. *J. Chem. Soc., Chem. Commun.* **1987**, 1675–1676.

(10) Wilczewski, T. *J. Organomet. Chem.* **1989**, 361, 219–229.

(11) Chinn, M. S.; Heinekey, D. M. *J. Am. Chem. Soc.* **1987**, 109, 5865–5867.

(12) Chinn, M. S.; Heinekey, D. M.; Payne, N. G.; Sofield, C. D. *Organometallics* **1989**, 8, 1824–1826.

(13) Chinn, M. S.; Heinekey, D. M. *J. Am. Chem. Soc.* **1990**, 112, 5166–5175.

(14) Jia, G.; Morris, R. H. *Inorg. Chem.* **1990**, 29, 581–582.

(15) Jia, G.; Morris, R. H. *J. Am. Chem. Soc.* **1991**, 113, 875–883.

(16) Jia, G.; Lough, A. J.; Morris, R. H. *Organometallics* **1992**, 11, 161–171.

\* Abstract published in *Advance ACS Abstracts*, July 1, 1995.

(1) Moore, D. S.; Robinson, S. D. *Chem. Soc. Rev.* **1983**, 12, 415–452.

(2) Pearson, R. G. *Chem. Rev.* **1985**, 85, 41–49.

(3) *Transition Metal Hydrides*; Dedieu, A., Ed.; VCH Publishers: New York, 1992.

(4) *Transition Metal Hydrides*; Muetterties, E. L., Ed.; Marcel Dekker: New York, 1971.

(5) Masters, C. *Homogeneous Transition-metal Catalysis—a gentle art*; Chapman and Hall: New York, 1981.

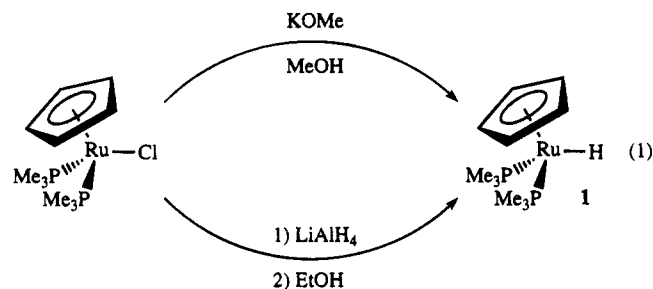
(6) Parshall, G. W.; Ittel, S. D. *Homogeneous Catalysis*, 2nd ed.; John Wiley & Sons: New York, 1992.

(7) Lemke, F. R. *J. Am. Chem. Soc.* **1994**, 116, 11183–11184.

hydride  $\text{Cp}(\text{PMe}_3)_2\text{RuH}$  and the dihydrides  $[\text{Cp}(\text{PMe}_3)_2\text{RuH}_2]\text{X}$  ( $\text{X} = \text{Cl}, \text{BF}_4, \text{B}[3,5-(\text{CF}_3)_2\text{C}_6\text{H}_3]_4$ ) and the crystal structures of  $\text{Cp}(\text{PMe}_3)_2\text{RuH}$  and  $[\text{Cp}(\text{PMe}_3)_2\text{RuH}_2]\text{BF}_4$ . The availability of these structures provides a unique opportunity to investigate the structural changes that occur upon converting a ruthenium(II) hydride to a ruthenium(IV) dihydride.

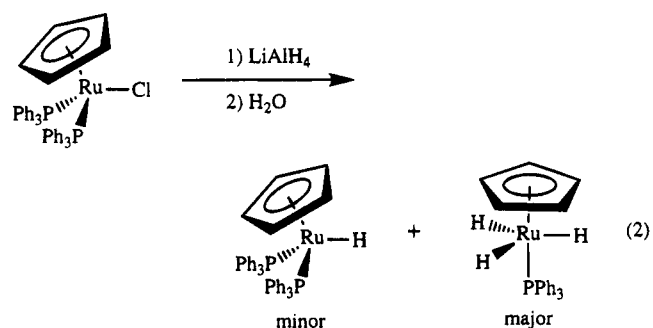
## Results and Discussion

**Synthesis of  $\text{Cp}(\text{PMe}_3)_2\text{RuH}$ .** The neutral hydride  $\text{Cp}(\text{PMe}_3)_2\text{RuH}$  (**1**) was prepared in high yields by a modification of the reported procedure.<sup>17</sup> Hydride **1** was readily prepared by reacting  $\text{Cp}(\text{PMe}_3)_2\text{RuCl}$  with KOMe in refluxing MeOH (eq 1). Due to the extreme solubility



of **1** in common organic solvents, crystallization of **1** from cold solvents results in low yields. However, hydride **1** readily sublimes and can be obtained as a bright yellow microcrystalline solid in high yields (ca. 90%). Similarly, reacting  $\text{Cp}(\text{PMe}_3)_2\text{RuCl}$  with  $\text{KOCD}_3$  in refluxing  $\text{CD}_3\text{OD}$  yields the deuteride  $\text{Cp}(\text{PMe}_3)_2\text{RuD}$  (**1-d<sub>1</sub>**) in good yields with ca. 90% deuterium incorporation at the metal hydride position. Hydride **1** can also be prepared by reacting  $\text{Cp}(\text{PMe}_3)_2\text{RuCl}$  with  $\text{LiAlH}_4$  in  $\text{Et}_2\text{O}$  followed by an EtOH quench (eq 1). Using  $\text{LiAlD}_4$  in  $\text{Et}_2\text{O}$  followed by an EtOD quench also produces **1-d<sub>1</sub>** but with only 70–75% deuterium incorporation at the metal hydride position.

The difference between the reactivity of  $\text{Cp}(\text{PMe}_3)_2\text{RuCl}$  and  $\text{Cp}(\text{PPh}_3)_2\text{RuCl}$  with  $\text{LiAlH}_4$  is noteworthy. Hydride **1** can be prepared in high yields (ca. 90%) from  $\text{Cp}(\text{PMe}_3)_2\text{RuCl}$  and  $\text{LiAlH}_4$  (eq 1). On the other hand, the reaction of  $\text{LiAlH}_4$  with  $\text{Cp}(\text{PPh}_3)_2\text{RuCl}$  generates the hydride  $\text{Cp}(\text{PPh}_3)_2\text{RuH}$  in low yields with the major product being the trihydride  $\text{Cp}(\text{PPh}_3)\text{RuH}_3$  (eq 2).<sup>18</sup>

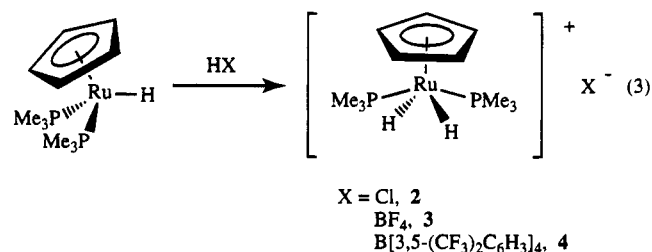


This difference in reactivity can be attributed to a difference in phosphine lability. The lability of the  $\text{PPh}_3$  ligands in  $\text{Cp}(\text{PPh}_3)_2\text{RuCl}$  is well documented, and  $\text{Cp}$ -

$(\text{PPh}_3)_2\text{RuCl}$  is a useful synthon for preparing a variety of other ruthenium(II) complexes,<sup>19</sup> including  $\text{Cp}(\text{PMe}_3)_2\text{RuCl}$ .<sup>20,21</sup> Furthermore, Nolan and co-workers, using anaerobic solution calorimetry, have recently determined that the Ru– $\text{PMe}_3$  bond is stronger than the Ru– $\text{PPh}_3$  bond by 7–8 kcal/mol.<sup>22</sup>

Hydride **1** is extremely air sensitive, turning blue upon exposure to air, and undergoes hydride/chloride metathesis with chlorocarbons. In  $\text{CDCl}_3$ , yellow **1** is completely converted to orange  $\text{Cp}(\text{PMe}_3)_2\text{RuCl}$  within minutes, while in  $\text{CD}_2\text{Cl}_2$  this conversion requires more than a day at room temperature. In the  $^1\text{H}$  NMR spectrum ( $\text{CD}_2\text{Cl}_2$ ), the hydride resonance of **1** is observed at –13.99 ppm as a triplet ( $^2J_{\text{PH}} = 36.8$  Hz). A broad band in the IR spectrum ( $\text{CH}_2\text{Cl}_2$ ) at  $1892\text{ cm}^{-1}$  is assignable to  $\nu(\text{Ru}-\text{H})$  (cf.  $\nu(\text{Ru}-\text{H}) = 1900\text{ cm}^{-1}$  in  $\text{KBr}$ <sup>17</sup>). This assignment is confirmed by the absence of this band in **1-d<sub>1</sub>** and the appearance of a band at  $1365\text{ cm}^{-1}$  assigned to  $\nu(\text{Ru}-\text{D})$ .  $\nu(\text{Ru}-\text{H})/\nu(\text{Ru}-\text{D}) = 1.39$  is observed, close to the calculated ratio of 1.41.

**Synthesis of  $[\text{Cp}(\text{PMe}_3)_2\text{RuH}_2]\text{X}$  ( $\text{X} = \text{Cl}, \text{BF}_4, \text{B}[3,5-(\text{CF}_3)_2\text{C}_6\text{H}_3]_4$ ).** Protonation of  $\text{Cp}(\text{PMe}_3)_2\text{RuH}$  with  $\text{HX}$  ( $\text{X} = \text{Cl}, \text{BF}_4, \text{B}[3,5-(\text{CF}_3)_2\text{C}_6\text{H}_3]_4$ ) in  $\text{Et}_2\text{O}$  or  $\text{CH}_2\text{Cl}_2$  (eq 3) produces the cationic dihydrides  $[\text{Cp}$ -



$(\text{PMe}_3)_2\text{RuH}_2]\text{X}$  [ $\text{X} = \text{Cl}$  (**2**),  $\text{BF}_4$  (**3**),  $\text{B}[3,5-(\text{CF}_3)_2\text{C}_6\text{H}_3]_4$  (**4**)], respectively, as white or light purple solids in high yields (ca. > 90%). Dihydride **2** was previously reported as a product from the reaction of **1** with chlorosilanes.<sup>7</sup> The isotopomers  $[\text{Cp}(\text{PMe}_3)_2\text{RuHD}]\text{BF}_4$  (**3-d<sub>1</sub>**) and  $[\text{Cp}(\text{PMe}_3)_2\text{RuD}_2]\text{BF}_4$  (**3-d<sub>2</sub>**) were prepared by protonating **1-d<sub>1</sub>** with  $\text{HBF}_4 \cdot \text{Et}_2\text{O}$  and  $\text{HBF}_4 \cdot \text{Et}_2\text{O}$  in  $\text{D}_2\text{O}$ , respectively. Deuterium incorporation at the metal hydride positions was 45% for **3-d<sub>1</sub>** and >95% for **3-d<sub>2</sub>**.

In the  $^1\text{H}$  NMR spectra ( $\text{CD}_2\text{Cl}_2$ ), the dihydride resonances for **2-4** are observed around –9.9 ppm (t,  $^2J_{\text{PH}} = 29$  Hz). A small dependence on the counterion is observed for the dihydride resonances [**2** (–9.87 ppm) > **3** (–9.90) > **4** (–9.93)] which parallels the coordinating ability of the counterions;<sup>23</sup> no effect on  $^2J_{\text{PH}}$  is observed. The HD isotopomer **3-d<sub>1</sub>** displayed a triplet at –9.88 ppm ( $^2J_{\text{PH}} = 29$  Hz), corresponding to a downfield isotopic shift of ~20 ppb, with no observable HD coupling.  $T_1$  measurements for **3** at 400 MHz in  $\text{CD}_2\text{Cl}_2$  gave a value of 9.41 s at 293 K which decreased to 1.96 s at 208 K. The broad bands in the IR spectra ( $\text{CH}_2\text{Cl}_2$ ) of **2-4** at  $\sim 1990\text{ cm}^{-1}$  are assigned to  $\nu(\text{Ru}-$

(19) Davies, S. G.; McNally, J. P.; Smallridge, A. J. In *Advances in Organometallic Chemistry*; Stone, F. G. A., West, R., Eds.; Academic Press: New York, 1990; Vol. 30, pp 1–76.

(20) Bruce, M. I.; Wong, F. S.; Skelton, B. W.; White, A. H. *J. Chem. Soc., Dalton Trans.* **1981**, 1398–1405.

(21) Treichel, P. M.; Komar, D. A. *Synth. React. Inorg. Met.-Org. Chem.* **1980**, *10*, 205–218.

(22) Cucullu, M. E.; Luo, L.; Nolan, S. P.; Fagan, P. J.; Jones, N. L.; Calabrese, J. C. *Organometallics* **1995**, *14*, 289–296.

(23) Strauss, S. H. *Chem. Rev.* **1993**, *93*, 927–942.

(17) Mayer, J. M.; Calabrese, J. C. *Organometallics* **1984**, *3*, 1292–1298.

(18) Davies, S. G.; Moon, S. D.; Simpson, S. J. *J. Chem. Soc., Chem. Commun.* **1983**, 1278–1279.

**Table 1.  $pK_a$  Values for Cationic  $[\text{Cp}^*\text{L}_2\text{RuH}_2]^+$  Dihydride Complexes**

complex <sup>a</sup>	$pK_a$	ref
$[\text{Cp}(\text{PPh}_3)_2\text{RuH}_2]^+$	8.3, <sup>b</sup> 8.0 <sup>c</sup>	15
$[\text{Cp}(\text{dpppp})\text{RuH}_2]^+$ <sup>d</sup>	8.4, <sup>b</sup> 8.6 <sup>c</sup>	15
$[\text{Cp}^*(\text{dppp})\text{RuH}_2]^+$ <sup>d</sup>	10.4 <sup>c</sup>	16
$[\text{Cp}^*(\text{PPh}_3)_2\text{RuH}_2]^+$	11.1 <sup>c</sup>	16
$[\text{Cp}^*(\text{PMePh}_2)_2\text{RuH}_2]^+$	12.2 <sup>c</sup>	15, 16
$[\text{Cp}(\text{PMe}_3)_2\text{RuH}_2]^+$	13.9 <sup>b</sup>	this work
$[\text{Cp}^*(\text{PMe}_2\text{Ph})_2\text{RuH}_2]^+$	14.3 <sup>c</sup>	16
$[\text{Cp}^*(\text{PMe}_3)_2\text{RuH}_2]^+$	16.3 <sup>c</sup>	16

<sup>a</sup> The complexes are listed in order of increasing  $pK_a$  value. <sup>b</sup> In  $\text{CH}_2\text{Cl}_2$ . <sup>c</sup> In THF. <sup>d</sup> dppp =  $\text{Ph}_2\text{P}(\text{CH}_2)_3\text{PPh}_2$ .

H). This band is absent in **3-d**<sub>2</sub> and has been replaced by a band at  $1422\text{ cm}^{-1}$  assigned to  $\nu(\text{Ru}-\text{D})$ . In the IR spectrum ( $\text{CH}_2\text{Cl}_2$ ) of the HD isotopomer **3-d**<sub>1</sub>, a weak broad  $\nu(\text{Ru}-\text{H})$  at  $1987\text{ cm}^{-1}$  as well as a strong  $\nu(\text{Ru}-\text{D})$  at  $1422\text{ cm}^{-1}$  is observed ( $\nu(\text{Ru}-\text{H})/\nu(\text{Ru}-\text{D}) = 1.40$ ). The spectroscopic data described above are consistent with a classical ruthenium(IV) dihydride configuration for complexes **2-4** with no evidence for a dihydrogen tautomer. Conroy-Lewis and Simpson had previously noted that  $[\text{Cp}(\text{PMe}_3)_2\text{RuH}_2]^+$  was a classical dihydride but without giving any supporting details.<sup>9</sup> The classical dihydride configuration was also confirmed by a single-crystal X-ray diffraction study on **3** (*vide infra*).

The  $pK_a$  of  $[\text{Cp}(\text{PMe}_3)_2\text{RuH}_2]^+$  in  $\text{CH}_2\text{Cl}_2$  was determined to be 13.9 using Proton Sponge as a reference base (see Experimental Section). Table 1 lists the  $pK_a$  values for several other classical ruthenium(IV) dihydrides. The low acidity of  $[\text{Cp}(\text{PMe}_3)_2\text{RuH}_2]^+$  is consistent with the electron-rich donor ligands (Cp and  $\text{PMe}_3$ ) present on the ruthenium. From the data in Table 1, several observations on ruthenium(IV) dihydride acidity can be made. First, replacing a Cp group with a Cp\* group decreases the acidity by 2–3 pH units. Second, replacing two  $\text{PPh}_3$  groups with two  $\text{PMe}_3$  groups decreases the acidity by 5–6 pH units. Third, replacing a Ph group on the phosphines with a Me group decreases the acidity by approximately 2 pH units.

The  $[\text{Cp}(\text{PMe}_3)_2\text{RuH}_2]^+$  fragment is readily deprotonated by a variety of strong bases such as  $\text{LiNR}_2$  ( $\text{R} = \text{Me}, \text{Pr}^i, \text{SiMe}_3$ ) (the  $pK_a$ 's for  $\text{HNR}_2$  cover the range 30–35<sup>24</sup>). Complications in this deprotonation reaction have been observed when halides ( $\text{Cl}^-$  in **2** and  $\text{F}^-$  from  $\text{BF}_4^-$  in **3**) are present. For example, the deprotonation of **2** with  $\text{LiN}(\text{SiMe}_3)_2$  produces a mixture of  $\text{Cp}(\text{PMe}_3)_2\text{RuH}$  and  $\text{Cp}(\text{PMe}_3)_2\text{RuCl}$ . This complication has been overcome by using excess KOMe as the deprotonating agent ( $pK_a$  of MeOH is 15.2<sup>25</sup>) in refluxing MeOH. Any  $\text{Cp}(\text{PMe}_3)_2\text{RuCl}$  which may form will then be converted to  $\text{Cp}(\text{PMe}_3)_2\text{RuH}$  as described in eq 1.

**Structures of  $\text{Cp}(\text{PMe}_3)_2\text{RuH}$  (1),  $[\text{Cp}(\text{PMe}_3)_2\text{RuH}_2]\text{BF}_4$  (3), and Related Metal Hydrides.** The

(24) Fraser, R. R.; Mansour, T. S. *J. Org. Chem.* **1984**, *49*, 3442–3443.

(25) Reeve, W.; Erikson, C. M.; Aluotto, P. F. *Can. J. Chem.* **1979**, *57*, 2747–2754.

(26) Glueck, D. S.; Winslow, L. J. N.; Bergman, R. G. *Organometallics* **1991**, *10*, 1462–1479.

(27) Klein, D. P.; Kloster, G. M.; Bergman, R. G. *J. Am. Chem. Soc.* **1990**, *112*, 2022–2024.

(28) Stoutland, P. O.; Bergman, R. G. *J. Am. Chem. Soc.* **1988**, *110*, 5732–5744.

(29) Smith, K.-T.; Rømming, C.; Tilset, M. *J. Am. Chem. Soc.* **1993**, *115*, 8681–8689.

(30) Buchanan, J. M.; Stryker, J. M.; Bergman, R. G. *J. Am. Chem. Soc.* **1986**, *108*, 1537–1550.

**Table 2. Atomic Coordinates ( $\times 10^4$ ) and Equivalent Isotropic Displacement Coefficients ( $\text{\AA}^2 \times 10^3$ ) for  $\text{Cp}(\text{PMe}_3)_2\text{RuH}$  (1)**

atom	x	y	z	$U(\text{eq})^a$
Ru	167(1)	2099(1)	2737(1)	26(1)
H	887(90)	2374(56)	3932(83)	60
P(1)	-929(3)	3469(1)	2425(2)	32(1)
P(2)	2211(2)	2520(2)	2235(2)	34(1)
C(1)	-491(10)	877(5)	3662(8)	41(4)
C(2)	434(10)	586(5)	2930(9)	49(4)
C(3)	-310(11)	798(5)	1636(9)	47(4)
C(4)	-1683(10)	1202(5)	1569(8)	39(3)
C(5)	-1759(10)	1244(5)	2824(8)	41(3)
C(11)	-1046(13)	4155(7)	1036(11)	80(6)
C(12)	-364(13)	4300(7)	3681(12)	96(9)
C(13)	-2887(12)	3444(6)	2271(12)	74(6)
C(21)	2109(13)	2950(8)	640(10)	84(6)
C(22)	3567(12)	1596(7)	2351(11)	69(5)
C(23)	3434(11)	3374(7)	3218(11)	69(5)

<sup>a</sup> Equivalent isotropic  $U$  defined as one-third of the trace of the orthogonalized  $U_{ij}$  tensor.

**Table 3. Atomic Coordinates ( $\times 10^4$ ) and Equivalent Isotropic Displacement Coefficients ( $\text{\AA}^2 \times 10^3$ ) for  $[\text{Cp}(\text{PMe}_3)_2\text{RuH}_2]\text{BF}_4$  (3)**

atom	x	y	z	$U(\text{eq})^a$
Ru	0	1975(1)	0	14(1)
P(1)	1006(1)	218(1)	394(1)	15(1)
P(2)	722(1)	3887(1)	738(1)	15(1)
C(1)	-1040(3)	2222(5)	-1704(4)	27(1)
C(2)	-1315(3)	3071(4)	-843(5)	28(1)
C(3)	-1528(3)	2268(5)	93(5)	30(1)
C(4)	-1377(3)	917(5)	-205(5)	30(1)
C(5)	-1068(3)	909(5)	-1302(4)	28(1)
C(11)	551(3)	-1108(4)	1199(4)	23(1)
C(12)	1264(3)	-647(4)	-886(3)	23(1)
C(13)	2180(3)	520(4)	1210(3)	20(1)
C(21)	-55(3)	4899(4)	1476(4)	25(1)
C(22)	1039(3)	5033(4)	-335(4)	27(1)
C(23)	1805(3)	3793(4)	1793(4)	23(1)
B	-1703(4)	7390(4)	-1394(5)	24(1)
F(1)	-806(3)	7714(4)	-1613(4)	49(1)
F(2)	-1792(4)	7867(3)	-294(3)	51(1)
F(3)	-2371(4)	7950(4)	-2253(5)	61(2)
F(4)	-1806(3)	6041(3)	-1410(3)	45(1)

<sup>a</sup> Equivalent isotropic  $U$  defined as one-third of the trace of the orthogonalized  $U_{ij}$  tensor.

crystal structures of  $\text{Cp}(\text{PMe}_3)_2\text{RuH}$  (1) and  $[\text{Cp}(\text{PMe}_3)_2\text{RuH}_2]\text{BF}_4$  (3) have been determined by low-temperature X-ray diffraction at 220 and 123 K, respectively. Atomic coordinates are listed in Tables 2 and 3, and pertinent interatomic distances and angles are presented in Table 4. The molecular structures of **1** and the cation of **3** are shown in Figures 1 and 2.

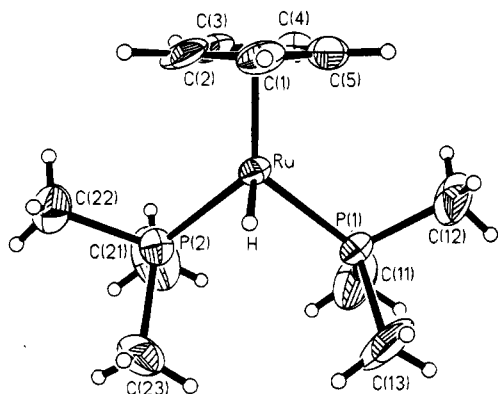
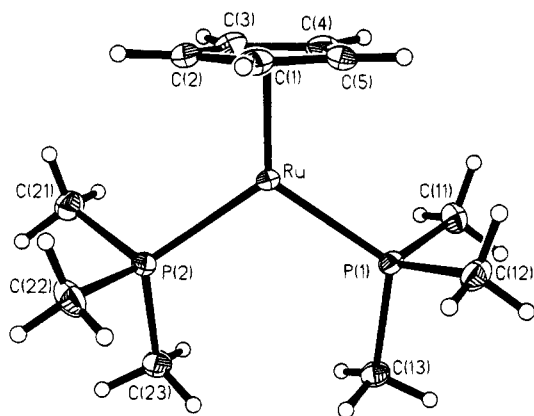
The geometries of **1** and the cation of **3** are best described in terms of "three- and four-legged piano stools", respectively, with the "legs" comprising the phosphine and hydride ligands. Both structures have approximate  $C_s$  symmetry. Although the hydride ligands were not located for **3**, from the comparison with related structures it can readily be inferred that the hydride ligands occupy a *trans* configuration (*vide infra*). Thus, the crystal structure of **3** confirms the absence of an  $\eta^2\text{-H}_2$  ligand as is indicated by the  $^1\text{H}$  NMR data (*vide supra*).

The geometries of related  $d^6\text{ Cp}^*\text{L}_2\text{MH}$ ,  $d^6\text{ Cp}^*\text{L}_2\text{M}(\eta^2\text{-H}_2)$ , and  $d^4\text{ Cp}^*\text{L}_2\text{MH}_2$  complexes are compared in Table 5 with those of **1** and **3**. Although there is some variation among complexes of each type, certain trends clearly emerge. In both the three-legged and four-legged piano stool geometries the plane of the ring



**Table 4. Selected Interatomic Distances (Å), Angles (deg), and Torsion Angles (deg) for Cp(PMe<sub>3</sub>)<sub>2</sub>RuH (1) and [Cp(PMe<sub>3</sub>)<sub>2</sub>RuH<sub>2</sub>]BF<sub>4</sub> (3)**

	1	3
Interatomic Distances <sup>a</sup>		
Ru-H	1.36(8)	
Ru-P(1)	2.248(2)	2.283(1)
Ru-P(2)	2.238(3)	2.288(1)
Ru-X	1.899	1.889
Ru-C(ring)	2.239(9)–2.271(8)	2.219(4)–2.274(5)
C-C	1.385(11)–1.430(12)	1.409(7)–1.433(7)
P(1)-C	1.806(11)–1.808(12)	1.809(4)–1.816(5)
P(2)-C	1.835(10)–1.845(11)	1.807(4)–1.826(5)
Angles <sup>a</sup>		
H-Ru-P(1)	88(4)	
H-Ru-P(2)	86(4)	
P(1)-Ru-P(2)	96.0(1)	110.6(1)
X-Ru-H	118.0	
X-Ru-P(1)	127.6	125.3
X-Ru-P(2)	128.2	124.1
Torsion Angles <sup>a</sup>		
X-Ru-P(1)-C(11)	-103.2	-55.5
X-Ru-P(1)-C(12)	13.3	61.5
X-Ru-P(1)-C(13)	128.8	-177.9
X-Ru-P(2)-C(21)	88.1	42.7
X-Ru-P(2)-C(22)	-30.6	-73.5
X-Ru-P(2)-C(23)	-147.0	163.8

<sup>a</sup> X refers to the Cp(centroid).**Figure 1.** Molecular structure of Cp(PMe<sub>3</sub>)<sub>2</sub>RuH (1) at 220 K shown with 50% probability ellipsoids for non-hydrogen atoms.**Figure 2.** Molecular structure of the cation of 3, [Cp(PMe<sub>3</sub>)<sub>2</sub>RuH<sub>2</sub>]<sup>+</sup>, at 123 K shown with 50% probability ellipsoids for non-hydrogen atoms.

centroid/metal atom/hydride ligand(s) lies perpendicular to the ML<sub>2</sub> plane. It is also evident that the two ligands, L and L' (in 1 and 3, L = L' = PMe<sub>3</sub>), must move away from the Cp' ring in order to accommodate the second hydride ligand. This is clearly demonstrated by con-

sidering the angle between the C<sub>5</sub> plane and the ML<sub>2</sub> plane. For the d<sup>6</sup> Cp'L<sub>2</sub>MH complexes this angle has a mean value of 67.6(13)<sup>o</sup> but has a mean value of 87.6-(4)<sup>o</sup> for the d<sup>4</sup> Cp'L<sub>2</sub>MH<sub>2</sub> complexes. The larger esd for the former reflects the larger distribution of observed angles. The geometries of d<sup>6</sup> Cp'L<sub>2</sub>M(η<sup>2</sup>-H<sub>2</sub>) complexes (mean value 56.1(8)<sup>o</sup>) can also be distinguished from those of the mono- and dihydride complexes on the basis of this interplanar angle. The corresponding interplanar angles for complexes 1 (67.1<sup>o</sup>) and 3 (87.3<sup>o</sup>) lie close to the means for the mono- and dihydride complexes, respectively (Figure 3). This observation confirms the formulation of 3 as a dihydride complex with a four-legged piano stool geometry, even in the absence of locating the hydride ligands crystallographically.

There is little evidence that in general the position of the first hydride ligand changes substantially relative to the cyclopentadienyl ring upon protonation to yield the dihydride species. However, repositioning of the L and L' ligands is quite evident from examination of the angle between the M-H vector(s) and the normal to the ML<sub>2</sub> plane. While the mean value of this angle is 7.9-(12)<sup>o</sup> for the d<sup>6</sup> Cp'L<sub>2</sub>MH complexes, the ML<sub>2</sub> plane moves toward the M-H vector by ca. 20<sup>o</sup> upon protonation to yield the corresponding d<sup>4</sup> Cp'L<sub>2</sub>MH<sub>2</sub> complexes with a mean angle of 30.0(20)<sup>o</sup>. The change in this angle is less dramatic when protonation yields the dihydrogen complexes d<sup>6</sup> Cp'L<sub>2</sub>M(η<sup>2</sup>-H<sub>2</sub>) (mean angle 15.5(18)<sup>o</sup>). Protonation of 1 to yield 3 also results in a reorientation of the methyl groups on phosphorus by a rotation of ca. 40–50<sup>o</sup> about the Ru-P bonds (Figure 3, Table 4).

Another identifiable structural trend is the increase in the L-M-L' angle in the course of the protonation reaction. Such angles for d<sup>6</sup> Cp'L<sub>2</sub>MH complexes are in the range 84–101<sup>o</sup> (mean 93.0(19)<sup>o</sup>), with the exception of a few complexes for which the angle is strongly constrained, as in the dppe ligand. The corresponding angle is enlarged to 101–111<sup>o</sup> (mean 107.2(10)<sup>o</sup>) in the d<sup>4</sup> Cp'L<sub>2</sub>MH<sub>2</sub> complexes, presumably to accommodate the *trans* hydride ligands.

Some complexes listed in Table 5 have geometries that deviate somewhat from the general trends described here. In some cases there appear to be chemical reasons for these deviations; in others these are probably ascribable to erroneous structures. Most notable are the structures of Cp(CO)(PPhFc)FeH (PPhFc = PhP-Fe(η<sup>5</sup>-C<sub>5</sub>H<sub>4</sub>)<sub>2</sub>)<sup>31</sup> and [Cp\*(dppe)FeD]PF<sub>6</sub>-CH<sub>2</sub>Cl<sub>2</sub> (dppe = Ph<sub>2</sub>P(CH<sub>2</sub>)<sub>2</sub>PPh<sub>2</sub>)<sup>38</sup>. In the former, the direction of

(31) Butler, I. R.; Cullen, W. R.; Rettig, S. J. *Organometallics* **1987**, *6*, 872–880.(32) Lister, S. A.; Redhouse, A. D.; Simpson, S. J. *J. Acta Crystallogr.* **1992**, *C48*, 1661.

(33) Lister, S. Ph.D. Thesis, University of Salford, 1992.

(34) Bruce, M. I.; Butler, I. R.; Cullen, W. R.; Koutsantonis, G. A.; Snow, M. R.; Tiekink, E. R. T. *Aust. J. Chem.* **1988**, *41*, 963–969.(35) Cotrait, M.; Bideau, J. P.; Gallois, B.; Ruiz, J.; Astruc, D. *Bull. Soc. Chim. Fr.* **1992**, *129*, 329.(36) Hitchcock, P. B.; Matos, R. M.; Nixon, J. F. *J. Organomet. Chem.* **1993**, *462*, 319–329.(37) Mingos, D. M. P.; Minshall, P. C.; Hursthouse, M. B.; Malik, K. M. A.; Willoughby, S. D. *J. Organomet. Chem.* **1979**, *181*, 169–182.(38) Hamon, P.; Toupet, L.; Hamon, J.-R.; Lapinte, C. *Organometallics* **1992**, *11*, 1429–1431.(39) Klooster, W. T.; Koetzle, T. F.; Jia, G.; Fong, T. P.; Morris, R. H.; Albinati, A. *J. Am. Chem. Soc.* **1994**, *116*, 7677–7681.(40) Herrmann, W. A.; Theiler, H. G.; Herdtweck, E.; Kiprof, P. *J. Organomet. Chem.* **1989**, *367*, 291–311.(41) Fernandez, M.-J.; Bailey, P. M.; Bentz, P. O.; Ricci, J. S.; Koetzle, T. F.; Maitlis, P. M. *J. Am. Chem. Soc.* **1984**, *106*, 5458–5463.

**Table 5. Geometries of d<sup>6</sup> Cp'L<sub>2</sub>MH, d<sup>6</sup> Cp'L<sub>2</sub>M(η<sup>2</sup>-H<sub>2</sub>), and d<sup>4</sup> Cp'L<sub>2</sub>MH<sub>2</sub> Complexes (deg)<sup>a</sup>**

compd	Cp'-ML <sub>2</sub> <sup>b</sup>	L-M-L'	X-M-H <sup>c</sup>	MH-ML <sub>2</sub> <sup>d</sup>	XMH-ML <sub>2</sub> <sup>e,e</sup>	CSD REFCODE <sup>f</sup>	ref
d <sup>6</sup> Cp'L <sub>2</sub> MH							
Cp*(PPh <sub>3</sub> )(OPr <sup>t</sup> )IrH	59.1	84.0	124.8	4.2	87.0	KIVPIO	26
Cp*(PMe <sub>3</sub> )(SBu <sup>t</sup> )IrH	60.5	87.4	129.5	10.7	84.0	KELDIO	27
Cp*(PMe <sub>3</sub> )(CH=CH <sub>2</sub> )IrH	61.3	85.8	127.5	8.0	88.5	DAMOS10	28
Cp(PPh <sub>3</sub> ) <sub>2</sub> RuH	65.5	100.7	124.8	16.4	76.5	PEYDUS	29
Cp*(PMe <sub>3</sub> )(C <sub>6</sub> H <sub>11</sub> )IrH <sup>g</sup>	66.8	89.2	122.8	9.0	85.2	DOPWAG	30
	67.1	88.6	118.6	5.2	86.1		
Cp(PMe <sub>3</sub> ) <sub>2</sub> RuH	67.1	96.0	118.0	4.9	88.8		this work
Cp(CO)(PPhFc)FeH	67.8	91.3	99.4	-13.3	89.9	FOHGEO	31
Cp(dppp)RuH	67.9	91.8	120.0	7.9	87.4	VUBXUL	32, 33
Cp(dppFc)RuH <sup>g</sup>	68.9	99.1				GIGCAA	34
	71.7	95.5					
Cp(PPh <sub>3</sub> ) <sub>2</sub> FeH	69.4	100.9	116.5	6.9	85.7	JUNYUM	35
Cp*(PPh <sub>3</sub> )LRhH <sup>h</sup>	69.8	94.5				WEHCAN	36
Cp(dppm)FeH	72.3	75.2	121.1	12.8	89.4	JUNYOG	35
[Cp*(PPh <sub>3</sub> ) <sub>2</sub> RhH]PF <sub>6</sub>	79.2	99.9				MCTPRH	37
[Cp*(dippe)FeD]PF <sub>6</sub> CH <sub>2</sub> Cl <sub>2</sub> <sup>i</sup>	89.6	88.4	120.4	28.4	83.2	KUCFET	38
mean dimensions <sup>j</sup>	67.6(13) <sup>k</sup>	93.0(19) <sup>l</sup>	122.4(15) <sup>k,m</sup>	7.9(12) <sup>k,m</sup>	85.9(12) <sup>k,m</sup>		
d <sup>6</sup> Cp'L <sub>2</sub> M(η <sup>2</sup> -H <sub>2</sub> )							
[Cp*(dppm)Ru(η <sup>2</sup> -H <sub>2</sub> )]PF <sub>6</sub> <sup>g</sup>	55.6	71.5	120.6, 128.9	9.2, 15.7	74.5, 81.9		33
	55.1	71.5	119.4, 124.2	14.3, 31.9	60.0, 75.7		
[Cp*(dppm)Ru(η <sup>2</sup> -H <sub>2</sub> )]BF <sub>4</sub> <sup>n</sup>	57.7	71.3	118.6, 119.4	18.8, 19.3	71.5, 71.8		39
mean dimensions <sup>j</sup>	56.1(8)		121.9(16)	15.5(18) <sup>o</sup>	72.6(29)		
d <sup>4</sup> Cp'L <sub>2</sub> MH <sub>2</sub>							
[Cp*(dippe)RuH <sub>2</sub> ]PF <sub>6</sub>	85.7	87.0	116.6, 117.2	22.6, 31.4	87.3, 88.4		33
Cp*(PPhMe <sub>2</sub> ) <sub>2</sub> ReH <sub>2</sub>	86.5	101.6	114.0, 115.1	23.8, 25.8	85.7, 88.0	SAWNUZ	40
Cp*(SiEt <sub>3</sub> ) <sub>2</sub> RhH <sub>2</sub> <sup>n</sup>	86.7	107.9	131.8, 133.4	37.7, 47.5	90.0, 90.0	CONFQ01	41
Cp*(SiEt <sub>3</sub> ) <sub>2</sub> IrH <sub>2</sub> <sup>n</sup>	87.2	109.5	129.8, 130.7	35.8, 44.7	90.0, 90.0	CIWJAT10	42
[Cp(PMe <sub>3</sub> ) <sub>2</sub> RuH <sub>2</sub> ]BF <sub>4</sub>	87.3	110.7					this work
[Cp(PPh <sub>3</sub> ) <sub>2</sub> OsH <sub>2</sub> ]CF <sub>3</sub> SO <sub>3</sub> CH <sub>2</sub> Cl <sub>2</sub>	87.5	105.7	118.1, 119.7	27.3, 31.7	82.7, 85.6	PESGEZ	43
[Cp*(dippe)FeH <sub>2</sub> ]BPh <sub>4</sub>	87.8	90.6	114.0, 115.1	21.1, 28.2	87.6, 88.2		44
[Cp*(PPh <sub>3</sub> ) <sub>2</sub> RuH <sub>2</sub> ]PF <sub>6</sub> CH <sub>2</sub> Cl <sub>2</sub>	88.9	105.6	111.8, 116.1	22.7, 25.4	85.9, 90.0		33
Cp(PPh <sub>3</sub> ) <sub>2</sub> ReH <sub>2</sub> C <sub>6</sub> H <sub>5</sub>	89.2	108.6	107.4, 114.6	16.0, 26.2	88.3, 87.5	FIZLUV	45
Cp*(SiHClMes)(PPR <sub>3</sub> )RuH <sub>2</sub>	89.6	107.7	121.9, 125.3	33.8, 38.6	73.5, 77.8	YAGKAS	46
mean dimensions <sup>j</sup>	87.6(4)	107.2(10) <sup>l</sup>	119.6(18)	30.0(20)	87.8(6) <sup>p</sup>		

<sup>a</sup> Cp' = Cp (C<sub>5</sub>H<sub>5</sub>), Cp\* (C<sub>5</sub>Me<sub>5</sub>), Cp<sup>†</sup> (C<sub>5</sub>H<sub>4</sub>Me); L = CO, PR<sub>3</sub>, PAR<sub>3</sub>, PR<sub>2</sub><sup>-</sup>, R<sup>-</sup>, OR<sup>-</sup>, SR<sup>-</sup>, SiR<sub>3</sub><sup>-</sup>; L<sub>2</sub> = diphosphines. PPhFc = PhP{Fe[(η<sup>5</sup>-C<sub>5</sub>H<sub>4</sub>)<sub>2</sub>]}, dppm = Ph<sub>2</sub>PCH<sub>2</sub>PPh<sub>2</sub>, dippe = Ph<sub>2</sub>P(CH<sub>2</sub>)<sub>2</sub>PPh<sub>2</sub>, dippe = Pr<sub>2</sub>P(CH<sub>2</sub>)<sub>2</sub>PPR<sub>2</sub>, dppFc = Fe(η<sup>5</sup>-C<sub>5</sub>H<sub>4</sub>PPH<sub>2</sub>)<sub>2</sub>. <sup>b</sup> Angle between mean planes of the C<sub>5</sub> ring and the ML<sub>2</sub> fragment. <sup>c</sup> Centroid(Cp')-M-H angle. X refers to the centroid. <sup>d</sup> Angle between the M-H vector and the normal to the ML<sub>2</sub> plane. A negative value indicates that the M-H vector points toward the Cp' ring when viewed from the ML<sub>2</sub> plane. <sup>e</sup> Angle between the XMH plane and the ML<sub>2</sub> plane. <sup>f</sup> Reference code for the Cambridge Structural Database (see: Allen, F. H.;

Kennard, O.; Taylor, R. *Acc. Chem. Res.* **1983**, *16*, 146). <sup>g</sup> Two crystallographically independent molecules. <sup>h</sup> L = (PPC(Bu<sup>t</sup>)PC(Bu<sup>t</sup>)). <sup>i</sup> Reported as d<sup>5</sup> Fe(III), may actually be d<sup>4</sup> [Cp\*(dippe)FeXD]<sup>+</sup> (see text). <sup>j</sup> Sample esd's, reported in the last significant digit, are calculated according to  $[\sum(d_i - \langle d \rangle)^2/n(n-1)]^{1/2}$ . <sup>k</sup> The value for [Cp\*(dippe)FeD]PF<sub>6</sub>CH<sub>2</sub>Cl<sub>2</sub> was excluded as this is believed to be incorrect (see text). <sup>l</sup> Compounds for which L<sub>2</sub> = diphosphine are excluded from the calculation of the mean. <sup>m</sup> The value for Cp(CO)(PPhFc)FeH was excluded as this is believed to be incorrect (see text). <sup>n</sup> Neutron diffraction studies. <sup>o</sup> The angle 31.9° was excluded on the basis that it is a statistical outlier. <sup>p</sup> The values for Cp\*(SiHClMes)(PPR<sub>3</sub>)RuH<sub>2</sub> were excluded on the basis that these are statistical outliers.

the M-H bond deviates by ca. 20° toward the Cp ring from that observed in all the other d<sup>6</sup> Cp'L<sub>2</sub>MH complexes, even though the relative positions of the other ligands fit the general trend very well. The authors report that the hydride was included in a calculated position. It appears that this calculated position is in error. Perhaps more interesting is the structure of the 17-electron d<sup>5</sup> [Cp\*(dippe)FeD]<sup>+</sup> cation. The unusual feature of the structure is that the FeP<sub>2</sub> plane is orthogonal (89.6°) to the plane of the C<sub>5</sub> ring, *i.e.* the geometry strongly resembles that of the d<sup>4</sup> Cp'L<sub>2</sub>MH<sub>2</sub> complexes rather than the d<sup>6</sup> Cp'L<sub>2</sub>MH complexes, even though only one hydride ligand is reported as present. The structure is also inconsistent with the structure of the related d<sup>5</sup> [Cp\*(dippe)Fe(CH<sub>2</sub>OMe)]<sup>+</sup> cation, in which

the Cp\*-FeP<sub>2</sub> interplanar angle is only 62.1°. <sup>47</sup> This suggests that the structure reported as [Cp\*(dippe)FeD]PF<sub>6</sub>CH<sub>2</sub>Cl<sub>2</sub> may in fact be [Cp\*(dippe)Fe(D)(X)]PF<sub>6</sub>CH<sub>2</sub>Cl<sub>2</sub>, where X = H or D, and was not observed crystallographically.

In all but two of the mono- and dihydride structures listed in Table 5, the M-H vector lies in a plane that is essentially perpendicular to both the C<sub>5</sub> ring plane and the ML<sub>2</sub> plane. In addition, little variation arises in the direction of the M-H vector within that plane, as is indicated by the relatively small esds calculated for the means of the X-M-H angle. This is consistent with the fact that, in general, X-ray diffraction has been successful in indicating the *direction* of the M-H bond, even though the M-H bond lengths may be subject to considerable inaccuracy. For the two structures in which the M-H vector lies out of the aforementioned plane, Cp(PPh<sub>3</sub>)<sub>2</sub>RuH<sub>2</sub><sup>29</sup> and Cp\*(PPR<sub>3</sub>)RuH<sub>2</sub>(SiHClMes),<sup>46</sup> it appears reasonable to suggest that the steric requirements of the ligands, L and L', give rise to the deviation of the hydride position from that in related structures.

(42) Ricci, J. S.; Koetzle, T. F.; Fernandez, M.-J.; Maitlis, P. M.; Green, J. J. *Organomet. Chem.* **1986**, *299*, 383-389.

(43) Rottnik, M.; Angelici, R. J. *J. Am. Chem. Soc.* **1993**, *115*, 7267-7274.

(44) Jiménez-Tenorio, M.; Puerta, M. C.; Valerga, P. *Organometallics* **1994**, *13*, 3330-3337.

(45) Jones, W. D.; Maguire, J. A. *Organometallics* **1987**, *6*, 1301-1311.

(46) Campion, B. K.; Heyn, R. H.; Tilley, T. D. *J. Chem. Soc., Chem. Commun.* **1992**, 1201-1203.

(47) Roger, C.; Toupet, L.; Lapinte, C. *J. Chem. Soc., Chem. Commun.* **1988**, 713-715.

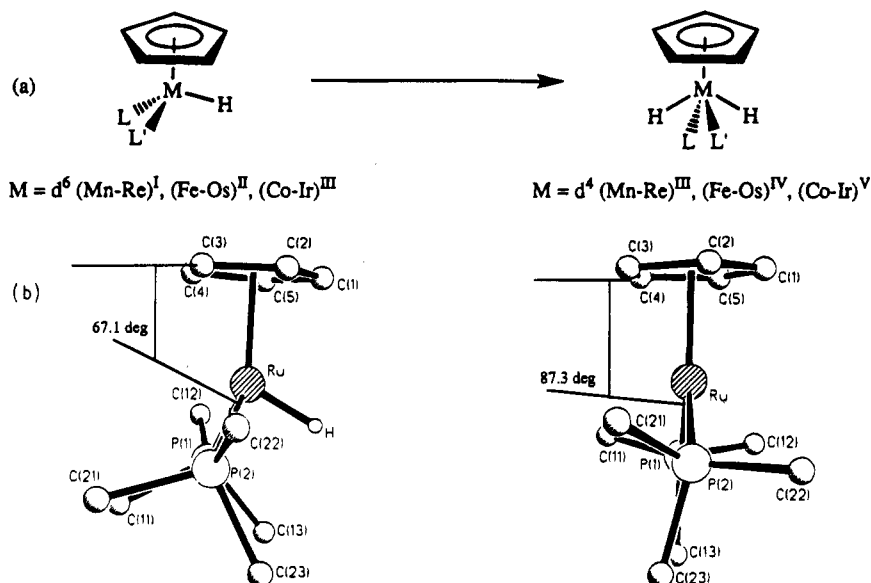


**Figure 3.** (a) Schematic representation of the change in geometry that occurs at the metal center during the protonation of a  $d^6$  Cp'L<sub>2</sub>MH complex. (b) Corresponding change in geometry that occurs in the protonation of **1** to give **3**. The Cp'-ML<sub>2</sub> interplanar angle is indicated; the corresponding mean angle in related dihydrogen complexes [Cp'(dppm)Ru( $\eta^2$ -H<sub>2</sub>)]<sup>+</sup> is 56.1(8)<sup>o</sup>.

### Conclusions

The protonation of the electron-rich hydride Cp(PMe<sub>3</sub>)<sub>2</sub>RuH (**1**) cleanly generates the cationic dihydride [Cp(PMe<sub>3</sub>)<sub>2</sub>RuH<sub>2</sub>]<sup>+</sup> in high yields. The classical dihydride configuration of [Cp(PMe<sub>3</sub>)<sub>2</sub>RuH<sub>2</sub>]<sup>+</sup> was confirmed spectroscopically and crystallographically. A quantitative relationship between the pK<sub>a</sub> of classical dihydrides [Cp'(PMe<sub>x</sub>Ph<sub>3-x</sub>)<sub>2</sub>RuH<sub>2</sub>]<sup>+</sup> (Cp' = C<sub>5</sub>H<sub>5</sub>, C<sub>5</sub>Me<sub>5</sub>;  $x = 0-3$ ) and the ancillary ligands (Cp' and PMe<sub>x</sub>Ph<sub>3-x</sub>) on ruthenium has been investigated. The structural changes that occur upon converting a "three-legged piano stool"  $d^6$  Cp'L<sub>2</sub>MH to either a "four-legged piano stool"  $d^4$  Cp'L<sub>2</sub>MH<sub>2</sub> complex or a  $d^6$  Cp'L<sub>2</sub>M( $\eta^2$ -H<sub>2</sub>) complex have been investigated. Several geometric trends have been established for these complexes. This study also confirms that X-ray diffraction is often useful for indicating the direction of the M-H bond, even though the M-H bond lengths may be subject to considerable systematic error.

### Experimental Section

**General Procedures.** All manipulations of oxygen- or water-sensitive compounds were carried out either under an atmosphere of argon by using Schlenk or vacuum-line techniques or under a helium/argon atmosphere in a Vacuum Atmospheres drybox.<sup>48</sup> <sup>1</sup>H NMR (400 and 250 MHz) spectra were recorded on a Varian VXr 400S and a Bruker AC-250 spectrometer, respectively. The PMe<sub>3</sub> resonances in these compounds do not appear as a simple first-order pattern in the <sup>1</sup>H NMR spectra. The PMe<sub>3</sub> resonances appear as a A<sub>9</sub>-XX'A<sub>9</sub> pattern; the appearance of which is a "filled-in-doublet" with the separation of the outer lines being equal to <sup>2</sup>J<sub>PH</sub> + <sup>4</sup>J<sub>PH</sub>.<sup>49,50</sup> The <sup>1</sup>H chemical shifts were referenced to the residual proton peak of the solvent: C<sub>6</sub>D<sub>6</sub>H,  $\delta$  7.15, and CDHCl<sub>2</sub>,  $\delta$  5.32. IR spectra were recorded on a Mattson Polaris FT-IR spectrometer or a Perkin-Elmer 1600 Series FT-

IR spectrometer. Elemental analyses were carried out by Oneida Research Services or Galbraith Laboratories.

**Materials.** Cp(PMe<sub>3</sub>)<sub>2</sub>RuCl was prepared by a modification of previously reported procedures.<sup>20,21</sup> Severe face rashes have been reported to result from exposure to Cp(PMe<sub>3</sub>)<sub>2</sub>RuCl, so adequate precautions should be taken.<sup>51</sup> [H(Et<sub>2</sub>O)<sub>2</sub>][B(3,5-(CF<sub>3</sub>)<sub>2</sub>C<sub>6</sub>H<sub>3</sub>)<sub>4</sub>] was prepared according to a literature procedure.<sup>52</sup> Anhydrous diethyl ether was stored over [Cp<sub>2</sub>TiCl]<sub>2</sub>ZnCl<sub>2</sub><sup>53</sup> and vacuum transferred immediately prior to use. Dichloromethane was distilled from and stored over CaH<sub>2</sub> and vacuum transferred immediately prior to use. Methanol and methanol-*d*<sub>4</sub> were dried over Mg and vacuum transferred immediately prior to use. Benzene-*d*<sub>6</sub> was dried over NaK and stored over P<sub>2</sub>O<sub>5</sub> and stored over CaH<sub>2</sub>. Acetonitrile-*d*<sub>3</sub> was dried over CaH<sub>2</sub>, stored over Cp<sub>2</sub>Zr(Me)Cl,<sup>54</sup> and vacuum transferred prior to use. Anhydrous HCl(g) was prepared by slowly adding H<sub>2</sub>SO<sub>4</sub>(l) to NaCl(s) and stored over anhydrous CaSO<sub>4</sub>(s) prior to use. KOMe was prepared by reacting solid K with excess MeOH in Et<sub>2</sub>O, collecting the solid by filtration, and drying the white solid under vacuum. KOC<sub>D</sub> was prepared *in situ* by reacting solid K with excess CD<sub>3</sub>OD. PMe<sub>3</sub> (Strem), LiAlH<sub>4</sub> (1 M in Et<sub>2</sub>O; Aldrich), LiAlD<sub>4</sub> (Aldrich), EtOD (Aldrich), HBF<sub>4</sub>·Et<sub>2</sub>O (85%, Aldrich), D<sub>2</sub>O (Cambridge Isotope Laboratories), and Proton Sponge (Aldrich) were used as received.

**Cp(PMe<sub>3</sub>)<sub>2</sub>RuH (1). Method A. From Cp(PMe<sub>3</sub>)<sub>2</sub>RuCl and KOMe.** This method involves a modification of the literature procedure.<sup>17</sup> MeOH (25 mL) was added by vacuum transfer to a flask charged with Cp(PMe<sub>3</sub>)<sub>2</sub>RuCl (840 mg, 2.38 mmol) and KOMe (675 mg, 9.63 mmol). The reaction mixture was heated to reflux 2-3 h, after which time the reaction mixture was evaporated to dryness under vacuum. The reaction residue was extracted with hexanes until the extracts were colorless. The combined hexane extracts were filtered through Celite and evaporated to dryness under vacuum. The yellow residue was sublimed at 60 °C (<0.03 mmHg) to give **1** as a bright yellow solid (675 mg, 88% yield). Typical yields were 85-95%.

(51) Selegue, J. P.; Koutantonis, G. A.; Lompfrey, J. R. *Chem. Eng. News* **1991**, 69, 2.

(52) Brookhart, M.; Grant, B.; Volpe, A. F., Jr. *Organometallics* **1992**, 11, 3920-3922.

(53) Sekutowski, D. G.; Stucky, G. D. *Inorg. Chem.* **1975**, 14, 2192-2199.

(54) Wailes, P. C.; Weigold, H.; Bell, A. P. *J. Organomet. Chem.* **1971**, 33, 181-188.

(48) Shriver, D. F.; Drezdson, M. A. *The Manipulation of Air-Sensitive Compounds*, 2nd ed.; Wiley-Interscience: New York, 1986.

(49) Harris, R. K. *Can. J. Chem.* **1964**, 42, 2275-2281.

(50) Harris, R. K.; Hayter, R. G. *Can. J. Chem.* **1964**, 42, 2282-2291.

**Method B. From Cp(PMe<sub>3</sub>)<sub>2</sub>RuCl and LiAlH<sub>4</sub>.** Et<sub>2</sub>O (30 mL) was added by vacuum transfer to a Schlenk flask charged with Cp(PMe<sub>3</sub>)<sub>2</sub>RuCl (1.531 g, 4.33 mmol) and cooled to -78 °C. LiAlH<sub>4</sub> (6.5 mL, 1.0 M in Et<sub>2</sub>O) was added dropwise by syringe under argon. The orange reaction mixture was allowed to warm to room temperature, during which time it became a yellow solution with a white solid. After 2 h, the yellow slurry was cooled in an ice-water bath, and EtOH (5 mL, 95%, degassed) was added slowly to decompose unreacted LiAlH<sub>4</sub>. Reaction volatiles were removed under vacuum. The yellowish residue was extracted with hexanes until the extracts were colorless. The hexane extracts were filtered through Celite and evaporated to dryness under vacuum. The yellow residue was sublimed at 60 °C (<0.03 mmHg) to give **1** as a bright yellow solid (1.245 g, 90% yield). Typical yields were 80–90%. <sup>1</sup>H NMR (400 MHz, CD<sub>2</sub>Cl<sub>2</sub>): δ 4.54 (s, 5H, Cp), 1.37 (filled-in-doublet, <sup>2</sup>J<sub>PH</sub> + <sup>4</sup>J<sub>PH</sub> = 8.0 Hz, 18H, PMe<sub>3</sub>), -13.99 (t, <sup>2</sup>J<sub>PH</sub> = 36.8 Hz, 1H, RuH). IR (CH<sub>2</sub>Cl<sub>2</sub>): ν(Ru-H) 1892 (br) cm<sup>-1</sup>. IR (KBr): ν(Ru-H) 1906 (br) cm<sup>-1</sup>. Anal. Calcd for C<sub>11</sub>H<sub>24</sub>P<sub>2</sub>Ru: C, 41.37; H, 7.58. Found: C, 41.57; H, 7.15. Crystals of **1** suitable for X-ray diffraction analysis were grown by slow sublimation at 50 °C under vacuum in a sealed tube.

**Cp(PMe<sub>3</sub>)<sub>2</sub>RuD (1-d<sub>1</sub>).** **Method A.** The reaction of Cp(PMe<sub>3</sub>)<sub>2</sub>RuCl (202 mg, 0.57 mmol) and KOCD<sub>3</sub> (190 mg, 2.6 mmol) in refluxing CD<sub>3</sub>OD (5 mL), as described in Method A for **1**, gave **1-d<sub>1</sub>** as a yellow sublimable solid (160 mg, 87% yield, >90% D by <sup>1</sup>H NMR).

**Method B.** The reaction of Cp(PMe<sub>3</sub>)<sub>2</sub>RuCl (200 mg, 0.57 mmol) and LiAlD<sub>4</sub> (35 mg, 0.83 mmol) in Et<sub>2</sub>O (20 mL) followed by an EtOD (2 mL, degassed) quench, as described in Method B for **1**, gave **1-d<sub>1</sub>** as a yellow sublimable solid (148 mg, 81% yield, 72% D by <sup>1</sup>H NMR). <sup>1</sup>H NMR (250 MHz, CD<sub>2</sub>Cl<sub>2</sub>): δ 4.55 (s, 5H, Cp), 1.37 (filled-in-doublet, <sup>2</sup>J<sub>PH</sub> + <sup>4</sup>J<sub>PH</sub> = 8.4 Hz, 18H, PMe<sub>3</sub>). IR (CH<sub>2</sub>Cl<sub>2</sub>): ν(Ru-D) 1365 (br) cm<sup>-1</sup>.

**[Cp(PMe<sub>3</sub>)<sub>2</sub>RuH<sub>2</sub>]Cl (2).** An excess of anhydrous HCl(g) was added to an ethereal solution (10 mL) of Cp(PMe<sub>3</sub>)<sub>2</sub>RuH (84 mg, 0.26 mmol) at -78 °C. A white precipitate formed immediately. After 1 h, the reaction mixture was evaporated to dryness and the residue washed with hexanes. Filtration of the solid followed by vacuum drying gave **2** (91 mg, 97% yield) as a white solid. <sup>1</sup>H NMR (400 MHz, CD<sub>2</sub>Cl<sub>2</sub>): δ 5.38 (s, 5H, Cp), 1.69 (filled-in-doublet, <sup>2</sup>J<sub>PH</sub> + <sup>4</sup>J<sub>PH</sub> = 10.9 Hz, 18H, PMe<sub>3</sub>), -9.87 (t, <sup>2</sup>J<sub>PH</sub> = 29.1 Hz, 2H, RuH). IR (CH<sub>2</sub>Cl<sub>2</sub>): ν(Ru-H) 1989 (br) cm<sup>-1</sup>. Anal. Calcd for C<sub>11</sub>H<sub>26</sub>Cl<sub>2</sub>P<sub>2</sub>Ru: C, 37.13; H, 7.08. Found: C, 36.11; H, 7.31. We were not successful at getting a good elemental analysis for this complex, even though the spectra indicated complete purity of the product.

**[Cp(PMe<sub>3</sub>)<sub>2</sub>RuH<sub>2</sub>]BF<sub>4</sub> (3).** Et<sub>2</sub>O (15 mL) was added by vacuum transfer to a flask charged with **1** (192 mg, 0.60 mmol). HBF<sub>4</sub>·Et<sub>2</sub>O (100 μL, 0.58 mmol) was added to this solution dropwise using a microliter syringe. The resulting precipitate was isolated by filtration, washed with Et<sub>2</sub>O, and dried under vacuum to give a light purple solid (232 mg, 99% yield). <sup>1</sup>H NMR (400 MHz, CD<sub>2</sub>Cl<sub>2</sub>): δ 5.31 (s, 5H, Cp), 1.64 (filled-in-doublet, <sup>2</sup>J<sub>PH</sub> + <sup>4</sup>J<sub>PH</sub> = 10.9 Hz, 18H, PMe<sub>3</sub>), -9.90 (t, <sup>2</sup>J<sub>PH</sub> = 29.3 Hz, 2H, RuH). IR (CH<sub>2</sub>Cl<sub>2</sub>): ν(Ru-H) 1989 (br) cm<sup>-1</sup>. Anal. Calcd for C<sub>11</sub>H<sub>25</sub>BF<sub>4</sub>P<sub>2</sub>Ru: C, 32.45; H, 6.19. Found: C, 32.25; H, 6.52. Crystals of **3** suitable for X-ray diffraction analysis were grown by vapor diffusion of Et<sub>2</sub>O into a CH<sub>2</sub>Cl<sub>2</sub> solution at room temperature.

**[Cp(PMe<sub>3</sub>)<sub>2</sub>RuHD]BF<sub>4</sub> (3-d<sub>1</sub>).** [Cp(PMe<sub>3</sub>)<sub>2</sub>RuHD]BF<sub>4</sub> was prepared from **1-d<sub>1</sub>** (49 mg, 0.15 mmol) and HBF<sub>4</sub>·Et<sub>2</sub>O (26 μL, 0.15 mmol) in Et<sub>2</sub>O as described for **3**. This gave a light purple solid (57 mg, 92% yield, 45% D by <sup>1</sup>H NMR). <sup>1</sup>H NMR (250 MHz, CD<sub>2</sub>Cl<sub>2</sub>): δ 5.31 (s, 5H, Cp), 1.65 (filled-in-doublet, <sup>2</sup>J<sub>PH</sub> + <sup>4</sup>J<sub>PH</sub> = 10.9 Hz, 18H, PMe<sub>3</sub>), -9.88 (t, <sup>2</sup>J<sub>PH</sub> = 29.2 Hz, 1H, RuH). IR (CH<sub>2</sub>Cl<sub>2</sub>): ν(Ru-H) 1987 (br w) cm<sup>-1</sup>, ν(Ru-D) 1422 (br s) cm<sup>-1</sup>.

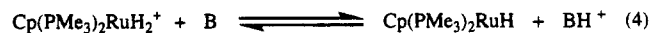
**[Cp(PMe<sub>3</sub>)<sub>2</sub>RuD<sub>2</sub>]BF<sub>4</sub> (3-d<sub>2</sub>).** DBF<sub>4</sub> (100 μL, prepared by mixing HBF<sub>4</sub>·Et<sub>2</sub>O and D<sub>2</sub>O in a 1:3 ratio by volume<sup>15</sup>) was

added dropwise to a solution of **1-d<sub>1</sub>** (56 mg, 0.17 mmol) in Et<sub>2</sub>O. The reaction mixture was evaporated to dryness. The reaction residue was dissolved in CH<sub>2</sub>Cl<sub>2</sub>, and then Et<sub>2</sub>O was added dropwise to initiate precipitation. The resulting solid was filtered out, washed with Et<sub>2</sub>O, and dried under vacuum. This gave **3-d<sub>2</sub>** as a light purple solid (54 mg, 77% yield, >95% D by <sup>1</sup>H NMR). <sup>1</sup>H NMR (250 MHz, CD<sub>2</sub>Cl<sub>2</sub>): δ 5.31 (s, 5H, Cp), 1.64 (filled-in-doublet, <sup>2</sup>J<sub>PH</sub> + <sup>4</sup>J<sub>PH</sub> = 10.9 Hz, 18H, PMe<sub>3</sub>). IR (CH<sub>2</sub>Cl<sub>2</sub>): ν(Ru-D) 1422 (br s) cm<sup>-1</sup>.

**[Cp(PMe<sub>3</sub>)<sub>2</sub>RuH<sub>2</sub>][B(3,5-(CF<sub>3</sub>)<sub>2</sub>C<sub>6</sub>H<sub>3</sub>)<sub>4</sub>] (4).** Methylene chloride (15 mL) was added by vacuum transfer to a flask charged with **1** (75 mg, 0.23 mmol) and [H(Et<sub>2</sub>O)<sub>2</sub>][B(3,5-(CF<sub>3</sub>)<sub>2</sub>C<sub>6</sub>H<sub>3</sub>)<sub>4</sub>] (238 mg, 0.24 mmol) at -78 °C. The reaction solution was allowed to warm to room temperature. After 30 min, the solution was concentrated, and hexane was added to initiate precipitation. The precipitate was isolated, washed with hexane, and dried under vacuum to give a white solid (246 mg, 90% yield). <sup>1</sup>H NMR (250 MHz, CD<sub>2</sub>Cl<sub>2</sub>): δ 7.72 (br, 8H, (CF<sub>3</sub>)<sub>2</sub>C<sub>6</sub>H<sub>3</sub>), 7.57 (br, 4H, (CF<sub>3</sub>)<sub>2</sub>C<sub>6</sub>H<sub>3</sub>), 5.24 (s, 5H, Cp), 1.60 (filled-in-doublet, <sup>2</sup>J<sub>PH</sub> + <sup>4</sup>J<sub>PH</sub> = 10.9 Hz, 18H, PMe<sub>3</sub>), -9.93 (t, <sup>2</sup>J<sub>PH</sub> = 29.4 Hz, 2H, RuH). IR (CH<sub>2</sub>Cl<sub>2</sub>): ν(Ru-H) 1992 (br) cm<sup>-1</sup>. Anal. Calcd for C<sub>43</sub>H<sub>37</sub>BF<sub>24</sub>P<sub>2</sub>Ru: C, 43.64; H, 3.15. Found: C, 43.58; H, 3.04.

**T<sub>1</sub> Measurements on [Cp(PMe<sub>3</sub>)<sub>2</sub>RuH<sub>2</sub>]BF<sub>4</sub> (3).** T<sub>1</sub> values for the hydride protons of **3** (34 mM in CD<sub>2</sub>Cl<sub>2</sub>, 400 MHz) were determined by using a 180-τ-90 pulse sequence. The T<sub>1</sub> value of 9.41 s at 293 K for the hydride resonance decreases to 6.33 s at 263 K and 1.96 s at 208 K.

**pK<sub>a</sub> of [Cp(PMe<sub>3</sub>)<sub>2</sub>RuH<sub>2</sub>]<sup>+</sup>.** For the equilibrium described in eq 4, where K<sub>eq</sub> = [Cp(PMe<sub>3</sub>)<sub>2</sub>RuH][BH<sup>+</sup>]/[Cp(PMe<sub>3</sub>)<sub>2</sub>RuH<sub>2</sub><sup>+</sup>]-



[B], the acidity of [Cp(PMe<sub>3</sub>)<sub>2</sub>RuH<sub>2</sub>]<sup>+</sup> (pK<sub>a</sub>) can be expressed by the equation

$$\text{pK}_a = \text{pK}_{\text{eq}} + \text{pK}_{\text{BH}^+}$$

For BH<sup>+</sup>, where B = Proton Sponge (1,8-bis(dimethylamino)naphthalene), a pK<sub>BH<sup>+</sup></sub> = 12.34 in H<sub>2</sub>O was determined by Alder *et al.*<sup>55</sup> Kristjánssdóttir and Norton observed the following relationship between acidities in aqueous and acetonitrile media: pK<sub>a</sub>(CH<sub>3</sub>CN) = pK<sub>a</sub>(H<sub>2</sub>O) + 7.5.<sup>56</sup> Dissolving equimolar quantities of **3** and Proton Sponge (pK<sub>a</sub>(CH<sub>3</sub>CN) = 19.8) in CD<sub>3</sub>CN gave a pK<sub>eq</sub> = 1.6, as determined by <sup>1</sup>H NMR spectroscopy using Si(SiMe<sub>3</sub>)<sub>4</sub> as an internal standard, and thus a pK<sub>a</sub>(CH<sub>3</sub>CN) = 21.4 for [Cp(PMe<sub>3</sub>)<sub>2</sub>RuH<sub>2</sub>]<sup>+</sup>. This corresponds to a pK<sub>a</sub>(CH<sub>2</sub>Cl<sub>2</sub>) = 13.9 for [Cp(PMe<sub>3</sub>)<sub>2</sub>RuH<sub>2</sub>]<sup>+</sup> assuming that pK<sub>a</sub>(H<sub>2</sub>O) approximately equals pK<sub>a</sub>(CH<sub>2</sub>Cl<sub>2</sub>).<sup>15</sup>

**Converting Dihydrides 2–4 to Hydride 1.** The dihydrides **2–4** may be deprotonated by a variety of strong bases, like LiNR<sub>2</sub> (R = Me, Pr<sup>i</sup>, SiMe<sub>3</sub>), but KOMe in MeOH worked the best. For example, MeOH (20 mL) was added by vacuum transfer to a flask charged with **2** (600 mg, 1.69 mmol) and KOMe (500 mg, 7.13 mmol) and equipped with a reflux condenser. The reaction mixture was heated to reflux for 1 h, after which time the reaction was evaporated to dryness under vacuum. The reaction residue was worked-up as described above for **1** in Method A. This gave **1** (496 mg, 92% yield) as a bright yellow solid.

**X-ray Crystal Structure Determinations of Cp(PMe<sub>3</sub>)<sub>2</sub>RuH (1) and [Cp(PMe<sub>3</sub>)<sub>2</sub>RuH<sub>2</sub>]BF<sub>4</sub> (3).** Both crystal structures were solved by direct methods and refined to convergence by full-matrix least-squares using the SHELXTL suite of programs.<sup>57</sup> Data for **3** were corrected for absorption

(55) Alder, R. W.; Bowman, P. S.; Steele, W. R. S.; Winterman, D. R. *Chem. Commun.* **1968**, 723–724.

(56) Kristjánssdóttir, S. S.; Norton, J. R. In *Transition Metal Hydrides*; Dedieu, A., Ed.; VCH Publishers: New York, 1992; pp 309–359.

(57) Sheldrick, G. SHELXTL 4.2. Siemens Analytical X-ray Instruments Inc., Madison, WI, 1991.

**Table 6. Data Collection, Structure Solution, and Refinement Parameters for Cp(PMe<sub>3</sub>)<sub>2</sub>RuH (1) and [Cp(PMe<sub>3</sub>)<sub>2</sub>RuH<sub>2</sub>]BF<sub>4</sub> (3)**

	1	3
cryst system	monoclinic	monoclinic
space group, <i>Z</i>	<i>P</i> 2 <sub>1</sub> / <i>n</i> , <i>Z</i> = 4	<i>C</i> c, <i>Z</i> = 4
<i>a</i> (Å)	9.429(4)	14.310(3)
<i>b</i> (Å)	14.719(7)	10.105(3)
<i>c</i> (Å)	11.002(5)	11.584(4)
$\beta$ (deg)	106.62(3)	99.73(2)
<i>V</i> (Å <sup>3</sup> )	1463.2(11)	1651.1(9)
density (g cm <sup>-3</sup> )	1.450	1.638
temp (K)	220(5)	123(5)
X-ray wavelength (Å)	0.710 73	0.710 73
$\mu$ (Mo K $\alpha$ ) (mm <sup>-1</sup> )	1.258	1.166
2 $\theta$ range (deg)	4.0–45.0	4.0–70.0
reflens colld	1935	3948
indepdt reflens ( <i>R</i> <sub>int</sub> )	1712 (0.072)	3769 (0.062)
obsd ( <i>F</i> > 3.0 $\sigma$ ( <i>F</i> ))	1478	3563
L. S. params	130	178
<i>R</i> ( <i>F</i> ), <i>R</i> <sub>w</sub> ( <i>F</i> )	0.046, 0.058	0.034, 0.040
<i>S</i> ( <i>F</i> )	1.26	1.04

by semi-empirical methods.<sup>57</sup> All non-hydrogen atoms were refined anisotropically; methyl and cyclopentadienyl hydrogens were included in calculated positions and refined using a riding model with fixed isotropic displacement parameters. The hydride ligand for **1** was located from the difference map and

refined with no positional constraints but with a fixed isotropic displacement parameter. Experimental data pertinent to both structure determinations are given in Table 6.

**Acknowledgment.** F.R.L. acknowledges the donors of the Petroleum Research Fund, administered by the American Chemical Society, for support of this research. F.R.L. also thanks Dr. Cathy Sultany of the Ohio University Instrument Center for help in obtaining <sup>1</sup>H (400 MHz) spectra and *T*<sub>1</sub> measurements. L.B. is grateful for funding from the Donors of the Petroleum Research Fund, administered by the American Chemical Society, and from the University of Missouri Research Board.

**Supporting Information Available:** Tables of X-ray crystallographic data, hydrogen positional and displacement parameters, anisotropic displacement parameters, and interatomic distances and angles (10 pages). This material is contained in many libraries on microfiche, immediately follows this article in the microfilm version of the journal, and can be ordered from the ACS; see any current masthead page for ordering information.

OM950146K

# Trimetallic Aluminum and Gallium Alkyl Complexes with Tetradentate (N<sub>2</sub>O<sub>2</sub>) Ligands

David A. Atwood\* and Drew Rutherford

Department of Chemistry, North Dakota State University, Fargo, North Dakota 58105

Received May 15, 1995<sup>⊙</sup>

The present work describes the synthesis and characterization of a series of complexes of formula LAlR(AIR<sub>2</sub>)<sub>2</sub> (R = Et, L = Salean (1), Salpan (2), Salophan (3), Salomphan (4); R = <sup>i</sup>Bu, L = Salean (5), Salpan (6), Salophan (7), Salomphan (8)). The use of the comparatively bulky <sup>i</sup>Bu group in 5 results in a complex which adopts a cis ligand configuration as shown by an X-ray structural analysis. The trimetallic complexes display <sup>1</sup>H NMR spectra that are consistent with a rigid solution-state geometry. The presence of a deshielding interaction between the protons on the alkyl group 13 reagent and the arylamine backbones of the Salophan and Salomphan ligands will be discussed. Additionally, the crystal structures of SalophanGaMe(GaMe<sub>2</sub>)<sub>2</sub> (9) and SalomphanGaMe(GaMe<sub>2</sub>)<sub>2</sub> (10) are reported.

## Introduction

Tetradentate Schiff base molecules, known generally as SalenH<sub>2</sub> (Figure 1a), have had a long, and continuing, history with the transition-metal elements.<sup>1</sup> Comparatively, main-group-element complexes with these ligands have been rare. There have been reports of Salen complexes with zinc,<sup>2</sup> aluminum alkyls<sup>3</sup> and alkoxides,<sup>4</sup> and gallium alkyls.<sup>5</sup> More recently, these ligands have been used to prepare a new class of aluminum cations which demonstrate catalytic activity for the oligomerization of oxiranes.<sup>6</sup>

The reduced form of this ligand (Figure 1b) should also be useful in the formation of unique main-group-element complexes. These ligands not only offer greater flexibility than the Schiff base analogs but also possess two additional sites capable of  $\sigma$  bonding. Previous reports have shown that all four  $\sigma$ -bonding sites can be used in the preparation of a new class of aluminum anions<sup>7</sup> and in the formation of trimetallic aluminum<sup>8</sup> and gallium<sup>9</sup> complexes of general formula LMR(MR<sub>2</sub>)<sub>2</sub> (L = Salean, Salpan, Salophan, Salomphan; R = alkyl).

The present work represents a continuation of the study of the structure and bonding in the trimetallic derivatives. In particular, the series of complexes of formula LAlR(AIR<sub>2</sub>)<sub>2</sub> (R = Et, L = Salean (1), Salpan (2), Salophan (3), Salomphan (4); R = <sup>i</sup>Bu, L = Salean (5), Salpan (6), Salophan (7), Salomphan (8)) are reported (SaleanH<sub>4</sub> = *N,N'*-bis(*o*-hydroxybenzyl)-1,2-diaminoethane, SalpanH<sub>4</sub> = *N,N'*-bis(*o*-hydroxybenzyl)-1,3-diaminopropane, SalophanH<sub>4</sub> = *N,N'*-bis(*o*-hydroxy-

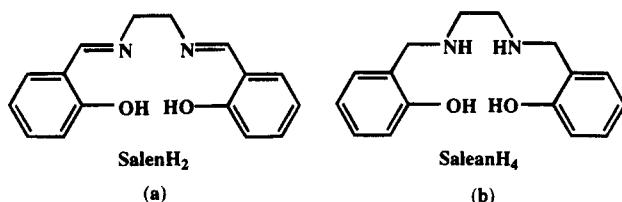
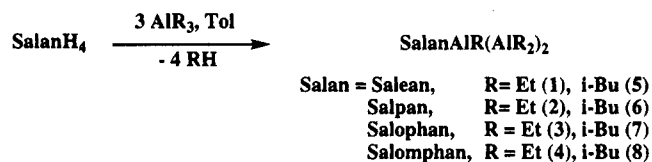


Figure 1. The Schiff base ligand SalenH<sub>2</sub> (a) and the reduced derivative SaleanH<sub>4</sub> (b).

## Scheme 1. General Syntheses of Compounds 1–8



benzyl)-1,2-diaminobenzene, SalomphanH<sub>4</sub> = *N,N'*-bis(*o*-hydroxybenzyl)-1,2-diamino-4,5-dimethylbenzene). These complexes, like those reported previously,<sup>8,9</sup> display <sup>1</sup>H NMR spectra that are consistent with a rigid solution-state geometry. The presence of a shielding ring current interaction between the protons on the alkyl group 13 moiety and the arylamine backbones of the Salophan and Salomphan ligands will be discussed. Additionally, the crystal structures of SaleanAl<sup>*i*</sup>Bu(Al<sup>*i*</sup>Bu<sub>2</sub>)<sub>2</sub> (5), SalophanGaMe(GaMe<sub>2</sub>)<sub>2</sub> (9), and SalomphanGaMe(GaMe<sub>2</sub>)<sub>2</sub> (10) are reported.

## Results and Discussion

**Synthesis and Characterization.** Compounds 1–8 were prepared by the exothermic reaction of the respective SalanH<sub>4</sub> ligand with trialkyl aluminum in a 1:3 stoichiometry (Scheme 1). The gallium derivatives 9 and 10 were prepared as previously reported.<sup>9</sup> The products were isolated in yields of 88–96%. Compounds 1–10 are moderately air sensitive and decompose on standing in air after 4 h. However, they react immediately with water. The <sup>27</sup>Al NMR for 1–8 consisted of two signals in the range  $\delta$  50–77 and 157–220 ppm, which could be attributed to the central and terminal aluminum atoms, respectively, in a trimetallic array (Table 1).

<sup>⊙</sup> Abstract published in *Advance ACS Abstracts*, July 15, 1995.  
 (1) (a) Holm, R. H.; Everett, G. W., Jr.; Chakravorty, A. *Prog. Inorg. Chem.* **1966**, *7*, 83. (b) Hobday, M. D.; Smith, T. D. *Coord. Chem. Rev.* **1972**, *9*, 311.  
 (2) (a) Hall, D.; Moore, F. H. *Proc. Chem. Soc.* **1960**, 256. (b) O'Connor, M. J.; West, B. O. *Aust. J. Chem.* **1967**, *20*, 2077.  
 (3) Dzigan, S. J.; Goedken, V. L. *Inorg. Chem.* **1986**, *25*, 2858.  
 (4) Gurian, P. L.; Cheatham, L. K.; Ziller, J. W.; Barron, A. R. *J. Chem. Soc., Dalton Trans.* **1991**, 1449.  
 (5) Chong, K. S.; Rettig, S. J.; Storr, A.; Trotter, J. *Can. J. Chem.* **1977**, *55*, 2540.  
 (6) Atwood, D. A.; Jegier, J. A.; Rutherford, D. *J. Am. Chem. Soc.*, in press.  
 (7) Atwood, D. A.; Rutherford, D. *Inorg. Chem.*, in press.  
 (8) Atwood, D. A.; Jegier, J. A.; Martin, K. J.; Rutherford, D. *Organometallics* **1995**, *14*, 1453.  
 (9) Atwood, D. A.; Rutherford, D. *Organometallics* **1995**, *14*, 2880.

Table 1. Selected NMR Data (ppm) for Compounds 1–8

compd	$^1\text{H}$				$^{27}\text{Al}$ ( $w_{1/2}$ , Hz)	
	PhCH <sub>2</sub>	NCH <sub>2</sub>	NCH <sub>2</sub> CH <sub>2</sub>	AlR <sub>H</sub>	Al (central)	AlR <sub>2</sub>
SaleanAlEt(AlEt <sub>2</sub> ) <sub>2</sub> (1)	3.42	2.52		0.21–1.72	69 (5200)	162 (5400)
	4.37	2.93				
SalpanAlEt(AlEt <sub>2</sub> ) <sub>2</sub> (2)	3.27	2.65	~1.15	0.13–1.56	77 (3120)	175 (14 560)
	4.50	2.95	2.18			
SalophanAlEt(AlEt <sub>2</sub> ) <sub>2</sub> (3)	4.04			-0.73 to +1.48	71 (5200)	159 (15 700)
	4.60					
SalomphanAlEt(AlEt <sub>2</sub> ) <sub>2</sub> (4)	4.13			-0.66 to +1.46	67 (6760)	157 (15 600)
	4.63					
SaleanAl <sup>i</sup> Bu(Al <sup>i</sup> Bu <sub>2</sub> ) <sub>2</sub> (5)	3.55	2.52		0.17–2.45	65 (8200)	180 (30 000)
	4.44	2.98				
SalpanAl <sup>i</sup> Bu(Al <sup>i</sup> Bu <sub>2</sub> ) <sub>2</sub> (6)	3.38	2.75	~1.15	0.21–2.46	50 (7200)	160 (25 000)
	4.57	3.02	~2.15			
SalophanAl <sup>i</sup> Bu(Al <sup>i</sup> Bu <sub>2</sub> ) <sub>2</sub> (7)	4.16			-0.89 to +2.31	55 (7100)	190 (35 000)
	4.69					
SalomphanAl <sup>i</sup> Bu(Al <sup>i</sup> Bu <sub>2</sub> ) <sub>2</sub> (8)	4.23			-0.94 to +2.38	55 (6500)	220 (32 000)
	4.71					

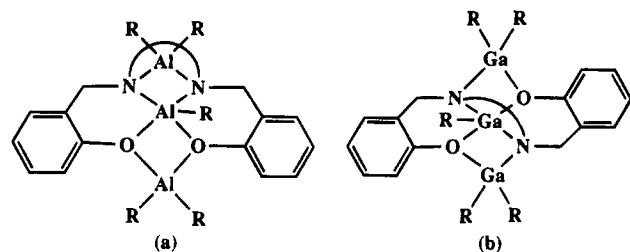


**Figure 2.** General depiction of the SalanMR(MR<sub>2</sub>)<sub>2</sub> molecules showing the cis disposition of the ligand for M = Al (a) and trans disposition of the ligand for M = Ga (b).

In general, the ligands adopt a cis orientation when bound to aluminum (Figure 2a) and a trans orientation when bound to gallium (Figure 2b). However, trimetallic complexes employing the SaleanH<sub>4</sub> ligand (with the ethylamine backbone) always adopt a trans geometry. This trans geometry is currently restricted to the trimetallic derivatives. A structurally characterized, monomeric complex, SaleanH<sub>2</sub>Sn, adopts the cis conformation.<sup>10</sup>

The  $^1\text{H}$  NMR data (Table 1) for these complexes display the doublet of doublet signals for the PhCH<sub>a</sub>H<sub>b</sub> groups which are a hallmark of these species<sup>8,9</sup> and demonstrate that the molecules maintain a rigid solution-state geometry. This type of coupling is also observed for the backbone alkylamine protons of **1**, **2**, **5**, and **6**. All of the complexes demonstrate a cis ligand geometry except **1** (see below). In **1–4** the Al–Et protons were manifested as a complex series of multiplets in the range  $\delta$  –0.73 to +1.72 ppm. Three unique resonances for these groups can be discerned for the Salean complex (**1**), which is indicative of a trans orientation for the ligand. This is the standard configuration for this ligand. In most cases it was difficult to assign the protons more accurately. However, the  $^1\text{H}$  NMR spectrum of **4** was interpretable and indicative of a cis configuration for the ligand (Figure 3). Each of the Et groups are in a unique environment, and there are four triplets for the CH<sub>3</sub> groups (c). Two of these resonances overlap. There are five quartets for the CH<sub>2</sub> groups (d). A similar situation was observed for **8**, although the spectrum was somewhat more complex (Figure 4). Compound **8** also possesses a rigid solution-state geometry, as indicated by the doublet of doublets

for the PhCH<sub>a</sub>H<sub>b</sub> group. Unique environments were also found for the ipso-CH<sub>2</sub> protons, as evidenced by five distinct doublets (c). The secondary CH groups were heavily coupled but still discernible as a series of five overlapping multiplets (d). There were four terminal CH<sub>3</sub> resonances (e) (two overlap). The spectra for the other complexes could be deciphered similarly, only differing in the degree to which the resonances in the range  $\delta$  0.5–1.3 ppm overlapped. As an exception, however, the proton NMR for **5** indicated that the ligand adopted a cis geometry. There were five resonances which could be attributed to the <sup>i</sup>Bu groups, indicating that all of the <sup>i</sup>Bu groups are inequivalent. This is the first instance where the Salean ligand adopts this geometry and may be attributed to the presence of the relatively more sterically demanding <sup>i</sup>Bu groups (compared to Me and Et).

Interestingly, the complexes possessing an arylamine backbone (i.e. **3**, **4**, **7**, and **8**) demonstrate two resonances that are shifted further upfield from those demonstrated for complexes possessing an alkylamine backbone. This trend was also present in the spectroscopic data for the Salophan and Salomphan derivatives of AlMe<sup>8</sup> and GaMe<sup>9</sup> (Table 2). This can be attributed to a ring current effect between the aryl group and the terminal alkyl group 13 moiety. It has been previously demonstrated that the relative shielding effect in these systems varies with the distance of the proton from the aryl group. An optimal value of H···aryl centroid was calculated to be 2.25 Å.<sup>11</sup> At this distance the chemical shift differential between the affected and unaffected protons ( $\Delta\delta$ ) would be maximized. In an extreme example, the chemical shift difference between the geminal hydrogens of the homotropylium cation was shown to be 5.8 ppm.<sup>12</sup> Similarly, the differences between the two methyls of the terminal GaMe<sub>2</sub> groups for **9** and **10** are  $\Delta\delta$  = 0.85 and 0.78 ppm, respectively (Table 2). The closest contact between the hydrogens of these methyl groups and the centroid of the aryl ring is in the range 2.82–3.19 Å. Due to the trans orientation of the ligand, only one set of resonances is observed for each molecule. However, the distances differ slightly in the solid state. When the ligand is in the cis conformation, there are two inequivalent sets of terminal M–Me resonances (as shown in Table 2 for Salo-

(10) Atwood, D. A.; Jegier, J. A.; Martin, K. J.; Rutherford, D. J. *Organomet. Chem.*, in press.

(11) Waugh, J. S.; Fessenden, R. W. *J. Am. Chem. Soc.* **1957**, *79*, 846.

(12) Keller, C. E.; Pettit, R. *J. Am. Chem. Soc.* **1966**, *88*, 604, 606.



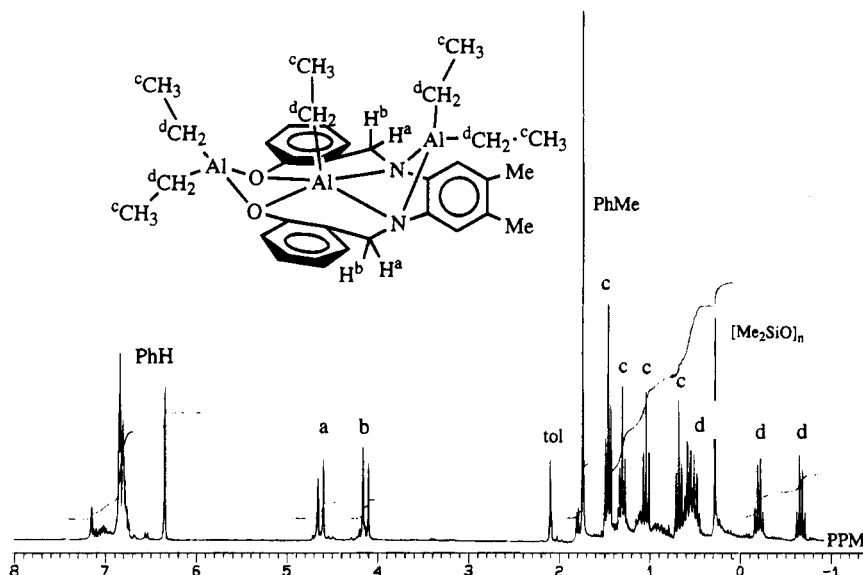


Figure 3.  $^1\text{H}$  NMR spectrum of **4** with chemical shift assignments.

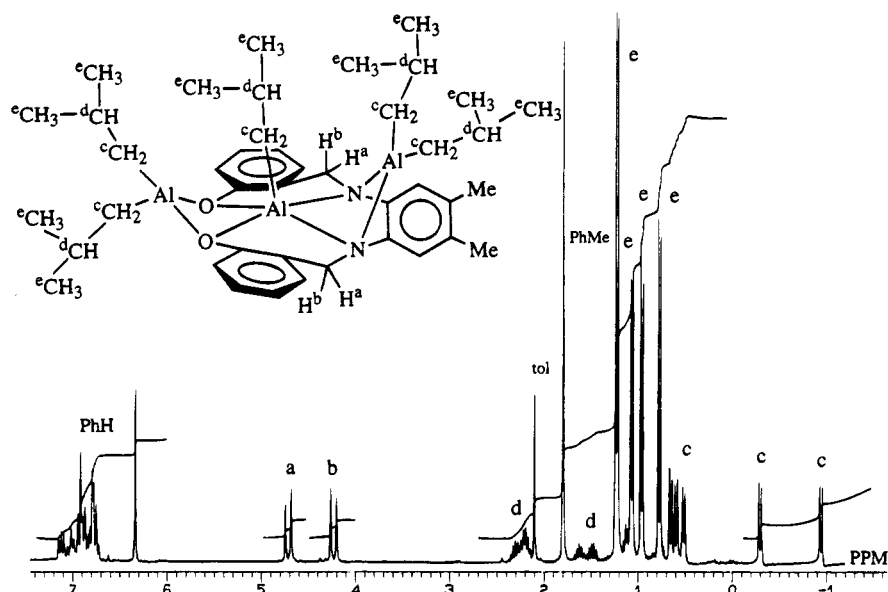


Figure 4.  $^1\text{H}$  NMR spectrum of **8** with chemical shift assignments.

Table 2. Comparison of Chemical Shifts Resulting from the Ring Current Effects of the Salan Ligands Possessing an Arylamine Backbone

compd (contact)	shift ( $\Delta\delta$ , ppm) <sup>a</sup>	dist (Å)	angle 1 (deg) <sup>b</sup>	angle 2 (deg) <sup>c</sup>
SalophanGaMe(GaMe <sub>2</sub> ) <sub>2</sub> ( <b>9</b> ) (Ga-CH <sub>3</sub> ·Ph)	0.85	2.82 2.93	72.6 65.3	82.1 81.4
SalomphanGaMe(GaMe <sub>2</sub> ) <sub>2</sub> ( <b>10</b> ) (Ga-CH <sub>3</sub> ·Ph)	0.78	3.01 3.19	59.5 55.1	80.4 79.6
SalophanAlMe(AlMe <sub>2</sub> ) <sub>2</sub> <sup>8</sup> (Al-CH <sub>3</sub> ·Ph)	0.80 1.00	2.97 3.03	90.8 92.5	64.5 97.7

<sup>a</sup> Defined by subtracting the chemical shift (ppm) of the deshielded group from that of the unaffected group on the same metal. <sup>b</sup> Vertical displacement from ring centroid (ideal 90°). An example of this angle for **9** is given in Figure 5a. <sup>c</sup> Lateral displacement from ring centroid (ideal 90°). An example of this angle for **9** is given in Figure 5b.

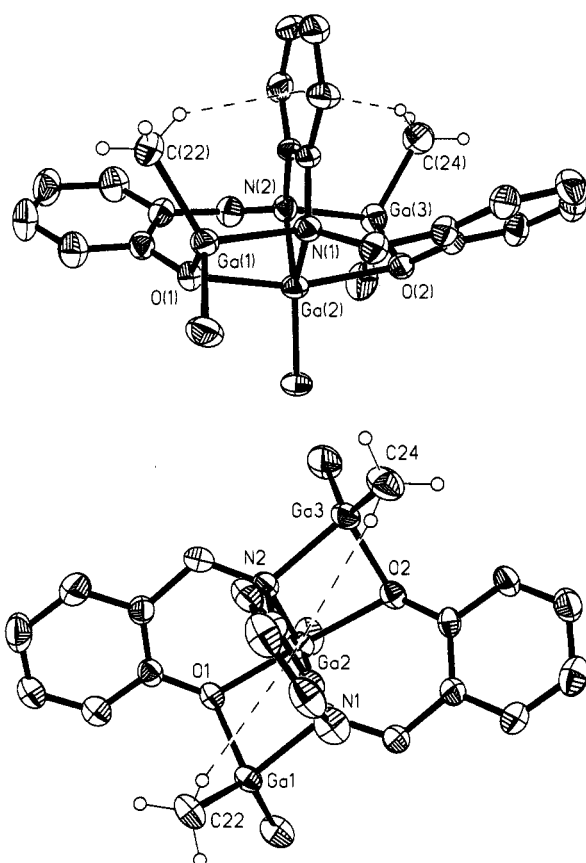
phanAlMe(AlMe<sub>2</sub>)<sub>2</sub>). This contact is maximized when the proton is centered above the aryl group. Thus, the angle that the C-H bond makes with the plane of the aryl group is also important. The greatest shielding would then occur at angles of 90°, directly in line with the magnetic field produced by the aryl ring. For **9** and **10**, these angles are oblique, and consequently the shift is not as pronounced. Views accentuating these two angles are shown in parts a and b of Figure 5, for

compound **9**. By comparison, the angles for Salophan-AlMe(AlMe<sub>2</sub>)<sub>2</sub><sup>9</sup> more closely approach 90° and the shift differential is correspondingly larger ( $\Delta\delta = 1.00$  ppm) (Table 2).<sup>8</sup>

**Structural Characterization.** In order to determine the geometry of complex **5**, an X-ray crystallographic study was undertaken. A summary of crystallographic data is given in Table 3. Selected bond distances and angles are given in Table 4, and positional

**Table 3. Crystal Data for SaleanAl<sup>i</sup>Bu(Al<sup>i</sup>Bu)<sub>2</sub> (5), SalophanGaMe(GaMe)<sub>2</sub> (9), and SalomphanGaMe(GaMe)<sub>2</sub> (10)**

compd	5	9	10
formula	C <sub>36</sub> H <sub>54</sub> Al <sub>3</sub> N <sub>2</sub> O <sub>2</sub>	C <sub>39</sub> H <sub>47</sub> Ga <sub>3</sub> N <sub>2</sub> O <sub>2</sub>	C <sub>27</sub> H <sub>35</sub> Ga <sub>3</sub> N <sub>2</sub> O <sub>2</sub>
fw	627.8	784.9	628.7
cryst syst	monoclinic	triclinic	monoclinic
space group	<i>P</i> 2 <sub>1</sub> / <i>n</i>	<i>P</i> 1	<i>P</i> 2 <sub>1</sub> / <i>n</i>
<i>a</i> (Å)	17.218(3)	9.528(1)	11.377(1)
<i>b</i> (Å)	9.657(2)	10.513(1)	14.294(1)
<i>c</i> (Å)	23.837(4)	17.686(2)	17.490(3)
α (deg)		99.60(1)	
β (deg)	101.070(10)	92.17(1)	100.59(1)
γ (deg)		113.98(1)	
<i>V</i> (Å <sup>3</sup> )	3889.8(12)	1584.9(3)	2796.1(6)
<i>Z</i>	4	2	4
<i>D</i> <sub>calc</sub> (g/cm <sup>3</sup> )	1.072	1.645	1.494
cryst size (mm)	1.8 × 0.4 × 0.3	1.6 × 0.4 × 0.2	1.2 × 0.4 × 0.4
temp (K)	223	298	298
2θ range (deg)	3.5–45	3.5–45	3.5–45
scan type	2θ–θ	2θ–θ	2θ–θ
scan speed (deg min <sup>-1</sup> )	8–60	8–60	8–60
scan range (deg)	0.41	0.46	0.41
no. of rflns collected	6511	4798	4686
no. of indep rflns	5097	3927	3631
no. of obs rflns	2798 ( <i>F</i> > 4.0σ( <i>F</i> ))	2889 ( <i>F</i> > 4.0σ( <i>F</i> ))	2646 ( <i>F</i> > 4.0σ( <i>F</i> ))
no. of params	382	325	307
<i>R</i>	0.0642	0.0564	0.0432
<i>R</i> <sub>w</sub>	0.0673	0.0594	0.0454
GOF	2.51	2.08	2.74
largest diff peak (e/Å <sup>3</sup> )	0.43	1.14	0.58

**Figure 5.** Molecular structure of **9** showing (a, top) the vertical angle between the C–H bond and the aryl ring centroid and (b, bottom) the lateral angle between the C–H bond and the aryl ring centroid.

parameters are given in Table 5. The molecular structure and atom-numbering scheme are shown in Figure 6. The data confirm that the solid-state structure corresponds to that found in solution. The Salean ligand is in a cis geometry with each of the Al<sup>i</sup>Bu<sub>2</sub> units bridging the two nitrogen and two oxygen atoms,

**Table 4. Bond Lengths (Å) and Angles (deg) for SaleanAl<sup>i</sup>Bu(Al<sup>i</sup>Bu)<sub>2</sub> (5)**

Bond Lengths			
Al(1)–Al(2)	2.855(3)	Al(2)–N(1)	1.967(5)
Al(1)–N(1)	1.977(6)	Al(2)–N(2)	1.971(5)
Al(1)–N(2)	1.974(5)	Al(2)–C(25)	1.964(7)
Al(1)–C(17)	1.961(7)	Al(3)–O(1)	1.854(4)
Al(1)–C(21)	1.972(7)	Al(3)–O(2)	1.863(5)
Al(2)–Al(3)	2.941(3)	Al(3)–C(29)	1.978(9)
Al(2)–O(1)	1.913(5)	Al(3)–C(33)	1.966(8)
Al(2)–O(2)	1.914(4)		
Bond Angles			
N(1)–Al(1)–N(2)	73.6(2)	O(1)–Al(3)–C(33)	115.3(3)
N(1)–Al(1)–C(17)	118.9(3)	O(2)–Al(3)–C(33)	111.4(3)
N(2)–Al(1)–C(17)	117.0(3)	C(29)–Al(3)–C(33)	124.4(3)
N(1)–Al(1)–C(21)	112.1(3)	Al(2)–O(1)–Al(3)	102.6(2)
N(2)–Al(1)–C(21)	115.4(3)	Al(2)–O(1)–C(1)	130.2(4)
C(17)–Al(1)–C(21)	114.0(3)	Al(3)–O(1)–C(1)	125.9(4)
O(1)–Al(2)–O(2)	76.2(2)	Al(2)–O(2)–Al(3)	102.3(2)
O(1)–Al(2)–N(1)	88.3(2)	Al(2)–O(2)–C(16)	130.1(4)
O(2)–Al(2)–N(1)	136.3(2)	Al(3)–O(2)–C(16)	124.4(4)
O(1)–Al(2)–N(2)	136.2(2)	Al(1)–N(1)–Al(2)	92.7(2)
O(2)–Al(2)–N(2)	89.5(2)	Al(1)–N(1)–C(7)	126.8(4)
N(1)–Al(2)–N(2)	73.9(2)	Al(2)–N(1)–C(7)	119.9(4)
O(1)–Al(2)–C(25)	104.7(2)	Al(1)–N(1)–C(8)	98.7(4)
O(2)–Al(2)–C(25)	109.7(2)	Al(2)–N(1)–C(8)	100.5(3)
N(1)–Al(2)–C(25)	113.7(2)	Al(1)–N(2)–Al(2)	92.7(2)
N(2)–Al(2)–C(25)	119.1(3)	Al(1)–N(2)–C(9)	99.2(3)
O(1)–Al(3)–O(2)	78.9(2)	Al(2)–N(2)–C(9)	100.0(4)
O(1)–Al(3)–C(29)	107.3(3)	Al(1)–N(2)–C(10)	128.8(4)
O(2)–Al(3)–C(29)	110.3(3)	Al(2)–N(2)–C(10)	119.1(4)

respectively. This leads to inequivalent <sup>i</sup>Bu resonances in the <sup>1</sup>H NMR. This is in contrast to the structures that were determined for SaleanAlMe(AlMe)<sub>2</sub><sup>8</sup> and SaleanGaMe(GaMe)<sub>2</sub>,<sup>9</sup> in which the ligand adopts a trans orientation. The trans orientation allows the hydrogens on the ethylamine backbone to adopt a staggered conformation. However, in **5** these atoms are in an energetically unfavorable eclipsed conformation (maximum deviation 0.015 Å). The strained structure that this implies may be the result of an increase of steric bulk in the series Me < Et < <sup>i</sup>Bu.

The structures of **9** and **10** exemplify the trans geometry found for the gallium trimetallic derivatives.

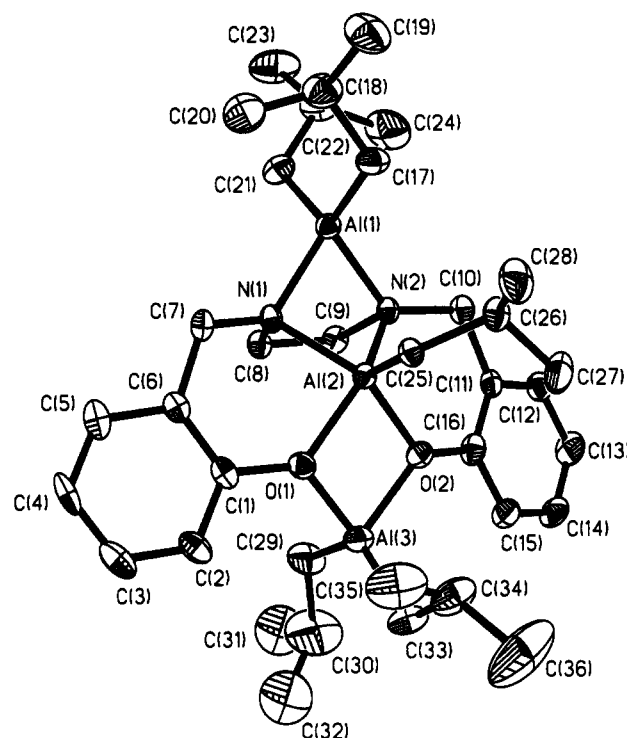
**Table 5. Atomic Coordinates ( $\times 10^5$ ) and Equivalent Isotropic Displacement Coefficients ( $\times 10^4$ ) for  $\text{SaleanAl}^i\text{Bu}(\text{Al}^i\text{Bu}_2)_2$  (5)**

atom	x	y	z	$U(\text{eq}) (\text{\AA}^2)$
Al(1)	10688(11)	7275(21)	84442(8)	341(7)
Al(2)	19221(11)	18854(20)	94837(8)	307(6)
Al(3)	24251(12)	17050(24)	107323(9)	428(8)
O(1)	16045(24)	23875(44)	101826(17)	372(16)
O(2)	27618(24)	12039(44)	100632(17)	381(16)
N(1)	8175(28)	13640(51)	91771(21)	315(18)
N(2)	19682(28)	1654(51)	90459(21)	314(18)
C(1)	8772(39)	28687(63)	102808(29)	366(25)
C(2)	8399(45)	33809(70)	108167(29)	461(28)
C(3)	1458(52)	38765(72)	109375(34)	547(33)
C(4)	-5416(47)	38332(67)	105131(35)	481(31)
C(5)	-5097(41)	32932(67)	99885(32)	452(27)
C(6)	2005(38)	27814(61)	98546(27)	335(24)
C(7)	1728(35)	22920(66)	92531(28)	370(24)
C(8)	7819(36)	-54(64)	94547(27)	354(23)
C(9)	15463(36)	-7969(65)	93744(28)	368(24)
C(10)	27414(35)	-3806(67)	89834(27)	372(24)
C(11)	33231(36)	-5729(71)	95411(28)	358(24)
C(12)	39036(39)	-15939(76)	95665(30)	467(27)
C(13)	44846(42)	-18140(90)	100462(35)	604(32)
C(14)	44939(42)	-10213(85)	105269(33)	556(31)
C(15)	39184(41)	-245(86)	105148(31)	527(29)
C(16)	33332(39)	1977(74)	100327(31)	433(27)
C(17)	12819(41)	21107(75)	78907(28)	483(27)
C(18)	5774(51)	25398(95)	74324(35)	700(35)
C(19)	8304(56)	35072(97)	69917(36)	876(43)
C(20)	-772(52)	31442(106)	76621(37)	899(43)
C(21)	3677(41)	-7892(77)	81016(30)	517(28)
C(22)	5562(52)	-14943(85)	75672(34)	654(35)
C(23)	-694(63)	-25525(96)	73144(39)	1001(47)
C(24)	13598(63)	-21462(109)	76904(42)	1077(53)
C(25)	22424(36)	36370(65)	91768(26)	338(23)
C(26)	29115(37)	37008(71)	88174(30)	415(26)
C(27)	37115(40)	34218(94)	91857(34)	683(34)
C(28)	29165(47)	50842(87)	85181(36)	702(36)
C(29)	20166(50)	681(85)	110822(32)	646(33)
C(30)	23653(95)	-3169(142)	116989(52)	1382(74)
C(31)	20344(113)	-16591(222)	118578(83)	1541(70)
C(32)	22776(119)	7332(223)	121305(87)	1613(76)
C(32A)	30906(178)	-5167(326)	119356(126)	1323(105)
C(33)	31234(47)	31134(86)	111606(31)	646(32)
C(34)	34066(54)	43001(93)	108299(39)	753(37)
C(35)	27873(67)	54130(101)	107070(46)	1111(55)
C(36)	41861(70)	48413(134)	111143(57)	1863(82)

A summary of crystallographic data is given in Table 3. Selected bond distances and angles are given in Table 6, and positional parameters are given in Tables 7 and 8, respectively. The molecular structure and atom-numbering scheme for **10** are shown in Figure 7. Two views of **9** are shown in Figure 5; it is isomorphous with **10**. The central gallium atoms adopt a trigonal-bipyramidal geometry with the oxygen atoms occupying the axial positions and the nitrogens and alkyl carbon making up the equatorial sites. As evidenced by the bond lengths and angles, there is essentially no difference between these molecules. Such distances and angles are in keeping with other structurally characterized examples.

### Conclusion

Trimetallic aluminum and gallium complexes formed using either SalophanH<sub>4</sub> or SalomphanH<sub>4</sub> demonstrate unusual chemical shifts due to ring current effects. The largest shift was observed to be  $\Delta\delta = 1.00$  ppm at a distance of 3.03 Å. The use of the relatively bulky <sup>i</sup>Bu ligand on aluminum leads to a complex (*SaleanAl*<sup>i</sup>Bu(*Al*<sup>i</sup>Bu<sub>2</sub>)<sub>2</sub>) (**5**) which adopts a highly strained cis ligand geometry. This geometry forces the ethylamine back-

**Figure 6.** Molecular structure and atom numbering scheme for **5**.**Table 6. Bond Lengths (Å) and Angles (deg) for Compounds **9** and **10****

	<b>9</b>	<b>10</b>
Bond Distances		
Ga(1)–N(1)	2.030(6)	2.032(6)
Ga(1)–O(1)	1.988(5)	1.982(7)
Ga(2)–O(1)	2.159(5)	2.102(5)
Ga(2)–O(2)	2.194(5)	2.190(5)
Ga(2)–N(1)	1.946(5)	1.961(9)
Ga(2)–N(2)	1.942(5)	1.968(8)
Ga(3)–O(2)	1.971(5)	1.968(6)
Ga(3)–N(2)	2.054(6)	2.071(6)
Bond Angles		
O(1)–Ga(1)–N(1)	82.2(2)	82.4(3)
O(1)–Ga(2)–O(2)	161.0(2)	163.2(3)
O(1)–Ga(2)–N(1)	79.9(2)	81.1(3)
O(1)–Ga(2)–N(2)	87.8(2)	88.5(2)
O(2)–Ga(2)–N(1)	87.2(2)	90.9(6)
O(2)–Ga(2)–N(2)	78.9(2)	80.5(2)
N(1)–Ga(2)–N(2)	92.9(2)	92.6(3)
Ga(2)–O(2)–Ga(3)	90.9(2)	91.9(2)
Ga(1)–N(1)–Ga(2)	97.1(2)	97.6(3)
O(2)–Ga(3)–N(2)	81.8(2)	83.5(2)
Ga(1)–O(1)–Ga(2)	91.8(2)	94.7(2)
Ga(2)–N(2)–Ga(3)	96.1(3)	95.6(3)

bone to adopt an energetically unfavorable eclipsed configuration. A trans geometry for the ligand was found in the crystal structures of SalophanGaMe(*GaMe*<sub>2</sub>)<sub>2</sub> (**9**) and SalomphanGaMe(*GaMe*<sub>2</sub>)<sub>2</sub> (**10**). Current research is focused on exploring the potential of the *SalanMR*(*MR*<sub>2</sub>)<sub>2</sub> complexes toward substitution at the M–C bonds. The indium analogs are also being synthesized and structurally characterized.

### Experimental Section

**General Considerations.** All manipulations were conducted using Schlenk techniques in conjunction with an inert-atmosphere glovebox. All solvents were rigorously dried prior to use. The ligands *Salean*H<sub>4</sub>, *Salpan*H<sub>4</sub>, *Salophan*H<sub>4</sub>, and

**Table 7. Atomic Coordinates ( $\times 10^5$ ) and Equivalent Isotropic Displacement Coefficients ( $\times 10^4$ ) for SalophanGaMe(GaMe<sub>2</sub>)<sub>2</sub> (9)**

atom	x	y	z	U(eq) (Å <sup>2</sup> )
Ga(1)	17662(11)	89639(10)	23575(6)	472(4)
Ga(2)	3215(12)	58508(10)	23940(6)	465(5)
Ga(3)	-28516(13)	37021(11)	25194(6)	554(5)
O(1)	17701(65)	77873(60)	31236(33)	499(27)
O(2)	-16483(66)	41380(58)	16429(34)	488(27)
N(1)	-643(79)	71517(72)	18276(40)	442(32)
N(2)	-13368(81)	57503(73)	30448(40)	464(32)
C(1)	16458(109)	82242(96)	38845(52)	506(44)
C(2)	27984(129)	94535(113)	42988(63)	712(54)
C(3)	27401(147)	99865(122)	50553(67)	821(60)
C(4)	15121(160)	92834(136)	54131(67)	852(67)
C(5)	3190(137)	79895(125)	50076(61)	760(60)
C(6)	3829(114)	74539(98)	42425(52)	533(45)
C(7)	-8731(112)	60074(99)	38636(54)	580(45)
C(8)	-19262(91)	67292(89)	27771(49)	411(37)
C(9)	-30705(110)	69769(104)	31599(62)	631(47)
C(10)	-37112(124)	77884(118)	28414(72)	708(56)
C(11)	-33072(123)	82273(111)	21911(73)	693(54)
C(12)	-21249(114)	80131(106)	18137(64)	641(50)
C(13)	-14562(96)	72294(87)	21557(50)	424(38)
C(14)	-2448(108)	66879(95)	9832(50)	534(44)
C(15)	-16751(107)	54095(95)	6284(51)	498(42)
C(16)	-24278(118)	54034(113)	-616(53)	597(50)
C(17)	-37506(132)	42440(136)	-4406(62)	763(64)
C(18)	-43117(124)	30330(120)	-1103(60)	675(52)
C(19)	-35995(113)	30310(102)	5636(57)	606(46)
C(20)	-22986(98)	42050(92)	9552(48)	445(40)
C(21)	34940(106)	91656(113)	17655(64)	688(51)
C(22)	12189(117)	104929(97)	28272(60)	648(48)
C(23)	17286(117)	49309(113)	23141(62)	710(55)
C(24)	-49256(111)	35443(119)	22830(68)	769(54)
C(25)	-22407(156)	24044(111)	29805(70)	918(67)
C(26)	112569(176)	5769(162)	3783(90)	1036(44)
C(27)	102942(401)	9569(310)	6865(167)	2314(117)
C(28)	90964(261)	12078(229)	8331(122)	628(54)
C(29)	85264(346)	2942(340)	2680(183)	2227(110)
C(30)	51326(427)	35133(384)	46375(206)	1236(107)
C(31)	56906(323)	45784(313)	51540(168)	951(80)
C(32)	35760(327)	44281(303)	42857(160)	955(79)
C(33)	64864(270)	39991(250)	53509(135)	1804(83)
C(34)	44015(202)	40007(181)	44992(93)	1160(50)

SalomphanH<sub>4</sub> were synthesized as previously described.<sup>13</sup> NMR data were obtained on JEOL GSX-400 and -270 instruments at 270.17 (<sup>1</sup>H), 62.5 (<sup>13</sup>C), and 104.5 (<sup>27</sup>Al) MHz. Chemical shifts are reported relative to SiMe<sub>4</sub> and are in units of ppm. Elemental analyses were obtained on a Perkin-Elmer 2400 analyzer. Mass spectral data were obtained on a Hewlett-Packard 5988 spectrometer using electron impact ionization (70 eV) with a direct ionization probe (DIP). Infrared data were recorded as KBr pellets on a Matheson Instruments 2020 Galaxy Series spectrometer and are reported in cm<sup>-1</sup>. For **5**, **9**, and **10**, crystals suitable for X-ray analysis were grown by dissolution in toluene and cooling to -30 °C.

**Preparation of SaleanAlEt(AIET<sub>2</sub>)<sub>2</sub>.** Triethylaluminum (5.50 mL, 1.0 M in hexanes, 5.50 mmol) was added to a rapidly stirred solution of SaleanH<sub>4</sub> (0.499 g, 1.83 mmol) in 50 mL of toluene at 25 °C. The exothermic reaction mixture was stirred at 25 °C until the evolution of gas ceased (15 min); then it was refluxed for 8 h. The toluene was removed in vacuo, leaving the title compound as a white solid (0.823 g, 91%): <sup>1</sup>H NMR (270 MHz, C<sub>6</sub>D<sub>6</sub>) δ 0.21–1.72 (m, 25H, CH<sub>2</sub>CH<sub>3</sub>), 2.52 (dd, *J* = 8, 16 Hz, 2H, NCH<sub>2</sub>), 2.93 (dd, *J* = 8, 16 Hz, 2H, NCH<sub>2</sub>), 3.42 (d, *J* = 17 Hz, 2H, PhCH<sub>2</sub>), 4.37 (d, *J* = 17 Hz, 2H, PhCH<sub>2</sub>), 6.61–6.98 (m, 8H, Ph *H*); <sup>13</sup>C NMR (65 MHz, C<sub>6</sub>D<sub>6</sub>) δ -1.2 (CH<sub>2</sub>CH<sub>3</sub>), -0.3 (CH<sub>2</sub>CH<sub>3</sub>), 1.6 (CH<sub>2</sub>CH<sub>3</sub>), 9.3 (CH<sub>2</sub>CH<sub>3</sub>), 9.7 (CH<sub>2</sub>CH<sub>3</sub>), 9.8 (CH<sub>2</sub>CH<sub>3</sub>), 42.0 (NCH<sub>2</sub>), 47.9 (PhCH<sub>2</sub>), 50.6 (PhCH<sub>2</sub>), 118.8 (Ph), 121.0 (Ph), 122.7 (Ph), 128.5 (Ph), 130.3 (Ph), 152.0 (Ph); <sup>27</sup>Al NMR (104.5 MHz, C<sub>6</sub>D<sub>6</sub>) δ

**Table 8. Atomic Coordinates ( $\times 10^5$ ) and Equivalent Isotropic Displacement Coefficients ( $\times 10^4$ ) for SalomphanGaMe(GaMe<sub>2</sub>)<sub>2</sub> (10)**

atom	x	y	z	U(eq) (Å <sup>2</sup> )
Ga(1)	-28054(7)	-42992(6)	-80956(5)	423(3)
Ga(2)	-8249(7)	-30166(5)	-83100(5)	396(3)
Ga(3)	17294(7)	-26111(6)	-76711(5)	476(3)
O(1)	-23608(40)	-30021(33)	-77460(27)	415(17)
O(2)	9416(41)	-33557(32)	-85687(29)	450(18)
N(1)	-10560(48)	-43545(37)	-81925(33)	375(20)
N(2)	1696(48)	-29046(37)	-72854(32)	362(20)
C(1)	-23968(60)	-27441(45)	-70082(42)	375(26)
C(2)	-34566(68)	-28746(49)	-67289(46)	469(29)
C(3)	-35430(79)	-26286(54)	-59790(50)	551(32)
C(4)	-26026(84)	-22420(57)	-54899(49)	587(34)
C(5)	-15362(75)	-21047(50)	-57670(44)	508(30)
C(6)	-14089(61)	-23590(46)	-65294(41)	379(25)
C(7)	-2304(62)	-21876(45)	-67689(44)	436(27)
C(8)	2038(56)	-38409(45)	-69623(39)	333(24)
C(9)	8148(62)	-40635(51)	-62294(41)	418(26)
C(10)	9158(61)	-49701(50)	-59371(42)	426(27)
C(11)	16136(78)	-51641(59)	-51311(44)	617(33)
C(12)	3619(64)	-56964(47)	-64091(41)	401(26)
C(13)	3908(84)	-66940(54)	-61328(51)	657(35)
C(14)	-2428(62)	-54820(44)	-71472(40)	369(25)
C(15)	-3490(57)	-45761(44)	-74517(38)	324(23)
C(16)	-7623(60)	-49332(50)	-88537(41)	416(26)
C(17)	5558(64)	-49807(51)	-88715(38)	399(25)
C(18)	10296(71)	-58515(51)	-90558(43)	475(29)
C(19)	22231(68)	-59556(57)	-91104(43)	495(29)
C(20)	29592(69)	-52003(58)	-89833(44)	517(30)
C(21)	25284(64)	-43301(52)	-87915(43)	452(28)
C(22)	13459(64)	-42205(51)	-87506(39)	404(26)
C(23)	-38119(72)	-41828(64)	-91235(47)	640(34)
C(24)	-31333(74)	-50712(55)	-72473(49)	600(33)
C(25)	-13673(77)	-21721(54)	-91641(45)	581(32)
C(26)	30882(70)	-32440(64)	-70585(55)	710(37)
C(27)	16625(79)	-13189(56)	-80554(54)	666(36)

69 ( $\omega_{1/2}$  = 5200 Hz), 162 ( $\omega_{1/2}$  = 5400 Hz); IR (KBr) 2932 s, 2862 vs, 1582 m, 1481 vs, 1451 s, 758 vs, 658 vs cm<sup>-1</sup>; MS (DIP/EI) *m/e* 494 (M<sup>+</sup>), 493 (M<sup>+</sup> - H), 465 (M<sup>+</sup> - Et), 379 (M<sup>+</sup> - Et - AlEt<sub>2</sub> - H), 351 (M<sup>+</sup> - 2Et - AlEt<sub>2</sub>), 322 (M<sup>+</sup> - 3Et - AlEt<sub>2</sub>), 293 (M<sup>+</sup> - Et - 2AlEt<sub>2</sub> - 2H), 85 (AlEt<sub>2</sub><sup>+</sup>), 57 (AlEtH<sup>+</sup>). Anal. Calcd (found): C, 63.14 (62.89); H, 8.36 (8.22); N, 5.66 (5.29).

**Preparation of SalpanAlEt(AIET<sub>2</sub>)<sub>2</sub>.** Triethylaluminum (5.25 mL, 1.0 M in hexanes, 5.25 mmol) was added to a rapidly stirred solution of SalpanH<sub>4</sub> (0.501 g, 1.75 mmol) in 50 mL of toluene at 25 °C. The exothermic reaction mixture was stirred at 25 °C until the evolution of gas ceased (15 min); then it was refluxed for 8 h. The toluene was removed in vacuo, leaving the title compound as a white solid (0.822 g, 93%): <sup>1</sup>H NMR (270 MHz, C<sub>6</sub>D<sub>6</sub>) δ 0.13–0.90 (m, 10H, CH<sub>2</sub>CH<sub>3</sub>), 1.08–1.56 (m, 16H, CH<sub>2</sub>CH<sub>3</sub> and CH<sub>2</sub>CH<sub>2</sub>), 2.08–2.29 (m, 1H, CH<sub>2</sub>CH<sub>2</sub>), 2.61–2.69 (m, 2H, NCH<sub>2</sub>), 2.90–3.00 (m, 2H, NCH<sub>2</sub>), 3.27 (d, *J* = 16 Hz, 2H, PhCH<sub>2</sub>), 4.50 (d, *J* = 16 Hz, 2H, PhCH<sub>2</sub>), 6.64–7.05 (m, 8H, Ph *H*); <sup>13</sup>C NMR (65 MHz, C<sub>6</sub>D<sub>6</sub>) δ -1.8 (CH<sub>2</sub>CH<sub>3</sub>), -0.5 (CH<sub>2</sub>CH<sub>3</sub>), 0.0 (CH<sub>2</sub>CH<sub>3</sub>), -0.7 (CH<sub>2</sub>CH<sub>3</sub>), 1.3 (CH<sub>2</sub>CH<sub>3</sub>), 9.5 (CH<sub>2</sub>CH<sub>3</sub>), 9.6 (CH<sub>2</sub>CH<sub>3</sub>), 10.0 (CH<sub>2</sub>CH<sub>3</sub>), 24.4 (CH<sub>2</sub>CH<sub>2</sub>), 48.0 (NCH<sub>2</sub>), 53.2 (PhCH<sub>2</sub>), 118.7 (Ph), 122.4 (Ph), 124.6 (Ph), 128.5 (Ph), 131.1 (Ph), 152.9 (Ph); <sup>27</sup>Al NMR (104.5 MHz, C<sub>6</sub>D<sub>6</sub>) δ 77 ( $\omega_{1/2}$  = 3120 Hz), 175 ( $\omega_{1/2}$  = 14 560 Hz); IR (KBr) 2938 vs, 2863 vs, 1604 w, 1580 w, 1491 vs, 1450 s, 1267 s, 1221 s, 1063 s, 878 s, 756 vs, 652 vs cm<sup>-1</sup>; MS (DIP/EI) *m/e* 508 (M<sup>+</sup>), 507 (M<sup>+</sup> - H), 479 (M<sup>+</sup> - Et), 421 (M<sup>+</sup> - 3Et), 393 (M<sup>+</sup> - Et - AlEt<sub>2</sub> - H), 365 (M<sup>+</sup> - 2Et - AlEt<sub>2</sub>), 307 (M<sup>+</sup> - Et - 2AlEt<sub>2</sub> - 2H), 85 (AlEt<sub>2</sub><sup>+</sup>), 57 (AlEtH<sup>+</sup>). Anal. Calcd (found): C, 63.76 (63.86); H, 8.52 (8.03); N, 5.51 (5.22).

**Preparation of SalophanAlEt(AIET<sub>2</sub>)<sub>2</sub>.** Triethylaluminum (4.78 mL, 1.0 M in hexanes, 4.78 mmol) was added to a rapidly stirred solution of SalophanH<sub>4</sub> (0.498 g, 1.59 mmol) in 50 mL of toluene at 25 °C. The exothermic reaction mixture was stirred at 25 °C until the evolution of gas ceased (15 min); then it was refluxed for 8 h. The toluene was removed in

(13) Atwood, D. A.; Benson, J.; Jegier, J. A.; Lindholm, N. F.; Martin, K. J.; Rutherford, D. *Main Group Chem.*, in press.

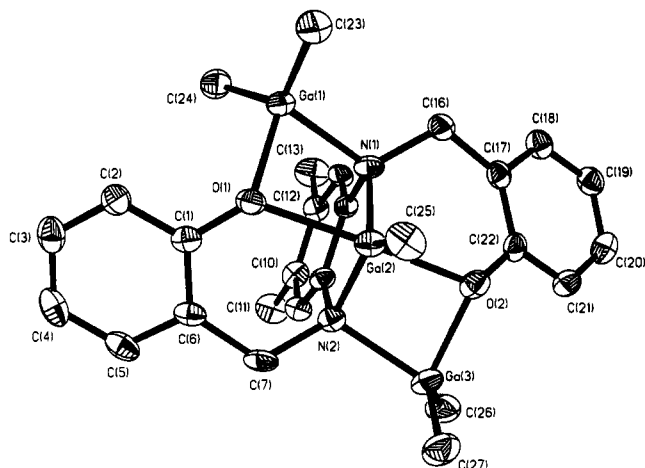


**Figure 7.** Molecular structure and atom numbering scheme for **10**.

vacuo, leaving the title compound as an off-white solid (0.833 g, 97%):  $^1\text{H}$  NMR (270 MHz,  $\text{C}_6\text{D}_6$ )  $\delta$  -0.73 (q,  $J$  = 8 Hz, 2H,  $\text{CH}_2\text{CH}_3$ ), -0.30 (q,  $J$  = 8 Hz, 2H,  $\text{CH}_2\text{CH}_3$ ), -0.12 to +1.48 (m, 21H,  $\text{CH}_2\text{CH}_3$ ), 4.04 (d,  $J$  = 17 Hz, 2H,  $\text{PhCH}_2$ ), 4.60 (d,  $J$  = 17 Hz, 2H,  $\text{PhCH}_2$ ), 6.39–7.05 (m, 12H, Ph *H*);  $^{13}\text{C}$  NMR (65 MHz,  $\text{C}_6\text{D}_6$ )  $\delta$  -9.6 ( $\text{CH}_2\text{CH}_3$ ), -4.2 ( $\text{CH}_2\text{CH}_3$ ), -2.8 ( $\text{CH}_2\text{CH}_3$ ), 1.3 ( $\text{CH}_2\text{CH}_3$ ), 1.8 ( $\text{CH}_2\text{CH}_3$ ), 8.8 ( $\text{CH}_2\text{CH}_3$ ), 8.9 ( $\text{CH}_2\text{CH}_3$ ), 9.2 ( $\text{CH}_2\text{CH}_3$ ), 9.4 ( $\text{CH}_2\text{CH}_3$ ), 9.5 ( $\text{CH}_2\text{CH}_3$ ), 46.7 (Ph $\text{CH}_2$ ), 114.1 (Ph), 119.1 (Ph), 122.5 (Ph), 122.9 (Ph), 123.2 (Ph), 128.6 (Ph), 129.3 (Ph), 129.7 (Ph), 138.8 (Ph), 151.6 (Ph);  $^{27}\text{Al}$  NMR (104.5 MHz,  $\text{C}_6\text{D}_6$ )  $\delta$  71 ( $w_{1/2}$  = 5200), 159 ( $w_{1/2}$  = 15 700); IR (KBr) 2934 vs, 2862 vs, 1584 m, 1495 s, 1451 s, 1215 vs, 752 vs, 653 vs  $\text{cm}^{-1}$ ; MS (DIP/EI)  $m/e$  513 ( $\text{M}^+$  - Et), 428 ( $\text{M}^+$  - Et -  $\text{AlEt}_2$ ), 399 ( $\text{M}^+$  - 2Et -  $\text{AlEt}_2$ ), 370 ( $\text{M}^+$  - 3Et -  $\text{AlEt}_2$ ), 341 ( $\text{M}^+$  - Et - 2 $\text{AlEt}_2$  - 2H), 237 (PhO $\text{CH}_2\text{NPhAl}^+$ ), 85 ( $\text{AlEt}_2^+$ ), 57 ( $\text{AlEtH}^+$ ). Anal. Calcd (found): C, 66.41 (66.79); H, 7.62 (7.43); N, 5.16 (5.10).

**Preparation of SalomphanAl<sup>i</sup>Bu(Al<sup>i</sup>Bu)<sub>2</sub>.** Triethylaluminum (4.30 mL, 1.0 M in hexanes, 4.30 mmol) was added to a rapidly stirred solution of SalomphanH<sub>4</sub> (0.500 g, 1.44 mmol) in 50 mL of toluene at 25 °C. The exothermic reaction mixture was stirred at 25 °C until the evolution of gas ceased (15 min); then it was refluxed for 8 h. The toluene was removed in vacuo, leaving the title compound as a tan solid (0.731 g, 89%):  $^1\text{H}$  NMR (270 MHz,  $\text{C}_6\text{D}_6$ )  $\delta$  -0.66 (q,  $J$  = 8 Hz, 2H,  $\text{CH}_2\text{CH}_3$ ), -0.21 (q,  $J$  = 8 Hz, 2H,  $\text{CH}_2\text{CH}_3$ ), 0.45–0.62 (m, 6H,  $\text{CH}_2\text{CH}_3$ ), 0.68 (t,  $J$  = 8 Hz, 3H,  $\text{CH}_2\text{CH}_3$ ), 1.04 (t,  $J$  = 8 Hz, 3H,  $\text{CH}_2\text{CH}_3$ ), 1.31 (t,  $J$  = 8 Hz, 3H,  $\text{CH}_2\text{CH}_3$ ), 1.46 (t,  $J$  = 8 Hz, 6H,  $\text{CH}_2\text{CH}_3$ ), 1.74 (s, 6H, Ph $\text{CH}_3$ ), 4.13 (d,  $J$  = 16 Hz, 2H, Ph $\text{CH}_2$ ), 4.63 (d,  $J$  = 16 Hz, 2H, Ph $\text{CH}_2$ ), 6.34 (s, 2H, Ph $\text{H}$ ), 6.75–6.85 (m, 8H, Ph *H*);  $^{13}\text{C}$  NMR (60 MHz,  $\text{C}_6\text{D}_6$ )  $\delta$  -4.0 ( $\text{CH}_2\text{CH}_3$ ), -2.4 ( $\text{CH}_2\text{CH}_3$ ), 1.1 ( $\text{CH}_2\text{CH}_3$ ), 1.4 ( $\text{CH}_2\text{CH}_3$ ), 2.2 ( $\text{CH}_2\text{CH}_3$ ), 8.7 ( $\text{CH}_2\text{CH}_3$ ), 9.2 ( $\text{CH}_2\text{CH}_3$ ), 9.6 ( $\text{CH}_2\text{CH}_3$ ), 19.6 (Ph $\text{CH}_3$ ), 46.8 (Ph $\text{CH}_2$ ), 115.6 (Ph), 119.0 (Ph), 122.9 (Ph), 128.5 (Ph), 128.6 (Ph), 129.7 (Ph), 131.0 (Ph), 136.3 (Ph), 151.7 (Ph);  $^{27}\text{Al}$  NMR (104.5 MHz,  $\text{C}_6\text{D}_6$ )  $\delta$  67 ( $w_{1/2}$  = 6760 Hz), 157 ( $w_{1/2}$  = 15 600 Hz); IR (KBr) 2934 s, 2862 vs, 1584 m, 1493 s, 1451 s, 1213 s, 752 vs, 663 vs, 621 s  $\text{cm}^{-1}$ ; MS (DIP/EI)  $m/e$  570 ( $\text{M}^+$ ), 541 ( $\text{M}^+$  - Et), 484 ( $\text{M}^+$  -  $\text{AlEt}_2$ ), 456 ( $\text{M}^+$  - Et -  $\text{AlEt}_2$ ), 427 ( $\text{M}^+$  - 2Et -  $\text{AlEt}_2$ ), 397 ( $\text{M}^+$  - 3Et -  $\text{AlEt}_2$ ), 369 ( $\text{M}^+$  - Et - 2 $\text{AlEt}_2$  - 2H), 85 ( $\text{AlEt}_2^+$ ), 57 ( $\text{AlEtH}^+$ ). Anal. Calcd (found): C, 67.35 (67.29); H, 7.95 (7.88); N, 4.91 (5.36).

**Preparation of SaleanAl<sup>i</sup>Bu(Al<sup>i</sup>Bu)<sub>2</sub>.** Triisobutylaluminum (1.09 g, 5.51 mmol) was added neat to a rapidly stirred solution of SaleanH<sub>4</sub> (0.500 g, 1.85 mmol) in 50 mL of toluene at 25 °C. The exothermic reaction mixture was stirred at 25 °C until the evolution of gas ceased (15 min); then it was refluxed for 8 h. After filtration and concentration, colorless crystals were grown at -30 °C (1.02 g, 87%):  $^1\text{H}$  NMR (270 MHz,  $\text{C}_6\text{D}_6$ )  $\delta$  0.17 (d,  $J$  = 5 Hz, 2H,  $\text{CH}_2\text{CH}$ ), 0.19 (d,  $J$  = 4 Hz, 2H,  $\text{CH}_2\text{CH}$ ), 0.35 (d,  $J$  = 7 Hz, 2H,  $\text{CH}_2\text{CH}$ ), 0.41 (d,  $J$  =

7 Hz, 2H,  $\text{CH}_2\text{CH}$ ), 0.78 (d,  $J$  = 7 Hz, 2H,  $\text{CH}_2\text{CH}$ ), 1.02 (d,  $J$  = 6 Hz, 6H,  $\text{CHCH}_3$ ), 1.04 (d,  $J$  = 6 Hz, 6H,  $\text{CHCH}_3$ ), 1.18 (d,  $J$  = 7 Hz, 6H,  $\text{CHCH}_3$ ), 1.20 (d,  $J$  = 7 Hz, 6H,  $\text{CHCH}_3$ ), 1.28 (d,  $J$  = 7 Hz, 6H,  $\text{CHCH}_3$ ), 1.97–2.15 (m, 4H,  $\text{CHCH}_3$ ), 2.30–2.45 (m, 1H,  $\text{CHCH}_3$ ), 2.52 (dd,  $J$  = 5, 10 Hz, 2H,  $\text{NCH}_2$ ), 2.98 (dd,  $J$  = 5, 10 Hz, 2H,  $\text{NCH}_2$ ), 3.55 (d,  $J$  = 16 Hz, 2H, Ph $\text{CH}_2$ ), 4.44 (d,  $J$  = 16 Hz, 2H, Ph $\text{CH}_2$ ), 6.64–7.08 (m, 8H, Ph *H*);  $^{13}\text{C}$  NMR (65 MHz,  $\text{C}_6\text{D}_6$ )  $\delta$  18.1 ( $\text{CH}_2\text{CH}$ ), 21.0 ( $\text{CH}_2\text{CH}$ ), 21.2 ( $\text{CH}_2\text{CH}$ ), 21.3 ( $\text{CH}_2\text{CH}$ ), 24.9 ( $\text{CHCH}_3$ ), 26.0 ( $\text{CHCH}_3$ ), 26.2 ( $\text{CHCH}_3$ ), 26.7 ( $\text{CHCH}_3$ ), 28.5 ( $\text{CH}_2\text{CH}$ ), 28.6 ( $\text{CH}_2\text{CH}$ ), 28.7 ( $\text{CH}_2\text{CH}$ ), 28.8 ( $\text{CH}_2\text{CH}$ ), 28.9 ( $\text{CH}_2\text{CH}$ ), 42.0 ( $\text{NCH}_2$ ), 50.9 (Ph $\text{CH}_2$ ), 119.5 (Ph), 122.9 (Ph), 123.8 (Ph), 128.4 (Ph), 130.3 (Ph), 151.8 (Ph);  $^{27}\text{Al}$  NMR (104 MHz,  $\text{C}_6\text{D}_6$ )  $\delta$  65 ( $w_{1/2}$  = 8200 Hz), 180 ( $w_{1/2}$  = 30 000 Hz); IR (KBr) 2951 vs, 2860 vs, 1584 vs, 1493 vs, 1452 vs, 1213 vs, 873 vs, 758 vs, 648 vs  $\text{cm}^{-1}$ . Anal. Calcd (found): C, 69.21 (69.35); H, 8.23 (7.95); N, 4.48 (5.00).

**Preparation of SalpanAl<sup>i</sup>Bu(Al<sup>i</sup>Bu)<sub>2</sub>.** Triisobutylaluminum (1.04 g, 5.24 mmol) was added neat to a rapidly stirred solution of SalpanH<sub>4</sub> (0.500 g, 1.75 mmol) in 50 mL of toluene at 25 °C. The exothermic reaction mixture was stirred at 25 °C until the evolution of gas ceased (15 min); then it was refluxed for 8 h. The toluene was removed in vacuo, leaving the title compound as a white solid (1.00 g, 88%):  $^1\text{H}$  NMR (270 MHz,  $\text{C}_6\text{D}_6$ )  $\delta$  0.21–0.83 (m, 10H,  $\text{CH}_2\text{CH}$ ), 0.92–1.52 (m, 31H,  $\text{CHCH}_3$  and  $\text{CH}_2\text{CH}_2$ ), 1.85–2.46 (m, 6H,  $\text{CHCH}_3$  and  $\text{CH}_2\text{CH}_2$ ), 2.65–2.85 (m, 2H,  $\text{NCH}_2$ ), 2.92–3.12 (m, 2H,  $\text{NCH}_2$ ), 3.38 (d,  $J$  = 16 Hz, 2H, Ph $\text{CH}_2$ ), 4.57 (d,  $J$  = 16 Hz, 2H, Ph $\text{CH}_2$ ), 6.62–7.35 (m, 8H, Ph *H*);  $^{13}\text{C}$  NMR (65 MHz,  $\text{C}_6\text{D}_6$ )  $\delta$  21.3 ( $\text{CH}_2\text{CH}$ ), 21.4 ( $\text{CH}_2\text{CH}$ ), 23.0 ( $\text{CH}_2\text{CH}$ ), 23.4 ( $\text{CH}_2\text{CH}$ ), 24.2 ( $\text{CH}_2\text{CH}$ ), 26.1 ( $\text{CHCH}_3$ ), 26.3 ( $\text{CHCH}_3$ ), 26.5 ( $\text{CHCH}_3$ ), 26.8 ( $\text{CHCH}_3$ ), 27.0 ( $\text{CHCH}_3$ ), 28.4 ( $\text{CH}_2\text{CH}$ ), 28.6 ( $\text{CH}_2\text{CH}$ ), 28.7 ( $\text{CH}_2\text{CH}$ ), 28.8 ( $\text{CH}_2\text{CH}$ ), 29.3 ( $\text{CH}_2\text{CH}$ ), 48.0 ( $\text{NCH}_2$ ), 53.6 (Ph $\text{CH}_2$ ), 119.1 (Ph), 122.5 (Ph), 124.8 (Ph), 127.6 (Ph), 130.0 (Ph), 152.7 (Ph);  $^{27}\text{Al}$  NMR (104 MHz,  $\text{C}_6\text{D}_6$ )  $\delta$  50 ( $w_{1/2}$  = 7200 Hz), 160 ( $w_{1/2}$  = 25 000 Hz); IR (KBr) 2949 vs, 2861 vs, 1605 s, 1491 s, 1458 vs, 1067 s, 869 vs, 762 vs, 677 vs  $\text{cm}^{-1}$ . Anal. Calcd (found): C, 69.57 (69.17); H, 8.36 (8.30); N, 4.39 (4.69).

**Preparation of SalophanAl<sup>i</sup>Bu(Al<sup>i</sup>Bu)<sub>2</sub>.** Triisobutylaluminum (11.22 g, 56.4 mmol) was added neat to a rapidly stirred solution of SalophanH<sub>4</sub> (6.00 g, 18.8 mmol) in 250 mL of toluene at 25 °C. The exothermic reaction mixture was stirred at 25 °C until the evolution of gas ceased (15 min); then it was refluxed for 10 h. The toluene was removed in vacuo, leaving the title compound as a white solid (12.15 g, 95%):  $^1\text{H}$  NMR (270 MHz,  $\text{C}_6\text{D}_6$ )  $\delta$  -0.89 (d,  $J$  = 7 Hz, 2H,  $\text{CH}_2\text{CH}$ ), -0.36 (d,  $J$  = 7 Hz, 2H,  $\text{CH}_2\text{CH}$ ), 0.52 (d,  $J$  = 7 Hz, 2H,  $\text{CH}_2\text{CH}$ ), 0.59 (d,  $J$  = 7 Hz, 2H,  $\text{CH}_2\text{CH}$ ), 0.66 (d,  $J$  = 7 Hz, 2H,  $\text{CH}_2\text{CH}$ ), 0.83 (d,  $J$  = 7 Hz, 6H,  $\text{CHCH}_3$ ), 0.94 (d,  $J$  = 7 Hz, 6H,  $\text{CHCH}_3$ ), 1.07 (d,  $J$  = 7 Hz, 6H,  $\text{CHCH}_3$ ), 1.21 (d,  $J$  = 7 Hz, 6H,  $\text{CHCH}_3$ ), 1.23 (d,  $J$  = 7 Hz, 6H,  $\text{CHCH}_3$ ), 1.45–1.53 (m, 2H,  $\text{CHCH}_3$ ), 2.17–2.31 (m, 3H,  $\text{CHCH}_3$ ), 4.16 (d,  $J$  = 16 Hz, 2H, Ph $\text{CH}_2$ ), 4.69 (d,  $J$  = 16 Hz, 2H, Ph $\text{CH}_2$ ), 6.40–7.14 (m, 12H, Ph *H*);  $^{13}\text{C}$  NMR (65 MHz,  $\text{C}_6\text{D}_6$ )  $\delta$  18.5 ( $\text{CH}_2\text{CH}$ ), 19.6 ( $\text{CH}_2\text{CH}$ ), 21.4 ( $\text{CH}_2\text{CH}$ ), 23.5 ( $\text{CH}_2\text{CH}$ ), 25.4 ( $\text{CH}_2\text{CH}$ ), 25.5 ( $\text{CHCH}_3$ ), 26.1 ( $\text{CHCH}_3$ ), 26.2 ( $\text{CHCH}_3$ ), 26.6 ( $\text{CHCH}_3$ ), 28.5 ( $\text{CH}_2\text{CH}$ ), 28.7 ( $\text{CH}_2\text{CH}$ ), 46.7 (Ph $\text{CH}_2$ ), 114.3 (Ph), 119.6 (Ph), 123.0 (Ph), 123.1 (Ph), 123.3 (Ph), 125.6 (Ph), 128.5 (Ph), 129.3 (Ph), 129.7 (Ph), 151.4 (Ph);  $^{27}\text{Al}$  NMR (104 MHz,  $\text{C}_6\text{D}_6$ )  $\delta$  55 ( $w_{1/2}$  = 7100 Hz), 190 ( $w_{1/2}$  = 35 000 Hz); IR (KBr) 2947 vs, 2860 vs, 1605 m, 1495 vs, 1452 vs, 1217 vs, 876 m, 760 vs, 667 vs  $\text{cm}^{-1}$ . Anal. Calcd (found): C, 71.41 (71.77); H, 7.64 (7.44); N, 4.16 (4.43).

**Preparation of SalomphanAl<sup>i</sup>Bu(Al<sup>i</sup>Bu)<sub>2</sub>.** Triisobutylaluminum (9.72 g, 48.8 mmol) was added neat to a rapidly stirred solution of SalomphanH<sub>4</sub> (5.66 g, 16.1 mmol) in 200 mL of toluene at 25 °C. The exothermic reaction mixture was stirred at 25 °C until the evolution of gas ceased (15 min); then it was refluxed for 10 h. The toluene was removed in vacuo, leaving the title compound as a tan solid (10.97 g, 96%):  $^1\text{H}$  NMR (270 MHz,  $\text{C}_6\text{D}_6$ )  $\delta$  -0.94 (d,  $J$  = 7 Hz, 2H,  $\text{CH}_2\text{CH}$ ), -0.30 (d,  $J$  = 7 Hz, 2H,  $\text{CH}_2\text{CH}$ ), 0.51 (d,  $J$  = 7 Hz, 2H,  $\text{CH}_2\text{CH}$ ), 0.59 (d,  $J$  = 7 Hz, 2H,  $\text{CH}_2\text{CH}$ ), 0.65 (d,  $J$  = 7 Hz, 2H,

$\text{CH}_2\text{CH}$ ), 0.77 (d,  $J = 7$  Hz, 6H,  $\text{CHCH}_3$ ), 0.96 (d,  $J = 7$  Hz, 6H,  $\text{CHCH}_3$ ), 1.06 (d,  $J = 7$  Hz, 6H,  $\text{CHCH}_3$ ), 1.22 (d,  $J = 7$  Hz, 12H,  $\text{CHCH}_3$ ), 1.42–1.70 (m, 2H,  $\text{CHCH}_3$ ), 1.80 (s, 6H,  $\text{PhCH}_3$ ), 2.15–2.38 (m, 3H,  $\text{CHCH}_3$ ), 4.23 (d,  $J = 17$  Hz, 2H,  $\text{PhCH}_2$ ), 4.71 (d,  $J = 17$  Hz, 2H,  $\text{PhCH}_2$ ), 6.33 (s, 2H, Ph  $H$ ), 6.72–7.15 (m, 8H, Ph  $H$ );  $^{13}\text{C}$  NMR (65 MHz,  $\text{C}_6\text{D}_6$ )  $\delta$  18.4 ( $\text{CH}_2\text{CH}$ ), 19.7 ( $\text{CH}_2\text{CH}$ ), 23.5 ( $\text{CH}_2\text{CH}$ ), 25.3 ( $\text{CH}_2\text{CH}$ ), 25.4 ( $\text{CH}_2\text{CH}$ ), 26.1 ( $\text{CHCH}_3$ ), 26.2 ( $\text{CHCH}_3$ ), 26.3 ( $\text{CHCH}_3$ ), 26.6 ( $\text{CHCH}_3$ ), 28.5 ( $\text{CH}_2\text{CH}$ ), 28.5 ( $\text{CH}_2\text{CH}$ ), 28.7 ( $\text{CH}_2\text{CH}$ ), 28.7 ( $\text{CH}_2\text{CH}$ ), 47.0 ( $\text{PhCH}_2$ ), 115.9 (Ph), 119.6 (Ph), 123.0 (Ph), 125.6 (Ph), 129.3 (Ph), 129.6 (Ph), 130.8 (Ph), 136.5 (Ph), 151.4 (Ph);  $^{27}\text{Al}$  NMR (104 MHz,  $\text{C}_6\text{D}_6$ )  $\delta$  55 ( $w_{1/2} = 6500$  Hz), 220 ( $w_{1/2} = 32\,000$  Hz); IR (KBr) 2951 vs, 2861 vs, 1586 m, 1493 vs, 1452 vs, 1267 vs, 1213 vs, 1014 vs, 808 vs, 752 vs, 651 vs  $\text{cm}^{-1}$ . Anal. Calcd (found): C, 71.98 (72.03); H, 7.91 (7.94); N, 4.00 (4.08).

**X-ray Experimental Details.** Details of the crystal data and a summary of data collection parameters for **5**, **9**, and **10** are given in Table 3. Data were collected on a Siemens P4 diffractometer using graphite-monochromated  $\text{Mo K}\alpha$  (0.710 73 Å) radiation. The check reflections, measured every 100 reflections, indicated a less than 5% decrease in intensity over the course of data collection, and hence, no correction was applied. All calculations were performed on a personal

computer using the Siemens software package SHELXTL-Plus. The structures were solved by direct methods and successive interpretation of difference Fourier maps, followed by least-squares refinement. All non-hydrogen atoms were refined anisotropically. The hydrogen atoms were included in the refinement in calculated positions using fixed isotropic parameters. For **5** there was some mild disorder of one of the  $^i\text{Bu}$  carbons (C(32)). It was refined as a partial occupancy between two positions weighted at 0.70 (C(32)) and 0.30 (C(32A)).

**Acknowledgment.** Gratitude is expressed to the National Science Foundation (Grant RII-861075) and the NDSU Grant-in-Aid program for generous financial support.

**Supporting Information Available:** Tables giving structure determination summaries, bond lengths and angles, positional parameters, and anisotropic thermal parameters and figures giving unit cell views for **5**, **9**, and **10** (33 pages). Ordering information is given on any current masthead page.

OM9503499

# Os(CO)<sub>4</sub>(η<sup>2</sup>-C<sub>2</sub>Me<sub>2</sub>)-Promoted Coupling of Alkynes and CO: Formation of (η<sup>4</sup>-C<sub>4</sub>Me<sub>2</sub>R<sub>2</sub>CO)Os(CO)<sub>3</sub> (R = Me, Et, <sup>n</sup>Pr) and Catalytic Activity of (η<sup>4</sup>-C<sub>4</sub>R<sub>4</sub>CO)Os(CO)<sub>3</sub> (R = Me, Ph)

John Washington, Robert McDonald,<sup>†</sup> and Josef Takats\*

Department of Chemistry and Structure Determination Laboratory, University of Alberta, Edmonton, Alberta, Canada T6G 2G2

Naim Menashe, Dvora Reshef, and Youval Shvo\*

School of Chemistry, Raymond and Beverly Sackler School of Exact Sciences, Tel Aviv University, Tel Aviv, Israel 69978

Received May 9, 1995<sup>⊗</sup>

Low-temperature photolysis of Os(CO)<sub>5</sub> in the presence of excess 2-butyne gives Os(CO)<sub>4</sub>(η<sup>2</sup>-C<sub>2</sub>Me<sub>2</sub>) (**1**) in moderate yield. Complex **1** undergoes facile alkyne-CO coupling with an additional alkyne ligand under mild thermal activation to give the cyclopentadienone-containing species (η<sup>4</sup>-C<sub>4</sub>Me<sub>2</sub>R<sub>2</sub>CO)Os(CO)<sub>3</sub> (R = Me (**2a**), Et (**2d**), <sup>n</sup>Pr (**2e**)). Isolation of the alkyne-carbonyl complex is not necessary to effect the transformation; *in situ* generated M(CO)<sub>4</sub>(η<sup>2</sup>-C<sub>2</sub>R<sub>2</sub>) provides a convenient method for the synthesis of (η<sup>4</sup>-C<sub>4</sub>R<sub>4</sub>CO)M(CO)<sub>3</sub> (M = Ru, Os; R = Me, Et, <sup>n</sup>Pr). On the basis of these observations, the proposed mechanisms for the formation of (η<sup>4</sup>-C<sub>4</sub>R<sub>4</sub>CO)M(CO)<sub>3</sub> complexes are discussed and evaluated. The solid-state structure of **2d** was determined and compared to the tetraphenyl analogue, (η<sup>4</sup>-C<sub>4</sub>Ph<sub>4</sub>CO)Os(CO)<sub>3</sub> (**4**). Compound **2d** crystallizes in the monoclinic space group P2<sub>1</sub>/c with *a* = 8.336(1) Å, *b* = 15.334(2) Å, *c* = 12.849(2) Å, β = 108.78(2)°, *Z* = 4, *R* = 0.040, and *R*<sub>w</sub> = 0.046. The use of **2a** and **4** as catalyst precursors for both Tishchenko and hydrogenation reactions was investigated and compared to the analogous ruthenium complex (η<sup>4</sup>-C<sub>4</sub>Ph<sub>4</sub>CO)Ru(CO)<sub>3</sub>.

## Introduction

The concept of alkyne coupling at a transition metal center is well documented in the literature.<sup>1</sup> Hübel contributed much to the early work in the field, studying the reactions of alkynes with iron carbonyl compounds.<sup>1a,2</sup> The reactions are complex and yield a myriad of products, with an often isolated component the well-known (cyclopentadienone)tricarbonyliron complexes, (η<sup>4</sup>-CPD)Fe(CO)<sub>3</sub> (CPD = substituted cyclopentadienone).<sup>2,3</sup> Recent interest in CPD complexes has been heightened by the discovery that (η<sup>4</sup>-C<sub>4</sub>Ph<sub>4</sub>CO)Ru(CO)<sub>3</sub> is a useful catalyst precursor for a number of organic

transformations,<sup>4</sup> and in conjunction with the work of Pearson on the reactions of Fe(CO)<sub>5</sub> with α,ω-diyne.<sup>5</sup>

The presence of Fe(CO)<sub>4</sub>(η<sup>2</sup>-RCCR) species along the reaction pathway to (η<sup>4</sup>-CPD)Fe(CO)<sub>3</sub> complexes has been postulated. However, these intermediates have not been detected, much less isolated. Indeed, although we have reported<sup>6</sup> a convenient synthesis for several M(CO)<sub>4</sub>(η<sup>2</sup>-C<sub>2</sub>R<sub>2</sub>) (M = Ru, Os; R = H, CF<sub>3</sub>, SiMe<sub>3</sub>) species, only one iron analogue, the bis(trimethylsilyl)acetylene derivative Fe(CO)<sub>4</sub>{η<sup>2</sup>-C<sub>2</sub>(SiMe<sub>3</sub>)<sub>2</sub>}, is known.<sup>7</sup> The Ru and Os complexes undergo interesting addition reactions with nucleophilic metal centers,<sup>6a-b,8</sup> yet no facile alkyne coupling reactions have been observed with these species.

Here, we report the synthesis of Os(CO)<sub>4</sub>(η<sup>2</sup>-C<sub>2</sub>Me<sub>2</sub>) (**1**) and its reaction with electron-rich alkynes to yield (η<sup>4</sup>-CPD)Os(CO)<sub>3</sub> complexes. In addition, a general

\* To whom inquiries regarding X-ray crystallographic results should be made.

<sup>⊗</sup> Abstract published in *Advance ACS Abstracts*, June 15, 1995.

(1) (a) Hübel, W. *Organic Syntheses via Metal Carbonyls*; Wender, I., Pino, P., Eds.; Wiley: New York, 1968; p 273. (b) Schore, N. E. *Chem. Rev.* **1988**, *88*, 1081. (c) Efraty, A. *Chem. Rev.* **1977**, *7*, 691. (d) Nicholas, K. M.; Nestle, M. O.; Seyferth, D. *Transition Metal Organometallics in Organic Synthesis*, Alper, H., Ed.; Academic Press: New York, 1978; Vol. 2, Chapter 1. (e) Parshall, G. W.; Ittel, S. D. *Homogeneous Catalysis*, 2nd ed.; Wiley: New York, 1992; Chapter 8. (f) Davidson, D. L. *Reactions of Coordinated Ligands*; Braterman, P. S., Ed.; Plenum Press: New York, 1986; pp 825-895. (g) Winter, M. J. *The Chemistry of the Metal-Carbon Bond*; Hartley, F. R., Patai, S., Eds.; Wiley: New York, 1985; Vol. 3, Chapter 5. (h) Otsuka, S.; Nakamura, A. *Adv. Organomet. Chem.* **1975**, *14*, 245.

(2) (a) Hübel, W.; Braye, B. H. *J. Inorg. Nucl. Chem.* **1959**, *10*, 250. (b) Hübel, W.; Braye, E. H.; Clauss, A.; Weiss, E.; Krüerke, D.; Brown, D. A.; King, G. S. D.; Hoogzand, C. *J. Inorg. Nucl. Chem.* **1959**, *9*, 204. (3) (a) Formals, D.; Pericas, M. A.; Serratos, F.; Vinaixa, J.; Font-Altaba, M.; Solans, X. *J. Chem. Soc., Perkin Trans. 1* **1987**, 2749. (b) Krespan, C. G. *J. Org. Chem.* **1975**, *40*, 261. (c) Boston, J. L.; Sharp, D. W. A.; Wilkinson, G. *J. Chem. Soc.* **1962**, 3488. (d) Wilcox, C.; Breslow, R. *Tetrahedron Lett.* **1980**, 3241.

(4) (a) Abed, M.; Goldbeg, Z.; Shvo, Y. *Organometallics* **1988**, *7*, 2054. (b) Shvo, Y.; Czarkie, D. *J. Organomet. Chem.* **1989**, *368*, 357. (c) Blum, Y.; Shvo, Y. *Isr. J. Chem.* **1984**, *24*, 144. (d) Shvo, Y.; Czarkie, D.; Rahamim, Y. *J. Am. Chem. Soc.* **1986**, *108*, 7400. (e) Shvo, Y.; Czarkie, D. *J. Organomet. Chem.* **1986**, *315*, C25. (f) Menashe, N.; Shvo, Y. *Organometallics* **1991**, *10*, 3885.

(5) (a) Pearson, A. J.; Shively, R. J. *Organometallics* **1994**, *13*, 578. (b) Pearson, A. J.; Shively, R. J.; Dubbert, R. A. *Organometallics* **1992**, *11*, 4096. (c) Pearson, A. J.; Dubbert, R. A. *J. Chem. Soc., Chem. Commun.* **1991**, 202.

(6) (a) Burn, M. J.; Kiel, G.-Y.; Seils, F.; Takats, J.; Washington, J. *J. Am. Chem. Soc.* **1989**, *111*, 6850. (b) Gagné, M. R.; Takats, J. *Organometallics* **1988**, *7*, 561. (c) Ball, R. G.; Burke, M. R.; Takats, J. *Organometallics* **1987**, *6*, 1918.

(7) Pannell, K. H.; Crawford, G. M. *J. Coord. Chem.* **1973**, *2*, 251.

(8) Takats, J.; Washington, J.; Santarsiero, B. *Organometallics* **1994**, *13*, 1078.



method utilizing *in situ* generated  $\text{M}(\text{CO})_4(\eta^2\text{-C}_2\text{R}_2)$  for the synthesis of a number of  $(\eta^4\text{-C}_4\text{R}_4\text{CO})\text{M}(\text{CO})_3$  ( $\text{M} = \text{Ru}, \text{Os}$ ;  $\text{R} = \text{Me}, \text{Et}, \text{}^i\text{Pr}$ ) compounds is presented. The solid-state X-ray structure of  $(\eta^4\text{-C}_4\text{Me}_2\text{Et}_2\text{CO})\text{Os}(\text{CO})_3$  (**2d**) was determined and a comparison made to the related  $(\eta^4\text{-C}_4\text{Ph}_4\text{CO})\text{Os}(\text{CO})_3$  (**4**). In addition, **2a** and **4** were evaluated as possible catalyst precursors in both Tishchenko and hydrogenation reactions, and the results of these studies are reported.

### Experimental Section

**General Procedures.** All synthetic procedures were carried out under purified nitrogen or argon atmospheres using standard Schlenk techniques. Pentane was stirred over concentrated  $\text{H}_2\text{SO}_4$  for several cycles, then washed with distilled water, and finally dried over sodium sulfate before distillation from  $\text{CaH}_2$ . Other solvents were distilled before use from appropriate drying agents. 2-Butyne, 3-hexyne, and 4-octyne were purchased from Aldrich Chemical Co. and used without further purification.  $\text{Ru}_3(\text{CO})_{12}$ <sup>9a</sup> and  $\text{Os}_3(\text{CO})_{12}$ <sup>9b</sup> were prepared by published procedures as were  $(\eta^4\text{-C}_4\text{Ph}_4\text{CO})\text{Ru}(\text{CO})_3$ <sup>10a</sup> and  $(\eta^4\text{-C}_4\text{Ph}_4\text{CO})\text{Os}(\text{CO})_3$ <sup>10b</sup>. Slight modifications were made to the reported procedures for the synthesis of  $\text{Ru}(\text{CO})_5$ <sup>11a</sup> and  $\text{Os}(\text{CO})_5$ <sup>11b</sup>. Specifically,  $\text{Ru}(\text{CO})_5$  was prepared by external photolysis ( $\lambda \geq 370$  nm) of a pentane suspension of  $\text{Ru}_3(\text{CO})_{12}$  under  $>1$  atm of CO. Also, in a typical experiment, 2.02 g of  $\text{Os}_3(\text{CO})_{12}$  was placed in a high-pressure autoclave under 200 atm of CO and heated to 280 °C for 9 h. The yield of  $\text{Os}(\text{CO})_5$  was 0.87 g along with 1.05 g of recovered  $\text{Os}_3(\text{CO})_{12}$ . The catalytic studies were carried out at Tel Aviv University, Tel Aviv, Israel.

Infrared spectra were recorded on Bomem MB-100 or Nicolet 205 Fourier transform spectrometers over the range 2200–1600  $\text{cm}^{-1}$ . NMR tubes were septa sealed under an inert atmosphere. The NMR spectra were collected on Bruker WP-400, WM-360, or WH-200 spectrometers. The mass spectra were obtained on AEI-12 (EI, 16 eV) or VG AUTOSPEC M-250 (FAB, 35 KV) mass spectrometers. Elemental analyses were carried out by the Microanalytical Laboratory at the University of Alberta (Department of Chemistry) or at The Hebrew University, Jerusalem, Israel.

**Preparation of  $\text{Os}(\text{CO})_4(\eta^2\text{-C}_2\text{Me}_2)$  (**1**).** A 100 mL immersion well fitted with a GWV (Glaswerk Vertheim,  $\lambda \geq 370$  nm) cut-off filter was charged with a pentane solution containing  $\text{Os}(\text{CO})_5$  (127.0 mg, 0.385 mmol) and excess 2-butyne (1.0 mL). The temperature of the solution was maintained at  $-60$  °C with a Lauda Klein-Kryomat circulating bath. The solution was photolyzed using a Philips HPK 125 W mercury vapor lamp, and the reaction was monitored using FT-IR spectroscopy. The reaction was complete in *ca.* 2 h after which time no  $\text{Os}(\text{CO})_5$  ( $\nu_{\text{CO}}$  2035, 1994  $\text{cm}^{-1}$ ) was present. An infrared spectrum taken at this time shows only bands due to  $(\eta^4\text{-C}_4\text{Me}_4\text{CO})\text{Os}(\text{CO})_3$  (**2a**) ( $\nu_{\text{CO}}$  2071, 2006, 1988  $\text{cm}^{-1}$ ;  $\nu_{\text{C}=\text{O}}$  1676  $\text{cm}^{-1}$ ) as a result of a facile thermal reaction between  $\text{Os}(\text{CO})_4(\eta^2\text{-C}_2\text{Me}_2)$  (**1**) and excess 2-butyne. The characterization of **1** is possible once excess alkyne is removed (*vide infra*). The solution was transferred by cannula to a flask precooled to  $-78$  °C. The solvent and excess 2-butyne were removed *in vacuo* at  $-78$  °C, and the product,  $\text{Os}(\text{CO})_4(\eta^2\text{-C}_2\text{Me}_2)$  (**1**) was sublimed at *ca.*  $-20$  °C to a dry ice cooled probe. The white, waxy solid was washed off the cold finger with cold pentane to yield a thermally sensitive, colorless solution. A yield of

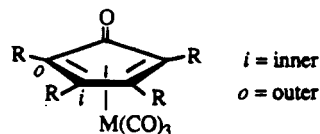
**Table 1. Mass Spectral Data ( $m/e$ ) and Elemental Analyses (%) for Complexes **2**, **3**, **7**, and **8****

compd	mass spectrum (EI, 16 eV) <sup>a</sup>			formula	calcd		found	
	$\text{M}^+$	% <sup>b</sup>	$\text{M}^+ - n\text{CO}$		C	H	C	H
<b>2a</b>	412	90.7	0-4	$\text{C}_{12}\text{H}_{12}\text{O}_4\text{Os}$	35.12	2.95	35.28	2.68
<b>2b</b>	468	43.6	0-4	$\text{C}_{16}\text{H}_{20}\text{O}_4\text{Os}$	41.19	4.32	41.30	4.42
<b>2c</b>	524	36.9	0-4	$\text{C}_{20}\text{H}_{28}\text{O}_4\text{Os}$	45.96	5.40	46.23	5.12
<b>2d</b>	440	23.4	0-4	$\text{C}_{14}\text{H}_{16}\text{O}_4\text{Os}$	38.34	3.68	38.33	3.60
<b>2e</b>	468	62.8	0-4	$\text{C}_{16}\text{H}_{20}\text{O}_4\text{Os}$	41.19	4.32	41.27	4.14
<b>3a</b>	322	24.8	0-4	$\text{C}_{12}\text{H}_{12}\text{O}_4\text{Ru}$	44.86	3.76	45.15	3.60
<b>3b</b>	378	29.6	0-4	$\text{C}_{16}\text{H}_{20}\text{O}_4\text{Ru}$	50.92	5.34	50.91	5.43
<b>3c</b>	434	24.5	0-4	$\text{C}_{20}\text{H}_{28}\text{O}_4\text{Ru}$	55.41	6.51	55.57	6.68
<b>7</b>	1265 <sup>c</sup>	100		$\text{C}_{62}\text{H}_{40}\text{O}_6\text{Os}_2$	59.05	3.17	58.86	2.99
<b>8</b>	633 <sup>c</sup>	45		$\text{C}_{31}\text{H}_{22}\text{O}_3\text{Os}$	58.84	3.48	59.17	3.52

<sup>a</sup> 130–180 °C. <sup>b</sup> Relative intensity. <sup>c</sup> FAB, 35 KV,  $\text{M}^+ - \text{H}$ .

61% (82.3 mg, 0.231 mmol) was obtained based upon titration with  $\text{Cp}^*\text{Rh}(\text{CO})_2$ . In further reactions absorption coefficients ( $\epsilon$ ) of the two strong terminal carbonyl bands were used to prepare pentane solutions of  $\text{Os}(\text{CO})_4(\eta^2\text{-C}_2\text{Me}_2)$  of known concentration. MS (*ca.*  $-20$  °C, 16 eV) [ $m/e$  (abundance)]:  $\text{M}^+$  (358, 17.2%),  $\text{M}^+ - \text{C}_2\text{Me}_2$  (304, 1.3%),  $\text{M}^+ - n\text{CO}$  ( $n = 0-4$ ). IR (pentane,  $\text{cm}^{-1}$ ):  $\nu(\text{CO})$  2106 (w), 2020 (vs) ( $\epsilon = 7.9 \times 10^3$   $\text{M}^{-1}\text{cm}^{-1}$ ), 1988 (m) ( $\epsilon = 5.0 \times 10^3$   $\text{M}^{-1}\text{cm}^{-1}$ ).  $^1\text{H}$  NMR (400 MHz, toluene- $d_8$ ,  $-70$  °C,  $\delta$ ): 2.03 ( $\text{CH}_3$ ).  $^{13}\text{C}$  NMR (100.6 MHz, toluene- $d_8$ ,  $-70$  °C,  $\delta$ ): 69.7 ( $\text{C}-\text{CH}_3$ ), 14.8 ( $\text{CH}_3$ ). Elemental analysis of this thermally sensitive compound could not be obtained.

**Preparation of  $(\eta^4\text{-CPD})\text{M}(\text{CO})_3$  Compounds.** The mass spectral data and elemental analyses for compounds **2–3** are listed in Table 1; IR and selected  $^{13}\text{C}$  NMR data are collected in Table 4. The designation “inner” and “outer” refers to the following diagram:



For **2–3**, NMR spectra were recorded in  $\text{CDCl}_3$  at 23 °C with the  $^1\text{H}$  NMR spectra acquired at 360 MHz and the  $^{13}\text{C}$  NMR spectra obtained at 90.5 MHz.

**$(\eta^4\text{-C}_4\text{Me}_4\text{CO})\text{Os}(\text{CO})_3$  (**2a**).** (a) **Using Isolated  $\text{Os}(\text{CO})_4(\eta^2\text{-C}_2\text{Me}_2)$  (**1**).** A round-bottomed flask, precooled to  $-78$  °C, was charged with a pentane solution containing 78.0 mg (0.219 mmol) of  $\text{Os}(\text{CO})_4(\eta^2\text{-C}_2\text{Me}_2)$  (**1**). An excess of 2-butyne (0.5 mL, 6.38 mmol) was added *via* syringe and the flask transferred to an ice bath. The solution was stirred at low temperature for 1 h and then at room temperature for an additional 0.5 h. The solvent and excess alkyne were removed *in vacuo* and the solid material extracted with pentane ( $2 \times 10$  mL). The volume of solvent was reduced to *ca.* 10 mL and the solution cooled to  $-80$  °C. The off-white, air stable precipitate was isolated and washed with 3 mL of cold pentane; the yield was 73.3 mg. Concentration of the mother liquor followed by crystallization at  $-80$  °C gave an additional 3.9 mg of **2a** for a total yield of 77.2 mg (0.188 mmol, 86%).  $^1\text{H}$  NMR ( $\delta$ ): 2.35 (6H, s, *i*- $\text{CH}_3$ ), 1.92 (6H, s, *o*- $\text{CH}_3$ ).  $^{13}\text{C}$  NMR ( $\delta$ ): 10.1 (*i*- $\text{CH}_3$ ), 8.9 (*o*- $\text{CH}_3$ ).

(b) **Using *In Situ* Generated  $\text{Os}(\text{CO})_4(\eta^2\text{-C}_2\text{Me}_2)$  (**1**).** A pentane solution containing  $\text{Os}(\text{CO})_5$  (88.0 mg, 0.266 mmol) and excess 2-butyne (0.5 mL) was photolyzed ( $\lambda \geq 370$  nm,  $-60$  °C) until no IR bands due to  $\text{Os}(\text{CO})_5$  were visible (*ca.* 2 h). The solution was transferred from the immersion well to a flask at 0 °C and stirred for 1 h. The solvent and 2-butyne were removed *in vacuo*, and the solid product was extracted with pentane ( $2 \times 10$  mL). The filtered extracts were combined and the volume reduced using an Ar stream until precipitation occurred. A small volume of pentane was then added to redissolve the precipitate and the solution placed in a  $-80$  °C freezer overnight. The resulting off-white solid was

(9) (a) Bruce, M. I.; Jensen, C. M.; Jones, N. L. *Inorg. Synth.* **1989**, 26, 259. (b) Johnson, B. F. G.; Lewis, J.; Kilty, P. A. *J. Chem. Soc.* **1968**, 2859.

(10) (a) Bruce, M. I.; Knight, J. R. *J. Organomet. Chem.* **1968**, 12, 411. (b) Burke, M.; Funk, T.; Takats, J. *Organometallics* **1994**, 13, 2109.

(11) (a) Johnson, B. F. G.; Lewis, J.; Twigg, M. V. *J. Organomet. Chem.* **1974**, 67, C75. (b) Rushman, P.; van Buuren, G. N.; Shiralian, M.; Pomeroy, R. K. *Organometallics* **1983**, 2, 693.

isolated and washed (2 × 5 mL) with cold pentane. The yield of ( $\eta^4$ -C<sub>4</sub>Me<sub>4</sub>CO)Os(CO)<sub>3</sub> (**2a**) was 60% (65.6 mg, 0.160 mmol) based on Os(CO)<sub>5</sub>.

( $\eta^4$ -C<sub>4</sub>Et<sub>4</sub>CO)Os(CO)<sub>3</sub> (**2b**). Using method b, Os(CO)<sub>5</sub> (76.5 mg, 0.232 mmol) and 3-hexyne (0.5 mL) gave ( $\eta^4$ -C<sub>4</sub>Et<sub>4</sub>CO)Os(CO)<sub>3</sub> (**2b**) in 56% yield (61.1 mg, 0.131 mmol). <sup>1</sup>H NMR ( $\delta$ ): 2.53 (4H, m, *i*-CH<sub>2</sub>CH<sub>3</sub>), 2.31 (2H, m, *o*-CH<sub>2</sub>CH<sub>3</sub>), 1.94 (2H, m, *o*-CH<sub>2</sub>CH<sub>3</sub>), 1.19 (12H, m, CH<sub>2</sub>CH<sub>3</sub>). <sup>13</sup>C NMR ( $\delta$ ): 18.7 (*i*-CH<sub>2</sub>CH<sub>3</sub>), 18.3 (*o*-CH<sub>2</sub>CH<sub>3</sub>), 16.8 (*i*-CH<sub>2</sub>CH<sub>3</sub>), 16.4 (*o*-CH<sub>2</sub>CH<sub>3</sub>).

( $\eta^4$ -C<sub>4</sub><sup>n</sup>Pr<sub>4</sub>CO)Os(CO)<sub>3</sub> (**2c**). Using method b, Os(CO)<sub>5</sub> (72.8 mg, 0.220 mmol) and 4-octyne (0.5 mL) gave ( $\eta^4$ -C<sub>4</sub><sup>n</sup>Pr<sub>4</sub>CO)Os(CO)<sub>3</sub> (**2c**) in 83% yield (95.2 mg, 0.182 mmol). <sup>1</sup>H NMR ( $\delta$ ): 2.43 (4H, m, *i*-CH<sub>2</sub>CH<sub>2</sub>CH<sub>3</sub>), 2.19 (2H, m, *o*-CH<sub>2</sub>CH<sub>2</sub>CH<sub>3</sub>), 1.82 (2H, m, *o*-CH<sub>2</sub>CH<sub>2</sub>CH<sub>3</sub>), 1.79 (2H, m, *i*-CH<sub>2</sub>CH<sub>2</sub>CH<sub>3</sub>), 1.52 (2H, m, *i*-CH<sub>2</sub>CH<sub>2</sub>CH<sub>3</sub>), 1.46 (2H, m, *o*-CH<sub>2</sub>CH<sub>2</sub>CH<sub>3</sub>), 1.22 (2H, m, *o*-CH<sub>2</sub>CH<sub>2</sub>CH<sub>3</sub>), 1.01 (6H, m, *i*-CH<sub>2</sub>CH<sub>2</sub>CH<sub>3</sub>), 0.98 (6H, m, *o*-CH<sub>2</sub>CH<sub>2</sub>CH<sub>3</sub>). <sup>13</sup>C NMR ( $\delta$ ): 27.8 (*i*-CH<sub>2</sub>CH<sub>2</sub>CH<sub>3</sub>), 27.7 (*o*-CH<sub>2</sub>CH<sub>2</sub>CH<sub>3</sub>), 25.9 (*i*-CH<sub>2</sub>CH<sub>2</sub>CH<sub>3</sub>), 25.5 (*o*-CH<sub>2</sub>CH<sub>2</sub>CH<sub>3</sub>), 14.8 (*i*-CH<sub>2</sub>CH<sub>2</sub>CH<sub>3</sub>), 14.7 (*o*-CH<sub>2</sub>CH<sub>2</sub>CH<sub>3</sub>).

( $\eta^4$ -C<sub>4</sub>Me<sub>2</sub>Et<sub>2</sub>CO)Os(CO)<sub>3</sub> (**2d**). Using method a, Os(CO)<sub>4</sub>( $\eta^2$ -C<sub>2</sub>Me<sub>2</sub>) (20.3 mg, 0.057 mmol) and 3-hexyne (0.5 mL) gave ( $\eta^4$ -C<sub>4</sub>Me<sub>2</sub>Et<sub>2</sub>CO)Os(CO)<sub>3</sub> (**2d**) in 78% yield (19.4 mg, 0.044 mmol). <sup>1</sup>H NMR ( $\delta$ ): 2.52 (2H, m, *i*-CH<sub>2</sub>CH<sub>3</sub>), 2.36 (3H, s, *i*-CH<sub>3</sub>), 2.31 (1H, m, *o*-CH<sub>2</sub>CH<sub>3</sub>), 2.02 (1H, m, *o*-CH<sub>2</sub>CH<sub>3</sub>), 1.94 (3H, s, *o*-CH<sub>3</sub>), 1.15 (6H, m, CH<sub>2</sub>CH<sub>3</sub>). <sup>13</sup>C NMR ( $\delta$ ): 18.7 (*i*-CH<sub>2</sub>CH<sub>3</sub>), 18.1 (*o*-CH<sub>2</sub>CH<sub>3</sub>), 16.8 (*i*-CH<sub>2</sub>CH<sub>3</sub>), 15.5 (*o*-CH<sub>2</sub>CH<sub>3</sub>), 10.1 (*i*-CH<sub>3</sub>), 9.1 (*o*-CH<sub>3</sub>).

( $\eta^4$ -C<sub>4</sub>Me<sub>2</sub><sup>n</sup>Pr<sub>2</sub>CO)Os(CO)<sub>3</sub> (**2e**). Using method a, Os(CO)<sub>4</sub>( $\eta^2$ -C<sub>2</sub>Me<sub>2</sub>) (34.4 mg, 0.097 mmol) and 4-octyne (0.5 mL) gave ( $\eta^4$ -C<sub>4</sub>Me<sub>2</sub><sup>n</sup>Pr<sub>2</sub>CO)Os(CO)<sub>3</sub> (**2e**) in 69% yield (31.1 mg, 0.067 mmol). <sup>1</sup>H NMR ( $\delta$ ): 2.46 (2H, m, *i*-CH<sub>2</sub>CH<sub>2</sub>CH<sub>3</sub>), 2.35 (3H, s, *i*-CH<sub>3</sub>), 2.19 (1H, m, *o*-CH<sub>2</sub>CH<sub>2</sub>CH<sub>3</sub>), 1.92 (3H, s, *o*-CH<sub>3</sub>), 1.89 (1H, m, *o*-CH<sub>2</sub>CH<sub>2</sub>CH<sub>3</sub>), 1.72 (1H, m, *i*-CH<sub>2</sub>CH<sub>2</sub>CH<sub>3</sub>), 1.51 (1H, m, *i*-CH<sub>2</sub>CH<sub>2</sub>CH<sub>3</sub>), 1.48 (1H, m, *o*-CH<sub>2</sub>CH<sub>2</sub>CH<sub>3</sub>), 1.27 (1H, m, *o*-CH<sub>2</sub>CH<sub>2</sub>CH<sub>3</sub>), 1.00 (3H, m, *i*-CH<sub>2</sub>CH<sub>2</sub>CH<sub>3</sub>), 0.97 (3H, m, *o*-CH<sub>2</sub>CH<sub>2</sub>CH<sub>3</sub>). <sup>13</sup>C NMR ( $\delta$ ): 27.7 (*i*-CH<sub>2</sub>CH<sub>2</sub>CH<sub>3</sub>), 27.5 (*o*-CH<sub>2</sub>CH<sub>2</sub>CH<sub>3</sub>), 25.9 (*i*-CH<sub>2</sub>CH<sub>2</sub>CH<sub>3</sub>), 24.5 (*o*-CH<sub>2</sub>CH<sub>2</sub>CH<sub>3</sub>), 14.8 (*i*-CH<sub>2</sub>CH<sub>2</sub>CH<sub>3</sub>), 14.3 (*o*-CH<sub>2</sub>CH<sub>2</sub>CH<sub>3</sub>), 10.5 (*i*-CH<sub>3</sub>), 9.1 (*o*-CH<sub>3</sub>).

**Preparation of ( $\eta^4$ -CPD)Ru(CO)<sub>3</sub> Compounds.** Due to the instability of Ru(CO)<sub>4</sub>( $\eta^2$ -C<sub>2</sub>R<sub>2</sub>), complexes **3a–c** were prepared exclusively *via* the *in situ* method b.

( $\eta^4$ -C<sub>4</sub>Me<sub>4</sub>CO)Ru(CO)<sub>3</sub> (**3a**). The immersion well was maintained at -5 °C, and Ru(CO)<sub>5</sub> (82.1 mg, 0.340 mmol) and excess 2-butyne (0.5 mL) gave ( $\eta^4$ -C<sub>4</sub>Me<sub>4</sub>CO)Ru(CO)<sub>3</sub> (**3a**) in 29% yield (31.3 mg, 0.097 mmol). <sup>1</sup>H NMR ( $\delta$ ): 2.13 (6H, s, *i*-CH<sub>3</sub>), 1.87 (6H, s, *o*-CH<sub>3</sub>). <sup>13</sup>C NMR ( $\delta$ ): 10.8 (*i*-CH<sub>3</sub>), 9.3 (*o*-CH<sub>3</sub>).

( $\eta^4$ -C<sub>4</sub>Et<sub>4</sub>CO)Ru(CO)<sub>3</sub> (**3b**). The immersion well was maintained at -60 °C, and Ru(CO)<sub>5</sub> (93.0 mg, 0.386 mmol) and 3-hexyne (0.5 mL) gave ( $\eta^4$ -C<sub>4</sub>Et<sub>4</sub>CO)Ru(CO)<sub>3</sub> (**3b**) in 53% yield (77.3 mg, 0.204 mmol). <sup>1</sup>H NMR ( $\delta$ ): 2.44 (4H, m, *i*-CH<sub>2</sub>), 2.30 (2H, m, *o*-CH<sub>2</sub>), 1.98 (2H, m, *o*-CH<sub>2</sub>), 1.19 (6H, m, *i*-CH<sub>3</sub>), 1.16 (6H, m, *o*-CH<sub>3</sub>). <sup>13</sup>C NMR ( $\delta$ ): 19.1 (*i*-CH<sub>2</sub>CH<sub>3</sub>), 17.6 (*o*-CH<sub>2</sub>CH<sub>3</sub>), 16.9 (*i*-CH<sub>2</sub>CH<sub>3</sub>), 15.7 (*o*-CH<sub>2</sub>CH<sub>3</sub>).

( $\eta^4$ -C<sub>4</sub><sup>n</sup>Pr<sub>4</sub>CO)Ru(CO)<sub>3</sub> (**3c**). The immersion well was maintained at -60 °C, and Ru(CO)<sub>5</sub> (91.1 mg, 0.378 mmol) and 4-octyne (0.5 mL) gave ( $\eta^4$ -C<sub>4</sub><sup>n</sup>Pr<sub>4</sub>CO)Ru(CO)<sub>3</sub> (**3c**) in 63% yield (103.4 mg, 0.238 mmol). <sup>1</sup>H NMR ( $\delta$ ): 2.34 (4H, m, *i*-CH<sub>2</sub>-CH<sub>2</sub>CH<sub>3</sub>), 2.15 (2H, m, *o*-CH<sub>2</sub>CH<sub>2</sub>CH<sub>3</sub>), 1.85 (2H, m, *o*-CH<sub>2</sub>-CH<sub>2</sub>CH<sub>3</sub>), 1.78 (2H, m, *i*-CH<sub>2</sub>CH<sub>2</sub>CH<sub>3</sub>), 1.53 (2H, m, *i*-CH<sub>2</sub>CH<sub>2</sub>-CH<sub>3</sub>), 1.46 (2H, m, *o*-CH<sub>2</sub>CH<sub>2</sub>CH<sub>3</sub>), 1.28 (2H, m, *o*-CH<sub>2</sub>CH<sub>2</sub>CH<sub>3</sub>), 1.01 (6H, m, *i*-CH<sub>2</sub>CH<sub>2</sub>CH<sub>3</sub>), 0.98 (6H, m, *o*-CH<sub>2</sub>CH<sub>2</sub>CH<sub>3</sub>). <sup>13</sup>C NMR ( $\delta$ ): 28.3 (*i*-CH<sub>2</sub>CH<sub>2</sub>CH<sub>3</sub>), 27.1 (*o*-CH<sub>2</sub>CH<sub>2</sub>CH<sub>3</sub>), 26.1 (*i*-CH<sub>2</sub>CH<sub>2</sub>CH<sub>3</sub>), 24.9 (*o*-CH<sub>2</sub>CH<sub>2</sub>CH<sub>3</sub>), 14.8 (*i*-CH<sub>2</sub>CH<sub>2</sub>CH<sub>3</sub>), 14.7 (*o*-CH<sub>2</sub>CH<sub>2</sub>CH<sub>3</sub>).

**Generation of Os(CO)<sub>4</sub>( $\eta^2$ -C<sub>2</sub>Ph<sub>2</sub>) and Attempted Thermal Reaction with C<sub>2</sub>Ph<sub>2</sub>.** A 100 mL immersion well fitted with a GWV (Glaswerk Vertheim,  $\lambda \geq 370$  nm) cut-off filter was charged with a pentane solution containing Os(CO)<sub>5</sub> (90.0 mg, 0.273 mmol) and excess diphenylacetylene (155.0 mg, 0.870 mmol). The temperature of the solution was maintained

**Table 2. Summary of Crystallographic Data for **2d****

formula	C <sub>14</sub> H <sub>16</sub> O <sub>4</sub> Os
fw	438.48
cryst size, mm	0.29 × 0.21 × 0.05
cryst system	monoclinic
space group	P2 <sub>1</sub> /c
a, Å	8.336(1)
b, Å	15.334(2)
c, Å	12.849(2)
$\beta$ , deg	108.78(2)
V, Å <sup>3</sup>	1555.0
Z	4
temp, °C	21
D <sub>calc</sub> , g cm <sup>-3</sup>	1.873
$\mu$ , cm <sup>-1</sup>	82.17
radiation ( $\lambda$ , Å)	Mo K $\alpha$ (0.710 73)
reflens measd	2849 ( $\pm h, k, l$ )
reflens used	1528 with $I > 3\sigma(I)$
variables	172
R <sup>a</sup>	0.040
R <sub>w</sub> <sup>b</sup>	0.046

$$^a R = \sum ||F_o| - |F_c|| / \sum |F_o|. \quad ^b R_w = (\sum w(|F_o| - |F_c|)^2 / \sum w F_o^2)^{1/2}.$$

at -50 °C, and the solution was photolyzed using a Philips HPK 125 W mercury vapor lamp. The reaction was complete in *ca.* 1.5 h after which time only bands due to Os(CO)<sub>4</sub>( $\eta^2$ -C<sub>2</sub>Ph<sub>2</sub>) ( $\nu_{CO}$  2117, 2037, 2024, 1991 cm<sup>-1</sup>) were present. The solution was transferred from the immersion well and filtered, at low temperature, to a precooled (-78 °C) flask. The pentane was removed at -50 °C, and the residue was redissolved in a hexane solution containing additional (91.4 mg, 0.513 mmol) diphenylacetylene. The resulting solution was warmed to room temperature. After 4 h only minimal amounts of ( $\eta^4$ -C<sub>4</sub>-Ph<sub>4</sub>CO)Os(CO)<sub>3</sub> (**4**) were detected by FT-IR spectroscopy. The complete preparation and characterization of Os(CO)<sub>4</sub>( $\eta^2$ -C<sub>2</sub>-Ph<sub>2</sub>) will be detailed in a forthcoming publication.

**Preparation of (Tetraphenylcyclopentadienyl)osmium Complexes.** The mass spectral data and elemental analyses for compounds **7** and **8** are listed in Table 1. The IR and <sup>1</sup>H and <sup>13</sup>C NMR data for **7** and **8**, along with the data for **5** and **6**, are listed in Table 6.

( $\eta^5$ -C<sub>4</sub>Ph<sub>4</sub>O)<sub>2</sub>( $\mu$ -H)<sub>2</sub>Os<sub>2</sub>(CO)<sub>4</sub> (**7**). A solution containing ( $\eta^4$ -C<sub>4</sub>Ph<sub>4</sub>CO)Os(CO)<sub>3</sub> (**4**) (140 mg, 0.212 mmol), sodium carbonate (300 mg), and water (1.0 mL) in THF (20 mL) was heated in a closed bomb under nitrogen at 110 °C for 4 h. After cooling, the solvent was removed *in vacuo* and the residue extracted with methylene chloride. Following drying (MgSO<sub>4</sub>) and evaporation, the residue was chromatographed on a silica column, using CH<sub>2</sub>Cl<sub>2</sub>-petroleum ether (3:1) as eluant, to give **7** as yellow platelets in 19% yield (25.0 mg, 0.020 mmol), mp 270–277 °C (dec). The second complex eluted (75 mg, 56%) was found to be identical with **8**.

( $\eta^5$ -C<sub>4</sub>Ph<sub>4</sub>COH)Os(CO)<sub>2</sub>H (**8**). A solution containing ( $\eta^4$ -C<sub>4</sub>Ph<sub>4</sub>CO)Os(CO)<sub>3</sub> (**4**) (70 mg, 0.106 mmol), sodium carbonate (150 mg), and water (0.5 mL) in THF (10 mL) was heated in a closed bomb under nitrogen at 110 °C for 1 h. After cooling, the solvent was removed *in vacuo* and the residue extracted with methylene chloride, which, after drying (MgSO<sub>4</sub>) and evaporation, was chromatographed on a silica column (CH<sub>2</sub>-Cl<sub>2</sub> eluant). Complex **8** was recovered as a white solid in 83% yield (56 mg, 0.088 mmol) which gave a single TLC spot (silica-methylene chloride), mp 200 °C (dec).

**X-ray Crystal Structure Analysis of ( $\eta^4$ -C<sub>4</sub>Me<sub>2</sub>Et<sub>2</sub>CO)Os(CO)<sub>3</sub> (**2d**).** A colorless, X-ray-quality crystal of **2d**, grown by cooling a hexane solution of **2d** to -5 °C, was mounted on the goniometer of a Enraf-Nonius CAD4 diffractometer. The crystal data and general conditions of data collection and structure refinement are given in Table 2. Three intensity and orientation standards were checked after every 120 min of exposure time and showed no appreciable decay. The position of the Os atom was determined using the direct

**Table 3. Positional ( $\times 10^3$ ) and Isotropic Thermal ( $\times 10^2$ ) Parameters<sup>a</sup> for Non-Hydrogen Atoms of **2d****

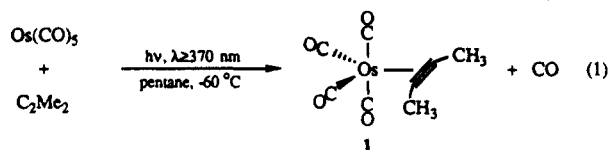
atom	x	y	z	U, Å <sup>2</sup>
Os	52.72(6)	-329.64(4)	-98.56(4)	4.73(1)
O1	53(1)	-174.5(6)	-300.2(7)	6.2(3)
O6	28(2)	-151.5(7)	-9(1)	11.8(6)
O7	345(1)	-393.7(9)	95.4(9)	10.4(5)
O8	-230(1)	-409.8(8)	-26.5(9)	10.0(5)
C1	-88(1)	-304.6(7)	-274.6(9)	4.1(4)
C2	-40(2)	-393.3(9)	-263(1)	6.1(5)
C3	145(2)	-394.4(9)	-220(1)	6.0(5)
C4	199(1)	-305.3(9)	-212(1)	5.2(5)
C5	57(1)	-249.5(8)	-268(1)	4.7(4)
C6	44(2)	-221.5(9)	-41(2)	8.8(7)
C7	228(2)	-371(1)	24(1)	7.6(6)
C8	-120(2)	-380(1)	-48(1)	7.1(6)
C11	-269(2)	-273(1)	-326(1)	7.6(6)
C21	-154(2)	-471(1)	-298(1)	9.3(7)
C31	253(2)	-474(1)	-205(1)	9.2(7)
C32	296(2)	-494(1)	-309(1)	12.2(8)
C41	378(2)	-276(1)	-185(1)	10.1(8)
C42	422(2)	-194(1)	-116(2)	12.3(9)

<sup>a</sup> Numbers in parentheses are the estimated standard deviations in the last significant digit.

methods program SHELXS-86,<sup>12</sup> and the remaining non-hydrogen atoms were located in difference Fourier maps after least squares refinement. Reflection data were corrected for absorption using the method of Walker and Stuart;<sup>13</sup> the minimum and maximum correction coefficients were 0.5077 and 1.5019. All H atoms were included at their idealized positions (calculated by assuming C-H = 0.95 Å and sp<sup>3</sup> geometry) and constrained to "ride" with the attached C atom. The H atoms were assigned fixed, isotropic thermal parameters 1.2 times those of the parent C atom. The final atomic coordinates are given in Table 3.

## Results and Discussion

**Synthesis and Characterization of Os(CO)<sub>4</sub>(η<sup>2</sup>-C<sub>2</sub>Me<sub>2</sub>) (1).** The synthesis of Os(CO)<sub>4</sub>(η<sup>2</sup>-C<sub>2</sub>Me<sub>2</sub>) is similar to that previously described for other osmium-alkyne compounds.<sup>6a-c</sup> Specifically, excess 2-butyne and Os(CO)<sub>5</sub> were photolyzed ( $\lambda \geq 370$  nm, -60 °C) to generate Os(CO)<sub>4</sub>(η<sup>2</sup>-C<sub>2</sub>Me<sub>2</sub>) (**1**) in moderate yield (eq 1). Low temperatures are required as **1** is thermally



unstable and will decompose to unidentified products at temperatures exceeding -25 °C. Owing to its unstable nature only spectroscopic data on Os(CO)<sub>4</sub>(η<sup>2</sup>-C<sub>2</sub>Me<sub>2</sub>) were obtained.

The mass spectrum of Os(CO)<sub>4</sub>(η<sup>2</sup>-C<sub>2</sub>Me<sub>2</sub>), obtained at ca. -20 °C, shows a peak due to the molecular ion, Os(CO)<sub>4</sub>(η<sup>2</sup>-C<sub>2</sub>Me<sub>2</sub>)<sup>+</sup>, at 358 amu followed by signals due to the successive loss of four carbonyl ligands. The fragment Os(CO)<sub>4</sub><sup>+</sup> is also observed, representing the loss of 2-butyne from **1**. Similar observations were made in the mass spectra of Os(CO)<sub>4</sub>(η<sup>2</sup>-HCCH) and Os(CO)<sub>4</sub>{η<sup>2</sup>-C<sub>2</sub>(SiMe<sub>3</sub>)<sub>2</sub>}.<sup>6a,c</sup>

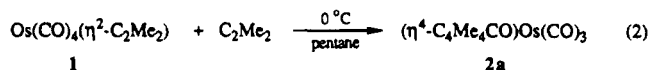
(12) Sheldrick, G. M. SHELXS-86. A Program for Crystal Structure Determination. Institut für Anorganische Chemie der Universität Göttingen, 1986.

(13) Walker, N.; Stuart, D. *Acta Crystallogr.* **1983**, *A39*, 158.

The FT-IR spectrum of **1** in the carbonyl region shows three bands, a characteristic high-frequency, low-intensity band due to the symmetrical stretch of the axial carbonyls at 2106 cm<sup>-1</sup> and two strong bands at 2020 and 1984 cm<sup>-1</sup>. For Os(CO)<sub>4</sub>(η<sup>2</sup>-alkyne) complexes with C<sub>2v</sub> symmetry, four terminal carbonyl bands are expected and often observed.<sup>6a-c</sup> In compound **1**, the band at 2020 cm<sup>-1</sup> is likely comprised of two overlapping IR-active bands.

The <sup>1</sup>H NMR and <sup>13</sup>C NMR spectra for **1** in toluene-d<sub>8</sub> (-70 °C) show methyl signals at 2.03 and 14.8 ppm, respectively, which are 0.50 and 11.6 ppm downfield of those of free 2-butyne. Coordination of an alkyne to a metal center reduces the C-C triple bond character of the alkyne, and this is usually reflected in a downfield <sup>13</sup>C NMR shift of the coordinated alkyne carbons.<sup>14</sup> Indeed, Templeton has reported an empirical relationship that correlates the number of electrons donated by an alkyne and its <sup>13</sup>C NMR chemical shift.<sup>14a</sup> The <sup>13</sup>C NMR results obtained for Os(CO)<sub>4</sub>(η<sup>2</sup>-C<sub>2</sub>Me<sub>2</sub>) are not in accord with these expectations as the alkyne carbons in **1** ( $\delta = 69.7$  ppm) are shifted upfield compared to those in free 2-butyne ( $\delta = 74.6$  ppm). However, within the series of Os(CO)<sub>4</sub>(η<sup>2</sup>-alkyne) complexes that we have prepared, there are precedents for such unusual results. For Os(CO)<sub>4</sub>{η<sup>2</sup>-C<sub>2</sub>(SiMe<sub>3</sub>)<sub>2</sub>}, an upfield coordination shift is observed,<sup>6c</sup> and Os(CO)<sub>4</sub>(η<sup>2</sup>-HCCH) undergoes only a small downfield coordination shift of 1.6 ppm.<sup>6a</sup> The unusual <sup>13</sup>C NMR chemical shifts may be related to a four-electron repulsive interaction between the coordinated alkyne and the d<sup>8</sup> transition metal center.<sup>15</sup>

**Thermal Reaction of M(CO)<sub>4</sub>(η<sup>2</sup>-C<sub>2</sub>R<sub>2</sub>) with Alkynes: Preparation of (η<sup>4</sup>-CPD)M(CO)<sub>3</sub> (M = Os (2), Ru (3)).** The observation that Os(CO)<sub>4</sub>(η<sup>2</sup>-C<sub>2</sub>Me<sub>2</sub>) reacts with alkynes was first noticed as an anomaly during infrared monitoring of the photochemical preparation of Os(CO)<sub>4</sub>(η<sup>2</sup>-C<sub>2</sub>Me<sub>2</sub>). As the reaction proceeded, only a decrease in the concentration of Os(CO)<sub>5</sub> coupled with an increased concentration of a species with three strong terminal carbonyl bands was observed in the FT-IR spectra at room temperature; bands due to **1** were not detected. Later it was discovered that a thermal reaction occurs in the IR cell between **1** and an additional molecule of 2-butyne to produce (η<sup>4</sup>-C<sub>4</sub>Me<sub>4</sub>CO)-Os(CO)<sub>3</sub> (**2a**). This was verified by deliberate reaction of 2-butyne with isolated **1** (eq 2).



The spectral characteristics of **2a** are in accord with previously reported (η<sup>4</sup>-CPD)M(CO)<sub>3</sub> compounds.<sup>3,10,16</sup> The IR spectrum consists of four carbonyl bands, three strong terminal carbonyl bands at 2071, 2006, and 1988 cm<sup>-1</sup> and a weak signal at 1676 cm<sup>-1</sup> due to the ketonic carbonyl. In the <sup>1</sup>H NMR spectrum, two singlets of equal intensity are observed. Similarly, two <sup>13</sup>C NMR resonances are observed for the methyl carbons. The

(14) (a) Templeton, J. L. *Adv. Organomet. Chem.* **1989**, *29*, 1. (b) Chisholm, M. H.; Clark, H. C.; Manzer, L. E.; Stothers, J. B. *J. Am. Chem. Soc.* **1972**, *94*, 5087.

(15) Marinelli, G.; Streib, W. E.; Huffman, J. C.; Caulton, K. G.; Gagné, M. R.; Takats, J.; Dartiguenave, M.; Chardon, C.; Jackson, S. A.; Eisenstein, O. *Polyhedron* **1990**, *9*, 1867.

(16) (a) Sappa, E.; Centini, G.; Gambino, O.; Valle, M. *J. Organomet. Chem.* **1969**, *20*, 201. (b) Sears, C. T.; Stone, F. G. A. *J. Organomet. Chem.* **1968**, *11*, 644.

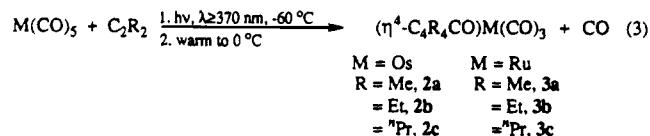
**Table 4. FT-IR and  $^{13}\text{C}$  NMR Data for  $\text{M}(\eta^4\text{-C}_4\text{R}_4\text{CO})(\text{CO})_3$  ( $\text{M} = \text{Ru}, \text{Os}$ ) Complexes**

compd	IR (pentane, $\text{cm}^{-1}$ )		$^{13}\text{C}$ NMR (23 $^\circ\text{C}$ , $\delta$ , ppm) <sup>a</sup>			
	$\nu(\text{CO})$	$\nu(\text{C}=\text{O})$	outer ( $\text{C}_o$ )	inner ( $\text{C}_i$ )	$\text{C}=\text{O}$	$\text{M}(\text{CO})$
<b>2a</b>	2071 (s), 2006 (s), 1988 (s)	1676 (w)	71.9	97.1	175.7	176.1
<b>2b</b>	2070 (s), 2004 (s), 1987 (s)	1669 (w)	80.7	101.1	177.0	175.4
<b>2c</b>	2069 (s), 2004 (s), 1987 (s)	1669 (w)	79.5	100.1	177.3	175.4
<b>2d</b>	2070 (s), 2005 (s), 1988 (s)	1672 (w)	73.4, <sup>b</sup> 80.5 <sup>c</sup>	96.4, <sup>d</sup> 101.4 <sup>e</sup>	175.2	175.2
<b>2e</b>	2071 (s), 2005 (s), 1988 (s)	1673 (w)	73.0, <sup>b</sup> 79.2 <sup>f</sup>	96.6, <sup>d</sup> 100.3 <sup>g</sup>	176.4	175.6
<b>3a</b>	2073 (s), 2016 (s), 1996 (s)	1670 (w)	77.5	101.2	175.4	196.0
<b>3b</b>	2072 (s), 2015 (s), 1996 (s)	1663 (w)	85.4	105.6	176.3	195.6
<b>3c</b>	2071 (s), 2014 (s), 1995 (s)	1662 (w)	84.2	104.6	176.3	195.7
<b>4<sup>h</sup></b>	2079 (s), 2015 (s), 1997 (s) <sup>i</sup>	1677 (w) <sup>i</sup>	78.4	102.0	173.9	173.6

<sup>a</sup> Recorded at 90.5 MHz; chemical shifts relative to TMS in  $\text{CDCl}_3$ . "Inner" and "outer" refer to the carbon atoms that belong to the closed and open ends of the 1,3-dienes. <sup>b</sup>  $\text{C}_o\text{-Me}$ . <sup>c</sup>  $\text{C}_o\text{-Et}$ . <sup>d</sup>  $\text{C}_i\text{-Me}$ . <sup>e</sup>  $\text{C}_i\text{-Et}$ . <sup>f</sup>  $\text{C}_o\text{-}^n\text{Pr}$ . <sup>g</sup>  $\text{C}_i\text{-}^n\text{Pr}$ . <sup>h</sup> Burke, M.; Funk, T.; Takats, J. *Organometallics* **1994**, *13*, 2109. <sup>i</sup> Recorded in cyclohexane.

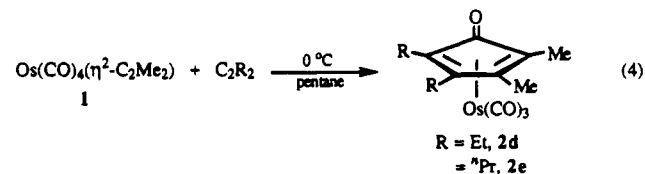
three terminal carbonyls give rise to a single  $^{13}\text{C}$  NMR resonance down to  $-60$   $^\circ\text{C}$ , indicating rapid carbonyl group scrambling,<sup>17</sup> consistent with previous work.<sup>10b</sup> Finally, two  $^{13}\text{C}$  NMR resonances are observed at 71.9 and 97.1 ppm which can be assigned to the CPD carbons and are in the region associated with coordinated diene-type structures.<sup>10b,17,18</sup>

The discovery of the facile alkyne coupling to produce  $(\eta^4\text{-C}_4\text{Me}_4\text{CO})\text{Os}(\text{CO})_3$  led to the development of a general synthesis for compounds of the type  $(\eta^4\text{-C}_4\text{R}_4\text{CO})\text{M}(\text{CO})_3$  ( $\text{M} = \text{Ru}, \text{Os}$ ;  $\text{R} = \text{Me}, \text{Et}, ^n\text{Pr}$ ).<sup>19</sup> This general method involves the low-temperature photolysis of  $\text{M}(\text{CO})_5$  ( $\text{M} = \text{Ru}, \text{Os}$ ) in the presence of an excess amount of the appropriate alkyne ( $\text{C}_2\text{R}_2$ ,  $\text{R} = \text{Me}, \text{Et}, ^n\text{Pr}$ ). After the photolysis is complete, as judged by the disappearance of  $\text{M}(\text{CO})_5$ , the solutions are warmed to  $0$   $^\circ\text{C}$ . This results in relatively clean conversions to the corresponding cyclopentadienone species in modest yields (eq 3).



The mass spectral and elemental analytical data for **2**–**3** are listed in Table 1; the IR and  $^{13}\text{C}$  NMR data listed in Table 4. The only exception to the above synthetic strategy involves the reaction of  $\text{Ru}(\text{CO})_5$  with excess 2-butyne. The extreme thermal instability of  $\text{Ru}(\text{CO})_4(\eta^2\text{-C}_2\text{Me}_2)$  necessitates that the photolysis reaction be carried out at  $-5$   $^\circ\text{C}$  so that any  $\text{Ru}(\text{CO})_4(\eta^2\text{-C}_2\text{Me}_2)$  formed reacts immediately with excess 2-butyne in solution.

In an effort to extend the method,  $\text{Os}(\text{CO})_4(\eta^2\text{-C}_2\text{Me}_2)$  was treated with different alkynes. Gratifyingly, **1** undergoes smooth copuling reactions with 3-hexyne and 4-octyne to yield the corresponding  $(\eta^4\text{-C}_4\text{Me}_2\text{R}_2\text{CO})\text{Os}(\text{CO})_3$  complexes (eq 4). The structures shown are those expected from simple alkyne–CO coupling.



It is interesting to note that, although  $\text{Os}(\text{CO})_4(\eta^2\text{-C}_2\text{Ph}_2)$  can be cleanly generated by low-temperature photolysis of  $\text{Os}(\text{CO})_5$  and diphenylacetylene ( $\text{DPA} = \text{C}_2\text{Ph}_2$ ), thermal reaction is not the method of choice for the preparation of  $(\eta^4\text{-C}_4\text{Ph}_4\text{CO})\text{Os}(\text{CO})_3$  (**4**). Indeed, stirring  $\text{Os}(\text{CO})_4(\eta^2\text{-C}_2\text{Ph}_2)$  with excess DPA at room temperature in hexane for several hours gives mostly unidentified decomposition products and only minimal amounts of  $(\eta^4\text{-C}_4\text{Ph}_4\text{CO})\text{Os}(\text{CO})_3$  (**4**). The lack of thermally induced alkyne coupling is consistent with our previous observation that  $\text{M}(\text{CO})_4(\eta^2\text{-CF}_3\text{C}_2\text{CF}_3)$  ( $\text{M} = \text{Ru}, \text{Os}$ ), containing the electron-deficient hexafluoro-2-butyne, also do not undergo such a reaction. A convenient synthesis of  $(\eta^4\text{-C}_4\text{Ph}_4\text{CO})\text{Os}(\text{CO})_3$  (**4**) is prolonged photolysis of  $\text{Os}_3(\text{CO})_{12}$  in the presence of excess DPA.<sup>10b</sup>

The FT-IR,  $^1\text{H}$  NMR, and  $^{13}\text{C}$  NMR data for **2d**–**3** are consistent with their formulation as  $(\eta^4\text{-CPD})\text{Os}(\text{CO})_3$  complexes (Tables 1 and 4), and this was also confirmed by an X-ray crystal structure analysis of complex **2d**. A perspective view of the molecule, with numbering scheme, is shown in Figure 1. Relevant bond distances and selected bond angles are listed in Table 5.

The formation of the CPD ring from coupling of the 2-butyne and 3-hexyne units is clearly visible. The structure of **2d** is consistent with other  $(\eta^4\text{-diene})\text{M}(\text{CO})_3$  type complexes.<sup>10b,20</sup> The geometry around the Os center can be described as a tetragonal pyramid. The apical carbonyl, C6–O6, occupies a site eclipsed by the ring ketone, C5–O1. The other two carbonyls and the midpoints of the  $\eta^4$ -coordinated cyclopentadienone ring form the four basal coordination sites.

The Os–C1, Os–C2, Os–C3, and Os–C4 distances are similar to those in related systems. Most notably, the solid-state structure of the tetraphenyl-substituted derivative  $(\eta^4\text{-C}_4\text{Ph}_4\text{CO})\text{Os}(\text{CO})_3$  (**4**) has been determined.<sup>10b</sup> The M–C distances in **2d** are essentially equal (range 2.19(2)–2.23(1) Å), whereas the corresponding distances in **4** range from 2.20(1) to 2.27(1) Å, with the Os-to-outer diene carbon distances being somewhat longer, as is commonly observed.<sup>10b</sup> The diene C–C distances in **2d** are C1–C2 = 1.41(2) Å, C2–

(17) Kruczynski, L.; Takats, J. *Inorg. Chem.* **1976**, *15*, 3140.

(18) (a) Mann, B. E.; Taylor, B. F.  *$^{13}\text{C}$  NMR Data for Organometallic Compounds*; Academic: New York, 1981. (b) Zobl-Ruh, S.; Von Philipsborn, W. *Helv. Chim. Acta.* **1980**, *63*, 773. (c) Zobl-Ruh, S.; Von Philipsborn, W. *Helv. Chim. Acta.* **1981**, *64*, 2378. (d) Mann, B. E. *Adv. Organomet. Chem.* **1974**, *12*, 135.

(19) (a) The synthesis of  $(\eta^4\text{-C}_4\text{Me}_4\text{CO})\text{Os}(\text{CO})_3$  has been reported although the spectroscopic data are not consistent with our results: Bruce, M. I.; Cooke, M.; Green, M.; Westlake, D. J. *J. Chem. Soc. A* **1969**, 987. (b)  $(\eta^4\text{-C}_4\text{Et}_4\text{CO})\text{Ru}(\text{CO})_3$  has been reported: ref 16b. (c) The synthesis of  $(\eta^4\text{-CPD})\text{Ru}(\text{CO})_3$  compounds with electron-withdrawing substituents ( $\text{R} = \text{CF}_3, \text{Ph}$ ) has been reported: ref 10a.

(20) LiShingMan, L. K. K.; Reuvers, J. G. A.; Takats, J.; Deganello, G. *Organometallics* **1983**, *2*, 28 and references therein.

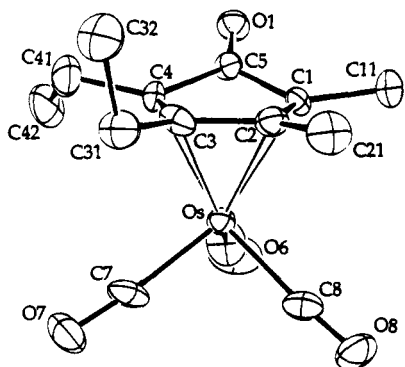


**Figure 1.** ORTEP view of **2d**. Probability ellipsoids are shown at the 50% level for non-hydrogen atoms.

**Table 5.** Selected Bond Lengths and Angles for **2d**

Bond Lengths (Å) <sup>a</sup>			
Os—C1	2.22(1)	C1—C2	1.41(2)
Os—C2	2.23(1)	C1—C5	1.46(2)
Os—C3	2.19(2)	C2—C3	1.46(2)
Os—C4	2.21(1)	C3—C4	1.43(2)
Os—C6	1.83(1)	C4—C5	1.45(2)
Os—C7	1.88(1)	O6—C6	1.18(2)
Os—C8	1.92(1)	O7—C7	1.15(2)
O1—C5	1.22(2)	O8—C8	1.13(1)

Bond Angles (deg) <sup>a</sup>			
C2—C1—C5	111(1)	O1—C5—C1	127(1)
C2—C3—C4	107(1)	O1—C5—C4	131(1)
C3—C4—C5	110(1)	Os—C6—O6	175(1)
C1—C5—C4	102(1)	Os—C7—O7	174(1)
C1—C2—C3	106(1)	Os—C8—O8	175(1)

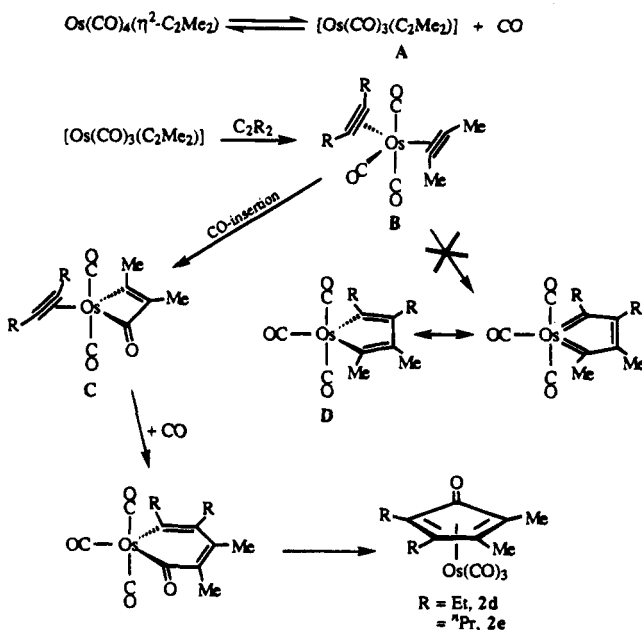
<sup>a</sup> Esd's given in parentheses.

C3 = 1.46(2) Å, and C3—C4 = 1.43(2) Å, while the corresponding C—C bond distances in **4** are 1.480(18), 1.428(15), and 1.456(17) Å. The long—short—long alternation in **4**, in contrast to the short—long—short alternation in **2d**, implies a stronger Os—CPD back-bonding interaction in **4** as compared to **2d**. This is as expected from the nature of the substituents on the respective CPD rings and is consistent with the slightly larger bending of the ring carbonyl away from the planar 1,3-diene moiety in **4** (20.4°) compared to that in **2d** (19.8°).

**Mechanism of Formation of  $(\eta^4\text{-CPD})\text{Os}(\text{CO})_3$  Complexes: A Proposal.** The observation that  $\text{Os}(\text{CO})_4(\eta^2\text{-C}_2\text{Me}_2)$  can be used as a starting point in alkyne—carbonylation reactions is significant for the overall mechanism for the formation of cyclopentadienones. Iron carbonyl mediated alkyne—carbonyl coupling reactions are thought to proceed *via* undetected  $\text{Fe}(\text{CO})_4(\eta^2\text{-alkyne})$  intermediates; thus, the thermal reaction of  $\text{Os}(\text{CO})_4(\eta^2\text{-C}_2\text{Me}_2)$  with alkynes is an important piece of the puzzle. Related alkyne coupling reactions at other  $d^8$  metal centers are known.<sup>1f,21</sup> Specifically, Britzinger and workers synthesized  $\text{CpCo}(\eta^4\text{-C}_4\text{Ph}_4\text{CO})$  from the photolysis of  $\text{CpCo}(\text{CO})_2$  in the presence of diphenylacetylene and suggested the intermediacy of  $\text{CpCo}(\text{CO})(\eta^2\text{-C}_2\text{Ph}_2)$ .<sup>21</sup> Although there was IR evidence for  $\text{CpCo}(\text{CO})(\eta^2\text{-C}_2\text{Ph}_2)$ , this species could not be isolated.

The proposed scenario for the formation of compounds **2d-e**, and by extension to the related  $(\eta^4\text{-CPD})\text{M}(\text{CO})_3$  ( $\text{M} = \text{Fe}, \text{Ru}, \text{Os}$ ) derivatives, is given in Scheme 1. The

**Scheme 1.** Proposed Mechanism for Formation of **2d-e**



initial step is dissociation of CO from complex **1**. This is consistent with other work in our laboratories which has shown that CO loss from  $\text{M}(\text{CO})_4(\eta^2\text{-RCCR}')$  ( $\text{M} = \text{Ru}, \text{Os}$ ) species is a common initiation step in their reactions with nucleophiles.<sup>6a-b,8,22</sup> To explain the lability of a CO ligand in  $\text{M}(\text{CO})_4(\eta^2\text{-RCCR}')$  complexes, one may invoke the ground-state four-electron destabilization that exists between the alkyne ligand and the  $d^8$  metal center.<sup>15</sup> In addition, there is potential stabilization of the " $\text{Os}(\text{CO})_3(\text{C}_2\text{Me}_2)$ " (**A**) intermediate with the alkyne ligand acting as a four-electron donor.<sup>15</sup> In this regard, we note the recent isolation and structural characterization of  $\text{Os}(\text{P}^i\text{Pr}_3)_2(\text{CO})(\text{C}_2\text{Ph}_2)$  where the two bulky,  $\sigma$ -donating phosphine ligands stabilize the molecule.<sup>23</sup> The isoelectronic  $\text{Ir}(\text{PMe}_2\text{Ph})_3(\text{DMAD})^+$  ( $\text{DMAD} = \text{C}_2(\text{CO}_2\text{Me})_2$ ) complex of  $C_s$  symmetry is stable, but it can add another DMAD ligand to yield the corresponding trigonal bipyramidal  $\text{Ir}(\text{PMe}_2\text{Ph})_3(\eta^2\text{-DMAD})_2^+$  species.<sup>15,24</sup> In contrast, the  $\text{Ir}(\text{triphos})^+$  ( $\text{triphos} = \text{MeC}(\text{CH}_2\text{PPh}_2)_3$ ) fragment has been shown to initiate alkyne cyclotrimerization reactions.<sup>24</sup> Related to this, the formation of cobaltacyclopentadienes from the isoelectronic  $\text{CpCo}(\text{alkyne})_2$  species has been observed by Yasufuku and Watatsuki.<sup>25</sup>

Coordination of a second alkyne molecule to " $\text{Os}(\text{CO})_3(\text{C}_2\text{Me}_2)$ " (**A**) is the proposed second step in the reaction. This finds precedent in the aforementioned iridium case.<sup>24</sup> The presence of *two* alkyne ligands in the 18-electron  $\text{Os}(\text{CO})_3(\eta^2\text{-C}_2\text{Me}_2)(\eta^2\text{-C}_2\text{R}_2)$  (**B**;  $\text{R} = \text{Et}, n\text{Pr}$ ) complex should result in an even larger destabilizing effect than in the starting complex, **1**, and provides the driving force for the next step. This could either be CO insertion into one of the  $\text{Os}(\eta^2\text{-alkyne})$  bonds to give the

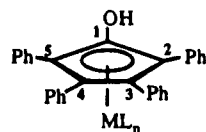
(22) Washington, J. Ph.D. Thesis, University of Alberta, 1994.

(23) Espuelas, J.; Estereulas, M. A.; Lahoz, F. J.; López, A. M.; Oro, L. A.; Valero, C. *J. Organomet. Chem.* **1994**, *468*, 223.

(24) Bianchini, C.; Caulton, K. G.; Chardon, C.; Doublet, M.-L.; Eisenstein, O.; Jackson, S. A.; Johnson, T. L.; Meli, A.; Peruzzini, M.; Streib, W. E.; Vacca, A.; Vizza, F. *Organometallics* **1994**, *13*, 2010.

(25) (a) Yasufuku, K.; Hamada, A.; Aoki, K.; Yamazaki, H. *J. Am. Chem. Soc.* **1980**, *102*, 4363. (b) Wakatsuki, Y.; Nomura, O.; Kitaura, K.; Morokuma, K.; Yamazaki, H. *J. Am. Chem. Soc.* **1983**, *105*, 1907.

(21) Lee, W.-S.; Britzinger, H. H. *J. Organomet. Chem.* **1977**, *127*, 93.

**Table 6.** FT-IR,  $^1\text{H}$  NMR, and  $^{13}\text{C}$  NMR Data for Tetraphenylcyclopentadienyl-Containing Os and Ru Complexes

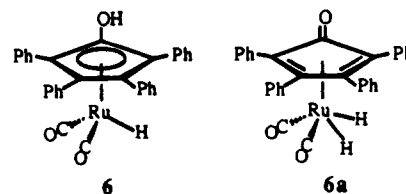
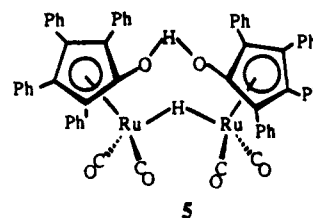
compnd	IR ( $\text{cm}^{-1}$ ) $\nu(\text{CO})$	$^1\text{H}$ NMR ( $\delta$ , ppm) <sup>c</sup>	$^{13}\text{C}$ NMR ( $\delta$ , ppm) <sup>d</sup>				
			$\text{C}_1$	$\text{C}_{2,5}$	$\text{C}_{3,4}$	Phenyl	M(CO)
5 (Ru)	2040 (s), 2010 (m), 1980 (s), 1970 (sh) <sup>a</sup>	7.10–7.73 (m, Ph), –17.7 (s, 1H)	154.3	87.8	103.5	132.0–127.0	200.8
6 (Ru)	2014 (s), 1955 (s) <sup>b</sup>	7.35–7.60 (m, Ph), –9.31 (s, 1H)	137.3	92.2	104.8	133.6–128.4	202.6
7 (Os)	2032 (s), 1998 (m), 1968 (s), 1952 (sh) <sup>a</sup>	6.69–7.50 (m, Ph), –21.5 (s, 1H)	157.1	84.5	99.4	132.0–127.0	181.3
8 (Os)	2000 (s), 1940 (s) <sup>b</sup>	7.05–7.46 (m, Ph), –13.1 (s, 1H)	134.5	88.4	101.5	134.5–125.9	183.1

<sup>a</sup> Measured in  $\text{CH}_2\text{Cl}_2$ . <sup>b</sup> Measured in THF. <sup>c</sup> Measured at 200.0 MHz in  $\text{C}_6\text{D}_6$ . <sup>d</sup> Measured at 50.3 MHz in  $\text{C}_6\text{D}_6$ .

osmacyclobutenone (**C**) or alkyne coupling to generate the osmacyclopentadiene (**D**). The proposed intermediates, unsaturated at first glance, can be stabilized by four-electron donation from the alkyne in **C** or contribution from the metallocyclopentatriene<sup>26</sup> resonance form in **D**. Both sequences of events have been postulated in alkyne–CO coupling processes.<sup>15,b,27</sup> Formation of stable metallacyclopentadienes with  $\pi$ -acidic alkynes (DMAD and HFB; HFB =  $\text{C}_2(\text{CF}_3)_2$ ) are well-known.<sup>28,29</sup> As shown in a recent study by Lindner and co-workers, an ionic alkyne coupling mechanism is favored due to the presence of an electron-rich metal center concomitant with alkynes bearing electron-withdrawing substituents.<sup>28a</sup> These electron-withdrawing groups can stabilize the negative charge which forms on the acetylenic carbon in the proposed reaction pathway. An ionic mechanism would be disfavored in the formation of **2** and **3** as alkyl substituents are attached to the acetylenic carbons. An oxidative alkyne coupling also seems to be unfavorable since, in a recent seminal paper, Bianchini, Caulton, and Eisenstein, using extended Hückel calculations, reported that the transformation from the trigonal bipyramidal bis(alkyne) complex  $\text{Ir}(\text{PH}_3)_3(\eta^2\text{-C}_2\text{H}_2)_2^+$ , isoelectronic to our proposed intermediate **B**, to the corresponding metallacyclopentadiene is a symmetry-forbidden process. We are thus left with the proposal that CPD ring formation with electron-rich alkynes proceeds along the alkyne–CO insertion route.

Supporting this postulate, we have discovered that CO insertion, promoted by bis(phosphines), into  $\text{Os}(\text{CO})_4(\eta^2\text{-HCCH})$  and  $\text{Os}(\text{CO})_4(\eta^2\text{-C}_2\text{Me}_2)$  is a very facile process.<sup>30</sup> Our proposed mechanism is in accord with this whereby the putative trigonal bipyramidal  $\text{Os}(\text{CO})_3(\eta^2\text{-C}_2\text{Me}_2)(\eta^2\text{-C}_2\text{R}_2)$  (**B**; R = Et, <sup>n</sup>Pr) intermediate, instead of alkyne coupling, undergoes a CO-insertion process which is driven by two four-electron destabilizing interactions. The formation of **2d–e** is completed by insertion of the second alkyne ligand followed by reductive coupling of the organic fragment.<sup>1f,h</sup>

**Catalytic Studies.** The dimeric ruthenium tetraphenylcyclopentadienyl complex, **5**, is currently the



best known catalyst for Tishchenko-type reactions. Its selectivity, rate, and turnover number allow the preparation of esters from aldehydes on a substantial scale.<sup>4f</sup> The stability of **5**, both in solution and in the solid state, makes it a convenient reagent. The recent introduction of formic acid as a promoter further simplifies the performance of this reaction.<sup>4f</sup> We have found that the key intermediate in the catalytic cycle of the Tishchenko reaction,<sup>4f</sup> using **5** as the charged catalyst, as well as hydrogenation reactions,<sup>4d</sup> is the mononuclear hydride **6**. It was experimentally demonstrated that this catalytic species transfers two hydrogen atoms to unsaturated organic substrates.<sup>4f</sup> Complex **6** has never been isolated, but spectroscopic data support the proposed structure rather than its tautomer **6a**. Complex **6** reverts to **5** upon exposure to air but is stable in solution under inert conditions.

Thus, due to its key role in several catalytic reactions, further insight into the structure and properties of **6** was desired. The isoelectronic Os complex (**8**), which has now been prepared from **4**, was pursued as a way of achieving this goal (eq 5). Treatment of the osmium compound **4**, after 1 h of reaction time, gave **8** as the sole product. Further heating leads to the formation of **7** as well. Complexes **7** and **8** can be separated by column chromatography using silica gel. Refluxing an acetone solution of **8** exposed to air slowly forms the dimer **7**, implying a sluggish oxidation process of the hydride. Complex **8**, in contrast to its ruthenium congener **6**, is stable in solution and in the solid state without the need for an inert atmosphere. The spectral data for the new osmium complexes **7** and **8** as well as their isoelectronic ruthenium complexes **5** and **6** are given in Table 6.

(26) Albers, M. O.; deWaal, P. J. A.; Liles, D. C.; Robinson, D. J.; Singleton, E.; Wiege, M. B. *J. Chem. Soc., Chem. Commun.* **1986**, 1680.

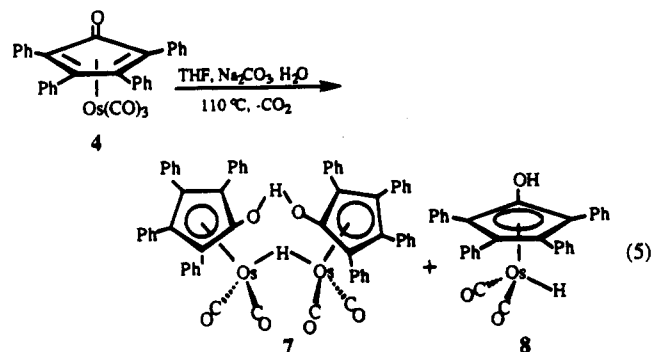
(27) Garlaschelli, L.; Malatesta, M. C.; Panzeri, S.; Albinati, A.; Ganazzoli, F. *Organometallics* **1987**, *6*, 63.

(28) (a) Lindner, E.; Kühbauch, H.; Mayer, H. A. *Chem. Ber.* **1994**, *127*, 1343. Lindner, E.; Kühbauch, H. *J. Organomet. Chem.* **1991**, *403*, C9. (c) Lindner, E.; Jansen, R.-M.; Mayer, H. A.; Hiller, W.; Fawzi, R. *Organometallics* **1989**, *8*, 2355. (d) Burke, M. R.; Takats, J. *J. Organomet. Chem.* **1986**, *302*, C25.

(29) Burt, R.; Cooke, M.; Green, M. *J. Chem. Soc. A* **1970**, 2981.

(30) Mao, T.-F.; Takats, J. Manuscript in preparation.





On the basis of the infrared carbonyl stretching frequencies, it may be concluded that **8** displays greater  $\text{M}\text{--CO}$  back-donation than **6**. The same trend can also be observed in the osmium and ruthenium dimers **5** and **7** (Table 6). Also, all the ring C atoms of **8** resonate at higher field than those of **6**, indicating a more extensive delocalization of the metal electronic charge into the CPD ring system in the osmium complex. Such phenomenon has been observed previously down the group VIII triad.<sup>10b</sup> Complex **8** has greater polarization of the  $\text{M}\text{--H}$  bond; the metal hydride resonance in **8** ( $-13.1$  ppm) is nearly 4 ppm upfield to that of **6** ( $-9.31$  ppm). A similar trend is also observed for the Os and Ru dimers **5** and **7** (Table 6). Although formally the osmium atom in **8** has a  $d^6$  electronic configuration, the increased electron donation to the carbonyl ligands and the CPD ring as compared to **6** causes it to be an inferior reducing agent relative to the Ru atom in **6**.

The catalytic activity of **8** was examined. Attempted hydrogenation of cyclohexanone with hydrogen (47 atm) at  $105^\circ\text{C}$  over a period of 4 h gave minimal conversion to the corresponding alcohol. A Tishchenko-type reaction with benzaldehyde with formic acid as a promoter was also attempted. Minimal product conversion, under toluene reflux, was seen over a 4 h period. Under the above conditions, the isoelectronic complex **6** catalyzes these reactions very efficiently.<sup>4f</sup> In addition, the hydrogenation of benzaldehyde at  $105^\circ\text{C}$  and 25 atm hydrogen gave only a low yield (30%) of benzyl alcohol after 96 h. Thus, not unexpectedly, **8** is a very sluggish hydrogenation catalyst compared to its Ru analogue.

Subjecting  $(\eta^4\text{-C}_4\text{Me}_4\text{CO})\text{Os}(\text{CO})_3$  (**2a**) to the reaction conditions of eq 5 gave back **2a**; no other complex could be detected in the reaction mixture by TLC and FT-IR analysis. This is in contrast to the facile formation of the isostructural complex **8** (eq 5) and must imply a diminished reactivity of the Os-bound CO groups in **2a** toward nucleophilic attack of hydroxide ion. Inspection of the IR stretching frequencies of the CO groups of **2a** and **4** (Table 4) reveals a shift to lower wavenumbers

in **2a** relative to **4**. This then implicates a stronger Os—CO bond in **2a** as a result of better Os—CO back-donation, consonant with the weaker  $\pi$ -acidity of tetramethylcyclopentadienone compared to tetraphenylcyclopentadienone.

**Summary.** Facile thermal reaction of  $\text{Os}(\text{CO})_4(\eta^2\text{-C}_2\text{Me}_2)$  (**1**) with excess alkyne offers an attractive method for the synthesis of (cyclopentadienone)tricarbonylosmium complexes and provides insights into the mode of formation of these species. The increased reactivity of **1** is due to a combination of enhanced CO lability and a weakly bound alkyne ligand, as compared to other  $\text{Os}(\text{CO})_4(\eta^2\text{-alkyne})$  species. We attribute this and subsequent facile alkyne coupling reactions involving **1** to the four-electron destabilization between 2-butyne and the  $d^8$  metal center. In addition, electron-rich alkynes such as 3-hexyne and 4-octyne may readily attack the pseudovacant coordination site left after CO loss from **1**. These alkynes can disrupt the four-electron interaction that stabilizes the putative  $\text{Os}(\text{CO})_3(\text{C}_2\text{Me}_2)$  intermediate, and the dramatic rise in electron density following coordination of a second electron-rich alkyne provides the impetus for the formation of the cyclopentadienone complexes. These features provided by electron-rich alkynes can also be exploited to effect the synthesis of a number of aliphatically substituted  $(\eta^4\text{-CPD})\text{M}(\text{CO})_3$  ( $\text{M} = \text{Ru}, \text{Os}$ ) complexes.

In addition, the synthesis of  $(\eta^5\text{-C}_4\text{Ph}_4\text{COH})\text{Os}(\text{CO})_2\text{H}$  (**8**) was also carried out and its catalytic activity was investigated. The increased thermal and air stability of this complex allowed for a more complete understanding of the role of the ruthenium analogue, **6**, in several catalytic cycles. Not unexpectedly, the increased stability of **8** resulted in minimal catalytic activity. Attempts to increase the catalytic potential of the osmium-based systems by increasing the donor ability of the CPD ring were unsuccessful. Thus, although the Ru-based complexes are superior catalysts, the Os analogues allow for the isolation and complete characterization of a key intermediate in the ruthenium-catalyzed reactions.

**Acknowledgment.** We wish to thank the Natural Sciences and Engineering Research Council of Canada for financial support of this work and a graduate scholarship to J.W. Support from the University of Alberta and Johnson-Mathey (loan of  $\text{OsO}_4$ ) is also gratefully acknowledged.

**Supporting Information Available:** Tables of anisotropic thermal parameters, least squares planes, torsional angles, and derived hydrogen atom positions and  $U$  values for **2d** (5 pages). Ordering information is given on any current masthead page.

OM950333I



# Reductive Dehalogenation of 4,8-Dihaloctakis(1,1,2-trimethylpropyl)tetracyclo[3.3.0.0<sup>2,7</sup>.0<sup>3,6</sup>]octasilanes with Sodium: Formation of Octasilacubane

Masafumi Unno, Hiroaki Shioyama, Masami Ida, and Hideyuki Matsumoto\*

Department of Applied Chemistry, Faculty of Engineering, Gunma University, Kiryu, Gunma 376, Japan

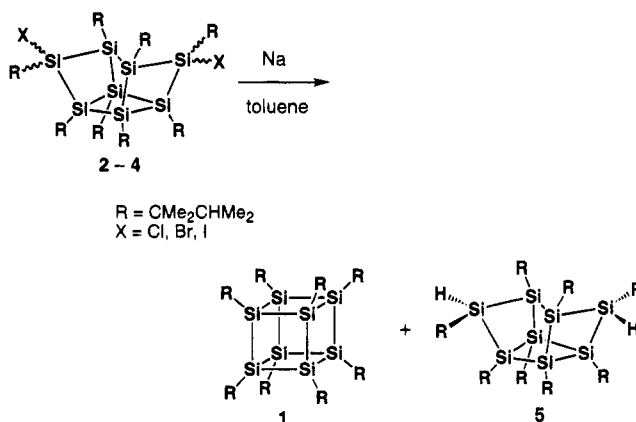
Received January 23, 1995\*

The reductive dehalogenation of 4,8-dichloro-, 4,8-dibromo-, and 4,8-diiodooctakis(1,1,2-trimethylpropyl)tetracyclo[3.3.0.0<sup>2,7</sup>.0<sup>3,6</sup>]octasilanes (**2-4**) with sodium resulted in unprecedented skeletal rearrangement to generate octakis(1,1,2-trimethylpropyl)octasilacubane (**1**), along with a reduced product, 4,8-dihydrooctakis(1,1,2-trimethylpropyl)tetracyclo[3.3.0.0<sup>2,7</sup>.0<sup>3,6</sup>]octasilane (**5**). The structure of **5** was determined by X-ray crystallography.

## Introduction

There is considerable interest in the syntheses and properties of [*n*]prismanes (where *n* = 3-5) of group 14 elements, Si, Ge, and Sn.<sup>1-3</sup> During our work on the chemistry of octasilacubanes and related compounds, we found that the chlorination of octakis(1,1,2-trimethylpropyl)octasilacubane (**1**)<sup>3</sup> with PCl<sub>5</sub> resulted in skeletal rearrangement with concomitant formation of stereoisomeric 4,8-dichlorooctakis(1,1,2-trimethylpropyl)tetracyclo[3.3.0.0<sup>2,7</sup>.0<sup>3,6</sup>]octasilanes (**2**).<sup>4</sup> Also we found that the halogenation of octasilacubane **1** with Br<sub>2</sub> or with I<sub>2</sub> produced stereoisomeric 4,8-dibromo- or 4,8-diiodooctakis(1,1,2-trimethylpropyl)tetracyclo[3.3.0.0<sup>2,7</sup>.0<sup>3,6</sup>]octasilanes (**3** or **4**), as described in the present manuscript. We have thus commenced an investigation of the behavior of these dihalooctasilanes toward active metals in hoping that they can serve as starting materials for a range of new silicon polyhedranes.<sup>5</sup> In this paper we report our finding that the reductive dehalogenation of **2-4** with sodium metal led to unusual skeletal rearrangement, forming octasilacubane **1**, along with a reduced product, 4,8-dihydrooctakis(1,1,2-trimethylpropyl)tetracyclo[3.3.0.0<sup>2,7</sup>.0<sup>3,6</sup>]octasilane (**5**) (Scheme 1).

## Scheme 1



## Results and Discussion

**Dechlorination of Dichlorooctasilane 2.** When a solution of stereoisomeric **2** in toluene was heated with a large excess sodium<sup>7</sup> at 110 °C for 4 h under an atmosphere of argon, 82% of **2** was dechlorinated and octasilacubane **1** was formed in 70% yield (based on the consumption of **2**) as red-orange crystals, along with reduced product **5** (18%). The identity of **1** was established by a comparison of its physical properties (HPLC retention time, mp, and NMR, IR, and UV spectra, etc.) with those of an authentic sample.<sup>3</sup> The solid structure of **5** was determined by X-ray crystallography. The ORTEP drawing is shown in Figure 1. Crystallographic data, positional parameters, and selected bond lengths and angles are given in Tables 1-3. Compound **5** crystallizes in the *P*2<sub>1</sub>/*a* space group with four molecules per unit cell. As indicated by the X-ray results, the SiH hydrogen atoms occupy *endo,endo* and the bulky 1,1,2-trimethylpropyl groups *exo,exo* positions (the positions relative to the bridged Si-Si bonds).

(6) A mixture of three isomers (*endo,exo-2/exo,exo-2/endo,endo-2* = 56/27/17) was used. The ratio of isomers for recovered dichlorides was 53/25/21, and the reactivities of three isomers toward dechlorination were thus thought to be basically similar.

(7) The reaction gave the highest yield of octasilacubane **1** when 12 equiv of sodium was used. An attempted dechlorination using 5 equiv of sodium resulted in the formation of trace amounts of **1**.

\* Abstract published in *Advance ACS Abstracts*, July 1, 1995.

(1) (a) Matsumoto, H.; Higuchi, K.; Hoshino, Y.; Koike, H.; Naoi, Y.; Nagai, Y. *J. Chem. Soc., Chem. Commun.* **1988**, 1083. (b) Sekiguchi, A.; Kabuto, C.; Sakurai, H. *Angew. Chem., Int. Ed. Engl.* **1989**, *28*, 55. (c) Nagase, S. *Angew. Chem., Int. Ed. Engl.* **1989**, *28*, 329. (d) Sita, L. R.; Kinoshita, I. *Organometallics* **1990**, *9*, 2865. (e) Sita, L. R.; Kinoshita, I. *J. Am. Chem. Soc.* **1991**, *113*, 1856. (f) Sekiguchi, A.; Yatabe, T.; Kamatani, H.; Kabuto, H.; Sakurai, H. *J. Am. Chem. Soc.* **1992**, *114*, 6260. (g) Wiberg, N.; Finger, C. M. M.; Polborn, K. *Angew. Chem., Int. Ed. Engl.* **1993**, *32*, 1054.

(2) For reviews: (a) Tsumuraya, T.; Batcheller, S. A.; Masamune, S. *Angew. Chem., Int. Ed. Engl.* **1991**, *30*, 902. (b) Nagase, S. *Polyhedron* **1991**, *10*, 1299. (c) Sekiguchi, A.; Sakurai, H. *Adv. Organomet. Chem.* **1995**, *37*, 1.

(3) Matsumoto, H.; Higuchi, K.; Kyushin, S.; Goto, M. *Angew. Chem., Int. Ed. Engl.* **1992**, *31*, 1354.

(4) Unno, M.; Higuchi, K.; Ida, M.; Shioyama, H.; Kyushin, S.; Matsumoto, H.; Goto, M. *Organometallics* **1994**, *13*, 4633.

(5) To our knowledge, no example has been reported for this type of skeletal rearrangement in the carbon system. For other types of skeletal rearrangements in carbon polyhedral compounds, see: (a) Griffin, G. W.; Marchand, A. P. *Chem. Rev.* **1989**, *89*, 997. (b) Marchand, A. P. *Chem. Rev.* **1989**, *89*, 1011.

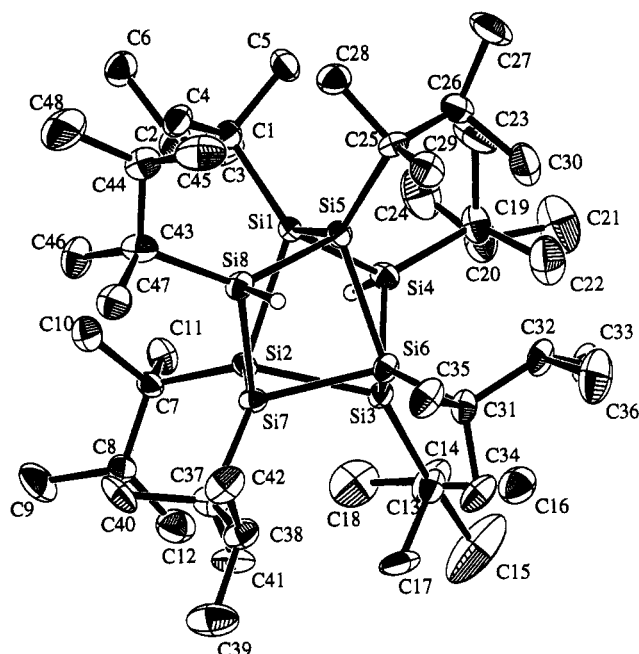


Figure 1. ORTEP drawing of **5**. Thermal ellipsoids are drawn at the 30% probability level.

Table 1. Summary of Crystal Data, Data Collection, and Refinement

Crystal Data	
formula	C <sub>48</sub> H <sub>106</sub> Si <sub>8</sub>
molecular weight	908.05
cryst description	colorless prisms
cryst size, mm	0.2 × 0.2 × 0.1
cryst system	monoclinic
space group	P2 <sub>1</sub> /a
a, Å	22.866(5)
b, Å	11.726(4)
c, Å	23.243(4)
β, deg	114.99(1)
V, Å <sup>3</sup>	5648(2)
Z	4
Data Collection	
diffractometer	Rigaku AFC7S
radiation (λ, Å)	Mo Kα (0.710 69)
μ, cm <sup>-1</sup>	2.19
variation of stds, %	0
2θ range, deg	3–55
range of h	0 to 30
range of k	0 to 15
range of l	–30 to 30
scan type	ω–2θ
scan width, deg	0.73 + 0.30 tan θ
no. of reflns measd	13 953
no. of indepdt reflns	13 620
no. of obsd reflns ( F <sub>o</sub>   ≥ 3σ(F <sub>o</sub> ))	2797
Refinement	
R	0.064
R <sub>w</sub>	0.044
weighting scheme	w = 1/σ <sup>2</sup> (F <sub>o</sub> )
S	1.54
(Δσ) <sub>max</sub>	0.00
(Δρ) <sub>max</sub> , e Å <sup>-3</sup>	0.38
(Δρ) <sub>min</sub> , e Å <sup>-3</sup>	–0.34
no. of params	513

In dihydrooctasilane **5**, the Si–Si bond lengths vary from 2.342(5) to 2.461(5) Å and the Si–Si–Si bond angles in the three fused cyclotetrasilane range from 79.9(1) to 94.2(2)°. These values are similar to those found in the corresponding isomer of dichlorooctasilane **2**, *exo,exo*-**2** (2.390(3)–2.452(3) Å and 81.2(1)–93.9(1)°).<sup>4</sup> The dihedral angles of the three cyclotetrasilane rings in **5**, however, are somewhat greater than the corre-

Table 2. Fractional Atomic Coordinates and Equivalent Isotropic Thermal Parameters for **5**

atom	x	y	z	B <sub>eq</sub> , Å <sup>2</sup>
Si(1)	0.3982(2)	0.5052(3)	0.7741(1)	2.53(9)
Si(2)	0.4208(2)	0.3074(3)	0.8127(1)	2.36(9)
Si(3)	0.3537(2)	0.2615(3)	0.7019(2)	2.68(9)
Si(4)	0.2982(2)	0.4319(3)	0.6981(2)	3.22(10)
Si(5)	0.4775(2)	0.5014(3)	0.7326(2)	2.84(9)
Si(6)	0.4550(2)	0.3045(3)	0.6960(2)	2.86(9)
Si(7)	0.5195(2)	0.2612(3)	0.8049(2)	2.65(9)
Si(8)	0.5773(2)	0.4303(3)	0.8139(2)	3.12(10)
C(1)	0.4013(6)	0.643(1)	0.8233(5)	3.1(3)
C(2)	0.3659(6)	0.633(1)	0.8680(6)	3.6(3)
C(3)	0.2939(6)	0.617(1)	0.8314(7)	5.6(4)
C(4)	0.4716(6)	0.6662(10)	0.8639(5)	4.0(4)
C(5)	0.3741(6)	0.741(1)	0.7764(5)	4.4(4)
C(6)	0.3758(5)	0.737(1)	0.9108(5)	4.5(4)
C(7)	0.4091(5)	0.2794(10)	0.8904(5)	3.1(3)
C(8)	0.4217(6)	0.159(1)	0.9140(6)	3.8(4)
C(9)	0.4257(7)	0.139(1)	0.9819(6)	6.9(5)
C(10)	0.4590(6)	0.356(1)	0.9402(5)	4.3(4)
C(11)	0.3414(5)	0.318(1)	0.8811(5)	4.1(4)
C(12)	0.3750(7)	0.073(1)	0.8718(6)	5.5(4)
C(13)	0.3026(6)	0.126(1)	0.6615(5)	3.4(3)
C(14)	0.2348(7)	0.132(1)	0.6631(7)	5.8(5)
C(15)	0.1920(7)	0.031(2)	0.6279(8)	12.7(8)
C(16)	0.2887(6)	0.127(1)	0.5924(6)	5.7(5)
C(17)	0.3413(6)	0.017(1)	0.6885(6)	6.1(4)
C(18)	0.2380(7)	0.128(1)	0.7264(8)	7.6(6)
C(19)	0.2327(6)	0.505(1)	0.6238(6)	3.9(4)
C(20)	0.1665(6)	0.479(1)	0.6210(6)	5.8(4)
C(21)	0.1108(6)	0.499(1)	0.5586(7)	8.6(5)
C(22)	0.2369(7)	0.452(1)	0.5664(6)	7.6(5)
C(23)	0.2453(7)	0.633(1)	0.6233(7)	6.6(5)
C(24)	0.1528(7)	0.547(1)	0.6694(7)	8.3(6)
C(25)	0.4904(6)	0.6318(10)	0.6862(5)	3.1(3)
C(26)	0.4264(6)	0.681(1)	0.6349(6)	4.0(4)
C(27)	0.4321(7)	0.794(1)	0.6067(7)	7.0(5)
C(28)	0.5216(6)	0.727(1)	0.7342(6)	4.5(4)
C(29)	0.5384(6)	0.598(1)	0.6585(6)	4.5(4)
C(30)	0.3929(6)	0.599(1)	0.5812(6)	6.0(4)
C(31)	0.4838(6)	0.250(1)	0.6322(5)	3.6(3)
C(32)	0.4537(6)	0.319(1)	0.5699(5)	4.0(4)
C(33)	0.3820(6)	0.308(1)	0.5348(5)	5.1(4)
C(34)	0.4706(6)	0.123(1)	0.6215(6)	5.1(4)
C(35)	0.5574(6)	0.266(1)	0.6615(5)	4.6(4)
C(36)	0.4854(7)	0.294(1)	0.5250(6)	7.8(5)
C(37)	0.5599(6)	0.116(1)	0.8403(6)	3.8(4)
C(38)	0.6054(6)	0.071(1)	0.8147(6)	4.1(4)
C(39)	0.6298(6)	–0.052(1)	0.8389(7)	7.1(5)
C(40)	0.5942(6)	0.128(1)	0.9142(6)	5.0(4)
C(41)	0.5041(6)	0.028(1)	0.8231(6)	5.1(4)
C(42)	0.6634(5)	0.145(1)	0.8271(6)	5.0(4)
C(43)	0.6411(6)	0.489(1)	0.8942(6)	3.9(4)
C(44)	0.6590(6)	0.613(1)	0.8899(6)	4.2(4)
C(45)	0.6890(6)	0.629(1)	0.8424(7)	6.4(5)
C(46)	0.6174(6)	0.475(1)	0.9458(6)	5.1(4)
C(47)	0.7012(5)	0.413(1)	0.9146(6)	4.7(4)
C(48)	0.7045(7)	0.665(1)	0.9532(7)	7.9(5)
H(Si4)	0.258(5)	0.406(9)	0.726(5)	7.0(7)
H(Si8)	0.616(4)	0.409(7)	0.782(4)	3.0(10)

$$^a B_{eq} = \frac{8}{3}\pi^2(U_{11}(aa^*)^2 + U_{22}(bb^*)^2 + U_{33}(cc^*)^2 + 2U_{12}aa^*bb^* \cos \gamma + 2U_{13}aa^*cc^* \cos \beta + 2U_{23}bb^*cc^* \cos \alpha).$$

sponding angles in **2** (31.7–41.5°), 44.7° between the Si(1)–Si(3)–Si(2) and Si(1)–Si(3)–Si(4) planes, 45.1° between the Si(2)–Si(4)–Si(1) and Si(2)–Si(4)–Si(3) planes, 33.0° between the Si(2)–Si(6)–Si(3) and Si(2)–Si(6)–Si(7) planes, 37.0° between the Si(3)–Si(7)–Si(2) and Si(3)–Si(7)–Si(6) planes, 41.6° between the Si(5)–Si(7)–Si(6) and Si(5)–Si(7)–Si(8) planes, and 43.0° between the Si(6)–Si(8)–Si(5) and Si(6)–Si(8)–Si(7) planes.

The formation of octasilacubane **1** is quite remarkable in light of previous work reported by Masamune and co-workers, who found that treatment of 4,8-dichlo-

**Table 3. Selected Bond Lengths (Å) and Angles (deg) for 5**

Bond Lengths			
Si(1)–Si(2)	2.461(5)	Si(1)–Si(4)	2.382(5)
Si(1)–Si(5)	2.388(4)	Si(1)–C(1)	1.96(1)
Si(2)–Si(3)	2.437(5)	Si(2)–Si(7)	2.403(5)
Si(2)–C(7)	1.96(1)	Si(3)–Si(4)	2.348(5)
Si(3)–Si(6)	2.431(5)	Si(3)–C(13)	1.96(1)
Si(4)–C(19)	1.94(1)	Si(5)–Si(6)	2.440(5)
Si(5)–Si(8)	2.414(5)	Si(5)–C(25)	1.96(1)
Si(6)–Si(7)	2.385(5)	Si(6)–C(31)	1.97(1)
Si(7)–Si(8)	2.342(5)	Si(7)–C(37)	1.94(1)
Si(8)–C(43)	1.95(1)	Si(4)–H(Si4)	1.37(9)
Si(8)–H(Si8)	1.39(8)		

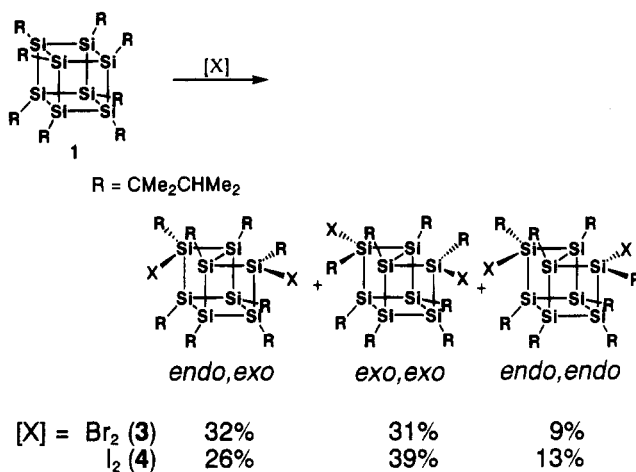
Bond Angles			
Si(2)–Si(1)–Si(4)	85.3(2)	Si(2)–Si(1)–Si(5)	93.0(2)
Si(2)–Si(1)–C(1)	127.7(4)	Si(4)–Si(1)–Si(5)	110.4(2)
Si(4)–Si(1)–C(1)	121.1(4)	Si(5)–Si(1)–C(1)	113.9(4)
Si(1)–Si(2)–Si(3)	83.2(2)	Si(1)–Si(2)–Si(7)	104.1(2)
Si(1)–Si(2)–C(7)	113.8(4)	Si(3)–Si(2)–Si(7)	93.6(2)
Si(3)–Si(2)–C(7)	131.8(4)	Si(7)–Si(2)–C(7)	122.0(4)
Si(2)–Si(3)–Si(4)	86.6(2)	Si(2)–Si(3)–Si(6)	79.9(1)
Si(2)–Si(3)–C(13)	131.9(4)	Si(4)–Si(3)–Si(6)	109.5(2)
Si(4)–Si(3)–C(13)	117.8(4)	Si(6)–Si(3)–C(13)	122.0(4)
Si(1)–Si(4)–Si(3)	86.8(2)	Si(1)–Si(4)–C(19)	129.6(5)
Si(3)–Si(4)–C(19)	127.7(5)	Si(1)–Si(5)–Si(6)	94.2(2)
Si(1)–Si(5)–Si(8)	108.6(2)	Si(1)–Si(5)–C(25)	121.5(4)
Si(6)–Si(5)–Si(8)	86.4(2)	Si(6)–Si(5)–C(25)	127.2(4)
Si(8)–Si(5)–C(25)	112.8(4)	Si(3)–Si(6)–Si(5)	104.0(2)
Si(3)–Si(6)–Si(7)	94.2(2)	Si(3)–Si(6)–C(31)	127.3(4)
Si(5)–Si(6)–Si(7)	83.5(2)	Si(7)–Si(6)–C(31)	118.9(4)
Si(7)–Si(6)–C(31)	118.4(4)	Si(2)–Si(7)–Si(6)	81.5(2)
Si(2)–Si(7)–Si(8)	108.4(2)	Si(2)–Si(7)–C(37)	117.2(4)
Si(6)–Si(7)–Si(8)	89.3(2)	Si(6)–Si(7)–C(37)	127.3(4)
Si(8)–Si(7)–C(37)	123.6(4)	Si(5)–Si(8)–Si(7)	84.9(2)
Si(5)–Si(8)–C(43)	134.9(4)	Si(7)–Si(8)–C(43)	123.4(4)

rocta-*tert*-butyltetracyclo[3.3.0.0<sup>2,7</sup>.0<sup>3,6</sup>]octasilane with lithium naphthalenide in toluene had provided only a reduced product, 4,8-dihydroocta-*tert*-butyltetracyclo[3.3.0.0<sup>2,7</sup>.0<sup>3,6</sup>]octasilane, after protolytic workup.<sup>8</sup> However, the choice of reaction conditions is crucial in our case: (1) When other active metals such as lithium powder were substituted for sodium, only starting materials were recovered and no octasilacubane was obtained. (2) When the reaction time was extended over several hours to attain the complete conversion of dichlorooctasilane **2**, the yield of **1** decreased and ring opening of **1** occurred during the reaction.

**Synthesis and Dehalogenation of Dibromooctasilane 3 and Diiodooctasilane 4.** We next examined the reductive dehalogenation of **3** and **4** with sodium. In the present work, these dihalooctasilanes were obtained by the reactions of octasilacubane **1** with Br<sub>2</sub> and with I<sub>2</sub> (Scheme 2). We found that in each case, the halogenation proceeded in a fashion similar to that observed for the chlorination using PCl<sub>5</sub>,<sup>4</sup> resulting in the exclusive formation of the rearranged products, **3** or **4**.<sup>9</sup> Thus, treatment of **1** with a slight excess of Br<sub>2</sub> in benzene at 5 °C to room temperature afforded a 75% yield of **3**. HPLC analysis indicates that **3** exists as a mixture of the three possible stereoisomers, **3a–c**.

(8) Kabe, Y.; Kuroda, M.; Honda, Y.; Yamashita, O.; Kawase, T.; Masamune, S. *Angew. Chem., Int. Ed. Engl.* **1988**, *27*, 1725. However, no crystal structure of the 4,8-dihydrooctasilane was given.

(9) An X-ray crystallographic determination was undertaken for isomer **3b**, and the preliminary results indicate the *exo,exo* structure. Crystal data for the compound: C<sub>48</sub>H<sub>104</sub>Br<sub>2</sub>Si<sub>8</sub>, monoclinic, C<sub>2</sub>/c; *a* = 27.907(2) Å, *b* = 11.783(2) Å, *c* = 22.302(1) Å, β = 127.431(2)°, *V* = 5823.6(10) Å<sup>3</sup>, *Z* = 4, *R* = 0.068, *R<sub>w</sub>* = 0.046 (for the ORTEP drawing of the compound, see the supporting information). We have, however, been unable to obtain crystals of compounds **3a,c** and **4a–c** suitable for X-ray crystallography.

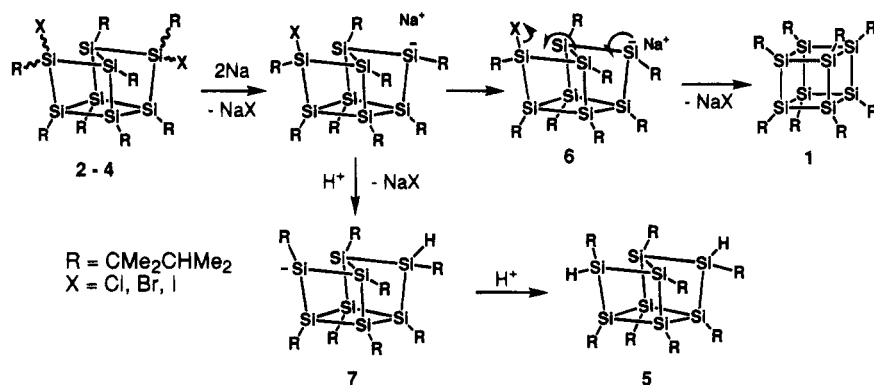
**Scheme 2**

These isomers could easily be separated by reverse-phase recycle-type HPLC (Scheme 2); yields were 32% (**3a**), 31% (**3b**), and 9% (**3c**). The diiodination of **1** was similarly accomplished as was the dibromination, resulting in the isolation of the three isomers in 26% (**4a**), 39% (**4b**), and 13% (**4c**) yields.

The structures of **3a–c** as *endo,exo*-, *exo,exo*-, and *endo,endo*-4,8-dibromooctakis(1,1,2-trimethylpropyl)tetracyclo[3.3.0.0<sup>2,7</sup>.0<sup>3,6</sup>]octasilanes were confirmed by IR, mass, and NMR (<sup>1</sup>H, <sup>29</sup>Si{<sup>1</sup>H}, and <sup>13</sup>C{<sup>1</sup>H}) spectroscopy (Experimental Section); the corresponding conformers of dichlorooctasilane **2**<sup>4</sup> can serve as precedents in determining the stereochemistry of isomers **3a–c**. Compound **3a** exhibits eight signals in the <sup>29</sup>Si{<sup>1</sup>H} NMR spectrum and 48 signals in the <sup>13</sup>C NMR spectrum, indicating that all eight silicon atoms and 1,1,2-trimethylpropyl groups are nonequivalent. The observed NMR patterns closely resemble those of the *endo,exo* isomer of **2**,<sup>4</sup> allowing the assignment of **3a** to the *endo,exo* structure. Both **3b** and **3c** exhibit four signals in the <sup>29</sup>Si{<sup>1</sup>H} NMR spectra and 24 signals in the <sup>13</sup>C NMR spectra, indicating the presence of C<sub>2</sub> symmetry in these molecules. These NMR results are consistent with the *exo,exo* and *endo,endo* structures, and the discrimination of the two structures was made from <sup>29</sup>Si NMR spectra of **3b** and **3c**. In **3b** the resonance of the <sup>29</sup>Si (SiBr) nuclei is observed at 46.59 ppm, and in **3c** the corresponding resonance is at 54.60 ppm. We previously showed that the <sup>29</sup>Si resonance of the Si(SiCl) atoms in the *exo,exo* isomer of **2** fell at higher field (51.49 ppm) than that of the *exo,exo* isomer (59.33 ppm).<sup>4</sup> Since the <sup>29</sup>Si (SiBr) resonance in **3b** is shifted upfield relative to the corresponding resonance in **3c**, **3b** is assigned as the *exo,exo* isomer,<sup>9</sup> and therefore **3c** is the *endo,endo* isomer. On a similar NMR basis, we assigned **4a–c** to the *endo,exo*, *exo,exo*, and *endo,endo* isomers.

Then, we examined the dehalogenation of bromide **3** and iodide **4** with sodium and observed the formation of **1** and **5**. Thus the treatment of **3** with a large excess of sodium at 120 °C for 4 h resulted in the formation of **1** and **5** in 68 and 29% yields, respectively. When **4** was treated with a large excess of sodium at 120 °C for 4 h, **1** and **5** formed in 45 and 22% yields, respectively. In both cases, the starting materials were completely consumed.

Scheme 3



### Possible Reaction Pathway for Dehalogenation.

The pathway leading to octasilacubane **1** is not clearly understood, but in Scheme 3 a possible reaction pathway is proposed to account for the formation of **1**. The initial process produces an anion species **6**, in a fashion similar to the reductive coupling of chloropolysilanes with alkali metals.<sup>10</sup> Then a rapid skeletal rearrangement follows wherein the central Si–Si bond is cleaved and the new Si–Si bonds are formed. Such a skeletal rearrangement is very unusual and has, to our knowledge, no precedent.<sup>11</sup> Although, this rearrangement may be associated with a high activation energy, the ring closure leading to **1** can be accomplished by employing the forced reaction conditions, as shown in the present work. In addition, releasing steric congestion in **2** due to the bulky 1,1,2-trimethylpropyl groups may provide a part of the driving force for the skeletal rearrangement. The generation of dihydrooctasilane **5** is also explained in the same scheme. The reason for the fact that only *endo,endo* isomer of **5** was obtained could also be demonstrated with the intermediate **7**. The steric repulsion of large 1,1,2-trimethylpropyl groups made *endo* conformation preferable.

### Summary

The reaction of 4,8-dihalo-octakis(1,1,2-trimethylpropyl)-tetracyclo[3.3.0.0<sup>2,7</sup>.0<sup>3,6</sup>]octasilane with sodium resulted the unprecedented rearrangement to give octasilacubane in good yields along with a reduced product, 4,8-dihydrooctakis(1,1,2-trimethylpropyl)tetracyclo[3.3.0.0<sup>2,7</sup>.0<sup>3,6</sup>]octasilane. The reductive dechlorination of **2** with sodium might offer an attractive route to **1**, otherwise available only in low yields from the reductive coupling of (1,1,2-trimethylpropyl)trichlorosilane with sodium.<sup>13</sup>

### Experimental Section

NMR spectra were recorded on a JEOL Model  $\alpha$ -500 (<sup>1</sup>H, 500.0 MHz; <sup>13</sup>C, 125.7 MHz; <sup>29</sup>Si, 99.3 MHz). Mass spectrom-

etry was performed by a JEOL JMS-D300. Infrared spectra were measured with a JASCO A-102 spectrometer. Analytical HPLC was done by JASCO 875UV/880PU and UV-970/880PU instruments with a Chemco 4.6 mm  $\times$  250 mm 5-ODS-H column. Preparative (recycle-type) HPLC was carried out using JAI LC-908 and LC-09 instruments with Chemco 20 mm  $\times$  250 mm 7-ODS-H columns. All reactions were carried out under an atmosphere of argon or nitrogen. All solvents were dried, distilled, and degassed, and all glassware was dried at 80 °C for several hours prior to use.

**Synthesis of Dibromooctasilane 3.** To a solution of octasilacubane **1** (24 mg, 0.025 mmol) in 6 mL of benzene was added 0.4 mL of 0.1 M benzene solution of Br<sub>2</sub> (0.04 mmol) around 5 °C, and the mixture was stirred at room temperature. After 2 h, an aliquot was taken from the mixture; HPLC showed the bromination to be complete. The reaction mixture was passed through a short silica gel column, and the solvent was removed by evaporation. A pale-yellow solid was obtained as a isomeric mixture of **3**. Each isomer of **3** was isolated by recycle-type preparative HPLC (ODS, MeOH/THF = 6/4 elution). Isomers **3a–c** were identified as *endo,exo*, *exo,exo*, and *endo,endo* conformers, respectively. The yields of **3a–3c** were 8.6 mg (32%), 8.4 mg (31%), and 2.3 mg (9%), respectively.

**3a:** colorless prisms, mp (sealed) 187 °C dec; <sup>1</sup>H NMR (CDCl<sub>3</sub>)  $\delta$  2.52 (sept, 2H,  $J = 6.7$  Hz), 2.40 (sept, 1H,  $J = 6.7$  Hz), 2.33 (sept, 2H,  $J = 6.7$  Hz), 2.29 (sept, 3H,  $J = 6.7$  Hz), 1.62 (s, 3H), 1.49 (s, 3H), 1.47 (s, 3H), 1.46 (s, 3H), 1.44 (s, 3H), 1.41 (s, 3H), 1.40 (s, 3H), 1.39 (s, 3H), 1.35 (s, 3H), 1.33 (s, 3H), 1.324 (s, 3H), 1.317 (s, 6H), 1.29 (s, 3H), 1.27 (s, 3H), 1.22 (s, 3H), 1.12 (d, 3H,  $J = 5.8$  Hz), 1.11 (d, 3H,  $J = 6.8$  Hz), 1.10 (d, 3H,  $J = 6.7$  Hz), 1.06 (d, 3H,  $J = 6.8$  Hz), 1.03 (d, 3H,  $J = 6.7$  Hz), 0.99 (d, 3H,  $J = 6.4$  Hz), 0.98 (d, 3H,  $J = 6.4$  Hz), 0.94 (d, 3H,  $J = 7.3$  Hz), 0.92 (d, 3H,  $J = 7.3$  Hz), 0.90 (overlap, d, 6H,  $J = 6.7$  Hz), 0.89 (overlap, d, 6H,  $J = 6.4$  Hz), 0.85 (overlap, d, 9H,  $J = 6.7$  Hz); <sup>13</sup>C{<sup>1</sup>H} NMR (CDCl<sub>3</sub>)  $\delta$  38.07, 37.38, 37.03, 36.39, 36.33, 36.19, 36.00, 35.66, 35.45, 35.36, 35.36, 35.01, 34.96, 34.43, 34.43, 34.19, 33.45, 30.43, 30.07, 29.68, 28.26, 27.93, 27.93, 27.22, 26.63, 26.55, 26.47, 25.43, 25.29, 23.96, 23.74, 23.45, 22.50, 22.24, 22.15, 21.91, 21.91, 21.12, 20.47, 20.40, 20.01, 19.79, 19.63, 18.77, 18.22, 18.03, 17.22, 16.08; <sup>29</sup>Si{<sup>1</sup>H} NMR (CDCl<sub>3</sub>)  $\delta$  51.39, 46.80, 19.94, 13.44, -0.76, -3.57, -18.59, -22.67; IR (KBr) 2960, 2860, 1460, 1370, 1120, 1080 cm<sup>-1</sup>; MS (30 eV)  $m/z$  980 (1, M<sup>+</sup> – C<sub>8</sub>H<sub>10</sub>), 895 (5), 811 (5), 727 (6), 643 (11), 559 (13), 475 (12), 391 (3), 69 (100); HRMS calcd for C<sub>48</sub>H<sub>104</sub>Si<sub>8</sub>Br<sub>2</sub>  $m/z$  1062.4664, found:  $m/z$  1062.4640.

**3b:** colorless prisms, mp (sealed) 191 °C dec; <sup>1</sup>H NMR (CDCl<sub>3</sub>)  $\delta$  2.41 (sept, 2H,  $J = 6.7$  Hz), 2.37 (sept, 4H,  $J = 6.7$  Hz), 2.33 (sept, 2H,  $J = 6.7$  Hz), 1.47 (s, 6H), 1.43 (overlap, s, 12H), 1.39 (overlap, s, 12H), 1.36 (s, 6H), 1.30 (s, 6H), 1.21 (s, 6H), 1.09 (d, 6H,  $J = 6.7$  Hz), 1.00 (d, 6H,  $J = 6.7$  Hz), 0.98 (d, 6H,  $J = 6.7$  Hz), 0.97 (overlap, d, 12H,  $J = 6.8$  Hz), 0.93 (d, 6H,  $J = 6.8$  Hz), 0.87 (d, 6H,  $J = 7.1$  Hz), 0.85 (d, 6H,  $J = 6.7$  Hz); <sup>13</sup>C{<sup>1</sup>H} NMR (CDCl<sub>3</sub>)  $\delta$  37.28, 36.61, 36.54, 35.62, 34.57, 34.57, 34.28, 33.67, 28.58, 27.80, 27.41, 26.79, 26.63, 26.49,

(10) Ruehl, K. E.; Davis, M. E.; Matyjaszewski, K. *Organometallics* **1992**, *11*, 788.

(11) In 1989, Weidenbruch et al. reported<sup>12</sup> the synthesis of 4,8-dibromoocta-*tert*-butyltetracyclo[3.3.0.0<sup>2,7</sup>.0<sup>3,6</sup>]octasilane. They described in their manuscript that the formation of an octagermacubane from it is not possible, since, in addition to the reductive elimination of the two bromine atoms, the cleavage and re-formation of a Ge–Ge bond is required.

(12) Weidenbruch, M.; Grimm, F.-T.; Pohl, S.; Saak, W. *Angew. Chem., Int. Ed. Engl.* **1989**, *28*, 198.

(13) We are now investigating the possibility of one-pot synthesis of the dichlorides **2** from 1,1,2-trimethylpropyltrichlorosilane.

26.20, 22.28, 22.02, 21.16, 20.75, 20.61, 20.55, 20.15, 19.07, 18.05;  $^{29}\text{Si}\{^1\text{H}\}$  NMR ( $\text{CDCl}_3$ )  $\delta$  46.59, 18.62, -4.29, -25.56; IR (KBr) 2960, 2860, 1460, 1370, 1120, 1080  $\text{cm}^{-1}$ ; MS (30 eV)  $m/z$  980 (1,  $\text{M}^+ - \text{C}_6\text{H}_{10}$ ), 895 (3), 811 (3), 727 (5), 643 (7), 559 (7), 475 (8), 391 (2), 69 (100); HRMS calcd for  $\text{C}_{42}\text{H}_{91}\text{Si}_8\text{Br}_2$  ( $\text{M}^+ - \text{CMe}_2\text{CHMe}_2$ )  $m/z$  977.3642, found  $m/z$  977.3655.

**3c:** pale yellow prisms, mp (sealed) 190 °C dec;  $^1\text{H}$  NMR ( $\text{CDCl}_3$ )  $\delta$  2.61 (sept, 2H,  $J = 7.0$  Hz), 2.47 (sept, 2H,  $J = 7.0$  Hz), 2.30 (sept, 2H,  $J = 7.0$  Hz), 2.29 (sept, 2H,  $J = 7.0$  Hz), 1.51 (s, 6H), 1.48 (s, 6H), 1.43 (s, 6H), 1.32 (overlap, s, 18H), 1.31 (s, 6H), 1.28 (s, 6H), 1.13 (d, 6H,  $J = 6.7$  Hz), 1.11 (d, 6H,  $J = 7.0$  Hz), 1.04 (d, 6H,  $J = 6.7$  Hz), 1.00 (d, 6H,  $J = 7.0$  Hz), 0.89 (d, 6H,  $J = 6.7$  Hz), 0.88 (d, 6H,  $J = 6.7$  Hz), 0.87 (d, 6H,  $J = 6.4$  Hz), 0.85 (d, 6H,  $J = 6.7$  Hz);  $^{13}\text{C}\{^1\text{H}\}$  NMR ( $\text{CDCl}_3$ )  $\delta$  37.22, 37.00, 36.10, 36.04, 35.44, 34.78, 34.54, 34.37, 30.28, 29.91, 28.54, 26.20, 26.11, 25.92, 24.29, 23.39, 23.06, 22.16, 21.81, 21.04, 19.15, 19.15, 17.66, 16.62;  $^{29}\text{Si}\{^1\text{H}\}$  NMR ( $\text{CDCl}_3$ )  $\delta$  54.60, 12.50, -1.52, -12.86; IR (KBr) 2960, 2860, 1460, 1370, 1120, 1080  $\text{cm}^{-1}$ ; MS (30 eV)  $m/z$  980 (1,  $\text{M}^+ - \text{C}_6\text{H}_{10}$ ), 895 (2), 811 (3), 727 (2), 643 (5), 559 (7), 475 (6), 391 (6), 69 (100); HRMS calcd for  $\text{C}_{42}\text{H}_{91}\text{Si}_8\text{Br}_2$  ( $\text{M}^+ - \text{CMe}_2\text{CHMe}_2$ )  $m/z$  977.3642, found  $m/z$  977.3610.

**Synthesis of Diiodooctasilane 4.** By a reaction analogous to that described for dibromooctasilane **3**, but using 22 mg (0.024 mmol) of octasilacubane **1** and 0.6 mL of a solution of 0.05 M iodine in benzene, a pale yellow solid was obtained after a 2.5 h reaction (at room temperature) and subsequent workup. Each isomer of **4** was isolated by recycle-type preparative HPLC (ODS, MeOH/THF = 6/4 elution). Isomers **4a-c** were identified as *endo,exo*, *exo,exo*, and *endo,endo* conformers, respectively. The yields of **4a-c** were 7.1 mg (26%), 10.6 mg (39%), and 3.6 mg (13%), respectively.

**4a:** pale yellow prisms, mp (sealed) 200 °C dec;  $^1\text{H}$  NMR ( $\text{CDCl}_3$ )  $\delta$  2.67 (sept, 1H,  $J = 7.0$  Hz), 2.54 (sept, 1H,  $J = 6.7$  Hz), 2.49 (sept, 1H,  $J = 6.7$  Hz), 2.40 (sept, 1H,  $J = 6.7$  Hz), 2.36-2.30 (m, 4H,  $J = 6.7$  Hz), 1.64 (s, 3H), 1.60 (s, 3H), 1.58 (s, 3H), 1.53 (s, 3H), 1.52 (s, 3H), 1.51 (s, 3H), 1.46 (s, 3H), 1.41 (s, 3H), 1.40 (s, 3H), 1.372 (s, 3H), 1.366 (s, 3H), 1.354 (s, 3H), 1.351 (s, 3H), 1.32 (s, 3H), 1.27 (s, 3H), 1.25 (s, 3H), 1.18 (d, 3H,  $J = 6.7$  Hz), 1.17 (d, 3H,  $J = 6.7$  Hz), 1.14 (d, 3H,  $J = 6.7$  Hz), 1.12 (d, 3H,  $J = 7.0$  Hz), 1.06 (d, 3H,  $J = 6.7$  Hz), 1.02 (d, 3H,  $J = 7.1$  Hz), 1.00 (d, 3H,  $J = 6.7$  Hz), 0.93-0.90 (m, 15H,  $J = 6.7$  Hz), 0.89 (d, 3H,  $J = 7.0$  Hz), 0.85 (d, 3H,  $J = 6.4$  Hz), 0.84 (d, 3H,  $J = 6.5$  Hz), 0.82 (d, 3H,  $J = 6.4$  Hz);  $^{13}\text{C}\{^1\text{H}\}$  NMR ( $\text{CDCl}_3$ )  $\delta$  38.48, 38.27, 37.37, 36.92, 36.69, 36.23, 35.99, 35.79, 35.55, 35.55, 34.82, 34.50, 34.05, 32.88, 32.29, 30.98, 30.88, 30.56, 30.19, 29.17, 28.77, 28.05, 27.98, 27.59, 27.52, 26.83, 26.10, 25.20, 24.58, 24.11, 24.06, 23.98, 23.56, 23.38, 23.06, 22.78, 22.78, 21.35, 20.93, 20.71, 20.11, 19.80, 19.03, 18.72, 18.27, 18.27, 16.89, 16.06;  $^{29}\text{Si}\{^1\text{H}\}$  NMR ( $\text{CDCl}_3$ )  $\delta$  31.00, 26.45, 18.57, 9.63, 1.44, 1.23, -5.48, -17.49; IR (KBr): 2960, 2860, 1460, 1370, 1120, 1080  $\text{cm}^{-1}$ ; MS (30 eV)  $m/z$  1074 (1,  $\text{M}^+ - \text{C}_6\text{H}_{13}$ ), 989 (1), 905 (1), 821 (2), 737 (4), 653 (5), 569 (5), 69 (base); HRMS calcd for  $\text{C}_{48}\text{H}_{104}\text{Si}_8\text{I}_2$   $m/z$  1158.4382, found  $m/z$  1158.4447.

**4b:** colorless prisms, mp (sealed) 207 °C dec;  $^1\text{H}$  NMR ( $\text{CDCl}_3$ )  $\delta$  2.51 (sept, 2H,  $J = 6.7$  Hz), 2.43 (sept, 2H,  $J = 6.7$  Hz), 2.41 (sept, 2H,  $J = 7.1$  Hz), 2.33 (sept, 2H,  $J = 6.7$  Hz), 1.57 (s, 6H), 1.49 (s, 6H), 1.46 (s, 6H), 1.43 (overlap, s, 12H), 1.40 (s, 6H), 1.37 (s, 6H), 1.24 (s, 6H), 1.14 (d, 6H,  $J = 6.7$  Hz), 1.02 (d, 6H,  $J = 6.7$  Hz), 1.01 (d, 6H,  $J = 7.3$  Hz), 0.98 (d, 6H,  $J = 6.7$  Hz), 0.95 (d, 6H,  $J = 6.7$  Hz), 0.93 (d, 6H,  $J = 6.8$  Hz), 0.88 (d, 6H,  $J = 6.7$  Hz), 0.84 (d, 6H,  $J = 6.8$  Hz);  $^{13}\text{C}\{^1\text{H}\}$  NMR ( $\text{CDCl}_3$ )  $\delta$  37.47, 37.33, 37.29, 25.49, 34.87, 34.80, 34.63, 32.30, 29.27, 28.34, 27.80, 27.63, 27.56, 27.24, 25.80, 24.21, 22.10, 21.57, 21.50, 21.14, 20.70, 19.72, 19.27, 18.33;  $^{29}\text{Si}\{^1\text{H}\}$  NMR ( $\text{CDCl}_3$ )  $\delta$  24.81, 16.32, -1.65, -18.85; IR (KBr) 2960, 2860, 1460, 1370, 1120, 1080  $\text{cm}^{-1}$ ; MS (30 eV)  $m/z$  1074 (1,  $\text{M}^+ - \text{C}_6\text{H}_{13}$ ), 989 (4), 905 (4), 821 (4), 737 (8), 653 (10), 569 (9), 485 (2), 69 (100); HRMS calcd for  $\text{C}_{48}\text{H}_{104}\text{Si}_8\text{I}_2$   $m/z$  1158.4382, found  $m/z$  1158.4428.

**4c:** pale yellow prisms, mp (sealed) 170 °C dec;  $^1\text{H}$  NMR ( $\text{CDCl}_3$ )  $\delta$  2.57 (sept, 2H,  $J = 6.7$  Hz), 2.48 (sept, 2H,  $J = 7.0$  Hz), 2.38 (sept, 2H,  $J = 6.7$  Hz), 2.33 (sept, 2H,  $J = 7.0$  Hz), 1.57 (s, 6H), 1.55 (s, 6H), 1.52 (s, 6H), 1.41 (s, 6H), 1.39 (s, 6H), 1.38 (s, 6H), 1.33 (s, 6H), 1.28 (s, 6H), 1.18 (d, 6H,  $J = 6.7$  Hz), 1.15 (d, 6H,  $J = 7.0$  Hz), 1.05 (d, 6H,  $J = 6.8$  Hz), 1.00 (d, 6H,  $J = 6.8$  Hz), 0.91 (d, 6H,  $J = 6.7$  Hz), 0.893 (d, 6H,  $J = 6.4$  Hz), 0.891 (d, 6H,  $J = 8.0$  Hz), 0.84 (d, 6H,  $J = 6.7$  Hz);  $^{13}\text{C}\{^1\text{H}\}$  NMR ( $\text{CDCl}_3$ )  $\delta$  47.37, 47.11, 45.73, 45.20, 45.04, 44.48, 43.54, 42.51, 40.24, 39.46, 38.32, 35.93, 35.83, 35.33, 33.72, 33.31, 33.05, 32.10, 31.32, 30.72, 28.71, 28.48, 27.62, 26.16;  $^{29}\text{Si}\{^1\text{H}\}$  NMR ( $\text{CDCl}_3$ )  $\delta$  35.00, 10.13, 0.48, -2.36; IR (KBr) 2960, 2860, 1460, 1370, 1120, 1080  $\text{cm}^{-1}$ ; MS (30 eV)  $m/z$  1074 (1,  $\text{M}^+ - \text{C}_6\text{H}_{13}$ ), 989 (2), 905 (3), 821 (4), 737 (7), 653 (9), 569 (10), 484 (2), 69 (100); HRMS calcd for  $\text{C}_{48}\text{H}_{104}\text{Si}_8\text{I}_2$   $m/z$  1158.4382, found  $m/z$  1158.4320.

**Reductive Dehalogenation of Dichlorooctasilane 2 with Sodium.** A suspension of sodium sand (8 mg, 0.35 mmol) in toluene (1 mL) was added to a solution of **2** (30 mg, 0.030 mmol, a mixture of the three isomers (*endo,exo-2*/*exo,exo-2*/*endo,endo-2* = 56/27/17)) in toluene (1 mL). The resulting mixture was stirred at 120 °C for 1.5 h. The color of the mixture changed from pale yellow to pink. The reaction mixture was passed through a short silica gel column, and the solvent was removed by evaporation. The residue was recrystallized from hexane to give 16 mg of red crystals, whose physical properties (HPLC retention time, mp, and NMR, IR, and UV spectra, etc.) were identical with those of an authentic sample of octasilacubane **1**.<sup>3</sup> The yield was 70% based on the dichlorooctasilane **2** consumed. Recycle-type preparative HPLC (ODS, MeOH/THF = 6/4 elution) of the supernatant liquid from the above recrystallization allowed isolation of reduced product **5** (4 mg, 18%) and unreacted **3** (*endo,exo-2*, 3 mg; *exo,exo-2*, 1 mg; *endo,endo-2*, 1 mg; total 18%).

**5:** colorless prisms, mp (sealed) 226-228 °C dec;  $^1\text{H}$  NMR ( $\text{C}_6\text{D}_6$ )  $\delta$  4.82 (s, 2H), 2.48 (sept,  $J = 6.7$  Hz, 2H), 2.45 (sept,  $J = 6.7$  Hz, 2H), 2.30 (sept,  $J = 6.7$  Hz, 4H), 1.63 (s, 6H), 1.63 (s, 6H), 1.49 (s, 6H), 1.43 (s, 6H), 1.43 (s, 6H), 1.42 (s, 6H), 1.39 (s, 6H), 1.37 (s, 6H), 1.38 (d,  $J = 6.7$  Hz, 6H), 1.28 (d,  $J = 6.7$  Hz, 6H), 1.15 (d,  $J = 6.7$  Hz, 6H), 1.12 (d,  $J = 6.7$  Hz, 6H), 1.09 (d,  $J = 6.7$  Hz, 6H), 1.06 (d,  $J = 6.7$  Hz, 6H), 1.02 (d,  $J = 6.7$  Hz, 6H), 0.99 (d,  $J = 6.7$  Hz, 6H);  $^{13}\text{C}\{^1\text{H}\}$  NMR ( $\text{C}_6\text{D}_6$ )  $\delta$  36.77, 36.56, 35.89, 35.81, 35.28, 34.36, 33.15, 30.77, 29.78, 28.49, 27.29, 26.55, 26.23, 25.38, 24.46, 24.08, 22.33, 21.43, 21.43, 19.33, 19.20, 18.76, 18.51, 18.15;  $^{29}\text{Si}\{^1\text{H}\}$  NMR ( $\text{C}_6\text{D}_6$ )  $\delta$  22.83, -7.20, -21.43, -32.16; IR (KBr) 2950, 2850, 2080, 1460, 1370, 1260, 1080, 800  $\text{cm}^{-1}$ ; MS (30 eV)  $m/z$  821 (14,  $\text{M}^+ - \text{C}_6\text{H}_{13}$ ), 737 (11), 653 (22), 569 (14), 485 (15), 401 (18), 317 (51), 233 (23), 69 (100); HRMS calcd for  $\text{C}_{48}\text{H}_{106}\text{Si}_8$   $m/z$  906.6449, found  $m/z$  906.6416.<sup>14</sup>

**Reductive Dehalogenation of Dibromooctasilane 3 with Sodium.** The same procedure as above with 22 mg (0.021 mmol) of **3**, 14 mg (0.61 mmol) of sodium sand, and 1.5 mL of toluene gave 13 mg (68% yield) of **1** and 5.6 mg (29% yield) of **5** after a 4 h reaction and subsequent workup including recycle-type preparative HPLC (ODS, MeOH/THF = 6/4 elution).

**Reductive Dehalogenation of Diiodooctasilane 4 with Sodium.** The same procedure as above with 45 mg (0.039 mmol) of **4**, 15 mg (0.65 mmol) of sodium sand, and 1.5 mL of toluene gave 16 mg (45% yield) of **1** and 8 mg (22% yield) of **5** after a 4 h reaction and subsequent workup including recycle-type preparative HPLC (ODS, MeOH/THF = 6/4 elution).

**X-ray Crystallographic Analysis of Reduced Product 5.** Colorless crystals of *endo,endo-4,8*-dihydrooctakis(1,1,2-trimethylpropyl)tetracyclo[3.3.0.0<sup>2,7</sup>.0<sup>3,6</sup>]octasilane were obtained from benzene by slow evaporation. A crystal specimen of dimensions 0.2 × 0.2 × 0.1 mm was sealed in a glass capillary and used for data collection on a Rigaku AFC7S

(14) SAPI91: Fan Hai-Fu. Structure Analysis Programs with Intelligent Control, Rigaku Corp., Tokyo, Japan, 1991.

diffractometer using graphite-monochromated Mo K $\alpha$  radiation. Cell parameters were refined by the least-squares method using 20 reflections ( $22.52 < 2\theta < 27.59^\circ$ ). The space group  $P2_1/a$  was uniquely determined from systematic absences ( $h0l, h \neq 2n; 0k0, k \neq 2n$ ). Intensity data were collected in the range of  $3 < 2\theta < 55^\circ$  by the  $\omega$ - $2\theta$  scan technique at a temperature of  $20 \pm 1^\circ\text{C}$ . Of the 13 953 reflections which were collected, 13 620 were unique ( $R_{\text{int}} = 0.101$ ). The intensities of three representative reflection were measured after every 150 reflections. No decay correction was applied. The linear absorption coefficient,  $\mu$ , for Mo K $\alpha$  radiation is  $2.2 \text{ cm}^{-1}$ . Azimuthal scans of several reflections indicated no need for an absorption correction. The data were collected for Lorentz and polarization effects. The structure was solved by SAPI91<sup>14</sup> and expanded using Fourier techniques.<sup>15</sup> The non-hydrogen atoms were refined anisotropically. Two of hydrogen atoms (Si-H) were refined isotropically, and the rest were included in fixed positions. The final cycle of full-matrix least squares refinement was based on 2797 observed reflections ( $|F_o| \geq 3\sigma(F_o)$ ) and 513 variable parameters and converged (largest

parameter was 0.01 times its esd) with unweighted and weighted factors of  $R = 6.4\%$  and  $R_w = 4.4\%$ . All calculations were carried out on a SiliconGraphics INDY computer. Details of crystal data, data collection and refinement are listed in Table 1.

**Acknowledgment.** This work was supported by a Grant-in-aid for Scientific Research (No. 05740405) and that on Priority Area of Reactive Organometallics (No. 05236102) from the Ministry of Education, Science, and Culture of Japan. We wish to thank Shin-Etsu Chemical Co. Ltd., Toshiba Silicon Co. Ltd., and Toagosei Co. Ltd. for financial support.

**Supporting Information Available:** Tables of anisotropic thermal parameters, atomic coordinates and isotropic thermal parameters involving H atoms, and bond lengths and angles for **5** and figures showing views of molecular packing and packing diagrams for **5** and an ORTEP drawing for **3b** (28 pages). Ordering information is given on any current masthead page.

OM950056F

(15) DIRDIF92: Beurskens, P. T.; Admiraal, G.; Beurskens, G.; Bosman, W. P.; Garcia-Granda, S.; Gould, R. O.; Smits, J. M. M.; Smykalla, C. The DIRDIF program system, Technical Report of the Crystallography Laboratory, University of Nijmegen, The Netherlands, 1992.

## Notes

Thermodynamic Studies of the Addition of N<sub>2</sub>, C<sub>2</sub>H<sub>4</sub>, and Alkynes to [Rh(P<sup>i</sup>Pr<sub>3</sub>)<sub>2</sub>Cl]<sub>2</sub>

Kun Wang and Alan S. Goldman\*

Department of Chemistry, Rutgers—The State University of New Jersey,  
New Brunswick, New Jersey 08903

Chunbang Li and Steven P. Nolan\*

Department of Chemistry, University of New Orleans, New Orleans, Louisiana 70148

Received March 27, 1995<sup>⊗</sup>

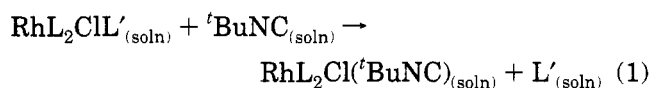
**Summary:** [Rh(P<sup>i</sup>Pr<sub>3</sub>)<sub>2</sub>Cl]<sub>2</sub> reacts with various small molecules L' to give complexes Rh(P<sup>i</sup>Pr<sub>3</sub>)<sub>2</sub>ClL'. The enthalpy of this reaction has been determined calorimetrically and/or by equilibrium methods for L' = N<sub>2</sub>, C<sub>2</sub>H<sub>4</sub>, diphenylacetylene, and 2-butyne. These values, in combination with the previously determined lower limit for the [Rh(P<sup>i</sup>Pr<sub>3</sub>)<sub>2</sub>Cl]<sub>2</sub> bridge strength, afford lower limits of the Rh–L' BDE's; the lower limits are probably only slightly less than the actual BDE's.

Rhodium phosphine complexes such as Wilkinson's Catalyst have played a major role in the development of "organometallic" catalysis and continue to reveal novel catalytic chemistry. If any species may be designated as the actual catalyst in much of this chemistry, it is bis(phosphine)rhodium chloride; this fragment, for example, is the key player in Rh(PPh<sub>3</sub>)<sub>3</sub>Cl-catalyzed olefin hydrogenation<sup>1</sup> and in alkane dehydrogenation catalyzed by Rh(PMe<sub>3</sub>)<sub>2</sub>(CO)Cl.<sup>2,3</sup> The need to develop a body of reliable organometallic thermodynamic data is particularly important for reactions of such catalytically relevant species. We have recently determined lower limits for the enthalpy of addition of CO, H<sub>2</sub>, and <sup>t</sup>BuNC to RhL<sub>2</sub>Cl (L = P<sup>i</sup>Pr<sub>3</sub>).<sup>4</sup> In this contribution we report the corresponding values for addition of C<sub>2</sub>H<sub>4</sub>, diphenylacetylene, 2-butyne, and N<sub>2</sub>.

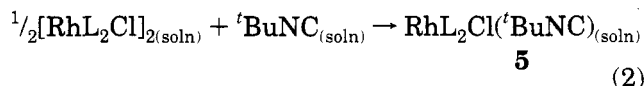
## Results and Discussion

[RhL<sub>2</sub>Cl]<sub>2</sub> (**1**) reacts in solution with N<sub>2</sub>, C<sub>2</sub>H<sub>4</sub>, and diphenylacetylene, respectively, to give the corresponding adducts RhL<sub>2</sub>ClL' (L' = N<sub>2</sub> (**2**), C<sub>2</sub>H<sub>4</sub> (**3**), and diphenylacetylene (**4**)),<sup>5</sup> which can be isolated as crys-

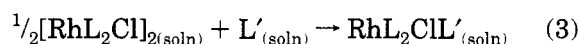
talline solids.<sup>6</sup> X-ray structures of **2**<sup>6,7</sup> and **3**<sup>6</sup> reveal square planar geometries with *trans*-phosphines; the C<sub>2</sub>H<sub>4</sub> ligand of **3** is perpendicular to the molecular plane.<sup>6</sup> Spectroscopic data indicate that the structure of **4** is analogous to that of **3**. Because C<sub>2</sub>H<sub>4</sub> and N<sub>2</sub> are gases (and, in the case of N<sub>2</sub>, because the reaction with **1** is quite slow) their addition reactions are not well suited to direct calorimetric measurement. In order to determine their bond disruption enthalpies we exploited a method previously reported for determination of the enthalpy of addition of H<sub>2</sub>. <sup>t</sup>BuNC reacts rapidly with complexes **2–4** to displace the respective ligands L'. These reactions (eq 1) were measured calorimetrically, and the resulting values were subtracted from those measured for the direct addition of <sup>t</sup>BuNC (eq 2) to give the enthalpies of addition of **1** (eq 3).<sup>8</sup> In the case of L'



L'	RhL <sub>2</sub> ClL'	ΔH <sub>1</sub> (kcal/mol)
N <sub>2</sub>	<b>2</b>	-25.9 ± 0.5
C <sub>2</sub> H <sub>4</sub>	<b>3</b>	-17.6 ± 0.3
PhC≡CPh	<b>4</b>	-19.9 ± 0.5



$$\Delta H_2 = -33.5 \pm 0.5 \text{ kcal/mol}$$



$$\Delta H_3 = \Delta H_2 - \Delta H_1$$

L'	RhL <sub>2</sub> ClL'	ΔH <sub>2</sub> - ΔH <sub>1</sub> (kcal/mol)
N <sub>2</sub>	<b>2</b>	-7.6 ± 0.7
C <sub>2</sub> H <sub>4</sub>	<b>3</b>	-15.9 ± 0.6
PhC≡CPh	<b>4</b>	-13.6 ± 0.7

= PhC≡CPh the addendum is not volatile. Thus the addition reaction could be directly measured, and doing so served as an internal consistency check for the method. The directly measured enthalpy of eq 4

(6) Busetto, C.; D'Alfonso, A.; Maspero, F.; Pergo, G.; Zazzetta, A. *J. Chem. Soc., Dalton Trans.* **1977**, 1828-1834.

<sup>⊗</sup> Abstract published in *Advance ACS Abstracts*, July 1, 1995.

(1) Halpern, J. *Inorg. Chim. Acta.* **1981**, *50*, 11-19 and references therein.

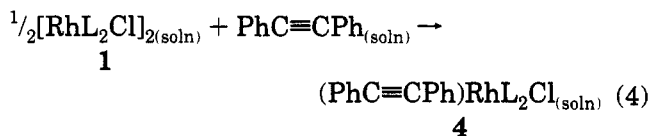
(2) (a) Maguire, J. A.; Boese, W. T.; Goldman, A. S. *J. Am. Chem. Soc.* **1989**, *111*, 7088-7093. (b) Maguire, J. A.; Boese, W. T.; Goldman, M. E.; Goldman, A. S. *Coord. Chem. Rev.* **1990**, *97*, 179-192.

(3) (a) Maguire, J. A.; Goldman, A. S. *J. Am. Chem. Soc.* **1991**, *113*, 6706-6708. (b) Maguire, J. A.; Petrillo, A.; Goldman, A. S. *J. Am. Chem. Soc.* **1992**, *114*, 9492-9498.

(4) Wang, K.; Rosini, G. P.; Nolan, S. P.; Goldman, A. S. *J. Am. Chem. Soc.* **1995**, *117*, 5082-5088.

(5) The closely related tricyclohexylphosphine analogs of these complexes were first reported by Van Gaal *et al.* (a) Van Gaal, H. L. M.; Moers, F. G.; Steggerada, J. J. *J. Organomet. Chem.* **1974**, *65*, C43-C45. (b) Van Gaal, H. L. M.; Van Den Bekerom, F. L. A. *J. Organomet. Chem.* **1977**, *134*, 237-248.



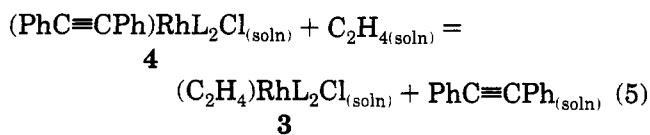


$$\Delta H_{4(\text{calcd})} = \Delta H_2 - \Delta H_1 = -13.6 \pm 0.7 \text{ kcal/mol}$$

$$\Delta H_{4(\text{exptl})} = -14.2 \pm 0.4 \text{ kcal/mol}$$

was found to be  $-14.2 \pm 0.4$  kcal/mol, equal within the limits of experimental error to the value of  $\Delta H_2 - \Delta H_1$ . (We will take  $\Delta H_4$  to be the average of the two values, i.e.,  $-13.9 \pm 0.8$  kcal/mol.) These results are indicated in Scheme 1.

The similar BDE's calculated for addition of  $\text{PhC}\equiv\text{CPh}$  and  $\text{C}_2\text{H}_4$  imply that it might be possible to spectroscopically observe an equilibrium between the two addenda. This is found to be the case. A variable temperature  $^{31}\text{P}$  NMR study of reaction 5 in toluene over



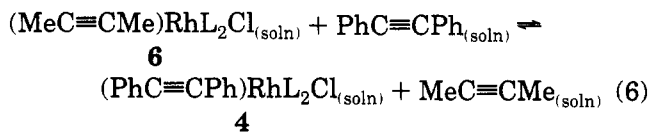
$$\Delta H_{5(\text{calorimetry})} = [\Delta H_3(L' = \text{C}_2\text{H}_4)] - \Delta H_4 =$$

$$-2.0 \pm 1.0 \text{ kcal/mol}$$

$$\Delta H_{5(\text{NMR})} = 0.1 \pm 0.2 \text{ kcal/mol}$$

the temperature range  $0-50$  °C was conducted. A van't Hoff plot gave a value for  $\Delta H_5$  of  $0.1 \pm 0.2$  kcal/mol ( $\Delta S = -5.3 \pm 0.6$  eu). This result is outside the limits of experimental error of the calorimetric data, but the deviation is fairly small, and, considering the very different nature of the two techniques, we do not consider it to be a very serious discrepancy. It may suggest, however, that the actual error limits are slightly greater than those calculated.

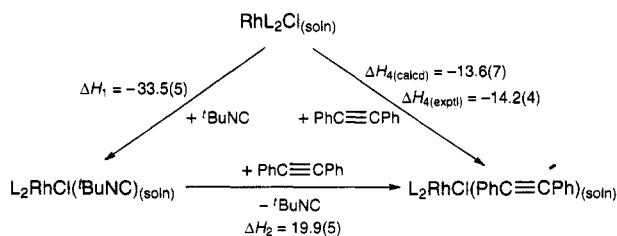
In another competition experiment, a mixture of 38 mM ( $\text{MeC}\equiv\text{CMe})\text{Rh}(\text{P}^i\text{Pr}_3)_2\text{Cl}$  (**6**) and 45 mM diphenylacetylene in  $\text{C}_6\text{D}_6$  (eq 6) at room temperature was



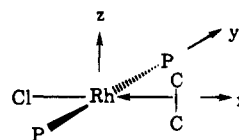
(7) The  $\text{N}_2$  ligand of  $\text{RhL}_2\text{Cl}(\text{N}_2)$  was originally characterized as binding in a "side-on" fashion<sup>8</sup>, but was later shown to be bound "end-on": Thorn, D. L.; Tulip, T. H.; Ibers, J. A. *J. Chem. Soc., Dalton Trans.* **1979**, 2022–2025.

(8) The ratio of solution to gas volume in the calorimetry cell is approximately 16 (4 mL: 0.25 mL). Since the solubility of ethylene in benzene is fairly high (ca. 0.14 M/atm at 20 °C,<sup>a</sup> in good agreement with a value reported for toluene, 3.19 cm<sup>3</sup> ( $\text{C}_2\text{H}_4$ )/(cm<sup>3</sup>(toluene)·atm) at 22 °C,<sup>b</sup> virtually all ethylene produced will remain in solution at equilibrium (ca. 98%); the actual percentage remaining in solution will of course be higher if equilibrium is not reached. The solubility of  $\text{N}_2$  is considerably lower (0.124 cm<sup>3</sup>( $\text{N}_2$ )/(cm<sup>3</sup>(benzene)·atm);<sup>c</sup> at equilibrium roughly equal amounts of  $\text{N}_2$  will be in gas and solution. However, as the heat of solution of  $\text{N}_2$  is undoubtedly very small (slightly positive as indicated by the observation that  $\text{N}_2$  solubility in benzene increases with increasing temperature<sup>d</sup>), this should have no significant effect on the determined reaction enthalpy. (a) Gerrard, W. *Solubility of Gases and Liquids*; Plenum Press: New York, 1976; p 141. (b) Waters, J. A.; Mortimer, G. A.; Clements, H. E. *J. Chem. Eng. Data* **1970**, *15*, 174–176. (c) Landolt–Bornstein. *Zahlenwerte und Funktionen*, 6th ed.; Springer-Verlag: Berlin, 1962; Vol. 2, Part 2b. (d) Burrows, G.; Preece, F. H. *Trans. Faraday Soc.* **1963**, *59*, 1293.

## Scheme 1



## Scheme 2



monitored by both  $^1\text{H}$  and  $^{31}\text{P}$  NMR spectroscopy. An equilibrium constant of 40(5) was measured; thus the Rh–alkyne BDE of **4** is about 2.2 kcal/mol greater than that in **6** (if  $\Delta S = 0$  is assumed). In a reciprocal experiment only a small fraction (ca. 2% of the total rhodium concentration) of diphenylacetylene was displaced by  $\text{MeC}\equiv\text{CMe}$  when a solution of **4** was treated with a 20-fold excess of  $\text{MeC}\equiv\text{CMe}$  in  $\text{C}_6\text{D}_6$ ; however, several unidentified species were observed (possibly due to replacement of  $\text{P}^i\text{Pr}_3$  by 2-butyne) and the results of this experiment are considered less meaningful.

Acetylenes typically bind more strongly than olefins,<sup>9</sup> particularly in the case of coordinatively unsaturated complexes like **4**. The greater (or at least comparable) binding affinity of  $\text{C}_2\text{H}_4$  in this case would not seem likely to result from steric factors; the phenyl groups of diphenylacetylene would be expected to lie in the plane perpendicular to the P–Rh–P axis to avoid interaction with the bulky  $\text{P}^i\text{Pr}_3$  ligands, while the  $\text{C}_2\text{H}_4$  hydrogen atoms could not do so.<sup>6</sup> Molecular mechanics (MM2) calculations support this hypothesis: if the Rh–L'(C–C midpoint) distance is fixed at 2.01 Å,<sup>6</sup> and L is varied from  $\text{PH}_3$  to  $\text{PMe}_3$  to  $\text{P}^i\text{Pr}_3$ , the calculated energy increases significantly less when  $L' = \text{PhC}\equiv\text{CPh}$  than when L' is either  $\text{MeC}\equiv\text{CMe}$  or  $\text{C}_2\text{H}_4$ . Accordingly, visual inspection of the calculated models ( $L = \text{P}^i\text{Pr}_3$ ) reveals significant crowding when L' is 2-butyne or  $\text{C}_2\text{H}_4$ , whereas the diphenylacetylene ligand neatly resides in a "cleft" between the two triisopropylphosphines.

The greater bonding affinity of  $\text{RhL}_2\text{Cl}$  for the olefin is not surprising if simple molecular orbital interactions are considered. If the complexes are viewed as  $d^8$  square-planar, with olefin or acetylene perpendicular to the  $\text{RhP}_2\text{Cl}$  plane,<sup>6</sup> the empty d(Rh) orbital is the  $x^2 - y^2$  (see Scheme 2 for labeling of axes). For both olefin and acetylene,  $\sigma$ -bond formation involves the  $\pi_{11}$  orbital while the  $d_{xz}$ (Rh) orbital is of correct symmetry to back-donate into the  $\pi_{11}^*$  orbital. However, the  $d_{xy}$  orbital of Rh and the  $\pi_{11}$  orbital of alkyne are both filled and therefore their interaction should weaken the Rh–alkyne bond. It has previously been suggested that  $D(\text{M} - \text{alkyne}) - D(\text{M} - \text{alkene})$  may be less for late than

(9) (a) Otsuka, S.; Nakamura, A. *Advances in Organometallic Chemistry*; Academic Press: New York, 1976; Vol. 14, pp 245–283. (b) Crabtree, R. H. *The Organometallic Chemistry of the Transition Metals*, 2nd ed.; John Wiley & Sons: New York, 1994; pp 111–112.

**Table 1. Enthalpy of Addition of L' to 1 in Solution and the Corresponding Minimum Rh-L' BDE's (kcal/mol)**

L'	$\Delta H$ (eq 3)	min Rh-L' BDE <sup>a</sup>
CO	-39.3(7) <sup>b</sup>	48.2 <sup>b</sup>
<sup>t</sup> BuNC	-33.5(5) <sup>b</sup>	42.4 <sup>b</sup>
H <sub>2</sub>	-23.6(6) <sup>b</sup>	32.5 <sup>b,c</sup>
C <sub>2</sub> H <sub>4</sub>	-15.9(6)	24.8
PhC≡CPh	-13.9(8) <sup>d</sup>	22.8 <sup>d</sup>
MeC≡CMe	-11.7(9)	20.6
N <sub>2</sub>	-7.6(7)	16.5

<sup>a</sup> Minimum enthalpy of addition of L' to monomeric RhL<sub>2</sub>Cl based on a minimum bridge strength of 1 of 17.8 kcal/mol (see ref 4). <sup>b</sup> Values from ref 4. <sup>c</sup> Minimum enthalpy of H<sub>2</sub> addition; this corresponds to an average Rh-H BDE of 68.4 kcal/mol. <sup>d</sup> Average of values obtained from direct (eqs 1 and 2) and indirect (eq 3) measurement.

for early transition metals;<sup>10</sup> similar MO-based considerations may be applicable generally.

**Comparison with Thermodynamics of Relevant Systems.** The bridge strength of 1 was previously determined to be at least 17.8 kcal/mol. While only a minimum value could be measured, on the basis of the estimated bridge strength of a closely related complex [Rh(P(4-Tol)<sub>3</sub>)<sub>2</sub>Cl]<sub>2</sub> (19.7 kcal/mol)<sup>11</sup> and the observed reactivity of 1,<sup>12</sup> we believe the actual value is not much greater. Addition of one-half of the minimum bridge strength to  $\Delta H_3$  gives the corresponding lower limits for the absolute Rh-L' BDE's. These values along with results from our previous study are shown in Table 1.

Thermodynamic measurements of other metal-nitrogen bonds have been made. Kubas and Hoff<sup>13</sup> reported the following M-N<sub>2</sub> BDE's in M(CO)<sub>3</sub>(PCy<sub>3</sub>)<sub>2</sub>(N<sub>2</sub>) (kcal/mol): Cr, 19.3; Mo, 19.0; W, 23.5; these values assume that the agostic interactions found in M(CO)<sub>3</sub>(PCy<sub>3</sub>)<sub>2</sub> are equal to 10 kcal/mol. Ru(dmpe)N<sub>2</sub> was studied by Scaiano *et al.*<sup>14</sup> using photoacoustic calorimetry, and the Ru-N<sub>2</sub> BDE was found to be 18.8 ± 2.0 kcal/mol. Using kinetic methods, Turner<sup>15</sup> determined the Ni-N<sub>2</sub> BDE in Ni(CO)<sub>3</sub>N<sub>2</sub> to be 10 kcal/mol. The lower limit of the Rh-N<sub>2</sub> BDE (16.5 kcal/mol) in 2 is thus consistent with other reported examples of metal-N<sub>2</sub> BDE's.

Addition of olefins and acetylenes to organometallic compounds is the subject of a large body of studies which have been reviewed.<sup>16,17</sup> The values reported in this work are not unusual. For example,  $\Delta H = -11.8$  kcal/mol for the addition of C<sub>2</sub>H<sub>4</sub> to Vaska's complex vs -9.3 kcal/mol for the addition of C<sub>2</sub>H<sub>2</sub>.<sup>18</sup> In view of the importance of bis(phosphine)rhodium chloride in olefin hydrogenation and alkane dehydrogenation catalysis,

a comparison of the enthalpy of binding of ethene with that of the addition of H<sub>2</sub> is worth noting. H<sub>2</sub> is found to add more readily by 7.7 kcal/mol (this value or any other differences in addition enthalpies resulting from this work are independent of the estimate of the bridge strength of 1). For alkenes other than ethene, the difference is presumably significantly greater for steric reasons.<sup>19</sup> Extrapolating such a comparison to complexes with different phosphines can only be done tentatively. With that proviso, we note that the greater binding enthalpy of H<sub>2</sub> is consistent with the mechanism proposed for Rh(PMe<sub>3</sub>)<sub>2</sub>(CO)Cl-catalyzed alkane photo-dehydrogenation:<sup>2</sup> the intermediate Rh(PMe<sub>3</sub>)<sub>2</sub>Cl(alkene)-H<sub>2</sub> is proposed to lose alkene, which should be thermodynamically more favorable than loss of H<sub>2</sub>.

## Experimental Section

**General Procedures.** All manipulations were conducted under an argon atmosphere either in a Vacuum Atmospheres Dry-Lab glovebox or by using standard Schlenk techniques. Nitrogen (99.99% grade) and ethylene (99.5% grade) were purchased from JWS Technologies, Inc., and used without further purification. 2-Butyne and *tert*-butyl isocyanide were purchased from Aldrich and freeze-pump-thawed prior to use. C<sub>6</sub>D<sub>6</sub> (99.5 atom % *d*, Cambridge Isotope Laboratories) was dried over Na and vacuum distilled prior to use. All other solvents were either distilled from dark purple solutions of benzophenone ketyl or dried over molecular sieves. [Rh(P<sup>*i*</sup>Pr<sub>3</sub>)<sub>2</sub>Cl]<sub>2</sub> (1) was synthesized according to Werner.<sup>20</sup> (<sup>*t*</sup>BuNC)Rh(P<sup>*i*</sup>Pr<sub>3</sub>)<sub>2</sub>Cl (5) was synthesized as reported earlier.<sup>4</sup>

NMR spectra were recorded on either a Varian VXR-200 or XL-400 MHz spectrometer. <sup>31</sup>P NMR chemical shift values are expressed in reference to 85% H<sub>3</sub>PO<sub>4</sub>. IR spectra were recorded on a Mattson Cygnus 100 FTIR spectrometer.

Only materials of high purity as indicated by IR and NMR spectroscopy were used in the calorimetric experiments. Calorimetric measurements were performed using a Calvet calorimeter (Setaram C-80) which was periodically calibrated using the TRIS reaction<sup>21</sup> or the enthalpy of solution of KCl in water.<sup>22</sup> The experimental enthalpies for these two standard reactions compared very closely to literature values. This calorimeter and the experimental procedures used have been previously described.<sup>23</sup> Typical procedures are described below. Experimental enthalpy data are reported with 95% confidence limits.

**Solution Calorimetry: Calorimetric Measurement of Reactions Between *t*-BuNC and L'/Rh(P<sup>*i*</sup>Pr<sub>3</sub>)<sub>2</sub>Cl (L' = N<sub>2</sub> (2), C<sub>2</sub>H<sub>4</sub> (3), and PhC≡CPh (4)).** The procedures for the measurement of this type of reactions are similar and represented by that of 4.

The mixing vessels of the Setaram C-80 were cleaned, dried in an oven maintained at 120 °C, and then taken into the glovebox. A 20–25 mg sample of 4 was accurately weighed into the lower vessel; it was closed and sealed with 1.5 mL of mercury. A 4 mL amount of a stock solution of *tert*-butyl isocyanide (25 μL of the isocyanide in 20 mL of freshly dried and distilled benzene) was added, and the remainder of the cell was assembled, removed from the glovebox, and inserted in the calorimeter. The reference vessel was loaded in an

(19) See for example: Hughes, R. P. In *Comprehensive Organometallic Chemistry*; Wilkinson, G., Stone, F. G. A., Abel, E. W., Eds.; Pergamon Press: Oxford, 1982; Vol. 5, pp 418–424.

(20) Werner, H.; Wolf, J.; Hohn, A. *J. Organomet. Chem.* **1985**, *287*, 395–407.

(21) Ojelund, G.; Wadsö, I. *Acta Chem. Scand.* **1968**, *22*, 1691–1699.

(22) Kilday, M. V. *J. Res. Natl. Bur. Stand. (U.S.)* **1980**, *85*, 467–481.

(23) Nolan, S. P.; Hoff, C. D.; Landrum, J. T. *J. Organomet. Chem.* **1985**, *282*, 357–362.

(10) Calhorda, M.; Carrondo, M.; Dias, A.; Galvão, A.; Garcia, M.; Martins, A.; Piedade, M.; Pinheiro, C.; Romão, C.; Simões, J.; Veiros, L. *Organometallics* **1991**, *10*, 483–494.

(11) (a) Pribula, A. J.; Drago, R. S. *J. Am. Chem. Soc.* **1976**, *98*, 2784–2788. (b) Drago, R. S.; Miller, J. G.; Hoselton, M. A.; Farris, R. D.; Desmond, M. J. *J. Am. Chem. Soc.* **1983**, *105*, 444–449.

(12) Shih, K.; Goldman, A. S. *Organometallics* **1993**, *9*, 3390–3392.

(13) (a) Gonzales, A. A.; Zhang, K.; Nolan, S. P.; Vega, R. L. d. l.; Mukerjee, S. L.; Hoff, C. D.; Kubas, G. J. *Organometallics* **1988**, *7*, 2429–2435. (b) Zhang, K.; Gonzales, A. A.; Mukerjee, S. L.; Chou, S.-J.; Hoff, C. D.; Kuba-Martin, K. A.; Barnhart, D.; Kubas, G. J. *J. Am. Chem. Soc.* **1991**, *113*, 9170–9176.

(14) Belt, S. T.; Scaiano, J. C.; Whittlesey, M. K. *J. Am. Chem. Soc.* **1993**, *115*, 1921–1925.

(15) Turner, J. J.; Simpson, M. B.; Poliakov, M.; Maier, W. B. *J. Am. Chem. Soc.* **1983**, *105*, 3898–3904.

(16) Mondal, J. U.; Blake, D. M. *Coord. Chem. Rev.* **1982**, *47*, 205–238.

(17) Hartley, F. R. *Chem. Rev.* **1973**, *73*, 163–190.

(18) Vaska, L. *Acc. Chem. Res.* **1968**, *1*, 335–344.

identical fashion with the exception that no organorhodium complex was added to the lower vessel. After the calorimeter had reached thermal equilibrium at 30.0 °C (about 2 h), the calorimeter was inverted, thereby allowing the reactants to mix. After the reaction had reached completion and the calorimeter had once again reached thermal equilibrium (ca. 2 h), the vessels were removed from the calorimeter. Conversion to  $(t\text{-BuNC})\text{Rh}(\text{P}^i\text{Pr}_3)_2\text{Cl}$  (**5**) was found to be quantitative under these reaction conditions. The enthalpy of reaction,  $-15.6 \pm 0.4$  kcal/mol, represents the average of five individual calorimetric determinations.

In order to consider all species in solution, the enthalpies of solution of **4** had to be directly measured. This was performed by using a procedure similar to the one described above with the exception that no isocyanide was added to the reaction cell. This enthalpy of solution represents the average of five individual determinations and is  $4.3 \pm 0.2$  kcal/mol.

**(N<sub>2</sub>)Rh(P<sup>i</sup>Pr<sub>3</sub>)<sub>2</sub>Cl (2).** Compound **2** was made by modification of a reported method.<sup>6</sup> Compound **1** (350 mg, 0.38 mmol) was dissolved in 30 mL of toluene, and the solution was stirred under 1 atm of N<sub>2</sub> at room temperature. The formation of **2** was monitored by <sup>31</sup>P NMR spectroscopy, and conversion was found to be complete after 30 h. The solvent was removed *in vacuo*, and the product was recrystallized from toluene/hexanes (330 mg, 90% yield). <sup>1</sup>H NMR (C<sub>6</sub>D<sub>6</sub>, 200 MHz):  $\delta$  1.31 (q, (<sup>3</sup>J<sub>P-H</sub> + <sup>5</sup>J<sub>P-H</sub>)/2 = J<sub>H-H</sub> = 6.6 Hz, 36 H), 2.45 (m, 6 H). <sup>31</sup>P NMR (C<sub>6</sub>D<sub>6</sub>, 162 MHz):  $\delta$  42.55 (d, J<sub>Rh-P</sub> = 122.06 Hz). IR (toluene): 2105.2 cm<sup>-1</sup> (s).

**(C<sub>2</sub>H<sub>4</sub>)Rh(P<sup>i</sup>Pr<sub>3</sub>)<sub>2</sub>Cl (3).** Compound **3** was prepared by modification of a literature method.<sup>6</sup> Compound **1** (350 mg, 0.38 mmol) was dissolved in 30 mL of toluene, and C<sub>2</sub>H<sub>4</sub> was bubbled through the solution for 30 seconds. The initially purple solution turned bright yellow immediately. The solvent was removed *in vacuo*, and the product was recrystallized from toluene/hexanes (330 mg, 90% yield). <sup>1</sup>H NMR (C<sub>6</sub>D<sub>6</sub>, 400 MHz):  $\delta$  1.26 (q, (<sup>3</sup>J<sub>P-H</sub> + <sup>5</sup>J<sub>P-H</sub>)/2 = J<sub>H-H</sub> = 6.6 Hz, 36 H), 2.32 (m, 6 H), 2.62 (pseudo q, 4 H, C<sub>2</sub>H<sub>4</sub>). <sup>31</sup>P NMR (C<sub>6</sub>D<sub>6</sub>, 162 MHz):  $\delta$  34.1 (d, J<sub>Rh-P</sub> = 120.03 Hz). IR (CH<sub>2</sub>Cl<sub>2</sub>): 1603.7 cm<sup>-1</sup> (w).

**(PhC≡CPh)Rh(P<sup>i</sup>Pr<sub>3</sub>)<sub>2</sub>Cl (4).** Compound **1** (350 mg, 0.38 mmol) was dissolved in 30 mL of toluene, and 136 mg (0.76 mmol) of diphenylacetylene was added. The initially purple solution turned bright yellow immediately. The mixture was stirred for 30 min, and the solvent was removed *in vacuo*. The product was recrystallized from toluene/hexanes (430 mg, 90% yield). <sup>1</sup>H NMR (C<sub>6</sub>D<sub>6</sub>, 200 MHz):  $\delta$  1.20 (q, (<sup>3</sup>J<sub>P-H</sub> + <sup>5</sup>J<sub>P-H</sub>)/2 = J<sub>H-H</sub> = 6.6 Hz, 36 H), 2.27 (m, 6 H), 8.27 (d, 4 H, Ph), 7.21 (t, 4 H, Ph), 7.05 (d, 2 H, Ph). <sup>31</sup>P NMR (C<sub>6</sub>D<sub>6</sub>, 162 MHz):  $\delta$  32.59 (d, J<sub>Rh-P</sub> = 116.13 Hz).

**Reaction of (N<sub>2</sub>)Rh(P<sup>i</sup>Pr<sub>3</sub>)<sub>2</sub>Cl (2) with *t*-BuNC.** A 0.45 mL amount of 25 mM **2** in C<sub>6</sub>D<sub>6</sub> was treated with 1.5  $\mu$ L (0.013 mmol) of *t*-BuNC in an NMR tube. The color of the solution changed from brownish-yellow to bright yellow immediately upon shaking, and the evolution of gas was observed. The <sup>31</sup>P NMR spectrum was observed immediately, and **2** had completely disappeared with the formation of **5** which was confirmed by IR, <sup>1</sup>H, and <sup>31</sup>P NMR. Excess (>1.1 equiv) *t*-BuNC led to uncharacterized species.

**Reaction of (C<sub>2</sub>H<sub>4</sub>)Rh(P<sup>i</sup>Pr<sub>3</sub>)<sub>2</sub>Cl (3) with *t*-BuNC.** A 0.45 mL amount of 25 mM **3** in C<sub>6</sub>D<sub>6</sub> was treated with 1.5  $\mu$ L (0.013 mmol) of *t*-BuNC in an NMR tube. The NMR tube was shaken gently, and the evolution of gas was observed. The <sup>31</sup>P NMR spectrum was recorded immediately, and **3** was found to have disappeared completely with the formation of **5**. Free C<sub>2</sub>H<sub>4</sub> was found in the <sup>1</sup>H NMR spectrum. As in the reaction of **2**, excess (>1.1 equiv) *t*-BuNC led to uncharacterized species.

**Reaction of (PhC≡CPh)Rh(P<sup>i</sup>Pr<sub>3</sub>)<sub>2</sub>Cl (4) with *t*-BuNC.** A 0.45 mL amount of 25 mM **4** in C<sub>6</sub>D<sub>6</sub> was treated with 1.5  $\mu$ L (0.013 mmol) of *t*-BuNC in an NMR tube. The NMR tube was shaken gently before the <sup>31</sup>P NMR spectrum was recorded, and complete conversion to **5** was observed within about 15 min. Free diphenylacetylene was observed in the <sup>1</sup>H NMR spectrum. Excess (>1.1 equiv) *t*-BuNC also leads to uncharacterized species in this reaction.

**Reaction of C<sub>2</sub>H<sub>4</sub> with (PhC≡CPh)Rh(P<sup>i</sup>Pr<sub>3</sub>)<sub>2</sub>Cl (4).** A 0.6 mL amount of a 66 mM solution of **4** in toluene was put in a J. Young NMR tube (which contained a sealed capillary of PPh<sub>3</sub> in acetone-*d*<sub>6</sub>) and placed under 840 Torr of C<sub>2</sub>H<sub>4</sub>. Variable temperature <sup>31</sup>P NMR spectroscopy was used to obtain a van't Hoff plot.

**Reaction of Diphenylacetylene with (MeC≡CMe)Rh(P<sup>i</sup>Pr<sub>3</sub>)<sub>2</sub>Cl (6).** Compound **6** was generated *in situ* by reacting 2 equiv of 2-butyne with **1**. <sup>1</sup>H NMR (C<sub>6</sub>D<sub>6</sub>, 400 MHz):  $\delta$  1.32 (q, (<sup>3</sup>J<sub>P-H</sub> + <sup>5</sup>J<sub>P-H</sub>)/2 = J<sub>H-H</sub> = 6.5 Hz, 36 H), 2.33 (m, 6 H), 2.01 (s, 6 H, C<sub>2</sub>Me<sub>2</sub>). <sup>31</sup>P NMR (C<sub>6</sub>D<sub>6</sub>, 162 MHz):  $\delta$  34.83 (d, J<sub>Rh-P</sub> = 122.62 Hz), IR (C<sub>6</sub>D<sub>6</sub>): 1953.8 cm<sup>-1</sup> (s). A mixture of 38 mM **6** and 45 mM diphenylacetylene in C<sub>6</sub>D<sub>6</sub> equilibrated at room temperature and was monitored with both <sup>1</sup>H and <sup>31</sup>P NMR spectroscopy.

**Acknowledgment.** Support for this research by the National Science Foundation (Grants CHE-9121695 to A.S.G. and CHE-9305492 to S.P.N.) and the Louisiana Education Quality Support Fund is gratefully acknowledged.

OM950225W

# Unexpected Reactivity of Functionalized Lewis Base Stabilized Silanediyl Transition Metal Complexes toward Organolithium Nucleophiles

Robert J. P. Corriu,\* Bhanu P. S. Chauhan, and Gérard F. Lanneau\*

Laboratoire des Précurseurs Organométalliques de Matériaux, UMR 44-Université Montpellier II, Case 007, Place Eugène Bataillon, 34095 Montpellier Cedex 05, France

Received March 14, 1995<sup>®</sup>

**Summary:** (Organosilanediyl)chromium(0) pentacarbonyl complexes,  $[2-(Me_2NCH_2)C_6H_4]RSi=Cr(CO)_5$  ( $R = Me, Ph, t-Bu, Ph-C\equiv C-, Me_3Si-C\equiv C-$ ), are obtained in good yield through the coupling reactions of (arylyhydrogenosilanediyl)chromium(0) pentacarbonyl complex  $[2-(Me_2NCH_2)C_6H_4]HSi=Cr(CO)_5$ , with the corresponding organolithium nucleophiles. Unexpectedly, the chloro- and bromosilanediyl complexes  $[2-(Me_2NCH_2)C_6H_4]XSi=Cr(CO)_5$  ( $X = Cl, Br$ ) are unreactive, but the fluorosilanediyl complex is even more reactive than the hydrogenosilanediyl complex with methylolithium. Possible geometries of the intermediate resulting in frontside attack of the nucleophile upon a zwitterionic silicon species are discussed.

In recent years, silylene(silanediyl)-transition metal complexes,<sup>1</sup>  $[R_2Si=ML_n]$  have been elusive synthetic targets in the rapidly developing field of the organometallic chemistry of silicon. This interest is associated with their invoked intermediacy in a number of chemical transformations<sup>2</sup> and also derives from the exciting reaction chemistry<sup>3</sup> related to them. Since 1987, after discovery of the first stable silylene-transition metal complexes,<sup>4</sup> a variety of synthetic strategies has been devised<sup>5-8</sup> to obtain such complexes stabilized by inter or intramolecular coordination of donor groups. The stabilizing influence of thiolate groups was also exploited to synthesize base-free tricoordinated silylene-

ruthenium or platinum complexes.<sup>9</sup> However, the reactivity of these complexes has not been extensively studied.<sup>10</sup>

We have recently described the preparation of arylhydrogenosilanediyl transition metal complexes<sup>11</sup> through the dehydrogenative coupling reaction of primary silanes  $ArSiH_3$  with transition metal carbonyls under

\* Authors to whom correspondence should be addressed. FAX Number: (33) 67 14 38 88.

<sup>®</sup> Abstract published in *Advance ACS Abstracts*, June 15, 1995.

(1) (a) Zybilla, C.; Handwerker, H.; Friedrich, H. *Adv. Organomet. Chem.* **1994**, *36*, 229. (b) Tilley, T. D. *Acc. Chem. Res.* **1993**, *26*, 22. (c) Lickiss, P. D. *Chem. Soc. Rev.* **1992**, *271*. (d) Tilley, T. D. In *The Chemistry of Organic Silicon Compounds*; Patai, S., Rappoport, Z., Eds.; Wiley: New York, 1989; pp 1415; *Ibid.*, 1991; pp 309. (e) Keith-Woo, L.; Smith, D. A.; Young, V. G., Jr. *Organometallics* **1991**, *10*, 3977. (f) Petz, W. *Chem. Rev.* **1986**, *86*, 1019. (g) Kawano, Y.; Tobita, H.; Ogino, H. *Angew. Chem., Int. Ed. Engl.* **1991**, *30*, 843. (h) Denk, M.; Hayashi, R. K.; West, R. J. *Chem. Soc., Chem. Commun.* **1994**, *33*. (i) Jutz, P.; Möhrke, A. *Angew. Chem., Int. Ed. Engl.* **1990**, *29*, 893. (j) Horng, K. M.; Wang, S. L.; Liu, C. S. *Organometallics* **1991**, *10*, 631. (k) Pi, Z.; Simons, R.; Tessier, C. XXVII Organosilicon Symposium, Troy, NY, 1994; A11.

(2) (a) Curtis, M. D.; Epstein, P. S. *Adv. Organomet. Chem.* **1981**, *91*, 213. (b) Ojima, I. In *The Chemistry of Organic Silicon Compounds*; Patai, S., Rappoport, Z., Eds.; Wiley: Chichester, U.K., 1989; pp 479. (c) Harrod, J. F.; Ziegler, T.; Tschinke, V. *Organometallics* **1990**, *9*, 897. (d) Yamashita, H.; Tanaka, M.; Goto, M. *Organometallics* **1992**, *11*, 3227. (e) Hengge, E.; Weinberger, M.; Jammeg, C. *J. Organomet. Chem.* **1991**, *410*, C1. (f) Corey, J. Y.; Chang, L. S.; Corey, E. R. *Organometallics* **1987**, *6*, 1595. (g) Brown-Wensley, K. A. *Organometallics* **1987**, *6*, 1590. (h) Aitken, C.; Harrod, J. F.; Samuel, E. *J. Am. Chem. Soc.* **1986**, *108*, 4059. (i) Hengge, E.; Weinberger, M. *J. Organomet. Chem.* **1993**, *443*, 167. (j) Ojima, I.; Inaba, S. I.; Kogure, T.; Nagui, Y. *J. Organomet. Chem.* **1973**, *55*, C7. (k) Chang, L. S.; Corey, J. Y. *Organometallics* **1989**, *8*, 1885. (l) Aitken, C.; Gill, U. S.; Harrod, J. F. *Can. J. Chem.* **1987**, *65*, 1804. (m) Harrod, J. F. *ACS Symp. Ser.* **1988**, *No. 360*, 89. (n) Clarke, M. P.; Davidson, I. M. T. *J. Organomet. Chem.* **1981**, *408*, 149. (o) Clarke, M. P. *J. Organomet. Chem.* **1989**, *376*, 165. (p) Clarke, M. P.; Davidson, I. M. T.; Eaton, G. *Organometallics* **1988**, *7*, 2076. (q) Okinoshima, H.; Yamamoto, K.; Kumada, M. *J. Am. Chem. Soc.* **1972**, *94*, 9263.

(3) (a) Pannell, K. H.; Cervantes, J.; Hernandez, C.; Cassias, J.; Vincenti, S. *Organometallics* **1986**, *5*, 1056. (b) Tobita, H.; Ueno, K.; Ogino, H. *Bull. Chem. Soc. Jpn.* **1988**, *61*, 2797. (c) Haynes, A.; George, M. W.; Haward, M. T.; Poliakoff, M.; Turner, J. J.; Boag, N. M.; Green, M. J. *Am. Chem. Soc.* **1991**, *113*, 2011. (d) Pannell, K. H.; Wong, L.-J.; Rozell, J. M. *Organometallics* **1989**, (e) Pannell, K. H.; Rozell, J. M.; Hernandez, C. *J. Am. Chem. Soc.* **1989**, *111*, 4482. (f) Seyferth, D.; Shannon, M. L.; Vick, S. C.; Lim, T. F. O. *Organometallics* **1985**, *4*, 57. (g) Sakurai, H.; Kamiyama, Y.; Nakadira, Y. *J. Am. Chem. Soc.* **1977**, *99*, 3879. (h) Marinetti-Mignani, A.; West, R. *Organometallics* **1987**, *6*, 141. (i) Jones, K. L.; Pannell, K. H. *J. Am. Chem. Soc.* **1993**, *115*, 11336. (j) Ueno, K.; Tobita, H.; Ogino, H. *Chem. Lett.* **1990**, 369. (k) Denk, M.; Lennon, R.; Hayashi, R.; West, R.; Belyakov, A. V.; Verne, H. P.; Haaland, A.; Wagner, M.; Metzler, N. *J. Am. Chem. Soc.* **1994**, *116*, 2691.

(4) (a) Straus, D. A.; Tilley, T. D.; Rheingold, A. L. *J. Am. Chem. Soc.* **1987**, *109*, 5872. (b) Zybilla, C.; Müller, G. *Angew. Chem., Int. Ed. Engl.* **1987**, *26*, 669.

(5) (a) Tilley, T. D. *Comments Inorg. Chem.* **1990**, *10*, 37. (b) Straus, D. A.; Zhang, C.; Quimbata, G. E.; Grumbine, S. D.; Hyne, R. H.; Tilley, T. D.; Rheingold, A. L.; Geib, S. J. *J. Am. Chem. Soc.* **1990**, *112*, 2673. (c) Straus, D. A.; Grumbine, S. D.; Tilley, T. D.; J. *Am. Chem. Soc.* **1990**, *112*, 7801. (d) Grumbine, S. D.; Chadha, R. K.; Tilley, T. D. *J. Am. Chem. Soc.* **1992**, *114*, 1518.

(6) (a) Zybilla, C.; Müller, G. *Organometallics* **1988**, *7*, 1368. (b) Zybilla, C.; Wilkinson, D. L.; Müller, G. *Angew. Chem., Int. Ed. Engl.* **1988**, *27*, 583. (c) Zybilla, C.; Wilkinson, D. L.; Leis, C.; Müller, G. *Angew. Chem., Int. Ed. Engl.* **1989**, *28*, 203. (d) Leis, C.; Wilkinson, D. L.; Handwerker, H.; Zybilla, C. *Organometallics* **1992**, *11*, 514. (e) Leis, C.; Zybilla, C.; Lachmann, J.; Müller, G. *Polyhedron* **1991**, *10*, 1163. (f) Handwerker, H.; Leis, C.; Gamper, S.; Zybilla, C. *Inorg. Chem. Acta.* **1992**, *200*, 763. (g) Zybilla, C. *Top. Curr. Chem.* **1991**, *160*, 1. (h) Handwerker, H.; Paul, M.; Riede, J.; Zybilla, C. *J. Organomet. Chem.* **1993**, *459*, 151. (i) Probst, R.; Leis, C.; Gamper, S.; Herdtweck, E.; Zybilla, C.; Auner, N. *Angew. Chem., Int. Ed. Engl.* **1991**, *30*, 1132.

(7) (a) Corriu, R. J. P.; Lanneau, G. F.; Priou, C. *Angew. Chem., Int. Ed. Engl.* **1991**, *30*, 1130. (b) Priou, C. Ph.D. Thesis, U. Montpellier II, Montpellier, France, 1990. (c) Corriu, R.; Lanneau, G.; Chauhan, B. *Münchener Silicontage* Munich, Germany, August, 1992. (d) Corriu, R. J. P.; Lanneau, G. F.; Chauhan, B. P. S. *Organometallics* **1993**, *12*, 2001. (e) Chauhan B. P. S.; Corriu, R. J. P.; Lanneau, G. F.; Priou, C.; Auner, N.; Handwerker, H.; Herdtweck, E. *Organometallics* **1995**, *14*(4), 1657.

(8) (a) Uno, K.; Tobita, H.; Shimoi, M.; Ogino, H. *J. Am. Chem. Soc.* **1988**, *110*, 4092. (b) Tobita, H.; Uno, K.; Shimoi, M.; Ogino, H. *J. Am. Chem. Soc.* **1990**, *112*, 3415. (c) Koi, J. R.; Tobita, H.; Ogino, H. *Organometallics* **1992**, *11*, 2479. (d) Uno, K.; Tobita, H.; Ogino, H. *J. Organomet. Chem.* **1992**, *430*, 93. (e) Uno, K.; Tobita, H.; Ogino, H. *Chem. Lett.* **1993**, 1723. (f) Uno, K.; Ito, S.; Endo, K.; Tobita, H.; Inomata, S.; Ogino, H. *Organometallics* **1994**, *13*, 3309.

(9) (a) Grumbine, S. D.; Tilley, T. D.; Rheingold, A. L. *J. Am. Chem. Soc.* **1993**, *115*, 358. (b) Grumbine, S. D.; Tilley, T. D.; Arnold, F. P.; Rheingold, A. L. *J. Am. Chem. Soc.* **1993**, *115*, 7884. (c) Grumbine, S. K.; Tilley, T. D.; Arnold, F. P.; Rheingold, A. L. *J. Am. Chem. Soc.* **1994**, *116*, 5495.

(10) (a) Kawano, Y.; Tobita, H.; Shimoi, M.; Ogino, H. *J. Am. Chem. Soc.* **1994**, *116*, 8575. (b) Grumbine, S. K.; Tilley, T. D. *J. Am. Chem. Soc.* **1994**, *116*, 6951. (c) Handwerker, H.; Leis, C.; Probst, R.; Bissinger, P.; Grohmann, A.; Kiprof, P.; Herdtweck, E.; Blümel, J.; Auner, N.; Zybilla, C. *Organometallics* **1993**, *12*, 2162. (d) Handwerker, H.; Paul, M.; Blümel, J.; Zybilla, C. *Angew. Chem., Int. Ed. Engl.* **1993**, *32*, 1313. (e) Zhang, C.; Grumbine, S. D.; Tilley, T. D. *Polyhedron*, **1991**, *10*, 1173.

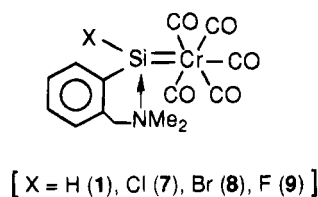
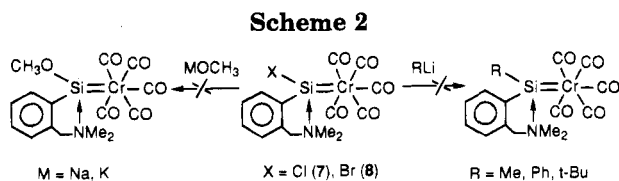
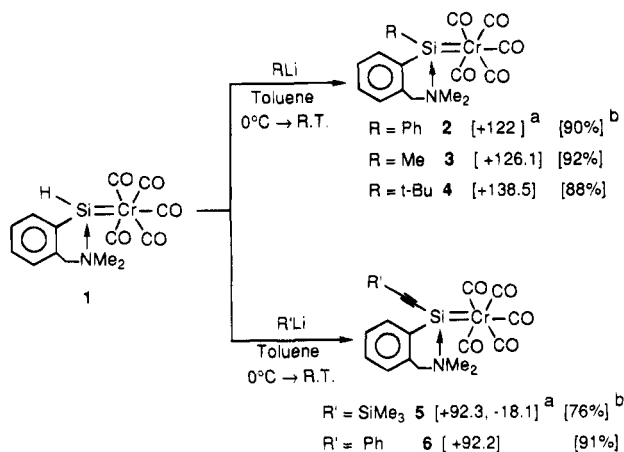


Figure 1.

**Scheme 1**

<sup>a</sup> Legend: (a) <sup>29</sup>Si-NMR chemical shifts in ppm (b) yields.

photolytic conditions. The photochemical displacement reactions of complex **1**, [2-(Me<sub>2</sub>NCH<sub>2</sub>)C<sub>6</sub>H<sub>4</sub>][HSi=Cr(CO)<sub>5</sub>], with various phosphines led either to cleavage of the silicon–metal bond [PR<sub>3</sub> = PPh<sub>3</sub>, P(OMe)<sub>3</sub>] or the displacement of two carbonyls on the metal moiety with (diphenylphosphino)ethane. Exchange reactions of complex **1** with Ph<sub>3</sub>CX afforded a series of functionalized complexes [2-(Me<sub>2</sub>NCH<sub>2</sub>)C<sub>6</sub>H<sub>4</sub>][XSi=Cr(CO)<sub>5</sub>] {X = Cl (**7**), Br (**8**), F (**9**)} (Figure 1).

In the present note, we wish to report the first successful coupling reactions of these complexes with organometallic nucleophiles.

To our knowledge, only one example of attempted<sup>12</sup> substitution reaction of a base-stabilized chlorosilane–transition metal carbonyl complex with organolithium reagent has been described, leading merely to decomposition products.

Reactions of complex **1** with organolithiums RLi (R = Me, Ph, *t*-Bu, Ph–C≡C–, Me<sub>3</sub>Si–C≡C–) at 0 °C in dry toluene, under argon, furnished the corresponding R-substituted silanediyl–chromium(0) pentacarbonyl complexes in good yields (Scheme 1).

Complex **2** has also been synthesized by the photochemical insertion reaction of Cr(CO)<sub>6</sub> with [2-[(dimethylamino)methyl]phenyl]phenyldihydrosilane<sup>7e</sup> or by reaction of Na<sub>2</sub>Cr(CO)<sub>5</sub> with [2-[(dimethylamino)methyl]phenyl]phenyldichlorosilane,<sup>10c</sup> but complexes **3–6** would be difficult to obtain by those methods.<sup>13,14</sup>

Spectroscopic properties of the complexes are consistent with the proposed structures. <sup>29</sup>Si-NMR chemical

(11) (a) Corriu, R.; Lanneau, G.; Chauhan, B. P. S. *16th International Conference on Organometallic Chemistry*, Brighton, U.K.; Royal Society of Chemistry: Cambridge, U.K., 1994; OB-10. (b) Corriu, R. J. P.; Chauhan, B. P. S.; Lanneau, G. F. *Organometallics* **1995**, *14*(4), 1646.

(12) Schmid, G.; Welz, E. *Angew. Chem., Int. Ed. Engl.* **1977**, *16*, 785.

(13) For example, reaction of [2-[(dimethylamino)methyl]phenyl]methylsilane with Cr(CO)<sub>6</sub> under photolytic conditions in pentane led to the formation of a mixture of three products, along with complex **3** in 10% yield.

shifts of complexes **2–6** fall in the range of +90 to +140 ppm, which is characteristic of Lewis base stabilized silanediyl metal complexes having at least one aromatic group on silicon atom.<sup>1</sup> As anticipated, <sup>1</sup>H-NMR and <sup>13</sup>C-NMR data confirmed the rigid coordination of dimethylamino groups to the silicon atom. <sup>1</sup>H-NMR spectra showed two signals for diastereotopic methyl groups on nitrogen. An AB system was observed for the methylene protons, indicating hindered rotation around the C–N bond. Two signals for diastereotopic methyl groups on nitrogen were also observed in <sup>13</sup>C-NMR spectra (see Experimental Section).

In light of the above results, we have attempted nucleophilic substitution reactions on the silicon atom of halogen-substituted silanediyl–chromium complexes<sup>11</sup> **7–9** with several nucleophiles. To our surprise, complexes **7** and **8** showed no reactivity toward organolithiums RLi (R = Me, Ph, *t*-Bu) and metal methoxides MOCH<sub>3</sub> (M = Na, K). For example, when methyllithium was added dropwise to the complex ([2-[(dimethylamino)methyl]phenyl]chlorosilane)chromium(0) pentacarbonyl, **7**, in a one-to-one ratio in toluene at 0 °C followed by stirring at room temperature, no reaction was observed even after 72 h. If the mixture was refluxed for 4 h in toluene, the decomposition of complex **7** to unidentified products was observed. In the case of the complex ([2-[(dimethylamino)methyl]phenyl]bromosilane)chromium(0) pentacarbonyl, **8**, reaction with methyllithium under identical conditions resulted in less than 10% conversion (calculated on the basis of <sup>1</sup>H-NMR of the mixture) to the corresponding methylsilanediyl complex **3**, but most of the starting material was recovered (Scheme 2). It should be noted that the nucleophilic addition of RLi onto a CO functionality, a well-known synthetic approach to carbenes,<sup>15</sup> is not observed in the present case.

The absence of reactivity of complexes **7** and **8** led us to investigate the chemical behavior of the fluoro-substituted silanediyl–chromium complex **9** toward various nucleophiles. In contrast to the results obtained with **7** and **8**, complex **9** reacted smoothly with organolithiums, giving rise to the corresponding organosilane–chromium complexes in good yields. For instance, reaction of methyllithium with complex **9** under identical reaction conditions (as for **1**, **7**, and **8**) afforded complex **3** in 98% yield in 12 h.

A comparison of the reactivity of complex **1** and complex **9** toward nucleophiles (MeLi as title example) has been carried out. In a complementary experiment, **1** and **9** were dissolved in toluene in equimolar amounts. This mixture was treated with 0.5 equiv of methyllithium at 0 °C and warmed to room temperature. The

(14) For comparison of the characteristic signals of acetylenic groups directly attached to a hypercoordinated silicon atom, see: Boyer-Elma, K.; Corriu, R. J. P.; Douglas, W. E. In *Silicon Containing Polymers*; Jones, R. G., Ed.; Royal Society of Chemistry: Cambridge, in press.

(15) Cardin, D. J.; Cetinkaya, B.; Lappert, M. F. *Chem. Rev.* **1972**, *72*, 545.

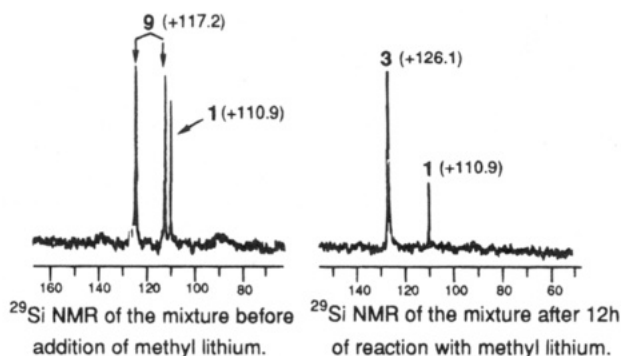


Figure 2.

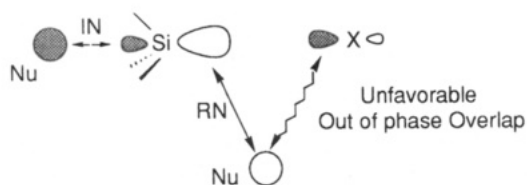


Figure 3.

course of the reaction was followed by IR and  $^{29}\text{Si}$ -NMR. After 12 h,  $^{29}\text{Si}$ -NMR of the reaction mixture indicated complete consumption of complex **9** and the appearance of a new peak at  $\delta$  +126.1, due to formation of complex **3** (Figure 2).

This reaction clearly demonstrates that fluorosilanediyl-chromium complex **9** is more reactive toward nucleophiles than is the hydrosilanediyl-chromium complex **1**. On the basis of the above studies, the following order of reactivity of Lewis base stabilized functional silanediyl-chromium complexes toward various nucleophiles can be proposed:



It is interesting to note that this order is unexpectedly different from the order of reactivity of the corresponding saturated silanes  $\text{R}_3\text{SiX}$  with nucleophiles ( $\text{Br}, \text{Cl} > \text{F} > \text{H}$ ), which essentially parallels the polarizability of the leaving group.<sup>16</sup> Such behavior could be related to the nature of the bond between the leaving group and the silicon atom of silanediyl complexes.

Anh and Minot<sup>17ab</sup> have tentatively rationalized the stereochemistry of nucleophilic attack at tetrahedral silicon by an extension of Salem's treatment of Walden inversion.<sup>17c</sup> Retention and/or inversion were considered to be the result of a fine balance between the in-phase and out-of-phase orbital overlap between the nucleophile and the LUMO of the substrate  $\sigma^* \text{Si-X}$  (Figure 3).

Hybridization arguments also explained the order of reactivity of cyclic systems (Figure 4).<sup>18</sup> Ring contraction decreases the *s* character of the intracyclic Si-C bonds which in turn increases the *s* character of the exocyclic Si-X bond. Both increased reactivity and displacement toward retention of configuration have been observed with such systems.

(16) (a) Corriu, R. J. P.; Guerin, C. *Adv. Organomet. Chem.* **1982**, *20*, 265. (b) Corriu, R. J. P.; Lanneau, G. F. *Bull. Soc. Chim. Fr.* **1973**, 3102. (c) Corriu, R. J. P.; Guerin, C.; Moreau, J. J. E. *Top. Stereochem.* **1984**, *15*, 43. (d) Brelriere, C.; Corriu, R. J. P.; DeSaxcé, A.; Royo, G. *J. Organomet. Chem.* **1979**, *166*, 153.

(17) (a) Anh, N. T.; Minot, C. *J. Am. Chem. Soc.* **1980**, *102*, 103. (b) Minot, C.; Anh, N. T. *Tetrahedron Lett.* **1975**, 3905. (c) Salem, L. *Chem. Ber.* **1969**, *5*, 449.

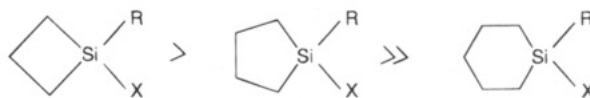


Figure 4.

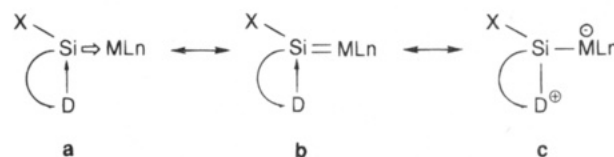


Figure 5.

Silanediyl-transition metal complexes can be represented by at least three resonance structures shown in Figure 5. With **a** and/or **b** as the formulated reactive species, there are no precedents in the literature for discussing the present data. On the other hand, if one supposes the zwitterionic structure **c** to be the reactive species involved in the nucleophilic substitution reaction, then geometrical arguments which have been earlier emphasized in the  $\text{S}_{\text{N}}2(\text{Si})$  reactions would favor here a retention pathway.

X-ray structure determination of two aminoaryl-silanediyl-transition metal complexes  $[2-(\text{Me}_2\text{NCH}_2)\text{-C}_6\text{H}_4]\text{C}_6\text{H}_5\text{Si}=\text{M}(\text{CO})_n$ , ( $\text{M} = \text{Cr}$ ,  $n = 5$ ;  $\text{M} = \text{Fe}$ ,  $n = 4$ ) are reported in the literature.<sup>6i,7e</sup> In the five-membered ring created through coordination of nitrogen to silicon, the bond angle  $\angle \text{NSiC}_1$  equals 85.7 and 86.8°, respectively, which liberates a large cone angle for frontside attack of the nucleophile, giving rise to retention of configuration (Figure 3). Such a pathway is not favorable for chlorine-silicon bond cleavage, which could explain the lower reactivity of chloro-, and bromosilanediyl-chromium complexes.

## Experimental Section

**General Comments.** All manipulations were performed under an atmosphere of dry argon by standard Schlenk tube techniques. Solvents were distilled from sodium benzophenone ketyl. Starting functionalized silanediyl-transition metal complexes **1** and **7-9** were prepared as previously reported.<sup>7c,11</sup> Commercially available chemicals were used as such without any further purification.  $^{29}\text{Si}$ ,  $^{13}\text{C}$ ,  $^1\text{H}$ , and  $^{31}\text{P}$  NMR spectra were recorded on Bruker WP 200 SY or AC 250 spectrometer.  $^1\text{H}$  and  $^{13}\text{C}$  chemical shifts were measured against  $\text{Me}_4\text{Si}$  using solvent resonances as standard locks.  $^{29}\text{Si}$  chemical shifts were referenced to external  $\text{Me}_4\text{Si}$  in the same solvent. IR spectra were recorded on Perkin Elmer 1600 FT as KBr pellets, Nujol suspensions, or solutions in  $\text{CaF}_2$  cells. The mass spectra were obtained on a JEOL JMS D100 apparatus by EI ionization at 30 or 70 eV. Elemental analyses were carried out by the Service Central de Microanalyse du CNRS or ENSC Montpellier.

**Preparation of Complexes 2-6.** Freshly prepared complex  $([2-[(\text{dimethylamino})\text{methyl}]\text{phenyl}]\text{hydrosilanediyl})\text{-chromium(0) pentacarbonyl}$ , **1**, (1.06 g, 3 mmol) was dissolved in 30 mL of toluene in a Schlenk tube and kept at 0 °C. To this cold solution was added  $\text{PhLi}$  (3.57 mL, 3 mmol) dropwise for 20 min. After 2 h lithium hydride salt started precipitat-

(18) (a) Hommer, G. D.; Sommer, L. H. *J. Am. Chem. Soc.* **1973**, *95*, 7700. (b) Corriu, R. J. P.; Henner, B. J. L. *J. Organomet. Chem.* **1975**, *102*, 407. (c) Hilderbrandt, R. L.; Hommer, G. D.; Boudjouk, P. *J. Am. Chem. Soc.* **1976**, *98*, 7476. (d) Cartledge, F. K.; McKinnie, B. G.; Wolcott, J. M. *J. Organomet. Chem.* **1976**, *118*, 7. (e) Corriu, R.; Fernandez, J. M.; Guerin, C. *J. Organomet. Chem.* **1978**, *152*, 21; 25. (f) Bassindale, A. R.; Taylor, P. In *The Chemistry of Organic Silicon Compounds*; Patai, S., Rappoport, Z., Eds.; Wiley: Chichester, U.K., 1989; pp 839.



ing. The course of the reaction was followed by  $^1\text{H-NMR}$ , which indicated complete consumption of complex **1** after 24 h of stirring at room temperature. The LiH salt was filtered out, and toluene was evaporated to give **2** in 90% yield. The same procedure and stoichiometric quantities of reactants were used for the preparation of **3-6**.

**Complex 2:** ([2-[(Dimethylamino)methyl]phenyl]phenylsilanediyl)chromium(0) Pentacarbonyl. Mp: 171 °C. Yield 90%. The compound has been identified by comparison of NMR characteristics with those of an authentic sample.<sup>7e,10c</sup>  $^{29}\text{Si-NMR}$  ( $\text{CDCl}_3$ ):  $\delta$  +121.9.  $^{13}\text{C-NMR}$  ( $\text{CDCl}_3$ ):  $\delta$  47.3 (N-CH<sub>3</sub>), 48.6 (N-CH<sub>3</sub>), 68.2 (N-CH<sub>2</sub>), 123.8, 128.85, 129.75, 134.6, 139.1, 142.8 (aromatics), 221.3 (CO, equatorial), 224.8 (CO, axial).

**Complex 3:** ([2-[(dimethylamino)methyl]phenyl]methylsilanediyl)chromium(0) pentacarbonyl. Yellow powder. Mp: 131 °C (decomp). Yield 92%. Anal. Calcd for  $\text{C}_{15}\text{H}_{15}\text{NO}_5\text{SiCr}$ : C, 48.78; H, 4.06; N, 3.79. Found: C, 48.82; H, 4.02; N, 3.81.  $^{29}\text{Si-NMR}$  ( $\text{CDCl}_3$ ):  $\delta$  +126.13.  $^{13}\text{C-NMR}$  ( $\text{CDCl}_3$ ):  $\delta$  7.36 (Si-CH<sub>3</sub>), 46.22 (N-CH<sub>3</sub>), 48.79 (N-CH<sub>3</sub>), 68.39 (N-CH<sub>2</sub>), 124.01, 128.96, 129.83, 133.53, 138.52, 145.03 (aromatics), 222.12 (CO, eq), 225.82 (CO, ax).  $^1\text{H-NMR}$  ( $\text{CDCl}_3$ ):  $\delta$  0.47 (s, 3H, Si-CH<sub>3</sub>), 1.73 (s, 3H, N-CH<sub>3</sub>), 1.97 (s, 3H, N-CH<sub>3</sub>), 2.58-2.63, 3.25-3.30 {dd, 2H, AB system,  $^2J_{\text{H-H}} = 14.26$  Hz, N-CH<sub>2</sub>}, 6.67, 7.05, 8.02 (m, 4H, aromatics). MS (EI, 30eV)  $m/e$  (relative intensity, %) 369 ( $\text{M}^+$ , 25), 341 (-CO, 10), 285 (-3CO, 04), 257 (-4CO, 46), 252 (15), 235 (18), 200 (38), 178 (100), 162 (22). IR ( $\text{C}_6\text{D}_6$ ,  $\text{cm}^{-1}$ ):  $\nu$ (CO) 1910 (br), 2034.

**Complex 4:** ([2-[(Dimethylamino)methyl]phenyl]tert-butylsilanediyl)chromium(0) Pentacarbonyl. Light brown powder. Mp: 153 °C (decomp) Yield 88%. Anal. Calcd for  $\text{C}_{18}\text{H}_{21}\text{NO}_5\text{SiCr}$ : C, 52.55; H, 5.10; N, 3.40. Found: C, 52.58; H, 5.13; N, 3.42.  $^{29}\text{Si-NMR}$  ( $\text{CDCl}_3$ ):  $\delta$  +139.5.  $^{13}\text{C-NMR}$  ( $\text{CDCl}_3$ ):  $\delta$  27.44 (\*C-CH<sub>3</sub>), 29.33 (C-C\*H<sub>3</sub>), 45.39 (N-CH<sub>3</sub>), 47.25 (N-CH<sub>3</sub>), 63.77 (N-CH<sub>2</sub>), 125.11, 126.82, 130.02, 134.13, 139.12, 145.40 (aromatics), 222.55 (CO, eq), 224.84 (CO, ax). MS (EI, 30eV)  $m/e$  (relative intensity, %) 411 ( $\text{M}^+$ , 10), 383 (-CO, 8), 356 (-2CO, 06), 327 (-3CO, 10), 299 (-4CO, 9), 271 (-5CO, 100), 220 (20), 192 (13), 162 (28), 135 (12), 119 (18), 91 (11). IR ( $\text{CDCl}_3$ ,  $\text{cm}^{-1}$ ):  $\nu$ (CO) 1907 (br), 2036.

**Complex 5:** ([2-[(Dimethylamino)methyl]phenyl]trimethylsilylethynylsilanediyl)chromium(0) Pentacarbonyl. Yield 76%. Anal. Calcd for  $\text{C}_{19}\text{H}_{21}\text{NO}_5\text{Si}_2\text{Cr}$ : C, 50.55; H, 4.65; N, 3.10. Found: C, 50.59; H, 4.71; N, 3.02.  $^{29}\text{Si-NMR}$  ( $\text{C}_6\text{D}_6$ ):  $\delta$  +92.31, -18.04.  $^{13}\text{C-NMR}$  ( $\text{C}_6\text{D}_6$ ):  $\delta$  0.26 (Si-CH<sub>3</sub>), 46.03 (N-CH<sub>3</sub>), 46.13 (N-CH<sub>3</sub>), 68.96 (N-CH<sub>2</sub>), 93.52 (C=C\*SiMe<sub>3</sub>), 113.12 (C\*CSiMe<sub>3</sub>), 124.05, 128.62, 130.24, 134.09, 139.83, 141.66 (aromatics), 220.76 (CO, eq), 224.96 (CO, ax).  $^1\text{H-NMR}$  ( $\text{C}_6\text{D}_6$ ):  $\delta$  0.15 (s, 9H, SiMe<sub>3</sub>), 1.85 (s, 3H, N-CH<sub>3</sub>), 2.10 (s, 3H, N-CH<sub>3</sub>), 2.55-2.65, 4.05-4.15 {dd, 2H, AB system,  $^2J_{\text{H-H}} = 13.40$  Hz, N-CH<sub>2</sub>}, 6.56, 6.92, 7.98 (m, 4H, aromatics). MS (EI, 30eV)  $m/e$  (relative intensity, %) 451 ( $\text{M}^+$ , 39), 395 (-2CO, 35), 367 (-3CO, 32), 339 (-4CO, 82), 311 (-5CO, 100), 287 (12), 268 (10), 244 (8), 162 (22), 135 (9), 119 (10), 91 (7). IR ( $\text{C}_6\text{D}_6$ ,  $\text{cm}^{-1}$ ):  $\nu$ (CO) 1831, 1909, 2043;  $\nu$ (C=C) 2025.

**Complex 6:** ([2-[(dimethylamino)methyl]phenyl]phenylethynylsilanediyl)chromium(0) Pentacarbonyl. Yield 91%. Anal. Calcd for  $\text{C}_{22}\text{H}_{17}\text{NO}_5\text{SiCr}$ : C, 58.02; H, 3.73; N, 3.07. Found: C, 58.14; H, 3.81; N, 3.01.  $^{29}\text{Si-NMR}$  ( $\text{CDCl}_3$ ):  $\delta$  +92.16.  $^{13}\text{C-NMR}$  ( $\text{CDCl}_3$ ):  $\delta$  46.46 (N-CH<sub>3</sub>), 46.48 (N-CH<sub>3</sub>), 69.05 (N-CH<sub>2</sub>), 92.72 (C=C\*Ph), 114.86 (Si-C\*CPH), 125.30, 127.61, 128.26, 129.03, 130.97, 132.07, 139.45, 141.47 (aromatics), 220.52 (CO, eq), 224.56 (CO, ax).  $^1\text{H-NMR}$  ( $\text{C}_6\text{D}_6$ ): 1.78 (s, 3H, N-CH<sub>3</sub>), 2.19 (s, 3H, N-CH<sub>3</sub>), 2.96-3.01, 3.87-3.92 {dd, 2H, AB system,  $^2J_{\text{H-H}} = 12.47$  Hz, N-CH<sub>2</sub>}, 7.19, 7.26, 7.29, 7.31, 7.44, 7.98 (m, 4H, aromatics). MS (EI, 30eV)  $m/e$  (relative intensity, %) 455 ( $\text{M}^+$ , 9), 399 (-2CO, 12), 371 (-3CO, 14), 343 (-4CO, 21), 315 (-5CO, 100), 272 (12), 262 (8), 248 (5), 219 (5), 162 (12). IR ( $\text{C}_6\text{D}_6$ ,  $\text{cm}^{-1}$ ):  $\nu$ (CO) 1821, 1906, 2044;  $\nu$ (C=C) 2143.

**Competition Experiment.** Compounds **1** (0.89 g, 2.5 mmol) and **9** (0.93 g, 2.5 mmol) were dissolved in 50 mL of toluene and kept at 0 °C. MeLi (2.4 mL, 3 mmol) was added dropwise to this mixture, and the solution was warmed to room temperature. After 12 h,  $^{29}\text{Si-NMR}$  indicated complete disappearance of the signal corresponding to complex **9** [ $\delta$  +117.2 (INVGATE, d,  $^1J_{\text{Si-F}} = 398.5$  Hz)], and a new signal at ( $\delta$  +126.1) for complex **3** was observed.

OM950193C



# Ab Initio MO Calculations of $^{29}\text{Si}$ - $^7\text{Li}$ NMR Coupling Constants in Silyllithiums

Terutake Koizumi, Kenji Morihashi, and Osamu Kikuchi\*

Department of Chemistry, University of Tsukuba, Tsukuba 305, Japan

Received April 21, 1995<sup>®</sup>

**Summary:** Ab initio calculations of  $^{29}\text{Si}$ - $^7\text{Li}$  coupling constants,  $^1J_{\text{SiLi}}$  in  $\text{H}_3\text{SiLi}$  and  $(\text{CH}_3)_3\text{SiLi}$ , using self-consistent perturbation theory have shown that the calculated  $^1J_{\text{SiLi}}$  values agree well with the experimental values observed in several (organosilyl)lithiums when three model solvents are coordinated at the lithium atom. Modeling the ionic Si-Li bond using the truncated lithium basis set gives  $^1J_{\text{SiLi}}$  values that are close to those of the solvated molecules, indicative of the ionic character of the Si-Li bond of (organosilyl)lithiums in solution.

## Introduction

(Organosilyl)lithium reagents are important synthetic intermediates,<sup>1-3</sup> and their structures and bonding have been studied experimentally<sup>4-13</sup> and theoretically.<sup>14-17</sup> Especially, in the last decade, the structures in solution have been investigated extensively by  $^{29}\text{Si}$  and  $^7\text{Li}$  NMR spectroscopies.<sup>5-10,18</sup> Moreover, the bonding character of the Si-Li bond is a matter of debate<sup>1-17</sup> as is that of the C-Li bond.<sup>19</sup>

The observed one-bond  $^{29}\text{Si}$ - $^7\text{Li}$  coupling constants,

$^1J_{\text{SiLi}}$ , in solution are in the range 33-51 Hz;<sup>5-10,20</sup> each  $^{29}\text{Si}$  NMR spectrum in these experiments shows a quartet pattern, reflecting the fact that one lithium atom interacts with one silicon atom. Although investigations of the energetics have been effected for (organosilyl)lithiums using several levels of calculations,<sup>14-17</sup> there have been no reports of theoretical studies of the  $^1J_{\text{SiLi}}$  values in (organosilyl)lithiums in connection with the molecular geometry in solution. In a previous study,<sup>21</sup> we calculated the one-bond  $^{13}\text{C}$ - $^7\text{Li}$  coupling constant  $^1J_{\text{CLi}}$  in  $(\text{CH}_3)_3\text{CLi}$  using self-consistent perturbation theory (SCPT) and found that this method gives excellent agreement with the experimental  $^1J_{\text{CLi}}$  values<sup>22</sup> when electron donor ligands are coordinated to the lithium atom. In the present study we have applied ab initio SCPT to silyllithiums  $\text{H}_3\text{SiLi}$  and  $(\text{CH}_3)_3\text{SiLi}$ , which are models for the experimentally-observed compounds, and have elucidated their molecular structures in solution on the basis of the calculated  $^1J_{\text{SiLi}}$  values.

## Calculations

Ab initio molecular orbital calculations were carried out with the MIDI-4 and MIDI-4\* basis sets.<sup>23</sup> The latter basis set includes the d-type polarization functions for each heavy (non-hydrogen) atom except for the lithium atom. For lithium, the Li(421/1) basis, in which the p-type polarization functions are added to the MIDI-4 basis set, was used. Moreover, Li(31), the truncated MIDI-4 basis set which includes only the 1s function and corresponds to the lithium cation,<sup>23d</sup> also was used to examine the nature of the Si-Li bond. All geometries were optimized under the restriction of the  $C_{3v}$  symmetry.

The  $^1J_{\text{SiLi}}$  values were calculated using the SCPT method,<sup>24</sup> in which the Fermi contact term was taken into account as the perturbation. The following formula<sup>24,25</sup> was used to calculate the  $^1J_{\text{SiLi}}$  values:

$$J_{\text{SiLi}} = \left[ \frac{16h\gamma_{\text{Si}}\gamma_{\text{Li}}\beta^2}{9} \right] \sum_{\lambda\sigma}^{\text{all AO}} \chi_{\lambda}(\text{R}_{\text{Si}})\chi_{\sigma}^*(\text{R}_{\text{Li}})e_{\lambda\sigma}^{(1)}$$

where  $\gamma$  is the magnetogyric ratio of the nucleus,  $\chi_{\lambda}(\text{R}_{\text{Si}})$  represents the function value of the atomic orbital  $\lambda$  evaluated

(20) Although the  $^{29}\text{Si}$ - $^6\text{Li}$  coupling constants also were measured for phenylsilyllithiums,<sup>5</sup> only the  $^1J_{\text{SiLi}}$  values are given in this note. The conversion to  $^1J_{\text{SiLi}}$  ( $^{29}\text{Si}$ - $^6\text{Li}$ ) is carried out using the relation  $^1J_{\text{SiLi}}(^{29}\text{Si}-^7\text{Li}) = (\gamma(^7\text{Li})/\gamma(^6\text{Li}))^2 J_{\text{SiLi}}(^{29}\text{Si}-^6\text{Li}) = 2.641^2 J_{\text{SiLi}}(^{29}\text{Si}-^6\text{Li})$ .<sup>5,18</sup>

(21) Koizumi, T.; Kikuchi, O. *Organometallics* 1995, 14, 987.

(22) Bauer, W.; Winchester, W. R.; Schleyer, P. v. R. *Organometallics* 1987, 6, 2371.

(23) (a) Tatewaki, H.; Huzinaga, S. *J. Comput. Chem.* 1980, 1, 205. (b) Sakai, Y.; Tatewaki, H.; Huzinaga, S. *J. Comput. Chem.* 1981, 2, 100. (c) Sakai, Y.; Tatewaki, H.; Huzinaga, S. *J. Comput. Chem.* 1981, 2, 108. (d) Huzinaga, S. *Gaussian Basis Sets for Molecular Calculations*; Elsevier: Amsterdam, 1984.

(24) (a) Blizard, A. C.; Santry, D. P. *J. Chem. Phys.* 1971, 55, 950. (b) Ditchfield, R.; Snyder, L. C. *J. Chem. Phys.* 1972, 56, 5823.

(25) Ostlund, N. S.; Newton, M. D.; McIver, J. W., Jr.; Pople, J. A. *J. Magn. Reson.* 1969, 1, 298.

<sup>®</sup> Abstract published in *Advance ACS Abstracts*, July 1, 1995.

(1) Bažant, V.; Chvalovský, V.; Rathouský, J. *Organosilicon Compounds*; Academic Press: New York, 1965; Part 1, p 93.

(2) Armitage, D. A. In *Comprehensive Organometallic Chemistry*, Wilkinson, G., Stone, F. G. A., Abel, E. W., Eds.; Pergamon Press: Oxford, England, 1982; Vol. 2, p 99.

(3) West, R. In *Comprehensive Organometallic Chemistry*, Wilkinson, G., Stone, F. G. A., Abel, E. W., Eds.; Pergamon Press: Oxford, England, 1982; Vol. 2, p 365.

(4) Buncel, E.; Venkatachalam, T. K.; Eliasson, B.; Edlund, U. *J. Am. Chem. Soc.* 1985, 107, 303.

(5) Edlund, U.; Lejon, T.; Venkatachalam, T. K.; Buncel, E. *J. Am. Chem. Soc.* 1985, 107, 6408. Buncel, E.; Venkatachalam, T. K.; Edlund, U. *Can. J. Chem.* 1986, 64, 1674.

(6) Heine, A.; Herbst-Irmer, R.; Sheldrick, G. M.; Stalke, D. *Inorg. Chem.* 1993, 32, 2694.

(7) Dias, H. V. R.; Olmstead, M. M.; Ruhlandt-Senge, K.; Power, P. P. *J. Organomet. Chem.* 1993, 462, 1.

(8) Becker, G.; Hartmann, H.-M.; Hengge, E.; Schrank, F. Z. *Anorg. Allg. Chem.* 1989, 572, 63.

(9) Ando, W.; Wakahara, T.; Akasaka, T.; Nagase, S. *Organometallics* 1994, 13, 4683.

(10) Belzner, J.; Dehnert, U.; Stalke, D. *Angew. Chem., Int. Ed. Engl.* 1994, 33, 2450.

(11) Schaaf, T. F.; Butler, W.; Glick, M. D.; Oliver, J. P. *J. Am. Chem. Soc.* 1974, 96, 7593. Schaaf, T. F.; Glick, M. D.; Oliver, J. P. *J. Am. Chem. Soc.* 1980, 102, 3769.

(12) Teclé, B.; Ilsley, W. H.; Oliver, J. P. *Organometallics* 1982, 1, 875.

(13) Becker, G.; Hartmann, H.-M.; Munch, A.; Riffel, H. Z. *Anorg. Allg. Chem.* 1985, 530, 29.

(14) Luke, B. T.; Pople, J. A.; Krogh-Jespersen, M.-B.; Apeloig, Y.; Chandrasekhar, J.; Schleyer, P. v. R. *J. Am. Chem. Soc.* 1986, 108, 260.

(15) Schleyer, P. v. R.; Clark, T. *J. Chem. Soc., Chem. Commun.* 1986, 1371.

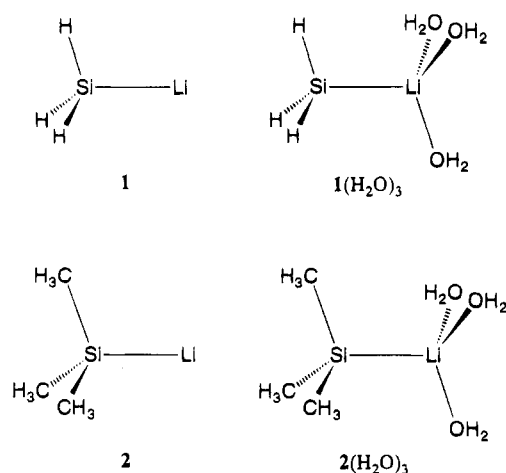
(16) Rajca, A.; Wang, P.; Streitwieser, A.; Schleyer, P. v. R. *Inorg. Chem.* 1989, 28, 3064.

(17) Moc, J.; Latajka, Z.; Rudzinski, J. M.; Ratajczak, H.; Szczeniak, M. M. *J. Chem. Soc., Perkin Trans. 2* 1989, 131.

(18) Bauer, W.; Schleyer, P. v. R. In *Advances in Carbanion Chemistry*, Snieckus, V., Ed.; JAI Press: Greenwich, CT, 1992; Vol. 1, p 89.

(19) Lambert, C.; Schleyer, P. v. R. *Angew. Chem., Int. Ed. Engl.* 1994, 33, 1129 and references cited therein.

Chart 1

**Table 1. Optimized Structures (Å and deg)<sup>a</sup> and Calculated <sup>1</sup>J(<sup>29</sup>Si-<sup>7</sup>Li) Values (Hz) for H<sub>3</sub>SiLi (1)**

	r(Si-Li)	r(Si-H)	∠(HSiH)	<sup>1</sup> J( <sup>29</sup> Si- <sup>7</sup> Li)
By the MIDI-4 Basis Set				
1 (unsolvated)	2.599	1.506	103.7	-137.8
1(H <sub>2</sub> O) <sub>3</sub>	2.827	1.525	99.8	-43.9
1 (truncated basis set)	2.444	1.511	102.9	-59.7
By the MIDI-4* Basis Set				
1 (unsolvated)	2.579	1.514	103.3	-133.8
1(H <sub>2</sub> O) <sub>3</sub>	2.777	1.529	99.9	-47.7
1 (truncated basis set)	2.425	1.521	102.3	-59.7
exptl <sup>b</sup>				±45

<sup>a</sup> All structures were optimized under the restriction of the C<sub>3v</sub> symmetry. <sup>b</sup> The value for (C<sub>6</sub>H<sub>5</sub>)<sub>3</sub>SiLi(THF)<sub>3</sub>,<sup>7</sup> the sign was not determined.

at the silicon nucleus,<sup>26</sup>  $\rho_{\text{Si}}^{(1)}$  are the first-order spin-density matrix elements perturbed by the Fermi contact interaction on the lithium atom and were calculated by the procedure given by Ditchfield and Snyder.<sup>24b</sup> The theory was incorporated into the ABINIT program written by our group.<sup>27</sup> All calculations were carried out on the HP-730 workstations.

## Results and Discussion

The optimized structures and calculated <sup>1</sup>J<sub>SiLi</sub> values for H<sub>3</sub>SiLi (1, Chart 1) are listed in Table 1 along with the experimental <sup>1</sup>J<sub>SiLi</sub> value in (C<sub>6</sub>H<sub>5</sub>)<sub>3</sub>SiLi(THF)<sub>3</sub>.<sup>7</sup> When solvation is not taken into account, the calculated <sup>1</sup>J<sub>SiLi</sub> value is much larger in magnitude than the experimental value. When three H<sub>2</sub>O molecules are coordinated at the lithium atom (1(H<sub>2</sub>O)<sub>3</sub>), on the other hand, the <sup>1</sup>J<sub>SiLi</sub> value is reduced remarkably to -43.9 Hz with the MIDI-4 calculation and to -47.7 Hz with the MIDI-4\* calculation and agrees well with the experimental value in (C<sub>6</sub>H<sub>5</sub>)<sub>3</sub>SiLi(THF)<sub>3</sub>, ±45 Hz.<sup>7</sup> A similar change caused by solvation had been observed in the calculated <sup>1</sup>J<sub>CLi</sub> values for H<sub>3</sub>CLi and (CH<sub>3</sub>)<sub>3</sub>CLi.<sup>21</sup> The conventional tetrahedral geometry about the lithium atom in 1(H<sub>2</sub>O)<sub>3</sub> is supported by the X-ray structures reported for ((CH<sub>3</sub>)<sub>3</sub>Si)<sub>3</sub>SiLi(THF)<sub>3</sub>,<sup>6,7</sup> ((C<sub>6</sub>H<sub>5</sub>)<sub>3</sub>Si)<sub>3</sub>SiLi(THF)<sub>3</sub>,<sup>7</sup> and (Li(THF)<sub>3</sub>)<sub>2</sub>(Si(C<sub>6</sub>H<sub>5</sub>)<sub>2</sub>)<sub>4</sub>.<sup>8</sup>

(26) Another procedure, in which  $\rho_{\text{Si}}^{(1)}$  is obtained by the Fermi contact interaction on the silicon atom and the function values are evaluated at the lithium atom, gives the same results.

(27) Kikuchi, O.; Nakano, T.; Morihashi, K. Unpublished results, 1988.

**Table 2. Optimized Structures (Å and deg)<sup>a</sup> and Calculated <sup>1</sup>J(<sup>29</sup>Si-<sup>7</sup>Li) Values (Hz) for (CH<sub>3</sub>)<sub>3</sub>SiLi (2)**

	r(Si-Li)	r(Si-C)	∠(CSiC)	<sup>1</sup> J( <sup>29</sup> Si- <sup>7</sup> Li)
By the MIDI-4 Basis Set				
2 (unsolvated)	2.632	1.947	104.3	-192.5
2(H <sub>2</sub> O) <sub>3</sub>	2.836	1.972	100.6	-51.2
2 (truncated basis set)	2.461	1.953	102.3	-72.4
By the MIDI-4* Basis Set				
2 (unsolvated)	2.600	1.932	104.4	-194.4
2(H <sub>2</sub> O) <sub>3</sub> <sup>b</sup>	2.833	1.955	100.9	-49.7
2 (truncated basis set)	2.434	1.942	102.2	-69.3
exptl <sup>c</sup>				±45

<sup>a</sup> All structures were optimized under the restriction of the C<sub>3v</sub> symmetry. Geometries for the methyl groups were fixed at the structures of those in (CH<sub>3</sub>)<sub>3</sub>SiH: r(C-H) = 1.095 Å, ∠(HCH) = 107.9°. <sup>29</sup> <sup>b</sup> Reference 32. <sup>c</sup> The value for (C<sub>6</sub>H<sub>5</sub>)<sub>3</sub>SiLi(THF)<sub>3</sub>.<sup>7</sup>

The Si-Li bond length in 1 also is influenced by solvation; this Si-Li bond becomes longer, from 2.6 to 2.8 Å, by the coordination of three H<sub>2</sub>O molecules (Table 1). It is noted, however, that the Si-Li bond elongation itself is not a key factor for decreasing the <sup>1</sup>J<sub>SiLi</sub> magnitude but that the coordination of solvent molecules is. We examined the dependence of <sup>1</sup>J<sub>SiLi</sub> on the Si-Li bond length for the unsolvated species in which the geometry of the silyl group was fixed.<sup>28</sup> The <sup>1</sup>J<sub>SiLi</sub> values in 1 calculated by MIDI-4\* basis set are -133.8 Hz for r(Si-Li) = 2.579 Å and -171.5 Hz for r(Si-Li) = 2.777 Å, indicating that a simple elongation of the Si-Li bond makes the magnitude of <sup>1</sup>J<sub>SiLi</sub> larger. Such a trend has been reported for <sup>1</sup>J<sub>CH</sub> in methane<sup>29a</sup> and isopropyl cation<sup>29b</sup> and for <sup>1</sup>J<sub>CLi</sub> in H<sub>3</sub>CLi.<sup>21</sup> Therefore, it is concluded that the solvation affects the electronic structure of the Si-Li bond, which reduces the magnitude of <sup>1</sup>J<sub>SiLi</sub> significantly. It may be accepted widely<sup>30</sup> that the one-bond coupling constant between two nuclei A and B, <sup>1</sup>J<sub>AB</sub>, decreases when the A-B distance increases. This is not always correct, and the important factor is not the length itself but the electronic nature of the A-B bond.

The calculations also were carried out using the truncated lithium basis set which models a purely ionic lithium atom. The calculated <sup>1</sup>J<sub>SiLi</sub> value in 1, -59.7 Hz, is close to that calculated for 1(H<sub>2</sub>O)<sub>3</sub>. This result strongly suggests that the Si-Li bond in H<sub>3</sub>SiLi with donor ligands is ionic, like the C-Li bond in H<sub>3</sub>CLi.<sup>21</sup>

Quite the same calculations were carried out for (CH<sub>3</sub>)<sub>3</sub>SiLi (2) in order to examine the effect of substitution at the silicon atom. Geometries of the methyl groups were fixed at the structure of those in (CH<sub>3</sub>)<sub>3</sub>SiH (r(C-H) = 1.095 Å, ∠(HCH) = 107.9°).<sup>31</sup> The results for 2 are listed in Table 2.<sup>32</sup> The optimized structure of 2 is similar to that of 1. The calculated <sup>1</sup>J<sub>SiLi</sub> for 2(H<sub>2</sub>O)<sub>3</sub> resembles that of 1(H<sub>2</sub>O)<sub>3</sub> and agrees well with the experimental value in (C<sub>6</sub>H<sub>5</sub>)<sub>3</sub>SiLi(THF)<sub>3</sub>.<sup>7</sup> The trend observed in the calculated <sup>1</sup>J<sub>SiLi</sub> values is not affected to any great degree by the substitution of alkyl groups on the silicon atom.

(28) The change in the geometry of the silyl group was not important for decreasing the magnitude of <sup>1</sup>J<sub>SiLi</sub>.

(29) (a) Sergeev, N. M.; Solkan, V. N. *J. Chem. Soc., Chem. Commun.* **1975**, 12. (b) Maciel, G. E. *J. Am. Chem. Soc.* **1971**, *93*, 4375.

(30) For the Si-Li bond, see ref 10.

(31) The Chemical Society of Japan. *Kagaku Binran (Chemical Handbook)*, 2nd ed.; Maruzen: Tokyo, 1975; p II-1395.

(32) For convenience, the d-type polarization functions on the oxygen atom were omitted in the MIDI-4\* calculation of 2(H<sub>2</sub>O)<sub>3</sub>.

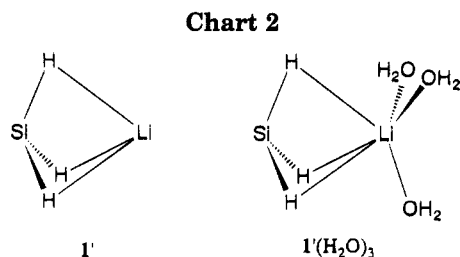


**Table 3. Optimized Structures (Å and deg)<sup>a</sup> and Calculated <sup>1</sup>J(<sup>29</sup>Si-<sup>7</sup>Li) Values (Hz) for the Inverted Geometries of H<sub>3</sub>SiLi (1')**

	r(Si-Li)	r(Si-H)	∠(HSiH)	<sup>1</sup> J( <sup>29</sup> Si- <sup>7</sup> Li)
By the MIDI-4 Basis Set				
1' (unsolvated)	2.554	1.589	89.0	18.6
1'(H <sub>2</sub> O) <sub>3</sub>	2.970	1.575	91.9	5.8
1' (truncated basis set)	2.514	1.595	86.5	11.1
By the MIDI-4* Basis Set				
1' (unsolvated)	2.462	1.586	89.3	15.4
1'(H <sub>2</sub> O) <sub>3</sub>	2.796	1.575	91.3	7.1
1' (truncated basis set)	2.408	1.583	88.5	9.5

<sup>a</sup> All structures were optimized under the restriction of the C<sub>3v</sub> symmetry.

Schleyer and Clark<sup>15</sup> calculated the inverted C<sub>3v</sub> geometry of H<sub>3</sub>SiLi (1', Chart 2) to be 2.4 kcal mol<sup>-1</sup> more stable than the conventional tetrahedral structure such as 1 at a very high level of calculation, MP4/SDTQ/6-31G\*\*//6-31G\*+ZEP. The stability of the inverted configuration like that in 1' in the crystalline state was

**Table 4. Total Energies (hartrees) and Relative Energies (kcal mol<sup>-1</sup>, in Parentheses) for H<sub>3</sub>SiLi Isomers 1 and 1' calculated with the MIDI-4\* Basis Set**

	HF/MIDI-4*/MIDI-4*		MP2/MIDI-4*/MIDI-4*	
1 (unsolvated)	-297.737085	(0.00)	-297.830689	(0.00)
1' (unsolvated)	-297.728989	(5.08)	-297.826335	(2.73)
1(H <sub>2</sub> O) <sub>3</sub>	-525.584866	(0.00)	-526.261359	(0.17)
1'(H <sub>2</sub> O) <sub>3</sub>	-525.581669	(2.01)	-526.261091	(0.00)

recently supported for H<sub>3</sub>SiNa.<sup>33</sup> Since the energy difference between two structures, 1 and 1', is expected to be very small, it may be difficult to determine the structure in solution on the basis of the calculated energies or the structures observed in the crystalline state. To examine the possibility of 1' for the structure of (organosilyl)lithiums in solution, the <sup>1</sup>J<sub>SiLi</sub> value was calculated for 1' and is listed in Table 3. The calculated energies for 1 and 1' are compared in Table 4. Table 3 shows that all <sup>1</sup>J<sub>SiLi</sub> values for 1' are positive and that their magnitudes are much smaller than the experimental ones, which are in the range of 33–51 Hz.<sup>5–10</sup> Although the energy difference between 1 and 1' is expected to be very small (Table 4), the <sup>1</sup>J<sub>SiLi</sub> calculations strongly suggest that the inverted geometry such as 1' is not an appropriate structure for alkyl- or aryl-substituted silyllithiums in solution.

OM950291Y

(33) Pritzkow, H.; Lobreyer, T.; Sundermeyer, W.; van Eikema Hommes, N. J. R.; Schleyer, P. v. R. *Angew. Chem., Int. Ed. Engl.* **1994**, *33*, 216.

# Convenient One-Pot Synthesis of Hexa-*n*-butylditin from Bis(tri-*n*-butyltin) Oxide

Helena McAlonan and Paul J. Stevenson\*

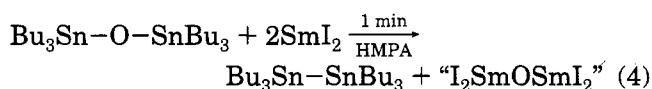
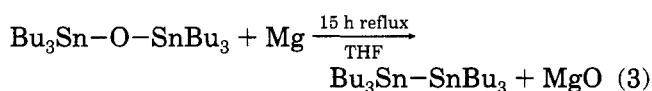
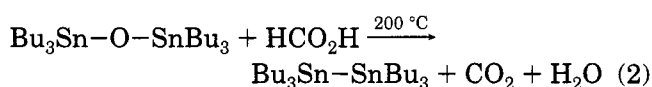
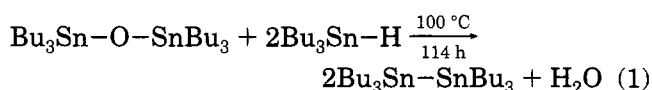
School of Chemistry, Queens University, Belfast, Northern Ireland BT9 5AG

Received February 24, 1995<sup>⊙</sup>

**Summary:** Hexa-*n*-butylditin is prepared in high yield (83%), by reduction of bis(tri-*n*-butyltin) oxide with sodium borohydride in ethanol. The first stage is reduction to tri-*n*-butyltin hydride (not isolated), which rapidly gives hexa-*n*-butylditin with the loss of hydrogen under the basic reaction conditions.

Over the past 20 years organotin compounds have emerged as versatile reagents in organic synthesis.<sup>1</sup> Hexa-*n*-butylditin has found widespread use in radical-mediated reactions,<sup>2</sup> in palladium-catalyzed cross-coupling reactions,<sup>3</sup> and as an intermediate for the syntheses of other tin metal-bound compounds.<sup>4</sup> A number of procedures are available for the synthesis of hexa-*n*-butylditin starting from bis(tri-*n*-butyltin) oxide, and these are summarized in Scheme 1. Thus, reactions of bis(tri-*n*-butyltin) oxide with tri-*n*-butyltin hydride (eq 1),<sup>5</sup> formic acid (eq 2),<sup>6</sup> magnesium sodium, or potassium in THF (eq 3),<sup>7</sup> and samarium diiodide in hexamethylphosphoramide (HMPA) (eq 4),<sup>8</sup> have all been utilized for preparing hexa-*n*-butylditin. Fairly harsh conditions or long reaction times are required in the first three cases (eq 1–3). The reaction conditions in eq 4 are mild, but expensive samarium diiodide and toxic HMPA are utilized.

## Scheme 1



We now report that hexa-*n*-butylditin can be prepared in 83% yield by reduction of bis(tri-*n*-butyltin) oxide with sodium borohydride in ethanol at room temperature for

2 h. The conditions are extremely mild, and the workup is simple, as hexa-*n*-butylditin is not very soluble in ethanol. In order to gain insight into what was happening mechanistically, the reaction was monitored by <sup>13</sup>C NMR spectroscopy. The first step in the process was the known reduction of tri-*n*-butyltin oxide with sodium borohydride to give tri-*n*-butyltin hydride.<sup>9</sup> This reduction was complete within 5 min, and tri-*n*-butyltin hydride was identified as the only product in the crude reaction mixture. As time proceeded, the NMR signals for tri-*n*-butyltin hydride diminished, the initially homogeneous reaction mixture became very cloudy, and a heavy oil precipitated. NMR analysis of this precipitated oil showed it to be hexa-*n*-butylditin. Within 2 h less than 2% of tri-*n*-butyltin hydride remained in the ethanol layer.

A wide variety of reagents and conditions are known to convert alkyltin hydrides to polyalkylditins. For example, transition-metal salts,<sup>10</sup> solvents such as dimethylformamide,<sup>11a</sup> bases such as pyridine,<sup>11b</sup> and even diborane<sup>12</sup> are known to facilitate this reaction.

At present, the mechanism, in our case, for the decomposition of tri-*n*-butyltin hydride to hexa-*n*-butylditin is unclear. To check if it was not solely a solvent effect, tri-*n*-butyltin hydride was dissolved in ethanol at room temperature. This solution was directly monitored by <sup>13</sup>C NMR spectroscopy, and after 24 h only tri-*n*-butyltin hydride was detected.

The other possibility was that ethoxide anion, generated by reaction of sodium borohydride with ethanol, was mediating the formation of hexa-*n*-butylditin. To check this, sodium borohydride was treated with 4 molar equiv of acetaldehyde, to give a solution of sodium tetraethoxyborate. This solution smoothly mediated the formation of hexa-*n*-butylditin from tri-*n*-butyltin hydride over 2 h, clearly demonstrating that tri-*n*-butyltin hydride is unstable in the presence of a boron ethoxide. The other possibility was that tri-*n*-butyltin ethoxide, generated by the reaction of a boron ethoxide with tri-*n*-butyltin hydride, was the true catalyst. It is known that sodium ethoxide reacts with tri-*n*-butyltin hydride, to give tri-*n*-butyltin ethoxide under reaction conditions similar to ours.<sup>13</sup> There is precedent for reactions of alkyltin hydrides with tin alkoxides to give alkylditins,<sup>13</sup> with hexa-*n*-butylditin often being formed as a byproduct in hydrostannation reactions of ketones.<sup>14</sup> In order

\* Abstract published in *Advance ACS Abstracts*, June 15, 1995.  
 (1) (a) Pereyre, M.; Quintard, J. P.; Rahm, A. *Tin in Organic Synthesis*; Butterworths: London, 1987. (b) Mitchell, T. N. *Synthesis* 1992, 803.  
 (2) (a) Keck, G. E.; Tafesh, A. M. *J. Org. Chem.* 1989, 54, 5845. (b) Snider, B. B.; Backman, B. O. *J. Org. Chem.* 1992, 57, 4883.  
 (3) Grigg, R.; Teasdale, A.; Shridharan, V. *Tetrahedron Lett.* 1991, 3859.  
 (4) Trost, B.; Walchli, R. *J. Am. Chem. Soc.* 1987, 109, 3487.  
 (5) (a) Sawyer, A. K. *J. Am. Chem. Soc.* 1965, 87, 537. (b) Neumann, W. P.; Schneider, B. *Angew. Chem., Int. Ed. Engl.* 1963, 3, 751.  
 (6) Jousseume, B.; Chanson, E.; Bevilacqua, M.; Saux, A.; Pereyre, M.; Barbe, B.; Petraud, M. *J. Organomet. Chem.* 1985, 294, C41.  
 (7) Jousseume, B.; Chanson, E.; Pereyre, M. *Organometallics* 1986, 5, 1271.  
 (8) Handa, Y.; Inanaga, J.; Yamaguchi, M. *J. Chem. Soc., Chem. Commun.* 1989, 298.

(9) Szammer, J.; Otvos, L. *Chem. Ind. London* 1988, 764.  
 (10) (a) Mitchell, T. N.; Killing, H.; Rutschow, D. *J. Organomet. Chem.* 1986, 304, 257. (b) Zhang, H. X.; Guibe, F.; Balavoine, F. B. *J. Org. Chem.* 1990, 55, 1857.  
 (11) (a) Puff, H.; Breuer, B.; Brinkmann, G.; Kind, P.; Reuter, H.; Schub, W.; Wald, W.; Weidenbruck, G. *J. Organomet. Chem.* 1989, 363, 265. (b) Davies, A. G.; Osei-Kiss, R. *J. Organomet. Chem.* 1994, 474, C8.  
 (12) Bury, A.; Speilman, J. R. *J. Org. Chem.* 1961, 83, 2667.  
 (13) (a) Kuivila, H. G.; Levins, P. *J. Am. Chem. Soc.* 1964, 86, 23. (b) Pommier, J. C.; Valade, J. *Bull. Soc. Chim. Fr.* 1965, 975.  
 (14) Creemer, H. M. J. C.; Noltes, J. G. *Recl. Trav. Chim. Pays-Bas* 1965, 84, 1589.

to test this hypothesis, tri-*n*-butyltin hydride was treated with tri-*n*-butyltin ethoxide in ethanol at room temperature. The tri-*n*-butyltin hydride was indeed quantitatively converted to hexa-*n*-butylditin (by NMR spectroscopy) inside 3 h, and the concentration of tri-*n*-butyltin ethoxide remained constant. Thus, tri-*n*-butyltin ethoxide is also capable of catalyzing formation of hexa-*n*-butylditin from tri-*n*-butyltin hydride. However, since a full 1 molar equiv of tri-*n*-butyltin ethoxide takes 3 h to catalyze the formation of hexa-*n*-butylditin, and in our reaction mixtures we cannot detect tri-*n*-butyltin ethoxide by NMR spectroscopy, then it seems unlikely that tri-*n*-butyltin ethoxide is the major catalytic entity.

Finally, the stability of tri-*n*-butyltin hydride in ethanol containing 0.1 molar equiv of sodium ethoxide was investigated. The reaction took 14 h, for a complete reaction of tri-*n*-butyltin hydride, giving hexa-*n*-butylditin in 86% yield.

Therefore, we conclude that ethoxide anion, generated by the reaction of sodium borohydride with ethanol, is catalyzing the formation of hexa-*n*-butylditin from tri-*n*-butyltin hydride. The ready availability of starting materials, and the simplicity of this procedure, should make it the method of choice for preparing hexa-*n*-butylditin.

### Experimental Section

Proton-decoupled  $^{13}\text{C}$  NMR spectra were recorded at 125 MHz on a General Electric Omega 500 MHz NMR spectrometer. Chemical shifts were reported in ppm units referenced to tetramethylsilane when deuteriochloroform was used as the solvent. Tin-carbon coupling constants are quoted as the average value of  $^{13}\text{C}-^{117}\text{Sn}$  and  $^{13}\text{C}-^{119}\text{Sn}$ , because for couplings other than  $^1J$  the multiplets were poorly resolved.

**Hexa-*n*-butylditin.** Sodium borohydride (143 mg, 3.8 mmol) was added in one portion to a magnetically stirred solution of bis(tri-*n*-butyltin) oxide (3 g, 5.0 mmol) in ethanol (6 mL). Inside 2 min all the sodium borohydride had dissolved and the solution was homogeneous. After 5 min,  $^{13}\text{C}$  NMR analysis showed the presence of only tri-*n*-butyltin hydride with no bis(tri-*n*-butyltin) oxide remaining. The solution was then stirred for a total of 2 h, after which time it had become

very cloudy and an oily layer had deposited. Water (10 mL) was added and the aqueous layer was extracted with methylene chloride ( $2 \times 10$  mL). The combined methylene chloride extracts were dried over magnesium sulfate, filtered, and concentrated. Vacuum distillation gave hexa-*n*-butylditin (2.42 g, 83%) as a clear oil, bp 150–152 °C/1 mmHg. The  $^{13}\text{C}$  NMR spectrum of this material was identical in every respect with that of an authentic sample of hexa-*n*-butylditin (purchased from Lancaster Synthesis), in good agreement with the literature spectrum.<sup>15</sup>  $^{13}\text{C}$  NMR spectrum of material obtained:  $\delta_{^{13}\text{C}}$  (125 MHz,  $\text{CDCl}_3$ ) 30.77 ( $^2J(\text{C}-\text{Sn}) = 16.6$  Hz), 27.56 ( $^3J(\text{C}-\text{Sn}) = 53.6$  Hz), 13.7, 10.01 ( $^1J(\text{C}-\text{Sn}) = 236.4$  Hz and  $^2J(\text{Sn}-\text{Sn}-\text{C}) = 38.8$  Hz).

For monitoring of the reaction,  $^{13}\text{C}$  NMR spectra of authentic samples of bis(tri-*n*-butyltin) oxide, tri-*n*-butyltin hydride, tri-*n*-butyltin ethoxide, and hexa-*n*-butylditin were recorded in ethanol unlocked and unshimmed. The  $\text{CH}_2$  signal for ethanol was set to 57.35 ppm, and the chemical shifts given are referenced to this. The quality of the spectra obtained was surprisingly good. Direct monitoring of crude reaction mixtures by  $^{13}\text{C}$  NMR spectroscopy allowed quantification of the species involved.

**Bis(tri-*n*-butyltin) oxide:**  $\delta_{^{13}\text{C}}$  (125 MHz, EtOH) 28.31 ( $^2J(\text{C}-\text{Sn}) = 20.7$  Hz), 27.45 ( $^3J(\text{C}-\text{Sn}) = 68.44$  Hz), 15.52 ( $^1J(\text{C}-\text{Sn}) = 405.1$  Hz), 13.5.

**Tri-*n*-butyltin hydride:**  $\delta_{^{13}\text{C}}$  (125 MHz, EtOH) 30.36 ( $^2J(\text{C}-\text{Sn}) = 21.2$  Hz), 27.48 ( $^3J(\text{C}-\text{Sn}) = 51.0$  Hz), 13.71, 8.23 ( $^1J(\text{C}-\text{Sn}) = 334.8$  Hz).

**Tri-*n*-butyltin ethoxide:**  $\delta_{^{13}\text{C}}$  (125 MHz, EtOH) 57.35, 28.48 ( $^2J(\text{C}-\text{Sn}) = 20.3$  Hz), 27.61 ( $^3J(\text{C}-\text{Sn}) = 64.7$  Hz), 18.15, 15.37 ( $^1J(\text{C}-\text{Sn}) = 387.51$  Hz), 13.59.

**Hexa-*n*-butylditin:**  $\delta_{^{13}\text{C}}$  (125 MHz, EtOH) 31.12 ( $^2J(\text{C}-\text{Sn}) = 13.6$  Hz), 27.81 ( $^3J(\text{C}-\text{Sn}) = 53.12$  Hz), 13.62, 10.30 ( $^1J(\text{C}-\text{Sn}) = 235.9$  Hz and  $^2J(\text{Sn}-\text{Sn}-\text{C}) = 38.8$  Hz).

Hexa-*n*-butylditin is not very soluble in ethanol. The last spectrum is essentially of neat hexa-*n*-butylditin contaminated with a small amount of ethanol.

**Acknowledgment.** We thank the Department of Education for Northern Ireland (DENI) for a studentship (H.M.) and Queens University for support.

OM9501485

(15) Mitchell, T. N. *J. Organomet. Chem.* **1973**, *59*, 189.

# In Situ Generation and Heck Coupling of Alkenes in Superheated Water

Jon Diminnie, Sean Metts, and Edith J. Parsons\*

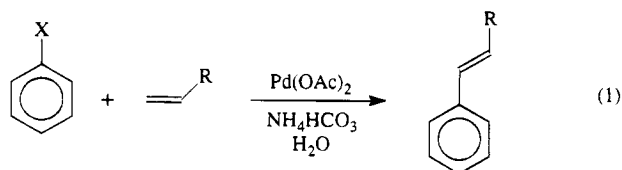
Department of Chemistry, Clemson University, Clemson, South Carolina 29634-1905

Received May 1, 1995\*

**Summary:** A series of 1,2-difunctionalized ethane derivatives were reacted with iodobenzene in the presence of PdCl<sub>2</sub> or Pd(OAc)<sub>2</sub> and NaOAc in superheated water (260 °C). The phenyl derivatives, 2-phenylethanol, 1-bromo-2-phenylethane, and 2-phenylethyl acetate, generated styrene which then coupled to the iodobenzene to form stilbene. The bromo derivatives, 1,2-dibromoethane, 1-bromo-2-chloroethane, 2-bromoethyl acetate, and 2-bromoethanol, lost bromide to form the respective vinyl compounds. With the exception of the vinyl alcohol which tautomerized to acetaldehyde, these also coupled to iodobenzene. Bromoethane did not couple under these conditions. The alcohol derivatives, ethanol, 2-chloroethanol, 2-chloroethyl acetate, ethylene glycol, ethylene glycol monoacetate, and ethylene glycol diacetate proved to be more inert under these relatively mild reaction conditions (260 °C water) and did not generate alkenes or undergo coupling to iodobenzene.

## Introduction

We have previously demonstrated that typical palladium-catalyzed alkene–arene coupling reactions of the Heck type will proceed in superheated water (260 °C, SW)<sup>1</sup> (eq 1). We are currently attempting to expand



X = I, Br, Cl, OTf

R = C<sub>6</sub>H<sub>5</sub>, CH<sub>2</sub>Y (Y = Br, Cl, OH), C(CH<sub>3</sub>)CO<sub>2</sub>CH<sub>3</sub>

this reaction by identifying additional, more unusual substrates which will undergo Heck coupling only under these conditions. One of our primary focuses has been the *in situ* generation of alkenes capable of undergoing coupling. Utilization of these “alkene synthons” relies on the unique properties associated with superheated and supercritical water and expands the scope of the Heck reaction to include alkane-based substrates in addition to the traditional alkene-based substrates.

The loss of functional groups from substituted alkyl compounds to yield alkenes is well-known in near-critical and supercritical water. In particular, the dehydration of alcohols in superheated and supercritical water has been thoroughly delineated.<sup>2</sup> Other func-

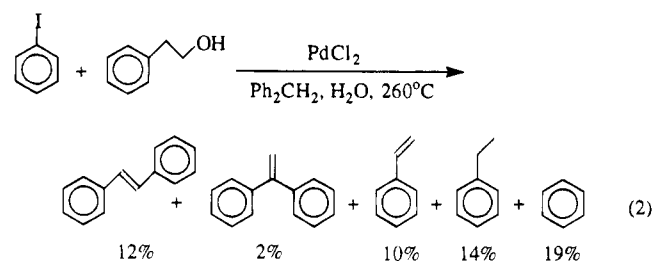
tional groups, including halides and carboxyl groups, can also be removed under supercritical water conditions to form alkenes.<sup>3,4</sup> These processes are generally acid catalyzed.

## Results and Discussion

A series of potential alkene synthons were examined in the Heck coupling reaction under SW conditions (Figure 1).

**Styrene Derivatives.** Styrene has been shown to couple with iodobenzene in superheated water in the presence of Pd(OAc)<sub>2</sub> and NH<sub>4</sub>HCO<sub>3</sub>.<sup>1</sup> The coupling is relatively clean at this temperature, yielding *trans*-stilbene (21% overall yield) and 1,1-diphenylethylene (3%). Recoveries were 91%, with no other organic products observed. This reaction was used as a benchmark in our previous studies of the Heck reaction, and so was utilized as our starting point in the synthon work.

Three compounds were examined as styrene synthons: 2-phenylethanol, 1-bromo-2-phenylethane, and 2-phenylethyl acetate. These reactants were substituted for styrene in the coupling reaction with iodobenzene, using PdCl<sub>2</sub> or Pd(OAc)<sub>2</sub> as the catalyst precursor and NaOAc as the base. Each reactant led to the desired *trans*-stilbene and 1,1-diphenylethylene products. The overall yields of these coupled products were slightly lower (see eq 2) than from the reaction of



styrene itself. Each reactant also produced styrene along with its hydrogenated analog, ethylbenzene. This indicates that the synthons were defunctionalized under the reaction conditions to form alkenes which then underwent coupling.

A closer examination of the reaction showed that only the 2-phenylethanol was actually responsible for formation of the styrene and coupled products. Both 1-bromo-

(3) (a) Crittendon, R.; Parsons, E. J. *Organometallics* 1994, 13, 2587.

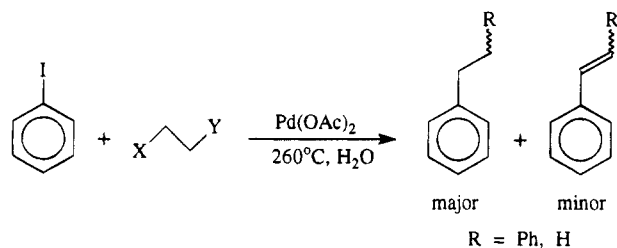
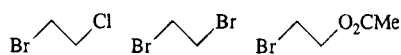
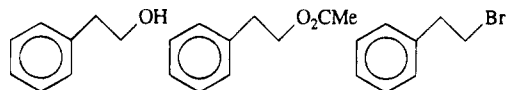
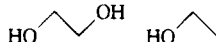
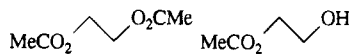
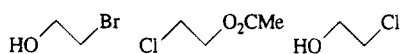
(b) Myrick, M. L.; Kolis, J.; Parsons, E.; Chilke, K.; Lovelace, M.; Scrivens, W.; Holliday, R.; Williams, M. J. *Raman Spectrosc.* 1994, 25, 59.

(4) (a) Houser, T. J.; Zhou, Y.; Tsao, C. C.; Liu, X. *ACS Symp. Ser.* 1993, 514, 327. (b) Li, L.; Egiebor, N. O. *Energy Fuels* 1992, 6, 35. (c) Jin, L.; Shah, Y. T.; Abraham, M. A. J. *Supercrit. Fluids* 1990, 3, 233. (d) Siskin, M.; Brons, G.; Katritzky, A. R.; Murugan, R. *Energy Fuels* 1990, 4, 482.

\* Abstract published in *Advance ACS Abstracts*, June 15, 1995.

(1) Reardon, P.; Metts, S.; Crittendon, C.; Daugherty, P.; Parsons, E. J. *Organometallics*, in press.

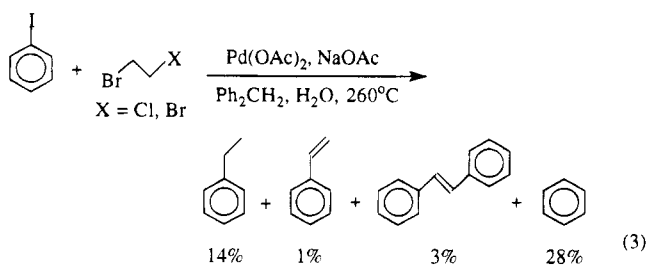
(2) (a) Xu, X.; De Almeida, C. P.; Antal, M. J., Jr. *Ind. Eng. Chem. Res.* 1991, 30, 1478. (b) Narayan, R.; Antal, M. J., Jr. *J. Am. Chem. Soc.* 1990, 112, 1927. (c) Xu, X.; DeAlmeida, C.; Antal, M. J., Jr. *J. Supercrit. Fluids* 1990, 3, 228. (d) West, M. A. B.; Gray, M. R. *Can. J. Chem. Eng.* 1987, 65, 645.

COUPLEDDID NOT COUPLE

**Figure 1.** Potential alkene synthons examined in the Heck coupling reaction in superheated water.

2-phenylethane and 2-phenylethyl acetate initially reacted by forming 2-phenylethanol via substitution or hydrolysis, respectively. Consequently, significant amounts of 2-phenylethanol were observed in the bromide and acetate reaction mixtures. The formation of 2-phenylethanol from both the phenylethyl bromide and acetate was also shown to occur in the absence of iodobenzene. Hydrolysis of the acetate was much slower than substitution of the bromide, thus the acetate required approximately twice the amount of time to produce coupled products. Increasing the acidity of the reaction mixture favored dehydration of the 2-phenylethanol.

**Vinyl Bromide Derivatives.** Vinyl species are reported to be very active at coupling to iodobenzene in normal organic solvent systems.<sup>5</sup> We therefore examined a series of functionalized vinyl derivatives in the superheated water coupling system. 1,2-Dibromoethane and 1-bromo-2-chloroethane each underwent coupling with loss of both functional groups to yield ethylbenzene and styrene (eq 3). Further coupling of the styrene with



iodobenzene to yield *trans*-stilbene was also observed.

However, neither 2-bromoethanol nor 1-bromoethane underwent coupling to iodobenzene under these SW conditions. 2-Bromoethyl acetate yielded a small amount of coupled products, but primarily it hydrolyzed to form 2-bromoethanol.

The active vinyl synthons underwent dehydrobromination to yield a substituted ethylene which then coupled to the iodobenzene prior to losing the second functional group. Evidence for this pathway includes the observation of rapid coupling by vinyl acetate under SW conditions and the complete lack of coupling by 1-bromoethane. Furthermore, under these conditions, 2-bromoethanol clearly underwent dehydrobromination, yielding large amounts of acetaldehyde. An alternative activation mechanism, involving substitution or hydrolysis of either functional group to form the respective alcohols followed by dehydration, is unlikely due to the lack of coupling observed with standards of these alcohols (2-bromoethanol, ethylene glycol monoacetate, and 2-chloroethanol).

**Vinyl Alcohol Derivatives.** Many vinyl alcohol derivatives (especially ethanol) are inexpensive and readily available, which makes them particularly desirable as alkene synthons. However, no coupling was observed after 20 min at 260 °C with ethanol, 2-chloroethanol, 2-chloroethyl acetate, ethylene glycol, ethylene glycol monoacetate, or ethylene glycol diacetate. Except for hydrolysis of the acetate groups, the substrates were recovered essentially unchanged from the reaction mixtures. This lack of coupling is attributed to a relative inertness of the alcohol group to dehydration under these conditions. (2-Phenylethanol is an exception, due to its activation by the phenyl ring.) Therefore, other means of activating alcohol derivatives will be explored, including running the reactions under harsher supercritical water (400 °C) conditions and adding specific dehydration catalysts.

### Summary

The set of substrates known to undergo Heck coupling with iodobenzene has been expanded to include  $\beta$ -derivatized phenylethyl and bromoethyl compounds. These substrates, called alkene synthons, generated alkene derivatives *in situ* in superheated (260 °C) water. The phenyl derivatives lost their second functional group to yield styrene, while the ethyl bromide derivatives underwent dehydrobromination to form their respective vinyl derivatives. These alkenes then coupled to iodobenzene. 2-Bromoethanol was an exception in that it formed vinyl alcohol which tautomerized to acetaldehyde instead of coupling. Alcohol derivatives without a bromide or phenyl substituent present are highly desirable as synthons. However, such alcohols proved generally inert under the mild conditions used in this study and did not dehydrate to form alkenes or undergo coupling.

### Experimental Section

Water was distilled from basic potassium permanganate. The reaction vessel consisted of coned and threaded 316SS

(5) (a) Heck, R. F. *Palladium Reagents in Organic Syntheses*; Academic Press: New York, 1985. (b) Colquhoun, H. M.; Holton, J.; Thompson, D. J.; Twigg, M. V. *New Pathways for Organic Synthesis*; Plenum Press: New York, 1984. (c) Davies, S. G. *Organotransition Metal Chemistry: Applications to Organic Synthesis*; Pergamon: New York, 1982. (d) Tsuji, J. *Organic Synthesis with Palladium Compounds*; Springer-Verlag: New York, 1980.



tubes, each fitted with an end cap, a valve, and a thermocouple. All parts were rated to 20 000 psi or greater and are commercially available from HiP.

**Reactions.** Substrates (1.0 mmol each) and water (3.5 mL) were placed in the reactor along with either Pd(OAc)<sub>2</sub> (0.1 mmol) and NaOAc (1.0 mmol) or PdCl<sub>2</sub> (0.1 mmol). Diphenylmethane (0.1 mmol) was added as an internal standard. The reactor was then sealed and placed in a tube furnace at a set temperature of 375 °C for 20–40 min. Monitoring the reaction by means of a thermocouple within the reactor showed a final temperature of 260 °C. After the designated time period, the reactor was cooled under a stream of water and the contents

were removed. The mixture was placed in a separatory funnel, and the organic layer was separated and dissolved in CDCl<sub>3</sub>. The water layer was extracted with CDCl<sub>3</sub>, and NMR spectra of both the water extract and the organic layer were obtained. Occasional reactions were also run in D<sub>2</sub>O, and the water layer was analyzed directly.

**Acknowledgment.** Support of this research by the EPA–EPSCoR program and by NSF (CHE-9403546) is gratefully acknowledged.

OM950317L

# [Al<sub>5</sub>(<sup>t</sup>Bu)<sub>5</sub>(μ<sub>3</sub>-O)<sub>2</sub>(μ<sub>3</sub>-OH)<sub>2</sub>(μ-OH)<sub>2</sub>(μ-O<sub>2</sub>CPh)<sub>2</sub>]: A Model for the Interaction of Carboxylic Acids with Boehmite

Yoshihiro Koide and Andrew R. Barron\*

Department of Chemistry, Harvard University, Cambridge, Massachusetts 02138

Received March 20, 1995<sup>⊗</sup>

**Summary:** Reaction of [(<sup>t</sup>Bu)Al(μ<sub>3</sub>-O)]<sub>6</sub> with benzoic acid affords the structurally characterized pentaaluminum compound [Al<sub>5</sub>(<sup>t</sup>Bu)<sub>5</sub>(μ<sub>3</sub>-O)<sub>2</sub>(μ<sub>3</sub>-OH)<sub>2</sub>(μ-OH)<sub>2</sub>(μ-O<sub>2</sub>CPh)<sub>2</sub>], in which the aluminums are five-coordinate and the benzoate ligands act as handles to the "basket" structure derived from the structure of [Al<sub>6</sub>(<sup>t</sup>Bu)<sub>6</sub>(μ<sub>3</sub>-O)<sub>4</sub>(μ<sub>3</sub>-OH)<sub>4</sub>]. The binding interaction between the benzoates is discussed with respect to the proposed interaction between carboxylates and an Al<sub>5</sub> fragment of the mineral boehmite, [Al(O)(OH)]<sub>n</sub>, and the benzoate alumoxane, [Al(O)<sub>x</sub>(OH)<sub>y</sub>(μ-O<sub>2</sub>CPh)<sub>z</sub>]<sub>n</sub>.

Recent work from this laboratory has been aimed at redefining the structural view of alumoxanes.<sup>1</sup> In place of the traditional chain or ring structure we have demonstrated that alumoxanes are three-dimensional cage compounds. Alkyl-substituted alumoxanes, [RAl(O)]<sub>n</sub>, have cage structures,<sup>2,3</sup> while alumoxanes with siloxide and carboxylate substituents, [Al(O)(OH)<sub>x</sub>(X)<sub>1-x</sub>]<sub>n</sub> (X = OR, OSiR<sub>3</sub>, O<sub>2</sub>CR), consist of an aluminum–oxygen core structure (I) with the organic substituents positioned on the periphery.<sup>4–6</sup> The Al–O core of the siloxide- and carboxylate-substituted alumoxanes is analogous to that found in the mineral boehmite, [Al(O)(OH)]<sub>n</sub>. On the basis of our knowledge of the boehmite-like core structure of hydrolytically stable alumoxanes, we proposed that alumoxanes should be readily prepared directly from the mineral boehmite. Such a "top-down" approach represents a departure from the traditional synthetic methodologies and was demonstrated for the carboxylate-substituted alumoxanes.<sup>7</sup>

Alumoxanes of the general formula [Al(O)<sub>x</sub>(OH)<sub>y</sub>(O<sub>2</sub>CR)<sub>z</sub>]<sub>n</sub> were prepared by refluxing boehmite, [Al(O)(OH)]<sub>n</sub>, with carboxylic acids under appropriate conditions.<sup>7</sup> These carboxylate alumoxanes were shown by SEM, TEM, and <sup>27</sup>Al NMR spectroscopy to consist of tiny particles (less than 0.1 μm in diameter) of boehmite. From <sup>13</sup>C NMR and IR spectroscopy, bridging carboxylate groups were proposed to encapsulate this boehmite-like core (i.e., II).<sup>7</sup>

In an effort to provide definitive evidence for the mode

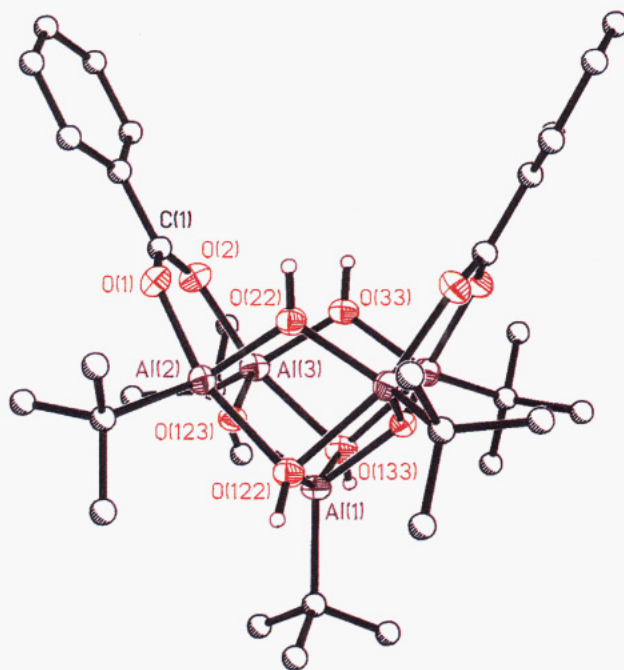
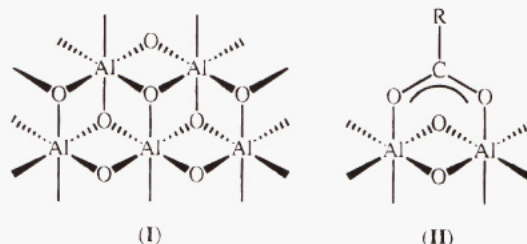


**Figure 1.** Molecular structure of [Al<sub>5</sub>(<sup>t</sup>Bu)<sub>5</sub>(μ<sub>3</sub>-O)<sub>2</sub>(μ<sub>3</sub>-OH)<sub>2</sub>(μ-OH)<sub>2</sub>(μ-O<sub>2</sub>CPh)<sub>2</sub>]. Thermal ellipsoids are drawn at the 30% level. The carbon atoms are shown as shaded spheres, and the organic hydrogen atoms are omitted for clarity. Aluminum and oxygen atoms are shown in purple and red, respectively.



of binding of a carboxylate to the surface of boehmite, we have investigated the synthesis and crystallographic characterization of low-molecular-weight carboxylate alumoxanes. As part of this study we have examined the reaction of [(<sup>t</sup>Bu)Al(μ<sub>3</sub>-O)]<sub>6</sub> with benzoic acid, and the results are presented herein.

## Results and Discussion

The reaction of [(<sup>t</sup>Bu)Al(μ<sub>3</sub>-O)]<sub>6</sub> with 1 molar equiv of benzoic acid allows for the isolation, upon recrystallization from acetonitrile, of a modest yield of the pentaaluminum compound [Al<sub>5</sub>(<sup>t</sup>Bu)<sub>5</sub>(μ<sub>3</sub>-O)<sub>2</sub>(μ<sub>3</sub>-OH)<sub>2</sub>(μ-OH)<sub>2</sub>(μ-O<sub>2</sub>CPh)<sub>2</sub>]·MeCN, the structure of which has been determined by X-ray crystallography and is wholly consistent with the <sup>1</sup>H and <sup>13</sup>C NMR and IR spectra.

The molecular structure of [Al<sub>5</sub>(<sup>t</sup>Bu)<sub>5</sub>(μ<sub>3</sub>-O)<sub>2</sub>(μ<sub>3</sub>-OH)<sub>2</sub>(μ-OH)<sub>2</sub>(μ-O<sub>2</sub>CPh)<sub>2</sub>] is shown in Figure 1; selected bond

\* To whom correspondence should be addressed at the Chemistry Department, Rice University, Houston, TX 77251.

⊗ Abstract published in *Advance ACS Abstracts*, June 15, 1995.

(1) The term alumoxane is often given to aluminum oxide macromolecules formed by the hydrolysis of aluminum compounds or salts, AlX<sub>3</sub> where X = R, OR, OSiR<sub>3</sub> or O<sub>2</sub>CR. See: Pasynkiewicz, S. *Polyhedron* **1990**, *9*, 429.

(2) Mason, M. R.; Smith, J. M.; Bott, S. G.; Barron, A. R. *J. Am. Chem. Soc.* **1993**, *116*, 4971.

(3) Harlan, C. J.; Mason, M. R.; Barron, A. R. *Organometallics* **1994**, *13*, 2957.

(4) Apblett, A. W.; Warren, A. C.; Barron, A. R. *Chem. Mater.* **1992**, *4*, 167.

(5) Landry, C. C.; Davis, J. A.; Apblett, A. W.; Barron, A. R. *J. Mater. Chem.* **1993**, *3*, 597.

(6) Apblett, A. W.; Barron, A. R. *Ceram. Trans.* **1991**, *35*.

(7) Landry, C. C.; Pappé, N.; Mason, M. R.; Apblett, A. W.; Tyler, A. N.; MacInnes, A. N.; Barron, A. R. *J. Mater. Chem.* **1995**, *5*, 331.



**Table 1. Selected Bond Lengths (Å) and Angles (deg) for****[Al<sub>5</sub>(<sup>t</sup>Bu)<sub>5</sub>(μ<sub>3</sub>-O)<sub>2</sub>(μ<sub>3</sub>-OH)<sub>2</sub>(μ-OH)<sub>2</sub>(μ-O<sub>2</sub>CPh)<sub>2</sub>]-MeCN**

Al(1)-O(122)	1.914(5)	Al(1)-O(123)	1.827(3)
Al(1)-O(133)	1.928(5)	Al(1)-C(11)	1.965(9)
Al(2)-O(122)	2.086(4)	Al(2)-O(123)	1.785(4)
Al(2)-O(22)	1.820(3)	Al(2)-C(21)	1.972(6)
Al(2)-O(1)	1.895(4)	Al(3)-O(123)	1.792(4)
Al(3)-O(33)	1.828(3)	Al(3)-O(133)	2.085(4)
Al(3)-C(31)	1.958(7)	Al(3)-O(2)	1.888(4)
O(1)-C(1)	1.267(7)	O(2)-C(1)	1.249(7)
O(122)-Al(1)-O(123)	82.2(2)	O(122)-Al(1)-O(133)	152.8(2)
O(123)-Al(1)-O(133)	81.3(2)	O(122)-Al(1)-C(11)	103.2(3)
O(123)-Al(1)-C(11)	127.6(1)	O(133)-Al(1)-C(11)	104.0(3)
O(122)-Al(2)-O(123)	78.6(2)	O(122)-Al(2)-O(22)	75.6(2)
O(123)-Al(2)-O(22)	108.3(2)	O(122)-Al(2)-C(21)	98.1(2)
O(123)-Al(2)-C(21)	127.1(2)	O(22)-Al(2)-C(21)	122.1(2)
O(122)-Al(2)-O(1)	162.5(2)	O(123)-Al(2)-O(1)	96.3(2)
O(22)-Al(2)-O(1)	90.5(2)	C(21)-Al(2)-O(1)	98.3(2)
O(123)-Al(3)-O(33)	109.4(2)	O(123)-Al(3)-O(133)	77.9(2)
O(33)-Al(3)-O(133)	75.5(2)	O(123)-Al(3)-C(31)	126.9(2)
O(33)-Al(3)-C(31)	121.2(3)	O(133)-Al(3)-C(31)	99.1(2)
O(123)-Al(3)-O(2)	97.3(2)	O(33)-Al(3)-O(2)	90.2(2)
O(133)-Al(3)-O(2)	162.1(2)	C(31)-Al(3)-O(2)	97.5(2)
Al(1)-O(122)-Al(2)	92.2(2)	Al(1)-O(123)-Al(2)	106.1(2)
Al(1)-O(123)-Al(3)	107.1(2)	Al(2)-O(123)-Al(3)	130.0(2)
Al(1)-O(133)-Al(3)	92.9(2)	Al(2)-O(1)-C(1)	134.2(4)
Al(3)-O(2)-C(1)	133.5(4)	O(1)-C(1)-O(2)	123.7(5)
O(1)-C(1)-C(2)	118.3(5)	O(2)-C(1)-C(2)	118.0(5)

lengths and angles are given in Table 1. A molecule of acetonitrile is found to cocrystallize with [Al<sub>5</sub>(<sup>t</sup>Bu)<sub>5</sub>(μ<sub>3</sub>-O)<sub>2</sub>(μ<sub>3</sub>-OH)<sub>2</sub>(μ-OH)<sub>2</sub>(μ-O<sub>2</sub>CPh)<sub>2</sub>] and is situated between the outstretched arms of the two carboxylate groups, pointing towards the Al<sub>5</sub> cage; however, the N···H-O distances are outside of those expected for hydrogen-bonding interactions. The overall molecular structure of [Al<sub>5</sub>(<sup>t</sup>Bu)<sub>5</sub>(μ<sub>3</sub>-O)<sub>2</sub>(μ<sub>3</sub>-OH)<sub>2</sub>(μ-OH)<sub>2</sub>(μ-O<sub>2</sub>CPh)<sub>2</sub>], as shown in Figure 1, may best be considered as an inverted square-based pyramid of aluminum atoms. The atoms Al(1), O(122), and O(133) are positioned on a crystallographic mirror plane. Each of the opposing triangular faces of the square-based pyramid are capped by either an oxide (O(123)) or hydroxide (O(122) and O(133)) oxygen, and the opposing edges of the square base are bridged by either a hydroxide oxygen (O(22) and O(33)) or a benzoate. All the aluminums are in distorted-trigonal-bipyramidal geometries, with Al(1) being the more distorted: O(122)-Al(1)-O(133) = 152.8(2)° versus O(122)-Al(2)-O(1) = 162.5(2)° and O(133)-Al(3)-O(2) = 162.1(2)°. The cage Al-O bond distances range from 1.785(4) to 2.086(4) Å, while those to the oxide ligands are at the short end of the range (1.785(4)-1.827(3) Å) and those to the hydroxide groups are the longest (1.823(3)-2.086(4) Å). As would be expected, the longest Al-O distances are to the capping hydroxides (O(122) and O(133)), which are situated axially with respect to each of the aluminum centers. The Al-O bonds to the benzoate ligands are within experimental error (Al(2)-O(1) = 1.895(4) Å and Al(3)-O(2) = 1.888(4) Å), as are the carboxylate's O-C bonds (O(1)-C(1) = 1.267(7), O(2)-C(1) = 1.249(7) Å), indicative of a symmetrically bound acid group.

As can be seen from Figure 2, the Al<sub>5</sub> cage structure of [Al<sub>5</sub>(<sup>t</sup>Bu)<sub>5</sub>(μ<sub>3</sub>-O)<sub>2</sub>(μ<sub>3</sub>-OH)<sub>2</sub>(μ-OH)<sub>2</sub>(μ-O<sub>2</sub>CPh)<sub>2</sub>] is clearly derived from that of [Al<sub>6</sub>(<sup>t</sup>Bu)<sub>6</sub>(μ<sub>3</sub>-O)<sub>4</sub>(μ<sub>3</sub>-OH)<sub>4</sub>], previously reported by us.<sup>8</sup> In fact, on the basis of the

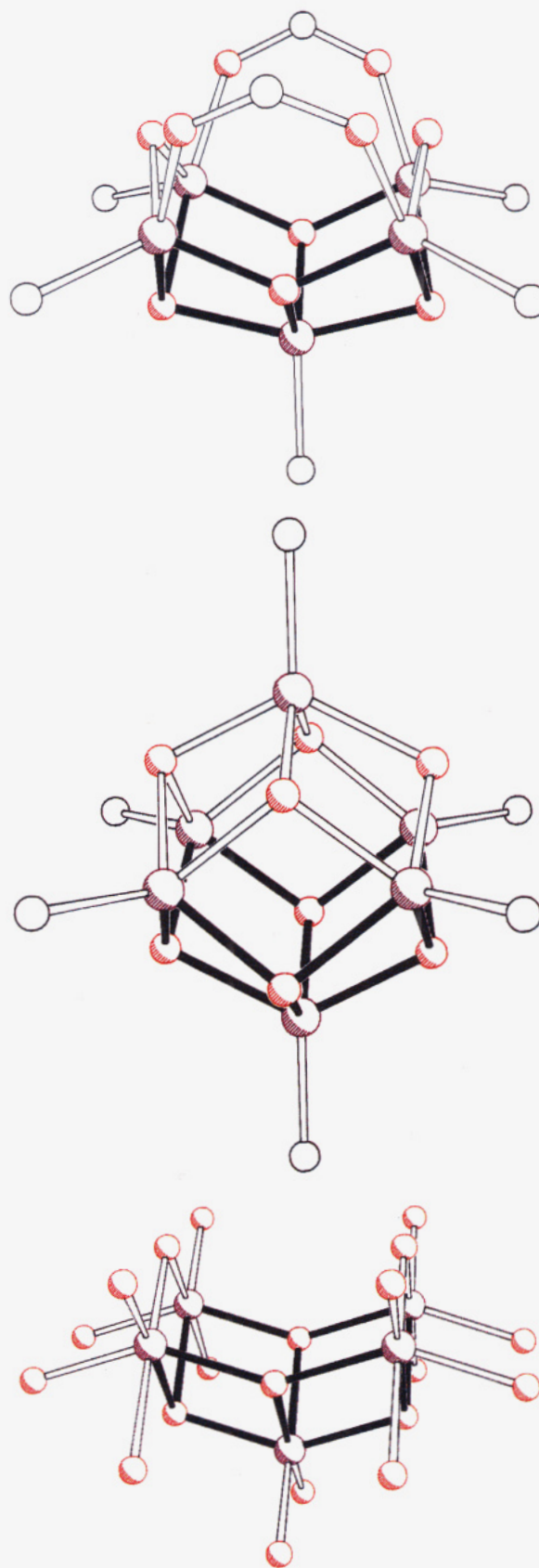
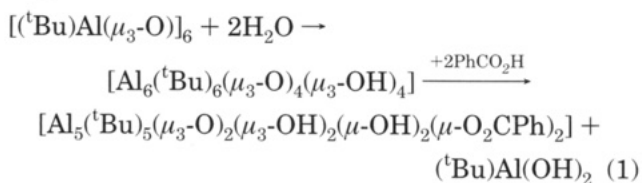


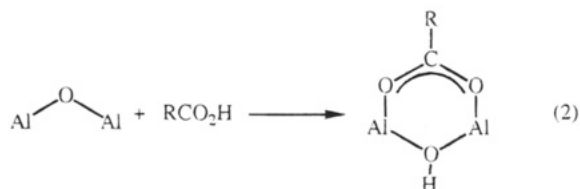
**Figure 2.** Core structures of [Al<sub>5</sub>(<sup>t</sup>Bu)<sub>5</sub>(μ<sub>3</sub>-O)<sub>2</sub>(μ<sub>3</sub>-OH)<sub>2</sub>(μ-OH)<sub>2</sub>(μ-O<sub>2</sub>CPh)<sub>2</sub>] (top), [Al<sub>6</sub>(<sup>t</sup>Bu)<sub>6</sub>(μ<sub>3</sub>-O)<sub>4</sub>(μ<sub>3</sub>-OH)<sub>4</sub>] (middle), and a fragment of boehmite, [Al(O)(OH)<sub>n</sub>] (bottom). The solid lines represent the common structural fragments present in each. Aluminum and oxygen atoms are shown in purple and red, respectively.

(8) Landry, C. C.; Harlan, C. J.; Bott, S. G.; Barron, A. R. *Angew. Chem., Int. Ed. Engl.* **1995**, *34*, 1199.

presence of traces of water in the benzoic acid,<sup>9</sup> and this structural relationship, a balanced equation for the formation of  $[\text{Al}_5(\text{}^t\text{Bu})_5(\mu_3\text{-O})_2(\mu_3\text{-OH})_2(\mu\text{-OH})_2(\mu\text{-O}_2\text{CPh})_2]$  may be written:



The reaction of a carboxylic acid with an oxo ligand to give an aluminum carboxylate and new hydroxide group *via* the protonation of an oxo ligand (eq 2) has been previously postulated.<sup>7</sup>



We have previously proposed that carboxylate groups exist as bridging ligands on the surface of boehmite.<sup>7</sup> The presence of bands in the IR spectra at 1596–1586 and 1473–1466  $\text{cm}^{-1}$  for  $[\text{Al}(\text{O})_x(\text{OH})_y(\mu\text{-O}_2\text{CR})_z]_n$ , and their similarity to those observed for  $[\text{Me}_2\text{Al}(\mu\text{-O}_2\text{CR})]_2$  (1546–1550 and 1480–1485  $\text{cm}^{-1}$ ) suggested the presence of bridging carboxylate groups.<sup>10</sup> Similarly, the IR spectrum of  $[\text{Al}_5(\text{}^t\text{Bu})_5(\mu_3\text{-O})_2(\mu_3\text{-OH})_2(\mu\text{-OH})_2(\mu\text{-O}_2\text{CPh})_2]$  shows bands at 1569 and 1496  $\text{cm}^{-1}$ , identical with those observed for  $[\text{Al}(\text{O})_x(\text{OH})_y(\mu\text{-O}_2\text{CPh})_z]_n$  (see Experimental Section), confirming the presence of bridging carboxylate moieties. In addition, the <sup>13</sup>C NMR spectral shift of the carboxylate  $\alpha$ -carbon ( $\text{O}_2\text{CR}$ ) were found to be similar for  $[\text{Al}(\text{O})_x(\text{OH})_y(\mu\text{-O}_2\text{CR})_z]_n$  and  $[\text{Me}_2\text{Al}(\mu\text{-O}_2\text{CR})]_2$ ,<sup>7</sup> and a similar correlation is observed for  $[\text{Al}_5(\text{}^t\text{Bu})_5(\mu_3\text{-O})_2(\mu_3\text{-OH})_2(\mu\text{-OH})_2(\mu\text{-O}_2\text{CPh})_2]$  and  $[\text{Al}(\text{O})_x(\text{OH})_y(\mu\text{-O}_2\text{CPh})_z]_n$ .

While the presence of bridging carboxylate groups in carboxylate alumoxanes is spectroscopically unambiguous, our proposal that the carboxylate would bridge adjacent edge-shared octahedra (see Scheme 1), had no structural precedent. However, as is clear from Figure 2, such a structure is indeed possible, since  $[\text{Al}_5(\text{}^t\text{Bu})_5(\mu_3\text{-O})_2(\mu_3\text{-OH})_2(\mu\text{-OH})_2(\mu\text{-O}_2\text{CPh})_2]$  is related to an  $\text{Al}_5$  section of boehmite, and the binding of the carboxylate is across the face as shown in Scheme 1. Thus,  $[\text{Al}_5(\text{}^t\text{Bu})_5(\mu_3\text{-O})_2(\mu_3\text{-OH})_2(\mu\text{-OH})_2(\mu\text{-O}_2\text{CPh})_2]$  represents the first crystallographic evidence for the binding of carboxylic acids to the surface of boehmite.

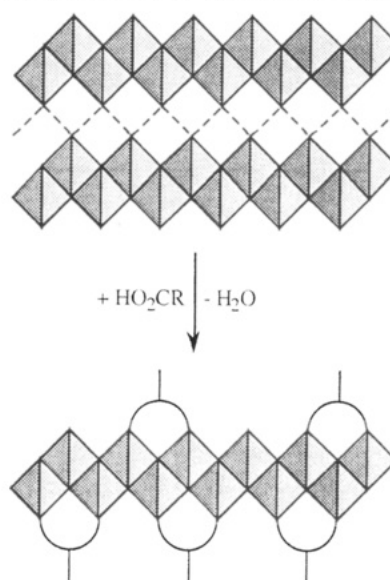
### Experimental Section

Mass spectra were obtained on a JEOL AX-505 H mass spectrometer operating with an electron beam

(9) The synthesis of  $[\text{Al}_5(\text{}^t\text{Bu})_5(\mu_3\text{-O})_2(\mu_3\text{-OH})_2(\mu\text{-OH})_2(\mu\text{-O}_2\text{CPh})_2]$  was repeated after the benzoic acid was doubly sublimed with no change in the product observed. Thermogravimetric measurements indicate that, despite sublimation, the benzoic acid was still "wet".

(10) Although aluminum carboxylate compounds,  $\text{Al}(\text{O}_2\text{CR})_3$ , and carboxylate alumoxanes have been proposed to contain chelating carboxylate groups, there has been no evidence for this mode of coordination to aluminum. In fact, our study of 1,3-diphenyltriazene complexes of aluminum, gallium, and indium, where the triazenes are exclusively chelating, has indicated that this mode is unavailable for carboxylates on aluminum, due to the ring strain which would be present in such a structure; see: Leman, J. T.; Braddock-Wilking, J.; Coolong, A. J.; Barron, A. R. *Inorg. Chem.* **1993**, *32*, 4324.

**Scheme 1. Pictorial Representation of the Reaction of Boehmite with Carboxylic Acids<sup>a</sup>**



<sup>a</sup> The shaded triangles represent a side view of the aluminum-oxygen fused octahedra, while the carboxylate groups are represented by a semicircle and bar.

energy of 70 eV for EI mass spectra. Infrared spectra (4000–400  $\text{cm}^{-1}$ ) were obtained using a Bio-Rad FTIR spectrometer; samples were prepared as mulls on KBr plates. <sup>1</sup>H and <sup>13</sup>C NMR spectra were obtained on a Bruker AM-400 spectrometer using  $\text{CDCl}_3$  solutions. Chemical shifts are reported relative to external TMS. Melting points were determined in sealed capillaries and are uncorrected. All procedures were performed under purified nitrogen. Solvents were distilled and degassed prior to use.  $[(\text{}^t\text{Bu})\text{Al}(\mu_3\text{-O})]_6$  was prepared as previously reported.<sup>2</sup> Research grade pseudo-boehmite (100%) was kindly provided by American Cyanamid.

$[\text{Al}_5(\text{}^t\text{Bu})_5(\mu_3\text{-O})_2(\mu_3\text{-OH})_2(\mu\text{-OH})_2(\mu\text{-O}_2\text{CPh})_2] \cdot \text{MeCN}$ . To  $[(\text{}^t\text{Bu})\text{Al}(\mu_3\text{-O})]_6$  (100 mg, 0.16 mmol) in hexane (2 mL) was added  $\text{HO}_2\text{CPh}$  (20 mg, 0.16 mmol) in hexane (5 mL). The solution was stirred vigorously for 10 min, at which point a white precipitate was formed. The volume of the solution was reduced by half, and the solution was allowed to stand in a freezer ( $-24^\circ\text{C}$ ) for 2 h. The resulting white precipitate was collected by filtration and recrystallized from  $\text{CH}_3\text{CN}$ ; yield ca. 40%; mp  $> 330^\circ\text{C}$  dec. MS (EI;  $m/z$  (%)): 705 ( $\text{M}^+ - \text{}^t\text{Bu}$ , 18).  $\mu\text{IR}$  ( $\text{cm}^{-1}$ ): 1569 (s), 1496 (w), 932 (w), 818 (m), 721 (m), 669 (m), 540 (m). <sup>1</sup>H NMR:  $\delta$  8.08 [4H, dd,  $J(\text{H-H}) = 8.0$  Hz,  $J(\text{H-H}) = 1.3$  Hz, *o-CH*], 7.58 [2H, dt,  $J(\text{H-H}) = 7.9$  Hz,  $J(\text{H-H}) = 1.3$  Hz, *p-CH*], 7.44 [4H, dd,  $J(\text{H-H}) = 8.0$  Hz,  $J(\text{H-H}) = 7.9$  Hz, *m-CH*], 3.67 (2H, s,  $\mu_3\text{-OH}$ ), 2.42 (2H, s,  $\mu\text{-OH}$ ), 1.00 [9H, s,  $\text{C}(\text{CH}_3)$ ], 0.97 [36H, s,  $\text{C}(\text{CH}_3)$ ]. <sup>13</sup>C NMR ( $\text{CDCl}_3$ ):  $\delta$  173.1 ( $\text{O}_2\text{CPh}$ ), 134.0, 131.5, 130.8, 128.6 ( $\text{C}_6\text{H}_5$ ), 31.0 [ $\text{C}(\text{CH}_3)$ ], 30.6 [ $\text{C}(\text{CH}_3)$ ].<sup>11</sup>

$[\text{Al}(\text{O})_x(\text{OH})_y(\mu\text{-O}_2\text{CPh})_z]_n$ . Boehmite (1.00 g, 16.7 mmol) and benzoic acid (0.85 g, 7.1 mmol) were refluxed in xylenes (60 mL) for 4 days to yield an off-white suspension. Addition of  $\text{Et}_2\text{O}$  (50 mL) followed by filtration and removal of the volatiles *in vacuo* yielded an off-white solid. IR ( $\text{cm}^{-1}$ ): 1568 (s), 1496 (w), 1067

(11) As is common for *tert*-butylaluminum compounds, the quaternary carbons,  $\text{Al}-\text{C}(\text{CH}_3)_3$ , are not observed due to their long relaxation delay and the quadrupole moment of aluminum.

**Table 2. Summary of X-ray Diffraction Data for  $[\text{Al}_5(\text{tBu})_5(\mu_3\text{-O})_2(\mu_3\text{-OH})_2(\mu\text{-OH})_2(\mu\text{-O}_2\text{CPh})_2]\cdot\text{MeCN}$** 

empirical formula	$\text{C}_{36}\text{H}_{62}\text{Al}_5\text{NO}_{10}$
cryst size, mm	$0.40 \times 0.25 \times 0.28$
cryst syst	orthorhombic
space group	<i>Pnma</i>
<i>a</i> , Å	20.533(8)
<i>b</i> , Å	21.533(8)
<i>c</i> , Å	10.610(6)
<i>V</i> , Å <sup>3</sup>	4696(9)
<i>Z</i>	4
<i>D</i> (calcd), g cm <sup>-3</sup>	1.137
$\mu$ , mm <sup>-1</sup>	0.165
radiation	Mo K $\alpha$ ( $\lambda = 0.71073$ Å), graphite monochromator
temp, K	298
$2\theta$ range, deg	4.0–40.0
no. of the collected	4269
no. of indep data	2275
no. of obsd data	1642 ( $ F_o  > 5.0\sigma F_o $ )
weighting scheme	$w^{-1} = \sigma^2( F_o )$
<i>R</i>	0.0498
<i>R<sub>w</sub></i>	0.0498
largest diff peak, e Å <sup>-3</sup>	0.33

(w), 1000 (m), 721 (s) 682 (w), 626 (w), 549 (m). <sup>13</sup>C CP-MAS NMR:  $\delta$  172.8 (O<sub>2</sub>CPh), 133.1, 131.1, 128.0, 126.0 (C<sub>6</sub>H<sub>5</sub>).

**Crystallographic Studies.** A crystal was mounted in a glass capillary attached to the goniometer head of a Nicolet R3m/V four-circle diffractometer. Data collection and unit cell and space group determination were all carried out in a manner previously described in detail.<sup>12</sup> The structures were solved using the direct methods program XS,<sup>13</sup> which readily revealed the positions of the Al and O and some of the C atoms. Subsequent difference Fourier maps revealed the position of all of the non-hydrogen atoms for  $[\text{Al}_5(\text{tBu})_5(\mu_3\text{-O})_2(\mu_3\text{-OH})_2(\mu\text{-OH})_2(\mu\text{-O}_2\text{CPh})_2]$ . After all of the non-hydrogen atoms were located and refined anisotropically, the *R* factor remained high; however, a difference map revealed three peaks consistent with a MeCN of crystallization. Subsequently, full refinement was successful. All the hydrogen atoms were placed in calculated positions ( $U_{\text{iso}} = 0.08$ ;  $d(\text{C-H}) = 0.96$  Å) for refinement. Neutral-atom scattering factors were taken from the usual source.<sup>14</sup> Refinement of positional and anisotropic thermal parameters led to convergence (see Table

(12) Healy, M. D.; Wierda, D. A.; Barron, A. R. *Organometallics* **1988**, *7*, 2543.

(13) Nicolet Instruments Corp., Madison, WI, 1988.

(14) *International Tables for X-Ray Crystallography*; Kynoch Press: Birmingham, U.K., 1974; Vol. 4.

**Table 3. Atomic Coordinates ( $\times 10^4$ ) and Equivalent Isotropic Thermal Parameters ( $\text{Å}^2 \times 10^3$ ) for  $[\text{Al}_5(\text{tBu})_5(\mu_3\text{-O})_2(\mu_3\text{-OH})_2(\mu\text{-OH})_2(\mu\text{-O}_2\text{CPh})_2]\cdot\text{MeCN}$** 

	<i>x</i>	<i>y</i>	<i>z</i>	$U_{\text{eq}}^a$
Al(1)	4366(1)	2500	-2357(2)	54(1)
Al(2)	4653(1)	3202(1)	-108(2)	53(1)
Al(3)	5570(1)	3203(1)	-2594(2)	57(1)
O(122)	4019(2)	2500	-682(4)	57(2)
O(123)	4812(1)	3172(1)	-1760(3)	51(1)
O(22)	4979(2)	2500	610(4)	52(2)
O(33)	6039(2)	2500	-2262(4)	56(2)
O(133)	5075(2)	2500	-3548(4)	61(2)
C(11)	3583(4)	2500	-3422(8)	75(4)
C(12)	2963(5)	2500	-2788(12)	271(14)
C(13)	3566(5)	3019(5)	-4259(12)	322(9)
C(21)	4012(3)	3732(3)	762(6)	70(3)
C(22)	4175(4)	4400(3)	606(11)	196(6)
C(23)	3321(4)	3650(5)	369(9)	200(6)
C(24)	4038(5)	3609(5)	2140(7)	187(6)
C(31)	5785(3)	3736(3)	-4030(6)	87(3)
C(32)	5485(5)	3577(5)	-5244(7)	218(7)
C(33)	5593(6)	4388(4)	-3759(10)	234(8)
C(34)	6521(4)	3761(5)	-4225(9)	199(6)
O(1)	5417(2)	3644(2)	336(3)	64(1)
O(2)	6049(2)	3638(2)	-1359(4)	65(2)
C(1)	5940(3)	3776(3)	-235(6)	57(2)
C(2)	6453(3)	4112(3)	466(6)	61(2)
C(3)	6324(4)	4334(3)	1651(6)	89(3)
C(4)	6809(5)	4636(3)	2317(7)	112(4)
C(5)	7408(5)	4722(3)	1794(8)	110(4)
C(6)	7543(3)	4510(3)	610(8)	96(3)
C(7)	7062(3)	4200(3)	-55(6)	78(3)
N(10)	6491(5)	2500	614(12)	146(6)
C(10)	6807(6)	2500	1463(15)	129(7)
C(20)	7242(7)	2500	2467(14)	336(18)

<sup>a</sup> Equivalent isotropic  $U_{\text{eq}}$ , defined as one-third of the trace of the orthogonalized  $U_{ij}$  tensor.

2). Final atomic positional parameters are given in Table 3.

**Acknowledgment.** Financial support for this work was provided by the Office of Naval Research. We gratefully acknowledge the assistance of Dr. Andrew N. Tyler (Harvard University) and Dr. Janet Braddock-Wilking (University of Missouri at St. Louis) with mass spectroscopic and CP-MAS NMR measurements, respectively.

**Supporting Information Available:** Full listings of bond lengths and angles, anisotropic thermal parameters, and hydrogen atom parameters (4 pages). Ordering information is given on any current masthead page.

OM950201P



# Additions and Corrections

---

1994, Volume 13

**Jianwei Ho, Roger Rousseau, and Douglas W. Stephan\***: Synthesis, Structure and Bonding in Zirconocene Primary Phosphido (PHR<sup>-</sup>), Phosphinidene (PR<sup>2-</sup>), and Phosphide (P<sup>3-</sup>) Derivatives.

Page 1918. One of the compounds reported in this paper is Cp<sub>2</sub>Zr(PH(2,4,6-C<sub>6</sub>H<sub>2</sub>Me<sub>3</sub>))Cl. The synthesis, structure, and some related reactivity were described. In fact, an earlier report of the preparation of this compound had appeared and was overlooked in the references (Hey, E.; Muller, U. *Z. Naturforsch.* **1989**, *44B*, 1538). In addition, we erroneously reported the <sup>31</sup>P chemical shift as 43.0 ppm; the chemical shift is -4.3 ppm in THF. The chemical shift of -5.7 ppm ( $|J_{P-H}| = 230$  Hz) in benzene was reported earlier by Hey and Muller.

OM950423N

**James D. Fisher, Ming-Yi Wei, Roger Willett, and Pamela J. Shapiro\***: Synthesis and Structural Characterization of Dicyclopentadienylaluminum Alkyl and Tricyclopentadienylaluminum Compounds: Crystal Structure of a Bis( $\eta^2$ -cyclopentadienyl)aluminum Alkyl Compound.

Pages 3328-3329. The <sup>27</sup>Al chemical shifts of compounds **2**, **4**, and **5** were misassigned. The correct values are  $\delta$  52 for compound **2**,  $\delta$  118 for compound **4**, and  $\delta$  110 for compound **5**.

OM950402T

1995, Volume 14

**Euro Solari, Fabrizio Musso, Emma Gallo, Carlo Floriani,\* Nazzareno Re, Angiola Chiesi-Villa, and Corrado Rizzoli**: Cationic Arylmanganese(II) Derivatives Occurring in Ion-Pair Forms with Tetraphenylborate Anions: Synthetic, Structural, and Magnetic Studies.

Page 2274. In the second paragraph in the Experimental Section, regarding the synthesis of **1**, the second line should read "...was added to a THF (500 mL) suspension of...".

OM950433O

# Additions and Corrections

---

1994, Volume 13

**Jianwei Ho, Roger Rousseau, and Douglas W. Stephan\***: Synthesis, Structure and Bonding in Zirconocene Primary Phosphido (PHR<sup>-</sup>), Phosphinidene (PR<sup>2-</sup>), and Phosphide (P<sup>3-</sup>) Derivatives.

Page 1918. One of the compounds reported in this paper is Cp<sub>2</sub>Zr(PH(2,4,6-C<sub>6</sub>H<sub>2</sub>Me<sub>3</sub>))Cl. The synthesis, structure, and some related reactivity were described. In fact, an earlier report of the preparation of this compound had appeared and was overlooked in the references (Hey, E.; Muller, U. *Z. Naturforsch.* **1989**, *44B*, 1538). In addition, we erroneously reported the <sup>31</sup>P chemical shift as 43.0 ppm; the chemical shift is -4.3 ppm in THF. The chemical shift of -5.7 ppm ( $|J_{P-H}| = 230$  Hz) in benzene was reported earlier by Hey and Muller.

OM950423N

**James D. Fisher, Ming-Yi Wei, Roger Willett, and Pamela J. Shapiro\***: Synthesis and Structural Characterization of Dicyclopentadienylaluminum Alkyl and Tricyclopentadienylaluminum Compounds: Crystal Structure of a Bis( $\eta^2$ -cyclopentadienyl)aluminum Alkyl Compound.

Pages 3328-3329. The <sup>27</sup>Al chemical shifts of compounds **2**, **4**, and **5** were misassigned. The correct values are  $\delta$  52 for compound **2**,  $\delta$  118 for compound **4**, and  $\delta$  110 for compound **5**.

OM950402T

1995, Volume 14

**Euro Solari, Fabrizio Musso, Emma Gallo, Carlo Floriani,\* Nazzareno Re, Angiola Chiesi-Villa, and Corrado Rizzoli**: Cationic Arylmanganese(II) Derivatives Occurring in Ion-Pair Forms with Tetraphenylborate Anions: Synthetic, Structural, and Magnetic Studies.

Page 2274. In the second paragraph in the Experimental Section, regarding the synthesis of **1**, the second line should read "...was added to a THF (500 mL) suspension of...".

OM950433O



# Additions and Corrections

---

1994, Volume 13

**Jianwei Ho, Roger Rousseau, and Douglas W. Stephan\***: Synthesis, Structure and Bonding in Zirconocene Primary Phosphido (PHR<sup>-</sup>), Phosphinidene (PR<sup>2-</sup>), and Phosphide (P<sup>3-</sup>) Derivatives.

Page 1918. One of the compounds reported in this paper is Cp<sub>2</sub>Zr(PH(2,4,6-C<sub>6</sub>H<sub>2</sub>Me<sub>3</sub>))Cl. The synthesis, structure, and some related reactivity were described. In fact, an earlier report of the preparation of this compound had appeared and was overlooked in the references (Hey, E.; Muller, U. *Z. Naturforsch.* **1989**, *44B*, 1538). In addition, we erroneously reported the <sup>31</sup>P chemical shift as 43.0 ppm; the chemical shift is -4.3 ppm in THF. The chemical shift of -5.7 ppm ( $|J_{P-H}| = 230$  Hz) in benzene was reported earlier by Hey and Muller.

OM950423N

**James D. Fisher, Ming-Yi Wei, Roger Willett, and Pamela J. Shapiro\***: Synthesis and Structural Characterization of Dicyclopentadienylaluminum Alkyl and Tricyclopentadienylaluminum Compounds: Crystal Structure of a Bis( $\eta^2$ -cyclopentadienyl)aluminum Alkyl Compound.

Pages 3328-3329. The <sup>27</sup>Al chemical shifts of compounds **2**, **4**, and **5** were misassigned. The correct values are  $\delta$  52 for compound **2**,  $\delta$  118 for compound **4**, and  $\delta$  110 for compound **5**.

OM950402T

1995, Volume 14

**Euro Solari, Fabrizio Musso, Emma Gallo, Carlo Floriani,\* Nazzareno Re, Angiola Chiesi-Villa, and Corrado Rizzoli**: Cationic Arylmanganese(II) Derivatives Occurring in Ion-Pair Forms with Tetraphenylborate Anions: Synthetic, Structural, and Magnetic Studies.

Page 2274. In the second paragraph in the Experimental Section, regarding the synthesis of **1**, the second line should read "...was added to a THF (500 mL) suspension of...".

OM950433O